

## New Publishing Arrangement Between AOCs and Springer

Eric J. Murphy

Published online: 13 January 2007  
© AOCs 2007

Dear *Lipids* readers,

This issue marks a major new direction for *Lipids* as AOCs embarks on a joint publishing arrangement with Springer, who is the second largest STM journals publisher in the world. Under the terms of this agreement, AOCs will maintain ownership and content control over *Lipids*, while Springer becomes responsible for production and lends significant marketing resources to promote our journal. At Springer, all marketing activities are tailored to directly reach the various target audiences including readers and authors, libraries and subscription agents. Springer's online platform SpringerLink currently serves 600 international consortia, comprising over 35,000 institutions, thereby enormously boosting the visibility of *Lipids*.

This new arrangement will result in significant upgrades to the electronic delivery of the content of *Lipids*. Springer's Online First capability will ensure speedy availability of articles ahead of your print subscription. Springer will also make the entire legacy content of *Lipids* available back to volume 1, issue #1 in 1966. We will also be implementing the use of the Manuscript Central peer review system, enabling more thorough and rapid communication among the editors of *Lipids* while enhancing the submissions process for contributing authors.

While we embrace modern electronic delivery systems for the content of *Lipids*, we remain dedicated to the science. As such, the *Lipids* editorial team will retain full authority over subject matter, peer review, and final acceptance–revision–rejection status of each submitted

manuscript. We will continue to welcome your submissions via the internet, so please go to <http://www.mc.manuscriptcentral.com/lipids> to submit your latest work.

On behalf of the American Oil Chemists' Society and *Lipids*, I salute this publishing arrangement with Springer. I fully expect that we will continue to fulfill *Lipids*' mandate by offering papers of the highest quality for the lipids research community. While I will maintain the broad emphasis of the Journal, by publishing papers on biochemistry, clinical nutrition, and metabolism, we will have an increasing emphasis on publishing novel methods for use in addressing questions involving lipids. The new invited thematic reviews will add substantially to the Journal, as leading experts will author timely reviews on a particular topic over three to four issues. The first topic is plant lipid biochemistry; future topics will include fatty acid binding proteins, acyl-CoA synthetases, and fatty acid desaturases. Combined, this new arrangement will make *Lipids* a stronger journal and one with a bright future.

Thank you for your interest in *Lipids*. On behalf of our editorial team, we look forward to continuing to provide you with a journal dedicated to publishing quality papers with a broad emphasis in lipid biochemistry.

Sincerely,



Eric J. Murphy  
Editor-in-Chief

E. J. Murphy (✉)  
Grand Forks, USA  
e-mail: emurphy@medicine.nodak.edu

## Recent Advances in Sterol Research

Presented at the 97th AOCs Annual Meeting and Expo in St. Louis, MO, USA,  
May 2006

Edward J. Parish · Robert A. Moreau ·  
Thomas J. Bach · W. David Nes · John R. Williams

Published online: 20 January 2007  
© AOCs 2007

The AOCs has been a regular host to sterol symposia since 1970. The history of this symposium series has been published [Weete JD, Parish EJ, Nes WD (2000) *Lipids* 35:241]. These symposia have focused on current research in the areas of sterol structure, biosynthesis, chemistry, regulation, and function.

The 2006 Sterol Symposium, "Recent advances in sterol research," was held at the AOCs Annual Meeting in Saint Louis, MO, USA. During the symposium, the third G.J. Schroepfer Jr. Award for steroid research was presented. The Award was established to honor the memory of Dr. George J. Schroepfer Jr., a prominent steroid biochemist and chemist who made major and lasting contributions to the steroid field. Much of his research dealt with the biosynthesis of cholesterol and its regulation. In addition, he maintained a strong organic synthesis program to support

his biochemical studies. A biography describing many of Dr. Schroepfer's contributions can be found in this journal [Wilson WK (2000) *Lipids* 35:242]. Dr. Schroepfer was scheduled to be the keynote speaker at the sterol symposium in Orlando, Florida, in 1999, but he unfortunately passed away on December 11, 1998.

The first two recipients of the Schroepfer Award were Professor Geoffrey F. Gibbons (2002) and Professor Jan B. Sjöval (2004). The third recipient of the G.J. Schroepfer Jr. Award, which was presented on May 2, 2006, was Professor Ingemar Björkhem of the Department of Laboratory Medicine, from the Karolinska Institutet in Stockholm, Sweden. Professor Björkhem has made major contributions to the steroid field, and we were pleased when we learned that he was chosen to receive this prestigious award. Professor Björkhem is well known for research on the metabolism of sterols and oxysterols.

As in past symposia, we are indebted to our corporate partners who helped make the symposium a success: Avanti Polar Lipids, Forbes Medi-Tech, Pfizer, and Seraloids, Inc. We appreciate their contribution and look forward to their continued support of our symposium series.

This symposium was sponsored by the Biotechnology Division of the AOCs. Speakers at the 2006 Sterol Symposium represented an international group of senior and junior scientists. We express here our appreciation to each of them for their cooperation during the planning process and for their participation in the symposium. By all accounts, the event was a success. We are looking forward to the next sterol symposium, which will be held at the 99th Annual Meeting and Expo of the American Oil Chemists' Society, May 18–21, 2008, in Seattle, Washington.

---

E. J. Parish  
Department of Chemistry, Auburn University,  
Auburn, AL 36849, USA

R. A. Moreau (✉)  
USDA, ARS, ERRC, Wyndmoor, PA 19038, USA  
e-mail: robert.moreau@ars.usda.gov

T. J. Bach  
Institut de Biologie Moléculaire des Plantes,  
Centre National de la Recherche Scientifique,  
67083 Strasbourg, France

W. D. Nes  
Department of Chemistry and Biochemistry,  
Texas Tech University, Lubbock, TX 79409, USA

J. R. Williams  
Department of Chemistry, Temple University,  
Philadelphia, PA 19122, USA

# Rediscovery of Cerebrosterol

Ingemar Björkhem

Received: 15 June 2006 / Accepted: 27 July 2006 / Published online: 23 January 2007  
© AOCs 2007

**Abstract** 24S-hydroxycholesterol was identified more than half a century ago and was initially given the name “cerebrosterol” due to the fact that it was abundant in the brain. A decade ago, we showed that the most important mechanism by which cholesterol is eliminated from the mammalian brain involves a hydroxylation into cerebrosterol followed by diffusion of this steroid over the blood–brain barrier. Using an  $^{18}\text{O}_2$  inhalation technique, we showed that about two-thirds of the cholesterol synthesis in rat brain is balanced by conversion into cerebrosterol. The hydroxylase responsible for the reaction was found to be dependent upon NADPH and oxygen, consistent with involvement of a species of cytochrome, P-450. The gene coding for the cytochrome P-450 responsible for the reaction was later cloned by the group of David Russell in Dallas and the enzyme was found to be located to neuronal cells in the brain. Recent studies by us and others on this new pathway for elimination of cholesterol from the brain have given new insights into the mechanisms by which cholesterol homeostasis is maintained in this organ. In addition, these studies have resulted in new diagnostic and prognostic tools in connection with neurological and neurodegenerative diseases. An overview of the studies is presented here and the possibility is discussed

that the cholesterol 24S-hydroxylase in the brain may be a new drug target in connection with neurodegenerative diseases.

## Introduction

I am deeply honoured to be the third recipient of the Schroepfer award.

I never met George Schroepfer in person, but I am very familiar with his work. He was one of the pioneers in the field of research on oxysterols, which is my major research interest at present. In addition to this, I have a personal link to George Schroepfer. My tutor, the late Professor Henry Danielsson, was a very good friend of George and often mentioned him. Both Henry and George had been working in the laboratory of Konrad Bloch.

I have learnt that the two previous recipients of the Schroepfer award have given broad overviews. Jan Sjövall, who received the award 2 years ago, described his 50 years with bile acids in health and disease [1]. I will be more selective and focus on a topic that I have been working on only during the last decade. However, given the interest of George Schroepfer in oxysterols, I think that the topic is appropriate.

## Oxysterols: General Properties

Oxysterols are defined as oxygenated derivatives of cholesterol (or precursors to cholesterol) that may be formed by autoxidation or by the action of specific monooxygenases (for details, see the classical very extensive review by Schroepfer [2]). Oxysterols may

---

I. Björkhem (✉)  
Department of Laboratory Medicine,  
Division of Clinical Chemistry,  
Karolinska Institutet,  
Huddinge 141 86, Sweden  
e-mail: ingemar.bjorkhem@hs.se

also be formed secondary to enzymatic or nonenzymatic lipid peroxidation. Most oxysterols are short-lived compounds which are rapidly oxidized to bile acids and eliminated from the body. The rapid degradation of these compounds, in particular side-chain oxidized oxysterols, is facilitated by their physical properties which allow them to pass lipophilic membranes orders of magnitude faster than cholesterol itself [3, 4].

An important feature of oxysterols is that they are present in trace amounts only in biological systems, and always in the presence of a great excess of cholesterol (most often this excess is in the range  $10^4$ – $10^6$ ). In some specific biological systems, as in the brain and in lipid-loaded macrophages, the excess of cholesterol may be somewhat lower than  $10^3$ . Exposing cultured cells to pure oxysterols at micromolar concentrations in the absence of cholesterol may be regarded as highly unphysiological. While such experiments may give some information concerning whether or not the system is sensitive to sterols, it is not possible to draw conclusions concerning the biological role of oxysterols under *in vivo* conditions.

Oxysterols have been ascribed important functions in connection with atherosclerosis, apoptosis, necrosis, inflammation, immunosuppression, development of gallstones (for a review, see [5]).

However, most of the evidence for this is still indirect and there is a clear discrepancy between the documented effects of the oxysterols under *in vitro* conditions and the studies demonstrating direct physiological effects *in vivo*.

The most obvious role of oxysterols is that they are precursor to bile acids. Another well established role is that they represent a transport form of cholesterol, allowing an elimination over biological membranes that is not dependent on specific transport proteins. To what extent oxysterols are of regulatory importance under *in vivo* conditions is still controversial. It is well documented that side-chain oxidized oxysterols are efficient ligands and activators of the nuclear receptors LXR $\alpha$  and LXR $\beta$  [6]. A knockout of these receptors leads to specific effects on cholesterol homeostasis. According to current concepts, oxysterols are the physiological activators of the above receptors, but this has not been established with certainty [5, 7].

### Cerebrosterol

More than half a century ago an oxysterol was isolated from horse and human brain by two Italian researchers, Ercoli and Ruggieri, that was given the name “cerebrosterol”. In 1953, they established the identity of this

oxysterol to be 24-hydroxycholesterol [8] (Fig. 1). The concentration of this oxysterol in the brain was found to be about 0.1–0.3% of that of cholesterol. About 20 years later, Leland L Smith and collaborators performed detailed studies on the occurrence of this compound in the brain and showed that it is only one of the two epimers of 24-hydroxycholesterol (24S) which is present (for a review, see [9]). This group also showed that 24S-hydroxycholesterol most probably originates from brain cholesterol. Homogenates and microsomal fractions from rat brain were thus shown to convert tritiated cholesterol into 24-hydroxycholesterol at a rate of about 0.01% per hour [10]. The extremely low degree of conversion prevented further characterization of the enzyme involved.

In retrospect it is interesting to note that Smith et al. draw the conclusion from their studies that “Our data on the levels of 24-hydroxycholesterol in several brain regions suggest that any physiological function of the trace steroid must be a generalized one, which is important to all major regions” [9].

In later work, 24S-hydroxycholesterol was found to be also present in adrenals, in the circulation, and as a sulphate in human meconium and infant faeces [11].

### A Surprising Discovery

As part of the general interest in oxysterols in our laboratory, accurate methods were developed for assay of oxysterols in plasma based on isotope dilution-mass spectrometry [12, 13]. 24S-hydroxycholesterol was found to be one of the major oxysterols in human circulation, ranging from 50–100 ng/ml. Using an  $^{18}\text{O}_2$ -inhalation technique to study oxygenation of cholesterol in the rat, we were able to show that most of the 24S-hydroxycholesterol present in the circulation is formed *in vivo*, most probably in an enzymatic reaction [14]. In view of this, it was considered to be of interest to have this oxysterol included in the panel of oxysterols that we measured.

A number of studies were performed in order to evaluate the possibility that oxysterols in the circulation may be used as biomarkers in different clinical conditions expected to have consequences for cholesterol homeostasis. We observed that some patients with atherosclerosis had increased levels of 27-hydroxycholesterol [15] and that patients with increased bile acid biosynthesis had increased levels of 7-hydroxycholesterol [16]. Up to 1995, only very small changes were seen in the levels of circulating 24S-hydroxycholesterol in any of all the different patients that we studied. Patients treated with the drug ketoconazole had

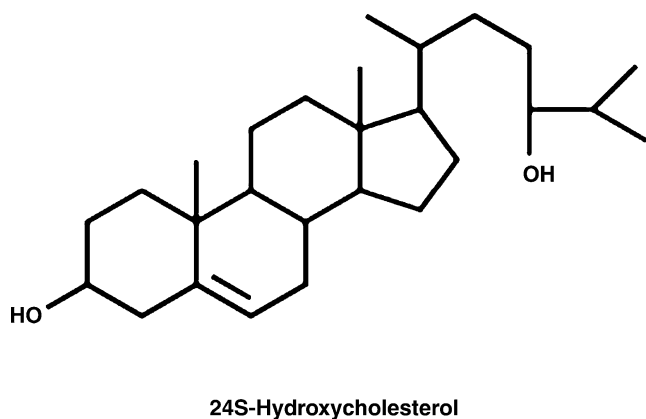


**Fig. 1** Structure of 24S-hydroxycholesterol

moderately increased levels of 24S-hydroxycholesterol, most probably due to a drug interference with its metabolism.

In 1995, a visiting scientist in my laboratory, Dr Dieter Lutjohann, analyzed plasma from a 14-year-old girl with sitosterolemia [17]. He found a level of 235 ng/ml of 24S-hydroxycholesterol—a level about three-fold the upper limit of the normal range that we had defined for adults. The younger sister of the patient had an even higher level, whereas the parents had normal plasma levels. It was not possible to couple this finding to sitosterolemia and so the obvious explanation was that infants have higher levels than adults. Analyses of a great number of plasma samples from subjects of different ages confirmed that this was the case (Fig. 2).

We considered the possibility that the increased levels of 24S-hydroxycholesterol in childhood were due

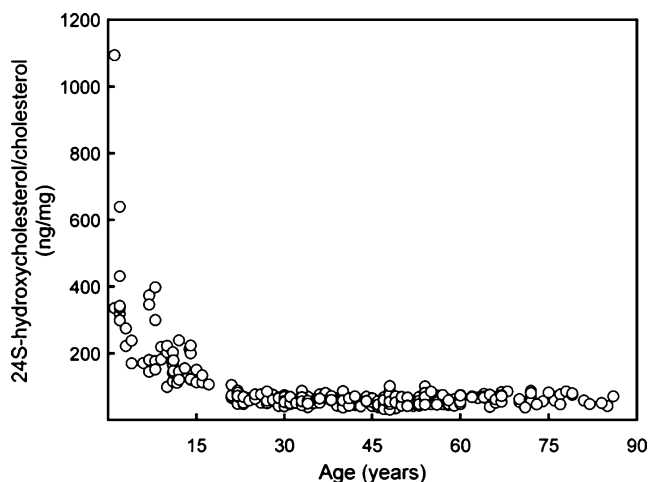


**Fig. 2** Age-dependent variations in plasma levels of 24S-hydroxycholesterol (modified from [18])

to effects of, e.g., growth hormone, or due to dietary factors (e.g., milk), but these possibilities were easily excluded. We then speculated that the high levels in infancy could be due to increased turnover of cholesterol in the brain of infants in relation to adults. The major fraction of cholesterol in the central nervous system is present in myelin, and it is known that the major portion of myelination occurs in the human brain during the first years of life.

Such a hypothesis must however be based on the assumption that the cerebrosterol present in human circulation originates from the brain.

### Demonstration that the Cerebrosterol Present in Human Circulation Originates from the Brain

We first confirmed the previous finding [8, 9] that the brain contains high levels of 24S-hydroxycholesterol. The level of 24S-hydroxycholesterol was found to vary between 4 and 15 ng/mg (wet weight) in different areas of the human brain. In contrast, the levels in all other organs, except the adrenals, was less than 0.2 ng/mg. In the adrenals, the level was about 3 ng/mg. When related to cholesterol levels, the ratio between 24S-hydroxycholesterol and cholesterol was found to vary between 0.7 and 2 ng/ $\mu$ g in the brain, but was only about 0.05 ng/ $\mu$ g in the circulation. It is evident that there is a marked concentration gradient between the brain and the circulation, consistent with the possibility of a flux of cerebrosterol in this direction. In accordance with a flux driven by the concentration gradient, the ratio between 24S-hydroxycholesterol and cholesterol in cerebrospinal fluid was between the corresponding ratio in the brain and in the circulation (about 0.3 ng/ $\mu$ g).

In order to measure the flux of 24S-hydroxycholesterol from the human brain into the circulation, we collaborated with two clinical physiologists who inserted catheters into the jugular vein, the hepatic vein, and the brachial artery of healthy volunteers. Almost all of the subjects had higher levels of 24S-hydroxycholesterol in the internal jugular vein than in the artery [18, 19], and this difference was highly significant from a statistical point of view. From the arteriovenous difference and an estimation of the blood flow through the brain, the net efflux of 24S-hydroxycholesterol was estimated to be about 6 mg/24 h. Most of the subjects had higher levels 24S-hydroxycholesterol in the artery than in the hepatic vein, and it was estimated that there was a net uptake of this oxysterol in the liver corresponding to about 7 mg/24 h. Since the secretion by the brain and the uptake in liver were found to be about

the same, the data are consistent with the possibility that most of the 24S-hydroxycholesterol present in human circulation originates from the brain (Fig. 3).

### Studies on Formation of 24S-Hydroxycholesterol in Rat Brain In vivo and In vitro

By exposing rats to  $^{18}\text{O}_2$  in the inhalation atmosphere, we had previously shown that 24S-hydroxycholesterol is formed by a monooxygenase that incorporates one of the two oxygen atoms in molecular oxygen in the product [14]. This technique was now used to measure the rate of incorporation of  $^{18}\text{O}$  in 24S-hydroxycho-

lesterol in the brain of rats exposed for some hours to  $^{18}\text{O}_2$  [20]. From the results obtained, it could be calculated that the rate of conversion of brain cholesterol into the oxysterol corresponded to about 0.02% of the total endogenous pool of cholesterol per hour. It was shown that there was also an incorporation of  $^{18}\text{O}$  in the 24S-hydroxycholesterol present in the circulation, although this incorporation was lower than that in the brain. This is consistent with a flux of the oxysterol from the brain into the circulation.

It was considered to be of interest to also measure the rate of synthesis of cholesterol in the brain of the above rats. We had previously demonstrated that it is possible to also use the  $^{18}\text{O}_2$ -technique for such measurements [21]. Thus the synthesis of cholesterol also requires a mixed function oxidation (the squalene oxidase step). As a consequence,  $^{18}\text{O}$  is incorporated in the  $3\beta$ -position under conditions when the de novo synthesis of cholesterol occurs in  $^{18}\text{O}_2$ -atmosphere. With use of this technique we could show that the rate of synthesis of cholesterol in the brain of a rat exposed to  $^{18}\text{O}_2$  corresponds to about 0.03% of the pool per hour. This means that the de novo synthesis of cholesterol in rat brain is balanced to about two-thirds by a metabolism into 24S-hydroxycholesterol.

Attempts were then made to set up a reliable in vitro assay for conversion of cholesterol into 24S-hydroxycholesterol in brain homogenates. In our hands, the assay described by Smith et al. [10], measuring the rate of conversion of added labeled cholesterol, was not reproducible, mainly due to the extremely low degree of conversion (about 0.01% of the pool per hour). A better assay was obtained by measuring the amount of endogenous 24S-hydroxycholesterol in the homogenate by isotope dilution-mass spectrometry before and after incubation. The best and most reliable assay was obtained by carrying out the incubation in  $^{18}\text{O}_2$  and measuring the incorporation of  $^{18}\text{O}$  in the 24S-hydroxycholesterol after the incubation [20]. By this technique, we could confirm the previous finding by Smith that the enzyme was located in the endoplasmic reticulum. We could also show that the reaction was dependent upon NADPH and oxygen. The rate of conversion was found to be comparable with the rate of conversion that we had found in vivo.

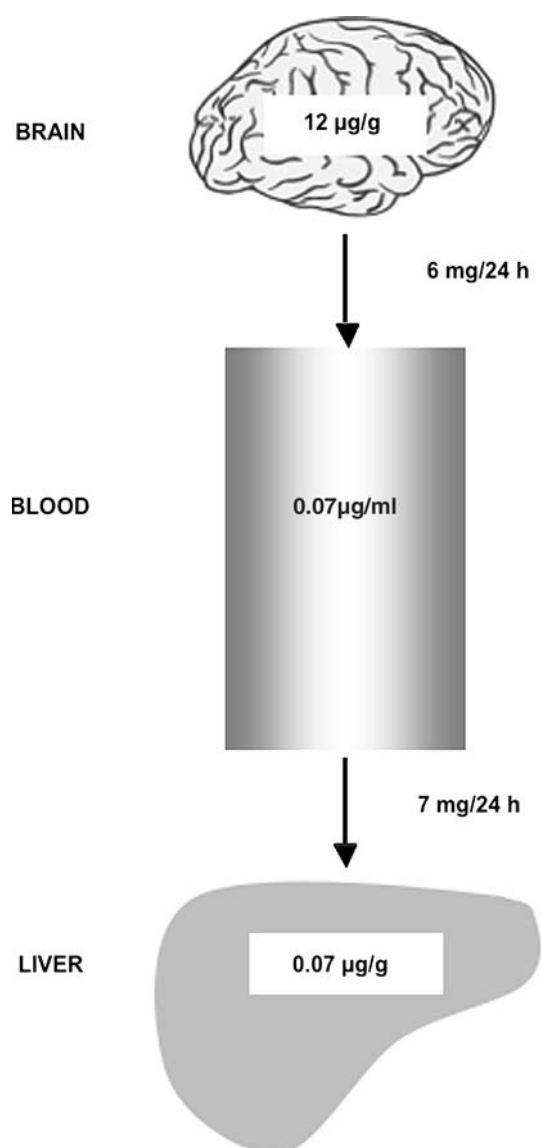


**Fig. 3** Flux of 24S-hydroxycholesterol from the brain to the circulation and liver (modified from [19])

### Attempts to Purify the Cholesterol 24-Hydroxylase and the Cloning of the Gene Coding for the Enzyme by the Group of David Russell

Several attempts were made in our laboratory to purify the microsomal cholesterol 24-hydroxylase from rat

and rabbit brain. It appeared most likely that the enzyme was a species of cytochrome P-450 and so some of the methods previously used for purification of such enzymes were tested. Unfortunately, all these attempts failed, and only a very modest degree of purification was obtained. Removal of the lipids from the membrane fractions by different methods almost invariably resulted in an irreversible loss of most of the enzymatic activity.

Meanwhile, my previous PhD student Erik Lund, working as a post-doctoral student in David Russell's laboratory in Dallas, cloned a new species of cytochrome P-450 from mouse liver by expression cloning [22]. This species of cytochrome, containing 500 amino acids, was expressed and found to be able to catalyze 24S-hydroxylation of cholesterol. Antibodies towards the enzyme were prepared, and it was confirmed that the enzyme was present almost exclusively in the brain in humans. The neuronal cells expressing the enzyme included pyramidal cells of the cortex and hippocampus, granule cells of the dentate gyrus and Purkinje cells of the cerebellum. The expression of the gene was low during the first year of life, but was then about constant during the rest of the life.

The new species of cytochrome P-450 was given the name CYP46.

The very successful work in the laboratory of David Russell not only confirmed and expanded our work, but also provided the necessary molecular tools for a further elucidation of the role of 24-hydroxylation of cholesterol in the brain. More recently, Drs Lund, Russell and collaborators developed a mouse model with a disruption of the gene coding for CYP46 [23]. The mice had no obvious biochemical phenotype, but had a reduction of cholesterol synthesis by about 40% in the brain. In accordance with our previous findings in the rat, the disruption of the gene resulted in a reduction of the flux of steroids from the mouse brain by about two-third [23].

### Characterization of the Cholesterol 24S-Hydroxylase (CYP46)

Due to the low enzymatic activity of the cholesterol 24S-hydroxylase in brain microsomes, it was difficult to characterize the enzyme in detail with such preparations. The cloning of the gene coding for the CYP46 protein by Lund et al. allowed a more detailed characterization by use of transfected mammalian cells and partially purified recombinant CYP46A1 protein. In collaboration with the group of Dr Irina Pikuleva at Galveston, it was shown that the enzyme was able to

further metabolize 24S-hydroxycholesterol into 24,25- and 24,27-dihydroxycholesterols [24]. C27-steroids other than cholesterol could undergo side-chain hydroxylation. Furthermore, the enzyme could introduce a hydroxyl group in the steroid nucleus of progesterone and testosterone and metabolize some xenobiotics. The physiological importance of the latter hydroxylations is, however, difficult to evaluate at the present state of knowledge. In spite of several attempts, we have only found trace amounts of the steroids 24,25- and 24,27-dihydroxycholesterols in the brain or cerebrospinal fluid.

### Studies on the Regulation of the Cholesterol 24S-Hydroxylase

In view of the obvious importance of the cholesterol 24S-hydroxylase for cholesterol homeostasis in the brain, we made a structural and functional characterization of the promoter of the human CYP46 gene [25]. No canonical TATA or CAAT boxes were found in the promoter region. Moreover, this region had a high GC content, a feature often found in genes considered to have a largely housekeeping function. A broad spectrum of different potential modulators using a variety of promoter constructs did not result in a significant transcriptional regulation, although oxidative stress caused a significant increase in transcriptional activity. The possibility of a substrate-dependent transcriptional regulation was explored in vivo in a sterol deficient model (*Dhcr24* null) [26] in which almost all cholesterol had been replaced with desmosterol, which is not a substrate for CYP46A. Compared to heterozygous littermates there was no statistically significant difference in the mRNA levels of the enzyme. However, during the first 2 weeks of life in the wild-type mouse, a significant increase of the mRNA levels was found, in parallel with an increase in 24S-hydroxycholesterol level and a reduction of cholesterol synthesis.

The most significant transcriptional effect on the gene was thus the induction of the enzyme during the neonatal stage. Attempts to define the factor(s) behind this induction have failed thus far, and we were able to exclude the possibility that growth hormone is involved in this effect.

The apparent resistance to regulation of the cholesterol 24S-hydroxylase at a transcriptional level is in marked contrast to the regulation of the rate-limiting enzyme for elimination of cholesterol from the liver, the cholesterol 7 $\alpha$ -hydroxylase (CYP7A1). The latter is subject to a highly sophisticated transcriptional

regulation by the flux of bile acids and cholesterol through the liver, and by a great number of dietary and hormonal factors [27]. It may be concluded that it is the synthesis rather than the metabolism of cholesterol that is regulated in the mammalian brain.

### Why is There a Need for Conversion of Cholesterol into 24S-Hydroxycholesterol by the Brain?

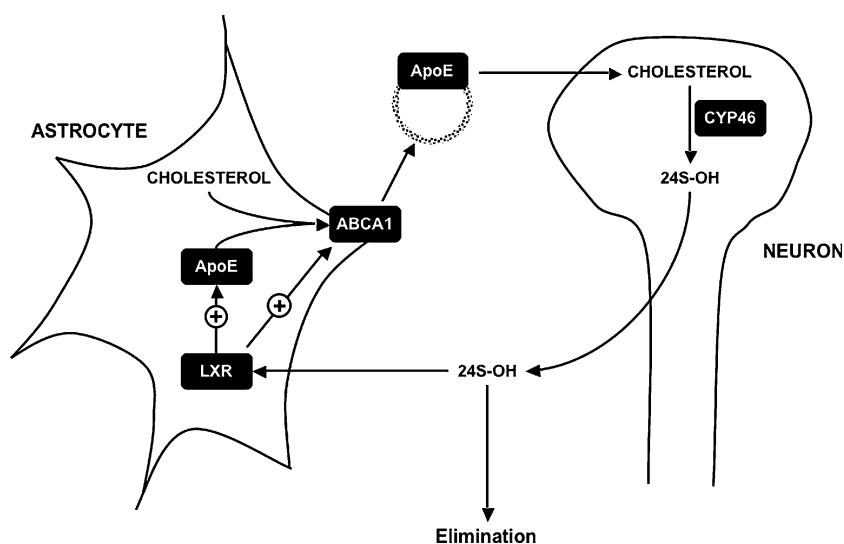
The rate of cholesterol synthesis in the brain of mammals is very low [19], and there appears to be a highly efficient reutilization of this compound. At the present state of knowledge, the most important role of the cholesterol 24S-hydroxylase system appears to be a compensation for the rate of de novo synthesis of cholesterol. Pfrieger has suggested a mechanism by which 24S-hydroxycholesterol may be involved in an interplay between neuronal and glial cells [28] (Fig. 4). Neuronal cells appear to have a low rate of synthesis of cholesterol in relation to glial cells, and there may be a flux of cholesterol in apoE bound form from the glial cells to the neuronal cells. This flux may in part be regulated by the cholesterol transporter ABCA1, which is under control of the nuclear receptor LXR [28]. 24S-hydroxycholesterol is an efficient activator of this receptor, and an increased flux of 24S-hydroxycholesterol from the neuronal cells to the glial cells would thus be expected to cause an increased flux of cholesterol to the neuronal cells. In accordance with a stimulatory effect of 24S-hydroxycholesterol on the efflux of cholesterol from glial cells, it was recently shown that 24S-hydroxycholesterol seems to have a direct effect on the production of apoE in glial cells [29].

The autoregulatory mechanism suggested by Pfrieger is conceptually attractive and is consistent with most experimental data. There is, however, a need for further testing of the hypothesis in other systems than those used thus far. A complicating factor in such studies is the extremely low rate of synthesis of 24S-hydroxycholesterol, and to our knowledge no cell culture experiments have been described at this point in time with a measurable reproducible production of 24S-hydroxycholesterol.

### Metabolism of 24S-Hydroxycholesterol

In view of the fact that a hydroxyl group is introduced in the 24-position during the normal conversion of cholesterol into bile acids, a conversion of 24-hydroxycholesterol into bile acids would be expected. In the major pathway for formation of bile acids, the first and rate-limiting step is the introduction of a hydroxyl group in the 7 $\alpha$ -position by the cytochrome P-450 enzyme CYP7A. In collaboration with the group of Dr Kjell Wikvall we could demonstrate that reconstituted human CYP7A has activity towards 24S-hydroxycholesterol [30]. In contrast, the cytochrome P-450 CYP7B, which is able to introduce a hydroxyl group in other side-chain oxidized C27-steroids like 25- and 27-hydroxycholesterol, had no such activity. The group of Dr David Russell cloned and characterized a novel species of cytochrome P-450 denoted CYP39 [31]. This enzyme was found to have a high 7 $\alpha$ -hydroxylase activity towards 24S-hydroxycholesterol. However, the relative importance of CYP39 and CYP7A in the metabolism of 24S-hydroxycholesterol is not known.

**Fig. 4** Regulatory effects of 24S-hydroxycholesterol on the flux of cholesterol from a glial cell to a neuronal cell (cf. [28, 29])





In a study on the metabolism of 24*S*-hydroxycholesterol in humans, we prepared tritium labeled 24*S*-hydroxycholesterol and incubated it with human primary hepatocytes, administered it to human volunteers and quantitated free and conjugated 24*S*-hydroxycholesterol and its neutral metabolites in ileocecal fluid from patients with ileal fistulae [32]. 24*S*-hydroxycholesterol, as well as the 24*R*-hydroxylated analog, were converted into the normal bile acids by human hepatocytes at a rate about 40% of that of the normal intermediate in bile acid synthesis, 7 $\alpha$ -hydroxycholesterol. There was also a conversion of the oxysterol into conjugates of the corresponding 27-hydroxylated derivative. The rate of the latter conversion was similar to that of the rate of conversion into bile acids. When administered to a human volunteer, labeled 24*S*-hydroxycholesterol was converted into bile acids at a rate about half that of simultaneously administered 7 $\alpha$ -hydroxycholesterol. Free, sulfated and glucuronidated 24*S*-hydroxycholesterol, as well as 27-hydroxylated 24*S*-hydroxycholesterol, were identified in ileocecal fluid. The excretion of these steroids was about 3.5 mg/24 h, amounting to about half of the production of 24*S*-hydroxycholesterol from the brain.

It was concluded from the above studies that 24*S*-hydroxycholesterol is a less efficient precursor to bile acids and that about half of it is conjugated and eliminated in bile as such or as a conjugate of a 27-hydroxylated metabolite [32]. The less efficient metabolism of 24*S*-hydroxycholesterol may explain the surprisingly high levels of this oxysterol in the circulation.

### **What is the Explanation for the High Levels of 24*S*-Hydroxycholesterol in the Circulation of Infants? Which Factors Other than Age are of Importance for the Levels?**

Our first hypothesis was that the high levels of 24*S*-hydroxycholesterol in infants are due to a higher rate of turnover of cholesterol in a developing brain. The high levels are apparently not related to the level of CYP46 in the brain, as reported by Lund and collaborators [22]. Measurement of 24*S*-hydroxycholesterol in the brain and circulation of experimental animals gave no information about the reason for the high levels in human infants. In this situation we measured the concentration of 24*S*-hydroxycholesterol in plasma of chondrodystrophic dwarfs [33]. The concentrations were increased in these subjects to a level similar to that seen in infants. The most likely explanation is that the levels of 24-hydroxycholesterol in the circulation

are dependent upon a balance between the secretion capacity of the brain and the metabolic capacity of the liver. Newborns have a size of the brain that is about three-fold that of the liver, whereas the size of the two organs is about the same in adults. In old age, the size of the liver is reduced to a greater extent than is the size of the brain. In accordance with this, there is a slight but significant increase in the plasma level of 24*S*-hydroxycholesterol after the age of 65. As expected from the relation between the size of the liver and the body surface, there is an inverse relationship between surface area and plasma 24*S*-hydroxycholesterol.

Since 24*S*-hydroxycholesterol is transported in plasma by the same lipoproteins as cholesterol, hypercholesterolemia would be expected to affect the circulating levels of this oxysterol. In accordance with this, there is a relationship between levels of cholesterol and levels of 24*S*-hydroxycholesterol [19, 33]. Reducing cholesterol levels by treatment with a statin causes a slight increase in the ratio between 24*S*-hydroxycholesterol and cholesterol in the circulation (unpublished observation).

In spite of the fact that the cholesterol level may affect the level of 24*S*-hydroxycholesterol in the circulation, this level is remarkably stable under most conditions. Thus, there is no diurnal variation and, with the exception of some efficient inhibitors of cytochrome P-450 enzymes (ketoconazol and itraconazol), there are surprisingly small effects of drugs on the levels. Except for very advanced stages of liver cirrhosis, liver diseases also appear to have little or no effect on the levels in the circulation.

### **24*S*-Hydroxycholesterol as a Marker for Neurological and Neurodegenerative Diseases**

Given the fact that almost all 24*S*-hydroxycholesterol present in human circulation is of cerebral origin, and the fact that hepatic metabolism appears to be constant during most conditions in adult life, we tested the possibility that 24*S*-hydroxycholesterol may be used as a surrogate marker for brain cholesterol homeostasis. We first tested the most drastic clinical situation possible, that of a brain-dead patient with little or no circulation in the brain [34]. As expected, the levels of 24*S*-hydroxycholesterol were low, and in accordance with our previous finding that the half-life of the oxysterol in the circulation is about 12 h, patients who had been brain-dead for about this period of time had a reduction in the concentration of 24*S*-hydroxycholesterol of about 50%. Patients with advanced Alzhei-

mer's disease were found to have significantly reduced plasma levels of the oxysterol, in accordance with the demonstration by Lund et al. that almost all of the enzyme is present in neuronal cells. A complicating factor in the interpretation, however, is that we could demonstrate some abnormal expression of the CYP46 enzyme in glial cells in the brain of patients with Alzheimer's disease [35], a finding that was recently confirmed by another group [36].

Patients with brain tumors and some severe CNS infections also have reduced levels of 24S-hydroxycholesterol. A few patients with multiple sclerosis in an active stage were found to have increased levels of 24S-hydroxycholesterol in the circulation. However, in the chronic situation, most patients have reduced plasma levels of the oxysterol [37].

From the low levels of 24S-hydroxycholesterol in the cerebrospinal fluid, it can be calculated that less than 1% of the oxysterol is excreted from the brain by this route. Surprisingly, this minor fraction appears to reflect neuronal damage and rate of neuronal loss rather than the total number of metabolically active neuronal cells [38]. Thus, patients with neurodegenerative disorders were found to have increased levels of 24S-hydroxycholesterol in cerebrospinal fluid, in parallel with decreased levels in the circulation. The changes in the cerebrospinal fluid were thus much more marked than those in the circulation. The diagnostic potential of the level of 24-hydroxycholesterol in cerebrospinal fluid is under investigation at present in our laboratory and in the laboratory of Dr Dieter Lutjohann. Levels of the tau protein, phosphorylated tau, and  $\beta$ -amyloid in cerebrospinal fluid are routinely used as biomarkers for neurodegenerative diseases and dementia. We recently showed that the level of 24S-hydroxycholesterol in cerebrospinal fluid appears to have about the same diagnostic sensitivity as these markers in connection with Alzheimer's disease and may be the most sensitive marker in early stages [39].

### Cholesterol 24S-Hydroxylase as a Potential Drug Target

We recently measured the levels of 24S-hydroxycholesterol and 27-hydroxycholesterol in brain materials from patients who had died from Alzheimer's disease and in the corresponding materials from control subjects [40]. The levels of 24S-hydroxycholesterol were decreased in most brain areas, whereas the levels of 27-hydroxycholesterol were increased. Interestingly, similar changes were observed in the brain of mice

with a mutation in the gene coding for Amyloid Precursor Protein (APP) (the Swedish mutation). The ratio between 24S-hydroxycholesterol and 27-hydroxycholesterol was markedly reduced in all the brain areas of both the AD patients and the transgenic mice.

The reduced levels of 24S-hydroxycholesterol may be due to the neuronal degeneration. We have shown that most of the 27-hydroxycholesterol present in the brain originates from the circulation [41, 42] and the increased levels may be due to increased flux over the blood–brain barrier. Another possibility is reduced metabolism.

According to a recent work by Brown et al. [36], 24S-hydroxycholesterol is an efficient inhibitor of the formation of  $\beta$ -amyloid under in vitro conditions. 27-hydroxycholesterol had a much lower capacity to inhibit the reaction. If the oxysterols are important for the generation of  $\beta$ -amyloid also under in vivo conditions, the reduced levels of 24S-hydroxycholesterol may accelerate the progress of the disease, and the increased levels of 27-hydroxycholesterol may not be able to compensate for this [43].

According to current concepts, cholesterol-rich membranes are more likely to lead to a primary cleavage of APP by  $\beta$ -secretase with subsequent generation of  $\beta$ -amyloid than membranes with a low concentration of cholesterol (for a review, see [44]). Theoretically, upregulation of the cholesterol 24S-hydroxylase may prevent formation of  $\beta$ -amyloid by two separate mechanisms: reduction of cholesterol in neuronal membranes and a direct inhibitory effect by the 24S-hydroxycholesterol [43]. On the other hand, high levels of 24S-hydroxycholesterol may have neurotoxic effects [45]. The possibility must be considered that pharmacological effects on the cholesterol 24S-hydroxylase may be utilized as a new therapeutic strategy in connection with neurodegenerating diseases. Such an approach would, however, require development of specific modulators of the enzyme activity which are able to cross the blood–brain barrier.

**Acknowledgments** The author is grateful to the previous PhD students (and, in some cases, later post doctoral students) in his laboratory working on different parts of the project: Karl Bodin, Olof Breuer, Ewa Ellis, Maura Heverin, Valerio Leoni, Erik Lund, Dieter Lutjohann, and Steve Meaney. In addition, he is grateful for the fruitful collaboration with his colleagues, Leonel Bretillon, Ulf Diczfalusy, Curt Einarsson, Elena Feinstein, Maria Norlin, Yoshihiko Ohyama, Irina Pikuleva, Lars-Olof Wahlund, John Wahren, Kjell Wikvall, Åke Wennmalm, Bengt Winblad, and Jan Sjövall. This work was supported by grants from the Swedish Science Council, the Swedish Heart-Lung Foundation, Foundation “Gamla Tjänarinnor”, Brain Power, Brain Foundation, and Pfizer.

## References

- Sjövall J (2004) Fifty years with bile acids and steroids in health and disease. *Lipids* 39:703–722
- Schroepfer GJ Jr (2000) Oxysterols: modulators of cholesterol metabolism and other processes. *Physiol Rev* 80:361–554
- Lange Y, Ye J, Strebel F Movement of 25-hydroxycholesterol from the plasma membrane to the rough endoplasmic reticulum in cultured hepatoma cells. *J Lipid Res* 36:1092–1097
- Meaney S, Bodin K, Diczfalussy U, Björkhem I (2002) On the rate of translocation in vitro and kinetics in vivo of the major oxysterols in human circulation: critical importance of the position of the oxygen function. *J Lipid Res* 43:2130–2135
- Björkhem I, Diczfalussy U (2002) Oxysterol. Friends, foes or just fellow passengers? *Arterioscl Thromb Vasc Biol* 22:734–742
- Lehmann JM, Kliewer SA, Moore LB, Smith-Oliver TA, Oliver BB, Su JL, Sundseth SS, Winegar DA, Blanchard SE, Spencer TA, Willson TM (1997) Activation of the nuclear receptor LXR by oxysterols defines a new hormone response pathway. *J Biol Chem* 272:3137–3140
- Björkhem I (2002) Do oxysterols control cholesterol homeostasis? *J Clin Invest* 110:725–730
- Ercoli IA, Ruggieri P (1953) The constitution of cerebrosterol, a hydroxycholesterol isolated from horse brain. *J Am Chem Soc* 75:3284
- Smith LL, Ray DR, Moody JA, Wells JD, Lier JE (1972) 24-Hydroxycholesterol in human brain. *J Neurochem* 19:899–904
- Lin YY, Smith LL (1974) Biosynthesis and accumulation of cholest-5-ene-3 $\beta$ , 24-diol (cerebrosterol) in developing rat brain. *Biochim Biophys Acta* 348:189–196
- Gustafsson JÅ, Sjövall J (1969) Identification of 22-, 24- and 26-Hydroxycholesterol in the steroid sulphate fraction of faeces from infants. *Eur J Biochem* 8:467–472
- Breuer O, Björkhem I (1990) Simultaneous quantification of several cholesterol autoxidation and monohydroxylation products by isotope dilution mass spectrometry. *Steroids* 55:185–192
- Dzeletovic S, Breuer O, Lund E, Diczfalussy U (1995) Determination of cholesterol oxidation products in human plasma by isotope dilution-mass spectrometry. *Anal Biochem* 225:73–803
- Breuer O, Björkhem I (1995) Use of an  $^{18}\text{O}_2$ -inhalation technique and mass isotopomer analysis to study oxygenation of cholesterol in rat: evidence for in vivo formation of 7-oxo, 7 $\beta$ -hydroxy, 24-hydroxy-, and 25-hydroxycholesterol. *J Biol Chem* 270:20278–20284
- Babiker A, Dzeletovic S, Wiklund B, Petterson N, Salonen J, Nyssönen K., Eriksson M, Diczfalussy U, Björkhem I (2005) Patients with atherosclerosis may have increased circulating levels of 27-hydroxycholesterol and cholestenic acid. *Scand J Clin Lab Invest* 65:365–376
- Björkhem I, Reihner E, Angelin B, Ewerth S, Åkerlund J.-E., Einarsson K (1987) On the possible use of 7 $\alpha$ -hydroxycholesterol as a marker for increased activity of the cholesterol 7 $\alpha$ -hydroxylase. *J Lipid Res* 28:889–894
- Lütjohann D, Björkhem I, Ose L (1996) Phytosterolemia in a Norwegian family: diagnosis and characterization of the first Scandinavian case. *Scand J Clin Lab Invest* 56:229–240
- Lütjohann D, Breuer O, Ahlborg G, Nennesmo I, Sidén Å, Diczfalussy U, Björkhem I (1996) Cholesterol homeostasis in human brain: evidence for an age-dependent flux of 24S-hydroxycholesterol from the brain into the circulation. *Proc Natl Acad Sci USA* 93:9799–9804
- Björkhem I, Lütjohann D, Diczfalussy U, Stähle L, Ahlborg G, Wahren J (1998) Cholesterol homeostasis in human brain: turnover of 24S-hydroxycholesterol and evidence for a cerebral origin of most of this oxysterol in the circulation. *J Lipid Res* 39:1594–1600
- Björkhem I, Lütjohann D, Breuer O, Sakinis A, Wennmalm Å (1997) Importance of a novel oxidative mechanism for elimination of brain cholesterol. Turnover of cholesterol and 24(S)-hydroxycholesterol in rat brain as measured with  $^{18}\text{O}_2$  techniques in vivo and in vitro. *J Biol Chem* 272:30178–30184
- Björkhem I, Lewenhaupt A (1979) Preferential utilization of newly synthesized cholesterol as substrate for bile acid biosynthesis. An in vivo study using  $^{18}\text{O}_2$ -inhalation technique. *J Biol Chem* 254:5252–5256
- Lund EG, Guileyardo JM, Russell DW (1999) cDNA cloning of cholesterol 24-hydroxylase, a mediator of cholesterol homeostasis in the brain. *Proc Natl Acad Sci USA* 96:7238–7243
- Lund EG, Xie C, Kotti T, Turley SD, Dietschy JM, Russell DW (2003) Knockout of the cholesterol 24-hydroxylase gene in mice reveals a brain-specific mechanism of cholesterol turnover. *J Biol Chem* 278:22980–22988
- Mast N, Norcross R, Andersson U, Shou M, Nakayama K, Björkhem I, Pikuleva I (2003) Broad substrate specificity of human cytochrome P-450 46A1 which initiates cholesterol degradation in the brain. *Biochemistry* 42:14284–14292
- Ohyama Y, Meaney S, Heverin M, Ekström L, Brafman A, Andersson U, Olin M, Eggertsen G, Diczfalussy U, Feinstein E, Björkhem I (2006) Studies on the transcriptional regulation of cholesterol 24-hydroxylase (CYP46A1): marked insensitivity towards different regulatory axes. *J Biol Chem* 281:3810–3820
- Wechsler A, Brafman A, Shafir M, Heverin M, Gottlieb H, Damari G, Gozlan-Kelner S, Spivak I, Moshkin O, Fridman E, Becker Y, Skaliter R, Einat P, Faerman A, Björkhem I, Feinstein E (2003) Generation of viable cholesterol-free mice. *Science* 302:2087
- Russell DW (2003) The enzymes, regulation, and genetics of bile acid synthesis. *Annu Rev Biochem* 72:137–174
- Pfriegeer FW (2003) Outsourcing in the brain: do neurons depend on cholesterol delivery by astrocytes? *Bioessays* 25:72–78
- Abildayeva K, Jansen PJ, Hirsch-Reinshagen V, Bloks VW, Bakker AHF, Ramackers FCS, deVente J, Groen AK, Wellington CL, Kuipers F, Mulder M (2006) 24S-Hydroxycholesterol participates in a liver X-receptor-controlled pathway in astrocytes that regulates apolipoprotein E-mediated cholesterol efflux. *J Biol Chem* (in press)
- Norlin M, Toll A, Björkhem I, Wikvall K (2000) 24-Hydroxycholesterol is a substrate for hepatic cholesterol 7 $\alpha$ -hydroxylase (CYP7A). *J Lipid Res* 41:1629–1639
- Li-Hawkins J, Lund E, Bronson AD, Russell DW (2000) *J Biol Chem* 275:16543–16549
- Björkhem I, Andersson U, Ellis E, Alvelius G, Ellegård L, Diczfalussy U, Sjövall J, Einarsson C (2001) From brain to bile. Evidence that conjugation and omega-hydroxylation are important for elimination of 24S-hydroxycholesterol (cerebrosterol) in humans. *J Biol Chem* 276:37004–37010
- Bretillon L, Lütjohann D, Stähle L, Widhe T, Bindl L, Eggertsen G, Diczfalussy U, Björkhem I (2000) Plasma levels of 24S-hydroxycholesterol reflect the balance between cerebral production and hepatic metabolism and are inversely related to body surface. *J Lipid Res* 41:840–845

34. Bretillon L, Sidén A, Wahlund LO, Lutjohann D, Minthon L, Crisby M, Hillert J, Groth CG, Diczfalusy U, Björkhem I (2000) Plasma levels of 24S-hydroxycholesterol in patients with neurological diseases. *Neurosci Lett* 331:163–166
35. Bogdanovic N, Bretillon L, Lund EG, Diczfalusy U, Lannfelt L, Winblad B, Russell DW, Björkhem I (2001) On the turnover of brain cholesterol in patients with Alzheimer's disease. Abnormal induction of the cholesterol-catabolic enzyme CYP46 in glial cells. *Neurosci Lett* 314:45–48
36. Brown J, Theisler C, Silberman S, Magnuson D, Gotthardt-Littell N, Lee JM, Yager D, Crowley J, Sambamurti K, Rahman MM, Wolozin (2004) Differential expression of cholesterol hydroxylases in Alzheimer's disease. *J Biol Chem* 279:34674–34681
37. Leoni V, Masterman T, Diczfalusy U, DeLuca G, Hillert J, Björkhem I (2002) Changes in human plasma levels of the brain specific oxysterol 24S-hydroxycholesterol during progression of multiple sclerosis. *Neurosci Lett* 331:163–166
38. Leoni V, Mastermann T, Mousavi FS, Wretling B, Wahlund LO, Diczfalusy U, Hillert J, Björkhem I (2004) Diagnostic use of cerebral and extracerebral oxysterols. *Clin Chem Lab Med* 42:186–191
39. Leoni V, Shafaati M, Salomon A, Kivipelto M, Björkhem I, Wahlund LO (2006) Are the CSF-levels of 24S-hydroxycholesterol a sensitive biomarker for mild cognitive impairment? *Neurosci Lett* 397:83–87
40. Heverin M, Bogdanovic N, Lutjohann D, Bayer T, Pikuleva I, Bretillon L, Diczfalusy U, Winblad B, Björkhem I (2004) Changes in the levels of cerebral and extracerebral sterols in the brain of patients with Alzheimer's disease. *J Lipid Res* 45:186–193
41. Leoni W, Masterman T, Patel P, Meaney S, Diczfalusy U, Björkhem I (2003) Side-chain oxidized oxysterols in cerebrospinal fluid and integrity of blood–brain barrier. *J Lipid Res* 44:793–799
42. Heverin M, Meaney S, Lutjohann D, Diczfalusy U, Wahren J, Björkhem I (2005) Crossing the barrier: net flux of 27-hydroxycholesterol into the human brain. *J Lipid Res* 46:1047–1052
43. Björkhem I, Heverin M, Leoni M, Meaney S, Diczfalusy U (2006) Oxysterols and Alzheimer's disease. *Acta Neurol Scand* 114 (Suppl 185):43–49
44. Björkhem I, Meaney S (2004) Brain cholesterol: long secret life behind a barrier. *Arterioscl Thromb Vasc Biol* 24:806–815
45. Kölsch H, Lutjohann D, Tulke A, Björkhem I, Rao ML (1999) The neurotoxic effect of 24-hydroxycholesterol on SH-SY5Y human neuroblastoma cells. *Brain Res* 818:171–175

# Sterol Biosynthesis Inhibitors: Potential for Transition State Analogs and Mechanism-Based Inactivators Targeted at Sterol Methyltransferase

Zhihong Song · W. David Nes

Received: 3 November 2006 / Accepted: 15 December 2006 / Published online: 14 February 2007  
© AOCs 2007

**Abstract** Sterol biosynthesis inhibitors (SBIs), discovered in the late 1960s and subsequently used commercially to treat ergosterol-dependent fungal diseases, represent a unique drug class targeted at an enzyme in a biosynthetic pathway. To date, few drugs have been commercialized as enzyme inhibitors; yet, prescription of SBIs has emerged as the gold standard for some cases of non-life-threatening antifungal chemotherapy and in crop protection. SBIs are not designed for their structural resemblance to the sterol molecule; they nonetheless can engender a curative effect by interfering with sterol production and homeostasis in the pathogenic organism. The increased use of SBIs in recent years, particularly the azole antifungals, has resulted in the development of resistance to those drugs, necessitating additional work to further our understanding of antifungal resistance and to explore opportunities to develop new enzyme inhibitors and uncover new enzyme targets that can regulate carbon flux in the post-lanosterol/cycloartenol pathway. This article reports general considerations for enzyme mechanism and active-site probes using inhibitors of the C-methylation reaction, including a potential new class of antifungal/antiparasitic agents of phytosterol synthesis tailored as mechanism-based inactivators. These steroid-based compounds prepared with different sterol side chain functionalities are designed to reversibly or irreversibly impair the sterol methyltransferase, an enzyme expressed in pathogenic microbes and plants but not in the human host. The salient aspects of these and related

topics directed toward the enzyme recognition of sterol structure, and the inhibitory properties and catalytic competence of a series of specifically modified substrate analogs that affect sterol methyltransferase action are discussed.

Primarily due to their impact upon plant and human health, the similarities and differences in sterol content between microbes of eukaryotic origin and more advanced systems, the functions of the various sterols and biosynthetic intermediates, as well as the characterization of the enzymatic reactions involved have all received substantial investigation. An important goal of most of these studies is to provide basic information about sterol biochemistry from which drugs, herbicides, etc., can be developed to exploit a fundamental difference in sterol homeostasis (involving the type and amount of cellular sterol) between the pathogenic microbe and its host, whether human or plant. Excellent reviews that cover the topic of sterol biosynthesis inhibitors are available [1–4]; the last time this subject was reviewed in the journal *Lipids* was in 1986 by the Strasbourg group, who made seminal contributions to the field [5].

## Ergosterol Homeostasis

The major sterol of microbes, ergosterol accumulates in the cell at ca. 20–100 fg/cell; this contrasts with the sterols of advanced plant and animal systems, sitosterol and cholesterol respectively, that occur at ca. 3,000 fg/cell [6] (Fig. 1). Ergosterol and sitosterol are regarded as phytosterols (sterols that contain a 24-alkyl

Z. Song · W. D. Nes (✉)  
Department of Chemistry and Biochemistry,  
Texas Tech University, Lubbock, TX 79409, USA  
e-mail: wdavid.nes@ttu.edu

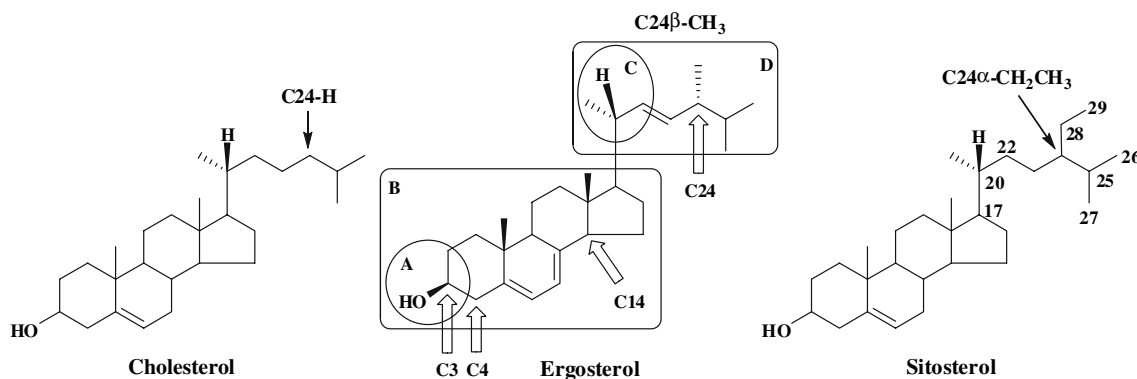


**Fig. 1** Representative zoosterol and phytosterols (24-alkyl sterols). The structure of ergosterol is boxed to show different domains of the nucleus and a side chain of functional significance; arrows indicate structural features of key importance

group in the sterol side chain), whereas cholesterol is regarded as a zoosterol (sterols that lack a 24-alkyl group in the sterol side chain) [6]. The physiological importance of ergosterol to fungal–plant/human interactions provide a biochemical paradigm that ergosterol-dependent diseases can be cured or eradicated through the disruption of ergosterol homeostasis. The key element of this paradigm is that *de novo* sterol synthesis and the structural features of ergosterol are important to fungal growth and that loss of the native ergosterol structure, such as through blockage of the addition of the C24-methyl group to the intermediate structure, will harm cell physiology.

The first evidence that disruption of ergosterol homeostasis can lead to impaired fungal growth was the study by Nes and coworkers, who in the 1970s cultured yeast anaerobically to generate sterol auxotrophy. By supplementing the culture medium with different sterols, they established the functional significance of the structural features of yeast ergosterol and demonstrated that lanosterol and other intermediates were harmful to cell proliferation and morphology [7, 8]. From a functional perspective, the structural features can be divided into the ring and side chain requirements (cf. the ergosterol structure in Fig. 1). For the ring, the 3 $\beta$ -OH group is obligatory for growth, whereas the presence of C4 and C14 methyl groups in the nucleus did not allow growth. There appeared to be little advantage in the presence of double bonds compared to the fully saturated B-ring sterol. In the side chain, the 24 $\beta$ -methyl group was obligatory for growth, but better growth still was observed with the natural side chain containing a 24 $\beta$ -methyl group and  $\Delta^{22}$ -double bond. By comparing the growth response to sterols with opposite configurations at C20 and C24, only sterols with the natural configuration at C20R- and C24 $\beta$ -methyl groups supported growth. This work

highlighted, for the first time, the importance of sterol specificity that can manifest itself in ergosterol-dependent diseases, and permitted a rational manipulation of ergosterol homeostasis that will lead to cell death. The importance of ergosterol to other microbial systems and sitosterol to plants in growth has been reported and confirms the original observations. In further work on this issue, several groups were able to show that sterol played a dual function in microbial physiology [1, 6, 7, 9–11]: the first as a bulk membrane component and the second as a “sparking” compound to signal cell proliferation; this second function uses orders of magnitude less sterol than that required in the membrane. Clearly, if those features that are essential for growth could be exploited as antifungal targets, then it should be possible to obtain an effective inhibitor for therapeutic purposes and for crop protection.

The study of ergosterol biosynthesis in fungi and protozoa became of particular interest after it was discovered that specifically acting compounds, the “azoles” [4], a diverse group of compounds including the imidazoles, triazoles, pyrimidines and pyridines, interfere quite precisely in fungal metabolism, mainly in one or three steps of the lanosterol–ergosterol pathway [viz., with the Erg11p, Erg24p and Erg2p]. The mechanism of action by which many of the azoles interrupt ergosterol synthesis is based on their ability to bind to the 14 $\alpha$ -demethylase enzyme [CYP51, Erg11p] with greater affinity in fungal cells than to the 14 $\alpha$ -demethylase in animal cells. A common structural feature of these compounds that promote enzyme inhibition is an unsubstituted imidazole ring or triazole ring, bound via the N-3 atom of the heterocycle to a carbon atom in the remainder of the molecule.

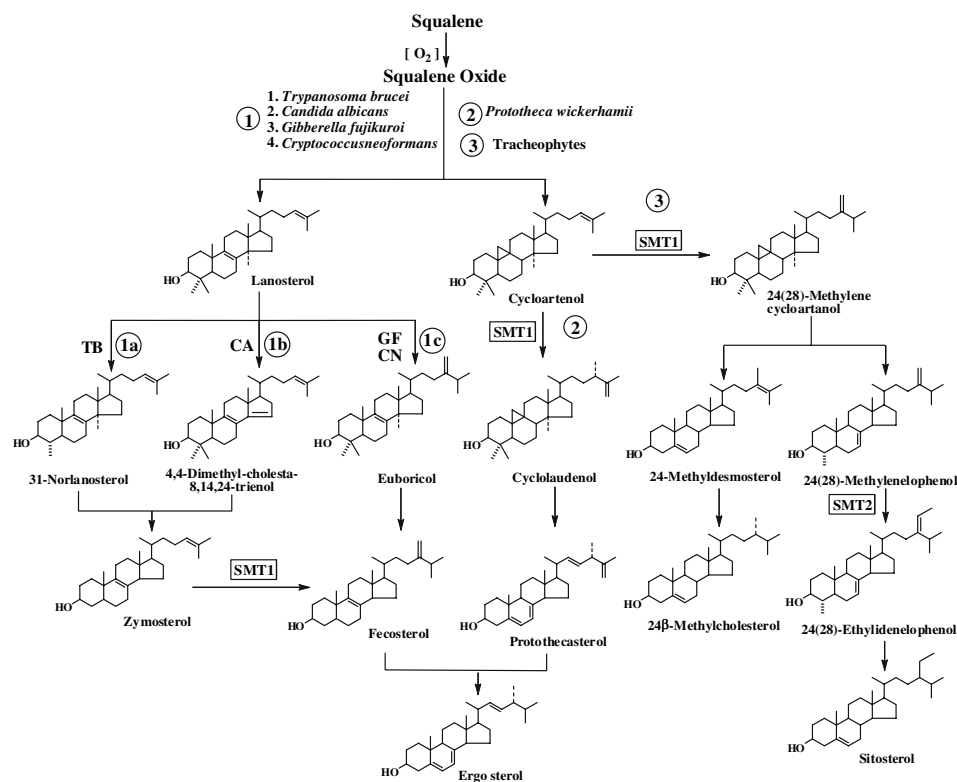
From a compound intervention standpoint, impaired activity that disrupts carbon flux would be

expected when substrates are produced on which the enzymes fail to catalyze; consequently, these substrates should become deleterious to the cell because they are present in abnormally high concentration and contain structural features harmful to membrane structure and function. This proposal has been confirmed in studies which show that impaired Erg11p activity can lead to an accumulation of lanosterol and 24(28)-methylene lanosterol in inhibitor-treated cells, causing these cells to die [4]. A related set of experiments has been performed with anaerobic yeast and a no-growth result occurred when cells were supplemented with lanosterol, consistent with the observations of the inhibitor-treated fungi. Although the activity of the 14 $\alpha$ -demethylase enzyme can be interrupted by azole treatment, thereby generating lanosterol in vivo, it is not necessarily the presence of the 14 $\alpha$ -methyl group [C32] on the back face of the sterol molecule that prevents proper sterol–lipid interactions in the lipid leaflet; rather it is more likely the presence of the C4-geminal methyl group on the sterol molecule that can perturb the hydrogen bonding ability of the C3-hydroxyl group in the membrane [12]. Removal of the C14-methyl group is necessary to allow for the introduction of the  $\Delta^5$ -bond in the nucleus, which can also have functional significance [10].

## Ergosterol Biosynthesis

In the early stages of formation, the synthetic pathway to fungal ergosterol uses an isoprenoid pathway to squalene oxide similar to the one involved in cholesterol formation (viz, the acetate–mevalonate pathway); thereafter the pathway can diverge into routes that are phylogenetically distinct based on whether the organism will synthesize lanosterol (animals and fungi) or cycloartenol (plants) (Fig. 2) [12, 13]. In most fungi and many protozoa, the following key transformations from lanosterol to ergosterol take place in the order: (1) methylation at C24; (2) demethylation at C4 followed by demethylation at C14; (3) double bond transformations in the nucleus from  $\Delta^8$  to  $\Delta^5$ , and (4) double bond transformations in the side chain at C24(28) and C22(23). The yeast *Saccharomyces cerevisiae* is an important exception; methylation at C24 occurs after C4-demethylation. In *Prototheca wickerhamii* there is an additional enzyme system not present in fungi that is involved in catalyzing the opening of the 9 $\beta$ ,19-cyclopropane ring in the cycloartenol structure characteristic of a plant pathway to ergosterol. Higher plants can also synthesize 24 $\beta$ -methyl sterols similar in structure to ergosterol but these are obtained through a different route (Path 3 in Fig. 2). They can also produce 24-ethyl sterols where the 24-ethyl group is stereochemically

**Fig. 2** Proposed general pathway for the biosynthesis of  $\Delta^5$ -phytosterols from the first tetracyclic sterol formed by the cyclization of squalene oxide, lanosterol or cycloartenol



opposite to the C24-methyl group in fungal sterol ergosterol (Path 3 in Fig. 2).

### Phytosterol Diversity

It has become increasingly evident that considerable variability can exist during the post-squalene stages of ergosterol (phytosterol) synthesis among microbes, and this may partially explain the different responses to sterol biosynthesis inhibitors in pathogenic organisms. In some cases, the organism's sterol content and/or composition and hence its synthetic pathway can undergo a marked change as a function of host–parasite interactions or from morphological switching of the single cell to the hyphal phase of growth. In order for these changes to occur in the sterol synthetic pathway, the relevant enzymes that compose the pathway must undergo a change in activity and/or transcript level accompanied by a change in protein level. In the parasite *Trypanosoma brucei*, which causes sleeping sickness, the protozoan form cultured on a lipid-deficient medium contains significant levels of 24-methyl sterols, whereas the main sterol is cholesterol in the bloodstream form; there are no detectable 24-methyl sterols in these cells [14]. Presumably, the cholesterol is absorbed from the host, causing the set of ergosterol enzymes in the parasite to be down-regulated. In a similar fashion, the opportunistic pathogen *Pneumocystis carinii*, isolated from its animal host, contains 31 sterols but no ergosterol; the main sterol cholesterol is also absorbed from the animal host [15].

In the phytopathogen *Gibberella fujikuroi*, 38 different sterols have been identified at different stages of development with multiple 24 $\beta$ -methyl sterol end-products produced, including ergosterol during mycelial growth [16]. In the fungal-like pathogen *P. wickerhamii*, the microbe can synthesize ergosterol by a cycloartenol-based pathway [13], whereas in the zygomycetous fungus *Mortierella alpina* [17], the major sterol synthesized by the mycelia is cholesta-5,24-dienol (desmosterol), with minor amounts of 24-alkyl sterols, suggesting that desmosterol is the membrane insert and the 24-alkyl sterol(s) is the “sparking” compound. In *M. alpina*, as reported for *P. carinii*, no ergosterol can be detected in the organism.

Several microbes have been found to utilize an unconventional phytosterol synthetic pathway that includes the ability to use a mevalonate-independent route to squalene [18, 19]. In the case of unconventional phytosterol side chain construction, multiple 24-alkyl sterol products are formed by sterol methyltransferase (SMT) catalysis in *T. brucei* [20], rather than a single

product as found in *S. cerevisiae* [21]. Other examples of unconventional phytosterol C-methylation pathways include formation of the  $\Delta^{25(27)}$ -olefins with a 24 $\beta$ -methyl group in *P. wickerhamii* [22] and in *T. brucei*, the formation of a 24-dimethyl group in trypanosomoid phytosterols [20], the formation of multiple C24-alkylated sterol side chains in *P. caranii* (analogous to the product outcome that has recently been found to be catalyzed by plant SMTs [23]), and the synthesis of the 24 $\beta$ -methyl group in 22,23-dihydrobrassicasterol in *G. fujikuroi* by a route distinct from the route to ergosterol [24].

A distinguishing feature of phytosterols is the SMT-catalyzed introduction of the 24-alkyl group. This class of catalyst can be appealing targets for the design of inhibitors to inhibit microbe growth, since they lie on a pathway that is essential to phytosterol formation and are absent from the sterol pathway in animals. SMTs are unique since they not only catalyze the C-methylation reaction stereospecifically and with a high degree of substrate specificity, but they can also provide a critical slow step that is used to regulate carbon flux in post-squalene pathway transformations [6]. Interestingly, when the SMT is blocked in certain pathogens it will promote the accumulation of lanosterol or cycloartenol analogous to the situation inazole-treated fungal cells [1–6]. Having identified the SMT as a biochemical target, we can now address what is known about its C-methylation reaction, enzymatic properties and tests involving substrate analogs, concluding with future directions that incorporate recent findings about reversible and irreversible inhibitors affecting SMT action and their potential use in medicine and agriculture.

### SMT: Steric–Electric Plug Model of Binding and Catalysis

The crucial C-methylation reactions that generate the parent phytosterol side chain skeletons are catalyzed by enzymes collectively known as sterol methyltransferases [25]. These enzymes bind a  $\Delta^{24}$ -sterol acceptor molecule and a methyl donor AdoMet cofactor to produce a 24-methylated (ethylated) sterol product and AdoHcy. The SMTs can be divided into two families based on their genetics and substrate preference for a sterol with a side chain structure of  $\Delta^{24(25)}$ -(SMT1) or  $\Delta^{24(28)}$ -(SMT2) [26]. However, largely based on our recent work which showed that SMT isoforms from different sources exhibit a high degree of substrate specificity for either zymosterol, cycloartenol, lanosterol and 24(28)-methylene lophenol, there has been a refinement of the



Enzyme Commission's (E.C.) classification of the reactions they catalyze [21]. By also considering the genetics and substrate specificity, the SMTs can be classed as follows; SMT1 zymosterol 24-methyltransferase (E.C. 2.1.1.41); SMT1 cycloartenol 24-methyltransferase (E.C. 2.1.1.142); (no E.C. number assigned for a lanosterol-binding SMT) and SMT2 24-methylene lophenol C-methyltransferase (E.C. 2.1.1.143). Therefore, in the E.C. classification of enzymes, SMT activity can be classified according to the catalytic mechanism of their active site into one of four mechanistic sets that involve the generation of a C-methyl- $\Delta^{24(28)}$ - and  $\Delta^{25(27)}$ -,  $\Delta^{23(24)}$ - and  $\Delta^{24(25)}$ -olefin. Although, as we will show below, SMT1 or SMT2 may be characterized by one of these catalytic mechanisms, this characteristic is not yet used in the E.C. nomenclature.

Since 1978, a series of investigations carried out using intact organisms and recombinant SMT by several research groups has greatly added to the present understanding of C-methyl transfer reactions catalyzed by SMT. In one case, the results support a nonstop (concerted) mechanism for the first  $C_1$ -transfer that produces a single product with a 24-methyl  $\Delta^{24(28)}$ -olefin, whereas the second series of studies provides the first evidence for a step-wise ionic mechanism for the second  $C_1$ -transfer, which generates multiple product sets such as those with a mixture of 24-methyl (or ethyl)  $\Delta^{24(28)}$ - and  $\Delta^{25(27)}$ -olefins. The stereochemical features on the path to the second  $C_1$ -transfer reaction were the same as those noted in the first  $C_1$ -transfer reaction [25]. Thus, the enzymatic transfer of a methyl group of AdoMet to a  $\Delta^{24(28)}$ -olefin acceptor sterol occurs on the *Si*-face of the original substrate double bond such that the C25 configuration obtained during the first  $C_1$ -transfer reaction is retained during the second  $C_1$ -transfer reaction. Based on the above considerations, related work with plant, fungal and protozoan SMT isoforms with unique sterol specificity, the results from other relevant biogenetic studies, and the conclusions drawn from model reactions [27], a general scheme for the first and second  $C_1$ -transfer methylation reactions has been proposed (Fig. 3) and embodied in the "steric–electric plug" model of sterol/AdoMet binding and catalysis [28] (Fig. 4).

This stereochemical model predicts the structural features of the sterol molecule needed to generate a productive Michaelis–Menten complex that includes a free  $3\beta$ -OH group, a planar tetracyclic nucleus, a side chain that orients to the "right" ( $C_{20R}$ -configuration) in a pseudocyclic conformation, and a double bond located at position C24. A related, central prediction of the model is that the ProE-26 of the  $\Delta^{24}$ -substrate derived from C2-MVA becomes the ProS-C26 of the

24-methyl(ene) product as a consequence of an  $S_N2$  type mechanism that involves  $\beta$ -face nucleophilic attack by the  $\pi$ -electrons of the  $\Delta^{24}$ -bond on the *S*-methyl group of AdoMet coupled to a stereospecific 1,2-hydride shift of H24 to C25 on the *Re*-face of the original substrate double bond (Fig. 4).

### C-Methylation Reaction Progress

The observed regiochemistry and stereochemistry of any particular sterol C-methylation reaction depends upon the precise amino acid contacts resulting in the active center with specific nucleophilic groups on the sterol acceptor. One approach to designing potent inhibitors of the SMT that can disrupt these interactions is to unmask the probable structure of the transition state of the chemical reaction catalyzed by the enzyme. Kinetic constants involved with catalytic efficiency,  $k_{cat}$  and  $k_{cat}/K_m$ , are measures of the stabilization of the catalytic transition state of the enzyme, where the  $K_d$ ,  $K_i$  and  $K_m$  values are measures of substrate/inhibitor binding affinity [29]; the term "transition state stabilization" is often used in the literature to refer to specific electrostatic interactions that are strengthened in the transition state. In the case of the yeast SMT-catalyzed reaction, one can envisage the involvement of a transient interaction in the activated complex between the C24 and C25 cationic intermediate(s) and the active site of the enzyme. Electrostatic interactions that occur in the SMT active site between enzyme and substrate can be disrupted by transition state analogs, such as 24(*R,S*)25-epiminocholest-8-enol, that possess a positively charged functional group at physiological pH. In our research laboratory we recently determined (for the first time for any enzyme that acts on sterol) the relevant kinetic constants to establish a free-energy diagram for an SMT enzyme-catalyzed reaction [6, 30]. As demonstrated schematically in Fig. 5, the reaction coordinate proceeds energetically uphill, from the binding interactions of the ground state (associating sterol and AdoMet) to the interactions of the activated complex (which involve stabilizing the making and breaking of chemical bonds associated with the methylation–deprotonation reaction, product formation, and then the release of the products from the enzyme)[6, 30].

In work carried out by the Strasbourg group [5], it was found that the high-energy intermediate [carbocation (**2** in Fig. 4)] generated at C25 during the methylation–deprotonation reaction could be replaced by a positively charged nitrogen atom (e.g., protonated form) introduced at C25 to mimic the structure of the

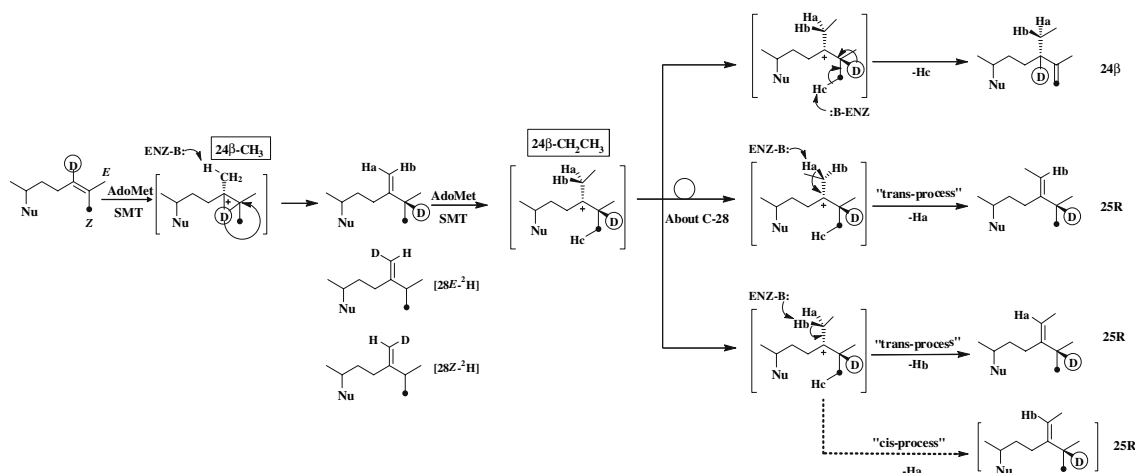
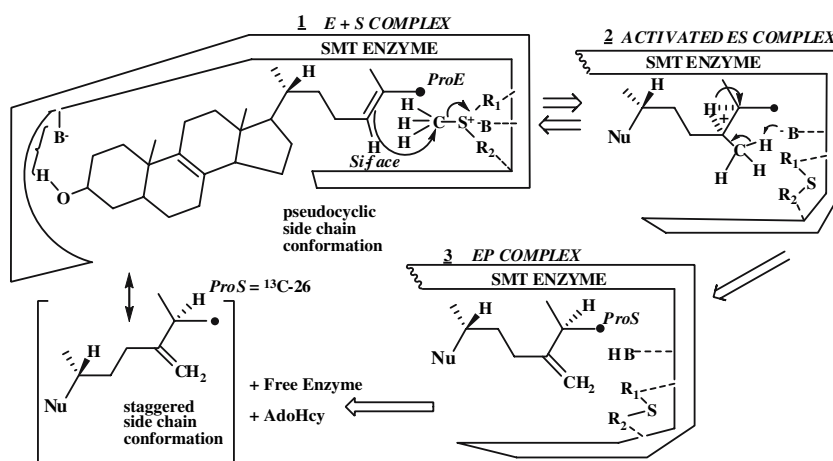


**Fig. 3** Proposed mechanism for the biosynthesis of phytosterols that generates successive mono and double C24-alkylation in the side chain from a  $\Delta^{24}$ -acceptor molecule. Deuterium-labeled

sterol side chains were studied to reveal the mechanism (adapted from [23, 32])

**Fig. 4** Steric–electric plug model of the sterol methyltransferase binding and catalysis of sterol and S-adenosyl-L-methionine (AdoMet). SMT sterol methyltransferase enzyme; *E* enzyme; *S* substrate or acceptor molecule; *P* C24-methylated product; *B* unidentified enzymic base; S-adenosyl-L-homocysteine (AdoHcy) (adapted from Parker and Nes in [28])



putative “charged” intermediate formed during catalysis. If the transition state stabilization is equated to the binding energy, a stable analog that mimics the structure of the transition state should bind to an enzyme more tightly than the native substrate, i.e., it should bind with a strength at least three orders of magnitude higher than that of the best substrate for the enzyme [5]. In support of this view, utilizing the yeast SMT we found that the  $K_m$  for zymosterol is 30  $\mu\text{M}$ , whereas a transition state analog and potent noncompetitive inhibitor of the C-methylation reaction, 24(*R,S*),25-epiminocholest-8-enol, generated a  $K_i$  value of 3 nM [31]. From the  $K_i/K_m$  values for the isostere cholest-8-enol and its “charged” counterpart 24(*R,S*),25-epiminocholest-8-enol [30], we calculate a  $\Delta(\Delta G)$  of 5.6 kcal/mol; this amount of binding energy reflects the contribution of electrostatic association to the total energy of formation of the inhibitor–enzyme complex in wild-type enzyme. In related work using a

plant SMT, Rahier et al. [5] reported a similar value for the  $K_m$  of cycloartenol and  $K_i$  values for 25-azacycloartenol in the micromolar and nanomolar range, respectively, as well as a value of 5.1 kcal/mol when comparing a similar set of inhibitors. However, the mechanistic work fails to show whether SMT actually lowers the activation energy for the making and breaking of bonds in the activated complex, or whether it simply forces the selection of a single reaction channel through the precise control of substrate conformation and the positions of counter ions that affect product outcome.

### SMT1 and SMT2 Isoforms

Over the past several years there have been remarkable advances in the study of SMT enzymes, because it has been possible to generate recombinant species of

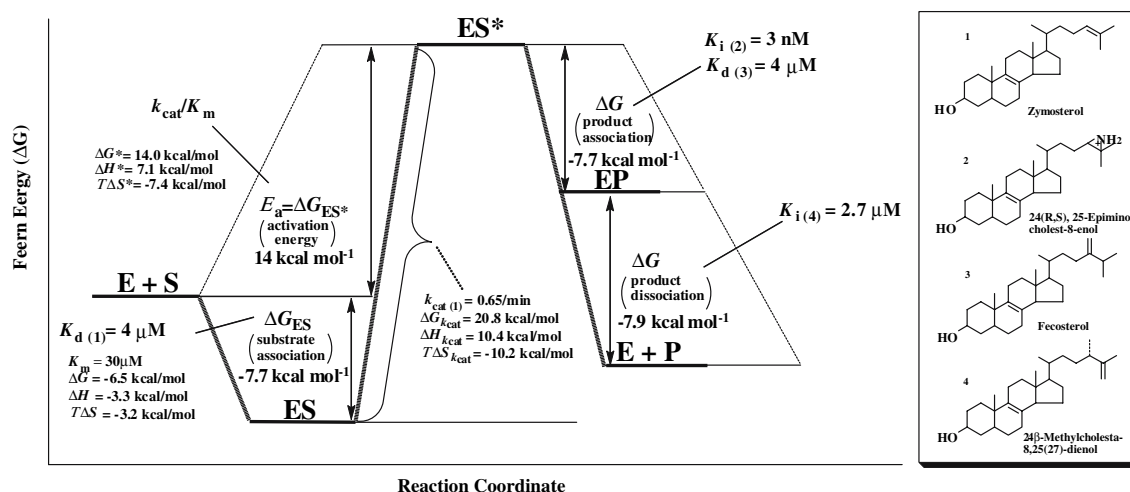


**Fig. 5** A hypothetical free energy profile for the sterol methyltransferase-catalyzed activity representing the C-methylation reaction that proceeds through the formation of a high-energy chemical intermediate (activated complex) by way of a C24-

methyl C25-cationic [or that of a C24(25)-bridged carbenium ion] intermediate. Compounds 1–4 assayed with the enzyme and the experimental values provided in the energy diagram are taken from [6, 30]

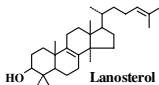
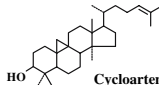
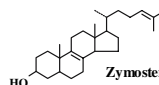
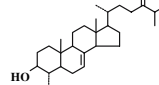
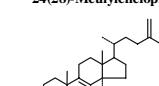
the native enzyme. Until now, the type and number of SMTs involved in catalyzing the product diversity observed in nature were not known. These enzymes had remained incompletely characterized until recently because of their low concentration in tissues, their membrane-bound nature and their lack of stability during purification efforts. Using cloned enzyme, it is now known that the pure SMT has unique properties that contribute to sterol specificity, kinetic and reaction properties, and to slow turnover, which serves to control carbon flux under physiological conditions. The cloned SMT from plant, fungi and protozoa possesses a pH that ranges from 6 to 8 with an optimum pH of 7.5, it is tetrameric with four identical subunits, and it has theoretical pI values that range from 5.4 to 7.5. The predicted molecular masses of the monomeric SMTs range from 38 to 43 kDa. The amino acid sequences deduced are reasonably similar to each other (21–78% identity), with 130–197 amino acids conserved in the primary structure [10, 21, 25, 27].

Fungi and protozoa have the genetics to express a single SMT (SMT1), whereas plants have a genome for SMT families and can express up to three SMT isoforms—one of the SMT1 type (C<sub>1</sub>-methylation activity) and two of the SMT2-type (C<sub>2</sub>-methylation activity) [21]; the different SMT activities possess different substrate properties and can produce various C24-methylated products. Both SMT1 and SMT2 from plants are currently known to be capable of performing either of the C<sub>1</sub>-transfer methylation activities, whereas the yeast SMT1 only performs the first C<sub>1</sub>-transfer methylation activity. The protozoa SMT1

can perform two C<sub>1</sub>-methyl transfers, but the doubly C24-alkylated product is different from that formed in plants [21]. There appear to be at least five sterol molecules that can serve as optimal substrate for the SMT, as shown in Fig. 6. In the case of fungi and protozoa, either lanosterol, 24(28)-methylene lanosterol (euboricol) or zymosterol are the preferred substrates of the enzyme. In the case of plants, cycloartenol or 24(28)-methylene lophenol are the preferred substrates for the enzyme. Equilibrium dialysis and time-dependent inhibition experiments indicate that the enzyme characteristically contains one active center with subsites for sterol and AdoMet. The turnover numbers for SMT1 and SMT2 are similarly slow, about 0.01 s<sup>-1</sup>, and the K<sub>m</sub> values for the optimal substrates for these enzymes are about the same, around 30 μM [20, 25, 27].

Biosynthetic pathways often involve enzymes that catalyze reversible bond formation, as determined for the Δ<sup>8</sup>- to Δ<sup>7</sup>-sterol isomerase. Alternatively, the plant SMT was found to act in an irreversible manner, with AdoMet binding predominantly in the forward direction. The enzyme activity responds to allostery; in soybean, the SMT1 is subject to down-regulation by the final product (K<sub>i</sub> of 65 μM), sitosterol (it is ergosterol in the case of yeast SMT1), but not by either cholesterol or ergosterol, and to up-regulation by physiological concentrations of ATP (400 μM) [25]. The position of SMT1 in, for instance, the soybean phytosterol pathway (in the first step), the relatively irreversible nature of the binding isotherm involving the cosubstrates, and the allosteric nature of the

**Fig. 6** Functional characteristics of the sterol methyltransferase in relation to sequence relatedness. SMT1 and SMT2 are distinguished by substrate specificity toward the  $\Delta^{24(25)}$ - and  $\Delta^{24(28)}$ -olefin side chain structure. The gene families are grouped into five distinct subfamilies based on sequence relatedness and substrate preference, as indicated in the figure (adapted from Nes et al. in [6, 21, 25])

SMT Classification	Substrate	Primary Catalytic Activity	Gene Family (Example)
SMT1	 Lanosterol	C <sub>1</sub> -transfer to 24,25-double bond	SMTc-fungal (Gibberella) (Cryptococcus)
SMT1	 Cycloartenol	C <sub>1</sub> -transfer to 24,25-double bond	SMTa-plant (Glycine)
SMT1	 Zymosterol	C <sub>1</sub> -transfer to 24,25-double bond	SMTb-fungal (Saccharomyces) SMTe-protzoan (Trypanosoma)
SMT2	 24(28)-Methylenlophenol	C <sub>1</sub> -transfer to 24(28)-double bond	
SMT2	 24(28)-Methylenlanosterol	C <sub>1</sub> -transfer to 24(28)-double bond	SMTc-fungal (Pneumocystis) (Glycine)

enzyme, together with the fact the SMT gives rise to the product diversity are all consistent with the SMT acting as the rate-limiting enzyme of phytosterol synthesis.

In cases where there is credible steady-state kinetic data for enzyme-catalyzed bisubstrate reactions, the yeast SMT1 is shown to proceed by a different reaction pathway than the one that operates for the plant SMT1 [23, 31]. In both cases, the cosubstrates, sterol and AdoMet, are bound to the enzyme at the same time at some point during the course of the reaction, forming a ternary complex. The possibility of the intervention of an X-group bound intermediate was eliminated experimentally; rather, for yeast a concerted addition–elimination C-methylation reaction was demonstrated kinetically [25]. In the yeast SMT1 case, a random ordered *bi bi* mechanism operates, where either substrate can bind first to the enzyme, and either product can leave first. For the plant SMT1, it was found that the AdoMet binds first to the SMT. Interestingly, the plant SMT1 can catalyze the second C<sub>1</sub>-transfer reaction in a mechanistically different way to the first C<sub>1</sub>-transfer, using a *bi ter* reaction to catalyze the  $\Delta^{24(28)}$ -substrate [32].

### SMT Sequence Relatedness

Over the past ten years, SMTs have been cloned, sequenced and purified from each of the major phylogenetic groups, including plant, fungi and protozoa.

Including the four families which represent enzymes of the SMT1 and SMT2 isoforms, sequences of another 60 SMTs are now available. Of the 383 amino acids in the *S. cerevisiae* SMT, 78 residues were completely conserved (21%) in those that we studied, including the SMT1-types *Glycine max*, *Cryptococcus neoformans*, and *Trypanosoma brucie* and the SMT2-type *Arabidopsis thaliana*. Overall, yeast SMT contains a distinct number of aromatic amino acids that are completely conserved (16 out of 47 with 34% identity), and two notable conserved regions of about ten amino acids each, referred to as Regions 1 and 3. In the yeast SMT, Region 1, which is highly hydrophobic with about 50% aromatic residues, spans Tyr81 to Phe91, and Region 3 spans Tyr192 to Pro201. Regions 1 and 3 are found only in the SMT, suggesting that they might have functional importance with respect to sterol biosynthesis. A third region that also contains ten amino acids, referred to as Region 2, spans Leu124 to Pro133. This signature motif is present in other AdoMet-dependent methyl transferases, where it is known to be part of the AdoMet binding site and therefore likely functions in the SMT structure in a similar fashion.

The possibility that several of the electron-rich aromatic residues with  $\pi$ -systems of indoles and phenyl groups might be part of the active center that directs the folding of the sterol side chain close to the AdoMet and contributes negative point charges that allow ion pairs to form, which could stabilize the developing cationic center(s) on the methylating substrate, was considered [25, 27]. The high degree of sequence

conservation in Regions 1–3 led us to perform leucine screening by site-directed mutagenesis of the aromatic residues in these regions [29–31]. We discovered that none of the conserved aromatic residues were essential to activity, but in the case of the *S. cerevisiae* SMT Tyr81 (Region 1) and Tyr192 (Region 3), substitution with a related aromatic amino acid can lead to altered substrate specificity, product formation and differential control of the first versus the second C<sub>1</sub>-transfer reaction, consistent with the hypothesis that aromatic amino acid residues at the active site play a crucial role in the C-methylation reactions. On the other hand, loss of activity was associated specifically with His-90 and Glu-195.

Chemical and photoaffinity labeling studies provided direct proof that Regions 1 and 3 are part of the sterol binding subsite and Region 2 is part of the AdoMet binding subsite. Supporting data, using site-directed mutagenesis, revealed that the aromatic amino acids of Regions 1 and 3 play a functional role in catalysis by managing reaction channeling that contributes to product diversity, whereas the histidine-90 residue in Region 1 and the glutamic acid-195 residue in Region 3 may act as the deprotonating agent and counter ion, respectively. According to Kyte–Doolittle hydrophathy plot analysis, the SMTs are moderately hydrophilic proteins without apparent membrane-spanning domains [25]. Thus, microsomal SMTs appear to associate weakly with membranes; this may explain the ease of solubilization from wild-type sources under mild conditions and their association with lipid droplets upon cell disruption.

### Substrate Analogs and Topological Considerations

Substrate, transition state and dead-end analogs tested with SMTs have long been useful for mapping the substrate specificity of the active site with regard to stereochemistry, three-dimensional shape, charge significance of functional groups or for determining the binding order of substrates and the molecular parameters of inhibition. In addition, we recently found that tight-binding SMT inhibitors can be used in an experimental strategy to determine the active enzyme concentration in wild-type cultured cells. The substrate specificity of SMT has been explored with a variety of analogs of zymosterol, cycloartenol and lanosterol. In a manner reminiscent of the forces involved in binding sterol to phospholipids in the membrane, the affinity of SMT for its substrates depends on polar interactions with the C3-hydroxyl group and C-24 double bond and nonpolar interactions with the nucleus and side chain.

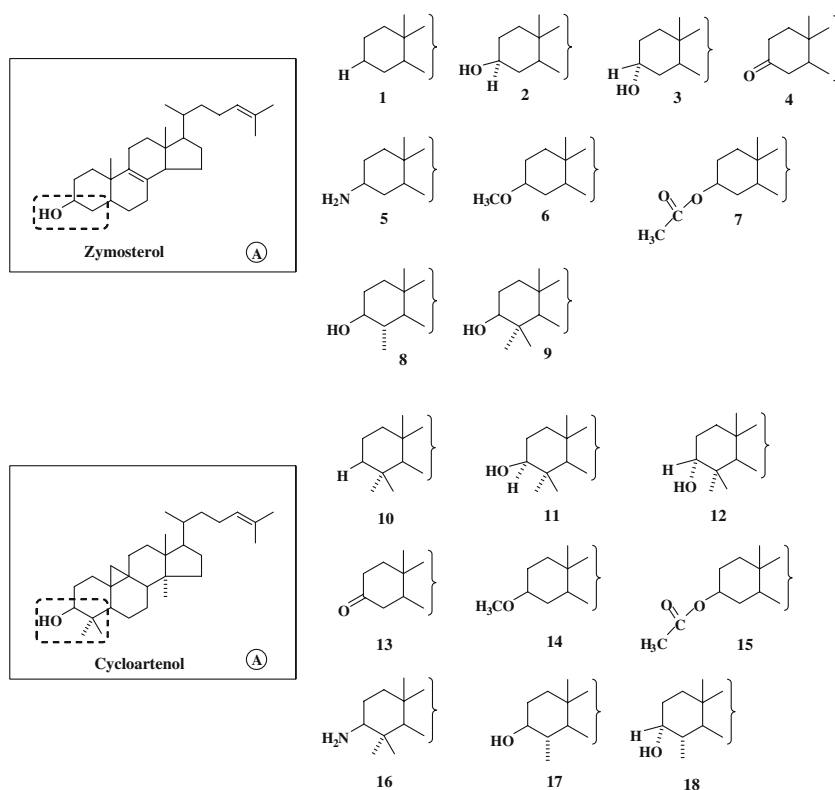
The molecule must be flat and the sterol side chain oriented to the “right-handed” conformation for optimal catalysis. The most extensive investigations of analogs used to test a specific region of the SMT1 and SMT2 were performed in this laboratory using compounds that differed in a single structural modification associated with a specific domain of the putative native substrate, referred to as Domain A, B, C or D (cf. Fig. 1), as summarized in Structures 1–5. The SMT1 can accept either a 4-demethyl sterol, such as zymosterol, or a 4,4-dimethyl sterol, such as cycloartenol, depending on the source of the enzyme (fungus or plant, respectively).

### Structure–Activity Studies: Substrates

When using  $V_{\max}/K_m$  determinations as the measure of catalytic competence for substrates assayed with the SMT, the SMT1 from a fungus and plant was found to recognize the stereochemistry, bulk and polarity at C3 (and at C4) [25]. Structure 1 shows substrates with modifications in Domain A. The yeast SMT1 prefers compound 2 with a 3 $\beta$ -hydroxyl group that is unhindered by a neighboring methyl group [3] at C4. It also accepts compounds 4 and 6 in which the 3-OH group has been replaced with a related oxygen-containing group. Alternatively, the plant SMT1 prefers a substrate that possesses the 3 $\beta$ -hydroxyl group with C4 substituted by a geminal methyl group, compound 10. The plant SMT1 will also accept compounds 13 and 15, but not the related methyl ether (compound 14), which is the case for the yeast SMT1. The results imply that the active sites of these SMT1 enzymes differ with respect to specific contact amino acids that are involved in hydrogen bonding to Domain A of the sterol molecule. The plant SMT2, which is not as extensively studied as the SMT1 isoforms because it is difficult to generate test sterols with a  $\Delta^7$ -nucleus, has been shown to prefer C4-monomethyl sterols with a 3 $\beta$ -hydroxyl group (e.g., compounds 17 vs. 18) [32].

In Structure 2, modifications of the sterol nucleus that refer to Domain B are explored. Sterols with a  $\Delta^{8(9)}$ ,  $\Delta^7$  or  $\Delta^5$  nucleus (monoene or diene) are good substrates for the plant or fungal enzyme, with  $\Delta^{8(9)}$ -sterols being the optimal substrates. Alternatively, sterols with a  $\Delta^{8(14)}$ -nucleus are poor substrates. Dredging models reveal that  $\Delta^{8(9)}$ -sterols are flatter than the other sterols tested with the SMT. An unexpected finding was that the yeast SMT1 utilized both of the 14 $\alpha$ -methyl sterols tested (compounds 25 and 26), converting them to C24(28)-methylene product (as judged by HPCL radiocounting against appropriate reference

## Structure 1

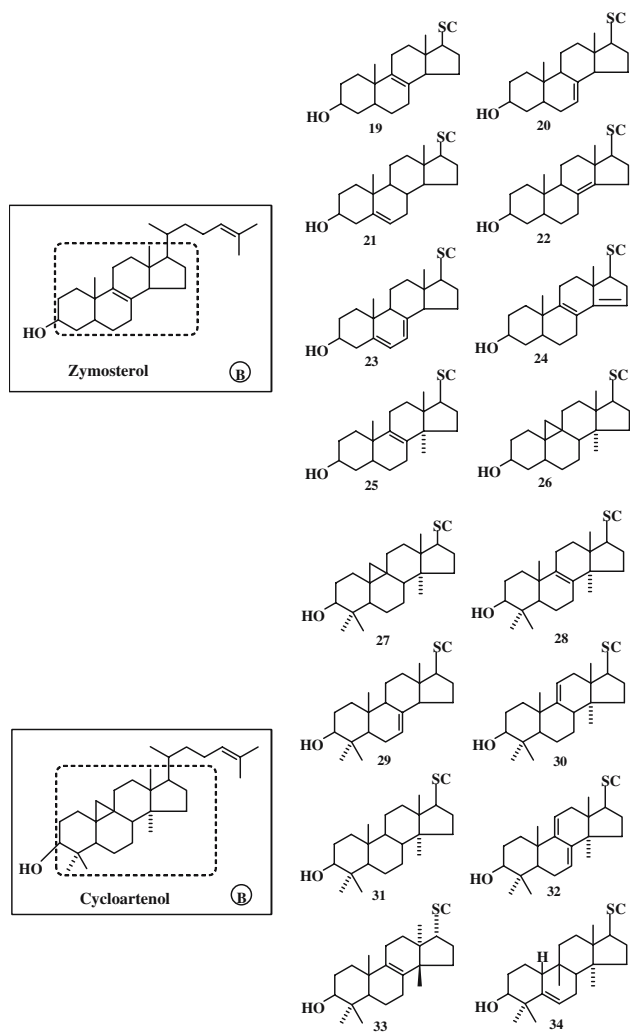


specimens and GC–MS). Earlier speculations [5] that  $9\beta,19$ -cyclopropane plant sterols are bent in shape, that they produce  $24\alpha$ -methyl sterols as a direct consequence of C-methylation, but that they cannot be converted to a  $24\beta$ -methyl sterol product because of their three-dimensional shape (Fig. 7), indicated that the ring structures in these substrates were similar [33]. Since plant sterols that contain a  $9\beta,19$ -cyclopropane ring structure have been found to be “flat” in solution and the solid state [39], the enzymatic results obtained with the two substrates (compounds **25** and **26**) are consistent with one another. In a second set of activity assays using plant SMT1 from soybean and sunflower [23, 34], we discovered that by assaying the structural isomers with a  $\Delta^{24}$ -bond and a  $9\beta,19$ -cyclopropane group,  $\Delta^9-\Delta^8-\Delta^7$  (compounds **27** to **30** and **32**) or no double bond in the nucleus (compound **31**), the optimal substrate for the SMT contained a  $9\beta,19$ -cyclopropyl group whereas the corresponding saturated sterol (lanostanol) that can flex somewhat into various physiological conformations failed to bind productively, suggesting that double bond character is important for locking the nucleus into a preferred conformation for binding. Further modification of the ring by changing the structure of the A/B ring system from flat to bent (compound **34**) or inverting the centers at C13, C14 and C17 to rearrange the methyl groups in C/D ring

junctions and the stereochemistry of the 17(20) bond (compound **33**) eliminated productive binding of the substrate. These results are keeping with the proposal that the substrate must possess a specific flat shape to be catalyzed by the SMT [25].

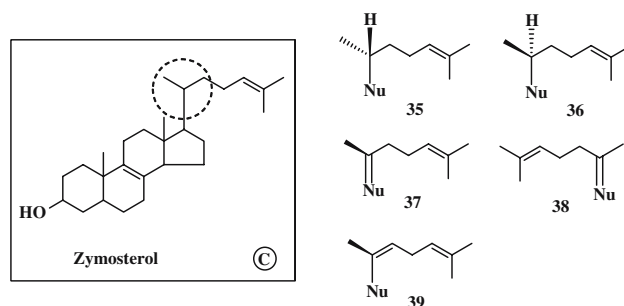
In Structure 3, the structure and stereochemistry at C20 were tested using SMTs from *S. cerevisiae* and *P. wickerhamii* [22, 35]. First, compounds **35** and **37** (which place the sterol side chain into the “right-handed” conformation) were converted to methylated product, whereas compounds **36** and **38** (which orient the sterol side chain into a “left-handed” conformation) were not accepted as substrates. These results suggest that the natural  $20R$  configuration in the sterol side chain is crucial to SMT-catalyzed reactions. The SMT enzyme can also catalyze a reaction with the planar  $\Delta^{20(22)E}, 24$ -dienol substrate (compound **39**), which proves that tetrahedral character at C20 is not essential for sterol binding to the SMT.

In Structure 4, the sterol side chain structure has been modified in terms of double bond position, double bond character, length and heteroatom substitution [22, 35, 36]. The presence of a  $\Delta^{24}$ -bond is crucial to catalysis. However, as found by studying the binding abilities of the substrate cholest-8-enol (compound **48**,  $K_d$  of 10  $\mu\text{M}$ ), it binds somewhat less effectively than zymosterol (cholesta-8,24-dienol; compound **40**,  $K_d$  of



### Structure 2

4  $\mu$ M) and it can impair catalytic activity since it has a  $K_i$  of ca. 100  $\mu$ M, suggesting that sterol can compete in the active site with native substrate. Activity is lost when the double bond in the side chain is moved to the



### Structure 3

$\Delta^{22}$ - (compound **41**) or  $\Delta^{25}$ - (compound **42**) position, but the  $\Delta^{24(25)}$ -sterol can undergo methylation to product (compound **44**) [20]. Steric hindrance produced by the addition of a methyl group at C24 (compounds **44** and **51**) can prevent methylation of the  $\Delta^{24}$ -substrate [33]. However, compounds **44** and **51** can both inhibit the yeast SMT, suggesting that the yeast SMT active site has limited freedom to accept added bulk to the side chain. Moving the substrate double bond from  $\Delta^{24(25)}$ - to generate a  $\Delta^{24(28)}$ -acceptor prevents the substrate from undergoing methylation by the wild-type yeast SMT, but in the case of the native SMT1 from plants, the  $\Delta^{24(28)}$ -acceptor is recognized in the second  $C_1$ -transfer reaction; both of the methylation activities can occur at the same active center in plant SMT1 and SMT2 isoforms, suggesting distinct subsites for binding the  $\Delta^{24(25)}$ - and  $\Delta^{24(28)}$ -olefins. Conjugated double bonds in the side chain at C22 and C24 or at C24 and C26 are not harmful to activity. Upon testing compound **45** with a truncated side chain, a requirement for the terminal branch in the side chain becomes apparent. Upon testing a homolog, compound **46**, a modest lengthening of the chain by one carbon was found to be tolerated by the SMT. The latter observation is worth noting, since in the case of the methylene cyclopropane (compound **47** [37]) the

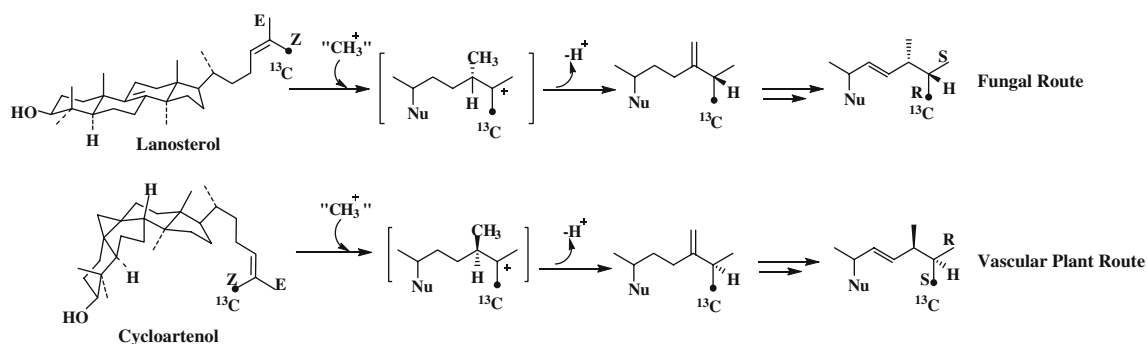
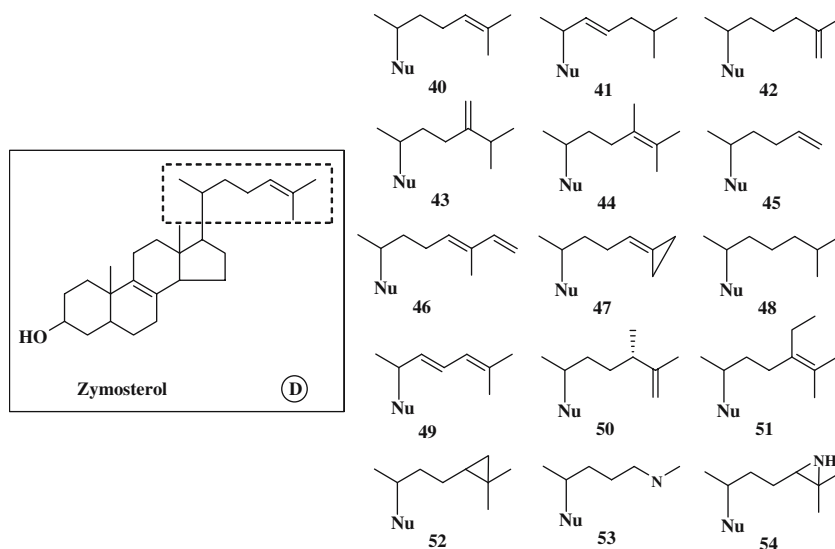


**Fig. 7** Alternative C-methylation reaction pathways that form  $24\alpha$ -methyl and  $24\beta$ -methyl sterols from substrates of possible distinct conformations: flat (lanosterol) or bent (cycloartenol);

work by the Nes research group discovered that the plant pathway illustrated does not operate in nature (adapted from Nes [25])

## Structure 4



substrate was methylated on the cyclopropane bridge-head C26 rather at C24, which is typical of all other  $\Delta^{24}$ -acceptor sterols. The  $\Delta^{24}$ -acceptor sterols catalyzed by the SMT were incorporated into the methylated sterol product regiospecifically; the methylene cyclopropane gave rise to a diene with double bonds at  $\Delta^{23}$  and  $\Delta^{25}$ , whereas all other  $\Delta^{24}$ -acceptors produced a  $\Delta^{24(28)}$ -olefin product.

The question of whether the 24,25-double bond in the sterol side chain could be replaced with an analog containing a fixed-locus nitrogen atom to mimic the developing olefin nucleophile of zymosterol by heteroatomic substitution of C24 or C25 has been examined with SMT from yeast, soybean and sunflower. Neither the azirdine-containing compound **54** nor its cyclopropane-containing surrogate (compound **52**) nor the 25-aza-containing side chain (compound **53**) were methylated by SMT, consistent with kinetic data that showed they were reversible inhibitors [35, 39].

The first studies directed at defining the structural parameters necessary for substrate recognition and subsequent initiation of the C-methylation reaction catalyzed by different SMT isoforms were confirmed and extended by examining the natures and magnitudes of inhibition (measured via experimentally determined  $K_i/K_m$  values) of a series of structurally related substrate analogs with nitrogen or sulfur introduced into the nucleus and/or side chain [35–40]. Using those nitrogen-containing analogs, which differ in a single structural feature but are otherwise similar to the natural substrate, and assuming that the recognition of an analog and natural substrate arises from a common set of enzyme interactions, it has been possible to identify and evaluate at least four critical structural elements of recognition involving the same

four domains reported before for the sterol structure. The principal determinant during binding appears to be associated with Domain A and the C3-hydroxyl group, since removal of the C3-hydroxyl group in the analog by replacement with hydrogen or by making a derivative of the C3-acetate alone is capable of non-competitively inhibiting the SMT at concentrations at least an order of magnitude lower than the inhibitor with the C3-hydroxyl group. The order of effectiveness of 25-azasteroids at inhibiting yeast SMT is 25-azazy-mosterol > 25-azalanosterol, and for plant SMT it is 25-azacycloartenol > 25-azacholesterol or 25-azalanosterol, consistent with the recognition of the sterol nucleus by the fungal and plant SMT1.

The stereochemistries at C20 and Domain C are also considered to be a major contributor to enzyme–substrate interactions for SMT isoforms. Consistent with earlier observations obtained using stereochemically varied substrates that show that the enzyme prefers 20*R*-sterols with the 20 $\beta$ -hydrogen atom (Structure 3), testing the diastereoisomeric pair of C20*R* and C20*S*-22-azacholesterols with side chain 20 $\alpha$ - or 20 $\beta$ -hydrogens, respectively (thereby placing the sterol side chain in a “left-handed” or “right-handed” conformation), revealed that the analog with the natural C20-configuration was a relatively potent noncompetitive inhibitor of SMT ( $K_i$  250 nM), whereas the analog with the unnatural C20 configuration was a weak competitive inhibitor of SMT ( $K_i$  1.2  $\mu$ M). The change in kinetic pattern suggests that the two inhibitors bind to different subsites in the active center of the enzyme.

The  $\Delta^{24}$ -bond associated with Domain D appears to be recognized electronically and specific to the natural side chain length, with a stringency paralleling that for the binding of the hydrophobic portion of the substrate



side chain. This follows from the observations that transition state analogs with a C25-nitrogen (in the salt form) inhibit the reaction three orders of magnitude more than the  $K_m$  for the natural substrate, as compared to the related inhibitor with an oxygen function (compound **64**) which failed to inhibit the reaction, and the 25-azasteroid with the terminal branch of the side chain was eliminated from the structure, producing a  $K_i/K_m$  value that was an order magnitude less than that of the corresponding natural 25-azasteroid.

### Structure–Activity Studies: Inhibitors

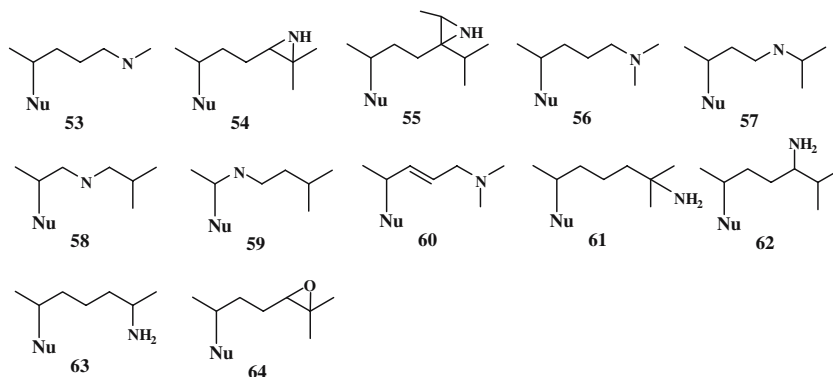
Structure 5 shows a set of inhibitors where modifications have been made to the structure and the location of the nitrogen atom along the lateral side chain. The “charged” aziridine compound **54** is more potent against the yeast SMT than any of the other inhibitors of similar structure for which compound **54** has been tested. The 24(28)-ethyl-containing aziridine, compound **55**, is less effective against the SMT than the 24(25)-aziridine inhibitor due to the added steric bulk at C24, which interferes with tight binding of the compound in the active site of the yeast SMT. The structure of the nitrogen—modified from a secondary amine (compound **54**) to a primary amine (e.g., compound **62**) to a tertiary amine (e.g., compound **61**)—had a significant effect on the inhibitor potency; the primary and tertiary amines were less potent by about an order magnitude than the secondary amine. Restricting rotation of the side chain by including a  $\Delta^{22}$ -bond (compound **60**) or by modifying the terminal branching in the side chain (e.g., compounds **61** and **63**) affected the binding such that these compounds were about an order magnitude less potent than the best inhibitor tested with the yeast SMT 24,(*R,S*),25-epiminocholest-8-enol. These results are consistent with the substrate preference for a  $\Delta^{24}$ -sterol and a distinct C-methylation mechanism performed by the yeast SMT; in this case,

the high-energy intermediate involves a bridged 24,25-carbenium ion, and the mechanism is short-lived and nonstop. On the other hand, in cases where the ionic C-methylation mechanism is rather long-lived and occurs step-wise to allow for a reversible hydride shift of H24 to C25, the C24,25-aziridine-containing inhibitor is less potent against the plant SMT than the 25-aza-containing compounds (e.g., compound **56**). When the C25-sulfur derivatives are prepared in the salt form [5, 35], they act in a similar fashion to C25-azasteroids and inhibit the SMT with equal effectiveness. The results described here provide strong suggestive evidence for the intermediacy of the predicted cationic species which the sulfonium and ammonium analogs were intended to mimic, and thus for the electrophilic nature and course of this reaction type.

The nitrogen atom can be moved toward the distal or proximal end of the sterol side chain, and the inhibitor will continue to bind quite well to the SMT. Inhibitors that contain a nitrogen function around C24–C25 usually impair catalysis between 1 and 50 nM. However, as the nitrogen atom is moved closer to C20, the inhibitor becomes less potent. When the inhibitor potency rises from the low nanomolar range to the low micromolar range, we observed that the kinetic pattern of inhibition changes from a noncompetitive-type to a competitive-type inhibition with respect to zymosterol. In a similar fashion the steroidal alkaloids solanidine and solasodine, which have the sterol side chain cyclized into a fifth ring and contain a nitrogen atom at about the equivalent of the C22–C23 position in the open extended side chain of cholesterol (Fig. 8), also generate a competitive-type kinetic pattern and will inhibit the enzyme in the low micromolar range [22, 36, 39]. The different  $K_i$  values and kinetic patterns of the various inhibitors tested with the SMT indicate that they possess different modes of binding in the active center.

It appeared possible that “charged” nitrogen-containing compounds (synthetically prepared or natural

### Structure 5



products) might serve as inhibitors of SMT until it was appreciated that these compounds lack specificity in terms of inhibiting enzymes of sterol biosynthesis, particularly during cholesterol synthesis [41–44]. For instance, the animal  $\Delta^{24}$ -reductase enzyme operates in a mechanistically similar way to the C-methylation reaction, so high-energy intermediate analogs with side chains shown in Structure 5 that inhibit SMT action should, and indeed have been found to, inhibit the animal  $\Delta^{24}$ -reductase. For instance, testing triparinol (a structural mimic of the natural products berberine and palmatine that inhibit SMT [45]) which, like 24(*R,S*),25-epiminolanosterol, can inhibit both the SMT and  $\Delta^{24}$ -reductase enzyme (Fig. 9) [33, 42], as an antihypercholesterolemic agent led to a range of side effects of sufficient severity to require withdrawal of the drug from the market [46]. The steroidal alkaloids from *Veratrum* (e.g., verazine) and *Solanum* steroidal alkaloids (e.g., solasodine) have good antifungal properties with  $IC_{50}$  values in the range 35–50  $\mu$ M [22, 47–49]. However, they can induce teratogenic effects in cows, causing malformations during embryonic development [50]. A further lack of specificity of these inhibitors is indicated by 25-azacholesterol binding to the human  $\Delta^8$ - to  $\Delta^7$ -isomerase with a  $K_i$  of 21  $\mu$ M [43], which might interrupt carbon flux in humans.

### Mechanism-Based Inhibition of SMT Catalysis

A final series of analogs related to the native  $\Delta^{24}$ -sterol acceptor molecule have been prepared for use

as possible mechanism-based inactivators to probe the topography of the active site, to serve as leader compounds for a new generation of antifungal/anti-parasitic agents, and for use as compounds to quantify active SMT concentrations in microbes and tissues. Figures 10 and 11 show hypothetical mechanisms for the inactivation of SMT by sterols with side chain modifications (including heteroatomic substitution with fluorine and sulfur or chemical alteration with novel olefin combinations to render them more electron-withdrawing), thereby allowing for the production of a unique reactive intermediate capable of trapping an enzyme nucleophile. Each of the side chain structures shown in Figs. 10 and 11 were prepared with a cycloartenol, lanosterol, desmosterol or zymosterol nucleus and the relevant inhibitor was tested with SMT from plant, fungus or protozoan [20, 32, 38, 40, 51–53, Song Z, Nes WD, unpublished data]. Our hypothesis is that mechanism-based inactivation of SMT requires ternary complex formation of the inhibitor followed by substrate methylation that undergoes rearrangement or delocalization to place a positive charge in a region of the active site that does not normally encounter electrophilic species. One or more of the resulting allylic cation species generated in the activated complex can serve as substrate to react with an active site base or nearby nucleophilic amino acid side chain, generating a covalent adduct with the enzyme. Alternatively, as in the case of the sulfur derivative (A, Fig. 11), the methylated intermediate may serve as a methyl donor to methylate an amino acid in the active site.

**Fig. 8** Representative natural products with a nitrogen in the structure that are found to inhibit fungal growth and to inhibit the sterol methyltransferase

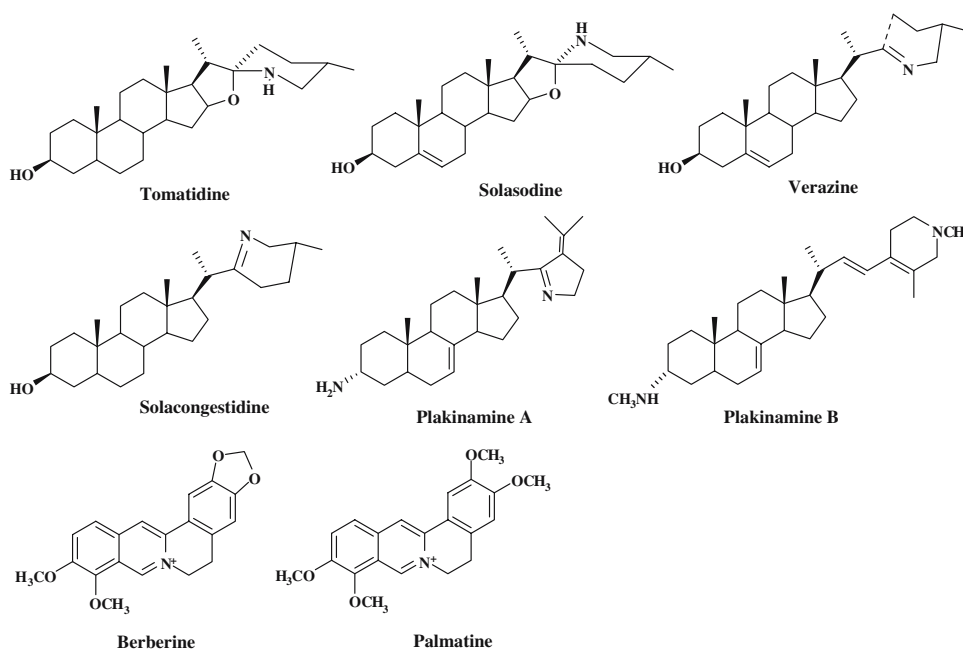


**Fig. 9** Postulated similarity between the C-24 alkylation and reduction of the sterol side chain  $\Delta^{24}$ -bond and inhibition by a hypothetical transition state analog of the reaction mechanism; the substrate mimic 24(*R,S*),25-epiminolanosterol and the related compound triparanol with structural features that can mimic the hydrophobic part of the sterol nucleus and a charged nitrogen at the tail portion of the molecule that can mimic the protonated nitrogen group in the tail portion of the 24(*R,S*),25-epiminolanosterol side chain

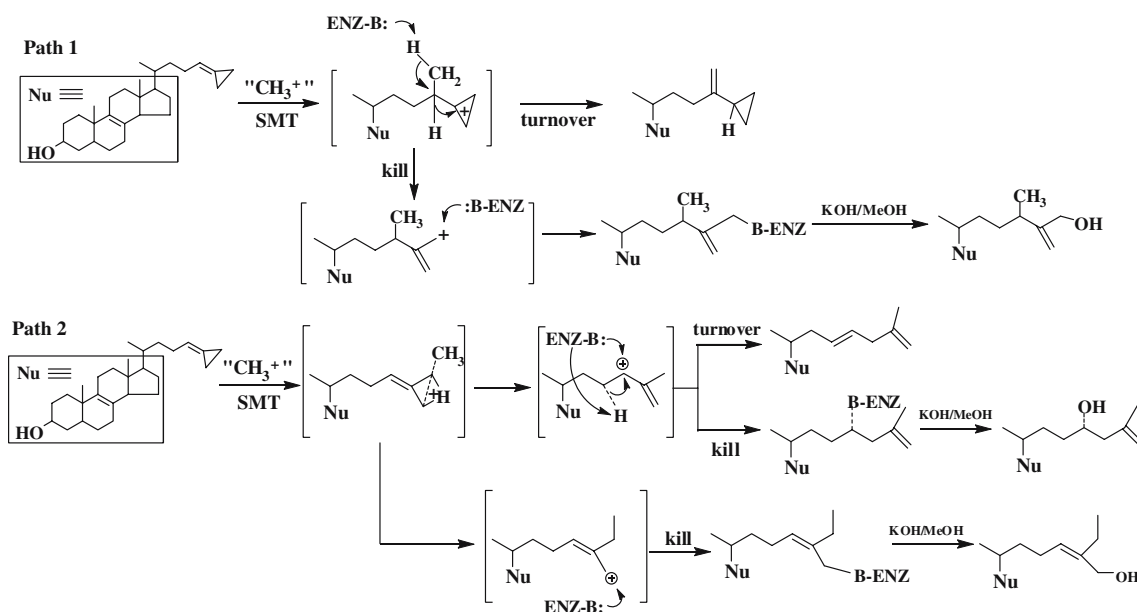
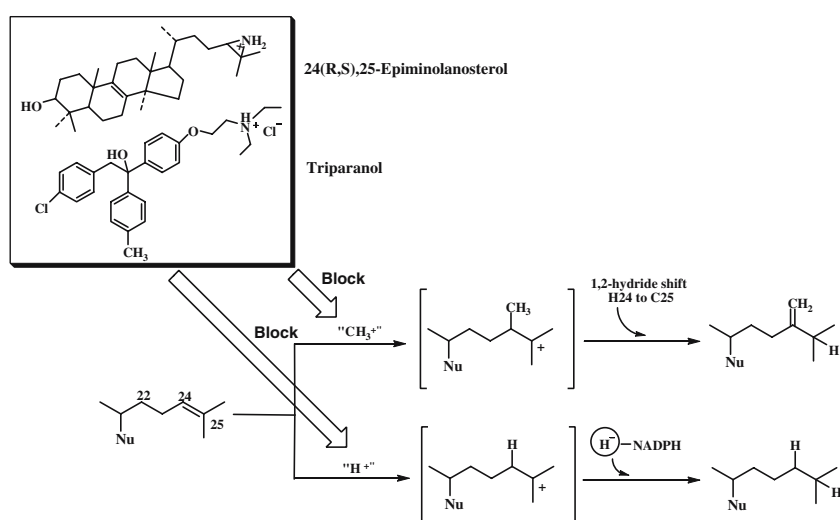
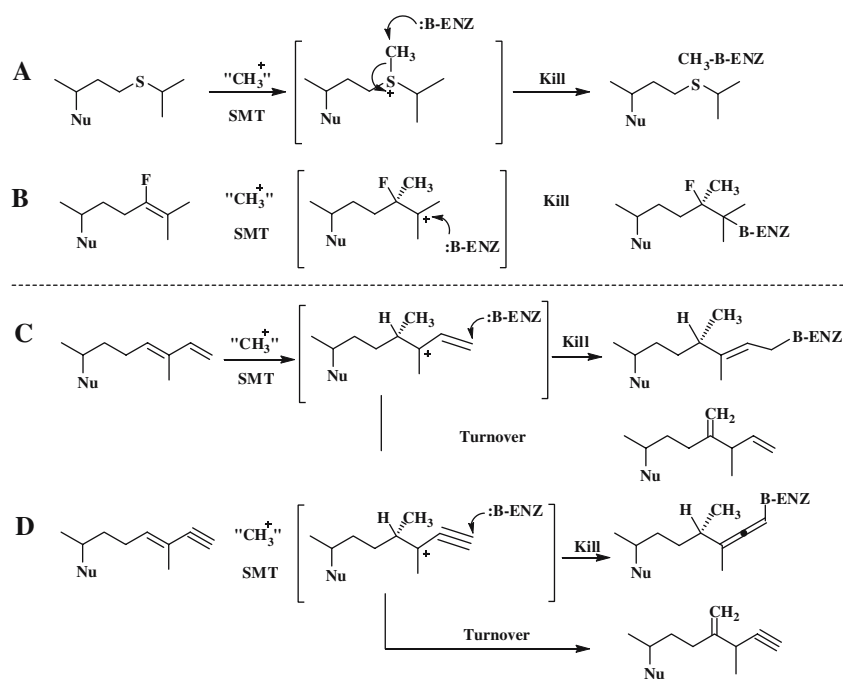


**Fig. 10** Two possible mechanisms for the conversion of 26,27-dehydrozymosterol (DHZ) to methylated product and potential modes of inactivation by DHZ; of the two alternatives, only Path 2 is catalyzed by the SMT (adapted from Nes et al. in [38, 51])

As shown in Fig. 10, two possible mechanisms for the inactivation of yeast SMT by activity assay with 26,27-dehydrozymosterol can be envisioned. In Path 1, the analog is expected to bind normally to the SMT and undergo C-methylation at C24, as with the natural substrate zymosterol. The resulting high-energy intermediate containing a cyclopropyl cation should undergo facile electrocyclic rearrangement to the more stable allylic cation, in which a positive charge is generated at C26. Presumably, the C26 cation can be placed in the immediate vicinity of the enzymic base involved with the normal C28-deprotonation step, which generates fecosterol [cholesta-8,24(28)-dienol]. Since the allylic

cation cannot be discharged directly by deprotonation, and it is presumably shielded from capture by water, alkylation of the SMT can proceed to inactivate the enzyme. The mechanism illustrated in Path 2 involves the nucleophilic attack of a methyl group from AdoMet on the C26 methylene cyclopropane, leading to a cyclopropyl cation followed by ring opening and ring expansion. In this case, an alternative set of high-energy intermediates can be predicted, including (1) the secondary carbonium ion at C24, which can eliminate a proton directly from C23 to produce a  $\Delta^{23(24)}$ -bond, or the positive charge can be eliminated through covalent attachment with an enzyme base, or (2) during the

**Fig. 11** Proposed modes of inactivation of the SMT by substrate analogs designed to be mechanism-based inactivators



initial rearrangement a second high-energy intermediate is formed with C26 methylated by AdoMet and C27 generating a cation, which can then interact with a base from the enzyme. Ring strain and the rich  $\pi$ -electron density associated with the overlapping  $sp^2$  system make the cyclopropanoid susceptible to C-methylation from AdoMet and nucleophilic rupture, leading to selectivity with respect to the direction of bond cleavage shown in Path 2. Recent studies performed using wild-type and a Tyr81Trp mutant of the yeast SMT indicate that the mechanism-based inactivation process for 26,27-dehydrozymosterol-treated SMT follows Path 2 in Fig. 11 [30, 38]. The wild-type yeast SMT does not appear to produce significant amounts of the C25(26)-methyl, C25-OH product. However, by using the Tyr81Trp yeast SMT mutant it has been possible to show that the alternate high-energy intermediate that leads to the C25(26)-methyl, C25-OH product together with the other high-energy intermediate that leads to the C25(27)–C24-OH product will associate with Regions 3 and 1, respectively, to covalently modify the enzyme [30]. The methylene cyclopropane-containing substrate analog has been attached to the zymosterol and cycloartenol nucleus and the resulting mechanism-based inactivator tested with SMT1 and SMT2 from fungi, plant and protozoa. The SMT from each group was shown to catalyze the inhibitor to a similar methylated product. In addition, the SMT1 from soybean, yeast and *Trypanosoma* was strongly inactivated, with  $k_{\text{inact}}$  values of 0.3, 1.5 and 0.3  $\text{min}^{-1}$  observed,

respectively [20, 38, 51], whereas the SMT2 from *Arabidopsis* was inactivated ( $k_{\text{inact}}$  of 0.60  $\text{min}^{-1}$ ), and the yeast-like *Prototheca* SMT1 was not inactivated by the inhibitor [51, 52]. The variation in the recognition of the inhibitor by the yeast and yeast-like SMTs suggests that subtle differences exist in the topographies of the active sites of these enzymes. The results reported here provide, for the first time, a route towards active site labeling involving a substrate mimic that is complementary to the previously described use of 24-sulfur-containing sterols [35, 40, 54]; it is mechanistically relevant that the location of the cations generated during the catalysis of 26,27-dehydrozymosterol become spatially distributed in a segment of inhibitor that is different from the region on the natural substrate that forms a C25 cation during catalysis. Thus, this class of inhibitor should not necessarily be harmful to a  $\Delta^{24}$ -reductase reaction (and hence, we discovered the long sought after differential specificity in enzyme mechanism that can be used in the design of second-generation mechanism-based inhibitors containing multiple sites in the sterol molecule modified either via heteroatomic substitution or with another site developed to inhibit additional enzyme targets in sterol synthesis, which can serve as dual action drugs). Finally, the generation of a covalent adduct using 26,27-dehydrozymosterol is entirely consistent with the postulated carbonium ion mechanism for the C<sub>1</sub>-(wild-type yeast SMT) and C<sub>2</sub>-transfer activities (Tyr81Phe yeast SMT mutant).

The inhibitory properties of a set of rationally designed analogs were tested recently with plant and yeast SMTs [40, 51–53, Song Z, Nes WD, unpublished data]. As shown in Fig. 11, two inhibitors were constructed with side chains of heteroatomic substitution at C24 (**A** and **B**), and two inhibitors were constructed with side chains of multiple olefin character involving a  $\Delta^{24}$ -bond conjugated to a double or triple bond attached to a C26 appendage (**C** and **D**). In each case, the test compound inhibited one or more SMTs. The inhibitors exhibited an irreversible-type and time-dependent inactivation kinetic pattern against the SMTs tested. For the soybean SMT, the sulfur and fluorine-derivatives generated  $k_{\text{inact}}$  values of 0.3 and 0.1  $\text{min}^{-1}$ , respectively, and the 24,26-diene compound and 24,26-triple bond-containing compounds generated  $k_{\text{inact}}$  values of 0.2 and 0.1  $\text{min}^{-1}$ , respectively. Marked specificity toward these inhibitors was observed between the fungal and plant SMTs. For instance, the inhibitor with the 24,26-dienol side chain attached to either the zymosterol or the cycloartenol nucleus to ensure optimal binding generated a  $k_{\text{inact}}$  value of 0.2  $\text{min}^{-1}$  for soybean SMT and 0.3  $\text{min}^{-1}$  for *P. wickerhamii* SMT, whereas no detectable enzyme inactivation was observed following the assay of the 24,26-dienol-containing inhibitor with the yeast SMT, although in the latter case the inhibitor was turned over to 24-methylated product, as determined by MS and NMR characterization. These results suggest that the SMT-active sites of the different enzymes are subtly different. The proposed mechanism for inhibiting the sulfur derivative is different from that of the other analogs; the sulfur derivative is considered to undergo methylation and then serve as a substrate to methylate the enzyme active site (**A**, Fig. 11) [53]. Alternatively, the other inhibitors are considered to form an adduct with the enzyme during catalysis (**B**, **C** and **D**, Fig. 11). The results indicate that, as with assays using the other substrate and transition state analogs, interactions between the enzyme and the  $\Delta^{24}$ -bond in the sterol side chain appear to be the major binding forces that affect product formation, and this therefore provides a key site in the sterol structure for chemical modification in rational drug design.

An exciting new analytical method of quantifying proteins crucial to phytosterol synthesis has emerged from our work, which uses the knowledge that the mechanism-based inhibitors bind to the SMT in stoichiometric fashion. Thus, it has become possible to use these inhibitors, especially sterols constructed with the methylene cyclopropane-containing side chain, to determine the concentration of *active* SMT in organisms/tissues and to use this information to establish the

turnover number ( $k_{\text{cat}}$  values) for a specific enzyme system in an intact system. In *S. cerevisiae* cultured to the onset of growth arrest, the active SMT concentration was measured at 0.7 fg/cell, which contrasts with the total SMT concentration measured from the same preparations by Western blotting at ca. 5.0 fg/cell, and the cellular ergosterol content, determined to be 40 fg/cell by GC–MS (Song Z, Nes WD, unpublished data). In separate work, the turnover numbers of the yeast and soybean SMTs from microsome preparations of wild-type material were found to be in excellent agreement with that shown for the corresponding pure enzyme, at ca. 0.01  $\text{s}^{-1}$  (Song Z, Nes WD, unpublished data).

## Summary

The past few years have seen major advances in the design and testing of SBIs. The first generation of SBIs that target ergosterol-dependent diseases are a defined class of highly effective antifungal agents, whose common structural features are the presence of a nitrogen atom in the molecule and a greasy nature, possessing limited volume to fit the active site. The structures and mechanisms of action of those drugs are unrelated to the class of lead compounds under review here, many of which contain a nitrogen atom in the steroid frame; however, several of the azasteroids tested so far, which show good specific activities in the low nanomolar range in vivo and in vitro toward the SMT, are not suitable for commercial use because cholesterol synthesis can be affected in animals, causing side effects. In order to avoid the biological and mechanistic concerns related to azasteroid-treatment of enzymes of the cholesterol pathway, a second generation of sterol biosynthesis inhibitors—mechanism-based inactivators of SMT—are being developed as new alternatives for plant protection and for use as therapeutics. Moreover, these compounds could potentially be used in biochemical diagnostics to quantify active enzyme isoforms, since they can be prepared for specific enzymes of the phytosterol pathway and they can be used to probe the uniformity and differences in active site topography amongst SMTs of different origins. With the arsenal of sterol analogs available to us now, we can begin to address the many challenging mechanistic and evolutionary questions about sterol enzymes that still remain:

- What are the substrate–enzyme interactions involved in the initiation and termination of C-methylation?

- How is the active center organized to recognize acceptor molecule and inhibitor?
- Is there a critical amino acid in the active center that can be targeted for blockage via ligand binding to provide a species-specific drug?
- How and in what way has nature modified structural motifs in the SMT during the evolution of this class of catalyst to make them more or less susceptible to a mechanism-based inactivator?

Studies in progress in this and other research laboratories around the world will provide rationales to develop new lead inhibitors of SMT action.

**Acknowledgments** One of us (WDN) thanks his students and post-doctoral fellows that participated in the synthesis and testing of the compounds described here and cited in the references. The work was supported by a Welch Foundation Grant (-D-1276), a National Science Foundation Grant (MCB-0417436) and a National Institutes of Health Grant (GM63477).

## References

1. Roberts CW, McLeod R, Rice DW, Ginger M, Chance ML, Goad JJ (2003) Fatty acid and sterol metabolism: potential antimicrobial targets in apicomplexan and trypanosomatid parasitic protozoa. *Mol Biochem Parasitol* 126:129–142
2. Burbiel J, Bracher F (2003) Azasteroids as antifungals. *Steroids* 68:587–594
3. Rahier A, Taton M (1997) Fungicides as tools in studying postsqualene sterol synthesis in plants. *Pest Biochem Physiol* 57:1–27
4. Berg D, Plempel M (1988) Sterol biosynthesis inhibitors: pharmaceutical and agrochemical aspects. Ellis Horwood, Chichester, UK, p 583
5. Rahier A, Taton M, Bouvier-Nave P, Schmitt P, Benveniste P, Schuber F, Narula AS, Cattell L, Anding C, Place P (1986) Design of high energy intermediate analogues to study sterol biosynthesis in higher plants. *Lipids* 21:52–62
6. Jayasimha J, Bowman CB, Pedroza JM, Nes WD (2006) Engineering pathway enzymes to understand the function and evolution of sterol structure and activity. *Rec Adv Phytochem* 40:211–251
7. Nes WR, Sekula BC, Nes WD, Adler JH (1978) The functional significance of structural features of ergosterol. *J Biol Chem* 253:6218–6225
8. Pinto WJ, Nes WR (1983) Stereochemical specificity for sterols in *Saccharomyces cerevisiae*. *J Biol Chem* 258:4472–4476
9. Nes WD (1987) Biosynthesis and requirement for sterols in the growth and reproduction of oomycetes. *Am Chem Soc Symp Ser* 325:304–328
10. Rodriguez RJ, Low C, Bottema CDK, Parks LW (1985) Multiple functions for sterols in *Saccharomyces cerevisiae*. *Biochim Biophys Acta* 837:336–343
11. Bloch KE (1983) Sterol structure and membrane function. *CRC Crit Rev Biochem* 14:47–82
12. Nes WR, Nes WD (1980) *Lipids in evolution*. Plenum, New York, p 244
13. Nes WD, Norton RA, Crumley FG, Madigan SJ, Katz ER (1990) Sterol phylogeny and algal evolution. *Proc Natl Acad Sci USA* 87:7565–7569
14. Zhou W, Cross GAM, Nes WD (2006) Cholesterol import fails to prevent catalyst-based inhibition of ergosterol synthesis and cell proliferation of *Trypanosoma brucei*. *J Lipid Res* (in press)
15. Zhou W, Nguyen TTM, Collins MS, Cushion MT, Nes WD (2002) Evidence for multiple sterol methyltransferase pathways in *Pneumocystis carinii*. *Lipids* 37:1177–1186
16. Nes WD, Xu X, Haddon WF (1988) Evidence for similarities and differences in the biosynthesis of fungal sterols. *Steroids* 53:533–558
17. Nes WD, Nichols SD (2006) Phytosterol biosynthesis pathway in *Mortierella alpina*. *Phytochemistry* 67:1716–1721
18. Zhou W, Nes WD (2000) Stereochemistry of hydrogen introduction at C-25 in ergosterol synthesized by the mevalonate-independent pathway. *Tetrahedron Lett* 41:2791–2795
19. Lichtenthaler HK (1999) The 1-deoxy-D-xylulose-5-phosphate pathway of isoprenoid biosynthesis in plants. *Annu Rev Plant Physiol Mol Biol* 50:47–65
20. Zhou W, Lepesheva GI, Waterman MR, Nes WD (2006) Mechanistic analysis of multiple product sterol methyltransferase implicated in ergosterol biosynthesis in *Trypanosoma brucei*. *J Biol Chem* 281:6290–6296
21. Nes WD (2005) Enzyme redesign and interactions of substrate analogues with sterol methyltransferase to understand phytosterol diversity, reaction mechanism and the nature of the active site. *Biochem Soc Trans* 33:1189–1196
22. Mangla A, Nes WD (2000) Sterol C-methyl transferase from *Prototheca wickerhamii*: mechanism, sterol specificity, and inhibition. *Bioorg Med Chem* 8:925–936
23. Nes WD, Song Z, Dennis AL, Zhou W, Nam J, Miller MB (2003) Biosynthesis of phytosterols: kinetic mechanism for the enzymatic C-methylation of sterols. *J Biol Chem* 278:34505–34516
24. Nes WD, Le PH (1990) Evidence for separate intermediates in the biosynthesis of 24 $\beta$ -methylsterol end products by *Gibberella fujikuroi*. *Biochim Biophys Acta* 1042:119–125
25. Nes WD (2003) Enzyme mechanisms for C-methylations. *Phytochemistry* 64:75–95
26. Bouvier-Nave P, Husselstein T, Benveniste P (1998) Two families of sterol methyltransferases are involved in the first and the second methylation steps of plant sterol biosynthesis. *Eur J Biochem* 256:88–96
27. Nes WD (2000) Sterol methyltransferase: enzymology and inhibition. *Biochim Biophys Acta* 1529:63–88
28. Parker SR, Nes WD (1992) Regulation of sterol biosynthesis and phylogenetic implications. *Am Chem Soc Symp Ser* 497:110–145
29. Nes WD, Jayasimha P, Zhou W, Kanagasabai R, Jin C, Jaradat TT, Shaw RW, Bujnicki JM (2004) Sterol methyltransferase: functional analysis of highly conserved residues by site-directed mutagenesis. *Biochemistry* 43:569–576
30. Jayasimha P (2006) Sterol methyltransferase: protein engineering, molecular mapping of adomet-binding site. Thermodynamic analysis and its phylogenetic implications. Ph.D. dissertation, Texas Tech University, p 193
31. Nes WD, Sinha A, Jayasimha P, Zhou W, Song Z, Dennis AL (2006) Probing the sterol binding site of soybean sterol methyltransferase by site-directed mutagenesis: functional analysis of conserved aromatic amino acids in region 1. *Arch Biochem Biophys* 448:23–30
32. Zhou W, Nes WD (2003) Sterol methyltransferase 2: purification, properties and inhibition. *Arch Biochem Biophys* 420:18–34
33. Venkatramesh M, Guo D, Jia Z, Nes WD (1996) Mechanism and structural requirements for transformation of substrates

- by the (*S*)-adenosyl-L methionine:  $\Delta^{24(25)}$ -sterol methyl transferase from *Saccharomyces cerevisiae*. *Biochim Biophys Acta* 1299:313–324
34. Nes WD, Janssen GG, Bergenstrahle A (1991) Structural requirements for transformation of substrates by the (*S*)-adenosyl-L-methionine:  $\Delta^{24(25)}$ -sterol methyl transferase. *J Biol Chem* 266:15202–15212
  35. Kanagasabai R, Zhou W, Liu J, Nguyen TTM, Veeramachaneni P, Nes WD (2004) Disruption of ergosterol biosynthesis, growth and the morphological transition in *Candida albicans* by sterol methyltransferase inhibitors containing sulfur at C-25 in the sterol side chain. *Lipids* 39:737–746
  36. Nes WD, Guo D, Zhou W (1997) Substrate-based inhibitors of the (*S*)-adenosyl-L-methionine  $\Delta^{24(25)}$ - to  $\Delta^{24(28)}$ -sterol methyltransferase from *Saccharomyces cerevisiae*. *Arch Biochem Biophys* 342:68–81
  37. Venkatramesh M, Guo D, Harman JG, Nes WD (1996) Sterol specificity of the *Saccharomyces cerevisiae* *ERG6* gene product expressed in *Escherichia coli*. *Lipids* 31:373–377
  38. Nes WD, Marshall JA, Jia Z, Jaradat TT, Song Z, Jayasimha P (2002) Active site mapping and substrate channeling in the sterol methyltransferase pathway. *J Biol Chem* 277:42549–42556
  39. Janssen GG, Nes WD (1992) Structural requirements for transformation of substrates by the S-adenosyl-L-methionine:  $\Delta^{24(25)}$ -sterol methyltransferase: inhibition of analogs of the transition state coordinate. *J Biol Chem* 267:25856–25863
  40. Zhou W, Song Z, Liu J, Miller MB, Nes WD (2004) 24-Thiacycloartanol, a potent mechanism-based inactivator of plant sterol methyltransferase. *Tetrahedron Lett* 45:875–878
  41. Malhotra HC, Nes WR (1971) The mechanism of introduction of alkyl groups at C-24 of sterols, IV. Inhibition by triparanol. *J Biol Chem* 246:4934–4937
  42. Popják G, Meenan A, Parish EJ, Nes WD (1989) Inhibition of cholesterol synthesis and cell growth by 24(*R,S*),25-epiminolanosterol and triparanol in cultured rat hepatoma cells. *J Biol Chem* 264:6230–6238
  43. Nes WD, Zhou W, Dennis AL, Li H, Jia Z, Keith RA, Piser TM, Furlong ST (2002) Purification, characterization, and catalytic properties of human sterol 8-isomerase. *Biochem J* 367:587–599
  44. Ator MA, Schmidt SJ, Adams JL, Dolle RE, Kruse LI, Frey CI, Barone JM (1992) Synthesis, specificity, and antifungal activity of inhibitors of the *Candida albicans*  $\Delta^{24}$ -sterol methyltransferase. *J Med Chem* 35:100–106
  45. Park KS, Kang KC, Kim JH, Adams DJ, Johng TN, Paik YK (1999) Differential inhibitory effects of protoberberines on sterol and chitin biosyntheses in *Candida albicans*. *J Antimicrob Chemother* 43:667–674
  46. Kirby TJ, Achor RWP, Perry HO, Winkelmann RK (1962) Cataract formation after triparanol therapy. *Arch Ophthalmol* 68:84–87
  47. Kusano G, Takahashi A, Sugiyama K, Nozoe S (1987) Antifungal properties of solanum alkaloids. *Chem Pharm Bull* 35:4862–4867
  48. Barrett-Bee K, Ryder N (1992) Biochemical aspects of ergosterol biosynthesis inhibition. In: Sutcliffe J, Georgopadakou NH (eds) *Emerging targets and antifungal therapy*. Routledge, Chapman and Hall, New York, pp 410–436
  49. Roddick JG (1987) Antifungal activity of plant sterols. *Am Chem Soc Symp Ser* 325:286–303
  50. Keeler RF (1984) Mammalian teratogenicity of steroidal alkaloids. In: Nes WD, Fuller G, Tsai L (eds) *Isopentenoids in plants: biochemistry and function*. Marcel Dekker, New York, pp 531–562
  51. Song Z, Zhou W, Liu J, Nes WD (2004) Mechanism-based active site modification of the soybean sterol methyltransferase by 26,27-dehydrocycloartenol. *Bioorg Med Chem Lett* 14:33–36
  52. Zhou W, Song Z, Kanagasabai R, Liu J, Jayasimha P, Sinha A, Veeramachaneni P, Miller MB, Nes WD (2004) Mechanism-based enzyme inactivators of phytosterol biosynthesis. *Molecules* 9:185–203
  53. Nes WD, Marshall JA, Zhou W, He L, Dennis AL (1998) Mechanism-based site modification of sterol methyltransferase by tritium-labeled 26-homocholesta-8,14,26-yn-3 $\beta$ -ol. *Tetrahedron Lett* 39:8575–8578
  54. Ator MA, Schmidt SJ, Adams JL, Dolle RE (1989) Mechanism and inhibition of delta 24-sterol methyltransferase from *Candida albicans* and *Candida tropicalis*. *Biochemistry* 28:9633–9640

# Syntheses of Ring C Oxysterols: Inhibitors of Sterol Biosynthesis

Edward J. Parish · Chi Luo · Thomas Webb ·  
John D. Gorden

Received: 1 September 2006 / Accepted: 18 November 2006 / Published online: 16 January 2007  
© AOCS 2007

**Abstract** Oxygenated derivatives of cholesterol and lanosterol, known as oxysterols, have consistently displayed significant activity as inhibitors of 3-hydroxy-3-methylglutaryl (HMG) CoA reductase, a key regulatory enzyme in sterol biosynthesis. We have developed the chemical syntheses of ring C oxysterols for evaluation as inhibitors of sterol biosynthesis. A key intermediate in the chemical synthesis was 3 $\beta$ -benzoyloxy-9 $\alpha$ , 1 $\alpha$ -epoxy-5 $\alpha$ -cholest-7-ene (**1**), whose structure was confirmed by X-ray crystallographic analysis and is presented herein.

**Keywords** Oxysterol · Steroid · Epoxide · Synthesis · X-ray · Crystallographic

## Abbreviations

HMG 3-hydroxy-3-methylglutaryl  
ORTEP Oak Ridge (National Laboratory) Thermal Ellipsoid Program  
THF Tetrahydrofuran  
*m*-CPBA *meta*-Perchlorobenzoic acid

## Introduction

As a class of compounds, oxysterols can be defined as sterols bearing a second oxygen function, in addition to that at carbon-3, and having an iso-octyl or modified

iso-octyl side chain. These compounds have demonstrated a variety of biological properties, including cytotoxicity, atherogenicity, carcinogenicity, mutagenicity, hypocholesterolemia, and effects on specific enzymes [1–3]. Widely distributed in nature, they have been found in animal tissues and food stuffs [1] and have been isolated from drugs used in folk medicines for the treatment of cancer [4–6]. A number of oxygenated derivatives of cholesterol and sterol intermediates in cholesterol biosynthesis in animal cell culture. The specific inhibition of cholesterol biosynthesis in mammalian cells by oxygenated derivatives of cholesterol and lanosterol has been shown in many cases to decrease cellular levels of HMG-CoA reductase, a key regulatory enzyme in sterol biosynthesis [7–12]. These observations suggest a regulatory mechanism which, by analogy to steroid hormone receptors and bacterial introduction-repression systems, requires a binding protein to recognize oxysterols and mediate subsequent cellular events. Evidence for the existence of a specific cytosolic receptor protein for oxysterols has been presented. After the activities of a number of sterol were evaluated, a good correlation was found between the actions of certain oxysterols on HMG-CoA reductase in L cells and their affinity for an oxysterol binding protein [11, 13, 14]. This oxysterol model for the regulation of cholesterol biosynthesis proposes that oxygenated derivatives of cholesterol or lanosterol are produced in cells as signal molecules that feedback and regulate enzymes of the cholesterol biosynthetic pathway [15–18].

The ring C oxysterols 5 $\alpha$ , 8 $\beta$ -cholest-7-ene-3 $\beta$ , 11 $\alpha$ -diol (**3**) and 3 $\beta$ -hydroxy-5 $\alpha$ -cholest-9-(11)-en-12-one (**8** and their 3-keto derivatives) were previously known to be effective inhibitors of HMG-CoA reductase [11, 19].

E. J. Parish (✉) · C. Luo · T. Webb · J. D. Gorden  
Department of Chemistry and Biochemistry,  
Auburn University, Auburn, AL 336849, USA  
e-mail: parishj@auburn.edu

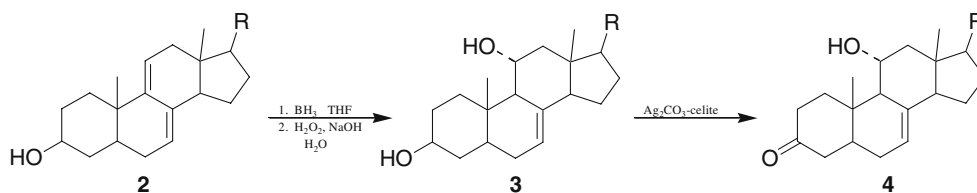


Lanosterol derivatives possessing a  $9\alpha$ -hydroxyl group were found to be less effective as inhibitors [19].  $3\beta$ -Hydroxy- $5\alpha$ -cholest-8-en-11-one (**12**), while demonstrating poor reductase inhibition, was found to be an effective inhibitor of tumor-cell growth and was shown to produce significant, but not sustained, hypocholesterolemic activity in laboratory animals [11, 20, 21].

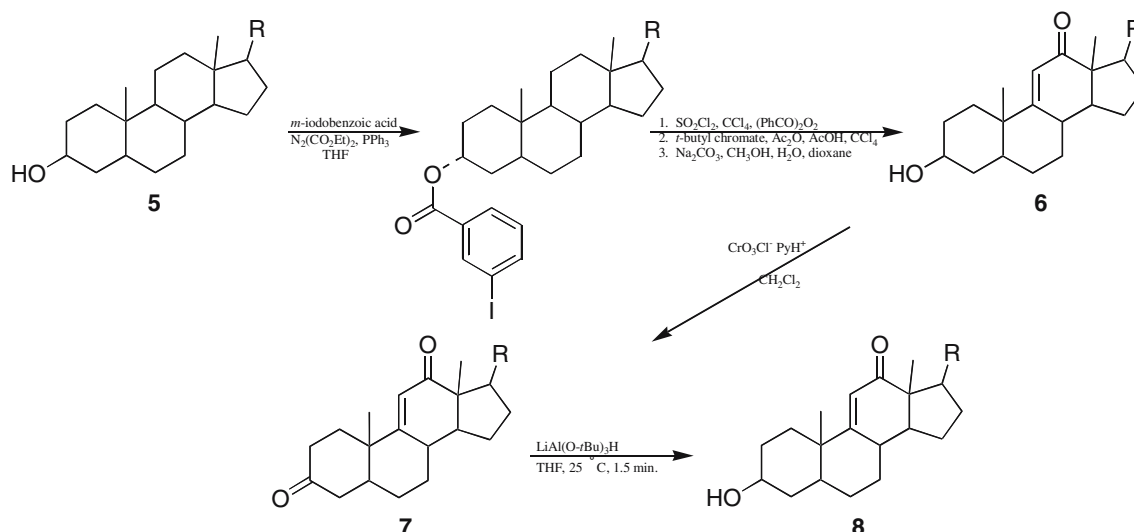
Scheme 1 shows the chemical synthesis of the  $3\beta,11\alpha$ -diol **3** and its corresponding 3-keto derivative **4** [19]. Diol **3** was obtained from the hydroboration–oxidation of 7,9(11)-diene **2**. The diene intermediate **2** was prepared from 7-dehydrocholesterol [19]. Scheme 2 shows the chemical synthesis of  $3\beta$ -hydroxy-12-ketone **8** and its corresponding 3-keto and  $3\alpha$ -hydroxy derivatives **7** and **8**, respectively [19]. These 12-keto sterols were prepared from cholesterol [5]. The ring C oxysterols shown in Schemes 1 and 2 were found to be significant inhibitors of sterol synthesis and reduction of levels of HMG-CoA reductase activity in L cells [19]. Their inhibitory activity is shown in Fig. 1 [19].

In our continuing study, we have sought to prepare oxysterols and observe their activity as potential inhibitors as HMG-CoA reductase and sterol biosynthesis. Oxysterols in ring C have not been studied to the same degree as those found on the side chain and other regions of the steroid nucleus [11, 18]. Since the C ring of steroids is associated with biochemical pathways essential for mammalian growth and development it appeared to be worthwhile to study the effects of oxysterols of ring C further and observe their inhibitory activity on HMG-CoA reductase and their effects as hypocholesterolemic agents.

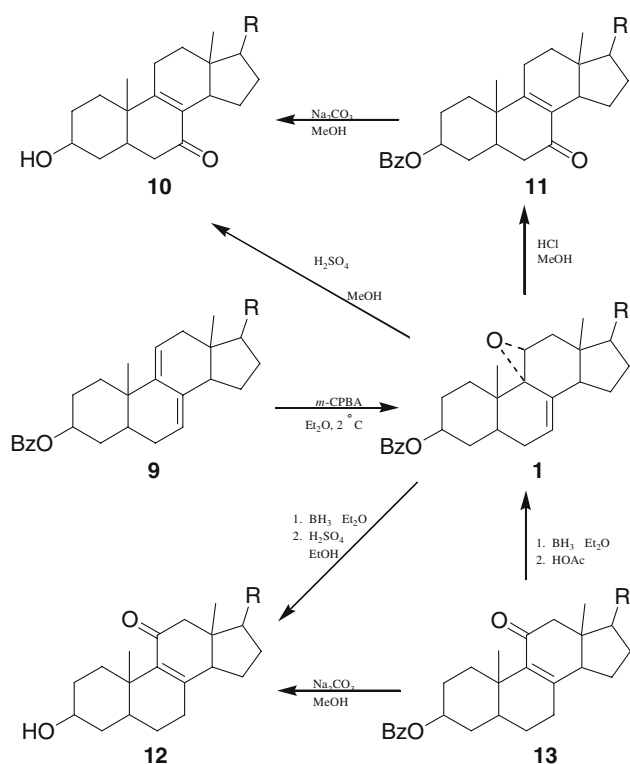
We have made additional examples of ring C oxysterols in our continuing studies of the hypocholesterolemic effects of 7-keto and 11-keto sterols [21]. The chemical synthesis of the key intermediate  $3\beta$ -benzoyloxy- $9\alpha,11\alpha$ -epoxy- $5\alpha$ -cholest-7-ene (**1**) and the corresponding 7-keto (**10**) and 11-keto (**12**) sterols derived from it are shown in Scheme 3 [21]. The key  $9\alpha,11\alpha$ -epoxide **1** was prepared from the corresponding 7,9(11)-diene **9**. The diene **9** was prepared from 7-dehydrocholesterol [21].



**Scheme 1** Synthesis of  $11\alpha$ -hydroxy- $\Delta^7$ -sterols and their derivatives (19)



**Scheme 2** Synthesis of  $11\alpha$ -hydroxy- $\Delta^7$ -sterols and their derivatives (19)



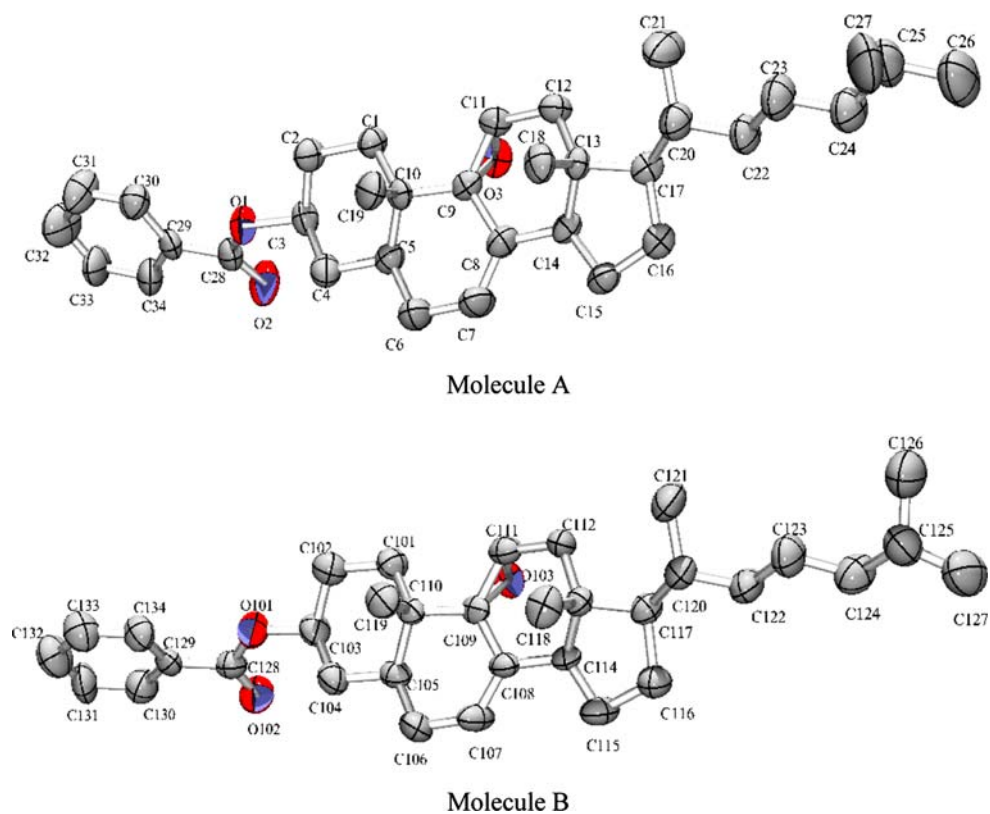
**Scheme 3** Chemical synthesis of ketosterols derived from 3β-benzoyloxy-9α,11α-epoxy-5α-cholest-7-ene (**1**) (R = C<sub>8</sub>H<sub>17</sub>)

In this present study, we were particularly interested in determining the absolute conformation of the epoxide in 3β-benzoyloxy-9α,11α-epoxy-5α-cholest-7-ene (**1**). Other steroids/epoxides in the C and O rings of steroids had been found to be in the α (down) configuration when they were obtained by peroxyacid oxidation of the corresponding alkene double bond (e.g. 3β-benzoyloxy-14α,15α-epoxy-5α-cholest-7-ene) [22, 23]. Based upon purely historical grounds, this was presumed to be an α-epoxide, although typical spectroscopic and chemical data were unable to confirm this. Since this epoxide is a sensible precursor for synthesis of additional ring C oxysterols and other related compounds, we initiated an X-ray crystallographic study of epoxide **1** to determine the configuration of the epoxy group as well as the orientation of the ancillary alkane (C<sub>8</sub>H<sub>17</sub>) side chain.

## Results and Discussion

Several cholesterol oxidation products and other oxidized sterol intermediates in cholesterol biosynthesis have been found to be potent inhibitors of sterol biosynthesis in various animal cells. The specific inhibition of cholesterol biosynthesis in mammalian cells by

**Fig. 1** Molecular structures of the two crystallographically independent molecules (**a** and **b**) present in the unit cell of 3β-benzoyloxy-9α,11α-epoxy-5α-cholest-7-ene (**1**) and their numbering scheme. The thermal ellipsoids are scaled to 50% probability



cholesterol oxidation products is thought to be an inhibition of 3-hydroxy-3-methylglutaryl coenzyme A (HMG-CoA) reductase activity, the key enzyme in cholesterol biosynthesis. These oxidation products appear to perturb cholesterol and fatty-acid homeostasis and contribute profoundly to the initiation of various diseases.

The three-dimensional structure of steroids plays a primary role in governing their interactions and activities. X-ray crystallographic studies provide the most reliable and precise data concerning molecular structure. By combining solid-state data with physical chemical data on structures in solution, a reasonable picture of the dynamic properties of steroids can be constructed. This information when combined with biochemical, pharmacological, and physiological data, give a better insight into the molecular mechanisms of biosynthesis, metabolism, membrane transport, receptor binding, and nuclear interaction [24].

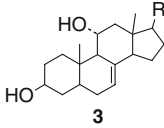
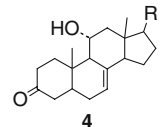
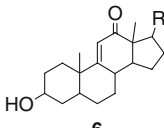
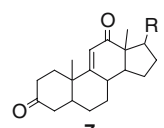
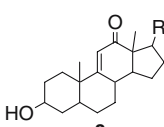
The three-dimensional structural details of hormones, drugs, and antibiotics determined by X-ray crystallographic techniques provide essential information on the global minimum-energy conformations of these molecules or local minimum-energy conformations that are very near the global minimum. X-ray data can be employed to define the most stable conformations of molecules, aid in the interpretation of solution spectra, and unambiguously assign the conformation of key intermediates allowing useful insight into the structure of further derivatives.

Indeed, **1** was confirmed to be an  $\alpha$ -epoxide with a C(9)-O(3)-C(11) angle of  $61.3^\circ$  which is consistent with other  $\alpha$ -epoxides [25]. As expected,  $\beta$ -epoxide conformation is disfavored due to the steric hindrance arising from the C(18) and C(19) angular methyl groups on the steroid nucleus. There are no unusually long contacts (e.g. hydrogen bonds) between the molecules in the unit cell and all bond lengths and angles are consistent with other structurally characterized oxysterols [25]. There are two independent molecules present in the unit cell that are nearly super-imposable with the only significant deviation being a  $67.9^\circ$  twist occurring at C25 (C125), C26 (C126) and C27 (C127) of the dimethylhexyl unit, which may be attributed to packing forces within the crystal.

## Methods and Materials

A small white oblique hexagonal prism was mounted on the end of a glass fiber. The unit cell was determined by centering 25 reflections in the  $2\theta$  range  $17$ – $28^\circ$ . Data were collected using the  $2\theta$ – $\theta$  scan

**Table 1** Inhibition of sterol synthesis and reduction of levels of HMG-CoA reductase activity in cells by C<sub>27</sub> ring C oxysterols ( $R = C_8H_{17}$ )

Inhibitor	Concentrations ( $\mu$ M) required for 50% inhibition	
	L cell cultures	
	Sterol synthesis	HMG-CoA reductase
 <b>3</b>	0.6	0.6
 <b>4</b>	2.0	0.5
 <b>6</b>	7.0	8.0
 <b>7</b>	1.0	1.0
 <b>8</b>	2.0	1.0

technique and processed on a computer-controlled four-circle Nicolet R3 m/V single-crystal diffractometer with Mo K $\alpha$  radiation. Two reflections established as standards were checked routinely for deviations of positions and intensities after every 100 reflections. Lorentz and polarization corrections and empirical absorption corrections based on  $\psi$  scans were performed. The positions of the atoms were located by direct methods and least-squares refinement<sup>1</sup>. The data

<sup>1</sup> All Computations were performed with SHELXTL PLUS VMS, Release 4.11, 1990 (Siemens Analytical X-Ray Instruments, Inc.), based on SHELX (G.M. Sheldrick). All hydrogens were included as calculated positions and refined using a riding model and a general isotropic thermal parameter.

**Table 2** Summary of crystallographic data for **1**

Empirical formula	C <sub>34</sub> H <sub>48</sub> O <sub>3</sub>
Space group	P1
Fw	504.7
Cell dimensions	
<i>a</i> (Å)	8.664(2)
<i>b</i> (Å)	11.637(2)
<i>c</i> (Å)	16.186(3)
$\alpha$	103.06(1)
$\beta$	100.30(1)
$\gamma$	105.23(1)
<i>Z</i>	2
<i>V</i> (Å <sup>3</sup> )	1483.8(5)
<i>T</i> (K)	294
Wavelength (Å)	0.71073
Calcd. density (g/cm <sup>3</sup> )	1.130
Absolute coefficient (cm <sup>-1</sup> )	0.065
Data collection range	3.0° ≤ 2σ ≤ 50.0°
No. of reflns. collected	5,624
Unique (merging <i>R</i> )	5248 (1.46%)
Observed ( <i>F</i> <sub>o</sub> > 4σ( <i>F</i> <sub>o</sub> ))	3479
<i>R</i> <sup>a</sup>	0.0629
<i>R</i> <sub>w</sub> <sup>a</sup>	0.0677
Goodness of fit	1.87

**Table 3** Selected bond lengths (Å) and bond angles (°) for **1**

	Bond length (Å)		Bond angle (°)
C(7)–C(8)	1.375 (13)	C(6)–C(7)–C(8)	122.6 (8)
C(8)–C(9)	1.509 (11)	C(7)–C(8)–C(14)	124.8 (7)
C(9)–C(11)	1.473 (12)	C(7)–C(8)–C(9)	119.8 (9)
C(9)–O(3)	1.460 (14)	C(8)–C(9)–C(10)	116.5 (8)
C(11)–O(3)	1.432 (12)	C(8)–C(9)–C(11)	117.6 (8)
C(9)–C(10)	1.530 (14)	C(10)–C(9)–O(3)	115.7 (8)
C(11)–C(12)	1.510 (14)	C(9)–O(3)–C(11)	61.3 (6)
		O(3)–C(9)–C(11)	58.4 (6)
		C(9)–C(11)–O(3)	58.4 (6)
		C(3)–C(11)–C(12)	117.4 (8)

were consistent with the space group P1 with two crystallographically independent molecules present in the unit cell. An Oak Ridge (National Laboratory) Thermal Ellipsoid Program (ORTEP) diagram of **1** is given in Fig. 1 and the crystallographic data and geometrical parameters are presented in Tables 1, 2 and 3.

## Conclusions

In summary, we have developed the chemical syntheses of ring C oxysterols utilizing 3β-benzoyloxy-9α,11α-epoxy-5α-cholest-7-ene (**1**). Since this epoxide has the potential to be a key intermediate for the chemical synthesis of additional ring C oxysterols and other related compounds, it was necessary to unambiguously assign the absolute configuration. The results of a single-crystal X-ray diffraction study of **1** is described.

biguously assign the absolute configuration. The results of a single-crystal X-ray diffraction study of **1** is described.

## References

- Smith LL (1981) Cholesterol autoxidation. Plenum Press, New York, pp 231–256
- Parish EJ, Nanduri UBB, Kohl HH, Taylor FR (1986) Oxysterols: chemical synthesis, biosynthesis and biological activities. *Lipids* 21(1):27–30
- Gibbons GF (1983) The role of oxysterols in the regulation of cholesterol biosynthesis. *Biochem Soc Trans* 11(6):649–651
- Cheng KP, Nagano H, Luu B, Ourisson G, Beck J-P (1977) Chemistry and biochemistry of Chinese drugs. Part I. Sterol derivatives cytotoxic to hepatoma cells, isolated from the drug *Bombyx cum Botryte*. *J Chem Res* 9:S217
- Nagano H, Poyser JP, Cheng K-P, Luu B, Ourisson G, Beck J-P (1977) Chemistry and biochemistry of Chinese drugs. Part II. Hydroxylated sterols, cytotoxic towards cancerous cells: synthesis and testing. *J Chem Res* 9:S218
- Zander M, Koch P, Luu B, Ourisson G, Beck J-P (1977) Chemistry and biochemistry of Chinese drugs. Part III Mechanism of action of hydroxylated sterols on cultured hepatoma cells. *J Chem Res* 9:S219
- Schroepfer GJ Jr (1981) Sterol biosynthesis. *Ann Rev Biochem* 50:585–621
- Schroepfer GJ Jr (1981) Sterol biosynthesis. *Ann Rev Biochem* 51:555–581
- Kandutsch AA, Taylor FR (1985) In: Straus JF, Menon KMJ (eds) Lipoprotein and cholesterol metabolism in steroidogenic tissues. George F. Stickley Co., Philadelphia, pp 194–219
- Gibbons GF (1983) In: Sabine JR (ed) 3-Hydroxy-3-methylglutaryl coenzyme A reductase. CRC, West Palm Beach, pp 153–232
- Taylor FR, Saucier SE, Shown EP, Parish EJ, Kandutsch AA (1984) Correlation between oxysterol binding to a cytosolic binding protein and potency in the repression of hydroxymethylglutaryl coenzyme A reductase. *J Biol Chem* 259(20):12382–12387
- Panini SR, Sexton RC, Gupta AK, Parish EJ, Chitrakorn S, Rudney H (1986) Regulation of 3-hydroxy-3-methylglutaryl coenzyme A reductase activity and cholesterol biosynthesis by oxysterols. *J Lipid Res* 27(11):1190–1204
- Kandutsch AA, Taylor FR, Shown EP (1984) Different forms of the oxysterol-binding protein. Binding kinetics and stability. *J Biol Chem* 259(20):12388–12397
- Morisaki M, Sonoda Y, Makino T, Ogihara N, Ikekawa N, Sato Y (1986) Inhibitory effect of 15-oxygenated sterols on cholesterol synthesis from 24,25-dihydrolanosterol. *J Biochem* 99(2):597–600
- Kandutsch AA, Chen HW, Heiniger HJ (1978) Biological activity of some oxygenated sterols. *Science* 201(4355):498–501
- Spencer TA (1994) The squalene dioxide pathway of steroid biosynthesis. *Acc Chem Res* 27(3):83–90
- Taylor FR (1992) In: Nes WD, Parish EJ (eds) Regulation of isopentenoid metabolism, ACS Symposium Series 497. American Chemical Society, Washington, pp 81–93
- Parish EJ, Parish SC, Li S (1995) Side-chain oxysterol regulation of 3-hydroxy-3-methylglutaryl coenzyme A reductase activity. *Lipids* 30(3):247–251

19. Schroepfer GJ Jr, Parish EJ, Kandutsch AA (1988) Inhibitors of sterol biosynthesis. Synthesis and activities of ring C oxygenated sterols. *Chem Phys Lipids* 46(2):147–154
20. Parish Edward J, Chitrakorn S, Luu B, Schmidt G, Ourisson G (1989) Studies of the oxysterol inhibition of tumor cell growth. *Steroids* 53(3–5):579–596
21. Parish EJ, Nanduri VBB, Seikel JM, Kohl HH, Nusbaum KE (1986) Synthesis of 3b-hydroxy-5a-cholest-8-en-7-one and 3b-hydroxy-5a-cholest-8-en-11-one: evaluation as potential hypocholesterolemic agents. *Steroids* 48(5–6):407–418
22. Parish EJ, Spike TE, Schroepfer GJ Jr (1977) Sterol synthesis. Chemical synthesis of 3b-benzoyloxy-14a, 15a-epoxy-5a-cholest-7-ene, a key intermediate in the synthesis of 15-oxygenated sterols. *Chem Phys Lipids* 18(3–4):233–239
23. Conner BN, Parish EJ, Schroepfer GJ Jr, Quioco FA (1977) Synthesis and crystal Structure of 3b-p-bromobenzoyloxy-14a, 15a-epoxy-5a-cholest-7-ene. *Chem Phys Lipids* 18(3–4):240–257
24. Duax WL, Griffin JF, Cheer C (1989) In: Nes WD, Parish EJ (eds) *Steroid conformational analyses based on X-ray crystal structure determination in analysis of sterols and other biologically significant steroids*. Academic, San Diego, pp 203–221
25. Huang X-C, Guo Y-W, Mollo E, Cimino G, Dysideasterols A-E (2005) Five new uncommon polyhydroxylated sterols from the south china sea sponge *Dysidea* sp. *Helv Chim Acta* 88(2):281–289

# Phytosterols, Cholesterol Absorption and Healthy Diets

Richard E. Ostlund Jr

Received: 31 July 2006 / Accepted: 23 November 2006 / Published online: 9 January 2007  
© AOCs 2007

**Abstract** The purpose of this review is to outline the emerging role of dietary phytosterols in human health. Dietary saturated fat, cholesterol and fiber are currently emphasized in the reduction of low-density lipoprotein cholesterol levels. However, other dietary components such as phytosterols may have equivalent or even larger effects on circulating cholesterol and need further study with respect to the potential for coronary heart disease risk reduction. Phytosterol effects were not considered in classic fat-exchange clinical trials and may account for some of the differences attributed to the food fats studied. Phytosterols reduce cholesterol absorption while being poorly absorbed themselves and the effects can be studied in human subjects in single-meal tests using stable isotopic tracers. Because phytosterols are insoluble and biologically inactive when purified, careful attention needs to be given to ensuring that commercial supplement products are rendered bioavailable by dissolution in fat or by emulsification. Recent work shows that phytosterols in natural food matrices are also bioactive. The retention of phytosterols during food manufacturing and the use of foods with high phytosterol content may constitute an alternative to the use of supplements.

## Introduction

There is a scientific consensus that reduction of low-density lipoprotein (LDL) cholesterol is important for coronary risk reduction and specific recommendations for cholesterol monitoring and treatment in the general population have been made by the United States National Cholesterol Education Program [1]. Lifestyle variables, including diet and dietary supplements, are an important part of this initiative. A better understanding of how dietary sterols may relate to LDL cholesterol can be gleaned from Fig. 1, which sketches the framework of whole body cholesterol metabolism [2]. Dietary cholesterol intake is variable but is often less than 300 mg/day and currently 200 mg/day is recommended. Biliary cholesterol is larger and is the principal component of intestinal cholesterol. Approximately 25% of the plasma cholesterol production rate is due to absorbed dietary cholesterol while 75% is accounted for by endogenously synthesized cholesterol [3]. However, dietary cholesterol appears to be quite important because it and endogenous cholesterol biosynthesis are inversely correlated, suggesting that they are coregulated [4]. In contrast to other nutrients, for which gastrointestinal absorption is nearly quantitative, cholesterol absorption averages only 56% (Fig. 2) and is variable between individuals [5]. However, when measured repeatedly in the same individual under standardized conditions, percentage cholesterol absorption is highly reproducible [6]. This indicates that there may be substantial inter-individual differences in susceptibility to dietary sterols. Since the principal route for cholesterol elimination is excretion in the stool, the efficiency of cholesterol absorption is a critical determinant of cholesterol catabolism and

---

R. E. Ostlund Jr (✉)  
Division of Endocrinology, Metabolism and Lipid Research,  
Washington University School of Medicine,  
660 South Euclid Ave, Box 8127, St. Louis, MO 63110, USA  
e-mail: ROstlund@im.wustl.edu

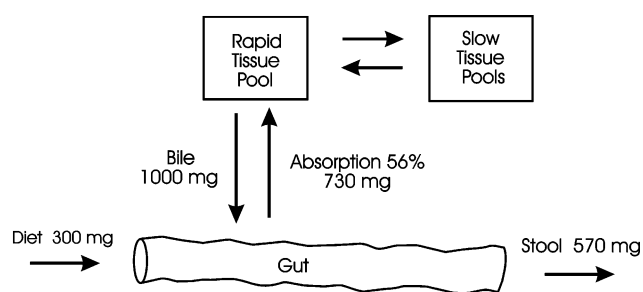


**Fig. 1** A model for cholesterol absorption and metabolism. Taken from [2]

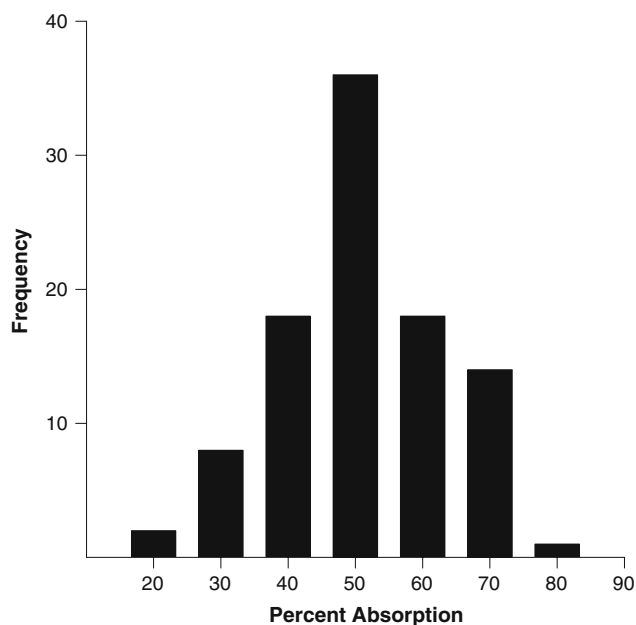


**Fig. 2** Distribution of percent cholesterol absorption in normal subjects. Taken from [5]

unabsorbed dietary and biliary cholesterol are the largest terminal components of what is often termed reverse cholesterol transport [2, 7, 8]. This model underscores the potential importance of increasing cholesterol catabolism and complements the pharmaceutical emphasis on reducing cholesterol biosynthesis with statin drugs.

### Types of Phytosterols

Phytosterols are structurally similar to cholesterol but have slight modifications of the aliphatic side chain [9, 10]. The principal molecular forms are sitosterol, campesterol and stigmasterol, and these may be esterified in the 3-position with fatty acids or ferulic acid. Since it is difficult to separate all the phytosterols in pure form in the amounts needed for clinical studies, there is relatively little information about the biological effects of

individual phytosterols and they are usually given as mixtures in clinical trials. Phytosterols are often categorized into classes consisting of  $\Delta^5$ -sterols and 5- $\alpha$ -reduced stanols, which appear to be equally effective in reducing LDL cholesterol [11]. Phytosterol glycosides are present in substantial quantities in many foods [12], but they are not cleaved efficiently by pancreatic enzymes *in vitro* so that their bioactivity has been questioned [13]. More work is needed to clarify the effectiveness of carefully purified and characterized phytosterols and their conjugates.

### Mechanism of Action

Phytosterols are thought to act primarily in the intestinal lumen. As cholesterol analogs they compete for cholesterol in absorptive micelles resulting in reduced solubility of cholesterol [14–16]. The affinity of plant sterols for micelles is greater than that of cholesterol [17]. In important human physiological studies the inclusion of phytosterols in a test meal resulted in the reduction of absorbable micellar cholesterol in duodenal aspirates [18]. An intraluminal site of action fits well with the small net systemic absorption of phytosterols, which varies by chemical structure.  $\Delta^5$ -Sterols such as campesterol and sitosterol have absorptions of 1.9 and 0.5% whereas stanols such as sitostanol have values as little as 0.04% [19]. A recent report of rapid and presumably transient absorption of phytosterols in an animal model [20] needs to be followed up since the low absorption figures cited above would not include those undergoing enterohepatic recycling with preferential biliary excretion. Although phytosterols have been proposed to have intracellular actions in enterocytes [21, 22], recent work has failed to show effects of phytosterols on cellular cholesterol transport proteins and the question of cell-based mechanisms remains open [23].

The reduction in cholesterol absorption by phytosterols is incomplete, with 30–40% decreases in absorption efficiency being reported even with high phytosterol doses [24, 25]. The prescription drug ezetimibe reduces cholesterol absorption by only 54% in humans [26]. These data open the possibility that there may be more than one pathway for cholesterol absorption and also suggest that more-effective methods of blocking cholesterol absorption need to be sought.

Phytosterols have a primary mechanism of action in the intestine, but these effects are mirrored in changes to circulating LDL cholesterol. Reduced delivery of absorbed cholesterol to the liver resulted in increased tissue LDL receptor expression as measured in

peripheral blood mononuclear cells [27]. In some subjects the production rate of LDL was decreased [28]. Further evidence of relative cholesterol deficiency after phytosterol treatment is the measured increase in whole body cholesterol biosynthesis of 38–53% [29]. This also demonstrates the rationale for using phytosterols with statin drugs.

### Phytosterol Supplements

Phytosterols, which are inherently hydrophobic and tend to form stable crystals, must be solubilized or formulated in order to become bioavailable [24]. Figure 3 demonstrates that dried unesterified sitostanol has very little immediate solubility in artificial bile salt micelles and even after many days the results are similar. But sitostanol emulsified with lecithin or other agents dissolves in the micelles in minutes. When unesterified sitostanol was administered to humans in pure crystalline form there was no significant effect on cholesterol absorption even at a dose of 1 g, but after formulation with lecithin cholesterol absorption was reduced by 37% [24].

Sitostanol/lecithin complexes reduced cholesterol absorption by 32–38% when administered to patients in test meals in nonfat beverages or egg whites and resulted in a 14.3% reduction in LDL cholesterol when taken for several weeks [30]. Other emulsifiers are also effective. Unesterified mixed phytosterols combined with sucrose ester and dispersed in milk reduced cholesterol absorption by 32% [31]. Food matrices themselves may be used as emulsifiers as demonstrated by direct addition of mixed unesterified phytosterols to orange juice at elevated temperature and pressure to

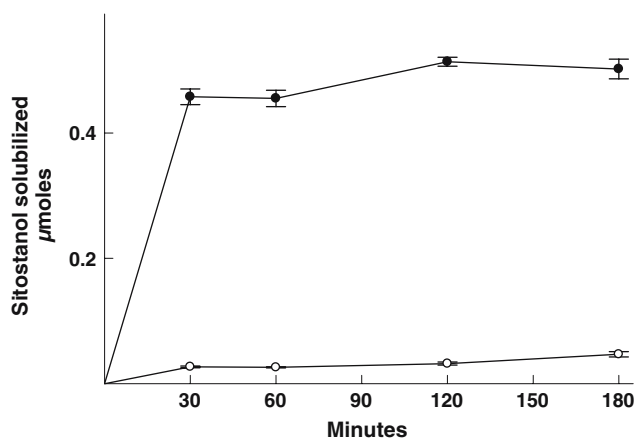


**Fig. 3** Solubility of dried sitostanol in artificial bile. Sitostanol was dried in either the absence (*open circles*) or presence (*closed circles*) of lecithin and then artificial bile was added for the time indicated. Taken from [24]

form a non-sedimenting product that reduced LDL cholesterol by 12.4% [32]. Since cholesterol needs to be in micellar form to be absorbed [33], it is likely that preparing phytosterols in micellar form would improve activity.

A common method of formulation is solubilization in fatty foods such as oils and margarines. In order to reduce the amount of fat needed the phytosterols are usually esterified with long-chain fatty acids to increase their solubility in food oils [34]. An analysis of cholesterol-lowering clinical trials showed a dose–response relationship with phytosterol dose and a maximum effect of about 10% lowering of LDL cholesterol at a dose of 2 g/day [10, 11]. The United States National Cholesterol Education program has recommended a dose of 2 g/day as a lifestyle change for reduction of LDL cholesterol and this is the level of effectiveness that can be expected from a properly formulated material. However, the consumer may not receive acceptable products because the United States Food and Drug Administration allows health claims for phytosterol supplements without requiring any demonstration of bioactivity.

Recent work has also focused on preparation of bioactive tablet or capsule formulations. Lecithin/stanol tablets reduced LDL cholesterol by 10.4% [35] and when added to statin drug treatment resulted in a further reduction of 9.1% in LDL cholesterol [36].

### Phytosterols Naturally Present in Foods

The quantity of phytosterols in natural diets is variable and values of 167–437 mg/day have been found in different populations [37–39]. Vegetable oils, breads and nuts have relatively large amounts while most fruits and vegetables have relatively little [40]. Whether or not food phytosterols would be important in achieving control of LDL cholesterol in communities is the subject of ongoing research, but existing work shows that cholesterol absorption can be significantly affected by the diet. The bioactivity of corn oil phytosterols was demonstrated by including corn oil containing 270 mg phytosterols in single-meal cholesterol absorption tests that also included labeled cholesterol [41]. Chemically purifying the corn oil triglycerides to remove phytosterols resulted in a 38% increase in cholesterol absorption and this was reduced to normal after adding the phytosterols back to purified oil. Corn oil containing as little as 150 mg phytosterols administered in a single meal had a statistically significant effect on reducing cholesterol absorption efficiency, suggesting that low levels might be more effective than previously thought. Similar results were obtained from



a study of the endogenous phytosterols of wheat germ. Cholesterol absorption was measured by including labeled cholesterol in a wheat germ muffin which contained 328 mg phytosterols [42]. Three single-meal tests were performed in the same individuals using either untreated wheat germ, selectively phytosterol-extracted wheat germ, or extracted wheat germ to which the phytosterols had been returned. Cholesterol absorption increased 42.8% when extracted wheat germ was used, and this was reduced to the original value when phytosterols were added back. These results show that phytosterols in low amounts in common foods can reduce cholesterol absorption (Fig. 4).

Many clinical trials have been performed to study the effect of food fats on serum LDL cholesterol levels. However, the phytosterol content of food oils, which is very high for vegetable oils and nil in animal fats [43], has been a confounding covariate which has not been adequately addressed in the literature [44]. For example, diets using polyunsaturated or monounsaturated fat often also contain increased amounts of phytosterols that might affect LDL cholesterol levels. Further complicating interpretation of diet studies is the lack of

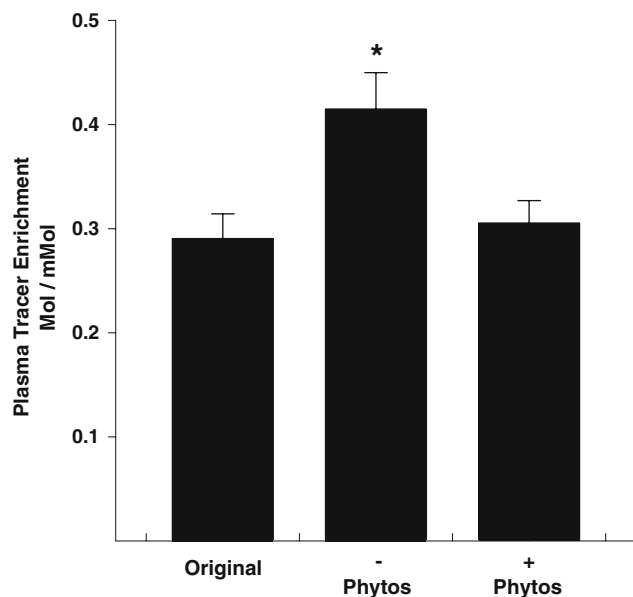


**Fig. 4** Effect of endogenous wheat germ phytosterols on cholesterol absorption. Percent cholesterol absorption was measured in 10 subjects in random order on three occasions using single-meal tests consisting of a wheat germ muffin and labeled cholesterol. The wheat germ used was either the original untreated material, wheat germ from which phytosterols had been selectively extracted, or extracted wheat germ reconstituted with the original phytosterols. Plasma tracer enrichment of cholesterol reflects cholesterol absorption. *Asterisk* denotes  $P < 0.01$  with respect to the original wheat germ. Taken from [42]

complete food database reference data on the phytosterol content of foods, which makes estimation of phytosterol content difficult.

## Conclusions

Phytosterols are recognized as an important component of healthy diets and diets designed to reduce hypercholesterolemia. The United States National Cholesterol Education Program recommends dietary phytosterol supplementation of 2 g/day as a lifestyle modification for cholesterol reduction, and this will lower LDL cholesterol by approximately 10%. Phytosterols are inactive as supplied in pure form and must be solubilized or emulsified to achieve biological activity. The principal mechanism of action appears to be competition for absorbable cholesterol in the intestine, resulting in reduced cholesterol absorption. Potentially more important than supplements are natural dietary phytosterols, which may be bioactive in their natural food matrices. Work is needed to add information about phytosterol content to existing food databases and to extend the evidence that feeding phytosterol-rich foods improves LDL cholesterol.

**Acknowledgments** This work was supported by NIH grant R01-50420. Dr. Ostlund and Washington University have an interest in Lifeline Technologies, Inc., a company providing emulsified phytosterols.

## References

- Expert panel on detection, evaluation, and treatment of high blood cholesterol in adults (2001) Executive summary of the third report of the national cholesterol education program (NCEP) expert panel on detection, evaluation and treatment of high blood cholesterol in adults (adult treatment panel III). *JAMA* 285:2486–2497
- Ostlund RE Jr (2002) Cholesterol absorption. *Curr Opin Gastroenterol* 18:254–258
- Ostlund RE Jr, Matthews DE (1993) [ $^{13}\text{C}$ ]cholesterol as a tracer for studies of cholesterol metabolism in humans. *J Lipid Res* 34:1825–1831
- Miettinen TA, Kesaniemi YA (1989) Cholesterol absorption: regulation of cholesterol synthesis and elimination and within-population variations of serum cholesterol levels. *Am J Clin Nutr* 49:629–635
- Bosner MS, Lange LG, Stenson WF, Ostlund RE Jr (1999) Percent cholesterol absorption in normal women and men quantified with dual stable isotopic tracers and negative ion mass spectrometry. *J Lipid Res* 40:302–308
- Bosner MS, Ostlund RE Jr, Osofisan O, Grosklos J, Fritschle C, Lange LG (1993) Assessment of percent cholesterol absorption in humans with stable isotopes. *J Lipid Res* 34:1047–1053
- Ostlund RE Jr (2004) Phytosterols and cholesterol metabolism. *Curr Opin Lipidol* 15:37–41

8. Spady DK (1999) Reverse cholesterol transport and atherosclerosis regression. *Circulation* 100:576–578
9. Moreau RA, Whitaker BD, Hicks KB (2002) Phytosterols, phytostanols, and their conjugates in foods: structural diversity, quantitative analysis, and health-promoting uses. *Prog Lipid Res* 41:457–500
10. Ostlund RE Jr (2002) Phytosterols in human nutrition. *Ann Rev Nutr* 22:533–549
11. Katan MB, Grundy SM, Jones P, Law M, Miettinen T, Paoletti R (2003) Efficacy and safety of plant stanols and sterols in the management of blood cholesterol levels. *Mayo Clin Proc* 78:965–978
12. Jonker D, van der Hoek GD, Glatz JFC, Homan C, Posthumus MA, Katan MB (1985) Combined determination of free, esterified and glycosylated plant sterols in foods. *Nutr Rep Int* 32:943–951
13. Moreau RA, Hicks KB (2004) The in vitro hydrolysis of phytosterol conjugates in food matrices by mammalian digestive enzymes. *Lipids* 39:769–776
14. Ikeda I, Tanaka K, Sugano M, Vahouny GV, Gallo LL (1988) Inhibition of cholesterol absorption in rats by plant sterols. *J Lipid Res* 29:1573–1582
15. Ikeda I, Tanaka K, Sugano M, Vahouny GV, Gallo LL (1988) Discrimination between cholesterol and sitosterol for absorption in rats. *J Lipid Res* 29:1583–1591
16. Ikeda I, Tanabe Y, Sugano M (1989) Effects of sitosterol and sitostanol on micellar solubility of cholesterol. *J Nutr Sci Vitamin* 35:361–369
17. Armstrong MJ, Carey MC (1987) Thermodynamic and molecular determinants of sterol solubilities in bile salt micelles. *J Lipid Res* 28:1144–1155
18. Nissinen M, Gylling H, Vuoristo M, Miettinen TA (2002) Micellar distribution of cholesterol and phytosterols after duodenal plant stanol ester infusion. *Am J Physiol* 282:G1009–G1015
19. Ostlund RE Jr, McGill JB, Zeng CM, Covey DF, Stearns J, Stenson WF, Spilburg CA (2002) Gastrointestinal absorption and plasma kinetics of soy Delta(5)-phytosterols and phytostanols in humans. *Am J Physiol Endocrinol Metab* 282:E911–E916
20. Igel M, Giesa U, Lutjohann D, von Bergmann K (2003) Comparison of the intestinal uptake of cholesterol, plant sterols, and stanols in mice. *J Lipid Res* 44:533–538
21. Plat J, Mensink RP (2002) Increased intestinal ABCA1 expression contributes to the decrease in cholesterol absorption after plant stanol consumption. *FASEB J* 16:1248–1253
22. Plat J, Nichols JA, Mensink RP (2005) Plant sterols and stanols: effects on mixed micellar composition and LXR (target gene) activation. *J Lipid Res* 46:2468–2476
23. Field FJ, Born E, Mathur SN (2004) Stanol esters decrease plasma cholesterol independently of intestinal ABC sterol transporters and Niemann-Pick C1-like 1 protein gene expression. *J Lipid Res* 45:2252–2259
24. Ostlund RE Jr, Spilburg CA, Stenson WF (1999) Sitostanol administered in lecithin micelles potently reduces cholesterol absorption in humans. *Am J Clin Nutr* 70:826–831
25. Lees AM, Mok HYI, Lees RS, McCluskey MA, Grundy SM (1977) Plant sterols as cholesterol-lowering agents: clinical trials in patients with hypercholesterolemia and studies of sterol balance. *Atherosclerosis* 28:325–338
26. Sudhop T, Lutjohann D, Kodal A, Igel M, Tribble DL, Shah S, Perevozskaya I, von Bergmann K (2002) Inhibition of intestinal cholesterol absorption by ezetimibe in humans. *Circulation* 106:1943–1948
27. Plat J, Mensink RP (2002) Effects of plant stanol esters on LDL receptor protein expression and on LDL receptor and HMG-CoA reductase mRNA expression in mononuclear blood cells of healthy men and women. *FASEB J* 16:258–260
28. Gylling H, Miettinen TA (1994) Serum cholesterol and cholesterol and lipoprotein metabolism in hypercholesterolaemic NIDDM patients before and during sitostanol ester-margarine treatment. *Diabetologia* 37:773–780
29. Jones PJ, Ntanos FY, Vanstone CA, Feng JY, Parsons WE (2000) Modulation of plasma lipid levels and cholesterol kinetics by phytosterol versus phytostanol esters. *J Lipid Res* 41:697–705
30. Spilburg CA, Goldberg AC, McGill JB, Stenson WF, Racette SB, Bateman J, McPherson TB, Ostlund RE Jr (2003) Fat-free foods supplemented with soy stanol-lecithin powder reduce cholesterol absorption and LDL cholesterol. *J Am Diet Assoc* 103:577–581
31. Shin MJ, Lee JH, Jang Y, Lee-Kim YC, Park E, Kim KM, Chung BC, Chung N (2005) Micellar phytosterols effectively reduce cholesterol absorption at low doses. *Ann Nutr Metab* 49:346–351
32. Devaraj S, Jialal I, Vega-Lopez S (2004) Plant sterol-fortified orange juice effectively lowers cholesterol levels in mildly hypercholesterolemic healthy individuals. *Arterioscler Thromb Vasc Biol* 24:e25–e28
33. Woollett LA, Wang Y, Buckley DD, Yao L, Chin S, Granholm N, Jones PJ, Satchell KD, Tso P, Heubi JE (2006) Micellar solubilisation of cholesterol is essential for absorption in humans. *Gut* 55:197–204
34. Mattson FH, Grundy SM, Crouse JR Jr (1982) Optimizing the effect of plant sterols on cholesterol absorption in man. *Am J Clin Nutr* 35:697–700
35. McPherson TB, Ostlund RE, Goldberg AC, Bateman JH, Schimmoeller L, Spilburg CA (2005) Phytostanol tablets reduce human LDL-cholesterol. *J Pharm Pharmacol* 57:889–896
36. Goldberg AC, Ostlund RE Jr, Bateman JH, Schimmoeller L, McPherson TB, Spilburg CA (2006) Effect of plant stanol tablets on low-density lipoprotein cholesterol lowering in patients on statin drugs. *Am J Cardiol* 97:376–379
37. Morton GM, Lee SM, Buss DH, Lawrance P (1995) Intakes and major dietary sources of cholesterol and phytosterols in the British diet. *J Hum Nutr Diet* 8:429–440
38. Ahrens EH Jr, Boucher CA (1978) The composition of a simulated American diet. *J Am Diet Assoc* 73:613–620
39. Cerqueira MT, Fry MM, Connor WE (1979) The food and nutrient intakes of the Tarahumara Indians of Mexico. *Am J Clin Nutr* 32:905–915
40. Normen L, Johnsson M, Andersson H, van Gameren Y, Dutta P (1999) Plant sterols in vegetables and fruits commonly consumed in Sweden. *Eur J Nutr* 38:84–89
41. Ostlund RE Jr, Racette SB, Okeke A, Stenson WF (2002) Phytosterols that are naturally present in commercial corn oil significantly reduce cholesterol absorption in humans. *Am J Clin Nutr* 75:1000–1004
42. Ostlund RE Jr, Racette SB, Stenson WF (2003) Inhibition of cholesterol absorption by phytosterol-replete wheat germ compared with phytosterol-depleted wheat germ. *Am J Clin Nutr* 77:1385–1389
43. Weihrauch JL, Gardner JM (1978) Sterol content of foods of plant origin. *J Am Diet Assoc* 73:39–47
44. Ostlund RE Jr, Racette SB, Stenson WF (2002) Effects of trace components of dietary fat on cholesterol metabolism: phytosterols, oxysterols, and squalene. *Nutr Rev* 60:349–359

# Molecular Genetics of Plant Sterol Backbone Synthesis

Masashi Suzuki · Toshiya Muranaka

Received: 3 July 2006 / Accepted: 13 September 2006 / Published online: 19 December 2006  
© AOCS 2006

**Abstract** Sterols, which are biosynthesized via the cytoplasmic mevalonate (MVA) pathway, are important structural components of the plasma membrane and precursors of steroid hormones in both vertebrates and plants. Ergosterol and cholesterol are the major sterols in yeast and vertebrates, respectively. In contrast, plants produce a wide variety of phytosterols, which have various functions in plant development. Although the general biosynthetic pathway to plant sterols has been defined, the details of the biochemical, physiological, and developmental functions of genes involved in the biosynthetic network and their regulation are not well understood. Molecular genetic analyses are an effective approach to use when studying these fascinating problems. Since three enzymes, 3-hydroxy-3-methylglutaryl CoA reductase, farnesyl diphosphate synthase, and lanosterol synthase, have been functionally characterized in planta, we reviewed recent progress on these enzymes. *Arabidopsis* T-DNA and transposon insertion mutants are now widely available. The use of molecular genetics, molecular biology, and bioorganic chemical approaches on these mutants, as well as inhibitors of the MVA pathway, should help us to understand plant sterol biosynthesis comprehensively.

**Keywords** Sterol · *Arabidopsis* · HMG-CoA reductase · Farnesyl diphosphate synthase · Oxidosqualene cyclase · Lanosterol · Cycloartenol · Phytosterol · Gene knockout · Isoprenoid

## Abbreviations

AACT	Acetoacetyl-CoA thiolase
CAS	Cycloartenol synthase
DMAPP	Dimethylallyl diphosphate
ER	Endoplasmic reticulum
FPS	Farnesyl diphosphate synthase
HMGR	3-Hydroxy-3-methylglutaryl-CoA reductase
HMGS	3-Hydroxy-3-methylglutaryl-CoA synthase
IPI	Isopentenyl diphosphate isomerase
IPP	Isopentenyl diphosphate
LAS	Lanosterol synthase
MVD	Mevalonate diphosphate decarboxylase
MEP	2-C-methyl-D-erythritol-4-phosphate
MK	Mevalonate kinase
MVA	Mevalonate
OSC	Oxidosqualene cyclase
PMK	Phosphomevalonate kinase
SQE	Squalene epoxidase
SQS	Squalene synthase

## Introduction

The occurrence of a wide variety of phytosterols demonstrates the diversity of plant species. To produce this variety of phytosterols, plants have evolved a steroid biosynthetic pathway that differs from that of vertebrates. All isoprenoids, including phytosterols, are biosynthesized from two common C5 isoprene units: isopentenyl diphosphate (IPP) and its isomer, dimethylallyl diphosphate (DMAPP). Unlike vertebrates, plants synthesize IPP and DMAPP via two

M. Suzuki · T. Muranaka (✉)  
Metabolic Diversity Research Team,  
RIKEN Plant Science Center, 1-7-22, Suehiro-cho,  
Tsurumi-ku, Yokohama, Kanagawa 230-0045, Japan  
e-mail: muranaka@riken.jp

pathways: the cytosolic mevalonate (MVA) and plastidial 2-C-methyl-D-erythritol-4-phosphate (MEP) pathways. Although metabolites flow between them [1–3], the MVA pathway is the main route to the production of steroidal backbones [4, 5]. As shown in Fig. 1, steroidal backbones are biosynthesized in 11 steps from acetyl-CoA: (a) the conversion of acetyl-CoA into acetoacetyl-CoA catalyzed by acetoacetyl-CoA thiolase (AACT); (b) the conversion of acetoacetyl-CoA into 3-hydroxy-3-methylglutaryl-CoA by 3-hydroxy-3-methylglutaryl-CoA synthase (HMGS); (c) the conversion of 3-hydroxy-3-methylglutaryl-CoA into MVA by 3-hydroxy-3-methylglutaryl-CoA reductase (HMGR); (d) the conversion of MVA into phosphomevalonate by mevalonate kinase (MK); (e) the conversion of phosphomevalonate into diphosphomevalonate by phosphomevalonate kinase (PMK); (f) the conversion of diphosphomevalonate into IPP by mevalonate diphosphate decarboxylase (MVD); (g) the isomerization of IPP to DMAPP by IPP isomerase (IPI); (h) the condensation of DMAPP with IPP to form farnesyl diphosphate by farnesyl diphosphate synthase (FPS); (i) the tail-to-tail condensation of two farnesyl diphosphate molecules to form squalene by squalene synthase (SQS); (j) the oxidation of squalene to 2,3-oxidosqualene by squalene epoxidase (SQE); and (k) the cyclization of 2,3-oxidosqualene into cycloartenol or lanosterol by cycloartenol synthase (CAS) or lanosterol synthase (LAS), respectively. Although the plant sterol biosynthetic route is similar to that in vertebrates, plant sterol biosynthesis has characteristic features. The 12 kinds of enzyme that

catalyze these steps are encoded by 24 genes in *Arabidopsis*; plants often have multiple genes in some steps, such as AACT, HMGR, MVD, IPI, FPS, SQS, and SQE (Fig. 1). This is a major difference between plant and vertebrate sterol biosynthesis, as mammals generally have only a single gene for each enzymatic step. The presence of multiple genes implies that these genes possess different biochemical or physiological functions. As summarized in Table 1, however, the functions of many of the genes in these 11 steps have been analyzed in vitro only or by expression in bacteria or yeast, while no functional analyses have been conducted in planta. Only three steps, those encoding HMGR, FPS, and LAS, have been analyzed for function in planta. In this review, we highlight recent progress in these genes using molecular genetic studies.

### 3-Hydroxy-3-Methylglutaryl-CoA Reductase (HMGR)

The plant HMGR gene was first isolated from *Arabidopsis* by two research groups. Learned and Fink [6] isolated it via expression cloning in a yeast mutant deficient in HMGR, and Caelles et al. [7] did so using classical hybridization methods. Upon isolation of the first plant HMGR gene (*Arabidopsis HMGI*), orthologous genes from a large variety of plant species were subsequently isolated. Expression analyses of these genes in the 1990s revealed features of the plant HMGRs that distinguish them from their mammalian counterparts. The protein structure of plant HMGR is

**Fig. 1** The putative pathway of sterol biosynthesis in *Arabidopsis thaliana*. Arrows indicate 12 reactions corresponding to 11 steps from acetyl-CoA to cycloartenol or lanosterol. Abbreviations for the enzymes that catalyze these reactions are shown under each arrow. The numbers correspond to the numbers annotated to each gene, which encode these biosynthetic enzymes in Table 1

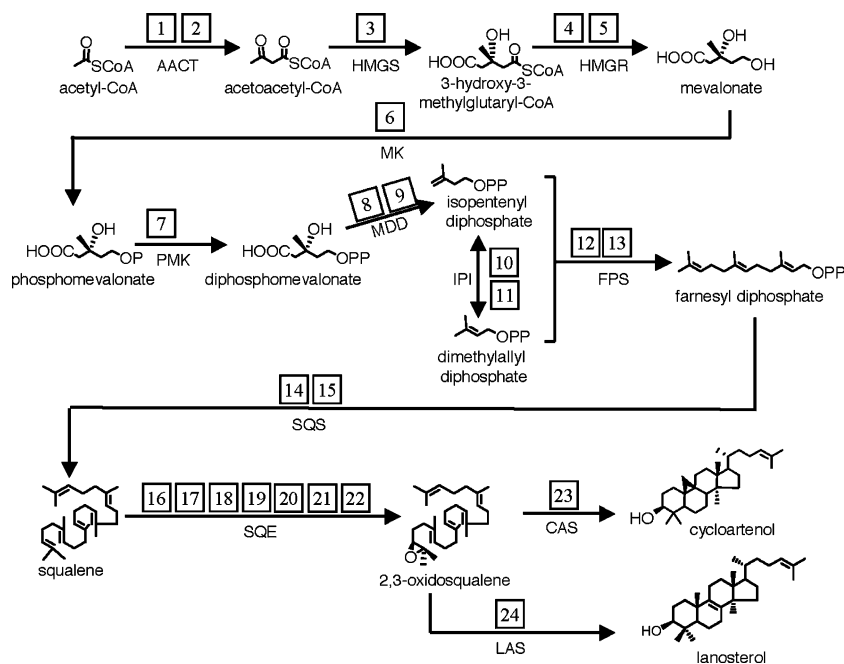


**Table 1** Enzymes involved in sterol backbone synthesis in *Arabidopsis*

Enzyme	Abbreviation for enzyme	Gene	AGI code	Cloning and expression analysis	In vitro or heterologous functional analysis	In planta functional analysis
Acetoacetyl-CoA thiolase	AACT	<i>AAT2</i>	At5g47720	–	–	–
Acetoacetyl-CoA thiolase	AACT	<i>AAT1</i>	At5g48230	–	–	–
3-Hydroxy-3-methylglutaryl-CoA synthase	HMGS	<i>HMGS</i>	At4g11820	[58]	[58]	–
3-Hydroxy-3-methylglutaryl-CoA reductase	HMGR	<i>HMG1</i>	At1g76490	[6]	[6, 59]	[14, 60]
3-Hydroxy-3-methylglutaryl-CoA reductase	HMGR	<i>HMG2</i>	At2g17370	[8]	–	[14]
Mevalonate kinase	MK	<i>MK</i>	At5g27450	[61]	[61]	–
Phosphomevalonate kinase	PMK	<i>PMK</i>	At1g31910	–	–	–
Mevalonate diphosphate decarboxylase	MVD	<i>MVD1</i>	At2g38700	[62]	[62]	–
Mevalonate diphosphate decarboxylase	MVD	<i>MVD2</i>	At3g54250	–	–	–
Isopentenyl pyrophosphate isomerase	IPI	<i>IPP2</i>	At3g02780	[63]	[63]	–
Isopentenyl pyrophosphate isomerase	IPI	<i>IPP1</i>	At5g16440	[63]	[63]	–
Farnesyl pyrophosphate synthase	FPS	<i>FPS1</i>	At5g47770	[21]	[21]	[25, 27]
Farnesyl pyrophosphate synthase	FPS	<i>FPS2</i>	At4g17190	[22]	[22]	–
Squalene synthase	SQS	<i>SQS1</i>	At4g34640	[64]	[64]	–
Squalene synthase	SQS	<i>SQS2</i>	At4g34650	[65]	[65]	–
Squalene epoxydase	SQE	<i>SQE1</i>	At1g58440	–	–	–
Squalene epoxydase	SQE	<i>SQE2</i>	At2g22830	–	–	–
Squalene epoxydase	SQE	<i>SQE3</i>	At4g37760	–	–	–
Squalene epoxydase	SQE	<i>SQE4/SQP2</i>	At5g24140	[66]	–	–
Squalene epoxydase	SQE	<i>SQE5/SQP1;1</i>	At5g24150	[66]	–	–
Squalene epoxydase	SQE	<i>SQE6</i>	At5g24155	–	–	–
Squalene epoxydase	SQE	<i>SQE7/SQP1;2</i>	At5g24160	[66]	–	–
Cycloartenol synthase	CAS	<i>CAS1</i>	At2g07050	[35]	[35]	–
Lanosterol synthase	LAS	<i>LAS1/LSS</i>	At3g45130	[49, 50]	[49, 50]	[50]

somewhat different from that of vertebrate HMGR. Although both plant and vertebrate HMGR are localized to the endoplasmic reticulum (ER), vertebrate HMGR possesses eight transmembrane domains, while plant HMGR possesses only two. Vertebrate HMGR is degraded through proteasomes after their transmembrane domains are ubiquitinated in response to high cholesterol levels. The mechanisms of plant HMGR homeostasis may differ from those of vertebrate HMGR.

First, plant HMGR genes constitute a multigene family [cf., two genes in *Arabidopsis* (*HMG1*, *HMG2*) [8], three in potato [9], and four in tomato [10], whereas HMGR is encoded by a single gene in mammals [11]. Second, plant HMGR genes are differentially regulated, which might lead to the biosynthesis of different types of isoprenoids; *HMG1* is expressed throughout the plant [8], whereas *HMG2* expression is restricted to meristematic and floral tissues, based on a tobacco heterologous expression system [12]. Choi and Bostock [13] reported that in potato, wounding and pathogens induce different antimicrobial isoprenoids (steroid glycoalkaloids and sesquiterpenoids, respectively), followed by the induction of different HMGR genes.

Despite these intensive studies, the role of each HMGR gene in plant development and metabolic

regulation of isoprenoid biosynthesis is unclear, as molecular genetics analyses of plant HMGRs have not been performed. Suzuki et al. [14] isolated *Arabidopsis* T-DNA insertion knockout mutants of *HMG1* and *HMG2*. *hmg1* mutant shows dwarfism, early senescence, and male sterility, which are consistent with its ubiquitous expression throughout the plant and a role as a housekeeping gene [8]. Brassinosteroids (BRs) and cytokinins (CKs) are isoprenoid-type phytohormones, which promote cell elongation and inhibit senescence, respectively. The dwarf and early senescence phenotype of *hmg1* is reminiscent of BR and CK deficiency in *hmg1*. However, *hmg1* did not show photomorphogenesis in the dark, the characteristic phenotype in BR-deficient mutants, indicating that *hmg1* is not a BR-deficient mutant [14]. Moreover, levels of CKs were not lower in *hmg1*, suggesting that CKs are not involved in the early senescence of *hmg1* [14]. Instead, these pleiotropic phenotypes were rescued by feeding the mutants with squalene, the precursor of sterols and triterpenoids. Indeed, levels of both sterols and triterpenoids were reduced in *hmg1* [14] (K. Ohya and T. Muranaka, unpublished data). Based on these results, it is clear that *HMG1*, which is shown to be responsible for the biosynthesis of sterols and triterpenoids, is important for plant development from vegetative through to reproductive stages.

What then is the function of *HMG2*? Based on the restriction of *HMG2* expression to meristematic and floral tissues, it was proposed that *HMG2* is important for cell division [12]. Under normal growth conditions, however, the *hmg2* mutant shows no obvious phenotype, suggesting that *HMG1* can compensate for the *HMG2* deficiency [14]. *HMGR2* seems to be a functional HMGR, as *hmg2* is more sensitive than the wild type to an HMGR inhibitor [14] and loss of both *HMG1* and *HMG2* is lethal (N. Nagata and T. Muranaka, unpublished data). *HMG2* might be involved in the production of specific isoprenoids in response to environmental stimuli such as light, drought, or pathogen attack. Metabolomic studies [15] on *HMG2*-overexpressing plants may be used to detect previously unknown isoprenoids. *HMG1* encodes two HMGR isoforms, *HMGR1S* and *HMGR1L* [16]. The subcellular localization of *HMGR1S* protein, a major isoform derived from *HMG1*, was recently analyzed in detail [17]. In contrast, the characteristics of *HMGR1L* and *HMGR2* have not been thoroughly investigated. Comparison of the subcellular localizations of these three proteins should prove interesting.

In vertebrates, HMGR is highly regulated on the transcriptional, post-transcriptional, and post-translational levels. The vertebrate HMGR gene contains an octameric *cis* sequence called the sterol regulatory element (SRE-1); sterol regulatory element binding proteins (SREBPs) are located in the ER but are cleaved in response to high cholesterol to produce active forms that migrate to the nucleus and regulate the expression of sterol regulatory genes such as HMGR [18]. SRE-1 and SREBP do not exist in plants, however, suggesting that the regulation of HMGR differs between the vertebrate and plant kingdoms.

Another approach to identifying the regulatory mechanism of HMGR is to isolate mutants that are resistant to the HMGR inhibitor, mevinolin (MEV). Rodríguez-Concepción et al. [19] screened for *Arabidopsis* MEV-resistant mutants based on leaf development. One of their MEV-resistant mutants, *rim1*, is a new allele of *phyB* (phytochrome B photoreceptor). The MEV-resistant phenotype of *rim1* resulted from the up-regulation of HMGR gene expression and thus increased enzymatic activity. The mutant is also resistant to fosmidomycin, which is an inhibitor of the MEP pathway. We are currently identifying and characterizing other mutants resistant to HMGR inhibitors based on a root elongation phenotype (K. Kobayashi and T. Muranaka, unpublished data), which will provide further insights into the unique HMGR regulation mechanism in plants.

## Farnesyl Diphosphate Synthase (FPS)

Farnesyl diphosphate (FPP) is formed by the sequential head-to-tail condensation of DMAPP and two molecules of IPP. The metabolic flow from IPP is slightly different between plants and vertebrates. In vertebrates, IPP is mainly metabolized to dolichols, ubiquinone, farnesylated proteins, and steroids via FPP but not isopentenyl adenine (tRNA). In plants, IPP is provided by both the cytosolic MVA and plastidic MEP pathways [20]. Plant IPP is metabolized to tRNA and CKs without going through FPP, but it is metabolized to dolichols, ubiquinone, farnesylated proteins, sesquiterpenes, and steroids via FPP. FPS is the great branching point in plants. Like HMGR, FPS is encoded by a multigene family in higher plants. Two genes, *FPS1* and *FPS2* [21, 22], encode three FPS isoforms, *FPS1S*, *FPS1L*, and *FPS2* [23], in *Arabidopsis*. *FPS1S* and *FPS1L* are both encoded by *FPS1*; *FPS1L* has an N-terminal extension of 41 amino acid residues with respect to *FPS1S* and is targeted to mitochondria [23]. *FPS1* was cloned by expression cloning in a yeast mutant deficient in FPS, *erg20*. The cDNA corresponding to *FPS2* was isolated using RT-PCR and its function was determined by complementation using *erg20*. The protein structure and molecular size of plant FPS are similar to those of vertebrate and yeast FPS.

The expression profiles of these two genes have been examined by Northern hybridization [22] and histochemical analyses using  $\beta$ -glucuronidase [24]. *FPS1S* is widely expressed in all plant tissues throughout development, suggesting a role for *FPS1S* in the synthesis of isoprenoids that are necessary for basic plant cell functions. In contrast, *FPS2* expression is restricted to specific organs at particular stages of development. The highest expression of *FPS2* has been observed in flowers, especially in pollen grains from the early stages of flower development. These results support a role for *FPS2* in the synthesis of specific isoprenoids with specialized functions. The expression profiles of *FPS1S* and *FPS2* are similar to those of *HMG1* and *HMG2*, suggesting that the physiological functions of *HMG1* and *FPS1S*, and of *HMG2* and *FPS2*, may be similar. If so, metabolites that are biosynthesized via HMGR1 and *FPS1* may be different from those produced via HMGR2 and *FPS2*.

When transgenic *Arabidopsis* plants overexpressing *FPS1S* were generated and characterized to investigate the physiological functions of *FPS1*, overexpression of *FPS1S* led to early senescence and reduced CK levels [25]. HMGR activity was not affected in this transgenic line. The CK zeatin, a phytohormone with strong antisenesescence activity, was biosynthe-

sized from IPP but not via FPP. These results indicate that reduced CK levels resulting from the overexpression of *FPS1S* may lead to early senescence. The details of CK biosynthesis were reported in 2004. While *trans*-zeatin, a bioactive form of CK, was predominantly biosynthesized via the MEP pathway, *cis*-zeatin, an inactive form, was biosynthesized via the MVA pathway [26].

In a subsequent paper examining *FPS1S* overexpression, Ferrer's group proposed a new hypothesis. As the activity of HMGR was not affected by *FPS1S* overexpression, the ratio of HMGR to FPS activity was drastically reduced in the transgenic plants. Because HMGR activity decreases with leaf age, the early senescence caused by *FPS1S* overexpression may be due to an imbalance between HMGR and FPS levels [27]. The authors demonstrated that the early senescence phenotype in the *FPS1S*-overexpressing *Arabidopsis* was rescued by co-overexpression of *HMG1*. *FPS1S* overexpression did not result in the overaccumulation of sterols, indicating that *FPS1S* is not limiting for sterol biosynthesis. It will be interesting to clarify which metabolites are affected by the imbalance of HMGR and FPS. Since the expression profiles of *FPS1S* and *FPS2* are different, suggesting different roles for *FPS1S* and *FPS2*, it will be important to examine knockout or knockdown mutants of these genes.

### Cycloartenol Synthase (CAS) and Lanosterol Synthase (LAS)

Sterols are 6,6,6,5-tetracyclic triterpene alcohols, which are formed by the cyclization of 2,3-oxidosqualene. This cyclization, which is catalyzed by oxidosqualene cyclases (OSCs), is one of the most complicated and fascinating reactions found in nature. While OSCs in vertebrates [28] and fungi [29] convert 2,3-oxidosqualene only to lanosterol, a sterol precursor, OSCs in plants convert 2,3-oxidosqualene to cycloartenol [30] and some other cyclic triterpenes [31]. Since plant triterpenes have diverse structures with more than 100 different carbon skeletons, plants have several genes encoding OSCs, including nine genes in rice and 13 genes in *Arabidopsis* [32]. Two of the 13 *Arabidopsis* OSCs are steroidal backbone synthases and others are nonsteroidal triterpenoid synthases [33].

For several decades, cycloartenol was thought to possibly replace lanosterol as the first cyclic triterpene during phytosterol biosynthesis [34]. The first cloned CAS gene was isolated from *Arabidopsis* in 1993 using a chromatographic screen of a heterologous expression

system [35]. This was the second OSC gene to be cloned, following the LAS gene from *Candida albicans* [36]. Following the cloning of *CAS1* from *Arabidopsis*, many cycloartenol synthase genes were isolated from dicotyledonous plants, such as *CASPEA* from *Pisum sativum* [37], *PNX* from *Panax ginseng* [38], *LcCAS1* from *Luffa cylindrical* [39], *GgCAS1* from *Glycyrrhiza glabra* [40], *CASBPX1* and *CASBPX2* from *Betula platyphylla* [41], *CPX* from *Cucurbita pepo* [42], and *OSCCCS* from *Centella asiatica*. Also isolated were *CSI* from *Avena strigosa* [43] and *CSOSCI* from *Costus speciosus* [44], both monocotyledonous plants, and *CAS1* from the gymnosperm *Abies magnifica*.

Despite the consensus that cycloartenol is the plant sterol precursor and the identification of CAS genes from many plant species, lanosterol has also been identified in some plants [45–47]. Since plants lack the ability to convert cycloartenol to lanosterol [48], lanosterol must be synthesized directly from oxidosqualene. In other words, LAS must be present in the plant kingdom. Very recently three laboratories independently identified LAS genes, including *LAS1* (also called as *LSS*) from *Arabidopsis* [49, 50], *PNZ* from *P. ginseng* [50], and *OSC7* from *Lotus japonica* [51]. *Arabidopsis* At3g45130 (*LAS1*) was previously postulated to be a CAS, based on its 77% similarity in amino acid sequence to *CAS1*. *LAS1* has been shown to complement LAS-deficient yeast [49, 50] and to function as a LAS in plant cells [50]. *LAS1* is the first plant OSC whose function has been verified in planta. *CAS1* mutant analyses demonstrated that Tyr410, His477, and Ile481 are important for CAS product specificity [52–55]. With just two amino acid substitutions, the CAS activity of *CAS1* (His477Asn and Ile481Val) is converted to LAS activity [56]. It is interesting to note that the amino acid residues of *LAS1*, *PNZ*, and *OSC7*, which correspond to His477 and Ile481 of *CAS1*, are Asn and Val, respectively. This is consistent with *LAS1*, *PNZ*, and *OSC7* having LAS rather than CAS activity.

Phylogenetic analyses showed that *LAS1*, *PNZ*, and *OSC7* belong to a branch that is most closely related to but distinct from the plant CAS branch (Fig. 2) [33, 42, 50, 57]. The plant LAS-type and CAS branches are different from other plant triterpenoid synthase branches. It has been proposed that other plant triterpenoid synthases, such as lupeol synthase and  $\beta$ -amyrin synthase, evolved in that order from ancestral CAS [41, 42]. Although CAS and LAS cyclize 2,3-oxidosqualene through chair–boat–chair conformations, other triterpenoid synthases cyclize 2,3-oxidosqualene through chair–chair–chair conformations. The differences in the primary structures of plant OSCs may reflect dif-

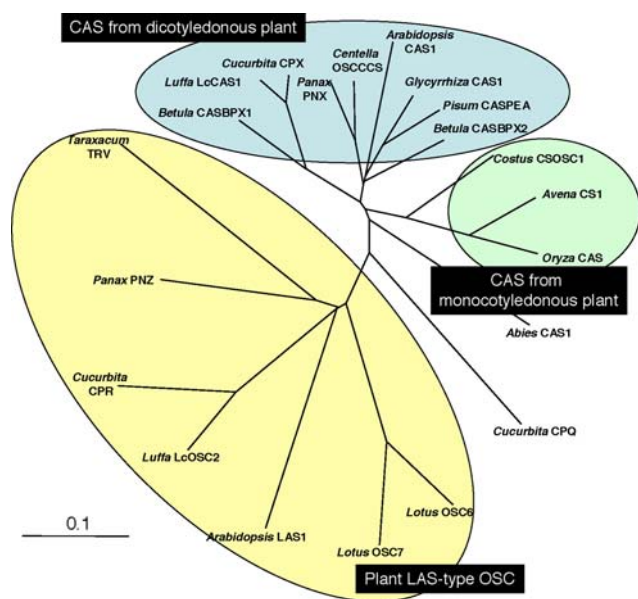


**Fig. 2** The phylogenetic tree of LAS1 homologous plant OSCs. The distance of each clone was calculated using the program CLUSTAL W. The indicated scale represents 0.1 amino acid substitution per site

ferences in their reaction mechanisms. Some other plant OSCs, such as TRV from *Taraxacum officinale*, CPR from *C. pepo*, LcOSC2 from *L. cylindrical*, and OSC6 from *L. japonica* belong to the plant LAS-type branch [49, 50, 57]. However, no LAS activity for these four OSCs has been identified [50, 51]. It may be worth noting that a conserved Asn residue is found in TRV (residue 451), CPR (residue 452), LcOSC2 (residue 453), and OSC6 (residue 454). The corresponding residue is a conserved Asp in other CAS and LAS enzymes (including plant, human, and yeast LAS), but is a conserved Asn in other triterpenoids synthases. TRV, CPR, LcOSC2, and OSC6 may thus represent intermediates in the evolution of plant LAS to other triterpenoid synthases.

Plant CAS and LAS genes have been cloned from many plant species, and their activities have been characterized in heterologous expression systems. Yet few biological functions of these genes have been determined. Only *Arabidopsis LAS1* has been characterized in planta. What determines whether 2,3-oxidosqualene is cyclized to cycloartenol, lanosterol, or other triterpenoids? What are the physiological and developmental functions of plant CAS and LAS? How are the expression patterns of the plant CAS and LAS regulated? All of these questions remain to be answered. Mutant analyses of *Arabidopsis cas1* suggested that the *cas1* homozygous mutant is lethal (M. Suzuki and T. Muranaka, unpublished data). This suggests

that the metabolites derived from cycloartenol are not necessarily the same as those derived from lanosterol. Whether sterol biosynthesis via lanosterol occurs in plants also remains to be determined.

In this review, we highlighted recent in planta molecular genetic studies of HMGR, FPS, and LAS. These three enzymes catalyze extremely important steps: HMGR is generally considered to be a regulatory enzyme in sterol biosynthesis, FPS acts at the important branching point in isoprenoid biosynthesis, and the presence of LAS shows the two routes of steroidal backbone synthesis in plants. However, previous research progress is insufficient for a comprehensive understanding of plant sterol biosynthesis. Important steps are highly regulated by multiple genes other than HMGR, FPS, and LAS. For example, seven genes encode SQE (Table 1; Fig. 1). Why does *Arabidopsis* need so many SQE genes? What are the differences between the biochemical and physiological functions of the SQE genes? Much research is needed to answer these questions. T-DNA and transposon insertion mutants of *Arabidopsis* are now widely available from several public services [67–69]. Studies of these mutants and inhibitors of the MVA pathway, using molecular genetics, molecular biology, and bioorganic chemistry, should help us to more fully understand the pathways of plant sterol biosynthesis.

**Acknowledgments** We thank Kiyoshi Ohyama (RIKEN) and Hubert Schaller (CNRS) for valuable discussions, and Robert Moreau (USDA) and Thomas Bach (CNRS) for the opportunity to review this topic. Part of this study was supported by a Grant-in-Aid for Scientific Research (C) (no. 17510188) to T.M. from the Japan Society for the Promotion of Science, the Japan Space Forum, and the Japan Society and Technology Agency.

## References

- Kasahara H, Hanada A, Kuzuyama T, Takagi M, Kamiya Y, Yamaguchi S (2002) Contribution of the mevalonate and methylerythritol phosphate pathways to the biosynthesis of gibberellins in *Arabidopsis*. *J Biol Chem* 277:45188–45194
- Nagata N, Suzuki M, Yoshida S, Muranaka T (2002) Mevalonic acid partially restores chloroplast and etioplast development in *Arabidopsis* lacking the non-mevalonate pathway. *Planta* 216:345–350
- Hemmerlin A, Hoeffler JF, Meyer O, Tritsch D, Kagan IA, Grosdemange-Billiard C, Rohmer M, Bach TJ (2003) Cross-talk between the cytosolic mevalonate and the plastidial methylerythritol phosphate pathways in tobacco bright Yellow-2 cells. *J Biol Chem* 278:26666–26676
- Benveniste P (2004) Biosynthesis and accumulation of sterols. *Annu Rev Plant Biol* 55:429–457
- Schaller H (2004) New aspects of sterol biosynthesis in growth and development of higher plants. *Plant Physiol Biochem* 42:465–476



6. Learned RM, Fink GR (1989) 3-Hydroxy-3-methylglutaryl-coenzyme A reductase from *Arabidopsis thaliana* is structurally distinct from the yeast and animal enzymes. *Proc Natl Acad Sci USA* 86:2779–2783
7. Caelles C, Ferrer A, Balcells L, Hegardt FG, Boronat A (1989) Isolation and structural characterization of a cDNA encoding *Arabidopsis thaliana* 3-hydroxy-3-methylglutaryl coenzyme A reductase. *Plant Mol Biol* 13:627–638
8. Enjuto M, Balcells L, Campos N, Caelles C, Arró M, Boronat A (1994) *Arabidopsis thaliana* contains two differentially expressed 3-hydroxy-3-methylglutaryl-CoA reductase genes, which encode microsomal forms of the enzyme. *Proc Natl Acad Sci USA* 91:927–931
9. Korth KL, Stermer BA, Bhattacharyya MK, Dixon RA (1997) HMG-CoA reductase gene families that differentially accumulate transcripts in potato tubers are developmentally expressed in floral tissues. *Plant Mol Biol* 33:545–551
10. Daraselia ND, Tarchevskaya S, Narita JO (1996) The promoter for tomato 3-hydroxy-3-methylglutaryl coenzyme A reductase gene 2 has unusual regulatory elements that direct high-level expression. *Plant Physiol* 112:727–733
11. Goldstein JL, Brown MS (1990) Regulation of the mevalonate pathway. *Nature* 343:425–430
12. Enjuto M, Lumbreras V, Marin C, Boronat A (1995) Expression of the *Arabidopsis HMG2* gene, encoding 3-hydroxy-3-methylglutaryl coenzyme A reductase, is restricted to meristematic and floral tissues. *Plant Cell* 7:517–527
13. Choi D, Bostock RM (1994) Involvement of de novo protein synthesis, protein kinase, extracellular  $Ca^{2+}$ , and lipoxygenase in arachidonic acid induction of 3-hydroxy-3-methylglutaryl coenzyme A reductase genes and isoprenoid accumulation in potato (*Solanum tuberosum* L.). *Plant Physiol* 104:1237–1244
14. Suzuki M, Kamide Y, Nagata N, Seki H, Ohyama K, Kato H, Masuda K, Sato S, Kato T, Tabata S, Yoshida S, Muranaka T (2004) Loss of function of 3-hydroxy-3-methylglutaryl coenzyme A reductase 1 (*HMG1*) in *Arabidopsis* leads to dwarfing, early senescence and male sterility, and reduced sterol levels. *Plant J* 37:750–761
15. Hirai MY, Yano M, Goodenowe DB, Kanaya S, Kimura T, Awazuhara M, Arita M, Fujiwara T, Saito K (2004) Integration of transcriptomics and metabolomics for understanding of global responses to nutritional stresses in *Arabidopsis*. *Proc Natl Acad Sci USA* 101:10205–12010
16. Lumbreras V, Campos N, Boronat A (1995) The use of an alternative promoter in the *Arabidopsis thaliana HMG1* gene generates an mRNA that encodes a novel 3-hydroxy-3-methylglutaryl coenzyme A reductase isoform with an extended N-terminal region. *Plant J* 8:541–549
17. Leivar P, González VM, Castel S, Trelease RN, López-Iglesias C, Arró M, Boronat A, Campos N, Ferrer A, Fernández-Busquets X (2005) Subcellular localization of *Arabidopsis* 3-hydroxy-3-methylglutaryl-coenzyme A reductase. *Plant Physiol* 137:57–69
18. Hampton RY (2002) Proteolysis and sterol regulation. *Annu Rev Cell Dev Biol* 18:345–378
19. Rodríguez-Concepción M, Forés O, Martínez-García JF, González V, Phillips MA, Ferrer A, Boronat A (2004) Distinct light-mediated pathways regulate the biosynthesis and exchange of isoprenoid precursors during *Arabidopsis* seedling development. *Plant Cell* 16:144–156
20. Lange BM, Ghassemian M (2003) Genome organization in *Arabidopsis thaliana*: a survey for genes involved in isoprenoid and chlorophyll metabolism. *Plant Mol Biol* 51:925–948
21. Delourme D, Lacroute F, Karst F (1994) Cloning of an *Arabidopsis thaliana* cDNA coding for farnesyl diphosphate synthase by functional complementation in yeast. *Plant Mol Biol* 26:1867–1873
22. Cunillera N, Arró M, Delourme D, Karst F, Boronat A, Ferrer A (1996) *Arabidopsis thaliana* contains two differentially expressed farnesyl-diphosphate synthase genes. *J Biol Chem* 271:7774–7780
23. Cunillera N, Boronat A, Ferrer A (1997) The *Arabidopsis thaliana FPS1* gene generates a novel mRNA that encodes a mitochondrial farnesyl-diphosphate synthase isoform. *J Biol Chem* 272:15381–15388
24. Cunillera N, Boronat A, Ferrer A (2000) Spatial and temporal patterns of gus expression directed by 5' regions of the *Arabidopsis thaliana* farnesyl diphosphate synthase genes *FPS1* and *FPS2*. *Plant Mol Biol* 44:747–758
25. Masferrer A, Arró M, Manzano D, Schaller H, Fernández-Busquets X, Moncaleán P, Fernández B, Cunillera N, Boronat A, Ferrer A (2002) Overexpression of *Arabidopsis thaliana* farnesyl diphosphate synthase (*fps1s*) in transgenic *Arabidopsis* induces a cell death/senescence-like response and reduced cytokinin levels. *Plant J* 30:123–132
26. Kasahara H, Takei K, Ueda N, Hishiyama S, Yamaya T, Kamiya Y, Yamaguchi S, Sakakibara H (2004) Distinct isoprenoid origins of *cis*- and *trans*-zeatin biosyntheses in *Arabidopsis*. *J Biol Chem* 279:14049–14054
27. Manzano D, Fernández-Busquets X, Schaller H, González V, Boronat A, Arró M, Ferrer A (2004) The metabolic imbalance underlying lesion formation in *Arabidopsis thaliana* overexpressing farnesyl diphosphate synthase (isoform 1s) leads to oxidative stress and is triggered by the developmental decline of endogenous HMGR activity. *Planta* 219:982–992
28. Corey EJ, Russey WE, Ortiz de Montellano PR (1966) 2,3-Oxidosqualene, an intermediate in the biological synthesis of sterols from squalene. *J Am Chem Soc* 88:4750–4751
29. Barton DHR, Gosden AF, Mellows G, Widdowson DA (1968) Lanosterol biosynthesis in *Saccharomyces cerevisiae*. *Chem Commun* 1067–1068
30. Rees HH, Goad LJ, Goodwin TW (1968) Cyclization of 2,3-oxidosqualene to cycloartenol in a cell-free system from higher plants. *Tetrahedron Lett* 9:723–725
31. Corey EJ, Ortiz de Montellano PR (1967) Enzymic synthesis of  $\beta$ -amyrin from 2,3-oxidosqualene. *J Am Chem Soc* 89:3362–3363
32. Husselstein-Muller T, Schaller H, Benveniste P (2001) Molecular cloning and expression in yeast of 2,3-oxidosqualene-triterpenoid cyclases from *Arabidopsis thaliana*. *Plant Mol Biol* 45:75–92
33. Phillips DR, Rasbery JM, Bartel B, Mastuda SPT (2006) Biosynthetic diversity in plant triterpene cyclization. *Curr Opin Plant Biol* 9:305–314
34. Benveniste P, Hirth L, Ourisson G (1966) La Biosynthèse des Stérols dans les Tissus de Tabac Cultivés in vitro—II.: Particularités de la Biosynthèse des Phytostérols des Tissus de Tabac Cultivés in vitro. *Phytochem* 5:45–58
35. Corey EJ, Matsuda SPT, Bartel B (1993) Isolation of an *Arabidopsis thaliana* gene encoding cycloartenol synthase by functional expression in a yeast mutant lacking lanosterol synthase by the use of a chromatographic screen. *Proc Natl Acad Sci USA* 90:11628–11632
36. Buntel CJ, Griffin JH (1992) Nucleotide and deduced amino acid sequence of the oxidosqualene cyclase from *Candida albicans*. *J Am Chem Soc* 114:9711–9713
37. Morita M, Shibuya M, Lee MS, Sankawa U, Ebizuka Y (1997) Molecular cloning of pea cDNA encoding cycloartenol synthase and its functional expression in yeast. *Biol Pharm Bull* 20:770–775

38. Kushiro T, Shibuya M, Ebizuka Y (1998)  $\beta$ -amyrin synthase. Cloning of oxidosqualene cyclase that catalyzes the formation of the most popular triterpene among higher plants. *Eur J Biochem* 256:238–244
39. Hayashi H, Hiraoka N, Ikeshiro Y, Yazaki K, Tanaka S, Kushiro T, Shibuya M, Ebizuka Y (1999) Molecular cloning of a cDNA encoding cycloartenol synthase from *Luffa cylindrical*. *Plant Physiol* 121:1383
40. Hayashi H, Hiraoka N, Ikeshiro Y, Kushiro T, Morita M, Shibuya M, Ebizuka Y (2000) Molecular cloning and characterization of a cDNA for *Glycyrrhiza glabra* cycloartenol synthase. *Biol Pharm Bull* 23:231–234
41. Zhang H, Shibuya M, Yokota S, Ebizuka Y (2003) Oxidosqualene cyclases from cell suspension cultures of *Betula platyphylla* var *japonica*: molecular evolution of oxidosqualene cyclases in higher plants. *Biol Pharm Bull* 26:642–650
42. Shibuya M, Adachi S, Ebizuka Y (2004) Cucurbitadienol synthase, the first committed enzyme for cucurbitacin biosynthesis, is a distinct enzyme from cycloartenol synthase for phytosterol biosynthesis. *Tetrahedron* 60:6995–7003
43. Haralampidis K, Bryan G, Qi X, Papadopoulou K, Bakht S, Melton R, Osbourn A (2001) A new class of oxidosqualene cyclases directs synthesis of antimicrobial phytoprotectants in monocots. *Proc Natl Acad Sci USA* 98:13431–13436
44. Kawano N, Ichinose K, Ebizuka Y (2002) Molecular cloning and functional expression of cDNAs encoding oxidosqualene cyclases from *Costus speciosus*. *Biol Pharm Bull* 25:477–482
45. Itoh T, Jeong MT, Hirano Y, Tamura T, Matsumoto T (1977) Occurrence of lanosterol and lanostenol in seeds of red pepper (*Capsicum annuum*). *Steroids* 29:569–577
46. Giner J-L, Djerassi C (1995) A reinvestigation of the biosynthesis of lanosterol in *Euphorbia lathyris*. *Phytochemistry* 39:333–335
47. Giner J-L, Berkowitz JD, Andersson T (2000) Nonpolar components of the latex of *Euphorbia peplus*. *J Nat Prod* 63:267–269
48. Rahier A, Cattel L, Benveniste P (1977) Mechanism of the enzymatic cleavage of the 9 $\beta$ ,19-cyclopropane ring of cycloartenol. *Phytochemistry* 16:1187–1192
49. Kolesnikova MD, Xiong Q, Lodeiro S, Hua L, Matsuda SPT (2006) Lanosterol biosynthesis in plants. *Arch Biochem Biophys* 447:87–95
50. Suzuki M, Xiang T, Ohyama K, Seki H, Saito K, Muranaka T, Hayashi H, Katsube Y, Kushiro T, Shibuya M, Ebizuka Y (2006) Lanosterol synthase in dicotyledonous plants. *Plant Cell Physiol* 47:565–571
51. Sawai S, Akashi T, Sakurai N, Suzuki H, Shibata D, Ayabe S, Aoki T (2006) Plant lanosterol synthase: divergence of the sterol and triterpene biosynthetic pathway in eukaryotes. *Plant Cell Physiol* 47:673–677
52. Hart EA, Hua L, Darr LB, Wilson WK, Pang JH, Matsuda SPT (1999) Directed evolution to investigate steric control of enzymatic oxidosqualene cyclization. An isoleucine-to-valine mutation in cycloartenol synthase allows lanosterol and parkeol biosynthesis. *J Am Chem Soc* 121:9887–9888
53. Herrera JBR, Wilson WK, Matsuda SPT (2000) A tyrosine-to-threonine mutation converts cycloartenol synthase to an oxidosqualene cyclase that forms lanosterol as its major product. *J Am Chem Soc* 122:6765–6766
54. Meyer MM, Xu R, Matsuda SPT (2002) Directed evolution to generate cycloartenol synthase mutants that produce lanosterol. *Org Lett* 4:1395–1398
55. Segura MJR, Lodeiro S, Meyer MM, Patel AJ, Matsuda SPT (2002) Direct evolution experiments reveal mutations at cycloartenol synthase residue His477 that dramatically alter catalysis. *Org Lett* 4:4459–4462
56. Lodeiro S, Schulz-Gasch T, Matsuda SPT (2005) Enzyme redesign: two mutations cooperate to convert cycloartenol synthase into an accurate lanosterol synthase. *J Am Chem Soc* 127:14132–14133
57. Sawai S, Shindo T, Sato S, Kaneko T, Tabata S, Ayabe S, Aoki T (2006) Functional and structural analysis of genes encoding oxidosqualene cyclases of *Lotus japonicus*. *Plant Sci* 170:247–257
58. Montamat F, Guilloton M, Karst F, Delrot S (1995) Isolation and characterization of a cDNA encoding *Arabidopsis thaliana* 3-hydroxy-3-methylglutaryl-coenzyme a synthase. *Gene* 167:197–201
59. Dale S, Arro M, Becerra B, Morrice NG, Boronat A, Hardie DG, Ferrer A (1995) Bacterial expression of the catalytic domain of 3-hydroxymethylglutaryl-coa reductase (isoform HMGR1) from *Arabidopsis thaliana*, and its inactivation by phosphorylation at Ser577 by *Brassica oleracea* 3-hydroxy-3-methylglutaryl-coa reductase kinase. *Eur J Biochem* 233:506–513
60. Re EB, Jones D, Learned RM (1995) Co-expression of native and introduced genes reveals cryptic regulation of HMG-CoA reductase expression in *Arabidopsis*. *Plant J* 7:771–784
61. Riou C, Tourte Y, Lacroute F, Karst F (1994) Isolation and characterization of a cDNA encoding *Arabidopsis thaliana* mevalonate kinase by genetic complementation in yeast. *Gene* 148:293–297
62. Cordier H, Karst F, Bergés T (1999) Heterologous expression in *Saccharomyces cerevisiae* of an *Arabidopsis thaliana* cDNA encoding mevalonate diphosphate decarboxylase. *Plant Mol Biol* 39:953–967
63. Campbell M, Hahn FM, Poulter CD, Leustek T (1997) Analysis of the isopentenyl diphosphate isomerase gene family from *Arabidopsis thaliana*. *Plant Mol Biol* 36:323–328
64. Nakashima T, Inoue T, Oka A, Nishino T, Osumi T, Hata S (1995) Cloning, expression, and characterization of cDNAs encoding *Arabidopsis thaliana* squalene synthase. *Proc Natl Acad Sci USA* 92:2328–2332
65. Kribii R, Arro M, DelArco A, Gonzalez V, Balcells L, Delourme D, Ferrer A, Karst F, Boronat A (1997) Cloning and characterization of the *Arabidopsis thaliana* SQS1 gene encoding squalene synthase—involverment of the C-terminal region of the enzyme in the channeling of squalene through the sterol pathway. *Eur J Biochem* 249:61–69
66. Schafer UA, Reed DW, Hunter DG, Yao K, Weninger AM, Tsang EWT, Reaney MJT, MacKenzie SL, Covello PS (1999) An example of intron junctional sliding in the gene families encoding squalene monooxygenase homologues in *Arabidopsis thaliana* and *Brassica napus*. *Plant Mol Biol* 39:721–728
67. TAIR(2006) Homepage. The arabidopsis information resource (TAIR), Stanford, CA (see <http://www.arabidopsis.org/>, last accessed 7th November 2006)
68. NASC(2006) The European arabidopsis stock center webpage. Nottingham Arabidopsis Stock Centre (NASC), Loughborough, UK (see <http://www.arabidopsis.info/>, last accessed 7th November 2006)
69. Experimental Plant Division, RIKEN Bioresource Center (2006) Arabidopsis Seed Catalogue webpage. Experimental Plant Division, RIKEN Bioresource Center, Tsukuba-shi, Ibaraki, Japan (see <http://www.brc.riken.go.jp/lab/epd/Eng/catalog/seed.shtml>, last accessed 7th November 2006)

# Formation of Triterpenoids throughout *Olea europaea* Fruit Ontogeny

Naim Stiti · Saïda Triki · Marie-Andrée Hartmann

Received: 5 October 2006 / Accepted: 30 November 2006 / Published online: 12 January 2007  
© AOCS 2007

**Abstract** Drupes were handpicked from olive (*Olea europaea* L.) trees, cv chemlali, at 13 distinct stages of fruit development, referred to as weeks after flowering (WAF), and analyzed for their free and esterified sterols and triterpenoids content. These two classes of compounds are synthesized via the acetate/mevalonate pathway and share common precursors up to oxidosqualene (OS). Cyclization of OS in either cycloartenol or  $\beta$ -amyirin constitutes a branch point between primary (sterol pathway) and secondary (triterpenoid pathway) metabolisms. At the onset of fruit development, i.e., between 12 and 18 WAF, drupes were found to contain high amounts of  $\alpha$ - and  $\beta$ -amyirins as well as more-oxygenated compounds such as triterpenic diols (erythrodiol and uvaol) and acids (oleanolic, ursolic and maslinic acids). Concomitantly, sterol precursors were barely detectable. From 21 WAF, when the olive fruit reached its final size and began to turn from green to purple,  $\alpha$ - and  $\beta$ -amyirins were no longer present, while 4,4-dimethyl- and 4 $\alpha$ -methylsterols started to be formed, indicating a redirection of the carbon flux from the triterpenoid pathway towards the sterol pathway. Between 21 and 30 WAF, sterol end products, mainly

represented by sitosterol, progressively accumulated and triterpenic diols were replaced by triterpenic acids, essentially maslinic acid. Interestingly, the developing olive fruit was found to accumulate significant amounts of parkeol as an ester conjugate. Whatever the stage of development, triterpenoids represent the major triterpenic compounds of the olive fruit.

**Keywords** *Olea europaea* · Olive fruit development · Triterpene synthases · Non-steroidal triterpenoids · Oleanane triterpenoids · Sterols · Ester conjugates

## Abbreviations

$\beta$ AS	$\beta$ -Amyrin synthase
CAS	Cycloartenol synthase
HPTA	Hydroxy pentacyclic triterpenic acid
OS	Oxidosqualene
RRT	Relative retention time
TAG	Triacylglycerol
WAF	Week after flowering

## Introduction

Besides sterols, higher plants produce a vast array of non-steroidal triterpenoids. Over 100 different carbon skeletons are known and further oxidative modifications and glycosylations generate even more diversity [1–3]. Despite the increasing interest in the wide range of biological properties of plant triterpenoids and their derivatives for human health [4–7], their roles and functions *in planta* still remain poorly understood. Sterols and non-steroidal triterpenoids are synthesized via the cytoplasmic acetate/mevalonate pathway and

Part of this work was presented at the 97th Annual Meeting of the AOCS in Saint Louis, Missouri, April 30–May 3, 2006.

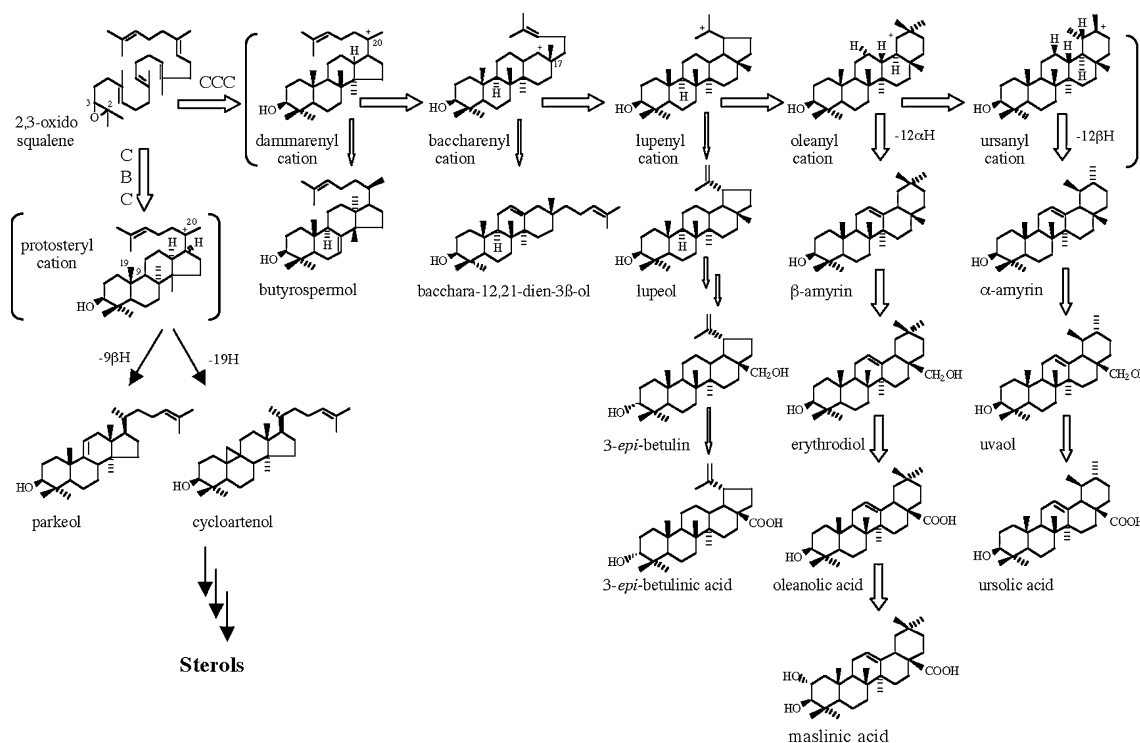
M.-A. Hartmann (✉)  
Département des Isoprénoides,  
Institut de Biologie Moléculaire des Plantes  
(CNRS UPR 2357), 28 rue Goethe,  
67083 Strasbourg Cedex, France  
e-mail: MA.Hartmann@ibmp-ulp.u-strasbg.fr

N. Stiti · S. Triki  
Laboratoire de Biochimie des Lipides,  
Faculté des Sciences, 1060 Tunis, Tunisia

share common biosynthetic precursors up to (3*S*)-2,3-oxidosqualene (OS) [8, 9]. Then, OS serves as a substrate for various OS cyclases, also called triterpene synthases. Cycloartenol synthase (CAS, EC 5.4.99.8) cyclizes OS folded in the pre-chair-boat-chair conformation via the protosteryl cation into cycloartenol, the first cyclic precursor of the sterol pathway, whereas non-steroidal triterpenoids are assumed to be formed from OS folded in the all-pre-chair conformation (see Scheme 1). As an example,  $\beta$ -amyrin synthase ( $\beta$ AS, EC 5.4.99) catalyzes the cyclization of OS into  $\beta$ -amyrin (olean-12-en-3 $\beta$ -ol), one of the most commonly occurring triterpenes. By generating four or five rings and several asymmetric centers in a single step, the OS cyclization reaction is thought to proceed through a series of rigidly held carbocationic intermediates [10]. As shown in Scheme 1, the proton-initiated cyclization first produces the tetracyclic dammarenyl C-20 cation, and the subsequent rearrangement leads to the pentacyclic oleanyl cation via the baccharenyl and lupenyl cationic intermediates. Finally, a series of 1,2-hydride shifts, with elimination of the 12-*pro-S* or 12-*pro-R* proton gives  $\beta$ - or  $\alpha$ -amyrin, respectively. Up to now, several triterpene synthase complementary deoxyribonucleic acids (cDNAs) have been cloned from plant sources and their enzyme functions identified by het-

erologous expression in yeast [11–14]. These studies have shown that most of these triterpene synthases, like other terpene synthases, are able to simultaneously form a vast array of products (up to 10) from OS [15]. They are called multifunctional and each product might result from the stabilization of a specific carbocationic intermediate [12]. Non-steroidal triterpenes are then metabolized into more-oxygenated compounds, which serve as substrates for synthesis of triterpenic saponins [16]. As the cyclization of OS to sterols and non-steroidal triterpenoids represents a branch point between primary and secondary metabolisms, triterpene synthases are attractive tools for investigating physiological roles of non-steroidal triterpenoids.

The aim of the present study is to shed more light on the biosynthetic relationships between sterol and triterpenoid pathways in *Olea europaea* L. throughout fruit development. The olive tree leaf and olive oil have been known for a long time to contain a variety of sterols and triterpenoids, including erythrodiol, oleanic acid and maslinic acid, which are oxygenated derivatives of  $\beta$ -amyrin [17–19]. However, very little attention has been paid so far to sterol and triterpenoid metabolism in developing drupes, mainly because of the low content of these compounds (around 1%)



**Scheme 1** Postulated biosynthetic pathway of non-steroidal triterpenoids in *Olea europaea* fruit. CCC and CBC refer to the all-pre-chair and pre-chair-boat-chair conformations of OS, leading to non-steroidal triterpenes and sterols, respectively. The

postulated carbocationic intermediates are represented in *brackets*. The width of the arrows reflects the relative proportions of the carbon flux between the different families of products

compared to triacylglycerols (TAGs) and the long maturation period of the olive fruit (6–7 months).

Batches of drupes were collected from olive trees belonging to the prominent Tunisian cultivar, Chemlali, at various stages of ripening, referred to as weeks after flowering (WAF), and analyzed for their content of free and esterified sterols and triterpenoids. The present results provide evidence for a complex regulation process of the carbon flux between sterol and triterpenoid pathways taking place at the OS cyclization step, a process also controlled by the acylation of intermediates and end products.

## Materials and Methods

### Plant Material

Batches of olives were handpicked from olive (*Olea europaea* L.) trees, cv Chemlali, at 13 distinct stages of development, referred to as WAF. Olive fruit were stored at  $-80\text{ }^{\circ}\text{C}$  until use. Fruit from two consecutive harvests (2003–2004) were analyzed, but data presented here correspond to only one set of analyses.

### Isolation of Total Lipids

After lyophilization, olives from each batch (between 1.4 and 2.7 g of dry weight) were ground in liquid nitrogen, and then homogenized with an ultra-turrax in the presence of dichloromethane/methanol (2:1 by volume). Total lipids were extracted twice by heating under reflux at  $65\text{ }^{\circ}\text{C}$ , for 2 h. The combined organic phases were filtrated and evaporated under reduced pressure. Analyses were performed on the third of each extract.

### Sterol Analysis

Free sterols and esterified sterols were isolated as previously described [20]. Briefly, total lipids were applied to 60 F<sub>254</sub> (Merck, Darmstadt, Germany) silica gel thin-layer chromatography (TLC) plates developed with dichloromethane (two runs). The bands corresponding to squalene and sterol esters ( $R_f$  0.95), to 4,4-dimethyl- ( $R_f$  0.4), 4 $\alpha$ -methyl- ( $R_f$  0.35) and sterols ( $R_f$  0.25) were scraped off and compounds eluted from silica with dichloromethane.

Squalene was separated from sterol esters by TLC with cyclohexane/toluene (19:1 by volume) as the developing solvent. Squalene ( $R_f$  0.4) was directly analyzed by gas chromatography (GC) whereas sterol

esters ( $R_f$  0.2) were hydrolyzed by heating at  $90\text{ }^{\circ}\text{C}$  for 1 h with 6% (wt/vol) KOH in methanol (2.5 mL). After addition of water (1 vol), sterols were extracted three times with hexane (3 vol) and separated into 4,4-dimethyl-, 4 $\alpha$ -methyl- and 4-desmethylsterols as described above.

Free sterols and sterols released from ester conjugates were acetylated with acetic anhydride/pyridine (2:1 by volume). Acetate derivatives were then purified and analyzed by GC using a Varian GC, model 8300, equipped with a flame ionization detector (FID) and a DB-1 capillary column (25 m  $\times$  0.32 mm i.d., 0.25  $\mu\text{m}$  thickness, J&W scientific), with H<sub>2</sub> as the carrier gas (2 mL/min). The temperature program included a fast rise from 60 to  $230\text{ }^{\circ}\text{C}$  ( $30\text{ }^{\circ}\text{C min}^{-1}$ ), a slow rise from 230 to  $280\text{ }^{\circ}\text{C}$  ( $2\text{ }^{\circ}\text{C min}^{-1}$ ), and a plateau at  $280\text{ }^{\circ}\text{C}$  for 10 min. Free cholesterol was used as an internal standard. The standard deviation (SD) for quantitative determinations was  $\pm 5\%$ . Sterol acetates were identified by gas-chromatography mass-spectrometry (GC-MS) analyses performed on an Agilent gas chromatograph equipped with an on-column injector and a DB-5 (J&W Scientific) capillary column (30 m  $\times$  0.25 mm, i.d.) and interfaced to a 5973 MSD using electron impact at 70 eV. Spectra were compared to those of authentic samples or our own reference sterols or to literature data [21].

### Triterpenoid Analysis

Free and esterified triterpenoids were isolated from the total lipid extract by TLC with dichloromethane as the solvent (two runs). Under these conditions, triterpenic diols ( $R_f$  0.1) were separated from free tetra- and pentacyclic triterpenes ( $R_f$  0.4) and esterified triterpenes ( $R_f$  0.95). Identification of lupenone ( $R_f$  0.6) and 3-*epi*-lupeol (3 $\alpha$ -lupeol) ( $R_f$  0.5) required the preliminary hydrolysis of TAGs.

Tetra- and pentacyclic triterpenes as well as triterpenic diols were acetylated, purified by TLC and identified by GC and GC-MS under similar conditions as sterol acetates, using free cholesterol as an internal standard. For triterpenic diacetates, the final temperature at  $280\text{ }^{\circ}\text{C}$  was held for 25 min instead of 10 min. Standards were prepared from commercially available uvaol (Sigma), erythrodiol and betulin (Extrasynthese).

Hydroxy pentacyclic triterpenic acids (HPTAs) were isolated according to the method of Pérez-Camino and Cert [22] with some modifications. Briefly, total lipids were firstly dissolved in tetrahydrofuran (THF), and then loaded on a bonded aminopropyl phase solid-phase extraction (SPE) cartridge, which

had been pretreated successively with methanol (3 mL), acetone (3 mL) and hexane (4 mL). The column was washed with hexane/dichloromethane (90:10 by volume), to eliminate hydrocarbons, waxes and TAGs, then with hexane/ethyl acetate (40:60 by volume), to discard alcohols, sterols, and diacylglycerols. Finally, HPTAs and free fatty acids were eluted from the cartridge with diethyl ether/acetic acid (98:2 by volume). The solvent was evaporated until dryness and the residue was treated with ethereal diazomethane, at 0 °C for 1 h. After removing the methylation reagent with a nitrogen flow, the corresponding methylesters were acetylated and purified by TLC (mono-acetoxymethylesters,  $R_f$  0.65; diacetoxymethylesters,  $R_f$  0.4). A standard of oleanolic acid methylester was run under the same conditions. Acetate derivatives of methyl esters were analyzed by GC under similar conditions as triterpene diacetates, but with oleanolic methylester as internal standard and a slightly different temperature program (from 60 to 240 °C, at 40 °C min<sup>-1</sup>, then from 240 to 300 °C at 2 °C min<sup>-1</sup> and a plateau at 300 °C for 25 min). Non-steroidal triterpenoids were identified by their relative retention time (RRT) in GC on DB-1 or DB-5 columns and by GC-MS. Spectra were compared to those of available authentic samples (acetate derivatives of oleanolic, ursolic and betulinic methyl esters prepared from the corresponding free acids provided by Sigma, Aldrich and Extrasynthese, respectively) or to literature data [23, 24].

#### Chemical Synthesis of 3-*epi*-lupeol

Lupenone (Extrasynthese, 10 mg) was dissolved in absolute ethanol and stirred in the presence of an excess of NaBH<sub>4</sub> for 2–3 h at room temperature. The reaction was stopped with addition of 3N HCl to eliminate NaBH<sub>4</sub>, and the mixture extracted with hexane. After TLC with dichloromethane as the solvent (two runs), 3-*epi*-lupeol ( $R_f$  0.5) was separated from lupeol ( $R_f$  0.4). The yield of the reaction was about 25%.

## Results and Discussion

Drupes (i.e. the whole fruit comprising the epicarp, the fleshy mesocarp and the endocarp or pit containing the seed) were harvested from *Olea europaea* L. trees, cv Chemlali, at 13 distinct stages of fruit growth and development corresponding to 12, 13, 15, 16, 18, 21, 23, 25, 27, 29, 30, 32 and 33 WAF. At the time of harvesting, the lignification of the olive endocarp had ended. Between 12 and 18 WAF, drupes were green

and progressively increased in size and fresh weight, but in the case of this cultivar, these changes were of limited amplitude compared to other olive varieties. At the end of this period, the final fruit size was almost fixed and from 21 WAF, epidermal color began to change, coinciding with the start of the synthesis of anthocyanins and loss of chlorophylls [25]. The olive fruit gradually turned from green to black. Complete maturity was observed after 29 WAF. The 33 WAF stage referred to an over-mature stage.

Drupes from the different batches were analyzed for their content of free and esterified sterols and triterpenoids, but only data obtained for olive fruit harvested at 12, 18, 21 and 30 WAF are presented here.

### The Olive Fruit Contains a Vast Array of Triterpenoids and Sterols

#### *Non-steroidal Compounds (Table 1)*

Most OS cyclase products co-migrate on TLC plates, including cycloartenol, 24-methylene cycloartanol and various tetra- and pentacyclic triterpenes. The resolution of such complex mixtures into individual compounds was not trivial, even by GC. Since most compounds were present in very low amounts, the use of <sup>1</sup>H NMR was excluded. All the compounds were identified as acetate derivatives by their RRT in GC and MS fragmentation pattern in GC-MS as described in the experimental section. Among the compounds found in the olive fruit (Tables 1, 2), at least 12 non-steroidal triterpenes and 4,4-dimethylsterols had the same molecular weight (MW) of 468 (acetate derivative) and, for many of them, very similar mass spectrometry (MS) fragmentation patterns. Besides 3 $\beta$ -OH triterpenes, we could also identify more-polar compounds with additional hydroxyl or carboxylic groups, corresponding to pentacyclic diols and mono- or di-HPTAs.

The different triterpenoids identified in the olive fruit are listed in Table 1 and their structures shown in Scheme 1. They include 18 pentacyclic triterpenoids arising from four different carbon skeletons: oleanane ( $\beta$ -amyirin,  $\beta$ -amyrone, 28-nor- $\beta$ -amyirin,  $\delta$ -amyirin, erythrodiol, oleanolic acid and maslinic acid), ursane ( $\alpha$ -amyirin, 28-nor- $\alpha$ -amyirin, uvaol, ursolic acid), lupane (lupeol, lupenone, 3-*epi*-lupeol, 3-*epi*-betulin and 3-*epi*-betulinic acid) and taraxane (taraxerol, D-fridoolean-14-ene-3 $\beta$ ,28-diol). Oleanane triterpenoids were largely predominant. We also found butyrospermol and traces of bacchar-12,21-dien-3 $\beta$ -ol, two tetracyclic triterpenes with euphane and baccharane carbon skeletons, respectively.

**Table 1** Triterpenoids of the Chemlali olive fruit: GC-MS analysis

Compound	MS (% relative abundance of molecular and characteristic fragment ions): experimental or literature data <sup>a</sup>
<b>Euphane group</b>	
Butyrospermol ( <i>5α</i> -eupha-7,24(25)-dien-3β-ol)	MS: <i>m/z</i> 468 [M <sup>+</sup> ] (22), 453 (100), 393 (68), 355 (18), 301 (7), 271 (8), 255 (10), 241 (12), 189 (20), 109 (38), 95 (41), 69 (79)
<b>Taraxane group</b>	
Taraxerol (D-friedoolean-14-en-3β-ol)	(24)
Taraxer-14-ene-3β,28-diol (D-friedoolean-14-ene-3β,28-diol)	(23)
<b>Oleanane group</b>	
β-Amyrin ( <i>5α</i> -olean-12-en-3β-ol)	(14)
β-Amyrone	MS: <i>m/z</i> 424 [M <sup>+</sup> ] (13), 409 (15), 406 (8), 355 (10), 218 (100), 207 (20), 203 (43), 189 (17), 163 (22)
28-Nor-β-amyrin (28-nor-5α-olean-12-en-3β-ol)	MS: <i>m/z</i> 454 [M <sup>+</sup> ] (3), 439 (2), 394 (2), 379 (2), 204 (100), 189 (39), 175 (17)
δ-Amyrin ( <i>5α</i> -olean-13(18)-en-3β-ol)	MS: <i>m/z</i> 468 [M <sup>+</sup> ] (35), 453 (17), 408 (3), 393 (8), 218 (43), 206 (43), 205 (100), 204 (37), 189 (78), 109 (78)
Erythrodiol ( <i>5α</i> -olean-12-ene-3β,28-diol)	(23)
Oleanolic acid (3β-hydroxy-5α-olean-12-en-28-oic acid)	MS: <i>m/z</i> 512 [M <sup>+</sup> ] (2.5), 453 (4), 452 (10), 262 (54), 249 (7), 203 (100), 189 (27), 175 (8), 133 (14)
Maslinic acid (2α,3β-dihydroxy-5α-olean-12-en-28-oic acid)	MS: <i>m/z</i> 570 [M <sup>+</sup> ] (3), 511 (6), 510 (9), 450 (8), 435 (11), 262 (50), 249 (10), 203 (100), 189 (28), 173 (13), 133(18)
<b>Lupane group</b>	
Lupeol ( <i>5α</i> -lup-20(29)-en-3β-ol)	(24)
Lupenone	MS: <i>m/z</i> 424 [M <sup>+</sup> ] (49), 409 (20), 382 (5), 369 (7), 342 (7), 314 (37), 245 (15), 232 (18), 218 (15), 205 (83), 189 (47), 175 (9), 149 (28), 109 (48), 69 (100)
3- <i>epi</i> -lupeol ( <i>5α</i> -lup-20(29)-en-3α-ol)	MS: <i>m/z</i> 468 [M <sup>+</sup> ] (23), 453 (3), 408 (9), 393 (4), 249 (10), 229 (8), 218 (17), 205 (20), 204 (23), 203 (18), 191 (43), 189 (100), 175 (22), 161 (25), 135 (40), 133 (20)
3- <i>epi</i> -betulin ( <i>5α</i> -lup-20(29)-ene-3β,28-diol)	MS: <i>m/z</i> 526 [M <sup>+</sup> ] (3), 466 (65), 453 (12), 451 (8), 423 (22), 406 (7), 393 (7), 391 (7), 249 (7), 213 (22), 203 (45), 189 (100), 187 (58), 175 (27)
3- <i>epi</i> -betulinic acid (3α-hydroxy-lup-20(29)-en-28-oic acid)	MS: <i>m/z</i> 512 [M <sup>+</sup> ] (2), 453 (13), 452 (30), 437 (7), 262 (34), 249 (17), 203 (39), 189 (100), 175 (21), 173 (24), 161 (33), 133 (31), 131 (18)
<b>Ursane group</b>	
α-Amyrin ( <i>5α</i> -urs-12-en-3β-ol)	(14)
28-Nor-α-amyrin (28-nor-urs-12-en-3β-ol)	MS: <i>m/z</i> 454 [M <sup>+</sup> ] (9), 439 (3), 394 (3), 379 (2), 207 (40), 204 (100), 189 (27), 175 (26)
Uvaol ( <i>5α</i> -urs-12-ene-3β,28-diol)	(19)
Ursolic acid (3β-hydroxyurs-12-en-28-oic acid)	MS: <i>m/z</i> 512 [M <sup>+</sup> ] (2), 497 (1), 453 (3), 452 (7), 437 (2.5), 393 (2), 262 (100), 249 (19), 233 (6), 215 (4), 203 (82), 189 (29), 133 (53), 119 (21)
<b>Baccharane group</b>	
Bacchar-12,21-dien-3β-ol	MS: <i>m/z</i> 468 [M <sup>+</sup> ] (3), 453 (3), 408 (2.5), 393 (5), 249 (7), 218 (100), 203 (38), 189 (23), 133 (87)

<sup>a</sup> Recorded MS correspond to either the monoacetate derivative of triterpenes or the diacetate derivative of triterpene diols or the mono or diacetate derivative of HPTA methylesters

To our knowledge, the occurrence of 3-*epi*-lupeol, with a 3α-hydroxyl group, and its oxygenated derivatives (3-*epi*-betulin and 3-*epi*-betulinic acid) in the *Olea europaea* fruit had not been reported yet. It should be pointed out that MS of 3-*epi*-acetate derivatives exhibit fragmentation patterns very similar to those of 3β-OH acetates, but both epimers of each pair have different RRTs in GC. As an example, the RRTs of 3α- and 3β-lupenyl acetates in a DB-5 column are 1.285 and 1.333, respectively, corresponding to a separation factor of 1.03, a result consistent with data reported for the

corresponding trimethylsilyl (TMS) derivatives [26]. Because of its lower polarity compared to β-lupeol, we initially missed 3-*epi*-lupeol. To check the presence of this compound in the olive fruit, we chemically synthesized a standard of 3-*epi*-lupeol by NaBH<sub>4</sub> reduction of an authentic sample of lupenone, as described in the experimental section. The 3-*epi*-epimer was found to co-migrate with TAGs. Evidence for the presence of 3-*epi*-lupeol and lupenone in the olive fruit was obtained after preliminary elimination of these very abundant compounds by alkaline hydrolysis.

**Table 2** Sterols of the Chemlali olive fruit: GC-MS analysis

Compound	MS (% relative abundance of molecular and characteristic fragment ions): experimental or literature data <sup>a</sup>
<b>4,4-Dimethylsterols</b>	
Cycloartenol	(21)
24-Methylenecycloartanol	(21)
Parkeol (5 $\alpha$ -lanosta-9(11),24-dien-3 $\beta$ -ol)	MS: <i>m/z</i> 468 [M <sup>+</sup> ] (23), 453 (90), 393 (72), 355 (6), 255 (10), 241 (11), 173 (16), 95 (41), 69 (100)
24-Methylene-lanost-9(11)-en-3 $\beta$ -ol	MS: <i>m/z</i> 482 [M <sup>+</sup> ] (8), 467 (55), 439 (30), 422 (8), 407 (68), 398 (10), 355 (100), 301 (8), 255 (20), 253 (22), 241 (20)
<b>4<math>\alpha</math>-Methylsterols</b>	
Cycloeucalenol	(21)
Obtusifoliol	(21)
24-Methylenelophenol	(21)
24-Methyllophenol	MS: <i>m/z</i> 456 [M <sup>+</sup> ] (100), 441 (18), 396 (7), 381 (14), 329 (13), 269 (86), 243 (16), 227 (31), 173 (15)
24-Ethyllophenol	MS: <i>m/z</i> 470 [M <sup>+</sup> ] (100), 455 (18), 410 (8), 395 (13), 355 (7), 329 (9), 287 (9), 269 (86), 243 (16), 227 (48)
24-Ethylidenelophenol	(21)
24-Ethyl- <i>E</i> -23-dehydrolophenol	MS: <i>m/z</i> 468 [M <sup>+</sup> ] (25), 453 (29), 408 (6), 393 (12), 327 (100), 297 (5), 269 (13), 267 (8), 241 (9), 227 (15)
4 $\alpha$ ,14 $\alpha$ -Dimethylstigmasta-8,24(24 <sup>1</sup> )-dien -3 $\beta$ -ol	MS: <i>m/z</i> 482 [M <sup>+</sup> ] (37), 467 (100), 439 (11), 407 (48), 369 (23), 329 (6), 309 (18), 269 (30), 241 (28)
24-Methylene-29-nor-9(11)-lanosterol	MS: <i>m/z</i> 468 [M <sup>+</sup> ] (8), 453 (36), 425 (19), 408 (5), 393 (33), 341 (100), 309 (11), 301 (12), 287 (19), 281 (15), 241 (22)
<b>Sterols</b>	
Cholesterol	(21)
Brassicasterol	(21)
24-Methylenecholesterol	(21)
Stigmasterol	(21)
Clerosterol (5 $\alpha$ -stigmasta-5,25-dien-3 $\beta$ -ol)	MS: <i>m/z</i> 454 [M <sup>+</sup> ], 394 (100), 379 (13), 296 (7), 253 (10), 228 (8), 213 (13)
Sitosterol	(21)
Sitostanol	(21)
$\Delta^5$ -Avenasterol (isofucosterol)	(21)
$\Delta^7$ -Avenasterol	MS: <i>m/z</i> 454 [M <sup>+</sup> ] (3), 394 (3), 379 (3), 356 (35), 341 (16), 313 (100), 296 (8), 288 (3), 255 (13), 253 (20), 227 (7), 213 (13)
$\Delta^{5,24}$ -Stigmastadienol	MS: <i>m/z</i> 454 [M <sup>+</sup> ], 394 (28), 379 (13), 315 (18), 296 (100), 281 (37), 253 (45), 213 (22)

<sup>a</sup> All the compounds have been identified by GC-MS, but only MS data, which have not been published before, are given here. Recorded MS spectra correspond to acetate derivatives

It is known that (3*S*)-2,3-OS is the precursor of both 3 $\alpha$ - and 3 $\beta$ -hydroxytriterpenes and that 3 $\alpha$ -epimers are biosynthesized from their 3 $\beta$ -isomers through reduction of the 3-oxo compounds [27]. The oxidation reaction can operate on the 3 $\beta$ -OH of a triterpene, a triterpenic diol or a triterpenic acid. Thus, the co-occurrence of lupeol, lupenone and 3-*epi*-lupeol as well as the absence of betulin, betulinic acid and the corresponding ketones, betulinone and betulinonic acid, strongly suggest that the change in the 3-OH group configuration takes place only at the level of lupeol in the olive fruit. No 3-*epi*-derivatives of  $\alpha$ - and  $\beta$ -amyrins have been detected.

#### Compounds of the Sterol Pathway (Table 2)

Free sterols and sterols released from ester conjugates were analyzed as described in [Materials and Methods](#).

They were identified as acetate derivatives by both their RRT in GC and their MS fragmentation by GC-MS analysis. The olive fruit was found to contain all the usual intermediates of the sterol pathway, from squalene up to sterol end products (Table 2). Sitosterol is by far the predominant sterol (95%), followed by 24-methylcholesterol, stigmasterol and isofucosterol ( $\Delta^5$ -avenasterol) (1–3%). We also detected other sterols such as brassicasterol, 24-methylenecholesterol,  $\Delta^{5,24}$ -stigmastadienol,  $\Delta^7$ -avenasterol and cholesterol. The classic sterol precursors, 4,4-dimethylsterols (cycloartenol and 24-methylenecycloartanol) and 4 $\alpha$ -methylsterols (obtusifoliol, cycloeucalenol, 24-methylene- and 24-ethylidenelophenol) were present, but also more unusual sterols such as (24*S*)-24-ethylcholesta-5,25-dien-3 $\beta$ -ol (clerosterol) and sterols with a double bond at C-23 ( $\Delta^{5,23}$ -stigmastadienol and 24-ethyl-*E*-23-dehydrolophenol) or C-11 (lanosta-9(11),24-dien-3 $\beta$ -ol or



parkeol). The acetate derivatives of cycloartenol and parkeol have very similar RRTs in DB-1 and DB-5 GC columns, but they can be easily discriminated by their MS fragmentation patterns [28]. Interestingly, parkeol was found only as an ester. Traces of a compound, which might be 24-methylene-lanost-9(11)-en-3 $\beta$ -ol, were detected.

All the compounds of the sterol pathway were also found as ester conjugates.

Thus, at least 20 compounds belonging to the sterol pathway have been identified in the olive fruit. Our results are consistent with previous reports about the sterol composition of olive oil [19, 29–31], especially that of the Chemlali cultivar [32].

### Changes in the Free Triterpenoid and Sterol Content Throughout Fruit Growth and Development

#### Total Lipids

Figure 1 shows the changes in total lipids during the whole period of olive fruit development. The olive mesocarp tissue begins to form large amounts of lipids from about 17 WAF until the end of the fruit ripening process. TAGs are by far the major compounds, accounting for 98–99% of total lipids. They progressively accumulate as lipid droplets, which progressively fuse to give a single large oil droplet [33].

#### Non-steroidal Triterpenoids

At the beginning of fruit ontogeny (i.e. between 12 and 18 WAF), the olive fruit was found to contain significant amounts of  $\alpha$ - and  $\beta$ -amyryns, in about a 3:2 ratio, as well as several more-oxygenated compounds with additional hydroxymethyl or carboxylic groups (Table 3; Scheme 1). The presence of a high content of

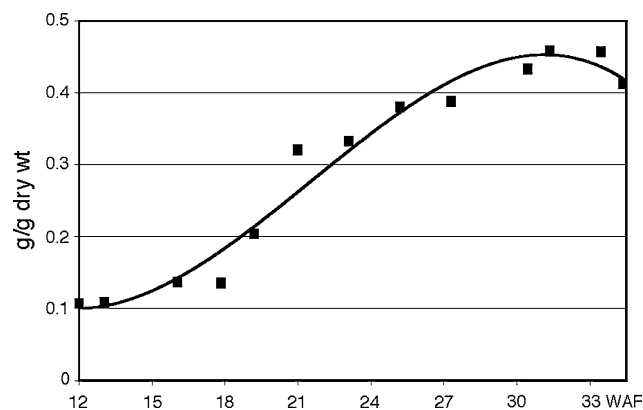


**Fig. 1** Changes in total lipids during olive fruit development

squalene was also observed (700  $\mu$ g/g dry wt at 13 WAF, data not shown), an unsurprising result since squalene is the direct precursor of OS needed for the synthesis of  $\alpha$ - and  $\beta$ -amyryns. Through several oxidation steps, the C-28 methyl group of  $\alpha$ - and  $\beta$ -amyryns might be sequentially converted into a hydroxymethyl, to give uvaol and erythrodiol, and then into a carboxylic group, to give ursolic and oleanolic acids (Scheme 1). The enzymes responsible for these oxidation reactions have not been characterized yet, but are likely to be cytochrome P-450 monooxygenases. Similar stepwise oxidations have been reported for the conversion of *ent*-kaurene into *ent*-kaurenic acid [34] or abietadienol into abietic acid [35], two series of reactions of diterpenoid metabolism, catalyzed by a unique multifunctional P-450 enzyme. If that holds true, this pathway does involve the intermediate formation of the aldehydes, 3 $\beta$ -hydroxy-5 $\alpha$ -urs-12-en-28-al and 3 $\beta$ -hydroxy-5 $\alpha$ -olean-12-en-28-al. The presence of these relatively unstable compounds in the olive fruit has not been verified. However, the triterpene fraction of the young olive fruit was found to contain significant amounts of 28-nor- $\alpha$ -amyryn (6%) and 28-nor- $\beta$ -amyryn (17%) (Table 3). These two compounds, which have no carbon at C-17, might arise from the decarbonylation *in planta* of both aforementioned aldehydes. Indeed, it has been reported that ursaldehyde can be partially converted to 28-nor- $\alpha$ -amyryn, when exposed to diffuse sunlight [36]. Both 28-nor- $\alpha$ - and 28-nor- $\beta$ -amyryns have also been identified in the leaves of *Nerium oleander* [37] and the resin of *Pistacia lentiscus* [38], among the whole series of ursane and oleanane triterpenoids, from  $\alpha$ - and  $\beta$ -amyryns to HPTAs via pentacyclic triterpene diols and aldehydes. In that context, it may be emphasized that uvaol and erythrodiol as well as ursolic and oleanolic acids have been found in the waxy epiderm of the olive fruit [39]. Thus, the complete sequence of oxidation reactions from triterpenes to pentacyclic acids via triterpenic diols and aldehydes might take place in the green epicarp of the fruit, which is directly exposed to the intense summer sunlight.

Between 12 and 18 WAF, maslinic acid, which differs from oleanolic acid by an additional hydroxyl group at the C-2 position, was also formed (Table 3). Its later accumulation suggests that the introduction of this additional hydroxyl group occurs after the oxidation of the C-28 methyl group and might involve a different P-450 enzyme.

Interestingly, taken together, these data indicate that, although  $\alpha$ -amyryn was present in excess compared to  $\beta$ -amyryn, oleanane compounds as a whole were produced in higher amounts than ursane com-

**Table 3** Changes in triterpenoids throughout olive fruit development

	Stage of development Compound	12 WAF μg/g dry wt	18 WAF μg/g dry wt	21 WAF μg/g dry wt	30 WAF μg/g dry wt
Pentacyclic triterpenes	28-Nor-β-amyrin	74	39	–	–
	β-Amyrin	139	65	4	4
	28-Nor-α-amyrin	25	11	–	–
	α-Amyrin	192	86	–	–
	Taraxerol	–	–	3	2
	Total	<b>430 (13)</b>	<b>201 (8)</b>	<b>7 (0.2)</b>	<b>6 (0.2)</b>
Pentacyclic dialcohols	D-Friedoolean-14-ene-3β,28-diol	8	<b>7</b>	<b>1</b>	1
	Erythrodiol	401	253	14	13
	Uvaol	245	161	3	0.4
	3- <i>epi</i> -betulin	11	6	1	0.8
	Total	<b>665 (21)</b>	<b>427(16)</b>	<b>19 (0.5)</b>	<b>15 (0.6)</b>
	Mono HPTAs	3- <i>epi</i> -betulinic acid	21	15	25
Oleanolic acid		1257	932	1616	929
Ursolic acid		6	6	9	4
Total		<b>1285 (40)</b>	<b>953 (37)</b>	<b>1650 (42)</b>	<b>946 (38)</b>
Di-HPTA	Maslinic acid	<b>830 (26)</b>	<b>1023 (39)</b>	<b>2250 (57)</b>	<b>1502 (61)</b>
Total amount		<b>3210</b>	<b>2604</b>	<b>3926</b>	<b>2469</b>

Numbers in brackets correspond to relative weight percentages of each class of compounds; the SDs for quantitative determinations are  $\pm 5\%$

pounds. Erythrodiol accounted indeed for about 60% of triterpenic dialcohols and oleanic and maslinic acids, for 98–99% of mono- and di-HPTAs (Table 3). Thus, the metabolic fate of  $\alpha$ -amyrin in the olive fruit remains to be elucidated.

Besides  $\alpha$ - and  $\beta$ -amyryns and the corresponding 28-nor compounds, no other tetra- or pentacyclic triterpenes were detected in the young olive fruit. However, the fractions of pentacyclic diols and acids were found to contain lupane derivatives, identified as 3-*epi*-betulin and 3-*epi*-betulinic acid, and a taraxane derivative, D-fridoolean-14-ene-3 $\beta$ ,28-diol. These compounds are likely to be formed through oxidation steps similar to those described above in the case of ursane and oleanane triterpenoids.

Between 21 and 30 WAF, a dramatic decrease in the content of  $\alpha$ - and  $\beta$ -amyryns and their derivatives was observed. Only  $\beta$ -amyrin remained detectable, with traces of taraxerol. During the same period, triterpenic diols were converted into mono- and di-HPTAs. Consequently, maslinic acid became the major triterpenoid (60% of total triterpenoids) and mono- and di-HPTAs together represented as much as 2.25 mg/g dry wt. At 30 WAF, a significant decrease in the content of all HPTAs was observed (Table 3), indicating that these compounds might be further metabolized, maybe into triterpenic saponins [16].

### Sterols

As described before, the very young olive fruit (between 12 and 18 WAF) was found to contain high

amounts of squalene, but the other usual sterol precursors such as 4,4-dimethyl- and 4 $\alpha$ -methylsterols were barely detectable. Sterol end products were present as a mixture in which sitosterol was largely predominant (95 wt% of total sterols), but the total free sterol content (about 220  $\mu\text{g g}^{-1}$  dry wt) was found not to change and even slightly decrease during this period, indicating that no significant sterol biosynthesis was occurring in the green olive fruit. The pre-existing  $\Delta^5$ -sterols in the young fruit arose from the floral ovary tissue as well as one of the two ovules, which gave the mesocarp and the seed after fertilization, respectively.

From 21 WAF, dramatic changes were observed in the sterol pathway. Early biosynthetic intermediates, i.e., 4,4-dimethyl- (cycloartenol and 24-methylene cycloartanol) and 4 $\alpha$ -methylsterols (cycloeucalenol, obtusifoliol, 24-methylene- and 24-ethylidene lophenol) as well as late precursors (isofucosterol) of the sterol pathway began to be detectable whereas a progressive increase in sterol end products was observed. Throughout the fruit ripening process, sterols continued to accumulate, with sitosterol remaining the major compound and no change in the relative proportions of the various sterols. At 33 WAF, the free sterol content of the olive fruit amounted to 720  $\mu\text{g g}^{-1}$  dry wt, corresponding to a three-fold total increase. At this stage, a significant increase in the content of some precursors, especially 24-methylene cycloartanol and 24-ethylidene lophenol, was observed, indicating a slowing down of the metabolic flux through the sterol pathway (Fig. 2a).

Taken together, these data indicate that a preferential channeling of available OS molecules towards

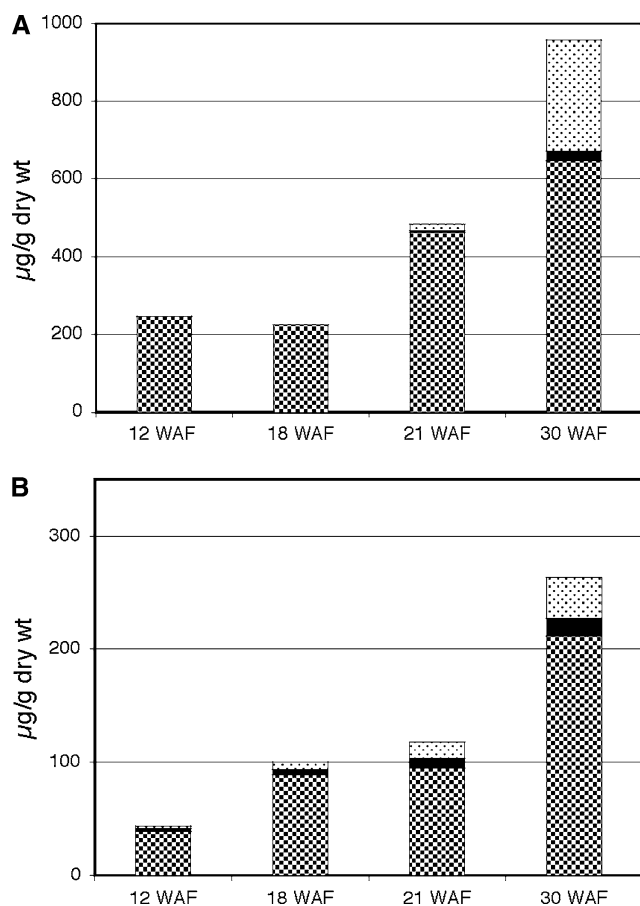


**Fig. 2** Changes in free (a) and esterified (b) sterols at four distinct stages of olive fruit development. (Medium shade square) sterols, (filled square) 4 $\alpha$ -methylsterols, (light shade square) 4,4-dimethylsterols

the triterpenoid pathway occurs in the very young olive fruit at the expense of the biosynthesis of housekeeping sterols, a situation which is reminiscent of that prevalent in pea (*Pisum sativum* L.) plantlets, where  $\beta$ -amyirin is actively produced just after germination and before sterol synthesis [40]. From 21 WAF,  $\alpha$ - and  $\beta$ -amyirins were no longer detected whereas sterol biosynthetic precursors began to appear (Fig. 3), clearly indicating a redirection of the carbon flux from the triterpenoid pathway towards the sterol pathway and the synthesis of membranes. Between 18 and 30 WAF, the total amount of free sterols was fivefold increased whereas mono- and di-HPTAs, mainly represented by maslinic acid, accumulated at the expense of non-steroidal triterpenes and diols (Table 3).

Thus, a complex regulation takes place at the level of OS cyclization. Studies of differential expression patterns of  $\beta$ AS and cycloartenol synthase at different stages of fruit development, which are currently in progress, should allow us to better understand the

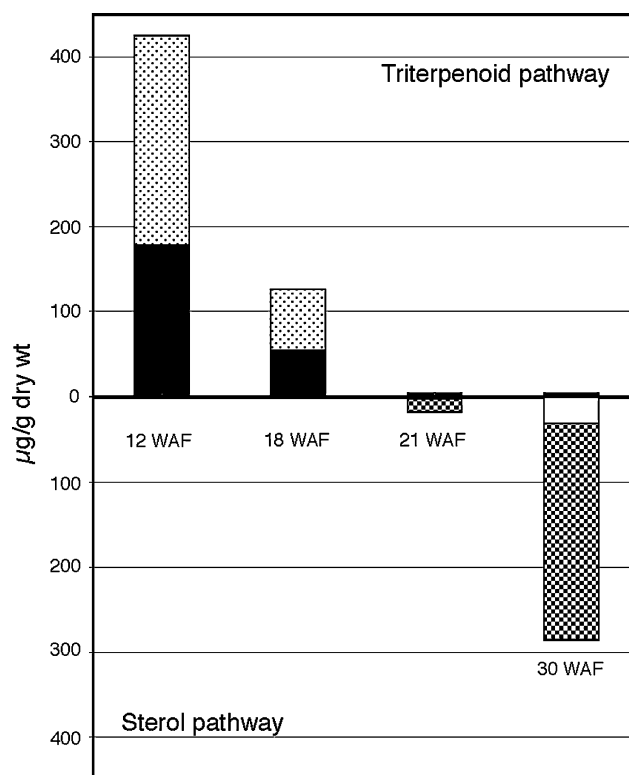


**Fig. 3** A redirection of the carbon flux from the triterpenoid pathway (free  $\alpha$ - and  $\beta$ -amyirins) towards the sterol pathway (free cycloartenol and 24-methylenecycloartenol) occurs between 18 and 21 WAF. (light-shaded square)  $\alpha$ -amyirin, (filled square)  $\beta$ -amyirin, (medium-shaded square) 24-methylene cycloartenol, (opensquare) cycloartenol

mechanisms underlying the sequential production of both sets of triterpenic compounds.

#### Changes in Esterified Sterols and Triterpenoids throughout Fruit Growth and Development

##### Triterpenoids

The young olive fruit (i.e. between 12 and 18 WAF) was found to contain only very low amounts of acylated non-steroidal triterpenes (Table 4), representing less than 2% of the corresponding free forms. This result indicates an almost complete metabolization of newly synthesized  $\alpha$ - and  $\beta$ -amyirin molecules into triterpenic diols and acids. Besides  $\alpha$ - and  $\beta$ -amyirins, esters of taraxerol,  $\delta$ -amyirin and lupeol were detected as traces.

From 21 WAF, when amyirins were not formed any longer, esterified triterpenes progressively accumulated (Table 4) and their content became higher than that of free non-steroidal triterpenes (Table 3). Concomitantly, a change in the profile of triterpenes could

**Table 4** Changes in esterified triterpenes throughout olive fruit development

Stage of development	12WAF		18WAF		21WAF		30WAF	
	$\mu\text{g/g}$ dry wt	%	$\mu\text{g/g}$ dry wt	%	$\mu\text{g/g}$ dry wt	%	$\mu\text{g/g}$ dry wt	%
Taraxerol	2	33	2	22	5	12	2	6
$\delta$ -Amyrin	1	10	2	22	6	16	8	23
$\beta$ -Amyrin	2	25	1	14	4	11	4	12
Butyrospermol	n.d.	–	n.d.	–	24	61	21	60
$\alpha$ -Amyrin	tr	5	tr	6	tr	–	tr	–
Lupeol	2	27	3	37	tr	–	tr	–
Total amount	7		9		39		35	

be noticed, mainly consisting in the appearance of a new compound, identified as butyrospermol, which represented up to 60% of total esterified triterpenes. Traces of esterified baccharadienol were detected only at late stages of ripening. As shown in Scheme 1, butyrospermol, baccharadienol as well as  $\delta$ -amyrin are likely to result from stabilization of carbocationic intermediates located on the route to  $\alpha$ -amyrin.

#### Sterols (Fig. 2b)

Between 12 and 18 WAF, the olive fruit was found to contain significant amounts of esterified sterols, with sitosterol being the major compound. The fraction of sterol esters contains the same compounds as free sterols, but in different proportions. For instance, an increase in the relative amounts of 24-methylcholesterol (2.5% vs. 0.4%) and stigmasterol (7–8% vs. 1.5%) was observed (data not shown). Only traces of 4,4-dimethyl- and 4 $\alpha$ -methylsterols were detected. Interestingly, despite the absence of sterol biosynthesis (Fig. 2a), a twofold increase in the total amount of sterol esters was observed (Fig. 2b), which occurred at the expense of sterol end products initially present in the fruit, indicating the presence of a functional sterol acyltransferase in the green olive. After the onset of free sterol biosynthesis, which takes place at around 21 WAF, sterol esters continue to accumulate, particularly between 27 and 30 WAF (Fig. 2b), with a total amount representing a sevenfold increase during the whole period of fruit development. All the usual sterol biosynthetic precursors (4,4-dimethyl- and 4 $\alpha$ -methylsterols) as well as end products were present as ester conjugates, but other compounds such as 24-ethyl-*E*-23-dehydrolophenol, 24-methyl- and 24-ethyl lophenol could also be detected. At the end of the ripening process, a specific accumulation of 24-methylene cycloartanol and 24-ethylidene lophenol was observed, in agreement with previous data about olive oil [29]. An interesting observation was the appearance of a new compound in the fraction of 4,4-dimethylsterols, which

has been identified to parkeol. This compound, which had been previously detected in olive oil [19], was formed concomitantly to cycloartenol, as shown in Fig. 4 and represented more than 50% of the total esterified 4,4-dimethylsterols.

A phospholipid:sterol acyltransferase (PSAT) involved in the acylation of free sterols has recently been identified in *Arabidopsis* [41]. This enzyme was shown to be able to acylate various sterols as well as sterol intermediates but not lupeol or  $\beta$ -amyrin [41], suggesting that a distinct enzyme would be involved in the acylation of non-steroidal triterpenes. During the period of active sterol biosynthesis, the physiological function of such a sterol acyltransferase might be to regulate the pool of free sterols as well as the amount of sterol biosynthetic intermediates in membranes [41]. In contrast, the role of sterol acylation at earlier stages of fruit development is less clear.

During the whole period of the olive fruit development, free sterols remained predominant compared to sterol esters (Fig. 2a, b).

Sterol esters, which are not membrane components, have been reported to be present with TAG in the core

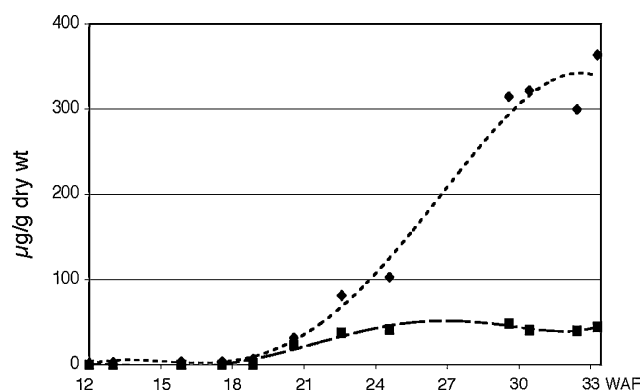


**Fig. 4** Changes in products arising from OS cyclization via the protosteryl cation throughout olive fruit development (dot) esterified parkeol, (dotted line) free and esterified (cycloartenol and 24-methylene cycloartanol)

of oil bodies [42], but the olive fruit contains oil droplets rather than proper lipid bodies [43]. Olive oil, which is comprised of 98–99% TAGs, is formed in the mesocarp of the developing fruit. TAG synthesis was found to begin between 16 and 17 WAF (Fig. 1), i.e. before sterol biosynthesis, and to depend on light [44]. The whole process involves the contribution of photoassimilates imported from adjacent leaves as well as those generated as the products of the photosynthesis taking place in the fruit itself [44]. Sterol esters thus appear to be formed concomitantly to TAGs and might therefore directly participate in oil droplet formation.

### Origin of the Structural Diversity of Triterpenoids in Olive Fruit

The present data provide evidence for the occurrence of a vast array of non-steroidal triterpenoids in the olive fruit, which might arise from the different carbocationic intermediates generated en route to  $\alpha$ -amyrin biosynthesis (Scheme 1). The question is now to elucidate whether the olive fruit contains one or several triterpenes synthases. In the young fruit,  $\alpha$ -amyrin is actively produced together with  $\beta$ -amyrin in a 3:2 ratio and these two pentacyclic triterpenes are by far the major products. As no monofunctional  $\alpha$ -amyrin synthase has been identified so far, one can postulate that in the olive fruit,  $\alpha$ - and  $\beta$ -amyrins could be formed by a mixed amyrin synthase similar to that of *Pisum sativum* [12]. Besides  $\alpha$ - and  $\beta$ -amyrins, the pea enzyme would be able to generate six other products including butyrospermol, lupeol and  $\delta$ -amyrin, which have been also identified in the olive fruit (Table 1). In this case, the amyrin synthase of the olive fruit would not belong to the family of monofunctional  $\beta$ AS [12, 45–48]. In addition to this mixed amyrin synthase, the olive fruit might contain a lupeol synthase, similar to that identified in olive leaves, catalyzing the formation of only lupeol [49]. The occurrence of other monofunctional lupeol synthases has been reported [46, 48–51], but it should be pointed out that lupeol can be also formed by multifunctional triterpene synthases [11, 13, 14]. These two classes of lupeol synthases are phylogenetically distinct [49].

An interesting point concerns the biosynthetic origin of parkeol in the olive fruit. In contrast to pentacyclic triterpenes, parkeol arises from the protosteryl C-20 cation, which is formed by cyclization of OS folded in the pre-chair-boat-chair conformation (Scheme 1). This cation undergoes a series of 1,2-methyl and hydride shifts with proton elimination to yield either cycloartenol (C-19 deprotonation), lanosterol (C-6

deprotonation), parkeol (C-11 deprotonation) or cucurbitadienol, the precursor of cucurbitacins [2].

The presence of parkeol has been reported in sea cucumbers [52, 53] and a few plants such as *Butyrospermum parkei* [54, 55] or *Neolitsea aciculata* [56]. Parkeol is not incorporated into sterols [57]. Some plants contain 24-alkyl- $\Delta^{9(11)}$ -sterols [58], which maybe result from metabolization of parkeol, but the question of whether or not parkeol is a by-product of sterol metabolism remains to be solved. No natural parkeol synthase has been cloned so far. It has been shown that wild-type *Arabidopsis* CAS, expressed in a yeast mutant, is able to produce 1% parkeol, but not lanosterol (<0.1%) [28]. Moreover, the possibility to generate an enzyme that makes parkeol as its major product from either CAS [28, 59, 60] or lanosterol synthase [61, 62] has been reported. As an example, the work by Segura et al. [60] has emphasized the critical role played by His477, which is strictly conserved in all CAS. The *Ath* H477Q mutant was shown indeed to form up to 73% parkeol. The natural occurrence of a nondiscriminating OS cyclase in the bacterium *Gemmata obscuriglobus*, producing both lanosterol and parkeol [63], has to be mentioned. Interestingly, in this organism, both lanosterol and parkeol are present exclusively as esters.

Parkeol seems not to be formed in young olive drupes. It appeared only from 21 WAF, concomitantly with cycloartenol (Fig. 4). Cycloartenol was rapidly converted into 24-methylenecycloartanol, which was then converted into ester. The fact that cycloartenol and parkeol were simultaneously formed during olive fruit ripening suggests the possible involvement of a single protein for production of both compounds. In this case, the olive fruit CAS would have evolved differently from other plant CAS. The fact that parkeol occurs in the olive fruit only as an ester conjugate suggests that it is not metabolized further on and is acylated immediately after release from the OS cyclase by a sterol acyltransferase similar to PSAT or by another sterol acyltransferase. Whether or not parkeol is a primary or secondary metabolite remains to be elucidated.

### Concluding Remarks

The present report represents the first detailed investigation into the triterpenoid composition of *Olea europaea* olive fruit and its changes occurring throughout the ripening process. Evidence is given for the presence of at least 23 sterols and 20 tetra- and pentacyclic non-steroidal triterpenoids. We have shown that the triterpenoid content of the olive fruit is closely dependent

on the stage of development and that a regulation process takes place at the OS cyclization step. Further work is now needed to investigate more deeply the non-steroidal triterpenoid biosynthetic pathway. Certainly, the rising interest in the valuable biological properties for human health of triterpenic acids, including maslinic acid (e.g., [64]), constitutes a strong motivation.

**Acknowledgment** We thank Prof. Z. Mighri (Faculté des Sciences, Monastir, Tunisia) for providing us with an authentic sample of maslinic acid and Dr. Pierrette Bouvier-Navé (IBMP, Strasbourg, France) for critical analysis of the work.

## References

- Mahato SB, Nandy AK, Roy G (1992) Triterpenoids. *Phytochemistry* 31:2199–2249
- Xu R, Fazio GC, Matsuda SPT (2004) On the origins of triterpenoid skeletal diversity. *Phytochemistry* 65:261–291
- Connolly JD, Hill RA (2005) Triterpenoids. *Nat Prod Rep* 22:230–248
- Akihisa T, Yasukawa K, Kimura Y, Takase S, Yamanouchi S, Tamura T (1997) Triterpene alcohols from camellia and sasanqua oils and their anti-inflammatory effects. *Chem Pharm Bull (Tokyo)* 45:2016–2023
- Ukiya M, Akihisa T, Tokuda H, Suzuki H, Mukainaka T, Ichiishi E, Yasukawa K, Kasahara Y, Nishino H (2002) Constituents of *Compositae* plants III. Anti-tumor promoting effects and cytotoxic activity against human cancer cell lines of triterpene diols and triols from edible *Chrysanthemum* flowers. *Cancer Lett* 177:7–12
- Popovich DG, Kitts DD (2002) Structure–function relationship exists for ginsenosides in reducing cell proliferation and inducing apoptosis in the human leukemia (THP-1) cell line. *Arch Biochem Biophys* 406:1–8
- Akihisa T, Franzblau SG, Ukiya M, Okuda H, Zhang F, Yasukawa K, Suzuki T, Kimura Y (2005) Anti-tubercular activity of triterpenoids from *Asteraceae* flowers. *Biol Pharm Bull* 28:158–160
- Benveniste P (2002) Sterol metabolism, American Society of Plant Biologists, Rockville. <http://www.bioone.org/archive/1543-8120/38/1/pdf/i1543-8120-38-1-1.pdf>
- Seo S, Yoshimura Y, Uomori A, Takeda K, Seto H, Ebizuka Y, Sankawa U (1988) Biosynthesis of triterpenes, ursolic acid, and oleanolic acid in tissue cultures of *Rabdosa japonica* Hara fed [ $5-^{13}\text{C}_2\text{H}_2$ ] mevalonolactone and [ $2-^{13}\text{C}_2\text{H}_3$ ] acetate. *J Am Chem Soc* 110:1740–1745
- Abe I, Rohmer M, Prestwich GD (1993) Enzymatic cyclization of squalene and oxidosqualene to sterols and triterpenes. *Chem Rev* 93:2189–2206
- Herrera JBR, Bartel B, Wilson WK, Matsuda SPT (1998) Cloning and characterization of the *Arabidopsis thaliana* Lupeol synthase gene. *Phytochemistry* 49:1905–1911
- Morita M, Shibuya M, Kushihiro T, Masuda K, Ebizuka Y (2000) Molecular cloning and functional expression of triterpene synthases from pea (*Pisum sativum*) new alpha-amyrin-producing enzyme is a multifunctional triterpene synthase. *Eur J Biochem* 26:3453–3460
- Segura MJ, Meyer MM, Matsuda SPT (2000) *Arabidopsis thaliana* LUP1 converts oxidosqualene to multiple triterpene alcohols and a triterpene diol. *Org Lett* 2:2257–2259
- Husselstein-Muller T, Schaller H, Benveniste P (2001) Molecular cloning and expression in yeast of 2,3-oxido-squalene-triterpenoid cyclases from *Arabidopsis thaliana*. *Plant Mol Biol* 45:75–92
- Ebizuka Y, Katsube Y, Tsutsumi T, Kushihiro T, Shibuya M (2003) Functional genomics approach to the study of triterpene biosynthesis. *Pure Appl Chem* 75:369–374
- Mahato SB, Sarkar SK, Poddar G (1988) Triterpenoid saponins. *Phytochemistry* 27:3037–3067
- Power FB, Tutin F (1908) The constituents of olive leaves. *J Chem Soc Trans* 93:891–904
- Caputo R, Mangoni L, Monaco P, Previtera L (1974) New triterpenes from the leaves of *Olea europaea*. *Phytochemistry* 13:2825–2827
- Itoh T, Yoshida K, Yatsu T, Tamura T, Matsumoto T (1981) Triterpene alcohols and sterols of Spanish olive oil. *J Am Oil Chem Soc* 58:545–550
- Hartmann MA, Benveniste P (1987) Plant membrane sterols: isolation, identification and biosynthesis. *Methods Enzymol* 148:632–650
- Rahier A, Benveniste P (1989) Mass spectral identification of phytosterols, In: Nes WD, Parish E (eds) *Analysis of sterols and other biologically significant steroids*, Academic, New York, pp 223–250
- Pérez-Camino MC, Cert A (1999) Quantitative determination of hydroxy pentacyclic triterpene acids in vegetable oils. *J Agric Food Chem* 47:1558–1562
- Budzikiewicz H, Wilson JM, Djerassi C (1963) Mass spectrometry in structural and stereochemical problems. XXXII Pentacyclic triterpenes. *J Am Chem Soc* 85:3688–3699
- Shiojima K, Arai Y, Masuda K, Takase Y, Ageta T, Ageta H (1992) Mass spectra of pentacyclic triterpenoids. *Chem Pharm Bull (Tokyo)* 40:1683–1690
- Roca M, Mínguez-Mosquera MI (2003) Carotenoid levels during the period of growth and ripening in fruits of different olive varieties (Hojiblanca, Picual and Arbequina). *J Plant Physiol* 160:451–459
- Mathe C, Culioli G, Archier P, Vieillescazes C (2004) Characterization of archaeological frankincense by gas chromatography-mass spectrometry. *J Chromatogr A* 1023:277–285
- Seo S, Tomita Y, Tori K (1981) Biosynthesis of oleanene- and ursene-type triterpenes from [ $4-^{13}\text{C}$ ] mevalonolactone and [ $1,2-^{13}\text{C}_2$ ] acetate in tissue cultures of *Isodon japonicus* Hara. *J Am Chem Soc* 103:2075–2080
- Hart EA, Hua L, Darr LB, Wilson WK, Pang J, Matsuda SPT (1999) Directed evolution to investigate steric control of enzymatic oxidosqualene cyclization. An isoleucine-to-valine mutation in cycloartenol synthase allows lanosterol and parkeol biosynthesis. *J Am Chem Soc* 121:9887–9888
- Chryssafidis D, Maggos P, Kiosseoglou V, Boskou D (1992) Composition of total and esterified 4 $\alpha$ -monomethylsterols and triterpene alcohols in virgin olive oil. *J Sci Food Agric* 58:581–583
- Reina RJ, White KD, Jahngen EG (1997) Validated method for quantitation and identification of 4,4-desmethylsterols and triterpene diols in plant oils by thin-layer chromatography-high resolution gas chromatography-mass spectrometry. *J AOAC Int* 80:1272–1280
- Casas JS, Bueno EO, Garcia AMM, Cano MM (2004) Sterol and erythrodiol + uvaol content of virgin olive oils from cultivars of extremadura (spain). *Food Chem* 87:225–230
- Stiti N, M'Sallem M, Triki S, Cherif A (2002) Etude de la fraction insaponifiable de l'huile d'olive de différentes variétés tunisiennes. *Riv Ital Sostanze Grasse* 79:357–363

33. Rangel B, Platt KA, Thomson WW (1997) Ultrastructural aspects of the cytoplasmic origin and accumulation of oil in olive fruit (*Olea europaea*). *Physiol Plant* 101:109–114
34. Helliwell CA, Poole A, Peacock WJ, Dennis ES (1999) Arabidopsis *ent*-Kaurene oxidase catalyzes three steps of gibberellin biosynthesis. *Plant Physiol* 119:507–510
35. Ro DK, Arimura G, Lau SY, Piers E, Bohlmann J (2005) Loblolly pine abietadienol/abietadienal oxidase PtAO (CYP720B1) is a multifunctional, multisubstrate cytochrome P450 monooxygenase. *Proc Natl Acad Sci USA* 102:8060–8065
36. Hota RK, Bapuji M (1994) Triterpenoids from the resin of *Shorea robusta*. *Phytochemistry* 35:1073–1074
37. Fu L, Zhang S, Li N, Wang J, Zhao M, Sakai J, Hasegawa T, Mitsui T, Kataoka T, Oka S, Kiuchi M, Hirose K, Ando M (2005) Three new triterpenes from *Nerium oleander* and biological activity of the isolated compounds. *J Nat Prod* 68:198–206
38. Assimopoulou AN, Papageorgiou VP (2005) GC-MS analysis of penta- and tetra-cyclic triterpenes from resins of *Pistacia* species. Part 1 *Pistacia lentiscus* var. Chia. *Biomed Chromatogr* 19:285–311
39. Bianchi G, Pozzi N, Vlahov G (1994) Pentacyclic triterpene acids in olives. *Phytochemistry* 37:205–207
40. Baisted DJ (1971) Sterol and triterpene synthesis in the developing and germinating pea seed. *Biochem J* 124:375–383
41. Banas A, Carlsson AS, Huang B, Lenman M, Banas W, Lee M, Noiriel A, Benveniste P, Schaller H, Bouvier-Navé P, Szyme S (2005) Cellular sterol ester synthesis in plants is performed by an enzyme (phospholipid:sterol acyltransferase) different from the yeast and mammalian acyl-CoA:sterol acyltransferases. *J Biol Chem* 280:34626–34634
42. Dyas L, Goad LJ (1994) The occurrence of free and esterified sterols in the oil bodies isolated from maize seed scutella and a celery cell suspension culture. *Plant Physiol Biochem* 32:799–805
43. Ross JHE, Sanchez J, Millan F, Murphy DJ (1993) Differential presence of oleosins in oleogenic seed and mesocarp tissues in olive (*Olea europaea*) and avocado (*Persea Americana*). *Plant Science* 93:203–210
44. Salas JJ, Sánchez J, Ramli US, Manaf AM, Williams M, Harwood JL (2000) Biochemistry of lipid metabolism in olive and other oil fruits. *Prog Lipid Res* 39:151–180
45. Kushiro T, Shibuya M, Ebizuka Y (1998) Beta-amyrin synthase-cloning of oxidosqualene cyclase that catalyzes the formation of the most popular triterpene among higher plants. *Eur J Biochem* 256:238–244
46. Hayashi H, Huang P, Takada S, Obinata M, Inoue K, Shibuya M, Ebizuka Y (2004) Differential expression of three oxidosqualene cyclase mRNAs in *Glycyrrhiza glabra*. *Biol Pharm Bull* 27:1086–1092
47. Suzuki H, Achnine L, Xu R, Matsuda SPT, Dixon RA (2002) A genomics approach to the early stages of triterpene saponin biosynthesis in *Medicago truncatula*. *Plant J* 32:1033–1048
48. Sawai S, Shindo T, Sato S, Kaneko T, Tabata S, Ayabe SI, Aoki T (2006) Functional and structural analysis of genes encoding oxidosqualene cyclases of *Lotus japonicus*. *Plant Science* 170:247–257
49. Shibuya M, Zhang H, Endo A, Shishikura K, Kushiro T, Ebizuka Y (1999) Two branches of the lupeol synthase gene in the molecular evolution of plant oxidosqualene cyclases. *Eur J Biochem* 266:302–307
50. Zhang H, Shibuya M, Yokota S, Ebizuka Y (2003) Oxidosqualene cyclases from cell suspension cultures of *Betula platyphylla* var. *japonica*: molecular evolution of oxidosqualene cyclases in higher plants. *Biol Pharm Bull* 26:642–650
51. Guhling O, Hobl B, Yeats T, Jetter R (2006) Cloning and characterization of a lupeol synthase involved in the synthesis of epicuticular wax crystals on stem and hypocotyl surfaces of *Ricinus communis*. *Arch Biochem Biophys* 448:60–72
52. Cordeiro ML, Djerassi C (1990) Biosynthetic studies of marine lipids. 25. Biosynthesis of  $\Delta^{9(11)}$ - and  $\Delta^7$ -sterols and saponins in sea cucumbers. *J Org Chem* 55:2806–2813
53. Makarieva TN, Stonik VA, Kapustina II, Boguslavsky VM, Dmitrenko AS, Kalinin VI, Cordeiro ML, Djerassi C (1993) Biosynthetic studies of marine lipids. 42. Biosynthesis of steroid and triterpenoid metabolites in the sea cucumber *Eupentacta fraudatrix*. *Steroids* 58:508–517
54. Itoh T, Tamura T, Matsumoto T (1975) 24-methylenelanost-9(11)-en-3 $\beta$ -ol, new triterpene alcohol from shea butter. *Lipids* 10:454–460
55. Khalid SA, Varga E, Szendrei K, Duddeck H (1989) Isolation of lanosta-9(11),24-dien-3 $\beta$ -yl acetate from *Leuzea carthamoides*. *J Nat Prod* 52:1136–1138
56. Yano K, Akihisa T, Tamura T, Matsumoto T (1992) Four 4 $\alpha$ -methylsterols and triterpene alcohols from *Neolisea aciculata*. *Phytochemistry* 31:2093–2098
57. Schaefer PC, De Reinach F, Ourisson G (1970) The conversion of parkeol into its 24,25-epoxide by tissue cultures of *Nicotiana tabacum*. *Eur J Biochem* 14:284–288
58. Akihisa T, Nishimura Y, Nakamura N, Roy K, Ghosh P, Thakur S, Tamura T (1992) Sterols of *Cajanus cajan* and three other leguminosae seeds. *Phytochemistry* 31:1765–1768
59. Matsuda SPT, Darr LB, Hart EA, Herrera JBR, McCann KE, Meyer MM, Pang J, Schepmann HG (2000) Steric bulk at cycloartenol synthase position 481 influences cyclization and deprotonation. *Org Lett* 2:2261–2263
60. Segura MJR, Lodeiro S, Meyer MM, Patel AJ, Matsuda SPT (2002) Directed evolution experiments reveal mutations at cycloartenol synthase residue His477 that dramatically alter catalysis. *Org Lett* 4:4459–4462
61. Meyer MM, Segura MJR, Wilson WK, Matsuda SPT (2000) Oxidosqualene cyclase residues that promote formation of cycloartenol, lanosterol, and parkeol. *Angew Chem Int Ed* 39:4090–4092
62. Wu TK, Yu MT, Liu YT, Chang CH, Wang HJ, Diau EW (2006) Tryptophan 232 within oxidosqualene-lanosterol-cyclase from *Saccharomyces cerevisiae* influences rearrangement and deprotonation but not cyclization reactions. *Org Lett* 8:1319–1322
63. Pearson A, Budin M, Brocks JJ (2003) Phylogenetic and biochemical evidence for sterol synthesis in the bacterium *Gemmata obscuriglobus*. *Proc Natl Acad Sci USA* 100:15352–15357
64. Xu HX, Zeng FQ, Sim KY (1996) Anti-HIV triterpene acids from *Geum japonicum*. *J Nat Prod* 59:643–645

# Synthetically Lethal Interactions Involving Loss of the Yeast *ERG24*: The Sterol C-14 Reductase Gene

M. Shah Alam Bhuiyan · James Eckstein ·  
Robert Barbuch · Martin Bard

Received: 16 May 2006 / Accepted: 14 August 2006 / Published online: 19 December 2006  
© AOCS 2006

**Abstract** *ERG2* and *ERG24* are yeast sterol biosynthetic genes which are targets of morpholine antifungal compounds. *ERG2* and *ERG24* encode the C-8 sterol isomerase and the C-14 reductase, respectively. *ERG2* is regarded as a non-essential gene but the viability of *ERG24* depends on genetic background, type of medium, and  $\text{CaCl}_2$  concentration. We demonstrate that *erg2* and *erg24* mutants are viable in the deletion consortium background but are lethal when combined in the same haploid strain. The *erg2erg24* double mutant can be suppressed by mutations in the sphingolipid gene *ELO3* but not *ELO2*. Suppression occurs on rich medium but not on synthetic complete medium. We also demonstrate that the suppressed *elo3erg2erg24* does not have a sterol composition markedly different from that of *erg24*. Further genetic analysis indicates that *erg24* combined with mutations in *erg6* or *erg28* is synthetically lethal but when combined with mutations in *erg3* is weakly viable. These results suggest that novel sterol intermediates probably contribute to the synthetic lethality observed in this investigation.

## Abbreviations

CSM	Synthetic complete media
GC	Gas chromatography
PCR	Polymerase chain reaction
YPAD	Yeast extract, peptone, adenine, dextrose

## Introduction

Synthesis of lanosterol is the first step in yeast sterol biosynthesis. The yeast *ERG24* gene encodes the C-14 reductase required to complete C-14 demethylation of lanosterol. This gene has been cloned and disrupted by several investigators who demonstrated that the C-14 reductase enzyme is essential for viability [1, 2]. Originally, *erg24* mutants were found to be lethal in wild-type genetic backgrounds but viable in genetic backgrounds containing mutations in *elo2/fen1* [1, 2]. Mutations in the *ELO2/FEN1* [3] gene result in resistance to the morpholine fenpropimorph [1, 2]. The morpholines inhibit both the C-8 isomerase and the C-14 reductase encoded by *ERG2* and *ERG24*, respectively [4, 5] possibly indicating a common target site on the two enzymes or an uncharacterized protein–protein interaction between them. Resistance to fenpropimorph because of a mutation in *FEN1* results in tolerance to accumulation of the sterol intermediate, ergosta-8,14-dienol, however. Lorenz and Parks [1] were able to construct a deletion mutation in the *ERG24* gene that was viable only in a *fen1* background. Similarly, Ladeveze et al. [6] also demonstrated that *ERG24* mutants were viable in a *fen1* background. Subsequent work by Baudry et al. [7] demonstrated

---

M. Shah Alam Bhuiyan · M. Bard (✉)  
Biology Department,  
Indiana University-Purdue University Indianapolis,  
723 West Michigan Street, Indianapolis,  
IN 46202, USA  
e-mail: mbard@iupui.edu

J. Eckstein · R. Barbuch  
Department of Drug Disposition,  
Eli Lilly and Co., Lilly Corporate Center,  
Indianapolis, IN 46285, USA



that *erg24* mutants were also suppressed by mutations in *elo3/sur4*. *ELO2/FEN1* and *ELO3/SUR4* encode enzymes that are involved in sphingolipid synthesis and are components of a fatty acid elongation system that elongates  $C_{16}/C_{18}$  to  $C_{24}/C_{26}$  [3]. Further analysis indicated that *erg24* mutants could be grown in some genetic backgrounds (wildtype for *ELO2* and *ELO3*) on synthetic complete or rich medium containing  $Ca^{2+}$  or  $Mg^{+2}$  [8, 9]. Thus replacement of ergosterol by ergosta-8,14-dienol is not lethal in itself but requires an adequate amount of these ions. Although both the C-8 isomerase and C-14 reductase enzymatic reactions are sensitive to morpholine antifungals, overexpression of the non-essential gene *ERG2* does not lead to fenpropimorph resistance whereas overexpression of the essential gene *ERG24* does [10]. Whereas *erg2* mutants have been generally isolated as non-essential in different genetic backgrounds, a single *erg2* mutant isolate in an FL100 wildtype genetic background was shown to be lethal but suppressible by mutations in either the *ELO2* or *ELO3* gene [3, 11].

We have previously demonstrated that *ERG24* is an essential gene in a wildtype Y294 genetic background [10] but the *erg24* mutant strain produced by the deletion consortium project using the S288C wildtype genetic background clearly indicates that viable *erg24* mutants can occur in genetic backgrounds not containing the *ELO2* or *ELO3* mutations. In this study we demonstrate the different synthetic lethal interactions that can occur with an *erg24* strain derived from the deletion consortium genetic (S288C) background.

## Materials and Methods

### Strains, Media, and Growth Conditions

Yeast strains used in this study are derived from W303; SCY325 strain (*MAT $\alpha$* , *ade2-1*, *his3-11,15*, *leu2-3,112*, *trp1-1*, *ura3-1*) and SCY328 (*MAT $\alpha$* , *ade2-1*, *his3-11,15*, *leu2-3,112*, *trp1-1*, *ura3-1*) are wildtype laboratory strains and were used to generate all ergosterol mutant strains other than *erg24*. The *erg24* strain was obtained from the deletion consortium [12] and the construction of other ergosterol deletion strains *erg2*, *erg3*, *erg4*, *erg5*, *erg6*, and *erg28* were as reported previously [13]. The deletion mutant strains *elo2* and *elo3* were generated by homologous recombination with PCR products [14] from plasmid-containing selectable marker genes [15] and from oligonucleotides containing gene-specific sequences. The *elo2* and *elo3* strains derived in the W303 background were isolated as *elo2::TRP1* and *elo3::TRP1* disruptions using the

forward and reverse primers (*ELO2* fwd: 5'-ATG AATTCACCTCGTTACTCAATATGCTGCTCCGTT GTTCGAGCGTTATCCCCAACTTCATTGGCGG GTGTCCGGGGCTGGC-3' and *ELO2* rev: 5'-TAGG AACGTTTTTCAAGTCAACGTTAACATACTCA TTAACCTTTGCGGGAACACCGCCGTTTGCCG ATTTCCGGCCTATTG-3' for *elo2::TRP1* and *ELO3* fwd: 5'-AGCTTACTTCTAGTTTATTTATTCGG CTTTTTCCGTTTGTGTTACGAAACATAAACAG TCGGCGGGTGTCCGGGGCTGGC-3' and *ELO3* rev: 5'-TAAGCAGCAGCAGCCTGAGTACCATAACA AGTACCCTTGTTTGGTAAAATACCGTCCAAG TTGCCGATTTCGGCCTATTG-3' for *elo3::TRP1*). Verification of the deletion was performed by PCR analysis using checking primers. Gene-specific oligonucleotides were obtained from Invitrogen. Disruptions containing the kanamycin (G418) resistance marker were obtained from deletion consortium or isolated as segregants from different crosses. Yeast strains were grown in either YPAD (1% yeast extract, 2% bacto-peptone, 2% glucose, and 0.012% adenine sulfate) or in synthetic complete media (CSM) containing 0.67% yeast nitrogen base (Difco) supplemented with appropriate amino acids and 2% glucose. Additional uracil (0.004%), leucine (0.02%), histidine (0.004%), and tryptophan (0.01%) were added when required. CSM lacking specific nutrients was used for selection of different marker genes. Ergosterol, when used, was added to autoclaved media at 20  $\mu\text{g mL}^{-1}$  to rescue synthetically lethal double mutant strains. For anaerobic growth, anaerobic jars containing the GasPaks system (BBL Microbiology System) were used. Sporulation media have been described previously [14]. All solid media for growth of yeast contained 2% Bacto Agar (Difco).

### Genetic Methods

Mating, sporulation, and genetic dissections to obtain double and triple mutants were as described previously [14]. Crosses and asci dissections of the four-spore meiotic products were performed on YPAD solid media supplemented with 20  $\mu\text{g mL}^{-1}$  ergosterol in 1:1 (v/v) Tween 80–ethanol solution and grown anaerobically. Briefly, diploids grown on YPAD medium were transferred to a 1% potassium acetate medium to induce sporulation. After a 1-h treatment with glucylase (Perkin–Elmer Life science), the four spored-asci were dissected under a microscope using a micromanipulator. All meiotic segregants were analyzed by replica plating on YPAD and CSM plates with and without ergosterol for synthetic lethal screening and the genotype confirmed by genetic markers.

## Sterol Analysis

Sterols were isolated as described previously [16]. Briefly, cells were grown for 20–24 h in YPAD liquid or solid media containing 20  $\mu\text{g mL}^{-1}$  cholesterol. Cells were pelleted, washed twice with Igepal (1%), and twice with distilled water, saponified with alcoholic KOH, and extracted in *n*-heptane. Sterols were first analyzed by gas chromatography (GC) with a Hewlett–Packard HP5890 series II chromatograph equipped with HP Chemstation software. The DB-5 capillary column (15 m  $\times$  0.25 mm  $\times$  0.25  $\mu\text{m}$  film thickness) with nitrogen as carrier gas (30 cm s<sup>-1</sup>) was programmed from 195 to 300 °C (3 min at 195 °C then increased at 5.5° min<sup>-1</sup> to 300 °C and held for 10 min). All injections were made in splitless mode with an inlet temperature of 280 °C. To identify novel sterols, gas chromatography–mass spectrometry (GC–MS) analysis was also performed, using an HP5890 GC coupled to a HP5972 mass-selective detector. GC separations were performed on a fused silica column (DB-5 15 m  $\times$  0.32 mm  $\times$  0.25  $\mu\text{m}$  film thickness), programmed from 40 to 300 °C (40 °C for 1 min, 30° min<sup>-1</sup> to 300 °C then held for 4 min). Helium was the carrier gas with a linear velocity of 50 cm s<sup>-1</sup> in the splitless mode. Mass spectra were generated in electron-impact mode with an electron energy of 70 eV and an ion-source temperature of 150 °C. The instrument was programmed to scan between 40 and 700 amu at 1-s intervals.

## Results

### Synthetic Lethality of *erg2erg24*

The observation that both *erg2* and *erg24* mutants could be suppressed by *elo2* or *elo3* mutations and the further observation that *erg24* was lethal in some genetic backgrounds but not in others led us to ask whether the *erg2erg24* double mutant strain was viable. The *erg2erg24* double mutant was obtained by mating viable *erg2* and *erg24* haploid strains to produce diploid heterozygotes; diploids were sporulated, and the four-spored asci were dissected on rich medium containing ergosterol (or cholesterol) and grown anaerobically. From a total of 100 tetrads, 83 *erg2erg24* double mutants were obtained, all of which could grow anaerobically with sterol supplement but failed to grow aerobically without sterol supplement (Table 1). In Fig. 1, wildtype, *erg2*, *erg24*, and *erg2erg24* strains were plated on both aerobic YPAD rich medium and synthetic complete medium (CSM). On YPAD medium,

*erg24* strains grew but growth was diminished at lower inocula; on YPAD medium, *erg2erg24* growth was completely absent. On CSM medium, however, both *erg2* and *erg24* strains grew normally but growth of the *erg2erg24* strain was minimal, indicating that it is not synthetically lethal on this medium. In the presence of ergosterol (which requires anaerobic growth conditions for sterol uptake) all four strains grew equally well. On YPAD or CSM media supplemented with 10 or 20 mmol L<sup>-1</sup> CaCl<sub>2</sub>, the growth responses were the same as without calcium. Results with 20 mmol L<sup>-1</sup> CaCl<sub>2</sub> (not shown) were exactly the same as with 10 mmol L<sup>-1</sup> CaCl<sub>2</sub> (Fig. 1).

### Suppression of *erg2erg24*

Mutations in *ELO2* and *ELO3* are known suppressors of *erg2* or *erg24* mutants [6, 7]. We generated *elo2erg2erg24* and *elo3erg2erg24* triple mutant strains to determine whether either or both suppressed the lethality of the *erg2erg24* strain. Figure 2 shows that only *elo3* suppressed *erg2erg24* lethality on YPAD medium as indicated by growth on this medium without ergosterol. On CSM medium, however, neither *elo2* nor *elo3* was found to be an efficient suppressor, because there was only small residual growth on this medium without ergosterol. Again, CaCl<sub>2</sub> supplementation in YPAD or CSM media did not rescue the synthetic lethality of *erg2erg24*.

### Sterol Analysis of *erg2erg24* and *erg2erg24elo3*

We proceeded to determine the sterol composition of each of these strains to assess whether a sterol composition difference could be attributable to the suppressed *erg2erg24elo3* strain. Table 2 indicates the sterol composition of the wildtype, *elo3*, *erg2*, *erg24*, *erg2erg24*, *erg2elo3*, *erg24elo3*, and the suppressed *erg2erg24elo3*

**Table 1** Genetic analysis to determine synthetic lethality of *erg24* double mutants in YPAD medium

Mating	Tetrads dissected	Viable double mutants <sup>a</sup>	Inviolate double mutants <sup>a</sup>
<i>erg2</i> $\times$ <i>erg24</i>	100	0	83
<i>erg3</i> $\times$ <i>erg24</i>	20	17 <sup>b</sup>	0
<i>erg4</i> $\times$ <i>erg24</i>	14	14	0
<i>erg5</i> $\times$ <i>erg24</i>	22	18 <sup>b</sup>	0
<i>erg6</i> $\times$ <i>erg24</i>	13	0	13
<i>erg28</i> $\times$ <i>erg24</i>	21	0	16

<sup>a</sup> Double mutants are *erg24* in combination with *erg2*, *erg3*, *erg4*, *erg5*, *erg6*, or *erg28*

<sup>b</sup> Poorly viable

**Fig. 1** Synthetic lethality of the *erg2erg24* double mutant strain. Cells were serially diluted and  $10^5$ – $10^2$  cells were sequentially spotted on to YPAD (upper panels) or CSM (lower panels) media with or without ergosterol or with  $10 \text{ mmol L}^{-1} \text{ CaCl}_2$ , to compare the phenotype of strains. The strains tested were wildtype, *erg2*, *erg24*, and *erg2erg24*. Plates containing ergosterol were incubated anaerobically, and those without ergosterol were incubated aerobically, both for 3 days at  $30^\circ \text{C}$ . The *erg2erg24* double mutant strain was able to grow only in presence of ergosterol

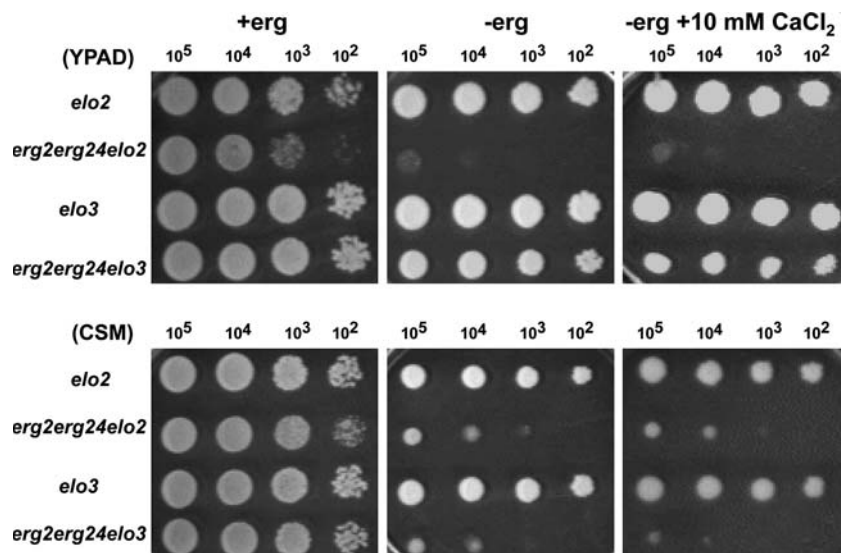
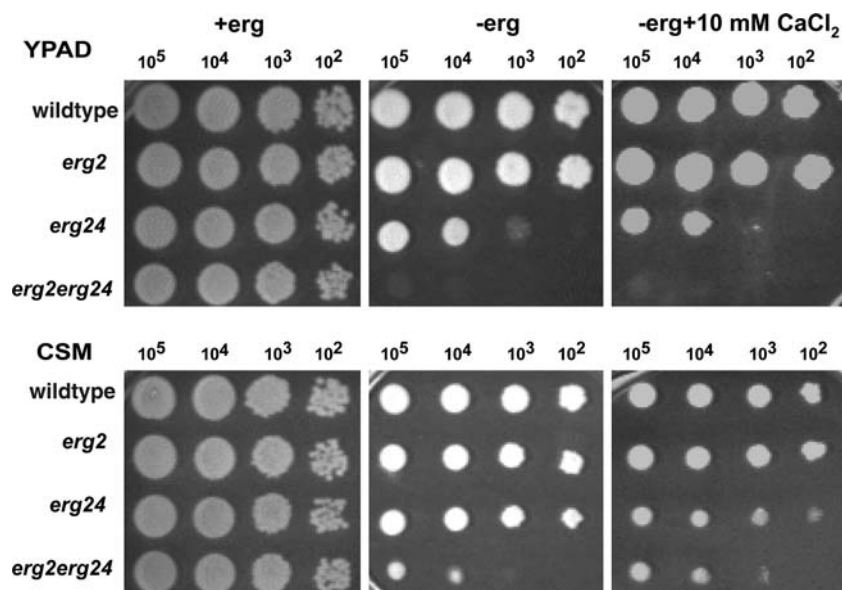


**Fig. 2** The mutation *elo3* but not the mutation *elo2* suppresses the *erg2erg24* double mutant. The growth response of strains *elo2*, *erg2erg24elo2*, *elo3*, and *erg2erg24elo3* was compared by spotting serial dilutions of  $10^5$ – $10^2$  cells of each strain on to YPAD (upper panels) or CSM (lower panels) media with or without ergosterol or with  $10 \text{ mmol L}^{-1} \text{ CaCl}_2$ . Plates containing

ergosterol were incubated anaerobically, and those without ergosterol were incubated aerobically, both for 3 days at  $30^\circ \text{C}$ . The *erg2erg24elo3* triple mutant strain was able to grow on YPAD but not on CSM media without ergosterol or with  $10 \text{ mmol L}^{-1} \text{ CaCl}_2$ . The *erg2erg24elo2* triple mutant strain was unable to grow on YPAD and grew very poorly on CSM media

strains grown in YPAD media under aerobic conditions. Identification of sterols was based on molecular ions and key fragment ions, and on comparison of standard sterol spectra and relative retention times (Table 3). The *erg2erg24* strain was grown anaerobically in the presence of cholesterol. There was essentially no difference between sterol profiles of the wildtype and *elo3* strains. The *erg2erg24* strain accumulated ergosta-8,14-diene sterols and squalene,

lanosterol, and the cholesterol provided in the growth medium. Sterol profiles from *erg24* and *erg2erg24elo3* strains were also similar in that 94 and 99% of the sterols accumulated in these two strains were ergosta-8,14 or cholesta-8,14 sterols, respectively, suggesting that the major effect of *elo3* suppression did not involve alteration of sterols. *erg2elo3* and *erg24elo3* usually reflected the sterol compositions of *erg2* and *erg24*, respectively.

**Table 2** Sterol analyses of *erg2erg24*, *erg2erg24elo3*, and related strains

Sterol	Percent sterol							
	Wildtype	<i>elo3</i>	<i>erg2</i>	<i>erg24</i>	<i>erg2 erg24<sup>a</sup></i>	<i>erg2 elo3</i>	<i>erg24 elo3</i>	<i>erg24 erg24 elo3</i>
Squalene	0.27	0.98	–	5.58	28.04	–	0.82	0.78
Cholesterol	–	–	–	–	47.84	–	–	–
Ergosta-5,8,22,24(28)-tetraen-3-ol	–	–	1.88	–	–	–	–	–
Zymosterol	18.73	18.46	1.30	–	–	–	–	–
Ergosterol	61.30	56.98	–	–	–	–	–	–
Ergosta-7,22-dien-3-ol	2.43	2.53	–	–	–	–	–	–
Ergosta-5,7,22,24(28)-tetraen-3-ol	1.59	1.97	–	–	–	–	–	–
Ergosta-8,14,24(28)-trien-3-ol	–	–	–	25.20	–	–	40.50	26.67
Ergosta-5,8,22-trien-3-ol	–	–	31.31	–	–	38.67	–	–
Ergosta-8,14-dien-ol	–	–	–	56.44	14.00	–	37.51	63.40
Ergosta-8-en-3-ol	–	–	11.21	–	–	17.05	–	–
Fecosterol	6.93	7.67	51.55	–	–	37.31	–	–
Ergosta-8,14-dien-3-one	–	–	–	1.85	–	–	–	–
Episterol	6.12	6.75	–	–	–	–	–	–
Lanosterol	0.51	2.54	0.61	–	8.19 <sup>b</sup>	–	9.20 <sup>b</sup>	–
4,4-Dimethylcholesta-8,14,22-trien-3-ol	–	–	–	10.53	–	–	–	3.61
4,4-Dimethylzymosterol	0.78	0.40	1.11	–	–	–	–	–
Ergosta-8,22-dien-3-ol	–	–	–	–	–	3.75	–	–
Ergostadien-3-one	–	–	–	–	–	–	0.45	–
Ergostatrien-3-one	–	–	–	–	–	–	0.31	–
Ergosta-5,8,14,22-tetraen-3-ol + cholesta-8,14,22-trien-3-ol	–	–	–	–	–	–	9.71	5.06

<sup>a</sup> Grown anaerobically in the presence of cholesterol<sup>b</sup> Consists of lanosterol and 4,4-dimethylcholesta-8,14,22-trien-3-ol**Table 3** GC–MS data for *erg2erg24*, *erg2erg24elo3*, and related strains

Sterol <sup>a</sup>	<i>m/z</i> (relative ion intensity)
Squalene	410 [M] (80), 367 (12), 341 (15), 136 (85), 123 (72), 121 (84), 109 (62), 107 (52), 95 (81), 93 (60), 81 (99), 69 (100)
Cholesterol	386 [M] (100), 371 (40), 368 (67), 353 (42), 301 (91), 275 (84), 255 (40), 231 (33), 213 (57), 145 (56)
Ergosta-5,8,22,24(28)-tetraen-3-ol	394 [M] (29), 379 (5), 376 (18), 361 (100), 268 (43), 251 (92), 235 (66), 209 (46)
Ergosta-8,22-dien-3-ol	398 [M] (37), 383 (21), 380 (2), 299 (6), 273 (40), 271 (41), 255 (23), 246 (37), 69 (100)
Ergosta-5,8,14,22-tetraen-3-ol	394 [M] (42), 379 (5), 361 (100), 297 (8), 268 (28)
Cholesta-8,14,22-trien-3-ol	382 [M] (100), 367 (35), 349 (41), 297 (53), 270 (18), 255 (28), 218 (32)
Zymosterol	384 [M] (97), 369 (75), 366 (2), 351 (13), 273 (10), 271 (22), 231 (22), 229 (23), 213 (42), 69 (100)
Ergosterol	396 [M] (96), 381 (4), 378 (5), 363 (100), 337 (41), 271 (17), 253 (43), 211 (36), 157 (37), 143 (52)
Ergosta-7,22-dien-3-ol	398 [M] (37), 383 (13), 300 (16), 271 (100), 255 (32), 213(17)
Ergosta-5,7,22,24(28)-tetraen-3-ol	394 [M] (49), 376 (7), 361 (78), 271 (18), 269 (29), 253 (46), 251 (58), 237 (41), 211 (45), 159 (43), 157 (57), 143 (92), 81 (100)
Ergosta- 8,14,24(28)-trien-3-ol	396 [M] (61), 381 (47), 378 (9), 363 (33), 353 (19), 311 (29), 297 (48), 270 (28), 269 (28), 255 (38), 55 (100)
Ergosta-8,14-dien-3-ol	398 [M] (100), 383 (49), 380 (2), 365 (13), 299 (2), 271 (15), 238 (11)
Fecosterol	398 [M] (100), 383 (60), 380 (3), 365 (12), 314 (6), 285 (18), 245 (23), 227 (34)
Ergosta-8-en-3-ol	400 [M] (100), 385 (47), 367 (7), 273 (35), 255 (17), 246 (13), 231 (22), 229 (31), 213 (36), 147 (35)
Ergosta-8,14-dien-3-one	396 [M] (100), 381 (34), 269 (56), 255 (37), 159 (32)
Episterol	398 [M] (33), 383 (12), 365 (18), 314 (29), 299 (7), 271 (100)
Lanosterol	426 [M] (58), 411 (87), 393 (47), 259 (21), 109 (61), 69 (100)
4,4 Dimethylcholesta-8,14,22-trien-3-ol	410 [M] (58), 395 (33), 377 (16), 325 (43), 313 (21), 298 (22), 283 (29), 246 (32), 69 (100)
4,4-Dimethylzymosterol	412 [M] (62), 397 (28), 394 (7), 379 (15), 299 (10), 259 (17), 135 (54), 69 (100)
4,4-Dimethylfecosterol	426 [M] (100), 411 (25), 408 (7), 393 (14), 342 (7), 327 (17), 299 (37), 281 (31)

<sup>a</sup> Sterols are listed from lowest to highest retention times

### Synthetic Lethality of *erg24* in Combination with Other Ergosterol Biosynthetic Mutants

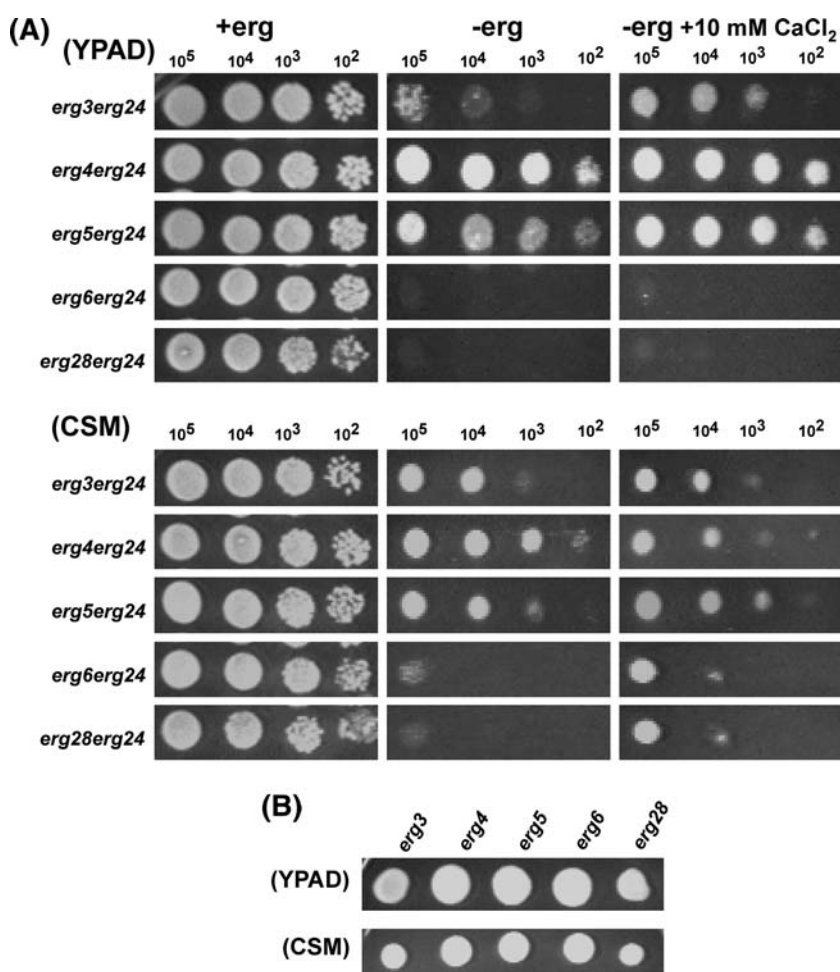
It was of interest to ascertain whether other ergosterol mutations, for example *erg3*, *erg4*, *erg5*, *erg6*, and *erg28*, would be synthetically lethal in combination with the *erg24* mutation. *ERG3* encodes the C-5 desaturase, *ERG4* encodes the C-24 reductase, *ERG5* encodes the C-22 desaturase, and *ERG6* encodes the C-24 trans-methylase; mutations in these genes are viable (Fig. 3b). *ERG28* encodes a scaffold protein required for complete C-4 demethylation and it, also, is non-essential for growth. We crossed all single mutants with the *erg24* strain to generate the haploid double mutants. All tetrads were dissected and grown anaerobically with ergosterol and then grown aerobically without ergosterol to assess viability (Fig. 3). Genetic analysis (Table 1) and spot-plating (Fig. 3) on YPAD medium demonstrated that the double mutants *erg4erg24* and *erg5erg24* were viable but the double mutants *erg6erg24* and *erg28erg24* were not. The *erg3erg24* double mutants

were only weakly viable, however. Addition of  $\text{CaCl}_2$  had a growth-enhancing effect on *erg5erg24* on YPAD medium but not on CSM medium; on CSM medium,  $\text{CaCl}_2$  also had a growth-enhancing effect on *erg6erg24* and *erg28erg24*. Finally, *elo3* failed to suppress *erg6erg24* or *erg28erg24* on YPAD or CSM media (data not shown). The observation that *elo3* did not suppress *erg6erg24* is expected, because Eisenkolb et al. [17] demonstrated that the double mutant *elo3erg6* is synthetically lethal.

### Discussion

The genes in the latter part of the yeast ergosterol pathway, *ERG6*, *ERG2*, *ERG3*, *ERG4*, and *ERG5*, are regarded as non-essential because the sterols produced by mutations of these genes function nearly as well as ergosterol and meet the biophysical and biochemical requirements of a sterol molecule. Mutations in *ERG24*, however, are lethal in some

**Fig. 3** An *erg24* mutation is synthetically lethal with *erg6* or *erg28* but not with *erg3*, *erg4*, or *erg5*. **A** Growth of the *erg24* mutant in combination with additional mutations in the ergosterol biosynthetic pathway—*erg3*, *erg4*, *erg5*, *erg6*, and *erg28*. Cells from the double mutants were serially spotted on to YPAD (*upper panels*) or CSM (*lower panels*) media with or without ergosterol or with 10 mmol L<sup>-1</sup> CaCl<sub>2</sub>. Plates containing ergosterol were incubated anaerobically, and those without ergosterol were incubated aerobically, both for 3 days at 30 °C. The *erg6erg24* and *erg28erg24* mutant strains did not grow on YPAD medium without ergosterol; the *erg3erg24* and *erg5erg24* mutant strains grew poorly; and the *erg4erg24* mutant strain grew well. All strains grew poorly or very poorly on CSM medium without ergosterol or with 10 mmol L<sup>-1</sup> CaCl<sub>2</sub>. **B** *erg3*, *erg4*, *erg5*, *erg6*, and *erg28* single mutant strains were viable on both YPAD and CSM media without ergosterol



genetic backgrounds but not others. The results presented here extend initial observations that the viability of *erg24* depends on factors such as type of medium, metal ion concentrations, and strain background. Studies by Parks and coworkers [8, 9] indicated that *erg24* could not grow on a rich medium (YPAD) but could grow on a synthetic complete medium, because of greater abundance of  $\text{Ca}^{2+}$  in the latter. Addition of  $\text{Ca}^{2+}$  to rich medium restored growth. Our studies confirm some of these findings but differ in that the deletion consortium *erg24* strain is viable on YPAD medium but growth is not enhanced by addition of  $\text{Ca}^{2+}$  (Fig. 1). Growth is enhanced on CSM medium, however. The combination of *erg2* and *erg24*, however, resulted in lethality on YPAD medium that was not rescued by  $\text{Ca}^{2+}$  supplementation. Growth of the *erg2erg24* strain was marginal on synthetic complete medium. Suppression of this lethality was achieved by introducing a third mutation, *elo3*. The *elo3* mutation has previously been found to individually suppress lethal isolates of *erg2* and *erg24*. Whereas *elo3* was able to restore growth of the *erg2erg24* strain on YPAD medium, however, it failed to restore growth on CSM medium (Fig. 2). Surprisingly *elo2* failed to suppress the lethality of *erg2erg24* on any medium, even media containing  $\text{Ca}^{2+}$  supplementation.

We next asked whether other ergosterol mutants were lethal in combination with *erg24* and the results indicated that *erg6erg24* and *erg28erg24* were also inviable on rich YPAD medium and this lack of growth was not suppressed by  $\text{Ca}^{2+}$  supplementation. The double mutant *erg3erg24* grew poorly and only *erg4erg24* and, to a lesser extent, *erg5erg24* was clearly growing on YPAD. On synthetic complete medium, however, we observed slightly better growth in the presence of  $\text{Ca}^{2+}$  (Fig. 3). All double mutants grew at least to some extent in synthetic complete medium if  $\text{Ca}^{2+}$  was added to the medium.

Crowley et al. [9] demonstrated that the concentration of  $\text{Ca}^{2+}$  was greater in a synthetic complete medium than on rich YPD medium and that increased  $\text{Ca}^{2+}$  resulted in resistance to fenpropimorph, suggesting that  $\text{Ca}^{2+}$  enhances membrane integrity in strains in which ergosterol is replaced by ergosta-8,14 sterol intermediates. It is not obvious why *erg2erg24* mutants are more compromised than *erg24* alone, because *erg24* mutants are epistatic to *erg2* and thus accumulate only C-8 sterols. Thus, in an *erg24* strain there is no evidence of Erg2p activity, because all accumulated sterols are C-8-sterols. Further work will reveal whether there is a regulatory sterol defect that must be taken into consideration. In considering the

synthetic lethality of *erg6erg24* and *erg28erg24* strains, however, each individual mutation should contribute to an altered sterol profile and thus may help explain why the double mutants in these cases are lethal.

**Acknowledgments** This work was supported by a NIH grant GM62104 to M.B.

## References

- Lorenz RT, Parks LW (1992) Cloning, sequencing, and disruption of the gene encoding sterol C-14 reductase in *Saccharomyces cerevisiae*. DNA Cell Biol 11:685–692
- Marcireau C, Guyonnet D, Karst F (1992) Construction and growth properties of a yeast strain defective in sterol 14-reductase. Curr Genet 22:267–272
- Oh CS, Toke DA, Mandala S, Martin CE (1997) *ELO2* and *ELO3*, homologues of the *Saccharomyces cerevisiae* *ELO1* gene, function in fatty acid elongation and are required for sphingolipid formation. J Biol Chem 272:17376–17384
- Mercer EI (1993) Inhibitors of sterol biosynthesis and their applications. Prog Lipid Res 32:357–416
- Baloch RI, Mercer EI (1987) Inhibition of Sterol  $\Delta^8$ – $\Delta^7$  isomerase and  $\Delta^{14}$  reductase by fenpropimorph, tridemorph, and fenpropidin in cell-free enzyme systems from *Saccharomyces cerevisiae*. Phytochem 26:663–668
- Ladeveze V, Marcireau C, Delourme D, Karst F (1993) General resistance to sterol biosynthesis inhibitors in *Saccharomyces cerevisiae*. Lipids 28:907–912
- Baudry K, Swain E, Rahier A, Germann M, Batta A, Rondet S, Mandala S, Henry K, Tint GS, Edlind T, Kurtz M, Nickless JT (2001) The effect of the *Erg26-1* mutation on the regulation of lipid metabolism in *Saccharomyces cerevisiae*. J Biol Chem 276:12702–12711
- Crowley JH, Smith SJ, Leak FW, Parks LW (1996) Aerobic isolation of an *ERG24* null mutant of *Saccharomyces cerevisiae*. J Bacteriol 178:2991–2993
- Crowley JH, Tove S, Parks LW (1998) A calcium-dependent ergosterol mutant of *Saccharomyces cerevisiae*. Curr Genet 34:93–99
- Lai MH, Bard M, Pierson CA, Alexander JF, Goebel M, Carter GT, Kirsch DR (1994) The identification of a gene family in the *Saccharomyces cerevisiae* ergosterol biosynthesis pathway. Gene 11:41–49
- Silve S, Leplatois P, Josse A, Dupuy PH, Lanau C, Kaghad M, Dhers C, Picard C, Rahier A, Taton M, Le Fur G, Caput D, Ferrara P, Loison G (1996) The immunosuppressant SR 31747 blocks cell proliferation by inhibiting a steroid isomerase in *Saccharomyces cerevisiae*. Mol Cell Biol 16:2719–2727
- Winzeler EA et al (1999) Functional characterization of the *S. cerevisiae* genome by gene deletion and parallel analysis. Science 6:901–906
- Valachovic M, Bareither BM, Bhuiyan MSA, Eckstein J, Barbuch R, Balderes D, Wilcox L, Sturley SL, Dickson RC, Bard M (2006) Cumulative mutations affecting sterol biosynthesis in the yeast *Saccharomyces cerevisiae* result in synthetic lethality that is suppressed by alterations in sphingolipid profiles. Genetics 173:1893–1908
- Adams A, Gottschling DE, Kaiser CA, Stearns T (1997) Methods in yeast genetics. Cold Spring Harbor Laboratory Press, New York

15. Sikorski RS, Hieter P (1989) A system of shuttle vectors and yeast host strains designed for efficient manipulation of DNA in *Saccharomyces cerevisiae*. *Genetics* 122:19–27
16. Gachotte D, Sen SE, Eckstein J, Barbuch R, Krieger M, Ray BD, Bard M (1999) Characterization of the *Saccharomyces cerevisiae* *ERG27* gene encoding the 3-keto reductase involved in C-4 sterol demethylation. *Proc Natl Acad Sci USA* 26:12655–12660
17. Eisenkolb M, Zenzmaier C, Leitner E, Schneiter R (2002) A specific structural requirement for ergosterol in long-chain fatty acid synthesis mutants important for maintaining raft domains in yeast. *Mol Biol Cell* 13:4414–4428

# Biological Activities and Syntheses of Steroidal Saponins: the Shark-Repelling Pavoninins

John R. Williams · Hua Gong

Received: 5 June 2006 / Accepted: 11 October 2006 / Published online: 19 December 2006  
© AOCS 2006

**Abstract** Steroidal saponins are complex compounds that have a steroid attached to a carbohydrate moiety. They are natural surfactants and detergents and exhibit a number of biological effects. Steroidal saponins have shown membrane-permeabilizing, hypocholesterolemic, immunostimulant, and anticancer properties. They have also been found to affect the growth, food intake and reproductive capabilities of animals. Furthermore, they have been shown to act as antiviral and antifungal agents. They have been isolated from many plants and some animals, especially sea cucumbers and starfish. Fish belonging to the species *Pardachirus pavoninus* excrete a mixture of six steroidal *N*-acetylglucosaminides, pavoninins 1–6, with shark-repelling properties. We report syntheses of the C-15 $\alpha$  pavoninin-4 by both direct synthesis from diosgenin and by remote functionalization. A general solution for the glycosylation of hindered alcohols was developed using glycosyl fluorides as good glycosyl donors. The syntheses of two C-16 $\beta$  structural analogs of OSW-1 are described.

**Keywords** Biological activities · Steroidal · Saponin · Aglycone · Sterol · Monosaccharide · Glycoside · Synthesis · Pavoninin · OSW-1

## Abbreviations

AgF	Silver fluoride
AgOTf	Silver triflate
Bn <sub>8</sub> Sn <sub>4</sub> Cl <sub>4</sub> O <sub>2</sub>	Bisdibutylchlorotin(IV) oxide
DAST	(Diethylamino)sulfur trifluoride

DDQ	2,3-Dichloro-5,6-dicyano-1,4-benzoquinone
DEAD	Diethyl azodicarboxylate
DIAD	Diisopropyl azodicarboxylate
DMSO	Dimethyl sulfoxide
LAH	Lithium aluminum hydride
LiDBB	Lithium di- <i>tert</i> -butylbiphenyl
MsCl	Methanesulfonyl chloride
Piv	Pivaloyl
TBAF	Tetrabutylammonium fluoride
TBSO	<i>t</i> -Butyldimethylsilyloxy

## Introduction

Steroidal saponins constitute a structurally and biologically diverse class of glycoconjugates, which have been isolated from a wide variety of both plant and animal species [1–3]. They consist of a hydrophobic aglycone (sapogenin) to which a sugar moiety is attached, usually containing a glucose, galactose, *N*-acetylglucosamine, glucuronic acid, xylose, rhamnose or methylpentose. The oligosaccharide is normally attached at the C-3 position but many are now known that have it attached at C-6, 7, 15, 16, 24, and 26. In this review we will survey some of the biological properties of saponins and report methods for the synthesis of 15 $\alpha$  and 16 $\beta$  steroidal saponins.

Steroidal saponins are natural surfactants, or detergents. They have been isolated from a great number of terrestrial plants, such as alliums, asparagus, aubergine, capsicum peppers, oats, tomato seeds, yams, and ginseng [2]. They are most abundant in the desert plants *Yucca* and *Quillaja*. They are common in plants used as herbs or for their health-promoting properties.

J. R. Williams (✉) · H. Gong  
Department of Chemistry, Temple University,  
13 and Norris Sts., Philadelphia, PA 19122-2585, USA  
e-mail: john.r.williams@temple.edu



Steroidal saponins are uncommon animal constituents. In the animal kingdom they are almost ubiquitous in sea cucumbers and starfish, while found only rarely in alcyonarians, gorgonians, sponges, and as shark-repelling compounds in fish. The shark-repelling pavoninins 1–6 (**1–5**) were isolated from fish belonging to the species *Pardachirus pavoninus* [4, 5]. The steroidal saponin OSW-1 (**6**) was isolated from the bulbs of the plant *Ornithogalum saundersiae*, and has been proven to be a highly potent anticancer agent [6, 7] (Fig. 1). Despite their different origins, they are both derivatives of cholesterol with additional hydroxyl functionalities on the B or D rings and a functionalized side chain. Pavoninins have the monosaccharide *N*-acetylglucosamine attached at the B ring C-7 $\alpha$  or D ring C-15 $\alpha$  hydroxyl group, and OSW-1 (**6**) has a disaccharide attached to the D-ring C-16 $\beta$  hydroxyl group. Due to their structural similarity to anticancer agents, it is believed that pavoninins could also have other important pharmacological properties beyond their shark-repelling properties.

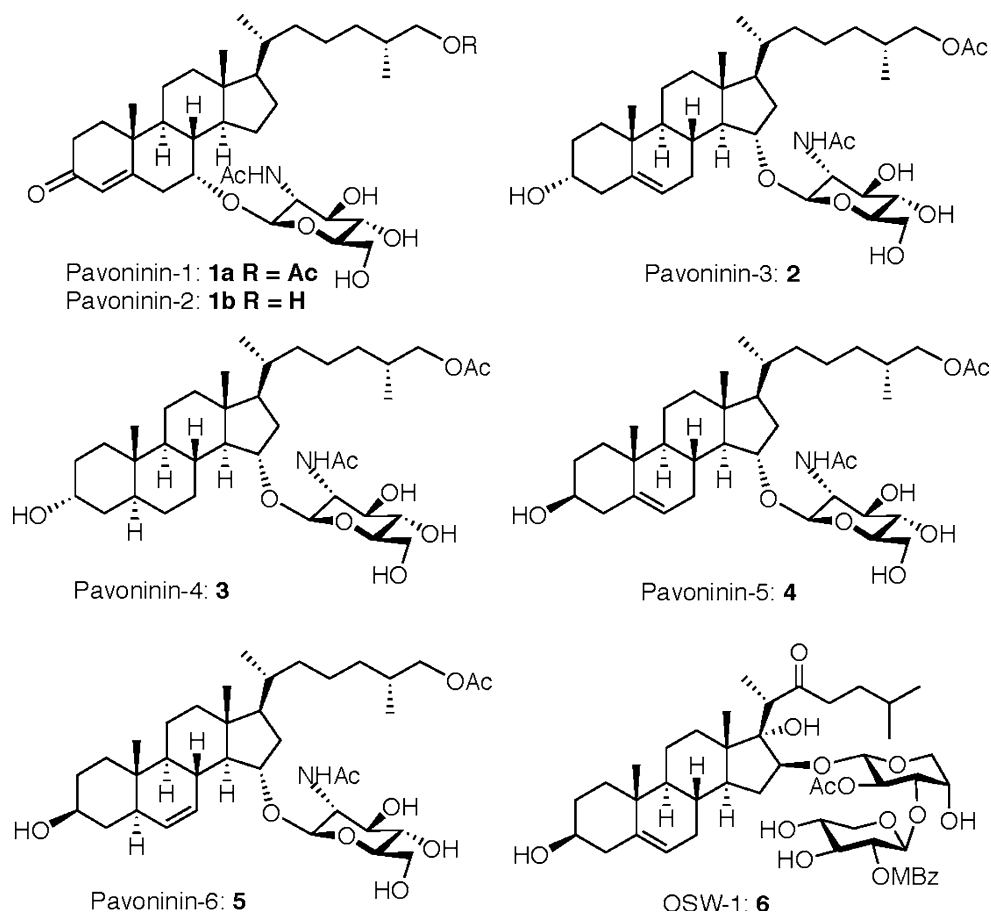
The effects of saponins in plants are not well understood. Many saponins are known to inhibit mold, to be antimicrobial, and to protect plants against insect

attack. Some can be considered to be part of a plant's defense system. This defensive property appears to carry over into animals, as some fish, such as the species *Pardachirus*, use saponins as defensive compounds in order to repel sharks [4, 5].

A broad range of biological effects have been ascribed to saponins: membrane-permeabilizing, hypocholesterolemic, immunostimulant, and anticancer properties [2]. They have also been found to affect growth and food intake in animals [8]. Furthermore, they have been shown to act as antiviral and antifungal agents.

Saponins have long been known to form pores in membranes, and this has resulted in their use in physiological research. There are a wide variety of saponin structures, as both the sapogenin and the sugar can be varied, and the site(s) and stereochemistry of conjugation on the sapogenin and the sugar can also be varied. This variation in saponin structure can lead to different biological mechanisms. For example, some steroidal saponins with a single monosaccharide were found to have strong hemolytic activity, whereas those with two sugars showed less activity [9]. However, this is not always the case and in some cases di- and triglycosides have been shown to have higher hemolytic activity [10].

**Fig. 1** Shark repellent pavoninins 1–6 (**1–5**) and the anticancer agent OSW-1, **6**



The exact details of the interactions between saponins and membranes needs more elucidation so that the molecular mechanisms involved can be better understood. It has been found that some saponins affect the permeability of the intestinal mucosa cells and thereby affect the uptake of nutrients through the intestinal membrane. The permeability of the brush border is apparently increased by sublethal levels of saponins and this has important implications for the uptake of macromolecules, such as allergens, whose passage through the epithelium is normally somewhat restricted [11].

Saponins from different sources have produced lower cholesterol levels in a variety of animals, including human subjects [12]. When saponin-rich foods are consumed, such as soybean, lucerne, and chickpeas, large mixed micelles are formed by the interaction of saponins with bile acids, which leads to their increased excretion [13]. Saponins also reduce the more harmful LDL-cholesterol selectively in the sera of rats, gerbils and human subjects [14].

The immune system is stimulated by saponins. *Quillaja* saponins have been reported to increase immune-cell proliferation in vitro, and to boost antibody production without producing any reagenic antibodies [15]. The mechanisms of the immune-stimulating actions of saponins are not clearly understood. Saponins reportedly induce the production of cytokines such as interleukins and interferons that might mediate their immunostimulant effects.

Saponins have been shown to inhibit the growth of cancer cells in vitro by unknown mechanisms. Saponin-induced apoptosis is primarily caused by stimulating the cytochrome *c*–caspase 9–caspase 3 pathway in the human cancer and other cell lines [16]. The tumor specificity of the cytotoxic action seems to be influenced by the structure of the sugar portion of the saponins after the hydrophobic aglycone core allowed saponins to traverse the mitochondrial membrane.

Saponins affect animal growth and feed intake. In ruminants and other domestic animals, dietary saponins have been found to improve growth, feed efficiency, and health [17]. Saponins are considered to have detrimental effects on protozoa through their binding with sterols on the protozoal surface [18]. Dietary saponins were often suspected of having a role in causing ruminant bloat, but clear experimental proof for this is lacking in the literature. Saponins damage the respiratory epithelia of some fish and are thus highly toxic [19]. However, fish belonging to the species *Pardachirus* excrete saponins that are ichthyotoxic and repel sharks and thus act as defensive compounds. Growth in common carp was significantly higher than control only when there was a continuous dietary

supply of saponins. Soybean saponins did not affect the growth of chicks when added at five times the concentration in a normal soybean-supplemented diet. Similarly in mice and rats, no effect on the growth response was observed on a soybean-supplemented diet. Dietary saponins depressed growth feed consumption in gerbils and egg production in poultry [20].

Saponins cause a reduction in protein digestibility, probably through the formation of sparingly soluble saponin–protein complexes [21]. The digestibility of bovine serum albumin–soyasaponin complex was much lower than that of free bovine serum albumin, indicating that complexing with saponins had an obstructing effect. Since a large number of foods and feed materials contain both saponins and proteins, the nature of the interactions between them would influence the nutritive value of the diet.

Due to the difficulty in isolating and purifying saponins, there is often very little pure material available. Since an understanding of the effects of these compounds will require significant amounts of the pure substances, methods for the isolation and preparation of target saponins need to be developed. Furthermore, the development of new synthetic methods frees the researcher from needing to use only naturally available saponins. Hopefully structure–activity relationships will lead researchers to design and synthesize new saponins in order to potentiate their desired biological activity. We apply these ideas to a study of the shark-repelling steroidal saponins called pavoninins.

Among the pavoninin family of steroidal saponins, the synthesis of pavoninin-1 (**1a**) [22], and the aglycone of pavoninin-1 (**1a**) and -2 (**1b**), have been reported [23]. Recently, we reported the syntheses of the aglycone of 26-*O*-deacetyl pavoninin-5 (**2b**) [24, 25], of pavoninin-4 (**3**) [26], and the aglycone of pavoninin-4 by remote functionalization [27]. The isolation and synthesis of shark-repelling saponins have recently been reviewed [28]. In this paper, we review our efforts in developing a good method for glycosylation of the hindered C-15 $\alpha$  and C-16 $\beta$  hydroxyl groups in a steroid, as well as the synthesis of the shark repellent pavoninin-4 (**3**). The synthesis of the structural analogs **32b** and **37** of the anticancer agent OSW-1 (**6**) are also reported.

## Results and Discussion

### Synthesis of the C-15 $\alpha$ Hydroxylated Steroid **14**

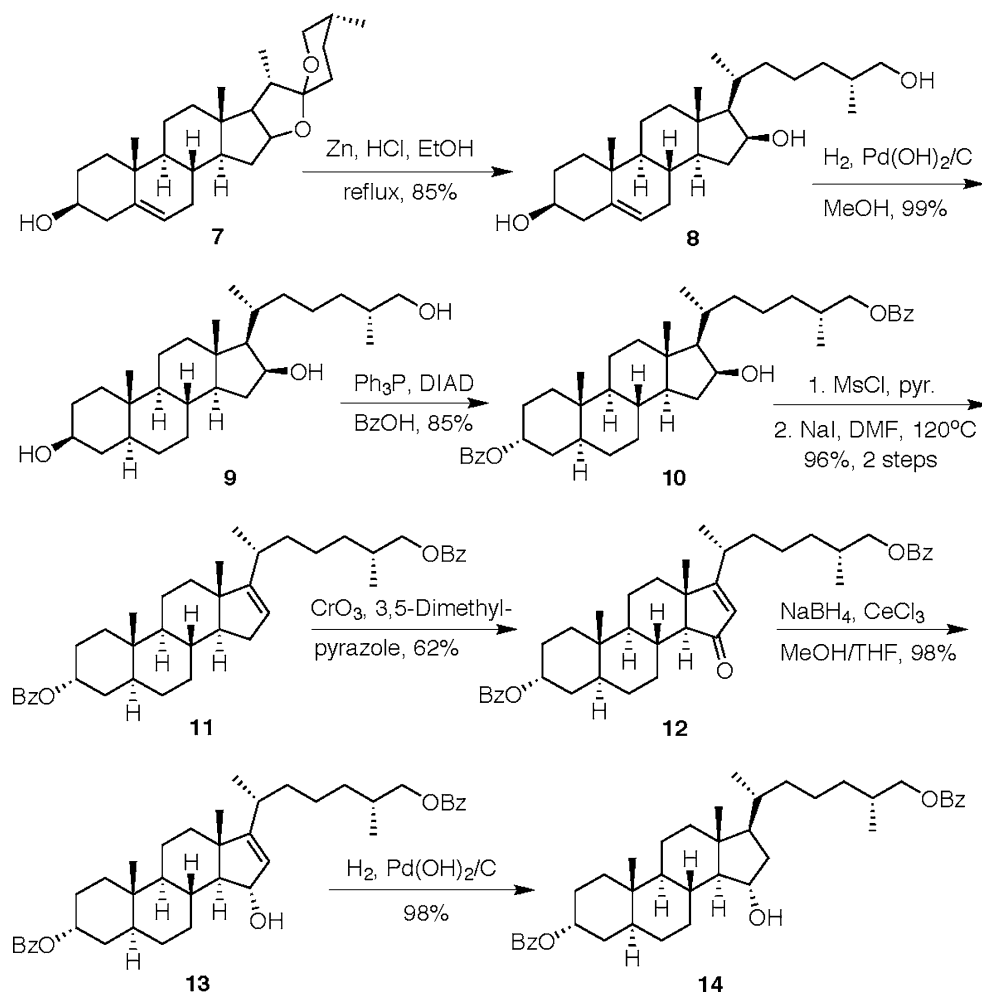
The synthesis of pavoninin-4 (**3**) presents three major problems: the presence of an *N*-acetylglucosamine moiety attached to a C-15 $\alpha$  hydroxylated cholesterol

and a C-26 acetate in the presence of three secondary and one primary alcohol. The synthesis of the C-15 $\alpha$  hydroxylated steroid **14** started from commercially available diosgenin **7**. Reduction of **7** using zinc and hydrochloric acid afforded (25*R*)-5-ene-cholesta-3 $\beta$ ,16 $\beta$ ,26-triol (**8**), which when subjected to a catalytic hydrogenation yielded the saturated (25*R*)-5 $\alpha$ -cholesta-3 $\beta$ ,16 $\beta$ ,26-triol (**9**). Subsequent Mitsunobu reaction [29] on the triol **9** afforded the 3 $\alpha$ ,26-dibenzoate **10** in 85% yield, and achieved several transformations. The C-3 and C-26 hydroxyl groups of triol **10** were chemoselectively protected, and at the same time the C-3 hydroxyl stereochemistry was inverted from  $\beta$  to  $\alpha$ , all in one step. We have reported a successful six-step method for transposing the C-16 $\beta$  hydroxyl in **8** to the 15 $\alpha$  position in our synthesis of the aglycone of 26-*O*-deacetyl pavoninin-5 [24, 25]. Oxidation of the C-16 alcohol afforded the ketone, which was converted to its silyl ether, and epoxidization followed by rearrangement yielded the 15 $\alpha$ -hydroxy-16-ketone. Protection of the C-15 $\alpha$  alcohol as its silyl ether followed by reduction of the ketone and chemoselective deoxygenation

of the C-16 alcohols using the Barton deoxygenation reaction afforded the 15 $\alpha$  alcohol [24, 25].

A very efficient four-step method for this transposition was developed via allylic oxidation and subsequent stereospecific reduction in our synthesis of (25*R*)-5 $\alpha$ -cholesta-3 $\beta$ ,15 $\alpha$ ,26-triol [30]. Using Kim's method [31], namely NaI in DMF, regiospecific dehydration of the hindered C-16 $\beta$  hydroxyl was achieved via a bis-protected 16-mesylate, to yield the disubstituted C-16 olefin, **11**, in 96% yield. Allylic oxidation at C-15 using chromium trioxide and 3,5-dimethylpyrazole yielded the 16-en-15-one, **12**. Stereospecific Luche reduction [32] proceeded quantitatively from the unexpected  $\beta$ -face to yield the 15 $\alpha$  allylic alcohol, **13**. The saturated alcohol **14** was prepared by catalytic hydrogenation. Comparison of the spectra of **14** with its 3 $\beta$  epimer (25*R*)-5 $\alpha$ -cholesta-3 $\beta$ ,15 $\alpha$ ,26-triol, whose structure has been determined by X-ray analysis [30], proved the  $\alpha$ -configuration of the C-15 hydroxyl group. Using this synthetic method, the C-15 $\alpha$  hydroxylated intermediate **14** was successfully achieved through an eight-step synthesis in a 41% overall yield from diosgenin, **7** (Scheme 1).

**Scheme 1** Synthesis of the C-15 $\alpha$  hydroxylated steroid **14**



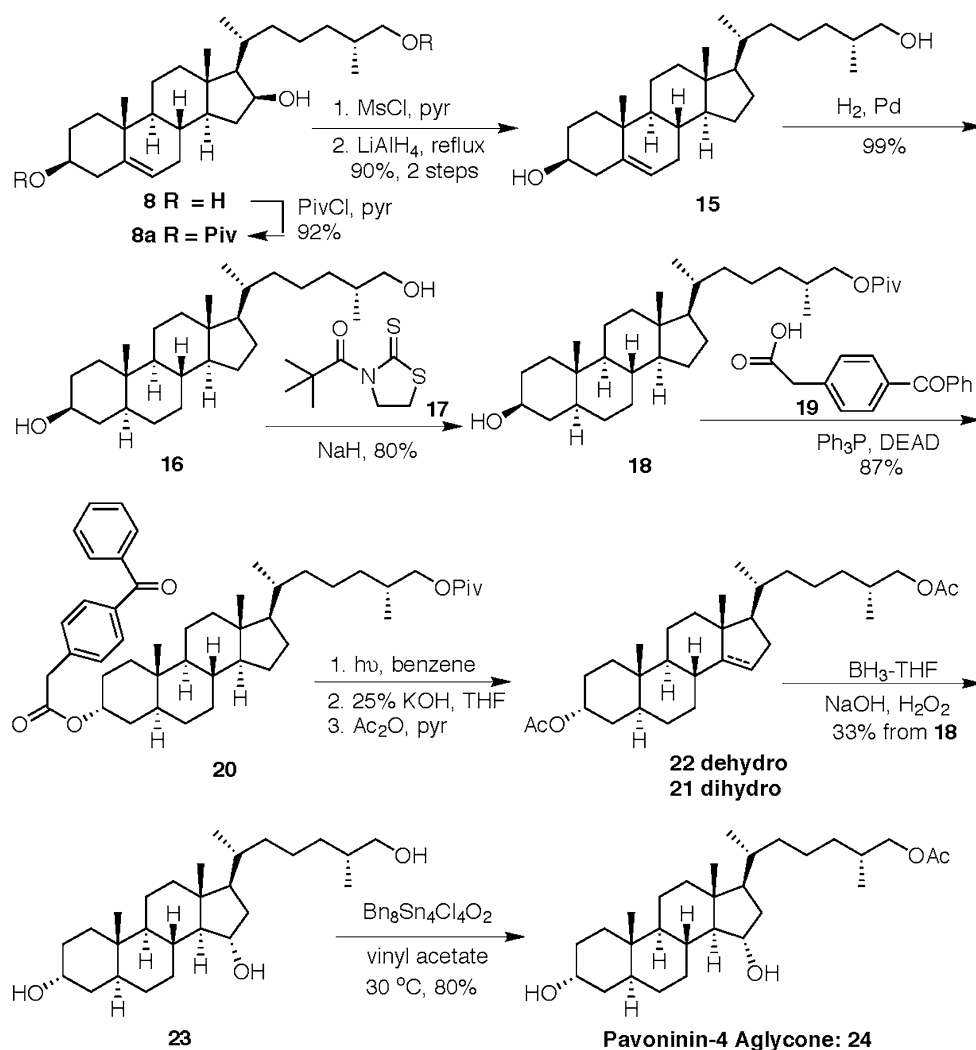
## Synthesis of the Aglycone of Pavoninin-4 **24**, Using Remote Functionalization

The aglycone of pavoninin-4 (**24**) can be also be synthesized from diosgenin **7** via (25*R*)-26-hydroxycholesterol (**15**) [33], using Breslow's remote functionalization [34] strategy, as shown in Scheme 2.

Triol **8** was chemoselectively protected as the hydroxy diester **8a**, as described in Scheme 2. Mesylation of the C-16 alcohol **8a** afforded a C-16 mesylate, which upon reduction with LAH yielded the diol **15** and effected deoxygenation at C-16. The unsaturated diol **15** was catalytically reduced to afford the saturated diol **16**. Chemoselective protection of the primary C-26 hydroxyl by 3-pivaloyl-1,3-thiazolidine **17** and sodium hydride [35] gave the 3β,26-diol 26-pivaloate **18** in 80% yield. The required 3α stereochemistry for pavoninin-4 (**3**) was introduced by treatment of the 3β alcohol **18** under Mitsunobu conditions with the known acid **19** [36] to yield the

inverted ester **20** in 85% yield. Photolysis of **20** using a 450-W medium-pressure Hanovia lamp with a Pyrex filter and subsequent hydrolysis of the C-3 and C-26 esters with potassium hydroxide under refluxing conditions gave the intermediate 3α,26-diol. Since this was difficult to separate, the diol was converted into a mixture of the unreacted saturated (25*R*)-5α-cholestan-3α,26-diol 3α,26-diacetate (**21**) and the desired (25*R*)-5α-cholest-14-ene-3α,26-diol 3α,26-diacetate (**22**) in a 2:3 ratio in 65% combined yield. Subsequent hydroboration and oxidation [37] on the above unsaturated and saturated mixture of **21** and **22**, accompanied by a simultaneous hydrolysis of bis-protected acetyl groups at C-3 and C-26 hydroxyl afforded the easy separation of the more polar (25*R*)-5α-cholestan-3α,15α,26-triol (**23**). Finally, selective acetylation of the primary C-26 hydroxyl by Otera's transesterification strategy [38], using vinyl acetate with distannoxane as a catalyst, afforded the aglycone of pavoninin-4 (**24**) in 80% yield.

**Scheme 2** Synthesis of the aglycone of the pavoninin-4 (**24**) by remote functionalization



### The First Attempt at the Glycosylation Reaction

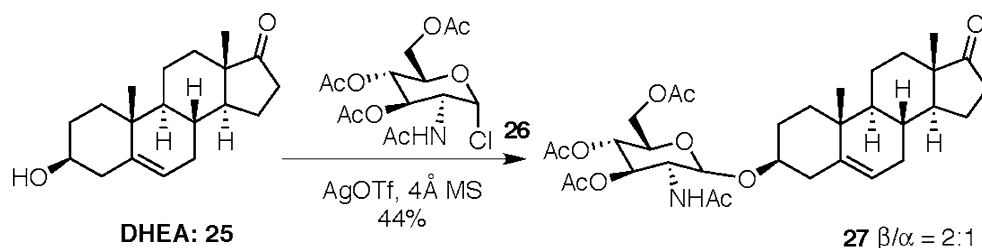
With both methods in place for making the C-15 $\alpha$  hydroxyl intermediate, we turned our attention to the glycosylation reaction on the steroid. We first tried to attach the *N*-acetylglucosamine to a C-16 $\beta$  hydroxyl steroid by using the commercially available 2-acetamido-2-deoxy- $\alpha$ -D-glucopyranosyl chloride 3,4,6-triacetate (**26**). Unfortunately, there was no reaction when using silver triflate as an activator [39]. So we tested the reaction conditions on 5-androsten-3 $\beta$ -ol-17-one (DHEA, **25**) as a model study. The result showed a successful glycosylation of DHEA that yielded the saponin **27** in 44% yield in a 2:1 ratio of  $\beta$ : $\alpha$  isomers (Scheme 3).

Many other activators have also been tried on this reaction. For example, iodine combined with DDQ [40], CdCO<sub>3</sub> [41], and thermal conditions as reported by Nishizawa et al. [42]. However, all these attempts failed, probably because the C-16 $\beta$  hydroxyl is so hindered by the steroid side chain that its reactivity is reduced in the glycosylation reaction. Therefore, we turned our attention to other glycosyl donors.

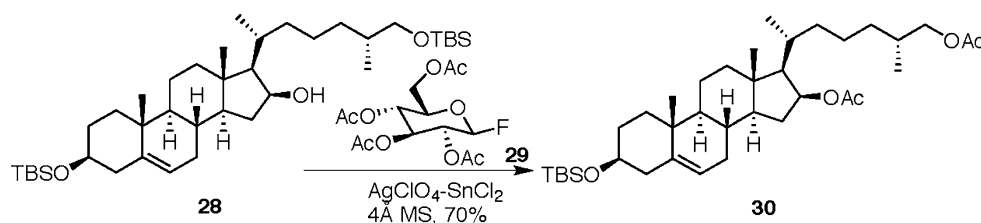
Because 2,3,4,6-*tetra-O*-acetyl-2-deoxy-D-glucopyranosyl fluoride (**29**) is commercially available, we decided to do another model study on the glycosylation

reaction using the glycosyl fluoride as a glycosyl donor. Following the procedure described by Mukaiyama et al. [43], we attempted to glycosylate the C-16 $\beta$  hydroxyl steroid (25*R*)-3 $\beta$ ,26-bis[(*tert*-butyldimethylsilyl)oxy]-cholest-5-en-16 $\beta$ -ol (**28**). However, the glycosylation reaction proceeded unexpectedly to yield (25*R*)-3 $\beta$ [(*tert*-butyldimethylsilyl)-oxy]-cholest-5-en-16 $\beta$ ,26-di-acetate (**30**) as an only product when glucosyl fluoride (**29**) was used as a glycosyl donor and AgClO<sub>4</sub>·SnCl<sub>2</sub> was used as an activator (Scheme 4). This result may be rationalized as a selective deprotection of the C-26 silyl protection group of **28** under the acidic glycosylation conditions, followed by an acetyl transfer between the resulting diol and the acetylated glucosyl fluoride **29**, due to catalyzation by the Lewis acid, SnCl<sub>2</sub>. Normally, the acetyl transfer can be avoided by using a less labile protection group [3]. Therefore, we tried the reaction by simply replacing the C-3 and C-26 bis-silyloxy groups with pivaloates (**31**). Under the same conditions, the glycosylation reaction went smoothly to afford the steroidal saponin **32** in 70% yield with a single  $\beta$  configuration based on proton NMR analysis of **32a**. When **32a** was treated with sodium methoxide in refluxing methanol, the C-16 $\beta$  analog of pavoninin-4, **32b**, was prepared in 90% yield (Scheme 5). Consequently, **32b** is also a structural analog of the OSW-1 [6], because

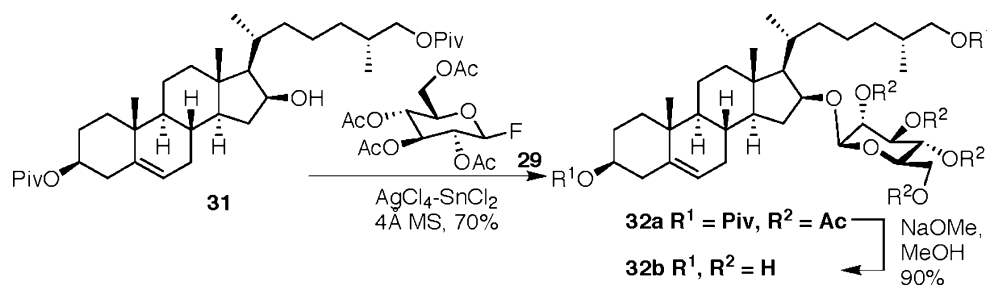
**Scheme 3** Glycosylation of DHEA using glycosyl chloride as a glycosyl donor



**Scheme 4** An unsuccessful glycosylation of the C-16 $\beta$  hydroxyl steroid, **3**



**Scheme 5** Synthesis of a C-16 $\beta$  analog of pavoninin-4 and OSW-1, **32b**



both are steroidal saponins with a sugar attachment on the same C-16 $\beta$  position of a steroid.

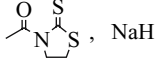
#### A Model Study on Selective Acetylation Reaction: Synthesis of a C-16 $\beta$ Analog of OSW-1 **32b** and **37**

Encouraged by the successful glycosylation of the hindered C-16 $\beta$  hydroxyl group, we turned our attention to selective acetylation at C-26 acetate of pavoninin-4 (**3**). In fact, five of the six pavoninins have an acetate group on the side chain at C-26 (see Fig. 1). The plan to introduce the C-26 acetate during a later stage of the synthesis would not work if the sugar alcohols were protected as acetates. Therefore, the benzyl group was used as a protecting group, since they could easily be removed by catalytic hydrogenation. We found that the benzyl-protected sugar fluoride, 2,3,4,6-tetra-*O*-benzyl-2-deoxy-D-glucopyranosyl fluoride (**33**) was commercially available, so we decided to pursue another model study on the chemoselective acetylation strategy (Scheme 6).

Under the same conditions, glycosylation of the hindered C-16 $\beta$  hydroxyl steroid **28** proceeded successfully to yield the saponin **34** in 70% yield, using the tetrabenzylated glucopyranosyl fluoride (**33**) as a donor. Subsequently, the C-3 and C-26 bis-silyl protection groups were removed with TBAF to afford a C-3 and C-26 diol **35**, which was then subjected to selective acetylation under three different conditions, as shown in Table 1.

Stork et al. achieved a selective acetylation of a primary alcohol in the presence of second alcohols by using 1.2 equiv. each of acetic anhydride and pyridine at  $-7^\circ\text{C}$ , in the total synthesis of prostaglandin  $F_{2\alpha}$  [44].

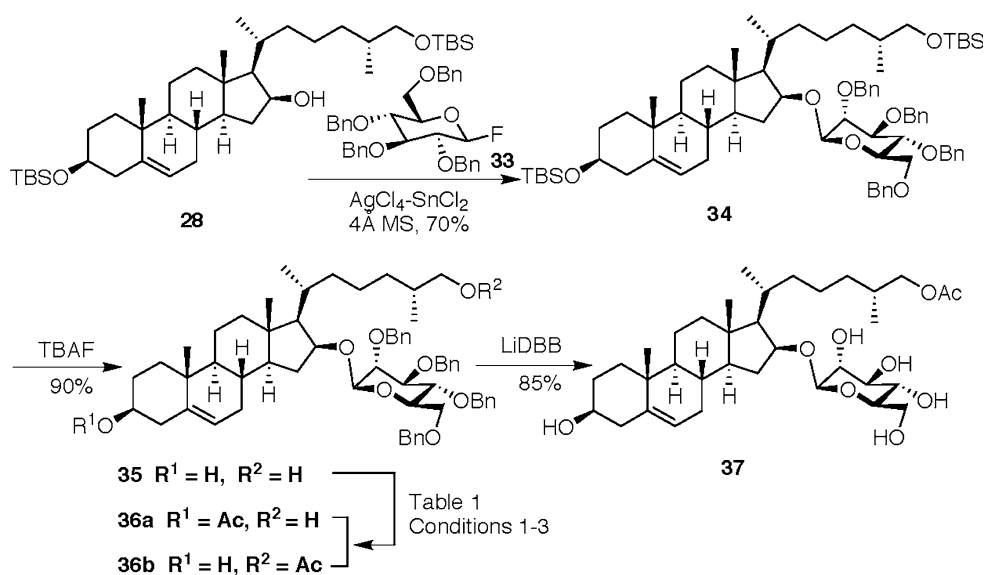
**Table 1** Selective acetylation of the saponin 3 $\beta$ ,26-diol **35**

Experiment	Condition	Yield (%)	Ratio (36a:36b)	Reference
1	Ac <sub>2</sub> O, pyr, 0–10 °C	N/A	N/A	Stork et al. [44]
2	 , NaH	50	~1:2	Yamada et al. [35]
3	Vinyl acetate, Bu <sub>8</sub> Sn <sub>4</sub> Cl <sub>4</sub> O <sub>2</sub>	80	~1:3	Otera et al. [38]

However, we found that the yield of chemoselective C-26 acetate **36** was poor when these conditions were used on the diol **35**, even after the reaction time was increased to three days. Therefore, Yamada's condition [35] for the highly selective acylation of di- and polyhydroxyl compounds by 3-acylthiazolidine-2-thiones was chosen as an alternative way to achieve the chemoselective acetylation of the C-3 and C-26 diol **35**. Results showed that two easily separated products **36a** and **36b** were prepared in 15% and 35% yields, respectively, which correspond to the selective acylation of C-3 and C-26 hydroxyls. This represents a considerable improvement over the yield obtained using Stork's conditions.

Otera used 1,3-dichlorodistannoxane as a catalyst for a highly selective acylation of alcohols [38]. When 1,3-dichlorodistannoxane was reacted with vinyl acetate in the presence of the diol **35**, the acetate group was transferred from the vinyl acetate to the C-3 (**36a**) or C-26 (**36b**) alcohol. The yield of the desired product

**Scheme 6** Synthesis of the C-16 $\beta$  analog of OSW-1 (**37**)



**36b** was dramatically increased to 60%. Furthermore, the ratio of **36b**:**36a** was increased from 2:1 to 3:1 with an 80% combined yield (Table 1).

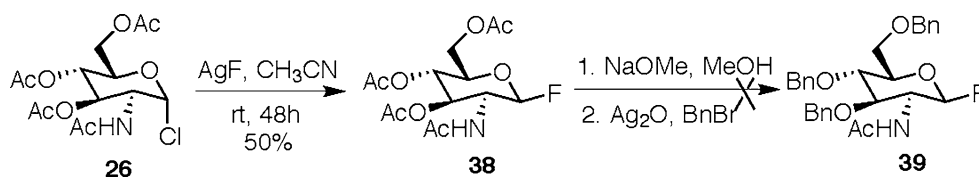
Finally, deprotection of benzyl groups on the sugar alcohols was achieved by LiDBB reduction [45], yielding **37**, the second C-16 $\beta$  analog of pavoninin-4 and OSW-1 in 85% yield (see Scheme 6).

#### Synthesis of 2-Acetamido-3,4,6-Tribenzyl-2-Deoxy-D-Glucopyranosyl Fluoride (**39**)

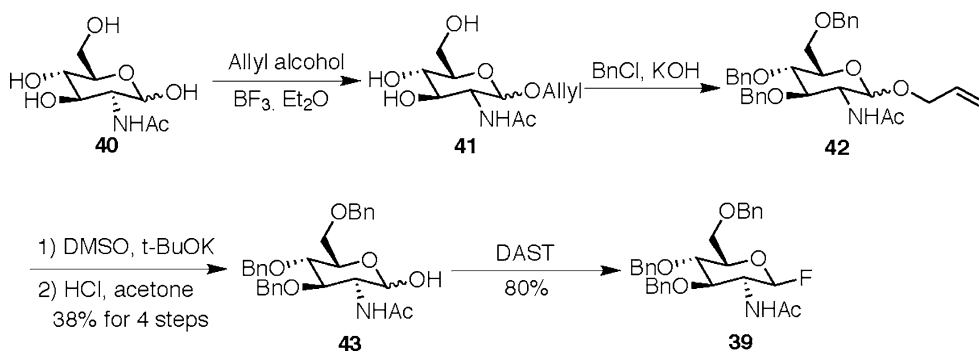
From the results of model studies on the glycosylation of the hindered alcohols and chemoselective acetylation, we have learned that the best sugar fluoride for the synthesis of pavoninin-4 should be a benzyl-protected *N*-acetyl sugar fluoride; that is, 2-acetamido-3,4,6-tribenzyl-2-deoxy-D-glucopyranosyl fluoride (**39**). Since this sugar product is not commercially available, we turned our attention to the synthesis of the desired glycosyl fluoride **39** (Scheme 7).

We first attempted to convert the 2-acetamido-3,4,6-triacetyl-2-deoxy-D-glucopyranosyl chloride (**26**) directly into a fluoride, 2-acetamido-3,4,6-triacetyl-2-deoxy-D-glucopyranosyl fluoride (**38**), by reaction of **26** with silver fluoride in dry acetonitrile [46]. The result showed a successful conversion and the expected fluoride **38** was prepared in 50% yield (Scheme 8). However, the following steps for replacing the acetate protecting groups with benzyl to synthesize **39** were difficult to achieve in high yield, probably due to the instability of the fluoride under the hydrolysis reaction conditions [46].

**Scheme 7** An unsuccessful synthesis of the glycosyl fluoride (**39**)



**Scheme 8** Synthesis of 2-acetamido-3,4,6-tribenzyl-2-deoxy-D-glucopyranosyl fluoride (**39**)

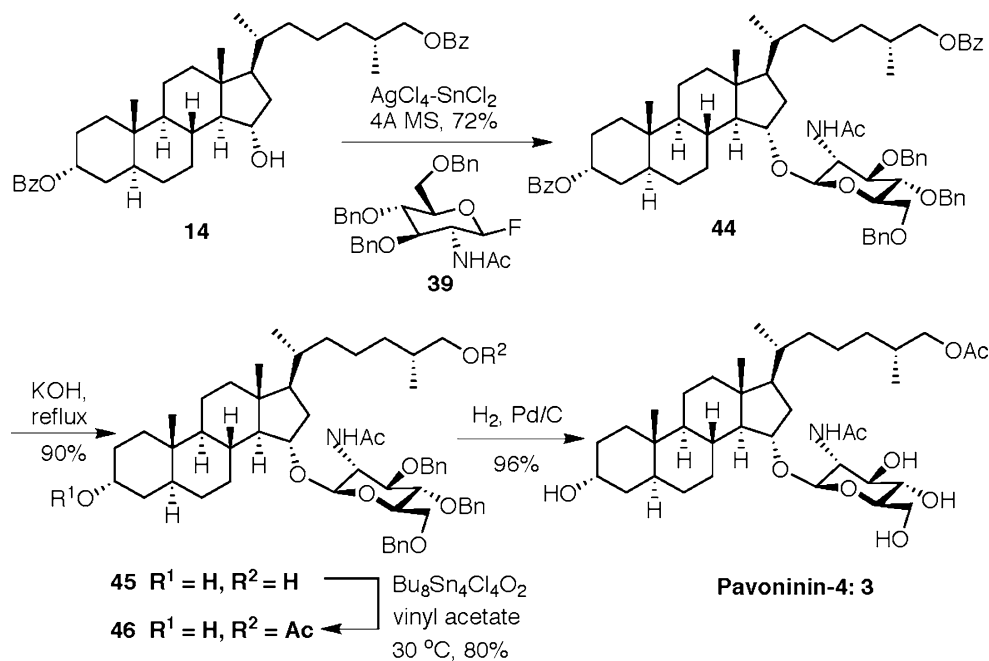


Alternatively, another commercially available sugar source, *N*-acetyl-D-glucosamine (**40**), was a readily available starting material. In four steps, **40** was converted into 2-acetamido-3,4,6-tribenzyl-2-deoxy-D-glucopyranose (**43**) in 38% yield [47]. Reaction of **43** with DAST afforded the 2-acetamido-3,4,6-tribenzyl-2-deoxy-D-glucopyranosyl fluoride **39** [48] as outlined in Scheme 8.

#### Synthesis of the Shark Repellent Pavoninin-4

Through the use of the fluoride **39**, glycosylation of the C-15 $\alpha$  hydroxyl intermediate **14**, with  $\text{AgClO}_4\text{-SnCl}_2$  used as an activator [43], proceeded very successfully to yield the saponin **44** in 72% yield plus 15% of recovered starting material. Exclusive formation of the  $\beta$ -glycoside may be explained by the intramolecular cyclization of the neighboring C-2 $\alpha$  acetamide function at the C-1 $\alpha$  position, directing the C-15 alcohol to attack  $\beta$  via an  $\text{S}_{\text{N}}2$  reaction to yield the  $\beta$ -glycoside **44**. Hydrolysis of C-3 and C-26 benzoyl-protecting groups using potassium hydroxide in methanol gave the expected C-3 and C-26 diol **45**. The C-26 acetate was selectively and efficiently introduced by Otera's transesterification using vinyl acetate under dioxane catalysis [35] to afford **46** in 80% yield. Deprotection of the benzyl ethers using catalytic hydrogenation afforded pavoninin-4 (**3**) (Scheme 9). The spectroscopic data for the synthetic pavoninin-4 were identical to those reported for the natural product [5].

**Scheme 9** Synthesis of the shark repellent pavoninin-4 (**3**)



## Conclusions

In summary, a broad range of biological effects have been ascribed to steroidal saponins: membrane-permeabilizing, hypocholesterolemic, immunostimulant, and anticancer properties. They have also been found to affect growth and food intake in animals and to act as antiviral and antifungal agents. Methods for the synthesis of C-15 $\alpha$  hydroxylated cholesterol were developed and applied to the synthesis of pavoninin-4 (**3**) starting from diosgenin **7**. The intermediate pavoninin-4 aglycone **24** was made by two routes: carbonyl reduction of an intermediate conjugated enone, and by remote functionalization. A general solution for glycosylation of hindered alcohols was explored using glycosyl fluorides as good glycosyl donors for the synthesis of steroidal saponins. A highly efficient method for the chemoselective acetylation of the C-26 primary alcohol of the cholesterol skeleton in the presence of *N*-acetylglucosamine is also reported. The syntheses of **32b** and **37**, structural analogs of OSW-1, are also described.

**Acknowledgment** Financial support for this research was provided by a grant from the Temple University Research Incentive Fund, GlaxoSmithKline, Pfizer, Bristol-Myers Squibb, Incyte and Merck.

## References

- Mahato SB, Ganguly AN, Sahu NP (1982) Steroid saponins. *Phytochemistry* 21:959–978
- Francis G, Kerem Z, Harinder MPS, Becker K (2002) The biological action of saponins in animal systems: a review. *Br J Nutr* 88:587–605
- Pellissier H (2004) The glycosylation of steroids. *Tetrahedron* 60:5123–5162
- Tachibana K, Sakaitani M, Nakanishi K (1984) Pavoninins: shark-repelling ichthyotoxins from the defense secretion of the Pacific sole. *Science* 226:703–705
- Tachibana K, Sakaitani M, Nakanishi K (1985) Pavoninins: shark-repelling and ichthyotoxic steroid *N*-acetylglucosaminides from the defense secretion of sole *Pardachirus pavoninus* (Soleidae). *Tetrahedron* 41:1027–1037
- Kubo S, Mimaki Y, Terao M, Sashida Y, Nikaida T, Ohmato T (1992) Acylated cholestane glycosides from the bulbs of *Ornithogalum saundersiae*. *Phytochemistry* 31:3969–3973
- Mimaki Y, Kuroda M, Kameyama A, Sashida Y, Hirano T, Oka K, Maekawa R, Wada T, Sugita K, Beutler JA (1997) Cholestane glycosides with potent cytostatic activities on various tumor cells from *Ornithogalum saundersiae* bulbs. *Bioorg Med Chem Lett* 7:633–636
- Makkar HPS, Becker K (1996) Effect of *Quillaja* saponins on in vitro rumen fermentation. In: Waller GR, Yamasaki Y (eds) *Saponinins used in food and agriculture*. Plenum, New York, pp 377–386
- Woldemichael GM, Wink M (2001) Identification and biological activities of triterpenoid saponins from *Chenopodium quinoa*. *J Agric Food Chem* 49:2327–2332
- Takechi M, Tanaka Y (1995) Haemolytic and time course differences between steroid and triterpenoid saponins. *Planta Med* 61:76–77
- Gee JM, Wortley GM, Johnson IT, Price KR, Rutten AAJJL, Houben GF, Penninks AH (1996) Effect of saponins and glycoalkaloids on the permeability and viability of mammalian intestinal cells and on the integrity of tissue preparations in vitro. *Toxicol In Vitro* 10:117–128
- Al-Habori M, Raman A (1998) Antidiabetic and hypocholesterolaemic effects of fenugreek (Review). *Phytother Res* 12:233–242



13. Oakenful DG, Sidhu GS (1990) Could saponins be a useful treatment for hypercholesterolaemia? *Eur J Clin Nutr* 44:79–88
14. Matsuura M (2001) Saponins in garlic as modifiers of the risk of cardiovascular disease. *J Nutr* 131:1000S–1005S
15. So HS, Yoon HS, Kwoon YS, Sung JH, Lee TG, Park EN, Cho HS, Lee BM, Cho JM, Ryu WS (1997) Effect of a novel adjuvant derived from *Quillaja saponaria* on immune response to recombinant hepatitis B surface antigen. *Mol Biol Cell* 7:176–186
16. Cai J, Liu M, Wang Z, Ju Y (2002) Apoptosis induced by dioscin in HeLa cells. *Biol Pharm Bull* 25:193–196
17. Mader TL, Brumm MC (1987) Effect of feeding sarsasaponin in cattle and swine diets. *J Anim Sci* 65:9–15
18. Lu CD, Jorgensen NA (1987) Alfalfa saponins affect site and extent of nutrient digestion in ruminants. *J Nutr* 117:919–927
19. Roy PK, Munshi JD, Dutta HM (1990) Effect of saponin extracts on morpho-history and respiratory physiology of an air breathing fish *Heteropneustes fossilis* (Bloch). *J Freshw Biol* 2:135–145
20. Jenkins KJ, Atwal AS (1994) Effects of dietary saponins on fecal bile acids and neutral sterols, and availability of vitamins A and E in the chick. *J Nutr Biochem* 5:134–138
21. Potter SM, Jimnez-Flores R, Pollack J, Lone TA, Berber-Jimenez MD (1993) Protein saponin interaction and its influence on blood lipids. *J Agric Food Chem* 41:1287–1291
22. Ohnishi Y, Tachibana K (1997) Synthesis of pavoninin-1, a shark repellent substance, and its structural analogues toward mechanistic studies on their membrane perturbation. *Bioorg Med Chem* 5:2251–2265
23. Kim HS, Kim IC, Lee SO (1997) Synthesis of two marine natural products: the aglycones of pavoninin-1 and -2. *Tetrahedron* 53:8129–8136
24. Williams JR, Chai D, Gong H, Zhao W, Wright D (2002) Studies toward the synthesis of the shark repellent pavoninin-5. *Lipids* 37:1193–1195
25. Williams JR, Chai D, Bloxton JD II, Gong H, Solvibile WR (2003) Synthesis of the aglycone of 26-*O*-deacetyl pavoninin-5. *Tetrahedron* 59:3183–3188
26. Williams JR, Gong H, Nathan H, Olubodun OI (2005) Synthesis of the shark repellent pavoninin-4. *J Org Chem* 70:10732–10736
27. Gong H, Williams JR (2006) Synthesis of the aglycone of the shark repellent pavoninin-4 using remote functionalization. *Org Lett* 8:2253–2255
28. Williams JR, Gong H (2004) Isolation and synthesis of shark-repelling saponins. *Lipids* 39:795–799
29. Dembinski R (2004) Recent advances in the Mitsunobu reaction: modified reagents and the quest for chromatography-free separation. *Eur J Org Chem* 2763–2772
30. Williams JR, Gong H, Nathan H, Olubodun OI, Carrol PJ (2004)  $\alpha$ -Hydroxylation at C-15 and C-16 in cholesterol: synthesis of (25*R*)-5 $\alpha$ -cholesta-3 $\beta$ ,15 $\alpha$ ,26-triol and (25*R*)-5 $\alpha$ -cholesta-3 $\beta$ ,16 $\alpha$ ,26-triol from diosgenin. *Org Lett* 6:269–271
31. Kim HS, Oh SH (1993) Chemical synthesis of 15-ketosterols. *Bioorg Med Chem Lett* 3:1339–1342
32. Luche J-L (1978) Lanthanides in organic chemistry. 1: Selective 1,2 reductions of conjugated ketones. *J Am Chem Soc* 100:2226–2227
33. Williams JR, Chai D, Wright D (2002) Synthesis of (25*R*)-26-hydroxycholesterol. *Steroids* 67:1041–1044
34. Breslow R, Baldwin S, Flechtner T, Kalicky P, Liu S, Washburn W (1973) Remote oxidation of steroids by photolysis of attached benzophenone groups. *J Am Chem Soc* 95:3251–3262
35. Yamada S (1992) Highly selective acylation of di- and polyhydroxyl compounds by 3-acylthiazolidine-2-thiones. *J Org Chem* 57:1591–1592
36. Zderic JA, Kubitschek MJ, Bonner WA (1961) Synthesis of *p*-benzoylmandelic acid. *J Org Chem* 26:1635–1637
37. Taylor EJ, Djerassi C (1977) Synthesis of cholest-5-ene-3 $\beta$ ,11 $\alpha$ ,15 $\beta$ -triol-7-one. A model for the steroid nucleus of oogoniol, a sex hormone of the water mold achlya. *J Org Chem* 42:3571–3579
38. Orita A, Mitsutome A, Otera J (1998) Distannoxane-catalyzed highly selective acylation of alcohols. *J Org Chem* 63:2420–2421
39. Saito S, Ichinose K, Sasaki Y, Sumita S (1992) Syntheses of glycyrrhetic acid  $\alpha$ -diglycosides and enol  $\alpha$ -glycosides. *Chem Pharm Bull* 40:3261–3268
40. Ravindranathan Kartha KP, Aloui M, Field RA (1996) Iodine: a versatile reagent in carbohydrate chemistry III. efficient activation of glycosyl halides in combination with DDQ. *Tetrahedron Lett* 37(48):8807–8810
41. Suzuki E, Namba S, Kurihara H, Goto J, Matsuki Y, Nambara T (1995) Synthesis of 15 $\alpha$ -hydroxyestrogen 15-*N*-acetylglucosaminides. *Steroids* 60:277–284
42. Nishizawa M, Shimomoto W, Momii F, Yamada H (1992) Stereoselective thermal glycosylation of 2-deoxy-2-acetamino-3,4,6-tri-*O*-acetyl- $\alpha$ -D-glucopyranosyl chloride. *Tetrahedron Lett* 33:1907–1908
43. Mukaiyama T, Murai Y, Shoda S (1981) An efficient method for glycosylation of hydroxy compounds using glucopyranosyl fluoride. *Chem Lett* 431–432
44. Stork G, Takahashi T, Kawamoto I, Suzuki T (1978) Total synthesis of prostaglandin F<sub>2 $\alpha$</sub>  by chirality transfer from D-glucose. *J Am Chem Soc* 100:8272–8273
45. Freeman PK, Hutchinson LL (1980) Alkylolithium reagents from alkyl halides and lithium radical anions. *J Org Chem* 45(10):1924–1930
46. Thiem J, Wiesner M (1988) Alkylation of glycosyl fluorides. *Synthesis* 2:124–127
47. Hoffmann M, Burkhart F, Hessler G, Kessler H (1996) C-Glycoside analogs of N4-(2-acetamido-2-deoxy- $\alpha$ -D-glucopyranosyl)-L-asparagine. Synthesis and conformational analysis of a cyclic C-glycopeptide. *Helv Chim Acta* 79:1519–1532
48. Posner GH, Haines SR (1985) A convenient, one-step, high-yield replacement of an anomeric hydroxyl group by a fluorine atom using DAST. Preparation of glycosyl fluorides. *Tetrahedron Lett* 26:5–8

# The Liebermann–Burchard Reaction: Sulfonation, Desaturation, and Rearrangement of Cholesterol in Acid

Quanbo Xiong · William K. Wilson · Jihai Pang

Received: 30 October 2006 / Accepted: 11 December 2006 / Published online: 18 January 2007  
© AOCS 2007

**Abstract** In the Liebermann–Burchard (LB) colorimetric assay, treatment of cholesterol with sulfuric acid, acetic anhydride, and acetic acid elicits a blue color. We studied the reactivity of cholesterol under LB conditions and provide definitive NMR characterization for approximately 20 products, whose structure and distribution suggest the following mechanistic picture. The major reaction pathways do not involve cholestadienes, i-steroids, or cholesterol dimers, as proposed previously. Instead, cholesterol and its acetate and sulfate derivatives undergo sulfonation at a variety of positions, often with skeletal rearrangements. Elimination of an  $\text{SO}_3\text{H}$  group as  $\text{H}_2\text{SO}_3$  generates a new double bond. Repetition of this desaturation process leads to polyenes and ultimately to aromatic steroids. Linearly conjugated polyene cations can appear blue but form too slowly to account for the LB color response, whose chemical origin remains unidentified. Nevertheless, the classical polyene cation model is not excluded for Salkowski conditions (sulfuric acid), which immediately generate consider-

able amounts of cholesta-3,5-diene. Some rearrangements of cholesterol in  $\text{H}_2\text{SO}_4$  resemble the diagenesis pathways of sterols and may furnish useful lipid biomarkers for characterizing geological systems.

**Keywords** Sterol · Colorimetric test · NMR · Mass spectrometry · Sulfone · Rearrangement · Diagenesis

## Abbreviations

ES	Electrospray
FAB	Fast-atom bombardment
HPLC	High-performance liquid chromatography
LB	Liebermann–Burchard
NBA	3-Nitrobenzyl alcohol
TLC	Thin-layer chromatography

## Introduction

Numerous colorimetric tests have been devised for the identification and quantitation of steroids [1]. Perhaps the foremost of these methods is the Liebermann–Burchard (LB) reaction, which was the leading assay for serum cholesterol in clinical laboratories during most of the twentieth century [2–4] and is still recommended by the USA Food and Drug Administration as a standard against which new methods are compared [5]. The LB reaction was first described in 1885 by Liebermann [6] and was later investigated extensively by Burchard [7]. Burchard developed the reaction into a quantitative test for cholesterol and used this assay to confirm the widespread presence of sterols in animal and plant tissues. The LB reaction has been studied for many other sterols; the color response varies markedly

---

Q. Xiong (✉)  
Department of Pharmaceutical Sciences,  
Texas Southern University, 3100 Cleburne Street,  
Houston, TX 77004, USA  
e-mail: xiongq@tsu.edu

Q. Xiong · W. K. Wilson · J. Pang  
Department of Biochemistry and Cell Biology,  
Rice University, Houston, TX, USA

*Present Address:*  
J. Pang  
Pharmaceutical Development Center,  
MD Anderson Cancer Center, University of Texas,  
Houston, TX, USA

depending on the double bond system [8], other functional groups, and the presence of a nonpolar side chain [9] (Fig. 1).

The mechanism that generates the LB color response has intrigued chemists for over 100 years, and much work was carried out even before the structure of sterols was established [10]. During the past 50 years, the color response has been attributed to polyene cations formed under LB conditions. Following Watanabe's [11] 1959 proposal of a tetraene dimer complexed with acid, Brieskorn and Hofmann [9] suggested the formation of a  $\Delta 4,6,8(14),15,17(20)$  steroid complex from cholesterol by a series of sulfonations with  $\text{SO}_3$ , coupled with elimination of  $\text{SO}_2$ . Key mechanistic analyses in 1974 [12, 13] supported and refined the polyene cation hypothesis, but extensive kinetic measurements failed to correlate  $\text{SO}_2$  evolution from the LB reaction with the color response. These and other mechanistic studies were summarized by Zuman [14] in 1991 in a comprehensive review covering the LB reaction and similar colorimetric assays.

A major weakness of the mechanistic work has been the lack of knowledge about the LB reaction pathways. Very few LB products have been characterized beyond UV and combustion analyses, and no polar intermediates have been reported apart from steryl sulfates and perchlorates. Investigators variously postulate cholesterol dimers [11, 15], cholestadienes [9, 12, 13], or epicholesterol derivatives [9] as pivotal intermediates without any evidence of their quantitative importance. As a result, the behavior of cholesterol in strongly acidic solution is still poorly understood.

We have now investigated the LB reaction with modern chromatographic and spectral methods. In situ NMR analysis and experiments with  $^{14}\text{C}$ -labeled cholesterol were used to trace the increasing levels of polar products as the reaction progresses. Preparative high-performance liquid chromatography (HPLC) and thin-layer chromatography (TLC) led to the isolation of numerous reaction products, whose structures were

determined by 2D NMR in conjunction with quantum-mechanical NMR calculations. The results indicated that cholesterol is rapidly converted to acetate and sulfate derivatives, which are slowly desaturated via sulfonic acids, eventually rearranging to aromatic steroids. These new insights into the behavior of cholesterol under LB conditions are discussed with regard to the chemical origin of the color response.

## Experimental Procedures

### Materials

Solvents and reagents were chromatography or reagent grade; chloroform was amylene-stabilized from bottles less than 6 months old unless otherwise specified. Deuterated reagents (acetic acid, acetic anhydride, and sulfuric acid) were obtained from Aldrich (Milwaukee, WI, USA). Commercial cholesterol (**1**) was purified via the dibromide and then recrystallized from methanol to remove oxysterol contaminants. [ $4\text{-}^{14}\text{C}$ ]Cholesterol was obtained from Amersham, and its purity was confirmed by radio-TLC (ethyl acetate/hexanes 2:7). A cholesteryl sulfate standard was purchased from Steraloids (Newport, RI, USA).

### LB Reaction

The LB color reagent was prepared freshly, as described by Abell et al. [16], by adding concentrated  $\text{H}_2\text{SO}_4$  to acetic anhydride at  $0\text{ }^\circ\text{C}$ , stirring for 10 min, adding acetic acid, and warming to room temperature. The proportion of  $\text{H}_2\text{SO}_4$ , acetic anhydride, and acetic acid is specified for each experiment, varying from the classic 1:20:10 (v/v) ratio to 8:20:10. Whereas the LB reagent is usually added directly to a dry residue in clinical protocols [16], we followed Burchard [7] in adding the reagent to a solution of cholesterol in chloroform; this facilitated in situ NMR studies and mixing in low-temperature experiments without qualitatively altering the color response.

### Spectral Methods

$^1\text{H}$  NMR and  $^{13}\text{C}$  NMR spectra of steroids were acquired at  $25\text{ }^\circ\text{C}$  in relatively dilute solution (1–20 mM) with Bruker AMX and Avance 500-MHz spectrometers. Proton spectra were referenced to tetramethylsilane;  $^{13}\text{C}$  spectra were referenced to  $\text{CDCl}_3$  at 77.0 ppm or  $\text{CD}_3\text{OD}$  at 49.0 ppm. Chemical shift reproducibility was about  $\pm 0.001$  ppm for  $^1\text{H}$  (except for protons near functional groups in  $\text{CD}_3\text{OD}$  solution)

	1 min	30 min	1 h
<b>LB conditions: conc. <math>\text{H}_2\text{SO}_4</math>, <math>\text{Ac}_2\text{O}</math>, <math>\text{AcOH}</math></b>			
cholesterol	colorless	blue	green
7-dehydrocholesterol	pink	blue	pale green
5 $\alpha$ -cholesta-8,14-dien-3 $\beta$ -ol	blue	intense blue	
19-norcholesta-5,7,9-trien-3 $\beta$ -ol	no color response		
C <sub>19</sub> steroids and bile acids	no color response		
<b>Salkowski conditions: conc. <math>\text{H}_2\text{SO}_4</math></b>			
cholesterol	pink	red	red

**Fig. 1** Colorimetric behavior of sterols under acidic conditions

and about  $\pm 0.03$  ppm for  $^{13}\text{C}$ . Mass spectra were obtained by direct probe using a ZAB-HF spectrometer with electron-impact ionization (70 eV) or fast-atom bombardment (FAB) in a matrix of glycerol or 3-nitrobenzyl alcohol (NBA). Higher-resolution mass spectra were acquired by infusing methanol solutions into a Waters (Micromass) Q-TOF Ultima with positive (ES+) or negative (ES-) electrospray ionization. Spectrophotometric analysis of LB reactions was done in 1.4- or 3.5-mL quartz cuvettes (10-mm path length) using a Shimadzu 1601 spectrophotometer. Radioactivity was measured with a Packard model 1500 liquid scintillation analyzer using ScintiVerse or toluene/2,5-diphenyloxazole.

### Quantum-Mechanical NMR Calculations

NMR shieldings were calculated with Gaussian 03 [17] by the gauge independent atomic orbital method at the B3P91/6-311G(d,p)//B3LYP/6-31G(d) level. The shieldings were converted to chemical shifts using empirical adjustments (L.-W. Guo, W. K. Wilson, and C. H. L. Shackleton, unpublished results). The structures of **10–20** were confirmed by comparing the observed  $^1\text{H}$  and  $^{13}\text{C}$  NMR chemical shifts with predicted shieldings, as described previously [18]. The agreement was generally within 0.1 ppm for  $^1\text{H}$  and within 1 ppm for  $^{13}\text{C}$ , except for systematic deviations affecting nuclei influenced by sulfonate groups. Sulfonates were modeled as sulfonic acids to compensate for hydrogen bonding; the model did not include solvation. The predicted shieldings greatly facilitated signal assignments, spectral interpretation, and positioning of sulfonate groups.

## Results

### Preliminary Studies of the LB Reaction

We initially explored many variations of the LB reaction. Under nearly all conditions, the reaction progressed from colorless, to pale blue, blue, bluish green, and green. A modified LB reagent with a 4:20:10 ratio (elevated amount of  $\text{H}_2\text{SO}_4$ ) increased the absorbance and was used in some studies. LB reactions with ethanol-stabilized chloroform were more sluggish than reactions with amylene-stabilized chloroform, producing the same sequence of colors but with lower absorbance. Omitting both acetic acid and anhydride, i.e., Salkowski conditions [19, 20], produced a red color, but other variations of LB conditions had no qualitative effect on color formation. Intermediate

stages of the LB reaction could be preserved for kinetic and NMR studies by maintaining the temperature below  $-20^\circ\text{C}$ . Substituting dichloromethane for chloroform reduced the reaction viscosity at low temperatures without affecting the color response. Quenching was explored by dropwise addition of cold 24% NaOH, ethanol, methanol, or pyridine, the last three reactions requiring subsequent neutralization with aqueous NaOH. Even nucleophilic quenching reagents generated only modest amounts of adducts with the nucleophile. The aim of quenching was to obtain stable products that reveal the structure of intermediates. Nevertheless, some workup conditions may have resulted in ester hydrolysis or further sulfonation.

### Studies of LB Reaction Products with $[4-^{14}\text{C}]$ Cholesterol

Reaction of  $[4-^{14}\text{C}]$ cholesterol (25 mg; 500,000 dpm) in chloroform (15 mL) with LB reagent (2.5 mL, 1:20:10 ratio) at room temperature produced a bluish-green color after 30 min. The mixture was immediately chilled to  $-70^\circ\text{C}$  and quenched by dropwise addition of cold 24% NaOH (10 mL). Scintillation counting of the resulting aqueous and organic layers and the precipitate indicated a 70:22:8 distribution of radioactivity. Chilling the aqueous layer to  $-20^\circ\text{C}$  produced more precipitate, corresponding to almost half the aqueous-layer radioactivity. A duplicate experiment gave similar results. With a more concentrated solution of cholesterol (250 mg) in chloroform (15 mL) and LB reagent (2.5 mL, 4:20:10 ratio), the distribution of the  $^{14}\text{C}$  label was 3:33:64 (aqueous layer, organic layer, precipitate). The precipitate was predominantly cholesteryl sulfate (see later). These results indicate that most of the cholesterol is converted to highly polar products that are insoluble in chloroform.

### Sterols Produced by LB Reaction A

To a solution of cholesterol (250 mg) in chloroform (25 mL; stabilized with 0.75% ethanol) was added LB reagent (1:20:10 ratio, 10 mL). The solution gradually turned blue and, before any appearance of green color, the reaction was quenched with 24% aqueous NaOH (3 mL) followed by water (20 mL). The precipitate that formed between the chloroform and the aqueous layers was identified as cholesteryl sulfate (**2**, 81 mg, above 99% purity). Evaporation of the chloroform layer gave a residue (201 mg) comprising cholesteryl acetate (**3**), with traces of *i*-steroids (3 $\alpha$ ,5 $\alpha$ -cyclocholestanes) and other sterols. This residue was subjected

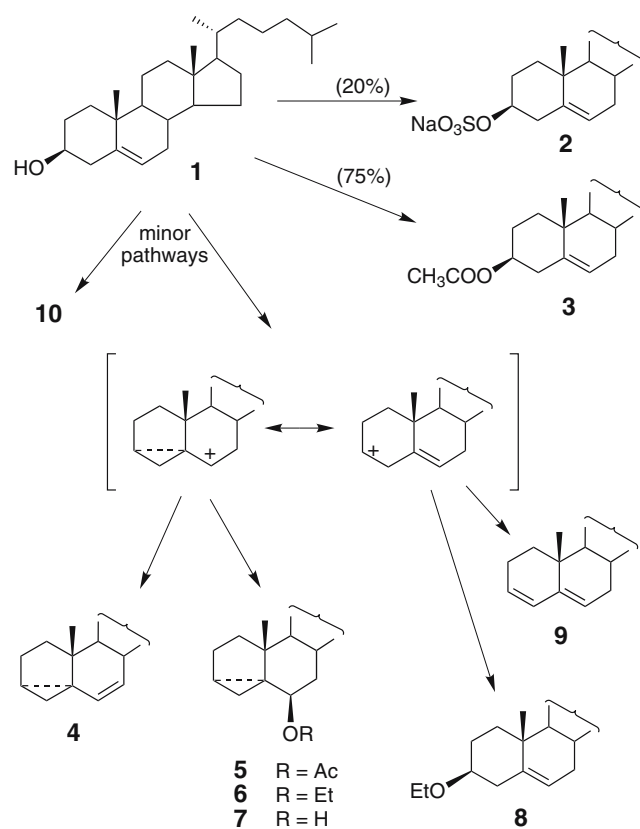


**Fig. 2** Products from Liebermann–Burchard (LB) reactions quenched at the blue stage. The initial major products **2** and **3** are subsequently converted to polar steroids

to repeated column chromatography and TLC (silica gel; ethyl acetate/hexane 1:5, 1:8, and 1:40); the products in order of increasing polarity were the Δ<sup>6</sup> i-steroid **4** (0.2 mg), **3** (130 mg), 6β-acetoxy i-steroid **5** (1 mg), 6β-ethoxy i-steroid **6** (1 mg), cholesteryl ethyl ether (**8**; 1 mg), and 6β-hydroxy i-steroid **7** (0.5 mg). These compounds, which were identified by NMR, are shown in Fig. 2.

NMR data: **2** (CD<sub>3</sub>OD, δ<sub>H</sub>) 0.718 (s), 0.877 (d, 6.6 Hz), 0.881 (d, 6.6 Hz), 0.943 (d, 6.6 Hz), 1.031 (s), 2.341 (dddd, 13.4, 11.7, 3.4, 2.8, 2.1 Hz), 2.530 (ddd, 13.4, 5.0, 2.4 Hz), 4.129 (tt, 11.5, 4.7 Hz), 5.385 (dt, 5.4, 2.1 Hz); **4** (CDCl<sub>3</sub>, δ<sub>H</sub>) 0.435 (dd, 8.0, 5.0 Hz), 0.718 (s), 0.863 (d, 6.6 Hz), 0.867 (d, 6.6 Hz), 0.897 (s), 0.903 (d, 6.6 Hz), 5.185 (dd, 9.8, 2.6 Hz), 5.522 (dd, 9.8, 1.9 Hz); **5** (CDCl<sub>3</sub>, δ<sub>H</sub>) 0.413 (dd, 8.3, 5.3 Hz), 0.499 (dd, 5.1, 3.8 Hz), 0.726 (s), 0.863 (d, 6.6 Hz), 0.867 (d, 6.6 Hz), 0.912 (d, 6.6 Hz), 1.009 (s), 2.048 (s), 4.508 (t, 3.0 Hz); **6** (CDCl<sub>3</sub>, δ<sub>H</sub>) 0.377 (dd, 8.3, 5.3 Hz), 0.616 (dd, 5.0, 3.7 Hz), 0.720 (s), 0.863 (d, 6.6 Hz), 0.868 (d, 6.6 Hz), 0.910 (d, 6.6 Hz), 1.013 (s), 1.148 (t, 7.0 Hz), 2.863 (t, 2.9 Hz), 3.377 (dq, 9.5, 7.0 Hz), 3.600 (dq, 9.5, 7.0 Hz); **7** (CDCl<sub>3</sub>, δ<sub>H</sub>) 0.291 (ddd, 8.1, 4.8, 0.8), 0.523 (dd, 4.8, 3.8 Hz), 0.721 (s), 0.863 (d, 6.6 Hz), 0.867 (d, 6.6 Hz),

0.912 (d, 6.6 Hz), 1.057 (s), 1.999 (dt, 12.7, 3.5 Hz), 3.261 (t, 3.0 Hz); **8** (CDCl<sub>3</sub>, δ<sub>H</sub>) 0.677 (s), 0.863 (d, 6.6 Hz), 0.867 (d, 6.6 Hz), 0.914 (d, 6.6 Hz), 1.002 (s), 1.200 (t, 7.0 Hz), 3.155 (tt, 11.3, 4.4 Hz), 3.52 (dq, 9.2, 7.0 Hz), 3.53 (dq, 9.2, 7.0 Hz), 5.345 (dt, 5.2, 2.1 Hz).

Similar LB reactions, carried out and quenched under a variety of mild conditions, also generated mainly **2** and **3**, often with traces of i-steroids, sultone **10** (see later), and Δ<sup>3,5</sup> diene **9**. NMR of **9**: (CDCl<sub>3</sub>, δ<sub>H</sub>) 0.704 (s), 0.864 (d, 6.6 Hz), 0.869 (d, 6.6 Hz), 0.921 (d, 6.6 Hz), 0.953 (s), 5.388 (br dd, 5, 2 Hz), 5.588 (br dd, 10, 5 Hz), 5.926 (dd, 9.8, 2.7 Hz). No other hydrophobic sterols were observed in LB reactions, apart from **11** and artifactual products like cholesteryl chloride [δ<sub>H</sub> 0.675 (s), 1.027 (s), 3.766 (tt), 5.370 (dt)] and esters of 7-hydroxycholesterol [e.g., δ<sub>H</sub> 0.689 (s), 1.055 (s), 5.606 (t, 2 Hz)].

### Sterols Produced by LB Reaction B

To a solution of cholesterol (2 g) in chloroform (40 mL) was added LB reagent (4:20:10 ratio, 20 mL). After 30 min at room temperature, the bluish-green solution was chilled and quenched with ethanol (60 mL) at −78 °C. The resulting yellowish-green mixture was evaporated in vacuo at 40 °C until there was no odor of acetic acid. Water (15 mL) and 24% aqueous NaOH (2–3 mL) were added to adjust the pH to 8. This solution was extracted with chloroform (2 × 20 mL); no precipitate was observed. The organic phase was evaporated to a brown residue (0.37 g); <sup>1</sup>H NMR indicated a complex mixture comprising mainly **1**, **3**, **10**, and **11**, with traces of i-steroids but no **9** or backbone rearrangement products [21]; reversed-phase chromatography (C<sub>18</sub> column, elution with 70–100% methanol in water) gave sultone **10** and (after further purification by C<sub>8</sub> HPLC) the phenanthrene derivative **11**, which were characterized by NMR (Tables 1, 2).

The aqueous phase was evaporated in vacuo to a solid, suspended in methanol (40 mL) with sonication, and centrifuged at 3,000 rpm for 10 min. The methanolic supernatant was evaporated to a residue (5.3 g), which was chromatographed on a 200-g C<sub>18</sub> column (50–100% methanol in water) to give, in order of elution, **15**, **18**, **12**, **17**, **19**, **20**, **13**, **14**, and **16**. Compounds **12–14** crystallized as colorless needles, but most other sterols were eluted as mixtures that were further purified by HPLC or TLC on C<sub>18</sub> media. Apart from **2**, the polar sterols comprised a multiplicity of minor products. In addition to compounds **12–20** (roughly 5–10 mg each), at least ten unidentified polar sterols were noted, together with a larger number of less abundant products.

**Table 1**  $^1\text{H}$  NMR chemical shifts of Liebermann–Burchard (LB) reaction products from cholesterol

	10	11	12	13	14	15	16	17	18	19	20
H-1 $\alpha$	2.269	8.569	2.449	2.430	2.529	1.434	1.893	2.331	2.356	8.080	7.942
H-1 $\beta$	1.741		2.288	2.275	2.219	2.298	1.302		2.615		
H-2 $\alpha$	2.678	7.501	1.467	1.530	1.524	3.233	2.138	6.988	7.190	7.471	7.349
H-2 $\beta$	1.909		2.196	1.737	1.844		2.21				
H-3 $\alpha$	5.056	7.393	4.651	3.977	5.052	4.359	5.787	7.004		7.489	7.297
H-4 $\alpha$	1.910		1.596	1.699	1.544	5.598	7.230	7.127		7.970	
H-4 $\beta$	2.084		3.127	2.714	3.019						
H-6 $\alpha$		7.903							7.200		7.813
H-6 $\beta$	3.206		2.789	2.791	2.782	3.619		5.089			
H-7 $\alpha$	1.509	7.751	2.079	1.941	1.928	1.260	2.008	3.202	6.505	8.406	8.543
H-7 $\beta$	2.229		1.940	2.083	2.086	2.439	2.652				
H-8 $\beta$	2.105		2.07	2.068	2.084	2.192	1.653	2.451			
H-9 $\alpha$						0.755	0.977	3.067	2.42		
H-11 $\alpha$	2.519	8.342	2.554	2.542	2.549	1.568	1.597	2.443	1.71	3.20 <sup>a</sup>	3.23 <sup>a</sup>
H-11 $\beta$	1.960		1.979	1.973	1.991	1.454	1.455	1.268	1.68	3.22 <sup>a</sup>	3.26 <sup>a</sup>
H-12 $\alpha$	1.177		1.113	1.096	1.116	1.155	1.213	1.490	1.301	1.993	2.005
H-12 $\beta$	1.960		2.051	2.053	2.059	2.035	2.065	2.014	2.126	2.255	2.259
H-14 $\alpha$	1.042		1.460	1.438	1.463	0.952	1.092	2.086			
H-15 $\alpha$	1.650	3.24 <sup>a</sup>	1.761	1.764	1.761	1.653	1.712	2.142	2.50 <sup>a</sup>		
H-15 $\beta$	1.170	3.26 <sup>a</sup>	1.158	1.158	1.162	1.245	1.175	1.234	2.36 <sup>a</sup>		
H-16 $\alpha$	1.867	2.20 <sup>a</sup>	1.871	1.871	1.875	1.854	1.888	1.940	1.964	3.120	3.122
H-16 $\beta$	1.310	2.22 <sup>a</sup>	1.292	1.294	1.299	1.290	1.319	1.312	1.529	2.666	2.678
H-17 $\alpha$	1.084	3.462	1.135	1.123	1.134	1.110	1.141	1.287	1.230	1.811	1.823
H-18	0.770	2.577	0.853	0.850	0.856	0.738	0.741	0.805	0.958	0.961	0.969
H-19	1.614	2.748	1.457	1.439	1.425	1.343	1.030	2.331	0.900	2.646	2.659
H-20	1.395	2.046	1.418	1.420	1.423	1.397	1.413	1.46	1.533	1.715	1.725
H-21	0.903	1.083	0.927	0.927	0.927	0.934	0.949	0.966	0.992	1.079	1.083
H-22R	1.335	0.95 <sup>a</sup>	1.37	1.38	1.37	1.38	1.39	1.40	1.40	1.52	1.52
H-22S	0.988	0.99 <sup>a</sup>	1.010	1.010	1.012	1.013	1.028	1.05	1.11	1.19	1.19
H-23R	1.33	1.28 <sup>a</sup>	1.37	1.38	1.37	1.38	1.38	1.40	1.38	1.47	1.47
H-23S	1.14	0.95 <sup>a</sup>	1.17	1.182	1.18	1.18	1.19	1.18	1.19	1.29	1.29
H-24	1.10	0.93	1.11	1.11	1.11	1.11	1.11	1.12	1.12	1.21	1.21
H-24	1.14	0.93	1.15	1.15	1.15	1.15	1.16	1.15	1.15	1.21	1.21
H-25	1.515	1.337	1.526	1.526	1.526	1.526	1.531	1.539	1.526	1.576	1.577
H-26	0.861	0.721 <sup>a</sup>	0.875	0.875	0.875	0.876	0.879	0.885	0.886	0.909 <sup>a</sup>	0.909 <sup>a</sup>
H-27	0.865	0.733 <sup>a</sup>	0.879	0.879	0.879	0.880	0.883	0.888	0.889	0.910 <sup>a</sup>	0.910 <sup>a</sup>

Chemical shifts were measured at 25°C in  $\text{CDCl}_3$  (**10**, **11**) or  $\text{CD}_3\text{OD}$  (**12–20**)

<sup>a</sup> Assignments of geminal or stereoisomeric pairs that may be interchanged. For ring A signals of **10**,  $\alpha$  denotes the sultone side. Coupling constants: H18 and H19 were singlets, H21, H26, and H27 were doublets (approximately 6.6 Hz), and H25 nonets (6.6 Hz); other notable couplings: **10**, H-1 $\alpha$ , dddd, 14.1, 12.5, 4.0, 1.6 Hz; H-1 $\beta$ , dddd, 14.1, 9.2, 5.3, 1.8 Hz; H-2 $\alpha$ , dddd, 13, 9, 4, 3 Hz; H-3 $\beta$ , ddd, 4.8, 3.1, 1.1 Hz; H-4 $\beta$ , dd, 13.5, 3.0 Hz; H-6 $\beta$ , ddd, 12.7, 2.2, 1.5 Hz; H-7 $\alpha$ , td, 12.9, 11.0 Hz; H-7 $\beta$ , ddd, 13.1, 6.1, 2.3 Hz; H-8 $\beta$ , br t, 11 Hz; H-11 $\alpha$ , ddd, 14.8, 4.6, 1.7 Hz; H-15 $\alpha$ , dddd, 12.2, 9.9, 7.1, 2.9 Hz; H-16 $\alpha$ , dtd, 13.4, 9.7, 6.1 Hz; **11**, H1, d, 8.4 Hz; H2, dd, 8.4, 7.0 Hz; H-3, dt, 7.0, 1.0 Hz; H6, br d, 9.2 Hz; H7, br d, 9.2 Hz; H-15, ddd, 16, 7, 6 Hz and 16, 9, 8 Hz; H17, ddd, 7, 4, 4 Hz; H20, dqdd, 10, 6.9, 3.3 Hz; **12**, H-1 $\alpha$ , dt, 14.2, 3.5 Hz; H-1 $\beta$ , br t, 14.4 Hz; H-2 $\alpha$ , br d, 12.5 Hz; H-3 $\alpha$ , quintet, 3.6 Hz; H-4 $\alpha$ , dd, 14.9, 3.8 Hz; H-4 $\beta$ , ddd, 14.9, 3.9, 2.4 Hz; H-6 $\alpha$ , dd, 12.9, 2.2 Hz; H-7 $\beta$ , td, 13.6, 6.7 Hz; H-11 $\alpha$ , dt, 13.5, 3.7, 2.8 Hz; H-11 $\beta$ , td, 13.6, 3.9 Hz; H-15 $\beta$ , dddd, 12.1, 9.8, 7.2, 2.5 Hz; H-16 $\beta$ , dddd, 12.9, 9.4, 8.7, 5.8 Hz; **13** and **14** had couplings similar to **12** ( $\pm 0.5$  Hz); **15**, H-1 $\alpha$ , t, 13.4 Hz; H-1 $\beta$ , dd, 12.9, 3.1 Hz; H-2 $\beta$ , ddd, 13.5, 9.2, 3.0 Hz; H-3 $\alpha$ , dd, 9.2, 2.6 Hz; H-4, d, 2.6 Hz; H-6 $\alpha$ , d, 7.2 Hz; H-7 $\beta$ , dd, 14.2, 3.7 Hz; H-9 $\alpha$ , ddd, 12.5, 10.7, 4.3 Hz; **16**, H3, br d, 10.4 Hz; H4, ddd, 10.4, 2.8, 1.5 Hz; H7 $\alpha$ , dd, 19, 11 Hz; H7 $\beta$ , dd, 19.4, 5.5 Hz; H8 $\beta$ , qd, 10.6, 5.5 Hz; **17**, H2, dd, 7.6, 2.1 Hz; H3, t, 7.4 Hz; H4, dd, 7.0, 2.1 Hz; H-6 $\alpha$ , dd, 3.3, 1.7 Hz; H-8 $\beta$ , td, 10.9, 3.4 Hz; H-9 $\alpha$ , td, 11.5, 3.2 Hz; H-12 $\beta$ , td, 12.8, 3.2 Hz; **18**, H-1 $\alpha$ , dd, 16.6, 3.1 Hz; H-1 $\beta$ , d, 16.7 Hz; H-2, d, 3.1 Hz; H6, d, 10.0 Hz; H7, d, 9.9 Hz; **19**, H1, dd, 8, 2 Hz; H2, ddd, 8.0, 6.8, 1.7 Hz; H3, ddd, 8.1, 6.9, 1.7 Hz; H4, dd, 8, 2 Hz; H12 $\alpha$ , ddd, 13.3, 10.0, 7.4 Hz; H12 $\beta$ , ddd, 13.3, 5.8, 3.8 Hz; H16 $\alpha$ , dd, 15.6, 7.9 Hz; H16 $\beta$ , dd, 16, 11 Hz; **20**, H1, d, 8.8 Hz; H2, dd, 8.5, 6.9 Hz; H3, d, 6.9 Hz; H6, d, 9.1 Hz; H7, d, 9.0 Hz; H12 $\beta$ , ddd, 13, 5, 4 Hz; H16 $\alpha$ , dd, 15.5, 7.9 Hz; H16 $\beta$ , dd, 16, 12 Hz

### Structure Elucidation of Compounds **10–20** by NMR and Mass Spectrometry

Because of the extensive rearrangements and/or presence of sulfonate groups, the structures of **10–20** were

not readily established by comparisons with NMR spectra of known compounds. Each of these steroids was analyzed by heteronuclear single quantum coherence, heteronuclear multiple bond correlation, correlation spectroscopy with F1 decoupling, and

**Table 2**  $^{13}\text{C}$  NMR chemical shifts of LB reaction products from cholesterol

	10	11	12	13	14	15	16	17	18	19	20
C-1	28.74	120.99	20.85	20.79	21.03	41.27	34.76	137.17	35.35	125.41	123.28
C-2	30.47	125.83	33.20	34.96	32.52	57.25	23.82	131.53	125.08	126.31	126.34
C-3	88.88	127.05	76.36	67.53	71.64	76.18	129.59	126.03	137.92	126.77	127.76
C-4	42.33	134.76	45.68	47.44	44.84	130.87	126.41	130.15	134.15	125.30	135.55
C-5	49.69	130.40	40.30	40.25	40.15	143.60	142.18	137.80	145.58	134.08	133.72
C-6	65.86	121.67	65.83	65.36	65.82	65.55	136.60	71.11	122.69	131.53	121.82
C-7	24.57	123.41	25.29	25.30	25.23	34.18	35.11	64.53	131.96	131.19	130.55
C-8	37.41	126.38	38.56	38.55	38.59	32.21	32.98	36.95	125.84	129.06	129.06
C-9	136.22	129.71	135.16	134.91	135.82	54.72	49.13	41.95	45.93	132.94	135.19
C-10	123.85	130.48	133.30	133.80	132.67	38.72	37.66	141.95	40.91	132.88	132.75
C-11	25.95	122.29	27.72	27.71	27.78	22.09	22.05	29.21	20.46	24.87	25.28
C-12	39.50	132.98	43.70	43.79	43.72	41.18	41.05	41.76	37.71	38.88	38.88
C-13	42.25	143.75	44.87	44.87	44.88	43.64	43.55	45.05	45.11	50.79	50.69
C-14	56.83	140.99	56.93	56.99	56.93	58.12	58.25	53.36	153.10	147.56	147.54
C-15	24.21	31.25	24.75	24.77	24.72	25.15	25.19	24.72	25.89	136.59	136.76
C-16	28.18	25.80	29.41	29.40	29.41	29.33	29.35	29.44	28.34	41.01	40.98
C-17	55.89	51.44	57.58	57.65	57.59	57.60	57.50	57.73	57.42	55.48	55.51
C-18	11.30	20.25	12.39	12.37	12.39	12.60	12.40	12.99	18.93	16.06	16.08
C-19	13.65	20.01	21.29	21.73	21.10	20.77	18.89	22.18	15.86	19.37	19.69
C-20	35.64	36.09	37.10	37.10	37.10	37.13	37.12	37.24	35.93	35.35	35.34
C-21	18.58	19.19	19.08	19.08	19.08	19.20	19.23	19.18	19.42	19.70	19.70
C-22	36.02	30.51	37.23	37.23	37.68	37.35	37.36	37.34	37.07	37.11	37.12
C-23	23.76	25.59	24.89	24.89	24.89	24.93	24.94	24.87	24.88	24.87	24.87
C-24	39.44	39.09	40.67	40.67	40.67	40.68	40.69	40.72	40.68	40.68	40.68
C-25	27.98	27.88	29.13	29.13	29.14	29.15	29.15	29.17	29.15	29.19	29.19
C-26	22.53	22.35 <sup>a</sup>	22.93	22.93	22.93	22.93	22.94	22.95	22.93	22.97	22.97
C-27	22.78	22.68 <sup>a</sup>	23.16	23.16	23.17	23.18	23.19	23.18	23.17	23.20	23.20

Chemical shifts were measured at 25 °C in  $\text{CDCl}_3$  (**10**, **11**) or in  $\text{CD}_3\text{OD}$  (**12**–**20**). Ethoxy signals for **15**:  $\delta$  15.89, 63.36

<sup>a</sup> Assignments that may be interchanged

distortionless enhanced polarization transfer experiments. Signal assignments were aided by quantum-mechanical NMR shielding predictions. These results, together with chemical shift comparisons, established the carbon skeleton and double-bond positions. The presence of  $-\text{SO}_3\text{Na}$  and  $-\text{OSO}_3\text{Na}$  substituents was established by mass spectrometry, and their location was inferred from NMR shielding patterns. In aromatic systems,  $-\text{SO}_3\text{Na}$  substitution deshields the *ipso* carbon by 10–20 ppm, and resonance-related carbons (e.g., *ortho* and *para*) are deshielded by a few parts per million. In aliphatic systems, the *ipso* carbon is strongly deshielded (by approximately 30–40 ppm), and nearby carbons are modestly deshielded. The exact position of sulfonate substitution in ring A could not be deduced for **18**, and the stereochemistry at C17 and C20 was not established for **11** (a single stereoisomer).

Mass spectral analyses were consistent with the structures shown in Fig. 3: **10** ( $\text{C}_{27}\text{H}_{44}\text{O}_3\text{S}$ ), electron impact  $m/z$  448 (97,  $\text{M}^+$ ), 433 (22), 384 (46), 366 (48), 335 (100), 253 (52), 159 (91); FAB (NBA) 449 (43,  $\text{M} + 1$ ), 367 (100,  $\text{M} - \text{HSO}_3$ ); **12** ( $\text{C}_{27}\text{H}_{44}\text{O}_7\text{Na}_2\text{S}_2$ ), ES+ 613.216 ( $\text{M} + \text{Na}$ ), ES- 567.229 ( $\text{M} - \text{Na}$ ); **13** ( $\text{C}_{27}\text{H}_{45}\text{O}_4\text{NaS}$ ), ES+ 511.285 ( $\text{M} + \text{Na}$ ), ES- 465.292 ( $\text{M} - \text{Na}$ ); **14** ( $\text{C}_{29}\text{H}_{47}\text{O}_5\text{NaS}$ ), ES+ 553.294 ( $\text{M} + \text{Na}$ ), ES- 507.291 ( $\text{M} - \text{Na}$ ); **15** ( $\text{C}_{29}\text{H}_{48}\text{O}_7\text{Na}_2\text{S}_2$ ), FAB (glycerol) 641 (30,  $\text{M} + \text{Na}$ ), 537 (100,  $\text{M} - \text{HSO}_3$ ); **16** ( $\text{C}_{27}\text{H}_{43}\text{O}_3\text{NaS}$ ), FAB (NBA) 493 (100,  $\text{M} + \text{Na}$ ); **17**

( $\text{C}_{27}\text{H}_{41}\text{O}_4\text{NaS}$ ), FAB (NBA) 507 (100,  $\text{M} + \text{Na}$ ); **18** ( $\text{C}_{27}\text{H}_{38}\text{O}_6\text{Na}_2\text{S}_2$ ), FAB (glycerol) 591 ( $\text{M} + \text{Na}$ ); **19** ( $\text{C}_{27}\text{H}_{35}\text{O}_3\text{NaS}$ ), FAB (NBA) 485 (100,  $\text{M} + \text{Na}$ ).

#### Reactivity of Cholesterol Under Salkowski Conditions

To cholesterol (1 mg) in  $\text{CDCl}_3$  (0.6 mL) in an NMR tube was added  $\text{D}_2\text{SO}_4$  (1  $\mu\text{L}$ ). The tube was inverted several times (the solution becoming pale pink), placed in the magnet, and maintained at 15 °C for 2 h while  $^{25}\text{H}$  NMR spectra were measured at 2–10-min intervals. NMR analysis indicated rapid formation of  $\Delta 3,5$  diene **9**. The ratio of  $\Delta 5$ ,  $\Delta 3,5$ , and other olefins was 74:25:1 after 4 min and 70:24:6 after 15 min, with little change thereafter. In contrast, cholesterol in LB reactions mainly underwent acetylation and sulfation, with little or no  $\Delta 3,5$  diene formation. Under both LB and Salkowski conditions, NMR showed no aromatic signals until later stages of the reaction, well after the blue or red color had fully developed.

Another Salkowski reaction was performed by adding  $\text{H}_2\text{SO}_4$  (512  $\mu\text{L}$ ) to a solution of cholesterol (1 g) in chloroform (50 mL). The mixture was shaken until a dark red color persisted, followed by chilling to  $-78$  °C and quenching with ethanol (25 mL;  $-78$  °C). To the resulting colorless solution was added 24% aqueous  $\text{NaOH}$  (10 mL). The precipitate contained **2**;

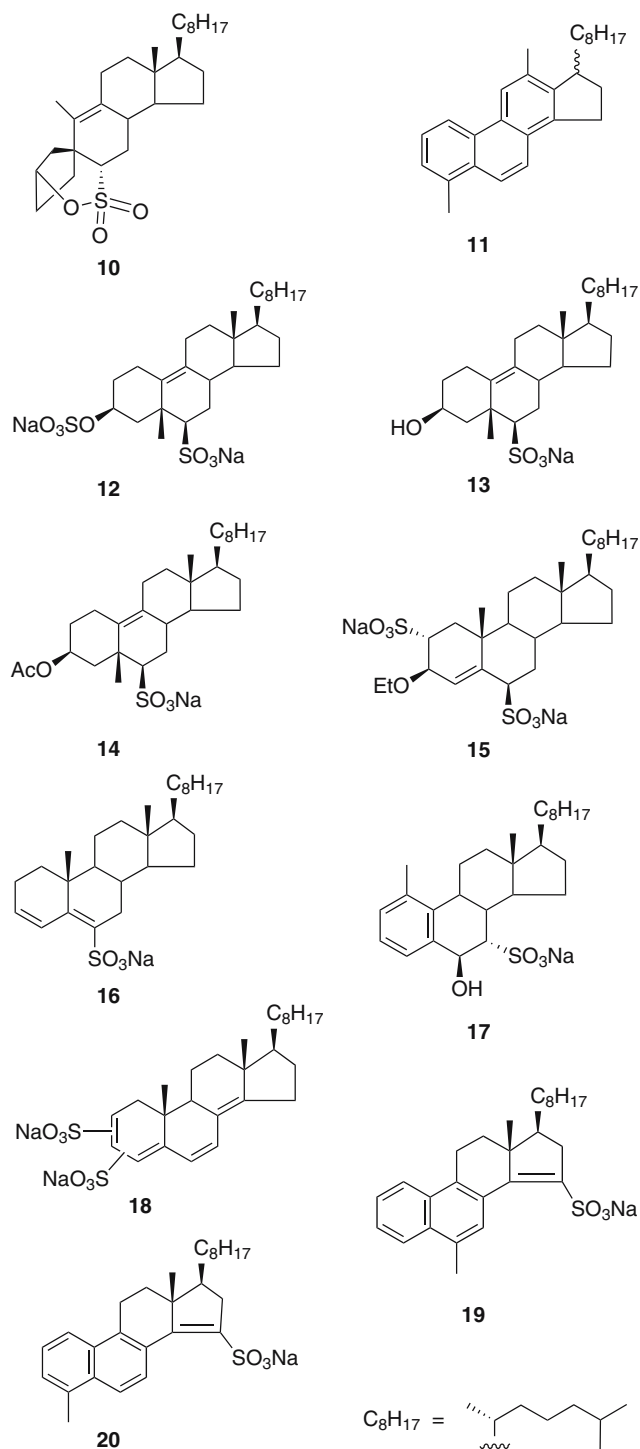


**Fig. 3** Products from a LB reaction quenched at the bluish-green stage (reaction B) and worked up under conditions permitting further reaction. The position of the sulfonate groups in **18** was not determined, but 2,4 or 3,4 substitution appeared likely

the organic phase was separated by preparative TLC (developed with CHCl<sub>3</sub>) into cholesterol (main component) and two backbone-rearrangement products

that were characterized by NMR: **21** (CDCl<sub>3</sub>,  $\delta_{\text{H}}$ ) 0.833 (d, 6.6 Hz), 0.838 (d, 6.6 Hz), 0.897 (s), 0.949 (d, 6.6 Hz), 1.080 (s), 4.093 (quintet, 2.9 Hz); **22** (CDCl<sub>3</sub>,  $\delta_{\text{H}}$ ) 0.851 (d, 6.6 Hz), 0.857 (d, 6.6 Hz), 0.897 (s), 0.903 (d, 6.6 Hz), 1.080 (s), 4.093 (quintet, 2.9 Hz). These products were identified, except for C10 stereochemistry, from NMR data reported for the 3-deoxy analogs [21]. The 10 $\alpha$ -H stereochemistry was assigned as shown in Fig. 4 on the basis of the H3 shieldings (matching calculated values much better for the 10 $\alpha$ -H than the 10 $\beta$ -H structure) and H3 coupling constants (indicating an axial  $\beta$ -hydroxy group and thus an AB-*trans* ring junction).

## Discussion

We have investigated the fate of cholesterol under strongly acidic conditions, with the ultimate goal of elucidating the origin of the color response in the LB reaction. The isolated products shown in Figs. 2 and 3 indicate the operation of several reaction pathways, summarized in Fig. 5. The LB mixture of sulfuric acid, acetic acid, and acetic anhydride in chloroform rapidly converts cholesterol to its acetate and sulfate derivatives, accompanied by small amounts of *i*-steroids, cholesta-3,5-diene, and other unsaturated species. The predominant  $\Delta^5$  species are then slowly converted to monounsaturated, diunsaturated, and polyunsaturated sulfonic acids. The polyene species gradually rearrange to aromatic steroids that are likely devoid of blue/green color, even as cations. We argue that none of these mainstream unsaturated species are responsible for the LB color response and that its chemical origin remains unknown.

The nature of the color-generating species in the LB reaction has received much attention. A neutral polyunsaturated steroid would not be colored, as judged by UV spectra of conjugated tetraenes [22], although only five C=C bonds are needed to generate the blue color of azulene. More likely candidates are linearly conjugated polyene cations; linear tetraenylic and pentaenylic cations (from a pentaene and hexaene) absorb in

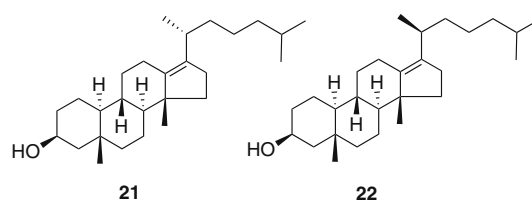


**Fig. 4** Structures for backbone rearrangement products formed under Salkowski conditions



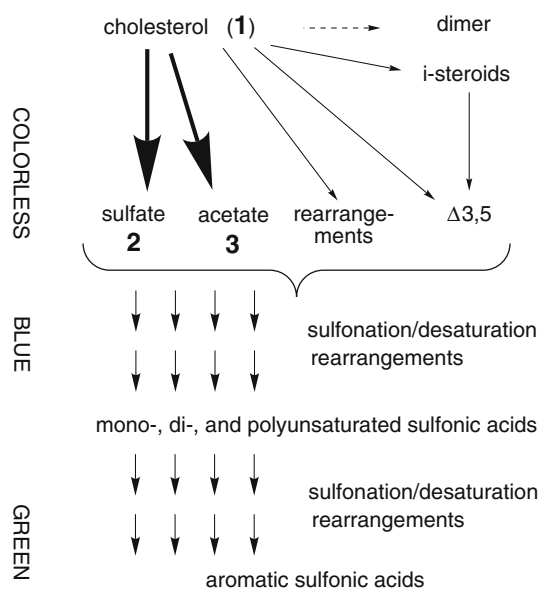


**Fig. 5** Major and minor pathways occurring in the LB reaction. The initial  $\Delta^5$  species **1–3** are slowly sulfonated and desaturated (oxidized) to form polyene sulfonic acids and aromatic steroids, as exemplified by **10–20**. The blue color appears at the nascent stage of polyene formation

the vicinity of 550 and 620 nm [23], respectively, whereas a tetraenylic cation containing a benzene ring absorbs at only 389 nm [24].

Desaturation of cholesterol to a polyene involves sulfuric acid, which is present in the reagents for the LB, Salkowski, and Zak colorimetric assays. The ability of concentrated  $\text{H}_2\text{SO}_4$  or  $\text{ClSO}_3\text{H}$  to convert sterols to polyunsaturated sulfonic acids with evolution of  $\text{SO}_2$  has long been known [25]. Brieskorn and Hofmann [9] noted that the dehydrating effects of the LB reagent would convert some  $\text{H}_2\text{SO}_4$  to  $\text{SO}_3$ , and their observation of  $\text{SO}_2$  evolution during the LB reaction confirmed the role of  $\text{H}_2\text{SO}_4$  in the desaturation of cholesterol.

Our characterization of numerous sulfonic acids from the LB reaction provides the first detailed insights into how the desaturation of cholesterol proceeds. Possible mechanisms for the conversion of  $\Delta^5$  species **1–3** to sulfonic acid derivatives are suggested in Fig. 6a. The modest concentration of  $\text{SO}_3$  and the unfavorable activation energy for attack of an isolated  $\text{C}=\text{C}$  on  $\text{SO}_3$  are consistent with the sluggishness of the LB color response. Moisture or alcohol (from ethanol-stabilized chloroform) would reduce the  $\text{SO}_3$  concentration and further retard the reaction, as is observed.

Our NMR analysis of hydrophobic sterol intermediates (Fig. 2) indicates that  $\Delta^5$  species are the major substrates in the LB reaction, as shown in Fig. 5. In contrast, Salkowski conditions produce substantial

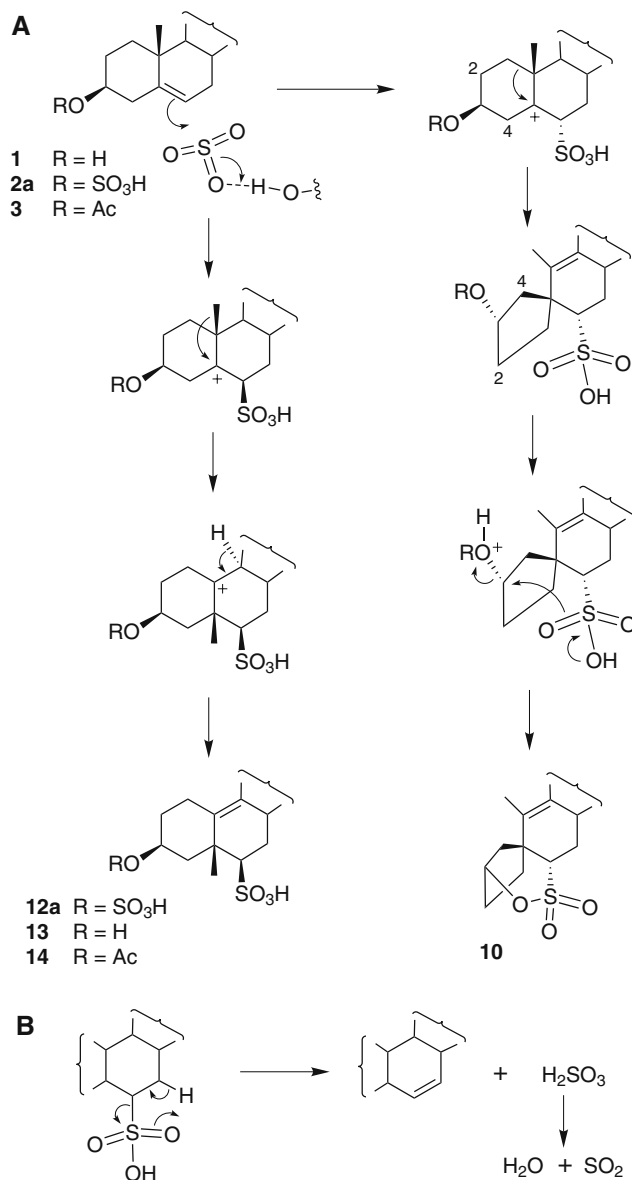


**Fig. 6** Suggested mechanisms for **A** the sulfonation of  $\Delta^5$  sterols and **B** oxidative elimination of  $\text{H}_2\text{SO}_3$  to give an olefin. Compounds **2** and **12** were isolated as sodium salts but are shown here as the sulfonic acids (**2a** and **12a**) that would exist in the LB reaction. For simplicity, the oxidative elimination in **B** is shown as a cyclic process, although the new O–H bond formation would normally proceed through an intervening solvent molecule

amounts of cholesta-3,5-diene (**9**), which would more readily attack  $\text{SO}_3$ , since an allylic cation would be formed. This is consistent with the rapid Salkowski color response. The Zak reaction (1:1.5  $\text{H}_2\text{SO}_4/\text{AcOH}$  with  $\text{Fe}^{3+}$ ) may similarly benefit from the absence of acetic anhydride, which favors 3-acetate formation over dehydration to **9**.

Cholesterol dimers have been proposed as the initial species in colorimetric reactions [11, 15]. As pointed

out by others [9, 12–14], the selectivity of the LB reaction (Fig. 1), the UV behavior, and the reaction kinetics (first order in cholesterol) indicate this to be a very minor pathway. We did not detect any sterol dimers in our analyses.

Our results raise serious doubts about the prevailing hypothesis that the LB color response is derived from linearly conjugated polyene cations. Our first concern with this hypothesis is the lack of intermediate colors in the LB reaction. Whereas the Zak reaction proceeds through distinct UV absorbance maxima separated by well-defined isosbestic points [13], our time-course UV analysis of the LB reaction (partially shown in Fig. 3 in [8]) and those of Burke et al. [12] indicated no intermediate species that absorb in the 300–500-nm range. Yellow and red colors are absent in the LB reaction, whereas sequentially yellow, red, blue, and green colors would be observed if double bonds are added one at a time to generate a polyene. Secondly, our NMR analysis showed only traces of sulfonic acids and polyenes at the stage of blue color. Thus, the formation of hexaunsaturated steroids seems too slow to account for the blue color response, even if the LB reagent is sufficiently acidic to protonate a linearly conjugated hexaene effectively. Finally, previous studies [12, 13] correlated the consumption of the oxidant ( $\text{Fe}^{3+}$  or  $\text{SO}_3$ ) with the color response in the Zak reaction but not the LB reaction. Taken together, these findings indicate that the LB color response does not stem from linearly conjugated polyene cations, although this mechanism may apply to the Zak reaction.

Some conceivable alternatives to the polyene cation model include charge-transfer complexes, phenol/quinone systems (e.g., a polycyclic analog of phenol red), and azulene systems (Fig. 7). Although these proposals are speculative and no such structures have been isolated, some of these systems contain structural features of **10–20** and might produce the observed color at trace levels. It is notable that the LB reaction produces a blue or green color, whereas the Zak and Salkowski assays are red.

Despite our advances in elucidating the mechanistic pathways of the LB reaction, the story is far from complete. We have not studied the elimination of  $\text{H}_2\text{SO}_3$  from sulfonic acids to generate olefins (Fig. 6b). This critical step appears to be slow under LB conditions, thus perhaps accounting for the paucity of polyunsaturated hydrocarbons and the predominance of sulfonic acid intermediates. Many more polar intermediates remain to be characterized and quantified; a comprehensive analysis would permit ranking the many sulfonation and rearrangement pathways in order of importance.

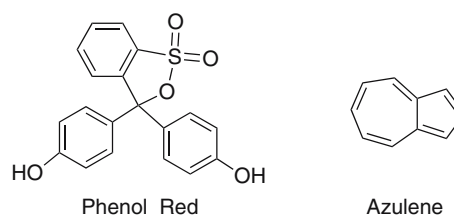


**Fig. 7** Polyunsaturated structures that produce intense color at low concentrations. Steroidal polyenes with some of these structural features might conceivably be responsible for the color response in the LB reaction

In summary, we have established the structures of many novel products of the LB reaction. In the presence of colorimetric reagents, cholesterol can variously undergo acetylation, i-steroid formation, backbone rearrangement, dimerization, sulfonation, oxidation/desaturation, and aromatization. Different kinetics among these pathways results in the different color responses observed for the LB, Zak, and Salkowski reactions. Although we have not identified the elusive color-producing species, our mechanistic insights and advances in methodology lay a sound foundation for future work. A resurrection of colorimetric assays is unlikely in clinical laboratories, but rapid and simple steroid assays continue to draw interest [26]. Some of the rearrangements observed for the LB and Salkowski reactions are similar to degradation pathways inferred from studies of sterol diagenesis under various geological conditions [27–29]. Modification of the LB reaction may provide conditions for accelerated ageing of sterols to produce lipid biomarkers that mimic specific geological processes. The behavior of sterols under acidic conditions is a fundamental, enduring topic of research, with many potential applications.

**Acknowledgements** This work was supported in part by startup funding from Texas Southern University for Q.X. We thank Alekha Kistic for supplying purified cholesterol. Quantum-mechanical calculations were carried out in part on the Rice Terascale Cluster funded by the NSF (EIA-0216467), Intel, and Hewlett-Packard and on the Rice Cray XD1 Research Cluster funded by the NSF (CNS-0421109) in partnership with AMD and Cray.

## References

1. Bartos J, Pesez M (1976) Colorimetric and fluorimetric analysis of steroids. Academic, London
2. Zak B (1980) Cholesterol methodology for human studies. *Lipids* 15:698–704
3. Zak B (1977) Cholesterol methodologies: a review. *Clin Chem* 23:1201–1214
4. Tonks DB (1967) The estimation of cholesterol in serum: a classification and critical review of methods. *Clin Biochem* 1:12–29

5. USA Food and Drug Administration. [http://www.fda.gov/cdrh/ode/605.html#toc\\_18](http://www.fda.gov/cdrh/ode/605.html#toc_18). Accessed Oct 2006
6. Liebermann C (1885) Ueber das Oxychinoterpen. *Chem Ber* 18:1803–1809
7. Burchard H (1889) Beiträge zur Kenntnis des Cholesterins. Inaugural-Dissertation, Universität Rostock [Chem Zentralbl 61-I:25–27 (1890)]
8. Xiong Q, Ruan B, Whitby FG, Tuohy RP, Belanger TL, Kelley RI, Wilson WK, Schroepfer GJ Jr (2002) A colorimetric assay for 7-dehydrocholesterol with potential application to screening for Smith-Lemli-Opitz syndrome. *Chem Phys Lipids* 115:1–15
9. Brieskorn CH, Hofmann H (1964) Beitrag zum Chemismus der Farbreaction nach Liebermann–Burchard. *Arch Pharm* 297:577–588
10. Rosenheim O (1929) A specific colour reaction for ergosterol. *Biochem J* 23:47–53
11. Watanabe T (1959) The colored intermediates and products of cholesterol by Liebermann–Burchard reaction, and its reaction mechanism. *Eisei Shikensho Hokoku* 77:87–94 (Chem Abstr 55:54430)
12. Burke RW, Diamondstone BI, Velapoldi RA, Menis O (1974) Mechanisms of the Liebermann–Burchard and Zak color reactions for cholesterol. *Clin Chem* 20:794–801
13. Velapoldi RA, Diamondstone BI, Burke RW (1974) Spectral interpretation and kinetic studies of the  $\text{Fe}^{3+}$ – $\text{H}_2\text{SO}_4$  (Zak) procedure for determination of cholesterol. *Clin Chem* 20:802–811
14. Zuman P (1991) A review of reactions of some sterols in strongly acidic media. *Microchem J* 43:10–34
15. Niiya T, Goto Y, Ono Y, Ueda Y (1980) Study on the correspondence of color change with polyenyl cation formation of cholesterol in strong acids. *Chem Pharm Bull* 28:1747–1761
16. Abell LL, Levy BB, Brodie BB, Kendall FE (1952) Simplified method for the estimation of total cholesterol in serum and demonstration of its specificity. *J Biol Chem* 195:357–366
17. Frisch MJ, Trucks GW, Schlegel HB, Scuseria GE, Robb MA, Cheeseman JR, Montgomery JA Jr, Vreven T, Kudin KN, Burant JC et al (2004) Gaussian 03, revisions C.02 and D.01. Gaussian, Wallingford, CT, USA
18. Shan H, Segura MJR, Wilson WK, Lodeiro S, Matsuda SPT (2005) Enzymatic cycliation of dioxidosqualene to heterocyclic triterpenes. *J Am Chem Soc* 127:18008–18009
19. Salkowski E (1872) Kleinere Mittheilungen physiologisch-chemischen Inhalts (II). *Archiv Gesamte Physiol Menschen Tiere* 6:207–222
20. Salkowski E (1908) Physiologisch-chemische Notizen. *Hoppe Seylers Z Physiol Chem* 57:515–528
21. Peakman TM, Ellis K, Maxwell JR (1988) Acid-catalyzed rearrangements of steroid alkenes. Part. 2 a re-investigation of the backbone rearrangement of cholest-5-ene. *J Chem Soc Perkin Trans* 1:1071–1075
22. Scott AI (1964) Interpretation of the ultraviolet spectra of natural products. Pergamon, New York, p 392
23. Sorensen TS (1965) The preparation and reactions of a homologous series of aliphatic polyenylic cations. *J Am Chem Soc* 87:5075–5084
24. Deno NC, Pittman CU Jr, Turner JO (1965) Cyclizations of pentadienyl and heptatrienyl cations. *J Am Chem Soc* 87:2153–2157
25. Yoder L, Thomas BH (1954) An antirachitic sulfonic acid derivative of cholesterol. *Arch Biochem Biophys* 50:113–123
26. Studer J, Purdie N, Krouse JA (2003) Friedel-Crafts acylation as a quality control assay for steroids. *Appl Spectrosc* 57:791–796
27. Rushdi AI, Ritter G, Grimalt JO, Simoneit BRT (2003) Hydrous pyrolysis of cholesterol under various conditions. *Org Geochem* 34:799–812
28. Schüpfer PY, Gülarar FO (2000) Relative stabilities of cholestadienes calculated by molecular mechanics and semi-empirical methods: application to the acid-catalyzed rearrangement reactions of cholesta-3,5-diene. *Org Geochem* 31:1589–1596
29. Chen J, Summons RE (2001) Complex patterns of steroidal biomarkers in tertiary lacustrine sediments of the Biyang basin, China. *Org Geochem* 32:115–126

# Enhancing Vitamin E in Oilseeds: Unraveling Tocopherol and Tocotrienol Biosynthesis

Sarah C. Hunter · Edgar B. Cahoon

Received: 11 December 2006 / Accepted: 17 January 2007 / Published online: 13 February 2007  
© AOCS 2007

**Abstract** Naturally occurring vitamin E, comprised of four forms each of tocopherols and tocotrienols, are synthesized solely by photosynthetic organisms and function primarily as antioxidants. These different forms vary in their biological availability and in their physiological and chemical activities. Tocopherols and tocotrienols play important roles in the oxidative stability of vegetable oils and in the nutritional quality of crop plants for human and livestock diets. The isolation of genes for nearly all the steps in tocopherol and tocotrienol biosynthesis has facilitated efforts to alter metabolic flux through these pathways in plant cells. Herein we review the recent work done in the field, focusing on branch points and metabolic engineering to enhance and alter vitamin E content and composition in oilseed crops.

**Keywords** Vitamin E · Tocopherols · Tocotrienols · Tocochromanols · Vitamin E biosynthesis · Oilseed · Soybean · Antioxidants · Metabolic engineering

## Abbreviations

DXP	1-Deoxy-D-xyulose-5-phosphate
GGDP	Geranylgeranyldiphosphate
GGR	Geranylgeranyl reductase
HGA	Homogentisate
HGGT	Homogentisate geranylgeranyl transferase

HPP	<i>p</i> -Hydroxyphenylpyruvate
HPPD	Hydroxyphenylpyruvate dioxygenase
HPT	Homogentisate phytyltransferase
PDP	Phytyldiphosphate
PK	Phytol kinase
PMP	Phytylmonophosphate
PrBQMT	2-Methyl-6-prenylbenzoquinol methyltransferase
PrDP	Prenyldiphosphate
SDP	Solanesyldiphosphate
TC	Tocopherol/tocotrienol cyclase
TMT	Tocopherol/tocotrienol methyltransferase

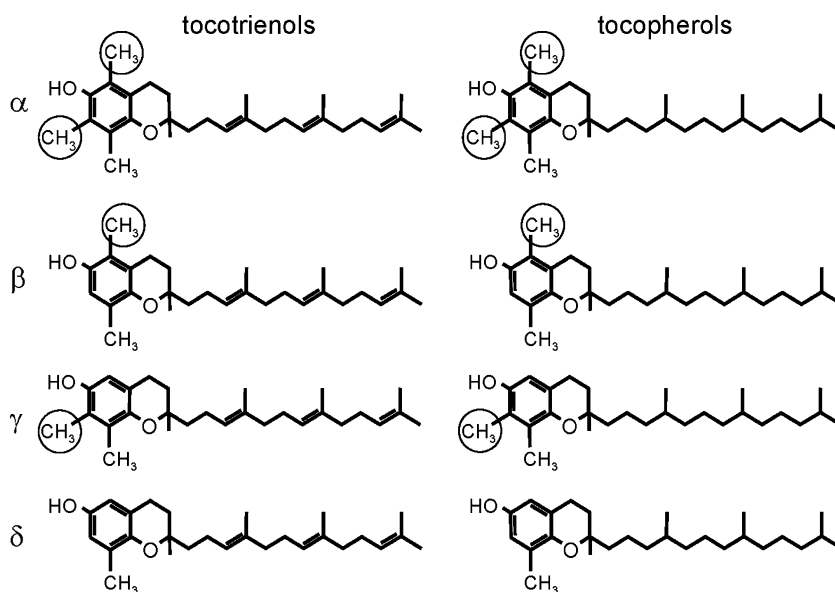
## Introduction

Tocopherols and tocotrienols comprise the vitamin E family of antioxidants and are synthesized by plants and other photosynthetic organisms. These molecules consist of a chromanol head group linked to an isoprenoid-derived hydrophobic tail. The aliphatic tail of tocopherols is fully saturated, while the side-chain of tocotrienols contains three *trans* double bonds (Fig. 1). Four different forms of tocopherols and tocotrienols occur in nature and differ by the numbers and positions of methyl groups on the aromatic portion of the chromanol head group (Fig. 1). The  $\alpha$  form of tocotrienols and tocopherols has three methyl groups, the  $\beta$  and  $\gamma$  forms have two methyl groups, and the  $\delta$  form has one methyl group on the aromatic ring. In the case of the  $\beta$  and  $\gamma$  forms, the methyl groups are at positions 5 and 8 or 7 and 8, respectively, of the chromanol head group. The  $\alpha$ ,  $\beta$ ,  $\gamma$ , and  $\delta$  forms of tocopherols and

S. C. Hunter · E. B. Cahoon (✉)  
United States Department of Agriculture,  
ARS, Plant Genetics Research Unit,  
Donald Danforth Plant Science Center,  
975 North Warson Road,  
Saint Louis, MO 63132, USA  
e-mail: ecahoon@danforthcenter.org

**Fig. 1** Naturally occurring vitamin E molecules (or tocochromanols) have one of eight forms, varying in the saturation of the prenyl group and methylation pattern on the chromanol ring.

Tocopherols contain fully saturated tails, while tocotrienol tails contain three *trans* double bonds. The hydrophilic head group has one, two, or three methyl groups. The hydrophobicity of the tail is greater than the hydrophilicity of the head group, thus vitamin E molecules are extracted with other lipids. Differences in methylation patterns are denoted by circles



tocotrienols are often referred to collectively as “tocochromanols.”

Tocopherols occur widely in plants, but the form of tocopherol often differs in the leaves and seeds of the same species.  $\alpha$ -Tocopherol is typically the primary form of tocopherols in leaves of plants and in photosynthetic prokaryotes such as *Synechocystis*. Seeds of different plant species, however, can be enriched in any of the four forms of tocopherol (Fig. 2). Soybean seeds, for example, contain primarily  $\gamma$ -tocopherol and lesser amounts of  $\delta$ - and  $\alpha$ -tocopherol. The occurrence of tocotrienols is more limited in plants. Tocotrienols are the principal tocochromanol of the seed endosperm of monocots, including important cereal grains such as wheat, rice, and barley (Fig. 2). Tocotrienols are also the major tocochromanol class in seeds of some dicots, including species of the Apiaceae (or Umbelliferae) family (e.g., coriander, celery) [1, 32]. Given their lipid soluble nature, tocopherols and tocotrienols are readily extracted as components of vegetable oils during the commercial processing of oilseeds. Soybean oil and palm oil, for example, are major commercial sources of tocopherols and tocotrienols, respectively.

Tocochromanols are potent lipid soluble antioxidants that protect plant cells against oxidative stresses. Tocopherols, for example, contribute to the maintenance of photosynthesis by mitigating photooxidative damage to photosystem II through the quenching of singlet oxygen [19]. In addition, seeds from *Arabidopsis* mutants that lack tocopherol display reduced storage life and accumulate increased amounts of compounds derived from the oxidation of stored oils [45]. The growth of these mutants at low temperatures is also reduced, suggesting that tocopherols contribute

to the cold-adaptation of plants [31]. It is likely that tocotrienols are also important for reducing oxidative stresses in plants, but the physiological role of these compounds in plants has yet to be established.

Tocopherols and tocotrienols are classified as vitamin E based on their ability to prevent the resorption of rat fetuses maintained on defined diets, the classical measure of “vitamin E activity.” In this assay,  $\alpha$ -tocopherol displays the greatest efficacy of the eight natural tocochromanols because of its ability to be more readily absorbed and retained by cells of the body [24]. As such,  $\alpha$ -tocopherol is considered to have the highest nutritional value of the different forms of tocopherols and tocotrienols, and has thus received the greatest attention for the vitamin E biofortification of crop plants. By comparison,  $\alpha$ -tocotrienol has about one-third of the vitamin E activity displayed by  $\alpha$ -tocopherol, while  $\gamma$ -tocopherol has only about one-tenth of the vitamin E activity of  $\alpha$ -tocopherol [24]. Regardless, all forms of tocochromanols are able to reduce free-radical damage to membrane lipids, and in model membrane studies, tocotrienols are better antioxidants than tocopherols [57, 48]. In addition, diverse health-promoting properties have been attributed to the various forms of tocochromanols. For example, low levels of  $\gamma$ -tocopherol, but not  $\alpha$ -tocopherol, in serum correlate with the incidence of coronary heart disease [34]. Likewise, tocotrienols have physiological properties that are distinct from those of  $\alpha$ -tocopherol. Tocotrienols inhibit cholesterol synthesis [39], and  $\gamma$ -tocotrienol is the most active inhibitor in studies with human hepatoma HepG2 cells [36]. Tocotrienols also reduce the *in vitro* growth of breast cancer cells [33], and  $\alpha$ -tocotrienol provides the

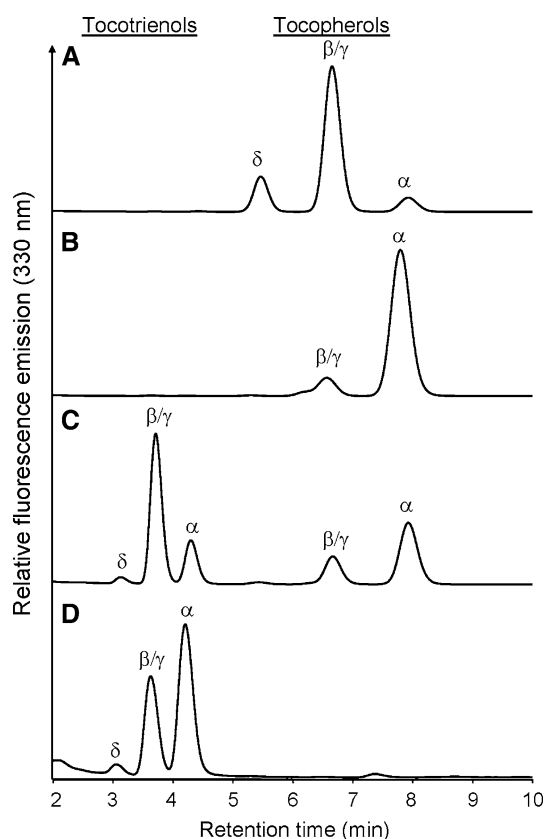


**Fig. 2** C18-reverse phase HPLC analysis of tocopherols in extracts from soybean seeds (**a**), sunflower seeds (**b**), rice seeds (**c**), and coconut endosperm (**d**). Tocopherols were detected in crude lipid extracts by fluorescence (292 nm excitation/330 nm emission). C18-reverse phase HPLC columns are typically unable to resolve  $\beta$  and  $\gamma$  forms of tocotrienols and tocopherols. These molecules can be resolved by normal phase (e.g., silica) HPLC columns. In the soybean seed extract (**a**), the  $\beta/\gamma$  tocopherol peak is composed almost entirely of  $\gamma$ -tocopherol, and in the rice seed extract (**c**), the  $\beta/\gamma$  tocotrienol peak is composed almost entirely of  $\gamma$ -tocotrienol

greatest protection against oxidative damage to neuronal cells of any of the tocopherols [35].

From a commercial standpoint, the oxidative stability that tocopherols confer to vegetable oils is perhaps their most important functional property. This property is especially valuable for reducing fatty acid oxidation and the formation of off-flavor compounds such as hexanals in foods fried or processed using vegetable oils [65, 67]. Of the different forms of tocopherol,  $\delta$ - and  $\gamma$ -tocopherols are the most effective at reducing the oxidative breakdown of vegetable oils in frying applications [65, 66]. In addition,  $\delta$ - and  $\gamma$ -tocotrienols have a slightly greater ability than the corresponding tocopherols to reduce the formation of fatty acid oxidation products during the frying of foods [66]. As interest in the use of vegetable oils as high-temperature lubricants grows [12], the ability to

genetically enhance the tocopherol content of oilseeds, particularly the  $\delta$  and  $\gamma$  forms, to improve oxidative stability will likely become increasingly important. Recent efforts to engineer oilseeds to produce long-chain  $\omega$ -3 polyunsaturated fatty acids (e.g., eicosapentaenoic acid), which are prone to oxidation, will also likely benefit from genetic enhancement of tocopherol content [11]. In addition to their contributions to the oxidative stability of vegetable oils, tocopherols are used commercially in cosmetics and sunscreens, and have potential value as livestock feed supplements to improve the quality and shelf-life of meats [30, 68].

Tocopherols are synthesized in plastids of plants from precursors that derive from the shikimate and methylerythritol phosphate pathways. The biosynthetic pathway for tocopherols and many of the associated enzymes were determined in the 1980s. Research during the past 8 years has uncovered nearly all of the genes that are required for the synthesis and modification of tocopherols and tocotrienols. This review summarizes recent advances in our understanding of the biochemistry and genetics of tocopherol and tocotrienol biosynthesis in plants and describes how this research has been applied for the biotechnological enhancement of the vitamin E content and composition of oilseed crops.

### Vitamin E Biosynthetic Enzymes

Vitamin E biosynthetic enzymes are found in chloroplasts [3, 21, 52, 55, 66] and chromoplasts [2], thus, presumably all plastids. Total vitamin E content increases during senescence [42], during chloroplast to chromoplast transition [2], and during seed development [15]. Although many of the enzymatic steps have been characterized for over 20 years [52], recent genetic work in dissecting the pathway has been facilitated by the availability of *Arabidopsis* mutants and the use of transgenic plants. Table 1 shows many of the available plant mutants and cloned genes. The generally accepted pathway for vitamin E biosynthesis is shown in Fig. 3 and major steps are summarized in Table 2. Only two steps are required to make a tocopherol: the prenylation of homogentisate (HGA) and a subsequent cyclization step. In this case, the vitamin E will be either  $\delta$ -tocopherol or  $\delta$ -tocotrienol. Additional methylation steps produce  $\alpha$ ,  $\beta$ , and  $\gamma$  forms of vitamin E.

Two substrates are required for vitamin E biosynthesis: HGA and a  $C_{20}$  prenyldiphosphate (PrDP). HGA supplies the aromatic ring of the chromanol head

**Table 1** Genes and mutants involved in vitamin E biosynthesis

Enzyme activity	Species	Gene identification	Mutants	References
Homogentisate phytyltransferase (HPT)	<i>Synechocystis</i>	slr1736		[7, 46, 47]
	<i>Arabidopsis</i>	VTE2, HPT1 At2g18950		[7, 46]
Homogentisate geranylgeranyl transferase (HGGT)	<i>Arabidopsis</i>		<i>vte2-1</i> , <i>vte2-2</i>	[45]
	Barley, rice, wheat			[5]
Homogentisate prenyldiphosphate transferase	<i>Arabidopsis</i>	VTE2-paralog, At3g11950		[43, 63]
2-Methyl-6-prenylbenzoquinol methyltransferase (PrBQMT)	<i>Synechocystis</i>	sll0418		[51]
	<i>Arabidopsis</i>	VTE3, At3g63410	<i>vte3-1</i> <i>vte3-1</i> , <i>vte3-2</i>	[62] [6]
Tocopherol/tocotrienol cyclase (TC)	Sunflower			[58]
	<i>Synechocystis</i>	slr1737		[44]
	<i>Arabidopsis</i>	VTE1, At4g32770	<i>vte1</i> <i>vte1-1</i> , <i>vte1-2</i>	[38] [44]
	Maize	SXD1	<i>sxd1</i>	[37]
Tocopherol/tocotrienol methyltransferase (TMT)	Potato	StSXD1		[21]
	<i>Synechocystis</i>	slr0089		[50]
	<i>Arabidopsis</i>	VTE4, At1g64970		[50]
	<i>Perilla</i>		<i>vte4-1</i> , <i>vte4-2</i>	[4]
Phytol kinase (PK)	Sunflower			[59]
	<i>Synechocystis</i>	slr1652		[18]
	<i>Arabidopsis</i>	VTE5, At5g04490	<i>vte5-1</i>	[61] [61]

group and is derived from tyrosine via the shikimate pathway. Tyrosine is deaminated to *p*-hydroxyphenylpyruvate (HPP), which in turn is oxygenated to HGA. HGA is also used in plastoquinone synthesis. The second required substrate is a prenyldiphosphate (PrDP), either phytyldiphosphate (PDP) or geranylgeranyldiphosphate (GGDP). These prenyl groups are supplied by the 1-deoxy-D-xyulose-5-phosphate (DXP) pathway, reviewed by Lichtenthaler [29]. GGDP can be used directly in tocotrienol synthesis or reduced to PDP for tocopherol biosynthesis. The proposed route for phytol synthesis has recently been revised [23, 61]. In the revised path, GGDP is incorporated into chlorophyll where the geranylgeranyl moiety is reduced to a phytyl moiety. Free phytol is released during chlorophyll breakdown [22]. One fate of this phytol may be phosphorylation and incorporation into tocopherols [23, 54, 61]. In addition to the two required substrates HGA and PrDP, tocopherols are mono-, di-, or trimethylated. The methyl donor is S-adenosyl-methionine [53]. The methylation pattern affects the bioavailability of the vitamin E as well as the antioxidant capabilities [24].

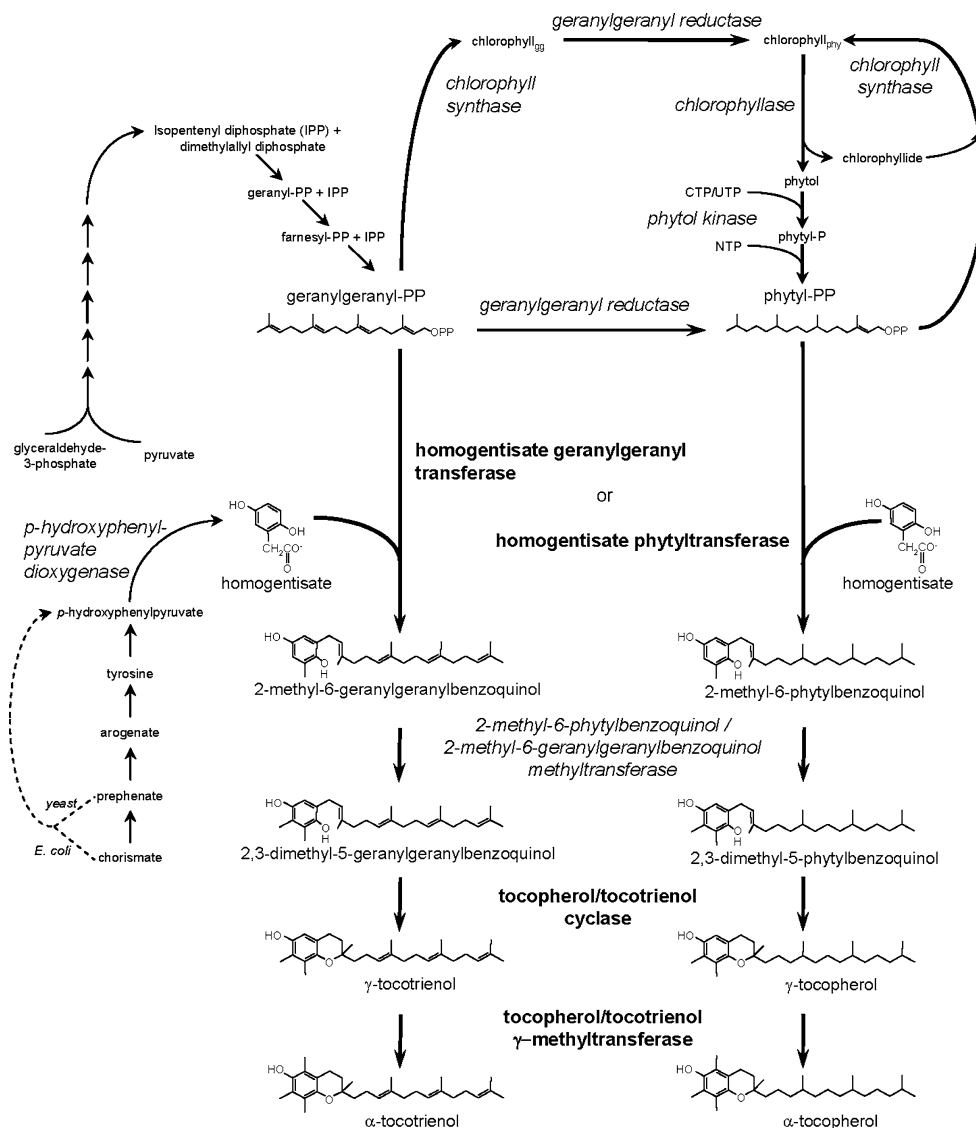
#### Homogentisate Prenyltransferases

The first step of vitamin E biosynthesis is the transfer of a prenyl group to HGA. This transfer, a condensation and decarboxylation [52], occurs via either homogentisate

phytyltransferase (HPT) or homogentisate geranylgeranyl transferase (HGGT). The substrate specificity of the prenyltransferase determines whether the final tocopherol will be a tocopherol or a tocotrienol. Tocopherols, with a phytyl tail, are more common in most plant tissues than tocotrienols, with a geranylgeranyl tail. Prenyltransferase activity was reported by Soll et al. [53] in 1980, working with spinach chloroplasts. To date, homogentisate prenyltransferase genes for vitamin E have been cloned from *Synechocystis* [7, 46, 47], *Arabidopsis* [7, 46], and the monocots barley, wheat, and rice [5]. The prenyltransferases are part of the ubiA prenyltransferase family and are predicted to be integral membrane proteins. Activity has been localized to the inner membranes of both chloroplasts [55] and chromoplasts [2] using cell fractionation methods.

The *Arabidopsis* HPT has been expressed in *E. coli*, where it has a strong substrate preference for PDP over GGDP [7, 43]. It shows no activity towards solanesyldiphosphate (SDP) [7, 43], a prenyltransferase activity required for phyloquinone biosynthesis. The *Synechocystis* enzyme has also been expressed in *E. coli* [7] and insect Sf-9 cells using a baculovirus system [46]. The *Synechocystis* HPT has activity for both PDP and GGDP, although in vitro GGDP activity is less than 20% of in vitro PDP activity [7]. No reports of HGGT expression have been made, and attempts to express the enzyme in *E. coli* have been unsuccessful [5]. However, HGGT is presumed to have

**Fig. 3** Biosynthesis of vitamin E occurs in plastids. The substrates, HGA and either GGDP (for tocotrienols) or PDP (for tocopherols) come from the shikimate and the deoxy-D-xylulose phosphate pathways, respectively. Enzymes in *bold* are specific to the synthesis of tocochromanols. Enzymes denoted in *italics*, while vital for vitamin E biosynthesis, are also used in other pathways. Neither methyltransferase step is required for tocochromanol synthesis. The figure shows the production of vitamin E molecules with  $\alpha$ - and  $\gamma$ -head groups.  $\delta$ -Head groups are produced when both methyltransferase steps are bypassed.  $\beta$ -Tocochromanols result when the first methylation step is omitted, but the second methylation step is included. The production of HPP varies. The pathway for plant synthesis is shown with *solid arrows*. Shunts, shown with *dashed lines*, have been used to manipulate vitamin E production in plants. In *E. coli* HPP is produced directly from chorismate by a bifunctional enzyme. In yeast, a prephenate dehydrogenase produces HPP



higher activity with GGDP than with PDP (as indicated in Fig. 3), based on the ability of the barley, wheat, and rice enzymes to confer tocotrienol biosynthetic ability to plant cells upon transgenic expression [5]. An additional prenyltransferase (referred to in Table 1 as “homogentisate prenyldiphosphate transferase”) has recently been identified [43, 65]. The recombinant enzyme expressed in *E. coli* shows strongest activity toward SDP, with minor activity for GGDP and PDP [43], however, the *in vivo* function of this prenyltransferase is not yet clear.

HPTs and HGGTs have been transgenically expressed in plants. Overexpression of HPT increases tocopherol content of *Arabidopsis* leaves [8], and antisense suppression of HPT expression in *Arabidopsis* seeds reduces levels up to ten-fold compared to seeds from non-transformed plants [46]. Expression of the barley HGGT in *Arabidopsis* leaves shifts toco-

chromanol biosynthesis toward the production of tocotrienols rather than tocopherols and increases total tocochromanol content [5]. This result clearly indicates that homogentisate prenyltransferases alone can dictate whether tocopherols or tocotrienols are produced by plant cells. In addition, the enhanced levels of tocochromanols that accompany HPT or HGGT overexpression suggest that homogentisate prenyltransferases can assert flux control through the vitamin E biosynthetic pathway. As such, these enzymes have been major targets for biotechnological efforts to fortify the tocochromanol content of oilseeds, as described below.

#### 2-Methyl-6-Prenylbenzoquinol Methyltransferase

In order to have  $\gamma$ - or  $\alpha$ -tocochromanols, the number 3 position on the benzoquinol ring must be methylated.



**Table 2** Summary of enzymes and major reactants found in vitamin E biosynthesis

Enzyme	Substrate(s)	Product(s)
<i>p</i> -Hydroxyphenylpyruvate dioxigenase (HPPD)	<i>p</i> -Hydroxyphenylpyruvate (HPP)	Homogentisate (HGA)
Geranylgeranyl reductase (GGR)	Geranylgeranyldiphosphate (GGDP)	Phytyldiphosphate (PDP)
Homogentisate phytyltransferase (HPT)	Chlorophyll <sub>geranylgeranyl</sub> HGA + PDP	Chlorophyll <sub>phytyl</sub> 2-Methyl-6-phytylbenzoquinol
Homogentisate geranylgeranyl transferase (HGGT)	HGA + GGDP (minor) HGA + GGDP	2-Methyl-6-geranylgeranyl-benzoquinol 2-Methyl-6-geranylgeranyl-benzoquinol
Prenylbenzoquinol methyltransferase (PrBQMT)	HGA + PDP (minor)	2-Methyl-6-phytylbenzoquinol
Tocopherol/tocotrienol cyclase (TC)	2-Methyl-6-phytylbenzoquinol 2-Methyl-6-geranylgeranyl-benzoquinol 2,3-Dimethyl-5-phytyl-benzoquinol 2,3-Dimethyl-5-geranylgeranyl-benzoquinol	2,3-Dimethyl-5-phytyl-benzoquinol 2,3-Dimethyl-5-geranylgeranyl-benzoquinol $\delta$ -Tocopherol $\delta$ -Tocotrienol $\gamma$ -Tocopherol $\gamma$ -Tocotrienol
Tocopherol/tocotrienol methyltransferase (TMT)	$\delta$ -Tocopherol $\delta$ -Tocotrienol $\gamma$ -Tocopherol $\gamma$ -Tocotrienol	$\beta$ -Tocopherol $\beta$ -Tocotrienol $\alpha$ -Tocopherol $\alpha$ -Tocotrienol
Phytol kinase (PK)	Phytol + CTP or UTP	Phytylmonophosphate (PMP)
Phytylmonophosphate kinase	PMP + NTP	PDP

This methylation step is omitted when  $\beta$ - and  $\delta$ -tocochromanols are produced. Methyltransferase activity was identified in 1980 [53] and a gene for 2-methyl-6-phytylbenzoquinol methyltransferase (PrBQMT) was cloned from *Synechocystis* in 2002 [51]. Since the production of  $\gamma$ - and  $\alpha$ -tocotrienols can be accomplished with the addition of the HGGT gene alone, PrBQMT appears to methylate either tocopherols or tocotrienols [5]. The enzyme has been localized to the chloroplast inner membrane [55] and the *Arabidopsis* gene has a putative transit peptide [6]. The *Synechocystis* gene was cloned via homology to the *Arabidopsis*  $\gamma$ -tocopherol methyltransferase (TMT) gene. The *Arabidopsis* PrBQMT gene has only 18% amino acid sequence identity to the *Synechocystis* gene [6], and was identified by forward genetics using screens for altered tocopherol composition [6, 62]. The *Arabidopsis* and cyanobacterial genes have been expressed in *E. coli*. In this system, the transferase activity does not appear to depend on the prenyl tail; both phytylbenzoquinols and solanesylbenzoquinols are used [6, 51, 62]. Although Soll and Schultz [53] reported methyltransferase activity with  $\beta$ -tocopherol, recent work has not duplicated that activity, activity assayed from *E. coli* expression experiments shows no activity toward  $\beta$ - and  $\delta$ -tocopherols [6, 51], thus, if the 3 position is to be methylated for either  $\gamma$ - or  $\alpha$ -tocochromanols, it appears that this methylation must happen before the cyclization. The main effect of overexpression of PrBQMT is to alter the composition, but not the total content of vitamin E. For example, overexpression in soybean seeds converts the pools of  $\delta$ - and  $\beta$ -tocopherols to  $\gamma$ - and

$\alpha$ -tocopherols but does not affect the total tocopherol content [62].

#### Tocopherol/Tocotrienol Cyclase

Tocopherol/tocotrienol cyclase (TC) is the second enzyme required for vitamin E biosynthesis (Fig. 3). It forms the chromanol head group from a benzoquinol intermediate. The product is either  $\gamma$ -tocochromanol or  $\delta$ -tocochromanol, depending on the methylation status of the chromanol head group. Unlike the other enzymes in the vitamin E pathway, TC has been localized to plastoglobules in chloroplasts [3, 64], but not to the inner membrane [52]. Since both  $\delta$ - and  $\gamma$ -tocochromanols are found in plants it is presumed that TC cyclizes both mono- and di-methylated prenylbenzoquinols. Cyclase genes from *Arabidopsis* [38, 44], potato [21], and maize [44] as well as cyanobacteria [56] have been cloned and expressed in *E. coli*. The activity shows little, if any, preference for phytylated substrates over geranylgeranylated substrates [21, 38]. Thus, TC produces both  $\gamma$ - and  $\delta$ -tocopherols and  $\gamma$ - and  $\delta$ -tocotrienols.

Although the cyclase gene was first identified as a vitamin E biosynthetic gene in 2002 [38], the *Arabidopsis* VTE1 gene is homologous to a maize gene *SXD1*. The maize mutant, *sxd1*, is deficient in sucrose transport [37]. Although further work has established that the maize gene complements the *Synechocystis* slr1737 knockout mutant [44] and affects tocopherol production in potato and *Arabidopsis* as well as maize and *Synechocystis* [21, 44], the *Arabidopsis* mutants do

not share the maize phenotype [38]. The link between vitamin E and sucrose transport is still under investigation.

When TC is constitutively overexpressed in *Arabidopsis*, the total leaf tocopherol content increases seven-fold, suggesting that TC, as well as the prenyltransferases, may play a role in flux control through the pathway [25].

#### Tocopherol/Tocotrienol Methyltransferase

Tocopherol/tocotrienol methyltransferase (TMT) catalyzes the final step in synthesis of  $\alpha$ - or  $\beta$ -tocochromanols: the methylation of the number 5 carbon on the chromanol ring (Fig. 3). This enzyme is often referred to as  $\gamma$ -tocopherol methyltransferase, but it also has activity with  $\delta$ -tocopherol,  $\delta$ -tocotrienol, and  $\gamma$ -tocotrienol. This methyltransferase activity was identified in 1980 and localized to the inner membrane of spinach chloroplasts [53], and the enzyme was purified from pepper chromoplasts [10]. The TMT gene was isolated from *Synechocystis* using homology to previously identified genes involved in vitamin E biosynthesis and looking for candidate genes on the same operon [50]. The *Arabidopsis* gene was then cloned via homology to the newly identified *Synechocystis* TMT [50]. *E. coli*-expressed *Arabidopsis* TMT methylates both  $\gamma$ - and  $\delta$ -tocopherol but has almost a three-fold preference for  $\gamma$ -tocopherol [50]. Overexpression of *Arabidopsis* TMT also converts nearly the entire content of  $\gamma$ -tocopherol in *Arabidopsis* seeds to  $\alpha$ -tocopherol [50]. Because most dicot seeds are enriched in  $\gamma$ -tocopherol, this result provides clear evidence that TMT activity is limiting for  $\alpha$ -tocopherol synthesis in dicot seeds, including major oilseeds such as canola and soybean.

#### Phytol Kinase and Phytylmonophosphate Kinase

While a phytol kinase (PK) activity had been reported in early work [54], conventional pathways had no source for PDP other than direct reduction of GGDP by geranylgeranyl reductase (GGR). However, recent work has demonstrated that a pathway from phytol to PDP exists [23] and a gene encoding PK has been identified and cloned [61]. Two separate kinase activities are required to synthesize PDP from phytol [23]. Free phytol increases during senescence as the phytyl moiety from chlorophyll is released by chlorophyllase [22]. Phytol from chlorophyll is phosphorylated by CTP or UTP [61, 23]. Using an *Arabidopsis* mutant with only 20% of wild type levels of total tocopherol Valentin et al. [61] cloned *VTE5*, which, when expressed in *E. coli*, phosphorylates free phytol. The

*Arabidopsis* phytol kinase gene contains a putative transit peptide and is predicted to be an integral membrane protein. A separate kinase activity phosphorylates phytylmonophosphate (PMP) to PDP using any of the four nucleotide triphosphates [23]. However, the gene that codes for PMP kinase activity has not yet been reported. Thus, phytol from chlorophyll breakdown can be used in tocopherol synthesis via direct phosphorylation of phytol and phytylmonophosphate.

#### Substrate Supply: Homogentisate and Prenyldiphosphates

The HGA used in tocochromanol biosynthesis is derived from HPP via a decarboxylation by hydroxyphenylpyruvate dioxygenase (HPPD) [17]. HPP, in turn, is derived from tyrosine via the shikimate pathway. HPP is synthesized differently in plants, bacteria, and yeast. In plants, chorismate, the end product of the shikimate pathway, is isomerized to prephenate. An aminotransferase creates aroenate from prephenate, and the aroenate is dehydrogenated to tyrosine. This aroenate-to-tyrosine step is subject to strong feedback regulation by tyrosine [9]. In *E. coli* and yeast, bifunctional enzymes bypass some or all of these steps. In *E. coli*, the precursor for tyrosine is chorismate [20], and in yeast the precursor is prephenate [41].

Overexpression of HPPD by itself has a negligible or only modest effect on increasing total tocopherol content in leaves and seeds of tobacco and *Arabidopsis* [14, 41]. Unlike the rest of the enzymes involved in vitamin E biosynthesis, HPPD is a cytosolic enzyme [17]. However, redirecting HPPD to plastids by addition of a transit peptide does not enhance tocopherol content over levels achieved by cytosolic expression [16]. In spite of this, feeding experiments in soybean suspension cultures indicate that HGA may limit vitamin E production, since addition of exogenous HGA doubles tocochromanol levels [26]. Thus, while the supply of HGA may be limiting, overexpression of HPPD alone does not result in large increases of tocochromanol content.

The prenyldiphosphate is supplied by the DXP pathway (also called the methylerythritol phosphate pathway), reviewed in [29]. Products of the DXP pathway are used in carotenoid, phyloquinone, terpenoid, and gibberellin biosyntheses as well as vitamin E biosynthesis [13]. Increased flux through the DXP pathway can increase vitamin E content. When 1-deoxy-D-xylulose-5-phosphate synthase, the gene for the first step in the DXP path, is overexpressed,

vitamin E content increases 1.5- to 2-fold [13]. Conversely, in deoxy-D-xylulose-5-phosphate synthase antisense plants, vitamin E content slightly decreases [13]. Additionally, competition for isoprenoid substrates between the vitamin E and other pathways can also decrease tocopherol content. For example, transgenic expression of a bacterial phytoene synthase, which uses GGDP as its substrate, results in a 50-fold increase in carotenoid levels in canola seeds, but the tocopherol content of these seeds is reduced by two-fold [49].

Four five-carbon isoprenoid moieties are required for the synthesis of the prenyldiphosphate moiety of tocochromanols. GGDP can be used directly in tocotrienol synthesis or reduced to PDP for tocopherol biosynthesis. Two paths for PDP synthesis have been proposed. In one, GGR reduces GGDP directly, and this PDP is available for incorporation into tocopherols [27, 55]. However, new evidence posits a second path for phytol synthesis through chlorophyll [23, 61]. In this pathway, GGDP is incorporated into chlorophyll, then reduced to phtylated chlorophyll. During chlorophyll breakdown, free phytol is released. This free phytol is then phosphorylated, creating PDP for incorporation into tocopherols. Kinase activity has been discovered as discussed above [23, 54, 61]. It is likely that both routes are used *in vivo*, since the phytol kinase mutant still has tocopherol [61], and many seeds that produce tocopherols lack detectable chlorophyll to support flux through the second pathway.

### Tocotrienol Biosynthesis

Tocotrienols occur principally in the endosperm of monocot seeds, and for the most part, tocotrienol biosynthesis differs little from tocopherol synthesis. The isolation of HGGT genes from barley, rice, and wheat provide a biochemical and genetic explanation for the occurrence of tocotrienols in monocot seeds [5]. The monocot HGGT identified to date share only 40–50% amino acid sequence identity with HPT, and the expression of the HGGT gene in barley was shown to be seed-specific, consistent with the location of tocotrienol accumulation in this plant [5]. Transgenic expression of the barley HGGT in tobacco callus and *Arabidopsis* leaves, which normally produce only tocopherols, results in the production of tocotrienols [5]. This result demonstrates that HGGT expression alone is sufficient to confer tocotrienol biosynthetic ability to plant cells. Seeds from some dicot species such as those of the Apiaceae family are also enriched in tocotrienols [1, 32]. Based on the monocot example, the simplest biosynthetic route that can account for tocotrienols in

these seeds is the activity of a yet to be identified HGGT-like enzyme.

The other enzymes of tocopherol biosynthesis have activity for both phtylated and geranylgeranylated compounds (Fig. 3). The *Arabidopsis* TC has about equal activity towards both forms of benzoquinols [38]. When tobacco callus is transformed with barley HGGT, all four forms of tocotrienols are detected [5], hence methyltransferase can use geranylgeranyl-derived substrates to produce different methylated forms of tocotrienols. However, it remains to be determined if variant forms of TC, PrBQMT, and TMT have evolved for the more efficient synthesis of tocotrienols in the endosperm of monocot seeds.

### HGGT-Independent Tocotrienol Synthesis

Several recent experiments in transgenic plants have uncovered an alternative route for tocotrienol synthesis. In these experiments, HGA synthesis is strongly upregulated by co-expression of HPPD with a yeast or bacterial enzyme that produces the HPP substrate for HPPD directly from the shikimate pathway. The yeast enzyme used in these studies was the prephenate dehydrogenase [41], and the bacterial enzyme used was the bifunctional chorismate mutase/prephenate dehydrogenase (encoded by the *tyrA* gene) [20, 26]. HPP is typically synthesized in two steps from tyrosine in plants (Fig. 3). The yeast and bacterial enzymes, however, shunt flux upstream of tyrosine (from prephenate or chorismate) toward the synthesis of HPP. This effectively bypasses steps in tyrosine synthesis that are normally negatively regulated by pool sizes of this amino acid [9, 20]. Through this strategy, high levels of tocotrienols were produced in tobacco leaves [20, 41], *Synechocystis* [26], and canola and soybean seeds [26], which normally accumulate only trace amounts of tocotrienols. In studies with soybean, HGA is increased to amounts high enough to alter the color of seeds [26]. Based on our current knowledge of vitamin E biosynthesis, it is unclear how greatly enhanced production of HGA results in tocotrienol synthesis. The *Arabidopsis* HPT, for example, displays relatively low activity with GGDP, the isoprenoid substrate for tocotrienol synthesis [7, 43]. Regardless, the production of tocotrienols, rather than tocopherols, through this alternative route suggests that available GGDP pools must greatly exceed those of PDP for tocochromanol synthesis. Although this transgenic method for production of tocotrienols is biochemically intriguing, it remains to be determined if this metabolic route normally contributes to tocotrienol synthesis in non-engineered plant cells.

## Genetic Enhancement of Vitamin E Composition and Content in Oilseeds

### Improvement of Tocochromanol Composition

The identification of vitamin E biosynthetic genes has facilitated biotechnological efforts to improve the nutritional value and antioxidant content of crop plants. One focus of this research has involved increasing the expression of methyltransferase genes to convert tocopherol in leaves or seeds into the more nutritious  $\alpha$  form. This approach has been of particular interest for the nutritional enhancement of seed oils from dicotyledonous grain crops (e.g., soybean and canola), which are typically enriched in  $\gamma$ -tocopherol. The ability to genetically convert the bulk of the tocopherol in plant organs from the  $\gamma$  to  $\alpha$  form was first demonstrated using the model plant *Arabidopsis thaliana* [50]. In this study, the tocopherol composition of *A. thaliana* seeds was shifted from 97%  $\gamma$ -tocopherol to 95%  $\alpha$ -tocopherol by genetic transformation with a cDNA for the *A. thaliana* TMT under control of a strong seed-specific promoter. Given that  $\alpha$ -tocopherol has ten-times greater vitamin E activity than  $\gamma$ -tocopherol, the net effect is an approximately nine-fold increase in the vitamin E activity of *Arabidopsis* seeds. Notably, this alteration in tocopherol composition is not accompanied by an increase in total tocochromanol content. The ability to increase relative amounts of  $\alpha$ -tocopherol by increased expression of TMT has subsequently been shown in seeds of crop plants including soybean [26, 59, 62] and *Brassica juncea* [69].

Soybean seeds offer an additional challenge for the generation of high levels of  $\alpha$ -tocopherol. The tocopherols of soybean seeds are composed of approximately 20%  $\delta$ -tocopherol and 65%  $\gamma$ -tocopherol. This is in contrast to the tocopherols of *A. thaliana* seeds, which are almost exclusively in the  $\gamma$  form. The conversion of  $\delta$ -tocopherol to  $\alpha$ -tocopherol requires two sequential enzymatic steps: (a) PrBQMT to convert  $\delta$ -tocopherol to  $\gamma$ -tocopherol and (b) TMT to convert the resulting  $\gamma$ -tocopherol to  $\alpha$ -tocopherol. Consistent with this, seed-specific co-expression of PrBQMT and TMT transgenes in soybean yields seeds with >90%  $\alpha$ -tocopherol [62]. In this study, enhanced expression of only PrBQMT results in seeds that contain exclusively the  $\gamma$  and  $\alpha$  forms of tocopherol, with a ratio of 80%  $\gamma$ -tocopherol and 20%  $\alpha$ -tocopherol. Increased expression of TMT alone yields seeds with approximately 75%  $\alpha$ -tocopherol and 25%  $\beta$ -tocopherol. These results demonstrate the utility of altering flux through PrBQMT and TMT to generate novel tocochromanol compositions.

Given that  $\delta$ - and  $\gamma$ -tocopherol confer greater oxidative stability to frying oils than  $\alpha$ -tocopherol [65, 66], it can be envisioned that suppression of methyltransferase expression may be of commercial value for generating improved vegetable oils for food processing and high-temperature lubricant applications. This is of particular significance with regard to sunflower. The tocopherols in seeds of this crop are composed of >90%  $\alpha$ -tocopherol. By mutational breeding, sunflower varieties have been generated with seeds that contain exclusively  $\delta$ - and  $\gamma$ -tocopherol [18, 58]. This composition was achieved by crossing lines with lesions in genes for PrBQMT and TMT [18, 58].

### Enhancement of Tocochromanol Content

A second focus of biotechnological efforts for vitamin E enhancement has been the production of increased total amounts of tocochromanols in seeds of crop species. As described in the “Introduction”, increasing the content of tocochromanols in seeds may be useful for enhancing the antioxidant capacity of vegetable oils. This, in turn, may improve the oxidative stability of vegetable oils in frying and other food processing applications and in high-temperature lubricants. This research to date has been successful in generating seeds with increased amounts of tocotrienols, but less successful in the enhancement of tocopherol levels in seeds. Attempts to increase the tocopherol content of seeds by use of a single transgene have centered on (a) increasing flux in the tocopherol biosynthetic pathway by overexpression of HPT or TC or (b) by increasing the supply of the HGA head group by overexpression of cDNAs for HPPD. Based on results obtained from overexpression studies in leaves, HPT and TC would appear to be logical targets for the enhancement of tocopherol levels in seeds. For example, overexpression of HPT and TC in leaves of *A. thaliana* results in a four- and seven-fold increase, respectively, in tocopherol content [7, 38]. However, expression of these enzymes using transgenes containing strong seed-specific promoters yields only modest increases (less than 1.5-fold) in the tocopherol content of seeds of *A. thaliana* [46], *B. napus* [28, 40], and soybean [26]. Similar results were also obtained with the overexpression of HPPD in seeds of these plants [26, 40, 60]. Only by co-expressing cDNAs for HPT, TC, and HPPD have increases in tocopherol content in the range 2- to 2.5-fold been achieved in *B. napus* seeds [40], which is the largest enhancement of tocopherol levels reported to date in an oilseed.

In contrast to the relatively small increases in tocopherol content attained by overexpression of HPT,

TC, or HPPD, seed-specific expression of an HGGT transgene resulted in up to a six-fold enhancement of the tocochromanol content of corn seeds, largely in the form of tocotrienols [5]. This is currently the largest increase in tocochromanol content in an engineered seed obtained by expression of only one transgene. A possible explanation for the success of this approach compared to HPT overexpression is that GGDP pools that support tocotrienol synthesis may greatly exceed those of PDP that are available for tocopherol synthesis.

The largest increase in total tocochromanol content achieved to date in genetically enhanced seeds was reported by Karunanandaa et al. [26]. In this study, co-expression of transgenes for HPPD, GGR, HPT, and a bacterial bifunctional chorismate mutase/prephenate dehydrogenase (encoded by the *tyrA* gene) increases total tocochromanol content in soybean seeds 10- to 15-fold. Although the goal of this experiment was to enhance tocopherol levels, the increase in tocochromanol content was largely due to the production of tocotrienols. In the highest tocochromanol-producing seeds, tocotrienols account for over 90% of the tocochromanols. Notably, tocotrienols are only trace components of the tocochromanols of non-engineered soybean seeds. The production of tocotrienols in vast preference to tocopherols in these seeds (in the apparent absence of HGGT) is also consistent with the existence of GGDP pools that greatly exceed those of PDP in seed plastids. Presumably under the metabolic conditions created in these seeds, HPT is able to use GGDP as a substrate despite its relatively low in vitro activity with this substrate [43].

The inability to engineer large increases in the tocopherol content of oilseeds points to a lack of understanding of the biosynthesis of PDP in seed plastids. The studies by Karunanandaa et al. [26] suggest that the availability of PDP limits the amounts of tocopherol synthesized. As described above, recent evidence points to a route of PDP synthesis involving the modification of geranylgeranyl-chlorophyll by the activity of GGR (Fig. 3) [61]. Developing metabolic engineering strategies to increase flux through this pathway may be necessary for increasing PDP pool sizes in plastids to support high levels of flux toward the synthesis of tocopherols rather than tocotrienols.

In conclusion, the isolation of genes for PrBQMT and TMT has facilitated biotechnological efforts to improve the nutritional value of vegetable oils. By increasing the expression of genes for one or both of these enzymes, it has been possible to shift the tocopherol content of oilseeds from the  $\delta$ ,  $\beta$ , and  $\gamma$  forms to the  $\alpha$  form, which has the highest vitamin E

activity of any of the naturally occurring tocochromanols. Efforts to engineer increased total tocopherol content in oilseeds, however, have met with only modest success. This appears to be due to the inability to generate enhanced pool sizes of the PDP substrate, because of gaps in our understanding of its synthesis from GGDP in seeds. The genetic enhancement of total tocotrienol content by expression of HGGT or by strong upregulation of HGA synthesis has proven to be a more successful strategy for generating seeds with increased amounts of vitamin E antioxidants. Through these approaches, corn and soybean seeds with 6- to 10-fold increases in total tocochromanol content have been produced. The availability of tocotrienol-enriched corn and soybean seeds should allow for functionality testing of the extracted oil to evaluate its performance in food processing, lubricants, and other commercial applications.

**Acknowledgments** The authors' work is supported by the National Research Initiative of the USDA Co-operative State Research, Education and Extension Service, grant number 2004-35318-14887.

## References

1. Aizetmüller K (1997) Antioxidative effects of *Carum* seeds. *J Am Oil Chem Soc* 74:185
2. Arango Y, Heise K (1998) Short communication. Localization of  $\alpha$ -tocopherol synthesis in chromoplast envelope membranes of *Capsicum annuum* L. *Fruits J Exp Bot* 49:1259–1262
3. Austin JR II, Frost E, Vidi PA, Kessler F, Staehelin LA (2006) Plastoglobules are lipoprotein subcompartments of the chloroplast that are permanently coupled to thylakoid membranes and contain biosynthetic enzymes. *Plant Cell* 18:1693–1703
4. Bergmüller E, Porfirova S, Dörmann P (2003) Characterization of an *Arabidopsis* mutant deficient in  $\gamma$ -tocopherol methyltransferase. *Plant Mol Biol* 52:1181–1190
5. Cahoon EB, Hall SE, Ripp KG, Ganzke TS, Hitz WD, Coughlan SJ (2003) Metabolic redesign of vitamin E biosynthesis in plants for tocotrienol production and increased antioxidant content. *Nat Biotechnol* 21:1082–1087
6. Cheng Z, Sattler S, Maeda H, Sakuragi Y, Bryant DA, DellaPenna D (2003) Highly divergent methyltransferases catalyze a conserved reaction in tocopherol and plastoquinone synthesis in cyanobacteria and photosynthetic eukaryotes. *Plant Cell* 15:2343–2356
7. Collakova E, DellaPenna D (2001) Isolation and functional analysis of homogentisate phytyltransferase from *Synechocystis* sp. PCC 6803 and *Arabidopsis*. *Plant Physiol* 127:1113–1124
8. Collakova E, DellaPenna D (2003) Homogentisate phytyltransferase activity is limiting for tocopherol biosynthesis in *Arabidopsis*. *Plant Physiol* 131:632–642
9. Coruzzi G, Last RL (2000) Amino acids (Chapter 8). In: Buchanan BB, Gruissem W, Jones RL (eds) *Biochemistry and molecular biology of plants*. American Society of Plant Physiologists, Rockville, pp 358–410

10. d'Harlingue A, Camara B (1985) Plastid enzymes of terpenoid biosynthesis. Purification and characterization of  $\gamma$ -tocopherol methyltransferase from *Capsicum* chromoplasts. *J Biol Chem* 260:15200–15203
11. Domergue F, Abbadi A, Heinz E (2005) Relief for fish stocks: oceanic fatty acids in transgenic oilseeds. *Trends Plant Sci* 10:112–116
12. Erhan SZ, Asadauskas S (2000) Lubricant basestocks from vegetable oils. *Ind Crops Prod* 11:277–282
13. Estévez JM, Cantero A, Reindl A, Reichler S, León P (2001) 1-Deoxy-D-xylulose-5-phosphate synthase, a limiting enzyme for plastidic isoprenoid biosynthesis in plants. *J Biol Chem* 276:22901–22909
14. Falk J, Andersen G, Kernebeck B, Krupinska K (2003) Constitutive overexpression of barley 4-hydroxyphenylpyruvate dioxygenase in tobacco results in elevation of the vitamin E content in seeds but not in leaves. *FEBS Lett* 540:35–40
15. Falk J, Krahnstöver A, van der Kooij TA, Schlenz M, Krupinska K (2004) Tocopherol and tocotrienol accumulation during development of caryopses from barley (*Hordeum vulgare* L.) *Phytochemistry* 65:2977–2985
16. Falk J, Brosch M, Schäfer A, Braun S, Krupinska K (2005) Characterization of transplastomic tobacco plants with a plastid localized barley 4-hydroxyphenylpyruvate dioxygenase. *J Plant Physiol* 162:738–742
17. Garcia I, Rodgers M, Pepin R, Hsieh TF, Matringe M (1999) Characterization and subcellular compartmentation of recombinant 4-hydroxyphenylpyruvate dioxygenase from *Arabidopsis* in transgenic tobacco. *Plant Physiol* 119:1507–1516
18. Hass CG, Tang S, Leonard S, Traber MG, Miller JF, Knapp SJ (2006) Three non-allelic epistatically interacting methyltransferase mutations produce novel tocopherol (vitamin E) profiles in Sunflower. *Theor Appl Genet* 113:767–782
19. Havaux M, Eymery F, Porfirova S, Rey P, Dörmann P (2005) Vitamin E protects against photoinhibition and photooxidative stress in *Arabidopsis thaliana*. *Plant Cell* 17:3451–3469
20. Herbers K (2003) Vitamin production in transgenic plants. *J Plant Physiol* 160:821–829
21. Hofius D, Hajirezaei MR, Geiger M, Tschiersch H, Melzer M, Sonnewald U (2004) RNAi-mediated tocopherol deficiency impairs photoassimilate export in transgenic potato plants. *Plant Physiol* 135:1256–1268
22. Hörtensteiner S (2006) Chlorophyll degradation during senescence. *Annu Rev Plant Biol* 57:55–77
23. Ischebeck T, Zbierzak AM, Kanwischer M, Dörmann P (2006) A salvage pathway for phytol metabolism in *Arabidopsis*. *J Biol Chem* 281:2470–2477
24. Kamal-Eldin A, Appelqvist LA (1996) The chemistry and antioxidant properties of tocopherols and tocotrienols. *Lipids* 31:671–701
25. Kanwischer M, Porfirova S, Bergmüller E, Dörmann P (2005) Alterations in tocopherol cyclase activity in transgenic and mutant plants of *Arabidopsis* affect tocopherol content, tocopherol composition, and oxidative stress. *Plant Physiol* 137:713–723
26. Karunanandaa B, Qi Q, Hao M, Baszis SR, Jensen PK, Wong YH, Jiang J, Venkatramesh M, Gruys KJ, Moshiri F, Post-Beittenmiller D, Weiss JD, Valentin HE (2005) Metabolically engineered oilseed crops with enhanced seed tocopherol. *Metab Eng* 7:384–400
27. Keller Y, Bouvier F, d'Harlingue A, Camara B (1998) Metabolic compartmentation of plastid prenyl lipid biosynthesis. Evidence for the involvement of a multifunctional geranylgeranyl reductase. *Eur J Biochem* 251:413–417
28. Kumar R, Raclaru M, Schübeler T, Gruber J, Sadre R, Lühs W, Zarhloul KM, Friedt W, Enders D, Frentzen M, Weier D (2005) Characterisation of plant tocopherol cyclases and their overexpression in transgenic *Brassica napus* seeds. *FEBS Lett* 579:1357–1364
29. Lichtenthaler HK (1999) The 1-deoxy-D-xylulose-5-phosphate pathway of isoprenoid biosynthesis in plants. *Annu Rev Plant Physiol Plant Mol Biol* 50:47–65
30. Liu Q, Lanari MC, Schaefer DM (1995) A review of dietary vitamin E supplementation for improvement of beef quality. *J Anim Sci* 73:3131–3140
31. Maeda H, Song W, Sage TL, DellaPenna D (2006) Tocopherols play a crucial role in low-temperature adaptation and phloem loading in *Arabidopsis*. *Plant Cell* 18:2710–2732
32. Matthaas B, Vosmann K, Pham LQ, Aizetmüller K (2003) FA and tocopherol composition of Vietnamese oilseeds. *J Am Oil Chem Soc* 80:1013–1020
33. Nesaretnam K, Stephen R, Dils R, Darbre P (1998) Tocotrienols inhibit the growth of human breast cancer cells irrespective of estrogen receptor status. *Lipids* 33:461–469
34. Öhrvall M, Sundlöf G, Vessby B (1996) Gamma, but not alpha, tocopherol levels in serum are reduced in coronary heart disease patients. *J Intern Med* 239:111–117
35. Osakada F, Hashino A, Kume T, Katsuki H, Kaneko S, Akaike A (2004)  $\alpha$ -Tocotrienol provides the most potent neuroprotection among vitamin E analogs on cultured striatal neurons. *Neuropharmacology* 47:904–915
36. Pearce BC, Parker RA, Deason ME, Qureshi AA, Wright JJ (1992) Hypocholesterolemic activity of synthetic and natural tocotrienols. *J Med Chem* 35:3595–3606
37. Porfirova S, Bergmüller E, Tropf S, Lemke R, Dörmann P (2002) Isolation of an *Arabidopsis* mutant lacking vitamin E and identification of a cyclase essential for all tocopherol biosynthesis. *Proc Natl Acad Sci USA* 99:12495–12500
38. Provencher LM, Miao L, Sinha N, Lucas WJ (2001) *Sucrose export defective1* encodes a novel protein implicated in chloroplast-to-nucleus signaling. *Plant Cell* 13:1127–1141
39. Qureshi AA, Burger WC, Peterson DM, Elson CE (1986) The structure of an inhibitor of cholesterol biosynthesis isolated from barley. *J Biol Chem* 261:10544–10550
40. Raclaru M, Gruber J, Kumar R, Sadre R, Lühs W, Zarhloul MK, Friedt W, Frentzen M, Weier D (2006) Increase of the tocopherol content in transgenic *Brassica napus* seeds by overexpression of key enzymes involved in prenylquinone biosynthesis. *Mol Breed* 18:93–107
41. Rippert P, Scimemi C, Dubald M, Matringe M (2004) Engineering plant shikimate pathway for production of tocotrienol and improving herbicide resistance. *Plant Physiol* 134:92–100
42. Rise M, Cojocaru M, Gottlieb HE, Goldschmidt EE (1989) Accumulation of  $\alpha$ -tocopherol in senescing organs as related to chlorophyll degradation. *Plant Physiol* 89:1028–1030
43. Sadre R, Gruber J, Frentzen M (2006) Characterization of homogentisate prenyltransferases involved in plastoquinone-9 and tocopherol biosynthesis. *FEBS Lett* 580:5357–5362
44. Sattler SE, Cahoon EB, Coughlan SJ, DellaPenna D (2003) Characterization of tocopherol cyclases from higher plants and cyanobacteria. Evolutionary implications for tocopherol synthesis and function. *Plant Physiol* 132:2184–2195
45. Sattler SE, Gilliland LU, Magallanes-Lundback M, Pollard M, DellaPenna D (2004) Vitamin E is essential for seed longevity and for preventing lipid peroxidation during germination. *Plant Cell* 16:1419–1432
46. Savidge B, Weiss JD, Wong YH, Lassner MW, Mitsky TA, Shewmaker CK, Post-Beittenmiller D, Valentin HE (2002) Isolation and characterization of homogentisate phytyl-

- transferase genes from *Synechocystis* sp. PCC 6803 and *Arabidopsis*. *Plant Physiol* 129:321–332
47. Schledz M, Seidler A, Beyer P, Neuhaus G (2001) A novel phytyltransferase from *Synechocystis* Sp. PCC 6803 involved in tocopherol biosynthesis. *FEBS Lett* 499:15–20
  48. Serbinova EA, Packer L (1994) Antioxidant properties of  $\alpha$ -tocopherol and  $\alpha$ -tocotrienol. *Meth Enzymol* 234:354–366
  49. Shewmaker CK, Sheehy JA, Daley M, Colburn S, Ke DY (1999) Seed-specific overexpression of phytoene synthase: increase in carotenoids and other metabolic effects. *Plant J* 20:401–412
  50. Shintani D, DellaPenna D (1998) Elevating the vitamin E content of plants through metabolic engineering. *Science* 282:2098–2100
  51. Shintani DK, Cheng Z, DellaPenna D (2002) The role of 2-methyl-6-phytylbenzoquinone methyltransferase in determining tocopherol composition in *Synechocystis* sp. PCC6803. *FEBS Lett* 511:1–5
  52. Soll J (1987)  $\alpha$ -Tocopherol and plastoquinone synthesis in chloroplast membranes. *Meth Enzymol* 148:383–392
  53. Soll J, Schultz G (1980) 2-Methyl-6-phytylquinol and 2,3-dimethyl-5-phytylquinol as precursors of tocopherol synthesis in spinach chloroplasts. *Phytochemistry* 19:215–218
  54. Soll J, Schultz G (1981) Phytol synthesis from geranylgeraniol in spinach chloroplasts. *Biochem Biophys Res Commun* 99:907–912
  55. Soll J, Kemmerling M, Schultz G (1980) Tocopherol and plastoquinone synthesis in spinach chloroplasts subfractions. *Arch Biochem Biophys* 204:544–550
  56. Stocker A, Fretz H, Frick H, Rüttimann A, Woggon WD (1996) The substrate specificity of tocopherol cyclase. *Bioorg Med Chem* 4:1129–1134
  57. Suzuki YJ, Tsuchiya M, Wassall SR, Choo YM, Govil G, Kagan VE, Packer L (1993) Structural and dynamic membrane properties of  $\alpha$ -tocopherol and  $\alpha$ -tocotrienol: implication to the molecular mechanism of their antioxidant potency. *Biochemistry* 32:10692–10699
  58. Tang S, Hass CG, Knapp SJ (2006) *Ty3/gypsy*-like retrotransposon knockout of a 2-methyl-6-phytyl-1,4-benzoquinone methyltransferase is non-lethal, uncovers a cryptic paralogous mutation, and produces novel tocopherol (vitamin E) profiles in sunflower. *Theor Appl Genet* 113:783–799
  59. Tavva VS, Kim YH, Kagan IA, Dinkins RD, Kim KH, Collins GB (2007) Increased  $\alpha$ -tocopherol content in soybean seed overexpressing the *Perilla frutescens*  $\gamma$ -tocopherol methyltransferase gene. *Plant Cell Rep* 26:61–70
  60. Tsegaye Y, Shintani DK, DellaPenna D (2002) Overexpression of the enzyme *p*-hydroxyphenylpyruvate dioxygenase in *Arabidopsis* and its relation to tocopherol biosynthesis. *Plant Physiol Biochem* 40:913–920
  61. Valentin HE, Lincoln K, Moshiri F, Jensen PK, Qi Q, Venkatesh TV, Karunanandaa B, Baszis SR, Norris SR, Savidge B, Gruys KJ, Last RL (2006) The *Arabidopsis* vitamin E pathway *gene5-1* mutant reveals a critical role for phytol kinase in seed tocopherol biosynthesis. *Plant Cell* 18:212–224
  62. Van Eenennaam AL, Lincoln K, Durrett TP, Valentin HE, Shewmaker CK, Thorne GM, Jiang J, Baszis SR, Levering CK, Aasen ED, Hao M, Stein JC, Norris SR, Last RL (2003) Engineering vitamin E content: from *Arabidopsis* mutant to soy oil. *Plant Cell* 15:3007–3019
  63. Venkatesh TV, Karunanandaa B, Free DL, Rottnek JM, Baszis SR, Valentin HE (2006) Identification and characterization of an *Arabidopsis* homogentisate phytyltransferase paralog. *Planta* 223:1134–1144
  64. Vidi PA, Kanwischer M, Baginsky S, Austin JR, Csucs G, Dörmann P, Kessler F, Bréhélin C (2006) Tocopherol cyclase (VTE1) localization and vitamin E accumulation in chloroplast plastoglobule lipoprotein particles. *J Biol Chem* 281:11225–11234
  65. Wagner KH, Elmadfa I (2000) Effects of tocopherols and their mixtures on the oxidative stability of olive oil and linseed oil under heating. *Eur J Lipid Sci Tech* 102:624–629
  66. Wagner KH, Wotruba F, Elmadfa I (2001) Antioxidative potential of tocotrienols and tocopherols in coconut fat at different oxidation temperatures. *Eur J Lipid Sci Tech* 103:746–751
  67. Warner K, Neff WE, Eller FJ (2003) Enhancing quality and oxidative stability of aged fried food with  $\gamma$ -tocopherol. *J Agric Food Chem* 51:623–627
  68. Waylan AT, O'Quinn PR, Unruh JA, Nelsens JL, Goodband RD, Woodworth JC, Tokach MD, Koo SI (2002) Effects of modified tall oil and vitamin E on growth performance, carcass characteristics, and meat quality of growing-finishing pigs. *J Anim Sci* 80:1575–1585
  69. Yusuf MA, Sarin NB (2007) Antioxidant value addition in human diets: genetic transformation of *Brassica juncea* with  $\gamma$ -TMT gene for increased  $\alpha$ -tocopherol content. *Transgenic Res* 16:109–113

## Dose-Dependent Effects of Docosahexaenoic Acid Supplementation on Blood Lipids in Statin-Treated Hyperlipidaemic Subjects

Barbara J. Meyer · Tone Hammervold ·  
Arild Chr. Rustan · Peter R. C. Howe

Received: 23 May 2006 / Accepted: 14 December 2006 / Published online: 8 February 2007  
© AOCS 2007

**Abstract** The objective of the study was to evaluate potential benefits of docosahexaenoic acid (DHA) rich fish oil supplementation as an adjunct to statin therapy for hyperlipidaemia. A total of 45 hyperlipidaemic patients on stable statin therapy with persistent elevation of plasma triglycerides (averaging 2.2 mmol/L) were randomised to take 4 g/day ( $n = 15$ ) or 8 g/day ( $n = 15$ ) of tuna oil or olive oil (placebo,  $n = 15$ ) for 6 months. Plasma lipids, blood pressure and arterial compliance were assessed initially and after 3 and 6 months in 40 subjects who completed the trial. Plasma triglycerides were reduced 27% by 8 g/day DHA-rich fish oil ( $P < 0.05$ ) but not by 4 g/day when compared with the placebo and this reduction was achieved by 3 months and was sustained at 6 months. Even though total cholesterol was already well controlled by the statin treatment (mean initial level 4.5 mmol/L), there was a further dose-dependent reduction with fish oil supplementation ( $r = -0.344$ ,  $P < 0.05$ ). The extent of total cholesterol reduction correlated ( $r = -0.44$ ) with the initial total cholesterol

levels ( $P < 0.005$ ). In the subset with initial plasma cholesterol above 3.8 mmol/L, plasma very low density lipoprotein (VLDL), intermediate-density lipoprotein (IDL) and low-density lipoprotein (LDL) were isolated and assayed for cholesterol and apolipoprotein B (apoB) at the commencement of the trial and at 3 months of intervention. Fish oil tended to lower cholesterol and apoB in VLDL and raise both in LDL. There were no changes in IDL cholesterol, IDL apoB and high-density lipoprotein cholesterol. The results demonstrate that DHA-rich fish oil supplementation (2.16 g DHA/day) can improve plasma lipids in a dose-dependent manner in patients taking statins and these changes were achieved by 3 months. Fish oil in addition to statin therapy may be preferable to drug combinations for the treatment of combined hyperlipidaemia.

**Keywords** Omega-3 polyunsaturated fatty acids · Statin therapy · Docosahexaenoic acid · Hyperlipidaemia · Combination therapy

### Abbreviations

ANOVA	Analysis of variance
CHD	Coronary heart disease
DHA	Docosahexaenoic acid
EPA	Eicosapentaenoic acid
HDL	High-density lipoprotein
HDL-C	High-density lipoprotein cholesterol
IDL	Intermediate-density lipoprotein
LDL	Low-density lipoprotein
LDL-C	Low-density lipoprotein cholesterol
PUFA	Polyunsaturated fatty acids
VLDL	Very low density lipoprotein
VLDL-C	Very low density lipoprotein cholesterol

B. J. Meyer (✉)  
School of Health Sciences, University of Wollongong,  
Wollongong, NSW 2522, Australia  
e-mail: bmeyer@uow.edu.au

T. Hammervold · A. Chr. Rustan  
Department of Pharmaceutical Biosciences,  
School of Pharmacy, University of Oslo, Oslo, Norway

P. R. C. Howe  
Nutritional Physiology Research Centre,  
School of Health Sciences, University of South Australia,  
Adelaide, SA 5000, Australia



## Introduction

Patients suffering from hyperlipidaemia with high plasma triglycerides, high low-density lipoprotein cholesterol (LDL-C) or low high-density lipoprotein cholesterol (HDL-C) are at increased risk of developing coronary heart disease (CHD) [1]. Patients newly diagnosed with hypercholesterolaemia are advised to adopt a cholesterol-lowering diet, e.g. National Cholesterol Education Program [2], in which replacement of saturated fat by polyunsaturated or monounsaturated fat results in lowering of plasma total and LDL-C. In cases where dietary management alone proves inadequate, hypocholesterolaemic drugs, primarily statins are prescribed. Statins inhibit cholesterol synthesis in the liver, subsequently reducing plasma total cholesterol and LDL-C levels, and have proven effective in counteracting CHD [3].

The potential benefit of triglyceride management is less clear, although lowering plasma triglyceride tends to improve HDL-C [4]. Omega-3 polyunsaturated fatty acids (PUFA) supplementation is now recognised as effective in lowering triglyceride, and fish oil extracts (e.g. Omacor) are indicated for hypertriglyceridaemia (American Heart Association guidelines). Both eicosapentaenoic acid (EPA) and docosahexaenoic acid (DHA) are effective at lowering plasma triglycerides [5, 6]. The extent of reduction correlates with initial plasma triglyceride levels and is usually accompanied by a modest rise in HDL-C and possibly transient elevation of LDL-C.

Omega-3 PUFA supplementation is also recommended for use in combined or mixed hyperlipidaemia, i.e. where both triglyceride and LDL-C are unacceptably high. This condition, estimated to occur in 60% of hypercholesterolaemic patients [7], is often treated with a combination of statin and fibrate drugs, the latter lowering plasma triglyceride. However, there are significant adverse effects associated with this drug combination [8], warranting further evaluation of the omega-3 PUFA supplementation as an alternative. Contacos et al. [9] demonstrated complementarity of the LDL-C lowering effect of pravachol and the triglyceride lowering effect of MaxEPA in subjects with combined hyperlipidaemia. Subsequent studies have also shown benefits of combining fish oil supplementation with statin treatment in combined hyperlipidaemic subjects [10–12].

Since then, newer statins with the ability to lower both LDL-C and triglyceride have been introduced [13, 14]. Nevertheless, a high proportion of statin-treated patients still have persistent hypertriglyceridaemia. Fish oil supplementation is indicated in hypertriglyceridaemia and in combined hyperlipidaemia as an adjunct to 3-hydroxy-3-methylglutarylcoenzyme A reductase inhibitors (statins) at daily doses of 3–4 g. To date, only EPA-rich fish oil has been evaluated in statin-treated subjects with combined hyperlipidaemia. Therefore, the purpose of the present study was to see whether such patients would derive further benefit from coadministration of a lower dose of fish oil, using, in this case, a DHA-rich fish oil supplement and to determine the duration of such achieved changes in plasma lipids.

Experimental Procedure

## Experimental Procedure

### Study Subjects and Study Design

Potential study subjects were recruited via the media (radio, newspaper and e-mail advertisements) in Wollongong, Australia. Entry criteria included subjects on stable statin treatment for hypercholesterolaemia (i.e. already taking statin drug for at least 3 months and expecting to continue on the same dosage during the study period) who had persistent hypertriglyceridaemia (greater than 1.6 mmol/L). Subjects were screened for fasting plasma triglyceride levels in fingerprick blood samples using a portable Accutrend instrument [15]. This study was approved by the University of Wollongong Human Ethics Research Committee and the subjects gave written informed consent.

Forty-five subjects who met the entry criteria were blocked for age, sex and entry plasma triglyceride levels and then randomly assigned to one of three treatments: DHA-rich tuna oil (HiDHA, Clover Corporation; 7% EPA, 27% DHA; 4 g/day, providing 1.08 g/day DHA) or DHA-rich tuna oil (8 g/day, providing 2.16 g/day DHA), or the olive oil group (placebo, half on 4 g/day and half on 8 g/day). DHA-rich tuna oil capsules comprise 27% saturated fats, 24.5% monounsaturated fats, 6% omega-6 polyunsaturated fats and 37.5% omega-3 polyunsaturated fats, of which 7% is EPA and 27% is DHA. The olive oil capsules comprise 14% saturated fats, 76% monounsaturated fats and 10% omega-6 polyunsaturated fats. The placebo group was matched to the fish oil group for dosage (4 and 8 g/day), but this difference in quantity is trivial compared to the dietary intake of monounsaturated fat. The subjects maintained their statin treatment throughout the study and consumed the capsules containing olive oil or DHA-rich tuna oil for 6 months. They attended the clinic on two consecutive days prior to the commencement of the trial and after 3 and 6 months of intervention to provide a fasted blood

sample and for the assessments of height (first clinic visit only), weight, arterial compliance and blood pressure.

### Plasma Lipids

Fasted blood samples were collected by venepuncture after an overnight fast in potassium EDTA tubes. Plasma was obtained after centrifugation at 3,000 rpm, 4 °C for 15 min. Plasma high-density lipoprotein (HDL) was isolated after precipitation with the dextran sulphate/magnesium chloride method [16]. Plasma total cholesterol, HDL-C and triglyceride were assessed by using the standard commercially available kits (from Roche Diagnostics) and an autoanalyser (Cobas Mira Plus). Plasma LDL-C was calculated by using the Friedewald calculation [17].

### Plasma Lipoproteins

In those subjects with plasma total cholesterol greater than 3.8 mmol/L, very low density lipoprotein (VLDL), intermediate-density lipoprotein (IDL) and low-density lipoprotein (LDL) were isolated from plasma. All lipoproteins were isolated using a 70Ti rotor at 35,000 rpm at 15 °C with polyallomer quick-seal centrifuge tubes (no. 342413, Beckman) in an L8 70 ultracentrifuge (Beckman).

Sequential ultracentrifugation was used to isolate VLDL, IDL and LDL from plasma. Briefly, 10 mL of plasma was overlaid with a 2 mL solution of  $d = 1.006$  g/mL per tube and subjected to ultracentrifugation for 16 h. VLDL particles were removed by tube slicing (approximately 2 mL), the remaining sample ( $d > 1.006$  g/mL) was adjusted to  $d = 1.019$  g/mL by the addition of  $d = 1.478$  g/mL solution, each tube was overlaid with 2 mL of  $d = 1.019$  g/mL solution and subjected to ultracentrifugation for 18 h. IDL was recovered by tube slicing (approximately 2 mL) and the remaining sample ( $d > 1.019$  g/mL) was adjusted to  $d = 1.063$  g/mL by the addition of  $d = 1.478$  g/mL solution, each tube was overlaid with 2 mL of  $d = 1.063$  g/mL solution and subjected to ultracentrifugation for 18 h. LDL was recovered by tube slicing (approximately 2 mL). VLDL, IDL and LDL were analysed for cholesterol and apolipoprotein B using standard commercially available kits.

### Arterial Compliance and Blood Pressure

Arterial compliance was assessed using a CR-2000 cardiovascular profiler instrument (Hypertension Diagnostic, Eagan, MN, USA), a noninvasive method

approved by the US Food and Drug Administration. It provides separate estimates of compliance in proximal or large arteries (C1, reflecting arterial capacitance) and in distal or small arteries (C2, reflecting resistance). These estimates correlate with aging and vascular disease (atherosclerosis), respectively. Three replicate assessments were taken at 5-min intervals whilst the patient was supine. Blood pressure (systolic, diastolic and mean arterial pressure) was assessed with the patient supine in the clinic while arterial compliance was measured using the cardiovascular profiler instrument.

### Statistical Analysis

Plasma triglyceride was the only variable that was not normally distributed; hence, data analysis was performed on the log transformation of plasma triglycerides. Other variables did not require transformation prior to data analysis. One-way analysis of variance (ANOVA) was used to determine the differences between the three groups (placebo, 4-g and 8-g dose). Multivariate correlation analysis was used to determine the correlation between the initial plasma total cholesterol levels and the change in plasma total cholesterol from 0 to 6 months. Repeated-measures ANOVA (Statistica for Windows, release 5.1) was used to compare the change of total cholesterol (after 3 and 6 months) from the baseline. Changes were considered significant when  $P < 0.05$ . All values are reported as the mean  $\pm$  the standard error of the mean.

### Results

Baseline characteristics of the 45 subjects enrolled in the study are shown in Table 1. The three groups were well matched for age, sex, body mass index and fasting plasma triglyceride levels and no significant differences between the groups were observed.

Forty subjects completed the 6-month trial (19 were taking simvastatin, 13 atorvastatin, 4 pravastatin, 2 cerivastatin and 2 fluvastatin). Table 2 and Fig. 1 show the effects of DHA-rich fish oil on plasma lipids in statin-treated subjects. The 8-g/day dosage of fish oil (providing 2.16 g/day DHA) was necessary to see a significant change (27% reduction) in plasma triglyceride levels as the 4-g/day dosage of fish oil (providing 1.08 g/day DHA) did not reach significance (Fig. 1). Although plasma total cholesterol levels were already well controlled by the statin therapy (average of 4.5 mmol/L), there was a trend toward a further reduction with the 8-g/day dosage of fish oil and a

**Table 1** Baseline characteristics

	Males/ females	Age (years)	BMI (kg/m <sup>2</sup> )	Plasma TG <sup>a</sup> (mmol/L)
Control	10, 5	59 ± 2	27.9 ± 1.2	2.77 ± 0.27
4 g/day DHA-rich fish oil	10, 5	58 ± 2	29.3 ± 0.3	2.70 ± 0.27
8 g/day DHA-rich fish oil	10, 5	53 ± 5	26.2 ± 0.2	2.62 ± 0.39

Values are the mean ± the standard error of the mean (SEM) BMI body mass index, TG triglycerides, DHA docosahexaenoic acid

<sup>a</sup> Using Accutrend TG screening [15]

**Table 2** Effects of DHA-rich fish oil on plasma lipids in statin-treated subjects

	TC (mmol/L)	HDL-C (mmol/L)	LDL-C (mmol/L)	TG (mmol/L)
Control ( <i>n</i> = 14)				
Baseline	4.41 ± 0.19	1.04 ± 0.13	2.45 ± 0.19	2.02 ± 0.24
3 months	4.47 ± 0.27	1.21 ± 0.15	2.60 ± 0.26	1.82 ± 0.19
6 months	4.47 ± 0.21	1.11 ± 0.10	2.49 ± 0.22	2.05 ± 0.20
4 g/day DHA-rich fish oil ( <i>n</i> = 13)				
Baseline	4.38 ± 0.19	1.11 ± 0.06	2.19 ± 0.20	2.20 ± 0.29
3 months	4.40 ± 0.23	1.18 ± 0.08	2.27 ± 0.20	2.08 ± 0.32
6 months	4.43 ± 0.23	1.16 ± 0.09	2.40 ± 0.21	1.92 ± 0.27
8 g/day DHA-rich fish oil ( <i>n</i> = 13)				
Baseline	4.63 ± 0.24	1.09 ± 0.04	2.58 ± 0.23	2.36 ± 0.37
3 months	4.31 ± 0.16	1.16 ± 0.04	2.48 ± 0.16	1.72 ± 0.29 <sup>a</sup>
6 months	4.18 ± 0.23	1.21 ± 0.05	2.35 ± 0.21	1.72 ± 0.20 <sup>a</sup>

Values are the mean ± SEM

TC total cholesterol, HDL-C high-density lipoprotein cholesterol, LDL-C low-density lipoprotein cholesterol

<sup>a</sup> One-way analysis of variance between the three groups, *P* < 0.05

significant correlation between dosage of fish oil and extent of cholesterol reduction ( $r = -0.344$ ,  $P < 0.05$ ). HDL-C and LDL-C were unaffected by fish oil supplementation in this statin-treated population. These changes in plasma total cholesterol and triglycerides were achieved by 3 months and were sustained at 6 months of intervention.

The reduction of plasma total cholesterol correlated with initial cholesterol levels ( $r = -0.44$ ,  $P < 0.05$ ). Given that there is a significant influence of initial cholesterol levels, the effects of treatment were reevaluated after excluding those subjects with low plasma total cholesterol (below 3.8 mmol/L) at the baseline after 3 months' intervention, as the 6-month data showed no further reduction in plasma lipids. This subset (ten subjects per group) showed a greater response to fish oil with marginal significance (13% reduction of total cholesterol with the 8 g/day dosage,

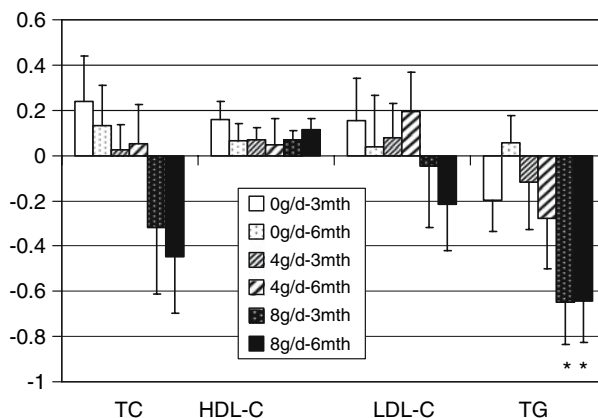


**Fig. 1** Changes in plasma lipids after 3 and 6 months for all subjects. Control group (white bars at 3 months, white bars with black dots at 6 months, *n* = 15), 4 g DHA-rich fish oil/day group (light hatched bars at 3 months, dark-hatched bars at 6 months, *n* = 15), 8 g DHA-rich fish oil/day group (black bars with white dots at 3 months, black bars at 6 months, *n* = 15). The asterisks indicate significantly different from the control,  $P < 0.005$ . DHA docosahexaenoic acid, TC total cholesterol, HDL-C high-density lipoprotein cholesterol, LDL-C low-density lipoprotein cholesterol, TG triglycerides

$P = 0.05$ , Fig. 2). In this subset VLDL, IDL and LDL were isolated and, although not significant, fish oil tended to lower plasma total cholesterol and apolipoprotein B in VLDL and raise both in LDL (Fig. 3).

There were no changes in blood pressure or in the indices of proximal (C1) or distal (C2) arterial compliance (results not shown) after DHA-rich fish oil treatment.

## Discussion

This study shows that, when administered as an adjunct to statin therapy in hypercholesterolaemic patients with persistent hypertriglyceridaemia, a tuna fish oil supplement yielding 2.16 g/day DHA can reduce plasma triglycerides by 27%, which is reflected in a reduction of VLDL. This reduction in plasma triglyceride levels were achieved by 3 months and was sustained to 6 months. There was a trend toward lowering plasma total cholesterol, which again is reflected in lowering circulating VLDL particles.

Drug combinations are usually prescribed for combined hyperlipidaemia. One such option is fibrate therapy in combination with a statin. Trials have tested this combination therapy with expected outcomes such as 50 [18] or 38% [19] reductions in plasma triglycerides. Despite the effectiveness of fibrates lowering plasma triglyceride levels, there have been reports of adverse side effects of the fibrates, such as liver and

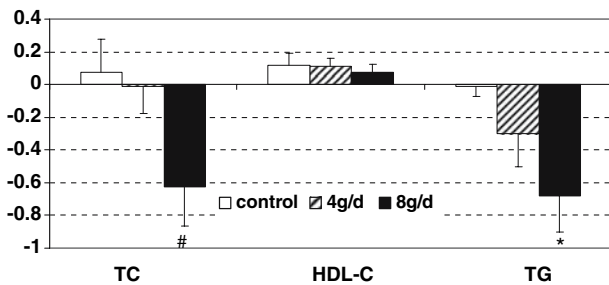


**Fig. 2** Changes in total cholesterol, high-density lipoprotein cholesterol and plasma triglycerides after 3 months of fish oil treatment in those subjects (ten per treatment group) with initial total cholesterol above 3.8 mmol/L. Control group (white bars  $n = 10$ ), 4 g DHA-rich fish oil/day group (hatched bars  $n = 10$ ), 8 g DHA-rich fish oil/day group (black bars  $n = 10$ ). The number sign indicates marginal significance compared with the control and the 4-g dose,  $P = 0.05$ . The asterisk indicates significantly different from the control,  $P < 0.05$

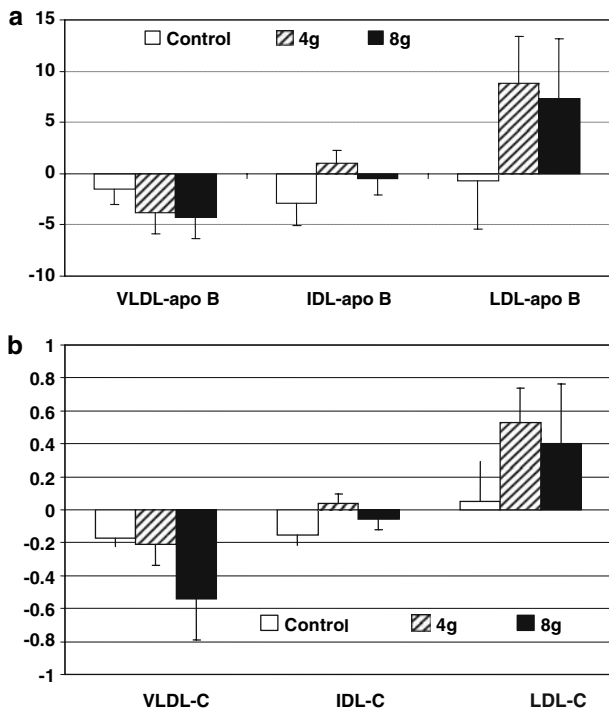


**Fig. 3** In the subset of subjects with plasma total cholesterol above 3.8 mmol/L (ten subjects per group) very low density lipoprotein (VLDL), intermediate-density lipoprotein (IDL) and low-density lipoprotein (LDL) were isolated. **a** The change in VLDL, IDL and LDL apolipoprotein B (apoB) levels from 0 to 3 months of intervention with the control group (white bars  $n = 10$ ), 4 g DHA-rich fish oil/day group (hatched bars  $n = 10$ ), 8 g DHA-rich fish oil/day group (black bars  $n = 10$ ). **b** The change in VLDL, IDL and LDL cholesterol levels (VLDL-C, IDL-C, LDL-C) from 0 to 3 months of intervention with the control group (white bars  $n = 10$ ), 4 g DHA-rich fish oil/day group (hatched bars  $n = 10$ ), 8 g DHA-rich fish oil/day group (black bars  $n = 10$ )

muscle toxicity [20, 21]. In particular, combined treatment of cerivastatin and gemfibrozil has been poorly tolerated and together with increased incidence of rhabdomyolysis led to the withdrawal of cerivastatin from the market [22]. Another option for treatment of statin-treated subjects with persistent hypertriglyceridaemia is niacin therapy in combination with a statin, where plasma triglyceride can be reduced by 40% [23]. However, there have been reported cases of hepatic toxicity [24], myopathy [25] and rhabdomyolysis [26] in patients primarily taking the sustained-release and twice-daily form of niacin [8].

An alternative approach to combined therapy for people with hyperlipidaemia is fish oil supplementation in combination with statin treatment. Contacos et al. [9] first demonstrated the potential of fish oil (3 g EPA/day) to substitute for fibrates as an adjunct to pravastatin therapy for mixed hyperlipidaemia. They found complementary effects of the oil and the statin on plasma triglycerides (27–30% reduction) and LDL-C (13–24% reduction), respectively. Despite its subsequent recommendation to general practitioners in the *National Heart Foundation Guide to Plasma Lipids for Doctors* (1997), this promising combination is hardly used, probably because of inadequate information on dose requirements, efficacy and availability.

In further examining the cardiovascular benefits of fish oil–statin treatment combinations, a preliminary observation was made that administration of EPA-rich fish oil not only reduced plasma triglycerides (by 36%), but also appeared to potentiate the hypocholesterolaemic effect of the statin [27], an effect that is not normally seen with fish oil supplementation alone. In the present study we have shown that an 8-g/day dosage of DHA-rich fish oil, when given as an adjunct to statin therapy, not only reduced plasma triglyceride levels but also potentially enhanced the cholesterol-lowering effect of the statin, especially in people with plasma total cholesterol levels greater than 3.8 mmol/L (Fig. 2). This cholesterol-lowering effect was primarily due to reduction in VLDL cholesterol (VLDL-C). These positive effects on plasma triglyceride and total cholesterol appeared to be dose-dependent and are achieved by 3 months' intervention with no further reduction at 6 months. The dose-dependent effect is consistent with studies conducted in statin-treated subjects using EPA-rich fish oil. Nordoy et al. [10] found a significant reduction of total cholesterol as well as plasma triglycerides in hyperlipidaemic patients when fish oil (3.3 g omega-3 PUFA/day, Omacor) was combined with simvastatin (20 mg/day) for 5 weeks. These effects were not seen in a subsequent study with a lower dose of fish oil (1.7 g/day), although a more

potent statin was being used [28]. Durrington et al. [11] reported reductions of 20–30% in plasma triglyceride, 30–40% in VLDL and 10% in total cholesterol following supplementation with 3.4 g long-chain omega-3 PUFA per day for 6 months.

People with combined hyperlipidaemia exhibit other dyslipidaemias, including an increased number of small, lipid-dense LDL particles that are highly susceptible to oxidation [10]. People with hypertriglyceridaemia have increased small, dense LDL particles [29], which are more atherogenic than normal-sized LDL particles [30]. Nordoy et al. [28] demonstrated a shift from small, dense LDL particles to larger, less dense LDL particles in combined hyperlipidaemics who were treated with atorvastatin and omega-3 PUFA, suggesting that supplementation with omega-3 PUFA may reduce cardiovascular risk by reducing the number of small, dense LDL particles. A limitation of this study was that LDL particle sizes were not measured, but certainly fish oil supplementation certainly did not result in significant increases of LDL-C levels.

Despite the apparent therapeutic benefits of omega-3 PUFA and other hypolipidemic nutrients, there have been few attempts to evaluate their role as adjunct therapy. Take the case of plant sterols. There are only four randomised clinical trials that test the hypocholesterolaemic potential of combining plant sterols with statins as a primary outcome measure [31–34]. These trials with plant sterol/stanol doses of 2–3 g/day for 4–8 weeks resulted in a 7–11% reduction of LDL-C over and above statin therapy [35]. The use of such nutrient combinations to reduce drug requirements may have avoided fatal adverse outcomes with cerivastatin, particularly if substituted for fibrate cotherapy. Despite the ability of plant sterols/stanols to further lower total cholesterol and LDL-C, they do not effectively reduce plasma triglycerides or improve HDL-C. Thus, combination therapy with omega-3 PUFA supplementation may be more suitable for people with combined hyperlipidaemia. Furthermore, statin therapy alone results in unfavourable changes in plasma fatty acids in that the arachidonic acid to EPA ratio and the arachidonic acid to DHA ratio are increased [36]. Although combination therapy of statins with omega-3 PUFA may result in a more favourable fatty acid profile, this awaits confirmation [36].

Apart from their cholesterol-lowering efficacy, statins may contribute to CHD risk reduction through proendothelial, antiplatelet and other mechanisms [37]. However, there are some disadvantages of statin use and risks at high doses. Initially in Australia around 30% of people prescribed statins lapsed within the first 6 months of therapy owing to a number of factors

including minor and major adverse reactions, indicating there are significant problems associated with statin treatment [33]. The most common adverse reactions to monotherapy are musculoskeletal (approximately 1–7% of reported cases) as well as constipation, indigestion, stomach pain, skin rashes and flatulence [38].

In summary, it appears from our study that a DHA intake of 2.16 g/day is effective in lowering plasma triglyceride levels in statin-treated patients with persistent hypertriglyceridaemia and this reduction is achieved by 3 months and is sustained at 6 months. Moreover, omega-3 PUFA supplementation may also reduce plasma total cholesterol (primarily VLDL-C reduction), especially if the plasma total cholesterol is greater than 3.8 mmol/L. These effects are dependent on the initial cholesterol levels and the omega-3 PUFA dose and are achieved within 3 months.

In conclusion, omega-3 PUFA supplementation as DHA-rich fish oil has the potential to further improve cardiovascular disease risk and potentially reduce medication in hyperlipidaemic patients taking statins. Taking omega-3 PUFA together with a statin may be preferable to combinations of drugs currently prescribed for mixed hyperlipidaemia as there are fewer side effects associated with omega-3 PUFA supplementation.

**Acknowledgements** The authors would like to acknowledge the study volunteers for their participation in the trial and Professor Dennis Calvert for the medical supervision of subject enrolment. The supply of placebo and DHA-rich fish oil capsules from Clover Corporation is gratefully acknowledged.

## References

- Hopkins PN, Heiss G, Ellison RC, Province MA, Pankow JS, Eckfeldt JH, Hunt SC (2003) Coronary artery disease risk in familial combined hyperlipidemia and familial hypertriglyceridemia: a case-control comparison from the National heart, lung, and blood Institute family heart study. *Circulation* 108:519–523
- Lichtenstein AH, Ausman LM, Carrasco W, Jenner JL, Gualtieri LJ, Goldin BR, Ordovas JM, Schaefer EJ (1993) Effects of canola, corn, and olive oils on fasting and postprandial plasma lipoproteins in humans as part of a National Cholesterol Education Program step 2 diet. *Arterioscler Thromb* 13:1533–1542
- Shepherd J, Cobbe SM, Ford I, et al (1995) Prevention of coronary heart disease with pravastatin in men with hypercholesterolemia. *N Engl J Med* 333:1301–1307
- Bruckert E, Baccara-Dinet M, McCoy F, Chapman J (2005) High prevalence of low HDL-cholesterol in a pan-European survey of 8,545 dyslipidaemic patients. *Curr Med Res Opin* 21:1927–1934
- Howe PRC, Clifton PM, James MJ (1999) Equal anti-thrombotic and triglycerides-lowering effectiveness of eicosapentaenoic acid-rich and docosahexaenoic acid-rich fish oil supplements. *Lipids* 34:S307–S308

6. Mori TA, Beilin LJ (2001) Long-chain omega 3 fatty acids, blood lipids and cardiovascular risk reduction. *Curr Opin Lipidol* 12:11–17
7. Packard CJ, Caslake MJ (1997) Mixed hyperlipidaemia and lipid turnover. In: *World of lipids*. LibraPharm, Newbury
8. Xydakis AM, Ballantyne CM (2002) Combination therapy for combined dyslipidemia. *Am J Cardiol* 90(Suppl):21K–29K
9. Contacos C, Barter PJ, Sullivan DR (1993) Effect of pravastatin and omega-3 fatty acids on plasma lipids and lipoproteins in patients with combined hyperlipidemia. *Arterioscler Thromb* 13:1755–1762
10. Nordoy A, Bonna KH, Nilsen H, Berge RK, Hansen JB, Ingebretsen OC (1998) Effects of simvastatin and omega-3 fatty acids on plasma lipoproteins and lipid peroxidation in patients with combined hyperlipidaemia. *J Intern Med* 243:163–170
11. Durrington PN, Bhatnagar D, Mackness MI, Morgan J, Julier K, Khan MA, France M (2001) An omega-3 polyunsaturated fatty acid concentrate administered for 1 year decreased triglycerides in simvastatin treated patients with coronary heart disease and persisting hypertriglyceridaemia. *Heart* 85:544–548
12. Chan DC, Watts GF, Mori TA, Barrett PHR, Beilin LJ, Redgrave TG (2002) Factorial study of the effects of atorvastatin and fish oil on dyslipidaemia in visceral obesity. *Eur J Clin Nutr* 32:429–436
13. Saklamaz A, Comlekci A, Temiz A, Caliskan S, Ceylan C, Alacacioglu A, Yesil S (2005) The beneficial effects of lipid-lowering drugs beyond lipid-lowering effects: a comparative study with pravastatin, atorvastatin, and fenofibrate in patients with type IIa and type IIb hyperlipidemia. *Metabolism* 54:677–681
14. McKenney JM (2005) Efficacy and safety of rosuvastatin in treatment of dyslipidemia. *Am J Health Syst Pharm* 62:1033–1047
15. Moses RG, Calvert D, Storlien LH (1996) Evaluation of the Accutrend GCT with respect to triglyceride monitoring. *Diabetes Care* 19:1305–1306
16. Warnick GR, Benderson J, Albers JJ (1982) Dextran sulphate–Mg<sup>2+</sup> precipitation procedure for quantitation of high-density lipoprotein cholesterol. *Clin Chem* 28:1379–1388
17. Freidewald WT, Levy RI, Fredrickson DS (1972) Estimation of the concentration of LDL cholesterol in plasma without the use of the preparative ultracentrifuge. *Clin Chem* 18:499–502
18. Athyros VG, Papageorgiou AA, Hatzikonstandinou HA, Didangelos TP, Carina MV, Kranitsas DF, Kontopoulos AG (1997) Safety and efficacy of long-term statin–fibrate combinations in patients with refractory familial combined hyperlipidemia. *Am J Cardiol* 80:608–613
19. Pauciullo P, Borgnino C, Paoletti R, Mariani M, Mancini M (2000) Efficacy and safety of a combination of fluvastatin and benafibrate in patients with mixed hyperlipidemia (FACT study). *Atherosclerosis* 150:429–436
20. Pierce LR, Wysowski DK, Gross TP (1990) Myopathy and rhabdomyolysis associated with lovastatin–gemfibrozil combination therapy. *JAMA* 264:71–75
21. Schectman G, Hiatt J (1996) Drug therapy for hypercholesterolemia in patients with cardiovascular disease: factors limiting achievement of lipid goals. *Am J Med* 100:197–204
22. Furberg CD, Pitt B (2001) Withdrawal of cerivastatin from the World market. *Curr Control Trials Cardiovasc Med* 2:205–207
23. Kashyap ML, McGovern ME, Berra K, Guyton JR, Kwitrovich PO Jr, Harper WL, Toth PD, Favrot LK, Kerzner B, Nash SD, Bays HE, Simmons PD (2002) Long-term safety and efficacy of a once-daily niacin/lovastatin formulation for patients with dyslipidemia. *Am J Cardiol* 89:672–678
24. Rader JI, Calvert RJ, Hathcock JN (1992) Hepatic toxicity of unmodified and time-release preparations of niacin. *Am J Med* 92:77–81
25. Norman DJ, Illingworth DR, Munson J, Hosenpud H (1988) Myolysis and acute renal failure in a heart-transplant recipient receiving lovastatin. *N Engl J Med* 318:46–47
26. Reaven P, Witzum JL (1988) Lovastatin, nicotinic acid, and rhabdomyolysis. *Ann Intern Med* 109:597–598
27. Howe PRC, Lungershausen YK, Abbey M, Anderson JL, Ablett MB (1998) Effects of pravastatin and omega-3 fatty acids in peripheral arterial occlusive disease. In: 24th annual scientific meeting of the Australian Atherosclerosis Society, Cairns, abstract P10
28. Nordoy A, Hansen JB, Brox J, Svensson B (2001) Effects of atorvastatin and omega-3 fatty acids on LDL subfractions and postprandial hyperlipemia in patients with combined hyperlipemia. *Nutr Metab Cardiovasc Dis* 11:7–16
29. Campos H, Genest JJ Jr, Blijlevens E, McNamara JR, Ordovas JM, Posner BM, Wilson PW, Castelli WP, Schaeffer EJ (1992) Low density lipoprotein particle size and coronary artery disease. *Arterioscler Thromb* 12:187–195
30. Packard CJ (1996) LDL subfractions and atherogenicity: an hypothesis from the University of Glasgow. *Curr Med Res Opin* 13:379–390
31. Blair SN, Capuzzi DM, Gottlieb SO, Nguyen T, Morgan JM, Cater NB (2000) Incremental reduction of serum total cholesterol and low-density lipoprotein cholesterol with the addition of plant stanol ester-containing spread to statin therapy. *Am J Cardiol* 86:46–52
32. Neil HA, Meijer GW, Roe LS (2001) Randomised controlled trial of use by hypercholesterolaemic patients of a vegetable oil sterol-enriched fat spread. *Atherosclerosis* 156:329–337
33. Simons LA (2002) Additive effect of plant sterol-ester margarine and cerivastatin in lowering low-density lipoprotein cholesterol in primary hypercholesterolemia. *Am J Cardiol* 90:737–740
34. O'Neill FH, Brynes A, Mandeno R, Rendell N, Taylor G, Seed M, Thompson GR (2004) Comparison of the effects of dietary plant sterol and stanol esters on lipid metabolism. *Nutr Metab Cardiovasc Dis* 14:133–142
35. Thompson GR (2005) Additive effects of plant sterol and stanol esters to statin therapy. *Am J Cardiol* 96(Suppl):37D–39D
36. Harris JI, Hibbeln JR, Mackey RH, Muldoon MF (2004) Statin treatment alters serum *n*-3 and *n*-6 fatty acids in hypercholesterolemic patients. *Prostaglandins Leukot Essent Fatty Acids* 71:263–269
37. Rosenson RS, Tangney CC (1998) Antiatherothrombotic properties of statins: implications for cardiovascular event reduction. *JAMA* 279:1643–1650
38. Evans M, Rees A (2002) The myotoxicity of statins. *Curr Opin Lipidol* 13:415–420

# A Docosahexaenoic Acid-Functional Food During Pregnancy Benefits Infant Visual Acuity at Four but not Six Months of Age

Michelle P. Judge · Ofer Harel ·  
Carol J. Lammi-Keefe

Received: 29 June 2006 / Accepted: 23 November 2006 / Published online: 19 January 2007  
© AOCS 2007

**Abstract** Within the visual system, docosahexaenoic acid (DHA, 22:6n-3) is an important structural component for retinal photoreceptors and cortical gray matter. There is a marked decrease in neural DHA accumulation in the face of DHA deficiency. DHA is accumulated at an accelerated rate during pregnancy, especially in the third trimester. However, pregnant women in the US and Canada have dietary DHA intakes that are significantly below the optimal level. The main objective of this study was to determine whether a DHA-functional food during pregnancy would benefit infant visual acuity at four and six months of age measured behaviorally using the acuity card procedure (ACP). In a randomized, longitudinal, double-blinded, and placebo-controlled trial, 30 pregnant women received either the DHA-functional food ( $n = 16$ ) or the placebo ( $n = 14$ ). There were significant main effects for visual acuity at four months of age ( $P = 0.018$ ). The mean acuity scores were  $3.8 \pm 1.1$  cycles/degree in the DHA group versus  $3.2 \pm 0.7$  cycles/degree in the

placebo group. At six months there were no group differences. Based on our results, we conclude that DHA supplemented during pregnancy plays a role in the maturation of the visual system.

**Keywords** Visual acuity · Infant visual development · Docosahexaenoic acid · Pregnancy · Functional food

## Introduction

The visual system comprises a complex signaling system involving the retina, thalamus and primary visual cortex. In addition, multiple other cortical regions are involved in the cognitive integration of visual information. Previous studies focused on the impact of long-chain polyunsaturated fatty acids (LCPUFA) on infant visual development have assessed two main aspects of the visual system: retinal development using electroretinogram (ERG), and visual processing at the level of the primary visual cortex. Cortical measures of resolution include sweep visual evoked potential (VEP) and behavioral assessments like the acuity card procedure (ACP). Of the resolution (grating) acuity measures, VEP measures cortical response directly and has less variability [1]. However, behavioral acuity measures provide a different measure of what an infant actually perceives, and normative data are well established for this procedure [1, 2]. Behavioral acuity measured with ACP is dependent on different brain regions controlling eye movements, attention, and other processes involved in generating the behavioral response [1].

Compared to other cells of the body, retinal photoreceptors have the highest docosahexaenoic acid

---

M. P. Judge · C. J. Lammi-Keefe  
Department of Nutritional Sciences,  
University of Connecticut, Storrs, CT 06269-4017, USA

O. Harel  
Department of Statistics, University of Connecticut,  
Storrs, CT 06269-4017, USA

C. J. Lammi-Keefe (✉)  
Division of Human Nutrition and Food,  
Louisiana State University, School of Human Ecology  
and Pennington Biomedical Research Center,  
297B Knapp Hall, Baton Rouge, LA 70803, USA  
e-mail: clammikeeefe@agcenter.lsu.edu

(DHA, 22:6 *n*-3) content. The gray matter in the visual cortex and multiple other cortical regions also have high levels of DHA. In an animal model, a diet deficient in LCPUFA during pregnancy impeded accumulation of DHA in these tissues [3]. A 50% reduction of DHA in retinal tissue and a 25% reduction in cerebral cortex DHA was reported for the offspring of rhesus monkeys fed a diet deficient in  $\alpha$ -linolenic acid (ALA, 18:3 *n*-3) during pregnancy compared to controls [3]. Deficient animals also had lower visual acuity using behavioral measures and a prolonged recovery time of the dark-adapted ERG after a saturating flash.

In full-term infants, improved visual function related to the provision of *n*-3 fatty acids during the postnatal period has been repeatedly reported based on the application of methods of visual acuity assessment [4–9]. There are no reports of improved infant visual acuity assessed using the ACP related to maternal dietary DHA intake. Malcolm et al. [10, 11] used VEP and ERG to assess visual acuity and retinal function after maternal DHA supplementation. In these studies, no significant treatment effect was reported for ERG in the first postnatal week [8] or VEP at 2.5 or 6.5 months of age [7].

Pregnant women in the US and Canada have DHA intakes well below the 300 mg/day recommended by the National Institutes of Health Workshop on the Essentiality of and Recommended Dietary Intakes for Omega-6 and Omega-3 Fatty Acids [12–17]. As the developing fetus has an extremely limited capacity to derive DHA from the 18-carbon precursor, the fetus is clearly at risk of a relative deficiency of DHA.

In the current study, we hypothesized that infants of mothers who consumed the DHA-functional food during pregnancy would have better visual acuity when assessed with ACP at four and six months of age compared to infants of mothers consuming a placebo.

## Methods

### Study Design

In a randomized, longitudinal, double-blinded, and placebo-controlled trial, 30 pregnant women 18–35 years of age and <20 weeks gestation were recruited. The cohort used to assess visual acuity was derived from a larger study (unpublished data) focused on the impact of maternal DHA supplementation on infant sleep patterning in the first two postnatal days. Ten ACP assessments were lost initially due to a delay in implementing the ACP. Once implemented, 50% of the infants of women originally recruited were assessed

for vision. Colored marbles representing each study group were selected at random for group assignments by an individual who did not work directly on the project. All other personnel involved with the project were blinded to group assignments. The placebo bars were packaged in exactly the same manner as the intervention bars, making detection of group assignments impossible for investigators or participants. Study groups received: (1) the DHA-containing cereal-based bars, *n* = 16 (300 mg DHA as low EPA fish oil: EPA:DHA, 1:8, per 92 kcal bar) or (2) the cereal-based placebo bars containing corn oil, *n* = 14. Within each group, women consumed three, five or seven bars weekly from 24 weeks of pregnancy to delivery. The consumption of an average of five bars per week provided 214 mg DHA/day via the functional food. The cereal-based bars did not differ in energy, carbohydrate, protein or total fat content (Table 1).

The initial blood draw and 24-h recall were collected at 20–22 weeks gestation prior to starting the intervention at 24 weeks. Women were instructed to consume bars beginning at 24 weeks gestation and continue until delivery. Bars were delivered to women once monthly. Women were given logs to record bar intakes and these were collected monthly. Four times throughout the pregnancy the women were interviewed using 24-h dietary recalls by a trained researcher. All maternal dietary data were evaluated using the Nutrition Data System for Research (NDS, 2005). Infant medical history and diet histories of infants' intakes were obtained at four and six months of age from the mother or primary caregiver. Visual assessments were conducted only on healthy infants and appointments were rescheduled if infants became ill prior to their scheduled appointments. Care was also taken to schedule appointments during the time of day that the infant was most alert/active.

### Subjects

Subject recruitment was conducted in accordance with IRB guidelines at Hartford Hospital and the

**Table 1** Nutritional content of the cereal-based bars used for the intervention and placebo groups

Nutrient per 23 g bar	Intervention	Placebo
Carbohydrate (g)	18	18
Dietary fiber (g)	0.3	0.3
Fat (g)	1.7 (300 mg DHA)	1.7
Protein (g)	1.3	1.3
Energy (kcal)	92	92



University of Connecticut. Women with a history of drug/alcohol addiction, smoking, hypertension, hyperlipidemia, renal disease, liver disease, diabetes or psychiatric disorder were excluded from study participation.

### Infant Visual Acuity Testing

Visual acuity assessments were conducted at four and six months of age by an individual trained in the ACP using Teller acuity cards [18, 19]. These rectangular cards each contain a square patch of black and white stripes; the cards are arranged from high to low stripe width or grating. One black and white stripe is referred to as one cycle and the frequency of the stripes is given in cycles per centimeter. The spatial frequency doubles stepwise every other card, and this increase in spatial frequency is referred to as an octave. Cards were presented to infants on a stage starting with 0.32 cycles/cm for the four-month assessment and 0.64 cycles/cm for the six-month assessment. Infants were seated 38 cm from the test stage at four months and 55 cm at six months of age. The distances from the stage based upon infant age were set according to the standard ACP procedure. Both groups were tested at identical distances from the stage at four and then at six months. A light meter was used to ensure that the lighting was consistent and adequate for all infants (minimum level of 10 candelas/m<sup>2</sup>).

The test administrator stood on the opposite side of the stage and observed the infants through a peephole in the cards. As the cards were presented to the infants, the tester was unaware of the location of the striped patch on the rectangular card, i.e., left or right. The high visual contrast of the black and white striped square provides a great deal of visual interest for young infants, causing them to look toward the grating pattern if it can be seen by the infant. The observer watched the infant's response to the card and made an assessment regarding whether the striped patch was located on the right or left side of the card based upon the infant's behavioral response. Cards were presented to infants from low to high visual frequency in 0.5 octave steps, and an assessment was made with each step as to whether the infant was able to see the stripes reliably. The observer repeated the presentation of each card; after the first presentation the card was typically flipped so that the stripes were on the opposite side (i.e., left versus right). If the infant could see the stripes, the observer expected the infant to look to the opposite side on alternate trials. The observer presented each card a sufficient number of times to

reliably answer the question, "Can the infant see the stripes?" (answer: yes or no). The card with the finest grating that the infant could see was defined as the threshold.

A single individual who was trained and validated in the procedure performed all visual assessments. All ACP assessments were completed at Hartford Hospital, ensuring that controlled conditions were used, e.g., lighting, sound, distance. Lastly, acuity scores in cycles/degree were converted to octaves, log (base 2), for all statistical analyses as a standard procedure associated with the ACP [18].

Previous studies of infants with diets supplemented with DHA demonstrated that significant differences between mean acuities were  $\geq 0.40$  octaves [20]. Because in the current study we were assessing dietary intake of pregnant mothers, rather than infants, we anticipated greater group differences (0.50 octaves). Using  $\alpha = 0.05$  and power = 0.80, the calculated sample size was 16 subjects per group.

### Statistical Analyses

All statistical analyses were conducted using the Statistical Analysis System (SAS) software [21]. The PROC GLM procedure was used for group comparisons of the log-transformed acuity scores. Analyses of baseline characteristics included the Student's *t*-test for numeric and chi-square for categorical variables. The Proc Mixed procedure was used to evaluate changes over time between four and six-month assessments.

### Results

Overall, groups were well randomized, as most group characteristics were similar between groups (Table 2). Total weight gain during pregnancy, infant gender and APGAR score at 5 min were significantly different between groups.

Information regarding maternal ethnicity and risk of depression was collected via a review of medical records, and there were no differences between groups. Incidence of venereal disease during pregnancy was low in both groups and there were no differences between groups.

The mean dietary DHA intake was not significantly different between groups, and the mean average DHA intake for our entire cohort was 80 mg/day. Thus, subjects in the intervention group received an average of 294 mg DHA/day with intervention and dietary intakes combined.

**Table 2** Visual acuity group characteristics of the DHA versus placebo groups

	DHA ( <i>n</i> = 16) <sup>a</sup>	Placebo ( <i>n</i> = 14)	<i>P</i> value
Maternal age (years) mean ± SD	23.9 ± 4.3	24.7 ± 4.8	0.643
Maternal education (years) mean ± SD	12.8 ± 2.2	12.2 ± 1.5	0.401
Parity mean ± SD	1.5 ± 0.8	1.8 ± 0.8	0.343
WIC participation	14	14	0.171
Single	13	10	0.775
Married	3	3	0.775
Pre-pregnancy BMI (kg/m <sup>2</sup> ) mean ± SD	25.4 ± 4.9 ( <i>n</i> = 15)	28.5 ± 6.1 ( <i>n</i> = 12)	0.151
Total pregnancy weight gain (kg) mean ± SD	17.3 ± 6.8	12.0 ± 5.2 ( <i>n</i> = 13)	0.027
Gestational age (weeks) mean ± SD	39.6 ± 1.3	39.3 ± 1.3	0.506
Infant gender	5 male 11 female	10 male 4 female	0.028
Birth weight (g) mean ± SD	3372 ± 749	3163 ± 657	0.213
Infant head circumference (cm) mean ± SD	34.6 ± 1.3	34.3 ± 3.5	0.605
Infant length (cm) mean ± SD	50.8 ± 3.3	49.5 ± 4.3	0.179
APGAR 1 min mean ± SD	8.0 ± 1.8	8.4 ± 1.2	0.247
APGAR 5 min mean ± SD	9.0 ± 0.0	8.8 ± 0.7	0.053

<sup>a</sup> Number of subjects used for comparison unless otherwise specified

Mode of infant feeding was categorized as: formula with DHA; formula containing no DHA; breast milk only; combination breast milk and formula no DHA; breastfed for 1–2 months, then changed to formula containing no DHA; breastfed for 2–4 months, then changed to formula containing no DHA. There were no differences between study groups for infant feeding type.

Groups were not different for timing of the ACP assessment at the four or six-month time points (133.2 ± 16.3 days, DHA intervention versus 126.7 ± 6.0 days, placebo at four months; 187.9 ± 7.5 days, DHA intervention versus 190.9 ± 9.6 days, placebo at six months of age). Mean visual acuity scores at four and six months of age for the DHA group compared to the placebo group are presented in Table 3.

The same regression model was used to evaluate infant visual acuity by group at four and six months. The main fixed factor was group (intervention, placebo). Independent and potentially confounding variables for the model were: infant gender, weight gain during pregnancy, APGAR score at 5 min, maternal hematocrit, participation in the WIC program and infant feeding type. Of these independent variables, infant gender and maternal weight gain were not

significant within the model (with significant group differences) and were therefore excluded. There was a significant group difference in visual acuity at four months of age after adjusting for potential confounding variables (*P* = 0.018). Using the same model, there was no significant group difference at six months of age.

There was an increase in ACP score over time for both groups between four and six months (*P* ≤ 0.0001); however, change over time was not significantly different between the DHA and placebo groups.

## Discussion

Our findings demonstrate that infants of mothers who consumed the DHA-functional food during pregnancy had higher ACP visual acuity scores at four months of age compared to controls. In principle, higher acuity scores indicate that the infant is able to resolve a finer grating and therefore demonstrate more mature sensory visual processing. Our finding suggests that the infants of mothers who consumed the DHA food during pregnancy had better visual development at four months than infants of women consuming the placebo, regardless of what the infants were fed post-natally. Group differences were not significant at six months of age.

Visual acuity improved from four to six months for both the DHA and placebo groups. An improvement in visual acuity from the four to the six-month time point was expected, as this is the pattern seen in normative ACP data [2]. These data can be interpreted from the standpoint that infants of mothers who consumed DHA during pregnancy had accelerated development of the visual system that occurred some time prior to four months of age, when we assessed it.

**Table 3** Visual acuity scores for DHA intervention and placebo groups at four and six months of age

	DHA	Placebo
Four-month mean acuity score	3.7 ± 1.3 cycles/degree ( <i>n</i> = 16)	3.2 ± 1.3 cycles/degree ( <i>n</i> = 14)
Six-month mean acuity score	5.9 ± 1.2 cycles/degree ( <i>n</i> = 15)	5.4 ± 1.3 cycles/degree ( <i>n</i> = 11)

Values are expressed as antilogs of the means of the original log transformed scores in mean ± SD

Although ACP has inherent subjectivity not associated with ERG and VEP, it provides an opportunity to evaluate the behavioral responses that require more integrated processing associated with the visual stimulus. As far as we know, this is the first report of the impact of DHA supplementation during pregnancy on infant visual acuity assessed with ACP.

Dietary DHA deficiency during pregnancy reduces the DHA content of photoreceptor membranes of the retina and induces subnormal visual acuity in offspring of nonhuman primates compared to controls [3]. In the absence of DHA, retinal tissue accumulated higher levels of *n*-6 derived docosapentaenoic acid (DPA, 22:5*n*-6), altering membrane characteristics [22]. Such changes in membrane properties interfere with cellular signaling pathways, leading to deficits in function. More specifically, impairment in the G protein-coupled receptor (GPCR) signal transduction was demonstrated in association with DHA deficiency in retinal rod outer segment membranes isolated from rats [22].

Alteration in GPCR signal transduction in the rat model provides a plausible mechanism for our findings of better visual acuity in those infants whose mothers consumed DHA during pregnancy. GPCR signal transduction also has been suggested as a likely basis for alterations in cortical processes related to suboptimal DHA status [23]. Like ACP, VEP is considered a functional measure, but it is a measure that is specific to the primary visual cortex. The ACP elicits a behavioral response, which requires integrative cortical processing. Future work should focus on evaluating (1) the maternal DHA status and the ability of infants to integrate visual stimuli, as in face and object recognition, and (2) the relationship of acuity assessed during infancy to vision at a later age, as well as to cognitive processes [24].

**Acknowledgments** We are grateful to so many who were instrumental in making this project a success: the staff at Hartford Hospital (Women's Ambulatory Health Services) especially, Brunella Ibarrola, Griselle Corcino, Lynn Deasy and Dr. John Greene who appreciated the importance of this work and supported us in establishing subject recruitment and follow-up procedures and provided us with an examination room to conduct our assessments; E. Eugenie Hartmann who provided us with the training and background necessary to establish reliability for the ACP procedures, interpreted results, and who kindly reviewed our manuscript; University of Connecticut graduate students Amber Courville, Charlotte DeMare, Melissa Keplinger, and Elizabeth McArthur, who worked collaboratively in recruitment and follow-up activities. A special thanks to the families from the greater Hartford area who took time from their busy lives to commit to participation in this longitudinal project. Supported in part by USDA IFAFS, Nestec, Ltd., the Hatch Act, the National Fisheries Institute and the American Dietetic Association Foundation.

## References

1. Neuringer M (2000) Infant vision and retinal function in studies of dietary long-chain polyunsaturated fatty acids: methods, results and implications. *Am J Clin Nutr* 71:256S–267S
2. Salomao SR, Ventura DF (1995) Large sample population age norms for visual acuities obtained with vistech-teller acuity cards. *Invest Ophthalmol Vis Sci* 36:657–670
3. Neuringer M, Connor WE, Barstad L, Luck S (1986) Biochemical and functional effects of prenatal and postnatal *n*-3 fatty acid deficiency on retina and brain in rhesus monkeys. *Proc Natl Acad Sci* 83:4021–4025
4. Carlson SE, Ford AJ, Werkman SH, Peeples JM, Koo WK (1996) Visual acuity and fatty acid status of term infants fed human milk and formulas with and without docosahexaenoate and arachidonate from egg yolk lecithin. *Pediatr Res* 39:882–888
5. Jorgensen HM, Hernell O, Lund P, Holmer G, Michaelsen KF (1996) Visual acuity and erythrocyte docosahexaenoic acid status in breast-fed and formula-fed term infants during the first four months of life. *Lipids* 31:99–105
6. Birch E, Birch DG, Hoffman DR, Hale L, Everett M, Uauy RD (1993) Breast feeding and optimal visual development. *J Pediatr Ophthalmol Strabismus* 30:33–38
7. Hoffman DR, Birch EE, Castaneda YS, Fawcett SL, Wheaton DH, Birch DG, Uauy R (2003) Visual function in breast-fed term infants weaned to formula with or without long-chain polyunsaturates at 4 to 6 months: a randomized clinical trial. *J Pediatr* 142:669–677
8. Makrides M, Simmer K, Goggin M, Gibson RA (1993) Erythrocyte docosahexaenoic acid correlates with the visual response of healthy, term infants. *Pediatr Res* 33:425–427
9. Makrides M, Neumann M, Simmer K, Pater J, Gibson R (1995) Are long-chain polyunsaturated fatty acids essential nutrients in infancy? *Lancet* 345:1463–1468
10. Malcolm CA, McCulloch DL, Montgomery C, Shepherd A, Weaver LT (2003) Maternal docosahexaenoic acid supplementation during pregnancy and visual evoked potential development in term infants: a double blind, prospective, randomized trial. *Arch Dis Childhood Fetal Neonatal Ed* 88:F383–F390
11. Malcolm CA, Hamilton R, McCulloch DL, Montgomery C, Weaver LT (2003) Scotopic electroretinogram in term infants born of mothers supplemented with docosahexaenoic acid during pregnancy. *Invest Ophthalmol Vis Sci* 44:3685–3691
12. Simopoulos AP, Leaf A, Salem N (2000) Workshop statement on the essentiality and recommended dietary intakes for omega-6 and omega-3 fatty acids. *Prostaglandins Leukot Essent Fatty Acids* 83:119–21
13. Lewis NM, Widga AC, Buck JS, Frederick AM (1995) Survey of omega-3 fatty acids in diets of midwest low-income pregnant women. *J Agromed* 2:49–56
14. Judge MP, Loosemore ED, DeMare CI, Keplinger MR, Mutungi G, Cote S, Ryan M, Ibarolla B, Lammi-Keefe CJ (2003) Dietary docosahexaenoic acid (DHA) intake in pregnant women. *J Am Diet Assoc* 103:A82
15. Judge MP, Loosemore ED, Farkas SL, DeMare CI, Keplinger MR, Mutungi G, Cote S, Ryan M, Ibarolla B, Lammi-Keefe CJ (2003) Dietary DHA intake across four ethnic groups. *FASEB J* 17:71–72
16. Innis SM, Elias SL (2003) Intakes of essential *n*-6 and *n*-3 polyunsaturated fatty acids among pregnant Canadian women. *Am J Clin Nutr* 77:473–478

17. Denomme J, Stark KD, Holub BJ (2005) Directly quantitated dietary (*n*-3) fatty acid intakes of pregnant Canadian women are lower than current dietary recommendations. *J Nutr* 135:206–211
18. Teller D (1990) Teller acuity cards (Tac) manual. Vistech Consultants, Inc., Dayton, OH
19. Hartmann EE, Ellis GS, Morgan KS, Love A, May JG (1990) The acuity card procedure: longitudinal assessments. *J Pediatr Ophthalmol Strabismus* 27:184–187
20. Mayer LD, Dobson V (1997) Grating acuity cards: validity and reliability in studies of human visual development. Academic, New York, pp 253–292
21. Freund RJ, Littell RD, Spector PC (2003) SAS System, v9 (TS M0). SAS Institute, Inc., Cary, NC
22. Nui SL, Mitchell DC, Lim SY, Wen ZM, Kim HY, Salem N, Litman BJ (2004) Reduced G protein-coupled signaling efficiency in retinal rod outer segments in response to *n*-3 fatty acid deficiency. *J Biol Chem* 279:31098–31104
23. Salem N Jr, Litman B, Kim HY, Gawrisch K (2001) Mechanisms of action of docosahexaenoic acid in the nervous system. *Lipids* 36:945–959
24. Neuringer M, Jeffrey BG (2003) Visual development: neural basis and new assessment methods. *J Pediatr* 143:S87–S95

## Butters Varying in *trans* 18:1 and *cis*-9,*trans*-11 Conjugated Linoleic Acid Modify Plasma Lipoproteins in the Hypercholesterolemic Rabbit

Dominique Bauchart · Alexandre Roy · Stephanie Lorenz · Jean-Michel Chardigny · Anne Ferlay · Dominique Gruffat · Jean-Louis Sébédio · Yves Chilliard · Denys Durand

Received: 6 June 2006 / Accepted: 15 December 2006 / Published online: 27 January 2007  
© AOCS 2007

**Abstract** The experiment was designed to study the effects of butters differing in conjugated linoleic acid (CLA) and *trans* 18:1 contents on lipoproteins associated with the risk of atherogenesis. New Zealand White male rabbits (9.6 weeks; 2.1 kg) were assigned for 6 or 12 weeks to three diets ( $n = 6$  per diet) made of conventional pellets with 0.2% cholesterol and with 12% fat provided from a butter poor in *trans*-10 and *trans*-11 18:1 and in CLA (standard group), or rich in *trans*-10 18:1 (*trans*-10 18:1 group) or rich in *trans*-11 18:1 and in *cis*-9,*trans*-11 CLA (*trans*-11 18:1/CLA group). Blood samples were collected at the end of dietary treatments. Lipoproteins were separated by gradient-density ultracentrifugation. Lipid classes were determined enzymatically and apolipoproteins A-I and B by radial immunodiffusion. Mainly in the 12-week rabbits, higher plasma triglycerides and apolipoprotein B levels shown in the standard and *trans*-10 18:1 groups compared with those in the

*trans*-11 18:1/CLA group are associated with higher plasma levels of very low density lipoproteins (VLDL) and low density lipoproteins (LDL) also shown in these two groups. In the 12-week rabbits, a shift towards denser LDL, considered as more atherogenic, was shown only in the *trans*-10 18:1 group. In these animals, the VLDL + LDL to HDL ratio was 1.7–2.3 times higher in the *trans*-10 18:1 group than in the other groups ( $P = 0.076$ ). These results suggest a rather neutral effect of *trans*-11 18:1/CLA butter towards the risk of atherogenesis, whereas *trans*-10 18:1 butter would tend to be detrimental.

**Keywords** Butter · *trans* 18:1 isomers · Conjugated linoleic acid · Cholesterol · Lipoproteins · Rabbit

### Abbreviations

CE	Cholesteryl esters
CETP	Cholesteryl ester transfer protein
CHD	Coronary heart disease
CLA	Conjugated linoleic acid
FC	Free cholesterol
HDL	High density lipoprotein
IDL	Intermediate density lipoprotein
INRA	Institut National de la Recherche Agronomique
LDL	Low density lipoprotein
NEFA	Nonesterified fatty acids
PHVO	Partially hydrogenated vegetable oils
PL	Phospholipids
PUFA	Polyunsaturated fatty acids
TC	Total cholesterol
TG	Triacylglycerols

D. Bauchart (✉) · S. Lorenz · D. Gruffat · D. Durand  
UR1213 Herbivores, Research Unit on Herbivores,  
Nutrients and Metabolisms Group, INRA,  
Site de Theix, 63122 Saint-Genès-Champanelle, France  
e-mail: bauchart@clermont.inra.fr

A. Roy · J.-M. Chardigny · J.-L. Sébédio  
INRA, UMR1019, Clermont-Ferrand 63001, France

A. Roy · J.-M. Chardigny · J.-L. Sébédio  
CRNH Auvergne, Clermont-Ferrand 63001, France

A. Ferlay · Y. Chilliard · A. Roy  
UR1213 Herbivores, Research Unit on Herbivores,  
Adipose Tissue and Milk Lipid Group, INRA,  
Site de Theix, 63122 Saint-Genès-Champanelle, France

VA Vaccenic acid  
VLDL Very low density lipoproteins

## Introduction

Atherosclerosis and its consequences are the main causes of mortality in industrialized countries, the incidence being related to increasing cholesterol and saturated fatty acid intake. The other factors linking saturated fatty acid and cholesterol intake with coronary heart disease (CHD) are thrombosis and insulin resistance [41]. Milk is often considered to be detrimental towards atherosclerosis because milk fat is rich in saturated fatty acid (especially C12, C14 and C16), and provides low but variable levels of cholesterol and *trans* monounsaturated fatty acids. However, different European prospective studies indicate that there is no evidence that milk [30] or milk fat [41] consumption is associated with CHD. Among different hypotheses, conjugated linoleic acid (CLA), which is sometimes abundant in milk fat, is reported to be potentially antiatherogenic owing to both its hypolipidemic [20] and its antioxidative properties [31].

CLA represents a group of positional and geometric isomers of linoleic acid (*cis*-9,*cis*-12 18:2). It is produced by ruminant animals, to a low degree, by biohydrogenation and *trans* isomerization of dietary polyunsaturated fatty acids (PUFA) by bacteria in the rumen and, to a high degree, by desaturation of *trans*-11 18:1 (vaccenic acid, VA, another intermediate in the ruminal PUFA biohydrogenation process) catalyzed by the stearoylcoenzyme A desaturase in the extrahepatic tissues [2]. Ruminant CLA, dominated by ruminic acid (*cis*-9,*trans*-11 CLA isomer), is preferentially incorporated into triglycerides of fat tissues and milk [12]. The composition and the level of CLA isomers in ruminant products are influenced by animal husbandry factors, mainly by feeding conditions [7, 9]. Products of ruminants represent the major dietary source of CLA for humans, ranging from 150 to 200 mg CLA per day [33].

Associated with CLA in ruminant products, *trans*-18:1 represent a mixture of positional isomers generally dominated by VA in meat or milk from animals offered conventional diets. However, *trans*-10 18:1 (putatively produced by the hydrogenation of *trans*-10,*cis*-12 CLA in the rumen, and/or from oleic acid isomerization [29], is low in traditional feeding systems, but was shown to be increased in milk fat of cows given corn silage-based or concentrate-rich diets supple-

mented with plant oils, especially linoleic-rich oils (sunflower or soybean oil), which tend to decrease milk fat content [4, 8]. For example, with the diet proposed by Bauman et al. [3] to increase CLA, there was an increase in milk *trans*-10 18:1 after 3 weeks, up to 7% of total fatty acids [34], despite the fact that this diet (460 g forage, 160 g hay and 310 g corn silage on a dry matter basis) was not a “high-concentrate diet”. This could contribute to increasing the mean percentage of *trans*-10 18:1 in commercial bulk milk, if farmers used this type of diet, in order to decrease milk saturated fatty acids, to increase milk CLA or to decrease milk fat content (especially in Europe with the milk fat quota regulation systems).

Generally, *trans* fatty acid intake is associated with CHD risk factors, but this link is still controversial [23]. Many studies in humans have shown a positive correlation between total *trans* fatty acid intake and myocardial infarction [32], but some others suggested that their potential for atherogenicity varies with the type of *trans* fatty acids consumed [5]. Indeed, *trans* fatty acids are provided in human foods not only by ruminant fat products (dominated by the *trans*-11 18:1 form) but, above all, by partially hydrogenated vegetable oils (margarines or shortenings) having high levels of several *trans* isomers of 18:1 ( $\Delta$ 6/8,  $\Delta$ 9,  $\Delta$ 10,  $\Delta$ 11,  $\Delta$ 12 and  $\Delta$ 13/14) [15].

To evaluate the specific impact of natural (milk) CLA and *trans*-18:1 on the risk of atherogenesis, three butters were prepared from cow milk fats that differed in their CLA (ruminic acid) and either *trans*-11 or *trans*-10 18:1 contents [35]. These butters, mixed in a conventional rabbit diet supplemented with 0.2% cholesterol, were given for 6 or 12 weeks to New Zealand White rabbits (a validated model for the study of lipoproteins–atherosclerosis interactions [10]) to compare the effects of butter fat containing either *cis*-9,*trans*-11 CLA associated with *trans*-11 18:1 or *trans*-10 18:1 on the blood lipids and lipoprotein profile, indicators of the risk of atherogenesis.

## Experimental Procedure

### Animals and Diets

All experimental procedures were approved by the Local Animal Ethics Committee of the Institut National de la Recherche Agronomique (INRA), in accordance with the French recommendations for the use of experimental animals (guidelines 18 April 1988). The experiment was performed in the experimental

unit of INRA Theix Research Center in France (approval number 06–02630; authorization number for animal experimentation 63 20). Thirty-six male New Zealand White rabbits (age  $9.6 \pm 0.5$  weeks, body weight  $2.1 \pm 0.1$  kg, Elevage Scientifique des Dombes, Chatillon sur Chalaronne, France) were divided according to diet into three groups of 12 animals on the age and body-weight basis. In the same experiment, the animals were given one of three diets either for 6 weeks ( $n = 6$  per treatment) or for 12 weeks ( $n = 6$  per treatment) to ensure a mean body weight gain of 20–25 g/day. The animals were housed in individual stainless steel cages in a temperature-controlled room (18°C) maintained on a 12-h light–dark cycle and were allowed free access to water. Food intake was measured daily and body weight was recorded every week. All rabbits were killed at the end of the experiment (6 or 12 weeks) after a food deprivation of 17 h.

The three experimental diets given to the rabbits (Tables 1, 2) were prepared and pelletized by the INRA (Station de Recherches Cunicoles, Toulouse, France). The butters having different fatty acid composition were prepared from milk from cows given rations varying in the composition of ingredients leading to modifications of the milk fatty acid composition (especially *trans* isomers of 18:1 and CLA contents) as described earlier [35]. They were incorporated into conventional pellets for rabbits (around 12% diet dry matter) which were supplemented with cholesterol (0.2% diet dry matter) (Table 1). The fatty acid composition of the three experimental diets (Table 3) was determined in total lipids extracted by chloroform/methanol (2:1, vol/vol) and then by hexane/ethanol/HCl (25:10:10, vol/vol/vol) [21] by gas–liquid chromatography using a PR 2100 chromatograph (Perichrom Society, Sault-les-Charreaux, France) equipped with a CP Sil 88 glass capillary column (length 100 m; inner diameter 0.25 mm) under conditions described earlier [37].

**Table 1** Mean composition of the experimental diets given to New Zealand White rabbits

Ingredients	Content (g/kg dry matter)
Butter	120
Corn oil	8
Cholesterol	2
Alfalfa flour	305
Beet pulp	100
Barley	65
Sunflower cake	50
Soya cake	233
Sucrose	102
Sodium chloride	5
Calcium hydrogen phosphate	5
Vitamin and mineral mix	5

**Table 2** Dry matter concentration and chemical composition of the diets with 0.2% cholesterol and 12% fat provided from a standard butter, a *trans*-10 18:1 butter or a *trans*-11 18:1/conjugated linoleic acid (CLA) butter

Diet	Standard	<i>trans</i> -10 18:1	<i>trans</i> -11 18:1/CLA
Dry matter (g/kg feed)	857	834	843
Composition of dry matter (g/kg)			
Organic matter	921	922	920
Crude cellulose	170	173	170
Protein (nitrogen $\times 6.25$ )	212	235	245
Lipid	135	136	131
Fatty acid	114	115	112

**Table 3** Fatty acid composition (wt% total fatty acid methyl esters) of a diet with 0.2% cholesterol and 12% fat provided from a standard butter, a *trans*-10 18:1 butter or a *trans*-11 18:1/CLA butter given to New Zealand White rabbits

Fatty acids (%)	Standard	<i>trans</i> -10 18:1	<i>trans</i> -11 18:1/CLA
<12	6.0	3.5	3.8
12:0	3.8	2.1	2.0
14:0	10.7	7.8	6.8
16:0	29.4	21.5	19.3
Sum 16:1	1.7	2.0	1.4
18:0	7.7	7.0	9.3
<i>trans</i> -9 18:1	0.3	0.6	0.9
<i>trans</i> -10 18:1	0.4	11.8	2.2
<i>trans</i> -11 18:1	1.1	1.8	7.0
<i>trans</i> -13 18:1	0.4	0.5	0.8
<i>cis</i> -9 18:1	16.6	16.8	20.9
<i>cis</i> -11 18:1	0.7	0.9	0.9
<i>cis</i> -12 18:1	0.2	0.3	0.6
<i>cis</i> -13 18:1	0.1	0.1	0.1
<i>cis</i> -14+15+16 18:1	0.2	0.3	0.4
<i>cis</i> -9, <i>cis</i> -12 18:2	9.8	10.1	11.0
<i>cis</i> -9, <i>cis</i> -12, <i>cis</i> -15 18:3	2.2	2.0	2.4
<i>cis</i> -9, <i>trans</i> -11 CLA	0.5	0.8	2.6
Others fatty acids	8.4	10.3	7.8
Sum saturated fatty acids	56.6	41.7	40.8
Sum <i>trans</i> -18:1	2.6	14.7	10.9
Sum <i>cis</i> -18:1	17.6	18.4	22.8
Sum n-3 FA	3.0	3.0	3.2
Sum n-6 FA	10.7	11.2	12.2
n-6/n-3 ratio	3.6	3.7	3.8
P/S ratio <sup>a</sup>	4.3	3.2	2.8

<sup>a</sup> Quotient of *cis*-9,*cis*-12 18:2+ *cis*-9,*cis*-12,*cis*-15 18 3: and 12:0 + 14:0 + 16:0 + 18:0

## Blood Samples

At the end of the two experiments and just before the morning meal, blood samples (50 mL) were collected by cardiac puncture into tubes containing Na<sub>2</sub>-EDTA, NaN<sub>3</sub> and merthiolate (final concentrations 3 mM, 0.1 and 0.01 g/L, respectively). Plasma was prepared by centrifugation of blood samples at 2,700g for 15 min at

15°C. Three 500- $\mu$ L fractions of plasma were stored at -20°C until analysis of lipid fractions and apolipoproteins B and A-I, and one fraction of 20 mL was treated immediately for lipoprotein fractionation.

### Lipoprotein Isolation

To determine the density distribution and the chemical composition of lipoprotein subfractions, plasma lipoproteins were separated by ultracentrifugation according to a three-step sequence in a Centrikon T-2060 ultracentrifuge equipped with a TST 41–14 swinging-bucket rotor (Kontron Analysis Division). First, chylomicrons ( $d < 0.950$  g/mL) were isolated by ultracentrifugal flotation at 103,000g for 46 min at 15°C. Second, very low density lipoproteins (VLDL,  $d < 1.006$  g/mL) were removed from plasma by ultracentrifugal flotation at 205,000g for 16 h at 15°C. Third, the lipoprotein fractions of  $d > 1.006$  g/mL were separated by ultracentrifugation in a discontinuous density gradient in saline solution for 46 h at 205,000g and at 15°C into 22 successive subfractions corresponding to a density from 1.018 to 1.180 g/mL according the procedure described earlier [1]. VLDL (including chylomicrons) were defined as lipoproteins of  $d < 1.018$  g/mL, low-density lipoproteins (LDL) (including intermediate-density lipoproteins, IDL, of  $d = 1.018$ – $1.026$  g/mL) as lipoproteins of  $d = 1.018$ – $1.060$  g/mL, light high-density lipoproteins (HDL) as lipoproteins of  $d = 1.060$ – $1.091$  g/mL, and heavy HDL as lipoproteins of  $d = 1.091$ – $1.180$  g/mL. Lipoprotein fractions were dialyzed at 4°C for 7 h against a buffer containing 0.02 M  $\text{NH}_4\text{HCO}_3$ , 1.5 mM  $\text{NaN}_3$  and 1 mM  $\text{Na}_2\text{-EDTA}$  pH 8.6 in a Gibco BRL microdialysis system (Bethesda Research Laboratories, Rockville, MD, USA) supplied with membranes with cutoff at 12–14 kDa.

### Chemical Analysis

The enzymatic methods used for the determination of lipid classes in plasma and in lipoprotein subfractions have been described previously [22]. Briefly, free cholesterol (FC) was measured by using the properties of the cholesterol oxidase and of the peroxidase. Total cholesterol (TC) was measured by using the reagent kit Cholesterol RTU (BioMérieux, Marcy l'Etoile, France). Cholesteryl ester (CE) content was calculated using the relationship  $\text{CE} = (\text{TC} - \text{FC}) \times 1.68$ . The triacylglycerol (TG) content was estimated from the total glycerol value by the enzymatic method using the reagent kit PAP 150 (reference 61236) supplied by BioMérieux (Marcy l'Etoile, France). Phospholipids (PL) were determined by the method of Trinder using

the BioDirect Phospholipids Kit (Bio Direct, La Villeneuve, France). Plasma nonesterified fatty acids (NEFA) were determined by the enzymatic method using the kit NEFA C WAKO (WAKO Oxoid, Dardilly, France). Protein concentration was determined in lipoprotein subfractions by the colorimetric method of the bicinchoninic acid protein assay reagent (Pierce, Rockford, USA).

### Immunological Analysis

Apolipoprotein A-I and apolipoprotein B in plasma and in lipoprotein subfractions were determined by radial immunodiffusion using polyclonal sheep antisera to rabbit apolipoprotein A-I (purified from HDL) and to rabbit apolipoprotein B (purified from LDL). The diameters of the precipitation rings were proportional to the logarithm of the antigen concentration given by a standard range (rabbit apolipoprotein A-I or apolipoprotein B).

### Statistical Analysis

All data were treated by analysis of variance using the general linear model procedure of SAS [36]. Treatment differences were considered significant at  $P < 0.10$ . Values of the body weight of animals, determined every week, were used in repeated measurements. When the effect of diet was considered to be statistically significant ( $P < 0.10$ ), treatment of means was compared between the kinetic points using a Student's  $t$  test of SAS [21].

## Results

### Diets and Animal Performance

Experimental diets given to rabbits differed in their content of saturated fatty acids (29% higher in the standard diet than in the two other diets) and more especially in their contents of *trans*-10 18:1 (11.8% in the *trans*-10 18:1 diet vs. 0.4 and 2.2% in the standard and *trans*-11 18:1/CLA diets, respectively), *trans*-11 18:1 (7.0 % in the *trans*-11 18:1/CLA diet vs. 1.1 and 1.8% in the standard and *trans*-10 18:1 diets, respectively) and *cis*-9,*trans*-11 CLA (2.6% in the *trans*-11 18:1/CLA diet vs. 0.5 and 0.8% in the standard and *trans*-10 18:1 diets, respectively) (Table 3). All rabbits in both experiments survived during the entire experiment, except for one animal from the standard group in 6-week rabbits which died owing to an accident



during blood sampling. The three diets were generally well accepted during the experiments. No significant differences in food intake were observed between diets, except for the rabbits fed the *trans*-10 18:1 diet in the last week of the experiment (12 weeks), the food intake of which was significantly lower than that in the two other groups (Fig. 1a, b). Rabbits given the three experimental diets for 6 weeks had similar variations of their body weight (Fig. 1a) and daily body weight gain (Table 4). On the other hand, rabbits fed the standard diet for 12 weeks had significantly higher ( $P < 0.05$ ) body weight (6% higher, Fig. 1b) and daily weight gain (15% higher, Table 5) than the rabbits fed the *trans*-10 18:1 or *trans*-11 18:1/CLA diets, the differences in the body weight generally being significant from 4 up to 12 weeks (Fig. 1b).

### Plasma Lipids and Apolipoproteins

In the 6-week rabbits, the plasma TC content of rabbits given the *trans*-10 18:1 diet was 2.4 and 1.8 times higher than that of rabbits given the standard and *trans*-11 18:1/CLA diets, respectively (Table 5). Plasma NEFA was higher in the *trans*-11 18:1/CLA group than in the standard group (+72%) and in the *trans*-10 18:1 group (+122%). Plasma apolipoprotein B, specifically

associated with non-HDL, was 2.0 and 1.8 times higher in the *trans*-10 18:1 group than in the standard and *trans*-11 18:1/CLA groups, respectively (Table 5).

In the 12-week rabbits, plasma TC, PL and apolipoprotein B were generally lower in the *trans*-11 18:1/CLA group than in the standard group and the *trans*-10 18:1 group (Table 5). Plasma NEFA were higher in the *trans*-10 18:1 (+125%) and *trans*-11 18:1/CLA groups (+110%) than in the standard group. Plasma apolipoprotein A-I was lower in the *trans*-10 18:1 and *trans*-11 18:1/CLA groups than in the standard group (Table 5).

### Density Distribution of Plasma Lipoproteins

Lipoprotein classes were separated into 22 subfractions by isopycnic density gradient ultracentrifugation according to their hydrated density (Fig. 2). Lipid classes and apolipoprotein B and A-I contents of each individual subfraction were determined to characterize lipoprotein chemical composition and plasma concentration (Table 6).

In both experiments, plasma VLDL (including chylomicrons) ( $d < 1.018$  g/mL), the most abundant lipoproteins (with LDL) of plasma New Zealand White rabbits (26.0–45.9% of lipoproteins of  $d < 1.180$  g/mL; 160–584 mg/dL), was 1.4–3.7 times ( $P < 0.05$ ) and

**Fig. 1** Variations with time of the diet intake (a, b) and the body weight (c, d) (expressed as mean  $\pm$  the standard error) of New Zealand White rabbits given a diet with 0.2% cholesterol and with 12% fat provided from a standard butter ( $n = 5$ ), a *trans*-10 18:1 butter ( $n = 6$ ) or a *trans*-11 18:1/conjugated linoleic acid (CLA) butter ( $n = 6$ ) for 6 weeks (a, c) or 12 weeks (b, d). The asterisks indicate the mean body weight values of rabbits fed the *trans*-10 18:1 diet or the *trans*-11 18:1/CLA diet significantly different from those of rabbits given the standard diet ( $P < 0.05$ )

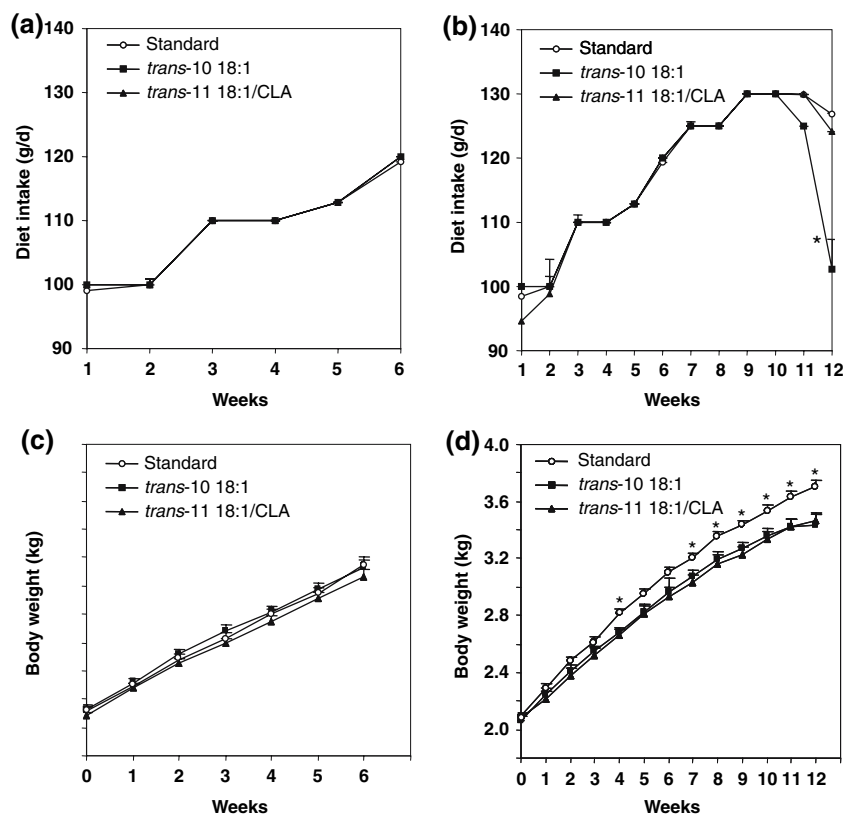


**Table 4** Mean body weight gain (g/day) of New Zealand White rabbits given a diet with 0.2% cholesterol and with 12% fat provided from a standard butter ( $n = 5$ ), a *trans*-10 18:1 butter ( $n = 6$ ) or a *trans*-11 18:1/CLA butter ( $n = 6$ ) for 6 or 12 weeks

	Standard	<i>trans</i> -10 18:1	<i>trans</i> -11 18:1/CLA	SEM	Diet effect
6 weeks	24.6	24.0	23.5	1.0	NS
12 weeks	19.2 <sup>a</sup>	16.4 <sup>b</sup>	16.2 <sup>b</sup>	0.6	0.006

Different *superscript letters* indicate significant differences between diets,  $P < 0.05$

SEM standard error of the mean, NS not significant

2.2–2.6 times ( $P < 0.05$ ) higher in the *trans*-10 18:1 group than in the standard and *trans*-11 18:1/CLA groups, respectively (Table 6, Fig. 2).

A similar trend was observed for total LDL (including IDL) particles ( $d = 1.018$ – $1.060$  g/mL), the other major rabbit lipoproteins (30–44% of total lipoproteins of  $d < 1.180$  g/mL; 159–512 mg/dL) (Table 6). In both 6-week and 12-week rabbits, plasma LDL concentration tended to be 1.8–2.6 times higher in animals given the *trans*-10 18:1 diet than the standard and *trans*-11 18:1/CLA diets, respectively ( $P = 0.086$ ) (Table 6). Total LDL was the lowest in the 12-week rabbits, especially in the *trans*-11 18:1/CLA group. The density profile of LDL subfractions was similar in the three groups in the 6-week rabbits, ranging from subfractions 2–10 (highest concentration in subfractions 6 and 7,  $d = 1.026$ – $1.035$  g/mL) (Fig. 2a, c). However, in the 12-week rabbits, a shift towards denser (putatively atherogenic) LDL particles (higher concentration in subfractions 8–12,  $d = 1.035$ – $1.068$  g/mL) was clearly observed in the *trans*-10 18:1 group, whereas a shift towards less dense (putatively nonatherogenic) LDL particles (higher values in subfractions 5 and 6,  $d = 1.023$ – $1.030$  g/mL) was noted in both the standard and the *trans*-11 18:1/CLA groups (Fig. 2b, d).

The total HDL (127–182 mg/dL) represented only 13–27% of total lipoproteins of  $d < 1.180$  g/mL in plasma of rabbits fed the three experimental diets (Table 6). They were dominated by heavy HDL

( $d = 1.091$ – $1.180$  g/mL) (64–72% of total HDL) compared with light HDL ( $d = 1.060$ – $1.091$  g/mL). The density profile of HDL subfractions (subfractions 11–22) was similar in plasma of 6-week rabbits given the three diets (Fig. 2a, e) and 12-week rabbits (Fig. 2b, f), with a maximal concentration for subfraction 17 ( $d = 1.108$ – $1.119$  g/mL). The mean concentrations of light and heavy HDL were generally not significantly influenced by the time of the experiments nor by the dietary treatments, except for the heavy HDL particularly in 6-week rabbits in which it was 1.3 times higher in the *trans*-10 18:1 group than in the *trans*-11 18:1/CLA group ( $P = 0.028$ ) (Table 6).

The ratio VLDL + LDL to HDL, an index of atherogenicity, tended to be modulated by the dietary treatments. It tended to be 2.3 and 1.7 higher in the *trans*-10 18:1 group than in the standard and the *trans*-11 18:1/CLA groups ( $P = 0.076$ ) (Table 6).

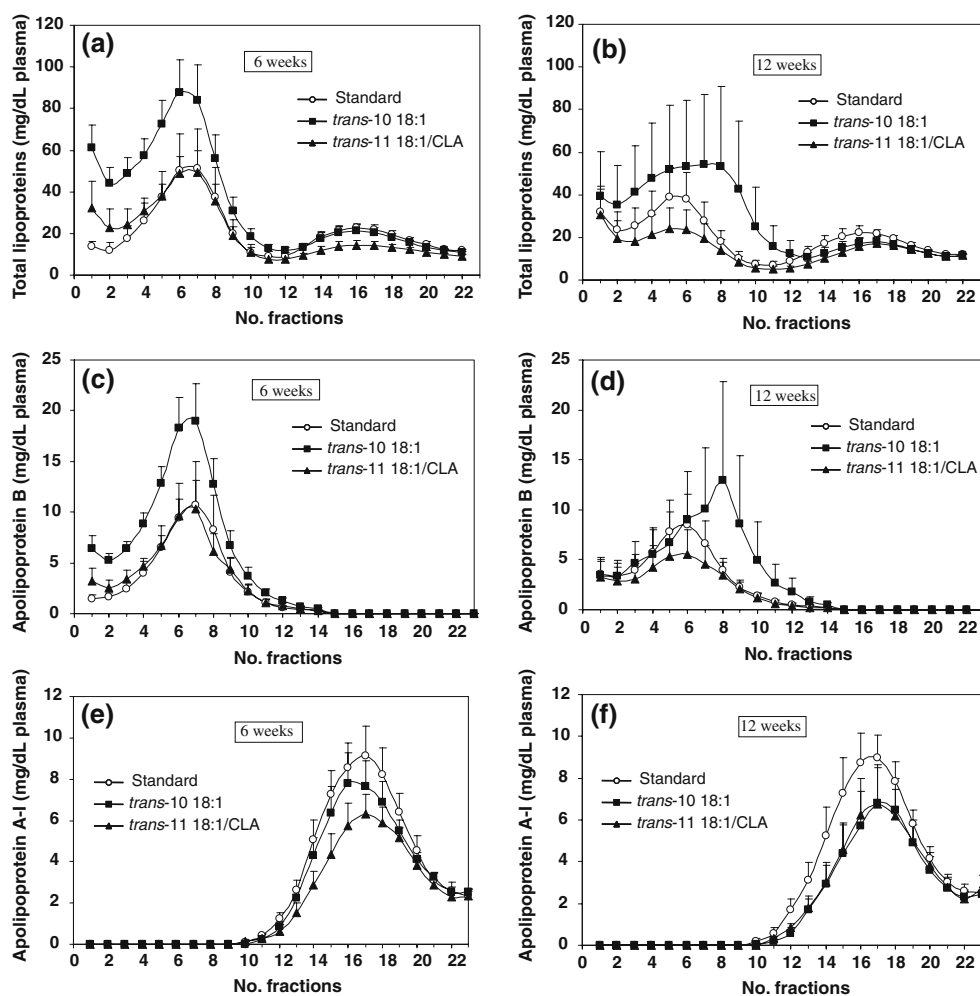
#### Chemical Composition of Plasma Lipoproteins

Analysis of lipid classes and total protein contents of the different lipoprotein classes showed more marked differences in the chemical composition of lipoprotein particles with the time of the experiments than with the dietary treatments (Table 6). Thus, the lipid core of VLDL and of LDL particles was, in the 12-week rabbits compared with the 6-week rabbits, 23–36% ( $P < 0.02$ ) and 8–32% ( $P < 0.04$ ) lower in the CE content in part to the benefit of TG. Similarly to TG, FC markedly increased (2.5–8.8 times) in VLDL particles in the 12-week rabbits compared with that in the 6-week rabbits ( $P = 0.004$ ). In the case of HDL particles, the same variations depending on the duration of the experiments were observed for lipids such as CEs (19–48% lower,  $P < 0.02$ ) and TG (11–82% higher,  $P < 0.01$ ). Finally, as for lipids, the protein content of LDL and HDL particles mainly varied with the duration of the experiments. Thus, the comparison of values determined for the 12-week rabbits with those determined for the 6-week rabbits showed a marked

**Table 5** Mean concentration (mg/dL) of the major plasma lipids and of plasma apolipoproteins B and A-I in New Zealand White rabbits given a diet with 0.2% cholesterol and with 12% fat

	Standard diet		<i>trans</i> -10 18:1 diet		<i>trans</i> -11 18:1/CLA diet		SEM	Diet effect	Time effect	Diet × time effect
	6 weeks	12 weeks	6 weeks	12 weeks	6 weeks	12 weeks				
Total cholesterol	197.9	290.8	475.0	384.2	271.4	172.7	98.7	0.089	0.697	0.574
Triglycerides	76.0	269.9	164.2	112.1	103.4	166.0	50.5	0.723	0.115	0.076
Phospholipids	169.4	241.1	324.8	261.0	193.5	146.6	57.8	0.110	0.789	0.474
Nonesterified fatty acids	9.9	11.6	7.7	26.1	17.1	35.9	6.41	0.069	0.022	0.352
Apolipoprotein B	66.5	68.4	133.4	89.1	74.4	47.1	23.0	0.072	0.323	0.674
Apolipoprotein A-I	137.5	135.5	124.3	96.7	104.7	97.2	14.9	0.072	0.233	0.618

**Fig. 2** Density distribution of lipoprotein subfractions (a, b) and of their apolipoproteins B (c, d) and A-I (e, f) of  $d > 1.018$  g/mL isolated by a single density-gradient ultracentrifugation. Mean lipoprotein, apolipoprotein B and apolipoprotein A-I masses (expressed in milligrams per plasma deciliter) were determined in New Zealand White rabbits given a diet with 0.2% cholesterol and with 12% fat provided from a standard butter ( $n = 5$ ), a *trans*-10 18:1 butter ( $n = 6$ ) or a *trans*-11 18:1/CLA butter ( $n = 6$ ) for 6 weeks (a, c, e) or 12 weeks (b, d, f). For details on lipoprotein isolation and determination, see “Experimental Procedure”



increase for proteins in LDL (9–43.3% higher,  $P = 0.004$ ) and in light HDL (13–24% higher,  $P = 0.008$ ) and, to a lower extent, in heavy HDL (6–8% higher,  $P = 0.009$ ) (Table 6).

## Discussion

This study using the experimental hypercholesterolemic rabbit model showed that feeding butter enriched in *cis*-9, *trans*-11 CLA and *trans*-11 18:1 (VA) did not modify the susceptibility of animals to atherosclerosis, whereas feeding butter enriched in *trans*-10 18:1 tended to modify plasma lipids and lipoproteins in a way which could increase the risk of atherosclerosis.

### The New Zealand White Rabbit, a Pertinent Model for Experimental Atherosclerosis

Among different animal species, including rat, mouse, hamster, pig and nonhuman primate, used as experimental models for the study of lipoprotein metabolism

related to atherosclerosis, rabbit has been frequently used because of size and easy handling but, above all, because of the high sensitivity of the response to dietary cholesterol [10]. Most strains of rabbits rapidly develop elevated hypercholesterolemia leading to atherosclerosis with deep lesions of blood vessels (aorta, coronary and cerebral arteries). This can be the consequence of gene mutations, such as in Watanabe heritable hyperlipidic line and St. Thomas' Hospital strains, or of the high sensitivity to dietary manipulations (fatty acid composition, cholesterol level) (New Zealand White strain [10]). Unlike rat, hamster or pig, rabbit shares with human a lipoprotein profile dominated by LDL particles and an abundant and active CE transfer protein (CETP) in plasma, conditions that naturally predispose rabbit to atherosclerosis.

### Dietary CLA or *trans* Fatty Acids and Growth Performance

The lack of effects of *cis*-9,*trans*-11 18:1/CLA diet on body weight gain and live weight of in our 6-week

**Table 6** Mean chemical composition (percentage of total mass) and plasma concentration (mg/dL) of lipoprotein classes in New Zealand White rabbits given a diet with 0.2% cholesterol and with 12% fat provided from a standard butter ( $n = 5$ ), a *trans*-10 18:1 butter ( $n = 6$ ) or a *trans*-11 18:1/CLA butter ( $n = 6$ ) for 6 or 12 weeks

Lipoprotein classes	Standard diet		<i>trans</i> -10 18:1 diet		<i>trans</i> -11 18:1/CLA diet		SEM	Diet effect	Time effect	Diet × time effect
	6 weeks	12 weeks	6 weeks	12 weeks	6 weeks	12 weeks				
<b>VLDL<sup>a</sup> (<math>d &lt; 1.018</math> g/mL)</b>										
Free cholesterol	0.9	7.9	1.2	3.0	0.9	6.0	1.8	0.465	0.004	0.083
Cholesteryl ester	56.6	43.8	66.1	50.4	60.9	38.8	7.9	0.506	0.016	0.842
Triglyceride	22.5	27.1	11.5	24.4	14.8	24.2	7.1	0.630	0.142	0.839
Phospholipid	15.8	17.1	19.3	25.2	17.1	17.2	3.1	0.136	0.342	0.504
Protein	4.3	4.0	4.0	5.0	3.9	5.8	0.6	0.530	0.124	0.227
VLDL concentration	159.6	337.8	583.5	484.9	268.2	190.3	131.2	0.049	0.995	0.531
Percentage of total lipoproteins ( $d < 1.180$ g/mL)	26.0	45.5	45.9	45.9	39.3	39.0				
<b>LDL<sup>b</sup> (<math>1.018 &lt; d &lt; 1.060</math> g/mL)</b>										
Free cholesterol	8.9	10.2	9.3	9.5	8.2	10.7	0.9	0.994	0.178	0.656
Cholesteryl ester	39.6	36.3	48.2	37.2	49.2	33.4	5.4	0.684	0.034	0.539
Triglyceride	6.3	9.7	5.4	10.6	3.3	10.9	3.0	0.942	0.039	0.798
Phospholipid	19.8	19.6	17.0	17.9	16.8	18.0	0.9	0.034	0.390	0.713
Protein	25.5	27.7	20.1	31.1	22.6	32.4	3.0	0.819	0.004	0.312
IDL + LDL concentration	272.7	227.6	512.2	419.9	287.7	159.0	88.8	0.086	0.358	0.938
Percentage of total lipoproteins ( $d < 1.180$ g/mL)	44.4	30.6	40.3	39.7	42.2	32.7				
<b>Light HDL (<math>1.060 &lt; d &lt; 1.091</math> g/mL)</b>										
Free cholesterol	5.1	5.6	6.3	4.5	4.4	5.8	0.8	0.940	0.981	0.313
Cholesteryl ester	23.7	19.3	27.7	23.0	27.9	14.5	3.7	0.465	0.020	0.406
Triglyceride	3.7	5.9	4.7	6.1	4.1	7.5	1.1	0.664	0.011	0.643
Phospholipid	21.6	19.5	18.6	18.8	18.6	19.0	1.3	0.281	0.643	0.579
Protein	45.9	51.6	42.7	50.7	45.2	56.1	3.5	0.530	0.008	0.757
Light HDL concentration	62.2	59.6	63.4	50.9	42.5	38.9	6.2	0.070	0.395	0.831
Percentage of total lipoproteins ( $d < 1.180$ g/mL)	10.1	8.0	5.0	4.8	6.2	8.0				
<b>Heavy HDL (<math>1.091 &lt; d &lt; 1.180</math> g/mL)</b>										
Free cholesterol	1.8	2.1	2.1	1.7	1.0	1.8	0.3	0.257	0.458	0.385
Cholesteryl ester	16.4	12.5	18.0	12.0	16.1	9.0	1.5	0.258	0.001	0.593
Triglyceride	3.4	4.9	4.4	5.4	4.1	6.4	0.5	0.089	0.005	0.446
Phospholipid	14.4	13.2	12.5	12.0	11.6	12.5	1.1	0.259	0.699	0.703
Protein	64.0	68.0	63.1	68.0	66.9	71.4	2.2	0.345	0.009	0.763
Heavy HDL concentration	119.4	117.9	111.5	101.7	84.2	98.7	6.6	0.028	0.894	0.433
Percentage of total lipoproteins ( $d < 1.180$ g/mL)	19.5	15.9	8.8	9.6	12.3	20.3				
LDL/HDL	1.46	1.24	3.06	2.75	2.43	1.14	0.53	0.126	0.333	0.738
VLDL + LDL/ HDL	2.32	3.00	6.60	5.96	4.65	2.64	1.55	0.076	0.612	0.700

Results are expressed as means ± the SEM

VLDL very low density lipoprotein, LDL low density lipoprotein, IDL intermediate density lipoprotein, HDL high density lipoprotein

<sup>a</sup> Including chylomicrons ( $d < 0.950$  g/mL)

<sup>b</sup> Including IDL ( $1.018 < d < 1.026$  g/mL)

cholesterol-fed New Zealand White rabbits confirmed general data obtained with CLA supplements to cholesterol-fed animals, i.e., hamsters (butter CLA [24]), rats (beef CLA or mixed synthetic CLA [28]) and New Zealand White rabbits (mixed synthetic CLA [18, 19]). However, as in our 12-week rabbits, experiments of

long duration can reduce growth performance in cholesterol-fed New Zealand White rabbits (13 weeks, mixed synthetic CLA [18]), but had no negative effects in cholesterol-fed hamsters (12 weeks, *cis*-9,*trans*-11 CLA [40]). Indeed, concerning their growth performance, New Zealand White rabbits appeared to be

more sensitive than other animals to dietary CLA since a decreasing weight gain was reported in these animals given from 0.1 to 1% of mixed synthetic CLA [18], whereas no such variations were noted in rats given 0.5–1.5% of mixed synthetic CLA [39].

In our study, the higher level of CLA (dominated by *cis-9,trans-11* CLA, ruminic acid) in the experimental *trans-11* 18:1/CLA butter is associated with the higher level of VA (*trans-11* 18:1), this latter fatty acid being known to be converted into *cis-9,trans-11* CLA by  $\Delta 9$  desaturation in the mammary gland or in extrahepatic tissues [2]. Therefore, such a decrease of the growth performance noted in the New Zealand White rabbits of the *trans-11* 18:1/CLA group could also be the result of the presence of the large amount of VA in the diet since a decrease was reported in the growth performance in rats given a diet enriched with a mixture of *trans* 18:1 isomers [13] and in mice given a diet enriched with VA [25]. However, a lower growth performance was not observed in cholesterol-fed hamsters given a butter enriched with VA compared with those given a standard butter [24], the lack of an effect probably being explained by the relatively short duration (4 weeks) of the experiment as also observed in our 6-week experiment, or by animal species differences (hamster/rabbit).

It is likely that the (generally moderate) reduction of growth performance following *trans* fatty acid consumption, which affected food intake as well as feed efficiency, was independent of the position of the *trans* double bond in the aliphatic chain of 18:1. Indeed, the same negative effect was noted in our experiment with New Zealand White rabbits given *trans-10* 18:1 or *trans-11* 18:1 and in rats given a mixture of 18:1 *trans* isomers [13].

#### Dietary CLA or *trans* Fatty Acids and Plasma Lipids and Lipoproteins

The lack of an additional effect of the butter rich in *trans-11* 18:1 and in *cis-9,trans-11* CLA given to our cholesterol-fed New Zealand White rabbits, to increase cardiovascular risk factors, is in agreement with recent data reporting the effects of butters enriched in *cis-9,trans-11* CLA on the lipoprotein profile in the hyperlipidemic hamster [40] or the effects of butters enriched in *trans-11* 18:1 and *cis-9,trans-11* CLA on the lipoprotein profile in the cholesterol-fed hamster [24]. Indeed, when expressing the data as the ratio VLDL + LDL to HDL, an index of atherogenicity, our rabbits given this butter tended, especially for the long-duration experiment (12 weeks), to have an improved profile of lipoproteins (in relation to health).

This butter being enriched in *trans-11* 18:1 and *cis-9,trans-11* CLA specifically to the detriment of three saturated fatty acids (C12, C14 and C16), it could be hypothesized that the favorable effect on the lipoprotein profile observed mainly resulted from a lower intake of these saturated fatty acids that were shown in some studies to be proatherogenic fatty acids [17]. However, Valeille et al. [40] provided direct evidence that adding *cis-9,trans-11* CLA in a high-fat diet reduced the early signs of atherosclerosis (lower LDL/HDL and aortic cholesterol loading) in hamster in comparison to the nonsupplemented animals given the same high-fat diet. Therefore, we can hypothesize that *trans-11* 18:1, which is the precursor of *cis-9,trans-11* CLA by  $\Delta 9$  desaturation [2], would also participate in the nonbeneficial or beneficial effects observed after feeding butter rich in *trans-11* 18:1 and *cis-9,trans-11* CLA as recently suggested [24].

Antiatherogenic properties attributed to *trans-11* 18:1 and *cis-9,trans-11* CLA are believed to be mainly the result of modifications of the LDL metabolism. First, it was reported that the decrease in plasma LDL cholesterol was consistent with a decrease in hepatic apolipoprotein B secretion [16], and a higher sequestration of cholesterol by the liver in a dose-dependent manner [38]. Additionally, it is well documented that *cis-9,trans-11* CLA can improve the protection of LDL from oxidation by favoring paraoxonase activity and by downregulation of inflammatory-related genes (TNF  $\alpha$ , IL-1 $\beta$ , cyclooxygenase 2) [40]. In contrast, the fact that *trans-11* 18:1 and *cis-9,trans-11* CLA decreased also plasma light and heavy HDL contents (not previously reported in the literature) in our hypercholesterolemic New Zealand White rabbits minimized the lowering effect of these fatty acids on plasma VLDL and LDL and therefore the protection towards atherosclerosis.

Our study using the hypercholesterolemic rabbit shows, for the first time, a trend for a specific detrimental effect of *trans-10* 18:1 on plasma lipoprotein metabolism leading to hyperlipidemia associated with higher plasma levels of LDL particles, which could be atherogenic. The metabolic effects of *trans-10* 18:1 on plasma lipoproteins related to atherosclerosis have not been previously studied, but have always been associated (only 17–19% of total *trans* 18:1 as *trans-10* 18:1, compared with 80% in the present study) with other *trans* 18:1 isomers in partially hydrogenated vegetable oils (margarines, spreads) [15], namely, in  $\Delta 6-8$  (23–26%),  $\Delta 9$  (17–18%),  $\Delta 11$  (16–17%) and  $\Delta 12$  (23–25%) positions [13, 24].

Generally, in numerous human studies, partially hydrogenated vegetable oils (PHVO) providing *trans* fatty acids at 4% of energy intake increased LDL

cholesterol, and at 5–6% of energy intake decreased HDL cholesterol when compared with dietary lipid sources very poor or deprived in *trans* 18:1 [15]. Such proatherogenic effects of *trans* fatty acids (produced by catalytic hydrogenation of plant oils) reported in humans were not confirmed in animal models such as rat [6, 11, 13] or hamster [40]. In these species, *trans* fatty acids from PHVO lowered plasma TC and LDL cholesterol and had less or no effect on HDL metabolism when compared with the effects of diets rich in *cis* 18:1 or in saturated fatty acids [11], in oleate or in stearate [13], in *trans*-11 18:1 and in *cis*-9,*trans*-11 CLA [24] or of diets poor in *trans* fatty acids and in CLA [24]. Indeed, such opposite effects of *trans* fatty acids on lipoprotein metabolism between humans and rats/hamsters could be explained by differences in the metabolism of apolipoprotein B lipoproteins (especially LDL) linked to the activity of CETP as previously proposed [11]. These authors suggested that the regulation of lipoprotein metabolism by dietary *trans* fatty acids can be masked in animal species exhibiting a very low plasma CETP activity (i.e., rat, mouse, hamster or pig) compared with that in humans [14]. However, the CETP activity, which results in a greater rate of transfer of CEs (and triglycerides) from HDL to other lipoproteins, was shown to be very high in rabbit (1.9 times higher than in human) [14]. Such similarities in lipoprotein metabolism in relation to CETP activity in rabbits compared with humans would explain, at least in part, the trend towards similar effects on LDL and HDL of *trans*-10 18:1 butter in our experiment and in PHVO present in human food items. Compared with previous data on *trans*-9 18:1 considered to be neutral in hamsters [42] and *trans*-11 18:1 proposed to be beneficial for atherosclerosis [24], we provide original data showing a trend towards a detrimental effect of *trans*-10 18:1 on atherosclerosis risk factors in New Zealand White rabbits, an animal model sharing important lipoprotein specificities with humans (predominance of plasma LDL, high plasma CETP activity). As reported for humans consuming diets enriched with soy bean oil based margarines [27], we observed a net shift of LDL particles towards small, dense LDL (which are known to be more atherogenic in humans) in the present rabbits given the *trans*-10 18:1 butter when compared with those given standard or *trans*-11 18:1/CLA-rich butters.

Indeed, since *trans*-10 18:1 and, possibly, other *trans* isomers mainly present in PHVO (i.e., *trans*-6–8 or *trans*-12 18:1) would favor atherosclerosis, different strategies to eliminate or greatly reduce *trans* 18:1 are being investigated by the food industry [15]. They are based on modifications of the hydrogenation treat-

ment, use of the interesterification process and selection of trait-enhanced oils. Similarly, in the case of ruminant milk products, attention must be paid in order to avoid the uncontrolled development of “new” feeding strategies that promote an increase of *trans*-10 18:1 production in the rumen and its secretion in milk, especially association of cereal-rich diets with plant oils [8, 26], initially proposed to increase the energy supplying producing animals and to increase PUFA (especially n-3 PUFA) in products.

**Acknowledgements** The authors wish to gratefully acknowledge Marinett Brunel and Anne-Sophie Bage for skillful technical assistance and Daniel Thomas and Philippe Gaydier for the excellent maintenance and care of the animals. The study was supported in part by the AQS CLA Program with financial aid from the French Research and Technology Ministry.

## References

- Bauchart D, Durand D, Laplaud PM, Forgez P, Goulinet S, Chapman MJ (1989) Plasma lipoproteins and apolipoproteins in the preruminant calf, bos spp: density distribution, physicochemical properties, and the in vivo evaluation of the contribution of the liver to lipoprotein homeostasis. *J Lipid Res* 30:1499–1514
- Bauman DE, Baumgard LH, Corl BA, Griinari JM (1999) Biosynthesis of conjugated linoleic acid in ruminants. *Proc Am Soc Anim Sci* 1–15
- Bauman DE, Barbano DM, Dwyer DA, Griinari JM (2000) Production of butter with enhanced conjugated linoleic acid for use in biomedical studies with animal model. *J Dairy Sci* 83:2422–2425
- Bauman JM, Griinari JM (2003) Nutritional regulation of milk fat synthesis. *Ann Rev Nutr* 23:203–227
- Baylin A, Kabagambe EK, Ascherio A, Spiegelman D, Campos H (2003) High 18:2 *trans*-fatty acids in adipose tissue are associated with increased risk of nonfatal acute myocardial infarction in costa rican adults. *J Nutr* 133:1186–1191
- Chiang MT, Lu YS (1996) Variation of plasma cholesterol levels in rats fed *trans* fatty acids or *cis* fatty acids. *Int J Vitam Nutr Res* 66:263–269
- Chilliard Y, Ferlay A, Mansbridge RM, Doreau M (2000) Ruminant milk fat plasticity: nutritional control of saturated, polyunsaturated, *trans* and conjugated fatty acids. *Ann Zootech* 49:181–205
- Chilliard Y, Ferlay A (2004) Dietary lipids and forages interactions on cow and goat milk fatty acid composition and sensory properties. *Reprod Nutr Dev* 44:467–492
- Enser M, Scollan ND, Choi NJ, Kurt E, Hallet K, Wood JD (1999) Effect of dietary lipid on the content of CLA in beef muscle. *Anim Sci* 69:143–146
- Fan J, Watanabe T (2000) Cholesterol-fed and transgenic rabbit models for the study of atherosclerosis. *J Atheroscler Thromb* 7:26–32
- Gatto LM, Lyons MA, Brown AJ, Samman S (2002) *Trans* fatty acids affect lipoprotein metabolism in rats. *J Nutr* 132:1242–1248
- Griinari JM, Bauman DE (1999) Biosynthesis of conjugated linoleic acid and its incorporation into meat and milk fat in

- ruminants. In: Yurawecz MP, Mossoba MM, Kramer JKG, Pariza MW, Nelson GJ (eds) *Advances in conjugated linoleic acid research*, vol 1. AOCS Press, Champaign, pp 180–200
13. Guidetti AM, Beynen AC, Lemmens AG, Gnoni G, Geelen JH (2003) Hepatic fatty acid metabolism in rats fed diets with different contents of C<sub>18:0</sub>, C<sub>18:1</sub> *Cis* and C<sub>18:1</sub> *trans* isomers. *Br J Nutr* 90:887–893
  14. Guyard-Dangremont V, Desrumaux C, Gambert P, Lallemand C, Lagrost L (1998) Phospholipid and cholesteryl ester transfer activities in plasma from 14 vertebrate species. Relation to atherogenesis susceptibility. *Comp Biochem Physiol* 120:517–525
  15. Hunter JE (2005) Dietary levels of trans-fatty acids: basis for health concerns and industry efforts to limit use. *Nutr Res* 25:499–513
  16. Khosla P, Fungwe T (2001) Conjugated linoleic acid : effects on plasma lipids and cardiovascular function. *Curr Opin Lipidol* 12:31–34
  17. Khosla P, Sundram K (1996) Effects of dietary fatty acid composition on plasma cholesterol. *Prog Lipid Res* 35(2):93–132
  18. Kritchevsky D, Tepper SA, Wright S, Tso P, Czarnecki SK (2000) Influence of conjugated linoleic acid (CLA) on establishment and progression of atherosclerosis in rabbits. *J Am Coll Nutr* 19:472S–477S
  19. Kritchevsky D, Tepper SA, Wright S, Czarnecki SK (2002) Influenced f graded levels on conjugated linoleic acid (CLA) on experimental atherosclerosis in rabbits. *Nutr Res* 22:1275–1279
  20. Lee KN, Kritchevsky D, Pariza MW (1994) Conjugated linoleic acid and atherosclerosis. *Atherosclerosis* 108:19–25
  21. Legay F, Bauchart D (1989) Distribution of bacteria in the rumen contents of dairy cows given a diet supplemented with soya-bean oil. *Br J Nutr* 61:725–740
  22. Leplaix-Charlat L, Bauchart D, Durand D, Laplaud PM, Chapman MJ (1996) Plasma lipoproteins in preruminant calves fed diets containing tallow or soybean oil with and without cholesterol. *J Dairy Sci* 79:1267–1277
  23. Lichtenstein A (2000) Trans fatty acids and cardiovascular disease risk. *Curr Opin Lipidol* 11:37–42
  24. Lock AL, Horne CAM, Baumann D, Salter AM (2005) Butter naturally enriched in conjugated linoleic acid and vaccenic alters tissue fatty acids and improves the plasma lipoprotein profile in cholesterol-fed hamsters. *J Nutr* 135:1934–1939
  25. Loor JJ, Lin X, Herbein JH (2003) Effects of dietary *cis*-9,*trans*-11 18:2, *trans*-10,*cis*-12 18:2, or vaccenic acid (*trans*-11 18:1) during lactation on body composition, tissue fatty acid profiles, and litter growth in mice. *Br J Nutr* 90:1039–1048
  26. Loor JJ, Ferlay A, Ollier A, Doreau M, Chilliard Y (2005) Relationship among trans and conjugated fatty acids and bovine milk fat yield due to dietary concentrate and linseed oil. *J Dairy Sci* 88:726–740
  27. Mauger J-F, Lichtenstein A, Ausman L, Jalbert SM, Jauhainen M, Ehnholm C, Lamarche B (2003) Effect of different forms of dietary hydrogenated fats on LDL particle size. *Am J Clin Nutr* 78:370–375
  28. Mir PS, Okine EK, Goonewardene L, He ML, Mir Z (2003) Effects of synthetic conjugated linoleic acid (CLA) or bio-formed CLA as high CLA beef on rat growth and adipose tissue development. *Can J Anim Sci* 83:583–592
  29. Moseley EE, Powell GL, Riley MB, Jenkins TC (2002) Microbial biohydrogenation of oleic acid to trans isomers in vitro. *J Lipid Res* 43:290–296
  30. Ness AR, Davey Smith G, Hart C (2001) Milk, coronary heart disease and mortality. *J Epidemiol Community Health* 55:379–382
  31. Nicolosi RJ, Laitinen L (1996) Dietary conjugated linoleic acid reduces aortic fatty streak formation greater than linoleic acid in hypercholesterolemic hamsters. *FASEB J Abst* 2751
  32. Oomen CM, Ocke MC, Feskens EJ, Van Erp-Baart MA, Kok FJ, Kromhout D (2001) Association between trans fatty acids intake and 10-year risk coronary heart disease in the Zutphen elderly study; a prospective population-based study. *Lancet* 357:746–751
  33. Ritzenthaler KL, McGuire MK, Falen R, Shultz TD, Dasgupta N, McGuire MA (2001) Estimation of conjugated linoleic acid intake by written dietary assessment methodologies underestimates actual intake evaluated by food duplicate methodology. *J Nutr* 131:1548–1554
  34. Roy A, Ferlay A, Shingfield KJ, Chilliard Y (2006) Examination of the persistency of milk fatty acid composition responses to plant oils in cows given different basal diets, with particular emphasis on trans-C18:1 fatty acids and isomers of conjugated linoleic acid. *Anim Sci* 82:479–492
  35. Roy A, Ferlay A, Chilliard Y (2006) Production of butter rich in trans-10 C18:1 for use in biomedical studies in rodents. *Reprod Nutr Dev* 46:211–218
  36. SAS/STAT (1989) *Guide for personal computers*. SAS Institute, Cary
  37. Scislawski V, Bauchart D, Gruffat D, Laplaud PM, Durand D (2005) Effects of dietary n-6 or n-3 PUFA protected or not against ruminal hydrogenations on plasma lipids and their susceptibility to peroxidation in fattening steers. *J Anim Sci* 83:2162–2174
  38. Sessions VA, Salter AM (1994) The effects of different dietary fats and cholesterol on serum lipoprotein concentrations in hamsters. *Biochim Biophys Acta* 1211:207–214
  39. Szymczyk B, Pisulewski P, Szczurek W, Hanczakowski P (2000) The effects of feeding conjugated linoleic (CLA) on rat growth performance, serum lipoproteins and subsequent lipid composition of selected rat tissues. *J Sci Food Agric* 80:1553–1558
  40. Valeille K, Férézou J, Amsler G, Quignard-Boulangé A, Parquet M, Grippois D, Dorosvska-Taran V, Martin JC (2005) A *Cis*-9, *trans* 11-conjugated linoleic acid-rich oil reduces the outcome of atherogenic process in hyperlipidemic hamster. *Am J Physiol Heart Circ Physiol* 289:H652–H659
  41. Warensjö E, Jansson J-H, Berglund L, Boman K, Åhrén B, Weinehall L, Lindhal B, Hallmans G, Vessby B (2004) Estimated intake of milk fat is negatively associated with cardiovascular risk factors and does not increase the risk of a first acute myocardial infarction. A prospective case-control study. *Br J Nutr* 91:635–642
  42. Woollet LA, Daumerie CM, Dietschy JM (1994) *Trans*-9 octadecenoic acid is biologically neutral and does not regulate the low-density-lipoprotein receptor as the *cis* isomer does in the hamster. *J Lipid Res* 35:1661–1673

## Rumenic Acid Significantly Reduces Plasma Levels of LDL and Small Dense LDL Cholesterol in Hamsters Fed a Cholesterol- and Lipid-Enriched Semi-Purified Diet

Martial LeDoux · Laurent Laloux ·  
Jean-Jacques Fontaine · Yvon A. Carpentier ·  
Jean-Michel Chardigny · Jean-Louis Sébédio

Received: 21 June 2006 / Accepted: 22 December 2006 / Published online: 14 February 2007  
© AOCS 2007

**Abstract** Conjugated linoleic acids (CLAs) consist of a series of positional and geometrical isomers of linoleic acid. CLA have been reported to beneficially affect cardiovascular risk factors in animal models. In order to assess the role of individual CLA isomers on lipoprotein cholesterol concentration, 30 hamsters were fed for 12 weeks an hyperlipidic diet containing pure *cis*-9,*trans*-11 CLA (*c9,t11*) or pure *trans*-10, *cis*-12 CLA (*t10,c12*) isomers given alone or as a mixture. Plasma total cholesterol, LDL and HDL cholesterol

concentrations were significantly lower in the *c9,t11* CLA isomer fed hamsters relative to the Control group, with the most substantially effect on LDL cholesterol (–56%;  $P < 0.05$ ). Plasma triacylglycerol concentrations did not differ significantly regarding those two groups. Plasma cholesterol parameters showed a tendency to decrease in the *t10,c12* CLA isomer and CLA mixture fed hamsters compared with the Control group, but differences were not significant. For the first time, the atherogenic fraction of small dense LDL was investigated. Plasma small dense LDL cholesterol concentration was lower in the *c9,t11* CLA relative to Control, while the *t10,c12* and CLA mixture groups showed only a non significant tendency to decrease. Taken together, these data indicate that feeding rumenic acid (*c9,t11* CLA) may beneficially affect lipoprotein profile in hamster fed a cholesterol- and lipid-enriched semi-purified diet, when *t10,c12* CLA isomer or CLA mixture would be less active.

M. LeDoux · L. Laloux  
Laboratoire d'Etudes et de Recherches sur la Qualité des  
Aliments et les Procédés Agroalimentaires,  
Agence Française de Sécurité Sanitaire des Aliments,  
94704 Maisons Alfort, France

M. LeDoux (✉)  
Laboratoire d'Etudes et de Recherches sur la Qualité  
des Aliments et les Procédés Agroalimentaires,  
Agence Française de Sécurité Sanitaire des Aliments,  
23 avenue du Général DeGaulle,  
94706 Maisons-Alfort Cédex, France  
e-mail: m.ledoux@afssa.fr

J.-J. Fontaine  
Unité d'Histologie et Anatomie Pathologique,  
Ecole Nationale Vétérinaire d'Alfort,  
94704 Maisons Alfort, France

Y. A. Carpentier  
L. Deloyers Laboratory for Experimental Surgery,  
Université Libre de Bruxelles, 1070 Brussels, Belgium

J.-M. Chardigny · J.-L. Sébédio  
INRA, UMR1019, Clermont-Ferrand 63000, France

J.-M. Chardigny · J.-L. Sébédio  
CRNH Auvergne, Clermont-Ferrand 63000, France

**Keywords** Conjugated linoleic acid · Lipoproteins ·  
LDL · Cholesterol · Hamster

### Abbreviations

CAD	Coronary artery disease
CLA	Conjugated linoleic acid
EDTA	Ethylenediaminetetracetic acid
HDL	High-density lipoprotein
HDL-C	High-density lipoprotein cholesterol
LDL	Low-density lipoprotein
LDL-C	Low-density lipoprotein cholesterol
SdLDL	Small dense low-density lipoprotein
TC	Total cholesterol
TAG	Triacylglycerol(s)



## Introduction

Conjugated linoleic acids (CLAs) refer to a group of positional and geometrical isomers of linoleic acid in which the double bonds are conjugated [1]. Some CLA isomers are naturally present in foods (especially in ruminant milk fat and dairy products as well as in ruminant meat), with rumenic acid (*c9,t11* 18:2) as the predominant isomer [2]. Chemical synthesis from linoleic acid leads to the formation of a complex mixture made of different isomers [3]. The older CLA preparations generally contained all four positional isomers from 8,10 to 11,13, while most of the current commercial preparations contain mainly both *c9,t11* and *t9,c12* CLA isomers [4]. Most experimental studies on health effects of dietary CLAs have used such synthetic mixtures.

Several beneficial effects of CLAs have been suggested from results of animal studies and include: carcinogenesis inhibition [5, 6], growth modulation [7] and body composition [8], prevention and treatment of type II diabetes [9], improved bone density [10] and reduced wasting in response to immune stimulation [11].

Synthetic mixtures of CLAs have also been suggested to decrease low-density lipoprotein cholesterol (LDL-C) and to reduce fatty streak formation in some (but not all) animal models [12–14]. Dietary intake may affect not only LDL-C and high-density lipoprotein cholesterol (HDL-C) levels but also low-density lipoprotein (LDL) size and the importance of the atherogenic small dense LDL (sdLDL) fraction [15]. However the effect of CLA supplementation on lipoprotein profile remains equivocal in man, especially regarding the specific effect of individual CLA isomers [16, 17]. Of interest, while mice and rats have a very low cholesteryl ester transfer (CETP) activity and therefore little if any cholesterol exchange between lipoproteins, hamsters show some CETP activity and a lipoprotein profile (with higher LDL-C levels and a fraction of sdLDL) more comparable to that in man.

In the present study, we prospectively analyzed the serum lipoprotein profile (including the different LDL subfractions) of hamsters fed a hypercholesterolemic diet with or without pure CLA isomers (*c9,t11* or *t10,c12*), or an equimolar mixture of both isomers.

## Materials and Methods

### Material

Pure *cis-9,trans-11* CLA (*c9,t11* 89.9%, *t10,c12* 2.8%, *c,c* isomers 0.8%, and *t,t* isomers 1.1%) and *trans-*

*10,cis-12*-CLA (*t10,c12* 96.5%, *c9,t11* 0.5%, *c10,c12* 1.25%, and *t,t* isomers 0.9%) isomers were commercially supplied as free fatty acids by Natural Lipids (Hovdebygda, Norway). Cholesterol and oleic acid were purchased from Sigma-Aldrich (Saint Quentin Fallavier, France). Triacylglycerol GPO-PAP and Cholesterol CHOD-PAP assay kits were purchased from Roche Diagnostics GmbH (Mannheim, Germany).

### Animals and Protocol

Forty golden Syrian male hamsters (Harlan, Gannat, France),  $82.5 \pm 0.67$  g body weight, 6–7 weeks old, were randomly allotted to four groups of ten animals. All hamsters were individually housed in stainless steel cages in an animal house maintained at  $26 \pm 1$  °C, with a 7:00 a.m.–5:00 p.m. light:dark cycle and free access to tap water. All animals were fed ad libitum a hypercholesterolemic diet consisting of 10% coconut oil, 1% safflower oil and 0.12% cholesterol (w:w), blended in a semi-purified diet containing wheat starch (342 g/kg DM), sucrose (246 g/kg DM), casein (219 g/kg DM), cellulose (33 g/kg DM), mineral mix (47 g/kg DM), and vitamin mix (14 g/kg DM). Supplementation of oleic acid as a control, *c9,t11* CLA (rumenic acid), *t10,c12* CLA, or a 50:50 (w:w) mixture of *c9,t11* CLA and *t10,c12* CLA, was added and accounted for 1% (by weight) of the hypercholesterolemic diet. Animal groups were designated as “control”, “*c9,t11* CLA”, “*t10,c12* CLA” and “CLA mixture” group, respectively. Body weight of the animals was monitored on a weekly basis throughout the study.

At the end of the 12-week experimental period, the hamsters were fasted overnight and anesthetized with isoflurane breathing. Blood sample was obtained from the *vena cava inferior* and collected on EDTA. Plasma was separated by centrifugation for 10 min at  $1,860 \times g$  at room temperature, frozen in liquid nitrogen and maintained at  $-80$  °C until analyzed within 2 months.

### Plasma Lipids and Lipoproteins Analyses

Plasma triacylglycerol (TAG) and total cholesterol (TC) concentrations were measured enzymatically in plasma and lipoprotein subclasses using Triacylglycerol GPO-PAP and Cholesterol CHOD-PAP assay kits.

Plasma lipoproteins were isolated by sequential ultracentrifugation at 4 °C using a Beckman TL-100 ultracentrifuge (Beckman Instruments Inc., Fullerton, CA, USA) equipped with a fixed angle rotor (TLA-100.2, Beckman Instruments Inc.) [18]. The LDL fraction was separated at density ranges between 1.019

and 1.063 g/mL and HDL at a density >1.063 g/mL. Subsequent separation of LDL subpopulations was performed by isopycnic ultracentrifugation [19] of the fraction ( $d = 1.019$ – $1.063$  g/mL) previously isolated. In brief, the LDL fraction was adjusted to  $d = 1.040$  g/mL (by dilution with water) and layered between potassium bromide solutions (containing EDTA and sodium azide 0.01%) of different densities [ $d = 1.019$  (1 mL), 1.025 (3 mL), 1.040 (3 mL LDL fraction), 1.054 (3.5 mL) and 1.085 g/mL (1 mL)] and then centrifuged for 40 h (40,000 rpm; 4 °C) in a Beckman XL-100K Ultracentrifuge using a swinging bucket rotor (SW41Ti, Beckman Instruments Inc.). A high density KBr solution (1.29 g/mL) was then injected through the bottom of the tube (2232 Microperpex S Peristaltic Pump, LKB, Bromma, Sweden) and 25 subfractions (450  $\mu$ l each) of increasing densities were recovered from the top of the tube. Density and cholesterol content were measured in each collected subfraction. LDL density profile was obtained by plotting cholesterol content versus density. The sdLDL fraction was considered as the sum of subfractions collected between 1.040 and 1.063 g/mL.

#### Aortic Fatty Streak

After blood collection, the aorta was perfused with 10% buffered formalin solution (pH 7.0). After a few minutes, the flow of fixative solution was slowed and fixation allowed for additional 30 min. The heart and the thoracic aorta were removed and immersed into fixative solution overnight. To study aortic fatty streak formation, a piece of aorta (between the heart and including the aortic arch) was cut and cleaned with phosphate buffer saline pH 7.4, and then rinsed with isopropanol. The aortic tissue was placed in a vial containing 5% Oil Red O stain in 70% isopropanol for 10 min. Then the aortic piece was rinsed consecutively with isopropanol and distilled water, and placed in a vial containing 1% toluidine blue in distilled water for a few seconds. Finally, the tissue was rinsed with distilled water. The arch was dissected vertically in two, then opened longitudinally, mounted on a glass slide, and observed under microscope at appropriate magnification. Samples were blind to examiners.

#### Statistics

Data were analyzed by one-way ANOVA with Statgraphics Plus, Version 5.1. When appropriate, pair wise comparisons of means were made by using Bonferroni test and the significance level set at  $P \leq 0.05$ .

#### Results

Body weight prior to and after the treatment period did not significantly differ between the four groups of hamsters (Table 1). However, body weight gain tended to be slightly higher ( $P < 0.1$ ) for the  $c9,t11$  CLA group as well for the control group than for the CLA mixture and the  $t10,c12$  CLA fed animals.

Plasma TAG concentrations tended to be higher in hamsters fed  $c9,t11$  CLA as well as for the  $t10,c12$  CLA fed animals compared to the control group (+11 and +22%, respectively), but these differences were not significant (Table 2). In contrast, plasma TAG concentration was significantly higher in hamsters fed the CLA mixture relative to the control group (+79%) ( $P < 0.05$ ).

Plasma TC and HDL-C concentrations were significantly lower (–35 and –40%, respectively;  $P < 0.05$ ) in the  $c9,t11$  CLA fed hamsters relative to control group (Table 2). No significant differences in the TC/HDL-C ratio were observed between the groups. In contrast, there were no significant differences for plasma TC and HDL-C concentrations between hamsters fed  $t10,c12$  CLA or those fed the CLA mixture, and the control group.

Plasma LDL-C concentration was significantly lower in the  $c9,t11$  CLA fed group relative to the control group (–56%;  $P < 0.05$ ) and tended to be lower for this  $c9,t11$  CLA group than for the CLA mixture and  $t10,c12$  CLA fed animals, but these differences were not significant (Table 2). No significant differences for LDL-C concentration were found between the groups fed the  $t10,c12$  CLA or the CLA mixture, and the control group.

The small dense LDL (sdLDL) subfraction was particularly high after dietary manipulation in the animal model used in the present study: the hamsters fed a cholesterol- and lipid-enriched semi-purified diet had significantly ( $P < 0.01$ ) higher sdLDL cholesterol concentrations compared to hamsters fed usual rodent

**Table 1** Initial and final body weight and weight gain (grams) of hamsters during the 12 weeks experiment

	<i>n</i>	Initial body weight	Final body weight	Weight gain
Control	7	80.6 $\pm$ 1.23 <sup>a</sup>	123.7 $\pm$ 2.78 <sup>a</sup>	43.1 $\pm$ 3.82 <sup>a</sup>
CLA Mixture	7	83.6 $\pm$ 1.15 <sup>a</sup>	119.6 $\pm$ 1.25 <sup>a</sup>	36.0 $\pm$ 1.56 <sup>a</sup>
$t10,c12$ CLA	7	82.3 $\pm$ 1.13 <sup>a</sup>	118.6 $\pm$ 2.48 <sup>a</sup>	36.3 $\pm$ 3.19 <sup>a</sup>
$c9,t11$ CLA	9	83.3 $\pm$ 1.55 <sup>a</sup>	123.7 $\pm$ 2.57 <sup>a</sup>	43.2 $\pm$ 1.45 <sup>a</sup>

Values are mean  $\pm$  SEM

Values in a column not sharing a superscript are significantly different ( $P < 0.05$ )

**Table 2** Plasma lipids and lipoprotein concentrations (mM/L) in hamsters after 12 weeks of dietary manipulation

Diet	<i>n</i> <sup>a</sup>	TAG	TC	HDL-C	LDL-C	sdLDL-C	TC/HDL-C
Control	7	0.86 ± 0.061 <sup>b</sup>	4.65 ± 0.247 <sup>b</sup>	3.03 ± 0.185 <sup>b</sup>	0.74 ± 0.106 <sup>b</sup>	0.32 ± 0.056 <sup>b</sup>	1.54 ± 0.038 <sup>b</sup>
Mixture	7	1.54 ± 0.164 <sup>c</sup>	4.28 ± 0.340 <sup>b</sup>	2.66 ± 0.212 <sup>b,c</sup>	0.57 ± 0.053 <sup>b,c</sup>	0.24 ± 0.038 <sup>b,c</sup>	1.62 ± 0.030 <sup>b</sup>
<i>t</i> -10, <i>c</i> -12	7	1.04 ± 0.114 <sup>b,c</sup>	3.80 ± 0.232 <sup>b,c</sup>	2.49 ± 0.163 <sup>b,c</sup>	0.53 ± 0.067 <sup>b,c</sup>	0.16 ± 0.042 <sup>b,c</sup>	1.53 ± 0.031 <sup>b</sup>
<i>c</i> -9, <i>t</i> -11	9	0.95 ± 0.130 <sup>b</sup>	3.00 ± 0.432 <sup>c</sup>	1.82 ± 0.281 <sup>c</sup>	0.33 ± 0.046 <sup>c</sup>	0.07 ± 0.014 <sup>c</sup>	1.69 ± 0.087 <sup>b</sup>

<sup>a</sup> See experimental part... Groups were initially constituted by *n* = 10 hamsters, but due to too small plasma volumes available for some animals, final “*n*” were reduced for plasma parameter analysis. Values are mean ± SEM

Values in a column not sharing a superscript are significantly different (*P* < 0.05; Bonferroni test)

chow diet (data not shown). This increased fraction of sdLDL cholesterol was not associated with high cholesterol or high triacylglycerol levels when compared to a group of normocholesterolemic animals fed regular diet (data not shown). Plasma sdLDL cholesterol concentrations were significantly lower in the hamsters fed *c*9,*t*11 CLA relative to control group (−75%; *P* < 0.05) and tended to be lower compared to the groups fed the *t*10,*c*12 CLA and the CLA mixture (−50 and −66%, respectively), but these differences were not significant (Table 2). The concentration of cholesterol in the sdLDL did not differ significantly between the group fed the CLA mixture and the control group. There was a substantial interindividual variability in plasma cholesterol concentrations within each animal group.

Histological studies under microscope after Oil Red O staining did not show any fatty streak formation in aortas of hamsters from any group.

## Discussion

Male Golden Syrian hamsters have been extensively used in studies involving lipoprotein metabolism. They are considered as a useful model for studying nutritional modulation of cholesterol and lipoprotein metabolism [20–24]. In the present study, four groups of hamsters were fed different diets in order to investigate the effects of CLA isomers on cholesterol concentration in total plasma and in atherogenic lipoproteins.

Plasma total cholesterol concentrations of about 3–5 mM/L are generally reported in normolipidic hamsters with 50–70% of this cholesterol carried out in the HDL fraction [22, 25–27]. On the other hand, when hamsters are fed a diet rich in cholesterol and lipids, total plasma cholesterol concentrations may increase fourfold within a month, with an inversion in HDL to LDL cholesterol ratios [24]. Hypercholesterolemic hamsters generally present plasma total cholesterol concentrations ranging from 6 to 20 mM/L, with

20–40% of this cholesterol in the HDL fraction [22, 27–29].

In our study, hamsters from the control group showed only slight differences in plasma lipids and lipoproteins when compared to animals fed a regular chow-based diet: plasma TC, LDL-C, and HDL-C concentrations were comparable between both groups. However, hamsters fed the cholesterol- and lipid-enriched diet had significantly (*P* < 0.01) higher sdLDL cholesterol concentrations than hamsters fed regular chow-based diet (0.09 mM/L). In man, such sdLDL particles are considered to be particularly atherogenic [15, 30]; the plasma lipoprotein profile accompanying a predominance of sdLDL particles is associated with a two- to threefold increased risk of coronary artery disease [31]. Despite these elevated sdLDL cholesterol concentrations, there was in our model no evidence of aortic atherosclerosis in the hamsters fed the cholesterol- and lipid-enriched semi-purified diet. In addition, the cholesteryl ester content in the liver remained rather low (3–4 mg lipids/g liver). Both the type of diet and the hamster strain may account for these unexpected findings. Some studies have suggested that semi-purified diets, as those used in the present studies are not as atherogenic in hamsters as non-purified diets [13, 14, 32]. On the other hand, different hamster strains were reported to have different responses to an atherogenic diet [27, 33, 34]. Considerable variations in plasma cholesterol concentrations were observed between animals from any given group; such interindividual variability was also reported in other studies of experimental atherosclerosis in hamster [24].

The effect of CLA on plasma cholesterol level is somewhat controversial (Table 3). Previous studies [12–14] have shown a reduction of cholesterol concentrations in animals fed a CLA mixture compared with controls in an atherogenic hamster model [12–14]; however no difference of plasma cholesterol lowering was observed between supplementation with a CLA mixture and linoleic acid. Other authors also reported that dietary CLA did not produce any significant differences in serum TC or HDL-C concentration in

C57BL/6 mice fed an atherogenic diet but increased HDL-C:TC ratio [35]. In another study, de Deckere et al. [25] showed that the CLA mixture could lower cholesterol concentrations in proatherogenic lipoproteins and that the active compound would be the *t10,c12* CLA isomer. On the contrary, Valeille et al. [36] showed the beneficial effect of rumenic acid (*c9,t11* CLA) on the cholesterolemia of hamsters fed a cholesterol- and lipid-enriched diet.

In the present study, hamsters fed rumenic acid (*c9,t11* CLA) showed lower plasma LDL and sdLDL cholesterol compared with the other groups. HDL-C was also reduced in animal fed *c9,t11* CLA, so TC:HDL-C ratio was not significantly increased in this group. In contrast, we did not observe any significant difference in plasma cholesterol concentrations between hamsters fed the CLA mixture or *t10,c12* CLA, and the control group. These results are not in agreement with those reported by de Deckere et al. [26], but the experimental conditions and design markedly differed between both studies with respects to hamster strain, duration, atherogenic diet, and amounts of added CLA isomers. However, our data are in good agreement with those obtained by Valeille et al. [36]

showing rumenic acid to improve plasma lipoprotein profile in hamsters. Both current findings and results of Valeille et al. [36] are based on much more purified CLA isomers than mixtures used in previous studies, this could explain why they are more consistent. It is increasingly evident the different CLA isomers have different biological and pathologic effects, and it is not surprising since they exhibited different physical and chemical properties [4].

In conclusion, the present results indicate that rumenic acid, a natural CLA isomer, fed at 1% of a cholesterol- and lipid-enriched semi-purified diet, may significantly decrease plasma total cholesterol but also HDL, LDL and sdLDL cholesterol concentrations. The strong decrease of sdLDL cholesterol suggests rumenic acid to have a greater potential than the other CLA isomers for reducing lipoprotein atherogenicity in hamsters. As far as we know, it is the first time that such a decrease in sdLDL cholesterol concentrations is reported related to rumenic acid consumption by hamsters. It would be of interest to investigate the specific effect of both CLA isomer on lipoprotein parameters, especially sdLDL, in using a hamster model developing aortic fatty streak.

**Table 3** Comparative effects of CLA on lipoprotein parameters in different hamster strains

Hamster	Regime	Effect	TC <sup>a</sup> (mM/L)	Reference
F1B	Atherogenous 10% coconut; 0.12% Chol control vs. 0.06 – 0.11 – 1.1% CLA vs. LA CLA <i>c9,t11</i> , <i>t9,c11</i> , <i>t10,c12</i>	CLA ↓ TC, TAG, nonHDL-C ↓ fatty streak	17.8	[12]
F1B	Atherogenous 20% coconut; 0,12% Chol control vs. 1% CLA vs. 1% LA CLA <i>c9,t11</i> , <i>t9,c11</i> , <i>t10,c12</i>	CLA ↓ TC, TAG, nonHDL-C ↓ fatty streak	8.5	[13]
CR	Atherogenous 10% coconut; 0.15% Chol 0.2% LA vs. 1% CLA with 0.2% <i>c9,t11</i> vs. 0.2% <i>c9,t11</i>	CLA ↓ TC, TAG <i>c9,t11</i> no difference vs. LA	6.5	[28]
F1B	Normolipidic (palm oil); 0.01% Chol control vs. 0.6% CLA <i>c9,t11</i> , <i>t9,c11</i> , <i>t10,c12</i> vs. 0.6% <i>c9,t11</i> vs. 0.5% <i>t10,c12</i>	CLA vs. control = no difference <i>10t,12c</i> vs. <i>c9,t11</i> ↓ LDL-C, HDL-C	3.4	[25]
LPN	Semi-synthetic diet + 33% mixed fat (energy) + 0.05% Chol control vs. 0,6% <i>c9,t11</i> vs. 1,2%, CLA <i>c9,t11</i> + <i>t10,c12</i> vs. 1,2% CLA + 1,2% fish oil vs. 1,2% fish oil	<i>c9,t11</i> , CLA, fish oil ↓ LDL-C, VLDL-C ↑ HDL-C ↑ HDL-C / LDL-C <i>c9,t11</i> > CLA > fish oil	4.0	[34]
Harlan	Purified diet 10% coconut, 1% safflower, 0.12% Chol control vs. 1% CLA <i>c9,t11</i> , <i>t10,c12</i> vs. 1% <i>c9,t11</i> vs. 1% <i>t10,c12</i>	CLA ↓ TC, LDL-C, sdLDL-C, HDL-C <i>c9,t11</i> > CLA = <i>t10,c12</i>	4.6	Present

<sup>a</sup> Values are average plasma total cholesterol content of the atherogenous control group for each experiment

**Acknowledgments** This study was funded by a grant from FunCLA (OLK1-1999-00076). The authors thank Marie COR-NU, Afssa-Lerpaz, for her support with statistical analyses.

## References

- Parodi PW (1976) Distribution of isomeric octadecenoic fatty acid in milk fat. *J Dairy Sci* 59:1870–1873
- Griinari JM, Bauman DE (1999) Biosynthesis of conjugated linoleic acid and its incorporation into meat and milk in ruminants. In: Yurawecz MP, Mossoba MM, Kramer JKG, Pariza MW, Nelson GJ (eds) *Advances in conjugated linoleic acid research*, vol 1. AOCS Press, Champaign, pp 180–200
- Christie WW (1997) Isomers in commercial samples of conjugated linoleic acid. *J Am Oil Chem Soc* 74:1231
- Kramer JKG, Cruz-Hernandez C, Deng Z, Zhou J, Jahreis G, Dugan MER (2004) Analysis of conjugated linoleic acid and trans 18:1 isomers in synthetic and animal products. *Am J Clin Nutr* 79(suppl):1137S–1145S
- Ha YL, Grimm NK, Pariza MW (1987) Anticarcinogens from fried ground beef: heat-altered derivatives of linoleic acid. *Carcinogenesis* 8:1881–1887
- Ip C, Singh M, Thompson HJ, Scimeca JA (1994) Conjugated linoleic acid suppresses mammary carcinogenesis and proliferative activity of the mammary gland in the rat. *Cancer Res* 54:1212–1215
- Ostrowska E, Muralitharan M, Cross RF, Bauman DE, Dunshea FR (1999) Dietary conjugated linoleic acids increase lean tissue and decrease fat deposition in growing pigs. *J Nutr* 129:2037–2042
- Park Y, Storkson JM, Albright KJ, Liu W, Pariza MW (1999) Evidence that the *trans*-10, *cis*-12 isomer of conjugated linoleic acid induces body composition changes in mice. *Lipids* 34:235–241
- Houseknecht KL, Vanden Heuvel JP, Moya-Camarena SY, Portocarrero CP, Peck LW, Nickel KP, Belury MA (1998) Dietary conjugated linoleic acid normalizes impaired glucose tolerance in the Zucker diabetic fatty *fa/fa* rat. *Biochem Biophys Res Commun* 244:678–682
- Li Y, Watkins BA (1998) Conjugated linoleic acids alter bone fatty acid composition and reduce *ex vivo* prostaglandin E2 biosynthesis in rats fed n-6 or n-3 fatty acids. *Lipids* 33:417–425
- Cook ME, Miller CC, Park Y, Pariza MW (1993) Immune modulation by altered nutrient metabolism: nutritional control of immune-induced growth depression. *Poult Sci* 72:1301–1305
- Lee KN, Kritchevsky D, Pariza MW (1994) Conjugated linoleic acid and atherosclerosis in rabbits. *Atherosclerosis* 108:19–25
- Nicolosi RJ, Rogers EJ, Kritchevsky D, Scimeca JA, Huth PJ (1997) Dietary conjugated linoleic acid reduces plasma lipoproteins and early aortic atherosclerosis in hypercholesterolemic hamsters. *Artery* 22:266–277
- Wilson TA, Nicolosi RJ, Chrysam M, Kritchevsky D (2000) Conjugated linoleic acid reduces early aortic atherosclerosis greater than linoleic acid in hypercholesterolemic hamsters. *Nutr Res* 20:1795–1805
- Krauss RM (1994) Heterogeneity of plasma low-density lipoproteins and atherosclerosis risk. *Curr Opin Lipidol* 5:339–349
- Benito P, Nelson GJ, Kelley DS, Bartolini G, Schmidt PC, Simon V (2001) The effect of conjugated linoleic acid on plasma lipoproteins and tissue fatty acid composition in humans. *Lipids* 36:229–236
- Tricon S, Burdge GC, Kew S, Banerjee T, Russel JJ, Jones EL, Grimble RF, Williams CM, Yaqoob P, Calder PC (2004) Opposing effects of *cis*-9, *trans*-11 and *trans*-10, *cis*-12 conjugated linoleic acid on blood lipids in healthy humans. *Am J Clin Nutr* 80:614–620
- Havel RJ, Eder HA, Bragdon JH (1955) The distribution and chemical composition of ultracentrifugally separated lipoproteins in human serum. *J Clin Invest* 34:1345–1353
- Chapman MJ, Laplaud PM, Luc G, Forgez P, Bruckert E, Goulinet S, Lagrange D (1988) Further resolution of the low density lipoprotein spectrum in normal human plasma: physicochemical characteristics of discrete subspecies separated by density gradient ultracentrifugation. *J Lipid Res* 29:442–458
- Billet MA, Bruce JS, White DA, Bennett AJ, Salter AM (2000) Interactive effects of dietary cholesterol and different saturated fatty acids on lipoprotein metabolism in the hamster. *Br J Nutr* 84:439–447
- Kris-Etherton PM, Dietschy JM (1997) Design criteria for studies examining individual fatty acid effects on cardiovascular disease risk factors: human and animal studies. *Am J Clin Nutr* 65(suppl):1590S–1596S
- Mangiapane EH, McAteer MA, Martin Benson G, White DA, Salter AM (1999) Modulation of the regression of atherosclerosis in the hamster by dietary lipids: Comparison of coconut oil and olive oil. *Br J Nutr* 82:401–409
- Spady DK (1999) Dietary fatty acids and atherosclerosis regression. *Br J Nutr* 82:337–338
- Nistor A, Bulla A, Filip DA, Radu A (1987) The hyperlipidemic hamster as a model of experimental atherosclerosis. *Atherosclerosis* 68:159–173
- Goulinet S, Chapman MJ (1993) Plasma lipoproteins in the golden syrian hamster: heterogeneity of apoB- and apoA-I-containing particles. *J Lipid Res* 34:943–959
- de Deckere EAM, van Amelsvoort JMM, McNeil GP, Jones P (1999) Effects of conjugated linoleic acids (CLA) isomers on lipid levels and peroxisome proliferation in the hamster. *Br J Nutr* 82:309–317
- Terpstra AHM, Holmes JC, Nicolosi RJ (1991) The hypocholesterolemic effect of dietary soybean protein vs. casein in hamsters fed a cholesterol-free or cholesterol-enriched semipurified diets. *J Nutr* 121:944–947
- Huang X, Fang C (2000) Dietary trans fatty acids increase hepatic acyl-coA: cholesterol acyltransferase activity in hamsters. *Nutr Res* 20:547–558
- Gavino VC, Gavino G, Leblanc M-J, Tuchweber B (2000) An isomeric mixture of conjugated linoleic acids but not pure *cis*-9, *trans*-11-octadecadienoic acid affects body weight gain and plasma lipids in hamsters. *J Nutr* 130:27–29
- Chancharme L, Théron P, Nigon F, Zarev S, Mallet A, Bruckert E, Chapman MJ (2002) LDL particle subclasses in hypercholesterolemia: molecular determinants of reduced lipid hydroperoxyde stability. *J Lipid Res* 43:453–462
- Austin MA, Breslow JL, Hennekens CH, Buring JF, Willett WC (1988) Low-density lipoprotein subclass patterns and risk of myocardial infarction. *JAMA* 260:1917–1921
- Nicolosi RJ, Wilson TA, Lawton C, Rogers EJ, Wiseman SA, Tjibburg LBM, Kritchevsky D (1998) The greater atherogenicity of nonpurified diets versus semipurified diet in hamsters is mediated via differences in plasma lipoprotein cholesterol distribution, LDL oxidative susceptibility, and plasma  $\alpha$ -tocopherol concentration. *J Nutr Biochem* 9:591–597
- Dorfman SE, Smith DE, Osgood DP, Lichtenstein AH (2003) Study of diet-induced changes in lipoprotein metab-

- olism in two strains of golden-syrian hamsters. *J Nutr* 133:4183–4188
34. Férézou J, Combettes-Souverain M, Souidi M, Smith JL, Boelher N, Milliat F, Eckhardt E, Blanchard G, Riottot M, Sérougne C, Lutton C (2000) Cholesterol, bile acid, and lipoprotein metabolism in two strains of hamster, one resistant, the other sensitive (LPN) to sucrose-induced cholelithiasis. *J Lipid Res* 41:2042–2054
35. Munday JS, Thompson KG, James KAC (1999) Dietary conjugated linoleic acids promote fatty streak formation in the C57BL/6 mouse atherosclerosis model. *Br J Nutr* 81:251–255
36. Valeille K, Gripois D, Blouquit M-F, Souidi M, Riottot M, Bouthegourd J-C, Sérougne C, Martin J-C (2004) Lipid atherogenic risk markers can be more favourably influenced by the *cis-9,trans-11*-octadecadienoate isomer than a conjugated linoleic acid mixture or fish oil in hamsters. *Br J Nutr* 91:191–199

## Postprandial Lipemia is Modified by the Presence of the *APOB*-516C/T Polymorphism in a Healthy Caucasian Population

Pablo Pérez-Martínez · Francisco Pérez-Jiménez · José María Ordovás · Juan Antonio Moreno · Carmen Marín · Rafael Moreno · Yolanda Jiménez-Gómez · Juan Antonio Paniagua · José López-Miranda

Received: 19 June 2006 / Accepted: 2 December 2006 / Published online: 10 February 2007  
© AOCS 2007

**Abstract** Apolipoprotein (apoB) plays a fundamental role in the transport and metabolism of plasma triacylglycerols (TAGs) and cholesterol. Several apoB polymorphic sites have been studied for their potential use as markers for coronary heart disease in the population. In view of the importance of apoB in postprandial metabolism, our objective was to determine whether the presence of the -516C/T polymorphism in the *APOB* gene promoter could influence postprandial lipoprotein metabolism in healthy subjects. Forty-seven volunteers who were homozygous for the E3 allele at the *APOE* gene were selected (30 homozygous for the common genotype (C/C) and 17 heterozygotes for the -516T allele (C/T). They were given a fat-rich meal containing 1 g fat and 7 mg cholesterol per kg body weight and vitamin A 60,000 IU/m<sup>2</sup> body surface. Fat accounted for 60% of calories, and protein and carbohydrates for 15 and 25% of energy, respectively. Blood samples were taken at time 0, every 1 h until 6 h, and every 2.5 h until 11 h. Total cholesterol and TAGs in plasma, and cholesterol, TAGs and retinyl palmitate in triacylglycerol-rich lipoproteins (large and small triacylglycerol-rich lipoproteins) were determined by ultracentrifugation.

Individuals carrying the C/T genotype presented greater postprandial concentrations of TAGs in small triacylglycerol-rich lipoproteins than did carriers of the C/C genotype ( $P = 0.022$ ). Moreover, C/T individuals presented higher concentrations of plasma TAGs during the postprandial period than did C/C subjects ( $P = 0.039$ ). No other statistically significant genotype-related differences for other parameters were observed. These results suggest that the presence of the genotype C/T is associated with a higher postprandial response. Thus, the allele variability in the -516C/T polymorphism in the *APOB* gene promoter may partly explain the interindividual differences in postprandial lipemic response in healthy subjects.

**Keywords** *APOB* polymorphism · Nutrigenetics · Postprandial lipemia · Triacylglycerol-rich lipoproteins

### Abbreviations

apoB	Apolipoprotein B
BMI	Body mass index
CHO	Carbohydrate
CHD	Coronary heart disease
LDL	Low-density lipoprotein
MUFA	Monounsaturated fatty acid
SFA	Saturated fatty acid
TAGs	Triacylglycerol
TRL	Triacylglycerol-rich lipoproteins

P. Pérez-Martínez (✉) · F. Pérez-Jiménez · J. A. Moreno · C. Marín · R. Moreno · Y. Jiménez-Gómez · J. A. Paniagua · J. López-Miranda  
Unit of Lipids and Atherosclerosis,  
Hospital Universitario Reina Sofía, Avda. Menéndez Pidal,  
s/n, 14004 Cordoba, Spain  
e-mail: pablopermar@yahoo.es

J. M. Ordovás  
Nutrition and Genomics Laboratory,  
JM-US Department of Agriculture Human Nutrition  
Research Center on Aging at Tufts University,  
Boston, MA, USA

### Introduction

The postprandial state constitutes the normal metabolic situation of human beings throughout the day in

developed societies, as the clearance of triacylglycerol (TAG)-rich lipoproteins (TRL) of intestinal or hepatic origin last for a period of 6–8 h. Determination of the postprandial response is a complex process, which makes it all the more challenging to assess the cardiovascular risk associated with postprandial lipemia than during fasting conditions. Previous studies have suggested that postprandial small TRL may predict the onset of coronary heart disease (CHD), and evidence supporting an association between postprandial lipemia and atherosclerosis has been provided by clinical trials [1–6]. Individual variability in the postprandial lipemic response is usually greater than that observed in the fasting state, and appears to be modulated by environmental and genetic factors [7, 8]. This concept is supported by studies showing that certain polymorphisms at candidate gene loci are associated with variability in postprandial clearance of lipoprotein [9].

Apolipoprotein (apoB) plays a fundamental role in the transport and metabolism of plasma TAG and cholesterol and it is synthesized primarily in hepatocytes and enterocytes. The human *APOB* gene is located on chromosome 2 and several *APOB* polymorphic sites have been studied for their potential use as markers for CHD in the population [10]. Moreover, some of them have been investigated for the inter-individual variability observed during postprandial lipemia (XbaI polymorphism, I/D polymorphism within the apoB signal peptide) [11–13]. Previously, a common functional polymorphism of the *APOB* promoter was described by van't Hooft et al. [14] involving a C to T change located at 516 base pairs upstream from the transcription start site. This polymorphism was found to induce significant increase in the transcription rate of the *APOB* gene and, consequently, in circulating levels of low-density lipoprotein (LDL) cholesterol. These findings are consistent with the fact that the *APOB* gene promoter plays a major role in cholesterol homeostasis [15]. Furthermore, we have demonstrated that healthy males carriers of the -516T allele, have a significant increase in insulin resistance after the consumption of diets with different fat content, but the difference is more pronounced after an SFA-enriched diet than following MUFA and CHO-rich diets [16].

In view of the insulin sensitivity of postprandial metabolism, it would be interesting to find out whether the presence of this polymorphism in the *APOB* gene could modulate postprandial lipemia, in the same way as it has already been observed in other genotypes.

## Material and Methods

### Subjects of the Study

Forty-seven healthy men were recruited from among 97 students at the University of Cordoba. The 47 subjects had a mean age ( $\pm$ SD) of  $23 \pm 4.12$  years. Of these, 30 were homozygotes for the -516C allele (C/C) and 17 heterozygotes for the -516T allele (C/T). The distribution of genotypes was as expected from the Hardy–Weinberg equilibrium. Informed consent was obtained from all participants. All the subjects were selected to have the *APOE* 3/3 genotype to avoid the potential confounder from the presence of the other common *APOE* alleles on postprandial lipemia [17]. All subjects underwent a comprehensive medical history, physical examination, and clinical chemistry analysis before inclusion in the study, and they did not show evidence of any chronic disease (hepatic, renal, thyroid, or cardiac dysfunction). None of the subjects were obese, nor did they perform unusually high levels of physical activity (e.g., sports training). In addition, none of the subjects had a family history of premature coronary artery disease or had taken medications or vitamin supplements in the 6 months prior to the study. Subjects were encouraged to maintain their regular physical activity and lifestyle and were asked to record in a diary any event that could affect the outcome of the study, such as stress, change in smoking habits and alcohol consumption in the week before the fat loading test. Previous to the fat loading test, the volunteers consumed a saturated fatty acid diet period as a baseline regimen, as this Western-style diet is frequently consumed by Western countries, including most areas of Spain. All studies were carried out in the Research Unit at the Reina Sofia University Hospital, and the experimental protocol was approved by the Hospital's Human Investigation Review Committee.

### Vitamin A and Fat Loading Test

After a 12-h fast, subjects were given a fatty meal enriched with 60,000 units of vitamin A per  $m^2$  of body surface area. The amount of fat given was 1 g of fat and 7 mg of cholesterol/kg of body weight. The meal contained 65% of energy as fat, 15% protein and 25% carbohydrates and was eaten in 20 min. We calculated the amount of each ingredient fed as a function of individual weight, so that although all the subjects consumed the same types of food, the quantities involved were different. The foods were bread, whole milk, eggs and butter. After the meal, the subjects had



no energy intake for 11 h, but were allowed to drink water. Blood samples were drawn before the meal, every hour until the sixth hour and then every 2 h and 30 min until the eleventh hour.

### Lipoprotein Separations

Blood was collected in tubes containing EDTA to give a final concentration of 0.1% EDTA. Plasma was separated from red cells by centrifugation at 1,500 g for 15 min at 4 °C. The chylomicron fraction of TRL (large TRL) was isolated from 4 mL of plasma obtained from EDTA tubes. Plasma was put in the bottom of a 13.4 mL polyallomer ultracentrifuge tube (UltraClear, Beckman Instruments, Palo Alto, CA, USA) and overlaid with a preservative solution consisting of NaCl (0.15 mol/L), sodium azide (0.05 g/L), chloramphenicol (0.05 g/L), gentamicin sulfate (40 mg/L) and EDTA (1 mmol/L), (pH 7.4,  $d < 1.006$  kg/L). Ultracentrifugation was performed in a type TY65 rotor (Beckman Instruments, Fullerton, CA, USA) at 36,200 $\times$ g and 4 °C for 30 min. Chylomicrons contained in the top layer were removed by aspiration, placed directly into individual vials and stored at –80 °C until assay for retinyl palmitate, biochemical determinations, apoB-48 and apoB-100. The infranatant fluid was centrifuged at a density of 1.019 kg/L and overlaid with the same preservative cocktail. The ultracentrifugation was performed for 24 h at 183,000 g in the same rotor. The nonchylomicron fraction (also referred to as small TRL) was removed from the top of the tube by aspiration, placed directly into individual vials and stored at –80 °C until assay for retinyl palmitate, biochemical determinations, apoB-48 and apoB-100. All operations were done under subdued light in order to prevent the degradation of retinyl palmitate (RP).

### Lipid Analysis

Cholesterol and TAGs in plasma and lipoprotein fractions were assayed by enzymatic procedures [18, 19]. Apo A-I and apo B were determined by turbidimetry [20]. HDL cholesterol (HDL-C) was measured by analyzing the supernatant obtained following precipitation of a plasma aliquot with dextran sulphate-Mg<sup>2+</sup>, as described by Warnick et al. [21]. The LDL cholesterol (LDL-C) was obtained as the difference between the cholesterol from the bottom part of the tube after ultracentrifugation at a density of 1.019 kg/L.

### Retinyl Palmitate Assay

The RP content of large and small TRL fractions was assayed using a method previously described [22]. Briefly, different volumes of the various fractions (100  $\mu$ L for chylomicrons and 100–500  $\mu$ L for remnant) were placed in 13  $\times$  100 mm glass tubes. The total volume in each tube was adjusted, as necessary, to 500  $\mu$ L using normal saline. Retinyl acetate (40 ng in 200  $\mu$ L of mobile phase buffer) was added to each tube as internal standard. Five hundred milliliter of methanol was added followed by the addition of 500  $\mu$ L of the mobile phase buffer for a total volume of 1.7 mL. The mobile phase buffer was prepared fresh on a daily basis by combining 90 mL of hexane, 15 mL *n*-butyl chloride, 5 mL acetonitrile, and 0.01 mL acetic acid (82:13:5 by volume with 0.01 mL of acetic acid). The tubes were thoroughly mixed after each step. The final mixture was centrifuged at 350 g for 15 min (room temperature) and the upper layer was carefully removed by aspiration and was injected into a high-performance liquid chromatography (HPLC) system. The autoinjector was programmed to deliver 100  $\mu$ L per injection and a new sample every 10 min in a custom prepackaged silica column SupelcoSil LC-SI (5 mm, 25 cm  $\times$  mm ID) provided by Supelco Inc. The flow was maintained at a constant rate of 2 mL/min and the peaks were detected at 330 nm. The peak of RP and retinyl acetate were identified by comparing its retention time with a purified standard (Sigma, St Louis, MO, USA) and the RP concentration in each sample was expressed as the ratio of the area under the RP peak to the area under the retinyl acetate peak [23]. All operations were performed in subdued light.

### Determination of ApoB-48 and ApoB-100

ApoB-48 and apoB-100 were determined by sodium dodecyl sulfate-polyacrylamide gel electrophoresis (SDS-PAGE) as described by Karpe et al. [24]. In brief, samples containing isolated lipoprotein fractions were delipidated in a methanol/diethyl ether solvent system and the protein pellet was dissolved in 100–500  $\mu$ L of 0.15 mol/L sodium phosphate, 12.5% glycerol, 2% SDS, 5% mercaptoethanol, and 0.001% bromophenol blue (pH 6.8), at room temperature for 30 min followed by denaturation at 80 °C for 10 min. Electrophoresis was performed with a vertical Hoefer Mighty Small II electrophoresis apparatus connected to an EPS 400/500 (Pharmacia) power supply on 3–20% gradient polyacrylamide gels. The upper and lower electrophoresis buffers contained 25 mmol/L

Tris, 192 mmol/L Glycine, and 0.2% SDS adjusted to pH 8.5. ApoB-100 derived from LDL was used as a reference protein and for standard-curve dilutions. A dilution curve ranging from 0.10 to 2 mg of apo B-100 was applied to four of the gel lanes. Electrophoresis was run at 60 V for the first 20 min and then at 100 V for 2 h. Gels were fixed in 12% trichloroacetic acid for at least 30 min and stained in 0.2% Coomassie G-250/40% methanol:10% acetic acid for at least 4 h. Destaining was done in 12% methanol:7% acetic acid with four changes of destaining solution for 24 h. Gels were scanned with a videodensitometer scanner (TDI, Madrid, Spain) connected to a personal computer for integration of the signals. Background intensity was calculated after scanning an empty lane. The coefficient of variation for the SDS-PAGE was 7.3% for apo B-48 and 5.1% for apo B-100.

#### DNA Amplification and Genotyping

DNA extraction was performed by standard procedures. Genotyping for the -516C/T polymorphism was carried out using the restriction enzyme Ear I (Biolabs, New England, Inc.) as described previously [14].

#### Statistical Analysis

Several variables were calculated in order to characterize the postprandial responses of plasma TAGs, large TRL and small TRL to the test meal. The area under the curve (AUC) is defined as the area between the plasma concentration versus time curve and a line drawn parallel to the horizontal axis through the 0 h concentration. This area was calculated by a computer program using the trapezoidal rule. Other variables were the normalized peak concentration above baseline and the peak time, which was the average of the time of peak concentration and the time to the second greatest concentration. Data were tested for statistical significance between genotypes, and between genotypes and time by analysis of variance for repeated measures and the Kruskal–Wallis test. In this analysis, we studied the statistical effects of the genotype alone, independent of the time in the postprandial study, the effect of time alone or of changes in the variable after ingestion of fatty food over the entire lipemic period, and the effect of the interaction of both factors, genotype and time, indicative of the magnitude of the postprandial response in each group of individuals with a different genotype. When statistical significance was found, the Tukey's post-hoc comparison test was used to identify group differences. A probability value less than 0.05 was considered significant.

All data presented in text and tables are expressed as means  $\pm$  SDs. SPSS 11.0 was used for the statistical comparisons.

#### Results

The basal characteristics by genotype are shown in Table 1. No differences for any of the variables examined were observed at baseline between genotype groups.

The postprandial response of plasma TAGs and TAGs in different lipoprotein fractions were analyzed. A significant effect of time in plasma for all variables measured except large TRL-RP was observed, with respect to baseline levels, indicating an increase of these parameters in the different groups of subjects during the postprandial period.

Individuals carrying the C/T genotype displayed greater postprandial concentrations of small-TRL TAGs than did carriers of the C/C genotype ( $P = 0.022$ ) (Fig. 1). C/T individuals also presented higher concentrations of plasma TAGs during the postprandial period than C/C subjects ( $P = 0.039$ ) (Fig. 1). No other statistically significant genotype-related differences for other parameters were observed.

The area under the postprandial curve in study participants according to the APOB -516C/T polymorphism was analyzed and no significant differences were observed between genotypes (Table 2).

#### Discussion

Our findings show that healthy male carriers of the T allele at the -516C/T polymorphism in the APOB gene

**Table 1** Baseline characteristics according to the -516C/T polymorphism in the ApoB gene promoter

	Genotype		<i>P</i>
	C/C [n = 30]	C/T [n = 17]	
Age (year)	23.40 $\pm$ 4.10	22.60 $\pm$ 3.98	0.504
BMI (kg/m <sup>2</sup> )	25.16 $\pm$ 3.62	24.70 $\pm$ 3.42	0.804
Total Cholesterol (mmol/L)	3.97 $\pm$ 0.6	3.90 $\pm$ 0.7	0.783
Triacylglycerol (mmol/L)	0.92 $\pm$ 0.3	0.87 $\pm$ 0.4	0.653
LDL-C (mmol/L)	2.36 $\pm$ 0.6	2.39 $\pm$ 0.6	0.858
HDL-C (mmol/L)	1.23 $\pm$ 0.2	1.19 $\pm$ 0.2	0.605
Apo B (g/L)	0.65 $\pm$ 0.1	0.66 $\pm$ 0.1	0.822
Apo A-I (g/L)	0.99 $\pm$ 0.2	0.95 $\pm$ 0.2	0.435
Large TRL-TAG (mmol/L)	0.20 $\pm$ 0.1	0.21 $\pm$ 0.1	0.921
Small TRL-TAG (mmol/L)	0.38 $\pm$ 0.1	0.36 $\pm$ 0.2	0.720

*Large TRL-TAG* large triacylglycerol-rich lipoprotein triacylglycerol

Data are mean  $\pm$  SD. There were no significant differences between genotypes (ANOVA)

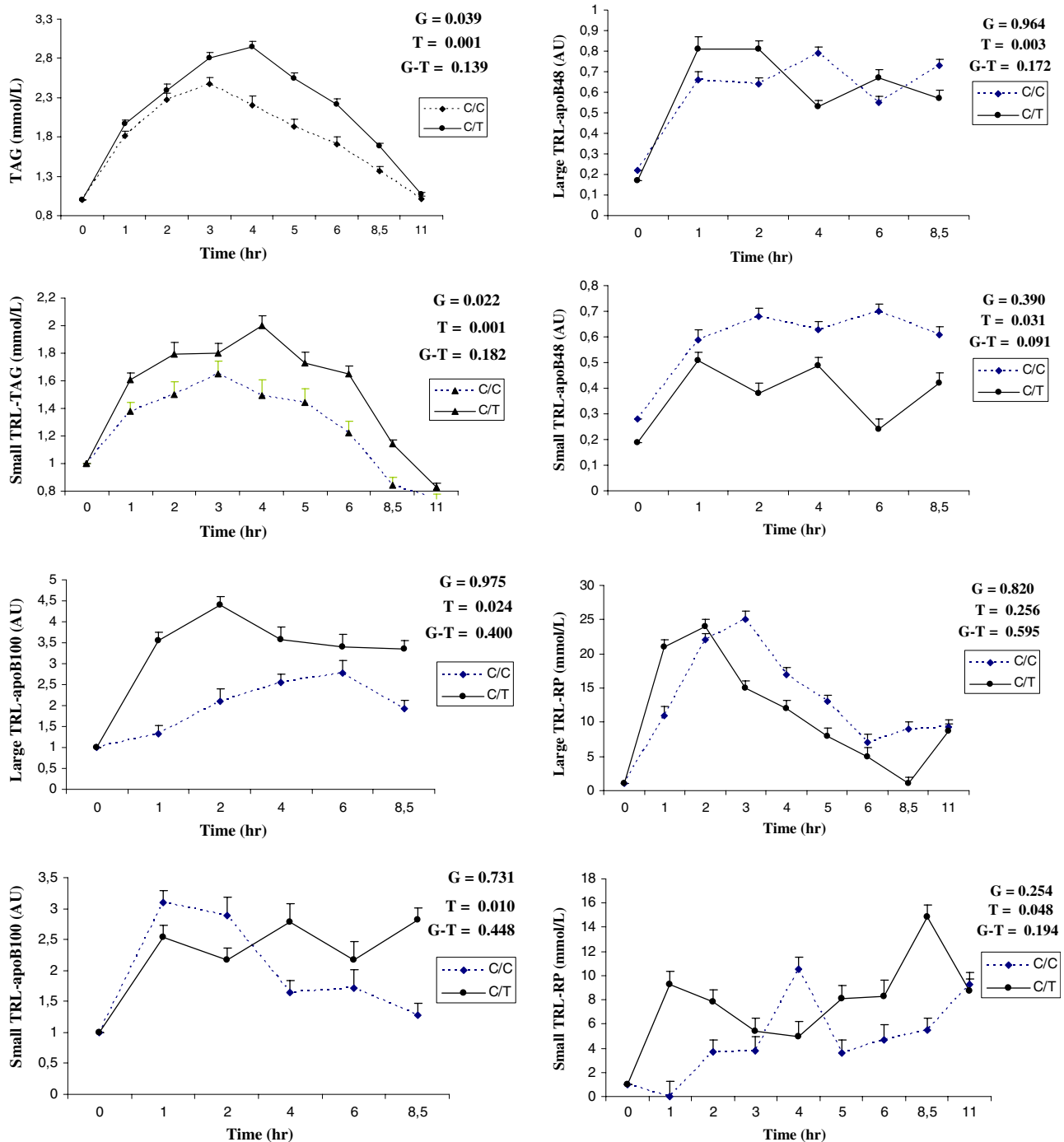


**Fig. 1** Line plots of postprandial triacylglycerol plasma, small TRL-TAG, large TRL-apoB100, small TRL-apoB100, large TRL-apoB48, small TRL-apoB48, large TRL-RP, small TRL-

RP in C/C subjects ( $n = 30$ , dashed line, black triangles), and C/T subjects ( $n = 17$ , continuous line, black circles). ANOVA for repeated measures

promoter have a greater postprandial response of TAGs in small TRL as compared with C/C individuals.

A growing body of experimental and clinical evidence suggests that TRL, and in particular small TRL, contribute to atherogenesis and consequently to cardiovascular disease progression and that high levels of

small TRL of both hepatic and intestinal origin are associated with the progression of coronary atherosclerosis [25, 26]. A study by Phillips et al. found that neither LDL-C nor TG fasting levels correlate highly with lesion progression or clinical events [26]. Small TRL-TG concentrations in plasma reflect postprandial

**Table 2** Area under the postprandial curve in study participants, according to the APOB -516C/T polymorphism

	Genotype	
	C/C	C/T
Large TRL Chol (mmol/L sg)	0.034 ± 0.011	0.039 ± 0.014
Small TRL Chol (mmol/L sg)	0.049 ± 0.024	0.049 ± 0.029
Large TRL RP (ng/mL sg)	827.53 ± 653.13	715.77 ± 521.26
Small TRL RP (ng/mL sg)	335.65 ± 229.31	311.29 ± 307.42
Large TRL Apo-B48 (AU)	408 ± 323	407 ± 348
Small TRL Apo-B48 (AU)	415 ± 442	245 ± 292
Large TRL Apo-B100 (AU)	600 ± 634	600 ± 735
Small TRL Apo-B100 (AU)	22075 ± 12471	24716 ± 22475

RP retinyl palmitate, AU arbitrary units, sg seconds

Values are mean ± SD. No significant differences were observed between genotypes

metabolism, and these did correlate with both lesion progression and cardiac events. Thus, smaller, partially catabolized TRL are believed to be more atherogenic or thrombogenic than larger, newly secreted TRLs, which makes our results of particular interest.

ApoB is required for the assembly secretion of chylomicrons in the intestine and very low-density lipoproteins (VLDL) in the liver, and it also acts as the ligand for LDL recognition by LDL receptors. Several studies have demonstrated an association between the C/T genotype and elevated plasma levels of LDL-C [27]. However, the influence of this polymorphism on postprandial lipemic response remains unknown. Our study is to our knowledge the first to examine the association between the -516C/T polymorphism in the APOB gene promoter and postprandial lipemic response in healthy subjects. We have observed a delayed postprandial clearance of TAGs in small TRL in subjects with the less common C/T genotype than in C/C individuals. A limitation of our study is that it includes a relatively small number of subjects. However, because the magnitude of postprandial lipemia is subject to considerable individual variability and is affected by several genetic factors [28, 29], our study sample was limited to healthy men with the Apo E3/E3 genotype, in order to avoid the variable postprandial lipid response of other apoE isoforms or gender [30].

Two mechanisms might explain the change observed in the catabolism of TRL in subjects with the -516C/T polymorphism. We have previously demonstrated that carriers of the -516T allele also have a significant increase in insulin resistance [16]. These data are in accordance with previous evidence demonstrating that small TRL concentrations are significantly higher in insulin-resistant healthy individuals with normal glucose tolerance [31]. In this context, a positive relation

between insulin resistance and altered postprandial lipemia has repeatedly been reported [32, 33]. Consequently, insulin resistance increases the hepatic synthesis of lipid substrates. These effects potentially increase the plasma concentrations of small TRL and increase competition for hepatic uptake between small TRL and VLDL remnants [34]. Nevertheless, postprandial lipemia is not a uniform abnormality and its pathophysiology has not yet been fully clarified; it is possible that the response to dietary fat is a multifactorial phenomenon. Previous studies suggest that the relationship between plasma insulin and TRL levels is partly influenced by other polymorphisms in the APOB gene (i.e., apoB XbaI polymorphism [11]). Furthermore, in our study C/T subjects showed a higher postprandial response of plasma TAGs than did carriers of the C/C genotype. In this context, subjects who display an increase in plasma TAGs concentrations have smaller and denser LDL particles and an enhanced degree of postprandial lipemia [35]. Previous data also suggest that individuals carrying the C/T genotype present significant increases in the transcription rate of the APOB gene and, consequently, in circulating levels of LDL cholesterol, a delayed postprandial clearance of TAGs in small TRL, and an increase in insulin resistance. On the other hand, the presence of this polymorphism is independently associated with the presence of carotid atherosclerotic disease [36]. Although these results are preliminary, the fact that our study was carried out on healthy individuals in a controlled interventional trial could be the key to a better understanding the effect of this polymorphism on postprandial lipoprotein metabolism.

Furthermore, because all the study subjects were young and healthy, it is possible that the effects on postprandial lipemia response observed in these individuals will be magnified as the subjects become older or obese, as has previously been shown with other polymorphisms (LPL HindIII polymorphism) [37].

In conclusion, allele variability in the -516C/T polymorphism in the APOB gene promoter could partly explain the interindividual differences in the postprandial lipemic response in healthy subjects.

**Acknowledgment** This work was supported by research grants from the CIBER CBO/6/03, Instituto de Salud Carlos III; Plan Nacional de Investigación (Ministerio de Educación y Ciencia) (SAF 01/2466-C05 04 to F P-J, SAF 01/0366 to J L-M); the Spanish Ministry of Health (FIS 01/0449); Consejería de Salud, Servicio Andaluz de Salud (00/212, 00/39, 01/239, 01/243, 02/64, 02/65, 02/78), Consejería de Educación, Plan Andaluz de Investigación, Universidad de Córdoba and by NIH/NHLBI grant no. HL54776 and contracts 53-K06-5-10 and 58-1950-9-001 from the US Department of Agriculture Research Service.

## References

- Kugiyama K, Doi H, Takazoe K, Kawano H, Soejima H, Mizuno Y, Tsunoda R, Sakamoto T, Nakano T, Nakajima K, Ogawa H, Sugiyama S, Yoshimura M, Yasue H (1999) Remnant lipoprotein levels in fasting serum predict coronary events in patients with coronary artery disease. *Circulation* 8:2858–2860
- Ooi TC, Cousins M, Ooi DS, Steiner G, Uffelman KD, Nakajima K, Simo IE (2001) Postprandial remnant-like lipoproteins in hypertriglyceridemia. *J Clin Endocrinol Metab* 86:3134–3142
- Boquist S, Ruotolo G, Tang R, Bjorkegren J, Bond MG, de Faire U, Karpe F, Hamsten A (1999) Alimentary lipemia, postprandial triglyceride-rich lipoproteins, and common carotid intima-media thickness in healthy, middle-aged men. *Circulation* 100:723–728
- Karpe F, Hellenius ML, Hamsten A (1999) Differences in postprandial concentrations of very-low-density lipoprotein and chylomicron remnants between normotriglyceridemic and hypertriglyceridemic men with and without coronary heart disease. *Metabolism* 48:301–307
- Fukushima H, Sugiyama S, Honda O, Koide S, Nakamura S, Sakamoto T, Yoshimura M, Ogawa H, Fujioka D, Kugiyama K (2004) Prognostic value of remnant-like lipoprotein particle levels in patients with coronary artery disease and type II diabetes mellitus. *J Am Coll Cardiol* 43:2219–2224
- Kolovou GD, Anagnostopoulou KK, Pavlidis AN, Salpea KD, Iraklianiou SA, Tsarpalis K, Damaskos DS, Manolis A, Cokkinos DV (2005) Postprandial lipemia in men with metabolic syndrome, hypertensives and healthy subjects. *Lipids Health Dis* 4:21
- Hamsten A, Silveira A, Boquist S, Tang R, Bond MG, de Faire U, Bjorkegren J (2005) The apolipoprotein CI content of triglyceride-rich lipoproteins independently predicts early atherosclerosis in healthy middle-aged men. *J Am Coll Cardiol* 45:1013–1017
- Ordovas JM (2001) Genetics, postprandial lipemia and obesity. *Nutr Metab Cardiovasc Dis* 11:118–133
- Lopez-Miranda J, Perez-Martinez P, Marin C, Moreno JA, Gomez P, Perez-Jimenez F (2006) Postprandial lipoprotein metabolism, genes and risk of CVD. *Curr Opin Lipidol* 17:132–138
- Genest JJ Jr, Ordovas JM, McNamara JR, Robbins AM, Meade T, Cohn SD, Salem DN, Wilson PW, Masharani U, Frossard PM (1990) DNA polymorphisms of the apolipoprotein B gene in patients with premature coronary artery disease. *Atherosclerosis* 82:7–17
- Lopez-Miranda J, Ordovas JM, Ostos MA, Marin C, Jansen S, Salas J, Blanco-Molina A, Jimenez-Perez JA, Lopez-Segura F, Perez-Jimenez F (1997) Dietary fat clearance in normal subjects is modulated by genetic variation at the apolipoprotein B gene locus. *Arterioscler Thromb Vasc Biol* 17:1765–1773
- Boerwinkle E, Chan L (1989) A three codon insertion/deletion polymorphism in the signal peptide region of the human apolipoprotein B (APOB) gene directly typed by the polymerase chain reaction. *Nucleic Acids Res* 25:4003
- Regis-Bailly A, Fournier B, Steinmetz J, Gueguen R, Siest G, Visvikis S (1995) Apo B signal peptide insertion/deletion polymorphism is involved in postprandial lipoparticles' responses. *Atherosclerosis* 118:23–34
- Van 't Hooft FM, Jormsjo S, Lundahl B, Tornvall P, Eriksson P, Hamsten A (1999) A functional polymorphism in the apolipoprotein B promoter that influences the level of plasma low density lipoprotein. *J Lipid Res* 40:1686–1694
- Olofsson SO, Boren J (2005) Apolipoprotein B: a clinically important apolipoprotein which assembles atherogenic lipoproteins and promotes the development of atherosclerosis. *J Intern Med* 258:395–410
- Perez-Martinez P, Perez-Jimenez F, Ordovas JM, Moreno JA, Moreno R, Fuentes F, Ruano J, Gomez P, Marin C, Lopez-Miranda J (2007) The APOB -516C/T polymorphism is associated with differences in insulin sensitivity in healthy males, during the consumption of diets with different fat contents. *Br J Nutr* (in press)
- Boerwinkle E, Brown S, Sharrett AR, Heiss G, Patsch W (1994) Apolipoprotein E polymorphism influences postprandial retinyl palmitate but not triglyceride concentrations. *Am J Hum Genet* 54:341–360
- Bucolo G, David H (1973) Quantitative determination of serum triglycerides by use of enzymes. *Clin Chem* 19:476–482
- Allain CC, Poon LS, Chang CSG, Richmond W, Fu PC (1974) Enzymatic determination of total serum cholesterol. *Clin Chem* 20:470–475
- Riepponen P, Marniemi J, Rautaoja T (1987) Immunoturbidimetric determination of apolipoproteins A-1 and B in serum. *Scand J Clin Lab Invest* 47:739–744
- Warnick R, Benderson J, Albers JJ (1982) Dextran Sulfate-Mg precipitation procedure for quantitation of high density lipoprotein cholesterol. *Clin Chem* 28:1379–1388
- Ruotolo G, Zhang H, Bentsianov V, Le NA (1992) Protocol for the study of the metabolism of retinyl esters in plasma lipoproteins during postprandial lipemia. *J Lipid Res* 33:1541–1549
- De Ruyter MGM, De Leecheer AP (1978) Simultaneous determination of retinol and retinyl esters in serum or plasma by reversed-phase high performance liquid chromatography. *Clin Chem* 24:1920–1923
- Karpe F, Hamsten A (1994) Determination of apolipoproteins B-48 and B-100 in triglyceride-rich lipoproteins by analytical SDS-PAGE. *J Lipid Res* 35:1311–1317
- Patsch JR, Miesenbock G, Hopferwieser T, Muhlberger V, Knapp E, Dunn JK, Gotto AM Jr, Patsch W (1992) Relation of triglyceride metabolism and coronary artery disease: studies in the postprandial state. *Arterioscler Thromb* 12:1336–1345
- Phillips NR, Waters D, Havel RJ (1993) Plasma lipoproteins and progression of coronary artery disease evaluated by angiography and clinical events. *Circulation* 88:2762–2770
- Perez-Martinez P, Perez-Jimenez F, Ordovas JM, Bellido C, Moreno JA, Gomez P, Marin C, Fernandez de la Puebla RA, Paniagua JA, and Lopez-Miranda J (2007) The APOB -516C/T polymorphism has no effect on lipid and apolipoprotein response following changes in dietary fat intake in a healthy population. *Nutr Metab Cardiovasc Dis* (in press)
- Pimstone SN, Clee SM, Gagné E., Miao L, Zhang H, Stein EA, Hayden MR (1996) A frequently occurring mutation in the lipoprotein lipase gene (Asn<sup>291</sup>Ser) results in altered postprandial chylomicron triglyceride and retinyl palmitate response in normolipidemic carriers. *J Lipid Res* 37:1675–1684
- Ostos MA, Lopez-Miranda J, Ordovas JM, Marin C, Blanco A, Castro P, Lopez-Segura F, Jimenez-Perez J, Perez-Jimenez F (1998) Dietary fat clearance is modulated by genetic variation in apolipoprotein A-IV gene locus. *J Lipid Res* 39:2493–2500
- Boerwinkle E, Brown S, Sharrett AR, Heiss G, Patsch W (1994) Apolipoprotein E polymorphism influences post-

- prandial retinyl palmitate but not triglyceride concentrations. *Am J Hum Genet* 54:341–360
31. Abbasi F, McLaughlin T, Lamendola C, Yeni-Komshian H, Tanaka A, Wang T, Nakajima K, Reaven GM (1999) Fasting remnant lipoprotein cholesterol and triglyceride concentrations are elevated in nondiabetic, insulin-resistant, female volunteers. *J Clin Endocrinol Metab* 84:3903–3906
  32. Ai M, Tanaka A, Ogita K, Sekine M, Numano F, Numano F, Reaven GM (2001) Relationship between insulin concentration and plasma remnant lipoprotein response to an oral fat load in patients with type 2 diabetes. *J Am Coll Cardiol* 38:1628–1632
  33. Harbis A, Perdreau S, Vincent-Baudry S, Charbonnier M, Bernard MC, Raccach D, Senft M, Lorec AM, Defoort C, Portugal H, Vinoy S, Lang V, Lairon D (2004) Glycemic and insulinemic meal responses modulate postprandial hepatic and intestinal lipoprotein accumulation in obese, insulin-resistant subjects. *Am J Clin Nutr* 80:896–902
  34. Tanaka A (2004) Postprandial hyperlipidemia and atherosclerosis. *J Atheroscler Thromb* 11:322–329
  35. Wilson DE, Chan IF, Buchi KN, Horton SC (1985) Post-challenge plasma lipoprotein retinoids: chylomicron remnants in endogenous hypertriglyceridemia. *Metabolism* 34:551–558
  36. Sposito AC, Gonbert S, Turpin G, Chapman MJ, Thillet J (2004) Common promoter C516T polymorphism in the ApoB gene is an independent predictor of carotid atherosclerotic disease in subjects presenting a broad range of plasma cholesterol levels. *Arterioscler Thromb Vasc Biol* 24:2192–2195
  37. Vohl MC, Lamarche B, Moorjani S, Prud'homme D, Nadeau A, Bouchard C, Lupien PJ, Despres JP (1995) The lipoprotein lipase *HindIII* polymorphism modulates plasma triglyceride levels in visceral obesity. *Arterioscler Thromb Vasc Biol* 15:714–720

# Absorption of Dietary Cholesterol Oxidation Products and Their Downstream Metabolic Effects Are Reduced by Dietary Apple Polyphenols

Yamato Ogino · Kyoichi Osada · Shingo Nakamura ·  
Yutaka Ohta · Tomomasa Kanda · Michihiro Sugano

Received: 30 June 2006 / Accepted: 28 November 2006 / Published online: 10 February 2007  
© AOCS 2007

**Abstract** Exogenous and endogenous cholesterol oxidation products (COPs) perturb various metabolic processes, and thereby they may induce various homeostasis-related disorders. Here, we observed that procyanidin-rich dietary apple polyphenol (APP) from unripe apples alleviates the perturbation of lipid metabolism by decreasing the exogenous COP levels in rats. Dietary COPs may be the greatest source of COPs found in the human body. Rats (4 weeks of age) were fed AIN-purified diets containing 0.3% COPs supplemented with 0.5 or 2.5% APP for 3 weeks. Dietary APP alleviated the growth inhibition action of the exogenous COPs. The modulations of the liver lipid profile by COPs remained unchanged. However, serum total cholesterol, high-density lipoprotein cholesterol, and triglyceride levels increased following the intake of

dietary APP. Further, dietary APP inhibited the increase in lipid peroxide levels in the liver and serum by COPs. The activity of hepatic  $\Delta 6$  desaturase was lowered by dietary APP in a dose-dependent manner, although exogenous COPs generally increased the activity of this enzyme. In keeping with this observation,  $\Delta 6$  desaturation indices in the phospholipids and cholesteryl esters of the liver and serum lipids were lower in the APP-fed groups than those in the control group. Dietary APP also promoted the excretion of exogenous COPs, cholesterol, and acidic steroids in feces. Therefore, the inhibition of intestinal absorption of COPs may partly contribute to the alleviation of the perturbation of lipid metabolism and lipid peroxidation levels. Thus, APP may be an important removal agent of exogenous toxic material such as COPs contained in processed or fast foods.

Y. Ogino · K. Osada (✉) · S. Nakamura  
Faculty of Agriculture and Life Science,  
Hirosaki University, 3 Bunkyo-cho, Hirosaki,  
Aomori 036-8561, Japan  
e-mail: kyochi@cc.hirosaki-u.ac.jp

Y. Ohta · T. Kanda  
Fundamental Research Laboratory,  
Asahi Breweries Ltd, 1-21 Midori 1-chome,  
Moriya, Ibaraki 302-0106, Japan

M. Sugano  
Faculty of Agriculture, Kyushu University,  
6-10-1 Hakozaki, Higashi-ku, Fukuoka 821-8581, Japan

*Present Address:*

Y. Ogino  
Fukushima Laboratory, TOAEIYO Co. Ltd,  
1 Tanaka, Yuno-aza, Izaka-cho,  
Fukushima 960-0280, Japan

**Keywords** Apple · Cholesterol oxidation products ·  
 $\Delta 6$  desaturase · Lipid metabolism · Polyphenol ·  
Procyanidin · Rat

**Abbreviations**

APP	Apple polyphenol
COP	Cholesterol oxidation product
FID	Flame ionization detector
GLC	Gas-liquid chromatography
HDL	High-density lipoprotein
HMG-CoA	3-Hydroxy-3-methylglutarylcoenzyme A
HPLC	High-performance liquid chromatography
6-Keto-PGF <sub>1<math>\alpha</math></sub>	6-Ketoprostaglandin F <sub>1<math>\alpha</math></sub>
mRNA	Messenger RNA
PC	Phosphatidylcholine

PE	Phosphatidylethanolamine
PGI <sub>2</sub>	Prostacyclin
SOD	Superoxide dismutase
TBARS	Thiobarbituric acid reactive substances

## Introduction

Cholest-5-en-3 $\beta$ -ol (cholesterol) in common foods is readily oxidized by exposure to oxygen, high temperature, irradiation with UV rays, and reaction with free radicals during processing or storage. Substantial amounts of cholesterol oxidation products (COPs) have been detected in a variety of processed foods [1] and fast foods [2, 3]. The major COPs were produced through the cholesterol oxidation process, as shown in Fig. 1. Previously, we observed that in rats approximately 30% of the major exogenous COPs are absorbed into the lymph from the intestine [4]. In addition, high levels of COPs were detected in the rat liver and sera following their oral administration at high doses (between 0.2 and 0.5%) [5–7]. COPs are produced in the human body by the attack of free radicals; however, dietary COPs may be the greatest

source of COPs found in the human body because of eating many processed foods containing high levels [1–3] of COPs from animals.

Many *in vitro* studies have shown that COPs exhibit specific deleterious effects such as cytotoxicity, mutagenicity, carcinogenicity, atherogenicity, inhibition of sterol biosynthesis, and modulation of immune function [8]. In previous studies, we observed that dietary COPs specifically disturbed growth, cholesterol metabolism, linoleic acid desaturation, and age-related changes in lipid metabolism [5, 6]. Thus, exogenous COPs appear to exert biologically deleterious effects on lipid metabolism. However, the regulation of COP-induced deleterious effects has not yet been explored. Recently, we observed that soybean protein partly alleviated some of the deleterious effects of exogenous COPs, including the promotion of hepatic linoleic acid desaturation and modulation of lipid parameters [9]. Dietary soybean protein exerted a modulatory effect via the inhibition of intestinal absorption of COPs and regulation of lipid metabolism.

Some reports indicated that dietary polyphenols exert a hypocholesterolemic action [10] and regulatory function on lipid metabolism [11]. The bioavailability of each polyphenol has not yet been completely

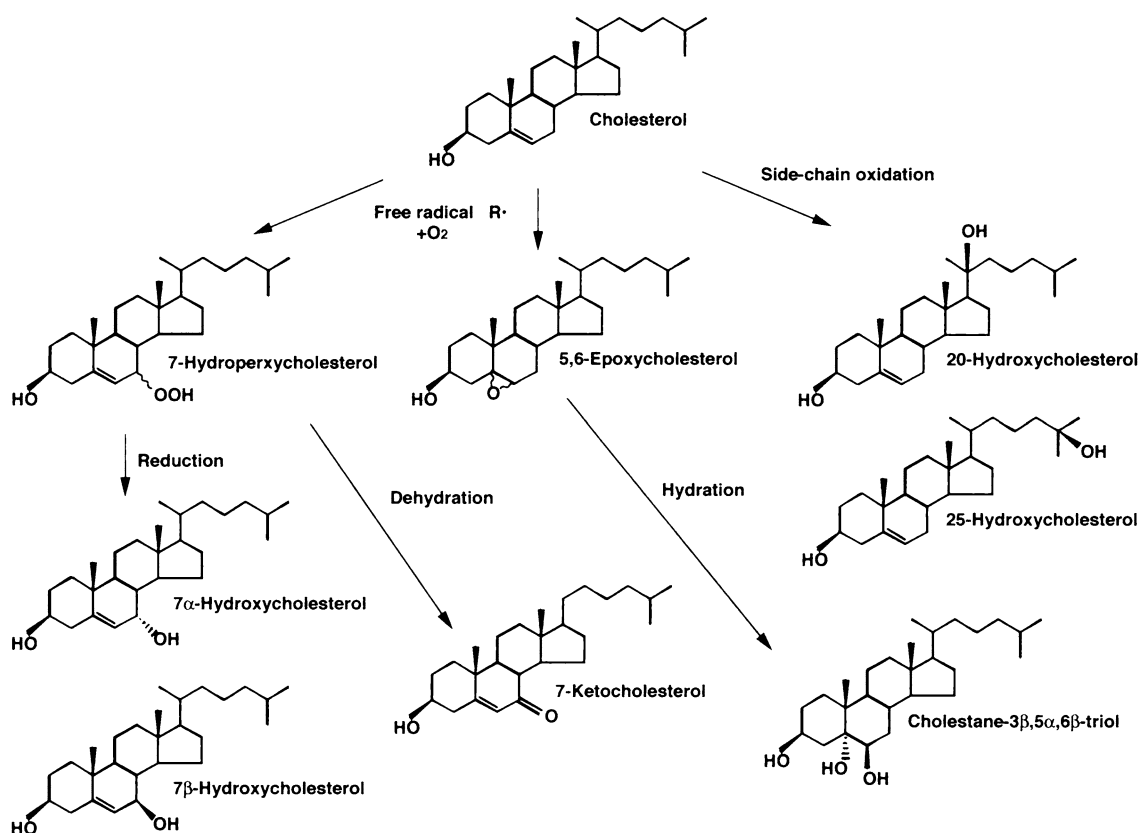


**Fig. 1** Common cholesterol oxidation pathways in foods



defined; however, they may not necessarily be absorbed at high levels as intact molecules from the intestine. Moreover, some reports found that tea catechins inhibit the intestinal absorption of sterols [12, 13]. These observations appear to be associated with the inhibition of the micellar solubility of sterols in the intestine. Therefore, it is possible that dietary polyphenols influence the intestinal absorption of exogenous COPs.

Leth and Jusrensen [14] evaluated that we consume approximately 28 mg polyphenols per day from various plant foods and beverages. The total polyphenol level in a typical fruit serving of 200 g is 50–500 mg [15]. Moreover, we consume tea and onions, etc.; therefore, our daily intake level of polyphenols may be much higher than 28 mg. Among fruits, apples have more than 200 mg polyphenols [15]. Compared with ripe apples, unripe apples contain a significantly higher level of procyanidins [16]; however, except for their antioxidative function, the nutritional function of these procyanidins has not yet been elucidated. Procyanidins in unripe apples consist of oligomeric (–)-epicatechins of 2–14 mer, and they comprise over 60% of total polyphenols [16]. Among procyanidins, low and intermediate molecular weight compounds are soluble in water, alcohol, and acetone [15]. Some of these compounds may be absorbed from the intestine, and their metabolites may influence lipid metabolism. In contrast, high molecular weight compounds are insoluble in the same solvents [15]. The bioavailability of these compounds may be low; however, they interfere with the micellar solubility of lipids. Therefore, the soluble fractions of apple polyphenol (APP), such as 2–4 mers of (–)-epicatechin, may alleviate various disturbances in lipid metabolism that are induced by COPs during metabolic processes. Moreover, the insoluble fractions, such as those over 5 mer of (–)-epicatechin, may inhibit the intestinal absorption of COPs. Since we usually consume many processed foods and fast foods in the modern diet, in the present study, we examined the effect of procyanidin-rich APP (approximately 64% procyanidins of 2–14 mer) on the perturbation of lipid metabolism induced by exogenous COPs in rats. Additionally, we aimed to evaluate the nutritional functions of procyanidin-rich APP as a preventive agent against toxic components in processed foods.

## Experimental Procedures

### Chemicals

[1-<sup>14</sup>C]Linoleic acid ( $\text{CH}_3(\text{CH}_2)_4\text{CH}=\text{CHCH}_2\text{CH}=\text{CH}(\text{CH}_2)_7^{14}\text{CO}_2\text{H}$ , 51 mCi/mmol) was purchased from

New England Nuclear (Boston, MA, USA), and it was purified by thin-layer chromatography prior to use [5]. Solvents and chemicals of reagent grade or better quality were purchased from Nacalai Tesque Co. (Kyoto, Japan) and Kanto Chemical Co. (Tokyo, Japan).

### Animals and Diet

Male Sprague–Dawley rats (3 weeks old, CLEA Japan, Co., Tokyo, Japan) were housed individually in a room with controlled temperature (20–23 °C) and light (0800–2000). After the rats had acclimatized for 1 week, they were divided into groups of seven and fed diets containing either 0.5 or 2.5% APP (99% purity, product of Fundamental Research Laboratory, Asahi Breweries) and 0.3% COPs. APP contained the following by weight percentage: (–)-epicatechin, 6.1; (+)-catechin, 1.1; phloridzin, 1.1; phloridzin xyloglucoside, 2.7; chlorogenic acid, 4.8; *p*-coumaroylquinic acid, 1.5; procyanidins (2 mer), 11.1; procyanidins (3 mer), 12.3; procyanidins (4 mer), 8.7; procyanidins (5 mer), 5.9; procyanidins (6 mer), 4.9; and procyanidins (above 7 mer), 39.8. The composition of added COPs is described in the section “Preparation of the Oxidized Cholesterol Mixture.” The diets were prepared according to the formula recommended by the American Institute of Nutrition [17]. They contained the following constituents by weight percentage: casein (Wako Pure Chemicals Co.), 20; safflower oil (Rinoru Oil Co.), 10; mineral mixture (AIN-76 mixture, Oriental Yeast Co.), 3.5; vitamin mixture (AIN-76 mixture, Oriental Yeast Co.), 1.0; choline bitartrate, 0.2; DL-methionine, 0.3; cellulose, 5.0; corn starch, 15; and sucrose to 100. COPs and APP were added at the expense of sucrose. COPs were added in the diet after emulsifying them into safflower oil. The experimental diet was prepared weekly, packed in a pouch containing an oxygen absorbent, and stored at 4 °C to prevent the autooxidation of lipids. The amount of diet given to the control and 0.5% APP diet-fed groups was the same as that consumed by the 2.5% APP-fed group because the high level of APP caused a significant reduction in food intake. After 3 weeks, the rats were decapitated; their liver was immediately excised and microsome was prepared at 4 °C. The plasma was separated by centrifugation after allowing the blood to clot at room temperature. These samples were maintained at –80 °C until analyses. In order to avoid oxidation, nitrogen gas was diffused through the samples. In order to analyze the fecal neutral and acidic steroids, feces were collected for 2 days, beginning 10 days prior to killing, and these were then lyophi-

lized. The Hirosaki University Animal Policy approved this animal study, and the rats were maintained according to the guidelines of Hirosaki University for the care and use of laboratory animals.

#### Preparation of the Oxidized Cholesterol Mixture

A COP-rich fraction was prepared from pure cholesterol (99.9%) by using the method described in a previous report [5]. The major COPs were identified by gas–liquid chromatography (GLC, Shimadzu GC-14B, Shimadzu Co., Kyoto, Japan) with a flame ionization detector (FID) and a C-R6A integrator after trimethylsilyl derivatization of the prepared fraction. The GLC conditions were as follows: a fused-silica capillary ULBON HR-1 column (0.25 mm × 50 m, Shimwa Chemical Industries, Kyoto, Japan) with a liquid-phase thickness of 0.25 μm; oven temperature, 270 °C; injector temperature, 300 °C; flow rate of helium, 0.7 mL/min; split ratio 1:10. This mixture contained the following by weight percentage: cholesterol, 6.8; cholest-5-en-3β,7α-diol (7α-hydroxycholesterol), 9.9; cholest-5-en-3β,7β-diol (7β-hydroxycholesterol) and 5,6β-epoxy-5β-cholestan-3β-ol (5β-epoxycholesterol), 13.3; 5,6α-epoxy-5α-cholestan-3β-ol (5α-epoxycholesterol), 4.4; 5α-cholestan-3β,5,6β-triol (cholestanetriol), 3.7; 3β-hydroxycholest-5-en-7-one (7-ketocholesterol), 10.2; cholest-5-en-3β,25-diol (25-hydroxycholesterol), 1.3; and identified oxysterols, 45. Unidentified oxysterols comprised more than ten unknown peaks. These may originate from slightly cleaved sterols, although we do not have an exact explanation.

#### Enzyme Activity

The activity of Δ6 desaturase in liver microsomes was measured by Sevansson's method [18]. The microsomal protein concentration was determined by the method of Lowry et al. [19].

#### Superoxide Dismutase Activity of Red Blood Cells

The activity of superoxide dismutase (SOD) in red blood cells was measured by the nitrite method according to the report of Oyanagui [20].

#### Lipid Peroxide Level

Liver and serum lipoperoxides were measured by the method of Yagi [21] and Ohokawa et al. [22], as thiobarbituric acid reactive substances (TBARS) are markers of lipid peroxide.

#### Lipid Analysis

Liver and serum lipids were extracted by the method of Folch et al. [23], and the concentrations of triglyceride, cholesterol, high-density lipoprotein (HDL) cholesterol, and phospholipids were measured as described previously [24]. The fatty acid compositions of liver phosphatidylcholine (PC) and phosphatidylethanolamine (PE) were analyzed by GLC (Shimadzu GC-8A) by using a FID and a Silar 10C column (2 mm × 3 m) [25].

#### Analysis of Fecal Steroids

Further, the levels of fecal acidic steroids were analyzed by GLC (Shimadzu GC-8A) with a FID by using a AN-600 column (2 mm × 3 m) using 23-nordeoxycholic acid (Steraloids, Wilton, NH, USA) as an internal standard [26]. The concentration of the sterols in the serum, liver, and feces were measured by GLC (Shimadzu GC-14B) by using a FID with a ULBON HR-1 column (0.25 mm × 50 m, 0.25 μm, Shinwa Chemical Industries) according to the condition described above. 5α-Cholestan (Sigma Chemical Co., St Louis, MO, USA) was used as an internal standard, and measurements were carried out after converting the sterol to a trimethylsilyl ester derivative [27].

#### Prostaglandin Analysis

For measurement of the aortic production of prostacyclin (PGI<sub>2</sub>), the thoracic aorta (approximately 25 mg) was incubated in Krebs–Henseleit bicarbonate buffer (pH 7.4) at 25 °C for 30 min, and the concentration of 6-ketoprostaglandin F<sub>1α</sub> (6-keto-PGF<sub>1α</sub>) in the medium was measured using a Shimadzu LC 10ADVP high-performance liquid chromatography (HPLC) system [28]. HPLC analysis of 6-keto-PGF<sub>1α</sub> was performed using a reversed-phase HPLC column (250 × 4.6 mm) at 195 nm by using a UV–vis detector. The contents of the column were eluted with acetonitrile/0.1% phosphoric acid (33:67 by volume) at a flow rate of 1 mL/min.

#### Identification of Major COPs

GLC–mass spectrometry was also performed to identify the major COPs according to a previous method [27]. The analysis was performed by using a Shimadzu GCMS-QP5050A mass spectrometer with a Shimadzu GC-17 gas chromatograph. The GLC–mass spectrometry conditions were as follows: a fused silica capillary ULBON HR-1 column (0.25 mm × 50 m) with a liquid-phase thickness of 0.25 μm; oven temperature,

270 °C; injector temperature, 300 °C; flow rate of helium, 0.7 mL/min; split ratio 1:50; make-up gas (helium), 40.1 mL/min. The mass spectra were measured within a mass range of  $m/z$  50–600. The scan speed was one scan per second. The ionization energy was 70 eV.

#### Effect of APP on Micellar Solubility of Cholesterol In Vitro

A mixed-micellar solution containing 6.6 mM sodium taurocholate, 0.6 mM egg yolk PC, 0.2 mg/mL COPs, 132 mM NaCl, and 15 mM sodium phosphate at pH 7.4 was prepared by sonication and kept at 37 °C for 24 h according to the method of Ikeda et al. [12]. A 100- $\mu$ L solution of various concentrations of APP (0.5, 1, and 2 mg/mL) was added to the 5-mL micellar solution. The mixed solution was incubated for 1 h at 37 °C after the addition of APP, and centrifuged at 1,000g for 10 min. The supernatant was filtered using a 220-nm Millex-GV filter (Japan Millipore, Tokyo). The COPs in each filtrate were identified by GLC as described above. The level of bile acid in the micelles was measured using a commercial kit (Enzabile-2, Daiichi Kagaku, Tokyo, Japan).

#### Statistical Analysis

Data were analyzed by Duncan's [29] new multiple range test to determine the exact nature of the difference ( $P < 0.05$ ) among the groups.

## Results

### Growth and Liver Weight

Compared with the control group, groups receiving dietary APP showed an increase in weight in a dose-dependent manner despite the pair-feeding protocol (Table 1). The relative liver weight was not influenced by dietary APP.

**Table 1** Effect of dietary apple polyphenol (APP) on growth in rats given cholesterol oxidation products (COPs)

Group	Initial body weight (g)	Weight gain (g/21 days)	Food intake (g/day)	Liver weight (g/100 g body weight)
Control	82 ± 1	119 ± 3 <sup>b</sup>	14.9 ± 0.1	4.58 ± 0.11
0.5% APP	82 ± 1	121 ± 39 <sup>bc</sup>	14.9 ± 0.2	4.57 ± 0.12
2.5% APP	82 ± 1	131 ± 4 <sup>c</sup>	14.9 ± 0.4	4.79 ± 0.30

Data are the mean ± the standard error (SE) of seven rats. Means with different letters in rows are significantly different ( $P < 0.05$ )

### TBARS Values of Serum and Liver

Table 2 shows the levels of serum and liver lipoperoxides that were measured as TBARS. A significant dose-dependent reduction in serum and liver TBARS values was observed in the groups receiving dietary APP when compared with the control group.

### SOD Activity of Red Blood Cells

The SOD activity of red blood cells was significantly lower in the APP-fed groups than in the control group (control group 574.5 ± 124.3 NU/mg protein, APP-0.5 group 254.9 ± 70.7 NU/mg protein, APP-2.5 group 284.0 ± 65.5 NU/mg protein).

### $\Delta 6$ Desaturase Activity of Liver Microsomes

The APP-fed groups showed lower hepatic  $\Delta 6$  desaturase activity than the control group (control group 1,138.1 ± 94.9 pmol/min/mg protein, AP-0.5 group 731.9 ± 142.8 pmol/min/mg protein, AP-2.5 group 496.1 ± 165.5 pmol/min/mg protein). In particular, this enzyme activity was significantly lower in the APP-2.5 group than in the control group.

### Concentration of Liver and Serum Lipids

Serum total cholesterol level was not changed by dietary APP; however, the HDL-cholesterol level was increased in a dose-dependent manner (Table 3). Further, dietary APP increased the serum triglyceride level in a dose-dependent manner. The liver total cholesterol level was not influenced by dietary APP. In contrast, the liver triglyceride level in the APP-fed groups was lower than that in the control group, particularly in the APP-2.5 group (Table 4). The liver phospholipid level in the APP-fed groups was lower than that in the control group; however, the serum phospholipid levels remained the same.

**Table 2** Effect of dietary APP on tissue the values of thiobarbituric reactive substances in rats given COPs

Group	Serum (nmol MDA/mL)	Liver (nmol MDA/g)
Control	3.43 ± 0.05 <sup>b</sup>	352.0 ± 12.6 <sup>b</sup>
0.5% APP	2.73 ± 0.30 <sup>c</sup>	290.1 ± 17.9 <sup>c</sup>
2.5% APP	2.69 ± 0.19 <sup>c</sup>	250.6 ± 16.7 <sup>c</sup>

Data are the mean ± SE of seven rats. Means with different letters in rows are significantly different ( $P < 0.05$ )

MDA malondialdehyde

**Table 3** Effect of dietary APP on serum lipid concentration in rats given COPs

Group	Total cholesterol (mg/dL)	HDL cholesterol (mg/dL)	Triglyceride (mg/dL)	Phospholipid (mg/dL)
Control	70.7 ± 4.9	45.6 ± 4.3 <sup>b</sup>	73.6 ± 19.6 <sup>b</sup>	130 ± 4
0.5% APP	75.2 ± 4.2	54.2 ± 2.9 <sup>b</sup>	111 ± 24 <sup>bc</sup>	126 ± 10
2.5% APP	74.0 ± 6.2	68.2 ± 4.3 <sup>c</sup>	169 ± 18 <sup>c</sup>	129 ± 9

Data are the mean ± SE of seven rats. Means with different letters in rows are significantly different ( $P < 0.05$ )

HDL high-density lipoprotein

**Table 4** Effect of dietary APP on liver lipid levels in rats given COPs

Group	Total cholesterol (mg/g)	Triglyceride (mg/g)	Phospholipids (mg/g)
Control	2.38 ± 0.14	28.3 ± 6.4 <sup>b</sup>	32.6 ± 0.9 <sup>b</sup>
0.5% APP	2.26 ± 0.14	18.7 ± 4.8 <sup>b</sup>	31.2 ± 0.6 <sup>b</sup>
2.5% APP	2.17 ± 0.10	5.68 ± 0.52 <sup>c</sup>	28.7 ± 1.0 <sup>c</sup>

Data are the mean ± SE of seven rats. Means with different letters in rows are significantly different ( $P < 0.05$ )

#### Δ6 Desaturation Index of Liver and Serum Lipids

The levels of linoleic acids (18:2n-6) in liver and serum lipids were higher in APP-fed rats than in the control group rats. In contrast to these observations, the levels of arachidonic acids (20:4n-6) in the liver and serum were lower in the APP-fed groups than that in the control group. These changes that were induced by

dietary APP occurred in a dose-dependent manner. In keeping with these results, the ratio of Δ6 desaturation indices (20:3n-6 + 20:4n-6)/18:2n-6 in liver PC and PE were lower in the APP-fed group than in the control group. This reduction occurred in a dose-dependent manner. Similar observations were made in the case of serum PC and CE (Table 5).

#### Level of PGI<sub>2</sub>

The aortic production of PGI<sub>2</sub> was significantly decreased by dietary APP (control group 9.90 ± 0.66 nmol/aorta mg, AP-0.5 group 7.56 ± 0.71 nmol/aorta mg, AP-2.5 group 5.95 ± 0.55 nmol/aorta mg).

#### Excretion of Acidic Steroids in Feces

The APP-fed group tended to show higher excretion of acidic steroids in the feces (Fig. 2) than the control group. Reflecting these observations, the total level of excreted acidic steroids in feces was significantly higher in the APP-fed rats than that in rats fed with a diet free of APP (control group 3.20 ± 0.35 mg/day, APP-0.5 group 3.55 ± 0.51 mg/day, APP-2.5 group 5.09 ± 0.35 mg/day).

#### The Levels of Major Oxidized Cholesterols in Tissues and Excreted Feces

Major COPs, including 7β-hydroxycholesterol, 25-hydroxycholesterol, 5α-epoxycholesterol, 5β-epoxycholesterol, cholestanetriol, and 7-ketocholesterol, were

**Table 5** Effect of dietary APP on tissue fatty acid compositions in rats fed COPs

Group	Fatty acids (%)							
	16:0	18:0	18:1	18:2(n-6)	20:3(n-6)	20:4(n-6)	22:6(n-3)	(20:3 + 20:4)/18:2
Liver phosphatidylcholine								
Control	18.2 ± 0.5 <sup>b</sup>	23.9 ± 0.5 <sup>b</sup>	7.2 ± 0.4	6.7 ± 0.3 <sup>b</sup>	0.9 ± 0.2	33.4 ± 0.4 <sup>b</sup>	1.7 ± 0.1	5.2 ± 0.2 <sup>b</sup>
0.5% APP	22.2 ± 0.9 <sup>c</sup>	22.7 ± 0.7 <sup>b</sup>	7.3 ± 0.4	8.7 ± 1.2 <sup>c</sup>	1.0 ± 0.1	29.5 ± 1.2 <sup>c</sup>	1.5 ± 0.2	3.9 ± 0.2 <sup>c</sup>
2.5% APP	20.9 ± 0.6 <sup>c</sup>	20.2 ± 0.8 <sup>c</sup>	7.0 ± 0.4	13.1 ± 1.6 <sup>d</sup>	0.7 ± 0.1	27.5 ± 0.8 <sup>c</sup>	1.7 ± 0.1	2.5 ± 0.2 <sup>d</sup>
Liver phosphatidylethanolamine								
Control	19.4 ± 0.9	25.5 ± 0.6	5.4 ± 0.3	3.2 ± 0.2 <sup>b</sup>	0.3 ± 0.1	28.0 ± 1.0	4.4 ± 0.5	9.0 ± 0.6 <sup>b</sup>
0.5% APP	18.9 ± 0.6	25.8 ± 0.7	5.3 ± 0.3	3.5 ± 0.3 <sup>b</sup>	0.4 ± 0.0	29.0 ± 0.7	4.5 ± 0.4	8.7 ± 0.8 <sup>c</sup>
2.5% APP	16.4 ± 1.8	23.8 ± 0.8	4.8 ± 0.4	4.5 ± 0.4 <sup>c</sup>	0.5 ± 0.1	27.2 ± 1.5	5.5 ± 0.5	6.4 ± 0.4 <sup>c</sup>
Serum phosphatidylcholine								
Control	23.4 ± 3.6 <sup>b</sup>	26.8 ± 4.7 <sup>b</sup>	5.5 ± 0.9	11.6 ± 1.7 <sup>b</sup>	2.8 ± 1.9	14.6 ± 0.8 <sup>b</sup>	3.7 ± 0.1 <sup>b</sup>	2.2 ± 1.0 <sup>b</sup>
0.5% APP	17.7 ± 3.9 <sup>c</sup>	13.6 ± 2.8 <sup>c</sup>	5.9 ± 1.1	11.8 ± 2.1 <sup>b</sup>	1.0 ± 0.4	11.1 ± 2.3 <sup>bc</sup>	2.3 ± 0.9 <sup>bc</sup>	1.0 ± 0.8 <sup>bc</sup>
2.5% APP	26.4 ± 0.8 <sup>b</sup>	23.7 ± 1.0 <sup>b</sup>	5.9 ± 0.3	18.7 ± 0.4 <sup>c</sup>	1.7 ± 0.6	11.8 ± 0.2 <sup>c</sup>	1.4 ± 0.1 <sup>c</sup>	0.7 ± 0.0 <sup>c</sup>
Serum cholesteryl ester								
Control	9.1 ± 1.5	2.9 ± 0.5	6.9 ± 2.3	12.1 ± 2.4 <sup>b</sup>	0.4 ± 0.1	59.8 ± 7.5	2.8 ± 0.9	5.3 ± 1.0 <sup>b</sup>
0.5% AP	8.2 ± 0.7	2.9 ± 0.2	6.8 ± 1.0	13.2 ± 1.5 <sup>b</sup>	0.8 ± 0.3	59.8 ± 2.1	3.0 ± 0.7	4.7 ± 0.7 <sup>bc</sup>
2.5% APP	9.0 ± 1.0	3.1 ± 0.7	6.3 ± 1.9	19.3 ± 2.2 <sup>c</sup>	0.4 ± 0.2	51.7 ± 7.0	2.9 ± 0.6	2.8 ± 0.6 <sup>c</sup>

Data are the mean ± SE of seven rats. Means with different letters in rows are significantly different ( $P < 0.05$ )

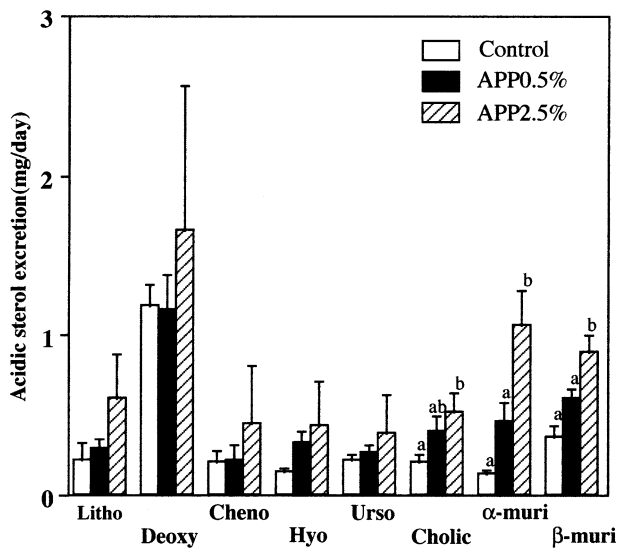


**Fig. 2** Effect of dietary apple polyphenol on excretion of fecal acidic steroids in rats given cholesterol oxidation products. Data are the mean ± the standard error of seven rats in each group. Means with different letters are significantly different at ( $P < 0.05$ ). APP apple polyphenol, litho lithocholic acid, deoxy deoxycholic acid, cheno chenodeoxycholic acid, hyo hydoxycholic acid, urso ursodeoxycholic acid, cholic cholic acid, α-muri α-muricholic acid, β-muri β-muricholic acid

detected in the serum and liver, irrespective of the consumption of APP (Table 6). The APP-fed group had lower accumulation of these COPs in the serum and liver than the control group. In contrast, the level of each COP in the feces tended to be significantly higher in the APP-fed groups than in the control group. Therefore, the levels of the major COPs that were excreted in the feces significantly increased in a dose-dependent manner.

**Effects of APP on Micellar Solubility of COPs and Bile Acids**

The addition of APP to a mixed-micellar solution containing COPs decreased the micellar solubility of COPs in a dose-dependent manner (Fig. 3). Further, the addition of APP reduces the levels of bile acid in micelles in a dose-dependent manner.

**Discussion**

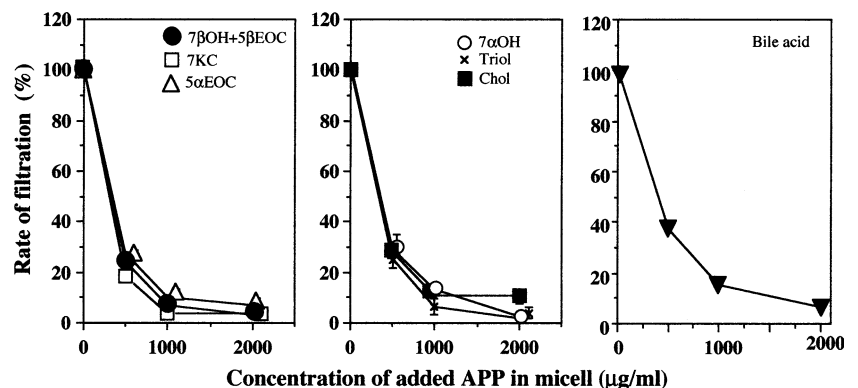
We consume various levels of COPs in daily food, especially processed food [1] and fast foods [2, 3] in our

**Table 6** Effect of dietary APP on serum, liver, and fecal neutral steroid levels in rats given COPs

Group	Oxysterols				
	7βOH + 5βEOC	5αEOC	Triol	7KC	25OH
<b>Serum (μg/mL)</b>					
Control	11.89 ± 1.04 <sup>b</sup>	5.61 ± 0.33 <sup>b</sup>	16.13 ± 1.64	23.63 ± 3.18 <sup>b</sup>	5.61 ± 0.66 <sup>b</sup>
0.5% APP	10.66 ± 1.59 <sup>bc</sup>	7.94 ± 0.84 <sup>c</sup>	14.73 ± 1.73	21.83 ± 1.75 <sup>b</sup>	3.47 ± 0.42 <sup>bc</sup>
2.5% APP	9.89 ± 8.72 <sup>c</sup>	4.86 ± 0.35 <sup>b</sup>	11.77 ± 2.11	14.18 ± 1.34 <sup>c</sup>	2.74 ± 0.80 <sup>c</sup>
<b>Liver (μg/g)</b>					
Control	117.49 ± 12.96	5.61 ± 0.33 <sup>b</sup>	16.13 ± 1.64	23.63 ± 3.18 <sup>b</sup>	5.61 ± 0.66 <sup>b</sup>
0.5% APP	100.50 ± 13.68	7.94 ± 0.84 <sup>c</sup>	14.73 ± 1.73	21.83 ± 1.75 <sup>b</sup>	3.47 ± 0.42 <sup>bc</sup>
2.5% APP	79.89 ± 8.72	4.86 ± 0.35 <sup>b</sup>	11.77 ± 2.11	14.18 ± 1.34 <sup>c</sup>	2.74 ± 0.80 <sup>c</sup>
<b>Feces (mg/g)</b>					
Control	0.76 ± 0.08 <sup>b</sup>	0.31 ± 0.04	0.40 ± 0.02	0.11 ± 0.01	0.04 ± 0.01
0.5% APP	1.01 ± 0.10 <sup>bc</sup>	0.39 ± 0.02	0.51 ± 0.02	0.19 ± 0.02	0.05 ± 0.01
2.5% APP	1.14 ± 0.17 <sup>c</sup>	0.40 ± 0.06	0.58 ± 0.05	0.18 ± 0.03	0.06 ± 0.02

Data are the mean ± SE of seven rats. Means with different letters in rows are significantly different ( $P < 0.05$ )  
 7βOH 7β-hydroxycholesterol,  
 5αEOC 5α-epoxycholesterol,  
 5βEOC 5β-epoxycholesterol,  
 triol cholestanetriol, 7KC 7-ketocholesterol, 25OH 25-hydroxycholesterol

**Fig. 3** Effect of apple polyphenols on micellar solubility of bile acids in vitro. Data are the mean ± the standard error of seven rats in each group. 7βOH 7β-hydroxycholesterol, 5βEOC 5β-epoxycholesterol, 7KC 7-ketocholesterol, 5αEOC 5α-epoxycholesterol, 7αOH 7α-hydroxycholesterol, triol cholestanetriol, chol cholesterol



modern diet. Compared with fatty acid oxidation products, these COPs are more easily absorbed from the intestine [30, 31]. Subsequently, they disturb lipid metabolism through their toxic effect [5, 7–9]. Thus, exogenous COPs from processed foods are hazardous to human health. However, no counterplan for this hazardous problem has been considered until now. We examined the preventive functions of dietary APP, which is an oligomeric (–)-epicatechin-rich polyphenol, on the perturbation of lipid metabolism by exogenous COPs. This was done because dietary APP may inhibit the intestinal absorption of COPs and their metabolites and regulates the disturbance of lipid metabolism by COPs without the various side effects caused by medicines.

Exogenous COPs generally inhibit growth and food intake [6, 32]; however, dietary APP appears to alleviate the growth inhibition induced by exogenous COPs. Recently, we observed that hepatic function including glutamate oxaloacetate transaminase (control  $41.5 \pm 1.9$  IU/L, APP-0.5  $25.5 \pm 1.6$  IU/L, APP-1.0  $18.4 \pm 1.7$  IU/L) and glutamate pyruvate transaminase (control  $20.1 \pm 0.9$  IU/L, APP-0.5  $10.6 \pm 0.8$  IU/L, APP-1.0  $7.7 \pm 0.8$  IU/L) was also alleviated by the consumption of APP in rats fed with 0.5% COP (unpublished data). Thus, dietary APP may alleviate the impairment of growth and hepatic function induced by exogenous COPs.

Exogenous COPs increase tissue lipoperoxide levels and disturb the biological antioxidative system [5, 7–9]. We observed that dietary APP decreased lipoperoxide levels (as TBARS values) in the liver and sera of rats that were fed COPs in this experiment. Moreover, the SOD activity of blood cells was higher in the control group than in the APP-fed groups. Dietary COPs may induce SOD activity because they elevated the TBARS value [7]. However, the metabolites from APP, particularly low molecular weight procyanidins, including 2–4 mers of (–)-epicatechin, may have antioxidative effect. Moreover, high molecular weight procyanidins such as greater than 4 mer in APP inhibited the absorption of COPs as described below. Therefore, SOD activity may not be induced in APP-fed groups. However, we observed that dietary APP prevented the exhaustion of tocopherols and SOD in rats fed a normal diet without COPs (unpublished data). We need to perform more experiments to explain this conflict. Analysis of the hydroperoxide levels of each lipid class or other more specific markers of lipid oxidation such as  $F_2$  isoprostanes is needed in future studies to more precisely evaluate the antioxidative effects of dietary APP.

We previously observed that exogenous COPs promoted the desaturation of linoleic acid through the

increase of  $\Delta 6$  desaturase activity [5, 7–9]. This promotive activity of the enzyme by COPs may be associated with the modulation of microsomal membrane fluidity [33, 34]. Moreover, the modulation of the messenger RNA (mRNA) level of  $\Delta 6$  desaturase may contribute to these modulations. The promotion of linoleic acid desaturation may cause an imbalance in the eicosanoid level because eicosanoids are metabolites of arachidonic acid. In fact, dietary COPs increase the production of  $PGI_2$  in the aorta. It has been reported that COPs influence arachidonic acid release from cell membrane phospholipids and cyclooxygenase activity in vitro [35, 36]. The imbalance in the eicosanoid level is associated with various homeostasis-related disturbances concerning lipid metabolism. Therefore, dietary APP may play an important role as a regulatory food factor in the perturbation of linoleic acid desaturation. Further study is needed to elucidate the relationship between dietary APP and the modulation of cyclooxygenase or lipoxygenase activities by exogenous COPs.

COPs generally perturb cholesterol biosynthesis; this reduces the cholesterol level in the liver and serum. In this study, dietary APP did not influence the liver cholesterol level. The metabolites from APP and COPs may inhibit hepatic 3-hydroxy-3-methylglutarylcoenzyme A (HMG-CoA) reductase; therefore, this may have been responsible for the unchanged liver cholesterol level in this experiment. In fact, we observed that dietary APP decreased the activity of hepatic HMG-CoA reductase in rats fed a cholesterol-free diet (polyphenol-free diet  $162.2 \pm 31.3$  pmol/min/mg protein, APP monomer diet  $122.7 \pm 18.1$  pmol/min/mg protein, APP oligomer fraction diet  $61.7 \pm 8.2$  pmol/min/mg protein, unpublished data). Further, the serum total cholesterol level was also the same in each group; however, the HDL cholesterol level increased in a dose-dependent manner. Therefore, the ratio of HDL cholesterol to total cholesterol significantly increased (control  $60.4 \pm 6.7\%$ , APP-0.5  $73.6 \pm 5.0\%$ , APP-1.0  $86.5 \pm 4.3\%$ ) and the atherosclerosis index [(total cholesterol–HDL cholesterol)/HDL cholesterol] significantly decreased owing to consumption of APP (control  $0.68 \pm 0.21$ , APP-0.5  $0.38 \pm 0.09$ , APP-1.0  $0.32 \pm 0.06$ ). Dietary APP increased the HDL cholesterol level in the rats fed a cholesterol-free diet (APP-free diet  $28.4 \pm 2.1$  mg/dL, APP-0.1 diet  $39.0 \pm 2.6$  mg/dL, APP-0.5 diet  $40.3 \pm 2.6$  mg/dL, unpublished data). The same observations were made in diabetic rats fed cocoa extract containing procyanidins [37]. Heat-epimerized tea catechins also increased the HDL cholesterol level in rats [38]. Dietary APP may increase the HDL cholesterol level through an increase of lecithin cholesterol acyl trans-

ferase, although we do not have exact explanation now. More study is needed to explain this mechanism. Thus, dietary APP may alleviate the modulation of the lipid profile by exogenous COPs, and therefore it may inhibit the induction of atherosclerosis by exogenous COPs.

In previous studies, we found that exogenous COPs inhibit hepatic cholesterol  $7\alpha$ -hydroxylase activity [5, 7–9]; however, dietary APP alleviated this inhibition effect in a dose-dependent manner. In fact, the total fecal acidic steroid level was significantly increased by dietary APP in a dose-dependent manner. We observed that dietary APP tended to increase the CYP7 mRNA in the liver and cholesterol  $7\alpha$ -hydroxylase activity [39]. Thus, the APP metabolite may modulate the perturbation of cholesterol catabolism by exogenous COPs.

Dietary APP also modulated the levels of serum and liver COPs in a diet containing 0.3% COPs. Major COPs in the serum and liver decreased in a dose-dependent manner when APP was consumed. In contrast to these observations, dietary APP increased the levels of the major COPs in the feces. These results refer to the inhibition of exogenous COPs from the intestine by dietary APP. Several studies have shown that tea catechins such as (–)-epigallocatechin gallate, which has gallate esters, decrease cholesterol absorption in the intestine [12]. Our *in vitro* study also demonstrated the possible mechanism by which COPs solubilized in mixed bile salt micelles are eliminated from the micelles by the addition of APP. In general, low and intermediate molecular weight polyphenolic compounds, such as hydrolysable tannins and procyanidins, can solubilize in water, alcohol, and acetone [15]. However, high molecular weight procyanidins remain insoluble in the same solvents. Some reports found that oligomeric procyanidins such as 2 mer, which have comparatively low molecular weight and are soluble in water and alcohol, were detected in the plasma [40]. Shoji et al. [41] observed that dietary procyanidins ranging from 2 mer to 5 mer were absorbed and detected in the plasma when rats were given apple condensed tannin. Our APP consists of 11.1% of 2 mer, 12.3% of 3 mer, 8.7% of 4 mer, 5.9% of 5 mer, 4.9% of 6 mer, 39.8% of greater than 7 mer, and 17.3% of other low molecular weight polyphenolic compounds. Therefore, the high molecular weight procyanidins in the added APP may form insoluble coprecipitates with COPs in a mixed-micellar solution similar to the relationship between (–)-epigallocatechin and cholesterol reported by Ikeda et al. [12]. Moreover, the addition of APP changed the concentration of bile acid in the micelles. This effect may be attributed

to the water-soluble complex of APP, particularly with low molecular weight polyphenolic compounds including procyanidins and bile acid. This complex may disrupt the micelles and then induce the precipitation of COPs in the intestinal lumen. The same observation was revealed in the case of water-soluble dietary fibers [42, 43]. Thus, dietary APP, especially high molecular weight procyanidins such as greater than 4 mer, may inhibit the intestinal absorption of hazardous COPs by disruption of the micelles and promote the excretion of procyanidins in feces. Recently, hypocholesterolemic function by dietary phytosterol such as  $\beta$ -sitosterol also has been investigated [44].  $\beta$ -Sitosterol also inhibited the absorption of dietary COPs; therefore, the combination of APP and  $\beta$ -sitosterol in the diet may be effective in the inhibition of absorption of hazardous materials such as COPs from the intestine.

Thus, dietary APP appears to alleviate the toxic action and perturbation of lipid metabolism by exogenous COPs. Two mechanisms may contribute to these alleviative functions. Firstly, high molecular weight procyanidins interfere with the intestinal absorption of exogenous COPs. Secondly, the metabolites from low molecular weight procyanidins such as procyanidins ranging from 2 mer to 4 mer and other monomeric polyphenols regulate the perturbation of lipid metabolism. In particular, the former may play an important role in our observed alleviatory effects against the hazardous effect of exogenous COPs. Rats were fed diets with high levels of COPs; however, this level may be not necessarily be at the physiological concentration. Dietary COP levels in the human diet have not yet been estimated, although we eat high levels of COPs in processed foods. Therefore, we must estimate the COP levels in the modern diet. In future, more animal feeding studies in which the subjects are fed with comparatively low levels of COPs are required. However, we can infer that procyanidin-rich diets and supplements or beverages containing high levels of APP containing high levels of procyanidins may be useful in inhibiting the absorption of hazardous COPs in diets such as those involving processed or fast foods. Thus, it will be possible to maintain a healthy condition while consuming a modern diet.

## References

1. Paniangvait P, King AJ, Jones AD, German BG (1995) Cholesterol oxides in foods of animal origin. *J Food Sci* 60:1159–1174
2. Lake RJ, Scholes P (1997) Quality and consumption of oxidized lipids from deep-frying fats and oils in New Zealand. *J Am Oil Chem* 74:1065–1068

3. Lake RJ, Scholes P (1997) Consumption of cholesterol oxides from fast foods fried in beef fat in New Zealand. *J Am Oil Chem* 74:1069–1075
4. Osada K, Sasaki E, Sugano M (1994) Lymphatic absorption of oxidized cholesterol in rats. *Lipids* 29:555–559
5. Osada K, Kodama T, Cui L, Ito Y, Sugano M (1994) Effects of dietary oxidized cholesterol on lipid metabolism in differently aged rats. *Biosci Biotechnol Biochem* 58:1062–1069
6. Osada K, Kodama T, Noda S, Yamada K, Sugano M (1995) Oxidized cholesterol modulates age-related change in lipid metabolism in rats. *Lipids* 30:405–413
7. Osada K, Kodama T, Yamada K, Nakamura S, Sugano M (1998) Dietary oxidized cholesterol modulates cholesterol metabolism in rats fed high-cholesterol diet. *Lipids* 33:757–764
8. Smith LL, Johnson BH (1989) Biological activities of oxysterols. *Free Radic Biol Med* 7:285–352
9. Osada K, Inoue T, Nakamura S, Sugano M (1999) Dietary soybean protein moderates the deleterious disturbance of lipid metabolism caused by exogenous oxidized cholesterol in rats. *Biochim Biophys Acta* 1427:337–350
10. Matsumoto N, Okushio K, Hara Y (1998) Effect of black tea polyphenols on plasma lipids in cholesterol-fed rats. *J Nutr Sci Vitaminol* 44:337–342
11. Vidal R, Hernandez-Vallejo S, Pauquai T, Texier O, Rousset M, Chambaz J, Demignot S, Lacorte JM (2005) Apple procyanidins decrease cholesterol esterification and lipoprotein secretion in Caco-2/TC7 enterocytes. *J Lipid Res* 46:258–268
12. Ikeda I, Imasato Y, Sasaki E, Nakayama M, Nagao H, Takeo T, Yayabe F, Sugano M (1992) Tea catechins decrease micellar solubility and intestinal absorption of cholesterol in rat. *Biochim Biophys Acta* 1127:141–146
13. Yang TT, Koo MW (2000) Chinese green tea lowers cholesterol level through an increase in fecal lipid excretion. *Life Sci* 66:411–423
14. Leth T, Jusensen U (1998) Analysis of flavonoids in fruits, vegetables and beverages by HPLC-UV and LC-MS and estimation of the total daily flavonoids intake in Denmark. In: Amado R, Andersson H, Bardocz S, Serra F (eds) Polyphenols in food. Office for official publications of the European communities, Luxembourg, pp 39–40
15. Macheix JJ, Fleuriet A, Billot J (1990) Changes and metabolism of phenolic compounds in fruits. In: Macheix JJ, Fleuriet A, Billot J (eds) Fruit phenolics. CRC, Boca Raton, pp 149–237
16. Ohnishi-Kameyama M, Yanagida A, Kanda K, Nagata T (1997) Identification of catechin oligomers from apple (*Malus pumila* cv. Fuji) in matrix-associated laser desorption/ionization time-of-flight mass spectrometry and fast-atom bombardment mass spectrometry. *Rapid Commun Mass Spectrom* 11:31–36
17. American Institute of Nutrition (1997) Report of the AIN Ad Hoc committee on standard for nutritional studies. *J Nutr* 107:1340–1348
18. Sevansson L (1988) The effect of dietary partially hydrogenated marine oils on desaturation of fatty acids in rats. *Lipids* 18:171–178
19. Lowry OH, Rosebrough NJ, Farr AL, Randall RJ (1951) Protein measurement with the Folin phenol reagent. *J Biol Chem* 193:265–275
20. Oyanagui Y (1984) Reevaluation of assay methods and establishment of kit for superoxide dismutase activity. *Anal Biochem* 142:290–296
21. Yagi K (1976) A simple fluorometric assay for lipoperoxides in blood plasma. *Biochem Med* 15:212–216
22. Ohkawa H, Ohishi N, Yagi K (1979) Assay for lipid peroxides in animal tissues by thiobarbituric acid reaction. *Anal Biochem* 95:351–358
23. Folch J, Lees M, Sloane-Stanley GH (1957) A simple method for the isolation and purification of total lipids from animal tissues. *J Biol Chem* 226:497–506
24. Kawakami Y, Tsurugasaki W, Yoshida Y, Igarashi Y, Nakamura S, Osada K (2004) Regulative actions of dietary soy isoflavone on biological antioxidative system and lipid metabolism in rats. *J Agric Food Chem* 52:1764–1768
25. Ikeda I, Tomari Y, Sugano M (1989) Interrelated effects of dietary fiber and fat on lymphatic cholesterol and triglyceride absorption in rats. *J Nutr* 119:1383–1387
26. Sugano M, Yamada Y, Yoshida K, Hashimoto Y, Matsuo T, Kimoto M (1988) The hypocholesterolemic action of the undigested fraction of soybean protein in rats. *Atherosclerosis* 72:115–112
27. Osada K, Kodama T, Yamada K, Sugano M (1993) Oxidation of cholesterol by heating. *J Agric Food Chem* 41:1198–1202
28. Bruckner GG, Lokesh B, German B, Kinsella JE (1984) Biosynthesis of prostanoids, tissue fatty acid composition and thrombotic parameters in rats fed diets enriched with docosahexaenoic (22:6n-3) or eicosapentaenoic (20:5n-3) acid. *Thromb Res* 34:479–497
29. Duncan DB (1955) Multiple range and multiple *F* test. *Biometrics* 11:1–42
30. Nakatsugawa K, Kaneda T (1980) Absorption of methyl linolate hydroperoxides in rabbit. *J Jpn Oil Chem Soc* 30:74–77
31. Nakatsugawa K, Kaneda T (1983) Absorption and metabolism of methyl linolate hydroperoxides in rat. *J Jpn Oil Chem Soc* 32:361–366
32. Kandutsch AA, Heiniger HJ, Chen HW (1977) Effects of 25-hydroxycholesterol and 7-ketocholesterol, inhibitor of sterol synthesis, administered orally to mice. *Biochim Biophys Acta* 486:260–272
33. Koba K, Wakamatsu K, Obata K, Sugano M (1993) Effects of dietary proteins on linoleic acid desaturation and membrane fluidity in rats liver microsomes. *Lipids* 28:457–464
34. Hochgraf E, Mokady S, Cogan U (1997) Dietary oxidized linoleic acid modifies lipid composition of rat liver microsomes and increases their fluidity. *J Nutr* 127:681–686
35. Lahous Z, Astruc ME, Crastes de Paulet A (1988) Serum-induced arachidonic acid release and prostaglandin biosynthesis are potentiated by oxygenated sterols in NRK 49F cells. *Biochim Biophys Acta* 958:396–404
36. Lahous Z, Vial H, Michel F, Crastes de Paulet A, Astruc ME (1991) Oxysterol activation of arachidonic acid release and prostaglandin E2 biosynthesis in NRK 49F cells is partially dependent on protein kinase C activity. *Cell Signal* 3:559–567
37. Ruzaidi A, Amin I, Nawalyah AG, Hamid M, Faizul HA (2005) The effect of Malaysian cocoa extract on glucose levels and lipid profiles in diabetic rats. *J Ethnopharmacol* 98:55–60
38. Kobayashi M, Unno T, Suzuki Y, Nozawa A, Sagesaka Y, Kakuda T, Ikeda I (2005) Heat-epimerized tea catechin disease prevention. In: Rodriguez H, Cutler RG (eds) Critical reviews of oxidative stress and aging, advances in basic science, diagnostics and intervention, vol 1. World Scientific, Singapore, pp 640–660
39. Osada K, Suzuki T, Sami M, Ohta Y, Kanda T, Ikeda M (2006) Dose-dependent hypocholesterolemic actions of dietary apple polyphenol in rats fed cholesterol. *Lipids* 41:133–140



40. Bagchi D, Preuss HG (2002) Oligomeric proanthocyanidins in human health and disease prevention. In: Rodriguez H, Cutler RG (eds) *Critical reviews of oxidative stress and aging, advances in basic science, diagnostics and intervention*, vol 1. World Scientific, Singapore, pp 640–660
41. Shoji T, Masumoto S, Moriichi N, Akiyama H, Kanda T, Ohtake Y, Goda Y (2006) Apple procyanidin oligomers absorption in rats after oral administration: analysis of procyanidins in plasma using the porter method and high-performance liquid chromatography/tandem mass spectrometry. *J Agric Food Chem* 54:884–892
42. Anderson JW, Gustafson NJ (1988) Hypocholesterolemic effects of oat and bean products. *Am J Clin Nutr* 48:749–753
43. Ogata S, Fujimoto K, Iwakiri R, Matsunaga C, Ogawa Y, Koyama T, Sakai T (1997) Effect of polydextrose on absorption of triglyceride and cholesterol in mesenteric lymph-fistula rats. *Proc Soc Exp Biol Med* 215:53–58
44. Hamada T, Goto H, Yamahira T, Sugawara T, Imaizumi K, Ikeda I (2006) Solubility in and affinity for the bile salt micelle of plant sterols are important determinants of their intestinal absorption in rats. *Lipids* 41:551–556

## Intestinal Epithelial Cells Absorb $\gamma$ -Tocotrienol Faster than $\alpha$ -Tocopherol

Wakako Tsuzuki · Ritsuko Yunoki ·  
Hiroyuki Yoshimura

Received: 11 September 2006 / Accepted: 28 December 2006 / Published online: 31 January 2007  
© AOCS 2007

**Abstract** To elucidate the transepithelial transport characteristics of lipophilic compounds, the cellular uptake of tocopherol and tocotrienol isomers were investigated in Caco2 cell monolayer models. These vitamin E isomers formed mixed micelles consisting of bile salts, lysophospholipids, free fatty acid, and 2-monoacylglycerols, then the micelles were supplied to Caco2 cells. The initial accumulation of tocotrienol isomers in Caco2 cells was larger than those of corresponding tocopherol isomers. There was little difference among the cellular accumulations of four tocopherol isomers. These findings suggested that the difference between the molecular structures of the C16 hydrocarbon chain tail in tocopherol and tocotrienol was strongly responsible for the rapid epithelial transport into the Caco2 cells membranes rather than the difference in the molecular structures of their chromanol head groups. Furthermore, the secretion of  $\alpha$ -tocopherol and  $\gamma$ -tocotrienol from Caco2 cells was investigated using Caco2 cells plated on a transwell. The time courses of their secretions from Caco2 cells showed that the initial secretion rate of  $\gamma$ -tocotrienol was also larger than that of  $\alpha$ -tocopherol. To investigate the intestinal uptake of  $\alpha$ -tocopherol and  $\gamma$ -tocotrienol in vivo, the mice were fed single doses of  $\alpha$ -tocopherol or  $\gamma$ -tocotrienol with triolein. The  $\gamma$ -tocotrienol responded faster in plasma than  $\alpha$ -tocopherol,

although the maximal level of  $\gamma$ -tocotrienol was lower than that of  $\alpha$ -tocopherol. This suggested that the intestinal uptake properties of administered  $\alpha$ -tocopherol and  $\gamma$ -tocotrienol would characterize their plasma level transitions in mice.

**Keywords** Tocopherol · Tocotrienol · Caco2 cells · Absorption

### Introduction

Vitamin E is known as a lipolytic antioxidant and is therefore important for people to take, whether through foods or supplements [1]. Vitamin E deficiency leads to severe degenerative diseases such as ataxia, infertility, and Duchine-like muscle degeneration [2]. Oxidative stress is a source of pathological problems [3, 4]. Vitamin E is a generic descriptor for all tocopherol and tocotrienol derivatives. Each tocopherol consists of a phytyl tail with three chiral centers in an R-configuration and a chromanol ring ( $\alpha$ -,  $\beta$ -,  $\gamma$ -, and  $\delta$ -) varying in the number and position of methyl groups on them. On the other hand, tocotrienol possesses an isoprenoid side chain [5]. Among these eight vitamin E derivatives,  $\alpha$ -tocopherol is known as the most abundant and the most powerful active form of vitamin E in vivo. Its high level of biological activity is supposed to be correlated with its strong affinity for  $\alpha$ -tocopherol transfer protein ( $\alpha$ -TTP) [6].

In addition to its lipophilic antioxidant activity, vitamin E was recently found to possess beneficial functions in human health that are independent of its antioxidant/radical scavenging abilities. These are called beyond-antioxidant functions. The roles of

W. Tsuzuki (✉) · R. Yunoki  
National Food Research Institute, Kannondai 2-1-12,  
Tsukuba, Ibaraki 305-8642, Japan  
e-mail: wakako@affrc.go.jp

H. Yoshimura  
Eisai Food and Chemical Co. Ltd., Nihonbashi 2-13-10,  
Chuo-ku, Tokyo 103-0027, Japan

vitamin E derivatives except  $\alpha$ -tocopherol have therefore received renewed attention [7, 8]. In particular, tocotrienol has exhibited widely varying degrees of biological effectiveness [9–11]. For example,  $\alpha$ -tocotrienol and  $\gamma$ -tocotrienol were more effective than  $\alpha$ -tocopherol in preventing glutamate-induced neuronal cell death by regulating signal transduction processes [12]. It has been pointed out that the superiority of these tocotrienol functions over those of  $\alpha$ -tocopherol against various cultured cell membranes would be responsible for the efficient transfer of tocotrienol into these cells [12–14].

Now more information on the absorption properties of dietary vitamin E derivatives by epithelial cells of the intestine is required to further understand their variations in biological actions. Since vitamin E is a lipophilic compound, it must be dissolved in mixed micelles before intestinal uptake [15]. Although the uptake by intestinal epithelial cells is a rate-limiting step throughout the entire process of dietary lipolytic component metabolism, the detailed absorption processes of vitamin E in mixed micelles have not been fully revealed. Previous reports suggested a simple diffusion mechanism for the cellular uptake of emulsified vitamin E by intestinal cells [16, 17]. Moreover, no transporter proteins for vitamin E absorption have been identified in intestinal cells so far.

In this study, we investigate the intestinal absorption properties of tocopherol and tocotrienol in the model system of Caco2 cells derived from human colonic carcinoma. In the previous studies, the serum concentration changes of the rat fed  $\alpha$ -tocopherol or  $\alpha$ -tocotrienol were traced [18]. In the other case,  $\alpha$ -tocotrienol and  $\gamma$ -tocotrienol were used for their uptake experiments by rats [19]. We here evaluate the plasmatic change of  $\alpha$ -tocopherol and  $\gamma$ -tocotrienol in mice fed each with oil in order to clarify the *in vivo* effect of the difference in molecular structure between them upon their intestinal uptake.

## Materials and Methods

### Materials

Several acylglycerols and free fatty acids were purchased from Funakoshi Co. (Tokyo, Japan). The micelle mixture components—lysophosphatidylcholine (1-palmitoyl-*sn*-glycero-3-phosphocholine) (LysoPC) and taurodeoxycholic acid sodium salt (Tau) were obtained from Sigma Chemical (St. Louis, MO, USA). Tocopherol and tocotrienol isomers were obtained from Merck (Darmstadt, Germany) and American River (Boston,

USA).  $\gamma$ -Tocotrienol was kindly supplied by Eisai Co. Ltd. (Tokyo, Japan). Other chemicals and solvents of analytical grade were purchased from Wako Pure Chemical (Osaka, Japan) and Kanto Chemical (Tokyo, Japan).

### Cell Culture

Caco2 cells (American Type Culture Collection, Rockville, MD, USA) were maintained in 10-cm dishes (Corning Glass Works, Corning, NY, USA) containing Dulbecco's modified Eagle's medium (DMEM) supplemented with 10% fetal bovine serum, 4 mmol/L L-glutamine, 40,000 U/L penicillin, 40 mg/L streptomycin, and 1% non-essential amino acids. The cells were kept at 37 °C in a humidified atmosphere of 95% air and 5% CO<sub>2</sub>. The growth medium was replenished every 2 or 3 days. Cells were reseeded when the cell monolayers became semiconfluent. For the experiments, cells at passages 25–50 were seeded in 12-well plates at  $1.2 \times 10^5$  cells per well and grown under the same conditions as those described above. For experiments on tocopherol and tocotrienol secretion from Caco2 cells, cells were seeded in 6-transwell filter chambers (polycarbonate membrane, 0.4  $\mu$ m pore size, Costar, Cambridge, MA, USA) at  $1.0 \times 10^6$  cells per well. The experiments were performed at 20–22 days post-seeding.

### Preparation of Mixed Micelles

Tocopherols and tocotrienols were delivered as mixed micelles prepared by modified versions of previously described procedures [20]. Briefly, appropriate volumes of stock solutions of the components of mixed micelle, bile salts, lysophospholipid, lipid metabolites and tocopherols, were transferred to glass tubes, and the organic solvent was removed under a stream of argon. The residue was dissolved in serum-free DMEM to eliminate amphiphilic activity of serum, because lipolytic compound were dissolved into the mixed micelle *in vivo*. The medium was sonicated using a micro-equipped Astrason ultrasonic processor model W-380 (Heat-System Ultrasonics, Inc., Farmingdale, NY, USA) until a predefined particle size distribution was achieved. The final concentration of each component in the medium was as follows: 2 mmol/L Tau, 0.2 mmol/L LysoPC, 0.1 mmol/L 2-monoacylglycerol, and 0.1 mmol/L free fatty acids. The resultant solutions were optically clear. The weight-averaged particle sizes of the mixed micelles were determined from quasi-elastic light-scattering measurements (NICOMP model 380 ZLS; Particle Sizing Systems, Santa Barbara, CA,

USA). The particle diameters of the mixed micelles ranged from 20–100 nm.

#### Incubation of Caco2 Cells with Micellar Lipids and Vitamin E Isomers

The differentiated monolayers of Caco2 cells in a 12-well plate or on a 6-transwell plate were washed twice with 1.0 mL serum-free DMEM. For the epithelial absorption experiments, 2 mL of the medium containing mixed micelles of lipid metabolites and vitamin E isomers was supplied to each well, and the Caco2 cells were incubated for 2 h. For the epithelial secretion experiments, 2 mL of the same medium was poured into each apical side of the transwell, and 2.5 mL serum-free medium was added to the basolateral one, followed by incubation for the defined periods.

#### Extraction of Vitamin E Isomers from Caco2 Cells and Medium

After the Caco2 cells on the wells were incubated for the indicated time, the medium was removed and the cells were washed twice with 1.0 mL PBS containing 4 mmol/L Tau to remove surface-bonded lipolytic compounds, followed by two additional washings with 1.0 mL PBS. The washed cells were harvested in 1 mL PBS and collected by centrifugation at 1,000×g for 5 min at 4 °C. The supernatants were discarded, and the cell pellets were homogenized with a microtube in 1.0 mL PBS. An aliquot of each cell homogenate was taken to determine the protein content according to the method of Lowry et al. [21]. Total lipolytic fractions containing Tocopherol and Tocotrienol from Caco2 cells were extracted by the method of Folch et al. [22]. Briefly, 0.75 mL chloroform/methanol (2:1, v/v) was added to the cell homogenate (0.25 mL) and mixed with the solution in a vortex shaker (NSD-12, Nissinrika Ltd., Tokyo, Japan) for 5 min following centrifugation at 1,000×g for 2 min. The resultant lower layer of chloroform was withdrawn and transferred to another tube. The upper layer was similarly extracted with 0.75 mL chloroform/methanol (2:1, v/v). The chloroform layer was combined with the initial extract. The combined extract was dried under a stream of argon gas.

#### HPLC Analysis of Vitamin E Isomers

Tocopherol and tocotrienol in the extracts from the Caco2 cells and medium were quantified with an HPLC system consisting of an EYELA Model PLC-5D (Tokyo Rika Kikai Co. Ltd., Tokyo, Japan), a JASCO Model FP-821 spectrofluorometer (Tokyo, Japan), an

AS-8020 autosampler (Tosoh, Tokyo, Japan), and a Chromatopack C-RIA integrator (Shimadzu, Kyoto, Japan). Vitamin E isomers were separated on a TSK gel ODS-80Tm column (Tosoh), 4.6 × 150 mm. Ethanol/acetonitrile (50:50, v/v) was used as a mobile phase for the analysis. An isocratic analysis was performed at a flow rate of 0.8 mL/min. Vitamin E isomers were monitored with a fluorescent detector (excitation at 295 nm and emission at 325 nm). They were quantified from their peak areas by use of the standard curves of reference compounds.

#### Animal Breeding and Vitamin E Administration

Animal breeding and experiments were entrusted to Sunplanet Co., Ltd. (Gifu, Japan). Male SicSD mice (6-weeks-old) obtained from Japan SLC Co. Ltd., (Shizuoka, Japan) were housed at 23 ± 2 °C on a 12 h light/dark cycle. The animals had free access to tap water and a commercially available diet (MF, Oriental Yeast Co. Ltd., Tokyo, Japan). The mice were handled according to the guidelines for experimental animals of Sunplanet Co. Ltd., Gifu, Japan.

After 7 days of feeding, the mice were divided into two groups ( $\alpha$ -tocopherol and  $\gamma$ -tocotrienol) according to the method of Statlight #11 (Yukmus Co. Ltd.). Fasting was not conducted before  $\alpha$ -tocopherol and  $\gamma$ -tocotrienol administration. Each group was fed  $\alpha$ -tocopherol (10 mg) or  $\gamma$ -tocotrienol (10 mg) diluted with 50 mg triolein. Mice in the zero-time control ( $n = 6$ ) and in two groups ( $n = 6$ /time point) at 2, 4, 6, 8, and 24 h after feeding were anesthetized with diethyl ether. Blood was collected from the caudal vena cava with a heparinized syringe. Plasma was immediately separated by centrifugation at 1,000×g for 15 min at 4 °C and then was immediately stored at –80 °C until analyzed.

#### Extraction from Plasma

$\alpha$ -Tocopherol and  $\gamma$ -tocotrienol were extracted from the plasma according to the procedures of Satomura et al. [23] with slight modifications. Briefly, the plasma (0.4 mL) was diluted to 0.8 mL with ice-cold deionized water, and 2.4 mL of chloroform/methanol (1:2, vol/vol) containing 0.2 pmol PMC (2,2,5,7,8-pentamethyl-6-hydroxy-chroman) as an internal standard for HPLC analysis was added and mixed vigorously using a vortex mixer. Then 1.2 mL of hexane was mixed with the solution. The resultant upper layer of hexane/chloroform was withdrawn. The extraction procedure was repeated for the lower layer one more time. The combined extract was evaporated until dry under a

stream of argon gas. The determination of  $\alpha$ -tocopherol and  $\gamma$ -tocotrienol in the plasma extracts was conducted by fluorometric HPLC as described above.

### Statistical Analysis

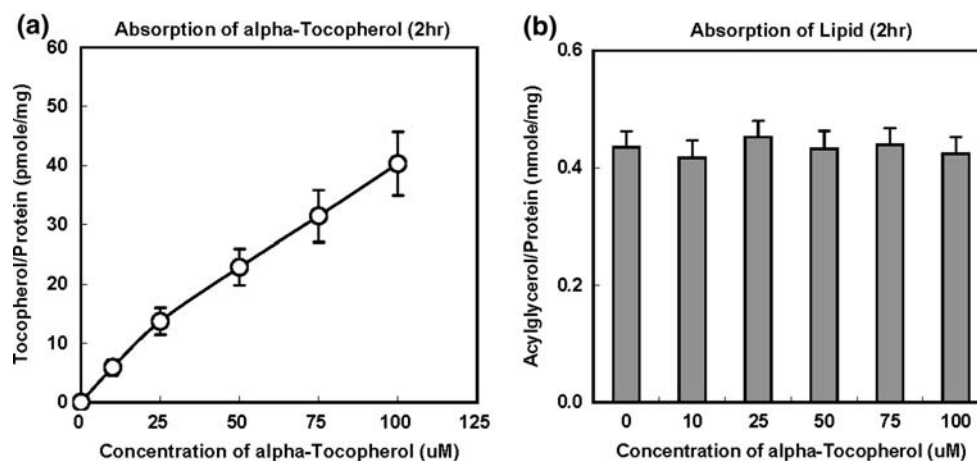
The data represent means  $\pm$ SD. Statistical analysis was made by one-way ANOVA and Dunnett's or Scheffe's F-test to identify significant differences between the groups.

## Results

### Effect of $\alpha$ -Tocopherol Concentration in the Mixed Micelles on its Absorption by Caco2 Cells

In vivo, lipophilic compounds such as a vitamin E are solubilized in mixed micelles before the intestinal uptake [15]. In this experiment, each vitamin E isomer formed mixed micelles with lipid metabolites, bile salts, and lysophospholipid, and the micelles were supplied to Caco2 cells monocultured in the wells to find the appropriate experimental condition of the absorption by Caco2 cells. The concentration of  $\alpha$ -tocopherol in the mixed micelles was varied from 0–100  $\mu$ M. After 2 h incubation with the mixed micelles, the cellular  $\alpha$ -tocopherol concentration was measured. As shown in Fig. 1a, the absorption of  $\alpha$ -tocopherol increased depending on its concentration in the mixed micelles. Based on this result, the concentration of  $\alpha$ -tocopherol in the mixed micelles was set at 50  $\mu$ M. In the examined concentration range of  $\alpha$ -tocopherol, no effect was detected on the absorption of lipid metabolites, as shown in Fig. 1b. This suggested that the transfer mechanism of lipid metabolites (oleic acid and 2-monoolein) to Caco2 cells from the mixed micelles was completely independent from that of  $\alpha$ -tocopherol.

**Fig. 1** The accumulation amount of the cellular  $\alpha$ -tocopherol (**a**) and acylglycerol (**b**) in the Caco2 cells incubated with various concentration of  $\alpha$ -tocopherol in the mixed micelles for 2 h. The mixed micelle was composed of 2-monoacylglycerols (0.1 mmol/L), oleic acid (0.1 mmol/L), bile salt (2.0 mmol/L) and lysophosphatidylcholine (0.2 mmol/L) in addition to  $\alpha$ -tocopherol (0, 20, 40, 60, 80, 100 mmol/L)



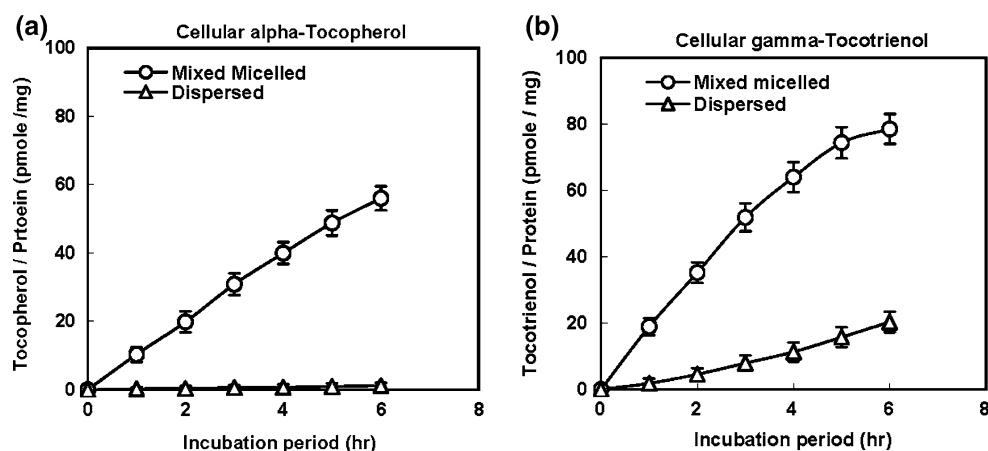
### Time Courses of the Absorption of $\alpha$ -Tocopherol and $\gamma$ -Tocotrienol by Caco2 Cells

To elucidate the comparative intake of  $\alpha$ -tocopherol and  $\gamma$ -tocotrienol by Caco2 cells, the time courses of their cellular concentrations were monitored. In the cases of  $\alpha$ -tocopherol and  $\gamma$ -tocotrienol contained in the mixed micelles, the cellular concentration of  $\gamma$ -tocotrienol increased more rapidly than that of  $\alpha$ -tocopherol (Fig. 2a, b). For example, the cellular concentrations of  $\alpha$ -tocopherol and  $\gamma$ -tocotrienol after 4 h incubation with each of the mixed micelles were 40.0  $\mu$ g/mg and 64.0  $\mu$ g/mg, respectively. The significant difference in the initial cellular accumulation between  $\alpha$ -tocopherol and  $\gamma$ -tocotrienol was more conspicuous in the case of Caco2 cells supplied by the dispersed  $\alpha$ -tocopherol and  $\gamma$ -tocotrienol than by the mixed-micellar ones (Fig. 2a, b). When the dispersed  $\alpha$ -tocopherol was supplied to the Caco2 cells, no increase was found in the cellular  $\alpha$ -tocopherol concentration, which meant that  $\alpha$ -tocopherol dispersed in the medium could scarcely transfer to the Caco2 cells (Fig. 2a). On the other hand, the cellular concentration of  $\gamma$ -tocotrienol increased gradually depending on the incubation period, when Caco2 cells were incubated with the dispersed  $\gamma$ -tocotrienol in the medium (Fig. 2b). This indicated that Caco2 cells could absorb not only the mixed-micellar  $\gamma$ -tocotrienol but also the dispersed one. However, the transfer rate of the dispersed  $\gamma$ -tocotrienol was considerably lower than that of the micellar one.

### Comparison of Absorption of Tocopherols and Tocotrienol Isomers by Caco2 Cells

Four tocopherol and tocotrienol isomers formed mixed micelles and were incubated with Caco2 cells to compare their initial absorption by Caco2 cells. After 2, 4 and 6 h incubation of mixed micelles, the cellular

**Fig. 2** Time course of accumulation of  $\alpha$ -tocopherol (a) and  $\gamma$ -tocotrienol (b) in Caco2 cells. The cells were incubated with mixed-micelled  $\alpha$ -tocopherol ((open circle) in a), with mixed-micelled  $\gamma$ -tocotrienol ((open circle) in b), with the dispersed  $\alpha$ -tocopherol ((open triangle) in a) and with the dispersed  $\gamma$ -tocotrienol ((open triangle) in b)



concentrations of these isomers were measured. As shown in Fig. 3a, there was a little difference in the incipient cellular concentrations among the four tocopherol isomers. Such tendency was also found among four tocotrienol isomers (Fig. 3b). Meanwhile, the cellular concentration of each tocotrienol isomer at each incubation period was significantly larger than those of the corresponding tocopherol isomers. This suggested that the molecular structure of C16 hydrocarbon chain tail, but not that of the chromanol ring of vitamin E isomers, was responsible for their initial transfer from mixed micelles to Caco2 cells.

#### Time Course of the Secretion of $\alpha$ -Tocopherol and $\gamma$ -Tocotrienol from Caco2 Cells

To characterize the secretion of vitamin E isomers from Caco2 cells, the cell monolayer fixed on a polycarbonated transmembrane was used.  $\alpha$ -Tocopherol

and  $\gamma$ -tocotrienol secreted into basolateral medium were measured at definite times after the mixed micelles were added in the apical medium. Both  $\alpha$ -tocopherol and  $\gamma$ -tocotrienol started to be secreted from Caco2 cells after 2 h incubation with the mixed micelles, as shown in Fig. 4. The secretion of  $\gamma$ -tocotrienol was quantitatively larger than that of  $\alpha$ -tocopherol in this initial period of secretion. Especially, the ratio of  $\gamma$ -tocotrienol to  $\alpha$ -tocopherol values secreted from Caco2 cells were 2.29-fold and 1.62-fold at 2 and 4 h after incubation, respectively (Fig. 4). In the absorption experiments using Caco2 cells described above,  $\gamma$ -Tocotrienol in the mixed micelles transferred into Caco2 cells more rapidly than  $\alpha$ -tocopherol. Such absorption of  $\alpha$ -tocopherol and  $\gamma$ -tocotrienol by Caco2 cells would characterize each secretion from Caco2 cells into the basolateral medium. This indicated that the  $\gamma$ -tocotrienol transferred throughout the membrane of Caco2 cells faster than  $\alpha$ -tocopherol did.

**Fig. 3** The accumulation amount of the tocopherol and tocotrienol isomers in the Caco2 cells. The cells were incubated with mixed-micelled each isomer for 0, 2, 4 and 6 h

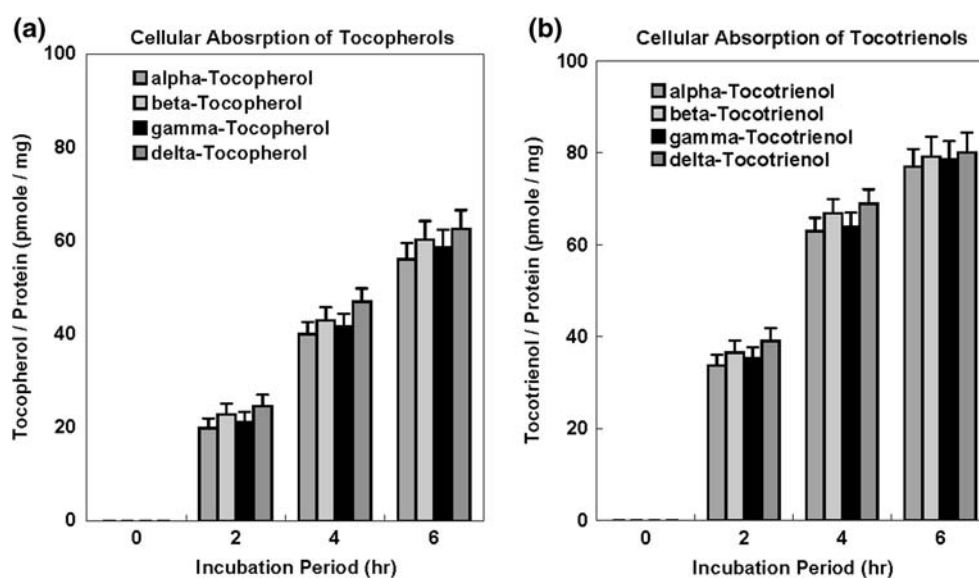
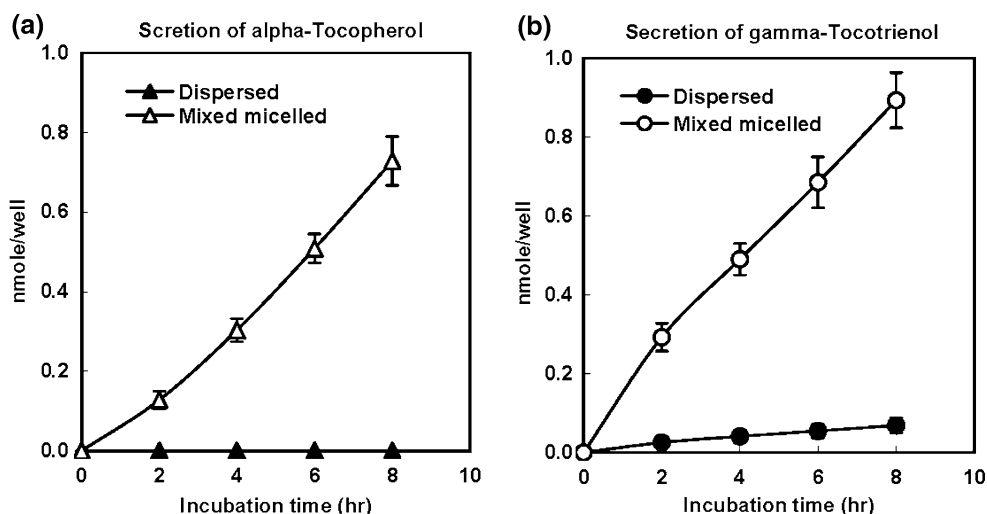


**Fig. 4** Time course of secretion of  $\alpha$ -tocopherol (a) and  $\gamma$ -tocotrienol (b) from Caco<sub>2</sub> cells to the basolateral medium. The cells were incubated with mixed-micelled  $\alpha$ -tocopherol ((open triangle) in a), with mixed-micelled  $\gamma$ -tocotrienol ((open circle) in b), with the dispersed  $\alpha$ -tocopherol ((filled triangle) in a) and with the dispersed  $\gamma$ -tocotrienol ((filled circle) in b)



When the Caco<sub>2</sub> cells were incubated with the dispersed  $\alpha$ -tocopherol instead of the micellar one, no  $\alpha$ -tocopherol was detected in the basolateral medium in the examined period (Fig. 4a). On the other hand, some  $\gamma$ -tocotrienol secretion from Caco<sub>2</sub> cells was detected, depending on the incubation period with the dispersed  $\gamma$ -tocotrienol (Fig. 4b). A quantitative comparison of the secreted  $\gamma$ -tocotrienol from Caco<sub>2</sub> cells supplied by the dispersed  $\gamma$ -tocotrienol with that supplied by the micellar one suggested that the solubilization of  $\gamma$ -tocotrienol into the mixed micelles was significant for its efficient transfer throughout the Caco<sub>2</sub> cells.

#### The Plasma Response of $\alpha$ -Tocopherol and $\gamma$ -Tocotrienol in Mice

To study the intestinal uptake of  $\alpha$ -tocopherol and  $\gamma$ -tocotrienol in mice administrated by them, their concentrations in plasma were monitored at 0, 1, 2, 4, 6, 8, and 24 h after oral administration (Fig. 5). Only  $\alpha$ -Tocopherol was detected in the plasma of mice in both groups at 0 h ( $20.5 \pm 0.5$  nM, data not shown), because no nutritional restraint was conducted in the mouse food prior to this experiment. During the initial 1–2 h after the administration, the increase of  $\gamma$ -tocotrienol level in plasma was abrupt, whereas the  $\alpha$ -tocopherol level in the plasma gradually increased with some lag time. The  $\alpha$ -tocopherol level in plasma was optimum ( $31.3 \pm 1.6$  nM) at 6–8 h after administration. On the other hand, the  $\gamma$ -tocotrienol level reached a maximum of  $7.96 \pm 0.89$  nM at 2–4 h, which suggested that the increase rate of the  $\gamma$ -tocotrienol level in plasma was larger than that of  $\alpha$ -tocopherol. The  $\gamma$ -tocotrienol level peaked at 6 h after administration and then immediately decreased. Thus, the faster response of the  $\gamma$ -tocotrienol

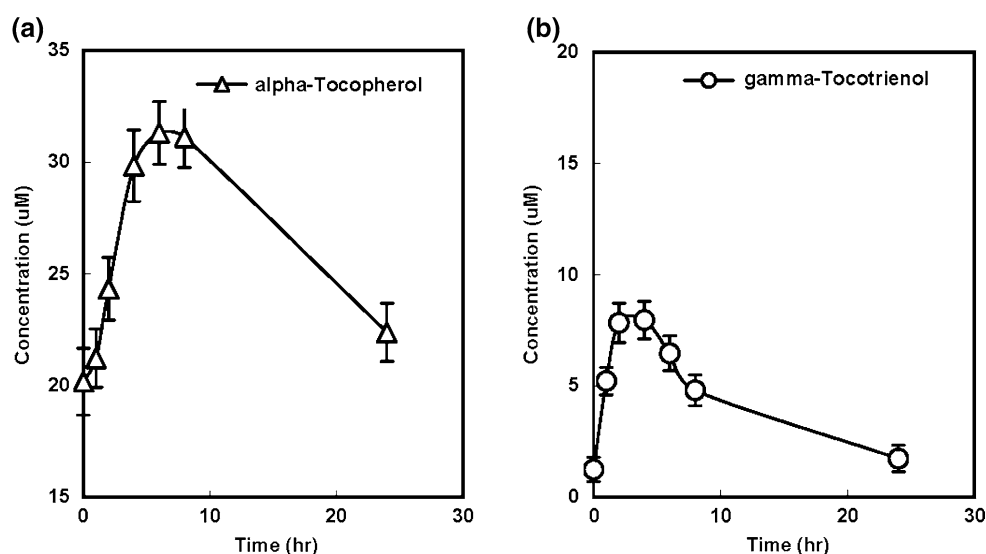
level in rat plasma compared to that of  $\alpha$ -tocopherol would reflect the rapid intestinal uptake of  $\gamma$ -tocotrienol.

#### Discussion

In the digestion processes, lipophilic compounds released from the food matrix are dispersed in lipid emulsion followed by solubilization into the mixed micelles containing bile salts. The mixed micelles move across the unstirred water layer adjacent to the cells of intestinal mucosa [15, 24]. The intestinal cellular uptake of tocopherol and tocotrienol isomers is thought to be mediated by a simple diffusion mechanism [16, 17]. Mixed micelle formation in the intestinal lumen plays an important role in the absorption not only of digested lipid but also of other lipophilic compounds.

In a previous study, the uptake and metabolism of isotope-labeled  $\alpha$ -tocopherol were compared with those of isotope-labeled  $\gamma$ -tocopherol using rats [18]. They concluded that the uptake of both tocopherols in rat was similar although there was a difference between the concentrations of them. Furthermore,  $\alpha$ -tocopherol and  $\alpha$ -tocotrienol concentrations of the plasma in the rats fed them were investigated and they found no difference between the uptake rates [19]. So, in the present study, the intestinal uptake of  $\alpha$ -tocopherol and  $\gamma$ -tocotrienol was compared. The most significant finding in this study was that  $\gamma$ -tocotrienol was more readily transferred to the intestinal cell membrane than  $\alpha$ -tocopherol in the Caco<sub>2</sub> cell model or in the rat administration experiments. This result is in accordance with the previous finding that tocotrienol isomers were more readily incorporated into various kinds of culture cells than tocopherol isomers [12, 14, 25–28]. Those studies concluded that the inter-membrane

**Fig. 5** Time course of concentrations of  $\alpha$ -tocopherol (a) and  $\gamma$ -tocotrienol (b) in the serum of the mice administered with these isomers



mobility of  $\gamma$ -tocotrienol was greater than that of tocopherol isomers [27]. The present study is the first to demonstrate the superior trans-membrane movement of tocotrienol isomers to tocopherol ones in Caco2 cells, human colonic carcinoma cells. In particular, these cells absorbed  $\gamma$ -tocotrienol dispersed in the medium but did not absorb dispersed  $\alpha$ -tocopherol isomers (Fig. 4). Even when tocopherol and tocotrienol isomers formed mixed micelles by bile salt and lysophospholipid, the transfer rate of tocotrienol isomers into Caco2 cells from the mixed micelles was faster than those of Tocopherol isomers (Fig. 4). On the other hand, there was no difference in the transfer rates of tocopherol isomers through the Caco2 cell membrane. This result was in good accordance with previous findings that the tocopherol isomers were taken up in equal amounts by epithelial cells in an unspecified process [29]. Tocopherol has a phytyl chain in its molecule, whereas tocotrienol possesses an isoprenoid chain with three double bonds at positions 3', 7', and 11'. A previous study suggested that the difference in the 16 carbonate chain between tocopherol and tocotrienol contributed to the larger inter-membrane mobility of tocotrienol compared with those of tocopherol isomers [27]. The results of the present study are supported by this previous explanation in the case of Caco2 cells.

Tocopherol and tocotrienol isomers are transported in chylomicrons from the intestine and subsequently in remnants to the liver. There, only  $\alpha$ -tocopherol is preferentially carried stereo-selectively by the cytosolic protein  $\alpha$ -tocopherol transfer protein ( $\alpha$ -TTP) to a very low-density lipoprotein, and then they are released into the circulation [32, 33]. These facts were confirmed by isotope-labeling studies [6, 30–32]. In fact, previous

studies reported that the  $\alpha$ -TTP binding affinity of  $\gamma$ -tocotrienol was about one-eighth of that of  $\alpha$ -tocopherol [6]. Tocotrienols are transported nonspecifically like other lipophilic compounds and the are dominantly found in a high-density lipoprotein fraction [15, 33, 34]. In the animal experiment in the present study, mice were administered an excessively large amount of non-isotope-labeled  $\alpha$ -tocopherol and  $\gamma$ -tocotrienol (10 mg per mouse), so that the time-dependent changes in their serum concentration could be successfully traced. The absolute serum concentration of  $\gamma$ -tocotrienol (from 1.24 to 7.96  $\mu\text{g}/\text{mL}$ ) in recipient mice was smaller than that of  $\alpha$ -tocopherol (from 20.1 to 31.3  $\mu\text{g}/\text{mL}$ ) as shown in Fig. 5. This comes from the difference in binding affinity  $\alpha$ -TTP between  $\alpha$ -tocopherol and  $\gamma$ -tocotrienol and in their circulation pathway in vivo between VLDL and HLD transports. However,  $\gamma$ -tocotrienol appeared in the mouse serum more rapidly than  $\alpha$ -tocopherol and increased at a faster rate. From the results of the present study, it was concluded that the epithelial transfer rates of  $\gamma$ -tocotrienol and  $\alpha$ -tocopherol in the absorption step in the intestine would reflect their serum circulation characteristics. On the other hand,  $\gamma$ -tocotrienol was cleared more rapidly from the plasma of mice than was the case with  $\alpha$ -tocopherol. That fact is probably due to the low affinity of tocotrienol to  $\alpha$ -TTP.

Because  $\alpha$ -TTP binds preferentially to  $\alpha$ -tocopherol compared to other tocopherol and tocotrienol isomers, the biological effectiveness of  $\alpha$ -tocopherol has been dominant [30, 32]. However, various bioactivities, beyond antioxidant functions, of tocopherol and tocotrienol isomers, have recently been reported [35, 36]. Several biological activities of tocotrienol isomers were reported to be more effective than those of tocopherol



isomers [12, 26–28]. Further information about the digestive behaviors of tocopherol and tocotrienol isomers will be needed in the near future so that their advanced use can be considered.

## References

- Halliwell B, Gutteridge JMC (1985) Free radicals in biology and medicine. Clarendon Press, Oxford
- Sies H (1991) Oxidative stress: oxidants and antioxidants. Academic, London
- IUPAC-IUB Joint Commission on Biochemical Nomenclature (JCBN) (1982) Nomenclature of tocopherols and related compounds. Recommendations 1981. Eur J Biochem 123:473–475
- Papas AM (1999) Antioxidant status, diet, nutrition, and health. CRC Press, Boca Raton
- Machlin LJ (1991) Handbook of vitamins. 2 edn. Marcel Dekker, New York, pp 99–144
- Hosomi A, Arita M, Sato Y, Kiyose C, Ueda T, Igarashi O, Arai H, Inoue K (1997) Affinity for  $\alpha$ -tocopherol transfer protein as a determinant of the biological activities of vitamin E analogs. FEBS Lett 409:105–108
- Servinova E, Kagan V, Han D, Parcke L (1991) Free radical recycling and intramembrane mobility in the antioxidant properties of  $\alpha$ -tocopherol and  $\alpha$ -tocotrienol. Free Rad Biol Med 10:263–275
- Suzuki YJ, Tsuchiya M, Wassall SR, Choo YM, Govil G, Kagan VE, Packer L (1993) Structural and dynamic membrane properties of  $\alpha$ -tocopherol and  $\alpha$ -tocotrienol: implication to the molecular mechanism of their antioxidant potency. Biochemistry 32:10692–10699
- Kamart JP, Devasagayam TP (1995) Tocotrienols from palm oil as potent inhibitors of lipid-peroxidation and protein oxidation in rat-brain mitochondria. Neurosci Lett 195:179–182
- Black TM, Wang R, Maeda N, Coleman RA (2000) Palm tocotrienols protect ApoE<sup>+/−</sup> mice from diet-induced atherosclerosis formation. J Nutr 130:2420–2426
- Xu AM, Hua N, Gadber JS (2001) Antioxidant activity of tocopherols, tocotrienols and  $\gamma$ -oryzanol components from rice bran against cholesterol oxidation accelerated by 2,2-azobis(2-methylpropionamide) dihydrochloride. J Agr Food Chem 49:2077–2081
- Sen CK, Khanna S, Roy S, Packer LJ (2000) Tocotrienol potently inhibits glucamine-induced pp60c-Src kinase activation and death of HT4 neuronal cells. Biol Chem 275:13049–13055
- McIntyre BS, Briski KP, Timenstein MA, Fariss MW, Gapor A, Sylvester PW (2000) Antiproliferative and apoptotic effects of tocopherols and tocotrienols on normal mouse mammary epithelial cells. Lipids 35:171–180
- Saito Y, Yoshida Y, Akazawa T, Takahashi K, Niki E, (2003) Cell death caused by selenium deficiency and protective effect of antioxidants. J Biol Chem 278:39428–39434
- Traber MG, Ingold KU, Burton GW, Kayden HJ (1988) Absorption and transport of deuterium-substituted 2R, 4'R, 8'R- $\alpha$ -tocopherol in human lipoproteins. Lipids 23:791–797
- Hopfer U (1992) Digestion and absorption of basic nutritional constituents. In: Devlin TM (eds) Textbook of biochemistry with clinical correlation. Wiley-Liss, New York, pp 1059–1091
- Verkade HJ, Tso P (2001) Biophysics of intestinal luminal lipids. In: Mansbach CM II, Tso P, Kuksis A (eds) Intestinal lipid metabolism. Kluwer Academic, Plenum, pp 1–18
- Peake IR, Biere JG (1971) Alpha- and gamma- tocopherol in the rat: in vitro and in vivo tissue uptake and metabolism. J Nutr 101:1615–1622
- Yamashita K, Ikeda S, Iizuka Y, Ikeda I (2002) Effect of sesaminol on plasma and tissue  $\alpha$ -tocopherol and  $\alpha$ -tocotrienol concentration in rats fed a vitamin E concentrate rich in tocotrienols. Lipids 37:351–358
- Garrett AD, Failla ML, Sarama RJ, Craft N (1999) Accumulation and retention of  $\beta$ -carotene and lutein by Caco-2 human intestinal cells. J Nutr Biochem 10:573–581
- Lowry OH, Rosebrough NJ, Farr AL, Randall RJ (1951) Protein measurement with the folin phenol reagent. J Biol Chem 193:265–275
- Folch J, Lees M, Sloane-Stanley GH (1957) A simple method for the isolation and purification of total lipids from animal tissues. J Biol Chem 226:497–509
- Satomura Y, Kimura M, Hiraike H, Iyokawa Y (1993) A method for simultaneous determination of retinol and tocopherol homologues and its application to biological specimens. Vitamins 67:111–119
- Murphy DJ, Mavis RD (1981) Membrane transfer of  $\alpha$ -tocopherol. J Biol Chem 256:10464–10468
- Kiyose C, Muramatsu R, Ueda T, Igarashi O (1995) Change in the distribution of  $\alpha$ -tocopherol stereoisomers in rats after intravenous administration. Biosci Biotech Biochem 59:791–795
- McIntyre BS, Briski KP, Timenstein MA, Fariss MW, Gapor A, Sylvester PW (2000) Antiproliferative and apoptotic effects of tocopherols and tocotrienols on normal mouse mammary epithelial cells. Lipids 35:171–180
- Yoshida Y, Niki E, Noguchi N (2003) Comparative study on the action of tocopherols and tocotrienols as antioxidant: chemical and physical effects. Chem Phys Lipids 123:63–75
- Kogure K, Fukazawa K (2004) Tocopheryl succinate-versatile functions due to its unique physicochemical properties. J Clin Biochem Nutr 35:29–34
- Gallo-Torres HE (1970) Obligatory role of bile for the intestinal absorption of vitamin E. Lipids 5:379–384
- Behrens WA, Madere R (1982) Transfer of  $\alpha$ -tocopherol to microsomes mediated by a purified liver  $\alpha$ -tocopherol binding protein. Nutr Res 2:611–618
- Ingold KU, Burton GW, Foster DO, Hughers L, Lindsay D, Webb A (1987) Biokinetics of discrimination between dietary RRR- and SRR- alpha-tocopherols in the male rat. Lipids 22:163–172
- Sato Y, Hagiwara K, Arai H, Inoue K (1991) Purification and characterization of the  $\alpha$ -tocopherol transfer protein from rat liver. FEBS Lett 288:41–45
- Burton GW, Traber MG, Acuff RV, Walters DN, Kayden H, Hughes L, Ingold KU (1988) Human plasma and tissue alpha-Tocopherol concentrations in response to supplementation with deuterated natural and synthetic vitamin E. Am J Clin Nutr 67:669–684
- Traber MG, Ingold KU, Burton GW, Ingold KU, Papas AM, Huffaker JE, Kayden HJ (1990) Impaired ability of patients with familial isolated vitamin E deficiency to incorporate alpha-tocopherol into lipoproteins secreted by the liver. J Clin Invest 85:397–407
- Sen CK, Khanna S, Roy S, Packer L (2000) Molecular basis of vitamin E action. J Biol Chem 275:13049–13055
- Khanna S, Roy S, Ryu H, Bahadduri P, Swaan PW, Ratan RR, Sen CK (2003) Molecular basis of vitamin E action. J Biol Chem 278:43508–43515

# Reaction of $\gamma$ -Tocopherol with Hypochlorous Acid

Quyên Nguyen · Peter T. Southwell-Keely

Received: 23 October 2006 / Accepted: 15 December 2006 / Published online: 27 January 2007  
© AOCS 2007

**Abstract** In addition to being a very good antioxidant,  $\gamma$ -tocopherol is also an excellent electrophile trap. This is a study of the reactivity of  $\gamma$ -tocopherol with hypochlorous acid/hypochlorite, a potential biological foe that is both an oxidant and an electrophile. Aqueous sodium hypochlorite (1.72 mmol; pH 7.4) was stirred with  $\gamma$ -tocopherol (0.12 mmol) in hexane for 2 min at room temperature. The following products were isolated:  $\gamma$ -tocopheryl quinone (0.6%), tocopherol (10%), 3-chloro- $\gamma$ -tocopheryl quinone (14%), an ether dimer of 3-chloro- $\gamma$ -tocopheryl quinone (0.4%), two isomers of 5-(5- $\gamma$ -tocopheryl)- $\gamma$ -tocopherol (3 and 2% respectively), 5-chloro- $\gamma$ -tocopherol (14%) and two chlorinated dimers (14 and 24% respectively) which were identified as diastereomers of (3*R*,10*R*)-11a-chloro-2,3,9,10-tetrahydro-3,5,6,10,12,13-hexamethyl-3,10-bis[(4*R*,8*R*)-4,8,12-trimethyltridecyl]-1*H*-pyrano(3,2*a*)-8*H*-pyrano(3,2*g*)-dibenzofuran-14(7*aH*)(14*aH*)-one. The chlorinated dimers, 5-chloro- $\gamma$ -tocopherol, 3-chloro- $\gamma$ -tocopheryl quinone and its ether dimer are new compounds.

**Keywords**  $\gamma$ -Tocopherol · Hypochlorous acid · Oxidation · Antioxidants · Electrophiles · Chlorinated dimers

## Introduction

Although  $\alpha$ -tocopherol is the most widely available form of vitamin E, and the form found in pharmaceutical preparations, probably the most common form in Western diets is  $\gamma$ -tocopherol (**1**, Fig. 1), because of the widespread use of soybean in many food products. Compound **1** is an excellent antioxidant, although slightly inferior to  $\alpha$ -tocopherol. However, **1** has another string to its bow in that it is an excellent scavenger of electrophiles due to the lack of substitution at the 5-position. Thus **1** has been shown to react rapidly with nitrite and nitric oxide to produce 5-nitro- $\gamma$ -tocopherol in high yield [1].

Another electrophile (and oxidant) that **1** may encounter is hypochlorous acid (HOCl), the major and most powerful oxidant produced by the myeloperoxidase of neutrophils [2]. HOCl has been shown to react rapidly with 2,2,7,8-tetramethyl-6-chromanol, the model compound of  $\gamma$ -tocopherol, to form a dichloropyrano-benzenedione [3].

This study was undertaken to determine whether **1** reacted in the same way as its model compound with HOCl.

## Experimental Procedures

### Instrumental

Ultraviolet spectra were determined on a Varian (Palo Alto, CA, USA) Cary IE spectrophotometer.  $^1\text{H}$  and  $^{13}\text{C}$  NMR spectra were recorded on a Bruker (Karlsruhe, Germany) AM-500 or a DMX-600 FT-NMR spectrometer and were taken in  $\text{CDCl}_3$  and are

Q. Nguyen · P. T. Southwell-Keely  
School of Chemistry, University of New South Wales,  
Sydney, NSW 2052, Australia

P. T. Southwell-Keely (✉)  
157 Hopetoun Avenue, Vaucluse, NSW 2030, Australia  
e-mail: p.southwellkeely@unsw.edu.au

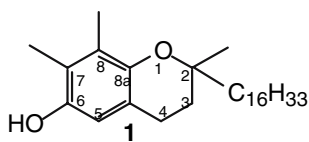


**Fig. 1**  $\gamma$ -Tocopherol

reported in parts per million downfield from tetramethylsilane used as internal standard. Heteronuclear single quantum correlation (HSQC) and heteronuclear multiple bond correlation (HMBC) techniques were used to assign correlations between  $^1\text{H}$  and  $^{13}\text{C}$  signals. Relative configuration was determined using nuclear Overhauser enhancement spectroscopy (NOESY).

Electron-impact mass spectra were determined on a Finnigan Polaris Q Ion-Trap mass spectrometer (Thermo Electron Corporation, Waltham, MA, USA), and ionisation was achieved with a 70 eV electron beam.

## Materials

*RRR*- $\gamma$ -Tocopherol and *RRR*- $\alpha$ -tocopheryl quinone (both from Acros Organics, Morris Plains, NJ, USA), sodium hypochlorite (NaOCl; 12.5% solution) and *n*-hexane (Spectrosol) (both from Asia Pacific Speciality Chemicals, NSW, Australia), and silica gel 60 GF254 (Merck, Darmstadt, Germany) were commercially available.

## Oxidation Reaction

In a typical reaction, **1** (50 mg, 0.12 mmol) was dissolved in hexane (3 mL) and stirred with NaOCl (128 mg, 1.72 mmol) in water (3 mL, adjusted to pH 7.4 with HCl) for 2 min at room temperature. The hexane layer was washed with water until neutral, dried ( $\text{Na}_2\text{SO}_4$ ), and the solvent removed in vacuo. The residue was chromatographed on thin layers of silica gel using light petroleum/ethyl acetate (19:1, v/v) as eluting solvent. Ten bands were observed with  $R_f$  values from 0.01 to 0.85. As all products were oily and complete removal of solvent from them could not be guaranteed, their yields were calculated using known molar extinction coefficients in ethanol, which were as follows (in units of  $\text{LM}^{-1}\text{cm}^{-1}$ ): for  $\gamma$ -tocopheryl quinone (**3**) at 262 nm, 19,000 (assumed similar to  $\alpha$ -tocopheryl quinone) [4], for tocored (**8**) at 281 nm (270 nm in hexane [5]) (6,500) [6], for 2,2,7,8-tetramethylchroman-5,6-dione, the model compound of **8**, at 467 nm (438 nm in hexane [5]), 1,200 [7], for 5-( $\gamma$ -tocopheryl)- $\gamma$ -tocopherol (**10**) ( $R_f$  0.48) at 300 nm 10,300

[6], and for its isomer (**5**) ( $R_f$  0.69) at 300 nm 10,500 [6]. The extinction coefficient of **1** at 298 nm, 3,802 [8], was also used to estimate 5-chloro- $\gamma$ -tocopherol (**4**) and the two chlorodimers, (**13** and **14**; bands 9 and 10). Both **8** and 3-chloro- $\gamma$ -tocopheryl quinone (**7**) have the same  $R_f$  values and are very difficult to separate, and both compounds absorb strongly at 270 nm. However, **8** can be estimated from its second, lower intensity, peak at 436 nm by using the molar extinction coefficient of 2,2,7,8-tetramethylchroman-5,6-dione at 467 nm (438 nm in hexane [5]), 1,200 [7]. From this amount and the known extinction coefficient of **8** at 281 nm (270 nm in hexane) (6,500) [6], the contribution of **8** to the total absorption at 270 nm can be calculated. The residual absorption is due to **7** and can be estimated using the extinction coefficient of **3**.

Compound **11** is believed to be an ether dimer of **7** and therefore an extinction coefficient of 38,000 for a molecular weight of 914 was used for it.

The yields thus calculated for all compounds are clearly approximate as most of the measurements were made in hexane solution rather than ethanol.

Band 1 ( $R_f$  0.01), which was not identified, had UV  $\lambda_{\text{max}}$  (in hexane) of 257 nm.

Band 2 ( $R_f$  0.03; pale yellow; 0.3 mg; 0.6%) was not completely pure but was identified as **3** ( $\gamma$ -tocopheryl quinone) on the basis of its spectral data: UV  $\lambda_{\text{max}}$  (in hexane) 257, 263 nm.  $^1\text{H}$  NMR  $\delta$  ( $\text{CDCl}_3$ ) 0.83–0.88, m, 12H,  $4 \times -\text{CH}_3$ ; 1.25, s, 3H,  $-\text{CH}_3$ ; 1.00–1.67, m, 23H,  $10 \times -\text{CH}_2 + 3 \times -\text{CH}$ ; 2.02, s, 3H,  $-\text{C}=\text{C}-\text{CH}_3$ ; 2.03, s, 3H,  $-\text{C}=\text{C}-\text{CH}_3$ ; 2.50, m, 2H, 2-(1'- $\text{CH}_2$ -); 6.54, s, 1H,  $-\text{C}=\text{C}-\text{H}$ .

Band 3 ( $R_f$  0.07; red) was identified as a mixture of **7** and **8**.

Compound **7** (3-chloro- $\gamma$ -tocopheryl quinone) (7.6 mg; 14%) had UV  $\lambda_{\text{max}}$  (in methanol) of 264 (sh) and 272 nm.  $^1\text{H}$  NMR  $\delta$  ( $\text{CDCl}_3$ ) 0.83–0.88, m, 12H,  $4 \times -\text{CH}_3$ ; 1.25, s, 3H,  $-\text{CH}_3$ ; 1.00–1.67, m, 23H,  $10 \times -\text{CH}_2 + 3 \times -\text{CH}$ ; 2.06, s, 3H,  $-\text{C}=\text{C}-\text{CH}_3$ ; 2.09, s, 3H,  $-\text{C}=\text{C}-\text{CH}_3$ ; 2.72, m, 2H, 2-(1'- $\text{CH}_2$ -). MS (ei)  $m/z$  (relative intensity) 452 (36), 451 (33), 450 (89), 244 (5), 243 (15), 242 (17), 241 (30), 227 (19), 225 (49), 200 (17), 199 (28), 198 (41), 187 (37), 186 (31), 185 (100), 184 (45).

Compound **8** (tocored) (5 mg; 10%) had UV  $\lambda_{\text{max}}$  (in hexane) of 268 and 436 nm.  $^1\text{H}$  NMR  $\delta$  ( $\text{CDCl}_3$ ) 0.83–0.88, m, 12H,  $4 \times -\text{CH}_3$ ; 1.00–1.67, m, 21H,  $9 \times -\text{CH}_2 + 3 \times -\text{CH}$ ; 1.32, s, 3H,  $-\text{CH}_3$ ; 1.74, m, 2H, 3- $\text{CH}_2$ ; 1.95, s, 3H,  $-\text{C}=\text{C}-\text{CH}_3$ ; 2.03, s, 3H,  $-\text{C}=\text{C}-\text{CH}_3$ ; 2.42, m, 2H, 4- $\text{CH}_2$ .

Band 4 ( $R_f$  0.24; colorless), was identified as **1**. It had UV  $\lambda_{\text{max}}$  (in hexane) of 294, 300 nm.  $^1\text{H}$  NMR  $\delta$  ( $\text{CDCl}_3$ ) 0.83–0.89, m, 12H,  $4 \times -\text{CH}_3$ ; 1.00–1.40, m,

19H, 8 × -CH<sub>2</sub> + 3 × -CH; 1.25, s, 3H, -CH<sub>3</sub>; 1.52, m, 2H, 1'-CH<sub>2</sub>; 1.71, m, 1H, (3-CH); 1.78, m, 1H, (3-CH); 2.12, s, 3H, Ar-CH<sub>3</sub>; 2.14, s, 3H, Ar-CH<sub>3</sub>; 2.68, m, 2H, 4-CH<sub>2</sub>; 4.23, s, 1H, -OH, 6.38, s, 1H, =C-H.

Band 5 (*R<sub>f</sub>* 0.42; 0.2 mg; 0.4%; colorless), was identified tentatively as **11**. It had UV λ<sub>max</sub> (in hexane) of 265 (sh) and 273 nm. <sup>1</sup>H NMR δ (CDCl<sub>3</sub>) 0.83–0.88, m, -CH<sub>3</sub>; 1.11, s, -CH<sub>3</sub>; 1.00–1.67, m, -CH<sub>2</sub> + -CH; 2.06, s, -C=C-CH<sub>3</sub>; 2.09, s, -C=C-CH<sub>3</sub>; 2.72, m, -(1'-CH<sub>2</sub>). MS (ei) *m/z* (relative intensity) 452 (14), 450 (33), 283 (17), 281 (54), 265 (19), 241 (7), 229 (26), 227 (50), 225 (74), 213 (16), 211 (67), 209 (100), 187 (12), 186 (10), 185 (35), 184 (15).

Band 6 (*R<sub>f</sub>* 0.48; colorless; 1.6 mg; 3%), was identified as **10** (5-(5-γ-tocopheryl)-γ-tocopherol) with “R” configuration. It had UV λ<sub>max</sub> (in hexane) 294 (sh), 302 nm. <sup>1</sup>H NMR δ (CDCl<sub>3</sub>) 0.83–0.88, m, 24H, 8 × -CH<sub>3</sub>; 1.00–1.40, m, 38H, 16 × -CH<sub>2</sub> + 6 × -CH; 1.24, s, 6H, 2 × -CH<sub>3</sub>; 1.52, m, 4H, 2 × (1'-CH<sub>2</sub>); 1.65, m, 2H, 2 × (3-CH); 1.68, m, 2H, 2 × (3-CH); 2.12, m, 2H, 2 × (4-CH); 2.18, s, 6H, 2 × Ar-CH<sub>3</sub>; 2.20, s, 6H, 2 × Ar-CH<sub>3</sub>; 2.29, m, 2H, 2 × (4-CH); 4.44, s, 2H, 2 × -OH. MS (ei) *m/z* (relative intensity) 830 (M<sup>+</sup>)(100), 564 (12), 299 (9), 285(14).

Band 7 (*R<sub>f</sub>* 0.69; colorless; 1 mg; 2%), was identified as **5** (5-(5-γ-tocopheryl)-γ-tocopherol) with “S” configuration. It had UV λ<sub>max</sub> (in hexane) of 301 nm. <sup>1</sup>H NMR δ (CDCl<sub>3</sub>) 0.83–0.88, m, 24H, 8 × -CH<sub>3</sub>; 1.00–1.40, m, 38H, 16 × -CH<sub>2</sub> + 6 × -CH; 1.22, s, 6H, 2 × -CH<sub>3</sub>; 1.52, m, 4H, 2 × (1'-CH<sub>2</sub>); 1.64, m, 2H, 2 × (3-CH); 1.71, m, 2H, 2 × (3-CH); 2.15, m, 2H, 2 × (4-CH); 2.18, s, 6H, 2 × Ar-CH<sub>3</sub>; 2.20, s, 6H, 2 × Ar-CH<sub>3</sub>; 2.27, m, 2H, 2 × (4-CH); 4.42, s, 2H, 2 × -OH. MS (ei) *m/z* (relative intensity) 830 (M<sup>+</sup>) (100), 564 (19).

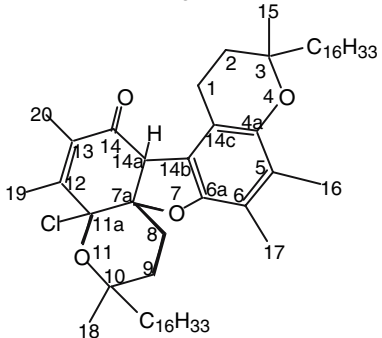
Band 8 (*R<sub>f</sub>* 0.76; colorless; 7.5 mg; 14%), was identified as **4** (5-chloro-γ-tocopherol). It had UV λ<sub>max</sub> (in hexane) of 299 nm. <sup>1</sup>H NMR δ (CDCl<sub>3</sub>) 0.83–0.88, m, 12H, 4 × -CH<sub>3</sub>; 1.00–1.40, m, 19H, 8 × -CH<sub>2</sub> + 3 × -CH; 1.24, s, 3H, -CH<sub>3</sub>; 1.52, m, 2H, 1'-CH<sub>2</sub>; 1.79, m, 1H, (3-CH); 1.81, m, 1H, (3-CH); 2.10, s, 3H, Ar-CH<sub>3</sub>; 2.20, s, 3H, Ar-CH<sub>3</sub>; 2.70, t, 2H, 4-CH<sub>2</sub>; 5.19, s, 1H, -OH. MS (ei) *m/z* (relative intensity) 452 (M+2)<sup>+</sup>(32), 450 (M<sup>+</sup>)(83), 227 (19), 225 (49), 187 (36), 185 (100), 184 (46).

Band 9 (*R<sub>f</sub>* 0.80; pale yellow; 7.3 mg; 14%), was identified as **13**, (3*R*,7*aR*,10*R*,11*aS*,14*aS*)-11*a*-chloro-2,3,9,10-tetrahydro-3,5,6,10,12,13-hexamethyl-3,10-*bis* [(4*R*,8*R*)-4,8,12-trimethyltridecyl]-1*H*-pyrano[3,2-*a*]-8*H*-pyrano[3,2*g*]dibenzofuran-14(7*aH*,14*aH*)-one. It had UV λ<sub>max</sub> (in hexane) of 292 nm. <sup>1</sup>H NMR δ (CDCl<sub>3</sub>) 0.83–0.88, m, 24H, 8 × -CH<sub>3</sub>; 1.00–1.40, m, 38H, 16 × -CH<sub>2</sub> + 6 × -CH; 1.21, s, 3H, 15-CH<sub>3</sub>; 1.35, s, 3H, 18-CH<sub>3</sub>; 1.61–1.62, m, 2H, 1 × (8-CH) + 1 ×

(9-CH); 1.71, s, 3H, 20-CH<sub>3</sub>; 1.75, m, 2H, 2-CH<sub>2</sub>; 1.99, s, 3H, 19-CH<sub>3</sub>; 2.08, s, 6H, 16-CH<sub>3</sub> + 17-CH<sub>3</sub>; 2.16, m, 1H, 1 × (8-CH); 2.31, m, 1H, 1 × (9-CH); 2.65, m, 1H, 1 × (1-CH); 3.06, m, 1H, 1 × (1-CH); 4.09, s, 1H, 14*a*-CH. <sup>1</sup>H and <sup>13</sup>C NMR δ (CDCl<sub>3</sub>) data for the pentacyclic nuclei of **13** and **14** are recorded in Table 1 for ease of comparison. MS (ei) *m/z* (relative intensity) 866 (M+2)<sup>+</sup>(22), 864 (M<sup>+</sup>) (38), 828 (100), 603 (33), 562 (15), 550 (26).

Band 10 (*R<sub>f</sub>* 0.85; pale yellow; 12.7 mg; 24%), was identified as **14**, (3*R*,7*aR*,10*R*,11*aR*,14*aS*)-11*a*-chloro-2,3,9,10-tetrahydro-3,5,6,10,12,13-hexamethyl-3,10-*bis* [(4*R*,8*R*)-4,8,12-trimethyltridecyl]-1*H*-pyrano[3,2-*a*]-8*H*-pyrano[3,2*g*]dibenzofuran-14(7*aH*,14*aH*)-one. It had UV λ<sub>max</sub> (in hexane) of 292 nm. <sup>1</sup>H NMR δ (CDCl<sub>3</sub>)

**Table 1** <sup>13</sup>C and <sup>1</sup>H NMR assignments of **13** and **14**



Position	<sup>13</sup> C NMR		<sup>1</sup> H NMR	
	<b>13</b>	<b>14</b>	<b>13</b>	<b>14</b>
1	19.6 <sup>a</sup>	20.5	3.06, 2.65	3.00, 2.69
2	31.5	30.8	1.75, 1.75	1.75, 1.75
3	74.9	74.9		
4a	146.3	146.2		
5/6	126.3	126.5		
6/5	123.0	123.0		
6a	142.4	142.3		
7a	68.4	68.3		
8	28.0	27.9	2.16, 1.61	2.19, 1.65
9	31.5	29.9	2.31, 1.62	2.32, 1.47
10	78.0	78.0		
11a	97.9	97.6		
12	147.2	147.8		
13	130.2	130.1		
14	193.3	193.3		
14a	57.0	56.9	4.09	4.10
14b	116.5	116.4		
14c	112.4	112.3		
15	24.1	23.6	1.21	1.16
16	11.9	11.7	2.08	2.08
17	11.9	11.9	2.08	2.09
18	29.6	27.4	1.35	1.46
19	12.9	13.1	1.99	1.97
20	11.1	11.2	1.71	1.71

<sup>a</sup> Chemical shifts in ppm downfield from tetramethylsilane

0.83–0.88, m, 24H,  $8 \times -\text{CH}_3$ ; 1.00–1.40, m, 38H,  $16 \times -\text{CH}_2 + 6 \times -\text{CH}$ ; 1.16, s, 3H,  $15-\text{CH}_3$ ; 1.46, s, 3H,  $18-\text{CH}_3$ ; 1.65, m, 1H,  $1 \times (8-\text{CH})$ ; 1.71, s, 3H,  $20-\text{CH}_3$ ; 1.75, m, 2H,  $2-\text{CH}_2$ ; 1.97, s, 3H,  $19-\text{CH}_3$ ; 2.08, s, 3H,  $16-\text{CH}_3$ ; 2.09, s, 3H,  $17-\text{CH}_3$ ; 2.19, m, 1H,  $1 \times (8-\text{CH})$ ; 2.32, m, 1H,  $1 \times (9-\text{CH})$ ; 2.69, m, 1H,  $1 \times (1-\text{CH})$ ; 3.0, m, 1H,  $1 \times (1-\text{CH})$ ; 4.10, s, 1H,  $14a-\text{CH}$ .  $^1\text{H}$  and  $^{13}\text{C}$  NMR  $\delta$  ( $\text{CDCl}_3$ ) data for the pentacyclic nuclei of **13** and **14** are recorded in Table 1 for ease of comparison. MS (ei)  $m/z$  (relative intensity) 866 ( $\text{M}+2$ )<sup>+</sup>(32), 864 ( $\text{M}^+$ ) (68), 828 (100), 603 (37), 562 (22), 550 (40).

$\alpha$ -Tocopheryl quinone has the following mass spectrum (ei;  $m/z$  (relative intensity) 446 ( $\text{M}^+$ )(12), 431 (8), 430 (13), 429 (16), 428 (17), 221 (64), 205 (19), 204 (18), 203 (100), 180 (51), 179 (69), 178 (58), 165 (75), 164 (25).

## Results and Discussion

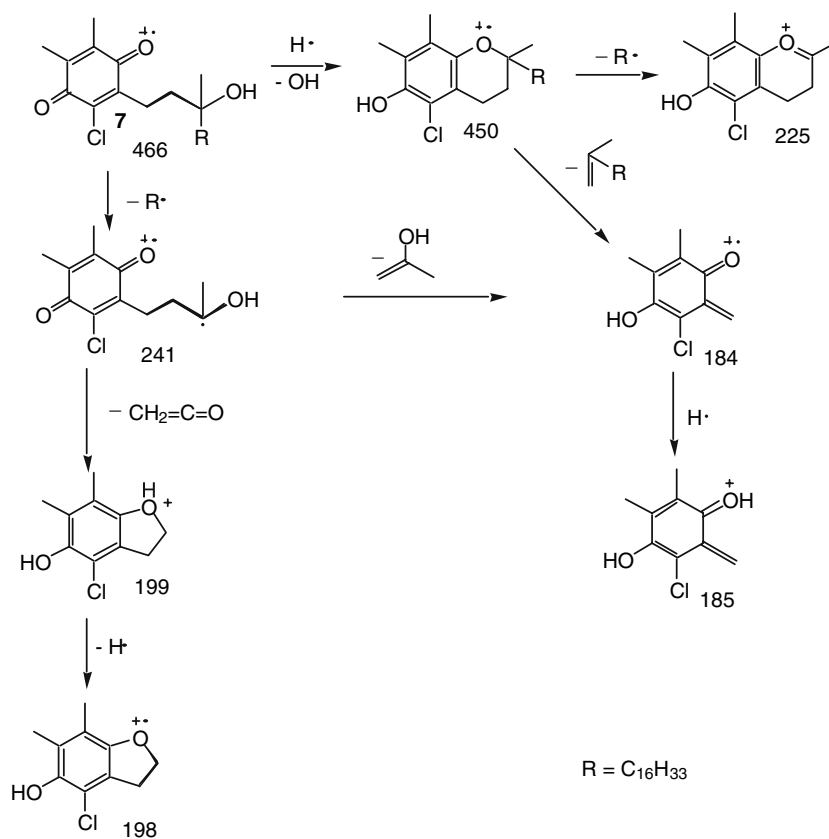
The method of ionisation used in the mass spectrometer proved a problem. Electrospray ionisation (ESI-MS) and atmospheric pressure chemical ionisation (APCI-MS) were attempted before settling on electron impact (EI-MS). Both ESI-MS and APCI-MS tended

to produce dimerisation in the source and unreliable results as a consequence.

The product with the lowest  $R_f$  (0.03) was **3**. It constituted only 0.6% of the total products and was the only product identified that was not substituted at the original position 5 of the aromatic ring of **1**. This gives some indication of the reactivity of position 5 of **1**.

Compound **7** (14% of the products), which had the same  $R_f$  as **8** and was very difficult to separate from **8**, does not seem to have been reported previously. Although **7** was clearly a quinone from its UV and  $^1\text{H}$  NMR spectra, and had a side-chain hydroxyl group, judging by its very low  $R_f$ , it did not give a molecular ion (mw 466) in the EI mass spectrum. However, the molecular weight of **7** is confirmed by a major chlorine-containing fragment of mw 241 which corresponds to the loss of the 4,8,12-trimethyltridecyl side chain from **7** (Scheme 1). This fragment is directly analogous to the 221 fragment of  $\alpha$ -tocopheryl quinone, whose EI mass spectrum is recorded above at the end of “[Experimental procedures](#)” for reference. Loss of ketene from the 241 fragment of **7** gives the cluster of ions at 198, 199, 200 (Scheme 1), which has its analogy in  $\alpha$ -tocopheryl quinone where the loss of ketene from the 221 fragment gives the cluster at 178, 179, 180. It appears that a major fragmentation pathway of **7** involves

**Scheme 1** Electron impact fragmentation pathways for **7** (3-chloro- $\gamma$ -tocopheryl quinone)

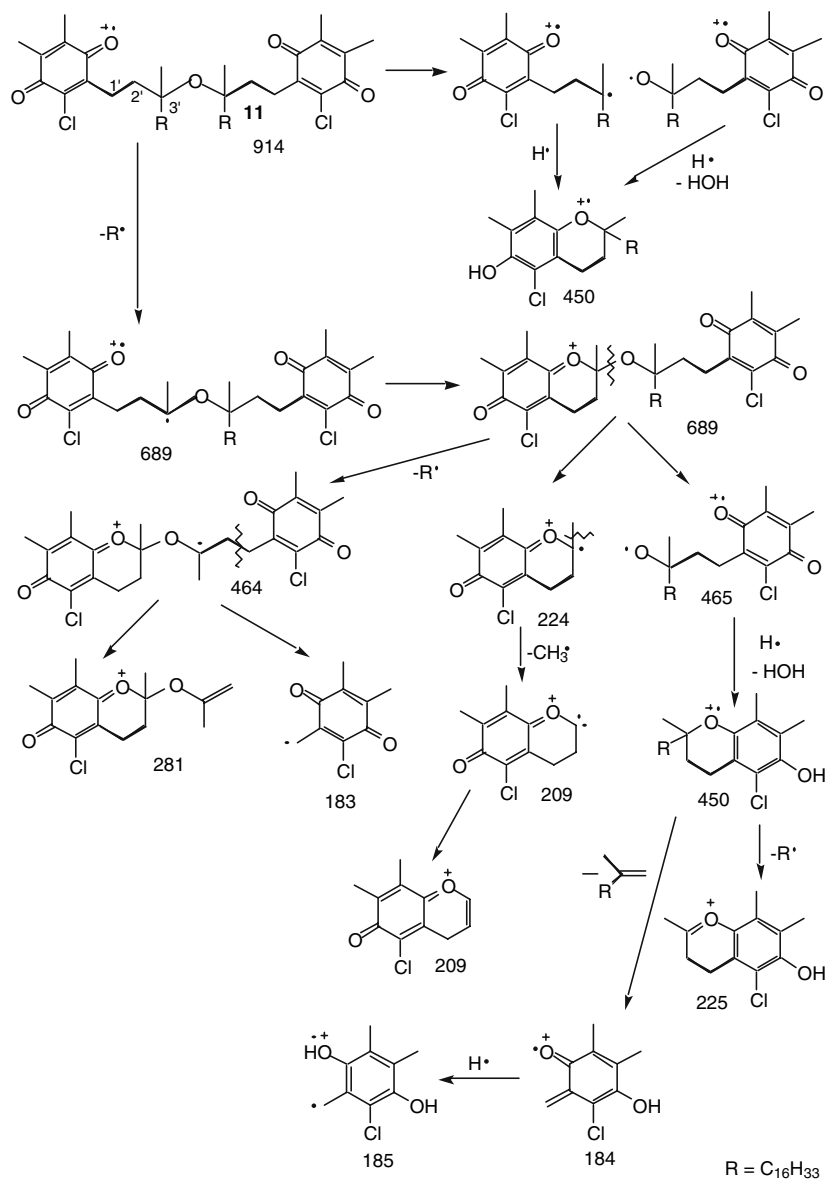


recyclisation in the source of the mass spectrometer to form **4** (mw 450) which then fragments to give major daughter peaks at 225 (loss of a 4,8,12-trimethyltridecyl group) and 184, 185 (loss of 2,6,10,14-tetramethyl-1-pentadecene) (Scheme 1). It seems that recyclisation of  $\alpha$ -tocopheryl quinone (mw 446) to form  $\alpha$ -tocopherol (mw 430) also occurs in the source of the mass spectrometer, but that this is a less prominent pathway than in **7**. Fragmentation of  $\alpha$ -tocopherol produces the fragment 205 corresponding to the 225 fragment of **7**. Loss of 2,6,10,14-tetramethyl-1-pentadecene from  $\alpha$ -tocopherol produces the cluster of ions at 164, 165, which corresponds to the 184, 185 ions from **7** (Scheme 1).

Compound **7** was obviously formed by the oxidation of **4** (14% of the products), which also does not seem to have been reported previously. The  $^1\text{H}$  NMR spectrum of **4** is very similar to that of 5-bromo-2,2,7,8-tetramethyl-6-chromanol [9]. It is interesting to note the deshielding effect of chlorine on the phenolic hydroxyl group of **4** (5.19 ppm) compared with that of **1** (4.23 ppm). The phenolic hydroxyl (5.04 ppm) of 5-bromo-2,2,7,8-tetramethyl-6-chromanol is also deshielded significantly compared to that of 2,2,7,8-tetramethyl-6-chromanol (4.24 ppm) [10].

Compound **8** is the best-known oxidation product of **1** but, in this reaction **8** only accounted for 10% of the products.

**Scheme 2** Electron impact fragmentation pathways for **11** (the ether dimer of (3-chloro- $\gamma$ -tocopheryl quinone)



The isomers **5** and **10** have been reported [6, 11, 12] and are clearly the precursors of **13** and **14** in this reaction. It seems likely that **5**, with the “S” configuration [12], is the immediate precursor. It is remarkable that these isomers are so easy to separate by TLC on silica gel. The lower  $R_f$  (0.48) isomer **10**, when kept in an NMR tube in the refrigerator, changed slowly into the higher  $R_f$  (0.69) isomer **5**, while **5** was unchanged.

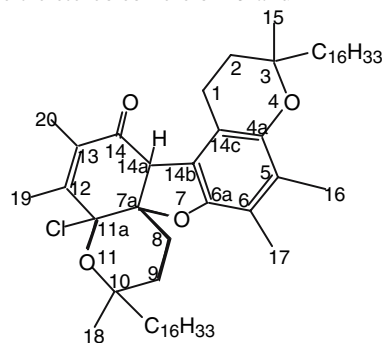
Compound **11** (band 5), a minor product, is believed to be an ether dimer of compound **7**. However the structure of **11** is speculative since the fragments in the EI mass spectrum are much smaller than the putative molecular weight of 914 (Scheme 2). However, the UV and  $^1\text{H}$  NMR spectra of **11** are virtually identical to those of **7**, suggesting that they are closely related quinones. However the  $R_f$  of **7** is 0.07, whereas that of **11** is 0.42, suggesting that **11** does not have an hydroxyl group. The mass spectra of **7** and **11** have several fragments in common and some of which are different. Both **7** and **11** have fragments at 450, 225 and 184, 185. In addition **7** has a cluster of ions at 198, 199, 200 not shared by **11**, while **11** has major fragments at 281 and 209 not shared by **7**. Schemes 1 and 2 attempt to explain how the differences in fragmentation arise.

Additional evidence for the ether dimer structure of **11** comes from its  $^1\text{H}$  NMR spectrum. The only difference between the  $^1\text{H}$  NMR spectra of **7** and **11** is the chemical shift of their 3' methyl protons, 1.25 and 1.11 ppm respectively. Molecular models show that, as the two halves of **11** rotate around the central ether bond, the 3' methyl groups are either very close to each other or to the first methylene group in the phytyl side chain on the other half of the molecule. The very close proximity of the methyl groups to each other or to a neighbouring methylene would result in strong shielding and therefore a shift to higher field.

Compounds **13** and **14**, which make up 38% of the products, have not been reported previously and their spectra are very similar in all respects. Table 1 shows that the chemical shifts of both protons and carbons near the dibenzofuranone centre of the pentacyclic nucleus are almost identical. The differences appear on the periphery, i.e. positions 1 (protons and carbons), 2 (carbons), 8 (protons), 9 (protons and carbons), 15 (protons and carbons) and 18 (protons and carbons).

Although **13** and **14** each have nine chiral carbon atoms, and thus  $2^9$  possible isomers, the side chains, together with their points of attachment to the pentacyclic nucleus, account for six chiral carbons and do not alter from isomer to isomer, and therefore the number of isomers simplifies down to eight, determined by positions 7a, 11a and 14a. The eight possible isomers are listed in Table 2.

**Table 2** Possible stereoisomers of **13** and **14**



Isomer number	Carbon positions		
	7a	11a	14a
1	S	R	R
2	R	S	S
3	R	R	S
4	S	S	R
5	R	R	R
6	S	S	S
7	R	S	R
8	S	R	S

Configurations at positions 3 and 10 of the nucleus and 4' and 8' in each  $\text{C}_{16}\text{H}_{33}$  side chain are all “R”

NOE spectroscopy (NOESY) allows one to eliminate four of these isomers. The proton on carbon 14a lies in a central position in the molecule, midway between the two peripheral pyran rings. The C14a proton has NOE correlations with both C1 protons and both C8 protons in **13** and **14**. This means that the only possible isomers are 1–4. Isomers 5–8 are excluded because the C1 and C8 protons in these isomers are further from the C14a protons than they are in isomers 1–4, and, in addition, the C14a protons in isomers 5–8 lie on the opposite surface of the ring system from the protons on C8.

One may eliminate two more isomers by using the chemical shift of the C18 methyl protons. Isomers 1 and 2 are diastereomers but, if one considers only positions 7a, 11a and 14a, may be thought of as pseudo-enantiomers. One may eliminate isomer 1 because its C18 methyl group would be expected to have a similar chemical shift to that of the C15 methyl, whereas, in isomer 2, the C18 methyl would be deshielded by the ethylenic double bond of the enone system. A similar argument applies to isomers 3 and 4. Isomer 4 may be eliminated because its C18 methyl group would be expected to have a similar chemical shift to that of the C15 methyl, whereas in isomer 3 the C18 methyl would be deshielded by the chlorine on C11a. The ability of chlorine to deshield may be seen in the chemical shift

of the phenolic hydrogen of compound **4** (5.19 ppm) compared to that of compound **1** (4.23 ppm).

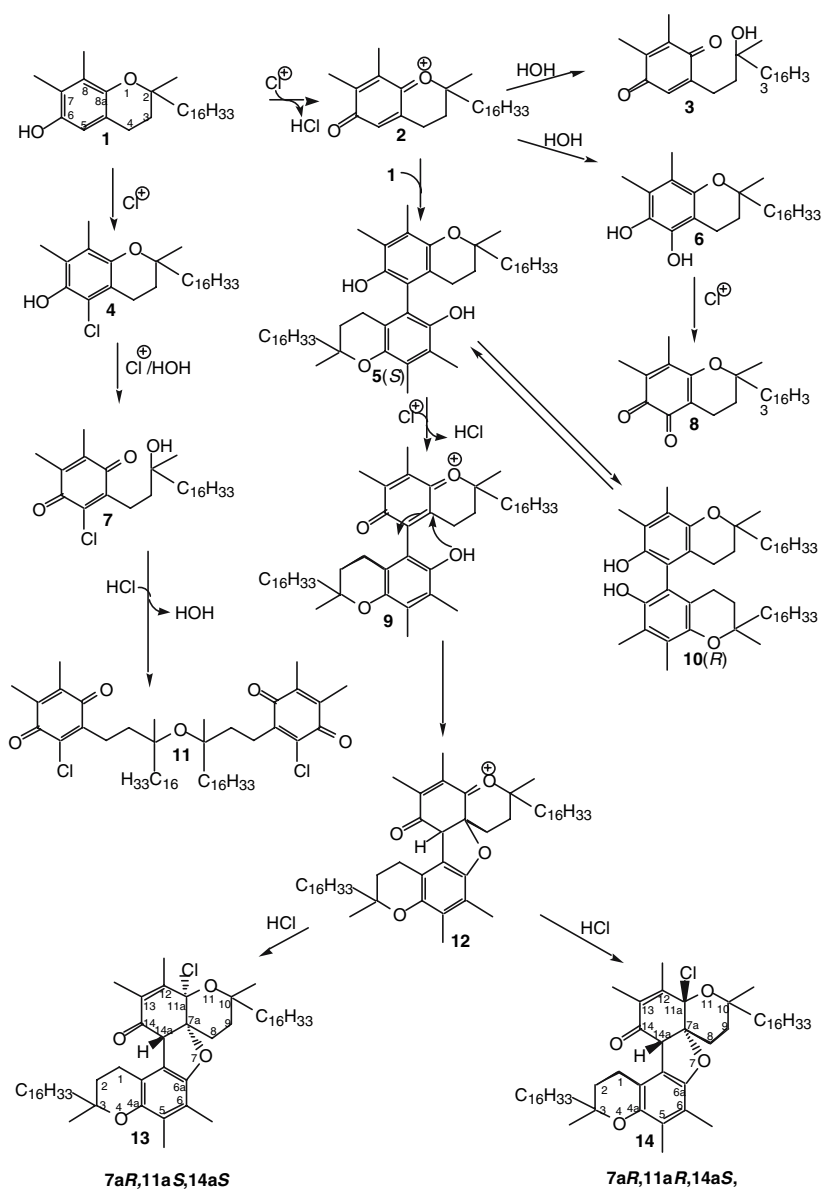
Molecular models suggest that **13** (Band 9;  $R_f$  0.80) is isomer 2. The reason for this is the chemical shifts of the C1a protons, which are close to the C14 carbonyl. In **13**, the C1a proton is at 3.06 ppm, whereas in **14** it is at 3.00 ppm. Molecular models of isomer 2 show that the C1a proton is significantly closer to the carbonyl, and hence more deshielded, than in isomer 3.

Scheme 3 shows how the products may be formed. The actual oxidising species is unknown but, since HOCl,  $\text{Cl}_2\text{O}$  and  $\text{Cl}_2$  are in equilibrium, it may be a mixture of all three [13]. At pH 7, HOCl is about 50% ionised ( $\text{p}K_a$  7.5), so each of the above chlorine species

would be present to some extent in the hexane layer. Whichever chlorine species is involved, it is almost certainly a two-electron oxidant and may be thought of as being equivalent to  $\text{Cl}^+$ , which it will be termed for the purposes of this discussion. It is acknowledged that  $\text{Cl}^+$  itself is not the actual species [13]. In the formation of **4**,  $\text{Cl}^+$  behaves as an electrophile. In the case of **7**,  $\text{Cl}^+$  is both an electrophile and an oxidant. In all other cases  $\text{Cl}^+$  behaves as an oxidant.

The key intermediate from which all other products derive is the oxonium ion **2** (see Scheme 3). Addition of water to **2** at position 8a produces **3**, while the addition of water at position 5 gives rise to the catechol **6**, which is then oxidised further to **8**. Compound **2** can

**Scheme 3** Products of the reaction of **1** ( $\gamma$ -tocopherol) with hypochlorous acid





also behave as an electrophile in an attack by another molecule of **1**, producing the two isomers **5** and **10**. Oxidation of **5** produces the chromanol-oxonium species **9** which then cyclises to form **12**. Compound **12** can react with hydrogen chloride to form the diastereomers **13** and **14**. Alternatively, **9** may react with HCl before cyclisation occurs.

The formation of **3**, **7** and **8** all require water. The fact that these three compounds made up less than 25% of the total products suggests that most of the reactions occurred within the hexane layer rather than at the hexane–water interface. Another reason for thinking this is that oxonium species such as **2** react very readily with water to the extent that the quinone of  $\alpha$ -tocopherol is its major oxidation product when water is present [14]. If the formation of **13** and **14** occurs within the hexane layer, it is likely that the source of chlorine in them is hydrogen chloride rather than chloride ion.

It was noted previously that 2,2,7,8-tetramethyl-6-chromanol, the model compound of **1**, reacted rapidly with HOCl to form a dichloro-pyrano-benzenedione [3]. There was no trace of the equivalent derivative of **1** in the present reactions. The reason for this may be related to the polarity of **1** and its model compound. Since the model compound lacks the phytyl side chain of tocopherol, it is considerably smaller and more polar than **1**. Thus a higher concentration of it at the water interface would be expected, leading to greater formation of 3-chloro-2-(3-hydroxy-3-methylbutyl)-5,6-dimethyl-1,4-benzoquinone (CIBQ), the model compound of **7** and the immediate precursor of the dichloro-pyrano-benzenedione. In addition, the side chain of CIBQ is much shorter, and presumably more flexible, than that of **7**, making it much easier to cyclise.

**Acknowledgments** Thanks are due to Dr. K. Fisher for running the mass spectra, to Mrs. H. Stender for the NMR spectra, and to Dr. J. Brophy for helpful discussions.

## References

1. Christen S, Woodall AA, Shigenaga MK, Southwell-Keely PT, Duncan MW, Ames BN (1997)  $\gamma$ -Tocopherol traps mutagenic electrophiles such as  $\text{NO}_x$  and complements  $\alpha$ -tocopherol: physiological implications. *Proc Natl Acad Sci USA* 94:3217–3222
2. Kettle AJ, Winterbourn CC (1997) Myeloperoxidase: a key regulator of neutrophil oxidant production. *Redox Rep* 3:3–15
3. Ho H, Soldevilla J, Hook JM, Southwell-Keely PT (2000) Oxidation of 2,2,7,8-Tetramethyl-6-chromanol, the model compound of  $\gamma$ -tocopherol, by hypochlorous Acid. *Redox Rep* 5:60–62
4. John W, Dietzel E, Emte W (1939) Über Einige Oxidationsprodukte der Tokopherole und Analoger Einfacher Modellkörper *Z. Physiol Chem* 257:173–189
5. Suarna C (1990) Studies on the oxidation of alpha-tocopherol and its model compound 2,2,5,7,8-pentamethyl-6-chromanol. Ph.D. Dissertation, The University of New South Wales, p 177
6. Yamauchi R, Matsui T, Kato K, Ueno Y (1990) Reaction products of  $\gamma$ -tocopherol with an alkylperoxyl radical in benzene. *Agric Biol Chem* 54:2703–2709
7. Smith LI, Irwin WB, Ungnade HE (1939) The chemistry of vitamin E. XVII. The oxidation products of  $\alpha$ -tocopherol and of related 6-hydroxychromans. *J Am Chem Soc* 61:2424–2429
8. Eggitt PWR, Norris FW (1955) The chemical estimation of vitamin-E activity in cereal products. III. *J Sci Food Agric* 6:689–695
9. Nilsson JLG, Sievertsson H, Selander H (1969) The directing effect of annulated rings in aromatic systems. *Acta Pharm Suec* 6:585–588
10. Suarna C (1990) Studies on the oxidation of alpha-tocopherol and its model compound 2,2,5,7,8-pentamethyl-6-chromanol. Ph.D. Dissertation, The University of New South Wales, p 242
11. Ha KH, Igarashi O (1990) The oxidation products from two kinds of tocopherols co-existing in autoxidation system of methyl linoleate. *J Nutr Sci Vitaminol* 36:411–421
12. Goh SH, Hew NF, Lee M (1992) Stereochemistry of bichromanyl dimers from  $\gamma$ -tocopherol and  $\gamma$ -tocotrienol. *Tetrahedron Lett* 33:4613–4616
13. Swain CG, Crist DR (1972) Mechanisms of chlorination by hypochlorous acid. *J Am Chem Soc* 94:3195–3200
14. Kohar I, Baca M, Suarna C, Stocker R, Southwell-Keely PT (1995) Is  $\alpha$ -tocopherol a reservoir for  $\alpha$ -tocopheryl hydroquinone? *Free Rad Biol Med* 19:197–207

# Engineering Oilseed Plants for a Sustainable, Land-Based Source of Long Chain Polyunsaturated Fatty Acids

Howard G. Damude · Anthony J. Kinney

Received: 22 December 2006 / Accepted: 7 February 2007 / Published online: 14 March 2007  
© AOCS 2007

**Abstract** Numerous clinical studies have demonstrated the cardiovascular and mental health benefits of including very long chain omega-3 polyunsaturated fatty acids, namely eicosapentaenoic acid (EPA) and docosahexaenoic acid (DHA) in the human diet. Certain fish oils can be a rich source of omega-3 long chain polyunsaturated fatty acids although processed marine oils are generally undesirable as food ingredients because of the associated objectionable flavors and contaminants that are difficult and cost-prohibitive to remove. Oilseed plants rich in omega-3 fatty acids, such as flax and walnut oils, contain only the 18-carbon omega-3 polyunsaturated fatty acid alpha-linolenic acid, which is poorly converted by the human body to EPA and DHA. It is now possible to engineer common omega-6 rich oilseeds such as soybean and canola to produce EPA and DHA and this has been the focus of a number of academic and industrial research groups. Recent advances and future prospects in the production of EPA and DHA in oilseed crops are discussed here.

## Abbreviations

LCPUFA	Long chain polyunsaturated fatty acids
DHA	Docosahexaenoic acid
EPA	Eicosapentaenoic acid
ARA	Arachidonic acid
COX-2	Cyclooxygenase-2
LNA	Linoleic acid

ALA	Alpha-linolenic acid
GLA	Gamma-linolenic acid
STA	Stearidonic acid
DGLA	Dihomo-gamma-linolenic acid
ETA	Eicosatetraenoic acid
EDA	Eicosadienoic acid
ERA	Eicosatrienoic acid
DPA	Docosapentaenoic acid
CoA	Coenzyme A
PtdCho	Phosphatidylcholine
LPAAT	Lysophosphatidic acid acyltransferase
SCA	Sciadonic acid
JUN	Juniperonic acid
PKS	Polyketide synthase

## Manipulating the Fatty Acid Content of the Human Diet

The main sources of oils and fats in the human diet are oilseed crop plants, mostly soy, canola (oilseed rape), palm, peanut and sunflower. Many of the oils from these crops are rich in 18-carbon omega-6 fatty acids. It has been demonstrated that excess consumption of omega-6 fatty acids leads to the depletion of omega-3 fatty acids in human body tissues, with numerous negative health consequences [1]. Hydrogenated or partially hydrogenated vegetable oils also contribute to the sensory characteristics of numerous processed food products. Edible vegetable oils are hydrogenated to improve shelf-life, maintain the flavor and provide the expected mouth-feel and consistency of oil-containing foods [2]. Hydrogenation leads to the formation of *trans* unsaturated fatty acids, which provide the

H. G. Damude · A. J. Kinney (✉)  
Crop Genetics Research, DuPont Experimental Station,  
Wilmington, DE 19880-0353, USA  
e-mail: Anthony.Kinney@USA.dupont.com

necessary solid-fat functionality for certain food applications. However, the negative health consequences of *trans* unsaturated fatty acid consumption on human health has become better understood in recent years [3].

The first successful attempts of genetically manipulating the fatty acid profile of omega-6 oilseed crops were focused on the redirection of fatty acid biosynthesis in the developing seed, either by blocking specific steps, such as fatty acid desaturation [4], or introducing single enzyme activities to redirect fatty acid synthesis to new end products that provided the required functionality [5]. By these means it was possible to improve the oxidative stability and provide a solid fat functionality in vegetable oils without the need for hydrogenation and the consequent formation of *trans* fatty acids [6, 7].

With advances in gene expression technology it is now possible to consider more complex manipulations of plant cell lipid metabolism, such as the introduction of entire metabolic pathways. Thus it is theoretically possible, for example, to transfer a metabolic pathway for EPA or DHA synthesis from a marine organism to an oilseed crop plant. This would provide an abundant, clean, sustainable and relatively inexpensive source of omega-3 long chain polyunsaturated fatty acids for the human diet. Here we discuss metabolic engineering efforts to achieve this goal.

### Long Chain Polyunsaturated Fatty Acids Human Health

Long chain polyunsaturated fatty acids (LCPUFA) are important components of cell membrane phospholipids in humans. Docosahexaenoic acid (DHA, 22:6 [4, 7, 10, 13, 16, 19]), for example, is an important component of mammalian retinal and brain membranes and has been shown to play a role in the cognitive development of infants as well as the mental health of adults [8, 9, 10]. Numerous studies [11–14] have shown cardiovascular health benefits arising from the consumption of eicosapentaenoic acid (EPA, 20:5 [5, 8, 11, 14, 17]). LCPUFA are also precursors to the eicosanoid family of metabolites which include prostaglandins, leukotrienes, thromboxanes [15, 16]. These molecules regulate certain key metabolic functions in the human body, such as inflammatory responses and the induction of blood clotting as well as the regulation of blood pressure [17]. Eicosanoids derived from omega-6 LCPUFA, such as arachidonic acid (ARA, 20:4 [5, 8, 11, 14]), are generally pro-inflammatory while those derived from omega-3 LCPUFA, such as eicosapentaenoic acid, are anti-inflammatory [12, 16, 18].

The first step in eicosanoid biosynthesis from LCPUFA is catalyzed by the cyclooxygenase-2 (COX-2) enzyme [16], which can utilize either ARA or EPA as a substrate.

Thus, in addition to the anti-inflammatory action of omega-3-derived eicosanoids themselves, the anti-inflammatory action of EPA can be attributed to its competitive inhibition of ARA for COX-2 [18]. Thus an optimal balance of omega-3 and omega-6 LCPUFA must be achieved to maintain a healthy state.

Direct inhibition of COX-2 activity is the mechanistic basis of a whole class of non-steroidal, anti-inflammatory pharmaceuticals used in the treatment of arthritis and similar conditions. However, while EPA and DHA are beneficial to cardiovascular health, preventing their conversion to eicosanoids by anti-arthritis pharmaceuticals can result in various negative cardiovascular side effects. Indeed negative cardiovascular side effects have been attributed to the use of some COX-2 selective inhibitors in some individuals [19]. It is apparent, therefore, that achieving a balanced dietary intake of omega-6 and omega-3 fatty acids is the most preferred means of preventing negative inflammation responses and of maintaining cardiovascular health for large segments of the population.

Eicosapentaenoic acid and ARA can be synthesized in the human body from the essential dietary fatty acids linoleic acid (LNA, 18:2 [9, 12]) or alpha-linolenic acid (ALA, 18:3 [9, 12, 15]), respectively [20]. The conversion of LNA and ALA to ARA and EPA is relatively inefficient and EPA, DHA and ARA can also be obtained more efficiently directly from the diet, mainly from the consumption of fish and fish-oil [16, 20]. In Western societies, the dietary ratio of omega-6 to omega-3 fatty acids has shifted heavily toward omega-6 fatty acids over the past 60 years [21]. This shift is the result of an overall decrease in the consumption of fish and fish oils, which contain high levels of omega-3 LCPUFA, as well as a large increase in the consumption of omega-6-containing foods, such as common vegetable oils or grain-fed meat and poultry [21]. By some estimate the current omega-6 to omega-3 intake in the human diet is as much as 30-fold too high [21, 23]. This has led to a general imbalance of ARA and EPA in the blood stream with numerous possible negative consequences [21]. Thus consumption of foods rich in omega-3 LCPUFA may help to correct this imbalance by shifting the omega-6 to omega-3 fatty acid ratio to more optimal levels in the human body.

An increasing demand for fish and fish oils high in omega-3 LCPUFA is putting an even greater stress on an already overexploited resource [24]. In addition, the cost associated with removing objectionable odors and flavors, as well as contaminants such as mercury and PCBs, generally limits the use of fish oils as food ingredients [25, 26]. Microalgal-derived omega-3 oils produced through fermentation are free from the contaminants found in fish oils but their high cost restricts their use to infant formula and medical foods and generally prohibit their inclusion in common food products.

A potentially cost-effective and sustainable alternative would be to engineer a biosynthetic pathway for omega-3 LCPUFA-production into a land-based host, such as a commercial oilseed crop. Since most cold water marine fish oils have very low levels of omega-6 fatty acids (2–5%) and a combined omega-3 LCPUFA content of 10–25% (EPA + DHA), this composition provides a suitable commercial target for omega-3 LCPUFA in plants.

### Engineering omega-3 LCPUFA into Plants: Polyketide Biosynthetic Pathways

Although many cold-water fish are capable of synthesizing LCPUFA from LNA and ALA, the typically high content of EPA and DHA found in their body oils can only be attained through their dietary intake of LCPUFA [27]. For large marine carnivores, such as tuna and salmon, substantial amounts of LCPUFA are obtained by eating smaller fish, such as Menhaden. For the small fish the main sources of LCPUFA are marine microorganisms such as diatoms, golden-brown algae, green algae, blue-green algae, microbial fungi and dinoflagellates, all of which are rich in LCPUFA synthesized *de novo* by one of two classes of biochemical pathway. These two classes are the anaerobic polyketide synthase pathways [28] and the aerobic fatty acid desaturation/elongation pathways [29].

Polyketides are a very broad group of secondary metabolites that are usually defined by their method of synthesis; that is, the iterative addition of carbon to a growing acyl-ACP chain catalyzed by a single enzyme complex known as a polyketide synthase (PKS). These PKS complexes catalyze reactions analogous to those of fatty acid metabolism [30]. But whereas aerobic fatty acid synthesis is the result of over 30 distinct enzyme activities, a PKS synthase consists of a single, multidomain enzyme with subunits encoded by only three or four open reading frames in the genome of the polyketide-producing organism [30]. While most PKS products, such as aflatoxins and antibiotics, are highly derivatized and cyclized acyl chains some marine organisms use PKS-type complexes to synthesize EPA or DHA. In general, the species of LCPUFA produced by these organisms is specific to the particular polyketide synthase they contain [28]. In some cases, a single organism may contain both PKS and fatty acid synthase pathways for EPA or DHA synthesis. For example, a complete PKS type DHA-synthase has been cloned and characterized from a number of Thraustochytrid species, as have various fatty acid synthase-type enzymes involved in EPA and DHA synthesis [31, 32].

Genes encoding the three subunits of a *Schizochytrium* PKS that catalyzes the synthesis of DHA from malonyl-CoA have been expressed in yeast. When co-expressed

with a phosphopantetheinyl transferase (PPT) from *Nostoc*, essential for activating the ACP domains of the DHA-synthase PKS, the yeast are able to produce small amounts (2.5%) of DHA [33]. Presumably, the ultimate intent is to transfer the *Schizochytrium* PKS and *Nostoc* PPT genes into an oilseed plant with the goal of producing DHA in the seed oil, although there are no published reports to date of the success or otherwise of this approach.

### Engineering omega-3 LCPUFA into Plants: Fatty Acid Biosynthetic Pathways

In contrast to PKS synthases, the pathways of aerobic ARA, EPA and DHA synthesis use a series of individual desaturase and elongase activities to catalyze the conversion of LNA and ALA to LCPUFA [34]. For ARA and EPA synthesis this requires the addition of two carbons and two double-bonds to LNA and ALA respectively. ARA can be converted to EPA by the action of a third (omega-3) desaturase [35].

Two converging ARA/EPA pathways have been identified in LCPUFA-producing organisms (Fig. 1); in both pathway types LNA and ALA are the metabolic precursors. In the first pathway type, LNA and ALA are first desaturated to gamma-linolenic acid (GLA, 18:3 [6, 9, 12]) and stearidonic acid (STA, 18:4 [6, 9, 12, 15]), respectively, by a delta-6 fatty acid desaturase. These fatty acids are then elongated to 20-carbons by a microsomal fatty acid elongation complex [28]. This elongation is initiated by a delta-6 specific beta-ketoacyl-CoA synthase enzyme (delta-6 elongase). The 20-carbon ketoacyl-CoA is then reduced, dehydrated and reduced again by the elongation complex to yield dihomo-gamma-linolenic acid (DGLA, 20:3 [8, 11, 14]) or eicosatetraenoic acid [ETA, 20:4 [8, 11, 14, 17]]. These fatty acids are then desaturated to ARA and EPA respectively by a delta-5 desaturase.

In the second pathway type, LNA and ALA are first elongated by a delta-9-specific elongase to eicosadienoic acid (EDA, 20:2 [11, 14]) and eicosatrienoic acid (ERA, 20:3 [11, 14, 17]), followed by delta-8 desaturation to DGLA and ETA, respectively. As in the first pathway, these fatty acids are then desaturated to ARA and EPA, respectively by a delta-5 desaturase.

Independent of the aerobic pathway utilized, some organisms have the added capability of efficiently converting omega-6 fatty acids to omega-3 fatty acids by the action of an omega-3 fatty acid desaturase [35–39]. This desaturation can occur on either 18-carbon or 20-carbon fatty acids.

In most organisms, conversion of EPA to DHA occurs by delta-5/C20 elongation of EPA to docosapentaenoic acid (DPA, 20:5 [7, 10, 13, 16, 19]) followed by delta-4

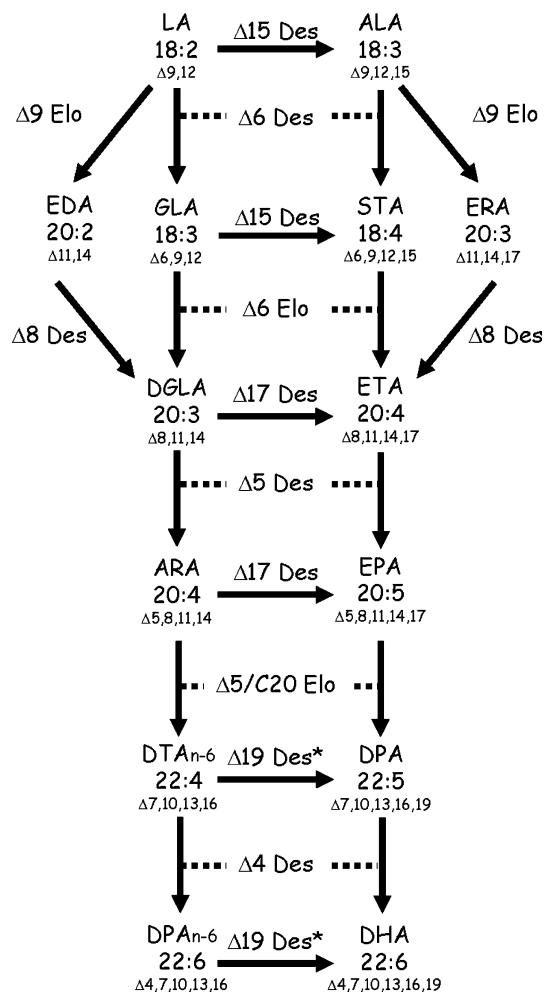


**Fig. 1** Aerobic LCPUFA biosynthetic pathways in marine microbes. The delta-6 pathway is shown with a delta-6 desaturase ( $\Delta 6$  Des) and delta-6 elongase ( $\Delta 6$  Elo) and the delta-9 pathway is shown with a delta-9 elongase ( $\Delta 9$  Elo) and a delta-8 desaturase ( $\Delta 8$  Des). Both pathways utilize a delta-5 desaturase ( $\Delta 5$  Des). All pathway enzymes utilize both omega-3 and omega-6 fatty acid substrates and this is indicated with a dotted line. Conversion of 18 carbon or 22 carbon omega-6 fatty acids to omega-3 fatty acids is catalyzed by the delta-15 desaturase ( $\Delta 15$  Des), delta-17 desaturase ( $\Delta 17$  Des) and possibly by a hypothetical delta-19 desaturase ( $\Delta 19$  Des\*), respectively. Elongation of ARA or EPA is catalyzed the  $\Delta 5/C20$  elongase ( $\Delta 5/C20$  Elo) and further delta-4 desaturation by the delta-4 desaturase ( $\Delta 4$  Des)

desaturation to DHA [29]. In humans and some other mammals, DHA synthesis is considerably more complex, involving two further elongations, a desaturation and beta-oxidation in a separate cellular compartment [34].

Among the first published descriptions of expression of a fatty acid-type LCPUFA pathway in plants was a report describing the constitutive expression of a delta-9 elongase pathway using genes from the microalgae *Isochrysis galbana* and *Euglena gracilis* and the microbial fungus *Mortierella alpina* in the model plant *Arabidopsis* [40]. Individual pathway genes (delta-9 elongase, delta-8

desaturase, delta-5 desaturase) were each linked to a Ca35S promoter and resulting EPA contents as high as 3.0% and ARA contents up to 6.6% were produced in *Arabidopsis* leaves. The ratio of omega-3 to omega-6 ratio fatty acids (2.2:1) was slightly lower in the transgenic plants than that for wild-type *Arabidopsis* leaves (3.5:1), but the new ratio was still in the range commonly found in fish oils [22]. A number of pathway intermediates and pathway by-products not commonly found in fish oils were also observed. These results were a significant proof-of-concept for expressing LCPUFA pathways in plants; however, *Arabidopsis* leaves could not be an economic production platform for these lipids.

In another report, published around the same time as the *Arabidopsis* study, Abbadi et al. [41] demonstrated very minor accumulation (less than 2%) of ARA and EPA in tobacco and flax seeds expressing a microbial delta-6 type pathway with genes from the diatom *Phaeodactylum tricornutum* and the fungus *Physcomitrella patens*. As in the *Arabidopsis* study there was substantial accumulation of pathway intermediates, mostly GLA and STA.

Thus, 18-carbon fatty acid elongation appeared to be limiting in the delta-6 pathway experiments (elongation was estimated to be around 10% in both tobacco and flax) but not in the delta-9 pathway experiments (where elongation in *Arabidopsis* was estimated to be about 36%). Poor elongation of delta-6 fatty acids was attributed to the low pool of the delta-6 acyl-CoA (GLA-CoA, STA-CoA) which are the main substrates for the delta-6 elongase. The low delta-6 acyl-CoA pools were probably the result of poor acyl-exchange of these lipids from the phospholipid substrates of the delta-6 desaturase to the acyl-CoA substrates for elongation. The pools of LNA-CoA and ALA-CoA for delta-9 elongation were presumably not limiting in the *Arabidopsis* study since these acyl species are the major fatty acids found in *Arabidopsis* leaf lipids. In a later study [42] the abundance of EPA in *Brassica juncea* expressing a delta-6 pathway was increased to as high as 15% partly by including a gene encoding a lysophosphatidyl acyltransferase from *Thraustochytrium* sp. This acyltransferase presumably increased the exchange of delta-6 acyl groups for acyl-phospholipids to acyl-CoAs for elongation.

However, a third report from 2004, describing commercially-significant amounts of LCPUFA in plant seeds reported good delta-6 elongation and a high abundance of EPA without the use of additional acyltransferases [43]. In this study, a delta-6 desaturase-type pathway from *M. alpina* was expressed in the agronomically-important oil-seed crop soybean, under control of strong, seed-specific promoters. In addition to the delta-6 pathway-genes (delta-6 desaturase, delta-6 elongase, delta-5 desaturase), the omega-6 ratio was increased from 0.2:1 (the normal soybean ratio) to 1.5:1 (a ratio close to that of many fish oils)

by concomitant expression of an *Arabidopsis* Fad 3 gene [44] and a *Saprolegnia diclina* delta-17 desaturase [39, 45].

The soybean study was the result of extensive characterization of multiple seed specific promoters and LCPUFA biosynthetic genes from different microbial sources, as well as optimization of promoter-gene cassette combinations and orientations in soy. Using this approach soybean seeds with an EPA content as high as 19.5% were produced with virtually no ARA. The low ARA content was attributed to the use of the *S. diclina* delta-17 desaturase. Additionally, the DHA precursor, DPA was found in high EPA lines at an abundance of about 4%, a result of the additional activity of the *M. alpina* delta-6 elongase towards the delta-5 fatty acid EPA. This same elongase had virtually no delta-5 EPA-elongating activity when expressed in yeast [46].

As in the other plant studies, pathway intermediates and by-products were present (35% in total). Unlike the flax and tobacco studies however, fatty acid elongation was not limiting in soybean. The total 20-carbon fatty acid content was as high as 40.2% representing 56% elongation of 18-carbon substrates.

In a more recent study, in which a similar set of LCPUFA biosynthetic genes for the same source were expressed (but without the omega-3 desaturases since the intent was to produce ARA), a very low abundance of total LCPUFA was observed (2.1%) in soy embryos [47]. The authors conclude that, as demonstrated in the soybean work of Kinney et al. [43], the careful combination of specific genes with individual promoters, gene cassette design and the screening of numerous events is crucial to obtaining the correct balance and a significant abundance of the desired LCPUFA in plants. Similar conclusions around the need for unique seed-specific promoters and pathway flux optimization were reached by Robert et al. [48] who expressed genes from a species of zebrafish (*Danio rerio*) and *Caenorhabditis elegans* in *Arabidopsis* seeds and observed a total LCPUFA content (ARA + EPA + DHA) of only 4.2%.

The flux to omega-3 fatty acids has since been further improved in soybean embryos [49] by the use of a novel, bifunctional delta-12/delta-15 desaturase from *Fusarium moniliforme* [39] in place of the *Arabidopsis* omega-3 desaturase. In the best events, the overall omega-3 fatty acid content was as high as 57% of total fatty acids. The *Fusarium* delta-15 desaturase was shown to be very active in soybean and when expressed alone, lead to ALA contents as high as 72%. It also had broad substrate specificity for numerous omega-6 fatty acids including LNA > GLA > DGLA > ARA [38], which further increases its usefulness in an LCPUFA pathway. Further LCPUFA pathway flux optimization and reduction in non-target fatty acids has since been achieved by further selection of the

types of desaturases and elongases used, codon optimization of microbial genes for plants and engineering optimal enzyme specificities (Damude and Kinney, unpublished data).

## Replacing Fish Oils with Transgenic Plant Oils

In the soybean study above, Kinney et al. [43] reported a relative abundance of DHA in soybean somatic embryo oil of up to 3.3%, which was the first demonstration of DHA in an oilseed plant. Soy somatic embryos are equivalent to the zygotic embryos of seeds [50]. This was achieved by the addition of a delta-5 elongase from *Pavlova* sp. [45] and a delta-4 desaturase from *Schizochytrium aggregatum* [51] in addition to the EPA biosynthetic pathway genes described above. The delta-4 desaturase used was highly active in plants with, in some cases, close to 100% conversion of DPA to DHA. In two other studies [42, 48], DHA was produced in a relative abundance of 0.5–1.5%. These are important milestones since all fish oils contain a mixture of EPA and DHA and thus the realization of a plant-based fish oil substitute appears to be on the horizon. Nevertheless, key challenges remain in obtaining a plant-based oil that is substantially similar to other commercially available fish oils. The first target will be to produce an EPA plus DHA plant oil with DHA comprising at least 10% of the total fatty acids, close to that of some marine oils. Although the highest abundance of DHA reported so far is less than 4%, current technology will allow for this abundance to be increased around threefold while maintaining an EPA abundance in the 10–15% range and this will provide an effective marine oils substitute. It will also be important to keep omega-6 fatty acids, pathway intermediates and pathway by-products to a minimum. It is now understood that by achieving the correct balance of relative gene expression and optimum metabolic flux through the engineered pathway it is possible to meet these criteria in commercial oilseed plants. Of course, once a seed oil having the desired target fatty acid composition has been achieved, there remains the key regulatory and agronomic challenges that face all new transgenic crop plants. However, the promising use of plant seed oils modified by biotechnology to produce n-3 long chain fatty acids will provide a readily available source of these important fatty acids in the future, overcoming the problems associated with obtaining n-3 LCPUFA from declining ocean fish supplies.

## References

1. Lands WEM (2005) Dietary fat and health: the evidence and the politics of prevention: careful use of dietary fats can improve life and prevent disease. *Ann NY Acad Sci* 1055:179–192

2. Stauffer CE (1996) Fats and Oils. Eagan Press, St Paul
3. Korver O, Katan MB (2006) The elimination of *trans* fats from spreads: how science helped to turn an industry around. *Nutr Rev* 64:275–279
4. Kinney AJ, Knowlton S (1998) Designer oils: the high oleic soybean. In: Roller S, Harlander S (eds) Genetic modification in the food industry. Blackie, London
5. Del Vecchio AJ (1996) High laurate canola. *Inform* 7:230–243
6. Voelker T, Kinney AJ (2001) Variations in the biosynthesis of seed-storage lipids. *Annu Rev Plant Physiol Mol Biol* 52:335–361
7. Coughlan SJ, Kinney AJ (2002) Transgenic plants as sources of modified oils. In: Oksman-Caldentey KM, Barz WH (eds) Plant biotechnology and transgenic plants. Marcel Dekker, New York
8. Willatts P, Forsyth JS (2000) The role of long-chain polyunsaturated fatty acids in infant cognitive development. *Prostaglandins Leukot Essent Fatty Acids* 63:95–100
9. Iribarren C, Markovitz JH, Jacobs DR Jr, Schreiner PJ, Daviglius M, Hibbeln JR (2004) Dietary intake of n-3, n-6 fatty acids and fish: relationship with hostility in young adults—the CARDIA study. *Eur J Clin Nutr* 58:24–31
10. Stoll AL, Damico KE, Daly BP, Severus WE, Marangell LB (2001) Methodological considerations in clinical studies of omega 3 fatty acids in major depression and bipolar disorder. *World Rev Nutr Diet* 88:58–67
11. Dyerberg J, Bang HO (1982) A hypothesis on the development of acute myocardial infarction in Greenlanders. *Scand J Clin Lab Inves Suppl* 161:7–13
12. Simopoulos AP (2006) Evolutionary aspects of diet, the Omega-6/Omega-3 ratio, and gene expression. In: Meskin MS, Bidlack WR, Randolph RK (eds) Phytochemicals. CRC Press LLC, Boca Raton
13. Napier JA, Beauoin F, Michaelson LV, Sayanova O (2004) The production of long chain polyunsaturated fatty acids in transgenic plants by reverse engineering. *Biochimie* 86:785–792
14. Napier JA, Sayanova O, Qi B, Lazarus CM (2004) Progress toward the production of long-chain polyunsaturated fatty acids in transgenic plants. *Lipids* 39:1067–1075
15. Funk C (2001) Prostaglandins and leukotrienes: advances in eicosanoid biology. *Science* 294:1871–1875
16. Smith W (2005) Cyclooxygenases, peroxide tone and the allure of fish oil. *Curr Opin Cell Biol* 17:174–182
17. Yaqoob P (2003) Fatty acids and the immune system: from basic science to clinical applications. *Proc Nutr Soc* 63:89–104
18. Calder PC (2003) n-3 polyunsaturated fatty acids and inflammation: from molecular biology to the clinic. *Lipids* 38:343–352
19. Mukherjee D, Nissen SE, Topol EJ (2001) Risk of cardiovascular events associated with selective COX-2 inhibitors. *JAMA* 286:954–959
20. Sprecher H (2000) Metabolism of highly unsaturated n-3 and n-6 fatty acids. *Biochim Biophys Acta* 1486:219–231
21. Hibbeln DR, Nieminen LRG, Lands WEM (2004) Increasing homicide rates and linoleic acid consumption among five Western countries, 1961–2000. *Lipids* 39:1207–1213
22. Sargent JR (1997) Fish oils and human diet. *Br J Nutr* 78:S5–S13
23. Simopoulos AP (1999) Essential fatty acids in health and chronic disease. *Am J Clin Nutr* 70:560S–569S
24. Pauly D, Christensen V, Guenette S, Pitcher TJ, Sumaila UR, Walters CJ, Watson R, Zeller D (2000) Towards sustainability in world fisheries. *Nature* 418:689–695
25. Jacobs MN, Covaci A, Gheorghe A, Schepens P (2004) Time trend investigation of PCBs, PBDEs, and organochlorine pesticides in selected n-3 polyunsaturated fatty acid rich dietary fish oil and vegetable oil supplements; nutritional relevance for human essential n-3 fatty acid requirements. *J Agric Food Chem* 52:1780–1788
26. Hites RA, Foran JA, Carpenter DO, Hamilton MC, Knuth BA, Schwage SJ (2004) Global assessment of organic contaminants in farmed salmon. *Science* 303:226–229
27. Bell JG, McGhee F, Campbell PJ, Sargent JR (2003) Rapeseed oil as an alternative to marine fish oil in diets of post-smolt Atlantic salmon (*Salmo salar*): changes in flesh fatty acid composition and effectiveness of subsequent fish oil “wash out”. *Aquaculture* 218:515–528
28. Metz JG, Roessler P, Facciotti D, Levering C, Dittrich F, Lassner M, Valentine R, Lardizabal K, Domergue F, Yamada A, Yazawa K, Knauf V, Browse J (2001) Production of polyunsaturated fatty acids by polyketide synthases in both prokaryotes and eukaryotes. *Science* 293:290–293
29. Sayanova O, Napier JA (2004) Eicosapentaenoic acid: biosynthetic routes and the potential for synthesis in transgenic plants. *Phytochemistry* 65:147–158
30. Bentley R, Bennett JW (1999) Constructing polyketides: from Collie to combinatorial biochemistry. *Annu Rev Microbiol* 53:411–456
31. Metz JG, Weaver CA, Barclay WR, Flatt JH (2004) Polyunsaturated fatty acid polyketide synthase genes and enzyme systems from *Thraustochytrium* and *Schizochytrium* and their use for preparation of bioactive molecules. *PCT Int Appl WO2004087879*
32. Qiu X, Hong H, Mackenzie SL (2001) Identification of a  $\Delta 4$  fatty acid desaturase from *Thraustochytrium* sp. involved in the biosynthesis of docosahexaenoic acid by heterologous expression in *Saccharomyces cerevisiae* and *Brassica juncea*. *J Biol Chem* 276:31561–31566
33. Metz JG, Kuner J, Weaver C, Zirkle R, Rosenzweig B, Havermale A, Lippmeier C (2006) PUFA synthases: biochemical characterization and heterologous expression in bacteria and yeast. In: 17th International symposium on plant lipids, Michigan State University, East Lansing
34. Wallis JG, Watts JL, Browse J (2002) Polyunsaturated fatty acid synthesis: what will they think of next? *Trends Biochem Sci* 27:467–473
35. Spychalla JP, Kinney AJ, Browse J (1997) Identification of an animal omega-3 fatty acid desaturase by heterologous expression in *Arabidopsis*. *Proc Natl Acad Sci USA* 18:1142–1147
36. Oura T, Kajiwara S (2004) *Saccharomyces kluyveri* FAD3 encodes an  $\omega 3$  fatty acid desaturase. *Microbiology* 150:1983–1990
37. Pereira SL, Huang YS, Bobik EG, Kinney AJ, Stecca KL, Packer JC, Mukerji P (2004) A novel omega3-fatty acid desaturase involved in the biosynthesis of eicosapentaenoic acid. *Biochem J* 378:665–671
38. Sakuradani E, Abe T, Iguchi K, Shimizu S (2005) A novel fungal  $\omega 3$ -desaturase with wide substrate specificity from arachidonic acid-producing *Mortierella alpina* 1S-4. *Appl Microbiol Biotechnol* 66:648–654
39. Damude HG, Zhang H, Farrall L, Ripp KG, Tomb JF, Hollerbach D, Yadav NS (2006) Identification of bifunctional  $\Delta 12/\omega 3$  fatty acid desaturases for improving the ratio of  $\omega 3$  to  $\omega 6$  fatty acids in microbes and plants. *PNAS* 103:9446–9451
40. Qi B, Fraser T, Mugford S, Dobson G, Sayanova O, Butler J, Napier JA, Stobart AK, Lazarus CM (2004) Production of very long chain polyunsaturated omega-3 and omega-6 fatty acids in plants. *Nat Biotechnol* 22:739–45
41. Abbadi A, Domergue F, Bauer J, Napier JA, Welti R, Zahringer U, Cirpus P, Heinz E (2004) Biosynthesis of very-long-chain polyunsaturated fatty acids in transgenic oilseeds: constraints on their accumulation. *Plant Cell* 16:2734–2748
42. Wu G, Truksa M, Datla N, Vrinten P, Bauer J, Zank T, Cirpus P, Heinz E, Qiu X (2005) Stepwise engineering to produce high yields of very long-chain polyunsaturated fatty acids in plants. *Nat Biotechnol* 23:1013–1017

43. Kinney AJ, Cahoon EB, Damude HG, Hitz WD, Kolar CW, Liu ZB (2004) Production of very long chain polyunsaturated fatty acids in oilseed plants. PCT Int Appl WO2004071467
44. Yadav NS, Wierzbicki A, Aegerter M, Caster CS, Perez-Grau L, Kinney AJ, Hitz WD, Booth JR Jr, Schweiger B et al (1993) Cloning of higher plant  $\omega$ -3 fatty acid desaturases. Plant Physiol 103:467–476
45. Pereira SL, Leonard AE, HuangYS, Chuang LT, Mukerji P (2004) Identification of two novel microalgal enzymes involved in the conversion of the  $\omega$ 3-fatty acid, eicosapentaenoic acid, into docosahexaenoic acid. Biochem J 384:357–366
46. Parker-Barnes JM, Das T, Bobik E, Leonard AE, Thurmond JM, Chaung YSH, Mukerji P (2000) Identification and characterization of an enzyme involved in the elongation of n-6 and n-3 polyunsaturated fatty acids. PNAS 97:8284–8289
47. Chen R, Matsui K, Ogaw M, Oe M, Ochiai M, Kawashima H, Sakuradani E, Shimizu S, Ishimoto M, Hayashi M, Murooka Y, Tanaka Y (2006) Expression of  $\Delta$ 6,  $\Delta$ 5 desaturase and GLELO elongase genes from *Mortierella alpina* for production of arachidonic acid in soybean [*Glycine max* (L.) Merrill] seeds. Plant Sci 170:399–406
48. Robert S, Singh SP, Zhou XR, Petrie JR, Blackburn SI, Mansour PM, Nichols PD, Liu Q, Green A (2005) Metabolic engineering of *Arabidopsis* to produce nutritionally important DHA in seed oil. Funct Plant Biol 32:473–479
49. Damude H, Yadav NS (2005) Cloning and sequences of fungal  $\Delta$ 15 desaturases suitable for production of polyunsaturated fatty acids in oilseed plants for food or industrial uses. PCT Int Appl WO2005047479
50. Kinney AJ (1996) Development of genetically engineered soybean oils for food applications. J Food Lipids 3:273–292
51. Mukerji P, Huang YS, Das T, Thurmond JM, Leonard AE, Pereira SL (2002) Protein and cDNA sequences of delta4-desaturases isolated from fungi and therapeutical uses thereof. PCT Int Appl WO2002090493



# Bovine Brain Diacylglycerol Lipase: Substrate Specificity and Activation by Cyclic AMP-dependent Protein Kinase

Thad A. Rosenberger · Akhlaq A. Farooqui ·  
Lloyd A. Horrocks

Received: 6 November 2006 / Accepted: 3 January 2007 / Published online: 31 January 2007  
© AOCS 2007

**Abstract** Diacylglycerol lipase (EC 3.1.1.3) was purified from bovine brain microsomes using multiple column chromatographic techniques. The purified enzyme migrates as a single band on SDS-PAGE and has an apparent molecular weight of 27 kDa. Substrate specificity experiments using mixed molecular species of 1,2-diacyl-*sn*-glycerols indicate that low concentrations of  $\text{Ca}^{2+}$  and  $\text{Mg}^{2+}$  have no direct effect on enzymic activity and 1,2-diacyl-*sn*-glycerols are the preferred substrate over 1,3-diacyl-*sn*-glycerols. The enzyme hydrolyzes stearate in preference to palmitate from the *sn*-1 position of 1,2-diacyl-*sn*-glycerols. 1-*O*-Alkyl-2-acyl-*sn*-glycerols are not a substrate for the purified enzyme. The native enzyme had a  $V_{\max}$  value of 616 nmol/min mg protein. Phosphorylation by cAMP-dependent protein kinase resulted in a three-fold increase in catalytic throughput ( $V_{\max} = 1,900$  nmol/min mg protein). The substrate specificity and catalytic properties of the bovine brain diacylglycerol lipase suggest that diacylglycerol lipase may regulate protein kinase C activity and 2-arachidonoyl-*sn*-glycerol levels by rapidly altering the intracellular concentration of diacylglycerols.

**Keywords** Diacylglycerols · 2-arachidonoyl-*sn*-glycerol · Lipase · Brain · Phosphorylation · Protein kinase A · Protein kinase C

## Abbreviations

DAG	Diacylglycerols
PKC	Protein kinase C
PKA	cAMP-dependent protein kinase
PLC	Phospholipase C
PLD	Phospholipase D
CB-1	Cannabinoid receptor 1
2-AG	2-Arachidonoyl- <i>sn</i> -glycerol
PtdIns(4,5)P <sub>2</sub>	Phosphatidylinositol-4,5-bisphosphate
Ins(1,4,5)P <sub>3</sub>	Inositol-1,4,5-trisphosphate
thioester substrate	<i>rac</i> -1,2- <i>S</i> , <i>O</i> -didecanoyl-1-mercapto-2,3-propanediol
physiologic substrate	1-Stearoyl-2-arachidonoyl- <i>sn</i> -glycerol

## Introduction

The phospholipid-derived second messenger, 1,2-diacyl-*sn*-glycerol, is an important bioactive molecule that plays a central role in the biosynthesis of phospholipids [1], is a physiological activator of protein kinase C [2], and is the precursor for the cannabinoid receptor (CB-1) agonist, 2-arachidonoyl-*sn*-glycerol [3–5]. Following cell stimulation, 1,2-diacyl-*sn*-glycerols are produced by mechanisms that involve either the G-protein-linked phospholipase C (PLC)  $\beta$ 1 and  $\beta$ 2 or the tyrosine kinase-linked PLC  $\gamma$ 1 and  $\gamma$ 2 (Fig. 3). These PLC isoforms preferentially hydrolyze phosphatidylinositol-

T. A. Rosenberger (✉)  
Department of Pharmacology, Physiology,  
and Therapeutics, University of North Dakota,  
School of Medicine and Health Sciences,  
501 North Columbia Road, Rm. 3742A,  
Grand Forks, ND 58203, USA  
e-mail: trosenberger@medicine.nodak.edu

A. A. Farooqui · L. A. Horrocks  
Department of Molecular and Cellular Biochemistry,  
The Ohio State University, 1645 Neil Avenue,  
Columbus, OH 43210, USA

4,5-bisphosphate (PtdIns(4,5)P<sub>2</sub>) producing 1,2-diacyl-*sn*-glycerols and inositol-1,4,5-trisphosphate [6]. An increase in the concentration of intracellular Ca<sup>2+</sup> can also activate PLC through voltage-dependent or receptor-mediated mechanisms. Further, sustained thyrotropin-releasing hormone stimulation in rat pituitary cells results in a biphasic release of intracellular 1,2-diacyl-*sn*-glycerols [7]. Following the transient hydrolysis of PtdIns(4,5)P<sub>2</sub> by PLC, sustained release is brought about by a Ca<sup>2+</sup>-independent mechanism that involves activation of both protein kinase C and phospholipase D (PLD)-mediated pathways in which PLD hydrolyzes phosphatidylcholine to choline and phosphatidic acid [7, 8]. Sustained levels of 1,2-diacyl-*sn*-glycerols are required for long-term responses such as cell growth and differentiation and are initiated by growth factors and phorbol esters [9].

Increased levels of 1,2-diacyl-*sn*-glycerols activate protein kinase C by binding to its C1 domain. This increases its affinity for the cellular membrane and removes the pseudo-substrate inhibition caused by the N-terminal of the protein kinase C polypeptide chain [10, 11]. The biological functions of protein kinase C are broad. The recurring themes attributed to its function include: receptor desensitization, modulation of membrane restructuring events, regulation of transcription, mediation of immune response, regulation of cell growth, and influencing learning and memory [10]. The product of the diacylglycerol lipase-catalyzed reaction, 2-arachidonoyl-*sn*-glycerol, also functions as an endogenous CB-1 receptor agonist [12, 13]. The endocannabinoid, 2-arachidonoyl-*sn*-glycerol, modulates intracellular Ca<sup>2+</sup> and results in the attenuation of voltage-gated Ca<sup>2+</sup> influx in differentiated NG108-15 cells [14, 15] and the transient release of intracellular Ca<sup>2+</sup> in non-differentiated NG108-15 cultures [12]. High frequency stimulation of hippocampal slices also increases brain 2-arachidonoyl-*sn*-glycerol levels fourfold and is dependent on neuronal depolarization and external Ca<sup>2+</sup> [16]. The coupling of calcium influx, diacylglycerol lipase activity, and 2-arachidonoyl-*sn*-glycerol is necessary and sufficient in controlling axonal growth and guidance in response to FGF receptor activation [17]. Unfortunately, the mechanism that couples the hydrolysis of 1,2-diacyl-*sn*-glycerols and the formation of 2-arachidonoyl-*sn*-glycerol to the calcium response is poorly understood.

To investigate the possibility that the activity of diacylglycerol lipase in the brain is regulated by phosphorylation and to investigate its function in the metabolism of 1,2-diacyl-*sn*-glycerols, we measured the substrate specificity and catalytic properties of the native (non-phosphorylated) and phosphorylated brain

microsomal enzyme. We report here that the  $V_{\max}$  values of bovine brain diacylglycerol lipase are increased threefold following phosphorylation by cAMP-dependent protein kinase, and that diacylglycerol lipase hydrolyzes stearate from the *sn*-1 position of 1,2-diacyl-*sn*-glycerols. Substrate specificity assays with the native enzyme show that microsomal diacylglycerol lipase shows a preference for 1,2-diacyl-*sn*-glycerols having arachidonic or linoleic acid esterified at the *sn*-2 position. These results suggest that native and phosphorylated diacylglycerol lipase can regulate both protein kinase C and CB-1 receptor activation by modulating the intracellular levels of 1,2-diacyl-*sn*-glycerols and 2-arachidonoyl-*sn*-glycerol. The data also suggest that protein phosphorylation tightly regulates brain diacylglycerol lipase activity, and that the metabolism of 1,2-diacyl-*sn*-glycerols following receptor-mediated cell stimulation may play an active role in organizing signaling responses following the initial stimulus.

## Materials and Methods

### Protein Purification

Bovine brain diacylglycerol lipase was purified to homogeneity using multiple column chromatographic procedures [18, 19]. Protein concentrations were determined with a dye-binding assay [20] using bovine serum albumin as standard. The purified protein was divided into aliquots and stored in 50 mM 3-(*N*-morpholino) propane sulfonic acid (MOPS) buffer, pH 7.4, containing 50% glycerol at –80 °C. Assays were performed on freshly thawed aliquots of enzyme. All chemicals used were of reagent grade and purchased from the Sigma Chemical Company (St Louis, MO) unless noted otherwise. The physiologic substrate, 1-stearoyl-2-arachidonoyl-*sn*-glycerol, was purchased from Matreya Inc. (Pleasant Gap, PA) and *rac*-1,2-*S,O*-didecanoyl-1-mercapto-2,3-propanediol (thioester substrate) was made as described previously [21].

### Substrate Preparation

Mixed molecular species of diacylglycerol were prepared from bovine brain phospholipid. Briefly, bovine brain phospholipid (200 mg), stored in *n*-hexane/2-propanol (3:2, by vol) was concentrated to zero under a steady-stream of N<sub>2</sub> at 45 °C and sonicated into solution in 50 mM MOPS buffer (pH 7.4) containing 5.0 mM CaCl<sub>2</sub>, 0.1% Triton X-100, and 0.25% essentially fatty acid free bovine serum albumin. The lipid suspension was incubated at room temperature in the

presence of 10,000 units phospholipase C (*Bacillus cereus*, Boehringer, Ridgefield, CT) to produce mixed molecular species of diacylglycerols. The reaction was stopped with the addition of 3.75 vol of chloroform/methanol (1:2, by vol) and extracted with the addition of 1.25 vol H<sub>2</sub>O. The lower phase containing the lipid was collected and purified with standards on TLC (silica gel G, Analtech) using heptane/isopropyl ether/acetic acid (60:40:4, by vol) [22]. Bands corresponding to 1,2-diacyl-*sn*-glycerols were extracted from the silica gel with *n*-hexane/2-propanol (3:2, by vol) and stored at -80 °C. The 1,3-diacyl-*sn*-glycerol isomers were produced by incubating 1,2-diacyl-*sn*-glycerols in methanol/H<sub>2</sub>O (1:1, by vol) for 24 h at 37 °C, and purified by TLC as outlined above. The diacylglycerol substrate isomers were re-purified using the above separation immediately prior to assay. Kinetic experiments were performed using a physiologic substrate, 1-stearoyl-2-arachidonoyl-*sn*-glycerol purchased from Matreya Inc. (Pleasant Gap, PA) or using a thioester substrate, *rac*-1,2-*S*,*O*-didecanoyl-1-mercapto-2,3-propanediol, prepared as described [21]. Substrate suspensions of known amounts of mixed molecular species of 1,2- or 1,3-diacyl-*sn*-glycerols, 1-stearoyl-2-arachidonoyl-*sn*-glycerol, or *rac*-1,2-*S*,*O*-didecanoyl-1-mercapto-2,3-propanediol were prepared via sonication of substrates in an assay buffer containing 6 mg lysophosphatidylcholine (Sigma).

#### Diacylglycerol Lipase Assay

Assays using mixed molecular species of diacylglycerol were performed at 37 °C in 50 mM MOPS buffer (pH 7.4) containing 0.25% essentially fatty acid free bovine serum albumin (BSA). Phosphorylated diacylglycerol lipase assays were preformed, using enzyme preparations that were pre-incubated at 37 °C for 10 min in 50 mM MOPS buffer pH 7.4 containing 0.25% BSA, 25 units of catalytic subunit of cAMP-dependent protein kinase (Promega, Madison, WI), 20 mM MgCl<sub>2</sub>, and 0.2 mM ATP. Parallel assays of “native” diacylglycerol lipase using both the physiologic substrate and the thioester substrate were performed, using those conditions outlined for the phosphorylated diacylglycerol lipase in the absence of the catalytic subunit of cAMP-dependent protein kinase. All diacylglycerol lipase assays (12.5 µg protein per assay), having a total volume of 0.5 ml, were initiated with the addition of suspensions containing known final amounts of substrate (18.75–300 µmol for kinetic analysis or 150 µmol for molecular species analysis) to the diacylglycerol lipase preparations. The reactions were stopped with the addition of 3.75 vol (2 ml) chloroform/methanol

(1:2, by vol) and samples were extracted as outlined above. The non-hydrolyzed diacylglycerols and non-esterified fatty acids released following incubation were isolated via TLC as outlined above then quantified by GLC. The molecular species preferences was determined using a subtraction assay in which the initial substrate and the substrate remaining following incubation were converted to their dinitrobenzoyl derivatives then isolated using silica Gel G developed with a solvent system of petroleum ether/ethyl ether/acetic acid (90:10:1, by vol) followed by second elution with toluene [23]. The 1,2-diacyl-*sn*-glycerols, 1,3-diacyl-*sn*-glycerols, and 1-*O*-alkyl-2-acylglycerols were extracted off the silica using hexane:2-propanol (3:2, by vol) and stored at -20 °C prior to analysis.

#### Molecular Species Determination

Molecular species analyses of the dinitrobenzoyl derivatives were isolated by HPLC on a Nucleosil C18 column (Phenomenex, Torrance, CA) using an isocratic elution of acetonitrile/2-propanol (80:20, by vol) as described in [23]. Fractions absorbing light at 254 nm were collected, methylated, and quantified by gas liquid chromatography.

#### Gas Liquid Chromatography (GLC)

Esterified fatty acids were converted to their methyl ester derivatives in 0.5 M methanolic KOH at 37 °C for 30 min and extracted in *n*-hexane. Non-esterified fatty acids were methylated in toluene/methanol (1:1, by vol) + 2% H<sub>2</sub>SO<sub>4</sub> at 60 °C for 2 h and extracted in petroleum ether following the addition of 0.5 vol H<sub>2</sub>O. Fatty acid methyl esters were quantified with a GLC (Shimadzu GLC-14A, Kyoto, Japan) equipped with a SP-2330 capillary column (0.32 mm ID × 30 m length, Supelco, Bellefonte, PA) and a flame ionization detector. Column temperature was maintained at 185 °C with nitrogen as the carrier gas at a pressure of 0.5 kg/cm<sup>2</sup>. Detector and injector temperatures were maintained at 220 °C. Known standards (NuChek Prep, Elysian, MN) were used to establish relative retention times and relative correction factors. The detector response was linear within the sample concentration range for all fatty acids of varying chain lengths and degree of saturation with correlation coefficients of 0.990 or greater.

#### Calculations

Reaction rates were determined by calculating the rate of hydrolysis of 1,2-diacyl-*sn*-glycerols, 1,3-diacyl-*sn*-

glycerols, or 1-*O*-alkyl-2-acyl-*sn*-glycerols or the formation of 2-arachidonoyl-*sn*-glycerol as a function of time compared to enzyme control blanks. One-way Analysis of Variance (ANOVA) with a Tukey-Kramer multiple comparison test (Instat<sup>®</sup> Ver. 3.05, GraphPad, San Diego, CA) was used to compare the hydrolysis rates of the enzyme towards different molecular species (Table 2), statistical significance was taken as  $p \leq 0.05$ . Data are presented as mean  $\pm$  SD.

## Results

### Molecular Species Specificity

Substrate specificity of native diacylglycerol lipase using mixed molecular species of 1,2-diacyl-*sn*-glycerols or 1,3-diacyl-*sn*-glycerols showed that diacylglycerol lipase cleaves primarily 1,2-diacyl-*sn*-glycerols (Fig. 1). Only trace amounts of the 1,3-diacyl-*sn*-glycerols or 1-*O*-alkyl-2-acyl-*sn*-glycerols were hydrolyzed. Due to the inability to separate 1-*O*-alkyl-2-acyl-*sn*-glycerols from 1,2-diacyl-*sn*-glycerols prior to their conversion to a dinitrobenzoyl derivative, the percent hydrolyzed was determined following the assay by measuring the amount of dinitrobenzoyl derivatives remaining of each species. In these experiments 1-*O*-alkyl-2-acyl-*sn*-glycerols composed approximately 7% of the total substrate being approximately 10.5  $\mu$ mol per assay and resulted in approximately 0.26 nmol hydrolyzed during

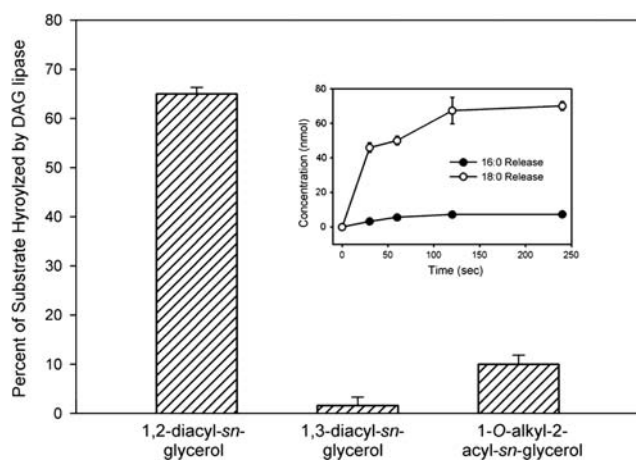


**Fig. 1** Specificity of diacylglycerol lipase toward different isomers of diacylglycerols. Bars represent the percent of substrate hydrolyzed by diacylglycerol lipase over a 4 min incubation period at 37 °C (values represent mean  $\pm$  SD,  $n = 5$ ). The inset represents reaction coordinates of free acid release during incubations performed using 1,2-diacyl-*sn*-glycerols, 1,3-diacyl-*sn*-glycerols, and 1-*O*-alkyl-2-acyl-*sn*-glycerols as substrate (values represent mean  $\pm$  SD,  $n = 5$ )

the 4.0 min incubation period. Substrate competition between the 1,2-diacyl-*sn*-glycerol and 1-*O*-alkyl-2-acyl-*sn*-glycerol molecular species was not determined. The rate of hydrolysis of 1-stearoyl-2-arachidonoyl-*sn*-glycerol or the substrate specificity of diacylglycerol lipase using the mixed molecular species assay was not affected following the addition of 25  $\mu$ M CaCl<sub>2</sub> or 25  $\mu$ M MgCl<sub>2</sub>.

### Fatty Acid Specificity

The reaction time course (Fig. 1, inset) shows the enzyme hydrolyzes stearate 35 times more readily than palmitate despite a 4.3-fold differential in the concentration ratio of these fatty acids in the substrate used (Table 1). These data were confirmed by directly quantifying the free fatty acid released following experiments using 150  $\mu$ mol of mixed molecular species of 1,2-diacyl-*sn*-glycerols. The release of palmitate was found in these assays; however the levels were near the detection limits of the gas chromatograph. Assays performed for 10 and 20 min resulted in the depletion of stearate-containing molecular species, but did not produce significant increases in the level of hydrolyzed palmitate nor a significant loss of palmitate-containing molecular species. Experiments were performed in which the 1,2-diacyl-*sn*-glycerols were depleted of stearate-containing molecular species by pre-incubating the substrate with diacylglycerol lipase then re-assaying the 18:0-depleted 1,2-diacyl-*sn*-glycerols. These experiments showed palmitate is hydrolyzed, but at a very slow rate compared to stearate (data not shown). Therefore, it was concluded that native diac-

**Table 1** Molecular species profile of the 1,2-diacyl-*sn*-glycerols purified from bovine brain phospholipid

Molecular species	nmol	mol %
16:0/22:6	46.2 $\pm$ 0.5	7.8
16:0/22:4	12.7 $\pm$ 0.3	2.1
16:0/20:5	17.3 $\pm$ 0.2	2.9
16:0/20:4	4.4 $\pm$ 0.3	0.7
16:0/18:1	30.6 $\pm$ 0.8	5.2
18:0/22:6	137.8 $\pm$ 0.2	23.3
18:0/22:5	60.9 $\pm$ 1.9	10.3
18:0/22:4	40.6 $\pm$ 0.3	6.9
18:0/20:4	96.7 $\pm$ 1.2	16.4
18:0/20:3	4.9 $\pm$ 0.6	0.8
18:0/18:2	12.0 $\pm$ 1.8	2.0
18:0/18:1	108.6 $\pm$ 0.04	18.4
18:0/18:0	18.1 $\pm$ 0.2	3.1
Total	590.61	99.9

Values are the mean  $\pm$  SD and represent the concentration (nmol) and mole percentage of individual species of 1,2-diacyl-*sn*-glycerols in aliquots of the mixed molecular species substrate ( $n = 6$ )

ylglycerol lipase does hydrolyze palmitate from 1,2-diacyl-*sn*-glycerols. Statistical analysis of the rates at which the different molecular species were hydrolyzed showed diacylglycerol lipase maintains a preference in the rate of hydrolysis of certain molecular species. This preference was 18:0/20:4 = 18:0/18:1 = 18:0/22:6 > 18:0/22:5 > 18:0/22:4 (Table 2).

### Enzyme Kinetics

The native enzyme displayed linear kinetic characteristics when incubated with varying concentrations between 300 and 18.75  $\mu\text{mol}$  of 1-stearoyl-2-arachidonoyl-*sn*-glycerol. The  $V_{\text{max}}$  values of native diacylglycerol lipase using 1-stearoyl-2-arachidonoyl-*sn*-glycerol or didecanoyl-1-thioglycerol were 616 and 120 nmol/min mg protein, respectively (Table 3). Experiments in which synthetic didecanoyl-1-thioglycerol was used, the decrease in the  $V_{\text{max}}$  of diacylglycerol lipase towards the thioester substrate suggests that the acyl chain length and degree of saturation of the fatty acids in the substrate may alter substrate presentation and catalysis. Phosphorylation of native diacylglycerol lipase by cAMP-dependent protein kinase increased the  $V_{\text{max}}$  of diacylglycerol lipase to 1,900 nmol/min mg protein, representing a threefold increase when compared to the native enzyme (Fig. 2).

**Table 2** Specificity of diacylglycerol lipase toward mixed molecular species of 1,2-diacyl-*sn*-glycerols

Molecular species	mol %	Activity (nmol/min)	SP activity (nmol/min/mg)
18:0/18:1	18.4	6.9 $\pm$ 1.2	548 $\pm$ 93
18:0/20:4	16.4	6.8 $\pm$ 0.7	540 $\pm$ 54
18:0/22:4	6.9	1.3 $\pm$ 0.5	103 $\pm$ 43
18:0/22:5	10.1	3.0 $\pm$ 0.4	237 $\pm$ 32
18:0/22:6	23.4	6.9 $\pm$ 1.1	552 $\pm$ 86

Values are the mean  $\pm$  SD of the activity and specific activity (SP activity) and represent the hydrolysis of 1,2-diacyl-*sn*-glycerols (150  $\mu\text{mol}$ ) over a 5 min incubation ( $n = 5$ ). Column 2 represents the mole percentage of the individual molecular species found in the substrate mixture

SP activity specific activity

### Discussion

It was found that bovine brain microsomal diacylglycerol lipase maintains a high level of substrate specificity in that the enzyme preferentially hydrolyzes stearate over palmitate from the *sn*-1 position of 1,2-diacyl-*sn*-glycerols. These experiments also demonstrated that  $\text{Ca}^{2+}$  and  $\text{Mg}^{2+}$ , at low concentrations, had no effect on the catalytic properties of the enzyme and that phosphorylation of native diacylglycerol lipase by cAMP-dependent protein kinase increased its  $V_{\text{max}}$  threefold. The presence of an actively regulated diacylglycerol lipase in the brain may serve several important functions in that it may regulate protein kinase C by modulating the intracellular levels of 1,2-diacyl-*sn*-glycerols as well as stimulate the cannabinoid receptor system by producing the CB-1 receptor ligand, 2-arachidonoyl-*sn*-glycerol.

The characterization and solubilization of membrane-bound diacylglycerol lipase using a thioester substrate has been reported. These studies show that the purified microsomal diacylglycerol lipase maintains a  $V_{\text{max}}$  of 182 nmol/min/mg protein [19]. Results found in these studies are similar to those found with the native microsomal diacylglycerol lipase using the thioester substrate (Table 3). The differing characteristics of the native diacylglycerol lipase toward the physiologic substrate suggest that the presence of an ester bond or the acyl-chain length of the esterified fatty acids influence the rate of hydrolysis of the substrate by the enzyme. Interestingly, assays using mixed molecular species show that the enzyme hydrolyzes palmitate esterified at the *sn*-1 position of the diacylglycerol molecule at a much slower rate compared to stearate. These results suggest that the acyl-chain length of the fatty acid found at the *sn*-1 position may influence the catalytic capacity. Therefore it is likely that the fivefold increase in the  $V_{\text{max}}$  of native diacylglycerol lipase toward the physiologic substrate is in part due to the presence of the ester bond and increased acyl chain length found at the *sn*-1 position of the native substrate.

**Table 3** Catalytic values for different substrates and different activation of diacylglycerol lipase

Substrate	Enzyme	$K_m$ ( $\mu\text{M}$ )	$V_{\text{max}}$ (nmol/min/mg protein)
1,2-Didecanoyl-1-thioglycerol	Non-phosphorylated (native)	38	120
1-Stearoyl-2-arachidonoyl - <i>sn</i> -glycerol	Non-phosphorylated (native)	63	616
1-Stearoyl-2-arachidonoyl - <i>sn</i> -glycerol	Phosphorylated	55	1,900

Values represent mean catalytic constants of non-phosphorylated (native) and phosphorylated enzyme when incubated with either 1,2-didecanoyl-1-thioglycerol or 1-stearoyl-2-arachidonoyl-*sn*-glycerol ( $n = 3$ ) experimental measures per concentration analyzed (18.75, 37.5, 75, 150, and 300  $\mu\text{mol}$ )

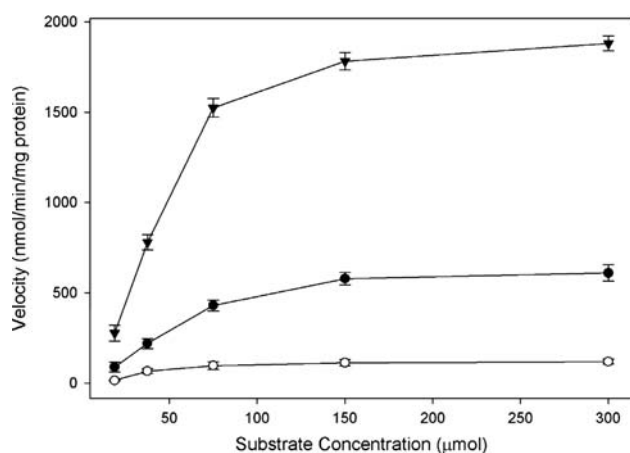


**Fig. 2** Plot of the velocity dependency as a function of substrate concentration of native (non-phosphorylated) and phosphorylated diacylglycerol lipase. (Open circles and closed circles represent assays performed on native enzyme using the thioester substrate, didecanoyl-1-thioglycerol or the physiologic substrate, 1-stearoyl-2-arachidonoyl-*sn*-glycerol, respectively). The plot showing closed triangles represent assays performed on phosphorylated enzyme preparations using 1-stearoyl-2-arachidonoyl-*sn*-glycerol. Values represent the mean  $\pm$  SD ( $n = 3$ )

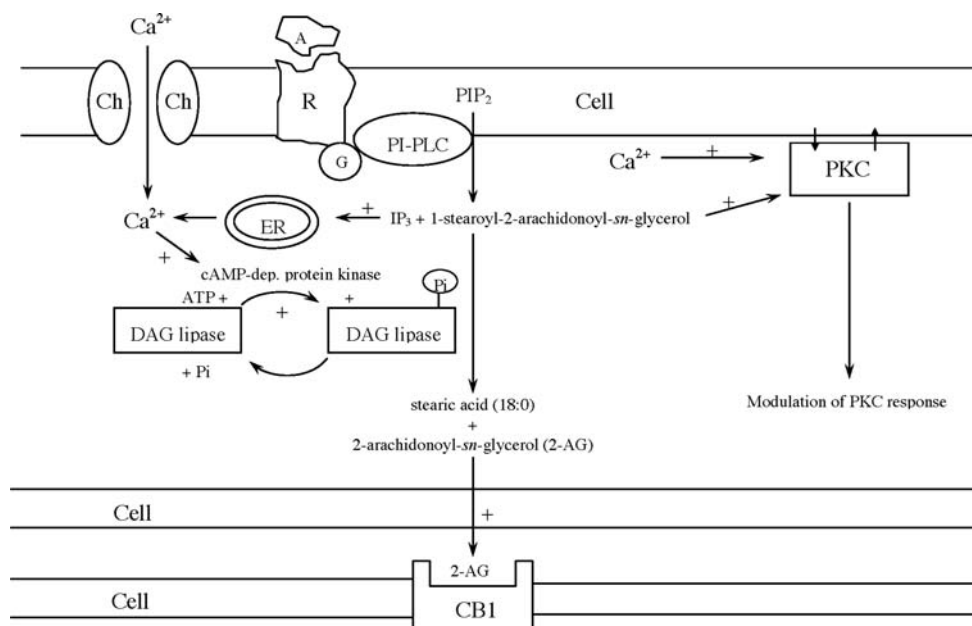
High calcium, magnesium, and manganese ions markedly stimulate the enzymic activity of the solubilized microsomal diacylglycerol lipase using the thioester substrate [19]. Diacylglycerol lipase activity in human platelet microsomes and the  $\alpha$  and  $\beta$  isoforms cloned from brain are also stimulated by  $\text{Ca}^{2+}$  ions [24–26]. However, we found that 25  $\mu\text{M}$  calcium or magnesium did not alter the enzymic activity of diacylglycerol lipase in assay using the physiologic substrate 1-stearoyl-2-arachidonoyl-*sn*-glycerol. These results suggest that the stimulation of diacylglycerol lipase by high concentrations of these ions in the presence of the thioester substrate may be due to the interaction with the thioester substrate rather than direct interactions with the protein molecule. The concentration-dependent stimulation by the non-ionic detergent Triton X-100 of the partially purified enzyme [18] supports the premise that the interfacial binding of the enzyme to the lipid bilayer is a crucial aspect of diacylglycerol lipase activity. The change in the bilayer organization of membrane lipids by calcium ions [27, 28] supports our previous assumption that the interaction of calcium ions with the thioester substrate reorganizes the aggregated structure of *rac*-1,2-*S,O*-didecanoyl-1-mercapto-2,3-propanediol [19]. Therefore, comparing the results from assays performed using the artificial and physiologic substrates suggests that the effect of increasing the concentration of positive ions on diacylglycerol lipase activity is probably due to contact of

the ions with the thioester substrate rather than a direct interaction with the protein.

As the cellular concentration of the biologically active 1,2-diacyl-*sn*-glycerols can modulate the activity of protein kinase C and is the precursor for the endocannabinoid, 2-arachidonoyl-*sn*-glycerol [27, 28], the amount of diacylglycerols in brain must be tightly regulated. Because the basal level of 2-arachidonoyl-*sn*-glycerol in brain is much lower than the binding affinity of anandamide with the CB1 receptor [29], a rapid equilibrium between formation and breakdown of this molecule is necessary to explain its action as a brain CB<sub>1</sub> receptor ligand [26, 30]. Several lines of evidence suggest that  $\text{Ca}^{2+}$ -dependent phosphorylation may act as a regulatory component in this system. The first is that treatment of neuron-enriched spinal cord cultures with NMDA and glutamate results in a dose- and time-dependent stimulation of diacylglycerol lipase activity [31, 32]. Further, diacylglycerol lipase activity and 2-arachidonoyl-*sn*-glycerol is necessary and sufficient in controlling axonal growth and guidance in response to FGF receptor activation [17]. Moreover, ATP increases the rate of 2-arachidonoyl-*sn*-glycerol formation in mouse astrocytes by a factor of 60, which is dependent on calcium and greater than any stimulus-induced increase in endocannabinoid production reported in brain to date [33]. Diacylglycerol lipase present in chicken adipose tissue is activated by cAMP-dependent protein kinase, which increases the catalytic capacity of the enzyme 1,000-fold [34, 35]. Therefore, the substrate specificity of the brain microsomal diacylglycerol lipase coupled to the positive regulatory effect of phosphorylation outlined above suggests that 2-arachidonoyl-*sn*-glycerol formation in brain is likely a result of activation of diacylglycerol lipases.

Two diacylglycerol lipase isoforms,  $\alpha$  and  $\beta$ , have been cloned when the sequence of a *Penicillium* diacylglycerol lipase is “blasted” against the human genome [26]. These isoforms have a molecular weight of 120 and 70 kDa, respectively, and thus do not correspond to the 27 kDa enzymatic activity studied here. Analyses of these isoforms show that they share similar substrate specificities with regard to the hydrolysis of fatty acid esterified to the *sn*-1 position of the diacylglycerol molecule, show a marked dependence on  $\text{Ca}^{2+}$  ions for activity, and demonstrate well-defined expression patterns during development. Thus, while it is at this point unclear, further studies are needed to determine whether the enzyme activity outlined in this manuscript represents a new diacylglycerol isoform or proteolytic cleavage of one of the cloned isoforms. Future studies to clone this enzyme and to produce

**Fig. 3** General schematic representing the hypothetical contribution that diacylglycerol lipase has following receptor-mediated signaling. Diacylglycerol lipase is phosphorylated by cAMP-dependent protein kinase (protein kinase A), but not protein kinase C.  $Ca^{2+}$  calcium, *Ch* calcium channel, *A* agonist, *R* receptor, + activation, *G* G-protein, *CB* cannabinoid receptor, *PI-PLC* phosphoinositide-specific phospholipase C, *PIP<sub>2</sub>* phosphatidylinositol-4,5-bisphosphate, *PKC* protein kinase C, *ER* endoplasmic reticulum *IP<sub>3</sub>* inositol-1,4,5-trisphosphate, *P<sub>i</sub>* phosphate, *DAG* diacylglycerols



antibodies against it will aid in determining the physiologic role this enzyme has in the brain.

Further, the common assumption that receptor-mediated activation of phospholipase C results in the release of arachidonic acid due to diacylglycerol lipase activation is not completely correct. Our results and others [26] support the idea that diacylglycerol lipase is not involved directly in the release of arachidonic acid from the *sn*-2 position of the diacylglycerol molecule (Fig. 3). The endocannabinoid, 2-arachidonoyl-*sn*-glycerol, is the primary product of the diacylglycerol lipase-mediated reaction. The majority of esterified arachidonic acid is located at the *sn*-2 position of the diacylglycerol moiety (Table 1) and the activation of the diacylglycerol lipase is able to release fatty acid only from the *sn*-1 position thereby forming primarily stearic acid and 2-arachidonoyl-*sn*-glycerol. Although several investigators have shown a relationship between ionomycin-induced activation of PLC and the subsequent release of arachidonic acid [36, 37], which can be inhibited with the diacylglycerol lipase inhibitor RHC 80267, our data suggest that this is more likely the result of subsequent hydrolysis by a monoacylglycerol lipase or possible overlapping PLA<sub>2</sub> activity. Therefore the more likely product of the diacylglycerol lipase reaction is the biologically active endocannabinoid, 2-arachidonoyl-*sn*-glycerol, followed by degradation by monoacylglycerol lipase [38]. Activation of diacylglycerol lipase by phosphorylation with cAMP-dependent protein kinase suggests that diacylglycerol lipase can be recruited by  $Ca^{2+}$ -dependent protein kinases to modulate cellular levels of 1,2-diacylglycerols.

Diacylglycerols derived from inositol glycerophospholipids are more effective in stimulating protein kinase C isoforms than the diacylglycerols derived from the hydrolysis of choline glycerophospholipids [2, 39].

In summary, these data support the premise that brain diacylglycerol lipase plays a role in regulating the intracellular levels of 1,2-diacyl-*sn*-glycerols. The diacylglycerol lipase activity can be modulated by phosphorylation by cAMP-dependent protein kinase. The microsomal diacylglycerol lipase in its phosphorylated form can produce the CB-1 receptor agonist, 2-arachidonoyl-*sn*-glycerol, at rates higher than previously appreciated. Therefore, the modulation of diacylglycerol lipase activity by phosphorylation can greatly influence its catalytic properties making it a more potent modulator of both protein kinase C and the cannabinoid receptor system in the brain.

**Acknowledgments** This work was supported in part by research grants NS-10165 and NS-29441 from the National Institutes of Health, US Public Health Service.

## References

1. Lee DP, Deonarine AS, Kienetz M, Zhu Q, Skrzypczak M, Chan M, Choy PC (2001) A novel pathway for lipid biosynthesis: the direct acylation of glycerol. *J Lipid Res* 42:1979–1986
2. Marignani PA, Epand RM, Sebaldt RJ (1996) Acyl chain dependence of diacylglycerol activation of protein kinase C activity in vitro. *Biochem Biophys Res Commun* 225:469–473
3. Sugiura T, Kobayashi Y, Oka S, Waku K (2002) Biosynthesis and degradation of anandamide and 2-arachidonoylglycerol

- and their possible physiological significance. Prostaglandins Leukot Essent Fatty Acids 66:173–192
4. Bisogno T, Sepe N, Melck D, Maurelli S, De Petrocellis L, Di Marzo V (1997) Biosynthesis, release and degradation of the novel endogenous cannabimimetic metabolite 2-arachidonoylglycerol in mouse neuroblastoma cells. *Biochem J* 322:671–677
  5. Bisogno T, Sepe N, De Petrocellis L, Di Marzo V (1997) Biosynthesis of 2-arachidonoyl-glycerol, a novel cannabimimetic eicosanoid, in mouse neuroblastoma cells. *Adv Exp Med Biol* 433:201–204
  6. Nakamura S, Nishizuka Y (1994) Lipid mediators and protein kinase C activation for the intracellular signaling network. *J Biochem (Tokyo)* 115:1029–1034
  7. Kiley SC, Parker PJ, Fabbro D, Jaken S (1991) Differential regulation of protein kinase C isozymes by thyrotropin-releasing hormone in GH<sub>4</sub>C<sub>1</sub> cells. *J Biol Chem* 266:23761–23768
  8. Exton JH (1994) Phosphatidylcholine breakdown and signal transduction. *Biochim Biophys Acta* 1212:26–42
  9. Farooqui AA, Farooqui T, Yates AJ, Horrocks LA (1988) Regulation of protein kinase C activity by various lipids. *Neurochem Res* 13:499–511
  10. Newton AC (1995) Protein kinase C: structure, function, and regulation. *J Biol Chem* 270:28495–28498
  11. Bell RM, Burns DJ (1991) Lipid activation of protein kinase C. *J Biol Chem* 266:4661–4664
  12. Sugiura T, Kodaka T, Kondo S, Tonegawa T, Nakane S, Kishimoto S, Yamashita A, Waku K (1996) 2-Arachidonoylglycerol, a putative endogenous cannabinoid receptor ligand, induces rapid, transient elevation of intracellular free Ca<sup>2+</sup> in neuroblastoma × glioma hybrid NG108–15 cells. *Biochem Biophys Res Commun* 229:58–64
  13. Parrish JC, Nichols DE (2006) Serotonin 5-HT receptor activation induces 2-arachidonoylglycerol release through a phospholipase c-dependent mechanism. *J Neurochem* 99:1164–1175
  14. Sugiura T, Kodaka T, Kondo S, Nakane S, Kondo H, Waku K, Ishima Y, Watanabe K, Yamamoto I, (1997) Is the cannabinoid CB1 receptor a 2-arachidonoylglycerol receptor? Structural requirements for triggering a Ca<sup>2+</sup> transient in NG108-15 cells. *J Biochem (Tokyo)* 122:890–895
  15. Sugiura T, Kodaka T, Kondo S, Tonegawa T, Nakane S, Kishimoto S, Yamashita A, Waku K (1997) Inhibition by 2-arachidonoylglycerol, a novel type of possible neuromodulator, of the depolarization-induced increase in intracellular free calcium in neuroblastoma x glioma hybrid NG108–15 cells. *Biochem Biophys Res Commun* 233:207–210
  16. Stella N, Schweitzer P, Piomelli D (1997) A second endogenous cannabinoid that modulates long-term potentiation. *Nature* 388:773–778
  17. Williams EJ, Walsh FS, Doherty P (2003) The FGF receptor uses the endocannabinoid signaling system to couple to an axonal growth response. *J Cell Biol* 160:481–486
  18. Farooqui AA, Taylor WA, Horrocks LA (1984) Separation of bovine brain mono- and diacylglycerol lipases by heparin sepharose affinity chromatography. *Biochem Biophys Res Commun* 122:1241–1246
  19. Farooqui AA, Rammohan KW, Horrocks LA (1989) Isolation, characterization, and regulation of diacylglycerol lipases from the bovine brain. *Ann NY Acad Sci* 559:25–36
  20. Bradford MM (1976) A rapid and sensitive method for the quantitation of microgram quantities of protein utilizing the principle of protein-dye binding. *Anal Biochem* 72:248–254
  21. Cox JW, Horrocks LA (1981) Preparation of thioester substrates and development of continuous spectrophotometric assays for phospholipase A<sub>1</sub> and monoacylglycerol lipase. *J Lipid Res* 22:496–505
  22. Breckenridge WC, Kuksis A (1968) Specific distribution of short-chain fatty acids in molecular distillates of bovine milk fat. *J Lipid Res* 9:388–393
  23. Nakagawa Y, Horrocks LA (1983) Separation of alkenylacyl, alkylacyl, and diacyl analogues and their molecular species by high performance liquid chromatography. *J Lipid Res* 24:1268–1275
  24. Bell RL, Kennerly DA, Stanford N, Majerus PW, (1979) Diglyceride lipase: a pathway for arachidonate release from human platelets. *Proc Natl Acad Sci USA* 76:3238–3241
  25. Majerus PW, Prescott SM (1982) Characterization and assay of diacylglycerol lipase from human platelets. *Methods Enzymol* 86:11–17
  26. Bisogno T, Howell F, Williams G, Minassi A, Cascio MG, Ligresti A, Matias I, Schiano-Moriello A, Paul P, Williams EJ, Gangadharan U, Hobbs C, Di Marzo V, Doherty P (2003) Cloning of the first sn1-DAG lipases points to the spatial and temporal regulation of endocannabinoid signaling in the brain. *J Cell Biol* 163:463–468
  27. Dawson RM, Hemington NL, Irvine RF (1983) Diacylglycerol potentiates phospholipase attack upon phospholipid bilayers: possible connection with cell stimulation. *Biochem Biophys Res Commun* 117:196–201
  28. Tilcock CP, Bally MB, Farren SB, Cullis PR, Gruner SM (1984) Cation-dependent segregation phenomena and phase behavior in model membrane systems containing phosphatidylserine: influence of cholesterol and acyl chain composition. *Biochemistry* 23:2696–2703
  29. Breivogel CS, Griffin G, Di Marzo V, Martin BR (2001) Evidence for a new G protein-coupled cannabinoid receptor in mouse brain. *Mol Pharmacol* 60:155–163
  30. Bazinet RP, Lee HJ, Felder CC, Porter AC, Rapoport SI, Rosenberger TA (2005) Rapid high-energy microwave fixation is required to determine the anandamide (*N*-arachidonylethanolamine) concentration of rat brain. *Neurochem Res* 30:597–601
  31. Farooqui AA, Horrocks LA (1997) Nitric oxide synthase inhibitors do not attenuate diacylglycerol or monoacylglycerol lipase activities in synaptoneurosomes. *Neurochem Res* 22:1265–1269
  32. Farooqui AA, Anderson DK, Horrocks LA (1993) Effect of glutamate and its analogs on diacylglycerol and monoacylglycerol lipase activities of neuron-enriched cultures. *Brain Res* 604:180–184
  33. Walter L, Dinh T, Stella N (2004) ATP induces a rapid and pronounced increase in 2-arachidonoylglycerol production by astrocytes, a response limited by monoacylglycerol lipase. *J Neurosci* 24:8068–8074
  34. Khoo JC, Steinberg D, Huang JJ, Vagelos PR (1976) Triglyceride, diglyceride, monoglyceride, and cholesterol ester hydrolases in chicken adipose tissue activated by adenosine 3':5'-monophosphate-dependent protein kinase. Chromatographic resolution and immunochemical differentiation from lipoprotein lipase. *J Biol Chem* 251:2882–2890
  35. Khoo JC, Steinberg D, Lee EY (1978) Activation of chicken adipose tissue diglyceride lipase by cyclic AMP-dependent protein kinase and its deactivation by purified protein phosphatase. *Biochem Biophys Res Commun* 80:418–423
  36. Mau SE, Vilhardt H, (1997) Cross talk between substance P and melittin-activated cellular signaling pathways in rat lactotroph-enriched cell cultures. *J Neurochem* 69:762–772



37. Bisogno T, Melck D, De Petrocellis L, Di Marzo V (1999) Phosphatidic acid as the biosynthetic precursor of the endocannabinoid 2-arachidonoylglycerol in intact mouse neuroblastoma cells stimulated with ionomycin. *J Neurochem* 72:2113–2119
38. Dinh TP, Carpenter D, Leslie FM, Freund TF, Katona I, Sensi SL, Kathuria S, Piomelli D (2002) Brain monoglyceride lipase participating in endocannabinoid inactivation. *Proc Natl Acad Sci USA* 99:10819–10824
39. Becker KP, Hannun YA (2004) Diacylglycerols. In: Nicolaou A, Kokotos G (eds) *Bioactive lipids*. The Oily Press, Bridgwater, pp 37–61

# Role of Liver X Receptor, Insulin and Peroxisome Proliferator Activated Receptor $\alpha$ on in Vivo Desaturase Modulation of Unsaturated Fatty Acid Biosynthesis

Mauro A. Montanaro · María S. González ·  
Ana M. Bernasconi · Rodolfo R. Brenner

Received: 17 August 2006 / Accepted: 3 December 2006 / Published online: 20 January 2007  
© AOCs 2007

**Abstract** We examined the in vivo contribution of insulin, T090137 (T09), agonist of liver X receptor (LXR), fenofibrate, agonist of peroxisome proliferator activated receptor (PPAR- $\alpha$ ) and sterol regulatory element binding protein-1c (SREBP-1c) on the unsaturated fatty acid synthesis controlled by  $\Delta 6$  and  $\Delta 5$  desaturases, compared with the effects on stearoyl-coenzyme A desaturase-1. When possible they were checked at three levels: messenger RNA (mRNA), desaturase protein and enzymatic activity. In control rats, only fenofibrate increased the insulinemia that was maintained by the simultaneous administration of T09, but this increase has no specific effect on desaturase activity. T09 enhanced SREBP-1 in control animals and the mRNAs and activity of the three desaturases in control and type-1 diabetic rats, demonstrating a LXR/SREBP-1-mediated activation independent of insulin. However, simultaneous administration of insulin and T09 to diabetic rats led to a several-fold increase of the mRNAs of the desaturases, suggesting a strong synergic effect between insulin and LXR/retinoic X receptor (RXR). Moreover, this demonstrates the existence of an interaction between unsaturated fatty acids and cholesterol metabolism performed by the insulin/SREBP-1c system and LXR/RXR. PPAR- $\alpha$  also increased the expression and activity of the three desaturases independently of the insulinemia since it was

equivalently evoked in streptozotocin diabetic rats. Besides, PPAR- $\alpha$  increased the palmitoylcoenzyme A elongase, evidencing a dual regulation in the fatty acid biosynthesis at the level of desaturases and elongases. The simultaneous administration of fenofibrate and T09 did not show additive effects on the mRNA expression and activity of the desaturases. Therefore, the results indicate a necessary sophisticated interaction of all these factors to produce the physiological effects.

**Keywords**  $\Delta 9$ ,  $\Delta 6$  and  $\Delta 5$  desaturases · Diabetes mellitus type 1 · Sterol regulatory element binding protein-1c · T091317 · Liver X receptor · Fenofibrate · Peroxisome proliferator activated receptor  $\alpha$

## Abbreviations

CoA	Coenzyme A
LXR	Liver X receptor
mRNA	Messenger RNA
PPAR- $\alpha$	Peroxisome proliferator activated receptor $\alpha$
RXR	Retinoic X receptor
SCAP	SREBP cleavage activating protein
SCD-1	Stearoylcoenzyme A desaturase-1
SREBP-1c	Sterol regulatory element binding protein-1c
T09	T0901317

M. A. Montanaro · M. S. González · A. M. Bernasconi ·  
R. R. Brenner (✉)

Instituto de Investigaciones Bioquímicas de La Plata  
(UNLP-CONICET), Facultad de Ciencias Médicas,  
Universidad Nacional de La Plata, 60 y 120,  
1900 La Plata, Argentina  
e-mail: rbrenner@atlas.med.unlp.edu.ar

## Introduction

Unsaturated fatty acids, either essential or nonessential, play a relevant role in animal metabolism and physiology, and as lipid components they determine

the structure and properties of membranes. Polyunsaturated fatty acids accomplish very important physiological functions when converted to eicosanoids and docosanoids, and they are important brain components. They are agonists in the expression of several nuclear receptors that activate or deactivate enzymes and proteins, modulating cellular signaling involved in human health and diseases.

Unsaturated fatty acids are provided by the diet, but the endogenous biosynthesis is another important way they are provided. It provides palmitoleic and oleic acids by  $\Delta 9$  desaturation of coenzyme A (CoA) thioesters of palmitic and stearic acids, respectively, whereas successive  $\Delta 6$  and  $\Delta 5$  desaturations evoked by the front-end  $\Delta 6$  and  $\Delta 5$  desaturases and elongation reactions of the CoA thioesters of the essential acids linoleic acid and  $\alpha$ -linolenic acid are necessary to biosynthesize the highly polyunsaturated acids of the n-6 and n-3 families.

These enzymes are expressed mainly in liver, which is the major site of polyunsaturated fatty acid biosynthesis and provision to other tissues.

The desaturating enzymes modulate the unsaturated fatty acid biosynthesis, and their activity is regulated by diet components, hormones and other factors as well as by competition among the different acids [1]. However, we have demonstrated that many hormones, like corticoids, testosterone and 17- $\beta$ -estradiol, upregulate  $\Delta 9$  desaturase and downregulate  $\Delta 6$  and  $\Delta 5$  desaturases. In the case of experimental diabetes mellitus type 1, unlike diabetes type 2 characterized by insulin deficiency, they have been known since the 1960s to depress the biosynthesis of unsaturated fatty acids of the n-6, n-3 and n-9 families. This was evoked by decreasing the gene expression of the corresponding messenger RNAs (mRNAs) and enzymatic activities of  $\Delta 9$ ,  $\Delta 6$  and  $\Delta 5$  desaturases [2–6] and that activity was recovered by insulin administration. Moreover, Waters and Ntambi [7] and Rimoldi et al. [8] have demonstrated that the insulin-dependent recovered expression of stearoyl-CoA desaturase-1 (SCD-1) (current name of one of the  $\Delta 9$  desaturases) and  $\Delta 6$  desaturase mRNAs is not a direct effect of insulin, but it is evoked by the previous biosynthesis of one or more proteins.

Since the studies by Shimomura et al. [9] and Matsuzaka et al. [10] and other authors, this protein has been considered to be mainly represented by the transcription factor sterol receptor element binding protein-1c (SREBP-1c) since insulin induces the transcription of the *srebp-1c* gene into the precursor SREBP-1c, which after a hydrolytic step is converted to the nuclear active form nSREBP-1c, which then

reaches the nucleus and activates the expression of the three desaturases.

In addition, peroxisome proliferator activated receptor  $\alpha$  (PPAR- $\alpha$ ) (NR1-C1), which together with PPAR- $\beta$ /PPAR- $\delta$  (NR1C2) and PPAR- $\gamma$ 1 and PPAR- $\gamma$ 2 (NR1C3) belongs to the nuclear receptor superfamily, is activated by xenobiotic agonists like fenofibrate and endogenous ligands like unsaturated fatty acids in general. Although the active PPAR- $\alpha$  is characterized by its catabolic effect on lipid metabolism, it has also been shown to enhance the activity of the fatty acid desaturases [11]. However, the effects are only evoked after heterodimerization with the retinoic X receptor (RXR).

*srebp-1c*, according to Repa et al. [12], is also a target gene of the nuclear liver X receptors (LXR) LXR- $\alpha$  (NR1-H3) and LXR- $\beta$  (NR1-H2), which are activated by oxysterol and are considered as intracellular cholesterol sensors. Also, LXR- $\alpha$ , the predominant liver isoform, and RXR- $\alpha$  form a heterodimer and the SREBP-1c gene promoter revealed a RXR/LXR-DNA binding site that is essential for this regulation.

Moreover, polyunsaturated fatty acids suppress SREBP-1c promoter activity, and according to Yoshikawa et al. [13], this effect is evoked by inhibition of LXR binding to LXR response elements. To complete this picture, Chen et al. [14] have demonstrated a central role for LXR in insulin-mediated activation of SREBP-1c transcription and stimulation of fatty acid synthesis in liver. Therefore, LXR activates genes involved in the catabolism of cholesterol to bile acids, but it indirectly enhances lipogenic enzymes by LXR-mediated induction of SREBP-1c.

This information mainly gathered through in vitro experiments led us to investigate the in vivo interactions among LXR, PPAR- $\alpha$ , SREBP-1c and insulin specifically in the modulation of hepatic  $\Delta 6$  and  $\Delta 5$  desaturases at three levels, the mRNA abundance, the amount of enzyme protein and the microsomal enzymatic activities, as well as the correlated fatty acid compositions, comparing them with the effects evoked on SCD-1.

The activation of LXR was achieved by administration of the exogenous agonist T091317 (T09) [15] and the activation of PPAR- $\alpha$  by fenofibrate. Both agonists were chosen because they are widely used in the activation of the aforementioned nuclear receptors. They were administered to streptozotocin diabetic and control rats. To assess the effect of these drugs on the nuclear receptors, peroxisomal acyl-CoA oxidase activity as well as SREBP-1 and nSREBP-1 were tested. In addition to the measurement of the desaturases, the effect on hepatic palmitoyl-CoA elongase was also investigated.

## Experimental Procedure

### Materials

[1-<sup>14</sup>C]Stearic acid (58 mCi/mmol), 98% radiochemically pure, [1-<sup>14</sup>C] $\alpha$ -linolenic acid (53 mCi/mmol), 97% radiochemically pure, and [1-<sup>14</sup>C]eicosa-8,11,14-trienoic acid (52 mCi/mmol), 97% radiochemically pure, were purchased from Amersham Biosciences (Little Chalfont, UK), PerkinElmer (Boston, MA, USA) and New England Nuclear (Boston, MA, USA), respectively. Unlabeled free fatty acids were provided by Doosan Serdary Research Laboratories (Toronto, Canada).

Cofactors used for enzymatic analysis and fenofibrate were obtained from Sigma Chemical Co. (St. Louis, MO, USA). Analytical grade solvents were purchased from Carlo Erba (Milan, Italy).

Rat complementary DNAs of SCD-1,  $\Delta 6$  desaturase and  $\Delta 5$  desaturase were kind gifts from Juris Ozols (Department of Biochemistry, University of Connecticut, Central Health, Farmington, CT, USA), Tsunehiro Aki (Department of Molecular Biotechnology, Hiroshima, Japan), and Reza Zolfaghari and Catharine Ross (Department of Nutritional Sciences, The Pennsylvania State University, University Park, PA, USA), respectively. Restriction enzymes and other molecular biology reagents were obtained from Promega (Madison, WI, USA). LXR agonist T09 was a kind gift from Amgen (South San Francisco, CA, USA).

### Animal Treatment

Male Wistar rats from our animal room, weighing 170–200 g, were used. Animal care followed international rules for experimentation with animals. They were fed on a complete commercial diet, containing 5.5% of lipids (Cargill, Buenos Aires, Argentina) and water ad libitum. The fatty acid composition of the food was 22.5 wt% 16:0, 1.1 wt% 16:1, 13.7 wt% 18:0, 25.9 wt% 18:1n-9, 2.5 wt% 18:1n-7, 30.7 wt% 18:2n-6 and 3.4 wt% 18:3n-3.

Diabetes type 1 was induced in nonfasted rats by intravenous injection of streptozotocin (70 mg/kg body weight) dissolved in 10 mM citrate buffer, pH 4.5, while control rats received only the vehicle. A week later, streptozotocin-treated rats were fasted for 12 h, and glycemia was determined by a commercial enzymatic method (Wiener Lab Test, Rosario, Argentina). Only animals with glycemia above 300 mg/dl were considered diabetic.

The rats were then separated into four control groups, three of which received the following by oral

gavage: first group, 10 mg/kg weight/day T09 for 6 days; second group, 100 mg/kg weight/day fenofibrate for 9 days; third group, same doses of both drugs, fenofibrate for 9 days and T09 for the last 6 days.

The streptozotocin diabetic rats were separated into four groups, of which three received the following by oral gavage, where appropriate: first group, T09 for 6 days as before; the second group was injected with 5 U/kg weight/day glargine insulin for 6 days; the third group received simultaneously the insulin and T09 treatment for 6 days.

After the periods indicated, the animals were fasted overnight and killed by decapitation without anesthesia, at the same time, in the morning to avoid circadian rhythm effects.

### Blood Parameters

Glycemia, insulinemia [16] and cholesterolemia (by a commercial enzymatic method, Wiener Lab Test, Rosario, Argentina) were measured.

### Liver Organelle Fractionation

After killing the animals, livers were excised and homogenized in a solution (1:3 wt/vol) composed of 0.25 M sucrose, 0.15 M KCl, 9.1 mM EDTA, 1.41 mM *N*-acetyl cysteine, 5 mM MgCl<sub>2</sub> and 62 mM phosphate buffer (pH 7.4). Samples were centrifuged at 10,000g for 30 min and postmitochondrial supernatant was used for fatty acyl-CoA oxidase assay. Microsomes were separately by differential ultracentrifugation at 100,000g (Beckman Ultracentrifuge) as usual. Protein concentration was measured according to the procedure of Lowry et al. [17].

### Lipid Analysis

Lipids were extracted from liver homogenate and microsomes according to the procedure of Folch et al. [18]. The samples were esterified with F<sub>3</sub>B at 64°C for 3 h.

The fatty acid composition of microsome total lipids was determined by gas-liquid chromatography of their methyl esters. They were injected into an Omega Wax 250 (Supelco, Bellefonte, PA, USA) capillary column of 39 m, 0.25-mm inner diameter and 0.25  $\mu$ m film. The temperature was programmed to obtain a linear increase of 3 °C/min from 175 to 230 °C. The chromatogram peaks were identified by comparison of their retention times with those of authentic standards.

## Enzymatic Activity Assays

Acyl-CoA oxidase was assayed in the liver postmitochondrial supernatant by measuring palmitoyl-CoA dependent  $\text{H}_2\text{O}_2$  production according to the spectrophotometric method of Small et al. [19].

The SCD-1 activity was estimated in hepatic microsomes using as a substrate  $30 \mu\text{M}$  [ $1\text{-}^{14}\text{C}$ ]stearic acid, the  $\Delta 6$  desaturation using  $40 \mu\text{M}$  [ $1\text{-}^{14}\text{C}$ ] $\alpha$ -linolenic acid and the  $\Delta 5$  desaturation using  $40 \mu\text{M}$  [ $1\text{-}^{14}\text{C}$ ]eicosa-8,11,14-trienoic acid. The acids were incubated with 2.5 mg of microsomal protein in a final volume of 1.5 ml at  $36^\circ\text{C}$  for 15 min. The reaction mixture consisted of 0.25 M sucrose, 0.15 M KCl, 1.41 mM *N*-acetyl-L-cysteine, 40 mM NaF, 60  $\mu\text{M}$  CoA (sodium salt), 1.3 mM ATP, 0.87 mM NADH, 5 mM  $\text{MgCl}_2$  and 40 mM potassium phosphate buffer (pH 7.4). After incubation, free fatty acids were dissolved in methanol/water/acetic acid (85:15:0.2 by volume), and fractionated by reversed-phase high-performance liquid chromatography on an Econosil C18, 10-mm particle size, reversed-phase column (250 mm  $\times$  4.6 mm) (Alltech Associates, Deerfield, IL, USA), coupled to a guard column (10.4 mm filled with pellicular C18). The mobile phase consisted of methanol/water/acetic acid (90:10:0.2 by vol) at a flow rate of 1 ml/min. The Merck–Hitachi (Darmstadt, Germany) L-6200 solvent delivery system was used. The eluate from the column was monitored by a UV spectrometer at 205 nm for fatty acid identification on the basis of retention times. The effluent was mixed with Ultima Flo-M scintillation cocktail (Packard Instruments, Downers Grove, IL, USA) at a 1:3 ratio, and the radioactivity was measured by passing the mixture through an online Radiomatic Instruments (Tampa, FL, USA) Flo-One- $\beta$  radioactivity detector fitted with a 0.5-ml cell.

The assay for the microsomal chain elongation of palmitoyl-CoA was performed by measuring the incorporation of [ $2\text{-}^{14}\text{C}$ ]malonyl-CoA into palmitoyl-CoA [20].

## Measurement of mRNA of Desaturases

Total liver RNA of different animals tested was isolated with a Wizard RNA isolation system (Promega, Madison, WI, USA) according to the manufacturer's instructions. Twenty micrograms of total RNA was size-fractionated on a 1% agarose/formaldehyde gel and then transferred to a Zeta-Probe nylon membrane (Bio-Rad, Richmond, CA, USA). SCD-1,  $\Delta 6$  desaturase and  $\Delta 5$  desaturase, and  $\beta$ -actin probes were prepared by incorporating [ $^{32}\text{P}$ ]deoxycytidine 5'-triphosphate by random prime labeling. Northern blot hybridization

analyses were performed as described by Sambrook et al. [21]. The radioactive signals for mRNAs of SCD-1,  $\Delta 6$  desaturase and  $\Delta 5$  desaturase were quantified using a Phosphorimager apparatus (Molecular Dynamics, Sunnyvale, CA, USA). They were normalized to mRNA for  $\beta$ -actin with all the mRNAs probed on the same gel. Northern blot analyses were performed using an unpaired *t* test.

## Western Blot Analysis

Following the method performed by D'Andrea et al. [22], a polyclonal anti-rat  $\Delta 6$  desaturase antibody was produced. The 131 N-terminal amino acid section of the enzyme was selected for the construction of the glutathione *S*-transferase/ $\Delta 6$  desaturase fusion protein, using PCR amplification with the forward primer 5'-CAGTGGATCCATGGGGGAAGGGAGGTA-3' and the reverse primer 5'-CTGCTCGAGTCACAGGTGGTTGGTTTTGAAAAGG-3'. The purified bacterial expressed fusion protein was used as an immunogen on rabbits.

Total microsomal protein samples (70  $\mu\text{g}$  per lane) were analyzed by sodium dodecyl sulfate polyacrylamide gel electrophoresis and blotted onto Hybond-ECL nitrocellulose membrane (Amersham Biosciences, Little Chalfont, UK). The membrane was probed with the anti- $\Delta 6$  serum obtained (1:33,000 dilution) and then with horseradish peroxidase conjugated anti-rabbit (Sigma) (1:5,000 dilution), using PBS-T buffer [11.5 g anhydrous disodium hydrogen orthophosphate, 2.96 g sodium dihydrogen orthophosphate, 5.84 g sodium chloride per liter, pH 7.5, with 0.1% (v/v) Tween 20], containing 5 and 1% nonfat dried milk, for saturation and incubation with antibodies, respectively. Washes were carried out using PBS-T buffer. Finally, peroxidase activity was revealed using Pierce ECL Western blotting substrate (Pierce, Rockford, IL, USA) and quantified using Kodak Digital Science software (Kodak, Rochester, NY, USA).

For SREBP-1 measurements, cytoplasmic and nuclear protein extracts were obtained using NE-PER nuclear and cytoplasmic extraction reagents (Pierce Biotechnology, Rockford, IL, USA). They were subjected to Western blot analysis as indicated above, except that anti-SREBP-1 antibody, K-10 (Santa Cruz Biotechnology, Santa Cruz, CA, USA), was used as the primary antibody (1:200 dilution).

## Statistical Methods

Data are expressed as means  $\pm$  standard deviation. Statistically significant differences among groups were

assessed by analysis of variance (Instat version 2.0, Graph Pad Software, San Diego, CA, USA). The Tukey–Kramer multiple-comparison test was used. Statistical significance was defined as  $P < 0.05$ .

## Results

### Effects of Fenofibrate and T09 on Acyl-CoA Oxidase and SREBP-1

To confirm that the administration of fenofibrate activated PPAR- $\alpha$ , we measured, as usual, the effect evoked on its specific hepatic target enzyme, the extramitochondrial acyl-CoA oxidase. Figure 1 shows clearly that fenofibrate evoked an eightfold increase of the enzyme activity, and that the addition of T09, a specific agonist of LXR, did not modify that increase. On the other hand, the activating effect of T09 administration on the LXR response was assessed by the induced expression of the LXR target gene *srebp-1* [15]. Figure 1b confirms that in our experimental conditions the administration of T09 to nondiabetic rats enhanced LXR activity as evidenced by a 7.3-fold increase of the hepatic 125-kD SREBP-1 precursor and a 3.8-fold increase of the nuclear active 68-kD n-SREBP-1. SREBP-2 was not measured because it is encoded by a different gene to that of SREBP-1, and it preferentially activates cholesterol synthesis [14].

### Effects of T09 and Fenofibrate on Insulinemia and Cholesterolemia

Both in control rats, in which the level of insulin is normal, and in diabetic animals with undetectable insulinemia, T09 administration in the doses tested did not modify significantly glycemia, cholesterolemia or the corresponding insulinemia after 6 days of treatment (data not shown). On the other hand, fenofibrate administration to control animals for 9 days significantly increased insulinemia from  $1.32 \pm 0.61$  to  $2.36 \pm 0.13$  ng/ml ( $P < 0.05$ ), confirming our previously published data [11], while it did not alter glycemia and cholesterolemia (data not shown). The simultaneous administration for the last 6 days of 10 mg/kg weight/day of T09 to the fenofibrate-treated control animals did not alter glycemia, while insulinemia increased ( $3.13 \pm 0.47$  ng/ml) ( $P < 0.001$ ).

Fenofibrate enhancement of the circulating insulin level in normal rats is attributed to increased expression and activity of PPAR- $\alpha$  in view of the fact that using the test usually employed by other authors we found an increase of the target enzyme acyl-CoA oxidase (Fig. 1).

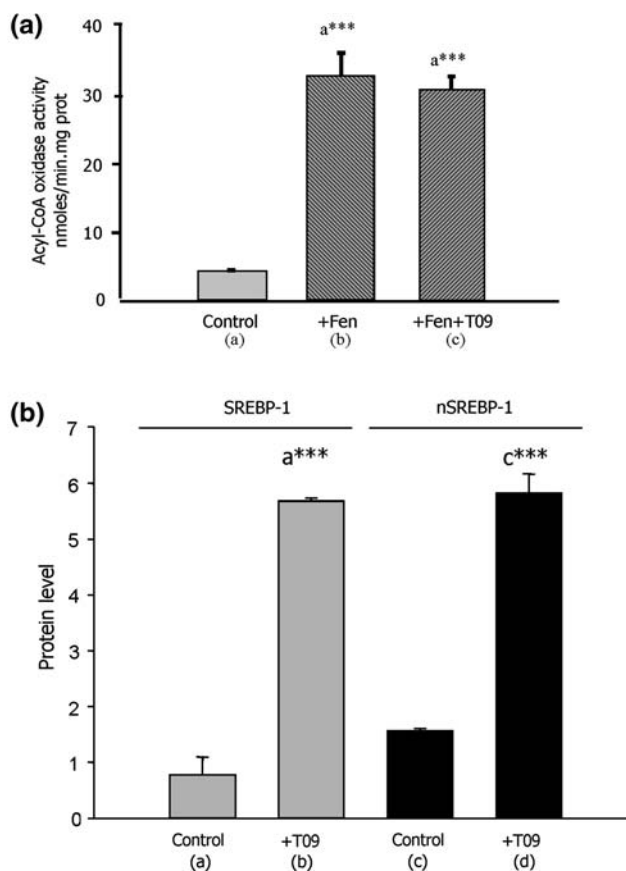


**Fig. 1** Assessment of the efficacy of fenofibrate and T0901317 (T09) in vivo activation of peroxisome proliferator activated receptor  $\alpha$  (PPAR- $\alpha$ ) and sterol regulatory element binding protein-1 (SREBP-1). **a** Effect of fenofibrate and T09 on extramitochondrial acylcoenzyme A oxidase activity in nondiabetic rats. Results expressed in nanomoles per minute per milligram of protein are the mean of four animals  $\pm$  the standard deviation (SD). **b** Effect of T09 on SREBP-1 precursor and nuclear active nSREBP-1 forms. Cytoplasmic and nuclear protein extracts were obtained using NE-PER nuclear and cytoplasmic extraction reagents and were subjected to Western blot analyses. Results expressed in arbitrary units are the mean of four animals  $\pm$  SD. Statistical differences were analyzed by analysis of variance (ANOVA).  $P < 0.001$

On the other hand, the addition of T09 to the control rats treated with fenofibrate evoked a specific depression of cholesterolemia from  $53.3 \pm 6.6$  mg/100 ml for the control rats,  $46.5 \pm 14.3$  mg/100 ml for control rats treated with T09 and  $60.9 \pm 6.6$  mg/100 ml for control rats treated with fenofibrate, to only  $25.7 \pm 5.7$  mg/100 ml ( $P < 0.001$ ) for control animals treated with fenofibrate and T09. In consequence, these results suggest an apparent interaction between PPAR- $\alpha$  and LXR in cholesterol-trafficking modulation.

Diabetic animals showed, as usual, significant increases of glycemia, no change of cholesterolemia and nearly undetectable insulinemia. T09 administration

did not significantly modify the levels of the aforementioned parameters as found in the diabetic animals and insulin increased insulinemia to about 0.20 mg/ml and normalized glycemia (data not shown).

#### Activating Effect of T09 and Fenofibrate on Fatty Acid Desaturase mRNA Levels

The effect of T09 and fenofibrate on control rats and that of T09 and insulin on the mRNAs levels of  $\Delta 6$  and  $\Delta 5$  desaturases and SCD-1 in diabetic animals are described in Fig. 2. It shows that not only the transcriptions of SCD-1 mRNA are modified but also that the mRNAs of  $\Delta 6$  and  $\Delta 5$  desaturases follow in general a similar pattern of changes.

Specifically Fig. 2 shows clearly that both in control and in diabetic rat livers, the mRNAs of SCD-1 and  $\Delta 6$  and  $\Delta 5$  desaturases were enhanced by the administration of LXR specific agonist T09, demonstrating that LXR activation evokes a similar insulin-independent increase of the three mRNAs. Therefore, these results support again, as found by Shulz et al. [15] and others, that LXR activates the *scd-1* liver expression, but now we add that this nuclear receptor also activates mRNA expression of  $\Delta 6$  and  $\Delta 5$  desaturases and the corresponding polyunsaturated fatty acid biosynthesis. Since

we found that LXR- $\alpha$  agonist T09 not only enhanced the expression of the three desaturases, but also the hepatic cytosolic SREBP-1 precursor (125-kD spot) and its nuclear active form nSREBP-1 (68-kD spot) (Fig. 1), our results are also consistent with a SREBP-1c mediated LXR- $\alpha$ /RXR- $\alpha$  dependent desaturase activation in which the secreted insulin through activation of SREBP cleaving activating protein (SCAP) [23] would cleave SREBP-1c to its nuclear active form.

Moreover, a large increase of the mRNA levels of  $\Delta 5$  and  $\Delta 6$  desaturases and SCD-1 was evoked by the T09 administration to the diabetic animals simultaneously treated with insulin (Fig. 2). This indicates an extraordinary hyperactivation of the expression of these enzyme mRNAs owing to a cooperative effect of LXR- $\alpha$  and insulin. Although LXR- $\alpha$  activates the expression of the mRNA of the three enzymes, both in normal rats having a normal insulin cycle secretion and in diabetic animals with undetectable insulinemia, only when LXR- $\alpha$  along with insulin were administered to the diabetic rats was the unexpectedly high synergic effect evoked. This effect could be explained by a SREBP-1c confluent stimulation.

In control rats, the administration of fenofibrate, a PPAR- $\alpha$  agonist, evoked an increase of  $\Delta 5$  desaturase and SCD-1 mRNAs (Fig. 2). A similar effect on  $\Delta 6$

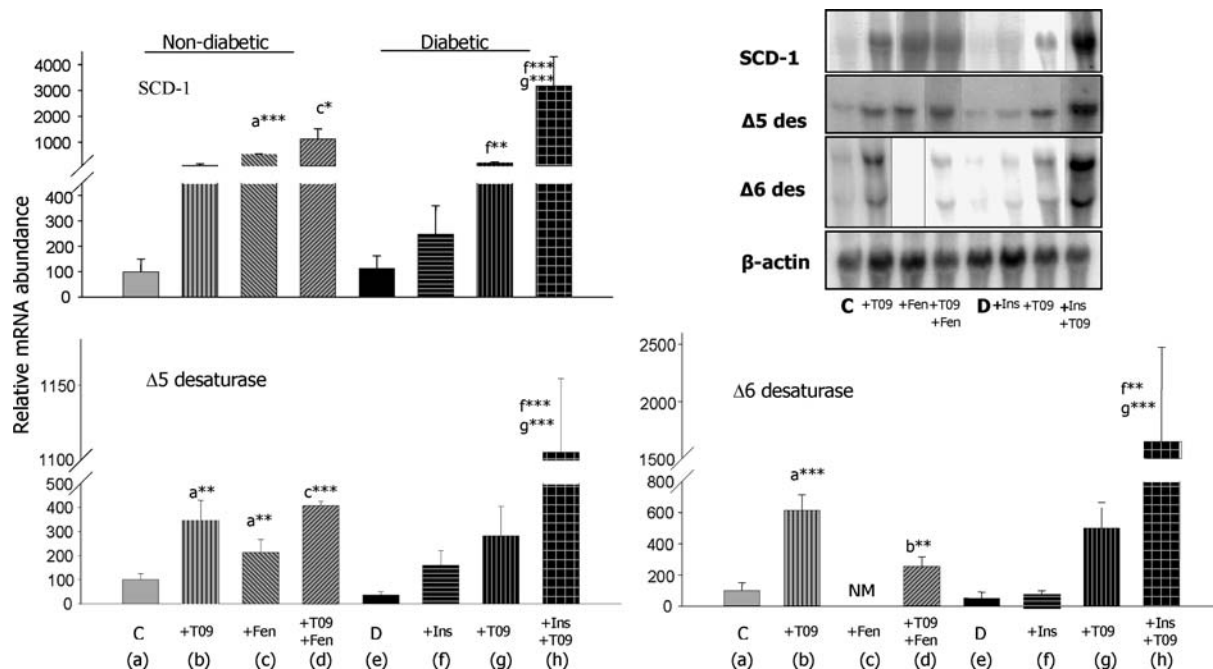


**Fig. 2** Effects of T09 and fenofibrate (*Fen*) on control rats (*C*) and T09 and insulin (*Ins*) on diabetic rats (*D*) on the messenger RNAs (*mRNAs*) of stearoylcoenzyme A desaturase-1 (*SCD-1*), and  $\Delta 5$  and  $\Delta 6$  desaturases. Hepatic mRNA signals of desaturases as described in the text were quantified using a Phosphorimager apparatus and normalized to mRNA of  $\beta$ -actin. They are

expressed in arbitrary units referred to control rats (100) as the mean of four animals  $\pm$  SD. Statistical differences were analyzed by ANOVA in nondiabetic and diabetic animals, respectively. Different superscript letters indicate differences between this value and that in the group indicated by that letter. \*\*\* $P < 0.001$ ; \*\* $P < 0.01$ . ND not determined

desaturase mRNA, though not measured here, has been found by Montanaro and Brenner in an independent experiment (personal communication). In addition, Montanaro et al. [11] found an enhancement of  $\Delta 5$  desaturase and SCD-1 mRNAs not only in nondiabetic but also in diabetic rat livers after forced feeding with fenofibrate for 9 days; therefore, they demonstrate that PPAR- $\alpha$  activation evoked an increase of the mRNAs of the three desaturases that is not related to the presence of insulin.

The simultaneous administration of T09 and fenofibrate to control rats also evoked an increase of mRNAs  $\Delta 6$  desaturase,  $\Delta 5$  desaturase and SCD-1. However, whereas the increases of  $\Delta 5$  desaturase and SCD-1 were on the same order as for those rats administered T09 alone, the enhancement of  $\Delta 6$  desaturase mRNA was smaller. Anyhow, this demonstrated the absence of an additive stimulating effect between LXR- $\alpha$ /RXR- $\alpha$  and PPAR- $\alpha$ /RXR- $\alpha$  in the transcription of mRNA of desaturases.

#### Activating Effect of T09 and Fenofibrate on Fatty Acid Desaturase Enzymatic Activities

Figure 3 displays the individual and combined effects of T09 and fenofibrate, as well as those induced by insulin, T09 and their combination on the three liver desaturase activities in control and diabetic rats, respectively.

In control rats the results show rather similar effects of T09 and fenofibrate on the SCD-1,  $\Delta 5$  desaturase and  $\Delta 6$  desaturase activities. On the other hand, they correlate fairly well with those changes evoked by the same factors on the mRNA expression of SCD-1,  $\Delta 5$  desaturase and  $\Delta 6$  desaturase in the same group of rats.

As in the case of these mRNAs, the three desaturating enzymes were activated by T09 both in control animals and in diabetic rats, confirming that LXR- $\alpha$  activation may evoke an insulin-independent increase of activities of hepatic SCD-1,  $\Delta 6$  desaturase and  $\Delta 5$  desaturase.

However, since the activations of SCD-1,  $\Delta 5$  desaturase and  $\Delta 6$  desaturase enzymes evoked in diabetic rats by T09 or T09 plus insulin as shown in Fig. 3 were quantitatively equivalent and no up-shooting was found by treatment with T09 plus insulin, we may deduce that the overexpression of the desaturase mRNAs did not produce enzyme-equivalent proteins synthesis and folding since this was not correlated by similar increases of the enzymatic activities.

The changes evoked by T09, fenofibrate and fenofibrate plus T09 treatment on the translation of the  $\Delta 6$  desaturase in the control nondiabetic rats were also

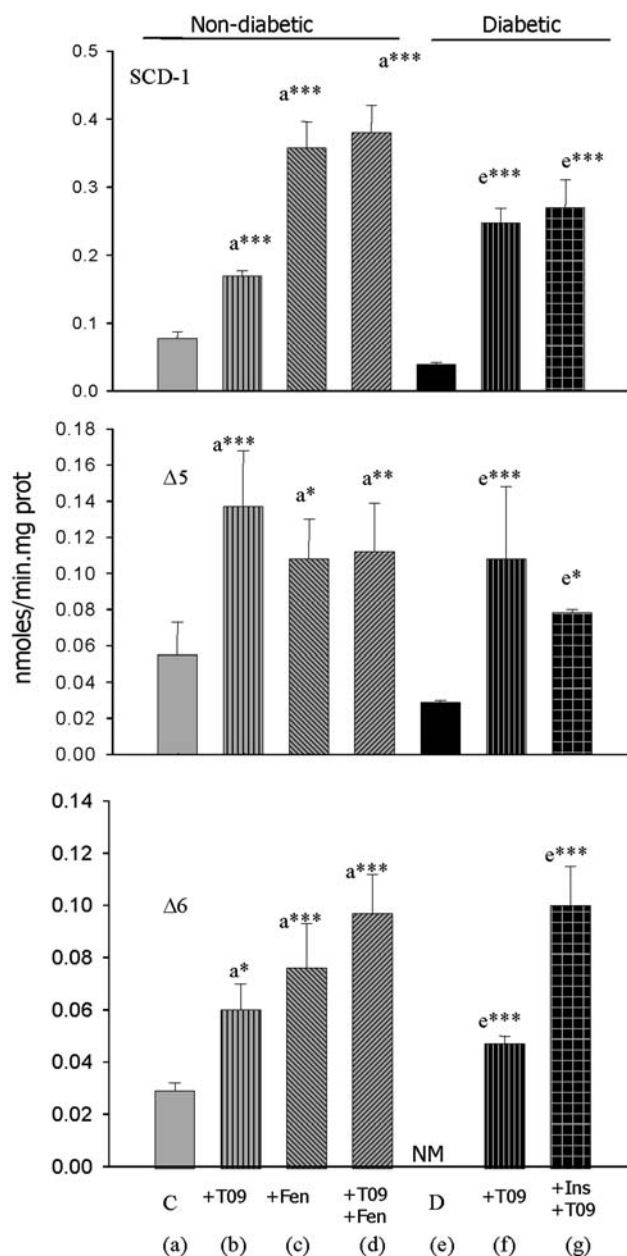


**Fig. 3** Enzymatic activities of hepatic SCD-1 and  $\Delta 6$  and  $\Delta 5$  desaturases in nondiabetic and diabetic rats after T09 and fenofibrate treatment in vivo. Activities were measured as described in “Experimental Procedures” and are expressed in nanomoles per minute per milligram of protein and are the mean of four animals  $\pm$  SD. Statistical differences were analyzed by ANOVA as described in the legend to Fig. 2. \*\*\* $P < 0.001$ ; \*\* $P < 0.01$ ; \* $P < 0.05$ . NM not measurable, ND not determined

monitored by measuring the amount of  $\Delta 6$  desaturase protein by immunoblotting (Fig. 4). Data show that T09, fenofibrate and T09 plus fenofibrate increased the amount of  $\Delta 6$  desaturase protein in control animals in correspondence to what happened with the mRNAs and with the enzymatic activity. In consequence, they



support the idea that the increased desaturase activity in these animals was due to an increase of the amount of enzyme and that PPAR- $\alpha$  competes with LXR- $\alpha$  in the activation of  $\Delta 6$  desaturase.

#### Effect of T09 and Fenofibrate on Fatty Acid Elongation

Fatty acid elongation is another reaction that modifies the fatty acid composition of animal lipids by converting palmitoyl-CoA to stearoyl-CoA and also the polyunsaturated fatty acids of 18 carbons to long-chain polyunsaturated acids of 20, 22 and 24 carbons.

Figure 5 shows that whereas T09 administered alone to control rats only evoked a statistically nonsignificant increase of the microsomal hepatic palmitoyl-CoA elongase, fenofibrate alone or fenofibrate plus T09 increased fivefold and eightfold, respectively, the activity of the enzyme.

In the diabetic rats the elongase activity was low, but neither insulin nor T09 administration increased significantly the palmitoyl-CoA conversion to stearoyl-CoA: however, the simultaneous administration of T09 and insulin to diabetic rats increased around tenfold

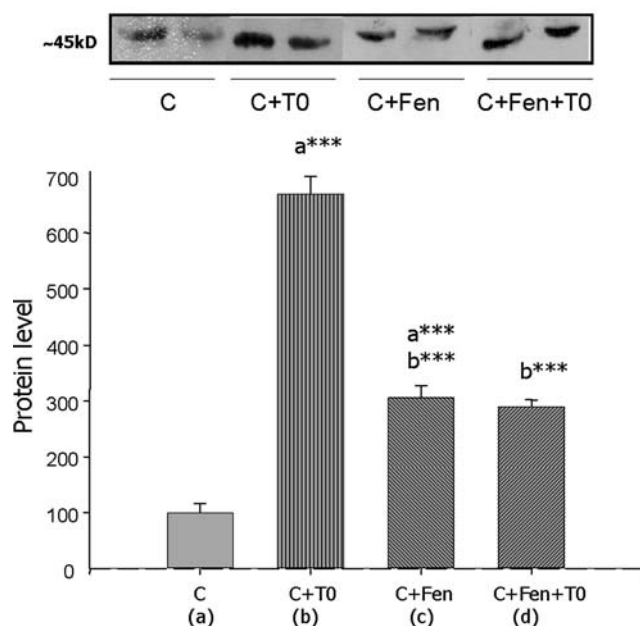


**Fig. 4** Western blot analysis of  $\Delta 6$  desaturase of nondiabetic rats (C) treated with T09 and fenofibrate (Fen). A polyclonal anti-rat  $\Delta 6$  desaturase antibody was produced and total microsomal protein samples (70  $\mu$ g per lane) were analyzed by sodium dodecyl sulfate polyacrylamide gel electrophoresis, blotted on a Hybond-ECL nitrocellulose membrane, and the 45-kD spots were quantified as described in “Experimental Procedures.” Results expressed in arbitrary units referred to nondiabetic rats (100) are the mean of three animals  $\pm$  SD. Statistical differences were analyzed by ANOVA. \*\* $P < 0.01$

the activity of the reaction, showing again a synergic effect. Therefore, these results suggest that both LXR plus PPAR- $\alpha$  and LXR plus insulin evoke an important cooperative effect that upregulates palmitoyl-CoA elongase.

#### Effect of T09 and Fenofibrate on Microsomal Liver Lipid Fatty Acid Composition

Changes in the microsomal liver lipid fatty acid composition are monitored and widely used to detect the effect of changes in the food fatty acid composition as well as alterations evoked in the endogenous biosynthesis of fatty acids that may modify the biological status of an animal.

Table 1 shows the changes evoked by the aforementioned metabolic agents in microsomal fatty acid composition after only 9 days of treatment. Throughout this short period of time, the fatty acid composition of microsomal liver lipids was in general poorly modified by the different factors tested. However, early changes evoked by PPAR- $\alpha$  could be detected.

In control rats, though T09 increased the activity of all the desaturating enzymes, it did not evoke significant changes in the percentage of the acids, but on the other hand fenofibrate, which also modified the activity of the desaturases, not only doubled the percentages of palmitoleic acid and oleic acid and increased arachidonic acid, but decreased by half the proportion of the biologically important docosahexaenoic acid (22:6n-3)

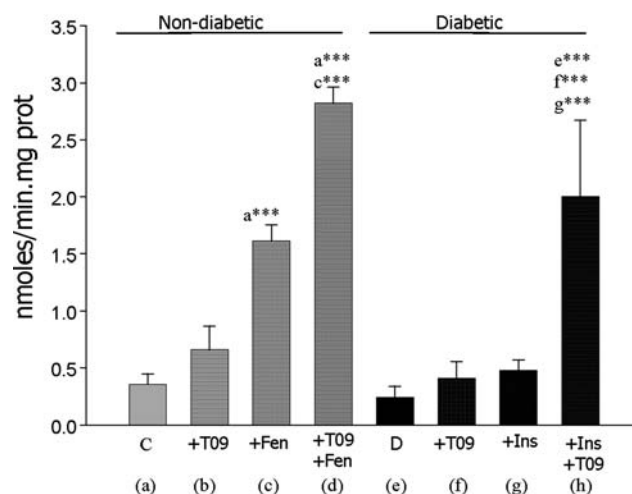


**Fig. 5** Effect of T09, fenofibrate and insulin in vivo on hepatic palmitoylcoenzyme A elongase activity of nondiabetic and diabetic rats. Results expressed in nanomoles per minute per milligram of protein are the mean of four animals  $\pm$  SD. Experimental conditions, abbreviations and statistical differences analyzed by ANOVA are as described in the legend to Fig. 2. \*\*\* $P < 0.001$

**Table 1** Fatty acid composition of liver microsomal lipids (weight percent)

Fatty acid	C	C + T09	C + Fen	C + Fen + T09	D	D + T09	D + Ins	D + Ins + T09
16:0	17.42 ± 1.66	20.75 ± 4.38	25.34 ± 0.56 <sup>b***</sup>	19.87 ± 1.02 <sup>c***</sup>	17.62 ± 0.59	19.77 ± 2.59	19.59 ± 2.82	17.94 ± 3.15
16:1	0.32 ± 0.10	0.58 ± 0.07	0.61 ± 0.10 <sup>a***</sup>	0.74 ± 0.05 <sup>a***</sup>	0.32 ± 0.08	0.46 ± 0.30	0.17 ± 0.13	1.10 ± 0.16 <sup>c***f,g***g***</sup>
18:0	28.97 ± 2.19	28.77 ± 6.65	23.14 ± 0.86 <sup>a***</sup>	27.78 ± 0.71 <sup>c***</sup>	29.83 ± 1.78	26.80 ± 2.18	31.48 ± 5.86	23.38 ± 1.23
18:1n-9	4.40 ± 0.07	6.06 ± 0.95	8.78 ± 1.30 <sup>b***</sup>	10.88 ± 0.54 <sup>b***</sup>	4.75 ± 0.54	6.02 ± 0.92	4.57 ± 0.85	12.65 ± 2.51 <sup>f,g***g***</sup>
18:1n-7	1.15 ± 0.09	1.44 ± 0.23	0.85 ± 0.02 <sup>a***</sup>	0.77 ± 0.09 <sup>a***</sup>	0.90 ± 0.07	1.22 ± 0.17	0.90 ± 0.14	1.82 ± 0.17
18:2 n-6	11.03 ± 0.88	9.09 ± 2.13	9.30 ± 0.93 <sup>a*</sup>	7.68 ± 0.69 <sup>a***</sup>	12.21 ± 0.96	9.33 ± 0.79	11.69 ± 2.20	11.34 ± 1.69
18:3n-3	0.58 ± 0.10	0.49 ± 0.18	0.51 ± 0.09	0.44 ± 0.16	0.39 ± 0.19	0.46 ± 0.16	0.52 ± 0.20	0.36 ± 0.18
20:3n-9	0.20 ± 0.02	0.17 ± 0.05	0.29 ± 0.08	0.27 ± 0.05	0.14 ± 0.01	0.15 ± 0.02	0.17 ± 0.09	0.25 ± 0.04
20:3n-6	0.35 ± 0.05	0.67 ± 0.02	1.71 ± 0.35 <sup>b***</sup>	1.90 ± 0.12 <sup>a***</sup>	0.76 ± 0.10	0.57 ± 0.03	0.74 ± 0.23	1.06 ± 0.27
20:4n-6	28.81 ± 2.61	24.33 ± 6.62	26.21 ± 1.84 <sup>b*</sup>	26.53 ± 0.69 <sup>b*</sup>	23.89 ± 1.30	23.87 ± 2.47	22.33 ± 2.75	20.85 ± 0.84
20:5n-3	0.51 ± 0.04	0.44 ± 0.13	0.15 ± 0.03 <sup>a***</sup>	0.14 ± 0.01 <sup>a***</sup>	0.56 ± 0.04	0.58 ± 0.07	0.51 ± 0.06	0.76 ± 0.15
22:4n-6	0.47 ± 0.10	0.38 ± 0.08	0.06 ± 0.11	0.09 ± 0.11	1.02 ± 0.38 <sup>a***</sup>	1.46 ± 0.64 <sup>b**</sup>	0.80 ± 0.21	1.28 ± 0.18
22:5n-3	0.72 ± 0.08	0.68 ± 0.17	0.27 ± 0.06 <sup>b***</sup>	0.21 ± 0.04 <sup>b***</sup>	0.59 ± 0.07	0.60 ± 0.07	0.58 ± 0.07	0.76 ± 0.14
22:6n-3	5.08 ± 0.45	6.17 ± 1.13	2.80 ± 0.63 <sup>a***</sup>	2.71 ± 0.24 <sup>a***</sup>	7.03 ± 0.88 <sup>a*</sup>	8.72 ± 1.52 <sup>b*</sup>	5.98 ± 1.09 <sup>f*</sup>	6.47 ± 0.81
Total fatty acid (mg fatty acid/mg protein)	0.27 ± 0.05	0.30 ± 0.02	0.32 ± 0.03	0.30 ± 0.02	0.33 ± 0.04	0.39 ± 0.07	0.29 ± 0.02	0.29 ± 0.03

Results are the mean of four animals ± the standard deviation. Statistical differences were analyzed by analysis of variance as described in the legend to Fig. 2

C control rats, T09 T0901317, Fen fenofibrate, D diabetic rats, Ins insulin

\*\*\* $P < 0.001$ ; \*\* $P < 0.01$ ; \* $P < 0.05$

and of the other n-3 polyunsaturated acids of 20 and 22 carbons. Also, it enhanced palmitic acid and depressed stearic acid.

The addition of T09 to fenofibrate did not much alter the effect of fenofibrate alone, and a similar increase of the percentages of palmitoleic acid and oleic acid, an equivalent depression of 22:6n-3 as well as the other changes were found. Therefore, it seems that in normal rats PPAR- $\alpha$ /RXR- $\alpha$  activation through the fenofibrate treatment was more effective than LXR- $\alpha$ /RXR- $\alpha$  activation through the T09 administration to evoke earlier changes in the fatty acid composition of liver lipids.

On the other hand, during the short period of diabetes tested, the only important change found was the increase of 22:6n-3, and insulin injection did not modify it significantly. This delayed action of diabetes and insulin agrees with their recognized time-dependent effect in the alteration of the fatty acid composition of different animal tissues [24]. T09 administration to diabetic animals did not modify the fatty acid composition, and the increase of 22:6n-3 was maintained. Besides, insulin and T09 when simultaneously administered to diabetic rats promoted a very significant increase of the monoenoic acids, palmitoleic and oleic, but not of other acids. Therefore, SCD-1 showed a stronger and more effective response than that of  $\Delta 5$  and  $\Delta 6$  desaturases to these combined effectors.

## Discussion

Since Burr and Burr demonstrated the essentiality of linoleic and  $\alpha$ -linolenic acids, it has been gradually shown that their biological effects are mainly produced through their conversion to the high polyunsaturated acids of 20 and 22 carbons of the n-6 and n-3 families and their derivatives, respectively. This conversion is mainly modulated by the  $\Delta 6$  and  $\Delta 5$  desaturases [1] that, therefore, play a key role in maintaining the healthy status of individuals. Their activity is altered in several diseases and it has been studied in depth in diabetes, in relation to inflammatory effects, oxidative stress, cholesterol metabolism, atherogenesis and, in general, cardiovascular diseases. However we have proved [1, 25] that the two main types of diabetes, type 1, evoked by insulin deficiency, and type 2, which shows normoglycemia or hyperglycemia, modify the activity of SCD-1 and  $\Delta 6$  and  $\Delta 5$  desaturases in opposite directions. In diabetes type 1, the three desaturases are downregulated, whereas in diabetes type 2, they are generally upregulated.

The downregulation evoked by diabetes type 1 is corrected by insulin, but we showed in the present

study that SREBP-1c, LXR and PPAR- $\alpha$  are also involved in this reactivation.

Firstly, we found that in control rats in which the cycle of blood insulin follows its normal rhythm of synthesis and degradation fenofibrate evoked an increase of insulinemia that exceeded the normal values. This effect was undoubtedly due to an activation of the PPAR- $\alpha$ /RXR heterodimer as usually tested by the enhancement of the peroxisomal specific target enzyme acyl-CoA oxidase; however, this hyperinsulinemia did not decrease the glycemia normal values, suggesting poor efficiency or the presence of compensatory metabolic effects.

The increasing fenofibrate effect on insulinemia in normal rats has already been shown and discussed in our previous publication [11] where it was found not to be evoked in insulin-treated diabetic rats. Therefore, the results suggest that PPAR- $\alpha$  stimulates pancreas insulin secretion and not decreased insulin degradation. However, while it is known [26] that PPARs are expressed in pancreatic  $\beta$  cells and many authors conclude that PPAR- $\alpha$  modulates insulin secretion of islets [27–29], there is no consensus on the mechanisms of action. In that respect, Tordzman et al. [30] have found by incubation of INS-1 cells, a rat insulinoma cell line, with clofibric acid for 48 h that this PPAR- $\alpha$  agonist decreased basal and glucose-stimulated insulin secretion. This effect would be evoked through a PPAR- $\alpha$  stimulated fatty acid oxidation that impairs  $\beta$ -cell function. However, Ravnskjaer et al. [29] proved that the expression of PPAR- $\alpha$ /RXR- $\alpha$  indeed potentiates glucose-stimulated insulin secretion in rat islets and INS-1E cells without affecting the mitochondrial membrane potential.

T09, which activates LXR- $\alpha$ , when administered to normal rats has no effect on insulinemia and glycemia, and it did not modify the hyperinsulinemia induced by fenofibrate, showing there was no interaction.

Notwithstanding this, Anderson et al. [31] and Ide et al. [32] found overlapping transcriptional programs regulated by PPAR- $\alpha$ , RXR and LXR- $\alpha$  in rodent liver and cross-talk between PPAR- $\alpha$  and LXR- $\alpha$  in nutritional regulation of fatty acid metabolism. These results suggested to the authors that LXR- $\alpha$  ligands evoked a reduction in the PPAR- $\alpha$ /RXR formation by competition of new LXR- $\alpha$  with PPAR- $\alpha$  for RXR in heterodimer formation, and therefore they decreased PPAR- $\alpha$ /RXR- $\alpha$  effects. This expected result, however, could not be detected in our experiment when administering T09 to these animals with increased fenofibrate-dependent insulinemia, suggesting an apparent lack of interaction in the case of pancreas insulin secretion.

The ineffectiveness of T09 to depress the normoglycemia in nondiabetic rats agrees with the results of Cao et al. [33] that showed that 1–100 mg/kg weight per day dosages of T09 were unable to evoke hypoglycemia. However, while we found that 10 mg/kg weight of T09 did not decrease hyperglycemia in our diabetic type 1 rats, they found significant decreases in hyperglycemia in obese insulin-resistant female Zucker (*fa/fa*) rats with doses from 3.0 to 30 mg/kg weight. That decrease was attributed by the authors to an increased insulin sensitivity and reduced gluconeogenesis derived from a depressed phosphoenolpyruvate carboxykinase. This apparent discrepancy might be due to the model of the diabetic animal studied. We used streptozotocin, insulin-deficient diabetic type 1 rats, whereas they used insulin-resistant diabetic type 2 animals [25].

However, the stimulation of LXR- $\alpha$  by T09 required the corresponding stimulation of PPAR- $\alpha$  by fenofibrate to depress the cholesterolemia that was decreased neither by LXR- $\alpha$  nor by PPAR- $\alpha$  separately. This cooperative effect between the two nuclear receptors on the depression of blood cholesterol level is due to the modulation of integrating factors of the PPAR/LXR cholesterol oxidation and efflux pathways [31, 34–36]. This suggests the convergence of the homeostatic mechanisms for cholesterol and fatty acid metabolism. In this respect, we demonstrated some time ago [37] an interaction of cholesterol with unsaturated fatty acid biosynthesis. It was shown that 1% of cholesterol in the diet for 21 days progressively activated hepatic SCD-1 mRNA transcription and activity, but it depressed enzymatic activity of  $\Delta 6$  and  $\Delta 5$  desaturases, modifying correlatively the fatty acid composition of liver lipids.

The present study of the effect of the mentioned nuclear receptors on liver fatty acid desaturase modulation showed, in the first place (Figs. 2, 3), that T09 administration by increasing LXR- $\alpha$  expression enhanced mRNA expression of hepatic SCD-1 and  $\Delta 6$  and  $\Delta 5$  desaturases as well as the activities of the same enzymes not only in control but also in diabetic rats with undetectable insulinemia.

The fact that LXR- $\alpha$  activation enhances the activity of SCD-1 has been already demonstrated in different ways in the last years by several authors [15, 38, 39], but in addition we prove here that LXR also activates  $\Delta 6$  and  $\Delta 5$  desaturases.

Moreover, Fig. 2 demonstrates a marked interaction between LXR- $\alpha$  and insulin in the modulation of the expression of fatty acid desaturases. In the first place, as indicated, LXR- $\alpha$  does not require the absolute assistance of insulin to evoke an enhancement of the desaturase expression, in view of the fact that in both normal and diabetic rats T09 administration increased

the mRNA expression of  $\Delta 6$  and  $\Delta 5$  desaturases and SCD-1 (Fig. 2). However, what is really remarkable, indicating an important insulin–LXR- $\alpha$  interaction, is that the activation of the LXR- $\alpha$  receptor not only increased per se the mRNA expression of  $\Delta 6$  and  $\Delta 5$  desaturases and SCD-1 in diabetic rats, but also the injection of insulin into the diabetic animals treated with T09 increased the expression strongly.

LXR- $\alpha$  not only enhanced the activity of the desaturases but also both SREBP-1 and nSREBP-1, and since Chen et al. [14] have already demonstrated the central role for LXR- $\alpha$  in the insulin activation of SREBP-1c transcription, and SREBP-1c per se has a pivotal role in expression and activity of desaturases [9, 10], the results obtained are easily explained by a collaborative effect of LXR- $\alpha$  and insulin in SREBP-1c activation that evokes the hyperexpression of the desaturases. The contribution of LXR- $\alpha$ /RXR- $\alpha$  is evoked through the induction of SREBP-1c gene expression as well as by an additional contribution of insulin through SCAP-dependent cleavage of the precursor SREBP-1c to the mature nuclear form nSREBP-1c [23].

This hyperexpression of the desaturase mRNAs by the joint action of LXR- $\alpha$  and insulin on the diabetic rats was, however, not correlated by a quantitatively similar increase of the desaturase enzymatic activities (Fig. 3), and therefore was not quantitatively transmitted to the ribosomal synthesis of desaturases.

PPAR- $\alpha$  activation by fibrates evokes also an increase of mRNAs and enzymatic activities of SCD-1 and  $\Delta 5$  and  $\Delta 6$  desaturases in control and diabetic rats as proved in this experiment and by Montanaro et al. [11]. In addition, Tang et al. [40] demonstrated that in rats, another PPAR- $\alpha$  activator, WY 14643, enhanced the transcription of hepatic  $\Delta 6$  desaturase by more than 500%. Moreover, they found that an imperfect direct repeat DR-1 element located at –385/–373 of the human  $\Delta 6$  desaturase gene possesses the ability to bind the heterodimer PPAR- $\alpha$ /RXR- $\alpha$  and subsequently to function as a PPAR- $\alpha$ -RE. The activation of  $\Delta 6$  desaturase mRNA expression by agonists of PPAR- $\alpha$  was also demonstrated by Matsuzaka et al. [10] and He et al. [41]. This fact that PPAR- $\alpha$  activation through fenofibrate administration activates both normal and diabetic rat [11] expression and activity of the desaturases demonstrates that the fenofibrate-dependent desaturase increase found in normal rats was not due to insulin in spite of the fact that insulinemia was enhanced by fenofibrate, but it was due to the genuine action of insulin-independent PPAR- $\alpha$ .

The simultaneous administration of T09 to fenofibrate-treated control rats did not further enhance significantly the activation of mRNA expression and

enzymatic activities of  $\Delta 5$  and  $\Delta 6$  desaturases and SCD-1 (Figs. 2, 3), and even the presence of fenofibrate reduced the enhancement of  $\Delta 6$  desaturase mRNA evoked by T09. Besides, Fig. 4 depicts a fenofibrate- and T09-dependent enhancement of the  $\Delta 6$  desaturase protein that follows a parallel pattern to the mRNA changes, but not the enzymatic activity. Therefore, we did not detect the existence, in control rats, of an additive effect of LXR- $\alpha$  and PPAR- $\alpha$  effects leading to an activation of unsaturated fatty acid biosynthesis through desaturase regulation.

The elongation of fatty acyl-CoAs is now considered another putative step in the control of polyunsaturated fatty acid biosynthesis [42]. PPAR- $\alpha$  as shown in Fig. 5 activates palmitoyl-CoA elongase in control rats and a simultaneous activation of LXR- $\alpha$  evokes a synergic effect. In that respect, according to Inagaki et al. [43] from two elongase genes identified in rats, rELO1 and rELO2, the rELO1 gene, a homologue of human ELOVL5, was shown to elongate monosaturated and polyunsaturated fatty acids of 16–20 carbons; however, its expression was little modified by fasting or rat re-feeding. On the other hand, the rELO2 gene expression in hepatocytes, which is responsible for palmitic acid elongation, was activated by fasting and refeeding cycles of the rats [42, 43]. Besides, a similar long chain fatty acid elongase that elongates saturated and monounsaturated acids was found to be activated in mouse liver by nSREBP-1c overexpression and T09 administration [44]. Therefore, a cross-talk exists between LXR- $\alpha$  and PPAR- $\alpha$  and LXR- $\alpha$  and insulin in elongase regulation. The mechanism and consequences of this activation are an interesting field for further investigation.

The translation of insulin, PPAR- $\alpha$ , LXR and SREBP activation of desaturase mRNA expression to the desaturases and their effects on liver fatty acid composition after a short treatment are depicted in Table 1. During this short period of time, the depressing effect of diabetes on the desaturase enzymatic activity was not found to be transferred to a statistically significant reduction of the unsaturated fatty acids. However, the activation of LXR- $\alpha$  by T09 and the simultaneous insulin administration to the diabetic rats, which evoked the highest desaturase expression, enhanced specifically palmitoleic and oleic acids synthesized by SCD-1, but not the  $\Delta 6$  and  $\Delta 5$  desaturase-dependent polyunsaturated acids. Therefore, that result is probably the consequence of a strong effect of LXR- $\alpha$  and insulin interaction on a SREBP-1c dependent activation specific for the SCD-1 desaturase reaction since it could not be detected after T09 administration to control and diabetic rats.

PPAR- $\alpha$ , in contrast, enhanced palmitic acid and depressed the amount of stearic acid, as already shown by Montanaro et al. [11], though it activated palmitoyl-CoA elongase (Fig. 5) and increased palmitoleic and oleic acids in correlation with an increase of SCD-1 activity (Fig. 3) [11, 45]. The increase of palmitic acid evoked by fenofibrate administration is difficult to understand, as attributed to an increased synthesis as already discussed by Montanaro et al. [11], in view of the antidyslipidemic, catabolic effect generally attributed to PPAR- $\alpha$  that would lead, as pointed out by Desvergne and Wahli [46], to the simultaneous activation of both anabolic and catabolic effects producing a futile cycle. However, in spite of the fact that the PPAR- $\alpha$  mediated activation of the malic enzyme gene generating the NADPH required for fatty acid synthesis might lead to lipid increases, on the other hand the coordinate genetic activation of acyl-CoA synthase, carnitine palmitoyl transferase I, medium-chain acyl-CoA dehydrogenase and liver fatty acid binding protein would evoke an increase of mitochondrial fatty acid oxidation [46], and we consider that the increase

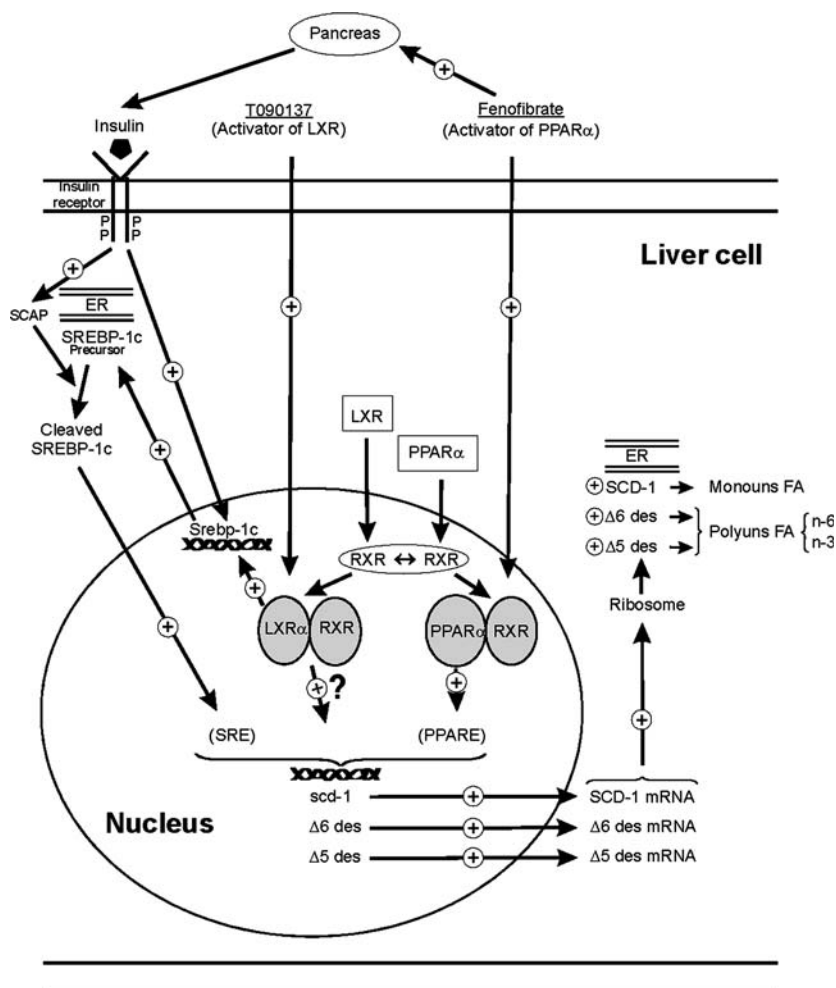
of palmitic acid in liver phospholipids does not necessarily indicate an enhanced fatty acid biosynthesis antagonistic to the catabolic effect. We suggest that a possible PPAR- $\alpha$  dependent activation of a specific acyl-CoA synthase in coordination with an acyl-CoA transferase could lead to a diversion of palmitic acid to interesterify membrane phospholipids without antagonizing the catabolic pathway.

PPAR- $\alpha$  activation depressed the highly polyunsaturated acids of the n-3 family, 20:5n-3, 22:5n-3 and 22:6n-3, as usually observed in some treatments in spite of the increase of desaturase activity [1, 11]; therefore, it would depress the anti-inflammatory, antioxidant and anti-atherogenic effects attributed to these acids as well as the beneficial effects in brain cognitive behavioral development and glucose uptake.

## Conclusions

As summarized in Fig. 6, we have been able to demonstrate the contribution of LXR- $\alpha$ , insulin, SREBP-1c and

**Fig. 6** LXR- $\alpha$ , PPAR- $\alpha$ , SREBP-1c and insulin interactions on modulation of liver fatty acid desaturases and unsaturated fatty acid biosynthesis



PPAR- $\alpha$  in vivo interaction in the sophisticated modulation of SCD-1 and  $\Delta 6$  and  $\Delta 5$  hepatic desaturases. Briefly, LXR- $\alpha$  activation increases Srebp-1c expression. Also insulin increases srebp-1c expression in addition to SREBP-1c hydrolysis to the nuclear active form. These increases enhance the mRNAs of SCD-1 and also of the  $\Delta 6$  and  $\Delta 5$  desaturases. LXR- $\alpha$  and insulin interact evoking a large cooperative enhancement of mRNAs of the desaturases. PPAR- $\alpha$  also activates the expression of the desaturases, but independently of the contribution of SREBP-1c and insulin. LXR- $\alpha$  and PPAR- $\alpha$  interact through the coparticipation of RXR- $\alpha$  in the formation of the corresponding heterodimers LXR- $\alpha$ /RXR- $\alpha$  and PPAR- $\alpha$ /RXR- $\alpha$  in the activation of mRNAs of the desaturases and the enzymatic activities reach levels not higher than those evoked by LXR- $\alpha$ . However, the level of expression and the enzymatic activities reached require some time to concomitantly modify the fatty acid composition of tissue lipids. Therefore, the biosynthesis of unsaturated fatty acids is modulated in vivo by the interplay of all these factors that may modify the specific effects of insulin and are very important in human physiology. They must be considered for an appropriate treatment of diabetes and cardiovascular diseases.

Anyhow, it is necessary to remark that in normal and even abnormal physiological conditions, in vivo, the real modulators of these factors are the unsaturated fatty acids and derivatives which also control their own biosynthesis and are supplied in foods [47]. The structure of the unsaturated fatty acids determines also their activity [48, 49], and they compete in their own biosynthesis and even evoke retroinhibitions as demonstrated a long time ago [50].

**Acknowledgements** This research is published in honor of the coauthor María S. González who passed away in October 2006. The gifts of T0901317 from Amgen and the SCD-1,  $\Delta 6$  desaturase and  $\Delta 5$  desaturase complementary DNA from J. Ozols, T. Aki and R. Zolfaghari and C. Ross, respectively, are greatly acknowledged. This work was partially supported by grant PIP 5724 from CONICET, Argentina.

## References

- Brenner RR (2003) Hormonal modulation of  $\Delta 6$  and  $\Delta 5$  desaturases: case of diabetes. *Prostaglandins Leukot Essent Fatty Acids* 68:151–162
- Gellhorn A, Benjamin W (1964) The intracellular localization of an enzymatic defect of lipid metabolism in diabetic rat. *Biochim Biophys Acta* 84:167–175
- Gellhorn A, Benjamin W (1964) Insulin action in alloxan diabetes modified by actinomycin D. *Sciences* 146:1166–1168
- Mercuri O, Peluffo RO, Brenner RR (1966) Depression of microsomal desaturation of linoleic to  $\gamma$ -linolenic acid in the alloxan-diabetic rat. *Biochim Biophys Acta* 116:409–411
- Mercuri O, Peluffo RO, Brenner RR (1967) Effect of Insulin on the oxidative desaturation of  $\alpha$ -linolenic, oleic, and palmitic acids. *Lipids* 2:284–285
- Brenner RR, Peluffo RO, Mercuri O, Restelli MA (1968) Effect of arachidonic acid in the alloxan-diabetic rat. *Am J Physiol* 215:63–70
- Waters KM, Ntambi JM (1994) Insulin and dietary fructose induce stearoyl-CoA desaturase-1 gene expression in liver of diabetic mice. *J Biol Chem* 269:27773–27777
- Rimoldi OJ, Finarelli GS, Brenner RR (2001) Effects of diabetes and insulin on hepatic  $\Delta 6$  desaturase gene expression. *Biochem Biophys Res Commun* 283:323–326
- Shimomura I, Bashmakov Y, Ikemoto S, Horton JD, Brown MS, Goldstein JL (1999) Insulin selectively increases SREBP-1c mRNA in the livers of rats with streptozotocin-induced diabetes. *Proc Natl Acad Sci USA* 96:13656–13661
- Matsuzaka T, Shimano H, Yahagi N, Amemiya-Kudo M, Yoshikawa T, Hasty AH, Tamura Y, Osuga J, Okazaki H, Iizuka Y, Takahashi A, Sone H, Gotoda T, Ishibashi S, Yamada N (2002) Dual regulation of mouse  $\Delta 5$  and  $\Delta 6$  desaturase gene expression by SREBP-1 and PPAR $\alpha$ . *J Lipid Res* 43:107–114
- Montanaro MA, Bernasconi AM, González MS, Rimoldi OJ, Brenner RR (2005) Effect of fenofibrate and insulin on the biosynthesis of unsaturated fatty acids in streptozotocin diabetic rats. *Prostaglandins Leukot Essent Fatty Acids* 73:369–378
- Repa JJ, Liang G, Ou J, Bashmakov WJ, Lobaccaro JMA, Shimomura I, Shan B, Brown MS, Goldstein JL, Mangelsdorf DJ (2000) Regulation of mouse sterol regulatory element-binding protein-1c gene (SREBP-1c) by oxysterol receptors, LXR $\alpha$  and LXR $\beta$ . *Genes Dev* 14:2819–2830
- Yoshikawa T, Shimano H, Yahagi N, Ide T, Amemiya-Kudo M, Matsuzaka T, Nakakuki M, Tomita S, Okazaki H, Tamura Y, Iizuka Y, Ohashi K, Takahashi A, Sone H, Osuga J, Gotoda T, Ishibashi S, Yamada N (2002) Polyunsaturated fatty acid suppress sterol regulatory element binding protein 1c promoter activity by inhibition of liver X receptor (LXR) binding to LXR response elements. *J Biol Chem* 277:1705–1711
- Chen G, Liang G, Ou J, Goldstein JL, Brown MS (2004) Central role for liver X receptor in insulin mediated activation of SREBP-1c transcription and stimulation of fatty synthesis in liver. *Proc Natl Acad Sci USA* 101:11245–11250
- Shulz JR, Tu H, Luk A, Repa JJ, Medina JC, Li L, Schwendner S, Wang S, Thoolen M, Mangelsdorf DJ, Lustig KD, Shan B (2000) Role of LXR in control of lipogenesis. *Genes Dev* 14:2831–2838
- Herbert V, Lau KS, Gottlieb CH, Bleicher S (1965) Coated charcoal immunoassay of insulin. *J Clin Endocrinol Metab* 25:1375–1384
- Lowry OH, Rosebrough NJ, Farr AL, Randall RJ (1951) Protein measurement with folin phenol reagent. *J Biol Chem* 193:265–275
- Folch J, Lees M, Sloane-Stanley GH (1957) A simple method for the isolation and purification of total lipids from animal tissues. *J Biol Chem* 226:497–509
- Small GM, Burdett K, Connock MJ (1985) A sensitive spectrophotometric assay for peroxisomal acyl-CoA oxidase. *Biochem J* 227:205–210
- Kudo N, Toyama T, Mitsumoto A, Kawashima Y (2003) Regulation by carbohydrate and clofibrate of palmitoyl-CoA chain elongation in the liver of rats. *Lipids* 38:531–537

21. Sambrook J, Frithch EF, Mamatis T (1989) Molecular cloning, a laboratory manual. Cold Spring Harbor Laboratory Press, New York, pp 938–957
22. D'Andrea S, Guillou H, Jan S, Catheline D, Thibault JN, Bouriel M, Legrand P (2002) The same rat  $\Delta 6$  desaturase acts not only on 18- but also on 24-carbon fatty acids in very long chain polyunsaturated fatty acid biosynthesis. *Biochem J* 364:49–55
23. Hegarty BD, Bobard A, Hainarelt I, Ferre P, Bossard P, Foufelle F (2005) Distinct roles of insulin and liver X receptor in the induction and cleavage of sterol regulatory element binding protein-C. *Proc Natl Acad Sci USA* 102:791–796
24. Hu R, Iskü E, Nakagawa Y (1994) Differential changes in relative levels of arachidonic acid in major phospholipids from rat tissues during progression of diabetes. *J Biochem* 115:405–408
25. Brenner RR (2006) Antagonism between Type 1 and Type 2 diabetes in unsaturated fatty acid biosynthesis. *Future Lipidol* (in press)
26. Zhou YT, Shimabujuro M, Wang MY, Lee Y, Higa M, Milburn JL, Newgard CB, Unger RH (1998) Role of peroxisome proliferator-activated receptor- $\alpha$  in disease of pancreatic  $\beta$ -cells. *Proc Natl Acad Sci USA* 95:8898–8903
27. Gremlich S, Nolan C, Rodiut R, Buealen R, Peyot ML, Delhingaro-Augusto V, Desvergne B, Michalik L, Prentki M, Wahli W (2005) Pancreatic islet adaptation to fasting is dependent on peroxisome proliferator-activated receptor ( $\alpha$ ) transcriptional up-regulation of fatty acid oxidation. *Endocrinology* 146:375–382
28. Bihan H, Rouault Ch, Reach G, Poitout V, Staels B, Guerre-Millo M (2005) Pancreatic islet response to hyperglycemia is dependent on peroxisome proliferator-activated receptor  $\alpha$  (PPAR- $\alpha$ ). *FEBS Lett* 579:2284–2288
29. Ravnskjaer K, Boergesen M, Rubi B, Larsen JK, Nielsen T, Fridriksson J, Maechler P, Mandrup S (2005) Peroxisome proliferator-activated receptor- $\alpha$  (PPAR- $\alpha$ ) potentiates whereas PPAR- $\gamma$  attenuates glucose-stimulated insulin secretion in pancreatic  $\beta$ -cells. *Endocrinology* 146:3266–3276
30. Tordzman K, Stanley KN, Bernal-Mizrachi C, Leone TS, Coleman T, Kelly DP, Semenkovich CF (2002) PPAR- $\alpha$  suppresses insulin secretion and induces UCP2 in insulinoma cells. *J Lipid Res* 43:936–943
31. Anderson SP, Dunn C, Laughter A, Yoon J, Swanson C, Stulnig TM, Steffensen KR, Chandraratna RAS, Gustafsson JA, Corton JCh (2004) Overlapping transcriptional programs regulated by the nuclear receptors peroxisome proliferator activated receptor  $\alpha$ , retinoic X receptor, and liver X receptor in mouse liver. *Mol Pharmacol* 66:1440–1452
32. Ide T, Shimano H, Yoshikawa T, Yahagi N, Amemiya-Kudo M, Matzuzaka T, Nakakuki M, Yatoh S, Iizuka Y, Tomita S, Ohashi K, Takahashi A, Sone H, Gotoda T, Osuga J, Ishibashi S, Yamada N (2003) Cross-talk between peroxisome proliferator-activated receptor (PPAR)  $\alpha$  and the liver X receptor (LXR) in nutritional regulation of fatty acid metabolism II LXRs suppress lipid degradation gene promoters through inhibition of PPAR signaling. *Mol Endocrinol* 17:1255–1267
33. Cao G, Liang Y, Broderick CL, Oldham BA, Beyer TP, Schmidt RJ, Zhang Y, Stayrook KR, Suen Ch, Otto KA, Miller AR, Dai J, Foxworthy P, Gao H, Ryan TP, Jiang X, Burris TP, Echo PI, Etgen GJ (2003) Antidiabetic action of a liver X receptor agonist mediated by inhibition of hepatic gluconeogenesis. *J Biol Chem* 278:1131–1136
34. Chinetti G, Lestavel S, Bocher V, Remaley AT, Neve B, Torra IP, Teissier E, Minnich A, Jaye M, Duverger N, Brewer HB, Fruchart JC, Clavey V, Setaels B (2001) PPAR- $\alpha$  and PPAR- $\gamma$  activators induce cholesterol removal from human macrophage foam cells through stimulation of the ABC A-1 pathway. *Nat Med* 7:53–58
35. Guan JZ, Tamasawa N, Murakami H, Matsui J, Yamato K, Suda T (2003) Clofibrate, a peroxisome proliferator enhances reverse cholesterol transport through cytochrome P450 activation and oxysterol generation. *Tohoku J Exp Med* 201:251–259
36. Li AC, Glass CK (2004) PPAR- and LXR-dependent pathways controlling lipid metabolism and the development of atherosclerosis. *J Lipid Res* 45:2161–2173
37. Brenner RR, Bernasconi AM, González MS, Rimoldi OJ (2002) Dietary cholesterol modulates  $\Delta 6$  and  $\Delta 5$  desaturase mRNAs and enzymatic activity in rats fed a low-EFA diet. *Lipids* 37:375–383
38. Chisholm JW, Hong J, Mills SA, Lacon RM (2003) The LXR ligand T0901317 induces severe lipogenesis in db/db diabetic mouse. *J Lipid Res* 44:2039–2048
39. Wang Y, Kurdi-Haidar B, Oram JF (2004) LXR-mediated activation of macrophage stearoyl-CoA desaturase generates unsaturated fatty acids that destabilize ABCA1. *J Lipid Res* 45:972–980
40. Tang Ch, Cho HP, Nakamura MT, Clarke SD (2003) Regulation of human  $\Delta 6$  desaturase gene transcription: identification of a functional direct repeat-1 element. *J Lipid Res* 44:686–695
41. He WS, Nara TY, Nakamura MT (2002) Delayed induction of  $\Delta 6$  and  $\Delta 5$  desaturases by peroxisome proliferator. *Biochem Biophys Res Commun* 299:832–838
42. Leonard AE, Pereira SL, Sprecher H, Huang Y-Sh (2004) Elongation of long-chain fatty acids. *Prog Lipid Res* 43:36–54
43. Inagaki K, Aki T, Fukuda Y, Kawamoto S, Shigeta S, Ono K, Suzuki O (2002) Identification and expression of a rat fatty acid elongase involved in the biosynthesis of C18 fatty acids. *Biosci Biotechnol Biochem* 66:613–621
44. Matsuzaka T, Shimano H, Yahagi N, Yoshikawa T, Amemiya-Kudo M, Hasty AH, Okasaki H, Tamura Y, Iizuka Y, Ohashi K, Osuga J, Takahashi A, Nato S, Sone H, Ishibashi S, Yamada N (2002) Cloning and characterization of a mammalian fatty acyl-CoA elongase as a lipogenic enzyme regulated by SREBPs. *J Lipid Res* 43:911–920
45. Miller CW, Ntambi JM (1996) Peroxisome proliferator induce mouse liver stearoyl-CoA desaturase 1 gene expression. *Proc Natl Acad Sci USA* 93:9443–9448
46. Desvergne B, Wahli W (1999) Peroxisome proliferator-activated receptors: nuclear control of metabolism. *Endocr Rev* 20:649–698
47. Sampath H, Ntambi JM (2005) Polyunsaturated fatty acid regulation of genes of lipid metabolism. *Annu Rev Nutr* 23:317–340
48. Botolin D, Wang Y, Christian B, Jump DB (2006) Docosahexaenoic acid (22:6n-3) regulates rat hepatocyte SREBP-1 nuclear abundance by Erk- and 26S proteasome-dependent pathways. *J Lipid Res* 47:181–192
49. Tobin AKR, Steiniger HH, Alberti HH, Spydevold S, Auwerx Ø, Gustafsson JA, Nebb HI (2000) Cross-talk between fatty acid and cholesterol metabolism mediated by liver X receptor- $\alpha$ . *Mol Endocrinol* 14:741–752
50. Brenner RR (1974) The oxidative desaturation of unsaturated fatty acids in animals. *Mol Cell Biochem* 3:41–52

# Lipid Metabolism in Rats is Modified by Nitric Oxide Availability Through a $\text{Ca}^{++}$ -Dependent Mechanism

Carlos A. Marra · Julio Nella · Damián Manti ·  
María J. T. de Alaniz

Received: 1 September 2006 / Accepted: 23 November 2006 / Published online: 19 January 2007  
© AOCS 2007

**Abstract** We studied lipid metabolism and the anti-oxidant defense system in plasma and liver of rats fed diets supplemented with  $L^{\omega}$ -nitro-L-arginine methyl ester (L-NAME), isosorbide dinitrate (DIS), L-arginine (Arg), or the associations of these drugs. Liver hydroperoxide and thiobarbituric-acid-reactive substance (TBARS) levels were decreased by Arg and increased by L-NAME or DIS treatments. Oxidized glutathione and conjugated dienes were increased by DIS. Nitrate + nitrite levels and serum calcium ( $[\text{Ca}^{++}]$ ) were incremented by Arg or DIS and reduced by L-NAME. Superoxide dismutase and catalase activities decreased under Arg treatment, while L-NAME or DIS caused stimulation. Liver high-density lipoprotein (HDL) cholesterol was increased by DIS or NAME (alone or associated with Arg). Free fatty acids and neutral and polar lipids were increased by Arg, L-NAME, and DIS. However, predominating phospholipid synthesis increased the neutral/polar ratio. Decreased levels of nitric oxide (NO) (low  $[\text{Ca}^{++}]$ ) was directly associated with increased fatty acid synthetase, decreased phospholipase  $A_2$ , carnitine-palmitoyl transferase, and fatty acid desaturase activities. Raised NO (high  $[\text{Ca}^{++}]$ ) inversely correlated with increased phospholipase- $A_2$  and acyl-coenzyme A (CoA) synthetase and decreased fatty acid synthetase and  $\beta$ -oxidation rate. Arg or DIS produced changes that were

partially reverted by association with L-NAME. Based on these observations, prolonged therapeutical approaches using drugs that modify NO availability should be carefully considered.

**Keywords** Oxidative stress · Calcium · Lipid metabolism · Rat liver · Nitric oxide

## List of Abbreviations

NO	Nitric oxide
$[\text{Ca}^{2+}]$	Calcium concentration
$[\text{NOx}]$	Nitrite plus nitrate concentration
Arg	L-arginine
CAT	Catalase
DIS	Isosorbide dinitrate
FAS	Fatty acid synthetase
GSHPx	Glutathione peroxidase
GSHRd	Glutathione reductase
GSHTTr	Glutathione transferase
LLC	Low-level chemiluminescence
L-NAME	$L^{\omega}$ -nitro-L-arginine methyl ester
NL	Neutral lipids
PL	Polar lipids (phospholipids)
PL- $A_2$	Phospholipase $A_2$
ROOHs	Lipid hydroperoxides
SOD	Superoxide dismutase

Julio Nella author in memoriam.

C. A. Marra (✉) · J. Nella · D. Manti · M. J. T. de Alaniz  
INIBIOLP (Instituto de Investigaciones Bioquímicas de La Plata), CONICET-UNLP. Cátedra de Bioquímica, Facultad de Ciencias Médicas, Universidad Nacional de La Plata, Calles 60 y 120 (1900), La Plata, Argentina  
e-mail: camarra@atlas.med.unlp.edu.ar

## Introduction

The central role of nitric oxide (NO) as a messenger molecule is well documented in various biochemical processes such as immune function [1, 2], inflammation [3–6], apoptosis and necrosis [7–10], neurotransmission



[11, 12], mitochondrial respiration [13, 14], and endothelial function [10, 15–19], among others. It has also been reported that NO production is involved in the regulation of carbohydrate metabolism [20, 21] and inhibition of the Krebs cycle [22]. Lipid metabolism is strongly influenced by antioxidant status, although the mechanism involved remains unknown. Previous works demonstrated that deficiency of ascorbate [23, 24],  $\alpha$ -tocopherol [25], and the oligoelements involved in the antioxidant system, such as selenium [26] or copper [27], were able to induce rapid and significant hyperlipidemia with a concomitant increase in liver very-low-density lipoprotein (VLDL) secretion [28]. A key study by Khedara et al [29] proved that serum concentration of nitrate negatively correlated with those of plasma triacylglycerides and total cholesterol. These authors concluded that lower NO levels in rats led to hyperlipidemia and that elevation in serum triacylglycerides might be due—at least in part—to reduced fatty acid (FA) oxidation [29, 30]. Taking into account that reduced NO production is one factor leading to hyperlipidemia and increased atherosclerotic risk [15–17, 29], we decided to further explore whether oxidative stress would affect lipid metabolism by either increasing or decreasing NO levels. Various enzymes of the antioxidant defense system and lipid metabolism, together with concentration of the major water- and lipid-soluble antioxidants, were also correlated with lipid composition in plasma and tissues of rats fed diets supplemented with  $L^{\omega}$ -nitro- $L$ -arginine methyl ester ( $L$ -NAME), isosorbide dinitrate (DIS)—usually employed as an antihypertensive drug in humans—and  $L$ -arginine (Arg) alone or in combination with other drugs. Considering the central role of lipid metabolism and antioxidant defense system in the pathogenesis of atherosclerotic lesions [6, 9, 15–17, 19, 31, 32], we investigated the mechanism by which changes in NO production might affect biochemical pathways involved in FA and complex lipid metabolisms.

## Materials and Methods

### Chemicals

The following chemicals were purchased from Sigma Chem. Co. (Buenos Aires, Argentina):  $L$ -NAME, Arg, standards for high-performance liquid chromatography (HPLC) (retinol, oxidized and reduced glutathione,  $\beta$ -carotene,  $\alpha$ - and  $\beta$ -tocopherols, FA methyl esters, glutathione, and ascorbate); snake venom (*Crotalus atrox* western diamondback rattlesnake); nicotinamide adenine dinucleotide (NAD)<sup>+</sup>, hydrogenated NAD

[NADH(H)], hydrogenated NAD phosphate [NADPH(H)], thiobarbituric acid; coenzyme A (CoA, lithium salt),  $N$ -ethylmaleimide, deferoxamine mesylate, organic and inorganic components for buffer preparations, triphenylphosphine; xylenol orange, tetraethoxypropane; sodium deoxycholate (grade II); delipidated serum albumin bovine serum albumin (BSA); fraction V from bovine); and butylated hydroxytoluene. DIS was purchased as Isordil from John Wyeth Lab. (Buenos Aires, Argentina). Sodium nitrite and nitrate were from Merck (Darmstadt, Germany). All solvents were HPLC grade and were provided by Carlo Erba, Milano, Italy. Silicagel G-60 plates for thin-layer chromatography (TLC) were provided by Fluka-Riedel-de Häen (Darmstadt, Germany). Lipid standards for TLC identification of neutral and polar lipids were from Serdary Research Laboratories (London, Ontario, Canada). Unlabeled FAs were provided by Nu-Chek Prep. (Elysian, MN, USA). Labeled [ $1\text{-}^{14}\text{C}$ ]FA (palmitic, linoleic,  $\alpha$ -linolenic, and eicosa-8,11,14-trienoic) (98–99% pure, 50–60 mCi/mmol) were obtained from Amersham Biosciences (Buckinghamshire, UK). All acids were stored in benzene under nitrogen atmosphere at  $-20\text{ }^{\circ}\text{C}$ . Concentrations and purities were routinely checked by both gas liquid chromatography (GLC) and liquid-scintillation counting. Other chemicals used were reagent grade from local commercial sources.

### Animal Treatment

Female Wistar rats from Comisión Nacional de Energía Atómica (Buenos Aires, Argentina) weighing  $170 \pm 10\text{ g}$  were bred and maintained on a control diet (Cargill type “C”, Rosario, Argentina) throughout gestation and lactation. Dams were housed in plastic cages (one animal per cage) in a vivarium kept at  $22 \pm 1\text{ }^{\circ}\text{C}$  with a 12-h light/dark cycle and relative humidity  $60 \pm 10\%$ . After weaning, 36 male pups (weighing  $46 \pm 4\text{ g/animal}$ ) were randomly divided into six groups of six animals fed ad libitum a balanced diet (group C) prepared in our laboratory as described in a previous paper [33]. Other groups were supplemented with Arg (40 g/kg) $L$ -NAME (200 mg/kg), DIS (10 mg/kg), or a combination of Arg +  $L$ -NAME or DIS +  $L$ -NAME. During the ad libitum feeding period (35 days), body weight, water consumption, and food intake were determined every day. Blood samples (100–150  $\mu\text{l}$ ) were collected from the tail vein once a week to determine plasma calcium and nitrite + nitrate ([NOx]) levels. Animals were sacrificed on day 35 after feeding. To avoid individual differences among animals that might result from an ad libitum feeding, on day 34,

all rats were fasted for 24 h, re-fed with the corresponding diet for 2 h, and then killed by rapid decapitation without prior anesthesia 12 h after the re-feeding period. All diet components used were purchased from Carlo Erba (Milano, Italy) or Mallinckrodt (New York, USA). Animal maintenance and handling were in accordance with the National Institutes of Health (NIH) Guide for the Care and Use of Laboratory Animals [34].

#### Sample Collection and Subcellular Fraction Preparation

Liver, heart, kidneys, lungs, and brain from all experimental groups were rapidly excised and immediately placed in an ice-cold homogenizing medium [35]. The homogenates were processed individually at 1°C. Microsomal suspensions and cytosols (soluble fractions) were separated by differential centrifugation at 110,000 g, as described previously [35]. Microsomal pellets were resuspended in cold homogenizing solution up to a final protein concentration of 30 mg/ml. Mitochondrial suspensions from liver homogenates were obtained as described by Kler et al. [36]. Blood was also collected after killing the rats by decapitation. Samples were individually dispensed into heparinized tubes and fractionated by centrifugation at 500 g (10 min). Plasmas were immediately processed for calcium determination following the method described elsewhere [37, 38] using the procedure of Tomlinson and Dhalla [39]. Nitrite plus nitrate levels were measured according to Verdon et al. [40]. Lipid analysis was performed as described above. Erythrocyte ghosts were prepared by hypotonic lysis according to the procedure of Dodge et al. [41] modified by Berlin et al. [42].

#### Oxidative Stress Biomarkers

Thiobarbituric-acid-reactive substance (TBARS) were measured by the fluorometric method of Yagi [43]. Organo peroxides were determined with the FOX version II assay for lipid hydroperoxides (ROOHs) (FOX2) according to Nourooz-Zadeh et al. [44]. Contents of oxidized glutathione (GSSG) were determined following the HPLC method of Asensi et al. [45], while reduced glutathione (GSH) was measured following the glutathione-S-transferase assay described by Brigelius et al. [46]. Samples for GSSG analyses were obtained in the presence of *N*-ethylmaleimide and deproteinized using trichloroacetic acid (15% final concentration) [45].  $\alpha$ - and  $\beta$ -tocopherols, lycopene, and  $\beta$ -carotene were determined by HPLC according to Butris and Diplock [47] as modified by Bagnati et al.

[48]. Ascorbate was determined in deferoxamine mesylate-treated samples by the method of Benzie et al. [49]. Catalase activity (CAT) was measured according to Aebi [50]. Cytosolic (Cu,Zn) and mitochondrial (Mn) superoxide dismutase (SOD) activities were assayed as described by Flohé and Ötting [51]. Glutathione peroxidase (GSHPx), glutathione transferase (GSHTTr), and glutathione reductase (GSHRd) were assayed according to Wheeler et al. [52], Habig et al. [53], and Carlberg et al. [54], respectively. Light emission by chemiluminescence from lipid peroxidation assays was measured following the procedure of Wright et al. [55] with some modification. Liver microsomal suspensions obtained from control Wistar rats (2 ml; 0.5 mg protein/ml) in 0.1 M TRIS-HCl buffer (pH 7.40) and 0.15 M KCl were incubated in glass vials at 25 °C with a solution containing 100  $\mu$ M Fe<sup>2+</sup> and 100  $\mu$ M sodium ascorbate to initiate nonenzymatic lipid peroxidation. Low-level light emission was continuously monitored in the dark over a 130-min period and recorded as constant photocurrent method (cpm) using a liquid scintillation counter (1214 Rackbeta Scintillation Counter, Turku, Finland) in the out-of-coincidence mode. At zero time, membrane preparations were supplemented with 0.5 mg cytosolic proteins from the different experimental groups. Other vials lacking ascorbate, Fe<sup>2+</sup>, or both were run as control assays in the same conditions. The sum of total chemiluminescence (areas under each curve) was used to calculate percent change in respect to the assay with no cytosol addition (reference curve).

#### Lipid Analysis and Enzyme Activities of Lipid Metabolism

Total lipids were extracted by the method of Folch et al. [56]. Phospholipid and neutral lipid fractions were separated from the Folch extracts by the microcolumn chromatography method described elsewhere [57] and/or TLC [58, 59]. GLC of fatty acid methyl esters (FAMES) was performed as indicated in our previous paper [60], except that in this case, we used a capillary column mounted on a Hewlett Packard HP 6890 Series GC System Plus (Avondale, PA, USA) equipped with a terminal computer integrator. The FAMES were identified by comparison of their relative retention times with authentic standards, and mass distribution was calculated electronically by quantification of the peak areas. Cholesterol content was enzymatically measured according to Allain et al. [61]. High-density lipoprotein (HDL) cholesterol was determined using a commercial kit (Wiener Lab. Rosario, Argentina). Total and neutral lipids were

estimated gravimetrically after evaporation of an aliquot of the corresponding lipid extract (Folch or silicic acid subfraction, respectively) up to constant weight [62]. Phospholipids were also measured as phosphorus content [63] after mineralization of an aliquot from the silicic acid partition. Phospholipase A<sub>2</sub> (PL-A<sub>2</sub>) activity was determined with [<sup>14</sup>C]phenylcyclohexene ([<sup>14</sup>C]PC) (24.0 mCi/mmol, 99% pure) as substrate according to the method of Hirata et al. [64] with the modifications described in our previous paper [65]. To determine FA desaturase activities in microsomal suspensions, each FA used as substrate [[1-<sup>14</sup>C] 16:0, [1-<sup>14</sup>C] 18:2 (n-6),  $\alpha$ -18:3 (n-3), or [1-<sup>14</sup>C] 20:3 (n-6)] was diluted to a specific activity of 0.20–0.25  $\mu$ Ci/mol with the respective pure unlabeled FA. In order to compare results, enzymatic assays were conducted at saturated substrate concentrations. Analyses were done as described in previous papers [65, 66]. Acyl-CoA synthetase assays were performed on cytosol fractions obtained as supernatants of 110,000 g, according to the method of Tanaka et al. [67] modified as described in our previous paper [38]. FA synthetase activity was assayed according to Horning et al. [68]. Carnitine-palmitoyl transferase activity was measured following the method of Bieber and Fiol [69], while the rate of  $\beta$ -oxidation was determined as the production of acid-soluble metabolites derived from [1-<sup>14</sup>C]palmitate in hepatic microsomal suspensions as described by Kler et al. [36]. Ketone bodies (acetoacetate plus 3-hydroxybutyrate) were measured according to Laun et al. [70] by an enzymatic assay using 3-hydroxybutyrate dehydrogenase. Free fatty acids (FFAs) were determined as described in the paper of Duncombe and Rising [71].

#### Other Methodologies

Calcium content was determined after sample mineralization by atomic absorption in a Shimadzu Atomic Absorption Spectrophotometer AA-630-12 (Shimadzu Corp., Kyoto, Japan) or calcium-sensitive electrode model 93-20 (Orion Res. Inc., Cambridge, MA, USA) as described elsewhere [37–39]. Protein content was determined by the micromethod of Bradford [72] with crystalline BSA as standard.

#### Graphic Software and Statistical Treatment of Data

All values represent the mean of six individual determinations (assayed in duplicate)  $\pm$ 1 standard error of the mean (SEM). Data were analyzed by either the Student's *t* test or by analysis of variance (ANOVA), with the aid of Systat (version 8.0 for Windows) from

SPSS Science (Chicago, IL, USA). Results were also plotted and analyzed using Sigma Scientific Graphing Software (version 8.0) from Sigma Chem. Co. (St. Louis, MO, USA) and/or GB-STAT Professional Statistics Program (version 4.0) from Dynamic Microsystems Inc. (Silver Springs, NV, USA).

## Results

### Animal Model

We found that the addition of L-NAME, Arg, or a combination of these drugs to the standard diet produced no significant differences in final body weight or water consumption among the experimental groups (data not shown). From day 15 to the end of the experiment, DIS or DIS + L-NAME groups showed a 16% increase and a 19% decrease (mean values compared to control group, not statistically significant) in the water and diet consumption, respectively, either expressed as milliliter water/body weight, milliliter water/rat, or grams food/body weight, grams food/rat.

### Oxidative Stress Biomarkers

Figure 1 shows the plasma [NO<sub>x</sub>] during the feeding period. Inclusion of DIS in the diet composition produced a rapid and sustained increase in [NO<sub>x</sub>] concentration detected 5 days after treatment. Values were maintained at this level up to the end of the experimental period. The effect of DIS was not significantly modified by association with L-NAME. Arg caused an increase in [NO<sub>x</sub>] levels 10 days after treatment, reaching a maximum (three-fold in respect to control values) on day 15. Then it tended to decline slightly. L-NAME decreased the [NO<sub>x</sub>] concentration from day 5 up to the end of the experimental period. However, when Arg was associated with L-NAME, [NO<sub>x</sub>] values were restored to control values after 10–15 days of the combined treatment. Levels of [NO<sub>x</sub>] in soluble (cytosolic) fractions from different tissues of control and treated rats are shown in Table 1. Arg-treated rats exhibited increased [NO<sub>x</sub>] concentrations in liver, heart, and lungs. Association with L-NAME completely abolished these increments. Supplementation with L-NAME alone caused a significant reduction of [NO<sub>x</sub>] levels in all tissues studied, but this effect did not impair the important increment produced by DIS treatment in all soluble fractions analyzed. As a measurement of the oxidant capacity of cytosol fractions obtained from the different experimental groups, we

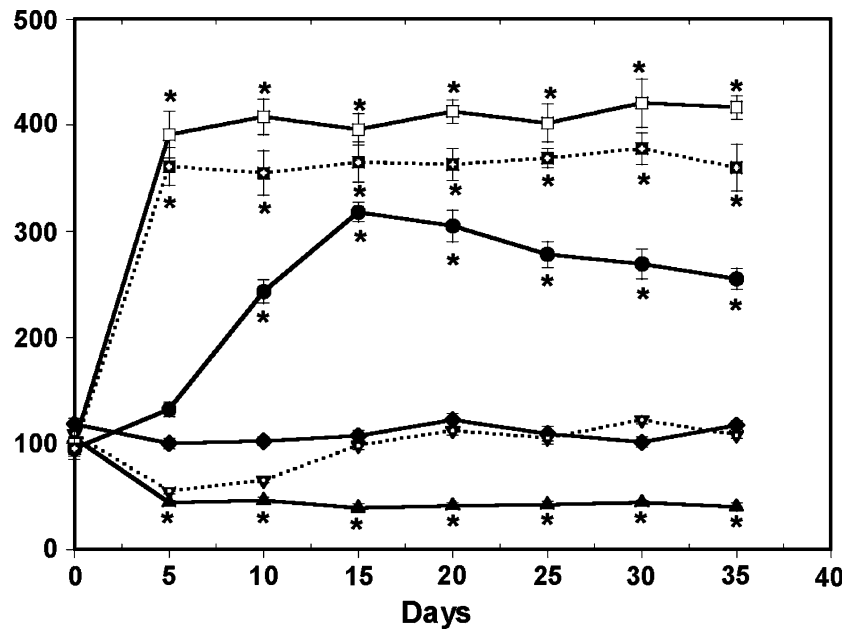


**Fig. 1** Nitrate + nitrite [NO<sub>x</sub>] concentration was determined in plasma samples obtained from the rats' tail vein every 5 days during the entire feeding period. Determination was based on reduction of nitrate to nitrite followed by Griess reaction (see "Materials and Methods"). Data are mean  $\pm$  1 standard error of the mean (SEM) (pmoles/mg protein) of duplicate or triplicate

measurements from six independent animals. Control group (filled diamond); L-*o*-nitro-L-arginine methyl ester (L-NAME) (filled triangle); L-arginine (Arg) + L-NAME (filled inverted triangle); Arg (filled circle); isosorbide dinitrate (DIS) + L-NAME (open square); DIS (open inverted triangle). (\*) Significantly different with respect to control data;  $P < 0.01$

**Table 1** Sum ( $\Sigma$ ) of nitrite + nitrate [NO<sub>x</sub>] in soluble fractions from tissues of treated rats

Treatment	Liver	Heart	Brain	Kidney	Lung
C	0.25 $\pm$ 0.02	1.12 $\pm$ 0.03	3.06 $\pm$ 0.18	0.44 $\pm$ 0.02	0.88 $\pm$ 0.03
Arg	0.39 $\pm$ 0.01*	1.69 $\pm$ 0.04	2.78 $\pm$ 0.26	0.48 $\pm$ 0.03	1.52 $\pm$ 0.04*
L-NAME	0.12 $\pm$ 0.01*	0.75 $\pm$ 0.02*	2.36 $\pm$ 0.11*	0.25 $\pm$ 0.01*	0.66 $\pm$ 0.03*
Arg + L-NAME	0.22 $\pm$ 0.02	1.23 $\pm$ 0.03	3.15 $\pm$ 0.09	0.46 $\pm$ 0.05	1.16 $\pm$ 0.04
DIS	1.08 $\pm$ 0.03*	2.50 $\pm$ 0.11*	4.74 $\pm$ 0.12*	0.76 $\pm$ 0.03*	1.55 $\pm$ 0.02*
DIS + L-NAME	0.81 $\pm$ 0.04*	2.23 $\pm$ 0.08*	4.11 $\pm$ 0.07*	0.52 $\pm$ 0.05	1.36 $\pm$ 0.03*

The sum ( $\Sigma$ ) of [NO<sub>x</sub>] was measured as described in "Materials and Methods". Results are expressed as pmoles/mg protein, and they are the mean of six independent determinations  $\pm$  1 standard error of the mean (SEM)

C control, Arg L-arginine, L-NAME L-*o*-nitro-L-arginine methyl ester, DIS isosorbide dinitrate

\*Significantly different with respect to the corresponding control value ( $P < 0.01$ )

tested the increase or decrease in low-level chemiluminescence (LLC) induced by Fe/ascorbate in vitro (Fig. 2). The curve indicated as "P" (without cytosol addition) showed the importance of endogenous components as antioxidants, as total CCL (area under the curve) increased 123% with respect to that obtained after the addition of control cytosol considered as the reference curve. Cytosols from DIS- or DIS + L-NAME-treated rats increased LLC by 250% and 259%, respectively, whereas cytosol from L-NAME-treated rats produced a 32% increase. Supplementation with Arg or Arg + L-NAME decreased LLC by -64% and -26%, respectively, with respect to the ref-

erence curve. "M" and "R" curves demonstrated that there was no spontaneous LLC—at least in a detectable extension—without induction by ascorbate or Fe/ascorbate.

Plasma from the Arg group showed increased values of TBARS, tocopherols, GSH, ascorbate, and carotene + glutathione, whereas retinol contents were decreased (Table 2) in comparison with the control group. L-NAME-treated rats showed increased levels of TBARS and ROOHs with respect to the control group. Ascorbate was also decreased in DIS- and DIS + L-NAME-treated rats and increased in Arg-supplemented animals. The combination of Arg +

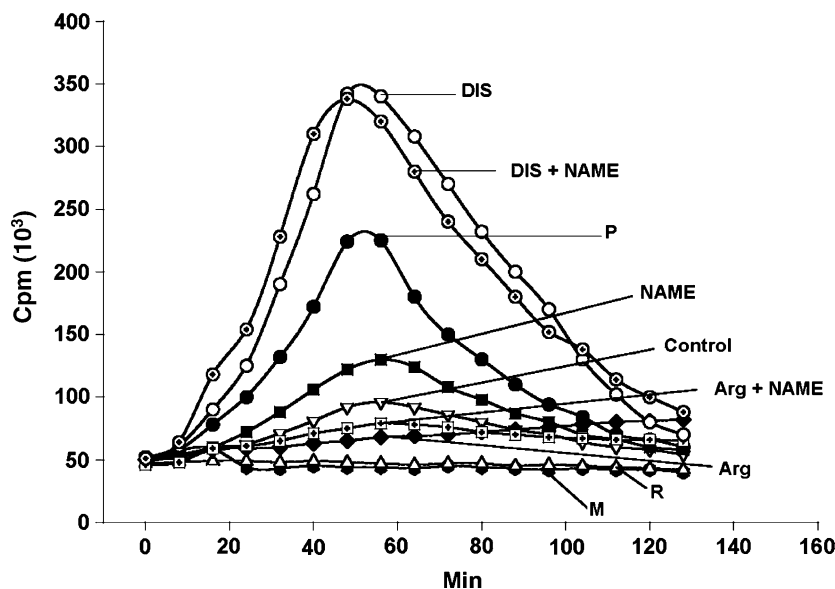


**Fig. 2** Low-level chemiluminescence [constant photocurrent method (cpm)  $10^3$ , mean of six determinations] induced by Fe/ascorbate in vitro at 25°C in control liver microsomes as a function of time. Control microsomes were incubated in a buffer solution (pH: 7.40) supplemented with cytosol fractions (0.5 mg protein/ml) obtained from liver of rats fed different experimental diets. Nonenzymatic peroxidation of lipids was induced by addition of Fe/ascorbate at zero time. Curve “P” represents data obtained in the presence of liver cytosol fraction from

nonsupplemented diet. *Control* corresponds to no cytosol addition. *M* and *R* are curves obtained without addition of cytosol and lacking Fe or ascorbate, respectively. Cytosol from L-arginine (Arg)- (filled diamond); Arg + L-nitro-L-arginine methyl ester (L-NAME)- (square with dot); L-NAME- (filled square); P- (filled circle); DIS + L-NAME- (circle with dot); and DIS- (open circle) treated animals. Standard errors of the mean (SEM) were omitted for simplicity, and they were between 5% and 8% of each mean value

L-NAME restored all values to control levels with the exception of GSH. Ratios of GSH/GSSG for Arg, L-NAME, and Arg + L-NAME groups were not modified with respect to control group. DIS or DIS + L-NAME treatments produced similar alterations in all biomarkers assayed. ROOHs and TBARS were increased, lipid soluble antioxidants were dramatically reduced, and ascorbate was decreased by  $27\% \pm 3\%$  with respect to the control group. The ratios of GSH/GSSG in DIS and DIS + L-NAME groups were decreased by 51% and 84%, respectively, compared with the control group. In DIS-treated rats, conjugated dienes also showed a marked increase with respect to other groups.

Table 3 shows the activities of some enzymes of the antioxidant defense system in plasma and erythrocytes from six experimental groups. Erythrocyte SOD and CAT activities were decreased by Arg treatment and increased by L-NAME supplementation. Glutathione-related enzymes were not significantly altered in either plasma or erythrocyte lysates from these experimental groups. Combined supplementation with Arg + L-NAME restored the activities of both enzymes to control values. DIS- or DIS + L-NAME-treated rats showed an important increase in SOD and GSHPx activities from plasma and erythrocytes, whereas CAT activity in erythrocytes was reduced by 41–45% with

respect to the control group. Characteristic stress biomarkers in liver from treated rats are shown in Table 4. The pattern of alterations was similar to that observed in plasma (Table 2). Livers from the Arg group exhibited decreased contents of tocopherols and increased amounts of  $\beta$ -carotene + glutathione. Arg caused a reduction in ROOHs and TBARS, whereas L-NAME supplementation produced an increment in both biomarkers with an elevation in diene conjugate concentration. In the Arg group, tocopherols were significantly decreased. The addition of L-NAME to the Arg diet neutralized all these alterations. However, L-NAME was ineffective in restoring the modifications caused by DIS, such as the elevation in ROOHs, TBARS, and diene conjugate levels and the concomitant decreased in tocopherol and ascorbate contents. The ratio GSH/GSSG decreased in DIS-treated rats compared with control rats.

Table 5 shows enzyme activities of the antioxidant defense system in liver of treated rats. SOD activity was measured using selective inhibitors for Mn-, Cu, and Zn-dependent isoforms [sodium cyanide and sodium dodecyl sulfate (SDS)]. Arg decreased both SOD isoforms and, as a consequence, total SOD activity. CAT was also diminished compared with controls. Glutathione-related enzymes were not significantly

**Table 2** Oxidative stress biomarkers in plasma from treated rats

Biomarkers	Treatments					
	C	Arg	L-NAME	Arg + L-NAME	DIS	DIS + L-NAME
Lipid hydroperoxidases (ROOHs)						
$\mu\text{M}$	4.6 $\pm$ 0.1	4.4 $\pm$ 0.3	5.5 $\pm$ 0.1*	4.7 $\pm$ 0.2	10.6 $\pm$ 2.1*	11.3 $\pm$ 1.9*
pmoles/mg protein	61.3 $\pm$ 4.4	58.4 $\pm$ 2.0	83.5 $\pm$ 2.8*	62.0 $\pm$ 1.1	137.7 $\pm$ 24.8*	148.7 $\pm$ 30.2*
pmoles/mg total lipids	1150 $\pm$ 41	927 $\pm$ 64	1522 $\pm$ 81*	1119 $\pm$ 55	1967 $\pm$ 123*	2288 $\pm$ 119*
Thiobarbituric-acid-reactive substance (TBARS)						
$\mu\text{M}$	1.3 $\pm$ 0.03	1.4 $\pm$ 0.1	2.9 $\pm$ 0.1*	1.4 $\pm$ 0.1	5.4 $\pm$ 0.3*	8.0 $\pm$ 0.3*
pmoles/mg protein	17.9 $\pm$ 1.0	28.6 $\pm$ 1.5*	22.4 $\pm$ 0.7*	18.2 $\pm$ 0.6	68.5 $\pm$ 1.9*	76.3 $\pm$ 2.0*
pmoles/mg total lipids	325 $\pm$ 16	348 $\pm$ 20*	644 $\pm$ 11*	334 $\pm$ 21	978 $\pm$ 61*	1089 $\pm$ 66*
$(\alpha + \gamma)$ tocopherols						
$\mu\text{M}$	16.1 $\pm$ 1.1	18.7 $\pm$ 0.6	13.9 $\pm$ 2.0	16.5 $\pm$ 1.2	9.8 $\pm$ 0.5*	9.1 $\pm$ 0.2*
pmoles/mg total lipids	4025 $\pm$ 133	4968 $\pm$ 84*	2106 $\pm$ 71*	3928 $\pm$ 107	1422 $\pm$ 61*	1404 $\pm$ 56*
Retinol						
$\mu\text{M}$	1.7 $\pm$ 0.1	1.8 $\pm$ 0.2	1.8 $\pm$ 0.3	1.7 $\pm$ 0.0	1.6 $\pm$ 0.2	1.5 $\pm$ 0.1
pmoles/mg total lipids	426 $\pm$ 24	285 $\pm$ 14*	273 $\pm$ 18*	407 $\pm$ 33	228 $\pm$ 21*	231 $\pm$ 12*
Oxidized glutathione (GSSG)						
nmoles/mg protein	65.5 $\pm$ 5.1	71.0 $\pm$ 4.2	54.3 $\pm$ 2.0*	68.6 $\pm$ 4.0	143.4 $\pm$ 3.0*	135.8 $\pm$ 2.7*
Reduced glutathione (GSH)						
nmoles/mg protein	833.0 $\pm$ 34.3	1041.6 $\pm$ 45.8*	841.5 $\pm$ 30.5	944.1 $\pm$ 42.1*	830.0 $\pm$ 55.0	839.4 $\pm$ 5.3
GSH/GSSG						
	12.7 $\pm$ 0.2	14.7 $\pm$ 0.2	15.5 $\pm$ 0.3	13.8 $\pm$ 0.4	5.8 $\pm$ 0.2*	6.2 $\pm$ 0.2*
Conjugated dienes						
ODU/mg total lipids	0.03 $\pm$ 0.0	0.03 $\pm$ 0.01	0.04 $\pm$ 0.01	0.02 $\pm$ 0.0	0.12 $\pm$ 0.01*	0.15 $\pm$ 0.01*
$\beta$ -carotene + glutathione						
$\mu\text{M}$	1.5 $\pm$ 0.2	1.6 $\pm$ 0.4	1.3 $\pm$ 0.3	1.4 $\pm$ 0.3	0.8 $\pm$ 1*	0.7 $\pm$ 0.1*
pmoles/ mg total lipids	375 $\pm$ 18	413 $\pm$ 11*	217 $\pm$ 24*	334 $\pm$ 28	114 $\pm$ 9*	108 $\pm$ 12*
Ascorbate						
$\mu\text{M}$	35.1 $\pm$ 1.3	44.6 $\pm$ 0.8*	32.3 $\pm$ 1.0	33.7 $\pm$ 0.4	27.4 $\pm$ 0.5*	26.0 $\pm$ 0.7*
pmoles/mg protein	468.0 $\pm$ 12.4	594.7 $\pm$ 15.7*	431.0 $\pm$ 16.4	443.4 $\pm$ 11.3	355.8 $\pm$ 10.2*	342.1 $\pm$ 9.8*

Biomarkers were determined according to the methods described in "Materials and Methods." Results were calculated in different ways and are expressed as the mean  $\pm$  1 standard error of the mean (SEM) of six independent determinations assayed in duplicate or triplicate

C control, Arg L-arginine, L-NAME L $\omega$ -nitro-L-arginine methyl ester, DIS isosorbide dinitrate

\*Significantly different with respect to the corresponding control value ( $P < 0.01$ )

modified. L-NAME supplementation produced increased total SOD activity at the expense of the cytosolic isoform, with no changes in the other enzymes assayed. Modifications observed for Arg or L-NAME were abolished by combination of these two drugs. DIS and DIS + L-NAME groups showed significant increments in SOD isoforms, GSHPx, and GSHPd activities with concomitant reduction of CAT activity.

#### Lipid Metabolism Parameters

Enzymatically determined total cholesterol and HDL cholesterol in plasma and liver microsomal suspensions are shown in Table 6. Total cholesterol was increased by supplementation with Arg, L-NAME, DIS, or

DIS + L-NAME. HDL cholesterol was reduced by DIS treatment either alone or in combination with L-NAME. As a result, the ratio HDL/total cholesterol was decreased in the Arg-, L-NAME-, DIS-, and DIS + L-NAME-treated groups. In liver microsomes only DIS supplementation produced a significant increase in cholesterol content that could not be reverted by simultaneous supplementation with L-NAME.

Supplements that modified NO levels also affected the absolute and relative amounts of neutral (NL) and polar (PL) lipids in liver microsomes and plasmas (Table 7). Liver NL and PL were increased by Arg, L-NAME, DIS, or DIS + L-NAME. The ratio NL/PL was decreased in the L-NAME-supplemented group. The same experimental groups exhibited elevated

**Table 3** Enzyme activities in plasma and erythrocytes from treated rats

Enzymes	Treatments					
	C	Arg	L-NAME	Arg + L-NAME	DIS	DIS + L-NAME
<b>Superoxide dismutase (SOD)</b>						
Erythrocytes	1843.5 ± 96.1	1197.3 ± 71.8*	2396.1 ± 153.5*	1806.9 ± 122.5	2673.8 ± 139.5*	2581.5 ± 135.6*
<b>Catalase</b>						
Erythrocytes	143.9 ± 12.2	98.5 ± 6.3*	193.3 ± 19.1*	135.0 ± 19.8	79.6 ± 6.1*	84.5 ± 7.7*
<b>Glutathione peroxidase (GSHPx)</b>						
Plasma	5.0 ± 0.4	4.2 ± 0.3	5.1 ± 0.3	4.7 ± 0.4	8.6 ± 0.5*	9.2 ± 0.6*
Erythrocytes	62.5 ± 10.4	59.7 ± 18.5	71.8 ± 11.8	66.4 ± 10.1	136.9 ± 15.1*	144.0 ± 17.1*
<b>Glutathione transferase (GSHTTr)</b>						
Plasma	2.7 ± 0.2	1.9 ± 0.3	2.5 ± 0.2	3.1 ± 0.4	3.0 ± 0.3	2.9 ± 0.2
Erythrocytes	15.3 ± 0.8	15.8 ± 0.7	14.3 ± 1.1	15.6 ± 0.9	16.2 ± 0.9	14.9 ± 0.8
<b>Glutathione reductase (GSHRd)</b>						
Plasma	2.1 ± 0.1	1.8 ± 0.2	2.2 ± 0.2	3.0 ± 0.3	2.7 ± 0.3	2.4 ± 0.2
Erythrocytes	8.8 ± 0.7	10.3 ± 0.6	9.1 ± 0.8	9.9 ± 0.6	10.1 ± 1.0	9.5 ± 0.9

Enzyme activities were determined as described in “Materials and Methods.” Results are expressed in units/mg protein (plasma) or units/g hemoglobin (erythrocytes) except for catalase, which is expressed in k instead of units. Each value represents the mean ± 1 standard error of the mean (SEM) of six independent determinations assayed in duplicate

C control, Arg L-arginine, L-NAME L $\omega$ -nitro-L-arginine methyl ester, DIS isosorbide dinitrate

\*Significantly different with respect to the corresponding control value ( $P < 0.01$ )

**Table 4** Oxidative stress biomarkers in liver from treated rats

Biomarkers	Treatments					
	C	Arg	L-NAME	Arg + L-NAME	DIS	DIS + L-NAME
<b>Lipid hydroperoxidases (ROOHs)</b>						
pmoles/mg protein	155.6 ± 23.1	106.1 ± 12.0*	253.2 ± 17.4*	134.8 ± 19.2	340.7 ± 31.2*	329.7 ± 26.2*
pmoles/mg total lipids	389 ± 45	176.8 ± 21.7*	442 ± 23*	321 ± 50	486 ± 29*	508 ± 43*
<b>Thiobarbituric-acid-reactive substance (TBARS)</b>						
pmoles/mg protein	86.1 ± 5.3	53.0 ± 2.1*	177.6 ± 12.5*	70.5 ± 7.7	188.1 ± 18.3*	170.0 ± 23.4*
pmoles/mg total lipids	215 ± 11	88.3 ± 15.4*	296.5 ± 20.2*	170.0 ± 16.4	269.2 ± 24.4*	261.7 ± 34.6*
<b>(<math>\alpha</math> + <math>\gamma</math>) tocopherols</b>						
pmoles/mg total lipids	1,505 ± 114	1349.1 ± 88.5*	920.6 ± 68.2*	1619.3 ± 106.7	741 ± 34*	809 ± 46*
<b>Reduced glutathione (GSH)</b>						
nmoles/mg protein	1,137 ± 72	1,095 ± 101	1,221 ± 135	1,088 ± 63	1,272 ± 66	1,304 ± 85
<b>Oxidized glutathione (GSSG)</b>						
nmoles/mg protein	53.0 ± 3.1	61.4 ± 4.3	40.5 ± 4.4*	60.0 ± 4.4	135.2 ± 4.0*	130.8 ± 5.1*
<b>GSH/GSSG</b>						
	21.5 ± 0.4	17.8 ± 0.3	30.1 ± 1.0*	18.1 ± 0.5	9.4 ± 0.2*	9.9 ± 0.3*
<b>Conjugated dienes</b>						
ODU/mg total lipids	0.06 ± 0.01	0.07 ± 0.01	0.110 ± 0.01*	0.06 ± 0.02	0.205 ± 0.03*	0.200 ± 0.02*
<b><math>\beta</math>-carotene + glutathione</b>						
pmoles/mg total lipids	1,095 ± 154	1,281 ± 46*	700 ± 52*	1,023 ± 95	551 ± 67*	590 ± 54*
<b>Ascorbate</b>						
pmoles/mg protein	12.6 ± 0.9	12.8 ± 0.5	11.3 ± 0.6	12.4 ± 0.8	8.1 ± 0.1*	7.5 ± 0.2*

Biomarkers were determined according to the methods described in “Materials and Methods.” Results were calculated in different ways and are expressed as the mean ± 1 standard error of the mean (SEM) of six independent determinations assayed in duplicate or triplicate

C control, Arg L-arginine, L-NAME L $\omega$ -nitro-L-arginine methyl ester, DIS isosorbide dinitrate

\*Significantly different with respect to the corresponding control value ( $P < 0.01$ )

**Table 5** Enzymes activities in liver from treated rats

Enzymes	Treatments					
	C	Arg	L-NAME	Arg + L-NAME	DIS	DIS + L-NAME
<b>SOD</b>						
Total	26.3 ± 0.5	21.2 ± 0.5*	30.6 ± 0.7*	25.8 ± 0.7	35.4 ± 0.9*	37.2 ± 1.1*
Mitochondrial (Mn-SOD)	5.5 ± 0.2	4.2 ± 0.1*	5.7 ± 0.3	5.1 ± 0.2	7.2 ± 0.2*	6.9 ± 0.3*
Cytosolic (Cu, Zn-SOD)	20.8 ± 0.4	17.0 ± 0.4*	24.9 ± 0.5*	20.7 ± 0.9	28.2 ± 0.8*	30.3 ± 0.5*
Catalase	0.9 ± 0.1	0.4 ± 0.1*	1.1 ± 0.2	0.9 ± 0.2	0.3 ± 0.05*	0.4 ± 0.1*
GSHPx	4.0 ± 0.2	3.8 ± 0.3	5.2 ± 0.3	4.1 ± 0.2	6.5 ± 0.3*	6.1 ± 0.2*
GSHT <sub>r</sub>	12.2 ± 0.3	13.1 ± 0.5	12.7 ± 0.6	10.1 ± 0.9	11.2 ± 0.6	10.7 ± 0.7
GSHR <sub>d</sub>	0.2 ± 0.03	0.2 ± 0.06	0.3 ± 0.03	0.2 ± 0.02	0.5 ± 0.10*	0.6 ± 0.20*

Enzyme activities were determined as described in “Materials and Methods.” Results are expressed in units per mg protein, except in the case of catalase, which are expressed in k/mg protein. Each value represents the mean ± 1 standard error of the mean (SEM) of six independent determinations assayed in duplicate

C control, Arg L-arginine, L-NAME L $\omega$ -nitro-L-arginine methyl ester, DIS isosorbide dinitrate, SOD superoxide dismutase, GSHPx glutathione peroxidase, GSHT<sub>r</sub> glutathione transferase, GSHR<sub>d</sub> glutathione reductase

\*Significantly different with respect to the corresponding control value ( $P < 0.01$ )

**Table 6** Cholesterol (CHO) content in plasma and liver microsomes from treated rats

Treatment	Plasma			Liver microsomes Total CHO
	Total CHO	HDL-CHO	HDL/total	
C	3.80 ± 0.10	2.40 ± 0.10	0.63 ± 0.01	0.14 ± 0.01
Arg	4.94 ± 0.20*	2.70 ± 0.15	0.55 ± 0.01*	0.16 ± 0.01
L-NAME	4.95 ± 0.04*	2.60 ± 0.10	0.52 ± 0.01*	0.13 ± 0.01
Arg + L-NAME	3.91 ± 0.06	2.80 ± 0.21	0.72 ± 0.03	0.14 ± 0.00
DIS	5.52 ± 0.03*	1.80 ± 0.10*	0.32 ± 0.01*	0.18 ± 0.02*
DIS + L-NAME	5.44 ± 0.02*	1.90 ± 0.12*	0.35 ± 0.01*	0.19 ± 0.02

Total cholesterol (CHO) and high-density lipoprotein (HDL)-CHO levels were determined enzymatically according to the method described in “Materials and Methods.” Results are expressed as nM concentration (plasma) or  $\mu$ moles/mg protein (liver microsomal suspensions) and are the mean ± 1 standard error of the mean (SEM) of six independent determinations assayed in duplicate

C control, Arg L-arginine, L-NAME L $\omega$ -nitro-L-arginine methyl ester, DIS isosorbide dinitrate

\*Significantly different from the corresponding control values ( $P < 0.01$ )

**Table 7** Neutral and polar lipids of liver microsomes and plasmas from treated rats

Treatment	Liver microsomes			Plasma		
	Neutral lipids	Polar lipids	Neutral lipids/ polar lipids	Neutral lipids	Polar lipids	Neutral lipids/ polar lipids
C	0.07 ± 0.01	0.47 ± 0.03	0.15 ± 0.01	1.60 ± 0.01	3.01 ± 0.02	0.53 ± 0.02
Arg	0.09 ± 0.01*	0.66 ± 0.02*	0.13 ± 0.02	2.58 ± 0.02*	5.60 ± 0.04*	0.46 ± 0.02*
L-NAME	0.11 ± 0.01*	0.88 ± 0.02*	0.12 ± 0.01*	2.72 ± 0.03*	5.70 ± 0.05*	0.47 ± 0.01*
Arg + L-NAME	0.07 ± 0.00	0.50 ± 0.02	0.14 ± 0.02	1.62 ± 0.06	3.07 ± 0.03	0.53 ± 0.02
DIS	0.13 ± 0.02*	0.92 ± 0.02*	0.14 ± 0.02	2.91 ± 0.05*	6.85 ± 0.05*	0.42 ± 0.01*
DIS + L-NAME	0.12 ± 0.03*	0.89 ± 0.01*	0.13 ± 0.02	2.69 ± 0.08*	5.78 ± 0.04*	0.46 ± 0.02*

Liver microsomal suspensions and plasma from treated rats were extracted by the method of Folch et al. [56] and fractionated into NL and PL subclasses using microcolumn silicic acid partition as described in “Materials and Methods.” Results are expressed as nmoles/mg protein (microsomes) or nM concentration (plasma) and are the mean ± 1 standard error of the mean (SEM) of six independent analyses. Representative molecular weights were considered for calculations of neutral and polar lipid concentrations (800 and 880, respectively)

C control, Arg L-arginine, L-NAME L $\omega$ -nitro-L-arginine methyl ester, DIS isosorbide dinitrate

\*Significantly with different respect to the corresponding control values ( $P < 0.01$ )



levels of NL and PL in plasma. The ratio NL/PL decreased significantly in Arg, L-NAME, DIS, and DIS + L-NAME groups.

Table 8 shows modifications in FFA and ketone bodies in plasma from treated rats. Increased production of NO by Arg, DIS, or DIS + L-NAME supplementation increased FFA concentration. Ketone bodies were elevated in DIS and DIS + L-NAME groups.

Some key enzymes of long-chain FA metabolism were measured under different experimental conditions (Table 9). Particulate PL-A<sub>2</sub> activity was diminished by the addition of L-NAME to control diet and elevated by DIS or DIS + L-NAME supplementation. Transport of FA into mitochondria was decreased by Arg, L-NAME, DIS, or DIS + L-NAME treatments. The rate of FA oxidation was also decreased in the same experimental groups. L-NAME supplementation increased acyl-CoA synthetase activity and decreased all FA desaturase activities measured. Groups treated with either DIS or DIS + L-NAME showed decreased activity of the fatty acid synthase (FAS) complex. We also analyzed the composition of fatty acyl chains in NL and PL from plasma and liver subfractions under the different experimental conditions. Figure 3 shows a typical fatty acyl pattern expressed in terms of FA ratios corresponding to PL in liver microsomal fractions. Similar modifications were observed in total lipids from plasma and liver homogenates and in NL from liver (data not shown). Monoenoic/saturated FA ratio was decreased in all experimental groups except the Arg-supplemented one with respect to control animals (which was taken as 0% change). The ratio of linoleic/arachidonic FA was significantly increased

only in the L-NAME group, whereas the docosahaenoic/docosapentaenoic ratio was elevated in all experimental groups.

#### Calcium Levels in Liver and Plasma from Treated Rats

Atomic absorption measurements of [Ca<sup>2+</sup>] in liver postmitochondrial supernatants and microsomal suspensions are shown in Table 10. Arg supplementation increased the concentration of calcium, whereas L-NAME produced a significant reduction. Combination of these supplements had no effect. DIS or DIS + L-NAME groups exhibited increased contents of [Ca<sup>2+</sup>]. Similar results were obtained in crude homogenates (data not shown). In liver microsomes, Arg, DIS, or DIS + L-NAME treatments elevated calcium levels, whereas L-NAME alone caused depletion. Total (free + linked to proteins) circulating [Ca<sup>2+</sup>] was not modified by any treatment (Table 10).

## Discussion

### Calcium Concentration and Oxidative Stress Biomarkers

It is well known that NO can both promote and inhibit lipid peroxidation [31]. By itself, it acts as an efficient scavenger of lipid peroxy radicals induced by a variety of oxidants, thus preventing the accumulation of oxidative chain propagators [73, 74]. However, in the presence of superoxide, NO forms peroxynitrite, which is a powerful oxidant capable of initiating lipid peroxidation and destroying water and lipid-soluble antioxidants and even deactivating antioxidant enzymes [74, 75]. We demonstrated that feeding rats with L-NAME decreased [NOx] levels in both plasma and homogenates from several tissues. Previous experimental data proved that more than 90% of [NOx] is derived from nitric oxide synthase (NOS) activity and that the contribution of the diet to [NOx] level is negligible [75]. Considering that the mean life of [NOx] in biological fluids is very short, the anion level indicates recent status in the activity of NOS isoforms [75]. We also observed how the level of [NOx] was increased after Arg supplementation in a more physiological way than that produced under the administration of pharmacological doses of DIS. This is very important, as supplementation with Arg reduces atherosclerotic risk, decreases platelet aggregation, and inhibits monocyte adhesion to endothelial cells [76–79], all of which are promising effects with therapeutic

**Table 8** Free fatty acids (FFA) and ketone bodies (KB) in plasma from treated rats

Treatments	FFA (nM)	KB (μM)
C	0.63 ± 0.01	223 ± 8
Arg	0.74 ± 0.01*	211 ± 10
L-NAME	0.79 ± 0.02*	230 ± 7
Arg + L-NAME	0.61 ± 0.02	214 ± 9
DIS	0.98 ± 0.02*	288 ± 12*
DIS + L-NAME	0.96 ± 0.03*	295 ± 15*

FFA and KB were determined as described in “Material and Methods.” Results are expressed as nmoles of palmitate/L (FFA) or μM of 3-OH-butyrate/L (KB), and are the mean ± 1 standard error of the mean (SEM) of six independent determinations assayed in duplicate

C control, Arg L-arginine, L-NAME Lω-nitro-L-arginine methyl ester, DIS isosorbide dinitrate

\*Significantly different with respect to the corresponding control value ( $P < 0.01$ )

**Table 9** Enzyme activities of lipid metabolism in liver from treated rats

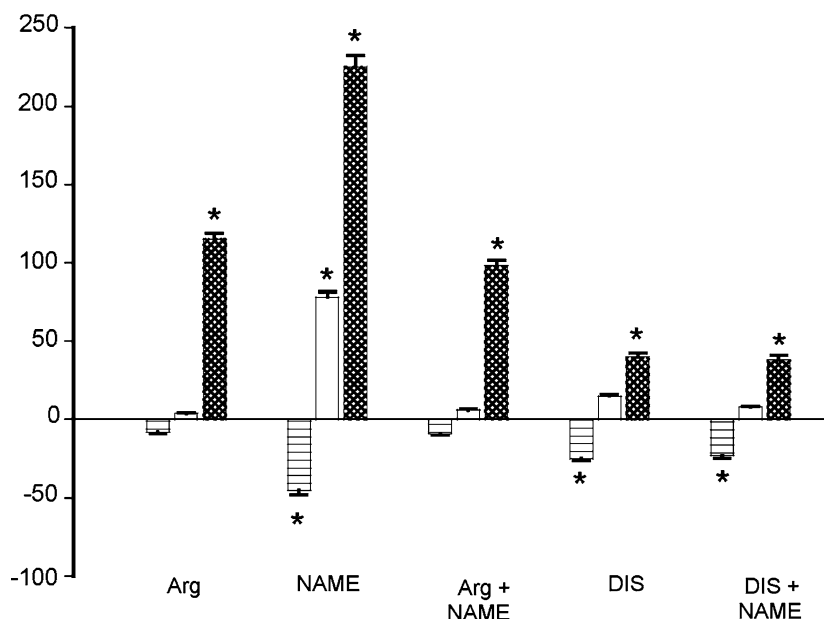
Enzyme specific activities	Treatments					
	C	Arg	L-NAME	Arg + L-NAME	DIS	DIS + L-NAME
Phospholipase A <sub>2</sub> (dpm/min mg protein)						
Soluble	403 ± 21	388 ± 22	452 ± 30	393 ± 19	431 ± 49	425 ± 47
Particulate	4,606 ± 77	5,215 ± 103	3,001 ± 64*	4,477 ± 105	6,815 ± 98*	5,907 ± 106*
Carnitine-palmitoyl transferase nmoles/min mg protein	3.26 ± 0.18	2.61 ± 0.11*	2.40 ± 0.08*	3.35 ± 0.21	1.66 ± 0.05*	1.78 ± 0.12*
Fatty acid β-oxidation rate nmoles acetate/min mg protein	4.12 ± 0.20	3.37 ± 0.10*	2.88 ± 0.06*	4.23 ± 0.16	1.95 ± 0.14*	1.91 ± 0.05*
Acyl-coenzyme A (CoA) synthetase nmoles/min mg protein	177.3 ± 7.8	168.5 ± 23.3	233.6 ± 14.0*	184.1 ± 15.2	161.7 ± 19.6	172.8 ± 11.5
Fatty acid synthetase ODU/ min mg protein	0.33 ± 0.02	0.30 ± 0.03	0.28 ± 0.04	0.36 ± 0.04	0.19 ± 0.02*	0.24 ± 0.03*
Fatty acid desaturases (nmoles/min mg protein)						
Δ9 (16:0 to > 16:1)	0.37 ± 0.02	0.33 ± 0.04	0.22 ± 0.03*	0.31 ± 0.06	0.34 ± 0.03	0.31 ± 0.03
Δ6 (18:2 n-6 to > 18:3 n-6)	0.72 ± 0.04	0.79 ± 0.03	0.36 ± 0.04*	0.77 ± 0.10	0.78 ± 0.10	0.75 ± 0.05
Δ6 (18:3 n-3 to > 18:4 n-3)	0.61 ± 0.03	0.65 ± 0.02	0.28 ± 0.03*	0.56 ± 0.05	0.60 ± 0.02	0.68 ± 0.05
Δ5 (20:3 n-6 to > 20:4 n-6)	1.02 ± 0.05	1.08 ± 0.07	0.69 ± 0.04*	0.98 ± 0.08	1.10 ± 0.09	1.06 ± 0.05

Enzyme activities were determined as described in “Material and Methods.” Results are expressed in the units indicated and represent the mean ± 1 standard error of the mean (SEM) of six independent determinations assayed in duplicate

C control, Arg L-arginine, L-NAME Lω-nitro-L-arginine methyl ester, DIS isosorbide dinitrate

\*Significantly different with respect to the corresponding control value ( $P < 0.01$ )

**Fig. 3** Percent change [mean of percent ± 1 standard error of the mean (SEM) of six independent analyses assayed in duplicate] calculated from the content (nmoles/mg protein) of selected fatty acids (FAs) of liver microsomal suspensions from rats fed different experimental diets. Within each grouped bars, the first one (horizontal pattern, rectangle with vertical lines) represents (16:1 + 18:1)/ (16:0 + 18:0) FA, the second one (no pattern, rectangle) 18:2 (n-2)/20:4 (n-6), and the third one (crossing pattern, rectangle with square) 22:6 (n-3)/22:5 (n-6). (\*) Significantly different with respect to control values,  $P < 0.01$  or less



implications [80–83]. Considering the dual behavior of NO as a pro- and an antioxidant [31, 84], it is not surprising that inhibition of NO with L-NAME is currently considered a neuroprotective strategy without undesirable side effects [82, 83]. However, our study also demonstrated that alterations in NO levels may induce dangerous modifications in other components

of the antioxidant defense system and in calcium concentration.

Although NO was first discovered as a mediator of vascular smooth relaxation, where it leads to a decrease in intracellular  $[Ca^{2+}]$  [85], other investigations carried out in several tissues demonstrated that treatments with NO and/or NO donors elicit increases in

**Table 10** Calcium levels in liver and plasma from treated rats

Treatment	Liver		Plasma
	Postmitoch.	Microsomes	
C	1.48 ± 0.02	2.54 ± 0.03	2.81 ± 0.02
Arg	1.79 ± 0.01*	2.86 ± 0.03*	2.96 ± 0.02
L-NAME	1.04 ± 0.03*	1.41 ± 0.05*	2.70 ± 0.04
Arg + L-NAME	1.52 ± 0.06	2.61 ± 0.04	2.85 ± 0.05
DIS	1.96 ± 0.03*	3.17 ± 0.03*	2.94 ± 0.03
DIS + L-NAME	1.89 ± 0.04*	2.99 ± 0.02*	2.91 ± 0.05

Postmitochondrial (Post-Mitoch.) and microsomal suspensions from liver homogenates and plasma from treated rats were analyzed for calcium contents using atomic absorption spectrometry as described in “Materials and Methods.” Results are expressed as nmoles/mg protein (liver) or mM concentration (plasma) and are the mean ± 1 standard error of the mean (SEM) of six independent determinations assayed in duplicate. C control, Arg L-arginine, L-NAME L $\omega$ -nitro-L-arginine methyl ester, DIS isosorbide dinitrate

\*Significantly different with respect to the corresponding control measurement ( $P < 0.01$ )

[Ca<sup>2+</sup>] [86]. This effect persists even in the absence of extracellular calcium and is dependent on ryanodine-sensitive calcium-release channels [86]. NO and peroxynitrite are responsible for [Ca<sup>2+</sup>] increase in the cytosolic compartment of various cell types [86–93]. Other reports suggested that peroxynitrite levels and, in general, NO availability determine calcium handling, especially from mitochondrial and endoplasmic reticulum stores [90, 91, 93]. Moreover, Berkels et al. [94] demonstrated a close correlation between NO and [Ca<sup>2+</sup>] by simultaneous detection using fluorometric probes. We found that there was a direct relationship between NO availability and [Ca<sup>2+</sup>] in liver homogenates, postmitochondrial supernatants, and microsomal suspensions. Perhaps this effect was produced through alterations in superoxide and/or peroxynitrite concentrations as suggested in previous reports [86, 88, 90, 93]. We observed unaltered total [Ca<sup>2+</sup>] in plasma. This may not be surprising and could be attributed to a compensatory mechanism that involves large calcium bone stores.

Modification in water- and lipid-soluble antioxidant levels may be an adaptive response to compensating peroxynitrite formation. It seems that there is an optimal concentration of NO that maintains antioxidant concentrations and GSH/GSSG ratio within the physiological range. Other authors suggested that there may be a relationship between NO availability and glutathione content [95, 96]. We also think that elevated NO may stimulate enzymes that synthesize glutathione, perhaps through a stimulatory effect of oxidative stress on  $\gamma$ -glutamyl-cysteinyl synthase

activity as previously reported for the central nervous system [96]. Changes described for antioxidant contents were reflected in the ability of cytosol fractions for quenching the low-level chemiluminescence signal derived from Fe/ascorbate-induced lipid peroxidation. It is feasible to speculate that such an in vitro effect may correlate with similar actions displayed in vivo.

ROOHs and TBARS are usually used as indicators of lipid peroxidation. A slight increase in NO production exerted a protective effect in liver homogenates but not in plasma. Decreasing or significantly increasing NO generation led to an opposite effect that was more evident in liver homogenates and plasma. These changes agree with previously discussed pro- and antioxidant actions of NO [31, 72–75, 84].

SOD is one of the key enzymes for controlling excessive superoxide production in both cellular compartments (mitochondrial matrix and cytosol) through activity of their specific isoforms. Hydrogen peroxide generated by these isoenzymes is further reduced to water by GSH peroxidase and by catalase. Thus, the content of GSH and SOD are both considered the predominant antioxidant defense, at least in liver [52]. The relative importance of CAT as a scavenger of peroxide depends—in consequence—on the availability of GSH, and conversely, levels of GSH are affected by the specific activity of CAT. SOD and CAT are inducible by oxidative stress and incremented NO levels [52]. GSHRd is also incremented by elevation of the GSSG/GSH ratio. We found that SOD isoforms were elevated in both plasma erythrocytes and liver homogenates by high levels of NO. On the contrary, SOD activities decreased in liver homogenates and erythrocytes under a mild increment of NO. This phenomenon may be the consequence of a minor superoxide production due to the antioxidant effect of NO and, as discussed before, may involve therapeutic implications for NO donors [74–83]. Thus, when L-NAME suppressed NO production, the oxidative status derived from this event significantly increased SOD activity. Oscillations in the activities of SOD isoforms were also in accordance with changes in the GSH/GSSG ratio. There was an inverse correlation between this ratio and the SOD activity that was more evident in DIS-treated animals. Results obtained may be analyzed in different ways, and multiple comparisons can be performed. However, if we focus the impact evoked by dietary supplements on liver biomarkers, some key conclusions can be obtained. The ratios [(GSHRd/GSHPx) × 10<sup>2</sup>], [CAT/SOD) × 10<sup>2</sup>], and [(GSHPx/SOD) × 10<sup>2</sup>] reflect the effort of the antioxidant defense system in maintaining the GSH/GSSG ratio between physiological values, neutralizing peroxide

overproduction, and reducing the formation of superoxide, respectively. Under excessive NO generation, the first ratio was increased significantly, as the stimulation of GSHRd observed in the DIS groups was insufficient to compensate for the level of SOD activity. Similarly, when NO levels were more physiological, CAT/SOD ratio was maintained at a mean value of 3.10. However, under excessive NO production, this ratio dropped to 0.90 because stimulation of CAT was unable to compensate for the SOD increase.

#### Lipid Metabolism and NO Availability

Diets that modified NO availability produced a major impact on lipid metabolism at both systemic and liver levels. Our findings concerning the changes in cholesterol content were in agreement with those previously reported by Khedara et al. [29, 30]. These authors suggested a relationship between cholesterol and the concentration of plasma nitrates. In addition, we found that the increase in plasma total cholesterol produced by either increased or decreased NO production was accompanied by elevated cholesterol levels in liver microsomes under DIS supplementation (not reverted by L-NAME). Interestingly, HDL cholesterol decreased in DIS groups and, as a result, a significant reduction in HDL/total cholesterol ratio was observed in experimental groups in which NO was decreased or increased by dietary manipulation. It is important to note that this finding was also observed under Arg or L-NAME treatment; both are currently used in human therapeutic approaches [74–83]. Our results suggest that careful consideration should be taken in prolonged administration of Arg or L-NAME in order to consider their real impact on one factors leading to hyperlipidemia and increased atherosclerotic risk. Hyperlipidemia induced by dietary manipulation was not mediated by renal dysfunction, as previous papers demonstrated that kidney size, serum creatinine, and albumin were not modified by prolonged administration of Arg or L-NAME [29, 30]. This study further demonstrated an important decrease in the NL/PL ratio especially observed in plasma under both NO depletion and increment of NO production. In these two conditions, alterations of the NL/PL ratio were the consequence of significant increments of both types of glycerolipids, with a predominant increase in PL concentration. These results showed for the first time that NO availability can simultaneously modify neutral and polar glycerolipid content in plasma and liver microsomes. Thus, in addition to the effects exerted on cholesterol metabolism, defective or excessive formation of NO should be considered a key point in

atherosclerotic patients receiving drugs that directly (or indirectly) modify NOS activity. The underlying mechanism that justifies these modifications is an issue that remains to be elucidated. Our study demonstrated that increased or decreased NO levels in plasma and tissues correlated with increased contents of plasma FFA and, in the case of NO overproduction, with a concomitant elevation of plasma ketone bodies. Misbalance in NO production established an oxidative stress condition that led to impairment of FA oxidation. In agreement with this, we found significant decreases in carnitine-palmitoyl transferase activity and acetate formation as an indicator of  $\beta$ -oxidation rate.

Interestingly, FA desaturase activities were inhibited in the L-NAME-treated rats in which availability of NO was depressed. This finding may be justified by our previous report concerning the general inhibitory effect exerted by deprivation of  $[Ca^{2+}]$  on FA desaturase enzymes [37]. Only L-NAME-treated animals underwent a constant low level of NO and exhibited diminished  $[Ca^{2+}]$  in liver homogenates and microsomal suspensions. In the same experimental group, acylation of FFAs was stimulated by calcium deprivation in accordance with our previous findings [38]. PL- $A_2$  is another key enzyme for glycerolipid metabolism. We found a direct correlation between NO levels,  $[Ca^{2+}]$ , and PL- $A_2$  activity. In the group in which  $[Ca^{2+}]$  was decreased, PL- $A_2$  was inhibited, and conversely, increased NO levels and  $[Ca^{2+}]$  stimulated PL- $A_2$  activity. This question is crucially important from the physiological point of view, as liberation of polyunsaturated fatty acids (PUFAs) (especially arachidonate) from PL stores plays a key role under different pathological conditions associated with modifications in local or systemic NO concentrations [97, 98]. We observed that the lipogenic enzyme FAS was inhibited when NO was generated in excess. Previous studies from other laboratories demonstrated that this enzyme was unaffected under discrete modifications of NO or administration of NO inhibitors [29]. However, DIS-treated animals showed a significant reduction of FAS activity, probably exerted via elevation of peroxynitrite and  $[Ca^{2+}]$  [99], and/or the strong accumulation of FFAs observed in these animals [100]. In addition, Mohr et al. [20] demonstrated that excessive NO formation inhibits glyceraldehydes-3-phosphate dehydrogenase. This fact may lead to depletion of the glycolytic route that in conjunction with the inhibitory effect exerted by NO on the Krebs cycle [22, 101] and mitochondrial respiration [13, 14, 102, 103] produced a general failure in availability of precursors and energy for FA synthesis.

All these modifications in lipid metabolism were reflected on the fatty acyl pattern of liver and plasma lipids. Alterations observed are difficult to analyze, as they depend on at least three factors: precursor desaturation–elongation rate, antioxidant influence, and selective  $\beta$ -oxidation (catabolism) and/or peroxidation (oxidative damage). In brief, we think that monoenoic/saturated FA ratio was diminished in the L-NAME group as a consequence of the inhibition of  $\Delta 9$  desaturase activity (via decrease in NO and  $[Ca^{2+}]$  availability) [37]. In DIS-treated rats, a less important decrease in this ratio may be attributed to a relative accumulation of saturated FA, perhaps due to a minor  $\beta$ -oxidation rate (the extension of which exceeded that of FAS inhibition). Decreased activities of  $\Delta 6$  and  $\Delta 5$  FA desaturases may account for the elevated linoleic/arachidonic FA ratio observed in L-NAME-treated animals. Biosynthesis of 22:6 (n-3) is carried out in mitochondria and depends critically on carnitine and  $\alpha$ -tocopherol levels [104]. In fact, this ratio was employed as an indicator of  $\alpha$ -tocopherol deficiency in mitochondria [105]. We found that there was a direct correlation between vitamin E levels and nmoles of 22:6 (n-3) per mg protein. However, the amount of 22:5 (n-3) also decreased at different proportions among the experimental groups, resulting in the ratios observed. Decrease of 22:5 (n-3) by peroxidation was intense in DIS-treated animals (data not shown). However, they exhibited minor values in the 22:6 (n-3)/22:5 (n-6)

ratios. This may be the consequence of the extensive drop in the amount of docosahexaenoic acid, which correlates with the important deficiency of  $\alpha$ -tocopherol in these experimental groups. Alterations in the ratio of PUFAs acylated to glycerolipids in general and to PL in particular should be considered of physiological relevance from at least two points of view: modifications in physicochemical properties of biomembranes (and indirectly most of their functions) as well as misbalance in the production of eicosenoids derived from the n-6 family (proinflammatory and proaggregating factors) and n-3 homologs (antiaggregating and anti-inflammatory) [106].

## Conclusions

Figure 4 depicts a general view of our findings. Oxidative damage can occur due to either increased or decreased NO levels through alterations in the antioxidant defense system (antioxidant depletion and/or modifications of antioxidant enzymes). Key enzymes in the lipid metabolism were also modified in a calcium- and NO-dependent way. A failure in the main producing energy routes was the consequence of changes in NO and in the oxidative-stress-derived condition. Decreased  $\beta$ -oxidation of FA was accompanied by increased production of ketone bodies and FFA concentration that may be channeled, at least in part, to

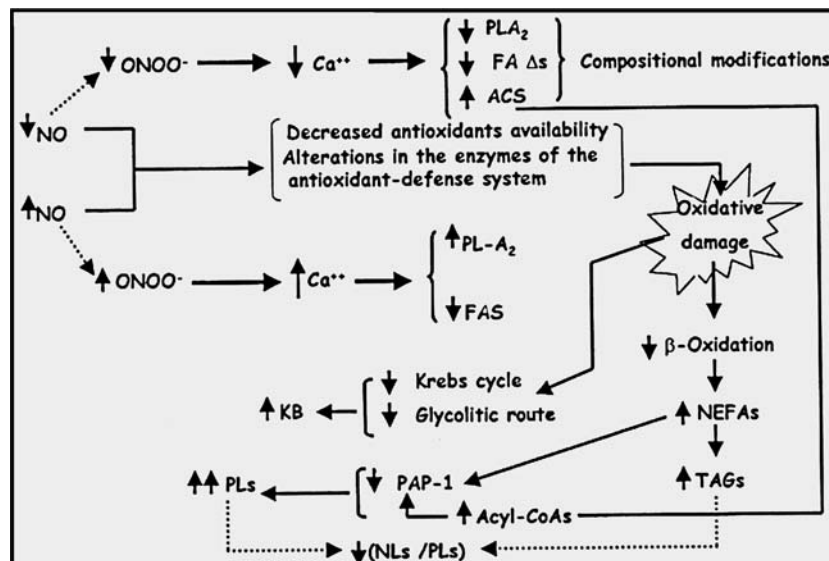


**Fig. 4** General scheme showing the main changes evoked by oxidative stress due to increased or decreased nitric oxide (NO) levels. Alterations in the antioxidant defense system and in the activities of enzymes are also shown in relation to calcium concentration ( $[Ca^{++}]$ ) and NO. ACS acyl-CoA-synthetase; FA

$\Delta s$  fatty acid desaturases, FA(s) fatty acid(s), FAS fatty acid synthetase, KB Krebs cycle, NEFAs nonesterified fatty acids, NLs neutral lipids, ONOO<sup>-</sup> peroxynitrite, PAP-1 phosphatidate-phosphohydrolase-1, PL-A<sub>2</sub> phospholipase A<sub>2</sub>, PLs polar lipids (phospholipids), TAGs triacylglycerides

glycerolipid biosynthesis. Accumulation of FFA and increased acylation of CoA inhibited phosphatidate-phosphohydrolase-1 activity [107]. Such a condition resulted in more availability of phosphatidate to be transformed into glycerophospholipids. Increased PL biosynthesis overcomes that of NL and, as a result, LN/PL ratio decreased. This metabolic situation should be considered in detail when modifications of NO levels are implemented in an attempt to ameliorate the consequences of graft rejection, immune disorders, septic shock, and cardiovascular and neurological pathologies [78–85], among others [108].

**Acknowledgments** This work was partially supported by grants from CONICET and CIC, República Argentina. The authors are grateful for the excellent technical assistance of Norma Cristalli and Elsa Claverie.

## References

- Bobé P, Benihoud K, Grandjon D, Opolon P, Pritchard LL, Huchet R (1999) Nitric oxide mediation of active immunosuppression associated with graft-versus-host reaction. *Blood* 94:1028–1037
- Barron JT, Gu L, Parrillo E (2001) Endothelial- and nitric oxide-dependent effects on oxidative metabolism of intact artery. *Biochim Biophys Acta* 1506:204–211
- Pavlick KP, Laroux FS, Fuseler J, Wolff RE, Gray L, Hoffman J, Grisham MB (2002) Role of reactive metabolites of oxygen and nitrogen in inflammatory bowel disease. *Free Radic Biol Med* 33:311–322
- Sakuma S, Fujimoto Y, Katoh Y, Fujita T (2003) The effects of nitric oxide and peroxynitrite on the formation of prostaglandin and arachidonoyl-CoA formed from arachidonic acid in rabbit kidney medulla microsomes. *Prostaglandins Leukot Essent Fatty Acids* 68:343–349
- Schopfer FJ, Baker PR, Freeman BA (2003) No-dependent protein nitration: a cell signaling event or an oxidative inflammatory response? *Trends Biochem Sci* 28:646–654
- Clapp BR, Hingorani AD, Kharbanda RK, Mohamed-Ali V, Stephens JW, Vallance P, MacAllister RJ (2004) Inflammation-induced endothelial dysfunction involves reduced nitric oxide bioavailability and increased oxidant stress. *Cardiovasc Res* 64:172–178
- Lipton SA, Nicotera P (1998) Calcium, free radicals and excitotoxins in neuronal apoptosis. *Cell Calcium* 23:165–171
- Bonfoco E, Krainc D, Ankarcona M, Nicotera P, Lipton SA (1995) Apoptosis and necrosis: two distinct events induced, respectively, by mild and intense insults with *N*-methyl-D-aspartate or nitric oxide/superoxide in cortical cell cultures. *Proc Natl Acad Sci USA* 92:7162–7166
- Heinloth A, Brüne B, Fischer B, Galle J (2002) Nitric oxide prevents oxidised LDL-induced p53 accumulation, cytochrome c translocation, and apoptosis in macrophages via guanylate cyclase stimulation. *Atherosclerosis* 162:93–101
- Murphy MP (1999) Nitric oxide and cell death. *Biochim Biophys Acta* 1411:401–414
- Leonard TO, Lydic R (1997) Pontine nitric oxide modulates acetylcholine release, rapid eye movement sleep generation, and respiratory rate. *J Neurosci* 17:774–785
- Kiss J, Zsilla G, Vizi ES (2004) Inhibitory effect of nitric oxide dopamine transporters: interneuronal communication without receptors. *Neurochem Int* 45:485–489
- Brown GC (1999) Nitric oxide and mitochondrial respiration. *Biochim Biophys Acta* 1411:351–369
- Valdez LB, Alvarez S, Arnaiz SL, Schöpfer F, Carreras MC, Poderoso JJ, Boveris A (2000) Reactions of peroxynitrite in the mitochondrial matrix. *Free Radic Biol Med* 34:349–356
- Abeywardena MY, Head RJ (2001) Long chain n-3 polyunsaturated fatty acids and blood vessel function. *Cardiovasc Res* 52:361–371
- Miatello R, Risler N, Castro C, González S, Rüttler M, Cruzado M (2001) Aortic smooth muscle cell proliferation and endothelial nitric oxide synthase activity in fructose-fed rats. *Am J Hypertens* 14:1135–1141
- Bilsborough W, Green DJ, Mamotte CD, Van Bockxmeer FM, ÓDriscoll GJ, Taylor RR (2003) Endothelial nitric oxide synthase gene polymorphism, homocysteine, cholesterol, and vascular endothelial function. *Atherosclerosis* 169:131–138
- Stoclet JC, Chataigneau T, Ndiaye M, Oak MH, Bedoui JE, Chataigneau M, Schini-Kerth VB (2004) Vascular protection by dietary polyphenols. *Eur J Pharmacol* 500:299–313
- Pereira AC, Sposito AC, Mota GF, Cunha RS, Herkenhoff FL, Mill JG, Krieger JE (2006) Endothelial nitric oxide synthase gene variant modulates the relationship between serum cholesterol levels and blood pressure in the general population: new evidence for a direct effect of lipids in arterial blood pressure. *Atherosclerosis* 18:193–200
- Mohr S, Stamler JS, Brune B (1994) Mechanism of covalent modification of glyceraldehydes-3-phosphate dehydrogenase at its active site thiol by nitric oxide, peroxynitrite and related nitrosating agents. *FEBS Lett* 348:223–227
- Gross SS, Wolin MS (1995) Nitric oxide pathophysiological mechanisms. *Annu Rev Physiol* 57:737–769
- Welsh N, Sandler S (1992) Interleukin-1 $\beta$  induces nitric oxide production and inhibits the activity of aconitase without decreasing glucose oxidation rates in isolated mouse pancreatic islets. *Biochem Biophys Res Commun* 182:333–340
- Ginter E (1979) Chronic marginal vitamin C deficiency: biochemistry and pathophysiology. *World Rev Nutr Diet* 33:104–141
- Nambisan B, Kurup PA (1975) Ascorbic acid and glycosaminoglycan and lipid metabolism in guinea pigs fed normal and atherogenic diets. *Atherosclerosis* 22:447–461
- Chupukdaroen N, Komaratat P, Wilairat P (1985) Effects of vitamin E deficiency on the distribution of cholesterol in plasma lipoproteins and the activity of cholesterol 7 $\alpha$ -hydroxylase in rabbit liver. *J Nutr* 115:468–472
- Stone WL, Scott RL, Stewart EM, Kheshti A (1994) Lipoprotein alterations in the spontaneously hypertensive rat fed diets deficient in selenium and vitamin E. *Proc Soc Exp Biol Med* 206:130–137
- Al-Othman AA, Rosenstein F, Lei KY (1993) Cooper deficiency increases in vivo hepatic synthesis of fatty acids, triacylglycerols, and phospholipids in rats. *Proc Soc Exp Biol Med* 204:97–103
- Scott RL, Kheshti A, Heimberg M, Wilcox HG, Stone WL (1991) The role of selenium in the secretion of very low density lipoprotein in the isolated perfused rat liver. *Biochem J* 279:741–745
- Khedara A, Kawai Y, Kayashita J, Kato N (1996) Feeding rats the nitric oxide synthase inhibitor, *l*-*n*<sup>o</sup>-nitroarginine, elevates serum triglyceride and cholesterol and lowers hepatic fatty acid oxidation. *J Nutr* 126:2563–2567

30. Khedara A, Goto T, Morishima M, Kayashita J, Kato N (1999) Elevated body fat in rats by the dietary nitric oxide synthase inhibitor, L-N-omega-nitroarginine. *Biosci Biotechnol Biochem* 63:698–702
31. Patel RP, McAndrew J, Sellak H, White CR, Jo H, Freeman BA, Darley-Usmar VM (1999) Biological aspects of reactive nitrogen species. *Biochim Biophys Acta* 1411:385–400
32. Hogg N, Kalyanaraman B (1999) Nitric oxide and lipid peroxidation. *Biochim Biophys Acta* 1411:378–384
33. Reeves PG, Nielsen FH, Fahey GC Jr (1993) AIN-93 Purified Diets for Laboratory Rodents: Final Report of the American Institute of Nutrition ad hoc Writing Committee on the Reformulation of the AIN-76A Rodent Diet. *J Nutr* 123:1939–1951
34. National Research Council, Guide for the Care and Use of Laboratory Animals (1985) Publication N° 85–23 (rev), National Institute of Health, Bethesda
35. Marra CA, Alaniz MJT de, Brenner RR (1986) Modulation of  $\Delta 6$  and  $\Delta 5$  rat liver microsomal desaturase activities by dexamethasone-induced factor. *Biochim Biophys Acta* 879:388–393
36. Kler RS, Jackson S, Barlett K, Bindoff LA, Eaton S, Pourfarzam M, Frerman FE, Goodman SI, Watmough NJ, Turnbull DM (1991) Quantitation of acyl-CoA and acyl-carnitine esters accumulated during abnormal mitochondrial fatty acid oxidation. *J Biol Chem* 266:22932–22938
37. Marra CA, Alaniz MJT de (2000) Calcium deficiency modifies polyunsaturated fatty acid metabolism in growing rats. *Lipids* 35:983–990
38. Marra CA, Alaniz MJT de (1999) Acyl-CoA synthetase activity in liver microsomes from calcium-deficient rats. *Lipids* 34:343–354
39. Tomlinson CW, Dhalla SN (1972) Myocardial contractility. II. Effect of changes in cardiac function on the subcellular distribution of calcium in the isolated perfused rat heart. *Can J Physiol Pharmacol* 50:853–859
40. Verdon CP, Burton BA, Prior RL (1995) Sample pretreatment with nitrate reductase and glucose-6-phosphate dehydrogenase quantitatively reduces nitrate while avoiding interference by  $\text{NADP}^+$  when the Griess reaction is used to assay for nitrite. *Anal Biochem* 224:502–508
41. Dodge JT, Mitchell C, Hanahan DJ (1963) The preparation and chemical characteristics of hemoglobin-free ghosts of human erythrocytes. *Arch Biochem Biophys* 100:119–130
42. Berlin E, Bhatena SJ, Judd JT, Nair PP, Jones DY (1989) Taylor, P.R. dietary fat and hormonal effects on erythrocyte membrane fluidity and lipid composition in adult women. *Metabolism* 38:790–796
43. Yagi K (1976) A simple fluorometric assay for lipoperoxide in blood plasma. *Biochem Med* 15:212–216
44. Nourooz-Zadeh J, Tajaddini-Sarmandi J, McCarthy S, Betteridge DJ, Wolff SP (1995) Elevated levels of authentic plasma hydroperoxides in NIDDM. *Diabetes* 44:1054–1058
45. Asensi M, Sastre J, Pallardo FV, García de la Asunción J, Estrela JM, Vina JA (1994) High-performance liquid chromatography method for measurement of oxidized glutathion in biological samples. *Anal Biochem* 217:323–328
46. Brigelius R, Muckel C, Akerboom TP, Sies H (1983) Identification and quantitation of glutathione in hepatic protein mixed disulfides and its relationship to glutathione disulfide. *Biochem Pharmacol* 32:2529–2534
47. Buttriss JL, Diplock AT (1984) High-performance liquid chromatography methods for vitamin E in tissues. *Methods Enzymol* 105:131–138
48. Bagnati M, Bordone R, Perugini C, Cau C, Albano E, Bellomo G (1998) Cu(I) availability paradoxically antagonizes antioxidant consumption and lipid peroxidation during the initiation phase of copper-induced LDL oxidation. *Biochem Biophys Res Commun* 253:235–240
49. Benzie IF (1996) An automated specific, spectrophotometric method for measuring ascorbic acid in plasma (EFTSA). *Clin Biochem* 29:111–116
50. Aebi H (1984) Catalase in vitro. *Methods Enzymol* 105:121–126
51. Flohé L, Ötting F (1984) Superoxide dismutase assays. *Methods Enzymol* 105:93–104
52. Wheeler MD, Nakagami M, Bradford BU, Uesugi T, Mason RP, Connor HD, Dikalova A, Kadiiska M, Thurman RG (2001) Overexpression of manganese superoxide dismutase prevents alcohol-induced liver injury in the rat. *J Biol Chem* 276:36664–36672
53. Habig WH, Pabst MJ, Jakoby WB (1984) Glutathione-S-transferases. The first enzymatic step in mercapturic acid formation. *J Biol Chem* 249:7130–7139
54. Carlberg I, Mannervick B (1985) Glutathione reductase. *Methods Enzymol* 113:484–490
55. Wright JR, Rumbaugh RC, Colby HD, Miles PR (1979) The relationship between chemiluminescence and lipid peroxidation in rat hepatic microsomes. *Arch Biochem Biophys* 192:344–351
56. Folch J, Lees M, Sloane GH (1957) A simple method for the isolation and purification of total lipids from animal tissues. *J Biol Chem* 226:497–509
57. Hanahan DJ, Dittner JC, Warashina E (1957) A column chromatographic separation of classes of phospholipides. *J Biol Chem* 228:685–690
58. Malins DC, Mangold HK (1960) Analysis of complex lipid mixtures by thin layer chromatographic and complementary methods. *J Am Oil Chem Soc* 37:576–582
59. Neskovic NM, Kostic DM (1968) Quantitative analysis of rat liver phospholipids by a two-step thin-layer chromatographic procedure. *J Chromatogr* 35:297–300
60. Marra CA, Alaniz MJT de (1989) Influence of testosterone administration on the biosynthesis of unsaturated fatty acids in male and female rats. *Lipids* 24:1014–1019
61. Allain CC, Poon LS, Chan CS, Richmond W, Fu PC (1974) Enzymatic determination of total serum cholesterol. *Clin Chem* 20:470–475
62. Marra CA, Alaniz MJT de (1990) Mineralocorticoids modify rat liver  $\Delta 6$  desaturase activity and other parameters of lipid metabolism. *Biochem Int* 22:483–493
63. Chen PS, Toribara TY, Warner H (1956) Microdetermination of phosphorus. *Anal Chem* 33:1405–1406
64. Hirata F, Schiffmann E, Venkatasubramanian K, Salomon D, Axelrod J (1980) A phospholipase  $A_2$  inhibitory protein in rabbit neutrophils induced by glucocorticoids. *Proc Natl Acad Sci USA* 77:2533–2536
65. Irazú CE, González-Rodríguez S, Brenner RR (1993)  $\Delta 5$  Desaturase activity in rat kidney microsomes. *Mol Cell Biochem* 129:31–37
66. López Jiménez J, Bordoni A, Hrelia S, Rossi CA, Turchetto E, Zamora Navarro S, Biagi PL (1993) Evidence for a detectable delta-6-desaturase activity in rat heart microsomes: aging influence on enzyme activity. *Biochem Biophys Res Commun* 192:1037–1041
67. Tanaka T, Hosaka K, Hoshimaru M, Numa S (1979) Purification and properties of long-chain acyl-coenzyme-A synthetase from rat liver. *Eur J Biochem* 98:165–172
68. Horning MG, Martin DB, Karmen A, Vagelos PR (1961) Fatty acid synthesis in adipose tissue. II. Enzymatic synthesis of branched chain and odd-numbered fatty acids. *J Biol Chem* 236:669–672

69. Bieber LL, Fiol C (1986) Purification and assay of carnitine acyltransferases. *Methods Enzymol* 123:276–284
70. Laun RA, Rapsch B, Abel W, Schroder O, Roher HD, Ekkerkamp A, Schulte KM (2001) The determination of ketone bodies: preanalytical, analytical and physiological considerations. *Clin Exp Med* 1:201–209
71. Duncombe WG, Rising TJ (1973) Quantitative extraction and determination of non-esterified fatty acids in plasma. *J Lipid Res* 14:258–261
72. Bradford MM (1976) A rapid and sensitive method for the quantitation of microgram quantities of protein utilizing the principle of protein-dye binding. *Anal Biochem* 72:248–254
73. Hogg N, Kalyanaraman B (1999) Nitric oxide and lipid peroxidation. *Biochim Biophys Acta* 141:378–384
74. Joshi MS, Ponthier JL, Lancaster JR Jr (1999) Cellular antioxidant and pro-oxidant actions of nitric oxide. *Free Rad Biol Med* 27:1357–1366
75. Moshage H (1997) Nitric oxide determinations: much ado about NO<sup>•</sup>-thing? *Clin Chem* 43:553–556
76. Adams MR, Phu CV, Stocker R, Celermajer DS (1999) Lack of antioxidant activity of the antiatherogenic compound L-arginine. *Atherosclerosis* 146:329–335
77. Tapiero H, Mathé G, Couvreur P, Tew KD (2002) Free aminoacids in human health and pathologies. (I) Arginine. *Biomed Pharmacother* 56:439–445
78. George J, Shmuel SB, Roth A, Her I, Izraelov S, Deutsch V, Keren G, Miller H (2004) L-Arginine attenuates lymphocyte activation and anti-oxidized LDL antibody levels in patients undergoing angioplasty. *Atherosclerosis* 174:323–327
79. Böger RH, Bode-Böger SM, Frölich JC (1996) The L-Arginine-nitric oxide pathway: role in atherosclerosis and therapeutic implications. *Atherosclerosis* 127:1–11
80. Slawinski M, Grodzinska L, Kostka-Trabka E, Bieron K, Goszcz A, Gryglewski RJ (1996) L-Arginine—substrate for NO synthesis—its beneficial effects in therapy of patients with peripheral arterial disease: comparison with placebo-preliminary results. *Acta Physiol Hung* 84:457–458
81. Bult H, Herman AG, Matthys KE (1999) Antiatherosclerotic activity of drugs in relation to nitric oxide function. *Eur J Pharmacol* 375:157–176
82. Moore PK, Handy RL (1997) Selective inhibitors of neuronal nitric oxide synthase—is no NOS really good NOS for the nervous system? *Trends Pharmacol Sci* 18:204–211
83. Ding-Zhou L, Marchand-Verrecchia C, Croci N, Plotkine M, Margail I (2002) L-NAME reduces infarction, neurological deficit and blood-brain barrier disruption following cerebral ischemia in mice. *Eur J Pharmacol* 457:137–146
84. Patel RP, Levonen AL, Crawford JH, Darley-Usmar VM (2000) Mechanisms of the pro- and anti-oxidant actions of nitric oxide in atherosclerosis. *Cardiovasc Res* 47:465–474
85. Willmott N, Sethi JK, Walseth TF, Lee HC, White AM, Galione A (1996) Nitric oxide-induced mobilization of intracellular calcium via the cyclic ADP-ribose signaling pathway. *J Biol Chem* 271:3699–3705
86. Guidarelli A, Sciorati C, Clementi E, Cantoni O (2006) Peroxynitrite mobilizes calcium ions from ryanodine-sensitive stores, a process associated with the mitochondrial accumulation of the cation and the enforced formation of species mediating cleavage of genomic DNA. *Free Radic Biol Med* 41:154–164
87. Szabó C, Salzman AL (1996) Inhibition of terminal calcium overload protects against peroxynitrite-induced cellular injury in macrophages. *Immunol Lett* 51:163–167
88. Zaidi A, Michaelis ML (1999) Effects of reactive oxygen species on brain synaptic plasma membrane Ca<sup>2+</sup>-ATPase. *Free Radic Biol Med* 27:810–821
89. Bapat S, Verkleij A, Post JA (2001) Peroxynitrite activates mitogen-activated protein kinase (MAPK) via a MEK-independent pathway: role for protein kinase C. *FEBS Lett* 499:21–26
90. Gutiérrez-Martín Y, Martín-Romero FJ, Henao F, Gutiérrez-Merino C (2002) Synaptosomal plasma membrane Ca<sup>2+</sup> pump activity inhibition by repetitive micromolar ONOO<sup>-</sup> pulses. *Free Rad Biol Med* 32:46–55
91. Pan BX, Zhao GL, Huang XL, Zhao KS (2004) Calcium mobilization is required for peroxynitrite-mediated enhancement of spontaneous transient outward currents in arteriolar smooth muscle cells. *Free Radic Biol Med* 37:823–838
92. Vicente S, Figueroa S, Pérez-Rodríguez R, González MP, Oset-Gasque MJ (2005) Nitric oxide donors induce calcium mobilisation from internal stores but do not stimulate catecholamine secretion by bovine chromaffin cells in resting conditions. *Cell Calcium* 37:163–172
93. Redondo PC, Jardín I, Hernández-Cruz JM, Pariente JA, Salido GM, Rosado JA (2005) Hydrogen peroxide and peroxynitrite enhance Ca<sup>2+</sup> mobilization and aggregation in platelets from Type 2 diabetic patients. *Biochim Biophys Res Commun* 333:794–802
94. Berkels R, Dachs C, Roesen R, Klaus W (2000) Simultaneous measurement of intracellular Ca<sup>2+</sup> and nitric oxide: a new method. *Cell Calcium* 27:281–286
95. Hsu HC, Lee YT, Chen MF (2001) Effects of fish oil and vitamin E on the antioxidant defense system in diet-induced hypercholesterolemic rabbits. *Prostaglandins Other Lipid Mediat* 66:99–108
96. Dringen R (2000) Metabolism and functions of glutathione in brain. *Progr Neurobiol* 62:649–671
97. Muralikrishna Adibhatla R, Hatcher JF (2006) Phospholipase A<sub>2</sub>, reactive oxygen species, and lipid peroxidation in cerebral ischemia. *Free Radic Biol Med* 40:376–387
98. White BC, Sullivan JM, DeGracia DJ, ÓNeil BJ, Neumar RW, Grossman LI, Rafols JA, Krause GS (2000) Brain ischemia and reperfusion: molecular mechanisms of neuronal injury. *J Neurol Sci* 179:1–33
99. Jensen B, Farach-Carson MC, Kenaley E, Akanbi KA (2004) High extracellular calcium attenuates adipogenesis in 3T3-L1 preadipocytes. *Exp Cell Res* 301:280–292
100. Schwartz RS, Abraham S (1982) Effect of dietary polyunsaturated fatty acids on the activity and content of fatty acid synthetase in mouse liver. *Biochim Biophys Acta* 711:316–326
101. Erecińska M, Silver IA (2001) Tissue oxygen tension and brain sensitivity to hypoxia. *Respir Physiol* 128:263–276
102. Brookes PS, Land JM, Clark JB, Heales SJR (1998) Peroxynitrite and brain mitochondria: evidence for increased proton leak. *J Neurochem* 70:2195–2202
103. Vatassery GT, Santa Cruz KS, DeMaster EG, Quach HT, Smith WE (2004) Oxidative stress and inhibition of oxidative phosphorylation induced by peroxynitrite and nitrite in rat brain subcellular fractions. *Neurochem Int* 45:963–970
104. Infante JP, Huszagh VA (2000) Secondary carnitine deficiency and impaired docosahexaenoic (22:6 n-3) acid synthesis: a common denominator in the pathophysiology of diseases of oxidative phosphorylation and β-oxidation. *FEBS Lett* 468:1–5



105. Infante JP (1999) A function for the vitamin E metabolite alpha-tocopherol quinone as an essential enzyme cofactor for the mitochondrial fatty acid desaturases. *FEBS Lett* 446:1–5
106. James MJ, Gibson RA, Cleland LG (2000) Dietary polyunsaturated fatty acids and inflammatory mediator production. *Am J Clin Nutr* 71:343S–348S
107. Elabbadi N, Day CP, Gamouh A, Ziad A, Yeaman SJ (2005) Relationship between the inhibition of phosphatidic acid phosphohydrolase-1 by oleate and oleoyl-CoA ester and its apparent translocation. *Biochimie* 87:437–443
108. Van Hove C, Carreer-Bruhwyler F, Géczy J, Herman AG (2005) Long-term treatment with the NO-donor molsidomine reduces circulating ICAM-1 levels in patients with stable angina. *Atherosclerosis* 180:399–405

## Inward Translocation of the Phospholipid Analogue Miltefosine across Caco-2 Cell Membranes Exhibits Characteristics of a Carrier-mediated Process

Cécile Ménez · Marion Buyse · Robert Farinotti · Gillian Barratt

Received: 6 November 2006 / Accepted: 9 January 2007 / Published online: 6 February 2007  
© AOCs 2007

**Abstract** Miltefosine (hexadecylphosphocholine, HePC) is the first effective oral agent for the treatment of visceral leishmaniasis. The characteristics of HePC incorporation into the human intestinal epithelial cell line Caco-2 were investigated in order to understand its oral absorption mechanism. The results provide evidence for the involvement of a carrier-mediated mechanism, since the association of HePC at the apical pole of Caco-2 cells was (1) saturable as a function of time with a rapid initial incorporation over 5 min followed by a more gradual increase; (2) saturable as a function of concentration over the range studied (2–200  $\mu\text{M}$ ) with a saturable component which followed Michaelis–Menten kinetics (apparent  $K_m$  15.7  $\mu\text{mol/L}$ ,  $V_{max}$  39.2 nmol/mg protein/h) and a nonspecific diffusion component; (3) partially inhibited by low temperature and ATP depletion, indicating the temperature and energy-dependence of the uptake process. Moreover, we demonstrated, by an albumin back-extraction method, that HePC is internalized via translocation from the outer to the inner leaflet of the plasma membrane and that HePC may preferentially diffuse through intact raft microdomains. In conclusion, our results

suggest that incorporation of HePC at the apical membrane of Caco-2 cells may occur through a passive diffusion followed by a translocation in the inner membrane leaflet through an active carrier-mediated mechanism.

**Keywords** Miltefosine · Hexadecylphosphocholine · Caco-2 · Cellular membrane incorporation · Intestinal absorption · Translocation

### Introduction

Miltefosine [hexadecylphosphocholine (HePC)], an alkylphosphocholine belonging to the antitumor ether lipids (AELs), is the first effective oral agent against *Leishmania donovani*, the parasite responsible for visceral leishmaniasis (VL), with a 98% cure rate of VL patients [1] with a dose of 2.5 mg/kg daily for 28 days [2]. This drug is considered as a breakthrough in antileishmanial treatment because of its high efficacy, its low toxicity and its high oral bioavailability which is a major advantage over currently employed antileishmanial drugs that require parenteral administration. Although the remarkable activity of HePC after oral administration has been demonstrated, little is known so far about HePC uptake by the intestinal epithelium. This question is all the more relevant since a previous *in vivo* study on the distribution of alkyl analogs of lysophosphatidylcholine in mice demonstrated a very remarkable depot effect at the sites of administration, especially after oral dosing where more than 80% of the drug remained in the gastro-intestinal tract 5 h after administration [3]. In this context, it was of particular interest to investigate the mechanism of

C. Ménez · G. Barratt (✉)  
Laboratoire de Physico-chimie, Pharmacotechnie et  
Biopharmacie, UMR CNRS 8612 Faculté de Pharmacie,  
Univ. Paris-Sud 11, IFR 141, Tour D5, 2ème étage,  
5 rue J.B. Clément, Châtenay-Malabry,  
Cedex 92296, France  
e-mail: gillian.barratt@u-psud.fr

M. Buyse · R. Farinotti  
Laboratoire de Pharmacie Clinique,  
UPRES 2706 Faculté de Pharmacie, Univ. Paris-Sud 11,  
IFR 141, Châtenay-Malabry 92296, France

HePC uptake by the intestinal epithelial cells in depth in order to elucidate the reason for this sequestration.

The intracellular distribution and metabolism of radiolabeled HePC was determined in MDCK cells [4], and found to be similar to that of other AELs which showed a high affinity for the plasma membrane and appeared to accumulate in the phospholipid bilayers of cellular membranes [5, 6], but not in the cytosolic fraction. Although the primary target of AELs is thought to be the plasma membrane, the mechanism of the cytotoxic action of AELs remains unknown. It has been demonstrated that after incorporation in the plasma membrane, they influence physical properties such as permeability [7] and fluidity [6, 8], inhibit normal phospholipid metabolism [9] and affect several membrane proteins including protein kinase C [10] and phospholipase C [11].

The mechanism of HePC accumulation within the enterocyte plasma membrane could be either passive diffusion or a specific and saturable process. Kelley et al. [12] proposed passive diffusion as the possible uptake mechanism of another ether lipid, edelfosine (ET-18-OCH<sub>3</sub>), by leukaemia cells, whereas other authors [13] suggested that internalization of ether lipids occurred through an endocytotic mechanism. On the other hand, there is strong evidence for the involvement of an active or carrier-mediated mechanism in the uptake of HePC into various membranes. Indeed, the transporters ligand-effect modulator 3 protein (Lem3p) [14] and LdMT (*L. donovani* putative Miltefosine Transporter) [15, 16] have recently been found to be required for the inward translocation of HePC into *Saccharomyces cerevisiae* yeast cells and *L. donovani* parasites, respectively.

The aim of this study was to investigate the mechanism(s) of HePC uptake by the human intestinal epithelial cells. The human colon carcinoma cell line Caco-2 was used as a suitable in vitro model system for studying intestinal uptake [17]. The objectives of this study were (1) to demonstrate whether the HePC association with these cells involved an active or passive mechanism and (2) to characterize the cellular accumulation by studying the kinetics of the cellular uptake and binding.

## Materials and Methods

### Materials

[<sup>3</sup>HC<sup>9</sup>-<sup>3</sup>HC<sup>10</sup>]HePC was synthesized as described previously [18, 19]. Its purity was monitored by  $\beta$ -imaging and was found to be 96%. Working solutions

were prepared with isotopic dilution and the specific activity was fixed at 50  $\mu$ Ci/mmol. HePC was obtained from Cayman Chemical Company (Ann Arbor, MI, USA). Solutions of HePC (10 mM) were freshly made in water or in Krebs modified buffer immediately before each experiment. Dulbecco's modified Eagle's medium (DMEM), phosphate-buffered saline (PBS), fetal bovine serum (FBS), non-essential amino acids solution (NEAA 10 mM, 100X), penicillin-streptomycin solution (10,000 units/ml penicillin and 10 mg/ml streptomycin), trypsin-EDTA solution (0.05% trypsin, 0.53 mM EDTA) were obtained from Invitrogen-Life Technologies. Transwell<sup>®</sup>-clear polyester membranes 12-well (1 cm<sup>2</sup> surface area, 0.4  $\mu$ m pore size) and 12-well cluster trays were purchased from the Costar Corning Corporation (NY, USA). The Cytotoxicity Detection Kit (LDH) was from Roche Diagnostics (Meylan, France). Ultima Gold<sup>™</sup> liquid scintillation was from Perkin Elmer Life Science Products (Boston, USA). All others chemical products were from Sigma-Aldrich (St Louis, MO, USA).

### Cell Culture

Caco-2 cells (passages 45–65) were cultured in DMEM supplemented with 20% FBS, 1% non-essential amino acids, 1% L-glutamine, and 1% penicillin–streptomycin mixture. Cells were kept at 37 °C in 5% CO<sub>2</sub> and 95% humidity. Every week, cells were trypsinized and seeded at  $5 \times 10^4$  cells per insert onto 12-well Transwells<sup>®</sup> or at  $5 \times 10^4$  cells per well in simple 12-well trays. Cells were then grown in the plates for a minimum of 14 days and used for experimentation between days 14 and 21. The medium was changed daily. The quality of the monolayers grown on the polyester membrane was assessed by measuring the transepithelial electrical resistance (TEER) using a EVOM Epithelial Tissue Voltohmmeter (World Precision Instrument, Sarasota, FL, USA). Monolayers that displayed a TEER of 200–300  $\Omega$  cm<sup>2</sup> were used in the experiments. For all the experimental conditions used, cell viability and plasma membrane integrity were checked using the MTT colorimetric assay [20] and the LDH release assay [21], respectively, as previously described [22].

### Cellular Accumulation Experiments

The incubation medium consisted of Krebs modified buffer: 5.4 mM KCl, 2.8 mM CaCl<sub>2</sub>, 1 mM MgSO<sub>4</sub>, 0.3 mM NaH<sub>2</sub>PO<sub>4</sub>, 137 mM NaCl, 0.3 mM KH<sub>2</sub>PO<sub>4</sub>, 10 mM glucose, and 10 mM HEPES/Tris (pH 7.4) or 10 mM MES/Tris (pH 6.0). For cellular incorporation studies from the apical side, Caco-2 cells were grown

on 12-well dishes for 14 days. Before experiments, the culture medium was removed and cells were washed three times with substrate-free incubation medium consisting of Krebs modified buffer pH 6.0. The compounds to be tested were dissolved in the same buffer. For cellular incorporation studies from the basolateral side, cells were grown on permeable supports (Transwell®) for 18 days. The pH of the incubation medium was adjusted to 6.0 in the apical compartment and 7.4 in the basolateral compartment. The culture medium in the apical and basolateral compartments was removed by aspiration, and monolayers were washed three times with substrate-free incubation medium at 37 °C, 30 min before the beginning of the experiment. At time 0, buffer containing [<sup>3</sup>H]HePC was added to the apical (0.5 ml) or basolateral (1.5 ml) compartment of the insert. At the end of the incubation period, the medium was immediately collected; the cells were washed three times with ice-cold Krebs modified buffer, solubilized with Triton-X100 at 1% and the amount of radiolabeled compound within Caco-2 cell monolayers was determined by counting the samples in a Beckman LS 6000TA liquid scintillation counter.

Unless otherwise indicated, 20 μM HePC was used for cellular accumulation studies, and incubations were carried out at 37 °C for 1 h in Krebs modified buffer. When the effect of endocytosis and metabolic inhibitors on HePC accumulation was investigated, cells were preincubated with Krebs modified buffer pH 6.0 containing the inhibitor for 30 min at 37 °C prior to the uptake study. When the influence of cholesterol on HePC accumulation was investigated, Caco-2 cells were incubated for 48 h in 20% FBS DMEM medium containing 25 μg/ml of cholesterol. This treatment has already been used to obtain cells with a high cell cholesterol concentration [23]. Cholesterol was dissolved in ethanol and added to the culture medium. The medium used for control incubation received the same amount of ethanol, at a concentration not exceeding 0.3% in the final incubation medium.

### Cellular Fractionation

The cell fractionation method used was adapted from previously described methods for different cell lines [24, 25]. Caco-2 cells, grown on 12-well dishes, were incubated for 1 h with [<sup>3</sup>H]HePC (20 μM, 0.1 μCi per well). At the end of the incubation period, cell monolayers were washed three times with ice-cold Krebs modified buffer and were then incubated 15 min at 4 °C with digitonin 0.01% in Krebs modi-

fied buffer for selective permeabilization of the plasma membrane. Cells in suspension were centrifuged 1 min at 16,000g. The supernatant, corresponding to the cytosolic fraction, was collected. The cell pellet was washed three times by resuspension in Krebs modified buffer and centrifugation (5 min, 500g). The pellet was then resuspended in Krebs modified buffer supplemented with 1% Triton X100 and incubated for 10 min at 4 °C to solubilize the cell membranes. The suspension was then centrifuged at 16,000g for 5 min at 4 °C and the resulting supernatant containing the cell membranes was referred as the Triton-soluble fraction. The pellet, containing the nucleus and cytoskeleton, was washed, solubilized in Chaps solution and referred as the Triton-insoluble fraction. The amount of radiolabeled compound in each fraction was determined by liquid scintillation counting.

Cytosolic lactate dehydrogenase (LDH), a stable cytoplasmic enzyme, was used as a cytosolic marker and the LDH activity was determined in each fraction. As described previously [26], a correct permeabilization protocol should result in than 80% of recovery of LDH in the cytosolic fraction. The amounts of LDH in the Triton-soluble and Triton-insoluble fractions were negligible, and 85.4 ± 3.2% of total cellular LDH were found, as expected, in the cytosolic fraction. The 100% value for LDH was determined by the addition of Triton 1% to control cells.

### Energy Depletion

To investigate whether the HePC incorporation was energy-dependent, the total intracellular ATP level was reduced using a method previously described [27]. Both the oxidative phosphorylation and the glycolytic pathways were blocked, by omitting glucose from the transport medium and supplementing it with sodium azide (NaN<sub>3</sub>, 10 mM), sodium fluoride (NaF, 2 mM) and 2-deoxyglucose (2-DG, 50 mM). After 30 min incubation at 37 °C, medium was removed, [<sup>3</sup>H]HePC (20 μM, 0.5 μCi per well) in Krebs modified buffer pH 6.0 was added and the cellular association was determined as described above.

### Evaluation of HePC Translocation Across the Cell Membrane

The assay for translocation was performed by using a method previously described for lysophosphatidylcholine [28]. This procedure is reported to remove the drug located in the outer leaflet of the plasma membrane. Briefly, after incubation with [<sup>3</sup>H]HePC,

back-extraction of HePC was performed by washing the cells three times with Krebs modified buffer with or without 1% (w/v) fatty acid-free bovine serum albumin (BSA). Radioactivity counted after saline washes alone was considered to represent the total HePC in both leaflets of the bilayer, while that measured after albumin washes was considered to represent HePC which was inaccessible due to translocation to the inner leaflet of the lipid bilayer of the intact cells. The difference between these two values represented HePC remaining in the outer leaflet.

#### Kinetics Analysis of HePC Incorporation

To estimate the kinetic parameters of the saturable cellular accumulation by Caco-2 cell monolayers, [ $^3\text{H}$ ]HePC accumulation across the apical membrane was determined after a 1-h incubation by adding increasing concentrations of unlabeled HePC (2–200  $\mu\text{M}$ ) to the apical compartment at 4 and 37  $^{\circ}\text{C}$  for binding and uptake measurements, respectively. Michaelis–Menten plots were constructed to calculate the kinetic parameters (the apparent Michaelis–Menten constant  $K_m$  and the maximal velocity  $V_{\text{max}}$ ) of HePC uptake in Caco-2 cells using a nonlinear least-square regression analysis by Prism 4 (GraphPad Software).

#### Determination of Protein Content

The amount of HePC incorporated was expressed as the amount of cell-associated HePC relative to the protein content. Therefore, for total protein extraction, Caco-2 cells pellets were homogenized at 4 $^{\circ}\text{C}$  in lysis buffer (Tris 10 mM, EDTA 5 mM, NaCl 126 mM, Triton 1% and SDS 0.1%) supplemented with 100  $\mu\text{mol/l}$  aprotinin, leupeptin and pepstatin. The homogenates were centrifuged at 12,000g for 20 min at 4  $^{\circ}\text{C}$ , the supernatants collected and proteins were quantified using the Bio-Rad Protein Assay Kit with BSA as reference (Bio-Rad Laboratories, Hercules, CA, USA).

#### Statistics

All experiments were conducted at least in triplicate and results are expressed as mean  $\pm$  standard deviation (SD). Statistical analysis was performed using one-way analysis of variance (ANOVA) with a Mann-Whitney non-parametric post-test for double comparisons or a Student's  $t$  test (GraphPad InStat, San Diego, CA, USA). Statistical significance was accepted as  $P < 0.05$ .

## Results

### Effect of pH, Localization and Albumin on HePC Incorporation

The effect of pH on 20  $\mu\text{M}$  [ $^3\text{H}$ ]HePC incorporation from the apical and from the basolateral side of Caco-2 cell monolayers was investigated. The pH on the apical side was changed from 6.0 to 7.4, while the basolateral pH was fixed at pH 7.4, corresponding to the physiological serosal pH of cells. Figure 1 showed that, at a concentration of 20  $\mu\text{M}$ , the change in apical pH did not significantly affect drug uptake, indicating that the HePC uptake process by Caco-2 cells was independent of the proton gradient. It should be noted that HePC is a zwitterion over the pH range studied.

In order to study the polarity of HePC uptake in the intestinal cell, the total amount of HePC incorporated into the Caco-2 monolayer was determined after incubation with HePC in the apical or basolateral medium (Fig. 1). The results show that the total amount of HePC associated with the cells after a 3-h incubation was almost twofold lower after incubation on the basolateral side ( $3.36 \pm 0.16$  nmol/monolayer) than on the apical side ( $5.66 \pm 0.09$  nmol/monolayer) of the Caco-2 cell monolayer ( $P < 0.01$ ). It is unlikely that the presence of the polyester membrane is

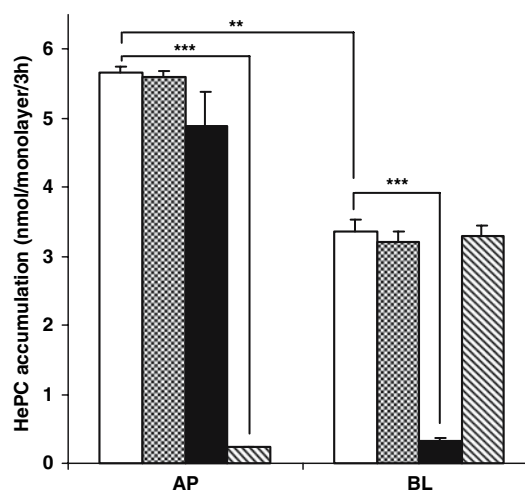


**Fig. 1** Effect of pH and albumin on cellular accumulation of HePC from the apical (AP) and the basolateral (BL) side of Caco-2 cells. AP pH 6.0 and BL pH 7.4 (white bar); AP pH 7.4 and BL pH 7.4 (grey bar); AP pH 6.0 and BL pH 7.4 with albumin in the BL compartment (black bar); AP pH 6.0 and BL pH 7.4 with albumin in the AP compartment (cross-hatched bar). Cells were incubated with [ $^3\text{H}$ ]HePC (20  $\mu\text{M}$ , 0.5  $\mu\text{Ci}$  per well) either at the apical or the basolateral membrane surfaces for 3 h. All measurements are expressed as mean  $\pm$  SD of three determinations with three different monolayers ( $n = 9$ ). \*\* $P < 0.01$ , \*\*\* $P < 0.001$

responsible for the lower basolateral uptake of such a small molecule as HePC (MW 408), since the filter pore size was 0.4  $\mu\text{m}$  and since the transport of HePC in the apical-to-basolateral and in the basolateral-to-apical directions was similar [29].

Furthermore, the influence of adding human serum albumin to the apical or basolateral compartment was studied. As shown in Fig. 1, albumin in the basolateral compartment had no effect on HePC cellular accumulation on the apical membrane surface, but strongly inhibited its cellular accumulation when the drug was loaded basolaterally ( $0.31 \pm 0.06$  vs.  $3.36 \pm 0.16$  nmol/monolayer,  $P < 0.001$ ). The apical uptake of HePC was also markedly reduced when human serum albumin was added to the AP compartment compared to the apical uptake under albumin-free conditions.

#### Time-course of Incorporation of HePC at the Apical Cell Surface

The apical incorporation of 20  $\mu\text{M}$  [ $^3\text{H}$ ]HePC by the Caco-2 cells was determined as a function of time over a 5-h period (Fig. 2). A profile with an extremely rapid initial linear accumulation over the first 5 min followed by a more gradual increase was observed. The initial incorporation rate, measured as the slope of the regression analysis during the linear phase, was 0.78 nmol/mg protein/min. This extremely rapid initial

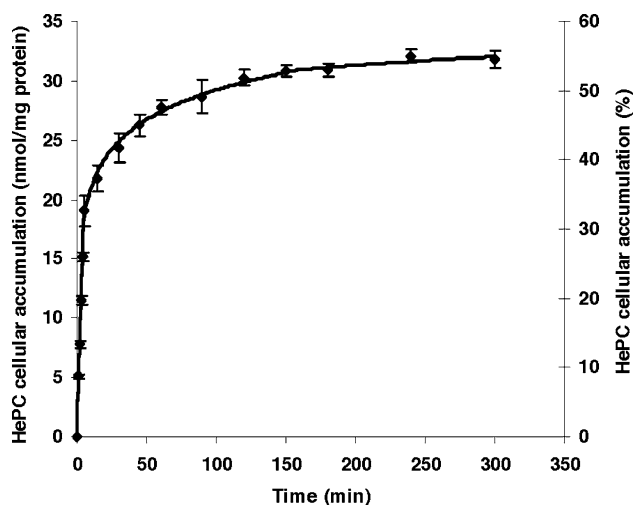


**Fig. 2** Time course of apical uptake of HePC by Caco-2 cell monolayers at 37 °C. Cells were incubated with incubation buffer containing [ $^3\text{H}$ ]HePC (20  $\mu\text{M}$ , 0.1  $\mu\text{Ci}$  per well) for 5 h. At various time intervals, the cellular accumulation was determined as described in the [Materials and Methods](#) section. All measurements were expressed as mean  $\pm$  SD ( $n = 12$ ). The equation of the linear regression analysis for the first 5 min was  $y = 3.8541x$ ,  $R^2 = 0.988$ . All measurements are expressed as mean  $\pm$  SD ( $n = 9$ )

incorporation suggested that association of the drug with the cell membrane was almost instantaneous. The accumulation of HePC was saturable and reached a plateau level of  $32.4 \pm 0.9$  nmol/mg protein after approximately 180 min, which persisted until at least 300 min. This slower increase in radioactivity could represent subsequent accumulation of HePC in cell membranes. The 1-h time point was used for all subsequent experiments to study both the concentration-dependence and the effect of various modulators on the apical association of HePC.

#### Subcellular Distribution of HePC

A previous study has shown that the accumulation of HePC within Caco-2 cells was very high compared with its transport across the monolayer, with more than 55% of the drug incorporated or sequestered within the cells after a 3-h incubation on the apical side [29].

The subcellular distribution of HePC in Caco-2 cells was investigated after a 1-h incubation (Table 1). The results show that more than 85% of the HePC incorporated into the cell was located in the membrane fraction whereas only 15% was located within the cytosol. No drug was found in the nucleus, in accordance with the observation that HePC does not interfere with DNA [30].

Taking into account our results and previous studies demonstrating that the cell plasma membrane is the main localization and site of action of HePC [5, 6], it is reasonable to assume that the majority of the HePC accumulated during our experiments was located within the plasma membrane.

#### Concentration-Dependence and Kinetics of HePC Incorporation at the Apical Surface

Cellular accumulation of HePC as a function of concentration was studied at 4 °C, a condition under which carrier-mediated processes are almost completely blocked and only nonspecific binding can take place. As shown in Fig. 3, this nonspecific binding of HePC was nonsaturable, since association of HePC with Caco-2 cells remained linear with respect to concentration in the range tested (2–200  $\mu\text{M}$ ). These results suggested that cell surface binding was not receptor-mediated (no extracellular membrane protein specific for HePC) and was more likely to occur by nonspecific insertion into the outer leaflet of the plasma membrane phospholipid bilayer.

At 37 °C, cellular accumulation of HePC was found to include a saturable component: the relationship between HePC accumulation rate and concentration

**Table 1** Subcellular distribution of HePC

Fraction	HePC (% <sup>a</sup> ) <sup>b</sup>
Cytosol	15.5 ± 1.9
Membranes	83.7 ± 3.4
Nucleus and cytoskeleton	0.8 ± 0.3

<sup>a</sup> Values are expressed as a percentage of total HePC accumulation in the cells

<sup>b</sup> Values are expressed as mean values ± SD of three separate experiments ( $n = 9$ )

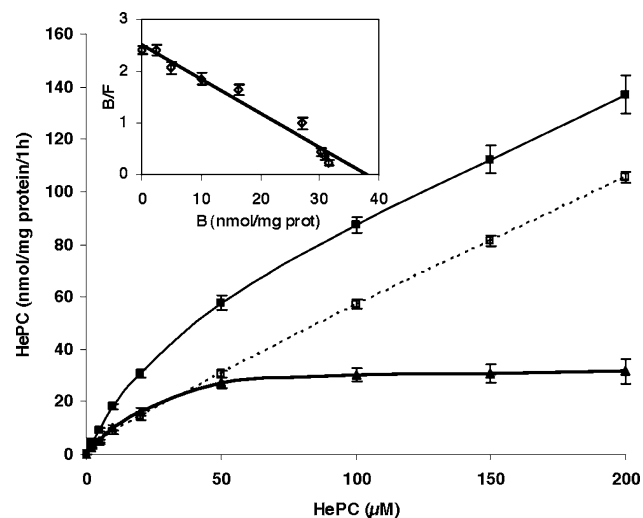


**Fig. 3** Concentration-dependence of apical binding and uptake of HePC in Caco-2 cell monolayers. Cells were incubated apically for 1 h with increasing concentrations of HePC from 2 to 200  $\mu\text{M}$ , keeping the concentration of [ $^3\text{H}$ ]HePC constant at 12.5 nM (0.1  $\mu\text{Ci/ml}$  per well) and adding unlabeled HePC to obtain the desired concentrations. The cumulative accumulation curve (filled square) with both saturable and nonsaturable components was obtained at 37 °C, the nonsaturable (nonspecific) component (open square) was obtained at 4 °C. This component was subtracted from total uptake to calculate the saturable component (filled triangle) (specific uptake) which was used in kinetic analysis. *Inset* Eadie-Hofstee plots of HePC uptake after correction for nonsaturable component ( $B/F$  vs.  $B$ ;  $B$  is the rate of HePC bound to cells and  $F$  is the rate of free HePC). Each value represents the mean  $\pm$  SD of three separate experiments ( $n = 9$ )

was non-linear, indicating that a process other than simple diffusion occurred. The cellular accumulation of HePC due to the saturable component was determined by subtracting incorporation by the nonsaturable component (4 °C) from the total accumulation (37 °C) at each HePC concentration examined. The result indicated that apical HePC cellular accumulation into Caco-2 cells could be explained by a Michaelis–Menten-like expression rather than by simple diffusion alone. The kinetic parameters of the saturable component were determined after one hour of uptake

and were found to be 15.7  $\mu\text{mol/L}$  and 39.2 nmol/mg protein/h for the apparent  $K_m$  and  $V_{max}$ , respectively. The value of the diffusion constant for the nonsaturable component  $K_D$ , calculated as the slope of the binding line at 4 °C, was  $0.51 \pm 0.02$  ml/mg protein/h.

### Translocation of HePC within the Cell Membrane

To examine the involvement of a carrier-mediated process in HePC incorporation into Caco-2 cells further, we investigated how HePC was internalized. The translocation of the drug from the outer to the inner membrane leaflet was evaluated by an albumin back-extraction method described previously for lysophosphatidylcholine [28]. HePC, because of its phospholipid-like structure (single long alkyl chain), easily inserts into the outer leaflet of the plasma membrane lipid bilayer. The strong binding of HePC to albumin was used to remove accessible HePC from the outer monolayer of the membrane, and therefore determine the fraction of the drug translocated into the inner face of the bilayer and into the cell. The translocated fraction of HePC into Caco-2 cells was determined after 1-min and 1-h incubation at 37 °C and compared to the total membrane accumulation observed at 37 °C or 4 °C (Fig. 4). The fact that some HePC remained associated with the membrane after albumin washing demonstrated that HePC was translocated across the cell membrane. Moreover, initially (at 1 min), most of the HePC associated with Caco-2 cells could be back-extracted by albumin, demonstrating that a high proportion of the drug remained in the outer leaflet of the plasma membrane. In contrast, after a 1-h incubation, almost 75% of HePC accumulated at 37 °C remained cell-associated after back-extraction, indicating that the majority of the drug was translocated or internalized and therefore situated within the cells or in the inner layer of the plasma membrane. This result demonstrated an increase in internalization and retention over the time and suggested translocation of the drug from the outer to the inner bilayer of the plasma membrane.

These results were then compared with cellular accumulation at 4 °C, when carrier-mediated transport was inhibited. The initial cellular amount of HePC, measured at 1 min, was not significantly decreased at 4 °C compared with 37 °C, further demonstrating that at 1 min the major part of HePC cellular accumulation occurred in the outer leaflet of the plasma membrane. On the other hand, after 1 h, incubation at 4 °C led to a decrease in cellular accumulation of HePC to less than 60% of control. Given that transmembrane transport mechanisms are far more sensitive to low temperature than cell surface binding, these data support our

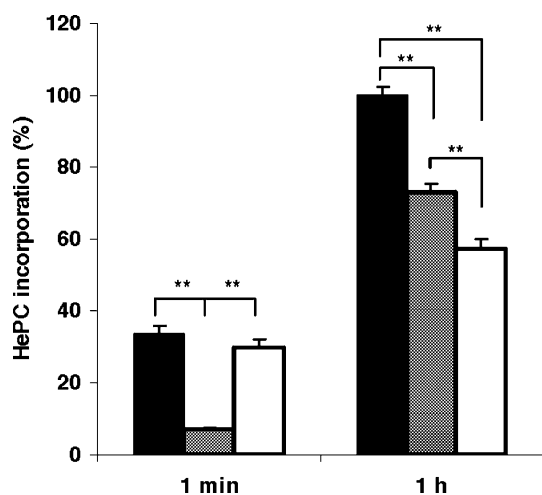


**Fig. 4** Assessment of internal and external HePC. [ $^3\text{H}$ ]HePC (20  $\mu\text{M}$ , 0.1  $\mu\text{Ci}$  per well) apical uptake by Caco-2 cells was determined after 1 min or 1 h incubation with saline washes at 37°C (black bar) or 4 °C (white bar), and with albumin washes at 37 °C (grey bar). Resistance to BSA back-extraction indicates movement of HePC from the outer membrane leaflet to another cellular location. Uptake at 37 °C without BSA back-extraction after a 1-h incubation was used as control. All measurements are expressed as mean  $\pm$  SD of three independent experiments with three monolayers ( $n = 9$ ). Values are expressed as a percentage of the control. \*\* $P < 0.01$

conclusion that a subsequent cellular incorporation through internalization occurred at 37 °C after 1 h.

#### Effect of Endocytosis and Metabolic Inhibitors on HePC Incorporation

To characterize the putative carrier responsible for HePC translocation in Caco-2 cells we examined the proportion of uptake that could be attributed to receptor-mediated endocytosis. We therefore used various endocytosis inhibitors such as colchicine, which disrupts microtubules, monensin, which acts by increasing endosomal pH, and cytochalasin B, which is an inhibitor of actin polymerization [31]. The extent of HePC uptake after these various treatments is given in Table 2. These treatments did not affect the amount of HePC associated with cells, suggesting that HePC internalization in Caco-2 cells did not occur via endocytosis but possibly by transbilayer movement.

In addition, the effect of ATP depletion was investigated. Therefore, cells were incubated with metabolic inhibitors, sodium fluoride, sodium azide and 2-deoxyglucose, a treatment that induces a rapid drop in the cellular ATP level by blocking both glycolysis and oxidative phosphorylation [27, 32]. This treatment did not totally abolish the accumulation of [ $^3\text{H}$ ]HePC into Caco-2 cells but inhibited it by almost 30%, demon-

strating that this process depended partially on cellular energy.

#### Effect of Cholesterol on HePC Incorporation

We investigated the influence of cholesterol on HePC incorporation in three different ways. Firstly, we used methyl- $\beta$ -cyclodextrin (Me- $\beta$ -CD) to remove cholesterol from cell plasma membrane and therefore disrupt the microdomain structures of the plasma membrane known as “rafts”, secondly, we pre-incubated Caco-2 cells for 48 h in 20% FBS DMEM medium containing 25  $\mu\text{g}/\text{ml}$  of cholesterol, in order to obtain Caco-2 cells with a high cell cholesterol concentration and, thirdly, we added cholesterol to HePC in the incubation medium. The results are depicted in Fig. 5. Pretreatment with Me- $\beta$ -CD led to a 30% inhibition of HePC internalization, demonstrating that cholesterol, and therefore the integrity of lipid rafts in the apical plasma membrane of enterocytes, seemed crucial for the incorporation process. This result is a further indication for the involvement of specialized membrane structures in HePC incorporation. Enrichment of Caco-2 cell membranes with cholesterol did not significantly affect the amount of HePC associated with the cells, whereas the presence of 25  $\mu\text{g}/\text{ml}$  of cholesterol and HePC together in the incubation medium led to a large decrease in HePC incorporation to approximately 30% of the control value.

#### Discussion

The aim of this study was to elucidate the mechanism of HePC incorporation by human enterocytes after the oral administration of this antileishmanial agent. We therefore used the human-derived intestinal epithelial cell line Caco-2 as a validated in vitro intestinal model system [17].

In this study, we showed that the membrane accumulation of HePC was higher when the drug was presented apically. This difference between total accumulation from apical and basolateral membranes cannot be ascribed to membrane surface area because it has been demonstrated that the relative apical and basolateral membrane surface areas of the Caco-2 cells was 1:3 [33], but might be the result of differences in the plasma membrane composition since it is known that apical and basal membranes of Caco-2 cells differ in lipid and protein composition. Furthermore, the lipid composition [34] and the cholesterol content [35] have been shown to influence the incorporation of AELs into the plasma membrane. This result should be



**Table 2** Effects of endocytosis and metabolic inhibitors on HePC incorporation into Caco-2 cells

Treatment	Drug concentration ( $\mu\text{M}$ )	HePC incorporation (percentage of control <sup>a</sup> ) <sup>b</sup>
Colchicine	10 $\mu\text{M}$	99.9 $\pm$ 2.2
Monensin	10 $\mu\text{M}$	94.4 $\pm$ 3.4
Cytochalasin B	50 $\mu\text{M}$	105.8 $\pm$ 3.7
ATP depletion	NaF 10 mM, NaN <sub>3</sub> 2 mM, 2-DG 50 mM	70.2 $\pm$ 4.0**

\*\* $P < 0.01$  versus control

<sup>a</sup> Krebs modified buffer pH 6.0 was used as control

<sup>b</sup> Values are expressed as mean values  $\pm$  SD of three separate experiments ( $n = 9$ )

correlated with previous data demonstrating that the effect of HePC on paracellular permeability was asymmetrical and much more pronounced when HePC was applied to the apical than when it was added to the basolateral side of Caco-2 cell monolayers [22]. Interestingly, these results are in accord with studies on the polarity of free fatty acid uptake in the enterocyte: the total uptake of palmitate was found to be 2-fold higher at the apical plasma membrane than at the basolateral one [33]. Thus, higher apical incorporation is likely to

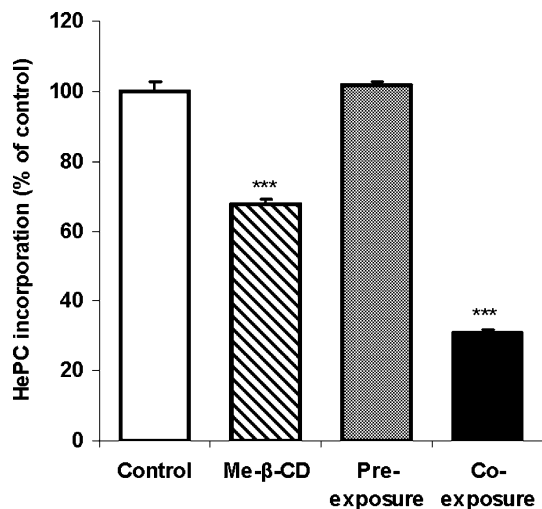


**Fig. 5** Effect of cholesterol status on HePC association with Caco-2 cells. *White bar* control cells. *Cross-hatched bar* cells were pre-incubated for 30 min with Me- $\beta$ -CD 10 mM to remove cholesterol from the plasma membrane. *Grey bar* (pre-exposure): cells were pre-incubated for 48 h with cholesterol (25  $\mu\text{g}/\text{ml}$ ) to enhance its content in the plasma membrane. *Black bar* (co-exposure): cholesterol (25  $\mu\text{g}/\text{ml}$ ) was added to [<sup>3</sup>H]HePC during the experiment. [<sup>3</sup>H]HePC (20  $\mu\text{M}$ , 0.1  $\mu\text{Ci}$  per well) was added to all groups and the amount of association with the cells was determined after 1 h incubation at 37 °C. All measurements are expressed as mean  $\pm$  SD ( $n = 12$ ). Values are expressed as a percentage of the control. \*\*\* $P < 0.001$  versus control

reflect specific HePC internalization mechanisms in the enterocyte.

The cellular accumulation at 37 °C from the basolateral side of Caco-2 monolayers was linear as a function of HePC concentration added to the basolateral compartment (data not shown), whereas it showed a saturable profile at the apical side, further arguing for a specific mechanism at the apical membrane of the enterocyte. Indeed, the cellular accumulation from the apical side included two components: one temperature-independent, with characteristics of nonspecific binding; and the other, saturable and temperature-dependent, with characteristics suggestive of specific internalization. The saturable component predominated for HePC concentrations below 50  $\mu\text{M}$ ; its kinetic constants were calculated to be  $V_{\text{max}}$ , 39.2 nmol/mg protein/h and  $K_m$ , 15.7  $\mu\text{mol}/\text{L}$ . This saturable process suggests that HePC incorporation into the enterocyte may occur in part by a protein-mediated pathway or a facilitated diffusion membrane transport process. This result could appear to be in contradiction with prior studies which have reported a nonsaturable uptake of edelfosine by two human leukemia cell lines, HL60 and K562 [36, 37]. However, the concentrations of the ether lipid that were used were extremely low (0–35 nM) and the uptake of this molecule could therefore appear to be nonsaturable in the concentration range used in these studies. It should be noted that the saturation of the incorporation process observed in our study occurs at concentrations which could easily be attained during therapy. The clinical dose of 100 mg/day administered orally [38] would lead to concentrations of 0.1–1 mg/ml in the intestine assuming that the fluid volume is 100–1,000 ml, which is about tenfold higher than the concentrations used in this study. In conclusion, the cellular incorporation of HePC occurs by both saturable and nonsaturable processes, suggesting that a carrier-mediated pathway coexists with the passive diffusion mechanism. HePC is a phospholipid analogue and it is interesting to note that our results are in accordance with the uptake process of micellar fatty acids by Caco-2 cells, which also include a dual mechanism by both saturable and nonsaturable diffusion processes [39, 40].

These results concerning association of HePC with Caco-2 cells have to be considered in conjunction with our previous study of the transepithelial transport of the drug in the same cell line [29]. Transport across the Caco-2 cell monolayer was found to occur, at least in part, by a passive paracellular mechanism. However, transport of HePC across the epithelial was found to be quantitatively much lower than the amount of drug accumulated within the cells. Release of labeled HePC

from the cells was slow and incomplete, even under sink conditions [29]. Therefore, in the in-vivo setting, these different mechanisms will co-exist. A part of the drug will be absorbed rapidly by the paracellular route, while another part will be accumulated within the enterocyte cell membranes. This cell-associated drug would be absorbed more slowly, giving rise to the delayed  $T_{\max}$  of about 48 h observed in mice [3]. It is difficult to predict from in-vitro experiments how much of the absorption will be by the paracellular route and how much by the slower transcellular pathway, since this will depend on the local HePC concentration. Given the affinity of HePC for albumin, binding to plasma proteins in the intestinal capillaries certainly plays an important role.

The cellular accumulation of HePC by Caco-2 cells was found to be partially inhibited by energy depletion and low temperature, suggesting the involvement, at least in part, of an energy-requiring component for HePC incorporation at the apical membrane of Caco-2 cells. These results are in agreement with previous studies on HePC uptake in various tumor cell lines [41], by MDCK cells [4], and for other AELs [42].

HePC incorporation into Caco-2 cells was found not to involve receptor-mediated endocytosis, since it was unaffected by inhibitors of this process. However, we cannot totally rule out the hypothesis of a caveolae-mediated endocytosis, although it has been demonstrated that Caco-2 cells do not express caveolin-1 and have very few caveolae [43]. In the literature, some investigators argue that endocytosis is a major pathway by which AELs are taken up [13, 42, 44], whereas others reach the opposite conclusion [12, 45, 46]. We cannot directly compare our results with studies arguing for the involvement of endocytosis because of differences in the drug used, in the incubation conditions and in the cell lines. The different cell types used may have dissimilar pathways of intracellular lipid trafficking or different membrane composition, leading to an alteration of the predominant pathway of AELs translocation. Moreover, it has been observed that the sensitivity of HePC uptake to compounds like chloroquine, monensin, cytochalasin B or colchicine was cell-line-dependent [47]. However, our results are consistent with a more recent study, which demonstrated that ether lipids are not internalized by endocytosis [14] and with the current understanding that the endocytotic uptake mechanism normally handles high-molecular-weight molecules, whereas ether lipids are much smaller molecules.

We also showed that HePC entry into Caco-2 cell plasma membrane was restricted by the presence of human serum albumin in the medium and that washing

with albumin removed a significant amount of HePC from cells. These results show that albumin plays an important role in HePC incorporation. As reported before, AELs bind to serum proteins [10, 12, 48] and a decrease edelfosine uptake by HL-60 cells [42], K562 cells [36] and *Trypanosoma cruzi* [49], caused by albumin, has already been observed. This binding to serum proteins, and especially albumin, would decrease the amount of HePC able to interact with the cells by lowering the concentration of free HePC in the medium. Taken together, these results suggest that HePC must be free in solution to be inserted in the plasma membrane of the cells and that the direct transfer from albumin to the plasma membrane is limited. HePC is a phospholipid analogue and our results can be correlated with previous studies using lipids and fatty acids, where similar competitive effects have been demonstrated with BSA-bound lipids [50]. Here we provide information that HePC behaves in the same way as fatty acid aggregates where albumin controls the lipid monomer concentration and therefore cell association.

We showed that removal of cholesterol from the cell plasma membrane using methyl- $\beta$ -cyclodextrin (Me- $\beta$ -CD) significantly decreased the capacity for HePC incorporation. This result could be explained by three hypotheses. Firstly, the incorporation of HePC might be correlated with the amount of cholesterol present in the plasma membrane, since HePC possesses a high affinity for the cholesterol molecule and forms a stable complex [51]. The reduction of HePC accumulation observed when cholesterol was present at high levels in the medium is in accordance with this hypothesis and with the formation of mixed aggregates between HePC and cholesterol. However, when the Caco-2 cell membranes were enriched in cholesterol, HePC accumulation was not enhanced. One can assume that the membrane rigidification induced by the enhancement of cholesterol content - since it is well established that cholesterol decreases the permeability of the lipid bilayer in membrane models—could inhibit HePC incorporation in the phospholipid bilayer and therefore counterbalance the affinity of HePC for cholesterol. The second hypothesis is that HePC may preferentially localize in rafts microdomains. Indeed, treatment by Me- $\beta$ -CD has been reported to disrupt these membrane domains, suggesting that intact rafts are required for the association of HePC to Caco-2 cell membranes, as demonstrated for the uptake of edelfosine by S49 cells [52]. Thirdly, the cholesterol content could affect the putative transporter activity. Finally, we have demonstrated, by albumin back-extraction of HePC and by low temperature treatment, that HePC is

translocated by Caco-2 cells from the outer to the inner leaflet of the plasma membrane bilayer.

Taken together, our results strongly suggested that HePC incorporation consists of passive absorption into the plasma membrane followed by translocation to the inner membrane leaflet by an active and saturable transport mechanism. The nonsaturable association may therefore represent the drug in the outer layer of the plasma membrane and the saturable component the drug which moves to inner membrane of the plasma membrane bilayer. The intriguing question is obviously the mechanism by which the translocation process occurs. Our results indicated that a protein-mediated translocation (“translocase activity”) is involved rather than a “spontaneous” flip-flop. Aminophospholipids and their fluorescent analogues are known to be actively translocated across cellular membranes, mediated by a specific translocase (“flippase”) [53]. In this respect, it is interesting to note that an HePC translocation process has been identified in *L. donovani* parasites [16] and the protein responsible has recently been cloned [15]. This novel P-type ATPase, belonging to the aminophospholipid translocase subfamily and called LdMT (*L. donovani* putative Miltefosine Transporter), was shown to be responsible for the inward translocation of HePC in the parasites [16]. LdMT has 47% homology with the human ATPase II and shares all the P-type ATPase consensus sequences and the APT subfamily-specific motifs from the mammalian homologues [15]. It is conceivable that this kind of transporter could take up HePC in the intestinal epithelium, as in vitro studies have suggested the presence of an aminophospholipid translocase in the plasma membrane of Caco-2 cells [54].

In summary, the present study indicates the involvement of a carrier-mediated process handling HePC at the apical membrane of Caco-2 cells. This conclusion is based on a number of observations that may be summarized as follows: (1) the accumulation of HePC was composed of both saturable and nonsaturable (specific and nonspecific) processes, (2) the saturable component followed Michaelis–Menten kinetics (15.7  $\mu\text{mol/l}$  and 39.2 nmol/mg protein/h for  $K_m$  and  $V_{max}$ , respectively), (3) cellular ATP depletion by treating cells with inhibitors of oxidative phosphorylation and the glycolytic pathway reduced the accumulation significantly, indicating the energy-dependence of this process, (4) reduction of the incubation temperature from 37 to 4 °C decreased the HePC accumulation. These observations fulfill the criteria for a carrier-mediated mechanism and provide good circumstantial evidence for the participation of a membrane protein, i.e., a carrier protein, responsible for the inward translocation of HePC in the

plasma membrane, after the nonspecific insertion of HePC into the outer leaflet of the plasma membrane. The fact that inhibitors of energy-dependent mechanisms only partially abolished the HePC accumulation may indicate that this carrier protein has a limited capacity to transport HePC compared with the amount of drug that can be incorporated into the outer leaflet of the membrane by passive diffusion. In parallel with this specific saturable mechanism, some HePC sequestered in the plasma membrane may enter intracellular membranes by the normal membrane recycling processes of the cell, as suggested by Fleer et al. [41]. Work remains to be done to determine the molecular mechanism of HePC uptake in intestinal epithelial cells, including localization of the saturable component and isolation of the protein, if any, that is involved.

**Acknowledgments** The authors are very grateful to Christophe Dugave for [ $^3\text{H}$ ]HePC synthesis and would like to thank H el ene Chacun for valuable help in radioactivity studies.

## References

- Sundar S, Makharia A, More DK, Agrawal G, Voss A, Fischer C, Bachmann P, Murray HW (2000) Short-course of oral miltefosine for treatment of visceral leishmaniasis. *Clin Infect Dis* 31:1110–1113
- Sundar S, Jha TK, Thakur CP, Engel J, Sindermann H, Fischer C, Junge K, Bryceson A, Berman J (2002) Oral miltefosine for Indian visceral leishmaniasis. *N Engl J Med* 347:1739–1746
- Arnold B, Reuther R, Weltzien HU (1978) Distribution and metabolism of synthetic alkyl analogs of lysophosphatidylcholine in mice. *Biochim Biophys Acta* 530:47–55
- Geilen CC, Wieder T, Haase A, Reutter W, Morre DM, Morre DJ (1994) Uptake, subcellular distribution and metabolism of the phospholipid analogue hexadecylphosphocholine in MDCK cells. *Biochim Biophys Acta* 1211:14–22
- Hoffman DR, Hoffman LH, Snyder F (1986) Cytotoxicity and metabolism of alkyl phospholipid analogues in neoplastic cells. *Cancer Res* 46:5803–5809
- Van Blitterswijk WJ, Hilkmann H, Storme GA (1987) Accumulation of an alkyl lysophospholipid in tumor cell membranes affects membrane fluidity and tumor cell invasion. *Lipids* 22:P820–P823
- Dive C, Watson JV, Workman P (1991) Multiparametric flow cytometry of the modulation of tumor cell membrane permeability by developmental antitumor ether lipid SRI 62-834 in EMT6 mouse mammary tumor and HL-60 human promyelocytic leukemia cells. *Cancer Res* 51:799–806
- Grunicke HH (1991) The cell membrane as a target for cancer chemotherapy. *Eur J Cancer* 27:281–284
- Modolell M, Andreesen R, Pahlke W, Brugger U, Munder PG (1979) Disturbance of phospholipid metabolism during the selective destruction of tumor cells induced by alkyllysophospholipids. *Cancer Res* 39:4681–4686
- Uberall F, Oberhuber H, Maly K, Zaknun J, Demuth L, Grunicke HH (1991) Hexadecylphosphocholine inhibits inositol phosphate formation and protein kinase C activity. *Cancer Res* 51:807–812

11. Powis G, Seewald MJ, Gratas C, Melder D, Riebow J, Modest EJ (1992) Selective inhibition of phosphatidylinositol phospholipase C by cytotoxic ether lipid analogues. *Cancer Res* 52:2835–2840
12. Kelley EE, Modest EJ, Burns CP (1993) Unidirectional membrane uptake of the ether lipid antineoplastic agent edelfosine by L1210 cells. *Biochem Pharmacol* 45:2435–2439
13. Bazill GW, Dexter TM (1990) Role of endocytosis in the action of ether lipids on WEHI-3B, HL60, and FDCP-mix A4 cells. *Cancer Res* 50:7505–7512
14. Hanson PK, Malone L, Birchmore J, Nichols J (2003) Lem3p is essential for the uptake and potency of alkylphosphocholine drugs, edelfosine and miltefosine. *J Biol Chem* 278:36041–36050
15. Perez-Victoria FJ, Gamarro F, Ouellette M, Castanys S (2003) Functional cloning of the miltefosine transporter. A novel P-type phospholipid translocase from *Leishmania* involved in drug resistance. *J Biol Chem* 278:49965–49971
16. Perez-Victoria FJ, Castanys S, Gamarro F (2003) *Leishmania donovani* resistance to miltefosine involves a defective inward translocation of the drug. *Antimicrob Agents Chemother* 47:2397–2403
17. Hidalgo IJ, Raub TJ, Borchardt RT (1989) Characterization of the human colon carcinoma cell line (Caco-2) as a model system for intestinal epithelial permeability. *Gastroenterology* 96:736–749
18. Geilen CC, Samson A, Wieder T, Wild H, Reutter W (1992) Synthesis of hexadecylphospho[methyl-14C]-choline. *J Labelled Compd Radiopharm* 31:1071–1076
19. Eibl H, Woolley P (1988) A general synthetic method for enantiomerically pure ester and ether lysophospholipids. *Chem Phys Lipids* 47:63–68
20. Mosmann T (1983) Rapid colorimetric assay for cellular growth and survival: application to proliferation and cytotoxicity assays. *J Immunol Methods* 65:55–63
21. Decker T, Lohmann-Matthes ML (1988) A quick and simple method for the quantitation of lactate dehydrogenase release in measurements of cellular cytotoxicity and tumor necrosis factor (TNF) activity. *J Immunol Methods* 115:61–69
22. Ménez C, Buyse M, Chacun H, Farinotti R, Barratt G (2006) Modulation of intestinal barrier properties by miltefosine. *Biochem Pharmacol* 71:486–496
23. Diomedea L, Colotta F, Piovani B, Re F, Modest EJ, Salmona M (1993) Induction of apoptosis in human leukemic cells by the ether lipid 1-octadecyl-2-methyl-rac-glycero-3-phosphocholine. A possible basis for its selective action. *Int J Cancer* 53:124–130
24. Garcia-Garcia E, Andrieux K, Gil S, Kim HR, Le Doan T, Desmaele D, d'Angelo J, Taran F, Georgin D, Couvreur P (2005) A methodology to study intracellular distribution of nanoparticles in brain endothelial cells. *Int J Pharm* 298:310–314
25. Galdiero M, Vitiello M, D'Isanto M, Peluso L (2001) Induction of tyrosine phosphorylated proteins in THP-1 cells by *Salmonella typhimurium*, *Pasteurella haemolytica* and *Haemophilus influenzae* porins. *FEMS Immunol Med Microbiol* 31:121–130
26. LeDoan T, Eto F, Tenu JP, Letourneux Y, Agrawal S (1999) Cell binding, uptake and cytosolic partition of HIV anti-gag phosphodiester oligonucleotides 3'-linked to cholesterol derivatives in macrophages. *Bioorg Med Chem* 7:2263–2269
27. Clarke BL, Weigel PH (1985) Recycling of the asialoglycoprotein receptor in isolated rat hepatocytes. ATP depletion blocks receptor recycling but not a single round of endocytosis. *J Biol Chem* 260:128–133
28. Mohandas N, Wyatt J, Mel SF, Rossi ME, Shohet SB (1982) Lipid translocation across the human erythrocyte membrane. Regulatory factors. *J Biol Chem* 257:6537–6543
29. Ménez C, Buyse M, Dugave C, Farinotti R, Barratt G (2006) Intestinal absorption of miltefosine: contribution of passive paracellular transport. *Pharm Res* (in press). <http://dx.doi.org/10.1007/s11095-006-9170-7>
30. Berkovic D, Fleer EA, Eibl H, Unger C (1992) Effects of hexadecylphosphocholine on cellular function. *Prog Exp Tumor Res* 34:59–68
31. Wolkers WF, Looper SA, Fontanilla RA, Tsvetkova NM, Tablin F, Crowe JH (2003) Temperature dependence of fluid phase endocytosis coincides with membrane properties of pig platelets. *Biochim Biophys Acta* 1612:154–163
32. Steinman RM, Silver JM, Cohn ZA (1974) Pinocytosis in fibroblasts. Quantitative studies in vitro. *J Cell Biol* 63:949–969
33. Trotter PJ, Storch J (1991) Fatty acid uptake and metabolism in a human intestinal cell line (Caco-2): comparison of apical and basolateral incubation. *J Lipid Res* 32:293–304
34. Chabot MC, Wykle RL, Modest EJ, Daniel LW (1989) Correlation of ether lipid content of human leukemia cell lines and their susceptibility to 1-O-octadecyl-2-O-methyl-rac-glycero-3-phosphocholine. *Cancer Res* 49:4441–4445
35. Diomedea L, Bizzi A, Magistrelli A, Modest EJ, Salmona M, Nosedà A (1990) Role of cell cholesterol in modulating antineoplastic ether lipid uptake, membrane effects and cytotoxicity. *Int J Cancer* 46:341–346
36. Heesbeen EC, Rijkssen G, van Heugten HG, Verdonck LF (1995) Influence of serum levels on leukemic cell destruction by the ether lipid ET-18-OCH<sub>3</sub>. *Leuk Res* 19:417–425
37. Heesbeen EC, Verdonck LF, Haagmans M, van Heugten HG, Staal GE, Rijkssen G (1993) Adsorption and uptake of the alkyllysophospholipid ET-18-OCH<sub>3</sub> by HL-60 cells during induction of differentiation by dimethylsulfoxide. *Leuk Res* 17:143–148
38. Sundar S, Rosenkaimer F, Makharia MK, Goyal AK, Mandal AK, Voss A, Hilgard P, Murray HW (1998) Trial of oral miltefosine for visceral leishmaniasis. *Lancet* 352:1821–1823
39. Murota K, Storch J (2005) Uptake of micellar long-chain fatty acid and sn-2-monoacylglycerol into human intestinal Caco-2 cells exhibits characteristics of protein-mediated transport. *J Nutr* 135:1626–1630
40. Trotter PJ, Ho SY, Storch J (1996) Fatty acid uptake by Caco-2 human intestinal cells. *J Lipid Res* 37:336–346
41. Fleer EA, Berkovic D, Eibl H, Unger C (1993) Investigations on the cellular uptake of hexadecylphosphocholine. *Lipids* 28:731–736
42. Small GW, Strum JC, Daniel LW (1997) Characterization of an HL-60 cell variant resistant to the antineoplastic ether lipid 1-O-octadecyl-2-O-methyl-rac-glycero-3-phosphocholine. *Lipids* 32:715–723
43. Vogel U, Sandvig K, van Deurs B (1998) Expression of caveolin-1 and polarized formation of invaginated caveolae in Caco-2 and MDCK II cells. *J Cell Sci* 111(Pt 6):825–832
44. Storch J, Munder PG (1987) Increased membrane permeability for an antitumoral alkyl lysophospholipid in sensitive tumor cells. *Lipids* 22:813–819
45. Mollinedo F, Fernandez-Luna JL, Gajate C, Martin-Martin B, Benito A, Martinez-Dalmau R, Modolell M (1997) Selective induction of apoptosis in cancer cells by the ether lipid ET-18-OCH<sub>3</sub> (Edelfosine): molecular structure requirements, cellular uptake, and protection by Bcl-2 and Bcl-X(L). *Cancer Res* 57:1320–1328
46. Zoeller RA, Layne MD, Modest EJ (1995) Animal cell mutants unable to take up biologically active glycerophospholipids. *J Lipid Res* 36:1866–1875

47. Fleer EA, Berkovic D, Unger C, Eibl H (1992) Cellular uptake and metabolic fate of hexadecylphosphocholine. *Prog Exp Tumor Res* 34:33–46
48. Kotting J, Marschner NW, Neumuller W, Unger C, Eibl H (1992) Hexadecylphosphocholine and octadecyl-methyl-glycero-3-phosphocholine: a comparison of hemolytic activity, serum binding and tissue distribution. *Prog Exp Tumor Res* 34:131–142
49. Santa-Rita RM, Santos Barbosa H, Meirelles MN, de Castro SL (2000) Effect of the alkyl-lysophospholipids on the proliferation and differentiation of *Trypanosoma cruzi*. *Acta Trop* 75:219–228
50. Ho SY, Storch J (2001) Common mechanisms of monoacylglycerol and fatty acid uptake by human intestinal Caco-2 cells. *Am J Physiol Cell Physiol* 281:C1106–1117
51. Rey Gomez-Serranillos I, Minones J Jr, Dynarowicz-Latka P, Minones J, Iribarnegaray E (2004) Miltefosine-Cholesterol interactions: a monolayer study. *Langmuir* 20:928–933
52. Van der Luit AH, Budde M, Ruurs P, Verheij M, Van Blitterswijk WJ (2002) Alkyl-lysophospholipid accumulates in lipid rafts and induces apoptosis via raft-dependent endocytosis and inhibition of phosphatidylcholine synthesis. *J Biol Chem* 277:39541–39547
53. Voelker DR (1990) Lipid transport pathways in mammalian cells. *Experientia* 46:569–579
54. Pomorski T, Herrmann A, Muller P, van Meer G, Burger K (1999) Protein-mediated inward translocation of phospholipids occurs in both the apical and basolateral plasma membrane domains of epithelial cells. *Biochemistry* 38:142–150

# Lymphatic Absorption and Deposition of Various Plant Sterols in Stroke-Prone Spontaneously Hypertensive Rats, a Strain Having a Mutation in ATP binding cassette transporter G5

Tadateru Hamada · Nami Egashira · Shoko Nishizono · Hiroko Tomoyori · Hideaki Nakagiri · Katsumi Imaizumi · Ikuo Ikeda

Received: 6 September 2006 / Accepted: 14 December 2006 / Published online: 23 January 2007  
© AOCS 2007

**Abstract** ATP binding cassette transporter G5 (ABCG5) and ATP binding cassette transporter G8 (ABCG8) have been suggested to transport absorbed plant sterols and cholesterol from enterocytes to the intestinal lumen and from hepatocytes to bile. It has been thought that mutations of *ABCG5* or *ABCG8* cause the deposition of plant sterols in the body. In the present study, lymphatic absorption of various plant sterols and their deposition in various tissues was investigated in stroke-prone spontaneously hypertensive rats (SHRSP), having a mutation in *Abcg5* and depositing plant sterols in the body. The order of

lymphatic 24-h recovery of plant sterols was as follows: campesterol > sitosterol > brassicasterol > stigmasterol = sitostanol. When SHRSP were fed a diet containing one of the plant sterols, the depositions of campesterol and sitosterol were comparatively higher than those of brassicasterol, stigmasterol and sitostanol. Highly positive correlations were obtained between lymphatic recovery of plant sterols and their levels in plasma, liver, adipose tissue and heart. The tendency of differential absorption of plant sterols to the lymph in SHRSP was similar to that in normal Wistar rats previously reported by us (Hamada et al. *Lipids* 41:551–556, 2006). These observations suggest that differential absorption of various plant sterols is kept in SHRSP in spite of a mutation in *Abcg5*.

T. Hamada · N. Egashira · H. Nakagiri · K. Imaizumi  
Laboratory of Nutrition Chemistry,  
Department of Bioscience and Biotechnology,  
Faculty of Agriculture, Graduate School,  
Kyushu University, Fukuoka 812-8581, Japan

S. Nishizono  
Cooperative Research Center,  
University of Miyazaki, Miyazaki 889-2192, Japan

H. Tomoyori  
Department of Environmental and Symbiotic Sciences,  
Faculty of Environmental and Symbiotic Sciences,  
Prefectural University of Kumamoto,  
Kumamoto 862-8502, Japan

I. Ikeda (✉)  
Laboratory of Food and Biomolecular Science,  
Department of Food Function and Health,  
Division of Bioscience and Biotechnology  
for Future Bioindustries,  
Graduate School of Agricultural Science,  
Tohoku University, Sendai 981-8555, Japan  
e-mail: iikeda@biochem.tohoku.ac.jp

**Keywords** ABCG5 · ABCG8 · Absorption · Brassicasterol · Campesterol · Plant sterol · Sitostanol · Sitosterol · Stigmasterol · Stroke-prone spontaneously hypertensive rats

## Abbreviations

ABCG5 ATP binding cassette transporter G5  
ABCG8 ATP binding cassette transporter G8  
ACAT Acylcoenzyme A:cholesterol  
acyltransferase  
NPC1L1 Niemann-Pick C1 like 1 protein  
SHRSP Stroke-prone spontaneously hypertensive  
rats

## Introduction

Plant sterols contained in plant foods and vegetable oils are less absorbable than cholesterol [1]. It is also

known that each plant sterol has a different absorption rate in humans [2, 3] and experimental animals [4–6]. In our study using Wistar rats, lymphatic 24-h recovery of campesterol given to the stomach was the highest among the plant sterols examined. Lymphatic recoveries of brassicasterol and sitosterol were intermediate and those of stigmasterol and sitostanol were extremely low [7]. The mechanisms of differential absorption of plant sterols are not well understood. Recently, various mutations in ATP binding cassette transporter G5 (*ABCG5*) and ATP binding cassette transporter G8 (*ABCG8*) have been found in sitosterolemic patients whose absorption and deposition of plant sterols are higher than those of normal subjects [8, 9]. *ABCG5* and *ABCG8* are mainly expressed in the intestine and the liver and form a heterodimer. They are thought to excrete sterols from intestinal epithelial cells to the intestinal lumen and from hepatocytes to bile [8–10]. Igel et al. [11] showed that plant sterols were once incorporated into the intestinal cell and then they were secreted to the intestinal lumen. They suggested that the secretion of plant sterols by *ABCG5* and *ABCG8* could be an important determinant for intestinal absorption of sterols. This means that *ABCG5* and *ABCG8* determine differential absorption of plant sterols.

In contrast, we suggested that solubility in and affinity for the bile salt micelle of plant sterols are important determinants for their intestinal absorption in rats [7]. We think that differential incorporation of plant sterols into the intestinal cell determines differential absorption of various plant sterols. Yu et al. [12] reported that differential absorption of cholesterol, campesterol and sitosterol was observed in *ABCG5*-/*ABCG8*-deficient mice. Observations by Yu et al. [12] and us [7] suggest that differential absorption of plant sterols is independent of the function of *ABCG5* and *ABCG8*.

It has been reported that stroke-prone spontaneously hypertensive rats (SHRSP) deposit plant sterols, in particular campesterol and sitosterol, in the body [13–15]. We showed that lymphatic absorption of radiolabeled sitosterol was higher and biliary excretions of campesterol and sitosterol were lower in SHRSP than in Wistar King-A rats [13]. Scoggan et al. [16] and Yu et al. [17] revealed that SHRSP have a mutation in *Abcg5*; therefore, it is thought that malfunction of *ABCG5*/*ABCG8* induces increased absorption and deposition of plant sterols in SHRSP [16, 17]. Because dietary plant sterols were rich in campesterol and sitosterol in the feeding study of SHRSP [13–15], it is not known whether plant sterols

other than campesterol and sitosterol can be absorbed in SHRSP.

In the present study, to reveal the relationship between differential absorption of plant sterols and the function of *ABCG5*/*ABCG8*, lymphatic absorption and deposition of various plant sterols were compared in SHRSP. There is a possibility that when a plant sterol mixture is given to rats, each plant sterol inhibits intestinal absorption of other plant sterols. Therefore, one of the purified plant sterols was given to rats in the present study.

## Experimental Procedure

### Materials

Brassicasterol (purity 93.5%), campesterol (94.4%), stigmasterol (97.7%) and sitosterol (98.6%) were kindly provided by Tama Biochemical Co. (Tokyo, Japan). Sitostanol (95.9%) and triolein were purchased from Sigma (Tokyo, Japan). Sodium taurocholate (purity better than 97%) was purchased from Nacalai Tesque (Kyoto, Japan).

### Lymphatic Absorption of Plant Sterols in SHRSP

Seven-week-old male SHRSP (SHRSP/Sea, inbred, SPF) ( $n = 35$ ) were obtained from Seac Yoshitomi, Fukuoka, Japan. The rat strain obtained from Seac Yoshitomi was proved to have a mutation in *Abcg5* by Scoggan et al. [16] and Yu et al. [17]. Rats were fed an AIN-93G purified diet [18] containing 10% lard for 5 weeks ad libitum. Since rat chow diets contain considerable amounts of plant sterols, SHRSP obtained from the breeder had already deposited plant sterols in the body. To reduce plant sterol levels in the body as low as possible, lard was used as the sole dietary fat, because the plant sterol content in lard is extremely low (sterol content in weight percent: cholesterol, 0.05%; campesterol, 0.0011%; sitosterol, 0.0013%). These rats were subjected to surgery. The average body weight at surgery was 273 g. After anesthetizing the animals with sodium pentobarbital given intraperitoneally (50 mg/kg body weight), the left thoracic lymphatic duct cephalad to the cisterna chili was cannulated as described previously [19]. A second indwelling catheter was placed in the stomach for administration of the test emulsion. After surgery, the animals were placed in restraining cages and intragastrically given a solution containing 139 mM glucose and 85 mM NaCl at a rate of 3.4 ml/h by an

infusion pump (Shinkoseiki, Fukuoka, Japan) continuously until the end of the experiment. The same solution was given as drinking water. The next morning, animals with a constant lymph flow rate were divided into five groups ( $n = 6-7$  rats per group) and used for sterol absorption study. Lipid emulsions composed of 67 mg sodium taurocholate, 17 mg fatty acid free bovine serum albumin (Serologicals, Kankakee, IL, USA), 67 mg triolein and 16.7 mg of highly purified plant sterol in 1 ml were prepared by sonication and administered into the stomach via the stomach tube at 1 ml per 100-g body weight. In this study, five types of highly purified plant sterols, brassicasterol, campesterol, stigmasterol, sitosterol and sitostanol, were used for preparing test emulsions. The chemical structures of the plant sterols and cholesterol are shown in Fig. 1. Lymph was collected on ice-chilled tubes containing EDTA and aliquots were subjected to sterol analysis. Because trace amounts of plant sterols were detected in lymph before the infusion of a test emulsion, the amounts of plant sterols in lymph before administration were used as the baseline. All animal studies were carried out under the guidelines for animal experiments of the Faculty of Agriculture, Graduate School of Kyushu University, and Law 105 and Notification 6 of the government of Japan.

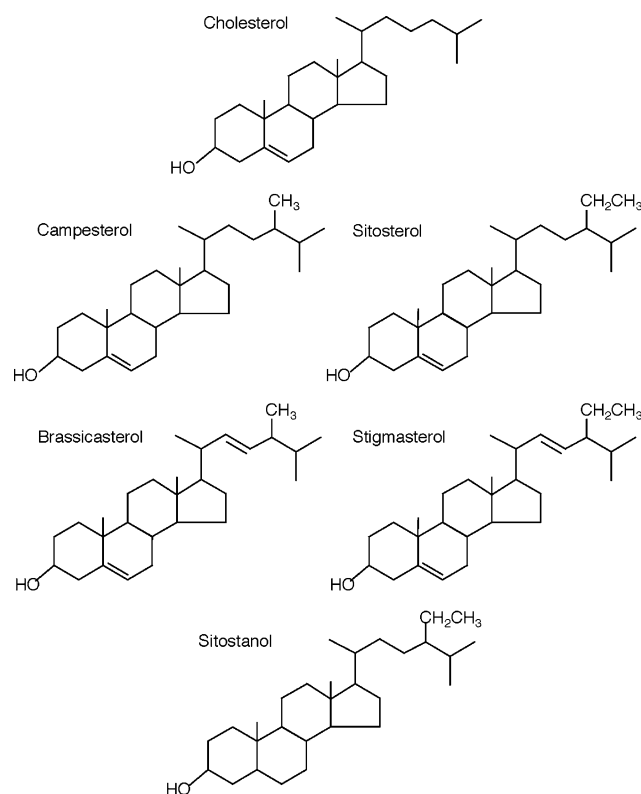


**Fig. 1** Chemical structures of the plant sterols and cholesterol

## Feeding Study of Plant Sterols in SHRSP

Four-week-old male SHRSP ( $n = 30$ ) were fed an AIN-93G purified diet containing 10% lard for 4 weeks. After that, 8-week-old SHRSP were separated into five groups ( $n = 6$  rats per group) and these rats were fed a purified diet containing 10% lard and 0.5% of one of the plant sterols for 10 days more. Five types of highly purified plant sterols, brassicasterol, campesterol, stigmasterol, sitosterol and sitostanol, were used. At the termination of the feeding period, the rats were fasted for 7 h and blood was withdrawn from the abdominal aorta under diethyl ether anesthesia. Liver, adipose tissue, heart and adrenals were excised and frozen at  $-40^{\circ}\text{C}$  until sterol analysis.

## Sterol Analysis

Lipids in plasma, liver, adipose tissue, heart, adrenals and lymph were extracted and purified by the method of Folch et al. [20]. After saponification of total lipids, unsaponifiable matter collected was derivatized to trimethylsilyl ethers and was quantified by gas-liquid chromatography using a SPELCO SPB-1<sup>TM</sup> column ( $0.25\text{ mm} \times 60\text{ m}$ ,  $0.25\text{-}\mu\text{m}$  film thickness, Sigma-Aldrich, Tokyo, Japan) and  $5\alpha$ -cholestane (Sigma) as an internal standard. Free and esterified sterols in total lipids were separated by thin-layer chromatography (hexane/diethyl ether/acetic acid, 83:16:1, by volume, as the developing solvent) and subjected to sterol analysis.

## Statistics

All data are expressed as the mean  $\pm$  the standard error. The Tukey–Kramer test was used and  $P < 0.05$  was considered significant.

## Results

### Lymphatic Recovery of Plant Sterols in SHRSP

As shown in Fig. 2 and Table 1, campesterol had the highest and stigmasterol and sitostanol the lowest lymphatic 24-h recovery among the five types of plant sterols. The lymphatic recoveries of brassicasterol and sitosterol were intermediate. The order of the absorption rates of each plant sterol was campesterol > sitosterol > brassicasterol > stigmasterol = sitostanol. The esterification ratio of campesterol in lymph was the highest and that of stigmasterol was the lowest among the five types of plant sterols. The order of esterification of each plant sterol was



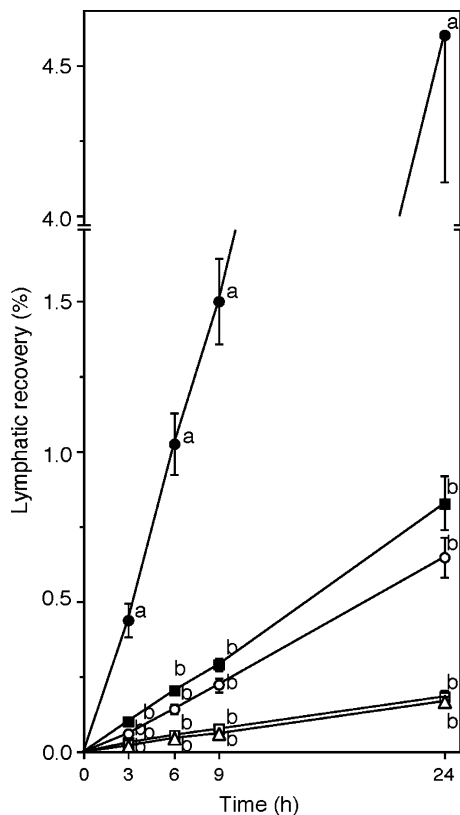


**Fig. 2** Lymphatic recovery of plant sterols in stroke-prone spontaneously hypertensive rats (SHRSP). Thoracic duct cannulated SHRSP were administered 1 ml/100 g body weight of a lipid emulsion containing 67 mg/ml triolein, 17 mg/ml fatty acid free bovine serum albumin, 6.7 mg/ml plant sterol and 67 mg/ml sodium taurocholate. Lymph was collected for 24 h. *Open circles* brassicasterol, *filled circles* campesterol, *open squares* stigmasterol, *filled squares* sitosterol, *triangle* sitostanol. Different letters show significant differences among plant sterols at  $P < 0.05$  in the Tukey–Kramer test

campesterol > brassicasterol > sitosterol = sitostanol > stigmasterol.

#### Plasma Sterol Levels in SHRSP

All of the dietary plant sterols fed to SHRSP were detected in plasma. The plasma level of campesterol was the highest and that of stigmasterol was the lowest

among the five types of plant sterols. The order of the plasma levels of each plant sterol was campesterol > sitosterol > sitostanol > brassicasterol > stigmasterol. The esterification ratio of sitostanol in plasma was the highest and the esterification ratios of brassicasterol and stigmasterol were the lowest among the five types of plant sterols. The order of esterification of each plant sterol was sitostanol > sitosterol > campesterol > brassicasterol = stigmasterol. There were no significant differences in plasma cholesterol levels among the groups. The percentages of cholesterol ester ranged from 70 to 75% (Table 2).

#### Sterol Levels of Various Tissues in SHRSP

All of dietary plant sterols fed to SHRSP were deposited in all of the tissues examined. On the basis of tissue weight, plant sterol levels in adrenals were the highest and those of adipose tissue were the lowest. In the liver, campesterol had the highest deposition and stigmasterol and sitostanol had the lowest deposition among the five types of plant sterols. The order was campesterol > sitosterol > brassicasterol > stigmasterol = sitostanol. The same tendency was obtained in adipose tissue and heart. In adrenals, the deposition of brassicasterol was higher than that of sitosterol and the order was campesterol > brassicasterol > sitosterol > stigmasterol > sitostanol (Table 2). The order of the cholesterol levels in liver was stigmasterol > sitostanol > campesterol > brassicasterol > sitosterol. The percentages of cholesterol ester in liver ranged from 15 to 45%. The orders of the cholesterol levels in adipose tissue and heart were similar, sitostanol > brassicasterol = stigmasterol > sitosterol > campesterol. The order of the cholesterol levels in adrenals was brassicasterol = sitostanol > stigmasterol > campesterol > sitosterol (Table 2).

#### Correlation Between Lymphatic Recovery and Plant Sterol Levels in SHRSP

As shown in Fig. 3, there was highly positive correlation between lymphatic recovery of plant sterols and

**Table 1** Lymphatic absorption and esterification ratio of plant sterols in stroke-prone spontaneously hypertensive rats (SHRSP) intragastrically infused with an emulsion containing one of the plant sterols

	Plant sterols administered				
	Brassicasterol	Campesterol	Stigmasterol	Sitosterol	Sitostanol
Recovery (%)	0.648 ± 0.068 <sup>a</sup>	4.60 ± 0.49 <sup>b</sup>	0.186 ± 0.017 <sup>a</sup>	0.828 ± 0.089 <sup>a</sup>	0.170 ± 0.015 <sup>a</sup>
Amount (mg/100 g body weight)	0.120 ± 0.012 <sup>a</sup>	0.862 ± 0.096 <sup>b</sup>	0.0348 ± 0.0031 <sup>a</sup>	0.145 ± 0.019 <sup>a</sup>	0.0325 ± 0.0026 <sup>a</sup>
Esterification (%)	28.2 ± 1.1 <sup>a</sup>	64.4 ± 1.9 <sup>b</sup>	10.7 ± 1.0 <sup>c</sup>	16.0 ± 0.7 <sup>c</sup>	15.8 ± 2.0 <sup>c</sup>

Data are the mean ± the standard error (SE) of six to seven rats per group. Different superscript letters show significant differences among plant sterols at  $P < 0.05$  in the Tukey–Kramer test

**Table 2** Plant sterol levels in plasma and various tissues of SHRSP fed a diet containing one of the plant sterols

	Plant sterols administered				
	Brassicasterol	Campesterol	Stigmasterol	Sitosterol	Sitostanol
<b>Plasma</b>					
Cholesterol (mg/dl)	43.7 ± 2.9	42.9 ± 1.6	44.3 ± 1.5	48.2 ± 2.1	47.7 ± 1.9
Cholesterol ester (%)	74.5 ± 1.2 <sup>a</sup>	70.4 ± 0.9 <sup>b</sup>	74.8 ± 0.4 <sup>a</sup>	71.0 ± 1.0 <sup>b</sup>	72.2 ± 0.4 <sup>ab</sup>
Plant sterol (mg/dl)	1.62 ± 0.18 <sup>a</sup>	26.5 ± 1.0 <sup>b</sup>	1.36 ± 0.14 <sup>a</sup>	12.0 ± 0.7 <sup>c</sup>	3.21 ± 0.22 <sup>a</sup>
Percentage of total sterol	3.49 ± 0.20 <sup>a</sup>	38.0 ± 0.6 <sup>b</sup>	2.93 ± 0.25 <sup>a</sup>	19.7 ± 0.3 <sup>c</sup>	6.22 ± 0.22 <sup>d</sup>
Esterification (%)	47.3 ± 1.6 <sup>a</sup>	67.3 ± 0.8 <sup>b</sup>	47.2 ± 0.8 <sup>a</sup>	70.8 ± 1.1 <sup>b</sup>	79.5 ± 0.4 <sup>c</sup>
<b>Liver</b>					
Cholesterol (mg/g)	2.66 ± 0.09 <sup>ab</sup>	2.76 ± 0.16 <sup>ab</sup>	3.14 ± 0.23 <sup>a</sup>	2.19 ± 0.14 <sup>b</sup>	2.90 ± 0.17 <sup>a</sup>
Cholesterol ester (%)	18.0 ± 0.8 <sup>a</sup>	44.9 ± 4.3 <sup>b</sup>	19.7 ± 2.8 <sup>a</sup>	14.6 ± 1.1 <sup>a</sup>	18.6 ± 3.0 <sup>a</sup>
Plant sterol (mg/g)	0.134 ± 0.005 <sup>a</sup>	1.17 ± 0.08 <sup>b</sup>	0.101 ± 0.004 <sup>a</sup>	0.360 ± 0.023 <sup>c</sup>	0.0807 ± 0.0066 <sup>a</sup>
Percentage of total sterol	4.77 ± 0.17 <sup>a</sup>	29.7 ± 0.8 <sup>b</sup>	3.16 ± 0.19 <sup>c</sup>	14.0 ± 0.2 <sup>d</sup>	2.69 ± 0.14 <sup>c</sup>
Esterification (%)	6.02 ± 0.53 <sup>ac</sup>	25.0 ± 3.0 <sup>b</sup>	3.16 ± 0.27 <sup>a</sup>	6.83 ± 0.53 <sup>ac</sup>	11.7 ± 0.8 <sup>c</sup>
<b>Adipose tissue</b>					
Cholesterol (mg/g)	0.408 ± 0.015 <sup>ac</sup>	0.303 ± 0.016 <sup>b</sup>	0.415 ± 0.017 <sup>ac</sup>	0.361 ± 0.016 <sup>ab</sup>	0.429 ± 0.007 <sup>c</sup>
Plant sterol (mg/g)	0.0184 ± 0.0012 <sup>a</sup>	0.0907 ± 0.0053 <sup>b</sup>	0.0110 ± 0.0007 <sup>a</sup>	0.0341 ± 0.0024 <sup>c</sup>	0.00912 ± 0.00075 <sup>a</sup>
Percentage of total sterol	4.26 ± 0.17 <sup>a</sup>	22.9 ± 1.1 <sup>b</sup>	2.59 ± 0.19 <sup>a</sup>	8.56 ± 0.37 <sup>c</sup>	2.07 ± 0.16 <sup>a</sup>
<b>Heart</b>					
Cholesterol (mg/g)	1.22 ± 0.03 <sup>ac</sup>	0.900 ± 0.029 <sup>b</sup>	1.16 ± 0.05 <sup>a</sup>	1.12 ± 0.04 <sup>a</sup>	1.34 ± 0.02 <sup>c</sup>
Plant sterol (mg/g)	0.0636 ± 0.0017 <sup>a</sup>	0.376 ± 0.016 <sup>b</sup>	0.0346 ± 0.0014 <sup>ad</sup>	0.135 ± 0.006 <sup>c</sup>	0.0282 ± 0.0017 <sup>d</sup>
Percentage of total sterol	4.91 ± 0.12 <sup>a</sup>	29.3 ± 0.8 <sup>b</sup>	2.89 ± 0.11 <sup>c</sup>	10.7 ± 0.3 <sup>d</sup>	2.05 ± 0.11 <sup>c</sup>
<b>Adrenals</b>					
Cholesterol (mg/g)	13.6 ± 0.7 <sup>a</sup>	9.70 ± 0.67 <sup>b</sup>	9.85 ± 0.80 <sup>b</sup>	8.32 ± 0.36 <sup>b</sup>	13.3 ± 1.0 <sup>a</sup>
Plant sterol (mg/g)	3.31 ± 0.19 <sup>a</sup>	4.87 ± 0.45 <sup>b</sup>	1.02 ± 0.07 <sup>c</sup>	1.37 ± 0.09 <sup>c</sup>	0.805 ± 0.053 <sup>c</sup>
Percentage of total sterol	19.4 ± 0.3 <sup>a</sup>	33.0 ± 1.0 <sup>b</sup>	9.33 ± 0.38 <sup>c</sup>	14.0 ± 0.4 <sup>d</sup>	5.74 ± 0.38 <sup>c</sup>

Data are the mean ± SE of six rats per group. Different *superscript letters* show significant differences among plant sterols at  $P < 0.05$  in the Tukey–Kramer test. The percentage of total sterol is the amount of the respective plant sterol to the sum of the plant sterols and cholesterol

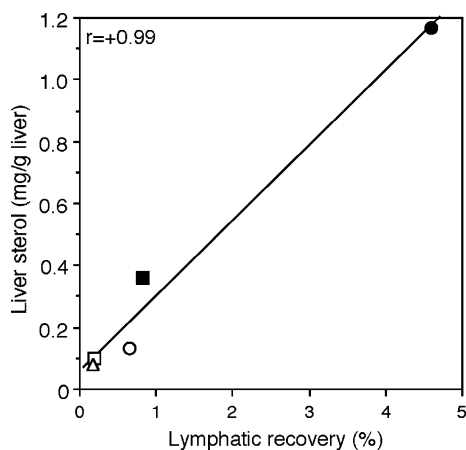


**Fig. 3** Correlation between lymphatic recovery of plant sterols and their levels in liver in SHRSP. *Open circle* brassicasterol, *filled circle* campesterol, *open square* stigmasterol, *filled square* sitosterol, *triangle* sitostanol. When the data for campesterol were omitted, the correlation coefficient between lymphatic recovery of plant sterols and their levels in liver was  $r = 0.84$  ( $P = 0.16$ )

the sterol levels in liver ( $r = 0.99$ ,  $P < 0.01$ ). The levels of plant sterols in plasma ( $r = 0.95$ ,  $P < 0.05$ ), adipose tissue ( $r = 0.99$ ,  $P < 0.01$ ) and heart ( $r = 0.99$ ,  $P < 0.01$ ) were also significantly correlated to the

lymphatic recovery, whereas those of adrenals were not significantly correlated ( $r = 0.86$ ,  $P = 0.06$ ). Since it was thought that correlations between lymphatic recovery of plant sterols and their levels in plasma and various tissues were biased by the data for campesterol, we also calculated correlation coefficients when the data for campesterol were omitted. The correlation coefficients were  $r = 0.69$  ( $P = 0.31$ ) in plasma,  $r = 0.84$  ( $P = 0.16$ ) in liver,  $r = 0.93$  ( $P = 0.07$ ) in adipose tissue,  $r = 0.91$  ( $P = 0.08$ ) in heart and  $r = 0.55$  ( $P = 0.45$ ) in adrenals, respectively.

## Discussion

The present study clearly showed that lymphatic recoveries and deposition in the body of various plant sterols were remarkably different from each other in SHRSP. Lymphatic recovery of campesterol was the highest and was 27 times higher than that of sitostanol, the least absorbable sterol. Lymphatic recovery of stigmasterol was also extremely low and comparable to that of sitostanol. Brassicasterol and sitosterol were about 4–5 times more absorbable than stigmasterol and sitostanol. We observed the same tendency of

differential absorption rates of plant sterols in Wistar rats, which have no mutation in *Abcg5* [7]; therefore, we can conclude that a mutation in *Abcg5* of SHRSP does not largely influence the differential absorption of the various plant sterols examined.

Our previous study showed that both the micellar solubility of plant sterols and their affinity for the bile salt micelle are important determinants for their intestinal absorption in Wistar rats [7]. The affinity of plant sterols for the bile salt micelle was assessed as sterol transfer from the bile salt micelle to triolein [7, 21]. If a sterol has a high affinity for the bile salt micelle, its transfer to the oil becomes low. Highly positive correlation ( $r = 0.88$ ,  $P < 0.05$ ) was observed between the lymphatic recovery of plant sterols and the multiplication product of their micellar solubility and the transfer rate [7]. In the present study, differential absorption of plant sterols in SHRSP was similar to that in normal Wistar rats. We calculated the correlation coefficient between the lymphatic recovery of plant sterols in SHRSP and the multiplication product of their micellar solubility and the transfer rate obtained in our previous study [7]. Again, highly positive correlation ( $r = 0.88$ ,  $P < 0.05$ ) was observed. The correlation coefficient between the lymphatic recovery rates of various plant sterols in SHRSP in the present study and in Wistar rats obtained in our previous study [7] was  $r = 0.995$ ,  $P < 0.001$ . The results strongly suggest that even in SHRSP, micellar solubility of plant sterols and their affinity for the bile salt micelle are important determinants for their differential absorption in the intestine. Yu et al. [12] reported that in *ABCG5*-/*ABCG8*-deficient mice, campesterol was more absorbable than sitosterol and suggested that differential absorption of plant sterols is largely independent of *ABCG5* and *ABCG8*. Our results support their observation.

Although Igel et al. [11] proposed that plant sterols are unselectively incorporated into the intestinal mucosal cells, we propose in the present study that less absorbable sterols are incorporated less into the intestinal mucosal cell. We think that the ability of secretion of various plant sterols from the intestinal cell to the intestinal lumen in SHRSP must be lowered at the same rate as in normal rats, because the pattern of differential absorption of plant sterols was similar between SHRSP and Wistar rats.

Altmann et al. [22] and Davis et al. [23] reported that Niemann-Pick C1 like 1 protein (NPC1L1) is involved in intestinal uptake of cholesterol and plant sterols. NPC1L1 contributes to about half of the intestinal absorption of cholesterol and plant sterols, because about half of the sterols are absorbed in

NPC1L1-deficient mice compared with wild-type mice [22, 23]. In addition, Yu et al. [24] showed that the administration of ezetimibe, a potential inhibitor of NPC1L1, to normal mice reduced the intestinal absorption of campesterol and sitosterol roughly to a half. The results suggest the possibility that NPC1L1 participates in differential incorporation of plant sterols into the intestinal cell. To clarify the role of NPC1L1 on differential absorption of plant sterols, intestinal absorption of various plant sterols should be measured in normal rats given ezetimibe or in NPC1L1-deficient mice.

Sterols are incorporated into enterocytes as their unesterified form and then they are subjected to esterification by microsomal acylcoenzyme A:cholesterol acyltransferase (ACAT) [25]. This process appears to be important for intestinal sterol absorption because esterification of absorbed sterols within the enterocyte promotes simple diffusion of unesterified sterols by maintaining their concentration gradient between the intestinal lumen and the intestinal cell [25]. In our previous study, about 80–90% of absorbed cholesterol was esterified in lymph, whereas the amount of sitosterol esterified was around 10% in rats [21]. Low absorbability of sitosterol is in part explained by less esterification by ACAT [26]. In the present study, although campesterol, the most absorbable plant sterol, showed the highest esterification rate among the plant sterols examined, the lymphatic absorption of the other plant sterols does not necessarily follow their esterification rates. For example, the esterification of sitostanol in lymph was almost the same as that of sitosterol (nearly 16%), whereas the absorbability of sitostanol (0.17%) was one fifth of that of sitosterol (0.83%). In addition, although the esterification of brassicasterol (28%) was about twice as high as that of sitosterol (16%), the absorbability of brassicasterol (0.64%) was almost comparable to that of sitosterol (0.83%) (Table 1). Therefore, there is no positive correlation between esterification rate and lymphatic recovery of less absorbable plant sterols, i.e., brassicasterol, stigmasterol, sitosterol and sitostanol. The results suggest that esterification of less absorbable plant sterols is not a determinant for their intestinal absorption.

In the present study, the percentages of the plant sterol esters in the liver were lower than those in plasma as shown in Table 2 and those in lymph as shown in Table 1. It is thought that absorbed plant sterols are partly esterified and incorporated into chylomicrons in the intestinal cell, secreted to lymph and then transported to the bloodstream. Chylomicrons are transformed to chylomicron remnants in the

bloodstream and are then incorporated into the liver. Since it is thought that plant sterol esters contained in chylomicrons and chylomicron remnants are not hydrolyzed in the bloodstream, plant sterol esters in chylomicrons are incorporated into the liver. There are some possibilities for the causes of the low esterification rates of plant sterols in the liver. One possibility is that plant sterol esters in chylomicron remnants are hydrolyzed in the liver and plant sterols are utilized as membrane components and substrates for bile acid synthesis, at least in SHRSP. There is a possibility that plant sterols incorporated into the cell membrane widely influence membrane functions. When SHRSP were fed a high plant sterol diet, stroke was induced at an early stage and their life span was shortened [14, 15]. Ratnayake et al. [15] suggested that plant sterols made the cell membrane more rigid in SHRSP and shortened the life span of SHRSP. It is also known that plant sterols are minor substrates for bile acid synthesis in rats [4, 27]. Another possibility is that plant sterol esters are preferentially secreted to plasma as very low density lipoproteins, and therefore the levels of plant sterol esters in plasma were higher than those in liver. The plant sterol esters are thought to be transported to extrahepatic tissues. It has been suggested that some plant sterols are utilized as substrates for steroid hormone synthesis [28, 29]. Since studies on the influence of plant sterols deposited in the body are scarce, SHRSP may be an appropriate model for those studies.

As we previously observed [13], the depositions of campesterol and sitosterol in SHRSP having a mutation in *Abcg5* were estimated to be higher than those in normal rats, because campesterol and sitosterol constituted 38 and 20% of total sterols in the plasma and 30 and 14% in the liver, respectively (Table 2). In contrast, the depositions of brassicasterol, stigmasterol and sitostanol were comparatively lower than those of campesterol and sitosterol. In the present study, significant positive correlations were observed between lymphatic recoveries of five types of plant sterols and their depositions in tissues examined, except for adrenals. It is thought that the positive correlations observed are biased by a high level of campesterol. Therefore, we calculated the correlations without the data for campesterol. Relatively high positive correlations were also found between lymphatic recoveries of plant sterols and their levels in liver, adipose tissue and heart even when the data for campesterol were omitted. These results suggest that intestinal absorption rates of plant sterols may be an important determinant for their deposition in the body.

Our results showed that deposition of brassicasterol in adrenals was relatively higher than that in other tissues and organs. The causes of the specific deposition of brassicasterol in adrenals cannot be explained at present. It is also not clear if the deposition is specific in SHRSP. Since it has been reported that the side chain of campesterol and sitosterol is cleaved by adrenal side chain cleavage enzyme and transformed into pregnenolone [28], brassicasterol may also be a substrate for steroid hormone. Yang et al. [30] suggested the possibility for the inhibition of cholesterol synthesis by specific plant sterols, campesterol, stigmasterol and brassicasterol, in the adrenal glands of *ABCG5*-/*ABCG8*-deficient mice; therefore, the deposition of brassicasterol in adrenals might influence steroid hormone synthesis. Further investigation is necessary to clarify the safety and functions of plant sterols accumulated in the body.

## References

1. Katan MB, Grundy SM, Jones P, Law M, Miettinen T, Paoletti R (2003) Efficacy and safety of plant stanols and sterols in the management of blood cholesterol levels. *Mayo Clin Proc* 78:965–978
2. Heinemann T, Axtmann G, Bergmann K (1993) Comparison of intestinal absorption of cholesterol with different plant sterols in man. *Eur J Clin Invest* 23:827–831
3. Connor WE, Lin DS (1981) Absorption and transport of shellfish sterols in human subjects. *Gastroenterology* 81:276–284
4. Ikeda I, Sugano M (1978) Comparison of absorption and metabolism of  $\beta$ -sitosterol and  $\beta$ -sitostanol in rats. *Atherosclerosis* 30:227–237
5. Vahouny GV, Connor WE, Subramaniam S, Lin DS, Gallo LL (1983) Comparative lymphatic absorption of sitosterol, stigmasterol, and fucosterol and differential inhibition of cholesterol absorption. *Am J Clin Nutr* 37:805–809
6. Vahouny GV, Connor WE, Roy T, Lin DS, Gallo LL (1981) Lymphatic absorption of shellfish sterols and their effects on cholesterol absorption. *Am J Clin Nutr* 34:507–513
7. Hamada T, Goto H, Yamahira T, Sugawara T, Imaizumi K, Ikeda I (2006) Solubility in and affinity for the bile salt micelle of plant sterols are important determinants of their intestinal absorption in rats. *Lipids* 41:551–556
8. Berge KE, Tian H, Graf GA, Yu L, Grishin NV, Schultz J, Kwiterovich P, Shan B, Barnes R, Hobbs HH (2000) Accumulation of dietary cholesterol in sitosterolemia caused by mutations in adjacent ABC transporters. *Science* 290:1771–1775
9. Lee MH, Lu K, Hazard S, Yu H, Shulenin S, Hidaka H, Kojima H, Allikmets R, Sakuma N, Pegoraro R, Srivastava AK, Salen G, Dean M, Patel SB (2001) Identification of a gene, *ABCG5*, important in the regulation of dietary cholesterol absorption. *Nature Genet* 27:79–83
10. Lu K, Lee MH, Patel SB (2001) Dietary cholesterol absorption; more than just bile. *Trends Endocrinol Metab* 12:314–320

11. Igel M, Giesa U, Lütjohann D, Bergmann K (2003) Comparison of the intestinal uptake of cholesterol, plant sterols, and stanols in mice. *J Lipid Res* 44:533–538
12. Yu L, Hammer RE, Li-Hawkins J, Bergmann K, Lütjohann D, Cohen JC, Hobbs HH (2002) Disruption of *Abcg5* and *Abcg8* in mice reveals their crucial role in biliary cholesterol secretion. *Proc Natl Acad Sci USA* 99:16237–16242
13. Ikeda I, Nakagiri H, Sugano M, Ohara S, Hamada T, Nonaka M, Imaizumi K (2001) Mechanisms of phytosterolemia in stroke-prone spontaneously hypertensive and WKY rats. *Metabolism* 50:1361–1368
14. Ratnayake WMN, Plouffe L, Hollywood R, L'Abbé MR, Hidioglou N, Sarwar G, Mueller R (2000) Influence of sources of dietary oils on the life span of stroke-prone spontaneously hypertensive rats. *Lipids* 35:409–420
15. Ratnayake WMN, L'Abbé MR, Mueller R, Hayward S, Plouffe L, Hollywood R, Trick K (2000) Vegetable oils high in phytosterols make erythrocytes less deformable and shorten the life span of stroke-prone spontaneously hypertensive rats. *J Nutr* 130:1166–1178
16. Scoggan KA, Gruber H, Lariviere K (2003) A missense mutation in the *Abcg5* gene causes phytosterolemia in SHR, stroke-prone SHR, and WKY rats. *J Lipid Res* 44:911–916
17. Yu H, Pandit B, Klett E, Lee MH, Lu K, Helou K, Ikeda I, Egashira N, Sato M, Klein R, Batta A, Salen G, Patel SB (2003) The rat *STSL* locus: characterization, chromosomal assignment, and genetic variations in sitosterolemic hypertensive rats. *BMC Cardiovasc Disord* 3:4
18. Reeves PG, Nielsen FH, Fahey GC (1993) AIN-93 purified diets for laboratory rodents: final report of the American Institute of Nutrition Ad Hoc Writing Committee on the reformulation of the AIN-76A rodent diet. *J Nutr* 123:1939–1951
19. Ikeda I, Matsuoka R, Hamada T, Mitsui K, Imabayashi S, Uchino A, Sato M, Kuwano E, Itamura T, Yamada K, Tanaka K, Imaizumi K (2002) Cholesterol esterase accelerates intestinal cholesterol absorption. *Biochim Biophys Acta* 1571:34–44
20. Folch J, Lees M, Sloane-Stanley GH (1957) A simple method for the isolation and purification of total lipides from animal tissues. *J Biol Chem* 226:497–509
21. Ikeda I, Tanaka K, Sugano M, Vahouny GV, Gallo LL (1988) Discrimination between cholesterol and sitosterol for absorption in rats. *J Lipid Res* 29:1583–1591
22. Altmann SW, Davis HR, Zhu L, Yao X, Hoos LM, Tetzloff G, Iyer SN, Maguire M, Golovko A, Zeng M, Wang L, Murgolo N, Graziano MP (2004) Niemann-Pick C1 Like 1 protein is critical for intestinal cholesterol absorption. *Science* 303:1201–1204
23. Davis HR, Zhu L, Hoos LM, Tetzloff G, Maguire M, Liu J, Yao X, Iyer SN, Lam M, Lund EG, Detmers PA, Graziano MP, Altmann SW (2004) Niemann-Pick C1 Like 1 (NPC1L1) is the intestinal phytosterol and cholesterol transporter and a key modulator of whole-body cholesterol homeostasis. *J Biol Chem* 279:33586–33592
24. Yu L, Bergmann K, Lütjohann D, Hobbs HH, Cohen JC (2005) Ezetimibe normalizes metabolic defects in mice lacking ABCG5 and ABCG8. *J Lipid Res* 46:1739–1744
25. Ros E (2000) Intestinal absorption of triglyceride and cholesterol. Dietary and pharmacological inhibition to reduce cardiovascular risk. *Atherosclerosis* 151:357–379
26. Field FJ, Mathur SN (1983)  $\beta$ -Sitosterol: esterification by intestinal acylcoenzyme A:cholesterol acyltransferase (ACAT) and its effect on cholesterol esterification. *J Lipid Res* 24:409–417
27. Subbiah MTR, Kuksis A (1973) Differences in metabolism of cholesterol and sitosterol following intravenous injection in rats. *Biochim Biophys Acta* 306:95–105
28. Tuckey RC, Cameron KJ (1993) Side-chain specificities of human and bovine cytochromes *P*-450<sub>SCC</sub>. *Eur J Biochem* 217:209–215
29. Arthur JR, Blair AF, Boyd GS, Mason JI, Suckling KE (1976) Oxidation of cholesterol and cholesterol analogues by mitochondrial preparations of steroid-hormone-producing tissue. *Biochem J* 158:47–51
30. Yang C, Yu L, Li W, Xu F, Cohen JC, Hobbs HH (2004) Disruption of cholesterol homeostasis by plant sterols. *J Clin Invest* 114:813–822

## Altered Lipid Parameters in Hepatic Subcellular Membrane Fractions Induced by Fumonisin B<sub>1</sub>

H.-M. Burger · S. Abel · P. W. Snijman ·  
S. Swanevelder · W. C. A. Gelderblom

Received: 1 August 2006 / Accepted: 16 December 2006 / Published online: 9 February 2007  
© AOCS 2007

**Abstract** Alteration of lipid constituents of cellular membranes has been proposed as a possible mechanism for cancer promotion by fumonisin B<sub>1</sub> (FB<sub>1</sub>). To further investigate this hypothesis a dietary dosage which initiates and promotes liver cancer (250 mg FB<sub>1</sub>/kg) was fed to male Fischer rats for 21 days and the lipid composition of plasma, microsomal, mitochondrial and nuclear subcellular fractions determined. The effect of FB<sub>1</sub> on the cholesterol, phosphatidylcholine (PC) and phosphatidylethanolamine (PE), as well as sphingomyelin (SM) and the phospholipids-associated fatty acid (FA) profiles, were unique for each subcellular membrane fraction. PE was significantly increased in the microsomal, mitochondrial and plasma membrane fractions, whereas cholesterol was increased in both the microsomal and nuclear fraction. In

addition SM was decreased and increased in the mitochondrial and nuclear fractions, respectively. The decreased PC/PE and polyunsaturated/saturated (P/S) FA ratio in the different membrane fractions suggest a more rigid membrane structure. The decreased levels in polyunsaturated fatty acids in PC together with a pronounced increase in C18:1 $\omega$ 9 and C18:2 $\omega$ 6 were indicative of an impaired delta-6 desaturase. The increased  $\omega$ 6/ $\omega$ 3 ratio and decreased C20:4 $\omega$ 6 PC/PE ratio due to an increase in C20:4 $\omega$ 6 in PE relatively to PC in the different subcellular fractions suggests a shift towards prostanoid synthesis of the E2 series. Changes in the PE and C20:4 $\omega$ 6 parameters in the plasma membrane could alter key growth regulatory and/or other cell receptors in lipid rafts known to be altered by FB<sub>1</sub>. An interactive role between C20:4 $\omega$ 6 and ceramide in the mitochondria, is suggested to regulate the balance between proliferation and apoptosis in altered initiated hepatocytes resulting in their selective outgrowth during cancer promotion effected by FB<sub>1</sub>.

H.-M. Burger (✉) · S. Abel · W. C. A. Gelderblom  
PROMEC Unit, Medical Research Council,  
P.O. Box 19070, Tygerberg 7505, South Africa  
e-mail: hester.burger@mrc.ac.za

S. Swanevelder  
Biostatistics Unit, Medical Research Council,  
P.O. Box 19070, Tygerberg 7505, South Africa

P. W. Snijman  
Department of Chemistry and Polymer Science,  
Physical Chemistry, University of Stellenbosch,  
Private Bag X1, Matieland 7602, South Africa

W. C. A. Gelderblom  
Department of Biochemistry, University of Stellenbosch,  
Private Bag X1, Matieland 7602, South Africa

**Keywords** Fumonisin B<sub>1</sub> · Microsomes · Mitochondria · Plasma membrane · Nuclei · Phospholipids · Fatty acids · Cholesterol · Sphingomyelin · Hepatocarcinogenesis

### Introduction

The structure, function and integrity of biological membranes are governed by the lipid composition of its bilayer [1–3]. Membranes show an asymmetric bilayer of aminophospholipids, such as phosphatidylethanolamine (PE) and phosphatidylserine located in the inner leaflet, whereas phosphatidylcholine (PC)

and the sphingolipid, sphingomyelin (SM), are located in the outer leaflet [4, 5]. The membrane structure and dynamics are important in maintaining cellular function that regulates signalling pathways related to cellular homeostasis [6, 7]. The role of cellular membranes during carcinogenesis has become more prominent and forms a part of subtle changes underlying epigenetic events [8, 9]. Isolated membrane fractions from tumour cells demonstrated alterations in their composition, structure and organization and thus in their functional properties [10, 11].

Fumonisin B<sub>1</sub> (FB<sub>1</sub>), a natural occurring mycotoxin with cancer promoting properties produced by the fungus *Fusarium verticillioides* in maize [12]. FB<sub>1</sub> causes several diseases in animals and is associated with a high incidence of human oesophageal and liver cancer in certain geographical areas in the world [13, 14], and the development of neural tube defects [15]. FB<sub>1</sub> is hepatotoxic and hepatocarcinogenic [16, 17] when chronically fed to rats and effects both cancer initiation and promotion properties in a short-term rat liver carcinogenesis model [18, 19]. This model provides an excellent opportunity to study the mechanisms associated with cancer induction by this “apparent” non-genotoxic compound as it lacks genotoxicity in the *Salmonella* mutagen and DNA repair assays [20–22]. However, FB<sub>1</sub> induces oxidative damage [23] and exhibited clastogenic properties [24], suggesting that the compound could either directly or indirectly, induce DNA damage. Short-term studies utilizing a cancer initiating/promoting model in rat liver indicated that FB<sub>1</sub> closely mimics the characteristics of other genotoxic carcinogens with respect to initiation [18]. With respect to cancer promotion, evidence supports a hypothesis that FB<sub>1</sub> effects a growth differential, during which initiated hepatocytes proliferate in an environment where the growth of normal cells is inhibited [25]. This became evident as FB<sub>1</sub> inhibits the epidermal growth factor (EGF) stimulatory response in primary hepatocytes in vitro [26] and hepatocyte regeneration following partial hepatectomy in vivo [18] suggesting that FB<sub>1</sub> induces a growth differential similar to most cancer promoters [27, 28].

The disruption of lipid metabolism and the subsequent affect on membrane integrity and function has been proposed as a possible mechanism for cancer promotion by fumonisin B<sub>1</sub> [25, 29, 30]. The present study described the effect of FB<sub>1</sub> on the lipid profiles of different rat hepatic subcellular membrane fractions including the microsomes, mitochondria, plasma membrane and the nuclei. The possible role of these changes during cancer promotion of FB<sub>1</sub> in rat liver is critically evaluated.

## Materials and Methods

### Chemicals and Reagents

Fumonisin B<sub>1</sub> was extracted and purified (>90%) according to the method described by Cawood et al. [31]. Fatty acid (FA) analytical standards (C14:0 to C24:1), used for calibration and identification, were obtained from Sigma Chemical Company (St Louis, MO, USA). All the chemical solvents were of analytical grade and glass distilled prior to use.

### Animals and Diets

Male Fischer rats (150 g body weight) were fed a modified AIN-76 diet after weaning [18] and housed individually in a controlled environment (23–25 °C) with a 12 h light/dark cycle with free access to feed and drinking water. FB<sub>1</sub> was dissolved in methanol prior to application on a subsample (200 g) of the AIN-76A diet and dried overnight. The subsample was mixed with the standard diet to obtain a concentration of 250 mg FB<sub>1</sub>/kg, a dose that both initiates [18] and promotes [19] cancer in rat liver. The diet was stored under nitrogen at 4 °C. A control diet was prepared in the same way using an equal volume of methanol. The control and FB<sub>1</sub>-containing diets were fed to the rats over a 21-day period. Following the feeding regimen, animals were sacrificed under sagatal anaesthesia after which the livers were harvested and stored in saline at –80 °C.

### Preparation of Membrane Subcellular Fractions

Membrane subcellular fractions were isolated at 4 °C according to the method of Bartoli et al. [32] and Loten and Redshaw-Loten [33] with modifications. In short, the livers were homogenized in a buffer containing 250 mM sucrose, 10 mM Tris–HCl, 1 mM EDTA (pH 7.4) and centrifuged at 1,500g for 10 min. Both the supernatant (S1) and the pellet (P1) were retained for further isolation of the different subcellular membrane fractions. The supernatant (S1) was centrifuged at 18,000g for 10 min to obtain the mitochondrial subcellular pellet (P2) whilst the microsomal fraction remained in the supernatant (S2). The microsomal subfractions were subsequently collected from the S2 fraction by ultra centrifugation at 105,000g for 60 min. The mitochondrial and microsomal subcellular fractions were suspended in 10 mM Tris–HCl buffer (pH 7.4) and centrifuged at 18,000g for 10 min and 105,000g for 30 min, respectively. All the subcellular fractions were stored at –80 °C until analysed.

Liver nuclear and plasma membrane subcellular fractions were prepared by fractionating the pellet (P1) on a self-forming Percoll (Sigma Chemical Co., St Louis, MO, USA) gradient by centrifugation at 35,000g for 20 min. By retaining the top layer and applying another Percoll gradient (45,000g for 30 min), the subsequent top and bottom layers, respectively, yielded the plasma membrane and nuclear fractions. The collected fractions were centrifuged in 10 mM Tris–HCl buffer and stored at  $-80^{\circ}\text{C}$  prior to analysis. The protein concentration of the different fractions was determined according to the method of Kaushal and Barnes [34].

### Lipid Analyses

The different subcellular membrane fractions were subjected to detailed lipid analysis; these included PC, PE, SM, total cholesterol and FA profiles of PC and PE. In short, the different subcellular fractions (1–2 mg protein/ml) were extracted with chloroform/methanol (2:1, v/v) containing 0.01% butylated hydroxytoluene as anti-oxidant [35, 36] and stored under nitrogen until analysed.

The sample extracts were analysed for cholesterol and subsequently for phospholipids by thin layer chromatography on  $20 \times 20$  silica plates [37] using chloroform–methanol–petroleum ether–acetic acid–boric acid (40:20:30:10:1.8, v/v/v/v/w) as developing solvent. Plates were developed for 90 min at room temperature followed by drying under  $\text{N}_2$  gas for 30 min, and the respective phospholipid concentrations and FA content determined.

### Phospholipids and Cholesterol

The phospholipid concentrations were quantified colourimetrically with malachite green dye [38] following digestion in saturated perchloric acid at  $170^{\circ}\text{C}$  for approximately 1 h. Total cholesterol was determined on aliquots of the original lipid extract by an enzymatic iodide method [39] with cholesterinoxidase and cholesterinesterase (Boehringer Mannheim, South Africa).

### Fatty Acids

The PC and PE fractions were transmethylated with 2.5 ml methanol:18 M sulphuric acid (95:5, v/v) at  $70^{\circ}\text{C}$  for 2 h as described by Tichelaar et al. [40]. The resultant FA methyl esters (FAME) were analysed on a Varian 3700 Gas Chromatograph equipped with 30 m fused silica megabore DB-225 columns of

0.53 mm internal diameter (J & W Scientific, Cat. No. 25-2232). The individual FAME were identified by comparison of the retention times with those of a standard mixture of free FA C14:0 to C24:1 and quantified with an internal standard (C17:0) as  $\mu\text{g}$  FA/mg protein.

### Statistical Analyses

For comparisons to test whether two independent diet groups with normal distributions had the same mean, the *t*-test was used. The pooled method was used if variances were equal, and the Satterthwaite method for unequal variances. Otherwise the non-parametric Wilcoxon Rank Sum test was used to compare the two independent diet groups with numerical observations that were not normally distributed.

## Results

### Cholesterol and Phospholipid Content

The  $\text{FB}_1$  treatment significantly increased the cholesterol content in the microsomal ( $P = 0.0001$ ) and nuclear ( $P = 0.05$ ) subcellular fractions, while no significant differences were observed in the mitochondrial and plasma membrane subcellular fractions. The phospholipid, PC was significantly increased in the microsomal ( $P = 0.003$ ) and decreased in the mitochondrial ( $P = 0.026$ ) fractions, respectively. PE was significantly increased in the microsomal ( $P = 0.0001$ ), mitochondrial ( $P = 0.026$ ), plasma membrane ( $P = 0.048$ ) fractions. The SM content was significantly decreased and increased in the mitochondrial ( $P = 0.013$ ), and nuclear ( $P = 0.01$ ) fractions, respectively, in the  $\text{FB}_1$ -treated rats (Table 1).

### Membrane Lipid Parameters

No significant change in the cholesterol/phospholipid (PC + PE) ratio was observed in any of the fractions of the  $\text{FB}_1$ -treated rats (data not shown). In contrast, a significant decrease in the PC/PE ratio was observed in the microsomal ( $P = 0.005$ ), mitochondrial ( $P = 0.005$ ) subcellular fractions of the  $\text{FB}_1$ -treated rats, mainly due to an increase in the phospholipid, PE (Table 1).

The polyunsaturated/saturated (P/S) FA ratio was significantly decreased in PC of the microsomal ( $P = 0.039$ ); mitochondria ( $P = 0.024$ ) and plasma membrane ( $P = 0.015$ ) fraction. In PE, the P/S ratio was only decreased in mitochondrial ( $P = 0.035$ ) and plasma membrane ( $P = 0.001$ ) fractions.



**Table 1** The effect of FB<sub>1</sub> treatment on the lipid and FA parameters of different membrane subcellular fractions from rat liver

Lipid and FA parameters	Control				FB <sub>1</sub> treated			
	Microsomes	Mitochondria	Plasma membrane	Nuclei	Microsomes	Mitochondria	Plasma membrane	Nuclei
Cholesterol ( $\mu\text{g}/\text{mg}$ protein)	23.53 $\pm$ 1.53	30.24 $\pm$ 3.22	34.03 $\pm$ 5.60	2.76 $\pm$ 0.82	<b>35.37 <math>\pm</math> 3.48</b> ( <i>P</i> = 0.0001)	31.36 $\pm$ 4.26	37.99 $\pm$ 4.13	<b>8.31 <math>\pm</math> 4.50</b> ( <i>P</i> = 0.05)
PC ( $\mu\text{g}/\text{mg}$ protein)	181.00 $\pm$ 34.50	276.20 $\pm$ 34.10	153.00 $\pm$ 25.90	24.89 $\pm$ 4.55	<b>246.20 <math>\pm</math> 21.50</b> ( <i>P</i> = 0.003)	<b>227.40 <math>\pm</math> 30.40</b> ( <i>P</i> = 0.026)	157.90 $\pm$ 38.10	22.94 $\pm$ 1.67
PE ( $\mu\text{g}/\text{mg}$ protein)	53.10 $\pm$ 9.40	85.10 $\pm$ 9.70	45.60 $\pm$ 12.30	9.70 $\pm$ 0.97	<b>122.80 <math>\pm</math> 13.10</b> ( <i>P</i> = 0.0001)	<b>122.30 <math>\pm</math> 9.50</b> ( <i>P</i> = 0.026)	<b>70.20 <math>\pm</math> 21.20</b> ( <i>P</i> = 0.048)	10.40 $\pm$ 2.31
SM ( $\mu\text{g}/\text{mg}$ protein)	10.80 $\pm$ 2.50	12.90 $\pm$ 2.50	7.40 $\pm$ 3.10	3.25 $\pm$ 0.72	9.80 $\pm$ 3.00	<b>8.80 <math>\pm</math> 2.20</b> ( <i>P</i> = 0.013)	8.10 $\pm$ 2.90	<b>7.95 <math>\pm</math> 2.94</b> ( <i>P</i> = 0.01)
PC/PE	3.23 $\pm$ 0.40	3.11 $\pm$ 0.50	2.80 $\pm$ 1.69	2.77 $\pm$ 0.58	<b>1.92 <math>\pm</math> 0.30</b> ( <i>P</i> = 0.005)	<b>1.76 <math>\pm</math> 0.22</b> ( <i>P</i> = 0.005)	2.24 $\pm$ 0.66	3.35 $\pm$ 0.18
P/S ratio								
PC	1.25 $\pm$ 0.12	1.24 $\pm$ 0.06	1.25 $\pm$ 0.10	1.12 $\pm$ 0.10	<b>1.12 <math>\pm</math> 0.12</b> ( <i>P</i> = 0.039)	<b>1.10 <math>\pm</math> 0.11</b> ( <i>P</i> = 0.024)	<b>1.07 <math>\pm</math> 0.09</b> ( <i>P</i> = 0.015)	1.03 $\pm$ 0.07
PE	1.33 $\pm$ 0.07	1.55 $\pm$ 0.17	1.55 $\pm$ 0.05	1.31 $\pm$ 0.40	1.40 $\pm$ 0.11	<b>1.35 <math>\pm</math> 0.10</b> ( <i>P</i> = 0.035)	<b>1.38 <math>\pm</math> 0.06</b> ( <i>P</i> = 0.001)	1.25 $\pm$ 0.08
PUFA								
PC ( $\mu\text{g}/\text{mg}$ protein)	55.27 $\pm$ 7.03	66.14 $\pm$ 4.00	73.96 $\pm$ 18.31	6.40 $\pm$ 0.70	55.79 $\pm$ 5.02	<b>49.32 <math>\pm</math> 1.50</b> ( <i>P</i> = 0.0001)	<b>50.99 <math>\pm</math> 10.93</b> ( <i>P</i> = 0.05)	<b>5.17 <math>\pm</math> 0.87</b> ( <i>P</i> = 0.04)
PC (% of total FA)	50.81 $\pm$ 1.50	50.52 $\pm$ 0.95	50.43 $\pm$ 2.21	46.60 $\pm$ 2.95	<b>46.21 <math>\pm</math> 1.79</b> ( <i>P</i> = 0.001)	<b>45.81 <math>\pm</math> 1.50</b> ( <i>P</i> = 0.0001)	<b>45.70 <math>\pm</math> 1.69</b> ( <i>P</i> = 0.002)	44.99 $\pm$ 1.50
PE ( $\mu\text{g}/\text{mg}$ protein)	22.56 $\pm$ 4.60	31.35 $\pm$ 6.10	30.31 $\pm$ 5.64	2.42 $\pm$ 0.70	<b>36.45 <math>\pm</math> 5.18</b> ( <i>P</i> = 0.001)	35.32 $\pm$ 3.02	33.20 $\pm$ 8.68	2.61 $\pm$ 0.78
PE (% of total FA)	52.71 $\pm$ 1.09	56.08 $\pm$ 2.40	55.89 $\pm$ 1.14	48.10 $\pm$ 8.04	53.24 $\pm$ 0.79	<b>52.70 <math>\pm</math> 1.23</b> ( <i>P</i> = 0.012)	<b>53.09 <math>\pm</math> 0.84</b> ( <i>P</i> = 0.001)	48.30 $\pm$ 2.86
$\omega 6/\omega 3$ ratio								
PC	23.61 $\pm$ 2.16	24.76 $\pm$ 2.26	21.51 $\pm$ 1.14	24.75 $\pm$ 4.47	27.73 $\pm$ 5.33	28.16 $\pm$ 5.10	<b>27.25 <math>\pm</math> 3.74</b> ( <i>P</i> = 0.01)	29.96 $\pm$ 2.97 ( <i>P</i> = 0.08)
PE	11.15 $\pm$ 1.33	10.57 $\pm$ 1.58	9.86 $\pm$ 1.19	15.62 $\pm$ 4.10	11.51 $\pm$ 2.82	11.12 $\pm$ 2.38	11.57 $\pm$ 2.13	16.63 $\pm$ 3.80
C20:4 $\omega 6$ PC/PE ratio $\mu\text{g}/\text{mg}$ protein	3.01 $\pm$ 0.73	2.66 $\pm$ 0.52	2.49 $\pm$ 1.30	3.20 $\pm$ 1.12	<b>1.64 <math>\pm</math> 0.16</b> ( <i>P</i> = 0.005)	<b>1.49 <math>\pm</math> 0.11</b> ( <i>P</i> = 0.005)	1.75 $\pm$ 0.31 ( <i>P</i> = 0.066)	2.10 $\pm$ 0.33
% of total FA	1.14 $\pm$ 0.04	1.10 $\pm$ 0.10	1.11 $\pm$ 0.06	1.11 $\pm$ 1.17	<b>0.92 <math>\pm</math> 0.05</b> ( <i>P</i> = 0.005)	<b>0.93 <math>\pm</math> 0.06</b> ( <i>P</i> = 0.008)	<b>0.96 <math>\pm</math> 0.10</b> ( <i>P</i> = 0.02)	0.96 $\pm$ 0.06 ( <i>P</i> = 0.09)

Values are means  $\pm$  STD of five determinations. Values in bold, differ significantly (*P* < 0.05) from the corresponding control subcellular fraction (actual *P* values are indicated in brackets)

Quantitatively ( $\mu\text{g FA}/\text{mg protein}$ ), the total PUFA ( $\omega 3$  and  $\omega 6$  PUFA) levels in PC decreased significantly in the mitochondria ( $P = 0.0001$ ); plasma membrane ( $P = 0.05$ ) and nuclear ( $P = 0.04$ ) fraction. In the microsomal fraction the total polyunsaturated fatty acid (PUFA) increased significantly ( $P = 0.001$ ) only in PE. Qualitatively, PUFA (expressed as the % of the total FA) decreased significantly in PC of the microsomal ( $P = 0.001$ ), mitochondrial ( $P = 0.0001$ ) and plasma membrane ( $P = 0.002$ ) subcellular fractions. In PE, PUFA was significantly decreased only the mitochondrial ( $P = 0.012$ ) and plasma membrane ( $P = 0.001$ ) subcellular fractions due to  $\text{FB}_1$  treatment.

The  $\omega 6/\omega 3$  PUFA ratios of the treated rats was significantly increased in the PC fraction of the plasma membrane ( $P = 0.01$ ) and marginally in the nuclei ( $P = 0.08$ ). The 20:4 $\omega 6$  PC/PE ratio was significantly reduced, quantitatively in the microsomal ( $P = 0.005$ ); mitochondrial ( $P = 0.008$ ) and marginally in the plasma membrane ( $P = 0.066$ ) fractions. Qualitatively, the 20:4 $\omega 6$  PC/PE ratio qualitative decreased significantly in the microsomal ( $P = 0.005$ ), mitochondria ( $P = 0.008$ ), plasma membrane ( $P = 0.02$ ) and only

marginally ( $P = 0.09$ ) in the nuclear fraction as a result of the  $\text{FB}_1$  treatment.

### Fatty Acids

Fatty acid profiles of the PE and PC phospholipids fractions of the different subcellular fractions are summarized in Tables 2, 3, 4 and 5. Data from the different subcellular fractions is expressed quantitatively ( $\mu\text{g}/\text{mg protein}$ ) and qualitatively as a percentage (%) of total FA content.

### Saturated Fatty Acid (C16:0 and C18:0)

The  $\text{FB}_1$  treatment significantly increased C16:0 ( $P = 0.023$ ) in the PC phospholipid fraction in the microsomes. The total saturated fatty acid (SFA) content of PE ( $P = 0.002$ ) increased significantly mainly due the increase in both C16:0 ( $P = 0.005$ ) and C18:0 ( $P = 0.002$ ). In the mitochondria, the SFA levels were decreased in PC ( $P = 0.005$ ) due to a significant decrease in C18:0 ( $P = 0.001$ ). In PE, the SFA levels were significantly increased ( $P = 0.001$ ) due to a sig-

**Table 2** Effect of  $\text{FB}_1$  on the SFA profiles of PC and PE phospholipids of different membrane subcellular fractions from rat liver

Subcellular fractions	Control				$\text{FB}_1$ treated			
	PC ( $\mu\text{g}/\text{mg protein}$ )	PC (%)	PE ( $\mu\text{g}/\text{mg protein}$ )	PE (%)	PC ( $\mu\text{g}/\text{mg protein}$ )	PC (%)	PE ( $\mu\text{g}/\text{mg protein}$ )	PE (%)
<b>Microsomes</b>								
C16:0	22.19 $\pm$ 3.06	20.00 $\pm$ 1.97	7.59 $\pm$ 1.21	17.93 $\pm$ 1.48	<b>27.17 <math>\pm</math> 3.36</b> ( $P = 0.023$ )	<b>22.42 <math>\pm</math> 1.38</b> ( $P = 0.033$ )	<b>10.71 <math>\pm</math> 1.79</b> ( $P = 0.005$ )	<b>15.60 <math>\pm</math> 0.57</b> ( $P = 0.015$ )
C18:0	22.02 $\pm$ 4.03	20.13 $\pm$ 1.40	9.22 $\pm$ 1.75	21.60 $\pm$ 1.05	23.11 $\pm$ 4.65	18.92 $\pm$ 2.11	<b>15.71 <math>\pm</math> 3.46</b> ( $P = 0.002$ )	22.69 $\pm$ 2.03
Total	44.20 $\pm$ 4.25	40.13 $\pm$ 1.93	16.81 $\pm$ 2.76	39.54 $\pm$ 1.23	50.28 $\pm$ 7.65	41.34 $\pm$ 2.67	<b>26.42 <math>\pm</math> 5.20</b> ( $P = 0.002$ )	38.28 $\pm$ 2.20
<b>Mitochondria</b>								
C16:0	25.63 $\pm$ 3.12	19.55 $\pm$ 1.64	7.61 $\pm$ 0.86	13.95 $\pm$ 2.70	24.70 $\pm$ 1.56	<b>22.94 <math>\pm</math> 1.42</b> ( $P = 0.003$ )	<b>10.80 <math>\pm</math> 0.54</b> ( $P = 0.001$ )	16.13 $\pm$ 1.01 ( $P = 0.09$ )
C18:0	27.70 $\pm$ 2.80	21.13 $\pm$ 1.50	12.60 $\pm$ 2.90	22.53 $\pm$ 0.71	<b>20.22 <math>\pm</math> 2.90</b> ( $P = 0.001$ )	18.75 $\pm$ 2.40 ( $P = 0.066$ )	<b>15.53 <math>\pm</math> 2.42</b> ( $P = 0.046$ )	23.07 $\pm$ 2.26
Total	53.32 $\pm$ 4.63	40.70 $\pm$ 1.33	20.20 $\pm$ 1.90	36.09 $\pm$ 2.30	<b>44.92 <math>\pm</math> 3.53</b> ( $P = 0.005$ )	41.69 $\pm$ 2.75	<b>26.30 <math>\pm</math> 2.75</b> ( $P = 0.001$ )	39.20 $\pm$ 2.06 ( $P = 0.056$ )
<b>Plasma membrane</b>								
C16:0	26.46 $\pm$ 7.25	8.71 $\pm$ 2.98	7.23 $\pm$ 2.64	13.30 $\pm$ 0.82	23.00 $\pm$ 5.26	21.17 $\pm$ 1.39 ( $P = 0.096$ )	8.94 $\pm$ 1.69	14.70 $\pm$ 1.90
C18:0	32.93 $\pm$ 8.39	22.19 $\pm$ 1.67	12.35 $\pm$ 1.96	23.35 $\pm$ 1.09	24.49 $\pm$ 6.28	21.68 $\pm$ 1.50	15.20 $\pm$ 4.72	23.88 $\pm$ 2.22
Total	59.39 $\pm$ 14.13	40.90 $\pm$ 1.52	19.58 $\pm$ 3.51	36.65 $\pm$ 1.01	48.17 $\pm$ 11.41	42.86 $\pm$ 2.20	24.15 $\pm$ 6.24	<b>38.58 <math>\pm</math> 1.39</b> ( $P = 0.02$ )
<b>Nuclei</b>								
C16:0	2.83 $\pm$ 0.26	20.75 $\pm$ 1.53	0.82 $\pm$ 0.27	17.33 $\pm$ 7.83	2.61 $\pm$ 0.53	22.65 $\pm$ 1.00 ( $P = 0.061$ )	0.95 $\pm$ 0.50	16.88 $\pm$ 4.21
C18:0	2.83 $\pm$ 0.35	20.69 $\pm$ 1.54	1.04 $\pm$ 0.19	21.42 $\pm$ 3.82	2.44 $\pm$ 0.36	21.27 $\pm$ 1.25	1.15 $\pm$ 0.30	21.73 $\pm$ 3.02
Total	5.66 $\pm$ 0.52	41.44 $\pm$ 1.82	1.86 $\pm$ 0.15	38.75 $\pm$ 8.47	5.05 $\pm$ 0.88	43.92 $\pm$ 1.75 ( $P = 0.065$ )	2.84 $\pm$ 0.70	38.61 $\pm$ 2.20

Values are means  $\pm$  STD of five determinations. Values in bold, differ significantly ( $P < 0.05$ ) from the corresponding control subcellular fraction (actual  $P$  values are indicated in brackets). Percentage (%) = % of total FA

**Table 3** The effect of FB<sub>1</sub> on the monounsaturated FA profiles of PC and PE phospholipids of different membrane subcellular fractions from rat liver

Subcellular fraction	Control				FB <sub>1</sub> treated			
	PC (μg/mg protein)	PC (%)	PE (μg/mg protein)	PE (%)	PC (μg/mg protein)	PC (%)	PE (μg/mg protein)	PE (%)
<b>Microsomes</b>								
C16:1	0.40 ± 0.09	0.85 ± 0.19	0.23 ± 0.06	0.56 ± 0.17	<b>1.81 ± 0.81</b> ( <i>P</i> = 0.008)	1.55 ± 0.89	0.27 ± 0.07	0.40 ± 0.15
C18:1	8.87 ± 0.78	8.21 ± 0.85	3.09 ± 0.74	7.20 ± 0.58	<b>13.22 ± 0.66</b> ( <i>P</i> = 0.0001)	<b>10.97 ± 0.64</b> ( <i>P</i> = 0.0001)	<b>5.41 ± 0.34</b> ( <i>P</i> = 0.001)	8.07 ± 1.58
Total	9.27 ± 0.77	9.06 ± 0.75	3.32 ± 0.72	7.76 ± 0.45	<b>15.03 ± 0.55</b> ( <i>P</i> = 0.0001)	<b>12.52 ± 1.38</b> ( <i>P</i> = 0.0003)	<b>5.67 ± 0.29</b> ( <i>P</i> = 0.0001)	8.47 ± 1.65
<b>Mitochondria</b>								
C16:1	0.89 ± 0.20	0.68 ± 0.12	0.19 ± 0.08	0.36 ± 0.16	1.67 ± 1.13	1.55 ± 1.06	0.27 ± 0.11	0.42 ± 0.20
C18:1	10.60 ± 1.02	8.12 ± 0.90	3.95 ± 0.80	7.10 ± 0.44	<b>11.77 ± 0.54</b> ( <i>P</i> = 0.033)	<b>10.94 ± 0.64</b> ( <i>P</i> = 0.0001)	<b>5.11 ± 0.64</b> ( <i>P</i> = 0.019)	7.68 ± 1.23
Total	11.50 ± 1.10	8.80 ± 0.89	4.15 ± 0.80	7.43 ± 0.50	<b>13.44 ± 1.60</b> ( <i>P</i> = 0.032)	<b>12.49 ± 1.60</b> ( <i>P</i> = 0.0005)	<b>5.40 ± 0.70</b> ( <i>P</i> = 0.015)	8.10 ± 1.40
<b>Plasma membrane</b>								
C16:1	0.79 ± 0.37	0.50 ± 0.27	0.25 ± 0.18	0.38 ± 0.32	1.03 ± 0.24	<b>0.98 ± 0.42</b> ( <i>P</i> = 0.037)	0.16 ± 0.09	0.28 ± 0.15
C18:1	11.16 ± 2.43	8.17 ± 1.14	3.74 ± 0.24	7.08 ± 0.52	11.62 ± 2.30	<b>10.46 ± 0.49</b> ( <i>P</i> = 0.001)	4.89 ± 0.92 ( <i>P</i> = 0.08)	8.05 ± 1.19 ( <i>P</i> = 0.096)
Total	11.95 ± 2.64	8.67 ± 1.07	3.99 ± 0.92	7.46 ± 0.62	12.65 ± 2.25	<b>11.44 ± 0.84</b> ( <i>P</i> = 0.0005)	5.05 ± 0.93	8.33 ± 1.26
<b>Nuclei</b>								
C16:1	0.23 ± 0.07	1.66 ± 0.53	0.11 ± 0.09	2.11 ± 1.69	0.15 ± 0.03 ( <i>P</i> = 0.066)	1.27 ± 0.09	0.14 ± 0.11	3.07 ± 2.56
C18:1	1.40 ± 0.40	10.32 ± 3.42	0.56 ± 0.31	11.05 ± 4.39	1.13 ± 0.19	9.83 ± 0.20	0.55 ± 0.34	10.01 ± 3.95
Total	1.62 ± 0.40	11.99 ± 3.41	0.66 ± 0.29	13.16 ± 3.71	1.30 ± 0.22	11.09 ± 0.26	0.70 ± 0.28	13.10 ± 4.26

Values are means ± STD of five determinations. Values in bold, differ significantly (*P* < 0.05) from the corresponding control subcellular fraction (actual *P* values are indicated in brackets). Percentage (%) = % of total FA

nificant increase in both C16:0 (*P* = 0.0001) and C18:0 (*P* = 0.046). Similar patterns were also noticed in the plasma membrane PE and PC fractions although differences were not significant. In the nuclear subcellular fraction no effects were observed.

Qualitatively total SFA in the microsomal fraction of the treated rats were not altered despite a significant decrease and increase of the percentage C16:0 in the PC (*P* = 0.033) and PE (*P* = 0.015) fractions, respectively. In the mitochondrial fraction, the percentage total SFA was marginally increased (*P* = 0.056) due to a marginal increase in C16:0, whereas in the plasma membranes it was significantly increased (*P* = 0.02) in the PE fraction. In the nuclei, C16:0 (*P* = 0.061) and the total SFA marginally (*P* = 0.065) increased in PC.

#### Monounsaturated Fatty Acid (C16:1 and C18:1)

The total monounsaturated fatty acid (MUFA) content of PC and PE was significantly elevated in the microsomal fraction (*P* = 0.0001) due to an increase in C16:1 (*P* = 0.008) and C18:1 (*P* = 0.0001) in PC and C18:1

(*P* = 0.0001) in PE. In the mitochondria, the total MUFA was increased in PC (*P* = 0.032) and PE (*P* = 0.015) due to an increase in C18:1 in PC (*P* = 0.033) and PE (*P* = 0.019) fractions. Only a marginally (*P* = 0.066) decrease of C16:1 was noticed in the nuclear PC. Except for a marginal (*P* = 0.08) increase in C18:1 in PE, no changes was noticed in the plasma membrane in the nuclear fraction.

In the PC fractions, the qualitative levels of the MUFA was significantly increased in the microsomal (*P* = 0.0003), mitochondrial (*P* = 0.0005) and plasma membrane (*P* = 0.0005) subcellular fractions due to an increase in C18 (*P* < 0.001 to *P* < 0.0001). In the plasma membrane fraction C16:1 (*P* = 0.037) was increased in PC. In the PE fraction C18:1 was marginally (*P* = 0.096) increased only in the plasma membrane fraction.

#### Polyunsaturated Fatty Acid

ω6 PUFA: (C18:2, C18:3, C20:3, C20:4, C22:4 and C22:5): In the microsomal subcellular fraction C18:2

**Table 4** FB<sub>1</sub> modulation of the  $\omega$ -6 FA profiles of the PC and PE phospholipids of different membrane subcellular fractions from rat liver

Subcellular fractions	Control					FB <sub>1</sub> treated				
	FA	PC ( $\mu$ g/mg protein)	PC (%)	PE ( $\mu$ g/mg protein)	PE (%)	PC ( $\mu$ g/mg protein)	PC (%)	PE ( $\mu$ g/mg protein)	PE (%)	
Microsomes	C18:2	9.54 $\pm$ 0.40	8.86 $\pm$ 0.92	2.84 $\pm$ 0.76	6.57 $\pm$ 0.64	<b>15.13 <math>\pm</math> 1.77</b> ( <i>P</i> = 0.0004)	<b>12.54 <math>\pm</math> 1.42</b> ( <i>P</i> = 0.0003)	<b>5.20 <math>\pm</math> 0.63</b> ( <i>P</i> = 0.0001)	<b>7.65 <math>\pm</math> 0.85</b> ( <i>P</i> = 0.033)	
	C20:4	36.76 $\pm$ 4.72	33.80 $\pm$ 1.20	12.71 $\pm$ 2.71	29.66 $\pm$ 1.18	32.48 $\pm$ 3.60	<b>26.83 <math>\pm</math> 1.35</b> ( <i>P</i> = 0.0001)	<b>20.06 <math>\pm</math> 3.27</b> ( <i>P</i> = 0.002)	29.23 $\pm$ 0.90	
	C22:4	1.02 $\pm$ 0.11	0.94 $\pm$ 0.06	1.06 $\pm$ 0.19	2.50 $\pm$ 0.11	0.93 $\pm$ 0.07	<b>0.78 <math>\pm</math> 0.11</b> ( <i>P</i> = 0.009)	<b>1.73 <math>\pm</math> 0.13</b> ( <i>P</i> = 0.0001)	2.56 $\pm$ 0.36	
	C22:5	4.84 $\pm$ 1.40	4.38 $\pm$ 0.76	3.80 $\pm$ 0.76	8.98 $\pm$ 1.37	4.17 $\pm$ 0.78	<b>3.43 <math>\pm</math> 0.41</b> ( <i>P</i> = 0.023)	<b>6.08 <math>\pm</math> 1.10</b> ( <i>P</i> = 0.002)	8.83 $\pm$ 0.05	
	Total	53.00 $\pm$ 6.65	48.74 $\pm$ 1.41	20.68 $\pm$ 4.20	48.33 $\pm$ 1.26	53.81 $\pm$ 5.00	<b>44.50 <math>\pm</math> 1.62</b> ( <i>P</i> = 0.001)	<b>33.44 <math>\pm</math> 4.92</b> ( <i>P</i> = 0.001)	48.83 $\pm$ 1.06	
Mitochondria	C18:2	11.35 $\pm$ 1.0	8.68 $\pm$ 0.80	3.71 $\pm$ 0.81	6.64 $\pm$ 0.70	<b>13.39 <math>\pm</math> 1.35</b> ( <i>P</i> = 0.014)	<b>12.45 <math>\pm</math> 1.39</b> ( <i>P</i> = 0.0002)	<b>4.80 <math>\pm</math> 0.17</b> ( <i>P</i> = 0.022)	<b>7.21 <math>\pm</math> 0.75</b> ( <i>P</i> = 0.022)	
	C20:4	44.63 $\pm$ 2.96	34.09 $\pm$ 1.20	17.33 $\pm$ 3.65	30.98 $\pm$ 1.88	<b>28.82 <math>\pm</math> 1.60</b> ( <i>P</i> = 0.0001)	<b>26.80 <math>\pm</math> 1.27</b> ( <i>P</i> = 0.0001)	<b>19.35 <math>\pm</math> 1.32</b> ( <i>P</i> = 0.0001)	<b>28.89 <math>\pm</math> 0.06</b> ( <i>P</i> = 0.041)	
	C22:4	1.20 $\pm$ 0.10	0.91 $\pm$ 0.05	1.52 $\pm$ 0.37	2.72 $\pm$ 0.38	<b>0.83 <math>\pm</math> 0.11</b> ( <i>P</i> = 0.0001)	<b>0.77 <math>\pm</math> 0.11</b> ( <i>P</i> = 0.015)	1.60 $\pm$ 0.20	2.41 $\pm$ 0.35	
	C22:5	5.40 $\pm$ 1.10	4.11 $\pm$ 0.74	5.59 $\pm$ 1.10	10.04 $\pm$ 1.42	<b>3.13 <math>\pm</math> 0.45</b> ( <i>P</i> = 0.004)	<b>3.34 <math>\pm</math> 0.36</b> ( <i>P</i> = 0.044)	6.17 $\pm$ 1.24	9.15 $\pm$ 1.16	
	Total	63.56 $\pm$ 3.91	48.55 $\pm$ 0.85	28.61 $\pm$ 5.62	51.16 $\pm$ 2.20	<b>47.58 <math>\pm</math> 1.43</b> ( <i>P</i> = 0.0001)	<b>44.19 <math>\pm</math> 1.40</b> ( <i>P</i> = 0.0001)	32.29 $\pm$ 2.42	<b>48.21 <math>\pm</math> 0.62</b> ( <i>P</i> = 0.02)	
Plasma Membrane	C18:2	11.95 $\pm$ 2.93	8.33 $\pm$ 0.56	3.56 $\pm$ 0.78	6.66 $\pm$ 0.58	12.64 $\pm$ 2.86	<b>11.38 <math>\pm</math> 1.19</b> ( <i>P</i> = 0.0002)	4.56 $\pm$ 0.96	7.44 $\pm$ 0.68 ( <i>P</i> = 0.056)	
	C20:4	49.50 $\pm$ 12.98	33.73 $\pm$ 1.83	16.38 $\pm$ 3.17	30.32 $\pm$ 0.76	<b>31.08 <math>\pm</math> 7.04</b> ( <i>P</i> = 0.02)	<b>27.78 <math>\pm</math> 1.58</b> ( <i>P</i> = 0.0001)	18.32 $\pm$ 5.17	29.18 $\pm$ 1.65	
	C22:4	1.47 $\pm$ 0.40	0.97 $\pm$ 0.10	1.57 $\pm$ 0.31	2.91 $\pm$ 0.14	<b>0.90 <math>\pm</math> 0.19</b> ( <i>P</i> = 0.02)	<b>0.82 <math>\pm</math> 0.15</b> ( <i>P</i> = 0.075)	1.62 $\pm$ 0.39	<b>2.61 <math>\pm</math> 0.11</b> ( <i>P</i> = 0.003)	
	C22:5	6.51 $\pm$ 1.29	4.41 $\pm$ 0.94	5.50 $\pm$ 0.85	10.00 $\pm$ 1.28	<b>3.59 <math>\pm</math> 0.85</b> ( <i>P</i> = 0.003)	<b>3.21 <math>\pm</math> 0.37</b> ( <i>P</i> = 0.016)	5.77 $\pm$ 1.65	9.15 $\pm$ 0.79	
	Total	70.65 $\pm$ 17.42	48.20 $\pm$ 2.00	27.48 $\pm$ 5.07	50.71 $\pm$ 0.77	<b>49.16 <math>\pm</math> 10.55</b> ( <i>P</i> = 0.05)	<b>44.05 <math>\pm</math> 1.57</b> ( <i>P</i> = 0.002)	30.52 $\pm$ 8.13	<b>48.76 <math>\pm</math> 1.41</b> ( <i>P</i> = 0.014)	
Nuclei	C18:2	1.36 $\pm$ 0.30	10.03 $\pm$ 2.21	0.47 $\pm$ 0.37	8.96 $\pm$ 5.52	1.27 $\pm$ 0.20	11.09 $\pm$ 1.01	0.54 $\pm$ 0.37	9.25 $\pm$ 3.60	
	C20:4	4.11 $\pm$ 0.70	30.04 $\pm$ 4.25	1.40 $\pm$ 0.46	27.95 $\pm$ 7.40	<b>2.95 <math>\pm</math> 0.50</b> ( <i>P</i> = 0.22)	25.70 $\pm$ 0.35 ( <i>P</i> = 0.054)	1.30 $\pm$ 0.36	24.51 $\pm$ 4.40	
	C22:4	0.08 $\pm$ 0.01	0.62 $\pm$ 0.11	0.10 $\pm$ 0.03	1.79 $\pm$ 0.48	0.14 $\pm$ 0.06	<b>1.15 <math>\pm</math> 0.29</b> ( <i>P</i> = 0.003)	<b>0.20 <math>\pm</math> 0.05</b> ( <i>P</i> = 0.001)	<b>3.83 <math>\pm</math> 1.10</b> ( <i>P</i> = 0.002)	
	C22:5	0.46 $\pm$ 0.11	3.36 $\pm$ 0.66	0.30 $\pm$ 0.20	5.80 $\pm$ 3.75	0.56 $\pm$ 0.11	<b>4.85 <math>\pm</math> 0.75</b> ( <i>P</i> = 0.011)	0.40 $\pm$ 0.15	7.34 $\pm$ 0.96	
	Total	6.11 $\pm$ 0.64	44.70 $\pm$ 2.70	2.26 $\pm$ 0.63	44.99 $\pm$ 7.35	<b>5.01 <math>\pm</math> 0.84</b> ( <i>P</i> = 0.044)	43.52 $\pm$ 1.54 ( <i>P</i> = 0.089)	2.46 $\pm$ 0.76	45.44 $\pm$ 3.16	

Values are means  $\pm$  STD of five determinations. Values in bold, differ significantly (*P* < 0.05) from the corresponding control subcellular fraction (actual *P* values are indicated in brackets). Percentage (%) = % of total FA

**Table 5** FB<sub>1</sub> modulation of the  $\omega$ -3 FA profiles of the PC and PE phospholipids of different membrane subcellular fractions from rat liver

Subcellular fractions	Control				FB <sub>1</sub> treated			
	PC ( $\mu$ g/mg protein)	PC (%)	PE ( $\mu$ g/mg protein)	PE (%)	PC ( $\mu$ g/mg protein)	PC (%)	PE ( $\mu$ g/mg protein)	PE (%)
<b>Microsomes</b>								
C22:5	0.19 $\pm$ 0.04	0.17 $\pm$ 0.03	0.14 $\pm$ 0.06	0.33 $\pm$ 0.09	<b>0.14 <math>\pm</math> 0.01</b> ( <i>P</i> = 0.019)	<b>0.12 <math>\pm</math> 0.02</b> ( <i>P</i> = 0.004)	<b>0.23 <math>\pm</math> 0.05</b> ( <i>P</i> = 0.033)	0.34 $\pm$ 0.10
C22:6	1.97 $\pm$ 0.40	1.80 $\pm$ 0.20	1.68 $\pm$ 0.38	3.92 $\pm$ 0.40	1.71 $\pm$ 0.33	<b>1.42 <math>\pm</math> 0.27</b> ( <i>P</i> = 0.018)	<b>2.66 <math>\pm</math> 0.66</b> ( <i>P</i> = 0.01)	3.90 $\pm$ 0.76
Total	2.27 $\pm$ 0.42	2.08 $\pm$ 0.21	1.88 $\pm$ 0.45	4.38 $\pm$ 0.46	1.99 $\pm$ 0.34	<b>1.65 <math>\pm</math> 0.29</b> ( <i>P</i> = 0.014)	<b>3.00 <math>\pm</math> 0.67</b> ( <i>P</i> = 0.006)	4.41 $\pm$ 0.82
<b>Mitochondria</b>								
C22:5	0.22 $\pm$ 0.04	0.17 $\pm$ 0.03	0.22 $\pm$ 0.07	0.40 $\pm$ 0.10	<b>0.13 <math>\pm</math> 0.04</b> ( <i>P</i> = 0.002)	0.12 $\pm$ 0.04	0.23 $\pm$ 0.04	0.34 $\pm$ 0.08
C22:6	2.22 $\pm$ 0.23	1.70 $\pm$ 0.20	2.44 $\pm$ 0.50	4.39 $\pm$ 0.57	<b>1.48 <math>\pm</math> 0.28</b> ( <i>P</i> = 0.0005)	<b>1.37 <math>\pm</math> 0.27</b> ( <i>P</i> = 0.038)	2.70 $\pm$ 0.80	4.00 $\pm$ 1.00
Total	2.58 $\pm$ 0.22	1.97 $\pm$ 0.19	2.74 $\pm$ 0.60	4.92 $\pm$ 0.70	<b>1.73 <math>\pm</math> 0.29</b> ( <i>P</i> = 0.0002)	<b>1.61 <math>\pm</math> 0.28</b> ( <i>P</i> = 0.027)	3.03 $\pm$ 0.80	4.50 $\pm$ 0.92
<b>Plasma membrane</b>								
C22:5	0.28 $\pm$ 0.10	0.18 $\pm$ 0.04	0.22 $\pm$ 0.05	0.42 $\pm$ 0.08	<b>0.14 <math>\pm</math> 0.03</b> ( <i>P</i> = 0.05)	<b>0.13 <math>\pm</math> 0.03</b> ( <i>P</i> = 0.032)	0.18 $\pm$ 0.03	<b>0.29 <math>\pm</math> 0.06</b> ( <i>P</i> = 0.012)
C22:6	2.73 $\pm$ 0.75	1.80 $\pm$ 0.27	2.37 $\pm$ 0.48	4.31 $\pm$ 0.54	<b>1.46 <math>\pm</math> 0.38</b> ( <i>P</i> = 0.009)	<b>1.31 <math>\pm</math> 0.20</b> ( <i>P</i> = 0.005)	2.34 $\pm$ 0.66	3.77 $\pm$ 0.75
Total	3.31 $\pm$ 0.92	2.23 $\pm$ 0.23	2.83 $\pm$ 0.63	5.17 $\pm$ 0.61	<b>1.83 <math>\pm</math> 0.45</b> ( <i>P</i> = 0.012)	<b>1.65 <math>\pm</math> 0.25</b> ( <i>P</i> = 0.002)	2.68 $\pm$ 0.70	4.33 $\pm$ 0.70 ( <i>P</i> = 0.051)
<b>Nuclei</b>								
C22:5	0.02 $\pm$ 0.01	0.12 $\pm$ 0.04	0.02 $\pm$ 0.02	0.32 $\pm$ 0.36	0.01 $\pm$ 0.01	0.13 $\pm$ 0.05	0.02 $\pm$ 0.01	0.32 $\pm$ 0.17
C22:6	0.18 $\pm$ 0.03	1.32 $\pm$ 0.21	0.12 $\pm$ 0.06	2.43.09	<b>0.13 <math>\pm</math> 0.03</b> ( <i>P</i> = 0.046)	1.16 $\pm$ 0.07	0.11 $\pm$ 0.04	2.05 $\pm$ 0.58
Total	0.26 $\pm$ 0.06	1.86 $\pm$ 0.40	0.16 $\pm$ 0.06	3.11 $\pm$ 1.11	<b>0.17 <math>\pm</math> 0.04</b> ( <i>P</i> = 0.041)	1.46 $\pm$ 0.12	0.15 $\pm$ 0.03	2.86 $\pm$ 0.67

Values are means  $\pm$  STD of five determinations. Values in bold, differ significantly (*P* < 0.05) from the corresponding control subcellular fraction in controls (actual *P* values are indicated in brackets). Percentage (%) = % of total FA

was significantly increased (*P* = 0.0004) in the PC fraction. The total  $\omega$ 6 PUFA content in the PE fraction was significantly (*P* = 0.001) increased due to a significant increase in the levels of C18:2 (*P* = 0.0001), C20:4 (*P* = 0.002), C22:4 (*P* = 0.0001) and C22:5 (*P* = 0.002).

In the mitochondria, the total  $\omega$ 6 PUFA content was significantly reduced in PC (*P* = 0.0001) due to a decrease in C20:4 (*P* = 0.0001), C22:4 (*P* = 0.0001) and C22:5 (*P* = 0.004) despite the fact that C18:2 (*P* = 0.014) increased. Except for a significant increase in C18:2 (*P* = 0.022), no other changes were noticed with respect to the PE fraction. In the plasma membrane PC, the total  $\omega$ 6 PUFA content was marginally (*P* = 0.05) decreased due to a decrease in C20:4 (*P* = 0.02), C22:4 (*P* = 0.02) and C22:5 (*P* = 0.003). In the nuclei, the total  $\omega$ 6 FA was decreased significantly in PC (*P* = 0.044) due to a decrease in C20:4 (*P* = 0.022). In PE, C22:4 (*P* = 0.001) increased significantly. Due to the low levels of C18:3 and C20:3 it was not included in Table 4 however; they were included in determining the total PUFA values.

Qualitatively the total  $\omega$ 6 PUFA decreased significantly (*P* < 0.005) in PC in the microsomal, mitochondrial and plasma membrane fractions due to a significant (*P* < 0.05) decrease in the long-chain  $\omega$ 6 PUFA (C20:4; C22:4 and C22:5), in spite of significant increases in C18:2 in the microsomes (*P* = 0.0003), mitochondria (*P* = 0.0002) and plasma membrane (*P* = 0.0002) fractions. In the nuclei the total  $\omega$ 6 PUFA only decreased marginally (*P* = 0.089) due to a marginal (*P* = 0.054) and significant (*P* = 0.011) decrease in C20:4 and C22:5, respectively, while C22:4 significantly (*P* = 0.003) increased. The total  $\omega$ 6 PUFA in the PE fraction was decreased significantly in the mitochondrial (*P* = 0.02) and plasma membrane (*P* = 0.014) fractions due to a decrease in the level of C20:4 (*P* = 0.041) and C22:4 (*P* = 0.003), respectively. C18:2 was significantly increased in both the microsomal fraction (*P* = 0.033) as well as the mitochondrial fraction (*P* = 0.022) and marginally in the plasma membrane (*P* = 0.056). In the nuclear fraction, only C22:4 (*P* = 0.002) was increased.

$\omega$ 3 PUFA: (C22:5, C22:6): The total  $\omega$ 3 FA in PC significantly decreased quantitatively in the mitochondrial ( $P = 0.0001$ ) and plasma membrane ( $P = 0.012$ ) due to a decrease in both C22:5 and C22:6 ( $P < 0.05$ ). In the microsomes, only C22:5 was significantly ( $P = 0.019$ ) decreased while in the nuclear fraction, the total  $\omega$ 3 FA decreased significantly ( $P = 0.041$ ) due to a decrease ( $P = 0.046$ ) in C22:6. In the microsomal PE the total  $\omega$ 3 FA ( $P = 0.006$ ) significantly increased due to an increase in C22:5 ( $P = 0.033$ ) and C22:6 ( $P = 0.01$ ).

Qualitatively the total  $\omega$ 3 PUFA decreased significantly in PC in the microsomal ( $P = 0.014$ ), mitochondria ( $P = 0.027$ ) and plasma membrane ( $P = 0.002$ ) fractions. This is due to a significant decrease in both C22:5 and C22:6 in the microsomal (C22:5,  $P = 0.004$ ; C22:6,  $P = 0.018$ ), mitochondria (C22:6,  $P = 0.038$ ) and plasma membrane (C22:5,  $P = 0.032$ ; C22:6,  $P = 0.005$ ) fractions. The total  $\omega$ 3 FA in the PE fraction, was marginally decreased ( $P = 0.051$ ) in the plasma membrane subcellular fraction due to a decrease in C22:5 ( $P = 0.012$ ). No changes were observed in PE for any of the other subcellular fractions.

## Discussion

FB<sub>1</sub> disrupts sphingolipid, phospholipids, FA and cholesterol metabolism in the liver and kidneys of different animal species. The disruption of the critical balance between proliferation and apoptosis by these different lipid parameters has been associated with cancer promotion by FB<sub>1</sub> in the liver and kidney of rats [25, 41]. However, it is unclear how changes in the lipid components of the different subcellular membrane fractions could create a growth differential in the liver that selectively stimulate the outgrowth of initiated cells. The current model and FB<sub>1</sub>-dose used promotes cancer in the liver [19] while a similar dose over a period of 5 weeks induces hepatocellular carcinoma in Fischer 344 rats [17].

Alterations to lipid components in the liver are associated with changes in membrane fluidity reflected by changes in the cholesterol/phospholipid (PC + PE) ratio, PC/PE and P/S ratios [42–44]. In the present study, the PC/PE ratio fluidity indicator, decreased significantly in the microsomal and mitochondrial subcellular fractions, mainly due to a significant increase in PE. The P/S ratio was decreased in PC from the microsomal, mitochondrial and plasma membrane subcellular membrane fractions and in PE in the mitochondrial and plasma membrane subcellular frac-

tions due to a significant decrease and increase in the qualitative levels of PUFA and SFA, respectively. Changes in these lipid parameters, which differ depending on the subcellular fraction, are likely to alter membrane fluidity. A reduction in the PC/PE and P/S ratios is associated with a more rigid membrane structure [42, 43], which could adversely affect many critical biological processes occurring at the membrane. Although the cholesterol/phospholipid (PC + PE) ratio was not altered significantly in the present study, the cholesterol was increased in the microsomal and nuclear membrane fraction, which will further increase the rigidity of the membrane structure as it stabilizes the fatty acyl groups [45].

Regarding the maintenance of cellular homeostasis, the organization of lipids and proteins into specialized clusters or microdomains on the outer leaflet in the plasma membrane is of importance. These microdomains, including lipid rafts and caveolae, are enriched with SM, cholesterol, C20:4 $\omega$ 6-containing plasmalogen ethanolamine and glycolipids serve as platforms for vesicular trafficking and the initiation and regulation of cell signalling processes [46, 47]. Many different growth factor receptors, including the endothelin, EGF, insulin receptor, insulin-like growth factor, platelet-derived growth factor, tumour necrosis factor (TNF) and folic acid receptor are lodged in lipid rafts/caveolae [48–51]. Lipid rafts/caveolae-associated signalling events affected by FB<sub>1</sub>, include the inhibition of folate receptor-mediated vitamin uptake [52], increased expression of TNF- $\alpha$ , TNF receptor-1, TNF-related apoptosis-induced ligand [53] and the inhibition of the EGF-induced mitogenic response [25]. The effect of FB<sub>1</sub> on these signalling processes has been related to the disruption of membrane integrity involving alterations in the sphingolipid [52, 53], cholesterol, phospholipid and FA metabolism [54]. Although, the plasma membrane concentrations of SM and cholesterol were not altered, the P/S ratio and PUFA were significantly reduced suggesting, as discussed above, a more rigid membrane structure, likely to affect membrane receptor and enzyme responses. The  $\omega$ 6/ $\omega$ 3 ratio was also increased due to a decrease in  $\omega$ 3 PUFA in PC which will impact on the prostaglandin synthesis by directing prostanoids synthesis more towards the E2-series associated with sustained cell proliferation [55]. In this regard the C20:4 $\omega$ 6 PC/PE ratio was significantly decreased, possibly due to the FB<sub>1</sub>-induced increase in the concentration of PE and the decrease in C20:4 $\omega$ 6 in PC. The increased level of C20:4 $\omega$ 6 in PE relative to PC has been implied as an important growth stimulus in hepatocyte nodules [44]. Changes in the content of C20:4 $\omega$ 6-enriched ethanolamine plasmalogens could

also be important during raft-mediated receptor responses and should be further investigated.

Changes to the major lipid parameters in the microsomal membrane fraction are similar to that reported previously [14]. Altered lipid parameters are known to impact on the activity of membrane enzymes relating to the synthesis of proteins, lipids and sterols [56]. The activity of cytochrome P450 isozymes [57], ceramide synthase [58], and the delta-6 desaturase [14] has been reported to be inhibited by FB<sub>1</sub>. Although FB<sub>1</sub> increased the level of cholesterol in the rat liver microsomal membrane fraction [14] the effect on 3-hydroxy-3-methylglutaryl coenzyme A reductase, the rate-limiting enzyme in endogenous cholesterol biosynthesis, has not been elucidated. The level of SM was not altered in the microsomal membrane fraction, which is in agreement with a previous report [24].

In the mitochondrial subcellular fraction, the PC/PE ratio was significantly reduced due to a decrease and increase in PC and PE, respectively. Disruption of the typical asymmetric lipid distribution of cell membranes could impact negatively on important physiological processes such as the induction of apoptosis [59]. In addition to the changes in PC and PE, SM was also reduced, presumably due to the disruption of the de novo sphingolipid biosynthesis by FB<sub>1</sub>. In this regard the presence of both ceramide synthase and ceramide has been observed in the mitochondrial membrane fraction [60, 61]. Ceramide regulates the generation of reactive oxygen species and the activation of mitochondrial apoptosis via several mechanisms, including glutathione peroxidase depletion and increased lipid peroxidation [62]. One of these mechanisms involves the down regulation of Bcl-2, an anti-apoptotic protein, which leads to the opening of the mitochondrial permeability transition pores (PTP) and apoptosis. Resistance to mitochondrial PTP opening is responsible for the promotion of initiated cells and an important event in the 2-acetylaminofluorene-induced hepatocarcinogenesis [63]. A moderate increase in lipid peroxidation was noticed in rat liver mitochondria after a dietary exposure of 250 mg FB<sub>1</sub>/kg [22], which could be related to the disruption of ceramide synthase.

It is unclear whether the depletion of ceramide in the mitochondria of altered hepatocytes is related to the cancer promoting properties of FB<sub>1</sub>. However, it was suggested that FB<sub>1</sub>-induced apoptosis may be due to the inhibition of ceramide synthase resulting in the depletion of ceramide and other complex sphingolipids and the accumulation of sphinganine and sphingosine [41, 64]. Cells sensitive to the proliferative effects of decreased ceramide and increased sphingosine 1-phosphate may have a selective growth advantage.

Although the liver is not normally a proliferative organ, it seems likely that the disruption of lipid and sphingolipid metabolism in the mitochondria by FB<sub>1</sub> could result in the impairment of apoptosis in the altered hepatocytes. The differential effect of FB<sub>1</sub> on mitochondrial oxidative damage in normal and initiated hepatocytes, therefore, could play an important role in their altered growth pattern. It has been postulated that, depending on the cell type, the disruptive effect of FB<sub>1</sub> on the sphingolipid metabolism, i.e. a decrease in ceramide and increased sphingosine 1-phosphate, will either favour proliferation or induce cell death [41, 65]. A recent study indicated that sphingosine accumulates in FB<sub>1</sub>-induced hepatocyte nodules suggesting it may be involved in the enhanced growth characteristics of these lesions via the formation of sphingosine 1-phosphate [66].

Lipid metabolism in the nuclear membrane fraction is considered to play an important role in signalling events that occur in this cellular compartment [67]. The effect of FB<sub>1</sub> on nuclear-associated membrane enzymes regarding lipid metabolism has not been established. In the present study the nuclear membrane fraction behaved very similarly to the microsomes regarding the increase in cholesterol with the exception that SM also increased. The presence of an SM cycle has been established in the rat liver nuclei [67], however the increase in SM in the nuclei due to FB<sub>1</sub> is unknown. As it was reported that similar levels of cholesterol and SM occur in the rat liver nuclei [67], the increase in SM could result from the corresponding increase in cholesterol. This increase and decrease of SM in the nuclei and mitochondria, respectively, could also explain why the level of SM was not affected by FB<sub>1</sub>-exposure when analysing whole liver [29]. The decrease in both  $\omega$ 3 and  $\omega$ 6 PUFA in the PC fraction could be due to an increase in lipid peroxidation in rat liver nuclei [23]. FB<sub>1</sub>-induced peroxidation of the membrane lipids was reported to induce oxidative DNA damage in isolated liver nuclei [68].

When considering the FA parameters, the observed changes differ for each subcellular membrane fraction as a result of the FB<sub>1</sub> exposure. Apart from the relative increase and decrease in SFA and PUFA, respectively, the total MUFA were moderately to significantly increased in PC and PE in the different subcellular fractions, except for the nuclear fraction. Of interest is the increase in C18:1 $\omega$ 9, the most abundant MUFA in membranes [69], which is associated with the modulation of the function of membrane-bound proteins in normal cells [1]. In addition, the increased in MUFA, specifically C18:1 $\omega$ 9 and C18:2 $\omega$ 6 is associated with the disruption of the delta-6 desaturase enzyme known to

be inhibited by  $FB_1$  [30]. The resultant increase in MUFA could also be due to an increase in delta-9 desaturase as observed in tumour growth in mouse mammary carcinoma cells [70], hepatoma cells [71], human leukemia and lymphoma cells [72]. The growth of mammary carcinogenesis in vitro was blocked by the addition of an inhibitor of delta-9 desaturase [73]. It is not known at present whether  $FB_1$  affects the activity of delta-9 desaturase. As C18:1 $\omega$ 9 is suggested to exhibit anti-oxidative properties [74] the accumulation thereof is likely to protect against the increased lipid peroxidation induced by  $FB_1$  in rat liver and subcellular fractions [74, 75]. The significant reduction in PUFA in most of the subcellular fractions indicated that apart from the inhibition of the delta-6 desaturase, the  $FB_1$ -induced lipid peroxidation also impacted on the status of the long chained FA such as C22:5 $\omega$ 6 and C20:6 $\omega$ 3. The increase lipid peroxidation and the resultant lipid breakdown products, especially in the nuclei, could be important in the cancer initiating properties of  $FB_1$  and in determining the extent of necrotic and/or apoptotic cell death.

Arachidonic acid (C20:4 $\omega$ 6) has been associated with the growth regulatory effects of  $FB_1$  in primary hepatocytes and cancer cells [24, 76]. It was hypothesized that the increase of C20:4 $\omega$ 6 in the PE phospholipids fraction together with the decrease of long-chain PUFA and associated low levels of lipid peroxidation are early events in the neoplastic transformation of hepatic nodules [44]. In the present study the C20:4 $\omega$ 6 PC/PE ratio was decreased in all the subcellular membrane fractions, due to an increased level of C20:4 $\omega$ 6 in PE. The importance of C20:4 $\omega$ 6 is further highlighted by the dual effect it has on cell proliferation or apoptosis via the formation of prostanoids or ceramide, respectively [77–79]. Recently a member of the phospholipase  $A_2$  ( $PLA_2$ ) enzyme-family, the type VI calcium-dependent  $iPLA_2$ , involved in C20:4 $\omega$ 6-generation and associated with C20:4 $\omega$ 6-induced apoptosis, was detected in close proximity of cyclooxygenase-2 (COX-2) in the mitochondria [80]. It has also been shown that  $FB_1$  stimulates cytoplasmic  $PLA_2$  activity, resulting in an increase in C20:4 $\omega$ 6 and its metabolites [81]. The suppression of apoptosis seems to be related to the conversion of C20:4 $\omega$ 6 to prostanoids by two isoforms of the enzyme COX, shown to be overexpressed in numerous human neoplasms [82]. In this regard the elevated expression of these COX isoform enzymes could be responsible for reduced availability for ceramide generation via the sphingomyelinase pathway [79]. The current study indicated that SM synthesis is also impaired by  $FB_1$  in the mitochondria through the inhibition of ceramide synthase.

The interaction between COX-2,  $PLA_2$  and ceramide synthase play a determining role in the regulation of apoptosis and cell proliferation during  $FB_1$  exposure. Therefore, the differential regulation of C20:4 $\omega$ 6 and ceramide levels in normal and altered hepatocytes are likely to be important determinants in the selective stimulation of preneoplastic lesion in the liver by  $FB_1$ .

**Acknowledgments** The authors wish to thank the Nutritional Intervention Research Unit for the use of their laboratory and gas-chromatography equipment. With thanks also to Johanna van Wyk for conducting the gas-chromatography analysis as well as Amelia Damons and John Moketary for washing and cleaning all the glassware. This project was funded by the Medical Research Council of South Africa and the National Research Foundation. Grant no FA2005032200026.

## References

1. Funari SS, Barceló F, Escribá PV (2003) Effects of oleic acid and its congeners, elaidic and stearic acids, on the structural properties of phosphatidylethanolamine membranes. *J Lipid Res* 44:567–575
2. Gudi S, Nolan JP, Frangos JA (1998) Modulation of GTPase activity of G proteins by fluid shear stress and phospholipid composition. *Proc Natl Acad Sci* 95:2515–2519
3. Fuller N, Rand RP (2001) The influence of lysolipids on the spontaneous curvature and bending elasticity of phospholipid membranes. *Biophys J* 81:243–254
4. Emoto K, Umeda M (2000) An essential role for a membrane lipid in cytokinesis: regulation of contractile ring disassembly by redistribution of phosphatidylethanolamine. *J Cell Biol* 149:1215–1224
5. Nyholm TKM, Nylund M, Slotte JP (2003) A calorimetric study of binary mixtures of dihydrosphingomyelin and sterols, sphingomyelin, or phosphatidylcholine. *Biophys J* 48:3138–3146
6. Brown RE (1998) Sphingolipid organization in biomembranes: what physical studies of model membranes reveal. *J Cell Sci* 111:1–9
7. Eriksson LC, Andersson GN (1992) Membrane biochemistry and chemical hepatocarcinogenesis. *Crit Rev Biochem Mol Biol* 27:1–55
8. Weisburger JH, Wynder EL (1984) The role of genotoxic carcinogens and of promoters in carcinogenesis and in human cancer causation. *Acta Pharmacol Toxicol (Copenh)* 55:53–68
9. Stern RG, Milestone BN, Gatenby RA (1999) Carcinogenesis and the plasma membrane. *Med Hypotheses* 52:367–372
10. Galeotti T, Borrello S, Minotti G, Masotti L (1986) Membrane alterations in cancer cells: the role of oxy radicals. *Ann NY Acad Sci* 488:468–480
11. Burns CP, Spector AA (1994) Biochemical effects of lipids on cancer therapy. *J Nutr Biochem* 5:114–123
12. Gelderblom WCA, Jaskiewicz K, Marasas WFO, Thiel PG, Horak MJ, Vlegaar R, Kriek NPJ (1988) Fumonisin—novel mycotoxin with cancer promoting activity produced by *Fusarium moniliforme*. *Appl Environ Microb* 54:1806–1811
13. Rheeder JP, Marasas WFO, Thiel PG, Sydenham EW, Shephard GS, Van Schalkwyk DJ (1992) *Fusarium moniliforme* and fumonisin in corn in relation to oesophageal cancer in Transkei. *Phytopathology* 82:353–357



14. Ueno Y, Iijima K, Wang SD, Sugiura Y, Sekijima M, Tanaka T, Chen C, Yu SZ (1997) Fumonisin as a possible contributory risk factor for primary liver cancer: a 3-year study of corn harvested in Haimen, China, by HPLC and ELISA. *Food Chem Toxicol* 35:1143–1150
15. Marasas WFO, Riley RT, Hendricks KA, Stevens VL, Sadler TW, Gelineau-van Waes J, Missmer SA, Cabrera J, Torres O, Gelderblom WCA, Allegood J, Martínez C, Maddox J, Miller JD, Starr L, Sullards MC, Roman AV, Voss KA, Wang E, Merrill AH (2004) Fumonisin disrupt sphingolipid metabolism, folate transport, and neural tube development in embryo culture and in vivo: a potential risk factor for human neural tube defects among populations consuming fumonisin-contaminated maize. *J Nutr* 134:711–716
16. Gelderblom WCA, Kriek NPJ, Marasas WFO, Thiel PG (1991) Toxicity and carcinogenicity of the *Fusarium moniliforme* metabolite, fumonisin B<sub>1</sub>, in rats. *Carcinogenesis* 12:1247–1251
17. Lemmer ER, Vessey CJ, Gelderblom WCA, Shephard EG, Van Schalkwyk DJ, Rochelle DJ, Van Wijk A, Marasas WFO, Kirsch RE, Hall P (2004) Fumonisin B<sub>1</sub>-induced hepatocellular and cholangiocellular tumors in male Fischer 344 rats: potentiating effects of 2-acetylaminofluorene on oval cell proliferation and neoplastic development in a discontinued feeding study. *Carcinogenesis* 25:1–8
18. Gelderblom WCA, Cawood ME, Snyman SD, Marasas WFO (1994) Fumonisin B<sub>1</sub> dosimetry in relation to cancer initiation in rat liver. *Carcinogenesis* 15:209–214
19. Gelderblom WCA, Snyman SD, Lebepe-Mazur S, van der Westhuizen L, Kriek NPJ, Marasas WFO (1996) The cancer promoting potential of fumonisin B<sub>1</sub> in rat liver using diethylnitrosamine as cancer initiator. *Cancer Lett* 109:101–108
20. Knasmueller S, Bresgen N, Kassie F, Merch-Sundermann V, Gelderblom WCA, Zohrer E, Eckl PM (1997) Genotoxic effects of three *Fusarium* mycotoxins, fumonisin B<sub>1</sub>, moniliformin and vomitoxin in bacteria and in primary rat hepatocytes. *Mutat Res* 391:39–48
21. Gelderblom WCA, Snyman SD (1991) Mutagenicity of potentially carcinogenic mycotoxins produced by *Fusarium moniliforme*. *Mycol Res* 7:46–52
22. Norred WP, Plattner RD, Vesonder RF, Bacon CW, Voss KA (1992) Effects of selected secondary metabolites of *Fusarium moniliforme* on unscheduled synthesis of DNA by rat primary hepatocytes. *Food Chem Toxicol* 30:233–237
23. Abel S, Gelderblom WCA (1998) Oxidative damage and fumonisin B<sub>1</sub>-induced toxicity in primary rat hepatocytes and rat liver in vivo. *Toxicology* 131:121–131
24. Ehrlich V, Darroudi F, Uhl M, Steinkellner H, Zsivkovits M, Knasmueller S (2002) Fumonisin B<sub>1</sub> is genotoxic in human derived hepatoma (HepG2) cells. *Mutagenesis* 17:257–260
25. Gelderblom WCA, Abel S, Smuts CM, Marnewick J, Marasas WFO, Lemmer ER, Ramljak D (2001) Fumonisin-induced hepatocarcinogenesis: mechanisms related to cancer initiation and promotion. *Environ Health Perspect* 109:291–300
26. Gelderblom WCA, Snyman SD, Van der Westhuizen L, Marasas WFO (1995) Mitoinhibitory effect of fumonisin B<sub>1</sub> on rat hepatocytes in primary culture. *Carcinogenesis* 16:625–631
27. Tsuda H, Lee G, Faber E (1981) Induction of resistant hepatocytes as a new principle for possible short-term *in vivo* test for carcinogens. *Cancer Res* 41:2096–2102
28. Faber E (1991) Clonal adaptation as an important phase of hepatocarcinogenesis. *Cancer Biochem Biophys* 12:157–165
29. Gelderblom WCA, Smuts CM, Abel S, Snyman SD, Van der Westhuizen L, Huber WW, Swanevelder S (1997) The effect of fumonisin B<sub>1</sub> on the levels and fatty acid composition of selected lipids in rat liver *in vivo*. *Food Chem Toxicol* 35:647–656
30. Gelderblom WCA, Moritz W, Swanevelder S, Smuts CM, Abel S (2002) Lipids and delta 6-desaturase activity alterations in rat liver microsomal membranes induced by fumonisin B<sub>1</sub>. *Lipids* 37:869–877
31. Cawood ME, Gelderblom WCA, Vleggaar R, Behrend Y, Thiel PG, Marasas WFO (1991) Isolation of the fumonisin mycotoxins: a quantitative approach. *J Agric Food Chem* 39:1958–1962
32. Bartoli GM, Bartoli S, Galeotti T, Bertoli E (1980) Superoxide dismutase content and microsomal lipid composition of tumours with different growth rates. *Biochim Biophys Acta* 620:205–211
33. Loten EG, Redshaw-Loten JC (1986) Preparation of rat liver plasma membranes in a high yield. *Anal Biochem* 154:183–185
34. Kaushal V, Barnes LD (1986) Effect of zwitterionic buffers on measurement of small masses of protein with bicinechonic acid. *Anal Biochem* 157:291–294
35. Folch J, Lees M, Stanley GHS (1957) A simple method for the isolation and purification of total lipids from animal tissues. *J Biol Chem* 226:497–509
36. Smuts CM, Weich HFH, Weight MJ, Faber M, Kruger M, Lombard CJ, Benadé AJ (1994) Free cholesterol concentrations in the high-density Lipoprotein subfraction-3 as a risk indicator in patients with angiographically documented coronary artery disease. *Coron Artery Dis* 5:331–338
37. Gilfillan AM, Chu AJ, Smart DA, Rooney SA (1983) Single plate separation of lung phospholipids including disaturated phosphatidylcholine. *J Lipid Res* 24:1651–1656
38. Itaya K, Ui M (1966) A new micromethod for the colorimetric determination of inorganic phosphate. *Clin Chim Acta* 14:361–366
39. Richmond W (1973) Preparation and properties of a cholesterol oxidase from *Nocardia* sp. and its application to the enzymatic assay of total cholesterol in serum. *Clin Chem* 19:1350–1356
40. Tichelaar HY, Benadé AJ, Daubitzer AK, Kotze TJ (1989) An improved rapid thin-layer chromatographic-gas-liquid chromatographic procedure for the determination of free fatty acids in plasma. *Clin Chim Acta* 183:207–216
41. Riley RT, Enongene E, Voss KA, Norred WP, Meredith FI, Sharma RP, Williams DE, Carlson DB, Spitsbergen J, Merrill AH Jr (2001) Sphingolipid perturbations as mechanisms for fumonisin carcinogenesis. *Environ Health Perspect* 109:301–308
42. Mahler SM, Wilce A, Shanley BC (1988) Studies on regenerating liver and hepatoma plasma membranes—I. Lipid and protein composition. *Int J Biochem* 20:605–611
43. Mahler SM, Wilce A, Shanley BC (1988) Studies on regenerating liver and hepatoma plasma membranes—II. Membrane fluidity and enzyme activity. *Int J Biochem* 20:613–619
44. Abel S, Smuts CM, De Villiers C, Gelderblom WCA (2001) Changes in essential fatty acid patterns associated with normal liver regeneration and the progression of hepatocyte nodules in rat hepatocarcinogenesis. *Carcinogenesis* 22:795–804
45. Ohvo-Rekila H, Ramstedt B, Leppimäki P, Slotte JP (2002) Cholesterol interaction with phospholipids in membranes. *Prog Lipid Res* 41:66–97
46. Sehgal PB, Guo GG, Shah M, Kumar V, Patel K (2002) Cytokine Signaling: STATS in plasma membrane rafts. *J Biol Chem* 277:12067–12074
47. Pike LJ (2003) Lipid rafts: bringing order to chaos. *J Lipid Res* 44:655–667

48. Huo H, Guo X, Hong S, Jiang M, Liu X, Liao K (2003) Lipid rafts/caveolae are essential for insulin-like growth factor-1 receptor signaling during 3T3-L1 preadipocyte differentiation induction. *J Biol Chem* 278:11561–11569
49. Pike LJ (2005) Growth factor receptors, lipid rafts and caveolae: an evolving story. *Biochim Biophys Acta* 1746:260–273
50. Cottin V, Doan JES, Riches DWH (2002) Restricted localization of the TNF receptor CD120a to lipid rafts: a novel role for the death domain. *J Immunol* 168:4095–4102
51. Kamen BA, Smith AK (2004) A review of folate receptor alpha cycling and 5-methyltetrahydrofolate accumulation with an emphasis on cell models in vitro. *Adv Drug Deliv Rev* 56:1085–1097
52. Stevens VL, Tang J (1997) Fumonisin B<sub>1</sub>-induced sphingolipid depletion inhibits vitamin uptake via the glycosylphosphatidylinositol-anchored folate receptor. *J Biol Chem* 272:18020–18025
53. He Q, Kim J, Sharma RP (2005) Fumonisin B<sub>1</sub> hepatotoxicity in mice is attenuated by depletion of Kupffer cells by gadolinium chloride. *Toxicology* 207:137–147
54. Gelderblom WC, Abel S, Smuts CM, Swanevelder S, Snyman SD (1999) Regulation of fatty acid biosynthesis as a possible mechanism for the mitoinhibitory effect of fumonisin B<sub>1</sub> in primary rat hepatocytes. *Prostaglandins Leukot Essent Fatty Acids* 61:225–234
55. Bagga D, Wang L, Farias-Eisner R, Glaspy JA, Reddy ST (2003) Differential effects of prostaglandin derived from w6 and w3 polyunsaturated fatty acids on COX-2 expression and IL-6 secretion. *Proc Natl Acad Sci USA* 100:1751–1756
56. Pahl HL (1999) Signal transduction from the endoplasmic reticulum to the cell nucleus. *Physiol Rev* 79:683–701
57. Spotti M, Maas RFM, De Nijs CM, Fink-Gremmels J (2000) Effect of fumonisin B<sub>1</sub> on rat hepatic P450 system. *Environ Toxicol Pharmacol* 8:197–204
58. Wang E, Norred WP, Bacon CW, Riley RT, Merrill AH Jr (1991) Inhibition of sphingolipid biosynthesis by fumonisins: implications for disease associated with *Fusarium Moniliforme*. *J Biol Chem* 266:14486–14490
59. Bevers EM, Comfurius P, Dekkers DWC, Zwaal RFE (1999) Lipid translocation across the plasma membrane of mammalian cells. *Biochem Biophys Acta* 1439:317–330
60. Ardail D, Popa I, Alcantara K, Pons A, Zanetta JP, Louisot P, Thomas L, Portoukalian J (2001) Occurrence of ceramides and neutral glycolipids with unusual long-chain base composition in purified rat liver mitochondria. *FEBS Lett*, 488:160–164
61. Bionda C, Portoukalian J, Schmitt D, Rodriguez-Lafresse C, Ardail D (2004) Subcellular compartmentalization of ceramide metabolism: MAM (mitochondria-associated membrane) and/or mitochondria? *Biochem J* 382:527–533
62. Won JS, Singh I (2006) Sphingolipid signaling and redox regulation. *Free Rad Biol Med* 40:1875–1888
63. Klöhn PC, Soriano ME, Irwin W, Penzo D, Scorrano L, Bitsch A, Neumann H-G, Bernardi P (2003) Early resistance to cell death and to onset of the mitochondrial permeability transition during hepatocarcinogenesis with 2-acetylaminofluorene. *Proc Natl Acad Sci USA* 100:10014–10019
64. Dragan YP, Bidlack WR, Cohen SM, Goldsworthy TL, Hard GC, Howard PC, Riley RT, Voss KA (2001) Implications of apoptosis for toxicity, carcinogenicity, and risk assessment: fumonisin B<sub>1</sub> as an example. *Toxicol Sci* 61:6–17
65. Lemmer ER, Hall PDM, Gelderblom WCA, Marasas WFO (1998) Poor reporting of oocyte apoptosis. *Nat Med* 4:373
66. Van der Westhuizen L, Gelderblom WCA, Shephard GS, Swanevelder S (2004) Disruption of sphingolipid biosynthesis in hepatocyte nodules: selective proliferative stimulus induced by fumonisin B<sub>1</sub>. *Toxicology* 200:69–75
67. Ledeen RW, Wu G (2004) Nuclear lipids: key signaling effectors in the nervous system and other tissues. *J Lipid Res* 45:1–8
68. Sahu AC, Epply RM, Page SW, Gray GG, Barton CN, O'Donnell MW (1998) Peroxidation of membrane lipids and oxidative DNA damage by fumonisin B<sub>1</sub> in isolated rat liver nuclei. *Cancer Lett* 125:117–121
69. Pala V, Krogh V, Muti P, Chajès V, Riboli E, Micheli A, Saadatian M, Sieri S, Berrino F (2001) Erythrocyte membrane fatty acids and subsequent breast cancer: a prospective Italian study. *J Natl Cancer Inst* 93:1088–1095
70. Lu J, Pei H, Kaeck M, Thompson HJ (1997) Gene expression changes associated with chemically induced rat mammary carcinogenesis. *Mol Carcinog* 20:204–215
71. De Alaniz MJ, Marra CA (1994) Role of delta 9-desaturase activity in the maintenance of high levels of monoenoic fatty acids in hepatoma cultured cells. *Mol Cell Biochem* 137:85–90
72. Marzo I, Martinez-Lorenzo MJ, Anel A, Desportes P, Alava MA, Naval J, Pineiro A (1995) Biosynthesis of unsaturated fatty acids in the main cell lineages of human leukemia and lymphoma. *Biochim Biophys Acta* 1257:140–148
73. Khoo DE, Fermor B, Miller J, Wood CB, Apostolov K, Barker W, Williamson RC, Habib NA (1991) Manipulation of body fat composition with stercularic acid can inhibit mammary carcinomas in vivo. *Br J Cancer* 63:97–101
74. Diplock AT, Balasubramanian KA, Manohar M, Mathan VI, Ashton D (1988) Purification and chemical characterization of the inhibitor of lipid peroxidation from intestinal mucosa. *Biochim Biophys Acta* 926:42–50
75. Abel S, De Kock M, Smuts CM, De Villiers C, Swanevelder S, Gelderblom WCA (2004) Dietary modulation of fatty acid profiles and oxidative status of rat hepatocyte nodules: effect of different n – 6/n – 3 fatty acid ratios. *Lipids* 39:963–976
76. Seegers JC, Joubert AM, Panzer A, Lottering ML, Jordan CA, Joubert F, Maree JL, Bianchi P, De Kock M, Gelderblom WCA (2000) Fumonisin B<sub>1</sub> influenced the effects of arachidonic acid, prostaglandins E<sub>2</sub> and A<sub>2</sub> on cell cycle progression, apoptosis induction, tyrosine- and CDC2-kinase activity in oesophageal cancer cells. *Prostaglandins Leukot Essent Fatty Acids* 62:75–84
77. Tapiero H, Ba GN, Couvreur P, Tew KD (2002) Polyunsaturated fatty acids (PUFA) and eicosanoids in human health and pathologies. *Biomed Pharmacother* 56:215–222
78. Cao Y, Pearman AT, Zimmerman GA, McUntyre TM, Prescott SM (2000) Intracellular unesterified arachidonic acid signals apoptosis. *Proc Natl Acad Sci USA* 97:11280–11285
79. Zhao S, Du XY, Chai MQ, Chen JS, Zhou YC, Song JG (2002) Secretory phospholipase A<sub>2</sub> induces apoptosis via a mechanism involving ceramide generation. *Biochem Biophys Acta* 1581:75–88
80. Liou JY, Aleksic N, Chen SF, Han TJ, Shyue SK, Wu KK (2005) Mitochondrial localization of cyclooxygenase-2 and calcium-independent phospholipase A<sub>2</sub> in human cancer cells: implication in apoptosis resistance. *Exp Cell Res* 306:75–84
81. Pinelli E, Poux N, Garren L, Pipy B, Castegnaro M, Miller DJ, Pfohl-Leszkowicz A (1999) Activation of mitogen-activated protein kinase by fumonisin B<sub>1</sub> stimulates cPLA<sub>2</sub> phosphorylation, the arachidonic acid cascade and cAMP production. *Carcinogenesis* 20:1683–1688
82. Shibata M, Kodani I, Osaki M, Araki K, Adachi H, Ryoke K, Ito H (2005) Cyclo-oxygenase-1 and -2 expression in human oral mucosa, dysplasias and squamous cell carcinomas and their pathological significance. *Oral Oncol* 41:304–312

## Expression Profiles of Genes Involved in Fatty Acid and Triacylglycerol Synthesis in Castor Bean (*Ricinus communis* L.)

Grace Q. Chen · Charlotta Turner · Xiaohua He · Tasha Nguyen · Thomas A. McKeon · Debbie Laudencia-Chingcuanco

Received: 5 October 2006 / Accepted: 24 December 2006 / Published online: 6 February 2007  
© AOCS 2007

**Abstract** Castor seed triacylglycerols (TAGs) contain 90% ricinoleate (12-hydroxy-oleate) which has numerous industrial applications. Due to the presence of the toxin ricin and potent allergenic 2S albumins in the seed, it is desirable to produce ricinoleate from temperate oilseeds. To identify regulatory genes or genes for enzymes that may up-regulate multiple activities or entire pathways leading to the ricinoleate and TAG synthesis, we have analyzed expression profiles of 12 castor genes involved in fatty acid and TAG synthesis using quantitative reverse transcription-polymerase chain reaction technology. A collection of castor seeds with well-defined developmental stages and morphologies was used to determine the levels of mRNA, ricinoleate and TAG. The synthesis of ricinoleate and TAG occurred when seeds progressed to stages of cellular endosperm development. Concomitantly, most of the genes increased their expression levels, but showed various temporal expression patterns and different maximum inductions ranging from 4- to 43,000-fold. Clustering analysis of the expression data indicated five gene groups with

distinct temporal patterns. We identified genes involved in fatty acid biosynthesis and transport that fell into two related clusters with moderate flat-rise or concave-rise patterns, and others that were highly expressed during seed development that displayed either linear-rise or bell-shaped patterns. Castor diacylglycerol acyltransferase 1 was the only gene having a higher expression level in leaf and a declining pattern during cellular endosperm development. The relationships among gene expression, cellular endosperm development and ricinoleate/TAG accumulation are discussed.

**Keywords** *Ricinus communis* · Gene transcription · Fatty acid · Triacylglycerol · Ricinoleate · Seed development · Temporal pattern

### Abbreviations

ACP	Acyl-carrier protein
ACBP	Acyl-CoA binding protein
BC	Biotin carboxylase
DAP	Day after pollination
DGAT1	Diacylglycerol acyltransferase 1
ER	Endoplasmic reticulum
EAR	Enoyl-ACP reductase
FAH	Fatty acid hydroxylase
FAME	Fatty acid methyl ester
FAS	Fatty acid synthase
KASA	46 kDa $\beta$ -ketoacyl-ACP synthase
KASB	50 kDa $\beta$ -ketoacyl-ACP synthase
PC	Phosphatidylcholine
PE	Phosphatidylethanolamine
RT-PCR	Reverse transcription-polymerase chain reaction

G. Q. Chen (✉) · C. Turner · X. He · T. Nguyen · T. A. McKeon · D. Laudencia-Chingcuanco  
Western Regional Research Center,  
Agricultural Research Service,  
U.S. Department of Agriculture,  
800 Buchanan St., Albany, CA 94710, USA  
e-mail: qhgc@pw.usda.gov

### Present Address:

C. Turner  
Department of Physical and Analytical Chemistry,  
Uppsala University, 75124 Uppsala, Sweden

SAD Stearoyl-acyl-carrier protein desaturase  
TAG Triacylglycerol

## Introduction

The castor plant (*Ricinus communis*) is a perennial shrub mainly cultivated in tropical and subtropical areas of India, China and Brazil as an oilseed crop. Its seeds accumulate 60% oil in the form of triacylglycerol (TAG) that serves as a major energy reserve for seed germination and seedling growth. Castor oil is unique in that 90% of its fatty acid content is ricinoleate, 12-hydroxyoleic acid. The hydroxy group imparts unique chemical and physical properties that make castor oil a vital industrial raw material for numerous products such as cosmetics, paints, coatings, plastics and anti-fungal products [1]. Castor oil is also used as an additive to prevent fuels and lubricants used in aircraft engines from freezing at extremely low temperatures [1], and its replacement for sulfur-based lubricity components in petroleum diesel helps to reduce sulfur emissions [2].

One of the problems associated with castor seeds is that they contain the toxin ricin and hyper-allergenic 2S albumins that are detrimental to growers and processors. Therefore it is highly desirable to develop a safe source for castor oil production. In the past decade scientists have sought to identify key genes responsible for the ricinoleate synthesis in order to develop temperate oilseeds to produce ricinoleate. A castor gene (FAH) for the hydroxylase which is directly responsible for synthesis of ricinoleate was successfully isolated [3], but transgenic expression of the FAH in the model oilseed *Arabidopsis* produced only 17% ricinoleate [4], which was too low to be useful. There are many examples of transgenic production of other unusual fatty acids by over-expression of a key gene in oilseeds. With the exception of lauric acid and gamma-linolenic acid, the amount of desired fatty acids in the transgenic oilseed has been considerably lower than in the wild species from which the transgene was obtained [5]. These results suggest that expressing a single key gene required for unusual fatty acid biosynthesis in transgenic plants is insufficient to produce a large amount of unusual fatty acids in seed.

Current efforts on metabolic engineering of new oilseeds have been shifted towards searching for additional genes [6] or general transcription factors [7] that may up-regulate multiple activities or entire pathways leading to oil biosynthesis. Therefore, knowledge of the expression of multiple genes and

their regulation during castor oil biosynthesis is needed to further understand the regulatory mechanisms controlling castor oil metabolism. In general, castor oil biosynthesis mostly follows the common biosynthetic pathways for fatty acid in the plastid as well as TAG in the endoplasmic reticulum (ER), although there is a modification step for ricinoleate formation in the latter pathway [8]. In this paper, we survey the available castor sequences in National Center for Biotechnology Information (<http://www.ncbi.nlm.gov>) to identify 12 genes that participate in different steps of the pathways leading to fatty acid and TAG synthesis. We characterize the expression profiles of these genes in developing castor seeds during the time-course of seed development and ricinoleate/TAG accumulation. Additionally, a leaf sample is included as vegetative control and for comparative studies. To further compare the temporal expression patterns among the genes, we perform a clustering analysis that reveals five groups with distinct temporal patterns. Our results provide not only the initial information on promoter activity for each gene, but also a first glimpse of the global patterns of gene expression and regulation, which are critical to metabolic engineering of transgenic oilseeds for safe castor oil production.

## Experimental Procedures

### Plant Material

Castor (*R. communis* L.) seeds, PI215769, were obtained from the USDA-Germplasm Resources Information Network, Southern Regional Plant Introduction Station (Griffin, GA). Plants were germinated and grown in a greenhouse at temperatures between 28 °C (day) and 18 °C (night), with supplemental metal halide lighting to provide a 15-h day length (1,000–1,250  $\mu\text{mol m}^{-2} \text{s}^{-1}$ ). Mature female flowers were individually pollinated and tagged, and the tagging dates were recorded as 0 day after pollination (0 DAP). Capsules were harvested at 7-day intervals from 12 to 61 DAP. Dissected seeds were frozen immediately in liquid nitrogen and stored at –80 °C. Leaf tissue was collected from a fully expanded young leaf in a mature castor plant.

### Isolation of Total RNA and Reverse Transcription

Total RNA was extracted using TRIzol Reagent (Invitrogen, Carlsbad, CA). RNA pellets were dissolved in DEPC-treated water, quantified by absorbance at 260 nm and checked for quality by ethidium bromide

gel electrophoresis. The total RNA samples were first treated with DNase I, and then reverse transcribed to first-strand cDNA using an Oligo(dT) primer and SUPERSRIPT III (Invitrogen, Carlsbad, CA). Finished cDNA products contained 50 ng/ $\mu$ L reverse transcribed total RNA, and were stored at  $-80^{\circ}\text{C}$ .

#### Primer Design and Standard Curve Construction

Putative primers were designed according to the SYBR Green Design criteria incorporated in the Beacon Designer 4.0 software (Premier Biosoft International Palo Alto, CA). To ensure maximum specificity and efficiency during quantitative PCR, putative primer pairs were further tested for linearity of response by constructing standard curves on five or six serial ten-fold dilutions. The templates used for the standard curve analysis were mixed cDNAs from 12 to 54 DAP samples with a starting concentration of 2.5 ng/ $\mu$ L. A standard reaction mixture (25  $\mu$ L) contained 10  $\mu$ L cDNA template, 1x iQ SYBR Green I Supermix (Bio-Rad, Hercules, CA) and 300 nM forward and reverse

primers. The Bio-Rad iCycler iQ-system was used for all amplifications. The PCR protocol consisted of an initial denaturing step of  $95^{\circ}\text{C}$  for 3 min, followed by 40 repeats of  $95^{\circ}\text{C}$  for 10 s and  $55^{\circ}\text{C}$  for 30 s. A melt-curve protocol immediately followed the amplification with heating to  $95^{\circ}\text{C}$  for 1 min and annealing at  $50^{\circ}\text{C}$  for 1 min, followed by 80 repeats of heating for 10 s, starting at  $50^{\circ}\text{C}$  with  $0.5^{\circ}\text{C}$  increments. The Bio-Rad iQ iCycler System software produced standard curves by plotting the  $\log_{10}$  of the starting quantity against the threshold cycle ( $C_T$ ). Correlation coefficients were determined from the standard regression formulas. Standard curves showing correlation coefficients of 0.99 or higher and PCR efficiencies between 90 and 110% were accepted. For each primer set, at least three independent standard curves were analyzed, and the average number was used in data analysis. PCR product specificity was confirmed by melting-curve analysis and by electrophoresis on 4% agarose gel to ensure that PCR reactions were free of primer dimers and non-specific amplicons. Information on optimized primer pairs is listed in Table 1.

**Table 1** Selection of lipid genes, primer sequences, size of amplification products, and PCR efficiencies

Lipid gene cellular location and activity	Abbreviated name	GenBank ID	Forward primer Reverse primer	Amplicon size (bp)	PCR efficiency
<b>Plastid location</b>					
Acetyl-CoA carboxylase biotin carboxylase subunit	BC	L39267	TTCCTACGACGATAGAATACC AACTCTGACCTTCAAATGTG	230	94.6
Acyl carrier protein	ACP	T15016	AAGGTCGTGGCATAAGTG TGATCCCAAATTCCTCCTC	142	93.8
46 kDa $\beta$ -ketoacyl-ACP synthase	KASA	L13241	GGGTAGGGAAAGGAGAATATGC GCCACAATGATGCGGAGAG	102	103.6
50 kDa $\beta$ -ketoacyl-ACP synthase	KASB	L13242	GAGTTGCTTGCTTATAGAG AGATAGACTTGATACTGAAATG	102	101.3
Enoyl-ACP reductase	EAR	CF981229	ACTCCTGCCACACAGATGAC TCTAAGCCTAGTCCAAGATGCC	120	96.4
Enoyl-reductase domain of type I-like FAS	FASI-like <sup>a</sup>	T15158	AATTCTGTGTAACACCATCAG ATTGTCCGGCAACCATTC	204	97.0
Stearoyl-acyl-carrier protein desaturase	SAD	M59857	GAGTCTACACAGCAAAGGATTATG TCTCTCCAGCCTTCTAATTCTTG	150	97.4
<b>Cytoplasm location</b>					
Acyl-CoA-binding protein	ACBP	Y08996	ACAAGCAAGCCACCGTTG CTTCCTCCGTAGATTTCCCTTC	114	95.6
<b>Endoplasmic reticulum location</b>					
Oleate 12-hydroxylase	FAH	U22378	TAACCAGCAACAACAGTGAG ATAGGCAACATAGGAGAATGAG	155	93.5
Diacylglycerol acyltransferase	DGAT1	AY366496	GACACCATTTCATAAGGAAG CTTTCTAATAAATGCTGTGC	144	101
Oleosin1	Ole1	AY360218	CTGCTGCCGTTGTTATG ATGCTTGTCCTTCC	205	97.2
Oleosin2	Ole2	AY360219	AGTCTCTATTTCTTTCTGG TGCTTTCTGTAAACATACC	209	95.5
<b>Constitutive control gene</b>					
Actin	Act	AY360221	GAATCCACGAGACTACATACAAC TTATGAAGGTTATGCTCTC	176	95.4

<sup>a</sup> Tentative assignments of the gene name and the cellular activity

## Quantitative RT-PCR Data Analysis

The method of Pfaffl [9] was applied to calculate comparative expression levels between samples. The castor actin gene (a house-keeping gene, [10]) was used as internal reference to normalize the relative amount of mRNAs for all samples. For each selected gene, triplicate sets of PCR reaction samples including the actin controls, and duplicate negative controls (reaction samples without cDNA templates), were prepared and run in a 96-well plate. The SYBR fluorescence was analyzed by iQ iCycler software and the  $C_T$  value for each sample was reported. The average  $C_T$  from 26 DAP measurements were calibrated as 100, 1,000 or  $10^5$  copy numbers, and the relative copy numbers of a gene were averaged over triplicates. The PCR experiments were repeated for each plate to ensure that similar results could be obtained.

## Data Clustering Analysis and Visualization

To partition the lipid genes into distinct groups such that genes assigned to the same cluster should have similar expression patterns, the quantitative expression data of each gene at various developmental stages were first normalized to the genes maximum expression (set at 100%) and then subjected to gene expression clustering analysis using the *k*-mean clustering method [11] provided within the software Expression Analyzer and DisplayER (EXPANDER, [12]). The *k*-mean clustering numbers, 4, 5 and 6 were tested (data not shown) and the clustering into five groups was selected because it gave the best scores for clustering quality. To view the expression patterns of clusters by a graph, the option of mean patterns with error bars operated by the EXPANDER was chosen that allows each cluster to be displayed in a separate panel with error bars representing standard deviations.

## Chemicals

Ricinoleic acid methyl ester and cyclohexane were obtained from Sigma–Aldrich (St. Louis, MO). Nonadecanoic acid methyl ester and GLC-68 FAME standard mixture were obtained from Nu-Chek Prep, Inc. (Elysian, MN). Heptadecanoic acid methyl ester and anhydrous acetyl chloride were purchased from Alltech (Deerfield, IL) and butylated hydroxytoluene (BHT) was obtained from Spectrum Chemical MFG Corp. (Gardena, CA). Anhydrous sodium sulfate was purchased from J.T. Baker Inc. (Philipsburg, NJ). 2-Propanol, methanol, hexane and toluene were obtained from Fisher Scientific (Fair Lawn, NJ).

Sodium chloride and potassium bicarbonate were obtained from Mallinckrodt Laboratory Chemicals (Philipsburg, NJ). Ethanol was purchased from AAPER Alcohol and Chemical Co. (Shelbyville, KY). The water used was double distilled, and all chemicals and solvents used were of reagent grade.

## Lipid Extraction, Seed Dry Weight and Water Content Measurement

Castor seeds were peeled and thoroughly homogenized using a mortar and a pestle. Seed samples were weighed (seed fresh weight) into Eppendorf tubes and dried under vacuum centrifugation over night. The dried samples were weighed and the water content was calculated. Triplicate samples were prepared by accurately weighing 0.01 g of dried seed sample into 10 mL glass tubes. The lipids were extracted using 2 mL of hexane/2-propanol (8:2) containing  $50 \mu\text{g mL}^{-1}$  of BHT. Internal standard (nonadecanoic acid methyl ester) was added and the extraction took place at  $55^\circ\text{C}$  for 30 min with shaking every 10 min. The extracts were filtered and dried over sodium sulfate, and the solvent was evaporated under nitrogen. The lipid weight was determined gravimetrically. After addition of 0.5 mL toluene, the lipids were methylated for 1 h at  $80^\circ\text{C}$  using methanolic hydrogen chloride (3%), as described by Christie [13]. The resulting FAMES were dissolved in 10 mL of cyclohexane (0.01% BHT) for GC analysis. The non-lipid dry weight was obtained by subtracting the lipid and water weight from the seed fresh weight.

## GC Analysis

Quantitative analysis was carried out by GC-FID using a Hewlett Packard 6890 GC system with split injection connected to a 7673 automatic liquid sampler, Agilent Technologies (Palo Alto, CA). Separation was achieved on a DB-WAX column (20 m  $\times$  0.12 mm i.d., 0.18  $\mu\text{m}$  film thickness) purchased from J & W Scientific, Agilent Technologies. The injector and detector temperatures were 250 and  $280^\circ\text{C}$ , respectively. The column temperature program was  $100^\circ\text{C}$  for 1 min,  $5^\circ\text{C min}^{-1}$  to  $250^\circ\text{C}$ , and hold 1 min. Standard solutions of a mixture of FAMES including methyl ricinoleate at three different concentrations in the range of  $40\text{--}400 \mu\text{g mL}^{-1}$  for methyl ricinoleate and  $5\text{--}150 \mu\text{g mL}^{-1}$  for the other FAMES were used for generating standard calibration curves.  $50 \mu\text{L}$  of methyl heptadecanoate ( $1 \text{ mg mL}^{-1}$ ) was added as internal standard to each 1-mL aliquot of standard sample. One microlitre injections were used, and

duplicate determinations were applied. Identification of peak components was achieved on a Hewlett Packard 5890 GC system connected to a 5970A mass selective detector, Agilent Technologies. Split injection was applied, and the same type of column and temperature program as described above was used. Comparison to mass spectra of known FAMES was used for identification of each peak. In addition, double-bond locations for the unsaturated fatty acids were determined by interpreting spectra from picolinyl derivatives of free fatty acids (FFAs), employing the methodology described by Christie [13].

## Results and Discussion

### Changes in Water, Lipid and Ricinoleate Content During Seed Development

A mature castor seed contains a mass of endosperm that synthesizes and stores oil and protein as major reserves [14]. We have previously characterized the morphological changes of developing castor seeds and established a time-course for assessing endosperm development [15]. Castor endosperm development has a nuclear endosperm development pattern that starts with a free-nuclear stage and then progresses into cellularization and maturation. The whole course takes about 54 DAP. At 61 DAP and after, seeds are completely mature and begin desiccation [15]. During the first 19 DAP, castor seeds grew rapidly to full size ([15], Fig. 1d), and consisted mostly of water at 90% of seed fresh weight and small amounts of lipid at about 5% (Fig. 1a). The endosperm stayed at free-nuclear stage and did not enter cellular endosperm development (Fig. 1d). Between 26 and 40 DAP, the endosperm underwent cellularization, expanding and eventually filling the most of the seed at 40 DAP ([15], Fig. 1d). Then the cellular endosperm continued maturation up to 54 DAP without showing visible changes [15]. During the course of cellular endosperm development (26–54 DAP), the seeds gradually lost water and gained storage lipid to a maximum level of 60% at 54 DAP (Fig. 1a) and maintained the same high level thereafter.

To examine the ricinoleate content, total fatty acid represented by FAME and ricinoleate was measured in seeds at various developmental stages. As shown in Fig. 1b, the ricinoleate and total FAME showed accumulation patterns parallel to each other, and the increase of the FAME was attributed predominantly to the increase of ricinoleate. At early stages (12 and 19 DAP) in free-nuclear endospermic seeds, the

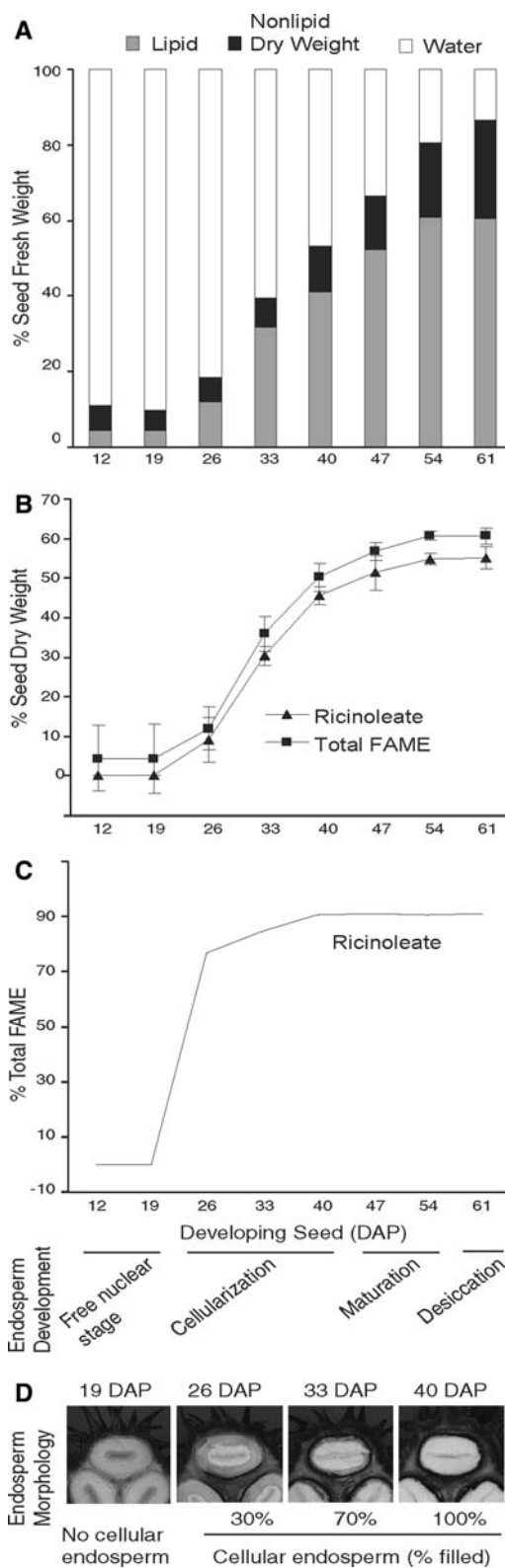


**Fig. 1** Changes in water, lipid and ricinoleate content during seed development. Each data point represents the mean ( $\pm$ SD) of three measurements and at least 20 seeds. **d** transverse cross section of developing castor seeds. Cellular endosperm is shown in opaque color. DAP days after pollination

ricinoleate was not detectable (Fig. 1c). However by 26 DAP when 30% of seed's volume filled with cellular endosperm (Fig. 1d), the ricinoleate accumulated immediately to 9.2% of seed dry weight (Fig. 1b) and accounted for 77% of fatty acid content (Fig. 1c). During the remaining stages of cellular endosperm development, the ricinoleate kept increasing and reached plateaus of 55% of seed dry weight at 54 DAP and 90% of total FAMES at 40 DAP (Fig. 1b, c). Besides ricinoleate, there were about seven minor fatty acids detected in seeds at all stages of the development, all of them accumulated at low background levels in a total amount of 2.8–6.5% of dry seed weight (data not shown). These fatty acids were probably components of structural lipids for maintaining the cell membrane and seed coat, in addition to being minor components of the oil. By using the same sets of developing seeds, similar results were observed by measuring changes in lipid classes, including acylglycerols, FFAs, phosphatidylcholine (PC) and phosphatidylethanolamine (PE) [16]. Before 19 DAP, there were considerable amounts of PC and PE present in seed lipid, and the acylglycerols contain less than 7% TAG. After 26 DAP, the relative amount of PC and PE dropped to negligible levels, and the fatty acids were almost exclusively in acylglycerols of which 77–89% was TAG [16]. It is known that ricinoleate accumulates almost exclusively as storage TAGs rather than as membrane lipids in castor seeds [8], therefore, the appearance of ricinoleate indicates the initiation of storage TAG synthesis. Taken together, the FAMES measured in seeds before 19 DAP (Fig. 1b) would represent mostly fatty acids from membrane lipids, whereas, after 26 DAP, the FAME are mostly of TAG origin. As shown in Fig. 1, ricinoleate and TAG synthesis started at 26 DAP, coinciding with the beginning of endosperm cellularization. Our previous studies in castor showed increased expression of ricin [17] and 2S albumins [15] genes that also started at 26 DAP. These results all suggest that the time between 19 and 26 DAP is a critical switchover stage for synthesizing both oil and storage proteins in castor. Moreover, these results also demonstrate that our series of developing seeds allows us to identify the initial timing and temporal pattern of different biochemical and cellular activities during seed development and to draw accurate comparisons between experiments.

#### Selection of Lipid Genes and Optimized PCR Primers

In order to find the lipid genes for castor oil biosynthesis, we searched the Genbank nucleotide database

(<http://www.ncbi.nlm.gov>) by using compound queries each consisting of *R. communis* and the nomenclature of genes involved in synthesis of fatty acid and TAG from a comprehensive lipid gene catalog [18], which lists 600 genes representing 210 cellular activities involved in various aspects of acyl lipid metabolic pathways including fatty acid and TAG biosynthesis from plant kingdom. We noticed that all hits were for cDNA clones from developing castor seeds, indicating their functional expression during seed lipid biosynthesis. In some cases, more than one accession exists because of multiple partial sequences submitted by different laboratories. We examined the candidate genes by multiple sequence alignment and selected the most complete sequence to represent the gene. The search also found a partial sequence (GenBank ID T15158) containing an enoyl-reductase domain of Type I fatty acid synthase (FAS). This sequence is tentatively designated as FASI-like gene in Table 1.

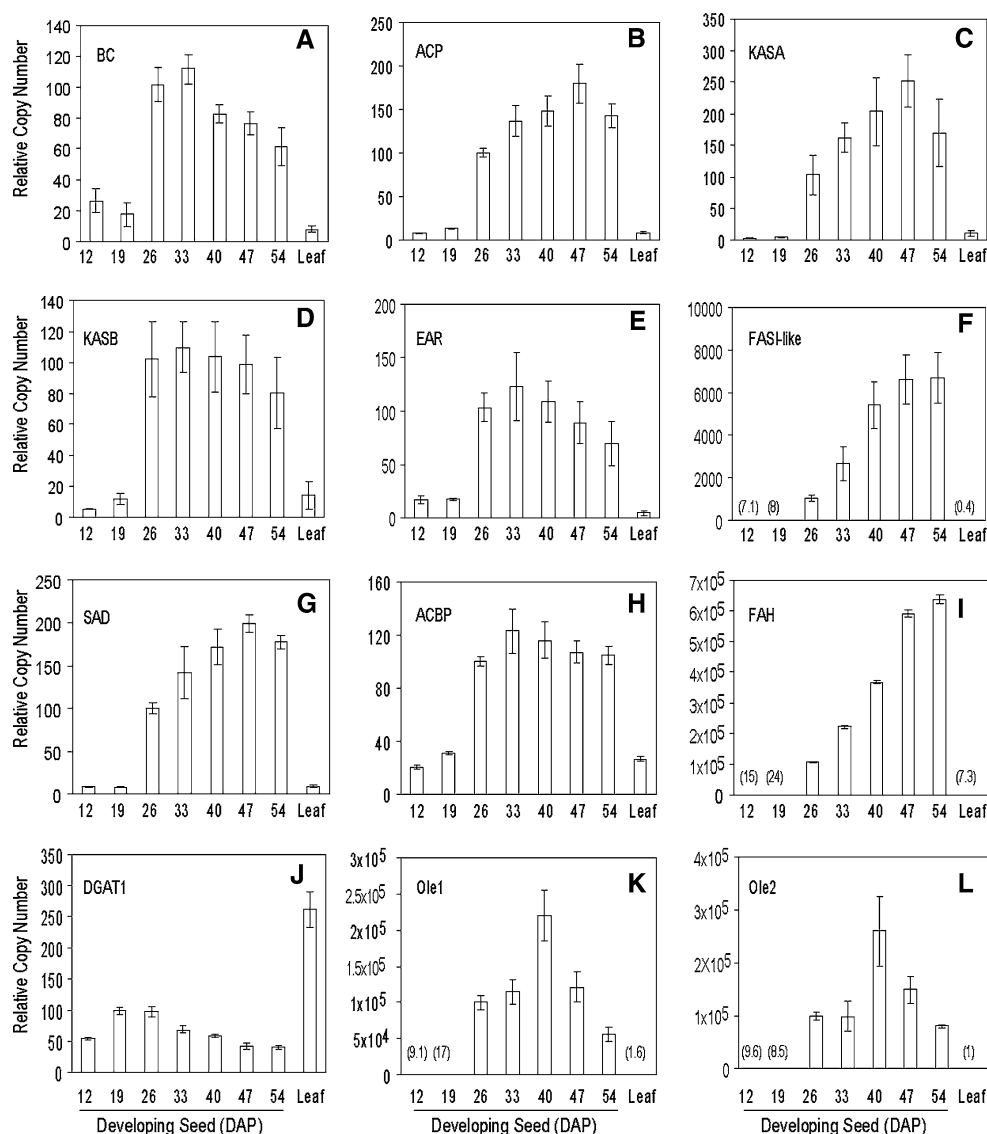
Quantitative PCR is one of the most sensitive and quantitative methods for measuring mRNA levels [19]. We optimized all assay conditions (“[Experimental Procedures](#)”), and the primer sets and PCR efficiencies are listed in Table 1. In addition, PCR products were designed to have similar sizes between 100 and 230 bp (Table 1). These optimized conditions allow simultaneous analysis of multiple genes on a 96-well plate and permit accurate comparison of relative copy numbers among genes.

#### General Expression Profiles of Lipid Genes and Lipid Gene Clusters

Using the quantitative RT-PCR technology, we examined the steady state mRNA levels of lipid genes in seed samples from various developmental stages. For convenience, these mRNA levels are referred to as ‘expression’ in this article. Expression profiles of the lipid genes are shown in Fig. 2. With the exception of the diacylglycerol acyltransferase 1 (DGAT1), we detected low background expression for the majority of lipid genes in leaf tissue and in young seeds at 12 and 19 DAP when endosperm was at the free-nuclear stage. When the seeds progressed to cellular endosperm development (26–54 DAP), the expression of the majority of lipid genes was induced to higher levels, displaying various temporal patterns; the maximum induction also varied dramatically, ranging from 4- to 43,000-fold (Fig. 2, Table 2). The results revealed that a major transcriptional activation of lipid gene expression occurred at the onset of cellular endosperm development, coinciding with the beginning of the storage TAG accumulation (Fig. 1b). It indicates a



**Fig. 2** Expression of lipid genes in developing seeds and leaf. Abbreviated names for the genes are described in Table 1. Each data point represents the mean  $\pm$  SD of three replicates. DAP days after pollination. Values in parentheses indicate relative copy number



primary role of gene transcription in regulating castor oil biosynthesis.

To examine relationships among the temporal expression patterns of the lipid genes, we performed clustering analysis (“[Experimental Procedures](#)”), which classified the lipid genes into five groups based on their pattern similarities. As expected, the DGAT1 itself formed a cluster showing a specific declining pattern (cluster 1 in Fig. 3a). The majority of the lipid genes showed various up-regulated patterns during seed development including flat-rise (cluster 2), concave-rise (cluster 3), bell-shaped (cluster 4) and linear-rise (cluster 5). The clusters are summarized in Fig. 3 and Table 2, together with their gene members and normalized mean pattern description, the changes in expression (maximum ratio) for each gene as well as

the maximum ratio between the developing seed and mature leaf.

#### Expression Profiles of the Lipid Genes Involved in Fatty Acid Biosynthesis

According to our current knowledge of castor seed TAG synthesis, oleic acid is synthesized in the plastid and then exported to cytoplasm following the standard fatty acid biosynthesis pathway [20]. Oleic acid is activated to oleoyl-CoA in the cytoplasm and imported into ER with help of acyl-CoA binding protein (ACBP) for TAG synthesis [20]. We have examined seven castor lipid genes involved in oleic acid biosynthesis and transport and found they belong to either cluster 2 or cluster 3. Cluster 2 has a flat-rise pattern

**Table 2** Summary of transcript profiles of lipid genes

Temporal pattern during seed development	Gene <sup>a</sup>	Maximum ratio of expression	
		Seed/seed <sup>b</sup>	Seed/leaf <sup>c</sup>
Cluster 1, decline	DGAT1	2.4	0.4
Cluster 2, flat rise	BC	4	12
	KASB	21	7.8
	EAR	7	28
	ACBP	6	4.7
Cluster 3, concave rise	ACP	22	20
	KASA	70	22
	SAD	23	23
Cluster 4, bell-shaped	Ole1	24,172	140,400
	Ole2	27,150	252,230
Cluster 5, linear rise	FASI-like	940	18,288
	FAH	43,083	86,990

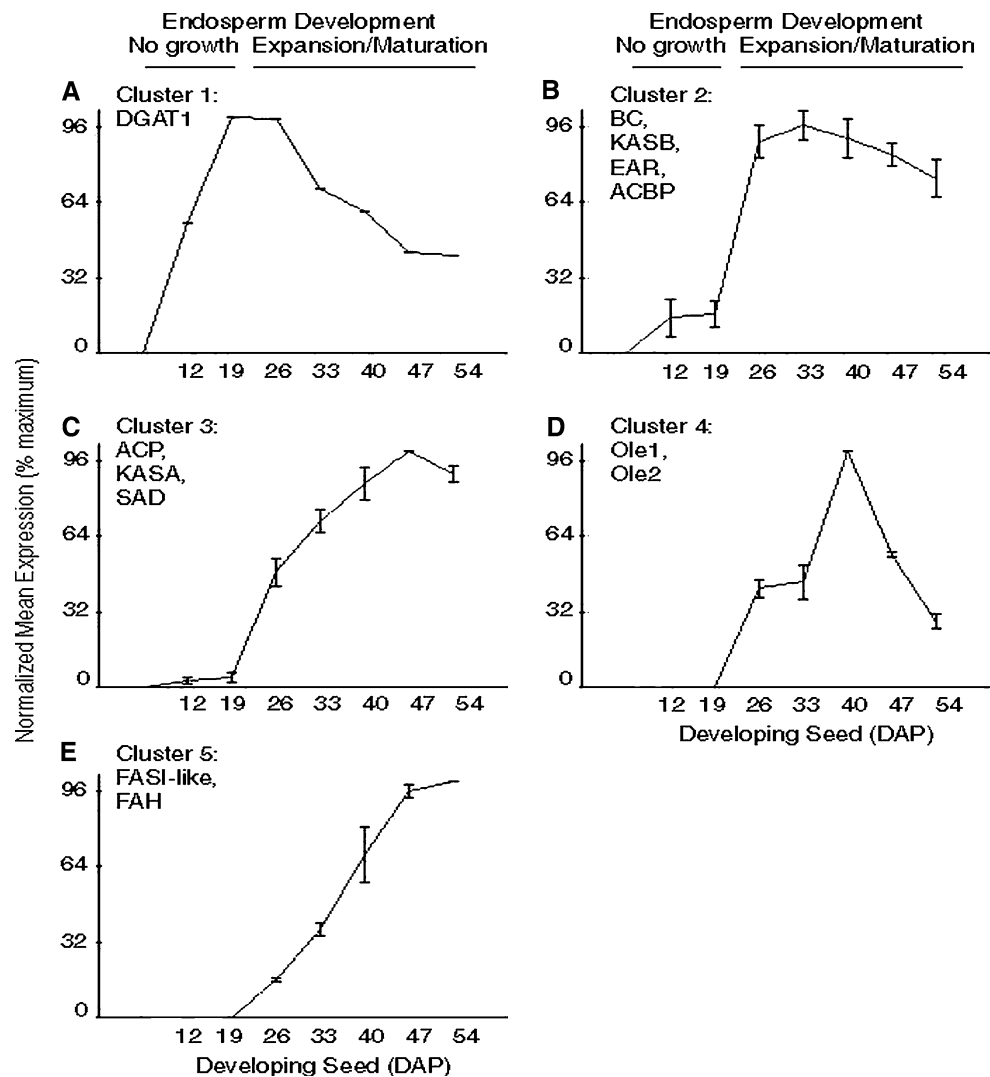
<sup>a</sup> The gene short names are described in the Table 1

<sup>b</sup> Ratio of the maximum to the minimum expression in seed

<sup>c</sup> Ratio of the maximum expression in seed to the expression in leaf

(Fig. 3b) with four members: acetyl-CoA carboxylase biotin carboxylase subunit (BC), 50 kDa  $\beta$ -ketoacyl-ACP synthase (KASB), enoyl-ACP reductase (EAR), and ACBP; while cluster 3 (Fig. 3c) includes three genes, acyl carrier protein (ACP), 46 kDa  $\beta$ -ketoacyl-ACP synthase (KASA), and stearoyl-acyl-carrier protein desaturase (SAD), all with a concave-rise pattern. Further comparisons among gene clusters reveal that cluster 2 and 3 share certain expression characteristics. First, the maximum induction ratios between seed and leaf in cluster 2 and 3 (4.7 to 28-fold) are much smaller than those in cluster 4 and 5 (18,288 to 252,230-fold). Second, during the time-course of seed development, cluster 2 and 3 have moderate maximum induction ratios (4 to 70-fold) compared to cluster 4 and 5 (940 to 43,083-fold). Third, the temporal patterns of cluster 2 and 3 are less dynamic than those of cluster 4 and 5; cluster 2 has a simple flat-rise, whereas cluster 3 has a quick rise that reaches its half-maximum at the

**Fig. 3** Expression patterns of lipid gene clusters during seed development. Abbreviated names are described in the Table 1. Each cluster is represented by the mean expression pattern over all the genes assigned to it. Error bars denote  $\pm$ SD. DAP days after pollination



beginning of cellular endosperm development, and increases slowly (<2 fold) during the rest of the seed development. As a consequence of these features, the levels of induction among clusters 2 and 3 at the onset of cellular endosperm development (26–33 DAP) are similar, ranging between 4 to 21 and 11 to 35 fold, respectively. These shared characteristics between clusters 2 and 3 suggest that common regulatory factors might be present to up-regulate the expression of these lipid genes in plastid. Moreover, the appearance of overall moderate expression and related patterns shared by clusters 2 and 3 would also suggest their house-keeping functions in cellular endosperm tissue. There is evidence that fatty acid biosynthesis is a house-keeping function and it undergoes coordinated regulation through gene expression to provide constant demands of fatty acids for membrane lipid biosynthesis, in addition to its involvement in storage TAG assembly. For instance, biochemical data show that individual enzymes required for fatty acid biosynthesis in the plastid may be retained as a functional unit, or a house-keeping metabolon [21]. Genes encoding components of the plastidic acetyl-CoA carboxylase in *Arabidopsis* [22] and the FAS in *Brassica* [23] are expressed at constant molar ratios both in different tissues of mature plants and throughout seed development. Furthermore, the microarray analysis of more than 100 *Arabidopsis* lipid genes demonstrates that 60% of them do not change in expression during the time-course of seed development, including some core enzymes of FAS, such as  $\beta$ -ketoacyl-ACP synthaseIII and isoforms of ACP [24]. In castor seed, cluster 2 and 3 may represent house-keeping genes and their boosted expressions obviously associated with the increasing demand of the oleic acid for TAG biosynthesis during cellular endosperm development. It is possible that cluster 2 and 3 genes also contribute to castor membrane lipid biosynthesis, because we have also observed low expression of cluster 2 and 3 in non-storage tissues such as leaf and young seeds at 12 and 19 DAP (Fig. 2). The low expression of cluster 2 and 3 in the vegetative tissues would correlate with the low demand for fatty acid in membrane lipid synthesis. Similar results were reported for the castor SAD gene expression using Northern blot analysis, showing highest expression in developing seed, moderate to low expression in leaf and low expression in root [25]. So probably there are two different mechanisms existing in castor to regulate the expression of genes involved in fatty acid biosynthesis, one at low levels for membrane function and the other at higher levels for reserve synthesis. Without castor whole genome information, other alternatives also exist, for example, isoforms of

cluster 2 and 3 may contribute to fatty acid biosynthesis in different tissues or at different developmental stages.

#### Expression Profiles of Castor Oleosin Genes

The clustering analysis groups two oleosin genes into cluster 4 showing a bell-shaped pattern (Fig. 3d). Oleosins are oil body-associated proteins that cover and stabilize oil bodies during TAG accumulation [26]. In most plants oleosins are encoded by multi-gene families and some of them are co-expressed [26]. We have observed that castor oleosin1 and oleosin2 genes were co-expressed during seed development with maximum induction ratios of 24,172 and 27,150-fold, respectively (Fig. 2k, l; Table 2). The oleosin proteins have been shown to accumulate in equal amounts [27] or different amounts with the oleosin1 at a higher level [10]. The difference in relative protein level between oleosin1 and oleosin2 could be due to genotype discrepancy among castor cultivars and/or post-transcriptional regulation involvement in oleosin protein accumulation. However our time-course data showed peaks at 40 DAP, a time point when cellular endosperm reached its full expansion (Fig. 1d). The peak expression of oleosins is probably driven by the demand for newly synthesized oil bodies resulting from the growing ER membranes during cellular endosperm expansion.

#### Expression Profiles of Castor FAH and FASI-Like Genes

The FAH and FASI-like genes are grouped into cluster 5 and display a linear rise pattern during seed development (Fig. 3e). As the enzyme responsible for ricinoleate biosynthesis, the FAH hydroxylates the *sn*-2 oleoyl chain of oleoyl PC to form *sn*-2 ricinoleate-PC [8]. The expression of the FAH gene was reported to be high in seed and very low in leaf [3]. Our data on the FAH gene expression is consistent with the previous report, but with new quantitative and detailed temporal expression profiles. In leaf and young seeds at free-nuclear endosperm stages (12 and 19 DAP), FAH is expressed at negligible levels (Fig. 2i). FAH is expressed at a high level when seeds progress into cellular endosperm development and storage TAG/ricinoleate biosynthesis during 26–54 DAP (Fig. 1b), showing an immediate 5,000-fold induction at the beginning (26 DAP, Fig. 2i) and continuous sharp increases during the rest of the stages. As a consequence, the FAH expression showed a linear-rise pattern and a maximum induction of 43,083-fold at the

end of the seed development (54 DAP, Fig. 2i; Table 2). These results would indicate that the FAH gene is transcriptionally expressed at similar high rates throughout the cellular endosperm development and, at the same time, the FAH transcripts are probably also very stable in cellular endosperm, resulting in its high accumulation. Furthermore, such high accumulation of the FAH gene transcript would suggest transcriptional regulation is the mechanism for maintaining high ricinoleate synthesis to fulfill the growing demand of TAG synthesis in developing cellular endosperm.

The function of the FASI-like gene remains unknown due to its incomplete sequence information. When searching the Genbank protein database with the truncate FASI-like protein sequence as a query, it retrieved a plant sequence encoding phenylpropenal double-bond reductase from *Pinus taeda* (Genbank accession: DQ829775.1) among five top hits (alignment score from 60 to 62). Although this enzyme is involved in phenylpropanoid metabolism for plant defense [28], it also shows sequence similarity to enzymes involved in plant lipid metabolism [28]: the enoyl acyl carrier protein reductase (Genbank accession: CAC41367) from *Brassica napus* and the 2-alkenal reductase (Genbank accession: At5g16970) from *Arabidopsis*. The castor FASI-like gene was highly expressed during seed development and oil synthesis, showing a maximum induction of 940-fold and a similar linear-rise pattern as that of FAH (Fig. 3e; Table 2). The results reveal intriguing information on the FASI-like gene, which should lead to future investigations on its enzymatic and cellular function during castor seed development.

#### Expression Profile of Castor DGAT1

Diacylglycerol acyltransferase catalyzes the final step in TAG synthesis that acylates diacylglycerol (DAG) with acyl-CoA to form TAG [29]. Castor DGAT1 has been shown to preferentially incorporate ricinoleate into diricinolein to form triricinolein [30]. Among the lipid genes examined, the DGAT1 is the only member in cluster 1 displaying a declining pattern. During seed development, the DGAT1 mRNA accumulated to highest level at early stages (19–26 DAP, Fig. 2j) and then decreased to lower levels over time (33–54 DAP), showing a maximum of 2.4-fold reduction from 26 to 54 DAP. The temporal pattern of DGAT1 (Fig. 3a) is in agreement with previous Northern data [16] and quantitative RT-PCR data [31]. However the DGAT1 protein level and enzymatic activity during seed development increased at 26 DAP, reached a maximum at 40 DAP, and both protein and activity were at

least 50% maximum level from 26 to 54 DAP [16], consistent with the pattern of TAG synthesis (Fig. 1a). The shifted pattern of DGAT1 protein/activity in comparison to its mRNAs was interpreted as post-transcriptional regulation contributing in part to the mechanism of TAG synthesis [16]. Since we observed the onset of cellular endosperm development that also started at 26 DAP (Fig. 1d), it is possible that the cellular endosperm plays a role in regulating the DGAT1 protein/activity by providing a micro-environment for its cellular function. The DGAT1-involved TAG synthesis takes place mainly in developing seed and pollen as storage reserves [29], but it also occurs in various vegetative tissues of *Arabidopsis*, such as root, stem, senescing leaf, flower and silique [32, 33]. We found that the DGAT1 mRNA in leaf tissue was higher than that in developing seeds (Fig. 2j; Table 2). Also, in cotyledons and true leaves of germinating castor seedlings, the DGAT1 mRNA, protein and enzyme activity were found to be expressed and temporally associated with increased levels of newly synthesized TAG [34]. These results suggest that DGAT1 may also play a regulatory role in balancing DAG and acyl-CoA molecules in membrane lipid metabolism to maintain membrane function in vegetative tissue. Besides DGAT1, there are at least other two independent reactions contributing to the final step of TAG synthesis in castor. A castor DGAT2 gene which has little amino sequence homology to DGAT1 but can also use diricinolein as acceptor and ricinoleoyl-CoA as the donor in TAG synthesis has been identified recently ([31], our unpublished data). Studies show that the DGAT2 displays a bell-shaped temporal pattern during seed development and is more highly expressed in seeds than in leaves ([31], our unpublished data). A castor enzyme, phospholipid:diacylglycerol acyltransferase (PDAT), has also been shown to contribute to TAG synthesis by acyl-CoA-independent acylation using ricinoleoyl-PC as acyl donors and ricinoleoyl-DAG as acceptors [35]. More independent gene families, such as bifunctional wax ester synthase/DGAT [36] and cytosolic DGAT [37] have been identified to catalyze the formation of TAG. It is possible that these gene families also participate in the final step in TAG synthesis in castor. Taken together, the final step in TAG synthesis in castor and other oilseeds is complicated and the question remains as to which of these genes and at what developmental stage do they play more or less important roles in TAG synthesis.

Overall, our series of seed studies, including endosperm development, storage TAG accumulation and gene expression, are all in parallel with the same

time-course, which provides integrative information for understanding their relationships during castor seed development. It is evident that synthesis of TAG requires coordinated regulation controlled by seed developmental programs at multiple levels, such as endosperm cellularization, gene transcription and post-transcriptional regulation. Obviously, gene transcription exerts a primary control in castor oil biosynthesis. The clustering analysis on temporal expression of lipid genes reveals five distinct patterns, indicative of different transcriptional regulatory mechanisms among these lipid genes. Our results of analysis of gene expression represent snapshots of a global transcriptional activities taking place during castor seed development and oil biosynthesis.

**Acknowledgments** The authors thank Susan Altenbach, Glenn Bartley and Paul Roessler for critical reading of the manuscript. This work was supported in part by the USDA-ARS Current Research Information System (CRIS) Project 5325-2100-012-00D, USDA Initiative for Future Agriculture and Food System Grant No. 2000-04820 and a cooperative agreement (No. 58-3K95-2-918) with Dow Chemical Company (Midland, MI).

## References

- Caupin HJ (1997) Products from castor oil: past, present, and future. In: Gunstone FD, Padley FB (eds) Lipid technologies and applications. Marcel Dekker, New York, pp 787–795
- Goodrum JW, Geller DP (2005) Influence of fatty acid methyl esters from hydroxylated vegetable oils on diesel fuel lubricity. *Bioresour Technol* 96:851–855
- Van De Loo F, Broun P, Turner S, Somerville C (1995) An oleate 12-hydroxylase from *Ricinus communis* L. is a fatty acyl desaturase homolog. *Proc Natl Acad Sci USA* 92:6743–6747
- Broun P, Somerville C (1997) Accumulation of ricinoleic, lesquerolic, and densipolic acids in seeds of transgenic *Arabidopsis* plants that express a fatty acyl hydroxylase cDNA from castor bean. *Plant Physiol* 113:933–942
- Thelen JJ, Ohlrogge JB (2002) Metabolic engineering of fatty acid biosynthesis in plants. *Metab Eng* 4:12–21
- Lu C, Fulda M, Wallis JG, Browse J (2006) A high-throughput screen for genes from castor that boost hydroxy fatty acid accumulation in seed oils of transgenic *Arabidopsis*. *Plant J* 45:847–856
- Cernac A, Benning C (2004) WRINKLED 1 encodes an AP2/EREB domain protein involved in the control of storage compound biosynthesis in *Arabidopsis*. *Plant J* 40:575–585
- Bafor M, Smith M, Jonsson L, Stobart K, Szymne S (1991) Ricinoleic acid biosynthesis and triacylglycerol assembly in microsomal preparations from developing castor-bean (*Ricinus communis*) endosperm. *Biochem J* 280:507–514
- Pfaffl MW (2001) A new mathematical model for relative quantification in real-time RT-PCR. *Nucleic Acids Res* 29:2002–2007
- Eastmond PJ (2004) Cloning and characterization of the acid lipase from castor beans. *J Biol Chem* 279:45540–45545
- Herwig R, Poustka A, Muller C, Bull C, Lehrach H, O'Brien J (1999) Large scale clustering of cDNA-fingerprinting data. *Genome Res* 9:1093–1105
- Shamir R, Maron-Katz A, Tanay A, Linhart C, Steinfeld I, Sharan R, Shiloh Y, Elkon R (2005) EXPANDER—an integrative program suite for microarray data analysis. *BMC Bioinformatics* 6:232
- Christie WW (1989) The preparation of derivatives of fatty acids. In: Christie WW (ed) Gas chromatography and lipids: a practical guide. The Oily Press Ltd, Dundee, pp 66–84
- Roberts LM, Lord JM (1981) Protein biosynthetic capacity in the endosperm tissue of ripening castor bean seeds. *Planta* 152:420–427
- Chen GQ, He X, Liao LP, McKeon TA (2004) 2S albumin gene expression in castor plant (*Ricinus communis*). *J Am Oil Chem Soc* 81:867–872
- He X, Chen GC, Lin JT, McKeon TA (2004) Regulation of diacylglycerol acyltransferase in developing seeds in castor. *Lipids* 39:865–871
- Chen GQ, He X, McKeon TA (2005) A simple and sensitive assay for distinguishing the expression of Ricin and *Ricinus communis* agglutinin genes, in developing castor seed (*Ricinus communis* L.) *J Agric Food Chem* 53:2358–2361
- Beisson F, Koo AJK, Ruuska S, Schwender J, Pollard M, Thelen JJ, Paddock T, Salas JJ, Savage L, Milcamps A, Mhaske VB, Cho Y, Ohlrogge JB (2003) *Arabidopsis* genes involved in acyl lipid metabolism. A 2003 census of the candidates, a study of the distribution of expressed sequence tags in organs, and web-based database. *Plant Physiol* 132:681–697
- Arya M, Shergill IS, Williamson M, Gommersall L, Arya N, Patel HRH (2005) Basic principles of real-time quantitative PCR. *Expert Rev Mol Diagn* 5:209–219
- Somerville C, Browse J, Jaworski JG, Ohlrogge JB (2000) Lipids. In: Buchanan B, Gruissem W, Jones R (eds) Biochemistry and molecular biology of plants. American Society of Plant Physiologists, Rockville, pp 456–527
- Roughan PG, Ohlrogge JB (1996) Evidence that isolated chloroplasts contain an integrated lipid-synthesizing assembly that channels acetate into long-chain fatty acids. *Plant Physiol* 110:1239–1247
- Ke J, Wen TN, Nikolau BJ, Wurtele ES (2000) Coordinate regulation of the nuclear and plastidic genes coding for the subunits of the heteromeric acetyl-coenzyme a carboxylase. *Plant Physiol* 122:1057–1071
- O'Hara P, Slabas AR, Fawcett T (2002) Fatty acid and lipid biosynthetic genes are expressed at constant molar ratios but different absolute levels during embryogenesis. *Plant Physiol* 129:310–320
- Ruuska SA, Girke T, Benning C, Ohlrogge JB (2002) Contrapuntal networks of gene expression during *Arabidopsis* seed filling. *Plant Cell* 14:1191–1206
- Shanklin J, Somerville C (1991) Stearoyl-acyl-carrier-protein desaturase from higher plants is structurally unrelated to the animal and fungal homologs. *Proc Natl Acad Sci USA* 88:2510–2514
- Murphy DJ (2005) Lipid-associated proteins. In: Murphy DJ (ed) Plant lipids: biology, utilisation and manipulation. CRC Press, Florida, pp 226–269
- Sadeghipour HR, Bhatla SC (2002) Differential sensitivity of oleosins to proteolysis during oil body mobilization in sunflower seedlings. *Plant Cell Physiol* 43:1117–1126
- Kasahara H, Jiao Y, Bedgar DL, Kim SJ, Patten AM, Xia ZQ, Davin LB, Lewis NG (2006) *Pinus taeda* phenylpropanal double-bond reductase: purification, cDNA cloning,

- heterologous expression in *Escherichia coli*, and subcellular localization in *P. taeda*. *Phytochemistry* 67:1765–1780
29. Weselake RJ (2005) Storage lipids. In: Murphy DJ (ed) *Plant lipids: biology, utilisation and manipulation*. CRC Press, Florida, pp 162–225
  30. He X, Turner C, Chen GQ, Lin JT, McKeon TA (2004) Cloning and characterization of a cDNA encoding diacylglycerol acyltransferase from castor bean. *Lipids* 39:311–318
  31. Kroon JTM, Wei W, Simon WJ, Slabas AR (2006) Identification and functional expression of a type 2 acyl-CoA:diacylglycerol acyltransferase (DGAT2) in developing castor bean seeds which has high homology to the major triglyceride biosynthetic enzyme of fungi and animals. *Phytochemistry* 67:2541–2549
  32. Kaup MT, Froese CD, Thompson JE (2002) A role for diacylglycerol acyltransferase during leaf senescence. *Plant Physiol* 129:1616–1626
  33. Lu CL, Bayon de Noyer S, Hobbs DH, Kang J, Wen Y, Krachtus D, Hills MJ (2003) Expression pattern of diacylglycerol acyltransferase-1, an enzyme involved in triacylglycerol biosynthesis, in *Arabidopsis thaliana*. *Plant Mol Biol* 52:31–41
  34. He X, Chen GQ, Lin JT, McKeon TA (2006) Diacylglycerol acyltransferase activity and triacylglycerol synthesis in germinating castor seed cotyledons. *Lipids* 41:281–285
  35. Dahlqvist A, Stahl U, Lenman M, Banas A, Lee M, Sandager L, Ronne H, Stymne S (2000) Phospholipid:diacylglycerol acyltransferase: an enzyme that catalyses the acyl-CoA-independent formation of triacylglycerol in yeast and plants. *Proc Natl Acad Sci USA* 97:6487–6492
  36. Kalscheuer R, Steinbuechel A (2003) A novel bifunctional wax ester synthase/acyl-CoA:diacylglycerol acyltransferase mediates wax ester and triacylglycerol biosynthesis in *Acinetobacter calcoaceticus* ADP1. *J Biol Chem* 278:8075–8082
  37. Saha S, Enugutti B, Rajakumari S, Rajasekharan R (2006) Cytosolic triacylglycerol biosynthetic pathway in oilseeds. Molecular cloning and expression of peanut cytosolic diacylglycerol acyltransferase. *Plant Physiol* 141:1533–1543

# Highly Sensitive Determination of Diverse Ceramides in Human Hair Using Reversed-Phase High-Performance Liquid Chromatography–Electrospray Ionization Mass Spectrometry

Yoshinori Masukawa · Hisashi Tsujimura

Received: 23 October 2006 / Accepted: 27 November 2006 / Published online: 19 January 2007  
© AOCS 2007

**Abstract** Since ceramides (CERs) play roles in signal transduction and cell regulation, CERs of human hair might be responsible for apoptosis during keratinization, in addition to their structural barrier and water-holding functions. Although, we previously developed a method for comprehensive profiling of the CERs in hair, that method was too insensitive to quantitatively characterize the CERs in a small amount of hair samples. The aim of this study was to develop a novel method for the highly sensitive determination of the diverse CERs. The method developed is negative ion electrospray ionization mass spectrometry (ESI-MS) coupled to reversed-phase high-performance liquid chromatography (RP-HPLC) using methanol containing 10 mM ammonium acetate as a mobile phase. By this method, 48 peaks derived from 73 kinds of CERs were simultaneously determined in selected ion monitoring measurement using one calibration line of the standard *N*-palmitoyl dihydrospingosine, based on extremely small differences in the molar responses among different species of CERs, followed by the calculation of the actual levels using corrections for  $^{13}\text{C}$  and  $^2\text{H}$  effects. This method had extremely high sensitivity as indicated in the limit of quantification being in the femtomolar range. Other quantitative validation data, such as reproducibility, linearity and recoveries, were all sufficient. The quantitative levels of CERs

determined by RP-HPLC–ESI-MS were comparable with those determined by thin-layer chromatography. This method was successfully applied to the characterization of levels of CERs in only 1-mm pieces derived from a single hair fiber and revealed the presence of interindividual and intraindividual variations of the CER composition. This RP-HPLC–ESI-MS method can be a powerful tool for future research on physicochemical and physiological roles of CERs in hair.

**Keywords** Ceramide · Determination · High sensitivity · Human hair · Reversed-phase high-performance liquid chromatography–electrospray ionization mass spectrometry · Selected ion monitoring · Simultaneous

## Abbreviations

% CV	Percentage coefficient of variation
ADS	Ceramides consisting of $\alpha$ -hydroxy fatty acid and dihydrospingosine moieties
APCI	Atmospheric pressure chemical ionization
AS	Ceramides consisting of $\alpha$ -hydroxy fatty acid and sphingosine moieties
CER	Ceramide
DAG	Diacylglycerol
ESI	Electrospray ionization
LC	Liquid chromatography
LOD	Limit of detection
LOQ	Limit of quantification
MS	Mass spectrometry
NDS	Ceramides consisting of non-hydroxy fatty acid and dihydrospingosine moieties

Y. Masukawa · H. Tsujimura  
Tochigi Research Laboratories, Kao Corporation,  
Ichikai, Haga, Tochigi 321-3497, Japan

Y. Masukawa (✉)  
Analytical Research Center, Kao Corporation,  
2606 Akabane, Ichikai, Haga, Tochigi 321-3497, Japan  
e-mail: masukawa.yoshinori@kao.co.jp

NS	Ceramides consisting of non-hydroxy fatty acid and sphingosine moieties
RP-HPLC	Reversed-phase high-performance liquid chromatography
SIM	Selected ion monitoring
TLC	Thin-layer chromatography

## Introduction

Ceramides (CERs) play roles in signal transduction and cell regulation [1–4] in addition to physicochemical roles as a barrier against cell permeability and as a matrix for the association of membrane proteins. Human cells/tissues predominantly include CERs consisting of even carbon atom containing non-hydroxy fatty acids and C<sub>18</sub> sphingosine moieties together with low levels of CERs consisting of even carbon atom containing  $\alpha$ -hydroxy fatty acids and C<sub>18</sub> sphingosine moieties [5–8]. In the human stratum corneum, there are diverse CERs with sphingosine, dihydrosphingosine, phytosphingosine and 6-hydroxysphingosine moieties [9, 10]. Those CERs and CER-related lipids may be involved not only with physicochemical roles in determining the barrier and water-holding functions in the intercellular spaces among the horny cells [11, 12], but also with physiological roles of differentiated keratinocytes where apoptosis occurs [13]. On the other hand, human hair also contains CERs which are predominantly composed of non-hydroxy or  $\alpha$ -hydroxy fatty acids and C<sub>18</sub> dihydrosphingosine moieties [14, 15]. We have hypothesized that CERs in hair might be responsible for apoptosis during keratinization, which proceeds from living hair matrix cells to dead cuticular or cortical cells, in addition to their contributions to the barrier function and the water-holding property of hair. To investigate this hypothesis, it was essential to have a method for the analysis of CERs.

While many conventional methods, such as gas chromatography–mass spectrometry (MS) [15], thin-layer chromatography (TLC) [16], diacylglycerol (DAG) kinase assay [17], liquid chromatography (LC)–evaporative light-scattering detection [18] and LC–UV detection using a derivatizing technique [19], have been used to determine CERs, Mano et al. [20], Gu et al. [21] and Couch et al. [22] reported MS using electrospray ionization (ESI) or atmospheric pressure chemical ionization (APCI) to be a valuable tool in the analysis of mixed CERs in 1997. Since the methods based on ESI-MS or APCI-MS were far superior to the

conventional methods in terms of sensitivity and selectivity, since after their articles, many methods using LC–MS and tandem MS (MS/MS) for the analysis of CERs have been developed. Among them, some methods have been applied to the determination of CERs in practically mixed samples including lipid extracts of human cells/tissues [5, 6, 23–30]. However, those methods could not be used for the determination of diverse CERs in hair because the analytes targeted by them were sphingosine-containing CERs and not the dihydrosphingosine-containing CERs that are predominantly present in hair. Therefore, we designed a new method to comprehensively profile diverse kinds of CERs, using reversed-phase high-performance liquid chromatography (RP-HPLC) coupled to APCI-MS [31]. We used this technique and found that there are at least 73 kinds of CERs, including isobaric and isomeric ones, in hair, which led to our interest in the biosynthesis of that diversity of CERs in hair matrix cells. However, this RP-HPLC–APCI-MS method was too insensitive to quantitatively characterize the CERs in a small amount of hair samples growing in a single hair follicle.

The aim of this study was to develop a method for the highly sensitive determination of diverse CERs in hair using LC–MS. We found that different deprotonated ions of monoisotopic molecules for standard CERs can be detected with extremely small differences in their molar responses when methanol containing ammonium acetate as the mobile phase in RP-HPLC combined with negative ion ESI-MS was used. Herein, we describe the successfully developed method using RP-HPLC–ESI-MS and its application to the analysis of the diverse CERs in hair samples collected from different subjects and among different 1-mm pieces derived from a single hair fiber. The application revealed that the high sensitivity of this method enables the characterization of the diverse CERs in only 1-mm pieces derived from a single hair fiber and that there are interindividual and intraindividual variations of CER composition, which demonstrates the applicability of this RP-HPLC–ESI-MS method for future research on physicochemical and physiological roles of CERs in hair.

## Experimental Procedure

### Nomenclature

CERs are termed according to previous reports [31, 32]. Briefly, non-hydroxy fatty acid,  $\alpha$ -hydroxy



fatty acid, dihydrosphingosine and sphingosine moieties are designated as N, A, DS and S, respectively. On the basis of this terminology, for example, a CER with a non-hydroxy fatty acid and dihydrosphingosine moieties is expressed as NDS. The number of fatty acid carbons and unsaturation (if present) is expressed following the letters N or A, while the number of sphingoid carbons is expressed following the letters DS or S, as shown in N24:1DS18 for a CER consisting of nervonic acid and C<sub>18</sub> dihydrosphingosine moieties.

## Chemicals

Methanol and chloroform, of infinity pure grade from Wako Pure Chemicals Industries (Tokyo, Japan), and *n*-hexane, of HPLC grade from Kanto Reagents (Tokyo, Japan), were used to prepare crude hair lipids. Methanol, of HPLC grade from Kanto Reagents (Tokyo, Japan), was used to prepare the mobile phase for RP-HPLC–ESI-MS. Ultrapure water prepared using a Milli-Q purification system (Millipore, Bedford, MA, USA) was used in all procedures. All other chemicals were of the highest analytical grade commercially available. Standard CERs, such as N-16:0 sphinganine (N16DS18), N-18:0 sphinganine (N18DS18), N-24:0 sphinganine (N24DS18), N24:1 sphinganine (N24:1DS18), CER C<sub>14:0</sub> (N14S18), CER C<sub>16:0</sub> (N16S18), CER C<sub>18:0</sub> (N18S18), CER C<sub>20:0</sub> (N20S18), CER C<sub>24:0</sub> (N24S18) and CER C<sub>24:1</sub> (N24:1S18) (purity above 98%) were from Avanti Polar Lipids (Alabaster, AL, USA). Other standard CERs, such as A16DS18, A24DS18, A16S18 and A24S18, were synthesized in the laboratory, with a slight modification of a method of Ramjit et al. [33]. Briefly, for the synthesis of A16DS18, 0.70 mmol C<sub>18</sub> dihydrosphingosine, 1.20 mmol 2-acetoxy palmitic acid, 1.30 mmol *N*-[3-(dimethylamino)propyl]-*N'*-ethylcarbodiimide hydrochloride and 1.30 mmol 1*H*-1,2,3-benzotriazol-1-ol hydrate were dissolved in chloroform and then were stirred at room temperature for 24 h under a nitrogen atmosphere. The resulting mixture was subjected to liquid–liquid extraction (700 ml chloroform and 700 ml 5% sodium hydrogen carbonate aqueous solution) and the separated organic phase was evaporated to dryness. About 40 ml of tetrahydrofuran/methanol (1:3, by volume) and potassium carbonate (0.415 g, 3.0 mmol) were added to the residue, which was then stirred at room temperature for 2 h. The solvent was evaporated again, followed by purification with silica gel column chromatography. The analysis by <sup>1</sup>H-NMR and <sup>13</sup>C NMR confirmed the structure of A16DS18 and the purity was determined as better than 98% by LC–UV

detection. The other CERs (A24DS18, A16S18 and A24S18) were synthesized and their purities were examined (better than 98%), similarly to the aforementioned CERs. Each standard solution was prepared as a molar solution using its average molecular weight (e.g., for N16DS18, not the monoisotopic mass 539.5 but rather the average mass 539.9 was used). Thus, individual standard stock solutions (1 mM each) were prepared by dissolving accurate amounts of the standard CERs in chloroform/methanol (1:9, by volume) and were stored at –4°C. Individual or mixed working standard solutions were obtained by further dilution of the stock solutions with methanol just prior to use.

## Hair Fibers and Preparation

Scalp hair fibers were collected from seven Japanese volunteers (designated as Hair-A for a 15-year-old female, Hair-F1 for a 10-year-old female, Hair-F2 for a 42-year-old female, Hair-F3 for a 76-year-old female, Hair-M1 for a 9-year-old male, Hair-M2 for a 25-year-old male and Hair-M3 for an 86-year-old male). None of these hair samples had been exposed to any chemical reactions, such as hair coloring or permanent waving. First of all, qualitative analyses of CERs in these hair samples were performed according to our previously reported RPLC–APCI-MS and RPLC–ESI-MS/MS methods [31]. Since the results showed that all the hair samples contained 73 kinds of CERs corresponding to our previous results [31], we did the quantitative analyses using full-length fibers from the proximal root end to the distal tip of Hair-A and five hair fibers of 2-cm-length each just from the root end (approximately 1 mg each in weight) of Hair-F1, Hair-F2, Hair-F3, Hair -M1, Hair-M2 and Hair-M3. These fibers were washed with plain shampoo for 1 min and rinsed with water for 10 min, which was repeated twice. The fibers were washed with *n*-hexane for approximately 1 min to remove contaminating CERs on the surface, which might come from the stratum corneum of the scalp, and their weights were measured accurately with an ultra-micro-balance (UTM2, Mettler Toledo, Tokyo, Japan) after drying at room temperature for more than 24 h. In a separate experiment, 1-mm pieces were cut with a knife from a single hair fiber (approximately 7 cm in length from the root end, Hair-M1). Thus, pieces (approximately 10 µg each in weight) of the hair fiber at 1–2, 13–14, 25–26, 37–38, 49–50 and 61–62 mm from the root end were obtained. The pieces were subjected to lipid extraction without any washing after their weights had been measured using the UTM2 instrument. The

preparative procedures were performed according to our previous reports [31, 34]. Briefly, the fibers were immersed successively into chloroform/methanol (2:1, 1:1, 1:2, by volume), followed by chloroform/methanol/water (18:9:1 by volume) each for 24 h at room temperature. The extracts were combined and dried using a nitrogen stream. The residues were then dissolved in methanol.

### MS Analysis

An Agilent 1100 series LC/MSD SL (single quadrupole) system equipped with an ESI or APCI source, ChemStation software, a 1100 well plate autosampler (Agilent Technologies, Palo Alto, CA, USA) and an L-column ODS separation column (2.1-mm inner diameter  $\times$  150 mm, Chemicals Evaluation and Research Institute, Tokyo, Japan) was used. In the case of flow-injection MS analysis, the column was uncoupled from the system. In this system, a 1100 binary pump was operated at a flow rate of 0.2 ml/min. The injection volume was 5  $\mu$ l each of standard solutions and extracted crude hair lipid solutions. The column temperature was maintained at 40°C. ESI measurements in the mass spectrometer were performed with the following settings: polarity, negative and positive; heater temperature of nitrogen gas, 350°C; flow of heated dry nitrogen gas, 8.0 l/min; nebulizer gas pressure, 30 psi; capillary voltage, -3,000 V for negative setting and 3,000 V for positive setting; fragmenter voltage (one of the parameters used in this mass spectrometer, which is the same as “cone voltage” used in others), 250 V. In contrast, APCI measurements were performed with the following settings: vaporizer temperature, 300°C; flow of heated dry nitrogen gas, 5.0 l/min; nebulizer gas pressure, 40 psi; corona current, 4.0  $\mu$ A; the other settings were the same as for ESI. These parameters were optimized in preliminary tests to get the highest abundance of the molecule-related ions for standard N16DS18. The selected ion monitoring (SIM) measurement in negative ion ESI was performed using unit mass resolution mode. To simultaneously detect 73 kinds of CERs in hair, 33 deprotonated ions of the monoisotopic molecules were used as follows (dwell time 36 ms each):  $m/z$  510.5 for N14DS18; 524.5 for N15DS18; 526.5 for A14DS18; 536.5 for N16:1DS18 and N16S18; 538.5 for N16DS18 (+N18DS16\*); 552.5 for A16S18 and N17DS18<sup>\$</sup> (+N18DS17\* + N16DS19\*); 554.5 for A16DS18; 564.5 for N18:1DS18 and N18S18; 566.6 for N18DS18; 568.5 for A17DS18; 580.6 for N19DS18<sup>\$</sup> (+N18DS19\*); 582.6 for A18DS18; 592.6 for N20S18; 594.6 for N20DS18 (+N18DS20\*); 608.6 for N21DS18<sup>\$</sup> (+N20DS19\*); 620.6 for N22:1DS18 and

N22S18; 622.6 for N22DS18 (+N20DS20\*); 634.6 for N23:1DS18; 636.6 for N23DS18<sup>\$</sup> (+N22DS19\*<sup>\$</sup>); 646.6 for N24:1S18; 648.6 for N24:1DS18 and N24S18; 650.6 for N24DS18 (+N22DS20\*); 662.7 for N25:1DS18<sup>\$</sup> (+N24:1DS19\*); 664.7 for A24:1DS18, A24S18 and N25DS18<sup>\$</sup> (+N24DS19\*<sup>\$</sup> + N23DS20\*); 666.6 for A24DS18 (+A22DS20\*); 674.7 for N26:1S18; 676.7 for N26:1DS18 (+N24:1DS20\*) and N26S18; 678.7 for N26DS18 (+N24DS20\*); 690.7 for N27:1DS18 (+N26:1DS19\*); 692.7 for N27DS18<sup>\$</sup> (+N26DS19\*<sup>\$</sup> + N25DS20\*<sup>\$</sup>); 704.7 for N28:1DS18 (+N26:1DS20\*); 706.7 for N28DS18 (+N26DS20\*); 732.7 for N30:1DS18 (+N28:1DS20\*). The asterisks and dollar signs indicate isobaric and isomeric CERs, respectively.

### Determination of CERs in Hair

Prior to the determination of the CERs, 1, 2.5, 5, 10, 25, 50, 100 and 250 fmol each of standard N16DS18 was injected into the RP-HPLC-ESI-MS system and then the calibration line was generated by plotting molar quantities corresponding to the monoisotopic molecule of standard N16DS18 (0.68, 1.7, 3.4, 6.8, 17, 34, 68 and 170 fmol) versus the peak areas obtained. Using the calibration line, we converted each peak area of the CER(s) in the SIM chromatogram to the levels of its (their) monoisotopic molecule(s). The levels were then converted to their actual levels by correction for <sup>13</sup>C and <sup>2</sup>H effects. To calculate isotopologue abundances of each CER, we used Microsoft Excel 2000 (Microsoft Corporation, Troy, NY, USA), based on the fundamental principles for obtaining mass spectral isotopic distributions previously reported by Yerger [35]. Every hair lipid sample was analyzed in triplicate. The means  $\pm$  the standard deviations of the levels are expressed as weights of lipids to that of hair fibers (micrograms per gram of hair). Recovery studies were performed by spiking the extracted crude hair lipids with 10 fmol of standard CERs. The levels of the CERs determined in spiked hair lipid were compared with those in nonspiked hair lipids.

### TLC Analysis

Hair lipid extracts (0.21 g) were obtained from approximately 10 g of Hair-A, following extraction with chloroform, methanol and water, as described already. The extracts were purified with silica gel column chromatography. The extracts dissolved in chloroform were injected onto the column, which had been previously equilibrated with chloroform, followed by the successive elution of 300 ml each of chloroform/methanol, 100:0, 99:1, 98:2, 96:4, 94:6, 92:8, 90:10, 85:15

and 80:20 (by volume). Comparison of  $R_f$  values of spots of the fractions with those of authentic N16DS18 and A16DS18 in the TLC analysis revealed that fractions of 98:2 and 96:4 included NDSs/NSs and ADSs/ASs, respectively. Their levels were determined using the standard N16DS18 by the TLC analysis, and their levels were compared with summed levels of individual CERs determined by RP-HPLC–ESI-MS. This TLC analysis was based on a slight modification of a previously reported method [15]. Briefly, high-performance TLC plates (silica gel 60, 20 cm × 10 cm, Merck) were used for the separation. After aliquots of concentrated fractions had been applied on the plate, it was developed with chloroform/methanol/acetic acid (190:9:1 by volume) twice. After drying, the plate was sprayed with 10% copper sulfate and 8% phosphoric acid solution and was charred by heating at 180°C for 5 min. Spots corresponding to NDSs/NSs and ADSs/ASs were densitometrically determined using a TLC Scanner 3 photodensitometer (Camag, Muttenz, Switzerland) and using the calibrated line of N16DS18.

## Results

### Optimization of Analytical Conditions

On the basis of our previous results [31], deprotonated ions  $[M - H]^-$  of monoisotopic molecules for standard NDSs and NSs were targeted in the SIM measurement of negative ion APCI and ESI, while protonated ions  $[M+H]^+$ , of monoisotopic molecules for standard NDSs and protonated ions with loss of 1 mol water  $[M + H - H_2O]^+$ , of monoisotopic molecules for standard NSs were selected in positive ion APCI and ESI. When equivalent numbers of moles of ten standard NDSs and NSs were subjected to flow-injection MS using methanol as a carrier, the intensities of the ions detected for the NDSs and NSs gradually decreased with increases in the chain lengths of fatty acid moieties in both negative ion and positive ion APCI, whereas the intensities were drastically decreased in both negative ion and positive ion ESI. Thus, as represented in Fig. 1a, the intensity of  $[M - H]^-$  for N24S18 was approximately 20% of that for N14S18 under conditions with negative ion ESI-MS. To improve the difference in intensities among the ten standard NDSs and NSs, effects of addition of acids or salts to methanol under conditions of different ionizations on the intensities of molecularly related ions derived from equivalent molar quantities of the ten NDSs and NSs were tested. Thus, we examined all combinations of addition of acids (formic acid or

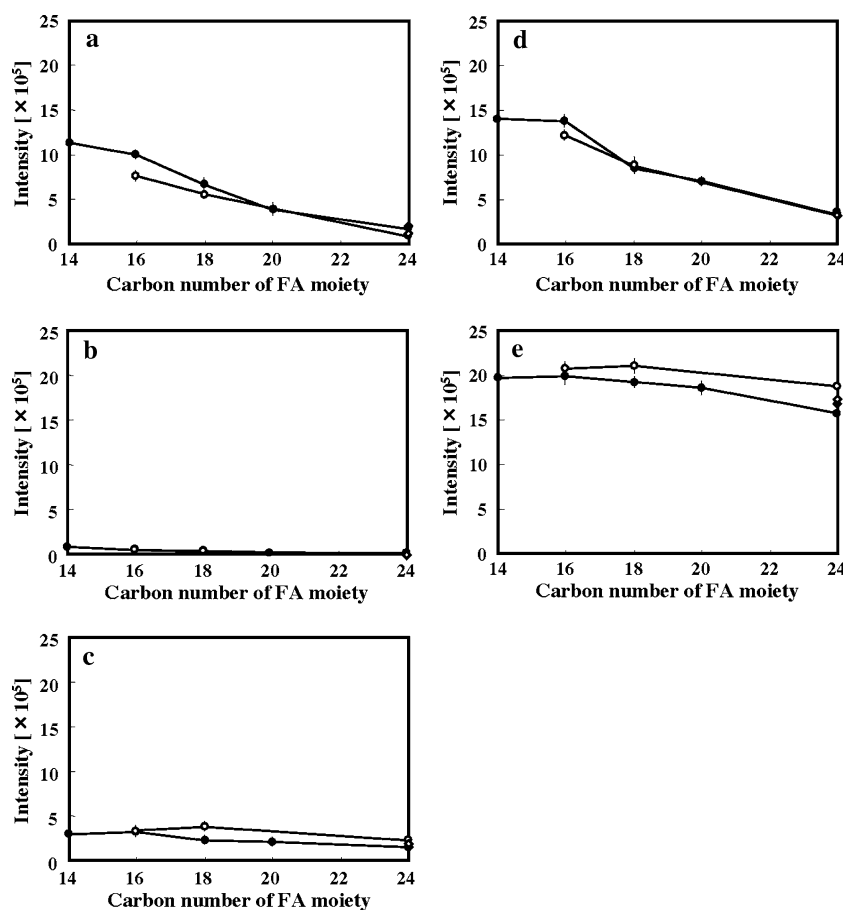
acetic acid) or salts (ammonium formate or ammonium acetate) and different ionization modes (negative ion ESI-MS, positive ion ESI-MS, negative ion APCI-MS or positive ion APCI-MS). Since we planned to couple MS with RP-HPLC using an octadecyl silica gel column after optimization of the MS conditions, acidic or neutral conditions but not basic ones were examined. It is known that silica gel is extremely unstable under basic conditions.

Of all the combinations tested, the addition of 50 mM ammonium acetate upon negative ion ESI-MS showed the highest mean of the intensities of the ten standard NDSs and NSs and the smallest difference in the intensities. This implies that the combination of ammonium acetate and negative ion ESI-MS provides the average highest sensitivity and the smallest difference in molar responses for the NDSs and NSs tested. The experimental data from negative ion ESI-MS are depicted in Fig. 1. In the case of the addition of 50 mM formic acid to methanol, the intensities for all the NDSs and NSs tested decreased to approximately 10% of those using methanol with no additives (Fig. 1a, b). When methanol containing 50 mM ammonium formate was used, the intensities of the NDSs and NSs with shorter chain lengths in the fatty acid moieties decreased to 30–40% of those using no additives, while the differences in the intensities tended to be rather small (Fig. 1a, c). Methanol containing 50 mM acetic acid yielded increased intensities up to 120–210% of those using no additives, while it hardly improved differences in the intensities (Fig. 1a, d). On the other hand, when 50 mM ammonium acetate was added to methanol, the differences in the intensities among the NDSs and NSs tested became the smallest (Fig. 1a, e). On the basis of those results, we selected the combination of negative ion ESI-MS and methanol containing ammonium acetate. Further, when the optimal concentration of ammonium acetate was examined in the range 1–200 mM, the maximal mean of the intensities for the ten standard NDSs and NSs was observed at a concentration of 1 mM, while the minimal difference in the intensities was observed at 10 mM. Since the mean was not improved much from 1 to 10 mM while the difference was greatly improved, 10 mM ammonium acetate was selected.

### Determination of CERs Using RP-HPLC–ESI-MS

Negative ion ESI-MS combined with RP-HPLC using a mobile phase of methanol containing 10 mM ammonium acetate and a stationary phase of L-column ODS was examined to develop a method for the highly sensitive determination of the diverse CERs. Figure 2

**Fig. 1** Effects of addition of acid or salt to the carrier on the intensities of deprotonated ion derived from 50 pmol each of standard NDSs and NSs in flow-injection mass spectrometry (MS) analysis with negative ion electrospray ionization (ESI). Carrier **a** methanol (no additives), **b** methanol containing 50 mM formic acid, **c** methanol containing 50 mM ammonium formate, **d** methanol containing 50 mM acetic acid, **e** methanol containing 50 mM ammonium acetate. *Open circles* NDS with saturated fatty acid moiety, *filled circles* NS with saturated fatty acid moiety, *open diamonds* N24:1DS18, *filled diamonds* N24:1S18. Error bars standard deviation ( $n = 3$ ). FA fatty acid. For an explanation of the ceramide names used, see “Nomenclature”



shows RP-HPLC–ESI-MS multi-SIM chromatograms of ten standard NDSs and NSs (dwell time 120 ms each). All monoisotopic molecules for the NDSs and NSs were detected as separate and distinct peaks in the chromatograms. There were five small peaks in the

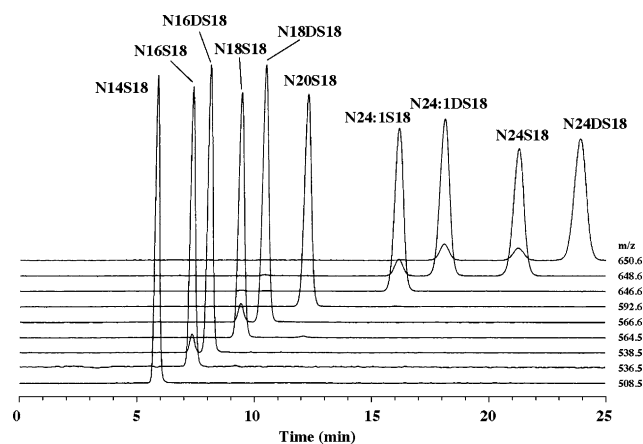


**Fig. 2** Reversed-phase high-performance liquid chromatography (RP-HPLC)–ESI-MS multiple selected ion monitoring (SIM) chromatograms of ten standard NDSs and NSs (250 fmol each, including all isotopic molecules)

$m/z$  538.5, 566.6, 648.6 and 650.6 SIM chromatograms in Fig. 2. Among the five, two small peaks were included in the  $m/z$  650.6 SIM chromatogram. The small peak that occurred in the  $m/z$  538.5 SIM chromatogram had identical retention times to those of the monoisotopic molecules of N16S18 that were eluted in the  $m/z$  536.5 SIM chromatogram. Therefore, the small peak was identified as an  $M + 2$  isotopologue of N16S18. Isotopic ions, such as  $M + 1$  and  $M + 2$  isotopologues, occurs naturally owing to the existence of  $^{13}\text{C}$  and  $^2\text{H}$ . Similarly, the small peaks in the  $m/z$  566.6 and 648.6 SIM chromatograms were identified as  $M + 2$  isotopologues of N18S18 and N24:1S18, respectively. As for the two small peaks in the  $m/z$  650.6 SIM chromatogram, the peaks having shorter and longer retention times were identified as  $M + 2$  isotopologues of N24:1DS18 and N24S18, respectively. The least hydrophobic CER of all those tested, N14S18, was eluted at approximately 6 min, while the most hydrophobic CER, N24DS18, was eluted at approximately 24 min. This indicates that isocratic elution with methanol containing 10 mM ammonium acetate may allow the appearance of N30:1DS18 or N28DS18 (one of the most hydrophobic CERs in hair) within a single

run, although it is slightly more time-consuming compared with the gradient elution system [31].

It is well known that MS can accurately provide isotopologue ratios of lipid molecules [25, 36–39]. By use of this property, individual lipid molecules are quantitatively determined even if more than two isotopologues derived from different lipid molecules have the same  $m/z$ . Therefore, under these RP-HPLC–ESI-MS conditions using unit mass resolution mode, it was validated whether monoisotopic molecules of targeted NDSs and NSs could be quantitatively detected. As representative standards, N16DS18 and N24DS18 were used in this experiment. The relative intensities of peak areas of four isotopologue ions ( $[M - H]$ ,  $[M + 1 - H]$ ,  $[M + 2 - H]$  and  $[M + 3 - H]$ ) for N16DS18 were obtained by simultaneously performing SIM on the four isotopologue ions and then comparing the peak areas in their SIM chromatograms. The same SIM measurement was performed for N24DS18. Those measured relative intensities were compared with theoretically calculated relative intensities, based on the isotopologue ratios of  $^{13}\text{C}$  and  $^2\text{H}$ . As a result, the measured relative intensities under the RP-HPLC–ESI-MS conditions were almost in agreement with the theoretical ones (Table 3). This implies that monoisotopic ions can be quantitatively detected even in the unit mass resolution mode of this RP-HPLC–ESI-MS method and that quantitative values of monoisotopic molecules for the CERs can be theoretically converted to their actual level, by correction for  $^{13}\text{C}$  and  $^2\text{H}$  effects. For example, if the level of the monoisotopic molecule for N16DS18 is obtained as 1.00  $\mu\text{g/g}$  hair, the actual level can be calculated as 1.47  $\mu\text{g/g}$  hair, because the monoisotopic molecule accounts for 67.9% of the total molar quantities for N16DS18.

#### Determination of 73 Kinds of CERs in Human Hair

There are 73 kinds of CERs, including many isobaric and isomeric ones, in hair, and these are divided into 33 molecular weights [31]. Therefore, to simultaneously detect the 73 kinds of CERs, multi-SIM measurement with 33 ions in this RP-HPLC–ESI-MS analysis was performed (dwell time 36 ms each). Prior to use of this method, crude hair lipids extracted from Hair-A were subjected to RPLC–APCI-MS and RPLC–ESI-MS/MS [31] and it was confirmed that Hair-A contains the 73 kinds of CERs. A set of multi-SIM chromatograms of the 73 kinds of CERs in hair (approximately 1 mg, Hair-A) is shown in Fig. 3, in which no peaks chromatographically interfere with the 48 peaks corresponding to the 73 kinds of CERs. The

identities of the 48 peaks were also confirmed using RP-HPLC–ESI-MS/MS [31] under identical RP-HPLC conditions, and were in complete agreement with the 73 kinds of CERs. The reproducibility (percentage coefficient of variation, % CV,  $n = 6$ ), limit of detection (LOD, signal-to-noise ratio of 3), limit of quantification (LOQ, signal-to-noise ratio of 10) and calibration lines for 13 standard CERs were obtained under conditions of simultaneous SIM of the 33 ions (Tables 1, 2). The % CVs of the peak areas of six consecutive analyses of 100 fmol were in the range 2.1–4.6%. The LOD and LOQ for 5  $\mu\text{l}$  of the standard solutions were in the ranges 0.14–0.40 and 0.46–1.37 fmol, respectively. As for their calibration lines, all determination correlations were greater than 0.9987 in the range between 1 and 250 fmol. There seemed to be a definite trend toward slightly larger slopes for the CERs with non-hydroxy fatty acid moieties than for those with  $\alpha$ -hydroxy fatty acid ones and with longer chain lengths in fatty acid ones. However, the % CV of the slopes of the 13 calibration lines corresponding to the 13 monoisotopic molecules was calculated to be 3.9%, implying there are extremely small differences in molar responses of monoisotopic ions among the 13 different CERs.

Recoveries were estimated by comparison of the determined levels of 13 standard CERs in spiked crude hair lipids with those in nonspiked hair lipids, using only one calibration line produced by the standard N16DS18 (Table 2). The average recoveries were in the range between 97.0 and 108.2% with the % CV being 1.9–5.1%. This demonstrated that our RP-HPLC–ESI-MS method using only one standard calibration line produced by the standard N16DS18 provides precise and accurate levels of the 13 CERs in hair, because of extremely small differences in molar responses of monoisotopic molecules between N16DS18 and the other CERs. Further, quantitative values obtained by RP-HPLC–ESI-MS were compared with those obtained by TLC. When fractions containing NDSs/NSs and ADSs/ASs obtained from hair lipid extracts of Hair-A were subjected to RP-HPLC–ESI-MS, the total levels of NDSs/NSs and ADSs/ASs were determined to be 352 and 47  $\mu\text{g/g}$  hair, respectively, where each of the 48 peaks corresponding to the 73 kinds of CERs was determined using a calibration line of the standard N16DS18 and the peaks were then summed up. In contrast, the TLC analysis showed 372 and 56  $\mu\text{g/g}$  hair as NDSs/NSs and ADSs/ASs, respectively. These results indicate that quantitative levels measured by RP-HPLC–ESI-MS are comparable with those determined by TLC.

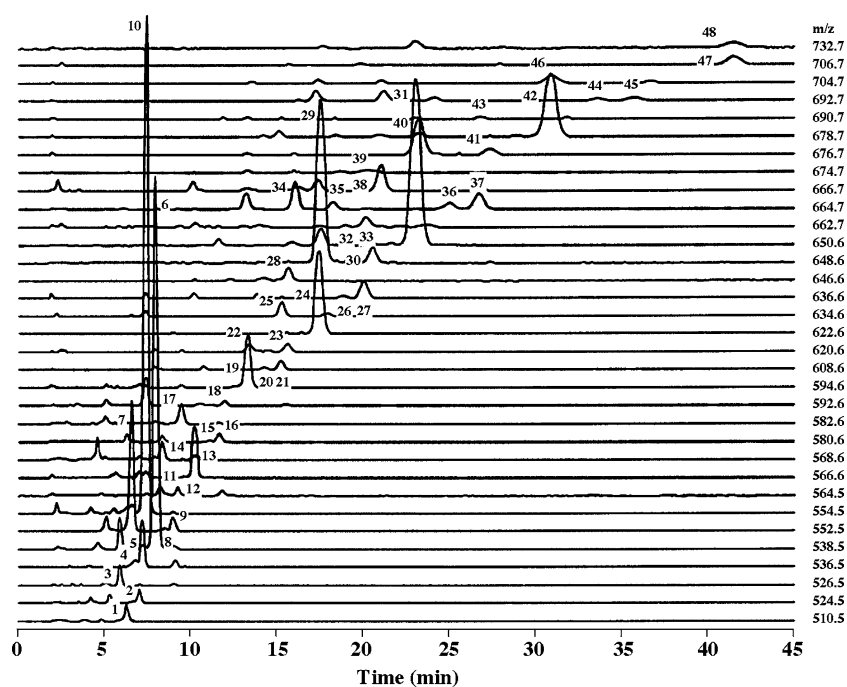


**Fig. 3** RP-HPLC-ESI-MS multi-SIM chromatograms of ceramides in extracted crude hair lipids. Peaks 1 N14DS18; 2 N15DS18; 3 A14DS18; 4 N16:1DS18; 5 N16S18; 6 N16DS18 (+N18DS16\*); 7 A16S18; 8 N17DS18<sup>S</sup>; 9 N17DS18<sup>S</sup> (+N18DS17\* + N16DS19\*); 10 A16DS18; 11 N18:1DS18; 12 N18S18; 13 N18DS18; 14 A17DS18; 15 N19DS18<sup>S</sup>; 16 N19DS18<sup>S</sup> (+N18DS19\*); 17 A18DS18; 18 N20S18; 19 N20DS18 (+N18DS20\*); 20 N21DS18<sup>S</sup>; 21 N21DS18<sup>S</sup> (+N20DS19\*); 22 N22:1DS18; 23 N22S18; 24 N22DS18 (+N20DS20\*); 25 N23:1DS18; 26 N23DS18<sup>S</sup> (+N22DS19\*<sup>S</sup>); 27 N23DS18<sup>S</sup> (+N22DS19\*<sup>S</sup>); 28 N24:1S18; 29 N24:1DS18; 30 N24S18; 31

N24DS18 (+N22DS20\*); 32 N25:1DS18<sup>S</sup>; 33 N25:1DS18<sup>S</sup> (+N24:1DS19\*); 34 A24:1DS18; 35 A24S18; 36 N25DS18<sup>S</sup> (+N24DS19\*<sup>S</sup>); 37 N25DS18<sup>S</sup> (+N24DS19\*<sup>S</sup> + N23DS20\*); 38 A24DS18 (+A22DS20\*); 39 N26:1S18; 40 N26:1DS18 (+N24:1DS20\*); 41 N26S18; 42 N26DS18 (+N24DS20\*); 43 N27:1DS18 (+N26:1DS19\*); 44 N27DS18<sup>S</sup> (+N26DS19\*<sup>S</sup> + N25DS20\*<sup>S</sup>); 45 N27DS18<sup>S</sup> (+N26DS19\*<sup>S</sup> + N25DS20\*<sup>S</sup>); 46 N28:1DS18 (+N26:1DS20\*); 47 N28DS18 (+N26DS20\*); 48 N30:1DS18 (+N28:1DS20\*). The asterisks and dollar signs indicate isobaric and isomeric ceramide molecules, respectively

## Applications

Similar to Hair-A, prior to the quantification, it was confirmed that Hair-F1, Hair-F2, Hair-F3, Hair-M1, Hair-M2 and Hair-M3 contain the 73 kinds of CERs by RPLC-APCI-MS and RPLC-ESI-MS/MS [31]. Table 3 shows the levels of CERs in different hair samples obtained from three females and from three males ( $n = 3$ , analysis in triplicate for each). In all the hair samples tested, 48 peaks corresponding to the 73 kinds of CERs were commonly observed. The following characteristics of the levels of CERs were observed among the subjects tested: (1) the levels of A16DS18 were greater in the hair samples derived from the males tested (Hair-M1, Hair-M2 and Hair-M3), while the levels of N22DS18 (+N20DS20), N23DS18 (+N22DS19), N24DS18 (+N22DS20) and A24DS were greater in those derived from the females tested (Hair-F1, Hair-F2 and Hair-F3); (2) the hair samples collected from the youngest female and the youngest male tested (Hair-F1 and Hair-M1) contained greater levels

of sphingosine-containing CERs (NSs and ASs), as seen in the levels of N16S18, A16S18, N22S18, A24S18 and N26S18; (3) there were other variations, such as the hair samples from two of the females tested (Hair-F1 and Hair-F3) had extremely high levels of N18DS18 and N20DS18 (+N18DS20).

In a separate experiment, the possibility to detect and determine the CERs using very small sample amounts of hair was examined. A set of the multi-SIM chromatograms of CERs in 1-mm pieces (approximately 10  $\mu\text{g}$  in weight) derived from a single hair fiber (Hair-M1) is shown in Fig. 4. Of the 48 peaks to be detected, 46 peaks of CERs were observed. No peaks originating from N16:1DS18 and N19DS18 were detected, probably owing to their extremely low level in this hair specimen, i.e., Hair-M1 (Table 3). Next, the levels of the CERs in six different pieces of 1-mm length (approximately 10  $\mu\text{g}$  each in weight) prepared from the fiber are listed in Table 4 ( $n = 1$ , analysis in triplicate for each). The six 1-mm pieces at intervals of 11 mm from the root end were analyzed. Since hair fibers generally grow approximately

**Table 1** Comparison of measured relative intensity of four isotopologue ions derived from 250 fmol each of standard N16DS18 and N24DS18 in selected ion monitoring (SIM) measurement of reversed-phase high-performance liquid chromatography–electrospray ionization mass spectrometry (RP-HPLC–ESI-MS) with theoretically calculated relative intensity based on  $^{13}\text{C}$  and  $^2\text{H}$  effects

Ceramide	Relative intensity <sup>a</sup>			
	[M – H]	[M + 1 – H]	[M + 2 – H]	[M + 3 – H]
<b>N16DS18<sup>b</sup></b>				
Measured	1.000	0.382	0.074	0.009
Theoretical	1.000	0.383	0.077	0.011
<b>N24DS18<sup>c</sup></b>				
Measured	1.000	0.465	0.107	0.016
Theoretical	1.000	0.472	0.115	0.019

Simultaneously run SIM on four isotopologue ions

For an explanation of the ceramide names used, see “[Nomenclature](#)”

<sup>a</sup> Calculated as intensity of [M – H] = 1.000 from the peak areas of the four isotopologue ions in their SIM chromatograms

<sup>b</sup> [M – H] = 538.5, [M + 1 – H] = 539.5, [M + 2 – H] = 540.5, [M + 3 – H] = 541.5

<sup>c</sup> [M – H] = 650.6, [M + 1 – H] = 651.6, [M + 2 – H] = 652.6, [M + 3 – H] = 653.6

12 mm/month [40], these pieces roughly correspond to monitoring 2.5 days of biosynthesis of CERs in a hair follicle at intervals of 1 month over 5 months. The levels

of the CERs tended to gradually decrease with the distance from the root end, as represented in A16DS18 and N24DS18 (+N22DS20). However, the levels of sphingosine-containing CERs (NSs and ASs), such as N16S18, A16S18, N18S18, N20S18, N22S18, A24S18, N26:1S18 and N26S18, were higher in the 49–50-mm piece than the root region (1–2 mm), while the levels of nervonic acid containing CERs, such as N24:1S18, N24:1DS18, A24:1DS18 and N26:1DS18 (+N24:1Ds20), were higher in the 25–26-, 49–50- and 61–62-mm pieces than in other regions (Table 4).

## Discussion

The aim of this study was to develop a method for the highly sensitive determination of the diverse CERs in hair. First, we found that a combination of methanol containing ammonium acetate and negative ion ESI-MS greatly improves molar sensitivity and differences in molar responses of monoisotopic molecules among different kinds of CERs, consisting of NDSs and NSs. When finally optimized RP-HPLC–ESI-MS with methanol containing 10 mM ammonium acetate as a mobile phase was applied to 13 standard CERs, including NDSs, NSs, ADSs and ASs, we observed definite differences in the molar responses of the

**Table 2** Reproducibility ( $n = 6$ ), limit of detection (LOD, signal-to-noise ratio of 3), limit of quantification (LOQ, signal-to-noise ratio of 10), calibration lines and recoveries obtained

Ceramide	Reproducibility <sup>a</sup> of peak area (% CV)	LOD <sup>b</sup> (fmol)	LOQ <sup>b</sup> (fmol)	Calibration line <sup>c</sup>		Recovery <sup>d</sup> (%)
				Equation	$R^2$	
N16DS18	2.1	0.20	0.65	$y = 6,848x + 2,107$	0.9989	102.2 ± 1.9
N18DS18	2.3	0.23	0.87	$y = 6,416x + 2,873$	0.9987	103.7 ± 2.2
N24DS18	4.1	0.31	1.03	$y = 7,056x + 1,089$	0.9993	98.3 ± 4.6
N24:1DS18	4.3	0.25	0.83	$y = 6,891x + 1,289$	0.9990	97.0 ± 3.8
N16S18	3.1	0.19	0.64	$y = 6,417x + 1,845$	0.9995	105.8 ± 3.0
N18S18	4.4	0.22	0.74	$y = 6,674x + 2,223$	0.9992	105.5 ± 4.4
N20S18	2.7	0.28	0.94	$y = 6,428x + 650$	0.9990	108.2 ± 5.1
N24S18	4.6	0.34	1.15	$y = 6,601x + 803$	0.9994	107.9 ± 4.5
N24:1S18	4.1	0.30	1.01	$y = 6,808x + 1,034$	0.9988	104.1 ± 3.8
A16DS18	2.0	0.14	0.48	$y = 6,652x + 2,095$	0.9989	106.0 ± 3.6
A24DS18	3.8	0.40	1.37	$y = 7,145x + 1,040$	0.9992	97.4 ± 4.9
A16S18	2.4	0.14	0.46	$y = 6,546x + 2,611$	0.9990	102.4 ± 3.2
A24S18	4.4	0.29	0.98	$y = 7,099x + 866$	0.9993	101.2 ± 4.4

Dwell time, 36 ms for each ceramide

% CV percentage coefficient of variation

<sup>a</sup> Presented as % CV of peak areas based on six consecutive analyses with injections of 100 fmol each for 13 standard ceramides

<sup>b</sup> Presented as molar quantities of monoisotopic molecules for 13 standard ceramides

<sup>c</sup>  $R^2$  is the determination coefficient,  $x$  is the injected molar quantities of monoisotopic molecules in femtomoles and  $y$  is the peak area. All calibration lines were produced by injections of 1, 2.5, 5, 25, 50, 100 and 250 fmol each for 13 standard ceramides

<sup>d</sup> Presented as the mean ± % CV. Three replicates were obtained following additions of 10 fmol each for 13 standard ceramides to extracted crude hair lipids

**Table 3** Levels of ceramides in six different hair samples obtained from three females and from three males

Peak <sup>a</sup>	Ceramide <sup>b</sup>	Level <sup>c</sup> (µg/g hair)					
		Hair-F1	Hair-F2	Hair-F3	Hair-M1	Hair-M2	Hair-M3
1	N14DS18	2.3 ± 0.2	2.5 ± 0.1	2.4 ± 0.1	2.2 ± 0.1	1.9 ± 0.0	3.7 ± 0.1
2	N15DS18	1.3 ± 0.1	1.4 ± 0.1	1.1 ± 0.0	1.6 ± 0.1	1.0 ± 0.0	1.3 ± 0.1
3	A14DS18	2.0 ± 0.1	2.6 ± 0.2	2.5 ± 0.1	3.3 ± 0.1	2.4 ± 0.1	3.1 ± 0.1
4	N16:1DS18	1.3 ± 0.2	0.7 ± 0.0	0.9 ± 0.0	0.2 ± 0.0	0.4 ± 0.0	0.7 ± 0.0
5	N16S18	5.4 ± 0.1	3.7 ± 0.1	3.7 ± 0.1	6.0 ± 0.2	3.8 ± 0.4	4.5 ± 0.2
6	N16DS18 (+N18DS16*)	44.7 ± 3.2	44.6 ± 2.0	50.3 ± 3.0	50.3 ± 2.3	46.2 ± 1.3	56.4 ± 1.6
7	A16S18	8.3 ± 0.2	5.1 ± 0.3	6.8 ± 0.2	12.4 ± 0.6	5.6 ± 0.2	5.3 ± 0.3
8	N17DS18 <sup>\$</sup>	0.5 ± 0.0	0.6 ± 0.0	0.6 ± 0.1	0.6 ± 0.0	0.4 ± 0.0	0.6 ± 0.0
9	N17DS18 <sup>\$</sup> (+N18DS17* + N16DS19*)	3.1 ± 0.2	3.5 ± 0.2	3.7 ± 0.1	3.7 ± 0.1	3.0 ± 0.1	3.1 ± 0.2
10	A16DS18	29.6 ± 1.8	33.7 ± 1.2	37.0 ± 2.0	62.3 ± 3.2	50.5 ± 2.2	45.7 ± 2.1
11	N18:1DS18	3.4 ± 0.2	1.0 ± 0.1	1.1 ± 0.0	1.5 ± 0.1	1.0 ± 0.1	1.2 ± 0.0
12	N18S18	2.5 ± 0.1	1.2 ± 0.0	1.6 ± 0.1	1.9 ± 0.1	1.2 ± 0.1	1.2 ± 0.1
13	N18DS18	24.2 ± 1.2	6.3 ± 0.5	32.3 ± 2.1	2.7 ± 0.2	7.7 ± 0.3	5.3 ± 0.2
14	A17DS18	1.3 ± 0.1	1.8 ± 0.1	2.1 ± 0.1	3.6 ± 0.2	1.8 ± 0.2	1.8 ± 0.1
15	N19DS18 <sup>\$</sup>	0.1 ± 0.0	0.1 ± 0.0	0.3 ± 0.1	0.1 ± 0.0	0.1 ± 0.0	0.1 ± 0.0
16	N19DS18 <sup>\$</sup> (+N18DS19*)	2.2 ± 0.2	1.1 ± 0.1	2.2 ± 0.1	2.2 ± 0.1	1.4 ± 0.1	1.0 ± 0.1
17	A18DS18	5.2 ± 0.3	1.5 ± 0.2	3.8 ± 0.3	3.9 ± 0.1	3.3 ± 0.2	1.7 ± 0.1
18	N20S18	1.5 ± 0.1	0.7 ± 0.1	1.4 ± 0.2	1.4 ± 0.2	0.8 ± 0.0	0.7 ± 0.1
19	N20DS18 (+N18DS20*)	29.0 ± 1.7	5.9 ± 0.3	22.7 ± 1.5	3.1 ± 0.3	8.1 ± 0.4	4.6 ± 0.3
20	N21DS18 <sup>\$</sup>	0.8 ± 0.1	0.5 ± 0.0	0.6 ± 0.0	1.3 ± 0.1	0.4 ± 0.0	0.2 ± 0.0
21	N21DS18 <sup>\$</sup> (+N20DS19*)	3.2 ± 0.3	1.5 ± 0.2	2.7 ± 0.2	3.4 ± 0.1	2.5 ± 0.3	1.5 ± 0.1
22	N22:1DS18	2.8 ± 0.2	2.8 ± 0.2	3.2 ± 0.1	3.2 ± 0.1	2.3 ± 0.1	3.5 ± 0.2
23	N22S18	2.4 ± 0.2	1.9 ± 0.2	1.4 ± 0.0	2.4 ± 0.1	1.6 ± 0.0	1.6 ± 0.1
24	N22DS18 (+N20DS20*)	30.0 ± 1.7	25.5 ± 1.3	28.5 ± 1.8	17.2 ± 0.8	23.0 ± 1.3	16.1 ± 1.4
25	N23:1DS18	3.1 ± 0.1	3.3 ± 0.3	3.1 ± 0.3	3.8 ± 0.2	3.4 ± 0.4	4.4 ± 0.3
26	N23DS18 <sup>\$</sup> (+N22DS19*)	1.1 ± 0.1	1.4 ± 0.1	1.3 ± 0.1	1.8 ± 0.0	1.1 ± 0.1	1.0 ± 0.0
27	N23DS18 <sup>\$</sup> (+N22DS19*)	8.9 ± 0.4	7.1 ± 0.7	6.2 ± 0.5	6.5 ± 0.3	5.1 ± 0.6	4.3 ± 0.4
28	N24:1S18	3.8 ± 0.1	3.4 ± 0.3	2.2 ± 0.2	3.6 ± 0.2	3.6 ± 0.2	3.9 ± 0.4
29	N24:1DS18	60.3 ± 2.5	58.0 ± 2.0	44.0 ± 1.0	42.7 ± 2.1	61.0 ± 3.6	63.0 ± 4.4
30	N24S18	6.5 ± 0.5	4.6 ± 0.3	2.8 ± 0.1	4.0 ± 0.3	4.2 ± 0.1	4.1 ± 0.1
31	N24DS18 (+N22DS20*)	63.5 ± 3.2	71.4 ± 4.3	63.0 ± 4.4	56.0 ± 3.0	53.7 ± 3.5	50.6 ± 2.7
32	N25:1DS18 <sup>\$</sup>	0.3 ± 0.0	0.6 ± 0.0	0.4 ± 0.0	0.5 ± 0.1	0.5 ± 0.0	0.7 ± 0.1
33	N25:1DS18 <sup>\$</sup> (+N24:1DS19*)	2.9 ± 0.3	2.8 ± 0.1	2.3 ± 0.3	3.3 ± 0.3	2.8 ± 0.2	3.1 ± 0.2
34	A24:1DS18	7.8 ± 0.4	6.6 ± 0.5	7.2 ± 0.2	2.5 ± 0.1	5.4 ± 0.3	6.2 ± 0.2
35	A24S18	3.5 ± 0.2	1.3 ± 0.1	1.9 ± 0.1	1.8 ± 0.0	1.3 ± 0.1	1.3 ± 0.1
36	N25DS18 <sup>\$</sup> (+N24DS19*)	2.5 ± 0.1	1.8 ± 0.2	1.9 ± 0.1	3.2 ± 0.3	2.1 ± 0.1	2.2 ± 0.2
37	N25DS18 <sup>\$</sup> (+N24DS19* + N23DS20*)	5.7 ± 0.6	7.2 ± 0.5	5.8 ± 0.2	8.3 ± 0.5	5.2 ± 0.3	5.3 ± 0.3
38	A24DS18 (+N22DS20*)	6.8 ± 0.2	8.9 ± 0.3	8.9 ± 0.3	4.9 ± 0.2	5.0 ± 0.2	6.2 ± 0.4
39	N26:1S18	3.4 ± 0.1	2.6 ± 0.3	2.3 ± 0.2	3.0 ± 0.1	3.0 ± 0.1	3.3 ± 0.1
40	N26:1DS18 (+N24:1DS20*)	12.5 ± 0.8	7.8 ± 0.3	6.9 ± 0.4	5.8 ± 0.2	9.9 ± 0.5	10.6 ± 0.7
41	N26S18	4.2 ± 0.1	2.6 ± 0.1	2.5 ± 0.0	4.2 ± 0.2	2.2 ± 0.1	2.0 ± 0.2
42	N26DS18 (+N24DS20*)	18.5 ± 0.5	22.9 ± 1.0	17.2 ± 0.8	17.5 ± 0.5	17.9 ± 1.1	14.8 ± 0.6
43	N27:1DS18 (+N26:1DS19*)	0.8 ± 0.2	0.7 ± 0.0	1.1 ± 0.1	1.7 ± 0.2	1.3 ± 0.1	0.9 ± 0.0
44	N27DS18 <sup>\$</sup> (+N26DS19* + N25DS20)	*1.2 ± 0.1	0.9 ± 0.0	0.7 ± 0.0	1.8 ± 0.2	1.3 ± 0.0	1.1 ± 0.1
45	N27DS18 <sup>\$</sup> (+N26DS19* + N25DS20*)	2.0 ± 0.2	1.9 ± 0.1	1.9 ± 0.1	2.6 ± 0.0	2.0 ± 0.1	2.0 ± 0.1
46	N28:1DS18 (+N26:1DS20*)	5.5 ± 0.4	3.7 ± 0.2	3.7 ± 0.2	5.2 ± 0.2	4.7 ± 0.3	6.0 ± 0.5
47	N28DS18 (+N26DS20*)	4.3 ± 0.2	4.5 ± 0.2	2.8 ± 0.2	3.9 ± 0.3	3.8 ± 0.3	3.5 ± 0.3
48	N30:1DS18 (+N28:1DS20*)	3.3 ± 0.1	2.4 ± 0.3	2.1 ± 0.1	2.5 ± 0.4	2.6 ± 0.2	4.7 ± 0.4

Every hair lipid sample was analyzed in triplicate for  $n = 3$  for each subject. Levels of means and the standard deviation (*SD*) are expressed as weights of lipids to the weight of hair fibers (µg/g hair)

<sup>a</sup> See the legend to Fig. 3 for an explanation of the peaks

<sup>b</sup> Asterisks and dollar signs indicate isobaric and isomeric ceramides, respectively

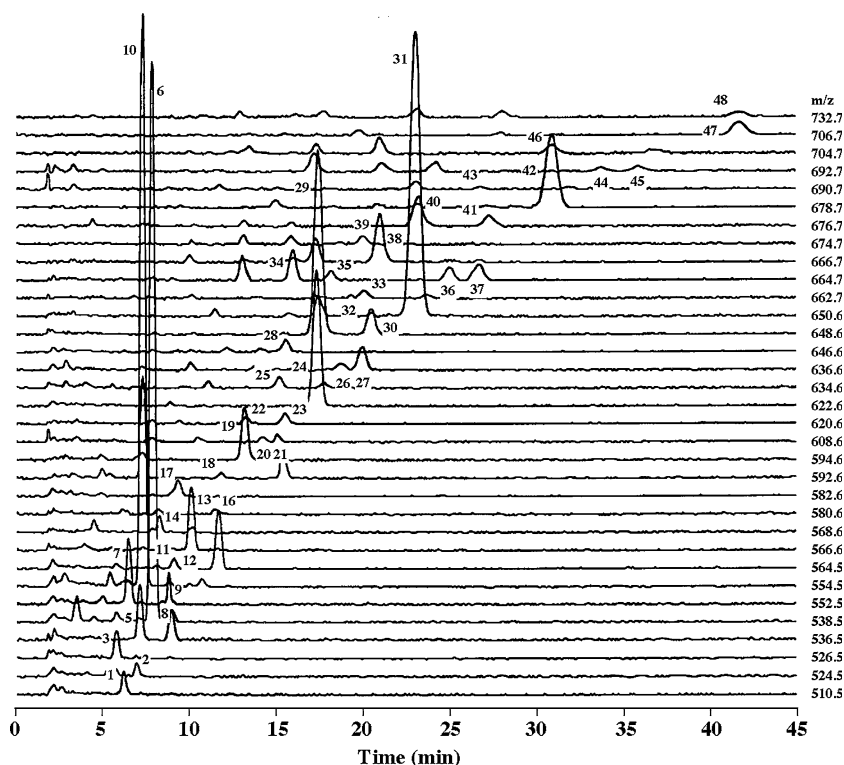
<sup>c</sup> Presented as the mean ± *SD*

monoisotopic molecules, i.e., the CERs with longer chain lengths and/or a hydroxyl group in the fatty acid moieties had slightly greater molar responses than those with shorter chains and/or no hydroxyl group.

However, the % CV of the slopes of the calibration lines among the 13 standard CERs was as low as 3.9%, which was comparable with 2.1–4.6% as the % CV of the peak areas in six consecutive injection analyses.



**Fig. 4** Detection of ceramides in a 1-mm piece derived from a single hair fiber at 1–2 mm from the proximal root end using RP-HPLC–ESI-MS. For the explanation of the peaks, see the legend to Fig. 3



This suggested that the extremely small differences in the molar responses of monoisotopic molecules among the 13 CERs may make it possible to determine any monoisotopic molecules of CERs in hair using only one calibration line generated by a monoisotopic molecule of a given standard CER. In this study, we selected N16DS18 for a calibration line, since N16DS18 is one of the predominant species in hair and other researchers can readily get it from suppliers if they want to use this method. The actual levels of the targeted CERs can be theoretically converted, because correction for  $^{13}\text{C}$  and  $^2\text{H}$  effects is available in this RP-HPLC–ESI-MS method using the unit mass resolution mode. This validity is corroborated by the fact that the recoveries of the crude hair lipids spiked with 13 standard CERs were close to 100% (97.0–108.2%) even when only standard N16DS18 was used for the determination.

From the % CVs of the slopes and the peak areas for the 13 standard CERs, the systematic error is theoretically estimated to be  $\pm 12.1\%$  [ $2\sigma = 2 \times (3.9^2 + 4.6^2)^{1/2}$ ] of the values determined. This theoretical error allows discrimination among the determined levels of CERs if their differences are more than 12%. We could not directly validate the quantitative recovery values for other CERs that are not available as standards but that are present in hair, because we had none of them as substantial materials. Also, we could not validate the

apparent quantitative values for peaks consisting of more than two kinds of isobaric CERs, which account for 21 of all 48 peaks. However, currently, we consider that the values determined for nonvalidated CERs would be roughly estimated within  $\pm 12\%$  as well as the 13 standard CERs, because of the experimental data that the summed quantitative levels of CERs by RP-HPLC–ESI-MS were comparable with those determined by TLC. Although an internal standard is generally used in MS analysis to determine targeted analytes, which enables one to normalize the absolute ion intensities that may be altered owing to ion suppression, we did not adopt an internal standard in our method. That was because, firstly, our method has been already normalized based on a characteristic that a molar response of the monoisotopic ion of N16DS18 is nearly equivalent to those of other CERs. Thus, in our method, monoisotopic ions derived from diverse CERs are determined using a calibration line of standard N16DS18 monoisotopic ion, produced just prior to the analysis. Secondly, since the recoveries of crude hair lipids spiked with standard CERs were nearly 100% (97.0–108.2%) and their % CV was less than 5.1% in three replicates, it is thought that there is no ion suppression in the analysis of CERs in crude hair lipids.

Here, we discuss how to use the newly developed RP-HPLC–ESI-MS. When RP-HPLC–ESI-MS is used for the determination of diverse CERs in hair, hair

**Table 4** Levels of ceramides in six different pieces of 1-mm length derived from a single hair fiber

Peak <sup>a</sup>	Ceramide <sup>b</sup>	Level <sup>c</sup> (µg/g hair)					
		1–2 mm	13–14	25–26	37–38	49–50	61–62
1	N14DS18	2.5 ± 0.3	2.6 ± 0.5	1.9 ± 0.2	2.2 ± 0.2	2.5 ± 0.4	2.2 ± 0.4
2	N15DS18	1.6 ± 0.2	1.5 ± 0.2	1.3 ± 0.2	1.4 ± 0.1	1.4 ± 0.2	1.3 ± 0.3
3	A14DS18	3.2 ± 0.3	3.1 ± 0.3	2.5 ± 0.3	2.5 ± 0.3	2.5 ± 0.0	2.4 ± 0.2
5	N16S18	5.9 ± 0.6	6.4 ± 0.3	5.5 ± 0.4	6.0 ± 0.4	8.0 ± 0.8	5.1 ± 0.4
6	N16DS18 (+N18DS16*)	62.0 ± 4.0	64.3 ± 5.0	58.3 ± 2.5	59.7 ± 3.5	62.1 ± 3.8	52.8 ± 5.3
7	A16S18	6.9 ± 0.5	6.9 ± 0.6	5.8 ± 0.4	6.3 ± 0.7	9.7 ± 0.7	6.7 ± 0.8
9	N17DS18 <sup>\$</sup> (+N18DS17* + N16DS19*)	3.7 ± 0.3	3.7 ± 0.5	3.6 ± 0.4	3.4 ± 0.4	2.9 ± 0.2	2.6 ± 0.2
10	A16DS18	64.3 ± 5.7	63.7 ± 5.5	58.8 ± 4.8	52.4 ± 4.1	55.0 ± 3.1	52.7 ± 4.0
12	N18S18	1.7 ± 0.2	1.6 ± 0.3	1.2 ± 0.1	1.3 ± 0.0	2.4 ± 0.1	1.6 ± 0.2
13	N18DS18	5.7 ± 0.7	5.9 ± 0.4	5.9 ± 0.3	6.5 ± 0.5	6.7 ± 0.5	5.3 ± 0.5
14	A17DS18	2.9 ± 0.3	2.3 ± 0.2	1.7 ± 0.2	1.7 ± 0.1	1.7 ± 0.1	1.5 ± 0.1
17	A18DS18	3.1 ± 0.3	2.7 ± 0.3	2.5 ± 0.4	2.1 ± 0.3	2.0 ± 0.3	2.0 ± 0.2
18	N20S18	1.2 ± 0.2	1.0 ± 0.2	0.9 ± 0.1	0.8 ± 0.1	1.8 ± 0.2	0.9 ± 0.2
19	N20DS18 (+N18DS20*)	6.1 ± 0.4	6.4 ± 0.4	6.5 ± 0.4	7.0 ± 0.3	6.7 ± 0.5	6.0 ± 0.4
23	N22S18	2.2 ± 0.2	2.3 ± 0.1	1.9 ± 0.2	2.3 ± 0.4	3.1 ± 0.7	2.0 ± 0.4
24	N22DS18 (+N20DS20*)	26.2 ± 1.6	26.3 ± 2.8	20.7 ± 2.1	22.2 ± 2.6	22.8 ± 2.7	22.5 ± 2.7
25	N23:1DS18	2.3 ± 0.2	2.1 ± 0.3	2.5 ± 0.4	2.0 ± 0.2	2.5 ± 0.4	2.2 ± 0.2
26	N23DS18 <sup>\$</sup> (+N22DS19*)	1.3 ± 0.1	1.2 ± 0.1	0.8 ± 0.1	0.9 ± 0.1	1.2 ± 0.0	0.9 ± 0.0
27	N23DS18 <sup>\$</sup> (+N22DS19*)	6.5 ± 0.3	5.4 ± 0.4	4.4 ± 0.6	4.5 ± 0.6	5.3 ± 0.5	5.0 ± 0.3
28	N24:1S18	3.0 ± 0.3	1.6 ± 0.2	3.9 ± 0.5	2.8 ± 0.4	4.8 ± 0.7	4.5 ± 0.5
29	N24:1DS18	38.8 ± 2.8	35.2 ± 3.3	49.2 ± 3.8	38.6 ± 4.8	55.1 ± 6.9	48.0 ± 2.5
30	N24S18	6.1 ± 0.4	6.3 ± 0.5	5.4 ± 0.4	5.3 ± 0.3	7.6 ± 0.9	5.7 ± 0.8
31	N24DS18 (+N22DS20*)	76.0 ± 5.6	70.3 ± 7.5	66.9 ± 5.5	62.0 ± 3.3	63.2 ± 5.7	60.0 ± 5.5
34	A24:1DS18	6.4 ± 0.4	6.6 ± 0.4	7.8 ± 0.8	6.1 ± 0.5	8.2 ± 0.5	8.4 ± 0.6
35	A24S18	2.3 ± 0.2	2.2 ± 0.1	1.5 ± 0.1	2.0 ± 0.4	4.1 ± 0.4	2.0 ± 0.2
36	N25DS18 <sup>\$</sup> (+N24DS19*)	3.2 ± 0.3	2.9 ± 0.3	2.9 ± 0.4	3.0 ± 0.3	3.2 ± 0.2	3.1 ± 0.1
37	N25DS18 <sup>\$</sup> (+N24DS19* + N23DS20*)	4.6 ± 0.3	5.4 ± 0.5	4.3 ± 0.3	4.4 ± 0.5	4.7 ± 0.2	4.1 ± 0.3
38	A24DS18 (+A22DS20*)	13.2 ± 0.8	11.4 ± 1.1	10.1 ± 0.5	11.2 ± 0.8	10.4 ± 0.8	10.7 ± 0.7
39	N26:1S18	2.1 ± 0.3	2.0 ± 0.1	2.0 ± 0.2	1.8 ± 0.1	2.7 ± 0.3	1.9 ± 0.4
40	N26:1DS18 (+N24:1DS20*)	5.5 ± 0.4	4.1 ± 0.7	8.9 ± 0.6	6.4 ± 0.9	8.6 ± 0.8	8.0 ± 0.6
41	N26S18	3.3 ± 0.2	2.9 ± 0.2	2.6 ± 0.1	3.0 ± 0.5	4.9 ± 0.4	3.3 ± 0.2
42	N26DS18 (+N24DS20*)	23.6 ± 1.8	20.6 ± 2.5	21.6 ± 1.3	23.3 ± 1.3	23.0 ± 1.9	19.8 ± 1.3
46	N28:1DS18 (+N26:1DS20*)	3.0 ± 0.2	2.5 ± 0.2	3.0 ± 0.2	2.4 ± 0.5	3.0 ± 0.5	3.1 ± 0.5
47	N28DS18 (+N26DS20*)	5.5 ± 0.3	4.9 ± 0.5	3.8 ± 0.3	4.4 ± 0.4	4.5 ± 0.4	4.0 ± 0.3
48	N30:1DS18 (+N28:1DS20*)	2.5 ± 0.3	2.5 ± 0.3	2.3 ± 0.2	1.9 ± 0.3	2.5 ± 0.5	2.2 ± 0.4

Every hair lipid sample ( $n = 1$ ) was analyzed in triplicate. Levels of means and SD are expressed as weights of lipids to the weight of hair fibers (µg/g hair)

<sup>a</sup> See the legend to Fig. 3 for an explanation of the peaks

<sup>b</sup> Asterisks and dollar signs indicate isobaric and isomeric ceramides, respectively

<sup>c</sup> Presented as the mean ± SD

samples that were previously subjected to RP-HPLC–APCI-MS and RP-HPLC–ESI-MS/MS for qualitative analyses [31] must be analyzed, as shown in our applications. Therefore, it should be noted that the presence of other kinds of CERs in a certain hair sample cannot be excluded when no qualitative analysis using RP-HPLC–APCI-MS and RP-HPLC–ESI-MS/MS is conducted owing to too small amounts of the hair samples collected. When other researchers want to use this method, especially in the case of mass spectrometers other than ours [Agilent 1100 series LC/MSD SL (single quadrupole) system], validation data must be acquired under ESI-MS conditions that seem to be equivalent to those described in the

“**Experimental Procedure.**” The most important point is that calibration lines of monoisotopic molecules derived from commercially available standard CERs (N16DS18, N18DS18, N24DS18, N24:1DS18, N16S18, N18S18, N20S18, N24S18 and N24:1S18) have nearly equivalent slopes to each other (roughly within 5.0% in CV), as represented in Table 2. On the basis of the validation data proving nearly equivalent molar responses in the standard CERs, other researchers can use this method. When the slopes are not equivalent to each other, ESI-MS conditions must be examined. In that case, first of all, the in-source collision energy, which greatly affects the transmission and the fragmentation of the targeted ions (“fragmenter

voltage” in our instrument or “cone voltage” in others), should be changed. That is because, in our experience, the intensities of different kinds of CERs greatly depend on in-source collision energies, while Xan [25] described effects of different collision energies on relative intensities among different molecular species of CERs despite neutral loss analyses in ESI-MS/MS being employed. If molar responses in the standard CERs are not improved, other parameters affecting ESI efficiencies, such as the flow of heated dry nitrogen gas, nebulizer gas pressure, dry gas temperature and capillary voltages, should be examined further.

Ammonium acetate as an additive to the mobile phase is generally used in RP-HPLC–ESI-MS analysis. Our method is not the first to use ammonium acetate for the analysis of CERs in RP-HPLC–ESI-MS, because Vietzke et al. [41, 42] already reported such a RP-HPLC–ESI-MS method. However, they used that method only to identify a few kinds of NSs and they did not examine the possibility to use it for the determination of diverse CERs, including NDSs, ASs and ADSs, whereas our method can be used to determine diverse kinds of CERs present in hair. Therefore, we can say that our RP-HPLC–ESI-MS method using the mobile phase of methanol containing ammonium acetate is quite different from the previous one [41, 42]. On the other hand, some methods to determine CERs using RP-HPLC–ESI-MS have been reported [26, 27, 30], while a method using RP-HPLC–thermospray MS has been described [28]. However, in those methods, quantitative targets were restricted to CERs available as standard materials and even the highest sensitivity was not sufficient, such as subpicomolar ranges of the LOD [26, 27]. Among the methods previously reported for the analysis of CERs, those close in performance to our RP-HPLC–ESI-MS method were reported by Han [25] and by Pettus et al. [29]. The method using direct MS/MS and neutral loss ion scan reported by Han [25] is superior to others because it can simultaneously determine NSs and ASs. Although the author described the applicability of that method to the analysis of NDSs and ADSs, this applicability is his speculation because there is no experimental evidence for the quantification of NDSs and ADSs. Therefore, we thought that method is for the quantitative analysis of only NSs and ASs but not NDSs and ADSs. As for the sensitivity, the LOD is approximately 10 fmol (consumed) as a standard CER. Another method using normal-phase HPLC–APCI-MS for NDSs and NSs reported by Pettus et al. [29] achieved the simultaneous determination of NDSs and NSs, but that method does not include ADSs and ASs as targets and

has low sensitivity and low linearity. Therefore, both methods are insufficient for the highly sensitive determination of diverse CERs, including NSs, NDSs, ASs and ADSs. In contrast, our method can achieve the comprehensive determination of the diverse CERs with extremely low LOD, such as in the subfemtomolar range at a signal-to-noise ratio of 3.

There are squalene, wax esters, triglycerides, free fatty acids, cholesterol, 18-methyleicosanoic acid and cholesterol sulfate within human hair fibers, in addition to CERs [34]. In the method developed in this study, it is obvious that these lipids do not interfere with the detection of CERs, because they are extremely different from CERs in terms of molecular weight and polarities. However, there is a possibility that DAGs produced by the hydrolysis of triglycerides may overlap with CERs in this method. For example, the molecular weights of palmitoyl-oleoyl DAG (16-18:1DAG) and N20DS18 are 594.6 and 595.6, respectively, whereas those of oleoyl-stearoyl DAG (18:1-18DAG) and N22DS18 are 622.6 and 623.6, respectively. Therefore, if 16-18:1DAG and 18:1-18DAG are predominantly detected as deprotonated ions  $[M - H]^-$  in negative ion ESI-MS, their isotopic ions  $[M+1 - H]^-$  would interfere with the monoisotopic ions  $[M - H]^-$  of N20DS18 and N22DS18 in their SIM chromatograms. When standard DAGs were subjected to this RP-HPLC–ESI-MS method, those DAGs yielded prominent acetate-adduct ions  $[M + CH_3COO]^-$  but no deprotonated ions  $[M - H]^-$  (data not shown). This may be due to an effect of ammonium acetate in the mobile phase used in this method. An examination of detected mass numbers of all possible DAGs with various constitutional fatty acids and 73 kinds of CERs present in hair led to the conclusion that the monoisotopic ions  $[M + CH_3COO]^-$  of DAGs and their isotopic ions, such as  $[M + 1 + CH_3COO]^-$  and  $[M + 2 + CH_3COO]^-$ , do not at all interfere with monoisotopic ions derived from the 73 kinds of CERs in hair. This indicates that the interference in the detection of CERs with other lipids, including DAGs, can be ignored and that the newly developed RP-HPLC–ESI-MS technique is specific for CERs in crude hair lipids.

Our previous report [31] showed that hair has 73 kinds of CERs and is unique in terms of the higher levels of NDSs and ADSs, compared with other human cells/tissues and human stratum corneum, which contain low levels of them [5–10]. In this study, the 73 kinds of CERs were qualified and then quantified in all hair samples collected from six subjects. Although it was roughly known that hair contains higher levels of NDSs/ADSs and lower levels of NSs/ASs [14, 15, 31], this RP-HPLC–ESI-MS analysis revealed quantitative

levels not only of predominant kinds but also of less abundant ones for the first time. The levels of CERs varied among the hair samples collected from three females and from three males. This interindividual variation in the CER composition suggests that there might be differences between females and males, or younger and older subjects, as described in “Results.” However, it should be noted that such differences in the levels of CERs between females and males, or between younger and older subjects, must be investigated further. On the other hand, the application to the analysis of CERs in 1-mm pieces of a single hair fiber demonstrates the high sensitivity of this RP-HPLC–ESI-MS method. The quantitative data of CERs show a tendency for gradual decreases in the levels of CERs in the direction from the root end to the tip. This is reasonable because of the interpretation of gradual loss by weathering effects during daily life activities [34, 43]. However, the levels of sphingosine-containing or nervonic acid containing CERs are obviously higher in regions more distant from the root end, which demonstrates the presence of intraindividual variation in the CER composition. Such variations might be related to the physicochemical properties or physiological phenomena of hair.

The de novo pathways for CERs are as follows [7]: (1) production of 3-ketosphinganine from palmitoyl-coenzyme A and L-serine by serine palmitoyltransferase; (2) production of dihydrosphingosine from 3-ketosphinganine by 3-ketosphinganine reductase; (3) production of NDS from dihydrosphingosine and fatty acylcoenzyme A by CER synthase; (4) production of NS from NDS by desaturase; (5) production of AS from NS by hydroxylase. Of all the hair samples tested, the levels of NDSs and ADSs are much higher than those of NSs and ASs. This fact suggests a lower activity of process 4 in hair matrix cells and a pathway for the production of ADSs directly from processes 3–5. Also, variation in the levels of sphingosine-containing CERs among different subjects and in different regions of a single hair fiber suggests that there might be differences in the activities of desaturase in process 4 in hair matrix cells among different individuals and among different periods during hair growth even in a single hair follicle. The fluctuation of NSs is of special interest because they might play a role in apoptosis of hair matrix cells [1, 2, 44, 45], related to the differentiation into cuticular or cortical cells.

Finally, we discuss the advantage of the newly developed method. There are two advantages: the applicability of the determination of CERs in small amounts of hair samples and the comprehensive property covering unusual CERs of humans [31]. As for the

first advantage, one can observe the CER composition even in the hair root region of a single hair follicle by use of this method. An individual hair fiber differs from others in terms of diameter, structure and physicochemical properties that might cause different regulation of hair growth even if they grow on the same scalp. The signal-to-noise ratio of the multi-SIM chromatograms in the 1-mm pieces of hair, as shown in Fig. 4, indicates that this method can be used for pieces shorter than 1 mm if minor species are ignored. According to the speed of hair growth [36], the analysis of CERs in each 400- $\mu$ m piece of hair corresponds to monitoring 1-day's production of CERs in hair matrix cells. Therefore, the first advantage may contribute to future research on hair science. As for the second advantage, this method can be used for the quantitative determination of unusual CER molecules of humans, such as odd-number CERs having odd carbons in sphingoid moieties and isomeric combinations assumed to have a branched acyl chain [31]. They are minor components but interest us in terms of their biosynthesis. The second advantage may contribute to future research on the physiology of CER metabolism of humans.

**Acknowledgements** We would like to express our cordial gratitude to Katsumi Kita of the Kao Corporation for his discussions and encouragement of this study. Our sincere thanks also go to Manabu Watanabe, Yoshiya Sugai and Yoshinori Nishizawa of the Kao Corporation for technical support in the synthesis of standard CERs.

## References

1. Fishbein JD, Dobrowsky RT, Bielawska A, Garrett S, Hannun YA (1993) Ceramide-mediated growth inhibition and CAPP are conserved in *Saccharomyces cerevisiae*. *J Biol Chem* 268:9244–9261
2. Riboni L, Prinetti A, Bassi R, Caminiti A, Tettamanti G (1995) A mediator role of ceramide in the regulation of neuroblastoma Neuro2a cell differentiation. *J Biol Chem* 270:26868–26875
3. Hannun YA (1996) Functions of ceramide in coordinating cellular responses to stress. *Science* 274:1855–1859
4. Pettus BJ, Chalfant CE, Hannun YA (2002) Ceramide in apoptosis: an overview and current perspectives. *Biochim Biophys Acta* 1585:114–125
5. Sullards MC, Wang E, Peng Q, Merrill AH (2003) Metabolomic profiling of sphingolipids in human glioma cell lines by liquid chromatography tandem mass spectrometry. *Cell Mol Biol* 49:789–797
6. Drobnik W, Liebisch G, Audebert F, Fröhlich -XD, Glück T, Vogel P, Rothe G, Schmitz G (2003) Plasma ceramide and lysophosphatidylcholine inversely correlate with mortality in sepsis patients. *J Lipid Res* 44:754–761
7. Merrill AH, Sweeley CC (1996) Sphingolipids: metabolism and cell signaling. In: Vance DE, Vance JE (eds) *Biochemistry of lipids, lipoproteins and membranes*. Elsevier, New York, pp 309–339

8. Alderson NL, Walla MD, Hama H (2005) A novel method for the measurement of in vivo fatty acid 2-hydroxylase activity by gas chromatography–mass spectrometry. *J Lipid Res* 46:1569–1575
9. Robson KJ, Stewart ME, Michelsen S, Lazo ND, Downing DT (1994) 6-Hydroxy-4-sphinganine in human epidermal ceramides. *J Lipid Res* 35:2060–2068
10. Farwanah H, Wohlrab J, Neubert RHH, Raith K (2005) Profiling of human stratum corneum ceramides by means of normal phase LC/APCI–MS. *Anal Bioanal Chem* 383:632–637
11. Elias PM (1983) Epidermal lipids, barrier, function, and desquamation. *J Invest Dermatol* 80:44s–49s
12. Imokawa G, Akasaki S, Hattori M, Yoshizuka N (1986) Selective recovery of deranged water-holding properties by stratum corneum. *J Invest Dermatol* 87:758–761
13. Hamanaka S, Nakazawa S, Yamanaka M, Uchida Y, Otsuka F (2005) Glucosylceramide accumulates preferentially in lamella bodies in differentiated keratinocytes. *Br J Dermatol* 152:426–434
14. Hussler G, Kaba G, Francois AM, Saint-Leger D (1995) Isolation and identification of human hair ceramides. *Int J Cosmet Sci* 17:197–206
15. Masukawa Y, Narita H, Imokawa G (2005) Characterization of the lipid composition at the proximal root regions of human hair. *J Cosmet Sci* 56:1–16
16. Imokawa G, Abe A, Jin K, Higaki Y, Kawashima M, Hidano A (1991) Decreased level of ceramides in stratum corneum of atopic dermatitis: an etiologic factor in atopic dry skin. *J Invest Dermatol* 96:523–526
17. van Veldhoven PP, Bishop WR, Yurivich DA, Bell RM (1995) Ceramide quantitation: evaluation of a mixed micellar assay using *E. coli* diacylglycerol kinase. *Biochem Mol Biol Int* 36:21–30
18. McNabb TJ, Cremesti AE, Brown PR, Fischl AS (1999) The separation and direct detection of ceramides and sphingoid bases by normal-phase high-performance liquid chromatography and evaporative light-scattering detection. *Anal Biochem* 276:242–250
19. Hoi U, Pei PT, Minard RD (1981) Separation of molecular species of ceramides as benzoyl and *p*-nitrobenzoyl derivatives by high performance liquid chromatography. *Lipids* 16:855–862
20. Mano N, Oda Y, Yamada K, Asakawa N, Katayama K (1997) Simultaneous quantitative determination method for sphingolipid metabolites by liquid chromatography/ion spray ionization tandem mass spectrometry. *Anal Biochem* 244:291–300
21. Gu M, Kerwin JL, Watts JD, Aebersold R (1997) Ceramide profiling of complex lipid mixtures by electrospray ionization mass spectrometry. *Anal Biochem* 244:347–356
22. Couch LH, Churchwell MI, Doerge DR, Tolleson WH, Howard PC (1997) Identification of ceramides in human cells using liquid chromatography with detection by atmospheric pressure chemical ionization–mass spectrometry. *Rapid Commun Mass Spectrom* 11:504–512
23. Liebisch G, Drobnik W, Reil M, Trümbach B, Arneche R, Olgemöller B, Roscher A, Schmitz G (1999) Quantitative measurement of different ceramide species from crude cellular extracts by electrospray ionization tandem mass spectrometry (ESI–MS/MS). *J Lipid Res* 40:1539–1546
24. Yamada Y, Kajiwara K, Yano M, Kishida E, Masuzawa Y, Kojo S (2001) Increase of ceramides and its inhibition by catalase during chemically induced apoptosis of HL-60 cells determined by electrospray ionization tandem mass spectrometry. *Biochim Biophys Acta* 1532:115–120
25. Han X (2002) Characterization and direct quantitation of ceramide molecular species from lipid extracts of biological samples by electrospray ionization tandem mass spectrometry. *Anal Biochem* 302:199–212
26. Fillet M, van Heugen J-C, Servais A-C, de Graeve J, Crommen J (2002) Separation, identification and quantitation of ceramides in human cancer cells by liquid chromatography–electrospray ionization tandem mass spectrometry. *J Chromatogr A* 949:225–233
27. Lee MH, Lee GH, Yoo JS (2003) Analysis of ceramides in cosmetics by reversed-phase liquid chromatography/electrospray ionization mass spectrometry with collision-induced dissociation. *Rapid Commun Mass Spectrom* 17:64–75
28. Yamane M (2003) Simultaneous quantitative determination method for ceramide species from crude cellular extracts by high-performance liquid chromatography–thermospray mass spectrometry. *J Chromatogr B* 783:181–190
29. Pettus BJ, Kroesen B-J, Szulc ZM, Bielawska A, Bielawski J, Hannun Y, A., Busman M (2003) Quantitative measurement of different ceramide species from crude cellular extracts by normal-phase high-performance liquid chromatography coupled to atmospheric pressure ionization mass spectrometry. *Rapid Commun Mass Spectrom* 18:577–583
30. Camera E, Picardo M, Presutti C, Catarcini P, Fanali S (2004) Separation and characterization of sphingoceramides by high-performance liquid chromatography–electrospray ionization mass spectrometry. *J Sep Sci* 27:971–976
31. Masukawa Y, Tsujimura H, Narita H (2006) Liquid chromatography–mass spectrometry for comprehensive profiling of ceramide molecules in human hair. *J Lipid Res* 47:1559–1571
32. Motta S, Monti M, Sesana S, Caputo R, Carelli S, Ghidoni R (1993) Ceramide composition of the psoriatic scale. *Biochim Biophys Acta* 1182:147–151
33. Ramjit HG, Newton R, Guare JP (2005) A novel coaxial electrospray ionization method for characterizing hexacosanoylceramides by Fourier transform ion cyclotron resonance mass spectrometry. *Rapid Commun Mass Spectrom* 19:1257–1262
34. Masukawa Y, Tsujimura H, Imokawa G (2005) A systematic method for the sensitive and specific determination of hair lipids in combination with chromatography. *J Chromatogr B* 823:131–142
35. Yergey JA (1983) A general approach to calculating isotopic distributions for mass spectrometry. *Int J Mass Spectrom Ion Phys* 52:337–349
36. Lieser B, Liebisch G, Drobnik W, Schmitz G (2003) Quantification of sphingosine and sphinganine from crude lipid extracts by HPLC electrospray ionization tandem mass spectrometry. *J Lipid Res* 44:2209–2216
37. Liebisch G, Lieser B, Rathenber J, Drobnik W, Schmitz G (2004) High-throughput quantification of phosphatidylcholine and sphingomyelin by electrospray ionization tandem mass spectrometry coupled with isotope correction algorithm. *Biochim Biophys Acta* 1686:108–117
38. Han X, Cheng H (2005) Characterization and direct quantitation of cerebroside molecular species from lipid extracts by shotgun lipidomics. *J Lipid Res* 46:163–175
39. Han X, Gross RW (2005) Shotgun lipidomics: electrospray ionization mass spectrometric analysis and quantitation of cellular lipidomes directly from crude extracts of biological samples. *Mass Spectrom Rev* 24:367–412
40. Robbins CR (1994) Chemical and physical behavior of human hair, 3rd edn. Springer, Heidelberg, pp 23–45
41. Vietzke J-P, Straßner M, Hinze U (1999) Separation and identification of ceramides in the human stratum corneum by

- high-performance liquid chromatography coupled with electrospray ionization mass spectrometry and electrospray multiple-stage mass spectrometry profiling. *Chromatographia* 50:15–20
42. Vietzke J-P, Brandt O, Abeck D, Rapp C, Strassner M, Schreiner V, Hinze U (2001) Comparative investigation of human stratum corneum ceramides. *Lipids* 36:299–304
  43. Masukawa Y, Tsujimura H, Tanamachi H, Narita H, Imokawa G (2004) Damage to human hair caused by repeated bleaching combined with daily weathering during daily life activities. *Exog Dermatol* 3:273–281
  44. Bieberich E, Silva J, Wang G, Krishnamurthy K, Condie BG (2004) Selective apoptosis of pluripotent mouse and human stem cells by novel ceramide analogues prevents teratoma formation and enriches for neural precursors in ES cell-derived neural transplants. *J Cell Biol* 167:723–734
  45. Venable ME, Webb-Froehlich LM, Sloan EF, Thomley JE (2006) Shift in sphingolipid metabolism leads to an accumulation of ceramide in senescence *Mech Ageing Dev* 127:473–480

# Synthesis of 1,3- and 1,2-Diphosphatidylglycerol

Moghis U. Ahmad · U. Murali Krishna ·  
Shoukath M. Ali · Sreeti Choudhury ·  
Imran Ahmad

Received: 20 March 2006 / Accepted: 2 January 2007 / Published online: 7 February 2007  
© AOCS 2007

**Abstract** A novel phosphonium salt methodology was utilized for the first time to synthesize 1,3-, and 1,2-diphosphatidylglycerol. Optically active 1,2-di-*O*-acyl-*sn*-glyceryl phosphate was coupled with unprotected glycerol in the presence of pyridiniumbromide perbromide and triethylamine to yield, after final removal of phosphate protecting group, the title compounds. The 1,2-diphosphatidylglycerol (1,2-isomer of cardiolipin) may be a member of a new class of phospholipids for industrial applications similar to other phosphocholines.

IR	Infra red
MS	Mass spectrometry
NMR	Nuclear magnetic resonance
PA	Phosphatidic acid
PBP	Pyridiniumbromide perbromide
PG	Phosphatidylglycerol
rt	Room temperature
TBHP	<i>tert</i> -Butylhydroperoxide
THF	Tetrahydrofuran
TLC	Thin layer chromatography

**Keywords** Cardiolipin · Cardiolipin isomer ·  
Diphosphatidylglycerol · Phosphitylation ·  
Phosphonium salt methodology

## Abbreviations

ATR	Attenuated total reflectance
CL	Cardiolipin
DIPEA	Diisopropylethylamine
ESI	Electron spray ionization

---

M. U. Ahmad · U. M. Krishna · S. M. Ali ·  
S. Choudhury · I. Ahmad  
NeoPharm, Inc., 1850 Lakeside Drive,  
Waukegan, IL 60085, USA

## Present Address:

M. U. Ahmad · S. M. Ali · I. Ahmad (✉)  
Jina Pharmaceuticals, Inc., 28100 N. Ashley Circle,  
Suite 103, Libertyville, IL 60048, USA  
e-mail: Imran@jinapharma.com

## Present Address:

U. M. Krishna  
New River Pharmaceuticals, 1881 Grove Ave.,  
Radford, VA 24141, USA

## Introduction

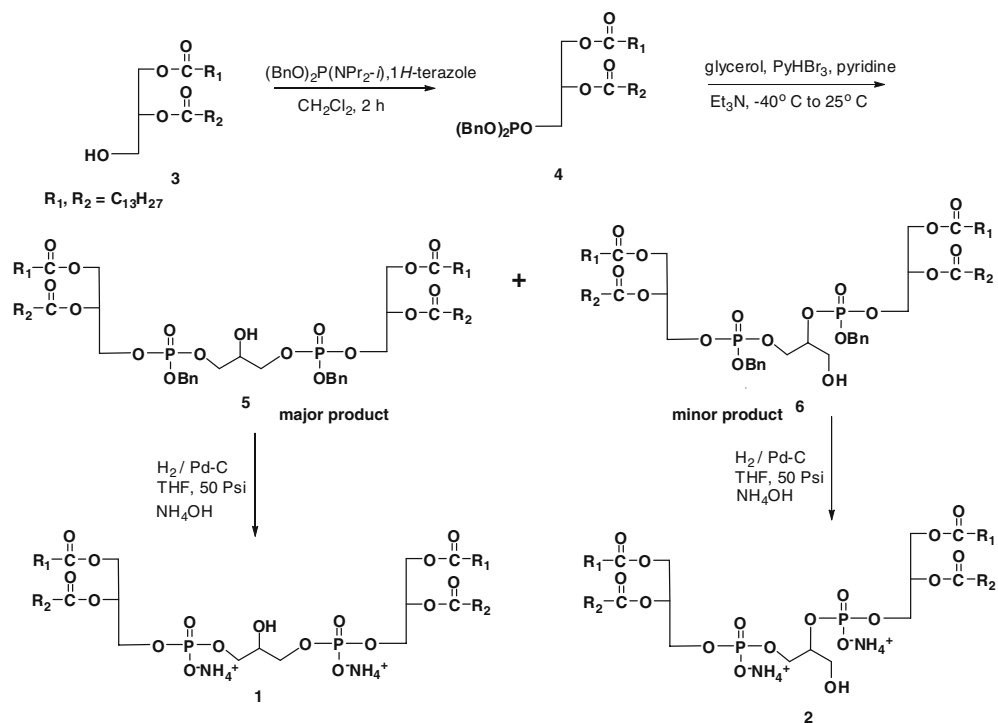
The most general methods used for the chemical synthesis of cardiolipin (CL) involve phosphatidic acid (PA) and phosphatidylglycerol (PG). Selective phosphorylation of the primary alcohol group of PG with PA, either by a semi-synthetic (by enzymes) method [1] or by condensation of PG or 2-*O*-protected glycerols with PA in the presence of 2,4,6-triisopropylbenzenesulfonyl chloride [2–5], will result in protected cardiolipin. Other synthetic approaches describe the use of phosphorylating agents such as cyclic enediol pyrophosphates [6–8], silver salts of PA [9, 10], phosphorus oxychloride [11], and 2-chlorophenyl phosphorodi-(1,2,4-triazolide) [12]. As part of our ongoing research towards the synthesis of cardiolipin and its analogues, we have developed and reported convenient alternative methodologies [13–15] based on phosphoramidite chemistry [16, 17]. However, all these methods utilize 2-*O*-protected glycerols along with the phosphorylation or condensation reagents. The synthesis of 2-*O*-protected glycerols in turn involves three additional steps starting from glycerol and

restrictions on the choice of protecting groups. We report herein a concise total synthesis of cardiolipin starting from unprotected glycerol via the phosphonium salt methodology [18, 19]. The versatility of this method was exemplified by the use of unprotected glycerol and completed in three steps (Structure 1). This method gives both 1,3-diphosphatidylglycerol (cardiolipin) and 1,2-diphosphatidylglycerol (1,2-isomer of cardiolipin). The synthetic method of 1,2-diphosphatidylglycerol is also developed (Structure 2) (Fig. 1).

## Experimental Section

Melting points were determined at atmospheric pressure and were uncorrected.  $^1\text{H}$ ,  $^{31}\text{P}$  NMR spectra were recorded using Varian Inova (500 MHz) NMR spectrometer at 500, 125 and 100 MHz, respectively.  $^1\text{H}$  chemical shifts are in ppm from internal tetramethylsilane. For  $^{31}\text{P}$  the external standard was 85%  $\text{H}_3\text{PO}_4$  calibrated to 0 ppm. Mass spectral analyses [electron spray ionization (ESI)] were carried out on Triple

### Structure 1



### Structure 2

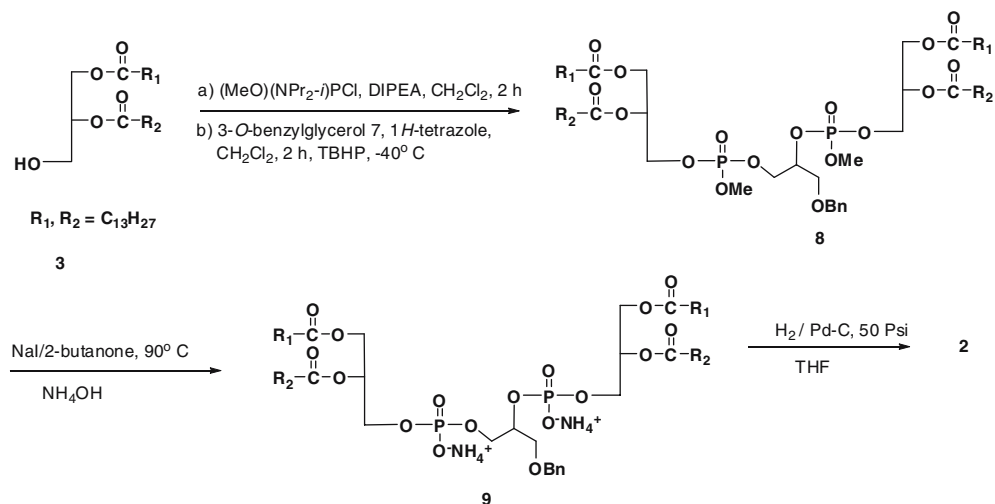
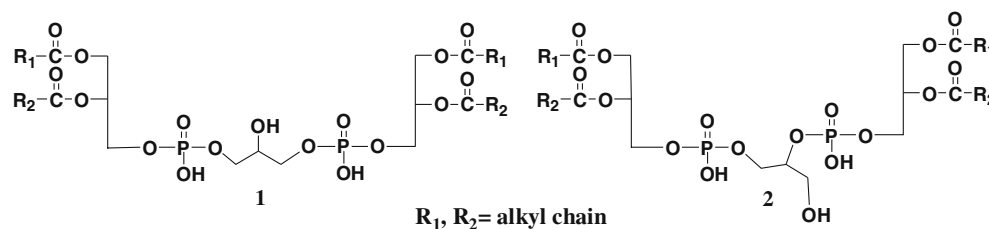




**Fig. 1** Chemical structures of 1,3-diphosphatidylglycerol (1,3-cardiolipin, **1**) and 1,2-diphosphatidylglycerol (1,2-cardiolipin, **2**)



Quadruple LC/MS/MS mass spectrometer API 4000 (Applied Biosystems). Infrared (IR) spectra were recorded on a Nicolet Nexus 470 FT-IR spectrophotometer. Samples were prepared by attenuated total reflectance (ATR) method. Thin layer chromatography (TLC) was carried out on Merck silica gel 60 F<sub>254</sub> plates (250  $\mu\text{m}$ ) and developed with the appropriate solvents. The TLC spots were visualized with either UV light or by heating plates stained with a solution of phosphomolybdic acid (5% ethanolic solution) or spraying with molybdenum blue (Sigma Chemical Co., St. Louis, MO, USA). Flash column chromatography was carried out on silica gel (230–400 mesh). All chemicals were purchased from Aldrich Chemical Co. (Milwaukee, WI, USA). All of the extracts were dried over anhydrous Na<sub>2</sub>SO<sub>4</sub>. Anhydrous dichloromethane (CH<sub>2</sub>Cl<sub>2</sub>) and tetrahydrofuran (THF) were used without further drying.

1,3-Bis [(1,2-Myristoyl-*sn*-Glycero-3)-Phosphoryl] Glycerol Dibenzyl Ester [5] and 1,2-Di [(1,2-Myristoyl-*sn*-Glycero-3)-Phosphoryl] Glycerol Dibenzyl Ester [6]

To a solution of 1,2-dimyristoyl-*sn*-glycerol **3** (7.35 g, 14.35 mmol) and 1*H*-tetrazole (8.4 mL of 0.45 M sol. in acetonitrile, 17.2 mmol) in 150 mL anhydrous CH<sub>2</sub>Cl<sub>2</sub>, dibenzyl diisopropyl phosphoramidite (5.45 g, 15.79 mmol) was added and stirred at room temperature for 1 h. The contents were diluted with 200 mL of CH<sub>2</sub>Cl<sub>2</sub> and then washed with 5% aqueous NaHCO<sub>3</sub> (2  $\times$  50 mL), brine (2  $\times$  50 mL), dried over Na<sub>2</sub>SO<sub>4</sub>, concentrated in vacuo and the oily residue **4** (10.84 g) was dried in a desiccator for 8 h and used as such in the next reaction.

A solution of the above phosphite **4**, glycerol (10.84 g, 14.35 mmol), pyridine (8.75 mL, 108.4 mmol) and Et<sub>3</sub>N (9.4 mL, 71.7 mmol) in CH<sub>2</sub>Cl<sub>2</sub> (150 mL) was cooled to  $-40^\circ\text{C}$  and pyridinium tribromide (6.88 g, 21.52 mmol) was added. The mixture was stirred at the same temperature for 1 h and gradually allowed to attain room temperature over a period of 2 h and treated with water (30 mL). The contents were diluted with EtOAc (250 mL) and the organic layer

was washed successively with aqueous 5% NaHCO<sub>3</sub> (2  $\times$  50 mL), water (50 mL) and brine (50 mL), dried (Na<sub>2</sub>SO<sub>4</sub>) and concentrated. The residue was purified on SiO<sub>2</sub> (8% acetone in CH<sub>2</sub>Cl<sub>2</sub>) to give 1.8 g (80%) of **5** as a colorless syrup as the major product. A minor product **6** (900 mg) was also obtained. <sup>1</sup>H NMR (CDCl<sub>3</sub>, 500 MHz) **5**:  $\delta$  0.88 (*t*, *J* = 7.0 Hz, 12H), 1.22–1.34 (*m*, 80H), 1.54–1.63 (*m*, 8H), 2.24–2.31 (*m*, 8H), 3.86–4.19 (*m*, 11H), 4.25–4.31 (*m*, 2H), 4.60–4.64 (*m*, 2H), 5.02–5.11 (*m*, 4H), 5.14–5.21 (*m*, 2H), 7.31–7.39 (*m*, 10H). **6**:  $\delta$  0.88 (*t*, *J* = 7.0 Hz, 12H), 1.22–1.34 (*m*, 80H), 1.54–1.62 (*m*, 8H), 2.23–2.31 (*m*, 8H), 4.02–4.31 (*m*, 12H), 4.60–4.64 (*m*, 1H), 5.02–5.11 (*m*, 4H), 5.14–5.21 (*m*, 2H), 7.31–7.39 (*m*, 10H).

1,3-Bis [(1,2-Dimyristoyl-*sn*-Glycero-3)-Phosphoryl] Glycerol Diammonium Salt [1]

A solution of protected cardiolipin [5] (1.5 g, 1.05 mmol) in tetrahydrofuran (30 mL) was hydrogenated at 50 psi over 10% Pd/C (350 mg) for 10 h. The catalyst was filtered off over a celite bed, treated with 5 mL of 30% ammonia solution and concentrated. The residue was dissolved in CHCl<sub>3</sub>, filtered through a 0.25  $\mu\text{m}$  filter and precipitated with acetone to give tetramyristoyl cardiolipin **1** (1.21 g, 90%) as a white solid. TLC (SiO<sub>2</sub>) CHCl<sub>3</sub>/MeOH/NH<sub>4</sub>OH (6.5:2.5:0.5) *R<sub>f</sub>* ~ 0.30. Mp 182–184°C FTIR (ATR) 3,214, 3,041, 2,956, 2,917, 2,849, 1,737, 1,467, 1,378, 1,328, 1,202, 1,091, 1,066 cm<sup>-1</sup>. <sup>1</sup>H NMR (CDCl<sub>3</sub>, 500 MHz):  $\delta$  0.88 (*t*, *J* = 7.0 Hz, 12H), 1.22–1.34 (*bs*, 80H), 1.52–1.66 (*m*, 8H), 2.26–2.34 (*m*, 8H), 3.06 (*bs*, 1H), 3.82–3.98 (*m*, 9H), 4.12–4.18 (*m*, 2H), 4.35–4.42 (*m*, 2H), 5.14–5.24 (*m*, 2H), 7.41 (*bs*, 8H). <sup>31</sup>P NMR (CDCl<sub>3</sub>, 161 MHz, 85% H<sub>3</sub>PO<sub>4</sub> as external standard)  $\delta$  0.78; ESI-MS (negative), *m/z* 1239.9 (M–2NH<sub>4</sub><sup>+</sup> + H<sup>+</sup>), 1011.9 (M–2NH<sub>4</sub><sup>+</sup>–RCOO<sup>-</sup>), 619.6 (M–2NH<sub>4</sub><sup>+</sup>)<sup>2-</sup>.

1,2-Di [(1,2-Dimyristoyl-*sn*-Glycero-3)-Phosphoryl] Glycerol Diammonium Salt [2]

Compound **2** was obtained from **6** in 88% yield as white solid following the procedure used for the synthesis of **1**. TLC (SiO<sub>2</sub>) CHCl<sub>3</sub>/MeOH/NH<sub>4</sub>OH

(6.5:2.5:0.5)  $R_f \sim 0.23$ . Mp 184–185 °C. FTIR (ATR) 3,220, 3,034, 2,956, 2,919, 2,851, 1,737, 1,416, 1,328, 1,202, 1,093, 1,063  $\text{cm}^{-1}$ .  $^1\text{H}$  NMR ( $\text{CDCl}_3$ , 500 MHz):  $\delta$  0.88 (*t*,  $J = 7.0$  Hz, 12H), 1.22–1.34 (*bs*, 80H), 1.52–1.63 (*m*, 8H), 2.25–2.33 (*m*, 8H), 2.92 (*bs*, 1H), 3.59–3.69 (*m*, 2H), 3.86–3.98 (*m*, 6H), 4.12–4.18 (*m*, 2H), 4.28–4.39 (*m*, 3H), 5.16–5.23 (*m*, 2H), 7.43 (*br s*, 8H).  $^{31}\text{P}$  NMR ( $\text{CDCl}_3$ , 161 MHz, 85%  $\text{H}_3\text{PO}_4$  as external standard)  $\delta$  0.34, 0.68; ESI-MS (negative),  $m/z$  1,239.9 ( $\text{M}-2\text{NH}_4^+ + \text{H}^+$ ), 1,011.8 ( $\text{M}-2\text{NH}_4^+ - \text{RCOO}^-$ ), 619.5 ( $\text{M}-2\text{NH}_4^+$ ) $^2$ .

### 3-*O*-Benzyl-1,2-Di[(1,2-*O*-Dimyristoyl-*sn*-Glycerol-3)Phosphoryl]Glycerol Dimethyl Ester [8]

To a solution of 1,2-*O*-dimyristoyl-*sn*-glycerol [3] (4.95 g, 9.66 mmol) and dry *N,N*-diisopropylethylamine (1.85 mL, 10.63 mmol) in anhydrous dichloromethane (80 mL) was added dropwise *N,N*-diisopropylmethylphosphonamidic chloride (2.06 mL, 10.63 mmol) at room temperature over a period of 30 min. After addition, the reaction solution was stirred at room temperature for 2 h and then 1*H*-tetrazole (25.76 mL, 11.59 mmol, 0.45 M sol. in acetonitrile) was added. To this reaction mixture, a solution of 3-*O*-benzylglycerol **7** (703 mg, 3.86 mmol) in  $\text{CH}_2\text{Cl}_2$  (20 mL) was added dropwise. The reaction mixture was stirred at room temperature for 3 h. The reaction mixture was then cooled to  $-40$  °C, and a solution of *tert*-butylhydroperoxide (2.9 mL, 14.49 mmol) was added such that the temperature of the reaction mixture was kept below 0 °C. The mixture was warmed to 25 °C before it was transferred to a separatory funnel and washed with 5%  $\text{Na}_2\text{S}_2\text{O}_3$  ( $2 \times 40$  mL), 5%  $\text{NaHCO}_3$  ( $2 \times 50$  mL), cold 1 N HCl ( $2 \times 20$  mL), Water and brine. The organic phase was dried over anhydrous  $\text{Na}_2\text{SO}_4$  and concentrated in vacuo to yield an oily residue. The residue was purified by flash chromatography on silica gel and eluted with hexane/ethyl acetate (2:1–3:2, vol/vol) to afford **8** as a colorless oil. Yield 4.19 g (85%). TLC (hexane/EtOAc 1:1, vol/vol),  $^1\text{H}$  NMR ( $\text{CDCl}_3$ , 500 MHz)  $\delta$  0.88 (*t*,  $J = 7$  Hz, 12H), 1.23–1.33 (*br s*, 80H), 1.59 (*m*, 8H), 2.28–2.34 (*m*, 8H), 3.66–3.71 (*d*,  $J = 5$  Hz, 2H), 3.73–3.80 (*dt*,  $J = 11.3, 3.0$  Hz, 6H), 3.84–3.89 (*m*, 1H), 4.12–4.37 (*m*, 10H), 4.55 (*br s*, 2H), 5.20–5.27 (*m*, 2H), 7.26–7.34 (*m*, 5H).

### 3-*O*-Benzyl-1,2-Di[(1,2-*O*-Dimyristoyl-*sn*-Glycerol-3)Phosphoryl]Glycerol Diammonium Salt [9]

To a stirred solution of **8** (2.45 g, 1.81 mmol) in 2-butanone (20 mL) was added sodium iodide (811 mg, 5.42 mmol), and the reaction mixture was refluxed at

90 °C for 3 h. The solvent was removed in vacuo and the resulting disodium salt was dissolved in cold  $\text{CHCl}_3$  (80 mL), MeOH (150 mL), and 0.1 N HCl (75 mL), and stirred at room temperature for 30 min. After addition of water (80 mL) and  $\text{CHCl}_3$  (80 mL), the  $\text{CHCl}_3$  layer was isolated and washed with  $\text{H}_2\text{O}$  (50 mL). The organic layer was neutralized with 10 mL of 10%  $\text{NH}_4\text{OH}$ . The organic layer was separated and concentrated to give a residue which was further purified by flash chromatography on silica gel and eluted with  $\text{CHCl}_3/\text{MeOH}/\text{NH}_4\text{OH}$  (7.0:2.0:0.5) to afford **9** as a white solid. Yield 1.92 g (72%).  $^1\text{H}$  NMR ( $\text{CDCl}_3$ , 500 MHz)  $\delta$  0.88 (*t*,  $J = 6.9$  Hz, 12H), 1.25–1.34 (*br s*, 80H), 1.56 (*br s*, 8H), 2.23–2.68 (*m*, 8H), 3.58 (*m*, 2H), 3.94 (*br s*, 6H), 4.07–4.16 (*m*, 3H), 4.28–4.36 (*dd*,  $J = 2$  Hz), 4.52 (*br s*, 2H), 5.22 (*m*, 2H), 7.24–7.30 (*m*, 5H), 9.26 (*br*, 8H,  $\text{NH}_4$ ).

### 1,2-Di [(1,2-Dimyristoyl-*sn*-Glycerol-3)-Phosphoryl]Glycerol Diammonium Salt [2]

Compound **9** (1.75 g, 1.28 mmol) was dissolved in tetrahydrofuran (50 mL) and 10% Pd/C (600 mg) was added. The solution was hydrogenated using a Parr hydrogenator at a pressure of 50 psi for 4 h. After filtration on celite to remove the catalyst, the solution was evaporated to dryness. The residue was dissolved in chloroform (10 mL) and precipitated using acetone (65 mL). The mixture was stored in a freezer overnight, and the white solid was filtered and washed with a small amount of cold acetone. After drying in a vacuum desiccator over phosphorus pentoxide overnight, 1,2-di [(1,2-dimyristoyl-*sn*-glycerol-3)-phosphoryl] glycerol diammonium salt [2] was obtained. Yield 1.3 g (85%). TLC ( $\text{SiO}_2$ )  $\text{CHCl}_3/\text{MeOH}/\text{NH}_4\text{OH}$  (6.5:2.5:0.5)  $R_f \sim 0.23$ ; Mp 184–185 °C,  $^1\text{H}$  NMR ( $\text{CDCl}_3$ , 500 MHz):  $\delta$  0.88 (*t*,  $J = 7.0$  Hz, 12H), 1.22–1.34 (*bs*, 80H), 1.52–1.63 (*m*, 8H), 2.25–2.33 (*m*, 8H), 2.92 (*bs*, 1H), 3.59–3.69 (*m*, 2H), 3.86–3.98 (*m*, 6H), 4.12–4.18 (*m*, 2H), 4.28–4.39 (*m*, 3H), 5.16–5.23 (*m*, 2H), 7.43 (*br s*, 8H).  $^{31}\text{P}$  NMR ( $\text{CDCl}_3$ , 161 MHz, 85%  $\text{H}_3\text{PO}_4$  as external standard)  $\delta$  0.34, 0.68; ESI-MS (negative),  $m/z$  1,240.21 ( $\text{M}-2\text{NH}_4^+ + \text{H}^+$ ), 1,011.9 ( $\text{M}-2\text{NH}_4^+ - \text{RCOO}^-$ ), 619.6 ( $\text{M}-2\text{NH}_4^+$ ) $^2$ .

### HPLC Method

Compounds **1** and **2** were analyzed at a concentration of 1 mg/mL on a prepacked DIOL cartridge column (ASTEC, 5  $\mu\text{m}$  particle size, 25 cm  $\times$  4.6 mm i.d.) using Agilent 1100 Series HPLC systems (Agilent Technology, Palo Alto, CA, USA). The column temperature was set at 40 °C and 50  $\mu\text{L}$  of sample was

injected into the HPLC for analysis and the sample temperature of the autosampler was maintained at 20 °C. The detection was done using evaporative light scattering detector (ELS1000, Polymer Laboratories Inc. Amherst, MA, USA). For the detector settings, nebulization occurred at 80–82 °C, evaporation temperature at 110 °C and the nitrogen flow was maintained at 1 mL/min. An isocratic mobile phase (MeOH:CHCl<sub>3</sub>, 9:1) was used at the flow rate of 0.8 mL/min.

## Results and Discussion

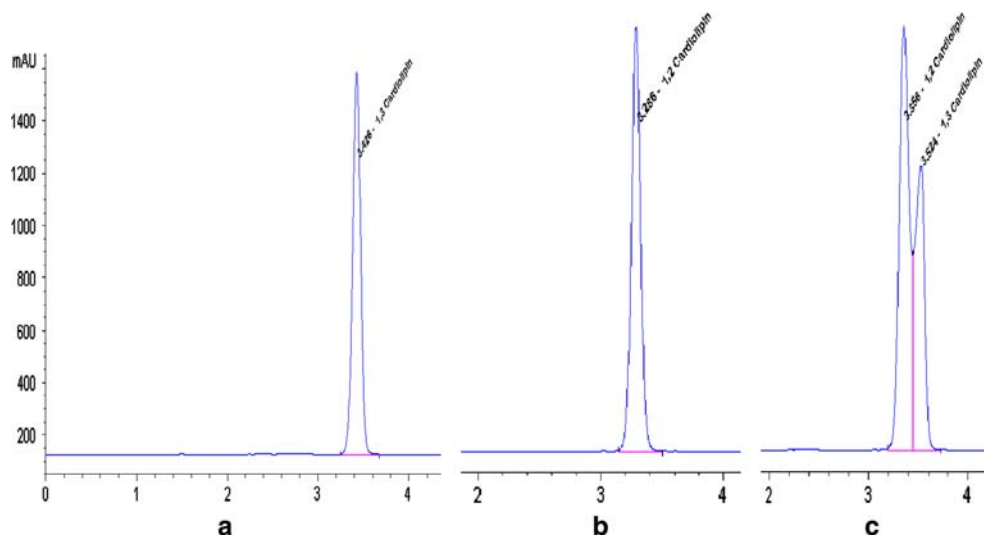
The new method presented here involves the treatment of unprotected glycerol with 1,2-diacyl-*sn*-glyceryl phosphite in the presence of pyridiniumbromide perbromide (PBP) and triethylamine in dichloromethane to afford a phosphoric triester. Removal of the phosphate protecting group will furnish the 1,3-diphosphatidylglycerol (cardiolipin). Accordingly, treatment of unprotected glycerol with dibenzyl 1,2-dimyristoyl-*sn*-glyceryl phosphate [4] prepared by a 1*H*-tetrazole mediated reaction of 1,2-dimyristoyl-*sn*-glycerol [3] with dibenzyl *N,N*-diisopropyl phosphoramidite in the presence of PBP and triethylamine afforded benzyl protected 1,3-diphosphatidylglycerol [5] along with the 1,2-phosphorylated product [6] (ratio of 6:1) in 75% yield (Structure 1). Both of these products were separated by silica gel chromatography and the structures were confirmed by NMR spectroscopy. The phosphates were individually subjected to hydrogenolysis with 10% Pd/C at 50 psi in tetrahydrofuran at room temperature to obtain tetramyristoyl cardiolipin [1] and 1,2-isomer of cardiolipin [2],

respectively, which were immediately converted to ammonium salt with the addition of ammonia. Alternatively, the crude phosphate mixture was subjected to hydrogenolysis and the products were separated at the final stage. The products (1 and 2) are easily separable on silica gel by flash chromatography with dichloromethane/methanol/ammonia (80:20:1) as eluent.

The identity and structure of 1,2-phosphorylated product 2 was further confirmed by an independent synthesis of the same (Structure 2). The synthesis of 2 was initiated by treating methyl *N,N*-diisopropylchlorophosphoramidite with 1,2-dimyristoyl-*sn*-glycerol [3] and 3-*O*-benzylglycerol [7] followed by in situ oxidation yielding the protected phosphate derivative [8]. The methyl group was deprotected by refluxing with sodium iodide (NaI) in 2-butanone to afford 9 and the debenzylation was accomplished by catalytic dehydrogenation yielding the 1,2-derivative 2 (1,2-isomer of cardiolipin) with a 76% yield (Structure 2). The products 1 and 2 were soluble in chloroform and showed clear <sup>1</sup>H NMR signals. The structures were characterized by NMR (<sup>1</sup>H, <sup>31</sup>P), IR and ESI-MS. Compound 2 is essentially a mixture of *sn*-1,2- and *sn*-2,3 isomers. Further purification of these regioisomers by chiral HPLC and with derivatization might be useful for the further synthesis of specific isomers of interesting compounds having biological importance.

Compound 1 and 2 were analyzed by HPLC on ASTEC diol column using an isocratic mobile phase (MeOH:CHCl<sub>3</sub>, 9:1) The detection was done using an evaporative light scattering detector. 1,3 Cardiolipin and 1,2-cardiolipin were well separated having retention times 3.42 and 3.28, respectively (Fig. 2). Both the cardiolipin were also injected together to observe the specification of the compounds, the peaks are found to

**Fig. 2** HPLC chromatograms **a** 1,3-diphosphatidylglycerol (1,3-cardiolipin), **b** 1,2-diphosphatidylglycerol (1,2-cardiolipin), **c** mixture of 1,3- and 1,2-diphosphatidylglycerol



be very close to each other indicative of two different compounds with similar structure as shown in Fig. 1.

In conclusion, the route used to make cardiolipin derivatives outlined here offers several advantages over other strategies used. The synthesis begins with readily available, 1,2-diacyl-*sn*-glycerols and dibenzyl phosphoramidites. Installation of the polar head group has been made easy by phosphate chemistry instead of cyclic enediol pyrophosphates and relatively labile PA. The present study has been aimed at the development of the 1,2-isomer of cardiolipin and also at a cost effective synthesis of 1,3-phosphatidylglycerol by reacting unprotected glycerol with 1,2-diacyl-*sn*-glyceryl phosphite. 1,2-Diphosphatidylglycerol may be a member of a new class of phospholipids for industrial applications similar to other natural or synthetic phosphocholines. Further, this method can be carried out on a gram scale with various types of metal ions and fatty acid chain lengths.

**Acknowledgments** We thank the Bioanalytical group of Pharmacokinetics, Safety and Efficacy (PSE) Department at NeoPharm for the Mass spectral analyses.

## References

1. Arrigo PD, Ferra LD, Fantoni GP, Scarcelli D, Servi S, Strini A (1996) Enzyme-mediated synthesis of two diastereoisomeric forms of phosphatidylglycerol and of diphosphatidylglycerol (cardiolipin). *J Chem Soc Perkin Trans 1*(21):2657–2660
2. Keana JFW, Shimiju M, Jernstedt KK (1986) A short, flexible route to symmetrically and unsymmetrically substituted diphosphatidylglycerols (cardiolipin). *J Org Chem* 51:2297–2299
3. Mishina IM, Vasilenko AE, Stepanov AE, Shvets VI (1987) Studies on complex lipids. Synthesis of diphosphatidylglycerol (cardiolipin) with unsaturated fatty acids. *Bioorg Khim* 13:1110–1115
4. Mishina IM, Vasilenko AE, Stepanov AE, Shvets VI (1984) Study of lipids. Synthesis of phosphatidylglycerol and diphosphatidylglycerol. *Zh Org Khim* 20:985–988
5. Mishina IM, Vasilenko AE, Stepanov AE, Shvets VI (1985) Synthesis of diphosphatidylglycerol (cardiolipin) with unsaturated fatty acids. *Bioorg Khim* 11:992–994
6. Ioannou PV, Marecek JF (1986) Studies on the chemical synthesis and stability of cardiolipins and related compounds. *Chem Chorn* 15:205–220
7. Ramirez F, Ioannou PV, Marecek JF, Dodd GH, Golding BT (1977) Synthesis of phospholipids by means of cyclic enediol pyrophosphates. *Tetrahedron* 33:599–608
8. Ramirez F, Ioannou PV, Marecek JF, Golding BT, Dodd GH (1976) Application of cyclic enediol pyrophosphates to the synthesis of phospholipids. Diphosphatidylglycerol (cardiolipin). *Synthesis* 11:769–770
9. Inoue K, Nojima S (1968) Immunochemical studies of phospholipids. II. Synthesis of cardiolipin and its analogues. *Chem Pharm Bull* 16:76–81
10. Inoue K, Nojima S (1963) On the cardiolipin analogues. Synthesis of dipalmitoyl-D,L- $\alpha$ -glycerylphosphoryl-propanol sodium salt and bis(dipalmitoyl-D,L- $\alpha$ -glycerylphosphoryl)-1,3-propanediol disodium salt. *Chem Pharm Bull* 11:1150–1156
11. Saunders RM, Schwarz HP (1966) Synthesis of phosphatidylglycerol and diphosphatidylglycerol. *J Am Chem Soc* 88:3844–3847
12. Duralski AA, Spooner PJR, Rankin SE, Watts A (1998) Synthesis of isotopically labelled cardiolipins. *Tetrahedron Lett* 39:11607–1610
13. Krishna UM, Ahmad MU, Ahmad I (2004) Phosphoramidite approach for the synthesis of cardiolipin. *Tetrahedron Lett* 45:2077–2079
14. Lin Z, Ahmad MU, Ali SM, Ahmad I (2004) An efficient and novel method for the synthesis of cardiolipin and its analogs. *Lipids* 39:285–290
15. Krishna UM, Ahmad MU, Ali SM, Ahmad I (2004) A short, concise route to diphosphatidylglycerol (cardiolipin) and its variants. *Lipids* 39:595–600
16. Browne JE, Driver MJ, Russel JC, Sammes PG (2000) Preparation of phospholipid analogues using the phosphoramidite route. *J Chem Soc Perkin Trans 1*(5):653–657
17. Beaucage SL, Iyer RP (1993) The synthesis of specific ribonucleotides and unrelated phosphorylated biomolecules by the phosphoramidite method. *Tetrahedron* 49:10441–10488
18. Watanaba Y, Hirofuji H, Ozaki S (1994) Synthesis of a phosphatidylinositol 3, 4, 5-triphosphate. *Tetrahedron Lett* 35:123–124
19. Watanaba Y, Nakamura T, Mitsumoto H (1997) Protection of phosphate with the 9-fluorenylmethyl group. Synthesis of unsaturated-acyl phosphatidylinositol 4, 5-bisphosphate. *Tetrahedron Lett* 38:7407–7410

# Leucine and Calcium Regulate Fat Metabolism and Energy Partitioning in Murine Adipocytes and Muscle Cells

Xiaocun Sun · Michael B Zemel

Received: 21 November 2006 / Accepted: 22 January 2007 / Published online: 20 February 2007  
© AOCS 2007

**Abstract** Dietary calcium modulation of adiposity is mediated, in part, by suppression of calcitriol, while the additional effect of dairy products is mediated by additional components; these include the high concentration of leucine, a key factor in the regulation of muscle protein turnover. We investigated the effect of leucine, calcitriol and calcium on energy metabolism in murine adipocytes and muscle cells and on energy partitioning between adipocytes and skeletal muscle. Leucine induced a marked increase in fatty acid oxidation in C2C12 muscle cells ( $P < 0.001$ ) and decreased FAS expression by 66% ( $P < 0.001$ ) in 3T3-L1 adipocytes. Calcitriol decreased muscle cell fatty acid oxidation by 37% ( $P < 0.001$ ) and increased adipocyte FAS gene expression by threefold ( $P < 0.05$ ); these effects were partially reversed by either leucine or calcium channel antagonism with nifedipine. Co-culture of muscle cells with adipocytes or incubation with 48-h adipocyte conditioned medium decreased muscle fatty acid oxidation by 62% ( $P < 0.001$ ), but treating adipocytes with leucine and/or nifedipine attenuated this effect. Leucine, nifedipine and calcitriol also modulated adiponectin production and thereby exerted additional indirect effects on fatty acid oxidation in C2C12 myotubes. Adiponectin increased IL-15 and IL-6 release by myotubes and partially reversed the inhibitory effects of calcitriol. Comparable effects of leucine, calcitriol and adiponectin were found in myotubes treated with conditioned medium derived

from adipocytes or co-cultured with adipocytes. These data suggest that leucine and nifedipine promote energy partitioning from adipocytes to muscle cells, resulting in decreased energy storage in adipocytes and increasing fatty acid utilization in muscle.

**Keywords** Calcium · Calcitriol · Leucine · Adiponectin

## Introduction

Adipose tissue has previously been perceived predominantly as a fuel reservoir that provides skeletal muscle and other organs with non-esterified fatty acids (NEFA) when exogenous nutrients are insufficient for their energy needs. Accordingly, many previous studies have focused on the development and metabolism of adipose tissue with the final aim of understanding the control of body fat stores. However, adipose tissue is now recognized as an active endocrine organ which synthesizes and secretes a variety of biological molecules, including adiponectin, leptin, tumor necrosis factor alpha (TNF $\alpha$ ), interleukins-6 (IL-6) and interleukins-15 (IL-15) [1–4]. The more recent recognition that skeletal muscle may also assume a similar role in response to various metabolic stimuli suggests a potential interaction between skeletal muscle and adipose tissue [5–6].

Previous data from this laboratory demonstrate that dietary calcium exerts an anti-obesity effect by inhibiting calcitriol secretion [7–10]. We have shown that calcitriol mediates increases in intracellular calcium ( $[Ca^{2+}]_i$ ) in adipocytes via the 1, 25(OH) $_2$ -D $_3$ -membrane associated rapid response steroid hormone

X. Sun · M. B. Zemel (✉)  
Department of Nutrition, University of Tennessee,  
1215 W. Cumberland Avenue, Knoxville,  
TN 37996-1920, USA  
e-mail: mzemel@utk.edu

(1, 25D<sub>3</sub>-MARRS) binding protein and stimulates lipogenesis and inhibits lipolysis via a calcium dependent mechanism [11–15]. We have also shown a dose responsive inhibition of uncoupling protein 2 (UCP2) expression by calcitriol in human adipocytes mediated by the nuclear vitamin D receptor (nVDR) [16]. Moreover, we have shown that suppression of circulating calcitriol levels by increasing dietary calcium suppresses adipocyte [Ca<sup>2+</sup>]<sub>i</sub>, increases UCP2 expression, promotes adipocyte apoptosis in white adipose tissue and reduces metabolic efficiency and adiposity in a mouse model of obesity [7–9], suggesting that dietary strategies designed to suppress circulating calcitriol levels may reduce adiposity.

In support of this concept, dietary calcium suppressed fat gain on eucaloric diets and accelerated fat loss on hypocaloric diets in both animals and humans [7–9]. Notably, providing calcium in the form of dairy, which also provides branch chain amino acids (BCAAs), exerted a greater effect on adiposity and protected muscle mass during energy restriction and increased muscle mass on eucaloric diets [17–18], suggesting that dietary calcium provided with BCAAs may regulate energy partitioning in a tissue selective manner and regulate energy metabolism by modulating endocrine function of both adipose tissue and skeletal muscle, favoring elevated energy expenditure in adipose tissue and promoting protein synthesis in skeletal muscle. However, the effect of BCAAs, specifically leucine, in regulating this process is unclear. Accordingly, the objective of the present study was to determine the role and mechanism of calcium, calcitriol and leucine in regulating cross-talk between adipose tissue and skeletal muscle, and in thereby modulating adiposity.

## Material and Methods

### Cell Culture

C2C12 and 3T3-L1 preadipocytes (American Type Culture Collection) were incubated at a density of 8,000 cells/cm<sup>2</sup> (10 cm<sup>2</sup> dish) and grown in Dulbecco's modified eagle's medium (DMEM) containing 10% fetal bovine serum (FBS), and antibiotics (adipocyte medium) at 37 °C in 5% CO<sub>2</sub>. Confluent 3T3-L1 preadipocytes were induced to differentiate with a standard differentiation medium consisting of DMEM (1:1, vol/vol) medium supplemented with 1% FBS, 1 μM dexamethasone, 3-isobutyl-1-methylxanthine (IBMX) (0.5 mM) and antibiotics (1% penicillin–streptomycin). Preadipocytes were maintained in this

differentiation medium for 3 days and subsequently cultured in adipocyte medium. Cultures were re-fed every 2–3 days to allow 90% cells to reach fully differentiation before conducting chemical treatment. For differentiation of C2C12 cells, cells were grown to 100% confluence, changed into differentiation medium (dexamethasone with 2% horse serum and 1% penicillin–streptomycin), and fed with fresh differentiation medium every day until myotubes were fully formed (3 days).

### Co-culture of Adipocyte and C2C12

Cells were co-cultured by using transwell inserts with a 0.4 μm porous membrane (Corning) to separate adipocytes and C2C12 muscle cells as described previously [19]. Each cell type was grown independently in the transwell plates. Following cell differentiation and growth to confluence, inserts containing adipocytes were transferred to myotube plates, and inserts containing myotubes were transferred to adipocyte plates. After incubation for 48 hours, the cells in the lower well were harvested for further analysis.

### Treatment of Cells

Calcitriol, leucine, nifedipine or/and adiponectin were freshly diluted in medium before treatment. Cells were incubated in serum free medium overnight and then washed with fresh medium, re-fed with medium containing the different treatments (2.5 mM leucine and/or 5 μM nifedipine with or without 10 nM calcitriol or 70 ng/ml adiponectin) and incubated at 37 °C in 5% CO<sub>2</sub> for 48 h before analysis. In some experiments, the supernatants of differentiated 3T3-L1 adipocytes were used to replace the medium of C2C12 myotubes. Cell viability was measured via trypan blue exclusion. At the end of the incubation, culture supernatants were collected and stored at –20 °C until assayed.

### Fat Oxidation

Muscle cell fat oxidation was measured as described previously [20], with minor modification. Briefly, C2C12 cell monolayers were rinsed twice with phosphate-buffered saline (PBS) and incubated in substrate mixture containing 22 μM unlabeled palmitate plus 5 μCi [<sup>3</sup>H]palmitate in Hank's basic salt solution containing 0.5 mg/ml BSA for 2 h. Negative controls were prepared by treating the monolayer with methanol for 30 s to abolish cellular metabolism. The reaction medium was then collected from cell monolayer and treated with 0.2 ml 10% trichloroacetic acid. The

protein precipitate was removed by centrifugation while supernatants were treated with 6 N NaOH and then applied to a poly-prep chromatography column with 1 ml Dowex-1. The  $^3\text{H}_2\text{O}$  passed through the column and the following 1 ml of water wash was collected and radioactivity was measured with a liquid scintillation counter.

To determine total cellular protein of cultures used for fatty acid oxidation assays, cell monolayers were harvested after removal of the reaction mixture and subjected to protein measurement using Bradford protein assay reagents.

#### Total RNA Extraction

A total cellular RNA isolation kit (Ambion, Austin, TX) was used to extract total RNA from cells according to manufacturer's instruction. The concentration and purity of the isolated RNA were measured spectrophotometrically ( $A_{280}/A_{260}$  between 1.9 and 2.1) and the integrity of RNA sample were analyzed via BioAnalyzer (Agilent 2100, Agilent Technologies).

#### Quantitative Real Time PCR

Adipocyte and muscle 18s, fatty acid synthase (FAS), peroxisome proliferator-activated receptor gamma (PPAR gamma) and mitochondrial uncoupling protein 3 (UCP3) were quantitatively measured using an ABI 7300 Real-Time PCR System (Applied Biosystems, Branchburg, NJ) with a TaqMan 1000 Core Reagent Kit (Applied Biosystems, Branchburg, NJ). The primers and probe sets were obtained from Applied Biosystems TaqMan® Assays-on-Demand™ Gene Expression primers and probe set collection according to manufacturer's instruction. Pooled adipocyte total RNA were serial-diluted in the range of 1.5625–25 ng and used to establish a standard curve; total RNAs for unknown samples were also diluted in this range. Reactions of quantitative RT-PCR for standards and unknown samples were also performed according to the instructions of ABI 7300 Real-Time PCR System and TaqMan Real Time PCR Core Kit. The mRNA quantitation for each sample were further normalized using the corresponding 18s quantitation.

#### Measurement of Secretion of Cytokines in Culture Supernatants

Concentrations of adiponectin, IL-15 and IL-6 in cell culture supernatants were determined by enzyme-linked immunosorbent assay (ELISA). ELISA kits were purchased from Assay Designs (Ann Arbor, MI)

and experiments were performed according to the manufacturer's instructions.

#### Statistical Analysis

All data were expressed as mean  $\pm$  SEM. Data from studies were evaluated by one-way or two-way ANOVA, and significantly different group means ( $P < 0.05$ ) were then separated by the least significant difference test using SPSS (SPSS Inc, Chicago, IL).

#### Results

Both leucine and nifedipine stimulated fatty acid oxidation in C2C12 muscle cells and this effect was attenuated by calcitriol ( $P < 0.001$ ) (Fig. 1a). Adiponectin markedly increased fatty acid oxidation in C2C12 myotubes and restored fatty acid oxidation suppressed by calcitriol in the presence of leucine (Fig. 1a). Comparable effects of leucine, calcitriol and adiponectin were found in myotubes co-cultured with adipocytes (Fig. 1b); however, the presence of adipocytes markedly suppressed fatty acid oxidation. This effect is attributable to secreted factor(s), as a comparable suppression resulted from exposure of the myotubes to adipocyte conditioned medium (Fig. 1c).

Consistent with this, the expression of UCP3 in C2C12 cells was significantly upregulated by leucine, and calcitriol partially inhibited this effect ( $P < 0.001$ ) (Fig. 2). However, nifedipine did not significantly affect UCP3 expression, indicating that leucine and calcitriol regulate UCP3 expression in a  $\text{Ca}^{2+}$ -independent manner. This is consistent with our previous data which demonstrates that calcitriol regulates uncoupling protein expression via the nVDR and is independent of  $\text{Ca}^{2+}$  signalling [16].

Leucine and calcitriol exerted complementary regulation on adipocytes. Leucine inhibited FAS ( $P < 0.001$ ) (Fig. 3a) and PPAR gamma ( $P < 0.001$ ) (Fig. 3b) expression in differentiated 3T3-L1 adipocytes while calcitriol stimulated both FAS and PPAR gamma expression and attenuated the effect of leucine on FAS expression and nifedipine exerted the opposite effect.

Our data also demonstrate that leucine, calcium and calcitriol regulate cytokine release from adipocytes and skeletal muscle and suggest that they may play a role in modulating their effect on energy metabolism. Leucine and nifedipine markedly increased adiponectin production in adipocytes while calcitriol exerted the opposite effect (Fig. 4). Adiponectin significantly enhanced IL-15 release in muscle cells compared to

**Fig. 1** The effect of leucine, nifedipine, adiponectin and calcitriol on fatty acid oxidation in C2C12 muscle cells. Fatty acid oxidation was determined by palmitate oxidation. C2C12 myotubes were treated with or without leucine (2.5 mM), nifedipine (10  $\mu$ M), adiponectin (70 ng/ml) or/and calcitriol (10 nM) for 48 h in basal medium (a), co-cultured with adipocytes (b) or in conditioned medium derived from 48-h incubation with adipocytes (c). Total cell numbers of cultures used for oxidation assays were evaluated by the DNA content. Values are presented as mean  $\pm$  SEM,  $n = 6$ . Means with different letter differ with  $P < 0.05$

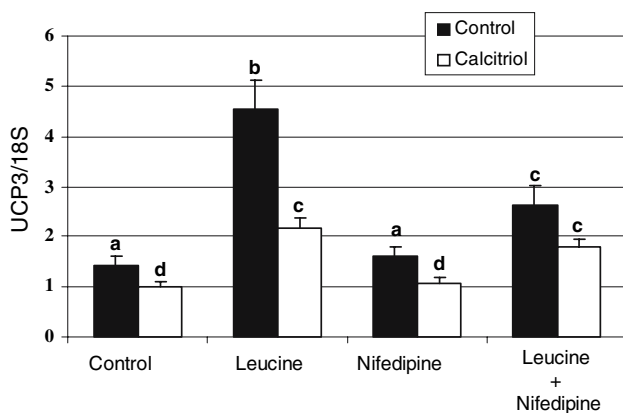
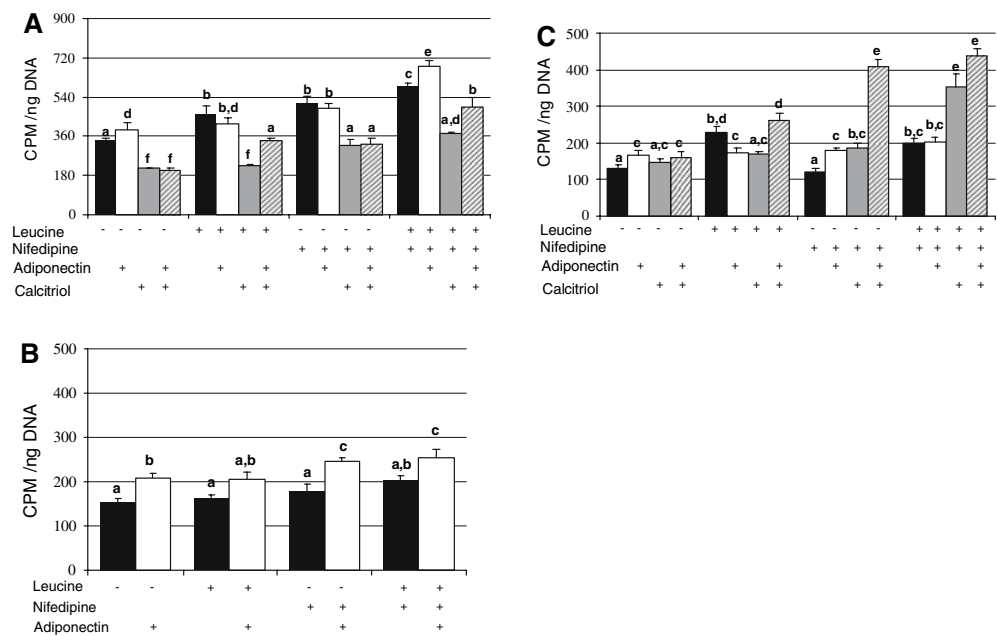


**Fig. 2** The effect of leucine, nifedipine and calcitriol on UCP3 to 18s expression ratio in C2C12 muscle cells. C2C12 myotubes were treated with or without leucine (2.5 mM), nifedipine (10  $\mu$ M), or/and calcitriol (10 nM) for 48 h. Values are presented as mean  $\pm$  SEM,  $n = 6$ . Means with different letter differ with  $P < 0.05$

basal medium and this effect was attenuated by addition of calcitriol (Fig. 5a). Leucine appeared to exert no additional effect on IL-15 release in basal medium with or without adiponectin while nifedipine alone promoted IL-15 release but adiponectin exerted no addition effect. Adiponectin also increased IL-15 release in muscle cells treated with both leucine and nifedipine and this effect was not attenuated by addition of calcitriol, indicating the effect of calcitriol is mediated, at least in part by calcium signaling. Comparable effects were found in myotubes co-cultured with adipocytes (Fig. 5b) or treated with conditioned medium derived from differentiated adipocytes (Fig. 5c).

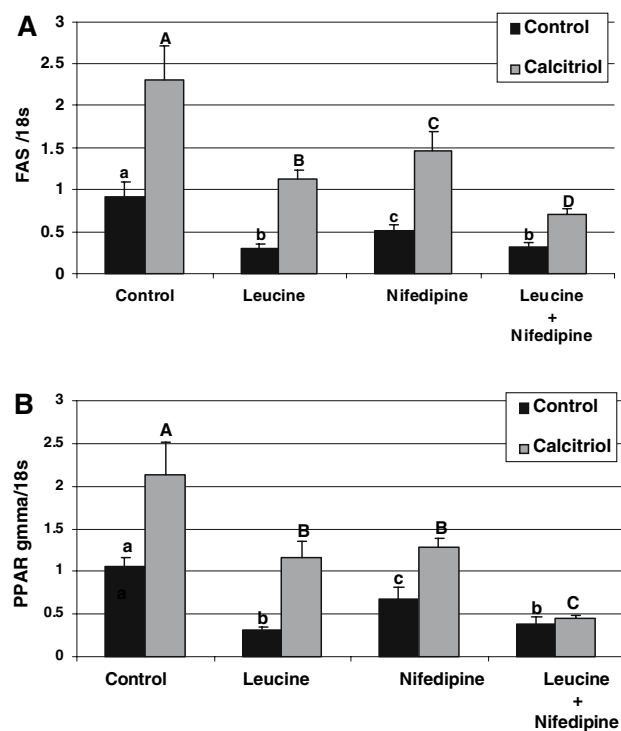


**Fig. 3** The effect of leucine, nifedipine and calcitriol on FAS to 18s expression ratio (a) and PPAR gamma to 18s expression ratio (b) in 3T3-L1 adipocytes. Adipocytes were treated with or without leucine (2.5 mM), nifedipine (10  $\mu$ M), or/and calcitriol (10 nM) for 48 h. Values are presented as mean  $\pm$  SEM,  $n = 6$ . Means with different letter differ with  $P < 0.05$

Similar observations were found in IL-6 production in muscle cells, with nifedipine stimulating IL-6 production, although leucine exhibited no effect (Fig. 6a).



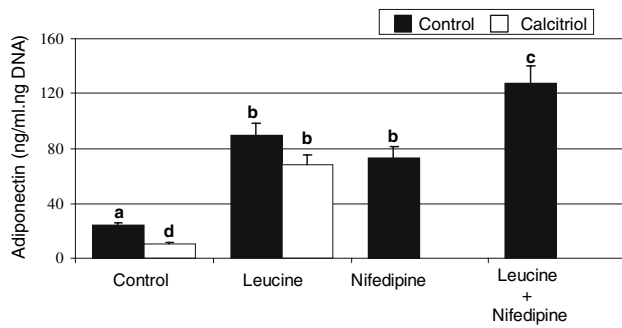


**Fig. 4** The effect of leucine, nifedipine and calcitriol on adiponectin production in 3T3-L1 adipocytes. Adiponectin was determined by ELISA as described in “Materials and methods” section. Adipocytes were treated with or without leucine (2.5 mM), nifedipine (10  $\mu$ M), or/and calcitriol (10 nM) for 48 h. Total cell numbers of cultures used for adiponectin production were evaluated by the DNA content. Values are presented as mean  $\pm$  SEM,  $n = 6$ . Means with different letter differ with  $P < 0.05$

Adiponectin increased IL-6 production and this effect was enhanced by nifedipine but not leucine. Although calcitriol exerted no significant effect on IL-6 production, it attenuated the effect of adiponectin on IL-6 production. Comparable effects were found in muscle cells co-cultured with adipocytes (Fig. 6b) or treated with conditioned medium derived from differentiated adipocytes (Fig. 6c).

## Discussion

The present data demonstrate independent roles of leucine and calcium antagonism in regulating energy partitioning between adipocytes and muscle cells, with both favoring fatty acid oxidation and UCP3 expression in C2C12 muscle cells. Calcitriol, a steroid hormone which has been shown to stimulate calcium influx via 1, 25D<sub>3</sub>-MARRS, suppressed fatty acid oxidation and attenuated the effects of leucine and nifedipine. Consequently, we hypothesize that this increase in muscle fat oxidation is coupled with decreased fat storage and increased fat catabolism in adipocytes. Consistent with this concept, we found that leucine inhibited FAS and PPAR gamma expression in differentiated 3T3-L1 adipocytes while calcitriol stimulated the expression of both genes and attenuated the effect of leucine on FAS expression, while nifedipine exerted the opposite effect. In addition, muscle cells treated with conditioned medium derived from adipocytes or co-cultured with adipocytes exhibited suppressed fatty acid oxidation, indicating that one or more factors derived from adipocytes regulate skeletal muscle energy metabolism. Indeed, leucine, nifedipine and calcitriol also modulate adiponectin production, with leucine and nifedipine increasing adiponectin production while calcitriol exerted the opposite effect. Consequently, we further evaluated the role of

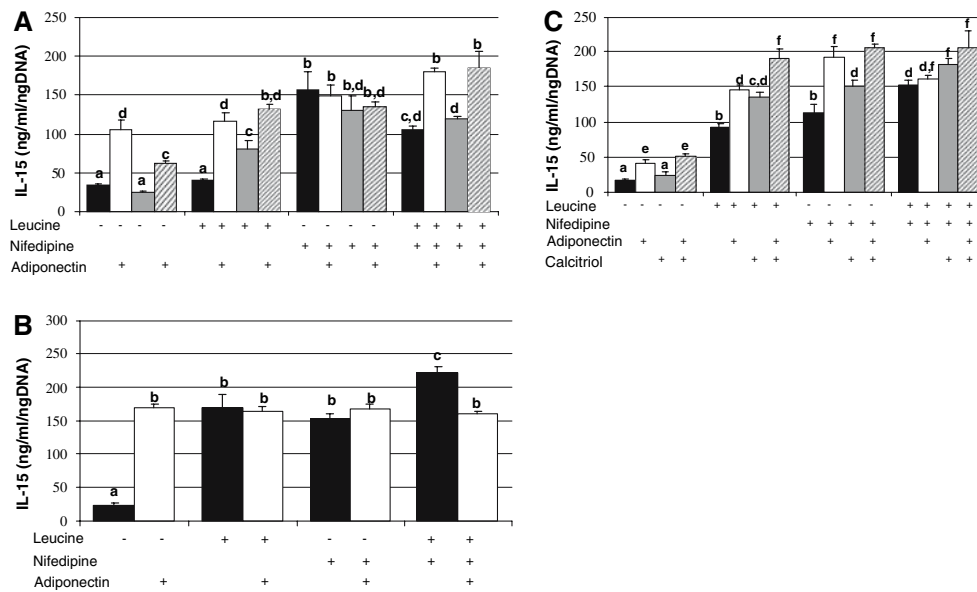


**Fig. 5** The effect of leucine, nifedipine, adiponectin and calcitriol on IL-15 production in C2C12 muscle cells. IL-15 production was determined by ELISA and C2C12 myotubes were treated with or without leucine (2.5 mM), nifedipine (10  $\mu$ M), adiponectin (70 ng/ml) or/and calcitriol (10 nM) for 48 h in basal

medium (a), co-cultured with adipocytes (b) or in conditioned medium derived from 48-h incubation with adipocytes (c). Total cell numbers of cultures used for oxidation assays were evaluated by the DNA content. Values are presented as mean  $\pm$  SEM,  $n = 6$ . Means with different letter differ with  $P < 0.05$

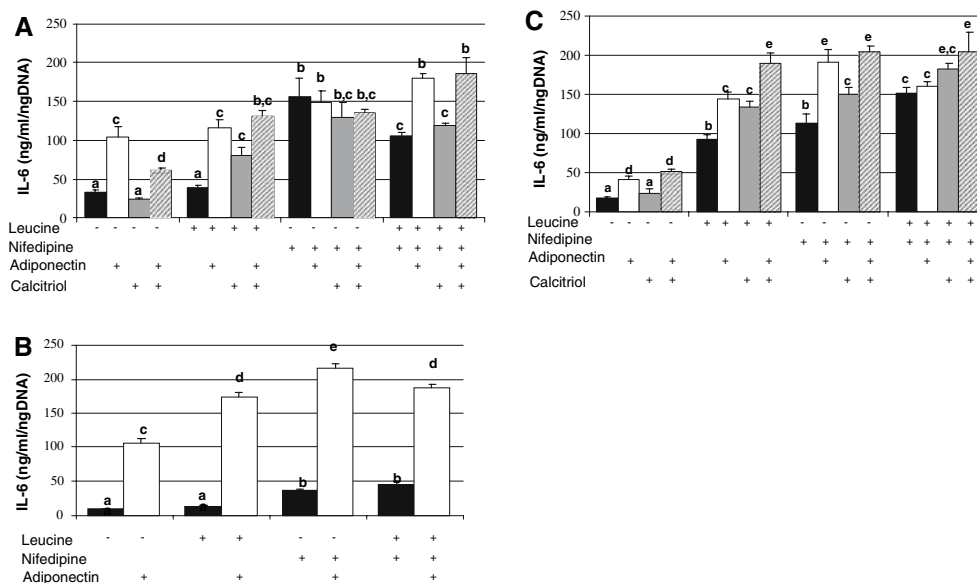


**Fig. 6** The effect of leucine, nifedipine, adiponectin and calcitriol on IL-6 production in C2C12 muscle cells. IL-6 production was determined by ELISA and C2C12 myotubes were treated with or without leucine (2.5 mM), nifedipine (10  $\mu$ M), adiponectin (70 ng/ml) or/and calcitriol (10 nM) for 48 h in basal

medium (a), co-cultured with adipocytes (b) or in conditioned medium derived from 48-h incubation with adipocytes (c). Total cell numbers of cultures used for oxidation assays were evaluated by the DNA content. Values are presented as mean  $\pm$  SEM,  $n = 6$ . Means with *different letter* differ with  $P < 0.05$

adiponectin in mediating the response to leucine, nifedipine and calcitriol. Adiponectin promoted fatty acid oxidation, consistent with previously reported data [21], and enhanced leucine and nifedipine stimulated fatty acid oxidation in muscle cells. This effect was accompanied by up-regulation of IL-15 and IL-6 production in muscle, both of which have been shown to stimulate fatty acid oxidation [22–24].

Adipose tissue excess is an important pathogenic mechanism underlying the obesity-associated metabolic syndrome [25–27]. However, weight loss through energy control is associated with the loss of lean body mass, contributing to decreased energy expenditure [28–29]. This decrease in energy expenditure is of sufficient magnitude to contribute to the very high recidivism following successful weight reduction. Thus, strategies to reduce body fat while also maintaining lean body mass may contribute to successful long-term management of obesity and associated disorders. Previous data demonstrate a role of calcium in regulating adipose tissue lipid metabolism and a role of BCAAs in maintenance of lean mass [18]. However, the effect of calcium and BCAAs in regulation of adipose-muscle cross-talk in modulating energy partitioning had not been evaluated. Data from this study suggest that both leucine and cellular calcium antagonism promote energy partitioning from adipocytes to muscle cells, resulting in decreased energy storage in adipocytes and increasing fatty acid utilization in muscle; moreover,

these effects appear to be partially attributable to modulation of cytokine production.

We have previously demonstrated that high calcium diets inhibit weight and fat gain in both mice and humans on obesigenic diets and accelerate weight and fat loss during energy restriction [17–18]. A key mechanism underlying this anti-obesity effect is suppression of calcitriol, which modulates intracellular  $\text{Ca}^{2+}$  signaling and mitochondrial uncoupling in adipocytes and consequently results in reduced adiposity and oxidative stress [10–16]. Notably, dairy sources of calcium exert a markedly greater effect on adiposity in both mice and humans [7–9, 30–31]. Moreover, unlike supplementary or fortified sources of calcium, utilization of intact dairy products as a calcium source resulted in a modest increase in muscle mass in the absence of energy restriction and substantially reduced the loss of lean mass which otherwise accompanies hypocaloric diets, while supplementary calcium was without effect on lean mass in either mice or humans. Accordingly, dairy appears to cause a significant change in energy partitioning between adipose tissue and muscle, resulting in reduced energy storage in adipose tissue and increased fat oxidation and energy utilization (presumably for protein synthesis) in skeletal muscle. Provision of BCAAs to skeletal mimics the effect of a complete mixture of amino acids in promoting protein synthesis both in vivo and in vitro [32–33]. For example, incubation of rat diaphragm with BCAAs results in similar

stimulation of protein synthesis to that found with a complete mixture of amino acids [34]. Similarly, perfusion of rat skeletal muscle with BCAAs produces a comparable stimulation of protein synthesis to that found with perfusion of a complete mixture of amino acids [35]. Conversely, perfusion with an amino acid mixture without BCAAs has no effect on protein synthesis. Of the BCAAs, leucine appears to be primarily responsible for this anabolic effect via both mammalian target of rapamycin (mTOR)-dependent and mTOR-independent signaling [36–39]. Leucine inhibits protein degradation in muscle and infusion of leucine in human subjects results in decreased plasma levels of other amino acids [40], indicating that leucine favors protein synthesis by either reducing protein breakdown or increasing amino acid disposal for protein synthesis. Recent data suggest that the effect of leucine in regulation of protein synthesis appears not to be limited to muscle and may regulate protein metabolism in adipose tissue as well [41–42].

Energy partitioning between adipose tissue and skeletal muscle has been previously demonstrated. Animals lacking myostatin exhibit markedly increased skeletal muscle mass and reduced body fat accumulation [43–44]. Comparable results can be achieved by blocking myostatin signaling via c-ski gene overexpression [45]. Moreover, stimulation of beta-adrenergic receptors produces a dramatic increase in skeletal muscle mass and a corresponding reduction body fat content [46–47]. These data suggest an important connection between adipose tissue and skeletal muscle, and *in vitro* evidence from the present study demonstrated that leucine, nifedipine and calcitriol regulate energy metabolism in both adipocytes and muscle cells. These data are consistent with previous *in vivo* observations that dairy increase fat loss but protect lean muscle mass [17]. However, whether leucine and calcium regulate energy partitioning between adipose tissue and skeletal muscle instead of modulating each tissue is yet unclear.

Adipocyte and skeletal muscle derived cytokines may play a key role in the adipocyte-muscle cross-talk in regulating energy partitioning. For example, TNF $\alpha$ , which is expressed and produced by adipocytes and increases in obesity, has been shown to induce muscle wasting via multiple mechanisms [48–50]. On the other hand, leptin and adiponectin, which are also synthesized and secreted by adipose tissue, alter lipid partitioning in skeletal muscle by increasing fat oxidation and decreasing fatty acid incorporation into triacylglycerols [21]. Moreover, adipocytes and muscle both produce IL-6 and *in vitro* studies suggest that IL-6 may stimulate adipocyte fatty acid release and muscle fatty

acid oxidation [22–23], although its *in vivo* effect remains unclear. Notably, IL-15, a cytokine highly expressed in skeletal muscle, decreases fat deposition in adipose tissue but increases skeletal muscle fiber growth [51–52]. Thus, a reciprocal regulation between adipose tissue and skeletal muscle may exist and may control adiposity by regulating the synthesis of fat and protein in adipose tissue and skeletal muscle respectively. Data from this study demonstrate that muscle cells cultured alone exhibit markedly higher fatty acid oxidation than those cultured in conditioned medium derived from adipocytes or co-cultured with adipocytes, suggesting that adipocyte-derived factor(s) participate in the regulation of muscle energy metabolism. In addition, leucine, nifedipine and calcitriol regulate adiponectin production in adipocytes and IL-15 and IL-6 in muscle cells. Administration of adiponectin at a comparable level to that derived from adipocytes stimulated significant increases in fatty acid oxidation and IL-15 and IL-6 production in muscle cells, indicating that adiponectin may play a key role in the metabolic connection between adipose tissue and skeletal muscle. However, the role of additional adipokines is not yet clear.

In conclusion, the present study demonstrates a role for leucine, calcium and calcitriol in the modulation of adipocyte-muscle cross talk in an *in vitro* system. We found leucine and nifedipine to suppress fat anabolism in adipocytes while they promote fatty acid oxidation in muscle cells. Calcitriol, which is increased by low-calcium diets, exerted the opposite effect. These results suggest a potential role of dietary calcium in modulation of energy partitioning between adipose tissue skeletal muscle and that leucine exerts an additional effect on this system.

## References

1. Coppack SW (2001) Pro-inflammatory cytokines and adipose tissue. *Proc Nutr Soc* 60:349–356
2. Trayhurn P, Beattie JH (2001) Physiological role of adipose tissue: white adipose tissue as an endocrine and secretory organ. *Proc Nutr Soc* 60:329–339
3. Ajuwon KM, Jacobi SK, Kuske JL, Spurlock ME (2004) Interleukin-6 and interleukin-15 are selectively regulated by lipopolysaccharide and interferon- $\gamma$  in primary pig adipocytes. *Am J Physiol Regul Integr Comp Physiol* 286:R547–R553
4. Okamoto Y, Kihara S, Funahashi T, Matsuzawa Y, Libby P (2006) Adiponectin: a key adipocytokine in metabolic syndrome. *Clin Sci (Lond)* 110:267–278
5. Chan MH, Carey AL, Watt MJ, Febbraio MA (2004) Cytokine gene expression in human skeletal muscle during concentric contraction: evidence that IL-8, like IL-6, is influenced by glycogen availability. *Am J Physiol Regul Integr Comp Physiol* 287:R322–R327

6. Steensberg A, Keller C, Starkie RL, Osada T, Febbraio MA, Pedersen BK (2002) IL-6 and TNF- $\alpha$  expression in, and release from, contracting human skeletal muscle. *Am J Physiol Endocrinol Metab* 283:E1272–E1278
7. Zemel MB (2005) Calcium and dairy modulation of obesity risk. *Obes Res* 13:192–193
8. Zemel MB, Richards J, Milstead A, Campbell P (2005) Effects of calcium and dairy on body composition and weight loss in African-American adults. *Obes Res* 13:1218–1225
9. Zemel MB, Shi H, Greer B, DiRienzo D, Zemel PC (2000) Regulation of adiposity by dietary calcium. *FASEB J* 14:1132–1138
10. Sun X, Zemel MB (2006) Dietary calcium regulates ROS production in ap2- agouti transgenic mice on high-fat/high-sucrose diets. *Int J Obes (Lond)* 30:1341–1346
11. Shi H, Halvorsen YD, Ellis PN, Wilkison WO, Zemel MB (2000) Role of intracellular calcium in human adipocyte differentiation. *Physiol Genomics* 3:75–82
12. Xue B, Greenberg AG, Kraemer FB, Zemel MB (2001) Mechanism of intracellular calcium ([Ca<sup>2+</sup>]<sub>i</sub>) inhibition of lipolysis in human adipocytes. *FASEB J* 15:2527–2529
13. Shi H, Norman AW, Okamura WH, Sen A, Zemel MB (2001) 1 $\alpha$ ,25-dihydroxyvitamin D<sub>3</sub> modulates human adipocyte metabolism via nongenomic action. *FASEB J* 15:2751–2753
14. Xue B, Moustaid N, Wilkison WO, Zemel MB (1998) The agouti gene product inhibits lipolysis in human adipocytes via a Ca<sup>2+</sup>-dependent mechanism. *FASEB J* 12:1391–1396
15. Kim JH, Mynatt RL, Moore JW, Woychik RP, Moustaid N, Zemel MB (1996) The effects of calcium channel blockade on agouti-induced obesity. *FASEB J* 10:1646–1652
16. Shi H, Norman AW, Okamura WH, Sen A, Zemel MB (2002) 1 $\alpha$ ,25- dihydroxyvitamin D<sub>3</sub> inhibits uncoupling protein 2 expression in human adipocytes. *FASEB J* 16:1808–1810
17. Zemel MB (2005) The role of dairy foods in weight management. *J Am Coll Nutr* 24:537S–546S
18. Zemel MB, Miller SL (2004) Dietary calcium and dairy modulation of adiposity and obesity risk. *Nutr Rev* 62:125–131
19. Suganami T, Nishida J, Ogawa Y (2005) A paracrine loop between adipocytes and macrophages aggravates inflammatory changes: role of free fatty acids and tumor necrosis factor alpha. *Arterioscler Thromb Vasc Biol* 25:2062–2068
20. Murase T, Haramizu S, Shimotoyodome A, Nagasawa A, Tokimitsu I (2005) Green tea extract improves endurance capacity and increases muscle lipid oxidation in mice. *Am J Physiol Regul Integr Comp Physiol* 288:R708–R715
21. Dyck DJ, Heigenhauser GJ, Bruce CR (2006) The role of adipokines as regulators of skeletal muscle fatty acid metabolism and insulin sensitivity. *Acta Physiol (Oxf)* 186:5–16
22. Path G, Bornstein SR, Gurniak M, Chrousos GP, Scherbaum WA, Hauner H (2001) Human breast adipocytes express interleukin-6 (IL-6) and its receptor system: increased IL-6 production by beta-adrenergic activation and effects of IL-6 on adipocyte function. *J Clin Endocrinol Metab* 86:2281–2288
23. Bruce CR, Dyck DJ (2004) Cytokine regulation of skeletal muscle fatty acid metabolism: effect of interleukin-6 and tumor necrosis factor- $\alpha$ . *Am J Physiol Endocrinol Metab* 287:E616–E621
24. Almendro V, Busquets S, Ametller E, Carbo N, Figueras M, Fuster G, Argiles JM, Lopez-Soriano FJ (2006) Effects of interleukin-15 on lipid oxidation: disposal of an oral [(14)C]-triolein load. *Biochim Biophys Acta* 1761:37–42
25. McPherson R, Jones PH (2003) The metabolic syndrome and type 2 diabetes: role of the adipocyte. *Curr Opin Lipidol* 14:549–553
26. Vega GL (2004) Obesity and the metabolic syndrome. *Minerva Endocrinol* 29:47–54
27. Weiss R, Dziura J, Burgert TS, Tamborlane WV, Taksali SE, Yockel CW, Allen K, Lopes M, Savoye M, Morrison J, Sherwin RS, Caprio S (2004) Obesity and the metabolic syndrome in children and adolescents. *N Engl J Med* 350:2362–2374
28. Ma SW, Foster DO (1986) Starvation-induced changes in metabolic rate, blood flow, and regional energy expenditure in rats. *Can J Physiol Pharmacol* 64:1252–1258
29. Milan G, Dalla, Nora. E., Pilon C, Pagano C, Granzotto M, Manco M, Mingrone G, Vettor R (2004) Changes in muscle myostatin expression in obese subjects after weight loss. *J Clin Endocrinol Metab* 89:2724–2727
30. Causey KR, Zemel MB (2003) Dairy augmentation of the anti-obesity effect of calcium in ap2-agouti transgenic mice. *FASEB J* 17:A746 (abstract)
31. Sun X, Zemel MB (2004) Calcium and dairy products inhibit weight and fat regain during ad libitum consumption following energy restriction in Ap2-agouti transgenic mice. *J Nutr* 134:3054–3060
32. Rennie MJ, Bohe J, Smith K, Wackerhage H, Greenhaff P (2006) Branched-chain amino acids as fuels and anabolic signals in human muscle. *J Nutr* 136:264S–268S
33. Kobayashi H, Kato H, Hirabayashi Y, Murakami H, Suzuki H (2006) Modulations of muscle protein metabolism by branched-chain amino acids in normal and muscle-atrophying rats. *J Nutr* 136:234S–236S
34. Fulks RM, Li JB, Goldberg AL (1975) Effects of insulin, glucose, and amino acids on protein turnover in rat diaphragm. *J Biol Chem* 250:290–298
35. Li JB, Jefferson LS (1978) Influence of amino acid availability on protein turnover in perfused skeletal muscle. *Biochim Biophys Acta* 544:351–359
36. Garlick PJ (2005) The role of leucine in the regulation of protein metabolism. *J Nutr* 135:1553S–1556S
37. Anthony JC, Anthony TG, Kimball SR, Vary TC, Jefferson LS (2000) Orally administered leucine stimulates protein synthesis in skeletal muscle of postabsorptive rats in association with increased eIF4F formation. *J Nutr* 130:139–145
38. Anthony JC, Yoshizawa F, Anthony TG, Vary TC, Jefferson LS, Kimball SR (2000) Leucine stimulates translation initiation in skeletal muscle of postabsorptive rats via a rapamycin-sensitive pathway. *J Nutr* 130:2413–2419
39. Lynch CJ, Hutson SM, Patson BJ, Vaval A, Vary TC (2002) Tissue- specific effects of chronic dietary leucine and nor-leucine supplementation on protein synthesis in rats. *Am J Physiol Endocrinol Metab* 283:E824–E835
40. Nair KS, Short KR (2005) Hormonal and signaling role of branched-chain amino acids. *J Nutr* 135:1547S–1552S
41. Roh C, Han J, Tzatsos A, Kandror KV (2003) Nutrient-sensing mTOR- mediated pathway regulates leptin production in isolated rat adipocytes. *Am J Physiol Endocrinol Metab* 284:E322–E330
42. Lynch CJ, Patson BJ, Anthony J, Vaval A, Jefferson LS, Vary TC (2002) Leucine is a direct-acting nutrient signal that regulates protein synthesis in adipose tissue. *Am J Physiol Endocrinol Metab* 283:E503–E513
43. Tobin JF, Celeste AJ (2005) Myostatin, a negative regulator of muscle mass: implications for muscle degenerative diseases. *Curr Opin Pharmacol* 5:328–332
44. McPherron AC, Lee SJ (2002) Suppression of body fat accumulation in myostatin-deficient mice. *J Clin Invest* 109:595–601
45. Suttrave P, Kelly AM, Hughes SH (1990) ski can cause selective growth of skeletal muscle in transgenic mice. *Genes Dev* 4:1462–1472

46. Yang YT, McElligott MA (1989) Multiple actions of beta-adrenergic agonists on skeletal muscle and adipose tissue. *Biochem J* 261:1–10
47. Spurlock ME, Cusumano JC, Ji SQ, Anderson DB, Smith CK 2nd, Hancock DL, Mills SE (1994) The effect of raclopramide on beta-adrenoceptor density and affinity in porcine adipose and skeletal muscle tissue. *J Anim Sci* 72:75–80
48. Coletti D, Moresi V, Adamo S, Molinaro M, Sassoon D (2005) Tumor necrosis factor-alpha gene transfer induces cachexia and inhibits muscle regeneration. *Genesis* 43:120–128
49. Meadows KA, Holly JM, Stewart CE (2000) Tumor necrosis factor-alpha-induced apoptosis is associated with suppression of insulin-like growth factor binding protein-5 secretion in differentiating murine skeletal myoblasts. *J Cell Physiol* 183:330–337
50. Fong Y, Moldawer LL, Marano M, Wei H, Barber A, Manogue K, Tracey KJ, Kuo G, Fischman DA, Cerami A (1989) Cachectin/TNF or IL-1 alpha induces cachexia with redistribution of body proteins. *Am J Physiol* 256:R659–R665
51. Busquets S, Figueras MT, Meijssing S, Carbo N, Quinn LS, Almendro V, Argiles JM, Lopez-Soriano FJ (2005) Interleukin-15 decreases proteolysis in skeletal muscle: a direct effect. *Int J Mol Med* 16:471–476
52. Carbo N, Lopez-Soriano J, Costelli P, Alvarez B, Busquets S, Baccino FM, Quinn LS, Lopez-Soriano FJ, Argiles JM (2001) Interleukin-15 mediates reciprocal regulation of adipose and muscle mass: a potential role in body weight control. *Biochim Biophys Acta* 1526:17–24

## Rapid Desensitization of Lipolysis in the Visceral and Subcutaneous Adipocytes of Rats

Shinobu Mori · Hiroshi Nojiri · Naonobu Yoshizuka · Yoshinori Takema

Received: 12 September 2006 / Accepted: 3 February 2007 / Published online: 7 March 2007  
© AOCS 2007

**Abstract** In adipocytes, short and long term stimulation of  $\beta$  adrenergic receptors ( $\beta$ AR) induces the desensitization to catecholamines, leading to a decrease in the intracellular accumulation of cAMP, but the roles played by this in lipolysis is not clear. In this study, we assessed the catecholamine-induced desensitization of lipolysis and compared this in adipocytes isolated from visceral and subcutaneous fat tissues of rats. When adipocytes were pretreated with isoproterenol (ISO), the norepinephrine (NE)-induced lipolysis was significantly reduced dose- and time-dependently. A similar reduction of the lipolytic response was also found in NE-, dobutamine-, terbutaline- or BRL37344-induced lipolysis. The ISO- and each  $\beta$ AR agonist-induced lipolysis in the visceral fat was not only higher than in the subcutaneous fat, but also markedly reduced by ISO- or NE-pretreatment. These results showed that short-term treatment of three subtypes of  $\beta$ AR by each agonist induces a rapid reduction in the lipolytic response to  $\beta$ AR stimulation. This suggests some common mechanism for the rapid desensitization of  $\beta$ AR-agonist-induced lipolysis, in contrast with previous reports on the characteristics of  $\beta$ AR subtypes. In addition, the regional difference of adipose tissue not only in inducing lipolysis but also in rapid desensitization was also apparent.

**Keywords** Rapid desensitization ·  $\beta$  adrenergic receptors · Isolated adipocytes · Lipolysis · Visceral fat · Subcutaneous fat

### Abbreviations

$\beta$ AR	$\beta$ adrenergic receptor
$\beta$ ARK	$\beta$ AR kinase
Gs	Stimulatory G protein
HSL	Hormone sensitive lipase
ISO	Isoproterenol
NE	Norepinephrine
PKA	Protein kinase A

### Introduction

The lipolytic reaction in adipocytes is mainly explained by the intracellular signaling mechanism using cAMP as a second messenger. That is, adrenaline and noradrenaline stimulate  $\beta$  adrenergic receptors ( $\beta$ AR) on the adipocyte cell surface and sequentially induce the activation of stimulatory G protein (Gs), increase cAMP due to the activation of adenylate cyclase, activate cAMP-dependent protein kinase A (PKA) and activate hormone-sensitive lipase (HSL), resulting in the hydrolysis of triglycerides in intracellular lipid droplets. There are at least three subtypes of  $\beta$ AR involved in lipolysis,  $\beta$ 1,  $\beta$ 2 and  $\beta$ 3, although their expression levels and functions are still controversial.

In addition to the acute Gs-mediated activation mechanism described above, the presence of inhibitory mechanisms that modify the activating reaction have also been known for  $\beta$ ARs. One is the attenuation of the response to short-term stimulation, that is, “acute desensitization”,

S. Mori · H. Nojiri · N. Yoshizuka · Y. Takema  
Biological Science Laboratories,  
Kao Corporation, Tochigi 321-3497, Japan

S. Mori (✉)  
Skin Care Products Research Laboratories,  
Kao Corporation, 2-1-3, Bunka Sumida-ku,  
Tokyo 131-8501, Japan  
e-mail: mori.shinobu@kao.co.jp

and the other is the down regulation of the  $\beta$ AR expression level by long-term stimulation of  $\beta$ ARs, that is, “chronic desensitization” [1–5]. In the former, the stimulated  $\beta$ ARs transmit intracellular activation signals, and at the same time, activate a negative regulatory mechanism. The following multistep inactivation mechanism has been proposed [6]. (1) The structure of the receptors is changed due to phosphorylation by PKA and  $\beta$ AR kinase ( $\beta$ ARK), and the affinity to G protein is decreased, resulting in dissociation. (2) Next,  $\beta$  arrestin binds to the phosphorylated receptors. (3) Finally, the receptors are incorporated into cells (internalization), and the number of agonist binding sites on the cell surface is reduced. In accordance with this mechanism, a marked reduction of the rise in the intracellular cAMP concentration in response to second stimulation after the first adrenaline stimulation has been reported in adipocytes [7, 8]. However, many problems remain unsolved, particularly whether the desensitization seen in the intracellular signal transduction system of adipocytes is correlated with any attenuated response in lipolysis. Also, the difference in desensitization among the three receptor subtypes has not been fully elucidated.

Adipocytes in different deposits of adipose tissue show similar lipolytic reactions, but their sensitivity to catecholamines or  $\beta$ AR agonists vary among regions, such as visceral and subcutaneous fat [9, 10]. However, no regional differences in desensitization have ever been investigated.

In this study, we investigated the rapid desensitization phenomenon of  $\beta$ AR-stimulated lipolysis in isolated adipocytes, by monitoring glycerol release, a final product and a direct index of lipolysis, rather than by monitoring cAMP formation. First, we confirmed the  $\beta$ AR stimulation-induced desensitization in lipolysis. Next, we investigated the receptor subtype lipolytic response to rapid desensitization. Different lipolytic responses between the visceral and subcutaneous fats were also examined with regard to the characteristics of the desensitization phenomenon.

## Experimental Procedures

### Preparation of Isolated Adipocytes

Isolated adipocytes were prepared from the epididymal and abdominal-inguinal subcutaneous fat pads of three male Wistar rats aged 9 weeks and weighing about 200–220 g, according to the method reported by Rodbell [11]. Briefly, the excised adipose tissue was cut into small pieces using ophthalmologic scissors, suspended and washed with Hank's buffer containing a 2% bovine serum albumin fraction (Sigma, MO, USA), and digested with collagenase (1 mg mL<sup>-1</sup>, Type I, Worthington Biochemical, NJ, USA) in the presence of 1 mg mL<sup>-1</sup> glucose for about 60 min at

37 °C. The digested tissue was filtered through a nylon mesh, and floating cells were collected and gently rinsed three times with Hank's buffer, and suspended in the same buffer.

### Pretreatment and Stimulation of Isolated Adipocytes

The isolated adipocyte suspension was pre-incubated with various concentrations of norepinephrine (NE) or isoproterenol (ISO, non-selective  $\beta$ AR agonist) in Hank's buffer at 37 °C for 0–30 min. The pretreated cells were gently rinsed three times with Hank's buffer, resuspended to approximately 10<sup>5</sup> cell mL<sup>-1</sup> and stimulated with NE, dobutamine ( $\beta$ 1AR agonist), terbutaline ( $\beta$ 2AR agonist) or BRL37344 ( $\beta$ 3AR agonist) at 37 °C for 2 h. The glycerol released into the buffer after stimulation was measured using the enzyme method [12]. Briefly, the buffer after stimulation was mixed with glycerol detecting solution and absorbance at 480 nm was measured. The composition of the glycerol detecting solution was 2.7 mM *p*-chlorophenyl, 0.04% Triton X-100, 2 mM magnesium sulfate, 2 mM ATP, 0.05 mM 4-amino antipiline, 1 mM EDTA, 0.5 U glycerokinase, 4 U glycerol-3-phosphate oxidase and 2 U peroxidase. Quantified glycerol concentration was normalized by number of isolated adipocytes and this was calculated using a hematocytometer. The data were statistically analyzed by ANOVA followed by Bonferoni method for multiple comparisons between pairs. All determined data are presented as the mean  $\pm$  SEM of triplicate incubation tubes for each condition. Each experiment was repeated three times with similar results.

## Results

### Time-Dependent Changes in NE-Induced Lipolysis

Time-dependent glycerol release was examined after the addition of 0.3 or 3  $\mu$ M NE in adipocytes isolated from the rat epididymal fat pad. As shown in Fig. 1, while the amounts of glycerol released were mostly stable without NE, they markedly increased with NE. The increase in the glycerol release was not linear with incubation time. The speed was higher when the incubation time was short, and moderated as the incubation time was prolonged according to stimulation time, showing that the amount of glycerol release per unit time decreased with time (Fig. 2). In adipocytes from subcutaneous fat, level of lipolysis were approximately 55% of that in the epididymal adipocytes (data for only one dose was shown in Fig. 1), and the releasing speed was gradually reduced, but the reduction was more moderate than with the epididymal adipocytes (Fig. 2).

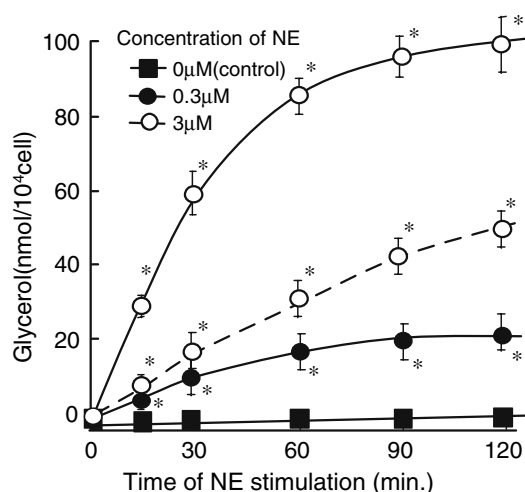


**Fig. 1** Glycerol release from isolated adipocytes after stimulation with NE. Adipocytes were stimulated with or without NE (0.3  $\mu$ M, 3  $\mu$ M) for 0–120 min. Epididymal adipocytes are shown by a *solid line*, and subcutaneous adipocytes with a *dashed line* (only one dose was shown). Each value represents the mean  $\pm$  SEM of three incubation tubes for each condition. \* $P < 0.05$ , compared with the value of the control

This phenomenon indicates that NE stimulation rapidly activates the signaling pathway to lipolysis, and that some inhibition mechanism subsequently reduces it; that is, the NE-induced desensitization of lipolysis. And amplitude of the inhibition is possibly different between the adipocytes from the visceral fat and the subcutaneous fat.

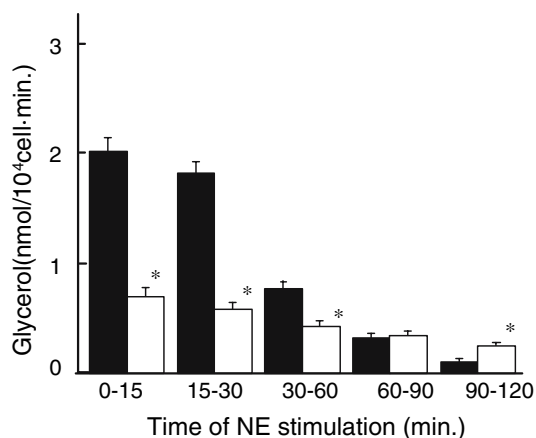


**Fig. 2** Glycerol releasing speed of isolated adipocytes after stimulation with NE. Adipocytes were stimulated with 3  $\mu$ M NE for 0–120 min. Epididymal adipocytes were shown by *black bars*, and subcutaneous adipocytes by *white bars*. Each value represents the mean  $\pm$  SEM of released glycerol per minutes from three incubation tubes for each condition. \* $P < 0.05$ , compared with the value of the epididymal adipocytes

### Effects of NE Pretreatment on NE-Induced Lipolysis

The lipolysis induced by NE was evaluated in adipocytes pretreated with 3  $\mu$ M NE for 0 (control), 10 and 30 min. As shown in Fig. 3, in the control epididymal adipocytes without pretreatment, the NE concentration-dependently induced lipolysis, showing a maximum response at 10  $\mu$ M. In the NE pretreated cells, the maximum response decreased as the time of pretreatment was increased, being 56% of that of the control in cells pretreated for 30 min. In the subcutaneous adipocytes, the lipolytic response to NE in the control cells was approximately 40% lower than that in the control epididymal adipocytes. The pretreatment with NE also reduced the response. Reduction rates, which are the values of released glycerol for pretreated cells relative to the control cells, were lower with statistically significance in the subcutaneous adipocytes than those in the epididymal adipocytes.

Thus, the pretreatment of adipocytes with NE reduces the lipolytic response to NE stimulation, indicating a rapid desensitization. This desensitization is more evident in adipocytes from the epididymal fat pad than subcutaneous adipocytes.

### Effects of $\beta$ AR Agonist Pretreatment on NE-Induced Lipolysis

The lipolytic response to NE was also investigated in adipocytes pretreated with a non-selective  $\beta$ AR agonist, ISO. In the same way as NE, ISO sufficiently induced lipolysis in adipocytes from both epididymal and subcutaneous fat (Fig. 4), showing maximum responses at 1  $\mu$ M, but to a lesser extent in adipocytes from subcutaneous fat (about 60% of that from the epididymal cells). When the cells were pretreated with 1  $\mu$ M ISO for 5–30 min (Fig. 5), the NE-induced lipolysis was reduced in a time-dependent manner. A significant reduction was observed after 10- and 30-min pretreatment of adipocytes from the epididymal and the subcutaneous fat, respectively. Reduction rates were significantly higher in the epididymal than the subcutaneous adipocytes.

The effects of 30-min pretreatment with varying concentrations of ISO were similarly evaluated. As shown in Fig. 6, the NE-induced lipolysis was reduced more in adipocytes pretreated with higher concentrations of ISO. At 100  $\mu$ M ISO-pretreatment, the maximum response was about 48 and 72% that of the controls in adipocytes from the visceral and subcutaneous fat, respectively. Their reduction rates were different with statistically significance.

Thus, transient treatment with ISO, as with NE, results in the desensitization of the lipolytic response to NE, more markedly or sensitive in the epididymal than in the subcutaneous fat.



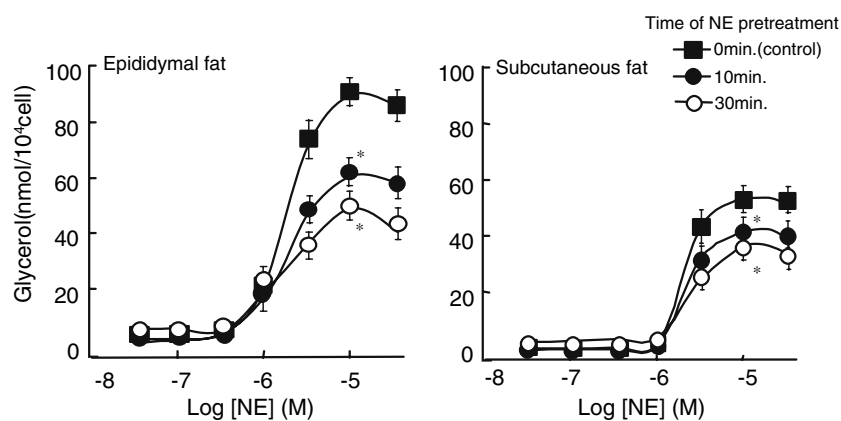


**Fig. 3** Effect of NE pretreatment on NE-induced lipolysis in adipocytes from epididymal fat and subcutaneous fat. Adipocytes were pretreated with NE (3  $\mu$ M) for 0–30 min, washed, and stimulated again with varying concentrations of NE. Each value

represents the mean  $\pm$  SEM of three incubation tubes for each condition. \* $P < 0.05$ , compared with the value of the control at the maximum effecting dose of NE treatment

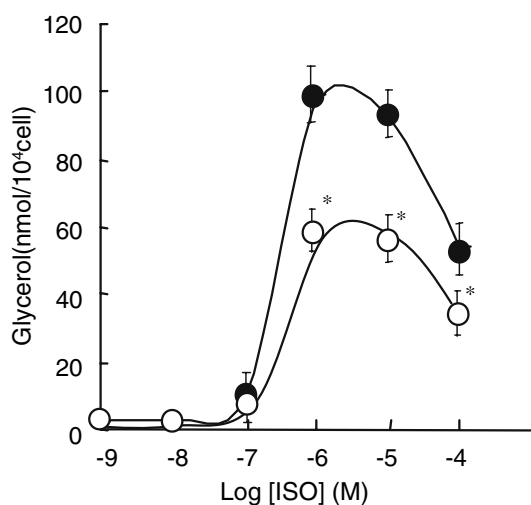


**Fig. 4** ISO-induced lipolysis in adipocytes. Adipocytes from the epididymal fat (filled circles) and subcutaneous fat (open circles) were stimulated with varying concentrations of ISO for 30 min. Each value represents the mean  $\pm$  SEM of three incubation tubes for each condition. \* $P < 0.05$ , compared with the value of the epididymal adipocytes at 1  $\mu$ M ISO

#### Lipolytic Response to Agonists for Individual $\beta$ ARs

Since all of the  $\beta$ AR subtypes,  $\beta_1$ ,  $\beta_2$  and  $\beta_3$ , are considered to be involved in the stimulation of lipolysis, the lipolytic response to the stimulation of each subtype was examined in adipocytes pretreated with 10 nM–100  $\mu$ M ISO for 30 min. As shown in Figs. 7, 8 and 9, dobutamine ( $\beta_1$ AR agonist), terbutaline ( $\beta_2$ AR agonist) and BRL37344 ( $\beta_3$ AR agonist) markedly stimulated lipolysis in the control untreated cells, and the maximum responses were at 10  $\mu$ M, 100  $\mu$ M and 300 nM, respectively, in adipocytes from the epididymal fat. In the subcutaneous adipocytes,

the responses were about 45, 55 and 60%, respectively, of those in the epididymal adipocytes.

When the cells were pretreated with ISO, the lipolytic response was reduced in an ISO concentration-dependent manner. In adipocytes from the epididymal fat, pretreatment with 100  $\mu$ M ISO reduced the responses to dobutamine, terbutaline and BRL37344 to about 10, 15 and 20% of the controls, respectively. In adipocytes from the subcutaneous fat, the pretreatment with ISO also reduced each lipolytic response, but the degrees of reduction were significantly smaller and the effective dose was higher than in the epididymal fat.

Thus, ISO-pretreatment induced reduction of  $\beta_1$ ,  $\beta_2$  and  $\beta_3$ AR agonist-induced lipolysis in similar manner, and the reduction was more marked in adipocytes from epididymal fat than from subcutaneous fat.

#### Discussion

Although there have been many reports of the acute and chronic desensitization of  $\beta$ AR-mediated responses [3–8], rapid desensitization in adipocytes has been focused on at the  $\beta$ AR level or coupled with adenylate-cyclase activity, which does not always parallel the final lipolytic reaction. In this study, we characterized the rapid desensitization in isolated adipocytes using lipolysis as an index. Our results showed  $\beta$ AR agonist-induced lipolysis was reduced after short-term pretreatment with NE or ISO. The degree of desensitization was dependent on the time and concentration of pretreatment with ISO. These results seem consistent with the previous reports that the  $\beta$ AR agonist-induced activation of adenylate cyclase was reduced by short-term (45–60 min) pretreatment with ISO in human adipocytes, and also in adipocyte membrane fractions.

**Fig. 5** NE-induced lipolysis in ISO-pretreated adipocytes: effects of pretreatment time. Adipocytes were pretreated with ISO (1  $\mu$ M) for 0–30 min, washed, and stimulated with varying concentrations of NE for 2 h. Each value represents the mean  $\pm$  SEM of three incubation tubes for each condition. \* $P < 0.05$ , compared with the value of the control at the maximum effecting dose of NE treatment

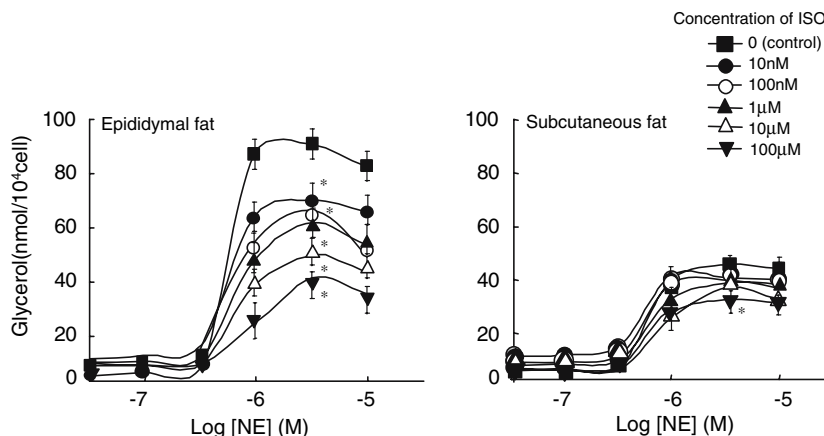
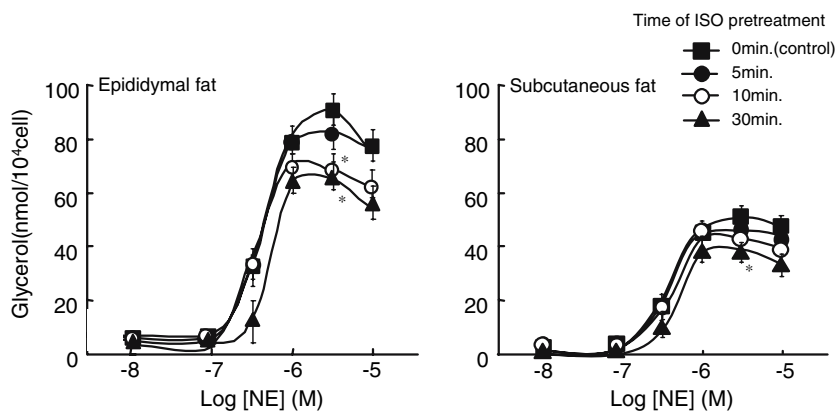


**Fig. 6** NE-induced lipolysis in ISO-pretreated adipocytes: Effects of ISO concentration. Adipocytes were pretreated with varying concentrations of ISO for 30 min, washed, and stimulated again with varying concentrations of NE for 2 h. Each value represents the mean  $\pm$  SEM

of three incubation tubes for each condition. \* $P < 0.05$ , compared with the value of the control at the maximum effecting dose of NE treatment. In the subcutaneous fat, statistically significance was shown in 10 and 100  $\mu$ M ISO- pretreated cells

**Fig. 7** Effect of ISO pretreatment on  $\beta$ 1AR agonist-induced lipolysis. Adipocytes were pretreated with varying concentrations of ISO for 30 min, washed, and stimulated again with varying concentrations of dobutamine for 2 h. Each value represents the mean  $\pm$  SEM of three incubation tubes for each condition. \* $P < 0.05$ , compared with the value of the control at the maximum effecting dose of dobutamine treatment

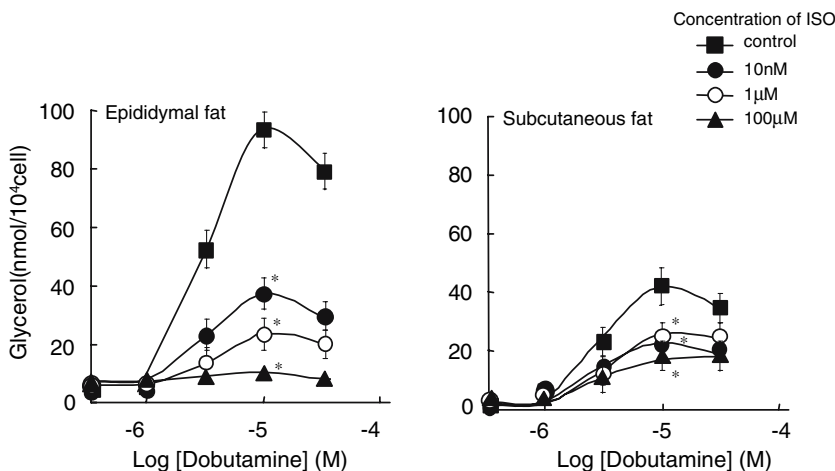


**Fig. 8** Effect of ISO pretreatment on  $\beta$ 2AR agonist-induced lipolysis. Adipocytes were pretreated with varying concentrations of ISO for 30 min, washed, and stimulated again with varying concentrations of terbutaline for 2 h. Each value represents the mean  $\pm$  SEM of three incubation tubes for each condition. \* $P < 0.05$ , compared with the value of the control at the maximum effecting dose of terbutaline treatment

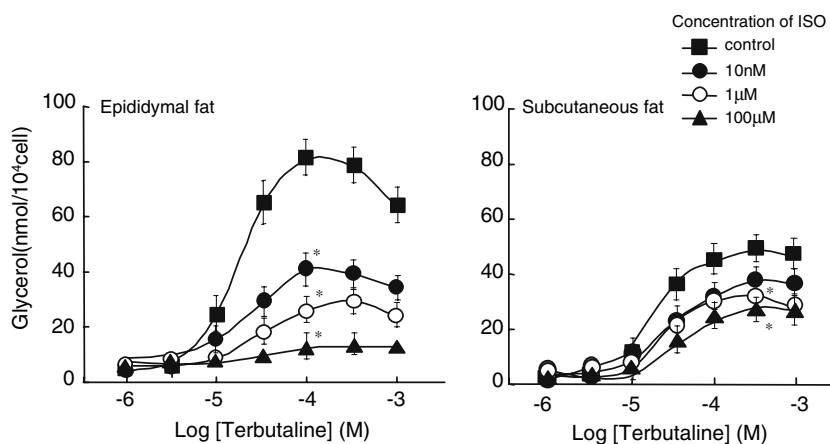
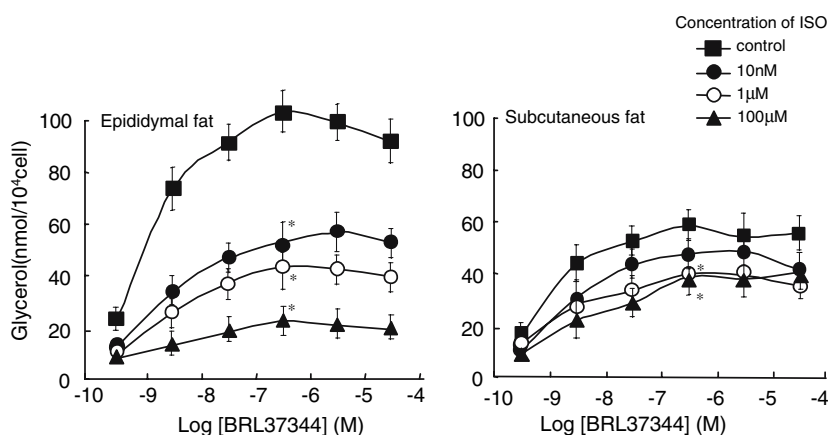


**Fig. 9** Effect of ISO pretreatment on  $\beta$ 3AR agonist-induced lipolysis. Adipocytes were pretreated with varying concentrations of ISO for 30 min, washed, and stimulated again with varying concentrations of BRL37344 for 2 h. Each value represents the mean  $\pm$  SEM of three incubation tubes for each condition. \* $P < 0.05$ , compared with the value of the control at the maximum effecting dose of BRL37344 treatment



There are at least three  $\beta$ AR subtypes,  $\beta$ 1,  $\beta$ 2 and  $\beta$ 3ARs, in adipocytes, all of which are known to be involved in the activation of lipolysis. Regarding the desensitization of individual  $\beta$ AR subtypes, it has been shown that rapid desensitization scarcely occurs in  $\beta$ 3AR compared to the other two subtypes. It is mainly considered that the weak desensitization of  $\beta$ 3AR is due to the structural characteristics of  $\beta$ 3AR [2, 7, 8], which lacks 3 of 11 PKA- and  $\beta$ ARK-phosphorylation sites present in  $\beta$ 1 and  $\beta$ 2ARs [13]. In contrast to these previous reports, our results showed rapid reduction of the lipolytic response to stimulation of the three subtypes, and some desensitization mechanism common to all of the subtypes. There may be, for example, common unidentified phosphorylation sites, co-factors, or mechanisms inhibiting lipolysis at levels downstream of the receptors, such as the activation of phosphodiesterase and perilipin. Further studies are needed, especially regarding the signal transduction cascade involved with this desensitization phenomenon.

The present study also revealed the regional differences in  $\beta$ AR agonist-induced lipolysis and desensitization between adipocytes from the epididymal and subcutaneous fats. This rapid desensitization has never been considered with regard to the differences between fat deposits. As many have previously reported, the lipolytic response to  $\beta$ AR stimulation was higher in the epididymal than in the subcutaneous adipocytes. The low lipolytic response in the subcutaneous fat may be due to the lower expression of  $\beta$ AR or the higher expression of  $\alpha$ 2 adrenergic receptors. However, any other differences, including the intracellular signal transduction and enzyme activity, have not appeared in detail [9, 14–20]. We expected that adipocytes from the subcutaneous fat may be desensitized more easily than the visceral fat, and thereby show a lower lipolytic response during a 2-h stimulation by  $\beta$ AR agonists. However, this is unlikely because the NE or  $\beta$ AR agonist-induced lipolysis in the visceral adipocytes was more strongly reduced by ISO pretreatment than it was in subcutaneous adipocytes. The visceral

fat around the digestive organs or cardiovascular system organs must rapidly and strongly respond to lipolytic hormones and neurotransmitters, but may be easily desensitized by these stimuli. This is the first finding about the regional differences of adipose desensitization.

The findings of the present study were obtained using rat adipocytes *in vitro*. There have been some reports suggesting similar desensitization *in vivo*. Marion-Latard et al. [21] reported that 60 min exercise stimulation desensitized the glycerol-releasing response to NE in adipose tissues in humans.

As for chronic desensitization *in vivo*, Ikezu et al. [22] reported that  $\beta$ 3AR agonist-induced lipolysis was less in adipocytes isolated from rats with burn injuries, while the expression levels of lipolysis-related protein, such as PKA and HSL, were not affected. In contrast, the up-regulation of  $\beta$ 3AR by chronic  $\beta$ AR stimulation has been reported [23–25], and it is considered that cAMP-response-element promotes the translation of the  $\beta$ 3AR gene.

In human adipocytes, the expression of  $\beta$ 3AR is rare and its physiological function has been controversial [13, 14]. Recently, it has been revealed that the coupling of  $\beta$ 3AR binding to the lipolytic reaction is weaker than the other  $\beta$ ARs, but it clearly shows active lipolysis *in vivo* or with the *in situ* microdialysis technique [26].

In conclusion, we demonstrated that short-term treatment of  $\beta$ AR agonists induce rapid reduction in the lipolytic response to  $\beta$ AR stimulation, regardless of the different  $\beta$ AR subtypes, and showed the regional differences not only in the lipolytic response, but also in the sensitivity of desensitization between the visceral and subcutaneous fat. The difference of metabolic character between these two types of adipocytes must be related to their physiological role of each fat deposit. Elucidation of the mechanisms of such rapid, as well as chronic, desensitization is important for a better understanding of the mechanism regulating fat and energy metabolism in adipose tissues. Moreover, it would be helpful for the development of  $\beta$ AR agonists and/or antagonists that are more effective and selective to adipocytes.

**Acknowledgments** The authors wish to express gratitude to Professor Masayuki Saito at the Graduate School of Veterinary Medicine, Hokkaido University.

## References

- Liggett SB (1991) Desensitization of the  $\beta$ -adrenergic receptor: distinct molecular determinants of phosphorylation by specific kinases. *Pharmacol Res* 24(Suppl 1):29–41
- Liggett SB, Freedman NJ, Schwinn DA, Lefkowitz RJ (1993) Structure basis for receptor subtype-specific regulation revealed by a chimeric  $\beta$ 3/ $\beta$ 2-adrenergic receptor. *Acad Sci USA Biochem* 90:3665–3669
- Liggett SB, Raymond JR (1993) Pharmacology and molecular biology of adrenergic receptors. *Baillieres Clin Endocrinol Metab* 7:279–306
- Carpene C, Galizky J, Collon P, Escalpez F, Dauzats M, Lafontan M (1993) Desensitization of beta-1 and beta-2, but not beta-3, adrenoceptor-mediated lipolytic responses of adipocytes after long-term norepinephrine infusion. *J Pharmacol Exp Ther* 265:237–247
- Seibold A, Williams B, Huang Z, Friedman J, Moore RH, Knoll BJ, Clark RB (2000) Localization of the sites mediating desensitization of the  $\beta$ 2-adrenergic receptor by the GRK pathway. *Mol Pharmacol* 58:1162–1173
- Jefkowitz RJ (1998) G protein-coupled receptors. III. New roles for receptor kinases and  $\beta$ -arrestins in receptor signaling and desensitization. *J Biol Chem* 273:18677–18680
- Granneman JG (1992) Effects of agonist exposure on the coupling of  $\beta$ 1 and  $\beta$ 3 adrenergic receptors to adenylyl cyclase in isolated adipocytes. *J Pharmacol Exp Ther* 261:638–642
- Jockers R, Issad T, Zilberfarb V, Copet P, Maullo S, Strosberg AD (1998) Desensitization of the  $\beta$ -adrenergic response in human brown adipocytes. *Endocrine Soc* 139:2676–2684
- Hellmer J, Marcus C, Sonnenfeld T, Arner P (1992) Mechanisms for differences in lipolysis between human subcutaneous and omental fat cells. *J Clin Endocrinol Metab* 75:15–20
- Tavernier G, Galitzky J, Valet P, Remaury A, Bouloumie A, Lafontan M, Langin D (1995) Molecular mechanisms underlying regional variations of catecholamine-induced lipolysis in rat adipocytes. *Am J Physiol* 268(6 Pt 1):E1135–E1142
- Rodbell M (1964) Metabolism of isolated fat cells I. Effects of hormones on glucose metabolism and lipolysis. *J Biol Chem* 239:375–380
- Kawano-Takahashi Y, Ohminaji H, Ubagai E, Okuda H (1984) Mechanism of action of mazindol in preventing onset and development of obesity induced by gold thioglucose injection. *Int J Obes* 8:655–664
- Emorine LJ, Marullo S, Briand-Sutren MM, Patey G, Tate K, Delavier-Klutchko C, Strosberg AD (1989) Molecular characterization of the human  $\beta$ 3-adrenergic receptor. *Science* 245:1118–1121
- Arner P (1996) Regulation of lipolysis in fat cells. *Diabetes Rev* 4:450–463
- Morimoto C, Tsujita T, Okuda H (1997) Norepinephrine-induced lipolysis in rat fat cells from visceral and subcutaneous sites: role of hormone-sensitive lipase and lipid droplets. *J Lipid Res* 38:132–138
- Harmelen V, Lonqvist F, Thorne A, Wennlund A, Large V, Reynisdottir S, Arner P (1997) Noradrenaline-induced lipolysis in isolated mesenteric, omental and subcutaneous adipocytes from obese subjects. *Int J Obes* 21:972–979
- Wajchenberg BL (2000) Subcutaneous and visceral adipose tissue: their relation to the metabolic syndrome. *Endocrine Rev* 21:697–738
- Montague CT, O'Rahilly S (2000) Causes and consequences of visceral adiposity. *Diabetes* 49:883–888
- Vidal-Puig A (2001) Gene expression in visceral and subcutaneous adipose tissue. *Ann Med* 33:547–555
- Lafontan M, Berlan M (2003) Do regional differences in adipocyte biology provide new pathophysiological insight? *Trends Pharmacol Sci* 24:276–283
- Marion-Latard F, Glisezinski I, Crampes F, Berlan M, Galitzky J, Suljkovicova H, Riviere D, Stich V (2001) A single bout of exercise induces  $\beta$ -adrenergic desensitization in human adipose tissue. *Am J Physiol Regul Integr Comp Physiol* 280:R166–R173
- Ikezu T, Yasuhara S, Granneman JG, Kraemer FB, Okamoto T, Tompkins RG, Martin JAJ (1999) A unique mechanism of

- desensitization to lipolysis mediated by  $\beta$ 3-adrenoceptor in rats with thermal injury. *Am J Physiol* 277:E316–E324
23. Thomas RF, Holt BD, Schwinn DA, Liggett SB (1992) Long-term agonist exposure induces upregulation of  $\beta$ 3-adrenergic receptor expression via multiple cAMP response elements. *Proc Natl Acad Sci USA* 89:4490–4494
  24. Atgie C, Faintrenie G, Carpenne C, Bukowiecki LJ, Geloan A (1998) Effects of chronic treatment with noradrenaline or a specific  $\beta$ 3-adrenergic agonist, CL316243, on energy expenditure and epididymal adipocyte lipolytic activity in rat. *Comp Biochem Physiol* 119A:629–636
  25. Login D, Tavernier G, Lafontan M (1995) Regulation of  $\beta$ -3 expression in white fat cells. *Fundam Clin Pharmacol* 2:97–106
  26. Hoffstedt J, Arner P, Hellers G, Lonnqvist F (1997) Variation in adrenergic regulation of lipolysis between omental and subcutaneous adipocytes from obese and non-obese men. *J Lipid Res* 38:795–804

## Effect of Interesterification of Palmitic Acid-rich Triacylglycerol on Postprandial Lipid and Factor VII Response

Sarah E. E. Berry · Rebecca Woodward ·  
Christabelle Yeoh · George J. Miller ·  
Thomas A. B. Sanders

Received: 15 August 2006 / Accepted: 21 December 2006 / Published online: 31 January 2007  
© AOCS 2007

**Abstract** The process of interesterification results in changes in triacylglycerol (TAG) structure and is used to increase the melting point of dietary fats. The acute health effects of this process on palmitic acid-rich fats are uncertain with regard to postprandial lipemia, insulin and factor VII activated (FVIIa) concentrations. Two randomized crossover trials in healthy male subjects compared the effects of meals containing 50 g fat [interesterified palm oil (IPO) versus native palm oil (NPO);  $n = 20$ , and IPO versus high-oleic sunflower oil (HOS);  $n = 18$ ], on postprandial changes in lipids, glucose, insulin, chylomicron composition and FVIIa. Compared with NPO, IPO decreased postprandial TAG and insulin concentrations. Both NPO and IPO increased FVIIa concentrations postprandially; mean increases at 6 h were 21 and 19%, respectively. Compared with HOS, IPO decreased postprandial TAG (47% lower incremental area under the curve) and reduced the postprandial increase in FVIIa concentration by 64% at 6 h; no significant differences in hepatic and total lipase activities or insulin concen-

trations were noted. All three test meals increased postprandial leukocyte counts (average 26% at 6 h). The fatty acid composition of the chylomicron TAG was similar to the test fats following all test meals. It is concluded that interesterification of palm oil does not result in adverse changes in postprandial lipids, insulin or FVIIa compared to high oleate and native palm oils.

**Keywords** Palm oil · Postprandial lipemia · Insulin · Chylomicron composition · Lipase activity · White blood cells

### Abbreviations

ABC-A1	ATP binding cassette transporter
DSC	Differential scanning calorimetry
FVIIa	Factor VII activated
GLC	Gas liquid chromatography
HOS	High-oleic sunflower oil
HL	Hepatic lipase
iAUC	Incremental area under curve
IPO	Interesterified palm oil
LPL	Lipoprotein lipase
NPO	Native palm oil
TAG	Triacylglycerol
WBC	White blood cells

George J. Miller: Deceased August 2006.

S. E. E. Berry (✉) · R. Woodward · C. Yeoh ·  
T. A. B. Sanders

Department of Nutrition and Dietetics,  
Nutritional Sciences Research Division,  
King's College London, Franklin-Wilkins Building,  
150 Stamford Street, London SE1 9NH, UK  
e-mail: sarah.e.berry@kcl.ac.uk

G. J. Miller  
Medical Research Council Cardiovascular Group,  
St. Bartholomew's and the Royal London  
School of Medicine and Dentistry,  
London EC1M 6BQ, UK

### Introduction

The positional composition of palmitic acid-rich triacylglycerol (TAG) varies between fats and oils and is believed to affect lipid metabolism. Fats from plant origin, such as cocoa butter and palm oil, generally have palmitic acid distributed in the outer positions of the TAG molecule (the *sn*-1 and *sn*-3 positions) whilst in

fats of animal origin, such as lard and human breast milk, palmitic acid is commonly found in the middle (*sn*-2) position. Random interesterification of vegetable fats, which is a technique being widely adopted by the food industry, results in the generation of TAG with a higher proportion of palmitic acid in the *sn*-2 position and a fat with a higher melting point.

Evidence from animal and human infant studies suggests that palmitic acid is better absorbed when found in the *sn*-2 position compared with the *sn*-1 and -3 positions [1], a phenomena that has been utilized by food manufacturers who have developed a fat with a high proportion of palmitic acid esterified to the *sn*-2 position of the TAG to produce a vegetable equivalent to human breast milk fat. It has also been claimed that palmitic acid in the *sn*-2 position of the TAG renders that TAG more atherogenic in animal models than when in the *sn*-1 or *sn*-3 positions [2]. The reason behind this is unclear as chronic studies in humans have not found an effect of positional composition of palmitic acid on cholesterol concentrations [3, 4].

A comparison of palmitic acid in the *sn*-2 position of TAG compared with the *sn*-1 or *sn*-3 positions, demonstrates superior absorption, a faster rate of chylomicron transport into lymph [5] and a slower chylomicron clearance rate [6, 7], suggesting a more pronounced and prolonged postprandial lipemia. However, this is not supported by a study comparing palm oil and Betapol<sup>TM</sup> [8] and one comparing meals rich in the TAG species 1, 3-oleyl, 2-palmityl glycerol and 1, 2-oleyl, 3-palmityl glycerol [9]. Furthermore, a small study in female subjects [10] reported a reduced postprandial lipemia following 50 g interesterified palm oil (IPO) compared with native palm oil (NPO).

Previous work indicates that compared with oleic acid-rich TAG, the postprandial increase in factor VII activated (FVIIa) concentrations is less marked following palmitic acid-rich TAG [11–13], and none have examined the effects of interesterification of palmitic acid-rich TAG on postprandial FVIIa concentrations. The present study tests the hypothesis that TAG structure of palmitic acid-rich TAG determines the extent to which plasma TAG and FVIIa increases postprandially. Palm oil was chosen as it has a unique TAG structure with almost all of the palmitic acid being present in the *sn*-1 and *sn*-3 position of the TAG as 1, 3-palmityl, 2-oleyl, and is the world's most important vegetable oil (accounting for over 30% of the total world production of oils and fats). The first study compares the postprandial response to NPO versus IPO. A subsequent study compares IPO versus high oleic sunflower oil (HOS).

## Experimental Procedures

### Subjects

Male subjects aged 18–60 years were recruited from among staff and students of King's College London. The subjects were healthy and exclusion criteria included history of cardiovascular disease, diabetes, body mass index <20 or >35 kg/m<sup>2</sup>, plasma cholesterol >7.8 mmol/l, plasma TAG >3 mmol/l, current use of antihypertensive or lipid lowering medication, and a self reported intake of alcohol of greater than 28 U/week (1 U = 10 mL ethanol). Fasting plasma lipoprotein lipid concentrations, body weight, blood pressure, blood cell count and liver function were confirmed to be within the prescribed limits prior to entry into the study. Habitual nutrient intake was assessed from a 3-day food intake diary and nutrients were estimated using the Microdiet programme (Downlee Systems Limited, UK). Twenty-one subjects were recruited for the first study and 18 subjects for the follow-up study, subject details are shown in Table 1. The characteristics of the subjects were broadly similar between both studies except that the subjects in the follow-up study were slightly heavier. One subject withdrew from the first study due to time constraints. Dietary intakes were close to recommended dietary guidelines for the UK [14].

### Study Design

A randomized crossover study design was used. Each subject received two experimental meals with at least 1 week between meals, such that treatment sequences were balanced. The day preceding each postprandial test, subjects were given advice to avoid consuming foods high in fat and were provided with a standardized low fat dinner (containing <10 g fat) to consume as their evening meal. To control for physical activity levels, subjects were asked to refrain from strenuous exercise, including cycling and sporting activities, and from the use of alcohol on the day before and on the day of the test meal. Subjects fasted overnight from 22:00 h and the following morning a cannula was inserted into the forearm (antecubital vein) of each subject between 08:00 and 10:00 h and fasting venous blood samples were obtained. The test meal was consumed within 15 min. Further venous blood samples were obtained at 15 min, 30 min, 1 h, 90 min, 2 h, 3 h, 4 h, 5 h and 6 h. In the follow-up study, an intravenous injection of heparin (100 IU heparin/kg body weight; Monoparin, CP Pharmaceuticals Ltd., UK) was given following the 6 h sample, and further blood samples

**Table 1** Subject characteristics

	Study	
	Native vs. interesterified palm oil <sup>a</sup>	Intesterified palm oil vs. high oleic sunflower oil <sup>b</sup>
Age (year)	28.8 ± 10.3	35.0 ± 14.4
Weight (kg)	73.0 ± 10.3	81.2 ± 9.8
BMI (kg/m <sup>2</sup> )	23.2 ± 2.6	24.8 ± 2.6
Serum cholesterol (mmol/l)	4.2 ± 0.9	4.7 ± 1.0
Serum LDL cholesterol (mmol/l)	2.3 ± 0.7	2.8 ± 0.9
Serum HDL cholesterol (mmol/l)	1.4 ± 0.3	1.3 ± 0.2
Serum triacylglycerol (mmol/l)	1.1 ± 0.6	1.2 ± 0.5
Dietary intake		
Energy (MJ)	8.5 ± 2.2	9.0 ± 2.2
Protein (% energy)	15.2 ± 3.1	15.4 ± 3.4
Carbohydrate (% energy)	45.2 ± 8.1	43.0 ± 9.4
Total fat (% energy)	35.7 ± 6.3	36.4 ± 5.9
Saturated fatty acids (% energy)	11.2 ± 3.1	10.9 ± 2.9
Monounsaturated fatty acids (% energy)	9.6 ± 3.0	10.3 ± 2.4
Polyunsaturated fatty acids (% energy)	3.9 ± 1.7	4.9 ± 2.2

Values are given as mean ± SD

<sup>a</sup> *n* = 20, <sup>b</sup> *n* = 18

were collected 5 and 15 min later. During the postprandial period, subjects refrained from the consumption of any food or drink except water, which they were asked to consume at regular intervals throughout, and following the 3 h blood sample when subjects received a standardized lunch (1.7 MJ) consisting of fresh fruit and a low fat yogurt (less than 1 g fat), which was given to make the procedure tolerable to the subjects. This has previously been shown not to interfere with the measurement of postprandial lipemia or the postprandial increase in FVIIa [12, 15]. The study protocol was reviewed and approved by King's College Research Ethics Committee, and all participants gave written informed consent.

#### Formulation of the Test Meals

The test fats consisted of NPO, IPO (ADM-Pura, Kent, UK) and HOS (Anglia Oils Ltd., Hull, UK). Differential scanning calorimetry (DSC) showed a major melting peak at 39 °C for the NPO and a broad melting endotherm for the IPO between 30 and 52 °C with two mean peak melting temperatures of 43 and 48 °C. All of the HOS was melted at approximately -8 °C. The proportion of unmelted fat determined by pulsed low-resolution nuclear magnetic resonance analysis (NMR) at body temperature (37 °C) of the NPO, IPO and HOS was 3.6, 15.2 and 0%, respectively. The fatty acid and positional composition and physical characteristics were determined, shown in Table 2.

The test meals consisted of two muffins (each containing 25 g test fat) and a milkshake and were formulated to provide 3.57 MJ (853 kcal), 50 g fat, 15 g protein and 89 g carbohydrate. The milkshake

consisted of 220 mL skimmed milk and 15 g Nesquick milkshake mix (Nestlé Ltd., Switzerland). The two muffins contained 50 g test fat, 28 g baking flour, 10 g cornflour, 28 g sugar, 38 mL skimmed milk, 4 g pasteurized egg white, 4 g vanilla essence, and 2 g baking powder. In the first study, the test fats consisted of NPO and IPO, and in the follow-up study they consisted of IPO and HOS. For each study, the muffins were made in a single batch, and stored at -20 °C. Before serving, muffins were defrosted and heated in a microwave to warm.

#### Collection and Handling of Blood Samples

Venous blood samples were collected from a cannula into a syringe and dispensed into vacutainers (Beckton Dickenson, UK). Blood samples were processed within 30 min of blood collection. Blood for lipid analysis (plasma fatty acid and TAG concentrations and chylomicron composition) was collected into 6 mL EDTA containing vacutainers and plasma was separated by centrifugation at 1,500g for 15 min at 4 °C. Blood for lipoprotein analysis (total and HDL cholesterol) was collected into 2 mL vacutainers containing no anti coagulant, centrifuged at 1,500g for 15 min at 4 °C. Blood for full blood counts was collected into 2 mL EDTA vacutainers for analysis on the same day. For FVIIa, blood was collected into 4.5 mL vacutainers containing 38 g/l trisodium citrate solution and centrifuged at 1,500g for 15 min at 18 °C. Blood for glucose analysis was collected into 4 mL fluoride oxalate tubes, and blood for insulin analysis was collected into 2 mL lithium heparin tubes, both were centrifuged at 1,500g for 15 min at 4 °C. Samples for lipid analysis were



**Table 2** Fatty acid composition and solid fat content of test fat triacylglycerol (TAG)

	Native palm oil		Interesterified palm oil		High oleic sunflower oil	
	TAG	<i>sn</i> -2	TAG	<i>sn</i> -2	TAG	<i>sn</i> -2
Fatty acid composition (mol %)						
Palmitic acid (16:0)	31.4	7.2	29.8	37.2	0.8	0.0
Stearic acid (18:0)	4.8	1.1	6.1	6.0	1.6	0.0
Oleic acid (18:1n-9)	51.3	70.9	51.2	45.3	84.9	91.2
Linoleic acid (18:2n-6)	11.1	19.0	11.7	10.7	8.0	8.7
Others	1.4	1.8	1.1	0.7	4.8	0.1
Solid fat content (%)						
32 °C	11.5		23.8		0.0	
37 °C	3.6		15.2		0.0	
42 °C	<1.0		10.2		0.0	
47 °C	<1.0		2.3		0.0	
52 °C	<1.0		<1.0		0.0	

collected at hourly intervals. Samples for lipoprotein analysis (2 mL no anti coagulant), full blood counts (2 mL EDTA) and FVIIa (4.5 mL Na Cit) were collected at 3 and 6 h postprandially. The chylomicron-rich fraction ( $S_f > 400$ ) was separated by ultracentrifugation from the EDTA plasma samples [16] at 2, 3, 4 and 5 h. Samples for glucose (4 mL fluoride oxalate) and insulin (2 mL lithium heparin) were collected at 15, 30, 60, 90 and 120 min postprandially. In the follow-up study, blood for lipoprotein lipase (LPL) and hepatic lipase (HL) activity was collected into 6 mL lithium heparin vacutainers 5 and 15 min following the heparin injection and centrifuged at 1,500g for 15 min at 4 °C.

### Analytical Methods

Melting characteristics of the test fats were determined by DSC using a Mettler-Toledo DSC 820 unit (Mettler-Toledo Ltd., Leicester, UK). The solid fat content profiles were measured by NMR using a QP<sup>20+</sup> pulsed NMR (Oxford instruments Ltd., Oxfordshire, UK) at five temperatures (32, 37, 42, 47 and 52 °C). A standard pre-conditioning procedure for fats showing polymorphisms was followed; samples were melted at 80 °C and kept at 60 °C for 5 min followed by storage in a water-bath at 26 °C for 40 h, prior to analysis samples were equilibrated for 90 min at 0 °C and at each measurement temperature for 60 min.

Plasma total, HDL cholesterol and TAG were determined by enzymatic assays [15]. Plasma insulin was measured by a solid-phase, two-site chemiluminescent immunometric assay on a DPC IMMULITE (Diagnostic products corporation, Caernarfon, UK). Plasma glucose was analyzed using the full enzymatic colorimetric procedure (GOD-PAP) using an automated instrument (Boehringer Hitachi 704 EC, Boehringer Mannheim, Lewes, UK). Plasma FVIIa was measured using a one-stage clotting assay as previously

described [17]. Plasma concentrations of palmitic, stearic, oleic and linoleic acid were determined by gas-liquid chromatography (GLC) using pentadecanoic acid (C15:0) as an internal standard [18] on a BP75 column (25 m × 220 μm × 0.25 μm SGE) on an Agilent 6890 (Agilent Technologies, Cheshire, UK). For determination of chylomicron TAG composition, lipids were extracted from the chylomicrons and the TAG fraction isolated by thin layer chromatography (TLC) and analyzed by GLC as described elsewhere [19]. The composition of the fatty acids in the *sn*-2 position of the test fats and the chylomicron TAG fraction were determined by specific enzymatic hydrolysis [16] followed by separation of the 2-monoacylglycerol by TLC and analysis of their fatty acid methyl esters by GLC.

LPL and HL activity were determined using an adaptation of the continuous fluorimetric lipase test (CONFLOULIP<sup>TM</sup>, Progen Biotechnik, Heidelberg, Germany) on a Cobas Fara II with a fluorescence measurement capability, fitted with a 400 nm emission filter, and a thermostatically controlled cuvette holder (37 °C). Two CONFLOULIP<sup>TM</sup> kits were used; the 'Total lipase test kit' and the 'Hepatic lipase select test kit'. The modification from the kit method was to use high and low salt concentration buffers both with a pH of 7.4. At low salt concentrations LPL and HL are active and total lipase activity is measured, at high salt concentrations LPL activity is inhibited so that only HL is active. LPL was then calculated by subtracting HL from total lipase activity.

### Statistical Analysis

Data that was not normally distributed was log transformed prior to analysis. Incremental area under the curves (iAUC) were calculated using GraphPad Prism (version 3.0) using the trapezoid rule. Statistical analysis of the data was carried out using repeated

measures analysis of variance (ANOVA) using SPSS PC version 10. Comparisons with fasting values were made using Dunnett's multiple comparison test.

## Results

Twenty subjects completed the first study and 18 subjects completed the follow-up study. Postprandial plasma TAG concentrations following IPO and NPO are shown in Fig. 1a. The incremental area under the curve (iAUC) was not significantly different between test fats [geometric mean with 95% CI; NPO; 138 (89, 214), IPO; 96 (64, 146),  $P = 0.075$ ]. However, the pattern of response differed (ANOVA; diet  $\times$  time interaction  $P = 0.002$ ), with the increase in plasma TAG concentrations being significantly greater at 1, 2, 5 and 6 h following the NPO compared with the IPO. The maximum increase occurred at 4 h for the NPO and IPO [geometric mean with 95% CI; 60% (38, 86) and 63% (43, 85) respectively, NS]. The postprandial increases in plasma palmitic and oleic acid concentrations (measured as iAUC) were not significantly different following IPO and NPO: geometric mean with 95% CI; 191.0 (145.2, 251.4) versus 235.6 (172.9, 320.9) for palmitic acid and 160.7 (117.7, 219.4) versus 208.4 (142.5, 304.6) for oleic acid. However, there was a significant diet  $\times$  time interaction for oleic and palmitic acid ( $P < 0.001$  for both), with the IPO showing a sharp rise and decline in concentrations compared with NPO, which remained significantly elevated above interesterified values at 6 h ( $P < 0.05$ ), similar to the plasma TAG response. There was no change in the proportion of fatty acids in the chylomicrons over time (ANOVA of diet  $\times$  time interaction; NS) consequently mean 2–6 h values are shown in Table 3. The proportion of palmitic, stearic, oleic and linoleic acid in the chylomicron TAG largely reflected those in the test fats, and was not significantly different between test fats except for oleic acid which was significantly lower in the chylomicron TAG ( $P = 0.005$ ) following the IPO compared with the NPO (mean  $\pm$  SD;  $40.9 \pm 1.4$  vs.  $42.3 \pm 1.3$  wt %, respectively). The distribution of fatty acids in the *sn*-2 position of the chylomicron TAG did not change with time (ANOVA of diet  $\times$  time interaction; NS) and broadly reflected that of the test fats, except for palmitic acid, which was higher in the *sn*-2 position of the chylomicrons compared to corresponding test fats. Furthermore, there was a significantly ( $P < 0.001$ ) higher proportion of palmitic acid in the *sn*-2 position in the chylomicrons following the IPO compared to NPO (mean  $\pm$  SD:  $44.6 \pm 1.5$  vs.  $23.6 \pm 1.9$  wt %, respectively).

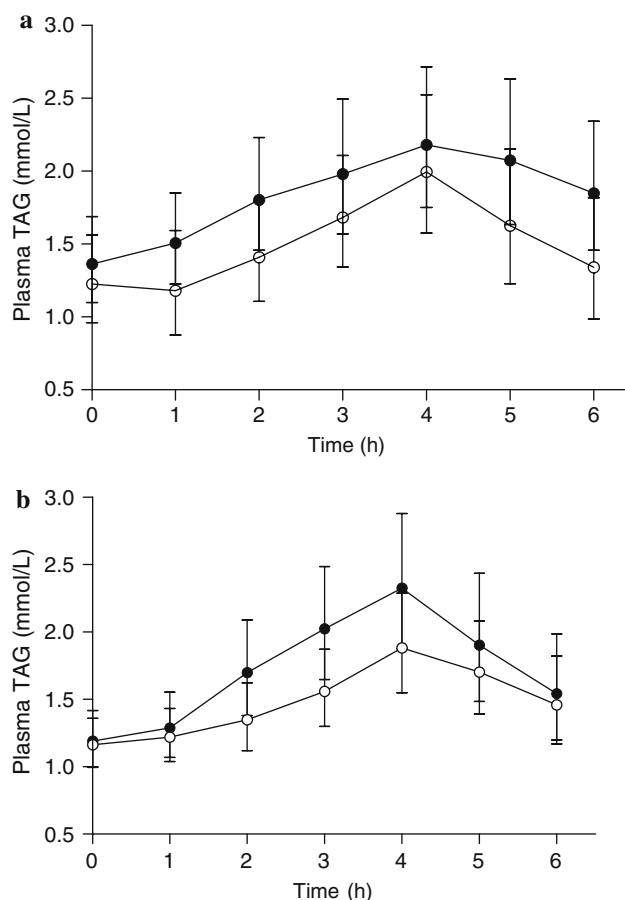


**Fig. 1** **a** Plasma triacylglycerol (TAG) concentrations following 50 g native palm oil (closed symbols) and interesterified palm oil (open symbols). Geometric mean with 95% CI,  $n = 20$ . Data was analyzed by ANOVA on deviations from fasting values: significant diet  $\times$  time interaction  $P = 0.002$ , diet effect  $P = 0.023$  and time effect  $P < 0.001$ . **b** Plasma triacylglycerol (TAG) concentrations following 50 g high oleic sunflower oil (closed symbols) and interesterified palm oil (open symbols). Geometric mean with 95% CI,  $n = 18$ . Data was analyzed by ANOVA on deviations from fasting values: significant diet  $\times$  time interaction  $P = 0.006$  and time effect  $P < 0.001$

In the follow-up study, plasma TAG concentrations increased to a lesser extent following the IPO compared with the HOS (Fig. 1b). Repeated measures ANOVA showed a significant diet  $\times$  time interaction for TAG concentrations ( $P = 0.003$ ) and for deviations of TAG from fasting ( $P = 0.006$ ). The incremental area under the curve for plasma TAG was significantly lower ( $P = 0.004$ ) following the IPO meal compared with the HOS meal (geometric mean with 95% CI): 120 (175, 192) versus 225 (159, 319), respectively. Peak 4 h increases in plasma TAG concentrations were 62% for IPO in the follow-up study compared with 63% in the first study, showing good reproducibility in postprandial responses between studies. Concentrations of plasma palmitic and oleic acid were significantly

**Table 3** Fatty acid composition (mol %) of the venous chylomicron triacylglycerol (TAG) and *sn*-2 position

	Chylomicron TAG <sup>a</sup>		<i>sn</i> -2 chylomicron fatty acids <sup>b</sup>	
	Interesterified	Native	Interesterified	Native
Palmitic acid (16:0)	44.6 ± 1.9	43.7 ± 1.2	44.0 ± 1.5 <sup>d</sup>	23.6 ± 1.9
Stearic acid (18:0)	4.5 ± 0.4	3.7 ± 1.1	5.9 ± 2.3 <sup>c</sup>	2.7 ± 1.2
Oleic acid (18:1n-9)	40.9 ± 1.4 <sup>c</sup>	42.3 ± 1.3	39.5 ± 2.7 <sup>c</sup>	58.2 ± 2.0
Linoleic acid (18:2n-6)	10.0 ± 1.1	10.3 ± 0.7	10.6 ± 1.3 <sup>c</sup>	15.5 ± 1.1

<sup>a</sup> Mean mol % ± SD; *n* = 20 (mean 2–6 h values)

<sup>b</sup> Mean mol % ± SD; *n* = 5 (mean of 2–6 h values, 5 pools of 4 subjects for each)

Significantly different from native palm oil, <sup>c</sup>*P* < 0.05; <sup>d</sup>*P* < 0.001 (paired *t* test)

different between test fats (diet × time interaction; *P* < 0.001 for both), with large increments from fasting values in palmitic acid [peak increase at 4 h of 40% (95% CI 26, 56)] following the IPO and a larger increase in oleic acid [peak increase at 4 h of 126% (95% CI 94, 165)] following the HOS. The proportion of fatty acids in the chylomicron TAG reflected that in the corresponding test fats and was significantly different between test meals, with a higher proportion of palmitic acid and lower proportion oleic acid (*P* < 0.001 for both) following the IPO compared with the HOS (mean ± SD: 43.5 ± 2.4 vs. 8.5 ± 1.9 for palmitic acid and 41.7 ± 2.9 vs. 79.4 ± 3.2 for oleic acid, respectively). There were no significant differences following the IPO compared with the HOS in post-heparin total lipase, LPL and HL activity (Table 4).

No differences were observed in postprandial serum cholesterol (total, HDL and LDL cholesterol) and glucose concentrations between the test fats in both studies. Following the IPO and NPO there was a significant diet × time interaction for insulin concentrations (*P* = 0.004) and for the deviations of insulin from fasting (*P* = 0.049) (Fig. 2a), with greater increases (difference in log transformed values) at 30, 90 and 120 min (*P* < 0.05 for all) following the NPO compared with the IPO, although the iAUC were not significantly different (*P* = 0.072). In the follow-up study, postprandial changes in insulin concentrations were not different between HOS and IPO (Fig. 2b).

**Table 4** Plasma post-heparin total lipase (TL), lipoprotein lipase (LPL) and hepatic lipase (HL) activity following test meals

	Interesterified palm oil	High oleic sunflower oil
TL	22.9 ± 7.0	24.2 ± 7.4
HL	19.3 ± 9.2	20.2 ± 7.1
LPL	3.3 ± 4.3	4.5 ± 4.1

Mean (pmol/mL/min) ± SD, *n* = 17

No differences between fats

FVIIa concentrations increased postprandially but the increase was not significantly different between the IPO and NPO (Fig. 3a). However, the increase in FVIIa was significantly lower following the IPO at 6 h (*P* = 0.006) compared with the HOS (Fig. 3b). White blood cell (WBC) counts did not differ postprandially between the test fats [for both IPO vs. NPO (Fig. 4a) and IPO vs. HOS (Fig. 4b)], but there was a significant time effect for WBC (*P* < 0.001) and neutrophils (*P* < 0.001), which increased at 3 and 6 h postprandially. No other significant differences were noted.

## Discussion

This study aimed to investigate whether the interesterification of a palmitic acid-rich fat resulted in adverse effects on postprandial lipemia, insulin and FVIIa concentrations. Previous work has suggested that palmitic acid-rich fats may increase insulin secretion [20] and delay the clearance of postprandial TAG [21] compared with unsaturated fats. However, not all studies have concurred with these findings [22] and some studies have not been able to demonstrate any significant difference between palm oil and an oleic acid rich oil [12, 15]. Both the present study, which was conducted in men, and a study in young women [10] indicate a blunted increase in plasma TAG following IPO versus NPO. The postprandial increase was also markedly lower following IPO compared with HOS (a 47% lower iAUC for plasma TAG).

Several possible explanations can be advanced for the lower postprandial rise in plasma TAG following the IPO, including differences in the rate of absorption, lipolysis and/or clearance. However, there were no differences in HL and LPL activities following the test fats, in agreement with a study by Tholstrup et al. [21], suggesting that differences in rates of chylomicron clearance or TAG lipolysis are unlikely to account for the differences observed. Furthermore, analysis of the

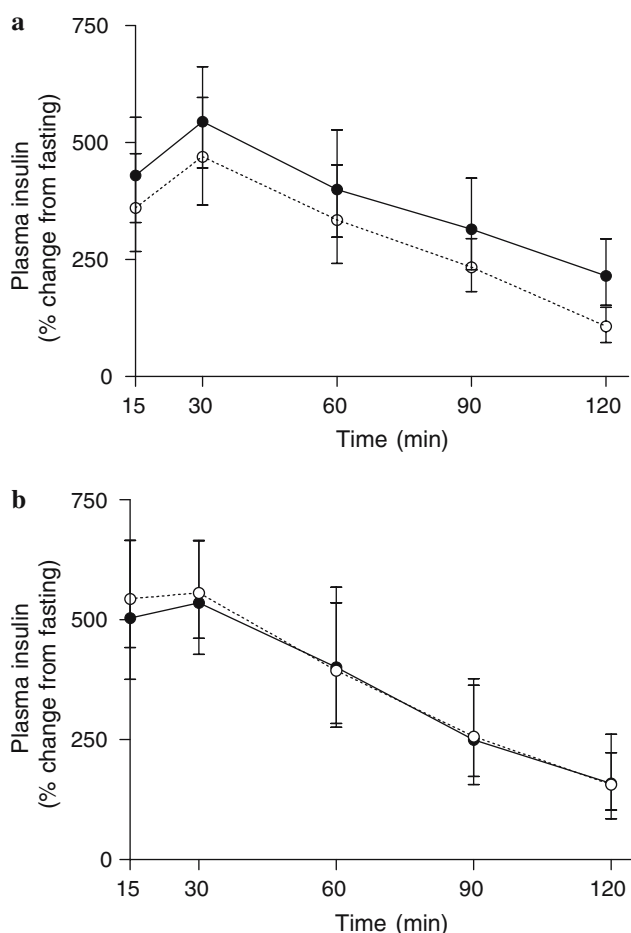


**Fig. 2** **a** Increase in plasma insulin concentrations from fasting following native palm oil (closed symbols) and interesterified palm oil (open symbols). Mean difference in log-transformed values with 95% CI,  $n = 20$ . Data was analyzed by ANOVA; diet  $\times$  time interaction  $P = 0.049$ , diet effect  $P < 0.001$  and time effect  $P < 0.001$ . **b** Increase in plasma insulin concentrations from fasting following high oleic sunflower oil (closed symbols) and interesterified palm oil (open symbols). Mean difference in log-transformed values with 95% CI,  $n = 18$ . Data was analyzed by ANOVA; time effect  $P < 0.001$

chylomicron TAG in plasma following the test meals revealed that the fatty acid composition and the proportion of palmitic acid in the *sn-2* position was broadly similar to the dietary fats, and as expected, the proportion of palmitic acid in the *sn-2* position of the chylomicron was greater following the IPO compared with the NPO. This would imply that there were unlikely to be differences in the extent of absorption of the different dietary fats, and this is supported by studies that have reported palmitic acid to be well digested in humans when in the outer positions [23, 24], randomly distributed on all three positions of the glycerol [25], or as tri-palmitin [26]. An alternative explanation may be that the IPO, which contains a higher proportion of solid fat at 37 °C compared with

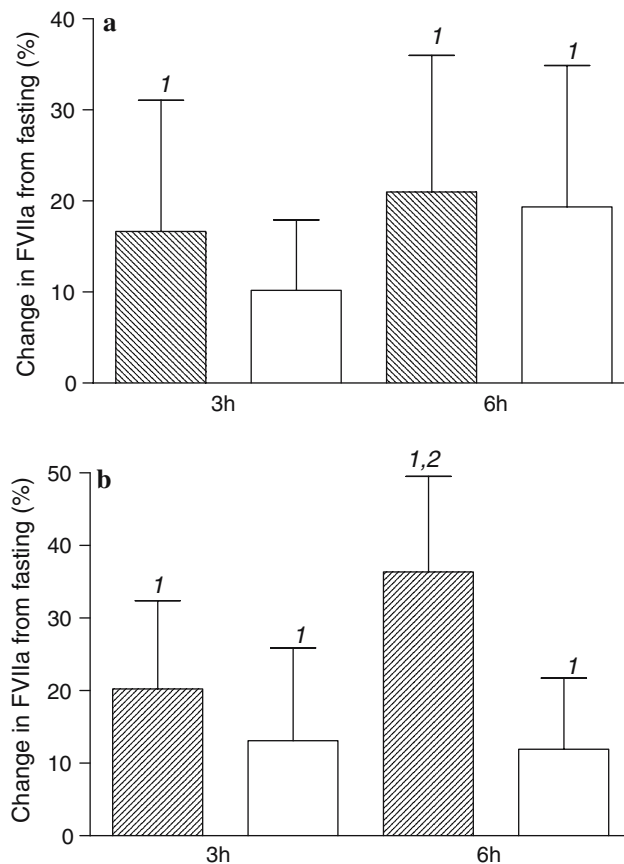


**Fig. 3** **a** Postprandial changes in plasma factor VII activated (FVIIa) concentrations following the native (hatched bars) and interesterified (open bars) palm oil, mean difference in log-transformed values with 95% CI,  $n = 20$ . <sup>1</sup>Significant increase from fasting values,  $P < 0.05$  (paired  $t$  test). No differences between fats. **b** Postprandial changes in plasma factor VII activated (FVIIa) concentrations following the high oleic sunflower oil (hatched bars) and interesterified palm oil (open bars), mean difference in log-transformed values with 95% CI,  $n = 18$ . <sup>1</sup>Significant increase from fasting values,  $P < 0.05$  (paired  $t$  test). <sup>2</sup>Significantly different from interesterified palm oil,  $P = 0.006$  (paired  $t$  test). Data was analyzed by ANOVA; significant diet  $\times$  time interaction  $P = 0.043$ , diet effect  $P = 0.02$  and time effect  $P = 0.017$

the NPO and HOS (IPO; 15%, NPO; 4% and HOS; 0%), may be emulsified less readily due to its high melting point [27], resulting in a slower increase in plasma TAG.

Saturated fatty acids are believed to have an adverse effect on plasma insulin concentrations and it has been reported that palm oil acutely increases plasma insulin concentrations to a greater extent compared to unsaturated fats [20]. A novel finding in the present study was that the IPO resulted in a lower increase in plasma insulin compared with NPO, mainly as a consequence of a lower initial rise in plasma insulin concentrations. As this occurs well before the increases in plasma TAG, it is likely that this effect is mediated by gut

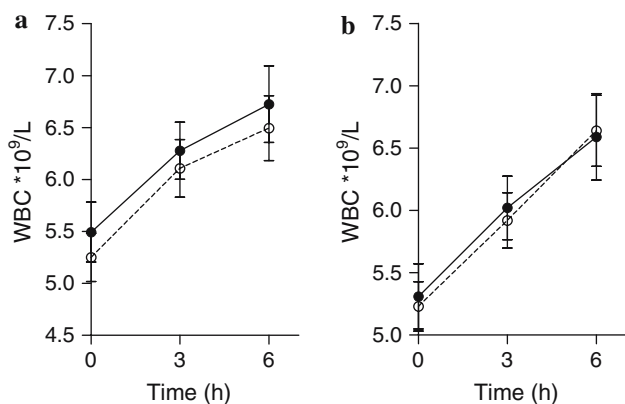


**Fig. 4** **a** Mean white blood cell counts (WBC  $\times 10^9/l$ ) following test meals containing native (closed symbols) and interesterified (open symbols) palm oil (with SEM;  $n = 20$ ). Data was analyzed by ANOVA; time effect  $P < 0.001$ , no effect of diet. **b** Mean white blood cell counts (WBC  $\times 10^9/l$ ) following test meals containing interesterified palm oil (open symbols) and high oleic sunflower oil (closed symbols) palm oil (with SEM;  $n = 18$ ). Data was analyzed by ANOVA; time effect  $P < 0.001$ , no effect of diet

hormones, whose release has previously been shown to be acutely influenced by dietary fat intake [28, 29]. Indeed, the NPO may be hydrolyzed more rapidly than the IPO, resulting in a rapid increase in the secretion of the gut hormone gastric inhibitory polypeptide and subsequent increase in insulin. This finding, taken together with the observation that there were no differences in the insulin response following IPO and HOS, suggests that interesterification may attenuate the postprandial rise in insulin observed following palm oil. This observation requires confirmation and further research on the mechanisms involved is warranted.

It is now well established that there is substantial increase in FVIIa concentrations 3–6 h following a meal high in fat [12, 15]. Both types of palm oil increased FVIIa but the increase in FVIIa was less marked for the IPO compared with HOS oil. The mechanism for the postprandial activation of FVII is uncertain but is believed to be associated with the process of lipolysis and lipid transfer reactions that occur in the postprandial period that generate a charged surface that activate FVII. It has been suggested that this might be a consequence of activation of the ABC-A1 transporter protein, which may be stimulated by unsaturated fatty acids, resulting in the expression of charged phospholipids on the outer surface of WBC and platelets [30]. In the present study, there was a substantial postprandial increase in WBC counts following all three test meals, probably a consequence of increased lymph output associated with chylomicron secretion, regardless of their ability to

increase FVIIa. The mechanism responsible for the postprandial activation of FVII requires further investigation.

In conclusion, the results of the present study indicate that interesterification of palm oil does not result in adverse changes in postprandial lipemia, insulin or factor VII activation compared with NPO or HOS.

**Acknowledgments** We thank ADM-Pura and Anglia Oils for providing and processing the test fats. We also thank David Howarth for the coagulation assays, Peter Lumb for the lipase assays, Roy Sherwood for the insulin and lipoprotein assays and Robbie Gray for technical help. Thomas A.B. Sanders and Sarah E.E. Berry conceived and devised the study and contributed to the analysis and writing of the manuscript. George J. Miller supervised the FVIIa analysis, Rebecca Woodward and Christabelle Yeoh organized and conducted the follow-up study. Sarah Berry was the recipient of King's College London Research Studentship Award and the project was institutionally funded. The authors have no financial or commercial interest in any company or organization sponsoring the research.

## References

- Tomarelli RM, Meyer BJ, Weaber JR, Bernhart FW (1968) Effect of positional distribution on the absorption of the fatty acids of human milk and infant formulas. *J Nutr* 95:583–590
- Kritchevsky D, Tepper SA, Chen SC, Meijer GW, Krauss RM (2000) Cholesterol vehicle in experimental atherosclerosis, 23. Effects of specific synthetic triglycerides. *Lipids* 35:621–625
- Zock PL, de Vries JH, de Fouw NJ, Katan MB (1995) Positional distribution of fatty acids in dietary triglycerides: effects on fasting blood lipoprotein concentrations in humans. *Am J Clin Nutr* 61:48–55
- Nestel PJ, Noakes M, Belling GB, McArthur R, Clifton PM (1995) Effect on plasma lipids of interesterifying a mix of edible oils. *Am J Clin Nutr* 62:950–955
- Aoe S, Yamamura J, Matsuyama H, Hase M, Shiota M, Miura S (1997) The positional distribution of dioleoyl-palmitoyl glycerol influences lymph chylomicron transport, composition and size in rats. *J Nutr* 127:1269–1273
- Redgrave TG, Kodali DR, Small DM (1988) The effect of triacyl-sn-glycerol structure on the metabolism of chylomicrons and triacylglycerol-rich emulsions in the rat. *J Biol Chem* 263:5118–5123
- Mortimer BC, Holthouse DJ, Martins IJ, Stick RV, Redgrave TG (1994) Effects of triacylglycerol-saturated acyl chains on the clearance of chylomicron-like emulsions from the plasma of the rat. *Biochim Biophys Acta* 1211:171–180
- Zampelas A, Williams CM, Morgan LM, Wright J, Quinlan PT (1994) The effect of triacylglycerol fatty acid positional distribution on postprandial plasma metabolite and hormone responses in normal adult men. *Br J Nutr* 71:401–410
- Summers LK, Fielding BA, Ilic V, Quinlan PT, Frayn KN (1998) The effect of triacylglycerol-fatty acid positional distribution on postprandial metabolism in subcutaneous adipose tissue. *Br J Nutr* 79:141–147
- Yli-Jokipii K, Kallio H, Schwab U, Mykkanen H, Kurvinen J, Savolainen M, Tahvonen R (2001) Effects of palm oil and transesterified palm oil on chylomicron and VLDL triacyl-

- glycerol structures and postprandial lipid response. *J Lipid Res* 42:1618–1625
11. Sanders TA, de Grassi T, Miller GJ, Humphries SE (1999) Dietary oleic and palmitic acids and postprandial factor VII in middle-aged men heterozygous and homozygous for factor VII R353Q polymorphism. *Am J Clin Nutr* 69:220–225
  12. Sanders TA, de Grassi T, Miller GJ, Morrissey JH (2000) Influence of fatty acid chain length and cis/trans isomerization on postprandial lipemia and factor VII in healthy subjects. *Atherosclerosis* 149:413–420
  13. Tholstrup T, Miller GJ, Bysted A, Sandstrom B (2003) Effect of individual dietary fatty acids on postprandial activation of blood coagulation factor VII and fibrinolysis in healthy young men. *Am J Clin Nutr* 77:1125–1132
  14. Henderson L, Gregory J, Irving K (2003) The national diet and nutrition survey: adults aged 19–64 years. H.M.Stationery Office 2, London
  15. Sanders TA, Oakley FR, Cooper JA, Miller GJ (2001) Influence of a stearic acid-rich structured triacylglycerol on postprandial lipemia, factor VII concentrations, and fibrinolytic activity in healthy subjects. *Am J Clin Nutr* 73:715–721
  16. Summers LK, Fielding BA, Herd SL, Ilic V, Clark ML, Quinlan PT, Frayn K (1999) Use of structured triacylglycerols containing predominantly stearic and oleic acids to probe early events in metabolic processing of dietary fat. *J Lipid Res* 40:1890–1898
  17. Morrissey JH, Macik BG, Neuenschwander PF, Comp PC (1993) Quantitation of activated factor VII levels in plasma using a tissue factor mutant selectively deficient in promoting factor VII activation. *Blood* 81:734–744
  18. Lepage G, Roy CC (1986) Direct transesterification of all classes of lipids in a one-step reaction. *J Lipid Res* 27:114–120
  19. Sanders TA, Berry SE, Miller GJ (2003) Influence of triacylglycerol structure on the postprandial response of factor VII to stearic acid-rich fats. *Am J Clin Nutr* 77:777–782
  20. Robertson MD, Jackson KG, Fielding BA, Williams CM, Frayn KN (2002) Acute effects of meal fatty acid composition on insulin sensitivity in healthy post-menopausal women. *Br J Nutr* 88:635–640
  21. Tholstrup T, Sandstrom B, Bysted A, Holmer G (2001) Effect of 6 dietary fatty acids on the postprandial lipid profile, plasma fatty acids, lipoprotein lipase, and cholesterol ester transfer activities in healthy young men. *Am J Clin Nutr* 73:198–208
  22. Pedersen A, Marckmann P, Sandstrom B (1999) Postprandial lipoprotein, glucose and insulin responses after two consecutive meals containing rapeseed oil, sunflower oil or palm oil with or without glucose at the first meal. *Br J Nutr* 82:97–104
  23. Shahkhalili Y, Duruz E, Acheson K (2000) Digestibility of cocoa butter from chocolate in humans: a comparison with corn-oil. *Eur J Clin Nutr* 54:120–125
  24. Denke MA, Grundy SM (1991) Effects of fats high in stearic acid on lipid and lipoprotein concentrations in men. *Am J Clin Nutr* 54:1036–1040
  25. Snook JT, Park S, Williams G, Tsai YH, Lee N (1999) Effect of synthetic triglycerides of myristic, palmitic, and stearic acid on serum lipoprotein metabolism. *Eur J Clin Nutr* 53:597–605
  26. Emken EA (1994) Metabolism of dietary stearic acid relative to other fatty acids in human subjects. *Am J Clin Nutr* 60:1023S–1028S
  27. Deuel HJ (1955) *The lipids*. Interscience Publishers, New York, vol 2, pp 216–221
  28. Costarelli V, Sanders TA (2001) Acute effects of dietary fat composition on postprandial plasma bile acid and cholecystokinin concentrations in healthy premenopausal women. *Br J Nutr* 86:471–477
  29. Yip RG, Wolfe MM (2000) GIP biology and fat metabolism. *Life Sci* 66:91–103
  30. Miller GJ, Cooke CJ, Nanjee MN (2002) Factor VII activation, apolipoprotein A-I and reverse cholesterol transport: possible relevance for postprandial lipaemia. *Thromb Haemost* 87:477–482

## Stearidonic Acid Increases the Red Blood Cell and Heart Eicosapentaenoic Acid Content in Dogs

William S. Harris · Maureen A. DiRienzo ·  
Scott A. Sands · Cherian George · Philip G. Jones ·  
Alex K. Eapen

Received: 19 December 2006 / Accepted: 7 February 2007 / Published online: 9 March 2007  
© AOCS 2007

**Abstract** Plant sources of omega-3 fatty acids (FA) are needed that can materially raise tissue levels of long-chain omega-3 FA [i.e., eicosapentaenoic acid (EPA; 20:5n-3) and docosahexaenoic acid (DHA; 20:6n-3)]. Stearidonic acid (SDA; 18:4n-3) is the delta-6 desaturase product of alpha-linolenic acid (ALA; 18:3n-3), and when fed to humans, increases red blood cell (RBC) content of EPA to a greater extent than does ALA. This study was undertaken to determine the dose-dependence and time course of the increase in the EPA and DHA content of the heart and RBC in dogs. Adult male Beagles were fed 21, 64, or 193 mg/kg of SDA in their food daily for up to 12 weeks. Positive and negative controls were given EPA (43 mg/kg) or high oleic acid sunflower oil, respectively. The baseline EPA content of RBC was  $0.38 \pm 0.03\%$  which increased ( $P < 0.01$ ) in a dose-dependent manner, with the high dose of SDA and EPA achieving levels of  $1.33 \pm 0.26$  and  $1.55 \pm 0.28\%$ , respectively. In the heart, the content of EPA rose from  $0.06 \pm 0.01$  to  $1.24 \pm 0.22\%$  in the EPA group and to  $0.81 \pm 0.32\%$  in the high SDA group (both  $P < 0.01$ ). In both tissues, DHA did not change. Compared

to dietary EPA, SDA was 20–23% as efficient in raising tissue EPA levels. In conclusion, SDA supplementation increased the EPA content of RBC and heart and may have utility as a plant-based source of omega-3 FA.

**Keywords** Omega-3 fatty acids · Eicosapentaenoic acid · Docosahexaenoic acid · Docosapentaenoic acid · Stearidonic acid · Dogs

### Abbreviations

FAME	Fatty acid methyl esters
GC	Gas chromatography
EPA	Eicosapentaenoic acid
DHA	Docosahexaenoic acid
SDA	Stearidonic acid
DPA	n-3 Docosapentaenoic acid
ALA	Alpha-linolenic acid
SFO	Sunflower oil
RBC	Red blood cells

W. S. Harris · S. A. Sands · P. G. Jones  
Mid America Heart Institute, Saint Luke's Hospital,  
Kansas City, MO, USA

M. A. DiRienzo · C. George  
Monsanto Company, St. Louis, MO, USA

A. K. Eapen  
WIL Research Laboratories, LLC, Ashland, OH, USA

W. S. Harris (✉)  
Sanford Research and School of Medicine of  
The University of South Dakota,  
1400 W. 22nd Street, Sioux Falls, SD 57105, USA  
e-mail: Bill.Harris@usd.edu

### Introduction

Omega-3 fatty acids, specifically eicosapentaenoic acid (EPA, 20:5) and docosahexaenoic acid (DHA, 22:6), have well-known cardioprotective properties. These include a decreasing risk of arrhythmias [1], inhibition of platelet aggregation [2], a reduction in serum triglyceride levels [3], and diminishing inflammatory responses [4]. The primary source of EPA and DHA is fish, especially oily fish such as sardines, salmon, mackerel and tuna. The American Heart Association has recommended that all adults eat at least two, preferably oily, fish meals per week, and that patients

with coronary heart disease (CHD) ingest about 1 g of EPA and DHA per day [5].

As concerns grow about the long-term sustainability of fish as the sole source of omega-3 fatty acids [6], interest has turned to the potentially infinite supply of plant-based forms of omega-3 fatty acids, notably alpha-linolenic acid (ALA) which is found in high concentration in flax seed oil, and at lower concentrations in canola and soybean oils. While epidemiological data suggest there may be a relationship between intake of ALA and reduced risk for heart disease, clinical evidence supporting a cause-and-effect relationship of ALA and reduce risk of heart disease is lacking [7–9]. In addition, ALA is poorly converted to EPA in humans and generates virtually no DHA [10]. The rate-limiting step in the conversion of ALA to EPA is the delta-6-desaturase, the enzyme that converts ALA to stearidonic acid (SDA). Previous work in animals and humans has shown that SDA is converted to EPA more efficiently than ALA [11], and increases the EPA content of human immune cells [12, 13], and RBC and plasma phospholipids [14]. The extent to which SDA will enrich heart cells (i.e., those cells in which the protective effects of omega-3 FA appear to reside) with EPA and DHA is unknown. In humans, supplementation with fish oil increases EPA and DHA in RBC and heart to the same extent [15].

The main purpose of this study was to determine the extent to which SDA feeding will increase EPA and DHA in RBC and heart in dogs. ALA is known to be converted to long-chain omega-3 FA in this species [16], and it is a model in which EPA and DHA (infused intravenously) have been shown to reduce risk for cardiac arrhythmias [17]. We also determined whether SDA per se accumulates in tissues, and we compared the relative efficiency with which various intakes of SDA are converted into EPA in vivo.

## Materials and Methods

### Animals and Diets

Eighty adult male, purpose-bred Beagle dogs (Ridgland Farms, Mt. Horeb, WI, USA) weighing 8–19 kg (17–33 months old) were housed individually at WIL Research Laboratories, LLC (Ashland, OH, USA). Animals were maintained in accordance with the Guide for the Care and Use of Laboratory Animals. The study was reviewed and approved by the Institutional Animal Care and Use Committee. Water was available ad libitum and the light cycle was 12 h on/off. One week prior to the initiation of the study, dogs were acclimated to the feeding procedure. Each morning after an overnight fast, dogs were offered one can (154 g) of Pet Pride Gourmet Beef flavor, to which about

13 mg of alpha-tocopherol acetate (Ameri-Pac, St. Joseph, MO, USA) and control oil (high oleic acid sunflower oil, SFO; ACH Food Companies Inc., USA) were added by dropper or syringe, respectively. For the next 2–4 h, 250 g of dry dog food pellets (Harlan Teklad 25% Lab Dog Diet #8653) was provided ad libitum. The former contained, by weight, 13.5% fat of with the following fatty acid composition: 25% palmitate, 6% palmitoleate, 11% stearate, 41% oleate, 13% linoleic, 2.5% arachidonate, and all others less than 1%. The latter contained, by weight, 10% fat and 1.4% linoleic acid. The volume of control oil added to each dog's food was based on his body weight and matched the volume of omega-3 test oil that would subsequently be added to his food. Control and omega-3 test oils were quantitatively ( $\pm 0.1$  ml) added to the canned food daily via calibrated syringe. The dogs readily and consistently consumed the entire portion of canned food, thus assuring complete consumption of the test oils. This regimen was followed throughout the entire study.

After 1 week of acclimation, 5 dogs were randomly set aside to serve as baseline controls (see below) and the remaining 75 dogs were randomized into five groups of 15 dogs each: low SDA (21.4 mg/kg), mid SDA (64.2 mg/kg), high SDA (192.9 mg/kg), EPA (42.9 mg/kg), and control SFO. The randomization was performed to achieve similar average and range of body weights across the five groups. The doses were chosen to provide the body-weight-based human equivalent of SDA (1.5, 4.5 and 13.5 g, low to high) or 3 g EPA, assuming an average human body weight of 70 kg. Dogs in the SDA and EPA groups also were given SFO so that all dogs received the same amount of added oil.

The test materials, SDA ethyl ester (76.7% purity) and EPA ethyl ester (90.6% purity) were purchased from KD Pharma (Bexbach GmbH, Germany.) These oils were maintained in small aliquots at  $-80^{\circ}\text{C}$ . They were thawed and stored refrigerated and under nitrogen prior to administration. No aliquot was used two days past its thawing. The SFO control oil was stored at room temperature. Individual food consumption was recorded daily and body weights were recorded weekly. Detailed physical examinations were conducted weekly, and animals were observed twice daily for mortality and morbidity.

Prior to the initiation of dosing, fasting blood samples were drawn from five dogs randomly selected to serve as baseline controls. These dogs were then euthanized and samples of heart muscle (right ventricle) were obtained for fatty acid analysis. At weeks 2, 4, 8 and 12, blood samples were collected from all surviving dogs, and at weeks 4, 8 and 12, five dogs per treatment group were euthanized to obtain tissue samples. Heart tissue samples were rapidly frozen in liquid nitrogen and stored at  $-70^{\circ}\text{C}$  until analyzed.



## Tissue and Cell Preparation/Lipid Extraction

RBC were separated from the plasma by centrifugation at  $1,500\times g$  for 20 min at  $4\text{ }^{\circ}\text{C}$ . Plasma and RBC were collected after discarding the buffy coat, and stored at  $-70\text{ }^{\circ}\text{C}$  until use. Packed RBC were thawed and  $50\text{ }\mu\text{l}$  were dried at  $45\text{ }^{\circ}\text{C}$  under nitrogen. Thereafter the samples were directly methylated by the addition of 0.5 ml boron trifluoride methanol (Sigma, St. Louis, MO, USA) and then heated at  $100\text{ }^{\circ}\text{C}$  for 10 min. This generated fatty acid methyl esters (FAME) from the glycerophospholipids in the RBC membranes [18]. After cooling, 1 ml water and 1 ml hexane containing 50 mg/l butylated hydroxytoluene (BHT, an antioxidant, Sigma) were added. Following manual-shaking for 30 s, the samples were centrifuged for 3 min at  $1,500\times g$  at room temperature. The hexane layer was collected, the solvent was evaporated  $45\text{ }^{\circ}\text{C}$  under nitrogen and the FAME thus generated were reconstituted with  $50\text{ }\mu\text{l}$  hexane and analyzed by flame ionization gas chromatography (GC).

Heart samples were first lyophilized (Savant Speed-Vac Plus) overnight. They were subsequently pulverized between two ground glass slides, returned to their test tubes in 1 ml saline and sonicated (4710 Ultrasonic homogenizer, Cole-Parmer, Chicago, IL, USA) for 10–15 s. Methanol and methylene chloride (both containing 50 mg/l BHT) were added, the samples were briefly agitated and centrifuged at  $1,500\times g$  for 10 min at  $4\text{ }^{\circ}\text{C}$ . The aqueous layer was discarded and the organic phase was dried under nitrogen in a  $45\text{ }^{\circ}\text{C}$  water bath. The samples were methylated and processed as described above for RBC.

## Gas Chromatography

The GC (GC-14A, Shimadzu, Columbia, MD, USA) was fitted with a fused silica capillary column (SP-2560, 100 m length, 0.25 mm internal diameter, 0.25  $\mu\text{m}$  film thickness) obtained from Supelco (Bellefonte, PA, USA). Hydrogen was used as the carrier gas and nitrogen as the make-up gas. The split ratio was 1:25, and the purge was set at 15–20 ml/min. The following temperature program was used: initial temperature,  $140\text{ }^{\circ}\text{C}$  held for 5 min; ramp to  $240\text{ }^{\circ}\text{C}$  at  $6.5\text{ }^{\circ}\text{C}/\text{min}$  and hold for 37 min. FAME are reported as percent of total and were identified by comparison with known standards.

## Statistical Analysis

Heart data were derived from independent samples within each treatment group and time point, and were analyzed using a general linear cell-means model, allowing for heterogeneity of variances. RBC data contained repeated measurements over time for surviving animals, and so were

analyzed using a general linear repeated measures model accounting for temporal within-animal correlations as well as heterogeneous variances. Analyses were conducted using SAS v9.1 (SAS Institute, Inc., Cary, NC, USA). Differences were considered significant when  $P < 0.01$  unless otherwise noted.

## Results

All animals survived to the scheduled necropsies. There were no test article-related clinical findings or effects on body weight or food consumption. SDA was undetectable (i.e., was less than 0.05% of total FA) in all of the tissues examined (data not shown).

### EPA

There was a dose- and time-dependent increase in the EPA content of RBC following SDA or EPA administration (Table 1, Fig. 1). By 12 weeks of treatment, the EPA had increased from  $0.38 \pm 0.03\%$  at baseline to  $1.55 \pm 0.28\%$  in the EPA group (308% increase) and to  $1.33 \pm 0.26\%$  in the high SDA group (249% increase) (Fig. 2). Both of these increases were significant ( $P < 0.007$ ), and values in the high SDA and EPA groups did not differ from each other. The low dose SDA maintained baseline RBC EPA levels, while the EPA levels in the SFO control group declined by 57% at 12 weeks. The mid and high SDA and EPA treatments significantly increased RBC EPA at all time points versus baseline. There was a significant dose–response relationship across treatment groups at each time point ( $P < 0.001$ ). In the heart, the content of EPA rose from  $0.06 \pm 0.02\%$  at baseline to  $1.24 \pm 0.22\%$  in the EPA group and to  $0.81 \pm 0.32\%$  in the high SDA group (Fig. 2). Again, both of the changes were significant ( $P < 0.001$ ), but unlike the RBC, heart EPA was higher after EPA than after high SDA ( $P = 0.004$ ). The mid- and high SDA and EPA treatments significantly increased the EPA content of the heart by 4 weeks, and it remained significantly elevated at all time points. Low dose SDA and the SFO control maintained baseline EPA levels. The correlation between RBC and heart EPA at the end of the experiment was 0.85 ( $P < 0.001$ ).

### DPA

The SFO control oil caused a decrease in RBC DPA, from  $0.29 \pm 0.05\%$  at baseline to  $0.10 \pm 0.02\%$  at week 12 ( $P < 0.01$ ). On the other hand, EPA produced an increase in RBC DPA which was evident at week 2 ( $0.51 \pm 0.11\%$ ,  $P < 0.01$ ) and persisted through week 12. Across all time points, high dose SDA did not significantly raise RBC DPA

**Table 1** Effect of three doses of SDA, EPA and sunflower oil control on RBC and heart EPA (% of total tissue FA)

	0 weeks		2 weeks		4 weeks		8 weeks		12 weeks		All weeks	
	Mean	SD	Mean	SD	Mean	SD	Mean	SD	Mean	SD	Mean	SD
<b>RBC</b>												
Baseline	0.38	0.03	–	–	–	–	–	–	–	–	–	–
SFO	–	–	0.35 <sup>b</sup>	0.09	0.26	0.11	0.2	0.03	0.16	0.03	0.27 <sup>c</sup>	0.11
Low SDA	–	–	0.49	0.07	0.57	0.1	0.48	0.09	0.32 <sup>b</sup>	0.02	0.50 <sup>c</sup>	0.11
Mid SDA	–	–	0.74	0.07	0.97	0.23	0.71	0.1	0.67	0.11	0.80 <sup>c</sup>	0.19
High SDA	–	–	1.23	0.25	1.39	0.33	1.58	0.43	1.33	0.26	1.37 <sup>c</sup>	0.34
EPA	–	–	1.28	0.12	1.5	0.25	1.61	0.3	1.55	0.28	1.46 <sup>c</sup>	0.26
<b>Heart</b>												
Baseline	0.06	0.01	–	–	–	–	–	–	–	–	–	–
SFO	–	–	–	–	0.09 <sup>b</sup>	0.02	0.1	0.03	0.07 <sup>b</sup>	0.02	0.09 <sup>c</sup>	0.02
Low SDA	–	–	–	–	0.10 <sup>b</sup>	0.03	0.28	0.29	0.18 <sup>b</sup>	0.04	0.19 <sup>c</sup>	0.17
Mid SDA	–	–	–	–	0.23	0.14	0.31	0.12	0.37	0.07	0.30 <sup>c</sup>	0.12
High SDA	–	–	–	–	0.62	0.12	0.63	0.16	0.81	0.32	0.69 <sup>c</sup>	0.22
EPA	–	–	–	–	0.86	0.46	0.86	0.23	1.24	0.22	0.99 <sup>c</sup>	0.35

<sup>a</sup> % difference from baseline

<sup>b</sup> Not significantly different from baseline group; all other means  $P < 0.01$  versus baseline

<sup>c</sup> Overall effect across all time points versus baseline,  $P < 0.001$

**Fig. 1** Effect on tissue EPA content (percent of total FA) of three doses of SDA (21.4, 64.2 and 192.9 mg/kg, respectively) versus EPA (42.9 mg/kg) and sunflower oil (control) in dogs. Values derive from five animals at each time point and each dose. Variances and significant differences are given in Table 1

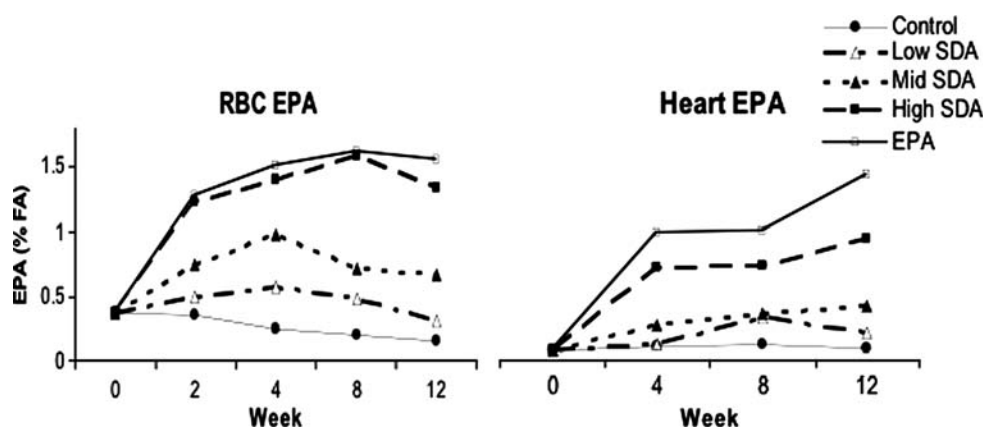
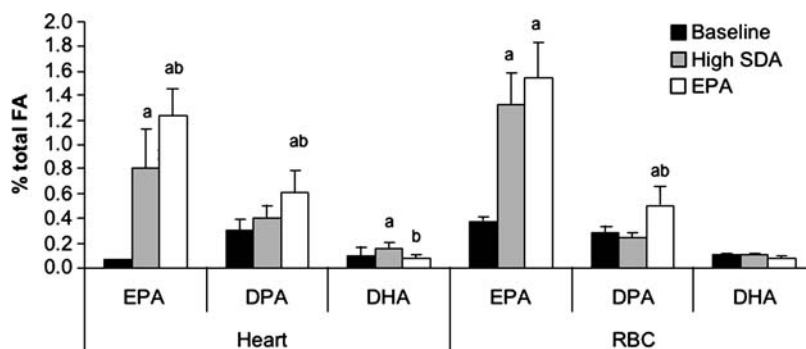


**Fig. 2** Effects of high dose SDA and EPA (vs. baseline) on individual omega-3 FA in RBC and heart tissue after 12 weeks of treatment. *a* different from baseline,  $P < 0.01$ ; *b* different from high SDA,  $P < 0.01$



(although at 4 weeks values were statistically higher than at baseline). At week 12, heart DPA was increased over baseline only with EPA feeding, and was significantly

higher than that observed with high dose SDA as well (Fig. 2). In RBC, DPA increased above baseline only in the EPA feeding group (Table 2, Fig. 2).

## DHA

The baseline DHA level in RBC was  $0.10 \pm 0.05$ . At week 12, DHA in heart was significantly increased only in the high dose SDA group ( $P < 0.01$ ; Fig. 2). Nevertheless, averaging across all time points and treatment groups, DHA levels were not affected in this study (Table 3).

## Relative Efficiency of Deposition of EPA in RBC and Heart by SDA versus EPA

Based on the data in Table 1, an estimate of the relative efficiency of deposition of EPA by SDA versus EPA can be made for each tissue (Table 4). For this analysis, RBC or heart EPA values from all available time points were included. For RBC EPA there were 45 data points from each treatment group: 5 at week 12, 10 at week 8, and 15 each at weeks 2 and 4. For the heart EPA, there were 15 points from each group: 5 each at weeks 4, 8 and 12. For each tissue, the overall percent increase in EPA (relative to baseline levels shown in Table 1) was first determined. The percent increase per gram of omega-3 FA (human equivalent) fed was calculated, and then the efficiency (with respect to EPA's ability to raise tissue EPA content) was determined for each SDA treatment group (Table 4). For example, RBC EPA at baseline was 0.38% of total fatty acids. For the EPA group, the mean RBC EPA level (averaging data from weeks 2–12) was 1.46%, which is an increase of 284%. The EPA dose fed to the dogs was equivalent to 3 g of EPA in a 70-kg human. Therefore, the incorporation efficiency (per gram of omega-3 FA fed) was

$284\%/3 \text{ g}$ , or  $95\%/g$ . Setting the  $95\%/g$  rate pure EPA as maximal (i.e., 100%) efficiency, then the  $20\%/g$  incorporation into RBC seen in the low SDA group was 22% of that observed with pure EPA ( $20\%/95\%$ ). This analysis revealed that the efficiency of deposition of EPA derived from SDA ranged from 15 to 27% in the heart and 20–26% in RBC. Averaging across doses within a tissue, the efficiency of deposition of EPA after SDA consumption was approximately 20–23% that of deposition of EPA after consumption of EPA.

## Discussion

Increased levels of EPA and DHA in RBC have been associated with a marked reduction in risk for sudden cardiac death both prospectively and cross-sectionally [19, 20], and RBC EPA and DHA content is highly correlated with that of the human heart [16]. Hence, if SDA feeding can materially raise RBC and heart EPA and DHA content, it may have clinical import.

Increasing RBC levels of EPA and DHA can readily be achieved by consuming fish [21] or fish oil [22], but many Americans do not consume adequate quantities of fish, and it seems unlikely that fish availability, affordability and consumption will increase markedly in the future. Thus, alternative, readily available dietary sources of omega-3 fatty acids are needed. While soybean, canola and flax seed oils contain the omega-3 fatty acid ALA, it has not been established that ALA favorably affects heart health, although substantial epidemiological support for this

**Table 2** Effect of three doses of SDA, EPA and sunflower oil control on RBC and heart DPA (% of total tissue FA)

	0 weeks		2 weeks		4 weeks		8 weeks		12 weeks		Overall <sup>b</sup>
	Mean	SD	Mean	SD	Mean	SD	Mean	SD	Mean	SD	
<b>RBC</b>											
Baseline	0.29	0.05	–	–	–	–	–	–	–	–	–
Control	–	–	0.03 <sup>a</sup>	0.04	0.20 <sup>a</sup>	0.04	0.13 <sup>a</sup>	0.04	0.10 <sup>a</sup>	0.02	<0.0001
Low SDA	–	–	0.28	0.07	0.35	0.10	0.21	0.07	0.15 <sup>a</sup>	0.01	0.20
Mid SDA	–	–	0.34	0.05	0.53 <sup>a</sup>	0.13	0.29	0.05	0.22	0.04	0.05
High SDA	–	–	0.34	0.07	0.46 <sup>a</sup>	0.19	0.30	0.08	0.24	0.05	0.09
EPA	–	–	0.51	0.11	0.51	0.11	0.54	0.18	0.51 <sup>a</sup>	0.16	<0.0001
<b>Heart</b>											
Baseline	0.30	0.09	–	–	–	–	–	–	–	–	–
Control	–	–	–	–	0.23	0.05	0.25	0.07	0.22	0.07	0.35
Low SDA	–	–	–	–	0.31	0.13	0.29	0.12	0.32	0.05	0.91
Mid SDA	–	–	–	–	0.32	0.16	0.33	0.06	0.40	0.09	0.48
High SDA	–	–	–	–	0.50 <sup>a</sup>	0.14	0.33	0.07	0.41	0.10	0.11
EPA	–	–	–	–	0.69 <sup>a</sup>	0.32	0.48 <sup>a</sup>	0.14	0.61 <sup>a</sup>	0.18	<0.0001

<sup>a</sup>  $P < 0.01$  versus baseline; <sup>b</sup> overall  $P$  value comparing baseline to each treatment across all time points

**Table 3** Effect of three doses of SDA, EPA and sunflower oil control on RBC and heart DHA (% of total tissue FA)

	0 weeks		2 weeks		4 weeks		8 weeks		12 weeks		Overall <sup>b</sup>	
	Mean	SD	Mean	SD	Mean	SD	Mean	SD	Mean	SD		
<b>RBC</b>												
Baseline	0.10	0.02	–	–	–	–	–	–	–	–	–	
Control	–	–	0.08	0.02	0.11	0.08	0.05 <sup>a</sup>	0.01	0.10	0.05	0.31	
Low SDA	–	–	0.11	0.11	0.09	0.04	0.07	0.02	0.09	0.02	0.62	
Mid SDA	–	–	0.08	0.01	0.23	0.33	0.07	0.02	0.18	0.22	0.24	
High SDA	–	–	0.10	0.03	0.11	0.05	0.09	0.03	0.10	0.02	0.62	
EPA	–	–	0.11	0.06	0.09	0.04	0.06	0.01	0.08	0.01	0.30	
<b>Heart</b>												
Baseline	0.09	0.08	–	–	–	–	–	–	–	–	–	
Control	–	–	–	–	0.08	0.03	0.09	0.04	0.08	0.02	0.57	
Low SDA	–	–	–	–	0.06	0.02	0.07	0.04	0.10	0.03	0.46	
Mid SDA	–	–	–	–	0.08	0.04	0.09	0.03	0.10	0.03	0.77	
High SDA	–	–	–	–	0.11	0.03	0.11	0.03	0.16 <sup>a</sup>	0.05	0.08	
EPA	–	–	–	–	0.11	0.04	0.08	0.02	0.08	0.02	0.83	

<sup>a</sup>  $P < 0.01$  versus baseline; <sup>b</sup> overall  $P$  value comparing baseline to each treatment across all time points

**Table 4** Estimated efficiency of deposition of EPA in tissues from consumption of SDA or EPA by dogs

n-3 FA fed	Dose <sup>b</sup>	% Increase vs. baseline	% Increase/g FA	Relative to EPA (%)
<b>Heart EPA<sup>a</sup></b>				
EPA	3	1,430	477	100
Low SDA	1.5	190	127	27
Mid SDA	4.5	368	82	17
High SDA	13.5	966	72	15
SDA average				20
<b>RBC EPA<sup>c</sup></b>				
EPA	3	284	95	100
Low SDA	1.5	31	20	22
Mid SDA	4.5	112	25	26
High SDA	13.5	262	19	20
SDA average				23

<sup>a</sup> Based on 15 heart EPA values per treatment group (including all weeks) versus baseline ( $n = 5$ )

<sup>b</sup> Human equivalent of the dose fed to the dogs in g/day

<sup>c</sup> Based on 45 RBC EPA values per treatment group (including all weeks) versus baseline ( $n = 5$ ). Data from Table 1

hypothesis exists [23–25]. In addition, the basis for any health benefit from ALA is unclear since its conversion to EPA via the rate-limiting enzymatic step, delta-6-desaturase, is highly inefficient [11]. Estimates of the fraction of ALA converted to EPA by humans range from 0.2% [10] to 7% [26]. Some of this inefficiency is also likely due to the high intake of linoleic acid which competes with ALA for the delta-6-desaturase.

A recent clinical study by Wilkinson et al. assessed the effects of feeding high doses of ALA-rich flax seed oil on RBC EPA and DHA content [27]. After 12 weeks of consuming 15 g/day ALA or 1.5 g/day EPA from fish oil, RBC EPA content increased by 153 or 124%, respectively. On a per-g of omega-3 FA-fed basis, EPA raised RBC EPA content by 82%/g and ALA, by 10%/g. Hence, ALA was 12% as efficient as EPA in raising RBC EPA levels in this study. This value is similar to that observed by James et al. [14] who gave humans an average of 1.125 g ALA, SDA or EPA for 6 weeks. Compared to EPA feeding, which raised RBC EPA by 192%/g omega-3 fed, SDA raised it by 44%/g and ALA, 13%/g. Therefore, in this study ALA was only 7% as efficient as EPA in raising RBC EPA levels.

Since SDA is the delta-6-desaturase product of ALA, its conversion to EPA should be more efficient. In the study by James et al. [14], the human efficiency of deposition of EPA from SDA into RBC was 23% of that seen for EPA itself. In our study in dogs we found the same, but since we did not include an ALA treatment group, the relative efficiency of ALA versus SDA in this species could not be evaluated. However, from the data of James et al., it can be estimated that EPA formed from SDA is deposited in tissues at about three times the rate at which it is from ALA (23 vs. 7%). Further studies are needed to confirm this estimate.

Both low- and mid-SDA treatment prevented the loss of DPA in RBC caused by the SFO control, but only EPA was effective in raising RBC and heart DPA levels. The role of DPA in myocardial metabolism and in cardiovascular disease risk remains unclear.

Neither SDA nor EPA feeding increased the DHA content of the heart. However, DHA content of RBC was slightly but significantly raised by high dose SDA but not by EPA. Nevertheless, the minimal impact of DHA precursors on tissue DHA reported by many investigators was generally confirmed here [10, 14, 28, 29].

The time course of incorporation of EPA differed somewhat in the RBC versus heart tissue following SDA feeding. In RBC stable levels were apparently achieved in about 8 weeks, whereas in heart tissue, there was a plateau between 4 and 8 weeks with a further increase at 12 weeks. This is similar to what has been observed with DHA in rat RBC and heart [30]. In the same study, EPA appeared to stabilize in the heart at 7 days but not until 6 weeks in RBC.

In this model, the degree of EPA deposition after omega-3 FA feeding was similar in RBC and the heart, with tissue EPA values reaching about 1.5% of total FA in both cases. In humans, similar percent increases in omega-3 fatty acid incorporation were observed in the human heart and RBC after 6 months of fish oil supplementation [15]. In contrast to EPA, there are marked differences in DHA in dog RBC and heart tissue, and as a consequence, the ratio of EPA to DHA differs in these two tissues. Dogs are known to have much lower levels of DHA in RBC than do rabbits, rats or humans [31, 32], and their heart DHA level is only one-third the level seen in guinea pigs (0.1 vs. 0.3%) [33]. Although baseline omega-3 FA levels are very low in this species, Beagles (like guinea pigs [33]) respond to fish oil feeding with robust increases in RBC EPA and DHA [34].

Although SDA increases tissue EPA levels, it is not clear that higher heart EPA alone affords cardiovascular benefit. When EPA and DHA are fed together (as in fish oils), cardiovascular events are reduced [35], and at high intakes (e.g., 3–4 g/day), serum triglycerides are lowered [3]. EPA alone has also been reported to lower serum TG [36] and remnant lipoproteins [37], to inhibit platelet aggregation [38–41] and to reduce in LDL peroxidation [37]. In vitro, EPA can block the toxic effects of ouabain in isolated rat cardiomyocytes [42, 43]. Similar benefits of EPA were observed using beta-adrenergic agonists [44] and acylcarnitine [45] to induce fibrillation. There is evidence that EPA acts on cardiac sodium, calcium and potassium channels, ultimately preventing calcium overload and prolonging the inactivated state of the channels [45–47].

The Japan EPA Lipid Intervention Study (JELIS) provided strong evidence for cardioprotective effects of EPA alone [results summarized in 48]. In this trial, over 18,000 hypercholesterolemic patients, all taking low-dose statins, were randomized to 1.8 g of EPA ethyl esters or usual care and followed for major adverse cardiac events for

4.5 years. There was a 19% reduction in risk observed in the EPA group ( $P = 0.01$ ). Complicating the interpretation (and extrapolation of these results to the US context) was the high background intake of EPA and DHA in the Japanese population [49]. Median intakes are approximately 1 g/day in this population compared to the 100–150 mg/day typical of the US population [50]. Nevertheless, the results of the JELIS trial indicate that increasing already high tissue levels of omega-3 FA with additional EPA confers additional protection against cardiovascular disease.

The western diet contains very little SDA, but there are natural sources, notably fish oils, which contains 1–2% SDA [51]. At present there are no commercially-viable plant sources for SDA. SDA is found in echium oil at about 12% [52], and feeding echium oil led to an increase in the EPA content of peripheral blood mononuclear cell phospholipids [12, 13]. Consumption of 15 g echium oil for 4 weeks decreased serum triacylglycerol concentrations by 21–30% and significantly increased EPA and DPA, but not DHA, in plasma and neutrophils in hypertriglyceridemic humans [52]. This suggests that echium oil possesses hypotriglyceridemic properties similar to those of fish oil whereas ALA does not [8]. However, echium oil is very limited in abundance compared to canola or soybean oil, and is not approved for consumption in the US. Other sources of SDA are also limited, and include evening primrose, borage and black currant seed oils. However, genetically enhanced soybeans can produce oils with about 20% SDA [51]. If suitable for commercialization and acceptable to consumers, SDA-enriched soybean oil could provide a substantial amount of omega-3 fatty acids in the human diet. Whether this would translate into health benefits remains to be seen.

**Acknowledgments** The authors thank Gulam Ahmed of Monsanto Company for his expert analysis of the test materials used in this study. This study was funded by a grant from Monsanto Company. WSH is a consultant to the Monsanto Company, Reliant Pharmaceuticals and OmegaMetrix, LLC.

## References

1. Leaf A, Kang JX, Xiao YF, Billman GE (2003) Clinical prevention of sudden cardiac death by n-3 polyunsaturated fatty acids and mechanism of prevention of arrhythmias by n-3 fish oils. *Circulation* 107:2646–2652
2. Knapp HR (1997) Dietary fatty acids in human thrombosis and hemostasis. *Am J Clin Nutr* 65(Suppl):1687S–1698S
3. Harris WS (1997) n-3 Fatty acids and serum lipoproteins: human studies. *Am J Clin Nutr* 65(Suppl):1645S–1654S
4. Calder PC (2003) n-3 polyunsaturated fatty acids and inflammation: from molecular biology to the clinic. *Lipids* 38:343–352
5. Kris-Etherton PM, Harris WS, Appel LJ (2002) Fish consumption, fish oil, omega-3 fatty acids, and cardiovascular disease. *Circulation* 106:2747–2757

6. Worm B, Barbier EB, Beaumont N, Duffy JE, Folke C, Halpern BS, Jackson JB, Lotze HK, Micheli F, Palumbi SR, Sala E, Selkoe KA, Stachowicz JJ, Watson R (2006) Impacts of biodiversity loss on ocean ecosystem services. *Science* 314:787–790
7. Wang C, Harris WS, Chung M, Lichtenstein AH, Balk EM, Kupelnick B, Jordan HS, Lau J (2006) n-3 Fatty acids from fish or fish-oil supplements, but not {alpha}-linolenic acid, benefit cardiovascular disease outcomes in primary- and secondary-prevention studies: a systematic review. *Am J Clin Nutr* 84:5–17
8. Wendland E, Farmer A, Glasziou P, Neil A (2006) Effect of alpha linolenic acid on cardiovascular risk markers: a systematic review. *Heart* 92:166–169
9. Sanderson P, Finnegan YE, Williams CM, Calder PC, Burdge GC, Wootton SA, Griffin BA, Joe MD, Pegge NC, Bemelmans WJ (2002) UK Food Standards Agency alpha-linolenic acid workshop report. *Br J Nutr* 88:573–579
10. Pawlosky RJ, Hibbeln JR, Novotny JA, Salem NJ (2001) Physiological compartmental analysis of alpha-linolenic acid metabolism in adult humans. *J Lipid Res* 42:1257–1265
11. Yamazaki K, Fujikawa M, Hamazaki T, Yano S, Shono T (1992) Comparison of the conversion rates of alpha-linolenic acid (18:3(n-3)) and stearidonic acid (18:4(n-3)) to longer polyunsaturated fatty acids in rats. *Biochim Biophys Acta* 1123:18–26
12. Miles EA, Banerjee T, Dooper MM, M'Rabet L, Graus YM, Calder PC (2004) The influence of different combinations of gamma-linolenic acid, stearidonic acid and EPA on immune function in healthy young male subjects. *Br J Nutr* 91:893–903
13. Miles EA, Banerjee T, Calder PC (2004) The influence of different combinations of gamma-linolenic, stearidonic and eicosapentaenoic acids on the fatty acid composition of blood lipids and mononuclear cells in human volunteers. *Prostaglandins Leukot Essent Fatty Acids* 70:529–538
14. James MJ, Ursin VM, Cleland LG (2003) Metabolism of stearidonic acid in human subjects: comparison with the metabolism of other n-3 fatty acids. *Am J Clin Nutr* 77:1140–1145
15. Harris WS, Sands SA, Windsor SL, Ali HA, Stevens TL, Magalski A, Porter CB, Borkon AM (2004) Omega-3 fatty acids in cardiac biopsies from heart transplant patients: correlation with erythrocytes and response to supplementation. *Circulation* 110:1645–1649
16. Dunbar BL, Bauer JE (2002) Conversion of essential fatty acids by Delta 6-desaturase in dog liver microsomes. *J Nutr* 132:1701S–1703S
17. Billman GE, Kang JX, Leaf A (1999) Prevention of sudden cardiac death by dietary pure w-3 polyunsaturated fatty acids in dogs. *Circulation* 99:2452–2457
18. Morrison WR, Smith LM (1964) Preparation of fatty acid methyl esters and dimethylacetals from lipids with boron fluoride-methanol. *J Lipid Res* 5:600–608
19. Siscovick DS, Raghunathan TE, King I, Weinmann S, Wicklund KG, Albright J, Bovbjerg V, Arbogast P, Smith H, Kushi LH, Cobb LA, Copass MK, Psaty BM, Lemaitre R, Retzlaff B, Childs M, Knopp RH (1995) Dietary intake and cell membrane levels of long-chain n-3 polyunsaturated fatty acids and the risk of primary cardiac arrest. *J Am Med Assoc* 274:1363–1367
20. Albert CM, Campos H, Stampfer MJ, Ridker PM, Manson JE, Willett WC, Ma J (2002) Blood levels of long-chain n-3 fatty acids and the risk of sudden death. *N Engl J Med* 346:1113–1118
21. Sands SA, Reid KJ, Windsor SL, Harris WS (2005) The impact of age, body mass index, and fish intake on the EPA and DHA content of human erythrocytes. *Lipids* 40:343–347
22. Harris WS, von Schacky C (2004) The omega-3 index: a new risk factor for death from coronary heart disease? *Prev Med* 39:212–220
23. Albert CM, Oh K, Whang W, Manson JE, Chae CU, Stampfer MJ, Willett WC, Hu FB (2005) Dietary alpha-linolenic acid intake and risk of sudden cardiac death and coronary heart disease. *Circulation* 112:3232–3238
24. Djousse L, Arnett DK, Carr JJ, Eckfeldt JH, Hopkins PN, Province MA, Ellison RC (2005) Dietary linolenic acid is inversely associated with calcified atherosclerotic plaque in the coronary arteries: the NHLBI family heart study. *Circulation* 111:2921–2926
25. Ascherio A, Rimm EB, Giovannucci EL, Spiegelman D, Stampfer MWWC (1996) Dietary fat and risk of coronary heart disease in men: cohort follow up study in the United States. *BMJ* 313:84–90
26. Goyens PL, Spilker ME, Zock PL, Katan MB, Mensink RP (2005) Compartmental modeling to quantify alpha-linolenic acid conversion after longer term intake of multiple tracer boluses. *J Lipid Res* 46:1474–1483
27. Wilkinson P, Leach C, Ah-Sing EE, Hussain N, Miller GJ, Millward DJ, Griffin BA (2005) Influence of alpha-linolenic acid and fish-oil on markers of cardiovascular risk in subjects with an atherogenic lipoprotein phenotype. *Atherosclerosis* 181:115–124
28. Francois CA, Connor SL, Bolewicz LC, Connor WE (2003) Supplementing lactating women with flaxseed oil does not increase docosahexaenoic acid in their milk. *Am J Clin Nutr* 77:226–233
29. Burdge GC, Jones AE, Wootton SA (2002) Eicosapentaenoic and docosapentaenoic acids are the principal products of alpha-linolenic acid metabolism in young men. *Br J Nutr* 88:355–363
30. Owen AJ, Peter-Przyborowska BA, Hoy AJ, McLennan PL (2004) Dietary fish oil dose- and time-response effects on cardiac phospholipid fatty acid composition. *Lipids* 39:955–961
31. Pekiner B, Pennock JF (1995) Fatty acids in plasma and red blood cell membranes in humans, rats, rabbits and dogs. *Biochem Mol Biol Int* 37:221–229
32. Giron MD, Mataix FJ, Suarez MD (1992) Long-term effects of dietary monounsaturated and polyunsaturated fatty acids on the lipid composition of erythrocyte membranes in dogs. *Comp Biochem Physiol Comp Physiol* 102:197–201
33. Abedin L, Lien EL, Vingrys AJ, Sinclair AJ (1999) The effects of dietary alpha-linolenic acid compared with docosahexaenoic acid on brain, retina, liver, and heart in the guinea pig. *Lipids* 34:475–482
34. Filburn CR, Griffin D (2005) Canine plasma and erythrocyte response to a docosahexaenoic acid-enriched supplement: characterization and potential benefits. *Vet Ther* 6:29–42
35. Marchioli R, Barzi F, Bomba E, Chieffo C, Di Gregorio D, Di Mascio R, Franzosi MG, Geraci E, Levantesi G, Maggioni AP, Mantini L, Marfisi RM, Mastrogiuseppe G, Mininni N, Nicolosi GL, Santini M, Schweiger C, Tavazzi L, Tognoni G, Tucci C, Valagussa F (2002) Early protection against sudden death by n-3 polyunsaturated fatty acids after myocardial infarction: time-course analysis of the results of the Gruppo Italiano per lo Studio della Sopravvivenza nell'Infarto Miocardico (GISSI)-Prevenzione. *Circulation* 105:1897–1903
36. Rambjor GS, Walen AI, Windsor SL, Harris WS (1996) Eicosapentaenoic acid is primarily responsible for the hypotriglyceridemic effect of fish oil in humans. *Lipids* 31:S45–S49
37. Ando M, Sanaka T, Nihei H (1999) Eicosapentaenoic acid reduces plasma levels of remnant lipoproteins and prevents in vivo peroxidation of LDL in dialysis patients. *J Am Soc Nephrol* 10:2177–2184
38. Dyerberg J, Bang HO (1979) Haemostatic function and platelet polyunsaturated fatty acids in Eskimos. *Lancet* 2(8140):433–435
39. Dyerberg J, Bang HO, Stoffensen E, Moncada S, Vane JR (1978) Eicosapentaenoic acid and prevention of thrombosis and atherosclerosis? *Lancet* 2(8081):117–119
40. Westerveld HT, de Graff JC, van Breugel HHHFI, Akkerman JWN, Sixma JJ, Erkelens DW, Banga JD (1993) Effects of low-

- dose EPA-E on glycemic control, lipid profile, lipoprotein (a), platelet aggregation, viscosity, and platelet and vessel wall interaction in NIDDM. *Diab Care* 16:683–688
41. Wojenski CM, Silver MJ, Walker J (1991) Eicosapentaenoic acid ethyl ester as an antithrombotic agent: comparison to an extract of fish oil. *Biochim Biophys Acta* 1081:33–38
  42. Hallaq H, Sellmayer A, Smith TW, Leaf A (1990) Protective effect of eicosapentaenoic acid on ouabain toxicity in neonatal rat cardiac myocytes. *Proc Natl Acad Sci USA* 87:7834–7838
  43. Kang JX, Leaf A (1994) Effects of long-chain polyunsaturated fatty acids on the contraction of neonatal rat cardiac myocytes. *Proc Natl Acad Sci USA* 91:9886–9890
  44. Kang JX, Leaf A (1995) Prevention and termination of beta-adrenergic agonist-induced arrhythmias by free polyunsaturated fatty acids in neonatal rat cardiac myocytes. *Biochem Biophys Res Commun* 208:629–636
  45. Kang JX, Leaf A (1996) Protective effects of free polyunsaturated fatty acids on arrhythmias induced by lysophosphatidylcholine or palmitoylecarnitine in neonatal rat cardiac myocytes. *Eur J Pharmacol* 297:97–106
  46. Honore E, Barhanin J, Attali B, Lesage F, Lazdunski M (1994) External blockade of the major cardiac delayed-rectifier K<sup>+</sup> channel (Kv1.5) by polyunsaturated fatty acids. *Proc Natl Acad Sci USA* 91:1937–1944
  47. Leaf A (2001) The electrophysiologic basis for the antiarrhythmic and anticonvulsant effects of n-3 polyunsaturated fatty acids: heart and brain. *Lipids* 36(Suppl):S107–S110
  48. Cleland JG, Freemantle N, Coletta AP, Clark AL (2006) Clinical trials update from the American Heart Association: REPAIR-AMI, ASTAMI, JELIS, MEGA, REVIVE-II, SURVIVE, and PROACTIVE. *Eur J Heart Fail* 8:105–110
  49. Iso H, Kobayashi M, Ishihara J, Sasaki S, Okada K, Kita Y, Kokubo Y, Tsugane S (2006) Intake of fish and n3 fatty acids and risk of coronary heart disease among Japanese: the Japan Public Health Center-based (JPHC) study cohort I. *Circulation* 113:195–202
  50. Kris-Etherton PM, Taylor DS, Yu-Poth S, Huth P, Moriarty K, Fishell V, Hargrove RL, Zhao G, Etherton TD (2000) Polyunsaturated fatty acids in the food chain in the United States. *Am J Clin Nutr* 71:179S–188S
  51. Ursin VM (2003) Modification of plant lipids for human health: development of functional land-based omega-3 fatty acids. *J Nutr* 133:4271–4274
  52. Surette ME, Edens M, Chilton FH, Tramposch KM (2004) Dietary echium oil increases plasma and neutrophil long-chain (n-3) fatty acids and lowers serum triacylglycerols in hypertriglyceridemic humans. *J Nutr* 134:1406–1411

# Longitudinal Assessment of Erythrocyte Fatty Acid Composition Throughout Pregnancy and Post Partum

Frances Stewart · Vanessa A. Rodie · Jane E. Ramsay ·  
Ian A. Greer · Dilys J. Freeman · Barbara J. Meyer

Received: 10 August 2006 / Accepted: 11 December 2006 / Published online: 27 March 2007  
© AOCS 2007

**Abstract** Transfer of fatty acids from mother to fetus during pregnancy is a requirement for optimal fetal growth. We report a longitudinal study of full maternal erythrocyte fatty acid profile assessed at each trimester of pregnancy [mean 12.5 (range 8–14), 26.1 (24–28) and 35.5 (33–38) weeks' gestation] and in the post partum period [18.1 (12–26) weeks]. The study recruited healthy women ( $n = 47$ ) from routine antenatal clinics at the Princess Royal Maternity Unit, Glasgow, Scotland. There were increases in 16:1 $n$ 7 (22%,  $p = 0.0005$ ), 24:1 $n$ 9 (13%,  $p = 0.0032$ ), 22:5 $n$ 6 (25%,  $p = 0.0003$ ), 18:3 $n$ 3 (41%,  $p = 0.0007$ ) and 22:6 $n$ 3 (20%,  $p = 0.0005$ ) concentrations during pregnancy. The greatest increases took place between gestations at sampling of 12.5 and 26.1 weeks. The change in 16:1 $n$ 7 concentration between gestations at sampling of 12.5 and 35.3 weeks was negatively associated with maternal booking body mass index ( $r = -0.40$ ,  $p = 0.006$ ). The change in 22:6 $n$ 3 concentration was correlated with the change in 24:1 $n$ 9 ( $r = 0.70$ ,  $p < 0.001$ ). In samples taken four months post partum, 14:0 concentration was lower (29%,  $p = 0.0002$ ) and 24:0 concentration (15%,  $p = 0.0009$ ) and  $n6/n3$  ratio (11%,  $p = 0.0019$ ) were higher than at a gestation at sampling of 12.5 weeks. In conclu-

sion, several fatty acids are specifically mobilised during pregnancy. The correlation between maternal 22:6 $n$ 3 and 24:1 $n$ 9 suggests that mobilisation of these fatty acids may be coordinated. The inverse relationship between 16:1 $n$ 7 and maternal central obesity warrants further investigation.

**Keywords** Fatty acid · Pregnancy · Obesity

## Abbreviations

12:0	Lauric acid
14:0	Myristic acid
16:0	Palmitic acid
18:0	Stearic acid
20:0	Arachidic acid
22:0	Behenic acid
24:0	Lignoceric acid
16:1 $n$ 7	Palmitoleic acid
18:1 $n$ 9	Oleic acid
20:1 $n$ 9	Eicosenoic acid
22:1 $n$ 9	Erucic acid
24:1 $n$ 9	Nervonic acid
18:2 $n$ 6	Linoleic acid
18:3 $n$ 6	Gamma-linolenic acid
20:3 $n$ 6	Dihomo-gamma-linolenic acid
20:4 $n$ 6	Arachidonic acid
22:4 $n$ 6	Adrenic acid
22:5 $n$ 6	Docosapentaenoic acid
18:3 $n$ 3	Alpha-linolenic acid
20:5 $n$ 3	Eicosapentaenoic acid
22:5 $n$ 3	Docosapentaenoic acid
22:6 $n$ 3	Docosahexaenoic acid
$n9$	Omega-9 monounsaturated fatty acids
$n7$	Omega-7 monounsaturated fatty acids
$n6$	Omega-6 polyunsaturated fatty acids
$n3$	Omega-3 polyunsaturated fatty acids

F. Stewart · V. A. Rodie · J. E. Ramsay · I. A. Greer ·  
D. J. Freeman  
Division of Developmental Medicine,  
University of Glasgow, Royal Infirmary,  
Glasgow G31 2ER, UK

B. J. Meyer (✉)  
School of Health Sciences, University of Wollongong,  
Northfields Avenue, Wollongong, NSW 2522, Australia  
e-mail: bmeyer@uow.edu.au



LC	Long chain
MUFA	Monounsaturated fatty acids
FA	Fatty acids
C20-22	Fatty acids with carbon chain lengths of 20–22 carbons
SCD	Stearyl CoA desaturase
WHR	Waist:hip ratio
BMI	Body mass index
DEPCAT	Deprivation score, which is a measure of socioeconomic status
PUFA	Polyunsaturated fatty acids
SAFA	Saturated fatty acids

## Introduction

Fatty acids are important constituents of cell membranes and are therefore essential for tissue formation (reviewed in [1]). The long chain polyunsaturated fatty acids (LCPUFA) commonly found in membranes, especially in the brain, are derived via elongation and desaturation from the essential fatty acids 18:2*n*6 (linoleic acid) and 18:3*n*3 (alpha-linolenic acid) (reviewed in [2]). In pregnancy, the fetus is reliant on placental transfer of fatty acids from the mother to support growth [2, 3]. The mother must therefore mobilise key fatty acids and make them available for accretion by the fetus [2]. Maternal LCPUFA status during pregnancy is critical to determining essential fatty acid status in the newborn [2, 4].

Al et al. have assessed the fatty acid statuses of mothers longitudinally throughout pregnancy by analysing plasma phospholipid fatty acid content [5]. Focussing mainly on the essential fatty acids and their long chain derivatives, they observed that the percentage of 18:2*n*6 did not change during pregnancy, whereas the percentage of 20:4*n*6 (arachidonic acid) decreased [5]. The maternal plasma phospholipid 22:6*n*3 (docosahexaenoic acid) percentage rose until 18 weeks and thereafter declined during pregnancy concomitant with an increase in umbilical plasma phospholipid 22:6*n*3 content [5]. These observations were consistent across populations selected from five different countries despite the variation in maternal essential fatty acid status between countries [6]. Similar changes in total plasma fatty acid compositions were observed longitudinally in pregnancy by Montgomery et al. [7]. It has been suggested [4, 8] that, in the populations studied and under their prevailing dietary conditions, the decline in plasma 22:6*n*3 in late gestation indicates that the mother may be unable to meet the fetal demand for essential long chain polyunsaturated fatty acids.

While plasma phospholipid fatty acid status has been used to indicate fatty acid mobilisation, these fatty acids

will be derived mainly from plasma lipoproteins, and their measurement is open to confounding by maternal fasting status. Erythrocyte fatty acid composition is most likely to represent an integrative measure of the fatty acid status over the preceding three months (the half life of an erythrocyte is 120 days), although new evidence indicates that erythrocyte fatty acid composition may reflect more recent changes in at least some plasma fatty acid concentrations [9]. It has been suggested that erythrocytes may act as a potential storage vehicle for 20:4*n*6 and 22:6*n*3 [10]. Montgomery [7] observed similar changes in erythrocyte fatty acids during pregnancy to those seen for plasma fatty acids. In a cross-sectional study, Ashby et al. [11] observed a second trimester increase in the erythrocyte content of the essential fatty acids 22:6*n*3, 20:5*n*3 (eicosapentaenoic acid), 20:4*n*6 and 18:2*n*6, followed by a decline in the third trimester in the absence of any significant changes in plasma fatty acids. Maternal plasma and erythrocyte 22:6*n*3 and 22:5*n*6 (docosapentaenoic acid) declined between 24 weeks' gestation and three months post partum in African-American women, while 20:5*n*3 and 20:4*n*6 increased over the same period [12].

Most longitudinal studies of changes in maternal fatty acid status in pregnancy have focused primarily on the LCPUFA changes during gestation and have not emphasised changes in shorter chain and saturated fatty acids; nor have changes in maternal fatty acid status across all trimesters been compared with the post partum period. In this study we report a full maternal erythrocyte fatty acid profile assessed at each trimester throughout pregnancy and at four months post partum.

## Methods

### Patient Recruitment and Sample Collection

Women ( $n = 47$ ) were recruited from the antenatal clinic, Princess Royal Maternity Unit, Glasgow Royal Infirmary, at their first antenatal appointment in the first trimester of pregnancy. None of the women had a medical history of cardiovascular or metabolic disease. None of the women recruited developed any metabolic complication of pregnancy which may affect fatty acid metabolism such as preeclampsia or gestational diabetes mellitus. None of them had hyperemesis gravidarum, and none reported significant vomiting. Ethical approval for this study was granted by the Glasgow Royal Infirmary Research Ethics Committee and all subjects gave informed consent to participate. The women were asked to attend for their first "study visit" during the first trimester. All women attended each visit after an overnight fast (>10 h) and

underwent testing between 0900 and 1100 hours. Patient characteristics were recorded at the first trimester visit from patient notes. Height, weight, waist circumference and hip circumference were measured by the same investigator (FS). Waist circumference was measured at the level of the umbilicus. Hip circumference was measured at the widest point over the buttocks. Waist and hip circumference were measured in duplicate to the nearest 0.5 cm. If the difference between the two measurements was greater than 2 cm, a third measurement was taken and the mean of the two closest measurements was calculated. Waist:hip ratio (WHR) was defined as waist circumference divided by hip circumference. Body mass index (BMI) was calculated as first trimester weight (kg) divided by height (m) squared. Deprivation category (DEPCAT score), a measure of socioeconomic status [13], was assigned using the Scottish Area Deprivation Index for Scottish postcode sectors, 1998. At this visit, further arrangements were made for the patient to attend in the second trimester and then again in the third trimester. At delivery, all patients were seen by the same investigator (FS) and arrangements made for a postnatal visit at circa three months. Details of gestation of delivery, mode of delivery, fetal sex, birth weight and placental weight were recorded from the patients' notes. Birthweights of offspring were normalised by gestation at birth, fetal sex and maternal parity [14], with a greater centile indicating a larger normalised birthweight. At each visit maternal venous blood was sampled into 1 mg/mL EDTA and packed blood cells collected by low-speed centrifugation. Blood samples were collected at a mean of 12.5 (range 8–14), 26.2 (range 24–28) and 35.5 (range 33–38) weeks' gestation. Post partum samples were collected at a mean of 18.1 (range 12–26) weeks after delivery.

#### Erythrocyte Membrane Fatty Acid Extraction

Preparation of a total fatty acid extract from erythrocyte membranes was performed by a modified Folch extraction [15, 16]. Packed red blood cells (400  $\mu$ L) were suspended in 10 mM *tris* buffer pH 7.0, and incubated at room temperature for 30 min. Suspensions were centrifuged in a Beckman (Fullerton, CA, USA) L8-60M Ultracentrifuge, Type 50.4 rotor, at 49,000 rpm and at 4 °C for 30 min. The erythrocyte pellet was resuspended in 200  $\mu$ L of distilled H<sub>2</sub>O and 150  $\mu$ L was transferred to a clean glass screw-top tube. Methanol:toluene (4:1, 2 mL) containing heneicosanoic acid internal standard (0.2 mg C<sub>21</sub>H<sub>42</sub>O<sub>2</sub>/mL toluene) was added, followed by 200  $\mu$ L of 100% acetyl chloride while mixing. Tubes were capped and sealed with teflon tape before heating at 100 °C for 1 h. After cooling, 10% K<sub>2</sub>CO<sub>3</sub> (3 mL) was

slowly added to each tube followed by 100  $\mu$ L toluene. After centrifugation at 3,000 rpm for 8 min at 5 °C, the upper toluene phase was transferred to gas chromatography (GC) vials and stored at –20 °C until ready for injection.

#### Gas Chromatography of Fatty Acids

Methyl fatty acids (FAs) were separated (1  $\mu$ L injection volume), identified and quantitated on a Shimadzu (Kyoto, Japan) GC 17A gas chromatograph with flame ionisation detection and Class VP software. A 30 m  $\times$  0.25 mm internal diameter DB-23 fused silica capillary column (J&W Scientific, Folson, CA, USA) with a film thickness of 0.25  $\mu$ m was used in conjunction with a Hewlett-Packard (Palo Alto, CA, USA) 7673B on-column auto-injector. Ultrahigh purity hydrogen and air were used as carrier gases at a flow rate of 2 mL/min. A temperature gradient programme was used with an initial temperature of 150 °C, increasing at 20 °C/min up to 190 °C, then at 5 °C/min up to 210 °C, then at 2 °C/min up to 230 °C and then at 4 °C/min up to 240 °C (final time 18.5 min), and with an equilibration time of 1 min. The total programme time was 22 min. Identification of fatty acid methyl esters was made by comparison with the retention times of authentic standard mixtures (fatty acid methyl ester mixture no. 189-19, product no. L9405, Sigma, Stockholm, Sweden).

#### Statistical Analysis

Values for biochemical variables are given as mean  $\pm$  standard deviation unless otherwise stated. Normality testing was carried out using the Ryan–Joiner test in Minitab (vs. 13.0). Percent 14:0, 16:0, 17:0, 18:0, 20:0, 24:0, 14:1*n*7, 16:1*n*7, 17:1*n*7, 18:1*n*9, 20:1*n*9, 20:2*n*6, 22:2*n*6, 22:5 *n*6, 20:5*n*3, and 22:3*n*3 were transformed to log values to achieve normality before significance testing. Absolute 12:0, 14:0, 17:0, 20:0, 20:1*n*9, 22:2*n*6 and 22:3*n*3 were transformed to log values and absolute 17:1*n*7, 18:2*n*6 and 20:5*n*3 were transformed to square root values to achieve normal distribution. For summary measures, percentage of MUFA, total *n*9, *n*6/*n*3 ratio and 20:4*n*6/22:6*n*3 were transformed to log values and total *n*7 transformed to square root values to achieve a normal distribution. Statistical analyses were performed using the JMP statistical analysis program (Version 5.1, SAS Institute, Cary, NC, USA). Each of the erythrocyte fatty acids were assessed for differences between the first, second and third trimesters by using one way analysis of variance, for repeated measures, with comparison for all

pairs using Tukey–Kramer HSD. Paired Student's *t*-tests were used for the comparison between the first trimester and the post partum values. Linear relationships between variables were estimated using Pearson's product moment correlation coefficients. Statistical significance was set at  $\alpha = 0.005$  for all analyses unless otherwise stated.

## Results

### Patient Characteristics

Baseline, first trimester, characteristics of the pregnant women studied are shown in Table 1. The characteristics of the women studied here are fairly typical for the Glasgow population when compared with first trimester characteristics of women enrolled in the Glasgow outcome APCR

**Table 1** Patient baseline and delivery characteristics for the current study and for women recruited to our previous Glasgow outcome APCR and LIPID (GOAL) pregnancy study [17]

Characteristic	Total ( <i>n</i> = 47)	GOAL [17] ( <i>n</i> = 4,218)
Age (years)	28.7 (5.0)	28.4 (5.8)
Smokers <i>n</i> (%)	17 (36.2)	1,701 (40.3)
Deprivation index <i>n</i> (%)		
Affluent (DEPCAT score 1–2) [13]	5 (10.6)	445 (10.6)
Intermediate (3–5)	17 (36.2)	1,788 (42.4)
Deprived (6–7)	24 (51.1)	1,754 (41.6)
Not known	1 (2.1)	231 (5.5)
Parity <i>n</i> (%)		
0	24 (51.1)	842 (43.7)
1–2	20 (42.6)	1,352 (32.1)
>2	3 (6.4)	289 (6.9)
Not known	0	735 (17.4)
BMI (kg/m <sup>2</sup> )	28.4 (6.1)	24.9 (4.7)
Waist (cm)	90.0 (15.5)	80.1 (10.5)
Waist:hip ratio	0.83 (0.11)	Not recorded
Gestation at delivery (days)	279 (10)	274 (15)
Mode of delivery <i>n</i> (%)		
Vaginal delivery	29 (61.7)	2,421 (57.4)
Assisted delivery	8 (17.0)	527 (12.5)
Caesarean section	10 (21.3)	874 (20.7)
Not recorded	0	419 (9.9)
Fetal sex <i>n</i> (%)		
Male	27 (57.4)	Not recorded
Female	20 (42.6)	
Birth weight centile	56.8 (33.2)	51.1 (29.6)
Placental weight (g)	770 (185)	674 (202)

and lipid (GOAL) pregnancy study [17] (Table 1) also carried out in our laboratory. However, the women studied here have a 3.5 kg/m<sup>2</sup> higher BMI than the mean for the Glasgow population.

### Gestational Changes in Maternal Erythrocyte Fatty Acid Composition

Maternal erythrocyte fatty acid profiles sampled at each trimester of pregnancy are shown expressed both as percentage total fatty acids (Table 2) and as absolute concentration (Table 3). There was a significant decrease in maternal 18:0 during pregnancy expressed as percentage total fatty acids; however, this was not reflected in a change in the absolute amount of this fatty acid. The significant increases in percentage of total fatty acids for 22:5*n*6, 18:3*n*3 and 22:6*n*3 were reflected in increases in the absolute amounts of these fatty acids of 25% ( $p = 0.0003$ ), 41% ( $p = 0.0007$ ) and 20% ( $p = 0.0005$ ), respectively. Furthermore, increases in the absolute amounts of 16:1*n*7 (22%,  $p = 0.0005$ ) and 24:1*n*9 (13%,  $p = 0.0032$ ) were observed in the absence of a significant change in their percentage contribution to total fatty acids. The rises in all of these fatty acids took place mostly between gestation at sampling of 12.5 weeks and gestation at sampling of 26.1 weeks, with the differences between the levels of fatty acids at 26.1 weeks' gestation and 35.5 weeks' gestation being nonsignificant upon post hoc testing.

### Correlation of Gestational Changes in Maternal Erythrocyte Fatty Acids with Maternal Characteristics

The change in absolute amount of 16:1*n*7 between a gestation at sampling of 12.5 weeks and a gestation at sampling of 35.3 weeks was inversely correlated with first trimester BMI ( $r = -0.41$ ,  $p = 0.005$ ) (Fig. 1) and first trimester waist circumference ( $r = -0.40$ ,  $p = 0.006$ ). Thus there appears to be a link between the accumulation of 16:1*n*7 and maternal central obesity. Change in 16:1*n*7 concentration was also weakly correlated with accumulation of 18:3*n*3 ( $r = 0.37$ ,  $p = 0.012$ ). There were weak correlations between change in 24:1*n*9 and 22:6*n*3 concentrations and placental weight ( $r = 0.33$ ,  $p = 0.024$  and  $r = 0.35$ ,  $p = 0.017$ , respectively). Finally, change in absolute amount of 22:6*n*3 was strongly associated with changes in absolute amounts of 24:1*n*9 and 22:5*n*6 ( $r = 0.70$ ,  $p < 0.001$  and  $r = 0.46$ ,  $p = 0.001$ , respectively) between gestations at sampling of 12.5 weeks and 35.3 weeks (Fig. 2). There were no relationships between changes in these fatty acids and maternal age, smoking status, deprivation category, parity, mode of delivery, gestation at delivery, fetal sex or birthweight centile.

**Table 2** Mean (SD) erythrocyte fatty acid composition (percentage of total fatty acids) in each trimester of pregnancy and four months post partum

Fatty acid (%)	SG 12.5 weeks (n = 46)	SG 26.1 weeks (n = 47)	SG 35.3 weeks (n = 47)	<i>p</i> *	18.1 weeks post partum (n = 38)	<i>p</i> ** SG 12.5 versus 18.1 weeks post partum
<b>SAFA</b>						
12:0	0.00 (0.00)	0.02 (0.09)	0.02 (0.08)	0.75	0.06 (0.18)	0.043
14:0	0.61 (0.27)	0.63 (0.30)	0.62 (0.26)	0.95	0.43 (0.21)	0.0002
16:0	21.9 (2.2)	22.0 (2.4)	22.2 (1.4)	0.70	20.3 (0.86)	<0.0001
17:0	0.35 (0.19)	0.31 (0.22)	0.33 (0.21)	0.81	0.40 (0.20)	0.98
18:0	15.7 (1.44)	14.8 (1.50)	14.5 (1.30)	<0.0001	15.3 (0.64)	0.08
20:0	0.72 (0.14)	0.70 (0.18)	0.63 (0.15)	0.0059	0.70 (0.18)	0.45
22:0	1.72 (0.41)	1.56 (0.36)	1.49 (0.37)	0.012	1.94 (0.28)	0.0061
24:0	3.20 (0.71)	3.30 (0.54)	3.29 (0.54)	0.54	3.64 (0.51)	0.0010
<b>MUFA</b>						
14:1 <i>n</i> 7	0.00 (0.03)	0.02 (0.10)	0.01 (0.05)	1.00	0.03 (0.10)	0.67
16:1 <i>n</i> 7	0.86 (0.23)	1.01 (0.27)	1.00 (0.23)	0.0057	0.74 (0.32)	0.0113
17:1 <i>n</i> 7	0.04 (0.11)	0.04 (0.11)	0.06 (0.13)	0.65	0.14 (0.23)	0.320
18:1 <i>n</i> 9	14.5 (1.7)	14.8 (2.0)	14.8 (1.7)	0.60	13.1 (1.0)	<0.0001
20:1 <i>n</i> 9	0.60 (0.13)	0.64 (0.23)	0.56 (0.12)	0.0088	0.55 (0.21)	0.0397
22:1 <i>n</i> 9	0.17 (0.24)	0.14 (0.23)	0.17 (0.23)	0.80	0.22 (0.24)	0.34
24:1 <i>n</i> 9	4.93 (0.75)	5.13 (1.00)	5.22 (0.80)	0.29	4.59 (0.57)	0.0275
<b>PUFA <i>n</i>6</b>						
18:2 <i>n</i> 6	8.60 (1.05)	8.91 (1.12)	8.90 (0.93)	0.27	9.76 (0.96)	<0.0001
18:3 <i>n</i> 6	0.17 (0.17)	0.11 (0.15)	0.11 (0.14)	0.16	0.08 (0.16)	0.023
20:2 <i>n</i> 6	0.38 (0.16)	0.41 (0.21)	0.41 (0.17)	0.36	0.29 (0.25)	0.47
20:3 <i>n</i> 6	1.83 (0.41)	2.03 (0.51)	1.95 (0.43)	0.12	1.97 (0.43)	0.13
20:4 <i>n</i> 6	13.7 (2.5)	12.7 (2.2)	12.9 (1.4)	0.054	15.4 (1.0)	0.0001
22:2 <i>n</i> 6	0.04 (0.15)	0.01 (0.07)	0.01 (0.05)	0.65	0.04 (0.13)	0.43
22:4 <i>n</i> 6	2.70 (0.75)	2.68 (0.79)	2.84 (0.70)	0.51	3.08 (0.46)	0.0088
22:5 <i>n</i> 6	0.54 (0.22)	0.67 (0.21)	0.68 (0.20)	0.0024	0.54 (0.22)	0.82
<b>PUFA <i>n</i>3</b>						
18:3 <i>n</i> 3	0.19 (0.15)	0.33 (0.20)	0.29 (0.18)	0.0009	0.23 (0.23)	0.31
20:5 <i>n</i> 3	0.80 (0.45)	0.85 (0.46)	0.71 (0.41)	0.32	0.88 (0.40)	0.21
22:3 <i>n</i> 3	0.37 (0.32)	0.38 (0.27)	0.41 (0.33)	0.73	0.50 (0.29)	0.069
22:5 <i>n</i> 3	2.01 (0.41)	2.01 (0.49)	2.08 (0.31)	0.65	2.23 (0.45)	0.021
22:6 <i>n</i> 3	3.29 (0.92)	3.79 (0.98)	3.85 (0.70)	0.0043	2.79 (0.68)	0.006

Gestation [mean (SD, range)] at sampling (SG): first trimester 12.5 (1.3, 8–14) weeks, second trimester 26.1 (1.3, 24–28) weeks, third trimester 35.3 (1.3, 33–38) weeks, post partum 18.1 (3.0, 12–26) weeks post delivery

SAFA saturated fatty acids, MUFA monounsaturated fatty acids, PUFA polyunsaturated fatty acids

\*One way analysis of variance for repeated measures, across gestations at sampling of 12.5, 26.1, and 35.3 weeks, with comparisons made for all pairs using Tukey–Kramer HSD.

\*\**t*-test, significance level  $p < 0.005$

### Comparison of Maternal Erythrocyte Fatty Acid Compositions at 12.5 Weeks' Gestation and at 18.1 Weeks Post Partum

In order to investigate whether fatty acids returned to baseline (gestation at sampling of 12.5 weeks) pregnancy levels within four months after delivery, the fatty acid composition after 12.5 weeks' gestation was compared with the erythrocyte fatty acid composition in samples collected a mean of 18 weeks after delivery (Tables 2, 3). The percentage contribution to total fatty acids was lower post partum than at 12.5 weeks' gestation for 14:0, 16:0 and 18:1*n*9, and higher post partum for 24:0, 18:2*n*6 and

20:4*n*6. However, a reduction in absolute amounts was only seen for 14:0. At a sampling time of 18.1 weeks post partum, 14:0 was 29% lower ( $p = 0.0002$ ) than for sampling at a gestation of 12.5 weeks. An increase in the absolute amount was only observed for 24:0, which was 15% higher ( $p = 0.0009$ ) than at a gestation at sampling of 12.5 weeks.

### Comparison of Summary Fatty Acid Measures During Pregnancy and Post Partum

Table 4 shows the summary measures during pregnancy and the post partum period. During pregnancy, the *n*6/*n*3

**Table 3** Mean (SD) erythrocyte fatty acid concentration (pmol/mL blood) in each trimester of pregnancy and four months post partum

Fatty acid (pmol/mL)	SG 12.5 weeks (n = 46)	SG 26.1 weeks (n = 47)	SG 35.5 weeks (n = 47)	<i>p</i> *	18.1 weeks post partum (n = 38)	<i>p</i> ** SG 12.5 versus 18.1 weeks post partum
<b>SAFA</b>						
12:0	0.0 (0.0)	0.8 (3.1)	0.7 (2.9)	0.81	2.0 (6.6)	0.048
14:0	16.8 (7.4)	17.6 (8.6)	19.1 (9.1)	0.64	12.0 (6.4)	0.0002
16:0	541.7 (90.5)	552.9 (94.2)	599.0 (114.1)	0.016	507.5 (77.7)	0.070
17:0	8.2 (4.5)	7.3 (5.4)	8.6 (5.8)	0.39	9.5 (5.0)	0.93
18:0	353.1 (69.0)	334.3 (58.8)	351.7 (63.0)	0.28	344.8 (53.7)	0.55
20:0	14.6 (3.5)	14.5 (4.5)	13.9 (3.7)	0.61	14.5 (4.3)	0.75
22:0	32.2 (9.5)	29.7 (8.0)	29.9 (7.8)	0.30	36.7 (7.2)	0.020
24:0	54.6 (10.6)	57.5 (11.0)	61.1 (11.5)	0.020	64.2 (14.9)	0.0009
<b>MUFA</b>						
14:1 <i>n</i> 7	0.1 (1.0)	0.7 (3.3)	0.4 (1.8)	0.55	0.8 (2.8)	0.17
16:1 <i>n</i> 7	21.3 (5.8)	25.5 (7.6)	27.2 (8.4)	0.0005	18.2 (8.3)	0.047
17:1 <i>n</i> 7	1.0 (2.8)	1.0 (2.8)	1.8 (3.7)	0.48	3.3 (5.4)	0.015
18:1 <i>n</i> 9	329.2 (78.3)	339.1 (72.1)	365.0 (80.5)	0.072	294.3 (47.1)	0.018
20:1 <i>n</i> 9	12.3 (3.4)	13.4 (4.8)	12.5 (3.5)	0.58	11.3 (4.8)	0.087
22:1 <i>n</i> 9	3.5 (4.7)	2.7 (4.3)	3.4 (4.6)	0.63	4.5 (4.9)	0.58
24:1 <i>n</i> 9	85.0 (15.7)	89.7 (20.0)	98.0 (19.0)	0.0032	80.6 (16.6)	0.22
<b>PUFA <i>n</i>6</b>						
18:2 <i>n</i> 6	196.2 (42.2)	206.6 (49.6)	219.7 (42.4)	0.041	222.6 (41.9)	0.0054
18:3 <i>n</i> 6	3.7 (3.8)	2.6 (3.3)	2.7 (3.7)	0.30	1.9 (3.8)	0.038
20:2 <i>n</i> 6	8.0 (3.4)	8.6 (4.5)	8.9 (4.1)	0.54	6.3 (5.3)	0.072
20:3 <i>n</i> 6	37.9 (9.5)	43.0 (13.1)	44.1 (10.9)	0.020	41.3 (11.1)	0.13
20:4 <i>n</i> 6	291.1 (81.4)	272.1 (65.5)	290.9 (53.8)	0.30	326.4 (57.2)	0.027
22:2 <i>n</i> 6	0.9 (2.9)	0.2 (1.4)	0.2 (1.0)	0.54	0.8 (2.5)	0.23
22:4 <i>n</i> 6	52.5 (17.9)	52.2 (16.5)	58.5 (15.7)	0.12	60.2 (12.7)	0.028
22:5 <i>n</i> 6	10.4 (4.3)	13.0 (4.5)	13.9 (3.7)	0.0003	10.8 (4.8)	0.70
<b>PUFA <i>n</i>3</b>						
18:3 <i>n</i> 3	4.4 (3.5)	7.7 (5.0)	7.4 (4.8)	0.0007	5.1 (5.4)	0.44
20:5 <i>n</i> 3	16.8 (9.9)	18.2 (10.1)	16.1 (9.1)	0.61	18.3 (9.0)	0.37
22:3 <i>n</i> 3	7.3 (6.6)	7.4 (5.1)	8.1 (6.7)	0.61	9.8 (5.5)	0.28
22:5 <i>n</i> 3	39.0 (10.6)	39.5 (10.9)	43.4 (8.7)	0.073	43.7 (11.1)	0.048
22:6 <i>n</i> 3	64.0 (19.7)	74.5 (21.0)	80.5 (19.4)	0.0005	54.6 (16.0)	0.021

Gestation [mean (SD, range)] at sampling (SG): first trimester 12.5 (1.3, 8–14) weeks, second trimester 26.1 (1.3, 24–28) weeks, third trimester 35.3 (1.3, 33–38) weeks, post partum 18.1 (3.0, 12–26) weeks post delivery

SAFA saturated fatty acids, MUFA monounsaturated fatty acids, PUFA polyunsaturated fatty acids

\*One way analysis of variance for repeated measures, across gestations at sampling of 12.5, 26.1, and 35.3 weeks, with comparisons made for all pairs using Tukey–Kramer HSD.

\*\**t* test, significance level  $p < 0.005$

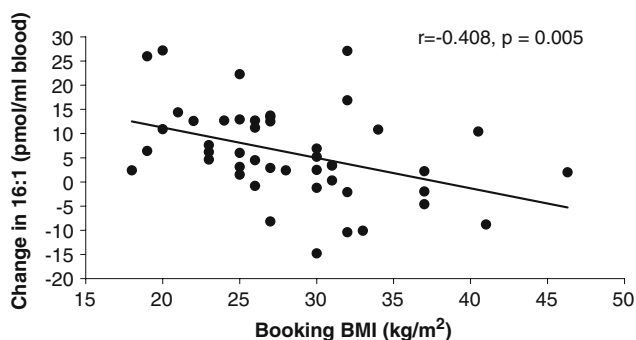


**Fig. 1** Relationship between first trimester BMI and change in 16:1*n*7 concentration (pmol/mL blood) between gestations at sampling of 12.5 and 35.3 weeks (SG 35.3–SG 12.5 weeks)

ratio decreased by 11% ( $p = 0.0019$ ) and the 20:4*n*6/22:6*n*3 ratio decreased by 23% ( $p < 0.0001$ ), but of these two ratios, only the 20:4*n*6/22:6*n*3 ratio increased by 24% in the post partum period ( $p < 0.0001$ ). The percent MUFA of total fatty acids decreased by 8% in the post partum period ( $p < 0.0001$ ), which is reflected in the total *n*9 fatty acids (9%,  $p < 0.0001$ ). Conversely, the percent PUFA of total fatty acids increased by 9% in the post partum period ( $p < 0.0001$ ), which is reflected in an increase in the *n*6 PUFA (11%,  $p < 0.0001$ ). The unsaturated index ( $p = 0.0013$ ), the average chain length ( $p = 0.0006$ ) and the C20–22 ( $p = 0.0005$ ) were all significantly higher in the post partum period.

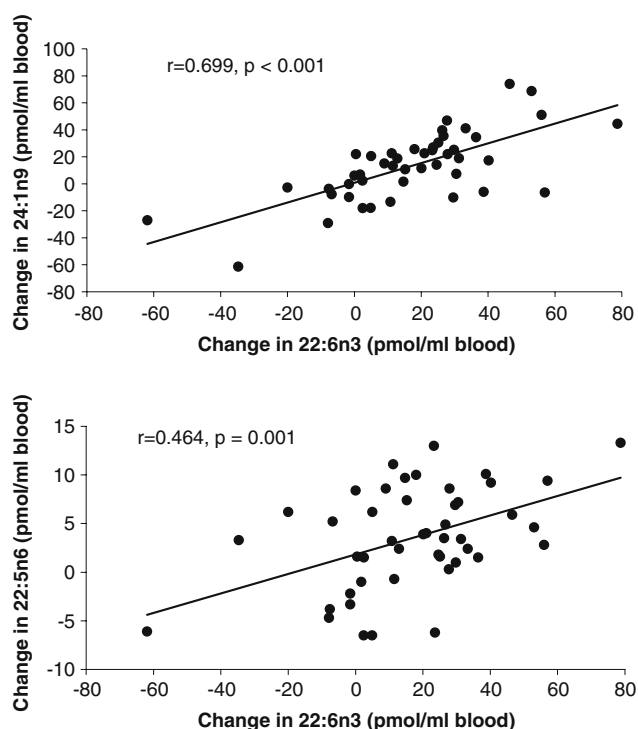


**Fig. 2** Relationship between change in 22:6n3 concentration (pmol/mL blood) and changes in 24:1n9 and 22:5n6 concentration (pmol/mL blood) between gestations at sampling of 12.5 and 35.3 weeks (SG 35.3–SG 12.5 weeks)

## Discussion

This paper clearly describes the changes in fatty acids that occur throughout pregnancy and during the post partum period. Comparison of our selected group with the large cohort of Glasgow women ( $n = 4218$ ) indicates that the women sampled were typical of the general Glasgow population apart from having a higher BMI (Table 1). The fatty acids that increased significantly during pregnancy were 18:3n3, 22:5n6, 22:6n3, 16:1n7 and 24:1n9 (Tables 2, 3). These changes were observed predominately between gestations at sampling of 12.5 and 26.1 weeks. If, as is commonly believed, changes in erythrocyte composition integrate changes in fatty acid metabolism over the preceding 120 days, then these changes must be initiated soon after implantation. However, recent evidence demonstrating a more rapid (two-week) equilibration between at least some fatty acids in plasma and erythrocyte membranes [9] might suggest later initiation of fatty acid mobilization. A combination of increased lipolysis, regulated by human placental lactogen [18], differential elongation and desaturation regulated by oestrogen [19, 20] and differential placental uptake of fatty acids [3, 21] could be potential mechanisms initiating and/or mediating these changes in pregnancy. Further studies of plasma and erythrocyte fatty acid composition in the early weeks of

**Table 4** Summary measures for fatty acids (%)

Fatty acids	SG 12.5 weeks ( $n = 46$ )	SG 26.1 weeks ( $n = 47$ )	SG 35.3 weeks ( $n = 47$ )	$p^*$	18.1 weeks post partum ( $n = 38$ )	$p^{**}$ SG 12.5 versus 18.1 weeks post partum
Saturated (%)	46.6 (3.7)	45.6 (3.0)	45.4 (2.4)	0.16	44.9 (1.1)	0.0077
Unsaturated (%)	53.4 (3.7)	54.4 (3.0)	54.6 (2.4)	0.16	55.1 (1.1)	0.0077
MUFA (%)	20.5 (1.7)	21.2 (1.8)	21.2 (1.7)	0.07	18.9 (1.1)	<0.0001
PUFA (%)	33.0 (4.3)	33.2 (3.9)	33.4 (2.5)	0.85	36.2 (1.4)	<0.0001
Total $n-9$	19.5 (1.6)	19.9 (1.7)	20.0 (1.5)	0.21	17.8 (1.0)	<0.0001
Total $n-7$	1.03 (0.29)	1.22 (0.38)	1.21 (0.32)	0.0062	1.03 (0.54)	0.63
Total $n-6$	27.0 (3.7)	26.7 (3.0)	26.9 (2.1)	0.82	30.3 (1.3)	<0.0001
Total $n-3$	6.0 (1.2)	6.6 (1.3)	6.6 (0.9)	0.0127	6.0 (0.9)	0.70
$n6/n3$ ratio	4.7 (1.0)	4.2 (0.8)	4.2 (0.6)	0.0019	5.2 (0.9)	0.0212
Unsaturated index	147.7 (16.8)	148.7 (16.4)	149.3 (10.8)	0.86	157.0 (5.5)	0.0013
Average chain length	18.6 (0.2)	18.6 (0.2)	18.6 (0.2)	0.86	18.7 (0.1)	0.0006
C20–22	29.31 (4.2)	28.9 (4.5)	28.9 (3.2)	0.96	31.7 (1.9)	0.0005
20:4n6/22:6n3	4.4 (1.4)	3.6 (1.0)	3.4 (0.7)	<0.0001	5.8 (1.4)	<0.0001

Gestation [mean (SD, range)] at sampling (SG): first trimester 12.5 (1.3, 8–14) weeks, second trimester 26.1 (1.3, 24–28) weeks; third trimester 35.3 (1.3, 33–38) weeks, post partum 18.1 (3.0, 12–26) weeks post delivery

SAFA saturated fatty acids, MUFA monounsaturated fatty acids, PUFA polyunsaturated fatty acids

\*One way analysis of variance for repeated measures, across gestations at sampling of 12.5, 26.1 and 35.3 weeks, with comparison made for all pairs using Tukey–Kramer HSD. \*\* $t$  test significance level  $p < 0.005$

pregnancy are required to clarify the timing of fatty acid mobilization.

The limitations of this study include the lack of maternal dietary intake data, maternal weight gain data and breastfeeding information. These data are recognized as potential confounding variables that could not have been adjusted for in our analysis. However, despite the lack of data, our results relating to a drop in 22:6n3 levels during the post partum period are in agreement with others outlined in a review by Makrides and Gibson [22].

Our data on changes in 22:6n3 are broadly consistent with previous observations that 22:6n3 is mobilised from maternal stores in order to supply the growing fetus [5–7]. However, we did not observe a decline in 22:6n3 levels between gestations at sampling of 26.1 and 35.3 weeks, which may indicate that our pregnant population is not deficient in 22:6n3 as has been suggested for other populations [4, 8]. This would be supported by the significant decline in the n6/n3 ratio during pregnancy, indicating an enrichment of maternal erythrocyte LC n3 PUFA. An increased ratio of 22:5n6/22:6n3 has been reported to reflect an omega-3 or 22:6n3 deficiency [23]. The calculated mol/mol 22:5n6/22:6n3 ratios in our population (gestation at sampling 12.5 weeks 0.16, 26.1 weeks 0.17, 35.3 weeks 0.17, and sampling at 18.1 weeks post partum 0.20 mol/mol) were normal according to the cut-off values of >0.22 mol/mol for 22:6n3 marginality and >0.48 mol/mol for 22:6n3 deficiency suggested by Fokkema et al. [23]. An increase in fish consumption during pregnancy by our subjects could account for the maintenance of 22:6n3 levels in maternal blood, but we have no information on diet to confirm or refute this.

The 41% ( $p = 0.0007$ ) increase in maternal erythrocyte 18:3n3 during pregnancy that we observed could be due to its role as a precursor for 22:6n3 synthesis. This large increase in 18:3n3 during pregnancy was either reported but not commented on [4, 6, 12] because the focus of the research involved was on LCPUFA, or it was not detected [7] or reported [5]. 18:3n3 can be derived from green vegetables or cooking oils such as canola oil in the diet. In the absence of detailed dietary information, changes in intake cannot be discounted as an explanation for increased 18:3n3 concentrations. An alternative explanation might be increased mobilisation of 18:3n3 from maternal stores in order to provide substrate for LC n3 PUFA synthesis. Women tend to partition less 18:3n3 to  $\beta$ -oxidation than men [19], thus increasing availability for conversion to LCPUFA. 18:3n3 can be elongated and desaturated to 20:5n3, 22:5n3 and 22:6n3 in women of childbearing age [20], but only to 20:5n3 and 22:5n3 in men [24]. Women taking synthetic oestrogens had an increased capacity to convert 18:3n3 to 22:6n3 [20]. This gender difference underlines the potential importance of the capacity to

synthesise 22:6n3 during pregnancy and lactation, and it is possible that the rise in oestrogen during pregnancy regulates the conversion of 18:3n3 to LCPUFA [19]. The physiological relevance of the conversion from 18:3n3 can be questioned, as 18:3n3 supplementation during pregnancy did not result in increased maternal or fetal DHA levels [25].

Nervonic acid (24:1n9) was also increased during pregnancy (Table 3), and it is well documented that 24:1n9 is important for neural development, particularly for myelination [26, 27]. The increased levels of 24:1n9 could be explained by an increased mobilization of this fatty acid for fetal neural development from mid-gestation and particularly during the post partum period [26]. 22:6n3 is also important for proper neural development (reviewed in [28, 29]) and is also increased during pregnancy (Table 3). The strong correlation between 22:6n3 and 24:1n9 ( $r = 0.70$ ,  $p < 0.001$ ) (Fig. 2) suggests that the regulation of the synthesis and/or transport of these two fatty acids may be coordinated. Interestingly, the change in concentrations of these fatty acids during pregnancy was correlated to placental weight.

Palmitoleic acid 16:1n7 was also increased during pregnancy and is reduced during the post partum period (Table 3). The change in 16:1n7 during pregnancy was negatively associated with first trimester BMI and waist circumference (Fig. 1), indicating a relationship between levels of this fatty acid and central obesity. This relationship may be apparent in our study due to the wide range of first trimester BMI (18.0–46.3 kg/m<sup>2</sup>, Fig. 1). 16:1n7 is synthesised from 16:0 by stearyl CoA desaturase (SCD) [30], an enzyme whose expression is downregulated by leptin [31] and whose activity is associated with obesity [32, 33]. Our observation in pregnancy of an inverse association between the product of SCD and obesity is at odds with these published data. This discrepancy could be explained if 16:1n7 were not a good index of SCD activity in pregnancy or if leptin metabolism were different in pregnancy. There is a well-recognised increase in maternal leptin in pregnancy [34, 35], which is even higher in obese pregnant women [36]. It has been suggested that maternal leptin resistance may occur in pregnancy [34, 37], possibly mediated by an increase in the amount of a soluble isoform of the leptin receptor derived from the placenta, resulting in an increased proportion of bound, and hence unavailable, leptin in the maternal circulation with advancing gestation [37, 38]. This potential for leptin resistance in pregnancy may account for the counterintuitive inverse association between 16:1n7 and obesity in pregnancy observed using the two independent measures of BMI and waist circumference. It has recently been observed that the expression of genes involved in hepatic lipogenesis, such as SCD and PPAR $\gamma$ , is increased by fenofibrate, a PPAR $\alpha$  agonist, in

virgin but not pregnant female rats [39]. Thus our observation of altered regulation of SCD in pregnancy is not unique. The association between fatty acid metabolism in pregnancy and obesity warrants further investigation, especially in light of the increased first trimester BMI observed over the last decade in our hospital [40].

**Acknowledgments** The fatty acid analysis conducted by Ann Brown and Liz Grigonis-Deane is gratefully acknowledged. We would like to acknowledge the following support: SCPMDE Clinical Research Fellowship (Vanessa Rodie), Chief Scientist's Office CZG/1/74, The Carnegie Trust, Lister Bellahouston Travelling Fellowship, Heart UK Sue McCarthy Travelling Fellowship, British Medical Association Obesity Research Award, and the University of Wollongong Australia for a study leave assistance grant.

## References

1. Uauy R, Mena P, Rojas C (2000) Essential fatty acids in early life: structural and functional role. *Proc Nutr Soc* 59(1):3–15
2. Sattar N, Berry C, Greer IA (1998) Essential fatty acids in relation to pregnancy complications and fetal development. *Br J Obstet Gynaecol* 105(12):1248–1255
3. Haggarty P (2002) Placental regulation of fatty acid delivery and its effect on fetal growth—a review. *Placenta* 23(Suppl A):S28–S38
4. van Houwelingen AC, Sorensen JD, Hornstra G, Simonis MM, Boris J, Olsen SF, et al. (1995) Essential fatty acid status in neonates after fish-oil supplementation during late pregnancy. *Br J Nutr* 74(5):723–731
5. Al MD, van Houwelingen AC, Kester AD, Hasaart TH, de Jong AE, Hornstra G (1995) Maternal essential fatty acid patterns during normal pregnancy and their relationship to the neonatal essential fatty acid status. *Br J Nutr* 74(1):55–68
6. Otto SJ, Houwelingen AC, Antal M, Manninen A, Godfrey K, Lopez-Jaramillo P, et al. (1997) Maternal and neonatal essential fatty acid status in phospholipids: an international comparative study. *Eur J Clin Nutr* 51(4):232–242
7. Montgomery C, Speake BK, Cameron A, Sattar N, Weaver LT (2003) Maternal docosahexaenoic acid supplementation and fetal accretion. *Br J Nutr* 90(1):135–145
8. Hornstra G, Al MD, van Houwelingen AC, Foreman-van Drongelen MM (1995) Essential fatty acids in pregnancy and early human development. *Eur J Obstet Gynecol Reprod Biol* 61(1):57–62
9. Skeaff CM, Hodson L, McKenzie JE (2006) Dietary-induced changes in fatty acid composition of human plasma, platelet, and erythrocyte lipids follow a similar time course. *J Nutr* 136(3):565–569
10. Ghebremeskel K, Min Y, Crawford MA, Nam JH, Kim A, Koo JN, et al. (2000) Blood fatty acid composition of pregnant and nonpregnant Korean women: red cells may act as a reservoir of arachidonic acid and docosahexaenoic acid for utilization by the developing fetus. *Lipids* 35(5):567–574
11. Ashby AM, Robinette B, Kay HH (1997) Plasma and erythrocyte profiles of nonesterified polyunsaturated fatty acids during normal pregnancy and labor. *Am J Perinatol* 14(10):623–629
12. Stark KD, Beblo S, Murthy M, Buda-Abela M, Janisse J, Rockett H, et al. (2005) Comparison of bloodstream fatty acid composition from African-American women at gestation, delivery, and postpartum. *J Lipid Res* 46(3):516–525
13. Carstairs V, Morris R (1989) Deprivation and mortality: an alternative to social class? *Community Med* 11(3):210–219
14. Altman DG, Coles EC (1980) Nomograms for precise determination of birth weight for dates. *Br J Obstet Gynaecol* 87(2):81–86
15. Folch J, Lees M, Sloane Stanley GH (1957) A simple method for the isolation and purification of total lipides from animal tissues. *J Biol Chem* 226(1):497–509
16. Hoving EB, Jansen G, Volmer M, Van Doormaal JJ, Muskiet FA (1988) Profiling of plasma cholesterol ester and triglyceride fatty acids as their methyl esters by capillary gas chromatography, preceded by a rapid aminopropyl-silica column chromatographic separation of lipid classes. *J Chromatogr* 434(2):395–409
17. Clark P, Sattar N, Walker ID, Greer IA (2001) The Glasgow outcome, APCR and lipid (GOAL) pregnancy study: significance of pregnancy associated activated protein C resistance. *Thromb Haemost* 85(1):30–35
18. Williams C, Coltart TM (1978) Adipose tissue metabolism in pregnancy: the lipolytic effect of human placental lactogen. *Br J Obstet Gynaecol* 85(1):43–46
19. Burdge G (2004) Alpha-linolenic acid metabolism in men and women: nutritional and biological implications. *Curr Opin Clin Nutr Metab Care* 7(2):137–144
20. Burdge GC, Wootton SA (2002) Conversion of alpha-linolenic acid to eicosapentaenoic, docosapentaenoic and docosahexaenoic acids in young women. *Br J Nutr* 88(4):411–420
21. Haggarty P (2004) Effect of placental function on fatty acid requirements during pregnancy. *Eur J Clin Nutr* 58(12):1559–1570
22. Makrides M, Gibson RA (2000) Long-chain polyunsaturated fatty acid requirements during pregnancy and lactation. *Am J Clin Nutr* 71(1 Suppl):307S–311S
23. Fokkema MR, Smit EN, Martini IA, Woltil HA, Boersma ER, Muskiet FA (2002) Assessment of essential fatty acid and omega-3-fatty acid status by measurement of erythrocyte 20:3omega9 (mead acid), 22:5omega6/20:4omega6 and 22:5omega6/22:6omega3. *Prostaglandins Leukot Essent Fatty Acids* 67(5):345–356
24. Burdge GC, Jones AE, Wootton SA (2002) Eicosapentaenoic and docosapentaenoic acids are the principal products of alpha-linolenic acid metabolism in young men. *Br J Nutr* 88(4):355–363
25. de Groot RH, Hornstra G, van Houwelingen AC, Roumen F (2004) Effect of alpha-linolenic acid supplementation during pregnancy on maternal and neonatal polyunsaturated fatty acid status and pregnancy outcome. *Am J Clin Nutr* 79(2):251–260
26. Martinez M, Mogan I (1998) Fatty acid composition of human brain phospholipids during normal development. *J Neurochem* 71(6):2528–2533
27. Sargent JR, Coupland K, Wilson R (1994) Nervonic acid and demyelinating disease. *Med Hypotheses* 42(4):237–242
28. Uauy R, Hoffman DR, Peirano P, Birch DG, Birch EE (2001) Essential fatty acids in visual and brain development. *Lipids* 36(9):885–895
29. Innis SM (2005) Essential fatty acid transfer and fetal development. *Placenta* 26(Suppl A):S70–S75
30. Dobrzyn A, Ntambi JM (2005) The role of stearoyl-CoA desaturase in the control of metabolism. *Prostaglandins Leukot Essent Fatty Acids* 73(1):35–41
31. Cohen P, Friedman JM (2004) Leptin and the control of metabolism: role for stearoyl-CoA desaturase-1 (SCD-1). *J Nutr* 134(9):2455S–2463S
32. Okada T, Furuhashi N, Kuromori Y, Miyashita M, Iwata F, Harada K (2005) Plasma palmitoleic acid content and obesity in children. *Am J Clin Nutr* 82(4):747–750
33. Dobrzyn A, Ntambi JM (2005) Stearoyl-CoA desaturase as a new drug target for obesity treatment. *Obes Rev* 6(2):169–174
34. Sattar N, Greer IA, Pirwani I, Gibson J, Wallace AM (1998) Leptin levels in pregnancy: marker for fat accumulation and mobilization? *Acta Obstet Gynecol Scand* 77(3):278–283



35. Highman TJ, Friedman JE, Huston LP, Wong WW, Catalano PM (1998) Longitudinal changes in maternal serum leptin concentrations, body composition, and resting metabolic rate in pregnancy. *Am J Obstet Gynecol* 178(5):1010–1015
36. Ramsay JE, Ferrell WR, Crawford L, Wallace AM, Greer IA, Sattar N (2002) Maternal obesity is associated with dysregulation of metabolic, vascular, and inflammatory pathways. *J Clin Endocrinol Metab* 87(9):4231–4237
37. Henson MC, Castracane VD (2006) Leptin in pregnancy: an update. *Biol Reprod* 74(2):218–229
38. Edwards DE, Bohm RP, Purcell J Jr, Ratterree MS, Swan KF, Castracane VD, et al. (2004) Two isoforms of the leptin receptor are enhanced in pregnancy-specific tissues and soluble leptin receptor is enhanced in maternal serum with advancing gestation in the baboon. *Biol Reprod* 71(5):1746–1752
39. Soria A, Gonzalez MC, Vidal H, Herrera E, Bocos C (2005) Triglyceridemia and peroxisome proliferator-activated receptor-alpha expression are not connected in fenofibrate-treated pregnant rats. *Mol Cell Biochem* 273(1–2):97–107
40. Kanagalingam MG, Forouhi NG, Greer IA, Sattar N (2005) Changes in booking body mass index over a decade: retrospective analysis from a Glasgow maternity hospital. *Br J Obstet Gynaecol* 112(10):1431–1433

## n-3 Polyunsaturated Fatty Acids and Atopy in Korean Preschoolers

Inkyung Hwang · Aeri Cha · Hyosun Lee ·  
Hyejung Yoon · Taeho Yoon · Byungmann Cho ·  
Suill Lee · Yongsoon Park

Received: 26 August 2006 / Accepted: 5 February 2007 / Published online: 20 March 2007  
© AOCS 2007

**Abstract** Atopy is a growing problem for Korean children. Since eicosapentaenoic acid is a precursor of less active inflammatory eicosanoids, n-3 polyunsaturated fatty acids (PUFA) may have a protective effect on atopy. This study was undertaken to determine whether n-3 PUFA in red blood cells (RBC) is lower in atopic than in non-atopic preschoolers. Three hundred and eight Korean children aged 4–6 years were enrolled. Total RBC fatty acid composition was measured by gas chromatography. The prevalence of atopic dermatitis, allergic rhinitis, or asthma was 29%. Total RBC n-3 PUFA were lower in preschoolers with atopy than controls ( $9.8 \pm 1.2$  vs.  $11.4 \pm 1.6\%$ ;  $P < 0.05$ ), while n-6 PUFA ( $33.0 \pm 1.4$  vs.  $32.2 \pm 1.0\%$ ;  $P < 0.05$ ) and n-6/n-3 PUFA ratio ( $3.4 \pm 0.6$  vs.  $2.8 \pm 0.5$ ;  $P < 0.05$ ) were greater. The following factors were also associated with an increase in atopy: higher saturated fatty acids ( $39.6 \pm 1.4$  vs.  $40.6 \pm 1.9$ ;  $P < 0.05$ ) and arachidonic acid ( $15.3 \pm 1.6$  vs.  $16.0 \pm 2.9$ ;  $P < 0.05$ ), and lower total PUFA ( $43.8 \pm 0.7$  vs.  $42.8 \pm 1.4$ ;  $P < 0.05$ ) and omega-3

index (EPA + DHA;  $9.1 \pm 0.8$  vs.  $7.8 \pm 0.5$ ;  $P < 0.05$ ) in RBC. Maternal history of atopy was a significant ( $P < 0.05$ ) risk factor, while lactation was not. The results suggest that a reduced content of n-3 PUFA in the RBC membrane could play a role in early children atopy.

**Keywords** Atopy · Children · Docosahexaenoic acid · Eicosapentaenoic acid · n-3 fatty acids

### Introduction

In keeping with the rising incidence of allergies worldwide [1], incidences of atopic diseases have been increasing for the last few decades, Korea included. Genetic factors such as family history and maternal age at birth have been proposed as the important risk factors for atopy [2, 3]. A number of environmental factors, including air pollution [2], cigarette smoking of parents, dust mites [2], formula feeding [4, 5], and diet [2, 6, 7] have been suggested as factors in the increasing prevalence of atopic dermatitis, allergic rhinitis, and asthma.

Many foods have been implicated in food allergies, and fish is a common food allergen causing atopy [8]. Some studies have reported that a decrease in the intake of n-3 PUFA, and an increase in the intake of n-6 PUFA, particularly linoleic acid may lead to an increase in atopic diseases [6, 9–14]. Linoleic acid is a precursor of arachidonic acid, which can be converted to prostaglandin E<sub>2</sub> (PGE<sub>2</sub>), whereas n-3 PUFA, eicosapentaenoic acid (EPA; C20:5) and docosahexaenoic acid (DHA; C22:6) inhibits the formation of PGE<sub>2</sub> [15, 16].

Kankaanpaa et al. [7] observed that atopic infants had less n-3 PUFA in serum cholesteryl esters, but not trigly-

I. Hwang · H. Lee · H. Yoon · T. Yoon · B. Cho ·  
S. Lee

Department of Preventive and Occupational Medicine,  
College of Medicine, Pusan National University,  
Pusan, South Korea

A. Cha  
Health Promotion Center,  
Samsung Heavy Industries H.S.E Medical Clinic,  
Geo-je, Kyung Nam, South Korea

Y. Park (✉)  
Department of Food and Nutrition,  
College of Human Ecology, Hanyang University,  
17 Haengdang-dong, Seongdong-gu,  
Seoul 133-791, South Korea  
e-mail: yongsoon@hanyang.ac.kr

cerides (TG) and phospholipids. Dunder et al. [17] and Yu et al. [18] also reported that serum n-3 PUFA was significantly lower in atopic children. Mihrshahi et al. [9] showed that supplementation with n-3 PUFA reduced the prevalence of wheezing in high risk children. However, other studies that failed to show an association between n-3 PUFA and asthma [19–21].

Most research on atopic diseases has been focused on maternal diet [7, 22–24] and breast milk fatty acid composition [25, 26] among infant or young children. In addition, there is limited information on the relationship between RBC n-3 PUFA of preschool aged children and atopy especially among Koreans. The omega-3 index is a new blood test that measure EPA and DHA content in RBC and provide a good reflection of systemic n-3 PUFA levels [27]. The purpose of this study was to measure RBC fatty acid composition and plasma lipid profiles for Korean children aged 4–6 with and without atopy.

## Experimental Procedures

### Subjects

A total of 497 children aged 4–6 years in one district hospital of Pusan, on the Southern tip of the Korean Peninsula, were recruited. Blood samples were taken to determine the fatty acid composition of RBC from only 398 children. This study was approved by Pusan National University Hospital Institutional Review Board, and informed, written consent was obtained from the parents of all participants.

### Protocol

Height, weight, and body fat were measured, and fasting blood samples were obtained after fasting for 8 h. Family history, age of parents at birth of the child, length of lactation, and allergy symptoms were obtained from both questionnaires completed by parents of the child and from medical charts. The children's fish intake was assessed by parental response to "how often does your child eat non-fried fish?" in a questionnaire with "never", "once a week or less", and "more than once a week" as possible answers.

### Procedure

Blood was centrifuged for 15 min at 3,000 rpm and after removing plasma, the RBC pellet was left in the bottom of the tube and used for fatty acid analysis. Plasma was analyzed for total cholesterol, TG and high-density lipoprotein (HDL) cholesterol concentrations using a

dry-chemistry method with Vitros 250 (Johnson and Johnson, USA); very-low density lipoprotein (VLDL) and low-density lipoprotein (LDL) cholesterol concentrations were estimated by the Friedewald equation [28].

Red blood cell lipids were isolated using 0.005% butylated hydroxytoluene containing isopropanol and hexane. Fatty acid methyl esters were made from RBC membrane by heating the lipid extract with boron trifluoride (BF<sub>3</sub>) methanol-benzene and analyzed with a 30-m SP2330 capillary column (Supelco, Bellefonte, PA; 33). Fatty acids were identified by comparison with known standards. Samples were analyzed in duplicate, and with each run, a quality control sample was included. The control was made from pooled RBC and the CV was 5%.

### Statistical Analysis

Independent *t*-test was used to compare lipid profile, RBC fatty acid composition, lactating period, family history, and age of parents at birth of the child between children with and without atopy. A two-tailed *P* value of <0.05 was required for statistical significance.

## Results

### General Characteristics and Atopic Disease Distribution of Subjects

Twenty-nine percent of the children were diagnosed with one of following atopic diseases: atopic dermatitis, allergic rhinitis, and asthma. Table 1 shows the prevalence of each atopic disease, and atopic dermatitis was the most common. Although, there was no statistical difference, more female children than male had atopic diseases (53.3 vs. 46.7%), and prevalence of atopic diseases decreased with age (Table 2). Height, weight, and body fat did not significantly differ between children with and without atopic disease (Table 2).

### Length of Lactation

Length of lactation was divided into <1 month (44 vs. 41%), 1–6 months (31 vs. 31%), and >6 months (25 vs. 28%). There was no significant relationship between length of lactation and atopic diseases within and between groups.

### Family History and Age of Parents at Birth

Table 2 shows the relationship between family history and atopic diseases. Maternal history of atopy was significantly (*P* < 0.001) associated with risk for atopy, while paternal and sibling history was not. Mean maternal and paternal

**Table 1** Distribution of atopic disease in subjects

Diseases	<i>n</i> (%)
None	218 (71)
Atopic dermatitis (AD)	65 (21)
Allergic rhinitis (AR)	24 (8)
Asthma (AA)	2 (<1)
AD + AR	7 (2)
AR + AA	1 (<1)
AD + AR + AA	1 (<1)
Total	308 (100)

*n* number of subjects

**Table 2** General characteristics in subjects

<i>n</i> (%)	Control ( <i>n</i> = 218)	Atopy ( <i>n</i> = 90)
Sex ( <i>n</i> , %)		
Male	117 (54)	42 (47)
Female	101 (46)	48 (53)
Age (years)		
4	15 (7)	8 (9)
5	86 (39)	40 (44)
6	117 (54)	42 (47)
Family history <sup>a</sup>		
Paternal	21 (9.6)	15 (41.7)
Mother <sup>a</sup>	12 (5.5)	16 (17.8)
Sibling	20 (9.2)	12 (13.3)
Anthropometric measurement*		
Height (cm)	110.9 ± 5.8	109.7 ± 6.1
Weight (kg)	19.3 ± 3.3	19.0 ± 3.6
Body fat (%)	20.4 ± 6.7	21.5 ± 7.2

*n* number of subjects

<sup>a</sup> *P* < 0.05 by independent *t*-test

\* Values are mean ± SD

age at birth were not significantly different between controls and atopic children.

#### Dietary Fish Intake

Overall, fish intake was not significantly associated with atopy, and 95% of children with and without atopy consume fish, more than a week.

#### Plasma Lipid Profile

There was no significant difference on total cholesterol (3.88 ± 0.60 vs. 3.87 ± 0.56 mmol/L), TG (1.04 ± 0.53 vs. 1.01 ± 0.49 mmol/L), HDL-cholesterol (1.41 ± 0.26 vs. 1.36 ± 0.28 mmol/L), and LDL-cholesterol concentrations

(1.99 ± 0.59 vs. 2.04 ± 0.51 mmol/L) between subjects with and without atopic diseases.

#### Red Blood Cell Fatty Acid Composition

Table 3 shows RBC fatty acid composition of subjects. PUFA was lower, while SFA was higher (*P* < 0.05) in subjects with than without atopic disease. MUFA was relatively low, and it was not significantly different in those with atopic disease and those without. Total n-3 PUFA was significantly higher, whereas total n-6 PUFA was significantly lower in children without atopic disease than those with. In addition, each n-3 PUFA such as EPA, DHA, docosapentaenoic acid (DPA, C22:5) and the omega-3 index (EPA + DHA) were significantly higher in subjects without atopic disease than those with. Stearic acid (C18:0) and arachidonic acid (C20:4) were significantly lower in subjects without atopic disease than those with atopic disease.

#### Discussion

The increased prevalence of atopy has been shown to coincide with the decreased intake of n-3 PUFA and the increased intake of n-6 PUFA [6, 9–14]. However, studies inconsistently show an improvement in asthmatics treated with fish oil [19–21]. Little information is available on the n-3 PUFA status of preschool aged children in relation to atopy.

In this study, we observed that RBC n-3 PUFA were significantly lower in preschoolers with atopy compared to those without, while n-6 PUFA and n-6/n-3 PFA ratios were significantly greater. These findings were consistent with the hypothesis that reduced tissue n-3 PUFA content (which naturally raises the n-6/n-3 PUFA ratio) is an important determinant of early childhood atopic diseases. Studies have suggested that n-3 PUFA affected immune response and expression of atopy by the modulation of the formation of cytokines and eicosanoids [22, 23, 29]. The levels of arachidonic acid, a precursor of PGE<sub>2</sub> were also higher in children with atopy than those without, suggesting an increased capacity for PGE<sub>2</sub> formation [15, 16].

Dunder et al. [17] reported that dietary fish intake was significantly lower in children (3–18 years old) with atopy than those without atopy. Similarly, serum cholesteryl ester DHA was significantly lower in those with atopic dermatitis. In addition, Yu et al. [18] observed that DHA (1.46 ± 0.54 vs. 1.90 ± 0.58%) and total n-3 PUFA (2.34 ± 0.67 vs. 2.80 ± 0.77%) in serum phospholipids were significantly lower in the allergic children aged 12–15 years than in the controls. Kankaanpaa et al. [7] also showed that atopic infants had less n-3 PUFA in serum

**Table 3** Fatty acid composition of red blood cell in subjects\*

%	Control ( <i>n</i> = 218)	Atopy ( <i>n</i> = 90)	Difference (%)
C12:0	0.8 ± 0.2	0.8 ± 0.2	2.5
C14:0	0.3 ± 0.1	0.3 ± 0.1	6.9
C15:0	1.8 ± 0.3	1.8 ± 0.3	2.2
C16:0	22.4 ± 1.2	22.8 ± 1.7	1.6
C17:0	0.3 ± 0.1	0.3 ± 0.1	9.7
C18:0	13.6 ± 0.8 <sup>a</sup>	14.0 ± 1.1	3.1
C16:1(n-7)	0.4 ± 0.1	0.3 ± 0.1	2.9
C18:1(n-9)	14.9 ± 1.3	14.9 ± 1.6	0.2
C24:1(n-9)	1.0 ± 0.3	1.0 ± 0.2	0
C18:2(n-6)	13.6 ± 1.3	13.5 ± 1.4	0.3
C20:2(n-6)	0.3 ± 0.1	0.3 ± 0.1	3.0
C20:4(n-6)	15.3 ± 1.6 <sup>a</sup>	16.0 ± 2.9	4.4
C20:5(n-3)	0.8 ± 0.3 <sup>a</sup>	0.7 ± 0.2	15.5
C22:3(n-3)	0.6 ± 0.3	0.5 ± 0.2	19.6
C22:4(n-6)	3.0 ± 0.6	3.1 ± 0.5	2.3
C22:5(n-3)	1.6 ± 0.3 <sup>a</sup>	1.4 ± 0.4	15.7
C22:6(n-3)	8.3 ± 1.3 <sup>a</sup>	7.1 ± 0.9	16.6
∑SFA	39.6 ± 1.4 <sup>a</sup>	40.6 ± 1.9	2.3
∑MUFA	16.6 ± 1.4	16.6 ± 1.7	0.2
∑PUFA	43.8 ± 0.7 <sup>a</sup>	42.8 ± 1.4	2.1
∑n-6 PUFA	32.2 ± 1.0 <sup>a</sup>	33.0 ± 1.4	2.2
∑n-3 PUFA	11.4 ± 1.6 <sup>a</sup>	9.8 ± 1.2	16.6
Omega-3 index	9.1 ± 0.8 <sup>a</sup>	7.8 ± 0.5	16.6

\* Values are mean ± SD, *n* number of subject, *SFA* saturated fatty acids, *MUFA* monounsaturated fatty acids, *PUFA* polyunsaturated fatty acids; omega-3 index = EPA + DHA

<sup>a</sup> *P* < 0.05 by independent *t*-test

cholesteryl ester (1.37 ± 0.47 vs. 1.63 ± 0.40%), but not in TG and phospholipid fractions. However, Mahrshahi et al. [9] did not find a relationship between plasma n-3 PUFA and atopy in children aged 18 months after n-3 PUFA supplementation. Meta-analysis by Van Gool et al. [24] showed that treatment trials have failed to show consistent improvement of atopic disease. Little information is available on the n-3 PUFA status of young children in relation to atopy. Pusan is a major port famous for its fish market, thus people may have higher fish consumption.

Oliwiecki et al. [30] reported that children with atopy had higher plasma and RBC linoleic acid, SFA, MUFA than the controls. We also observed higher SFA, but linoleic acid and MUFA were not significantly different in the present study.

The prevalence of atopy has been shown to be lower in male children than in female children, and also to decrease with age [31]. However, we could not confirm this. The role of exclusive breast feeding in protecting against asthma is controversial. Businco et al. [32] and Gruskay et al. [33] found that breast feeding decreased the risk of

atopy in high-risk newborns. However, some studies reported that the effect of breast feeding in children diminished several years later [34, 35]. In the present study, breast feeding was not associated with the prevalence of atopy, which may be due to either the age of our children (4–6 years) as previous studies reported, or to short breast-feeding periods of most children (<1 month in 44% of control and 41% of children with atopy).

A family history of atopy is an important risk factor for atopy, and a maternal history of atopy is more important than paternal [36]. We also found that maternal history of atopy was significantly associated with atopy in children.

In summary, the amounts of RBC n-3 PUFA were significantly lower in preschoolers with atopy compared to those without atopy, while the amounts of n-6 PUFA were significantly higher, suggesting that the n-3 PUFA status of the RBC membrane could play a role in atopy in early childhood. Thus, membrane fatty acid disturbances may be an important determinant of early childhood atopic diseases. There is a need for further research into the role of n-3 PUFA supplementation in atopy, particularly for children.

**Acknowledgments** This work was supported by the research fund of Hanyang University (HY-2005-N).

## Reference

1. Thomsen SF, Ulrik CS, Larsen K, Backer V (2004) Change in prevalence of asthma in Danish children and adolescents. *Ann Allergy Asthma Immunol* 92:506–511
2. von Mutius E, Schmid S, the PASTURE Study Group (2006) The PASTURE project: EU support for the improvement of knowledge about risk factors and preventive factors for atopy in Europe. *Allergy* 61:407–413
3. Bohme M, Wickman M, Lennart NS, Svartengren M, Wahlgren CF (2003) Family history and risk of atopic dermatitis in children up to 4 years. *Clin Exp Allergy* 33:1226–1231
4. Gdalevich M, Mimouni D, Mimouni M (2001) Breast feeding and the high risk of bronchial asthma in childhood: a systematic review with meta-analysis of prospective studies. *J Pediatr* 139:261–266
5. Oddy WH, Holt PG, Sly PD, Read AW, Landau LI, Stanley FJ, Kendall GE, Burton PR (1999) Association between breast feeding and asthma in 6-year-old children: findings of prospective birth cohort study. *BMJ* 319:815–819
6. Murray CS, Simpson B, Kerry G, Woodcock A, Custovic A (2006) Dietary intake in sensitized children with recurrent wheeze and healthy controls: a nested case-control study. *Allergy* 61:438–442
7. Kankaanpää P, Nurmela K, Erkkilä A, Kalliomäki M, Holmberg-Marttila D, Salminen S, Isolauri E (2001) Polyunsaturated fatty acids in maternal diet, breast milk, and serum lipid fatty acids of infants in relation to atopy. *Allergy* 56:633–638
8. Zapatero Remon L, Alonso Lebrero E, Martin Fernandez E, Martinez Molero MI (2005) Food protein-induced enterocolitis syndrome caused by fish. *Allergol Immunopathol* 33:312–316
9. Mahrshahi S, Peat JK, Webb K, Oddy W, Marks GB, Mellis CM (2004) CAPS Team. Effect of omega-3 fatty acid concentrations

- in plasma on symptoms of asthma at 18 months of age. *Pediatr Allergy Immunol* 15:517–522
10. KanKaapaa P, Sutas Y, Salminen S, Lichtenstein A, Isolauri E (1999) Dietary fatty acids and allergy. *Ann Med* 31:282–287
  11. Woods RK, Raven JM, Walters EH, Abramson MJ, Thien FC (2004) Fatty acid levels and risk of asthma in young adults. *Thorax* 59:105–110
  12. Duchon K (2001) Are human milk polyunsaturated fatty acids (PUFA) related to atopy in the mother and her child? *Allergy* 56:587–592
  13. Hoppu U, Kalliomaki M, Isolauri E (2005) Maternal diet rich in saturated fat during breast feeding is associated with atopic sensitization of the infant. *Eur J Clin Nutr* 54:702–705
  14. Prescott SL, Calder PC (2004) *N*-3 polyunsaturated fatty acids and allergic disease. *Curr Opin Clin Nutr Metab Care* 7:123–129
  15. Duchon K, Bjorksten B (2001) Polyunsaturated n-3 fatty acids and the development of atopic disease. *Lipids* 36:1033–1042
  16. Sperling RI, Benincaso AI, Knoell CT, Larkin JK, Austen KF, Robinson DR (1993) Dietary omega-3 polyunsaturated fatty acids inhibit phosphoinositide formation and chemotaxis in neutrophils. *J Clin Invest* 91:651–660
  17. Dunder T, Kuikka L, Turtinen J, Rasanen L, Uhari M (2001) Diet, serum fatty acids, and atopic diseases in childhood. *Allergy* 56:425–428
  18. Yu G, Bjorksten B (1998) Polyunsaturated fatty acids in school children in relation to allergy and serum IgE levels. *Pediatr Allergy Immunol* 8:133–138
  19. Thien FCK, Woods RK, Walters EH (1996) Oily fish and asthma: a fishy story? *Med J Aust* 164:135–136
  20. Kirsch CM, Payan DG, Wong MYS, Dohlman JG, Blake VA, Petri MA, Offenberger J, Goetzl EJ, Gold WM (1988) Effect of eicosapentaenoic acid in asthma. *Clin Allergy* 18:177–187
  21. Thien FCK, Mercia-Huerta JM, Lee TH (1993) Dietary fish oil effects on seasonal hay fever and asthma in pollen sensitive subjects. *Am Rev Respir Dis* 147:1138–1143
  22. Dunstan JA, Mori TA, Barden A, Belin LJ, Holt PG, Prescott SL (2003) Maternal fish oil supplementation in pregnancy reduces interleukin-13 levels in cord blood of infants at high risk of atopy. *Clin Exp Allergy* 33:442–448
  23. Dunstan JA, Mori TA, Barden A, Belin LJ, Holt PG, Prescott SL (2003) Fish oil supplementation in pregnancy modifies neonatal allergen-specific immune responses and clinical outcomes in infants at high risk of atopy: a randomized, controlled trial. *J Allergy Clin Immunol* 112:1178–1184
  24. Van Gool CJAW, Zeegers MPA, Thijs C (2004) Oral essential fatty acid supplementation in atopic dermatitis—a meta-analysis of placebo-controlled trials. *British Journal of Dermatology* 150:728–740
  25. Thijs C, Houwelingen A, Poorterman I, Mordant A, van den Brandt P (2000) Essential fatty acids in breast milk of atopic mothers: comparison with non-atopic mothers, and effect of borage oil supplementation. *Eur J Clin Nutr* 54:234–238
  26. Stoney RM, Woods RK, Hosking CS, Hill DJ, Abramson MJ, Thien FC (2004) Maternal breast milk long-chain n-3 fatty acids are associated with increased risk of atopy in breast-fed infants. *Clin Exp Allergy* 34:194–200
  27. Harris WS, Von Schacky C (2004) The omega-3 index: a new risk factor for death from coronary heart disease? *Prev Med* 39:212–20
  28. Fridewald WT, Levy RI, Fedreicson DS (1979) Estimation of concentration of low density lipoprotein cholesterol in plasma without use of the preparative ultracentrifuge. *Clin Chem* 18:499–502
  29. Ferrucci L, Cherubini A, Bandinelli S, Bartali B, Corsi A, Lauretani F, Martin A, Andres-Lacueva C, Senin U, Guralnik JM (2006) Relationship of plasma polyunsaturated fatty acids to circulating inflammatory markers. *J Clin Endocrinol Metab* 91:439–446
  30. Oliwiecki S, Burton JL, Elles K, Horrobin DF (1991) Levels of essential and other fatty acids in plasma and red cell phospholipids from normal controls and patients with atopic eczema. *Acta Derm Venereol* 71:224–228
  31. Mandhane PJ, Greene JM, Cowan JO, Taylor DR, Sears MR (2005) Sex differences in factors associated with childhood- and adolescent-onset wheeze. *Am J Respir Crit Care Med* 172:45–54
  32. Businco L, Marchetti F, Pellegrini G (1983) Perception of atopic disease in “at risk newborns” by prolonged breast-feeding. *Ann Allergy* 51:296–299
  33. Gruskay FI (1982) Comparison of breast, cow and soy feeding in the prevention of onset of allergic disease: a 15-year prospective study. *Clin Pediatric* 21:486–491
  34. Faith-magnusson K, Kjellman NI (1992) Allergy prevention by maternal elimination diet during late pregnancy 5-year follow-up of a randomized study. *J Allergy Clin Immunol* 89:709–713
  35. Zeiger RS, Heiler S (1995) The development and prediction of atopy in high risk children: follow up at age seven years in a prospective randomized study of combined maternal and infant food allergen avoidance. *J Allergy Clin Immunol* 95:1179–1190
  36. Forastiere F, Sunyer J, Farchi S, Corbo G, Pistelli R, Baldacci S, Simoni M, Agabiti N, Perucci CA, Viegi G (2005) Number of offspring and maternal allergy. *Allergy* 60:510–514

# Dynamic Features of the Rumen Metabolism of Linoleic Acid, Linolenic Acid and Linseed Oil Measured in Vitro

Jean-Pierre Jouany · Bernadette Lassalas · Michel Doreau · Frédéric Glasser

Received: 11 September 2006 / Accepted: 19 January 2007 / Published online: 8 March 2007  
© AOCs 2007

**Abstract** The lipid quality of ruminant products is largely determined by the extent of rumen microbial biohydrogenation (BH) of polyunsaturated fatty acids (FAs) and the substances formed thereby. In vitro batch incubations with mixed rumen bacteria were tracked over 24 h to characterize the profiles and kinetics of the BH products from three lipid sources: pure linoleic acid (*c*9,*c*12–18:2), pure linolenic acid (*c*9,*c*12,*c*15–18:3) and linseed oil (mainly *c*9,*c*12,*c*15–18:3 in triacylglycerols). After 24 h of incubation biohydrogenation was more complete for *c*9,*c*12–18:2, which gave mainly stearic acid (18:0), than for *c*9,*c*12,*c*15–18:3, which yielded mainly *trans*-18:1 FAs. This suggests inhibition of the final BH step (18:1 to 18:0). Incubations of *c*9,*c*12–18:2 resulted in high levels of carbon 10- and 12-desaturated 18:1, *t*10,*c*12- and *c*9,*t*11-CLAs. Incubations of *c*9,*c*12,*c*15–18:3 resulted in high levels of *t*11–18:1, carbon 13- and 15-desaturated 18:1 as well as *t*11,*c*15–18:2 and 11,13-CLAs. A comparative study of linolenic acid and linseed oil kinetics revealed that the BH process was not significantly slowed by the esterification of polyunsaturated FAs, but may have been limited by the isomerization step in which the *cis*12 double bond goes to the *trans*11 position. The disappearance rates of *c*9,*c*12–18:2 and *c*9,*c*12,*c*15–18:3 ranged from 23.6 to 44.6%/h. The wide variety of BH intermediates found here underlines the large number of possible BH pathways. These data help provide a basis for dynamic approaches to BH processes.

**Keywords** Rumen · Biohydrogenation · Polyunsaturated fatty acids · Linoleic acid · Linolenic acid · Linseed oil

## Abbreviations

BH Biohydrogenation  
LA Linoleic acid  
LN Linolenic acid  
LO Linseed oil

## Introduction

In the anaerobic rumen microbial ecosystem, unsaturated fatty acids (FAs) can be used as electron sinks. The metabolites resulting from biohydrogenation (BH) are therefore specific to ruminants. Ruminant products such as milk and meat are thus richer in saturated FAs than products from monogastric animals [1]. The rumen microbial ecosystems also yields a range of BH intermediates such as monounsaturated *trans* FAs and conjugated linoleic acids (CLAs) that are transferred into ruminant products. These intermediates have varied nutritional properties. The ruminal BH of dietary 18-carbon unsaturated FA sources is a sequential process, beginning with lipolysis and followed by isomerization and hydrogenation of the double bonds, finally yielding saturated stearic acid (C18:0) together with a wide variety of monounsaturated, dienoic or trienoic intermediates with either a *cis* or *trans* stereoisomeric positioning of the double bonds. Rumen metabolism of linoleic acid (*c*9,*c*12–18:2) starts with a shift in the double bond position from carbon 12 to carbon 11, and then transisomerization to yield the CLA *c*9,*t*11–18:2, which is then reduced to vaccenic acid (*t*11–18:1) and finally to C18:0 [2, 3]. Similarly, BH of  $\alpha$ -linolenic acid (*c*9,*c*12,*c*15–18:3) yields the conjugated triene *c*9,*t*11,*c*15–18:3,

J.-P. Jouany (✉) · B. Lassalas · M. Doreau · F. Glasser  
INRA, UR1213 Herbivores, Site de Theix,  
63122 Saint-Genès-Champanelle, France  
e-mail: jouany@clermont.inra.fr

which is then sequentially hydrogenated into *t*11,*c*15–18:2, *t*11–18:1 and C18:0 [4]. These are the main known pathways for linoleic and  $\alpha$ -linolenic acids, but biohydrogenation, in fact, yields a wide variety of other BH intermediates, in particular *cis* and *trans* isomers of C18:1 and C18:2. The yield of BH intermediates depends on the amounts of dietary FAs, but may also depend on whether they are supplied in the free or esterified form. In the case of plant oils (compared with free FAs), the additional step of lipolysis may delay the process of microbial BH of polyunsaturated FAs and alter the formation of the various intermediates before saturated C18:0 is reached.

We sought to obtain a detailed description of the products of rumen microbial BH and isomerization of two pure unsaturated free FAs (*c*9,*c*12–18:2 and *c*9,*c*12,*c*15–18:3) in an in vitro batch system with mixed rumen bacteria and protozoa, and to examine the kinetics of these products over a 24 h incubation period. Linseed oil, which contains both *c*9,*c*12–18:2 and *c*9,*c*12,*c*15–18:3 in triacylglycerol form, was also monitored under similar conditions. In linseed oil, the amounts of unsaturated FAs and the preliminary lipolysis step were both different compared with the incubations of free FAs, and may modify the type and/or amount of BH intermediates and products. The rate of FA addition chosen (about 3% of substrate DM) was designed to mimic real animal feeding conditions.

## Materials and Methods

### In Vitro Batch Culture System

Each batch incubator was a 120 mL serum bottle closed by a crimped butyl septum containing rumen juice mixed with a buffer solution, substrates, and with or without supplementation with a FA source. Two sheep fitted with rumen cannulae were used as ruminal fluid donors. They were fed 1,200 g per day of a mixed diet composed of meadow hay (45%) and barley grain (55%) given in two equal meals at 9 AM and 4 PM. Rumen content was sampled through the cannula before the morning meal and then filtered on a metal grid (2 mm mesh size) in a low-oxygen environment to obtain rumen fluid. First, 15 mL of the filtrate was mixed with 25 mL Coleman buffer (Simplex type) [5] at 39 °C and introduced into the incubators, which had been previously filled with pure CO<sub>2</sub>.

Second, 500 mg of a ground substrate made of the same ingredients as the animals' diet was introduced into each incubator to feed the microbes. It consisted of a mixture of meadow hay and barley (45:55), with the following composition on a DM basis: organic matter 88.1%, crude protein 15.0%, NDF 43.0% and ADF 22.0%. This substrate supplied 1.15 mg *c*9,*c*12–18:2 and 0.23 mg *c*9,*c*12,*c*15–18:3

per incubator. Each series of incubations comprised four incubators for each incubation time: three experimental incubators supplemented with either pure *c*9,*c*12–18:2 (LA), pure *c*9,*c*12,*c*15–18:3 (LN) or linseed oil (LO), and one non-supplemented incubator used as control. About 13 mg of pure *c*9,*c*12–18:2 (99% pure; Biovalley, Marne-La-Vallée, France) was introduced into the LA incubators, 14 mg of pure *c*9,*c*12,*c*15–18:3 (99% pure; Biovalley, Marne La Vallée, France) into the LN incubators, and 13 mg of linseed oil obtained by cold pressing (Vandeputte, 7700 Mouscron, Belgium) into the LO incubators. The linseed oil contained 60.9% of *c*9,*c*12,*c*15–18:3, 15.0% of *c*9,*c*12–18:2, 15.0% of *c*9–18:1, 4.7% of 16:0 and 2.8% of 18:0. The filled incubators were gassed with CO<sub>2</sub> to eliminate oxygen and maintain anaerobic condition during fermentation, and were placed in a water bath at 39 °C. Fermentation gases were collected and analyzed every time incubators were removed to check for the absence of oxygen. The medium in each incubator was regularly mixed with a magnetic stirring bar (30 s every 4 min). One control incubator and one incubator from each experimental set (LA, LN and LO) were simultaneously removed after 0, 0.5, 2, 5 and 24 h of incubation. Four series were run on four different days. Samples were taken at the 0.5 h time point in only two of the four series.

### Extraction and Transmethylation of Lipids

These two steps were carried out on the whole content of the incubators immediately after removal from the water bath. Lipids were extracted according to the method described in Folch et al. [6]. As an internal standard, 500  $\mu$ L of pure methyl tricosanoate (400  $\mu$ g/mL in hexane) (Sigma, Saint-Quentin-Fallavier, France) was added to the tubes containing the final solution of lipids. Lipids were then transmethylated at ambient temperature using sodium methanolate followed by BF<sub>3</sub>-methanol according to the method described in Christie et al. [7].

The solutions of methyl esters were bleached through florisil columns and eluted with 10 mL of a mixture of hexane and diethyl ether (95/5 vol/vol). The solvents were evaporated under a gaseous nitrogen flow. The methyl esters were weighed and dissolved in 3 mL of hexane, and kept at –20 °C until analysis.

### Analysis of Methyl Esters

Fatty acid composition was determined by gas-liquid chromatography (GLC). Samples were injected by means of an autosampler into a Varian CP-3800 gas chromatograph equipped with a flame ionization detector. Methyl esters of FAs were separated on a 100 m  $\times$  0.25 mm i.d. CP-Sil 88 fused silica capillary column (Varian, Les Ulis, France). A mixture of 37 pure methyl esters



(Supelco™ 37 Component FAME Mix No. 47885-U, Supelco Inc., Saint-Quentin-Fallavier, France), a CLA isomer standard mixture composed of *c9,t11-*, *t10,c12-*, *c11,t13-*, *c9,c11-* and *t9,t11-18:2* (Matreya Inc., Pleasant Gap, PA), and pure *c9,c12-18:2* and *c9,c12,c15-18:3* (Matreya Inc., Pleasant Gap, PA) were used for peak identification and for quantitative calibration of response factors for individual FAs.

Fatty acid analyses were performed under the following conditions: 0.5–1  $\mu$ L methyl esters in hexane injected at a 50:1 to 90:1 split ratio, with injector temperature maintained at 250 °C and detector temperature set at 255 °C. The initial oven temperature was held at 70 °C for 1 min, then increased at a heating rate of 5 °C/min to 100 °C (held for 2 min), then increased at a heating rate of 10 °C/min to 175 °C (held for 40 min), and finally increased at 5 °C/min to the final temperature of 225 °C (held for 25 min) [8]. Hydrogen was used as the carrier gas. Injector pressure was held constant at 23 psi. Satisfactory separation of most *cis* and *trans* C18:1 and CLA isomers was obtained with a single chromatographic run.

#### Control of O<sub>2</sub> Absence in the Gas Phase of Incubators

Fermentation gases were collected in a syringe [9], and oxygen was quantified by gas-solid chromatography using a 2.3 m  $\times$  2.1 mm i.d. stainless steel column filled with 60/80 mesh Carboxen 1000 (Supelco), a thermal conductivity detector, with argon as the carrier gas.

#### Animal Care

The use of cannulated sheep was approved by the Ethics Committee of the INRA research center. The scientists and technicians involved in the experiment were licensed by the French Ministry of Agriculture to conduct experiments on living animals.

#### Computation and Statistics

Using the individual values measured for each FA at the different sampling times, the mean amounts of FAs over the 24 h incubation period were computed as the area under the curve divided by the total duration of incubation. Positive or negative balances of the different FAs were computed as the difference between the initial content and the incubator content following 24 h of incubation. The number of double bonds in the C18 FAs was computed for each sample based on the amount of each FA in moles and the number of double bonds in each FA molecule. To compare the BH kinetics of the different lipid sources, the quantities of double bonds and substrate FAs (*c9,c12-18:2*

and *c9,c12,c15-18:3*) remaining at the various sampling times were expressed as a proportion of their initial quantities. The evolutions of these proportions were adjusted to an exponential model. Given the shape of the curves and the aberrant values obtained with adjustment of the models integrating a lag time, we opted to use the following model without lag time:

$$Q_t(\text{quantity at time } t \text{ in \% of initial amount}) \\ = 100 - a \times (1 - e^{-b \times t})$$

where *a* is the maximum extent of BH (expressed in % of initial amount) and *b* is the disappearance rate (expressed in %/h). Parameters *a* and *b* were adjusted using the NLIN procedure of the SAS software package [10].

The individual values measured at the different sampling times were analyzed using the MIXED procedure of the SAS software package, with a fixed effect of lipid source, a random effect of repetition (series) and the REPEATED statement for time (unequally spaced measures, power covariance structure). Multiple comparison of means among sampling times and lipid sources was performed using Tukey's method. The mean amounts, balance data and kinetic parameters were compared using the MIXED procedure of the SAS software package, with a fixed effect of lipid source and a random effect of repetition. The significance level was set at *P* = 0.05.

#### Results

At the start of incubations, LA incubators contained a mean amount of 15.4 mg of *c9,c12-18:2*, LN incubators contained 2.1 mg of *c9,c12-18:2* and 15.8 mg of *c9,c12,c15-18:3*, and LO incubators contained 3.2 mg of *c9-18:1*, 4.5 mg of *c9,c12-18:2* and 8.6 mg of *c9,c12,c15-18:3*. None of the other C18 FAs were significantly different from the control incubators.

#### Mean Amounts of the C18 FAs

Table 1 gives the mean amounts of the different C18 FAs over the 24 h incubation period calculated from the areas under the kinetic curves (see Computations and statistics). In the LA incubations, the addition of *c9,c12-18:2* to the medium gave higher levels of nine 18:1 isomers (*t4-*, *t5-*, *t6 + 7 + 8-*, *t9-*, *t10-*, *t12-*, *c10 + t15-*, *c12-* and *c13-18:1*) and six 18:2 isomers (*t9,t11-*, *c9,t11-*, *c9,c12-*, *c9,t12-*, *c10,c12-* and *t10,c12-18:2*) compared with the control incubations. The isomer *t9,t11-18:2* may have been mixed with *t8,t10-18:2*, since these two FAs were not separated by the GLC method. Several C18:1 isomers and most of the C18:2 isomers had significantly different values between

**Table 1** Mean values ( $\mu\text{g}/\text{incubator}$ ) of C18 FAs during 24 h incubations with different lipid sources

		CO	LA	LN	LO	SEM	<i>P</i>
18:0		13789	16673	13917	13850	843	0.10
18:1	<i>t</i> 4	19.8 <sup>b</sup>	32.2 <sup>a</sup>	23.1 <sup>ab</sup>	24.0 <sup>ab</sup>	2.4	0.03
	<i>t</i> 5	6.3 <sup>c</sup>	16.9 <sup>a</sup>	14.0 <sup>ab</sup>	10.1 <sup>bc</sup>	1.3	0.002
	<i>t</i> 6 + 7 + 8	57 <sup>b</sup>	273 <sup>a</sup>	228 <sup>a</sup>	118 <sup>b</sup>	26	0.0008
	<i>t</i> 9	40 <sup>b</sup>	178 <sup>a</sup>	160 <sup>a</sup>	86 <sup>b</sup>	18	0.002
	<i>t</i> 10	87 <sup>b</sup>	981 <sup>a</sup>	312 <sup>b</sup>	171 <sup>b</sup>	91	0.0003
	<i>t</i> 11	748 <sup>b</sup>	1971 <sup>ab</sup>	2942 <sup>a</sup>	1145 <sup>b</sup>	383	0.02
	<i>t</i> 12	85 <sup>b</sup>	390 <sup>a</sup>	321 <sup>a</sup>	189 <sup>b</sup>	36	0.0008
	<i>t</i> 13 + 14	163 <sup>b</sup>	579 <sup>b</sup>	1884 <sup>a</sup>	586 <sup>b</sup>	163	0.0002
	<i>c</i> 9	632 <sup>b</sup>	512 <sup>b</sup>	629 <sup>b</sup>	1971 <sup>a</sup>	91	<0.0001
	<i>c</i> 10 + <i>t</i> 15	97 <sup>c</sup>	278 <sup>b</sup>	463 <sup>a</sup>	293 <sup>b</sup>	37	0.0006
	<i>c</i> 11	118	130	190	181	21	0.09
	<i>c</i> 12	34 <sup>b</sup>	230 <sup>a</sup>	92 <sup>b</sup>	73 <sup>b</sup>	23	0.001
	<i>c</i> 13	5 <sup>c</sup>	18 <sup>b</sup>	40 <sup>a</sup>	19 <sup>b</sup>	3	0.0003
	<i>c</i> 14 + <i>t</i> 16	103 <sup>b</sup>	236 <sup>ab</sup>	314 <sup>a</sup>	208 <sup>ab</sup>	37	0.02
	<i>c</i> 15	49 <sup>b</sup>	65 <sup>b</sup>	321 <sup>a</sup>	80 <sup>b</sup>	51	0.02
18:2 (non-conjugated)	<i>t</i> 8, <i>c</i> 13	170 <sup>a</sup>	144 <sup>b</sup>	161 <sup>a</sup>	141 <sup>b</sup>	5	0.007
	<i>c</i> 9, <i>c</i> 12	811 <sup>b</sup>	5783 <sup>a</sup>	689 <sup>b</sup>	1424 <sup>b</sup>	425	<0.0001
	<i>c</i> 9, <i>t</i> 12	20 <sup>c</sup>	76 <sup>a</sup>	46 <sup>b</sup>	44 <sup>b</sup>	6	0.002
	<i>t</i> 9, <i>c</i> 12	7 <sup>b</sup>	54 <sup>ab</sup>	63 <sup>a</sup>	19 <sup>ab</sup>	12	0.04
	<i>t</i> 9, <i>t</i> 12	4 <sup>b</sup>	15 <sup>b</sup>	31 <sup>a</sup>	10 <sup>b</sup>	4	0.006
	<i>c</i> 9, <i>t</i> 13	4 <sup>b</sup>	8 <sup>b</sup>	60 <sup>a</sup>	20 <sup>b</sup>	6	0.0002
	<i>c</i> 9, <i>c</i> 15	9 <sup>b</sup>	11 <sup>b</sup>	32 <sup>a</sup>	13 <sup>b</sup>	4	0.02
	<i>t</i> 11, <i>c</i> 15	30 <sup>b</sup>	26 <sup>b</sup>	1459 <sup>a</sup>	460 <sup>b</sup>	117	<0.0001
CLAs	<i>c</i> 9, <i>c</i> 11	8 <sup>b</sup>	12 <sup>b</sup>	87 <sup>a</sup>	42 <sup>b</sup>	12	0.004
	<i>c</i> 9, <i>t</i> 11	19 <sup>b</sup>	214 <sup>a</sup>	39 <sup>b</sup>	81 <sup>b</sup>	22	0.0007
	<i>t</i> 9, <i>c</i> 11	4	10	6	4	3	0.47
	<i>t</i> 8, <i>t</i> 10 + <i>t</i> 9, <i>t</i> 11	7 <sup>b</sup>	200 <sup>a</sup>	35 <sup>b</sup>	29 <sup>b</sup>	32	0.008
	<i>c</i> 10, <i>c</i> 12	2.8 <sup>b</sup>	13.0 <sup>a</sup>	6.6 <sup>b</sup>	1.5 <sup>b</sup>	1.6	0.003
	<i>c</i> 10, <i>t</i> 12	3.7 <sup>ab</sup>	11.7 <sup>a</sup>	0.4 <sup>b</sup>	2.8 <sup>ab</sup>	2.4	0.04
	<i>t</i> 10, <i>c</i> 12	9 <sup>b</sup>	356 <sup>a</sup>	10 <sup>b</sup>	15 <sup>b</sup>	34	<0.0001
	<i>c</i> 11, <i>t</i> 13	2.3 <sup>b</sup>	3.2 <sup>b</sup>	12.5 <sup>a</sup>	4.2 <sup>b</sup>	1.6	0.006
	<i>t</i> 11, <i>t</i> 13	6 <sup>b</sup>	9 <sup>b</sup>	425 <sup>a</sup>	79 <sup>b</sup>	27	<0.0001
18:3	<i>c</i> 9, <i>c</i> 12, <i>c</i> 15	192 <sup>c</sup>	161 <sup>c</sup>	4085 <sup>a</sup>	2544 <sup>b</sup>	269	<0.0001
	<i>C</i> 6, <i>c</i> 9, <i>c</i> 12	2	5	9	11	4	0.38
	<i>Trans</i>	9 <sup>b</sup>	8 <sup>b</sup>	37 <sup>a</sup>	43 <sup>a</sup>	4	0.0005

CO Control (no lipids added), LA linoleic acid, LN linolenic acid, LO linseed oil. Results are expressed as LS means, *P* values indicate lipid substrate effect, and different superscript letters in the same row indicate significantly different values (*P* < 0.05)

the LA and LN incubations. Compared with the LN incubations, LA had significantly higher levels of *c*9,*c*12–18:2 (substrate), *t*10- and *c*12–18:1, *c*9,*t*11-, *c*9,*t*12-, *t*10,*c*12-, *c*10,*t*12-, *c*10,*c*12- and *t*9,*t*11–18:2. In the LA incubations, the two main C18:1 intermediates (*t*10 and *t*11) together accounted for about 50% of the total 18:1 intermediates, while the two main 18:2 intermediates (*c*9,*t*11 and *t*10,*c*12) similarly accounted for about 50% of the total C18:2 intermediates.

In the LN incubations, the addition of *c*9,*c*12,*c*15–18:3 gave higher levels of ten 18:1 isomers (*t*5-, *t*6 + 7 + 8-, *t*9-,

*t*11-, *t*12-, *t*13 + 14-, *c*10 + *t*15, *c*13-, *c*14 + *t*16- and *c*15–18:1) and nine 18:2 isomers (*c*9,*c*11-, *c*9,*t*12-, *c*9,*t*13-, *c*9,*c*15-, *t*9,*c*12-, *t*9,*t*12-, *c*11,*t*13-, *t*11,*t*13- and *t*11,*c*15–18:2) compared with the control incubations. Compared with the LA incubations, the LN incubations had much higher levels of *t*11,*c*15–18:2, and significantly higher levels of *t*13 + 14-, *c*10 + *t*15-, *c*13- and *c*15–18:1, *t*9,*t*12-, *c*9,*t*13-, *t*8,*c*13-, *c*9,*c*15-, *c*11,*t*13-, *c*9,*c*11- and *t*11,*t*13–18:2. Addition of pure  $\alpha$ -linolenic acid to incubators yielded high levels of *c*9,*c*12,*c*15–18:3 (substrate) and *trans*-18:3 (undetermined isomer(s) of C18:3 with at least one

*trans* double bond). In the LN incubations, the two main 18:1 products (*t*11 and *t*13 + 14) accounted for 61% of the total 18:1 intermediates, while the two main 18:2 products (*t*11,*c*15 and *t*11,*t*13) accounted for 75% of the total 18:2 intermediates. The other 18:1 and 18:2 BH intermediates showed no differences between the LA and LN incubations. Mean amounts of FAs in LO incubations ranged between control and LN values, except for *c*9–18:1 and *c*9,*c*12–18:2, which were supplied by linseed oil, thus giving higher levels in the LO than in the LN incubations. Mean levels of BH intermediates (18:1 and 18:2 isomers except *c*9–18:1 and *c*9,*c*12–18:2) were significantly lower in the LO incubations than in the LN incubations (4150 vs 9805 µg/incubator). After 24 h of incubation, the proportions of the main C18 FA (in % of total C18) were: 65% of 18:0, 6% of *c*9–18:1, 17% of other 18:1 isomers, 3% of *c*9,*c*12–18:2, 6% of other 18:2 isomers and 4% of *c*9,*c*12,*c*15–18:3.

### FA Balances

Table 2 presents C18 FA balances between start and end of incubations. In the LA incubations, the disappearance of *c*9,*c*12–18:2 (substrate) was mainly balanced by an increase in 18:0 (indicating complete BH of the substrate) and, to a lesser extent, in *t*10–18:1, *cis*-18:1 except *c*9–18:1, and in all CLAs. None of the other FAs had balances significantly different from zero.

In the LN incubations, the disappearance of 18:3 was mainly balanced by an increase in *trans*- and *cis*-18:1 except for *c*9–18:1, in *t*11,*c*15–18:2 and other non-conjugated 18:2, and mainly in 11,13 CLAs. The increase in 18:0 (complete BH) was close to significance ( $P = 0.056$ ), and was numerically higher than the increase in *t*11–18:1 (4.43 vs 3.43 mg/incubator).

The balance in the LO incubations was characterized by decreases in *c*9–18:1, *c*9,*c*12–18:2 and 18:3, which were all present in linseed oil. The main BH product was 18:0, but there were also significant increases in *trans*-18:1, *t*11,*c*15–18:2, and other 18:2 isomers. The increase in *t*11–18:1 during incubation was not significantly different from zero.

For all three lipid substrates, the overall balance of total C18 FA was negative, but not significantly different from zero.

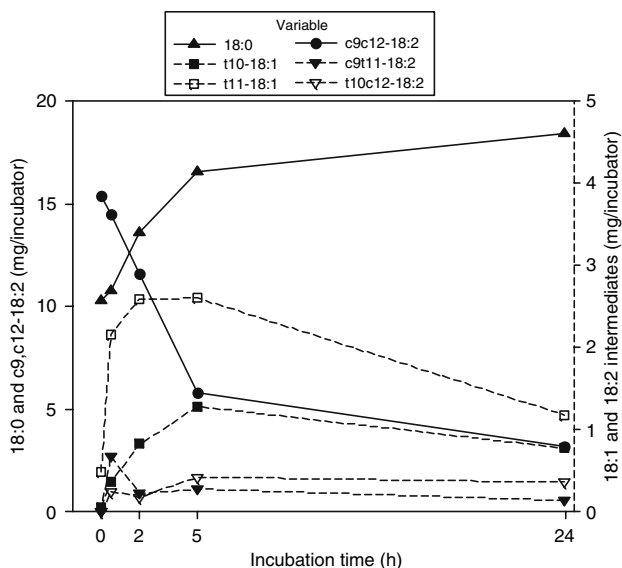
### Dynamic Features

Figure 1 depicts the time course of the most characteristic FAs produced in the LA incubations. The levels of the substrate (*c*9,*c*12–18:2) were not significantly modified during the first 0.5 h ( $P = 0.41$  for the difference between 0 and 0.5 h) but then dropped rapidly to 5 h of incubation, and more slowly to the end of incubation ( $P = 0.02$  for the difference between 5 and 24 h). The CLA *c*9,*t*11–18:2 reached a peak (0.7 mg/incubator) at 0.5 h, and then remained constant between 2 and 24 h of incubation ( $P = 0.12$ ). The CLA *t*10,*c*12–18:2 also increased during the first 0.5 h ( $P < 0.0001$ ) and remained constant thereafter, always below 0.5 mg/incubator or 1.5% of the total C18 FAs. Vaccenic acid (*t*11–18:1) increased rapidly during the first 0.5 h ( $P = 0.002$ ), peaked between 2 and 5 h of incubation (2.6 mg/incubator), and slowly decreased thereafter ( $P = 0.04$ ) to reach 1.2 mg/incubator at 24 h. The amount of *t*10–18:1 increased from 0.5 to 5 h, and then decreased ( $P = 0.02$ ) to reach levels similar to *t*11–18:1 after 24 h. The amount of 18:0 did not significantly change during the first 0.5 h. It then increased to 2 h of incubation ( $P = 0.004$ ), and also increased between 2 and 24 h ( $P = 0.02$ ; the value after 5 h was intermediate, not significantly different from values at 2 and 24 h).

**Table 2** Balances of the C18 FAs (mg/incubator) between start and end of 24 h incubations with different lipid sources

LA Linoleic acid, LN linolenic acid, LO linseed oil. Positive values correspond to a net production of the FA whereas negative values correspond to a net disappearance of the FA. The last column gives  $P$  values for the lipid source effect, and different superscript letters in the same row indicate significant differences among LS means

	LA	LN	LO	SEM	$P$
C18:0	+8.18	+4.43	+4.99	1.87	0.37
<i>c</i> 9–18:1	–0.51	–0.35	–1.81	0.44	0.07
Other <i>cis</i> -18:1	+0.42 <sup>a</sup>	+1.70 <sup>b</sup>	+0.43 <sup>a</sup>	0.14	0.0001
<i>t</i> 10–18:1	+0.72 <sup>c</sup>	+0.39 <sup>b</sup>	+0.20 <sup>a</sup>	0.07	0.0003
<i>t</i> 11–18:1	+0.69 <sup>a</sup>	+3.43 <sup>b</sup>	+0.82 <sup>a</sup>	0.63	0.02
Other <i>trans</i> -18:1	+1.00 <sup>a</sup>	+4.03 <sup>b</sup>	+1.25 <sup>a</sup>	0.42	0.0003
<i>c</i> 9, <i>c</i> 12–18:2	–12.17 <sup>a</sup>	–1.77 <sup>b</sup>	–3.82 <sup>b</sup>	1.70	0.009
<i>t</i> 11, <i>c</i> 15–18:2	0.00 <sup>a</sup>	+0.99 <sup>b</sup>	+0.78 <sup>b</sup>	0.15	0.005
Other non conj. 18:2	+0.03 <sup>a</sup>	+0.23 <sup>b</sup>	+0.07 <sup>a</sup>	0.02	0.0009
<i>c</i> 9, <i>t</i> 11–18:2	+0.13 <sup>b</sup>	0.00 <sup>a</sup>	+0.09 <sup>b</sup>	0.03	0.03
<i>t</i> 10, <i>c</i> 12–18:2	+0.35	0.00	+0.02	0.10	0.08
Other CLAs	+0.18 <sup>a</sup>	+0.62 <sup>b</sup>	+0.21 <sup>a</sup>	0.07	0.008
<i>c</i> 9, <i>c</i> 12, <i>c</i> 15–18:3	–0.37 <sup>c</sup>	–13.98 <sup>a</sup>	–7.62 <sup>b</sup>	0.61	<0.0001
Total C18	–1.36	–0.28	–4.28	2.76	0.47



**Fig. 1** Kinetics of the main FAs during linoleic acid incubations (mg/incubator). C18:0 and *c9,c12-18:2* (lipid source) are presented in solid lines on the left scale. The biohydrogenation intermediates (*t10-* and *t11-18:1*, *c9,t11-* and *t10,c12-18:2*) are presented in dotted lines on the right scale

Table 3 presents the kinetic parameters describing the disappearance of substrate FAs (*c9,c12-18:2* and *c9,c12,c15-18:3*) and double bonds during incubations. In the LA incubations, *c9,c12-18:2* and *c9,c12,c15-18:3* showed similar maximum extents of disappearance (78.7 and 80.0% of the initial amount, respectively) and disappearance rates (23.6 and 33.9%/h, respectively), but the extent and rate of disappearance of double bonds had lower values (67.5 and 11.6%/h, respectively).

**Table 3** Adjusted parameters of kinetic models of the disappearance of *c9,c12-18:2*, *c9,c12,c15-18:3* and double bonds measured during incubations of different lipid sources

Variable measured	Parameter	LA	LN	LO	SEM	<i>P</i>
<i>c9,c12-18:2</i>	a	78.7	81.8	85.9	9.2	0.74
	b	23.6	41.9	33.6	8	0.34
<i>c9,c12,c15-18:3</i> <sup>d</sup>	a	80	86.9	91.2	5.4	0.21
	b	33.9	44.6	26.8	6.3	0.20
Double bonds	a	67.5	61.7	71.1	11.1	0.78
	b	11.6	32.4	28.7	5.2	0.06

LA Linoleic acid, LN linolenic acid, LO linseed oil. The model used is  $Q_t$  (quantity at time *t* expressed in %  $Q_0$ ) =  $100 - a \times (1 - e^{-b \times t})$ , where *a* is the maximum extent of BH (expressed in % of the initial amount) and *b* is the disappearance rate (expressed in %/h). Values are LS means of the adjusted parameters

<sup>d</sup> There were only two adjustable curves for *c9,c12,c15-18:3* in LA incubations, so the corresponding SEM has to be multiplied by 1.41 for this lipid source

Figure 2 depicts the time course of the most characteristic FAs produced in the LN incubations. The substrate *c9,c12,c15-18:3* decreased as early as 0.5 h of incubation, dropped rapidly during the first 5 h of incubation, and then fell at a slower rate to 24 h. The *trans-18:3* remained low and constant throughout the incubation period (mean content 0.04 mg/incubator). The 18:2 isomers showed two main time course patterns. In the first pattern, as exemplified by *t11,c15-18:2* (see Fig. 2), the FAs peaked after about 2 h of incubation and decreased thereafter. The isomers *c9,t13-*, *c9,c15-*, *c9,c11-*, *c9,t11-*, *c10,t12-* and *c10,c12-18:2* also followed this pattern. In the second pattern, as exemplified by *t11,t13-18:2* (see Fig. 2), the FAs also increased at the beginning of incubation, but instead of decreasing after 5 h of incubation, they remained constant to 24 h. The isomers *c9,t12-*, *t9,c12-*, *t9,t12-*, *c11,c13-* and *c11,t13-18:2* followed this pattern. All 18:1 isomers increased steadily for the whole 24 h incubation period (e.g. *t11-* and *t13 + 14-18:1* in Fig. 2). Stearic acid (C18:0) increased slightly ( $P = 0.06$ ) during the first 0.5 h, and then remained constant throughout the 24 h incubation period.

The disappearance rates of *c9,c12-18:2* and *c9,c12,c15-18:3* were higher ( $P < 0.1$ ) in the LN incubations (41.9 and 44.6%/h, respectively) than in the LA incubations (23.6 and 33.9%/h, respectively) (Table 3). The substrate decreased as early as 0.5 h in the LN incubations, and less substrate remained at 2 h in the LN than in the LA incu-

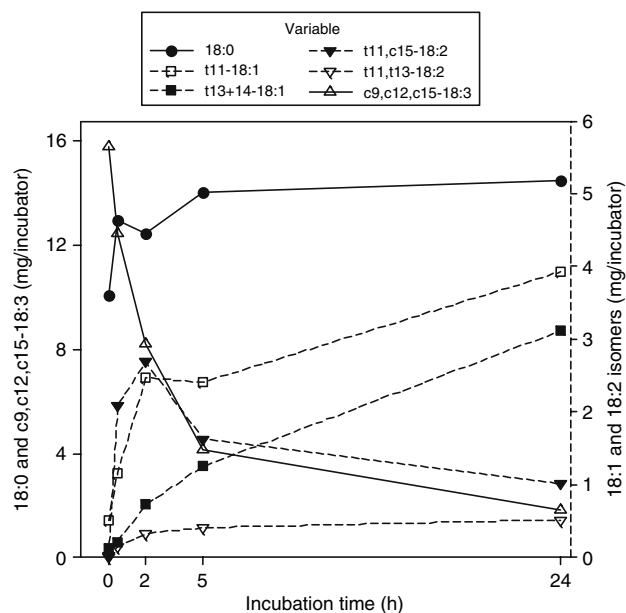


**Fig. 2** Kinetics of the main FAs during linolenic acid incubations (mg/incubator). C18:0 and *c9,c12,c15-18:3* (lipid source) are presented as solid lines on the left scale. The biohydrogenation intermediates (*t11-* and *t13 + 14-18:1*, *t11,c15-* and *t11,t13-18:2*) are presented as dotted lines on the right scale

bations (52% of initial amount remained for *c9,c12,c15-18:3* in LN vs 74% for *c9,c12-18:2* in LA incubations;  $P = 0.07$ ). This was confirmed by a higher disappearance rate of double bonds ( $P = 0.03$ ) in LN (32.4%/h) than in LA incubations (11.6%/h). Most of the double bonds in the LN incubations disappeared during the first 5 h (the double bond numbers were not significantly different between 5 and 24 h of incubation;  $P = 0.30$ ). By contrast, the number of double bonds in LA incubations remained unchanged ( $P = 0.60$ ) during the first 2 h of incubation, decreased rapidly between 2 and 5 h of incubation ( $P = 0.02$ ), and continued to decrease at a lower rate between 5 and 24 h ( $P = 0.02$ ).

The LO incubations (Fig. 3) followed a general pattern similar to the LN incubations, i.e. a rapid increase in 18:2 BH intermediates and a steady increase in *trans*-18:1 throughout the 24 h incubation period, but yielded lower levels of all the BH intermediates. After 24 h of incubation, the C18 FAs were composed of 65% of 18:0, 6% of *c9-18:1*, 17% of other 18:1 isomers, 3% of *c9,c12-18:2*, 6% of other 18:2 isomers and 4% of *c9,c12,c15-18:3*. The kinetics of *c9,c12-18:2*, *c9,c12,c15-18:3* and double bonds were also very similar between the LO and LN incubations (Table 3), except that the disappearance rate of *c9,c12,c15-18:3* tended to be lower in LO (26.8%/h in LO vs 44.6%/h in LN;  $P = 0.1$ ).

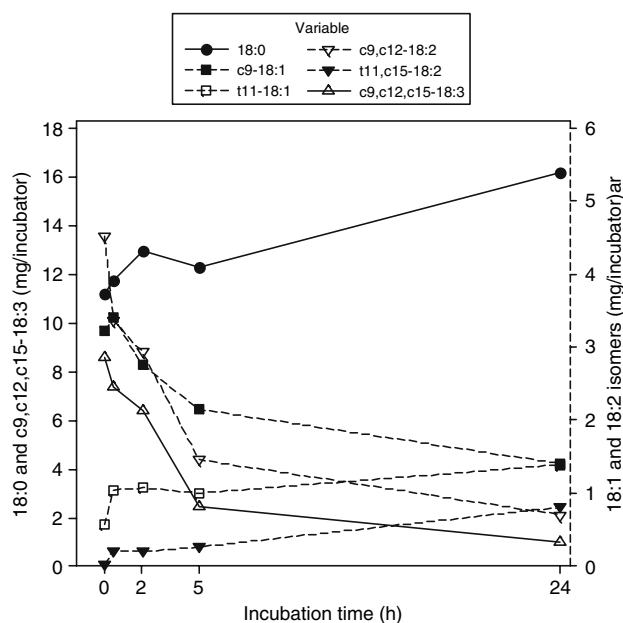


**Fig. 3** Kinetics of the main FAs during linseed oil incubations (mg/incubator). C18:0 and *c9,c12,c15-18:3* (main lipid source) are presented in solid lines on the left scale. The 18:1 and 18:2 isomers (*c9-* and *t11-18:1*, *c9,c12-* and *t11,c15-18:2*) are presented as dotted lines on the right scale

## Discussion

### Validity of the in Vitro Model

In vitro incubations used to study the rumen metabolism of unsaturated FA often produce much higher levels of BH than those occurring in in vivo conditions. Several hypotheses can be put forward to account for these discrepancies: the absence of particulate matter may enhance the inhibiting effect of added lipids on microbes [11], the presence of oxygen in the medium may disrupt microbe metabolism, very high doses of supplemental lipids are sometimes used, and an excessive duration of incubations may induce a loss of activity of the microbes. We took precautions with regard to these factors to make the results more realistic. Thus we added particulate matter to the incubations (DM represented a mean 5.25% of incubator contents). We ensured by gas analysis that oxygen was not present in the incubators. We added only moderate amounts of lipids to the incubators (equivalent to 3% of DM), and limited the duration of incubations to 24 h. In these conditions, the composition of C18 FAs at the end of the LO incubations was comparable to that obtained in the duodenum of animals fed a high forage diet containing 3% of linseed oil (12): 65% (in the LO incubations) vs 66% (in [12]) of 18:0, 6% vs 3% of *c9-18:1*, 17% vs 23% of other 18:1 isomers, 3 vs 3% of *c9,c12-18:2*, 6 vs 3% of other 18:2 isomers, and 4 vs 2% of *c9,c12,c15-18:3*. The final products of in vitro BH were thus consistent with in vivo results, showing that the conditions used for the incubations allowed a normal microbial metabolism.

### Specificity of BH Products of *c9,c12-18:2* and *c9,t11,c15-18:3*

During the 24 h incubation period, results for the main FAs (Table 1) were consistent with the main metabolic pathways, with *c9,c12-18:2* generating *c9,t11-18:2* and *t11-18:1*, and *c9,c12,c15-18:3* producing *t11,c15-18:2* and *t11-18:1* [13]. However, a large number of 18:1 and 18:2 isomers were identified here, showing that there are several other “minor” BH pathways. This agrees with BH data obtained with plant oil supplements rich in unsaturated FAs in both in vitro [14] and in vivo [12, 15] studies. In the LA incubations, the fact that the two main C18:1 and C18:2 BH intermediates accounted for only 50% of total intermediates indicates that the “minor” pathways may in fact account for half of the total BH of *c9,c12-18:2*. The BH pathways of *c9,c12,c15-18:3* were probably less diversified than the 18:2 BH pathways, since the sum of the two main 18:1 and 18:2 BH intermediates accounted for 60–75% of the total intermediates.

The detailed examination of the BH products showed the specificity of most BH products: addition of *c9,c12-18:2* to the medium gave higher levels of nine 18:1 isomers and six 18:2 isomers compared with the control incubations. The main 18:1 isomers were those with double bonds in positions 10 and 12, while the main 18:2 isomers were 9,11- and 10,12- CLAs. Absolute amounts of *trans-18:1* with double bonds on carbon 4–9 also increased, but their proportions of total C18 FAs were similar to those of the control incubations. Such profiles are consistent with duodenal FA profiles already observed in vivo on animals fed diets supplemented with 18:2-rich plant oils [16–18]. In the LN incubations, in addition to the main products *t11,c15-18:2* and *t11-18:1*, the formation of *t13 + 14-*, *c13-*, *c10 + t15-*, *c15-18:1*, as well as several 11,13 CLAs and other 18:2 intermediates with a double bond on carbon 13 or carbon 15, was also promoted. This indicates that besides the most extensively described metabolic pathways involving carbon 11-desaturated FAs, the carbon 13- and carbon 15-metabolic pathways can be considered specific to the ruminal metabolism of *c9,c12,c15-18:3*. The accumulation of carbon 13- and carbon 15-desaturated metabolites confirms the low BH of the double bonds in these positions in both *cis* and *trans* configurations already reported by other authors [19, 20]. Among the 9,12–18:2 isomers, *c9,t12-* and *t9,c12-18:2* were increased by both *c9,c12-18:2* and *c9,c12,c15-18:3* supplementations, in accordance with the in vivo data [12, 15, 21], whereas *t9,t12-18:2* was only increased by *c9,c12,c15-18:3* and not by *c9,c12-18:2*.

#### Differences in BH Dynamics and Extent Between *c9,c12-18:2* and *c9,t11,c15-18:3*

The disappearance rate of *c9,c12-18:2* in the LA incubations was lower than the disappearance rate of *c9,c12,c15-18:3* in the LN incubations (Table 3). This result was confirmed by a lower disappearance rate of double bonds in the LA than in the LN incubations. The BH process had almost reached its maximum after 5 h of incubation in the LN and LO incubations, whereas significant amounts were still being hydrogenated between 5 and 24 h in the LA incubations. The slower BH of *c9,c12-18:2* compared with *c9,c12,c15-18:3*, which has already been reported (for example in [22]), may be due to a preferential uptake of *c9,c12-18:2* by bacteria [23], thus protecting it against BH, or to differences in microbial isomerase or saturase affinity between the two FAs. The disappearance rate of *c9,c12-18:2* found in this study was similar to that reported by Troegeler-Meynadier et al. [24] in very similar in vitro conditions (23.6 and 22.5%, respectively). The maximum extent of disappearance of *c9,c12-18:2* and *c9,c12,c15-18:3* (78.7–85.9% and 80–91.2% of initial amount,

respectively) was not significantly different among the three lipid sources, and was similar to mean in vivo BH data reviewed in [25].

The kinetics of the main FAs during incubations showed that 18:2 intermediates appeared first and were followed by a later increase in 18:1 intermediates, which fits the logical sequence of the BH process. In LA incubations, *t11-18:1* showed an earlier increase than *t10-18:1*, and the *t11/t10-18:1* ratio decreased over time, probably reflecting a short-term modification in the balance between the different metabolic pathways. The main difference between the LN and LA incubations was that the increase in 18:1 was transitory in the LA incubations, whereas the 18:1 intermediates accumulated between 5 and 24 h in the LN incubations, a feature also observed, though to a lesser extent, in the LO incubations. The balances of C18 FAs after a 24 h incubation period confirmed that the BH of *c9,c12-18:2* was more complete than that of *c9,c12,c15-18:3*: the main product of *c9,c12-18:2* BH was C18:0, whereas the main products of *c9,c12,c15-18:3* BH were *trans-18:1* isomers (Table 2). Two reasons may explain this result: some *trans-18:1* isomers specific to *c9,c12,c15-18:3* BH (for example carbon 13- or carbon 15-desaturated 18:1) are probably more resistant to BH than those specific to *c9,c12-18:2* BH [19]; for other intermediates (as *t11-18:1* present in both the LA and LN incubations), a partial inhibition of the last step of BH (from *trans-18:1* to 18:0) probably occurred in the LN incubations. This step is under the control of group B bacteria [26]. The inhibition may be due to a direct toxic effect of *c9,c12,c15-18:3* itself or of one of its BH intermediates on these microbes. Since the fastest increase in C18:0 occurred at the start of the incubations, when *c9,c12,c15-18:3* was at its maximum level, it is unlikely that *c9,c12,c15-18:3* was responsible for the inhibition. The hypothesis of inhibition by one or several BH intermediates is thus more probable, but no published data are currently available to confirm this hypothesis.

#### Effects of FA Esterification (Free FAs vs Linseed oil)

Since the amounts of unsaturated FAs supplied in free or triacylglycerol form in the medium of each incubator were similar for all the lipid sources, we were able to compare free FAs and triacylglycerols, and assess the production of the various BH intermediates according to the FA source.

The disappearance rate of *c9,c12,c15-18:3* in the LN incubations was slightly higher than in the LO incubations, which may be a consequence of the necessary prior lipolysis of the triacylglycerol form of C18:3 in linseed oil, causing a slow release of free FAs used as substrates in the subsequent steps of isomerization and BH. The LN and LO incubations differed not only in the esterification of FAs, but also in the fact that linseed oil contained significant

amounts of *c9,c12*–18:2. However, the disappearance rate of double bonds was similar between the LN and LO incubations, so the global BH was not slowed by the esterification in our conditions. This is confirmed by the similar disappearance rates of *c9,c12*–18:2 between the LA and LO incubations. The lipolysis was thus not a limiting factor, and the disappearance of the substrates was probably limited by one of the subsequent steps in the BH process. The slower disappearance of *c9,c12,c15*–18:3 in LO compared with LN may arise from competition between *c9,c12,c15*–18:3 and *c9,c12*–18:2 for the initial step of BH in the LO incubations, already hypothesized by other authors [24]. The isomerization of the *cis*12 double bond into *trans*11 is an obligatory step before saturation [2, 27], and is probably performed on the same site for *c9,c12*–18:2 and *c9,c12,c15*–18:3 [27]. Since LO contains both FAs, we can hypothesize that they compete for the sites, causing a slowing of *c9,c12,c15*–18:3 disappearance in the LO incubations at their start, without affecting the global BH (disappearance of double bonds). With a lipid supplementation level of about 3% of DM, the limiting step of LO hydrogenation seems to be the first isomerization step (*c12* to *t11*-double bond) rather than the lipolysis step.

## Conclusion

This in vitro study with moderate levels of added lipids was designed to be representative of in vivo BH in diets supplemented with realistic amounts of unsaturated FAs. It showed that for a similar amount of supplemental FAs, more 18:0 (corresponding to complete BH) and less intermediates were produced from *c9,c12*–18:2 than from *c9,c12,c15*–18:3. Incubations of *c9,c12,c15*–18:3 produced higher amounts of 18:1 intermediates, 74% of which were *t11*- and *t13* + 14–18:1. Esterification of *c9,c12,c15*–18:3 in the LO had no effect on BH rate or on maximum extent of BH, which suggests that the initial step of BH (*cis*12 double bond isomerization) was more limiting than the lipolysis step in these conditions. The detailed description of 18:1 and 18:2 isomers produced from *c9,c12*–18:2 and *c9,c12,c15*–18:3 BH underlines that the main isomers commonly described (*t11*–18:1, *c9,t11*- and *t11,c15*–18:2) give only a very partial view of overall BH products. There is a need for more mechanistic approaches to the BH that take into account all the various metabolic pathways and reflect the full diversity of the isomers produced in the rumen, which in turn influence the lipid profiles of animal products.

**Acknowledgments** This research was funded by the European Union (*HealthyBeef* Project QLK1-CT-2000-01423) and INRA. The authors thank J. J. Loor and D. Bauchart for their scientific advice and support, the team of the *Annexe Elevage* experimental unit for animal

care and rumen content sampling, D. Durand for surgery on cannulated sheep, and J. Portelli and S. Laverroux for technical assistance with the GLC analyses of FAs.

## References

- Demeyer D, Doreau M (1999) Targets and products for altering ruminant meat and milk lipids. *Proc Nutr Soc* 58:593–607
- Kepler C, Hirons K, McNeill JJ, Tove SB (1966) Intermediates and products of the biohydrogenation of linoleic acid by *Butyrivibrio fibrisolvens*. *J Biol Chem* 241:1350–1354
- Polan CE, McNeill JJ, Tove CB (1964) Biohydrogenation of Unsaturated fatty acids by rumen bacteria. *J Bacteriol* 88:1056–1064
- Harfoot CG, Hazlewood GP (1997) Lipid metabolism in the rumen. In: Hobson PN, Stewart CS (eds) *The rumen microbial ecosystem*. Blackie Academic & Professional, London, pp 382–426
- Coleman GS (1978) Rumen endotiniomorphid protozoa. In: Baker JR, Taylor AER (eds) *Methods of cultivating parasites in vitro*. Academic, London, pp 39–54
- Folch J, Lees M, Sloane Stanley GH (1957) A simple method for the isolation and purification of total lipids from animal tissues. *J Biol Chem* 226:497–509
- Christie WW, Sebedio JL, Juaneda P (2001) A practical guide to the analysis of conjugated linoleic acid *Inform* 12:147–152
- Loor JJ, Herbein JH (2001) Alterations in blood plasma and milk fatty acid profiles of lactating Holstein cows in response to ruminal infusion of a conjugated linoleic acid mixture. *Anim Res* 50:463–476
- Jouany J-P, Lassalas B (2002) Gas pressure inside a rumen in vitro system stimulates the use of hydrogen. *Reproduction nutrition development* 42(Suppl 1): S64
- Sas institute (2000) *Sas user's guide: statistics*. Version 8.1, Cary
- Henderson C (1973) The effects of fatty acids on pure cultures of rumen bacteria. *J Agric Sci* 81:107–112
- Loor JJ, Ueda K, Ferlay A, Chilliard Y, Doreau M (2004) Biohydrogenation, duodenal flow, and intestinal digestibility of *trans* fatty acids and conjugated linoleic acids in response to dietary forage: concentrate ratio and linseed oil in dairy cows *J Dairy Sci* 87:2472–2485
- Dawson RMC, Kemp P (1970) Biohydrogenation of dietary fats in ruminants. In: Phillipson AT (ed) *Physiology of digestion and metabolism in the ruminant*, Oriel Press, Newcastle upon Tyne, pp 504–518
- Loor JJ, Bandara ABPA, Herbein JH (2002) Characterization of 18:1 and 18:2 isomers produced during microbial biohydrogenation of unsaturated fatty acids from canola and soya bean oil in the rumen of lactating cows. *J Anim Physiol Anim Nutr* 86:422–432
- Loor JJ, Ferlay A, Ollier A, Ueda K, Doreau M, Chilliard Y (2005) High-concentrate diets and polyunsaturated oils alter *trans* and conjugated isomers in bovine rumen, blood, and milk. *J Dairy Sci* 88:3986–3999
- Atkinson RL, Scholljegerdes EJ, Lake SL, Nayigihugu V, Hess BW, Rule DC (2006) Site and extent of digestion, duodenal flow, and intestinal disappearance of total and esterified fatty acids in sheep fed a high-concentrate diet supplemented with high-linoleate safflower oil. *J Anim Sci* 84:387–396
- Loor JJ, Ueda K, Ferlay A, Chilliard Y, Doreau M (2005) Intestinal flow and digestibility of *trans* fatty acids and conjugated linoleic acids (cla) in dairy cows fed a high-concentrate diet supplemented with fish oil, linseed oil, or sunflower oil, *anim. Feed Sci Technol* 119:203–225

18. Duckett SK, Andrae JG, Owens FN (2002) Effect of high-oil corn or added corn oil on ruminal biohydrogenation of fatty acids and conjugated linoleic acid formation in beef steers fed finishing diets. *J Anim Sci* 80:3353–3360
19. Kemp P, Lander DJ (1984) The hydrogenation of some *cis*- and *trans*-octadecenoic acids to stearic acid by a rumen *Fusocillus* Sp. *Br J Nutr* 52:165–170
20. Body DR (1976) The occurrence of *cis*-octadec-15-enoic acid as a major biohydrogenation product from methyl linoleate in bovine rumen liquor. *Biochem J* 157:741–744
21. AbuGhazaleh AA, Schingoethe DJ, Hippen AR, Kalscheur KF, Whitlock LA (2002) Fatty acid profiles of milk and rumen digesta from cows fed fish oil, extruded soyabeans or their blend. *J Dairy Sci* 85:2266–2276
22. Sinclair LA, Cooper SL, Chikunya S, Wilkinson RG, Hallett KG, Enser M, Wood JD (2005) Biohydrogenation of N-3 polyunsaturated fatty acids in the rumen and their effects on microbial metabolism and plasma fatty acid concentrations in sheep. *Anim Sci* 81:239–248
23. Bauchart D, Legay-Carmier F, Doreau M, Gaillard B. (1990) Lipid metabolism of liquid-associated and solid-adherent bacteria in rumen contents of dairy cows offered lipid-supplemented diets. *Br J Nutr* 63:563–578
24. Troegeler-Meynadier A, Nicot MC, Bayourthe C, Moncoulon R, Enjalbert F (2003) Effects of pH and concentrations of linoleic and linolenic acids on extent and intermediates of ruminal biohydrogenation in vitro. *J Dairy Sci* 86:4054–4063
25. Doreau M, Ferlay A (1994) Digestion and utilisation of fatty acids by ruminants. *Anim Feed Sci Technol* 45:379–396
26. Kemp P, Lander DJ (1984) Hydrogenation in vitro of alpha-linolenic acid to stearic acid by mixed cultures of pure strains of rumen bacteria. *J Gen Microbiol* 130:527–533
27. Kepler C, Tove CB (1967) Biohydrogenation of unsaturated fatty acids, III, purification and properties of a linoleate delta12 *cis*-delta11 *trans* isomerase from *Butyrvibrio Fibrisolvans*. *J Biol Chem* 242:5686–5692



## Total Lipids of Sarda Sheep Meat that Include the Fatty Acid and Alkenyl Composition and the CLA and *Trans*-18:1 Isomers

Viviana Santercole · Rina Mazzette · Enrico P. L. De Santis ·  
Sebastiano Banni · Laki Goonewardene · John K. G. Kramer

Received: 29 August 2006 / Accepted: 3 December 2006 / Published online: 16 February 2007  
© AOCS 2007

**Abstract** The total lipids of the *longissimus dorsi* muscle were analyzed from commercial adult Sarda sheep in Sardinia taken from local abattoirs, and in the subsequent year from three local farms in the Sassari region that provided some information on the amount and type of supplements fed to the pastured sheep. The complete lipid analysis of sheep meat included the fatty acids from *O*-acyl and *N*-acyl lipids, including the *trans*- and conjugated linoleic acid (CLA) isomers and the alk-1-enyl ethers from the plasmalogenic lipids. This analysis required the use of a combination of acid- and base-catalyzed methylation procedures, the former to quantitate the *O*-acyl, *N*-acyl and alkenyl ethers, and the latter to determine the content of CLA isomers and their metabolites. A combination of gas chromatographic and silver-ion separation techniques was necessary to quantitate all of the meat lipid constituents, which included a prior separation of the *trans*-octadecenoic acids (18:1) and a separation of fatty acid methyl

esters and the dimethylacetals (DMAs) from the acyl and alk-1-enyl ethers, respectively. The alk-1-enyl moieties of the DMAs were analyzed as their stable cyclic acetals. In general, about half of the meat lipids were triacylglycerols, even though excess fat was trimmed from the meat. The higher fat content in the meat appears to be related to the older age of these animals. The variation in the *trans*-18:1 and CLA isomer profiles of the Sarda sheep obtained from the abattoirs was much greater than in the profiles from the sheep from the three selected farms. Higher levels of 10*t*-18:1, 7*t*9*c*-18:2, 9*t*11*c*-18:2 and 10*t*12*c*-18:2 were observed in the commercial sheep meat, which reflected the poorer quality diets of these sheep compared to those from the three farms, which consistently showed higher levels of 11*t*-18:1, 9*c*11*t*-18:2 and 11*t*13*c*-18:2. In the second study, sheep were provided with supplements during the spring and summer grazing season, which contributed to higher levels of 11*t*-18:1 and 9*c*11*t*-18:2. The farm that provided a small amount of supplements during the spring had the better lipid profile at both time periods. The polyunsaturated fatty acid (PUFA) content was higher in the meat from Sarda sheep from the three farms than in the meat from those sheep obtained from commercial slaughter operations. The plasmalogenic lipid content ranged from 2 to 3% of total lipids, the alk-1-enyl ethers consisted mainly of saturated and monounsaturated moieties, and the *trans*-18:1 profile was similar to that of the FA. The n-6 (6–8%) and n-3 PUFA (2–3%) contents, the n-6/n-3 ratio (3:1), as well as the saturated fatty acid (SFA) content (42–45%) and the SFA to PUFA ratio (4:1 to 5:1) of the Sarda sheep from the three farms were comparable to sheep meat lipids

V. Santercole · R. Mazzette · E. P. L. De Santis  
Faculty of Veterinary Medicine, University of Sassari,  
07100 Sassari, Italy

S. Banni  
Department of Experimental Biology,  
University of Cagliari, 09042 Monserrato, Cagliari, Italy

L. Goonewardene  
Alberta Agriculture, Food and Rural Development,  
Agricultural Research Division, Edmonton, AB, Canada

J. K. G. Kramer (✉)  
Agriculture and Agri-Food Canada,  
Food Research Program, N1G 5C9 Guelph, ON, Canada  
e-mail: kramerj@em.agr.ca

found in similar commercial operations in Europe. Inclusion of small amounts of supplements for the grazing Sarda sheep resulted in improved quality of sheep meat lipids.

### Abbreviations

Ag <sup>+</sup> -HPLC	Silver ion-high performance liquid chromatography
Ag <sup>+</sup> -TLC	Silver ion-thin layer chromatography
CLA	Conjugated linoleic acid
DHA	Docosahexaenoic acid
EPA	Eicosapentaenoic acid
FA	Fatty acid
FAME	Fatty acid methyl ester
FFA	Free fatty acid
FID	Flame ionization detector
GC	Gas chromatography
HPLC	High-performance liquid chromatography
LC	Long-chain
MUFA	Monounsaturated fatty acid
PUFA	Polyunsaturated fatty acid
SFA	Saturated fatty acid
TFA	<i>Trans</i> fatty acid

### Introduction

In the last 50 years, meat and dairy products from ruminants have received a negative image, largely based on their contents of cholesterol, total fat, and specifically saturated fatty acids (SFAs), which have been related to an increased risk of coronary heart disease [1]. However, meat is also a good source of essential amino acids, fat-soluble (A, D, E and K) and B-complex vitamins (riboflavin, niacin, B6 and B12), and minerals (Zn, Fe, Mg). In addition, it is a good source of essential fatty acids and their long-chain n-3 polyunsaturated fatty acid (LC n-3 PUFA) metabolites, such as eicosapentaenoic (EPA) and docosahexaenoic acids (DHA) that are related to improved health [2]. In the last few years there has also been an increased awareness of the potential benefits of conjugated linoleic acid (CLA) present in the fats of ruminants, specifically rumenic acid (9*c*11*t*-CLA), and vaccenic acid (11*t*-18:1), its metabolic precursor [3]. CLA has been shown to protect against cancer, inflammation and diabetes in experimental animals and cell models [4, 5], and some

recent studies suggest that it reduces the risk of certain cancers [6, 7] and acute myocardial infarctions in humans [8].

There are only a few reports that provide a comprehensive fatty acid (FA) composition of beef muscle, including all the *trans*-octadecenoic acids (18:1), CLA isomers, and the long-chain PUFAs [9–13]. The FA composition of sheep meat is generally less complete [14–19], except for a recent report by Bessa et al. [20]. The accurate determination of the LC n-3 PUFAs in meat lipids is essential for assessing their contribution to our diet. The current concern over *trans* fatty acids (TFAs) and their association with coronary heart disease [1, 21] and inflammation [22] includes meat and dairy products of ruminants, since they also contain TFAs. Even though at this time the TFA regulation excludes CLA from mandatory labeling [23], the exclusion does not apply to 11*t*-18:1, the metabolic precursor of 9*c*11*t*-CLA. Since the TFA isomers responsible for the negative effects have not been identified, it is difficult to assess whether the TFAs from industrial and ruminant fats pose a similar health risk [24]. Therefore, accurate analyses of the CLA, *trans*-18:1, *cis/trans*-18:2 and LC PUFAs are needed to provide a more reliable database that can be used to assess the possible involvement of these TFAs in health-related issues. Currently many feeding studies are designed to decrease the content of SFAs and increase the content of the n-3 PUFAs and CLA in the meat of ruminants [25–27]. However, this requires an accurate determination of all the CLA and TFA isomers, since dietary manipulations may not necessary increase the desirable isomers, i.e., 9*c*11*t*-CLA and 11*t*-18:1 [28, 29].

Diaz et al. [16] reported the FA compositions of lamb meat from different production systems, including lambs fed mainly pasture in Uruguay, high-concentrate diets in Spain, or a combination of the two systems in the United Kingdom and Germany. They reported individual PUFAs and total CLA contents, but not TFA and CLA isomer compositions. Very little is known about the FA composition of meat from sheep reared on marginal grasslands, and for this reason Sarda sheep raised in Sardinia were investigated. About 40% of the sheep industry in Italy is located in Sardinia, where over three million Sarda sheep are raised on about 15,000 farms (data from the Italian Institute of Statistics for 2002; see <http://www.istat.it>). The estimated value of this industry is about 350 million Euros/year. Eighty percent of the income from Sarda sheep derives from milk (350 × 10<sup>6</sup> L/year) and cheese production (56 × 10<sup>6</sup> kg/year), and 20% from the sale of meat of one-year-old lambs (12,600 heads)

(data from 2003 from [30]). However, about 1,000 muttons and 77,000 ewes are slaughtered every year and their meat is only used to a limited extent for human consumption.

The main purpose of the present study was to describe comprehensive methods for the complete analysis of total meat lipids. We chose to analyze the meat from adult Sarda sheep raised under typical commercial settings in Sardinia, because such information is not currently available and the results will serve to assess the quality of this meat in preparation for its potential use. The first group of sheep meat was sampled from commercial abattoirs, and the second group comprised sheep meat obtained from three larger commercial farm establishments with good feeding practices. A combination of methods was used to analyze the TFA and CLA isomers; a combination of GC with long polar capillary columns and silver-ion TLC ( $\text{Ag}^+$ -TLC) techniques was used to analyze the TFA isomers [28, 29, 31, 32], and  $\text{Ag}^+$ -HPLC was used to determine the CLA isomers [28, 33, 34]. In addition, we report here for the first time the complete lipid composition of the plasmalogenic lipids in meat. Plasmalogenic lipids are ubiquitous constituents in all meat products [35]. However, in recent years their content in meat appears to have been overlooked because of the widespread use of base-catalyzed methylation procedures to avoid isomerization of CLA during methylation [36]. The alk-1-enyl ether bond in plasmalogenic lipids is stable under alkali-catalyzed methylations, but not under acid-catalyzed methylation procedures [28, 29, 32, 37].

## Materials and Methods

### Materials

Several pure free fatty acids (FFAs) were obtained from Sigma-Aldrich (St. Louis, MO, USA) including

arachidonic (20:4n-6), linoleic (18:2n-6),  $\alpha$ -linolenic (18:3n-3), eicosatrienoic (20:3n-9), vaccenic (11t-18:1), and erucic acids (13c-22:1). In addition, several *trans*-18:1 (6t-, 7t-, 9t-, 11t-, 12t-, 13t- and 15t-), *cis*-18:1 (6c-, 7c-, 9c-, 11c-, 12c-, 13c- and 15c-) isomers and 20:3n-9 were obtained from Sigma-Aldrich. A GC reference standard (#463), a mixture of four positional CLA isomers (#UC-59M) and long-chain saturated fatty acid methyl esters (FAMES) (17:0, 21:0, 23:0, and 26:0) were obtained from Nu-Chek Prep. Inc., (Elysian, MN, USA). All chemicals and solvents were of analytical grade. Trimethylsilyl-diazomethane (TMS-DAM) was purchased from TCI America (Portland, OR, USA).

### Animals and Diets

In the first study, 80 adult Sarda sheep were randomly selected at several abattoirs in the northern regions of Sardinia during the months of April, May, June and July 2002. The sheep ranged in age from two to seven years. Samples of *longissimus dorsi* muscle were obtained 24 h post-slaughter and stored at  $-20^\circ\text{C}$  until analyzed. No information was available on the amount and type of feed supplements they received, if any. In the second study, 36 sheep were sampled from three established farms in the Sassari region during April and July 2003. The farms were selected based on location, good management practices, and knowledge of the supplement provided (Table 1). Even though the farms reported the type and average amount of supplement per sheep during the spring and early summer, this should be considered to be an estimate since actual consumption data were not measured and the switchover between diets was a transition and was not the same at all farms. In addition, the feed supplement was not analyzed. All muscles (*longissimus dorsi*) samples were obtained 24 h post-slaughter and stored at  $-20^\circ\text{C}$  until analyzed. The sheep ranged in age from three to eight years, had grazed freely, and

**Table 1** Supplements provided to pasture-fed sheep at three farm operations in the Sassari region of Sardinia

Time	Diet	Farms in the Sassari region		
		Muzzoni (M)	Area (A)	Piras (P)
Before April 2003	Pasture	Ad libitum	Ad libitum	Ad libitum
	Supplement	Corn/peas/barley	Barley	Commercial
	Amount (g/sheep/d)	300 g	100 g	300 g
April–July 2003	Pasture	Ad libitum	Ad libitum	Ad libitum
	Supplement	None	None	Commercial
	Amount (g/sheep/d)	–	–	200 g

had been provided with a limited amount of concentrate (Table 1).

#### Lipid Extraction and Preparation of FAs for UV Determination

To investigate the CLA metabolites, sheep meat (0.3–0.4 g) was ground using a mechanical grinder (Ultra-Turrax T8, S8N-8G, IKA-Werke, Staufen, Germany), and the total lipids were extracted [38] and stored in chloroform at  $-20^{\circ}\text{C}$ . The total lipids were quantitated using the method described by Chiang et al. [39]. Briefly, 0.25 mL of the lipid extract were added to a 1.5 mL potassium dichromate solution (2 g  $\text{K}_2\text{Cr}_2\text{O}_7$  and 4 mL  $\text{H}_2\text{O}$  were made up to 100 mL with concentrated  $\text{H}_2\text{SO}_4$ ) and heated for 30 min at  $100^{\circ}\text{C}$ . After cooling, 1.5 mL  $\text{H}_2\text{O}$  was added and the UV absorbance was measured at 600 nm.

An aliquot of the total lipids (3 mL) was mildly saponified in 5 mL of ethanol to which 100  $\mu\text{L}$  of Desferal (25 mg/mL  $\text{H}_2\text{O}$ ), 1 mL ascorbic acid (10 g/40 g  $\text{H}_2\text{O}$ ), and 0.5 mL 10 N KOH was added [40]. The solution was left at room temperature in the dark for 14 h. After the addition of hexane (10 mL) and  $\text{H}_2\text{O}$  (7 mL), and acidification with 37% HCl to pH 3–4, the hexane layer was clarified by centrifugation. The hexane phase was collected, and after removal of the solvent, the FFA residue was dissolved in 0.5 mL of 0.14%  $\text{CH}_3\text{COOH}$  in  $\text{CH}_3\text{CN}$ . Conjugated and unsaturated FFAs were analyzed using an HPLC system (Model 1100, Agilent Technologies, Palo Alto, CA, USA) equipped with a quaternary pump (G1311A), an autosampler (G1313A), and a diode array detector (G1315B). A reversed-phase C-18 column was used (Inertsil ODS-2, 5  $\mu\text{m}$  particle size,  $150 \times 4.6$  mm; GL Sciences Inc., CPS Analytica, Milan). The mobile phase was  $\text{CH}_3\text{CN}/\text{H}_2\text{O}/\text{CH}_3\text{COOH}$  (70/30/0.12) operated isocratically at a flow rate of 1.5 mL/min. Unsaturated unconjugated FFAs were detected at 200 nm and conjugated diene FA at 234 nm. The latter were confirmed via their second-derivative UV spectra generated using the Phoenix 3D HP ChemStation software (Hewlett-Packard, Palo Alto, CA, USA) [41, 42]. The second-derivative UV spectra showed two typical negative peaks at about 233–238 nm and 244–247 nm [41]. In addition, the presence of hydroperoxy-octadecatrienoic acids were identified at 234 nm in sheep meat lipids by RP-HPLC; these had been previously characterized by UV and mass spectrometry [43]. The FFAs were also converted to their FAMES using TMS-DAM for total FA determination [44].

#### Lipid Extraction and Preparation of FAMES for GC Determination

In the second study, total lipids were extracted from about 5 g of sheep meat using  $\text{CHCl}_3/\text{CH}_3\text{OH}$  (1:1) after pulverization at dry ice temperature [45]. The total lipids were then partitioned in  $\text{CHCl}_3/\text{CH}_3\text{OH}/\text{H}_2\text{O}$  (1:1:0.9) to remove any nonlipid material [46]. The chloroform layer was collected, and after removal of the solvent the total lipids were weighed and then dissolved in 15 mL chloroform and stored at  $-70^{\circ}\text{C}$  until analyzed. An aliquot of total lipids was saponified and analyzed by RP-HPLC as described above. Several sheep muscle lipids (3–4 mg) were analyzed by three-directional TLC to assess the relative distributions of all the sheep meat lipids, and test for the presence of plasmalogenic lipids after exposure of the TLC plates to HCl fumes following the first development [47].

Total sheep muscle lipids were separately methylated using acid- and base-catalyzed procedures. Acid-catalyzed methylations were performed to derivatize all lipids by reacting about 30 mg total lipids with 1 mL anhydrous HCl/ $\text{CH}_3\text{OH}$  (5% w/v) for 1 h at  $80^{\circ}\text{C}$ . The base-catalyzed methylation procedure was used to retain the CLA isomer profile [36] by reacting 2 mg of total lipids with 0.5 mL  $\text{NaOCH}_3$ /methanol solution (0.5 N methanolic base #33080, Supelco Inc., Bellefonte, PA, USA) in a 2 mL autosampler vial for 15 min at  $50^{\circ}\text{C}$  [28, 48]. The methylated products from the base method and one-tenth of those from the acid-catalyzed method were purified on precoated Silica G TLC plates (Fisher Scientific Inc., Ottawa, ON, Canada) using the developing solvent hexane/diethyl ether/acetic acid (85:15:1). The bands corresponding to FAMES in the base-catalyzed product, and FAMES plus dimethylacetals (DMAs) in the acid-catalyzed methylation, were located using UV light after spraying the plate with a 2',7'-dichlorofluorescein solution in methanol. After removal of the bands, the methylated products were eluted from the silica gel with hexane and concentrated for analysis by GC.

The remaining acid-catalyzed methylation products (about 28 mg of FAMES and DMAs) were applied onto a precoated Silica G plate using a TLC applicator (Applied Science, State College, PA, USA). The developing solvent was 1,2-dichloroethane in which FAMES eluted just ahead of the DMAs [49]. The bands corresponding to the FAMES and DMAs were removed with hexane after they were visualized by spraying with 2',7'-dichlorofluorescein and detected under UV light. The FAME and DMA fractions were analyzed separately by GC using the same column and chromatographic conditions.

### Analysis of Dimethylacetals (DMAs) by GC

The DMAs produced during acid-catalyzed methylation of the plasmalogenic lipids were not stable at the injector temperature of 250 °C in the GC, resulting in the partial loss of one methanol to form alk-1-enyl methyl ethers (AMEs) [50]. The AMEs can occur in both the *cis* and the *trans* configurations [51]. The more stable cyclic acetals were prepared by reacting the isolated DMAs with 1,3-propanediol in the presence of catalytic amounts of *p*-toluenesulfonic acid [52]. The GC elution order of a given alk-1-enyl ether moiety is AME < DMA < cyclic acetal.

### Gas Chromatography (GC)

The gas chromatograph (Model 5890, Series II, Hewlett-Packard, Palo Alto, CA, USA) was equipped with splitless injection port (flushed after 0.3 min), a flame ionization detector (FID), an autosampler (Hewlett-Packard, Model 7673), a 100 m CP-Sil 88 fused capillary column (Varian Inc., Mississauga, ON, Canada), and a Hewlett-Packard ChemStation software system (Version A.09). The injector and detector temperatures were both set at 250 °C, H<sub>2</sub> served as carrier gas (1 mL/min), and the FID gases were H<sub>2</sub> (40 mL/min), N<sub>2</sub> (30 mL/min), and purified air (300 mL/min). The temperature program was as follows: initial temperature was 45 °C held for 4 min, programmed at 13 °C/min to 175 °C and held for 27 min, then programmed at 4 °C/min to 215 °C and held for 35 min [28, 32].

### Analyses of *Trans* 18:1 FA Isomers by Ag<sup>+</sup>-TLC/GC

For complete separation and identification of all *trans*-18:1 isomers, the total FAME mixture of meat lipids was fractionated into saturated, mono-*trans*, and mono-*cis* plus conjugated FAMES using silver-ion-impregnated Silica G TLC plates [28, 32, 53, 54]. The developing solvent was hexane/diethyl ether (90:10). The bands were visualized under UV light after spraying with 2',7'-dichlorofluorescein, eluted from the silica gel and analyzed by GC. The FAME fractions were analyzed using a stepwise temperature program starting at 120 °C [28, 32]. In addition, the *cis* and *trans* fractions were analyzed at high and low sample loads to resolve the minor and major FAME isomers.

### Analyses of CLA Isomers by Ag<sup>+</sup>-HPLC

The FAMES obtained by base-catalyzed methylation were used to determine the CLA isomer composition by

Ag<sup>+</sup>-HPLC, because this methylation procedure retained the original CLA profile [36]. The HPLC system was similar to that described above for the UV analysis of free and conjugated FAs. The diode array detector was operated at 233 nm for CLA and at 205 nm for unsaturated FAMES. Three ChromSpher 5 Lipids analytical silver-ion impregnated columns (Varian Inc.) were used in series [33]. The mobile phase was hexane/acetonitrile/*tert*-butylmethyl ether (99.4:0.1:0.5) operated isocratically at a flow rate of 1.0 mL/min. A small amount of toluene was added to each sample to estimate the void volume and aid the identification of the CLA isomers relative to 9*c*11*t*-18:2 [34].

### Identification and Quantitation of FAMES and DMAs

The FAMES were identified by comparison with known FAME standards, which included GC standard mixture #463, CLA mixture #UC-59M with all four positional isomers, plus other FAMES (21:0, 23:0 and 26:0), all available from Nu-Chek Prep. (Elysian, MN, USA) [28, 32, 55, 56]. The DMAs were identified by their ease of cleavage under HCl fumes [47], their selective reactivity to only acid-catalyzed methylation [28, 32], their characteristic separation from FAMES by TLC using 1,2-dichloroethane as developing solvent [49], and by their GC chromatographic profiles. The individual DMAs were identified after conversion to cyclic acetals [52] and subsequent analysis by GC. No standards of DMAs or their cyclic acetals were available. Identification of the cyclic acetals was based on their relative elution order and their similarity to the FAME profiles. The structures of the major DMAs and cyclic acetals were confirmed by GC/MS.

Quantitation of the FAMES and DMAs was based on the FID response of the acid-catalyzed methylation products. The CLA isomers were quantitated using the GC FID response, while the relative proportion of most CLA isomers was complemented using the Ag<sup>+</sup>-HPLC separation [28]. Quantitation of the unresolved *trans* 18:1 isomers required a prior separation by Ag<sup>+</sup>-TLC and subsequent analysis of the *trans* fraction using a GC temperature program starting at 120 °C. The *trans*-18:1 isomers 6*t*- to 11*t*-18:1 were well separated and free of interferences after using both GC programs and therefore served as internal comparisons [28]. The sum of all DMA and AME peaks in the GC chromatogram from the acid-catalyzed methylation mixture was used to quantitate the total alk-1-enyl content of the meat lipids. The composition of the alk-1-enyl moieties was obtained by GC analysis of the cyclic acetals.

## Statistical Analysis

The data from the second study was analyzed as six separate treatments using the GLM procedure of SAS [57]. Farm and sampling times were not used as factors given that true farm and time effects could not be determined due to confounding dietary differences between farms. In addition, the amount of feed provided per sheep was an estimate based on the amount of feed provided to the herd, and no analysis of the feed was determined. Statistical differences between the groups were identified at  $P < 0.05$  using Duncan's multiple range test.

## Results

In the first study, 80 sheep were sampled with a mean age of  $4.5 \pm 1.1$  years (range 2–7 years), a mean live weight of  $42.5 \pm 5.7$  kg (range 30–56.5 kg), and a carcass mean weight of  $18.0 \pm 3.1$  kg (range 12–25.2 kg) after 1 h, and  $17.6 \pm 3.1$  kg (range 11.7–24.9 kg) after 24 h following slaughter. The slaughter yield was  $42.3 \pm 3.9\%$  and  $41.3 \pm 3.6\%$  after 1 and 24 h, respectively. The mean carcass pH after 1 h was  $6.7 \pm 0.2$  (range 5.5–7.5) and  $5.7 \pm 0.1$  (range 5.2–6.3) after 24 h. The pH declined markedly in the first 5 h after slaughter, from 6.4 to 5.9, and more slowly thereafter, reaching a final value of 5.7. The mean temperature of the carcasses was  $32.1 \pm 1.9$  °C (range 27.3–36.2 °C) after 1 h and  $3.8 \pm 1.9$  °C (range 1.1–9.0 °C) after 24 h. The cooling curve was regular, with the temperature falling below 7 °C in about 8 h and below 4 °C in about 12 h. For more detailed information on the characteristics of the Sarda sheep meat, see Mazzette et al. [58].

The mean total meat lipid contents of the 80 sheep randomly sampled at the abattoir in 2002 were  $47.1 \pm 26.0$  mg/g of wet weight of tissue in April,  $56.40 \pm 19.5$  in May,  $54.51 \pm 32.0$  in June and  $59.15 \pm 26.0$  in July. The variability among samples was high, and there were no significant differences among different time periods. The rainfall from January to July 2002 was 310 mm (<http://www.sar.sardegna.it>). The sheep were randomly selected after being raised in Northern Sardinia, and no diet information was available. In the following year (2003), Sarda sheep were sampled from three farm operations near Sassari, where information on the type and amount of feed supplemented was reported (Table 1), but the detailed FA composition was not determined. The total lipid content in the meat sampled in April was significantly higher than in July from farms M and A,

while farm P showed no significant differences between time periods (Table 2). In 2003 more rainfall was reported from January to July (355 mm) compared to the same period in 2002.

In this study, we report the FA and alkenyl ether compositions of total sheep meat available in a specific cut of *longissimus dorsi* muscle from sheep. No attempt was made to analyze neutral and phospholipids separately, or the individual lipid class, but superficial fat was trimmed. This was done to more accurately reflect the total lipids available in a common cut of Sarda sheep meat. The total meat lipids from a few sheep were analyzed for their complete lipid compositions in order to assess the relative lipid profile. The lipid subclasses were resolved using a three-directional TLC system (Fig. 1), and individual lipid classes were estimated by densitometry [47]. The major neutral lipids in sheep meat were triacylglycerol (TAG; ~50%) and free cholesterol (C; ~4%), while the major phospholipids were phosphatidylcholine (PC; ~23%), followed by phosphatidylethanolamine (PE; ~13%), diphosphatidylglycerol (DPG; ~4%) and sphingomyelin (SM; ~3%). There were small amounts of phosphatidylserine (PS), phosphatidylinositol (PI) and cholesterol esters (CEs). Each of the phospholipids may include different proportions of the 1,2-diacyl- and 1-alk-1-enyl, 2-acyl- structures that were not resolved by TLC. FFAs were present in the meat lipids since the cuts were obtained 24 h after slaughter, which would have caused some lipid autolysis. Every effort was made in the second study to minimize further endogenous lipase activity by freezing and storing the tissue, and pulverizing the meat tissue at dry ice temperatures [45]. Plasmalogenic lipids were detected, mainly in the PE and much less in the PC fractions of sheep meat lipids as determined by exposing the separated lipids on the TLC plate to HCl fumes after the first development and before the second TLC development [47]; these results are not shown here.

The variation in the FA compositions of Sarda sheep randomly selected from April to July 2002 study was extensive. Only selected data from the first study will be presented here to demonstrate these wide differences, even though it could be argued that they more accurately reflect the FA composition of Sarda sheep from Sardinia. The FA compositions of the *longissimus dorsi* muscles from the 36 sheep sampled in the second trial are shown in Table 2. The relative concentrations of *trans*-18:1, CLA and plasmalogenic lipids were corrected by combining the results from different chromatographic techniques; see the “Materials and methods” section. In general, the FA profiles for the muscles of the sheep in the second study showed only

**Table 2** Total lipid composition (% of total FID response) of Sarda sheep muscle sampled at three farms (Muzzoni, Area, and Piras) and at two time periods (April and July)

Fatty acid	April			July			SEM
	M	A	P	M	A	P	
14:0	1.64	1.64	1.64	2.03	1.75	1.84	0.06
15:0 iso	0.14	0.10	0.13	0.12	0.11	0.14	0.01
15:0 ai	0.12	0.10	0.16	0.12	0.12	0.14	0.02
15:0	0.32	0.29	0.34	0.32	0.29	0.36	0.03
16:0 iso	0.11 <sup>a</sup>	0.08 <sup>a</sup>	0.10 <sup>a</sup>	0.03 <sup>b</sup>	0.05 <sup>b</sup>	0.05 <sup>b</sup>	0.01
16:0	24.06 <sup>a</sup>	22.38 <sup>ab</sup>	22.89 <sup>ab</sup>	24.25 <sup>a</sup>	21.40 <sup>b</sup>	23.54 <sup>a</sup>	0.44
Σ16:1 <i>trans</i>	0.28 <sup>bc</sup>	0.38 <sup>a</sup>	0.34 <sup>ab</sup>	0.26 <sup>c</sup>	0.31 <sup>bc</sup>	0.28 <sup>bc</sup>	0.02
7c-16:1	0.29	0.27	0.34	0.26	0.26	0.34	0.02
9c-16:1	1.17	1.21	1.11	1.21	1.04	1.19	0.04
17:0 iso	0.48	0.41	0.49	0.44	0.43	0.50	0.02
17:0 ai	0.57	0.54	0.59	0.51	0.57	0.56	0.02
17:0	0.94	0.95	0.95	0.94	0.95	0.99	0.02
9c-17:1	0.40	0.47	0.46	0.47	0.46	0.47	0.02
18:0 iso	0.17	0.13	0.15	0.14	0.16	0.16	0.01
18:0	16.35	15.37	16.82	16.49	16.29	16.01	0.30
10t-18:1	0.22	0.32	0.31	0.29	0.24	0.21	0.03
11t-18:1	1.19 <sup>b</sup>	1.88 <sup>a</sup>	1.86 <sup>a</sup>	1.34 <sup>ab</sup>	1.92 <sup>a</sup>	1.46 <sup>ab</sup>	0.13
Σ18:1 <i>trans</i>	3.12 <sup>ab</sup>	3.96 <sup>a</sup>	3.84 <sup>a</sup>	2.80 <sup>b</sup>	3.86 <sup>a</sup>	3.11 <sup>ab</sup>	0.20
9c-18:1	34.73	36.53	34.32	33.77	34.46	35.46	0.40
11c-18:1	0.75	0.74	0.77	0.67	0.71	0.74	0.03
12c-18:1	0.25	0.20	0.22	0.24	0.20	0.21	0.02
13c-18:1	0.12	0.13	0.11	0.11	0.14	0.13	0.01
14c-18:1	0.20	0.19	0.17	0.19	0.18	0.18	0.01
15c-18:1	0.18	0.20	0.15	0.18	0.19	0.16	0.01
16c-18:1	0.11	0.13	0.11	0.12	0.11	0.12	0.01
19:0	0.14	0.13	0.15	0.16	0.15	0.15	0.01
9c13t/8t13c-18:2	0.47	0.60	0.48	0.49	0.51	0.47	0.03
8t12c/9c12t-18:2	0.28 <sup>ab</sup>	0.33 <sup>a</sup>	0.24 <sup>b</sup>	0.27 <sup>ab</sup>	0.29 <sup>ab</sup>	0.26 <sup>ab</sup>	0.02
9t12c-18:2	0.03	0.05	0.05	0.03	0.05	0.04	0.01
11t15c-18:2	0.25 <sup>b</sup>	0.43 <sup>a</sup>	0.34 <sup>ab</sup>	0.30 <sup>ab</sup>	0.41 <sup>a</sup>	0.32 <sup>ab</sup>	0.03
18:2n-6	4.21	3.52	4.63	4.28	4.61	3.97	0.17
20:0	0.09	0.08	0.08	0.10	0.09	0.09	0.01
11c-20:1	0.08	0.08	0.08	0.07	0.08	0.07	0.01
18:3n-3	1.51	1.23	1.14	1.42	1.39	1.34	0.06
Σ CLA	0.63 <sup>c</sup>	1.01 <sup>a</sup>	0.82 <sup>bc</sup>	0.63 <sup>c</sup>	0.93 <sup>ab</sup>	0.74 <sup>c</sup>	0.06
20:2n-6	0.04	0.04	0.05	0.04	0.04	0.04	0.01
9c11t15c-18:3	0.16 <sup>b</sup>	0.19 <sup>ab</sup>	0.21 <sup>a</sup>	0.16 <sup>b</sup>	0.22 <sup>a</sup>	0.18 <sup>ab</sup>	0.01
22:0	0.03	0.03	0.03	0.04	0.04	0.03	0.01
20:3n-6	0.04	0.04	0.04	0.04	0.03	0.04	0.01
20:4n-6	1.00	0.84	0.96	1.03	1.06	0.94	0.04
20:5n-3	0.31 <sup>ab</sup>	0.37 <sup>ab</sup>	0.23 <sup>b</sup>	0.35 <sup>ab</sup>	0.49 <sup>a</sup>	0.35 <sup>ab</sup>	0.04
24:0	0.03	0.03	0.02	0.04	0.04	0.02	0.01
22:4n-6	0.06	0.04	0.05	0.05	0.05	0.05	0.01
22:5n-6	0.39 <sup>ab</sup>	0.44 <sup>ab</sup>	0.31 <sup>b</sup>	0.45 <sup>ab</sup>	0.56 <sup>a</sup>	0.49 <sup>ab</sup>	0.04
22:6n-3	0.12 <sup>ab</sup>	0.11 <sup>ab</sup>	0.07 <sup>b</sup>	0.13 <sup>a</sup>	0.12 <sup>ab</sup>	0.15 <sup>a</sup>	0.02
Σ DMA	2.29	2.36	2.30	2.29	2.94	1.91	0.16
Σ SFA	45.21 <sup>a</sup>	42.28 <sup>b</sup>	44.58 <sup>ab</sup>	45.80 <sup>a</sup>	42.48 <sup>b</sup>	44.64 <sup>ab</sup>	0.62
Σ branched-chain FA	1.57	1.37	1.61	1.37	1.44	1.55	0.05
Σ <i>cis</i> -MUFA	41.41 <sup>ab</sup>	44.15 <sup>a</sup>	41.70 <sup>ab</sup>	40.45 <sup>b</sup>	41.47 <sup>ab</sup>	42.11 <sup>ab</sup>	0.58
Σ n-6 PUFA	5.40	4.56	5.82	5.53	5.92	5.14	0.22
Σ n-3 PUFA	2.37	2.19	1.78	2.39	2.59	2.37	0.13
Σ LC n-6 PUFA	1.15	1.01	1.16	1.22	1.28	1.13	0.06
Σ LC n-3 PUFA	0.86 <sup>ab</sup>	0.96 <sup>ab</sup>	0.64 <sup>b</sup>	0.97 <sup>ab</sup>	1.20 <sup>a</sup>	1.03 <sup>ab</sup>	0.10
n-6/n-3 PUFA	2.30 <sup>b</sup>	2.10 <sup>b</sup>	3.37 <sup>a</sup>	2.33 <sup>b</sup>	2.31 <sup>b</sup>	2.20 <sup>b</sup>	0.15
SFA/PUFA	5.93	6.57	5.98	6.08	5.16	6.04	0.22
14:0/9c-14:1	40.1	38.1	50.3	41.4	50.7	42.0	2.20
16:0/9c-16:1	20.7	18.7	20.9	20.5	21.3	20.0	0.43
17:0/9c-17:1	2.3	2.0	2.1	2.0	2.1	2.1	0.07

**Table 2** continued

Fatty acid	April			July			SEM
	M	A	P	M	A	P	
18:0/9c-18:1	0.47	0.43	0.50	0.50	0.48	0.46	0.03
11t-18:1/9c11t-CLA	3.59	3.03	3.68	3.59	3.16	3.17	0.13
Total fat (mg/g wet wt)	71.1 <sup>a</sup>	72.6 <sup>a</sup>	43.4 <sup>b</sup>	43.4 <sup>b</sup>	39.2 <sup>b</sup>	58.5 <sup>ab</sup>	6.05

Values are means of six sheep sampled per farm and per time period. Means with different superscript letters are significantly different at  $P < 0.05$ . 9c-18:1 contains very small amounts of 10c-18:1, LC n-6 PUFAs include 20:2n-6, 20:3n-6, 20:4n-6 and 22:4n-6, and LC n-3 PUFAs include 20:5n-3, 22:5n-3 and 22:6n-3

Abbreviations: Branched-chain fatty acid (FA) iso and anteiso (ai), CLA conjugated fatty acid, DMA dimethyl acetal, FID flame ionization detector, LC long-chain, MUFA monounsaturated fatty acid, PUFA polyunsaturated fatty acid, SEM standard error of the mean, SFA saturated fatty acid

minor differences since all of the sheep were mainly pasture-fed, with minor differences occurring between the type and amount of supplements provided; climate and grazing conditions were also similar.

### Saturated Fatty Acids (SFAs)

The total SFA content ranged from 42 to 45% of total FA, and consisted mainly of 16:0 (21–24%) and 18:0 (15–17%), with minor amounts of 14:0 (1.6–2.0%), 17:0 (1%) and 15:0 (0.3%), and trace amounts of long-chain SFA (19:0, 20:0, 22:0, and 24:0). There were significant differences between the farms. Farm A consistently showed lower levels of total SFA than farm M,

specifically in 16:0 (Table 2). The difference in SFA could be related to the amount of supplement provided on farm M compared to farm A before April (300 vs. 100 g/sheep) (Table 1); both barley and peas contain appreciable amounts (about 23%) of 16:0. The relative difference in SFA and 16:0 persisted into the results obtained in July, which indicates that the actual switchover from supplement to pasture after April appears uncertain.

Branched-chain FAs are common constituents in the fat of ruminants. The sheep meat in the present study contained small amount of iso and anteiso FAs that ranged from 1.4 to 1.6% of total FAs. There were no differences in the contents of branched-chain FAs between the farms and sampling times. The feeding of cereal starches (mixtures of peas, barley and corn) is known to increase the level of branched-chain FAs in ruminants [59].

### Monounsaturated Fatty Acids (MUFAs)

The total content of *cis*-MUFA in the sheep meat ranged from 40 to 44% (Table 2), and consisted mainly of 18:1 (35–38%) and 16:1 (1.4–1.6%), with trace amounts of 20:1 and 24:1. Except for a higher content of total *cis*-MUFA at farm A in April, there were no significant differences in the *cis*-MUFA contents between farms and sampling times. The *trans*-MUFA consisted mainly of 18:1 (3–4%) and 16:1 (0.3–0.4%). In this case, farm A, which had the lowest supplementation of a barley concentrate, consistently showed the highest *trans*-18:1 and *trans*-16:1 contents in sheep meat, while farm M had the lowest TFA contents (Table 2).

### *Cis*- and *Trans*-18:1 Isomers

There was extensive overlap of the geometric and positional 18:1 FAME isomers in the sheep meat fat

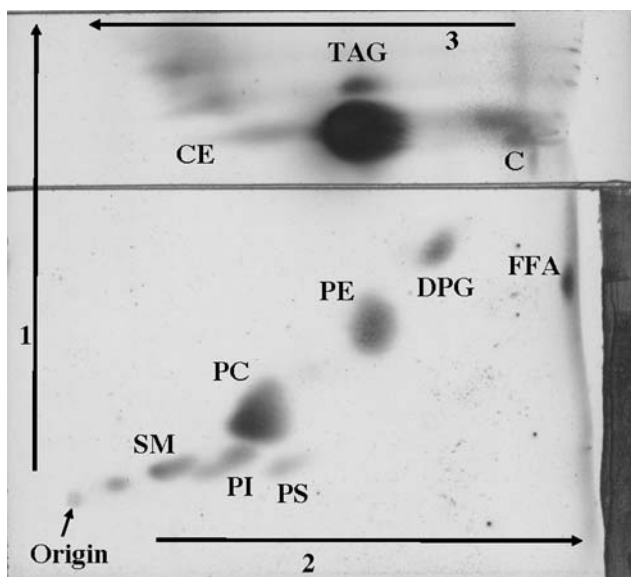


**Fig. 1** Three-directional TLC separation of total sheep muscle lipid classes on silica gel H plates. Solvent 1: chloroform/methanol/ammonium hydroxide (65:25:4), solvent 2: chloroform/acetone/methanol/acetic acid/water (50:20:10:15:5), solvent 3: hexane/diethyl ether/acetic acid (85:15:1). For the identities of the abbreviated lipid classes, see the “Results” section



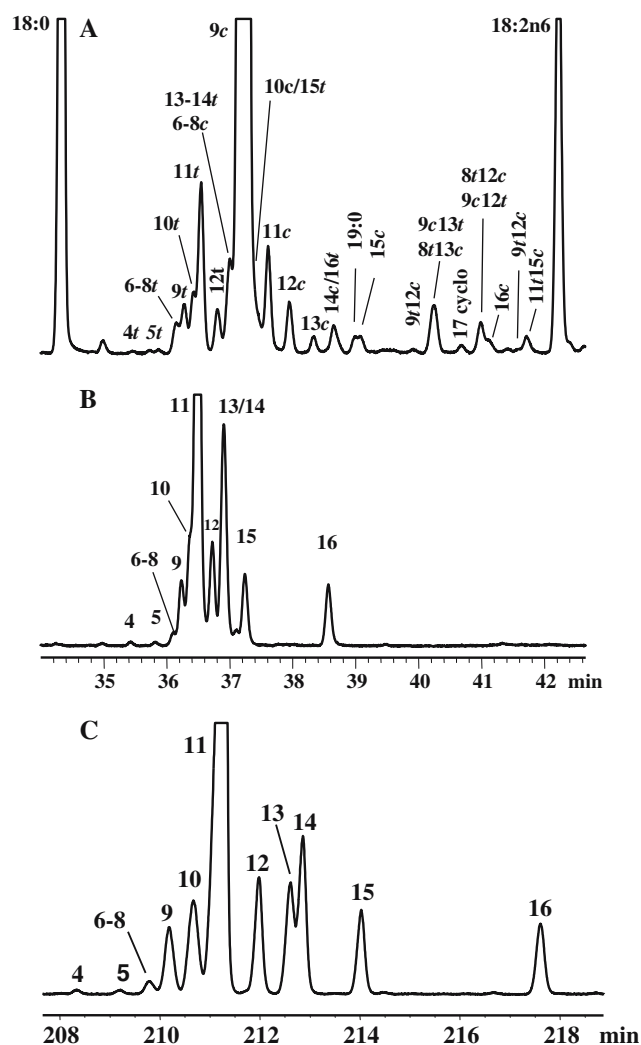


**Fig. 2A–C** A partial GC chromatogram of the 18:0 to 18:2n-6 region of total FAME from sheep muscle fat (**A**), and the isolated *trans* band isolated by  $\text{Ag}^+$ -TLC (**B**), analyzed using a GC temperature program from 45 to 215 °C. The same *trans* band was analyzed by GC using an isothermal low temperature program starting at 120 °C (**C**)

(Fig. 2A), despite using a 100 m highly polar capillary GC column. The resolution of several 18:1 isomers was slightly improved by applying lower sample loads onto the GC. The content of 13*t*-/14*t*-18:1 is often overestimated because of a lack of baseline resolution from the dominant 9*c*-18:1 peak in ruminant fats, while 15*t*- and 16*t*-18:1 were not resolved from 9*c*-18:1 and 14*c*-18:1, respectively. Depending on the relative concentrations of 10*t*- or 11*t*-18:1 isomers, the quantitation of 6*t*-8*t*- to 11*t*-18:1 isomers is also an estimate (Fig. 2A). A more reliable analysis of all the *trans*- and *cis*-18:1 isomers requires prior separation of the FAMES by  $\text{Ag}^+$ -TLC followed by low-temperature GC analyses [28, 31, 32, 54, 55]. Figure 2B shows a GC separation of the isolated *trans* band of total sheep meat FAMES by

$\text{Ag}^+$ -TLC using the same temperature program, while Fig. 2C shows the improved separation of the *trans* band achieved by using a low-temperature GC program starting at 120 °C.

The relative compositions of the individual *trans*-18:1 isomers are presented in Table 3. The major *trans*-18:1 isomer was 11*t*-18:1, which ranged from 34 to 48% of the total *trans* 18:1 isomers, or 1.2–1.9% of total methylated lipids (Table 2). The content of 11*t*-18:1 was significantly ( $P < 0.001$ ) lower in sheep muscle from farm M compared to A and P at both sampling periods. The second most abundant *trans*-18:1 isomers were the combined 13*t*-/14*t*-18:1 pair that were significantly lower ( $P < 0.01$ ) in the July than in the April samples at farms A and P when expressed as percent of total *trans*-18:1 (Table 3), and significantly higher ( $P < 0.05$ ) at farm M compared to the other two farms when expressed as percent of total FAME (0.83 vs 0.77%). Of the remaining *trans*-18:1 isomers, five isomers ranged in content from 5 to 9% (9*t*-, 10*t*-, 12*t*-, 15*t*- and 16*t*-18:1), while the unresolved isomers 6*t*- to 8*t*-18:1 were present at 3–4%, and trace amounts of 4*t*- and 5*t*-18:1 were observed.

Figure 3 (top) shows a partial GC chromatogram of 6*t*-8*t*- to 13*t*-/14*t*-18:1 from selected sheep meat lipids, representing the maximum range in the *trans*-18:1 isomer distributions observed in the 2003 samples. In all cases 11*t*-18:1 was the dominant *trans*-18:1 isomer. This was in contrast to the larger variation in *trans*-18:1 isomer compositions observed in the sheep meat lipids from the 2002 study (Fig. 3, bottom) in which 10*t*-18:1 was the second most abundant *trans*-18:1 isomer. In addition, the total *trans*-18:1 content was significantly lower in the 2002 meat samples (2.7%) compared to 2003 (3.8%). The difference in the total *trans*-18:1 contents and relative distributions of the individual *trans*-18:1 isomers appears to reflect lower quality feed supplementation and/or consumption of poorer quality pasture. *Trans*-18:1 isomers are the products of partial biohydrogenation of precursor dietary PUFAs [3].

Of the *cis*-18:1 isomers, oleic acid (9*c*-18:1) accounted for 33–36% of the total methylated lipids (Table 2), or 95–96% relative to the other *cis*-18:1 isomers; there were no significant time and farm differences. The second most abundant *cis*-18:1 isomer was 11*c*-18:1 at 0.7–0.8% of total lipids, while the remaining *cis*-18:1 isomers were present at about 0.2% (12*c*-, 14*c*- and 15*c*-18:1) and 0.1% (13*c*- and 16*c*-18:1) of total lipids (Table 2). In general there were no significant time differences for any of the isomers, but farm A consistently showed higher values of 13*c*- and 15*c*-18:1 and a lower value of 12*c*-18:1 compared to the other two farms.

**Table 3** Relative distributions (%) of total *trans*-18:1 isomers in Sarda sheep muscle fat

Fatty acid	April			July			SEM
	M	A	P	M	A	P	
4 <i>t</i> -18:1	0.64	0.55	0.51	0.55	0.64	0.57	0.05
5 <i>t</i> -18:1	0.76	0.81	0.62	0.82	0.72	0.60	0.07
6 <i>t</i> -8 <i>t</i> -18:1	4.06 <sup>ab</sup>	3.32 <sup>b</sup>	3.66 <sup>ab</sup>	4.47 <sup>a</sup>	3.71 <sup>ab</sup>	3.86 <sup>ab</sup>	0.32
9 <i>t</i> -18:1	8.31	7.42	7.14	7.32	7.14	8.06	0.35
10 <i>t</i> -18:1	6.46 <sup>ab</sup>	7.39 <sup>ab</sup>	7.66 <sup>ab</sup>	7.93 <sup>a</sup>	6.07 <sup>b</sup>	6.22 <sup>b</sup>	0.56
11 <i>t</i> -18:1	34.58 <sup>c</sup>	44.12 <sup>ab</sup>	44.77 <sup>ab</sup>	37.13 <sup>c</sup>	47.97 <sup>a</sup>	41.92 <sup>b</sup>	1.62
12 <i>t</i> -18:1	8.70 <sup>ab</sup>	7.04 <sup>c</sup>	6.66 <sup>c</sup>	9.01 <sup>a</sup>	7.20 <sup>c</sup>	8.07 <sup>b</sup>	0.69
13 <i>t</i> /14 <i>t</i> -18:1	25.20 <sup>a</sup>	20.42 <sup>b</sup>	20.67 <sup>b</sup>	22.02 <sup>b</sup>	17.41 <sup>c</sup>	19.95 <sup>c</sup>	1.42
15 <i>t</i> -18:1	5.72 <sup>a</sup>	4.36 <sup>b</sup>	4.21 <sup>b</sup>	5.28 <sup>a</sup>	4.50 <sup>b</sup>	5.46 <sup>a</sup>	0.40
16 <i>t</i> -18:1	5.65 <sup>a</sup>	4.47 <sup>b</sup>	4.15 <sup>b</sup>	5.37 <sup>a</sup>	4.57 <sup>b</sup>	5.37 <sup>a</sup>	0.39
∑18:1 <i>trans</i> (% of total FID response)	3.12 <sup>ab</sup>	3.96 <sup>a</sup>	3.84 <sup>a</sup>	2.80 <sup>b</sup>	3.86 <sup>a</sup>	3.11 <sup>ab</sup>	0.20

Values are means for six sheep sampled per farm and per time period. Three farms (Muzzoni, Area, and Piras) were sampled at two time periods (April and July). Means with different superscript letters are significantly different at  $P < 0.05$ . For abbreviations see Table 2

### 16:1 Isomers

Total *trans*-16:1 contents ranged from 0.26 to 0.38% of total FAME in sheep muscle (Table 2). In general, the

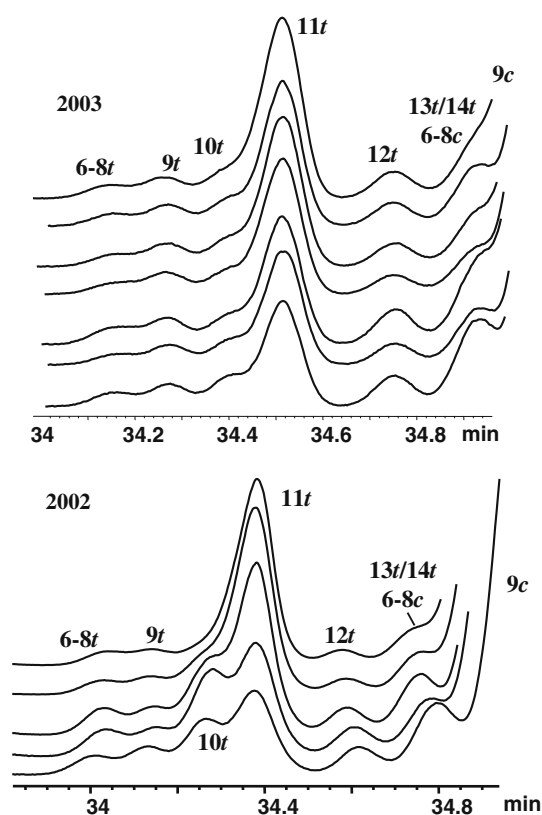


**Fig. 3** Partial GC chromatograms of the *trans*-18:1 isomers from 6*t*/7*t*/8*t*-18:1 to 13*t*/14*t*-18:1. The total sheep meat FAMES were selected from the 2002 and 2003 studies that represent the maximum variations in the relative abundances of these *trans*-18:1 isomers

values appeared higher during the April than the July sampling, and higher at farm A than farm M. These differences in *trans*-16:1 content were similar to those observed for the *trans*-18:1 isomers. The relative contents of the *cis*-16:1 isomers showed no regional and time differences and ranged from 1.4 to 1.6% of total methylated lipids. The most abundant *cis*-16:1 isomer was 9*c*-16:1, and its relative abundance ranged from 31 to 35% of the total *cis*-16:1 isomers (data not shown).

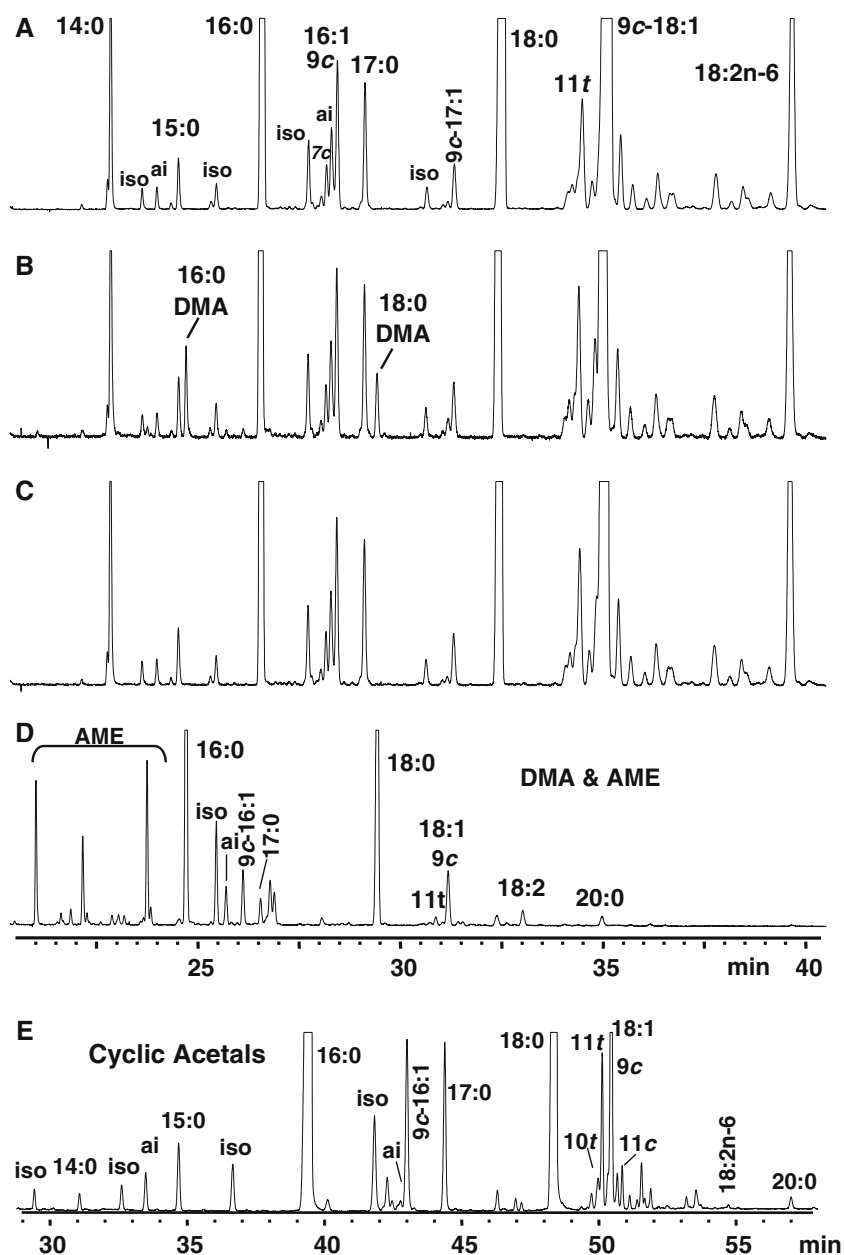
### Δ9 Desaturase Activities

The Δ9 desaturase activity was determined for a number of FA pairs, including 14:0/9*c*-14:1, 16:0/9*c*-16:1, 17:0/9*c*-17:1, 18:0/9*c*-18:1, and 11*t*-18:1/9*c*11*t*-18:2. There were no significant differences in the Δ9 desaturase ratios for each of the FA pairs (Table 2). Differences in amount and type of supplement added had little effect on the Δ9 desaturase activities.

### Dimethylacetals (DMAs) Derived from Plasmalogenic Lipids

A partial GC chromatogram of the 12:0 to 18:2*n*-6 FAMES from total sheep meat lipids is shown in Fig. 4. The total base- and acid-catalyzed methylation products are shown in Fig. 4A and B respectively, while the isolated FAME and DMA fractions obtained after TLC separation from the acid-catalyzed methylated meat mixture are shown in Fig. 4C and D, respectively. The same GC temperature program was used for all separations. The results clearly indicate that the base catalyst did not methylate plasmalogenic lipids (Fig. 4A), while the acid catalyst did (Fig. 4B). Thermal degradation of the DMAs [RCH<sub>2</sub>-CH(OCH<sub>3</sub>)<sub>2</sub>] in

**Fig. 4A–E** Partial GC chromatograms of total sheep lipids methylated using a base- (**A**) or an acid-catalyzed procedure (**B**). The acid-catalyzed methylation mixture (**B**) was resolved by TLC (developing solvent, 1,2-dichloroethane) into the FAMES derived from *O*-acyl lipids (**C**) and dimethylacetals (DMAs) from the plasmalogenic lipids (**D**). The DMA mixture was converted to the more stable cyclic acetals (**E**) used to determine the alk-1-enyl composition. All GC separations were performed using the same GC column and temperature program; see the “Materials and Methods” section. The temperature of the injection port (250 °C) caused partial loss of one methanol from the DMAs to form a mixture of alk-1-enyl methyl ethers (AMEs) and DMAs



the injection port during GC analysis resulted in the loss of methanol from DMA to form alk-1-enyl methyl ethers [AMEs;  $\text{RCH}=\text{CH}(\text{OCH}_3)$ ], as previously reported [50]. The identification of the resultant AMEs is complicated since they occur as mixtures of *cis* and *trans* conformations [51]. The extent of AME formation from DMA is a function of a number of variables, including the GC injection temperature, injection parameters, and mode of injection. Separation of the FAMES from the DMAs by TLC followed by GC analysis of the fractions permitted the identification of the peaks associated with the DMAs and AMEs (Fig. 4). The elution order for any specific alk-1-enyl

chain length was FAME > DMA > AME. On the 100 m CP Sil 88 column, the saturated 18:0 and 16:0 DMAs eluted at CN 17.05 and 15.05 relative to FAME, respectively, while the monounsaturated 9c-18:1 and 9c-16:1 DMA eluted at CN 17.68 and CN 15.68, respectively.

The plasmalogenic lipids in the total methylated reaction mixture were quantitated by adding the total area response for all DMA and AME peaks in Fig. 4B. These peaks were identified by comparing the GC results of the isolated DMAs obtained by TLC (Fig. 4D) to the total acid-catalyzed FAMES (Fig. 4B). To identify the alk-1-enyl moieties of the plasmalogenic

**Table 4** Relative percent (%) of alk-1-enyl ether moieties in the plasmalogenic lipids from Sarda sheep muscle analyzed as their cyclic acetals; see the “Materials and methods” section

Alk-1-enyl ethers	April			July			SEM
	M	A	P	M	A	P	
16:0 iso	0.78	0.92	0.89	0.97	0.92	0.81	0.05
16:0	36.37 <sup>b</sup>	36.20 <sup>b</sup>	36.93 <sup>b</sup>	41.38 <sup>a</sup>	36.90 <sup>b</sup>	38.38 <sup>b</sup>	0.80
17:0 iso	3.04	3.70	3.40	3.56	3.98	3.55	0.14
17:0 ai	5.37	4.85	4.92	4.19	4.61	4.55	0.18
17:0	7.22 <sup>a</sup>	5.07 <sup>bc</sup>	5.69 <sup>b</sup>	5.16 <sup>bc</sup>	5.91 <sup>b</sup>	4.59 <sup>c</sup>	0.37
9 <i>c</i> -17:1	0.08 <sup>c</sup>	0.14 <sup>bc</sup>	0.34 <sup>a</sup>	0.11 <sup>bc</sup>	0.24 <sup>ab</sup>	0.11 <sup>bc</sup>	0.04
18:0 iso	0.46	0.40	0.36	0.43	0.48	0.51	0.02
18:0	31.23	31.41	28.88	31.57	32.52	32.69	0.56
9 <i>t</i> -18:1	0.18	0.29	0.19	0.30	0.23	0.29	0.02
10 <i>t</i> -18:1	0.34	0.60	0.52	0.44	0.40	0.39	0.04
11 <i>t</i> -18:1	0.84 <sup>c</sup>	2.18 <sup>ab</sup>	1.77 <sup>b</sup>	1.08 <sup>c</sup>	2.63 <sup>a</sup>	1.33 <sup>bc</sup>	0.28
12 <i>t</i> -18:1	0.33	0.51	0.38	0.37	0.41	0.36	0.02
15 <i>t</i> -18:1	0.46	0.66	0.48	0.51	0.40	0.48	0.04
9 <i>c</i> -18:1	5.51 <sup>b</sup>	6.92 <sup>a</sup>	6.65 <sup>a</sup>	5.03 <sup>b</sup>	4.48 <sup>b</sup>	6.46 <sup>a</sup>	0.40
11 <i>c</i> -18:1	0.25	0.30	0.29	0.21	0.23	0.31	0.02
12 <i>c</i> -18:1	0.12	0.10	0.15	0.11	0.07	0.12	0.01
13 <i>c</i> -18:1	0.11	0.12	0.12	0.09	0.07	0.11	0.02
14 <i>c</i> /16 <i>t</i> -18:1	0.08	0.08	0.08	0.09	0.09	0.10	0.03
15 <i>c</i> -18:1	0.03	0.06	0.06	0.04	0.03	0.04	0.01

Values are means of six sheep sampled per farm and per time period. Three farms (Muzzoni, Area, and Piras) were sampled at two time periods (April and July). Means with different superscript letters are significantly different at  $P < 0.05$ . 9*c*-18:1 contains minor amounts of 13*t*-14*t*- and 10*c*-18:1. For abbreviations, see Table 2

lipids, the DMAs were converted to stable 1,3-dioxolane derivatives that are stable under GC conditions [52]. The plasmalogenic lipid content was determined by combining all the DMA and AME peaks in the acid-catalyzed mixture. The alk-1-enyl ether composition was obtained by analyzing the 1,3-dioxolane derivatives (Fig. 4E).

The total DMAs accounted for 1.9–2.9% of the total lipids in the sheep meat (Table 2). The relative composition of the alk-1-enyl chains of the plasmalogenic lipids in sheep meat is shown in Table 4. The alkenyl chains consisted mainly of saturated moieties (83–86%), mostly 16:0 and 18:0 (67–69%), but substantial amounts of iso (4.8%) and anteiso chains (4.7%) were also present. There were some significant differences between samplings but they were not consistently related to farm or time period. The *trans*-18:1 contents ranged from 2.2 to 4.9% with 11*t*-18:1 being the major isomer, and farm A showing consistently higher levels than farm M. The pattern for the *trans*-18:1 isomers and the relatively increased amounts of 11*t*-18:1 were similar to those observed for the *trans*-18:1 FAMES; see below. The total *cis*-18:1 alkenyl ethers ranged from 5.0 to 7.6% with 9*c*-18:1 being the predominant *cis*-18:1 isomer (87–92%); there were no consistent time or farm differences in any of the *cis*-18:1 isomers. Only trace amounts of 18:2 were detected. No peaks could be identified in the expected conjugated 18:2

region, but that was difficult to ascertain since no standards were available.

#### Conjugated Linoleic Acid (CLA) Isomers

Figure 5 shows a comparison of the GC (5B) and Ag<sup>+</sup>-HPLC (5D) separations of a representative total sheep muscle FAME mixture. Only the base-catalyzed methylation mixtures were used for the assessment of the CLA region since acid-catalyzed methylation caused extensive isomerization [36]. The CLA isomers were identified by comparison to a CLA standard analyzed by GC (Fig. 5A) and Ag<sup>+</sup>-HPLC (Fig. 5C) that was spiked with 21:0 FAME [28]. The peak eluting between 9*c*11*t*- and 7*t*9*c*-18:2 by Ag<sup>+</sup>-HPLC was examined to see if it was 8*t*10*c*-18:2, or a conjugated triene. A conjugated triene would give a characteristic triplet absorption centered at 270 nm. As seen in the inset next to Fig. 5D, there appeared to be no evidence of a conjugated triene coeluting with 8*t*10*c*-18:2 in sheep meat lipids. Similar results were obtained when another milk fat was examined previously [34].

The total CLA contents ranged from 0.63% to 1.01% of total sheep muscle (Table 2). Table 5 shows the relative percentage of the CLA isomers in sheep meat collected during the April and July sampling. The 9*c*11*t*-18:2 isomer was the major CLA isomer of Sarda sheep muscle, accounting for 0.41–0.74% of total lipids

**Fig. 5A–D** Partial GC chromatogram of the CLA region of the standard CLA mixture (A) and a sheep meat total FAME mixture using a 100 m highly polar capillary column (B). Partial Ag<sup>+</sup>-HPLC separation of the CLA standard (C) and sheep meat total FAME (D) using three Ag<sup>+</sup>-HPLC columns in series. The UV spectra of several CLA isomers and the unknown peak eluting between 9*c*11*t*- and 7*t*9*c*-18:2 are shown in the inset of the lower Ag<sup>+</sup>-HPLC separation

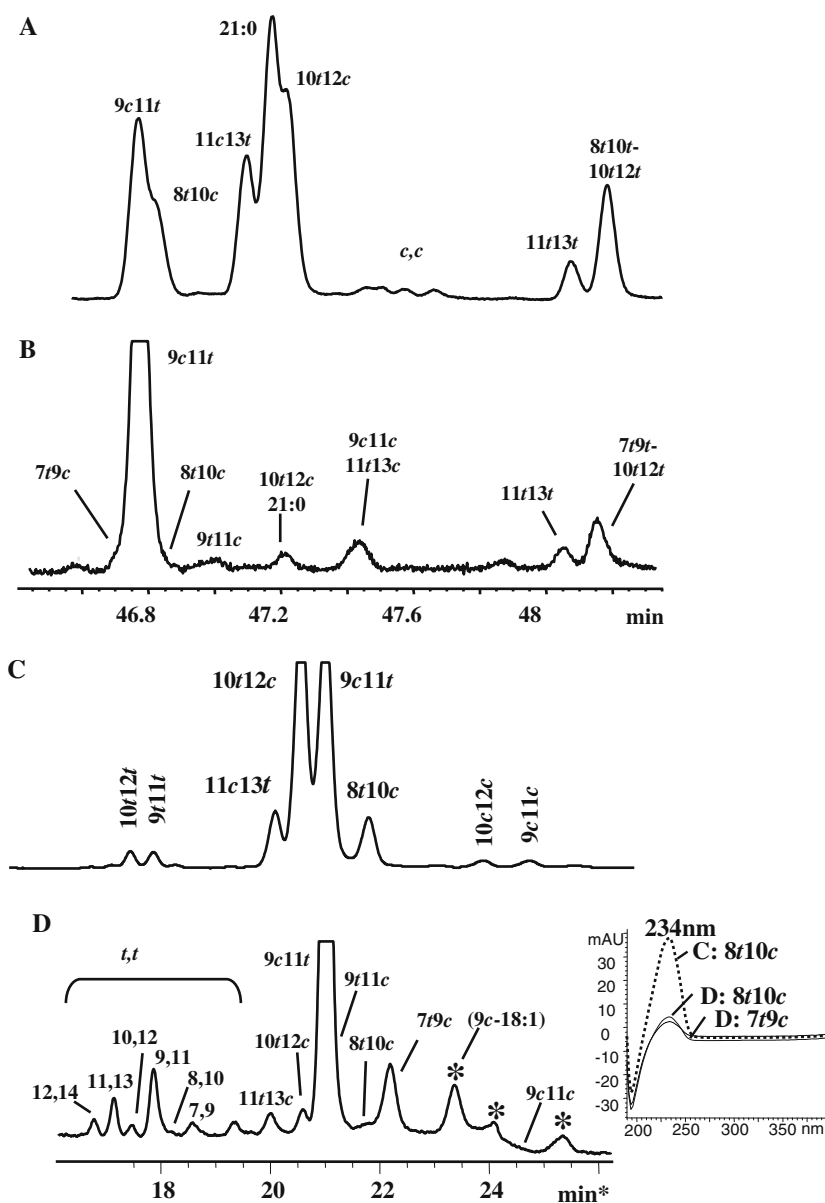


(Table 2), or 60–71% of the relative CLA isomers (Table 5). The remaining CLA isomers of the sheep meat were those generally associated with either pasture (11*t*13*c*- and 11*t*13*t*-18:2; 8–12%) or concentrate feeding of ruminants (7*t*9*t*-, 9*t*11*c*-, 10*t*12*c*- and 9*t*11*t*-18:2; 12–16%) [28, 56, 60–63]. In general, farm A had the highest levels of 9*c*11*t*-18:2 and 11*t*13*c*-18:2 and the lowest levels of 7*t*9*c*-18:2, 9*t*11*c*-18:2 and 10*t*12*c*-18:2 compared to farm M during the April sampling, while the values were more similar in July, consistent with the claim that both herds were fed pasture. The difference in the contents of 9*c*11*t*-18:2 at these farms was also reflected in their relative contents of 11*t*-18:1 (Table 3). The conjugated metabolite derived from

18:3*n*-3, 9*c*11*t*15*c*-18:3, was identified in sheep meat, which eluted just before 22:0 using the 100 m CP Sil GC column and conditions. This GC peak was first thought to be 20:3*n*-9 based on the expected elution of this FA, but it was clearly distinguishable based on coinjection with a known standard of 20:3*n*-9. The identity of this conjugated 18:3 isomer was confirmed by reversed-phase HPLC analysis; see below.

Figure 6 shows a partial GC chromatogram of the wide differences in the CLA profiles of Sarda sheep meat encountered in commercial markets in Sardinia in 2002. The data from the first study showed that some sheep were mainly pasture-fed, characterized by high levels of 11*t*13*c*- and 11*t*13*t*-18:2 and 21:0 (uppermost

**Table 5** Relative percent (%) of CLA isomers in Sarda sheep muscle lipids

CLA isomers	April			July			SEM
	M	A	P	M	A	P	
12 <i>t</i> 14 <i>t</i> -	2.90	2.64	2.04	3.50	2.52	3.06	0.20
11 <i>t</i> 13 <i>t</i> -	8.14	4.94	4.25	8.15	4.63	7.19	0.74
10 <i>t</i> 12 <i>t</i> -	0.85	0.75	0.58	0.85	0.62	0.73	0.05
9 <i>t</i> 11 <i>t</i> -	4.56 <sup>b</sup>	4.25 <sup>b</sup>	3.68 <sup>b</sup>	4.82 <sup>b</sup>	4.46 <sup>b</sup>	6.04 <sup>a</sup>	0.32
8 <i>t</i> 10 <i>t</i> -	0.32	0.09	0.13	0.31	0.10	0.35	0.05
7 <i>t</i> 9 <i>t</i> -	0.94 <sup>ab</sup>	0.60 <sup>b</sup>	0.94 <sup>ab</sup>	0.92 <sup>ab</sup>	0.79 <sup>ab</sup>	1.32 <sup>a</sup>	0.10
Σ <i>t,t</i> -CLA	17.71	13.27	11.61	18.56	13.12	18.69	1.29
12 <i>t</i> 14 <i>c</i> -	1.73	0.93	0.92	1.70	0.92	1.27	0.16
12 <i>c</i> 14 <i>t</i> -	0.84 <sup>a</sup>	0.39 <sup>b</sup>	0.28 <sup>b</sup>	0.40 <sup>b</sup>	0.28 <sup>b</sup>	0.45 <sup>b</sup>	0.08
11 <i>t</i> 13 <i>c</i> - <sup>d</sup>	4.10	4.28	3.85	3.76	3.41	4.09	0.13
10, 12 <i>c/t</i> - <sup>e</sup>	3.45	1.83	1.96	2.68	2.85	2.00	0.26
9 <i>t</i> 11 <i>c</i> -	3.21	2.26	2.90	2.89	2.98	2.97	0.13
9 <i>c</i> 11 <i>t</i> -	60.25 <sup>b</sup>	70.24 <sup>a</sup>	70.13 <sup>a</sup>	62.14 <sup>b</sup>	70.80 <sup>a</sup>	64.14 <sup>b</sup>	1.91
8 <i>t</i> 10 <i>c</i> -	1.82	1.26	1.86	1.65	1.55	1.85	0.10
7 <i>t</i> 9 <i>c</i> -	5.25 <sup>ab</sup>	3.92 <sup>b</sup>	4.46 <sup>b</sup>	6.12 <sup>a</sup>	4.02 <sup>b</sup>	4.56 <sup>b</sup>	0.34
Σ <i>c,t</i> -CLA	80.65	85.09	86.36	81.33	86.81	81.31	1.14
11 <i>c</i> 13 <i>c</i> -	0.60	0.30	1.21	0.05	0.07	0.00	0.19
9 <i>c</i> 11 <i>c</i> -	1.05 <sup>a</sup>	1.35 <sup>a</sup>	0.82 <sup>a</sup>	0.06 <sup>b</sup>	0.00 <sup>b</sup>	0.00 <sup>b</sup>	0.25
Σ <i>c,c</i> -CLA	1.64 <sup>a</sup>	1.64 <sup>a</sup>	2.03 <sup>a</sup>	0.12 <sup>b</sup>	0.07 <sup>b</sup>	0.00 <sup>b</sup>	0.09
Total CLA (% total FID response)	0.63 <sup>c</sup>	1.01 <sup>a</sup>	0.82 <sup>bc</sup>	0.63 <sup>c</sup>	0.93 <sup>ab</sup>	0.74 <sup>c</sup>	0.06

Values are means for six sheep sampled per farm and per time period. Three farms (Muzzoni, Area, and Piras) were sampled at two time periods (April and July). Means with different superscript letters are significantly different at  $P < 0.05$ . For abbreviations, see Table 2

CLA profile). On the other hand, other sheep meats contained less of the above and increasing amounts of 9*t*11*c*-, 10*t*12*c*- and 7*t*9*c*-18:2, typical of sheep fed concentrate or poor-quality pasture (lower CLA profiles). The complete identifications of 9*c*11*t*- and 7*t*9*c*-18:2, 11*t*13*c*- and 9*c*11*c*-18:2, and 10*t*12*c*-18:2 and 21:0 were achieved by comparing the GC and Ag<sup>+</sup>-HPLC separations, as shown in Fig. 5. The CLA isomer distribution in the sheep meat in the second study was less diverse, as shown in Table 5.

## PUFAs

The total n-6 and n-3 PUFA contents of Sarda sheep meat were averaged, yielding 5.4 and 2.3%, respectively (Table 2). The main n-6 and n-3 PUFAs in sheep meat were 18:2n-6 and 18:3n-3, present at about 4.2 and 1.3%, respectively, with a relative ratio of about 3:1 (18:2n-6/18:3n-3). There were some differences between farms and time periods, but the differences were not significant. The content of LC n-6 PUFAs (20:2n-6, 20:3n-6, 20:4n-6, and 22:4n-6) ranged from 1.0 to 1.3% of total lipids, and generally showed no

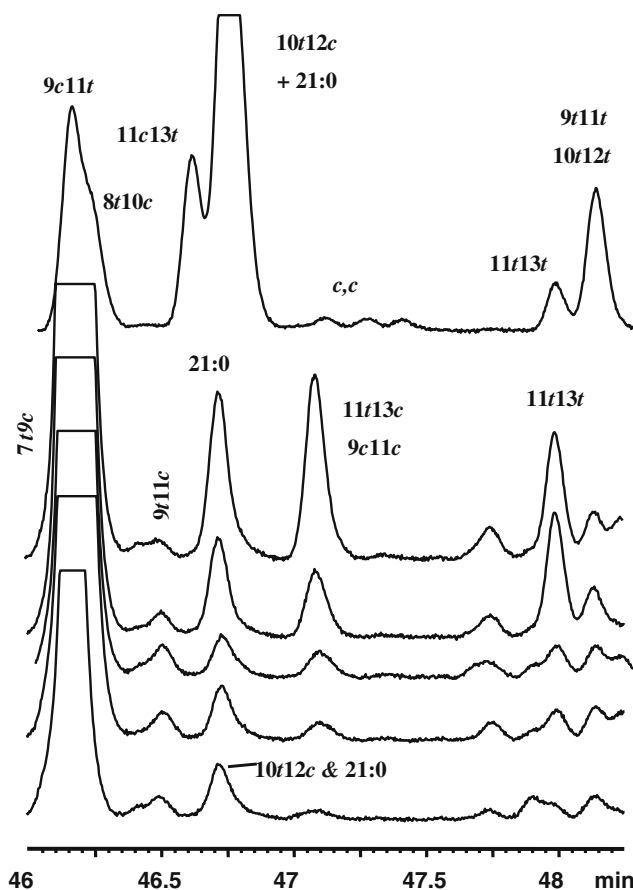


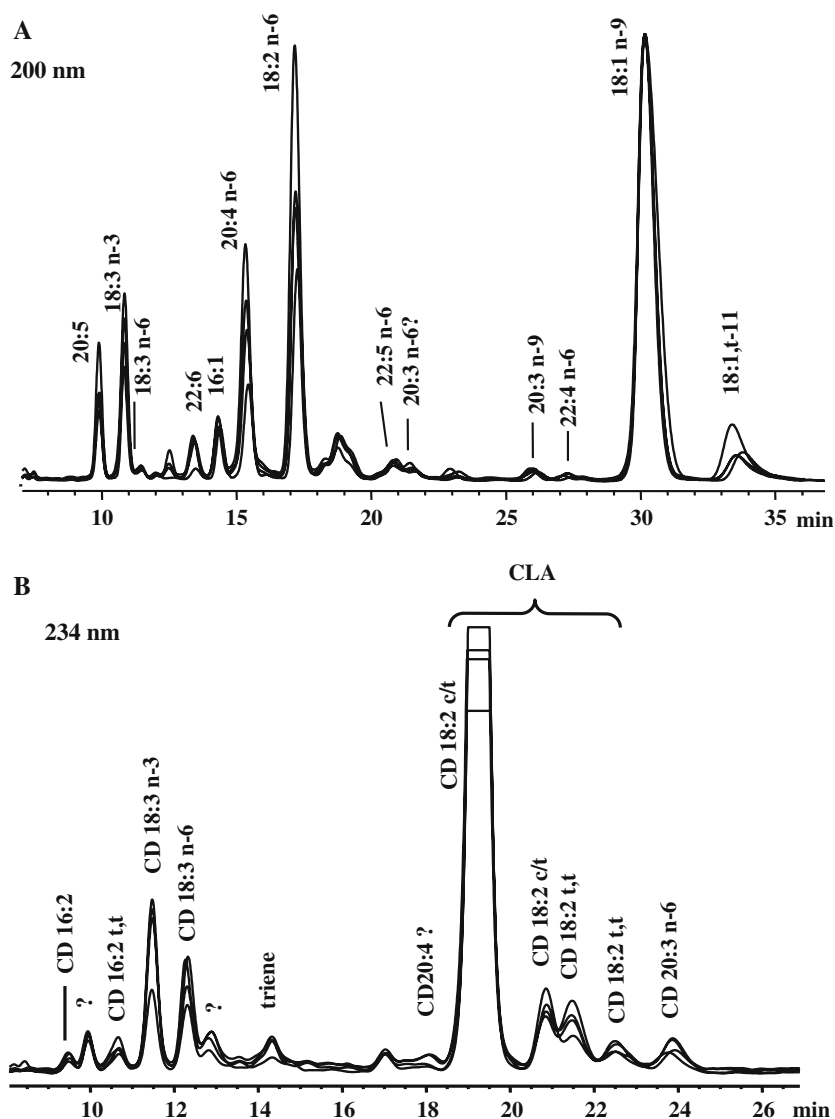
**Fig. 6** Partial GC chromatograms of the CLA region of the standard CLA mixture (upper graph) and five typical sheep meat total FAME mixtures, which represent the maximum variation observed in the CLA profiles in the 2002 study

significant farm or time differences. However, the total content of LC n-3 PUFAs (20:5n-3, 22:5n-3, 22:6n-3) in July (1.06%) was generally higher than in April (0.82%) (Table 2), which reflected the greater exposure of sheep to pasture during the early summer. The ratio of LC n-6 PUFA to LC n-3 PUFA ranged from 1.1:1 to 1.8:1. The content of LC-PUFAs relative to their essential FA precursors in sheep was 3.6:1 for the n-6 and 1.6:1 for the n-3 PUFAs.

## CLA Metabolites

The CLA metabolites were resolved by reversed-phase HPLC of their FFAs prepared from total sheep meat fat and detected using a diode array detector at 233 nm. Figure 7 shows typical separations of four total sheep muscle lipids in which the unsaturated FAs were recorded at 200 nm (Fig. 7A) and the conjugated dienes (CD) at 234 nm (Fig. 7B). The contents of the CLA metabolites in Sarda sheep muscle are summarized in Table 6. The major CD FA was 9*c*11*t*-18:2, and it was

**Fig. 7A–B** Partial RP-HPLC chromatograms showing the variation in unsaturated unconjugated FA contents recorded at 200 nm (**A**) and conjugated diene contents recorded at 234 nm (**B**) for four representative sheep muscle samples. Operating conditions: C18 reversed-phase column, mobile phase: CH<sub>3</sub>CN/H<sub>2</sub>O/CH<sub>3</sub>COOH (70/30/0.12)



significantly higher in the sheep meat from farm A than in that from farm M, consistent with the GC results (Table 2). Two separate CD 18:3 FA metabolites were identified derived from the n-3 or n-6 series of FA, as previously observed [41]. The CD derived from 18:3n-3 was the second most abundant CD FA in sheep meat, and it was identified as 9*c*11*t*15*c*-18:3 by GC. A number of additional minor CD metabolites were detected in sheep meat, including CD 16:2, CD 16:3, CD 18:3 and CD 20:3; their concentrations increased with increased levels of 9*c*11*t*-18:2 in the meat tissue.

## Discussion

The present study provides the first complete and detailed FA composition of meat from a ruminant animal

that includes the CLA and TFA isomers and their metabolites and the LC PUFAs, as well as the alk-1-enyl ethers from the plasmalogenic lipids and the long-chain SFAs from the sphingolipids in meat. Such an analysis requires a combination of several derivatization and separation techniques to obtain the complete profile of all acyl and alkenyl groups present in ruminant meats.

Commercial Sarda sheep were selected since their total lipid composition has not yet been reported. The meat from adult Sarda sheep have been used only to a limited extent for human consumption, and an evaluation of the quality of their meat lipids may open up potential uses for this product. The total fat content of the Sarda sheep meat was somewhat higher in the sheep randomly selected in 2002 (6–9%) compared to those raised in the Sassari region and sampled in 2003

**Table 6** Contents of conjugated dienes (mg/g total lipid) in Sarda sheep muscle

CD mg/g total lipid	April			July			SEM
	M	A	P	M	A	P	
D16:2( <i>c,t</i> )	0.137 <sup>b</sup>	0.259 <sup>a</sup>	0.250 <sup>a</sup>	0.181 <sup>b</sup>	0.291 <sup>a</sup>	0.266 <sup>a</sup>	0.02
CD 16:3	0.051	0.077	0.073	0.064	0.088	0.088	0.03
CD18:3n-3	0.702 <sup>c</sup>	1.054 <sup>b</sup>	1.043 <sup>b</sup>	0.949 <sup>bc</sup>	1.244 <sup>a</sup>	1.144 <sup>ab</sup>	0.03
CD18:3n-6	0.228	0.575	0.395	0.326	0.580	0.456	0.02
CD20:3(?)	0.091 <sup>c</sup>	0.157 <sup>b</sup>	0.209 <sup>a</sup>	1.436 <sup>bc</sup>	0.222 <sup>a</sup>	0.168 <sup>ab</sup>	0.02
CD 18:2 (CLA)	4.531 <sup>c</sup>	15.375 <sup>a</sup>	8.954 <sup>bc</sup>	5.288 <sup>c</sup>	11.068 <sup>ab</sup>	9.057 <sup>b</sup>	0.45

Values are means for six sheep sampled per farm and per time period. Three farms (Muzzoni, Area, and Piras) were sampled at two time periods (April and July). Means with different superscript letters are significantly different at  $P < 0.05$ . For abbreviations, see Table 2

(4–7%). These values compare to ranges of 1.5–2.5% reported in some experimental sheep herds [14, 66], to 2–4% in others [17, 67, 68], and values as high as 5–6% [15, 69]. The high lipid content in the Sarda sheep appears to be related mainly to their age, with older sheep showing higher fat levels [16], and less to diet supplementation [14]. The high lipid content in Sarda sheep meat largely accounted for the higher levels of TAG in the sheep meat (TLC separation of total lipids Fig. 1), even though every effort was made to trim the excess fat from the sheep meat before analysis.

#### Acyl and Plasmalogenic Lipids in Meat

Meat lipids of ruminants are known to contain mainly acyl lipids in the form of TAG and phospholipids that are easily converted to their FAMES using base-catalyzed methylations. However, meat lipids also contain plasmalogenic lipids, mainly in the PE fractions that are stable to alkali conditions. Sheep muscle was reported to contain 31% as alk-1-enyl acyl PE and 5% as alk-1-enyl acyl PC [35]. Ignoring this amount of plasmalogenic lipids substantially underestimates the total lipid content of meat. Aldehydes released from the dietary plasmalogenic lipids in meats are readily oxidized to their corresponding FAs and enter the general FA pool. Characterization and analysis of plasmalogenic lipids is generally based on their stability to base-catalyzed methanolysis, and rapid conversion to their dimethylacetals under acid-catalyzed methanolysis conditions [28, 48, 69].

#### Methylation Procedures that Include Plasmalogenic and Sphingolipids

It would appear that the present attempts to avoid acid-catalyzed isomerization of CLA in ruminant fats [36] has resulted in the preferred use of base-catalyzed methanolysis for the analysis of meat (and milk) lipids. The attempt to successfully analyze the naturally

occurring CLA profile unfortunately ignored the presence of non-*O*-acyl lipids in meats. The initial concern over avoiding isomerization and artifact formation of CLA during methylation [36] was never intended to exclude major lipid classes such as plasmalogens and sphingomyelin [28, 32, 37, 56]. The exclusion of these two lipid classes applies to all base-catalyzed methylation procedures such as NaOCH<sub>3</sub>, trimethylsilyldiazomethane (TMS-DAM) or tetramethylguanidine [28, 32]. Alkali saponification has occasionally been used as an alternative method to prepare total FAMES from meat lipids. In that procedure, total meat lipids are first saponified using KOH/ethanol (or NaOH/ethanol) and then analyzed as such [41, 42], or converted to their FAMES using BF<sub>3</sub> [67, 70, 71], HCl [72, 73], or TMS-DAM [68] as catalysts. Even though the saponification/methylation method appears suitable since it retains the CLA isomer profile, it also lacks quantitation since the plasmalogenic and sphingolipids are again excluded from the total meat lipids. Occasionally acid-catalyzed methylation procedures were used to methylate meat lipids, but the expected DMAs were not reported [15, 16, 18, 74, 75], while others reported total DMAs in muscle phospholipids from two breeds of cattle (7.3–12.8%) but no TFA and CLA isomers [76]. Pork meat also contains plasmalogenic lipids [77]. On the other hand, Wolff [78] isolated plasmalogenic lipids from sheep heart and characterized the alk-1-enyl composition.

The general omission of both plasmalogenic lipids and sphingomyelins from the total lipids of meats underestimates the total lipid content in ruminant meats by about 8–15%, depending on the total meat lipids examined, and the relative content of phospholipids to TAG in the meat lipids since plasmalogenic lipids are present mainly in the phospholipid fraction. The plasmalogenic lipid contents of the Sarda sheep in the present study ranged from 2 to 3% of total lipids and there appears to be no difference in the meats selected (Table 2). If all the plasmalogenic lipids were



derived from PE this would represent about 15–20% in the PE fraction based on a PE content about 13% of total lipids (Fig. 1); no direct PE determinations were performed. The alkenyl composition of the plasmalogenic lipids of Sarda sheep meat consisted mainly of saturated and monounsaturated alkenyl moieties, with trace amounts of 18:2, which is consistent with previous findings [35, 78]. There was no evidence to indicate the presence of alk-1-enyl ethers containing conjugated moieties, which would suggest that CLA was not incorporated into plasmalogenic lipids. However, it was clearly evident that the *trans*-18:1 FA moieties were incorporated into the plasmalogenic lipids, since the isomer profiles of acyl and alkenyl ethers were very similar.

Sphingomyelins are generally present at about 3% in all muscular tissue from ruminants [79]. The *N*-acyl bond in sphingomyelin is stable under base-catalyzed conditions and requires an acid catalyst and extensive heating (i.e., 80 °C for 1 h) for complete methylation to FAMES [28, 32]. Therefore, this lipid fraction is also ignored when only base-catalyzed methylation procedures are used. The content of sphingomyelin in the Sarda sheep meat was estimated to be about 3–5% based on several meat lipids examined by TLC (Fig. 1). It should be noted that exclusion of sphingolipids from total meat lipid would also underestimate the SFA content, since this lipid fraction consists mainly of long-chain SFAs from 18:0 to 26:0 (data not included).

#### Recommended Methylation Procedures for Total Meat Lipids

The analytical approach used in this study for total meat lipid analysis consisted of a cold-temperature pulverization of the meat tissue to avoid lipid lipolysis, followed by extraction of total lipids using chloroform/methanol [45]. Three separate derivatization procedures were conducted. The first was an acid-catalyzed methylation using HCl/methanol at 80 °C for 1 h to obtain the total acyl and alk-1-enyl profile of meat lipids, i.e., FAMES from *O*- and *N*-acyl lipids, and DMAs from the alk-1-enyl ether lipids. This methylated mixture provided the quantitative composition of the total lipid content in meats. The second was a base-catalyzed methylation procedure using NaOCH<sub>3</sub>/methanol at 50 °C for 15 min to ensure retention of the CLA isomer profile. The third preparation involved a mild alkali hydrolysis of total lipids overnight at room temperature to prepare FFAs that were used to measure the conjugated FA metabolites using reversed-phase HPLC [41, 42]. This method provided confirmatory evidence of the CLA content, and the presence

of chain-elongated, desaturated and chain-shortened metabolites of CLA in ruminant meats. Both base-catalyzed procedures, unlike acid-catalyzed methylation, caused no isomerization of the conjugated double bonds or methoxy artifact formation [36]. However, the methylation products cannot be used to quantitate meat lipids since neither NaOCH<sub>3</sub>-catalyzed methylation or mild alkali hydrolysis included the plasmalogenic and sphingolipids.

#### *Trans* FA and CLA Isomers

Meat fat from ruminants contain TFA and CLA isomers formed as metabolic intermediates by isomerization and reduction of PUFAs in rumen bacteria [3]. The TFAs may be further metabolized by rumen bacteria to SFA, or taken up in rumen tissue lipids where some of the TFA isomers are converted to more unsaturated FAs by desaturases. All possible *trans* MUFAs from 16:1 to 22:1 have been found in ruminant fats including *trans* containing di- and tri-unsaturated FAs (28, 80, 81). The *trans*-18:1 and CLA isomer composition depends on the dietary source of PUFAs and on the amount and type of concentrate fed. Pasture-fed ruminants generally yield a high content of 11*t*-18:1, 9*c*11*t*-18:2 and 11*t*13*c*-18:2 compared to ruminants fed concentrate [56, 61, 63]. Grasses contain both essential fatty acids (18:3*n*-3 > 18:2*n*-6) that act as precursors for 11*t* containing FAs. Supplementing small amount of concentrate rich in 18:2*n*-6 and 18:3*n*-3 increases the levels of 11*t*-18:1 and 9*c*11*t*-18:2 in milk [62, 64, 82] and sheep meat lipids [19, 20, 68, 72, 74]. On the other hand, feeding concentrates high in digestible starch leads to increased levels of 10*t*- relative to 11*t*-18:1 in both meat [15, 20, 83, 84] and milk lipids [28, 61, 62, 85–87]. These changes are due to a reduction in the cellulolytic bacteria in the rumen population, specifically *Butyrivibrio fibrisolvens* [88–90] known to produce 11*t*-18:1 [91, 92], and a concurrent increase in the lactate-producing (*Streptococcus bovis*) and lactate-utilizing bacteria (*Selenomonas ruminantium* and *Megasphaera elsdenii*) that lead to the formation of 10*t*-containing FAs such as 10*t*-18:1 and 10*t*12*c*-18:2 [93, 94].

The sheep selected in the 2002 study indicated a wider range in the *trans*-18:1 (4.0–5.1%), total CLA (0.54–1.35%) and 9*c*11*t*-18:2 isomer (0.34–0.99%) contents. Some sheep appeared to have had access to good pasture, as evidenced by a relatively high level of 11*t*-18:1 compared to 10*t*-18:1, while other sheep had a relatively high 10*t*-18:1 to 11*t*-18:1 ratio. In addition to higher 10*t*-18:1, these sheep meats also contained higher levels of 7*t*9*c*-, 9*t*11*c*- and 10*t*12*c*-18:2, while

pasture-fed sheep had higher levels of 11*t*-18:1 and 9*c*11*t*-18:2 and 11*t*13*c*-18:2. Comparison of the present results for the *trans* 18:1 and CLA isomers in sheep meat with those reported by others was generally not possible, since a clear separation of 10*t*- and 11*t*-18:1 was not reported [14–19, 66–68, 70] and 9*c*11*t*-18:2 was generally overestimated by the amount of the coeluting 7*t*9*c*-18:2 isomer; the latter could only be resolved using a complementary Ag<sup>+</sup>-HPLC technique [28, 32, 33, 95]. The 7*t*9*c*-18:2 isomer generally occurs as the second most abundant isomer in bovine milk [60, 62, 95] and beef fat [9, 10, 12, 13, 95] when concentrate diets are fed, while in pasture-fed ruminants the second most abundant CLA isomer is 11*t*13*c*-18:2, and 7*t*9*c*-18:2 is greatly reduced [56, 61]. Bessa et al. [20] recently reported a more complete *trans*-18:1 composition for sheep meat that clearly showed increased levels of 10*t*-18:1 and 10*t*12*c*-18:2 in sheep meat when concentrates were fed and soybean oil was included in a forage diet.

These results from the 2002 study stand in contrast to the compositions found in the sheep selected in the 2003 study, when all the sheep meats showed 11*t*-18:1 as the predominant *trans*-18:1 isomer, and 9*c*11*t*-18:2 and 11*t*13*c*-18:2 as the major CLA isomers; the total contents of the *trans*-18:1 and the CLA isomers ranged from 3.44 to 4.25% and 0.63 to 1.01%, respectively. These results indicate the importance of good management practices where pasture-fed sheep are supplemented with moderate amounts of concentrate to provide additional PUFAs. The corn, peas and barley mixture given to the sheep at the Sassari farms provided about 51–56% 18:2*n*-6 from all three ingredients, and peas (9%) and barley (6%) provided additional 18:3*n*-3. Among the three farms, farm A generally showed the highest levels of 11*t*-18:1, 9*c*11*t*-18:2 and 11*t*13*c*-18:2, and the lowest levels of 7*t*9*c*-, 9*t*11*c*- and 10*c*12*t*-18:2. These results suggest that farm A was more successful in producing sheep meat that maximized the content and composition of *trans*-18:1 and CLA isomers, yielding a healthier image than the other two farms. The feeding records show that farm A achieved this by provided a smaller amount of supplement of barley rich in 18:2*n*-6 and 18:3*n*-3 in the spring, unlike farm M that provided a larger amount of supplement in the spring, or farm P that supplied a higher supplement throughout the whole period. A balanced feeding approach of adding supplements to pasture-fed ruminants resulted in improved meat quality based on the *trans*-18:1 and CLA isomer content and composition. A similar approach was successfully used to increase the 11*t*-18:1 and 9*c*11*t*-18:2 in milk fat by supplementing pasture fed cows with a minimum of crushed oil seeds or vegetable oil in the

diet [61, 64, 65], and similarly in meat lipids [19, 20, 68, 72, 74]. On the other hand, feeding consistently high levels of concentrates generally result in high levels of undesirable 10*t*-18:1 and CLA isomers, such as 10*t*12*c*-, 9*t*11*c*- and 7*t*-9*c*-18:2.

#### CLA Metabolites

The content of the conjugated FAs other than 9*c*11*t*-18:2 was significantly higher in sheep slaughtered in July than April, reflecting the higher content of pasture feeding during the early summer period. These non-CLA conjugated FAs were present in trace amounts and were identified as their FFAs by UV at 233 nm using RP-HPLC (Table 6). Generally these minor conjugated FAs could not be identified by GC, except for the conjugated 18:3 metabolite 9*c*11*t*15*c*-18:3 that was identified by RP-HPLC as well as GC. The 9*c*11*t*-18:2 CLA isomer was previously shown to convert to CD 18:3, CD 20:3 and CD 20:4 metabolites by endogenous desaturation and elongation in ruminants [41], rats [96, 97], and humans [98], or to CD 16:2 and CD 16:3 FAs by peroxisomal  $\beta$ -oxidation [43].

#### Essential Fatty Acids

The contents and relative compositions of the essential FAs and their LC derivatives are of interest when assessing the quality of meat lipids, since these PUFAs from meat serve as a source of essential FAs in our diet. The meat from the Sarda sheep provided both *n*-6 (6–8%) and *n*-3 PUFAs (2–3%), as well as their LC *n*-6 (1–1.3%) and *n*-3 (0.6–1.2%) PUFA derivatives. The *n*-6/*n*-3 ratio in the Sarda meat lipids from the selected farms in 2003 averaged 3.2 for all the PUFAs and 1.3 for the LC PUFAs; the latter included the C20 and C22 PUFAs. The results from the sheep randomly selected during the 2002 season showed greater variation and their *n*-6/*n*-3 PUFA (2.3) and LC *n*-6/LC *n*-3 PUFA ratios (0.8) were not as good. A number of factors contributed to the improved essential FA status in the meat lipids in 2003, such as the higher precipitation recorded in 2003 compared to 2002, possibly better forage quality, and management practices that included the addition of some supplements to provide dietary 18:2*n*-6 and 18:3*n*-3. Based on the amount and *n*-6/*n*-3 ratio of the PUFAs, most of the Sarda meat would appear to qualify as an acceptable source of essential FAs. However, it should be noted that meat quality characteristics such as tenderness, moisture and taste were not addressed in this study.

The PUFA contents in the sheep meat would have been influenced by the FA composition of the herbage

and supplemented diets provided, but that information was not available. A recent survey on the FAs available in several botanical groups typically found in Mediterranean pastures during the growth and reproductive stages of the plants [99] was helpful. The 18:3n-3 contents in all of the five forage species reported by Cabiddu et al. [99] were more than 60%, with a range of 18:3n-3/18:2n-6 of 3–7. However, this data was of limited value since such pastures might not have been available to the sheep, particularly during the dry spells common in Sardinia. Furthermore, supplements of unknown composition may have been provided to the sheep in the first study.

Despite the semiarid climate in Sardinia, the 18:2n-6 (4.2%) and 18:3n-3 (1.2%) contents in the commercial Sarda sheep compared well with those of commercial lambs surveyed from Germany (5.5 and 1.5%), the United Kingdom (3.9 and 1.6%) and Uruguay (5.1 and 3.3%) [16]. The average contents of 18:2n-6 and 18:3n-3 in three breeds of sheep raised on dried grass in the United Kingdom also showed similar levels (4.1 and 2.0%) [68]. However, the total LC PUFA content (2%; 20:3n-6, 20:4n-6, 22:4n-6, 20:5n-3, 22:5n-3 and 22:6n-3) in the Sarda sheep (2%) was less than that found in commercial sheep in Germany (2.7%), the United Kingdom (3.3%) and Uruguay (3.7%) [16], and in the study by Washira et al. [68] (3.9%). Lambs fed exclusively fresh pasture generally showed increased levels of C18 PUFAs and LC PUFAs, as observed in the Marino Branco lambs fed a lucerne grass diet in Portugal [20], and in a study conducted by Nuernberg et al. [66]. On the other hand, the feeding of concentrates enhanced the dietary FAs and their LC metabolites: 18:2n-6 and LC n-6 PUFAs when soybean oil was included [20], 18:3n-3 and LC n-3 PUFAs when linseed was included [68], the C18 PUFAs and the LC PUFAs when cereal grains were fed [16, 66], and LC n-3 PUFAs when fish oil was included in the diet [68]. Based on these findings, it is clear that the FA profile of Sarda sheep meat can be improved by optimizing the type and amount of concentrate provided to the pasture-fed sheep.

### Saturated Fatty Acids

The ratios of SFA to PUFA in the Sarda sheep ranged from 4:1 to 5:1, which is similar to the FA compositions of commercial sheep in different countries [16, 17, 68], but unlike sheep fed, under controlled conditions, diets rich in PUFA or exclusively rich pastures [20, 66, 68]. The high ratio of SFA to PUFA reflects the high content of TAG in Sarda sheep meat lipids and the inclusion of sphingolipids in the analysis.

**Acknowledgments** The current work was financially supported by the Ministero dell'Istruzione dell'Università e della Ricerca. The authors wish to acknowledge the technical assistance of Marta Hernandez. Contribution number S290 from the Food Research Program, Agriculture and Agri-Food Canada, Guelph, ON, Canada.

### References

- Mensink RP, Zock PL, Kester ADM, Katan MB (2003) Effects of dietary fatty acids and carbohydrates on the ratio of serum total to HDL cholesterol and on serum lipids and apolipoproteins: a meta-analysis of 60 controlled trials. *Am J Clin Nutr* 77:1146–1155
- Gebauer S, Harries WS, Kris-Etherton PM, Etherton TD (2005) Dietary n-6: n-3 fatty acid ratio and health. In: Akoh CC, Lai O-M (eds) *Healthful lipids*. AOCS Press, Champaign, IL, pp 221–248
- Bauman DE, Griinari JM (2003) Nutritional regulation of milk fat synthesis. *Ann Rev Nutr* 23:203–227
- Pariza MW, Park Y, Cook ME (2001) The biologically active isomers of conjugated linoleic acid. *Progr Lipid Res* 40:283–298
- Belury M (2002) Dietary conjugated linoleic acid in health: physiological effects and mechanisms of action. *Ann Rev Nutr* 22:505–531
- Aro A, Männistö S, Salminen I, Ovaskainen M-L, Kataja V, Uusitupa M (2000) Inverse association between dietary and serum conjugated linoleic acid and risk of breast cancer in postmenopausal women. *Nutr Cancer* 38:151–157
- Larsson SC, Bergkvist L, Wolk A (2005) High-fat dairy food and conjugated linoleic acid intakes in relation to colorectal cancer incidence in the Swedish mammography cohort. *Am J Clin Nutr* 82:894–900
- Warensjö E, Jansson J-H, Berglund L, Boman K, Åhrén B, Weinehall L, Lindahl B, Hallmans G, Vessby B (2004) Estimated intake of milk fat is negatively associated with cardiovascular risk factors and does not increase the risk of a first acute myocardial infarction. A prospective case—control study. *Br J Nutr* 91:635–642
- Fritsche S, Rumsey TS, Yurawecz MP, Ku Y, Fritsche J (2001) Influence of growth promoting implants on fatty acid composition including conjugated linoleic acid isomers in beef fat. *Eur Food Res Technol* 212:621–629
- Nuernberg K, Nuernberg G, Ender K, Lorenz S, Winkler K, Rickert R, Steinhart H (2002) *N*-3 fatty acids and conjugated linoleic acids of *Longissimus* muscle in beef cattle. *Eur J Lipid Sci Technol* 104:463–471
- Scollan ND, Enser M, Gulati SK, Richardson I, Wood JD (2003) Effect of including a ruminally protected lipid supplement in the diet on the fatty acid composition of beef muscle. *Br J Nutr* 90:709–716
- Dannenberger D, Nuernberg G, Scollan N, Schabbel W, Steinhart H, Ender K, Nuernberg K (2004) Effect of diet on the deposition of *n*-3 fatty acids, conjugated linoleic and C18:1 *trans* fatty acid isomers in muscle lipids of German holstein bulls. *J Agr Food Chem* 52:6607–6615
- Dannenberger D, Nuernberg K, Nuernberg G, Scollan N, Steinhart H, Ender K (2005) Effect of pasture versus concentrate diet on CLA isomer distribution in different tissue lipids of beef cattle. *Lipids* 40:589–598
- Arousseau B, Bauchart D, Calichon E, Micol D, Priolo A (2004) Effect of grass on concentrate feeding systems and rate of growth on triglyceride and phospholipid and their

- fatty acids in the *M. longissimus thoracis* of lambs. *Meat Sci* 66:531–541
15. Daniel ZCTR, Wynn RJ, Salter AM, Buttery PJ (2004) Differing effects of forage and concentrate diets on the oleic acid and conjugated linoleic acid content of sheep tissue: the role of stearoyl-CoA desaturase. *J Anim Sci* 82:747–758
  16. Diaz MT, Álvarez I, De la Fluente J, Sañudo C, Campo MM, Oliver MA, Font i Furnols M, Montossi F, San Julián R, Nute GR, Cañeque V (2005) Fatty acid composition of meat from typical lamb production systems of Spain, United Kingdom, Germany and Uruguay. *Meat Sci* 71:256–263
  17. Maranesi M, Bochicchio D, Montellato L, Zaghini A, Paggiuca G, Badiani A (2005) Effect of microwave cooking or broiling on selected nutrient contents, fatty acid patterns and true retention values in separable lean from lamb rib-loins, with emphasis on conjugated linoleic acid. *Food Chem* 90:207–218
  18. Priolo A, Bella M, Lanza M, Galofaro V, Biondi L, Barbagallo D, Ben Salem H, Pennisi P (2005) Carcass and meat quality of lambs fed fresh sulla (*Hedysarum coronarium* L.) with or without polyethylene glycol or concentrate. *Small Rumin Res* 59:281–288
  19. Santos-Silva J, Mendes IA, Portugal PV, Bessa RJB (2004) Effect of particle size and soybean oil supplementation on growth performance, carcass and meat quality and fatty acid composition of intermuscular lipids of lambs. *Livest Prod Sci* 90:79–88
  20. Bessa RJB, Portugal PV, Mendes IA, Santos-Silva J (2005) Effect of lipid supplementation on growth performance, carcass and meat quality and fatty acid composition of intramuscular lipids of lambs fed dehydrated lucerne or concentrate. *Livest Prod Sci* 96:185–194
  21. Lemaitre RN, King IB, Mozaffarian D, Sotoodehnia N, Rea TD, Kuller LH, Tracy RP, Siscovick DS (2006) Plasma phospholipids trans fatty acids, fatal ischemic heart disease, and sudden cardiac death in older adults. The cardiovascular health study. *Circulation* 114:209–215
  22. Lopez-Garcia E, Schulze MB, Meigs JB, Manson JE, Rifai N, Stampfer MJ, Willett WC, Hu FB (2005) Consumption of *trans* fatty acids is related to plasma biomarkers of inflammation and endothelial dysfunction. *J Nutr* 135:562–566
  23. Ratnayake WMN, Zehaluk C (2005) *Trans* fatty acids in foods and their labeling regulations. In: Akoh CC, Lai O-M (eds) *Healthful lipids*. AOCS Press, Champaign, IL, pp 1–32
  24. Weggemans RM, Rudrum M, Trautwein EA (2004) Intake of ruminant *versus* industrial *trans* fatty acids and risk of coronary heart disease—What is the evidence? *Eur J Lipid Sci Technol* 106:390–397
  25. Demeyer D, Doreau M (1999) Targets and procedures for altering ruminant meat and milk lipids. *Proc Nutr Soc* 58:593–607
  26. Khanal RC, Olsen KC (2004) Factors affecting conjugated linoleic acid (CLA) content in milk, meat, and eggs: a review. *Pak J Nutr* 3:82–98
  27. Schmid A, Collomb M, Sieber R, Bee G (2006) Conjugated linoleic acid in meat and meat products: a review. *Meat Sci* 73:29–41
  28. Cruz-Hernandez C, Deng Z, Zhou J, Hill AR, Yurawecz MP, Delmonte P, Mossoba MM, Dugan MER, Kramer JKG (2004) Methods for analysis of conjugated linoleic acid and *trans*-18:1 isomers in dairy fats by using a combination of gas chromatography, silver-ion thin-layer chromatography/gas chromatography, and silver-ion liquid chromatography. *J AOAC Int* 87:545–562
  29. Cruz-Hernandez C, Kramer JKG, Kraft J, Santercole V, Or-Rashid M, Deng Z, Dugan MER, Delmonte P, Yurawecz MP (2006) Systematic analysis of *trans* and conjugated linoleic acids in the milk and meat of ruminants. In: Yurawecz MP, Kramer JKG, Gudmundsen O, Pariza MW, Banni S (eds) *Advances in conjugated linoleic acid research*, vol. 3. AOCS Press, Champaign, IL, pp 45–93
  30. FAO (2006) Website. Food and Agriculture Organization of the United Nations, Rome (see <http://www.fao.org>, last accessed 22nd December 2006)
  31. Precht D, Molketin J (2000) Identification and quantitation of *cis/trans* C16:1 and C17:1 fatty acid positional isomers in German human milk lipids by thin-layer chromatography and gas chromatography/mass spectrometry. *Eur J Lipid Sci Technol* 102–113
  32. Kramer JKG, Cruz-Hernandez C, Zhou J (2001) Conjugated linoleic acid and octadecenoic acids: analysis by GC. *Eur J Lipid Sci Technol* 103:600–609
  33. Sehat N, Rickert R, Mossoba MM, Kramer JKG, Yurawecz MP, Roach JAG, Adlof RO, Morehouse KM, Fritsche J, Eulitz KD, Steinhart H, Ku Y (1999) Improved separation of conjugated fatty acid methyl esters by silver ion-high-performance liquid chromatography. *Lipids* 34:407–413
  34. Delmonte P, Yurawecz MP, Mossoba MM, Cruz-Hernandez C, Kramer JKG (2004) Improved identification of conjugated linoleic acid isomers using silver-ion HPLC separations. *J AOAC Int* 87:563–568
  35. Horrocks LA (1972) Content, composition, and metabolism of mammalian and avian lipids that contain ether groups. In: Snyder F (ed) *Ether lipids*. Academic, New York, pp 177–272
  36. Kramer JKG, Fellner V, Dugan MER, Sauer FD, Mossoba MM, Yurawecz MP (1997) Evaluating acid and base catalysts in the methylation of milk and rumen fatty acids with special emphasis on conjugated dienes and total *trans* fatty acids. *Lipids* 32:1219–1228
  37. Kramer JKG (1980) Comparative studies on composition of cardiac phospholipids in rats fed different vegetable oils. *Lipids* 15:651–660
  38. Chiang SD, Gessert CF, Lowry OH (1957) Colorimetric determination of extracted lipids, an adaptation for microgram amounts of lipids obtained from cerumen. *Curr List Med Lit Res* 33:56–64
  39. Folch J, Lees M, Sloane Stanley GH (1957) A simple method for the isolation and purification of total lipid from animal tissues. *J Biol Chem* 226:497–509
  40. Banni S, Day BW, Evans RW, Corongiu FP, Lombardi B (1994) Liquid chromatography-mass spectrometric analysis of conjugated diene fatty acids in a partly hydrogenated fat. *J Am Oil Chem Soc* 71:1321–1325
  41. Banni S, Carta G, Contini MS, Angioni E, Deiana M, Dessì MA, Melis MP, Corongiu FP (1996) Characterization of conjugated diene fatty acids in milk, dairy products, and lamb tissues. *J Nutr Biochem* 7:150–155
  42. Banni S, Carta G, Angioni E, Murru E, Scanu P, Melis MP, Bauman DE, Fischer SM, Ip C (2001) Distribution of conjugated linoleic acid and metabolites in different lipid fractions in the rat liver. *J Lipid Res* 42:1056–1061
  43. Banni S, Petroni A, Blasevich M, Carta G, Angioni E, Murru E, Day BW, Melis MP, Spada S, Ip C (2004) Detection of conjugated C16 PUFAs in rat tissues as possible partial beta-oxidation products of naturally occurring conjugated linoleic acid and its metabolites. *Biochim Biophys Acta* 1682:120–127
  44. Sehat N, Yurawecz MP, Roach JAG, Mossoba MM, Kramer JKG, Ku Y (1998) Silver ion high-performance liquid chromatographic separation and identification of conjugated linoleic acid isomers. *Lipids* 33:217–221

45. Kramer JKG, Hulan HW (1978) A comparison of procedures to determine free fatty acids in rat heart. *J Lipid Res* 19:103–106
46. Bligh EG, Dyer WJ (1959) A rapid method of total lipid extraction and purification. *Can J Biochem Physiol* 37:911–917
47. Kramer JKG, Fouchard RC, Farnworth ER (1983) A complete separation of lipid by three-directional thin layer chromatography. *Lipids* 18:896–899
48. Kramer JKG, Zhou J (2001) Conjugated linoleic acid and octadecenoic acids: extraction and isolation of lipids. *Euro J Lipid Sci Technol* 103:594–600
49. Winterfeld M, Debuch H (1966) Die Lipoide einiger Gewebe und Organe des Menschen. *Hoppe Seylers Z Physiol Chem* 345:11–21
50. Mahadevan V, Viswanathan CV, Phillips F (1967) Conversion of fatty acid aldehyde dimethyl acetals to the corresponding alk-1-enyl methyl ethers (substituted vinyl ethers) during gas-liquid chromatography. *J Lipid Res* 8:2–6
51. Stein RA, Slawson V (1966) A model for fatty aldehyde dimethyl acetal gas-liquid chromatography. The conversion of octadecanal dimethyl acetal to methyl 1-octadecenyl ether. *J Chromatogr* 25:204–212
52. Venkata Rao P, Ramachandran S, Cornwell DG (1967) Synthesis of fatty acid aldehydes and their cyclic acetals (new derivatives for the analysis of plasmalogens). *J Lipid Res* 8:380–390
53. Wolff RL, Bayard CC, Fabien RJ (1995) Evaluation of sequential methods for the determination of butterfat fatty acid composition with emphasis on *trans*-18:1 acids. Application to the study of seasonal variations in french butters. *J Am Oil Chem Soc* 72:1471–1483
54. Precht D, Molkentin J (1996) Rapid analysis of the isomers of *trans*-octadecenoic acid in milk fat. *Int Dairy J* 6:791–809
55. Kramer JKG, Blackadar CB, Zhou J (2002) Evaluation of two GC columns (60-m SUPELCOWAX 10 and 100-m CP Sil 88) for analysis of milkfat with emphasis on CLA, 18:1, 18:2 and 18:3 isomers, and short- and long-chain FA. *Lipids* 37:823–835
56. Kramer JKG, Cruz-Hernandez C, Deng Z, Zhou J, Jahreis G, Dugan MER (2004) Analysis of conjugated linoleic acid and *trans*-18:1 isomers in synthetic and animal products. *Am J Clin Nutr* 79(Suppl.):1137S–1145S
57. SAS Institute (1990) SA user's guide, version 6. SAS Institute, Inc., Cary, NC
58. Mazzette R, Meloni D, De Santis EPL, Santercole V, Scarno C, Cosseddu AM (2005) Characterization of Sarda sheep carcasses used in the processing of meat products. *Vet Res Commun* 29(Suppl. 2):335–338
59. Smith A, Calder AG, Lough AK, Duncan WRH (1979) Identification of methyl-branched fatty acids from the triacylglycerols of subcutaneous adipose tissue of lambs. *Lipids* 14:953–960
60. Piperova LS, Teter BB, Bruckental I, Sampugna J, Mills SE, Yurawecz MP, Fritsche J, Ku K, Erdman RA (2000) Mammary lipogenic enzyme activity, *trans* fatty acids and conjugated linoleic acids are altered in lactating dairy cows fed a milk fat-depressing diet. *J Nutr* 130:2568–2574
61. Kraft J, Collomb M, Möckel P, Sieber R, Jahreis G (2003) Differences in CLA isomers distribution of cow's milk lipids. *Lipids* 38:657–664
62. Shingfield KJ, Reynolds CK, Lupoli B, Toivonen V, Yurawecz MP, Delmonte P, Griinari JM, Grandison AS, Bever DE (2005) Effects of forage type and proportion of concentrate in the diet on milk fatty acid composition in cows given sunflower oil and fish oil. *Anim Sci* 80:225–238
63. Kramer JKG, Cruz-Hernandez C, Or-Rashid M, Dugan MER (2004) The use of total *trans*-11 containing FA, rather than total “n-7” FA, is recommended to assess the content of FA with a positive health image in ruminant fats. *Lipids* 39:693–695
64. Fearon AM, Mayne CS, Beattie JA, Bruce DW (2004) Effect of level of oil inclusion in the diet of dairy cows at pasture on animal performance and milk composition and properties. *J Sci Food Agric* 84:497–504
65. Rego OA, Rosa HJD, Portugal PV, Franco T, Vouzela CM, Borba AES, Bessa RJB (2005) The effect of supplementation with sunflower and soybean oils on the fatty acid profile of milk fat from grazing dairy cows. *Anim Res* 54:17–24
66. Nürnberg K, Grumbach S, Zupp W, Hartung M, Nürnberg G, Ender K (2001) Erhöhung der n-3 Fettsäuren und der konjugierten linolsäure (CLA) im lammfleisch durch weidehaltung. *Fleischwirtschaft* 81:120–122
67. Ponnampalam EN, Sinclair AJ, Egan AR, Blakeley SJ, Lery BJ (2001) Effect of diets containing n-3 fatty acids on muscle long-chain n-3 fatty acid content in lambs fed low and medium-quality roughage diets. *J Anim Sci* 79:698–706
68. Washera AM, Sinclair LA, Wilkinson RG, Enser M, Wood JD, Fisher AV (2002) Effects of dietary fat source and breed on the carcass composition, n-3 polyunsaturated fatty acid and conjugated linoleic acid content of sheep meat and adipose tissue. *Br J Nutr* 88:697–709
69. Hanahan DJ (1972) Ether linked lipids: chemistry and methods of measurement. In: Snyder F (ed) *Ether lipids*. Academic, New York, pp 25–50
70. Knight TW, Knowles SO, Death AF, Cummings TL, Muir PD (2004) Conservation of conjugated linoleic, *trans*-vaccenic and long chain omega-3 fatty acid content in raw and cooked lamb from two cross-breeds. *New Zeal J Agric Res* 47:129–135
71. Giuffrida de Mendoza M, Arenas de Moreno L, Huerta-Leidenz N, Uzcátegui-Bracho, Beriain MJ, Smith GC (2005) Occurrence of conjugated linoleic acid in *longissimus dorsi* muscle of water buffalo (*bubalus bubalis*) and zebu-type cattle raised under savannah conditions. *Meat Sci* 69:93–100
72. Bolte MR, Hess BW, Means WJ, Moss GE, Rule DC (2002) Feeding lambs high-oleate or high-linoleate safflower seeds differentially influences carcass fatty acid composition. *J Anim Sci* 80:609–616
73. Rule DC, Broughton KS, Shellito SM, Maiorano G (2002) Comparison of muscle fatty acid profiles and cholesterol concentrations of bison, beef cattle, elk, and chicken. *J Anim Sci* 80:1202–1211
74. Kucuk O, Hess BW, Ludden PA, Rule DC (2001) Effect of forage: concentrate ratio on ruminal digestion and duodenal flow of fatty acids in ewes. *J Anim Sci* 79:2233–2240
75. Murrieta CM, Hess BW, Rule DC (2003) Comparison of acidic and alkaline catalysts for preparation of fatty acid methyl esters from ovine muscle with emphasis on conjugated linoleic acid. *Meat Sci* 65:523–529
76. Malau-Aduli AEO, Siebert BD, Bottema CDK, Pitchford WS (1998) Breed comparison of the fatty acid composition of muscle phospholipids in jersey and limousin cattle. *J Anim Sci* 76:766–773
77. Estévez Garcia M, Cava R (2004) Plasmalogens in pork: aldehyde composition and changes in aldehyde profile during refrigerated storage of raw and cooked meat. *Food Chem* 85:1–6
78. Wolff RL (2002) Characterization of *trans*-monounsaturated alkenyl chains in total plasmalogens (1-O-alk-1'-enyl-2-acyl glycerophospholipids) from sheep heart. *Lipids* 37:811–816

79. White DA (1973) The phospholipid composition of mammalian tissue. In: Ansell GB, Hawthorne JN, Dawson RMC (eds) Form and function of phospholipids. Elsevier, Amsterdam, pp 441–482
80. Precht D, Molkentin J (2000) Recent trends in the fatty acid composition of German sunflower margarines, shortenings and cooking fats with emphasis on individual C16:1, C18:1, C18:2, C18:3 and 20:1 *trans* isomers. *Nahrung* 44:222–228
81. Precht D, Hagemeister H, Kanitz W, Voigt J (2002) *Trans* fatty acids and conjugated linoleic acids in milk fat from dairy cows fed a rumen-protected linoleic acid rich diet. *Kieler Milchwirtschaftliche Forschungsberichte* 54:225–242
82. Bauman DE, Barbano DM, Dwyer DA, Griinari JM (2000) Production of butter with enhanced conjugated linoleic acid for use in biomedical studies with animal models. *J Dairy Sci* 83:2422–2425
83. Madron MS, Peterson DG, Dwyer DA, Corl BA, Baumgard LH, Beermann DH, Bauman DE (2002) Effect of extruded full-fat soybeans on conjugated linoleic acid content of intramuscular, intermuscular, and subcutaneous fat in beef steers. *J Anim Sci* 80:1135–1143
84. Gillis MH, Duckett SK, Sackmann JR (2004) Effects of supplemental rumen-protected conjugated linoleic acid or corn oil on fatty acid composition of adipose tissues in beef cattle. *J Anim Sci* 82:1419–1427
85. Griinari JM, Dwyer DA, McGuiere MA, Bauman DE, Palmquist DL, Nurmela KVV (1998). *Trans*-octadecenoic acids and milk fat depression in lactating dairy cows. *J Dairy Sci* 81:1251–1261
86. Jurjanz S, Monteils V, Juaneda P, Laurent F (2004) Variations of *trans* octadecenoic acid in milk fat induced by feeding different starch-based diets to cows. *Lipids* 39:19–24
87. Loor JJ, Ferlay A, Ollier A, Doreau M, Chilliard Y (2005) Relationship among *trans* and conjugated fatty acids and bovine milk fat yield due to dietary concentrate and linseed oil. *J Dairy Sci* 88:726–740
88. Latham MJ, Storry JE, Sharpe ME (1972) Effect of low-roughage diets on the microflora and lipid metabolism in the rumen. *Appl Microbiol* 24:871–877
89. Elias A, Garcia R, Cordero J, Gomez E. (1996) Change in the population of some physiological groups of ruminal bacteria of grazing cows supplemented with concentrates. *Cuban J Agric Sci* 30:165–170
90. Klieve AV, Hennessy D, Ouwerkerk D, Forster RJ, Mackie RI, Attwood GT (2003) Establishing populations of *Megasphaera elsdenii* YE 34 and *Butyrivibrio fibrisolvens* YE 44 in the rumen of cattle fed high grain diets. *J Appl Microbiol* 95:621–630
91. Kepler CR, Hirons KP, McNeill JJ, Tove SB (1966) Intermediates and products of the biohydrogenation of linoleic acid by *Butyrivibrio fibrisolvens*. *J Biol Chem* 241:1350–1354
92. Kim YJ, Liu RH, Bond DR, Russell JB (2000) Effect of linoleic acid concentration on conjugated linoleic acid production by *Butyrivibrio fibrisolvens* A38. *Appl Environ Microbiol* 66:5226–5230
93. Tajima K, Aminov RI, Nagamine T, Matsui H, Nakamura M, Benno Y (2001) Diet-dependent shifts in the bacterial population of the rumen revealed with real-time PCR. *Appl Environ Microbiol* 67:2766–2774
94. Kim YJ, Liu RH, Rychlik JL, Russell JB (2002) The enrichment of a ruminal bacterium (*Megasphaera elsdenii* YJ-4) that produces the *trans*-10, *cis*-12 isomer of conjugated linoleic acid. *J Appl Microbiol* 92:976–982
95. Yurawecz MP, Roach JAG, Sehat N, Mossoba MM, Kramer JKG, Frische J, Steinhart H, Ku Y (1998) A new conjugated linoleic acid isomer, 7 *trans*, 9 *cis*-octadecadienoic acid, in cow milk, cheese, beef and human milk and adipose tissue. *Lipids* 33:803–809
96. Sébédio J-L, Juaneda P, Dobson G, Ramilison I, Martin JC, Chardigny JM, Christie WW (1997) Metabolites of conjugated isomers of linoleic acid (CLA) in the rat. *Biochim Biophys Acta* 1345:5–10
97. Sébédio J-L, Chardigny JM, Berdeaux O (2003) Metabolism of conjugated linoleic acids. In: Sébédio J-L, Christie WW, Adlof R (eds) *Advances in conjugated linoleic acid research*, vol 2. AOCS Press, Champaign, IL, pp 259–266
98. Lucchi L, Banni S, Melis MP, Angioni E, Carta G, Casu V, Rapana R, Ciuffreda A, Corongiu FP, Albertazzi A (2000) Changes in conjugated linoleic acid and its metabolites in patients with chronic renal failure. *Kidney Int* 58:1695–1702
99. Cabiddu A, Decandia M, Addis M, Piredda G, Pirisi A, Molle G (2005) Managing mediterranean pastures in order to enhance the level of beneficial fatty acids in sheep milk. *Small Rumin Res* 59:169–180

# Comparison of the Structures of Triacylglycerols from Native and Transgenic Medium-Chain Fatty Acid-Enriched Rape Seed Oil by Liquid Chromatography–Atmospheric Pressure Chemical Ionization Ion-Trap Mass Spectrometry (LC–APCI–ITMS)

Christopher Beermann · Nadine Winterling ·  
Angelika Green · Michael Möbius ·  
Joachim J. Schmitt · Günther Boehm

Received: 30 November 2006 / Accepted: 8 December 2006 / Published online: 27 January 2007  
© AOCS 2007

**Abstract** The *sn* position of fatty acids in seed oil lipids affects physiological function in pharmaceutical and dietary applications. In this study the composition of acyl-chain substituents in the *sn* positions of glycerol backbones in triacylglycerols (TAG) have been compared. TAG from native and transgenic medium-chain fatty acid-enriched rape seed oil were analyzed by reversed-phase high performance liquid chromatography coupled with online atmospheric-pressure chemical ionization ion-trap mass spectrometry. The transformation of summer rape with thioesterase and 3-ketoacyl-[ACP]-synthase genes of *Cuphea lanceolata* led to increased expression of 1.5% (*w/w*) caprylic acid (8:0), 6.7% (*w/w*) capric acid (10:0), 0.9% (*w/w*) lauric acid (12:0), and 0.2% (*w/w*) myristic acid (14:0). In contrast, linoleic (18:2n6) and alpha-linolenic acid (18:3n3) levels decreased compared with the original seed oil. The TAG *sn* position distribution of fatty acids was also modified. The original oil included eleven unique TAG species whereas the transgenic oil contained sixty. Twenty species were common to both oils. The transgenic oil included trioctadecenoyl-glycerol (18:1/18:1/18:1) and trioctadecatrienoyl-glycerol (18:3/18:3/18:3) whereas the native oil included only the latter. The transgenic TAG were dominated by combinations of caprylic, capric, lauric, myristic, palmitic (16:0), stearic (18:0), oleic (18:1n9), linoleic, arachidic (20:0), behenic (22:0), and lignoceric acids (24:0), which accounted for 52% of the total fat. In the original TAG palmitic, stearic, oleic, and

linoleic acids accounted for 50% of the total fat. Medium-chain triacylglycerols with capric and lauric acids combined with stearic, oleic, linoleic, alpha-linolenic, arachidic, and gondoic acids (20:1n9) accounted for 25% of the transgenic oil. The medium-chain fatty acids were mainly integrated into the *sn*-1/3 position combined with the essential linoleic and alpha-linolenic acids at the *sn*-2 position. Eight species contained caprylic, capric, and lauric acids in the *sn*-2 position. The appearance of new TAG in the transgenic oil illustrates the extensive effect of genetic modification on fat metabolism by transformed plants and offers interesting possibilities for improved enteral applications.

**Keywords** Ion trap · Liquid chromatography · Mass spectrometry · *sn* position · Transgenic plant · Triacylglycerol

## Abbreviations

ACP	Acyl carrier protein
APCI	Atmospheric pressure chemical ionization
AUC	Area under the curve
arb	Auxiliary gas pressure unit
CGC	Capillary gas chromatography
ESI	Electrospray ionization
FAME	Fatty acid methyl ester
HPLC	High-performance liquid chromatography
ITMS	Ion-trap mass spectrometry
MS <sup>n</sup>	Multistage sequenced mass spectrometry
MCFA	Medium-chain fatty acids
MCT	Medium-chain triacylglycerol
MUFA	Monounsaturated fatty acids
LC	Liquid chromatography
LCFA	Long-chain fatty acids

C. Beermann (✉) · N. Winterling · A. Green ·  
M. Möbius · J. J. Schmitt · G. Boehm  
Numico Research, 61381 Friedrichsdorf, Germany  
e-mail: Christopher.Beermann@Milupa.de

RP	Reversed phase
RT	Retention time
SAFA	Saturated fatty acids
<i>sn</i> -	Stereospecific numbering
TAG	Triacylglycerol
TIC	Total-ion chromatogram

## Introduction

The effort to refine vegetable oils for dietary, cosmetic or technical applications often requires alteration of the fatty acid composition. In this study the molecular structures of triacylglycerols (TAG) of native and transgenic rape seed oils enriched with medium-chain triacylglycerols (MCT), and the physiological consequences for dietary applications, are discussed. MCT oils, containing caprylic acid (8:0), capric acid (10:0), lauric acid (12:0), and myristic acid (14:0) have been used therapeutically since the 1950s. In the treatment of epilepsy with ketogenic diets, fat malabsorption of cystic fibrosis patients, human immune deficiency virus infected patients, and premature infants, MCT oils have been widely accepted. Physiologically, medium-chain fatty acids (MCFA) are digested, absorbed, transported, and metabolized more rapidly than long-chain fatty acids (LCFA) [1]. Milk formulas with MCT reduced lipid and lipoprotein oxidation in preterm infants [2]. In athletics, MCT are used as an ergogenic aid [3]. Recent studies have indicated the effective use of MCT in weight-reducing diets, because they enhance catabolic fat metabolism and modulate adipocyte accumulation and lipolysis [4–6].

MCT are synthetic oils based on coconut and palm kernel oil. Preparation requires acyl group modification by lipase-mediated transesterification or ester synthesis [7]. Rape seeds (*Brassica* sp.) are a frequent source of traditional or modified vegetable oils and raw material for margarine formulations. To provide new viable sources, several studies have been conducted to alter the expression pattern of MCT in rape seeds [8]. Unusual fatty acids in crop seed oils with industrial properties often occur in non-agronomic plant species which could be gene pools for biotechnological applications [9]. Transformation with medium-chain thioesterases derived from bay (*Umbellularia californica*), which inhibit acyl-chain elongation, has been found to efficiently increase MCFA in storage TAG [8, 10]. The bay MCFA-acyl carrier protein thioesterase, which induces fatty acid oxidation and biosynthesis, has been

expressed in rape to enhance MCT accumulation in the seeds [11]. In rape seed phospholipids and TAG are synthesized from the same diacylglycerol pool. Thus, the transformation of lysophosphatidic acid acyltransferase or diacylglycerol acyltransferase, both capable of efficiently incorporating MCFA into TAG, must be introduced in MCT-enriched transgenic systems [12]. The catabolic pathway, especially, has been suggested as a mechanism for engineering and controlling the fatty acid composition [12]. Different acyltransferases incorporate different MCFA at the *sn*-2 position, however [13, 14]. As a consequence, TAG structures of transgenic plants are modified. Transgenic expression of a yeast *sn*-2 acyltransferase gene or a lysophosphatidic acid acyltransferase from meadow foam into *Brassicaceae* has been reported to modify the stereospecific acyl distribution of TAG in seed oil [15, 16]. Knutzon et al. [13] increased the total laurate level of rape seed oil by transforming the lysophosphatidic acid acyltransferase of coconut endosperm, which mediates the insertion of laurate at the *sn*-2 position of TAG.

The regiospecificity of dietary TAG fatty acids affects lipid metabolism in humans. Several studies have shown that the fatty acid composition of blood and organs, for example the heart and liver, is affected by nutritional or pharmacological use of lipids [17]. In such applications the specific *sn* position of fatty acids can also determine metabolic processing. For example, digestibility in the gastrointestinal tract, absorption by intestinal enterocytes, and metabolic clearance of blood lipids might be accelerated, or the lipoprotein transport pathways of the portal or lymph system might be affected [18, 19]. In contrast with LCFA, which are transported via the lymph system, MCFA are transported via the portal vein directly to the liver for catabolism. Carvajal et al. [20] suggested that the *sn*-2 position of MCFA shifts the transport of dietary TAG to the lymphatic pathway with several consequences for lipid metabolism.

In addition to common methods for determination of the *sn* position of fatty acids by specific enzymatic digestion and subsequent liquid or gas chromatographic analysis [21], a variety of mass spectrometric methods are also available. Atmospheric-pressure chemical ionization (APCI) is a gentle ionization technique for amphiphilic molecules [22]. Multistage sequenced mass spectrometry experiments ( $MS^n$ ) with ion-trap detection enable fragmentation of defined ions and detailed analysis of molecular structure [23, 24]. Marzilli et al. [25] have analyzed TAG structures using an electrospray-ionization (ESI) source and  $MS^n$  experiments with ion-trap mass spectrometric (ITMS)



detection. This determination is based on the formation of *sn* position-specific acyl product ions and related acyl fragments, which are subject to a collision potential in MS<sup>3</sup> experiments. The ratio of the signal intensity of distinct fragment ions has been used to distinguish between *sn* position. To analyze the regio-specificity of neutral ether lipids of complex native matrices pre-separation of the TAG species is required. Hartvigsen et al. [26] suggested performing such analysis by reversed-phase high-performance liquid chromatography (RP-HPLC) coupled with single-quadrupole MS detection. The composition of TAG in rape seeds and several other vegetable oils has been characterized by RP-HPLC combined with APCI-MS [27].

In this study the molecular structures of TAG in rape-seed oil were analyzed after transformation with thioesterase and acyl-chain-condensing enzyme genes from the cigar flower (*Cuphea lanceolata*). The regio-specificity of TAG fatty acids was characterized by RP LC coupled with APCI-ITMS. The relative amounts of TAG species in original and transgenic rape oils were compared by RP-HPLC.

## Material and Methods

### Rape Seed Oils

The original oilseed was from *Brassica napus* L. variety Drakkar (summer rape). The transgenic oilseed was from the original-type Drakkar carrying the acyl-[ACP]-thioesterase gene *C/FatB4* and the 3-ketoacyl-[ACP]-synthase *KAS III* from *Cuphea lanceolata* (cigar flower) for control of the native seed-specific *Napin* promoter according to the gene construct description of the Federal Centre for Breeding Research on Cultivated Plants, Institute for Stress Physiology and Quality of Raw Materials, 18190 Gross Lüsewitz, Germany [28, 29].

### Lipid Extraction from Rape Seed

Rape seeds (300 mg) were homogenized in 3 mL petroleum ether by use of an Ultra Turrax homogenizer (IKA Werke; Janke-Kunkel, Staufen, Germany). After incubation for 30 min the clear supernatant was transferred into the exsicator. Total lipids were obtained by Soxhlet extraction assisted by ultrasound, in accordance with the method of Luque-Garcia and Luque de Castro [30]. The organic solvent was totally evaporated under vacuum. The remaining oil was used for the analysis.

### Fatty Acid Methyl Ester (FAME) Analysis by Capillary Gas Chromatography (CGC)

For derivatization, 100  $\mu$ L seed oil was dissolved in 2 mL methanol–hexane (4:1, *v/v*) plus 0.5% pyrogallol and methylation was conducted, in accordance with Lepage and Roy [31], with 200  $\mu$ L acetyl chloride at 100°C for 1 h. K<sub>2</sub>CO<sub>3</sub> (6%, 5 mL) was added and the mixture was centrifuged for 10 min at 2,200 $\times$ g. The upper hexane phase containing the FAME was removed. The FAME were analyzed by CGC with a 6890 N gas chromatograph (Agilent Technologies, Waldbronn, Germany) fitted with a cold on column injector to prevent fatty acid discrimination [32]. A chemically bonded DB23 (50% cyanopropyl methylpolysiloxane) capillary column, 60 m, I.D. 0.25 mm, film 0.25  $\mu$ m (JW Scientific, Agilent Technologies, USA) was used for separation of the fatty acids. The chromatographic conditions were: injector (COC): 65–270°C; carrier gas: hydrogen at a flow of 40 cm s<sup>-1</sup> flow. Compounds were monitored by flame-ionization detection at 250°C. Fatty acids were identified by comparison of their retention times with those of standards (GLC 85 standard mix; NuChekPrep, Elysian, MN, USA). The column oven temperature was maintained at 60°C for 0.5 min after injection then programmed at 40° min<sup>-1</sup> to 180°C (held for 2 min) then at 2° min<sup>-1</sup> to 210°C (held for 3 min) and finally at 3° min<sup>-1</sup> to 240°C (held for 10 min).

### Statistical Analysis

Data are given as mean  $\pm$  standard deviation. Inter-group comparisons between the two tested groups were performed by use of an unpaired *t*-test, using the software Statview 4.5 (SAS, USA). The *P*-value <0.05 was regarded as statistically significant.

### Determination of the *sn* Position of Fatty Acids in Linked TAG by LC–APCI-ITMS

Analysis of the *sn* position was performed by liquid chromatography–mass spectrometry with an LCQ Deca (Thermo Electron Corporation, San Jose, CA, USA). The distinct TAG subclasses were separated by reversed-phase chromatography on a 250 mm  $\times$  2.1 mm ODS-AQ C<sub>18</sub> RP column (YMC, Schermbeck, Germany). The mobile phase is described below. The flow rate was 0.2 mL min<sup>-1</sup>. The liquid chromatograph was coupled to the mass spectrometer by means of an online APCI source. To ionize the molecules 10% ammonium acetate was infused directly into the ion source, by syringe application, at a flow of 1  $\mu$ L min<sup>-1</sup>. The discharge

current was 5  $\mu\text{A}$ , the capillary potential 46 V, the capillary temperature 130°C, the vaporizer temperature 350°C, and the sheath gas flow rate 60 arbitrary units. Separation of the TAG species was visualized by use of the total ion chromatogram (TIC). The ion collision energy in the multistage sequenced MS experiments was adjusted to between 30 and 35%. The measurement range was between  $m/z$  200 and 1,500. The total measurement time was 50 min.

#### Separation of the TAG Species by RP-HPLC

The oil was dissolved in 1:1 ( $v/v$ ) chloroform–methanol at a concentration of 0.5–2.5  $\text{mg mL}^{-1}$ . HPLC separation of the TAG species was achieved with an Alliance 2695 chromatograph (Waters, Eschborn, Germany) coupled with a PL-ELS 1000 evaporative light-scattering detector (Polymer Laboratories, Darmstadt, Germany). Detection was performed at 30°C for the nebulizer and 35°C for the evaporator. Compounds were separated on a 250 mm  $\times$  4.6 mm, 5  $\mu\text{m}$  particle, end-capped ODS-AQ  $\text{C}_{18}$  RP column (YMC Europe, Schermbeck, Germany). The mobile phase was a gradient prepared from acetonitrile (component A) and isopropanol (component B) as described by Ando et al. [33]. All solvents were HPLC-grade or supra-solvent quality (Merck Eurolab, Darmstadt, Germany). The gradient was: start A–B (%) 80:20, 0–30 min A–B (%) 80:20 to 20:80, 30–40 min A–B (%) 20:80, 40–45 min A–B (%) 20:80 to 80:20, 45–50 min A–B (%) 80:20. The flow rate was 0.85  $\text{mL min}^{-1}$ . The distinct species were characterized by retention time and mass spectrometric

analysis. The standards used were: tridecanoyl-glycerol, tridodecanoyl-glycerol, 1,2-didodecanoyl -3-tetradecanoyl-rac-glycerol, tridecanoyl-glycerol, 1,2-ditetradecanoyl-3-dodecanoyl-rac-glycerol, tritetradecanoyl-glycerol, rac-1,2-ditetradecanoyl-3-octadecenoyl-glycerol, rac-1,2-di tetradecanoyl-3-hexadecanoyl-glycerol, tri(*cis*-9-octadecenoyl)-glycerol, 1,2-dioctadecenoyl-3-hexadecanoyl-rac-glycerol, 1,2-hexadecanoyl-3-octadecenoyl-rac-glycerol, trihexadecanoyl-glycerol, 1,2-dioctadecanoyl-3-hexadecanoyl-rac-glycerol, and trioctadecanoyl-glycerol (all Sigma Aldrich Chemie, Taufkirchen, Germany).

## Results

### Analysis of Fatty Acid Composition

Transformation of summer rape led to increased expression of caprylic, capric, lauric and myristic acids. In contrast, amounts of linoleic acid (18:2n6) and alpha-linolenic acid (18:3n3) decreased significantly ( $P \leq 0.0001$ ) compared with the original seed oil (Table 1). As a consequence of this the total amount of polyunsaturated fatty acids in transgenic rape seed oil decreased substantially compared with the original oil; the difference was 47.3% ( $P \leq 0.0001$ ). Efficient expression of MCFA reduced the amount of essential linoleic acid and alpha-linolenic acid.

The total saturated fatty acid content of the transgenic rape seed oil increased; the difference was 153% ( $P \leq 0.0001$ ) compared with the original oil. The total

**Table 1** Comparison of the fatty acid composition of original and transgenic rape seed oil

Fatty acids	Original rape seed oil (% , w/w)	Transgenic seed oil (% , w/w)	Difference (%)	<i>P</i> -value
8:0		1.5 $\pm$ 0.0166	1.5	
10:0		6.7 $\pm$ 0.0424	6.7	
12:0		0.9 $\pm$ 0.0168	0.9	
14:0	0.04 $\pm$ 0.0001	0.2 $\pm$ 0.0022	0.16	
16:0	3.7 $\pm$ 0.0618	3.4 $\pm$ 0.0228	0.3 (8.1 $\downarrow$ )	0.031
16:1n7	0.2 $\pm$ 0.0016	0.1 $\pm$ 0.0002	0.1	
17:0	0.1 $\pm$ 0.0003	0.1 $\pm$ 0.0001	0	
17:1n7	0.1 $\pm$ 0.0038	0.1 $\pm$ 0.0014	0	
18:0	1.7 $\pm$ 0.0328	2.6 $\pm$ 0.0167	0.9 (53.0 $\uparrow$ )	$\leq 0.0001$
18:1n7/9	66.9 $\pm$ 0.0378	69.9 $\pm$ 0.0957	3 (4.5 $\uparrow$ )	$\leq 0.0001$
18:2n6	15.4 $\pm$ 0.1990	7.0 $\pm$ 0.0811	8.4 (45.5 $\downarrow$ )	$\leq 0.0001$
18:3n3	8.9 $\pm$ 0.0805	4.5 $\pm$ 0.0140	4.4 (50.6 $\downarrow$ )	$\leq 0.0001$
20:0	0.6 $\pm$ 0.0049	0.9 $\pm$ 0.0169	0.3	$\leq 0.0001$
20:1n9	1.0 $\pm$ 0.0198	1.1 $\pm$ 0.0083	0.1	0.022
22:0	0.3 $\pm$ 0.0015	0.5 $\pm$ 0.0027	0.2	$\leq 0.0001$
22:1n9	0.5 $\pm$ 0.0038	0.2 $\pm$ 0.0009	0.3 (40.0 $\downarrow$ )	$\leq 0.0001$
24:0	0.1 $\pm$ 0.0048	0.2 $\pm$ 0.0046	0.1	$\leq 0.0001$
24:1n9	0.1 $\pm$ 0.0024	0.1 $\pm$ 0.0008	0	
SAFA saturated fatty acids,	SAFA	17.0 $\pm$ 0.0420	10.3 (153.0 $\uparrow$ )	$\leq 0.0001$
MUFA monounsaturated	MUFA	71.3 $\pm$ 0.1065	2.5 (3.6 $\uparrow$ )	$\leq 0.0001$
fatty acids, PUFA	PUFA	11.6 $\pm$ 0.0669	12.9 (47.3 $\downarrow$ )	$\leq 0.0001$
polyunsaturated fatty acids				

mono-unsaturated fatty acid content decreased slightly; the difference was 3.5% ( $P \leq 0.0001$ ). The amount of dominant oleic acid (18:1n9) of transgenic oil increased (the difference was 4.5%;  $P \leq 0.0001$ ) whereas the erucic acid (22:1n9) content decreased (the difference was 40.0%;  $P \leq 0.0001$ ) compared with the original oil. All other detected monounsaturated fatty acids were unaffected. The amount of palmitic acid (16:0) of transgenic oil decreased whereas stearic (18:0), arachidic (20:0), behenic (22:0), and lignoceric acids (24:0) increased compared with the original oil. No fatty acids with epoxy or hydroxy functions, conjugated double bonds, or branched structures could be detected after transformation.

### Analysis of TAG Structures

To determine whether this induced atypical accumulation of MCFA in rape seeds affects the TAG structure of transgenic oil, the *sn* position of associated fatty acids was determined by LC-APCI-ITMS (Fig. 1 and Table 2). The molecular species and the *sn* position of the acyl substituents were identified using product-ion spectra of major precursor ions. These were selected from the mass spectra averaged across the peaks in the TIC, utilizing the preferential loss of the acyl group in the *sn*-1 or *sn*-3 position. During the APCI process ammonium acetate was infused by syringe to enhance the reproducibility of *sn* position-specific cleavage of fatty acids. Acidification destabilizes the ester linkage between the fatty acid and glycerol. Possible effects on the cleavage properties of molecular structure, for example carbon-chain length and degree of saturation of the fatty acids, might be reduced.

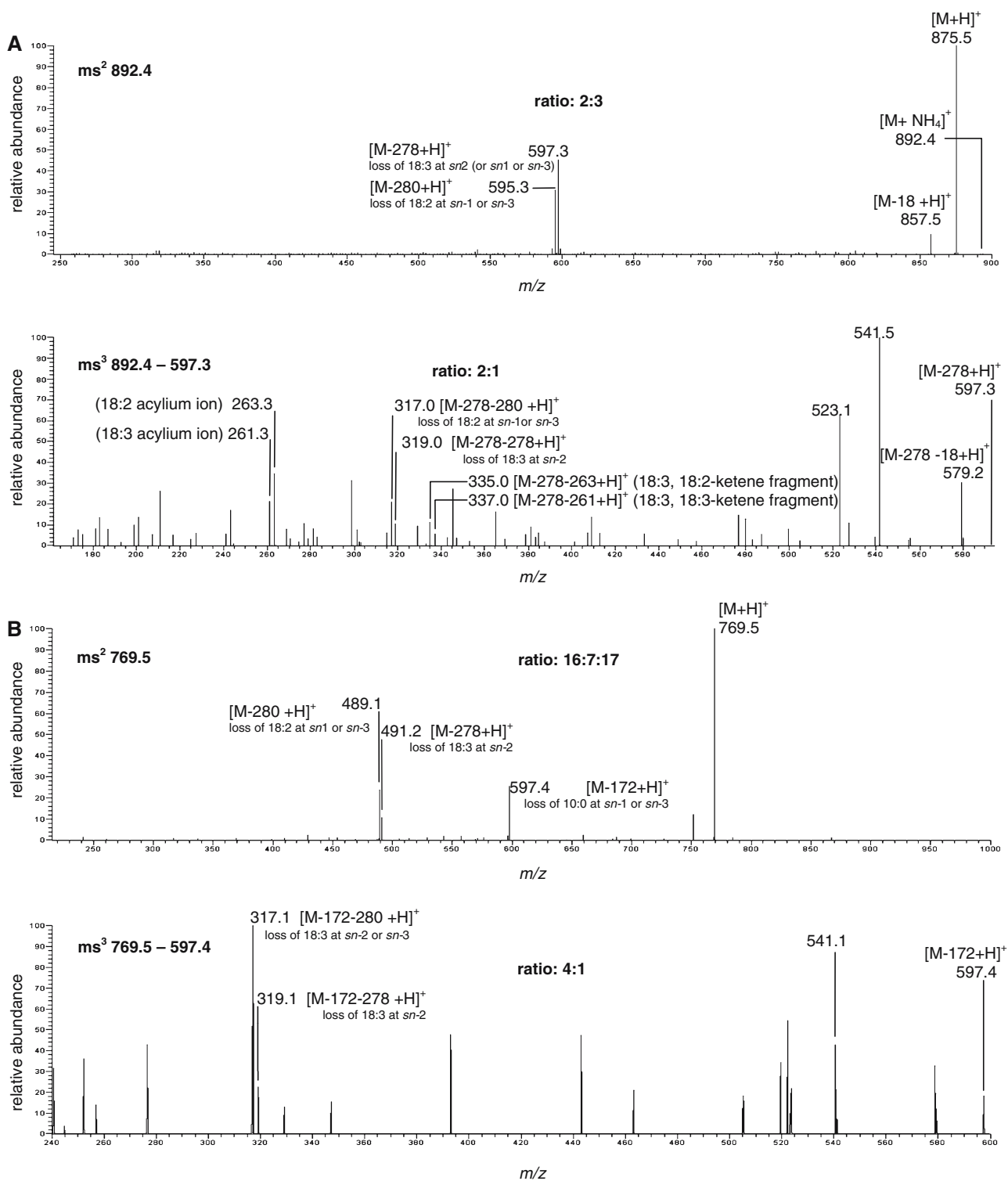
Because the location of integrated double bond fatty acids was not detectable by ITMS, the *n*-3, *n*-6, and *n*-9 families of the respective fatty acids were determined by CGC analysis. Figure 1a shows the MS<sup>2</sup> and MS<sup>3</sup> spectra of 1,2-dioctadecatrienoyl-3-octadecadienoyl-glycerol or 1-octadecadienoyl-2,3-dioctadecatrienoyl-glycerol (geometric isomer) derived from native rape seed oil. Fragmentation of the ion with an *m/z* of 892 revealed loss of ammonia resulting in a triacylglycerol ion of *m/z* 875. Because the samples were acidified with ammonium acetate during APCI, ammonium adducts of precursor ions were obtained from the TAG, in accordance with the literature [22]. The *m/z* 595 and *m/z* 597 fragments arose from cleavage of octadecadienoic acid  $[M - 280 + H]^+$  and octadecatrienoic acid  $[M - 278 + H]^+$ , respectively. Fatty acids at the *sn*-1 and *sn*-3 positions are preferentially cleaved from the glycerol backbone. In MS<sup>2</sup> experiments Marzilli et al. [25] observed different

relative abundance ratios of diacylglycerol ions derived from TAG containing two similar and one different saturated or monounsaturated fatty acid depending on their specific *sn* positioning. The predicted statistical ratio of such TAG fragments would be expected to be less than 1:2, because loss from the *sn*-2 position is energetically disfavored. The 2:3 ratio between the *m/z* 595 and *m/z* 597 fragments shown in Fig. 1a indicated that the octadecadienoic acid was mostly in the *sn*-1 and *sn*-3 positions whereas octadecatrienoic acid was in the *sn*-2 position. Laakso and Voutilainen [34] have demonstrated that the number of fatty acid double bonds affects the energetically favored fractionation pattern. Although the high unsaturation of octadecadienoic and octadecatrienoic acid might affect the fragmentation pattern, detection of the specific ratios was not affected. Differentiation between the *sn*-1 and *sn*-3 positions is impossible.

The MS<sup>3</sup> fragmentation of the *m/z* 597 ion (1–2 dioctadecatrienoyl-glycerol) resulted in fragments at *m/z* 317 and *m/z* 319, indicative of loss of octadecadienoic  $[M - 278 - 280 + H]^+$  and octadecatrienoic  $[M - 278 - 278 + H]^+$  acids, respectively. The 2:1 ratio between these fragments indicates that octadecadienoic acid was located at the *sn*-1 or *sn*-3 position and the octadecatrienoic acid at the *sn*-2 position.

Cleavage of the ester linkage between the fatty acids and the glycerol during APCI could result in the loss of acid fragments RCOOH and ketene fragments RCHCO, described in detail by Hsu and Turk [35]. In accordance to this, we observed signals of acylium ions of the cleaved fatty acids with *m/z* 261 for octadecatrienoic acid  $[R_{2/3}CO]^+$  and *m/z* 263 for octadecadienoic acid  $[R_1CO]^+$ . The corresponding *m/z* 335 and *m/z* 337 glycerol backbone-containing fragments  $[R_nCO+74]^+$  indicated loss of the octadecadienoic ketene fragment  $[M - 278 - 263 + H]^+$  and the octadecatrienoic ketene fragment  $[M - 278 - 261 + H]^+$ , respectively. Again, the type of fragmentation depended on the degree of saturation of the associated fatty acids. Linoleic, alpha-linolenic, and long-chain polyunsaturated fatty acids with more than three double bonds tended to form acylium ions during the APCI fragmentation process. More acylium ions resulted in fewer acid ions and vice versa.

The degree of saturation and the carbon-chain length of fatty acids seems to affect the binding energy of the TAG ester linkage. Analyses of neutral lipids by triple quadrupole FAB-MS and ESI-MS demonstrated, for increased chain length and number of double bonds, reduced loss of fatty acids [26]. We reduced the collision energy to suppress such ion formation (data not shown), because the ratios of acylium ions and corresponding



glycerol backbone-containing fragments do not reflect the *sn* position.

Interestingly, the released fatty acids seem to have reacted with each other to form anhydrides presented by *m/z* 541, [278 + 280 - 17 + H]<sup>+</sup>. The suggested

anhydride formation, which occurs irrespective of the degree of saturation of fatty acids and the collision energy, might be specific for APCI applications. Interpretation of these data needs further investigation, however.

◀ **Fig. 1** Determination, by LC–APCI–ITMS, of the *sn* position of 1,2-dioctadecatrienoyl-3-octadecadienoyl-glycerol (18:3/18:3/18:2), or geometric isomers, of original summer rape seed oil (**a**) and 1-decanoyl-2-octadecatrienoyl-3-octadecadienoyl-glycerol (10:0/18:3/18:2), or geometric isomers, of transgenic seed oil (**b**) transformed with medium-chain thioesterase. The compounds were separated on an end-capped ODS-AQ C<sub>18</sub> column. The mobile phase was a gradient prepared from acetonitrile (component A) and isopropanol (component B). The gradient was: start A–B (%) 80:20, 0–30 min A–B (%) 80:20 to 20:80, 30–40 min A–B (%) 20:80, 40–45 min A–B (%) 20:80 to 80:20, 45–50 min A–B (%) 80:20. The flow rate was 0.85 mL min<sup>-1</sup>. The mass spectra were acquired on a mass spectrometer with an on-line APCI source. The discharge current was 5 μA, the capillary potential 46 V, the capillary temperature 130°C, the vaporizer temperature 350°C, and the sheath gas flow rate 60 arbitrary units. The ion collision energy in the multistage sequenced MS experiments was adjusted to between 30 and 35%. The measurement range was between *m/z* 200 and 1,500

By using MS<sup>2</sup>, the 1-dodecanoyl-2-octadecatrienoyl-3-octadecadienoyl-glycerol (10:0/18:3/18:2) or the geometric isomer with *m/z* 769, derived from the transgenic seed oil was fragmented into *m/z* 489, *m/z* 491, and *m/z* 597 signals which represented a loss of dodecanoic (10:0), octadecatrienoic, and octadecadienoic acids, respectively (Fig. 1b). The corresponding 16:7:17 fragmentation ratios were a preliminary indication of respective *sn* positioning. The fragmentation of the *m/z* 597 ion in the MS<sup>3</sup> experiment revealed a 4:1 ratio between *m/z* 317 and *m/z* 319 fragments which represented a loss of octadecadienoic acid [M – 172 – 280 + H]<sup>+</sup> and octadecatrienoic acid [M – 172 – 278 + H]<sup>+</sup> corresponding to the *sn*-1/3 and *sn*-2 position, respectively. Again, the released fatty acids might form anhydrides, represented by *m/z* 541 [278 + 280 – 17 + H]<sup>+</sup>.

Table 2 gives an overview of different TAG species from native and transgenic seed oil. Although the objective of this rape transformation was MCT production, octanoyl (8:0/8:0/8:0), decanoyl (10:0/10:0/10:0), and dodecanoyl-glycerol (12:0/12:0/12:0) could not be detected in the transgenic oil. These data indicated that the acyltransferases link MCFA to the glycerol only in combination with LCFA. In consequence, the *sn* position distribution of fatty acids of storage TAG was modified. The original oil contained eleven unique distinct TAG species, the transgenic oil sixty. Twenty species were common to both oils (Table 2). The original and transgenic oil contained trioctadecenoyl-glycerol (18:1/18:1/18:1) and trioctadecatrienoyl-glycerol (18:3/18:3/18:3) whereas the native oil included only the latter. Although no trioctadecenoyl-glycerol could be detected in the origi-

nal, in the transgenic oil octadecenoic acid dominates in heterogeneous TAG structures.

### Quantification of Distinct TAG Species

Because the occurrence of new TAG species might affect the quantitative distribution of all TAG, the original and transgenic storage TAG were compared by analytical RP-HPLC (Fig. 2 and Table 2). Quantification of lipids by total-ion chromatography with ion-trap detection depends on the ionization properties of the molecule. To determine the relative amount (area under the curve, AUC) of neutral lipids irrespective of their ionization properties, which might restrict quantification, evaporative light-scattering detection was used. This technique enables quantification irrespective of the ionization or absorption properties of the mobile phase or samples [36].

Characterization of the TAG profile by RP-HPLC was based on the identical TIC of the MS experiments controlled with external standards (data not shown).

The original rape seed oil furnished 15 peaks, the transgenic oil 22 peaks; 14 peaks were common to both oils. The distribution of TAG fatty acids of the transgenic oil was more heterogeneous than that of the original. In the transgenic oil the new peaks were 1, 2, 3, 5, 8, 9, 12, and 16 (eight new peaks) and peak 6 of the original oil disappeared. The dominant peak 19 represented 50.2% of original oil and 52.2% of the transgenic oil, i.e. was approximately unchanged, whereas peak 17 which accounted for 27.5% of the original oil was reduced to 6.7% in the transgenic oil. Peak 11 represented 0.1% in the original oil and increased to 25.5% in transgenic oil. Peak 14 decreased from 11.1% in the original oil to 2.3% in the transgenic oil.

Because one peak included several co-eluting TAG species, distinct peaks of the oils represent several different clusters of TAG species. The transgenic oil mainly contained combinations of caprylic, capric, lauric, myristic, palmitic, stearic, oleic, linoleic, arachidic, behenic, and lignoceric acids representing 52% of the total fat content. The original oil was dominated by TAG combining palmitic, stearic, oleic, and linoleic acids to form 50% of the total fat content. The structural combination of palmitic, stearic, linoleic, and alpha-linolenic acids which accounted for 27% of the original oil TAG was reduced to 6.7%. In the transgenic oil new MCFA combinations with palmitic, stearic, and linoleic acids were detected. MCT with capric, and lauric acids combined with stearic, oleic, linoleic, alpha-linolenic, arachidic, and gondoic

**Table 2** Relative amounts of triacylglycerol species and *sn* position of integrated fatty acids of original and transgenic rape seed oil analyzed by LC–APCI–ITMS and RP–HPLC

	RT (min)	TAG species			Amount (% of AUC)	
		Original	Common for both oils	Transgenic	Original	Transgenic
1	17.4			8:0/18:1/10:0 8:0/18:3/18:3 10:0/18:2/10:0	10:0/18:3/10:0 10:0/18:3/18:3	0.1
2	19.3			10:0/18:3/18:2 10:0/18:2/18:3	18:1/8:0/18:3	0.1
3	19.4			8:0/8:0/22:1 10:0/18:1/10:0		0.5
4	21.1	18:3/18:3/18:3	18:3/18:3/18:2	10:0/18:2/18:2		0.1
5	21.5			10:0/18:1/12:0 10:0/18:3/16:0	10:0/18:3/18:1	0.1
6	22.2	18:3/18:3/16:0				0.1
7	22.5		18:1/18:3/18:3 18:2/18:3/18:2			0.4
8	23.3			8:0/18:1/16:0 10:0/18:1/14:0		3.1
9	23.7			8:0/18:1/18:1 10:0/18:2/18:1	10:0/18:3/18:0 18:0/8:0/18:2	0.1
10	24.5	16:0/18:3/18:2 16:1/18:2/18:2	18:1/18:3/18:2 18:2/18:2/18:2			2.5
11	25.3		18:0/18:3/18:3	10:0/18:2/20:1 10:0/18:3/20:0	12:0/18:2/18:1 12:0/18:3/18:0	0.1
12	25.6			8:0/18:1/18:0 10:0/18:1/16:0	10:0/18:1/18:1	0.3
13	26.1		16:0/18:3/18:1			2.7
14	26.5		16:0/18:2/18:2	10:0/18:0/18:1 12:0/18:1/16:0	14:0/18:1/14:0	11.1
15	27.0		18:1/18:3/18:1 18:1/18:2/18:2	18:1/18:1/18:3		0.4
16	27.5			8:0/18:1/20:0 10:0/20:1/18:1	10:0/20:0/18:2 12:0/18:1/18:1	0.2
17	28.3		16:0/18:3/18:0 16:0/18:2/18:1	8:0/18:1/22:0 8:0/18:1/24:1 10:0/18:1/20:0 10:0/18:2/22:0 12:0/18:1/18:0	14:0/18:0/18:2 14:0/18:1/18:1 16:0/16:1/18:1 16:0/14:0/18:1 16:0/18:2/16:0	27.5
18	28.7		18:0/18:2/18:2 18:0/18:3/18:1 18:1/18:2/18:1	10:0/18:3/24:0 18:3/12:0/22:0		1.3
19	30.1	18:0/18:2/18:1	16:0/18:1/16:0 16:0/18:1/18:1 16:0/18:2/18:0 18:1/18:1/18:1	10:0/18:2/24:0 14:0/18:0/18:1 18:1/8:0/24:0	18:1/10:0/22:0 18:1/12:0/20:0	50.2
20	30.5		18:1/18:1/18:1	18:0/18:3/18:0		3.0
21	31.8	18:0/18:2/18:0	18:0/18:1/18:1	18:0/18:1/18:0		0.2
22	32.2	16:0/18:1/20:1 16:0/18:2/20:0		10:0/18:1/24:0 18:1/12:0/22:0	18:1/14:0/20:0	0.7
23	33.9	16:0/18:0/18:0 16:0/20:0/18:0 18:0/16:0/20:0		18:0/16:1/20:0 18:1/12:0/24:0 18:1/16:0/20:0		0.1
Sum of TAG		11	20	60		

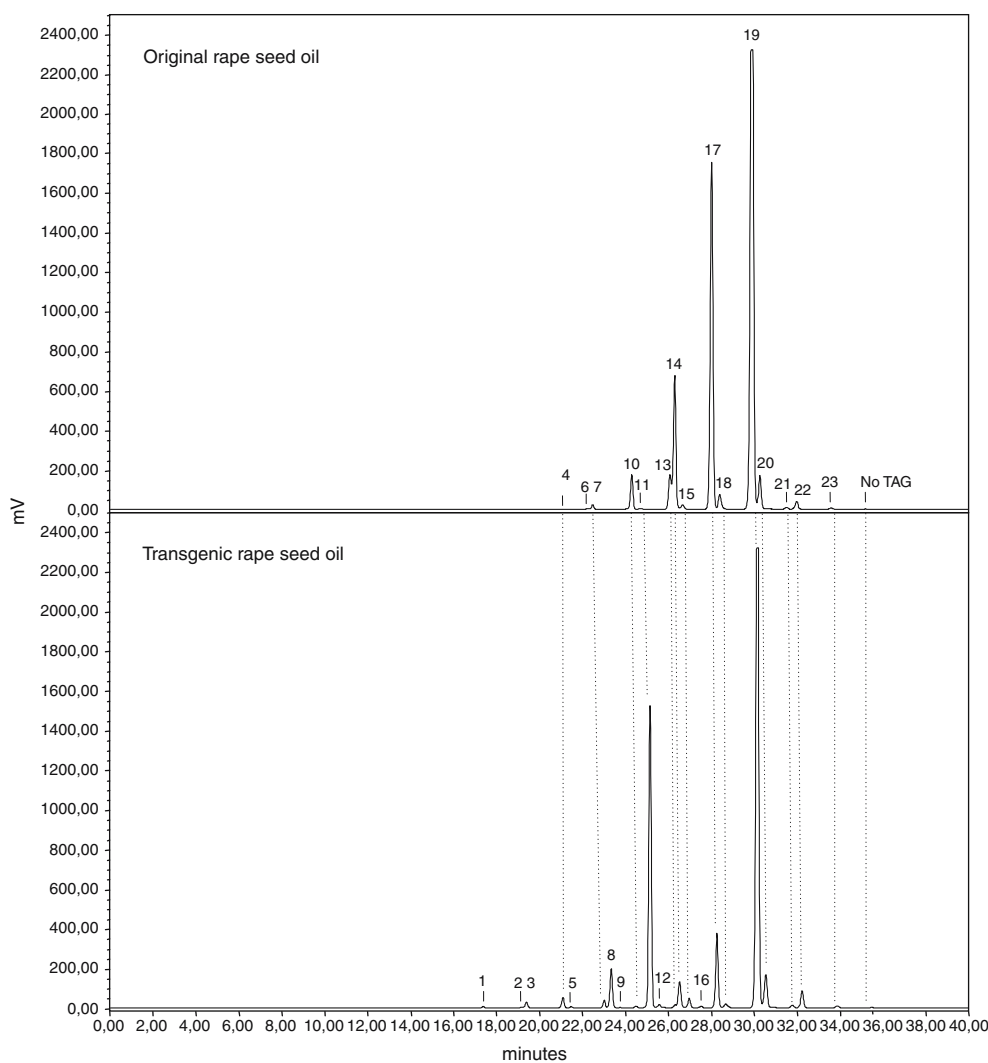
The TAG species were measured by LC–APCI–ITMS. The relative amounts of the TAG were measured by analytical RP–HPLC as percentages of the area under the curve (AUC)

acids dominated, and accounted for 25% of the total fat in the transgenic oil. We conclude that transformation of seed oil results in different TAG species with modified fatty acid compositions.

## Discussion

Stepwise metabolic engineering is one strategy for enhancing the capacity of plants to produce special

**Fig. 2** RP-HPLC separation of TAG species of original and transgenic rape seed oil. The compounds were separated on an end-capped ODS-AQ C<sub>18</sub> column. The mobile phase was a gradient prepared from acetonitrile (component A) and isopropanol (component B). The gradient was: start A–B (%) 80:20, 0–30 min A–B (%) 80:20 to 20:80, 30–40 min A–B (%) 20:80, 40–45 min A–B (%) 20:80 to 80:20, 45–50 min A–B (%) 80:20. The flow rate was 0.85 mL min<sup>-1</sup>. The samples were measured by evaporative light-scattering detection. TAG, triacylglycerol



foods or pharmaceutical compounds. For example, the over-expression of MCFA-specific thioesterase, alone or in combination with the respective chain-length-specific condensing enzyme, can affect the composition and positional distribution of fatty acids in growing and ripe transgenic rape seeds [37]. In this study the fat composition of seed oil from transgenic summer rape, modified with the acyl-[ACP]-thioesterase gene *CIFatB4* from *Cuphea lanceolata* (cigar flower) and the native seed-specific *Napin* promoter, was investigated. Mature seeds of cigar flowers contain up to 83% capric acid in storage TAG [38]. The thioesterase hydrolyzes the thioester linkage between synthesized fatty acids and the acyl carrier protein to inhibit acyl-chain elongation [28]. In this study the fatty acid composition of transgenic rape could be altered in favor of MCFA. The efficient expression of MCFA reduced the amount of essential linoleic acid and alpha-linolenic acid. This finding might diminish the nutritional value of this

transgenic oil for dietary applications. The same phenomenon has been described for transformation of rape plants to produce very-long-chain polyunsaturated fatty acids [39]. Because of the expression of eicosapentaenoic acid (20:5n3) a reduced amount of essential fatty acids of the transgenic seed oil was determined.

Although medium-chain thioesterase has been reported to inhibit acyl-chain elongation, the amounts of several monounsaturated and saturated fatty acids up to 18 carbon atoms in chain length increased in the transgenic oil. This might be because of limited expression of the engineered transgenes or because the carbon-chain elongation pathway is appropriately regulated [8, 10].

In addition to the induced over-expression of transgenic enzymes, other factors affecting the expression pattern of fatty acids might be relevant. Effects on anabolic and catabolic pathways might be

especially relevant in affecting fatty acid profiles of storage oils. Dittrich et al. [40] suggested that fatty acid elongation in yeast depends on the availability of malonyl-CoA, nicotinamide adenine-dinucleotide phosphate, and the chain-length of acyl primers, but not on respiratory competence. This offers several possibilities of affecting the composition of storage fat. Metabolic regulation, genetic prerequisites that encode fatty acid biosynthetic enzymes, and movement of fatty acids in the cell, determine the effect of transgenes on the phenotype and lipid composition of rape seed oils [41]. Thus, the whole metabolic environment of the synthesis should be considered for successful metabolic engineering.

The detailed analysis of TAG structures of native and transgenic vegetable oils in this study illustrates that APCI-ITMS is suitable for direct determination of the structures of TAG derived from native matrices. Because of the complex TAG pattern, however, pre-separation with a coupled LC is required. In contrast, in studies such as that described by Han and Gross [42] triple-quadrupole MS was used with direct infusion into the ion-source. Direct application of the sample with a syringe pump was unsuitable for our ITMS measurement, however. Ion suppression or space-charging overpopulation of the ion trap probably impaired efficient signal recognition by this technique. Thus, determination of the *sn* position of TAG-associated fatty acids was achieved by coupling MS measurement with RP LC to separate the different molecular species. The TIC was scanned manually or automatically (triple-play mode) within the range  $m/z$  200–1,500 to select specific ion signals. MS<sup>n</sup> experiments based on selected ions were then used to identify molecular species and the position of the acyl substituents. Although MS coupled RP-HPLC is sometimes a compromise in chromatographic and ionization requirements, sufficient separation of TAG species enables production of distinct molecular species for subsequent MS<sup>n</sup> experiments. Unexpected co-elution of TAG with different equivalent carbon numbers might occur because of matrix effects or because of the inadequate separating power of the microcolumn.

The appearance in the transformed seed oil of distinctive TAG species with dissimilar regioselectivities of associated fatty acids, compared to the original oil, is indicative of possible implications of genetic modification on the general fat metabolism of the transformed plant. The two inserted transgenes which are not involved in the biosynthesis of the TAG structure itself affected the acylation profile and *sn* positioning of the fatty acids of storage TAG. As recently discussed by several authors, distribution of the *sn* posi-

tions of MCFA might depend on different substrate affinities of acyltransferases in TAG biosynthesis, for example lysophosphatidic acid, diacylglycerol, and lysophosphatidylcholine acyltransferase [12, 14]. Although the transgenes inserted are not directly involved in TAG assembly, they are relevant to fatty acid synthesis. Introduction of new fatty acid species into the pool might affect the TAG composition. The non-physiological MCFA might therefore displace TAG associated LCFA, resulting in new heterogeneous TAG species. Analysis of control–transformation experiments with the vector but without the transgenes would exclude TAG alterations resulting from the transformation procedure itself, however.

In transgenic oil MCFA were mainly integrated into the *sn*-1/3 position in combination with essential linoleic or alpha-linolenic acids. Eight species were detected with caprylic, capric and lauric acids in the *sn*-2 position. In the transgenic and original oils polyunsaturated fatty acids were mainly associated with the *sn*-2 position of TAG. These structures afford interesting possibilities for improved enteral applications. Several studies have shown that the fatty acid composition of blood and organs, for example the heart or liver, can be affected by treatment with nutritional or pharmacological lipids [17]. Further studies have revealed that the specific *sn* position of fatty acids determines metabolic processing [18, 19]. LCFA are transported via the lymph, MCFA are transported via the portal vein directly to the liver for catabolism. It has been suggested that the *sn*-2 position of MCFA shifts transport of dietary TAG to the lymphatic pathway and modifies the chemical composition of chylomicrons with several consequences for lipid metabolism [20]. With animal models it has been demonstrated that structured TAG increase lymphatic absorption of tocopherol and retinol, both of which are important fat-soluble vitamins and anti-oxidants [43]. Because MCT are absorbed independently from lipases, they have beneficial effects on fat malabsorption or disturbed fat digestion. The remaining fatty acid at the *sn*-2 position after digestion of TAG with intestine-lipases is absorbed as monoacyl-glycerol. Structured TAG with a combination of MCFA at the *sn*-1 and *sn*-3 positions and long-chain fatty acids at the *sn*-2 position therefore support fat supply with reduced soap formation [7]. Preterm milk formulas with structured *sn*-2 palmitate TAG are targeted at reducing insoluble calcium soap formation and release of free fatty acids in the gut [44]. In a rat model dietary application of a structured lipid with LCFA combined with MCFA resulted in enhanced lymphatic absorption of these fatty acids [45]. In this respect, TAG found in the transgenic oil containing LA, ALA



primarily in the 2 *sn* position, and MCFA in the 1 or 3 *sn* position, may have the same physiologic effects. Such oils might have beneficial effects during malabsorption, within a postoperative phase or tube-feeding period. It has been suggested that structured TAG based on MCFA and LCFA reduce liver dysfunction in patients with long-term parenteral nutrition [46]. The current effort to establish structured MCFA with docosahexaenoic acid (22:6n3) and arachidonic acid (20:4n6) in algal single-cell oils for dietary use emphasizes the relevance of setting up non-synthetic sources for structured lipids with MCFA [47]. The transgenic oil analyzed in this study contains TAG species which could be suitable for those applications.

Analysis of TAG structures by use of LC coupled with ITMS might therefore be useful for characterizing the physiological value of oils. As a result of the use of ammonium acetate during the APCI process, 10–80 µg fat extract was sufficient for determination of TAG species with fatty acids up to 0.04% (*w/w*). Although the detection limit of LC–APCI–ITMS analysis of *sn* position is not comparable with that of enzyme/CGC analysis, the technique enables reproducible, sensitive, and rapid routine determination of the *sn* position of TAG-associated fatty acids.

Analysis of more than 50 different transformation experiments with summer rape and gene constructs containing thioesterases in combination with alpha 3-ketoacyl-[ACP]-synthase has indicated that the different distribution of regiospecific fatty acid linkages and the appearance of new TAG species in transformed seed oil, compared to the original oil, is distinctive for this type of transformation (data not shown).

## Conclusion

It can be concluded that APCI–ITMS is an applicable strategy for direct structural determination of TAG. Transformation of rape plants with two enzymes which are not directly involved in the biosynthesis of TAG but in the elongation of acyl chains alters the distribution of the *sn* position in TAG-associated fatty acids of the seed oil. The *sn* position-specific distribution of fatty acids in TAG of oils is important nutritionally, biochemically, technologically, and with regard to quality. Detailed analysis of end-products and possible contamination is therefore required. The appearance of different TAG species in the transgenic oil illustrates the extensive effect of genetic modification on the general fat metabolism of transformed plants and

affords interesting possibilities for improved enteral applications.

**Acknowledgments** The authors would like to thank Professor W. Friedt and Mr Christof Stoll, University of Giessen, Department of Agricultural Science, for providing the native and transgenic rape seed oils. The work for this publication was supported by the Federal Ministry for Consumer Protection, Nutrition and Agriculture under the grant number 22008801.

## References

- Ramirez M, Amate L, Gil A (2001) Absorption and distribution of dietary fatty acids from different sources. *Early Hum Dev* 65(Suppl):S95–S101
- Rodriguez M, Funke S, Fink M, Demmelmair H, Turini M, Crozier G, Koletzko B (2003) Plasma fatty acids and [13C] linoleic acid metabolism in preterm infants fed a formula with medium-chain triglycerides. *J Lipid Res* 44:41–48
- Kern M, Lagomarcino ND, Misell LM, Schuster V (2000) The effect of medium-chain triacylglycerols on the blood lipid profile of male endurance runners. *J Nutr Biochem* 11:288–292
- Beermann C, Jelinek J, Reinecker T, Hauenschild A, Boehm G., Klör HJ (2003a) Short term effects of dietary medium-chain fatty acids and N-3 long-chain polyunsaturated fatty acids on the fat metabolism of healthy volunteers. *Lipids Health Dis* 2(1):1–10
- Lei T, Xie W, Han J, Corkey BE, Hamilton JA, Guo W (2004) Medium-chain fatty acids attenuate agonist-stimulated lipolysis, mimicking the effects of starvation. *Obes Res* 12:599–611
- Matsuo T, Takeuchi H (2004) Effects of structured medium- and long-chain triacylglycerols in diets with various levels of fat on body fat accumulation in rats. *Brit J Nutr* 91:219–225
- Iwasaki Y, Yamane T (2004) Enzymatic synthesis of structured lipids. *Adv Biochem Eng Biotechnol* 90:151–171
- Wiberg E, Banas A, Szymne S (1997) Fatty acid distribution and lipid metabolism in developing seeds of laurate-producing rape. *Planta* 203:341–348
- Jaworski J, Cahoon EB (2003) Industrial oils from transgenic plants. *Curr Opin Plant Biol* 6:178–184
- Voelker TA, Worrell AC, Anderson L, Bleibaum J, Fan C, Hawkins DJ, Radke SE, Davis HM (1992) Fatty acid biosynthesis redirected to medium chains in transgenic oilseed plants. *Science* 257:72–74
- Eccleston VS, Ohlroge JB (1998) Expression of lauroyl-acyl carrier protein thioesterase in *Brassica napus* seeds induces pathways for both fatty acid oxidation and biosynthesis and implies a set point for triacylglycerol accumulation. *Plant Cell* 10:613–622
- Larson TR, Edgell T, Byrne J, Dehesh K, Graham IA (2002) Acyl CoA profiles of transgenic plants that accumulate medium-chain fatty acids indicate inefficient storage lipid synthesis in developing oilseeds. *Plant J* 32:519–527
- Knutzon DS, Hayes TR, Wyrick A, Xiong H, Maelor Davies MH, Voelker TA (1999) Lysophosphatidic acid acyltransferase from coconut endosperm mediates the insertion of laurate at the *sn*-2 position of triacylglycerols in lauric rapeseed oil and can increase total laurate levels. *Plant Physiol* 120:739–746
- Furukawa, Stoffer TL, Boyle RM, Thomson AL, Sarna MA, Weselake RJ (2003) Properties of lysophosphatidylcholine

- acyltransferase from brassica napus cultures. *Lipids* 38:651–656
15. Lassner MW, Levering CK, Davies HM, Knutzon DS (1995) Lysophosphatidic acid acyltransferase from meadowfoam mediates insertion of erucic acid at the sn-2 position of triacylglycerol in transgenic rapeseed oil. *Plant Physiol* 109:1389–1394
  16. Zou J, Katavic V, Giblin EM, Barton DL, MacKenzie SL, Keller WA, Hu X, Taylor DC (1997) Modification of seed oil content and acyl composition in the brassicaceae by expression of a yeast sn-2 acyltransferase gene. *Plant Cell* 9:909–923
  17. Calder PC, Deckelbaum RJ (1999) Dietary lipids: more than just a source of calories. *Curr Opin Clin Nutr Metab Care* 2:105–107
  18. Tso P, Karlstad MD, Bistrrian BR, DeMichele SJ (1995) Intestinal digestion, absorption, and transport of structured triglycerides and cholesterol in rats. *Am J Physiol* 268:568–577
  19. Hunter JE (2001) Studies on effects of dietary fatty acids as related to their position on triglycerides. *Lipids* 36:655–668
  20. Carvajal O, Sakono M, Sonoki H, Nakayama M, Kishi T, Sato M, Ikeda I, Sugano M, Imaizumi K (2000) Structured triacylglycerol containing medium-chain fatty acids in sn-1(3) facilitates the absorption of dietary long-chain fatty acids in rats. *Biosci Biotechnol Biochem* 64:793–798
  21. Christie WW (1982) *Lipid analysis*, 2nd edn. Pergamon Press, Elmsford, New York
  22. Byrdwell WC (2001) Atmospheric pressure chemical ionization mass spectrometry for analysis of lipids. *Lipids* 36:327–346
  23. Wilm M, Mann M (1996) Analytical properties of the nano-electrospray ion source. *Anal Chem* 68:1–8
  24. Creaser CS, Stygall JW (1998) Recent developments in analytical ion trap mass spectrometry. *Trends Anal Chem* 17:583–593
  25. Marzilli LA, Fay LB, Dionisi F, Vouros P (2003) Structural characterization of triacylglycerols using electrospray ionization-MSn ion trap MS. *J Am Oil Chem Soc* 80(3):195–202
  26. Hartvigsen K, Ravandi A, Bukhave K, Holmer G, Kuksis A (2001) Regiospecific analysis of neutral ether lipids by liquid chromatography/electrospray ionization/single quadrupole mass spectrometry: validation with synthetic compounds. *J Mass Spectrom* 36:1116–1124
  27. Holcapek M, Jandera P, Zderadicka P, Hruby L (2003) Characterization of triacylglycerol and diacylglycerol composition of plant oils using high-performance liquid chromatography-atmospheric pressure chemical ionization mass spectrometry. *J Chromatogr A* 1010:195–215
  28. Rudloff E, Wehling P (1997) Release of transgenic oilseed rape (*Brassica napus* L.) with altered fatty acids. *Acta Hort* 459:379–385
  29. Schutt BS, Brummel M, Schuch R, Spener F (1998) The role of acyl carrier protein isoforms from *Cuphea lanceolata* seeds in the de-novo biosynthesis of medium-chain fatty acid. *Planta* 205:263–268
  30. Luque-Garcia JL, Luque de Castro MD (2004) Ultrasound-assisted soxhlet extraction: an expeditive approach for solid sample treatment. application to the extraction of total fat from oleaginous seeds. *J Chromatogr A* 1034:237–242
  31. Lepage G, Roy CC (1984) Improved recovery of fatty acid through direct transesterification without prior extraction or purification. *J Lipid Res* 25:1391–1396
  32. Beermann C, Möbius M, Winterling N, Schmitt JJ, Boehm G (2005) SN-position determination of phospholipid linked fatty acids derived from erythrocytes by liquid chromatography electrospray ionization ion-trap mass spectrometry LC/ESI-ITMS. *Lipids* 40:211–218
  33. Ando Y, Oomi Y (2001) Positional distribution of highly unsaturated fatty acids in triacyl-sn-glycerols of *Artemia nauplii* enriched with docosahexaenoic acid ethyl ester. *Lipids* 36:733–740
  34. Laakso P, Voutilainen P (1996) Analysis of triacylglycerols by silver-ion high-performance liquid chromatography-atmospheric pressure chemical ionization mass spectrometry. *Lipids* 31:1311–1322
  35. Hsu FF, Turk J (1999) Structural characterization of triacylglycerols as lithiated adducts by electrospray ionization mass spectrometry using low-energy collisionally activated dissociation on a triple stage quadrupole instrument. *J Am Mass Spectrom* 10:587–599
  36. Beermann C, Green A, Möbius M, Schmitt JJ, Boehm G (2003b) Lipid class separation by HPLC combined with GC FA analysis: comparison of seed lipid compositions from different *Brassica napus* L. varieties. *J Am Oil Chem Soc* 80:747–753
  37. Wiberg E, Edwards P, Byrne J, Stymne S, Dehesh K (2000) The distribution of caprylate, caprate, and laurate in lipids from developing and mature seeds of transgenic *Brassica napus* L. *Planta* 212:33–40
  38. Graham SA (1989) Cuphea: a new plant source of medium-chain fatty acids. *Crit Rev Food Sci Nutr* 28:139–173
  39. Wu G, Truksa M, Datla N, Vrinten P, Bauer J, Zank T, Cirpus P, Heinz E, Qui X (2005) Stepwise engineering to produce high yields of very long-chain polyunsaturated fatty acids in plants. *Nature Biotech* 23:1013–1017
  40. Dittrich F, Zajonc D, Huhne K, Hoja U, Ekici A, Greiner E, Klein H, Hofmann J, Bessoule JJ, Sperling P, Schweizer E (1998) Fatty acid elongation in yeast-biochemical characteristics of the enzyme system and isolation of elongation-defective mutants. *Eur J Biochem* 252:477–485
  41. Kinney AJ, Cahoon EB, Hitz WD (2002) Manipulating desaturase activities in transgenic crop plants. *Biochem Soc Trans* 30:1099–1103
  42. Han X, Gross RW (1994) Electrospray ionization mass spectrometric analysis of human erythrocyte plasma membrane phospholipids. *Proc Natl Acad Sci USA* 91:10635–10639
  43. Tso P, Lee T, DeMichele SJ (2001) Randomized structured triglycerides increase lymphatic absorption of tocopherol and retinol compared with the equivalent physical mixture in a rat model of fat malabsorption. *J Nutr* 131:2157–2163
  44. Lucas A, Quinlan P, Abrams S, Ryan S, Meah S, Lucas PJ (1997) Randomized controlled trial of a synthetic triglyceride milk formula for preterm infants. *Arch Dis Child Fetal Neonatal Ed* 77:F178–F184
  45. Nagata JI, Kasai M, Watanabe S, Ikeda I, Saito M (2003) Effects of highly purified structured lipids containing medium-chain fatty acids and linoleic acid on lipid profiles in rats. *Biosci Biotechnol Biochem* 67:1937–1943
  46. Rubin M, Moser A, Vaserberg N, Greig F, Levy Y, Spivak H, Ziv Y, Lelcuk S (2000) Structured triacylglycerol emulsion, containing both medium- and long-chain fatty acids, in long-term parenteral nutrition: a double-blind randomized cross-over study. *Nutrition* 16:95–100
  47. Hamam F, Shahidi F (2004) Production and stability of structured lipids from algal oils and capric acid. *Biofactors* 22:315–317

## Two New Monogalactosyl Diacylglycerols from Brown Alga *Sargassum thunbergii*

Young Hwan Kim · Eun-Hee Kim · Chulhyun Lee ·  
Mi-Hee Kim · Jung-Rae Rho

Received: 29 January 2007 / Accepted: 1 February 2007 / Published online: 7 March 2007  
© AOCS 2007

**Abstract** Two new monogalactosyl diacylglycerols (MGDGs) along with two known glycolipids were isolated from the moderate polar fraction of the methanolic extract of the brown alga *Sargassum thunbergii* by using reversed silica flash chromatography. Two new MGDGs were identified as (2*S*)-1-*O*-(5*Z*,8*Z*,11*Z*,14*Z*,17*Z*-eicosapentaenoyl)-2-*O*-(9*Z*,12*Z*,15*Z*-octadecatrienoyl)-3-*O*- $\beta$ -D-galactopyranosyl-*sn*-glycerol (**1**) and (2*S*)-1-*O*-(9*Z*,12*Z*,15*Z*-octadecatrienoyl)-2-*O*-(6*Z*,9*Z*,12*Z*,15*Z*-octadecatetraenoyl)-3-*O*- $\beta$ -D-galactopyranosyl-*sn*-glycerol (**2**) by FAB tandem mass spectrometry, NMR techniques, and specific enzyme-catalyzed hydrolysis of the *sn*-1 fatty acyl linkage. The regiochemical attachment of the acyl chains in the glycerol moiety was established by 2D NMR correlations and confirmed by enzymatic hydrolysis.

**Keywords** *Sargassum thunbergii* · Monogalactosyl diacylglycerols (MGDGs) · Collision-induced dissociation (CID) · Fast atom bombardment (FAB) · Heteronuclear multiple bond coherence (HMBC) · Chromatography · Regiospecificity · ( $\omega$ -3) Polyunsaturated fatty acid

Y. H. Kim · M.-H. Kim  
Proteomics Team, Korea Basic Science Institute,  
52 Eoun-Dong Yuseong-Gu, Daejeon 305-333, South Korea

E.-H. Kim · C. Lee  
Magnetic Resonance Team,  
Korea Basic Science Institute,  
52 Eoun-Dong Yuseong-Gu,  
Daejeon 305-333, South Korea

J.-R. Rho (✉)  
Department of Oceanography, Kunsan National University,  
San 68 Miryong-dong, Kunsan,  
Jeonbuk 573-701, South Korea  
e-mail: jrrho@kunsan.ac.kr

### Abbreviation

CID	Collision-induced dissociation
COSY	Correlation spectroscopy
FAB	Fast atom bombardment
HMBC	Heteronuclear multiple bond coherence
NOE	Nuclear Overhauser enhancement
HPLC	High performance liquid chromatography

### Introduction

The brown alga *Sargassum thunbergii* is widely distributed in the coastal areas of Korea. This alga produces biologically active substances such as antitumor polysaccharides [1], and peroxynitrite scavengers [2]. In addition, glyceroglycolipids, the major lipid components of the photosynthetic membrane in plants, algae and various bacteria [3, 4] were isolated. In our search for novel bioactive compounds from marine macro algae, we recently observed that the acetone fraction of the brown alga *Sargassum thunbergii* collected from the offshore area of the West Sea in Korea exhibited moderate antifungal effects on *Candida albicans*. We examined these antifungal effects by using the agar diffusion disk method and isolated two new monogalactosyl diacylglycerols (MGDGs), along with two known glycolipids. This paper describes the elucidation of the complete structure of these compounds by using tandem mass spectrometry, NMR techniques and hydrolysis of the specific enzyme, Lipase XI.

### Experimental Procedures

#### General Experimental Procedures

Optical rotations were measured on a JASCO DIP-1000 digital polarimeter. IR spectra were obtained on a Mattson

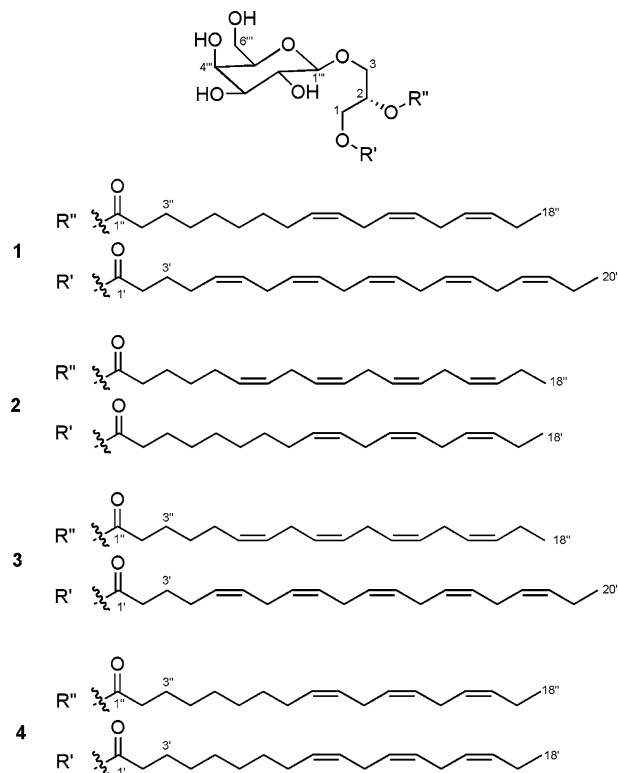
Galaxy spectrometer. The 1D and 2D NMR spectra were obtained on a Varian UNITY500 spectrometer working at 500 MHz for proton and 125 MHz for carbon. The  $^1\text{H}$  and  $^{13}\text{C}$  NMR chemical shifts were attributed to  $\text{CD}_3\text{OD}$  at 3.30 and 49.0 ppm, respectively. For all experiments, the temperature was stabilized at 297 K. The parameters used for 2D NMR spectra were as follows; The gradient COSY spectra were collected with a spectral width of 2,567 Hz in a  $512 (t1) \times 1,024 (t2)$  matrix, a pulse gradient with strength of 10 G/m for 1 ms and processed with a sinebell function. The gradient HSQC spectra were measured in a  $128 (t1) \times 1,024 (t2)$  matrix with  $J_{\text{CH}} = 140$  Hz, and to obtain a higher resolution, processed in a  $256 (t1) \times 1,024 (t2)$  matrix by a linear prediction method. The gradient HMBC experiment was optimized for a long-range coupling constant of 7 Hz. To reduce the artifacts in the spectra, the HSQC and HMBC experiments were utilized by the pulse gradients with strength of 10 G/m for 1 ms.

All mass spectrometric analyses were performed using a four-sector tandem mass spectrometer (JMS-HX110/110A, JEOL) with mass resolution set at 1,000 (10% valley). The ion source was operated in the positive-ion mode at 10 kV accelerating voltage. Ions were produced by FAB using the cesium ion beam, which was generated from the ion gun and accelerated to 22 kV. The samples were dissolved in a  $\text{CHCl}_3/\text{CH}_3\text{OH}$  (2:1, by vol) solution. The solution of 1  $\mu\text{L}$  was mixed with 1  $\mu\text{L}$  of 3-nitrobenzyl alcohol saturated with NaI on the FAB probe tip. Precursor ions selected by the first mass spectrometer ( $E_1B_1$ ) were subjected to CID in the collision cell located between  $B_1$  and  $E_2$  and were floated at 3.0 kV. The resultant product ions were analyzed by B/E scan method of the second mass spectrometer ( $E_2B_2$ ). The collision gas, helium, was introduced into the collision chamber at a pressure that was sufficiently high to reduce the precursor ion signal by 70%.

#### Extraction and Isolation

The dried brown alga (1.5 kg), collected from the offshore area of the West Sea in Korea was subjected to extraction at room temperature using MeOH. The MeOH extract was partitioned between the *n*-BuOH and  $\text{H}_2\text{O}$  layers. The butanolic layer was evaporated under conditions of reduced pressure and repartitioned between a MeOH/ $\text{H}_2\text{O}$  (85:15, by vol) solvent system and *n*-hexane. The aqueous MeOH portion was subjected to reversed-phase flash chromatography using polar solvents that were ordered (MeOH: $\text{H}_2\text{O}$  = 70:30, 80:20, 90:10; 100% MeOH; acetone; EtOAc) to yield six fractions. The acetone fraction that showed strong signals of unsaturated protons in  $^1\text{H}$  NMR and a moderate antifungal effect on *C. albicans* (diffusion disk method, a clear zone of 9 mm), was separated by reversed-phase HPLC (YMC-A, 250 mm  $\times$  10 mm) with 100%

MeOH as an eluent. This separation yielded the four constituents, namely, the compound **1** (5.6 mg), **2** (4.2 mg), **3** (5.0 mg), and **4** (4.2 mg) at retention times of 68, 78, 64, and 84 min, respectively.



(i) Compound **1**  $[\alpha]_{\text{D}}^{25} -4.0$  (*c* 1.2, MeOH); IR  $\nu_{\text{max}}$  ( $\text{cm}^{-1}$ ) 3,360, 2,921, 2,860, 1,734;  $^1\text{H}$  NMR (500 MHz,  $\text{CD}_3\text{OD}$ ) 5.35 (16H, m, H-5', -6', -8', -9', -11', -12', -14', -15', 17', -18', -9'', -10'', -12'', -13'', -15'', -16''), 2.82 (12H, m, H-7', -10', -13', -16', -11'', -14''), 2.32 ( $\times 2$ ) (4H, t,  $J = 7.2$ , H-2', -2''), 2.12 (2H, m, H-4'), 2.07 (4H, m, H-19', -17''), 2.06 (2H, m, H-8''), 1.66 (2H, m, H-3'), 1.60 (2H, m, H-3''), 1.35 (8H, m, H-4'', -5'', -6'', -7''), 0.96 (6H, t,  $J = 7.6$ , H-20', 18''),  $^{13}\text{C}$  NMR (125 MHz,  $\text{CD}_3\text{OD}$ ) 175.0 (C-1'), 174.8 (C-1''), 132.8, 132.7, 131.1, 130.0 ( $\times 2$ ), 129.5, 129.2 ( $\times 4$ ), 129.1 ( $\times 2$ ), 128.9 ( $\times 2$ ), 128.2 ( $\times 2$ ) (C-5', -6', -8', -9', -11', -12', -14', -15', 17', -18', -9'', -10'', -12'', -13'', -15'', -16''), 35.1, 34.3 (C-2', 2''), 30.7, 30.3, 30.2, 30.1 (C-4'', -5'', -6'', -7''), 28.2 (C-8''), 27.5 (C-4'), 26.6 ( $\times 4$ ), 26.4 ( $\times 2$ ) (C-7', -10', -13', -16', -11'', -14''), 26.0 (C-3''), 25.9 (C-3'), 21.5 ( $\times 2$ ) (C-19', -17''), 14.7 ( $\times 2$ ) (C-20', 18'').

(ii) Compound **2**  $[\alpha]_{\text{D}}^{25} -4.5$  (*c* 0.9, MeOH); IR  $\nu_{\text{max}}$  ( $\text{cm}^{-1}$ ) 3,380, 2,930, 2,860, 1,735;  $^1\text{H}$  NMR (500 MHz,  $\text{CD}_3\text{OD}$ ) 5.35 (14H, m, H-9', -10', -12', -13', -15', -16', -6'', -7'', -9'', -10'', -12'', -13'', -15'', -16''), 3.83 (10H, m, H-11', -14', -8'', -11'', -14''), 2.33 (2H, t,  $J = 7.4$ , H-2''), 2.30 (2H, t,  $J = 7.4$ , H-2'), 2.10 (2H, m, H-5''), 2.08 (2H, m, H-8''), 2.06 (4H, m, H-17', -17''), 1.65 (2H, m, H-3''), 1.60 (2H, m, H-3'), 1.40 (2H, m, H-4''), 1.32 (8H, m,

H-4',-5',-6',-7'), 0.97 (6H, t,  $J = 7.6$ , H-18', 18"),  $^{13}\text{C}$  NMR (125 MHz,  $\text{CD}_3\text{OD}$ ) 175.0 (C-1'), 174.7 (C-1''), 132.8, 132.7, 131.1, 130.6, 129.5, 129.3 ( $\times 2$ ), 129.2 ( $\times 2$ ), 129.1, 129.0, 128.9, 128.3, 128.2 (C-9', -10', -12', -13', -15', -16', -6'', -7'', -9'', -10'', -12'', -13'', -15'', -16''), 35.0 (C-2''), 34.9 (C-2'), 30.5, 30.3, 30.2, 30.1 ( $\times 2$ ) (C-4', -5', -6', -7', -4''), 28.2 (C-8'), 27.9 (C-5''), 26.6 ( $\times 3$ ), 26.4 ( $\times 2$ ) (C-11', -14', -8'', -11'', -14''), 26.0 (C-3'), 25.6 (C-3''), 21.5 ( $\times 2$ ) (C-17', -17''), 14.7 ( $\times 2$ ) (C-18', 18'').

#### Preparation of *sn*-2 Acyl Lysogalactolipids

A solution of both the MGDG and Lipase XI (from *Rhizopus arrhizus*, Sigma: 1800 unit) in the presence of Triton X-100 (2.5 mg) in boric acid–borax buffer (0.63 ml, pH 7.7) was stirred for 1 h at 37 °C [5]. The reaction solution was adjusted to pH 4 by adding acetic acid, and subsequently quenched by adding 2 mL of  $\text{CHCl}_3/\text{CH}_3\text{OH}$  (2:1, by vol) solution. The extracted organic phase was washed using 1 mL of 0.2 M  $\text{H}_3\text{PO}_4/1$  M KCl solution. The aqueous phase was re-extracted into  $\text{CHCl}_3$ , and the resulting organic phases were combined, dried, and redissolved in a minimal volume of the  $\text{CHCl}_3/\text{CH}_3\text{OH}$  (2:1, by vol). The resulting products were separated into lysogalactolipids and fatty acids by thin-layer chromatography (TLC) performed on a silica gel plate (K6 Silica Gel 60 Å; Whatman, Hillsboro, OR, USA) with  $\text{CHCl}_3/\text{CH}_3\text{OH}/\text{H}_2\text{O}$  (65:25:4, by vol). *Sn*-2 Acyl lyso components were identified by spraying the TLC plate with 0.01% primuline in a mixture of  $\text{Ac}_2\text{O}$  and  $\text{H}_2\text{O}$  (4:1, by vol) followed by illumination of the plate with ultraviolet light. The *sn*-2 acyl lyso components were located on the lowest part of the TLC plate.

#### Results and Discussion

Compound **1** was isolated in the form of an amorphous gum. From the sodium-adducted ion peak of  $[\text{M} + \text{Na}]^+$  at  $m/z$  821.5179 ( $\Delta -0.1$  mmu) in the high resolution FAB mass spectrum, the molecular formula of **1** was determined to be  $\text{C}_{47}\text{H}_{74}\text{O}_{10}$ . Its IR spectrum exhibited absorption bands corresponding to the hydroxyl ( $3,360\text{ cm}^{-1}$ ) and ester ( $1,734\text{ cm}^{-1}$ ) groups. The  $^1\text{H}$  and  $^{13}\text{C}$  NMR spectra of **1** showed the signals for carbon chains bearing a high number of methylene-interrupted double bonds, a sugar moiety, and two carbonyl groups. Further, from the results of the analysis of the  $^1\text{H}$ - $^1\text{H}$  COSY spectrum, it was deduced that compound **1** was a monoglycosyl diacylglycerol (Table 1).

As mentioned in a previous study, high-energy CID of the sodium-adducted molecular ions ( $[\text{M} + \text{Na}]^+$ ) of glycosyl diacylglycerol enabled the complete structural

analysis of the fatty acyl residues and the head group [6–8]. In particular, fragmentation along the hydrocarbon chains remote from the charge site allowed the determination of the position of the double-bond in the polyunsaturated fatty acyl groups. As shown in Fig. 1a, the fragmentation pattern observed in CID-MS/MS of compound **1** was very similar to that of the MGDG investigated in our previous work [8]. The fragmentation pathways and labeled product ions are also illustrated in Fig. 2. The  $^{15}\text{A}$ , B', B and C-2H ions at  $m/z$  157, 169, 185 and 201, respectively, provided the information on the monosaccharide as the head group. The fatty acyl composition in **1** was determined by a pair of G ion peaks resulting from the loss of free fatty acid moieties from each acyl group. Therefore, two strong ion peaks at  $m/z$  519  $[\text{M} + \text{Na}-\text{C}_{19}\text{H}_{31}\text{COOH}]^+$  and 543  $[\text{M} + \text{Na}-\text{C}_{17}\text{H}_{29}\text{COOH}]^+$  were indicative of the presence of C20:5 and C18:3 (carbon atoms:double bonds), respectively.

As shown in Fig. 1b, the positions of the double-bond in the fatty acyl chains were also determined by fragmentations occurring along the chains of fatty acids observed in the high mass region of the CID spectrum. The fragmentation of each fatty acid chain resulted in a series of product ions generated by the loss of  $\text{C}_n\text{H}_{2n+2}$  with neighboring peaks in the series separated by 14 u. The presence of a double bond in the chain reduced the separation between neighboring peaks to 12 u. Thus, homologous ions generated by the fragmentations of two different fatty acid chains can be divided into two groups in addition to the ions at  $m/z$  805, 791, 779 (=), where “=” represents the double-bond, 765, 751, 739 (=), 725, 711, 699 (=), 685 and 671 ions arising from cleavages of both fatty acid chains;

**Table 1** NMR spectral data for common glycerol and sugar parts within compounds **1** and **2**

Number	$^{13}\text{C}^{\text{a, b}}$	$^1\text{H}$ (multiplicity, $J$ in Hz) <sup>a, b</sup>
1	64.0, t	4.43 (dd, 12.0, 2.9) 4.21 (dd, 12.0, 6.8)
2	71.8, d	5.25 (m)
3	68.7, t	3.98 (dd, 11.1, 5.6) 3.74 (dd, 11.1, 5.9)
1'''	105.4, d	4.22 (d, 7.6)
2'''	72.4, d	3.50 (dd, 9.7, 7.6)
3'''	74.9, d	3.45 (dd, 9.7, 3.2)
4'''	70.2, d	3.82 (dd, 3.2, 0.6)
5'''	76.8, d	3.51 (m)
6'''	62.5, d	3.76 (dd, 11.4, 6.8) 3.71 (dd, 11.4, 5.6)

<sup>a</sup> Measured at 500 MHz in  $\text{CD}_3\text{OD}$

<sup>b</sup> Assignments are based on the COSY, HSQC, and HMBC correlation data

**Fig. 1** **a** High-energy (7 kV) CID spectrum of  $[M + Na]^+$  ion (at  $m/z$  821) generated by the positive-ion FAB of compound **1** in a 3-nitrobenzyl alcohol matrix saturated with NaI. **b** High-mass region of the CID spectrum where the ion peaks were obtained by the fragmentations occurring along the hydrocarbon chains of two fatty acyl groups. The equals signs above the peaks indicate the double-bond positions

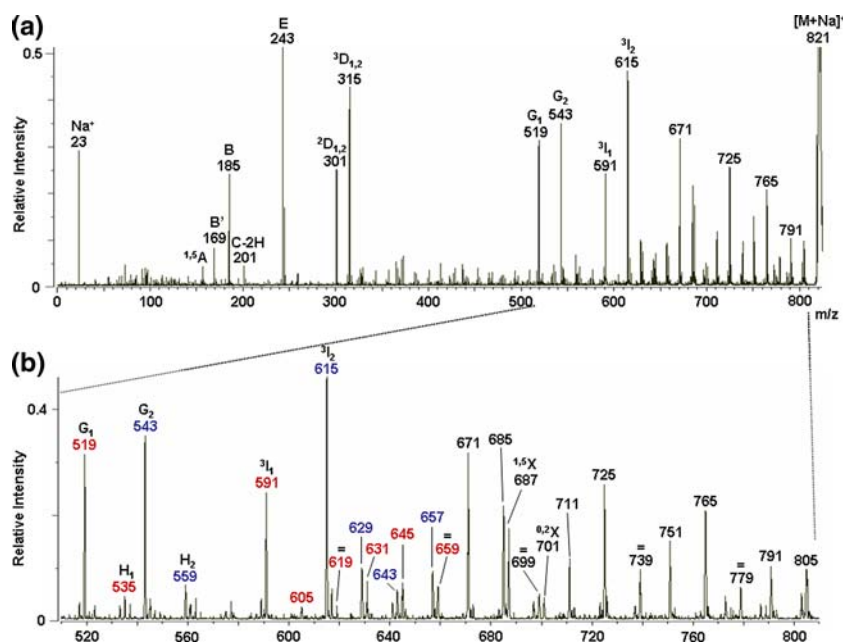
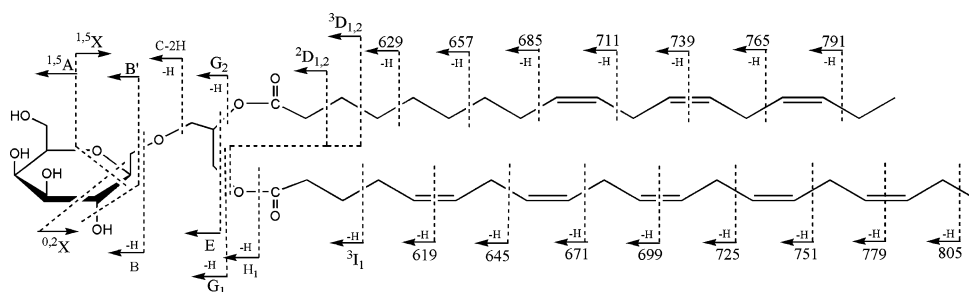


**Fig. 2** The fragmentation pathways and labeling product ions observed in the CID spectrum of  $[M + Na]^+$  ion (at  $m/z$  821) shown in Fig. 1



$m/z$  657, 643, 629 and 615 ( $^3I_2$ ) due to 9,12,15-octadecatrienoic acid chain (i.e.,  $\alpha$ -linolenic acid) and  $m/z$  659 (=), 645, 631, 619 (=), 605 and 591 ( $^3I_1$ ) due to 5,8,11,14,17-eicosapentaenoic acid (EPA) chain.

The linkage of two different fatty acid residues in the glycerol moiety was identified by a combination of the  $^1H$ - $^1H$  COSY and HMBC experiments. First, the proton signals of the three methylene units (H-2'-4') in the C20:5 chain were apparently resolved in the  $^1H$  NMR spectrum and readily assignable by the  $^1H$ - $^1H$  COSY spectrum. Next, the methylene protons at  $\delta$  1.65 (H-3') exhibited HMBC correlations with the carbonyl carbon at  $\delta$  175.0 (C-1') on the C20:5 chain, which showed further HMBC correlations with the methylene protons at  $\delta$  4.43 and 4.21 (H-1) in the glycerol moiety. On the other hand, in the HMBC spectrum, the methylene protons at  $\delta$  1.60 (H-3'') in the C18:3 chain were correlated with the carbonyl carbon at  $\delta$  174.7 (C-1''). This observation indicated that the C20:5 and C18:3 acyl chains were attached at positions C-1 and C-2 of the glycerol moiety, respectively. To confirm the

regiospecificity of the fatty acyl linkages, compound **1** was subjected to a regioselective enzymatic hydrolysis using Lipase XI (from *Rhizopus arrhizus*) that specifically cleaves the ester bond between the glycerol backbone and *sn*-1 fatty acyl group. FAB mass spectrum of the hydrolyzed product indicated that the peak at  $m/z$  537 corresponded to *sn*-2 acyl lysoglycerolipid with  $\alpha$ -linolenic acid at the *sn*-2 position.

As revealed by the HMBC correlation between the anomeric proton at  $\delta$  4.22 ( $J = 7.6$  Hz) and C-3, the sugar residue was linked to the C-3 of the glycerol moiety. Based on the information of the coupling constants for H-1'''/H-2''' ( $J = 7.6$  Hz), H-2'''/H-3''' ( $J = 9.7$  Hz) and H-3'''/H-4''' ( $J = 3.2$  Hz), and the NOE peaks H-1'''/H-3''' and H-1'''/H-5''', we classified the sugar as a  $\beta$ -galactopyranose; it was also shown that its  $^{13}C$  NMR resonances was identical to that reported for similar compounds [9].

The treatment of **1** with 15% NaOMe in MeOH afforded a glyceryl galactoside and a mixture of two fatty acid methyl esters. After partitioning, the optical rotation of the

aqueous fraction was measured to be  $[\alpha]_D^{25} \sim -6.0^\circ$  (*c* 0.15 H<sub>2</sub>O), which was very similar to that measured for (2*R*)-1-*O*-glyceryl- $\beta$ -D-galactopyranoside [10]. Based on this comparison, the stereochemistry of both the sugar and glycerol groups of **1** was established. Further, on the basis of chemical shifts of the allylic carbons ( $\delta$  25.6–28.2), the geometry of all the double bonds was determined to be in the *Z* form [11].

Accordingly, the structure of **1** was determined to be (2*S*)-1-*O*-(5*Z*,8*Z*,11*Z*,14*Z*,17*Z*-eicosapentaenoyl)-2-*O*-(9*Z*,12*Z*,15*Z*-octadecatrienoyl)-3-*O*- $\beta$ -D-galactopyranosyl-*sn*-glycerol.

Compound **2** was also isolated in the form of as an amorphous gum. The exact mass measurement of its  $[M + Na]^+$  at *m/z* 795 revealed the elemental composition to be C<sub>45</sub>H<sub>72</sub>O<sub>10</sub>Na (observed *m/z*, 795.5018; theoretical *m/z*, 795.5023). <sup>1</sup>H, <sup>13</sup>C NMR, and MS/MS spectra for **2** were closely similar to those observed for compound **1**. From the fragmentation patterns observed in the CID spectrum of its  $[M + Na]^+$ , compound **2** was observed to contain two polyunsaturated fatty acyl groups from the G<sub>1</sub> and G<sub>2</sub> ions at *m/z* 517 and 519, respectively; it contained the 9,12,15-octadecatrienoyl and 6,9,12,15-octadecatetraenoyl (i.e., stearidoenoyl) groups.

Similarly, the locations of two fatty acids in compound **2** were established by the correlations of HMBC and were confirmed by enzymatic hydrolysis. The key HMBC correlations in **2** also revealed the positions of two different acyl chains in the glycerol moiety. The methylene protons at  $\delta$  2.30 (H-2') within C18:3 chain were correlated with the carbonyl carbon at  $\delta$  175.0 (C-1'), which further exhibited the HMBC correlation with the methylene protons at  $\delta$  4.43 and 4.21 (C-1) on the glycerol group. This observation indicated the attachment of 9,12,15-octadecatrienoyl chain (C18:3) at the *sn*-1 position of **2**. The regiospecificity of the two fatty acyl groups was also confirmed by the specific enzyme-catalyzed hydrolysis of *sn*-1 fatty acyl linkage.

As mentioned above, compound **2** was determined to be (2*S*)-1-*O*-(9*Z*,12*Z*,15*Z*-octadecatrienoyl)-2-*O*-(6*Z*,9*Z*,12*Z*,15*Z*-octadecatetraenoyl)-3-*O*- $\beta$ -D-galactopyranosyl-*sn*-glycerol.

Compounds **3** and **4** were identified by comparing their spectral and physical data with compounds that were reported earlier.

The ( $\omega - 3$ ) family of polyunsaturated fatty acids present in these components occurs widely in algae. However, glycolipid compounds containing two useful ( $\omega - 3$ ) polyunsaturated fatty acids are not commonly observed. And in this case, the linkage of the polyunsaturated fatty acids in the glycerol moiety could be readily determined by the NMR techniques; this technique was preferred over both the enzymatic and alkaline hydrolysis that followed the LC–MS method.

**Acknowledgments** This research was financially supported by MarineBio21, Ministry of Maritime Affairs and Fisheries and also in part by a grant funded to Dr. Y. H. Kim from Korea research council of fundamental science & technology, South Korea.

## References

- Ito H, Sugiura M (1976) Antitumor polysaccharide fraction from *Sargassum thunbergii*. Chem Pharm Bull 24:1114–1115
- Seo Y, Lee H-J, Park KE, Kim YA, Ahn JW, Yoo JS, Lee B-J (2004) Peroxynitrite-scavenging constituents from the brown alga *Sargassum thunbergii*. Biotechnol Bioprocess Eng 9:211–216
- Murata N, Siegenthaler P-A (1998) Lipids in photosynthesis: an overview. In: Siegenthaler P-A, Murata N (eds) Lipids in photosynthesis: structure, function and genetics. Kluwer, Dordrecht
- Joyard J, Block MA, Malherbe A, Maréchal E, Douce R (1993) Origin and synthesis of galactolipid and sulfolipid head groups. In: Moore TS Jr (ed) Lipid metabolism in plants. CRC, Boca Raton
- Murakami N, Imamura H, Morimoto T, Ueda T, Nagai S, Sakakibara J, Yamada N (1991) Selective preparation of *sn*-1 and *sn*-2 lysogalactolipids by enzymatic hydrolysis using lipase (from *Rhizopus arrhizus*). Tetrahedron Lett 32:1331–1334
- Kim YH, Choi J-S, Yoo JS, Park Y-M, Kim MS (1999) Structural identification of glycerolipid molecular species isolated from Cyanobacterium *Synechocystis* PCC 6803 using fast atom bombardment tandem mass spectrometry. Anal Biochem 267:260–270
- Kim YH, Choi J-S, Hong J, Yoo JS, Kim MS (1999) Identification of acylated glycolipids from a cyanobacterium, *Synechocystis* sp., by tandem mass spectrometry. Lipids 34:847–853
- Kim YH, Gil JH, Hong J, Yoo JS (2001) Tandem mass spectrometric analysis of fatty acyl groups of galactolipid molecular species from wheat flour. Microchem J 68:143–155
- Jung JH, Lee H, Kang SS (1996) Diacylglycerylgalactosides from *Arisaema amurense*. Phytochemistry 42:447–452
- Oshima Y, Yamada S-H, Matsunaga K, Moriya T, Ohizumi Y (1994) A monogalactosyl diacylglycerol from a cultures marine dinoflagellate, *Scrippsiella trochoidea*. J Nat Prod 57:534–536
- Stothers JB (1972) Carbon-13 NMR spectroscopy. Academic, New York

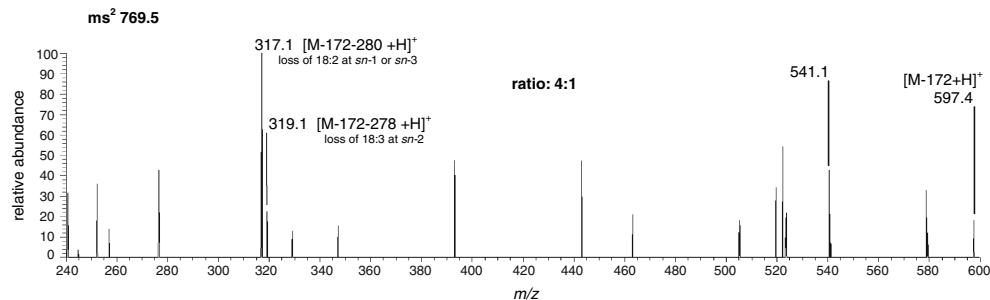
## Comparison of the Structures of Triacylglycerols from Native and Transgenic Medium-Chain Fatty Acid-Enriched Rape Seed Oil by Liquid Chromatography–Atmospheric Pressure Chemical Ionization Ion-Trap Mass Spectrometry (LC–APCI–ITMS)

Christopher Beermann · Nadine Winterling ·  
Angelika Green · Michael Möbius ·  
Joachim J. Schmitt · Günther Boehm

Published online: 1 March 2007  
© AOCS 2007

**Erratum to: Lipids**  
**DOI 10.1007/s11745-006-3009-1**

Figure 1b illustrates the specific fragmentation pattern of 1-decanoyl-2-octadecatrienoyl-3-octadecadienoyl-glycerol (10:0/18:3/18:2) or geometric isomer of transgenic seed oil within a sequenced MS experiment. The mass of  $m/z$  317  $[M - 172 - 280 + H]^+$  represents the loss of 18:2 at the *sn*-1 or *sn*-2 position of the acylglycerol not the loss of 18:3 at the *sn*-2 or *sn*-3 position as stated in the text.



The online version of the original article can be found at  
<http://dx.doi.org/10.1007/s11745-006-3009-1>.

C. Beermann (✉) · N. Winterling · A. Green ·  
M. Möbius · J. J. Schmitt · G. Boehm  
Numico Research, 61381 Friedrichsdorf, Germany  
e-mail: Christopher.Beermann@Milupa.de



# Plasma Lipoproteins and Triacylglycerol are Predictors of Small, Dense LDL Particles

Vasilis Tsimihodimos · Irene Gazi · Christina Kostara ·  
Alexandros D. Tselepis · Moses Elisaf

Received: 6 March 2007 / Accepted: 8 March 2007 / Published online: 11 April 2007  
© AOCs 2007

**Abstract** Recently published data suggest that the assessment of LDL subfraction profiles may contribute to the determination of the cardiovascular risk. In this study, we tested the ability of various metabolic parameters to estimate the presence or the preponderance of small, dense LDL particles (sdLDL). One hundred and fifty individuals attending the Outpatient Clinics of the University Hospital of Ioannina for suspected metabolic abnormalities were included in the study. Individuals were excluded if they were found to be diabetic or if they had a history of cardiovascular disease. Patients with thyroid dysfunction, liver or kidney diseases as well as those receiving drugs that may interfere with lipids or glucose metabolism were also excluded from the study. The ability of the various parameters to identify individuals with pattern B LDL phenotype or, alternatively, with measurable quantities of sdLDL particles was tested with the calculation of the areas under the ROC curves. The ratio of triglycerides to HDL-C was the best predictor of the presence of the pattern B LDL phenotype. Nevertheless, when the variable of interest was the presence of measurable quantities of sdLDL subfractions, the ratio of apoB to apoAI had the best predictive

ability. In conclusion the ratios of apoB to apoAI and of triglycerides to HDL-C can reliably predict the presence of measurable quantities of sdLDL particles and of the pattern B LDL phenotype, respectively. However, since the quantitative determination of sdLDL concentrations may contribute to the determination of the cardiovascular risk, whereas the role of the LDL particle size remains controversial, apoB to apoAI ratio could provide more valuable information compared to markers that simply predict the presence of the pattern B LDL phenotype.

**Keywords** LDL particle diameter · LDL subfractions · Apolipoprotein B · Apolipoprotein AI

## Introduction

Low-density lipoprotein (LDL) concentrations represent a well-established predictor of cardiovascular morbidity and mortality [1]. Previously published studies have shown that LDLs are not the sum of identical particles but rather they consist of discrete subfractions that differ in respect to their size, density, composition, and other physicochemical properties [2]. These differences are, at least in part, responsible for the differences observed in the biological behaviour of LDL subfractions and more specifically in their ability to promote atherosclerosis [3]. Experimental studies suggest that the small, dense LDL particles (sdLDL) may exhibit greater atherogenic potential compared to larger and more buoyant LDL subfractions. This increased atherogenicity has been attributed to a number of biological properties of these particles, such as their increased permeability to the subendothelial space [4], their increased affinity for intimal proteoglycans [5, 6], their lower resistance to oxidative modification [7] as well

V. Tsimihodimos · I. Gazi · M. Elisaf (✉)  
Department of Internal Medicine, Medical School,  
University of Ioannina, 45110 Ioannina, Greece  
e-mail: egepi@cc.uoi.gr

C. Kostara  
Laboratory of Clinical Chemistry, Medical School,  
University of Ioannina, Ioannina, Greece

A. D. Tselepis  
Laboratory of Biochemistry, Department of Chemistry,  
University of Ioannina, Ioannina, Greece

as to their higher residence time in the plasma due to their decreased affinity for LDL receptors [8].

The clinical studies that tested the contribution of LDL subfraction profile in the determination of the total cardiovascular risk revealed contradictory results. Thus, some studies supported that an LDL subfraction profile characterized by a preponderance of sdLDL particles may represent an independent risk factor for the subsequent development of cardiovascular events [9–11], whereas others failed to reveal an independent predictive value of the LDL subfraction profile when other common risk factors were included in the analysis [12–14]. Recently, the Quebec cardiovascular study as well as the Veterans Affairs High-Density Lipoprotein Intervention Trial (VA-HIT) results showed a strong independent linear relationship between sdLDL particle concentration and the risk for ischemic events, thus indicating that the determination of the concentrations of these particles may be of great clinical significance [15, 16]. More specifically in the Quebec study patients with elevated sdLDL concentrations (third vs. first tertile) had a relative risk of 2.5 for the development of cardiovascular events, whereas in the VA-HIT study the odds ratio for new events associated with a 1-SD (standard deviation) increment in the concentration of sdLDL particles was 1.44. Thus, it is evident that the increased concentrations of sdLDL subfractions (which do not necessarily represent a “preponderance” of these particles) may significantly contribute to the determination of the cardiovascular risk [15, 16].

Several methodologies have been developed for the subfractionation of apolipoprotein B (apoB)-containing lipoproteins and the assessment of the LDL subfraction profile. The most widely used technique in clinical studies was the determination of the peak LDL particle diameter (LDL-PPD) by gradient electrophoresis [17]. Based on the peak particle diameter individuals can be subdivided into those with a preponderance of dense particles (referred as pattern B LDL phenotype) and into those with a preponderance of large, buoyant particles (pattern A LDL phenotype) [18]. However, the peak LDL particle size is an indirect, qualitative marker of the relative distribution of LDL subfractions that does not provide direct information for the concentration of the atherogenic sdLDL particles. On the contrary, other methodologies [such as density gradient ultracentrifugation [19], nuclear magnetic resonance (NMR) spectroscopy [14], gradient electrophoresis followed by quantification of the individual subfractions [20, 21] and recently Lipoprint [22]] allow the direct determination of the concentrations of LDL subfractions and thus they could be more feasible for the study of LDL subfraction profiles. Indeed, it has been proposed that the quantitative assessment of LDL particles may provide more valuable information for the determination of cardiovascular risk than the simple determination of LDL

particle size. Thus, in a number of studies where LDL particle concentration and size were evaluated simultaneously multivariate analyses revealed that sdLDL concentrations were independently associated with the risk of cardiovascular events, whereas LDL size was not a significant predictor of cardiovascular risk [16, 23]. Similarly, in the Quebec cardiovascular study the LDL particle size did not differ significantly between patients with ischemic heart disease and control individuals [15].

Since most of the methodologies that have been used so far for the characterization of lipoprotein subfraction profile are expensive, time consuming and technically demanding their application in every day clinical practice remains limited. Thus, efforts have been made for the identification of simple serum markers that could predict with acceptable sensitivity and specificity the presence of elevated concentrations of the atherogenic sdLDL particles. The aim of our study was to evaluate the ability of various metabolic parameters to predict the presence of phenotype B or, alternatively, the presence of measurable quantities of sdLDL subfractions in a group of individuals referred to the outpatient clinics of our hospital for suspected metabolic abnormalities. The identification of a simple inexpensive marker of the presence of sdLDL particles may provide a useful screening tool that could guide the decision for a more definitive subfraction analysis.

## Methods

### Patients

The study population was consisted of individuals attending the Outpatient Clinics of the University Hospital of Ioannina for suspected metabolic abnormalities. Individuals were excluded if they were found to be diabetic (fasting glucose levels greater than 7 mmol/l) or if they had a history of cardiovascular disease. Patients with thyroid dysfunction, liver or kidney diseases (defined as a positive medical history or a threefold increase in serum aminotransferases and serum creatinine levels greater than 92  $\mu$ mol/l, respectively) as well as those receiving drugs that may interfere with lipids or glucose metabolism were also excluded from the study. After the application of these exclusion criteria a total of 150 patients were included in the study. All study participants gave a written informed consent prior to their enrollment in the study, which was approved by the Ethics Committee of the University Hospital of Ioannina.

### Analytical Methods

All samples for lipid and lipoprotein determinations were collected after an overnight fast. Serum levels of total

cholesterol, HDL-C and triglycerides were determined enzymatically on the Olympus AU600 Clinical Chemistry analyzer (Olympus Diagnostica, Hamburg, Germany). Serum LDL-C was calculated using the Friedewald formula (provided that triglyceride levels were lower than 3.95 mmol/l). In individuals with serum triglyceride concentrations greater than 3.95 mmol/l ( $n = 9$ ) LDL-C was not determined. Serum apolipoproteins AI and B (apoAI and apoB, respectively) levels were measured with a Behring Holding GmbH BN 100 Nephelometer (Liederbach, Germany).

#### LDL Subclass Analysis

Electrophoresis was performed using the Lipoprint LDL System (Quantimetrix, Redondo Beach, CA, USA) as previously described [24]. By definition (according to the manufacturer's instructions) a concentration of sdLDL-cholesterol greater than 0.16 mmol/l was considered to be representative of the presence of "measurable" quantities of sdLDL particles in the serum. LDL-PPD was determined using the  $R_f$  at the highest peak of LDL bands according to the equation proposed by Kazumi et al: LDL-PPD =  $(1.429 - R_f) \times 25$  [23]. Individuals with an LDL-PPD <25.8 nm were considered to have a pattern B LDL subfraction profile [25]. It should be noted that the subfractionation of apoB-containing lipoproteins was performed within 24 h after sample collection. Meanwhile the samples were stored at 4 °C.

#### Statistical Analysis

All values were checked for normality with the Kolmogorov–Smirnov test and were found to be normally distributed. Correlations between sdLDL particle indices and other metabolic parameters were estimated using linear regression analysis, whereas, multiple regression analysis was used for the multivariate assessment of the correlations between those variables. In all cases a  $P$  level of less than 0.05 was considered statistically significant. To test the ability of various measures to predict the presence of sdLDL particles we constructed Receiver Operating Characteristic (ROC) curves and calculated the areas under the curve (AUC). The best cut-off points in apoB to apoAI and triglyceride to HDL-C ratios were determined using the Youden's index [26].

#### Results

The clinical characteristics and the lipid profile of the study individuals are shown in Table 1. Most subjects were

**Table 1** Clinical and laboratory characteristics of the study population

	Mean $\pm$ SD	Range
Age (years)	50.3 $\pm$ 11.4	21–78
Sex (males/females)	63/87	
Waist circumference (cm)		
Men	107.7 $\pm$ 11.1	87–152
Women	98.2 $\pm$ 11.4	61–147
BMI (Kgr/m <sup>2</sup> )	27.2 $\pm$ 4.8	23.4–33.2
Insulin ( $\mu$ U/ml)	13.8 $\pm$ 8.6	2.7–56.8
Total cholesterol (mmol/l)	6.1 $\pm$ 1.2	2.9–9.4
Triglycerides (mmol/l)	2.1 $\pm$ 1.2	0.5–7.9
HDL-C (mmol/l)	1.3 $\pm$ 0.3	0.7–2.3
LDL-C (mmol/l)	3.8 $\pm$ 0.9	2.1–6.9
Non-HDL-C (mmol/l)	4.7 $\pm$ 1.1	2.5–7.6
ApoB (g/l)	1.1 $\pm$ 0.3	0.5–1.8
ApoAI (g/l)	1.3 $\pm$ 0.3	0.4–2.1
Pattern B LDL phenotype <sup>a</sup> (%)	39	
Patients with measurable quantities of sdLDL subfractions (%)	69	

<sup>a</sup> LDL-Peak particle diameter <25.8 nm

LDL-C LDL-cholesterol, HDL-C HDL-cholesterol, non-HDL-C non-HDL-cholesterol, Apo apolipoprotein

middle-aged, whereas 58% of the study participants were women. Study individuals exhibited a wide spectrum of serum lipid concentrations (Table 1). As shown in the table, 39% of study subjects displayed a LDL-PPD lower than 25.8 nm (pattern B LDL phenotype). However, when study participants were evaluated for the presence of sdLDL particles 69% of them were found to have measurable quantities of these particles in their serum.

Table 2 displays the univariate, unadjusted correlations between sdLDL particle indices and various metabolic parameters. As shown, the serum concentrations of sdLDL particles were positively correlated with the concentrations of total, LDL and non-HDL cholesterol as well as with triglycerides and apoB. In addition, a significant negative correlation between sdLDL values and apoAI was also observed. The concentration of sdLDL particles was also positively correlated with the ratios of apoB to apoAI and triglycerides to HDL-C, whereas it was negatively correlated with the ratio of total cholesterol to triglycerides. As it is shown in Table 2 serum triglycerides along with the non-HDL cholesterol values showed the strongest correlations with the concentrations of sdLDL particles. Multivariate analysis (which included triglycerides, LDL-C, HDL-C and serum concentrations of apolipoproteins AI and B as predictors) revealed that serum triglycerides and LDL-C concentrations were the only important independent determinants of sdLDL cholesterol values (beta values

**Table 2** Correlations between small, dense LDL subfraction indices and various metabolic parameters

	Concentrations of sdLDL particles	LDL-PPD
TC	0.44**	-0.29**
TRG	0.53**	-0.53**
HDL-C	-0.14	0.25**
LDL-C	0.27**	-0.12
Non-HDL-C	0.53**	-0.39**
ApoB	0.50**	-0.33**
ApoAI	-0.18*	0.17**
ApoB/ApoAI	0.46**	-0.40**
TRG/HDL-C	0.43**	-0.46**
TC/TRG	-0.42**	0.47**
LDL-C/ApoB	-0.21**	0.28**

Data represent Pearson's correlation coefficients (*r*). \*  $P < 0.05$  and \*\*  $P < 0.01$ , respectively

sdLDL Small dense LDL, LDL-PPD LDL-peak particle diameter, TC total cholesterol, TRG triglycerides, HDL-C HDL-cholesterol, LDL-C LDL-cholesterol, Non-HDL-C non-HDL-cholesterol, Apo apolipoprotein

0.5 and 0.31 for triglycerides and LDL-C, respectively;  $P < 0.01$  for both correlations).

On the other hand LDL-PPD was positively correlated with the serum concentrations of HDL-C and apoAI as well as with the ratio of total cholesterol to triglycerides (Table 2). Conversely, LDL particle diameter was negatively correlated with total, LDL and non-HDL cholesterol, triglycerides and apoB as well as with the ratios of apoB to apoAI and triglycerides to HDL-C. Again, serum triglyceride concentration exhibited the strongest correlation with LDL-PPD. Surprisingly, the ratio of LDL-C to apoB [a marker widely used as indicative of the presence of sdLDL particles [27–29]] was only weakly correlated with the indices of sdLDL subfractions (Table 2). In multivariate analysis the serum concentration of triglycerides was the only significant independent determinant of LDL-PPD (beta value -0.46,  $P < 0.01$ ).

The ability of the lipoprotein variables that were most closely related to the concentrations of sdLDL particles to predict the presence of measurable quantities of sdLDL subfractions was evaluated with ROC analysis. The corresponding AUCs, their confidence intervals as well as their level of significance are displayed in Table 3. As can be seen, the AUC was greatest for the ratio of apoB to apoAI, whereas the serum concentration of triglycerides and the ratio of triglycerides to HDL-C gave slightly lower values. The same variables were also tested for their ability to predict the presence of the pattern B LDL phenotype. As shown in Table 3, the strongest predictor was the ratio of triglycerides to HDL-C, whereas serum triglycerides and the apoB to apoAI ratio revealed lower AUC values. In

**Table 3** Areas under the receiver-operating characteristic curves and 95% confidence intervals for the prediction of the presence of measurable quantities of small, dense LDL subfractions and the pattern B LDL subfraction phenotype

	Presence of sdLDL		Presence of pattern B phenotype	
	AUC	CI	AUC	CI
TRG	0.76	0.70–0.84	0.78	0.68–0.88
ApoB	0.73	0.65–0.81	0.69	0.58–0.81
Non-HDL-C	0.75	0.69–0.85	0.70	0.59–0.81
ApoB/ApoAI	0.80	0.73–0.88	0.73	0.64–0.81
TRG/HDL-C	0.78	0.71–0.85	0.81	0.71–0.90
LDL-C/ApoB	0.62	0.54–0.72	0.70	0.57–0.82
TC/TRG	0.73	0.65–0.82	0.71	0.64–0.78

AUC Area under the curve, CI confidence interval, TC total cholesterol, TRG triglycerides, HDL-C HDL-cholesterol, LDL-C LDL-cholesterol, Non-HDL-C non-HDL-cholesterol, Apo apolipoprotein. The level of significance was less than 0.01 for all parameters

agreement with the results of linear regression analysis, the ratio of LDL-C to apoB (which has been widely used as a marker for the presence of sdLDL) gave AUC values for the presence of sdLDL that differ substantially from those observed for the other parameters (Table 3).

The selection of a cut-off point for a particular test is a complicated procedure that is largely affected by two factors: disease prevalence and the relative “cost” of errors (false-positive and false-negative results) [30]. The Youden index is a prevalence-independent index that optimises the summary measures of sensitivity and specificity [26]. According to this index the best cut-off value for the ratio of apoB to apoAI was 0.687. This value predicted the presence of measurable quantities of sdLDL particles with a sensitivity of 86% and a specificity of 69%, respectively, whereas the corresponding positive (PPV) and negative predictive values (NPV) were 68 and 67%, respectively. Similarly, according to the Youden's index the best cut-off point for the ratio of triglycerides to HDL-C was 3.69 (when both parameters were expressed in mg/dl). This value predicted the presence of the pattern B LDL phenotype with a sensitivity of 81% and a specificity of 66%, whereas the corresponding PPV and NPV were 33 and 94%, respectively. Although the Youden index represents a useful tool for the comparison of multiple tests, it does not provide cut-off points that can be easily applied in every day clinical practice. Thus, if the surrogate markers of the presence of sdLDL particles are to be used as screening tools for deciding which subjects have a high probability of having measurable quantities or a preponderance of sdLDL subfractions (and thus are eligible for a more definitive subfraction analysis) cut-off values with higher specificity should be selected. In this context, the values of the ratios of apoB to apoAI and of triglycerides to HDL-C that

provide a specificity of 90% for the identification of individuals with measurable quantities or a preponderance of sdLDL particles were 0.85 and 5.45, respectively. The corresponding sensitivities, PPVs and NPVs were 56, 91 and 46% for the ratio of apoB to apoAI and 62, 53 and 92% for the ratio of triglycerides to HDL-C, respectively. On the other hand, if the aim of these screening tools is to identify nearly all the individuals with measurable quantities or a preponderance of sdLDL subfractions, a cut-off point with high sensitivity should be selected. The values of the ratios of apoB to apoAI and of triglycerides to HDL-C that gave a sensitivity of 90% were 0.61 and 2.77, respectively. The corresponding specificities, PPVs and NPVs were 38, 77 and 62% for the ratio of apoB to apoAI and 48, 27 and 97% for the ratio of triglycerides to HDL-C, respectively.

It must be noted that in our population, a ratio of triglycerides to HDL-C of 3.5 [that was shown to have the greatest discriminative value in previous studies [31]] predicted the presence of the pattern B LDL phenotype with a sensitivity of 80% and a specificity of 61%.

## Discussion

Previous studies have shown that LDLs comprise a heterogeneous group of particles that differ in respect to their physicochemical properties and to their biological behaviour [2]. Experimental and clinical data suggest that sdLDL subfractions exhibit greater atherogenic potential as compared to large, buoyant LDL particles [3]; consequently, the assessment of LDL subfraction profile may substantially contribute to the determination of the total cardiovascular risk. However, since most of the techniques currently used for the subfractionation of apoB-containing lipoproteins are expensive, time-consuming and technically demanding their application in every day clinical practice seems very difficult. In this study we tested the ability of various common metabolic parameters to predict the presence (or the preponderance) of sdLDL particles. In agreement with previously published studies we found that the ratio of triglycerides to HDL-C was the best predictor of the presence of pattern B LDL subfraction distribution [31, 32]. Nevertheless, when the variable of interest was the presence of measurable quantities of sdLDL subfractions in the serum (irrespective of LDL subfraction profile) the ratio of apoB to apoAI had the best predictive ability.

The determination of LDL-PPD with gradient gel electrophoresis, although more convenient for use in every day clinical practice compared to other techniques (NMR, density gradient ultracentrifugation), does not provide direct information concerning the concentration of the atherogenic sdLDL particles. On the contrary, it represents a rough, indirect, qualitative marker of LDL particles'

relative distribution and can be modified by changes not only in the concentrations of sdLDL subfractions, but also in the concentrations of large, buoyant particles as well as in the concentrations of subfractions of intermediate density. Although the LDL-PPD was the most widely used marker of LDL subfraction profile in the past, recently developed methodologies (NMR, Lipoprint) focus on the direct determination of the concentrations of the atherogenic sdLDL particles. Since recently published studies revealed that the increased concentration of these particles (which do not necessarily represent a preponderance) may contribute to the determination of the total cardiovascular risk [15, 16], whereas the LDL particle size is not an independent predictor of ischemic events [16, 23] this approach seems to be more sensitive and precise. Indeed, based on the LDL-PPD, a substantial proportion of subjects in our study (about 30%) would have been misclassified as having low cardiovascular risk (since they did not exhibit a pattern B LDL phenotype), whereas, Lipoprint analysis revealed that these patients had measurable quantities of sdLDL subfractions in their serum and thus, they may deserve further quantitative determination of the sdLDL concentration for the precise determination of their future cardiovascular risk. Consequently, the determination of the ratio of apoB to apoAI that predicts the presence of sdLDL particles seems to be more valuable than markers that simply predict the presence of a pattern B LDL phenotype.

The determination of the LDL subfraction profile is a complicated process involving the production and catabolism of apoB-containing lipoproteins as well as the intravascular remodelling of lipoprotein particles [33, 34]. Experimental and clinical studies have shown that the most important determinant of this process is the concentration of triglyceride-rich lipoproteins [18, 35]. As a consequence, patients with elevated triglyceride values usually exhibit a preponderance of dense LDL particles (pattern B LDL phenotype), whereas individuals with normal concentrations of triglycerides usually have a predominance of buoyant LDL particles (pattern A LDL phenotype) [17]. In this context it is not surprising that the ratio of triglycerides to HDL-C was the most important predictor of the presence of the type B phenotype, since triglycerides significantly affect the distribution of LDL particles. On the other hand, when the variable of interest was more "quantitative" i.e. the presence of measurable quantities of sdLDL particles the ratio of apoB to apoAI had the best predictive ability. A possible explanation for this difference could be that the numerator of this later ratio (which represents a marker of the sum of apoB-containing particles) includes, in addition to the "driving force" for the generation of sdLDL particles (triglyceride-rich lipoproteins), the substrate that is available for this generation (LDL particles). Thus, it could be expected that patients with high LDL values could

exhibit measurable quantities (but not predominance) of sdLDL particles even in the absence of elevated triglyceride concentrations. This assumption is indirectly supported by our data showing that LDL-C concentrations were significantly correlated with the concentrations of sdLDL particles, but not with the LDL-PPD that represents an indirect, qualitative measure of LDL subfraction distribution.

Another important issue that deserves special attention is the inverse relationship between the measures of high-density lipoproteins (HDL-C and apoAI) and sdLDL particle indices (sdLDL concentrations and LDL-PPD). Although this relationship has been observed in many studies [20, 29, 36] there is a discrepancy as to whether this correlation remains significant after the inclusion of triglycerides in the multivariate analyses. Thus, it is not known if HDL particles are directly implicated in the generation of sdLDL particles or if this correlation merely represents a consequence of the well-known inverse correlation between the concentration of triglycerides and that of HDL-C. Our data indicates that the incorporation of HDL indices in the ratios of triglycerides to HDL-C and apoB to apoAI, respectively, improves the ability of apoB and triglycerides to predict the presence of sdLDL particles. Nevertheless, further studies are needed to delineate the role of HDL in the process that generates sdLDL particles.

Recently published studies indicate that the ratio of apoB to apoAI is a very strong predictor of cardiovascular risk [37, 38]. Although pathophysiologically the prognostic ability of this measure can be easily explained by the inclusion of markers of the atherogenic apoB-containing particles and of the reverse cholesterol transport process (apoB and apoAI, respectively), it could be assumed that the significant relationship of this ratio with the concentrations of sdLDL particles may also contribute to its predictive value. In this context, Jungner et al. [29] recently proposed that the failure of LDL particle size to add predictive information to the apoB to apoAI ratio may just reflect that this ratio also captures the risk related to LDL size.

A potential limitation of our study is that a significant proportion of the study participants exhibited an abnormal lipid profile and elevated concentrations of sdLDL particles. Consequently, our sample is not representative of the general population. However, the predictive ability of the various metabolic parameters was assessed using measures that are not affected by the prevalence of the tested variable in the study population (such as sensitivity, specificity and AUC). In addition, our study population is representative of the individuals usually referred to outpatient clinics with suspected metabolic abnormalities; in this population the assessment of LDL subfraction profile is of potential clinical interest for the determination of the total cardio-

vascular risk. On the contrary, since the concentrations of sdLDL particles are significantly correlated with serum lipids, an LDL subfraction profile characterized by elevated concentrations of these particles can only exceptionally be observed in individuals with normal lipid values. This observation along with the lack of clinical guidelines and specific treatments for the reduction of sdLDL particle concentrations in otherwise healthy individuals, significantly limit the clinical value of the determination of LDL subfraction profile in the general population.

Recently published studies revealed a substantial heterogeneity of results and interpretations among the methodologies currently used for the analysis of LDL subfractions [39]. Thus, another potential limitation of our study is the use of the Lipoprint system which does not allow the comparison of our results with those in the literature obtained by other techniques. However, in the absence of a standardization program the same is also true for the other methodologies currently used for the subfractionation of apolipoprotein B-containing lipoproteins [39].

In conclusion, the ratios of apoB to apoAI and of triglycerides to HDL-C can reliably predict the presence of measurable quantities of sdLDL particles and of the pattern B LDL phenotype, respectively. However, since the increased concentrations of sdLDL particles may substantially contribute to the determination of the total cardiovascular risk, whereas the role of the LDL particle size remains controversial, the apoB to apoAI ratio may provide more valuable information compared to markers that simply predict the presence of a pattern B LDL phenotype.

## References

1. Siegel RD, Cupples A, Schaefer EJ, Wilson PW (1996) Lipoproteins, apolipoproteins, and low-density lipoprotein size among diabetics in the Framingham offspring study. *Metabolism* 45:1267–1272
2. Teng B, Thompson GR, Sniderman AD, Forte TM, Krauss RM, Kwiterovich PO Jr (1983) Composition and distribution of low density lipoprotein fractions in hyperapobetalipoproteinemia, normolipidemia, and familial hypercholesterolemia. *Proc Natl Acad Sci USA* 80:6662–6666
3. Austin MA, Breslow JL, Hennekens CH, Buring JE, Willett WC, Krauss RM (1988) Low-density lipoprotein subclass patterns and risk of myocardial infarction. *JAMA* 260:1917–1921
4. Nielsen LB (1996) Transfer of low density lipoprotein into the arterial wall and risk of atherosclerosis. *Atherosclerosis* 123:1–15
5. Anber V, Millar JS, McConnell M, Shepherd J, Packard CJ (1997) Interaction of very-low-density, intermediate-density, and low-density lipoproteins with human arterial wall proteoglycans. *Arterioscler Thromb Vasc Biol* 17:2507–2514
6. Anber V, Griffin BA, McConnell M, Packard CJ, Shepherd J (1996) Influence of plasma lipid and LDL-subfraction profile on the interaction between low density lipoprotein with human arterial wall proteoglycans. *Atherosclerosis* 124:261–271

7. Chait A, Brazg RL, Tribble DL, Krauss RM (1993) Susceptibility of small, dense, low-density lipoproteins to oxidative modification in subjects with the atherogenic lipoprotein phenotype, pattern B. *Am J Med* 94:350–356
8. Lund-Katz S, Laplaud PM, Phillips MC, Chapman MJ (1998) Apolipoprotein B-100 conformation and particle surface charge in human LDL subspecies: implication for LDL receptor interaction. *Biochemistry* 37:12867–12874
9. Griffin BA, Freeman DJ, Tait GW et al (1994) Role of plasma triglyceride in the regulation of plasma low density lipoprotein (LDL) subfractions: relative contribution of small, dense LDL to coronary heart disease risk. *Atherosclerosis* 106:241–253
10. Gardner CD, Fortmann SP, Krauss RM (1996) Association of small low-density lipoprotein particles with the incidence of coronary artery disease in men and women. *JAMA* 276:875–881
11. Lamarche B, Lemieux I, Despres JP (1999) The small, dense LDL phenotype and the risk of coronary heart disease: epidemiology, patho-physiology and therapeutic aspects. *Diabetes Metab* 25:199–211
12. Stampfer MJ, Krauss RM, Ma J et al (1996) A prospective study of triglyceride level, low-density lipoprotein particle diameter, and risk of myocardial infarction. *JAMA* 276:882–888
13. Blake GJ, Otvos JD, Rifai N, Ridker PM (2002) Low-density lipoprotein particle concentration and size as determined by nuclear magnetic resonance spectroscopy as predictors of cardiovascular disease in women. *Circulation* 106:1930–1937
14. Kathiresan S, Otvos JD, Sullivan LM et al (2006) Increased small low-density lipoprotein particle number: a prominent feature of the metabolic syndrome in the Framingham Heart Study. *Circulation* 113:20–29
15. St Pierre AC, Cantin B, Dagenais GR et al (2005) Low-density lipoprotein subfractions and the long-term risk of ischemic heart disease in men: 13-year follow-up data from the Quebec Cardiovascular Study. *Arterioscler Thromb Vasc Biol* 25:553–559
16. Otvos JD, Collins D, Freedman DS et al (2006) Low-density lipoprotein and high density lipoprotein particle subclasses predict coronary events and are favourably changed by gemfibrozil therapy in the Veterans Affairs High-Density Lipoprotein Intervention Trial. *Circulation* 113:1556–1563
17. Nichols AV, Krauss RM, Musliner TA (1986) Nondenaturing polyacrylamide gradient gel electrophoresis. *Meth Enzymol* 128:417–431
18. Austin MA, King MC, Vranizan KM, Krauss RM (1990) Atherogenic lipoprotein phenotype. A proposed genetic marker for coronary heart disease risk. *Circulation* 82:495–506
19. Tsimihodimos V, Karabina S-A., Tambaki A, et al (2003) Effect of atorvastatin on the concentration, relative distribution, and chemical composition of lipoprotein subfractions in patients with dyslipidemias of type IIA and IIB. *J Cardiovasc Pharmacol* 42:304–310
20. Skoglund-Andersson C, Tang R, Bond MG, de Faire U, Hamsten A, Karpe F (1999) LDL particle size distribution is associated with carotid intima-media thickness in healthy 50-year-old men. *Arterioscler Thromb Vasc Biol* 19:2422–2430
21. St-Pierre AC, Ruel IL, Cantin B, Dagenais GR, Bernard PM, Despres JP, Lamarche B (2001) Comparison of various electrophoretic characteristics of LDL particles and their relationship to the risk of ischemic heart disease. *Circulation* 104:2295–2299
22. Gazi I, Lourida ES, Filippatos T, Tsimihodimos V, Elisaf M, Tselepis AD (2005) Lipoprotein-associated phospholipase A2 activity is a marker of small, dense LDL particles in human plasma. *Clin Chem* 51:2264–2273
23. Blake GJ, Otvos JD, Rifai N, Ridker PM (2002) LDL particle concentration and size as determined by NMR spectroscopy as predictors of cardiovascular disease in women. *Circulation* 106:1930–1937
24. Gazi I, Tsimihodimos V, Filippatos T, Bairaktari E, Tselepis AD, Elisaf M (2006) Concentration and relative distribution of low-density lipoprotein subfractions in patients with metabolic syndrome defined according to the National Cholesterol Education Program criteria. *Metabolism* 55:885–891
25. Kazumi T, Kawaguchi A, Hozumi T et al (1999) Low density lipoprotein particle diameter in young, nonobese, normolipidemic Japanese men. *Atherosclerosis* 142:113–119
26. Youden WJ (1950) Index for rating diagnostic tests. *Cancer* 3:32–35
27. Wagner AM, Jorba O, Rigla M, Alonso E, Ordonez-Lianos J, Perez A (2002) LDL-cholesterol/apolipoprotein B ratio is a good predictor of LDL phenotype B in type 2 diabetes. *Acta Diabetol* 39:215–220
28. Garin MC, Kalix B, Morabia A, James RW (2005) Small, dense lipoprotein particles and reduced paraoxonase-1 in patients with the metabolic syndrome. *J Clin Endocrinol Metab* 90:2264–2269
29. Jungner I, Sniderman AD, Furberg C, Aastveit AH, Holme I, Walldius G (2006) Does low-density lipoprotein size add to atherogenic particle number in predicting the risk of fatal myocardial infarction? *Am J Cardiol* 97:943–946
30. Zweig MH, Campbell G (1993) Receiver-operating characteristic (ROC) plots: a fundamental evaluation tool in clinical medicine. *Clin Chem* 39:561–577
31. McLaughlin T, Reaven G, Abbasi F et al (2005) Is there a simple way to identify insulin-resistant individuals at increased risk of cardiovascular disease? *Am J Cardiol* 96:399–404
32. Maruyama C, Imamura K, Teramoto T (2003) Assessment of LDL particle size by triglyceride/HDL-cholesterol ratio in non-diabetic, healthy subjects without prominent hyperlipidemia. *J Atheroscler Thromb* 10:186–191
33. Packard CJ, Shepherd J (1997) Lipoprotein heterogeneity and apolipoprotein B metabolism. *Arterioscler Thromb Vasc Biol* 17:3542–3556
34. Berneis KK, Krauss RM (2002) Metabolic origins and clinical significance of LDL heterogeneity. *J Lipid Res* 43:1363–1379
35. Watson TD, Caslake MJ, Freeman DJ et al (1994) Determinants of LDL subfraction distribution and concentrations in young normolipidemic subjects. *Arterioscler Thromb* 14:902–910
36. Benton JL, Blumenthal RS, Becker DM, Yanek LR, Moy TF, Post W (2005) Predictors of low-density lipoprotein particle size in a high-risk African-American population. *Am J Cardiol* 95:1320–1323
37. Meisinger C, Loewel H, Mraz W, Koenig W (2005) Prognostic value of apolipoprotein B and A-I in the prediction of myocardial infarction in middle-aged men and women: results from the MONICA/KORA Augsburg cohort study. *Eur Heart J* 26:271–278
38. Lind L, Vessby B, Sundstrom J (2006) The apolipoprotein B/AI ratio and the metabolic syndrome independently predict risk for myocardial infarction in middle-aged men. *Arterioscler Thromb Vasc Biol* 26:406–410
39. Ensign W, Hill N, Heward CB (2006) Disparate LDL phenotypic classification among 4 different methods assessing LDL particle characteristics. *Clin Chem* 52:1722–1727

## Deposition of Free Cholesterol in the Blood Vessels of Patients with Coronary Artery Disease: a Possible Novel Mechanism for Atherogenesis

Ricardo D. Couto · Luís A. O. Dallan ·  
Luiz A. F. Lisboa · Carlos H. Mesquita ·  
Carmen G. C. Vinagre · Raul C. Maranhão

Received: 16 August 2006 / Accepted: 7 February 2007 / Published online: 19 April 2007  
© AOCs 2007

**Abstract** A cholesterol-rich nanoemulsion (LDE) that mimics the composition of low-density lipoprotein (LDL) acquires apoE in the plasma and is taken-up by the cells by LDL receptors. In this study, to verify whether free cholesterol (FC) and the cholesteryl ester (CE) components of LDL are taken-up differently by the vessels. LDE labeled with  $^3\text{H}$ -cholesterol and  $^{14}\text{C}$ -cholesteryl oleate was injected into 20 coronary artery disease patients 24 h before a scheduled myocardial coronary artery bypass grafting. The plasma kinetics of both radiolabels was determined from plasma samples collected over 24 h, and fragments of vessels discarded during surgery were collected and analyzed for radioactivity. LDE FC was removed faster than CE. The radioactive counting of LDE CE was greater than that of LDE FC in the blood, but the uptake of FC was markedly greater than that of CE in all fragments: fivefold greater in the aorta ( $p = 0.04$ ), fourfold greater in the internal thoracic artery ( $p = 0.03$ ), tenfold greater in the saphenous vein ( $p = 0.01$ ) and threefold in the radial artery ( $p = 0.05$ ). In conclusion, the greater removal from plasma

of FC compared with CE and the remarkably greater vessel tissue uptake of FC compared with CE suggests that, in the plasma, FC dissociates from the nanoemulsion particles and precipitates in the vessels. Considering LDE as an artificial nanoemulsion model for LDL, our results suggest that dissociation of FC from lipoprotein particles and deposition in the vessel wall may play a role as an independent mechanism in atherogenesis.

**Keywords** LDL metabolism · Nanoparticles · Emulsions · Lipids and atherosclerosis · Free cholesterol · Cholesteryl esters · Coronary artery disease · Lipoproteins · Lipoprotein kinetics

### Introduction

The low-density lipoprotein (LDL) quasispherical particle is basically composed of a core of cholesteryl esters (CE) with residual triglycerides surrounded by a phospholipid monolayer that also contains free cholesterol (FC). Apolipoprotein B100, the single protein molecule on the particle surface mediates the removal of the lipoprotein from the circulation through binding of the particle to specific cell membrane receptors. In the circulation, CE molecules may shift from LDL to other lipoprotein classes by means of the cholesterol ester transfer protein, that can also transfer triglycerides and phospholipids [1]. In contrast, FC is able to freely diffuse from LDL to the surrounding aqueous medium. Therefore, FC is less stable in the lipoprotein structure than CE [1].

Cholesterol is esterified in the intravascular compartment by the action of lecithin cholesterol acyl transferase (LCAT) using apo A1 as a co-factor [2]. This reaction occurs mainly in HDL, which is the central esterification

R. D. Couto · L. A. O. Dallan · L. A. F. Lisboa  
C. G. C. Vinagre · R. C. Maranhão  
Lipid Metabolism Laboratory and the Surgical Division,  
The Heart Institute (INCOR) of the Medical School Hospital,  
University of São Paulo, Sao Paulo, Brazil

R. D. Couto · C. H. Mesquita · R. C. Maranhão  
Faculty of Pharmaceutical Sciences, University of São Paulo,  
Sao Paulo, Brazil

R. C. Maranhão (✉)  
Instituto do Coração (InCor) do Hospital das Clínicas da USP,  
Laboratório de Metabolismo de Lípidos, Avenida Dr Enéas C.  
Aguiar 44, 1° Subsolo, CEP-05403-000 Sao Paulo-SP, Brazil  
e-mail: ramarans@usp.br



site in the plasma. In LDL, the esterification reaction may occur only at very slow rates [2]. Cholesterol trapped by the cells of the vessel wall is esterified by acyl-CoA:cholesterol acyltransferase catalysis. The phenomena related with the uptake of the cholesterol contained in lipoproteins such as LDL by the arterial wall are of fundamental importance in the understanding of the mechanism of the lipid deposition and accumulation in the artery and atherogenesis.

Lipoproteins can be modeled by artificially made lipid emulsions [3–7]. We have shown that nanoemulsions (LDE) roughly resembling the lipidic structure of LDL particles, as described above, but made without protein, are taken-up by LDL receptors [3, 6]. In contact with plasma, LDE acquires apo E and other apolipoproteins from native lipoproteins. Apo E can be also recognized by LDL receptors and allows binding of the artificial emulsion to the receptors. Compared to native LDL, LDE is more rapidly removed from the plasma due to the differences in apolipoprotein profile on the surface of those particles. Apo E that binds to the LDE particle surface has been shown to possess several times greater affinity for the receptor than the unique LDL apolipoprotein, namely apo B100. In fact, when apo B100 was incorporated to LDE before the injection into rats, the removal from the plasma of the emulsion was markedly slowed down [8].

Compared with native LDL, the shorter testing period, uniformity of the preparation and ease of labeling with isotopic, fluorescent or other means are advantages of the LDE model that facilitate the performance of plasma kinetic studies. Thus, LDE has been used to investigate in subjects defects in the process of LDL removal from the plasma. Recently, we observed that after intravenous injection the removal of LDE FC was faster in patients with coronary artery disease (CAD) than in controls without the disease [9]. On the other hand, the removal of the CE of the nanoemulsion did not differ between CAD and non-CAD subjects. This suggests that in CAD, dissociation of the free form of cholesterol from the nanoemulsion particles, and for extension of native LDL, occurs with potential pathophysiological implications. In this study, the question was posed whether or not the two forms of cholesterol constituting the nanoemulsion particles are taken up at different rates by the blood vessels of CAD patients. To answer this question, LDE labeled with both  $^{14}\text{C}$ -cholesteryl oleate and  $^3\text{H}$ -cholesterol was injected intravenously in CAD patients that were scheduled for coronary bypass surgery within the next ensuing 24 h. After the injection, blood samples were taken and the arterial and venous fragments that were discarded during the surgical procedure were analyzed for radioactive counting.

## Methods

### Patients

Twenty patients (3 females and 17 males) with CAD who were scheduled for coronary artery bypass grafting (CABG) were selected from the infirmary of the Heart Institute. They were aged 41–79 years ( $59 \pm 9$ , mean  $\pm$  S.D.). The patients did not have concomitant metabolic diseases, renal or hepatic dysfunction, as evaluated by clinical and laboratory criteria. The patients had (in  $\text{mg dl}^{-1}$ ) total cholesterol  $204 \pm 12$ , LDL cholesterol was  $129 \pm 11$ , HDL was  $41 \pm 3$ , triglycerides  $170 \pm 23$ , and glucose  $114 \pm 9$  (mean  $\pm$  S.D.).

### Plasma Biochemical Determinations

Blood samples for determination of plasma lipids were collected after a 12-h fast on the same day the kinetic studies were performed. Commercial enzymatic methods were used for the determination of total cholesterol (Boehringer-Mannheim, Penzberg, Germany) and triglycerides (Abbott Laboratories, USA). HDL cholesterol was determined by the same method used for total cholesterol after lipoprotein precipitation with magnesium phosphotungstate. LDL cholesterol was calculated by the formula of Friedewald [10].

### LDE Preparation

LDE was prepared from a lipid mixture composed of 40 mg cholesteryl oleate, 20 mg egg phosphatidylcholine, 1 mg triolein and 0.5 mg cholesterol purchased from Nu-Check Prep (Elysian, USA).  $^{14}\text{C}$ -cholesteryl oleate and  $^3\text{H}$ -cholesterol purchased from Amersham International (Amersham, UK) were added to the mixture. Emulsification of lipids by prolonged ultrasonic irradiation in aqueous media and the procedure of two-step ultracentrifugation of the crude emulsion with density adjustment by addition of KBr to obtain LDE microemulsion was performed as described previously [3, 6]. LDE was dialyzed against saline solution and passed through a  $0.22\text{-}\mu\text{m}$  millipore membrane filter for injection into the patients.

### Dissociation of FC and CE from LDE and from Native LDL

To verify whether or not the dissociation of lipids from the LDE particles is similar to dissociation from native LDL, both LDE and LDL labeled with  $^{14}\text{C}$ -cholesteryl oleate and  $^3\text{H}$ -cholesterol were dialyzed against human plasma for

measurement of the radioactivity remaining in the dialysis bags during a 48-h period.

For this experiment, LDE was obtained and labeled with the radioactive lipids as described above. Native LDL was obtained from a healthy normolipidemic donor by sequential ultracentrifugation of the plasma aliquot using a SW41 rotor (Beckman, Palo Alto, CA, USA). For labeling with the radioactive lipids, the obtained LDL fraction was incubated with 1Ci  $^{14}\text{C}$ -cholesteryl oleate and 1Ci  $^3\text{H}$ -cholesterol dissolved in ethanol at 37 °C for 48 h [11, 12]. LDL was then separated from the unbound radioactive lipids using the same ultracentrifugation procedure described above. Five 0.5 ml aliquots of the labeled LDE and five of the native LDL were transferred to five dialysis bags, each one designed to the sequential dialysis times: 5 min and 1, 2, 8 and 48 h. After the dialysis against plasma, the volumes of the bags were transferred to counting vials for radioactive counting in a scintillation counter. The data of the radioactivity remaining in the LDE and LDL fractions into the dialysis bags were plotted against time and the AUC was calculated.

#### LDE Plasma Kinetics and Cholesterol Esterification

On the day preceding surgery, at approximately 9:00 a.m., the labeled emulsion (roughly 130 kBq  $^{14}\text{C}$ -cholesteryl oleate and 158 kBq  $^3\text{H}$ -cholesterol, 4 mg total lipid mass) was injected intravenously in a bolus, with the participants fasting for 12 h. During the study, they were allowed two standard meals, at approximately 12:30 p.m. and 7 p.m. Plasma samples were collected over 24 h, at intervals of 5 min and 1, 2, 4, 6, 8 and 24 h after the injection. Aliquots (1.0 ml) of blood plasma were transferred to counting vials containing 7.0 ml of scintillation solution (Ultima Gold XR, Packard, Groningen, The Netherlands). Radioactivity was counted using a Packard 1660 TR (Meriden, CT, USA) spectrometer.

To verify the kinetics of cholesterol esterification in the LDE remaining in the plasma after the injection into the patients, the sequential plasma samples collected for the clearance experiments were submitted to lipid extraction and resolved into lipid classes by thin-layer chromatography as described in our previous study [9]. Bands corresponding to free and esterified cholesterol were scraped and transferred into vials for  $^3\text{H}$  radioactivity counting.

#### Estimation of Fractional Catabolic Rate

Fractional catabolic rates (FCR) of the LDE  $^{14}\text{C}$ -cholesteryl oleate and  $^3\text{H}$ -cholesterol, were calculated according to the method described by Matthews [13] as FCR, where  $a_1$ ,  $a_2$ ,  $b_1$  and  $b_2$  were estimated from

biexponential curves obtained from the remaining radioactivity found in plasma after injection, fitted by least squares procedure, as  $y = (a_1 \cdot e^{-b_1 t}) + (a_2 \cdot e^{-b_2 t})$  where  $y$  represents the radioactivity plasma decay as a function of time ( $t$ );  $a$  indicates the linear coefficient and  $b$ , the angular coefficient, which represents the FCR in  $\text{h}^{-1}$ . The FCR were estimated from parameters  $a_1$ ,  $b_1$  and  $b_2$  by the following equation:  $\text{FCR} = (a_1/b_1 + a_2/b_2)^{-1}$ . Calculations were performed using the ANACOMP software [14]. The compartment model used is illustrated in Fig. 1.

#### LDE Uptake by the Vascular Tissues

During the surgery, which occurred 20–24 h after LDE injection, the removed fragments of CABG were collected, separated and put into 0.9% cold saline solution and immediately transported to the laboratory for analysis. The fragments of vascular (aorta, radial, internal thoracic arteries and saphenous vein) and pericardium were then chopped and lipids from 0.1 g of both tissues were extracted with chloroform/methanol (2:1, v/v) and the radioactivity was measured in a scintillation solution.

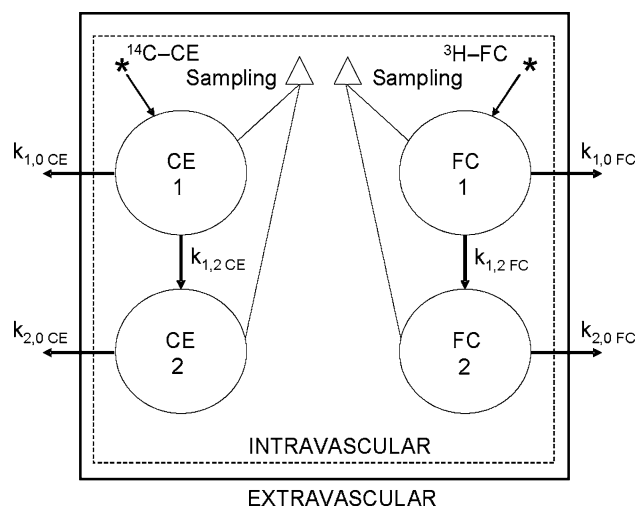


**Fig. 1** Compartmental model used to analyze the kinetics of LDE FC and CE. The model consists of four discrete compartments: two for  $^{14}\text{C}$ -CE and two for  $^3\text{H}$ -FC labels. All compartments are in the intravascular space ( $I_{\text{CE}}$ ,  $2_{\text{CE}}$ ,  $I_{\text{FC}}$  and  $2_{\text{FC}}$ ). LDE  $^{14}\text{C}$ -CE and  $^3\text{H}$ -FC were injected intravenously in a bolus (arrow with asterisk) into compartment  $I_{\text{CE}}$  and  $I_{\text{FC}}$ , respectively. A fraction  $k_{1,0\text{CE}}$  and  $k_{1,0\text{FC}}$  of the labeled lipids is removed to the extravascular space. Competitively, fractions  $k_{1,2\text{CE}}$  and  $k_{1,2\text{FC}}$  of the injected lipids are converted into compartments  $2_{\text{CE}}$  and  $2_{\text{FC}}$  due to the incorporation of apolipoproteins available in the plasma. Subsequently, the materials of those compartments are transferred to the extravascular space following the  $k_{2,0\text{CE}}$  and  $k_{2,0\text{FC}}$  routes. The samplings, represented by triangles correspond to the indiscriminate combination of compartments 1 and 2

## Informed Consent and Radiological Safety

The experimental protocol was approved by the Ethical Committee of the Heart Institute and a written informed consent was given by all participants. The safety of the radioactive dose intravenously injected into the patients was assured according to the regulations of the International Commission on Radiological Protection, ICRP [15]. The injected dose in each experiment was 0.03 mSv, well below the 50 mSv annual limit for intake of radionuclides as described in our previous study [14].

## Statistical Analysis

Data normality was tested by the Kolmogorov–Smirnov procedure. Data are expressed as mean  $\pm$  standard error of the mean except for FCR and the constants ( $k$ ) of transference that are expressed as median and percentiles (25th; 75th) (Table 1). The FCRs of  $^{14}\text{C}$ -cholesteryl oleate and  $^3\text{H}$ -cholesterol were compared by the Mann–Whitney's rank sum test. Parametric tests, analysis of variance, were performed to compare the decay curves points of LDE radioactive labels, and the amount of  $^{14}\text{C}$  and of  $^3\text{H}$  radioactivity measured in fragments. In all analysis, difference of two tail  $p < 0.05$  was considered statistically significant.

## Results

Figure 2 shows the curves of disappearance from the dialysis bags of LDE and native LDL labeled with both  $^3\text{H}$ -FC and  $^{14}\text{C}$ -CE. It is apparent that there was no difference between LDE and LDL regarding the rates of desorption of

**Table 1** Fractional catabolic rate (FCR, in  $\text{h}^{-1}$ ) and the transfer constants ( $k$ ) of the  $^{14}\text{C}$ -cholesteryl oleate ( $^{14}\text{C}$ -CE) and  $^3\text{H}$ -cholesterol ( $^3\text{H}$ -FC) labels of LDE

Kinetic parameters	Labeled lipids	Median (25th;75th)	$p$ -value <sup>a</sup>
FCR	14C-CE	0.0773 (0.0606–0.0843)	0.181
	3H-FC	0.0566 (0.0071–0.0862)	
$k_{1,0}$	14C-CE	0.3400 (0.0525–0.7040)	0.058
	3H-FC	0.5970 (0.4050–0.7990)	
$k_{1,2}$	$^{14}\text{C}$ -CE	2.0140 (0.6380–4.0000)	0.007
	3H-FC	0.6550 (0.1950–1.1580)	
$k_{2,0}$	$^{14}\text{C}$ -CE	0.0558 (0.0297–0.0072)	0.006
	3H-FC	0.0287 (0.0236–0.0057)	

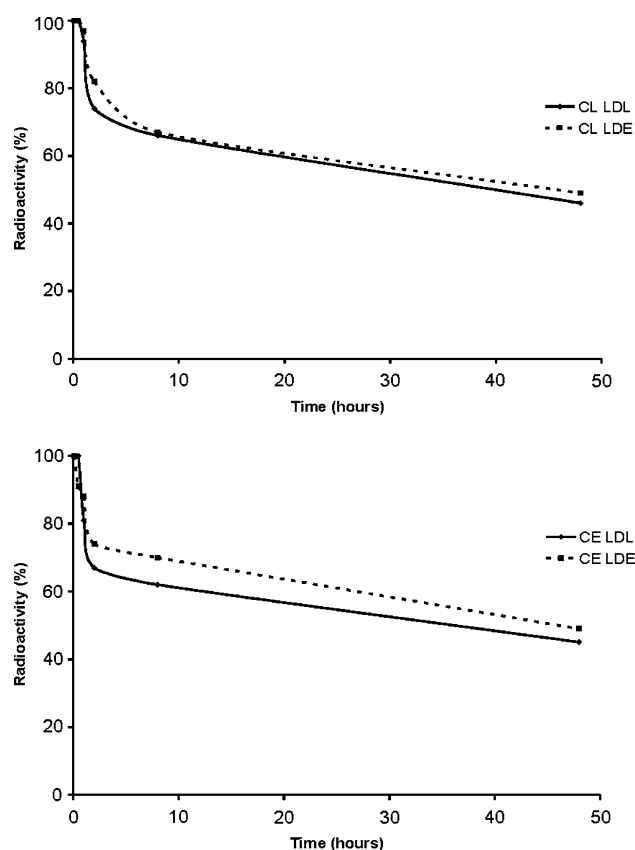
Data are expressed as median and percentiles (25th; 75th)

<sup>a</sup> Mann–Whitney rank sum test comparing the parameters of the CE with those of FC decay curve

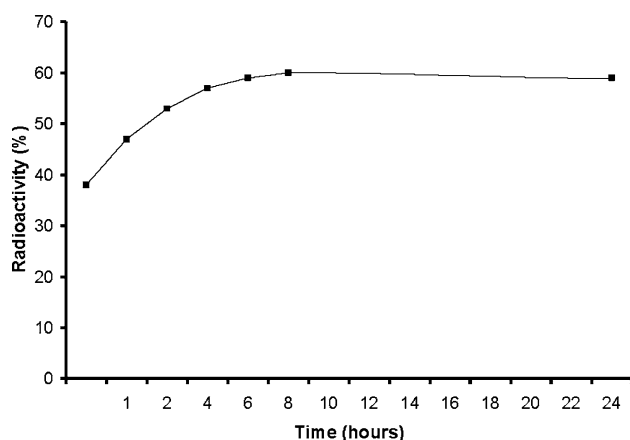
the two radioactive lipids from the dialyzed preparations. As expected from the curve behavior, the AUC of the FC and CE of LDE were not different of those of native LDL.

Figure 2 shows the decay curves of the LDE radioactive labels. It appears that in the first 6 h the decay of  $^3\text{H}$ -FC is faster than that of the  $^{14}\text{C}$ -CE ( $p < 0.05$ ). Subsequently, the incline of both curves seems to be equal. Table 1 shows that the FCR of both labels is not different, presumably due to the trend of the two curves to become equal after the 6-h point. This could be ascribed to recirculation of the LDE-labeled lipids. Table 1 also shows the kinetic parameters derived from both the decay curves.

Figure 3 shows the average esterification curve of the LDE FC injected into the blood stream of the subjects. There was increasing esterification of FC so that by 8 h



**Fig. 2** Dissociation of FC and CE from LDE and native LDL. LDE and LDL, both labeled with  $^{14}\text{C}$ -cholesteryl oleate and  $^3\text{H}$ -cholesterol were dialyzed against human plasma at for measurement of the radioactivity remaining in the dialysis bags during a 48-h period. After the dialysis, the volumes of the six bags, each one corresponding to a different period of dialysis (5 min and 1, 2, 8 and 48 h) were transferred to counting vials for radioactive counting. The data of the radioactivity remaining in the LDE and LDL fractions into the dialysis bags were plotted against time and the AUC was calculated. Experiments were performed in duplicate.



**Fig. 3** Kinetics of cholesterol esterification in the LDE remaining in the plasma after the intravenous injection. The sequential plasma samples collected over 24 h were submitted to lipid extraction and resolved into lipid classes by thin-layer chromatography;  $^3\text{H}$  radioactivity was measured in the bands corresponding to free and esterified cholesterol. In the average curve obtained from 12 patients, %  $^3\text{H}$  FC that was transformed into  $^3\text{H}$  CE is plotted against time

almost 60% of the FC of the LDE remaining in the plasma had been esterified, but thereafter a plateau was attained.

Figure 4 shows the amount of  $^{14}\text{C}$  and of  $^3\text{H}$  radioactivity measured in fragments of the aorta, internal thoracic and radial artery and saphenous vein. In all vessel tissues the amount of the LDE  $^3\text{H}$ -FC was greater than that of the  $^{14}\text{C}$ -CE: roughly fivefold greater in the aorta, four-

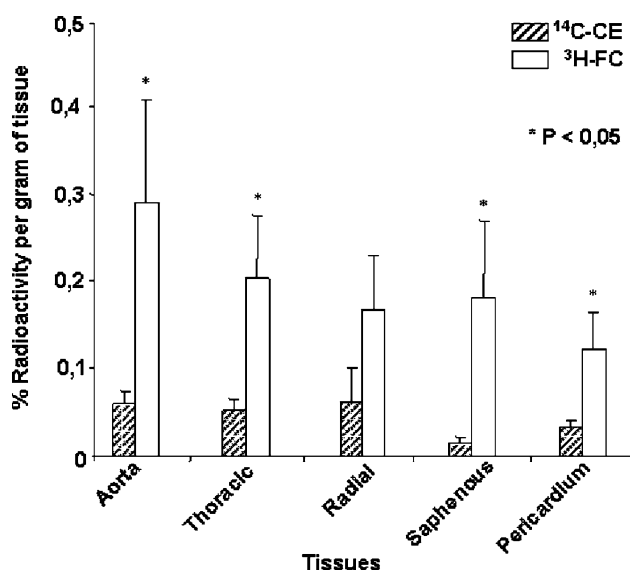


**Fig. 4** LDE  $^3\text{H}$ -cholesterol and  $^{14}\text{C}$ -cholesteryl oleate labels taken up 24 h after the injection into the patients submitted to coronary artery bypass grafting by the following fragments: 1 aorta ( $n = 7$ ); 2 internal thoracic artery ( $n = 14$ ); 3 radial artery ( $n = 7$ ); 4 saphenous vein ( $n = 10$ ) and 5 pericardium ( $n = 8$ ). Results are % of the radioactivity injected recovered per gram of tissue. Mean  $\pm$  standard error of the mean, asterisk represents  $p < 0.05$ , ANOVA

fold in the internal thoracic, threefold in the radial artery and tenfold in the saphenous vein ( $p < 0.05$ ). Comparing the uptakes of CE by the arterial tissues with that of the saphenous vein, they tended to be greater in the arteries, but this difference was statistically significant only between the aorta and the saphenous vein ( $p = 0.05$ ). There was no difference in the FC uptake between the saphenous vein and the arterial tissues. The uptake of FC was also greater than that of CE in the pericardium.

## Discussion

In this study, after the injection of doubly labeled LDE into CAD patients, the removal from the plasma of the FC was faster than that of CE in the first 6 h and, conversely, more FC than CE was taken up by the vessels.

In lipoprotein structure, FC, which is located in the particle surface, is more unstable than the CE located in the particle core. The esterified form largely depends on transfer proteins to exit the lipoprotein particle when is shuttled to other lipoprotein particles. Thus, CE is continuously kept sequestered into a more stable plasma cholesterol pool which exists in the lipoprotein core. Despite the action of transfer proteins, CE is a tracer of the lipoprotein particles and in fact the plasma kinetics of CE as a component of LDL is similar to that of apolipoprotein B [17]; apo B does not dissociate from the lipoprotein and is in fact the LDL marker in the circulation. In contrast, the unesterified form may diffuse into the surrounding aqueous media and thereafter may precipitate in the vessel wall.

Thus, since in the study patients, FC tended to be removed faster than CE of LDE, it can be assumed that the FC was being dissociated from the LDE particles in the circulation. FC that leaks from LDE may incorporate into other lipoprotein classes, a process that can be facilitated by phospholipid transfer proteins. In our study, however, it is unlikely that this had happened at substantial rates; native lipoproteins such as VLDL, LDL or HDL are removed from the plasma slower than LDE. If LDE FC were transferred to the native lipoproteins, the removal from plasma would be slower and not faster than that of LDE CE, as observed in this study. By showing that LDE releases FC and CE at rates similar to those of native LDL, the dialysis experiment illustrated in Fig 2 indicates that LDE is appropriate for exploring the phenomenon of FC dissociation that occurs in the plasma decaying curves of CAD patients (Fig 5).

It is likely that the precipitation of the dissociated molecules in the arterial wall would be the cause of the accelerated removal of the FC from the plasma. This is confirmed by the vessel tissue uptake experiments wherein there is more free than esterified cholesterol in the vessels.

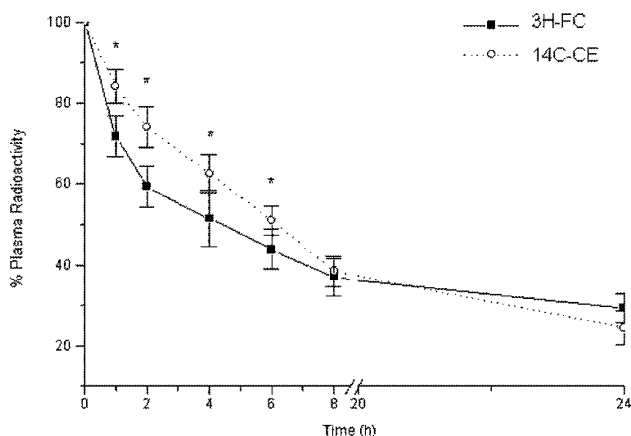


**Fig. 5** Plasma decay curves of LDE  $^3\text{H}$ -cholesterol and  $^{14}\text{C}$ -cholesteryl oleate obtained from 20 patients. Labeled LDE was injected intravenously the day before the scheduled coronary artery bypass grafting and plasma samples were taken at predetermined intervals over 24 h for radioactive counting in a liquid scintillation solution. Data are expressed as mean  $\pm$  standard error of the mean, asterisk represents  $p < 0.05$ , ANOVA

Conceivably, the excess FC in the vessels corresponds to the direct deposition of FC dissociated from the LDE particles. On the other hand, the LDE CE present in the vessels should correspond to the whole particles taken-up by the cells via receptor-mediated endocytosis [16, 18–21].

It is also possible that, in addition to the deposition in the vessel wall, the LDE FC could also be trapped by blood cells. These were removed from the blood samples taken from the patients for the radioactive plasma counting and were not evaluated. In the pericardium, a greater uptake of FC than CE was found which suggests that in tissues other than vessels, this could be occurring. For ethical reasons this was not examined in our patients. Another important limitation of the study consisted of the impossibility of performing the vessel uptake experiments in non-CAD control subjects for comparison with the data of the CAD patients.

Nonetheless, in our previous study we compared the plasma kinetics of LDE FC and CE determined in CAD patients with the data of control non-CAD subjects [9]. In CAD patients there was leakage of FC from the LDE particles, as suggested by the increased removal of the FC relative to the esterified form, but this did not occur in the non-CAD controls. Because excess FC in the vessels is consequent to the loss of this component in the blood, it is not likely that the greater deposition of FC than CE could also be occurring in non-CAD subjects. Therefore, it is reasonable to presume that FC would be more prone to dissociate from the particles in patients with CAD than in subjects without the disease, and then precipitate this cholesterol in the vessel wall. It is difficult to ascertain whether or not this phenomenon is a consequence of the

atherosclerosis process or, otherwise, participate in mechanisms that originate the disease.

The plasma disappearance curve of the LDE FC was faster than that of CE in just the first 8 h after injection (Fig 5). This was translated into a greater  $k_{1,0}$  of FC than that of CE and suggests that FC dissociation from LDE would occur only in that initial period. However, lipoproteins are continuously being synthesized and introduced into the plasma compartment, so that there would be continuous, uninterrupted release of FC from lipoproteins in subjects predisposed to CAD, as pointed out in our previous study. Another interesting point is that also in the first 8 h after injection there was a progressive esterification of the  $^3\text{H}$  FC in the LDE particles remaining in the plasma that thereafter reached a plateau. This coincides with the behavior of the FC plasma decay curve that was faster than that of CE only in the first 8 h, suggesting a possible causal link between esterification and the desorption of FC from the lipoprotein particles.

Dissociation of the plasma kinetics of the two forms of cholesterol was also documented in our recent study involving patients with familial hypercholesterolemia (FH) [22]. As expected, the removal of the LDE CE was delayed in the hypercholesterolemic patients, as occurs with the kinetics of apo B of native LDL in this condition. As to the removal of FC, it was equal to that of the CE but the reduction in FH patients was not so marked as that of the CE. On the other hand, whereas the treatment with simvastatin normalized the removal of cholesterol esters, that of the FC was accelerated but at smaller rates. Those findings support the assumption that the two forms of cholesterol composing the structure of the same lipoprotein particles may undergo different metabolic fates.

The established mechanisms for the lipid deposition in atherosclerosis involve the arterial deposition of the entire lipoprotein particles. In the lipoprotein peroxidation mechanism, the most well known and documented proposal for the lipid deposit in atherogenesis, after peroxidation of the protein and lipid components of LDL, a process that occurs mainly in the subendothelial space, the modified lipoprotein is taken-up by the macrophages after recognition by the scavenger receptors [19–21]. Macrophage lipid plethora originate the foam cells that make-up the fatty streaks, the precursor lesions in atherogenesis [20–23].

The possibility that LDL FC may detach from the lipoprotein and move by aqueous diffusion to cellular membranes was raised by Lundberg and Suominen in an in vitro study with fibroblasts [24]. They postulated that unesterified cholesterol from LDL can move by aqueous transport, despite its low water solubility, and this transfer is facilitated by the addition of albumin to the medium. Ohmura et al. [25] showed that the FC content in the small dense LDL

subfraction particles is relatively depleted. Because this subfraction is considered the most atherogenic, this might suggest that FC impoverishment could be a contributing factor to the disease development.

In the past, many authors have been concerned with the form of cholesterol deposited in the arterial wall [ 26–31]. In the current study, the use of LDE double labeled with the two cholesterol forms and injected into the bloodstream allows the identification in the vessel of the original cholesterol form present into the nanoemulsion structure and injected into the patients, regardless of whether it was esterified or hydrolyzed subsequently to the injection [31].

It is interesting that not only in the artery the uptake of the FC of the injected LDE was greater than that of CE, but this also happens in the veins analyzed. In the vein, the FC/CE ratio seems greater than in the arteries, probably because the CE uptake, i.e., whole particle uptake, was smaller. Thus, the uptake of the LDE particles was smaller whereas the deposition of the dissociated FC was similar to that of the arteries. Although the vein is not prone to atherosclerosis, when grafted to the arterial system as in coronary artery saphenous bypass surgery may develop atherogenesis rapidly so that most grafted veins become occluded within 10 years in a typical atherosclerosis process. Nonetheless, the fact that the vein also shows a >1 FC/CE ratio may suggest that the FC deposit is not consequent to the atherosclerosis process.

Dissociation of the FC from lipoprotein particles may occur by several mechanisms, such as the activity of LCAT. FC is continuously esterified by the action of this enzyme, and a deficit in this action may facilitate dissociation. In severe cases of LCAT deficiency, precocious atherosclerosis develops. Likewise, other humoral or rheologic factors or combination of them may facilitate dissociation of FC.

The direct deposition of FC may disturb the metabolism of endothelial or smooth muscle cells such that secretion of pro-inflammatory factors or apoptosis may be induced. FC accumulation is a potent inducer of inflammatory cytokines and apoptosis in macrophages which represent two important features of advanced unstable plaques.

In conclusion, and in accordance with our previous study that showed greater removal of FC in CAD patients than in non-CAD subjects, there was a relatively greater deposition of the LDE <sup>3</sup>H-cholesterol than the LDE <sup>14</sup>C-CE in the vascular tissues. This result suggests that what may be occurring is dissociation of the FC from the LDE and for an extension from the LDL particles and deposition of this cholesterol in the vessel wall.

**Acknowledgments** This study was supported by Fundação do Amparo à Pesquisa do Estado de São Paulo (FAPESP) and The Zerbini Foundation, both in São Paulo, Brazil. Dr Maranhão has a

research award from the Conselho Nacional de Desenvolvimento Científico e Tecnológico (CNPq), Brasília, Brazil.

## References

- Stein O, Stein Y (2005) Lipid transfer proteins (LTP) and atherosclerosis. *Atherosclerosis* 178:217–230
- Dobiasova M, Frohlich J (1998) Understanding the mechanism of LCAT reaction may help to explain the high predictive value of LDL/HDL cholesterol ratio. *Physiol Res* 47:387–397
- Maranhão RC, Roland IA, Toffoletto O, Ramires JA, Goncalves RP, Mesquita CH, Pileggi F (1997) Plasma kinetic behavior in hyperlipidemic subjects of a lipidic microemulsion that binds to low density lipoprotein receptors. *Lipids* 32:627–633
- Sposito AC, Lemos PA, Santos RD, Hueb W, Vinagre CG, Quintella E, Carneiro O, Chapman MJ, Ramires JA, Maranhão RC (2004) Impaired intravascular triglyceride lipolysis constitutes a marker of clinical outcome in patients with stable angina undergoing secondary prevention treatment: a long-term follow-up study. *J Am Coll Cardiol* 43:2225–2232
- Puk CG, Vinagre CG, Bocchi E, Bacal F, Stolf N, Maranhão RC (2004) Plasma kinetics of a cholesterol-rich microemulsion in patients submitted to heart transplantation. *Transplantation* 78:1177–1181
- Maranhão RC, Garicochea B, Silva EL, Dorliac-Llacer P, Cadena SM, Coelho IJ, Meneghetti JC, Pileggi FJ, Chamone DA (1994) Plasma kinetics and biodistribution of a lipid emulsion resembling low-density lipoprotein in patients with acute leukemia. *Cancer Res* 54:4660–4666
- Maranhão RC, Feres MC, Martins MT, Mesquita CH, Toffoletto O, Vinagre CG, Gianinni SD, Pileggi F (1996) Plasma kinetics of a chylomicron-like emulsion in patients with coronary artery disease. *Atherosclerosis* 126:15–25
- Hirata RD, Hirata MH, Mesquita CH, Cesar TB, Maranhão RC (1999) Effects of apolipoprotein B-100 on the metabolism of a lipid microemulsion model in rats. *Biochim Biophys Acta* 1437:53–62
- Santos RD, Hueb W, Oliveira AA, Ramires JA, Maranhão RC (2003) Plasma kinetics of a cholesterol-rich emulsion in subjects with or without coronary artery disease. *J Lipid Res* 44:464–469
- Friedewald WT, Levy RI, Fredrickson DS (1972) Estimation of the concentration of low-density lipoprotein cholesterol in plasma, without the use of the preparative ultracentrifuge. *Clin Chem* 18:499–502
- Nishikawa O, Yokoyama S, Kurasawa T, Yamamoto A (1986) A method for direct incorporation of radiolabeled cholesteryl ester into human plasma low-density lipoproteins: preparation of tracer substrate for cholesteryl ester transfer reaction between lipoproteins. *J Biochem* 99:295–301
- Dobiášová M, Adler L, Ohta T, Frohlich J (2000) Effect of labeling of plasma lipoproteins with [<sup>3</sup>H]cholesterol on values of esterification rate of cholesterol in apolipoprotein B-depleted plasma. *J Lipid Res* 41:1356–1357
- Matthews CME (1957) The theory of tracer experiments with I labelled plasma proteins. *Phys Med Biol* 2:36–42
- Marchese SRM, Mesquita CH, Cunha IL (1998) Anacom program application to calculate <sup>13</sup>C transfer rates in marine organisms and dose in man. *J Radioanal Nucl Chem* 232:233–236
- Sowby FS (1984) Radiation protection. In: Limits for intakes of radionuclides by workers. ICRP publication 30. Part I. Pergamon, Oxford
- Maranhão RC, Graziani SR, Yamaguchi N, Melo RF, Latrilha MC, Rodrigues DG, Couto RD, Schreier S, Buzaid CA (2002)

- Association of carmustine with a lipid emulsion: in vitro, in vivo and preliminary studies in cancer patients. *Cancer Chemother Pharmacol* 49:487–498
17. Schwartz CC, Van den Broek JM, Cooper PS (2004) Lipoprotein cholesteryl ester production, transfer, and output in vivo in humans. *J Lipid Res* 45:1594–1607
  18. Liao JK (1998) Endothelium and acute coronary syndromes. *Clin Chem* 44:1799–1808
  19. Kataoka H, Kume N, Miyamoto S, Minami M, Moriwaki H, Murase T, Sawamura T, Masaki T, Hashimoto N, Kita T (1999) Expression of lectinlike oxidized low-density lipoprotein receptor-1 in human atherosclerotic lesions. *Circulation* 99:3110–3117
  20. Llorente-Cortés V, Martínez-González J, Badimon L. (2000). LDL receptor-related protein mediates uptake of aggregated LDL in human vascular smooth muscle cells. *Arterioscler Thromb Vasc Biol* 20:1572–1579
  21. Ricciarelli R, Zingg J-M, Azzi A (2000) Vitamin E reduces the uptake of oxidized LDL by inhibiting CD 36 scavenger receptor expression in cultured aortic smooth muscle cells. *Circulation* 102:82–87
  22. Santos RD, Chacra AP, Morikawa A, Vinagre CG, Maranhão RC (2005) Plasma kinetics of free and esterified cholesterol in familial hypercholesterolemia: effects of simvastatin. *Lipids* 40:737–743
  23. Libby P (1990) Inflammatory and immune mechanisms in atherogenesis. In: Leaf A, Weber P (eds) *Atherosclerosis reviews*. Raven Press, New York, pp 70–89
  24. Lundberg BB, Suominen LA (1985) Physicochemical transfer of [<sup>3</sup>H]cholesterol from plasma lipoproteins to cultured human fibroblasts. *Biochem J* 228:219–225
  25. Ohmura H, Mokuno H, Sawano M, Hatsumi C, Mitsugi Y, Watanabe Y, Daida H, Yamaguchi H (2002) Lipid compositional differences of small, dense low-density lipoprotein particle influence its oxidative susceptibility: possible implication of increased risk of coronary artery disease in subjects with phenotype B. *Metabolism* 51:1081–1087
  26. Dayton S (1959) Turnover of cholesterol in the artery walls of normal chickens. *Circ Res* 7:468
  27. Newman HAI, Mccandless EL, Zilversmit DB (1961) The synthesis of C14-lipids in rabbit atheromatous lesions. *J Biol Chem* 236:1264
  28. Smith EB, Slater PB (1973) Lipids and low density lipoproteins in intima in relation to its morphological characteristics. *Ciba Found Symp* 12:39–53
  29. Stender S, Christensen S, Nyvad O (1978) Uptake of labelled free and esterified cholesterol from plasma by the aortic intima—media tissue measured in vivo in three animal species. *Atherosclerosis* 31: 279–293
  30. Bondjers G, Bjorkerud S (1977) Arterial repair and atherosclerosis after mechanical injury. VI. Cholesterol elimination in vitro from experimental atherosclerotic lesions. *Exp Mol Pathol* 26:341–349
  31. Day AJ, Wahlqvist ML, Campbell DJ (1970) Differential uptake of cholesterol and of different cholesterol esters by atherosclerotic intima in vivo and in vitro. *Atherosclerosis* 11:301–320

## Relationship Between Apolipoprotein Concentrations and HDL Subclasses Distribution

Li Tian · Mingde Fu · Lianqun Jia · Yanhua Xu ·  
Shiyin Long · Haoming Tian · Ying Tian

Received: 22 November 2006 / Accepted: 21 January 2007 / Published online: 8 March 2007  
© AOCs 2007

**Abstract** Alterations in plasma apolipoproteins levels can influence the composition, content, and distribution of plasma lipoproteins that affect the risk of atherosclerosis. This study assessed the relationship between plasma apolipoproteins levels, mainly apoAI, and HDL subclass distribution. The contents of plasma HDL subclasses were determined by two-dimensional gel electrophoresis coupled with immunodetection in 545 Chinese subjects. Compared with a low apoAI group, the contents of all HDL subclasses increased significantly both in middle and high apoAI group, and the contents of large-sized HDL<sub>2b</sub> increased more significantly relative to those of small-sized pre $\beta$ <sub>1</sub>-HDL in a high apoAI group. When apoAI and HDL-C levels increased simultaneously, in comparison to a low apoAI along with HDL-C concentration group, a significant increase (116%) was shown in HDL<sub>2b</sub> but only a slight increase (26%) in pre $\beta$ <sub>1</sub>-HDL. In addition, Pearson correlation analysis revealed that apoAI levels were positively and significantly correlated with all

HDL subclasses. Multiple liner regression demonstrated that the apoAI concentrations were the most powerful predictor for HDL subclass distribution. With the elevation of apoAI concentrations, the contents of all HDL subclasses increased successively and significantly, especially, an increase in large-sized HDL<sub>2b</sub>. Further, when apoAI and HDL-C concentrations increased simultaneously, the shift to larger HDL size was more obvious. Which, in turn, indicated that HDL maturation might be enhanced and, the reverse cholesterol transport might be strengthened along with apoAI levels which might be a more powerful factor influencing the distribution of HDL subclasses.

**Keywords** Apolipoproteins · Lipoproteins · Plasma lipids · Arteriosclerosis

### Introduction

Most prospective epidemiological studies have firmly established that high density lipoprotein (HDL) as assessed by its cholesterol content is inversely correlated with the incidence and prevalence of atherosclerosis [1–3]. In recent years, it has been considered that changes in the distribution of HDL subclasses might be an important marker for susceptibility to the development of coronary heart disease (CHD) [4]. This anti-atherogenic action of HDL is probably related to the reverse cholesterol transport (RCT) by which excess peripheral cholesterol is returned to the liver.

HDL is highly heterogeneous with respect to the hydrated density, size, shape, charge and physiologic functions [5]. Using two-dimensional gel electropho-

---

L. Tian · M. Fu (✉) · L. Jia · H. Tian  
Laboratory of Endocrinology and Metabolism,  
West China Hospital, Sichuan University,  
New building 6, Room 902, #16 Section 3,  
People South Road, Chengdu, 610041 Sichuan,  
People's Republic of China  
e-mail: fumingde@126.com

Y. Xu  
Chengdu Hoist Biotechnology Co., LTD,  
Sichuan, People's Republic of China

S. Long · Y. Tian  
Department of Biochemistry and Molecular Biology,  
Nanhua University, Hengyang, Hunan  
People's Republic of China



resis and subsequently the immunoblotting method, HDL can be subdivided into large-sized (HDL<sub>2a</sub> and HDL<sub>2b</sub>) and small-sized subclasses (pre $\beta$ <sub>1</sub>-HDL, HDL<sub>3c</sub>, HDL<sub>3b</sub>, and HDL<sub>3a</sub>) and pre $\beta$ <sub>2</sub>-HDL [6, 7]. The protein components of HDL include apolipoprotein AI (apoAI; 70%), apoAII (20%), and small amounts of apoE and apoC<sub>s</sub>. As the principal carrier protein of HDL apoAI is believed to mediate the change of HDL size [8]. ApoAI is the activator of lecithin: cholesterol acyltransferase (LCAT) and LCAT may catalyze unesterified cholesterol to cholesterol ester and promote the conversion of pre $\beta$ <sub>1</sub>-HDL and HDL<sub>3</sub> to HDL<sub>2</sub> thus playing a functional role in the maturation process of HDL subclasses [9]. In addition, apoAI is a critical ligand of the HDL receptor scavenger receptor BI (SR-BI) and the interaction of apoAI and SR-BI may facilitate hepatic selective uptake of HDL-C in the RCT pathway [10]. Therefore, apoAI plays a vital role in the maturation and metabolism of HDL as well as the whole RCT process.

Our laboratory investigated the influence of plasmid lipids on the HDL subclass distribution and results suggested that with the increase of plasma triglyceride(TG), total cholesteryl (TC), and low density lipoprotein cholesteryl (LDL-C) levels as well as TG/HDL-C and TC/HDL-C ratios, or the decrease of plasma HDL-C levels, there was a general shift toward smaller-sized HDL [7, 11–14]. This indicated that HDL maturation might be abnormal and RCT might be weakened. In this work, we investigated the characteristic distribution of HDL subclasses along with relationship between apolipoproteins concentrations in particularly apoAI and alteration of HDL subclass distribution in the Chinese population. This might provide additional information about the potential role of HDL subclasses in the risk for CHD.

## Subjects and Methods

### Subjects

Six-hundred and twelve Chinese adults being either current or retired staff of the university were recruited to participate in a study examining plasma lipid and apolipoprotein concentrations. The study protocol was approved by an ethics committee, and all subjects gave informed consent. Exclusion criteria included the following: (1) presence of nephrosis, diabetes mellitus, hypothyroidism, hepatic impairment; (2) presence of major cardiovascular event (myocardial infarction, severe surgery), stroke; (3) taking lipid-altering

medications in the previous 1 month; (4) consuming alcohol, and smoking cigarettes in the previous week before the study. In addition, the women had not undergone administration of hormone replacement therapy or used oral contraceptives and were not pregnant. After applying the exclusions, 545 subjects (347 males mean age  $56.4 \pm 9.5$  years, 198 females mean age  $56.9 \pm 9.0$  years), 395 subjects were from the West China University of Medical Science, Sichuan University and Sichuan Normal University, in Chengdu, Sichuan Province, PR China. 150 subjects were from Nan Hua University, in Hengyang Hunan Province, PR China were included in our present study.

In order to investigate the impact of plasma apoAI levels on the distribution of the HDL subclasses, we divided the subjects into three groups according to apoAI concentrations. Firstly, frequency distribution of apoAI using the Kolmogorov–Smirnov test showed a normal distribution (Fig. 1). Considering that about 68% scores fell in the range of the mean (1248.1) plus or minus 1 SD (204.5), we used 1043.6 mg/L (1248.1–204.5) and 1452.6 mg/L (1248.1 + 204.5) as the two cut-out points. So, the subjects were further subdivided into a low apoAI group (apoAI  $\leq$  1043.6 mg/L), a middle apoAI group (apoAI 1043.6–1452.6 mg/L) and a high apoAI group (apoAI  $\geq$  1452.6 mg/L). To investigate further the influence of plasma apoAI and HDL-C levels on the distributions of HDL subclasses, we divided the subjects described above into three groups according to plasma HDL-C levels, that is, high ( $\geq$ 1.55 mmol/L), middle (1.03–1.55 mmol/L), and low ( $<$ 1.03 mmol/L). The HDL-C levels selected for classifica-

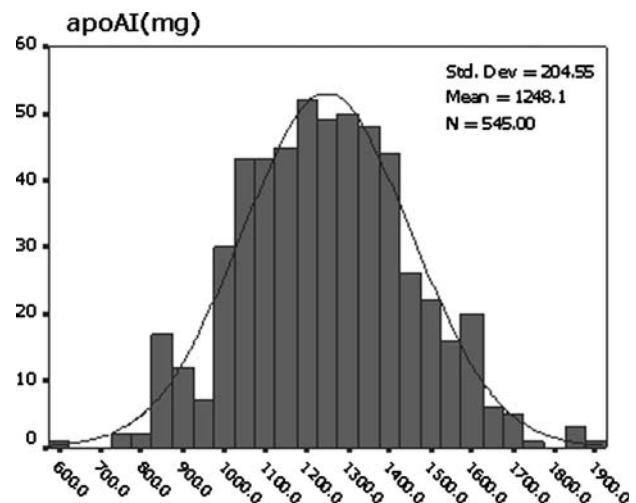


**Fig. 1** Frequency distribution of apoAI in total subjects

tion generally conform to Adult Treatment Panel III guidelines [15].

### Specimens

Whole blood specimens were drawn, after a 12-h overnight fast, into EDTA-containing tubes. Plasma was separated within 1–2 h. The plasma was then stored at 4 °C and used within 24 h for lipid and apolipoprotein analyses. An aliquot of plasma was stored at –70 °C for the determination of HDL subclasses.

### Plasma Lipid and Apolipoprotein Analyses

Plasma TG, TC and HDL-C were measured by standard techniques. TC and TG were determined with enzymatic kits (Beijing Zhongsheng Biotechnological Corporation, Beijing). HDL-C was determined after precipitation of the apolipoprotein (apo)B-containing lipoproteins by phosphotungstate/magnesium chloride [16]. LDL-C was calculated using the Friedwald formula ( $TG < 4.52 \text{ mmol/L}$ ) [17]. When plasma  $TG \geq 4.52 \text{ mmol/L}$ , LDL-C was determined using the precipitation method with polyvinylsulfate (enzymatic kits). Plasma apoAI, B100, CII, CIII and E were determined by radial immunodiffusion methods [18] using kits developed at the Apolipoprotein Research Laboratory, West China Medical Center, Sichuan University. The intra-assay CV for apolipoprotein concentrations was between 2.1 and 4.8%, inter-assay CV was 3.5–7.9% [19].

### HDL Subclass Analyses

For each of the enrolled subjects, apoAI-containing HDL subclasses were measured by nondenaturing two-dimensional gel electrophoresis associated with the immunodection method as described previously [7]. Briefly, 10  $\mu\text{l}$  of plasma was first separated by charge on 0.7% agarose gel, into  $\text{pre}\beta$  and  $\alpha$  mobility particles. After electrophoretic separation of lipoproteins in agarose gels, the developed lipoproteins on agarose gels along with a mixture of standard proteins (bovine serum albumin, ferritin, and thyroglobulin obtain from Pharmacia Uppsala, Sweden) were further separated by electrophoresis in 2–30% nondenaturing polyacrylamide gradient gel in the second dimension. In fact, after 2-D gel electrophoresis, plasma proteins and molecular markers were electrophoretically transferred to PVDF membranes, stained with 0.1% ponceau S, and the position of

molecular standard protein bands labeled by pencil, and destained by diffusion, then, using 5% dyllipid milk, recovered from the membrane, following interaction with horseradish peroxidase-labeled goat anti-human apo-AI-IgG. The relative concentration of each subclass was calculated as the percentage of plasma apoAI (%) according to the density of each spot. Particle diameters of the HDL subclasses were assessed by comparing the mobility of the sample with the mobility of calibration standard proteins. Then the relative percentage concentration of each HDL subclass was multiplied by apoAI concentrations in sample individuals, respectively. The result was the relative concentration of each HDL subclasses of apoAI(mg/L, apoAI in the subclasses). The inter assay CVs of relative content of  $\text{pre}\beta_1$ -HDL,  $\text{pre}\beta_2$ -HDL, HDL<sub>3c</sub>, HDL<sub>3b</sub>, HDL<sub>3a</sub>, HDL<sub>2a</sub> and HDL<sub>2b</sub> in plasma sample were 9.4, 9.8, 4.9, 6.2, 7.3, 11.1 and 7.9%, respectively ( $n = 5$ ).

### Statistical Analyses

All statistical analyses were performed using the statistical package SPSS Version 11.0 (SPSS Inc). The Kolmogorov–Smirnov test was applied to test normal distribution. Data were expressed as the mean  $\pm$  SD. The significant differences between two groups were analyzed by one-way analysis of variance (ANOVA). Multiple liner correlation and regression were calculated to study correlation. Differences were considered significant at  $P < 0.05$ .

## Results

### Concentrations of Plasma Lipids, Apolipoproteins and Contents of HDL Subclasses

Table 1 showed that in the population, the concentration of TG was  $2.4 \pm 1.7 \text{ (mmol/L)}$  which exceeds normal TG levels recommended in the third Report of the National Cholesterol Education Program (NCEP) (ATPIII) guidelines, which indicated a substantial proportion of subjects with hypertriglyceridemia. Meanwhile, concentrations of plasma lipids, lipoproteins along with contents of HDL subclasses were similar change in this population and the subjects with endogenous hypertriglyceridemia [12].

Furthermore, concentrations of TG, and the ratios of TG/HDL-C, TC/HDL-C were significantly lower while those of HDL-C, apoAI, HDL<sub>2a</sub> and HDL<sub>2b</sub> were significantly higher in female than in male.

**Table 1** Concentrations of serum lipids, apolipoproteins and contents of HDL subclasses in total subjects

	Total (n = 545)	Males (n = 347)	Females (n = 198)
Age (year)	56.6 ± 9.3	56.4 ± 9.5	56.9 ± 9.0
BMI (kg/m <sup>2</sup> )	23.6 ± 3.0	23.7 ± 3.1	23.4 ± 2.9
TG (mmol/L)	2.4 ± 1.7	2.5 ± 1.9	2.2 ± 1.4 <sup>a,b</sup>
TC (mmol/L)	5.6 ± 0.9	5.6 ± 0.9	5.5 ± 1.0
HDL-C (mmol/L)	1.2 ± 0.4	1.2 ± 0.4	1.3 ± 0.4 <sup>a,c</sup>
LDL-C (mmol/L)	3.3 ± 0.9	3.3 ± 0.9	3.2 ± 1.1
apoAI (mg/L)	1248.1 ± 204.6	1230.7 ± 202.5	1278.6 ± 205.1 <sup>a,c</sup>
apoB100(mg/L)	909.5 ± 218.7	906.7 ± 221.6	914.4 ± 214.0
apoCII(mg/L)	69.8 ± 40.0	71.0 ± 42.8	67.5 ± 34.6
apoCIII(mg/L)	160.5 ± 73.3	159.9 ± 73.1	161.5 ± 73.7
apoE(mg/L)	53.9 ± 21.6	53.6 ± 22.0	54.3 ± 20.8
TG/HDL-C	2.4 ± 2.1	2.5 ± 2.0	2.1 ± 1.9 <sup>a,b</sup>
TC/HDL-C	4.9 ± 1.6	5.1 ± 1.6	4.7 ± 1.7 <sup>a,c</sup>
Preβ <sub>1</sub> -HDL(mg/L)	118.0 ± 41.6	121.6 ± 48.2	114.6 ± 43.6
Preβ <sub>2</sub> -HDL(mg/L)	59.8 ± 21.7	57.9 ± 21.2	60.6 ± 22.6
HDL <sub>3c</sub> (mg/L)	74.3 ± 30.1	74.6 ± 29.5	73.8 ± 31.1
HDL <sub>3b</sub> (mg/L)	149.2 ± 54.1	152.7 ± 52.5	143.1 ± 56.4
HDL <sub>3a</sub> (mg/L)	291.0 ± 86.6	294.4 ± 84.6	285.1 ± 89.8
HDL <sub>2a</sub> (mg/L)	253.2 ± 75.1	245.5 ± 78.9	266.7 ± 66.2 <sup>a,c</sup>
HDL <sub>2b</sub> (mg/L)	310.0 ± 113.2	291.6 ± 112.3	342.4 ± 107.6 <sup>a,d</sup>

Values are expressed as Mean ± SD

<sup>a</sup> Between female and male

<sup>b</sup> *P* < 0.05

<sup>c</sup> *P* < 0.01

<sup>d</sup> *P* < 0.001

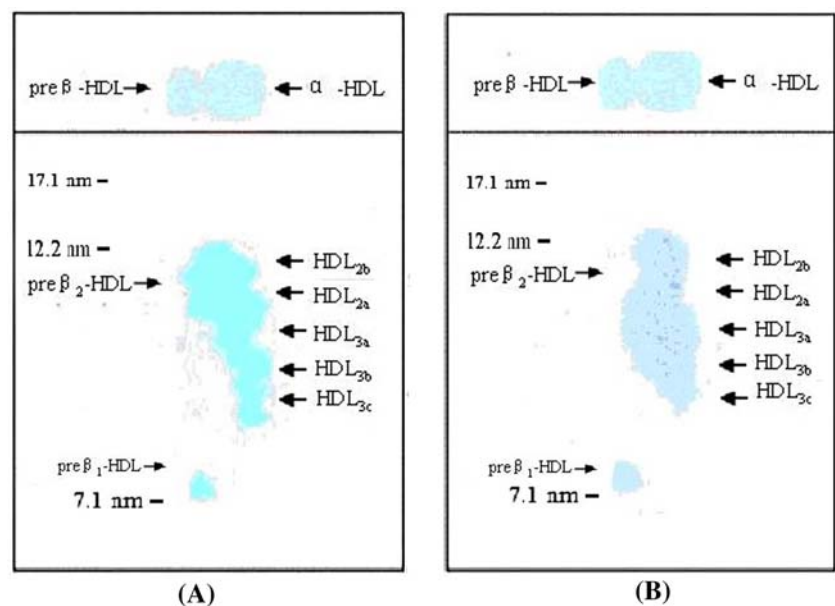
### ApoA-I Contents of HDL Subclasses

Figure 2 shows the distributions of HDL subclasses for representative subjects from the group having normolipidemic (A) and from the hyperlipidemic groups. In the hyperlipidemic subjects, spots for the small-sized subclasses (preβ<sub>1</sub>-HDL, HDL<sub>3a</sub>, HDL<sub>3b</sub>, and HDL<sub>3c</sub>) were larger, whereas large-sized HDL<sub>2</sub> (HDL<sub>2a</sub> and HDL<sub>2b</sub>) had spots that were smaller in comparison with the normolipidemic subjects.

### Concentrations of Plasma Lipids, Apolipoproteins and Contents of HDL Subclasses According to the Levels of apoAI

As shown in Table 2, with the elevation of apoAI levels, concentrations of HDL-C significantly increased while those of TG decreased significantly. Moreover, all HDL subclasses increased successively and significantly both in males and females. In addition, compared with males in the middle and low apoAI group, the contents

**Fig. 2** Electrophoretic comparisons of apoA1-containing HDL subclasses. High-density lipoprotein (B) protein subclasses were separated by nondenaturing two-dimensional gel electrophoresis and immunodetection with a goat antihuman apoA1-IgG labeled with horseradish peroxidase.  
**a** Normolipidemic.  
**b** Hyperlipidemic subjects



**Table 2** Concentrations of serum lipids, apolipoproteins and contents of HDL subclasses according to the levels of apolipoproteinAI in the total number of subjects

	Low apoAI group		Middle apoAI group		High apoAI group	
	Males ( <i>n</i> = 60)	Females ( <i>n</i> = 24)	Males ( <i>n</i> = 242)	Females ( <i>n</i> = 140)	Males ( <i>n</i> = 45)	Females ( <i>n</i> = 34)
TG(mmol/L)	3.1 ± 1.7	2.7 ± 1.2 <sup>a,b</sup>	2.5 ± 1.9 <sup>e,b</sup>	2.3 ± 1.6 <sup>a,b,e,b</sup>	2.3 ± 1.2 <sup>e,d</sup>	2.0 ± 1.4 <sup>a,b,e,d</sup>
TC(mmol/L)	5.4 ± 0.9	4.8 ± 1.1 <sup>a,b</sup>	5.6 ± 0.9	5.6 ± 0.9 <sup>e,c</sup>	5.8 ± 0.9 <sup>e,b</sup>	5.7 ± 1.0 <sup>e,c</sup>
HDL-C(mmol/L)	0.9 ± 0.2	1.1 ± 0.3 <sup>a,b</sup>	1.2 ± 0.4 <sup>e,c</sup>	1.3 ± 0.5 <sup>a,b,e,b</sup>	1.4 ± 0.3 <sup>e,d</sup>	1.5 ± 0.4 <sup>a,b,e,c</sup>
LDL-C(mmol/L)	3.1 ± 0.8	2.8 ± 0.9 <sup>a,c</sup>	3.2 ± 0.9	3.1 ± 1.1	3.3 ± 0.8 <sup>e,b</sup>	3.2 ± 1.1 <sup>e,b</sup>
apoAI(mg/L)	920.9 ± 77.1	953.7 ± 95.7 <sup>a,b</sup>	1233.3 ± 113.4 <sup>e,d</sup>	1267.8 ± 112.6 <sup>a,c,e,d</sup>	1575.7 ± 103.1 <sup>e,d</sup>	1585.4 ± 83.8 <sup>e,d</sup>
apoB100(mg/L)	939.0 ± 191.7	912.0 ± 181.5	909.5 ± 227.6	904.7 ± 208.1	955.1 ± 219.4 <sup>e,b</sup>	848.9 ± 256.4 <sup>a,b</sup>
apoCII(mg/L)	72.9 ± 40.5	68.0 ± 29.4	68.7 ± 44.7	66.9 ± 36.3	67.8 ± 31.9	65.2 ± 31.1
apoCIII(mg/L)	157.1 ± 82.7	162.3 ± 58.3	154.9 ± 72.7	156.6 ± 71.5	153.1 ± 53.7	155.6 ± 87.6
apoE(mg/L)	56.9 ± 19.9	54.6 ± 15.7	53.6 ± 23.5	52.5 ± 21.4	51.1 ± 15.2	50.1 ± 20.4
Preβ <sub>1</sub> -HDL(mg/L)	95.1 ± 28.2	92.4 ± 26.5	114.9 ± 49.9	104.4 ± 42.4	130.9 ± 52.7 <sup>e,c</sup>	131.9 ± 43.7 <sup>e,c</sup>
Preβ <sub>2</sub> -HDL(mg/L)	44.6 ± 14.0	43.3 ± 17.1	56.5 ± 17.0	59.6 ± 17.9	73.3 ± 27.7 <sup>e,d</sup>	76.5 ± 31.7 <sup>e,d</sup>
HDL <sub>3c</sub> (mg/L)	60.6 ± 23.3	60.4 ± 15.9	74.8 ± 27.8	74.7 ± 28.3	92.3 ± 35.8 <sup>e,d</sup>	89.9 ± 37.3 <sup>e,d</sup>
HDL <sub>3b</sub> (mg/L)	118.6 ± 34.5	104.1 ± 30.4	150.2 ± 44.3 <sup>e,c</sup>	140.9 ± 51.1 <sup>e,c</sup>	211.3 ± 64.9 <sup>e,d</sup>	186.6 ± 60.3 <sup>e,d</sup>
HDL <sub>3a</sub> (mg/L)	245.4 ± 63.8	224.5 ± 61.9	294.4 ± 76.2 <sup>e,c</sup>	277.8 ± 81.8 <sup>e,c</sup>	365.1 ± 82.2 <sup>e,d</sup>	359.6 ± 107.0 <sup>e,d</sup>
HDL <sub>2a</sub> (mg/L)	179.9 ± 53.1	209.7 ± 36.7 <sup>a,b</sup>	245.5 ± 63.3 <sup>e,d</sup>	262.4 ± 56.9 <sup>a,b,e,d</sup>	324.6 ± 75.0 <sup>e,d</sup>	332.8 ± 97.7 <sup>e,d</sup>
HDL <sub>2b</sub> (mg/L)	209.8 ± 90.1	238.5 ± 71.8 <sup>a,b</sup>	296.2 ± 102.2 <sup>e,d</sup>	346.1 ± 103.0 <sup>a,c,e,d</sup>	375.5 ± 137.3 <sup>e,d</sup>	400.7 ± 96.9 <sup>e,d</sup>

Values are expressed as Mean ± SD

<sup>a</sup> Between females and males in the same apoAI group

<sup>b</sup> *P* < 0.05

<sup>c</sup> *P* < 0.01

<sup>d</sup> *P* < 0.001

<sup>e</sup> Between high, middle and low apoAI in the same gender

of HDL<sub>2a</sub> and HDL<sub>2b</sub> were significantly higher for the females in the same apoAI group. In the high apoAI group, the contents of all HDL subclasses had no significant difference between males and females.

#### Characteristics of HDL Subclass Contents and Frequency Distribution According to apoAI Along with HDL-C

To further investigate the influence of plasma apoAI combined with HDL-C levels on the distributions of HDL subclasses, we designated apoAI ≥ 1452.6 mg/L together with HDL-C ≥ 1.55 mmol/L as the high concentrations group, apoAI 1043.6–1452.6 mg/L to-

gether with HDL-C 1.03–1.55 mmol/L as the middle concentrations group, and apoAI ≤ 1043.6 mg/L together with HDL-C < 1.03 mmol/L as the low concentrations group. As shown in Fig. 3, there were 180 (approximately 33%) subjects in the middle concentrations group and they occupied the highest percentage of the population.

Table 3 presented that with elevation of apoAI combined with HDL-C concentrations, all HDL subclasses increased significantly and successively; further compared to the low concentrations group, a significant increased (116%) in large-sized HDL<sub>2b</sub> but only a slight increase (26%) in small-sized preβ<sub>1</sub>-HDL were found in high concentrations group.

**Fig. 3** Frequency distribution of subjects according to apoAI together with HDL-C levels

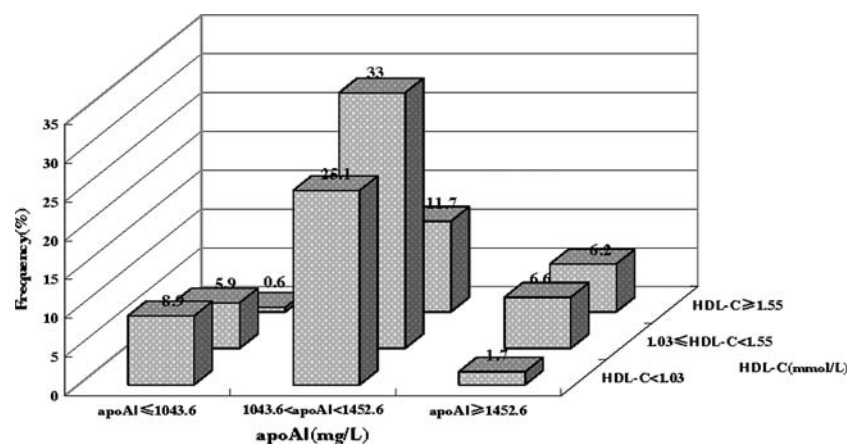


**Table 3** Contents of HDL subclasses according to apoAI together with HDL-C Levels

	Low concentrations group (n = 49)	Middle concentrations group (n = 180)	High concentrations group (n = 34)
Pre $\beta_1$ -HDL	96.8 ± 27.1	98.5 ± 41.3	121.6 ± 48.9 <sup>a,c</sup>
Pre $\beta_2$ -HDL	46.2 ± 14.9	55.6 ± 17.5	74.5 ± 26.9 <sup>a,d</sup>
HDL <sub>3c</sub>	56.4 ± 23.2	73.4 ± 27.2 <sup>a,b</sup>	88.1 ± 43.3 <sup>a,d</sup>
HDL <sub>3b</sub>	113.2 ± 36.4	137.7 ± 44.2 <sup>a,b</sup>	208.9 ± 68.9 <sup>a,d</sup>
HDL <sub>3a</sub>	252.6 ± 64.4	282.3 ± 72.2 <sup>a,c</sup>	339.5 ± 91.9 <sup>a,d</sup>
HDL <sub>2a</sub>	170.5 ± 46.4	252.5 ± 60.6 <sup>a,d</sup>	359.3 ± 99.3 <sup>a,d</sup>
HDL <sub>2b</sub>	194.8 ± 66.5	338.2 ± 94.9 <sup>a,d</sup>	420.3 ± 122.7 <sup>a,d</sup>

<sup>a</sup> Compared to apoAI ≤ 1403.6 mg/L, HDL-C < 1.03 mmol/L group

<sup>b</sup> *P* < 0.05

<sup>c</sup> *P* < 0.01

<sup>d</sup> *P* < 0.001

### Correlation Coefficients Between Apolipoproteins and Contents of Plasma HDL Subclasses

Correlation analysis revealed that apoAI levels were positively and significantly correlated with all HDL subclasses. Furthermore, apoB100, apoCII, apoCIII and apoE showed positive correlations with pre $\beta_1$ -HDL and HDL<sub>3a</sub> as well as negative correlations with HDL<sub>2a</sub>, HDL<sub>2b</sub>. No significant difference was noted between males and females (Table 4).

### Multiple Liner Regression Correlation Between Contents of Plasma HDL Subclasses and Apolipoproteins

Multiple liner regression showed that apoAI was associated independently and positively with all HDL subclasses and it was the most powerful predictor (SRC from 0.321 to 0.605, *P* < 0.001) for alterations of HDL subclass distributions. In contrast, other apolipoproteins showed positive correlation with pre $\beta_1$ -HDL but negative correlation with HDL<sub>2b</sub> (Table 5).

## Discussion

Numerous clinical and epidemiological studies have demonstrated the inverse and independent association between HDL-C and the risk of CHD [20]. HDL exerts various potentially antiatherogenic properties and until recently, the protective features of HDL had been attributed primarily to its classical function of removing cholesterol from peripheral tissues and transferring it to the liver in a process known as RCT. In vitro experiments as well as genetic family and population studies and the investigation of transgenic animal models have revealed that plasma HDL cholesterol levels do not necessarily reflect the efficacy and anti-atherogenicity of RCT [20–23]. Instead, the contents of HDL subclasses are important determinants of RCT and the risk of atherosclerosis [24]. Moreover, the physiologic basis of HDL subclasses has not been elucidated completely. It is necessary to disclose the alterations of distribution of HDL subclasses with the change of plasma apolipoproteins especially apoAI concentrations.

Our results showed that, with the elevation of apoAI levels, all HDL subclasses increased successively and significantly both in males and females. Studies in human apoAI transgenic mice have showed that the distribution of apoAI among the HDL subclasses was similar, suggesting that the content of apoAI in the major HDL subspecies was fixed and that excess apoAI was not present in HDL particles [25]. Kunitake et al. observed that pre $\beta$ -HDL (discoid shape) generally contain 2 copies, and other studies found that pre $\beta_1$ -HDL contain 1 copy whereas large-sized HDL<sub>2</sub> contain four copies of apoAI per particles [26–28]. Hence, apoAI levels might reflect the number of HDL particles, and with the elevation of apoAI levels, molecules of apoAI distributed to each of the subclasses increased which resulted in all HDL subclasses tending to increase. It has been postulated that RCT is

**Table 4** Correlation coefficients between contents of plasma HDL subclasses and apolipoprotein

	Male					Female				
	apoAI	apoB100	apoCII	apoCIII	apoE	apoAI	apoB100	apoCII	apoCIII	apoE
Pre $\beta_1$ -HDL	0.29 <sup>b</sup>	0.27 <sup>b</sup>	0.44 <sup>b</sup>	0.46 <sup>b</sup>	0.42 <sup>b</sup>	0.44 <sup>b</sup>	0.39 <sup>b</sup>	0.39 <sup>b</sup>	0.44 <sup>b</sup>	0.35 <sup>b</sup>
Pre $\beta_2$ -HDL	0.48 <sup>b</sup>	0.001	0.04	0.15 <sup>b</sup>	0.09	0.39 <sup>b</sup>	0.03	0.12	0.16 <sup>a</sup>	0.13
HDL <sub>3c</sub>	0.31 <sup>b</sup>	0.03	0.05	0.04	-0.02	0.44 <sup>b</sup>	0.17 <sup>a</sup>	0.15 <sup>a</sup>	0.08	0.04
HDL <sub>3b</sub>	0.49 <sup>b</sup>	0.02	0.04	0.05	0.01	0.58 <sup>b</sup>	0.16 <sup>a</sup>	-0.001	0.05	0.08
HDL <sub>3a</sub>	0.49 <sup>b</sup>	0.17 <sup>b</sup>	0.19 <sup>b</sup>	0.17 <sup>b</sup>	0.13 <sup>b</sup>	0.53 <sup>b</sup>	0.19 <sup>b</sup>	0.26 <sup>b</sup>	0.25 <sup>b</sup>	0.21 <sup>b</sup>
HDL <sub>2a</sub>	0.58 <sup>b</sup>	-0.21 <sup>b</sup>	-0.26 <sup>b</sup>	-0.26 <sup>b</sup>	-0.20 <sup>b</sup>	0.59 <sup>b</sup>	-0.05	-0.17 <sup>a</sup>	-0.14 <sup>a</sup>	-0.19 <sup>a</sup>
HDL <sub>2b</sub>	0.49 <sup>b</sup>	-0.33 <sup>b</sup>	-0.40 <sup>b</sup>	-0.46 <sup>b</sup>	-0.37 <sup>b</sup>	0.40 <sup>b</sup>	-0.27 <sup>b</sup>	-0.26 <sup>b</sup>	-0.21 <sup>b</sup>	-0.26 <sup>b</sup>

<sup>a</sup> *P* < 0.05

<sup>b</sup> *P* < 0.01

**Table 5** Multiple liner regression correlation between contents of plasma HDL subclasses and apolipoprotein

	Pre $\beta_1$ -HDL		Pre $\beta_2$ -HDL		HDL <sub>3c</sub>		HDL <sub>3b</sub>		HDL <sub>3a</sub>		HDL <sub>2a</sub>		HDL <sub>2b</sub>	
	$\beta$	P	$\beta$	P	$\beta$	P	$\beta$	P	$\beta$	P	$\beta$	P	$\beta$	P
<b>Male</b>														
apoAI	0.377	<0.001	0.508	<0.001	0.321	<0.001	0.519	<0.001	0.540	<0.001	0.553	<0.001	0.423	<0.001
apoB100	0.120	<0.05	–	–	–	–	–	–	–	–	–	–	–0.099	<0.05
apoCII	0.154	<0.05	–0.14	<0.05	–	–	–	–	0.151	<0.05	–	–	–	–
apoCIII	0.206	<0.01	0.321	<0.01	–	–	–	–	–	–	–	–	–0.232	<0.05
apoE	0.198	<0.01	–	–	–	–	–	–	–	–	–	–	–	–
<b>Female</b>														
apoAI	0.401	<0.001	0.396	<0.001	0.440	<0.001	0.574	<0.001	0.529	<0.001	0.605	<0.001	0.420	<0.001
apoB100	0.168	<0.05	–	–	–	–	0.180	<0.05	–	–	–	–	–0.198	<0.05
apoCII	–	–	–	–	0.263	<0.05	–	–	0.266	<0.05	–	–	–	–
apoCIII	–	–	–	–	–	–	–	–	–	–	–	–	–	–
apoE	–	–	–	–	–	–	–	–	–	–	–	–	–0.221	<0.05

$\beta$ : standardized regression coefficients

indeed the mature and metabolic process that nascent pre $\beta$ -HDL converted to mature  $\alpha$ -HDL. Consequently, the contents of all HDL subclasses increased suggesting that speed of RCT might be enhanced.

Furthermore, the present study showed that the contents of large-sized HDL<sub>2b</sub> increased more obviously relative to those of the small-sized pre $\beta_1$ -HDL with the elevation of apoAI. In comparison to the same gender subjects in the low apoAI levels, there was an increase in HDL<sub>2b</sub> (79% in males; 68% in females) and an increase in pre $\beta_1$ -HDL (38% in males; 43% in females) for the subjects with high apoAI levels, which suggests that plasma apoAI levels have significantly important effects on the distributions of HDL subclasses. The variations of HDL subclass distributions are probably related to an increase in HDL-C concentrations and a decrease in TG concentrations for the subjects with high apoAI levels. Several studies have shown that enhanced LCAT, lipoprotein lipase (LPL) activities and impeded hepatic lipase (HTGL) are consistent with lower plasma TG levels [9, 29, 30]. The LCAT may catalyze unesterified TC to cholesteryl and promote the conversion of pre $\beta_1$ -HDL and HDL<sub>3</sub> to HDL<sub>2</sub>. LPL plays an important role in hydrolyzing TG transported in chylomicrons and very low density lipoprotein (VLDL) particles. When catabolized by LPL, chylomicrons (CM) and VLDL release TG, TC, PL, apoAI, and apoCs. Subsequent binding of these products to HDL<sub>3</sub> results in formation of HDL<sub>2</sub> particles. The HTGL activities promote the conversion of HDL<sub>2</sub> to HDL<sub>3</sub>, and furthermore, excess surface phospholipids and apoAI dissociated from HDL<sub>2</sub>, impaired HTGL activity must lead to the increase of large-sized HDL<sub>2</sub> particles and decrease of small-sized pre $\beta_1$ -HDL particles. In addition, it was demonstrated that LCAT activities also increased with high plasma

HDL-C levels [29]. Hence, with the increase of apoAI levels, not only the number of HDL particles increased but a lot of large-sized HDL<sub>2b</sub> was generated which indicated the speed and efficiency of RCT had been enhanced.

We further analyzed the combined impact of plasma apoAI and HDL-C levels on the alterations of HDL subclass distribution. Data obtained in the present study suggested that, with elevation of apoAI along with HDL-C levels, all HDL subclass levels increased gradually and significantly, meanwhile, compared with low the concentrations group (apoAI  $\leq$  1043.6 together with HDL-C < 1.03), the contents of large-sized HDL<sub>2b</sub> (116%) increased more significantly than those of small-sized pre $\beta_1$ -HDL (26%) which resulted in an elevation of the HDL<sub>2b</sub>/pre $\beta_1$ -HDL ratio (2.0 vs. 3.5) in the high concentrations group (apoAI  $\geq$  1452.6 together with HDL-C > 1.55). It indicated that alteration of the number of large-sized HDL particles might be more obvious with the increase of apoAI and HDL-C levels.

The correlation analysis also showed that the concentrations of apoAI had a significant positive correlation with all HDL subclasses and multiple liner regression revealed that apoAI might be a more powerful factor influencing the distribution of HDL subclasses. HDL is known to serve as a reservoir for apoC<sub>s</sub>, apoE. ApoCII is the activator protein for LPL. In contrast, apoCIII could inhibit the LPL activity. Evidently, changes in concentrations of other apolipoproteins (including apoB100, apoCII, apoCIII, apoE) may affect HDL subclass distribution.

In summary, our results reported in this work showed that with the increase of plasma apoAI concentrations, the contents of all the HDL subclasses rose gradually and significantly, especially, an increase in

large-sized HDL<sub>2b</sub> was very striking. Furthermore, when apoAI and HDL-C concentrations increased simultaneously, the trend toward larger HDL size was more obvious. Which, in turn indicated that the maturation of HDL might be enhanced and that RCT might be improved. In addition, Pearson correlation and multiple linear regression analysis revealed that apoAI levels revealed that apoAI levels might be a more powerful factor influencing the distributions of HDL subclasses.

**Acknowledgments** We thank technician Yu Liu, master students Jia Yao and Xuemei Zhang for the collection of blood sample and technical support in the lipid and apolipoprotein assays.

## References

- Gordon T, Castelli WP, Hjortland MC, Kannel WB, Dawber TR (1977) High density lipoprotein as a protective factor against coronary heart disease: Framingham study. *Am J Med* 62:707–62714
- Watkins LO, Neaton JD, Kuller L H. (1986) Racial differences in high density lipoprotein cholesterol and coronary heart disease incidence in the usual care group of the multiple risk factor intervention trial. *Am J Cardiol* 57:538–57545
- Gordon DJ, Probstfield JL, Garrison RJ, Bangdiwala S, Tyroler HA (1989) High density lipoprotein cholesterol and cardiovascular disease. Four prospective American studies. *Circulation* 79:8–815
- Atger V, Giral P, Simon A, Cambillau M, Levenson, Garipey J, Megnien JL, Moatti N (1995) High-density lipoprotein subfractions as markers of early atherosclerosis. *Am J Cardiol* 75:127–131
- Von Eckardstein A, Huang Y, Assmann G (1994) Physiological role and clinical relevance of high-density lipoprotein subclasses. *Curr Opin Lipidol* 15:404–15416
- Wu XW, Fu MD, Lin BW (1999) Study on the immunodetection method of HDL subclasses in human serum. *Chin J Arterioscler* 7:253–255
- Xu Y, Fu MD (2003) Alterations of HDL subclasses in hyperlipidemia. *Clinica Chimica Acta* 332:95–102
- Jonas A, Kezdy KE, Wald JH (1989) Defined apolipoprotein A-I conformations in reconstituted high density lipoprotein discs. *J Biol Chem* 264:4818–4824
- Rye KA, Clay MA, Barter PJ (1999) Remodelling of high density lipoproteins by plasma factors. *Atherosclerosis* 145:227–238
- Kwiterovich Jr PO (1998) The antiatherogenic role of high-density lipoprotein cholesterol. *Am J Cardiol* 82:13Q–21Q
- Yuye Yang, Bingyu Yan, Mingde Fu, Yanhua Xu, Ying Tian (2005) Relationship between plasma lipid concentrations and HDL subclasses. *Clinica Chimica Acta* 354:49–58
- Lantu Gou, Mingde Fu, Yanhua Xu, Ying Tian, Bingyu Yan, Luchuan Yang (2005) Alterations of HDL subclasses in endogenous hypertriglyceridemia. *Am Heart J* 150:1039–1045
- Lianqun Jia, Shiyin Long, Mingde Fu, Bingyu Yan, Ying Tian, Yanhua Xu, Lantu Gou (2006) Relationship between total cholesterol/high-density lipoprotein cholesterol ratio, triglyceride/high-density lipoprotein cholesterol ratio, and high-density lipoprotein subclasses. *Metabol Clin Exp* (in press)
- Li Tian, Lianqun Jia, Mingde Fu, Ying Tian, Yanhua Xu, Haoming Tian, Yuye Yang (2006) Alterations of high density lipoprotein subclasses in obese subjects. *Lipids* 41:789–796
- Executive summary of the third report of NCEP (2001) Expert panel on detection, evaluation and treatment of high blood cholesterol in adults. Adult Treatment Panel III. *JAMA* 285:486–497
- Warnick GR, Nguyen T, Albers AA (1985) Comparison of improved precipitation methods for quantification of high-density lipoprotein cholesterol. *Clin Chem* 31:217–222
- Friedwald WF, Levy RI, Fredrickson DS (1972) Estimation of the concentration of low-density lipoprotein cholesterol in plasma, without use of the preparative ultracentrifuge. *Clin Chem* 18:499–502
- Labeur C, Shepherd J, Rosseneu M (1990) Immunological assays of apolipoproteins in plasma: methods and instrumentation. *Clin Chem* 36:591–597
- Liu B (1995) Immunoassay of human plasma apolipoproteins and clinical applications. In: Wang KQ (ed) *Lipoproteins and atherosclerosis*. People's Health Press, Beijing, pp 359–368
- Gordon D, Rifkin BM (1989) Current concepts: high density lipoproteins—the clinical implications of recent studies. *N Engl J Med* 321:1311–1315
- Hirano K, Yamashita S (1995) Atherosclerotic disease in marked hyperalphalipoproteinemia: combined reduction of cholesteryl ester transfer protein and hepatic triglyceride lipase. *Arterioscler Thromb Vasc Biol* 15:1849–1856
- Berard AM, Foger B (1997) High plasma HDL concentrations associated with enhanced atherosclerosis in transgenic mice overexpressing lecithin-cholesteryl acyltransferase. *Nat Med* 3:744–749
- Hoeg JM, Santamarina-Fojo S (1996) Overexpression of lecithin:cholesterol acyltransferase in transgenic rabbits prevents diet-induced atherosclerosis. *Proc Natl Acad Sci USA* 93:11448–11453
- Arnold Von Eckardstein (2001) High density lipoproteins and Arteriosclerosis. *Arterioscler Thromb Vasc Biol* 21:13
- Edward M, Rubin Y, Ishida, Shirley M, Clift, Ronald M, Kranss (1991) Expression of human apolipoprotein A-I in transgenic mice results in reduced plasma levels of murine apolipoprotein A-I and the appearance of two new high density lipoprotein size subclasses. *Biochemistry* 88:434–438
- Kunitake STm Ka La Sala KJ, Kane JP (1985) Apolipoprotein A-I-containing lipoproteins with pre-beta electrophoretic mobility. *J Lipid Res* 26:549–555
- Asztalos BF, Sloop CH, Wong L (1993) Two-dimensional electrophoresis of plasma lipoproteins: recognition of new apo A-I-containing subpopulations. *Biochim Biophys Acta* 1169:291–300
- Castro GR, Fielding CJ (1988) Early incorporation of cell derived cholesterol into pre $\beta$ -migrating high-density lipoprotein. *Biochemistry* 27:25–29
- Miida T, Kawano M, Fielding CJ (1992) Regulation of the concentration of pre $\beta$  high-density lipoprotein in normal plasma by cell membranes and lecithin:cholesterol acyltransferase activity. *Biochemistry* 31:11112–11117
- Miida T, Yamaguchi T, Tsuda T, Okada M (1998) High prebeta1-HDL levels in hypercholesterolemia are maintained by probucol but reduced by a low-cholesterol diet. *Atherosclerosis* 138:128–134

## Metabolic Syndrome: Effects of n-3 PUFAs on a Model of Dyslipidemia, Insulin Resistance and Adiposity

Yolanda B. Lombardo · Gustavo Hein ·  
Adriana Chicco

Received: 7 December 2006 / Accepted: 12 February 2007 / Published online: 17 March 2007  
© AOCs 2007

**Abstract** Both genetic and environmental factors (e.g. nutrition, life style) contribute to the development of the plurimetabolic syndrome, which has a high prevalence in the world population. Dietary n-3 PUFAs specially those from marine oil (EPA and DHA) appear to play an important role against the adverse effects of this syndrome. The present work examined the effectiveness of fish oil (FO) in reversing or improving the dyslipidemia, insulin resistance and adiposity induced in rats by long-term feeding a sucrose-rich diet (SRD). We studied several metabolic and molecular mechanisms involved in both lipid and glucose metabolisms in different tissues (liver, skeletal muscle, fat pad) as well as insulin secretion patterns from perfused islets under the stimulation of different secretagogues. Dietary FO reverses dyslipidemia and improves insulin action and adiposity in the SRD fed rats. FO reduces adipocytes cell size and thus, the smaller adipocytes are more insulin sensitive and the release of fatty acids decreases. In muscle, FO normalizes both the oxidative and non-oxidative glucose pathways. Moreover, FO modifies the fatty acid composition of membrane phospholipids. In isolated  $\beta$  cells, lipid contents and glucose oxidation return to normal. All these effects could contribute to the normalization of glucose-stimulated insulin secretion and muscle insulin insensitivity.

**Keywords** n-3 PUFAs · Metabolic syndrome · Sucrose-rich diet · Dyslipidemia · Insulin resistance · Visceral adiposity

### Introduction

Both genetic and environmental factors (e.g. nutrition, life style) contribute to the development of the plurimetabolic syndrome. This syndrome, which has a high prevalence in the world population, refers to a cluster of metabolic abnormalities including among others: insulin resistance, dyslipidemia [increased triglyceride and decreased high density lipoprotein cholesterol (HDL) levels], hypertension, central obesity, glucose intolerance and type 2 diabetes. All of them are well-documented risk factors for cardiovascular disease [1].

The composition of the macronutrients in the diet plays an important role in modifying several key factors of this syndrome. In this regard, numerous clinical and animal studies on n-3 polyunsaturated fatty acids (PUFAs), especially those from marine oil—eicosapentaenoic acid (20:5n-3 EPA) and docosahexaenoic acid (22:6n-3, DHA)—have shown their beneficial effects impacting on normal health and chronic diseases (e.g. the plurimetabolic syndrome). In addition to their use as fuels and structural components of the cell, the dietary intake of marine n-3 PUFAs (fish oil) has proven to be effective in lowering both triglyceride (Tg) and VLDL-Tg concentration in experimental animals and normal and hypertriglyceridemic men (see review) [2, 3]. It has been shown that fish oil (FO) in rats decreases the mRNA encoding of several enzymes proteins involved in “the novo” hepatic lipogenesis suppressing the nuclear abundance and expression of sterol regulatory element binding protein 1 (SREBP-1),

Y. B. Lombardo (✉) · G. Hein · A. Chicco  
Department of Biochemistry, School of Biochemistry,  
University of Litoral, Ciudad Universitaria Paraje  
“EL Pozo”.C.C.242 (3000), Santa Fe, Argentina  
e-mail: ylombard@fcb.unl.edu.ar



and enhances fatty acid oxidation throughout a peroxisome proliferator-activated receptor (PPAR $\alpha$ )—stimulated process [4, 5]. Moreover, the effects of n-3 PUFAs includes the alteration of the fatty acid composition of membrane phospholipids that modify membrane-mediated processes such as insulin transduction signals, activities of lipases and biosynthesis of eicosanoids [6].

Numerous studies from our group (see review [2]) and others [7–10] have shown that normal rats fed a sucrose-rich diet for a short period (3–5 weeks) develop hypertriglyceridemia, increase plasma free fatty acid (FFA) levels and enhanced triglyceride accumulation in liver and heart muscle. This is accompanied by normoglycemia with hyperinsulinemia, insulin resistance, increase in the first peak of glucose stimulated insulin secretion in perfused islets and hypertension. A different picture emerges after a long-term feeding (15–40 weeks) of a sucrose-rich diet. In addition to the altered lipid metabolism and ectopic fat deposition in several non adipose tissues, rats develop visceral adiposity with a moderate increase in body weight, hyperglycemia with normoinsulinemia and a lack of the first peak with an increase in the second phase of glucose stimulated insulin secretion from perfused islets [2, 11–14]. Interestingly, this animal model exhibits many of the hallmarks present in the plurimetabolic syndrome in humans. Moreover, the temporal metabolic changes described may reflect the early start of type 2 diabetes mellitus, since many patients have chronically elevated plasma FFA and Tg levels, altered peripheral insulin sensitivity and loss of the first peak of insulin in response to glucose.

Most experimental studies examining the effect of dietary nutrients (e.g. n-3 fatty acids from marine source) on dyslipidemia and insulin resistance have focused on the development of the impairment. In this vein, it has been shown that FO prevents the onset of insulin resistance and dyslipidemia when fed to rats with high fat [2, 15–17] or high sucrose diets [2, 18, 19]. However, relatively few studies have examined the effectiveness of FO in reversing diet-induced insulin resistance [20–23]. Therefore, the rats fed a long-term sucrose-rich diet seem to be an appropriate experimental model to investigate the effect of dietary n-3 PUFAs (fish oil) to improve or reverse these metabolic abnormalities.

The present study was conducted on rats fed a SRD during 8 months, in which a stable dyslipidemia and insulin resistance had been present before the source of fat in the diet (corn oil) was replaced by an isocaloric amount of FO for the last 2 months. We analyzed several aspects of lipid and glucose metabolism in the liver, skeletal muscle and adipose tissue of these rats. In addition, we studied the insulin secretion patterns from “in vitro” perfused isolated islets under the stimulation of different secretagogues (glucose, palmitate) and peripheral insulin sensitivity (euglycemic–hyperinsulinemic clamp).

## Materials and Methods

### Animal Model and Diets

Two months old male Wistar rats, initially weighting 170–185 g were maintained under controlled temperature ( $22 \pm 1$  °C), humidity and air flow conditions, with a fixed 12 h light:dark cycle (light 07:00–19:00). After a 1-week acclimation period, the rats were randomly divided into two groups: experimental and control. The first group received a purified sucrose-rich diet (SRD) containing by weight 62.5% sucrose, 17% of vitamin free casein, 8% corn oil, 7.5% cellulose, 3.5% salt mixture (AIN-93-MX), 1% vitamin mixture (AIN-93M-VX), 0.2% choline chloride, and 0.3% methionine. The control group received the same semisynthetic diet but with sucrose replaced by starch (CD). The experimental group received the SRD for 6 months after which the rats were randomly divided into two subgroups. The rats of the first subgroup continued on the SRD up to 8 months. The second subgroup, SRD + fish oil, (SRD + FO) received the SRD in which the source of fat (corn oil 8/100 g) had been replaced by cod liver oil (7/100 g) plus (1/100 g) of corn oil during the last 2 months on the diet. The control group received the CD throughout the experimental 8-month period. The SRD without the addition of FO used from months 6 to 8 and the CD were balanced for cholesterol and vitamins D and A, present in the FO. Diets were isoenergetics, providing approximately 16.3 kJ/g of food and were available ad libitum. Diets were prepared every day by adding the oils and base mixture containing the other nutrients. The oils and base mixture were separately stored at 4 °C until preparation of the diet. Fish oil was kept under a nitrogen atmosphere during storage. The weight of each rat was assessed twice each week during the experimental period. At the end of the 8 months dietary period, except as otherwise indicated, the food was removed and experiments were performed between 09:00 and 12:00 h. The Human and Animal Research Committee of the School of Biochemistry, University of Litoral, Santa Fe, Argentina, approved the experimental protocol.

### Analytical Methods

Rats were anesthetized with intraperitoneal pentobarbital sodium (60 mg/kg body weight). Blood samples were obtained from the jugular vein, rapidly centrifuged, and plasma was either immediately assayed or stored at  $-20$  °C. Plasma triglyceride, FFA, glucose, leptin and adiponectine as well as immunoreactive insulin levels were determined as previously described [23]. Liver, pancreas, gastrocnemius muscle and white adipose tissue (epididymal and retroperitoneal) were rapidly removed from the

anesthetized rats, and except otherwise indicated they were frozen, clamped in liquid nitrogen and stored at  $-80^{\circ}\text{C}$ . The weight of the epididymal and retroperitoneal adipose tissue was recorded.

#### *Liver Tissue Assays*

Homogenates of frozen liver were used for the determination of triglyceride content [23]. A cytosolic fraction of liver homogenates samples was obtained by centrifugation at  $100,000\times g$ , and the fatty acid synthase (FAS) activity was assayed immediately as described by Halestrap [24]. Carnitine palmitoyltransferase I (CPT-I) activity was determined spectrophotometrically following the release of CoA-SH from palmitoyl-CoA in liver homogenates in the presence and absence of L-carnitine [25]. The fatty acid oxidase activity (FAO) was measured by a modification of the procedure reported by Vamecq [26] and the  $\text{H}_2\text{O}_2$  release was determined spectrophotometrically from a coupled peroxidative reaction [27]. The malic enzyme (ME) activity was assayed by the method proposed by Ochoa with a minor modification according to Hsu et al. [28]. Pyruvate dehydrogenase complex (PDHc), and glucose-6-P-dehydrogenase (G-6-PDH) activities were analyzed as previously described [21]. The triglyceride secretion rate (VLDL-Tg secretion) was evaluated in 12-h fasting rats following the procedure described by Lombardo et al. [20].

#### *Gastrocnemius Muscle Assays*

Triglyceride, long-chain acyl-CoA (LC ACoA), diacylglycerol (DAG), malonyl-CoA, glycogen, and glucose-6-phosphate content as well as the activities of glycogen synthase (GSa), PDHc and PDH kinase were analyzed in muscle homogenate as previously described [29]. Gastrocnemius lipids were extracted, total phospholipids separated by TLC and their fatty acid analyzed by a procedure described in detail by Brenner et al. [14]. The protein mass expression of nPKC $\theta$  in the cytosol and membrane fraction of the gastrocnemius muscle were measured as described by D'Alessandro et al. [29].

#### *Euglycemic Hyperinsulinemic Clamp Studies*

Whole body peripheral insulin sensitivity was measured using the euglycemic hyperinsulinemic clamp technique as described in detail elsewhere [12]. At the end of the second hour of the clamp studies, gastrocnemius muscles were quickly removed, frozen and stored at  $-80^{\circ}\text{C}$  for the assay of both glycogen and glucose-6-phosphate concentration and GSa activity [12].

#### *Adipose Tissue Assays*

##### *Preparation of Isolated Adipocytes*

The adipocytes were isolated from the epididymal fat pad according to the method described by Robdell [30]. Fat cell size, number and triglyceride content were determined in the isolated adipocytes [31]. Aliquots of isolated epididymal fat cells were incubated in a shaking Dubnoff water bath at  $37^{\circ}\text{C}$  for 1 h; glycerol release was measured under these experimental conditions as an index of basal lipolysis. More details of the methodology employed have been previously described [31]. Lipoprotein lipase (LPL) and G-6-PDH activities in epididymal fat pads were also measured as previously described [31].

##### *Total RNA Preparation and Relative Quantitative RT-PCR Analysis*

Adipose tissue total RNA was prepared from fat pad tissue (epididymal and retroperitoneal) of each dietary group. Total RNA samples were stored at  $-80^{\circ}\text{C}$  until quantification of the target mRNAs (ob mRNA and adiponectin mRNA). A real time, two-step RT-PCR assay was developed for mRNA relative quantification as previously described [23]. The relative-quantitative data were expressed as the ratio of the level of adiponectin or leptin mRNA to that of 18S rRNA in arbitrary units.

#### *Pancreas Tissue Assays*

##### *Perifusion of Isolated Islets*

Islets were isolated by collagenase digestion and collected under a stereoscopic microscope. After a 30 min prewash period, a group of 30–40 islets were perifused with a Krebs Ringer buffer pH 7.4 at  $37^{\circ}\text{C}$  ( $\text{O}_2$  95:CO $_2$  5) containing high glucose concentration (16.5 mM) or glucose 16.5 mM plus palmitate 0.5 mM until the end of the perifusion (40 min). In all the experiments, aliquots from the effluent for insulin assays were collected after different periods of time and stored at  $-20^{\circ}\text{C}$  until insulin analysis. More details of the methodology employed have been previously described [22]. Islet triglyceride content and PDHc activity were assayed in isolated islets as previously described [22].

#### *Statistical Analysis*

Results were expressed as mean  $\pm$  SEM. The statistical significant between groups was determined by one way analysis of variance followed by the inspection of all differences between pairs of means by the Newman Keul's

**Table 1** Blood variables in rats fed a control (CD), sucrose-rich (SRD) or SRD + fish oil (SRD + FO) diets

	Triglycerides (mmol/L)	Free fatty acids ( $\mu\text{mol/L}$ )	Glucose (mmol/L)
CD	0.64 $\pm$ 0.04 <sup>b</sup>	287.2 $\pm$ 18.0 <sup>b</sup>	6.40 $\pm$ 0.12 <sup>b</sup>
SRD	2.23 $\pm$ 0.10 <sup>a</sup>	794.0 $\pm$ 30.0 <sup>a</sup>	8.18 $\pm$ 0.10 <sup>a</sup>
SRD + FO	0.60 $\pm$ 0.06 <sup>b</sup>	295.1 $\pm$ 38.0 <sup>b</sup>	6.52 $\pm$ 0.20 <sup>b</sup>

Values are expressed as mean  $\pm$  SEM,  $n = 6$ . Values in a column that do not share the same superscript letter are significantly different ( $p < 0.05$ ) when one variable at a time was compared by the Newman Keul's test

SRD + FO group consumed the sucrose-rich diet for 6 months and the SRD diet containing FO for the last 2 months of the experiment

test.  $P$  values lower than 0.05 were considered to be statistically significant.

## Results

### Blood Variables

At the end of the dark period (7 AM), plasma triglyceride, FFA and glucose concentration were higher ( $p < 0.05$ ) in rats fed a SRD compared with age-matched controls fed a CD (Table 1). A complete normalization of all of these variables occurred in rats fed a SRD + FO during the last 2 months of the experimental period. Moreover plasma insulin levels did not differ between the groups (data not shown).

### Liver Tissue

#### *Main Effects of FO (n-3 PUFAs) on the Hepatic Liver Metabolism of SRD-fed Rats*

Both triglyceride content and VLDL-triglyceride secretion were significantly higher in the liver of rats fed a SRD

**Table 2** Liver triglyceride content, triglyceride secretion rate (VLDL-Tg) and enzyme activities in rats fed a control (CD), sucrose-rich (SRD) or SRD + fish oil (SRD + FO) diets

Diets	CD	SRD	SRD + FO
Triglyceride ( $\mu\text{mol/g}$ wet tissue)	12.60 $\pm$ 0.28 <sup>b</sup>	23.83 $\pm$ 2.35 <sup>a</sup>	11.20 $\pm$ 0.52 <sup>b</sup>
VLDL-Tg [nmol/(min $\times$ g body weight)]	161.5 $\pm$ 3.0 <sup>b</sup>	194.6 $\pm$ 8.5 <sup>a</sup>	120.3 $\pm$ 9.5 <sup>c</sup>
Fatty acid synthase (mU/mg protein)	1.21 $\pm$ 0.02 <sup>c</sup>	5.78 $\pm$ 0.49 <sup>a</sup>	2.41 $\pm$ 0.08 <sup>b</sup>
Malic enzyme (mU/mg protein)	1.14 $\pm$ 0.01 <sup>c</sup>	2.15 $\pm$ 0.15 <sup>a</sup>	1.68 $\pm$ 0.06 <sup>b</sup>
Glucose-6-phosphate dehydrogenase (mU/mg protein)	26.06 $\pm$ 2.19 <sup>b</sup>	36.00 $\pm$ 0.95 <sup>a</sup>	23.10 $\pm$ 2.00 <sup>b</sup>
PDHa (% PDHt)	35.02 $\pm$ 1.61 <sup>b</sup>	50.55 $\pm$ 3.04 <sup>a</sup>	36.33 $\pm$ 1.54 <sup>b</sup>
Carnitine palmitoyltransferase I (mU/mg protein)	1.20 $\pm$ 0.13 <sup>b</sup>	0.70 $\pm$ 0.03 <sup>c</sup>	1.92 $\pm$ 0.15 <sup>a</sup>
Fatty acid oxidase (mU/mg protein)	2.40 $\pm$ 0.17 <sup>b</sup>	2.45 $\pm$ 0.13 <sup>b</sup>	5.33 $\pm$ 0.35 <sup>a</sup>

Values are expressed as mean  $\pm$  SEM,  $n = 6$ . Values in a line that do not share the same superscript letter are significantly different ( $p < 0.05$ ) when one variable at a time was compared by the Newman Keul's test

PDHa active form of PDH complex, expressed as percentage of total PDHc activity (PDHa basal activity  $\times$  100/total activity). Total PDH activity (mU/mg protein) 8.01  $\pm$  0.99 for CD, 7.46  $\pm$  0.87 for SRD and 8.00  $\pm$  1.00 for SRD + FO

compared to those fed a CD (Table 2). The activities of the enzymes related to the "novo lipogenesis" were significantly increased in the SRD-fed rats, whereas the fatty acid oxidase (FAO) activity was similar and CPT-1 activity was significantly decrease compared to that in the control group fed a CD. The presence of FO in the SRD collectively acted to normalize or improve liver triglyceride contents and the VLDL-Tg secretion rate as well as the lipogenic enzyme activities, while increasing the mitochondrial and peroxisomal fatty acid oxidation (CPT-1 and FAO activities).

### Skeletal Muscle

#### *Effects of FO on Metabolite Concentrations, Enzyme Activities and PKC $\theta$ Mass Expression in Gastrocnemius Muscle of SRD-fed Rats*

Compared to CD-fed rats, the gastrocnemius muscle of dyslipemic insulin-resistant, SRD-fed rats at the basal state (ex vivo) shows a significant increase ( $p < 0.05$ ) of triglyceride, LC ACoA and DAG contents without changing malonyl-CoA levels (Table 3). Qualitative and quantitative analyses of Western blots showed that the relative abundance of nPKC $\theta$  isozyme was also significantly increased in the membrane fraction of the gastrocnemius muscle of the SRD, whereas the cytosol fraction was slightly but not significantly decreased. Moreover, both a reduced active form of PDHc and an increase in PDH kinase activities were observed in SRD-fed animals, suggesting an impaired glucose oxidation. Table 3 also shows that FO reduced the increased triglyceride contents to basal levels within the skeletal muscle cells, and restored the PDHc activity. Besides, FO improved long-chain acyl CoA and DAG concentration and the nPKC $\theta$  mass expression in the membrane fraction of the skeletal muscle of SRD-fed rats.

**Table 3** Gastrocnemius muscle metabolites, protein mass expression of nPKC $\theta$  and PDHc and PDH kinase activities of rats fed control (CD), sucrose-rich (SRD) or SRD + fish oil (SRD + FO) diets

Diets	CD	SRD	SRD + FO
Triglyceride ( $\mu\text{mol/g}$ wet tissue)	3.34 $\pm$ 0.44 <sup>b</sup>	8.01 $\pm$ 0.40 <sup>a</sup>	3.44 $\pm$ 0.51 <sup>b</sup>
LC ACoA ( $\mu\text{mol/l}$ )	8.72 $\pm$ 0.23 <sup>b</sup>	15.08 $\pm$ 1.44 <sup>a</sup>	10.14 $\pm$ 0.33 <sup>c</sup>
DAG (nmol/g wet tissue)	116.1 $\pm$ 10.0 <sup>c</sup>	177.2 $\pm$ 9.1 <sup>a</sup>	143.5 $\pm$ 7.2 <sup>b</sup>
Malonyl-CoA (nmol/g wet tissue)	1.36 $\pm$ 0.43	1.30 $\pm$ 0.58	1.05 $\pm$ 0.19
nPKC $\theta$ (densitometric units relative to control diet) Cytosol	100.0 $\pm$ 4.1	84.2 $\pm$ 6.2	88.3 $\pm$ 5.0
Membrane	100.0 $\pm$ 3.1 <sup>c</sup>	174.1 $\pm$ 8.0 <sup>a</sup>	143.2 $\pm$ 7.0 <sup>b</sup>
PDHa (% PDHt)	34.51 $\pm$ 1.20 <sup>a</sup>	18.70 $\pm$ 1.81 <sup>b</sup>	32.52 $\pm$ 1.60 <sup>a</sup>
PDH kinase (K/min <sup>-1</sup> )	1.55 $\pm$ 0.12 <sup>b</sup>	3.30 $\pm$ 0.24 <sup>a</sup>	1.60 $\pm$ 0.14 <sup>b</sup>

Values are expressed as mean  $\pm$  SEM,  $n = 6$ . Values in a line that do not share the same superscript letter are significantly different ( $p < 0.05$ ) when one variable at a time was compared by the Newman Keul's test

Long-chain acyl-CoA is expressed as  $\mu\text{mol/L}$  assuming that 80% of the tissue was water, PDHa active form of PDH complex (see Table 2), PDH kinase activity was assayed as determining the adenosine triphosphate-dependent inactivation of PDHc activity as a function of time (K/min<sup>-1</sup>) and was calculated from the first order kinetic constant

Values were still higher than those observed in the CD-fed rats.

On the other hand, dietary FO reversed the impaired insulin-stimulated glucose-6-phosphate concentration, glycogen storage and glycogen synthase activity during the euglycemic hyperinsulinemic clamp (Fig. 1). Moreover, the glucose infusion rate (GIR), which measures whole body peripheral insulin action "in vivo", was lower ( $p < 0.01$ ) in the SRD-fed group [ $24.17 \pm 4.34 \mu\text{mol}/(\text{kg min})$ ,  $n = 6$ ] compared to CD-fed rats [ $64.45 \pm 5.00 \mu\text{mol}/(\text{kg min})$ ,  $n = 6$ ]. However, in the SRD + FO group, the GIR did not differ from the controls [ $68.10 \pm 6.30 \mu\text{mol}/(\text{kg min})$ ,  $n = 6$ ].

The normalization of peripheral insulin sensitivity in the SRD + FO fed rats was accompanied by a significant increase in the n-3 PUFAs, specially EPA and DHA, in the

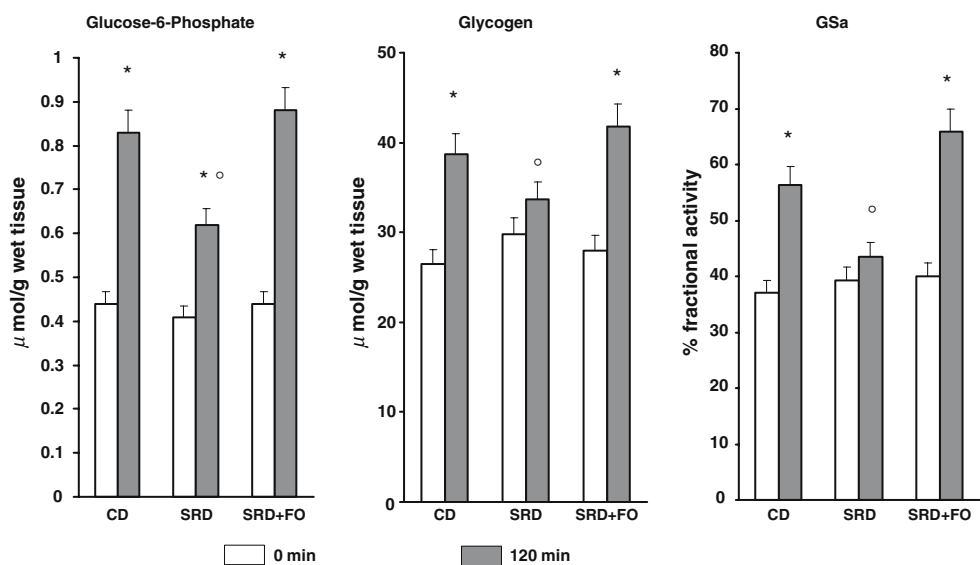
phospholipids of the gastrocnemius muscle. The n-3/n-6 ratio was significantly higher ( $p < 0.05$ ). Values were as follows: % fatty acids; n-3PUFAs (mean  $\pm$  SEM  $n = 6$ ): 13.61  $\pm$  0.44 in CD, 5.58  $\pm$  0.58 in SRD and 22.23  $\pm$  0.61 in SRD + FO. The ratio n-3/n-6 was 0.35 in CD, 0.14 in SRD and 0.81 in SRD + FO, respectively.

#### Adipose Tissue

##### Effects of Dietary FO on Body Weight, Fat Pad Morphology, Triglyceride Content and Enzyme Activities

Rats fed a SRD developed visceral adiposity (increase in epididymal and retroperitoneal fat tissues) and a moderate increase in body weight (Table 4). Isolated adipocyte from epididymal fat tissue showed a significant increase in

**Fig. 1** Glucose-6-phosphate and glycogen concentration and glycogen synthase (GSa) activity in gastrocnemius muscle at the start (*open bars* 0 min) and at the end (*closed bars* 120 min) of the clamp studies in rats fed control (CD), sucrose-rich (SRD) or SRD + fish oil (SRD + FO). Values are expressed as mean  $\pm$  SEM,  $n = 6$ . \* $p < 0.05$  120 versus 0 min in CD, SRD or SRD + FO; (*open circles*)  $p < 0.05$  SRD 120 versus CD and SRD + FO 120 min



triglyceride contents, and cell volume without changes in total cell number compared to CD-fed rats. Lipoprotein lipase and glucose-6-phosphate dehydrogenase activities were significantly increased ( $p < 0.05$ ) in the SRD. Dietary FO markedly reduced the fat pad mass and the hypertrophy of fat cells (decreased cell volume and triglyceride contents). However, only a slight but not significant decrease of total body weight was observed. In addition, we previously reported [31] that the histograms of adipose size distribution that showed a significant increase (37%) of the mean cell diameters in the SRD-fed rats compared to CD-fed animals were significantly improved in the group of rats fed the SRD + FO. The presence of FO in the SRD reduced the high levels of lipoprotein lipase and glucose-6-phosphate dehydrogenase activities. Basal lipolysis, which was significantly increased in isolated adipocytes of SRD-fed rats, was improved when FO replaced corn oil as a source of fat in the diet. Values were as follows (mean  $\pm$  SEM  $n = 6$ )  $\mu\text{mol glycerol}/(10^6 \text{ cells} \times \text{h})$ ;  $0.7 \pm 0.1$  in CD;  $3.4 \pm 0.3$  in SRD and  $1.3 \pm 0.2$  in SRD + FO,  $p < 0.05$  SRD versus CD and SRD + FO;  $p < 0.05$  SRD + FO versus CD.

#### Plasma Leptin and Adiponectin Levels and Gene Expression in White Adipose Tissue

Both plasma leptin and adiponectin levels were significantly decreased in the SRD-fed rats. By shifting the source of fat in the diet to FO, the plasma levels of both adipokines reached values similar to those found in the rats fed a CD (Fig. 2a). Figure 2b shows obmRNA in adipose tissue (epididymal and retroperitoneal) of various dietary groups. Ob mRNA in both adipose tissues did not change between the different groups. Adiponectin mRNA showed a similar profile in both white adipose tissues. The presence of FO

after the installation of insulin resistance induced by the SRD (Fig. 2b) had not additional effects. Therefore, Fig. 2b represents the obmRNA and adiponectin mRNA levels of both adipose tissues.

#### Pancreas

##### Insulin Secretion from Perfused Isolated Islets. Effect of Dietary Fish Oil

Perfused islets from SRD-fed rats showed an alteration in the biphasic patterns of glucose stimulated insulin secretion with an absence of the first peak and an increase in the second phase of hormone secretion compared to CD-fed rats. Dietary FO completely normalized glucose induced insulin secretion in the SRD-fed rats (Fig. 3a). Furthermore, as expected, a short-term exposure of  $\beta$  cell to 0.5 mmol/L of palmitate in the perfused fluid enhanced glucose stimulated insulin secretion in rats fed a CD. In the SRD-fed group, the presence of palmitate diminished both the first peak and the second phase of insulin secretion when compared to the CD group. Dietary FO enhanced the first and second phase of hormone secretion, which was greater ( $p < 0.05$ ) than those in the SRD group and comparable to the control group fed a CD (Fig. 3b).

##### Triglyceride Concentration and PDHc Activity in Isolated Islets

Figure 4a shows an increase ( $p < 0.05$ ) in the triglyceride content in SRD-fed rats that was accompanied by a decrease ( $p < 0.05$ ) in the PDHc activity (Fig. 4b). However, in the SRD + FO fed group neither variable differed from the CD group.

**Table 4** Body weight, adipose tissue weight, cell volume and number, triglyceride content and LPL and G-6-PDH activities in rats fed a control (CD), sucrose-rich (SRD) or SRD + fish oil (SRD + FO) diets

Diets	CD	SRD	SRD + FO
Body weight (g)	442.5 $\pm$ 10.0 <sup>b</sup>	513.1 $\pm$ 19.0 <sup>a</sup>	487.3 $\pm$ 6.4 <sup>a</sup>
Epididymal fat (g)	7.29 $\pm$ 0.63 <sup>c</sup>	14.00 $\pm$ 0.89 <sup>a</sup>	10.40 $\pm$ 0.50 <sup>b</sup>
Epididymal relative weight (g/100 g body weight)	1.58 $\pm$ 0.10 <sup>c</sup>	2.80 $\pm$ 0.13 <sup>a</sup>	2.09 $\pm$ 0.06 <sup>b</sup>
Cell volume (pl)	264.1 $\pm$ 15.4 <sup>c</sup>	488.9 $\pm$ 10.5 <sup>a</sup>	360.0 $\pm$ 20.5 <sup>b</sup>
Cell number $\times 10^6$ /g tissue	4.03 $\pm$ 0.18 <sup>a</sup>	2.30 $\pm$ 0.15 <sup>c</sup>	3.10 $\pm$ 0.14 <sup>b</sup>
Triglyceride (nmol/cell)	0.31 $\pm$ 0.03 <sup>c</sup>	0.61 $\pm$ 0.04 <sup>a</sup>	0.42 $\pm$ 0.03 <sup>b</sup>
LPL (pkat/cell number $\times 10^6$ )	660.0 $\pm$ 95.1 <sup>b</sup>	1360.2 $\pm$ 170.4 <sup>a</sup>	820.2 $\pm$ 110.2 <sup>b</sup>
G-6-PDH (mU/cell number $\times 10^6$ )	43.50 $\pm$ 1.91 <sup>b</sup>	80.42 $\pm$ 3.71 <sup>a</sup>	30.60 $\pm$ 2.60 <sup>c</sup>
Retroperitoneal fat (g)	6.05 $\pm$ 0.40 <sup>c</sup>	12.98 $\pm$ 0.94 <sup>a</sup>	9.94 $\pm$ 0.49 <sup>b</sup>
Retroperitoneal relative weight (g/100 g body weight)	1.23 $\pm$ 0.16 <sup>c</sup>	2.65 $\pm$ 0.18 <sup>a</sup>	2.07 $\pm$ 0.08 <sup>b</sup>

LPL: Lipoprotein lipase, G-6-PDH: glucose-6-phosphate dehydrogenase

Values are expressed as mean  $\pm$  SEM,  $n = 6$ . Values in a line that do not share the same superscript letter are significantly different ( $p < 0.05$ ) when one variable at a time was compared by the Newman Keul's test

**Fig. 2** Plasma leptin and adiponectin levels (**a**) and white adipose tissue (WAT) (retroperitoneal and epididymal) ob and adiponectin mRNAs expression (**b**) of rats fed a control (CD), sucrose-rich (SRD) or SRD + fish oil (SRD + FO). Levels of mRNA were determined by real-time quantitative RT-PCR. The values are expressed as mean  $\pm$  SEM,  $n = 6$ . \* $p < 0.05$  SRD versus CD and SRD + FO

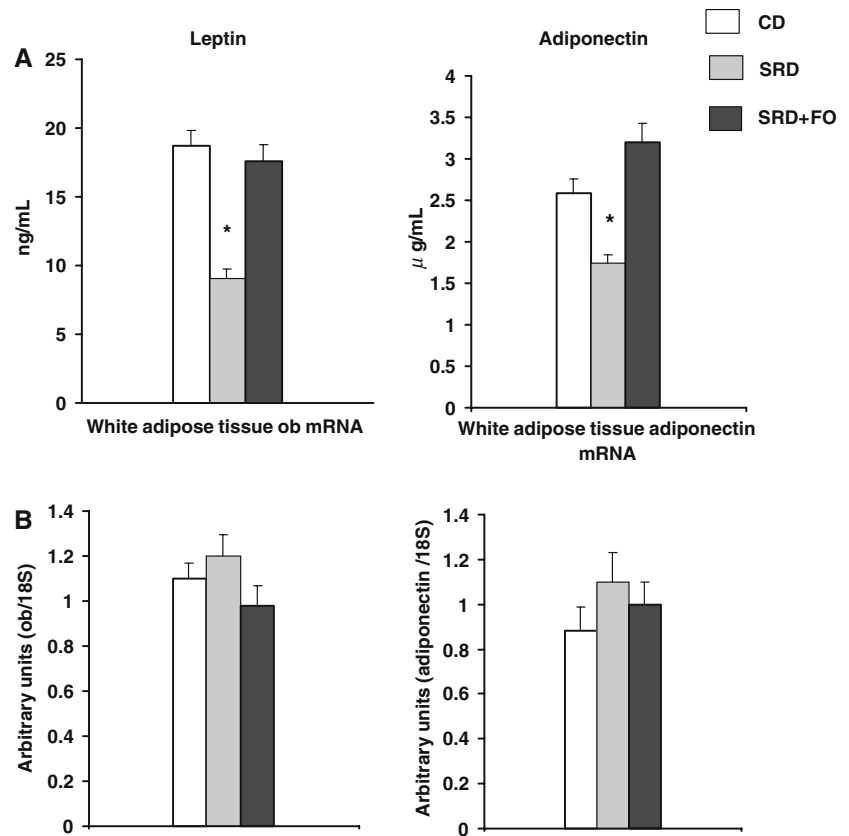
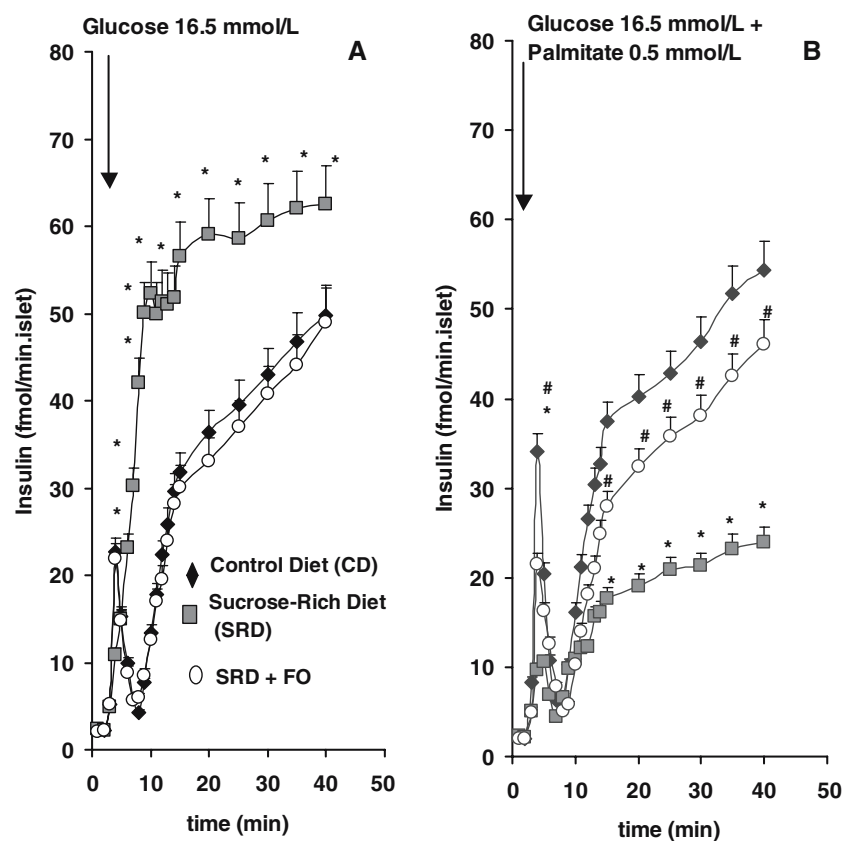


**Fig. 3** Insulin secretion in perfused pancreatic islets from rats fed control (CD), sucrose-rich (SRD) or SRD + fish oil (SRD + FO) diets under the stimulus of glucose **a** or glucose + palmitate **b**. Values are expressed as mean  $\pm$  SEM,  $n = 6$ ; \* $p < 0.05$  SRD versus CD and SRD + FO at each time point in **a** and **b**; # $p < 0.05$  SRD + FO versus CD at each time point in **b**



## Discussion

This work focused on the analyses of several metabolic and molecular mechanisms concerning the effect of fish oil (FO) on the reversion or improvement of dyslipidemia and insulin resistance ensuing a long-term feeding of a sucrose-rich diet to normal rats. The study shows that in this experimental model dietary FO is associated with a number of effects that collectively act to reduce dyslipidemia and improve insulin action.

### Effects on the Liver

The liver plays a central role in whole body carbohydrate and lipid metabolism and several metabolic pathways may be regulated by PUFAs through changes in the activity or abundance of different transcription factor families, among them, PPARs, SREBPs, and LXR  $\alpha$  and  $\beta$ . FO decreases plasma and liver triglyceride levels, VLDL-Tg secretion, and return plasma triglyceride to basal levels in SRD fed rats. Moreover, by shifting the source of fat in the SRD from corn oil to FO, the enzymatic activities of FAS, G-6-PDH, ME and PDHc, all of them involved with “the novo” lipogenesis, decreased to values similar to those recorded in the control fed rats while FAO and CPT1 activities were enhanced. Neschen et al. [32] have recently demonstrated that dietary n-3 PUFAs administered to rats increases the fatty acid oxidation capacity of tissues through their ability to function as ligand activators of transcription factor PPAR $\alpha$  and thereby induces the transcription of several gene-encoding proteins affiliated with fatty acid oxidation. Besides, the suppression of “the novo” lipogenesis and MUFA synthesis by n-3 PUFAs requires that the

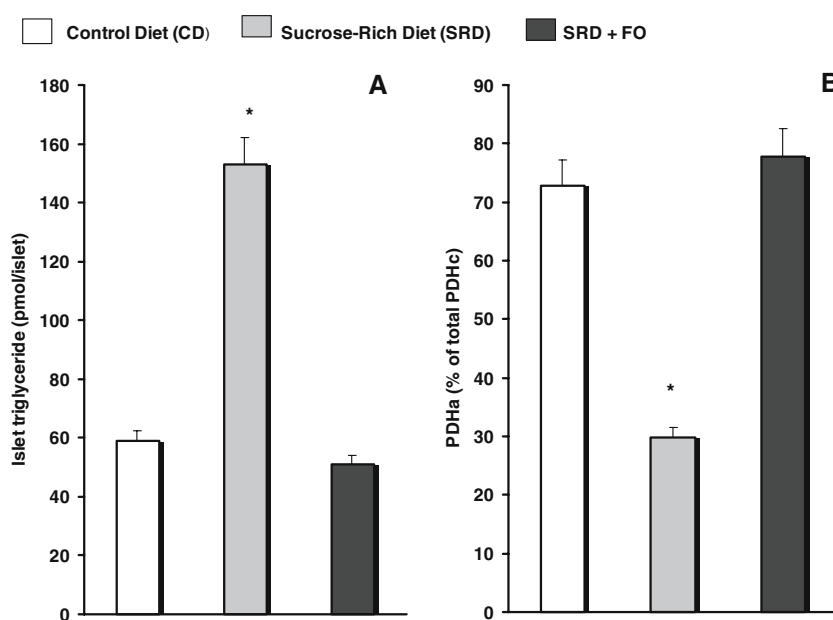
transcription factor SREBP-1c [4]. Thus, in the SRD-fed rats, the normalization of plasma and liver triglyceride levels suggests that the principal action of FO on hepatic lipid metabolism involves a shift from lipid synthesis and storage to lipid oxidation and therefore, both mechanisms, thus contributing to the hypolipemic effect of FO.

### Effects on Skeletal Muscle

In the skeletal muscle, the regulation of the glucose metabolism involves a complex interplay with the other fuels, especially free fatty acids. Studies in rats and humans [33] have shown that the degree of insulin resistance is strongly correlated with the muscle accumulation of triglycerides, and especially with LC ACoA. In the SRD-fed rats, D'Alessandro et al. [29] have recently demonstrated a significant increase in both triglyceride and LC ACoA contents within the gastrocnemius muscle which was accompanied by a significant increase in DAG and nPKC $\theta$  protein mass expression in the cell membrane fraction and a decrease in PDHc activity. LC ACoA by their esterification to DAG stimulate the PKC activity. Indeed, PKC disrupts the insulin signal via serine or threonine phosphorylation of insulin receptors, insulin receptor substrate 1, and potentially, other proteins such as glycogen synthase [34]. An increase in the LC ACoA concentration could also affect translocation of the glucose transport Glut 4 by acylating proteins involved in membrane fusion processes [35]. In addition, a significant reduction of flux through PDHc may limit glucose oxidation via the glucose–fatty acid cycle [29].

Fish oil normalizes and/or improves lipid storage and glucose oxidation within the skeletal muscle as well as

**Fig. 4** Triglyceride content **a** and pyruvate dehydrogenase complex (PDHc) activity **b** in isolated islets from rats fed control (CD), sucrose-rich (SRD) or SRD + fish oil (SRD + FO) diets. Values are mean  $\pm$  SEM,  $n = 6$ . \* $p < 0.05$  SRD versus CD and SRD + FO. PDHa, the active form of PDHc, was expressed as percentage of total PDHc activity (PDHt) (PDHa: basal activity  $\times$  100/total activity). To convert triglyceride contents to pmol, multiply ng by 1.13



nPKC $\theta$  proteins mass expression in the membrane fraction. Moreover, FO reversed the impaired insulin stimulated glycogen storage, glucose-6-phosphate concentrations, GSa activity and whole body insulin insensitivity, and returned plasma glucose and FFA levels to normal without changes in insulin levels.

The hypolipidemic effect of FO decreases the availability of the lipid fuel within the skeletal muscle and could, in turn, restore glucose oxidation and help to normalize insulin resistance. A recent study in healthy humans fed a high fat diet (75% fat) for 3 days showed an increase in PDH kinase and reduced PDHc activities in the skeletal muscle. In these people, the replacement of 15% of the fat by n-3 PUFAs decreased triglycerides and improved PDH kinase without changes in PDHc activities [36]. Moreover, Aas et al. [37] showed that the chronic exposure of EPA increased the uptake and oxidation of glucose despite a marked increase in fatty acid uptake and synthesis of complex lipids in cultured human skeletal muscle.

Increasing evidence suggests that the fatty acid composition of membrane phospholipids in the skeletal muscle and other target tissues is a critical factor that may induce changes in the structure and fluidity of cell membranes that could, in turn, directly affect insulin action. An increase in n-3 EPA and DHA as well as the n-3/n-6 ratio in the gastrocnemius muscle was observed after FO administration to SRD-fed rats, and this could also contribute to improve muscle insulin insensitivity. Moreover, Simonicova et al. [38] also demonstrated that substitution of fish oil into a high fat diet in rats led to an improvement of “in vivo” insulin action. The insulin sensitive effect of FO was accompanied by a decrease of plasma FFA, triglyceride and glycerol levels and a decrease of lipid content in liver and skeletal muscle. However, another study by Podolin et al. [18] demonstrated that when the sucrose diet containing menhaden oil was given to insulin-resistant rats, insulin action on the glucose metabolism remained impaired. Differences in the amount of FO present in the diet as well as the n-3/saturated ratio between the oils employed may contribute to the effectiveness of FO in reversing insulin insensitivity.

#### Effects on Adipose Tissue

Dietary FO was able to reverse the preexisting metabolic and morphological changes of visceral fat pad tissue, reduce the hypertrophy of fat pad cells and improve their altered size distribution in the SRD fed rats. We have also recently observed that both the inhibitory effect of high sucrose upon the antilipolytic action of insulin and the impaired insulin stimulated glucose transport were completely normalized (unpublished results). The changes induced by FO could be possibly via mechanisms that

include FO (specially EPA) binding and activation of the PPAR- $\gamma$ 2 isoform expression in white adipose tissue. PPAR- $\gamma$ 2 results in a coordinated increase in a large number of genes involved in lipid metabolism [39]. Moreover, PPAR- $\gamma$  remodels the adipose tissue in adult animals, driving the formation of small insulin sensitive white adipocytes. Rossi et al. [23] have recently shown that the adiposity and insulin resistance present in the SRD-fed rats were accompanied by a decrease of plasma leptin and adiponectin levels, while no changes in the gene expression of both adipokines in visceral fats (epididymal and retroperitoneal) were observed. Leptin and adiponectin play an important role in the lipid and glucose metabolism and their regulation by FO might be implicated in the functional and morphological changes present in the adipose tissue of SRD-fed rats. Indeed, by shifting the source of fat to FO, the plasma levels of both adipokines were increased without changes in their gene expression, while insulin insensitivity and dyslipidemia were reversed and adiposity improved. Although the mechanisms by which FO increase plasma leptin and adiponectin are still unclear, these results suggest that the normal levels reached by both adipokines might play an essential role in the normalization of insulin resistance and adiposity [23]. Recently, Yamauchi et al. [40] demonstrated that insulin resistance in lipoatrophic mice was completely reversed by a combination of physiological doses of adiponectin and leptin, but only partially when either adipokine was given alone, suggesting that leptin and adiponectin may work hand in hand to sensitize peripheral tissues to insulin. Although we cannot extrapolate these results to humans, Skurnick-Minot et al. [41] demonstrated a decrease of whole body adiposity and adipocyte size in type 2 diabetic insulin resistant patients after 2 months of treatment with FO capsules (1.8 g of n-3 PUFAs). In these patients, plasma adiponectin tended to increase without any deterioration or amelioration of insulin sensitivity at this stage.

#### Effects on $\beta$ Cell Function

A chronic exposure to hyperglycemia and high levels of plasma FFA has been shown to have a deleterious effect on both insulin secretion and action, a concept termed glucolipotoxicity. Several mechanisms have been proposed that could contribute to the dysfunction of the  $\beta$  cell such as changes in glucose oxidation, increase in triglyceride content within the islets, down regulation of several genes including glut 2 and glucokinase, stimulation of SREBP-1c and PPAR $\gamma$  among others (See [42] for a review). In long-term SRD-fed rats, we have recently demonstrated [22] highly deteriorated insulin secretion patterns in response to glucose stimulus. Furthermore, the islets acute exposure to palmitate in the perfusion medium did not improve insulin



release [22]. This was accompanied by an increase in the triglyceride storage within the islets that occurred concomitantly with a reduction of the PDHc activity. A decreased flux through the PDHc is associated with lower PDHa levels, and could involve activation of the PDH kinase. The inhibition of PDHc limits the oxidative glucose metabolism, a signal for insulin secretion and synthesis. These could play a key role in the abnormal insulin secretion of rats chronically fed a SRD. Moreover, the beneficial hypolipidemic effect of dietary FO on  $\beta$  cell dysfunction becomes evident since after FO administration all the above alterations were completely normalized. Interestingly, an improvement by fish oil of both insulin sensitivity and i.v glucose tolerance has been shown in patients with primary hypertriglyceridemia [43].

Finally, dietary FO appears to play an important protecting role against the adverse symptoms of the pluri-metabolic syndrome. The present work suggests some possible mechanisms through which FO improve or reverse dyslipidemia,  $\beta$  cell dysfunction and adiposity in rats fed a long-term a SRD. However, some effects of n-3 PUFAs on physiological processes such as the nature of the intracellular signal responsible for regulating the various affected transcription factors, both in human and experimental models, still remain unclear. Future research in this area will contribute to our understanding of how these singular lipids impact upon human health and disease.

**Acknowledgments** This investigation was carried out with the financial support of the Agencia Nacional de Promoción Científica y Tecnológica (ANPCYT) and CONICET, Grants N° PICTO # 05-13260/BID 1201/OC-AR, PIP # 5619/2005. The authors thank A.M. Bernasconi, Instituto de Investigaciones Bioquímicas de La Planta (INIBIOLP) for her technical assistance in the determination of muscle phospholipids.

## References

1. Cheal KL, Abbasi F, Lamendola C, McLaughlin T, Reaven GM, Ford ES (2004) Relationship to insulin resistance of the adult treatment panel III diagnostic criteria for identification of the metabolic syndrome. *Diabetes* 53:1195–1200
2. Lombardo YB, Chicco A (2006) Effects of dietary polyunsaturated n-3 fatty acids on dyslipidemia and insulin resistance in rodents and humans. *A Rev J Nutr Biochem* 17:1–13
3. Connor WE (2000) Importance of n-3 fatty acids in health and disease. *Am J Clin Nutr* 71(suppl):171S–175S
4. Jump DB, Botolin D, Wang Y, Xu J, Christian B, Demeure O (2005) Fatty acid regulation of hepatic gene transcription. *J Nutr* 135:2503–2506
5. Clarke SD (2001) Polyunsaturated fatty acid regulation of gene transcription: a molecular mechanism to improve the metabolic syndrome. *J Nutr* 131:1129–1132
6. Clamp AG, Ladha S, Clark DC, Grimble RF, Lund EK (1997) The influence of dietary lipids on the composition and membrane fluidity of rat hepatocyte plasma membrane. *Lipids* 32:179–184
7. Reaven GM (1984) Diabetic hypertriglyceridemia in the rat: animal models simulating the clinical syndromes of impaired glucose tolerance, noninsulin-dependent diabetes and insulin-dependent diabetes. In: Shafir E, Renold AS (eds) *Lessons from animal diabetes*. Libby, London, pp. 531–536
8. Pagliassotti MJ, Prach PA, Koppenhafer TA, Pan DA (1996) Changes in insulin action, triglycerides, and lipid composition during sucrose feeding in rats. *Am J Physiol* 271:R1319–R1326
9. Bezerra RMN, Ueno M, Silva MS, Tavares DQ, Carvalho CRO, Saad MJA (2000) A high fructose diet affects the early steps of insulin action in muscle and liver of rats. *J Nutr* 130:1531–1535
10. Luo J, Rizkalla SW, Lerer-Metzger M, Boillot J, Ardeleanu A, Bruzzo F, Desplanque N, Dalix AM, Durand G, Slama G (1995) A fructose-rich diet decreases insulin-stimulated glucose incorporation into lipids but not to glucose transport in adipocytes of normal and diabetic rats. *J Nutr* 125:164–171
11. Chicco A, Soria A, Fainstein-Day P, Gutman R, Lombardo YB (1994) Multiphasic metabolic changes in the heart of rats fed a sucrose-rich diet. *Horm Metab Res* 26:397–403
12. Chicco A, D'Alessandro ME, Karabatas L, Pastorale C, Basabe JC, Lombardo YB (2003) Muscle lipid metabolism and insulin secretion are altered in insulin-resistant rats fed a high sucrose diet. *J Nutr* 133:127–133
13. Lombardo YB, Drago S, Chicco A, Fainstein-Day P, Gutman R, Gagliardino JJ, Gomez Dumm CL (1996) Long-term administration of a sucrose-rich diet to normal rats: relationship between metabolic and hormonal profiles and morphological changes in the endocrine pancreas. *Metabolism* 45:1527–1532
14. Brenner RR, Rimoldi OJ, Lombardo YB, Gonzalez MS, Bernasconi AM, Chicco A, Basabe JC (2003) Desaturase activities in rat model of insulin resistance induced by a sucrose-rich diet. *Lipids* 38:733–742
15. Storlien LH, Jenkins AB, Chisholm DJ, Pascoe WS, Khouri S, Kraegen EW (1991) Influence of dietary fat composition on development of insulin resistance in rats. Relationship to muscle triglycerides and w-3 fatty acids in muscle phospholipid. *Diabetes* 40:280–289
16. Taouis M, Dagou C, Ster C, Durand G, Pinault M, Delarue J (2002) n-3 Polyunsaturated fatty acids prevent the defect of insulin receptor signaling in muscle. *Am J Physiol* 282:E664–E671
17. Storlien LH, Kraegen EW, Chisholm DJ, Ford GL, Bruce DG, Pascoe WS (1987) Fish oil prevents insulin resistance induced by high-fat feeding in rats. *Science* 237:885–888
18. Podolin DA, Gayles EC, Wei Y, Thresher JS, Pagliassotti MJ (1998) Menhaden oil prevents but does not reverse sucrose-induced insulin resistance in rats. *Am J Physiol* 274:R840–R848
19. Peyron-Caso E, Fluteau-Nadler S, Kabir M, Guerre-Millo M, Quignard-Boulangé A, Slama G, Rizkalla SW (2002) Regulation of glucose transport and transporter 4 (Glut-4) in muscle and adipocytes of sucrose-fed rats: effects of n-3 poly- and mono-unsaturated fatty acids. *Horm Metab Res* 34:362–366
20. Lombardo YB, Chicco A, D'Alessandro ME, Martinelli M, Soria A, Gutman R (1996) Dietary fish oil normalizes dyslipidemia and glucose intolerance with unchanged insulin levels in rats fed a high sucrose diet. *Biochem Biophys Acta* 1299:175–182
21. D'Alessandro ME, Chicco A, Karabatas L, Lombardo YB (2000) Role of skeletal muscle on impaired insulin sensitivity in rats fed a sucrose-rich diet: effect of moderate levels of dietary fish oil. *J Nutr Biochem* 11:273–280
22. Pighin D, Karabatas L, Rossi A, Chicco A, Basabe JC, Lombardo YB (2003) Fish oil affects pancreatic fat storage, pyruvate dehydrogenase complex activity and insulin secretion in rats fed a sucrose-rich diet. *J Nutr* 133:4095–4101
23. Rossi A, Lombardo YB, Lacorte JM, Chicco A, Rouault C, Slama G, Rizkalla SW (2005) Dietary fish oil positively regulates

- plasma leptin and adiponectin levels in sucrose-fed, insulin-resistant rats. *Am J Physiol* 289:R486–R494
24. Halestrap AP, Denton RM (1973) Insulin and the regulation of adipose tissue acetylCoA carboxylase. *Biochem J* 132:509–517
  25. Karlic H, Lohninger S, Koeck T, Lohninger A (2002) L-carnitine stimulates carnitine acyltransferases in the liver of aged rats. *J Histochem Cytochem* 50:205–212
  26. Vamecq J (1990) Fluorometric assay of peroxisomal oxidase. *Anal Biochem* 186:340–349
  27. Xing Xian Y, Drackley JK, Odle J (1998) Food deprivation changes peroxisomal  $\beta$  oxidation activity but not catalase activity during postnatal development in pig tissues. *J Nutr* 128:1114–1121
  28. Hsu TH, Lardy HA (1969) Method of enzymatic analysis, Vol XIII, pp 230
  29. D'Alessandro ME, Chicco A, Lombardo YB (2006) A long-term sucrose-rich diet increases diacylglycerol content and membrane nPKC $\theta$  expression and alters glucose metabolism in skeletal muscle of rats. *Nutr Res* 26:289–296
  30. Rodbell M (1964) Metabolism of isolated fat cells. I. Effects of hormones on glucose metabolism on lipolysis. *J Biol Chem* 239:375–380
  31. Soria A, Chicco A, D'Alessandro ME, Rossi A, Lombardo YB (2002) Dietary fish oil reverse epididymal tissue adiposity, cell hypertrophy and insulin resistance in dyslipemic sucrose fed rat model. *J Nutr Biochem* 13:209–218
  32. Neschen S, Moore I, Regittnig W, Yu CL, Wang Y, Pypaert M, Petersen KF, Shulman GI (2002) Contrasting effects of fish oil and safflower oil on hepatic peroxisomal and tissue lipid content. *Am J Physiol* 282:E395–E401
  33. Ellis BA, Poynten A, Lowy AJ, Furler SM, Chisholm DJ, Kraegen EW, Cooney GJ (2000) Long chain acyl-CoA esters as indicators of lipid metabolism and insulin sensitivity in rat and human muscle. *Am J Physiol* 279:E554–E560
  34. Yu C, Chen Y, Cline GW, Zhang D, Zong H, Wang Y, Bergeron T, Kim JK, Cushman SW, Cooney GJ, Cooney BA, White MF, Kraegen EW, Shulman GI (2002) Mechanism by which fatty acid inhibits insulin activation of insulin receptor substrate-1 (IRS-1)-associated phosphatidylinositol-3-kinase activity in muscle. *J Biol Chem* 277:50230–50236
  35. Sleeman MW, Donegan NP, Heller-Harrison R, Lane WS, Czeck MP (1998) Association of acyl-CoA synthetase-1 with Glut4-containing vesicle. *J Biol Chem* 273:3132–3135
  36. Turvey EA, Heigenhauser JF, Parolin M, Peters SJ (2005) Elevated n-3 fatty acids in a high-fat diet attenuate the increase in PDH kinase activity but not PDH activity in human skeletal muscle. *J Appl Physiol* 98:350–355
  37. Aas V, Rokling-Andersen H, Kase ET, Thoresen GH, Rustan AC (2006) Eicosapentaenoic acid (20:5 n-3) increases fatty acid and glucose uptake in cultured human skeletal muscle cells. *J Lipid Res* 47:366–374
  38. Simoncikova P, Wein S, Gasperikova D, Ukropec J, Certik M, Klimes I, Sebkova E (2002) Comparison of the extrapancreatic action of gamma-linolenic acid and n-3 PUFAs in the high fat diet-induced insulin resistance. *Endocr Regul* 36:143–149
  39. Brun RP, Spiegelman BM (1997) Obesity and the adipocyte. *J Endocrinol* 155:217–218
  40. Yamauchi T, Kamon J, Waki H, Terauchi Y, Kubota N, Hara K, Mori Y, Ide T, Murakami K, Tsuboyama-Kasaoka N, Ezaki O, Akunuma Y, Gavrilova O, Vinson C, Reitman M, Kagechika H, Shudo K, Yoda M, Nakano Y, Tobe K, Nagai R, Kimura S, Tomita M, Froguel P, Kadowaki T (2001) The fat-derived hormone adiponectin reverses insulin resistance associated with both lipotrophy and obesity. *Nat Med* 7:887–888
  41. Skurnick-Minot G, Laromiguiere M, Oppert JM, Quignard-Boullange A, Boillot J, Rigoir A, Slama G, Rizkalla SW (2004) Whole-body fat mass and insulin sensitivity in type 2 diabetic women: effect of n-3 polyunsaturated fatty acids. In: 64th ADA Meeting, Orlando, June 4th–8th, Diabetes 53, Suppl 2, A44 (0159)
  42. Poitout V (2004)  $\beta$ -cell lipotoxicity: burning fat into heat? *Endocrinology* 145:3563–3565
  43. Zak A, Zeman E, Tvrzicka E, Pisarikova A, Sindelkova E, Vrana A (1993) Glucose tolerance, insulin secretion, plasma lipid fatty acids, and the hypolipidemic effects of fish oil. In: Klimes I, Howard BU, Storlien LH, Sebkova E (eds) Dietary lipids and insulin action, vol 683. New York Academy of Sciences, New York, pp 378–379

## Levels of Lipid Peroxidation in Human Plasma and Erythrocytes: Comparison between Fatty Acids and Cholesterol

Yasukazu Yoshida · Yoshiro Saito · Mieko Hayakawa ·  
Yoko Habuchi · Yasuharu Imai · Yoshiyuki Sawai ·  
Etsuo Niki

Received: 28 November 2006 / Accepted: 10 February 2007 / Published online: 15 March 2007  
© AOCS 2007

**Abstract** Lipid peroxidation has gained renewed attention with increasing evidence showing its biological role in producing toxic compounds and cellular signaling mediators. The assessment of lipid peroxidation levels in vivo is difficult partly because lipids are oxidized by different oxidants by different mechanisms to give versatile types of products, which may undergo metabolism and secondary reactions. In the present study, total hydroxyoctadecadienoic acids (tHODE) and  $7\alpha$ - and  $7\beta$ -hydroxycholesterol (t7-OHCh) from 44 healthy human subjects were assessed as biomarkers after reduction with sodium borohydride followed by saponification with potassium hydroxide comparing with the prevailing standard 8-isoprostaglandin  $F_{2\alpha}$  (t8-iso-PGF $_{2\alpha}$ ). The average concentrations of tHODE, total 8-isoprostaglandin  $F_{2\alpha}$  (t8-iso-PGF $_{2\alpha}$ ), t7 $\alpha$ -OHCh, and t7 $\beta$ -OHCh were 203, 0.727, 87.1, and 156 nmol/l plasma and 1,917, 12.8, 1,372, and 3,854 nmol/l packed erythrocytes, respectively. The ratios of tHODE and t7-OHCh to the parent substrates were 194 and 3,519  $\mu$ mol tHODE/mol linoleates and 40.9 and 686  $\mu$ mol t7-OHCh/mol cholesterol in plasma and erythrocytes, respectively. It was found that (1) t7-OHCh in blood was unexpectedly high, as high as or even higher than tHODE, (2) the amounts of tHODE was

more than 100 fold higher than t8-iso-PGF $_{2\alpha}$  (3) the level of lipid oxidation products in erythrocytes was higher than that in plasma, and (4) lipid peroxidation products level tended to increase while antioxidant level decrease with age. These products may be used as potential biomarker for assessment of lipid peroxidation and oxidative stress in vivo.

**Keywords** Antioxidant · Oxidative stress · Total hydroxyoctadecadienoic acid · Total 7-hydroxycholesterol · Coenzyme Q $_{10}$  · Total 8-iso-prostaglandin  $F_{2\alpha}$

### Abbreviations

BHT	2, 6-Di- <i>tert</i> -butyl-4-methylphenol
BOSS	Biomarkers of oxidative stress study
BSTFA	N,O-Bis(trimethylsilyl)trifluoroacetamide
CoQ10	Coenzyme Q $_{10}$ (ubiquinol-10 + ubiquinone-10);
HV	Hematocrit value
9-HODE-d $_4$	9S-Hydroxy-10E, 12Z-octadecadienoic-9,10,12,13-d $_4$ acid
HPODE	Hydroperoxyoctadecadienoic acid
t8-iso-PGF $_{2\alpha}$	Total 8-iso-prostaglandin $F_{2\alpha}$
8-iso-PGF $_{2\alpha}$ -d $_4$	8-Iso-prostaglandin $F_{2\alpha}$ -d $_4$ ;
7-KCh	7-Ketocholesterol
LDL	Low density lipoprotein
PBS	Phosphate-buffered saline
SeP	Selenoprotein P
tCh	Total cholesterol
7-OOHCh	7-Hydroperoxycholesterol
t7-OHCh	Total 7-hydroxycholesterol
t18:2	Total linoleate
tHODE	Total hydroxyoctadecadienoic acid
Q $_{10}$ H $_2$	Ubiquinol-10

Y. Yoshida (✉) · Y. Saito · M. Hayakawa ·  
Y. Habuchi · E. Niki  
Human Stress Signal Research Center,  
National Institute of Advanced Industrial Science  
and Technology (AIST), 1-8-31 Midorigaoka, Ikeda,  
Osaka 563-8577, Japan  
e-mail: yoshida-ya@aist.go.jp

Y. Imai · Y. Sawai  
Department of Internal Medicine, Ikeda Municipal Hospital,  
3-1-18 Johnan, Ikeda, Osaka 563-8510, Japan

Q <sub>10</sub>	Ubiquinone-10
αT	α-Tocopherol
ZE/EE	Stereoisomer ratio of HODE (9- and 13-(Z,E)-HODE/9- and 13-(E,E)-HODE)

## Introduction

Lipid peroxidation has been implicated in oxidative stress and accepted to be involved in various diseases [1]. It induces disruption of membrane organization, causing changes in fluidity and permeability, inhibition of metabolic processes, and alterations of ion transport. It oxidatively modifies low density lipoprotein (LDL) to become pro-atherogenic. It gives potentially toxic compounds. It has been also shown that lipid peroxidation products act as signaling mediators and induce adaptive response [2, 3]. It was found recently that various lipid peroxidation products induce phase II antioxidant proteins and enzymes by Nrf2-dependent pathway to enhance the defense capacity against subsequent oxidative stress [4–6]. Thus, lipid peroxidation in vivo has received renewed attention.

Lipid peroxidation gives vast numbers of products and the measurement of lipid peroxidation levels in vivo is not easy. Various products have been measured by diverse methods and techniques for that purpose. The oxidation of both fatty acids and cholesterol proceeds by enzymatic and non-enzymatic mechanisms [1]. Lipoxygenases and cyclooxygenases oxidize polyunsaturated fatty acids, while cytochrome P450s oxidize cholesterol specifically. The non-enzymatic oxidation by singlet oxygen and ozone proceeds stoichiometrically, while that by free radicals proceeds by chain mechanism. Importantly, the effectiveness of antioxidants depends on the type of oxidation. Isoprostanes are isomeric to prostaglandins but are formed via the free radical-mediated oxidation of arachidonic acid. Since their first discovery in 1990 [7], isoprostanes have emerged as an excellent biomarker of oxidative damage in vivo [8]. We have been interested in measuring the products from linoleates and cholesterol to measure the lipid peroxidation level in vivo [9]. The biological samples are first reduced and then saponified to convert hydroperoxides and ketones as well as hydroxides of both free and ester forms of linoleic acid and cholesterol to hydroxyoctadecadienoic acid (HODE) and hydroxycholesterol (OHCh), respectively. HODE and OHCh thus measured account for much of oxidized linoleates and cholesterol, respectively.

The mechanisms and products of linoleate oxidation have been studied extensively and are now well understood [10]. The oxidation of free linoleic acid and esters proceeds by the same mechanism to give the same products, although the rate may depend on the substrates and reaction

milieu. The oxidation by 12/15-lipoxygenase proceeds by regio-, stereo-, and enantio-specific mechanisms to give 13S-hydroperoxy-9Z, 11E-octadecadienoic acid (13(S)-(Z, E)-HPODE), while singlet oxygen-mediated oxidation gives 9-, 10-, 12-, and 13-(Z, E)-HPODE. On the other hand, the oxidation induced by free radicals yields both 9- and 13-(Z, E) and (E, E)-HPODE as primary products. They are racemic. HPODEs are readily reduced in vivo by reducing enzymes to give HODE. Thus, 9- and 13-(E, E)-HODE are specific products for free radical-mediated oxidation, while 10- and 12-HODE are specific markers for singlet oxygen oxidation. Cholesterol is oxidized by specific cytochrome P450: CYP7A1 oxidizes cholesterol to give 7α-hydroxycholesterol (7α-OHCh) [11]. Singlet oxygen oxidizes cholesterol to yield 5α-OOHCh, which undergoes isomerization to 7α-OOHCh [12]. On the other hand, free radical-mediated oxidation of free and esterified cholesterol gives several products including 7α- and 7β-hydroperoxycholesterol (7α- and 7β-OOHCh), 7α- and 7β-OHCh and 7-ketocholesterol (7-KCh). These products are converted to free 7α- and 7β-OHCh by the analytical procedures employed in this study.

In the present study, 9- and 13-(Z, E) and (E, E)-HODE and 7α- and 7β-OHCh as well as isoprostanes in plasma and erythrocytes of healthy human subjects were measured and compared. The total amounts of linoleates and cholesterol and low molecular weight antioxidants were also measured to compare the level of oxidation in plasma and erythrocytes and also antioxidant. It was found that the lipids in erythrocytes were oxidized relatively more than those in plasma and that cholesterol oxidation products were found as much as those from linoleates.

## Materials and Methods

### Materials

8-Iso-prostaglandin F<sub>2α</sub> (8-iso-PGF<sub>2α</sub>), 8-iso-prostaglandin F<sub>2α</sub>-d<sub>4</sub> (8-iso-PGF<sub>2α</sub>-d<sub>4</sub>), 13-hydroxy-9(Z), 11(E)-octadecadienoic acid (13-(Z,E)-HODE), 13-hydroxy-9(E), 11(E)-octadecadienoic acid (13-(E,E)-HODE), 9-hydroxy-10(E), 12(Z)-octadecadienoic acid (9-(E,Z)-HODE), 9-hydroxy-10(E), 12(E)-octadecadienoic acid (9-(E,E)-HODE), and 9S-hydroxy-10E, 12Z-octadecadienoic-9,10,12,13-d<sub>4</sub> acid (9-HODE-d<sub>4</sub>) were obtained from Cayman Chemical Company (MI, USA). Other materials were of the highest grade available commercially.

### Subjects

Forty-four healthy volunteers [male = 20, female = 24, age varying from 25 to 82 years (mean ± SD = 57.2 ± 15.2),

body mass index (BMI);  $22.4 \pm 2.8$ ] were enrolled in this study. None of the subjects had a history of any diseases or antioxidant supplements. BMI was not dependent on age in this study ( $r = -0.079$ ,  $P > 0.05$ ). This study was conducted in accordance with the principles of the Declaration of Helsinki and was approved by the local ethics committees of the National Institute of Advanced Industrial Science and Technology and Ikeda Municipal Hospital. All volunteers gave written informed consent after a complete explanation of the purpose of this study.

### Specimen Processing

Blood samples were collected in ethylenediaminetetraacetic acid (EDTA)-containing tubes after overnight fasting. The samples were placed on ice immediately after the collection. Plasma was obtained by centrifugation at  $1,580\times g$  for 10 min at  $4^\circ\text{C}$  and subjected to the analysis immediately. The erythrocytes were washed twice with a fourfold volume of saline and adjusted to hematocrit value (HV) around 40% with saline. Accurate HV was later determined by a hematocrit capillary (Cosmo-bio Ltd. Tokyo, Japan). The erythrocyte sample (HV ca 40%) was extracted with fourfold volume of methanol containing  $100\ \mu\text{mol/l}$  2, 6-di-*tert*-butyl-4-methylphenol (BHT) by vortexing and centrifugation ( $20,400\times g$  at  $4^\circ\text{C}$  for 10 min) and subjected to the analysis immediately.

### Analyses of Total HODE, 8-iso-PGF<sub>2x</sub>, and 7-OHCh

Total HODE (tHODE) and 8-iso-PGF<sub>2x</sub> were measured using a previously reported method, which was slightly modified [9]. Internal standards—8-iso-PGF<sub>2x</sub>-d<sub>4</sub> (50 ng for plasma and 100 ng for erythrocytes), 9-HODE-d<sub>4</sub> (50 ng for plasma and 100 ng for erythrocytes)—and 1 ml of methanol containing  $100\ \mu\text{mol/l}$  BHT were added to the 2 ml plasma and 1 ml extracts from the erythrocytes sample, followed by reduction of hydroperoxides and ketones with large amounts of sodium borohydride (4 mg) at room temperature for 5 min. Next, the reduced sample was mixed with potassium hydroxide in methanol (1 mol/l, 1 ml) under nitrogen and incubated for 30 min in darkness at  $40^\circ\text{C}$  on a shaker. The sample was centrifuged ( $3,000\times g$  at  $4^\circ\text{C}$  for 10 min); the supernatant was diluted with a fourfold volume of water (pH 3) and adjusted to pH 3 with HCl (2 mol/l). The acidified sample was centrifuged ( $3,000\times g$  at  $4^\circ\text{C}$  for 10 min) and the supernatant was subjected to solid phase extraction [9]. The eluent obtained was evaporated under nitrogen and  $30\ \mu\text{l}$  of the silylating agent N,O-bis(trimethylsilyl)-trifluoroacetamide (BSTFA) was added to the dried residue. The solution was

vigorously mixed by vortexing for 1 min and incubated for 1 h at  $60^\circ\text{C}$  to obtain trimethylsilyl esters and ethers. An aliquot of this sample was injected into the gas chromatograph (GC 6890 N, Agilent Technologies, Palo Alto, CA, USA) equipped with a quadrupole mass spectrometer (5973 Network, Agilent Technologies). A fused-silica capillary column (HP-5MS, 5% phenyl methyl siloxane,  $30\ \text{m} \times 0.25\ \text{mm}$ , Agilent Technologies) was used. Helium, at a flow rate of 1.2 ml/min, was used as the carrier gas. Temperature programming was performed from 60 to  $280^\circ\text{C}$  at  $10^\circ\text{C}/\text{min}$ . The injector temperature was set at  $250^\circ\text{C}$ ; the temperatures of transfer line to mass detector and ion source were 250 and  $230^\circ\text{C}$ , respectively. Electron energy was set at 70 eV. 8-Iso-PGF<sub>2x</sub> and HODE were identified based on their retention times and mass patterns ( $m/z = 571$  and 481 for 8-iso-PGF<sub>2x</sub>, and 440, 369, and 225 for HODE). The amounts of 8-iso-PGF<sub>2x</sub> and HODE were determined by using the fragment ions of 481 and 440, respectively. 8-Iso-PGF<sub>2x</sub>-d<sub>4</sub> ( $m/z = 485$ ) and 9-HODE-d<sub>4</sub> ( $m/z = 444$ ) were used as internal standards for quantifications of 8-iso-PGF<sub>2x</sub> and HODE, respectively.

Total 7-OHCh in plasma and erythrocyte was also measured as follows. The internal standards, 16-hydroxyhexadecanoic acid (70 ng), 7 $\alpha$ -OHCh-d<sub>7</sub> (180 ng), and 7 $\alpha$ -OHCh-d<sub>7</sub> (180 ng), and 500  $\mu\text{l}$  methanol containing  $100\ \mu\text{mol/l}$  BHT were added to plasma (500  $\mu\text{l}$ ) and the extracts from erythrocytes (500  $\mu\text{l}$ ). We have confirmed that the quantified values by using these internal standards did not differ among themselves and the more convenient 16-hydroxyhexadecanoic acid was used in further study. Reduction of 7-OOHCh and 7-KCh was carried out by the addition of large amounts of sodium borohydride (4 mg) to the solution followed by saponification under nitrogen. The reduced sample was suspended in potassium hydroxide in methanol (1 mol/l, 1 ml) and pure ether (2 ml) and mixed for 30 min in darkness at  $40^\circ\text{C}$  in a shaker. The mixture was acidified with 20% acetic acid in water (2 ml) and extracted with hexane (3 ml). The sample was evaporated to dryness under nitrogen and derivatized with BSTFA for 1 h at  $60^\circ\text{C}$ . An aliquot of this solution was injected into the same gas chromatograph equipped with a quadrupole mass spectrometer as mentioned above. The identification of 7-OHCh was conducted by retention time and mass pattern ( $m/z = 546$ , 456) and ions at 456 were selected for the quantification. 7 $\alpha$ -OHCh and 7 $\beta$ -OHCh were identified with retention times of 28.5 and 30.9 min, respectively. Ch ( $m/z = 458$ ) and linoleic acid ( $m/z = 337$ ) were simultaneously measured by this method.

Artificial oxidation of lipids during sample work-up was kept minimal by adding antioxidant and carrying out analytical procedures under nitrogen as much as possible. It was confirmed that the experimental errors were within  $\pm 10\%$  [9].

## HPLC Analysis

Plasma antioxidants were extracted by chloroform/methanol (2/1, by volume).  $\alpha$ - and  $\gamma$ -Tocopherol (T) were measured using an HPLC by an amperometric electrochemical detector (NANOSPACE SI-1, Shiseido Co. Ltd., Tokyo, Japan) set at 800 mV, with an octadecyl-bonded silica (ODS) column (LC-18, 5  $\mu$ m, 250  $\times$  4.6 mm, Sigma-Aldrich Japan, Tokyo, Japan) and methanol/*tert*-butyl alcohol (95/5 by volume) containing 50 mmol/l sodium perchlorate as an eluent at a rate of 1 ml/min. Plasma concentration of ascorbic acid was measured by an HPLC with UV detector (SPD-10AV, Shimadzu Corp., Kyoto, Japan, 263 nm). An NH<sub>2</sub> column (Wakosil 5NH<sub>2</sub>, 5  $\mu$ m, 250  $\times$  4.6 mm, Wako Pure Chemical Ind. Ltd., Tokyo, Japan) was used and 40 mmol/l phosphate-buffered saline (PBS)/methanol (1/9, by volume) was delivered as the eluent at a rate of 1 ml/min. Plasma was diluted with methanol (1/4, by volume) and mixed vigorously by a vortex mixer for 1 min, followed by centrifugation (20,400 $\times$ g at 4 °C for 10 min) and immediately an aliquot of the upper layer was injected into the HPLC column. Ubiquinols and ubiquinones in plasma were also measured by using HPLC with the same amperometric electrochemical detector (NANOSPACE SI-1), set at 700 mV. The samples were passed through a reverse phase column (LC-8, 5  $\mu$ m, 250  $\times$  4.6 mm, Sigma-Aldrich Japan, Tokyo, Japan), followed by a reducing column (RC-10, 30  $\times$  4 mm, Shiseido Co. Ltd., Tokyo, Japan). Methanol/*tert*-butyl alcohol (85/15, by volume) containing 50 mM sodium perchlorate was used as an eluent at a rate of 1 ml/min. Plasma was diluted with methanol and hexane (1/5/10, by volume) and mixed vigorously by a vortex mixer for 1 min followed by centrifugation (20,400 $\times$ g at 4 °C for 10 min) and immediately an aliquot of the upper layer was injected into the HPLC column.

## Measurements of Selenoprotein P (SeP)

Plasma SeP concentrations were determined with a sandwich ELISA using rat anti-human SeP monoclonal antibody BD1 and AH5 as described previously [13]. The optical density of the plates was measured at 450 nm using a Multiskan Ascent plate reader (Thermo Labsystems, Helsinki, Finland). All measurements were made in duplicate, and the average value was adopted.

## Statistics

Statistical analyses were performed on a Microsoft personal computer. Correlations were analyzed using the Pearson test, a *P* value of less than 0.05 was considered significant. Data are presented as the mean  $\pm$  SD.

## Results

### Lipid Peroxidation Level in Human Plasma and Erythrocytes

The levels of total HODE, 7-OHCh and 8-iso-PGF<sub>2 $\alpha$</sub>  were measured by the methods described above for plasma and erythrocytes from 44 healthy human subjects. The total HODE in plasma and erythrocytes ranged from 86.2 to 350 nmol/l plasma and 797 to 5,630 nmol/l packed cells, while total 7-OHCh ranged from 72.3 to 542 nmol/l plasma and from 1,860 to 11,100 nmol/l packed cells, respectively. The average concentrations of tHODE, t8-iso-PGF<sub>2 $\alpha$</sub> , and t7-OHCh were obtained as 203, 0.727, and 243 nmol/l in plasma, while those in erythrocytes were 1,917, 12.8, and 5,226 nmol/l packed cells for tHODE, t8-iso-PGF<sub>2 $\alpha$</sub> , and t7-OHCh, respectively (Table 1). Relatively more oxidation products were found in erythrocytes than in plasma, the ratio being 9.4, 18, and 22 fold for tHODE, t8-iso-PGF<sub>2 $\alpha$</sub> , and t7-OHCh, respectively. The stereo-isomer ratio of HODE, (*Z,E/E,E*), was lower than 1 in plasma, but higher than 1 in erythrocytes. More 7 $\beta$ -OHCh was found than 7 $\alpha$ -OHCh in both plasma and erythrocytes.

In order to compare the extent of oxidation more quantitatively, the ratio of oxidation products to the parent substrates was measured. The total linoleate (t18:2) and cholesterol (tCh) in plasma and erythrocytes were determined after saponification to measure both free and ester forms. Unfortunately, total arachidonate could not be measured. The results are summarized in Table 2. A statistically significant correlation was observed between tHODE/t18:2 and t7-OHCh/tCh for both plasma and erythrocytes (Fig. 1). The average molar ratio of products to parent substrates tHODE/t18:2 and t7-OHCh/tCh were obtained as  $1.94 \times 10^{-4}$  and  $4.09 \times 10^{-5}$  for plasma and  $3.52 \times 10^{-3}$  and  $6.86 \times 10^{-4}$  for erythrocytes, respectively. These results show that the relative oxidation ratio of plasma to erythrocytes is 1/18.1 for linoleates and 1/16.8 for cholesterol, showing that relative oxidation level in erythrocytes was much higher than that in plasma. Furthermore, the relative extent of oxidation of linoleates to cholesterol is 4.74 and 5.13 in plasma and erythrocytes, respectively. This may not necessarily suggest that linoleates are about five times more oxidizable than cholesterol *in vivo*, since the observed concentrations of products depend on the rates of metabolism and excretion as well as formation (see Discussion).

### The Antioxidant Level

The concentrations of representative antioxidants measured in plasma and erythrocytes are also included in Table 1. The concentrations of  $\alpha$ - and  $\gamma$ -tocopherol, ascorbic acid,

**Table 1** Concentrations of lipid peroxidation products and antioxidants in plasma and erythrocytes and their correlations with age of healthy human

	Number studied (range of age)	Concentrations (Mean $\pm$ SD)	Correlation with age, <i>r</i> and significance
<i>Lipid peroxidation products</i>			
Plasma (nmol/l except ratio)			
tHODE	*	203 $\pm$ 76	0.247 (NS)
9-and 13-( <i>ZE</i> )-HODE	*	74.5 $\pm$ 27	-0.068 (NS)
9-and 13-( <i>EE</i> )-HODE	*	128 $\pm$ 55	0.375 ( $P < 0.05$ )
HODE ratio ( <i>ZE/EE</i> )	*	0.635 $\pm$ 0.207	-0.686 ( $P < 0.001$ )
t8-iso-PGF <sub>2<math>\alpha</math></sub>	*	0.727 $\pm$ 0.604	0.152 (NS)
t7-OHCh	26 (51–82)	243 $\pm$ 130	0.383 (NS)
7 $\alpha$ -OHCh	26 (51–82)	87.1 $\pm$ 50	0.328 (NS)
7 $\beta$ -OHCh	26 (51–82)	156 $\pm$ 102	0.325 (NS)
Erythrocytes (nmol/l packed cell except ratio)			
tHODE	*	1917 $\pm$ 1004	0.004 (NS)
9-and 13-( <i>ZE</i> )-HODE	*	1221 $\pm$ 656	0.047 (NS)
9-and 13-( <i>EE</i> )-HODE	*	696 $\pm$ 388	-0.068 (NS)
HODE ratio ( <i>ZE/EE</i> )	*	1.84 $\pm$ 0.45	0.164 (NS)
t8-iso-PGF <sub>2<math>\alpha</math></sub>	*	12.8 $\pm$ 7.9	0.212 (NS)
t7-OHCh	23 (25–76)	5226 $\pm$ 2008	0.190 (NS)
7 $\alpha$ -OHCh	23 (25–76)	1372 $\pm$ 461	0.196 (NS)
7 $\beta$ -OHCh	23 (25–76)	3854 $\pm$ 1844	0.063 (NS)
<i>Antioxidants</i>			
Plasma ( $\mu$ mol/l, otherwise stated)			
$\alpha$ -tocopherol	*	23.9 $\pm$ 8.7	-0.262 (NS)
$\gamma$ -tocopherol	*	1.99 $\pm$ 1.02	0.155 (NS)
ascorbic acid	*	40.5 $\pm$ 17.8	-0.068 (NS)
Ubiquinol-10 (A)	*	1.05 $\pm$ 0.71	-0.515 ( $P < 0.01$ )
Ubiquinone-10 (B)	*	0.24 $\pm$ 0.17	-0.463 ( $P < 0.01$ )
Reduced/total (A)/(A) + (B)	*	79.2 $\pm$ 10.8%	-0.097 (NS)
Selenoprotein P	30 (41–82)	6.87 $\pm$ 1.92 $\mu$ g/ml	-0.158 (NS)
Erythrocytes ( $\mu$ mol/l packed cell)			
$\alpha$ -tocopherol	40 (25–82)	2.49 $\pm$ 1.13	-0.431 ( $P < 0.01$ )
$\gamma$ -tocopherol	40 (25–82)	0.37 $\pm$ 0.19	-0.285 (NS)

NS not significant

\**n* = 44, ranging from 25 to 82 years**Table 2** Concentrations of total linoleic acid (18:2) and cholesterol (Ch) and their oxidation products, tHODE and t7-OHCh, in plasma and erythrocytes

	Total linoleate (t18:2) (mmol/l)	tHODE/t18:2 ( $\mu$ mol/mol)	Total cholesterol (tCh) (mmol/l)	t7-OHCh/tCh ( $\mu$ mol/mol)	Relative oxidizability of 18:2 against Ch
Plasma	1.28 $\pm$ 0.54	194 $\pm$ 123 (A)	6.87 $\pm$ 2.82	40.9 $\pm$ 23.5 (B)	A/B 4.74
Erythrocytes	0.66 $\pm$ 0.61	3519 $\pm$ 1980 (C)	11.0 $\pm$ 11.5	686 $\pm$ 433 (D)	C/D 5.13
Relative ratio of plasma to erythrocytes		A/C 1/18.1		B/D 1/16.8	

ubiquinol-10 (Q<sub>10</sub>H<sub>2</sub>) and ubiquinone-10 (Q<sub>10</sub>) are in agreement with the values in the literatures reported previously. The ratio of Q<sub>10</sub>H<sub>2</sub> to Q<sub>10</sub> is also in reasonable

agreement with the literature values. It has been accepted that the stereo-isomer ratio, (*Z,E/E,E*)-HODE, is a good measure of antioxidant capacity [14]. It was found that this

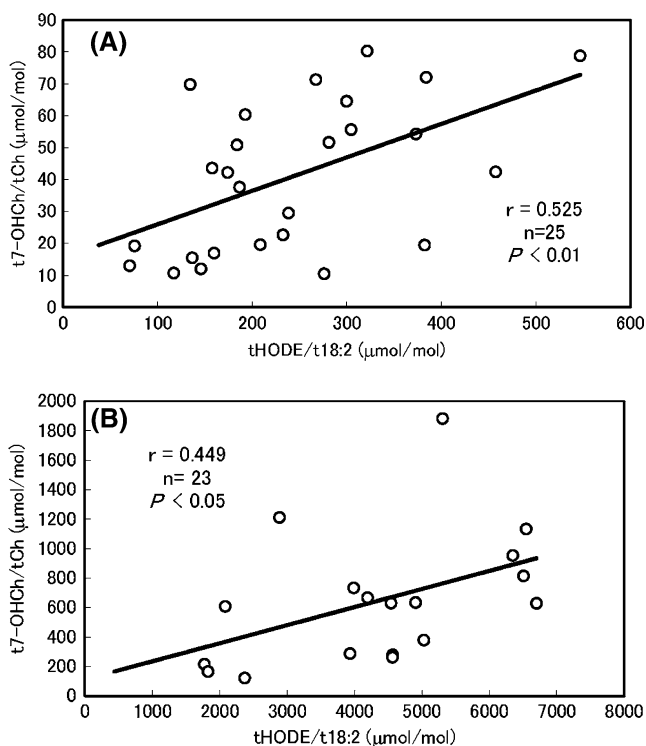


**Fig. 1** The plots of molar ratios of tHODE/total linoleate (t18:2) and t7-OHCh/total cholesterol (tCh) in plasma (a) and erythrocytes (b). The number studied, correlation coefficient,  $r$ , and  $P$ -values are shown in the figure

ratio correlated significantly with  $Q_{10}H_2$  (Fig. 2a) and total coenzyme Q (Fig. 2b), but not with tocopherols (data not shown).

#### Effect of Age on Oxidation Products and Antioxidant

The age of the human subjects tested in this study ranged from 25 to 82 years old. The effects of age on the lipid peroxidation products and antioxidants in plasma and erythrocytes are included in Table 1 and shown in Fig. 3. As a whole, the lipid peroxidation products tended to increase with age, while antioxidants decreased, although the statistical significance was observed only for 9- and 13- ( $E,E$ )-HODE (Fig. 3a), stereo-isomer ratio ( $Z/E/E,E$ )-HODE (Fig. 3b),  $Q_{10}H_2$  (Fig. 3c) and  $Q_{10}$  (Fig. 3d) in plasma and for  $\alpha$ -tocopherol ( $\alpha T$ ) (Fig. 3e) in erythrocytes. Furthermore, a statistical significance was observed for the correlation of tHODE/t18:2 ( $r = 0.483$ ,  $n = 39$ ,  $P < 0.01$ ) and t7-OHCh/tCh ( $r = 0.483$ ,  $n = 25$ ,  $P < 0.05$ ) in plasma with age (data not shown).

#### Discussion

Lipid peroxidation has gained renewed attention since its products can exert versatile beneficial functions and

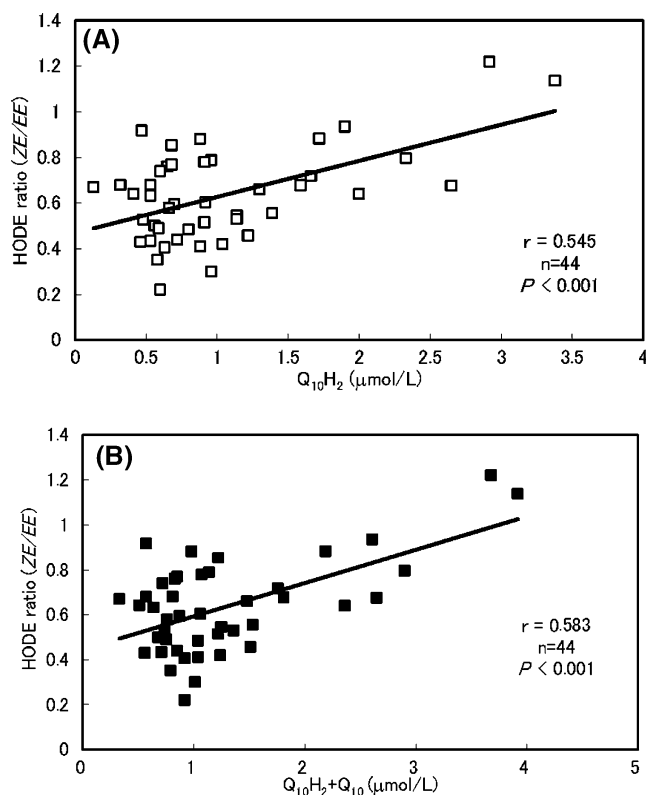


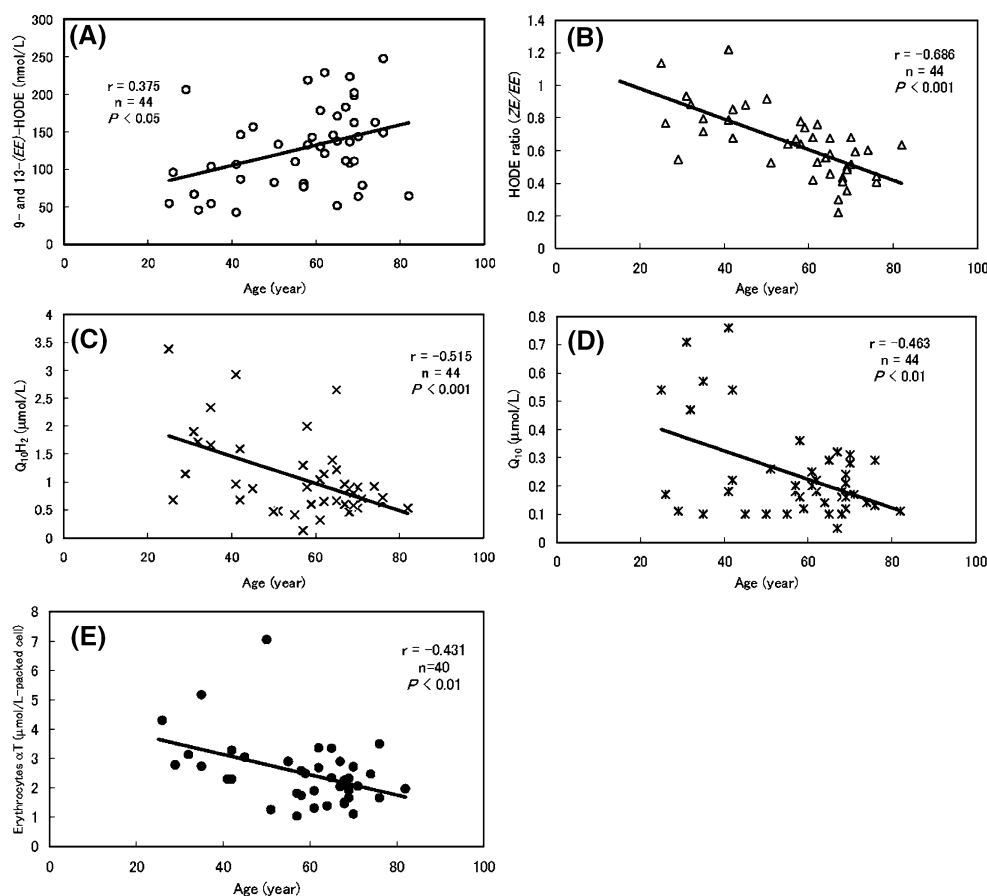
**Fig. 2** The plots of stereo-isomeric ratio of HODE ( $ZE/EE$ ) against ubiquinol-10 ( $Q_{10}H_2$ ) (a) and total CoQ10 ( $Q_{10}H_2 + Q_{10}$ ) (b) in plasma from healthy humans ( $n = 44$ ). Correlation coefficient,  $r$ , and  $P$ -values are shown in the figure

deleterious effects [2, 3]. Various biomarkers have been proposed and applied for assessment of lipid peroxidation in vivo. Isoprostanes, non-enzymatic oxidation products from arachidonic acid and its esters, are accepted to be the most reliable available marker of lipid peroxidation in vivo [8]. They are present in vivo in the free and esterified forms. In the present study, the plasma and erythrocytes were first reduced with sodium borohydride and then saponified with KOH to convert hydroperoxides and ketones as well as hydroxides of both free and esterified linoleic acid and cholesterol to tHODE and t7-OHCh, respectively. t8-Iso-PGF<sub>2 $\alpha$</sub>  was also measured similarly. The results thus obtained reveal several interesting facts.

Firstly, the amount of t7-OHCh was unexpectedly high. The absolute amounts decreased in the order of t7-OHCh  $\geq$  tHODE  $\gg$  t8-iso-PGF<sub>2 $\alpha$</sub>  in both plasma and erythrocytes. The ratios (tHODE/t18:2)/(t7-OHCh/tCh) = 4.74 and 5.13 in plasma and erythrocytes, respectively (Table 2) show that linoleates are oxidized about five times more than cholesterol in blood. It had been previously observed in the free radical-mediated oxidation of isolated LDL that the relative oxidizability decreased with decreasing number of double bond, that is, 22:6 > 20:4 > 18:2 > 18:1 > 16:0, and that cholesterol was oxi-



**Fig. 3** Age-related plots of 9- and 13-(*EE*)-HODE concentration (a), stereo-isomer ratio of HODE (*ZE/EE*) (b), concentrations of  $Q_{10}H_2$  (c) and ubiquinone-10 ( $Q_{10}$ ) (d) in plasma, and concentration of  $\alpha$ -tocopherol ( $\alpha T$ ) in erythrocytes from healthy humans [ $n = 44$ , except for  $\alpha T$  ( $n = 40$ )]. Correlation coefficient,  $r$ , and  $P$ -values are shown in the figure



dized only after most of unsaturated fatty acids were depleted [15]. However, we found in this study that the concentrations of  $t7$ -OHCh were higher than those of  $t$ HODE in both plasma and erythrocytes. Cholesterol is oxidized by three mechanisms: namely an enzymatic mechanism, a non-enzymatic, stoichiometric mechanism, and a free radical-mediated chain mechanism [12]. The typical oxidants for these three mechanisms are cytochrome P450, singlet oxygen, and peroxy radicals, respectively. The major products from the free radical oxidation of cholesterol are  $7\alpha$ - and  $7\beta$ -OOHCh,  $7\alpha$ - and  $7\beta$ -OHCh,  $7$ -KCh,  $5\alpha,6\alpha$ -EpoxyCh,  $5\beta,6\beta$ -EpoxyCh, and  $5,6$ -di-OHCh [12, 16–18]. The levels of oxysterols in human plasma or serum have been compiled by Brown and Jessup [17]. In the present study,  $7\alpha$ - and  $7\beta$ -OOHCh and  $7$ -KCh as well as  $7\alpha$ - and  $7\beta$ -OHCh were measured as  $t7$ -OHCh, but  $5,6$ -EpoxyCh and  $5,6$ -diOHCh were not assessed.  $24$ -,  $25$ -, and  $27$ -OHCh which are formed by cytochrome P450 were not assessed either in this study. Singlet oxygen oxidizes cholesterol to yield  $5\alpha$ -OOHCh, which may undergo isomerization to give  $7\alpha$ -OOHCh. However, the oxidation by singlet oxygen may not be important in vivo, except for skin. CYP7A1, cholesterol  $7\alpha$ -hydroxylase, is a microsomal liver-specific enzyme that

converts cholesterol to  $7\alpha$ -OHCh [11]. It has been reported that  $7\alpha$ -OHCh formed in the liver by CYP7A1 is leaked into the circulation and  $7\alpha$ -OHCh in serum was proposed to be a potential marker for the activity of this enzyme [19]. CYP7A1 only oxidizes the free form of cholesterol, not cholesterol esters in the lipoproteins. Thus, total  $7$ -OHCh measured in this study must contain  $7\alpha$ -OHCh formed by CYP7A1. It has been reported also that  $7$ -KCh is reduced stereo-specifically to  $7\beta$ -OHCh by  $11$ -betahydroxysteroid dehydrogenase type 1 [20–22]. These data suggest that  $t7\beta$ -OHCh may be a better marker for non-regulated oxidation of cholesterol in vivo. However, the correlation between  $t7$ -OHCh and  $t7\beta$ -OHCh was quite strong both for plasma (Fig. 4a) and erythrocytes (Fig. 4b).

The observed level of lipid peroxidation products is determined by a balance between the rates of formation, secondary reactions, metabolism, and excretion. Lipid hydroperoxides are reduced to the corresponding hydroxides by glutathione peroxidases and SeP. The oxidized phospholipids are metabolized by phospholipases. It has been shown that the rate of reduction of hydroperoxides by glutathione peroxidase decreases in the order of free fatty acid hydroperoxides > phospholipid hydroperoxides > cholesteryl ester hydroperoxides > cholesteryl

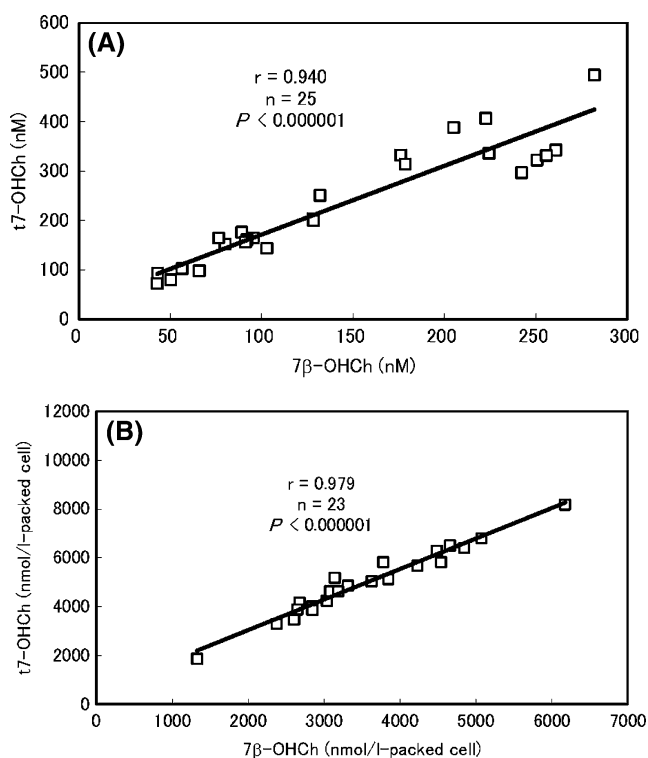


**Fig. 4** The correlations of  $7\beta$ -OHCh with  $t7$ -OHCh in plasma (a) and erythrocytes (b). The number studied, correlation coefficient,  $r$ , and  $P$ -values are shown in the figure

hydroperoxide [23]. The metabolism of oxidized cholesterol may be slower than oxidized fatty acids, which may account, at least in part, for the observed relatively high concentrations of oxidized cholesterol compared with oxidized fatty acids in plasma and erythrocytes.

Secondly, the concentrations of tHODE were more than 100 times higher than those of  $t8$ -iso-PGF<sub>2α</sub>. This is reasonable since the content of  $t18:2$  is much higher than that of  $t20:4$  in blood and linoleates are oxidized by a straightforward mechanism to give products which are counted as HODE, whereas the oxidation of arachidonates proceeds by a complicated routes and 8-iso-PGF<sub>2α</sub> is only one of the many minor products.

Like cholesterol, linoleates are oxidized by three mechanisms. Several subclasses of human lipoxygenases are known [24] and 15-LOX oxidizes linoleates to give 13(S)-(Z,E)-HPODE selectively. Singlet oxygen oxidizes linoleates to give 9-, 10-, 12-, and 13-(Z,E)-HPODE. The free radical-mediated oxidation of linoleates gives both 9- and 13-, (Z,E) and (E,E)-HPODE as the primary products, these four HPODEs being racemic. Thus, tHODE measured in this study may originate from these different mechanisms. The relative contribution of these mechanisms is difficult to evaluate from tHODE. It was reported previously that the ratio of enantio isomers 13(S)-HODE/

13(R)-HODE in human plasma was below 0.60 [25], implying that the 15-LOX-induced oxidation is at best 20%. However, it may be also added that the enantio specificity in the oxidation of plasma by mammalian 15-LOX was considerably lower than that in simple aqueous solution [24, 26]. In general, the free radical oxidation of linoleates gives same amounts of 9- and 13-HODE. But it was reported recently that the oxidation of linoleic acid bound to human serum albumin induced by free radicals was regio-selective with a larger accumulation of 13-HPODE with more *E, E*-stereoisomers [27]. It may be said that  $t9$ - and 13-(*E, E*)-HODE are a better marker for free radical-mediated oxidation of linoleates. It was found, however, that the correlation between (*E, E*)-HODE and tHODE was remarkably well (Figs. 5a, b).

Thirdly, this study showed that erythrocytes contained more oxidation products than plasma, the ratio of (tHODE/ $t18:2$ ) and ( $t7$ -OHCh/ $tCh$ ) in erythrocytes to that in plasma being 18.1 and 16.8, respectively (Table 2). This result was rather surprising, since it was observed before that plasma lipids were oxidized by free radicals faster than erythrocyte lipids in the oxidation of whole blood [28]. The reason is not clear at present, but this may be ascribed to a lower rate of metabolism for oxidized lipids in erythrocytes than those in plasma.

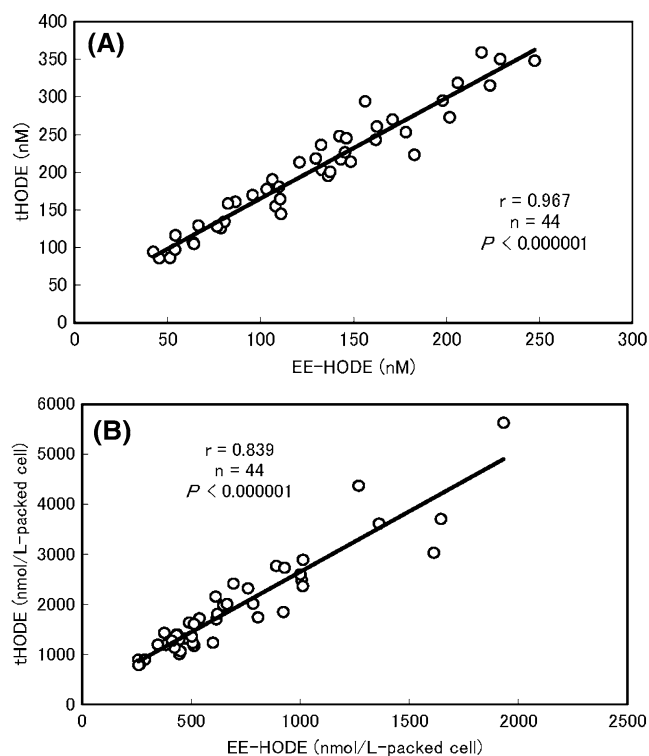


**Fig. 5** The correlations of 9- and 13-(*EE*)-HODE with tHODE in plasma (a) and erythrocytes (b). The number studied, correlation coefficient,  $r$ , and  $P$ -values are shown in the figure

## Lipid Peroxidation Products as Biomarker

An appropriate biomarker has been looked for to assess the extent of oxidative stress under normal physiological conditions and also to evaluate the antioxidant efficacy *in vivo*. Apparently, the oxidative stress is brought about by different oxidants and mechanisms, and it is quite difficult to develop a single biomarker which is valid for various oxidative stress. Among others, isoprostanes have been widely accepted as the most reliable marker of lipid peroxidation *in vivo* and applied for the assessment of oxidative injury (8 and references cited therein). Increased levels of isoprostanes, especially 8-iso-PGF<sub>2α</sub>, have been detected in tissues and fluids from human patients with various diseases [8]. The extensive multi laboratory work termed the Biomarkers of Oxidative Stress Study (BOSS) coordinated by National Institute of Health (NIH) of the USA shows promising results [29, 30]. We have proposed tHODE and t7-OHCh as potential biomarkers for oxidative stress and shown that they are useful for assessment of oxidative stress in several animal experiments induced by carbon tetrachloride [31], choline-deficient diet [32], light-exposure [33], and free radicals [34]. They have been also applied for the assessment of antioxidant efficacy *in vivo* [35]. Furthermore, we have recently reported that tHODE and t7-OHCh increased with increasing oxidation of LDL in healthy humans [36]. It may be said that tHODE and t7-OHCh could be good biomarkers for the early detection of adult diseases as well as the evaluation of disease progression which involves oxidative stress. It is recommended that BOSS should be expanded to include both tHODE and t7-OHCh as biomarkers. It may be also added that relative amounts of tHODE, t8-iso-PGF<sub>2α</sub>, and t7-OHCh depend on tissues. For example, the ratio of tHODE/ t8-iso-PGF<sub>2α</sub> is much smaller in the brain than in plasma (Yoshida et al., unpublished results).

One of the concerns about tHODE and t7-OHCh as biomarkers is that they are formed by different oxidants and by different mechanisms, some of which may not be relevant to oxidative stress. As described above, 13-HODE may be derived from both enzymatic and non-enzymatic oxidation. 10- and 12-HODE may be specific to singlet oxygen-mediated oxidation, while 9- and 13-(*E,E*)-HODE to free radical-mediated oxidation. The significance of isomerization from 9-(*Z,E*)-HPODE and 13-(*Z,E*)-HPODE to 13-(*E,E*)-HPODE and 9-(*E,E*)-HPODE, respectively, *in vivo* is not known. The levels of 9- and 13-(*E,E*)-HODE correlated quite well with those of tHODE (Figs. 5a, b), implying that both tHODE and t9- and 13-(*E,E*)-HODE may be appropriate biomarker for lipid peroxidation *in vivo*.

7α-OHCh is formed also by both enzymatic and free radical-mediated oxidation. Hepatic 7α-hydroxylation of

cholesterol by CYP7A1 is the rate-limiting step for bile acid synthesis [19], and this may not be relevant to oxidative stress. Therefore, 7β-OHCh may be a better biomarker for oxidative stress than 7α-OHCh, although quite a strong correlation was observed between the levels of 7β-OHCh and t7-OHCh for both plasma (Fig. 4a) and erythrocytes (Fig. 4b).

## Effects of Age on the Levels of Lipid Peroxidation and Antioxidants

It was observed that, as a whole, lipid peroxidation level increased and antioxidant decreased with age, although the statistical significance was observed for only five markers out of 25 (Table 1). The stereo-isomer ratio of HODE (*ZE/EE*) in plasma decreased quite significantly with age, suggesting a decrease in antioxidant capacity with age. The decrease in αT and ascorbic acid with age was not statistically significant, but both reduced and oxidized forms of Coenzyme Q<sub>10</sub> (CoQ10) significantly decreased with age. It was reported that the capability of tissues to synthesize CoQ10 decreased during aging [37]. The results of the present study on CoQ10 are in good agreement with this report. However, the effects of age on CoQ10 levels are still controversial [38, 39], and Miles et al. [40] found that plasma CoQ10 concentrations in healthy human adults were relatively constant independent of age (*n* = 148, ranging from 30 to 75 years). Kaikkonen et al. [41] reported from a wide-range epidemiological study (*n* = 518, aged 45–70 years) that plasma CoQ10 concentrations were affected by gender, lipid level, alcohol-consumption as well as age. Apparently, more studies are necessary with larger numbers to elucidate the effects of aging on lipid peroxidation and antioxidant levels.

## References

1. Niki E, Yoshida Y, Saito Y, Noguchi N (2005) Lipid peroxidation: mechanisms, inhibition, and biological effects. *Biochem Biophys Res Commun* 338:668–676
2. Leonarduzzi G, Arkan MC, Basaga H, Chiarpotto E, Sevanian A, Poli G (2000) Lipid oxidation products in cell signaling. *Free Rad Biol Med* 28:1370–1378
3. Ceaser EK, Moellering DR, Shiva S, Ramachandran A, Landar A, Venkartraman A, Crawford J, Patel R, Dickinson DA, Ulasova E, Ji S, Darley-USmar VM (2004) Mechanisms of signal transduction mediated by oxidized lipids: the role of the electrophile-responsive proteome. *Biochem Soc Trans* 32:151–155
4. Chen ZH, Saito Y, Yoshida Y, Sekine A, Noguchi N, Niki E (2005) 4-Hydroxynonenal induces adaptive response and enhances PC12 cell tolerance primarily through induction of thiorodoxin reductase 1 via activation of Nrf2. *J Biol Chem* 280:41921–41927
5. Chen ZH, Yoshida Y, Saito Y, Sekine A, Noguchi N, Niki E (2006) Induction of adaptive response and enhancement of PC12

- cell tolerance by 7-hydroxycholesterol and 15-deoxy-delta-prostaglandin J2 through up-regulation of cellular glutathione by different mechanisms. *J Biol Chem* 281:14440–14445
6. Gao L, Wang J, Sekhar KR, Yin H, Yared NF, Schneider SN, Sasi S, Dalton TP, Anderson ME, Chan JY, Morrow JD, Freeman ML (2007) Novel N-3 fatty acid oxidation products activate Nrf2 by destabilizing the association between Keap1 and Cullin3. *J Biol Chem* 282:2529–2537
  7. Morrow JD, Hill KE, Burk RF, Nammour TM, Badr KF, Roberts LJ II (1990) A series of prostaglandin F2-like compounds are produced in vivo in humans by a non-cyclooxygenase, free radical-catalyzed mechanism. *Proc Natl Acad Sci USA* 87:9383–9387
  8. Musiek ES, Yin H, Milne GL, Morrow JD (2005) Recent advances in the biochemistry and clinical relevance of the isoprostane pathway. *Lipids* 40:987–994
  9. Yoshida Y, Niki E (2004) Detection of lipid peroxidation in vivo: total hydroxyoctadecadienoic acid and 7-hydroxycholesterol as oxidative stress marker. *Free Rad Res* 38:787–794
  10. Porter NA, Caldwell SE, Mills KA (1995) Mechanisms of free radical oxidation of unsaturated lipids. *Lipids* 30:277–290
  11. Pikuleva IA (2006) Cholesterol-metabolizing cytochromes P450. *Drug Metab Dispos* 34:513–520
  12. Smith LL, Johnson BH (1989) Biological activities of oxysterols. *Free Rad Biol Med* 7:285–332
  13. Saito Y, Watanabe Y, Saito E, Honjoh T, Takahashi K (2001) Production and application of monoclonal antibodies to human selenoprotein P. *J Health Sci* 47:346–352
  14. Barclay LRC, Vinquist MR, Antunes F, Pinto RE (1997) Antioxidant activity of vitamin E determined in a phospholipid membrane by product studies: avoiding chain transfer reactions by vitamin E radicals. *J Am Chem Soc* 119:5764–5765
  15. Noguchi N, Numano R, Kaneda H, Niki E (1998) Oxidation of lipids in low density lipoprotein particles. *Free Rad Res* 29:43–52
  16. Sevanian A, Seraglia R, Traldi P, Rossato P, Ursini F, Hodis H (1994) Analysis of plasma cholesterol oxidation products using gas- and high-performance liquid chromatography/mass spectrometry. *Free Rad Biol Med* 17:397–409
  17. Brown AJ, Jessup W (1999) Oxysterols and atherosclerosis. *Atherosclerosis* 142:1–28
  18. Diczfalussy U (2004) Analysis of cholesterol oxidation products in biological samples. *J AOAC Int* 87:467–473
  19. BjÖkhem I, Reihner E, Angelin B, Ewerth S, Akerlund JE, Einarsson K (1987) On the possible use of the serum level of 7 $\alpha$ -hydroxycholesterol as a marker for increased activity of the cholesterol 7 $\alpha$ -hydroxylase in humans. *J Lipid Res* 28:889–894
  20. Schweizer RA, Zurcher M, Balazs Z, Dick B, Odermatt A (2004) Rapid hepatic metabolism of 7-ketocholesterol by 11 beta-hydroxysteroid dehydrogenase type 1: species-specific differences between the rat, human, and hamster enzyme. *J Biol Chem* 279:18415–18424
  21. Hult M, Elleby B, Shafiqat N, Svensson S, Rane A, Jornvall H, Abrahamson L, Oppermann U (2004) Human and rodent type 11 beta-hydroxysteroid dehydrogenases are 7beta-hydroxycholesterol dehydrogenases involved in oxysterol metabolism. *Cell Mol Life Sci* 61:992–999
  22. Arampatzis S, Kadereit B, Schuster D, Balazs Z, Schweizer RA, Frey FJ, Langer T, Odermatt A (2005) Comparative enzymology of 11 beta-hydroxysteroid dehydrogenase type 1 from six species. *J Mol Endocrinol* 35:89–101
  23. Thomas JP, Maiorino M, Ursini F, Girotti AW (1990) Protective action of phospholipid hydroperoxide glutathione peroxidase against membrane-damaging lipid peroxidation. In situ reduction of phospholipid and cholesterol hydroperoxides. *J Biol Chem* 265:454–461
  24. Kühn H, Borchert A (2002) Regulation of enzymatic lipid peroxidation: the interplay of peroxidation and peroxide reducing enzymes. *Free Rad Biol Med* 33:154–172
  25. Kühn H, Heydeck D, Hugou I, Gniwotta C (1997) In vivo action of 15-lipoxygenase in early stages of human atherogenesis. *J Clin Invest* 99:888–893
  26. Yamashita H, Nakamura A, Noguchi N, Niki E, Kühn H (1999) Oxidation of low density lipoprotein and plasma by 15-lipoxygenase and free radicals. *FEBS Lett* 445:287–290
  27. Dufour C, Loonis M (2005) Regio- and stereoselective oxidation of linoleic acid bound to serum albumin: identification by ESI-mass spectrometry and NMR of the oxidation products. *Chem Phys Lipids* 138:60–68
  28. Niki E, Yamamoto Y, Takahashi M, Yamamoto K, Yamamoto Y, Komuro E, Miki M, Yasuda H, Mino M (1988) Free-radical mediated damage of blood and its inhibition by antioxidants. *J Nutr Sci Vitaminol* 34:507–512
  29. Kadiiska MB, Gladen BC, Baird DD, Germolec D, Graham LB, Parker CE, Nyska A, Wachsmann JT, Ames BN, Basu S, Brod N, FitzGerald GA, Floyd RA, George M, Heinecke JW, Hatch GE, Hensley K, Lawson JA, Marnett LJ, Morrow JD, Murray DM, Plastaras J, Roberts II LJ, Rokach J, Shigenaga MK, Sohal RS, Sun J, Tice RR, Van Thiel DH, Wellner D, Walter PB, Tomer KB, Mason RP, Barrett JC (2005) Biomarkers of oxidative stress study II. Are oxidation products of lipids, proteins, and DNA markers of CCl4 poisoning? *Free Rad Biol Med* 38:698–710
  30. Kadiiska MB, Gladen BC, Baird DD, Graham LB, Parker CE, Ames BN, Basu S, FitzGerald GA, Lawson JA, Marnett LJ, Morrow JD, Murray DM, Plastaras J, Roberts II LJ, Rokach J, Shigenaga MK, Sun J, Walter PB, Tomer KB, Barrett JC, Mason RP (2005) Biomarkers of oxidative stress study III. Effects of the nonsteroidal anti-inflammatory agents indomethacin and meclofenamic acid on measurements of oxidative products of lipids in CCl4 poisoning. *Free Rad Biol Med* 38:711–718
  31. Yoshida Y, Itoh N, Hayakawa M, Piga R, Cynshi O, Jishage K, Niki E (2005) Lipid peroxidation induced by carbon tetrachloride and its inhibition by antioxidant as evaluated by an oxidative stress marker, HODE. *Toxicol Appl Pharmacol* 208:87–97
  32. Yoshida Y, Itoh N, Hayakawa M, Habuchi Y, Inoue R, Chen ZH, Cao J, Cynshi O, Niki E (2006) Lipid peroxidation in mice fed choline-deficient diet and its inhibition by antioxidants as evaluated by an oxidative stress marker, HODE. *Nutrition* 22:303–311
  33. Tanito M, Yoshida Y, Kaidzu S, Ohira A, Niki E (2006) Detection of lipid peroxidation in light-exposed mouse retina assessed by oxidative stress markers, total hydroxyoctadecadienoic acid and 8-iso-prostaglandin F<sub>2 $\alpha$</sub> . *Neurosci Lett* 398:63–68
  34. Yoshida Y, Hayakawa M, Niki E (2005) Total hydroxyoctadecadienoic acid as a marker for lipid peroxidation in vivo. *BioFactors* 24:7–15
  35. Yoshida Y, Hayakawa M, Habuchi Y, Niki E (2006) Evaluation of the dietary effects of coenzyme Q in vivo by the oxidative stress marker, hydroxyoctadecadienoic acid and its stereoisomer ratio. *Biochim Biophys Acta* 1760:1558–1568
  36. Kitano S, Yoshida Y, Kawano K, Hibi N, Niki E (2007) Oxidative status of human low density lipoprotein isolated by anion-exchange high-performance liquid chromatography—assessment by total hydroxyoctadecadienoic acid, 7-hydroxycholesterol, and 8-iso-prostaglandin F<sub>2 $\alpha$</sub> . *Anal Chim Acta* 585:86–93
  37. Kalen A, Appelkvist EL, Dallner G (1989) Age-related changes in the lipid compositions of rat and human tissues. *Lipids* 24:579–584
  38. Komorowski J, Muratsu K, Nara Y, Willis R, Folkers K (1988) Significance of biological parameters of human blood levels of CoQ10. *BioFactors* 1:67–69

39. Zita C, Overvad K, Mortensen SA, Sindberg CD, Moesgaard S, Hunter DA (2003) Serum coenzyme Q10 concentrations in healthy men supplemented with 30 mg or 100 mg coenzyme Q10 for two months in a randomised controlled study. *BioFactors* 18:185–193
40. Miles MV, Horn PS, Morrison JA, Tang PH, DeGrauw T, Pesce AJ (2003) Plasma coenzyme Q<sub>10</sub> reference intervals, but not redox status, are affected by gender and race in self-reported healthy adults. *Clin Chim Acta* 332:123–132
41. Kaikkonen J, Kosonen L, Nyyssonen K, Ristonmaa U, Salonen JT (1998) Effect of combined coenzyme Q10 and d- $\alpha$ -tocopheryl acetate supplementation on exercise-induced lipid peroxidation and muscular damage: a placebo-controlled double-blind study in marathon runners. *Free Rad Res* 29:85–92

## Apolipoprotein E $\epsilon 4$ Genotype is Independently Associated with Increased Intima-Media Thickness in a Recessive Pattern

M. Wohlin · J. Sundström · Lars Lannfelt ·  
Tomas Axelsson · A. C. Syvänen · B. Andrén ·  
S. Basu · L. Lind

Received: 6 February 2006 / Accepted: 23 February 2007 / Published online: 11 April 2007  
© AOCs 2007

**Abstract** Polymorphisms in the apolipoprotein E (Apo E) gene have been associated with lipid levels, carotid intima media thickness (CCA-IMT), inflammation and cardiovascular disease (CVD). Earlier findings suggested an association of the Apo E alleles with increased CCA-IMT following a recessive pattern. Whether associations might be independent of C-reactive protein (CRP), lipid levels and other CVD risk factors is not known. We investigated the relationships between Apo E ( $\epsilon 2$ ,  $\epsilon 3$  and  $\epsilon 4$  alleles) and CCA-IMT, measured by B-mode ultrasound, in dominant and recessive models in a community-based sample of 437 men 75 years of age. In men homozygous for the  $\epsilon 4$  allele CCA-IMT was significantly increased by 0.13 mm to  $0.86 \pm 0.16$  mm compared to  $0.73 \pm 0.19$  mm in non- $\epsilon 4$ -carriers ( $P = 0.0012$ ) and  $0.73 \pm 0.21$  mm in  $\epsilon 4$  heterozygous ( $P = 0.0044$ ) in unadjusted recessive models. The association between Apo E  $\epsilon 4$  genotype and CCA-IMT was independent of Apo E  $\epsilon 2$  and Apo E  $\epsilon 3$  alleles, CRP, lipid variables (TG, LDL, HDL) and other CVD risk factors (smoking, hypertension, body mass index, diabetes) ( $P = 0.018$ ). No relations between Apo E genotype and CCA-IMT were observed in dominant models. No significant associations between the Apo E  $\epsilon 2$  and  $\epsilon 3$  alleles and CCA-IMT were found. In this study, men homozygous with the ApoE  $\epsilon 4$  allele had thicker CCA-IMT, independently of Apo E  $\epsilon 2$  and  $\epsilon 3$  alleles, CRP, lipid variables (TG, LDL,

HDL) and other CVD risk factors (smoking, hypertension, body mass index, diabetes), suggesting CCA-IMT to be modified by the ApoE  $\epsilon 4$  genotype in a recessive pattern.

**Keywords** Ultrasound · Apolipoprotein E · Intima-media · Genotype · Carotid

### Introduction

Cardiovascular disease (CVD) is the leading cause of morbidity and mortality in industrialized countries and atherosclerosis is the main underlying pathology. Common carotid artery (CCA) intima-media thickness (IMT) is commonly used as a surrogate measure of atherosclerosis [1].

Apolipoprotein E (Apo E) is a plasma protein of 299 amino acids, with a mass of 34 kDa and is produced mainly by the liver, brain, skin and tissue macrophages. The primary metabolic role for ApoE is to transport and deliver lipids from one tissue or cell type to another. It has three common isoforms (E2, E3 and E4) which are the products of three alleles ( $\epsilon 2$ ,  $\epsilon 3$  and  $\epsilon 4$ ). Allele  $\epsilon 3$  is most common and from which  $\epsilon 2$  and  $\epsilon 4$  differ by a single amino acid, although the  $\epsilon 4$  seems to be the ancestral one [2]. Associations between Apo E alleles and plasma lipid levels and cardiovascular risk have been well established [3]. Studies investigating associations between Apo E alleles and CCA-IMT have reported discordant results [4–19]. The larger, earlier, population-based studies of the association between Apo E genotype and CCA-IMT [4, 5, 9, 20] have regarded Apo E allele variations from a dominant Mendelian perspective. That is all carriers (not regarding the number of alleles) are at greater risk compared to  $\epsilon 3$  homozygous. We aimed to investigate the association between Apo E genotype and CCA-IMT in both dominant and recessive

M. Wohlin (✉) · L. Lannfelt · S. Basu  
Department of Public Health and Caring Sciences/Geriatrics  
and Clinical Nutrition, Faculty of Medicine, Uppsala University,  
Uppsala Science Park, 751 85 Uppsala, Sweden  
e-mail: martin.wohlin@pubcare.uu.se

J. Sundström · T. Axelsson · A. C. Syvänen ·  
B. Andrén · L. Lind  
Medical Sciences, Uppsala University, Uppsala, Sweden

models. This based on the findings of earlier studies that the Apo E  $\epsilon$ 4-homozygous tend to have increased disease burden [21], has been shown to suffer greater risk of cardiovascular death [22] and increased CCA-IMT [4, 5, 9, 20] compared to other variations of the Apo E genotype [4–19]. To study Apo E and CCA-IMT associations we used a community-based sample of 437 elderly men 75 years of age.

## Methods

### Study Sample

In 1970–1973, all men born in 1920–1924 and residing in Uppsala County were invited to a health survey aimed at identifying risk factors for cardiovascular disease. Of the invited subjects, 82% participated. The present study sample consists of the consecutive last 437 out of 1,221 to attend a re-investigation 20 years later in which an examination of the carotid arteries by ultrasound was performed on average 55 months following the major investigation [23]. The men investigated in this study were healthier than the consecutive first 784 men in all variables (anthropometrical, blood pressure, smoking, and diabetes) except regarding hyperlipidemia (serum cholesterol  $>6.5$  mmol/l and/or serum triglycerides  $>2.3$  mmol/l and/or lipid-lowering medications). Hyperlipidemia prevalence in the last 437 men was 40% and the first 784 men 33% [23]. All subjects gave written informed consent, and the Ethics Committee of Uppsala University approved the study. All procedures were performed in accordance with department guidelines.

### Clinical Examinations

Diabetes mellitus was defined as fasting plasma glucose  $\geq 7$  mmol/l or oral glucose tolerance test value  $\geq 11.1$  mmol/l or diabetes medication. Hypertension was defined as systolic blood pressure  $\geq 140$  mmHg or diastolic blood pressure  $\geq 90$  mmHg or hypertension treatment. CRP measurements were performed by latex enhanced reagent (Dade Behring, Deerfield, IL, USA) using a Behring BN ProSpec analyzer (Dade Behring). The intra-assay CV of the CRP method was 1.4% at both 1.23 and 5.49 mg/l. Assessment of smoking prevalence, blood pressures, anthropometrical measurements, fasting glucose and lipids levels were made as recently published [24] and on: <http://www.pubcare.uu.se/ULSAM>.

### Carotid B-Mode Ultrasound

A comprehensive two-dimensional Doppler ultrasound examination of the carotid arteries was performed with a

Sonos 1500 ultrasound unit (Hewlett Packard). A 7.5 MHz linear transducer was used for the B-mode examinations. All examinations were made with the subject in a supine position and the face directed away from the investigated side. The three technically best registrations were chosen and their average was calculated. All measurements were made on-line and stored in the computer of the ultrasonic unit for later printout. Three experienced vascular technologists performed the recordings. The readings of the images were done by one physician (B.A.), unaware of the clinical data of the subjects. CCA-IMT was measured using the leading edge-to-leading edge convention in the far wall of the CCA approximately 1 cm proximal to the carotid bulb [25]. The individual values used are the means of measurements of the two carotid arteries. The intra-observer variability of IMT was 2.6%.

### Genetic Analysis

We investigated relations of Apo E genotype to CCA-IMT using two sets of models: dominant and recessive.

1. Dominant models: To be consistent with previous publications, we defined three dominant ApoE genotype groups: (a) the ApoE  $\epsilon$ 2 group includes those men carrying the  $\epsilon$ 2/ $\epsilon$ 2 or  $\epsilon$ 2/ $\epsilon$ 3 genotype; (b) the ApoE  $\epsilon$ 3 group includes those men carrying the  $\epsilon$ 3/ $\epsilon$ 3 genotype; and (c) the ApoE  $\epsilon$ 4 group includes those carrying the  $\epsilon$ 3/ $\epsilon$ 4 or  $\epsilon$ 4/ $\epsilon$ 4 genotype. By this definition participants with the  $\epsilon$ 4/ $\epsilon$ 2 genotype ( $n = 5$ ) were excluded from the analyses.
2. Recessive models: To investigate Apo E genotype and CCA-IMT also in recessive models we divided the men by number of alleles of Apo E  $\epsilon$ 2,  $\epsilon$ 3 and  $\epsilon$ 4. No participants were excluded in this analysis.

The ApoE112 (rs429358) and ApoE158 (rs7412) SNPs were genotyped using a single-base primer extension assay with fluorescence polarization detection [26] using reagents from Perkin-Elmer. As two SNPs were genotyped the Apo E alleles are therefore unambiguous. The PCR primers (5'–3') were GCGGGCACGGCTGTCCAA (forward) and GCAGGTCATCGGCATCGC (reverse) for Apo E112 and, GGCCAGAGCACCGAGGAG (forward) and CACGCGGCCCTGTTCCAC (reverse) for ApoE158. The “minisequencing” primers were CTGGGC GCGGACAT GGAGGACGTG for ApoE112 and CCGGATGCCG ATGACCTGCAG AAG for ApoE158. Both minisequencing primers detected the nucleotides C and T in the coding DNA strand. The overall genotype call rate was 95.6%, and the accuracy was 99.2% according to duplicate analysis of 17% of the genotypes (347/2011). The genotype data from both SNPs conferred to Hardy–Weinberg equilibrium.

## Statistical Analyses

Univariate analyses were conducted to assess the distributional properties of the baseline variables. Skewed variables were logarithmically transformed to promote normal distribution. *T*-test and ANOVA was used to investigate CCA-IMT and covariates differences by Apo E groups and by number of alleles. Both unadjusted and multivariable-adjusted models were used adjusting for lipid variables (TG, LDL and HDL), CRP and clinical variables (body mass index [BMI], smoking, hypertension and diabetes prevalence). We also investigated interaction terms to evaluate variation in the relation of Apo E alleles to CCA-IMT outcomes according to all used variables. Two-tailed confidence intervals were used, with  $P < 0.05$  regarded as significant. Stata 8.2 software was used for calculations (Stata Corporation, College Station, TX).

## Results

The clinical characteristics of the study sample are shown in Table 1.

### Recessive Models

CCA-IMT was significantly increased by 0.13 mm to  $0.86 \pm 0.16$  mm in  $\epsilon 4$  homozygous compared to  $0.73 \pm 0.19$  mm in non- $\epsilon 4$ -carriers ( $P = 0.001$ , Table 1) and to  $0.73 \pm 0.21$  mm in  $\epsilon 4$  heterozygous ( $P = 0.004$ , Table 1). CCA-IMT was significantly associated with the Apo E  $\epsilon 4$  allele in the unadjusted recessive model ( $P = 0.006$ , Table 3) and this association also remained in the multivariable adjusted ANOVA model with Apo E  $\epsilon 2$  and  $\epsilon 3$  alleles, TG, LDL and HDL, CRP, smoking, hypertension, BMI and diabetes ( $P = 0.02$ , Table 3).

### Dominant Models

There were no significant differences in CCA-IMT between Apo E groups in unadjusted or multivariable adjusted dominant models (Table 2).

## Discussion

### Principal Findings

The principal finding of this study is the independent association in recessive models between Apo E  $\epsilon 4$  homozygous and increased CCA-IMT seen also after adjustment for lipid levels (TG, LDL and HDL), inflammation (CRP) and established CVD risk factors (smoking, hypertension, BMI and diabetes).

**Table 1** Clinical characteristics in the total study sample according to alleles of Apolipoprotein E

	Total	Apolipoprotein E $\epsilon 2$		$\epsilon 2/\epsilon 2$		$\epsilon 2$ carriers		Apolipoprotein E $\epsilon 3$		$\epsilon 3/\epsilon 3$		Apolipoprotein E $\epsilon 4$		$\epsilon 4/\epsilon 4$		$\epsilon 4$ carriers
		0 $\epsilon 2$ allele	1 $\epsilon 2$ allele	1 $\epsilon 2$ allele	1 $\epsilon 2$ allele	0 $\epsilon 3$ allele	1 $\epsilon 3$ allele	0 $\epsilon 4$ allele	1 $\epsilon 4$ allele	0 $\epsilon 4$ allele	1 $\epsilon 4$ allele	0 $\epsilon 4$ allele	1 $\epsilon 4$ allele			
n/%	437/100	378/86	54/12	5/1	59/13	26/6	169/39	242/55	293/67	130/30	14/3	144/33				
IMT	$0.73 \pm 0.20$	$0.73 \pm 0.20$	$0.71 \pm 0.11$	$0.79 \pm 0.21$	$0.72 \pm 0.12$	$0.73 \pm 0.20$	$0.71 \pm 0.11$	$0.79 \pm 0.21$	$0.73 \pm 0.19$	$0.73 \pm 0.21$	$0.86 \pm 0.16$	$0.74 \pm 0.21$				
CRP	$3.03 \pm 4.08$	$2.91 \pm 3.92$	$3.79 \pm 5.12$	$3.19 \pm 2.70$	$3.74 \pm 4.94$	$2.30 \pm 2.56$	$2.95 \pm 4.28$	$3.14 \pm 4.09$	$3.27 \pm 4.31$	$2.58 \pm 3.59$	$1.96 \pm 2.53$	$2.52 \pm 3.51$				
TG	$1.44 \pm 0.75$	$1.42 \pm 0.73$	$1.54 \pm 0.86$	$2.13 \pm 0.94$	$1.59 \pm 0.87$	$1.62 \pm 0.94$	$1.43 \pm 0.75$	$1.43 \pm 0.73$	$1.45 \pm 0.74$	$1.43 \pm 0.78$	$1.30 \pm 0.57$	$1.42 \pm 0.77$				
LDL	$3.92 \pm 0.89$	$3.98 \pm 1.51$	$3.54 \pm 0.76$	$3.40 \pm 1.51$	$3.52 \pm 0.83$	$3.92 \pm 1.06$	$3.94 \pm 0.87$	$3.90 \pm 0.89$	$3.83 \pm 0.90$	$4.07 \pm 0.84$	$4.32 \pm 0.99$	$4.09 \pm 0.86$				
HDL	$1.29 \pm 0.34$	$1.28 \pm 0.34$	$1.31 \pm 0.34$	$1.28 \pm 0.19$	$1.31 \pm 0.33$	$1.33 \pm 0.32$	$1.31 \pm 0.35$	$1.27 \pm 0.34$	$1.28 \pm 0.34$	$1.31 \pm 0.36$	$1.36 \pm 0.29$	$1.32 \pm 0.35$				
Chol	$5.86 \pm 1.01$	$5.9 \pm 1.00$	$5.54 \pm 1.00$	$5.64 \pm 1.81$	$5.55 \pm 1.06$	$5.98 \pm 1.19$	$5.90 \pm 1.02$	$5.81 \pm 0.99$	$5.76 \pm 1.01$	$6.03 \pm 0.98$	$6.26 \pm 1.11$	$6.05 \pm 1.00$				
BMI	$26.2 \pm 3.1$	$26.1 \pm 3.1$	$26.7 \pm 3.1$	$27.1 \pm 4.6$	$26.7 \pm 3.2$	$26.5 \pm 4.0$	$26.1 \pm 3.1$	$26.3 \pm 3.0$	$26.3 \pm 3.0$	$26.0 \pm 3.3$	$25.6 \pm 3.7$	$26.0 \pm 3.3$				
DM	19	20	19	0	17	15	17	21	20	18	14	17				
Smok	18	18	16	20	16	20	16	18	18	15	23	16				
HT	69	69	69	60	68	65	69	70	70	66	79	69				

Figures in the table are mean and ( $\pm$ ) standard deviation except when percent (%)

CRP C-reactive protein in mg/l, TG triglycerides, LDL Low-density lipoprotein, HDL High-density lipoprotein, Chol cholesterol. All lipids in mmol/l. BMI Body mass index in kg/m<sup>2</sup>, IMT common carotid artery intima-media thickness in mm, HT hypertension, MS metabolic syndrome, DM diabetes mellitus, Smok smokers



**Table 2** Dominant models for associations between CCA-IMT and Apo E groups

Apo E groups	$\epsilon 2/\epsilon 2$ and $\epsilon 2/\epsilon 3$ , $\epsilon 3/\epsilon 3$ , $\epsilon 3/\epsilon 4$ and $\epsilon 4/\epsilon 4$	$\epsilon 3/\epsilon 4$ and $\epsilon 4/\epsilon 4$ versus $\epsilon 3/\epsilon 3$	$\epsilon 2/\epsilon 2$ and $\epsilon 2/\epsilon 3$ versus $\epsilon 3/\epsilon 3$
	<i>P</i>	<i>P</i>	<i>P</i>
Unadjusted	0.63	0.36*	0.69*
Multivariable adjusted	0.57	0.35	0.56

Calculations by ANOVA or *t*-test (=\*). CCA-IMT = Common carotid artery intima-media thickness. Multivariate models adjusted for: Apo E groups ( $\epsilon 2/\epsilon 2$  and  $\epsilon 2/\epsilon 3$  together,  $\epsilon 3/\epsilon 3$ ,  $\epsilon 3/\epsilon 4$  and  $\epsilon 4/\epsilon 4$  together), C-reactive protein, triglycerides, LDL-cholesterol, HDL-cholesterol, body mass index, diabetes, smoking and hypertension

**Table 3** Recessive ANOVA models of associations of CCA-IMT and Apo E alleles

Apo E genotypes	Apo E $\epsilon 4$ <i>P</i>	Apo E $\epsilon 3$ <i>P</i>	Apo E $\epsilon 2$ <i>P</i>
Unadjusted	0.0058	0.13	0.61
Multivariable adjusted	0.018	0.26	0.36

CCA-IMT = common carotid artery intima-media thickness. Covariates in multivariate model: Apo E  $\epsilon 2$ ,  $\epsilon 3$ ,  $\epsilon 4$  (for 0, 1 or 2 alleles), C-reactive protein, triglycerides, LDL-cholesterol, HDL-cholesterol, body mass index, diabetes, smoking and hypertension

### Recessive Models

When comparing the results of the present study with the findings of major studies [4, 5, 9, 20] there are noteworthy similarities suggesting recessive associations between the Apo E genotype and CCA-IMT. In the ARIC Study among Afro-American men,  $\epsilon 4/\epsilon 4$ -homozygous subjects had a statistically significant increased CCA-IMT. In the Rotterdam Study, men with the  $\epsilon 4/\epsilon 4$  genotype had slightly (not statistically significant) increased CCA-IMT, and also in the CUDAS study the bivariate analysis showed borderline significance ( $P = 0.07$ ) for increased CCA-IMT in  $\epsilon 4/\epsilon 4$ -homozygous men.

### Dominant Models

In the present study, no associations were found in dominant models. In the Framingham Offspring Study men suffering from diabetes in the Apo E4 group were associated with increased CCA-IMT. Also in women, a statistically significant increase in CCA-IMT was found in the Apo E 4 group in Framingham.

### Comparisons with Previous Studies

In the presented study, the investigated variables vary by a number of Apo  $\epsilon 4$  alleles in both recessive (CCA-IMT) and

dominant (lipids, diabetes) manners (Table 1). The findings in previous studies (as described above) and the presented study suggest that associations of the Apo E genotype with covariates should be investigated in both recessive and dominant models. That is, both as carrier-groups in dominant models (see Table 2) and by the number of alleles in recessive models (see Tables 1, 3). The difference in the findings presented among earlier studies are most likely due to differences in Apo E allele groupings, the use of  $\epsilon 3/\epsilon 3$ -carriers as controls and study material (age, sex, race, size, recruitment procedures), CCA-IMT measurement criteria (measurement sites, left, right or mean values) and data analysis (recessive/dominant models). The four major population-based studies with large samples (ARIC, Rotterdam, Framingham and Perth) all analyzed the associations of the Apo E genotype with CCA-IMT in dominant models with  $\epsilon 3/\epsilon 3$ -carriers as controls in all analyses. The reason for this grouping is probably the high frequency of  $\epsilon 3/\epsilon 3$ -carriers in western populations and the use of the lipid levels of the  $\epsilon 3/\epsilon 3$ -carriers as normal values, and a wish to maximize power by constructing as large E2 and E4 groups as possible.

The participants in the presented study were all men of 75 years of age and the mean ages in the larger population-based studies mentioned above were 54, 59, 69 and 53 years [4, 5, 9, 20]. This might partly explain the lack of significant associations in the studies above as CCA-IMT continuously increases with age [27] and increased CCA-IMT in the samples might not yet have reached significant levels for the Apo E genotype associations.

When comparing the man to woman ratio in the studies mentioned above they range from 41 to 59%. As findings of associations between CCA-IMT and Apo E genotypes differ between sexes in these studies one might assume mixed sample decreases the possibility of revealing significant associations.

The Framingham Offspring Study and the CUDAS/Perth papers report a diabetes mellitus prevalence of 14% in men and 10% in women (Framingham) and 2.2 and 2.0% in men and women (CUDAS/Perth). In this study the diabetes prevalence is 19%. Since the Framingham study reported an association in diabetic men between CCA-IMT and the Apo E4 group, one might assume this association becomes stronger as the number of diabetics increases to the levels of this presented study.

The Framingham and the CUDAS/Perth studies report the hypertension prevalence to be 31% in men and 26% in women (Framingham) and 24% in both men and women (CUDAS/Perth). In the present study, the hypertension prevalence is 69%. As an increased CCA-IMT is strongly associated with hypertension [4, 5, 9, 20] this study's sample have an increased disease burden and therefore increased CCA-IMT compared to healthier samples and significant associations might be easier to detect.

## Possible Mechanisms

The primary role for Apo E is lipid transport in an ‘‘endocrine-like’’ function and the different Apo E alleles have definite impacts on lipid levels [28]. The LDL-receptor family is a growing transmembrane receptor family composed of more than ten receptors with the very low density lipoprotein (VLDL) receptor and the Apolipoprotein E receptor 2 being most similar to the LDL-receptor structurally [29]. Growing experimental evidence suggests that members of the LDL-receptor family activate kinase-dependent intracellular signalling cascades after binding to adaptor proteins, often interacting with more than one receptor [30]. The reverse cholesterol transport is a critical way for maintaining cholesterol homeostasis in cells and Apo E uniquely facilitates this pathway by increasing the size of HDL particles as a component of a subclass of HDL (HDL with Apo E) [31] and recent findings suggest Apo E redistributes lipids in a ‘‘paracrine-like’’ function. Mice which only produce Apo E in macrophages were protected against atherosclerosis, even though plasma levels of Apo E were low and cholesterol levels high [32] and further, mice with the expression of Apo E normal except in macrophages were susceptible to increased atherosclerosis [33].

Apo E also influences the metabolism of lipoproteins not only as a receptor ligand. Accumulation of Apo E on the surface lipoproteins slows the lipolysis by lipase [34] and affects VLDL levels directly as increased Apo E synthesis by the liver is associated with increased VLDL synthesis [35].

CRP has also been shown to be a predictor of cardiovascular events [36] and immune system defects have been described in ApoE knockout mice [37]. In this study CRP was inversely related to the  $\epsilon 4$  alleles (Table 1). This relation has recently been shown in a sample of patients recruited at a coronary angiography center, where the presence of at least one  $\epsilon 4$  allele decreased CRP by 19% [38]. This raises the possibility that production, release or catabolism of CRP is related to the mevalonate pathway in the liver, as statins (inhibiting the rate limiting step of the mevalonate pathway) have been shown to lower CRP [39]. However, as CRP did not markedly attenuate the relationship between the ApoE  $\epsilon 4$  and CCA-IMT in the multivariable adjusted model, it is likely that the Apo E genotype influences CCA-IMT by other means than by a general inflammatory response.

## Strength and Limitations

The men investigated in this study are a part of a well-characterized population-based sample and this reinvesti-

gation includes 437 men 75 years of age to attend a reinvestigation 20 years after the first investigation. The so-called healthy cohort effect: dropout of the least healthy subjects and a selective survival may have influenced the investigated associations. The men included in this study were healthier than excluded men in all variables (anthropometrical, blood pressure, smoking, and diabetes) with the exception of hyperlipidemia [23]. However, both of these circumstances could only bias us toward the null hypothesis, and not lead to false positive results. Our homogenous sample makes it not possible to generalize the presented associations to any group other than white elderly men. The results obtained in this study are observational, thus no cause and effect conclusions of the presented associations can be made.

In conclusion, this study suggests ApoE  $\epsilon 4$  homozygous to be associated with thicker CCA-IMT, independent of inflammation, lipid levels and CVD risk factors in a population-based sample of elderly men, suggesting CCA-IMT to be modified by the ApoE  $\epsilon 4$  genotype in a recessive pattern.

**Acknowledgments** The SNPs were genotyped by the Wallenberg Consortium North (WCN) SNP technology platform. We thank Kristina Larsson for performing the genotyping assays. We thank the Swedish Heart and Lung Foundation for their support.

## References

1. Cheng KS, Mikhailidis DP, Hamilton G, Seifalian AM (2002) A review of the carotid and femoral intima-media thickness as an indicator of the presence of peripheral vascular disease and cardiovascular risk factors. *Cardiovasc Res* 54(3):528–538
2. Hanlon CS, Rubinsztein DC (1995) Arginine residues at codons 112 and 158 in the apolipoprotein E gene correspond to the ancestral state in humans. *Atherosclerosis* 112(1):85–90
3. Mahley RW, Rall SC Jr (2000) Apolipoprotein E: far more than a lipid transport protein. *Annu Rev Genomics Hum Genet* 1:507–537
4. Elosua R, Ordovas JM, Cupples LA, Fox CS, Polak JF, Wolf PA et al (2004) Association of APOE genotype with carotid atherosclerosis in men and women: the Framingham Heart Study. *J Lipid Res* 45(10):1868–1875 Epub 2004 Jul 16
5. Beilby JP, Hunt CC, Palmer LJ, Chapman CM, Burley JP, McQuillan BM et al (2003) Apolipoprotein E gene polymorphisms are associated with carotid plaque formation but not with intima-media wall thickening: results from the Perth Carotid Ultrasound Disease Assessment Study (CUDAS). *Stroke* 34(4):869–874 Epub 2003 Mar 13
6. Karvonen J, Kauma H, Kervinen K, Ukkola O, Rantala M, Paivansalo M et al (2002) Apolipoprotein E polymorphism affects carotid artery atherosclerosis in smoking hypertensive men. *J Hypertens* 20(12):2371–2378
7. Haraki T, Takegoshi T, Kitoh C, Wakasugi T, Saga T, Hirai JI et al (2002) Carotid artery intima-media thickness and brachial artery flow-mediated vasodilation in asymptomatic Japanese male subjects amongst apolipoprotein E phenotypes. *J Intern Med* 252(2):114–120

8. Djousse L, Myers RH, Province MA, Hunt SC, Eckfeldt JH, Evans G et al (2002) Influence of apolipoprotein E, smoking, and alcohol intake on carotid atherosclerosis: National Heart, Lung, and Blood Institute Family Heart Study. *Stroke* 33(5):1357–1361
9. Sliotoer AJ, Bots ML, Havekes LM, del Sol AI, Cruts M, Grobbee DE et al (2001) Apolipoprotein E and carotid artery atherosclerosis: the Rotterdam study. *Stroke* 32(9):1947–1952
10. Ilveskoski E, Loimaala A, Mercuri MF, Lehtimäki T, Pasanen M, Nenonen A et al (2000) Apolipoprotein E polymorphism and carotid artery intima-media thickness in a random sample of middle-aged men. *Atherosclerosis* 153(1):147–153
11. Horejsi B, Spacil J, Ceska R, Vrablik M, Haas T, Horinek A (2000) The independent correlation of the impact of lipoprotein(a) levels and apolipoprotein E polymorphism on carotid artery intima thickness. *Int Angiol* 19(4):331–336
12. Hanon O, Girerd X, Luong V, Jeunemaitre X, Laurent S, Safar ME (2000) Association between the apolipoprotein E polymorphism and arterial wall thickness in asymptomatic adults. *J Hypertens* 18(4):431–436
13. Zannad F, Visvikis S, Gueguen R, Sass C, Chapet O, Herbeth B et al (1998) Genetics strongly determines the wall thickness of the left and right carotid arteries. *Hum Genet* 103(2):183–188
14. Sass C, Zannad F, Herbeth B, Salah D, Chapet O, Siest G et al (1998) Apolipoprotein E4, lipoprotein lipase C447 and angiotensin-I converting enzyme deletion alleles were not associated with increased wall thickness of carotid and femoral arteries in healthy subjects from the Stanislas cohort. *Atherosclerosis* 140(1):89–95
15. Kogawa K, Nishizawa Y, Hosoi M, Kawagishi T, Maekawa K, Shoji T et al (1997) Effect of polymorphism of apolipoprotein E and angiotensin-converting enzyme genes on arterial wall thickness. *Diabetes* 46(4):682–687
16. Vauhkonen I, Niskanen L, Ryyanen M, Voutilainen R, Partanen J, Toyry J et al (1997) Divergent association of apolipoprotein E polymorphism with vascular disease in patients with NIDDM and control subjects. *Diabet Med* 14(9):748–756
17. Cattin L, Fiscaro M, Tonizzo M, Valenti M, Danek GM, Fonda M et al (1997) Polymorphism of the apolipoprotein E gene and early carotid atherosclerosis defined by ultrasonography in asymptomatic adults. *Arterioscler Thromb Vasc Biol* 17(1):91–94
18. Terry JG, Howard G, Mercuri M, Bond MG, Crouse JR 3rd (1996) Apolipoprotein E polymorphism is associated with segment-specific extracranial carotid artery intima-media thickening. *Stroke* 27(10):1755–1759
19. de Andrade M, Thandi I, Brown S, Gotto A Jr, Patsch W, Boerwinkle E (1995) Relationship of the apolipoprotein E polymorphism with carotid artery atherosclerosis. *Am J Hum Genet* 56(6):1379–1390
20. Volcik KA, Barkley RA, Hutchinson RG, Mosley TH, Heiss G, Sharrett AR et al (2006) Apolipoprotein E polymorphisms predict low density lipoprotein cholesterol levels and carotid artery wall thickness but not incident coronary heart disease in 12,491 ARIC study participants. *Am J Epidemiol* 164(4):342–348
21. Stengard JH, Zerba KE, Pekkanen J, Ehnholm C, Nissinen A, Sing CF (1995) Apolipoprotein E polymorphism predicts death from coronary heart disease in a longitudinal study of elderly Finnish men. *Circulation* 91(2):265–269
22. Davignon J, Gregg RE, Sing CF (1988) Apolipoprotein E polymorphism and atherosclerosis. *Arteriosclerosis* 8(1):1–21
23. Wohlin M, Sundstrom J, Arnlov J, Andren B, Zethelius B, Lind L (2003) Impaired insulin sensitivity is an independent predictor of common carotid intima-media thickness in a population sample of elderly men. *Atherosclerosis* 170(1):181–185
24. Sundstrom J, Lind L, Nystrom N, Zethelius B, Andren B, Hales CN et al (2000) Left ventricular concentric remodeling rather than left ventricular hypertrophy is related to the insulin resistance syndrome in elderly men. *Circulation* 101(22):2595–2600
25. Wikstrand J, Wendelhag I (1994) Methodological considerations of ultrasound investigation of intima-media thickness and lumen diameter. *J Intern Med* 236(5):555–559
26. Hsu TM, Chen X, Duan S, Miller RD, Kwok PY (2001) Universal SNP genotyping assay with fluorescence polarization detection. *Biotechniques* 31(3):560, 562, 564–568 passim
27. Salonen JT, Salonen R (1993) Ultrasound B-mode imaging in observational studies of atherosclerotic progression. *Circulation* 87(3 Suppl):II56–II65
28. Sing CF, Davignon J (1985) Role of the apolipoprotein E polymorphism in determining normal plasma lipid and lipoprotein variation. *Am J Hum Genet* 37(2):268–285
29. Takahashi S, Sakai J, Fujino T, Miyamori I, Yamamoto TT (2003) The very low density lipoprotein (VLDL) receptor—a peripheral lipoprotein receptor for remnant lipoproteins into fatty acid active tissues. *Mol Cell Biochem* 248(1–2):121–127
30. Gotthardt M, Trommsdorff M, Nevitt MF, Shelton J, Richardson JA, Stockinger W et al (2000) Interactions of the low density lipoprotein receptor gene family with cytosolic adaptor and scaffold proteins suggest diverse biological functions in cellular communication and signal transduction. *J Biol Chem* 275(33):25616–25624
31. Mahley RW, Huang Y, Weisgraber KH (2006) Putting cholesterol in its place: apoE and reverse cholesterol transport. *J Clin Invest* 116(5):1226–1229
32. Bellosta S, Mahley RW, Sanan DA, Murata J, Newland DL, Taylor JM et al (1995) Macrophage-specific expression of human apolipoprotein E reduces atherosclerosis in hypercholesterolemic apolipoprotein E-null mice. *J Clin Invest* 96(5):2170–2179
33. Fazio S, Babaev VR, Murray AB, Hasty AH, Carter KJ, Gleaves LA et al (1997) Increased atherosclerosis in mice reconstituted with apolipoprotein E null macrophages. *Proc Natl Acad Sci USA* 94(9):4647–4652
34. Huang Y, Liu XQ, Rall SC Jr, Taylor JM, von Eckardstein A, Assmann G et al (1998) Overexpression and accumulation of apolipoprotein E as a cause of hypertriglyceridemia. *J Biol Chem* 273(41):26388–26393
35. van Dijk KW, van Vlijmen BJ, van't Hof HB, van der Zee A, Santamarina-Fojo S, van Berkel TJ et al (1999) In LDL receptor-deficient mice, catabolism of remnant lipoproteins requires a high level of apoE but is inhibited by excess apoE. *J Lipid Res* 40(2):336–344
36. Ridker PM, Rifai N, Rose L, Buring JE, Cook NR (2002) Comparison of C-reactive protein and low-density lipoprotein cholesterol levels in the prediction of first cardiovascular events. *N Engl J Med* 347(20):1557–1565
37. Persson L, Boren J, Nicoletti A, Hansson GK, Pekna M (2005) Immunoglobulin treatment reduces atherosclerosis in apolipoprotein E low-density lipoprotein receptor mice via the complement system. *Clin Exp Immunol* 142(3):441–445
38. Marz W, Scharnagl H, Hoffmann MM, Boehm BO, Winkelmann BR (2004) The apolipoprotein E polymorphism is associated with circulating C-reactive protein (the Ludwigshafen risk and cardiovascular health study). *Eur Heart J* 25(23):2109–2119
39. Albert MA, Danielson E, Rifai N, Ridker PM (2001) Effect of statin therapy on C-reactive protein levels: the pravastatin inflammation/CRP evaluation (PRINCE): a randomized trial and cohort study. *JAMA* 286(1):64–70

# Spin-Probe Investigations of Head Group Behavior in Aqueous Dispersions of a Nonionic Amphiphilic Compound

Kouichi Nakagawa

Received: 1 August 2006 / Accepted: 23 February 2007 / Published online: 27 March 2007  
© AOCS 2007

**Abstract** Head group behavior of nonionic amphiphilic compound, (poly(oxyethylene) hydrogenated castor oil, HCO), in aqueous dispersions were investigated by EPR (electron paramagnetic resonance) in conjunction with a modern slow-tumbling simulation. The aliphatic spin probes, 5-doxylstearic acid (5-DSA) and 3 $\beta$ -doxyl-5 $\alpha$ -cholestane (CHL), were used to obtain fluidity of the surface region of the membrane. The order parameter ( $S_0$ ) using the simulation for 5-DSA and CHL in the region were approximately 0.4 and 0.2, respectively. The ordering results suggest that the head group region of the membrane is somewhat fluid. The rotational diffusion coefficients ( $R_{\perp} \approx 1/(6\tau_R)$ ) for the probes were  $3.4 \times 10^7$  and  $7.1 \times 10^7$  s $^{-1}$ , respectively. Activation energies, calculated using the temperature dependence of diffusion coefficients, were 18 and 17 kJ/mol for the probes. The EPR results imply that the CHL probe in the HCO membrane has quite different behavior in comparison with that of PC (phosphatidylcholine) from egg. Thus, the present EPR analyses have provided quantitative insight into the surface region of the amphiphilic membrane.

**Keywords** EPR · Spin probe · Rotational diffusion coefficients · Activation energy · Amphiphilic compound

## Introduction

Behavior of the surface region of amphiphilic membranes provides very important clues for understanding the phys-

icochemical characteristics of the membranes. Knowledge of regional behavior is crucial for quantitatively understanding the membrane properties. Reliable information of the surface region can be obtained by EPR (electron paramagnetic resonance) as well as fluorescence spectroscopies [1, 2]. Investigations of the surface region have been performed using fluorescence in conjunction with aromatic molecular probes. The fluorescence probes, having a large aromatic ring and very different chemical structure relative to the lipid components, are normally used. Furthermore, the sensitivity of the fluorescence techniques is low because of the micromolar concentration of the probe. On the other hand, the 9 GHz EPR is not only sensitive to micro to nanomolar concentration but also the chemical structures of the aliphatic spin probes are more similar to the lipids. Thus, EPR is an excellent technique for investigating insights into regional behavior of the membranes. The probe tumbling times in the lipids are generally on the order of  $10^{-8}$ – $10^{-7}$  s. A modern slow-tumbling simulation analysis in conjunction with the spin probe method can extract detailed information regarding various probe motions in the membranes [3].

For over 25 years the various properties of biological membranes, in conjunction with the spin probes (doxylstearic acids), have been discussed as the results of conventional analysis using the so-called spectral parameter and order parameter [4, 5]. The conventional method determined the chain ordering of biological membranes employing EPR hyperfine-coupling constants of lipid incorporated probes [6, 7]. The conventional analysis of the membrane organization, such as order parameter, provides qualitative information about the membrane. The values do not reflect small changes of the EPR spectral pattern. The values only change when the hyperfine coupling constants are changed. Therefore, the detailed membrane character-

K. Nakagawa (✉)  
RI Research Center, Fukushima Medical University,  
1 Hikarigaoka, Fukushima 960-1295, Japan  
e-mail: nakagawa@fmu.ac.jp

istics should be extensively investigated by means of careful analysis of the corresponding EPR observations.

Nonionic surface-active agents have been of great interest in the fields of cosmetics as well as pharmaceuticals. In drug encapsulation, vesicle formation of the agent is necessary. Nontoxic and naturally degradable substances are also desired. Recently, poly(oxyethylene) hydrogenated castor oil (termed HCO), which is derived from one of the lipids and related natural products, was found to form vesicles [7]. A stable multi-lamellar vesicle with an average diameter of ~500 nm was observed. HCO is a physiologically nontoxic and naturally degradable substance. Furthermore, HCO has a unique chemical structure among triglyceride derivatives. It consists of a uniform fatty-portion structure embodying oxyethylene groups unlike most naturally occurring triglycerides, which are composed of mixed fatty-portions. Hence, HCO is a very interesting compound for investigation of lipid motions [1, 8, 9].

Detailed motions of aliphatic spin probes in the membrane were investigated [1, 9]. The activation energies obtained for the 7-, 12-, and 16-DSA are 19, 24, and 37 kJ/mol, respectively. The values indicate that the various probe moieties have a different temperature sensitivity in the range 20–50 °C. The area near the end of the membrane chain is sensitive to temperature. Furthermore, physicochemical characterization of the vesicle for the nonionic amphiphilic compound HCO could lead to detailed understanding of the bilayer behavior as well as its characteristics. Temperature dependence in relation to dynamic structure of membranes is an important subject in colloid interface and membrane sciences. Recently, it has been found that quantitative EPR investigations (e.g. an EPR spectral simulation) will lead to detailed understanding of the bilayer behavior directly related to characteristics of the membrane [1, 10].

In this investigation, a modern slow-tumbling simulation for EPR spectra was applied to reveal detailed probe behavior in the head group region of the HCO membrane. Detailed rotational diffusion coefficients of spin probes in aqueous dispersions of HCO membrane were analyzed as a function of temperature. The slow-tumbling simulation is advantageous for investigation of the head group behavior of the membrane. The results are also discussed in comparison with those for PC from egg.

## Materials and Methods

### Materials and Sample Preparations

Poly(oxyethylene) hydrogenated castor oil (HCO) of the highest quality was donated by Nikko Chemicals Co. Ltd. (Tokyo, Japan) and used as received. The HCO had about

ten oxyethylene groups per molecule. The molecular structures of HCO and the spin probes used in this study are depicted in Fig. 1. The oxyethylene groups attach to the 12th carbon from the carbonyl carbon of the main chain.

The spin probes 5-(4, 4-dimethyl-3-oxazolidinyl)oxy-octadecanoic acid, the so called 5-doxyloctadecanoic acid (5-DSA), and 3 $\beta$ -doxyl-5 $\alpha$ -cholestane (CHL) were obtained from Aldrich Chemical Co. (Tokyo, Japan). Lecithin (phosphatidylcholine, PC) from egg was purchased from Wako Pure Chemical Ind. Ltd., Japan. All chemicals were of the highest grade obtainable and used as received.

Sample solutions were prepared as follows: a weighed amount of HCO was dissolved in a few milliliters of chloroform. The spin probe was dissolved in ~0.3 ml of chloroform and mixed with the HCO solution. After evaporation of the chloroform in a rotary evaporator, a 10 wt% dispersion of HCO/spin probe in distilled water (Wako Pure Chemical Ind. Ltd., Japan) was prepared.

The spin probes were incorporated into the PC from egg in the same manner as the HCO. A ~0.8 wt% dispersion of PC/probe in 1 mM Tris-HCl buffer solution under a nitrogen atmosphere was prepared. The test tube containing the dispersion solution was agitated on a vortex mixer until completely dispersed. An aliquot of the dispersion was used for EPR measurements. The final concentration of the spin probe was approximately 100  $\mu$ mol for the measurements. A detailed description of the sample preparation is also presented elsewhere [1, 9].

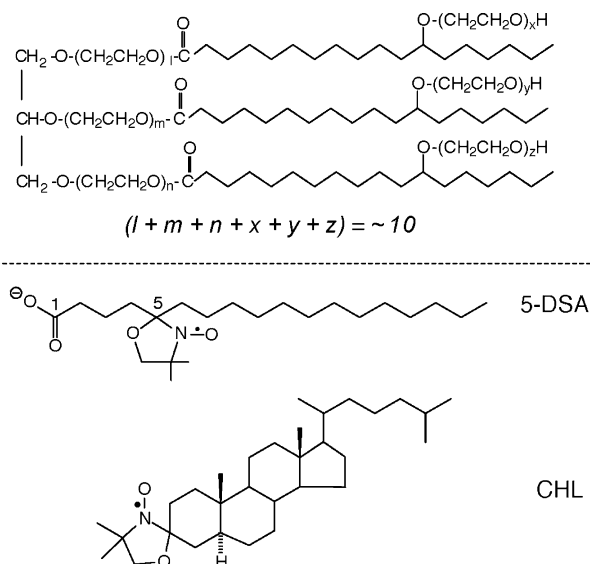


**Fig. 1** Chemical structures of poly(oxyethylene) [11] HCO and the spin probes (5-DSA and CHL) used are depicted. It is notable that the fatty portion of HCO is composed of 18 carbon atoms

## Deoxygenation

The sample solutions (~0.15 ml) were deoxygenated for about 15 min in an AtmosBag (Aldrich) and the solutions were put into capillaries (i.d., 0.9 mm; o.d., 1.4 mm; Nippon Rikagaku Kikai Co. Ltd., Japan). A sample capillary was inserted in a 3-mm EPR tube (JEOL Datum Co. Ltd., Japan) in the AtmosBag and taped around the tube cap.

## EPR Measurements

EPR signals were measured by a JEOL FE1X X-band EPR spectrometer. This spectrometer is equipped with a TE<sub>011</sub> mode cavity. The sample temperature was controlled by nitrogen gas flow through the Dewar using a JEOL ES-DVT system. The EPR signals were digitized using a Scientific Software Services data acquisition system (Illinois, USA). The microwave frequency was measured using an EMC-14 X-band microwave frequency counter (Echo Electronics Co., Ltd., Japan). Typical EPR conditions were the following: microwave frequency, 9.18 GHz; microwave power, 5 mW; modulation amplitude, 0.32 G (Gauss); time constant, 1 s; scan rate, 3.125 G per min. All sample solutions were measured under identical conditions.

## Calculation of the Slow-Tumbling Spin Probe

The slow-tumbling motions ( $10^{-8}$ – $10^{-7}$  s) of the aliphatic spin probes were calculated using the nonlinear least-squares fitting program called NLLS to analyze the EPR spectra based on the stochastic Liouville equation [3, 11]. The simulation of the EPR spectra for spin probes incorporated into multilamellar vesicles was carried out using a microscopically ordered but macroscopically disordered (MOMD) model [12]. This model is based on the characteristics of the dynamic structure of lipid dispersions. For example, lipid molecules are preferentially oriented by the local structure of the bilayer, but the lipid bilayer fragments are distributed randomly overall. The spectrum from the sample can be regarded as a superposition of the spectra from all of the fragments.

The lipid and the probe molecules in the membrane bilayer experience ordering potentials, which restrict the amplitude of the rotational motion. The ordering potential in a lipid bilayer,  $U(\Omega)$ , determines the orientational distribution of molecules with respect to the local ordering axis of the membrane bilayer. It can be expressed in generalized spherical harmonics [13],

$$-U/kT = c_0^2 D_{00}^2(\Omega) + c_2^2 (D_{02}^2(\Omega) + D_{-2}^2(\Omega)) + \dots, \quad (1)$$

where  $\Omega = (\alpha, \beta, \gamma)$  are the Euler angles between the molecular frame of the rotational diffusion tensor and the local director frame. The  $c_0^2$  and  $c_2^2$  are dimensionless potential energy coefficients,  $k$  is the Boltzmann constant, and  $T$  is the absolute temperature.

There are two axes systems in the calculation of the rotational dynamics and orientational ordering of the spin probe. In the magnetic frame, the  $z$ -axis is parallel to the  $2P_z$  orbital of the N atom for doxylstearic acid, which is perpendicular to the N–O bond of the nitroxide probe as shown in Fig. 2. Then, the  $y$ -axis in the magnetic frame is perpendicular to both  $x$ - and  $z$ -axes, forming a right-handed axis frame. In the molecular frame, the  $z$ -axis is parallel to the symmetry axis of the probe molecule. For the spin probe doxylstearic acid, obviously, the  $z$ -axis is parallel to the long hydrocarbon chain, which coincides with the  $z$ -axis in the magnetic frame.

The rigidity (chain ordering),  $S_0$ , is defined as

$$S_0 = \langle D_{00}^2 \rangle = \left\langle \frac{1}{2} (3 \cos^2 \gamma - 1) \right\rangle = \frac{\int d\Omega \exp(-U/kT) D_{00}^2}{\int d\Omega \exp(-U/kT)}, \quad (2)$$

which measures the angular extent of the rotational diffusion of the nitroxide moiety. Gamma ( $\gamma$ ) is the angle between the rotational diffusion symmetry axis and the  $z$ -axis of the nitroxide axis system. The local or microscopic ordering of the nitroxide spin probe in the membrane is

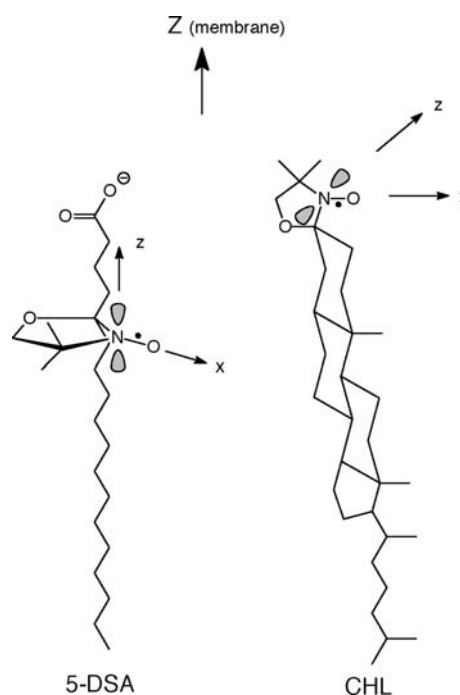


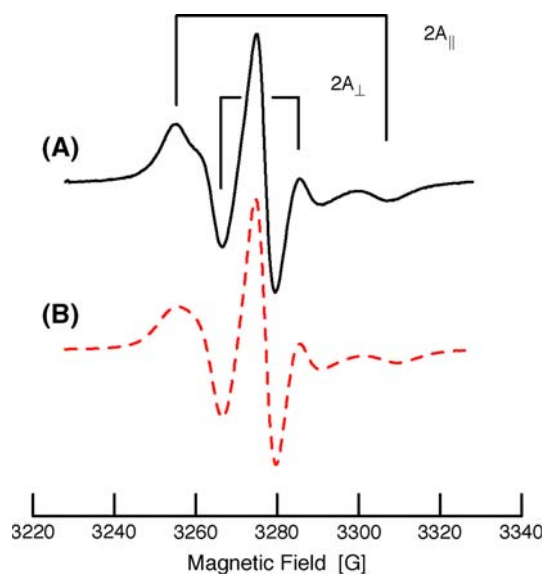
**Fig. 2** Coordination of the spin probes, 5-DSA and CHL, for the NLLS calculations are presented. The  $z$ -axis is the membrane director

characterized by the  $S_0$  value. A larger  $S_0$  value indicates a more restricted motion. Therefore,  $S_0$  reflects the local ordering of bilayer molecules in the membrane.

Dynamics of the probe are described by the following parameters: rotational diffusion rates ( $R_{\perp}$  and  $R_{\parallel}$ ) along axes perpendicular and parallel to the molecular symmetry axes [13]. The perpendicular component ( $R_{\perp}$ ) represents the rotational wagging motion of the long axis of the hydrocarbon chain. This component can be correlated with the rotational correlation time ( $\tau_R \approx 1/(6R_{\perp})$ ) [11]. In the calculation of experimental spectra, the principal components for the probes obtained by the previous values were used [14, 15].

## Results and Discussion

In order to reveal the motional behaviors in the head group region, 5-DSA and CHL were used as the probes. Figure 3a shows the typical EPR spectrum of HCO/5-DSA in an aqueous dispersion at 20 °C. The EPR spectrum shows that the nitroxide probe is immobilized in the membrane and the parallel ( $2A_{\parallel}$ ) and perpendicular ( $2A_{\perp}$ ) hyperfine components as presented in the figure are clearly recognized. The anisotropic EPR spectral pattern is slightly different from the rigid spectral pattern, which was published previously [1]. The perpendicular hyperfine component was clearly observed. This indicates that the head group region is relatively flexible. The amphiphilic property may be due to hydration in the head group region.



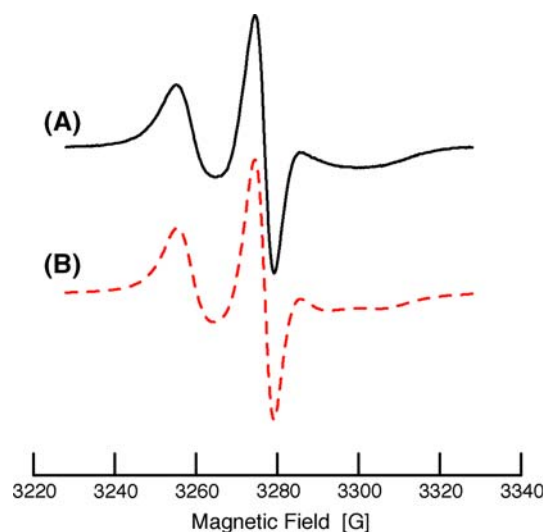
**Fig. 3** Experimental (solid line) and simulated (dotted line) EPR spectra of 5-DSA in aqueous dispersions of HCO at 20 °C are presented. The conventional parallel ( $2A_{\parallel}$ ) and perpendicular ( $2A_{\perp}$ ) hyperfine couplings are depicted for reference

Figure 3b shows the EPR slow-tumbling simulation for the observed spectrum. The perpendicular rotational diffusion coefficient ( $R_{\perp}$ ) obtained at 20 °C was  $3.4 \times 10^7 \text{ s}^{-1}$ . The value of the chain ordering ( $S_0$ ) was approximately 0.3–0.4 which suggests comparatively low rigidity of the region in the membrane.

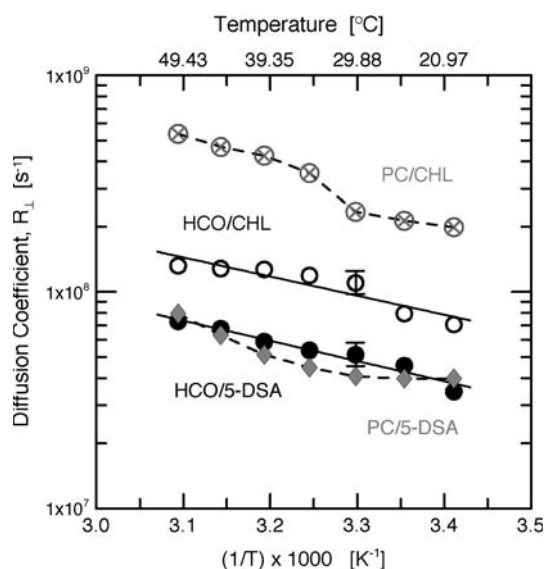
The values of  $R_{\perp}$  for 5-DSA probe are similar for both HCO and PC in the temperature range examined. It is interesting to note that the  $R_{\perp}$  value for PC from egg starts to increase slightly at around 30 °C. The results imply that the motion of the probe changes as the temperature increases.

Figure 4a shows the typical EPR spectrum of HCO/CHL in an aqueous dispersion at 20 °C. The spectral pattern obtained for CHL is similar to that previously reported [15]. The EPR spectral pattern also suggests that the head group region is relatively flexible. This is consistent with the low  $S_0$ -value (–0.2) obtained. The flexibility can be due to hydration induced by the oxyethylene groups in the region. Figure 4b shows the EPR slow-tumbling simulation of the observed spectrum. The perpendicular rotational diffusion coefficient for HCO/CHL obtained at 20 °C was  $7.1 \times 10^7 \text{ s}^{-1}$ .

Figure 5 presents perpendicular components of the diffusion coefficients for 5-DSA and CHL as a function of the temperature examined. The values of  $R_{\perp}$  for CHL have slightly faster diffusion coefficients than the one for 5-DSA. These results can be associated with the probe orientation as well as the moiety in the membrane (Fig. 2). The diffusion coefficients for both probes show similar temperature dependence.



**Fig. 4** Representative experimental (solid line) and simulated (dotted line) EPR spectra of CHL in aqueous dispersions of HCO at 20 °C are presented



**Fig. 5** Plot of the rotational diffusion coefficients ( $R_{\perp}$ ), 5-DSA (filled circles) and CHL (open circles), in aqueous dispersions of HCO as a function of the inverse of the absolute temperature. The 5-DSA (diamonds) and CHL (crossed circles) indicate the  $R_{\perp}$  values for PC from egg

The  $R_{\perp}$  value for HCO/CHL obtained at 50 °C was  $1.3 \times 10^8 \text{ s}^{-1}$ . The  $R_{\perp}$  value of  $3.6 \times 10^7 \text{ s}^{-1}$  for DPPC/CSL obtained at 50 °C is reported [16]. The value for HCO/CHL suggests a slightly faster motion. It is interesting to note that the values of  $R_{\perp}$  for PC/CHL are much higher than those of HCO/CHL and show that the rate of the probe motion is faster than that of HCO. The values for PC/CHL increase significantly at approximately 30 °C. The results obtained are consistent with those for HCO/5-DSA. The change can be correlated with a phase transition.

The activation energies using the diffusion coefficients resulting from the respective MOMD calculation were calculated based on the slope of the plot (Fig. 5). An Arrhenius type equation gives the activation energy ( $E_a$ ) for the spin probe in the HCO membrane [1],

$$R_{\perp} = R_{\perp}^0 \exp\left(\frac{-E_a}{RT}\right), \quad (3)$$

where  $E_a$  is the activation energy,  $R$  is the gas constant, and  $T$  is the absolute temperature. The activation energies for 5-DSA and CHL in the membrane are  $18 \pm 0.5$  and  $17 \pm 0.4 \text{ kJ/mol}$ , respectively. The higher activation energy calculated implies that the perpendicular motion of 5-DSA has a similar value to 19 kJ/mol of 7-DSA [1]. The activation energies are associated with the micro-viscosity around the spin probes.

In addition, these results can be associated with the amphiphilic membrane properties. Most likely  $\text{H}_2\text{O}$  easily

reaches the inner head group region. Because of the oxyethylene group in the region, significant dehydration may not occur even at higher temperatures. The surface region of the membrane can always make contact with  $\text{H}_2\text{O}$ . The rest of the lipids will change to a hydrophobic environment as the temperature rises. Therefore, the present EPR shows that the fluidity of the head group region does not change considerably throughout the temperatures examined.

## Conclusions

The current results obtained by the advanced EPR simulation provided quantitative insight into the behavior of the head group region of the nonionic amphiphilic membrane. The order parameter and rotational diffusion coefficients for the 5-DSA probe in the region were approximately 0.4 and  $3.4 \times 10^7 \text{ s}^{-1}$ , respectively. No abrupt change of the  $R_{\perp}$  value was observed for HCO/5-DSA and HCO/CHL. The activation energy of the probe in the range of 20–50 °C is close to the one in 7-DSA but the order parameter is lower than that of 7-DSA. The  $R_{\perp}$  values obtained for HCO/CHL implies that the probe moiety in the membrane is slow motion in comparison with PC/CHL. The results suggest that physicochemical dynamics of the HCO membrane is distinctive. Thus, the present evidence provides insights into quantitative understanding of the regional probe behavior as well as the amphiphilic membrane characteristics.

**Acknowledgments** The author thanks E. Yagi of Shiseido Research Center for useful suggestions of the sample preparations and Dr. Mingtao Ge of Cornell University for helpful discussions concerning the simulation. The latest version of the NLLS program was provided by Cornell University. Part of this research was supported by a Grant-in-Aid for Scientific Research (C) (18500347) from JSPS.

## References

- Nakagawa K (2003) Diffusion coefficient and relaxation time of aliphatic spin probes in a unique triglyceride membrane. *Langmuir* 19:5078–5082
- Crosas E, Egea MA, Reig F (2006) Spectroscopic techniques applied to the study of laminin fragments inserted into model membranes. *J Colloid Interface Sci* 295:264–269
- Budil DE, Lee S, Saxena S, Freed JH (1996) Nonlinear-least-squares of slow-motion EPR spectra in one and two dimensions using a modified Levenberg. *J Magn Reson Ser A* 120:155–189
- Shimshick EJ, McConnell HM (1973) Lateral phase separation in phospholipid membranes. *Biochemistry* 12:2351–2360
- Hubbell WL, McConnell HM (1971) Molecular motion in spin-labeled phospholipids and membranes. *J Am Chem Soc* 93:314–326
- Ligeza A, Tikhonov AN, Hyde JS, Subczynski WK (1998) Oxygen permeability of thylakoid membrane: electron paramagnetic resonance spin labeling study. *Biochim Biophys Acta* 1365:453–463



7. Tanaka M, Fukuda H, Horiuchi T (1990) Properties of the aqueous vesicle dispersion formed with poly(oxyethylene)hydrogenated castor oil. *J Am Oil Chem Soc* 67:55–60
8. Nakagawa K (2002) Spin-lattice relaxation times of aliphatic probes in a unique triglyceride membrane. *Chem Lett*, 666–667
9. Nakagawa K (2004) ESR spin probe investigation of chain ordering of triglycerol membrane. *Bull Chem Soc Jpn* 77:269–273
10. Freed JH (2000) New technologies in electron spin resonance. *Annu Rev Phys Chem* 51:655–689
11. Freed JH (1976) Theory of slow tumbling ESR spectra for nitroxides. In: Berliner LJ (ed) *Spin labeling, theory and applications*, vol 3. Academic, New York, pp 53–132
12. Meirovitch E, Nayeem A, Freed JH (1984) Analysis of protein–lipid interactions based on model simulations of spin resonance spectra. *J Phys Chem* 88:3451–3465
13. Ge M, Freed JH (1998) Polarity profiles in oriented and dispersed phosphatidylcholine bilayers are different, an ESR study. *Biophys J* 74:910–917
14. Ge M, Rananavare SB, Freed JH (1990) ESR studies of stearic acid binding to bovine serum albumin. *Biochim Biophys Acta* 1036:228–236
15. Shin Y-K, Freed JH (1989) Dynamic imaging of lateral diffusion by electron spin resonance and study of rotational dynamics in model membrane effect of cholesterol. *Biophys J* 55:537–550
16. Costa-Filho AJ, Shimoyama Y, Freed JH (2003) A 2D-ELDOR study of liquid ordered phase in multilamellar vesicle membrane. *Biophys J* 84:2619–2633

## Evaluation of Lipophilic Antioxidant Efficacy in Vivo by the Biomarkers Hydroxyoctadecadienoic Acid and Isoprostane

Yasukazu Yoshida · Mieko Hayakawa ·  
Yoko Habuchi · Nanako Itoh · Etsuo Niki

Received: 3 January 2007 / Accepted: 21 February 2007 / Published online: 27 March 2007  
© AOCS 2007

**Abstract** The evaluation of antioxidant activity in vivo is difficult. In this study, the effects of dietary natural and synthetic antioxidants on the lipid peroxidation in mice were assessed using a biomarker, total hydroxyoctadecadienoic acid (tHODE). Biological samples such as plasma, erythrocytes, and tissues were first reduced and then saponified to convert various oxidation products of linoleates to tHODE. Subsequently, the absolute concentration of tHODE and its stereoisomer ratio, [9- and 13-(*Z,E*)-HODE]/[9- and 13-(*E,E*)-HODE], which is a measure of the hydrogen donor capacity of antioxidants, were determined by gas chromatography–mass spectrometry (GC–MS) analyses. These were then compared with total 8-iso-prostaglandin  $F_{2\alpha}$  (t8-iso-PGF $_{2\alpha}$ ) which was also assessed after reduction and saponification. Remarkable increases in tHODE and t8-iso-PGF $_{2\alpha}$  levels were observed in the plasma, erythrocytes, liver, and brain of mice that were fed an  $\alpha$ -tocopherol ( $\alpha$ T)-stripped (E-free) diet for 1 month when compared with those of mice that were fed a standard diet ( $\alpha$ T = 0.002 wt%). When mice were fed for 1 month on an E-free diet supplemented with a lipophilic antioxidant (0.04 wt%), namely,  $\alpha$ T,  $\alpha$ -tocotrienol ( $\alpha$ T3),  $\gamma$ -tocopherol ( $\gamma$ T), or 2,3-dihydro-5-hydroxy-4,6-di-*tert*-butyl-2,2-dipentylbenzofuran (BO-653), a potent synthetic antioxidant, the increases of tHODE and t8-iso-PGF $_{2\alpha}$  in the plasma, erythrocytes, liver, and brain were suppressed to the levels lower than those of mice fed a standard diet. The (*Z,E/E,E*) HODE ratio was decreased in the plasma and erythrocytes

of mice fed the E-free diet when compared with that in mice fed the standard diet. This stereo-isomeric ratio was significantly recovered by the addition of  $\alpha$ T and BO-653. These results show that the tHODE level and the (*Z,E/E,E*) HODE ratio are useful biomarkers for the assessment of antioxidant capacity in vivo and that the antioxidant capacity decreased in the order: BO-653 >  $\alpha$ T3  $\geq$   $\alpha$ T,  $\gamma$ T, as assessed by tHODE levels from blood, liver, and brain.

**Keywords** Antioxidant · tHODE · Isoprostanes · Vitamin E · Vitamin C · Coenzyme Q · BO-653

### Abbreviations

BSTFA	<i>N,O</i> -bis(trimethylsilyl)trifluoroacetamide
BO-653	2,3-Dihydro-5-hydroxy-4,6-di- <i>tert</i> -butyl-2,2-dipentylbenzofuran
GPT	Glutamic pyruvic transaminase
tHODE	Total hydroxyoctadecadienoic acid
( <i>Z,E/E,E</i> ) HODE ratio	Molar ratio of HODE stereoisomer, [9- and 13-( <i>Z,E</i> )-HODE]/[9- and 13-( <i>E,E</i> )-HODE]
HPODE	Hydroperoxyoctadecadienoic acid
t8-iso-PGF $_{2\alpha}$	Total 8-iso-prostaglandin $F_{2\alpha}$
PBS	Phosphate-buffered saline
$\alpha$ T	$\alpha$ -Tocopherol
$\gamma$ T	$\gamma$ -Tocopherol
$\alpha$ T3	$\alpha$ -Tocotrienol
TBARS	Thiobarbituric acid reactive substances

Y. Yoshida (✉) · M. Hayakawa · Y. Habuchi ·  
N. Itoh · E. Niki

Human Stress Signal Research Center, National Institute of Advanced Industrial Science and Technology (AIST), 1-8-31 Midorigaoka Ikeda, Osaka 563-8577, Japan  
e-mail: yoshida-ya@aist.go.jp

### Introduction

Currently, it is generally accepted that lipid peroxidation is involved in the in vivo oxidative damage and pathogenesis

of several disorders and diseases that are induced by reactive oxygen and nitrogen species. Lipid peroxidation may directly damage biological molecules and membranes and may also induce the generation of toxic and signaling molecules [1, 2]. Accordingly, the potential role of antioxidant nutrients has been investigated in the prevention of cancer, cardiovascular disease, cataract, age-related macular degeneration, and aging. From this viewpoint, lipid peroxidation products have received considerable attention as biomarkers for the evaluation of antioxidants. Lipid hydroperoxides are formed as the major primary products during the oxidation of polyunsaturated fatty acids and their esters. However, these hydroperoxides are the substrates for many enzymes such as glutathione peroxidases and phospholipases, and they may readily undergo non-enzymatic secondary reactions [3]. Therefore, the amount of lipid hydroperoxides measured does not always reflect the extent of in vivo lipid peroxidation. F<sub>2</sub>-isoprostanes formed from arachidonic acid have been reported as the gold standard for the in vivo assessment of oxidative injury [4–6]; however, they are only one of the several minor products formed from arachidonates. Further, the use of thiobarbituric acid (TBA)-reactive substances (TBARS) is often debatable since TBA reacts with several oxidation products as well as with malonaldehyde to yield a pigment [7]. We have recently developed a method for the in vivo measurement of lipid peroxidation wherein total hydroxyoctadecadienoic acid (tHODE) is determined by gas chromatography–mass spectrometry (GC–MS) analysis of physiological samples after reduction with sodium borohydride followed by saponification with potassium hydroxide [8]. In this method, hydroperoxides and ketones as well as hydroxides of both the free and ester forms of linoleic acid are measured as tHODE. Further, both free and ester forms of 8-iso-prostaglandin F<sub>2α</sub> (8-iso-PGF<sub>2α</sub>), one of the major forms of F<sub>2</sub>-isoprostanes, can be assessed simultaneously with tHODE by using GC–MS. Linoleates are the major in vivo polyunsaturated fatty acids and their oxidation proceeds via a straightforward mechanism to yield 9- and 13-hydroperoxyoctadecadienoates (HPODE) as the major products [9]. Therefore, the tHODE measured by this method may account for a considerable amount of the in vivo lipid peroxidation.

Another advantage of using tHODE as a biomarker is that, in addition to its higher concentration than F<sub>2</sub>-isoprostanes, its regional and stereoisomers can be measured separately [8]. It is known that lipid peroxidation proceeds by different mechanisms depending on the oxidants to yield different isomers, and importantly, the efficacy of the antioxidants depends on the oxidants [10]. For example, the free radical-mediated oxidation of linoleates gives equal amounts of 9- and 13-HODE with both *cis*–*trans* and *trans*–*trans* isomers. The ratio of *cis*–*trans* to *trans*–*trans*

HODE is a measure of the capacity of hydrogen atom donation at the site of oxidation. This measurement, i.e., the (*Z,E,E,E*) HODE ratio, is practically important for the assessment and evaluation of the in vivo antioxidant capacity of natural and synthetic compounds, foods, and beverages as well as supplements and their components.

Vitamin E is a generic description of four isomers of tocopherol (T) and tocotrienol (T<sub>3</sub>) derivatives.  $\alpha$ -Tocopherol ( $\alpha$ T) is the most abundant form of vitamin E in vivo, although the level of  $\gamma$ -tocopherol ( $\gamma$ T) is often almost the same as or even higher than that of  $\alpha$ T in the diet and in plants. The role of  $\gamma$ T and tocotrienols has recently received considerable attention [11]. The synthetic antioxidant 2,3-dihydro-5-hydroxy-4,6-di-*tert*-butyl-2,2-dipentylbenzofuran (BO-653) has been designed to function as a potent radical-scavenging antioxidant [12]. It has been observed that BO-653 scavenges free radicals as rapidly as  $\alpha$ T; the aryloxy radical derived from BO-653 is considerably more stable than the  $\alpha$ -tocopheroxy radical [13], and BO-653 inhibits the oxidation of low-density lipoproteins [14] and plasma [15] more efficiently than  $\alpha$ T.

In the present study, we assessed the effects of the dietary lipophilic antioxidants mentioned above on experimental animals by the comparison of the tHODE level and the (*Z,E,E,E*) HODE ratio with those of total 8-iso-prostaglandin F<sub>2α</sub> (t8-iso-PGF<sub>2α</sub>).

## Experimental Procedures

### Reagents

BO-653 was kindly supplied by Chugai Pharmaceutical Co. Ltd. (Tokyo, Japan). Natural forms of  $\alpha$ T,  $\alpha$ T<sub>3</sub>, and  $\gamma$ T were kindly supplied by Eisai Co. Ltd. (Tokyo, Japan). 8-iso-PGF<sub>2α</sub>, 8-iso-prostaglandin F<sub>2α</sub>-d<sub>4</sub> (8-iso-PGF<sub>2α</sub>-d<sub>4</sub>), 13-hydroxy-9(*Z*),11(*E*)-octadecadienoic acid [13-(*Z,E*)-HODE], 13-hydroxy-9(*E*),11(*E*)-octadecadienoic acid [13-(*E,E*)-HODE], 9-hydroxy-10(*E*),12(*Z*)-octadecadienoic acid [9-(*E,Z*)-HODE], 9-hydroxy-10(*E*),12(*E*)-octadecadienoic acid [9-(*E,E*)-HODE], and 9(*S*)-hydroxy-10(*E*),12(*Z*)-octadecadienoic-9,10,12,13-d<sub>4</sub> acid (9-HODE-d<sub>4</sub>) were obtained from Cayman Chemical Company (MI, USA). Other materials were of the highest commercially available grade.

### Animals and Protocols

Male mice (specific pathogen free, C57BL/6J, weighing 19–24 g, and 11 weeks old) were purchased from Nippon Clea Co. (Tokyo, Japan). They were divided into six groups by the types of diet: a control diet containing 0.002 wt%  $\alpha$ T (cont), vitamin E-free (E-free) diet

(Funabashi Nojyo, Chiba, Japan), an E-free diet fortified with 0.04 wt%  $\alpha$ T (aT),  $\alpha$ T3 (aT3),  $\gamma$ T (gT), or BO-653 (BO). The composition of the E-free diet was summarized in our previous report [16]. The mice were kept under standardized conditions of light (7 a.m.–7 p.m.), temperature (22 °C), and humidity (70%). After 1 month, the animals were sacrificed under anesthesia with diethyl ether. The experimental protocols were approved by the Institutional Animal Care and Use Committee (IACUC) of the National Institute of Advanced Industrial Science and Technology.

#### HPLC Analysis

Plasma lipophilic antioxidants were extracted with chloroform–methanol (2:1, v/v). Mouse liver and brain were homogenized in saline (liver:saline = 1:3, w/w) with a Polytron PT3100 tissue homogenizer (Kinematica AG, Lucerne, Switzerland). Chloroform–methanol (100  $\mu$ L, 2:1, v/v) was added to the homogenized suspension (50  $\mu$ L, 25 w/w%) and the lipids and vitamin E were extracted by centrifugation (20,400 $\times$ g, 4 °C, 10 min) after mixing vigorously with a vortex mixer. Subsequently,  $\alpha$ T,  $\gamma$ T, and BO-653 were measured by an HPLC with an amperometric electrochemical detector (NANOSPACE SI-1, Shiseido Co. Ltd., Tokyo, Japan) set at 800 mV combined with an octadecyl-bonded silica (ODS) column (LC18, 5  $\mu$ m, 250  $\times$  4.6 mm, Sigma-Aldrich Japan Com., Tokyo, Japan); methanol-*tert*-butyl alcohol (95:5, v/v) containing 50 mM sodium perchlorate was used as the eluent at a rate of 1 mL/min. The level of vitamin C in the plasma and homogenates of liver and brain was measured by using an HPLC equipped with a UV detector (SPD-10AV, Shimadzu Corp., Kyoto, Japan; 263 nm). An NH<sub>2</sub> column (Wakosil 5NH<sub>2</sub>, 5  $\mu$ m, 250  $\times$  4.6 mm, Wako Pure Chemical Ind. Ltd., Tokyo, Japan) was used with 40 mM PBS-methanol (1:9, v/v) as the eluent delivered at a rate of 1 mL/min. Vitamin C was extracted from the samples with methanol (sample:methanol = 1:4, v/v) by the same method mentioned above; an aliquot of the upper layer was immediately injected into the HPLC column. Ubiquinols and ubiquinones were also measured simultaneously according to the method reported previously [17]. Briefly, they were measured by an HPLC with a NANOSPACE SI-1 set at 700 mV. The samples were passed through a reverse phase column (LC8, 5  $\mu$ m, 250  $\times$  4.6 mm, Sigma-Aldrich Japan Co., Tokyo, Japan) followed by a reducing column (RC-10, 30  $\times$  4 mm, Shiseido Co. Ltd., Tokyo, Japan); methanol-*tert*-butyl alcohol (85:15, v/v) containing 50 mM sodium perchlorate was used as the eluent at a rate of 1 mL/min. Ubiquinols and ubiquinones were extracted from the plasma and homogenates of liver and brain with methanol–hexane (sample:methanol:hexane = 1:5:10, v/v); an aliquot of the upper layer was immediately injected into the HPLC column.

#### Analyses of tHODE and 8-iso-PGF<sub>2x</sub> in the Plasma, Erythrocytes, Liver, and Brain

The tHODE and t8-iso-PGF<sub>2x</sub> were measured as follows by a slightly modified method reported previously [8]. Animal blood was collected from the inferior vena cava by using a heparinized syringe, and the erythrocytes and plasma were separated by centrifugation (1,580 $\times$ g, 10 min). Immediately after collection, the plasma (0.2 mL) was used for the analysis. The liver was also collected and stored at –80 °C until analysis. Internal standards—8-iso-PGF<sub>2x</sub>-d<sub>4</sub> (100 ng) and 9-HODE-d<sub>4</sub> (100 ng)—and 1 mL of methanol were added to the plasma (200  $\mu$ L) followed by reduction with an excessive amount of sodium borohydride at room temperature for 5 min under nitrogen. The liver and brain homogenates (25 wt%, 300  $\mu$ L) were diluted with saline (1,700  $\mu$ L). The internal standards and 1 mL of methanol were added to this solution followed by the reduction as described above. Subsequently, the reduced sample was mixed with 1 M KOH in methanol (1 mL) under nitrogen and incubated in a shaker at 40 °C for 30 min in the dark. The sample was centrifuged (1,580 $\times$ g, 4 °C, 10 min) and the supernatant was diluted with a fourfold volume of water (adjusted to pH 3, beforehand) and acidified (pH 3) using 2 N HCl. The acidified sample was centrifuged (1,580 $\times$ g, 4 °C, 10 min) and the supernatant was subjected to solid-phase extraction [8]. The eluted solution was evaporated with nitrogen gas and 30  $\mu$ L of a silylating agent, i.e., (*N,O* bis) trimethylsilyl trifluoroacetamide (BSTFA), was added to the dried residue. The solution was vigorously mixed with a vortex mixer for 1 min and incubated at 60 °C for 60 min to obtain trimethylsilyl esters and ethers. This solution was diluted with 70  $\mu$ L of acetone and an aliquot of this sample was then injected into the gas chromatography system (GC 6890 N, Agilent Technologies Co. Ltd., Palo Alto, CA, USA) equipped with a quadrupole mass spectrometer (5973 Network, Agilent Technologies Co. Ltd.). A fused-silica capillary column (HP-5MS, 5% phenyl methyl siloxane, 30 m  $\times$  0.25 mm, Agilent Technologies Co. Ltd.) was used. Helium was used as the carrier gas at a flow rate of 1.2 mL/min. The temperature was programmed to increase from 60 to 280 °C at 10 °C/min. The injector temperature was set at 250 °C and temperatures of the transfer lines to the mass detector and ion source were 250 and 230 °C, respectively. Electron energy was set at 70 eV. The amounts of t8-iso-PGF<sub>2x</sub> and tHODE were determined by using fragment ions of *m/z* 481 and 440, respectively. The internal standards used for the quantification of 8-iso-PGF<sub>2x</sub> and HODE were 8-iso-PGF<sub>2x</sub>-d<sub>4</sub> (*m/z* = 485) and 9-HODE-d<sub>4</sub> (*m/z* = 444), respectively.

## Statistical Analysis

Statistical analyses were performed on a Microsoft personal computer by variance analysis of using Tukey's test for multiple comparisons (ANOVA). Data are expressed as mean value  $\pm$  standard deviation (SD).

## Results

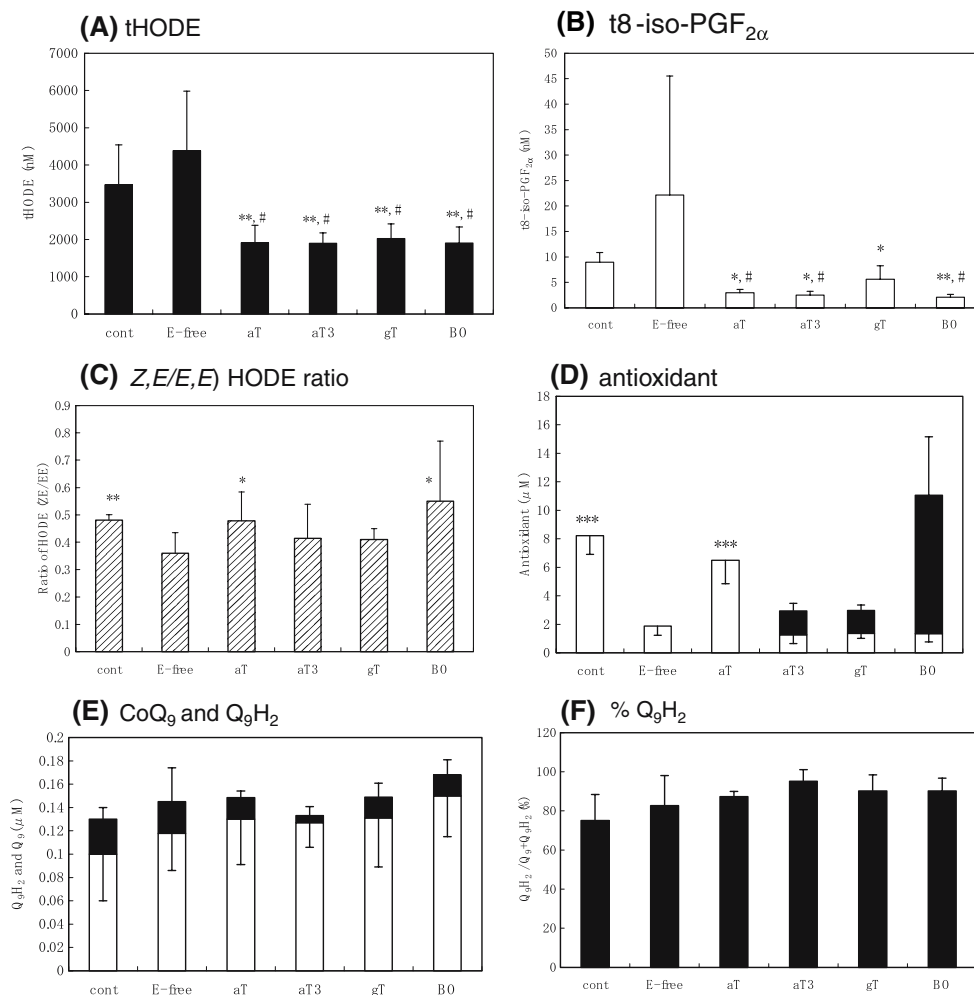
### Body Weight and Glutamic Pyruvic Transaminase (GPT) in Plasma

For 1 month, mice were fed either an E-free diet, a standard diet (cont-diet,  $\alpha$ T = 0.002 wt%), or an antioxidant-fortified diet that was prepared by the addition of  $\alpha$ T,  $\alpha$ T3,  $\gamma$ T, or BO-653 to the E-free diet. The body weight of the mice was measured once a week for 1 month, and it was found that among the six dietary groups, neither the weight nor the plasma GPT levels increased (data not shown).

### Plasma Levels of tHODE, t8-iso-PGF<sub>2 $\alpha$</sub> , and Antioxidants

As shown in Fig. 1, the E-free diet increased the plasma levels of both tHODE and t8-iso-PGF<sub>2 $\alpha$</sub> , while the antioxidants fortified decreased them. Thus, it was confirmed that the decrease in vitamin E increased lipid peroxidation in vivo. The tHODE concentrations were higher than those of t8-iso-PGF<sub>2 $\alpha$</sub>  by a factor of more than 100. It is noteworthy that the tHODE levels in the 0.04 wt% antioxidant-fortified groups were lower than that in the cont-diet (0.002 wt%  $\alpha$ T) group, suggesting every antioxidant tested was effective in reducing lipid peroxidation in vivo. The plasma levels of the antioxidants, namely,  $\alpha$ T,  $\alpha$ T3,  $\gamma$ T, BO-653, vitamin C, ubiquinol, and ubiquinone, were also assessed. The results are summarized in Fig. 1d–f. BO-653 and  $\alpha$ T were incorporated more efficiently than  $\alpha$ T3 and  $\gamma$ T. The fortified  $\alpha$ T3,  $\gamma$ T and BO-653 reduced the  $\alpha$ T level (Fig. 1d). There was no significant difference in the plasma levels of vitamin C among the different dietary groups

**Fig. 1** The plasma levels of tHODE (a), t8-iso-PGF<sub>2 $\alpha$</sub>  (b), the (Z,E/E,E) HODE ratio (c) and  $\alpha$ T (open bars) and the antioxidants corresponding to the diet types (solid bars) (d), ubiquinol-9 (open bars) and ubiquinone-9 (solid bars) (e), and ubiquinol-9 percentage (f) of mice fed either the standard diet (cont,  $\alpha$ T = 0.002 wt%,  $n = 10$ ), the E-free diet ( $n = 9$ ), or the antioxidant-fortified diet ( $n = 5$  in each group) for 1 month.  $\alpha$ T,  $\alpha$ T3,  $\gamma$ T, and BO-653 (0.04 wt%) were added to the E-free diet. Tukey's test for multiple comparisons (ANOVA) was carried out. Data are expressed as mean value  $\pm$  SD. The symbols \*, \*\*, and \*\*\* indicate  $P < 0.05$ ,  $P < 0.005$ , and  $P < 0.001$ , respectively, as compared to the E-free diet group and the symbol # indicates  $P < 0.05$  as compared to control diet group



(data not shown). The stereoisomer ratio (*Z,E/E,E*) HODE which is a measure of the hydrogen donor capacity of antioxidants decreased by the depletion of  $\alpha$ T, but recovered by the antioxidant, especially by  $\alpha$ T and BO-653 (Fig. 1c). The effect of  $\alpha$ T depletion and antioxidant supplementation did not affect coenzyme Q level.

#### Erythrocyte Levels of tHODE, t8-iso-PGF<sub>2 $\alpha$</sub> , and Antioxidants

Similar results were observed for erythrocytes as those for plasma. Vitamin E removal from diet increased both tHODE and t8-iso-PGF<sub>2 $\alpha$</sub>  and antioxidants fortified decreased them. The effects on t8-iso-PGF<sub>2 $\alpha$</sub>  were less significant than those for tHODE. BO-653 was incorporated into the erythrocytes to a considerable extent, although this level was lower than that of  $\alpha$ T (Fig. 2d). The (*Z,E/E,E*) HODE ratios in the cont-,  $\alpha$ T-,  $\alpha$ T3-,  $\gamma$ T-, and BO-diet groups were significantly higher than that in the E-free diet group (Fig. 2c).

#### Liver Levels of tHODE, t8-iso-PGF<sub>2 $\alpha$</sub> , and Antioxidants

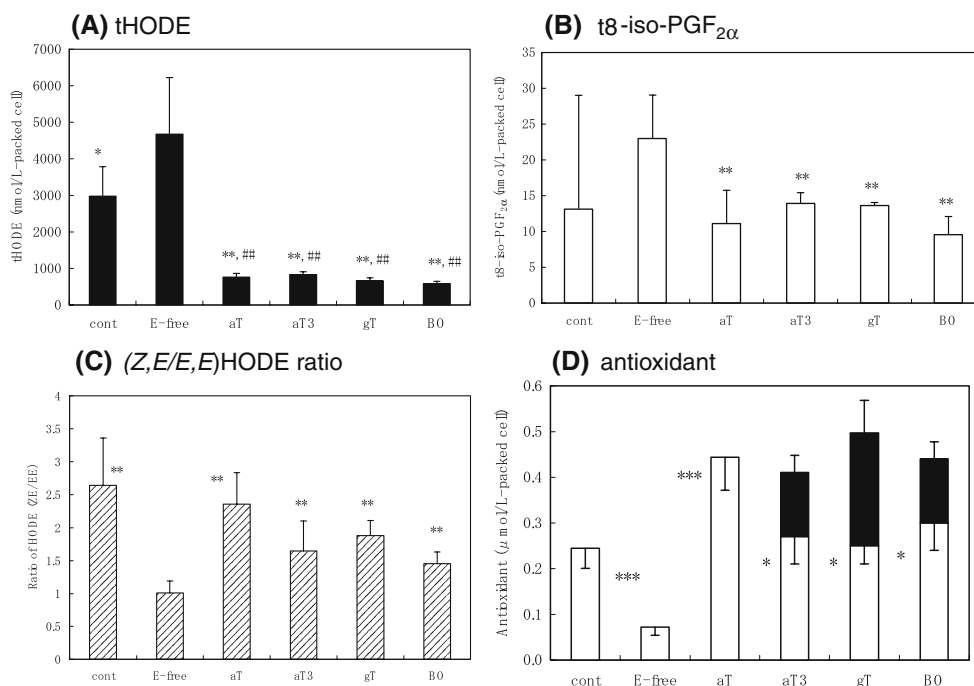
The effects of the antioxidants were clearly observed in the liver. As shown in Fig. 3a and b, the liver levels of tHODE and t8-iso-PGF<sub>2 $\alpha$</sub>  showed a significant increase by vitamin E depletion from diet, while the antioxidants lowered these lipid peroxidation products to the level less than those of

the control diet group. The liver levels of the antioxidants  $\alpha$ T,  $\alpha$ T3,  $\gamma$ T, BO-653, vitamin C, ubiquinol, and ubiquinone were also assessed and the data are summarized in Fig. 3d and e and Table 1. There was no significant difference among the dietary groups with regard to the liver levels of ubiquinol-9 or ubiquinone-9 (Table 1). The concentration of BO-653 in the liver of BO-653-diet group was much higher than that of  $\alpha$ T in the  $\alpha$ T-diet group (Fig. 3d), as observed previously [18]. The (*Z,E/E,E*) HODE ratios in the  $\alpha$ T3- and BO-653-diet groups were significantly lower than that in the E-free diet group (Fig. 3c).

#### Brain Levels of tHODE, t8-iso-PGF<sub>2 $\alpha$</sub> , and Antioxidants

The effects of antioxidants on the brain are of interest in connection with their potential use for neuronal diseases. The vitamin E removal from diet increased both tHODE and t8-iso-PGF<sub>2 $\alpha$</sub>  and the antioxidant fortification attenuated such increase (Fig. 4a, b). However, compared with plasma, erythrocytes, and liver, the effects of antioxidant removal and fortification were small in brain. For example, the vitamin E-free diet for 1 month decreased  $\alpha$ T concentration to less than 1/3 for plasma and erythrocytes and 1/10 in liver, but only 4/5 for brain. A few interesting data may be pointed out for brain. Firstly, the ratio of tHODE/t8-iso-PGF<sub>2 $\alpha$</sub>  in brain (35.6 mol/mol) was much smaller than that in plasma, erythrocytes and liver (387, 226, 278 mol/mol, respectively) in the control diet group.

**Fig. 2** The erythrocyte levels of tHODE (a), t8-iso-PGF<sub>2 $\alpha$</sub>  (b), the (*Z,E/E,E*) HODE ratio (c), and  $\alpha$ T (open bars) and the antioxidants corresponding to the diet types (solid bars) (d) in mice. The symbols and experimental conditions are the same as those in Fig. 1 except for the number of mice in E-free diet group ( $n = 7$ ). Tukey's test for multiple comparisons (ANOVA) was carried out. Data are expressed as mean values  $\pm$  SD. The symbols \* and \*\* indicate  $P < 0.01$  and  $P < 0.001$ , respectively, as compared to the E-free diet group and the symbol ## indicates  $P < 0.01$  as compared to control diet group



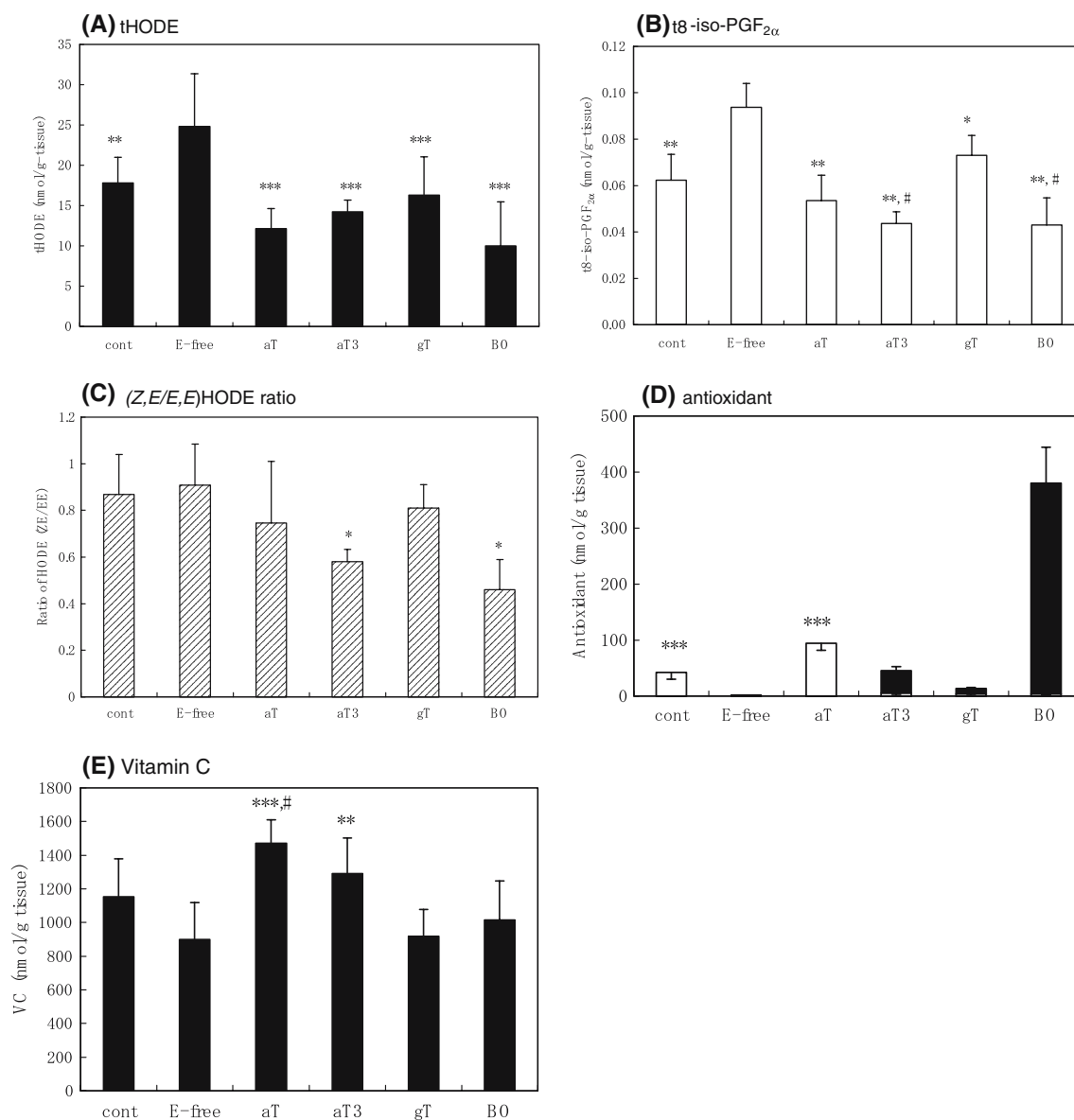


**Fig. 3** The liver levels of tHODE (a), t8-iso-PGF<sub>2α</sub> (b), the (Z,E/E,E)HODE ratio (c), αT (open bars) and the antioxidants corresponding to the diet types (solid bars) (d), and vitamin C (e) in mice. The symbols and experimental conditions are the same as those in Fig. 1 except for the number of mice in E-free diet group ( $n = 10$ ). Tukey's test for

multiple comparisons (ANOVA) was carried out. Data are expressed as mean value  $\pm$  SD. The symbols \*, \*\*, and \*\*\* indicate  $P < 0.05$ ,  $P < 0.005$ , and  $P < 0.001$ , respectively, as compared to the E-free diet group and the symbol # indicates  $P < 0.05$  as compared to control diet group

Secondly, the percentage of reduced form ubiquinol in total coenzyme Q is much smaller in brain than in liver and plasma (Table 1). Thirdly, the brain level of αT was higher than that of the other antioxidants. But, it is interesting that the net increase in αT3 was higher than that in αT (Fig. 4d).

## Discussion

The reactivity of radical-scavenging antioxidants in vitro may be determined quantitatively by several methods

and the correlation with structure has been documented extensively for various antioxidants. However, the antioxidant efficacy in vivo is determined by several factors such as concentration, localization, and mobility at the microenvironment, fate of antioxidant-derived radical, interaction with other antioxidants, bioavailability, that is, uptake, retention, metabolism, and excretion, as well as the chemical reactivity toward radicals [10, 19]. Therefore, the evaluation of antioxidant efficacy in vivo is difficult. One potential approach is to measure the effects of antioxidant supplementation or removal on the

**Table 1** Concentrations of ubiquinol-9 (Q<sub>9</sub>H<sub>2</sub>) and ubiquinone-9 (Q<sub>9</sub>) in plasma, liver, and brain of mice

Tukey's test for multiple comparison (ANOVA) was carried out. Data for Q<sub>9</sub>H<sub>2</sub> ratio are expressed as mean value ± standard deviation (SD). Significant difference against E-free diet, \*  $P < 0.01$ , \*\*  $P < 0.005$

Diet	Cont	E free	αT	αT3	γT	BO-653
Concentrations (Q <sub>9</sub> H <sub>2</sub> + Q <sub>9</sub> , mean)						
Plasma (μM)	0.130	0.145	0.149	0.133	0.149	0.168
Liver (nmol/g tissue)	63.1	63.3	76.8	71.2	69.2	84.5
Brain (nmol/g tissue)	35.5	28.7	50.4	42.8	35.7	40.1
Q <sub>9</sub> H <sub>2</sub> /Q <sub>9</sub> H <sub>2</sub> + Q <sub>9</sub> (%)						
Plasma	75.1 ± 13.3	82.7 ± 15.4	87.3 ± 2.7	95.2 ± 5.9	90.2 ± 8.2	90.2 ± 6.5
Liver	55.5 ± 6.6	45.5 ± 5.2	52.8 ± 3.7	52.5 ± 3.1	48.9 ± 5.8	51.9 ± 4.5
Brain	24.0 ± 5.7	15.5 ± 1.8	26.2 ± 4.7**	20.8 ± 0.8*	21.3 ± 2.3*	23.5 ± 2.6*

oxidative status by using biomarkers. In the present study, the effects of αT removal from the diet and also of fortification of other antioxidants on the level of lipid peroxidation products, tHODE and t8-iso-PGF<sub>2x</sub> were investigated.

The effects of different diets on the increase or decrease in tHODE and t8-iso-PGF<sub>2x</sub> relative to control diet are summarized in Table 2. It can be easily seen that vitamin E removal from the diet increased both tHODE and t8-iso-PGF<sub>2x</sub> and every antioxidant decreased them. The tHODE and 8-iso-PGF<sub>2x</sub> patterns were largely the same in the plasma, erythrocytes, and liver, where the concentration of tHODE was approximately two orders larger than that of 8-iso-PGF<sub>2x</sub>. However, it is interesting that in accordance with the fact that the brain contains relatively higher amounts of arachidonic acid, the level of tHODE in the brain is only 10 to 30-fold higher than that of t8-iso-PGF<sub>2x</sub>. As mentioned previously [8, 20], this is reasonable since linoleates are the major in vivo lipids although they are less reactive toward free radicals than arachidonates; further, the oxidation of linoleates proceeds by a straightforward mechanism to give much simpler products than arachidonates [21, 22], thus the selectivity for the formation of HPODE is much higher than that of 8-iso-PGF<sub>2x</sub>.

The ratio of *cis-trans* to *trans-trans* HODE is a measure of the capacity of hydrogen atom donation at the site of oxidation [23, 24]. We were able to evaluate the in vivo site-specific efficacy of the antioxidants based on the stereoisomer ratio (*Z,E/E,E*) HODE as observed in the previous reports [16, 24, 25]. For example, when compared with the E-free diet, the potent natural antioxidant αT resulted in low levels of tHODE and a high (*Z,E/E,E*) HODE ratio in the plasma, erythrocytes, liver, and brain. αT3, which is another potent isoform of vitamin E, was also found to be effective in vivo. It should be noted that the (*Z,E/E,E*) HODE ratio was clearly increased by αT, αT3,

and BO-653 in the plasma and erythrocytes depending on the antioxidant capacity; however, no increase was observed in the liver or brain. Further, αT3 as well as BO-653 induced a low (*Z,E/E,E*) HODE ratio only in the liver, although the tHODE levels were decreased in both groups when compared with that in the E-free diet group. The reason for this is unclear at present; however, the inhibition of enzymatic lipid oxidation may be at least partially responsible. In fact, 15-lipoxygenase is known to yield the regiospecific, stereospecific, and enantiospecific product 13(*S*)-(*Z,E*)-HPODE [26]. Khanna et al. [27] observed that a small amount of αT3, but not αT, suppressed glutamate-induced cell death by binding to the catalytic site of 12-lipoxygenase. Further studies are needed to clarify this observation.

The present study clearly shows that the efficacy of antioxidants in vivo can be evaluated reasonably well based on the tHODE level and its stereoisomer ratio and that the antioxidant capacity decreased in the order: BO-653 > αT3 ≥ αT, γT when tHODE levels in blood, liver, and brain were compared. However, needless to say, further study is required to evaluate the role and efficacy of antioxidants and nutrients in humans. The effects of αT on human health remain debatable since certain epidemiological and intervention studies have reported contradictory results [28, 29]. This may not be surprising because the lipid peroxidation must proceed by different mechanisms in vivo and the antioxidant activity must be determined based on several factors as mentioned above. The present study showed that tHODE and its stereoisomer ratio are promising tools for such evaluations.

In conclusion, this study shows that tHODE and its stereoisomer distribution as well as isoprostanes are appropriate biomarkers for the assessment of the antioxidant capacity of various foods, beverages, and supplements in vivo. Further studies are required to verify their efficacy in humans.



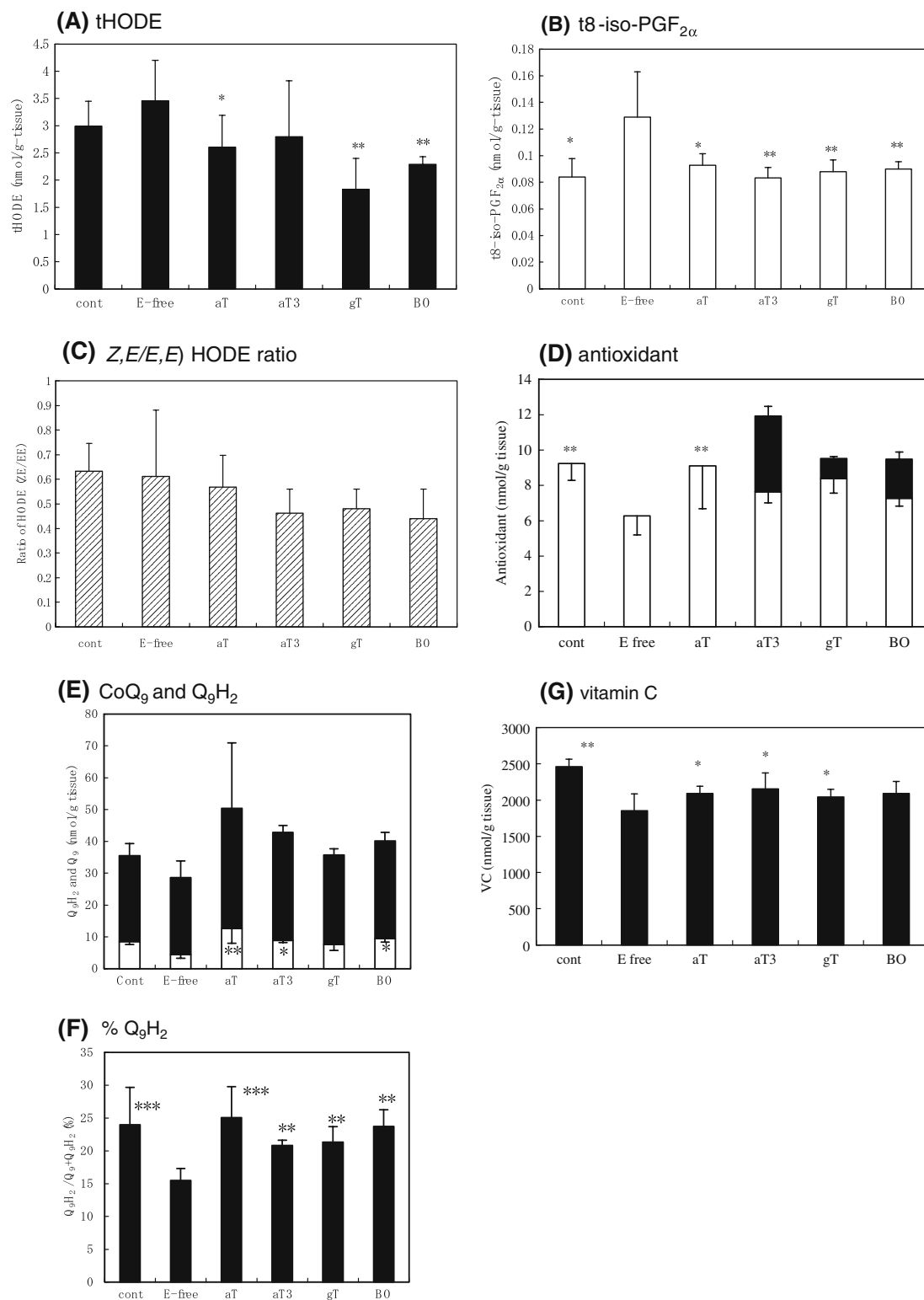


**Fig. 4** The brain levels of tHODE (a), t8-iso-PGF<sub>2α</sub> (b), the (Z,E/E,E) HODE ratio (c), αT (open bars) and the antioxidants corresponding to the diet types (solid bars) (d), ubiquinol-9 (open bars) and ubiquinone-9 (solid bars) (e), and ubiquinol-9 percentage (f), and vitamin C (g) in mice. The symbols and experimental

conditions are the same as those in Fig. 1 except for the number of mice in E-free diet group ( $n = 5$ ). Tukey's test for multiple comparisons (ANOVA) was carried out. Data are expressed as mean value  $\pm$  SD. The symbols \*, \*\*, and \*\*\* indicate  $P < 0.05$ ,  $P < 0.01$ , and  $P < 0.005$ , respectively, as compared to the E-free diet group

**Table 2** Relative ratio of tHODE and t8-iso-PGF<sub>2α</sub> in antioxidant-fortified (0.04 wt%) and vitamin E-free diet groups to that in control-diet (α-tocopherol, 0.002 wt%) group

	Plasma		Erythrocytes		Liver		Brain	
	tHODE	t8-iso-PGF <sub>2α</sub>	tHODE	t8-iso-PGF <sub>2α</sub>	tHODE	t8-iso-PGF <sub>2α</sub>	tHODE	t8-iso-PGF <sub>2α</sub>
Cont	1 (3,468)	1 (8.97)	1 (2,978)	1 (13.2)	1 (17.3)	1 (0.0623)	1 (2.99)	1 (0.0840)
–E	1.26	2.47	1.56	1.74	1.43	1.50	1.16	1.54
+aT	0.55	0.33	0.26	0.49	0.61	0.86	0.75	0.72
+aT3	0.55	0.28	0.28	0.60	0.64	0.47	0.81	0.64
+gT	0.58	0.62	0.22	0.60	0.66	0.78	0.53	0.68
+BO	0.55	0.23	0.20	0.42	0.40	0.46	0.66	0.70

The value in the parenthesis shows the absolute concentration (plasma, nM; erythrocytes, nmol/L packed cell; liver and brain, nmol/g tissue). The number of mice is shown in the legends of Figs. 1, 2, 3, and 4

**Acknowledgments** We would like to gratefully acknowledge the generous gift of the natural forms of α- and γ-tocopherol and α-tocotrienol from the Eisai Co. Ltd., and that of the synthetic antioxidant BO-653 from the Chugai Pharmaceutical Co. Ltd. This study was partially supported by a grant from the AOB Research Committee, by a Grant-in-Aid for Scientific Research (C) from the Ministry of Education, Science, Sports and Culture (17500495, 2006), by a grant from the Foundation, Oil and Fat Industry Kaikan, and by a donation from Eisai Food and Chemical Co. Ltd.

## References

- Leonarduzzi G, Arkan MC, Basaga H, Chiarotto E, Sevanian A, Poli G (2000) Lipid oxidation products in cell signaling. *Free Radic Biol Med* 28:1370–1378
- Tang DG, La E, Kern J, Kehrer JP (2002) Fatty acid oxidation and signaling in apoptosis. *Biol Chem* 383:425–442
- Girotti AW (1998) Lipid hydroperoxide generation, turnover, and effector action in biological systems. *J Lipid Res* 39:1529–1542
- Morrow JD, Hill KE, Burk RF, Nammour TM, Badr KF, Roberts LJ II (1990) A series of prostaglandin F<sub>2</sub>-like compounds are produced in vivo in humans by a non-cyclooxygenase, free radical-catalyzed mechanism. *Proc Natl Acad Sci* 87:9383–9387
- Pratico D, Rokach J, Lawson J, FitzGerald GA (2004) F<sub>2</sub>-isoprostanes as indices of lipid peroxidation in inflammatory diseases. *Chem Phys Lipids* 128:165–171
- Musiek ES, Yin H, Milne GL, Morrow JD (2005) Recent advances in the biochemistry and clinical relevance of the isoprostane pathway. *Lipids* 40:987–994
- Kikugawa K (1997) Use and limitation of thiobarbituric acid (TBA) test for lipid peroxidation. *Recent Res Dev Lipid Res* 1:73–96
- Yoshida Y, Niki E (2004) Detection of lipid peroxidation in vivo: total hydroxyoctadecadienoic acid and 7-hydroxycholesterol as oxidative stress marker. *Free Radic Res* 38:787–794
- Porter NA, Caldwell SE, Mills KA (1995) Mechanisms of free radical oxidation of unsaturated lipids. *Lipids* 30:277–290
- Niki E (2004) Antioxidants and atherosclerosis. *Biochem Soc Trans* 32:156–159
- Yoshida Y, Niki E, Noguchi N (2003) Comparative study on the action of tocopherols and tocotrienols as antioxidant: chemical and physical effects. *Chem Phys Lipids* 123:63–75
- Noguchi N, Iwaki Y, Takahashi M, Komuro E, Kato Y, Tamura K, Cynshi O, Kodama T, Niki E (1997) 2,3-Dihydro-5-hydroxy-2,2-dipentyl-4,6-di-*tert*-butylbenzofuran: design and evaluation as a novel radical-scavenging antioxidant against lipid peroxidation. *Arch Biochem Biophys* 342:236–243
- Watanabe A, Noguchi N, Fujisawa A, Kodama T, Tamura K, Cynshi O, Niki E (2000) Stability and reactivity of aryloxy radicals derived from a novel antioxidant BO-653 and related compounds. Effects of substituent and side chain in solution and membranes. *J Am Chem Soc* 122:5438–5442
- Noguchi N, Okimoto Y, Tsuchiya J, Cynshi O, Kodama T, Niki E (1997) Inhibition of oxidation of low-density lipoprotein by a novel antioxidant, BO-653, prepared by theoretical design. *Arch Biochem Biophys* 347:141–147
- Itoh N, Yoshida Y, Hayakawa M, Noguchi N, Kodama T, Cynshi O, Niki E (2004) Inhibition of plasma lipid peroxidation by anti-atherogenic antioxidant BO-653, 2,3-dihydro-5-hydroxy-4,6-di-*tert*-butyl-2,2-dipentylbenzofuran. *Biochem Pharmacol* 68:813–818
- Yoshida Y, Hayakawa M, Habuchi Y, Niki E (2006) Evaluation of the dietary effects of coenzyme Q in vivo by the oxidative stress marker, hydroxyoctadecadienoic acid and its stereoisomer ratio. *Biochim Biophys Acta* 1760:1558–1568
- Yamashita S, Yamamoto Y (1997) Simultaneous detection of ubiquinol and ubiquinone in human plasma as a marker of oxidative stress. *Anal Biochem* 250:66–73
- Yoshida Y, Itoh N, Hayakawa M, Piga R, Cynshi O, Jishage K, Niki E (2005) Lipid peroxidation induced by carbon tetrachloride and its inhibition by antioxidant as evaluated by an oxidative stress marker, HODE. *Toxicol Appl Pharmacol* 208:87–97
- Niki E, Noguchi N (2000) Evaluation of antioxidant capacity. What capacity is being measured by which method? *IUBMB Life* 50:323–329
- Yoshida Y, Hayakawa M, Niki E (2005) Hydroxyoctadecadienoic acid as free radical-induced oxidative stress marker in vivo. *Biofactors* 24:7–15
- Tallman KA, Pratt DA, Porter NA (2001) Kinetic products of linoleate peroxidation: rapid? β-fragmentation of non-conjugated peroxy radicals. *J Am Chem Soc* 123:11827–11828
- Roschek B Jr, Tallman KA, Rector CL, Gillmore JG, Pratt DA, Punta C, Porter NA (2006) Peroxyl radical clocks. *J Org Chem* 71:3527–3532
- Barclay LRC, Vinqvist MR, Antunes F, Pinto RE (1997) Antioxidant activity of vitamin E determined in a phospholipid membrane by product studies: avoiding chain transfer reactions by vitamin E radicals. *J Am Chem Soc* 119:5764–5765
- Yoshida Y, Niki E (2006) Review: bio-markers of lipid peroxidation in vivo; hydroxyoctadecadienoic acid and hydroxycholesterol. *Biofactors* 27:195–202
- Yoshida Y, Itoh N, Hayakawa M, Habuchi Y, Inoue R, Chen ZH, Cao J, Cynshi O, Niki E (2006) Lipid peroxidation in mice fed

- choline-deficient diet and its inhibition by antioxidants as evaluated by an oxidative stress marker, HODE. *Nutrition* 22:303–311
26. Yamashita H, Nakamura A, Noguchi N, Niki E, Kuhn H (1999) Oxidation of low density lipoprotein and plasma by 15-lipoxygenase and free radicals. *FEBS Lett* 445:287–290
  27. Khanna S, Roy S, Ryu H, Bahadduri P, Swaan PW, Ratan RR, Sen CK (2003) Molecular basis of vitamin E action: tocotrienol modulates 12-lipoxygenase, a key mediator of glutamate-induced neurodegeneration. *J Biol Chem* 278:43508–43515
  28. Micheletta F, Natoli S, Misuraca M, Sbarigia E, Diczfalusy U, Iuliano L (2004) Vitamin E supplementation in patients with carotid atherosclerosis: reversal of altered oxidative stress status in plasma but not in plaque. *Arterioscler Thromb Vasc Biol* 24:136–140
  29. Miller III ER, Pastor-Barriuso R, Dalal D, Riemersma RA, Appel LJ, Guallar E (2005) Meta-analysis: high-dosage vitamin E supplementation may increase all-cause mortality. *Ann Intern Med* 142:37–46

# Rapid Analysis of Acylglycerols in Low Molecular Weight Milk Fat Fractions

R. J. Craven · R. W. Lencki

Received: 1 September 2006 / Accepted: 21 February 2007 / Published online: 3 April 2007  
© AOCS 2007

**Abstract** A suitable analytical method was required to facilitate development of an industrial-scale short-path distillation (SPD) process. Short-path distillation produces milk fat distillates (MFD) enriched in low molecular weight milk fat components—viz. free fatty acids, monoacylglycerols, diacylglycerols, cholesterol and low molecular weight triacylglycerols. In this case, solid-phase extraction (SPE) was considered a better alternative than thin-layer chromatography for separating polar and apolar lipid components in MFD samples due to its speed and near-complete recoveries. Solid-phase extraction of MFDs yielded two fractions, both of which are sufficiently pure for subsequent analysis by gas chromatography. This procedure provided rapid and complete chemical characterization (including mass balances) of low-molecular weight milk-fat fractions.

**Keywords** Minor lipids · Milk fat · Short-path distillation · Diacylglycerol · Gas chromatography

## Abbreviations

DAG	Diacylglycerol
FA	Fatty acid
FFA	Free fatty acid
FID	Flame ionization detector
GC	Gas chromatograph(y)
MAG	Monoacylglycerol
MF	Milk fat
MFD	Milk fat distillate

MFD170	MFD collected at 170 °C
MFD185	MFD collected at 185 °C
MFD195	MFD collected at 195 °C
MFD200	MFD collected at 200 °C
MW	Molecular weight
RT	Retention time
SE	Standard error
SP	Short-path
SPD	Short-path distillation
SPE	Solid-phase extraction
SPE-1	First SPE fraction
SPE-2	Second SPE fraction
TAG	Triacylglycerol
TLC	Thin-layer chromatography
TMS	Trimethyl silyl
TMSI	Trimethyl silyl imidazole

## Introduction

Milk fat (MF) is more challenging to characterize than most natural lipids due to its compositional diversity. Detailed chromatographic analysis is difficult due to the wide range of FA in MF acylglycerols and the presence of minor components—specifically cholesterol, DAG, MAG and FFA [1–3].

Milk fat contains many compounds with novel functionality (e.g. short-chain fatty acids) [4–7], and industrial-scale short-path distillation (SPD) is a popular technique for their separation and purification [8–10]. The development, optimization and control of a commercial MF SPD system requires an analysis technique that is fast, accurate and economical. Fractionation of MF by SPD enriches the

R. J. Craven · R. W. Lencki (✉)  
Department of Food Science, University of Guelph,  
N1G 2W1 Guelph, ON, Canada  
e-mail: rlencki@uoguelph.ca

distillate fraction not only with low-MW TAG, but also with the minor components (*viz.* cholesterol, MAG, DAG and FFA) that have similar MW [8, 11–14]. Since low-MW TAG and DAG have similar retention times, their peaks overlap in the resulting gas chromatogram making their simultaneous analysis by GC-FID impractical [15].

No current analytical technology can easily achieve the simultaneous determination of both apolar (TAG) and polar (DAG, MAG, FFA and cholesterol) lipid fractions in MF. For this reason, methodologies generally rely on an initial separation of apolar and polar lipid fractions prior to chromatographic analysis [11, 14–21]. For instance, Itabashi, Myher and Kuksis [14] used thin layer chromatography (TLC) to separate TAG, DAG and MAG from a mixture produced by partial Grignard degradation of hydrogenated low MW MF TAG prior to analysis of the resulting DAG fractions by chiral-phase HPLC.

Classical lipid analysis techniques can provide excellent separations; however, these TLC-based methods are time-consuming and samples are subject to possible degradations and rearrangements (e.g. acyl migration) [18, 19, 22]. In addition, TLC is a subjective technique requiring a high degree of expertise and attention; it is not easily reduced to a set of uniform and repeatable steps, as is required for routine analysis. In recent years, solid-phase extraction (SPE) techniques have supplanted many TLC-related separations and liquid–liquid extractions due to their ease, reliability and near-complete recoveries [23–25]. Consequently, several approaches have been developed for the separation of lipid classes by SPE in vegetable and seed oils [26–28], and model biological extracts [25].

Thin layer chromatography has the unmatched flexibility and resolving power necessary for analyzing samples of unknown composition. On the other hand, SPE excels where samples are known to have similar composition and processing speed or the number of samples to be analyzed is important. A suitable SPE method for the analysis of milk fat distillate (MFD) produced by SPD would streamline laboratory, pilot plant scale-up, and quality control processes.

## Materials and Methods

Milk fat (Gay Lea, Guelph, ON, Canada) distillate (MFD) was produced in a 2" SPD unit (Pope Scientific, Menomonee Falls, WI, USA). All solvents were HPLC grade and all reagents and analytical standards were of the highest practical grade (Fisher Scientific, Mississauga ON; Sigma-Aldrich, St Louis, MO, USA). TLC bands and GC retention times were determined for FFA, MAG, DAG, cholesterol and TAG using appropriate standards (Sigma-Aldrich).

## Thin-Layer Chromatography

TLC plates, 20 × 20 cm with a 250 μm layer of silica G (Analtech Inc., Newark, DE, USA) were sprayed with a saturated solution of boric acid in water/methanol (25:75, by volume) and dried in a 120 °C oven for 30 min. Up to 10 mg of sample, dissolved in 200 μl chloroform, was applied in a thin line one inch from the bottom of the plate. Plates were developed with chloroform/acetone (96:4, by volume) and allowed to dry. To prepare samples for GC analysis, TLC plates were sprayed with a 0.05% solution of primuline (Sigma-Aldrich) in methanol. Lipid fractions were visible as blue bands when viewed under UV light. Lipid bands were marked, scraped from plates and extracted with chloroform. For direct observation of TLC separations, this procedure was followed with the following exceptions: small spots of sample were applied to the boric acid treated TLC plates; once developed and dried, plates were sprayed with 50% sulphuric acid and placed in a 180 °C oven for one hour [22, 29].

## Solid-Phase Extraction: Load Limit Determination

Known quantities of MFD (starting with 100 mg) were eluted through two stacked cartridges. These cartridges were treated as a single unit until the first lipid fraction (SPE-1) had been eluted. Afterwards, the cartridges were separated and eluted independently—the top cartridge for the second lipid fraction (SPE-2), and the bottom cartridge for SPE-1 and then for SPE-2. These steps were repeated with successively smaller samples until MAG and DAG were no longer detected in the SPE-2 fraction from the bottom cartridge [24].

## Solid-Phase Extraction: Sample Preparation

The MFD samples were separated on 3 ml SPE cartridges containing a 500 mg bed-weight of diol bonded phase (Supelco, Bellefonte, PA, USA). The packing material in each diol cartridge was washed with 4 ml of hexane and was not allowed to dry. MFD dissolved in approximately 500 μl hexane was transferred quantitatively to the top of each hexane-washed SPE cartridge and two fractions were collected: SPE-1—eluted with 6 ml of hexane/methylene chloride/diethyl ether (89:10:1, by volume); and SPE-2—eluted with 4 ml of chloroform/methanol (2:1, by volume). The solvent in each fraction was evaporated under a stream of nitrogen and samples were analyzed by GC. SPE-1 was dissolved in iso-octane and analyzed directly for TAG content, TMS derivatives were prepared for SPE-2 prior to GC analysis. Diol bonded phases are preferred for the isolation of DAG because they do not promote acyl migration [27, 28].

### Fatty Acid Methyl Ester Analysis

The SPE-1 samples were dissolved in 1 ml iso-octane and 100  $\mu$ l 2N sodium methoxide in methanol was added. Samples and reactants were thoroughly mixed using a vortex mixer for 1 min, then allowed to react at room temperature. After 5 min, 250 mg sodium bisulphate monohydrate was added and the sample vial was centrifuged for 3 min. For SPE-2 samples, half the amount of solvent and reagents was used. 2  $\mu$ l was injected onto a custom-made (1.5 m  $\times$  1/8") stainless steel column containing 10% Silar 9CP on 80/100 Chromosorb b WAW (Supelco) housed in a Hewlett Packard 5890 (Agilent, Palo Alto, CA, USA) GC equipped with FID. The carrier gas was nitrogen at 10 psi, the inlet and detector temperature were set at 235  $^{\circ}$ C, and the temperature was held at 34  $^{\circ}$ C for 2.5 min, increased to 155  $^{\circ}$ C at 17.5  $^{\circ}$ C/min, increased to 190  $^{\circ}$ C at 2.0  $^{\circ}$ C/min, increased to 230  $^{\circ}$ C at 17.5  $^{\circ}$ C/min, and held at 230  $^{\circ}$ C for 8 min [30–32].

### Trimethyl-Silyl Derivatives

Identification and quantification of FFA, MAG and DAG is greatly improved by preparing their trimethyl-silyl (TMS) derivatives. SPE-2 samples and TLC fractions were dissolved in 400  $\mu$ l pyridine, a vortex mixer being used to ensure complete dissolution. Then, 100  $\mu$ l trimethyl silylimidazole (TMSI; 98+%, Sigma-Aldrich) was added and the reaction mixture was once again blended thoroughly with a vortex mixer. The reaction was conducted in a dry nitrogen atmosphere and can be considered virtually complete within 5 min at room temperature [33]. For samples less than 10 mg, half the volume of pyridine and TMSI was used.

### GC Analysis of Acylglycerols

Fractions obtained by SPE and TLC were analyzed on a polarizable capillary column (30 m  $\times$  0.25 mm) (Restek MXT-65TG from Chromatographic Specialties, Brockville ON) with a crosslinked 65% diphenyl/35% dimethyl polysiloxane stationary phase that is stable to 370  $^{\circ}$ C. Polarizable columns separate acylglycerols primarily by carbon number and secondarily by their degree of unsaturation [34, 35]. The column was housed in a Hewlett Packard 6890 (Agilent) GC equipped with FID. 1  $\mu$ L of sample was injected manually and optimal sample loading was obtained by adjusting the split ratio manually. The split was adjusted so that for SPE-1 fractions the highest TAG peak was approximately 150 picoamperes (pA), and for SPE-2 fractions the highest peak (apart from cholesterol) was approximately 100 pA. Hydrogen carrier gas flowed at a rate of 2.8 ml/min, the injector and detector

were held at 330 and 370  $^{\circ}$ C, respectively, and the oven temperature was held for 2 min at 60  $^{\circ}$ C, increased to 275  $^{\circ}$ C at 15  $^{\circ}$ C/min, increased to 340  $^{\circ}$ C at 4  $^{\circ}$ C/min, increased to 360  $^{\circ}$ C at 30  $^{\circ}$ C/min, and held at 360  $^{\circ}$ C for 5 min. The extraordinarily large number of peaks in a MF chromatogram makes identification, integration and quantification exceedingly difficult—consequently, acylglycerols are typically identified and grouped by the number of acyl carbon atoms [19].

### Results and Discussion

To investigate the application of SPE to the analysis of low MW MF fractions prepared by SPD, four representative samples were selected. These MFD were collected at 170, 185, 195 and 200  $^{\circ}$ C and a pressure of approximately 6 mtorr—their corresponding yields were 2.26, 4.67, 6.64 and 17.17% (by mass) respectively. These samples were collected at the lowest (MFD170 collected at 170  $^{\circ}$ C), highest (MFD200 collected at 200  $^{\circ}$ C) and typical (MFD185 and MFD 195 collected at 185 and 195  $^{\circ}$ C, respectively) operating temperatures.

Load limit determination experiments are necessary to evaluate any SPE procedure prior to use. The load limit for a 500 mg diol bonded phase SPE cartridge was determined to be 12 mg of MAG and DAG. For analyses, samples weighing approximately 30 mg were separated by SPE—this is well below the load limit for 500 mg of bonded phase but 3 times the capacity of standard 20  $\times$  20 cm (250  $\mu$ m) TLC plates [18, 22].

Both qualitative and quantitative data are available from the same SPE experiment; complete mass balances are easily obtained and sample losses due to SPE are extremely low. This is demonstrated by high recovery and reproducibility of SPE separations reported in Table 1. Quantitative SPE data is determined gravimetrically—this non-destructive measurement leaves SPE fractions intact and unaltered for subsequent qualitative analysis. In contrast, quantitative and qualitative TLC are separate methodologies requiring dedicated technologies and sample treatments [18, 22]. Even when dedicated TLC techniques are applied, good

**Table 1** Yields of fractions obtained by solid-phase extraction (SPE-1 and SPE-2) of milk fat distillates (MFD) collected at 170, 185, 195 and 200  $^{\circ}$ C (average  $\pm$  SE,  $n = 6$ )

Fraction	Yield (mass %)			
	170 $^{\circ}$ C	185 $^{\circ}$ C	195 $^{\circ}$ C	200 $^{\circ}$ C
SPE-1	68.06 $\pm$ 0.16	78.23 $\pm$ 0.20	79.21 $\pm$ 0.65	86.65 $\pm$ 0.29
SPE-2	29.88 $\pm$ 0.38	20.51 $\pm$ 0.20	19.49 $\pm$ 0.08	12.25 $\pm$ 0.26
Total	97.94	98.74	98.70	98.90

quantitative accuracy is still difficult to achieve [18] and the various manipulations (e.g. plate-scraping, extraction, washing and the addition of acid and dye) required for qualitative TLC limit yields (to as little as 80%) and hinder precise quantitation [25].

The purity of SPE fractions produced from MFD was investigated by TLC. A sample of each MFD was separated by SPE and a boric acid treated TLC plate was spotted with each of the resulting fractions (Fig. 1). After development with chloroform/acetone (96:4, by volume), the plate was sprayed with 50% sulfuric acid and charred at 180 °C for one hour; this method makes as little as 1 µg of lipid visible [22, 29]. TLC spots were identified by comparison with standards and by referring to the current literature [14]. These experiments indicate that SPE-1 is mainly composed of TAG (fraction a), with additional spots in distillates collected at 185 and 170 °C (fraction c) indicating the presence of FFA and cholesterol. Between these, an extremely light band was observed (it is, however, not

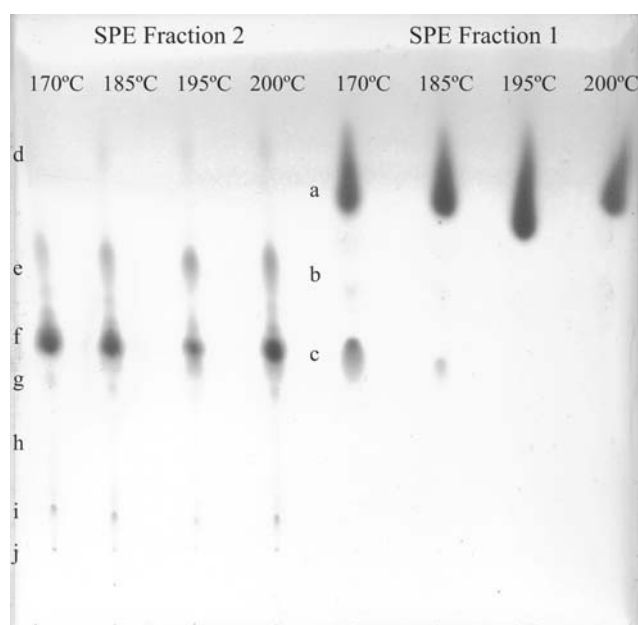


**Fig. 1** Boric acid TLC analysis of fractions obtained by solid-phase extraction (SPE-1 and SPE-2) of milk fat distillates (MFDs) collected at 170, 185, 195 and 200 °C. For a typical boric acid TLC analysis these bands would be identified as: **a** TAG; **b** DAG (if present); **c** DAG (if present), cholesterol and FFA; **d** TAG (if present); **e** DAG; **f**, **g** DAG, cholesterol and FFA; **h** unknown; **i** 1- and 2-MAG; and **j** glycerol. They are, however, according to GC analysis (with their relative quantity in mass percent presented in brackets): **a** TAG (51.2); **b** TAG and cholesterol (5.0); **c** cholesterol (9.4); **d** TAG (0.7); **e** DAG with two long acyl chains (predominantly 1,2-DAG) and cholesterol (13.4); **f** DAG with one long and one short acyl chain (predominantly 1,3-DAG), cholesterol and FFA (14.7); **g** DAG with one long and one short acyl chain (1,3- and 1,2(2,3)-DAG), cholesterol and FFA (0.5); **h** nothing; **i** MAG and cholesterol (4.9); and **j** nothing

discernible in the printed figure) for distillates collected at 170 and 185 °C (fraction b). Though light, this band cannot be dismissed since it may indicate the presence of DAG in SPE-1 and thus, an incomplete separation by SPE—in which case this method may not be suitable for its intended purpose. For this reason, replicate samples of the SPE-1 fraction of MFD170 were separated by preparative TLC and analyzed in greater detail by GC.

Figure 1 also shows that SPE-2 fractions had high concentrations of cholesterol (fraction f) and DAG (fraction e), smaller quantities of MAG (fraction i) and FFA (fraction g), and very small quantities of TAG (fraction d). This last band (fraction d) cannot be dismissed since it indicates the presence of TAG in SPE fraction 2. This band indicates incomplete separation by SPE and if the concentration of TAG is too high, this may interfere with proper integration of SPE-2 fractions during GC analysis. Consequently, MFD170 SPE-2 samples were also separated by preparative TLC and analyzed in greater detail by GC.

The SPE-1 and SPE-2 fractions of MFD170 were separated by preparative boric acid TLC and analyzed by GC to verify and quantify the potential impurities observed in Fig. 1. MFD170 was chosen because it has the highest proportion of SPE-2 (Table 1) and therefore the highest concentration of MAG and DAG. Three MFD170 SPE-1 fractions were separated by boric acid TLC—by dividing each fraction between two plates the sample load did not exceed 10 mg per plate. Plates were developed in chloroform/acetone (96:4, by volume) and TLC bands became visible under UV light after spraying with a solution of primuline. Whether visible or not, all three regions (i.e. fractions a, b and c) of the TLC plates were scraped, extracted, weighed and analyzed by GC. For the DAG region (fraction b) of the plates, silica gel scraped from all six TLC plates was combined to increase sample concentration, and the likelihood of detecting contaminants. Likewise, four SPE-2 samples were separated by boric acid TLC—since each of these samples was approximately 10 mg, only one TLC plate was required for each SPE-2 fraction. After spraying with primuline, then viewing and marking bands under UV light, all seven regions (fractions d through j) of each plate were scraped, extracted, weighed and analyzed by GC. For the TAG region (fraction d) and for fractions g, h and j of the plates, the silica gel from all four plates was combined to increase sample concentration and aid in detection.

Chromatograms of the main TLC fractions isolated from SPE-2 of MFD170 are provided in Fig. 2. For a typical lipid the length of acyl chains in DAG plays no role in their separation by TLC [30]. Boric acid TLC separates these DAG on the basis of their positional isomerism into two bands: 1,3-DAG and 1,2(2,3)-DAG. In native milk fat, however, the acyl chain lengths for 1,3- and 1,2-DAG are

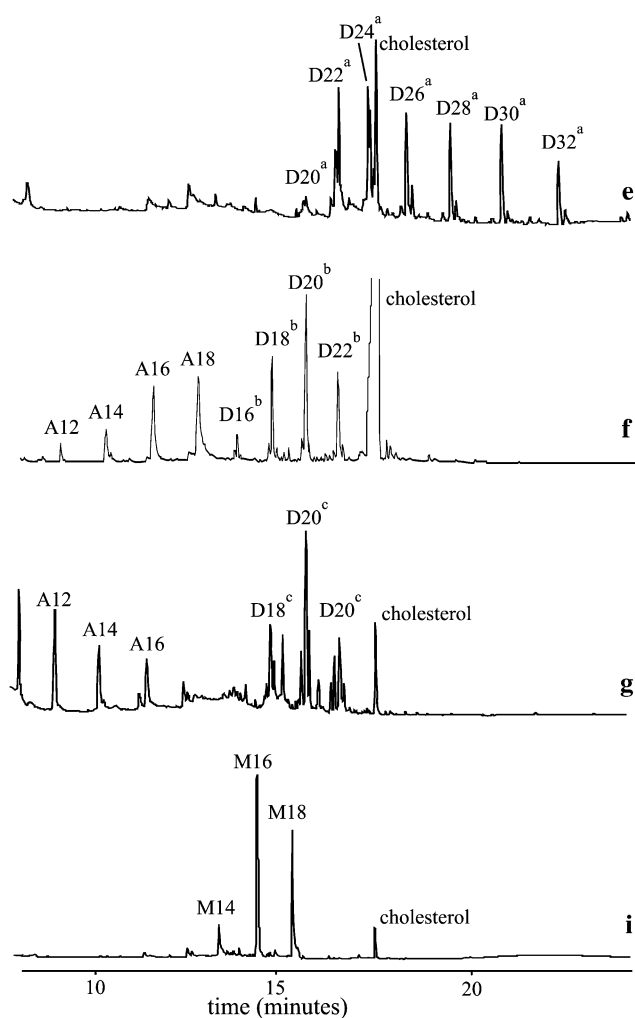


**Fig. 2** Gas chromatographic analysis of boric acid TLC fractions isolated from the second solid-phase extraction fraction (SPE-2) of MFD collected at 170 °C (MFD170). Chromatograms labeled *e*, *f*, *g* and *i* correspond to TLC spots as they appear in Fig. 1. Fractions *e*, *f* and *i* are single samples, whereas, for fraction *g*, silica gel from four plates was combined and extracted. Peaks are identified by a single-letter prefix (*A* for FFA, *M* for MAG, *D* for DAG) followed by the total number of carbon atoms in the FA residues. <sup>a</sup>DAG with two long acyl chains (predominantly 1,2-DAG). <sup>b</sup>DAG with one long and one short acyl chain (predominantly 1,3-DAG). <sup>c</sup>DAG with one long and one short acyl chain (1,3- and 1,2(2,3)-DAG)

different due to the positional specificity with which acyl chains are placed on the glycerol backbone during milk fat biosynthesis [2]. In addition, TLC separation of milk fat DAG is based primarily on differences of acyl chain length and secondarily on positional isomerism. Thus, milk fat DAG produce an upper band containing DAG with two long acyl chains: 1,3-DAG (if present) above 1,2-DAG, and a lower band containing DAG with one long and one short acyl chain: 1,3-DAG above 1,2-DAG (if present). A detailed explanation of this phenomenon is provided by Itabashi, Myher and Kuksis [14]. Chromatograms for

fractions *e*, *f* and *g* in Fig. 2 show that these TLC bands each contain a portion of the complete DAG profile in addition to cholesterol and FFA. TLC band *e* contains the long- and medium-chain 1,2-DAG whereas TLC bands *f* and *g* contain DAG having at least one short chain and therefore, lower carbon numbers. Band *f* contains 1,3-DAG and in theory band *g* should contain pure 1,2-DAG formed, for the most part, from 1,3-DAG that have undergone acyl migration. However, it appears band *g* has been contaminated with material from band *f* and thus, contains both 1,2- and 1,3-DAG. This was difficult to avoid given the lack of clear delineation between bands *f* and *g* on the TLC plate, the relatively high concentration of band *f* (Table 2) and the fact that the chromatogram for band *g* was produced by combining and extracting the silica gel from four plates in order to increase its concentration.

Chromatograms for fractions *e*, *f* and *g* also show that FFA is not distributed evenly on boric acid treated TLC plates—longer FFA are concentrated in fractions *e* and *f* while fraction *g* is enriched in shorter FFA. The chromatogram for fraction *i* shows this fraction contains the MAG (positional isomer was not determined) and some cholesterol.

The distribution of mass between the various TLC fractions is reported in the caption for Fig. 1. Based on differences in their relative sizes, the potential contamination of SPE-1 by DAG (fraction *b*) would be of greater concern than contamination of SPE-2 by TAG (fraction *d*). Chromatograms for both fractions of interest are shown in Fig. 3 (fractions *b* and *d*) along with a pure TAG fraction (*a*) and DAG fraction (*e*). Comparison of these four chromatograms demonstrates that there is no detectable DAG in fraction *b*; therefore, SPE-1 can be considered DAG-free. SPE-2, however, cannot be considered TAG-free since TAG are detectable in the chromatogram for fraction *d*. Nevertheless, peaks corresponding to TAG account for less than 33% (by mass) of those present in fraction *d*; therefore, the SPE-2 fraction is at most 0.67% (by mass) TAG. Since this mass is distributed over more than 100 peaks, the presence of TAG at these levels is unlikely to interfere

**Table 2** FFA determined by GC analysis of fractions obtained by SPE (SPE-1 and SPE-2) of MFDs collected at 170, 185, 195 and 200 °C (average  $\pm$  SE,  $n = 3$ )

Fraction	Relative response (%)			
	170 °C	185 °C	195 °C	200 °C
SPE-1	10.57 $\pm$ 0.03	1.14 $\pm$ 0.47	0.08 $\pm$ 0.03	–
SPE-2	17.09 $\pm$ 0.91	27.34 $\pm$ 1.86	30.90 $\pm$ 2.19	27.44 $\pm$ 1.88
MFD (total)	12.30	6.50	6.09	3.36



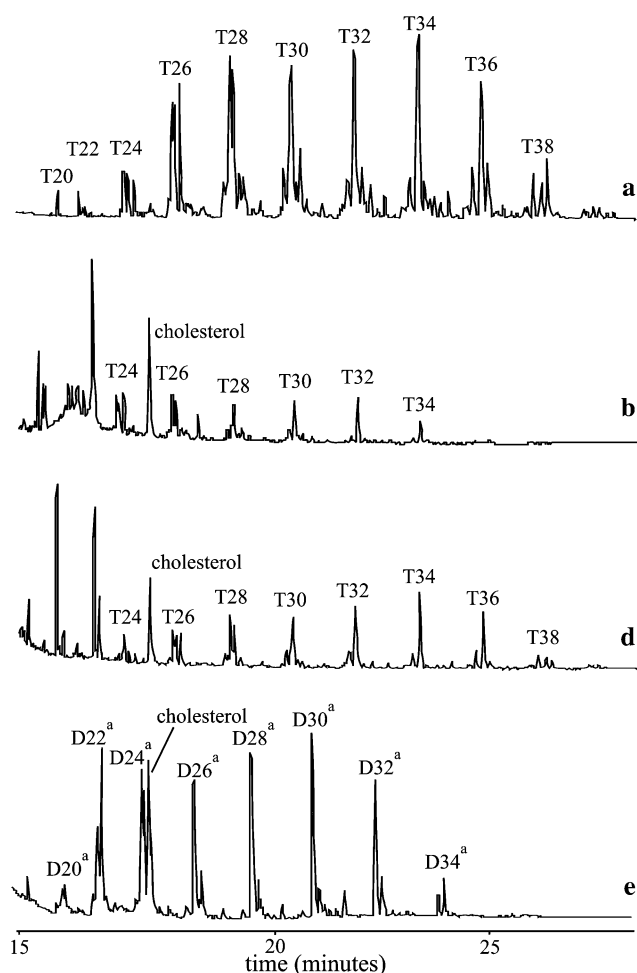


**Fig. 3** Gas chromatographic analysis of boric acid TLC fractions isolated from fractions obtained by SPE of MFD collected at 170 °C (MFD170). Labels for chromatograms correspond to TLC spots as they appear in Fig. 1 and are (from top to bottom): **a** TAG band for the first solid-phase extraction fraction (SPE-1) (one sample), **b** any potential DAG in SPE-1 (three samples combined), **d** any potential TAG in the second solid-phase extraction fraction (SPE-2) (four samples combined), **e** DAG band for SPE-2 (one sample). TAG peaks are identified by the letter T followed by the total number of carbon atoms in the FA residues. Other peaks are identified as described for Fig. 2

markedly with detection or integration of MAG, DAG and cholesterol in SPE-2 fractions.

As demonstrated in the preceding experiments, SPE is effective for the separation of TAG from DAG, MAG and cholesterol. SPE-1 fractions contain TAG and some FFA, whereas SPE-2 fractions contain MAG, DAG, cholesterol and some FFA. Thus, following SPE, MAG, DAG, cholesterol and TAG can all be accurately resolved by GC. To measure the precision of SPE for the fractionation of MFDs, three replicates of each MFD were separated by SPE and each fraction (SPE-1 and SPE-2) was analyzed by GC-FID. Gas chromatograms for SPE fractions

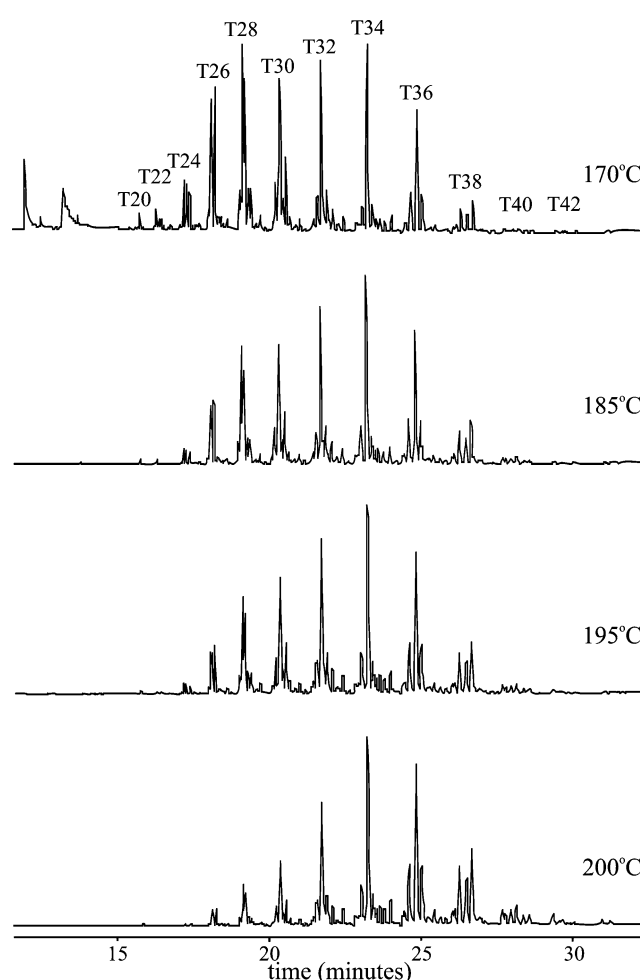


**Fig. 4** Gas chromatographic analysis for the first solid-phase extraction fractions (SPE-1) of MFDs collected at 170, 185, 195 and 200 °C. Peaks are identified as described for Figs. 2 and 3

obtained from MFD170, 185, 195 and 200 are shown in Figs. 4 and 5.

Free fatty acid is present in both SPE-1 and SPE-2 fractions, and thus, it appears that FFA is distributed between, rather than separated into the two SPE fractions. When lipid samples are separated on untreated silica TLC plates developed with acid-free solvent the same thing happens; FFA are not separated, instead they produce vertical streaks [18]. Consequently, the FFA content of replicate fractions prepared by SPE will not be consistent and it is best to view integration for FFA as an estimate (Table 2). Also, TMS derivatives were not prepared for SPE-1 fractions, whereas they were prepared for SPE-2 fractions. Thus, integration for SPE-2 FFA content should be more accurate than integration for SPE-1 FFA. Additionally, to allow the many small MAG and DAG peaks in chromatograms for SPE-2 to be integrated automatically, integration of FFA was conducted manually afterwards, thereby introducing errors inherent in such processes. The

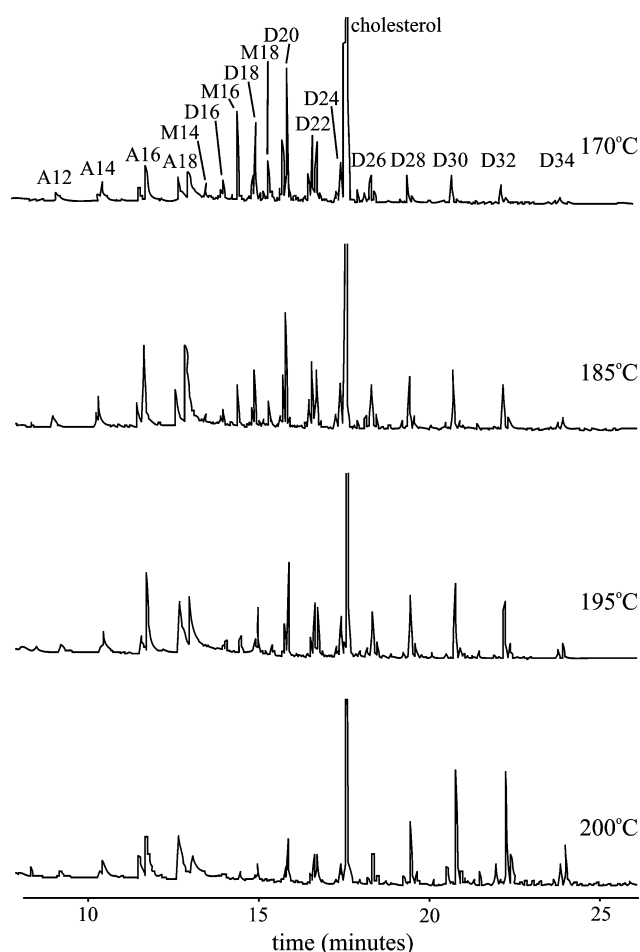


**Fig. 5** Gas chromatographic analysis for the second solid-phase extraction fractions (SPE-2) of MFDs collected at 170, 185, 195 and 200 °C. Peaks are identified as described for Figs. 2 and 3

standard errors for FFA in SPE-2 are high by GC analysis standards; nevertheless, when compared to those encountered in quantitative TLC (with relative errors as high as 20%) they appear quite reasonable [18]. If an accurate and rapid appraisal of overall FFA content is required, it may be better to obtain this by titration with sodium hydroxide (AOCS Official Method, Ca 5a-40).

Integration results for TAG in SPE-1, and MAG, DAG and cholesterol in SPE-2 fractions are presented in Tables 3 and 4. The relative detector response (in percent) has been reported in order to facilitate the comparison of standard errors. The standard errors reported demonstrate that the method presented is indeed precise. To quantify acylglycerols on a mass or molar basis, however, empirical response factors should be employed.

Triacylglycerol with extremely low carbon numbers of 20 and 22 are clearly delineated in the chromatograms of SPE-1 for MFD170 (Fig. 4), and of the TLC fraction of

SPE-1 for this same MFD (Fig. 3a). The detection of TAG with such low MW is not without precedent; Myher, Kuksis and Marai [13] have previously detected traces of T20 in a MFD sample using reversed-phase HPLC/MS.

Diacylglycerol with low carbon numbers of 16 and 18 are discernable in the chromatograms of all SPE-2 fractions (Fig. 5), and a TLC fraction (Fig. 2f) of SPE-2 for MFD170. These low MW DAG are most likely 1,3-DAG with a butyryl or acetyl group in the *sn*-3 position [14].

Monoacylglycerols were isolated by boric acid TLC from the SPE-2 fraction of MFD170 (Fig. 2i) and could be identified in three of the chromatograms for SPE-2 fractions (Fig. 5: 170, 185 and 195 °C). In these chromatograms, the MAG14 peak is super-imposed on the FFA18 peak. Baselines (drawn across the FFA18 peak) among sample replicates are not identical because the FFA18 content is not consistent between samples (see discussion above). As a result, the standard error for integration of MAG14 is quite high (Table 4), especially for the SPE-2 fraction of the MFD170.

FAME analysis results for SPE fractions of MFD are presented in Table 5. Methyl esters were prepared with methanolic sodium methoxide at room temperature. This procedure does not lead to the esterification of free fatty acid; therefore, proportions of FAME are for acyl groups on the glycerol backbone: i.e. TAG for SPE-1, and MAG and DAG for SPE-2 [31]. Proportions of FAME in SPE-1 and SPE-2 are different and changes in distillation temperature have different effects on their compositions. For example, the 4:0 content for SPE-2 changes radically over the four distillation temperatures, whereas for SPE-1 it changes very little. Thus, FAME profiles for TAG, MAG and DAG in MFD are different, and FAME analysis for a complete MFD is not indicative of the fatty acid profile of any single class of acylglycerol.

Methyl acetate (FAME of 2:0) was not quantified in the FAME analysis for SPE-1 or SPE-2 fractions (Table 5), although a peak corresponding to (or coincident with) methyl acetate was detected in all FAME analyses for the present study. This peak was confirmed by separate injection and co-injection of ethyl acetate transesterified with methanolic sodium methoxide. However, anything beyond detection, such as precise and accurate integration, of this volatile component would be difficult.

In conclusion, SPE provided accurate and precise results for resolving the acylglycerol composition of MFD. Accurate mass balances are critical for process development and were easily obtained by non-destructive means using SPE. Consequently, this method is well-suited to applications where speed is vital yet accuracy and detail must not be compromised (e.g. pilot plant trials).

**Table 3** Composition of the first fraction obtained by solid-phase extraction (SPE-1) of MFDs Collected at 170, 185, 195 and 200 °C (average  $\pm$  SE,  $n = 3$ )

Component	RT <sup>a</sup>	Relative response (%)			
		170 °C	185 °C	195 °C	200 °C
TAG20	15.6	0.03 $\pm$ 0.01			
TAG22	16.1	0.45 $\pm$ 0.01	0.17 $\pm$ 0.02	0.07 $\pm$ 0.00	0.04 $\pm$ 0.00
TAG24 <sup>b</sup>	17.0	1.15 $\pm$ 0.02	0.39 $\pm$ 0.02	0.20 $\pm$ 0.00	–
TAG26	18.0	4.28 $\pm$ 0.07	1.71 $\pm$ 0.15	1.11 $\pm$ 0.01	1.01 $\pm$ 0.10
TAG28	19.0	12.29 $\pm$ 0.05	6.70 $\pm$ 0.34	4.74 $\pm$ 0.02	1.72 $\pm$ 0.02
TAG30	20.3	17.31 $\pm$ 0.04	12.80 $\pm$ 0.32	10.30 $\pm$ 0.04	4.31 $\pm$ 0.03
TAG32	21.6	16.25 $\pm$ 0.10	15.28 $\pm$ 0.18	14.15 $\pm$ 0.06	7.84 $\pm$ 0.02
TAG34	23.2	15.13 $\pm$ 0.15	17.06 $\pm$ 0.24	17.47 $\pm$ 0.07	13.75 $\pm$ 0.03
TAG36	24.9	14.84 $\pm$ 0.12	18.94 $\pm$ 0.35	20.81 $\pm$ 0.03	22.16 $\pm$ 0.01
TAG38	26.8	11.36 $\pm$ 0.03	15.82 $\pm$ 0.17	18.18 $\pm$ 0.04	24.41 $\pm$ 0.05
TAG40	28.3	5.16 $\pm$ 0.22	7.95 $\pm$ 0.30	9.13 $\pm$ 0.06	15.07 $\pm$ 0.06
TAG42	29.6	1.41 $\pm$ 0.19	2.55 $\pm$ 0.18	2.91 $\pm$ 0.05	5.98 $\pm$ 0.03
TAG44	31.2	0.33 $\pm$ 0.06	0.63 $\pm$ 0.11	0.78 $\pm$ 0.05	2.20 $\pm$ 0.02
TAG46	32.9			0.16 $\pm$ 0.02	0.89 $\pm$ 0.01
TAG48	34.1				0.62 $\pm$ 0.01

<sup>a</sup> Retention time of the main peak in minutes<sup>b</sup> Integration includes even-numbered and next consecutive odd-numbered TAG for TAG24 to TAG46**Table 4** Composition of second fraction obtained by solid-phase extraction (SPE-2) of MFDs Collected at 170, 185, 195 and 200 °C (average  $\pm$  SE,  $n = 3$ )

Component	RT <sup>a</sup>	Relative response (%)			
		170 °C	185 °C	195 °C	200 °C
MAG14	13.5	0.85 $\pm$ 0.12	0.55 $\pm$ 0.06	0.23 $\pm$ 0.02	0.10
DAG16	14.0	1.57 $\pm$ 0.10	1.31 $\pm$ 0.08	1.27 $\pm$ 0.06	0.97 $\pm$ 0.06
MAG16	14.4	4.44 $\pm$ 0.09	2.42 $\pm$ 0.11	1.54 $\pm$ 0.06	0.51 $\pm$ 0.01
DAG18	15.0	5.75 $\pm$ 0.05	4.54 $\pm$ 0.11	4.05 $\pm$ 0.33	2.14 $\pm$ 0.07
MAG18	15.4	3.11 $\pm$ 0.02	2.20 $\pm$ 0.03	1.23 $\pm$ 0.11	0.32 $\pm$ 0.05
DAG20 <sup>b</sup>	15.9	11.10 $\pm$ 0.10	9.32 $\pm$ 0.05	7.97 $\pm$ 0.18	4.43 $\pm$ 0.11
DAG22	16.7	9.96 $\pm$ 0.08	9.67 $\pm$ 0.03	8.55 $\pm$ 0.05	5.34 $\pm$ 0.09
DAG24	17.4	3.64 $\pm$ 0.03	4.76 $\pm$ 0.04	5.13 $\pm$ 0.20	3.02 $\pm$ 0.13
Cholesterol	17.8	46.25 $\pm$ 0.17	37.87 $\pm$ 0.46	36.76 $\pm$ 0.76	26.92 $\pm$ 0.49
DAG26	18.4	4.32 $\pm$ 0.01	5.90 $\pm$ 0.04	6.58 $\pm$ 0.15	5.18 $\pm$ 0.01
DAG28	19.5	3.02 $\pm$ 0.06	6.19 $\pm$ 0.02	7.32 $\pm$ 0.08	8.19 $\pm$ 0.16
DAG30	20.8	2.81 $\pm$ 0.06	6.87 $\pm$ 0.03	8.73 $\pm$ 0.10	15.31 $\pm$ 0.14
DAG32	22.3	2.18 $\pm$ 0.04	5.90 $\pm$ 0.06	7.54 $\pm$ 0.12	17.97 $\pm$ 0.23
DAG34	24.0	0.82 $\pm$ 0.03	2.16 $\pm$ 0.04	2.68 $\pm$ 0.04	7.81 $\pm$ 0.26
DAG36	25.8	0.19 $\pm$ 0.01	0.34 $\pm$ 0.01	0.36 $\pm$ 0.04	1.41 $\pm$ 0.15
DAG38	27.8			0.03 $\pm$ 0.02	0.29 $\pm$ 0.03
DAG40	29.6			0.04 $\pm$ 0.00	0.12 $\pm$ 0.04

<sup>a</sup> Retention time of the main peak in minutes<sup>b</sup> Integration includes even-numbered and next consecutive odd-numbered DAG for DAG20 to DAG36

**Table 5** FAME analysis for fractions obtained by solid-phase extraction (SPE-1 and SPE-2) of MFDs collected at 170, 185, 195 and 200 °C

FA	Composition (mole %)							
	SPE-1				SPE-2			
	170 °C	185 °C	195 °C	200 °C	170 °C	185 °C	195 °C	200 °C
4:0	23.37	22.66	20.53	20.56	20.89	15.42	14.06	9.25
5:0	0.08	0.08	0.07	0.07	–	–	–	–
6:0	10.03	9.04	8.37	7.86	8.92	7.39	6.45	3.93
7:0	0.11	0.10	0.28	0.07	–	–	–	–
8:0	6.83	5.61	5.09	3.72	4.69	4.33	3.66	3.07
9:0	0.19	0.17	0.14	0.10	0.13	–	–	–
10:0	9.86	8.65	7.99	6.21	7.91	8.51	7.83	5.77
11:0	0.93	0.86	0.79	0.63	0.89	0.98	0.86	0.68
12:0	7.86	7.22	7.11	6.06	6.69	7.42	7.34	5.90
14:0	13.24	13.66	14.37	14.17	13.94	14.96	15.71	15.61
14:1	0.88	0.96	1.08	1.13	1.60	1.69	1.82	1.91
15:0	1.07	1.07	1.31	1.11	1.08	1.24	1.28	1.39
16:0	17.19	19.78	21.78	24.86	20.24	23.27	25.62	31.82
16:1	0.71	1.40	1.69	1.79	2.10	2.21	3.02	3.60
17:0	–	–	0.11	–	–	–	–	–
18:0	1.71	2.07	2.40	2.99	1.41	1.87	1.92	3.13
18:1	4.86	5.50	5.74	7.40	7.84	8.85	8.99	11.57
18:2	0.55	0.63	0.66	0.75	1.22	1.34	1.14	1.75
18:3	0.24	0.33	0.38	0.33	0.44	0.51	0.28	0.62

**Acknowledgments** We gratefully acknowledge the financial support of the Dairy Farmers of Ontario, Ontario Ministry of Agriculture, Food and Rural Affairs, Ontario Ministry of Training, Colleges and Universities, and National Sciences and Engineering Research Council of Canada.

## References

- Jensen RG (2002) The composition of bovine milk lipids: January 1995 to December 2000. *J Dairy Sci* 85:295–350
- Jensen RG, Newburg DS (1995) Bovine milk lipids. In: Jensen RG (eds) *Handbook of milk fat composition*. Academic, San Diego, pp 543–575
- Christie WW (1987) The analysis of lipids with special reference to milk fat. In: Hamilton RJ, Bhati A (eds) *Recent advances in chemistry and technology of fats and oils*. Elsevier, New York, pp 57–77
- Burgess KJ (2001) Milk fats as ingredients. *Int J Dairy Tech* 54(2):56–60
- Rajah KK (1994) Milk fat developments. *J Soc Dairy Tech* 47(3):81–83
- Jimenez-Flores R (1997) Trends in research for alternative uses of milk fat. *J Dairy Sci* 80:2644–2650
- Lencki RW, Smink N, Snetling H, Arul J (1988) Increasing short-chain fatty acid yield during lipase hydrolysis using a butterfat fraction and periodic aqueous extraction. *J Am Oil Chem Soc* 75(9):1195–1200
- Arul J, Boudreau A, Makhlof J, Tardif R, Bellavia T (1988) Fractionation of anhydrous milk fat by short-path distillation. *J Am Oil Chem Soc* 65(10):1642–1646
- Lanzani A, Bondioli P, Mariani C, Folegatte L, Venturini S, Fedeli E, Barreteau P (1994) A new short-path distillation system applied to the reduction of cholesterol in butter and lard. *J Am Oil Chem Soc* 71(6):297–303
- Campos RJ, Litwinenko JW, Marangoni AG (2003) Fractionation of milk fat by short-path distillation. *J Dairy Sci* 86:735–745
- Myher JJ, Kuksis A, Marai L (1988) Identification of the more complex triacylglycerols in bovine milk fat by gas chromatography-mass spectrometry using polar-capillary columns. *J Chromatogr* 452:93–118
- McCarthy MJ, Kuksis A, Beveridge JMR (1962) Gas-liquid chromatographic analysis of the triglyceride composition of molecular distillates of butter oil. *Can J Biochem* 40:1693–1703
- Myher JJ, Kuksis A, Marai L (1993) Identification of the less common isologous short-chain triacylglycerols in the most volatile 2.5% molecular distillate of butter oil. *J Am Oil Chem Soc* 70(12):1183–1191
- Itabashi Y, Myher JJ, Kuksis A (1993) Determination of positional distribution of short-chain fatty acids in bovine milk fat on chiral columns. *J Am Oil Chem Soc* 70(12):1177–1181
- Fagan P, Wijesundera C, Watkins P (2004) Determination of mono- and di-acylglycerols in milk lipids. *J Chromatogr A* 1054:251–259
- Mottram HR, Evershed RP (2001) Elucidation of the composition of bovine milk fat triacylglycerols using high-performance liquid chromatography-atmospheric pressure chemical ionization mass spectrometry. *J Chromatogr A* 926:239–253
- Mariani C, Contarini G, Zucchetti S, Toppino PM (1990) Significance of minor components of milk fat. *J High Res Chromatogr* 13:356–360
- Hammond EW (1993) *Chromatography for the analysis of lipids*. CRC Press, Boca Raton

19. Christie WW (1982) *Lipid analysis: isolation, separation, identification and structural analysis of lipids*. 2nd edn. Pergamon Press, Oxford
20. Christie WW (1989) *Gas chromatography and lipids; a practical guide*. The Oily Press Ltd, Ayr
21. Kuksis A, Myher JJ, Sandra P (1990) Gas-liquid chromatographic profiling of plasma lipids using high-temperature-polarizable capillary columns. *J Chromatogr* 500:427–441
22. Christie WW (2003) *Lipid analysis: isolation, separation, identification and structural analysis of lipids*. 3rd edn. The Oily Press, Bridgewater
23. Hennion MC (1999) Solid-phase extraction: method development, sorbents, and coupling with liquid chromatography. *J Chromatogr A* 856:3–54
24. Sigma-Aldrich (1998) Supelco bulletin 910: guide to solid phase extraction. Supelco, Bellefonte
25. Kaluzny MA, Duncan LA, Merritt MV, Epps DE (1985) Rapid separation of lipid classes in high yield and purity using bonded phase columns. *J Lipid Res* 26:135–140
26. Hopia AI, Piironen VI, Koivistoinen PE, Hyvonen LET (1992) Analysis of lipid classes by solid-phase extraction and high-performance size-exclusion chromatography. *J Am Oil Chem Soc* 69(8):772–776
27. Perez-Camino MC, Moreda W, Cert A (1996) Determination of diacylglycerol isomers in vegetable oils by solid-phase extraction followed by gas chromatography on a polar phase. *J Chromatogr A* 721:305–314
28. Ruiz-Gutierrez V, Perez-Camino MC (2000) Update on solid-phase extraction for the analysis of lipid classes and related compounds. *J Chromatogr A* 885:321–341
29. Thomas AE III, Scharoun JE, Ralston H (1965) Quantitative estimation of isomeric monoglycerides by thin-layer chromatography. *J Am Oil Chem Soc* 42:789–792
30. Ulberth F (1997) milk fat—determination of the fatty acid composition by gas-liquid chromatography, in ISO proposed methods
31. Christie WW (1992) Preparation of fatty acid methyl esters. *Inform* 3(9):1031–1034
32. Bannon CD, Craske JD, Hilliker AE (1985) Analysis of fatty acid methyl esters with high accuracy and reliability. iv. fats with fatty acids containing four or more carbon atoms. *J Am Oil Chem Soc* 62(10):1501–1507
33. Goh EM, Timms RE (1985) Determination of mono- and diglycerides in palm oil, olein and stearin. *J Am Oil Chem Soc* 62(4):730–734
34. Geeraert E, Sandra P (1985) Capillary GC of triglycerides in fats and oils using a high temperature phenylmethylsilicone stationary phase, part I. *J High Res Chromatogr* 8(August):415–422
35. Geeraert E, Sandra P (1987) Capillary GC of triglycerides in fats and oils using a high-temperature phenylmethylsilicone stationary phase. part ii. the analysis of chocolate fats. *J Am Oil Chem Soc* 64(1):100–105

## Validation of Two Methods for Fatty Acids Analysis in Eggs

Mônica R. Mazalli · Neura Bragagnolo

Received: 6 July 2006 / Accepted: 26 February 2007 / Published online: 28 March 2007  
© AOCS 2007

**Abstract** A comparative study between two methods (lipid extraction followed by saponification and methylation, and direct methylation) to determine the fatty acids in egg yolk was evaluated. Direct methylation of the samples resulted in lower fatty acid content and greater variation in the results than the lipid extraction followed by saponification and methylation. The low repeatability observed for the direct HCl methylation method was probably due to a less efficient extraction and conversion of the fatty acids into their methyl esters as compared to the same procedure starting with the lipid extract. As the lipid extraction followed by esterification method was shown to be more precise it was validated using powdered egg certified as reference material (RM 8415, NIST) and applied to samples of egg, egg enriched with polyunsaturated omega-3 fatty acids (n-3 PUFA), and commercial spray-dried whole egg powder.

**Keywords** GC · Fatty acids · Eggs

### Abbreviations

n-3 PUFA	Polyunsaturated omega-3 fatty acids
BF <sub>3</sub>	Methanolic boron trifluoride
FAME	Fatty acids methyl ester
EPA	Eicosapentaenoic acid
DHA	Docosahexaenoic acid
SFA	Saturated fatty acid
RSD%	Relative standard deviation

### Introduction

Fatty acids in foods are mostly analysed by gas chromatography (GC) of their methyl esters [1]. The most common method of sample preparation used for the determination of fatty acids in eggs is lipid extraction with chloroform-methanol [2] followed by conversion of the fatty acids into methyl esters [3]. This methodology involves two steps; first, the lipid is heated with NaOH in methanol, forming glycerol and free fatty acids in approximately 5 min, and secondly, the free fatty acids are then esterified with methanolic boron trifluoride (BF<sub>3</sub>) for 2 min at 100 °C. This method has been adopted as the official method [4, 5]. However, transesterification of intact fats can be very quick in the presence of alkali in methanol, even at room temperature, producing methyl esters in 2–3 min [6]. With additional time or heat, the base will start saponifying the already formed esters, and part of the sample will be converted back into free fatty acids. Additionally it was observed that in the two-step method with BF<sub>3</sub> required 20 min of heating time to esterify 99% of the fatty acids. Apart from this, Ackman [6] recommended it because no alkali transesterification is needed. Over the years the work of Metcalfe et al. [3] has undergone modifications, giving rise to methods using other methanolic solutions of bases and acids [7–9]. However, the methylation methods using methanolic BF<sub>3</sub> are amongst those presenting the best results [9].

Recently, various other methods (direct HCl methylation, saponification, extraction with chloroform-methanol followed by saponification) have been compared for the determination of fatty acids in egg yolk [10]. The results showed less variation using the method of direct methylation than using the other methods. Direct methylation was more precise than extraction of lipids followed by saponification, due

M. R. Mazalli · N. Bragagnolo (✉)  
Department of Food Science, Faculty of Food Engineering,  
State University of Campinas, 13083-862 Campinas, SP, Brazil  
e-mail: neura@fea.unicamp.br

to the smaller number of steps involved in the extraction and sample preparation processes. It consequently demonstrated better recovery and was also quicker and less costly [11].

The analysis of methyl esters by GC requires high resolution in order to separate the positional and configurational isomers. The fused silica capillary columns typically used in this type of analysis normally vary from 25 to 100 m [12]; 100 m columns with highly polar stationary phases, such as those filled with cyanoalkyl polysiloxane are the most recommended for the separation of isomers of conjugated, monounsaturated and polyunsaturated linolenic fatty acids as well as many of the 18:2n-6 and 18:3n-3 artifact isomers [13]. A more accurate analysis of *trans* fatty acids can be obtained from the association of gas chromatography with silver-nitrate thin-layer chromatography or silver-ion liquid chromatography [14].

Identification of the fatty acids present in foods is carried out by comparing the retention times of the methyl esters of the sample with those of the standards. For the non-identified compounds, some studies use equivalent chain length (ECL) values [15–17]. However, the combination of parameters such as retention time with structural information obtained from mass spectrometry constitutes one of the most precise methods for identifying complex organic compounds [12, 18, 19].

An internal standard is used to quantify the fatty acids in mg/100 g samples; nervonic (24:1n-9) and tricosanoic (23:0) fatty acids are the most commonly used internal standards, due to the similar response obtained by both with the ionisation detector. The nervonic fatty acid has the additional advantage of being highly soluble, although it is an unstable compound and can suffer losses by autoxidation [20]. On the other hand, tricosanoic fatty acid is stable but it has limited solubility [20,21]. However, 19:0 and 21:0 improved the accuracy and precision for the analysis of the PUFAs compared to 23:0 [22].

In the present study, the method involving lipid extraction with chloroform-methanol [2] followed by saponification and methylation with  $\text{BF}_3$  [21] was compared with direct sample HCl methylation [10], using GC with internal standardisation. Precision and accuracy was validated with reference material (RM 8415, NIST) and applied to samples of egg, egg enriched with polyunsaturated omega-3 fatty acids (n-3 PUFA) and commercial spray-dried whole egg powder.

## Material and Methods

### Solvents and Chemicals

The solvents sodium hydroxide (NaOH), methanol, isooctane and methanolic boron trifluoride ( $\text{BF}_3$ ) were of

analytical grade (Merck, Darmstadt, Germany) and *n*-hexane was HPLC grade (Mscience, Darmstadt, Germany). A total of 37 fatty acid methyl ester (FAME) standards from 4:0 to 24:0 (Supelco, Bellefonte, PA, USA) were used for identification. The internal standards used for quantification were the methyl esters of tricosanoic acid (23:0) and tridecanoic (13:0) acid (Sigma, St Louis, MO, USA) of 99% purity. The reference material (RM 8415), acquired from NIST (Gaithersburg, MD, USA) was used to verify the accuracy and precision of the method.

### Samples

Fresh eggs enriched with n-3 PUFA was used for the comparative study between the two methods. Commercial spray-dried whole egg powder (recently prepared), fresh eggs and eggs enriched with n-3 PUFA were used to verify the method. The fresh eggs and eggs enriched with n-3 PUFA were purchased directly from a local egg-processing plant and the commercial spray-dried whole egg powder was acquired directly from the factory (Mizumotu Alimentos Ltda, Guapirama, Paraná, São Paulo). In all the experiments, one pool of 12 yolks and one kg of spray-dried egg were homogenised in beakers, stirred with glass rods and analyzed in triplicate. The commercial laying hens were fed with base diets containing yellow corn, soybean meal and 3.00% of deodorized fish oil (diet 1) or 1.18% of soybean oil (diet 2) for production of the eggs enriched with n-3 PUFA or eggs, respectively (Table 1). Commercial spray-dried whole egg powder was produced with eggs of the laying hens that received diet 2.

### Experimental Correction Factor for the Fatty Acids EPA and DHA

The chemical and instrumental parameters were optimised to verify the detector response for a saturated fatty acid (16:0) in relation to the internal standard (23:0). The experimental correction factors for the fatty acids EPA and DHA were calculated in relation to the internal standard and compared to the theoretical correction factors [5, 23].

### Comparison of the Methods and Validation of the Method to Determine the Fatty Acid Composition

A comparative study between lipid extraction according to Folch et al. [2] followed by preparation of the methyl esters according to Joseph and Ackman [21] by saponification and methylation with  $\text{BF}_3$ , and direct sample methylation according to Wang et al. [10], was conducted. The method presenting the best results regarding accuracy and precision was validated using powdered egg certified reference

**Table 1** Percentage of diet composition

Ingredient	Diet 1 <sup>a</sup>	Diet 2 <sup>b</sup>
Yellow corn	59.19	61.44
Soybean meal (46%)	25.99	25.81
Dicalcium phosphate (18% P, 21% Ca)	1.94	1.93
Limestone	8.86	8.87
Salt	0.34	0.34
Fish oil	3.00	–
Soybean oil	–	1.18
Choline chloride (60%)	0.05	0.05
DL methionine	0.13	0.13
Sand	0.25	–
Vitamin-mineral premix <sup>c</sup>	0.25	0.25
Metabolizable energy (kcal/kg)	2.800	2.800
Crude protein	17.07	17.18
Calcium	3.90	3.90
Sodium	0.17	0.17
Available phosphorus	0.45	0.45
Methionine	0.40	0.40
Methionine + cystine	0.69	0.69
Lysine	0.89	0.89

<sup>a</sup> Production eggs enriched with n-3 PUFA

<sup>b</sup> Production eggs

<sup>c</sup> Supplied per kilogram of diet: vitamin A (6.250 IU); vitamin D (2.500 IU); vitamin E (12 IU); vitamin K (0.04 mg); thiamin (0.25 mg); riboflavin (3.4 mg); vitamin B6 (0.25 mg); vitamin B12 (20 µg); pantothenic acid (3.8 mg); niacin (9.9 mg); biotin (0.1 mg); folic acid (0.25 mg); copper (6 mg); iron (52.5 mg); iodine (0.33 mg); selenium (0.21 mg); manganese (48 mg); zinc (60.23 mg); ethoxyquin (0.313 mg)

material (RM 8415, NIST) and applied to fresh samples of egg, egg enriched with n-3 PUFA, and commercial spray-dried whole egg powder.

#### GC Equipment and Conditions

A Varian 3400 CX gas chromatograph (Walnut Creek, California, USA) was used, equipped with a flame ionisation detector, split injector, CP-SIL 88 column (100 m, 0.25 mm, 0.20 µm) (Chrompack, Netherlands) and star workstation. The chromatographic conditions were: detector temperature 280 °C; injector temperature 250 °C; initial column temperature 120 °C for 8 min, programmed to increase at a rate of 15 °C per minute up to 160 °C and then at 4 °C per minute up to 195 °C, maintaining this temperature for 12 min and then increasing again at 15 °C per minute up to the final temperature of 220 °C, maintained for 12 min. The carrier gas was hydrogen at 1 mL/min with linear velocity of 33.95 cm/s, with a make-up gas of nitrogen at 30 mL/min and synthetic air at 300 mL/min. Split injection (1:50) and a volume of 1 µL were used. The split

injection mode was to empty the needle by, quick injection and a 5 s dwell time. Fatty acids were identified by comparing the retention times and relative retention times of the standards with those of the samples (Table 2). The quantification was by internal standardisation using the methyl esters of tricosanoic and tridecanoic acids as the internal standards. The results obtained in mg/100 g of the sample were calculated according to AOCS methodology [5].

#### Determination of the Lipid and Moisture Contents

Total lipids were determined using the gravimetric method of Folch et al. [2] and moisture content using the AOAC methodology [4].

#### Statistical Analysis

The Statistica 5.0 programme was used to analyse the experimental data. ANOVA was used for the results obtained and the means were compared by Tukey's test, with significance based on a 0.05 probability level.

## Results and Discussion

#### Experimental Correction Factor for the Fatty Acids Eicosapentaenoic (EPA) and Docosapentaenoic (DHA)

The methyl ester of palmitic acid (16:0) was used to verify the detector response for a saturated fatty acid with regard to the internal standard (23:0). The experimental correction factor for the detector response was  $1.004 \pm 0.03$ ; similar to the theoretical correction factor [5], demonstrating that the conditions for the application of the methodologies were optimal. The experimental correction factors for EPA and DHA obtained in relation to the methyl ester of tricosanoic acid, used as the internal standard, were  $1.07 \pm 0.12$  and  $0.97 \pm 0.01$ , respectively, values considered to be satisfactory since the theoretical correction factors [5] are 0.99 for EPA and 0.97 for DHA. The theoretical correction factors were used for the calculations of mg/100 g EPA and DHA in regard to the internal standard used. The other fatty acids were calculated according to AOCS methodology [5]. However, the AOCS method does not strictly demand the application of these factors by indicating that they only should be used for optimum accuracy. In addition, when theoretical correction factors are applied, systematic errors will usually be beyond 1%, whereas errors of more than 5% must be accepted with 23:0 as internal standard especially for EPA, even when the injection system is optimized [22].



**Table 2** Retention time (RT, min) and relative retention time (RRT) of methyl esters of fatty acids (FAME) on CP-SIL 88 column

	FAME (standard)	Samples (RT)			FAME (standard)	Samples (RRT)		
		n-3 PUFA egg	Egg	Spray-drier eggs		n-3 PUFA egg	Egg	Spray-drier eggs
4:0 <sup>a</sup>	–	–	–	–	–	–	–	–
6:0 <sup>a</sup>	–	–	–	–	–	–	–	–
8:0	7.58	ND	ND	ND	0.40	ND	ND	ND
10:0	10.18	ND	ND	ND	0.53	ND	ND	ND
11:0	11.63	ND	ND	ND	0.61	ND	ND	ND
12:0	13.15	ND	ND	ND	0.69	ND	ND	ND
13:0 <sup>b</sup>	14.67	14.64	14.62	14.65	0.77	0.76	0.77	0.77
14:0	16.16	16.11	16.10	16.13	0.85	0.84	0.84	0.84
14:1n-9	17.33	17.29	17.28	17.07	0.91	0.90	0.91	0.89
15:0	17.61	17.56	17.56	17.58	0.92	0.91	0.92	0.92
15:1n-5	17.99	17.72	17.83	17.89	0.94	0.92	0.93	0.93
16:0	19.04	19.21	19.09	19.14	1.00	1.00	1.00	1.00
16:1n-7	20.04	20.04	20.00	20.05	1.05	1.04	1.05	1.05
17:0	20.50	20.46	20.45	20.46	1.08	1.07	1.07	1.07
17:1n-7	21.58	21.69	21.45	21.48	1.13	1.13	1.12	1.12
18:0	22.07	22.38	22.14	22.17	1.16	1.17	1.16	1.16
<i>trans</i> 18:1n-9	22.79	22.46	22.83	22.78	1.20	1.17	1.20	1.19
18:1 n-9	23.22	23.47	23.26	23.32	1.22	1.22	1.22	1.22
<i>trans</i> 18:2n-6 <sup>c</sup>	24.07	23.96	24.03	24.05	1.26	1.25	1.26	1.26
18:2n-6	24.91	25.02	24.93	25.02	1.31	1.30	1.31	1.31
20:0	25.80	25.74	26.05	26.02	1.35	1.34	1.36	1.36
18:3n-6	26.42	26.39	26.35	26.43	1.39	1.37	1.38	1.38
20:1n-9	27.16	27.11	27.09	27.15	1.43	1.41	1.42	1.42
18:3n-3	27.34	27.34	27.26	27.34	1.44	1.42	1.43	1.43
21:0	28.13	28.00	28.02	28.02	1.48	1.46	1.47	1.46
20:2n-6	29.61	29.52	29.51	29.61	1.55	1.54	1.55	1.55
22:0	30.96	31.03	30.91	30.98	1.63	1.62	1.62	1.62
20:3n-6	31.64	31.58	31.64	31.66	1.66	1.64	1.66	1.65
22:1n-9	32.29	32.32	32.28	32.29	1.70	1.68	1.69	1.69
20:3n-3	32.37	32.36	32.38	32.38	1.70	1.68	1.70	1.69
20:4n-6	32.64	32.61	32.65	32.66	1.71	1.70	1.71	1.71
23:0 <sup>b</sup>	33.11	33.36	33.16	33.15	1.74	1.74	1.74	1.73
22:2n-6	34.17	33.79	34.16	33.90	1.79	1.76	1.79	1.77
24:0	35.05	35.00	35.06	35.04	1.84	1.82	1.84	1.83
20:5n-3	35.24	35.26	35.20	35.24	1.85	1.84	1.84	1.84
24:1n-9	36.52	36.39	36.10	36.22	1.92	1.89	1.89	1.89
22:6n-3	41.55	41.45	41.43	41.55	2.18	2.16	2.17	2.17

Relative to 16:0

ND not determined

<sup>a</sup> Eluated with solvent peak<sup>b</sup> Internal standard<sup>c</sup> (9-*trans*, 12-*trans*)

As the split injection mode used was optimized in this study, discrimination was not expected. Split injection at 250 °C and a split rate of 1:50 is recommended as the preferred injection technique, especially in vaporizing injectors, since it is the main source of error in quantitative analysis of the long-chain saturated fatty acids (internal standards) to a different extent to PUFAs [24]. In addition,

on-column injection as well as optimized split injection produced accurate results for PUFAs [22].

DHA in this work was submitted to brief exposure times and a mild column temperature not causing thermal losses. On the other hand, when the column temperature was programmed to 170 °C for 0.5 min, then 10 °C per minute to 240 °C for 22 min, a shortfall in

DHA of 10% was observed using ethyl or methyl esters 23:0 [25].

#### Comparison of the Methodologies of Joseph and Ackman [21] and Wang et al. [10] for the Determination of Fatty Acids in Egg

Table 3 shows the results of the comparative study between extracting the lipids according to Folch et al. [2] followed by preparation of the methyl esters according to Joseph and Ackman [21], and direct methylation of the sample according to Wang et al. [10]. Direct methylation of the samples [10] resulted in significantly lower ( $P < 0.05$ ) fatty acid contents and greater variation in the results when compared to the method of first extracting the lipids with chloroform-methanol [2], followed by saponification and methylation [21]. Despite the fact that the method of Joseph and Ackman [21] presented a greater number of steps, consequently increasing the time and cost of the analysis, it presented better repeatability, observed from the relative standard deviation (RDS%) (Table 3). The low repeatability observed for the direct methylation method proposed by Wang et al. [10] was probably due to a less efficient recovery and conversion of the fatty acids in the lipids into their methyl esters as compared to the same procedure but starting with the lipid extract. The present results, disagreed with the results of both Wang et al. [10] and Lepage and Roy [11].

The main problem for the analysis of n-3 PUFA is that PUFAs are rather unstable, so that calibration cannot be performed by using stored or opened containers of quantitative standards [22]. With official methods recommending 23:0 as the internal standard, however, it can lead to systematic overestimation of n-3 PUFAs, since the standard deviations of 22:6n-3 versus 21:0 and 20:5n-3 versus 19:0 were considerably smaller compared to 17:0 and 23:0 [22]. The aim of the present study was to compare the official method [5, 23] with the results of Wang et al. [10].

**Table 3** EPA and DHA contents of fresh eggs enriched with n-3 PUFA, determined by different methods

Fatty acid <sup>c</sup>	Joseph and Ackman[21]		Wang et al. [10]	
	M ± SD <sup>a</sup>	RDS (%) <sup>b</sup>	M ± SD <sup>a</sup>	RDS (%) <sup>b</sup>
EPA <sup>d</sup>	9.56 ± 0.4 a	4.2	4.78 ± 0.9 b	18.8
DHA <sup>e</sup>	118.20 ± 4.8 a	4.1	77.10 ± 15.0 b	19.5

<sup>a</sup> Mean ± standard deviation  $n = 10$ , Means followed by the same letter do not differ according to the Tukey test ( $P > 0.05$ )

<sup>b</sup> RDS (%) = relative standard deviation

<sup>c</sup> (mg/100 g of yolk, dry basis)

<sup>d</sup> (EPA, 20:5n-3)

<sup>e</sup> (DHA, 22:6n-3)

In addition, 21:0 was found in the eggs, so it will be impossible to use it as an internal standard. In order to improve the quantification 13:0 was also used as an internal standard.

#### Validation of the Methodology for the Determination of Fatty Acids in Eggs by Gas Chromatography Using Internal Standardisation

Since the method of Joseph and Ackman [21] was shown to be more precise, this method was validated using powdered egg certified reference material (RM 8415, NIST). Table 4 shows the results obtained for the fatty acids of the powdered egg reference material using the Joseph and Ackman method [21] and comparing these results with the values declared in the certificate. The results obtained were the same as those specified for the reference material.

#### Determination of the Total Lipid and Moisture Contents

Table 5 shows the results for total lipids and moisture content in eggs, eggs enriched with n-3 PUFA and whole spray-dried egg powder. The values for lipids in the egg

**Table 4** A comparison of fatty acids and total lipids by method of Joseph and Ackman [2] using whole egg powder (RM 8415, NIST)

Fatty acids	(RM 8415, NIST) <sup>a</sup>	Joseph and Ackman[21]
14:0	0.191 ± 0.013	0.189 ± 0.016
15:0	0.050 ± 0.03	0.051 ± 0.03
16:0	12.36 ± 0.45	12.36 ± 0.45
16:1	1.59 ± 0.37	1.50 ± 0.46
17:0	0.156 ± 0.029	0.156 ± 0.027
18:0	4.21 ± 0.26	4.19 ± 0.29
18:1n-9	23.0 ± 2.4	23.5 ± 2.2
18:2n-6	4.69 ± 0.38	4.67 ± 0.40
20:3	0.064 ± 0.007	0.064 ± 0.005
20:4	0.496 ± 0.045	0.499 ± 0.040
22:6n-3	0.266 ± 0.062	0.262 ± 0.064
Lipids	48.0 ± 5.0	48.1 ± 5.2

<sup>a</sup> Values declared on the certificate (% weight, dry basis)

**Table 5** Total lipids and moisture in eggs

Sample	Total lipids <sup>a</sup>	Moisture <sup>a</sup>
n-3 PUFA egg <sup>b</sup>	69.01 ± 2.02	50.02 ± 1.62
Egg <sup>b</sup>	61.59 ± 1.56	50.87 ± 1.59
Whole spray-dried egg powder <sup>c</sup>	36.72 ± 1.11	2.98 ± 0.10

<sup>a</sup> Mean ± standard deviation  $n = 3$

<sup>b</sup> mg/100 g yolk, dry basis

<sup>c</sup> mg/100 g, dry basis

yolk and those of the eggs enriched with n-3 PUFA were lower and the values of the whole spray dried powder higher than the values cited by the USDA [26]. The results for moisture content for all the egg samples were similar to those found by the USDA [26].

#### Application of the Methodology to Eggs

Table 6 shows the results calculated on the dry weight basis obtained for the composition of saturated, monounsaturated and polyunsaturated fatty acids and of *trans* fatty acids in eggs, eggs enriched with n-3 PUFA and whole spray-dried egg powder. Twenty-nine fatty acids were identified, and 14:0, 16:0, 18:0, 16:1n-7, 18:1n-9, 18:2n-6 and 18:3n-3 were found to be the principal fatty acids in all samples. In the whole spray-dried egg powder, the major fatty acids were *trans* fatty acids 18:1n-9. The following fatty acids were not identified in any of the egg samples: 4:0; 6:0; 8:0; 10:0; 11:0; 12:0; 13:0 and 23:0 and only traces (<1 mg/100 g) of the following: 15:1n-5, 22:1n-9

and 22:2n-6 were found. Although, the 18:0 was 23% higher, the other saturated fatty acids (SFA) showed a reduction of 31% in the eggs enriched with n-3 PUFA. The concentration of these acids in the eggs are little influenced by the lipid content of the diet [27, 28]. The concentration of 18:3n-3 and 22:6n-3 in the eggs enriched with n-3 PUFA were 30 and 100% higher, respectively, than the amounts found in other eggs. Among the important monounsaturated fatty acids, 16:1n-7 was 54% and 18:1n-9 was 37% higher than in other eggs. In contrast, production of a polyunsaturated fatty acid egg does not appear to be practical using dietary influences as well as strains of the hens [29].

In fresh eggs enriched with n-3 PUFA and eggs *trans* fatty acids (18:1n-9 and 18:2n-6) were found. As the concentration of *trans* fatty acids in eggs was low, it is probably due to the diet of the hens since the laying hens received a diet with soybean oil and deodorised fish oil (Table 1). Guardiola et al. [30] observed a good relationship between the proportion of commercial feed in the

**Table 6** Saturated, monounsaturated and polyunsaturated fatty acids and *trans* fatty acids (*trans* FA) in eggs<sup>a</sup>

Fatty acids	n-3 PUFA egg <sup>b</sup>	Egg <sup>b</sup>	Whole spray-dried egg powder <sup>c</sup>
14:0	640 ± 11 b	660 ± 10 b	939 ± 18 a
15:0	90 ± 2 b	100 ± 2 b	157 ± 6 a
16:0	4250 ± 61 c	6520 ± 74 a	5951 ± 60 b
17:0	280 ± 11 c	350 ± 9 b	428 ± 19 a
18:0	1750 ± 19 b	1340 ± 15 c	4197 ± 101 a
20:0	100 ± 2 c	180 ± 4 a	124 ± 3 b
21:0	tr <sup>e</sup>	tr	174 ± 3
22:0	100 ± 2 c	120 ± 2 b	203 ± 4 a
24:0	16 ± 0 c	26 ± 1 b	67 ± 2 a
14:1n-9	110 ± 3 b	100 ± 3 b	169 ± 2 a
16:1n-7	4690 ± 62 a	3040 ± 48 b	1206 ± 16 c
17:1n-7	240 ± 4 a	110 ± 2 b	tr c
18:1n-9	6640 ± 75 b	4850 ± 55 c	7986 ± 88 a
20:1n-9	340 ± 9 a	110 ± 3 b	39 ± 1 c
24:1n-9	tr	tr	62 ± 2
18:2n-6	5310 ± 74 b	9296 ± 102 a	4161 ± 50 c
18:3n-6	16 ± 0 b	16 ± 0 b	34 ± 1 a
20:2n-6	290 ± 3 a	48 ± 2 b	38 ± 1 b
20:3n-6	25 ± 0 b	35 ± 1 a	33 ± 1 a
20:4n-6	200 ± 3 b	340 ± 8 a	343 ± 10 a
18:3n-3	1630 ± 38 a	1250 ± 23 b	680 ± 13 c
20:3n-3	tr	tr	36 ± 1
20:5n-3	14 ± 0 b	tr	55 ± 1 a
22:6n-3	170 ± 3 b	85 ± 2 c	806 ± 16 a
<i>trans</i> 18:1n-9	34 ± 2 c	95 ± 3 b	1777 ± 73 a
<i>trans</i> 18:2n-6 <sup>d</sup>	13 ± 1 b	16 ± 0 b	31 ± 1 a
PUFA / SFA	1.1	1.2	0.5
PUFA n-6/PUFA n-3	3.2	7.3	2.9

<sup>a</sup> Mean ± standard deviation  $n = 3$ , Means followed by the same letter in the same line do not differ according to the Tukey test ( $P > 0.05$ )

<sup>b</sup> mg/100 g yolk, dry basis

<sup>c</sup> mg/100 g, dry basis

<sup>d</sup> (9-*trans*, 12-*trans*)

<sup>e</sup> tr = traces (less than 1 mg/100 g)

hens' diet and the total content of *trans* monounsaturated fatty acid (16:1n-7 and 18:1n-9) in eggs. It is now well known that during deodorisation and/or refining of oil *cis-trans* isomerisation reactions could have occurred [31, 32]. Recent research has recommended that the deodorisation of marine oils should be conducted at a maximum temperature of 180 °C to avoid geometrical isomerisation [33, 34]. However the *trans* fatty acid isomers of EPA and DHA was not the subject of research in this study.

High concentrations of *trans* 18:1n-9 were observed in the whole spray dried egg powder, probably due to the high temperature required for the processing of these eggs [35] and the presence of the catalysts, nitric and nitrous oxides, produced during the spray-drying process by the direct heating of the air by gas combustion [36]. When heated in the presence of catalysts such as nitrogen oxides, unsaturated *cis* fatty acids are transformed into their *trans* stereo-isomers. In addition, nitrous oxide is considered to be a free radical, known to initiate the oxidation of unsaturated lipids in model systems [37].

From these results, it can be concluded that quantification of the fatty acids by internal standardisation according to the method of Joseph and Ackman [21] is more accurate and precise than the direct methylation method. Although it is necessary to extract the total lipids, this is easily carried out. By applying this methodology, it was shown that eggs enriched with n-3 PUFA showed a better lipid profile from the nutritional point of view than standard eggs. In addition, high contents of *trans* fatty acids were found in the whole spray dried egg powder. Considering that whole spray dried egg powder is used in the formulation of a variety of products, mainly infant foods, the presence of *trans* fatty acids represents a public health problem.

**Acknowledgments** The authors are grateful to the São Paulo State Research Foundation (FAPESP) and the Brazilian National Research Foundations (CAPES and CNPq) for their financial support.

## References

- Eder K (1995) Gas chromatographic analysis of fatty acid methyl esters. *J Chromatogr B* 671:113–131
- Folch J, Less M, Stanley GHS (1957) A simple method for the isolation and purification of total lipids from animal tissues. *J Biol Chem* 226:497–509
- Metcalfe LD, Schmitz AA, Pelka JR (1966) Rapid preparation of fatty acid esters from lipids for gas chromatographic analysis. *Anal Chem* 38:514–515
- AOAC (1997) Official methods of analysis of AOAC international. In: Arlington (ed) Association of official agricultural chemists, 16th edn. Official Method 963. 33, Gaithersburg, Maryland, USA
- AOCS (1997) In: Firestone D (ed) Official methods and recommended practices of the American oil chemists' society, 5th edn. Official Method Ce 1b-89. American Oil Chemists' Society Press, Champaign
- Ackman RG (1998) Remarks on official methods employing boron trifluoride in the preparation of methyl esters of the fatty acids of fish oils. *J Am Oil Chem Soc* 75:541–545
- Hartman L, Lago RCA (1973) Rapid preparation of fatty acid methyl esters from lipids. *Lab Prac* 22:475–476
- Slover HT, Lanza E (1979) Quantitative analysis of food fatty acids by capillary gas chromatography. *J Am Oil Chem Soc* 56:933–943
- Craske JD (1993) Separation of instrumental and chemical errors in the analysis of oils by gas chromatography—a collaborative evaluation. *J Am Oil Chem Soc* 70:325–334
- Wang Y, Sunwoo H, Cherian G, Sim JS (2000) Fatty acid determination in chicken egg yolk: a comparison of different methods. *Poult Sci* 79:1168–1171
- Lepage G, Roy CC (1986) Direct transesterification of all classes of lipids in a one step reaction. *J Lipid Res* 27:114–120
- Gutnikov G (1995) Fatty acid profiles of lipids samples. *J Chromatogr B* 671:71–89
- Kramer JKG, Blackadar CB, Zhou JQ (2002) Evaluation of two GC columns (60-m SUPELCOWAX 10 and 100-m CP Sil 88) for analysis of milk fat with emphasis on CLA, 18:1, 18:2 and 18:3 isomers, and short- and long-chain FA. *Lipids* 37:823–835
- Ratnayake WMN (2004) Overview of methods for the determinations of *trans* fatty acids by gas chromatography, silver-ion thin-layer chromatography, silver-ion liquid chromatography, and gas chromatography/mass spectrometry. *J AOAC Int* 87:523–539
- Stránský K, Jursík T, Vitek A (1997) Standard equivalent chain length values of monoenoic and polyenoic (methylene interrupted) fatty acids. *J High Resol Chromatogr* 20:143–158
- Bragagnolo N, Rodriguez-Amaya DB (2001) Total lipid, cholesterol, and fatty acids of farmed freshwater prawn (*Macrobrachium rosenbergii*) and wild marine shrimp (*Penaeus brasiliensis*, *Penaeus schimitti*, *Xiphopenaeus kroyeri*). *J Food Comp Anal* 14:359–369
- Bragagnolo N, Rodriguez-Amaya DB (2002) Simultaneous determination of total lipid, cholesterol and fatty acids in meat and back fat of suckling and adult pigs. *Food Chem* 79:255–260
- Woollard PM, Mallet AI (1984) Lipoygenase products—a novel gas—chromatography mass—spectrometric assay for monohydroxy fatty acids. *J Chromatogr* 306:1–21
- Kuksis A, Myher JJ (1995) Application of tandem mass—spectrometry for the analysis of long-chain carboxylic acids. *J Chromatogr B* 671:35–70
- Shantha NC, Ackman RG (1990) Nervonic acids versus tricosanoic acid as internal standards in quantitative gas—chromatographic analysis of fish oil longer-chain n-3 polyunsaturated fatty acid methyl esters. *J Chromatogr B* 533:1–10
- Joseph JD, Ackman RG (1992) Capillary column gas chromatographic method for analysis of encapsulated fish oils and fish oil ethyl esters: collaborative study. *J AOAC Int* 75:488–506
- Schreiner M (2005) Quantification of long chain polyunsaturated fatty acids by gas chromatography—evaluation of factors affecting accuracy. *J Chromatogr A* 1095:126–130
- Ackman RG, Sipos JC (1964) Application of specific response factors in the gas chromatographic analysis of methyl esters of fatty acids with flame ionization detectors. *J Am Oil Chem Soc* 41:377–378
- Grob K, Biedermann M (2002) The two options for sample evaporation in hot GC injectors: thermospray and band formation. Optimization of conditions and injector design. *Anal Chem* 74:10–16
- Tande T, Breivik H, Aasoldsen T (1992) Validation of a method for gas chromatographic analysis of eicosapentaenoic acid and docosahexaenoic acid as active ingredients in medicinal products. *J Am Oil Chem Soc* 69:1124–1130

26. USDA (2000) Nutrient database for standard reference. Release 13, NDB No. 13390, No. 01125, No. 01133
27. Li-Chan ECY, Powrie WD, Nakai S (1995) The chemistry of eggs and egg products, in *Egg Science and Technology*. In: Stadelman WJ, Cotterill OJ (eds) 4th edn. Food Products Press, New York, p 591
28. Mazalli MR, Faria DE, Salvador D, Ito DT (2004) A comparison of the feeding value of different sources of fat for laying hens: 2. lipid, cholesterol, and vitamin E profiles of egg yolk. *J Appl Poult Res* 13:280–290
29. Kuksis A (1992) Yolk lipids. *Biochem Biophys Acta* 1124:205–222
30. Guardiola F, Codony R, Rafecas M, Boatella J, López A (1994) Fatty acid composition and nutritional value of fresh eggs, from large- and small-scale farms. *J Food Comp Anal* 7:171–180
31. Camacho ML, Méndez MVR, Constante EG (2003) Cinética de la reacción de elaidización del ácido oléico durante la desodorización y/o refinación física de las grasas comestibles. *Grasas y Aceites* 54:138–144
32. Wolff RL (1993) Heat-induced geometrical isomerization of  $\alpha$ -linolenic acid: effect of temperature and heating time on the appearance of individual isomers. *J AOCS* 70:425–430
33. Mjos SA, Solvang M (2006) Geometrical isomerisation of eicosapentaenoic and docosahexaenoic acid at high temperatures. *Eur J Lipid Sci Technol* 108:589–597
34. Fournier V, Destailats F, Juanéda P, Dionisi F, Lambelet P, Sébédio JL, Berdeaux O (2006) Thermal degradation of long-chain polyunsaturated fatty acids during deodorization of fish oil. *Eur J Lipid Sci Technol* 108:33–42
35. Fontana A, Antoniazzi F, Ciavatta ML, Trivellone E, Cimino G (1993) H-NMR study of cholesterol autooxidation in egg powder and cookies exposed to adverse storage. *J Food Sci* 58:1286–1290
36. Wheeler WH (1980) Chemical and engineering aspects of low NO<sub>x</sub> concentration. *Chem Eng* 362:693–699
37. Pryor WA, Lightsey JW (1981) Mechanism of nitrogen dioxide reactions: initiation of lipid peroxidation and the production of nitrous acid. *Sci* 214:435–437

## Epidermal Lipoxygenase Products of the Hepoxilin Pathway Selectively Activate the Nuclear Receptor PPAR $\alpha$

Zheyong Yu · Claus Schneider · William E. Boeglin · Alan R. Brash

Received: 23 January 2007 / Accepted: 16 February 2007 / Published online: 14 April 2007  
© AOCs 2007

**Abstract** Arachidonic acid can be transformed into a specific epoxyalcohol product via the sequential action of two epidermal lipoxygenases, 12R-LOX and eLOX3. Functional impairment of either lipoxygenase gene (*ALOX12B* or *ALOXE3*) results in ichthyosis, suggesting a role for the common epoxyalcohol product or its metabolites in the differentiation of normal human skin. Here we tested the ability of products derived from the epidermal LOX pathway to activate the peroxisome proliferator-activated receptors PPAR $\alpha$ ,  $\gamma$ , and  $\delta$ , which have been implicated in epidermal differentiation. Using a dual luciferase reporter assay in PC3 cells, the 12R-LOX/eLOX3-derived epoxyalcohol, 8R-hydroxy-11R, 12R-epoxyeicosa-5Z,9E,14Z-trienoic acid, activated PPAR $\alpha$  with similar in potency to the known natural ligand, 8S-hydroxyeicosatetraenoic acid (8S-HETE) (both at 10  $\mu$ M concentration). In contrast, the PPAR $\gamma$  and PPAR $\delta$  receptor isoforms were not activated by the epoxyalcohol. Activation of PPAR $\alpha$  was also observed using the trihydroxy hydrolysis products (trioxilins) of the unstable epoxyalcohol. Of the

four trioxilins isolated and characterized, the highest activation was observed with the isomer that is also formed by enzymatic hydrolysis of the epoxyalcohol. Formation of a ligand for the nuclear receptor PPAR $\alpha$  may be one possibility by which 12R-LOX and eLOX3 contribute to epidermal differentiation.

**Keywords** Lipoxygenase · 12R-LOX · eLOX3 · HETE · PPAR · Ichthyosis · Epidermis · Epoxyalcohol · Hepoxilin · Trioxilin

### Abbreviations

HETE	Hydroxyeicosatetraenoic acid
HPETE	Hydroperoxyeicosatetraenoic acid
LOX	Lipoxygenase
8R,11R,12R-epoxyalcohol	8R-Hydroxy-11R,12R-epoxyeicosa-5Z,9E,14Z-trienoic acid
PPAR	Peroxisome proliferator-activated receptor
RP-HPLC	Reversed phase high performance liquid chromatography
SP-HPLC	Straight phase high performance liquid chromatography
CP-HPLC	Chiral phase high performance liquid chromatography
TMS	Trimethylsilyl
NCIE	Non-bullous ichthyosiform erythroderma

Z. Yu · C. Schneider · W. E. Boeglin · A. R. Brash (✉)  
Division of Clinical Pharmacology,  
Department of Pharmacology,  
Vanderbilt University School of Medicine,  
23rd Ave. at Pierce, Nashville,  
TN 37232-6602, USA  
e-mail: alan.brash@vanderbilt.edu

### Present Address:

Z. Yu  
Howard Hughes Medical Institute,  
Washington University, St Louis,  
MO 63110, USA

## Introduction

Genetic evidence suggests that a pathway for the transformation of arachidonic acid by two lipoxygenases (12R-LOX and eLOX3) plays a crucial role in epidermal differentiation [1, 2], as recently reviewed [3]. Inactivating mutations of either LOX have been found to result in a severe type of ichthyosis, (NCIE, non-bullous ichthyosiform erythroderma) associated with the loss of a functional epidermal water barrier. Initially, the lipoxygenases were identified through genetic screening of affected patients [1, 2], and their role in the formation of a specific epoxyalcohol product (hepoxilin), 8*R*,11*R*,12*R*-epoxyeicosa-5*Z*,9*E*,14*Z*-trienoic acid, was elucidated in biochemical studies using the recombinant enzymes [4, 5]. The primary hepoxilin product of the two LOX enzymes is enzymatically hydrolyzed in cells to a specific trihydroxy derivative (trioxilin) [5]. Several hepoxilin and trioxilin isomers have been detected in human skin [6–8], although the specific 12*R*-LOX/eLOX3 derived products have yet to be identified.

At the present state of knowledge, there are multiple potential mechanisms of action of the 12*R*-LOX/eLOX3 pathway products, and these include an action via a putative membrane receptor (ichthyin) implicated through genetic studies in ichthyosis patients [9], or an activity via activation of PPAR receptors, a possibility that we have initially evaluated in this study. There is accumulating evidence that peroxisome proliferator-activated receptors (PPAR) are important regulators of epidermal differentiation [10–12]. All three subtypes have been identified in human keratinocytes. Whereas PPAR $\delta$  is the predominant subtype expressed, PPAR $\alpha$  and PPAR $\gamma$  are present at lower levels but are upregulated during keratinocyte differentiation (e.g. Refs. [13, 14]). PPAR $\beta/\delta$  is not implicated in differentiation but is activated in inflammation and wound repair [15, 16]. The PPAR subtypes are activated by diverse lipid-derived molecules including fatty acids and eicosanoids [17, 18]. Here, we tested the hypothesis that the 12*R*-LOX/eLOX3-derived epoxyalcohol could be an activating ligand for the PPAR nuclear receptors. We also tested the trioxilin hydrolysis products of the unstable epoxyalcohol.

## Experimental Procedures

### Materials

12*R*-HPETE and 8*S*-HPETE were prepared by autoxidation of arachidonic acid and isolation using reversed phase and chiral phase HPLC as described previously [4]. [1-<sup>14</sup>C]12*R*-HPETE was prepared by the reaction of

[1-<sup>14</sup>C]arachidonic acid with recombinant human 12*R*-LOX [19]. The eLOX3-derived epoxyalcohol, 8*R*,11*R*,12*R*-epoxyeicosa-5*Z*,9*E*,14*Z*-trienoic acid (8*R*,11*R*,12*R*-epoxyalcohol), was prepared by the reaction of 12*R*-HPETE with recombinant human eLOX3 in Tris buffer (pH 6.0) as described [4]. 8*S*-HETE was prepared from 8*S*-HPETE by reduction with triphenylphosphine and purification using RP-HPLC. The synthetic ligands GW7647 (PPAR $\alpha$  ligand), GW7845 (PPAR $\gamma$  ligand) and GW1516 (PPAR $\delta$  ligand) were gifts from Dr. Raymond N. Dubois, who obtained these synthetic ligands from GlaxoSmithKline. PC-3 cells (ATCC CRL-1435) were cultured in Ham's F12K medium containing 10% fetal bovine serum (BioWhittaker, Walkersville, MD) at 37 °C, 5% CO<sub>2</sub>. Cells were typically split in a ratio of 1:6 every 3 days.

### Quantification of 8*R*,11*R*,12*R*-Epoxyalcohol

8*R*,11*R*,12*R*-epoxyalcohol exhibits only end absorbance in the UV and no synthetic standard is available, making it difficult to quantify. Here the quantitation was based on knowing the specific activity of a radioactive sample of its hydroperoxy precursor, [<sup>14</sup>C]12*R*-HPETE ( $\epsilon = 23,000$  at 235 nm [20]), and converting this to [<sup>14</sup>C]8*R*,11*R*,12*R*-epoxyalcohol using eLOX3, and using the HPLC-purified <sup>14</sup>C product as the quantified authentic standard. Triol hydrolysis products were quantified assuming an equimolar absorbance of hepoxilin and trioxilin at 205 nm measured on RP-HPLC.

### Acid-Catalyzed Hydrolysis of 8*R*,11*R*,12*R*-Epoxyalcohol

The 8*R*,11*R*,12*R*-epoxyalcohol was quantitatively hydrolyzed by treatment with 1% acetic acid in water at room temperature for 30 min. The mixture of diastereomeric trihydroxy-eicosatrienoic acids (trioxilins) was analyzed by RP-HPLC using a Waters Symmetry C18 5- $\mu$ m column (0.46  $\times$  25 cm) eluted with methanol/water/acetic acid (80/20/0.01, by volume) at a flow rate of 1 mL/min and monitoring at UV 205 nm. Products eluting between 5 and 6 min were collected and further resolved by SP-HPLC using a Beckman Ultrasphere 5- $\mu$ m silica column (0.46  $\times$  25 cm) eluted with hexane/isopropanol/acetic acid (90/10/0.1, by volume) at a flow rate of 1 mL/min. Further purification was achieved by chiral phase HPLC using a Chiralpak AD column (0.46  $\times$  25 cm) eluted with hexane/methanol/ethanol/acetic acid (95/5/10/0.1, by volume) at a flow rate of 0.5 mL/min. The position of the hydroxy groups along the carbon chain was determined by GC-MS after hydrogenation (Pd/H<sub>2</sub>) and derivatization to the methyl esters TMS ethers as described previously [5].

## PPAR Activation Using a Dual-Luciferase Assay

PPRE-tk-luc (PPAR reporter plasmid expressing firefly luciferase), pRL-SV40 (control plasmid expressing *Renilla* luciferase), and the expression plasmids containing full-length cDNAs for PPAR $\alpha$  in pBKCMV, PPAR $\gamma$ /pCDNA3.1 and PPAR $\delta$ /pCDNA3.1 were kindly provided by Dr. Raymond N. DuBois (Vanderbilt University, Nashville, TN). Assays were performed using PC-3 cells [21]; theoretically the dual luciferase assay can use any cell line because the proteins involved are over-expressed from the transfected plasmids, not endogenous proteins. PC-3 cells ( $1.0 \times 10^5$  cells/well using 24-well plates) were transfected using FuGENE 6 (Roche Molecular Biochemicals) at a lipid/DNA ratio of 3:1. Cells were exposed to a mix containing 150 ng/mL PPRE-tk-luc, 150 ng/mL of one of the three PPAR plasmids (PPAR $\alpha$ , PPAR $\gamma$ , or PPAR $\delta$ ), and 1.0 ng/mL pRL-SV40 in Ham's F12K medium. The transfection mixture was replaced after 4–5 h with 10% charcoal-stripped FBS containing media supplemented with either 0.1% vehicle (DMSO or ethanol) or the indicated compound. After 24 h, cells were harvested in 100  $\mu$ L/well  $1\times$  luciferase lysis buffer (Promega) for 20 min at room temperature using an orbital shaker. Relative light units from firefly luciferase activity were determined using a luminometer (MGM Instruments, Hamden, CT) and normalized to the relative light units from *Renilla* luciferase, which served as internal control for transfection efficiency (Promega). The effects of various compounds on activation of PPARs are presented as “fold activation” relative to the vehicle control values.

## Statistical Analysis

All data were analyzed using Prism 4 software (Graphpad software, Inc), and results are expressed as means and standard deviations; all tests were two-tailed. The unpaired Student *t* test was used to compare reporter activities between control and sample-treated groups. Differences were considered significant when *P* values were less than 0.05.

## Results

Activation of PPAR $\alpha$  by 8*R*,11*R*,12*R*-Epoxyalcohol

A PPAR transactivation assay was used to test whether the 12*R*-LOX/eLOX3-generated epoxyalcohol 8*R*-hydroxy-11*R*,12*R*-epoxyeicosa-5*Z*,9*E*,14*Z*-trienoic acid (8*R*,11*R*,12*R*-epoxyalcohol) could serve as an activating ligand for PPARs. In the assay, PC-3 cells are transiently co-transfected with PPRE-tk-luc plasmid (a PPAR reporter plasmid expressing firefly luciferase), pRL-SV40 plasmid (a control

plasmid expressing *Renilla* luciferase) and one of the three full length PPAR plasmids (PPAR $\alpha$ , PPAR $\gamma$ , or PPAR $\delta$ ). The transfected cells are treated with a synthetic ligand specific for each receptor or with increasing concentrations of the 8*R*,11*R*,12*R*-epoxyalcohol (0.1, 1.0, 5.0 and 10  $\mu$ M) and the relative activation over control cells is determined.

The 8*R*,11*R*,12*R*-epoxyalcohol showed dose-dependent activation of PPAR $\alpha$  at 5 and 10  $\mu$ M concentration (2.2- and 2.6-fold activation, respectively) (Fig. 1a). The specific synthetic ligand GW7647 (1.0  $\mu$ M) produced about five-fold activation relative to vehicle control. The known natural ligand 8*S*-HETE [22] showed a maximum activation of about 3.5-fold at 10  $\mu$ M concentration. In contrast to PPAR $\alpha$ , the isoforms PPAR $\gamma$  or PPAR $\delta$  were not transactivated by the 8*R*,11*R*,12*R*-epoxyalcohol (0.1–10  $\mu$ M) while the synthetic ligands GW7845 (100 nM) activated PPAR $\gamma$  about 12-fold and GW1516 (100 nM)

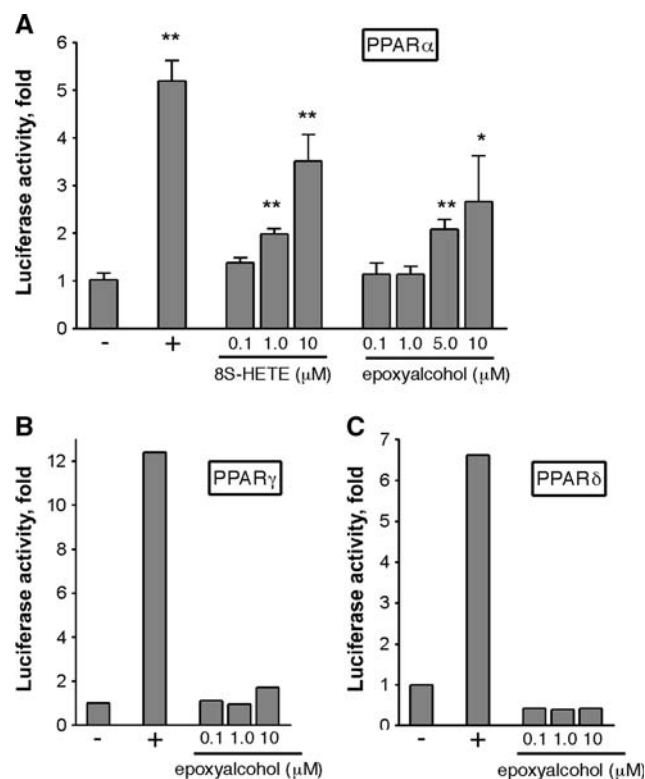


**Fig. 1** Activation of PPAR isoforms by the 8*R*,11*R*,12*R*-epoxyalcohol. **a** Activation of PPAR $\alpha$  by the epoxyalcohol and the natural ligand 8*S*-HETE is dose-dependent. One micromolar of the synthetic ligand GW7647 was used as a positive control (+). **b** The PPAR isoforms  $\gamma$  and  $\delta$  are not activated by the epoxyalcohol (0.1–10  $\mu$ M); the positive controls (+) are GW7845 (for PPAR $\gamma$ ) and GW1516 (for PPAR $\delta$ ), 100 nM each. The dual luciferase assay was performed using transiently transfected PC3 cells. Results are plotted as fold activation versus the DMSO control (mean  $\pm$  SD of three experiments each performed in triplicate). *P* values versus the DMSO control are presented in the figure. \* *P* < 0.05, \*\* *P* < 0.01



activated PPAR $\delta$  about six- to seven-fold, respectively (Fig. 1b, c)

In an earlier experiment we had used a chimeric receptor containing only the ligand-binding domain of PPAR $\alpha$  fused with the DNA-binding domain of the yeast GAL4 transcription factor. Neither the positive control 8S-HETE nor the epoxyalcohol activated the chimeric PPAR $\alpha$  receptor in PC-3 cells using this construct, although the synthetic ligand GW7647 was active (data not shown).

#### Hydrolysis of the 8*R*,11*R*,12*R*-Epoxyalcohol to Trioxilins

Acid-catalyzed hydrolysis of the 8*R*,11*R*,12*R*-epoxyalcohol gave a mixture of four trihydroxy products (designated 1–4) that were not resolved by RP-HPLC and only partially resolved using SP-HPLC (Fig. 2a, b). Using CP-HPLC as an alternative normal phase chromatography system a different elution pattern was achieved and products 1 and 3 were clearly resolved while products 2 and 4 eluted as a single early peak (Fig. 2c). Re-chromatography of the early peak collected from CP-HPLC using SP-HPLC resolved products 2 and 4 (Fig. 2d). LC-MS analysis in the negative ion mode of the crude hydrolysis mixture revealed a molecular ion of  $m/z$  353 ( $[M-H]^-$ ) for all four hydrolysis products, an increase of 18 mass units over the starting epoxyalcohol, compatible with a trihydroxy derivative of a C20 fatty acid containing three double bonds. GC-MS analysis of the reduced methyl ester, TMS ether derivatives proved that all of the four hydrolysis products are trihydroxy derivatives, and allowed assignment of the location of the hydroxy groups from the EI-MS fragmentation patterns (data not shown) [5]. Products 1 and 2 are 8,9,12-triols and products 3 and 4 are 8,11,12-triols.

We tentatively assigned the absolute configuration of the four triols according to observations made by Hamberg [23, 24]. Epoxyalcohols containing a 1-hydroxy-2,3-ene-4,5-epoxy structure are attacked by the solvent at carbons 2 and 4, giving 1,2,5- and 1,4,5-triol products. As a result, the configuration of carbons 1 and 5 is retained in the hydrolysis products. Thus, each of the four triols that are formed by acid hydrolysis of the 8*R*,11*R*,12*R*-epoxyalcohol are expected to retain the 8*R* and 12*R* configurations. In addition, according to Morris [25] and Hamberg [23, 24], the three diastereomers of trihydroxy fatty acids are less polar than the corresponding erythro compounds, which will result in an earlier elution time using SP-HPLC. Thus, the elution order on SP-HPLC was used to assign the absolute configuration of the third hydroxy group at C-9 and C11, respectively (Fig. 2b, d). Therefore, given that the 5*Z* and 14*Z* double bonds are unaffected by the hydrolysis reaction, peak 1 from SP-HPLC was tentatively identified

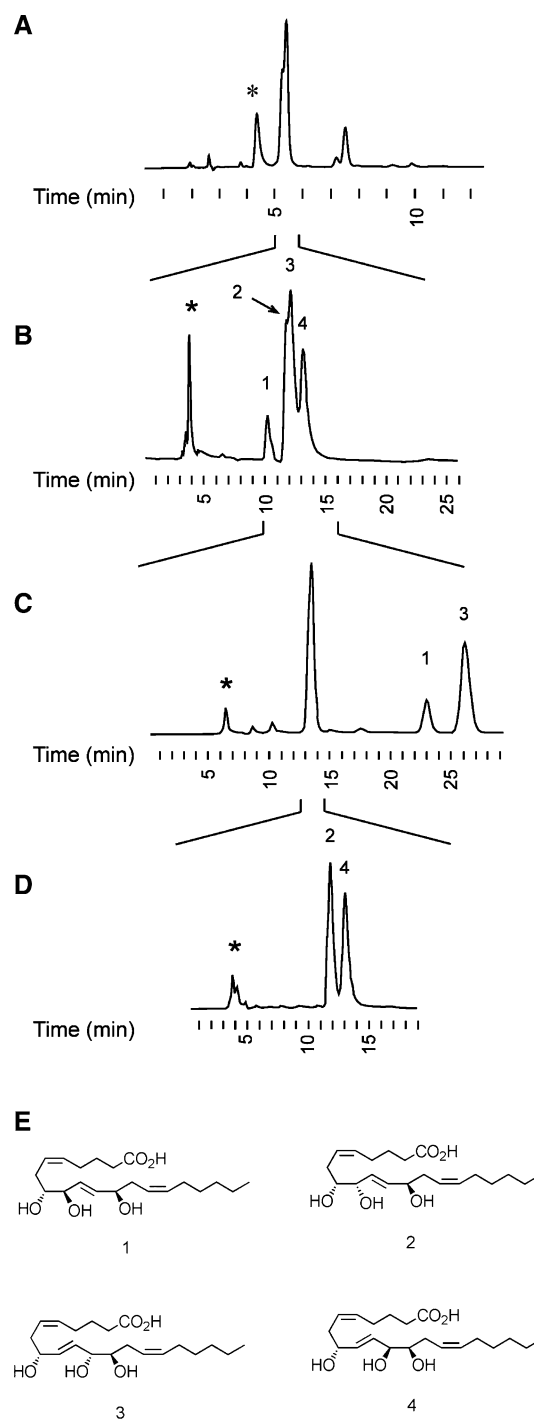


**Fig. 2** HPLC analysis of the acid-catalyzed hydrolysis of the 8*R*,11*R*,12*R*-epoxyalcohol. **a** RP-HPLC of the crude hydrolysis reaction; the trioxilin hydrolysis products elute at ~5.5 min; the epoxyalcohol starting material is quantitatively hydrolyzed (expected retention time ~10 min). **b** SP-HPLC of the crude hydrolysis reaction shows four partially resolved trioxilin products. **c** Chiral-phase HPLC analysis was used to resolve products 1 and 3. **d** SP-HPLC of the early peak collected from CP-HPLC resolved products 2 and 4. **e** Structures of the trihydroxy hydrolysis products 1–4. The HPLC conditions are described in Experimental Procedures. Detection: UV absorbance at 205 nm. The *asterisk* marks an injection artifact

as the *8R,9R,12R*-diastereomer and peak 2 as the *8R,9S,12R*-diastereomer of *8,9,12*-trihydroxy-*5Z,10E,14Z*-eicosatrienoic acid. Similarly, peak 3 was tentatively identified as *8R,11R,12R*-trihydroxy-*5Z,9E,14Z*-eicosatrienoic acid and peak 4 as *8R,11S,12R*-trihydroxy-*5Z,9E,14Z*-eicosatrienoic acid (Fig. 2e). The hydrolysis product of the *8R,11R,12R*-epoxyalcohol formed by incubation with homogenates of human keratinocytes [5] co-chromatographed on SP-HPLC with triol 4 indicating that *8R,11S,12R*-trihydroxy-*5Z,9E,14Z*-eicosatrienoic acid is the likely endogenous metabolite in human skin.

#### Activation of PPAR $\alpha$ by Trihydroxy Metabolites of the *8R,11R,12R*-Epoxyalcohol

Although rather limited quantities were available, we tested the ability of the trihydroxy hydrolysis products of the *8R,11R,12R*-epoxyalcohol to activate PPAR $\alpha$ , initially by using a mixture of all four hydrolysis products and then by testing the individual isomers. Using the mixture of hydrolysis products a dose-dependent activation of PPAR $\alpha$  was observed; at 10  $\mu$ M concentration, the triols were as active as the natural PPAR $\alpha$  ligand, 8S-HETE (Fig. 3a). When the triols were tested individually, each product was found to be active although triols 1 and 4 showed the highest activity (Fig. 3b).

#### Discussion

Our finding that a specific hepoxilin isomer, *8R*-hydroxy-*11R,12R*-epoxyeicosa-*5Z,9E,14Z*-trienoic acid, can selectively activate the PPAR $\alpha$  subtype has significance both for functions in the epidermis and beyond. As a large class of fatty acid derivatives, the hydroperoxide-derived epoxyalcohols and related metabolites have not been tested as PPAR ligands, partly because they are not commercially available. One of the enzymes involved in the biosynthesis of epoxyalcohols, eLOX3, is not a functional LOX enzyme, but has catalytic activity as a hydroperoxide isomerase [4]. The hydroperoxide isomerase (epoxyalcohol synthase) activity was initially discovered for the transformation of the *12R*-LOX derived *12R*-HPETE. Since eLOX3 can also transform other fatty acid hydroperoxides like *12S*-HPETE and *15S*-HPETE, tissue-specific formation of a wide variety of epoxyalcohols from the coupling of eLOX3 with other lipoxygenases is possible yet unproven so far [26]. Although skin is where eLOX3 is most strongly expressed as judged by RT-PCR, selected other organs give positive signals [27]. For example, a recent report has implicated eLOX3 expression in facilitating the early stages of a classic model system, the PPAR $\gamma$ -induced differentiation of preadipocytes [26, 28].

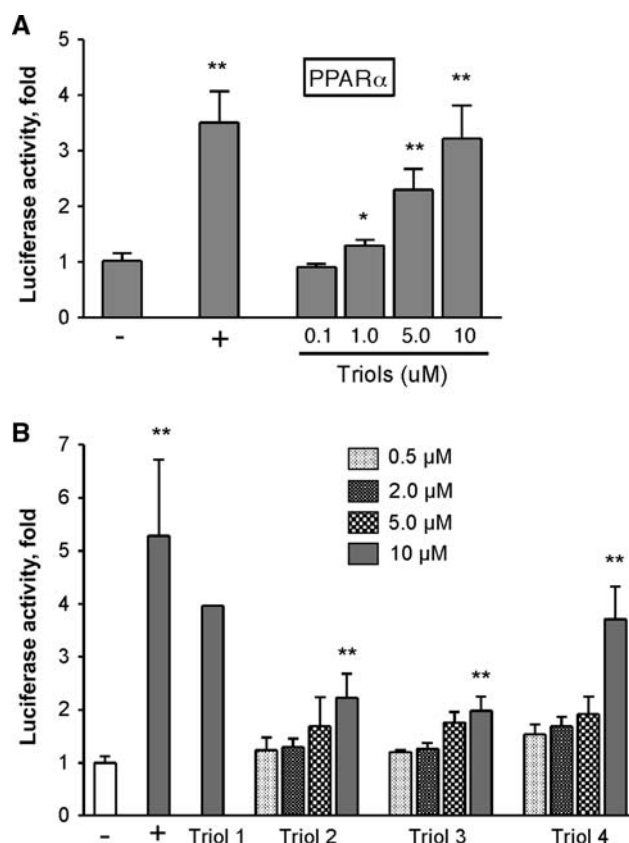


**Fig. 3** Activation of PPAR $\alpha$  by trihydroxy hydrolysis products of the *8R,11R,12R*-epoxyalcohol. **a** Dose-dependent activation of PPAR $\alpha$  by a mixture of the 4 hydrolysis products. **b** Analysis of the activation of PPAR $\alpha$  by the four individual trihydroxy isomers shown in Fig. 2e. For triol 1, only 10  $\mu$ M concentration was tested due to limited availability of the compound. 8S-HETE (10  $\mu$ M) was used as a positive control (+). Results are plotted as fold activation versus the DMSO control (mean  $\pm$  SD of three experiments each performed in triplicate). *P* values versus the DMSO control are presented in the figure. \*\* *P* < 0.01

Epoxyalcohols are chemically unstable molecules and will be hydrolyzed in a cellular system either non-enzymatically or by the enzymes soluble epoxide hydrolase or hepoxilin hydrolase that are widely expressed [29]. Enzymatic hydrolysis of the *8R,11R,12R*-epoxyalcohol yields a specific triol, with the tentative structure of *8R,11S,12R*-trihydroxy-*5Z,9E,14Z*-eicosatrienoic acid, and this product showed among the highest activation of PPAR $\alpha$  in our studies. Whether only the hydrolysis products or also the parent epoxyalcohol (or both) are activators of PPAR $\alpha$  would be dependent on their relative stabilities and accumulation in vivo. Hepoxilin and trioxilin isomers have been detected in human epidermis and are elevated in psoriasis [7, 8], although the specific stereo configurations have yet to be assigned [3].

The *8R,11R,12R*-epoxyalcohol is comparable in potency to the known natural PPAR $\alpha$  activator, 8S-HETE, a product

of the 8S-LOX in mouse skin, and there is evidence that both the 8-LOX enzyme and its 8-HETE product are involved in murine epidermal differentiation [14, 30–32]. Additional genetic studies on ichthyosis patients have shown that inactivating mutations in an uncharacterized cytochrome P450 (CYP4F22, a putative fatty acid omega-hydroxylase) give a similar phenotype to that seen with the 12R-LOX or eLOX3 mutations [33]. The omega-hydroxylation of other eicosanoids such as the epoxyeicosatrienoic acids (EETs) strongly enhances their activity as PPAR activators [34]. In the case of the 8R,11R,12R-epoxyalcohol and its trioxilin hydrolysis product there is also the distinct possibility that metabolic activation could enhance the bioactivity, potentially a function of the CYP4F22 also involved in ichthyosis [33]. The formation of an activating ligand for PPAR $\alpha$  is one possibility of how the epidermal lipoygenases 12R-LOX and eLOX3 can contribute to epidermal differentiation. Whether there are other cellular targets for the epoxyalcohols or their downstream metabolites, for example a putative hepoxilin receptor [9] has yet to be established.

**Acknowledgments** This work was supported by National Institutes of Health grant AR051968.

## References

- Jobard F, Lefèvre C, Karaduman A, Blanchet-Bardon C, Emre S, Weissenbach J, Özgüç M, Lathrop M, Prud'homme JF, Fischer J (2002) Lipoygenase-3 (*Aloxe3*) and 12(*R*)-Lipoygenase (*Alox12b*) are mutated in non-bullous congenital ichthyosiform erythroderma (Ncie) linked to chromosome 17p13.1. *Hum Mol Genet* 11:107–113
- Eckl KM, Krieg P, Kuster W, Traupe H, Andre F, Wittstruck N, Fürstenberger G, Hennies HC (2005) Mutation spectrum and functional analysis of epidermis-type lipoygenases in patients with autosomal recessive congenital ichthyosis. *Hum Mutat* 26:351–361
- Brash AR, Yu Z, Boeglin WE, Schneider C (2007) The hepoxilin connection in the epidermis. *FEBS J* (in press)
- Yu Z, Schneider C, Boeglin WE, Marnett LJ, Brash AR (2003) The lipoygenase gene *Aloxe3* implicated in skin differentiation encodes a hydroperoxide isomerase. *Proc Natl Acad Sci USA* 100:9162–9167
- Yu Z, Schneider C, Boeglin WE, Brash AR (2005) Mutations associated with a congenital form of ichthyosis (NCIE) inactivate the epidermal lipoygenases 12R-LOX and eLOX3. *Biochim Biophys Acta* 1686:238–247
- Antón R, Abian J, Vila L (1995) Characterization of arachidonic acid metabolites through the 12-lipoygenase pathway in human epidermis by high-performance liquid chromatography and gas chromatography/mass spectrometry. *J Mass Spectrom Rapid Commun Mass Spectrom* S169–S182
- Antón R, Puig L, Esgleyes T, de Moragas JM, Vila L (1998) Occurrence of hepoxilins and trioxilins in psoriatic lesions. *J Invest Dermatol* 110:303–310
- Antón R, Vila L (2000) Stereoselective biosynthesis of hepoxilin B<sub>3</sub> in human epidermis. *J Invest Dermatol* 114:554–559
- Lefèvre C, Bouadjar B, Karaduman A, Jobard F, Saker S, Ozguc M, Lathrop M, Prud'homme JF, Fischer J (2004) Mutations in ichthyin a new gene on chromosome 5q33 in a new form of autosomal recessive congenital ichthyosis. *Hum Mol Genet* 13:2473–2482
- Elias PM, Feingold KR (2001) Coordinate regulation of epidermal differentiation and barrier homeostasis. *Skin Pharmacol Appl Skin Physiol* 14(Suppl 1):28–34
- Kuenzli S, Saurat JH (2003) Peroxisome proliferator-activated receptors in cutaneous biology. *Br J Dermatol* 149:229–236
- Di-Poi N, Michalik L, Desvergne B, Wahli W (2004) Functions of peroxisome proliferator-activated receptors (PPAR) in skin homeostasis. *Lipids* 39:1093–1099
- Hanley K, Jiang Y, He SS, Friedman M, Elias PM, Bikle DD, Williams ML, Feingold KR (1998) Keratinocyte differentiation is stimulated by activators of the nuclear hormone receptor PPAR $\alpha$ . *J Invest Dermatol* 110:368–375
- Muga SJ, Thuillier P, Pavone A, Rundhaug JE, Boeglin WE, Jisaka M, Brash AR, Fischer SM (2000) 8S-lipoygenase products activate peroxisome proliferator-activated receptor  $\alpha$  and induce differentiation in murine keratinocytes. *Cell Growth Differ* 11:447–454
- Tan NS, Michalik L, Desvergne B, Wahli W (2003) Peroxisome proliferator-activated receptor (PPAR)-beta as a target for wound healing drugs: what is possible? *Am J Clin Dermatol* 4:523–530
- Tan NS, Michalik L, Noy N, Yasmin R, Pacot C, Heim M, Fluhmann B, Desvergne B, Wahli W (2001) Critical roles of PPAR  $\beta/\delta$  in keratinocyte response to inflammation. *Genes Dev* 15:3263–3277
- Forman BM, Chen J, Evans RM (1996) The peroxisome proliferator-activated receptors: ligands and activators. *Ann N Y Acad Sci* 804:266–275
- Hiji AK, Michalik L, Wahli W (2002) PPARs: transcriptional effectors of fatty acids and their derivatives. *Cell Mol Life Sci* 59:790–798
- Boeglin WE, Kim RB, Brash AR (1998) A 12R-lipoygenase in human skin: mechanistic evidence, molecular cloning and expression. *Proc Natl Acad Sci USA* 95:6744–6749
- Gibian MJ, Vandenberg P (1987) Product yield in oxygenation of linoleate by soybean lipoygenase: the value of the molar extinction coefficient in the spectrophotometric assay. *Anal Biochem* 163:343–349
- Shappell SB, Gupta RA, Manning S, Whitehead R, Boeglin WE, Schneider C, Case T, Price J, Jack GS, Wheeler TM, Matusik RJ, Brash AR, DuBois RN (2001) 15-Hydroxyeicosatetraenoic acid (15-HETE) activates peroxisome proliferator activated receptor gamma (PPAR $\gamma$ ) and inhibits proliferation in PC3 prostate carcinoma cells. *Cancer Res* 61:497–503
- Yu K, Bayona W, Kallen CB, Harding HP, Ravera CP, McMahon G, Brown M, Lazar MA (1995) Differential activation of peroxisome proliferator-activated receptors by eicosanoids. *J Biol Chem* 270:23975–23983
- Hamberg M (1991) Regiochemical and stereochemical analysis of trihydroxyoctadecenoic acids derived from linoleic acid 9-hydroperoxide and 13-hydroperoxide. *Lipids* 26:407–415
- Hamberg M (1999) An epoxy alcohol synthase pathway in higher plants: biosynthesis of antifungal trihydroxy oxylipins in leaves of potato. *Lipids* 34:1131–1142
- Morris LJ (1963) Separation of isomeric long-chain polyhydroxy fatty acids by thin layer chromatography. *J Chromatogr* 12:321–328
- Fürstenberger G, Epp N, Eckl KM, Hennies HC, Jorgensen C, Hallenborg P, Kristiansen K, Krieg P (2007) Role of epidermis-type lipoygenases for skin barrier function and adipocyte differentiation. *Prostaglandins Other Lipid Mediat* 82:128–134

27. Krieg P, Marks F, Fürstenberger G (2001) A gene cluster encoding human epidermis-type lipoxygenases at chromosome 17p13.1: cloning, physical mapping, and expression. *Genomics* 73:323–300
28. Madsen L, Petersen RK, Sorensen MB, Jorgensen C, Hallenborg P, Pridal L, Fleckner J, Amri EZ, Krieg P, Fürstenberger G, Berge RK, Kristiansen K (2003) Adipocyte differentiation of 3T3-L1 preadipocytes is dependent on lipoxygenase activity during the initial stages of the differentiation process. *Biochem J* 375:539–549
29. Newman JW, Morisseau C, Hammock BD (2005) Epoxide hydrolases: their roles and interactions with lipid metabolism. *Prog Lipid Res* 44:1–51
30. Fürstenberger G, Hagedorn H, Jacobi T, Besemfelder E, Stephan M, Lehmann WD, Marks F (1991) Characterization of an 8-lipoxygenase activity induced by the phorbol ester tumor promoter 12-*O*-tetradecanoylphorbol-13-acetate in mouse skin in vivo. *J Biol Chem* 266:15738–15745
31. Schneider C, Strayhorn WD, Brantley DM, Nanney LB, Yull FE, Brash AR (2004) Upregulation of 8-lipoxygenase in the dermatitis of IKB- $\alpha$ -deficient mice. *J Invest Dermatol* 122:691–698
32. Kim E, Rundhaug JE, Benavides F, Yang P, Newman RA, Fischer SM (2005) An antitumorigenic role for murine 8S-lipoxygenase in skin carcinogenesis. *Oncogene* 24:1174–1187
33. Lefèvre C, Bouadjar B, Ferrand V, Tadini G, Mégarbané A, Lathrop M, Prud'homme JF, Fischer J (2006) Mutations in a new cytochrome P450 gene in lamellar ichthyosis type 3. *Hum Mol Genet* 15:767–776
34. Cowart LA, Wei S, Hsu MH, Johnson EF, Krishna MU, Falck JR, Capdevila JH (2002) The CYP4A isoforms hydroxylate epoxyeicosatrienoic acids to form high affinity peroxisome proliferator-activated receptor ligands. *J Biol Chem* 277:35105–35112

# Identification and Characterization of a Novel Bovine Stearoyl-CoA Desaturase Isoform with Homology to Human SCD5

Andrea J. Lengi · Benjamin A. Corl

Received: 25 January 2007 / Accepted: 16 March 2007 / Published online: 28 April 2007  
© AOCS 2007

**Abstract** Stearoyl-CoA desaturase (SCD) is an enzyme responsible for the production of *cis*-9, *trans*-11 conjugated linoleic acid in ruminant fats, and for the synthesis of palmitoleoyl-CoA and oleoyl-CoA. To date, only one SCD isoform has been described in ruminant species, although multiple isoforms have been found in many other mammalian species. In this paper, we describe for the first time a second SCD isoform in cattle, which appears to be an ortholog of human SCD5 rather than a homolog of bovine SCD1 or any of the described murine SCD isoforms. As described in other SCD proteins, the predicted amino acid sequence of bovine SCD5 includes four transmembrane domains and three conserved histidine motifs. The amino-terminus of the predicted protein sequence of SCD5 lacks the PEST sequences typically found in SCD1 homologs, which are thought to target proteins for rapid degradation. Similar to human SCD5, the bovine SCD5 gene is organized into five exons and four introns, and is highly expressed in the brain. In other tissues examined, mRNA expression of SCD5 was minimal. Furthermore, the expression levels of SCD5 between brain gray and white matter are not different. This is the first description of a homolog of human SCD5 in a non-primate species.

**Keywords** Conjugated linoleic acid · Ruminants · Genomic organization · Expression profile

## Abbreviations

bp	Base pair(s)
cDNA	DNA complementary to RNA
CLA	Conjugated linoleic acid
kb	Kilobase(s) or 1000 bp
PCR	Polymerase chain reaction
RACE	Rapid amplification of cDNA ends
RT	Reverse transcription
SCD	Stearoyl-CoA desaturase
UTR	Untranslated region

## Introduction

Conjugated linoleic acids (CLA) are an isomeric family of 18 carbon fatty acids with two conjugated double bonds. Several CLA isomers have been shown to exhibit beneficial health properties in animal models [1, 2]. For example, *cis*-9, *trans*-11 CLA, an isomer found in ruminant fats, is anticarcinogenic and antiatherogenic in animal models [3–5]. In ruminant species, stearoyl-CoA desaturase (SCD), a membrane bound protein of the endoplasmic reticulum, catalyzes the desaturation of *trans*-11 18:1, producing *cis*-9, *trans*-11 CLA [6, 7]. Although SCD produces CLA in several species [8, 9], this enzyme is mainly responsible for catalyzing the desaturation of saturated fatty acyl-CoA substrates, including palmitoyl-CoA and stearoyl-CoA, at the delta-9 position, resulting in the synthesis of palmitoleoyl-CoA and oleoyl-CoA [10].

A. J. Lengi · B. A. Corl  
Department of Dairy Science,  
Virginia Polytechnic Institute and State University,  
Blacksburg, VA 24061, USA

B. A. Corl (✉)  
2020 Litton Reaves Hall, Blacksburg, VA 24061-0315, USA  
e-mail: bcorl@vt.edu

Homologues of the *SCD* gene have been characterized in many mammalian species, including mouse, rat, hamster, sheep, goat, pig, cow, and human. Some mammalian genomes have been shown to contain multiple *SCD* isoforms. To date, four isoforms have been described in mice [11–14], and two isoforms have been described in humans [15, 16]. While the reason for the existence of multiple isoforms in some species is unclear, there is evidence for divergent tissue-specific expression of different isoforms. For example, in the mouse, *SCD1* is expressed predominantly in lipogenic tissues [13], *SCD2* is preferentially expressed in brain and neuronal tissues [11], *SCD3* is expressed in sebocytes, preputial gland and Harderian gland [14], and *SCD4* expression is restricted to the heart [12]. In humans, *SCD1* is most highly expressed in adipose tissue and liver while a second *SCD* gene, termed *hSCD5*, is highly expressed in brain and pancreas [15]. In addition to tissue specific expression, there is evidence to suggest that some *SCD* isoforms may differ in their preferred substrate specificity. For example, murine *SCD1*, *SCD2* and *SCD4* have been shown to desaturate both palmitoyl-CoA and stearoyl-CoA, while murine *SCD3* desaturates palmitoyl-CoA but not stearoyl-CoA [17]. The tissue and substrate specificity of *SCD* isoforms suggests that each may have a distinct physiological role.

Although the mouse and human genomes both contain multiple *SCD* isoforms, there appear to be differences in the evolutionary origins of these genes. In the mouse, all four *SCD* isoforms are contained within a 200 kb region of chromosome 19 and appear to have arisen from tandem gene duplication events [12]. In the human, the *SCD1* and *SCD5* genes are on separate chromosomes, suggesting that they are not the result of a similar gene duplication event. Furthermore, while the human *SCD1* gene appears to be an ortholog of mouse *SCD1*, *hSCD5* appears to be a distinct stearoyl-CoA desaturase gene rather than an ortholog of any of the mouse *SCD* isoforms [15].

Unlike humans and mice, only one *SCD* isoform has been characterized in the ruminant species examined, including goats [18], sheep [19], and cattle [20]. Because genome sequence information is incomplete in these species, we hypothesized that additional undiscovered *SCD* isoforms might exist. Here we describe a second bovine stearoyl-CoA desaturase gene that shares 90.1% identity to human *SCD5* at the amino acid level. As is the case in humans, the novel *SCD* gene is on a separate chromosome (chromosome 6) from *SCD1*, which in cattle is located on chromosome 26 [21]. This is the first report of a human *SCD5* ortholog in a non-primate species, and the first report of multiple *SCD* isoforms in a ruminant species. To be consistent with current proposed nomenclature, we have termed this new gene bovine *SCD5*.

## Experimental Procedures

### Animals

Adipose and liver samples were collected from cows slaughtered at a packing plant (Gaffney, SC). Adipose, liver, heart, brain, lung, spleen, and skeletal muscle tissues were collected from three bulls slaughtered by the Food Science Department at Virginia Tech. Brain white matter and gray matter samples were each collected from five animals (three steers and two cows) slaughtered at a packing plant (Rich Creek, VA). All tissues were snap frozen in liquid nitrogen and stored at  $-80^{\circ}\text{C}$  until use.

### cDNA Isolation and Characterization

Total RNA was isolated from bovine adipose tissue and liver using TRI reagent (Molecular Research Center Inc, Cincinnati, OH) according to the manufacturer's instructions. RNA pellets were resuspended in RNase-free water, and quantified using a spectrophotometer. 5' RACE-ready cDNA and 3' RACE-ready cDNA were synthesized using the SMART RACE cDNA Amplification Kit (Clontech, Mountain View, CA) according to the manufacturer's instructions. The resulting first strand cDNAs were used in 5' and 3' RACE PCR reactions with gene-specific primers localized to the known portions of *SCD5* sequence in conjunction with universal primers included in the RACE kit. Resulting PCR products were cloned using the TOPO TA Cloning Kit for sequencing (Invitrogen, Carlsbad, CA) and sequenced, and the cDNA sequence was submitted to GenBank with the accession number EF014951. Gene specific RACE primers are shown in Table 1. For GC-rich regions in exon one, PCR reactions were performed using the Advantage-GC 2 PCR Kit (Clontech, Mountain View, CA) according to the manufacturer's instructions.

### Genomic DNA Analysis

Genomic DNA was isolated from bovine blood using DNAzol (Molecular Research Center, Cincinnati, OH) according to the manufacturer's instructions. To confirm intron/exon boundaries, PCR was performed using intronic primers spanning each exon (Table 1). Reaction conditions were as follows: 35 cycles of  $94^{\circ}\text{C}$  for 30 s,  $58^{\circ}\text{C}$  for 30 s, and  $72^{\circ}\text{C}$  for 1 min. Resulting PCR products were sequenced to confirm the sequence at the splice junctions.

### Real Time PCR

Total RNA was extracted from snap-frozen tissues using TRI Reagent (Molecular Research Center, Cincinnati, OH) and was reverse transcribed (500 ng per reaction) into

**Table 1** PCR primers

Primer	Forward primer	Reverse primer	Prod. size
RACE PCR primers			
5' RACE	tagcggaggatggaggccaggaagta		
3' RACE	ggacgtcattgagaagggagggaagc		
Genomic PCR primers			
Exon 1	gtgtactccctgggtctcatccccaaa	gagcaggagagaaggcgaaccgagag	206
Exon 2	tgtccaaggtcccagtttc	ggcctagaattggtgtgaa	456
Exon 3	agtggtaggatggaagtgg	gacgagcagtgaggaaaac	612
Exon 4	gcgtgggtttcacctgtact	tgagtggttctctatttc	793
Exon 5	tgtcaccagttcatgggaaa	gcgtgattctgttctctcc	838
Real-time PCR primers			
SCD5	284F: agaaggggaggaagcttgac	450R:ggaggccaggaagtaggagt	166
SCD1	1608F:cccttccttgagctgtctg	1788R:atgctgactctctcccctga	180
Myelin	1120F:ccgcgacgacctatttcta	1286R:aggggttagtgcttctgtg	166
Actin	820F:ctcttcagccttctctct	997R:ggcgagtgatctcttctgc	178

cDNA using the Omniscript reverse transcription kit (Qiagen, Valencia, CA) according to the manufacturer's instructions. Real-time PCR reactions were performed using the Quantitect SYBR Green PCR kit (Qiagen, Valencia, CA) and an Applied Biosystems 7300 Real-time PCR machine (Applied Biosystems, Foster City, CA). Each reaction was performed in duplicate wells. Beta actin was used as an endogenous control gene. Spleen was used as the calibrator for making relative comparisons between tissues for the tissue distribution studies, and gray matter was used as the calibrator for the brain tissue comparison study. Fold change was calculated using the  $2^{-\Delta\Delta C_T}$  method [22]. For adipose, brain, heart, liver, lung, skeletal muscle, and spleen, data from three animals were used to calculate fold change. Data from five animals were used to calculate fold change between brain gray matter and white matter. Primer pairs are shown in Table 1 and reaction conditions were as follows: 35 cycles of 94 °C for 30 s, 58 °C for 30 s, and 72 °C for 1 min.

#### Phylogenetic Analysis

The phylogram was drawn using Molecular Evolutionary Genetic Analysis software MEGA version 3.1, available at <http://www.megasoftware.net>. The following amino acid sequences were included in the phylogenetic tree reconstruction: bovine SCD1 (GenBank Accession No. AAF22305.1), goat SCD1 (AAK01666.1), hamster SCD (AAC42058.1), human SCD1 (CAA73998.1), human SCD5 (AAP31443.1), mouse SCD1 (AAA40103.1), mouse SCD2 (AAH40384.1), mouse SCD3 (NP\_077770.1), mouse SCD4 (AAR06950.1), rat SCD1 (AAM34746.1), rat SCD2 (AAH61737.1), sheep SCD1 (NP\_001009254.1), and swine SCD1 (NP\_998946.1). The yeast SCD protein,

OLE1 (NP\_011460) was used as an out-group to root the tree. Bootstrap analysis with 500 replicates was performed to assess the statistical significance of the tree.

#### Statistical Analysis

The tissue distribution was statistically analyzed as an analysis of variance using the General Linear Model procedure of SAS (version 9.1.3) with animal and tissue included in the model. Treatment means were separated by Tukey's multiple comparison procedure. Gray and white matter data were compared similarly to tissue distribution with animal and brain matter type included in the model using the General Linear Model procedure of SAS.

## Results

#### Nucleotide Sequence of the Bovine *SCD5* Transcript

By BLAST searching the Ensembl bovine genome database (Btau 2.0), we were able to identify a region on chromosome 11 with homology to exons five and six of bovine *SCD1*. In addition, we located a region with homology to exons three and four of bovine *SCD1* on an unmapped "scaffold" (a set of ordered, oriented contigs). By performing RT PCR with bovine liver and adipose RNA, we demonstrated that these two regions were part of the same transcript. These results were confirmed by DNA sequencing of the amplified PCR product. Further BLAST searching of the Bovine Genome Project at the Human Genome Sequencing Center at Baylor College of Medicine (v.3.1) revealed that the *SCD5* gene is located on chromosome 6 (accession number CM000182), suggesting that

the portion of sequence we originally located on chromosome 11 was incorrectly assigned.

In order to examine the transcript of this putative new bovine desaturase gene, we performed 5' and 3' rapid amplification of cDNA ends, or RACE reactions and sequenced the resulting products (Fig. 1). During the time that this work was performed, a complete cDNA clone isolated from a Hereford cow hypothalamus cDNA library was submitted to Genbank under the accession number BC112711. This clone matched the cDNA sequence that we obtained by RACE amplification and included an additional 195 upstream base pairs of the 5' untranslated region of exon one, making the transcript 2.583 kb in length. The sequence we obtained by RACE PCR differs at two nucleotide positions from this cDNA clone, but neither of these potential nucleotide sequence polymorphisms results in an amino acid sequence change. Because the coding region of the transcript was found to have 89.4% homology to the human *SCD5* nucleotide sequence, we have named this novel desaturase gene bovine *SCD5*.

#### Amino Acid Sequence and Conserved Protein Features

The predicted amino acid sequence for bovine *SCD5*, shown in Fig. 2a, shares many of the characteristic features that are highly conserved among stearoyl-CoA desaturase

proteins, including three histidine motifs (HXXXXH and HXXHH) that are catalytically essential to fatty-acyl desaturase activity [23]. Sequence alignment shows 90.1% identity between bovine *SCD5* and human *SCD5* at the amino acid level. A Kyte-Doolittle hydrophathy plot (Fig. 2b) drawn from the amino acid sequence highlights the location of the four conserved transmembrane domains [24, 25]. The N-terminus of the bovine *SCD5* protein lacks the conserved PEST sequences that are present in mammalian *SCD1* proteins and are thought to play a role in their rapid degradation (Fig. 2c).

#### Phylogenetic Relationship of Mammalian SCD Isoforms

To determine the likely evolutionary relationship between bovine *SCD5* and mammalian *SCD1* orthologs, we compared the predicted protein sequence of bovine *SCD5* with the sequences of other mammalian SCD proteins. As shown in Table 2 and Fig. 3, bovine *SCD5* clearly shares much greater amino acid sequence identity and appears to have a much closer evolutionary relationship with human *SCD5* than with any other SCD protein, including bovine *SCD1*. Human and bovine *SCD5* share 90.1% sequence identity at the amino acid level. While the *SCD1* orthologs from ruminant species share significant homology

```

ggggagccggcagccgagggcaagggggcgccctttctcttaagagcctcaagggcgaccctgattggctgtagct
atgcaggtcttttcccccgctccctccgagcagtcctcccccgccgctctcagctcttccacaccccccccc
ccccccggcggccccctccccccggcgctcgccccctctctctggcggcggcaggttcttccggcagccgagc
gggtgatgcccagcaacagatgcccgggacccaagatggcctccttaggccacgctgaagccctgaagaagcgagaa
ggaagcagagcagggcggggaagggggacagaggtgcccggagatccccctaccacaaatcccccaaaaaagggca
ggaagccggcccccaaccggagagctccgctcctcggagatcggcggtcgtgccaactgcccggggcgctaggtct
ccccagccATGCCAGGCCCGGCCGCTGGACCGGAGAAGGTCCTTCCCGAGCCCAAGGAGAGATCCGTCGGGG
GTAGGGTCGAGGGCTCGGAGGGCGGGCGGGCGGGCGGGGAGAGGGCCGGCGGGCGGGCACCCGAGGAC
ATCGTCTGGAGGAACGTGTTCCTGATGAGCCTGCTCCACTTGGCGGCGGTACTCCCTGGTGTCTATCCCCAAGCC
CAGCCGCTCACTCTGCTCTGGCCCTACTTCTGCTTCCCTCTGACTGCTCTGGGTGTGACAGCTGTTGCCATCGTTTG
TGGACCCACAGTCTCAACAGGCTAAGCTACCCCTGAGGATATTTCTGGCTGCTGCCAATCCATGGCTTTCCAGAA
GACATCTTCAGTGTGCGAGGGACCCAGGTCATCAACAAGTACTCGGAGACGGACGCTGACCCACACAATGCCCCG
CGGGCTTCTTCTCTCCACATCGGCTGGCTGTTTTCGCAAGCATCGGGACGTCATTGAGAAGGGGAGGAAAGCTT
GACGTCACCGACTTGTGGCTGACCCCTGGTCCGGTTCAGAGAAAGTACTACAAGATCACCGTGGTGTCTCATGTG
CTTCGTAGTCCCACGCTGGTGCCTGGTACATCTGGGGAGAAAGCCTGTGGAACCTCACTTCTGGCCCTCATCTC
CGCTACACCACTCACTCAACCTCACTGGCTGGTGAACAGTGTGCGCACATGTACCGAAACCGGCCCTATGACA
AGCACATCAGCCCTCGGAGAACCCGCTCGTCAACCTGGTGCATTGGTGAAGGTTCCATAACTACCATCACCTT
TCCCTTTGACTACTCTGCGAGTGAATTTGGCTTAAATTTCAACCCAACCACTGGTTCATTGACTTTCATGTGTTGGC
TGGGCTAGCCACTGACCGAACCGGGCAACCAAGCAGATGATCGAAGCCCGAAAGCCCGGACTGGAGACGGGAGCG
CTTGA)ctctggatcctccatctgcccgcctgtcaacgaagcctccgttcatggccttggtaactacacttctcttg
tccatggatcgtgggagggggcgcaagctggggagagaacagaatccacgagcttgggggttttttctggtggctc
caaaaatgtcaagatacaaaactacaatgaaaagaatttttaaagtcagtgtaactatgcttcaactagaaac
gggacatgtgatttaacgctgtagctacaacatgctcatcaaacatacatcgtcatgtgctggtactgtacgtga
tgttaaccctgacagatgaaggaatttcatattcttccagtgatcagggagagccttggtttctgttttaaac
caacctattttaaacagactactgaagggcagagagggcaggggtggaagacaaaagagagttcaagtagtaagga
aagaatgttctgctttgtaattattgtgtgtgtgtgtgtgtgttttaaagtaagaaaatgaaaatgttaaaaatg
agaatcaggaatggctctcttattttttgcccctgtgcccagctgtttaatgttcccgttctcttgctcaagggg
ctgttcaactgctcagctagttttgtgtcctgagctgtccgctcagctgacctataatcagtgctgttttaagtg
ttgattttctctcttctgctattgtcgttttaaggtgtagaactcagaagtcaggaacatcaagtagaactcaagga
agctctcattcaatgtttagacacctaatttatatttcaatgtatcctagcactgggtgcatgtacttaccactct
ctgctaaaataagcattataattttccacaccaggtcactcagatctgaataaccaacagttatctagaactcaggtctc
acaaatgttccactgcatggccctcatgtattttgcaagacataaagtgatcatatgtagcctctggattt
taaaaaaatctgtgtgttaagtgtcctgttaagagcagctgcaaatcaatgggacagcgtgccccttggtttagatg
tagagcaaaagagaccttatagtttggcatcagagcactcgaagatagtgctgcaagataggggaagatgtagga
ttaaattttacatttttgaagaagtgacccggtaggggaattgtcattaaatgaagttctctcatccagcaggtgtttaa
cggtgttatttttgccattaatatgtgtaaactatgagtgatcacaataaagattatgaatgcaaaaaaa
aaaaaaaaaaaaaa

```

**Fig. 1** Nucleotide sequence of bovine *SCD5* cDNA. Shaded region indicates additional 5' untranslated nucleotide sequence from a cDNA clone submitted to Genbank (accession number BC112711). Lower case letters indicate untranslated regions, while capital letters denote the coding sequence. Start and stop codons are enclosed in boxes. Bold letters indicate single nucleotide differences between sequence

obtained by RACE PCR and the sequence of the cDNA clone. These potential polymorphisms do not change the amino acid sequence. Possible mRNA destabilization motifs (ATTTA) in the 3' UTR are underlined, while the consensus polyadenylation signal (AATAAA) is double underlined



**Fig. 2 a** Amino acid sequence alignment of bovine SCD5 and human SCD5. *Asterisk* indicates matching residues. *Double dot* indicates conserved amino acid substitutions. *Dot* indicates semi-conserved substitutions. Boxed sequences indicate the location of the three conserved histidine motifs (one HXXXXH and two HXXHH). **b** Kyte Doolittle Hydrophathy Plot drawn with a window size of 19. Positive scores correlate to the degree of hydrophobicity. *Bold* regions indicate the location of the four conserved transmembrane domains. **c** Comparison of the first 66 amino acid residues from bovine SCD5, murine SCD1, and bovine SCD1. Potential PEST sequences, as determined using the PESTfind algorithm (<http://www.at.embnet.org/embnet/tools/bio/PESTfind>), are *underlined*

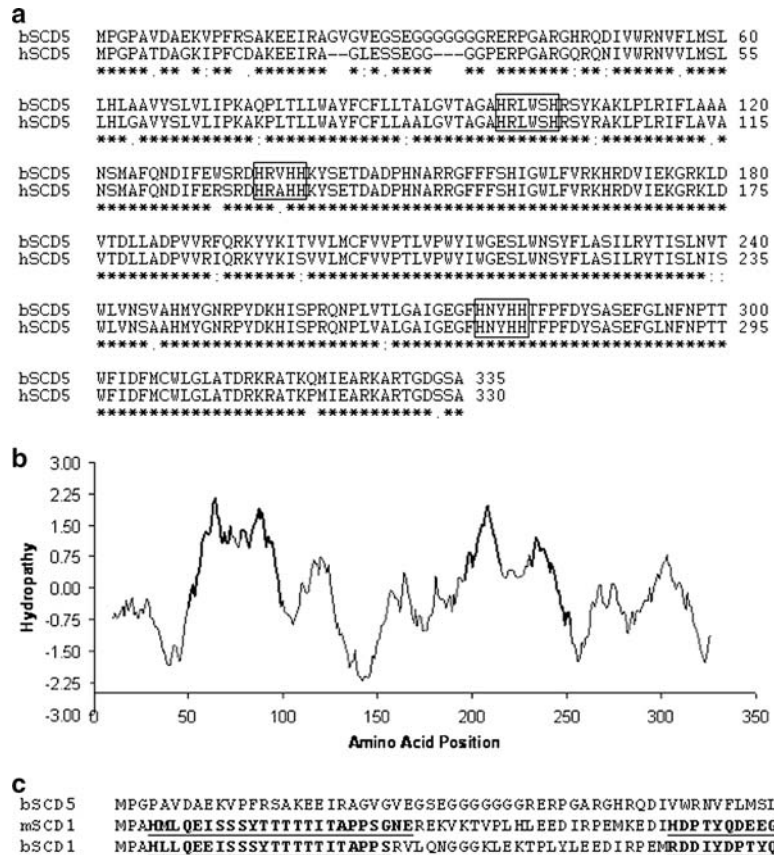


**Table 2** Comparison of % identity between SCD isoforms/species

	cSCD	oSCD	pSCD	bSCD1	bSCD5	hSCD1	hSCD5	mSCD1	mSCD2	mSCD3	mSCD4
cSCD	100										
oSCD	98.1	100									
pSCD	88.0	88.3	100								
bSCD1	94.4	93.6	88.3	100							
bSCD5	65.0	65.0	66.4	65.0	100						
hSCD1	86.6	86.6	86.9	86.1	65.0	100					
hSCD5	65.5	65.5	66.9	65.1	90.1	65.1	100				
mSCD1	82.7	82.1	84.1	81.0	64.3	84.1	64.4	100			
mSCD2	81.1	80.5	82.5	78.3	63.6	82.5	63.7	85.4	100		
mSCD3	83.0	82.2	83.6	80.2	62.9	82.7	63.0	87.7	84.7	100	
mSCD4	75.7	75.7	75.7	74.6	60.1	77.4	60.6	78.9	79.0	78.5	100

Percent identities were calculated by the ExPASy SIM Alignment Tool for Protein Sequences, using the BLOSUM62 comparison matrix with a Gap Open penalty of 12 and a Gap Extension penalty of 4

c caprine, o ovine, p porcine, b bovine, h human, m murine

(93.6–98.1%), none share greater than 65% identity with bovine SCD5. Phylogenetic analysis of mammalian SCD protein sequences shows that bovine SCD5 and human SCD5 are grouped together and are much more closely related to each other than to any mammalian SCD1 sequence (Fig. 3).

#### Genomic Organization of the Bovine SCD5 Gene

By comparing the cDNA sequence obtained from the RACE PCR to the available published bovine genomic DNA sequence, we determined that bovine SCD5 is organized into five exons and four introns (Fig. 4), spanning

**Fig. 3** Phylogenetic tree of selected mammalian SCD amino acid sequences. The scale bar indicates the unit of amino acid Poisson distance. The percentage bootstrap values are indicated. Yeast OLE1 was used as an outgroup to root the tree

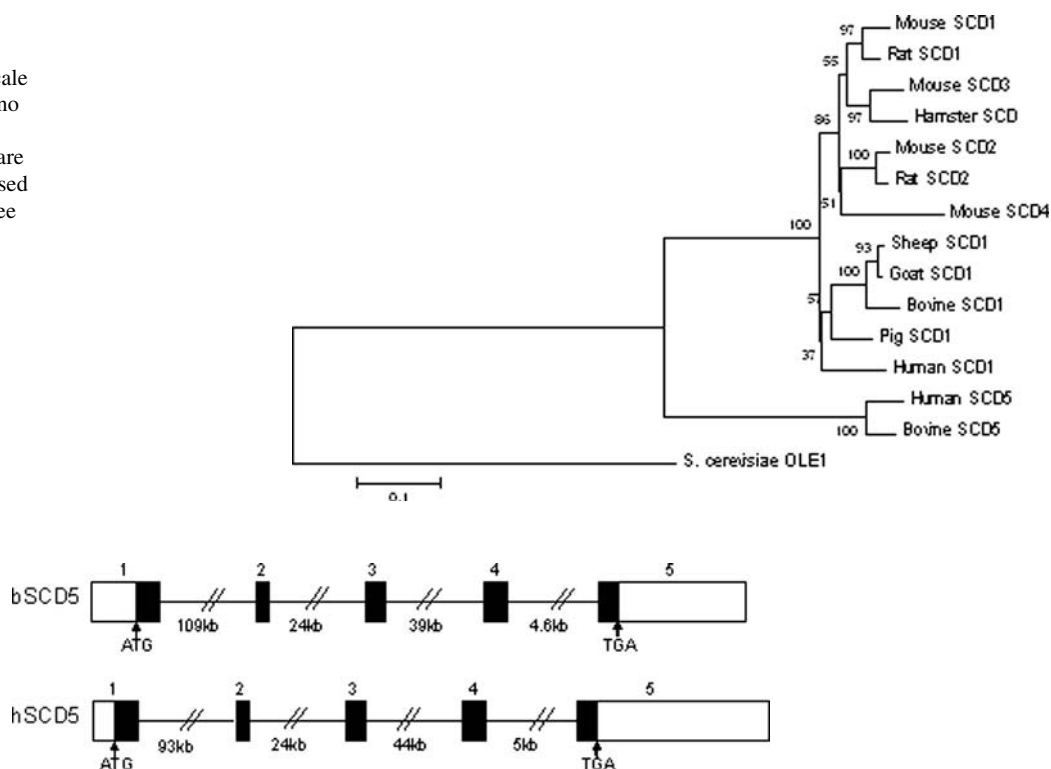


**Fig. 4** Genomic structure of bovine *SCD5* deduced from known bovine genomic DNA sequence. Lines represent introns and boxes represent exons. White boxes represent untranslated regions, while black boxes represent the open reading frame

**Table 3** Exon–intron junctions of bovine *SCD5*

Exon	Exon size (bp)	5' splice donor	Intron size (kb)	3' splice acceptor
1	723	CTCTGGG <b>gt</b> gagtactctg	109	tgtgtcttgc <b>ag</b> CCTACTT
2	131	TTTCCAG <b>gt</b> gggaatggag	23.9	ttctccctgc <b>ag</b> AATGACA
3	206	AGAGAA <b>gt</b> taagtgagcaa	39	tctcttcc <b>ag</b> GTACTAC
4	233	GCCATTG <b>gt</b> gagtgcggg	4.6	tttgtctcc <b>ag</b> GTGAAGG
5	1497			

Exon sequences are denoted by capital letters, and intronic sequences are in lowercase. The canonical dinucleotide gt (splice donor) and ag (splice acceptor) sequences are in bold

more than 175 kb. Splice site sequences were determined by PCR amplification of genomic DNA spanning each exon based on the published genomic sequence. Amplified products were sequenced to confirm the intron–exon junctions (Table 3).

#### Tissue Specific Expression of Bovine *SCD5*

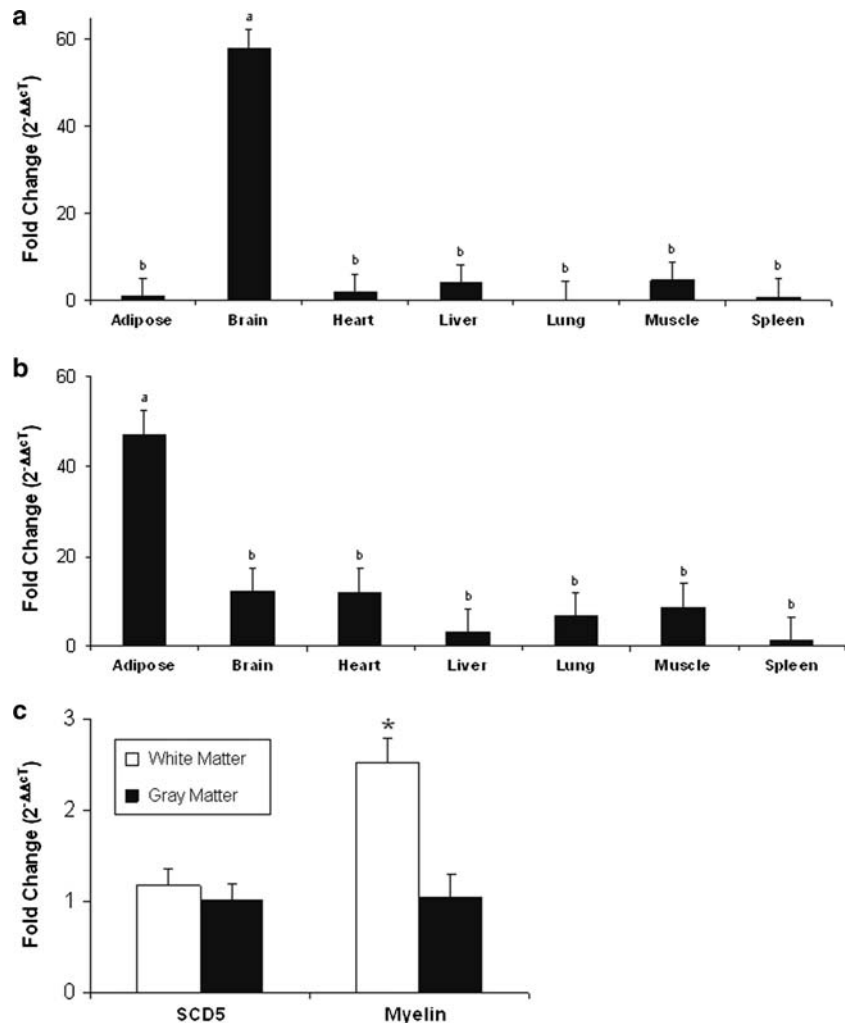
Because it has been shown that different *SCD* isoforms in mice have different tissue expression profiles, we examined a panel of bovine tissues (adipose, liver, heart, brain, lung, spleen, and skeletal muscle) using quantitative real-time PCR to determine tissue-specific expression of bovine *SCD5* and *SCD1*. The mRNA expression of *SCD5* was significantly greater in the brain compared to all other

tissues examined (Fig. 5a), whereas the mRNA expression of *SCD1* was significantly higher in adipose tissue (Fig. 5b). We next investigated whether *SCD5* expression differs between white matter and gray matter regions of the bovine brain. The mRNA expression of myelin basic protein was used as a control to validate separation of white matter and gray matter. No significant difference was found in *SCD5* mRNA abundance between these tissues (Fig. 5c).

#### Discussion

Ruminant fats are rich in saturated fatty acids as a result of the ruminal biohydrogenation of dietary unsaturated fatty acids. Stearoyl-CoA desaturase reduces the saturated fatty

**Fig. 5** Analysis of **a** bovine *SCD5* gene expression and **b** bovine *SCD1* gene expression using real-time PCR. Real-time PCR was performed using RNA extracted from bull tissues (adipose, brain, heart, liver, lung, muscle, spleen;  $n = 3$ ). Beta actin was used as the endogenous control gene, and spleen was used as the calibrator for making relative comparisons between tissues. Fold change was calculated using the  $2^{-\Delta\Delta C_T}$  method. Bars not sharing a common superscript letter differ ( $P < 0.001$ ). **c** Real-time PCR analysis of bovine *SCD5* gene expression using total RNA from brain white matter and gray matter ( $n = 5$ ). Myelin basic protein mRNA expression was used to validate separation of white matter and gray matter. Beta actin was used as the endogenous control gene, and gray matter was used as the calibrator for making relative comparisons between tissues. Fold change was calculated using the  $2^{-\Delta\Delta C_T}$  method. \* $P < 0.05$  within a transcript



acid content of ruminant fats and is important in determining ruminant fatty acid composition for this reason. Many mammalian genomes contain multiple stearoyl-CoA desaturase isoforms. Ruminant species, however, have so far been found to have only one *SCD* gene. In this paper, we describe for the first time a second *SCD* gene in cattle, which we have named bovine *SCD5*. This novel bovine desaturase gene appears to be an ortholog of the recently described human *SCD5* gene. In addition to humans, partial *SCD5* cDNA sequences have been found in other primate species such as chimpanzees and orangutans [15]. This is the first report of an *SCD5* ortholog in a non-primate species.

It has been hypothesized that the four *SCD* isoforms found in mice may be the result of multiple gene duplication events while human *SCD5* is a distinct stearoyl-CoA desaturase created by a single gene duplication event. This gene duplication event could have occurred prior to the divergence of mammals, and *SCD5* was then lost during the evolution of some species, such as rodents [15]. An alternate hypothesis is that the *SCD5* gene was acquired

only in primates later during evolution. Evidence to support the first hypothesis includes the fact that all four mouse isoforms are found within a 200 kb span of the same chromosome and share considerable amino acid sequence homology, and are therefore likely to be derived from relatively recent gene duplication events, while human *SCD1* and *SCD5* are on separate chromosomes and share much less sequence identity than the mouse isoforms. Further, while human *SCD1* appears to be an ortholog of mouse *SCD1* and other mammalian *SCD1* genes, human *SCD5* does not appear to be an ortholog of any of the four mouse isoforms or of any other mammalian *SCD1* gene.

The genomic organization of bovine *SCD5* closely resembles that of the human *SCD5* gene [26] and diverges from the highly conserved six exon, five intron structure of the bovine, caprine [18], porcine [27], and human [16], *SCD1* genes as well as all four murine *SCD* genes [11–14]. Further, phylogenetic analysis shows that bovine *SCD5* and human *SCD5* protein sequences are much more closely related to each other than to any mammalian *SCD1* protein. Taken together, these data support the idea that *SCD5* is a

distinct desaturase gene that existed before the divergence of mammals but was lost during the evolution of some species, and refutes the possibility that *SCD5* is a gene acquired later during the evolution of primates.

The human *SCD5* isoform was previously shown to be most highly expressed in brain and pancreas [15, 26]. Similarly, our results show that bovine *SCD5* is most highly expressed in the brain. We did not test the expression of *SCD5* in bovine pancreas, but *SCD5* message was detectable by RT PCR in all tissues examined, indicating that this transcript may be expressed at low levels in many tissues (data not shown). Within the brain, it has been shown that white matter tends to have much greater phospholipid concentrations of monoenoic fatty acids compared to gray matter [28]. However, the expression of *SCD5* mRNA does not appear to be different between bovine brain white matter and gray matter.

Mammalian SCD1 proteins have a short half-life of 3–4 h [29, 30] and are rich in PEST sequences made up of local high concentrations of proline, glutamic acid, serine, threonine, and aspartic acid residues, which are thought to target proteins for rapid degradation by the ubiquitin-proteasome pathway [31]. The PEST-rich 66 N-terminal amino acids of mammalian SCD1 proteins have been shown to play an important role in their rapid proteasomal degradation, and when this region is deleted, the half-life of the resulting protein increases significantly [32, 33]. Additionally, a conserved lysine residue at amino acid position 33 of the rat SCD1 protein has been shown to be important for conferring instability to the protein [34]. Interestingly, this N-terminal region of SCD1 is also the region of greatest sequence divergence between SCD1 and SCD5 proteins. In contrast to mammalian SCD1 proteins, the N-terminus of bovine SCD5 contains neither PEST sequences nor the conserved lysine residue. This suggests that SCD5 may exhibit greater protein stability than SCD1, or that its degradation may be regulated differently than SCD1.

The expression of rodent SCD1 is sensitive to dietary manipulations, being highly induced under fat-restricted diets, and rapidly down regulated by diets high in polyunsaturated fatty acids [33, 35] and regulation is facilitated by its short half-life [36]. Stearoyl-CoA desaturase 5 is highly expressed in the brain, a tissue enriched with long chain polyunsaturated fatty acids [28], and this may indicate that SCD5 is not as sensitive to polyunsaturated fatty acids as SCD1. The lack of PEST sequences in SCD5 suggests this protein may be more stable and therefore less sensitive to dietary regulation. The half-life of SCD5 is currently unknown, but future studies expressing the full-length protein will allow us to address the question of stability, as well as to determine substrate specificity of the enzyme. Different tissue-specific expression and N-termi-

nal sequences of SCD1 and SCD5 may reflect differences in the regulation and physiological roles of these isoforms.

Stearoyl-CoA desaturase produces almost all the mono-unsaturated fatty acids present in ruminant fats and is the major source of *cis*-9, *trans*-11 CLA in the milk fat of lactating dairy cows [6, 7]. Diet plays a major role in determining the CLA content of milk fat, and the concentration of *cis*-9, *trans*-11 CLA in milk fat increases as much as eight fold when cows are switched to a CLA inducing diet [37]. However, significant variation also occurs among cows on the same diet and this appears to be driven by variation in mammary desaturase activity [38]. Abundant SCD activity is present in the mammary gland of lactating dairy cows [39], but the relative expression of SCD isoforms in the mammary gland has not been examined. It is not currently known if SCD5 contributes to mammary SCD activity to account for some of the observed variation in CLA and desaturase activity in lactating cows.

One potential role for SCD activity in the brain may be to maintain optimal levels of oleic acid. Evidence suggests that oleic acid in the brain is not supplied by the diet, but rather is produced exclusively by de novo synthesis in the brain itself. Rats fed a diet devoid of oleic acid had much lower concentrations of oleic acid in many tissues, but not in brain, nerve endings, or myelin [40]. Experiments using deuterated fatty acids in milk substitute fed to rat pups during the developmental period of brain growth spurt prior to myelination showed that oleic acid in the brain was not supplied via circulation, but by de novo biosynthesis in the brain [41]. These data suggest that the nervous system synthesizes the oleic acid that it needs, regardless of dietary intake, thereby indicating a need for SCD activity in this tissue.

Oleic acid has several critical functions in the brain. First, oleic acid is a major component of myelin, which forms an insulating sheath around nerve fibers in both the central and peripheral nervous systems to greatly increase electrical impulse speed [42]. Demyelination of neurons is associated with several devastating neurodegenerative diseases, including multiple sclerosis, transverse myelitis, and chronic inflammatory demyelinating polyneuropathy. Second, oleic acid is a neurotrophic factor in the developing brain, promoting axonal growth and neural clustering, and inducing the expression and activation of growth associated protein-43 (GAP-43), a marker for neural differentiation and regeneration [43, 44]. These data indicate that the oleic acid synthesized by SCD is important for normal brain structure and development.

In conclusion, we have identified a second stearoyl-CoA desaturase isoform in cattle, which contains the conserved transmembrane domains and histidine residues characteristic of desaturase enzymes. Unlike other SCD isoforms, bovine SCD5 lacks PEST sequences, which are thought to

target proteins for rapid degradation, thereby facilitating rapid transcriptional regulation. This isoform has high sequence homology and similar gene structure to human *SCD5*, and, like human *SCD5*, does not have high homology with other isoforms identified in rodents. Furthermore, this is the first homologue identified outside primates. Like human *SCD5*, bovine *SCD5* exhibits significantly greater expression in the brain than lipogenic tissues.

**Acknowledgments** We thank Hengjian Wang and Kim Waterman of the Department of Food Science and Technology at Virginia Tech and Smith Valley Meats for tissue samples, and the Virginia Bioinformatics Institute for sequencing work. This research was supported by the Virginia Agricultural Experiment Station.

## References

- Ip MM, Masso-Welch PA, Ip C (2003) Prevention of mammary cancer with conjugated linoleic acid: role of the stroma and the epithelium. *J Mammary Gland Biol Neoplasia* 8:103–118
- Brown JM, McIntosh MK (2003) Conjugated linoleic acid in humans: regulation of adiposity and insulin sensitivity. *J Nutr* 133:3041–3046
- Corl BA, Barbano DM, Bauman DE, Ip C (2003) *cis-9*, *trans-11* CLA derived endogenously from *trans-11* 18:1 reduces cancer risk in rats. *J Nutr* 133:2893–2900
- Lock AL, Corl BA, Barbano DM, Bauman DE, Ip C (2004) The anticarcinogenic effect of *trans-11* 18:1 is dependent on its conversion to *cis-9*, *trans-11* CLA by delta9-desaturase in rats. *J Nutr* 134:2698–2704
- Lock AL, Home CA, Bauman DE, Salter AM (2005) Butter naturally enriched in conjugated linoleic acid and vaccenic acid alters tissue fatty acids and improves the plasma lipoprotein profile in cholesterol-fed hamsters. *J Nutr* 135:1934–1939
- Corl BA, Baumgard LH, Dwyer DA, Griinari JM, Phillips BS, Bauman DE (2001) The role of delta(9)-desaturase in the production of *cis-9*, *trans-11* CLA. *J Nutr Biochem* 12:622–630
- Kay JK, Mackle TR, Auldust MJ, Thomson NA, Bauman DE (2004) Endogenous synthesis of *cis-9*, *trans-11* conjugated linoleic acid in dairy cows fed fresh pasture. *J Dairy Sci* 87:369–378
- Mosley EE, McGuire MK, Williams JE, McGuire MA (2006) *cis-9*, *trans-11* conjugated linoleic acid is synthesized from vaccenic acid in lactating women. *J Nutr* 136:2297–2301
- Santora JE, Palmquist DL, Roehrig KL (2000) *trans*-Vaccenic acid is desaturated to conjugated linoleic acid in mice. *J Nutr* 130:208–215
- Enoch HG, Catala A, Strittmatter P (1976) Mechanism of rat liver microsomal stearyl-CoA desaturase. Studies of the substrate specificity, enzyme–substrate interactions, and the function of lipid. *J Biol Chem* 251:5095–5103
- Kaestner KH, Ntambi JM, Kelly TJ Jr, Lane MD (1989) Differentiation-induced gene expression in 3T3-L1 preadipocytes. A second differentially expressed gene encoding stearyl-CoA desaturase. *J Biol Chem* 264:14755–14761
- Miyazaki M, Jacobson MJ, Man WC, Cohen P, Asilmaz E, Friedman JM, Ntambi JM (2003) Identification and characterization of murine SCD4, a novel heart-specific stearyl-CoA desaturase isoform regulated by leptin and dietary factors. *J Biol Chem* 278:33904–33911
- Ntambi JM, Buhrow SA, Kaestner KH, Christy RJ, Sibley E, Kelly TJ Jr, Lane MD (1988) Differentiation-induced gene expression in 3T3-L1 preadipocytes. Characterization of a differentially expressed gene encoding stearyl-CoA desaturase. *J Biol Chem* 263:17291–17300
- Zheng Y, Prouty SM, Harmon A, Sundberg JP, Stenn KS, Parimoo S (2001) Scd3—a novel gene of the stearyl-CoA desaturase family with restricted expression in skin. *Genomics* 71:182–191
- Wang J, Yu L, Schmidt RE, Su C, Huang X, Gould K, Cao G (2005) Characterization of HSCD5, a novel human stearyl-CoA desaturase unique to primates. *Biochem Biophys Res Commun* 332:735–742
- Zhang L, Ge L, Parimoo S, Stenn K, Prouty SM (1999) Human stearyl-CoA desaturase: alternative transcripts generated from a single gene by usage of tandem polyadenylation sites. *Biochem J* 340(Pt 1):255–264
- Miyazaki M, Bruggink SM, Ntambi JM (2006) Identification of mouse palmitoyl-coenzyme A Delta9-desaturase. *J Lipid Res* 47:700–704
- Bernard L, Leroux C, Hayes H, Gautier M, Chilliard Y, Martin P (2001) Characterization of the caprine stearyl-CoA desaturase gene and its mRNA showing an unusually long 3'-UTR sequence arising from a single exon. *Gene* 281:53–61
- Ward RJ, Travers MT, Richards SE, Vernon RG, Salter AM, Buttery PJ, Barber MC (1998) Stearyl-CoA desaturase mRNA is transcribed from a single gene in the ovine genome. *Biochim Biophys Acta* 1391:145–156
- Chung M, Ha S, Jeong S, Bok J, Cho K, Baik M, Choi Y (2000) Cloning and characterization of bovine stearyl CoA desaturase cDNA from adipose tissues. *Biosci Biotechnol Biochem* 64:1526–1530
- Campbell EM, Gallagher DS, Davis SK, Taylor JF, Smith SB (2001) Rapid communication: mapping of the bovine stearyl-coenzyme A desaturase (SCD) gene to BTA26. *J Anim Sci* 79:1954–1955
- Livak KJ, Schmittgen TD (2001) Analysis of relative gene expression data using real-time quantitative PCR and the 2(-Delta Delta C(T)) method. *Methods* 25:402–408
- Shanklin J, Whittle E, Fox BG (1994) Eight histidine residues are catalytically essential in a membrane-associated iron enzyme, stearyl-CoA desaturase, and are conserved in alkane hydroxylase and xylene monooxygenase. *Biochemistry* 33:12787–12794
- Kyte J, Doolittle RF (1982) A simple method for displaying the hydropathic character of a protein. *J Mol Biol* 157:105–132
- Man WC, Miyazaki M, Chu K, Ntambi JM (2006) Membrane topology of mouse stearyl-CoA desaturase 1. *J Biol Chem* 281:1251–1260
- Zhang S, Yang Y, Shi Y (2005) Characterization of human SCD2, an oligomeric desaturase with improved stability and enzyme activity by cross-linking in intact cells. *Biochem J* 388:135–142
- Ren J, Knorr C, Huang L, Brenig B (2004) Isolation and molecular characterization of the porcine stearyl-CoA desaturase gene. *Gene* 340:19–30
- Svennerholm L (1968) Distribution and fatty acid composition of phosphoglycerides in normal human brain. *J Lipid Res* 9:570–579
- Oshino N, Sato R (1972) The dietary control of the microsomal stearyl CoA desaturation enzyme system in rat liver. *Arch Biochem Biophys* 149:369–377
- Heinemann FS, Ozols J (1998) Degradation of stearyl-coenzyme A desaturase: endoproteolytic cleavage by an integral membrane protease. *Mol Biol Cell* 9:3445–3453
- Rechsteiner M, Rogers SW (1996) PEST sequences and regulation by proteolysis. *Trends Biochem Sci* 21:267–271
- Mziaut H, Korza G, Ozols J (2000) The N terminus of microsomal delta 9 stearyl-CoA desaturase contains the sequence determinant for its rapid degradation. *Proc Natl Acad Sci USA* 97:8883–8888

33. Kato H, Sakaki K, Mihara K (2006) Ubiquitin-proteasome-dependent degradation of mammalian ER stearoyl-CoA desaturase. *J Cell Sci* 119:2342–2353
34. Mziaut H, Korza G, Benraiss A, Ozols J (2002) Selective mutagenesis of lysyl residues leads to a stable and active form of delta 9 stearoyl-CoA desaturase. *Biochim Biophys Acta* 1583:45–52
35. Jones BH, Maher MA, Banz WJ, Zemel MB, Whelan J, Smith PJ, Moustaid N (1996) Adipose tissue stearoyl-CoA desaturase mRNA is increased by obesity and decreased by polyunsaturated fatty acids. *Am J Physiol* 271:E44–49
36. Heinemann FS, Ozols J (2003) Stearoyl-CoA desaturase, a short-lived protein of endoplasmic reticulum with multiple control mechanisms. *Prostaglandins Leukot Essent Fatty Acids* 68:123–133
37. Peterson DG, Kelsey JA, Bauman DE (2002) Analysis of variation in *cis*-9, *trans*-11 conjugated linoleic acid (CLA) in milk fat of dairy cows. *J Dairy Sci* 85:2164–2172
38. Kelsey JA, Corl BA, Collier RJ, Bauman DE (2003) The effect of breed, parity, and stage of lactation on conjugated linoleic acid (CLA) in milk fat from dairy cows. *J Dairy Sci* 86:2588–2597
39. McDonald TM, Kinsella JE (1973) Stearyl-CoA desaturase of bovine mammary microsomes. *Arch Biochem Biophys* 156:223–231
40. Bourre JM, Dumont OL, Clement ME, Durand GA (1997) Endogenous synthesis cannot compensate for absence of dietary oleic acid in rats. *J Nutr* 127:488–493
41. Edmond J, Higa TA, Korsak RA, Bergner EA, Lee WN (1998) Fatty acid transport and utilization for the developing brain. *J Neurochem* 70:1227–1234
42. Garbay B, Boiron-Sargueil F, Shy M, Chbihi T, Jiang H, Kamholz J, Cassagne C (1998) Regulation of oleoyl-CoA synthesis in the peripheral nervous system: demonstration of a link with myelin synthesis. *J Neurochem* 71:1719–1726
43. Granda B, Taberero A, Tello V, Medina JM (2003) Oleic acid induces GAP-43 expression through a protein kinase C-mediated mechanism that is independent of NGF but synergistic with NT-3 and NT-4/5. *Brain Res* 988:1–8
44. Velasco A, Taberero A, Medina JM (2003) Role of oleic acid as a neurotrophic factor is supported in vivo by the expression of GAP-43 subsequent to the activation of SREBP-1 and the up-regulation of stearoyl-CoA desaturase during postnatal development of the brain. *Brain Res* 977:103–111

## Comparing Subcutaneous Adipose Tissue in Beef and Muskox with Emphasis on *trans* 18:1 and Conjugated Linoleic Acids

Michael E. R. Dugan · John K. G. Kramer ·  
Wayne M. Robertson · William J. Meadus ·  
Noelia Aldai · David C. Rolland

Received: 3 January 2007 / Accepted: 5 March 2007 / Published online: 10 May 2007  
© Her Majesty the Queen in Right of Canada, as represented by the Minister of Agriculture and Agri-Food, Canada 2007

**Abstract** Muskox (*Ovibos moschatus*) are ruminant animals native to the far north and little is known about their fatty acid composition. Subcutaneous adipose tissue (backfat) from 16 wild muskox was analyzed and compared to backfat from 16 barley fed beef cattle. Muskox backfat composition differed substantially from beef and the most striking difference was a high content of 18:0 (26.8 vs. 9.77%). This was accompanied by higher levels of most other saturated fatty acids except beef had more 16:0. Muskox backfat also had a lower level of *cis*-18:1 and this was related to a lower expression of steroyl-CoA desaturase mRNA. Beef backfat had a higher level of total *trans*-18:1 (4.25 vs. 2.67%). The most prominent *trans*-18:1 isomers in beef backfat were 10*t*-18:1 (2.13%) and 11*t*-18:1 (0.77%) whereas the most prominent isomers in muskox backfat were 11*t*-18:1 (1.41%), 13*t*/14*t*- (0.27%) and 16*t*-18:1 (0.23%). The total conjugated linoleic acid (CLA) content was higher in beef backfat than muskox (0.67 vs. 0.50%) with 9*c*,11*t*-18:2 as the most abundant CLA isomer. The second most abundant CLA isomer in beef backfat was 7*t*,9*c*-18:2 (0.10%) whereas in muskox it was 11*t*13*c*-18:2 (0.04%). Muskox backfat had a higher content of 18:3n-3 and its elongation and desaturation products 20:5n-3, 22:5n-3 and 22:6n-3 and a lower n-6/n-3 ratio. Overall, the high forage diet of muskox seemed to produce a healthier fatty acid profile and highlighted the need to develop feeding

strategies for intensively raising beef that will not negatively impacting fatty acid composition.

**Keywords** Beef · Muskox · Conjugated linoleic acid · *trans* 18:1 · Stearic acid · Saturated fatty acids · Stearyl-CoA desaturase

### Abbreviations

ACO	Acyl CoA oxidase
CLA	Conjugated linoleic acid
FAME	Fatty acid methyl esters
FAS	Fatty acid synthase
MUFA	Monounsaturated fatty acids
PUFA	Polyunsaturated fatty acids
SFA	Saturated fatty acids
SCD-1	Stearyl CoA desaturase-1
SFA	Saturated fatty acids

### Introduction

Muskox (*Ovibos moschatus*) are ruminant animals native to the far north and along with goats and sheep fall into the sub-family Caprinae of the Bovidae family. In Canada, muskox are found mainly on the Arctic islands and the majority of these can be found on Banks Island. Banks Island is the most western island in the Canadian Arctic Archipelago and covers an area of 70,266 km<sup>2</sup> and has a muskox population of approximately 65,000, representing about 47% of the total population of the Canadian Northwest Territories [1]. Muskox are harvested for local use, for export of highly valued quiviut and hides and also for developing markets for their meat. The nutritive value of

M. E. R. Dugan (✉) · W. M. Robertson ·  
W. J. Meadus · N. Aldai · D. C. Rolland  
Lacombe Research Centre, Agriculture and Agri-Food Canada,  
6000 C&E Trail, Lacombe, AB, Canada T4L 1W1  
e-mail: duganm@agr.gc.ca

J. K. G. Kramer  
Food Research Program, Agriculture and Agri-Food Canada,  
Guelph, ON, Canada

the meat is in part related to its fatty acid composition, but little is known about muskox lipid composition and nothing is known about the conjugated linoleic acid (CLA) or *trans*-18:1 content of its tissues. Adamczewski et al. [2] reported the content of lean, fat and bone in muskox and the percent lipid class distribution, but not their fatty acid compositions. Baker et al. [3] only reported the fatty acid composition of milk fat from muskox but did not include total nor individual CLA or *trans*-18:1 isomers.

Conjugated linoleic acid has many purported roles in the prevention and possible treatment of several diseases including diabetes, obesity and some types of cancer [4, 5]. Rumenic acid (9*c*,11*t*-18:2), the major CLA isomer in ruminant fats has been associated with beneficial effects, while the other CLA isomers, notably 10*t*,12*c*-18:2, have not [6–8]. In addition, vaccenic acid (11*t*-18:1), the major *trans*-18:1 isomer generally present in ruminant fats is equally effective in cancer prevention [9], because of its endogenous conversion to 9*c*,11*t*-18:2 in animals [10], humans [11], and human cell lines [12]. The health effects of several *trans*-18:1 isomers other than 11*t*-18:1, notably 9*t*- and 10*t*-18:1, were shown to be associated with negative plasma lipid and lipoprotein profiles [13, 14]. However, butter fat enriched in 11*t*-18:1 and 9*c*,11*t*-18:2 improved the plasma cholesterol profile in hamsters [15] and natural beef fat reduced the growth of human cancer cells [16].

The present communication reports the comprehensive fatty acid composition of subcutaneous adipose tissue (backfat) from wild muskox and compares it to the most commonly consumed adipose tissue of ruminant origin in Canada (i.e., beef) finished on a high barley diet at the Lacombe Research Centre. Additional mRNA analysis of fatty acid metabolizing enzymes was then conducted to help explain differences in the levels of saturated (SFA) and monounsaturated fatty acids (MUFA) between these ruminant species.

## Experimental Procedures

### Animals, Diets and Sample Collection

Sixteen muskox and 16 beef animals were used in this study. Beef animals were raised and both beef and muskox were slaughtered in accordance to principles and guidelines of the Canadian Council of Animal Care. The average age of the muskox was estimated to be 2.5 years and the beef animals 1.5 years. Wild muskox were harvested from Banks Island where a high proportion of their diet consists of sedges (*Carex aquatilis*, *Eriophorum* spp.; [17]) which are similar to grasses in composition with high fiber levels and relatively low protein contents [18]. Post-slaughter, muskox carcasses were rapidly chilled outdoors (–20 to

–25 °C with a wind chill of approximately –40 °C) and frozen carcasses were shipped to the Lacombe Research Centre. The beef animals were raised under typical cow/calf and feedlot conditions for Western Canada at the Lacombe Research Centre. In the last 75 days prior to slaughter, beef animals had ad libitum access to a finishing diet consisting of 22.0% barley silage, 73.3% barley grain, 1.6% molasses, 3.1% feedlot supplement (32% crude protein) and 22 mg/kg sodium monensin. Beef animals were slaughtered and processed at the Lacombe Research Centre abattoir and adipose tissue samples were collected from both muskox and beef animals between the fifth and sixth ribs at 5 cm off the midline and these samples remained frozen at –80 °C until analyzed.

### Feed Fatty Acid Analysis

Fatty acid methyl esters (FAME) from the beef feedlot diet and sedges grab sampled from Banks Island (i.e., muskox diet) were prepared according to Sukhija and Palmquist [19] and using a Varian 3800 GC (Varian, Walnut Creek, CA, USA) equipped with a Varian 8100 autosampler and a 30 m SP2340 capillary column (Supelco, Bellefonte, PA, USA). The system was operated under constant pressure (15 psi) using hydrogen as the carrier gas and a 20:1 split ratio. The injector and detector were held at 250 °C and the FAME were quantified using a flame ionization detector. Samples were injected (1 µl, 0.5 µg/µl) and the column temperature was held initially at 50 °C for 30 s, increased to 170 °C at 25 °C/min, held for 3 min, increased to 180 °C at 2 °C/min, then increased to 230 °C at 10 °C/min. Chromatograms were integrated using Varian Star Chromatography Workstation software.

### Adipose Tissue Analyses

Subcutaneous adipose tissue was directly methylated with sodium methoxide and the FAME were analyzed using the GC and Ag<sup>+</sup>-HPLC equipment and methods outlined by Cruz-Hernandez et al. [20]. The *trans*-18:1 isomers were, however, analyzed using two complementary GC temperature programs instead of a preparatory Ag<sup>+</sup>-TLC separation followed by GC separation at 120 °C. The first temperature program was as previously described (temperature program A; 45 °C held for 4 min, increased at 13 °C/min to 175 °C and held for 27 min, then increased at 4 °C/min to 215 °C and held for 35 min) [20]. The second program (temperature program B; 45 °C held for 4 min, increased at 13 °C/min to 150 °C and held for 47 min, then increased at 4 °C/min to 215 °C and held for 35 min) improved the resolution of some *trans*-18:1 isomers (6-8*t*- to 11*t*-18:1) and allowed for analysis of the remaining *trans*-18:1 isomers by difference.



For the identification of FAME by GC, the reference standard no. 461 from Nu-Check Prep Inc. (Elysian, MN, USA) was used. Branch-chain FAME were identified using a GC reference standard BC-Mix1 purchased previously from Applied Science (State College, PA, USA). All the geometric isomers of linoleic and linolenic acids were prepared by mild iodine isomerization [20]. The CLA isomers no. UC-59M from Nu-Chek Prep Inc. was used since it contained all four positional CLA isomers, and they were analyzed by GC and Ag<sup>+</sup>-HPLC [20]. Individual CLA isomers were obtained from Matreya Inc. (Pleasant Gap, PA, USA) and isomerized using iodine to obtain all geometric CLA isomers [20]. All chemicals and solvents were of analytical grade.

#### mRNA Analysis of Fatty Acid Metabolizing Enzymes

Total RNA was isolated from muskox ( $n = 8$ ) and beef ( $n = 8$ ) adipose tissue in ten volumes of the guanidium thiocyanate based TRI reagent solution in accordance with the manufacturer's specifications (Sigma, St Louis, MO, USA). A prior clean-up step was required after the adipose samples were dissolved in the TRI reagent to remove excess lipid by centrifugation at 10,000  $g$  at 20 °C and removal of the upper lipid fraction prior to addition of chloroform. Pools of cDNA were generated from each sample at 42 °C for 60 min (Sigma, St Louis, MO, USA) using: 5  $\mu$ g of total RNA primed with 300 ng of random hexamers, 200 U of MMLV-reverse transcriptase (RT) enzyme, 1 mM of dATP, dGTP, dTTP and dCTP, 10 mM DTT, and 10 U of RNase inhibitor in the manufacturer's RT buffer. The yield of cDNA was measured according to the polymerase chain reaction signal generated from the internal house keeping gene  $\beta$ -actin [21].

To generate PCR primers for the "comparative gene expression studies", new cDNAs were cloned and

sequenced from the muskox adipose RNA for the stearyl CoA desaturase-1 (SCD1), fatty acid synthase (FAS), acyl CoA oxidase (ACO) and  $\beta$ -actin mRNAs. To help standardized the gene expression analysis studies, PCR primers were designed to have 100% homology with their equivalent beef mRNAs, SCD1 (Gb no. AY241932), FAS (Gb no. AF285607), ACO (Gb no. BF230141), and 96% homology with  $\beta$ -actin (Gb no. AY141970) (Table 1). Sequence homologies between muskox and beef cDNAs were analyzed using the ClustalW program [22]. Primer sequences, which matched both muskox and beef cDNAs, were generated using the Primer3 program [23] and validated using the BLASTn program [24].

Gene expression activity in the beef and muskox adipose samples was measured using SYBR green labeled Real-time quantitative RT-PCR analysis method in a Stratagene Mx4000 machine (Stratagene, La Jolla, CA, USA). For each sample, cDNA was added to 1X Brilliant SYBR green QPCR master mix and then aliquoted into 20  $\mu$ L fractions. The specific gene primers were added to their independent fraction and run simultaneously in the Mx4000 machine. Gene expression activity was estimated by the number of PCR cycles required to reach a minimum threshold for cycle detection (Ct value). The signal for  $\beta$ -actin was used as an internal standard to normalize the estimates of FAS, ACO and SCD1 mRNA levels between species.

#### Statistical Analysis

Data were analyzed by ANOVA using the GLM procedure of SAS© software (SAS Systems, Release 8.2, SAS Institute Inc., Cary, NC, USA). Results were expressed as mean  $\pm$  SEM, and a  $P$  value of 0.05 was considered significant.

**Table 1** Primers, Genbank accession numbers, and the expected product size from PCR amplification of cDNA and genomic DNA templates of muskox and bovine adipose samples

Gene	Muskox cDNA (bp)	Muskox genomic DNA (bp)	Bovine cDNA (bp)	Forward reverse	Muskox Genbank <sup>a</sup> accession number
SCD1	214	214	214	5'-cctaccaggataaggagggc-3' 5'- ttttaggttcggtgactcc-3'	AY530631
FAS	393	482	373	5'-agcgggaagcgtgtgatgg-3' 5'-ttccggctgtgtgccac-3'	AY768701
ACO	217	519	217	5'-gtggaacctaacgtccattg-3' 5'-cctgggtgatctgagact-3'	AY766151
$\beta$ -actin	231	343	224	5'-ggactctgagcaggatgg-3' 5'-gcaccgtgtggcgtagagg-3'	DQ017256

SCD1 Stearyl CoA desaturase-1, FAS fatty acid synthase, ACO acyl CoA oxidase

<sup>a</sup> Genbank, National Institute of Health, Bethesda

## Results and Discussion

### Diet

The fatty acid composition of the beef diet was typical for barley grain lipids with high levels of linoleic acid (18:2n-6; 48.9%), substantial amounts of linolenic acid (18:3n-3; 7.63%) and an 18:2n-6/18:3n-3 ratio of 6.4 (Table 2). The beef diet also contained intermediate amounts of 9c-18:1 and 16:0. The sedge lipids consisted mainly of SFAs (55.9%) that included 16:0 (23.3%), 18:0 (3.8%) and the long-chain SFAs 20:0 (6.4%), 22:0 (14.8%) and 24:0 (4.7%) (Table 2) which would be indicative of a high content of waxy cuticle [25] and a reduced feeding value for this forage. The sedges contained a higher level of 18:3n-3 relative to the beef diet, but the amount was lower than that reported in other leaf lipids [26]. Sedge lipids also contained substantial amounts of 18:2n-6 (15.9%) and had an 18:2n-6/18:3n-3 ratio of 1.4.

### Adipose Tissue SFA

Muskox subcutaneous adipose tissue had higher total SFAs than beef including most of the individual SFAs except beef adipose tissue had more 16:0 ( $P < 0.05$ ; Table 3), which may be indicative of a higher plane of nutrition and

**Table 2** Dietary fatty acid content and percent composition

	Beef diet	Sedges <sup>a</sup>
Dietary fat (mg FAME/g DM)	29.3	8.6
Fatty acid (FAME, %)		
14:0	0.33	1.65
15:0	0.08	0.52
16:0	17.7	23.3
9c-16:1	0.28	1.35
17:0	0.11	0.58
18:0	1.31	3.80
9c-18:1	20.5	10.9
11c-18:1	1.27	1.57
18:2n-6	48.9	15.9
20:0	0.28	6.41
18:3n-3	7.63	11.08
11c-20:1	0.72	0.21
22:0	0.23	14.89
13c-22:1	0.13	0.94
24:0	0.12	4.70
15c-24:1	0.08	0.59

Diets were analyzed in duplicate

FAME fatty acid methyl esters, DM dry matter

<sup>a</sup> Sedges are a major component of the muskox diet

**Table 3** Muskox and beef subcutaneous adipose tissue saturated fatty acid composition ( $n = 16$  in each group)

Percentage of total fatty acids	Beef	Muskox	SEM
10:0	0.05**	0.15	0.01
12:0	0.07	0.13	0.03
14iso	0.03**	0.07	0.00
14:0	3.38*	4.30	0.31
15iso	0.10**	0.33	0.01
15ai	0.15**	0.29	0.02
15:0	0.52	0.53	0.05
16 iso	0.15**	0.21	0.01
16:0	25.4*	23.4	0.56
17iso	0.33**	0.42	0.01
17ai	0.59**	0.94	0.03
17:0	1.18*	1.39	0.07
18:0 iso	0.15*	0.17	0.01
18:0	9.77**	26.8	0.67
19:0	0.05**	0.24	0.01
20:0	0.07**	0.64	0.02
21:0	0.01**	0.12	0.01
22:0	0.01**	0.33	0.01
23:0	0.02**	0.12	0.01
24:0	0.01**	0.16	0.01
26:0	0.00**	0.06	0.00
Sum SFA	42.0**	60.9	1.11
Sum iso and anteiso	1.49**	2.42	0.07

SEM standard error of the mean, SFA saturated fatty acids

\* $P < 0.05$ , beef differs from muskox, \*\* $P < 0.01$ , beef differs from muskox

increased rates of de novo fatty acid synthesis in beef fat. Of particular interest, muskox adipose tissue had higher levels of long-chain SFAs ( $\geq 18:0$ ;  $P < 0.05$ ), specifically 18:0 (26.8 vs. 9.8% in beef fat). High 18:0 levels were previously reported in the milk fat of muskox [3]. Finding a high SFA content in muskox adipose tissue was unusual since decreased levels of SFA are generally observed in animals living at low ambient temperatures, as expected in the Arctic, which maintains their fat in a liquid or semi-liquid state [27]. The high insulation value of the coat may negate their need for desaturation, as well as their higher content of low melting point branch-chain FAs (noted below). Sheep and goats are more closely related to muskox than beef cattle, and they also have been found to deposit high levels of 18:0 when grazing forages [28], but 18:0 is lower in lambs when fed a high-energy corn diet [29]. Comparably high levels of 18:0 have been found in other wild ruminants (elk, deer and antelope) under natural grazing conditions [30]. The high level of 18:0 in the fat of muskox could be related to the diet, to more extensive biohydrogenation of dietary polyunsaturated fatty acids

(PUFAs) compared to beef cattle and/or to reduced rates of 18:0 desaturation.

### Branched-Chain Fatty Acids

Muskox adipose tissue was found to contain higher levels of C14 to C18 branched-chain (iso and anteiso) fatty acids ( $P < 0.05$ ; Table 3). Short branched-chain fatty acids arise from deamination of branched-chain amino acids by rumen microorganisms [31] or by carboxylation of propionyl-CoA to form methylmalonyl-CoA [32]. These branched-chain fatty acids can then be incorporated during fat synthesis in ruminants to form longer chain branched-chain fatty acids [33]. Higher levels of branch-chain fatty acids typically result when readily fermentable carbohydrate sources are available, causing an increase in propionate production [27]. Given the relatively poor quality of forage available to muskox and lack of grain in their diet, synthesis of branched-chain fatty acids through carboxylation of propionyl-CoA seems unlikely. Furthermore, muskox may be predisposed to deposit higher levels of branched-chain FAs similar to sheep and goats who were shown to deposit greater levels of branched-chain FAs compared to cattle when fed the same diet [32].

### *cis*- and *trans*-MUFA

The separation of the *cis* and *trans*-MUFA, particularly of the 18:1 isomers remains a challenge, as evident from the partial GC chromatograms of beef (Fig. 1) and muskox backfat (Fig. 2). When *cis* and *trans*-MUFA are not pre-fractionated using  $\text{Ag}^+$ -TLC prior to GC, one deals with partial resolution of 10*t*- and 11*t*-18:1 because of the large differences in their relative abundance, and overlap of 13*t*- to 16*t*-18:1 with *cis*-18:1 isomers. To avoid this, two separate GC temperature programs were employed in this study to improve the resolution of 6-8*t*- to 11*t*-18:1 isomers by lowering the temperature during the plateau region from 175 to 150 °C (see inserts in Figs. 1, 2), and to determine the remaining *trans*-18:1 isomers by difference between the two separate GC chromatograms.

The most abundant *cis*-MUFAs in both beef and muskox adipose tissue were 9*c*-16:1 and 9*c*-18:1 and the latter contained trace amounts of 10*c*-18:1 (Table 4). The adipose tissue of beef contained much more 9*c*-18:1 (38.0 vs. 27.4%) and correspondingly less 18:0 than found in muskox (9.8 vs. 26.8%). Beef adipose tissue also contained significantly higher levels of most of the other *cis*-MUFA, some arising from  $\Delta 9$  desaturation of their SFA precursors, while others are possible intermediates of rumen biohydrogenation of PUFAs [34].

Beef adipose tissue contained more total *trans*-18:1 relative to muskox ( $P < 0.01$ ; Table 4) and this was

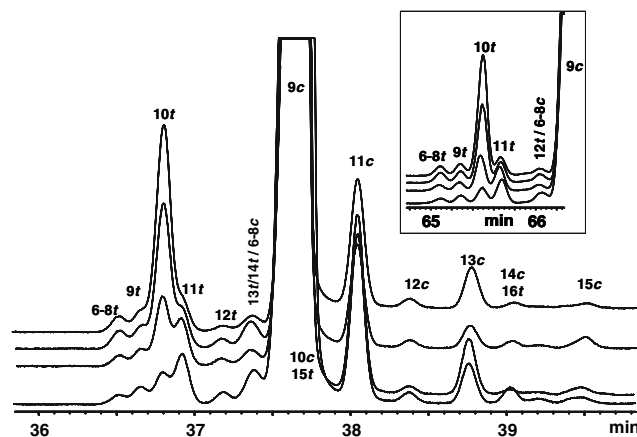


**Fig. 1** Partial GC chromatograms of the 18:1 region from representative adipose tissue FAME of barley fed beef adipose tissue showing the maximum range of 10*t*- and 11*t*-18:1 isomer distribution among samples using GC temperature program A (details in M&M section). *Insert* shows separation of partial *trans*-18:1 isomers of the same beef samples using GC temperature program B

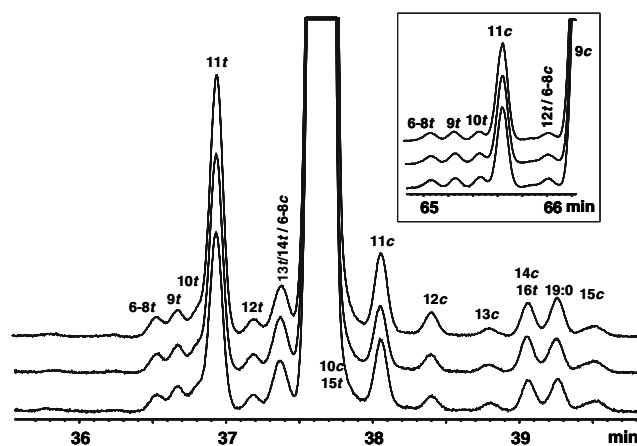


**Fig. 2** Partial GC chromatograms of the 18:1 region from representative adipose tissue FAME of wild muskox adipose tissue showing the maximum range of 10*t*- and 11*t*-18:1 isomer distribution among samples using GC temperature program A (details in M&M section). *Insert* shows separation of partial *trans*-18:1 isomers of the same muskox samples using GC temperature program B

primarily due to a higher level of 10*t*-18:1 and slightly greater levels of 6-8*t*, 9*t* and 12*t*-18:1 ( $P < 0.01$ ; Fig. 3). Conversely, the most abundant *trans*-18:1 isomer in muskox adipose tissue was 11*t*-18:1 and its level was greater than that found in beef fat ( $P < 0.01$ ). The *trans*-18:1 content and composition was also more variable in beef than muskox fat as evident from the partial GC chromatograms presented in Figs. 1 and 2 demonstrating the range in *trans*-18:1 compositions encountered in beef and muskox, respectively.

Feeding high levels of concentrate significantly increases 10*t*-18:1 in adipose tissue of ruminants making it

**Table 4** Muskox and beef subcutaneous adipose tissue monounsaturated fatty acid composition ( $n = 16$  in each group)

Percentage of total fatty acids	Beef	Muskox	SEM
9c-14:1	1.27*	0.14	0.08
Sum 16:1 <i>t</i>	0.10	0.11	0.00
Total 16:1c	5.39**	2.53	0.34
7c-	0.20**	0.59	0.03
9c-	4.78**	1.85	0.31
11c-	0.30**	0.03	0.02
13c-	0.12**	0.07	0.01
9c-17:1	1.11**	0.47	0.04
Total 18:1 <i>t</i>	4.25**	2.67	0.24
Total 18:1c	41.3**	28.4	0.86
6c-8c-	0.14**	0.09	0.01
9c/10c-	38.0**	27.4	0.81
11c-	1.91**	0.46	0.08
12c-	0.12**	0.09	0.01
13c-	0.58**	0.06	0.04
14c-	0.04**	0.00	0.01
15c-	0.16**	0.08	0.01
16c-	0.09*	0.07	0.00
17-	0.18	0.19	0.01
9c-20:1	0.11*	0.10	0.01
11c-20:1	0.31**	0.21	0.02
15c-24:1	0.01**	0.06	0.01
9c-14:1/14:0	0.34**	0.03	0.02
9c-16:1/16:0	0.17**	0.07	0.01
9c-17:1/17:0	0.93**	0.31	0.06
9c-18:1/18:0	3.85**	1.00	0.19
9c/11 <i>t</i> -18:2/11 <i>t</i> -18:1	0.55**	0.23	0.04

SEM standard error of the mean

\* $P < 0.05$ , beef differs from muskox, \*\* $P < 0.01$ , beef differs from muskox

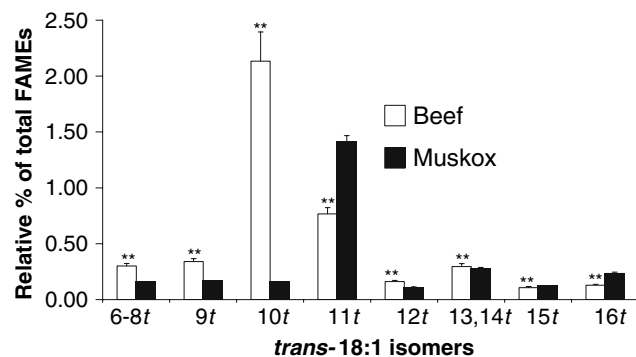


**Fig. 3** Muskox and beef subcutaneous adipose tissue *trans*-18:1 composition. Bars and vertical lines represent mean  $\pm$  SEM,  $n = 16$  for each species. For each isomer, bars with asterisks are significantly different ( $P < 0.01$ )

the predominant *trans*-18:1 isomer irrespective of the grain type fed, whether corn [35], barley [36], a barley/oat mixture [37], or a mixture to several ingredients [38]. On the other hand, feeding a lower concentrate to forage ratio increases both 11*t*- and 10*t*-18:1, but 11*t*-18:1 remains the major *trans*-18:1 isomer [39–42]. Comparable changes in 10*t*-18:1 levels in milk fat have also been found when dairy cows are fed differing concentrate to forage ratios [43–46]. A recent study shows that the shift toward 10*t*-18:1 production can be eliminated by feeding a grass/hay basal diet supplemented with linseed oil when the forage to concentrate ratio is 64:36 [47]. The ionophore monensin has also been shown recently to increase 10*t*-18:1 in milk fat when dairy cows are fed a concentrate containing supplementary sunflower seed oil [48]. High levels of 10*t*-18:1 appear to be related to changes (and instability) in the rumen environment and altered bacterial populations when highly fermentable (i.e., pH reducing) diets are fed [36, 49, 50].

### CLA

The complete analysis of the CLA isomers in beef and muskox required a combination of GC and Ag<sup>+</sup>-HPLC, reference standard no. UC-59M from Nu Chek Prep Inc., and isomerization of individual CLA standards using iodine [20]. Peaks were identified by comparison to previously established elution orders by GC and Ag<sup>+</sup>-HPLC [20, 34, 51, 52]. The 7*t*,9*c*-18:2 isomer was observed as a distinct shoulder on the 9*c*,11*t*-18:2 peak in the GC chromatogram but by Ag<sup>+</sup>-HPLC these isomers were clearly resolved (Fig. 4). On the other hand, 9*c*,11*t*- and 9*t*,11*c*-18:2 were resolved by GC but co-eluted with using Ag<sup>+</sup>-HPLC (Fig. 4). The relatively high content of 21:0 observed in muskox lipids eluted in the region of the minor CLA isomers in the GC chromatogram and the presence of these isomers was confirmed using Ag<sup>+</sup>-HPLC (Fig. 4) [20, 34].

The adipose tissue of beef had significantly more total CLA than muskox (Table 5). The most abundant CLA isomer in both beef and muskox was 9*c*, 11*t*-18:2, which was significantly higher in beef than in muskox as a percent of total FAME (Fig. 5), but both had ~67% 9*c*,11*t*-CLA in total CLA. There were, however, significant differences in the remaining CLA isomers. Among the minor CLA isomers present, beef had significantly greater amounts of amounts of 7*t*,9*c*- and 9*t*,11*c*-18:2 ( $P < 0.01$ ; Fig. 5) and contained trace amounts of 10*t*,12*c*-18:2 (data not presented). The CLA profile of beef fat in this study was similar to that reported by others in beef [40, 53] and dairy cows [44, 54] fed concentrates. Muskox adipose tissue had significantly greater amounts of 11*t*,13*c*-18:2 ( $P < 0.01$ ; Fig. 5) and 11*t*,13*t*-18:2 (Fig. 4, Ag<sup>+</sup>-HPLC). For details regarding the identification of the CLA isomers see reference by Cruz-Hernandez et al. [20]. The minor *trans*, *trans*-CLA isomers

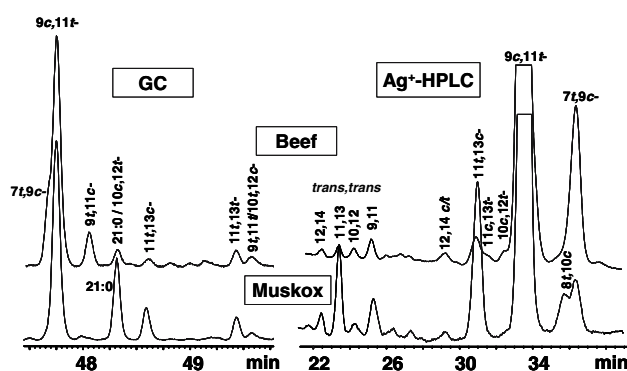


**Fig. 4** Partial GC and  $\text{Ag}^+$ -HPLC chromatograms of the CLA region of adipose tissue FAME from wild muskox and barley fed beef. Details of GC temperature program A and silver-ion HPLC separation are given in the M&M sections

(<0.02%) shown in Fig. 4 ( $\text{Ag}^+$ -HPLC separation) were included in total CLA, but are not reported or discussed separately.

The metabolic origin of some, but not all the different CLA isomers is understood. The  $9c,11t$ - and  $7t,9c$ -18:2 CLA isomers are synthesized in the tissues of ruminants from their respective *trans*-18:1 precursors by stearyl-CoA desaturase [55, 56]. The rate of their formation is considerably slower in muskox than in beef based on the lower desaturation ratio of  $9c,11t$ -18:2/ $11t$ -18:1 in muskox (Table 4). It has been suspected that the  $11t,13c$ -18:2 isomer was derived from  $18:3n-3$  [54] and this has now been confirmed showing  $9c,11t,15c$ -18:3 and  $11t,15c$ -18:2 are intermediates and the latter is then isomerized to  $11t,13c$ -18:2 [57].

#### Non-Conjugated *c/t* 18:2 Isomers

Although the content of the non-conjugated *c/t* 18:2 isomers is less than 1% of total adipose FAME in these two ruminants (Table 5), their occurrence and concentration does provide an indication of their respective metabolism of PUFAs by rumen bacteria, or subsequent tissue synthesis. Beef subcutaneous fat contained more *c/t* 18:2 metabolites than muskox supporting the suggestion that biohydrogenation is more complete in muskox than in beef. Most of the identified *c/t* 18:2 isomers were more abundant in beef, except the minor isomers  $8t,13c$ - and  $9t,12c$ -18:2 (Table 5). The relative high content of the  $18:3n-3$  metabolite  $11t,15c$ -18:2 was not surprising since both beef and muskox had access to feed containing  $18:3n-3$  (i.e., barley and sedges, respectively). The higher  $\Delta 9$  desaturation activity in beef (see below) would also explain the higher amounts of  $9c,13t$ - and  $9c,12t$ -18:2 in the adipose tissue of beef derived from the corresponding *trans*-18:1 precursors. The identity of some of the *c/t*-18:2 and *c/c/t*-18:3 isomers were

confirmed by comparison with iodine isomerized products of linoleic and linolenic acids [58].

#### PUFA

Dietary differences in the content of the essential fatty acid ( $18:2n-6$  and  $18:3n-3$ ) between these two ruminants (Table 1) were also reflected in the PUFA content in their adipose tissue (Table 5). Beef adipose tissue had more  $18:2n-6$  and its elongation and desaturation product  $20:3n-6$  ( $P < 0.05$ ), however, beef and muskox had similar levels of  $20:4n-6$ . On the other hand, muskox adipose tissue had significantly higher levels of  $18:3n-3$  and its elongation and desaturation products  $20:5n-3$ ,  $22:5n-3$  and  $22:6n-3$

**Table 5** Muskox and beef subcutaneous adipose tissue polyunsaturated fatty acid composition ( $n = 16$  in each group)

Percentage of total fatty acids	Beef	Muskox	SEM
Total 18:2 <i>c/t</i>	0.83**	0.46	0.04
9c13t/ 8t12c-	0.29**	0.10	0.01
8t13c-	0.04**	0.07	0.00
9c12t-	0.13**	0.04	0.01
9t12c-	0.00**	0.13	0.00
11t15c-	0.24**	0.05	0.02
9c15c 18:2	0.12**	0.02	0.00
18:2n-6	1.62**	1.04	0.09
Total 18:3 <i>c/c/t</i> <sup>a</sup>	0.04**	0.10	0.01
18:3n-3	0.27**	0.77	0.03
Total CLA	0.67**	0.50	0.03
20:2n-6	0.03	0.04	0.00
20:3n-6	0.07**	0.02	0.00
20:4n-6	0.05	0.07	0.01
22:2n-6	0.00**	0.09	0.00
20:5n-3	0.00**	0.02	0.00
22:4n-6	0.03*	0.04	0.00
22:5n-3	0.04**	0.37	0.02
22:6n-3	0.00**	0.02	0.00
Sum n-6 PUFA	1.82**	1.32	0.09
Sum n-3 PUFA	0.18**	0.26	0.02
Sum LC n-6 PUFA	0.31**	1.18	0.03
Sum LC n-3 PUFA	0.04**	0.41	0.02
n-6/n-3	10.2**	5.33	0.51

SEM standard error of the mean, CLA conjugated linoleic acid, includes all the major *c/t*-CLA isomers in Fig. 5 and all the trace amounts of *t/t*-CLA isomers, LC long-chain

<sup>a</sup> The major  $18:3$  *c/c/t* isomers were  $9c,12c,15t$ - and  $9t,12c,15c$ -18:3 in about equal proportions, while  $9c,12t,15c$ -18:3 was present in trace amounts

\* $P < 0.05$ , beef differs from muskox

\*\* $P < 0.01$ , beef differs from muskox

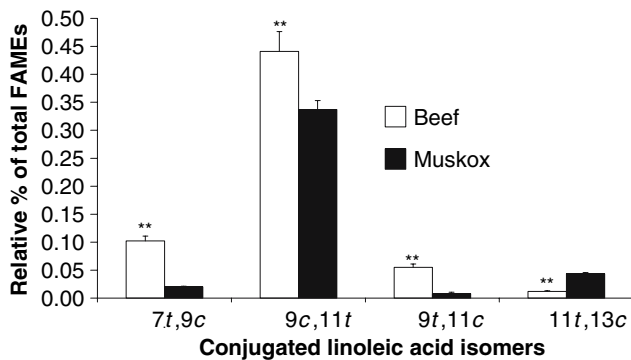


**Fig. 5** Muskox and beef subcutaneous adipose tissue conjugated linoleic acid (CLA) composition of selected CLA isomers. Bars and vertical lines represent mean  $\pm$  SEM,  $n = 16$  for each group. For each isomer, bars with asterisks are significantly different ( $P < 0.01$ )

(Table 5). As a consequence, muskox adipose tissue had a lower n-6/n-3 ratio ( $P < 0.05$ ) and could contribute toward fulfilling dietary recommendations for improved cardiovascular health [59].

#### mRNA Analysis of Fat Metabolizing Enzymes

The higher than expected level of SFAs in muskox, particularly 18:0 (Table 3), was further investigated using mRNA analysis. Stearyl-CoA desaturase-1 (SCD1) desaturates 18:0 to 9*c*-18:1 and is the key enzyme in regulating levels of desaturation in de novo fat biosynthesis. We isolated and sequenced the muskox SCD1 mRNA to examine if it could further explain the lack of unsaturation in muskox adipose tissue. The cloned fragment of the muskox SCD1 mRNA (Genbank no. AY530631) had 99% homology with goat and sheep versions of the SCD1 mRNA and 96% homology with beef SCD1. This agreed with earlier phylogeny studies relating the muskox as a closer relative to Caprinae than Bovinae. Semi-quantitative measures of SCD1 mRNA in muskox adipose tissue showed one-third less expression than standardized bovine adipose tissue when measured against the house keeping gene  $\beta$ -actin (Genbank no. DQ017256).

A more intensive investigation compared the expression of SCD1 against the fat metabolic and catabolic indicator enzymes, palmitoyl fatty acid synthase (FAS) [60] and palmitoyl CoA oxidase (ACO) [61] in both muskox and beef samples (Fig. 6). Muskox adipose tissue again expressed lower levels of SCD1 mRNA relative to FAS and ACO mRNA when compared to bovine adipose tissue. This confirmed that muskox SCD1 expression was selectively lower relative to bovine adipose tissue, which would in large part explain the higher level of 18:0 in muskox. A lower expression of SCD1 might also in part

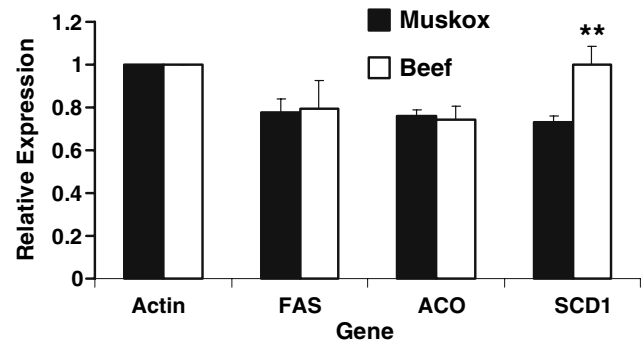


**Fig. 6** Relative gene expression of the lipid metabolizing enzymes fatty acid synthase (FAS), acyl CoA oxidase (ACO) and steroyl CoA desaturase (SCD1) in muskox and beef adipose tissue. The mRNA expression levels were adjusted relative to the  $\beta$ -actin signal (asterisks indicates difference  $P < 0.01$ ). Values  $\pm$  SEM,  $n = 16$  for each group

explain why muskox had a lower adipose tissue level of 9*c*, 11*t*-, 9*c*, 13*t*- and 9*c*, 12*t*-18:2 (Table 5), a higher SFA to MUFA ratio, and lower desaturation index for 14:0, 16:0, 17:0 and 18:0, as well as 9*c*, 11*t*-18:1 to 11*t*-18:1 (Table 4).

In summary, the fatty acid composition of wild muskox adipose tissue was substantially different from that of beef finished on a high barley diet. Even though the adipose tissue of wild muskox had a substantially higher content of SFAs and branch-chain fatty acids than beef, this was offset by a healthier fatty acid profile of *trans*-18:1 and CLA isomers, a higher n-3 PUFA content and a lower n-6 to n-3 ratio. On the other hand, beef adipose tissue had a significantly greater level 10*t*-18:1, which has been shown to negatively effect plasma lipoprotein profiles in rabbits [14], and had higher levels of 7*t*, 9*c*-CLA [44] and 9*t*, 11*c*-CLA [62] which have been linked to milk fat depression. Regarding current beef production practices, feeding higher levels of forage as opposed to grain should be encouraged to promote a healthier fatty acid profile and/or greater emphasis needs to be placed on developing feeding strategies to take advantage of intensive production without negatively impacting beef fatty acid composition. Specific areas that need further investigation include studying the effects of grain type, processing and how added oils interact with the dietary matrix in the production and deposition of individual CLA and *trans*-18:1 isomers.

**Acknowledgments** The kind assistance of Sigrid Lohmann in the collection and transport of sedge samples from Banks Island is gratefully acknowledged. The technical assistance of Marta Hernandez (FRP, AAFC, Guelph) is also gratefully acknowledged. The Education, University and Research Department of the Basque Government (Spain) is also acknowledged for the support of N. Aldai through a postdoctoral fellowship.

## References

- Fournier B, Gunn A (1998) Muskox numbers and distribution in the Northwest Territories, 1997. Northwest Territories Department of Renewable Resources, Canada, file report no. 121, p 55
- Adamczewski JZ, Flood PF (1995) Body composition of muskox (*Ovibos moschatus*) and its estimation from condition index and mass measurements. *Can J Zool* 73:2021–2034
- Baker BE, Cook HW, Teal JJ (1970) Muskox (*Ovibos moschatus*) milk composition, fatty acid, and mineral constitution. *Can J Zool* 48:1345–1347
- Belury MA (2002) Dietary conjugated linoleic acid in health: physiological effects and mechanisms of action. *Annu Rev Nutr* 22:505–531
- Ip MM, Masso-Welch PA, Ip C (2003) Prevention of mammary cancer with conjugated linoleic acid: role of the stroma and the epithelium. *J Mammary Gland Biol Neoplasia* 8:103–118
- Larsen TM, Toubro S, Astrup A (2003) Efficacy and safety of dietary supplements containing CLA for the treatment of obesity: evidence from animal and human studies. *J Lipid Res* 44:2234–2241
- Terpstra AHM (2004) Effect of conjugated linoleic acid on body composition and plasma lipids in humans: an overview of the literature. *Am J Clin Nutr* 79:352–361
- Tricon S, Burdge GC, Kew S, Banerjee T, Russell JJ, Jones EL, Grimble RF, Williams CM, Yaqoob P, Calder PC (2004) Opposing effects of *cis-9,trans-11* and *trans-10,cis-12* conjugated linoleic acid on blood lipids in healthy humans. *Am J Clin Nutr* 80:614–620
- Banni S, Angioni E, Murru E, Carta G, Melis MP, Bauman DE, Dong Y, Ip C (2001) Vaccenic acid feeding increases tissue levels of conjugated linoleic acid and suppresses development of pre-malignant lesions in rat mammary gland. *Nutr Cancer* 41:91–97
- Lock AL, Bauman DE (2004) Modifying milk fat composition of dairy cows to enhance fatty acids beneficial to human health. *Lipids* 39:1197–1206
- Turpeinen AM, Mutanen M, Aro A, Salminen I, Basu S, Palmquist DL, Griinari JM (2002) Bioconversion of vaccenic acid to conjugated linoleic acid in humans. *Am J Clin Nutr* 76:504–510
- Miller A, McGrath E, Stanton C, Devery R (2003) Vaccenic acid (*t11-18:1*) is converted to *c9,t11-CLA* in MCF-7 and SW480 cancer cells. *Lipids* 38:623–632
- Hodgson JM, Wahlqvist ML, Boxall JA, Balazs ND (1996) Platelet *trans* fatty acids in relation to angiographically assessed coronary artery disease. *Atherosclerosis* 120:147–154
- Roy A, Chardigny J-M, Bauchart D, Ferlay A, Lorenz S, Durand D, Gruffat D, Faulconnier Y, Sébédio J-L, Chilliard Y (2007) Butter rich in *trans-10-C18:1* plus *cis-9,trans-11-CLA* differentially affects plasma lipids and aortic streak in experimental atherosclerosis in rabbits. *Animal* 1 (in press)
- Lock AL, Horne CAM, Bauman DE, Salter AM (2005) Butter naturally enriched in conjugated linoleic acid and vaccenic acids alter tissue fatty acids and improves the plasma lipoprotein profile in cholesterol-fed hamsters. *J Nutr* 135:1934–1939
- De La Torre A, Debiton E, Juanéda P, Durand D, Chardigny J-M, Barthelemy C, Bauchart D, Gruffat D (2006) Beef conjugated linoleic acid isomers reduce human cancer cell growth even when associated with other beef fatty acids. *Br J Nutr* 95:346–352
- Larter NC, Nagy JA (1997) Peary caribou, muskox and Banks Island Forage: assessing seasonal diet similarities. *Rangifer* 17:9–16
- National Research Council (1984) Nutrient requirements of beef cattle, 6th edn. National Academic, Washington
- Sukhija PS, Palmquist DL (1988) Rapid method for determination of total fatty acid content and composition of feedstuffs and feces. *J Agric Food Chem* 36:1202–1206
- Cruz-Hernandez C, Deng Z, Zhou J, Hill AR, Yurawecz MP, Delmonte P, Mossoba MM, Dugan MER, Kramer JKG (2004) Methods to analyze conjugated linoleic acids (CLA) and *trans-18:1* isomers in dairy fats using a combination of GC, silver ion TLC-GC, and silver ion HPLC. *J AOAC Int* 87:545–560
- Meadus WJ (2003) A semi-quantitative RT-PCR method to measure the in vivo effect of dietary conjugated linoleic acid on porcine muscle PPAR gene expression. *Biol Proced Online* 5:20–28
- Higgins D, Thompson J, Gibson T, Thompson JD, Higgins DG, Gibson TJ (1994) CLUSTAL W: improving the sensitivity of progressive multiple sequence alignment through sequence weighting, position-specific gap penalties and weight matrix choice. *Nucleic Acids Res* 22:4673–4680
- Rozen S, Skaletsky HJ (2000) Primer3 on the WWW for general users and for biologist programmers. In: Krawetz S Misener S (eds) Bioinformatics methods and protocols: methods in molecular biology, Humana, Totowa, pp 365–386
- Altschul SF, Madden TL, Schaffer AA, Zhang J, Zhang Z, Miller W, Lipman DJ (1997) Gapped BLAST and PSI-BLAST: a new generation of protein database search programs. *Nucleic Acids Res* 25:3389–3402
- Post-Beittenmiller D (1996) Biochemistry and molecular biology of wax production in plants. *Ann Rev Plant Physiol Plant Mol Biol* 47:405–430
- Gunstone FD, Harwood JL Padley FB (1995) The lipid handbook, 2nd edn. Chapman & Hall, New York, pp 202–204
- Wood JD (1984) Fat deposition and the quality of fat tissues in meat animals. In: Wiseman J (ed) Fats in animal nutrition, Butterworths, Toronto, pp 407–436
- Casey NH, van Niekerk WA, Spreeth EB (1988) Fatty acid composition of subcutaneous fat of sheep grazed on eight different pastures. *Meat Sci* 23:55–63
- Busboom JR, Miller GJ, Field RA, Crouse JD, Riley ML, Nelms GE, Ferrell CL (1981) Characteristics of fat from heavy ram and wether lambs. *J Anim Sci* 52:83–92
- Cordain L, Watkins BA, Florant GI, Kelher M, Rogers I, Li Y (2002) Fatty acid analysis of wild ruminant tissues: evolutionary implications for reducing diet-related chronic disease. *Eur J Clin Nutr* 56:181–191
- El-Shazly K (1952) Degradation of protein in the rumen of the sheep. 2. The action of rumen micro-organisms on amino-acids. *Biochem J* 51:647–653
- Duncan WRH, Garton GA (1978) Differences in the proportion of branched-chain fatty acids in subcutaneous triacylglycerols of barley-fed ruminants. *Br J Nutr* 40:29–33
- Horning MG, Martin DB, Karmen A, Vagelos PR (1961) Fatty acid synthesis in adipose tissue II. Enzymatic synthesis of branched chain and odd-numbered fatty acids *J Biol Chem* 236:669–672
- Kramer JKG, Cruz-Hernandez C, Deng Z, Zhou J, Jahreis G, Dugan MER (2004) The analysis of conjugated linoleic acid and *trans 18:1* isomers in synthetic and animal products. *Am J Clin Nutr* 79(Suppl):1137S–1145S
- Gillis MH, Duckett SK, Sackmann JR (2006) Effects of supplemental rumen-protected conjugated linoleic acid or corn oil on fatty acid composition of adipose tissues in beef cattle. *J Anim Sci* 82:1419–1427
- Hristov AN, Kennington LR, McGuire MA, Hunt CW (2005) Effect of diets containing linoleic acid- or oleic acid-rich oils on ruminal fermentation and nutrient digestibility, and performance and fatty acid composition of adipose tissue and muscle tissues of finishing cattle. *J Anim Sci* 83:1312–1321
- Daniel ZCTR, Wynn RJ, Salter AM, Buttery PJ (2004) Differing effects of forage and concentrate diets on the oleic acid and

- conjugated linoleic acid content of sheep tissues: the role of stearyl-CoA desaturase. *J Anim Sci* 82:747–758
38. Bessa RJB, Portugal PV, Mendes IA, Santos-Silva J (2005) Effect of lipid supplementation on growth performance, carcass and meat quality and fatty acid composition of intramuscular lipids of lambs fed dehydrated lucerne or concentrate. *Livestock Prod Sci* 96:185–194
  39. Madron MS, Peterson DG, Dwyer DA, Corl BA, Baumgard LH, Beermann DH, Bauman DE (2002) Effect of extruded full-fat soybeans on conjugated linoleic acid content of intramuscular, intermuscular, and subcutaneous fat in beef steers. *J Anim Sci* 80:1135–1143
  40. Dannenberger D, Nuernberg G, Scollan N, Schabbel W, Steinhart H, Ender K, Nuernberg K (2004) Effect of diet on the deposition of *n*-3 fatty acids, conjugated linoleic and C18:1 *trans* fatty acid isomers in muscle lipids of German Holstein bulls. *J Agric Food Chem* 52:6607–6615
  41. Raes K, Fievez V, Chow TT, Ansorena D, Demeyer D, de Smet S (2004) Effect of diet and dietary fatty acids on the transformation and incorporation of C18 fatty acids in double-muscled Belgian blue young bulls. *J Agric Food Chem* 52:6035–6041
  42. Lee MRF, Tweed JKS, Moloney AP, Scollan ND (2005) The effects of fish oil supplementation on rumen metabolism and the biohydrogenation of unsaturated fatty acids in beef steers given diets containing sunflower oil. *Anim Sci* 80:361–367
  43. Griinari JM, Dwyer DA, McGuire MA, Bauman DE, Palmquist DL, Nurmela KVV (1998) *trans*-Octadecenoic acids and milk fat depression in lactating dairy cows. *J Dairy Sci* 81:1251–1261
  44. Piperova LS, Teter BB, Bruckental I, Sampugna J, Mills SE, Yurawecz MP, Fritsche J, Ku K, Erdman RA (2000) Mammary lipogenic enzyme activity, *trans* fatty acids and conjugated linoleic acids are altered in lactating dairy cows fed a milk fat-depressing diet. *J Nutr* 130:2568–2574
  45. Bradford BJ, Allen MS (2004) Milk fat responses to a change in diet fermentability vary by production level in dairy cattle. *J Dairy Sci* 87:3800–3807
  46. Shingfield KJ, Reynolds CK, Lupoli B, Toivonen V, Yurawecz MP, Delmonte P, Griinari JM, Grandison AS, Beever DE (2005) Effect of forage type and proportion of concentrate in the diet on milk fatty acid composition in cows given sunflower oil and fish oil. *Anim Sci* 80:225–238
  47. Roy A Ferlay A, Shingfield KJ, Chilliard Y (2006) Examination of the persistency of milk fatty acid composition responses to plant oils in cows given different basal diets, with particular emphasis on *trans*-C<sub>18:1</sub> fatty acids and isomers of conjugated linoleic acid. *Anim Sci* 82:479–492
  48. Cruz-Hernandez C, Kramer JKG, Kennelly JJ, Okine EK, Weselake RJ (2006) Effect of sunflower oil and monensin on the CLA and 18:1 isomer composition of milk fat in dairy cattle, 4th Euro Fed Lipid Congress, Madrid, Spain, 1–4 October 2006. Abstract. [https://va.gdch.de/wwwdata/abstracts/5860/5860\\_0434.pdf](https://va.gdch.de/wwwdata/abstracts/5860/5860_0434.pdf)
  49. Klieve AV, Hennessy D, Ouwerkerk D, Forster RJ, Mackie RI, Attwood GT (2003) Establishing populations of *Megasphaera elsdenii* YE 34 and *Butyrivibrio fibrisolvens* YE 44 in the rumen of cattle fed high grain diets. *J Appl Microbiol* 95:621–630
  50. AbuGhazaleh AA, Riley MB, Thies EE, Jenkins TC (2005) Dilution rate and pH effects on the conversion of oleic acid to *trans* C<sub>18:1</sub> positional isomers in continuous culture. *J Dairy Sci* 88:4334–4341
  51. Delmonte P, Roach JAG, Mossoba MM, Losi G, Yurawecz MP (2004) Synthesis, isolation and GC analysis of all 6,8- to 13,15-*cis/trans* conjugated linoleic acid isomers. *Lipids* 39:185–191
  52. Delmonte P, Kataoka PA, Corl BA, Bauman DE, Yurawecz MP (2004) Relative retention order of all *cis/trans* conjugated linoleic acid FAME from the 6,8- to 13,15-positions using silver ion HPLC with two elution systems. *Lipids* 40:507–514
  53. Fritsche S, Rumsey TS, Yurawecz MP, Ku Y, Fritsche J (2001) Influence of growth promoting implants on fatty acid composition including conjugated linoleic acid isomers in beef. *Eur Food Res Technol* 212:621–629
  54. Kraft J, Collomb M, Möckel P, Sieber R, Jahreis G (2003) Differences in CLA isomer distribution of cow's milk lipids. *Lipids* 38:657–664
  55. Griinari JM, Corl BA, Lacy SH, Chouinard PY, Nurmela KVV, Bauman DE (2000) Conjugated linolenic acid is synthesized endogenously in lactating dairy cows by  $\Delta$ 9-desaturase. *J Nutr* 130:2285–2291
  56. Corl BA, Baumgard LH, Griinari JM, Delmonte P, Morehouse KM, Yurawecz MP, Bauman DE (2002) *trans*-7,*cis*-9 CLA is synthesized endogenously by  $\Delta$ 9-desaturase in dairy cows. *Lipids* 37:681–688
  57. Hino T, Fukuda S (2006) Biohydrogenation of linoleic and linolenic acids, and production of conjugated isomers by *Butyrivibrio fibrisolvens*, 4th Euro fed lipid congress, Madrid, Spain, 1–4 October 2006, Abstract. [https://va.gdch.de/wwwdata/abstracts/5860/5860\\_0593.pdf](https://va.gdch.de/wwwdata/abstracts/5860/5860_0593.pdf)
  58. Kramer JKG, Blackadar CB, Zhou J (2002) Evaluation of two GC columns (60-m SUPELCOWAX 10 and 100-m CP Sil 88) for analysis of milkfat with emphasis on CLA, 18:1, 18:2 and 18:3 isomers, and short- and long-chain FA. *Lipids* 37:823–835
  59. Gebauer S, Harris WS, Kris-Etherton PM, Etherton TD (2005) Dietary *n*-6:*n*-3 fatty acid ratio and health. In: Akoh CC, Lai O-M (eds) *Healthful lipids*, AOCS, Champaign, pp 221–248
  60. Clarke SD (1993) Regulation of fatty acid synthase gene expression: an approach for reducing fat accumulation. *J Anim Sci* 71:1957–1965
  61. Osumi T, Ishii N, Miyazawa S, Hashimoto T (1987) Isolation and structural characterization of the rat acyl-CoA oxidase gene. *J Biol Chem* 262:8138–8143
  62. Perfield II JW, Lock AL, Sæbø A, Griinari JM, Bauman DE (2005) *trans*-9,*cis*-11 Conjugated linoleic acid (CLA) reduces milk fat synthesis in lactating dairy cows (Abstract 284). *J Dairy Sci* 88 (Suppl 1):211



# Novel Cyclopropane Fatty Acids from the Phospholipids of the Caribbean Sponge *Pseudospongosorites suberitoides*

Néstor M. Carballeira · Nashbly Montano ·  
Jan Vicente · Abimael D. Rodriguez

Received: 9 November 2006 / Accepted: 27 December 2006 / Published online: 14 March 2007  
© AOCs 2007

**Abstract** The cyclopropane fatty acids 17-methyl-*trans*-4,5-methyleneoctadecanoic acid, 18-methyl-*trans*-4,5-methylenonadecanoic acid, and 17-methyl-*trans*-4,5-methylenonadecanoic acid were characterized for the first time in nature in the phospholipids (mainly PE, PG and PS) of the hermit-crab sponge *Pseudospongosorites suberitoides*. Pyrrolidine derivatization was the key in identifying the position of the cyclopropyl and methyl groups in the acyl chains and  $^1\text{H}$  NMR was used to determine the *trans* stereochemistry of the cyclopropane ring. The phospholipids from the sponge also contained an interesting series of *iso-anteiso*  $\Delta^{5,9}$  fatty acids with chain-lengths between 17 and 21 carbons, with the fatty acids (5*Z*,9*Z*)-18-methyl-5,9-nonadecadienoic acid and the (5*Z*,9*Z*)-17-methyl-5,9-nonadecadienoic acid being described for the first time in sponges. The *anteiso*  $\alpha$ -methoxylated fatty acid 2-methoxy-12-methyltetradecanoic acid was also identified for the first time in nature in the phospholipids of this interesting marine sponge. The novel cyclopropyl fatty acids could have originated from the phospholipids of a cyanobacterium living in symbiosis with the sponge.

**Keywords** Cyanobacteria · Cyclopropane · Fatty acids · Phospholipids · *Pseudospongosorites suberitoides* · Pyrrolidides · Sponges

## Abbreviations

ATCC	American type culture collection
ECL	Equivalent chain length
FAME	Fatty acid methyl ester
GC–MS	Gas chromatography–mass spectrometry
PE	Phosphatidylethanolamine
PG	Phosphatidylglycerol
PS	Phosphatidylserine

## Introduction

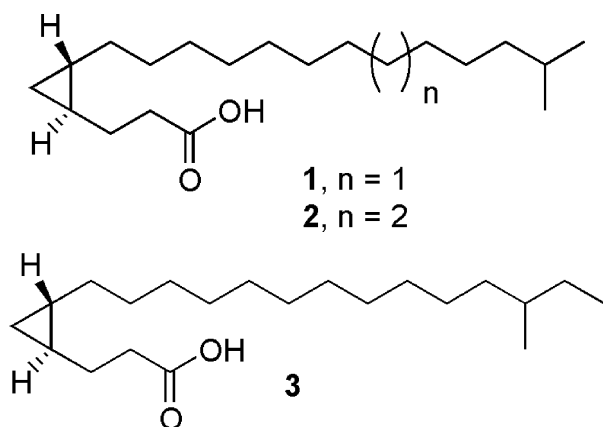
Cyclopropane fatty acids (FA) are quite ubiquitous in seed oils, bacteria, and other microorganisms [1]. Since the discovery of lactobacillic acid (*cis*-11,12-methyleneoctadecanoic acid) in 1951, several interesting cyclopropyl FA have been identified in both Gram-negative and Gram-positive bacteria [2]. For example, the acid 9,10-methylenehexadecanoic acid was reported in the Gram-negative bacterium *Pseudomonas cepacia* [3]. The protozoan *Herpetomonas megaseliae* synthesizes de novo the *iso*-branched FA 17-methyl-*cis*-9,10-methyleneoctadecanoic acid [4], while the acids 9,10-methylene-5-hexadecenoic acid and 11,12-methylene-5-octadecenoic acid are present in the slime mould *Polysphondylium pallidum* [5]. The *cis*-9,10-methyleneoctadecanoic acid has been identified in the seeds of *Litchi chinensis*, in longan seed oil, and in trypanosomatids and is preferentially located at the *sn*-2 position of triglycerides [6–7]. At present there is no known role for these cyclopropane FA.

Although less ubiquitous, cyclopropane FA have also been reported in marine organisms. Sponges have provided some interesting examples. For example, the acid

N. M. Carballeira (✉) · N. Montano · J. Vicente ·  
A. D. Rodriguez  
Department of Chemistry, University of Puerto Rico,  
Río Piedras Campus, PO Box 23346,  
San Juan 00931-3346, Puerto Rico  
e-mail: nmcarballeira@uprrp.edu

19,20-methylenehexacosanoic acid was identified in the phospholipids of the sponge *Calyx niceansis* [8], while the sponge *Amphimedon* sp., collected in Australia, contains the acid 10,11-methyleneheptacosanoic acid, a topoisomerase I inhibitor with an  $IC_{50} = 1.2 \mu\text{M}$  [9]. More recently, majusculoic acid, a brominated diunsaturated cyclopropyl fatty acid with a *trans* cyclopropane ring between carbons 4 and 5, was isolated from a cyanobacterial mat assemblage [10]. Majusculoic acid exhibited antifungal activity against *Candida albicans* ATCC 14503 with a MIC of  $8 \mu\text{M}$  [10].

Aimed at discovering other unusual cyclopropyl FA in marine sponges, we investigated herein, for the first time, the phospholipid FA composition of the hermit-crab sponge *Pseudospongisorites suberitoides* (Class Demospongiae, Family Suberitidae) [11] and report on the occurrence of the novel cyclopropane FA **1–3** with an uncommon *trans* cyclopropyl group between carbons 4 and 5 of the acyl chain [12]. In addition, other previously unidentified phospholipid FA containing either the  $\alpha$ -methoxy substitution or the  $\Delta 5,9$  diunsaturation were also identified for the first time in nature in *P. suberitoides*.



## Materials and Methods

### Instrumentation

Fatty acid methyl esters (FAME) and pyrrolidides were analyzed by direct ionization using GC–MS (Hewlett-Packard 5972A MS ChemStation) at 70 eV equipped with a  $30 \text{ m} \times 0.25 \text{ mm}$  special performance capillary column (HP-5MS). The GC-temperature program was:  $130 \text{ }^\circ\text{C}$  for 1 min, increased at a rate of  $3 \text{ }^\circ\text{C}/\text{min}$  to  $270 \text{ }^\circ\text{C}$ , and maintained for 30 min at  $270 \text{ }^\circ\text{C}$ .  $^1\text{H-NMR}$  spectra were recorded on a Bruker DPX-300 spectrometer.  $^1\text{H-NMR}$  chemical shifts are reported with respect to internal  $\text{Me}_4\text{Si}$ , and chemical shifts are given in parts per million (ppm).

### Sponge Collection

The sponge *Pseudospongisorites suberitoides* (Class Demospongiae, Family Suberitidae) (Díaz, van Soest and Pomponi 1993) (Sandford and Kelly-Borges 1997) was collected from Mona Island (near Monito), Puerto Rico in July 2006 at 26 m depth by scuba. The sponge was freeze-dried and stored at  $-20 \text{ }^\circ\text{C}$  until extraction. A voucher specimen (IM06-06) is stored at the Chemistry Department of the University of Puerto Rico, Río Piedras campus.

### Extraction and Isolation of Phospholipids

The sponge (74 g of dry weight) was carefully cleaned and cut into small pieces. Extraction with  $2 \times 200 \text{ ml}$  of  $\text{CHCl}_3/\text{MeOH}$  (1:1) yielded the total lipids (8.4 g). The neutral lipids, glycolipids, and phospholipids (3.9 g) were separated by column chromatography on Si gel (60–200 mesh) using the procedure of Privett et al. [13]. The phospholipid classes were identified by  $R_f$  values using thin-layer chromatography using Si gel H plates and  $\text{CHCl}_3/\text{MeOH}/\text{NH}_4\text{OH}$  (65:30:5) as developing solvent. The main phospholipids identified were phosphatidylethanolamine (PE), phosphatidylglycerol (PG), and phosphatidylserine (PS).

### Derivatives

The fatty acyl components of the phospholipids were obtained as their methyl esters by reaction of the phospholipids with methanolic HCl followed by column chromatography on Si gel eluting with hexane/ether (9:1). An aliquot of the methyl esters were hydrogenated in 10 ml methanol with catalytic amounts of Pd/C (10%). The double-bonds, methyl-branching, and cyclopropane positions in these compounds were determined by pyrrolidide derivatization of an aliquot of the methyl esters following the preparation procedure previously described [14]. Mass spectral data for the novel compounds follows and/or are presented in Table 1.

### Methyl 2-methoxy-12-methyltetradecanoate

ECL = 15.93; GC–MS  $m/z$  (relative intensity)  $\text{M}^+$  286 (2), 228 (17), 227 (100), 139 (4), 138 (2), 125 (15), 123 (3), 111 (34), 109 (8), 104 (7), 99 (5), 97 (63), 95 (18), 87 (9), 85 (17), 83 (71), 81 (26), 79 (5), 75 (9), 71 (79), 70 (10), 69 (72), 67 (27), 59 (12), 58 (24), 57 (91), 56 (13), 55 (77).

### Methyl 18-methyl-5,9-nonadecadienoate

ECL = 19.09; GC–MS  $m/z$  (relative intensity)  $\text{M}^+$  322 (6), 199 (3), 181 (4), 164 (4), 154 (4), 150 (10), 143 (7), 141

**Table 1** Mass spectral data (70 eV) for the novel cyclopropane compounds and their pyrrolidide derivatives

Compound	ECL	<i>m/z</i> (relative intensity)
Methyl 17-methyl- <i>trans</i> -4,5-methyleneoctadecanoate	19.15	M <sup>+</sup> 324 (1), 293 (2), 292 (9), 250 (16), 237 (2), 208 (3), 194 (3), 180 (1), 166 (2), 165 (2), 155 (3), 152 (3), 151 (3), 141 (5), 139 (4), 137 (6), 128 (16), 127 (6), 125 (8), 123 (9), 114 (8), 111 (19), 110 (15), 109 (14), 101 (54), 97 (39), 96 (36), 95 (25), 87 (23), 85 (29), 83 (43), 82 (29), 81 (36), 74 (66), 71 (28), 69 (60), 67 (51), 59 (65), 57 (61), 55 (100)
<i>N</i> -17-methyl- <i>trans</i> -4,5-methyleneoctadecanoylpyrrolidine		M <sup>+</sup> 363 (9), 349 (3), 348 (12), 321 (2), 320 (7), 307 (1), 306 (3), 292 (3), 279 (1), 278 (5), 265 (1), 264 (5), 251 (1), 250 (5), 237 (2), 236 (6), 223 (2), 222 (10), 210 (1), 209 (3), 208 (11), 195 (3), 194 (12), 181 (4), 180 (12), 167 (10), 166 (31), 154 (7), 152 (7), 139 (5), 138 (34), 126 (15), 114 (13), 113 (100), 98 (59), 91 (8), 85 (19), 79 (11), 70 (38), 67 (21), 57 (19), 55 (82)
Methyl 18-methyl- <i>trans</i> -4,5-methylenenonadecanoate	20.14	M <sup>+</sup> 338 (1), 306 (9), 264 (13), 263 (3), 141 (6), 139 (4), 137 (5), 128 (14), 127 (5), 125 (8), 123 (7), 114 (6), 111 (17), 110 (14), 109 (16), 101 (41), 97 (36), 96 (33), 95 (25), 87 (22), 85 (26), 83 (40), 82 (26), 81 (40), 74 (57), 71 (29), 69 (54), 67 (52), 59 (52), 57 (57), 55 (100)
<i>N</i> -18-methyl- <i>trans</i> -4,5-methylenenonadecanoylpyrrolidine		M <sup>+</sup> 377 (8), 363 (4), 362 (13), 335 (2), 334 (8), 320 (3), 306 (3), 292 (4), 278 (5), 264 (6), 250 (6), 237 (2), 236 (7), 223 (3), 222 (13), 209 (3), 208 (14), 195 (4), 194 (16), 181 (7), 180 (21), 167 (14), 166 (41), 153 (7), 152 (10), 139 (8), 138 (44), 127 (5), 126 (17), 114 (11), 113 (94), 98 (72), 85 (17), 83 (15), 72 (22), 70 (38), 57 (31), 55 (100)
Methyl 17-methyl- <i>trans</i> -4,5-methylenenonadecanoate	20.24	M <sup>+</sup> 338 (1), 306 (6), 264 (10), 141 (4), 139 (4), 137 (6), 128 (15), 127 (5), 125 (9), 123 (10), 114 (7), 111 (18), 110 (14), 109 (16), 101 (41), 97 (36), 96 (30), 95 (28), 87 (21), 85 (24), 83 (40), 82 (26), 81 (41), 74 (53), 71 (32), 69 (51), 67 (51), 59 (51), 57 (88), 55 (100)
<i>N</i> -17-methyl- <i>trans</i> -4,5-methylenenonadecanoylpyrrolidine		M <sup>+</sup> 377 (7), 363 (3), 362 (11), 348 (5), 321 (2), 320 (7), 307 (2), 306 (3), 292 (4), 278 (4), 264 (5), 250 (5), 237 (2), 236 (5), 223 (3), 222 (11), 209 (3), 208 (11), 195 (4), 194 (15), 181 (5), 180 (17), 167 (14), 166 (36), 153 (7), 152 (10), 139 (7), 138 (39), 127 (5), 126 (15), 114 (11), 113 (100), 98 (68), 97 (11), 85 (17), 83 (10), 81 (10), 72 (18), 70 (37), 57 (52), 55 (92)

ECL Equivalent chain-length

(21), 136 (10), 135 (9), 123 (7), 121 (10), 110 (18), 109 (45), 107 (8), 99 (17), 97 (21), 95 (24), 87 (23), 85 (10), 83 (29), 81 (100), 79 (27), 74 (41), 71 (16), 69 (51), 67 (73), 57 (50), 55 (85).

*N*-18-methyl-5,9-nonadecadienoylpyrrolidine

GC-MS *m/z* (relative intensity) M<sup>+</sup> 361 (3), 348 (3), 320 (2), 306 (1), 292 (1), 278 (2), 264 (2), 250 (2), 236 (2), 234 (3), 222 (3), 208 (4), 194 (4), 182 (2), 180 (19), 166 (10), 154 (1), 152 (3), 140 (3), 126 (20), 113 (100), 98 (31), 85 (14), 72 (15), 71 (14), 57 (16), 55 (53).

Methyl 17-methyl-5,9-nonadecadienoate

ECL = 19.21; GC-MS *m/z* (relative intensity) M<sup>+</sup> 322 (1), 237 (3), 163 (5), 150 (9), 141 (17), 136 (12), 135 (9), 123 (12), 121 (12), 110 (19), 109 (40), 107 (10), 99 (16), 97 (24), 95 (31), 87 (14), 85 (15), 83 (29), 81 (100), 79 (31), 74 (30), 71 (21), 69 (48), 67 (72), 57 (60), 55 (89).

## Results and Discussion

*Pseudospongosorites suberitoides* presented a typical sponge phospholipid profile where PE, PG, and PS were the most abundant phospholipids. Acid methanolysis of the

total phospholipids provided a rather complex and unusual phospholipid FA composition of around 51 identifiable FA as shown in Table 2. FA chain lengths ranged between 14 and 27 carbons, mainly consisting of methyl-branched fatty acids (75% of the total FA mixture). The  $\Delta$ 5,9 FA were particularly abundant in this sponge (25% of the total FA) but their chain lengths were atypical with respect to other sponge phospholipid  $\Delta$ 5,9 FA inasmuch as here the most abundant  $\Delta$ 5,9 FA had chain lengths between 17 and 20 carbons. Among the  $\Delta$ 5,9 FA the even-chain (5*Z*,9*Z*)-5,9-octadecadienoic acid was particularly abundant (7.8% relative abundance), a most unusual finding for sponges [15]. Around 66% of the total FA contained odd carbon chains. The isoprenoid FA 4,8,12-trimethyltridecanoic acid was also present in *P. suberitoides*. It is important to mention that this FA is a common constituent of the phospholipids of the sponge families Spirastrellidae and Clionidae [16].

The most interesting series of FA from *P. suberitoides* were the cyclopropane fatty acids 17-methyl-*trans*-4,5-methyleneoctadecanoic acid (**1**), 18-methyl-*trans*-4,5-methylenenonadecanoic acid (**2**), and 17-methyl-*trans*-4,5-methylenenonadecanoic acid (**3**), all FA with an unusual *trans* cyclopropane ring between carbons 4 and 5. The relative GC retention times and mass spectra of the methyl esters, the mass spectra of the corresponding pyrrolidide derivatives, catalytic hydrogenation, and <sup>1</sup>H NMR of the whole FAME mixture provided the basis for their characterization. For

**Table 2** Identified phospholipid FA from *Pseudospongosorites suberitoides*

FA	Relative abundance (wt %)
Tetradecanoic (14:0)	0.6
4,8,12-Trimethyltridecanoic (16:0)	4.3
6-Methyltetradecanoic ( <i>br</i> -15:0)	2.0
13-Methyltetradecanoic ( <i>i</i> -15:0)	3.3
12-Methyltetradecanoic ( <i>ai</i> -15:0)	3.2
Pentadecanoic ( <i>n</i> -15:0)	0.7
14-Methylpentadecanoic ( <i>i</i> -16:0)	1.3
( <i>Z</i> )-9-Hexadecenoic (16:1n-7)	1.0
2-Methoxy-12-methyltetradecanoic (2-OMe- <i>ai</i> -15:0) <sup>a</sup>	1.5
Hexadecanoic ( <i>n</i> -16:0)	3.2
(5 <i>Z</i> ,9 <i>Z</i> )-15-Methyl-5,9-hexadecadienoic ( <i>i</i> -17:2n-7)	0.9
( <i>Z</i> )-15-Methyl-9-hexadecenoic ( <i>i</i> -17:1n-7)	3.8
(5 <i>Z</i> ,9 <i>Z</i> )-14-Methyl-5,9-hexadecadienoic ( <i>ai</i> -17:2n-7)	0.5
10-Methylhexadecanoic ( <i>br</i> -17:0)	4.6
15-Methylhexadecanoic ( <i>i</i> -17:0)	2.5
14-Methylhexadecanoic ( <i>ai</i> -17:0)	1.2
( <i>Z</i> )-9-Heptadecenoic (17:1n-8)	0.8
(5 <i>Z</i> ,9 <i>Z</i> )-5,9-Octadecadienoic (18:2n-9)	7.8
( <i>Z</i> )-9-Octadecenoic (18:1n-9)	2.1
( <i>Z</i> )-11-Octadecenoic (18:1n-7)	1.7
Octadecanoic ( <i>n</i> -18:0)	2.3
(5 <i>Z</i> ,9 <i>Z</i> )-17-Methyl-5,9-octadecadienoic ( <i>i</i> -19:2n-9)	2.2
11-Methyloctadecanoic ( <i>br</i> -19:0)	7.6
12-Methyloctadecanoic ( <i>br</i> -19:0)	7.0
(5 <i>Z</i> ,9 <i>Z</i> )-16-Methyl-5,9-octadecadienoic ( <i>ai</i> -19:2n-9)	3.5
17-Methyloctadecanoic ( <i>i</i> -19:0)	1.7
16-Methyloctadecanoic ( <i>ai</i> -19:0)	0.7
(5 <i>Z</i> ,9 <i>Z</i> )-18-Methyl-5,9-nonadecadienoic ( <i>i</i> -20:2n-10) <sup>a</sup>	1.0
17-Methyl- <i>trans</i> -4,5-methyleneoctadecanoic ( <i>i</i> - <i>cy</i> -20:0) <sup>a</sup>	5.5
(5 <i>Z</i> ,9 <i>Z</i> )-17-Methyl-5,9-nonadecadienoic ( <i>ai</i> -20:2n-10) <sup>a</sup>	0.6
5,8,11,14-Eicosatetraenoic (20:4n-6)	1.9
(5 <i>Z</i> ,9 <i>Z</i> )-Eicosadienoic (20:2n-11)	3.8
Eicosanoic ( <i>n</i> -20:0)	1.3
(5 <i>Z</i> ,9 <i>Z</i> )-19-Methyl-5,9-eicosadienoic ( <i>i</i> -21:2n-11)	1.5
18-Methyl- <i>trans</i> -4,5-methylenonadecanoic ( <i>i</i> - <i>cy</i> -21:0) <sup>a</sup>	0.9
(5 <i>Z</i> ,9 <i>Z</i> )-18-Methyl-5,9-eicosadienoic ( <i>ai</i> -21:2n-11)	0.6
17-Methyl- <i>trans</i> -4,5-methylenonadecanoic ( <i>ai</i> - <i>cy</i> -21:0) <sup>a</sup>	0.9
19-Methyleicosanoic ( <i>i</i> -21:0)	0.5
18-Methyleicosanoic ( <i>ai</i> -21:0)	0.5
Heneicosanoic ( <i>n</i> -21:0)	0.4

**Table 2** continued

FA	Relative abundance (wt %)
Methylheneicosanoic ( <i>br</i> -22:0)	0.2
Docosanoic ( <i>n</i> -22:0)	0.1
21-Methyldocosanoic ( <i>i</i> -23:0)	0.6
20-Methyldocosanoic ( <i>ai</i> -23:0)	0.1
Methyltricosanoic ( <i>br</i> -24:0)	0.3
Tetracosanoic (24:0)	0.2
23-Methyltetracosanoic ( <i>i</i> -25:0)	0.7
22-Methyltetracosanoic ( <i>ai</i> -25:0)	0.2
(5 <i>Z</i> ,9 <i>Z</i> )-25-Methyl-5,9-hexacosadienoic ( <i>i</i> -27:2n-17)	1.6
(5 <i>Z</i> ,9 <i>Z</i> )-24-Methyl-5,9-hexacosadienoic ( <i>ai</i> -27:2n-17)	0.4
Heptacosanoic (27:0)	0.1

<sup>a</sup> Unprecedented in nature

example, methyl 17-methyl-*trans*-4,5-methyleneoctadecanoate exhibited unusual chromatographic properties, namely an equivalent chain length (ECL) value of 19.15, for which the fractional value is well in agreement with a highly branched FA structure. The mass spectrum of methyl 17-methyl-*trans*-4,5-methyleneoctadecanoate contained a molecular ion peak at  $m/z$  324 ( $C_{21}H_{40}O_2$ ) and an intense peak at  $m/z$  101 (54%) as well as the classical McLafferty rearrangement peak at  $m/z$  74 (66%). Upon mild catalytic hydrogenation (Pd/C) the molecular ion of this methyl ester remained the same, while other monoenes and dienes in the FAME mixture incorporated hydrogen. Therefore, this experiment excluded the possibility of a monounsaturated methyl ester and suggests the presence of a cyclopropyl ring in the fatty acyl chain.

Pyrrolidide derivatization was instrumental in elucidating the basic structure of this FA. For example, in the mass spectrum of *N*-17-methyl-*trans*-4,5-methyleneoctadecanoylpyrrolidine the presence of a cyclopropyl group between carbons 4 and 5 was indicated from a difference of 12 amu between fragments at  $m/z$  126 ( $C_3$ ) and  $m/z$  138 ( $C_4$ ), and confirmed by a strong fragmentation peak at  $m/z$  166 ( $C_6$ ) arising from cleavage between carbons 5 and 6 at the other end of the cyclopropane ring. Previous work by Andersson on the mass spectra of pyrrolidides of FA containing cyclopropyl groups indicates that if an interval of 12 amu, instead of the regular 14, is observed between the most intense peaks of clusters of fragments containing  $n-1$  and  $n$  carbon atoms of the acid moiety, a cyclopropane ring occurs between carbon atoms  $n$  and  $n+1$  in the molecule [17]. However, caution should be exercised when dealing with pyrrolidides since the cyclopropane ring can

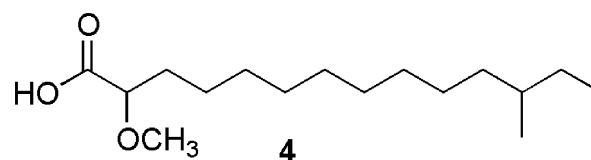
be located within one carbon position of its true location if the ring lies between carbons 6,7 and 16,17, but in our case such an exception does not apply since the ring lies between carbons 4,5 [17]. The presence of the *iso* terminal methyl branching in this compound was also clearly observed in the pyrrolidide mass spectrum since a diminished peak (and/or absent peak) at  $m/z$  334 with the corresponding intense peaks at  $m/z$  320 and 348 were also observed.

In order to corroborate the presence of the cyclopropyl group as well as to assign its *trans* stereochemistry  $^1\text{H}$  NMR was used [18]. Since the  $^1\text{H}$  NMR signals of a cyclopropane ring normally resonate at high-field it was possible to observe these signals in the  $^1\text{H}$  NMR spectrum of the whole FAME mixture without interference from other peaks. Proton signals were indeed observed as multiplets at  $\delta$  0.29 ppm and at  $\delta$  0.66 ppm, while no absorption was observed at  $-0.3$  ppm. This observation is indicative of a *trans* stereochemistry for the cyclopropane rings, since FA with a cyclopropane ring in *cis* configuration normally show absorptions at 0.6 ppm and at  $-0.3$  ppm for the two methylene cyclopropane hydrogens [18]. In the case of a *trans* cyclopropane ring these two methylene hydrogens are similar, due to a pseudo- $\text{C}_{2v}$  symmetry, and both resonate at around 0.2 ppm [10, 18]. Therefore, we can unequivocally assign as methyl 17-methyl-*trans*-4,5-methylenooctadecanoate our methyl ester in question.

The other cyclopropane fatty acids **2** and **3**, as well as their corresponding derivatives, displayed similar spectral characteristics as **1** that allowed their characterization as isomeric  $\text{C}_{21}$  members of the same family of cyclopropane FA. A slight difference in the spectral data was observed for methyl 17-methyl-*trans*-4,5-methylenonadecanoate, inasmuch as an ECL value of 20.24 indicated the presence of an *anteiso*  $\text{C}_{21}$  isomer. This structural assignment was further confirmed in the mass spectrum of *N*-17-methyl-*trans*-4,5-methylenonadecanoylpyrrolidine ( $\text{M}^+ = 377$ ) where a diminished peak (and/or absent peak) at  $m/z$  334 confirmed the C-17 methyl substitution.

Among the studied FA from *P. suberitoides* a novel  $\alpha$ -methoxylated fatty acid, namely **4**, was also characterized using GC–MS as well as gas chromatographic ECL values as compared to synthetic standards [14, 19]. The mass spectrum of the methyl ester of **4** displayed a molecular ion peak at  $m/z$  286 and a strong  $\text{M}^+ - 59$  peak at  $m/z$  227 (100%), together with a small peak at  $m/z$  104 (McLafferty rearrangement), all typical mass fragments for  $\alpha$ -methoxylated saturated methyl esters [14, 19]. The  $\alpha$ -methoxylation was further confirmed by  $^1\text{H}$  NMR spectroscopy since it was also possible to observe the characteristic signals of the  $\alpha$ -methoxy methyl ester in the  $^1\text{H}$  NMR spectrum of the whole FAME mixture without interference

from other peaks. In this case, the methoxy protons resonated as a singlet at  $\delta$  3.66 ppm, while the methine  $\alpha$ -hydrogen resonated as a multiplet at  $\delta$  3.75 ppm, all chemical shift values in agreement with other  $\alpha$ -methoxylated methyl esters [20]. The GC retention time of the methyl ester of **4** (ECL value of 15.93) suggested it to be an *anteiso* methyl-branched fatty acid [14]. A normal chain  $\alpha$ -methoxylated  $\text{C}_{15}$  FA methyl ester displays an ECL value of 16.20, while an *iso*  $\alpha$ -methoxylated  $\text{C}_{15}$  FA methyl ester displays an ECL value of 15.86. Therefore, based on this evidence the most logical structural assignment for the original acid is that of 2-methoxy-12-methyltetradecanoic acid (**4**), which has not been identified before in sponges. It should be pointed out that pyrrolidide derivatization has limited usefulness in locating methyl branching in  $\alpha$ -methoxylated fatty acids [14].



As we mentioned before *P. suberitoides* also contained a complete series (11% of the total phospholipid fatty acid composition) of *iso* and *anteiso*  $\text{C}_{17}$ – $\text{C}_{21}$  FA with the typical  $\Delta 5,9$  diunsaturation pattern of “demospongiac” acids [21]. Among these  $\Delta 5,9$  fatty acids the 18-methyl-5,9-nonadecadienoic acid (*i*-20:2 $\Delta 5,9$ ) and the 17-methyl-5,9-nonadecadienoic acid (*ai*-20:2  $\Delta 5,9$ ) appear not to have been identified before in sponges. In mass spectrometry the methyl esters of *i*-20:2 $\Delta 5,9$  and *ai*-20:2  $\Delta 5,9$  displayed the same molecular ion ( $\text{M}^+$ ) at  $m/z$  322. In addition, the  $\Delta 5,9$  diunsaturation was readily recognized from the characteristic base peak at  $m/z = 81$ , the allylic cleavage fragmentation between C-7 and C-8 at  $m/z$  141, and the fragmentation at  $m/z$  109 which results from the loss of methanol from the  $m/z$  141 fragment [22]. Pyrrolidides were also informative in characterizing these FA [22]. For example, in the mass spectrum of *N*-18-methyl-5,9-nonadecadienoylpyrrolidine the characteristic allylic cleavage between C-7 and C-8 was observed at  $m/z$  180 as well as cleavage between C-11 and C-12 at  $m/z$  234 [22]. Catalytic hydrogenation of methyl 18-methyl-5,9-nonadecadienoate and methyl 17-methyl-5,9-nonadecadienoate afforded methyl 18-methylnonadecanoate and methyl 17-methylnonadecanoate, respectively, as confirmed by their GC retention times and mass spectrometry, thereby confirming the terminal *iso-anteiso* methyl branching in these compounds. The mass spectrum of *N*-18-methyl-5,9-nonadecadienoylpyrrolidine also confirmed the *iso* methyl branching whereby a diminished (or absent peak) at  $m/z$  334 was also observed.

The results obtained for *P. suberitoides* are interesting for several reasons. The phospholipid FA composition of *P. suberitoides* is unusual in the sense that the main  $\Delta 5,9$  fatty acids present in the sponge have chain lengths between 17 and 21 carbons, in contrast to the typical FA composition of many sponges belonging to the Demospongiae where very long-chain  $\Delta 5,9$  FA with chain lengths between 25 and 29 carbons predominate [21, 23]. This finding could have significance in the chemotaxonomy of sponges belonging to the Suberitidae family.

The characterization of the novel cyclopropyl FA 1–3 in the phospholipids of *P. suberitoides* is also a rare finding, inasmuch as these fatty acids possess a *trans* cyclopropyl ring attached to carbons 4 and 5. This unusual 4,5 cyclopropane substitution seems to be specific for marine cyanobacteria since it has only been identified before in complex FA containing metabolites from the marine cyanobacterium *Lyngbya majuscula* and from other cyanobacterial communities [10, 12]. Our findings indicate that the more classical *iso-anteiso* FA can also exist with this type of 4,5 cyclopropyl substitution. Moreover, based on the highly methyl-branched nature of these FA it is very likely that they also originate from symbiotic microorganisms (bacteria or cyanobacteria) within *P. suberitoides*. If the latter is true, then we could be dealing with a novel marine bacterial strain previously unidentified since, to the best of our knowledge, there are no known marine bacteria with *iso-anteiso* FA with a 4,5 cyclopropyl substitution. More interesting could be the biological potential of these cyclopropyl FA as antimycobacterial agents (in particular against *Mycobacterium tuberculosis*) [24] or even against pathogenic fungi such as *Candida albicans* [10]. Further research is thus needed to put in perspective the pharmacological potential of these compounds.

**Acknowledgments** This work was supported by a grant from the SCORE program of the National Institutes of Health (grant no. S06GM08102). J. Vicente thanks the NIH-MARC program for an undergraduate fellowship.

## References

- Gunstone FD (1994) Cyclic acids, In: Gunstone FD, Harwood JL, Padley FB (eds) The lipid handbook, 2nd edn, Chapman and Hall, London, pp 13–14
- Grogan DW, Cronan JE Jr (1997) Cyclopropane ring formation in membrane lipids of bacteria. *Microbiol Mol Biol Rev* 61:429–441
- Cox AD, Wilkinson SG (1989) Polar lipids and fatty acids of *Pseudomonas cepacia*. *Biochim Biophys Acta* 1001:60–67
- Holz GG Jr, Beach DH, Singh BN, Fish WR (1983) Biosynthesis of the novel fatty acid, 17-methyl-*cis*-9,10-methyleneoctadecanoic acid, by the parasitic protozoan *Herpetomonas megaseliae*. *Lipids* 18:607–610
- Saito T, Ochiai H (1998) Fatty acid composition of the cellular slime mold *Polysphondylium pallidum*. *Lipids* 33:327–332
- Gontier E, Boussouel N, Terrasse C, Jannoyer M, Menard M, Thomasset B, Bourgaud F (2000) *Litchi chinensis* fatty acid diversity: occurrence of the unusual cyclopropanoic fatty acids. *Biochem Soc Trans* 28:578–580
- Fish WR, Holz GG Jr, Beach DH, Owen E, Anekwe GE (1981) The cyclopropane fatty acid of trypanosomatids. *Mol Biochem Parasitol* 3:103–115
- Lankelma J, Ayanoglu E, Djerassi C (1983) Double-bond location in long-chain polyunsaturated fatty acids by chemical ionization-mass spectrometry. *Lipids* 18:853–858
- Nemoto T, Yoshino G, Ojika M, Sakagami Y (1997) Amphiphilic acids and related long-chain fatty acids as DNA Topoisomerase I inhibitors from an Australian sponge, *Amphimedon* sp.; isolation, structure, synthesis, and biological evaluation. *Tetrahedron* 53:16699–16710
- MacMillan JB, Molinski TF (2005) Majusculoic acid, a brominated cyclopropyl fatty acid from a marine cyanobacterial mat assemblage. *J Nat Prod* 68:604–606
- Diaz MC, Pomponi SA, Van Soest RWM (1993) A systematic revision of the Central West Atlantic Halichondrida (Demospongiae, Porifera). Part III: description of valid species. *Sci Mar* 57:283–306
- Sitachitta N, Gerwick WH (1998) Grenadadiene and grenadamide, cyclopropyl-containing fatty acid metabolites from the marine *Cyanobacterium Lyngbya majuscula*. *J Nat Prod* 61:681–684
- Privett OS, Dougherty KA, Erdahl WL, Stolyhwo A (1973) Lipid composition of developing soybeans. *J Am Oil Chem Soc* 50:516–520
- Carballeira NM, Alicea J (2001) The first naturally occurring  $\alpha$ -methoxylated branched-chain fatty acids from the phospholipids of *Amphimedon complanata*. *Lipids* 36:83–87
- Djerassi C, Lam WK (1991) Sponge Phospholipids. *Acc Chem Res* 24:69–75
- Carballeira NM, Maldonado ME, Rivera E, Porras B (1989) The fatty acid 4,8,12-trimethyltridecanoic as a common constituent of the phospholipids of the sponge families Spirastrellidae and Clionidae. *Biochem Syst Ecol* 17:311–314
- Andersson BA (1978) Mass spectrometry of fatty acid pyrrolidides. *Prog Chem Fats Lipids* 16:279–308
- Knothe G (2006) NMR characterization of dihydrosterculic acid and its methyl ester. *Lipids* 41:393–396
- Carballeira NM, Alicea J (2002) Novel methoxylated FA from the Caribbean sponge *Sphaciospongia cuspidifera*. *Lipids* 37:305–308
- Carballeira NM, Cruz H, Kwong CD, Wan B, Franzblau S (2004) 2-Methoxylated fatty acids in marine sponges: defense mechanism against Mycobacteria? *Lipids* 39:675–680
- Bergquist PR, Lawson MP, Lavis A, Cambie RC (1984) Fatty acid composition and the classification of the Porifera. *Biochem Syst Ecol* 12:63–84
- Walkup RD, Jamieson GC, Ratcliff MR, Djerassi C (1981) Phospholipid studies of marine organisms: 2. Phospholipids, Phospholipid-bound fatty acids and free sterols of the sponge *Aplysina fistularis* (Pallas) forma *fulva* (Pallas) (= *Verongia thiona*). Isolation and structure elucidation of unprecedented branched fatty acids *Lipids* 16:631–646
- Thiel V, Blumenberg M, Hefter J, Pape T, Pomponi SA, Reed J, Reitner J, Wörheide G, Michaelis W (2002) A chemical view of the most ancient metazoa-biomarker chemotaxonomy of hexactinellid sponges. *Naturwissenschaften* 89:60–66
- Hartmann S, Minnikin DE, Römmling HJ, Baird MS, Ratledge C, Wheeler PR (1994) Synthesis of Methyl 3-(2-octadecylcyclopropen-1-yl)propanoate and methyl 3-(2-Octadecylcyclopropen-1-yl)pentanoate and cyclopropane fatty acids as possible inhibitors of mycolic acid biosynthesis. *Chem Phys Lipids* 71:99–108

## Fatty Acids in Liver, Muscle and Gonad of three Tropical Rays including Non-Methylene-Interrupted Dienoic Fatty Acids

Mohamed Vall Ould El Kebir · Gilles Barnathan ·  
Emile M. Gaydou · Yves Siau · Joseph Miralles

Received: 2 January 2007 / Accepted: 12 February 2007 / Published online: 3 April 2007  
© AOCS 2007

**Abstract** Scientific investigation of lipids in Elasmobranchs has been conducted mainly on shark species. Because rays seem to be neglected, this study was performed to examine the complete fatty acid (FA) composition with a particular interest for long-chain polyunsaturated FA (PUFA) content in different tissues of three ray species including parts usually discarded. The total FA and PUFA profiles of total lipids were determined in muscle, liver, and gonad of *Rhinobatos cemiculus*, *Rhinoptera marginata*, and *Dasyatis marmorata*, the most often caught ray species from the East Tropical Atlantic Ocean. Fifty FA were characterized as methyl esters and *N*-acyl pyrrolidides by gas chromatography/mass spectrometry, showing significant levels of 20:5n-3 (EPA) (up to 5.3%) and 22:5n-3 (DPA) (up to 7.3%), high levels of 20:4n-6 arachidonic

(ARA) (4.8–8.6% of total FA) and 22:6n-3 (DHA) (up to 20.0%). The results show that muscle, liver and gonad of rays can provide high amounts of essential PUFA, specially DHA, for direct human nutrition or the food processing industry. High proportions of DHA were particularly found in all samples of *R. cemiculus* (11.6–20.0%), and in muscle and liver of *D. marmorata* (11.1–16.1%). Regarding the high amounts of (n-3) PUFA, this study shows that these rays deserve a better up-grading, including the normally discarded parts, and describes the occurrence of unusual NMID FA in all tissues studied. Five non-methylene-interrupted dienoic fatty acids (NMID FA) (0–3.4%) were reported, including previously known isomers, namely 20:2  $\Delta$ 7,13, 20:2  $\Delta$ 7,15, 22:2  $\Delta$ 7,13, 22:2  $\Delta$ 7,15, and new 22:2  $\Delta$ 6,14. These acids are quite unusual in fish and unprecedented in rays. The 22:2  $\Delta$ 6,14 acid occurred in gonads of male specimens of *R. cemiculus* at 2.9%.

M. V. O. E. Kebir · E. M. Gaydou  
Laboratoire de Phytochimie de Marseille,  
UMR CNRS 6171, Faculté des Sciences et Techniques  
de Saint-Jérôme, Université Paul Cézanne, Case 531,  
Avenue Escadrille Normandie-Niémen,  
13397 Marseille Cedex 20, France

M. V. O. E. Kebir · J. Miralles  
Laboratoire de Biochimie, Faculté des Sciences,  
Nouakchott, République Islamique de Mauritanie

G. Barnathan (✉)  
Laboratoire de Chimie Marine, Groupe SMAB, EA 2160,  
Pôle Mer et Littoral, Université de Nantes, ISOMer, BP 92208,  
2 rue La Houssinière, 44322 Nantes Cedex 3, France  
e-mail: Gilles.Barnathan@univ-nantes.fr

Y. Siau  
Laboratoire d'Ichthyologie, Case 102,  
Université de Montpellier II, Place Eugène Bataillon,  
34095 Montpellier Cedex 5, France

**Keywords** DHA · 6,14-Docosadienoic acid · EPA ·  
Fatty acids · Fishes · Non-methylene-interrupted dienoic  
fatty acids · Polyunsaturated fatty acids · Rays

### Abbreviations

amu	Atomic mass unit
ARA	Arachidonic acid
DHA	Docosahexaenoic acid (22:6n-3)
DPA	22:5n-3
DUFA	Diunsaturated FA
EPA	Eicosapentaenoic acid (20:5n-3)
FA	Fatty acid
FAME	Fatty acid methyl ester
GC/MS	Gas chromatography–mass spectrometry
MUFA	Monounsaturated FA
NMID FA	Non-methylene-interrupted dienoic FA

PUFA	Polyunsaturated FA
SFA	Saturated FA
TLC	Thin layer chromatography

## Introduction

In Mauritania, a small amount of ray flesh is consumed only after being air-dried or salted, a major part is commonly exported to South West African countries [1, 2]. The selected ray species for this study have not yet been investigated, although they are the most commonly caught. The main part of these rays caught is wasted.

The lipid content of fish has been studied for a long time mainly in the liver and edible parts such as muscles. The n-3 long-chain polyunsaturated fatty acids (PUFA), particularly eicosapentaenoic acid (20:5n-3/EPA) and docosahexaenoic acid (22:6n-3/DHA), have been proven to display a variety of beneficial effects for human health and nutrition in areas ranging from foetal brain development to alleged cancer prevention [3–12]. Fish are recognized as excellent sources of PUFA, particularly of the long-chain n-3 series [3, 9, 10, 12]. In the new millennium, there is a growing demand for marine fish oils, the main source of n-3 PUFA for the use in human food, nutraceuticals and pharmaceuticals [3, 12]. Due to the general decline of fish stocks, the investigation of unfished or less-exploited fish species is needed, and a better use of raw material is required, involving the evaluation of by-products from fisheries [12].

The coasts of Senegal and Mauritania, with alternating cold and warm marine currents, are the richest areas of West Africa for seafood resources, mainly fish [13]. Only a few detailed chemical reports of the lipid and fatty acid (FA) content of fish from this area are available, even for fish species most often locally consumed. We have investigated fish from these waters, e.g. *Sardinella maderensis*, *S. aurita* and *Cephalopholis taeniops* [14]. The flesh of the latter species contains high concentrations of n-3 PUFA, up to 29% including EPA and DHA as major components [14]. Furthermore, parts of fish such as skin, often discarded when fish are prepared for consumption, were found to be rich in these PUFA [14]. Thus, it was of great interest to evaluate the potential in lipids and essential PUFA of different organs of rays. For the ray fishery, only the caudal fins are utilized, since they are very much appreciated by Asian consumers in shark-soup. The head and viscera, including the liver, are thrown back into the sea. There is little information on lipids and FA composition of rays, although these are closely related to sharks [15]. Both species are members of the Class Chondrichthyes, or

cartilaginous fish, and belong to the Subclass Elasmobranchii [15]. We recently reported on FA distribution in muscle, liver and gonads of the Mauritanian rays *Dasyatis marmorata*, *Rhinobatos cemiculus* and *Rhinoptera marginata* commonly fished from the East Tropical Atlantic [16]. Considerable data are available on lipids and FA in shark tissues [17–19]. Published work on lipids of sharks and rays is often centered on the liver oil where it is assumed that fish concentrate fats. The liver oil of deep-sea sharks has attracted much attention, mainly for the often large amount of hydrocarbons including squalene, and also alkyldiacylglycerols [17, 18]. Studies on pelagic shark species revealed that the liver lipids contained high levels of n-3 PUFA, especially DHA (up to 28.4%) [18]. Lipids and natural antioxidants were recently reported in the liver oil of *Dasyatis brevis* and *Gymnura marmorata* rays captured in the Gulf of California and high levels of EPA and DHA were observed [20]. The liver lipid composition of the ray *Dasyatis bleekeri* from India was reported [21]. Lipid profiles and occurrence of carotenes and tocopherols have been reported in the liver oil of the ray *Rhinoptera steindechneri* [22]. As an important fishing resource along the Galician coast, the ray *Raja clavata* was studied for lipid changes in muscle tissue during processing and frozen storage [23, 24].

Our recent results regarding the three Mauritanian rays showed that rays are potential sources of n-3 PUFA and should be used in the diet of local populations [16]. These rays are found both in coastal waters and far out to sea [13]. Rays of various families are effectively known to migrate [25]. Thus, though mostly observed in inshore waters, Rhinobatidae can enter deep waters. In Californian waters, the guitarfish *Rhinobatos productus* shows seasonal variations in abundance [26], while reproduction-related migrations are observed in *Rhinoptera bonasus* from Chesapeake Bay [27].

On the basis of phylogenetic relationships, rays are divided into five groups [10]. The genus *Rhinobatos* belongs to the Rhibatoid group, while the genera *Dasyatis* and *Rhinoptera* belong to the Myliobatoid group. Principal component analysis allowed us to reveal significant differences in various FA distribution, related to the species and sex of the sampled fish [16]. About fifty FA were identified by gas chromatography–mass spectrometry (GC–MS) from muscles, livers and gonads of these species. Muscle is the major edible part of fish but liver oil is known as a good source of interesting FA. Therefore, we studied ray livers even if they represent a lower part of the fish mass than in sharks. The only complete FA compositions reported in our previous paper were that in male muscle for these species [16]. Therefore, the present report deals with the FA composition of different tissues, and describes the characterization of unusual FA with emphasis on the non-methylene-interrupted diunsaturated FA (NMID FA).



## Materials and Methods

### Fish Species and Sampling

Fish specimens were obtained from local Mauritanian fish markets in autumn and winter (i.e. November to February, 1996–1998). Fish specimens were mainly caught off Nouakchott, in the same area, in the South part of the Banc d'Arguin. They were identified as detailed in our previous paper [13, 16]. Samples were kept on ice from the market to the laboratory in Nouakchott before lipid extraction.

**Lipid extraction.** For each analysis, ~10 g of muscle, liver, and gonad were homogenized separately using a Waring Blender. Muscles were sampled under the skin on the dorsal side. Lipids were extracted according to a modification of the Bligh and Dyer method [28] using a mixture of 20 mL of methanol and 10 mL of chloroform for 5 min. After centrifugation, the lower chloroform phase was collected, dried with anhydrous sodium sulfate, and evaporated under vacuum to give the total lipids. A small amount of BHT was added to the lipid extracts and these were kept in dry ice during transfer to the laboratory in Marseille, France.

### Saponification and Fatty Acid Derivatives

Fatty acid methyl esters (FAME) were prepared by saponification of the total lipids (50 mg) with KOH-ethanol, 2 M (1 mL) [29] followed by recovery of the fatty acids, and acid-catalyzed methylation with methanolic hydrogen chloride. *N*-Acyl pyrrolidides were prepared by direct treatment of methyl esters with pyrrolidine/acetic acid (10:1, v/v) for 2 h under reflux and purified by TLC on silica gel layers using hexane/diethyl ether (1:2, v/v) [30].

### Gas Chromatography (GC)

A Delsi gas chromatograph equipped with a flame ionization detector (FID) and a fused silica capillary column (25 m × 0.28 mm i.d.) coated with Carbowax 20 M (0.2 μm phase thickness) was used for analyses (Delsi Instruments, Suresnes, France). Temperatures used were 180 °C for 10 min, then raised at 2 °C min<sup>-1</sup> to 220 °C for the column, and 250 °C for the inlet and detector.

### Gas Chromatography–Mass Spectrometry (GC–MS)

Fatty acids (FA) were characterized as their methyl esters and *N*-acyl pyrrolidides using gas chromatography and gas chromatography–mass spectrometry. Compounds are listed as saturated (SFA), monounsaturated (MUFA), diunsaturated (DFA), and polyunsaturated fatty acids (PUFA), and in the increasing order of chromatographic retention times

of their FAME on a DB1 column. Double bond positions were established by GC–MS of *N*-acyl pyrrolidides [16, 30]. GC–MS was performed on a Hewlett-Packard HP-5890 chromatograph linked to a HP-5989-A mass spectrometer (70 eV) equipped with a HP-9000/345 integrator, using a 30 m × 0.32 mm i.d. fused silica capillary column coated with DB-1 (0.25 μm phase thickness) (Palo Alto, CA). The carrier gas was He. The column temperature was programmed from 170 °C (4 min hold) to 300 °C at 3 °C min<sup>-1</sup> for methyl esters, and from 200 °C (4 min hold) to 310 °C for *N*-acyl pyrrolidides.

### Statistic Analysis

Statistical analysis of the data has been made as described in our previous paper [16]. Fifty-four samples were taken into account, i.e. three species, three years, three parts (gonad, muscle and liver), male and female. Fish specimens have been obtained for 4 months (November, December, January and February) including three replicates for each collect.

## Results

The livers of the three rays contained high amounts of lipids (30–50%) except female *R. marginata* with 16.2% (relative percentage of whole fresh organ), lipid contents were up to 1.7% for muscle and up to 5.4% for gonad [16]. Tables 1, 2 and 3 provide the FA profiles of muscle, liver and gonads of the three rays (male and female), respectively.

Analysis of the FA compositions from different organs of the rays revealed similarities and significant differences (Tables 1–3). The most abundant individual FA in all samples were myristic (14:0), palmitic (16:0), stearic (18:0), palmitoleic (16:1n-7), oleic (18:1n-9), vaccenic (18:1n-7), ARA, EPA, DHA and DPA. Odd numbered saturated and monounsaturated C<sub>15</sub> and C<sub>17</sub> FA are present in all samples and included *iso*-pentadecanoic, *iso*-heptadecanoic and *anteiso*-heptadecanoic acids.

### Saturated Fatty Acids (SFA)

SFA ranged from tetradecanoic to docosanoic acid in almost all the samples analysed. Palmitic (14.1–34.9% of total FA) and stearic (3.6–25.0%) were generally the most abundant saturated FA. Myristic acid was found at high level in gonads of *D. marmorata* (male and female, up to 19%), and *R. cemiculus* (female, 12%). 4,8,12-Trimethyltridecanoic acid, often present in marine organisms and known to originate from the degradation of the phytol in plants, was found in all samples at low amounts (0.05–2.54%) except in *D. marmorata* (3.7–4.6%).

**Table 1** Fatty acids from muscle of three Mauritanian rays

Fatty acid	<i>Dasyatis marmorata</i>		<i>Rhinoptera marginata</i>		<i>Rhinobatos cemiculus</i>	
	M	F	M	F	M	F
<b>Saturated fatty acids</b>						
14:0	2.24 ± 0.14	6.93 ± 0.19	1.54 ± 0.05	1.76 ± 0.05	5.83 ± 0.21	5.64 ± 0.33
TMTD <sup>a</sup>	0.60 ± 0.08	0.70 ± 0.01	0.13 ± 0.02	0.11 ± 0.01	0.43 ± 0.04	0.29 ± 0.02
i-15:0	0.26 ± 0.02	1.59 ± 0.04	0.28 ± 0.03	0.42 ± 0.03	0.31 ± 0.03	1.03 ± 0.02
15:0	0.29 ± 0.02	4.76 ± 0.22	0.59 ± 0.01	0.77 ± 0.03	0.34 ± 0.02	3.41 ± 0.14
16:0	19.4 ± 1.3	15.6 ± 0.98	25.9 ± 2.9	18.8 ± 2.4	21.0 ± 2.0	21.8 ± 0.95
i-17:0	0.98 ± 0.15	2.67 ± 0.10	1.39 ± 0.54	1.73 ± 0.03	0.73 ± 0.08	0.15 ± 0.02
ai-17:0	0.22 ± 0.02	–	0.03 ± 0.01	–	0.45 ± 0.18	–
17:0	0.18 ± 0.01	0.49 ± 0.01	0.14 ± 0.11	0.37 ± 0.01	0.41 ± 0.02	0.15 ± 0.01
18:0	9.23 ± 0.61	7.73 ± 0.19	25.0 ± 1.7	21.8 ± 1.6	13.3 ± 0.7	8.70 ± 0.50
20:0	0.21 ± 0.01	0.36 ± 0.02	0.15 ± 0.01	0.60 ± 0.03	0.13 ± 0.01	0.40 ± 0.01
22:0	0.42 ± 0.03	–	0.15 ± 0.01	–	0.60 ± 0.03	–
<b>Monounsaturated fatty acids</b>						
16:1n-10	0.34 ± 0.10	0.25 ± 0.01	0.77 ± 0.05	0.45 ± 0.03	0.28 ± 0.02	0.45 ± 0.02
16:1n-7	2.85 ± 0.20	3.25 ± 0.14	3.23 ± 0.18	3.63 ± 0.15	1.9 ± 0.10	1.92 ± 0.10
16:1n-6	0.53 ± 0.01	0.66 ± 0.02	tr	tr	0.8 ± 0.02	0.25 ± 0.01
17:1n-11	0.68 ± 0.03	0.82 ± 0.04	1.02 ± 0.05	0.35 ± 0.02	0.26 ± 0.02	0.76 ± 0.01
17:1n-8	0.30 ± 0.01	0.82 ± 0.06	2.60 ± 0.13	0.75 ± 0.03	0.44 ± 0.02	2.08 ± 0.13
18:1n-12	1.48 ± 0.04	1.29 ± 0.06	0.90 ± 0.01	2.10 ± 0.06	1.81 ± 0.05	0.55 ± 0.02
18:1n-9	8.61 ± 0.50	3.79 ± 0.05	6.60 ± 0.40	8.72 ± 0.47	8.00 ± 0.50	8.04 ± 0.32
18:1n-7	3.49 ± 0.20	2.63 ± 0.15	6.25 ± 0.19	2.94 ± 0.13	0.44 ± 0.02	2.88 ± 0.10
20:1n-13	tr	0.36 ± 0.20	tr	0.80 ± 0.05	tr	0.21 ± 0.01
20:1n-10	0.18 ± 0.03	–	0.10 ± 0.01	–	0.46 ± 0.02	–
20:1n-9	0.50 ± 0.02	0.44 ± 0.02	0.33 ± 0.03	0.73 ± 0.03	0.21 ± 0.01	0.19 ± 0.01
20:1n-7	0.15 ± 0.01	0.61 ± 0.03	0.66 ± 0.05	0.76 ± 0.02	0.63 ± 0.06	0.55 ± 0.02
22:1n-15	0.22 ± 0.01	–	0.08 ± 0.01	–	0.42 ± 0.02	–
22:1n-14	0.20 ± 0.01	0.28 ± 0.02	0.13 ± 0.01	0.25 ± 0.01	0.60 ± 0.03	0.21 ± 0.01
<b>Diunsaturated fatty acids</b>						
18:2 Δ <sup>9,12</sup>	1.09 ± 0.45	0.38 ± 0.21	0.52 ± 0.06	0.30 ± 0.28	0.40 ± 0.23	0.69 ± 0.06
20:2 Δ <sup>7,13</sup>	–	–	tr	tr	–	–
20:2 Δ <sup>7,15</sup>	0.80 ± 0.01	2.03 ± 0.09	0.95 ± 0.00	1.40 ± 0.30	0.43 ± 0.03	0.16 ± 0.01
22:2 Δ <sup>6,14</sup>	0.19 ± 0.02	–	0.80 ± 0.04	–	0.23 ± 0.01	–
22:2 Δ <sup>7,13</sup>	3.46 ± 0.14	3.01 ± 0.29	0.07 ± 0.01	1.35 ± 0.57	2.28 ± 0.15	2.00 ± 0.10
22:2 Δ <sup>7,15</sup>	3.46 ± 0.60	0.43 ± 0.03	0.73 ± 0.03	0.11 ± 0.01	0.35 ± 0.02	0.39 ± 0.02
<b>Polyunsaturated fatty acids</b>						
16:3n-4	0.56 ± 0.00	0.48 ± 0.01	0.07 ± 0.01	tr	0.53 ± 0.03	0.21 ± 0.03
18:4n-3	0.67 ± 0.03	1.31 ± 0.06	2.34 ± 0.12	2.37 ± 0.10	0.68 ± 0.03	0.53 ± 0.03
18:3n-6	0.10 ± 0.01	0.41 ± 0.02	0.04 ± 0.01	0.09 ± 0.01	0.75 ± 0.05	0.15 ± 0.02
20:5n-3	4.95 ± 0.13	2.89 ± 0.10	2.26 ± 0.18	4.35 ± 0.21	4.63 ± 0.24	5.32 ± 0.28
20:4n-6	5.57 ± 0.16	5.74 ± 0.19	8.00 ± 0.60	6.77 ± 0.47	7.32 ± 0.40	6.39 ± 0.35
22:4n-6	–	6.40 ± 0.34	–	1.00 ± 0.05	–	1.05 ± 0.05
22:5n-6	–	2.13 ± 0.15	–	0.55 ± 0.02	–	0.79 ± 0.04
22:5n-3	9.37 ± 0.58	7.26 ± 0.52	2.36 ± 0.12	2.58 ± 0.13	3.91 ± 0.16	2.18 ± 0.10
22:6n-3	16.1 ± 1.5	11.1 ± 0.34	3.74 ± 0.17	9.98 ± 0.84	18.7 ± 1.8	20.0 ± 2.0

M Male, F female, tr trace (<0.01%). Other FA present in traces: 16:1n-8/18:1n-6/22:1n-14

Relative percentage obtained using Carbowax 20 M results. Mean of three adult rays collected between November and February 1996, 1997, and 1998

<sup>a</sup> 4,8,12-Me<sub>3</sub>-13 :0

**Table 2** Fatty acids from liver of three Mauritanian rays

Fatty acid	<i>Dasyatis marmorata</i>		<i>Rhinoptera marginata</i>		<i>Rhinobatos cemiculus</i>	
	M	F	M	F	M	F
<b>Saturated fatty acids</b>						
14:0	5.77 ± 0.31	3.05 ± 0.11	4.02 ± 0.17	2.94 ± 0.17	0.05 ± 0.01	2.94 ± 0.19
TMTD <sup>a</sup>	0.51 ± 0.13	1.41 ± 0.06	0.12 ± 0.04	0.51 ± 0.07	0.21 ± 0.04	0.05 ± 0.01
i-15:0	0.33 ± 0.02	0.91 ± 0.12	0.16 ± 0.08	0.47 ± 0.02	0.22 ± 0.01	0.24 ± 0.17
15:0	0.18 ± 0.02	0.55 ± 0.02	3.17 ± 0.07	2.16 ± 0.11	0.12 ± 0.01	0.44 ± 0.02
16:0	14.1 ± 1.1	17.3 ± 1.59	27.1 ± 2.2	17.61 ± 0.34	20.7 ± 0.17	17.26 ± 1.15
i-17:0	0.32 ± 0.19	1.12 ± 0.07	0.86 ± 0.42	2.99 ± 0.12	0.37 ± 0.02	0.87 ± 0.23
ai-17:0	0.37 ± 0.01	–	0.12 ± 0.08	–	0.06 ± 0.02	–
17:0	0.27 ± 0.05	1.51 ± 0.04	0.69 ± 0.02	0.78 ± 0.02	0.19 ± 0.01	0.89 ± 0.03
18:0	5.51 ± 0.19	12.3 ± 1.21	15.4 ± 1.3	14.4 ± 0.48	19.4 ± 1.2	18.9 ± 1.3
20:0	0.11 ± 0.01	0.52 ± 0.03	0.25 ± 0.02	1.28 ± 0.03	0.23 ± 0.03	0.59 ± 0.06
22:0	–	0.41 ± 0.02	–	0.17 ± 0.05	–	0.16 ± 0.03
<b>Monounsaturated fatty acids</b>						
16:1n-10	0.58 ± 0.03	1.03 ± 0.06	0.49 ± 0.02	0.65 ± 0.04	0.24 ± 0.01	0.24 ± 0.02
16:1n-7	11.6 ± 1.8	6.98 ± 0.08	6.03 ± 0.74	6.18 ± 0.35	9.42 ± 0.74	9.17 ± 0.83
16:1n-6	0.66 ± 0.03	1.46 ± 0.06	tr	0.13 ± 0.01	0.59 ± 0.03	0.07 ± 0.01
17:1n-11	0.11 ± 0.01	0.69 ± 0.11	0.71 ± 0.06	0.72 ± 0.04	0.87 ± 0.06	0.08 ± 0.03
17:1n-8	1.14 ± 0.01	1.19 ± 0.06	0.55 ± 0.03	1.25 ± 0.04	0.99 ± 0.01	0.66 ± 0.01
18:1n-12	1.18 ± 0.07	1.25 ± 0.05	1.29 ± 0.08	1.93 ± 0.05	0.13 ± 0.01	0.66 ± 0.01
18:1n-9	6.59 ± 0.25	4.00 ± 0.15	4.76 ± 0.13	4.50 ± 0.21	6.54 ± 0.17	7.20 ± 0.10
18:1n-7	5.63 ± 0.28	4.49 ± 0.17	4.78 ± 0.09	4.94 ± 0.18	0.35 ± 0.06	3.56 ± 0.06
18:1n-6	0.24 ± 0.03	0.33 ± 0.01	tr	tr	0.05 ± 0.01	0.10 ± 0.02
20:1n-13	2.25 ± 0.13	1.03 ± 0.05	0.86 ± 0.02	1.48 ± 0.13	0.09 ± 0.01	0.22 ± 0.04
20:1n-9	1.02 ± 0.04	0.51 ± 0.02	0.44 ± 0.04	0.71 ± 0.01	0.61 ± 0.04	0.49 ± 0.02
20:1n-7	1.30 ± 0.07	3.87 ± 0.20	0.83 ± 0.04	1.62 ± 0.06	0.60 ± 0.10	0.53 ± 0.01
<b>Diunsaturated fatty acids</b>						
18:2 Δ9,12	1.08 ± 0.52	0.25 ± 0.05	3.92 ± 0.42	0.86 ± 0.63	0.39 ± 0.18	1.17 ± 0.58
20:2 Δ7,13	–	–	tr	tr	–	–
20:2 Δ7,15	2.96 ± 0.27	1.86 ± 0.15	1.12 ± 0.13	2.37 ± 0.02	1.30 ± 0.03	1.42 ± 0.07
22:2 Δ6,14	–	tr	–	tr	–	tr
22:2 Δ7,13	2.20 ± 0.30	2.29 ± 0.20	0.10 ± 0.01	1.03 ± 0.12	1.94 ± 0.00	1.00 ± 0.01
22:2 Δ7,15	–	2.31 ± 0.18	–	0.21 ± 0.01	–	0.65 ± 0.03
<b>Polyunsaturated fatty acids</b>						
16:3n-4	1.04 ± 0.05	0.78 ± 0.05	0.16 ± 0.02	0.32 ± 0.00	0.53 ± 0.04	0.05 ± 0.01
18:4n-3	1.15 ± 0.05	1.31 ± 0.06	3.74 ± 0.04	2.37 ± 0.10	0.81 ± 0.05	0.53 ± 0.03
18:3n-6	0.95 ± 0.09	0.32 ± 0.02	0.33 ± 0.01	0.31 ± 0.01	0.87 ± 0.04	1.07 ± 0.08
20:5n-3	3.41 ± 0.12	1.88 ± 0.13	3.35 ± 0.15	4.63 ± 0.40	5.01 ± 0.10	2.92 ± 1.12
20:4n-6	5.66 ± 0.30	5.07 ± 0.37	7.81 ± 0.09	7.66 ± 0.86	6.63 ± 0.26	7.75 ± 0.18
22:4n-6	1.40 ± 0.05	1.74 ± 0.15	0.14 ± 0.01	0.32 ± 0.01	1.00 ± 0.07	0.99 ± 0.11
22:5n-6	1.30 ± 0.20	1.27 ± 0.03	0.15 ± 0.01	0.16 ± 0.01	0.76 ± 0.03	0.74 ± 0.16
22:5n-3	5.24 ± 0.42	2.42 ± 0.27	0.90 ± 0.05	1.69 ± 0.06	4.76 ± 0.24	2.78 ± 0.10
22:6n-3	13.4 ± 1.1	11.6 ± 2.3	5.64 ± 0.96	10.0 ± 0.25	13.2 ± 0.69	13.1 ± 3.1

M male, F Female, tr Trace (<0.01%)

Acids 20:1n-3, 22:1n-15, and 22:1n-14 occurred in traces in livers of females

Relative percentage obtained using Carbowax 20 M results. Mean of three adult rays collected between November and February 1996, 1997, and 1998

<sup>a</sup> 4,8,12-Me<sub>3</sub>-13:0

**Table 3** Fatty acids from gonad of three Mauritanian rays

Fatty acid	<i>Dasyatis marmorata</i>		<i>Rhinoptera marginata</i>		<i>Rhinobatos cemiculus</i>	
	M	F	M	F	M	F
<b>Saturated fatty acids</b>						
14:0	15.1 ± 1.2	18.94 ± 1.12	2.11 ± 0.08	3.43 ± 0.12	3.56 ± 0.17	12.10 ± 0.76
TMTD <sup>a</sup>	4.62 ± 0.43	3.74 ± 0.04	0.08 ± 0.01	0.32 ± 0.03	0.32 ± 0.04	2.54 ± 0.08
i-15:0	0.43 ± 0.13	0.14 ± 0.04	0.27 ± 0.04	0.29 ± 0.01	0.71 ± 0.06	0.89 ± 0.03
15:0	0.88 ± 0.03	0.41 ± 0.03	0.76 ± 0.04	1.44 ± 0.05	0.84 ± 0.04	0.31 ± 0.01
16:0	16.4 ± 0.2	21.8 ± 1.7	33.1 ± 1.3	34.3 ± 1.4	17.2 ± 1.1	24.5 ± 1.6
i-17:0	0.14 ± 0.06	0.24 ± 0.07	1.20 ± 0.11	1.75 ± 0.58	0.82 ± 0.14	0.62 ± 0.10
ai-17:0	–	tr	–	0.56 ± 0.20	–	tr
17:0	tr	0.12 ± 0.01	tr	0.05 ± 0.01	tr	0.64 ± 0.03
18:0	12.0 ± 1.1	5.21 ± 0.19	22.6 ± 1.5	18.20 ± 1.18	11.9 ± 0.8	3.62 ± 0.16
20:0	1.37 ± 0.07	tr	0.35 ± 0.03	0.27 ± 0.01	1.08 ± 0.05	tr
22:0	0.10 ± 0.03	tr	0.15 ± 0.01	tr	0.55 ± 0.02	tr
<b>Monounsaturated fatty acids</b>						
16:1n-10	0.12 ± 0.01	0.23 ± 0.02	0.12 ± 0.01	0.09 ± 0.01	0.50 ± 0.02	0.37 ± 0.01
16:1n-7	7.4 ± 0.30	8.95 ± 0.82	2.99 ± 0.11	3.64 ± 0.13	2.97 ± 0.09	6.14 ± 0.27
16:1n-6	0.26 ± 0.01	0.45 ± 0.02	1.58 ± 0.04	2.80 ± 0.11	0.52 ± 0.03	0.51 ± 0.05
17:1n-11	0.49 ± 0.02	0.57 ± 0.02	0.13 ± 0.01	0.15 ± 0.01	0.21 ± 0.01	0.70 ± 0.06
17:1n-8	0.12 ± 0.01	0.18 ± 0.01	0.63 ± 0.02	0.39 ± 0.01	0.67 ± 0.03	0.38 ± 0.01
18:1n-12	3.82 ± 0.18	3.41 ± 0.06	0.35 ± 0.01	0.92 ± 0.03	2.29 ± 0.13	1.35 ± 0.05
18:1n-9	7.27 ± 0.50	7.52 ± 0.09	9.85 ± 0.18	4.06 ± 0.14	9.65 ± 0.60	11.3 ± 1.0
18:1n-7	5.50 ± 0.17	7.03 ± 0.12	5.40 ± 0.14	1.94 ± 0.05	6.04 ± 0.18	1.43 ± 0.11
18:1n-6	–	1.05 ± 0.04	–	tr	–	tr
20:1n-13	tr	0.37 ± 0.02	0.61 ± 0.04	0.27 ± 0.01	0.18 ± 0.01	1.03 ± 0.06
20:1n-9	0.12 ± 0.01	0.91 ± 0.03	0.44 ± 0.03	0.75 ± 0.04	0.74 ± 0.03	tr
20:1n-7	0.11 ± 0.01	tr	0.51 ± 0.05	tr	0.82 ± 0.03	tr
22:1n-14	0.10 ± 0.01	0.31 ± 0.01	0.01 ± 0.01	0.05 ± 0.01	1.09 ± 0.05	1.64 ± 0.06
<b>Diunsaturated fatty acids</b>						
20:2 Δ <sup>9,12</sup>	–	0.11 ± 0.01	–	0.08 ± 0.01	–	0.58 ± 0.03
20:2 Δ <sup>7,15</sup>	1.33 ± 0.30	–	0.51 ± 0.10	–	0.87 ± 0.05	–
22:2 Δ <sup>6,14</sup>	0.26 ± 0.01	tr	0.01 ± 0.01	tr	2.95 ± 0.10	tr
22:2 Δ <sup>7,13</sup>	0.26 ± 0.01	0.19 ± 0.02	1.15 ± 0.30	0.43 ± 0.05	1.33 ± 0.07	1.04 ± 0.05
22:2 Δ <sup>7,15</sup>	1.68 ± 0.06	0.50 ± 0.03	0.01 ± 0.01	tr	1.17 ± 0.06	0.36 ± 0.01
<b>Polyunsaturated fatty acids</b>						
16:3n-4	–	0.17 ± 0.01	–	0.10 ± 0.01	–	0.35 ± 0.02
18:4n-3	0.17 ± 0.01	0.47 ± 0.02	1.85 ± 0.10	2.58 ± 0.77	2.47 ± 0.09	0.86 ± 0.05
18:3n-6	0.95 ± 0.05	0.15 ± 0.01	0.18 ± 0.01	0.04 ± 0.00	1.42 ± 0.04	0.54 ± 0.01
20:5n-3	3.53 ± 0.16	3.57 ± 0.77	3.18 ± 0.13	3.71 ± 0.86	3.03 ± 0.10	4.78 ± 0.21
20:4n-6	4.76 ± 0.32	5.07 ± 0.66	5.98 ± 0.37	8.61 ± 1.17	6.92 ± 0.87	7.07 ± 1.11
22:4n-6	–	0.65 ± 0.03	–	0.01 ± 0.00	–	1.27 ± 0.04
22:5n-3	3.58 ± 0.22	1.14 ± 0.15	0.15 ± 0.01	0.84 ± 0.05	3.11 ± 0.11	1.47 ± 0.05
22:6n-3	6.28 ± 0.33	5.77 ± 0.86	3.67 ± 0.19	7.93 ± 0.26	13.9 ± 1.4	11.6 ± 0.6

M Male, F female, tr trace (<0.01%). Other FA in traces: 16:1n-8 and 22:1n-9 in all samples, and 20:1n-10 and 22:1n-15 in gonads of females. Relative percentage obtained using Carbowax 20M results. Mean of three adult rays collected between November and February 1996, 1997, and 1998

<sup>a</sup> 4,8,12-Me<sub>3</sub>-13:0

### Monounsaturated Fatty Acids (MUFA)

Twenty MUFA were found in the samples. Several isomers were identified for each of the monoenoic 16:1, 17:1, 18:1, 20:1 and 22:1 FA by analysis of their pyrrolidide derivatives, whose mass spectra displayed the expected corresponding molecular ion, and a corresponding gap of 12 amu, instead of the usual gap of 14 amu, indicating the location of the double bond [16, 30]. Thus, the acids 16:1n-6, 16:1n-7, 16:1n-8 and 16:1n-10 were readily identified from their GC mobilities, a molecular ion peak at  $m/z$  307 and gaps of 12 amu instead of 14 amu between respectively,  $m/z$  210 and 222,  $m/z$  196 and 208,  $m/z$  182 and 194,  $m/z$  154 and 166. Palmitoleic acid 16:1n-7 (1.9–11.6%), oleic acid 18:1n-9 (3.8–11.3%), and vaccenic acid 18:1n-7 (0.5–7.3%) were the dominant MUFA identified. Other unusual FA such as 20:1n-10 and 22:1n-14 were identified with the same procedure. Palmitoleic acid was found at high levels in the liver of *D. marmorata* (up to 12%) and *R. cemiculus* (up to 9%), and to a lesser extent in the gonads of *D. marmorata* (up to 9%). Oleic acid was found at high levels in gonads of *R. cemiculus* (male and female, up to 11%), and in male *R. marginata* (about 10% vs. 4% for the female specimens). Several 22:1 isomers occurred, including the unusual 22:1n-14 and 22:1n-15 acids. The latter FA were found as a trace level except for the gonads of *R. cemiculus* (up to 1.7% for the males).

### Diunsaturated Fatty Acids (DUFA)

Seven DUFA were identified as pyrrolidides by GC–MS. Two methylene-interrupted FA occurred, namely linoleic acid 18:2n-6, and the rare 20:2n-8 (or 20:2  $\Delta$ 9,12). Linoleic acid (18:2n-6) was present in all liver and muscle of the three rays, while the eicosadienoic acid (20:2n-8) occurred only in female gonads of the three rays at very low levels. Mass spectra of these FA displayed the molecular ion at  $m/z$  333 and 361, respectively, and gaps of 12 amu between

$m/z$  196 and 208, and between  $m/z$  236 and 248, confirming the location of the double bonds between C-9 and C-10, and between C-12 and C-13, respectively.

The other DUFA identified in the FA mixtures were non-methylene-interrupted dienoic FA (NMID FA) as determined by mass spectrometry of their pyrrolidide derivatives and their GC mobility.

The already known 20:2  $\Delta$ 7,13, 20:2  $\Delta$ 7,15, 22:2  $\Delta$ 7,13 and 22:2  $\Delta$ 7,15 FA were identified as pyrrolidide derivatives from their mass spectra (Table 4). The ECL values found for the 22:2 NMID FA (GC phase: Carbowax 20 M) were similar to those reported on similar polar phases, e.g. 22.47 for 22:2  $\Delta$ 7,13, and 22.50 for 22:2  $\Delta$ 7,15 [31], and 22.44 for 22:2  $\Delta$ 7,15 [32] (Table 4).

An additional 22:2 NMID FA was identified from the mass spectrum of its pyrrolidide (Fig. 1). This mass spectrum displayed an abundant molecular ion at  $m/z$  389 (22:2 acid structure). The locations of the double bonds were established as  $\Delta$ 6 and  $\Delta$ 14, with the spectrum showing two gaps of 12 amu between the fragment ions at  $m/z$  154 and 166, and at  $m/z$  264 and 276, respectively (Table 4, Fig. 1). Thus, the novel NMI FA was 6,14-docosadienoic acid.

### Polyunsaturated Fatty Acids (PUFA)

All the PUFA present in all specimens belonged to the n-3 and n-6 series, except 16:3n-4 (Tables 1, 2, 3). All PUFA were identified as their pyrrolidide derivatives, whose mass spectra displayed the corresponding molecular ions, and the expected gaps of 12 amu the series of homologous fragment ions.

As examples, pyrrolidides of the 16:3n-4 and 18:3n-6 acids displayed molecular ions at  $m/z$  303 and 331, respectively, and the same gaps of 12 amu between  $m/z$  154 and 166 ( $\Delta$ 9), between  $m/z$  194 and 206 ( $\Delta$ 9), and between  $m/z$  234 and 246 ( $\Delta$ 12). In addition, GC mobilities of these derivatives were in good concordance with the standard FA structures.

**Table 4** ECL values and principal diagnostic fragment ions in the mass spectra of *N*-acyl pyrrolidides, and of non-methylene-interrupted dienoic fatty acids identified in the rays

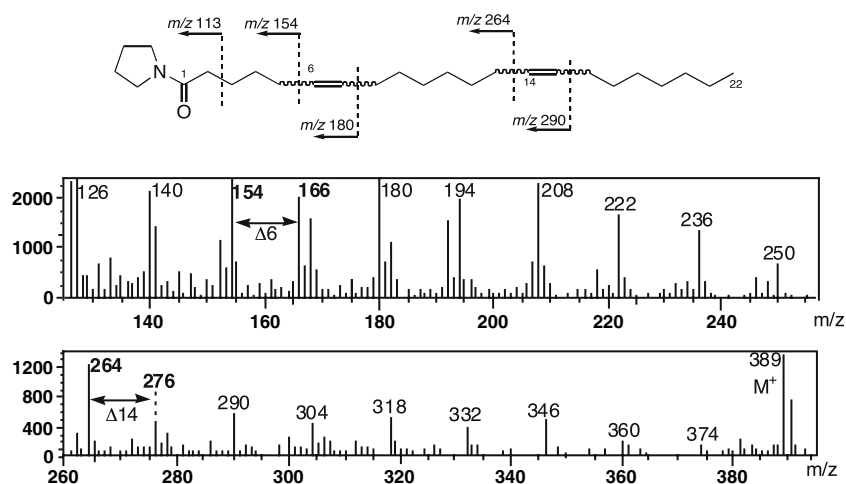
Structure	ECL <sup>c</sup>	M <sup>++a</sup>	First double bond <sup>b</sup>	Second double bond <sup>b</sup>
Fragment-ions with a gap of 12 amu <sup>a,b</sup>				
20:2 $\Delta$ 7,13	20.94	361	168 (C <sub>6:0</sub> )/180 (C <sub>7:1</sub> )	250 (C <sub>12:1</sub> )/262 (C <sub>13:2</sub> )
20:2 $\Delta$ 7,15	20.97	361	168 (C <sub>6:0</sub> )/180 (C <sub>7:1</sub> )	278 (C <sub>14:1</sub> )/290 (C <sub>15:2</sub> )
22:2 $\Delta$ 7,13	22.24	389	168 (C <sub>6:0</sub> )/180 (C <sub>7:1</sub> )	250 (C <sub>12:1</sub> )/262 (C <sub>13:2</sub> )
22:2 $\Delta$ 7,15	22.35	389	168 (C <sub>6:0</sub> )/180 (C <sub>7:1</sub> )	278 (C <sub>14:1</sub> )/290 (C <sub>15:2</sub> )
22:2 $\Delta$ 6,14	22.20	389	154 (C <sub>5:0</sub> )/166 (C <sub>6:1</sub> )	264 (C <sub>13:1</sub> )/276 (C <sub>14:2</sub> )

<sup>a</sup>  $m/z$  (e.i. 70 eV)

<sup>b</sup> Observed into the usual increasing series of homologous ions separated by 14 amu

<sup>c</sup> ECL equivalent chain length determined on Carbowax 20 M (see “Materials and Methods”)

**Fig. 1** Partial mass spectrum of the pyrrolidide derivative of 6,14-docosadienoic acid (Abundance vs.  $m/z$ ; base peak:  $m/z$  113)



DHA was the major PUFA, especially in the muscle of *R. marginata*, occurring at 18.7% (males) and at 20.0% (females). It should be noted that DHA was also present at high levels in liver (13.4% in of *D. marmorata*, male, and 13.1 and 13.2% in of *R. cemiculus*, male and female, respectively), and gonad (11.6–13.9% in gonads of *R. cemiculus*). ARA was the second most abundant PUFA, accounting for 5.5–8.0% in muscle of the rays, 5.1–7.8% in the liver, and 5.1–8.6% in the gonad. EPA occurred at levels of 2.2–5.3% in muscle, of 1.9–5.0% in liver, and of 3.0–4.9% in gonad. DPA was identified in all samples (up to 7.2%) with the exception for the male muscles of the three rays.

## Discussion

The percentages of n-3 PUFA found in the three rays were similar to those in fish used commercially as sources of PUFA and may be useful in the diet of local populations, including EPA, DHA and DPA [16]. This study shows that muscle of the rays contain high levels of DHA ranged from 10 to 20% of the total FA, with the exception for the males of *R. marginata* (3.74%). Thus, muscle seems suitable for consumption, and may provide an important amount of DHA as compared to the commercial fish oil [9, 10]. Furthermore, this study demonstrates that usually discarded parts of the rays, such as liver and gonad, contain high levels of lipid and of PUFA of current interest, e.g. EPA and DHA. DPA occurred in some FA mixtures analyzed and it could be noted that it is known to can be easily retroconverted to EPA [33]. The isomeric DPA and 22:5n-6 occurred only in muscle of females for the three rays. Livers of rays represent a relatively small part of the body but contain a considerable amount of lipids [20, 21], and they also contain high proportions of DHA except in the case of males of *R. marginata*. 16:3n-4 and 22:4n-6

occurred only in gonads of females suggesting a possible specific biological role. Occurrence of branched saturated and unsaturated C<sub>15</sub> and C<sub>17</sub> FA in the samples suggest a possible contribution of bacteria [34–36].

One of the most striking result of the present study is the finding of several NMID FA. Four previously known NMID FA were found in the selected tissues of the rays, namely 20:2  $\Delta$ 7,13, 20:2  $\Delta$ 7,15, 22:2  $\Delta$ 7,13 and 22:2  $\Delta$ 7,15 acids. The new 22:2  $\Delta$ 6,14 acid occurred as a minor component except in the muscle of male *R. cemiculus* (2.95%). The NMID were observed in all samples, and it is the first time that such FA are known to occur in rays. 20:2  $\Delta$ 7,13 was not present in the rays except as a trace level in muscle and liver of *R. marginata*. 20:2  $\Delta$ 7,15 was present in all FA mixtures except in female gonads of the three rays. 22:2  $\Delta$ 7,13 was identified in all FA mixtures, and it is the same for 22:2  $\Delta$ 7,15 except in male livers of the three rays.

NMID FA such as 20:2  $\Delta$ 5,11, 20:2  $\Delta$ 5,13 were not detected in any samples by means of a accurate GC–MS analysis of the corresponding expected area, even as trace amounts.

NMID FA are even quite rare in fish [42], although they are well known in other marine organisms [31, 32, 37–56]. They are widely represented in sponges, albeit with a high number of carbon atoms including dienoic and trienoic FA with the  $\Delta$ 5,9 unsaturation pattern [31, 32, 37–40]. In addition to these typical bis-methylene-interrupted 5,9-unsaturated FA, some sponges also contained FA such as 20:2  $\Delta$ 5,11, 20:2  $\Delta$ 5,13, 20:2  $\Delta$ 7,13, 22:2  $\Delta$ 7,13 and 22:2  $\Delta$ 7,15 [31, 32]. These last FA were also reported mainly from molluscs and other invertebrates [41–56]. Marine invertebrates in the Bivalvia and Gastropoda groups usually contain NMID FA in large amounts [50]. Marine bivalve molluscs were shown to have active FA elongation and desaturation systems and to be able to synthesize the acids 22:2  $\Delta$ 7,13 and 22:2  $\Delta$ 7,15 from acetate de novo [51, 52].

A recent study reported on fatty acid composition of some tissues from the deep-sea hydrothermal vent tube-worm *Riftia pachyptila*, including 20:2 and 22:2 NMID at high levels (up to 13% of total FA) and from other vent organisms [55, 56]. These deep-sea organisms are now well known to contain chemosynthetic microbes such as sulphur-oxidising bacteria. Recently, GC–MS characterization of FA from marine aerobic anoxygenic phototrophic bacteria showed, high amounts of the very unusual octadeca-5,11-dienoic acid present in 9 of the 12 strains analyzed [57].

Rays usually have been thought to obtain nutrition solely from ingestion of photosynthetically-derived plant material, but it is now known that rays primarily feed on benthic invertebrates (molluscs, crustaceans, worms), and occasionally smaller fish [58–61].

However, the preferred prey varies with the species: in Rhinobatidae, *Rhinobatos cemiculus* feed on various benthic organisms including sponges, mollusks and crustaceans, but they also eat small fishes [62–64] but *Rhinobatos percellens* prefers crustaceans [64]. Rhinopteridae eat bottom-living mollusks, crustaceans and fishes [63] but *Rhinoptera marginata* is known to prefer mollusks with hard shells, mainly bivalves, and large crustaceans [63]. Dasyatidae feed on benthic invertebrates: bivalves, crustaceans and worms but they also eat teleosts [65]. Some rays crush their prey between their blunt teeth. Thus, the stingray (*Dasyatis*) is known to be an active hunter that finds its food supply among invertebrates, small crustaceans and molluscs [65]. Thus, it appears that the three species of fish studied in the present work can feed on a great variety of items, mostly benthic invertebrates. However Rhinobatidae and Dasyatidae are also known to eat fish while these enter rarely the diet of Rhinopteridae.

Thus, the presence of NMI FA likely indicates a dietary contribution from invertebrates. As noted above, it is also possible that identified NMID FA arise from a symbiotic relationship of bacteria with the host cells of marine invertebrates [57].

In further studies, it will be interesting to examine which lipid classes contain these NMI-FA and to examine their specific role more precisely. Is there a distribution of NMI FA in rays dependent on taxonomic position, and the season of harvest? In addition, it would be interesting to expand the range of marine animals investigated.

**Acknowledgments** Thanks are due to A. Ould Haouba (Nouakchott University, Mauritania) for administrative facilities and Z. Mint Sid’Oumou (Biology Department, Nouakchott University, Mauritania) for the collection and species identification, also to G. Nourrisson, Laboratory of Organic Synthesis, UMR 6513 CNRS, University of Nantes, France, for GC–MS experiments. Financial support by the French Government (Grant for MVEK from the Cooperation Ministry) is gratefully acknowledged.

## References

1. Fisher W, Bianchi G, and Scott WB (1981) FAO species identification sheets for fishery purposes: Eastern Central Atlantic fishing area. vol 1–7. Department of Fisheries and Oceans, Ottawa, Canada, p 34, 47
2. El Kebir MV, Mirallès J, Arabi S, Siau Y (1995) Exploitation of guitarfishes in Mauritania, E C Fisheries Cooperation. Fish Bull 8:15–17
3. Arts MT, Ackman RG, Holub BJ (2001) ‘Essential fatty acids’ in aquatic ecosystems: a crucial link between diet and human health and evolution. Can J Fish Aquat Sci 58:122–137
4. Connor WE (2000) Importance of n-3 fatty acids in health and disease. Am J Clin Nutr 71(Suppl. 1):171S–175S
5. von Schacky C, Angerer P, Kothny W, Theisen K, Mudra H (1999) The effect of dietary omega-3 fatty acids on coronary atherosclerosis. A randomized, double-blind, placebo-controlled trial. Ann Intern Med 130:554–562
6. Lapillonne A, Carlson SE (2001) Polyunsaturated fatty acids and infant growth. Lipids 36:901–911
7. Salem Jr N, Litman B, Kim H-Y, Gawrisch K (2001) Mechanisms of action of docosahexaenoic acid in the nervous system. Lipids 36:945–959
8. Diggle CP (2002) In vitro studies on the relationship between polyunsaturated fatty acids and cancer: tumour or tissue specific effects? Prog Lipid Res 41:240–253
9. Li D, Bode O, Drummond H, Sinclair AJ (2003) Omega-3 (n-3) fatty acids. In: Gunstone FD (ed) Lipids for functional foods and nutraceuticals. vol 13. The Oily Press, UK, pp 225–262
10. Calder PC, Burdge GC (2004) Fatty acids. In: Nicolaou A, Kokotos G (eds) Bioactive lipids. vol 17. The Oily Press, UK, pp 1–36
11. Stillwell W, Wassall SR (2003) Docosahexaenoic acid: membrane properties of a unique fatty acid. Chem Phys Lipids 126:1–27
12. Bergé JP, Barnathan G (2005) Fatty acids from lipids of marine organisms: molecular biodiversity, roles as biomarkers, biologically active compounds, and economical aspects, Adv Biochem Eng/Biotechnol 96. Springer, Heidelberg, pp 49–126
13. Maigret J, Ly B (1986) Les Poissons de Mer de la Mauritanie. Centre National de Recherches Océanographiques et des Pêches (CNROP). Ed. Compiègne, France, 213 pp
14. Njinkoué JM, Barnathan G, Mirallès J, Gaydou EM, Samb A (2002) Lipids and fatty acids in muscle, liver and skin of three edible fish from the Senegalese coast: *Sardinella maderensis*, *Sardinella aurita* and *Cephalopholis taeniops*, Comp. Biochem Physiol 131B:395–402
15. Compagno LJV (1977) Phyletic relationships of living sharks and rays. Amer Zool 17:303–322
16. Ould El Kebir MV, Barnathan G, Siau Y, Mirallès J, Gaydou EM (2003) Fatty acid distribution in muscle, liver and gonads of rays (*Dasyatis marmorata*, *Rhinobatos cemiculus* and *Rhinoptera marginata*) from the East tropical Atlantic Ocean. J Agric Food Chem 51:1942–1947
17. Wetherbee BM, Nichols PD (2000) Lipid composition of the liver oil of deep-sea sharks from the Chatham Rise, New Zealand. Comp Biochem Physiol 125B:511–521
18. Navarro-García G, Pacheco-Aguilar R, Vallejo-Cordova B, Ramirez-Suarez JC, Bolaños A (2000) Lipid composition of the liver oil of shark species from the Caribbean and Gulf of California waters. J Food Comp Anal 13:791–798
19. Jayasinghe C, Gotoh N, Wada S (2003) Variation in lipid classes and fatty acid composition of salmon shark (*Lamna ditropis*) liver with season and gender. Comp Biochem Physiol 134B:287–295
20. Navarro-García G, Pacheco-Aguilar R, Bringas-Alvarado L, Ortega-García J (2004) Characterization of the lipid composition

- and natural antioxidants in the liver oil of *Dasyatis brevis* and *Gymnura marmorata* rays. Food Chem 87:89–96
21. Pal D, Banerjee D, Patra TK, Patra A, Ghosh A (1998) Liver lipids and fatty acids of the sting ray *Dasyatis bleekeri* (Blyth). J Am Oil Chem Soc 75:1373–1378
  22. Navarro-García G, Bringas-Alvarado L, Pacheco-Aguilar R, Ortega-García J (2004) Oxidative resistance, carotenes, tocopherols and lipid profile of liver oil of the ray *Rhinoptera steindechneri*. J Food Comp Anal 17:699–706
  23. Fernández-Reiriz MJ, Pastoriza L, Sampedro G (1992) Lipid changes in muscle tissue of Ray (*Raja clavata*) during processing and frozen storage. J Agric Food Chem 40:484–488
  24. Fernández-Reiriz MJ, Pastoriza L, Sampedro G, Herrera JJ (1994) Effects of processing and ice storage on lipid classes and fatty acids of ray muscle (*Raja clavata*). Food Chem 51:95–98
  25. Smith MM, Heemstra PC (1986) Smith's sea fishes. Springer, Berlin, pp 599
  26. Talent LG (1985) The occurrence, seasonal distribution, and reproductive condition of elasmobranch fishes in Elkhorn Slough, California. Calif Fish Game 71:210–219
  27. Blaylock RA (1993) Distribution and abundance of the cownose ray, *Rhinoptera bonasus*, in lower Chesapeake Bay. Estuaries 16:255–263
  28. Bligh EG, Dyer W (1959) A rapid method of total lipid extraction and purification. Can J Biochem Physiol 37:911–917
  29. Wolff JP (1968) Manuel d'Analyse des Corps Gras. Azoulay, Paris, 524
  30. Andersson BA (1978) Mass spectrometry of fatty acid pyrrolidides. Progr. Chem Fats Other Lipids 16:279–308
  31. Christie WW, Brechany EY, Stefanov K, Popov S (1992) The fatty acids of the sponge *Dysidea fragilis* from the Black Sea. Lipids 27:640–644
  32. Nechev J, Christie WW, Robaina R, de Diego F, Popov S, Stefanov K (2004) Chemical composition of the sponge *Hymeniacidon sanguinea* from the Canary Islands. Comp Biochem Physiol 137A:365–374
  33. Bénistant C, Achard F, Ben Slama S, Lagarde M (1996) Docosapentaenoic acid (22:5n-3): metabolism and effect on prostacyclin production in endothelial cells. Prost Leukotr Essent Fatty Acids 55:287–292
  34. Kates M (1964) Bacterial lipids. Adv Lipid Res 2:17–90
  35. Kaneda T (1977) Fatty acids of the genus *Bacillus*: an example of branched-chain preference. Bacteriol Rev 41:391–418
  36. Bobbie RJ, White D (1980) Characterization of benthic microbial community structure by high-resolution gas chromatography of fatty acid methyl esters. Appl Environ Microbiol 39:1212–1222
  37. Djerassi C, Lam WK (1991) Sponge phospholipids. Acc Chem Res 24:69–75
  38. Carballeira NM, Pagan M, Rodriguez AD (1998). Identification and total synthesis of novel fatty acids from the Caribbean sponge *Calyx podatypa*. J Nat Prod 61:1049–1052
  39. Barnathan G, Kornprobst JM, Doumenq P, Mirallès J (1996) New unsaturated long-chain fatty acids in the phospholipids from the Axinellidae sponges *Trikenion loeve* and *Pseudaxinella cf. lunaecharta*. Lipids 31:193–200
  40. Barnathan G, Genin E, Nongonierma R, Al-Lihaibi S, Velosaotsy NE, Kornprobst JM (2003) Phospholipid fatty acids and sterols of two *Cinachyrella* from Saudi Arabia Red Sea. Comparative study with *Cinachyrella* sponges species from other origins. Comp Biochem Physiol 135B:297–308
  41. Ackman RG, Hooper SN (1973) Non-methylene-interrupted fatty acids in lipids of shallow-water marine invertebrates: a comparison of two molluscs (*Littorina littorea* and *Lunatia triseriata*) with the sand shrimp (*Crangon septempinosus*). Comp Biochem Physiol 46B:153–165
  42. Ackman RG (1990) Fatty acids. In: Ackman RG (ed) Marine biogenic lipids, fats and oils. vol 1. CRC Press Inc., Boca Raton, Florida, pp 103–137
  43. Ackman RG, Lamothe F (1990) Marine mammals. In: Ackman RG (ed) Marine biogenic lipids, fats and oils, vol 2. CRC Press Inc., Boca Raton, Florida, pp 179–381
  44. Klingensmith JS (1982) Distribution of methylene and nonmethylene-interrupted dienoic fatty acids in polar lipids and triacylglycerols of selected tissues of the Hardshell Clam (*Mercenaria mercenaria*). Lipids 17:976–981
  45. Fang J, Comet PA, Brooks JM, Wade TL (1993) Nonmethylene-interrupted fatty acids of hydrocarbon seep mussels: occurrence and significance. Comp Biochem Physiol 104B:287–291
  46. Pazos AJ, Sánchez JL, Román G, Luz Pérez-Parallé M, Abad M (2003) Seasonal changes in lipid classes and fatty acid composition in the digestive gland of *Pecten maximus*. Comp Biochem Physiol 134B:367–380
  47. Kraffe E, Soudant P, Marty Y (2004) Fatty acid composition of serine, ethanolamine and choline plasmalogens in some marine bivalves. Lipids 39:56–66
  48. Freites L, Fernández-Reiriz MJ, Labarta U (2002) Fatty acid profiles of *Mytilus galloprovincialis* (Lmk) mussel of subtidal and rocky shore origin. Comp Biochem Physiol 132B:453–461
  49. Abad M, Ruiz C, Martínez D, Mosquera G, Sánchez JL (1995) Seasonal variations of lipid classes and fatty acids in flat oyster, *Ostrea edulis*, from San Cibrán (Galicia, Spain). Comp Biochem Physiol 110C:109–118
  50. Zhukova NV, Svetashev VI (1986) Non-methylene-interrupted dienoic fatty acids in molluscs from the sea of Japan. Comp Biochem Physiol 83B:643–646
  51. Zhukova NV (1986) Biosynthesis of non-methylene-interrupted dienoic fatty acids from [<sup>14</sup>C] acetate in molluscs. Biochim Biophys Acta 878:131–133
  52. Zhukova NV (1991) The pathway of the biosynthesis of non-methylene-interrupted dienoic fatty acids in molluscs. Comp Biochem Physiol 100B:801–804
  53. Takagi T, Kaneniwa M, Itabashi Y, Ackman RG (1986) Fatty acids in Echinoidea: unusual *cis*-5-olefinic acids as distinctive lipid components in sea urchins. Lipids 21:558–565
  54. Howell KL, Pond DW, Billett DSM, Tyler PA (2003) Feeding ecology of deep-sea seastars (Echinodermata: Asteroidea): a fatty-acid biomarker approach. Mar Ecol Prog Ser 255:193–206
  55. Fullarton JG, Dando PR, Sargent JR, Southward AJ, Southward EC (1995) Fatty acids of hydrothermal vent *Ridgeia piscesae* and inshore bivalves containing symbiotic bacteria. J Mar Biol Ass UK 75:455–468
  56. Phleger CF, Nelson MN, Groce AK, Cary SC, Coyne KJ, Nichols PD (2005) Lipid composition of deep-sea hydrothermal vent tubeworm *Riftia pachyptila*, crabs *Munidopsis subsquamosa* and *Bythograea thermydron*, mussels *Bathymodiolus* sp. and limpets *Lepetodrilus* spp. Comp Biochem Physiol 141B:196–210
  57. Rontania JF, Christodoulou S, Koblizek M (2004) GC-MS structural characterization of fatty acids from marine aerobic anoxygenic phototrophic bacteria. Lipids 40:97–108
  58. Capapé C, Zaouli J (1979) Diet of two selachians common to the Gulf of Gabes (Tunisia): *Rhinobatos rhinobatos* (Linné, 1758) and *Rhinobatos cemiculus* (Geoffroy Sainte-Hilaire, 1817). Arch Inst Pasteur Tunis 56:285–306
  59. Abdel-Aziz SH, Khalil AN, Abdel-Maguid SA (1993) Food and feeding habits of the common guitarfish, *Rhinobatos rhinobatos* in the Egyptian Mediterranean waters. Indian J Mar Sci 22:287–290
  60. Wilga CD, Motta PJ (1998) Feeding mechanism of the Atlantic guitarfish *Rhinobatos lentiginosus*: modulation of kinematic and motor activity. J Exp Biol 201:3167–3183



61. Ebert DA, Cowley PD (2003) Diet, feeding behaviour and habitat utilization of the blue stingray *Dasyatis chrysonota* (Smith, 1828) in Southern African waters. *Mar Freshw Res* 54:957–965
62. Whitehead PJP, Bauchot M-L, Hureau J-C, Nielsen J, Tortonese E (1986) Fishes of the North–Eastern Atlantic and the Mediterranean. *Copeia* 1:266–267
63. Quéro JC, Hureau J-C, Karrer C, Post A, Saldanha L (1990) Checklist of the fishes of the Eastern tropical Atlantic. Junta Nacional de Investigação Científica e Tecnológica, Lisbon, SEI, UNESCO, Paris, Springer 2(2), pp 182–184
64. Shibuya A, de Souza Rosa R, Soares MC (2005) Note on the diet of the guitarfish *Rhinobatos percellens* (Walbaum (Elasmobranchii, Rhinobatidae) from the coast of Paraíba, Brazil. *Acta Biologica Leopoldensia* 27:63–64
65. Capapé C, Zaouali J (1992) The diet of the marbled stingray *Dasyatis marmorata* (Pisces, Dasyatidae) from Tunisian waters (Fr.). *Vie Milieu Paris* 42:269–276

# Authenticating Production Origin of Gilthead Sea Bream (*Sparus aurata*) by Chemical and Isotopic Fingerprinting

Douglas J. Morrison · Tom Preston · James E. Bron ·  
R. James Hemderson · Karen Cooper · Fiona Strachan ·  
J. Gordon Bell

Received: 9 February 2007 / Accepted: 16 March 2007 / Published online: 27 April 2007  
© AOCS 2007

**Abstract** Recent EU legislation (EC/2065/2001) requires that fish products, of wild and farmed origin, must provide consumer information that describes geographical origin and production method. The aim of the present study was to establish methods that could reliably differentiate between wild and farmed European gilthead sea bream (*Sparus aurata*). The methods that were chosen were based on chemical and stable isotopic analysis of the readily accessible lipid fraction. This study examined fatty acid profiles by capillary gas chromatography and the isotopic composition of fish oil ( $\delta^{13}\text{C}$ ,  $\delta^{18}\text{O}$ ), phospholipid choline nitrogen ( $\delta^{15}\text{N}$ ) and compound specific analysis of fatty acids ( $\delta^{13}\text{C}$ ) by isotope ratio mass spectroscopy as parameters that could reliably discriminate samples of wild and farmed sea bream. The sample set comprised of 15 farmed and 15 wild gilthead sea bream (*Sparus aurata*), obtained from Greece and Spain, respectively. Discrimination was achieved using fatty acid compositions, with linoleic acid (18:2n-6), arachidonic acid (20:4n-6), stearic acid (18:0), vaccenic acid (18:1n-7) and docosapentaenoic acid (22:5n-3) providing the highest contributions for discrimination. Principle components analysis of the data set highlighted good discrimination between wild and farmed fish. Factor 1 and 2 accounted for >70% of the variation in

the data. The variables contributing to this discrimination were: the fatty acids 14:0, 16:0, 18:0, 18:1n-9, 18:1n-7, 22:1n-11, 18:2n-6 and 22:5n-3;  $\delta^{13}\text{C}$  of the fatty acids 16:0, 18:0, 16:1n-7, 18:1n-9, 20:5n-3 and 22:6n-3; Bulk oil fraction  $\delta^{13}\text{C}$ ; glycerol/choline fraction bulk  $\delta^{13}\text{C}$ ;  $\delta^{15}\text{N}$ ; % N; % lipid.

**Keywords** Sea bream · Product authentication · Fatty acid compositions · Isotope ratio mass spectrometry (IRMS) · Flesh oil  $\delta^{13}\text{C}$  · Flesh oil  $\delta^{18}\text{O}$  · Glycerol choline fraction  $\delta^{15}\text{N}$  · Principal components analysis

## Introduction

The global demand for finfish and shellfish is increasing in line with the demands of increasing global populations. However, the food-grade capture fisheries have reached, or exceeded, their sustainable limits and increasingly the shortfall in supply must be met by aquaculture produce [1, 2]. While landings from capture fisheries are static, aquaculture production worldwide is increasing at around 10% per annum [2] and for this reason much more aquaculture produce is currently available to consumers. Currently, more than 30% of world seafood production is derived from aquaculture and this is likely to increase in the future [2].

Within the production chain, similar fish products can arise from different points of origin and there is consequently potential for fraud due to product mislabelling. As a result, in October 2002, the EC issued Commission regulation no. 2065/2001 to ensure that more details on labelling, packaging and traceability of fishery and aquaculture products would be available to retailers and consumers. The reason for this additional legislation is to

D. J. Morrison (✉) · T. Preston · K. Cooper  
Stable Isotope Biochemistry Laboratory,  
Scottish Universities Environmental Research Centre (SUERC),  
Rankine Avenue, Scottish Enterprise Technology Park,  
East Kilbride G75 0QF, UK  
e-mail: D.Morrison@suerc.gla.ac.uk

J. E. Bron · R. J. Hemderson · F. Strachan · J. G. Bell  
Institute of Aquaculture, University of Stirling,  
Stirling FK9 4LA, UK

provide more and clearer information to retailers and consumers who are currently more aware of the food they eat and the consequences of different food production methods on nutritional quality and safety.

A number of recent reports have suggested that farmed salmon may contain higher levels of persistent organic contaminants, such as dioxins and PCBs [3], although the levels were well within the accepted range [4]. However, there is considerable evidence that suggests the benefits of eating fish, particularly oily fish, significantly outweigh any perceived risks [5, 6]. Highly unsaturated fish oils, and eicosapentaenoic acid (20:5n-3; EPA) in particular, are under clinical investigation to determine their therapeutic benefit in immunomodulated disease [7–10]. However, while the anti-inflammatory effects of EPA are well documented the functional activity of docosahexaenoic acid (22:6n-3; DHA) is also vital for normal cellular function. DHA is required for the normal growth and development of neural tissue in infants and is also essential for maintaining normal brain function in adults [11]. The importance of DHA is evidenced by the fact that over 20% of the brain dry weight is DHA and this is the most abundant fatty acid in neural tissues [12, 13]. As well as being linked with brain function, DHA deficiencies are also linked to reduced visual acuity, attention deficit hyperactivity disorder, cystic fibrosis, unipolar and bipolar depression, aggression and dysfunctions of the immune system [4, 14, 15].

In addition, the fishmeal and fish oil which have been used by the aquaculture industry as the basis of aquafeed formulations for over 30 years have reached limits of sustainable production [16] and new sustainable raw materials are now being tested and introduced in commercial aquafeeds. However, while the use of plant-derived raw materials can reduce the concentrations of organic contaminants in fish [17, 18] the concentrations of beneficial n-3 highly unsaturated fatty acids (HUFA), particularly EPA and docosahexaenoic acids (22:6n-3; DHA), are reduced as the cheaper vegetable oils likely to be used do not contain these n-3 HUFA [19]. Thus, farmed fish, cultured on diets containing lower levels of marine-derived raw materials, may have different lipid compositions compared with fish from wild capture fisheries [20, 21].

The present study examined whether farmed and wild gilthead sea bream (*Sparus aurata*) could be discriminated, in terms of their production origin, using a range of analytical measurements that have the potential to discriminate source terms, on flesh samples including fatty acid composition,  $\delta^{13}\text{C}$  of individual fatty acids,  $\delta^{13}\text{C}$  and  $\delta^{18}\text{O}$  of total flesh oil and  $\delta^{15}\text{N}$  of the choline fraction of phospholipid.

**Table 1** Source and average weight gilthead sea bream

Species	Source	Country of origin	Average weight (g)
Farmed sea bream	Bernard Corrigan Ltd <sup>a</sup>	Greece	545
Wild sea bream	University of Cadiz <sup>b</sup>	Spain	192

<sup>a</sup> Bernard Corrigan Ltd, Glasgow (Fish wholesaler) <http://www.bernardcorrigan.com>

<sup>b</sup> Professor Gabriel Mourente, Dept. de Biologia, University of Cadiz, caught by gill netting in the Bay of Cadiz

## Methods

### Samples

Farmed sea bream from Greece were supplied by Bernard Corrigan Ltd, Glasgow. Samples of wild sea bream were caught by gill net in the Bay of Cadiz in Spain and were supplied by Prof. Gabriel Mourente of the University of Cadiz. Details of the fish analysed in this survey are given in Table 1.

### Sample Preparation and Extraction of Lipids

The compositional and isotopic analyses were performed on the oil fraction obtained from sea bream flesh after evisceration using 0.88% KCl, filtration and extraction using isohexane:isopropanol (3:2 v/v). The lipid content (% lipid) was determined by the weight of oil extracted from a known weight of fish flesh. The flesh oil fraction was used to determine stable isotope ratios for  $^{18}\text{O}/^{16}\text{O}$  and  $^{13}\text{C}/^{12}\text{C}$  by elemental analyser-pyrolysis-isotope ratio mass spectrometry (EA-Py-IRMS) and elemental analyser-combustion-isotope ratio mass spectrometry (EA-IRMS [22]), respectively.  $^{15}\text{N}/^{14}\text{N}$  was determined on a concentrated glycerol/choline fraction by EA-IRMS. The glycerol/choline fraction was prepared by mixing 2–5 g of flesh oil with 50 ml of 1M KOH in ethanol followed by reflux extraction for 2 h at 100 °C. After cooling and addition of 25 ml distilled water the solution was acidified to ~pH 1 by dropwise addition of 37% (w/v) HCl. Twenty milliliter of distilled water was added to dissolve KCl salts and following four washes with 25 ml of cyclohexane the aqueous phase was dried by rotary evaporation at 50 °C. The resulting glycerol/choline was dissolved in 30 ml ethanol, filtered and washed with small amounts of ethanol and dried first by rotary evaporation and then for 1 h at 70 °C under vacuum. The sample was further dried under a stream of nitrogen for 1 h before the weight of the glycerol/choline fraction was determined. A portion of the oil fraction was saponified and the free fatty acids transmethylated to produce fatty acid methyl esters (FAMES),

which were analysed for fatty acid content by GC and  $^{13}\text{C}$  abundance by GC combustion IRMS (GC-C-IRMS).

#### Fatty Acid Analysis by GC

Fatty acid methyl esters (FAMES) were prepared from a small quantity (50–100 mg) of the dried flesh oil by alkali-catalysed transmethylation. Briefly, the oil was placed in a test tube with 2 ml of iso-hexane and 0.2 ml of 2M KOH in methanol. After shaking for 2 min the tube was centrifuged for 5 min at 1,000×g. One milliliter of the upper phase was removed and made to 10 ml with methanol in a volumetric flask. One milliliter of this diluted solution was mixed with 4  $\mu\text{L}$  of 200 g/mL butylated hydroxytoluene (internal standard) in iso-hexane in a GC vial. The sample was then ready for injection on the GC. FAMES were separated and quantified by gas chromatography (GC) in the presence of an internal standard. Separation of fatty acids and detection by flame ionisation detection (FID) was developed to quantify the composition of FAME in the fish lipid extracts on a percentage weight basis. FAMES were separated and quantified by GC using a Thermo Finnigan Trace 2000 GC (Thermoquest, Hemel Hempstead, UK) equipped with a fused silica capillary column (Chrompack CPWAX52CB, 30 m  $\times$  0.32  $\mu\text{m}$   $\times$  0.25 mm i.d.; Chrompak, London, UK) using hydrogen as carrier gas (2.0 ml/min constant flow mode) and detected by FID at 250 °C. The GC temperature program was: initial temperature: 50 °C, ramp 1: 40 °C/min to 150 °C, ramp 2: 2 °C/min to 225 °C, hold for 5 min at 225 °C. Cold on column injection was used (1  $\mu\text{L}$  of 1 mg/mL in iso-hexane). Thirteen peaks, identified as contributing to >95% of the FAME weight, were used. These were: 14:0, 16:0, 16:1, 18:0, 18:1n-7, 18:1n-9, 18:2n-6, 20:1n-9, 20:4n-6, 20:5n-3, 22:1n-11, 22:5n-3 and 22:6n-3. The identification was carried out in comparison to a standard solution composed of 12 of the above FAME (without 20:4n-6) in equal weights. The standard solution was a custom preparation from Supelco Inc. (Bellafonte, PA, USA).

#### Bulk IRMS Analysis of Fish Lipid Components

Isotope ratios ( $^{13}\text{C}/^{12}\text{C}$ ,  $^{18}\text{O}/^{16}\text{O}$ ,  $^{15}\text{N}/^{14}\text{N}$ ) determined by IRMS are expressed on a relative scale as the deviation, referred to in delta ( $\delta$ ) units with the notation ‰, parts per thousand or per mil with respect to the isotope ratio content of an international standard,  $R_{\text{std}}$ . The primary references standards are VSMOW (Vienna—standard mean ocean water) for  $\delta^{18}\text{O}$ ‰, PDB (Pee Dee Belemnite, a calcium carbonate) for  $\delta^{13}\text{C}$ ‰, and air for  $\delta^{15}\text{N}$ ‰. These international standards, or secondary standards calibrated against the primary standards, are produced and certified by the International Atomic Energy Agency (IAEA) in Vienna.

This  $\delta$  notation is routinely used by laboratories working in food and beverage authenticity using isotopic measurements by IRMS. The deviation of a measured isotope ratio from the ratio of a calibrated standard is given by

$$\delta_i [\text{‰}] = \left[ \frac{R_i}{R_{\text{std}}} - 1 \right] \times 1000$$

where  $R_i = ^{13}\text{C}/^{12}\text{C}$ ,  $^{18}\text{O}/^{16}\text{O}$ , or  $^{15}\text{N}/^{14}\text{N}$

Fish oil ( $\delta^{13}\text{C}$  and  $\delta^{18}\text{O}$ ), glycerol/choline ( $\delta^{13}\text{C}$  and  $\delta^{15}\text{N}$ ) and free fatty acids ( $\delta^{13}\text{C}$ ), produced from the oil fraction were analysed for their isotopic fingerprint.  $\delta^{13}\text{C}$  and  $\delta^{15}\text{N}$  provide information on the diet of the fish and the  $\delta^{18}\text{O}$  affords information on the geographical environment of the fish.

#### $\delta^{13}\text{C}$ and $\delta^{15}\text{N}$ Determinations

$\delta^{13}\text{C}$  (‰) and  $\delta^{15}\text{N}$  (‰) were measured separately using an elemental analyser (Carlo Erba 1500 N) coupled to an isotope ratio mass spectrometer (IRMSr; ThermoFinnigan, TracerMAT). Samples were weighed into tin capsules (4  $\times$  8 mm; Elemental Microanalysis, Okehampton, UK) and these were dropped automatically into the ‘‘hot-zone’’ of the reactor where they were oxidised at a temperature of 1,060 °C in a quartz reactor. The combustion gases ( $\text{CO}_2$ ,  $\text{H}_2\text{O}$ ,  $\text{NO}_x$ ) were swept by a flow of helium carrier gas through a bed of chromium oxide and silvered cobalt oxide granules. Nitrogen oxides were reduced to  $\text{N}_2$  over a bed of reduced copper wires, held at 650 °C and water vapour was removed by a chemical trap containing magnesium perchlorate, and, for nitrogen analysis,  $\text{CO}_2$  was removed using a carbosorb trap. The combustion gases then passed through a packed GC column filled with Porapak Q to separate  $\text{N}_2$  from  $\text{CO}_2$ . A portion of the effluent was allowed to flow into the ion source of the IRMSr. For  $\delta^{13}\text{C}$  determinations, the ratio of the ions at mass to charge ratio ( $m/z$ ) 45 ( $^{13}\text{C}^{16}\text{O}^{16}\text{O}$ ) to the ions at  $m/z$  44 ( $^{12}\text{C}^{16}\text{O}^{16}\text{O}$ ) in  $\text{CO}_2$  was determined (including correction for the contribution of  $^{17}\text{O}$  at  $m/z$  45; the Craig correction [23]) by comparison with a calibrated reference of known  $\delta^{13}\text{C}$  value. The working standard used was menhaden oil ( $\delta^{13}\text{C} = -24.96$ ‰; Sigma-Aldrich, Poole, UK), which was span-calibrated against international reference materials IAEA CH6 and CH7 [24].

For  $\delta^{15}\text{N}$  determinations the ratio of the ions at  $m/z$  29 ( $^{15}\text{N}^{14}\text{N}$ ) to the ions at  $m/z$  28 ( $^{14}\text{N}^{14}\text{N}$ ) in  $\text{N}_2$  was determined by comparison with a calibrated reference of known  $\delta^{15}\text{N}$  value. The working standard used was ammonium sulphate ( $\delta^{15}\text{N} = -0.86$ ‰; BDH, UK), which had been span calibrated against the international reference materials IAEA N1 and N2 [24]. The nitrogen content of the sample (% N) was determined by weighing the samples when

dispensed into tin capsules and relating the absolute amount of nitrogen (calculated from the nitrogen peak area relative to the ammonium sulphate standard of known nitrogen content) to the amount of sample.

### $\delta^{18}\text{O}$ IRMS Determinations

Samples were weighed into silver capsules ( $4 \times 6$  mm; Elemental Microanalysis, Okehampton, UK) and these are dropped automatically into the “hot-zone” of the reactor where they were pyrolysed at a temperature of  $1,080^\circ\text{C}$  in a quartz reactor (Carlo Erba, 1500N). The pyrolysis gases ( $\text{CO}$ ,  $\text{H}_2$ ,  $\text{N}_2$ ) were swept by a flow of helium carrier gas through a bed of nickelised carbon grit (50% nickel). The pyrolysis gases then passed through a carbosorb/magnesium perchlorate trap to remove traces of  $\text{CO}_2$  and water respectively and thereafter through a packed  $50\text{ cm} \times 6\text{ mm}$  ID GC column filled with molecular sieves of  $5\text{ \AA}$  held at  $30^\circ\text{C}$  to separate  $\text{H}_2$ ,  $\text{N}_2$ , and  $\text{CO}$ . A portion of the effluent was allowed to flow into the ion source of the IRMSr (ThermoFinnigan, TracerMAT) and the  $^{18}\text{O}/^{16}\text{O}$  ratio of  $\text{CO}$  was used to determine  $\delta^{18}\text{O}$ .  $\text{N}_2$  was clearly resolved from  $\text{CO}$ .

The ratio of the ions at  $m/z$  30 ( $^{12}\text{C}^{18}\text{O}$ ) to the ions at  $m/z$  28 ( $^{12}\text{C}^{16}\text{O}$ ) was determined by comparison with a calibrated working standard (menhaden oil,  $\delta^{18}\text{O}$  16.85‰ vs. VSMOW) which had been calibrated against a secondary international standard (IAEA CH6,  $\delta^{18}\text{O}$  36.4 vs. VSMOW). Preliminary work revealed a strong matrix specific effect which resulted in drift of the measured  $\delta^{18}\text{O}$  values throughout the analytical cycle, which was not apparent and could not be easily corrected for when using a carbohydrate standard (glucose  $\delta^{18}\text{O}$ , 29.32‰ vs. VSMOW). The use of a matrix standard allowed correction for this drift in addition to the normal drift correction, specific to the IRMSr. Samples were drift and linearity corrected against laboratory standards that were interspersed throughout the analytical cycle [25].

### $\delta^{13}\text{C}$ (‰) GC-C-IRMS Determinations of Individual Fatty Acids

FAMES were analysed by GC-C-IRMS to derive  $\delta^{13}\text{C}$  of the free fatty acids. Briefly, this technique uses gas chromatography to separate individual analytes in a continuous stream of helium, which passes through a combustion interface (to convert all analyte carbon to  $\text{CO}_2$ ) and subsequent analysis of ions  $m/z$  44, 45 and 46 in an IRMSr. Samples were analysed on an Isochrom III GC-C-IRMS system (GV Instruments, Manchester, UK). Briefly, the instrument consisted of an Agilent 6890 gas chromatograph coupled to an isotope ratio mass spectrometer, through a combustion interface. The gas chromatograph was

operated in splitless injection mode and was installed with a capillary column (Zebron ZB-Wax,  $30\text{ m} \times 0.32\text{ }\mu\text{m} \times 0.25\text{ mm}$  i.d.; Phenomenex, UK) to effect analyte separation. The injector temperature was  $250^\circ\text{C}$  and the carrier gas (helium) was controlled to maintain a constant column flow of  $2\text{ ml/min}$ . The GC operating conditions were as follows: initial temperature of  $80^\circ\text{C}$  held for  $4\text{ min}$ , ramp  $7.5^\circ\text{C/min}$  to  $150^\circ\text{C}$ , ramp  $2^\circ\text{C/min}$  to  $225^\circ\text{C}$ , hold  $5\text{ min}$ . The column flow was directed to a FID, via the heart-split valve (a pressure balanced micro-needle valve for directing column flow to either FID or IRMS), until the bulk of the solvent peak had eluted. The heart-split valve was closed to direct the column flow through the combustion interface, held at  $350^\circ\text{C}$ , and through the combustion furnace. The combustion furnace was made of similar materials as the oxidative furnace for bulk  $^{13}\text{C}$  analysis but of  $0.5\text{ mm}$  bore. It was held at  $800^\circ\text{C}$ . Downstream from the combustion furnace was the open split, where a portion of the gas stream was allowed to enter the IRMSr capillary. A cryogenic trap was operated ( $-100^\circ\text{C}$ , liquid  $\text{N}_2$ ), between the open split and the IRMS, to remove water from the carrier stream. The IRMS continuously monitored ions of  $m/z$  44, 45 and 46 and the proprietary software (Isochrom, GV instruments, UK) was used to integrate the major and minor peak areas with appropriate corrections for background and isotopic shift.

An internal standard [pentadecanoic acid (C15:0); Sigma-Aldrich, Poole, Dorset] was used as both chemical and isotopic standard. A portion of the standard was derivatised using acid catalysed transmethylation and the free fatty acid (FFA) and FAME form were analysed by bulk EA-IRMS (Costech EA—ThermoFinnigan, Delta XP) to determine  $\delta^{13}\text{C}$  and from the data,  $\delta^{13}\text{C}$  of the methyl carbon added by derivatisation by mass balance. Span calibration [24] against the international standards IAEA CH6 and IAEA CH7 resulted in  $\delta^{13}\text{C}$  FFA =  $-34.3\text{‰}$  and  $\delta^{13}\text{C}$  FAME =  $-34.94\text{‰}$  producing a derived  $\delta^{13}\text{C}$  =  $-44.53\text{‰}$  for methanol used in derivatisation. The methanol used for this calibration was also the same methanol used in all transmethylation reactions. Ten microliter of  $20\text{ mM}$  internal standard in isooctane were added to each  $100\text{ }\mu\text{L}$  of sample and samples were diluted to attain  $1\text{ mg FAME/mL}$  solvent.  $0.5\text{ }\mu\text{L}$  of analyte mix was injected, equivalent to  $200\text{ pMol}$  of C15:0 on column. Over a mean area ratio range of sample to internal standard of  $1.1\text{--}0.4$  (max  $1.62$ , min  $0.22$ ), a precision of  $0.3\text{‰}$  was attained ( $n = 12$ ). Over the area ratio range  $0.3\text{--}0.1$  (max  $0.4$ , min  $0.1$ ), a precision of  $1.2\text{‰}$  was attained. In practice, peaks with an area ratio of  $<0.2$  were not reliably quantifiable in terms of peak area and therefore in terms of isotopic composition. Samples were linearity corrected as previously described [25].

Statistical analysis: parameters were analysed by ANOVA with post-hoc analysis to determine parameters of

significant difference between wild and farmed sea bream. Principal components were conducted using the XLSTAT add-in for Microsoft Excel (Addinsoft France, Paris, France).

## Results

Wild sea bream had a significantly lower lipid content than farmed sea bream ( $P < 0.01$ ) with a concomitant higher nitrogen content in wild sea bream compared with farmed sea bream ( $P < 0.01$ ). A bivariate plot of the compositional data yielded discrimination simply on lipid and nitrogen content (Fig. 1). In terms of the fatty acid profiles, farmed sea bream contained significantly more 14:0, 16:1n-7, 20:1n-9, 22:1n-11, 18:2n-6, 20:5n-3 and 22:6n-3 but significantly less 16:0, 18:0, 18:1n-9, 18:1n-7 and 20:4n-6 compared with wild sea bream (Table 2). Wild sea bream contained significantly higher levels of 20:4n-6 and significantly lower levels of 18:2n-6 compared with their farmed counterparts. In addition, the wild fish contained higher 16:0 and 18:1n-9. The isotopic data showed that free fatty acid  $\delta^{13}\text{C}$  exhibited significant differences in  $\delta^{13}\text{C}$  values in 16:0, 18:0, 16:1n-7, 18:1n-9 and 18:1n-7 between farmed and wild sea bream (Fig. 2). Bulk  $\delta^{13}\text{C}$  analysis of the total oil fraction (Fig. 3) and glycerol/choline fraction (Fig. 4) yielded highly significant differences with farmed fish lighter than wild fish. Significant differences were also observed in the nitrogen content (Fig. 5) and  $\delta^{15}\text{N}$  (Fig. 6) of farmed versus wild sea bream. Analysis of  $\delta^{18}\text{O}$  from total oil extracted from flesh lipid of sea bream exhibited significant differences between farmed and wild sea bream (Fig. 7).

Principal components analysis (PCA) was used to examine the multivariate structure of the bream data set. Table 3 demonstrates that the first two factors account for over 70% of the variability within the data, with Table 4 indicating the contribution of the variables to the selected

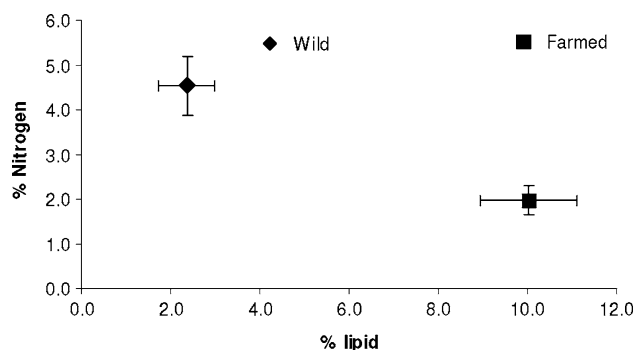


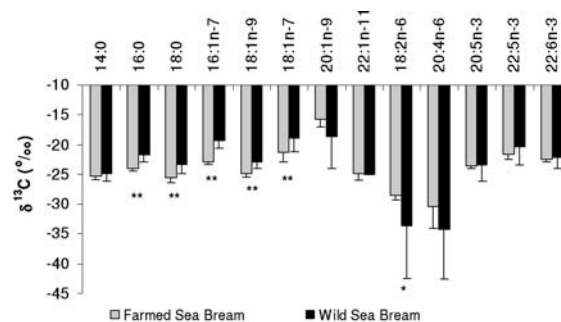
**Fig. 1** Bivariate plot of mean (and standard deviation) lipid versus nitrogen (choline) content of wild and farmed sea bream

**Table 2** Selected fatty acid compositions (weight % of total fatty acids) of farmed and wild gilthead sea bream flesh

Fatty acid	Farmed	Wild	<i>P</i> value
14:0	5.5 ± 0.1	2.7 ± 0.3	<0.0001
16:0	17.4 ± 0.2	24.9 ± 0.7	< 0.0001
18:0	3.2 ± 0.2	8.4 ± 0.3	<0.0001
16:1n-7	8.3 ± 0.1	7.7 ± 0.6	0.0007
18:1n-9	18.8 ± 0.6	25.3 ± 3.0	<0.0001
18:1n-7	3.2 ± 0.1	3.5 ± 0.3	0.001
20:1n-9	2.8 ± 0.1	1.1 ± 0.1	<0.0001
22:1n-11	2.6 ± 0.1	0.2 ± 0.1	<0.0001
18:2n-6	8.0 ± 0.0	1.0 ± 0.2	<0.0001
20:4n-6	0.8 ± 0.0	4.3 ± 1.0	<0.0001
20:5n-3	4 ± 0.1	6.5 ± 1.1	<0.0001
22:5n-3	4.2 ± 0.1	4.0 ± 0.7	NS
22:6n-3	15.9 ± 0.4	10.3 ± 1.5	<0.0001

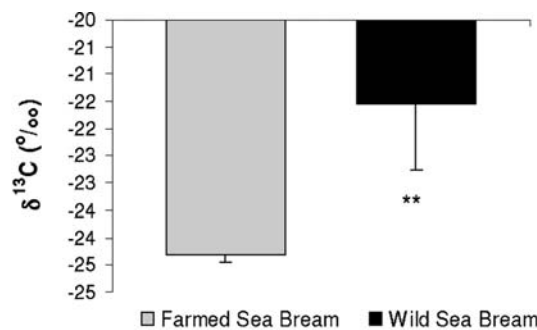
Values are mean ± SD,  $n = 15$

NS not significant ( $P > 0.05$ ) as determined by Student's *t* test (two-tailed, paired samples)



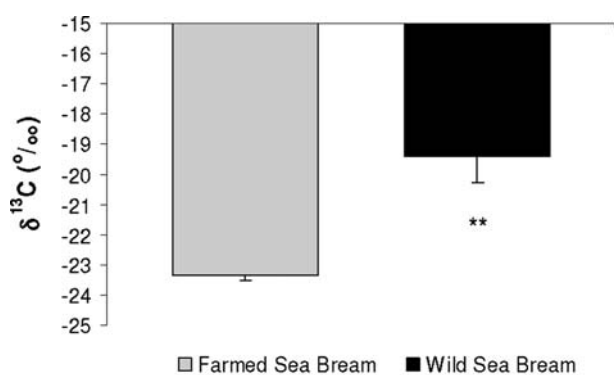
Columns assigned either one or two asterisks are significantly different between farmed and wild samples ( $P < 0.05$  and  $0.01$ , respectively).

**Fig. 2** Compound specific  $\delta^{13}\text{C}$  analysis of fatty acids from farmed and wild sea bream determined by GC-C-IRMS of flesh lipid



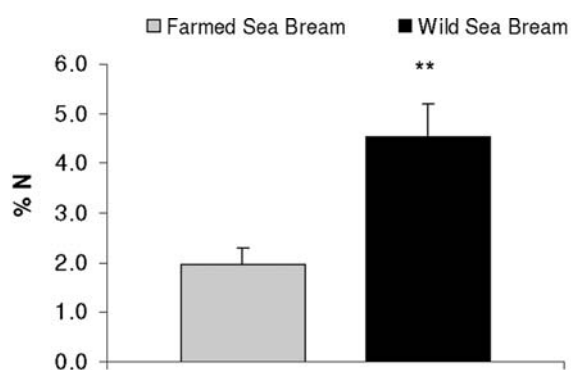
Column assigned \*\* signifies a significant difference between farmed and wild samples ( $P < 0.05$ ).

**Fig. 3**  $\delta^{13}\text{C}$  of the bulk oil fraction from total lipid extracted from flesh of wild and farmed sea bream determined by EA-IRMS



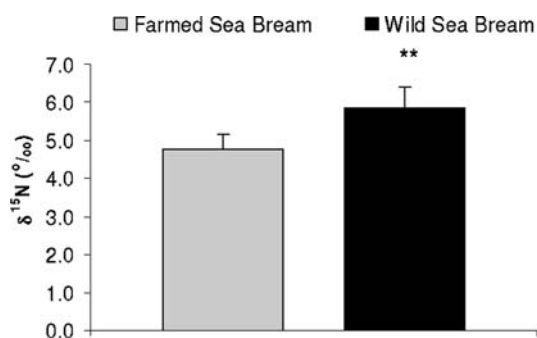
Column assigned \*\* signifies a significant difference between farmed and wild samples ( $P < 0.05$ ).

**Fig. 4**  $\delta^{13}\text{C}$  of glycerol/choline concentrated from flesh lipid extract in wild and farmed sea bream determined by EA-IRMS



Column assigned \*\* signifies a significant difference between farmed and wild samples ( $P < 0.05$ ).

**Fig. 5** Percentage nitrogen (% N) determined by weight from N analysis of the concentrated glycerol/choline fraction of wild and farmed sea bream by EA-IRMS



Column assigned \*\* signifies a significant difference between farmed and wild samples ( $P < 0.05$ ).

**Fig. 6**  $\delta^{15}\text{N}$  of the glycerol/choline fraction concentrated from flesh lipid extract of wild and farmed sea bream determined by EA-IRMS

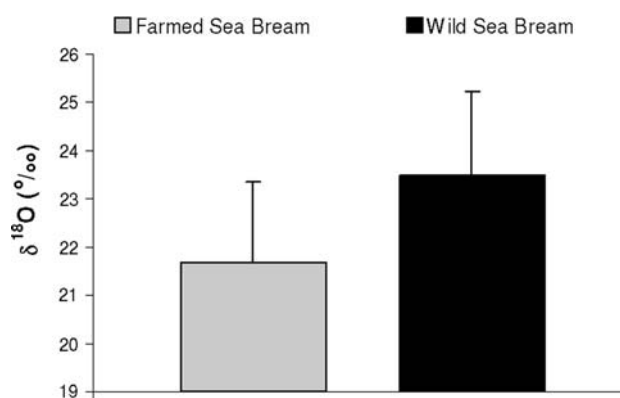


**Fig. 7**  $\delta^{18}\text{O}$  of total lipid extract from flesh of wild and farmed sea bream determined by EA-pyrolysis-IRMS

**Table 3** Table of eigenvalues for principle components analysis (PCA) of chemical and isotopic data from sea bream

	Eigenvalue	Variability (%)	Cumulative eigenvalue	Cumulative (%)
F1	15.63	55.84	15.63	55.84
F2	5.21	18.60	20.84	74.44
F3	1.81	6.45	22.65	80.89
F4	1.23	4.38	23.88	85.27
F5	0.99	3.52	24.86	88.79
F6	0.92	3.28	25.78	92.07
F7	0.49	1.76	26.27	93.84

factors. Plots of Factor 1 versus Factors 2, 3 and 4 all demonstrate clear separation of wild and farmed bream with factor 1 providing greatest discrimination (Fig. 8).

## Discussion

Recent EU legislation has dictated that the production origin of food must be clearly and verifiably defined for the consumer. The increase in aquaculture production to meet consumer demand for finfish has resulted in a number of farmed species entering the marketplace in the last decade. This includes gilthead sea bream (*Sparus aurata*). Gilthead sea bream were first cultured in Italy in 1970. Production has grown steadily over the past two decades with 2004 production reaching 91,000 metric tonnes with Greece, Turkey and Spain being the major producers [2]. The temptation to label farmed fish as wild fish by unscrupulous fish merchants, retailers and restaurateurs is significant because of the price premium commanded by wild fish. In order to combat such mislabelling and conform with the legislation, verifiable methods of distinguishing farmed from wild fish are required for consumer confidence and for local authority enforcement purposes. This study

**Table 4** Factor loadings for bream PCA

Variable	F1	F2
14:0	<b>-0.946</b>	0.149
16:0	<b>0.914</b>	-0.337
18:0	<b>0.955</b>	-0.260
18:1n-9	<b>0.705</b>	-0.665
18:1n-7	<b>0.805</b>	0.079
22:1n-11	<b>-0.969</b>	0.229
18:2n-6	<b>-0.925</b>	0.340
22:5n-3	0.347	<b>0.797</b>
16:0 $\delta^{13}\text{C}$	<b>0.923</b>	0.315
18:0 $\delta^{13}\text{C}$	<b>0.826</b>	0.401
16:1n-7 $\delta^{13}\text{C}$	<b>0.966</b>	0.163
18:1n-9 $\delta^{13}\text{C}$	<b>0.867</b>	0.360
20:5n-3 $\delta^{13}\text{C}$	0.227	<b>0.796</b>
22:6n-3 $\delta^{13}\text{C}$	0.300	<b>0.804</b>
Bulk $\delta^{13}\text{C}$	<b>0.931</b>	0.240
G/C bulk $\delta^{13}\text{C}$	<b>0.982</b>	0.019
$\delta^{15}\text{N}$	<b>0.706</b>	-0.396
% N	<b>0.949</b>	-0.049
% lipid	<b>-0.964</b>	0.125

Bold type indicates loadings > 0.7 and < -0.7

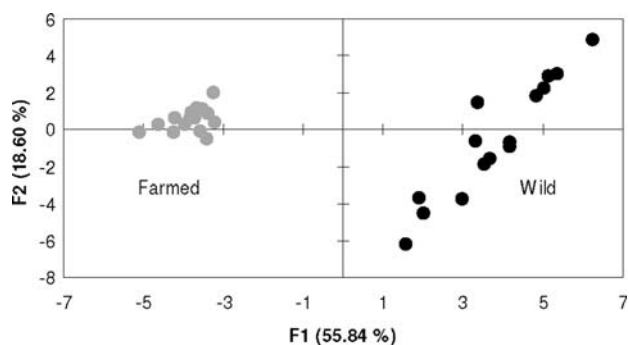


**Fig. 8** Principle component analysis (PCA) plot of combined chemical and isotopic data measured from farmed and wild sea bream. Factor 1 and 2 combined account for 74.4% of the variation between data sets and afford discrimination of production origin

establishes the utility of chemical and isotopic fingerprinting as robust methodologies for distinguishing the production origin of gilthead sea bream (*Sparus aurata*).

Analysis of the fatty acid composition showed marked differences in the lipid profiles and lipid content of the fish. Farmed fish contained significantly more lipid (~5-fold more lipid) as a fraction of flesh composition. This may partly be due to the larger average weight of the farmed bream, although, while larger fish generally accumulate more flesh lipid it is also the case that wild fish are generally leaner than their farmed counterparts [26, 27]. Farmed fish also exhibited a lower nitrogen content com-

pared with wild fish. The lower nitrogen content cannot be simply explained by the dilution effect of higher lipid content and probably reflects a lower phosphatidylcholine:triacylglycerol ratio in farmed fish and a higher protein content of wild fish due to greater muscle mass. The fatty acid composition reflected the dietary sources of, particularly polyunsaturated fatty acids. The n-3/n-6 ratio was higher for wild fish compared with farmed fish [4.0 (0.4) vs. 3.4 (0.1)] although there were marked differences in the n-3 and n-6 profiles between production origin reflecting dietary intake of plant-derived 18:2n-6 and marine fish oil-derived 22:6n-3 in farmed fish and marine derived 20:4n-6 in wild fish. The commercial diet formulations for sea bream utilise a range of marine and terrestrial products. The terrestrial products can include soybean, wheat, maize, sunflower, pea, lupin and rapeseed meals, which can contain a significant lipid component [28]. The plant lipid, either from the plant meals described above or added directly as vegetable oil, explains the higher levels of 18:2n-6 in the farmed bream flesh compared to wild fish [29]. Wild fish also contained higher 16:0, 18:1n-9 and 20:4n-6 and evidence suggests that bream that tend to feed in inshore and estuarine waters often have fatty acid compositions that reflect the dietary fauna from those areas, whereas aquafeeds contain fish products obtained from the open oceans, which are quite different in their fatty acid compositions [30, 31].

Bulk  $\delta^{13}\text{C}$  analysis of the total oil fraction and glycerol/choline fraction yielded highly significant differences with farmed fish isotopically lighter than wild fish reflecting the lighter  $^{13}\text{C}$  content of farmed fish diets, probably containing significant terrestrial carbon input from vegetable meals and oils, as also evidenced by their fatty acid compositions as described above. Marine fish diets are isotopically heavier due to the source of carbon (dissolved inorganic carbon pool,  $\delta^{13}\text{C} \sim 0\text{‰}$ ) used by macroalgae and phytoplankton, which form the lower trophic levels of the marine food web, compared with terrestrial photosynthesis from atmospheric  $\text{CO}_2$  ( $\delta^{13}\text{C} \sim -7.8\text{‰}$ ). Furthermore, marine vertebrates, through their trophic sequestration of zooplankton and Crustacea, further enrich the isotopic signature to produce heavier  $\delta^{13}\text{C}$  values. The source of dietary lipids in farmed feed reflects a significant terrestrial signature of plant oils and appears largely to be of C3 origin, the photosynthetic pathway used by temperate plants, such as cereals likely to be used in aquaculture feeds [32].

The compound specific data highlight differences in the carbon isotope signatures of the major fatty acids between wild and farmed species. Whatever the route to C16:0 in wild fish, dietary or de novo synthesis, the source will be heavier than farmed fish, which will have a significant dietary input of C16:0 from terrestrial plant origin. The desaturation of the major saturated fatty acids appears to



reflect dietary origin of the saturated fatty acid. Significant differences were observed with the most abundant fatty acids probably reflecting the increased precision of analysis of the major analytes. Lower abundance analytes have poorer precision of analysis because they suffer to a greater proportion from baseline perturbations and present less  $\text{CO}_2$  to the ion source, which has a significant effect on precision. The choice of the internal standard method for quantitation ensured that accuracy was maintained (against an externally calibrated isotopic standard) and furthermore allowed the quantitation of analyte concentration because of the excellent area ratio response of the IRMSr to  $\text{CO}_2$  concentration [33]. This approach would not have been possible using the reference gas configuration, as is commonly used in GC-C-IRMS, and thus the analysis of compound specific fatty acid analysis also yields the fatty acid composition of the sample. Further analysis allows accurate reconstruction of the bulk  $\delta^{13}\text{C}$  value using mass balance equations (data not shown). Thus, the utility of compound specific analysis is clear, yielding fatty acid composition, individual fatty acid  $\delta^{13}\text{C}$  and bulk  $\delta^{13}\text{C}$ .

The expectation that wild fish are isotopically heavier than their farmed counterparts was observed in  $\delta^{15}\text{N}$ . This heavier signal reflects the higher trophic level of wild sea bream within marine food webs and, for farmed fish,  $\delta^{15}\text{N}$  reflects probably significant input of plant protein from terrestrial sources that are commonly included in aquafeed formulations [28]. However, extrapolating these observations across species should be undertaken with care because  $\delta^{15}\text{N}$  may be influenced by other factors including, maturity or growth rate, seasonal variations in  $\delta^{15}\text{N}$  in coastal marine environments and possible spoilage of the fish sample between collection and analysis. The sample fractions processed for choline analysis did not undergo a thorough 'clean-up' and may as a result be prone to contamination by spoilage amines of varying  $^{15}\text{N}$  natural abundance. The differences observed between farmed and wild sea bream  $\delta^{18}\text{O}$  may reflect the latitudinal differences in mean ocean  $\delta^{18}\text{O}$ , which will be in isotopic equilibrium with fish metabolic water and therefore may discriminate between fish caught in different geographical locations. This may have influenced the values in sea bream in the present study where farmed bream were from the Mediterranean while wild bream were from the Atlantic. Furthermore, although the geographical location of farmed fish is controlled, wild fish may migrate over large geographical regions, over the course of their life cycles, and the utility of using  $\delta^{18}\text{O}$  as a discriminatory factor between farmed and wild fish across species must be carefully considered.

These analytical methodologies provide the basis for discriminating between wild and farmed fish and have the potential to be used across species, particularly the isotopic fingerprinting of individual fatty acids. The decreasing

stocks of marine derived feedstuffs for the aquaculture industry entails that there will be an ever increasing terrestrial  $\delta^{13}\text{C}$  input to farmed fish diets, providing greater isotopic discrimination. As the industry strives to deliver a farmed product that reflects the wild product, sources and blends of terrestrial plants may be produced that mimic the fatty acid composition of wild fish more closely although the isotopic signature would still provide firm discriminatory evidence. The utility of nitrogen and oxygen isotopes, whilst useful, may be complicated by maturity, growth rate and regional variations in fish. The application of compound specific isotope analysis appears to provide robust and confirmatory data, which may be used in addition to, or in place of, simple fatty acid composition analysis. However, it is noteworthy that the present study is based on a relatively small sample set and future studies should seek to assess the usefulness of the described methods on fish samples derived from different species and geographical locations, from both the farmed and wild production sectors.

**Acknowledgement** We thank Paul Gorman of SUERC for his technical assistance. This work was funded by the UK Food Standards Agency, London (Project no. Q02067).

## References

1. Sargent JR, Tacon AGJ (1999) Development of farmed fish: a nutritionally necessary alternative to meat. *Proc Nutr Soc* 58:377–383
2. FAO (2005a) FAO Fisheries Department, Fishery Information, Data and Statistics Unit, Fishstat Plus: Universal software for fishery statistical time series, Aquaculture production: quantities 1950–2003, Aquaculture production: values 1984–2003, Capture production: 1950–2003, Commodities production and trade: 1950–2003, Total production: 1970–2003, Vers. 2.30
3. Hites RA, Foran JA, Carpenter DO, Hamilton MC, Knuth BA, Schwager SJ (2004) Global assessment of organic contaminants in farmed salmon. *Science* 303:226–229
4. European Commission Regulation 199/2006a amending Regulation (EC) 466/2001 setting maximum levels for certain contaminants in foodstuffs as regards dioxins and dioxin-like PCBs
5. Scientific Advisory Committee on Nutrition and Committee on Toxicology (SACN/COT) (2004) Advice on fish consumption: benefits and risks. The Stationary Office, Norwich. Available online at <http://www.food.gov.uk/news/newsarchive/2004/jun/fishreport2004>
6. EFSA (European Food Safety Authority) (2005) EFSA J 236:123 pages. Available online at [http://www.efsa.eu.int/science/contam/contam\\_opinions/1007\\_en.html](http://www.efsa.eu.int/science/contam/contam_opinions/1007_en.html)
7. Barber MD, Ross JA, Preston T, Shenkin A, Fearon KC (1999) Fish-oil enriched nutritional supplement attenuates progression of the acute phase response in weight-losing patients with advanced pancreatic cancer. *J Nutr* 129:1120–1125
8. Barber MD, McMillan DC, Preston T, Ross JA, Fearon KCH (2000) Metabolic response to feeding in weight-losing pancreatic cancer patients and its modulation by a fish-oil-enriched nutritional supplement. *Clin Sci* 98:389–399
9. Barber MD, Preston T, McMillan DC, Slater C, Ross JA, Fearon KCH (2004) Modulation of the liver export protein synthetic

- response to feeding by an n-3 fatty-acid-enriched nutritional supplement is associated with anabolism in cachectic cancer patients. *Clin Sci* 106(4):359–364
10. Moses AWG, Slater C, Preston T, Barber MD, Fearon KCH (2004) The reduced total energy expenditure and physical activity in cachectic patients with pancreatic cancer can be modulated by energy and protein dense oral supplements enriched with n-3 fatty acids. *Br J Cancer* 90(5):996–1002
  11. Horrocks LA, Yeo YK (1999) Health benefits of docosahexaenoic acid (DHA). *Pharmacol Res* 40:211–225
  12. Sastry PS (1985) Lipids of nervous tissue: composition and metabolism. *Prog Lipid Res* 24:69–176
  13. Simopoulos AP (1991) Omega-3 fatty acids in health and disease and in growth and development. *Am J Clin Nutr* 54:438–463
  14. Calder PC (2001) Polyunsaturated fatty acids, inflammation and immunity. *Lipids* 36:1007–1024
  15. Young G, Conquer J (2005) Omega-3 fatty acids and neuropsychiatric disorders. *Reprod Nutr Dev* 45:1–28
  16. Tacon AGJ (2004) Use of fish meal and fish oil in aquaculture: a global perspective. *Aquatic Resour Cult Dev* 1:18–19
  17. Bell JG, McGhee F, Dick JR, Tocher DR (2005) Dioxin and dioxin-like polychlorinated biphenyls (PCBs) in Scottish farmed salmon (*Salmo salar*): effects of replacement of dietary marine fish oil with vegetable oils. *Aquaculture* 243:305–314
  18. Berntssen MHG, Lundebye A-K, Torstensen BE (2005) Reducing the levels of dioxins and dioxin-like PCBs in farmed Atlantic salmon by substitution of fish oil with vegetable oil in the feed. *Aquac Nutr* 11:219–231
  19. Torstensen BE, Bell JG, Sargent JR, Rosenlund G, Henderson RJ, Graff IE, Lie Ø, Tocher DR (2005) Tailoring of Atlantic salmon (*Salmo salar* L.) flesh lipid composition and sensory quality by replacing fish oil with a vegetable oil blend. *J Agric Food Chem* 53:10166–10178
  20. Periago MJ, Ayala MD, Lopez-Albors O, Abdel I, Matinez C, Garcia-Alcazar A, Ros G, Gil F (2005) Muscle cellularity and flesh quality of wild and farmed sea bass *Dicentrarchus labrax* L. *Aquaculture* 249:175–188
  21. Blanchet C, Lucas M, Julien P, Morin R, Gingras S, Dewailly E (2005) Fatty acid composition of wild and farmed Atlantic salmon (*Salmo salar*) and rainbow trout (*Oncorhynchus mykiss*). *Lipids* 40:529–531
  22. Preston T (1992) The measurement of stable isotope natural abundance variations. *Plant Cell Environ* 15:1091–1097
  23. Craig H (1957) Isotopic standards for carbon and oxygen and correction factors for mass-spectrometric analysis of carbon dioxide. *Geochim Cosmochim Acta* 12:133–149
  24. Coplen TB, Brand WA, Gehre M, Groning M, Meijer HA, Toman B, Verkouteren RM (2006) New guidelines for delta(13)C measurements. *Anal Chem* 78:2439–2441
  25. Morrison DJ, Cooper K, Slater C, Waldron S, Weaver LT, Preston T (2004) A streamlined approach to the analysis of volatile fatty acids and its application to the measurement of whole body flux. *Rapid Commun Mass Spectrom* 18:2593–2600
  26. Grigorakis K, Taylor KDA, Alexis MN (2003) Organoleptic and volatile aroma compounds comparison of wild and cultured gilthead sea bream (*Sparus aurata*): sensory differences and possible chemical basis. *Aquaculture* 225:109–119
  27. Mnari A, Buhlel I, Chraief I, Hammami M, Rondhane MS, El Cafsi M, Chaouch A (2007) Fatty acids in muscles and liver of Tunisian wild and farmed gilthead sea bream, *Sparus aurata*. *Food Chem* 100:1393–1397
  28. Gomez-Requeni P, Mingarro M, Kirchner S, Caldach-Giner JA, Medale F, Martin SAM, Houlihan DF, Kaushik SJ, Perez-Sanchez J (2004) Protein growth performance, amino acid utilisation and somatotrophic axis responsiveness to fish meal replacement by plant protein sources in gilthead sea bream (*Sparus aurata*). *Aquaculture* 232:493–510
  29. Mourente G, Good JE, Bell JG (2005) Partial substitution of fish oil with rapeseed, linseed and olive oils in diets for European sea bass (*Dicentrarchus labrax* L.) effects on flesh fatty acid composition, plasma prostaglandins E<sub>2</sub> and F<sub>2α</sub>, immune function and effectiveness of a fish oil finishing diet. *Aquac Nutr* 11:25–40
  30. Farndale BM, Bell JG, Bruce MP, Bromage NR, Oyen F, Zanuy S, Sargent JR (1999) Dietary lipid composition affects blood leucocyte fatty acid compositions and plasma eicosanoid concentrations in European sea bass (*Dicentrarchus labrax*). *Aquaculture* 179:335–350
  31. Bell MV, Dick JR, Thrush M, Navarro JC (1996) Decreased 20:4n-6/20:5n-3 ratio in sperm from cultured sea bass, *Dicentrarchus labrax*, broodstock compared with wild fish. *Aquaculture* 144:189–199
  32. O'Leary MH, Madhavan S, Paneth P (1992) Physical and chemical basis of carbon isotope fractionation in plants. *Plant Cell Environ* 15:1099–1104
  33. Preston T, Slater C (1994) Mass spectrometric analysis of stable isotope labelled amino acid tracers. *Proc Nutr Soc* 53:363–372

## Replacement of Dietary Fish Oils by Alpha-Linolenic Acid-Rich Oils Lowers Omega 3 Content in Tilapia Flesh

Ioannis T. Karapanagiotidis · Michael V. Bell ·  
David C. Little · Amararatne Yakupitiyage

Received: 17 November 2006 / Accepted: 20 March 2007 / Published online: 1 May 2007  
© AOCS 2007

**Abstract** A 20-week feeding trial was conducted to determine whether increasing linolenic acid (18:3n-3) in vegetable oil (VO) based diets would lead to increased tissue deposition of 22:6n-3 in Nile tilapia (*Oreochromis niloticus*). Five isonitrogenous and isoenergetic diets were supplemented with 3% of either linseed oil (LO), a mixture of linseed oil with refined palm olein oil (PO) (LO–PO 2:1) and a mixture of refined palm olein oil with linseed oil (PO–LO 3:2) or with fish oil (FO) or corn oil (CO) as controls. The PO–LO, LO–PO and LO diets supplied a similar amount of 18:2n-6 (0.5% of diet by dry weight) and 0.5, 0.7 and 1.1% of 18:3n-3, respectively. Increased dietary 18:3n-3 caused commensurate increases in longer-chain n-3 PUFA and decreases in longer-chain n-6 PUFA in the muscle lipids of tilapia. However, the biosynthetic activities of fish fed the LO-based diets were not sufficient to raise the tissue concentrations of 20:5n-3, 22:5n-3 and 22:6n-3 to those of fish fed FO. The study suggests that tilapia (*O. niloticus*) has a limited capacity to synthesise 20:5n-3 and 22:6n-3 from dietary 18:3n-3. The replacement of FO in the diet of farmed tilapia with vegetable oils could therefore lower tissue concentrations of 20:5n-3 and 22:6n-3, and consequently produce an aquaculture product of lower lipid nutritional value for the consumer.

**Keywords**  $\alpha$ -Linolenic acid · Polyunsaturated fatty acids · Linseed oil · Tilapia · *Oreochromis niloticus*

### Abbreviations

CO	Corn oil
FCR	Food conversion ratio
FAME	Fatty acid methyl ester
FO	Fish oil
LO	Linseed oil
MUFA	Monounsaturated fatty acid
PER	Protein efficiency ratio
PO	Palm olein oil
PUFA	Polyunsaturated fatty acid
SFA	Saturated fatty acid
SGR	Specific growth rate
TL	Total lipid
VO	Vegetable oil

### Introduction

Polyunsaturated fatty acids (PUFA) are essential for normal growth, development and reproduction in all vertebrates, including fish and humans [1, 2]. The requirement is usually met by dietary linoleic acid (18:2n-6) and  $\alpha$ -linolenic acid (18:3n-3) which are then converted to the functionally essential C20 and C22 homologues, 20:4n-6, 20:5n-3 and 22:6n-3. For some species unable to perform the metabolic conversions at a sufficient rate the dietary EFA are the longer chain homologues.

The intake of n-3 PUFA, and specifically 20:5n-3 and 22:6n-3, is considered to be beneficial against many human health disorders. There is now compelling evidence from clinical and epidemiological research that increased intakes

I. T. Karapanagiotidis · M. V. Bell (✉) ·  
D. C. Little  
Institute of Aquaculture, University of Stirling,  
Stirling FK9 4LA, Scotland  
e-mail: m.v.bell@stir.ac.uk

A. Yakupitiyage  
School of Environment, Resources and Development,  
Asian Institute of Technology, Pathumthani 12120, Thailand

of 20:5n-3 and 22:6n-3 are effective in the prevention or attenuation of many cardiovascular problems and inflammatory conditions [3]. The balance between dietary n-3 and n-6 PUFA is as important as the amount of PUFA and an altered n-3/n-6 ratio affects the haemostatic balance as well as the inflammatory and immune responses [4]. Today industrialised societies are characterised by an increase in energy intake, saturated fat and n-6 PUFA and a decrease in n-3 PUFA intake [5]. This has been linked with the occurrence of many health disorders, once considered a problem primarily of western societies, but rapidly becoming a major health problem in other parts of the world, including Asia [5, 6]. It is, therefore, recommended to increase the intake of n-3 PUFA, and particularly 20:5n-3 and 22:6n-3, and decrease the dietary intake of n-6 PUFA in the human diet [7].

Fish and marine mammals are by far the richest source of long chain n-3 PUFA in nature. Fish products comprise an important part of the human diet and demand is expected to increase [8]. Given static or declining wild fisheries [8], aquaculture has a significant role in ensuring fish supplies. Tilapia farming makes a large and growing contribution to global fish supplies [9]. As the farming of fish is becoming a major contributor to world fish supplies, it is important to maintain the high lipid nutritional quality of the product and continue to provide large amounts of the health-promoting n-3 PUFA for the consumer.

Freshwater fish species, generally, have higher capacities for the conversions of C18 PUFA to the longer C20 and C22 homologues than marine species, although this should not be treated as a general rule [2]. Tilapias are known to possess some ability to elongate and desaturate 18:3n-3 to 20:5n-3 and 22:6n-3 [10, 11]. Studies with salmonids have shown that the PUFA metabolic pathways are induced after removing C20 and C22 PUFA from VO-rich diets [12, 13]. Linseed oil has a high content (up to 56%) of 18:3n-3 and a much lower content of 18:2n-6 compared to other vegetable oils, so dietary LO has the potential for enhancing the n-3 content in fish flesh.

The aims of this study were: (1) to study the effects of variation in dietary n-3 and n-6 PUFA on the lipid nutritive value of tilapia (*Oreochromis niloticus*) for the human consumer and (2) to elevate the levels of elongation and desaturation products, 20:5n-3 and 22:6n-3, as well as of the n-3/n-6 PUFA ratio, in tilapia muscle tissue by feeding fish on diets high in 18:3n-3.

## Materials and Methods

### Experimental Diets

Five isonitrogenous (32% crude protein) and isoenergetic (17 KJ/g diet) diets were formulated (Table 1) to satisfy

the nutritional requirements of tilapia (*O. niloticus*). Dietary ingredients used in the five diets were identical except the natural oil or the mixture of oils used as the lipid source, which was added at a level of 3% of the total diet (by dry weight). The dietary fatty acid composition is shown in Table 2. Diets were prepared at the Charoen Pokphand Foods feed mill (Samut Sakorn, Thailand) by feed mill personnel and these were in the form of a water stable sinking pellet of 3 mm size. Portions of diet for analysis were stored at  $-20^{\circ}\text{C}$  otherwise bulk diets were stored in air-tight polyethylene bags at  $4^{\circ}\text{C}$  and used within 4 weeks. Proximate analysis of experimental diets was performed for moisture, protein, lipid, ash, crude fibre and energy according to the methods of AOAC [14].

### Experimental Fish and Culture System

Male sex-reversed tilapia fry (*O. niloticus*) of initial weight 0.5–2 g were obtained from the Asian Institute of Technology's hatchery (Pathumthani, Thailand). The fish were randomly distributed into 30 groups of 100 fry each and stocked into 30 net cages (3 m  $\times$  1.8 m  $\times$  0.8 m, 3 mm mesh size) that were suspended in an earthen pond (40 m  $\times$  40 m  $\times$  1 m). Each cage was covered with an anti-predator net (mesh size of 5 cm) and provided with a plastic feeding tray (55 cm length  $\times$  30 cm width  $\times$  25 cm height) attached and submerged to one side of the cage. Wooden walkways connected the cages to the pond bank. Water depth in the pond was maintained at 1 m throughout the experiment by adding water biweekly to replace evaporation and seepage losses. After initial stocking into the cages, fry were allowed to acclimatise for 1 day without feeding. The feeding trial was conducted for 20 weeks. Fish were bulk weighed biweekly and the daily food rations were adjusted accordingly. The daily feeding ration was divided into 4 equal portions (08.00, 11.00, 14.00, 17.00 h) until the end of the 6th week, then into 3 portions (08.00, 11.00, 16.00 h) until end of 14th week and into 2 portions (08.00, 15.00 h) thereafter. On the days of bulk weighing no feed was given as fish experienced stress. Feeding rates were 12% of body weight (b.w.) per day for the first 4 weeks, 10% of b.w. until the 6th week, 9% of b.w. until the 8th week, 6% of b.w. until the 10th week, 5% of b.w. until the 12th week, 3.5% of b.w. until the 14th week, 2.5% of b.w. until the 16th week, 2% of b.w. until the 18th week and 1% of b.w. until the end of the 20-week trial. No fertiliser was added to the experimental pond, neither prior to, nor during, the dietary trial in order to keep levels of pond natural food to a minimum and diminish their influence on dietary intake.

**Table 1** Formulation (g/100g diet) and composition (%) of the diets

Composition	PO–LO	LO–PO	LO	FO	CO
Soybean meal	61.0	61.0	61.0	61.0	61.0
Fishmeal	5.0	5.0	5.0	5.0	5.0
Cassava flour (food-grade)	22.24	22.24	22.24	22.24	22.24
Fine rice husks	4.0	4.0	4.0	4.0	4.0
DCP	2.5	2.5	2.5	2.5	2.5
DL-methionine	0.25	0.25	0.25	0.25	0.25
Ethoxyquin	0.0125	0.0125	0.0125	0.0125	0.0125
Vitamin premix <sup>a</sup>	1.0	1.0	1.0	1.0	1.0
Mineral premix <sup>b</sup>	1.0	1.0	1.0	1.0	1.0
Linseed oil	1.2	2.0	3.0	–	–
Refined olein oil	1.8	1.0	–	–	–
Fish oil	–	–	–	3.0	–
Corn oil	–	–	–	–	3.0
Proximate composition					
Dry matter (%)	93.1 ± 0.3	93.0 ± 0.4	93.0 ± 0.3	93.1 ± 0.4	93.1 ± 0.3
Crude protein (%)	32.0 ± 1.0	32.0 ± 1.0	32.0 ± 1.0	32.1 ± 0.8	32.1 ± 1.1
Crude lipid (%)	3.5 ± 0.4	3.5 ± 0.3	3.5 ± 0.4	3.5 ± 0.4	3.4 ± 0.5
Carbohydrates (%)	41.8 ± 0.9	41.2 ± 1.0	41.7 ± 1.0	41.3 ± 0.7	41.3 ± 1.1
Ash (%)	9.6 ± 0.6	9.6 ± 0.6	9.6 ± 0.7	9.5 ± 0.6	9.7 ± 0.7
Crude fibre (%)	6.2 ± 0.7	6.6 ± 0.6	6.2 ± 0.9	6.8 ± 1.1	6.7 ± 1.1
Gross energy (KJ g <sup>-1</sup> )	17.4 ± 0.1	17.1 ± 0.5	17.2 ± 0.0	17.1 ± 0.0	17.3 ± 0.1

Values for proximate composition and energy represent means ±SD ( $n = 10$ ). Values presented for the different oils are in ml/100 g diet. All feed ingredients, mineral/vitamin premixes and oils (except linseed oil) were provided by CP Foods Plc, Bangkok, Thailand. Soybean meal is solvent extracted (defatted, 49% crude protein). Linseed oil was from ICN (Basingstoke, Hampshire, UK)

DCP dicalcium phosphate

<sup>a</sup> 1 kg of vitamin premix contained 0.26% vitamin B<sub>1</sub>, 0.31% vitamin B<sub>2</sub>, 0.1% vitamin B<sub>6</sub>, 0.24% vitamin B<sub>12</sub>, 2.86% vitamin C, 0.5% biotin, 6.67% choline, 0.26% folic acid, 2.51% nicotinic acid, 0.5% inositol, 0.1% pantothenic acid, 0.2% vitamin A, 0.1% vitamin D, 1% vitamin E, 0.59% vitamin K and 83.8% refined cassava flour

<sup>b</sup> 1 kg of mineral premix contained 10% magnesium, 6.67% potassium, 0.94% iron, 0.4% manganese, 0.2% copper, 0.1% chromium, 6.6% zinc and 75.09% refined cassava flour

### Fish Sampling

Prior to stocking, a total number of 20 fry from the initial stock were randomly sampled. After weighing, the dorsal muscle tissue of each fish was dissected, skin and blood-stains removed, and the muscle tissue frozen inside airtight clip bags at  $-20^{\circ}\text{C}$  until lipid analysis. A second sampling of the experimental fish was made on day 32 when the fish had reached a size of around 15 g. A total of six fish randomly selected from each cage (30 fish in total per treatment) were killed by a blow to the head and transferred straight to the laboratory for muscle tissue dissection as before. At the end of the 20-week feeding period a final sampling was made again of six fish from each cage.

### Water Quality

Water quality analysis was conducted biweekly by taking integrated water column samples at 10.00 h from three

points of the open water and three cages randomly chosen. Samples were also taken before the start of the experiment (day 0). Water samples were analysed for total ammonium nitrogen (TAN), total alkalinity, chlorophyll  $\alpha$ , total suspended solids (TSS) and total volatile solids (TVS) using standard methods [15]. Dissolved oxygen (DO), temperature and pH were measured at three different depths (25 cm below the water surface, middle, and 25 cm above pond bottom) at 06.00, 10.00, 14.00 and 18.00 h using a YSI model 54 oxygen meter (Yellow Springs Instruments, Yellow Springs, OH, USA) and a Hanna model HI8424 pH meter (Hanna Instruments, Rhode Island, USA), respectively. At the time of collecting water samples, Secchi disk visibility was measured in open water.

### Chemicals and Materials

Chloroform, methanol, iso-hexane and diethyl ether were HPLC grade from Fisher (Loughborough, Leicestershire,

**Table 2** The fatty acid composition of the diets

Fatty acids	PO–LO	LO–PO	LO	FO	CO
14:0	0.20 ± 0.05 <sup>a</sup>	0.16 ± 0.04 <sup>a</sup>	0.09 ± 0.01 <sup>b</sup>	0.99 ± 0.16 <sup>c</sup>	0.10 ± 0.02 <sup>b</sup>
15:0	0.03 ± 0.01 <sup>a</sup>	0.03 ± 0.01 <sup>a</sup>	0.03 ± 0.00 <sup>a</sup>	0.10 ± 0.01 <sup>b</sup>	0.03 ± 0.00 <sup>a</sup>
16:0	5.70 ± 1.28 <sup>a</sup>	4.31 ± 0.68 <sup>b</sup>	2.40 ± 0.38 <sup>c</sup>	4.21 ± 0.58 <sup>b</sup>	3.53 ± 0.95 <sup>bc</sup>
18:0	1.11 ± 0.19	1.03 ± 0.16	1.08 ± 0.21	1.12 ± 0.17	0.88 ± 0.29
20:0	0.07 ± 0.02 <sup>a</sup>	0.06 ± 0.01 <sup>a</sup>	0.05 ± 0.01 <sup>a</sup>	0.06 ± 0.01 <sup>a</sup>	0.11 ± 0.03 <sup>b</sup>
22:0	0.06 ± 0.03 <sup>ab</sup>	0.04 ± 0.01 <sup>a</sup>	0.05 ± 0.01 <sup>ab</sup>	0.06 ± 0.01 <sup>ab</sup>	0.08 ± 0.03 <sup>b</sup>
Total SFA	7.16 ± 1.52 <sup>a</sup>	5.63 ± 0.89 <sup>ab</sup>	3.70 ± 0.62 <sup>c</sup>	6.55 ± 0.92 <sup>a</sup>	4.72 ± 1.31 <sup>bc</sup>
16:1n-9	ND	ND	ND	0.05 ± 0.01 <sup>b</sup>	ND
16:1n-7	0.16 ± 0.03 <sup>a</sup>	0.17 ± 0.07 <sup>a</sup>	0.14 ± 0.05 <sup>a</sup>	1.36 ± 0.23 <sup>b</sup>	0.16 ± 0.04 <sup>a</sup>
18:1n-9	6.67 ± 1.35 <sup>a</sup>	5.65 ± 0.83 <sup>ab</sup>	4.13 ± 0.74 <sup>b</sup>	4.06 ± 0.59 <sup>b</sup>	6.41 ± 1.64 <sup>a</sup>
18:1n-7	0.35 ± 0.14 <sup>a</sup>	0.28 ± 0.11 <sup>a</sup>	0.28 ± 0.11 <sup>a</sup>	0.77 ± 0.10 <sup>b</sup>	0.40 ± 0.18 <sup>a</sup>
20:1n-11/n-9	0.07 ± 0.02 <sup>a</sup>	0.06 ± 0.04 <sup>a</sup>	0.05 ± 0.01 <sup>a</sup>	0.32 ± 0.05 <sup>b</sup>	0.08 ± 0.03 <sup>a</sup>
20:1n-7	ND	ND	ND	0.05 ± 0.01	ND
22:1n-11/n-9	ND	ND	ND	0.15 ± 0.05 <sup>b</sup>	ND
24:1n-9	0.01 ± 0.01 <sup>a</sup>	0.01 ± 0.01 <sup>a</sup>	0.01 ± 0.01 <sup>a</sup>	0.09 ± 0.02 <sup>b</sup>	0.01 ± 0.01 <sup>a</sup>
Total MUFA	7.26 ± 1.41 <sup>a</sup>	6.12 ± 0.99 <sup>ab</sup>	4.61 ± 0.83 <sup>b</sup>	6.86 ± 1.02 <sup>a</sup>	7.06 ± 1.68 <sup>a</sup>
18:2n-6	4.46 ± 0.82 <sup>a</sup>	4.56 ± 0.72 <sup>a</sup>	4.86 ± 0.84 <sup>a</sup>	2.76 ± 0.33 <sup>b</sup>	11.13 ± 2.20 <sup>c</sup>
18:3n-6	ND	ND	ND	0.02 ± 0.01	0.04 ± 0.05
20:2n-6	ND	ND	ND	0.05 ± 0.01	ND
20:3n-6	ND	ND	ND	0.03 ± 0.01	ND
20:4n-6	0.06 ± 0.01 <sup>a</sup>	0.06 ± 0.01 <sup>a</sup>	0.06 ± 0.01 <sup>a</sup>	0.17 ± 0.03 <sup>b</sup>	0.05 ± 0.01 <sup>a</sup>
22:4n-6	ND	ND	ND	0.04 ± 0.01 <sup>b</sup>	ND
22:5n-6	0.03 ± 0.01 <sup>a</sup>	0.03 ± 0.01 <sup>a</sup>	0.03 ± 0.01 <sup>a</sup>	0.07 ± 0.01 <sup>b</sup>	0.03 ± 0.01 <sup>c</sup>
Total n-6 PUFA	4.55 ± 0.83 <sup>a</sup>	4.64 ± 0.74 <sup>a</sup>	4.95 ± 0.86 <sup>a</sup>	3.15 ± 0.39 <sup>b</sup>	11.25 ± 2.19 <sup>c</sup>
18:3n-3	4.41 ± 1.32 <sup>a</sup>	6.58 ± 1.03 <sup>b</sup>	11.01 ± 2.66 <sup>c</sup>	0.61 ± 0.16 <sup>d</sup>	0.68 ± 0.22 <sup>d</sup>
18:4n-3	ND	ND	ND	0.19 ± 0.06	ND
20:3n-3	ND	ND	ND	ND	ND
20:4n-3	ND	ND	ND	0.18 ± 0.04	ND
20:5n-3	0.08 ± 0.02 <sup>a</sup>	0.08 ± 0.02 <sup>a</sup>	0.08 ± 0.01 <sup>a</sup>	1.47 ± 0.34 <sup>b</sup>	0.08 ± 0.02 <sup>a</sup>
22:4n-3	ND	ND	ND	ND	ND
22:5n-3	0.03 ± 0.01 <sup>a</sup>	0.03 ± 0.01 <sup>a</sup>	0.03 ± 0.01 <sup>a</sup>	0.67 ± 0.15 <sup>b</sup>	0.03 ± 0.01 <sup>a</sup>
22:6n-3	0.29 ± 0.17 <sup>a</sup>	0.26 ± 0.10 <sup>a</sup>	0.29 ± 0.05 <sup>a</sup>	2.14 ± 0.42 <sup>b</sup>	0.31 ± 0.08 <sup>a</sup>
Total n-3 PUFA	4.82 ± 1.40 <sup>a</sup>	6.95 ± 1.12 <sup>b</sup>	11.41 ± 2.73 <sup>c</sup>	5.26 ± 1.08 <sup>ab</sup>	1.12 ± 0.34 <sup>d</sup>
Total PUFA	9.37 ± 2.14 <sup>ab</sup>	11.60 ± 1.85 <sup>ab</sup>	16.36 ± 3.58 <sup>c</sup>	8.41 ± 1.43 <sup>a</sup>	12.37 ± 2.49 <sup>b</sup>
(n-3)/(n-6)	1.05 ± 0.10 <sup>a</sup>	1.50 ± 0.05 <sup>b</sup>	2.28 ± 0.16 <sup>c</sup>	1.66 ± 0.12 <sup>b</sup>	0.10 ± 0.02 <sup>d</sup>
Total FA	23.81 ± 4.75	23.40 ± 3.68	24.66 ± 4.96	21.82 ± 3.34	24.16 ± 5.42

Data are expressed as mg of FA/g of diet. Values represent means ± SD ( $n = 10$ ). Values in the same row, which do not share the same superscript letters are significantly different at  $\alpha = 0.01$

ND not detected (values <0.01)

UK). Concentrated sulphuric acid (Aristar grade) and Merck silica gel 60 thin layer chromatography (TLC) plates (no. 5721) and high performance TLC (HPTLC) plates (no. 5633) were obtained from VWR (Lutterworth, Leicestershire, UK). All other chemicals were from Sigma (Poole, Dorset, UK).

#### Lipid Extraction and Fatty Acid Analysis

The total lipid from wet muscle tissue and from diets was extracted and measured gravimetrically according to the method of Folch et al. [16]. Wet muscle samples and diets were homogenised in chloroform/methanol (C:M 2:1, by

vol.) using an Ultra-Turrax tissue disrupter (Fisher Scientific, Loughborough, UK). The homogenates were filtered and a Folch extract prepared. Samples were kept on ice under nitrogen between procedures and lipid extracts stored in C:M (2:1, by vol.) at a final concentration of 10 mg lipid/ml at  $-20\text{ }^{\circ}\text{C}$  under nitrogen. Solvents contained 0.01% (w/v) butylated hydroxy-toluene (BHT) as an antioxidant.

Lipid class analysis was performed using double development HPTLC as described by Olsen and Henderson [17]. Samples were chromatographed in methyl acetate: propan-2-ol: chloroform: methanol: 0.25% (w/v) KCl (25:25:25:10:9, by vol.) to separate phospholipid classes and iso-hexane: diethyl ether: glacial acetic acid (80:20:2, by vol.) to separate neutral lipids and cholesterol. Lipid classes were visualised by spraying with 3% cupric acetate (w/v) in 8% phosphoric acid (by vol.) and charred at  $160\text{ }^{\circ}\text{C}$  for 15 min. Lipid classes were quantified by scanning densitometry (370 nm) using a CAMAG TLC scanner 3 (version Firmware 1.14.16) and scanned images were recorded automatically in a computer using a special software (winCATS Planar Chromatography Manager, version 1.2.0).

Fatty acid methyl esters (FAME) were prepared by acid-catalysed transesterification of 1 mg total lipid plus 0.1 mg heptadecanoic acid (Sigma Chemical Company, St. Louis, USA) as internal standard using 2 ml of 1% (by vol.) sulphuric acid in methanol and 1 ml of toluene under nitrogen at  $50\text{ }^{\circ}\text{C}$  for 16 h [18]. Crude FAME were purified by TLC in iso-hexane: diethyl ether: acetic acid (90:10:1, by vol.) and visualised by spraying lightly the edge of the plate with 1% (w/v) iodine in  $\text{CHCl}_3$ . FAME were scraped from the plate and eluted with iso-hexane: diethyl ether (1:1, by vol.). Purified FAME were re-dissolved in iso-hexane containing 0.01% BHT and stored under nitrogen at  $-20\text{ }^{\circ}\text{C}$  prior to gas liquid chromatography.

Fatty acid methyl esters were separated and quantified by gas liquid chromatography (Fisons 8000 series, Thermo-Finnegan, Hemel Hempstead, UK) using a CP Wax 52CB fused silica capillary column ( $30\text{ m} \times 0.32\text{ mm}$  i.d.,  $0.25\text{ }\mu\text{m}$  film thickness) (Chrompak, London, UK). Hydrogen was used as carrier gas at a flow rate of 2.5 ml/min and temperature programming was from  $50$  to  $150\text{ }^{\circ}\text{C}$  at  $40\text{ }^{\circ}\text{C}/\text{min}$  and from  $150$  to  $225\text{ }^{\circ}\text{C}$  at a rate of  $2\text{ }^{\circ}\text{C}/\text{min}$  and the final temperature of  $225\text{ }^{\circ}\text{C}$  was maintained for 5 min. Individual methyl esters were identified by comparison to known standards (marine fish oil) and by reference to published data. Peak areas of fatty acids were quantified with reference to the peak area of 17:0 internal standard and computed automatically by a computing integrator (Chromcard for Windows, ThermoQuest, Milan, Italy).

## Statistical Analysis

Data from individual fish were treated as independent samples. Proximate composition of the diets, growth performance and feed utilisation efficiency parameters, muscle total lipid and fatty acid composition were all subjected to one-way analysis of variance (ANOVA) and differences were considered significant at an alpha value of 0.01. Analyses were performed using SPSS statistical package (version 10.0.1, SPSS Inc., Chicago, USA). Data that were identified as non-homogeneous (using Levene's test of homogeneity) were subjected to either log or power transformation before analysis. Differences between means were determined by Tukeys' test.

Data of the water quality parameters for cages and open water were analysed statistically with independent-sample *t*-test and data from the different sampling periods were analysed with paired-sample *t*-test. Differences were considered significant at an alpha level of 0.01.

## Results

### Growth Performance

All the parameters of water quality that were monitored during the course of the study were within the ranges considered suitable for the growth and survival of tilapia (*Oreochromis niloticus*). Values of water quality parameters between the cages and open water were not significantly different, indicating the homogeneous water environment that fish were reared during the course of the study.

At the end of the 20-week experimental period, the growth performance of fish fed the different diets and the feed utilisation were evaluated using a number of parameters that are shown in Table 3. There was no significant difference among dietary treatments in any of the performance parameters examined. Fish appeared healthy at the end of the trial with survival ranging from 86.2 to 92.3% among all groups of fish, while there were a number of mortalities unrelated to diet. Weight gain and specific growth rate (SGR) were in the ranges of 170.0–186.9 g and 3.42–3.46 (%/day), respectively. However, fish fed the FO diet displayed a slightly higher weight gain, but not significantly so, compared to the other groups of fish throughout the feeding trial. Protein efficiency ratios (PER) were within the range 1.52–1.55 and food conversion ratios (FCR) within the range 2.01–2.06 among all five dietary treatments.

**Table 3** Growth performance and feed utilisation efficiency of fish

Performance parameters <sup>a</sup>	PO–LO	LO–PO	LO	FO	CO
Initial weight (g)	1.09 ± 0.08	1.13 ± 0.08	1.06 ± 0.06	1.09 ± 0.05	1.18 ± 0.06
Final weight (g)	170.0 ± 12.4	177.7 ± 14.8	174.0 ± 10.8	186.9 ± 12.0	175.9 ± 11.3
Weight gain <sup>b</sup> (g)	168.9 ± 12.4	176.5 ± 14.8	172.9 ± 10.9	185.8 ± 12.1	174.7 ± 11.3
SGR <sup>c</sup> (%/day)	3.44 ± 0.10	3.44 ± 0.08	3.43 ± 0.05	3.46 ± 0.08	3.42 ± 0.08
FCR <sup>d</sup>	2.05 ± 0.11	2.04 ± 0.12	2.06 ± 0.08	2.03 ± 0.10	2.01 ± 0.07
PER <sup>e</sup>	1.53 ± 0.08	1.54 ± 0.09	1.52 ± 0.06	1.54 ± 0.07	1.55 ± 0.05
Survival (%)	91.5 ± 3.2	90.8 ± 1.8	86.2 ± 9.6	86.8 ± 8.8	92.3 ± 5.1

<sup>a</sup> Values for weight gain, SGR, FCR, PER and survival are the means of 6 replicate groups of 6 fish. Values for the initial fish body weight are the means of 100 fish (initial fish population), while values for the final fish body weight are the means of all individual fish within the same group that survived after the 20-week course of the study. There was no significant difference ( $\alpha = 0.01$ ) between the treatments in any of the parameters examined

<sup>b</sup> Weight gain = mean final body weight (g) – mean initial body weight (g)

<sup>c</sup> Specific growth rate (SGR, %/day) =  $100 \times [(\text{Ln}(\text{mean final body weight}) - \text{Ln}(\text{mean initial body weight})) / \text{culture period (days)}]$

<sup>d</sup> Feed conversion ratio (FCR) = total dry weight of feed given (g)/wet weight gain (g)

<sup>e</sup> Protein efficiency ratio (PER) = wet weight gain (g)/crude protein fed (g)

### Total Lipid and Lipid Class Composition

The different groups of fish contained similar total lipid contents (TL) at both time points ranging from 9.11 to 9.84 mg/g wet weight tissue at day 32 and 7.03–7.82 mg/g wet weight tissue after 20 weeks (Table 4) with no significance between time points. There was also no significant difference in lipid class composition between the five dietary treatments. Triacylglycerol and cholesterol were the major neutral lipid classes found in the muscle tissues of all groups of fish, which accounted for 23.8–26.9% and 17.2–18.4% of TL, respectively. Phosphatidylcholine (PC) and phosphatidylethanolamine (PE) were the major polar lipid classes found in the muscle tissues of all groups of fish and these were in the range of 24.7–27.6% of TL and 13.3–15.8% of TL, respectively (data not shown).

### Fatty Acid Composition of Muscle Total Lipid

The fatty acid composition of the fish at the start of the feeding trial reflected the composition of the commercial weaning diet. Palmitic acid was the major FA followed by 22:6n-3 and 18:1n-9, smaller amounts of 18:0 and 18:2n-6 with 20:4n-6, 18:1n-7, 16:1n-7, 22:5n-3 and 22:5n-6 the only other FA present at more than 10 µg/mg TL (Table 5).

The FA composition of the fish quickly reflected that of the different diets and the FA composition was similar at day 32 and at the end of the trial at 20 weeks (Tables 5, 6). Fish from the five treatments contained similar amounts of 16:0, 18:0, 20:0, 22:0 and total saturated fatty acids (SFA), both after 32 days of feeding (Table 5) and at the end of the trial (Table 7), despite the fact that the five diets supplied significantly different amounts of these FA (Table 2). The concentrations of 14:0 and 15:0, however, were significantly higher in FO-fed fish at the end of the trial, due to the much higher supply of these two FA in the FO diet.

The amounts of total monounsaturated fatty acids (MUFA) were also not significantly different between the five dietary treatments (Tables 5, 6). 18:1n-9 was the most abundant MUFA in the muscle lipids of fish fed all five diets with no differences between treatments (Tables 5, 6). However, there were significant differences in the concentration of the individual monoenes among the five dietary treatments. FO-fed fish contained significantly higher amounts of 16:1n-7 than LO-fed fish and CO-fed fish (Table 6) and also significantly higher concentrations of 18:1n-7, 22:1n-11/n-9 and 24:1n-9 than in the other four treatments. Additionally, FO-fed fish contained increased amounts of the twenty carbon MUFA (20:1n-9 + 20:1n-7). The higher concentrations of all the above MUFA in the

**Table 4** Total lipid content of muscle tissue from tilapia after 32 and 140 days on the experimental diets (mg/g wet weight tissue)

	PO–CO	LO–PO	LO	FO	CO
Day 32	9.57 ± 1.24	9.31 ± 0.59	9.11 ± 0.62	9.84 ± 0.69	9.57 ± 0.63
Day 140	7.67 ± 1.58	7.82 ± 0.89	7.09 ± 0.50	7.28 ± 0.56	7.03 ± 1.36

Mean ± SD,  $n = 6$



**Table 5** The fatty acid compositions ( $\mu\text{g}/\text{mg}$  of total lipid) of muscle TL of the initial fish population (day 0) and of fish fed the five diets after 32 days of feeding

Fatty acid	Initial fish group	PO–LO	LO–PO	LO	FO	CO
14:0	$6.1 \pm 2.1^a$	$6.8 \pm 0.8^a$	$7.0 \pm 0.8^a$	$6.2 \pm 1.1^a$	$10.1 \pm 0.6^b$	$6.3 \pm 0.7^a$
15:0	$2.4 \pm 0.5^a$	$1.9 \pm 0.4^{ab}$	$1.9 \pm 0.3^{ab}$	$1.7 \pm 0.3^b$	$2.4 \pm 0.2^a$	$1.6 \pm 0.3^b$
16:0	$105.1 \pm 10.6$	$110.6 \pm 8.0$	$112.4 \pm 8.3$	$100.9 \pm 13.1$	$117.4 \pm 8.8$	$110.5 \pm 11.9$
18:0	$49.6 \pm 4.4^a$	$34.9 \pm 2.0^b$	$34.9 \pm 2.5^b$	$34.2 \pm 3.4^b$	$37.2 \pm 2.8^b$	$35.6 \pm 4.3^b$
20:0	$1.3 \pm 0.3^a$	$0.7 \pm 0.1^b$	$0.8 \pm 0.4^b$	$0.7 \pm 0.1^b$	$0.8 \pm 0.1^b$	$0.8 \pm 0.0^b$
22:0	$1.5 \pm 0.4$	$1.2 \pm 0.2$	$1.2 \pm 0.3$	$1.0 \pm 0.2$	$1.0 \pm 0.1$	$1.2 \pm 0.2$
Total SFA	$166.0 \pm 14.4$	$156.0 \pm 10.4$	$158.2 \pm 10.9$	$144.8 \pm 17.4$	$168.9 \pm 11.9$	$156.0 \pm 16.5$
16:1n-9	$2.1 \pm 0.8^a$	$3.4 \pm 0.3^b$	$3.6 \pm 0.3^b$	$2.5 \pm 0.3^{ab}$	$3.2 \pm 0.3^b$	$3.2 \pm 0.2^b$
16:1n-7	$11.9 \pm 4.1^a$	$18.4 \pm 2.4^{cd}$	$20.5 \pm 1.6^{bc}$	$16.4 \pm 2.7^{acd}$	$23.8 \pm 1.8^b$	$15.0 \pm 1.3^d$
18:1n-9	$63.7 \pm 14.1^a$	$83.4 \pm 16.3^{ab}$	$90.5 \pm 9.8^b$	$75.0 \pm 11.5^{ab}$	$75.3 \pm 8.8^{ab}$	$86.1 \pm 14.4^{ab}$
18:1n-7	$17.7 \pm 2.4^a$	$17.2 \pm 4.2^{abc}$	$17.7 \pm 4.1^{ab}$	$12.0 \pm 0.7^c$	$20.0 \pm 3.5^{ab}$	$14.2 \pm 2.0^{abc}$
20:1n-9	$4.0 \pm 1.5^a$	$2.9 \pm 0.6^{ab}$	$3.1 \pm 0.5^{ab}$	$2.2 \pm 0.3^b$	$3.6 \pm 0.4^a$	$3.7 \pm 0.7^a$
20:1n-7	$0.3 \pm 0.2^{ab}$	$0.4 \pm 0.2^{ab}$	$0.4 \pm 0.2^{ab}$	ND	$0.6 \pm 0.2^a$	$0.2 \pm 0.1^b$
22:1 n-11/n-9	$1.0 \pm 0.4$	$0.7 \pm 0.5$	$0.6 \pm 0.3$	$0.4 \pm 0.2$	$1.0 \pm 0.6$	$0.5 \pm 0.2$
24:1n-9	$1.9 \pm 0.6^a$	$0.9 \pm 0.1^{bc}$	$0.8 \pm 0.1^c$	$0.7 \pm 0.1^c$	$1.3 \pm 0.6^b$	$0.7 \pm 0.1^c$
Total MUFA	$102.5 \pm 20.9$	$127.2 \pm 20.3$	$137.3 \pm 15.3$	$109.2 \pm 15.2$	$128.7 \pm 14.7$	$123.7 \pm 16.6$
18:2n-6	$39.2 \pm 7.8^a$	$36.6 \pm 4.9^a$	$39.1 \pm 4.3^a$	$38.8 \pm 5.9^a$	$25.2 \pm 1.8^b$	$76.1 \pm 6.1^c$
18:3n-6	$1.1 \pm 0.3^a$	$1.7 \pm 0.2^b$	$1.7 \pm 0.1^b$	$1.4 \pm 0.2^{ab}$	$1.1 \pm 0.1^a$	$2.9 \pm 0.4^c$
20:2n-6	$3.4 \pm 0.8^c$	$2.8 \pm 0.4^{bc}$	$2.8 \pm 0.3^{bc}$	$2.3 \pm 0.4^{ab}$	$2.0 \pm 0.1^a$	$5.6 \pm 0.7^d$
20:3n-6	$4.5 \pm 0.9^c$	$3.9 \pm 0.5^{bc}$	$3.7 \pm 0.4^{bc}$	$3.0 \pm 0.5^{ab}$	$2.8 \pm 0.2^a$	$6.5 \pm 1.1^d$
20:4n-6	$19.7 \pm 6.7^a$	$14.8 \pm 3.3^{abc}$	$12.1 \pm 1.0^{abc}$	$11.6 \pm 1.8^c$	$12.8 \pm 1.9^{abc}$	$16.0 \pm 1.8^b$
22:4n-6	$4.1 \pm 0.9^a$	$4.7 \pm 0.6^a$	$3.9 \pm 0.2^a$	$3.5 \pm 0.5^a$	$4.0 \pm 0.6^a$	$6.5 \pm 1.0^b$
22:5n-6	$10.6 \pm 2.5^a$	$9.2 \pm 1.4^a$	$8.1 \pm 1.3^{ab}$	$6.5 \pm 0.8^b$	$6.7 \pm 0.6^b$	$16.7 \pm 1.9^c$
Total n-6 PUFA	$82.6 \pm 17.5^c$	$73.6 \pm 7.2^{bc}$	$71.4 \pm 6.8^{bc}$	$67.1 \pm 8.1^b$	$54.6 \pm 3.5^a$	$130.2 \pm 11.6^d$
18:3n-3	$5.8 \pm 1.7^a$	$25.7 \pm 3.9^b$	$29.6 \pm 4.4^b$	$54.1 \pm 8.2^c$	$6.1 \pm 0.3^a$	$7.1 \pm 1.3^a$
18:4n-3	$0.7 \pm 0.2^{ab}$	$0.9 \pm 0.2^b$	$1.1 \pm 0.2^{bc}$	$1.3 \pm 0.3^c$	$1.1 \pm 0.1^{bc}$	$0.4 \pm 0.1^a$
20:3n-3	$1.7 \pm 0.4^a$	$4.5 \pm 0.5^b$	$4.6 \pm 0.7^b$	$8.3 \pm 1.4^c$	$1.1 \pm 0.2^a$	$1.4 \pm 0.2^a$
20:4n-3	$1.5 \pm 0.4^a$	$1.5 \pm 0.2^a$	$1.5 \pm 0.2^a$	$2.2 \pm 0.4^b$	$1.9 \pm 0.1^{ab}$	$0.5 \pm 0.1^c$
20:5n-3	$8.5 \pm 2.0^a$	$3.8 \pm 0.9^b$	$3.5 \pm 0.6^b$	$4.2 \pm 0.6^b$	$8.2 \pm 0.5^a$	$1.9 \pm 0.5^c$
22:4n-3	ND	$0.6 \pm 0.4$	$0.7 \pm 0.2$	$0.7 \pm 0.2$	$0.3 \pm 0.3$	$0.5 \pm 0.5$
22:5n-3	$13.1 \pm 2.4^b$	$11.0 \pm 2.3^{bc}$	$9.7 \pm 0.6^{cd}$	$11.5 \pm 1.6^{bc}$	$20.8 \pm 1.5^a$	$6.8 \pm 1.4^d$
22:6n-3	$65.6 \pm 12.6^b$	$49.0 \pm 6.6^c$	$46.7 \pm 7.3^{cd}$	$50.0 \pm 6.5^c$	$88.2 \pm 7.2^a$	$34.0 \pm 4.6^d$
Total n-3 PUFA	$96.9 \pm 17.3^b$	$97.1 \pm 11.1^b$	$97.3 \pm 12.0^b$	$132.2 \pm 17.1^a$	$127.8 \pm 8.3^a$	$52.5 \pm 6.8^c$
Total PUFA	$179.5 \pm 32.5$	$170.7 \pm 18.2$	$168.7 \pm 18.1$	$199.4 \pm 25.1$	$182.4 \pm 10.7$	$182.8 \pm 16.3$
(n-3)/(n-6)	$1.2 \pm 0.2^a$	$1.3 \pm 0.0^a$	$1.4 \pm 0.1^a$	$2.0 \pm 0.1^b$	$2.3 \pm 0.1^c$	$0.4 \pm 0.1^d$
Total DMA	$11.6 \pm 3.7$	$10.4 \pm 1.4$	$10.6 \pm 1.5$	$9.6 \pm 1.0$	$9.9 \pm 0.5$	$9.8 \pm 1.1$
20:4n-6/20:5n-3	$2.3 \pm 0.4^b$	$3.9 \pm 0.1^c$	$3.5 \pm 0.3^c$	$2.8 \pm 0.2^b$	$1.6 \pm 0.2^a$	$8.4 \pm 1.6^d$
Total FA	$459.5 \pm 51.8$	$464.2 \pm 45.5$	$474.8 \pm 44.3$	$463.0 \pm 57.6$	$489.8 \pm 34.9$	$470.0 \pm 47.0$

Values are the mean of 6 replicate groups of 6 fish ( $\pm$ SD). ND not detected. Values in the same row, which do not share the same superscript letter are significantly different at  $\alpha = 0.01$

lipids of FO-fed fish reflected the higher concentrations of 18:1n-7, 20:1n-9, 20:1n-7, 22:1 and 24:1n-9 in this diet compared to the other diets (Table 2).

The amounts of the individual PUFA varied greatly between the five dietary treatments (Tables 5, 6). The CO-fed fish contained the highest amounts of all n-6 PUFA, namely 18:2n-6, 18:3n-6, 20:2n-6, 20:3n-6, 20:4n-6, 22:4n-

6 and 22:5n-6 (Tables 5, 6), despite the fact that this diet contained similar amounts of all n-6 PUFA, except 18:2n-6, to the three LO-based diets. In contrast, FO-fed fish contained the lowest amounts ( $P < 0.01$ ) of 18:2n-6, 18:3n-6, 20:2n-6 and 20:3n-6 in their muscle lipids, and significantly decreased amounts of 22:4n-6 and 22:5n-6 compared to fish fed the PO–LO and CO diets (Tables 5, 6).

**Table 6** The fatty acid compositions ( $\mu\text{g}/\text{mg}$  of total lipid) of muscle TL of the initial fish population (day 0) and of fish fed the five diets after 140 days of feeding

Fatty acid	Initial fish group	PO–LO	LO–PO	LO	FO	CO
14:0	6.1 $\pm$ 2.1 <sup>a</sup>	6.6 $\pm$ 1.6 <sup>ab</sup>	7.1 $\pm$ 1.2 <sup>ab</sup>	5.9 $\pm$ 1.5 <sup>a</sup>	9.9 $\pm$ 1.5 <sup>b</sup>	6.1 $\pm$ 2.3 <sup>a</sup>
15:0	2.4 $\pm$ 0.5 <sup>a</sup>	0.8 $\pm$ 0.1 <sup>c</sup>	0.9 $\pm$ 0.1 <sup>c</sup>	0.9 $\pm$ 0.1 <sup>c</sup>	1.4 $\pm$ 0.2 <sup>b</sup>	0.9 $\pm$ 0.2 <sup>c</sup>
16:0	105.1 $\pm$ 10.6 <sup>a</sup>	129.2 $\pm$ 12.0 <sup>b</sup>	126.2 $\pm$ 12.2 <sup>b</sup>	114.5 $\pm$ 9.5 <sup>ab</sup>	130.8 $\pm$ 6.8 <sup>b</sup>	121.2 $\pm$ 17.3 <sup>ab</sup>
18:0	49.6 $\pm$ 4.4 <sup>a</sup>	41.2 $\pm$ 5.3 <sup>b</sup>	41.8 $\pm$ 2.5 <sup>b</sup>	43.5 $\pm$ 4.6 <sup>ab</sup>	45.0 $\pm$ 1.5 <sup>ab</sup>	44.6 $\pm$ 5.3 <sup>ab</sup>
20:0	1.3 $\pm$ 0.3	0.9 $\pm$ 0.1	0.9 $\pm$ 0.1	1.0 $\pm$ 0.2	1.0 $\pm$ 0.1	1.1 $\pm$ 0.1
22:0	1.5 $\pm$ 0.4	1.4 $\pm$ 0.4	1.4 $\pm$ 0.4	1.4 $\pm$ 0.2	1.2 $\pm$ 0.1	1.3 $\pm$ 0.1
Total SFA	166.0 $\pm$ 14.4	180.0 $\pm$ 18.0	178.2 $\pm$ 16.1	167.2 $\pm$ 14.5	189.2 $\pm$ 9.4	175.1 $\pm$ 24.2
16:1n-9	2.1 $\pm$ 0.8	1.6 $\pm$ 0.6	1.6 $\pm$ 0.9	1.6 $\pm$ 1.0	1.9 $\pm$ 0.6	1.5 $\pm$ 0.3
16:1n-7	11.9 $\pm$ 4.1 <sup>a</sup>	13.0 $\pm$ 2.7 <sup>ab</sup>	13.6 $\pm$ 2.9 <sup>ab</sup>	10.7 $\pm$ 2.6 <sup>a</sup>	18.0 $\pm$ 2.3 <sup>b</sup>	10.5 $\pm$ 3.0 <sup>a</sup>
18:1n-9	63.7 $\pm$ 14.1 <sup>a</sup>	124.9 $\pm$ 21.8 <sup>b</sup>	117.2 $\pm$ 17.5 <sup>b</sup>	96.4 $\pm$ 11.6 <sup>b</sup>	98.1 $\pm$ 7.6 <sup>b</sup>	108.3 $\pm$ 22.8 <sup>b</sup>
18:1n-7	17.7 $\pm$ 2.4 <sup>a</sup>	11.4 $\pm$ 1.1 <sup>b</sup>	11.7 $\pm$ 1.7 <sup>b</sup>	10.4 $\pm$ 1.1 <sup>b</sup>	18.1 $\pm$ 3.4 <sup>a</sup>	11.4 $\pm$ 1.3 <sup>b</sup>
20:1n-9	4.0 $\pm$ 1.5 <sup>abc</sup>	3.5 $\pm$ 0.5 <sup>ac</sup>	3.6 $\pm$ 0.5 <sup>ab</sup>	2.9 $\pm$ 0.3 <sup>b</sup>	4.8 $\pm$ 0.3 <sup>c</sup>	4.5 $\pm$ 0.9 <sup>ac</sup>
20:1n-7	0.3 $\pm$ 0.2 <sup>ab</sup>	0.4 $\pm$ 0.2 <sup>ab</sup>	0.3 $\pm$ 0.2 <sup>ab</sup>	0.1 $\pm$ 0.0 <sup>a</sup>	0.5 $\pm$ 0.2 <sup>b</sup>	0.3 $\pm$ 0.1 <sup>ab</sup>
22:1 n-11/n-9	1.0 $\pm$ 0.4 <sup>a</sup>	0.2 $\pm$ 0.2 <sup>b</sup>	0.3 $\pm$ 0.3 <sup>b</sup>	0.3 $\pm$ 0.2 <sup>b</sup>	1.0 $\pm$ 0.3 <sup>a</sup>	0.8 $\pm$ 0.1 <sup>a</sup>
24:1n-9	1.9 $\pm$ 0.6 <sup>a</sup>	1.0 $\pm$ 0.1 <sup>b</sup>	1.0 $\pm$ 0.2 <sup>b</sup>	0.9 $\pm$ 0.1 <sup>b</sup>	1.4 $\pm$ 0.3 <sup>a</sup>	1.0 $\pm$ 0.1 <sup>b</sup>
Total MUFA	102.5 $\pm$ 20.9	156.3 $\pm$ 26.0	149.3 $\pm$ 22.9	123.3 $\pm$ 16.2	143.8 $\pm$ 9.7	138.2 $\pm$ 27.9
18:2n-6	39.2 $\pm$ 7.8 <sup>a</sup>	59.7 $\pm$ 6.4 <sup>b</sup>	58.8 $\pm$ 5.2 <sup>b</sup>	61.8 $\pm$ 2.5 <sup>b</sup>	38.8 $\pm$ 2.7 <sup>a</sup>	109.0 $\pm$ 16.2 <sup>c</sup>
18:3n-6	1.1 $\pm$ 0.3 <sup>a</sup>	1.5 $\pm$ 0.2 <sup>b</sup>	1.5 $\pm$ 0.2 <sup>b</sup>	1.2 $\pm$ 0.1 <sup>ab</sup>	0.9 $\pm$ 0.1 <sup>a</sup>	2.6 $\pm$ 0.4 <sup>c</sup>
20:2n-6	3.4 $\pm$ 0.8 <sup>bc</sup>	4.6 $\pm$ 0.4 <sup>a</sup>	4.1 $\pm$ 0.3 <sup>ab</sup>	3.9 $\pm$ 0.2 <sup>b</sup>	2.8 $\pm$ 0.2 <sup>c</sup>	9.1 $\pm$ 1.1 <sup>d</sup>
20:3n-6	4.5 $\pm$ 0.9 <sup>ab</sup>	5.2 $\pm$ 0.6 <sup>a</sup>	4.6 $\pm$ 0.2 <sup>ab</sup>	3.9 $\pm$ 0.4 <sup>b</sup>	3.1 $\pm$ 0.2 <sup>c</sup>	9.1 $\pm$ 1.4 <sup>d</sup>
20:4n-6	19.7 $\pm$ 6.7 <sup>a</sup>	11.1 $\pm$ 1.7 <sup>b</sup>	9.7 $\pm$ 0.9 <sup>b</sup>	9.0 $\pm$ 1.1 <sup>b</sup>	9.6 $\pm$ 0.7 <sup>b</sup>	19.2 $\pm$ 3.2 <sup>a</sup>
22:4n-6	4.1 $\pm$ 0.9 <sup>b</sup>	3.4 $\pm$ 0.4 <sup>bc</sup>	2.8 $\pm$ 0.2 <sup>cd</sup>	2.3 $\pm$ 0.3 <sup>d</sup>	2.6 $\pm$ 0.3 <sup>d</sup>	6.8 $\pm$ 0.8 <sup>a</sup>
22:5n-6	10.6 $\pm$ 2.5 <sup>b</sup>	6.0 $\pm$ 0.9 <sup>c</sup>	4.9 $\pm$ 0.4 <sup>cd</sup>	4.2 $\pm$ 0.8 <sup>d</sup>	4.2 $\pm$ 0.4 <sup>d</sup>	15.6 $\pm$ 2.4 <sup>a</sup>
Total n-6 PUFA	82.6 $\pm$ 17.5 <sup>a</sup>	91.5 $\pm$ 9.2 <sup>a</sup>	86.2 $\pm$ 6.7 <sup>a</sup>	86.2 $\pm$ 4.3 <sup>a</sup>	62.0 $\pm$ 4.0 <sup>b</sup>	171.3 $\pm$ 21.9 <sup>c</sup>
18:3n-3	5.8 $\pm$ 1.7 <sup>a</sup>	25.3 $\pm$ 3.7 <sup>b</sup>	37.0 $\pm$ 5.7 <sup>c</sup>	54.6 $\pm$ 5.9 <sup>d</sup>	6.0 $\pm$ 1.2 <sup>a</sup>	4.9 $\pm$ 1.1 <sup>a</sup>
18:4n-3	0.7 $\pm$ 0.2 <sup>a</sup>	0.6 $\pm$ 0.1 <sup>a</sup>	0.9 $\pm$ 0.2 <sup>a</sup>	0.9 $\pm$ 0.2 <sup>a</sup>	0.8 $\pm$ 0.1 <sup>a</sup>	0.1 $\pm$ 0.1 <sup>b</sup>
20:3n-3	1.7 $\pm$ 0.4 <sup>b</sup>	5.5 $\pm$ 0.9 <sup>c</sup>	7.5 $\pm$ 0.9 <sup>d</sup>	11.1 $\pm$ 0.6 <sup>e</sup>	1.1 $\pm$ 0.2 <sup>a</sup>	1.3 $\pm$ 0.2 <sup>a</sup>
20:4n-3	1.5 $\pm$ 0.4 <sup>ab</sup>	1.4 $\pm$ 0.2 <sup>a</sup>	1.8 $\pm$ 0.2 <sup>b</sup>	2.3 $\pm$ 0.2 <sup>c</sup>	1.7 $\pm$ 0.2 <sup>ab</sup>	0.2 $\pm$ 0.2 <sup>d</sup>
20:5n-3	8.5 $\pm$ 2.0 <sup>a</sup>	2.8 $\pm$ 0.4 <sup>c</sup>	3.2 $\pm$ 0.4 <sup>bc</sup>	4.0 $\pm$ 0.4 <sup>b</sup>	8.5 $\pm$ 0.5 <sup>a</sup>	1.1 $\pm$ 0.3 <sup>d</sup>
22:4n-3	ND	0.5 $\pm$ 0.2 <sup>a</sup>	0.7 $\pm$ 0.2 <sup>ab</sup>	0.9 $\pm$ 0.1 <sup>b</sup>	0.1 $\pm$ 0.1 <sup>c</sup>	ND
22:5n-3	13.1 $\pm$ 2.4 <sup>b</sup>	7.4 $\pm$ 0.8 <sup>c</sup>	8.2 $\pm$ 0.8 <sup>c</sup>	9.0 $\pm$ 0.8 <sup>c</sup>	20.4 $\pm$ 2.0 <sup>a</sup>	4.6 $\pm$ 1.1 <sup>d</sup>
22:6n-3	65.6 $\pm$ 12.6 <sup>b</sup>	41.0 $\pm$ 5.5 <sup>cd</sup>	42.1 $\pm$ 3.0 <sup>c</sup>	45.0 $\pm$ 6.5 <sup>c</sup>	87.0 $\pm$ 8.7 <sup>a</sup>	29.2 $\pm$ 4.4 <sup>d</sup>
Total n-3 PUFA	96.9 $\pm$ 17.3 <sup>b</sup>	84.4 $\pm$ 9.9 <sup>b</sup>	101.3 $\pm$ 10.5 <sup>b</sup>	127.7 $\pm$ 7.3 <sup>c</sup>	125.5 $\pm$ 10.1 <sup>c</sup>	41.3 $\pm$ 6.1 <sup>a</sup>
Total PUFA	179.5 $\pm$ 32.5 <sup>ab</sup>	175.9 $\pm$ 19.0 <sup>a</sup>	187.5 $\pm$ 17.0 <sup>ab</sup>	213.9 $\pm$ 10.6 <sup>b</sup>	187.5 $\pm$ 13.3 <sup>ab</sup>	212.6 $\pm$ 22.6 <sup>b</sup>
(n-3)/(n-6)	1.2 $\pm$ 0.2 <sup>c</sup>	0.9 $\pm$ 0.0 <sup>d</sup>	1.2 $\pm$ 0.1 <sup>c</sup>	1.5 $\pm$ 0.1 <sup>b</sup>	2.0 $\pm$ 0.1 <sup>a</sup>	0.3 $\pm$ 0.1 <sup>e</sup>
Total DMA	11.6 $\pm$ 3.7	14.2 $\pm$ 2.4	13.7 $\pm$ 1.6	14.5 $\pm$ 0.7	13.1 $\pm$ 0.9	13.3 $\pm$ 2.0
20:4n-6/20:5n-3	2.3 $\pm$ 0.4 <sup>c</sup>	4.0 $\pm$ 0.2 <sup>a</sup>	3.0 $\pm$ 0.2 <sup>b</sup>	2.2 $\pm$ 0.1 <sup>c</sup>	1.1 $\pm$ 0.0 <sup>d</sup>	17.7 $\pm$ 4.8 <sup>e</sup>
Total FA	459.5 $\pm$ 51.8	526.4 $\pm$ 52.0	528.6 $\pm$ 55.7	518.9 $\pm$ 37.6	533.7 $\pm$ 27.1	539.2 $\pm$ 67.4

Values are the mean of 6 replicate groups of 6 fish ( $\pm$ SD). *ND* not detected. Values in the same row, which do not share the same superscript letter are significantly different at  $\alpha = 0.01$

However, at the end of the 20-week feeding trial, FO-fed fish had similar concentrations of 20:4n-6 to fish fed the three LO-based diets, and about half the concentration of CO-fed fish (Table 6). The amounts of all n-6 PUFA increased as the amount of dietary LO decreased. Thus, LO-fed fish contained significantly lower amounts of 20:2n-6, 20:3n-6, 22:4n-6 and 22:5n-6 compared to those found in

PO–LO-fed fish (Tables 5, 6). LO-fed fish also contained decreased amounts of 18:3n-6 and 20:4n-6 compared to fish fed the PO–LO and LO–PO diets, but these were not significantly different.

The n-3 PUFA content of the muscle lipids of fish also showed significant differences between dietary treatments. Fish fed the CO diet contained the lowest amounts

**Table 7** The percentage retention of dietary fatty acids in the tissues of fish fed the five experimental diets for 140 days

Fatty acid	PO–LO	LO–PO	LO	FO	CO
14:0	11.3 ± 1.8 <sup>a</sup>	19.7 ± 7.8 <sup>ab</sup>	27.0 ± 7.6 <sup>b</sup>	4.2 ± 0.9 <sup>c</sup>	27.3 ± 17.3 <sup>ab</sup>
15:0	7.8 ± 0.9 <sup>ab</sup>	10.7 ± 4.1 <sup>a</sup>	11.2 ± 1.4 <sup>a</sup>	5.6 ± 1.2 <sup>b</sup>	12.5 ± 4.2 <sup>a</sup>
16:0	8.0 ± 0.5 <sup>a</sup>	12.1 ± 3.8 <sup>ab</sup>	18.5 ± 2.1 <sup>b</sup>	12.5 ± 1.3 <sup>b</sup>	13.7 ± 4.5 <sup>b</sup>
18:0	12.9 ± 1.0 <sup>a</sup>	16.2 ± 4.5 <sup>ab</sup>	15.4 ± 1.6 <sup>ab</sup>	15.9 ± 1.3 <sup>ab</sup>	19.7 ± 5.1 <sup>b</sup>
20:0	4.9 ± 0.1 <sup>ab</sup>	6.6 ± 2.5 <sup>ab</sup>	7.5 ± 1.5 <sup>a</sup>	6.9 ± 1.2 <sup>a</sup>	4.0 ± 1.4 <sup>b</sup>
22:0	8.4 ± 0.2 <sup>ab</sup>	11.7 ± 4.4 <sup>a</sup>	10.0 ± 2.1 <sup>a</sup>	7.7 ± 1.0 <sup>ab</sup>	6.6 ± 1.5 <sup>b</sup>
16:1n-9	>100	>100	>100	14.7 ± 5.3	>100
16:1n-7	27.4 ± 3.1 <sup>a</sup>	35.2 ± 15.3 <sup>a</sup>	31.0 ± 8.2 <sup>a</sup>	5.5 ± 1.1 <sup>b</sup>	27.4 ± 14.6 <sup>a</sup>
18:1n-9	6.5 ± 0.6	8.9 ± 3.3	9.3 ± 1.4	10.0 ± 1.6	7.0 ± 3.0
18:1n-7	11.2 ± 0.5 <sup>ab</sup>	17.3 ± 5.6 <sup>a</sup>	14.3 ± 2.0 <sup>a</sup>	9.5 ± 1.9 <sup>b</sup>	11.2 ± 3.3 <sup>ab</sup>
20:1n-9	20.0 ± 2.3 <sup>a</sup>	25.3 ± 9.5 <sup>a</sup>	24.2 ± 3.1 <sup>a</sup>	6.1 ± 0.8 <sup>b</sup>	23.2 ± 9.4 <sup>a</sup>
20:1n-7	>100	>100	>100	4.1 ± 1.3	>100
22:1	>100	>100	>100	2.7 ± 0.9	>100
24:1n-9	33.9 ± 2.2 <sup>a</sup>	37.9 ± 12.9 <sup>a</sup>	41.2 ± 6.2 <sup>a</sup>	5.9 ± 1.3 <sup>b</sup>	47.3 ± 10.7 <sup>a</sup>
18:2n-6	4.8 ± 0.3	5.2 ± 1.5	4.9 ± 0.4	5.6 ± 0.6	3.9 ± 1.1
18:3n-6	>100	>100	>100	17.7 ± 3.3	25.7 ± 8.1
20:2n-6	>100	>100	>100	22.2 ± 2.3	>100
20:3n-6	>100	>100	>100	35.9 ± 3.7	>100
20:4n-6	67.8 ± 5.3 <sup>a</sup>	61.4 ± 15.8 <sup>a</sup>	56.8 ± 6.7 <sup>a</sup>	21.3 ± 2.4 <sup>b</sup>	>100
22:4n-6	>100	>100	>100	26.4 ± 4.1	>100
22:5n-6	78.1 ± 6.1 <sup>a</sup>	68.0 ± 21.2 <sup>a</sup>	60.7 ± 11.6 <sup>a</sup>	23.5 ± 3.4 <sup>b</sup>	>100
18:3n-3	2.1 ± 0.2 <sup>a</sup>	2.4 ± 0.9 <sup>ab</sup>	1.9 ± 0.3 <sup>a</sup>	4.0 ± 1.2 <sup>b</sup>	2.8 ± 1.0 <sup>ab</sup>
18:4n-3	>100	>100	>100	1.8 ± 0.4	>100
20:3n-3	>100	>100	>100	>100	>100
20:4n-3	>100	>100	>100	>100	>100
20:5n-3	11.8 ± 0.8 <sup>a</sup>	15.5 ± 4.2 <sup>ab</sup>	19.5 ± 1.7 <sup>b</sup>	2.2 ± 0.2 <sup>c</sup>	4.8 ± 1.3 <sup>d</sup>
22:4n-3	>100	>100	>100	>100	>100
22:5n-3	81.8 ± 4.9 <sup>a</sup>	96.3 ± 28.3 <sup>a</sup>	>100	12.1 ± 1.7 <sup>b</sup>	48.4 ± 12.4 <sup>c</sup>
22:6n-3	51.0 ± 1.6 <sup>a</sup>	61.4 ± 16.7 <sup>a</sup>	56.8 ± 7.0 <sup>a</sup>	15.9 ± 1.7 <sup>b</sup>	35.6 ± 5.8 <sup>c</sup>

Values represent means of six cages ± SD. Percentage retention >100 indicates tissue concentration higher than the dietary supply and implies synthesis and/or high retention of the tissue reserves. Values in the same row, which do not share the same superscript letter are significantly different at  $\alpha = 0.01$

Calculation:

For each FA,

FA assimilated in fish (g) = final FA content (g) – initial FA content (g) (1)

and therefore for each group of fish reared in a hapa

Initial total FA content (g) = average initial concentration of FA (g/g muscle tissue) × initial fish biomass (g) (2)

Final total FA content (g) = average final concentration of FA (g/g muscle tissue) × final fish biomass (g) (3)

Therefore FA assimilated by total biomass of fish/hapa = Eq. (3) – Eq. (2) (4)

Feed was provided on a tray and pellets rarely remained inside the tray so only a small proportion of feed was wasted. Therefore, assuming that 90% of total feed given was eaten,

Total amount of FA eaten (g) = 0.9 × total amount of FA given (g) (5)

Where total amount of FA given = concentration of FA in diet (g/g of diet) × total feed given to that hapa (g)

% Assimilation/hapa = Eq. (4) × 100/Eq. (5)

( $P < 0.01$ ) of all n-3 PUFA, namely 18:3n-3, 18:4n-3, 20:3n-3, 20:4n-3, 20:5n-3, 22:5n-3 and 22:6n-3 (Tables 5, 6). FO-fed fish had significantly decreased amounts of 18:3n-3 compared to the three LO-based treatments

(Tables 5, 6) due to the lower concentration of 18:3n-3 in the FO diet. Also, FO-fed fish contained significantly lower amounts of 20:3n-3 and 22:4n-3 compared to the three LO-based treatments, and significantly lower amounts of

20:4n-3 compared to the LO-fed fish (Tables 5, 6), despite the fact that the FO diet supplied a higher amount of the latter FA compared to the LO-based diets (Table 2). On the other hand, FO-fed fish had the highest contents ( $P < 0.01$ ) of 20:5n-3, 22:5n-3 and 22:6n-3 in their muscle lipids, both at day 32 of the feeding period (Table 5) and at the end of the dietary trial (Table 6).

The inclusion of increasing levels of LO at the cost of PO in the basal diet resulted in significant increases in tissue 18:3n-3, 20:3n-3 and 20:4n-3 (Table 6). However, the amounts of 18:4n-3, 22:5n-3 and 22:6n-3 were not significantly different ( $P > 0.01$ ) in the muscle lipids of fish fed the three LO-based diets, though in an increasing order with the higher inclusion of LO in the diet (Table 6). The amounts of 20:5n-3 and 22:4n-3 were also in an increasing order in fish fed the PO–LO diet to fish fed the LO–PO and LO diets and the concentrations of these two FA in the LO-fed fish were significantly higher than those found in PO–LO-fed fish (Table 6).

The n-3/n-6 PUFA ratio was the highest in FO-fed fish and LO-fed fish contained a significantly higher n-3/n-6 PUFA ratio compared to fish fed the PO–LO, LO–PO and CO diets (Table 6). The lowest n-3/n-6 PUFA ratio ( $P < 0.01$ ) was found in the muscle lipids of fish fed the CO diet and reflected the lower ratio supplied by this diet (Table 2). The ratio of 20:4n-6/20:5n-3, predictive of the production of series 2 and series 3 eicosanoids, was found to be the highest ( $P < 0.01$ ) in CO-fed fish, while FO-fed fish exhibited the lowest 20:4n-6/20:5n-3 value ( $P < 0.01$ , Tables 5, 6). Fish fed the three LO-based diets had moderate 20:4n-6/20:5n-3 ratios, which were in a significantly decreasing order in PO–LO-fed fish to LO-fed (Table 6).

## Discussion

The present study suggests that linseed oil and its blends with palm olein oil could totally replace fish oil without any negative effects on the growth and feed efficiency of tilapia (*O. niloticus*), consistent with the current trend towards replacement of fish oil in fish feeds. Survival rates of fish were high and consistent between treatments, while values of SGR were relatively high, without any signs of growth cessation. The relatively high values of FCR observed could be related to overfeeding and/or to the lower digestibility caused by the high inclusion level of soybean meal.

The study was not designed to define the precise requirements of tilapia for n-6 and/or n-3 PUFA but, nevertheless, suggests that both series of PUFA may be important for maximum growth of this species. Since the FO diet provided only 0.3% (by dry weight) of dietary n-6 PUFA and led to similar growth as the CO diet that pro-

vided 1.1% of n-6 PUFA, it appears that the requirement for n-6 PUFA may be as low as 0.3% of diet by dry weight. The FO diet with the highest content of long-chain n-3 PUFA gave the highest weight gain, although not significantly so, indicating that 20:5n-3 and 22:6n-3 may also have a growth promoting effect. Furthermore, the similar growth rates among fish fed the three LO-based diets suggest that the increases in dietary 18:3n-3 (from 0.5 to 1.1%) are not associated with depressed growth as reported in previous studies [19].

The TL content of the muscle tissue was not significantly affected by the different dietary treatments suggesting that the different oils did not have any significant effect upon muscle tissue adiposity, in agreement with previous studies (e.g. [20, 21]). However, other workers found differences in fillet and whole-body lipid levels of Nile tilapia (*O. niloticus*) depending on the source of dietary oil [22, 23], as was shown in salmonids [24].

Incorporation of FA into tissues is under various metabolic influences such as preferential incorporation,  $\beta$ -oxidation, lipogenic activity, and fatty acid elongation and desaturation processes [25] and may also be affected by environmental factors [26] or size or age of animals [27]. A mass balance approach can be used to give an insight into the catabolism or deposition of different fatty acids since the dietary intake of the different groups of fish was known accurately. For each dietary fatty acid, it is assumed that, from the total amount of this FA eaten, a proportion is retained in tissues and the rest is metabolised. Retention of a FA in fish tissues will also include de novo synthesis in the case of a SFA or MUFA. Utilisation includes the degradation of a fatty acid via  $\beta$ -oxidation for energy, and/or its utilisation as a substrate for desaturation and chain elongation to longer chain PUFA. In addition, utilisation (not retention) in this simplified model includes the proportion of the dietary FA that was not digested/absorbed.

In general, all groups of fish displayed low percentage retention of their dietary SFA (Table 7). However, the FA composition of the diet affected the extent to which the different SFA were retained (or synthesised de novo) by the fish. There was a distinct trend in which fish receiving a lower dietary amount of a certain SFA tended to retain this FA at a higher level compared to fish receiving a higher dietary amount of this SFA (Table 7). This was true for all individual SFA, including the two major saturates 16:0 and 18:0. These findings are consistent with a previous study with tilapia sampled from various culture systems and sites, where, despite differences in feed inputs, fish displayed similar levels of SFA in their muscle tissues [28]. Similar findings have been reported for salmonids [24, 29] and for a red hybrid of tilapia [23]. The pattern of retention was similar for MUFA. Again fish with a lower dietary intake of a certain MUFA tended to retain this at a higher level

compared to fish with a higher dietary intake and this trend was observed for all individual MUFA (Table 7). In general, all groups of fish metabolised the majority of their dietary MUFA. 18:1n-9 is known to be a preferred substrate for  $\beta$ -oxidation in fish [25].

Irrespective of the diet fed, fish showed a very low retention of dietary 18:3n-3 and 18:2n-6 (Table 7). Dietary 18:3n-3 was extensively utilised by fish and its retention was the lowest of any dietary FA. In rainbow trout the great majority of ingested 18:3n-3 was catabolised [13, 30]. Dietary 18:2n-6 was the next most utilised FA after 18:3n-3 (Table 7). The  $\beta$ -oxidation of FA in fish tissues is known to be a selective process [25], where, in general, SFA, MUFA and 18:2n-6 are preferred over C20 and C22 PUFA. Fish fed the LO-based diets retained dietary 20:4n-6 and 22:5n-6 at high levels, while the CO-fed fish retained these two FA at levels higher than their dietary supply (Table 7), perhaps implying synthesis from shorter chain n-6 PUFA. Fish fed the FO diet retained 20:4n-6 and 22:5n-6, as well as all other n-6 PUFA except 18:2, at higher levels than those of their dietary n-3 PUFA. The preferential retention of 20:4n-6 and 22:5n-6, irrespective of the diet fed, indicates the nutritional importance of these FA for tilapia. Those n-6 PUFA that were in very low concentrations (not detected) in the VO diets, such as 18:3n-6, 20:2n-6, 20:3n-6 and 22:4n-6, were preferentially retained by these fish (Table 7, values >100%). Similarly, those PUFA of the n-3 series that were in low concentrations in all diets, such as 20:3n-3, 20:4n-3 and 22:4n-3, were also preferentially retained by fish (Table 7). Dietary 20:5n-3 was retained at relatively low levels in all groups of fish (Table 7). However, fish fed the linseed oil-based diets retained their dietary 20:5n-3 to a greater extent than the FO- and CO-fed fish, suggesting a synthesis of this FA from 18:3n-3. On the other hand, fish fed the VO diets preferentially retained 22:5n-3 and 22:6n-3, while FO-fed fish retained these two FA at higher levels than other dietary n-3 PUFA. The best retained of the major FA in all four VO diets were 20:4n-6 and 22:6n-3 which are known to have essential roles in cellular physiology and membrane structure, and 22:5n-3 and 22:5n-6 which have not. While 22:5n-3 is an intermediate in the synthesis of 22:6n-3 and may accumulate because of the inherent inefficiency of the pathway, the accumulation of 22:5n-6 may indicate that this PUFA can partially substitute for 22:6n-3 in tilapia.

The muscle content of 18:2n-6 and 18:3n-3 strongly reflected dietary intake with the highest amounts of 18:2n-6 in fish fed the CO diet and 18:3n-3 in fish fed the LO diets, while fish fed the FO diet contained the highest amounts of long-chain n-3 PUFA. Fish fed the three LO-diets contained significantly higher amounts of all other individual n-3 PUFA compared to CO-fed fish, although all four VO diets supplied similar amounts of individual n-3 PUFA

except 18:3n-3. This indicates that there was desaturation and elongation of dietary 18:3n-3 in fish fed the three LO-based diets. Similarly fish fed the 18:2n-6-rich CO diet displayed the highest contents of all n-6 PUFA despite the fact that the CO diet and the three LO based diets differed only in their levels of 18:2n-6. This also suggests that there was a significant desaturation and elongation of dietary 18:2n-6 in the CO-fed fish. These findings are consistent with previous studies, which showed that Nile tilapia (*O. niloticus*) [10, 11], redbelly tilapia (*Tilapia zillii*) [31], and blue tilapia (*O. aureus*) [19] all possessed some ability to elongate and desaturate 18:3n-3 and 18:2n-6 to their longer chain derivatives.

The inclusion of increasing levels of LO in the diet, and thus graded amounts of dietary 18:3n-3, resulted in commensurate increases in tissue 18:3n-3 and all n-3 PUFA pathway anabolites, though the increases in 18:4n-3, 22:5n-3 and 22:6n-3 were not significant. The largest increase was in the elongation product 20:3n-3 which mirrored the change in 18:3n-3 content. Studies in animals [32, 33] and humans [34] have shown that there is an optimal amount of dietary 18:3n-3 that gives a peak in the synthesis of 22:6n-3 with a plateau or decline thereafter. Although we could not confirm this from the present experiment, it is clear that in tilapia the conversion of 18:3n-3 to longer chain n-3 PUFA derivatives is not efficient, and particularly the synthesis of 22:5n-3 and 22:6n-3 is low. When comparing the fish fed PO-LO and LO diets a 2.29-fold increase in dietary 18:3n-3 resulted in a 2.16-fold increase in tissue 18:3n-3 that in turn gave a 1.41-fold increase in tissue 18:4n-3, a 1.61-fold increase in tissue 20:4n-3, a 1.45-fold increase in tissue 20:5n-3, a 1.21-fold increase in tissue 22:5n-3 and only a 1.10-fold increase in tissue 22:6n-3. Thus, progressively less substrate reaches the end products indicating that further increases in dietary 18:3n-3 will not give meaningful increases in tissue 22:6n-3. The final muscle concentration of 22:6n-3 in the LO-fed fish fell compared to the FO-fed fish indicating a net loss of 22:6n-3. These findings are in agreement with studies in other fish species [13, 24, 30] and tilapia (*O. niloticus*) [11], which suggested that fish fed a vegetable oil diet were unable to maintain the tissue concentration of 20:5n-3, 22:5n-3 and 22:6n-3. This is a conclusion of great importance indicating that the replacement of FO with VO in diets for farmed fish lowers their content of the nutritionally important long-chain n-3 PUFA.

In fish fed the CO diet, where there was a large amount of 18:2n-6 and a small amount of 18:3n-3, the synthesis of 22:6n-3 will have been minimal, and all the tissue 22:6n-3 was probably derived from the fish meal in the diets. The CO-fed fish showed a weight gain of 175 g with a FCR of 2.01 and had a 22:6n-3 concentration of 29.2  $\mu\text{g}/\text{mg}$  TL with 7.03 mg TL/wet weight carcase. Assuming a uniform

body concentration of 22:6n-3 equivalent to the value found in muscle gives 35.9 mg 22:6n-3 per fish. The intake of 22:6n-3 from the diet was 105 mg so there was a turnover/ $\beta$ -oxidation equivalent to about twice the body 22:6n-3 content. Using the increment of 22:6n-3 concentration in the PO–LO-fed fish and LO-fed fish over the CO-fed fish it is possible to calculate the increment of 22:6n-3 due to synthesis in the LO-fed fish. In PO–LO-fed fish this gives 10 mg 22:6n-3 synthesised/g 18:3n-3 eaten and in the LO-fed fish 5.0 mg 22:6n-3 synthesised/g 18:3n-3 eaten confirming that the more 18:3n-3 ingested the less is converted to 22:6n-3.

Another finding of the study was that in FO-fed fish, tissue concentrations of 20:5n-3 were lower than the dietary concentration. This confirmed the findings of an in vivo study with Nile tilapia (*O. niloticus*) [10], and this FA is also extensively oxidised in Atlantic salmon [35]. This is consistent with our findings in a previous study where tilapia that had been raised on commercial diets containing high levels of fishmeal and FO contained low concentrations of 20:5n-3 (0.3–1.1% of total FA) compared to the concentrations of 22:6n-3 (7–10% of total FA) [28]. It is likely, therefore, that 20:5n-3 is selectively used as a substrate for  $\beta$ -oxidation in tilapia. While the retention of 20:5n-3 was low in all dietary groups, the concentration of 22:6n-3 in the FO-fed fish was higher than that supplied by the FO diet indicating selective retention.

Tilapia is a tropical non-migratory fish and the muscle lipid content of <1% wet weight lipid is low compared to a salmonid and some other migratory fishes but similar to a gadoid such as cod. Thus, although the intake of long-chain n-3 PUFA from consuming tilapia is low relative to a salmonid, it is a widely consumed fish species in many parts of the world and an important dietary resource for those populations who do not have access to oily fish or PUFA supplements. It is recommended that vegetable oil alternatives that are rich in 18:3n-3 and low in 18:2n-6 are used if the replacement of FO in fish feeds become inevitable. The inclusion of LO can maximise the retention of desirable 20:5n-3 and 22:6n-3 and can minimise the deposition of undesirable long-chain n-6 PUFA in the edible muscle tissue of fish compared to a vegetable oil that is rich in 18:2n-6. A possible solution could be that a diet containing LO is used to promote the growth of tilapia and a finishing diet containing FO is used to restore the levels of long-chain n-3 PUFA as this strategy has been shown to have promising results in salmonids [35].

**Acknowledgments** We thank James Dick for help with the fatty acid analysis, the staff of the Asian Institute of Technology (Pathumthani, Thailand) and Charoen Pokphand Foods feed mill (Samut Sakorn, Thailand) for their assistance with this experiment.

## References

- Innis SM (1991) Essential fatty acids in growth and development. *Prog Lipid Res* 30:39–103
- Sargent JR, Tocher DR, Bell JG (2002) The lipids. In: Halver JE, Hardy RW (eds) *Fish nutrition*, 3rd edn. Academic, San Diego, pp. 181–257
- Connor WE (2000) Importance of n-3 fatty acids in health and disease. *Am J Clin Nutr* 71:171S–175S
- Leaf A, Weber PC (1988) Medical progress. Cardiovascular effects of n-6 fatty acids. *New Eng J Med* 318:549–557
- Simopoulos AP (1999) Evolutionary aspects of omega-3 fatty acids in the food supply. *Prost Leuk Ess Fatty Acids* 60:421–429
- Bulliyya G (2000) Key role of dietary fats in coronary heart disease under progressive urbanization and nutritional transition. *Asia Pacific J Clin Nutr* 9:289–297
- Okuyama, H, Kobayashi T, Watanabe S (1997) Dietary fatty acids—the n-6/n-3 balance and chronic elderly diseases. Excess linoleic acid and relative n-3 deficiency syndrome seen in Japan. *Prog Lipid Res* 35:409–457
- Sargent JR, Tacon AGJ (1999) Development of farmed fish: a nutritionally necessary alternative to meat. *Proc Nutr Soc* 58:377–383
- FAO (Food and Agriculture Organisation of the United Nations) (2004) *The State of World Fisheries and Aquaculture (SOFIA)*. Food and Agriculture Organization of the United Nations, Rome, 153 p
- Olsen RE, Henderson RJ, McAndrew BJ (1990) The conversion of linoleic acid and linolenic acid to longer chain polyunsaturated fatty acids by *Tilapia (Oreochromis nilotica)* in vivo. *Fish Physiol Biochem* 8:261–270
- Tocher DR, Agaba M, Hastings N, Bell JG, Dick JR, Teale AJ (2002) Nutritional regulation of hepatocyte fatty acid desaturation and polyunsaturated fatty acid composition in zebrafish (*Danio rerio*) and tilapia (*Oreochromis niloticus*). *Fish Physiol Biochem* 24:309–320
- Buzzi M, Henderson RJ, Sargent JR (1996) The desaturation and elongation of linolenic acid and eicosapentaenoic acid by hepatocytes and liver microsomes from rainbow trout (*Oncorhynchus mykiss*) fed diets containing fish oil or olive oil. *Biochim Biophys Acta* 1299:235–244
- Bell MV, Dick JR (2004) Changes in capacity to synthesise 22:6n-3 during development in rainbow trout (*Oncorhynchus mykiss*). *Aquaculture* 235:393–409
- AOAC (Association of Official Analytical Chemists) (1990) *Official Methods of Analysis*. In: Helrich K (ed) AOAC. Arlington, 684 p
- APHA (American Public Health Association) (1985) *Standard methods for examination of water and wastewater*, 16th edn. American Public Health Association, American Water Works Association, and Water Pollution Control Federation, Washington, 1268 p
- Folch J, Lees M, Sloane-Stanley GH (1957) A simple method for the isolation and purification of total lipid from animal tissues. *J Biol Chem* 226:497–509
- Olsen RE, Henderson RJ (1989) The rapid analysis of neutral and polar marine lipids using double-development HPTLC and scanning densitometry. *J Exp Mar Biol Ecol* 129:189–197
- Christie WW (2003) *Lipid analysis: isolation, separation, identification and structural analysis of lipids*, 3rd edn. The Oily Press, Bridgwater
- Stickney RR, McGeachin RB (1983) Responses of *Tilapia aurea* to semipurified diets of differing fatty acid composition. In: Fishelson L, Yaron Z (eds) *Proceedings of the international sym-*

- posium on tilapia in aquaculture. Tel Aviv University Press, Tel Aviv, pp 346–355
20. Huang CH, Huang MC, Hou PC (1998) Effect of dietary lipids on fatty acid composition and lipid peroxidation in sarcoplasmic reticulum of hybrid tilapia, *Oreochromis niloticus* × *O. aureus*. *Comp Biochem Physiol* 120B:331–336
  21. Justi KC, Hayashi C, Visentainer JV, de Souza NE, Matsushita M (2003) The influence of feed supply time on the fatty acid profile of Nile tilapia (*Oreochromis niloticus*) fed on a diet enriched with n-3 fatty acids. *Food Chem* 80:489–493
  22. Santiago CB, Reyes OS (1993) Effects of dietary lipid source on reproductive performance and tissue lipid levels of Nile tilapia *Oreochromis niloticus* (Linnaeus) broodstock. *J Appl Ichthyol* 9:33–40
  23. Ng WK, Lim PK, Sidek H (2001) The influence of a dietary lipid source on growth, muscle fatty acid composition and erythrocyte osmotic fragility of hybrid tilapia. *Fish Physiol Biochem* 25:301–310
  24. Bell JG, Henderson RJ, Tocher DR, McGhee F, Dick JR, Porter A, Smullen RP, Sargent JR (2002) Substituting fish oil with crude palm oil in the diet of Atlantic Salmon (*Salmo salar*) affects muscle fatty acid composition and hepatic fatty acid metabolism. *J Nutr* 132:222–230
  25. Henderson RJ (1996) Fatty acid metabolism in freshwater fish with particular reference to polyunsaturated fatty acids. *Arch Anim Nutr* 49:5–22
  26. Tocher DR, Sargent JR (1990) Effect of temperature on the incorporation into phospholipid classes and metabolism via desaturation and elongation of n-3 and n-6 polyunsaturated fatty acids in fish cells in culture. *Lipids* 25:435–442
  27. Kiessling A, Pickova J, Johansson L, Asgard T, Storebakken T, Kiessling KH (2001) Changes in fatty acid composition in muscle and adipose tissue of farmed rainbow trout (*Oncorhynchus mykiss*) in relation to ration and age. *Food Chem* 73:271–284
  28. Karapanagiotidis IT, Bell MV, Little DC, Yakupitiyage A, Rakshit SK (2006) Polyunsaturated fatty acid content of wild and farmed tilapias in Thailand: effect of aquaculture practices and implications for human nutrition. *J Agric Food Chem* 54:4304–4310
  29. Greene DHS, Selivonchick DP (1990) Effects of dietary vegetable, animal and marine lipids on muscle lipid and haematology or rainbow trout (*Oncorhynchus mykiss*). *Aquaculture* 89:165–182
  30. Bell MV, Dick JR, Porter AEA (2001) Biosynthesis and tissue deposition of docosahexaenoic acid (22:6n-3) in rainbow trout (*Oncorhynchus mykiss*). *Lipids* 36:1153–1159
  31. Kanazawa A, Teshima SI, Sakamoto M, Awal MA (1980) Requirements of *Tilapia zillii* for essential fatty acids. *Bull Jap Soc Sci Fish* 46(11):1353–1356
  32. Blank C, Neumann MA, Makrides M, Gibson RA (2002) Optimizing DHA levels in piglets by lowering the linoleic acid to  $\alpha$ -linolenic acid ratio. *J Lipid Res* 43:1537–1543
  33. Morise A, Combe N, Boue C, Legrand P, Catheline D, Delplanque B, Fenart E, Weill P, Hermier D (2004) Dose effect of  $\alpha$ -linolenic acid on PUFA conversion, bioavailability, and storage in the hamster. *Lipids* 39:325–334
  34. Gerster H (1998) Can adults adequately convert  $\alpha$ -linolenic acid (18:3n-3) to eicosapentaenoic acid (20:5n-3) and docosahexaenoic acid (22:6n-3)? *Int J Vitam Nutr Res* 68:159–173
  35. Bell JG, Tocher DR, Henderson RJ, McGhee F, Dick JR, Crampton VO (2003) Altered fatty acid compositions in Atlantic salmon (*Salmo salar*) fed diets containing linseed and rapeseed oils can be partially restored by a subsequent fish oil finishing diet. *J Nutr* 133:2793–2801

# Investigating the Location of Propyl Gallate at Surfaces and Its Chemical Microenvironment by $^1\text{H}$ NMR

Anja Heins · Tobias Sokolowski · Heiko Stöckmann · Karin Schwarz

Received: 22 March 2006 / Accepted: 13 March 2007 / Published online: 20 April 2007  
© AOCs 2007

**Abstract** The location and the resulting chemical microenvironment of the antioxidant propyl gallate (PG) was studied in micellar solutions using the cationic emulsifier cetyl trimethyl ammonium bromide (CTAB), the anionic emulsifier sodium dodecyl sulphate (SDS) and the non-ionic emulsifier Brij 58 (polyoxyethylene-20-cetyl ester).  $T_1$  relaxation time of the aromatic protons of PG was investigated in micellar solutions and compared with that in aqueous solution in the absence of emulsifier. The relaxation time of the PG portion that is solubilized in the micelle ( $T_{1,\text{eff}}$ ) was calculated from the partition behavior of PG in micellar solution. From the 1D- $^1\text{H}$  spectrum, the alteration in the electron density of the aromatic protons and the alteration in the peak shape of the emulsifier headgroup and alkyl chain proton signals were indicative of the location of propyl gallate in the different micelles. Nuclear Overhauser effects (NOE) made it possible to deduce the exact location of PG by calculation of the relative NOEs. Marked differences were found for the location of PG in CTAB, SDS and Brij 58 micelles. PG was found to be located in the palisade layer of CTAB micelles, in the region of the polyoxyethylene chain of Brij micelles and in the Stern layer of SDS micelles. For careful study of the location of antioxidants and therefore to be able to characterize the chemical microenvironment of the antioxidants is crucial for understanding differences in anti-

oxidant activities as a function of lipid surfaces. The application of spectroscopic methods may help to optimize the antioxidant activity to inhibit lipid oxidation at surfaces that are formed in a wide range of foods (emulsions), cosmetics, pharmaceuticals (emulsions and carrier systems) and of biological membranes (LDL-particles).

**Keywords** Solubilization · Antioxidant activity · Emulsifier · Surface active agent · CTAB · SDS · Brij · Propyl gallate · Stern layer · Palisade layer

## Abbreviations

alk	Alkyl chain protons of emulsifiers
Brij 58	Polyoxyethylene-20-cetyl ester
CTAB	Cetyltrimethylammonium bromide
$\text{H}_a\text{--H}_d$	Protons of propyl gallate
hg	Headgroup protons of emulsifiers
NOE	Nuclear Overhauser effect
PG	Propyl gallate
SDS	Sodium dodecyl sulfate

## Introduction

Many studies demonstrated that the activity of antioxidants can vary strongly depending on the systems in which they have been tested [1–8]. Pryor et al. [4], for example, observed that Trolox showed a fourfold higher protection of the oxidation of linoleic acid in hexadecyltrimethylammonium bromide micelles (HDTBr, positively charged) than in negatively charged micelles of sodium dodecyl sulphate micelles (SDS). The more hydrophilic ascorbic acid showed a 13-fold higher protection in HDTBr

A. Heins (✉) · H. Stöckmann · K. Schwarz  
Institute of Human Nutrition and Food Science,  
University of Kiel, Heinrich- Hecht-Platz 10,  
24118 Kiel, Germany  
e-mail: info@foodtech.uni-kiel.de

T. Sokolowski  
Beiersdorf AG, Physical Analytics,  
Unnastr. 48, 20245 Hamburg, Germany



micelles. Barclay and Vinqvist [5] demonstrated that Trolox significantly inhibited the oxidation of positively charged liposomes (dilinoleoylphosphatidylcholine with stearylamine) at pH 4.0 and 7.0 but had no effect when the surface of the liposome (dilinoleoylphosphatidyl glycerol at pH 7.0) was negative, and had low activity at pH 4.0 when the liposome was neutral. These results indicate that the positive charge of the surface increases and a negative charge decreases the activity of hydrophilic antioxidants. In contrast Stöckmann et al. [3] reported the strongest activity of propyl gallate (PG) in SDS emulsion and no activity in CTAB emulsion. Only little work has been done to characterize the function of antioxidants at surfaces regarding their interactions with surface active molecules on a molecular level. One parameter which has been well investigated is the partitioning of antioxidants, which offers information on a ‘phase level’. This means that the proportion of antioxidants was estimated present in aqueous environments vs. lipid particles or droplets and membranes [1–3, 6–8]. Furthermore, it was possible to differentiate between the proportion of an antioxidant solubilized by oil vs. surface active compounds (e.g. emulsifiers) [2].

As lipid oxidation is considered to occur at interfaces due to the polarity of the radicals involved in the reaction [4, 5], it was found to be crucial to understand the parameters which may affect the functionality of antioxidants at interfaces. Results reported by Stöckmann et al. [3] showed that the partitioning of antioxidants into interfaces does not provide enough information. E.g. the order of the antioxidant PG showed decreasing activity in the order SDS emulsion > Brij emulsion and CTAB emulsion. In contrast, the partitioning behaviour indicated an increasing proportion of PG in the opposite order, which should have resulted in higher antioxidant concentration and thus in a higher efficiency towards lipid radicals. Due to the two-state model, small molecules are dissolved either in the micellar interior or associated with the hydrophilic interface (palisade layer and Stern layer) [9, 10], which results in different types of chemical microenvironments for the small molecules. Therefore, characterizing the location, the chemical microenvironment and resulting interaction of small molecules at surfaces is a fundamental subject in lipid sciences. Careful analyses can provide detailed information on the functionality of small molecules at surfaces.

To characterize the location and the interactions, various studies on solubilization of solutes in micellar systems were carried out [11–22]. A number of techniques were found to be suitable to investigate solubilization properties [23]. Using spectroscopic methods like different NMR techniques, quantitative measurements of the interactions between emulsifier and solute are possible [19, 22, 24, 25].

$T_1$  relaxation measurements give direct information about interactions with the chemical environment due to the transfer of energy from the spin system to the medium [26–28]. In particular, nuclei on the surface like protons are dominated by intermolecular interactions with new available dipoles [29, 30] which lead to an interference of their local motion and can be observed by a strong reduction in the relaxation time [22, 24, 26, 31–33]. In the case of antioxidants in dispersed systems alterations in  $T_1$  relaxation times are indicative of the interactions in different phases or pseudophases. Alterations in the chemical shift give information on the electron density in the closed chemical environment of the solute. Solubilization of a solute in a hydrophobic environment causes a shift to lower frequencies compared to a hydrophilic environment [11, 12, 34]. This allows a differentiation in whether a solute is solubilized in the more hydrophilic or hydrophobic layer [11–16]. Likewise, the shape and width of the peaks of the 1D spectrum are of interest. In particular, emulsifier proton signal shapes give hints of a deposition or intercalation of a solute with increasing solute concentration [17, 18, 35, 36].

Nuclear Overhauser effects (NOEs) provide information on the location of solutes since this technique allows the characterization of the intensities of interaction and arrangement of several molecules in close proximity ( $\leq 5 \text{ \AA}$ ) [19–22]. Determining the volumes of the cross peak signal compared to its corresponding diagonal signal, the relative NOEs can be calculated [29].

The aim of this study was to evaluate the location and the chemical environment of antioxidants in model systems in order to extract information regarding the resulting interactions between antioxidants and surfaces. Propyl gallate was used as an antioxidant and SDS, CTAB and Brij to model surfaces with different chemical microenvironments. The experimental design should help to provide tools for biological systems and complex dispersed matrices such as foods.

## Experimental Procedures

### Samples

Cationic CTAB (cetyl trimethyl ammonium bromide,  $\geq 99\%$ ), non-ionic Brij 58 (polyoxyethylene-20-cethyl ether,  $>98\%$ ) and propyl gallate (trihydroxy benzoic acid propyl ester,  $>99\%$ ) were obtained from Sigma-Aldrich, Germany.  $D_2O$  ( $>99.8\%$ ) and anionic SDS (sodium dodecyl sulphate,  $\geq 99\%$ ) were purchased from Carl Roth, Germany. All chemicals were used without further purification.

Micellar stock solutions of 1.1% emulsifier were prepared in 50 mmol/l acetic buffer solution in bidistilled water, pH 5.00. The required amount of antioxidants was weighed (1–3.5 mg) and filled up with either buffer (control) or micellar solution to 900 mg, finally D<sub>2</sub>O were supplemented to 1,000 mg.

### <sup>1</sup>H NMR Measurements

<sup>1</sup>H NMR measurements were performed on a Bruker DRX500 ( $B_0 = 11.75$  T) spectrometer in a 5 mm multinuclear inverse probe and at a constant temperature of  $300 \pm 0.1$  K. Samples were measured in 5-mm sample tubes with deuterium lock and without spinning. Using the 180° pulse length, the pulse length of the 90° excitation were determined to periods between 9.8 and 12 s according to the individual sample. The acquisition and the processing of the spectra were carried out by XWinNMR software (Bruker). To get information about possible interactions between emulsifier and antioxidants, the NMR measurements were performed in the individual micellar solutions and referred to the corresponding measurements in buffer solution (control). Standard methods included in the Bruker pulse sequence library were modified and used to acquire the individual NMR spectra by different pulse programs. Since all samples contained 90% H<sub>2</sub>O, each NMR experiment was carried out with suppression of the HDO signal which allowed a pure phase NMR spectrum with a fundamental low and smaller HDO signal, at the highest possible sensitivity to be obtained. This approach (watergate, water suppression by gradient-tailored excitation) consisted of a gradient echo 3-9-19-pulse sequence [37, 38].

### Chemical Shift

1D <sup>1</sup>H spectra were acquired in 8 scans with a 30° pulse. Spectra were Fourier transformed and subsequently phase corrected. All chemical shifts of the proton signals were referenced to the CH<sub>3</sub>-signal of acetic acid (HAc = 2 ppm). The chemical shifts obtained are given with an accuracy of  $\pm 0.003$  ppm.

### <sup>1</sup>H $T_1$ Relaxation

The saturation-recovery method was used where a non-periodic sequence of 90° pulses was applied to achieve the saturation of the spin system. After the waiting time  $\tau$ , the decreased magnetization  $M_Z$  was transferred by a 90° pulse to the  $x$ - $y$  plane and detected. The period of the waiting time  $\tau$ , was randomly varied in the pulse sequence in order to minimize possible drift-effects during the measuring time [39, 40]. The spectra were recorded as a set of 1D

spectra in a 2D dataset and were processed accordingly. An experimental error was calculated by investigating the  $T_1$  relaxation of 0.2% PG in triplicate both in buffer solution and in the several micellar solutions. The  $T_1$  relaxation was collected for each proton signal and the relative experimental error for all  $T_1$  relaxation measurements were estimated to about 10%.

### NOESY

NOEs were obtained by 2D homonuclear correlation experiments. The pulse program consisted of three 90° pulses; the delay for the evolution time  $\tau_1$  was systematically varied to provide chemical shift information in the  $F_1$  domain. Mixing time  $\tau_m$  was set to 750 ms according to the highest signal intensity. During acquisition, 512 data points were recorded in  $t_1$  and 2,048 data points in  $t_2$ . Time domain data were processed with a squared cosine-function in  $F_1$  and  $F_2$  and zero-filled to a final matrix of  $1 \times 1$  k data points. 1D phase corrections were carried out for the  $F_1$  and  $F_2$  domain as well as for the base lines. The cross peaks were referred to the projection of the 1D <sup>1</sup>H spectrum in the  $F_1$  and the  $F_2$  domain. By integration of the cross-peaks and the related diagonal peaks by XWinNMR tools, the intensities of the NOEs were determined.

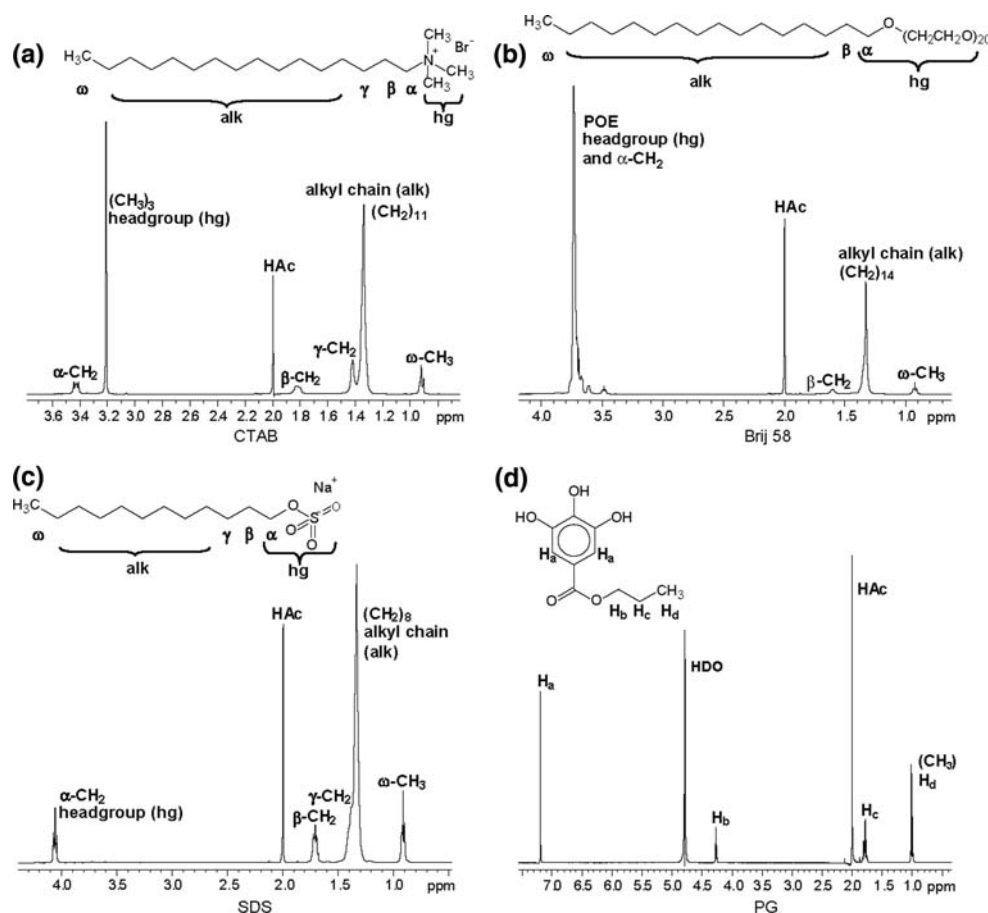
## Results and Discussion

1D <sup>1</sup>H reference spectra of the applied emulsifiers CTAB, Brij, and SDS as well as of the antioxidant PG in buffer solution are shown in Fig. 1 with the respective nomenclature. The emulsifiers showed signals for the specific headgroup region (hg) and the alkyl chain (alk) as well as for the individual methylene and methyl protons that split into a single multiplet ( $\alpha$ ,  $\beta$ ,  $\gamma$  and  $\omega$ ). The individual proton signals of PG were marked by H<sub>a</sub>–H<sub>d</sub> started on the aromatic ring with the protons closest to the hydroxyl groups H<sub>a</sub>. Assignment was continued for the gallate ester alkyl chain according to the number of methylene and methyl groups. The hydroxyl groups underwent exchanges with the surrounding water molecules so quickly that separate signals could not be detected. The protons H<sub>a</sub> were used as the indicator for the phenolic OH-groups, which demonstrate the antioxidant properties by radical-quenching.

### <sup>1</sup>H- $T_{1,eff}$ Relaxation Time

Since the exchanging process of the solute among the different phases is very fast, the observed relaxation time ( $T_{1,obs}$ ) is an average of the relaxation times in all different

**Fig. 1** 1D  $^1\text{H}$  reference spectra of the emulsifier CTAB (1%, **a**), Brij 58 (1%, **b**), SDS (1%, **c**), and of the antioxidant PG (0.25%, **d**). HAc is the acetate buffer peak; HDO is the water-deuterium peak



phases [32]. The portion of PG that is solubilized in the different micelles ( $f_{\text{sol}}$ ) was determined by ultra filtration method described by Stöckmann and Schwarz [2] and found in CTAB micelles of about 0.989, in Brij micelles of about 0.893, and in SDS micelles of about 0.735. Provided that the free mobility is the same for the portion of PG in the aqueous phase of the micellar solution as for PG in buffer solution  $T_{1,\text{sol}}$  the relaxation rate for PG solubilized in the micellar phase ( $T_{1,\text{eff}}$ ) was calculated by [41–45]

$$\frac{1}{T_{1,\text{obs}}} = \frac{1 - f_{\text{sol}}}{T_{1,\text{con}}} + \frac{f_{\text{sol}}}{T_{1,\text{eff}}} \quad (1)$$

Comparison of the  $T_{1,\text{con}}$  relaxation time of the  $\text{H}_a$  protons of PG in the aqueous phase with the  $T_{1,\text{eff}}$  relaxation time in the micellar phase showed reduced relaxation times in all emulsifier solutions (Fig. 2). This reduction could result from restricted motion of the antioxidant molecule caused by spatial proximity of the antioxidant and the emulsifier present [22, 24, 26, 31–33]. It could also be caused by the loss of tumbling of PG achieved by adopting the rotation of the micelle [27] or by molecular interactions [41]. Also differences in the solubilized proportion of PG could be observed for the different types of emulsifier. While  $\text{H}_a$  had

a relaxation time of 1.9 s in buffer solution, relaxation became significantly shorter when solubilized in micelles. Whereas in anionic SDS micelles a  $T_{1,\text{eff}}$  time constant of 1.6 s was found and in non-ionic Brij micelles it was 1.1 s, the  $T_{1,\text{eff}}$  time in CTAB micelles was reduced to 0.8 s. From the quantitative reduction of the  $T_{1,\text{eff}}$  relaxation time the strength and location of interaction or solubilization can be obtained [46, 47]. The different strength of interactions between PG and the emulsifiers were in the order CTAB > Brij > SDS. This clearly indicates different solubilization environments for PG offered by the emulsifier moieties. The region of the SDS micelles that solubilizes PG resembles the characteristics of the buffer solution, i.e. being very polar. In contrast, the environment offered by CTAB can be assumed to be markedly different of a buffer solution, since CTAB apparently formed much stronger interactions than SDS, causing a 50% reduction of the  $T_{1,\text{eff}}$  relaxation times relative to SDS. The differences in solubilization are due to molecular interactions which includes different kinds of intermolecular forces. These interactions include electrostatic interactions or Coulomb forces, H-bonds, and dispersion forces, which are all modulated by hydration effects [48]. However, it is impossible to correlate certain effects with individual forces due to an overlap

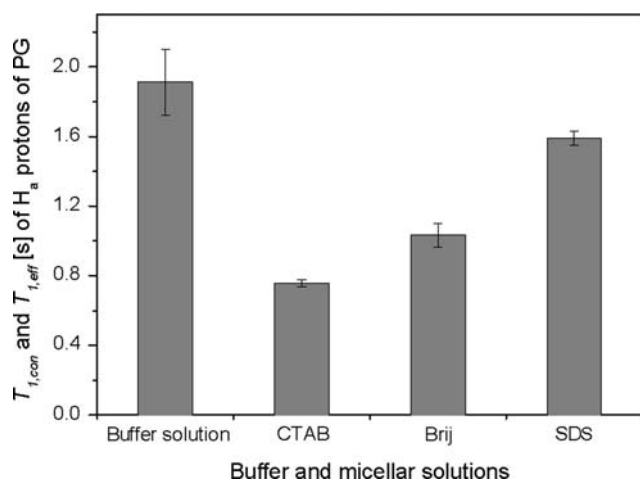


**Fig. 2** Comparison of the  $T_1$  relaxation time of the aromatic protons  $H_a$  of 0.25% PG in buffer solution ( $T_{1,con}$ ) and in the micellar phase of 1% CTAB, Brij, and SDS micellar solutions ( $T_{1,eff}$ )

of different interactions involved in the micellar environment of the headgroup, counterions and different segments of the alkyl chain [48].

To investigate the concentration dependency of the  $T_{1,eff}$  relaxation time, the  $T_1$  relaxation ratio was calculated using the following equation

$$T_{1,AH} = \frac{T_{1,eff}}{T_{1,con}} \quad (2)$$

This compares the effective relaxation times of the antioxidant solubilized in micelles  $T_{1,eff}$  with the relaxation times of the freely movable antioxidant in the aqueous phase  $T_{1,con}$ . The corresponding relaxation ratio for the emulsifier protons  $T_{1,em}$  is given by the equation

$$T_{1,em} = \frac{T_{1,AH\text{ present}}}{T_{1,AH\text{ absent}}} \quad (3)$$

and compares the relaxation time in the presence and absence of antioxidants. A  $T_1$  relaxation ratio value of 1 shows that the relaxation time of the antioxidant is the same in the micellar phase as in the aqueous phase, while lower  $T_1$  relaxation ratio values indicate a reduction of the relaxation time of antioxidants solubilized in the micelle.

For the different concentrations (0.1–0.35%) of PG investigated, no significant difference in the  $T_{1,AH}$  relaxation ratios could be observed between the individual emulsifiers and antioxidant protons, exemplifying the aromatic protons  $H_a$  of PG (Fig. 3a).

The interactions of the emulsifier protons with those of antioxidants were also investigated as a function of different antioxidant concentrations. The  $T_{1,em}$  relaxation ratios (Eq. 3) for the headgroup (hg) in the presence and absence of PG are shown in Fig. 3b. The headgroup

protons showed the same tendency of decreasing interaction strength as the PG aromatic protons in the order CTAB > Brij > SDS for the impact of PG. The CTAB headgroup protons revealed a significant reduction of the  $T_{1,em}$  relaxation ratio, i.e. below 1, but this was independent of the antioxidant concentration indicating a close proximity of PG and the CTAB headgroup protons [26–28]. In contrast, no significant reduction was observed for the headgroup protons of Brij and SDS. Since the  $T_{1,con}$  relaxation time is assumed to be constant in the different micellar solutions, this ratio is influenced only by the  $T_{1,eff}$  relaxation time of the portion of antioxidants solubilized in the emulsifier pseudophase. For a concentration range from 0.1 to 0.35% PG, the  $T_{1,AH}$  relaxation ratio of the portion solubilized in the emulsifier pseudophase showed no dependence on the antioxidant/emulsifier ratio of PG for all emulsifiers employed. This demonstrates a qualitative equivalence of interactions in the complete investigated concentration range.

#### Chemical Shift

The chemical shift of antioxidant signals, which is altered in micellar solution, is shown as the difference between the positions of a signal in the presence and absence of emulsifiers (Fig. 4). Positive differences in the chemical shift indicate a shift to lower frequencies (shielding) owing to electron density enhancement. In the opposite case of negative chemical shifts, a lower electron density of the proton is indicated by a shift to higher frequencies (deshielding) [49]. In general, shifts of the PG and emulsifier proton signals became stronger with increasing PG concentration (Fig. 4) since the concentration was not corrected by the partitioning of PG and the observed chemical shifts are the average of the shifts in all phases. Alteration in the chemical shift was strongly pronounced for  $H_a$  in CTAB, less in Brij and the least in SDS micellar solution (Fig. 4a).

In Brij and CTAB micellar solutions, the position of the aromatic proton signals were shifted to lower frequencies corresponding to an increasing electron density. This is caused by the change in the chemical environment of the aromatic protons from the buffer solution to the less polar environment [11, 12, 34] offered by Brij and CTAB micelles. Since larger shifts were observed for PG in CTAB, PG can be assumed to be solubilized in a more water-deficient environment in CTAB than in Brij. The water content in micelles ranges from 40 to 53% [50], whereby water penetration into ionic micelles is markedly lower than in non-ionic micelles [51, 52]. In the headgroup region of Brij, which can be described as a concentrated solution of polyoxyethylene groups [53, 54], the main portion of the water is bounded as H-bond donors to the polyether oxygen

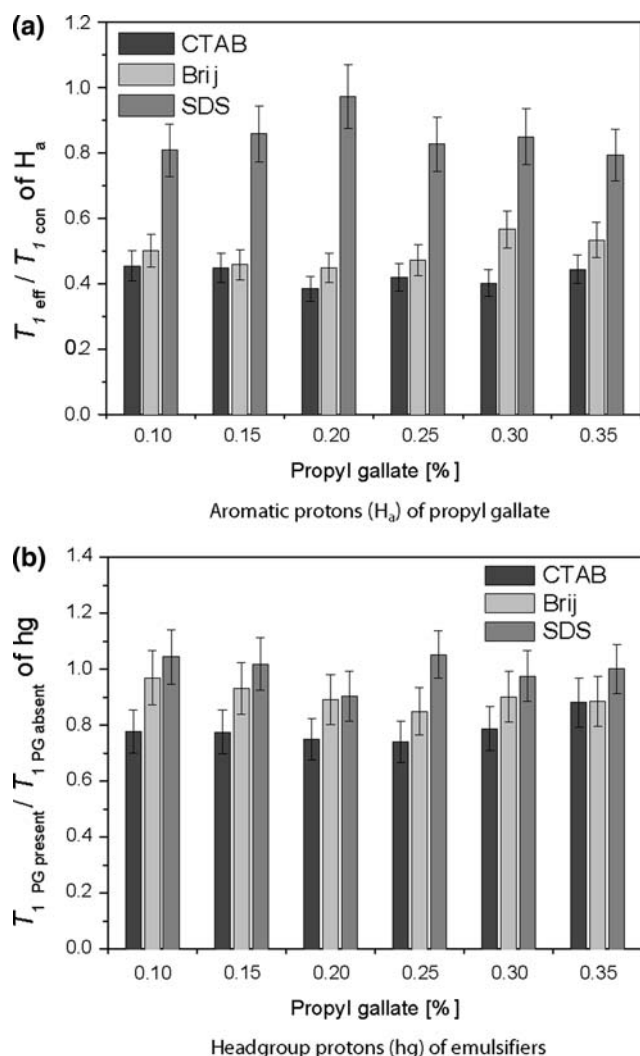


**Fig. 3** Comparison of the  $T_{1, \text{AH}}$  relaxation ratio for the aromatic protons  $H_a$  of different PG concentrations in buffer solution and in the micellar phase of 1% CTAB, Brij, and SDS micellar solution (a). Comparison of the  $T_{1, \text{em}}$  relaxation ratio of the corresponding emulsifier headgroup protons hg (b)

[55]. In addition, the larger volume of Brij than that of CTAB micelles offers a greater space to the solubilized PG in Brij micelles so that PG may not accumulate locally with increasing PG concentration. This in turn may explain why the aromatic proton signals of PG shifted uniformly in Brij micelles (Fig. 4a).

In SDS micellar solutions, the  $H_a$  proton signals of PG at a concentration of 0.1–0.2% were shifted to higher frequencies. At a PG concentration of 0.25%, the shift was the same as for the control and at 0.3–0.35% PG, a shift to lower frequencies was observed. This deshielding can be attributed to a decrease in the electron density of the aromatic protons. The surface of SDS micelles is strongly hydrophilic with adsorbed counterions, which are generally separated by a layer of water molecules [56]. Solubilized

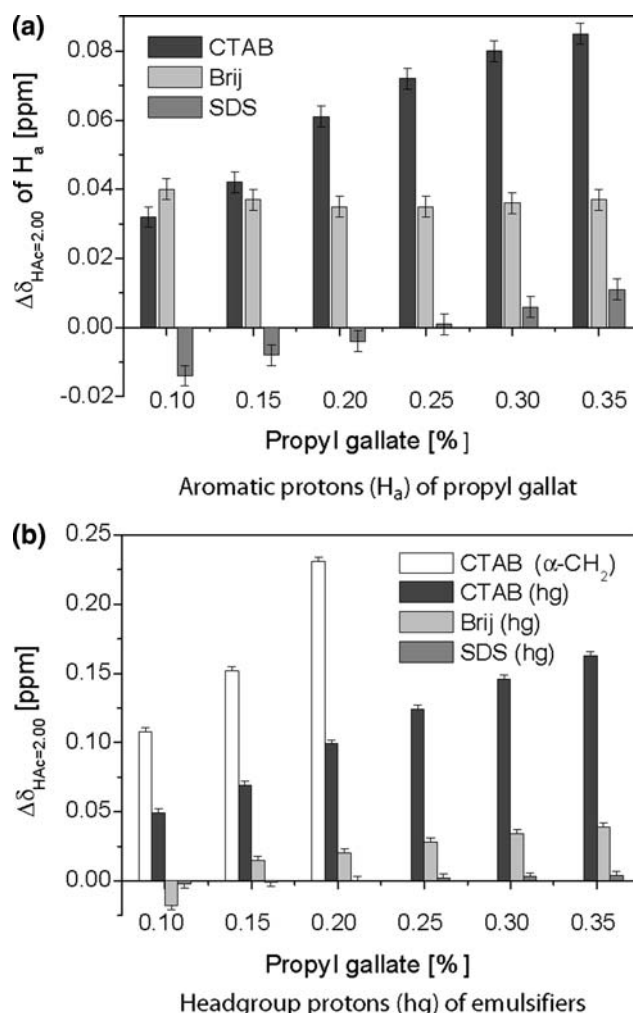


**Fig. 4** Difference in the chemical shift of the aromatic protons  $H_a$  of PG in buffer and a 1% micellar solution of CTAB, Brij and SDS with different concentrations of PG (a) and of the corresponding headgroup (hg) proton signals (b). Positive differences in the chemical shift indicate a shielding (shift to lower frequencies), while negative differences in the chemical shift indicate a deshielding (shift to higher frequencies)

PG may alter the solvent structure in the Stern layer [57] accompanied with a displacement of counterions and dehydration [58]. That is, fewer dipoles are located in the Stern layer and the dielectric constant decreases [57, 59–61]. The deficiency of dipoles may lead in turn to a deshielding of the antioxidant protons and this may cause the decrease in the electron density of the aromatic protons. With increasing PG concentration, more PG molecules accumulate in the Stern layer, which may be associated with the  $\text{--SO}_3^-$  group of SDS by  $\pi\text{--}\pi$  interactions [51], leading again to an increase in electron density, so that a shielding was observed.

Alteration in the chemical shift that occurred for the emulsifier proton signals in the presence of PG is shown in Fig. 4b. CTAB showed the greatest difference in chemical

shift, but it was more pronounced for the  $\alpha$ -CH<sub>2</sub> group than for the headgroup signal entering into one peak with increasing PG concentration. Generally, increasing antioxidant concentration led to a greater positive shift for CTAB and Brij headgroup proton signals, whereas those of SDS were not shifted regardless of the PG concentration. This could indicate an electron density enhancement by the antioxidant aromatic ring in the palisade layer of CTAB, particularly in the region of the  $\alpha$ -CH<sub>2</sub> signal. The headgroup signals of SDS were not shifted, which is in accordance with a localization of PG in the outer region of the SDS micelle (Stern layer).

### Peak Shape

Increasing concentrations of PG influenced the peak shape of the emulsifier headgroup (hg) and the alkyl chain (alk) proton signals. Alterations in these peak shapes differed strongly for all emulsifiers employed. This makes conclusions possible on the type of interaction taking place between the emulsifier and antioxidant and, as a consequence, on the solubilization of the antioxidant. The peak shape of the alkyl chain and headgroup proton signal of CTAB, SDS, and Brij is shown in the presence of PG in concentrations varying from 0.1 to 0.35% (Fig. 5).

The CTAB alkyl chain signal (Fig. 5a, A) was found to be separated into a main alkyl chain signal and a small one at higher frequencies for the  $\gamma$ -CH<sub>2</sub> group (Fig. 1a). In the presence of the lowest PG concentration, the  $\gamma$ -CH<sub>2</sub> merged into the main signal. Upon addition of 0.15% PG, a new peak emerged at lower frequencies from the alkyl chain signal. When the PG concentration was increased further, the split alkyl chain peak broadened out and its intensity decreased. The signals of the headgroup and  $\alpha$ -CH<sub>2</sub> group (B) showed the clearest separation in the control CTAB solution. With addition of PG, the distance between them became smaller. Finally, both signals merged into one peak that broadened and decreased in intensity with increasing PG concentration. Both observations could be related to a strong electron density increase in the palisade layer owing to the intercalation of the aromatic ring into this region [17, 18, 35, 36]. Thereby, the aromatic ring is located closer to the  $\alpha$ -CH<sub>2</sub> group than to the headgroup protons indicated by a stronger shift of the  $\alpha$ -CH<sub>2</sub> proton signal and the final merge of both signals. The extreme broadening of both signals at higher PG concentration is accompanied by an increasing viscosity caused by a sphere-to-rod transition of the micelle [62]. A higher viscosity leads to a longer correlation time  $\tau_c$ , which is associated with shorter  $T_2$  relaxation times and ends up with broader signals in the spectrum.

The alkyl chain signal of Brij appeared in the pure micellar solution as a single peak (Fig. 5b, A). In the

presence of 0.15% PG, the alkyl chain signal split into two peaks with the second smaller peak appearing at lower frequencies. The line widths of the split signal were slightly broadened and the second peak became more intense with further increase in the PG concentration. The headgroup signal (B) resulting from a polyoxyethylene chain showed extensive broadening of the line width with higher PG concentrations. This indicates the intercalation of PG into the hydrophobic part of the Brij micelle [17, 18, 35, 36]. Since the viscosity of the Brij micellar solution was not affected in the presence of PG [62], the broadening of the headgroup signal may be due to a restriction of the motion of the Brij headgroup by the intercalation of PG into the headgroup region.

In the absence of antioxidants, the SDS alkyl chain signal (Fig. 5c, A) appeared as one signal with the  $\gamma$ -CH<sub>2</sub> signal indicated as a small shoulder at higher frequencies (Fig. 1c). This  $\gamma$ -CH<sub>2</sub> signal separated more and more from the alkyl chain signal with increasing PG concentration. Also the headgroup signal (B) had a higher resolution with increasing concentrations of PG. The triplets were narrower and the lines within the triplet were closer to the baseline. Generally, a higher resolution of the NMR spectrum at the same field strength and without exchanging processes is the result of a higher mobility. Higher mobility is associated with smaller molecule aggregates [57, 60, 61] that may result from a lower dielectric constant of the Stern layer [57, 59–61] by solubilization of PG resulting in a displacement of counterions.

### Nuclear Overhauser Effects (NOEs)

From the intensities of the NOEs between antioxidants and emulsifiers, their stereoscopic arrangement can be derived. ROESY (NOE in the rotating frame) measurements exemplarily performed for PG and CTAB (data not shown) indicated that the appearance of cross-peaks is due to direct through-space dipolar coupling and not caused by spin diffusion [63]. When PG was solubilized in CTAB micellar solution, several NOEs were observed between the antioxidant and the emulsifier (Fig. 6a). All proton signals of PG demonstrated a distance smaller than 5 Å to the CTAB protons and in particular to the alkyl chain (alk) and the headgroup signal (hg). By integrating the cross peaks and placing them in relationship to the volume of the corresponding diagonal signal, the relative NOE or the strength of the interaction could be calculated (Table 1).

The strongest interactions were observed between the aromatic protons H<sub>a</sub> and first methylene group H<sub>b</sub> of PG and the alkyl chain of CTAB, whereas these PG protons showed less interaction with the headgroup protons. However, the headgroup protons of CTAB showed the highest NOE intensity with the H<sub>c</sub> proton of PG. The

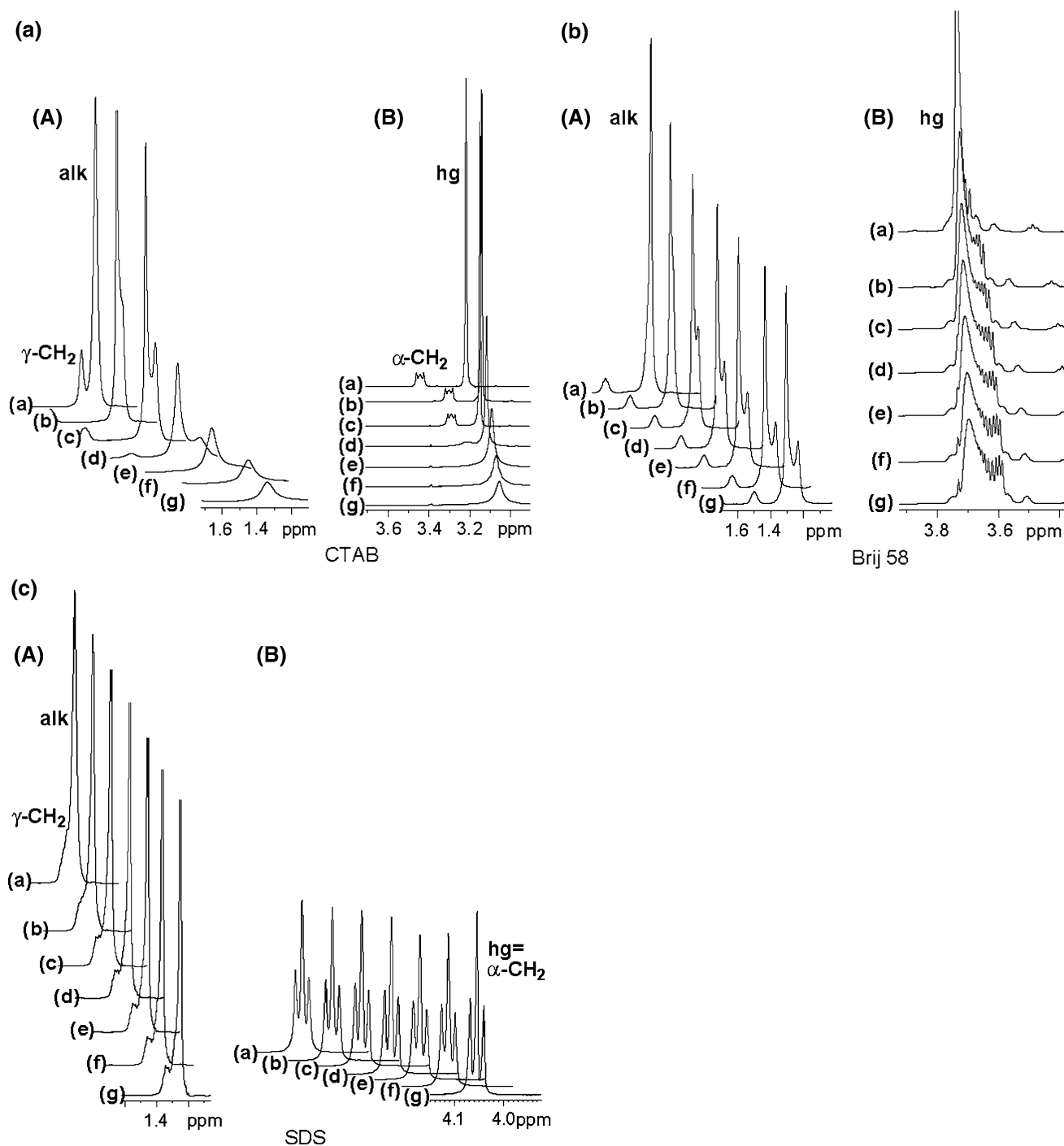


**Fig. 5** Alteration in the peak shape of the alkyl chain (alk and  $\gamma$ -CH<sub>2</sub>) (A) and the headgroup (hg and  $\alpha$ -CH<sub>2</sub>) (B) proton signals of 1% CTAB (a), Brij 58 (b), and SDS (c) in the presence of increasing PG

concentration [control (a), 0.1% PG (b), 0.15% PG (c), 0.2% PG (d), 0.25% PG (e), 0.3% PG (f), 0.35% PG (g)]

arrangement derived from this data shows a definitive intercalation of PG into the CTAB micelle with the aromatic ring is located next to the alkyl chain of CTAB [19, 22, 64]. It may be possible, that PG may be aligned with the aromatic ring towards the interior of the micelle, while the alkyl chain of PG may be positioned at the headgroup

of the CTAB micelle, although from the partial lipophilicity of the antioxidant the opposite alignment would be expected.

Likewise, intermolecular NOEs between all protons of the antioxidant and the alkyl chain (alk) as well as the headgroup (hg) protons of the Brij micelle were observed

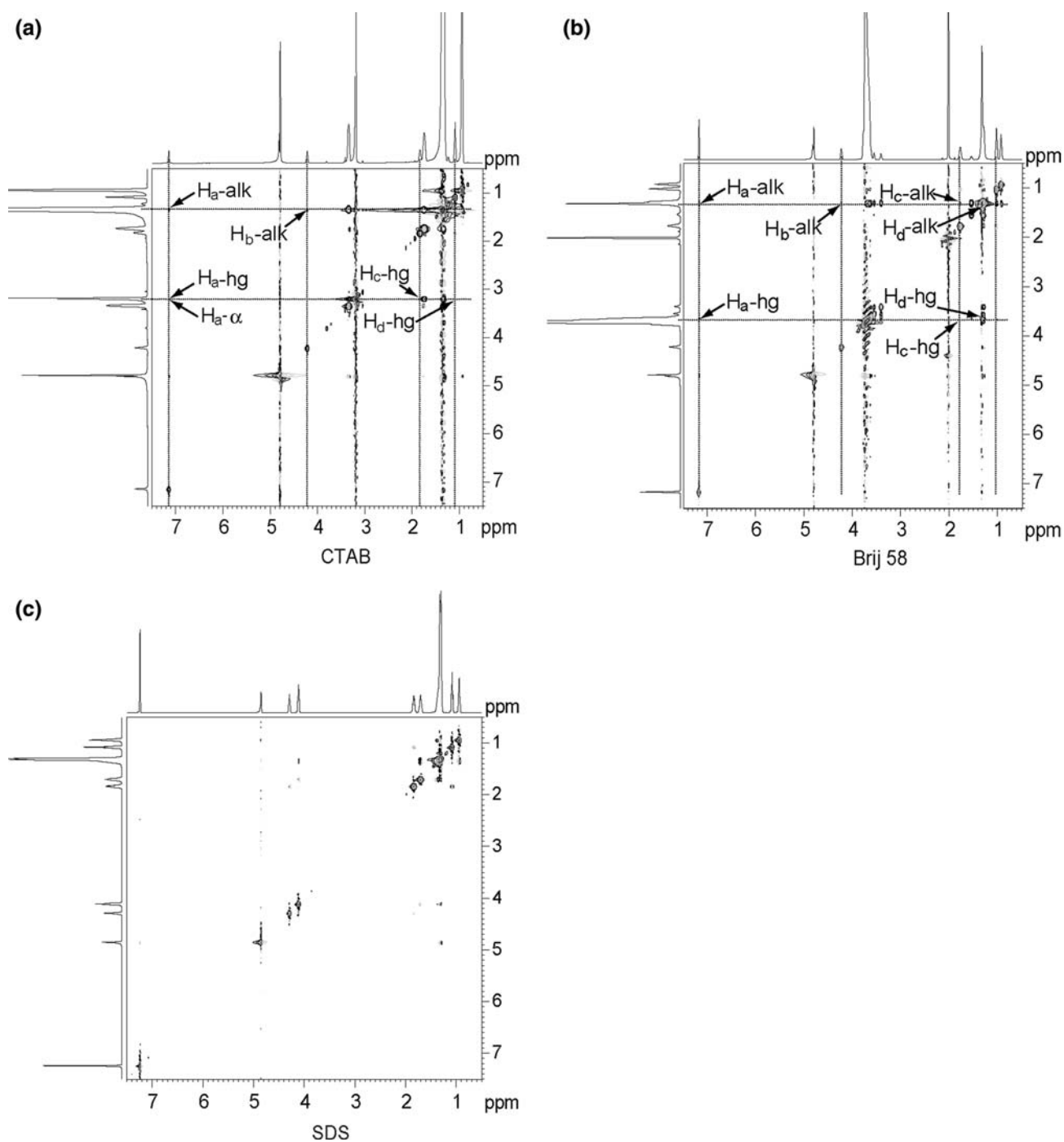


**Fig. 6** Intermolecular NOEs ( $\tau_m = 750$  ms) between individual PG (0.25%) and CTAB (1%) protons (a) or Brij (1%) protons (b). NOEs could not be observed between PG (0.6%) and SDS (1%) protons (c)

for PG in Brij micellar solution (Fig. 6b). The intensities of the NOEs were weaker than those in CTAB micelles (Table 1). The interactions of the Brij alkyl chain with  $H_a$  to  $H_c$  were equivalent but increased by a factor of two with  $H_d$ . The intensities of the NOEs of the headgroup signals were generally lower and showed the strongest interaction with the aromatic proton  $H_a$  of PG. The uniform strength of

NOEs between Brij protons and the individual PG protons indicates a random orientation of the antioxidant in the headgroup region and the palisade layer. This in turn would mean a greater ability of PG to diffuse freely in these regions.

Contrary to the experiments in CTAB and Brij micellar solutions, no NOEs could be found between the protons of



**Table 1** Relative NOEs between PG Protons ( $H_a$ – $H_d$ ) and the Headgroup (hg) and Alkyl Chain (alk) Protons of CTAB and Brij ( $\tau_m = 750$  ms)

	Relative NOEs for corresponding diagonal-peak (%)			
	$H_a$	$H_b$	$H_c$	$H_d$
CTAB (hg)	0.90		3.99	0.89
CTAB (alk)	7.09	6.13		
Brij (hg)	1.95		0.85	1.12
Brij (alk)	2.59	2.37	2.49	4.60

PG and SDS micelles (Fig. 6c). PG could therefore be located in the outer hydrated layer of the SDS micelles like the Stern layer where it was not in close proximity to the alkyl chain or the headgroup protons ( $\alpha$ -CH<sub>2</sub>) of SDS.

## Conclusion

The present study demonstrates that differences in the chemical characteristics of the microenvironment of surfaces will result in a different location of PG in the surface due to interactions with the surfactant molecule. PG is found to be solubilized in the palisade layer of CTAB micelles orientated with its aromatic ring towards the hydrophobic interior. This results in a fixed position of PG due to very strong interactions particular between the aromatic protons of PG and the first adjacent methylene groups of the CTAB alkyl chain. Intercalation of PG in Brij micelles is suggested as taking place in the headgroup region and at higher concentrations additionally in the alkyl chain region. Brij reveals intermediate interactions with antioxidants relative to CTAB and SDS micelles. Antioxidant may still have the ability to diffuse freely within the Brij micelle. PG is located in the Stern layer of the SDS micelle undergoing only weak interactions, which are half as strong as those in CTAB micelles but probably changing the hydration of the SDS micelle. The location of PG in different surfaces will affect the functionality of antioxidants towards radicals. Moreover the polarity of radicals may also result in different location in interfaces. ESR experiments [65] showed different activity of antioxidants towards hydrophilic and lipophilic radicals. Although radical and antioxidants are both incorporated into the micelle the specific location within the micelle (surface) determines the functionality. Propyl gallate is able to reduce the lipophilic radical galvinoxyl to a higher extent in CTAB micelles than in SDS or Brij micelles. Further, MacFaul and co-workers [66] demonstrated that the H-abstraction kinetic of antioxidants in solvents strongly depends on the protic character of the solvent and thus on the chemical environment of the antioxidant. To study the

location of antioxidants and their chemical microenvironment carefully is therefore crucial to understand differences in antioxidant activities as a function of lipid surfaces. The application of spectroscopic methods may help to optimize the antioxidant activity and to inhibit lipid oxidation at surfaces that are present in a wide range of foods, cosmetics, pharmaceuticals (emulsions and carrier systems) and of biological membranes and surfaces (LDL-particles).

## References

- Schwarz K, Frankel EN, German JB (1996) Partition behaviour of antioxidative phenolic compounds in heterophasic systems. *Fett / Lipid* 98:115–121
- Stöckmann H, Schwarz K (1999) Partitioning of low molecular weight compounds in oil-in-water emulsions. *Langmuir* 15:6142–6149
- Stöckmann H, Schwarz K, Huynh-Ba T (2000) The influence of various emulsifiers on partitioning and antioxidant activity of hydrobenzoic acids and their derivatives in oil-in-water emulsions. *JAACS* 77:535–542
- Pryor WA, Cornicelli JA, Devall LJ, Tait B, Trivedi BK, Witiak DT, Wu M (1993) A rapid scanning test to determine the antioxidant potencies of natural and synthetic antioxidants. *J Org Chem* 58:3521–3532
- Barclay LCR, Vinqvist MR (1994) Membrane peroxidation: inhibiting effects of water-soluble antioxidants on phospholipids of different charge types. *Free Rad Biol Med* 16:779–788
- Huang SW, Hopia AI, Schwarz K, Frankel EN, German B (1996) Antioxidant activity of  $\alpha$ -tocopherol and Trolox in different lipid substrates: bulk oils vs. oil-in-water emulsions. *J Agric Food Chem* 44:2496–2502
- Huang SW, Frankel EN, Schwarz K, Aeschebach R, German B (1996) Antioxidant activity of carnosic acid and methyl carnosate in bulk oil and in oil-in-water emulsions. *J Agric Food Chem* 44:2951–2956
- Pekkarinen SS, Stöckmann H, Schwarz K, Heinonen M, Hopia AI (1999) Antioxidant activity and partitioning of phenolic acids in bulk and emulsified methyl linoleate. *J Agric Food Chem* 47:3036–3043
- Cardinale JR, Mukerjee P (1978) Solvent effects on the ultraviolet spectra of benzene derivatives and naphthalene. Identification of polarity sensitive spectral characteristics. *J Phys Chem* 82:1614–1627
- Mukerjee P, Ko JS (1992) Solubilization of ethyl *o*-, *m*-, and *p*-aminobenzoates in micelles of different charge types: interfacial adsorption and orientation effects. *J Phys Chem* 96:6090–6094
- Eriksson JC, Gillberg G (1965) NMR-studies of the solubilization of aromatic compounds in cetyltrimethylammonium bromide solution. *Surf Chem*, pp 148–156
- Eriksson JC, Gillberg G (1966) NMR-studies of the solubilization of aromatic compounds in cetyltrimethylammonium bromide solution II. *Acta Chem Scand* 20:2019–2027
- Bunton CA, Minch MJ (1974) Micellar effects on the ionization of carboxylic acids and interactions between quaternary ammonium ions and aromatic compounds. *J Phys Chem* 78:1490–1498
- Fendler JH, Fendler EJ, Infante GA, Shih P-S, Patterson LK (1975) Absorption and proton magnetic resonance spectroscopic investigation of environment of acetophenone and benzophenone in aqueous micellar solutions. *J Am Chem Soc* 97:89–95
- Kreke PJ, Magid LJ, Gee JC (1996) <sup>1</sup>H and <sup>13</sup>C NMR studies of mixed counterion, cetyltrimethylammonium bromide/cetyltri-

- thylammonium dichlorobenzoate, surfactant solutions: the intercalation of aromatic counterions. *Langmuir* 12:699–705
16. Vermathen M, Stiles P, Bachofer SJ, Simonis U (2002) Investigations of monofluoro-substituted benzoates at the tetradecyltrimethylammonium micellar interface. *Langmuir* 18:1030–1042
  17. Manohar C, Rao URK, Valaulikar BS, Iyer RM (1986) On the origin of viscoelasticity in micellar solutions of cetyltrimethylammonium bromide and sodium salicylate. *J Chem Soc Chem Commun*, pp 379–381
  18. Rao URK, Manohar C, Valaulikar BS, Iyer RM (1987) Micellar chain model for origin of the viscoelasticity in dilute surfactant solutions. *J Phys Chem* 91:3286–3291
  19. Bachofer SJ, Simonis U, Nowicki TA (1991) Orientational binding of substituted naphthoate counterions to the tetradecyltrimethylammonium bromide micellar interface. *J Phys Chem* 95:480–488
  20. Lee S, Kim Y (1999) Solution structure of neuromedin B by  $^1\text{H}$  nuclear magnetic resonance spectroscopy. *FEBS Lett* 460:263–269
  21. Wymore T, Wong TC (1999) Molecular dynamics study of substance *p* peptides partitioned in a sodium dodecylsulfate micelle. *Biophys J* 76:1213–1227
  22. Momot KI, Kuchel PW, Chapman BE, Deo P, Whittaker D (2003) NMR study of the association of propofol with non-ionic surfactants. *J Am Chem Soc* 125:2088–2095
  23. Marangoni DG, Kwak JCT (1995) Comparison of experimental methods for the determination of the partition coefficients of *n*-alcohols in SDS and DTAB micelles. In: Christian S, Scamehorn J (eds) *Solubilization in surfactant aggregates*. Vol. 55 of *Surfactant science series*, Marcel Dekker, New York, pp 455–490
  24. Calzolari L, Gaggelli E, Maccotta A, Valensin G (1996) Interaction of daunomycin with dipalmitoylphosphatidylcholine model membranes. A  $^1\text{H}$  NMR study. *J Magn Res B* 112:228–235
  25. Yuan H-Z, Cheng G-Z, Zhao S, Miao X-J, Yu J-Y, Shen L-F, Du Y-R (2000) Conformational dependence of Triton X-100 on environment studies by  $^2\text{D}$  NOESY and  $^1\text{H}$  NMR relaxation. *Langmuir* 16:3030–3035
  26. Stark RE, Kasakevich ML, Granger JW (1982) Molecular motion of micellar solutes: a  $^{13}\text{C}$  NMR relaxation study. *J Phys Chem* 86:335–340
  27. Casaratto MG, Craik DJ (1991) Carbon-13 and proton NMR studies of the interaction of tricyclic antidepressant drugs with micellar aggregates. *J Phys Chem* 95:7093–7099
  28. Levy GC, Cargioli JD, Anet FAL (1973) Carbon-13-spin lattice relaxation in benzene and substituted aromatic compounds. *J Am Chem Soc* 95:1527–1535
  29. Ellena JF, Hutton WC, Cafiso DS (1985) Elucidation of cross-relaxation pathways in phospholipid vesicles utilizing two-dimensional  $^1\text{H}$  NMR spectroscopy. *J Am Chem Soc* 107:1530–1537
  30. Turov VV, Bogiollo VI, Utlenko EV (1994) NMR investigation of the interaction of carbon black with water, benzene and acetonitrile molecules. *J Appl Spectrosc* 61:514–520
  31. Eriksson JC, Henriksson U, Klason T, Ödberg L (1982) In: Mittal K, Fendler E (eds) *Solution behaviour of surfactants*, Vol 2. Plenum, New York, pp 907
  32. Stilbs P (1995) Solubilization, as studied by nuclear spin relaxation and NMR-based self diffusion techniques. In: Christian SD, Scamehorn JF (eds) *Solubilization in surfactant aggregates*, Vol. 55 of *surfactant science series*. Marcel Dekker, New York, pp 367–381
  33. Jayasundera S, Schmidt WF, Hapeman CJ, Torrents A (2003) Examination of molecular interaction sites of acetanilides with organic matter surrogates using nuclear magnetic resonance techniques. *J Agric Food Chem* 51:3829–3835
  34. Jacobs JJ, Anderson RA, Watson TR (1971) Interaction in phenol-sodium dodecyl sulphate-water systems. *J Pharm Pharmacol* 23:148–149
  35. Vermathen M, Louie EA, Chodosh AB, Ried S, Simonis U (2000) Interactions of water-insoluble tetraphenylporphyrins with micelles probed by UV-visible and NMR spectroscopy. *Langmuir* 16:210–221
  36. Suratkar V, Mahapatra S (2000) Solubilization site of organic perfume molecules in sodium dodecyl sulfate micelles: new insights from proton NMR studies. *J Colloid Interf Sci* 225:32–38
  37. Piotta M, Saudek V, Sklenar V (1992) Gradient-tailored excitation for single-quantum NMR spectroscopy of aqueous solutions. *J Biomol NMR* 2:661–666
  38. Sklenar V, Piotta M, Leppik R, Saudek V (1993) Gradient-tailored water suppression for H-1-N-15 experiments optimized to retain full sensitivity. *J Magn Res Ser A* 102:241–245
  39. Dietrich W, Bergmann G, Gerhards R (1976) Neues Verfahren zur Bestimmung der longitudinalen Relaxationszeit in der Kernresonanzspektroskopie. *Zeitschr anal Chem* 279:177–181
  40. Frye JS (1989) Comparison of inversion-recovery methods for measuring longitudinal relaxation rates. *Conc Magn Res* 1:27–33
  41. Bonechi C, Donati A, Picchi MP, Rossi C, Tiezzi E (1996) DNA-ligand interaction detected by proton selective and non-selective spin-lattice relaxation rate analysis. *Colloid Surf A* 115:89–95
  42. Blieser DM, Sentell KB (1993) Deuterium nuclear magnetic resonance spectroscopy as a probe for reversed-phase liquid chromatographic bonded phases solvation. 2. Aqueous solvation in methanol and acetonitrile binary mobile phase. *Anal Chem* 65:1819–1826
  43. Marshall DB, McKenna WP (1984) Deuterium nuclear magnetic resonance relaxation study of mobile phase-stationary phase interactions in reversed-phase-high-performance liquid chromatography. *Anal Chem* 56:2090–2093
  44. Gao Z, Wasylishen RE, Kwak JCT (1991) Distribution equilibrium of poly(ethylene oxide) in sodium dodecyl sulfate micellar solutions: a NMR paramagnetic study. *J Phys Chem* 95:462–467
  45. Tanaka M, Asahi Y, Masuda S, Ota T (1991) Binding position of azathioprine with bovine serum albumin determined by measuring nuclear resonance relaxation time. *Chem Pharmacol Bull* 39:2771–2774
  46. Yushmanov VE, Imasato H, Perussi J, Tabak M (1995) Proton relaxation and spin label studies of papaverine localization in ionic micelles. *J Magn Res B* 106:236–244
  47. Yushmanov VE, Tabak M (1997) Dipyrindamole interacts with the polar part of cationic reversed micelles in chloroform:  $^1\text{H}$  NMR and ESR evidence. *J Colloid Interf Sci* 191:384–390
  48. Engberts JBFN (1992) Catalysis by surfactant aggregates in aqueous solutions. *Pure Appl Chem* 64:1653–1660
  49. Herzog W, Messerschmidt M (1995) *NMR-Spektroskopie für Anwender. Die Praxis der instrumentellen Analytik*, VCH Verlagsgesellschaft, Weinheim
  50. Hartland GV, Grieser F, White LR (1987) Surface potential measurements in pentanol-sodium dodecyl sulphate micelles. *J Chem Soc Faraday Trans 1*(83):591–613
  51. Diaz Garcia ME, Sanz-Medel A (1986) Dye-surfactants interactions: a review. *Talanta* 33:255–264
  52. Bruce CD, Berkowitz ML, Perera L, Forbes MDE (2002) Molecular dynamics simulation of sodium dodecyl sulfate micelle in water: micellar structural characteristics and counterions distribution. *J Phys Chem B* 106:3788–3793
  53. Mulley BA, Metcalf AD (1956) Non-ionic surface active agents. Part I: The solubility of chloroxylenol in aqueous solutions of polyethylene glycol 1000 monocetyl ether. *J Pharm Pharmacol* 8:774–779
  54. Mukerjee P (1971) Solubilization of benzoic acid derivatives by nonionic surfactants: location of solubilizates in hydrocarbon

- core of micelles and polyoxyethylene mantle. *J Pharm Sci* 60:1528–1530
55. Leisner D (1996) Kinetik nukleophiler Reaktionen mit Benzylbromid in Mikroemulsionen. PhD Thesis, University of Bielefeld
56. Buchner R, Baar C, Fernandez P, Schrödle W, Kunz S (2005) Dielectric spectroscopy of micelle hydration and dynamics in aqueous ionic surfactant solutions. *J Mol Liq* 118:179–187
57. Caponetti E, Martino E, Floriano MA, Triolo R (1997) Localization of *n*-alcohols and structural effects in aqueous solutions of sodium dodecyl sulfate. *Langmuir* 13:3277–3283
58. Ruasse MF, Blagoeva IB, Ciri R, Garcia-Rio L, Leis JR, Marques A, Mejuto J, Monnier E (1997) Organic reactions in micro-organized media: why and how? *Pure Appl Chem* 69:1923–1932
59. Alonso B, Harris RK, Kenwright AM (2002) Micellar solubilization: structural and conformational changes investigated by  $^1\text{H}$  and  $^{13}\text{C}$  liquid-state NMR. *J Colloid Interf Sci* 251:366–375
60. Zana R (1995) Aqueous surfactant-alcohol systems: a review. *Adv Colloid Interf Sci* 57:1–64
61. Førland GM, Samseth J, Gjerde MI, Høiland M, Jensen AØ, Mortensen K (1998) Influence of alcohol on the behavior of sodium dodecylsulfate micelles. *J Colloid Interf Sci* 203:328
62. Heins A, Garamus VM, Steffen B, Stöckmann H, Schwarz K (2006) Impact of phenolic antioxidants on structural properties of micellar solutions. *Food Biophys* 1:189–201
63. Günther H (1992) NMR-Spektroskopie: Grundlagen, Konzepte und Anwendungen in der Protonen- und Kohlenstoff-13-Kernresonanz-Spektroskopie in der Chemie, 3rd edn. Georg Thieme Verlag
64. Rakin AR, Pack GR (2005) Necessity of aromatic carboxylate anions to be planar to induce growth of cationic micelles. *Langmuir* 21:837–840
65. Heins A, McPail DB, Sokolowski T, Stöckmann H, Schwarz K (2007) The location of phenolic antioxidants and radicals at interfaces determines their activity. *Lipids* doi:10.1007/s11745-007-3052-6
66. MacFaul PA, Ingold KU, Lusztyk J (1996) Kinetic solvent effects on hydrogen atom abstraction from phenol, aniline, and diphenylamine. The importance of hydrogen bonding on their radical-trapping (antioxidant) activities. *J Org Chem* 61:1316–1321

# The Location of Phenolic Antioxidants and Radicals at Interfaces Determines Their Activity

Anja Heins · Donald B. McPhail · Tobias Sokolowski ·  
Heiko Stöckmann · Karin Schwarz

Received: 15 December 2006 / Accepted: 13 March 2007 / Published online: 1 May 2007  
© AOCs 2007

**Abstract** To characterize parameters influencing the antioxidant activity at interfaces a novel ESR approach was developed, which facilitates the investigation of the reaction stoichiometry of antioxidants towards stable radicals. To relate the activity of antioxidants towards the location of radicals at interfaces NMR experiments were conducted. Micellar solutions of SDS, Brij and CTAB were used to model interfaces of different chemical nature. The hydrophilic Fremy's radical was found to be solubilized exclusively in the aqueous phase of SDS micellar solution but partitioned partly into the hydrophilic headgroup area of Brij micelles. In contrast the hydrophobic galvinoxyl was exclusively located in the micellar phase with the increasing depth of intercalation in the order SDS < Brij < CTAB. Gallates revealed a higher stoichiometric factor towards galvinoxyl in CTAB systems, which is accounted to a concentration effect of antioxidant and radical being both solubilized in the palisade layer. In contrast, in SDS solutions hardly any reaction between galvinoxyl and gallates was found. SDS acted as a physical barrier between radical (palisade layer) and antioxidant (stern layer). The influence of the hydrophobic properties of the antioxidant was clearly seen in Brij micelles. Elongation

of the alkyl chain in gallate molecule resulted in increasing stoichiometric factors in the presence of galvinoxyl being located in the deeper region of the bulky headgroup area. The reverse trend was found in the presence of Fremy's radical being located in the hydrated area of the micelles.

**Keywords** Solubilization · Antioxidant activity · Emulsifier · Gallates · CTAB · SDS · Brij · ESR · Interfaces

## Abbreviations

alk	Alkyl chain protons of emulsifiers
BG	Butyl gallate
Brij 58	Polyoxyethylene-20-cetyl ester
CTAB	Cetyltrimethylammonium bromide
EG	Ethyl gallate
ESR	Electron spin resonance spectroscopy
$f_{sol}$	Portion of the antioxidant that is solubilized in the emulsifier pseudophase
GA	Gallic acid
hg	Headgroup protons of emulsifiers
MG	Methyl gallate
OG	Octyl gallate
PG	Propyl gallate
SDS	Sodium dodecyl sulfate
$S_{con}$	Stoichiometric factor in the control system
$S_{eff}$	Effective stoichiometric factor of the antioxidant in the emulsifier pseudophase
$S_{obs}$	Observed stoichiometric factor of the entire complex system

## Introduction

It is of current interest to understand the parameters that influence the activity of antioxidants in complex systems

A. Heins (✉) · H. Stöckmann · K. Schwarz  
Institute of Human Nutrition and Food Science,  
University of Kiel, Heinrich-Hecht-Platz 10,  
24118 Kiel, Germany  
e-mail: info@foodtech.uni-kiel.de

D. B. McPhail  
Rowett Research Institute, Greenburn Road, Bucksburn,  
Aberdeen AB21 9SB Scotland, UK

T. Sokolowski  
Beiersdorf AG, Physical Analytics, Unnastr. 48, 20245  
Hamburg, Germany

and to develop methods that allow a systematic approach focusing on interfaces. Electron spin resonance experiments (ESR) allow estimating the potency of hydrogen atom donation of antioxidants in various systems measuring the reaction rate with stable radicals [1–3] or unstable radicals in the presence of spin trapping probes [4]. Since the ESR spin probe is applicable for investigating the actions of antioxidants in membranes and lipoproteins [1, 5], it can be likewise used for emulsions and micellar solutions [2, 3, 6, 7]. Stable radicals that are excellent spin probes for either lipophilic or hydrophilic phases and show good reactivity towards antioxidants are the hydrophilic Fremy's radical [2, 8, 9] and the lipophilic galvinoxyl [10, 11]. Alteration of the microenvironment are indicated by changes of line shape, width and intensity [12] changes in the hyperfine splittings of spectra give information on the solubilization of radicals in dispersed systems.

Fremy's radical can be used as a probe for the peroxy radical because of their similar reaction mechanism, their isoelectronically structure and their large dipole moment [2, 13]. This probe is of negative charge and posses a well-defined and sharp spectrum in an aqueous solution at room temperature. Galvinoxyl is a resonance-stabilized and sterically protected radical that is particularly applied to test the activity of lipophilic antioxidants [11]. In the presence of phenolic compounds it is reduced by hydrogen atom transfer, where the process is governed by O–H bond dissociation enthalpy of the donor group [14]. A comparison of antioxidant assays based on radical scavenging and lipid oxidation showed good correlations between the inhibition of oxidation products in lipids and the reaction with stable radicals like DPPH, Fremy's radical and galvinoxyl. It was concluded that investigation of stable radical scavenging is a suitable method to predict the antioxidant activity in bulk lipids [15]. However, in complex dispersed systems like emulsions, antioxidant activity is related to various parameters determined by the interface. Depending on the particular emulsifier used, an accumulation of antioxidants at the interface can be achieved [16, 17]. Although the interface is the main site of lipid oxidation [18–21] enrichment of antioxidants at the interface does not necessarily result in an enhancement of antioxidant activity [22]. The loss of efficiency may be related to interactions between antioxidants and emulsifiers at the interface, which may be hydrophobic in origin or due to hydrogen bonding [22]. These interactions may influence the characteristics of the phenolic OH-bond, thereby affecting the hydrogen atom transfer process from the antioxidant to the free radical [22–24]. Further, the location of radicals in the interface is not well known. Only a few data based on the dipole moment are available in the literature, suggesting that alkyl radicals are buried in the interface whereas hydroxy radicals are close to the aqueous environment [18, 19, 21].

The aim of this study was to investigate effects of different interfaces on the antioxidant efficiency. For this purpose, a novel ESR approach was developed using stable radicals with definite solubilization sites characterized by NMR. Interfaces were modeled by micellar solutions using cationic CTAB, anionic SDS and non-ionic Brij 58. Gallates with different alkyl chain length were used to vary the location of antioxidants in the interface.

## Experimental Procedures

### Chemicals

Cationic CTAB (cetyltrimethylammonium bromide,  $\geq 99\%$ ), non-ionic Brij 58 (polyoxyethylene-20-cethyl ether,  $>98\%$ ) and the gallates (Fig. 1): gallic acid ( $>99.9\%$ ), methyl gallate ( $\geq 98\%$ ), ethyl gallate ( $\sim 98\%$ ), propyl gallate ( $>99\%$ ), butyl gallate ( $>98\%$ ), and octyl gallate ( $\geq 99\%$ ) were obtained from Sigma-Aldrich, Germany. Fremy's radical (potassium nitrosodisulfate) and galvinoxyl (2,6-di-*tert*-butyl- $\alpha$ -(3,5-di-*tert*-butyl-4-oxo-2,5-cyclohexadiene-1-ylidene)-*p*-tolyl-oxy) were purchased from Sigma-Aldrich, UK. Anionic SDS (sodium dodecyl sulphate,  $\geq 99\%$ ) was obtained from Carl Roth, Germany. All chemicals were used without further purification.

### ESR Analysis

Electron spin resonance (ESR) measurements were carried out on a Bruker ECS 106 spectrometer at room temperature. It was operating at approximately 9.7 GHz (ECS 041 MR, microwave bridge X-band) and equipped with a TM<sub>110</sub> cavity. Spectra were analyzed using WinEPR software (Bruker). Spectra of the previously unreacted radical were recorded by ESR static measurements, after the required time by which the reaction had gone to completion from the mixing of the radical with the sample. Concentrations of the remaining radicals were calculated by double integration of the spectrum and referred to that of the individual control system consisting of buffer (ethanolic) or micellar solution and radical without any antioxidant present. After plotting the applied concentrations of

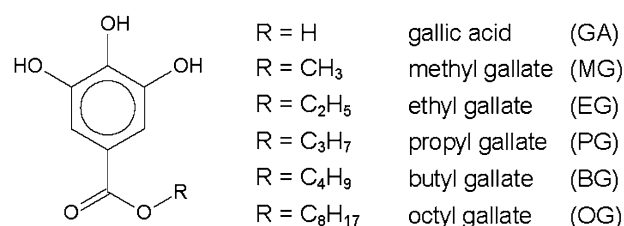


**Fig. 1** Structures of gallates

antioxidants against the remaining radical concentration the reaction stoichiometry could be obtained by linear fit. Reproducibility of the individual decay curves was in good accordance. The relative standard deviation for the antioxidant Trolox, a hydrophilic derivative of  $\alpha$ -tocopherol, was measured in triplicate. Two percentages were added for safety to determine an experimental error as a function of the system (Fremy's radical in buffer (3%), in SDS (4%) and in Brij (5%) solution; Galvinoxyl in ethanolic (3%), CTAB (3%), SDS (5%) and Brij (8%) solution).

#### Fremy's Radical

Stock solution (2 mmol/l) of Fremy's radical, 4% of SDS and Brij micellar solutions, and 4 mmol/l stock solutions of antioxidants in acetic buffer solution (0.2 mol/l, pH 5.00) were prepared (exception octyl gallate: 2 mmol/l and 2% micellar stock solution). At first the antioxidants were mixed in varying concentrations (0.1–0.5 mmol/l) either with 1.5 ml micellar solution or buffer solution to a volume of 3 ml. Equal volume of Fremy's radical stock solution were added. After 5 min of shaking and transferring into an ESR static quartz cell, the spectra of the low-field peak of the previously unreacted Fremy's radical were recorded [8, 9]. The spectra were obtained by following machine settings: centerfield: 3449.95 G, sweep width: 4.0 G, microwave frequency: approx. 9.73 GHz, microwave power: 2.01 mW, modulation frequency: 100 kHz, modulation amplitude:  $9.51 \times 10^{-2}$  G, receiver gain:  $2.5 \times 10^{+3}$ , conversion time: 20.48 s, time constant: 10.24 s.

#### Galvinoxyl

Stock solutions of 4 mmol/l galvinoxyl in ethanol, 2% micellar solution of SDS, Brij, and CTAB in buffer solution as well as 4 mmol/l antioxidants in ethanol were prepared. An aliquot of 500  $\mu$ l ethanolic galvinoxyl stock solution were filled up with micellar solution to 50 ml. For investigations in bulk solutions (control) the galvinoxyl stock solution was only diluted tenfold in ethanol. Dilution was repeated for the ethanolic antioxidant stock solutions. Buffer solution and antioxidant solution were premixed in varying concentrations in a total volume of 3 ml and finally an equal volume of the galvinoxyl containing micellar solution was added. After 5 min the reaction had reached completion [11] and the spectra were able to be recorded under the following conditions: centerfield: 3464.45 G, sweep width: 30.0 G (40.0 G in ethanol; The ethanolic solution was not deoxygenated for better handling, therefore the spectrum was getting broader), microwave frequency: approx. 9.73 GHz, microwave power: 2.01 mW, modulation frequency: 100 kHz, modulation amplitude: 1.07 G, receiver gain:  $8 \times 10^4$  ( $86.3 \times 10^4$  in ethanol),

conversion time: 81.92 s (40.96 s in ethanol), time constant: 40.96 s (20.48 s in ethanol).

#### $T_1$ Relaxation Time

$T_1$  relaxation time were performed on a Bruker DRX500 ( $B_0 = 11.75$  T) spectrometer in a 5 mm multinuclear inverse probe and at a constant temperature of  $300 \pm 0.1$  K. Performance of NMR-measurements is previously described in detail [25]. Experimental errors were calculated for each proton signal and were set on 10%. The individual emulsifier protons are shown in Fig. 2 their respective nomenclature for the specific headgroup region (hg), the alkyl chain (alk) as well as for the individual methylene and methyl protons that split into a single multiplet ( $\alpha$ ,  $\beta$ ,  $\gamma$  and  $\omega$ ).

## Results and Discussion

### Solubilization Sites of Fremy's Radical

The isotropic spectrum of Fremy's radical consists of three single narrow peaks that arise from the interaction of the unpaired electron spin with the nuclear spins of nitrogen ( $I = 1$ ) (Fig. 3a). The anisotropic spectrum is characterized by axial symmetry; the peaks correspond to the extreme case of orientation of the principle axis parallel to the field (Fig. 3b).

Peak shapes and width of the spectra of Fremy's radical in buffer solution and SDS or Brij micellar solutions were equal and showed typical isotropic spectra (Fig. 4). In contrast, the spectrum of Fremy's radical in CTAB micellar solution showed anisotropic effects (Fig. 3b) due to the

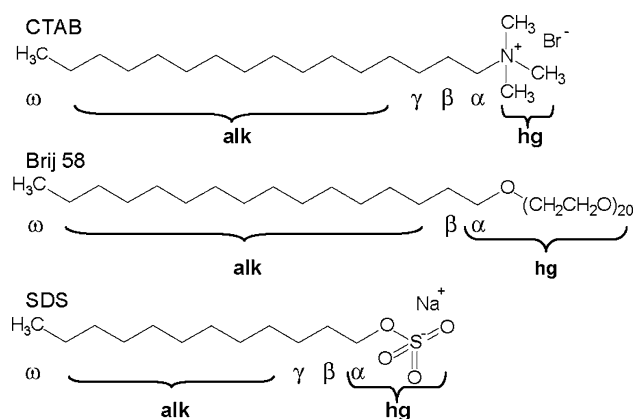


**Fig. 2** Structures and nomenclature of the emulsifiers CTAB, Brij 58 and SDS: headgroup protons (hg), alkyl chain protons (alk), individual methylene and methyl protons ( $\alpha$ ,  $\beta$ ,  $\gamma$  and  $\omega$ )

**Fig. 3** Spectra and structure of Fremy's radical including  $g$  and  $A$  values, **a** isotropic spectrum of Fremy's radical in buffer solution at 20 °C, **b** anisotropic spectrum of Fremy's radical at -77 °C

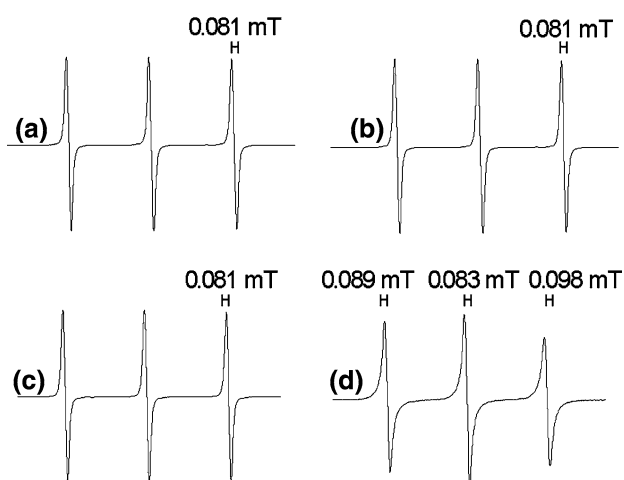
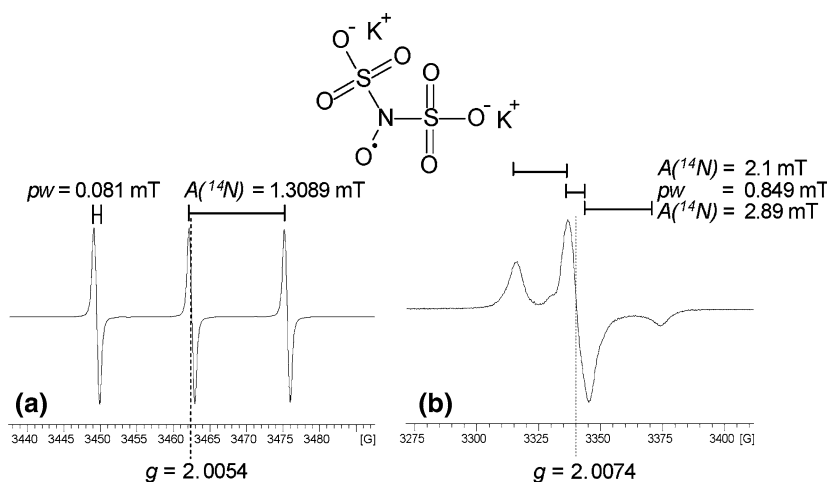


**Fig. 4** Spectra of Fremy's radical in different micellar solutions including the peak width **a** in buffer solution, **b** in SDS solution, **c** in Brij solution, **d** in CTAB solution

broadening of the peaks (Fig. 4), particularly the first and the third peak.

To obtain additional information on the location of Fremy's radical, the  $T_1$  relaxation time of the individual emulsifier proton signals was measured in the presence of Fremy's radicals by NMR [25] (Fig. 5). The  $T_{1,r}$  relaxation ratio was defined by the relationship of the  $T_1$  relaxation time in the presence and absence of radicals by the following equation:

$$T_{1,r} = \frac{T_{1,\text{radical present}}}{T_{1,\text{radical absent}}} \quad (1)$$

None of the SDS emulsifier proton signals showed significant alteration in the  $T_{1,r}$  ratio. i.e., Fremy's radical is solubilized exclusively in the aqueous environment of SDS micellar solution. As the headgroups of SDS are negatively charged, a repulsive effect [2] in addition to the strong

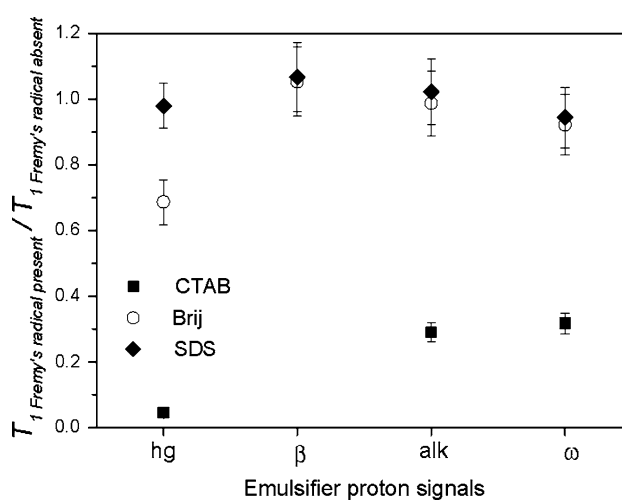


**Fig. 5**  $T_{1,r}$  relaxation ratio of single emulsifier proton signals in the presence to the absence of Fremy's radical. [Emulsifier protons: headgroup protons ( $hg$ ),  $\beta$ -CH<sub>2</sub> protons ( $\beta$ ), alkyl chain protons ( $alk$ ) and  $\omega$ -CH<sub>3</sub> protons ( $\omega$ )]

polarity of Fremy's radicals determined the solubilization in the aqueous phase.

The Brij headgroup signal showed a marked reduction of the  $T_{1,r}$  relaxation ratio relative to that in pure buffer solution (Fig. 5), while the other signals had the same  $T_1$  relaxation time in the presence and absence of Fremy's radical. This provided evidence that Fremy's radical is partly solubilized in the large headgroup region of Brij. The headgroup region of Brij offers an environment resembling a concentrated solution of polyoxyethylene groups [26] with a high water content [27]. i.e. the hydrophilic Fremy's radical may partition between the aqueous environment and the headgroup area of Brij.

A precipitation of Fremy's radical was observed in CTAB micellar solution seen in the strong reduction of the  $T_{1,r}$  relaxation ratio of all CTAB proton signals (Fig. 5). This was in all likelihood caused by strong electrostatic

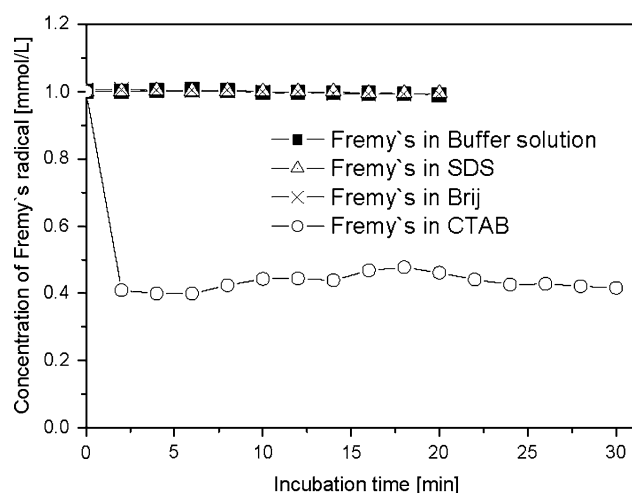


**Fig. 6** Concentration of Frey's radical in different micellar solutions as a function of time

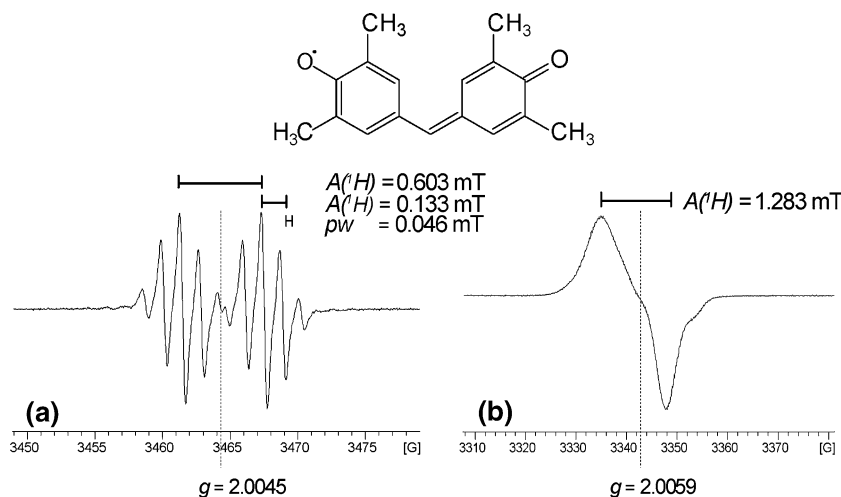
interaction between the negatively charged Frey's radical and the positively charged headgroup of CTAB [2]. Therefore, systems containing Frey's radical and CTAB systems were excluded from further investigations.

Observation of the remaining concentration of Frey's radical in buffer and micellar solutions over a period of 20 and 30 min indicated a sufficient stability of the radical in buffer, SDS, and Brij micellar solutions. In contrast, Frey's radical content was reduced immediately by 60% in CTAB solution due to precipitation (Fig. 6).

#### Solubilization Sites of Galvinoxyl

Galvinoxyl demonstrates in ethanolic solution a characteristic isotropic spectrum consisting of a doublet of quintets which arise from the interaction of the unpaired electron with the nuclear spins of the proton on the central carbon and the four equivalent protons on the aromatic ring

**Fig. 7** Spectra and structure of galvinoxyl including  $g$ ,  $A$  values and peak width ( $pw$ ), **a** isotropic spectrum of galvinoxyl in deoxygenated ethanol solution at 20 °C, **b** anisotropic spectrum of galvinoxyl at -77 °C



( $I = 1/2$ ) (Fig. 7a). The anisotropic spectrum of galvinoxyl shows an enormous broadening of two large signals. The hyperfine splitting of the four aromatic ring protons completely disappeared and the distance between the left doublet signals was doubled compared to the isotropic spectrum (Fig. 7b).

The isotropic hyperfine splitting of galvinoxyl (Fig. 2a) was found to be particularly sensitive to changes in the microenvironment. The presence of oxygen interfered with the aromatic ring protons so that the hyperfine splitting nearly disappeared (Fig. 8). Therefore, it was necessary to deoxygenate the ethanol system prior to the addition of galvinoxyl. To dissolve galvinoxyl in micellar solutions and emulsions, an organic solvent was used as the carrier. In order to minimize interfering effects of the carrier solvent the volume had to be kept at minimum. Different solvents were tested for their impact on galvinoxyl. In hexane, the maximum amount of galvinoxyl that could be dissolved was fivefold and in octanol threefold higher than in ethanol (ethanol 20 mmol/l < octanol 33 mmol/l < hexane 100 mmol/l). The spectra of galvinoxyl dissolved in deoxygenated hexane or octanol, showed a similar hyperfine splitting compared to that in deoxygenated ethanolic solution (Fig. 9).

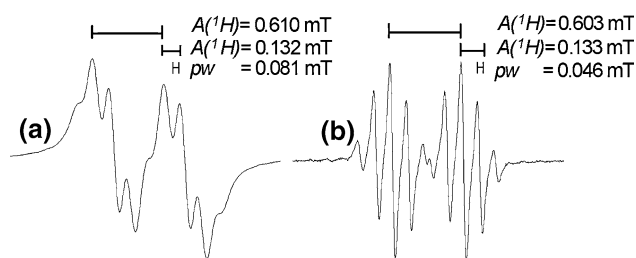


**Fig. 8** Spectra of galvinoxyl in ethanolic solution in the presence (a) and absence (b) of oxygen, including  $A$  values and peak width ( $pw$ )



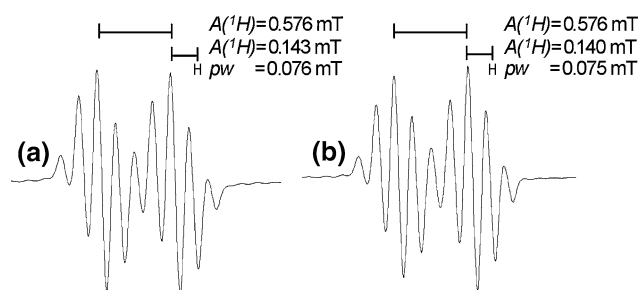


**Fig. 9** Spectra of galvinoxyl in hexane (a) and octanol (b) including  $A$  values and peak width ( $pw$ )

Ethanol (1%) or octanol (0.6%) as carrier solvent in Brij micellar solution altered only slightly the hyperfine splitting compared with that of galvinoxyl dissolved in deoxygenated ethanolic solution. The distance between both doublet signals and the single quintet signals tended to increase and the separation was not as sharp as in ethanolic solution. Transfer of galvinoxyl into Brij micellar solution using hexane (0.2% carrier solvent was required) led to a completely different spectrum and the solution slowly became turbid accompanied by increasing viscosity (Fig. 10).

The reduction of the galvinoxyl concentration resulted in increasing sharpness of the hyperfine splitting. A tenfold lower concentration of galvinoxyl showed a spectrum quite similar to that in deoxygenated ethanolic solution (Fig. 11) as spin–spin interactions of galvinoxyl are reduced at lower concentration due to decreasing proximity.

When galvinoxyl was added in ethanol to the buffer solution without any emulsifier present, the hyperfine splitting was lost (Fig. 12) and brownish particles were formed, which were indicative of precipitation of galvinoxyl in aqueous solution. However, when it was added to micellar solutions, the hyperfine splitting was retained and

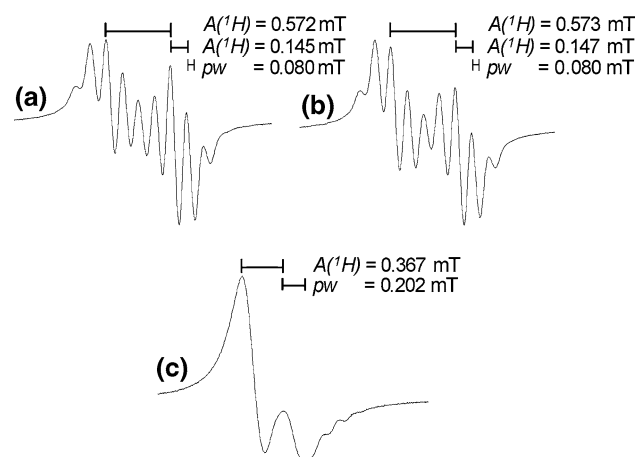


**Fig. 10** Spectra of 0.2 mmol/l galvinoxyl dissolved first in ethanol (a), octanol (b) or hexane (c) and subsequently transferred into Brij micellar solution

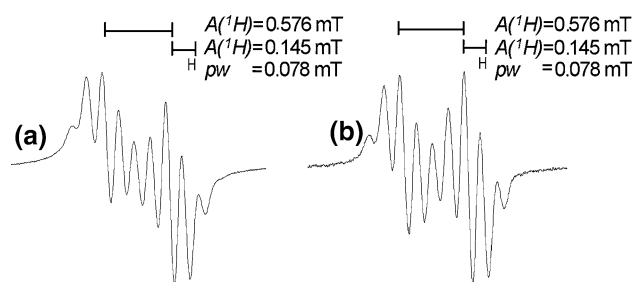


**Fig. 11** Spectra of galvinoxyl dissolved in ethanol and then transferred into Brij micellar solutions, recorded in the presence of 0.2 mmol/l (a) and 0.02 mmol/l (b) of galvinoxyl in micellar solutions including  $A$  values and peak width ( $pw$ )

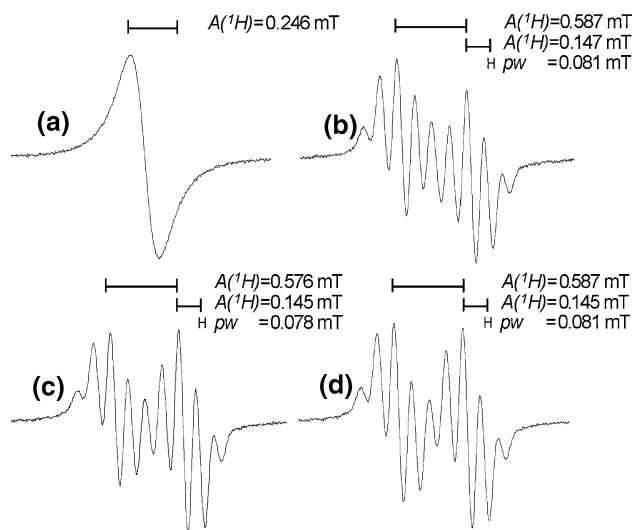


**Fig. 12** Spectra of the galvinoxyl in buffer solution and different micellar solutions with the  $A$  values and peak width ( $pw$ ): a in buffer solution, b in SDS solution, c in Brij solution, d in CTAB solution

comparable to that of galvinoxyl dissolved in deoxygenated ethanol indicating that galvinoxyl is solubilized in the micelles of CTAB, SDS and Brij. The spectrum of galvinoxyl in CTAB micellar solution showed the most similarity compared with that recorded in deoxygenated ethanol. Small changes of the hyperfine splitting were observed in SDS micellar solution.

Further indication of the solubilization sites of galvinoxyl were found by the  $T_{1,r}$  relaxation ratio of single surfactant proton signals in the presence and absence of galvinoxyl (Eq. 1). This ratio decreased for all emulsifiers from the hydrophilic headgroup with approximately 1 to the lipophilic  $\omega$ -CH<sub>3</sub> signal indicating stronger interactions with galvinoxyl the more lipophilic the emulsifier protons. Whereas the  $\omega$ -CH<sub>3</sub> of CTAB decreased to 0.4, the same proton signal of Brij was only significantly reduced to 0.7 and that of SDS roughly to 0.9 (Fig. 13). As these data demonstrated that galvinoxyl is solubilized in the deeper

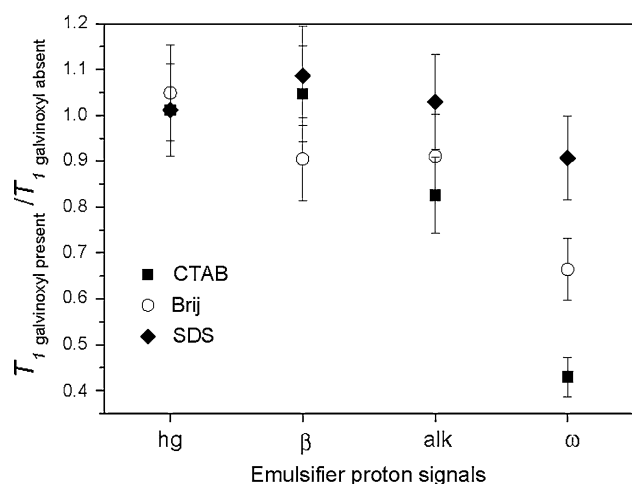


**Fig. 13**  $T_{1,r}$  relaxation ratio of single emulsifier proton signals in the presence of galvinoxyl. [Emulsifier protons: headgroup protons (*hg*),  $\beta$ -CH<sub>2</sub> protons ( $\beta$ ), alkyl chain protons (*alk*) and  $\omega$ -CH<sub>3</sub> protons ( $\omega$ )]

region of the palisade layer, it can be concluded that galvinoxyl is completely solubilized in the micelles of CTAB, SDS and Brij.

#### Activity of Gallates Solubilized in the Emulsifier Pseudophase of Micellar Solutions

Reaction stoichiometries for gallates were determined towards the hydrophilic Frey's radical and the lipophilic galvinoxyl. The exchange process of the solute between the different phases is very fast, so that the observed stoichiometry is actually an average of the ones in all different phases [28]. To calculate the effective stoichiometric factor  $S_{\text{eff}}$  of gallates in the interface (modeled by the surfactant micelles) the stoichiometric factor of the entire system  $S_{\text{obs}}$ , the portion of the antioxidant that is solubilized in the micellar pseudophase  $f_{\text{sol}}$  as well as the stoichiometric factor in the control system  $S_{\text{con}}$  need to be considered as expressed in Eq. 2 [29]:

$$S_{\text{obs}} = S_{\text{con}}(1 - f_{\text{sol}}) + S_{\text{eff}}f_{\text{sol}} \quad (2)$$

Thus, the values listed in the tables describe the antioxidant activities either of the entire system, i.e. micellar solution, buffer or ethanolic solution (control). For antioxidants partly partitioning into the micelles the effective stoichiometric factors  $S_{\text{eff}}$  are compared in Fig. 14a, b. For antioxidants that are only solubilized in the aqueous phase, comparison of the effective parameters obtained in individual phases was not useful and instead the observed stoichiometric factors  $S_{\text{obs}}$  (Table 1) were used for comparison.

The stoichiometric factors were equal for all gallates but gallic acid in buffer solution (Table 1). One gallate ester

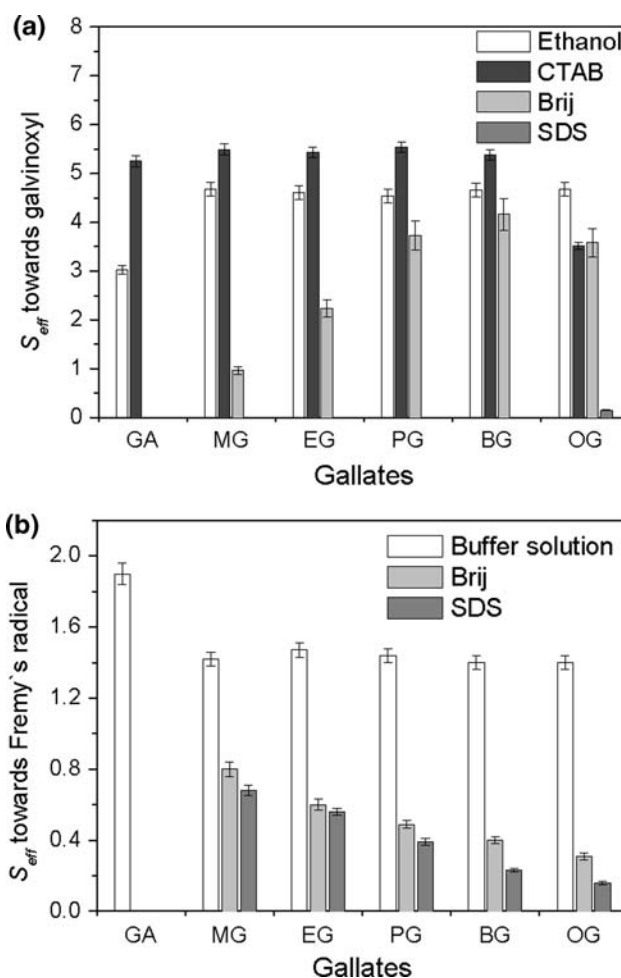


**Fig. 14** Stoichiometric factors of various gallates towards Frey's radical in buffer solution and in the emulsifier pseudophases  $S_{\text{eff}}$  of SDS and Brij micellar solutions (a), and towards galvinoxyl radical in ethanol and in the emulsifier pseudophases  $S_{\text{eff}}$  of CTAB, SDS, and Brij micellar solutions (b).  $S_{\text{eff}}$  is calculated according to Eq. 2 including the following values for  $f_{\text{sol}}$  [30]: CTAB with GA = 0.493, MG = 0.86, EG = 0.939, PG = 0.989, BG = 0.996, OG = 1; Brij with GA = 0.226, MG = 0.5, EG = 0.654, PG = 0.861, BG = 0.951, OG = 1; SDS with GA = 0, MG = 0.297, EG = 0.506, PG = 0.689, BG = 0.824, OG = 1

molecule reacted on average with 1.4–1.5 molecules of Frey's radical, while GA was able to reduce on average 1.9 molecules of Frey's radical. Also all gallates with the exception of GA showed the same activity towards the lipophilic galvinoxyl radical in ethanolic solution and reduced on average 4.5–4.7 molecules galvinoxyl per molecule gallate. In the case of GA,  $S_{\text{eff}}$  was lower and amounted on average to 3.0.

#### Activity of Gallates in CTAB Systems

Solubilized in the CTAB emulsifier pseudophase, all gallates but OG showed the same activity of about

**Table 1** Observed stoichiometry  $S_{\text{obs}}$  of the reaction between various antioxidants and Fremy's radical or galvinoxyl in the control and in micellar solutions

	$S_{\text{obs}}$ towards Fremy's radical			$S_{\text{obs}}$ towards galvinoxyl			
	Control	Brij	SDS	Control	CTAB	Brij	SDS
GA	1.9 ± 0.06	1.8 ± 0.09	1.9 ± 0.08	3.0 ± 0.09	4.1 ± 0.08	1.2 ± 0.10	0.0 ± 0.00
MG	1.4 ± 0.04	1.1 ± 0.06	1.2 ± 0.05	4.7 ± 0.14	5.4 ± 0.11	2.8 ± 0.23	0.1 ± 0.00
EG	1.5 ± 0.04	0.9 ± 0.05	1.0 ± 0.04	4.6 ± 0.14	5.4 ± 0.11	3.1 ± 0.24	0.1 ± 0.01
PG	1.4 ± 0.04	0.6 ± 0.03	0.7 ± 0.03	4.5 ± 0.14	5.5 ± 0.11	3.8 ± 0.30	0.2 ± 0.01
BG	1.4 ± 0.04	0.5 ± 0.02	0.4 ± 0.02	4.7 ± 0.14	5.4 ± 0.11	4.2 ± 0.33	0.2 ± 0.01
OG	1.4 <sup>a</sup> ± 0.04	0.3 ± 0.02	0.2 ± 0.01	4.7 ± 0.14	3.5 ± 0.07	3.6 ± 0.29	0.2 ± 0.01

<sup>a</sup> Octyl gallate could not be dissolved in buffer solution. However, the stoichiometric factor was assumed to be equal to that of the other gallates

$S_{\text{eff}} = 5.4$  but being higher than in the control (Fig. 14a). As we found in studies investigating the location of antioxidants in dispersed systems [25, 31] the main proportion of these gallates partitioned into the CTAB emulsifier pseudophase and was solubilized in the palisade layer of CTAB (see caption of Fig. 14). Consequently, gallates can be in very close proximity to galvinoxyl, which is exclusively solubilized in the interior of CTAB micelles. Thus, the accelerated activity towards galvinoxyl may be attributed to a local concentration effect that can occur by the accumulation of both gallates and galvinoxyl in the CTAB micellar phase resulting in an increase of their collision frequency [32]. The stoichiometric factor for OG towards galvinoxyl indicated a deeper intercalation into the micellar interior. Deeper intercalation can be accompanied by stronger specific interactions with CTAB than found between the other gallates and CTAB [33].

#### Activity of Gallates in SDS Systems

The stoichiometric factors of the solubilized proportion of gallates towards galvinoxyl in SDS micelles solution were close to zero (Fig. 14a). This may be accounted to the difference in solubilization sites of gallates and galvinoxyl. Gallates were found to be solubilized in the Stern layer of SDS micelles [25, 31] and the galvinoxyl is located in the micellar interior (Figs. 12, 13). Thus, it can be concluded that the SDS micelle acted as a physical barrier, i.e. providing different environments and thereby segregating the radicals and the antioxidants [34–36]. The reduced antioxidant activities in SDS micellar systems were consistent with results of studies that investigated the influence of increasing chain length of vitamin C derivatives [2, 3, 37] and vitamin E derivatives [2, 3, 38].

Reaction of the solubilized proportions of gallates with Fremy's radical in the emulsifier pseudophase of SDS micelles decreased with increasing chain length (Fig. 14b). This may also be attributed to the solubilization of the

gallate ester in the Stern layer where two different processes may influence the radical quenching activity. Since Fremy's radical is negatively charged, it may be electrostatically repelled by the anionic headgroup of SDS, and solubilization of Fremy's radical in the Stern layer is not feasible. The longer the ester alkyl chain, the deeper the aromatic ring could be located in this layer reducing contact with Fremy's radical.

#### Activity of Gallates in Brij Systems

In the Brij emulsifier pseudophase, the stoichiometric factors of the different gallate esters towards galvinoxyl were found to be enhanced with increasing ester alkyl chain length up to PG, whereas the reaction stoichiometry from PG to OG was constant (Fig. 14a). Our studies showed that antioxidants were located in the headgroup region of Brij (polyoxyethylene chain) [25, 31] and with stronger antioxidant lipophilicity additionally in the palisade layer. Since the gallate esters up to PG were located closer to the micellar interior with increasing alkyl chain [33], this is consistent with the assumption that a closer proximity of antioxidant and radical would facilitate their reaction.

The stoichiometric factor of the solubilized proportions of gallates with hydrophilic Fremy's radical in the emulsifier pseudophase of Brij micelles gradually decreased with increasing gallate lipophilicity (Fig. 14b). Because the proportions of the individual gallates solubilized in the Brij emulsifier pseudophase were higher than in the SDS emulsifier pseudophase, this provided additional evidence that Fremy's radical is partly located in the hydrophilic region of the Brij headgroup (Fig. 5). Consequently, Fremy's radical and gallates were in closer proximity than in SDS micellar solutions. OG may penetrate deeper into the polyoxyethylene region, because of the longer alkyl chain and thus form stronger H-bonds with the oxygens of the polyether groups of Brij that reduce the H-atom abstraction kinetic [26, 39, 40].

The observed stoichiometric factor (Table 1) of GA in Brij micellar solution were the same as in pure buffer solution, as the majority of GA is solubilized outside the micelle and the effect of closer proximity in the micelle is not significant.

## Conclusion

The solubilization sites of the hydrophilic Fremy's radical and hydrophobic galvinoxyl at interfaces were characterized by ESR and NMR experiments. It was shown that the close proximity of radical and antioxidant is a crucial prerequisite for the radical reducing action of antioxidants. The depth of intercalation for galvinoxyl in the interface depended on the surfactant used and increased in the order SDS < Brij < CTAB. CTAB increased the antioxidant efficiency due to solubilization of antioxidant and hydrophobic radical in close proximity in the micelle interior and thereby elevating their concentrations. In interfaces modeled by Brij a longer alkyl chain of the antioxidant (from methyl to butyl) resulted in increasing antioxidant efficiency. In contrast, interfaces modeled by SDS micelles caused a segregation of galvinoxyl (palisade layer) and antioxidant (stern layer), thus no antioxidant action took place. The hydrophilic Fremy's radical was exclusively solubilized in the aqueous environment of SDS systems but partitioned partly into the large headgroup region of Brij micelles. As gallates were solubilized to substantial amounts in micelles, the antioxidant efficiency was higher in Brij than in SDS micellar systems. The data clearly demonstrated that information on the solubilization sites of antioxidants and radicals are essential to control the antioxidant activity at interfaces present in a wide range of foods, cosmetics, pharmaceuticals (emulsions and carrier systems) and of biological membranes.

## References

- Niki E (1995) Action of antioxidants as studied by electron spin resonance. In: Ohya-Nishiguchi H, Packer L (eds) Bioradicals detected by ESR spectroscopy. Birkhäuser Verlag, Basel, pp 277–283
- Liu ZL, Han ZX, Chen P, Liu YC (1990) Stopped-flow ESR study on the reactivity of vitamin E, vitamin C and its lipophilic derivatives towards Fremy's salt in micellar systems. *Chem Phys Lipids* 56:73–80
- Liu Z (1995) Antioxidant activity of vitamin E and vitamin C derivatives in membrane mimetic systems. In: Ohya-Nishiguchi H, Packer L (eds) Bioradicals detected by ESR spectroscopy. Birkhäuser Verlag, Basel, pp 259–275
- Noda Y, Kaneyuki T, Mori A, Packer L (2002) Antioxidant activities of pomegranate fruit extract and its anthocyanidins: delphinidin, cyanidin and pelargonidin. *J Agric Food Chem* 50:166–171
- Packer L (1995) Vitamin E and antioxidant interactions in biological systems. In: Ohya-Nishiguchi H, Packer L (eds) Bioradicals detected by ESR spectroscopy. Birkhäuser Verlag, Basel, pp 237–257
- Bansal K, Patterson L (1971) Reaction of hydrated electrons, hydrogen atoms and hydroxyl radicals in micellar systems. *Intern J Phys Chem* 3:321–331
- de la Vega R, Pérez-Tejeda P, López-Cornejo P, Sánchez F (2004) Kinetic study of the oxidation of  $[\text{Ru}(\text{NH}_3)_5\text{pz}]^{2+}$  by  $[\text{Co}(\text{C}_2\text{O}_4)_3]^{3-}$  in AOT-oil-water microemulsions and in CTAC micellar solutions. *Langmuir* 20:1558–1563
- Gardner PT, McPhail DB, Duthie GG (1998) Electron spin resonance spectroscopic assessment of the antioxidant potential of teas in aqueous and organic media. *J Sci Food Agric* 76:257–262
- McPhail DB, Gardner PT, Duthie GG, Steele GM, Reid K (1999) Assessment of antioxidant potential of scotch whiskeys by electron spin resonance spectroscopy: relationship to hydroxyl containing aromatic components. *J Agric Food Chem* 47:1937–1941
- Burns J, Gardner PT, O'Neil J, Crawford S, Morecroft I, McPhail DB, Lister C, Matthews D, MacLean MR, Lean MEJ, Duthie GG, Crozier A (2000) Relationship among antioxidant activity, vasodilation capacity, and phenolic content of red wines. *J Agric Food Chem* 48:220–230
- McPhail DB, Hartley RC, Gardner PT, Duthie GG (2003) Kinetic and stoichiometric assessment of the antioxidant activity by electron spin resonance spectroscopy. *J Agric Food Chem* 51:1684–1690
- Pedrielli P, Skibsted LH (2002) Antioxidant synergy and regeneration effect of quercetin, (–)-epicatechin, and (+)-catechin on  $\alpha$ -tocopherol in homogeneous solutions of peroxidating methyl linoleate. *J Agric Food Chem* 50:7138–7144
- Barclay LRC, Ingold KU (1981) Autoxidation of biological molecules. 2. The autoxidation of a model membrane. A comparison of autoxidation of egg lecithin phosphatidylcholine in water and in chlorobenzene. *J Am Chem Soc* 103:6478–6485
- Lucarini M, Pedulli GF (1994) Bond dissociation enthalpy of  $\alpha$ -tocopherol and other phenolic antioxidants. *J Org Chem* 59:5063–5070
- Schwarz K, Bertelsen G, Nissen LR, Gardner PT, Heinonen M, Hopia AI, Huynh-Ba T, Lambelet P, McPhail DB, Skibsted LH, Tijburg L (2001) Investigation of plant extracts for the protection of processed foods against lipid oxidation. Comparison of antioxidant assays based on radical scavenging, lipid oxidation and analysis of the principal antioxidant compounds. *Eur Food Res Technol* 212:319–328
- Schwarz K, Frankel EN, German B (1996) Partition behaviour of antioxidative phenolic compounds in heterophasic systems. *Fett/Lipid* 98:115–121
- Stöckmann H, Schwarz K (1999) Partitioning of low molecular weight compounds in o/w emulsions. *Langmuir* 15:6142–6149
- Fessenden RW, Hitachi A, Nagarajan V (1984) Measurement of the dipole moment of a peroxy radical by microwave dielectric absorption. *J Phys Chem* 88:107–110
- Boyd LS, Boyd RJ, Barclay LRC (1990) A theoretical investigation of the structures and properties of peroxy radicals. *J Am Chem Soc* 112:5724–5730
- Pryor WA, Cornicelli JA, Devall LJ, Tait B, Trivedi BK, Witiak DT, Wu A (1993) A rapid screening test to determine the antioxidant potencies of natural and synthetic antioxidants. *J Org Chem* 110:2224–2229
- Barclay LRC, Vinqvist MR (1994) Membrane peroxidation: inhibiting effects of water-soluble antioxidants on phospholipids of different charge types. *Free Radic Biol Med* 16:779–788
- Stöckmann H, Schwarz K, Huynh-Ba T (2000) The influence of various emulsifiers on partitioning and antioxidant activity of

- hydrobenzoic acids and their derivatives in oil-in-water emulsions. *JAOCS* 77:535–542
23. Iwatsuki M, Tsuchiya J, Komuro E, Yamamoto Y, Niki E (1994) Effects of solvents and media on the antioxidant activity of  $\alpha$ -tocopherol. *Biochim Biophys Acta* 1200:19–26
  24. Polewski K, Kniat S, Slawinska D (2002) Gallic acid, a natural antioxidant, in aqueous and micellar environment: spectroscopic studies. *Curr Top Biophys* 26:217–227
  25. Heins A, Sokolowski T, Stöckmann H, Schwarz K (2007) Investigating the location of propyl gallate at surfaces and its chemical microenvironment by  $^1\text{H}$  NMR. *Lipids* (in press)
  26. Mukerjee P (1971) Solubilization of benzoic acid derivatives by nonionic surfactants: location of solubilizates in hydrocarbon core of micelles and polyoxyethylene mantle. *J Pharm Sci* 60:1528–1530
  27. Leisner D (1996) Kinetik nukleophiler Reaktionen mit Benzylbromid in Mikroemulsionen. Ph.D. Universität Bielefeld
  28. Stilbs P (1995) Solubilization, as studied by nuclear spin relaxation and NMR-based self diffusion techniques. In: Christian SD, Scamehorn JF (eds) *Solubilization in surfactant aggregates*, vol 55. Surfactant science series, Marcel Dekker Inc., New York, pp 367–381
  29. Marangoni DG, Kwak JCT (1995) Comparison of experimental methods for the determination of the partition coefficients of *n*-alcohols in SDS and DTAB micelles. In: Christian SD, Scamehorn JF (eds) *Solubilization in surfactant aggregates*, vol 55. Surfactant science series. Marcel Dekker Inc., New York, pp 455–490
  30. Stöckmann H (2000) Untersuchungen zum Einfluß des Verteilungs- und Solubilisierungsverhaltens auf die Aktivität von Wirkstoffen in dispersen Systemen am Beispiel von Antioxidantien in O/W Emulsionen. Ph.D. Thesis, Universität Hannover
  31. Heins A, Garamus VM, Steffen B, Stöckmann H, Schwarz K (2006) Impact of phenolic antioxidants on structural properties of micellar solutions. *Food Biophys* 1:189–201
  32. Reščič J, Vlady V, Bhuiyan LB, Outhwaite CW (2005) Theoretical study of catalytic effects in micellar solutions. *Langmuir* 21:481–486
  33. Heins A (2005) Localisation and activity of antioxidants in dispersed systems characterised by NMR and ESR spectroscopy. Ph.D. Thesis, University of Kiel
  34. Coupland JN, McClements DJ (1996) Lipid oxidation in food emulsions. *Trends Food Sci Technol* 7:83–91
  35. McClements DJ, Decker EA (2000) Lipid oxidation in oil-in-water emulsions: impact of molecular environment on chemical reactions in heterogeneous food systems. *J Food Sci* 65:1270–1282
  36. Decker EA (1998) Strategies for manipulating the prooxidative/antioxidative balance of foods to maximize oxidative stability. *Food Sci Technol* 9:241–248
  37. Wen XL, Zhang J, Liu ZL, Han ZX, Rieker A (1998) Micellar effects on the oxidative electrochemistry of lipophilic vitamin C derivatives. *J Chem Soc Perkin Trans* 2:905–910
  38. Castle C, Perkins MJ (1986) Inhibition kinetics of chain-breaking phenolic antioxidants in SDS micelles. Evidence that intermicellar diffusion rates may be rate-limiting for hydrophobic inhibitors such as  $\alpha$ -tocopherol. *J Am Chem Soc* 108:6381–6382
  39. Mulley BA, Metcalf AD (1956) Non-ionic surface active agents. Part I: The solubility of chloroxylenol in aqueous solutions of polyethylene glycol 1000 monocetyl ether. *J Pharm Pharmacol* 8:774–779
  40. Fendler EJ (1982) Membrane mimetic chemistry: characterization and applications of micelles, microemulsions, monolayers, bilayers, vesicles, host-guest systems, and polyions. Wiley, New York

## Macadamia Nut Consumption Modulates Favourably Risk Factors for Coronary Artery Disease in Hypercholesterolemic Subjects

Manohar L. Garg · Robert J. Blake · Ron B. H. Wills · Edward H. Clayton

Received: 11 January 2007 / Accepted: 17 February 2007 / Published online: 17 April 2007  
© AOCs 2007

**Abstract** Macadamia nuts are rich source of monounsaturated fats (oleic and palmitoleic acids) and contain polyphenol compounds, therefore, their consumption can be expected to impart health benefits to humans. This study was conducted to examine the effects of consuming macadamia nuts in hypercholesterolemic male individuals on plasma biomarkers of oxidative stress, coagulation and inflammation. Seventeen hypercholesterolemic male subjects were given macadamia nuts (40–90 g/day), equivalent to 15% energy intake, for a period of 4 weeks. As expected, monounsaturated fatty acids (16:1n-7, 18:1n-9 and 20:1n-9) were elevated in the plasma lipids of all volunteers following intervention with macadamia nuts. Plasma markers of inflammation (leukotriene,  $LTB_4$ ) and oxidative stress (8-isoprostane) were significantly lower ( $1,353 \pm 225$  vs.  $1,030 \pm 129$  pg/mL and  $876 \pm 97$  vs.  $679 \pm 116$  pg/mL, respectively) within 4 weeks following macadamia nut intervention. There was a non-significant (23.6%) reduction in the plasma  $TXB_2/PGI_2$  ratio following macadamia nut consumption. This study demonstrates, for the first time, that short-term macadamia nut consumption modifies favourably the biomarkers of oxidative stress, thrombosis and inflammation, the risk factors for coronary artery disease, despite an increase in dietary fat intake. These data, combined with our previous results on cholesterol-lowering effects of macadamia nuts, suggest that

regular consumption of macadamia nuts may play a role in the prevention of coronary artery disease.

**Keywords** Macadamia nuts · Oxidative stress · Monounsaturated fatty acids · Prostacyclin · Leukotrienes · Hypercholesterolemia · Thromboxane · 8-Isoprostane

### Abbreviations

PUFA Polyunsaturated fatty acids  
MUFA Monounsaturated fatty acids

### Introduction

Dietary factors known to alleviate lipid peroxidation and oxidative stress levels in humans include carotenoids, flavonoids, antioxidant vitamins (vitamin A, C and E), glutathione, uric acid and ubiquinone Q10. n-6 and n-3 Polyunsaturated fatty acids (PUFA) have been shown to favourably modify plasma lipid levels but are vulnerable to oxidative damage and may increase requirements for antioxidants to protect them from auto-oxidation and minimise oxidative damage in the body [1–3]. Saturated fatty acids in the diet, although not susceptible to oxidative deterioration, have been associated with an increase in total and LDL-cholesterol. Monounsaturated fatty acids (MUFA), shown to be cholesterol neutral or even cholesterol-lowering in several studies [4, 5], also have the potential to reduce demands for anti-oxidants, thus help reducing oxidative stress in vivo [6–8]. Research on whole foods containing factors with antioxidant activity is sparse.

The macadamia nut, a tree nut native to Australia, contains approximately 75% fat (w/w) and more than 85%

M. L. Garg (✉) · R. J. Blake · R. B. H. Wills · E. H. Clayton  
Nutraceuticals Research Group, School of Biomedical Sciences,  
Faculty of Health, University of Newcastle,  
305C Medical Science Building, Callaghan,  
NSW 2308, Australia  
e-mail: manohar.garg@newcastle.edu.au

of its energy from fat. Macadamia nuts contain higher levels of monounsaturated fatty acids than any other food source known to-date (more than 60 g/100 g of edible whole nuts) [9]. Curb et al. [10] demonstrated that a macadamia nut-based diet is nearly as effective as a moderately low-fat diet (American Heart Association Step 1 diet) in reducing total plasma cholesterol and LDL cholesterol, in comparison to a typical American diet. We have recently demonstrated that replacing 15% dietary energy intake by macadamia nuts (40–90 g/day) lowers total and LDL-cholesterol and increases HDL-cholesterol in hypercholesterolemic subjects within 4 weeks [11]. In general, research on tree nuts has been limited to their ability to modulate plasma lipid levels and information on their potential to modulate other health risk factors, including oxidative damage, inflammation and clotting tendency, is lacking in the literature.

The current study was conducted to examine the effects of consuming macadamia nuts on plasma biomarkers of oxidative stress, coagulation and inflammation in subjects with an increased risk of coronary artery disease.

## Experimental Procedures

### Subjects

Seventeen male hypercholesterolemic subjects with a cholesterol range of 6.1–7.5 mmol/L were advised to maintain their regular lifestyle especially their physical activity throughout the study period.

### Study Design

Freshly roasted lightly salted and unsalted macadamia nut kernels (*Macadamia integrifolia*) were purchased from the Suncoast Gold Macadamias Ltd (QLD, Australia). Participants consumed macadamia nuts contributing an equivalent of approximately 15% of the total daily energy intake for a 4-week period. The absolute amount of macadamia nuts consumed ranged between 40–90 g/day, depending on subject's energy intake. Nuts were packed in separate bags containing only 1-day supply/bag. An extra colour-coded bag of macadamia nuts was given to the volunteers to share with family and friends in order to improve compliance. Compliance was measured by examining the incorporation of palmitoleic acid (16:1n-7) into plasma lipids following the 4 weeks intervention period. Fasting blood samples were collected by venipuncture on entry to the study and at the conclusion of the intervention. Fatty acid composition of macadamia nuts and nutrient intake of the study participants has been reported previously [11].

### Markers of Inflammation and Oxidative Stress

Venous blood for 8-iso-prostaglandin F<sub>2α</sub> (8-isoprostane) analysis was collected in tubes pre-coated with EDTA and containing 1 mg/mL whole blood of reduced glutathione (GSH) (Sigma Chemical Company, St Louis, MI, USA) as an antioxidant in order to prevent in vitro production of isoprostanes. Separated plasma was transferred to storage tubes, pre-coated with butylated hydroxytoluene as an antioxidant in order to further prevent in vitro production of isoprostanes, and stored at –70 °C until analysis. 8-Iso-PGF<sub>2x</sub> was determined using an 8-isoprostane EIA kit (Cayman Chemical Company, Ann Arbor, MI, USA). The ability of this assay to measure 8-iso-PGF<sub>2x</sub> was validated using a series of known amounts of 8-iso-PGF<sub>2x</sub> and a high correlation was found between the known positive control concentrations and the values determined using the kit.

Plasma leukotriene B<sub>4</sub> (LTB<sub>4</sub>) levels were determined on venous blood collected into tubes coated with EDTA using a commercially available LTB<sub>4</sub> EIA kit (Cayman Chemical Company, Ann Arbor, MI, USA).

### Thromboxane and Prostacyclin Assays

Plasma thromboxane (TXB<sub>2</sub>) concentrations were determined using a commercially available thromboxane B<sub>2</sub> EIA kit (Cayman Chemical Company, Ann Arbor, MI, USA). Venous blood was collected into an indomethacin coated blood tube, mixed gently by inversion, and then centrifuged at 3,000×g for 10 min at 4 °C. The plasma fraction was removed and stored at –70 °C until analysis.

An aliquot of <sup>3</sup>H-TXB<sub>2</sub> equivalent to 5,000 cpm was added to a 500 μL aliquot of plasma. The samples were deproteinated by the addition of 2 mL of ethanol, followed by vigorous mixing. Samples were allowed to stand at 4 °C prior to being centrifuged at 1,500×g for 10 min. 8 mL of 0.1 mM phosphate buffer (pH 4.0) was added to the ethanolic supernatant, followed by vigorous vortex mixing.

Samples were further purified by solid phase extraction. A reverse phase (C18) Sep Pak cartridge (Waters) was first activated by washing with 5 mL of ethanol followed by 5 mL of ultra-pure water. Samples were loaded onto the cartridge and purified by washing with 5 mL of ultra-pure water followed by 5 mL of hexane. The TXB<sub>2</sub> was eluted from the cartridge into a glass tube with 5 mL of ethyl acetate:methanol (99:1). The elute was evaporated to dryness under a stream of nitrogen and then dissolved in assay buffer.

Fifty microlitre aliquots of sample, standard or buffer were added to wells of a microwell plate coated with Mouse Anti-rabbit IgG, followed by 50 μL of TXB<sub>2</sub> acetylcholinesterase tracer, and then TXB<sub>2</sub> antiserum. The plate was then covered with plastic film and incubated at

room temperature for 18 h. The wells were then emptied and washed five times with wash buffer. About 200  $\mu\text{L}$  of Ellman's reagent was added to each well and the plate was covered with plastic film. The plate developed in the dark on an orbital shaker for between 60–90 min. Absorbance was read at 412 nm on a microplate reader and TXB<sub>2</sub> concentration determined from a standard calibration curve in pg/mL.

Plasma prostacyclin I<sub>2</sub> levels were determined on venous blood collected into tubes coated with EDTA using a commercially available prostacyclin EIA kit (Cayman Chemical Company, Ann Arbor, MI, USA).

### Fatty Acid Analysis

The lipid profile of the plasma was determined according to a modification of the method of Lepage & Roy using an acetyl chloride methylation procedure, as detailed previously [12]. Fatty acid methyl esters were quantified using a Hewlett Packard 6890 gas chromatograph and quantified by comparison with authentic fatty acid methyl ester standards (Nu Chek Prep).

### Statistical Analysis

Mean and standard error of mean are presented for each measurement. Data for TXB<sub>2</sub> and prostacyclin (PGI<sub>2</sub>) were not normally distributed and were transformed using square root transformation prior to analysis. The Student *t* test (paired, two-tailed) was used to compare baseline values with post-intervention values. Differences were considered significant at  $P < 0.05$ .

## Results

The average age of the hypercholesterolemic subjects was 54 years and a BMI of 26.24 at baseline. A high degree of compliance was evident from the increase in MUFA content in the plasma samples following intervention with macadamia nuts. Specifically, the levels of palmitoleic acid (16:1n-7), for which the unique dietary source is macadamia nut, were elevated in all volunteers (Table 1). Plasma saturated and polyunsaturated fatty acids (n-6 and n-3) were not affected by the intervention.

LTB<sub>4</sub> levels in the plasma were lower ( $P = 0.024$ ) post-intervention ( $679 \pm 116$  pg/mL) compared with the baseline values ( $876 \pm 97$  pg/mL) (Fig. 1). 8-Isoprostane concentration was significantly ( $P = 0.032$ ) reduced from  $1,353 \pm 225$ – $1,030 \pm 129$  pg/mL following the feeding of macadamia nuts to hypercholesterolaemic subjects.

**Table 1** Plasma fatty acid composition (% of total fatty acids) of hypercholesterolaemic subjects ( $n = 17$ ) at baseline and post-intervention with macadamia nuts

Fatty acid	Baseline	Post-intervention
C14:0	1.05 $\pm$ 0.09	0.90 $\pm$ 0.06 <sup>a</sup>
C14:1n-7	0.13 $\pm$ 0.01	0.10 $\pm$ 0.01 <sup>a</sup>
C16:0	21.13 $\pm$ 0.46	19.95 $\pm$ 0.43 <sup>a</sup>
C16:1n-7	2.30 $\pm$ 0.17	3.14 $\pm$ 0.14 <sup>a</sup>
C18:0	7.85 $\pm$ 0.13	7.52 $\pm$ 0.09 <sup>a</sup>
C18:1n-9	22.93 $\pm$ 0.56	24.83 $\pm$ 0.62 <sup>a</sup>
C18:1n-7	1.76 $\pm$ 0.05	2.13 $\pm$ 0.06 <sup>a</sup>
C18:2n-6	25.75 $\pm$ 0.88	24.71 $\pm$ 0.75
C18:3n-6	0.53 $\pm$ 0.04	0.52 $\pm$ 0.03
C18:3n-3	0.62 $\pm$ 0.05	0.51 $\pm$ 0.04
C20:0	0.28 $\pm$ 0.02	0.36 $\pm$ 0.01 <sup>a</sup>
C20:1n-9	0.15 $\pm$ 0.01	0.23 $\pm$ 0.02 <sup>a</sup>
C20:2n-6	0.15 $\pm$ 0.01	0.15 $\pm$ 0.01
C20:3n-6	1.70 $\pm$ 0.09	1.61 $\pm$ 0.13
C20:4n-6	6.38 $\pm$ 0.31	6.07 $\pm$ 0.47
C20:5n-3	1.15 $\pm$ 0.10	1.40 $\pm$ 0.30
C22:0	0.81 $\pm$ 0.06	0.92 $\pm$ 0.05
C22:1n-9	0.00 $\pm$ 0.00	0.07 $\pm$ 0.07
C22:5n-3	0.67 $\pm$ 0.04	0.59 $\pm$ 0.04
C22:6n-3	2.25 $\pm$ 0.19	2.00 $\pm$ 0.18
C24:0	0.79 $\pm$ 0.07	0.84 $\pm$ 0.07
C24:1n-9	1.17 $\pm$ 0.08	1.08 $\pm$ 0.08
Total SFA	32.015 $\pm$ 0.41	30.56 $\pm$ 0.41 <sup>a</sup>
Total MUFA	28.433 $\pm$ 0.61	31.58 $\pm$ 0.68 <sup>a</sup>
Total n-6 PUFA	34.516 $\pm$ 0.86	33.07 $\pm$ 0.74
Total n-3 PUFA	5.036 $\pm$ 0.32	4.79 $\pm$ 0.29

<sup>a</sup> Means ( $\pm$ sem) are significantly different from the pre-intervention means ( $\pm$ sem) ( $P < 0.05$ )

TXB<sub>2</sub> and PGI<sub>2</sub> concentrations were not significantly lower ( $122 \pm 23$  vs.  $90 \pm 14$  pg/mL;  $P = 0.177$  and  $192 \pm 31$  vs.  $177 \pm 26$  pg/mL;  $P = 0.269$ , respectively) following macadamia nut consumption for 4 weeks (Fig. 1). The mean thromboxane TXB<sub>2</sub> to prostacyclin ratio was reduced by 23.6% following macadamia nut consumption, however, this change was not significant (from  $0.82 \pm 0.12$  to  $0.62 \pm 0.10$ ;  $P = 0.094$ ).

## Discussion

Hypercholesterolemia is a major risk factor for coronary artery disease and reducing plasma cholesterol levels, in particular LDL cholesterol, reduces the risk of this disease. In addition, an increase in the plasma levels of biomarkers



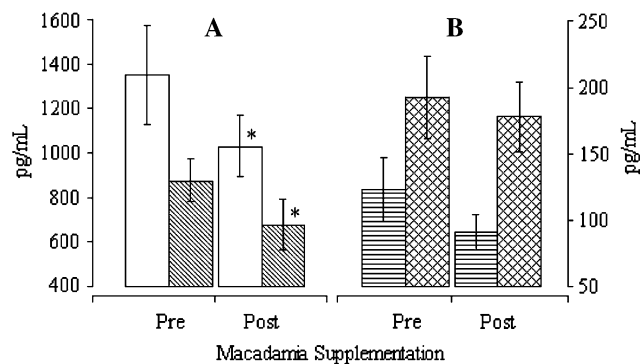


**Fig. 1** Plasma markers of oxidative stress and inflammation including *A* isoprostane (empty squares) and leukotriene B<sub>4</sub> (squares with diagonal lines) and *B* thromboxane (B<sub>2</sub>) (squares with horizontal lines) and prostacyclin I<sub>2</sub> (hatched squares) in hypercholesterolemic ( $n = 17$ ) subjects prior to and following the consumption of macadamia nuts (15% of energy) for 4 weeks. Values are means  $\pm$  standard error of the means (pg/mL). Asterisks indicate significantly different values from pre-supplementation value analysed by paired *t* test (isoprostane and prostacyclin) or Wilcoxin ranked sums test (leukotriene and thromboxane)

of clotting tendency, lipid peroxidation and inflammation also contribute to the development and progression of atherosclerosis. Dietary strategies have been focussed mainly to reduce circulating levels of cholesterol, LDL-cholesterol and to date very little attention has been paid to other biomarkers of coronary artery disease. In a recent study, we demonstrated that replacing 15% of daily energy intake by macadamia nuts for 4 weeks results in a significant reduction in plasma and LDL-cholesterol with a concomitant increase in HDL-cholesterol [11]. In the current study, we report, for the first time, the risk factors (biomarkers of oxidative stress, clotting tendency and inflammation) other than plasma/LDL cholesterol in subjects with elevated levels of plasma cholesterol following the consumption of macadamia nuts for 4 weeks.

8-Isoprostane produced from arachidonic acid by a free-radical catabolized reaction is a reliable in-vivo marker of oxidative stress [13, 14]. Plasma levels of 8-isoprostane were reduced by 18.9% following macadamia nut intervention. Previous studies have demonstrated that diets rich in MUFA reduce oxidisability of LDL and lower plasma 8-isoprostanes [15] and, therefore, may be cardio-protective. It is, therefore, likely that MUFA present in the macadamia nuts are responsible for the reduction in 8-isoprostane levels in hypercholesterolaemic subjects. It is also possible that the phenolic compounds present in macadamia nuts contribute to the reduction in plasma isoprostane levels [16].

LTB<sub>4</sub> derived from arachidonic acid by the action of lipo-oxygenase are highly chemotactic substance and elevated levels are suggestive of increased inflammation.

Replacing 15% of daily energy intake for 4 weeks resulted in a 22.5% reduction of LTB<sub>4</sub> concentration in the plasma. Anti-inflammatory effects of tree nuts, including macadamia nuts, have not previously been reported. A recent study using walnuts as an intervention in hypercholesterolemic subjects reported 64% increase in endothelium dependent vasodilation (EDV) with a concomitant reduction of the vascular cell adhesion molecule (VCAM-1) by 20% [17]. The authors attributed the change in VCAM-1 and EDV to changes in the plasma lipid profile and  $\alpha$ -linolenic acid present in walnuts. However, it is also likely that components of nuts, yet unidentified, may be responsible for the observed anti-inflammatory effects.

TXB<sub>2</sub> is a potent pro-aggregatory and PGI<sub>2</sub> is an anti-aggregatory substance, and the plasma ratio of TXB<sub>2</sub>:PGI<sub>2</sub> is a reliable indicator of clotting tendency which has been reported to be increased in hypercholesterolaemic individuals [18]. Although not significantly different, TXB<sub>2</sub>/PGI<sub>2</sub> ratio was lowered by 23.6% by macadamia nut intervention. This reduction in biomarkers of clotting tendency may be due to the presence of MUFA and/or vitamin E present in macadamia nuts [19, 20]. It is also likely that macadamia nuts contain compounds yet unidentified that may reduce the levels of these eicosanoids. In this context, examination of other biomarkers of clotting tendency, such as fibrinogen and ex-vivo measurements of platelet or whole blood aggregation, may be worthy of further investigation.

Taken together, the results presented suggest that consumption of macadamia nuts as part of a healthy diet is associated with a reduction in biomarkers of coronary artery disease. Combined with our previous study on cholesterol lowering effects of macadamia nuts [11], this study demonstrates that short-term consumption of macadamia nuts, despite increasing the fat content of the diet, may be used as an adjunct to drug therapy to reduce risk of coronary artery disease. Jenkins et al. [21] demonstrated that diets low in saturated fat and high in viscous fibers and phytosterols, when combined with vegetable protein foods and nuts, reduce plasma cholesterol and C-reactive protein similarly to the initial therapeutic dose of first generation statin. This study demonstrates that macadamia nuts may make an important contribution to the heart healthy diet. Long-term health benefits of macadamia nut consumption remain to be elucidated. The constituents of macadamia nuts responsible for the reduction in biomarkers remain to be identified. In this respect, palmitoleic acid (16:1n-7) present in high amounts (approximately 20% of total fatty acids) in macadamia nuts may appear promising. Effects of palmitoleic acid on eicosanoid metabolism are not known at present and are worthy of further investigations. The current study not only provides a pathophysiological explanation for the beneficial effects of consuming

macadamia nuts on the heart, but it also clearly shows that this beneficial effect was independent of any other lifestyle factors.

**Acknowledgments** Supported by a grant from the Horticultural Research and Development Corporation.

## References

1. Bulur H, Ozdemirler G, Oz B, Toker G, Ozturk M, Jysal M (1995) High cholesterol diet supplemented with sunflower seed oil but not olive oil stimulates lipid peroxidation in plasma, liver and aorta of rats. *J Nutr Biochem* 6(10):547–550
2. Nair PP, Judd JT, Berlin E, Taylor PR, Shami S, Sainz E, Bhagavan HN (1993) Dietary fish oil-induced changes in the distribution of alpha-tocopherol, retinol, and beta-carotene in plasma, red blood cells, and platelets: modulation by vitamin E. *Am J Clin Nutr* 58(1):98–102
3. Karlsson J (1997) Exercise, muscle metabolism and the antioxidant defense. In: Simopoulos AP, Pavlou KN (eds) *World reviews on nutrition and dietetics*, vol 82. Karger, Basel, pp 81–100
4. Grundy SM (1986) Comparison of monounsaturated fatty acids and carbohydrates for lowering plasma cholesterol. *N Engl J Med* 314(12):745–748
5. Kris-Etherton PM, Pearson TA, Wan Y, Hargrove RL, Moriarty K, Fishell V, Etherton TD (1999) High-monounsaturated fatty acid diets lower both plasma cholesterol and triacylglycerol concentrations. *Am J Clin Nutr* 70(6):1009–1015
6. Lopez-Miranda J, Gomez P, Castro P, Marin C, Paz E, Bravo MD, Blanco J, Jimenez-Perez J, Fuentes F, Perez-Jimenez F (2000) Mediterranean diet improves low density lipoprotein susceptibility to oxidative modifications. *Med Clin* 115(10):361–365
7. Parthasarathy S, Khoo JC, Miller E, Barnett J, Witztum JL, Steinberg D (1990) Low density lipoprotein rich in oleic acid is protected against oxidative modification: implications for dietary prevention of atherosclerosis. *Proc Natl Acad Sci USA* 87(10):3894–3898
8. Berry EM, Eisenberg S, Haratz D, Friedlander Y, Norman Y, Kaufmann NA, Stein Y (1991) Effects of diets rich in monounsaturated fatty acids on plasma lipoproteins—the Jerusalem nutrition study: high MUFAs vs. high PUFAs. *Am J Clin Nutr* 53(4):899–907
9. Holland B, Unwin ID, Buss DH (1992) *Fruits and nuts: the composition of foods*, McCance and Widdowson's 5th edn. Xerox Ventura, Cambridge
10. Curb JD, Wergowske G, Dobbs JC, Abbott RD, Huang B (2000) Serum lipid effects of a high-monounsaturated fat diet based on macadamia nuts. *Arch Intern Med* 160(8):1154–1158
11. Garg ML, Blake RJ, Wills RB (2003) Macadamia nut consumption lowers plasma total and LDL cholesterol levels in hypercholesterolemic men. *J Nutr* 133(4):1060–1063
12. Lepage G, Roy CC (1986) Direct transesterification of all classes of lipids in a one-step reaction. *J Lipid Res* 27(1):114–120
13. Mueller T, Dieplinger B, Gegenhuber A, Haidinger D, Schmid N, Roth N, Ebner F, Landl M, Poelz W, Haltmayer M (2004) Serum total 8-iso-prostaglandin F2alpha: a new and independent predictor of peripheral arterial disease. *J Vasc Surg* 40(4):768–773
14. Wood LG, Gibson PG, Garg ML (2003) Biomarkers of lipid peroxidation, airway inflammation and asthma. *Eur Respir J* 21(1):177–186
15. Nansen C, Vessby B, Berglund L, Uusitupa M, Hermansen K, Riccardi G, Rivellese A, Storlien L, Erkkila A, Yla-Herttuala S, Tapsell L, Basu S (2006) Dietary (n-3) fatty acids reduce plasma F2-isoprostanes but not prostaglandin F2alpha in healthy humans. *J Nutr* 136(5):1222–1228
16. Visioli F, Caruso D, Galli C, Viappiani S, Galli G, Sala A (2000) Olive oils rich in natural catecholic phenols decrease isoprostane excretion in humans. *Biochem Biophys Res Commun* 278(3):797–799
17. Ros E, Nunez I, Perez-Heras A, Serra M, Gilabert R, Casals E, Deulofeu R (2004) A walnut diet improves endothelial function in hypercholesterolemic subjects: a randomized crossover trial. *Circulation* 109(13):1609–1614
18. Osterud B, Elvevoll EO, Brox J, Olsen JO (2002) Cellular activation responses in blood in relation to lipid pattern: healthy men and women in families with myocardial infarction or cancer. *Blood Coagul Fibrinolysis* 13(5):399–405
19. Kelly CM, Smith RD, Williams CM (2001) Dietary monounsaturated fatty acids and haemostasis. *Proc Nutr Soc* 60(2):161–170
20. Ferroni P, Basili S, Falco A, Davi G (2004) Oxidant stress and platelet activation in hypercholesterolemia. *Antioxid Redox Signal* 6(4):747–756
21. Jenkins DJA, Kendall CWC, Marchie A, Faulkner DA, Wong JMW, de Souza R, Emam A, Parker TL, Vidgen E, Lapsley KG, Trautwein EA, Josse RG, Leiter LA, Connelly PW (2003) Effects of a dietary portfolio of cholesterol-lowering foods versus lovastatin on serum lipids and C-reactive protein. *J Am Med Assoc* 290(4):502–510

## Incorporation of Arachidonic and Stearic Acids Bound to L-FABP into Nuclear and Endonuclear Lipids from Rat Liver Cells

Sabina M. Maté · Juan P. Layerenza · Ana Ves-Losada

Received: 13 January 2007 / Accepted: 9 April 2007 / Published online: 6 June 2007  
© AOCs 2007

**Abstract** The incorporation of exogenous fatty acids bound to L-FABP into nuclei was studied. Rat liver cell nuclei and nuclear matrices (membrane depleted nuclei) were incubated in vitro with [1-<sup>14</sup>C]18:0 and 20:4n-6 either free or bound to L-FABP, ATP and CoA. FA esterification in whole nuclei and endonuclear lipids was ATP-CoA-dependent, and with specificity regarding fatty acid type and lipid class. 18:0 and 20:4n-6, free or L-FABP bound, showed the same incorporation and esterification pattern in lipids of whole nuclei. Only 20:4n-6 L-FABP bound was less incorporated into TAG with respect to free 20:4n-6. In the nuclear matrix, 18:0 free or L-FABP bound was esterified with a higher specific activity (SA) into: PtdEtn > PtdIns, PtdSer > PtdCho. 20:4n-6 free or L-FABP bound was esterified into: PtdIns > PtdEtn > PtdCho. 20:4n-6: L-FABP was esterified in endonuclear total-PL and PtdIns with a greater SA with respect to free 20:4n-6 and with a minor one as FFA. To summarize, trafficking of FA to nuclei includes esterification of 18:0 and 20:4n-6 either free or L-FABP-bound, into nuclear and endonuclear lipids by an ATP-CoA-dependent pathway. Endonuclear fatty acid esterification was more active than that in whole nuclei, and independent of the nuclear membrane. Esterification patterns of fatty acids L-FABP-bound or free into whole nuclear lipids were the same whereas in the nuclear matrix, L-FABP could play an important role in the

mobilization of 20:4n-6 into specific sites of utilization such as the PtdIns pools.

**Keywords** Cell nuclei · Nuclear matrix · Endonuclear lipids · Arachidonic acid · Stearic acid · Fatty acid incorporation · L-FABP

### Introduction

The biological function of fatty acids has long been considered only as a source of nutrients, substrates of metabolic energy and structural components in membranes when esterified in glycerolipids, sphingolipids and cholesterol. Currently we are aware that fatty acids have per se physiological and pharmacological properties; they also regulate gene expression.

Gene expression regulation is an event, which develops within the nucleus of eukaryotic cells. It may be produced by a direct effect of fatty acids (FA) or acyl-CoAs on the regulation of the genetic expression, or through the activation of transcription factors that are translocated to the nucleus [1, 2]. The regulation of gene transcription by FA may be due to changes in the activity or abundance of at least four transcript factor families: PPAR, LXR, HNF-4 $\alpha$  and SREBP [1, 2].

Fatty acids are molecules of hydrophobic nature and poor water solubility. They are strongly reactive and easily esterified to other lipids, moving about within the cell when bound to the fatty acid binding protein (FABP). FABP is involved in fatty acid metabolism by modulating their cellular import, their distribution and the activity of enzymes.

Fatty acid binding proteins (FABPs) belong to a family of cytosolic fatty acid chaperones specifically localized in

S. M. Maté · J. P. Layerenza · A. Ves-Losada (✉)  
Facultad de Ciencias Médicas, Instituto de Investigaciones Bioquímicas de La Plata (INIBIOLP), CONICET-UNLP, 60 y 120, 1900 La Plata, Argentina  
e-mail: avlosada@biol.unlp.edu.ar

A. Ves-Losada  
Dto. de Ciencias Biológicas, Facultad de Ciencias Exactas, UNLP, 1900 La Plata, Argentina

different animal tissues [3]; only the so-called L-FABP is biosynthesized in rat liver [4], and it is located in the cytoplasm as well as in the nucleus of hepatocytes. FABPs have evolved over millenniums from ancestral forms, and their cellular role and mechanism of action are being visualized. L-FABP is a soluble low molecular weight protein (14.3 kDa) that corresponds to approximately 5% of cytosolic liver proteins [5]. It has a tertiary structure consisting of ten antiparallel  $\beta$ -strands that form a  $\beta$ -barrel, which is capped by two short  $\alpha$ -helices arranged as a helix–turn–helix segment [6]. L-FABP, different to other FABPs contains two FA binding sites [6], but it can also bind other hydrophobic ligands even acyl-CoAs [7].

Studies with a fluorescent analogue of FAs showed that transfer of FA from the L-FABP to phospholipid membranes is consistent with an aqueous mediated diffusion model mechanism and differs from heart H-FABP and adipocyte A-FABP that form a transient collisional complex with membrane-like acceptors [4, 8].

Fatty acids of cellular nuclei may come from cytosol where they are synthesized, incorporated from the diet, or generated from the hydrolysis of other nuclear lipid pools. Although we have previously demonstrated that arachidonic acid is also synthesized in the nucleus by  $\Delta 5$  desaturation of 20:3n-6 acid, 20:3n-6 fatty acid must have originated in the cytosol (ER) [9]. These days, the precise trafficking of fatty acids from cytosol to nuclear receptors, where they participate in the regulation of gene expression, has not been fully elucidated.

We have demonstrated that in nuclei isolated from rat liver cells, exogenous acyl-CoAs, saturated and polyunsaturated fatty acids are incorporated in the nuclei by an esterification mechanism by means of an acyl-CoA-dependent pathway [10, 11]. FA are mainly esterified in phospholipids, to a minor proportion in triacylglycerols, and also incorporated as free fatty acid (FFA) [11]. In addition, we have demonstrated that arachidonic acid synthesized in the nucleus by  $\Delta 5$  desaturation of 20:3n-6 is rapidly esterified into nuclear lipids [12]. We have also reported that in nuclei, phosphatidylcholine fatty acids can be remodeled by an acyl-CoA-dependent process, in which cytosolic proteins would be involved [13]. It is still unknown whether cytosolic FABP or ACBP is involved in this process, though the existence of L-FABP and ACBP in the nucleus was corroborated [14, 15]. It was also found that PPAR- $\alpha$  is activated by L-FABP bound fatty acids [7, 16].

Taking into account that the available information is poor, the aim of this work was to study the role of L-FABP in the trafficking of fatty acids from the cytosol to the nuclei. Metabolizable fatty acids were chosen as they are closely related to lipid pools as already demonstrated, through interactions, esterification and hydrolysis. 18:0 and

20:4n-6 fatty acids were chosen as they are the major saturated and polyunsaturated acids in rat liver cell nuclear and endonuclear lipid pools [17].

## Materials and Methods

### Materials

[1-<sup>14</sup>C] Arachidonic acid (55 mCi/mmol 98.1% radiochemically pure) and [1-<sup>14</sup>C] stearic acid (56 Ci/mmol, 99% radiochemically pure) were purchased from New England Nuclear Co., Boston, MA. Rat liver fatty acid binding protein (L-FABP) was a kind gift from Betina Córscico (INIBIOLP, La Plata, Argentina). The recombinant rat pET11-a-L-FABP plasmid was kindly provided by Dr. Alan Kleinfeld and Dr. Ron Ogata (Torrey Pines Institute for Molecular Studies, San Diego, CA). The protein was expressed in the *E. coli* BL21 (DER) expression system and purified as described by Hsu and Storch [19]. Cofactors were provided by Sigma Chemical Co. (St Louis, MO). Chemicals and solvents were of analytical and HPLC grade. TLC precoated silica gel G 20 × 20 cm plates with a concentrated zone of 2.5 × 20 cm was from Merck (Argentina).

### Animals

Experiments were performed on male Wistar rats of 60–70 days of age, weighing 180–200 g. Rats were housed in rooms with 12–12 h light–dark cycle (midnight being the midpoint of the dark period), and the experiments were performed in accordance with the Guide of Care and Use of Laboratory Animals (1996, National Academy Press). Animals were maintained on a commercial standard pellet diet (Cargill mouse and rat chow, Pilar, Argentina) and tap water *ad libitum*. The diet contained 24% proteins and 8% of total lipids with a fatty acid composition (wt%) of 1.7% 14:0, 20.3% 16:0, 1.8% 16:1, 11.4% 18:0, 27.5% 18:1n-9, 2.1% 18:1n-7, 31.4% 18:2n-6, 3.1% 18:3n-3, 0.2% 20:4n-6, and 0.6% 22:6n-3.

### Preparation of Homogenate, Subcellular Fractions and Membrane-Depleted Nuclei

Rats were killed at 8 a.m. to equalize circadian rhythm effects [18], and livers pooled from 3–5 animals were homogenized in 0.25 M sucrose TKM [0.05 M Tris–HCl, (pH 7.5), 0.0025 M KCl, 0.005 M MgCl<sub>2</sub>] 1:2 (w/v). Highly purified nuclei were isolated from liver homogenate by sucrose-gradient ultracentrifugation using the method of Blobel and Potter modified by Kasper as described in a previous publication [9]. All steps were carried out at 4 °C.

To obtain the nuclear matrix (the membrane-depleted nucleus), a quantitative removal of the nuclear envelope was performed as already described [17]. The double nuclear membrane was solubilized with the non-ionic detergent Triton TX-100 followed by separation over a sucrose gradient using the method of Vann et al. [19] slightly modified as follows: 0.5 ml aliquot of nuclei (8 mg prot/ml) in solution A [10 mM Tris-HCl (pH 7.5); 2 mM MgCl<sub>2</sub>; 0.25 M sucrose] was mixed with 20 ml of ice-cold suspension buffer [5 mM Tris-HCl (pH 7.4), 5 mM MgCl<sub>2</sub>, 1.5 mM KCl, 0.29 M sucrose, 1 mM EGTA] and incubated on ice for 20 min. TX-100 was added to this buffer before the addition of the nuclei to yield a final concentration of 0.08% (w/v). The nuclei were pelleted at 165×g for 6 min (4 °C), and the supernatant removed. The pellet was resuspended in solution A (5 ml) and a 10 ml cushion of [10 mM Tris-HCl (pH 7.5), 2 mM MgCl<sub>2</sub>, 0.5 M sucrose] was carefully laid beneath it and then centrifuged at 165×g for 6 min (4 °C). This procedure was repeated once again. Membrane-depleted nuclei were then resuspended in 25% glycerol, [10 mM Tris-HCl (pH 7.9)] and stored at -80 °C until used. Concentration of nuclei and nuclear matrices in terms of proteins was determined by the method of Lowry et al. [20] using crystalline bovine serum albumin as standard.

#### Criteria of Nuclear Purity

Nuclei and membrane-free nuclei preparations were checked for purity by electron microscopy as described previously [10, 17].

#### Fatty Acids Bound to L-FABP (FA:L-FABP)

FAs concentrations bound to L-FABP were chosen so as to saturate the first high affinity binding site of L-FABP [21, 22]. Therefore, equivalent concentrations of 2 μM [1-<sup>14</sup>C] arachidonic, or [1-<sup>14</sup>C] stearic acid and 2 μM L-FABP were incubated for 1 min at 36 °C in a solution of 0.15 M KCl, 0.25 M sucrose, 5 mM MgCl<sub>2</sub>, 1.6 mM *N*-acetylcysteine, and 41.7 mM potassium phosphate buffer (pH 7.4).

#### Incorporation of [1-<sup>14</sup>C] FA into Nuclear and Endonuclear Lipid Pools

Incorporation of [1-<sup>14</sup>C] arachidonic and [1-<sup>14</sup>C] stearic acids in rat liver cell whole nuclei and nuclear matrices was performed by incubating 6 mg proteins from each nuclear source. The incubation medium contained 0.15 M KCl, 0.25 M sucrose, 5 mM MgCl<sub>2</sub>, 1.6 mM *N*-acetylcysteine, 41.7 mM potassium phosphate buffer (pH 7.4) with 2 μM [1-<sup>14</sup>C]FA free or bound L-FABP in the presence or ab-

sence of 60 μM CoA and 1.3 mM ATP. The open tubes were incubated by gentle shaking at 36 °C with a total volume of 1.6 ml, for 1, 5 and 10 min. After incubation, the nuclei were separated from the incubation mixture by centrifugation at 2,000×g at 4 °C for 10 min.

#### Lipid Analyses

Lipids were extracted from rat liver cell nuclei by the procedure of Folch et al. [24]. Lipids were recovered from the original chloroform extract; phospholipids, triacylglycerols, diacylglycerols and free fatty acids were separated by thin-layer chromatography (TLC) on precoated silica gel G plates with a concentration zone, using hexane-diethyl ether-acetic acid (80:20:2 v/v/v) as the mobile phase. The different phospholipid classes were also separated by TLC on the same type of plates, but using chloroform-methanol-acetic acid-water (50:37.5:3.5:2 v/v/v/v) as the mobile phase [17]. They were located and identified by comparison with known lipid standards and visualized by exposure to iodine vapor. For individual phospholipid analysis, spots of unexposed sections were extracted from the plates for quantification by phosphorus spectrophotometric determination as already described [17]. Radioactivity incorporated in the different lipids was measured by radiochromatographic scanning on a Berthold Ld 2723, Dünnschicht Scanner (Wildbad, Germany).

#### Data Presentation and Statistical Analyses

Biochemical analyses were run in duplicate. All the experiments were carried out five times. Data are shown as mean ± SE. Significance was determined by Student's *t*-test for unpaired samples. Differences were considered significant at *P* < 0.05.

## Results

#### Experimental Conditions

In order to study the role of L-FABP in the trafficking of fatty acids from cytosol to the nuclei, two metabolizable fatty acids and nuclear fractions were chosen. 18:0 and 20:4n-6 fatty acids were selected as they are the major saturated and polyunsaturated acids in rat liver cell nuclear and endonuclear lipid pools as already described [17]. Whole nuclei and nuclear matrices isolated from rat liver cells were chosen as nuclear and endonuclear lipid pools. FAs concentrations bound to L-FABP were chosen so as to saturate the first high affinity binding site of L-FABP, considering that *K<sub>D</sub>* for 18:0 and 20:4n-6 are 9 and 110 μM, respectively [21, 22]. The fatty acid concentration utilized

was 2  $\mu$  M as in a previous work [11], since it corresponds to the fatty acid physiological concentration range of rat liver cell cytosol (20:4n-6 is 2–5  $\mu$ M [23] and 18:0 17.6  $\mu$ M [24]). FABPs cytosol concentrations in liver cells range from 0.2 to 1 mM [25–27], and under physiological conditions only 2% L-FABP would have a ligand bound [25–27]. Therefore our experimental conditions at 2- $\mu$ M L-FABP concentration with the high affinity binding site saturated by the fatty acid, would be within the physiological range conditions.

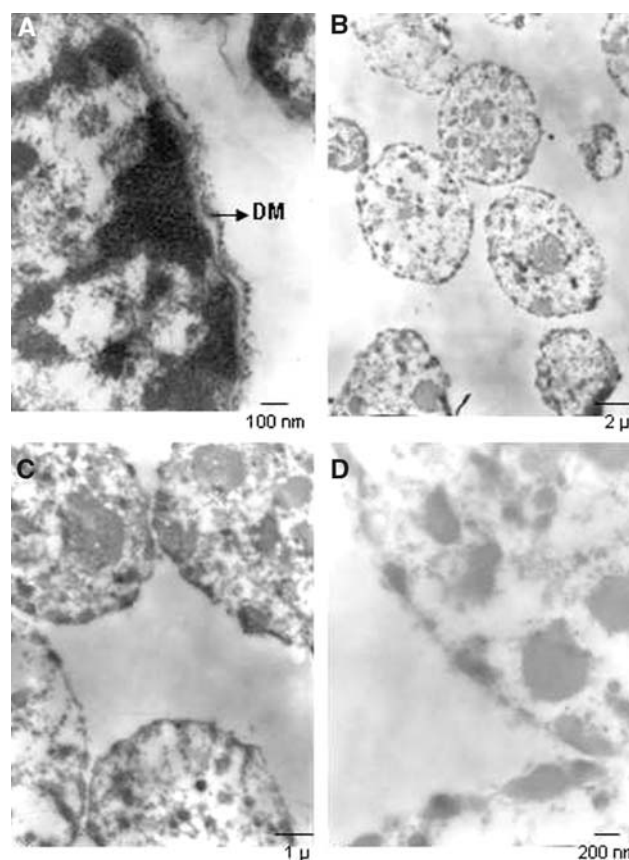
#### Electron-Microscopic Analysis of the Rat Liver Nuclear Matrix

Nuclear matrices were obtained from rat liver nuclei isolated as described previously [17], according to the procedure described by Vann et al. (1997). Mild concentrations of TX-100 were applied when the matrices were isolated from nuclei of rat liver cells. Rat liver nuclei were first isolated as described elsewhere [9], and the nuclear envelope was quantitatively removed with 0.08% (w/v) concentrations of TX-100, followed by separation over a sucrose gradient. The nuclear membrane removal was checked by electron microscopy as shown in Fig. 1. The isolated control nuclei (without TX-100 incubation) corresponded to whole nuclei with all their characteristic structures that include the double nuclear membrane, chromatin zones and nucleoli; ribosomes can also be observed associated to the external nuclear membrane, as shown in Fig. 1a. Figure 1b, c, and d, observed at different magnification powers, correspond to nuclear matrices; they show that the detergent removed the nuclear double membrane without visible alterations of the remaining endonuclear structure. Nuclear matrices were not collapsed nor deformed and conserved a spherical shape. These results were similar to those obtained by Vann et al. (1997) [19].

#### Incorporation of [1-<sup>14</sup>C]18:0 Acid Free and Bound to L-FABP into Nuclear Lipid Pools

Incorporation and esterification of exogenous [1-<sup>14</sup>C]18:0 fatty acid L-FABP-bound in nuclear lipid pools were studied by incubation in vitro of nuclei isolated from rat liver in the presence of either 2  $\mu$ M [1-<sup>14</sup>C]18:0 or [1-<sup>14</sup>C]18:0:L-FABP, ATP and CoA (Figs. 2, 3).

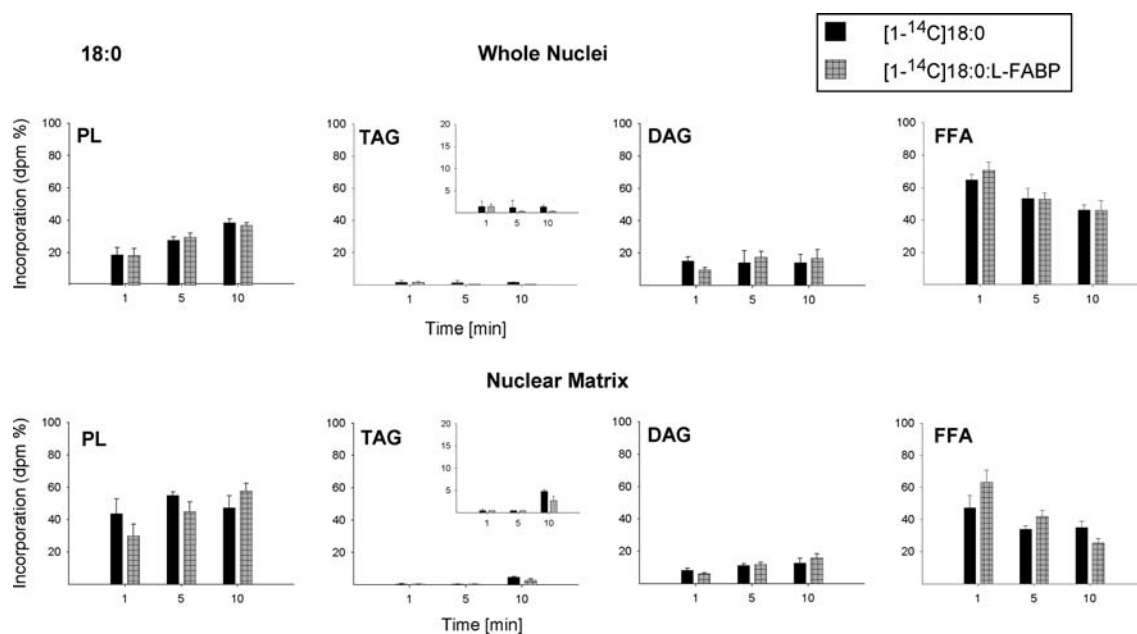
Under these experimental conditions [1-<sup>14</sup>C]18:0:L-FABP was esterified to PL (20%), DAG (10–15%), and mainly incorporated as FFA (60%) in rat liver cell nuclei (Fig. 2). After 10 min incubation, the radioactivity incorporated as FFA decreased as it was mainly esterified to PL (40%). DAG esterification was saturated from the starting point, and TAG esterification was very low (2%).



**Fig. 1** Electron micrographs of nuclear preparations. **a** Control rat liver cell nuclei (scale bar 0.10  $\mu$ M). The classical double membrane (DM) surrounds the nucleus. **b** Nuclear matrix obtained by treatment of nucleus with 0.08% (w/v) TX-100 (scale bar 2  $\mu$ M) that removes nuclear DM. **c** and **d** The nuclear matrix at higher magnification shows no nuclear envelope (scale bar 1.0  $\mu$ M and 0.2  $\mu$ M, respectively)

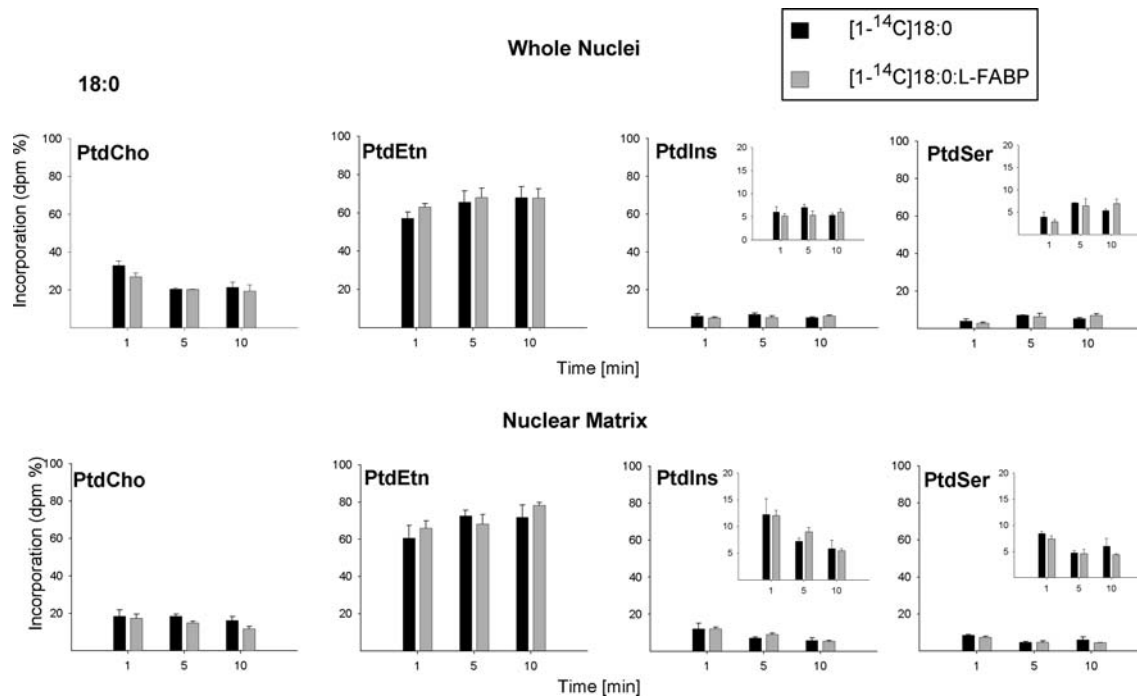
[1-<sup>14</sup>C]18:0 fatty acid, either free or bound to L-FABP was incorporated with the same pattern to nuclear lipid pools, as no significant differences were found between both groups. Table 2 shows the incorporation of 18:0 acid in nuclear lipid pools as nmol.mg total lipid (TL)<sup>-1</sup>. For the calculation it was taken into account that nuclei contain  $0.206 \pm 0.03$  mg TL.mg prot<sup>-1</sup> (data not shown).

Figure 3 shows the esterification of [1-<sup>14</sup>C]18:0 either free or bound to L-FABP in nuclear PL in the presence of ATP and CoA. Esterification percentages of [1-<sup>14</sup>C]18:0 either free or bound to L-FABP in each nuclear PL were not correlated with their relative mass. As already reported [17], liver cell nuclei have the following phospholipid composition: PtdCho (64%), PtdEtn (22%), PtdIns (10%), SM (1.9%) and PtdSer (1.6%). Figure 3 shows that 18:0 acid was esterified mainly in PtdEtn, though it is not the major nuclear PL. Esterification percentages of 18:0 acid in PL were as follows: PtdEtn (60–70%) > PtdCho (20–30%) whereas the lowest proportion was found in PtdIns (6%)



**Fig. 2** Time-course incorporation of  $[1-^{14}\text{C}]18:0$  and  $[1-^{14}\text{C}]18:0\text{:L-FABP}$  into nuclear and endonuclear lipid classes. Whole nuclei or nuclear matrices isolated from rat liver cells were incubated with  $[1-^{14}\text{C}]18:0$  or  $[1-^{14}\text{C}]18:0\text{:L-FABP}$  with ATP and CoA. At different time points, the incubation mixture was centrifuged to separate whole nuclei or nuclear matrices. Lipids were extracted and separated

by thin-layer chromatography (TLC). Scanning of thin-layer plates was performed as described in “Materials and Methods”.  $^{14}\text{C}$  was recovered in PL and in NL as TAG, DAG and FFA. Results are the mean of five experiments  $\pm$  SE. Statistical analysis was performed by the Student’s *t* test between results from incubations with FA bound to L-FABP (FA: L-FABP) with respect to free FA (FA)



**Fig. 3** Time-course esterification of  $[1-^{14}\text{C}]18:0$  and  $[1-^{14}\text{C}]18:0\text{:L-FABP}$  into nuclear and endonuclear phospholipids. Whole nuclei or nuclear matrices isolated from rat liver cells were incubated with  $[1-^{14}\text{C}]18:0$  or  $[1-^{14}\text{C}]18:0\text{:L-FABP}$  with ATP and CoA. Lipids were extracted and separated by thin-layer chromatography (TLC).

Scanning of thin-layer plates was performed as described in “Materials and Methods”.  $^{14}\text{C}$  was recovered in PtdCho, PtdEtn, PtdIns and PtdSer. Results are the mean of five experiments  $\pm$  SE. Statistical analysis was performed by the Student’s *t* test between FA bound to L-FABP (FA: L-FABP) with respect to free FA (FA)

and PtdSer (5%). Under the present experimental conditions [ $1\text{-}^{14}\text{C}$ ]18:0 acid, free or bound to L-FABP was esterified in all nuclear PL except in SM. These results are quite difficult to be explained as SM molecular species are characterized by an esterified saturated or monounsaturated fatty acid [28]. In addition, 18:0 acid was esterified in PtdSer, which is a minor nuclear PL as SM in nuclei, as we have already reported [17]. Then, one could discard the idea that the absence of 18:0 esterified in SM may be due to the low amount of SM in liver nuclei. It is clear that, 18:0 was selectively esterified to nuclear PtdEtn with respect to the other nuclear PL.

Table 3 displays esterification of 18:0 either free or bound to L-FABP as *specific activity* (SA). For the calculation it was taken into account that rat liver cell nuclei have  $39.2 \pm 0.1$  nmol PL mg prot $^{-1}$ , and the PL distribution already described [18]. 18:0 was esterified into each nuclear PL as follows: PtdEtn/PtdSer > PtdIns > PtdCho. These results confirmed that 18:0 was selectively esterified into nuclear PtdEtn and PtdSer regarding the total nuclear PL.

When the incubations were performed without ATP and CoA [ $1\text{-}^{14}\text{C}$ ]18:0 or [ $1\text{-}^{14}\text{C}$ ]18:0, L-FABP was not esterified in any nuclear lipid pool as it was exclusively incorporated as FFA (100%) (Table 1). Then 18:0 free or bound to L-FABP was esterified into nuclear lipid pools by an acyl-CoA mechanism as already reported for the free fatty acid [11].

#### Incorporation of [ $1\text{-}^{14}\text{C}$ ] 20:4n-6 Acid Free and Bound to L-FABP into Nuclear Lipid Pools

Figures 4 and 5 show the incorporation and esterification of exogenous 20:4n-6 acid into nuclear lipid pools, after in vitro incubation of nuclei isolated from rat liver cells in the presence of either 2  $\mu\text{M}$  [ $1\text{-}^{14}\text{C}$ ]20:4n-6 or [ $1\text{-}^{14}\text{C}$ ]20:4n-6:L-FABP, ATP and CoA.

Firstly, [ $1\text{-}^{14}\text{C}$ ]20:4n-6:L-FABP was mainly esterified in PL (40%) and incorporated as FFA (45%). After 10 min

incubation, 20:4n-6 decreased (30%) as FFA after esterification to PL (50%), and in a minor proportion to TAG (20%). [ $^{14}\text{C}$ ] was not found esterified in DAG. When [ $1\text{-}^{14}\text{C}$ ]20:4n-6 acid was bound to L-FABP, the fatty acid was esterified into nuclear TAG in a minor proportion with respect to free fatty acid.

Incorporation of 20:4n-6 fatty acid free or bound to L-FABP into nuclear lipid pools as nmol mg TL $^{-1}$  is described in Table 4. The comparison of Tables 2 and 4, showed that the amount (nmol.mg TL $^{-1}$ ) of arachidonic and stearic acids, esterified to nuclear PL was similar. When comparing the esterification of 20:4n-6 to that of 18:0 in nuclear lipid pools (nmol.mg LT $^{-1}$ ; Tables 2, 4), it was observed that 20:4 was mainly esterified in PL and TAG with respect to 18:0. Only 18:0 acid was esterified into nuclear DAG under the experimental conditions assayed.

The amount of 20:4n-6 esterified to nuclear TAG was greater than that of 18:0, but it was lower than the amount of 20:4n-6 that remained as FFA with respect to 18:0.

Figure 5 displays the esterification percentage of [ $1\text{-}^{14}\text{C}$ ]20:4n-6 acid either free or bound to L-FABP in each nuclear PL in the presence of ATP and CoA. No significant differences in nuclear PL esterification pattern were observed when 20:4n-6 acid was free or bound to L-FABP. 20:4n-6 acid was esterified into nuclear PL as follows: PtdCho (50–60%) > PtdEtn (20–30%) > PtdIns ( $\approx$  15%), and in a very low proportion PtdSer (1–2%). Under the present experimental conditions, [ $1\text{-}^{14}\text{C}$ ]20:4n-6 acid, either free or bound to L-FABP, was esterified to all PL nuclear classes except SM. It is well documented that SM molecular species have a saturated or monounsaturated fatty acid esterified in the molecule, but not a polyunsaturated fatty acid, such as 20:4n-6 acid [28].

It is interesting to note that exogenous 20:4n-6, free or bound to L-FABP, was esterified to nuclear PtdIns with a SA ([ $1\text{-}^{14}\text{C}$ ]20:4n-6 nmol. nmol PtdIns $^{-1}$ ) that doubles that of PtdCho and PtdEtn after 10 min of incubation (Table 5).

**Table 1** Effect of ATP and CoA on [ $1\text{-}^{14}\text{C}$ ]fatty acid free and bound to L-FABP incorporation into nuclear and endonuclear lipids pools

Incubation conditions	Incorporation of radioactivity as FFA (dpm%)							
	Whole nuclei				Nuclear matrix			
	18:0		20:4n-6		18:0		20:4n-6	
[ $1\text{-}^{14}\text{C}$ ] Fatty acid	FA	FA:L-FABP	FA	FA:L-FABP	FA	FA:L-FABP	FA	FA:L-FABP
With ATP and CoA	46	46	30	27	32	28	70	65
Without ATP and CoA	100	100	100	100	100	100	100	100

Liver nuclei or membrane-depleted nuclei were incubated with [ $1\text{-}^{14}\text{C}$ ]18:0 (FA), [ $1\text{-}^{14}\text{C}$ ]18:0:L-FABP (FA:L-FABP), [ $1\text{-}^{14}\text{C}$ ]20:4n-6 or [ $1\text{-}^{14}\text{C}$ ]20:4n-6:L-FABP fatty acids with or without ATP and CoA. After 10 min, the incubation mixture was centrifuged to separate whole nuclei or the nuclear matrices from the incubation mixture. Lipids were extracted and separated by TLC.  $^{14}\text{C}$  was recovered in PL and in NL when ATP and CoA were added as shown in Figs. 2, 3, 4, and 5.  $^{14}\text{C}$  was only recovered in NL as FFA (100%) when ATP and CoA were omitted. Results are presented as the percentage of total  $^{14}\text{C}$  radioactivity incorporated as FFA into nuclear and endonuclear lipid pools



**Table 2** Incorporation of [ $1-^{14}\text{C}$ ]18:0 free and bound to L-FABP into nuclear and endonuclear lipid classes

Time	PL		TAG		DAG		FFA	
	FA	FA: L-FABP	FA	FA: L-FABP	FA	FA: L-FABP	FA	FA: L-FABP
Whole nuclei (nmol.mg TL <sup>-1</sup> )								
1	0.41 ± 0.10	0.41 ± 0.10	0.03 ± 0.03 <sup>c</sup>	0.03 ± 0.01 <sup>a</sup>	0.33 ± 0.05	0.21 ± 0.03	1.41 ± 0.08 <sup>a</sup>	1.57 ± 0.11 <sup>a</sup>
5	0.58 ± 0.04	0.62 ± 0.06 <sup>c</sup>	0.03 ± 0.03 <sup>a</sup>	0.03 ± 0.02 <sup>c</sup>	0.30 ± 0.16	0.36 ± 0.08	1.12 ± 0.13 <sup>c</sup>	1.10 ± 0.08 <sup>b</sup>
10	0.80 ± 0.05	0.79 ± 0.04	0.03 ± 0.01 <sup>a</sup>	0.03 ± 0.02 <sup>a</sup>	0.29 ± 0.11	0.36 ± 0.11	0.96 ± 0.07 <sup>a</sup>	0.98 ± 0.13 <sup>b</sup>
Nuclear matrix (nmol.mg TL <sup>-1</sup> )								
1	6.26 ± 0.65 <sup>a</sup>	4.22 ± 1.01	0.07 ± 0.04	0.07 ± 0.04	1.19 ± 0.34	0.87 ± 0.10	6.79 ± 0.50 <sup>a</sup>	8.88 ± 1.08
5	6.72 ± 0.30 <sup>a</sup>	6.38 ± 0.85 <sup>b</sup>	0.07 ± 0.04 <sup>a</sup>	0.07 ± 0.04 <sup>a</sup>	1.59 ± 0.17	1.70 ± 0.17	4.84 ± 0.30 <sup>a</sup>	5.94 ± 0.57 <sup>b</sup>
10	6.50 ± 0.32 <sup>a</sup>	8.15 ± 0.68 <sup>a</sup>	0.66 ± 0.14 <sup>b</sup>	0.38 ± 0.14 <sup>b</sup>	1.75 ± 0.41	2.24 ± 0.37	4.82 ± 0.44 <sup>a</sup>	3.60 ± 0.40 <sup>a</sup>

Whole liver nuclei or nuclear matrices (membrane-depleted nuclei) were incubated with [ $1-^{14}\text{C}$ ]18:0 or [ $1-^{14}\text{C}$ ]18:0:L-FABP, ATP and CoA for 1, 5 and 10 min. After incubation samples were assayed as described in ‘‘Materials and Methods’’. Results are presented as nmol of [ $1-^{14}\text{C}$ ]18:0 incorporated/mg total lipids<sup>-1</sup> (TL) and are the mean of five experiments ± SE. Statistical analysis was performed by the Student’s *t* test. No significant differences were found in FA:L-FABP respect FA. A letter denotes significant differences between 18:0 data (Table 2) vs. the same 20:4n-6 data from Table 4, either incorporated or esterified: <sup>a</sup> *P* < 0.001, <sup>b</sup> *P* < 0.01 and <sup>c</sup> *P* < 0.05

**Table 3** Esterification of [ $1-^{14}\text{C}$ ]18:0 free and bound to L-FABP into nuclear and endonuclear phospholipid classes

Time (min)	PtdCho		PtdEtn		PtdIns		PtdSer	
	FA	FA: L-FABP	FA	FA: L-FABP	FA	FA: L-FABP	FA	FA: L-FABP
Whole nuclei (pmol.nmol each PL <sup>-1</sup> )								
1	1.1 ± 0.3	0.9 ± 0.38	5.6 ± 1.7	6.1 ± 1.6	1.4 ± 0.6 <sup>b</sup>	1.2 ± 0.4 <sup>a</sup>	4.9 ± 2.5	3.5 ± 1.6
5	1.0 ± 0.2 <sup>b</sup>	1.0 ± 0.2 <sup>c</sup>	9.1 ± 1.5	9.9 ± 1.6 <sup>b</sup>	2.2 ± 0.4 <sup>c</sup>	1.8 ± 0.5	12.6 ± 2.2	12.1 ± 4.1
10	1.4 ± 0.3 <sup>b</sup>	1.2 ± 0.3 <sup>b</sup>	12.9 ± 1.9 <sup>b</sup>	12.7 ± 1.5 <sup>b</sup>	2.3 ± 0.4 <sup>c</sup>	2.6 ± 0.42 <sup>a</sup>	13.0 ± 4.2	16.7 ± 3.2
Nuclear matrix (pmol.nmol each PL <sup>-1</sup> )								
1	10.2 ± 2.9	6.4 ± 2.4	70.8 ± 15.2 <sup>a</sup>	51.9 ± 15.6 <sup>a</sup>	32.6 ± 11.4 <sup>a</sup>	21.63 ± 6.98	25.2 ± 3.8	15.0 ± 3.4
5	12.8 ± 1.2	8.3 ± 1.7	106.1 ± 8.4 <sup>a</sup>	81.3 ± 16.8 <sup>a</sup>	24.0 ± 2.9	24.51 ± 5.45	17.7 ± 2.2	14.1 ± 5.6
10	9.3 ± 1.6	8.5 ± 1.6 <sup>c</sup>	87.1 ± 12.2 <sup>a</sup>	118.9 ± 12.1 <sup>a</sup>	16.1 ± 5.2	18.77 ± 2.95	18.7 ± 5.6	17.2 ± 2.2

Whole liver nuclei or nuclear matrix were incubated with [ $1-^{14}\text{C}$ ]18:0 or [ $1-^{14}\text{C}$ ]18:0:L-FABP, ATP and CoA for 1, 5 and 10 min. After incubation samples were assayed as described in ‘‘Materials and Methods’’. Results are presented as pmol of [ $1-^{14}\text{C}$ ]18:0 incorporated/nmol each PL class, and are the mean of five experiments ± SE. Statistical analysis was performed by the Student’s *t* test. No significant differences were found in FA:L-FABP respect FA. A letter denotes significant differences between data of 18:0 (Table 3) vs. the same data of 20:4n-6 in Table 5: <sup>a</sup> *P* < 0.001, <sup>b</sup> *P* < 0.01 and <sup>c</sup> *P* < 0.05

It was also observed that 20:n-6 was esterified with a greater SA in nuclear PtdCho and PtdIns with respect to 18:0, but in a minor proportion in PtdEtn and PtdSer (Tables 3, 5).

When incubations were performed without ATP and CoA in the incubation medium, [ $1-^{14}\text{C}$ ]20:4n-6 or [ $1-^{14}\text{C}$ ]20:4n-6: L-FABP was not esterified in any nuclear lipid pools; it was exclusively incorporated as FFA (100%) (Table 1). Then 20:4n-6, free or bound to L-FABP, was esterified to nuclear lipid pools by an acyl-CoA mechanism, as we have already reported for free 20:4n-6 [11].

#### Incorporation of [ $1-^{14}\text{C}$ ]18:0 Acid, Free and Bound to L-FABP, into Endonuclear Lipid Pools

In order to determine the mechanism of incorporation and esterification of FA into endonuclear lipids, nuclear

matrices were incubated in vitro in the presence of [ $1-^{14}\text{C}$ ]18:0 or [ $1-^{14}\text{C}$ ]18:0:L-FABP, ATP and CoA (Figs. 2, 3). Each nuclear matrix was isolated by removing the double nuclear membrane, solubilized at low concentrations using a non-ionic detergent (TX-100) as indicated elsewhere (Fig. 1).

Exogenous 18:0 acid, free or L-FABP bound, was mainly esterified to PL (30–40%), a minor proportion to DAG (7%), and the remainder was incorporated as FFA (50–60%) into the nuclear matrices from rat liver cells (Fig. 2). After 10 min incubation, the incorporated radioactivity decreased as FFA since it was being esterified to PL (50–60%), to DAG (15%), and to TAG (3–5%).

The fact that 18:0 acid was free or bound to L-FABP did not modify the general pattern of incorporation and esterification of fatty acids in endonuclear lipid pools (Figs. 2,

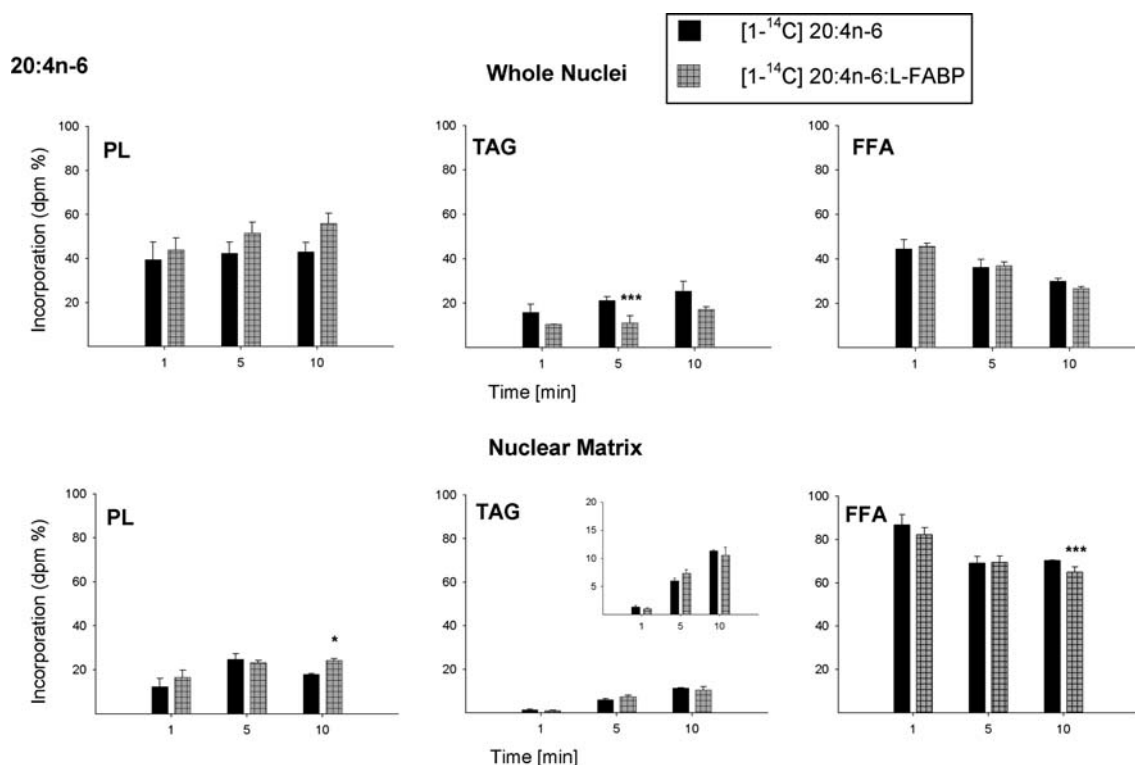


**Fig. 4** Time-course incorporation of  $[1-^{14}\text{C}]20:4n-6$  and  $[1-^{14}\text{C}]20:4n-6\text{:L-FABP}$  into nuclear and endonuclear lipid classes. Whole nuclei or nuclear matrices isolated from rat liver cells were incubated with  $[1-^{14}\text{C}]20:4n-6$  or  $[1-^{14}\text{C}]20:4n-6\text{:L-FABP}$  with ATP and CoA. After the incubation samples were assayed as described in Fig. 2.  $^{14}\text{C}$

was recovered in PL and in NL as TAG and FFA. Results are the mean of five experiments  $\pm$ SE. Statistical analysis was performed by the Student's *t* test. FA: L-FABP significantly different from FA: \* $P < 0.001$  and \*\*\* $P < 0.05$

3). However, there was less dispersion of data over the incubation time when  $[1-^{14}\text{C}]18:0$  was bound to L-FABP compared with the free acid.

These results imply that esterification of fatty acids to endonuclear lipid pools, is an autonomous matrix mechanism, since it still occurs after the removal of the double nuclear membrane. Consequently, all the enzymes and factors involved must also have an endonuclear localization.

As reported in a previous work, endonuclear lipid pools have a relatively different composition with respect to whole nuclei [17]. Liver nuclear matrices contain 0.5 mg proteins.g liver<sup>-1</sup> and 8.5 nmol PL.mg prot<sup>-1</sup>. As already reported [17], they represent 25.8 and 22.6% of the respective whole nuclei components.

Table 2 shows FA incorporation and esterification into endonuclear lipid pools (nmol incorporated mg TL<sup>-1</sup>). It must be taken into account that nuclear matrices contain 0.032  $\pm$  0.01 mg TL.mg prot<sup>-1</sup> (data not shown). Results show that exogenous 18:0, either free or bound to L-FABP, was esterified to PL and DAG, and incorporated as FFA in a greater amount in the nuclear matrix than in the whole nucleus. Therefore, nuclear matrices have a more active fatty acid metabolism than that of whole liver nuclei.

As already observed in nuclear pools, esterification of exogenous 18:0 acid, free or bound to L-FABP, in each endonuclear PL did not correspond to their relative masses (Fig. 2). As previously described elsewhere rat liver cell matrices contained the following phospholipid composition: PtdCho (43%), PtdEtn (20%), PtdIns (9%)m SM (9%) and PtdSer (8%) and LysoPtdCho (10%) [17]. Esterification percentage of  $[1-^{14}\text{C}]18:0$  into each PL (Fig. 3) was as follows: PtdEtn (63%) > PtdCho (18%) > PtdIns (12%) > PtdSer (4–8%). We must bear in mind that nuclear matrices are enriched in SM with regard to nuclei, since the matrix contains 9% SM whereas the whole nucleus only 1.9% [17]. In spite of this, 18:0 acid, free or bound to L-FABP, was esterified in all endonuclear PL except SM (Fig. 3). These results corroborate that fatty acids are incorporated into SM during the de novo synthesis, which has been reported to take place in the cytosol [28].

Table 3 shows esterification of 18:0 acid, free or L-FABP bound, in each PL as specific activity (SA, pmol.nmol each PL<sup>-1</sup>). 18:0 acid either free or L-FABP bound was esterified in endonuclear PL with the following SA: PtdEtn > PtdIns/PtdSer > PtdCho. This esterification pattern of 18:0 acid free or L-FABP bound in each endo-

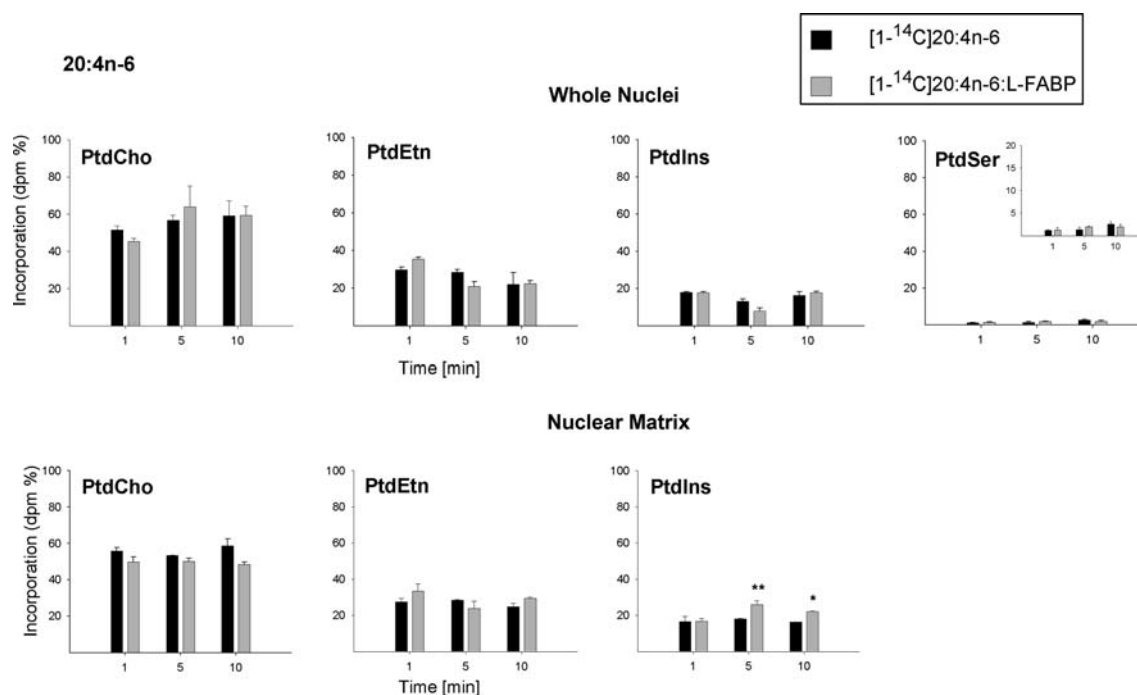


**Fig. 5** Time-course esterification of  $[1-^{14}\text{C}]20:4n-6$  and  $[1-^{14}\text{C}]20:4n-6:L-FABP$  into nuclear and endonuclear phospholipids. Whole nuclei or nuclear matrices isolated from rat liver cells were incubated with  $[1-^{14}\text{C}]20:4n-6$  or  $[1-^{14}\text{C}]20:4n-6:L-FABP$  with ATP and CoA. Lipids were extracted and separated by TLC. Scanning of thin-layer

plates was performed as described in ‘‘Materials and Methods’’.  $^{14}\text{C}$  was recovered in PtdCho, PtdEtn, PtdIns and PtdSer. Results are the mean of five experiments  $\pm$ SE. Statistical analysis was performed by the Student’s *t* test. FA: L-FABP significantly different from FA: \* $P < 0.001$  and \*\* $P < 0.01$

**Table 4** Incorporation of  $[1-^{14}\text{C}]20:4n-6$  free and bound to L-FABP into nuclear and endonuclear lipid classes

Time (min)	PL		TAG		FFA	
	FA	FA: L-FABP	FA	FA: L-FABP	FA	FA: L-FABP
Whole nuclei (nmol.mg TL <sup>-1</sup> )						
1	0.68 $\pm$ 0.136	0.71 $\pm$ 0.087	0.27 $\pm$ 0.07	0.17 $\pm$ 0.020	0.77 $\pm$ 0.07	0.74 $\pm$ 0.021
5	0.80 $\pm$ 0.098	0.88 $\pm$ 0.082	0.40 $\pm$ 0.03	0.19 $\pm$ 0.053 <sup>b</sup>	0.68 $\pm$ 0.07	0.63 $\pm$ 0.029
10	0.84 $\pm$ 0.082	0.90 $\pm$ 0.073	0.50 $\pm$ 0.08	0.28 $\pm$ 0.018 <sup>a</sup>	0.59 $\pm$ 0.02	0.43 $\pm$ 0.012 <sup>a</sup>
Nuclear matrix (nmol.mg TL <sup>-1</sup> )						
1	1.60 $\pm$ 0.23	2.00 $\pm$ 0.24	0.17 $\pm$ 0.04	0.12 $\pm$ 0.02	11.31 $\pm$ 0.61	9.89 $\pm$ 0.40
5	3.17 $\pm$ 0.31	2.73 $\pm$ 0.12	0.76 $\pm$ 0.06	0.85 $\pm$ 0.08	8.86 $\pm$ 0.38	8.12 $\pm$ 0.35
10	2.37 $\pm$ 0.36	3.01 $\pm$ 0.12	1.49 $\pm$ 0.13	1.31 $\pm$ 0.19	9.26 $\pm$ 0.40	8.06 $\pm$ 0.29 <sup>c</sup>

Whole liver nuclei or nuclear matrices were incubated with  $[1-^{14}\text{C}]20:4n-6$  or  $[1-^{14}\text{C}]20:4:L-FABP$ , ATP and CoA. After incubation samples were assayed as described in ‘‘Materials and Methods’’. Results are presented as nmol of  $[1-^{14}\text{C}]20:4n-6$  incorporated.mg TL<sup>-1</sup> and are the mean of five experiments  $\pm$  SE. Statistical analysis was performed by the Student’s *t* test. FA:L-FABP significantly different from FA : <sup>a</sup>  $P < 0.001$ , <sup>b</sup>  $P < 0.01$  and <sup>c</sup>  $P < 0.05$

nuclear PL was different to that of the whole nucleus as already analyzed. It is important to note that 18:0 esterifies into endonuclear PtdEtn, PtdIns and PtdCho with a greater SA than in whole nuclei. These results imply that PL fatty acid remodeling in the nuclear matrix is a very active process.

When the incubations were performed without ATP and CoA,  $[1-^{14}\text{C}]18:0$  or  $[1-^{14}\text{C}]18:0:L-FABP$  was not esteri-

fied in any endonuclear lipid pools; it was exclusively incorporated as FFA (100%) (Table 1). Then 18:0, free or bound to L-FABP, could only be esterified into endonuclear lipid pools by an acyl-CoA mechanism. This mechanism appears to be independent of the double nuclear membrane and would also imply a matrix localization of nuclear long chain acyl-CoA synthetase, as already described in whole nuclei [10].

**Table 5** Esterification of [ $1\text{-}^{14}\text{C}$ ]20:4n-6 free and bound to L-FABP into nuclear and endonuclear phospholipid classes

Time (min)	PtdCho		PtdEtn		PtdIns	
	FA	FA: L-FABP	FA	FA: L-FABP	FA	FA: L-FABP
Whole nuclei (pmol.nmol each PL <sup>-1</sup> )						
1	2.83 ± 0.69	2.59 ± 0.41	4.81 ± 1.13	5.96 ± 0.92	6.77 ± 1.50	6.91 ± 1.08
5	3.65 ± 0.62	4.56 ± 1.22	5.40 ± 0.93	4.39 ± 0.95	5.76 ± 1.28	3.85 ± 1.24
10	4.00 ± 0.93	4.33 ± 0.71	4.37 ± 1.68	4.80 ± 0.77	7.59 ± 1.62	8.83 ± 1.16
Nuclear matrices (pmol.nmol each PL <sup>-1</sup> )						
1	7.89 ± 1.44	8.74 ± 1.58	8.22 ± 1.80	12.47 ± 2.99	11.29 ± 3.70	14.23 ± 3.08
5	14.93 ± 2.14	12.03 ± 0.92	16.81 ± 2.45	12.15 ± 2.55	24.45 ± 4.26	30.13 ± 3.85
10	12.27 ± 2.14	12.87 ± 0.85	10.96 ± 2.10	16.57 ± 1.64	16.48 ± 2.94	28.28 ± 3.09 <sup>a</sup>

Whole liver nuclei or nuclear matrices were incubated with [ $1\text{-}^{14}\text{C}$ ]20:4n-6 or [ $1\text{-}^{14}\text{C}$ ]20:4:L-FABP, ATP and CoA for 1, 5 and 10 min. After incubation the samples were assayed as described in “Materials and Methods”. Results are presented as pmol of [ $1\text{-}^{14}\text{C}$ ]20:4n-6 incorporated/nmol of each PL and are the mean of five experiments ± SE. Statistical analysis was performed by the Student's *t* test. FA:L-FABP significantly different from FA : <sup>a</sup>  $P < 0.05$

#### Incorporation of [ $1\text{-}^{14}\text{C}$ ]20:4n-6 Acid either Free or Bound to L-FABP into Endonuclear Lipid Pools

Figures 4 and 5 display the incorporation and/or esterification of exogenous 20:4n-6 acid, free or bound to L-FABP, into endonuclear lipid pools. Nuclear matrices were incubated in vitro in the presence of [ $1\text{-}^{14}\text{C}$ ] 20:4n-6, [ $1\text{-}^{14}\text{C}$ ] 20:4n-6:L-FABP, ATP and CoA.

[ $1\text{-}^{14}\text{C}$ ] 20:4n-6 acid free or bound to L-FABP was primarily incorporated into endonuclear lipid pools, either directly as FFA (89%) or esterified in PL (15%). After 10 min incubation, incorporated FA continues its esterification in PL (20%), and only in a minor proportion in TAG (10%). As already observed in whole nuclei, when 20:4n-6 acid was incubated with nuclear matrices, no [ $^{14}\text{C}$ ] could be detected in DAG. When 20:4n-6 acid is either free or bound to L-FABP, the percentage of fatty acid esterified in endonuclear TAG increased during the incubation time.

After 10 min incubation, 20:4n-6 acid bound to L-FABP displayed a greater esterification in endonuclear PL with respect to the free 20:4n-6, since it diminished as FFA (Fig. 4).

Table 4 shows that exogenous 20:4n-6 acid, free or L-FABP bound, was esterified (PL and TAG) and incorporated as FFA to a greater degree in endonuclear lipids pools than with whole liver nuclei.

In endonuclear lipid pools, the amount of 20:4n-6, free or bound to L-FABP, that esterifies in TAG was greater than with respect to 18:0. On the other hand, the amount of 18:0, free or bound to L-FABP, that esterifies in PL and DAG was greater with respect to 20:4n-6 (Tables 2, 4).

20:4n-6 acid free or L-FABP bound was esterified in all endonuclear PL, except in SM. Under the present conditions, neither 18:0 nor 20:4 acid were esterified in SM of

nuclear or endonuclear pools (Figs. 3, 5). These results imply that SM fatty acid remodeling does not occur in both nuclear fractions. Moreover, as we have already reported, 20:4-CoA was not incorporated into nuclear SM pools either [13].

Figure 5 shows that exogenous 20:4n-6 acid, free or L-FABP bound, was esterified in endonuclear PL as follows: PtdCho (≈55%) > PtdEtn(25–30%) > PtdIns (15–25%).

Table 5 shows that free or L-FABP-bound 20:4n-6 acid was esterified with greater specific activity in endonuclear PtdIns with respect to PtdCho and PtdEtn. These results are similar to those observed in whole nuclear pools (Table 5).

It is interesting to note that only when 20:4n-6 acid was bound to L-FABP, the fatty acid was esterified with a greater specific activity in endonuclear PtdIns than with respect to the free fatty acid (Table 5). It is evident that selectivity of 20:4n-6 acid for PtdIns is greater when the fatty acid is bound to L-FABP.

When the incubations were performed without ATP and CoA [ $1\text{-}^{14}\text{C}$ ]20:4 or [ $1\text{-}^{14}\text{C}$ ]20:4 L-FABP was not esterified in any endonuclear lipid pool; it was exclusively incorporated as FFA (100%) (Table 1). Then 20:4, free or bound to L-FABP, could only be esterified into endonuclear lipid pools by an acyl-CoA mechanism. This mechanism would be independent of the double nuclear membrane.

## Discussion

The aim of this work was to study the incorporation of exogenous fatty acids bound to L-FABP into nuclei.

We have demonstrated that exogenous fatty acids, either free or bound to L-FABP, were mostly incorporated as

FFA, and esterified in polar and neutral lipid pools by an acyl-CoA-dependent mechanism of whole nuclear and endonuclear lipid pools.

Although the mechanism through which cytosolic fatty acids reach the cellular nucleus is still unknown, it is postulated that FABPs could be the proteins involved in fatty acid cytoplasmic-nucleus transport. The size of the L-FABP with or without ligand would facilitate its transport to the cellular nucleus through the nuclear pore complex by means of simple diffusion as the active and regulated transport operates when molecules are greater than 60 kDa [16].

#### Whole Nuclei

The first experimental approach was done by incubating rat liver cell nuclei *in vitro* in the presence of the most abundant nuclear fatty acids, the [ $1\text{-}^{14}\text{C}$ ]18:0 and 20:4n-6, bound to L-FABP and in the presence of ATP and CoA.

Under these experimental conditions, 18:0 and 20:4n-6 acids, either free or bound to L-FABP, showed the same pattern of incorporation and/or esterification in polar and neutral lipids of whole nuclei. Only 20:4n-6 when bound to L-FABP was incorporated into TAG in a minor proportion when 20:4n-6 was free.

The free fatty acid nuclear pool where 18:0 and 20:4n-6 acids were incorporated, was metabolically active, and it decreased with incubation time when ATP and CoA were present (Figs. 2, 3, and 4). These results showed that this pool must be related to nuclear long chain acyl-CoA synthetase as already described, which would activate fatty acids to the respective acyl-CoAs prior to their esterification into nuclear lipids [10].

Esterification of fatty acids into nuclear lipid pools was found to be specific for the type of exogenous fatty acid tested and the lipid class.

These results imply that fatty acids, free or L-FABP bound, are incorporated into the nuclear FFA pool or trapped by acyl-CoA synthetase, and then an acyl-CoA transferase downstream from acyl-CoA synthetase would determine the metabolic fate of each fatty acid. Thus, 18:0 was esterified in PL with the greatest SA in PtdEtn and PtdSer whereas 20:4n-6 was esterified in PtdIns. These results suggest that nuclear PtdEtn and PtdSer present an active remodeling of 18:0, and still the biological implications of these results must be elucidated. On the other hand, in the neutral lipid pool, 18:0 acid was mainly esterified in DAG whereas 20:4n-6 was found to be in TAG. It is interesting to note that the fatty acid composition of nuclear neutral lipids is characterized by a much higher proportion of 18:0 than 20:4n-6, as already reported [13].

The high rate of esterification of arachidonic acid into PtdIns is consistent with the fact that PtdIns is the phos-

pholipid with greater affinity to esterify 20:4n-6 acid [29]. Moreover, around 80% of rat liver PtdIns molecular species contained 18:0–20:4 [29]. This process would account for the characteristic composition of the main PtdIns molecular species, 18:0–20:4 [37], since nuclear PtdIns would be transported from the cytosol where it is synthesized [37].

Huang et al. reported an increment in the nuclear uptake of fluorescent saturated and unsaturated fatty acids of medium and long chain in cells overexpressing L-FABP with respect to control cells that can not overexpress that protein [30]. In fact, the increment of fluorescence was mainly located on the internal face of the nuclear membrane, but it was not associated with the nuclear interior. It must be noted that the fatty acids utilized by these authors could not be esterified in the nuclear lipid pools like those used in our experiments. One could infer that the location of fluorescent fatty acids, observed by Huang et al, matches that of the pool of [ $1\text{-}^{14}\text{C}$ ] 18:0 and [ $1\text{-}^{14}\text{C}$ ] 20:4n-6, which remains as free fatty acids in the present experimental model [7].

Under the experimental conditions, L-FABP does not seem to specifically favor the interaction between FA and whole nuclei lipid pools. These results are consistent with those previously observed when nuclei isolated from rat liver cells were incubated *in vitro* with [ $^{14}\text{C}$ ] fatty acids and hepatic cytosol proteins [12]. The presence of cytosol in the incubation medium did not change the incorporation and esterification patterns of 18:0, 18:2n-6 and 20:4n-6 acids in nuclear lipid pools [12]. It must be noted that L-FABP was present in the incubation medium, since that binding protein corresponds to approximately 5% of total hepatic cytosolic proteins [14].

#### Nuclear Matrices (Membrane Depleted Nuclei)

In a second step, experiments were done with membrane depleted nuclei (nuclear matrices) in order to assess if fatty acids either free or bound to L-FABP could be incorporated and re-distributed in endonuclear lipid pools, disregarding their trafficking mechanism through the double nuclear membrane. With this purpose, rat liver nuclear matrices were incubated *in vitro* in the presence of the most abundant endonuclear FA, the [ $1\text{-}^{14}\text{C}$ ]18:0 and [ $1\text{-}^{14}\text{C}$ ] 20:4n-6 acids, either free or bound to L-FABP, ATP and CoA.

Exogenous fatty acids, either free or bound to L-FABP, were found to be incorporated mostly as free fatty acid, and esterified in polar and neutral endonuclear lipid pools by an acyl-CoA-dependent mechanism. Our results indicate that long chain acyl-CoA synthetase would be associated to the nuclear matrix, as well as the enzymes involved in FA esterification to endonuclear lipid pools. Both 18:0 and 20:4n-6 fatty acids, either free or bound to L-FABP, were

incorporated and esterified to endonuclear lipids, showing a larger SA than that in whole nuclei. It is evident that the nuclear matrix, a site of second messenger generation from compartmentalized lipid pools, has a more active lipid metabolism than that of whole liver cell nuclei.

As already shown in whole nuclei, the endonuclear FFA pool was a metabolically active lipid pool. It decreased during the incubation when ATP and CoA were present (Figs. 2, 3, and 4). Fatty acid esterification in endonuclear lipid pools showed specificity regarding the fatty acid type and the lipid class.

18:0 acid, either free or bound to L-FABP, was incorporated and esterified with the same pattern in endonuclear lipids (Figs. 2, 3, 4, and 5) as already observed in whole nuclei. 18:0 acid was esterified not only to PL and TAG, but also to DAG. In endonuclear PL, 18:0 either free or L-FABP bound, was esterified with a greater SA to PtdEtn, followed by PtdIns, PtdSer and PtdCho (Table 3).

The highest percentage of esterification of 20:4n-6, free or bound to L-FABP, in the different endonuclear phospholipid classes was observed in PtdCho, followed by PtdEtn and PtdIns (Table 5). This is not surprising since PtdCho was the major PL in matrices as previously reported [17]. As already shown in whole nuclei, 20:4n-6 was esterified with a higher SA in endonuclear PtdIns, with respect to total PL (Table 5).

In the matrix, L-FABP would seem to play an important role in the mobilization and redistribution of 20:4n-6 within nuclear lipid pools. When 20:4n-6 was bound to L-FABP, arachidonic acid was esterified to a greater degree in endonuclear total PL, particularly in PtdIns; then it diminished in the FFA pool, with respect to free 20:4 (Fig. 4). Under the experimental conditions assayed, we were unable to observe the same results when the nuclei were surrounded by the double nuclear membrane. These results suggest that L-FABP facilitates the mobilization of 20:4n-6 to specific sites of utilization. First L-FABP delivers 20:4n-6 to an acyl-CoA synthetase located in the nuclear matrix, and then to those enzymes (acyl-transferases) responsible for its esterification in PI.

An active endonuclear PtdIns metabolism is not something new, and according to the present results, L-FABP should be included as an important component of it. Nuclear signal transduction system of PtdIns was described a long time ago, and it was found to have protein and lipid components that are mostly associated or anchored to the nuclear matrix [32–33]. Yet, this endonuclear transduction system of PtdIns showed a cytosol-independent regulation [34].

Endonuclear arachidonic acid mobilized by L-FABP could be delivered to different fates other than esterification into glycerolipids within the nuclei. 20:4n-6 could be

metabolized to prostaglandins or leukotrienes [35]. Also it could activate PPAR- $\alpha$ , taking into account that the existence of a nuclear co-localization between L-FABP and PPAR- $\alpha$  has also been reported [16].

Hunt suggested that PtdEtn was the PL responsible for the supply of unsaturated fatty acids in nuclear matrices from neuroblastoma culture cells. However, our results showed that in rat liver cell matrices 18:0 and not 20:4n-6 fatty acid had the highest specific activity of esterification in PtdEtn [36, 37]. Esterification is a necessary step in fatty acid mobilization and remodeling; it is involved in fatty acid utilization. The apparent difference between our results in rat liver nuclei and those of others showing low levels of polyunsaturated acids in the cell nuclei is, in many cases, the consequence of using neoplastic cells. These cultured cell lines are generally characterized by low levels of essential fatty acids, and high levels of saturated and monoenoic fatty acids in their lipid pools [38, 39]. So the fatty acid composition of their nuclear lipid pools would be the consequence of the characteristic metabolism of neoplastic cells, and not the consequence of a specific and generalized nuclear localization as suggested [37].

Lawrence et al. [40] have studied the role of L-FABP in the transport of 18:1 toward the nuclear matrices of rat liver cells obtained using a concentration of 1% (wt/v) TX-100. One must take into account that these authors added neither ATP nor CoA to the *in vitro* incubation medium, and as demonstrated in the present work (Table 1), the exogenous FA can not be esterified into endonuclear lipid pools as they remained as FFA. On the other hand, they utilized 18:1 acid as exogenous FA, which is a minor component in the nuclear and endonuclear FA lipid pool of rat liver cells as already described [17].

Summarizing, esterification of exogenous 18:0 and 20:4n-6 fatty acids either free or L-FABP bound, into whole nuclear and endonuclear lipid pools is an ATP and CoA-dependent mechanism. In the nuclear matrix, fatty acid esterification is a more active process than that in the whole nucleus, and it is independent of the nuclear double membrane. The esterification patterns of fatty acids, either L-FABP-bound or free, into whole nuclear lipid pools showed no difference. L-FABP facilitates the mobilization of 20:4n-6 within nuclei from the FFA pool to PtdIns. First 20:4n-6 must be activated to acyl-CoA and then a downstream acyl-CoA transferase will determine its esterification into PtdIns.

**Acknowledgments** This work was financially supported by grants of Universidad Nacional de La Plata (UNLP) and Agencia de Promoción Científica y Tecnológica (ANPCyT) from Argentina. The authors are grateful to Norma Tedesco for her secretarial assistance.

## References

- Pegorier JP, Le May C, Girard J (2004) Control of gene expression by fatty acids. *J Nutr* 134:2444S–2449S
- Xu Z, Bernlohr DA, Banaszak LJ (1992) Crystal structure of recombinant murine adipocyte lipid-binding protein. *Biochemistry* 31:3484–3492
- Santomé JA, Di Pietro SM, Cavagnari BM Córdoba OL, Dell Ángelica EC (1998) Fatty acid-binding proteins. Chronological description and discussion of hypothesis involving their molecular evolution. *Trends Comp Biochem Physiol* 4:23–38
- Hsu KT, Storch J (1996) Fatty acid transfer from liver and intestinal fatty acid-binding proteins to membranes occurs by different mechanisms. *J Biol Chem* 271:13317–13323
- Ockner RK, Manning JA, Kane JP (1982) Fatty acid binding protein. Isolation from rat liver, characterization, and immunochemical quantification. *J Biol Chem* 257:7872–7878
- Thompson J, Winter N, Terwey D, Bratt J, Banaszak L (1997) The crystal structure of the liver fatty acid-binding protein. A complex with two bound oleates. *J Biol Chem* 272:7140–7150
- Huang H, Starodub O, McIntosh A, Atshaves BP, Woldegiorgis G, Kier AB, Schroeder F (2004) Liver fatty acid-binding protein colocalizes with peroxisome proliferator activated receptor alpha and enhances ligand distribution to nuclei of living cells. *Biochemistry* 43:2484–2500
- Corsico B, Liou HL, Storch J (2004) The alpha-helical domain of liver fatty acid binding protein is responsible for the diffusion-mediated transfer of fatty acids to phospholipid membranes. *Biochemistry* 43:3600–3607
- Ves-Losada A, Brenner RR (1995) Fatty acid delta 5 desaturation in rat liver cell nuclei. *Mol Cell Biochem* 142:163–170
- Ves-Losada A, Brenner RR (1996) Long-chain fatty acyl-CoA synthetase enzymatic activity in rat liver cell nuclei. *Mol Cell Biochem* 159:1–6
- Ves-Losada A, Mate SM, Brenner RR (2001) Incorporation and distribution of saturated and unsaturated fatty acids into nuclear lipids of hepatic cells. *Lipids* 36:273–282
- Ves-Losada A, Brenner RR (1998) Incorporation of delta 5 desaturase substrate (dihomogammalinolenic acid, 20:3 n-6) and product (arachidonic acid 20:4 n-6) into rat liver cell nuclei. *Prostaglandins Leukot Essent Fatty Acids* 59:39–47
- Mate SM, Brenner RR, Ves-Losada A (2004) Phosphatidylcholine fatty acid remodeling in the hepatic cell nuclei. *Prostaglandins Leukot Essent Fatty Acids* 70:49–57
- Bordewick U, Heese M, Borchers T, Robenek H, Spener F (1989) Compartmentation of hepatic fatty-acid-binding protein in liver cells and its effect on microsomal phosphatidic acid biosynthesis. *Biol Chem Hoppe Seyler* 370:229–238
- Elholm M, Garras A, Neve S, Tornehave D, Lund TB, Skorve J, Flatmark T, Kristiansen K, Berge RK (2000) Long-chain acyl-CoA esters and acyl-CoA binding protein are present in the nucleus of rat liver cells. *J Lipid Res* 41:538–545
- Wolfrum C, Borrmann CM, Borchers T, Spener F (2001) Fatty acids and hypolipidemic drugs regulate peroxisome proliferator-activated receptors alpha- and gamma-mediated gene expression via liver fatty acid binding protein: a signaling path to the nucleus. *Proc Natl Acad Sci USA* 98:2323–2328
- Mate SM, Brenner RR, Ves-Losada A (2006) Endonuclear lipids in liver cells. *Can J Physiol Pharmacol* 84:459–468
- Actis Dato SM, Catala A, Brenner RR (1973) Circadian rhythm of fatty acid desaturation in mouse liver. *Lipids* 8:1–6
- Vann LR, Wooding FB, Irvine RF, Divecha N (1997) Metabolism and possible compartmentalization of inositol lipids in isolated rat-liver nuclei. *Biochem J* 327(Pt 2):569–576
- Lowry OH, Rosebrough NJ, Farr AL, Randall RJ (1951) Protein measurement with the Folin phenol reagent. *J Biol Chem* 193:265–275
- Richieri GV, Ogata RT, Kleinfeld AM (1994) Equilibrium constants for the binding of fatty acids with fatty acid-binding proteins from adipocyte, intestine, heart, and liver measured with the fluorescent probe ADIFAB. *J Biol Chem* 269:23918–23930
- Norris AW, Spector AA (2002) Very long chain n-3 and n-6 polyunsaturated fatty acids bind strongly to liver fatty acid-binding protein. *J Lipid Res* 43:646–653
- Suruga K, Mochizuki K, Suzuki R, Goda T, Takase S (1999) Regulation of cellular retinol-binding protein type II gene expression by arachidonic acid analogue and 9-cis retinoic acid in caco-2 cells. *Eur J Biochem* 262:70–78
- Sakuma S, Fujimoto Y, Katoh Y, Kitao A, Fujita T (2001) The effects of fatty acyl CoA esters on the formation of prostaglandin and arachidonoyl-CoA formed from arachidonic acid in rabbit kidney medulla microsomes. *Prostaglandins Leukot Essent Fatty Acids* 64:61–65
- McArthur MJ, Atshaves BP, Frolov A, Foxworth WD, Kier AB, Schroeder F (1999) Cellular uptake and intracellular trafficking of long chain fatty acids. *J Lipid Res* 40:1371–1383
- Tipping E, Ketterer B (1981) The influence of soluble binding proteins on lipophile transport and metabolism in hepatocytes. *Biochem J* 195:441–452
- Glatz JF, Borchers T, Spener F, van der Vusse GJ (1995) Fatty acids in cell signalling: modulation by lipid binding proteins. *Prostaglandins Leukot Essent Fatty Acids* 52:121–127
- Masserini M, Ravasi D (2001) Role of sphingolipids in the biogenesis of membrane domains. *Biochim Biophys Acta* 1532:149–161
- Holub BJ, Kuksis A (1971) Differential distribution of orthophosphate- 32 P and glycerol- 14 C among molecular species of phosphatidylinositols of rat liver in vivo. *J Lipid Res* 12:699–705
- Huang H, Starodub O, McIntosh A, Kier AB, Schroeder F (2002) Liver fatty acid-binding protein targets fatty acids to the nucleus. Real time confocal and multiphoton fluorescence imaging in living cells. *J Biol Chem* 277:29139–29151
- Irvine RF (2006) Nuclear inositide signalling—expansion, structures and clarification. *Biochim Biophys Acta* 1761:505–508
- D'Santos CS, Clarke JH, Divecha N (1998) Phospholipid signalling in the nucleus. Een DAG uit het leven van de inositide signaling in de nucleus. *Biochem Biophys Acta* 1436:201–232
- Payrastra B, Nievers M, Boonstra J, Breton M, Verkleij AJ, van Bergen en Henegouwen PM (1992) A differential location of phosphoinositide kinases, diacylglycerol kinase, and phospholipase C in the nuclear matrix. *J Biol Chem* 267:5078–5084
- Martelli AM, Gilmour RS, Bertagnolo V, Neri LM, Manzoli L, Cocco L (1992) Nuclear localization and signalling activity of phosphoinositidase C beta in Swiss 3T3 cells. *Nature* 358:242–245
- Luo M, Flamand N, Brock TG (2006) Completing the cycles; the dynamics of endonuclear lipidomics. *Biochim Biophys Acta* 1761:577–87
- Hunt AN, Clark GT, Attard GS, Postle AD (2001) Highly saturated endonuclear phosphatidylcholine is synthesized in situ and colocalized with CDP-choline pathway enzymes. *J Biol Chem* 276:8492–8499
- Hunt AN (2006) Dynamic lipidomics of the nucleus. *J Cell Biochem* 97:244–251

38. Marra CA, de Alaniz MJ (1992) Incorporation and metabolic conversion of saturated and unsaturated fatty acids in SK-Hep1 human hepatoma cells in culture. *Mol Cell Biochem* 117:107–118
39. Albino L, Polo MP, de Bravo MG, de Alaniz MJ (2001) Uptake and metabolic conversion of saturated and unsaturated fatty acids in Hep2 human larynx tumor cells. *Prostaglandins Leukot Essent Fatty Acids* 65:295–300
40. Lawrence JW, Kroll DJ, Eacho PI (2000) Ligand-dependent interaction of hepatic fatty acid-binding protein with the nucleus. *J Lipid Res* 41:1390–1401



# Respective Hydrolysis and Esterification of Esterified and Free Plant Stanols Occur Rapidly in Human Intestine After Their Duodenal Infusion in Triacyl- or Diacylglycerol

Markku J. Nissinen · Matti Vuoristo ·  
Helena Gylling · Tatu A. Miettinen

Received: 29 January 2007 / Accepted: 12 April 2007 / Published online: 6 June 2007  
© AOCS 2007

**Abstract** Esterification of dietary phytosterols and glycerols may affect intestinal absorption of cholesterol and non-cholesterol sterols. We infused plant stanol esters in triacylglycerol (TAG) (F1) and diacylglycerol (DG) (F2) oils, and free plant stanols in F1 and F2 (F3) to the duodenum of healthy human subjects and sampled the contents from the proximal jejunum (PJ). Free and ester sterols were analysed from the infusates, and intestinal contents before and after ultracentrifuge separation of oil, micelle and sediment phases. During the 60-cm intestinal passage, over 40% of plant stanol esters were hydrolysed ( $P < 0.05$ ) but around 30% of the infused free plant stanols ( $P < 0.05$ ) and up to 40% of cholesterol ( $P < 0.05$ ) were esterified in PJ after infusions. TAG in F1 favoured accumulation of plant stanol esters in the oil phase of the PJ aspirates as compared with respective values of F2 and F3 ( $P < 0.05$  for both). About one third of free plant stanols of F3 had been esterified ( $P < 0.05$ ) and 17% precipitated mainly in free form in the PJ aspirates ( $P < 0.05$  compared with F1 and

F2). In conclusion, DG- and TAG-oils had no profound superiority over each other as intestinal carriers regarding hydrolysis/esterification of administered plant stanol esters and cholesterol and their partition in oil, micellar and sediment phases in the PJ. The unesterified plant stanols experienced partial esterification and sedimentation during their intestinal passage, which might influence their biochemical properties in that segment of the gut where cholesterol is absorbed.

**Keywords** Campestanol · Cholesterol · Intestinal absorption · Micellar solubility · Phytosterols · Sitostanol

## Abbreviations

ABC	ATP-binding cassette transporter proteins
EST%	Esterification percentage
DG	Diacylglycerol
F1	Plant stanol esters in triacylglycerol formula
F2	Plant stanol esters in diacylglycerol formula
F3	Free plant stanols in triacylglycerol and diacylglycerol formulas
LDL-C	Low-density lipoprotein cholesterol
PJ	Proximal jejunum
TAG	Triacylglycerol
TC	Total cholesterol

M. J. Nissinen  
Department of Medicine, Division of Gastroenterology,  
University of Helsinki, Helsinki 00029, Finland

M. Vuoristo · T. A. Miettinen  
Department of Medicine, Division of Internal Medicine,  
University of Helsinki, Helsinki 00029, Finland

H. Gylling  
Department of Clinical Nutrition,  
University of Kuopio and Kuopio University Hospital,  
Kuopio, Finland

M. J. Nissinen (✉)  
Biomedicum Helsinki, C422, University of Helsinki,  
P.O.B. 700, Helsinki 00029, Finland  
e-mail: markku.nissinen@dlc.fi

## Introduction

The amount and degree of esterification of dietary phytosterols affect the sterol composition of duodenal mixed micelles [1–3], which are crucial for the intestinal absorption of dietary and biliary cholesterol and fat-soluble

vitamins in the upper part of the human intestine [4]. The mixed micelles present cholesterol and phytosterols to the epithelial Niemann-Pick C1 Like 1 transporter proteins, which have been suggested to be one factor for their uptake from the intestinal lumen into the enterocyte [5]. Also ATP-binding cassette (ABC) transporter proteins, formed by the expression of *ABCG5* and *ABCG8* genes, are essential in determining the net absorption of sterols as they secrete plant sterols from the enterocyte back to the intestinal lumen and from the hepatocyte to the bile [6]. This may partly explain why the absorption efficiencies of campesterol (1.9–9.6%) and sitosterol (0.5–4.2%) are very low in short-term studies [7, 8], and their serum concentrations are normally about 0.2–0.005% of that of cholesterol [8]. The  $5\alpha$ -saturated derivatives of plant sterols—campestanol and sitostanol, have much lower absorption efficiencies (below 0.2%) and serum concentrations than the respective plant sterols [8]. Several putative mechanisms for the inhibitory effect of phytosterols on cholesterol absorption have been suggested: (1) displacing cholesterol from mixed micelles [1, 2, 9], (2) competitive blocking of cholesterol absorption from intestinal contents [7], (3) promoting cholesterol efflux from enterocytes back into the intestinal lumen [10] and (4) decreasing cholesterol esterification rate in the intestinal epithelium [11, 12]. Due to better fat-solubility of esterified derivatives of plant stanols and sterols as compared with crystalline or poorly soluble ones, they are particularly effective in inhibiting intestinal cholesterol absorption, which results in lowering of serum levels of total (TC) and low-density lipoprotein cholesterol (LDL-C) during short-term and long-term usage [13]. Addition of plant stanols in daily diet also lowers the absorption of plant sterols and their serum levels, while that of plant sterols increases their serum values [13]. This may be an important finding as plant sterols are recovered from the atheromatous plaques in relation to their serum levels [14].

Earlier findings indicate that, the magnitude of postprandial lipemia can be reduced by displacing dietary triacylglycerols (TAG) with diacylglycerols (DG) [15–18]. Animal studies with rabbits suggest that phytosterols dissolved in DG are more effective than respective TAG-based solutions in decreasing serum TC and preventing development of atherosclerotic lesions in the aorta [18]. A randomized crossover study showed that dissolution of phytosterols in DG had a better serum TC and LDL-C lowering effect than dissolution in TAG [19]. Phytosterols may have higher solubility in DG than in TAG, which is beneficial in their competition with dietary and biliary cholesterol in intestinal micelles. Furthermore, controlled feeding studies suggest that DG as opposed to TAG reduced abdominal fat accumulation, and, thus, DG might reduce the risks of visceral obesity [20]. According to this

data, an intriguing option would be to supply dietary plant stanols in DG oil-based products.

The aim of this gastrointestinal perfusion study was to elucidate the effects of esterified versus free phytosterols in TAG versus DG-based liquid formula phytosterol test meals on intestinal solubility of cholesterol and plant sterols in the upper part of the small intestine among healthy human subjects.

## Subjects and Methods

### Subjects

Fifteen healthy medical students (ten females, five males) with a mean ( $\pm$ SE) age of  $24 \pm 1$  years (range 19–35 years) volunteered for the study. Their body mass indexes were within normal limits (19–23 kg/m<sup>2</sup>). The study protocol followed the principles of the Helsinki declaration. The subjects were informed of the nature and purpose of the investigation, and a written informed consent was obtained from each subject. During X-ray guidance of the nasojejunal tube, the genitals of the subjects were covered with lead shielding. The study was approved by the Ethics Committee of the Department of Medicine, Helsinki University Central Hospital.

### Experimental Design

A double-lumen radiopaque tube (Medi-Line S.A, Angieur, Belgium) was used for the infusion of the liquid test meal formulas and for collection of samples from the proximal jejunum (PJ) for sterol analysis. The study subjects were fasted overnight. The tube was placed under X-ray control such that the proximal (infusion) outlet was in the middle of the second part of duodenum, i.e., adjacent to the ampulla of Vater (Fig. 1). The distal outlet was located 60 cm below the first one. The following liquid formulas were infused via the tube. The liquid formula 1 (F1) was TAG oil formula and it was prepared by sonication of 0.45 g of plant stanols (sitostanol/campestanol = 2.3) as their esters in 5 g of rapeseed oil (TAG) (Raisio Benecol Ltd, Raisio, Finland), half of an egg yolk, and to make the formula more soluble 2.5 g of glycerol-L-mono-oleate (Fluka AG, Switzerland), and 100 ml of water in a final volume of 110 ml. The liquid formula 2 (F2) was prepared otherwise similar to F1, but rapeseed oil was replaced by 5 g of DG oil (Kao Co, Tokyo, Japan). Two kinds of free (unesterified) plant stanol formulas (in DG- and in TAG-oils) were prepared identically to those of F1 and F2, but plant stanol esters were replaced by 0.45 g of plant stanols (sitostanol/campestanol = 2.3). For clarity and to enable statistical comparison with F1 and F2, the infusion results of suc-

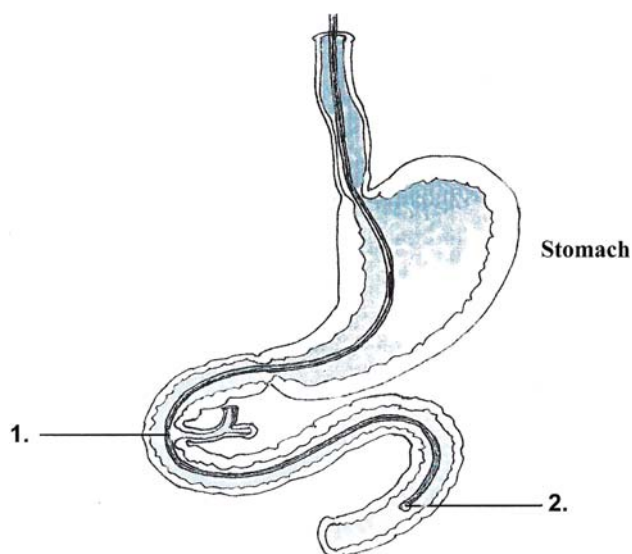


**Fig. 1** Schematic drawing of the upper gastrointestinal tract showing the location of the nasojejunal perfusion tube and its proximal (1) and distal (2) outlets

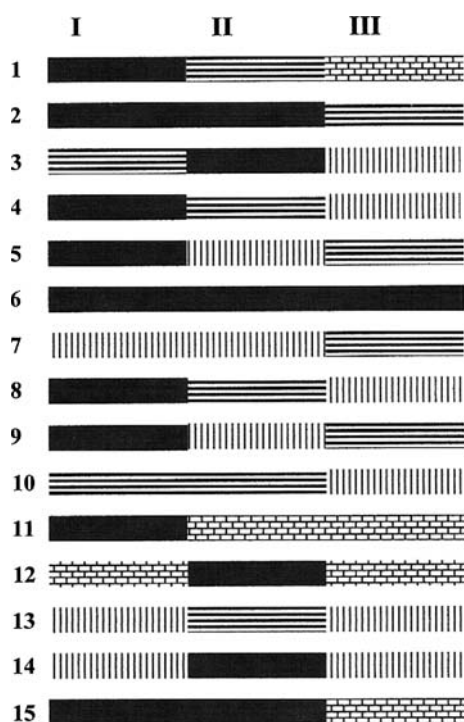


**Fig. 2** Order of infusions of the test meal formulas F1 (*horizontal pattern*) ( $n = 11$ ), F2 (*vertical pattern*) ( $n = 12$ ) and F3 (*brick pattern*) ( $n = 6$ ) according to each study subject [1–15], each of whom received three infusions (I–III). Formula infusions with no data obtained and three plant sterol formula infusions are marked with black (see “Subjects and Methods”)

successful (volume sufficient in each case for ultracentrifugation, i.e., sample size more than 3 ml) DG- ( $n = 3$ ) and TAG ( $n = 3$ )-based free plant stanol formulas were com-

bined and called F3. Combination was considered appropriate, because the number of infusates was low, and the results of the aspirates of single DG- and TAG-based infusions were equally (in both groups) distributed above and below their combined mean values. In addition, plant sterol formulas (sitosterol/campesterol = 1.8), prepared identical to those of the plant stanol ones, were infused. All formulas were infused at a constant rate of 50 ml/h through the proximal outlet of the tube using an infusion pump (type 871 102, Braun B, Melsungen AG, Germany). The formulas were infused consecutively without a washout period each for 1 h in a different previously planned order (Fig. 2), so that each subject received three test meal infusions. Altogether 45 test meal infusions were given (15 subjects, each receiving three infusions), but 13 of them were excluded because of scanty intestinal fluid samples most probably due to bending of the tube in mucosal folds. During the infusions, four 15-minutes samples were collected from each subject at the PJ, starting aspiration 15, 30, 45 and 60 min from the beginning of each infusate via the distal lumen. As the first 15 min at the beginning of each infusion were needed to wash out the previous infusion, the first aspirated sample (at the 15-min) was not used for calculations. Samples aspirated at 30-, 45- and 60-min were pooled. The PJ samples (typical volume 5–6 ml) were placed in a water bath at 80 °C for 10 min to destroy the lipase and hydrolase activities, and then stored at –20 °C until analyzed. The total number of successful test meal infusions used for final analysis were 11, 12 and 6 in F1, F2 and F3, respectively. As only three of the infused sitosterol test meals (one sitosterol ester in TAG oil, one sitosterol ester in DG oil and one unesterified sitosterol in TAG oil) were sampled successfully, their results were omitted. Results from F1, F2 and F3 infusions were used for final statistical calculations as described below. The term phytoosterol will mean in the text saturated ( $5\alpha$ ) or unsaturated ( $\Delta^5$ ) sterols or their mixture.

#### Chemical Analysis

Separation of oil, micellar and sediment phases of total intestinal fluid were obtained by ultracentrifugation of samples for 1 h at 37 °C using a Beckman rotor type 50.4 Titan at a speed of 20,000 rpm corresponding to a  $g$ -force of 36,000 $g$  (the diameter and the length of the sample tube were 13 and 64 mm, respectively). Samples from both the total intestinal fluid and, after ultracentrifugation, from the oil droplet on the surface of the ultracentrifuged sample and from the micellar phase were collected. After removal of the oil phase and most of the micellar phase, sediment in a measured amount of micellar phase was also sampled.  $5\alpha$ -cholestane and epicoprostanol were added for internal markers to the samples and those of the three infusates,

which were then extracted with chloroform–methanol, evaporated and subjected to thin-layer chromatography in diethyl ether:heptane (50:50) solution to separate free and esterified sterols. The fractions were extracted from the silica gel plate with diethyl ether, and the ester fraction, containing also 5 $\alpha$ -Cholestane was saponified with 2 M KOH in 90% ethanol, and non-saponifiable lipids were extracted from the alkaline alcoholic–water medium with hexane. The sterol fractions were silylated, and free and ester sterols were quantified by gas–liquid chromatography on a 50-m long SE-30 capillary column (Ultra 1 column, Agilent Technologies, Wilmington, DE) with an automated electronic integrator (Sigma 10, Hewlett-Packard, Palo Alto, CA) for measurement of peak areas [21–23]. Epico-prostanol served as the internal standard for free sterols and 5 $\alpha$ -cholestane for ester sterols.

### Calculations

The esterification percentages of cholesterol, cholestanol, plant sterols (sitosterol and campesterol), stanols (sitostanol and campestanol), and their free, esterified and total concentrations were calculated in formulas, total intestinal fluids, and in micellar, oil and sediment phases of aspirated samples from the PJ (distal outlet). Since sitostanol was the largest phytosterol fraction in the formulas F1–F3 and was probably negligibly absorbed during the passage of the short upper intestinal segment, it was used as internal marker to correct dilutions [3, 7, 24, 25]. Sitostanol may be transiently taken up by the mucosa, but this occurs equally with each formula infusion. Thus, the absolute values (concentrations) of sterols and their esterified forms were calculated as ratios to respective sitostanol in order to evaluate the effects of the different infusate compositions and the duodenal transit. Free sterols in the micellar phase and sterols in the sediment phase of the PJ samples were calculated as percentage of the total amount of the corresponding sterol.

The hourly cholesterol flow in the PJ was calculated according to the following equation: net cholesterol flow in the PJ = sitostanol input (mg/h)  $\times$  cholesterol (mg) to sitostanol (mg) ratio in PJ – infused cholesterol (mg/h) [24, 25]. Thus, the net cholesterol flow in PJ is given by the difference between biliary cholesterol secretion and absorption of cholesterol during the 60-cm long passage. For campesterol and sitosterol this equation gives practically the difference between their biliary secretion and loss during the duodenal transit (absorption and transient mucosal uptake). Because each subject received his/her three infusates during the first three hours, and not in a steady state of biliary secretion, which begins after 6 h [24], the main emphasis of this study was not to measure biliary secretion of sterols or absorption of cholesterol.

The data were analyzed for significance and normality with the Number Crunching Statistical Software™ (NCSS™, Statistical Solutions Ltd, 2,000, Kaysville, Utah). Statistical analyses were carried out using Student's unpaired and paired *t* test. Logarithmic transformations were used with skewed distributions. Comparisons between the groups (F1–F3) were performed with one-way analysis of variance (ANOVA) and Kruskal-Wallis nonparametric ANOVA when the data were not normally distributed, with Bonferroni adjustment in both of them. The differences between the means were considered statistically significant if *P*-value was < 0.05. Mean  $\pm$  SE values are given.

## Results

### Test Meal Formulas

The contents of cholesterol, cholestanol and plant stanols were similar in the three formulas (Table 1). Plant stanols formed the predominant sterol proportion in the formulas, as their percentage amount varied from 71 to 74% of the total amount of sterols. It was due to rapeseed oil in F1 that its campesterol and sitosterol contents were higher than in F2. In F1–F3, cholesterol (90–94%), cholestanol (90–98%) and phytosterols (over 99%) were in the oil phase, whereas the micellar and sediment phases lacked phytosterols.

### Sterol Levels in Proximal Jejunal Contents

Comparison of the phytosterol content of the infusates with that of the PJ aspirates indicated that during the duodenal transit the infused phytosterols experienced a 5- to 7-fold dilution (Table 1). Use of sitostanol as an unabsorbable marker showed that cholesterol, in terms of mg/mg of sitostanol, increased by 3.8-, 3.7- and 3.3-fold (and that of cholestanol by twofold) from infusate to PJ in formulas F1–F3, respectively, probably due to biliary secretion of cholesterol. Due to biliary secretion also the respective ratios of campesterol and sitosterol increased (Table 1), while those of campestanol were unchanged in PJ as compared with the infusates. Biliary cholesterol secretion (mg/h) for campesterol was 17  $\pm$  14 with F1, 2  $\pm$  1 with F2, and 7  $\pm$  4 with F3 (NS), and for sitosterol 27  $\pm$  23 with F1, 3  $\pm$  1 with F2, and 11  $\pm$  8 with F3 (NS).

Hourly net cholesterol flow in the PJ (mg/h) was 172  $\pm$  46 with F1, 126  $\pm$  36 with F2, and 123  $\pm$  32 with F3 infusions (NS).

### Sterol and Stanol Esters During Duodenal Transit

Comparison of infusate cholesterol EST% (5%) in F1–F3 with their respective EST% in PJ aspirates revealed similar,

**Table 1** Concentrations of sterols in infusates and proximal jejunum and differences of their ratios to sitostanol between proximal jejunum and infusate

	F1 ( <i>n</i> = 11)		F2 ( <i>n</i> = 12)		F3 ( <i>n</i> = 6)	
	Infusate	PJ	Infusate	PJ	Infusate	PJ
Cholesterol	91.3 ± 9.7	51.0 ± 6.9 <sup>a</sup>	91.0 ± 2.2	58.1 ± 6.8 <sup>a</sup>	103.1 ± 8.0	61.2 ± 14.4
Δ ratio		+134 ± 36 <sup>a</sup>		+114 ± 32 <sup>a</sup>		+106 ± 26 <sup>a</sup>
Cholestanol	2.0 ± 0.1	0.6 ± 0.1 <sup>a</sup>	1.9 ± 0.0	0.7 ± 0.1 <sup>a</sup>	2.0 ± 0.1	0.8 ± 0.2 <sup>a</sup>
Δ ratio		+1.1 ± 0.3 <sup>a</sup>		+1.0 ± 0.3 <sup>a</sup>		+0.9 ± 0.2 <sup>a</sup>
Campesterol	15.1 ± 0.9	2.8 ± 0.5 <sup>a</sup>	8.0 ± 0.1 <sup>b</sup>	2.8 ± 0.5 <sup>a</sup>	8.5 ± 2.0 <sup>b</sup>	3.4 ± 0.9 <sup>a</sup>
Δ ratio		+3.0 ± 2.2		+2.2 ± 0.5 <sup>a</sup>		+5.9 ± 3.1
Campestanol	100 ± 3.1	15.9 ± 2.5 <sup>a</sup>	100 ± 2	22.4 ± 3.6 <sup>a</sup>	115 ± 5	23.5 ± 7.3 <sup>a</sup>
Δ ratio		+0.8 ± 1.4		+0.6 ± 0.5		-0.3 ± 0.5
Sitosterol	18.4 ± 1.3	3.5 ± 0.6 <sup>a</sup>	10 ± 0 <sup>b</sup>	3.5 ± 0.7 <sup>a</sup>	14 ± 2	5.2 ± 1.4 <sup>a</sup>
Δ ratio		+4.0 ± 2.8		+2.5 ± 0.5 <sup>a</sup>		+9.3 ± 5.8
Sitostanol	216 ± 5	34 ± 5 <sup>a</sup>	218 ± 3	48 ± 8 <sup>a</sup>	231 ± 10	48 ± 15 <sup>a</sup>

Values are mean ± SE, concentrations are mg/dl, Δ ratios are differences of sterol to sitostanol ratios (mg of sterol per mg of respective sitostanol × 100) between PJ and infusate

F1 stanol esters in triacylglycerol formula, F2 stanol esters in diacylglycerol formula, F3 free stanol formula, PJ proximal jejunum

<sup>a</sup> *P* < 0.05, compared with the respective infusate

<sup>b</sup> *P* < 0.05, compared with corresponding value of F1

**Table 2** Esterification percentages of sterols in test meal formulas and in proximal jejunum

Sterols	F1 ( <i>n</i> = 11)		F2 ( <i>n</i> = 12)		F3 ( <i>n</i> = 6)	
	Infusate (%)	PJ (%)	Infusate (%)	PJ (%)	Infusate (%)	PJ (%)
Cholesterol	4.9 ± 0.3	35.6 ± 4.4 <sup>a</sup>	5.0 ± 0.2	41.7 ± 3.7 <sup>a</sup>	4.8 ± 0.7	40.2±3.5 <sup>a</sup>
Cholestanol	61.8 ± 1.7	46.1 ± 4.3 <sup>a</sup>	64.4 ± 0.9	53.1 ± 3.3 <sup>a</sup>	4.3 ± 0.9	43.6±3.5 <sup>a</sup>
Campesterol	68.0 ± 1.7	49.2 ± 3.7 <sup>a</sup>	72.2 ± 1.0	55.4 ± 2.7 <sup>a</sup>	55.8 ± 5.0	42.8±3.2
Campestanol	95.8 ± 1.2	57.2 ± 3.5 <sup>a</sup>	97.1 ± 0.4	60.0 ± 2.3 <sup>a</sup>	0.5 ± 0.0 <sup>b</sup>	30.2±3.6 <sup>a,b</sup>
Sitosterol	61.2 ± 1.8	43.5 ± 3.3 <sup>a</sup>	63.9 ± 0.4	47.0 ± 2.8 <sup>a</sup>	51.5 ± 4.7	40.5±3.2
Sitostanol	95.8 ± 1.8	58.0 ± 3.6 <sup>a</sup>	97.1 ± 0.4	60.2 ± 2.2 <sup>a</sup>	0.4 ± 0.0 <sup>b</sup>	31.8±5.0 <sup>a,b</sup>

Value are means ± SE

F1 stanol esters in triacylglycerol formula, F2 stanol esters in diacylglycerol formula, F3 free stanol formula, PJ proximal jejunum

<sup>a</sup> *P* < 0.05, compared with corresponding value of infusate

<sup>b</sup> *P* < 0.05, compared with corresponding values of F1 and F2

i.e., about eightfold increases during the intestinal passage (*P* < 0.05) (Table 2). However, plant stanol, plant sterol and cholestanol esters had been hydrolyzed by ~39, ~28 and ~22%, respectively (*P* < 0.05 for all), during the intestinal passage of formulas F1 and F2 (Table 2). Opposite to those, almost one third of the practically unesterified plant stanols of the F3 infusate were esterified in PJ (*P* < 0.05), while the respective values of plant sterols remained practically unchanged, and that of cholestanol increased tenfold.

The respective EST%:s of sitostanol and campestanol were 59.7 ± 2.0 and 59.2 ± 2.0 in PJ during the F1 and F2 stanol ester formula infusions (calculated together, *n* = 23),

whereas the respective values during F3 were significantly lower, about 30% (Table 2).

The absolute concentrations of esterified cholesterol (mg/dl) were 4–5 times higher in PJ than the infusates F1–F3, but when standardized by infused total sitostanol the respective PJ-ratios were 29-, 20- and 27-times higher in F1–F3 (*P* < 0.05 for all), respectively (Table 3). The concentrations of all plant sterol and stanol esters decreased during the transfer to PJ. The PJ-ratios of esterified cholestanol were in F1 and F2 1.5- and 1.7-times (*P* < 0.05 for both), and in F3 25-times (*P* < 0.05 compared with the increase in F1 and F2) higher than the respective ratios in infusates.

**Table 3** Concentrations of esterified sterols in infusates and proximal jejunum and differences of their ratios to sitostanol between proximal jejunum and infusate

	F1 ( <i>n</i> = 11)		F2 ( <i>n</i> = 12)		F3 ( <i>n</i> = 6)	
	Infusate	PJ	Infusate	PJ	Infusate	PJ
Cholesterol	4.5 ± 0.6	18.9 ± 3.0 <sup>a</sup>	6.7 ± 2.1	24.7 ± 3.7 <sup>a</sup>	4.9 ± 1.0	24.1 ± 5.2 <sup>a</sup>
Δ ratio		+58.0 ± 11.0 <sup>a</sup>		+58.7 ± 9.6 <sup>a</sup>		+58.3 ± 13.0 <sup>a</sup>
Cholestanol	1.3 ± 0.1	0.3 ± 0.04 <sup>a</sup>	1.2 ± 0.0	0.4 ± 0.1 <sup>a</sup>	0.1 ± 0.0 <sup>b</sup>	0.3 ± 0.1 <sup>a</sup>
Δ ratio		+3.0 ± 1.2 <sup>a</sup>		+3.7 ± 1.0 <sup>a</sup>		+7.1 ± 1.1 <sup>a,b</sup>
Campesterol	10.4 ± 0.7	1.4 ± 0.2 <sup>a</sup>	5.6 ± 0.2	1.6 ± 0.3 <sup>a</sup>	5.0 ± 1.4	1.5 ± 0.4 <sup>a</sup>
Δ ratio		-0.2 ± 0.8		+0.6 ± 0.3 <sup>a</sup>		+2.2 ± 1.8 <sup>b</sup>
Campestanol	96.4 ± 3.7	9.7 ± 1.7 <sup>a</sup>	91.5 ± 5.5	13.5 ± 2.2 <sup>a</sup>	0.5 ± 0.0 <sup>b</sup>	6.8 ± 1.9 <sup>a,c</sup>
Δ ratio		-17.6 ± 1.4 <sup>a</sup>		-14.4 ± 2.7 <sup>a</sup>		+13.9 ± 2.0 <sup>a,b</sup>
Sitosterol	11.5 ± 0.9	1.5 ± 0.3 <sup>a</sup>	6.2 ± 0.3 <sup>d</sup>	1.7 ± 0.3 <sup>a</sup>	7.1 ± 1.7 <sup>d</sup>	2.2 ± 0.7 <sup>a</sup>
Δ ratio		-0.2 ± 1.1		+0.4 ± 0.3 <sup>d</sup>		+3.6 ± 3.4 <sup>b</sup>
Sitostanol	207.1 ± 7.4	21.0 ± 3.7 <sup>a</sup>	199.8 ± 11.5	29.2 ± 4.7 <sup>a</sup>	1.0 ± 0.1 <sup>b</sup>	13.7 ± 4.1 <sup>a</sup>
Δ ratio		-37.8 ± 3.7 <sup>a</sup>		-31.6 ± 6.0 <sup>a</sup>		+27.6 ± 3.9 <sup>a,b</sup>

Values are mean ± SE, concentrations are mg/dl, Δ ratios are differences of esterified sterol to sitostanol ratios (mg of esterified sterol per mg of respective total sitostanol (×1,000 for cholestanol and ×100 for other sterols)) between PJ and infusate

F1 stanol esters in triacylglycerol formula, F2 stanol esters in diacylglycerol formula, F3 free stanol formula, PJ proximal jejunum

<sup>a</sup> *P* < 0.05, compared with corresponding value of infusate

<sup>b</sup> *P* < 0.05, compared with corresponding values of both F1 and F2

<sup>c</sup> *P* < 0.05, compared with corresponding value of F2

<sup>d</sup> *P* < 0.05, compared with corresponding value of F1

During the intestinal passage, ratios of esterified plant stanols decreased in F1 and F2 infusions by 39 and 34% (*P* < 0.05 for both) for campestanol and by 39 and 34% (*P* < 0.05 for both) for sitostanol, respectively. In F3 infusion, esterified campestanol and sitostanol ratios increased by 71- and 70-fold (*P* < 0.05 for both), respectively (Table 3).

Respective ratios of plant sterols slightly increased.

#### Sterols in Sediment, Micellar and Oil Phases of Intestinal Contents

Calculations of sediment phase sterols in PJ aspirates showed that relative amounts of sedimented campestanol and sitostanol were higher with infusion of F3 than with infusions of the stanol ester formulas (Table 4, Fig. 3), and with F3 these stanols were predominantly hydrolyzed. Relative amount of sedimented cholesterol with infusion of F3 in PJ aspirates was lower than with the two stanol ester formulas F1 and F2, as calculated together (1.9 ± 0.4 vs. 5.1 ± 1.5; *P* < 0.05) (Fig. 3). Percentages of sterols and their EST% in the micellar phase were equal in the PJ as F1–F3 were compared with each other (Fig. 3).

Comparison of sterols in the oil phase of the PJ aspirates revealed 65–79% higher (*P* < 0.05 for both) relative amounts of sitostanol during the stanol ester than during free stanol infusion (Fig. 3). Furthermore, 86.9 ± 1.6% of

the oil phase sitostanol in PJ was esterified in F1, while the respective value was lower, 77.2 ± 1.9% in F2 and the lowest 65.3 ± 5.3% in F3, (*P* < 0.05 for all, compared with each other).

#### Discussion

The main new results of the present study were that, first, plant stanol ester hydrolysis and esterification of cholesterol were chiefly similar in TAG- and DG- based formulas F1 and F2 during the intestinal transit as compared with each other. In contrast, second, free plant stanols of F3 (mean of 3F1 and 3F2) were partly esterified during the transit, but to a lesser degree than remaining after hydrolysis of the two stanol ester formulas. Third, sedimentation of sitostanol and campestanol in PJ, mainly in free form, was more profound with the free than ester plant stanol formulas.

Accumulation of sterols and stanols in the oil phase of the infusates in F1–F3 is rational in the absence of bile salts, which are crucial for the intestinal micelle formation, and it parallels our earlier findings [1, 3], indicating that differences between stanol ester and unesterified stanol formulas reported here occurred during the duodenal transit. In our previous intestinal perfusion study [3] analogous to the present one, we compared biochemical

**Table 4** Percentages of sedimented sterols of total amount of respective sterol and esterification percentages of sediment phase sterols in proximal jejunum

Sterol	Percentage(%) <sup>a</sup>			EST% <sup>b</sup>		
	F1 (n = 11)	F2 (n = 12)	F3 (n = 6)	F1 (n = 11)	F2 (n = 12)	F3 (n = 6)
Cholesterol	5.2 ± 2.5	5.0 ± 1.8	1.9 ± 0.4 <sup>c</sup>	51.4 ± 6.2	47.8 ± 5.3	27.1 ± 10.7
Cholestanol	5.2 ± 2.3	5.1 ± 1.8	5.5 ± 1.8	64.1 ± 4.7	67.0 ± 5.2	17.7 ± 13.1 <sup>d,e</sup>
Campesterol	5.2 ± 1.7	5.1 ± 1.8	5.2 ± 1.7	55.3 ± 8.6	64.8 ± 3.5	18.3 ± 11.6 <sup>d,e</sup>
Campestanol	4.4 ± 1.6	5.2 ± 1.7	16.9 ± 5.9 <sup>d</sup>	75.2 ± 3.0	72.0 ± 3.3	1.7 ± 1.2 <sup>d,e</sup>
Sitosterol	5.9 ± 2.2	5.1 ± 1.8	6.4 ± 2.3	53.7 ± 8.2	55.0 ± 3.7	17.0 ± 11.5 <sup>d,e</sup>
Sitostanol	4.4 ± 1.6	5.1 ± 1.7	17.6 ± 5.4 <sup>d,e</sup>	77.6 ± 3.5	72.0 ± 3.2	1.6 ± 1.1 <sup>d,e</sup>

Values are mean ± SE (%)

EST% esterification percentage, F1 stanol esters in triacylglycerol formula, F2 stanol esters in diacylglycerol formula, F3 free stanol formula

<sup>a</sup> Sediment phase sterols as percentages of total intestinal sterols

<sup>b</sup> Esterification percentage of respective sterols

<sup>c</sup>  $P < 0.05$  compared with F1 + F2 (calculated together)

<sup>d</sup>  $p < 0.05$  compared with F1

<sup>e</sup>  $P < 0.05$  compared with F2

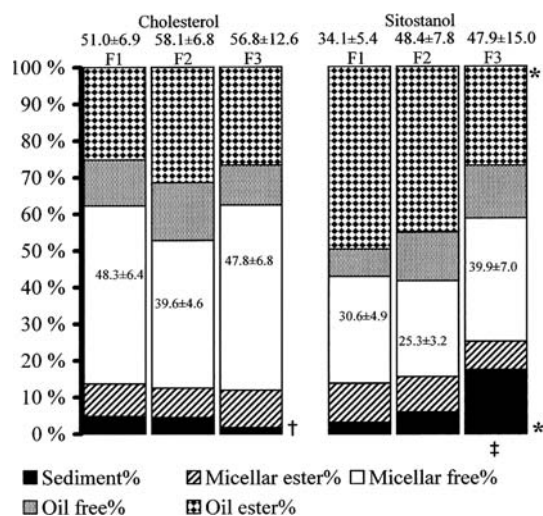


**Fig. 3** Columns show the amounts of sedimented sterols and esterified and free sterols in micellar and oil phases in PJ aspirates of test meal formulas F1–F3 as percentages. Concentrations of sterols (mg/dl) in total intestinal fluid samples are at the tops of the columns (mean ± SE). Free micellar sterols, percentage of total intestinal sterols, are marked in the columns (mean ± SE). Asterisks and daggers on the right-hand side of the columns indicate statistical significances ( $P < 0.05$ ) in percentages of oil and sediment phase sterols of total intestinal sterols in F3 compared with respective values of F1 and F2 separately (single asterisk) or with F1 and F2 calculated together (dagger), and respectively, a double dagger below the columns indicates esterification percentages of total intestinal sterols compared separately with F1 and F2 ( $P < 0.05$ , for both F1 and F2)

changes of sterols of a control rapeseed oil formula (very low phytosterol concentration) with a plant stanol ester formula during their duodenal transit. We found that the high micellar cholesterol fraction in the PJ after the control

infusion was 32% lower with the plant stanol ester formula, but, respectively, cholesterol fraction in the oil phase was over three times higher [3]. This suggested that mechanism of action of plant stanols might be displacement of cholesterol from the micellar phase [3]. In the present study, the micellar cholesterol fractions were of the same magnitude in each formula (Fig. 3) indicating that their efficacy with this respect remained equal. Net cholesterol flow in PJ tended to be ~38% higher (NS) with F1 infusion compared with F2 and F3 infusions. Thus, no significant difference could be seen in inhibition of cholesterol absorption between TAG- or DG-based stanol solutions. The reason for the relatively high values of particularly net cholesterol flow rate, but also of net campesterol and sitosterol flow rates in the PJ is that the administration of the test meal formulas caused a prandial state with gallbladder contractions and enhanced biliary secretion. These results are in accordance with those of Grundy and Metzger [24], who showed that a steady state in biliary output is reached after 4–6 h from the beginning of a formula infusion. Therefore, the hourly biliary secretion rate of phytosterols given in this study should not be considered as a daily secretion. As the physiological state was the same with infusions of the formulas studied here, the experimental setting used in this study allows their comparisons with each other.

Postprandial lipemia has been implicated in the risk of coronary artery disease and development of atherosclerosis [26]. Thus a rationale to consume DG instead of TAG in diet arises from the findings that DG could reduce the magnitude of postprandial lipemia [17]. Furthermore, hypolipidemic effects of dietary plant sterols dissolved in DG-based oil were better than in a control group using

TAG-based oil presumably due to better solubility of free plant sterols in DG [17]. With this respect our findings of very similar distribution of plant stanols and cholesterol in different intestinal fluid phases (higher oil phase stanol EST% in F1 than F2 and respective cholesterol EST% tended to be smaller) in these two oil solutions suggest that a putative difference in their hypolipidemic action is neither in micellar competition of plant stanols with cholesterol nor in precipitation of cholesterol. Murata and associates [15, 16] have suggested that the favorable effect of dietary DG on postprandial lipemia might be due to decreased intestinal re-esterification and chylomicron formation, to reduced secretion of chylomicrons into the circulation, and to altered fatty acid metabolism in the liver.

Numerous studies with Caco-2 cells, in experimental animals and in human subjects have tried to resolve the role of carboxyl ester lipase (CEL; also called as pancreatic cholesterol esterase) and acyl CoA cholesterol acyltransferase (ACAT) in intestinal absorption of cholesterol with controversial results (for a review see [27]). The former one is capable of hydrolyzing e.g., cholesterol and phytosterol esters, and it has been shown to mediate the intestinal absorption of esterified cholesterol in mice [28]. Dietary esterified cholesterol needs to be rapidly hydrolyzed by CEL during the intestinal passage in order to get penetrated into the micellar phase, which further presents cholesterol to the epithelial transporter proteins for absorption into the enterocytes. Results of our present and previous studies [3] indicate that esterified plant stanols are hydrolyzed by ~40% in the 60-cm long segment of the upper small intestine. Contrary to that, esterified fraction of infused free cholesterol was increased relatively and absolutely during the duodenal transit by factors 4–8. One putative explanation to the esterification could be reversed intraluminal action of pancreatic CEL and absorption of free cholesterol. This phenomenon favors free plant stanols to displace free cholesterol from the micellar phase, as cholesterol becomes esterified during the duodenal transit, and is accumulated into the oil phase. One could suggest that unesterified plant stanol preparations would be more beneficial with this respect, as their action would not depend on extensive hydrolysis [29]. However, the results of the present study showed that during the duodenal transit of the unesterified plant stanol formula F3, free plant stanols were esterified 70-fold. This suggests indirectly that they may lose part of their capacity to inhibit cholesterol absorption as compared to the optimal situation, in which administered free plant stanols would remain in their free form also in the PJ. Our results are in agreement with an earlier perfusion study among human subjects, which documented 3.5 times higher EST% of infused free sitosterol in the PJ compared to the infusate [1]. We are not able to provide clear explanation to the esterification of free

phytosterols, but reversed action of CEL could be suspected. Another possibility could be that the intestinal mucosa takes up free phytosterol in the short term thus increasing the intraluminal EST%. It is interesting to note that the EST% of cholesterol increased from about 5 to about 40% after F1, F2 and F3 in the PJ despite the fact that F3 contained virtually no plant stanol esters. Thus, the presumed reversed CEL action in cholesterol ester formation was not dependent on plant stanol esters. Duodenal esterification of free cholesterol and non-cholesterol sterols documented in our previous [3] and the present study needs further laboratory and clinical examination to reveal its biochemical background. Furthermore, a relatively high percentage of plant stanols in F3 infusion was lost in the sediment phase.

In addition to an average 40% hydrolysis of plant stanol esters in the upper part of the small intestine, their hydrolysis also continues more distally in the gut. This was evidenced in a study with colectomized subjects consuming daily 2 g of plant stanol esters with a spread, as their fecal analysis indicated total hydrolysis of 85% during the intestinal passage [30]. During the treatment period of 1 week, this led to average reductions of 16 and 40% in serum TC level and in cholesterol absorption efficiency, respectively [30]. Earlier human studies with normal intestinal tracts had showed that stanol esters were virtually absent in feces [31] indicating that only ~10% of their hydrolysis occurs in the colon. That hydrolysis of plant stanol esters occurs predominantly in a relatively short segment of the upper small intestine is crucial with respect to their desired action, as cholesterol is absorbed in that segment of the gut [25]. Also the type of plant stanol ester carrying vehicle and amount of dietary fat affect their hydrolysis [32]. Interesting with this respect is the finding that when plant stanol esters were consumed in pastilles having a fat free matrix by colectomized subjects, their hydrolysis was only about 60% in the whole small intestine [32]. This was probably due to low release of the stanol esters from the pastilles as compared with a spread, and presumably also to their fat free matrix. Parallel to this was also the finding that high amount of dietary fat favors the hydrolysis [32]. However, despite the reduced intestinal hydrolysis when plant stanol esters were consumed with pastilles, reductions in serum levels of TC and LDL-C and absorption efficiency of cholesterol were 9, 14 and 42%, respectively, in 1 week long study period [32]. This further indicates that only partial hydrolysis of plant stanol esters during the intestinal passage is sufficient. The amount of fat in the formulas examined in the present and our previous [3] study was relatively high with a prominent proportion of glycerol-L-mono-oleate. The results may not be applicable to a low-fat diet or to a diet with different fat composition.



Although plant sterols and stanols are differentially absorbed in the intestine, they have frequently been applied as internal markers in perfusion studies. Their differential absorption has to be taken into account when comparing the data based on sterol ratios. However, also sitosterol as a marker sterol has limitations as it is taken up by the intestinal mucosa in the short term, although to a lesser extent than other phytosterols [33]. In the setting of our study, this has most probably occurred to the same extent with F1–F3, and thus, has no influence on comparison between the formulas. However, mucosal uptake of a stanol marker may lead to overestimation of biliary secretion of sterols (according to the equation used [24]). It may also skew the change in EST% during the duodenal transit, as mucosal uptake may prefer the unesterified form.

In conclusion, plant stanol ester preparations were equally hydrolyzed in TAG- and DG-based formulas during their 60 cm long duodenojejunal transit, thus allowing equal formation of their free form, which is considered to be essential in micellar competition with cholesterol. Contrary to that, part of the free fraction of administered unesterified plant stanols are lost with their esterification and sedimentation.

**Acknowledgments** This study was supported by grants from the Paavo Nurmi Foundation, Raisio Scientific Foundation and Helsinki University EVO grant. The phytosterol and oil preparations were kindly provided by Raisio Benecol Ltd, Raisio, Finland.

## References

- Miettinen TA, Siurala M (1971) Bile salts, sterols, sterol esters, glycerides and fatty acids in micellar and oil phases of intestinal contents during fat digestion in man. *Z Klin Chem Klin Biochem* 9:47–52
- Armstrong MJ, Carey MC (1987) Thermodynamic and molecular determinants of sterol solubilities in bile salt micelles. *J Lipid Res* 28:1144–1155
- Nissinen M, Gylling H, Vuoristo M, Miettinen TA (2002) Micellar distribution of cholesterol and phytosterols after duodenal plant stanol ester infusion. *Am J Physiol Gastrointest Liver Physiol* 282:G1009–G1015
- Siperstein MD, Chaikoff IL, Reinhardt WO (1952) C<sup>14</sup>-cholesterol. V. obligatory function of bile in intestinal absorption of cholesterol. *J Biol Chem* 198:111–114
- Altmann SW, Davis Jr HR, Zhu L, Yao X, Hoos LM, Tetzloff G, Iyer SPN, Maguire M, Golovko A, Zeng M, Wang L, Murgolo N, Graziano MP (2004) Niemann–Pick C1 like 1 protein is critical for intestinal cholesterol absorption. *Science* 303:1201–1204
- Graf GA, Yu L, Li W-P, Gerard R, Tuma PL, Cohen JC, Hobbs HH (2003) ABCG5 and ABCG8 are obligate heterodimers for protein trafficking and biliary cholesterol excretion. *J Biol Chem* 278:48275–48282
- Heinemann T, Axtmann G, von Bergmann K (1993) Comparison of intestinal absorption of cholesterol with different plant sterols in man. *Eur J Clin Invest* 23:827–831
- Ostlund RE Jr, McGill J, Zeng C-M, Covey DF, Stearns J, Stenson WF, Spilburg CA (2002) Gastrointestinal absorption and plasma kinetics of soy  $\Delta^5$ -phytosterols and phytosterols in humans. *Am J Physiol Endocrinol Metab* 282:E911–E916
- Ikeda I, Tanaka K, Sugano M, Vahouny GV, Gallo LL (1988) Inhibition of cholesterol absorption in rats by plant sterols. *J Lipid Res* 29:1573–1582
- Plat J, Mensink RP (2002) Increased intestinal ABCA1 expression contributes to the decrease in cholesterol absorption after plant stanol consumption. *FASEB J* 16:1248–1253
- Child P, Kuksis A (1983) Critical role of ring structure in the differential uptake of cholesterol and plant sterols by membrane preparations in vitro. *J Lipid Res* 24:1196–1209
- Ikeda I, Sugano M (1983) Some aspects of mechanism of inhibition of cholesterol absorption by b-sitosterol. *Biochim Biophys Acta* 732:651–658
- Katan MB, Grundy SM, Jones P, Law M, Miettinen TA, Paoletti R (2003) For the stresa workshop participants. Efficacy and safety of plant stanols and sterols in the management of blood cholesterol levels. *Mayo Clin Proc* 78:965–978
- Miettinen TA, Railo M, Lepäntalo M, Gylling H (2005) Plant sterols in serum and in atherosclerotic plaques of patients undergoing carotid endarterectomy. *J Am Coll Cardiol* 45(11):1794–1801
- Murata M, Hara K, Ide T (1994) Alteration by diacylglycerols of the transport and fatty acid composition of lymph chylomicrons in rats. *Biosci Biotech Biochem* 58:1416–1419
- Murata M, Ide T, Hara K (1997) Reciprocal responses to dietary diacylglycerol of hepatic enzymes of fatty acid synthesis and oxidation in the rat. *Br J Nutr* 77:107–121
- Taguchi H, Watanabe H, Onizawa K, Nagao T, Gotoh N, Yasukawa T, Tsushima R, Shimasaki H, Itakura H (2000) Double-blind controlled study on the effects of dietary diacylglycerol on postprandial serum and chylomicron triacylglycerol responses in healthy human. *J Am Coll Nutr* 19(6):789–796
- Meguro S, Hase T, Otsuka A, Tokimitsu I, Itakura H (2003) Effect of phytosterols in dietary diacylglycerol on atherosclerosis in cholesterol-fed rabbits. *Nutrition* 19:670–675
- Meguro S, Higashi K, Hase T, Honda Y, Otsuka A, Tokimitsu I, Itakura H (2001) Solubilization of phytosterols in diacylglycerol versus triacylglycerol improves the serum cholesterol-lowering effect. *Eur J Clin Nutr* 55:513–517
- Nagao T, Watanabe H, Goto N, Onizawa K, Taguchi H, Matsuo N, Yasukawa T, Tsushima R, Shimasaki H, Itakura H (2000) Dietary diacylglycerol suppresses accumulation of body fat compared to triacylglycerol in men in a double-blind controlled trial. *J Nutr* 130:792–797
- Miettinen TA (1988) Cholesterol metabolism during ketoconazole treatment in man. *J Lipid Res* 29:43–51
- Miettinen TA, Koivisto P (1983) Non-cholesterol sterols and bile acid production in hypercholesterolaemic patients with ileal bypass. In: Paumgartner G, Stiehl A, Gerok W (eds) *Bile acids and cholesterol in health and disease*. MTP Press, Lancaster, pp 183–187
- Miettinen TA, Kesäniemi YA, Järvinen H, Hästbacka J (1986) Cholesterol precursor sterols, plant sterols, and cholestanol in human bile and gallstones. *Gastroenterology* 90:858–864
- Grundy SM, Metzger AL (1972) A physiological method for estimation of hepatic secretion of biliary lipids in man. *Gastroenterology* 62:1200–1217
- Mok HYI, von Bergmann K, Grundy SM (1979) Effects of continuous and intermittent feeding on biliary lipid outputs in man: application for measurements of intestinal absorption of cholesterol and bile acids. *J Lipid Res* 20:389–398
- Zilversmit DB (1979) Atherogenesis: a postprandial phenomenon. *Circulation* 60:473–485
- Lu K, Lee M-H, Patel SB (2001) Dietary cholesterol absorption; more than just bile. *Trends Endocrin Met* 12(7):314–320

28. Howles PN, Carter CP, Hui DY (1996) Dietary free and esterified cholesterol absorption in cholesterol esterase (bile salt-stimulated lipase) gene-targeted mice. *J Biol Chem* 271(12):7196–7202
29. Sudhop T, Lütjohann D, Agna M, von Ameln C, Prange W, von Bergmann K (2003) Comparison of the effects of sitostanol, sitostanol acetate, and sitostanol oleate on the inhibition of cholesterol absorption in normolipemic healthy male volunteers. *Arzneimittelforschung* 53(10):708–713
30. Miettinen TA, Vuoristo M, Nissinen M, Järvinen H, Gylling H (2000) Serum, biliary, and fecal cholesterol and plant sterols in colectomized subjects before and during consumption of stanol ester margarine. *Am J Clin Nutr* 71:1095–1102
31. Miettinen TA, Gylling H (1979) Serum cholesterol lowering properties of plant sterols, in Bioactive inositol phosphates and phytosterols in foods, proceedings of COST 916, 2nd workshop, European community office of official publications, Luxemburg pp 85–91
32. Nissinen MJ, Gylling H, Miettinen TA (2006) Effects of plant stanol esters supplied in a fat free milieu by pastilles on cholesterol metabolism in colectomized human subjects. *Nutr Metab Cardiovasc Dis* 16(6):426–435
33. Igel M, Giesa U, Lütjohann D, von Bergmann K (2003) Comparison of the intestinal uptake of cholesterol, plant sterols, and stanols in mice. *J Lipid Res* 44:533–538

## Absorption Properties of Micellar Lipid Metabolites into Caco2 Cells

Wakako Tsuzuki

Received: 16 February 2007 / Accepted: 10 May 2007 / Published online: 21 June 2007  
© AOCS 2007

**Abstract** To elucidate the absorption characteristics of dietary lipids in the human intestine, we investigated the cellular uptake of lipid metabolites using a differential monolayer of the Caco2 cells. As lipid metabolites, several free fatty acids and 2-monoacylglycerols, were formed a mixed micelle by bile salts and lysophospholipids and they were supplied to the Caco2 cells. To estimate the effect of the mixed micelles on the permeability of cells' membranes during incubation with the mixed micelles, the transepithelial electrical resistance (TEER) value was monitored, and no pronounced changes of TEER was detected. This suggested that mixed micelles did not affect their cellular properties of the barrier measured by TEER. The lipid metabolites transferred from the mixed micelle into the Caco2 cells were determined quantitatively by an enzymatic colorimetric method and were done by thin layer chromatography (TLC) for a species of acylglycerols. These highly sensitive methods enabled us to monitor the transepithelial transports of various kinds of non-isotope-labeled various lipid metabolites. Newly re-synthesized triacylglycerols were accumulated in Caco2 cells after 30 min incubation with the mixed micelles, and their amounts increased gradually for 4 h. The secretion of re-esterified triacylglycerols into a basolateral medium from the Caco2 cells began at 2 h after the mixed micelles were added to the apical medium. The intake of external lipid metabolites by the Caco2 cells were evaluated by an initial 2-h incubation with the mixed micelles. For example, 2-monomyristin and 2-monopalmitin were more rapidly transferred into the Caco2 cells from the mixed micelles

than 2-monocaprin was. On the other hand, the absorption rates of capric acid, lauric acid and myristic acid by the cells were larger than those of stearic acid and oleic acid. It revealed that the side-chain structure of these lipid metabolites affected their absorption by the Caco2 cells. The results of this study suggested that the Caco2 cell monolayer could be a useful model for investigating the involvement of dietary lipids in the transepithelial absorption in the human intestine.

**Keywords** Lipid metabolites · Absorption · Caco2 cell · Mixed micelle

### Introduction

Studies on the metabolism of lipids in the diet have become more important because of the increasing corpulence of populations around the world. The excess intake of dietary lipids induces several clinical diseases, especially in adult humans. On the other hand, the consumption of lipids is essential for the ingestion not only of energy but also of several essential fatty acids. Furthermore, the efficient uptake of lipophilic vitamins is strongly related to the simultaneous coexistence of lipids [1]. The appropriate intake of lipids is thus desirable from a nutritional viewpoint.

In the duodenum, dietary lipids, emulsified with physiological surfactants, such as bile salts and phospholipids, are hydrolyzed by a pancreatic lipase to produce 2-monoacylglycerols and free fatty acids. The latter two lipolytic products are then formed into mixed micelles by lysophospholipids, bile salts, and cholesterols, followed by absorption into the intestinal lumen. Their uptake by intestinal epithelial cells, the final step in the digestive

W. Tsuzuki (✉)  
National Food Research Institute, Kannondai 2-1-12,  
Tsukuba, Ibaraki 305-8642, Japan  
e-mail: wakako@affrc.go.jp

phase, is a rate-limiting step throughout the entire process of dietary lipid metabolism [2]. The transfer of lipid metabolites across the enterocyte membrane is thought to take place via facilitated diffusion and/or a membrane associated binding protein [3]. However, many aspects of the mechanisms underlying the intestinal absorption of lipid metabolites remain unknown.

The Caco2 cell line was established from a human colonic adenocarcinoma, expressing many phenotypic features of adult differentiated small intestinal enterocytes [4]. The cells have been used as a model for reproducing physiological events involving dietary nutrients at the small intestine. Previously, lipid metabolism was also studied in the Caco2 cells model for elucidating transcellular trafficking and intracellular compartmentalization of intestinal lipid metabolism. For example, the lipid metabolic capabilities of the Caco2 cells include absorption of lipid metabolites, re-synthesis of triacylglycerol and its secretion as triacylglycerol-rich lipoproteins. However, the amount of lipid metabolites, free fatty acids and 2-monoacylglycerols were too small to be monitored in the Caco2 cells model. In the previous studies, specific fatty acids, such as unsaturated fatty acids, 13-hydroxy octadecadienoic, were isotope-labeled and served in the Caco2 cells to monitor their behaviors [5–8]. Non isotope-labeled fatty acids were used in this cells model, only when their effects on transcellular permeation of other components, ions, proteins and so on, had been evaluated [9–12]. Therefore, little information has been available for the comparative study of transepithelial transport of various structured lipid metabolites in the Caco2 cells, because the kinds of isotope-labeled lipids metabolites used in the experiments were limited.

Recently, various structured lipids, defined as particular molecular species of triacylglycerols with specific fatty acids at specific positions of glycerol hydroxyl moieties, have been designed and produced. Their characteristic metabolic fates have been investigated in experimental animals [13–16]. These studies demonstrated that the intramolecular structure of a dietary triacylglycerol was strongly related to its nutritional and pharmaceutical property. The functional transepithelial transports of these structured lipids in intestinal absorption processes should be considered.

In this study, we firstly examined the introduction of one of the bile salts and lysophospholipid for making mixed micelles with lipid metabolites in order to enhance their uptake potentials by Caco2 cells. The previous study reported that absorption of the lipid metabolites by the Caco2 cells depended on the dissociation of micelles, the permeability coefficient and their monomer concentrations of lipid metabolites [16]. The formation of mixed micelles by several surfactants was expected to increase markedly the

monomer concentration of lipid metabolites exposed to the enterocyte membrane. Secondly, we investigated the intercellular trafficking property of each lipid metabolite in the Caco2 cells model system using non-isotope labeled 2-monoacylglycerols and free fatty acids. The object of the present study was to characterize the relationship between the lipid structure and its absorption property by the enterocytes. We then discussed the feasibility of the Caco2 cells as a model for studying the epithelial transport of dietary lipids.

## Materials and Methods

### Materials

Several acylglycerols and free fatty acids were purchased from Funakoshi Co. (Tokyo, Japan). The micelle mixture components—lysophosphatidylcholine (1-palmitoyl-*sn*-glycero-3-phosphocholine) (LysoPC) and taurodeoxycholic acid sodium salt (Tau)—were obtained from Sigma Chemical (St Louis, MO). The LDH-cytotoxic test kit was purchased from Wako Pure Chemical (Osaka, Japan). Other chemicals and solvents of analytical grade were purchased from Wako Pure Chemical and Kanto Chemical (Tokyo, Japan).

### Cell Culture

Caco-2 cells (American Type Culture Collection, Rockville, MD) were maintained in 10-cm dishes (Corning Glass Works, Corning, NY) containing Dulbecco's modified Eagle's medium (DMEM) supplemented with 10% fetal bovine serum, 4 mmol/L L-glutamine, 40,000 U/L penicillin, 40 mg/L streptomycin, and 1% non-essential amino acids. DMEM medium contained 1 g/L glucose and the concentration of glucose was constant throughout the absorption experiments using the mixed micelles. The cells were kept at 37 °C in a humidified atmosphere of 95% air and 5% CO<sub>2</sub>. The growth medium was replenished every 2 or 3 days. Cells were reseeded when the cell monolayers became semiconfluent. For the experiments, cells at passages 25–50 were seeded in 12-well plates at  $1.2 \times 10^5$  cells per well and grown under the same conditions as those described above. For experiments on the secretion of lipids from Caco2 cells, the cells were seeded in transwell filter chambers (polycarbonate membrane, 0.4- $\mu$ m pore size, Costar, Cambridge, MA) at  $1.0 \times 10^6$  cells per well. The experiments were performed at 20–22 days post-seeding. Transepithelial electrical resistance (TEER) was measured at the end of the culture period using a voltmeter equipped with a chopstick-type electrode (EVOMX and STX2 electrode, World Precision Instruments, Sara-

sota, FL). The TEER value of Caco2 cultured in each transwell chamber was around  $330 \pm 26 \Omega$  indicating the formation of tight monolayers. At the end of the experiment for transepithelial transport of lipid metabolites, the TEER values were measured again. No pronounced changes of TEER could be observed, comparing with those values gained before the experiment. It was suggested that the incubation with the mixed micelles did not affect the physical property of the barrier measured by TEER.

#### Preparation of Mixed Micelles

Lipid metabolites were delivered as mixed micelles prepared by modified versions of previously described procedures [17–19]. Briefly, appropriate volumes of stock solutions of components were transferred to glass tubes, and the organic solvent was removed under a stream of argon. The residue was dissolved in serum-free DMEM (the concentration of glucose was constant (1.0 g/L)) and sonicated using a micro-equipped Astrason ultrasonic processor model W-380 (Heat-System Ultrasonics, Inc., Farmingdale, NY) until a predefined particle size distribution was achieved. The final concentration of each component in the medium was as follows: 2 mmol/L Tau, 0.2 mmol/L LysoPC, 0.1 mmol/L 2-monoacylglycerol, and 0.1 mmol/L free fatty acids. The resultant solutions were optically clear. The weight-averaged particle sizes of mixed micelles were determined from quasielastic light-scattering measurements (NICOMP model 380 ZLS; Particle Sizing Systems, Santa Barbara, CA). The particle diameters of the mixed micelles ranged from 20 to 100 nm.

#### Uptake of Micellar Lipids by Caco2 Cells

The differentiated monolayers of the Caco2 cells in a 12-well plate or on a 6-transwell plate were washed twice with 0.5 mL serum-free DMEM medium and then supplemented with 2 ml of the medium containing micellar lipids. For the epithelial absorption experiments, 2 ml of the medium containing micellar lipids was supplied into each well and the Caco2 cells were routinely incubated for 2 h. For the epithelial secretion experiments, 2 ml of the same medium was poured into each apical side of the transwell, and the 2.5 ml serum-free medium was added in the basolateral one.

#### Extraction of Lipids from Caco2 Cells or from a Basolateral Medium and Their Analyses

After incubation of the Caco2 cells with the mixed micelles, the cell monolayers were washed twice with 0.5 mL PBS containing 4 mmol/L Tau to remove surface-bonded lipids, followed by two additional washings with 0.5 mL

PBS. The washed cells were harvested in 1 mL PBS and collected by centrifugation at  $1,000 \times g$  for 5 min at 4 °C. The supernatants were discarded, and the cell pellets were homogenized with a microtube homogenizer in 0.5 mL PBS. An aliquot of each cell homogenate was taken to determine the protein content, according to the method of Lowry et al. [20]. Total lipids contained in the Caco2 cells were extracted by the method of Folch et al. [21]. Briefly, 0.75 mL chloroform/methanol (2:1, v/v) was added to the cell homogenate and mixed with the solution in a vortex shaker (NSD-12, Nissinrika Ltd., Tokyo, Japan) for 5 min following centrifugation at  $1,000 \times g$  for 2 min. The resultant lower layer of chloroform was withdrawn and transferred to another tube. The upper layer was similarly extracted with 0.75 mL chloroform/methanol (2:1, v/v). The chloroform layer was combined with the initial extract. The combined extract was dried under a stream of argon gas and dissolved in 0.5 mL chloroform/methanol (2:1, v/v). Then, 0.2 mL solvent was used for quantitative determination of acylglycerols by the Triglyceride-E Test Wako kit (Wako Pure Chemical). For the secretion experiments of lipid from the Caco2 cells, lipids in the basolateral medium was extracted and analyzed according to the methods described above.

#### Statistical Analysis

The data represent mean  $\pm$  SD. Statistical analysis were made by one-way ANOVA and Dunnett's or Scheffe's *F* test to identify significant differences between the groups.

#### Thin-layer Chromatography Analyses

To identify the acylglycerols species, the total lipid extracted from Caco2 cells were applied to a silica thin-layer chromatography (TLC) plate (silica gel 60, Merck) and developed in hexane/diethylether/acetic acid (8:2:0.1, by vol.) or chloroform/methanol (6:4, v/v). Lipid was visualized by the vapor off iodine or by spray with 50% phosphomolybdic acid/ethanol solution followed by charring at 200 °C.

## Results

#### Potential Cytotoxic Effects of Tau and LysoPC on Caco2 Cells Culture

In the previous works, lipid metabolites were dispersed or emulsified in the medium containing serum albumin before being supplied to the Caco2 cells [10–12]. In this study, the mixed micelles were formed by physiological surfactants, Tau and LysoPC to monitor the epithelial transport of the

**Table 1** Cellular acylglycerols/protein (nmol/mg) after 4 h incubation

	nmol	% <sup>a</sup>
Medium	0.162 ± 0.041	0.0
2 mmol/L Taurodeoxycholic acid sodium salt (Tau)	0.219 ± 0.030	7.6
0.2 mmol/L Lysophosphatidylcholine (LysoPC)	0.312 ± 0.038	20.1
2 mmol/L Tau + 0.2 mmol/L LysoPC (mixed micelles)	0.279 ± 0.033	15.6
0.1 mmol/L Oleic acid (dispersed)	0.352 ± 0.039	25.4
0.1 mmol/L Oleic acid/Tau + LysoPC (mixed micelles)	0.447 ± 0.040	38.1
0.1 mmol/L 2-Monoolein (dispersed)	0.371 ± 0.038	27.9
0.1 mmol/L 2-Monoolein/Tau + LysoPC (mixed micelles)	0.492 ± 0.046	44.1
0.1 mmol/L Oleic acid + 0.1 mmol/L 2-Monoolein (dispersed)	0.563 ± 0.049	53.6
0.1 mmol/L Oleic acid + 0.1 mmol/L 2-Monoolein/Tau + LysoPC (mixed micelles)	0.910 ± 0.052	100.0

<sup>a</sup> The relative values were calculated in comparison with that of the cellular TG re-synthesized from mixed micellar 2-monoolein and oleic acid, which was taken 100%

lipid metabolites into the Caco2 cells from mixed micelles. Previous work pointed out that these physiological surfactants affected the viability of the Caco2 cells [22]. We evaluated the toxicity of these surfactants, which were used as the components of mixed micelle in the epithelial transport of lipid metabolites in the Caco2 cells model in a pilot study. Actually, the release of cytoplasmic lactate dehydrogenase (LDH) from the Caco2 cells into the medium was measured during incubation with the medium containing 0.2 mmol/L LysoPC and 2.0 mmol/L Tau. Based on the values of LDH release, the loss of viability of the Caco2 cells was less than 1.0% of the cells after 2 h incubation, which suggested that injury of the cells was small. The concentrations of Tau and LysoPC for use in micelle mixtures were set at 2.0 mmol/L and 0.2 mmol/L, respectively. In addition, the concentration ranges of these physiological surfactants were not contradictory to those in the digestive organs *in vivo* [1].

#### Effects of the Components of the Mixed Micelle on the Re-esterification of Acylglycerols in Caco2 Cells

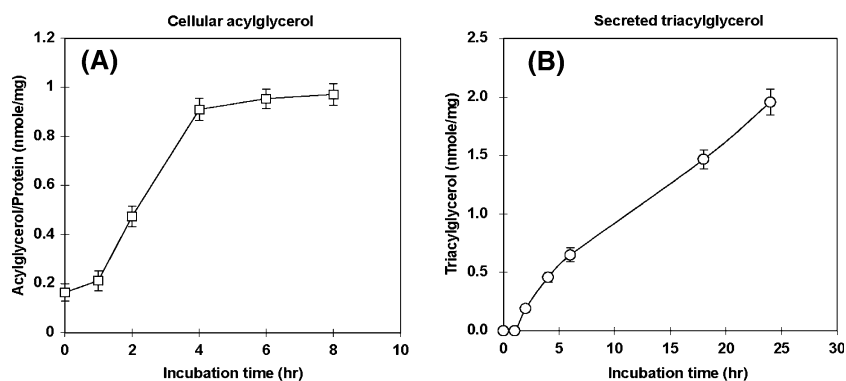
In this study, lipolytic products were mixed-micelled with Tau and LysoPC and then were supplied to the Caco2 cells plated on the wells. Previous works revealed that incubation with Tau or LysoPC alone involved the newly synthesis of lipids in the Caco2 cells [23, 24]. The effects of these micellar components on intercellular lipid levels in the Caco2 cells and on triacylglycerol secretion from the cells were to be addressed. We first evaluated the cellular acylglycerol amounts induced by each component of the mixed micelle. When both of lipolysis products, oleic acid and 2-monoolein, were mixed-micelled by Tau and LysoPC simultaneously followed by addition to the Caco2 cells, a considerable amount of triacylglycerol re-synthesis was induced in the cells for 4 h (0.910 nmol per mg of protein, which was taken 100%), as shown in Table 1. The addition of LysoPC, Tau and both induced an increase of

cellular acylglycerols by a modest 20%, 7%, and 15%, respectively (Table 1). Oleic acid dispersed in the medium was partially absorbed into Caco2 cells and stimulated corresponding triacylglycerol re-synthesis at the level of 25%. This result was consistent with the previous ones that only oleic acid stimulated lipoprotein production by increasing the synthesis and accumulation of cellular triacylglycerol [12, 25]. The other lipolysis product, 2-monoolein dispersed in the medium also facilitated the triacylglycerol re-synthesis in the Caco2 cells (27%). Meanwhile, the absorption amounts of the mixed-micellar oleic acid and 2-monoolein by the Caco2 cells were larger than those of the dispersed ones (Table 1). This result suggested that the formation of mixed micelle in the intestinal lumen would play an essential role in an efficient absorption of lipid metabolites.

#### Time Courses of the Uptake of Lipid Metabolites and the Secretion of Triacylglycerols by Caco2 Cells' Model

When the mixed micellar 2-monoolein and oleic acid were incubated with the Caco2 cells plated on wells or on transwells, the accumulation of re-synthesized triacylglycerols in the Caco2 cells and their secretion from the cells were traced in each defined incubation period. As shown in Fig. 1a, the cellular triacylglycerols in the Caco2 cells started to accumulate within 30 min after they were incubated with the mixed micellar lipids, and a proportional increase was found until around 4 h of incubation. After 2 h of incubation with micellar oleic acid and 2-monoolein, their transfers into the Caco2 cells was analyzed by the TLC method. As shown in Fig. 2a, neither oleic acid nor 2-monoolein existed in the Caco2 cells in this initial period of the incubation. The quick conversion process of these lipid metabolites into corresponding triacylglycerols by the Caco2 cells suggested that the absorption processes but not the re-synthesis of triacylglycerol processes was the rate

**Fig. 1** Time course of accumulation of cellular lipid in Caco2 cells (a) and that of the secretion of lipid from Caco2 cells (b) incubated with mixed micellar 2-monoolein and oleic acid. The data represent the mean  $\pm$  SD of six wells. Replicated experiments demonstrated a similar trend



limiting of whole processes of the accumulation of cellular triacylglycerol during the initial 2-h incubation. It could be concluded that the cellular triacylglycerol accumulation in the Caco2 cells during an initial 2 h was regarded as the absorption amounts of these lipid metabolites.

On the other hand, the secretion of newly re-synthesized triacylglycerols from the cells into the basolateral medium was detected after 2 h of incubation with the micellar

lipolytic products and increased gradually for at least 24 h. (Fig. 1b). The secreted lipids were also checked by the TLC method. Only triacylglycerol re-synthesized by the Caco2 cells was detected.

Based on the time course data of the cellular acylglycerol accumulation and of their secretion, the initial 2-h incubation with micellar lipolytic products was appropriate for the evaluation of their initial absorption of lipid metabolites by the Caco2 cells.

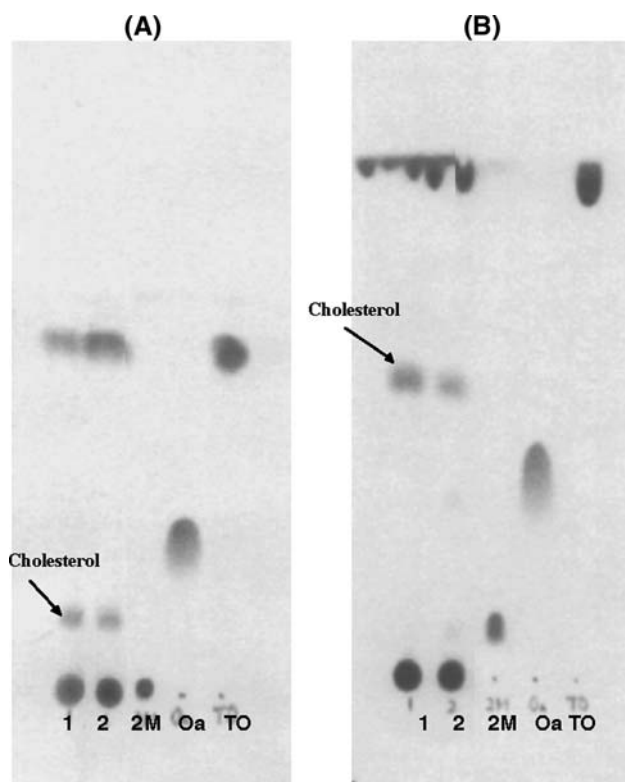


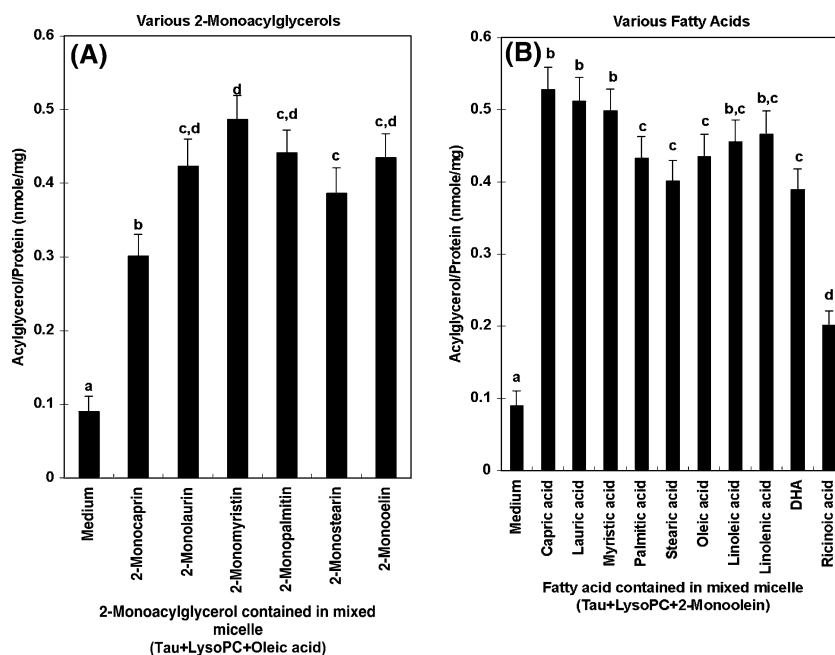
**Fig. 2** Thin layer chromatography of lipid extracted from the intact Caco2 cells, which were incubated with the medium alone [1], with the medium containing mixed micellar 2-monoolein and oleic acid [2]. The same sample were developed by hexane/diethyl ether/acetic acid (8:3:0.1, v/v) (a) and by chloroform/methanol (6:4, v/v) (b). 2Mmonoolein (2M), oleic acid (Oa) and triolein (TO) were also developed as references

#### Uptake of Lipolytic Products with Various Molecular Structures into the Caco2 Cells

Since absorption of non-isotope-labeled 2-monoolein and oleic acid in the Caco2 cells model were able to be evaluated, 2-monoacylglycerols with various length side chains were examined. In addition to 2-monoolein, 2-monocaprin, 2-monolaurin, 2-monomyristin, 2-monopalmitin, and 2-monostearin formed mixed micelle with Tau and LysoPC in the presence of oleic acid, followed by the addition to the Caco2 cells. Little difference was found in the accumulation amount of re-synthesized triacylglycerols using 2-monopalmitin, 2-monostearin, and 2-monoolein. Whereas, the accumulation of triacylglycerols re-synthesized by the Caco2 cells incubated with 2-monocaprin, 2-monolaurin, and 2-monomyristin, increased in this order (Fig. 3a).

In the next experiment, caprylic acid, capric acid, stearic acid, oleic acid, linoleic acid, linolenic acid, *cis*-4,7,10,13,16,19-docosahexanoic acid (DHA) and ricinoic acid were each introduced to be formed the mixed micelle with 2-monoolein, Tau and LysoPC. No free fatty acid could be detected by TLC methods in the initial 2-h incubation and all of them were re-synthesized into corresponding triacylglycerols (data not shown). It was concluded that the absorption amounts of lipid metabolites could be estimated by the measurements of cellular re-synthesized triacylglycerol one. As shown in Fig. 3b, epithelial transfer rates of middle length chain fatty acids (capric acid, lauric acid and myristic acid) to the Caco2

**Fig. 3** The accumulation amount of the cellular lipids of the Caco2 cells incubated with various 2-monoacylglycerols and oleic acid formed mixed micelles for 2 h (a). The accumulation amount of the cellular lipids of the intact Caco2 cells incubated with various free fatty acids and 2-monoolein formed mixed micelles for 2 h (b). The data represent the mean  $\pm$  SD of six wells. Replicated experiments demonstrated a similar trend. Statistical comparisons were made by Scheffe's *F*-test. Values not sharing a common letter in each line are significantly different from others ( $P < 0.05$ )



cells from the mixed micelles was larger than those of the long length and saturated fatty acids. (palmitic acid and stearic acid).

## Discussion

The final step in the lipid digestion process was the uptake of lipolytic products from the micelle mixture into the cell membranes of enterocytes *in vivo*. Due to the lipophilic nature of lipid metabolites, a passive diffusion and/or a protein-mediated energy-dependent uptake process, was thought to be their uptake pathways by enterocytes [3, 24]. However, these complicated uptake mechanisms of lipolytic compounds at the luminal cell surface, have not been resolved fully. The most significant finding in this work was that the behaviors of non-isotope-labeled lipolysis products could be monitored in the Caco2 cell model. This has allowed us to investigate the relationship between the molecular structures of lipids and their absorptive and secreting properties in the Caco2 cell model, using various kinds of lipolytic products. The introduction of non-isotope-labeled lipid metabolites into the Caco2 cell model was accomplished by following two improvements in the experimental procedures.

The first improvement was the successful introduction of highly sensitive detection methods to determine trace amounts of acylglycerols extracted from the Caco2 cells. The quantitative determination of acylglycerols was based on a commercially available kit. In addition, the TLC method was useful for discriminating among molecular species of acylglycerols. The detection limits of these

methods were at the level of 1–10 pmol. Because these methods were sensitive enough to measure the amount of the cellular lipid compounds, non-isotope-labeled lipid metabolites in the Caco2 cell model could be evaluated. Based on these methodological improvements, the absorption of other lipophilic nutrients materials in relation to the behavior of lipid metabolites, will be able to be analyzed in this Caco2 model in future.

In the second improvement in this study, all the lipolytic products were afforded as mixed micelles with physiological surfactants (Tau and LysoPC) to the Caco2 cells. Although 2-monoacylglycerols and free fatty acids with short or middle length chains can partially exist as free monomers in an aqueous solution, most of lipid metabolites have poor water-solubilities. It has long been known that the uptake by enterocytes depends on their monomer concentration in an aqueous phase and on that in the intermicellar concentration [2]. Previously, several surfactants, such as bovine serum albumin and phosphatidylcholine, were examined as materials for making micelles with lipid metabolites to increase the lipid metabolites absorbed by Caco2 cells [9, 22, 23]. In this study, Tau and LysoPC were successfully introduced to be components of mixed micelles. The enhancement of the monomerization of lipolytic products by the formation of mixed micelles contributes to their efficient transfer into the Caco2 cells.

This study revealed that 2-monoacylglycerol and fatty acid transferred from the mixed micelles were converted quickly into corresponded triacylglycerols in the cells and that very low amounts of intact types of lipolytic metabolites were contained in the cells in the initial incu-



bation (2 h). The initial accumulation rate of triacylglycerols re-synthesized by the Caco2 cells was taken as the initial absorption of exogenous 2-monoacylglycerol and fatty acid. Comparison of the absorption in using various lipid metabolites suggested that the molecular structure of lipolytic metabolites affected their absorption by the Caco2 cells. Thus information would help to consider the absorption properties of the structured lipids.

The absorption mechanism of lipids *in vivo* would be more complicated than that in the Caco2 cell model, because the contribution of an unstirred water layer and a mucin layer on the surface of the intestinal lumen should be considered in intestinal absorption *in vivo* [1]. In studies of the complicated absorption mechanisms in the intestine, information about transepithelial absorption processes of lipolytic products through the enterocyte membranes will be supplied using this Caco2 cell model. The cells have been widely utilized as an enterocyte absorption model for various dietary materials. As for lipid digestion, further investigation into the relationship between the molecular structures of lipolytic products and their absorption into the Caco2 cells will be undertaken in our laboratory using various structured lipids.

## References

1. Thomson ABR, Dietschy JM (1981) Intestinal lipid absorption : major extracellular and intercellular events. In: Johnson LR (ed) *Physiology of the gastrointestinal tract*. Ravan Press, New York pp 1147–1220
2. Linscheer WG, Vergroesen AJ (1981) Lipids. In: Shils EM, Olson JA, Shike M (eds) *Modern nutrition in health and disease*, eighth edition. Academic, New York pp 47–83
3. Storch J, Thumser AEA (2000) The fatty acid transport function of fatty acid-binding proteins. *Biochim Biophys Acta* 1486:28–44
4. Fogh J, Fogh JM, Orfeo T (1977) One hundred and twenty-seven cultured human tumor cell lines producing tumors in nude mice. *J Natl Cancer Inst* 59:221–226
5. Murthy S, Born E, Mathur S, Field FJ (1998) 13-Hydroxy octadecadienoic acid (13-HODE) inhibits triacylglycerol-rich lipoprotein secretion by CaCo-2 cells. *J Lipid Res* 39:1254–1262
6. Gedde-Dahl A, Bakillah A, Hussain MM, Rustan AC (1999) Tetradecylthioacetic acid (a 3-tha fatty acid) impairs secretion of oleic acid-induced triacylglycerol-rich lipoproteins in Caco2 cells. *Biochim Biophys Acta* 1438:73–84
7. Levy E, Yotov W, Seidman EG, Garofalo C, Delven E, Menard D (2000) Caco-2 cells and human fetal colon: a comparative analysis of their lipid transport. *Biochim Biophys Acta* 1439:353–362
8. Meaney CM, O'Driscoll CM (2000) A comparison of the permeation enhancement potential of simple bile salt and mixed bile salt : fatty acid micellar system using the Caco-2 cell culture model. *Int J Pharm* 207:21–30
9. Milovic V, Turchanowa L, Stein J, Caspary WF (2001) Trans-epithelial transport of putrescine across monolayers of the human intestinal epithelial cell line, Caco-2. *World J Gastroenterol* 7:193–197
10. Zerounian NR, Linder MC (2002) Effects of copper and ceruloplasmin on iron transport in the Caco2 cell intestinal model. *J Nutr Biochem* 13:138–148
11. Usami M, Komurasaki T, Hanada A, Kinoshita K, Ohata A (2003) Effect of gamma-linolenic acid or docosahexaenoic acid on tight junction permeability in intestinal monolayer cells and their mechanism by protein kinase C activation and/or eicosanoid formation. *Nutrition* 19:150–156
12. Jewell C, Cusack S, Cashman KD (2005) The effect of conjugated linoleic acid on transepithelial calcium transport and mediators of paracellular permeability in human intestinal-like Caco-2 cells. *Prostaglandins, Leukot Essent Fatty Acids*, 72:163–171
13. Kishi T, Carvajai O, Tomoyon H, Ikeda I, Sugano M, Imaizumi K (2002) Structured triglycerides containing medium-chain fatty acids and linoleic acid differently influenced clearance rate in serum of triglycerides in rats. *Nutr Res* 22:1343–1351
14. Hartvigsen MS, Mu H, Hoy C-E (2003) Influence of maternal dietary n-3 fatty acids on breast milk and liver lipids of rat dams and offspring—a preliminary study. *Nutr Res* 23:747–760
15. Matulka RA, Noguhi O, Nosaka N (2006) Safety evaluation of a medium- and long-chain triacylglycerol oil produced from medium-chain triacylglycerols and edible vegetable oil. *Food Chem Toxicol* 44:1530–1538
16. Engle MJ, Mahmood A, ad Alpers DH (2001) Regulation of surfactant-like particle secretion by Caco-2 cells. *Biochim Biophys Acta* 1511:369–380
17. Wickham M, Garrood M, Leney J, Wilson PDG, Fillery-Travis A (1998) Modification of a phospholipid stabilized emulsion interface by bile salts: effect on pancreatic lipase activity. *J Lipid Res* 38:623–632
18. Wickham M, Wilde P, Fillery-Travis A (2002) A physicochemical investigation of two phosphatidylcholine/bile salt interfaces : implications for lipase activation. *Biochim Biophys Acta* 1580:110–122
19. Garrett AD, Failla ML, Sarama RJ, Craft N (1999) Accumulation and retention of  $\beta$ -carotene and lutein by Caco-2 human intestinal cells. *J Nutr Biochem* 10:573–581
20. Lowry OH, Rosebrough NJ, Farr AL, Randall RJ (1951) Protein measurement with the folin phenol reagent. *J Biol Chem* 193:265–275
21. Folch J, Lees M, Sloane-Stanley GH (1957) A simple method for the isolation and purification of total lipids from animal tissues. *J Biol Chem* 226:497–509
22. Lapre JA, Termont DSML, Groen AK, van der Meer R (1992) Lytic effect of mixed micelles of fatty acids and bile acids. *Am J Physiol* 263:G333–G337
23. Mathur SN, Born E, Murthy S, Field FJ (1996) Phosphatidylcholine increases the secretion of triacylglycerol-rich lipoproteins by Caco-2 cells. *Biochem J* 314:569–575
24. Trotter PJ, Ho SY, Storch J (1996) Fatty acid uptake by Caco-2 human intestinal cells. *J Lipid Res* 37:336–346
25. Kamp F, Hamilton JA (1993) Movement of fatty acids, fatty acid analogues and bile acids across phospholipid bilayers. *Biochemistry* 32:11074–11086

# A Green Tea Catechin Extract Upregulates the Hepatic Low-Density Lipoprotein Receptor in Rats

Christina A. Bursill · Paul D. Roach

Received: 15 February 2007 / Accepted: 16 May 2007 / Published online: 21 June 2007  
© AOCs 2007

**Abstract** Green tea extracts have hypocholesterolaemic properties in epidemiological and animal intervention studies. Upregulation of the low-density lipoprotein (LDL) receptor may be one mechanism to explain this as it is the main way cholesterol is removed from the circulation. This study aimed to determine if a green tea extract could upregulate the hepatic LDL receptor in vivo in the rat. A green tea extract (GTE) enriched in its anti-oxidant constituents, the catechins, was fed to rats ( $n = 6$ ) at concentrations of either 0, 0.5, 1.0 or 2.0% (w/w) mixed in with their normal chow along with 0.25% (w/w) cholesterol for 12 days. Administration of the GTE had no effect on plasma total or LDL cholesterol concentrations but high-density lipoprotein significantly increased (41%;  $p < 0.05$ ). Interestingly, there was a significant increase in LDL receptor binding activity (2.7-fold) and LDL receptor protein (3.4-fold) in the 2% (w/w) treatment group compared to controls. There were also significant reductions in liver total and unesterified cholesterol (40%). Administration of the GTE significantly reduced cholesterol absorp-

tion (24%) but did not affect cholesterol synthesis. These results show that, despite no effect on plasma cholesterol, the GTE upregulated the LDL receptor in vivo. This appears to be via a reduction in liver cholesterol concentration and suggests that the green tea extract was able to increase the efflux of cholesterol from liver cells.

**Keywords** Green tea · LDL receptor · Cholesterol synthesis · Cholesterol absorption · Lathosterol · Phytosterols

## Introduction

The low-density lipoprotein (LDL) receptor is a cell surface protein that is present on the outer surface of most cells, but in particular liver cells. It is the main mechanism by which cholesterol-carrying LDL can be removed from the circulation [1]. There is, therefore, much interest in agents that increase LDL receptor activity and subsequently lower plasma cholesterol concentrations. Elevated LDL cholesterol levels are associated with increased risk of heart disease, one of the biggest killers in western societies [2].

There is evidence to suggest that green tea and its anti-oxidant constituents, the catechins, can upregulate the LDL receptor. This has evolved from epidemiological studies [3–5] showing that drinking between 5 and 10 cups of green tea per day is associated with lower plasma cholesterol concentrations. Intervention studies in rats, mice and hamsters have also found that green tea and green tea extracts enriched in catechins exhibit hypocholesterolaemic effects [6–10]. An increase in the LDL receptor may be one mechanism by which to explain this observed cholesterol-lowering ability of green tea extracts.

---

C. A. Bursill (✉)  
Heart Research Institute, University of Sydney,  
114 Pyrmont Bridge Road, Camperdown,  
NSW 2050, Australia  
e-mail: bursillc@hri.org.au

P. D. Roach  
Applied Sciences, School of Environmental and Life Sciences,  
The University of Newcastle, P.O. Box 127,  
Ourimbah, NSW 2258, Australia

C. A. Bursill · P. D. Roach  
CSIRO Human Nutrition, Adelaide, SA 5000, Australia

C. A. Bursill  
University of Adelaide, Adelaide, SA 5000, Australia

Studies in vitro [11–13] have provided more direct evidence that green tea extracts and its catechin constituents can upregulate the LDL receptor and modulate cholesterol metabolism in HepG2 cells. Indirect evidence that the LDL receptor may be upregulated by green tea extracts in vivo has also been found [14]. When rats were fed EGCG, the main catechin in green tea, the removal of intravenously injected  $^{14}\text{C}$ -cholesterol from the plasma was enhanced. This increase in the plasma clearance of cholesterol may be due to the upregulation of the LDL receptor [1] but was not assessed.

Currently, the inhibition of cholesterol absorption has been proposed as the mechanism to explain the cholesterol lowering effects of green tea in vivo. This is because the faecal excretion of total lipids and cholesterol were found to be higher in animals consuming green tea extracts [6, 7, 9]. The EGCG has also been observed to inhibit the uptake of  $^{14}\text{C}$ -cholesterol from the intestine [14]. This apparent reduction in intestinal cholesterol absorption has been ascribed to EGCG reducing the solubility of cholesterol into mixed bile salt micelles [15]. It has also been found that hamsters and rats fed green tea extracts had increased faecal excretion of bile acids [9, 10]. A study in rabbits found that a green tea extract also inhibited cholesterol synthesis [16]. Despite these effects on cholesterol absorption and synthesis, it does not rule out the possibility that an upregulation of the LDL receptor could also contribute to the hypocholesterolaemic effects of green tea. Evidence for this has been found in recently published work, where the administration of a green tea extract to rabbits significantly increased the hepatic LDL receptor in vivo [16].

The aims of this study were to determine if administration of a crude catechin extract from green tea could upregulate the hepatic LDL receptor in rats and subsequently lower plasma cholesterol in the rat.

## Experimental Procedures

### Catechin Extract

The crude catechin extract was prepared from commercially available “Special Gunpowder” green tea, packaged by the China National Native Products and Animal By-products Import and Export Corporation, Zhejiang Tea Branch, China. The method used was based on the method of Huang et al. [17]. Briefly, 15 kg of green tea was extracted with three volumes (v/v) of methanol at 50 °C for 3 h. Solvent was removed from the extract using a reduced pressure rotary evaporator. The residue was dissolved in two volumes of water (v/v) at 50 °C and extracted twice

with equal volumes of hexane (v/v) and once with an equal volume of chloroform (v/v). The remaining aqueous phase was then extracted once with an equal volume of ethyl acetate (v/v) which extracts the polyphenolic compounds including the catechins. The ethyl acetate was then evaporated, the residue redissolved in the minimum amount of warm water (50 °C) and freeze dried. The extract contained at least 58% (w/w) catechins and the composition of the measured constituents was: 30% EGCG, 21% ECG, 10% caffeine, 6% moisture, 4% EGC, 2% GCG and 0.5% theanine.

### Animal Study

Twenty-four male Sprague Dawley rats (IMVS, Gillies Plains, SA, Australia) were housed at the CSIRO Health Sciences and Nutrition Animal Facility (Kintore Avenue, Adelaide, SA, Australia) in surroundings of controlled temperature ( $20 \pm 1$  °C) and a 12 h light cycle (0600 to 1800). Ethics approval for the study was obtained from the University of Adelaide and CSIRO Health Sciences and Nutrition Animal Ethics Committees.

After an initial plasma collection from the tail vein, the rats were randomised into four different treatment groups. The crude catechin extract was mixed in with their normal rat chow at concentrations of 0, 0.5, 1 or 2% (w/w) along with 0.25% (w/w) cholesterol and fed to the rats for a period of 12 days. The rats were weighed every 2 days. After the 12 days dietary intervention the rats were fasted overnight prior to sacrifice.

Blood was collected into tubes containing EDTA (final concentration 1 g/L) from the abdominal aorta of rats under halothane anaesthesia. Plasma was isolated by centrifugation at  $1,500 \times g$  for 10 min and 1 mL aliquots were frozen at  $-20$  °C for later analysis. Liver tissue was also excised and immediately frozen in liquid nitrogen.

### Plasma Lipid Determinations

The LDL fraction ( $d = 1.019\text{--}1.063$  g/mL) was isolated from 2 mL of plasma by sequential ultracentrifugation. The high-density lipoprotein (HDL) fraction was obtained after precipitating apoB containing lipoproteins with polyethylene glycol 6000 (BDH Chemicals, Kilsyth, Victoria, Australia). Cholesterol in whole plasma and in the LDL and HDL fractions was measured on the Cobas Bio automated centrifugal analyser (Roche, Basel, Switzerland) by enzymatic methods using test kits (Roche Diagnostica, Basel, Switzerland) [18]. The triglyceride concentration of the whole plasma was also determined using enzymatic methods (Roche Diagnostica) on the Cobas Bio.

## Cholesterol Synthesis and Intrinsic Capacity to Absorb Dietary Cholesterol

Plasma lathosterol and phytosterols (campesterol and  $\beta$ -sitosterol) were measured by gas chromatography (GC) [19]. The ratios of serum lathosterol and phytosterol concentrations in the plasma to plasma cholesterol concentration, have been found to correlate with whole body cholesterol synthesis [20] and the intrinsic capacity to absorb dietary cholesterol [21], respectively.

## Hepatic LDL Receptor Binding Assay

To prepare LDL–gold conjugates, normolipidemic human blood (Australian Red Cross, Adelaide, Australia) was used to isolate LDL ( $1.025 < d < 1.050$ ) by sequential ultracentrifugation. Colloidal gold was prepared and the isolated LDL was then conjugated to the colloidal gold as previously described [22].

A 2–3 g piece of liver was homogenised and microsomal membranes (800–100,000 $\times$ g centrifuge fraction) were prepared and solubilised with 1% (w/v) Triton X-100, 5 mM phenylmethylsulfonyl fluoride and 5 mM *N*-ethylmaleimide, to prevent degradation and dimerisation of the rat LDL receptor protein. Once solubilised, Triton X-100 was removed using Amberlite XAD-2 [23] and the protein content of the microsomal membranes was determined.

To measure LDL receptor binding activity, 8  $\mu$ g of the solubilised liver membranes were applied to nitrocellulose paper (Schleicher and Schuell, Westborough, MA, USA) which was then blocked with 4% (w/v) bovine serum albumin solution [22, 24]. The nitrocellulose membranes were then incubated in buffer containing either 20  $\mu$ g/mL LDL–gold in the absence and presence of 20 mM EDTA to determine total and non-specific binding, respectively. The nitrocellulose paper was soaked in water for 30 min and then incubated with intense BL silver enhancement kit (Amersham, UK) for further 30 min. This was washed with water, dried and scanned using an LKB Ultrascan XL enhanced laser densitometer (Pharmacia LKB Biotechnology, North Ryde, NSW, Australia). The specific binding (total minus the non-specific binding) was taken to be the LDL receptor binding activity which is expressed as peak height, determined from the laser densitometer scan.

## Quantification of LDL Receptor Protein

To determine relative amounts of LDL receptor protein, solubilised rat liver membranes (150  $\mu$ g) were subjected to electrophoresis on 3–15% SDS polyacrylamide gradient gels and electrotransferred onto nitrocellulose paper. The membranes were then overlaid with a polyclonal antibody [24] against the LDL receptor (1:2,000) followed by an

anti-rabbit IgG antibody conjugated to horseradish peroxidase (Sigma, St Louis, MO, USA). The LDL receptor band was then detected on X-ray film (Hyperfilm-ECL, Amersham, North Ryde, NSW, Australia) using enhanced chemiluminescence (Amersham, North Ryde, NSW, Australia). Quantification of LDL receptor protein was performed by laser densitometry. Results are expressed as peak area, determined from the densitometer scan.

## Liver Lipid Determinations

Total cholesterol, unesterified cholesterol and triglycerides were measured on the liver homogenates. Liver preparations were initially sonicated then diluted 1:1 with a 2% (w/w) Triton X-100 and 2 mM  $\text{CaCl}_2$  solution. This was agitated on a rotating wheel for 30 min at 4 °C and protein content determined. Lipid measurements were performed using enzymatic methods on the Cobas Bio and expressed relative to the protein concentrations.

## Statistical Analyses

Results are expressed as mean  $\pm$  SEM. Percentage changes were calculated by determining the percentage change in the highest dose treatment group (2% w/w) relative to the control group. Similarly, fold changes were calculated by dividing the mean of the 2% (w/w) treatment group by the control group.

Statistical evaluation was done using a one way analysis of variance (ANOVA) and a Tukey's posthoc test. A value of  $p < 0.05$  was the criterion of significance. The statistics were performed using the SPSS statistics package.

## Results

### Crude Catechin Extract from Green Tea has No Effect on Plasma Lipids in Rats

There were no significant differences in plasma total cholesterol concentration between groups before intervention with the crude catechin extract (data not shown). There was also no significant changes in body weight between groups throughout the treatment period. This would indicate that there was no variability in food intake between groups, although this was not systematically measured. The inclusion of a green tea catechin extract to regular rat chow did not therefore affect the appetite of the rats.

Administration of the crude catechin extract along with 0.25% cholesterol for 12 days did not significantly change plasma total cholesterol, LDL cholesterol or triglyceride concentrations compared to the control group (Table 1). The HDL cholesterol concentrations were however,

**Table 1** Plasma lipid concentrations in rats after the administration of a crude catechin extract

	Crude catechin extract (%) (w/w)			
	0	0.5	1	2
Total cholesterol (mmol/L)	1.01 ± 0.10	1.39 ± 0.21	1.20 ± 0.12	1.49 ± 0.23
Triglycerides (mmol/L)	0.55 ± 0.04	0.68 ± 0.08	0.40 ± 0.03	0.52 ± 0.04
LDL cholesterol (mmol/L)	0.32 ± 0.06	0.39 ± 0.10	0.35 ± 0.07	0.44 ± 0.08
HDL cholesterol (mmol/L)	0.66 ± 0.05	0.87 ± 0.10	0.77 ± 0.05	0.93* ± 0.10

Values given as mean ± SEM. Twenty-four Sprague Dawley rats were divided into four different treatment groups of six rats each. The different treatment groups were fed a crude catechin extract for 12 days at concentrations of either 0, 0.5, 1.0, 2.0% (w/w) mixed in with normal rat chow and 0.25% cholesterol. Plasma lipids were determined using sequential ultracentrifugation and enzymatic methods on the Cobas Bio

\*  $p < 0.05$  (significant difference to control)

significantly increased (41%;  $p < 0.05$ ) in rats supplemented with the highest dose of crude catechin extract (2%) when compared with the control rats (Table 1).

#### Crude Catechin Extract from Green Tea Decreases Cholesterol Absorption

The ratio of plasma phytosterol to cholesterol was used as an index of the intrinsic capacity to absorb dietary cholesterol. Administration of the crude catechin extract was found to significantly decrease cholesterol absorption (24%) in the highest dose treatment group compared to controls (Table 2). No significant changes were seen in cholesterol synthesis between treatment groups.

#### Crude Catechin Extract from Green Tea Upregulates the Hepatic LDL Receptor

The calcium-dependant, LDL–gold binding capacity of solubilised liver membranes was used to determine hepatic LDL receptor binding activity. Administration of the highest dose of crude catechin extract (2% w/w) significantly increased (2.7-fold;  $p < 0.05$ ) the hepatic LDL receptor binding activity compared to the control (Fig. 1). Using a polyclonal antibody against the LDL receptor of liver homogenates, the relative amounts of LDL receptor protein was found to be significantly higher ( $p < 0.05$ ) in all the treatment groups compared to the control. It was at

its highest in the in the 2% (w/w) treatment group (3.4-fold higher than control) (Fig. 1).

#### Crude Catechin Extract from Green Tea Lowers Liver Cholesterol

Administration of the crude catechin extract significantly reduced ( $p < 0.05$ ) total and unesterified cholesterol in liver homogenates (40% for both) in the 2% (w/w) treatment group compared to controls (Fig. 2). Unesterified cholesterol constituted approximately 70% of the total cholesterol content and consumption of the crude catechin extract did not alter this percentage significantly. Administration of the crude catechin extract also significantly lowered triglyceride concentrations in liver homogenates by 40% (control:  $80.4 \pm 6.8$ , 0.5%: $74.7 \pm 10.0$ , 1.0%: $65.4 \pm 8.0$ , 2.0%: $49.0 \pm 4.0$  mmol/L;  $p < 0.05$ ).

## Discussion

The aim of this study was to investigate if administration of a crude catechin extract, from green tea, could increase the hepatic LDL receptor in vivo in the rat. An upregulation of the LDL receptor would provide a mechanism to explain the hypocholesterolaemic effects of green tea that have been observed in epidemiological and animal intervention studies. In contrast with previous studies, administration of

**Table 2** Effect of a crude catechin extract on cholesterol absorption and cholesterol synthesis

	Crude catechin extract (%) (w/w)			
	0	0.5	1	2
Phytosterols/cholesterol ( $\mu\text{M}/\text{mM}$ )	21.92 ± 2.12	23.93 ± 2.85	19.75 ± 3.34	16.74* ± 1.70
Lathosterol/cholesterol ( $\mu\text{M}/\text{mM}$ )	0.11 ± 0.01	0.07 ± 0.005	0.10 ± 0.020	0.10 ± 0.032

Values given as mean ± SEM. Twenty-four Sprague Dawley rats were divided into four treatment groups of six rats each. The different treatment groups were fed a crude catechin extract for 12 days at concentrations of either 0, 0.5, 1.0, 2.0% (w/w) mixed in with normal rat chow and 0.25% cholesterol. Phytosterols, lathosterol and cholesterol were measured using gas chromatography

\*  $p < 0.05$  (significant difference compared to the control)

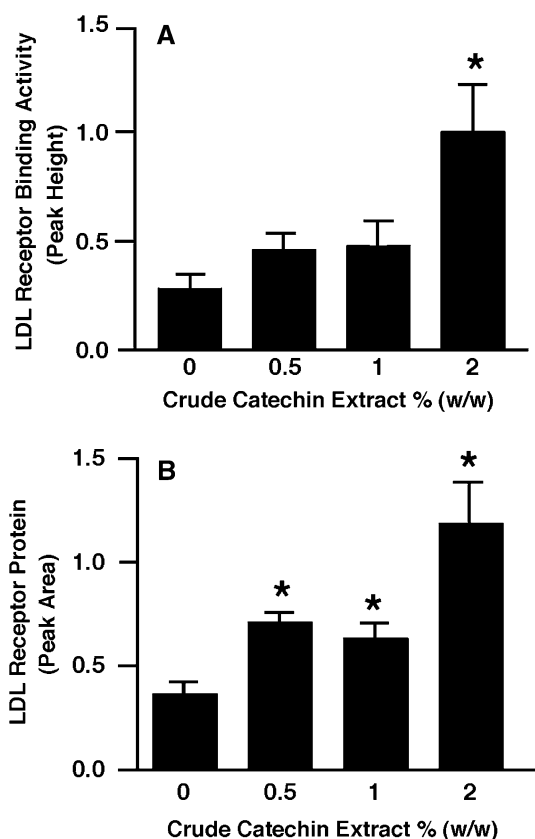


**Fig. 1** Green tea extract upregulates the LDL receptor. Twenty-four Sprague Dawley rats were divided into four treatment groups of six rats each. The different treatment groups were fed a crude catechin extract for 12 days at concentrations of either 0, 0.5, 1.0, 2.0% (w/w) mixed in with normal rat chow and 0.25% cholesterol. **a** Calcium-dependant LDL receptor binding activity was measured using solubilised livers dot-blotted onto nitrocellulose membranes and colloidal-gold LDL. **b** Relative amounts of LDL receptor protein were measured using a polyclonal antibody and western blotting. \* $p < 0.05$  (significant difference compared to the control)

the crude catechin extract did not alter plasma total or LDL cholesterol concentrations. There was, however, a significant increase in HDL cholesterol. Interestingly, administration of the highest dose (2% w/w) of extract was able to significantly increase both LDL receptor binding activity and the relative amounts of LDL receptor protein. There were also significant reductions in liver total and unesterified cholesterol concentrations. In accordance with previous studies, there was a significant reduction in the intrinsic capacity to absorb cholesterol. Despite no effect on plasma cholesterol concentrations, the crude catechin extract used in this study upregulated the LDL receptor. This appears to be via a reduction in liver cholesterol concentrations, suggesting that the crude catechin extract increases the efflux of cholesterol from liver cells.

Upregulation of the LDL receptor is triggered when there is a reduction in intracellular cholesterol concentrations [1]. Administration of the crude catechin extract

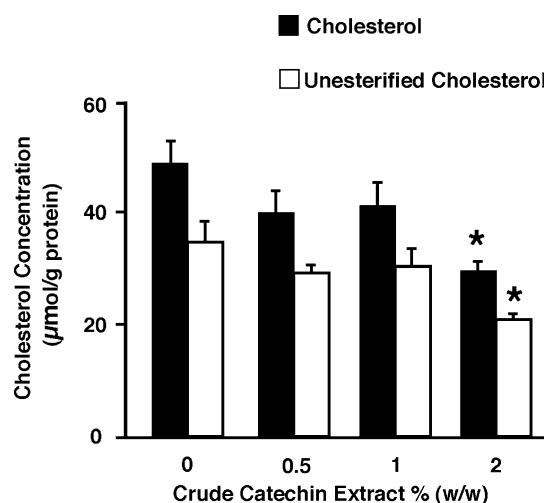


**Fig. 2** Green tea extract lowers liver cholesterol. Twenty-four Sprague Dawley rats were divided into four treatment groups of six rats each. The different treatment groups were fed a crude catechin extract for 12 days at concentrations of either 0, 0.5, 1.0, 2.0% (w/w) mixed in with normal rat chow and 0.25% cholesterol. Total and unesterified cholesterol concentrations were measured on homogenised livers using enzymatic methods on the Cobas Bio. \* $p < 0.05$  (significant difference compared to the control)

lowered liver cholesterol and increased the hepatic LDL receptor. In particular there was a reduction in liver unesterified cholesterol which is thought to be the regulatory form of cholesterol [25]. These results are consistent with in vitro studies which found that incubation with green tea or ECGC increased the LDL receptor and decreased intracellular cholesterol concentrations in HepG2 cells [11, 12]. This work is also consistent with a recent study, which found that administration of a green tea extract to rabbits increased the hepatic LDL receptor and lowered intracellular liver cholesterol [16].

Liver cellular cholesterol concentration can be lowered by three main mechanisms: (1) a decrease in cholesterol entry to the cell, (2) an increase in the packaging of cholesterol into lipoproteins and secretion or, (3) an increase in bile acid production. The first mechanism is unlikely as there should have been an increase in cholesterol entry into the cell due to the increase in the LDL receptor. The third mechanism is possible. However, if bile acid production and excretion had increased, it would have been expected that the plasma cholesterol concentration would have subsequently decreased. As there was no change in plasma cholesterol concentrations it would seem that an increase in packaging of cholesterol into lipoproteins and secretion from the liver cells is most likely. So despite the increased entry of cholesterol into the cell via the upregulation of the LDL receptor, plasma cholesterol levels may not have been lowered due to the increased secretion of cholesterol back into the circulation. This apparent increase in LDL recycling

may be a beneficial effect of the crude catechin extract as the LDL particle would be in the circulation for less time, thus reducing its chances of being oxidised. Oxidised LDL has been found to be pro-atherogenic [26, 27].

An increase in cholesterol efflux from the liver cells is also consistent with *in vitro* HepG2 cell studies [11, 12]. Incubation with green tea and EGCG appeared to increase cholesterol efflux from the cells as cholesterol concentration in the cell media was significantly increased.

Administration of the crude catechin extract increased HDL cholesterol concentration. This increase in HDL concentration may have offset any potential reduction in plasma total cholesterol concentration. However, an increase in HDL cholesterol could potentially be an athero-protective effect of the crude catechin extract. The HDL is involved in a process called reverse cholesterol transport where it transfers cholesterol from the tissues and arteries and transports it back to the liver for processing [28]. Large clinical trials have also found that there is a strong inverse correlation between heart disease and plasma HDL concentrations [29, 30]. The mechanism for the increase in HDL cholesterol by the green tea extract is not known. It is possible that the crude catechin extract is able to upregulate the factors involved in the transfer of cholesterol from cells to HDL. The results from this study suggest that there is an increased efflux of cholesterol from liver cells. It is therefore likely that the crude catechin extract may have this effect in other cells, for example, in the tissues and arteries. This is supported in a recently published study [16] that found administration of a green tea extract to rabbits decreased cholesterol concentrations in the thoracic aorta. In this study, however, plasma cholesterol concentrations were significantly reduced which would also contribute to a lowering of cholesterol in the thoracic aorta.

Consistent with previous studies the crude catechin extract significantly reduced the intrinsic capacity of cholesterol to be absorbed. This was measured by the plasma ratio of phytosterols to cholesterol. Other studies have found that faecal excretion of total lipids and cholesterol were higher in animals consuming green tea extracts [6, 7, 9] and EGCG has been observed to inhibit the uptake of  $^{14}\text{C}$ -cholesterol from the intestine [14]. This apparent reduction in intestinal cholesterol absorption has been ascribed to EGCG reducing the solubility of cholesterol into mixed bile salt micelles [15]. It has also been found that hamsters and rats fed green tea extracts had increased faecal excretion of bile acids [9, 10]. Despite the reduction in cholesterol absorption, there was no reduction in plasma cholesterol concentrations. A reduction in plasma cholesterol concentration may have been expected as less cholesterol was entering the circulation. The reduction in cholesterol absorption is consistent, however, with the reduction in liver cholesterol concentrations and reinforces

that the crude catechin extract was increasing the efflux of cholesterol from the liver cells.

In contrast to previous studies, we did not find a hypo-cholesterolaemic effect with green tea. This indicates that the crude catechin extract used in this study, for this time period, must affect lipid metabolism differently in rats than observed in other studies. Previous studies have found that green tea extracts fed to rats, mice, hamsters and rabbits have significantly lowered plasma cholesterol concentrations [6–10]. It is possible that the 12 days dietary intervention was not sufficient as other studies tended to be longer (4–8 weeks). It may also be due to the particular strain of rats used in the present study having a different response [31].

The green tea extract used in this study contained 10% caffeine. There is evidence in the literature that unfiltered coffee has cholesterol-raising effects. This is thought to be due to components called diterpenes [32]. However, the effects of caffeine alone, as present in the green tea extract, are inconclusive [32]. It has been found, however, that caffeine can inhibit cholesterol absorption [33]. It is possible, therefore that caffeine had a minor effect on cholesterol absorption in this study. Catechins, particularly EGCG are also known to inhibit cholesterol absorption [6, 7, 9, 14], consistent the current study.

There is certainly no evidence that caffeine has an effect on the LDL receptor. In addition to this, previous studies by our group have found that purified, commercially purchased, catechins upregulate the LDL receptor [12]. This would suggest that it is the catechin constituents in the green tea extract and not the caffeine that are upregulating the LDL receptor in rats.

In conclusion, administration of a crude catechin extract from green tea upregulated the hepatic LDL receptor in the rats. This appeared to be due to an increase in the efflux of cholesterol from the liver cells into the circulation, as there was a decrease in liver intracellular cholesterol and no change in plasma cholesterol.

**Acknowledgments** We would like to thank the University of Adelaide for providing Christina Bursill with a postgraduate scholarship and additional funding.

## References

1. Brown MS, Goldstein JL (1986) A receptor-mediated pathway for cholesterol homeostasis. *Science* 232:34–47
2. Glass CK, Witztum JL (2001) Atherosclerosis: the road ahead. *Cell* 104:503–516
3. Kono S, Shinchi K, Ikeda N, Yanai F, Imanishi K (1992) Green tea consumption and serum lipid profiles: a cross-sectional study in northern Kyushu, Japan. *Prev Med* 21:526–531
4. Stensvold I, Tverdal A, Solvoll K, Foss OP (1992) Tea consumption: relationship to cholesterol, blood pressure, and coronary and total mortality. *Prev Med* 21:546–553

5. Imai K, Nakachi K (1995) Cross sectional study of effects of drinking green tea on cardiovascular and liver diseases. *BMJ* 310:693–696
6. Muramatsu K, Fukuyo M, Hara Y (1986) Effect of green tea catechins on plasma cholesterol level in cholesterol-fed rats. *J Nutr Sci Vitaminol (Tokyo)* 32:613–622
7. Matsuda H, Chisaka T, Kubomura Y, Yamahara J, Sawada T, Fujimura H, Kimura H (1986) Effects of crude drugs on experimental hypercholesterolemia. I. Tea and its active principles. *J Ethnopharmacol* 17:213–224
8. Yang TT, Koo MW (1997) Hypocholesterolemic effects of Chinese tea. *Pharmacol Res* 35:505–512
9. Anonymous (2000) Chinese green tea lowers cholesterol level through an increase in fecal lipid excretion. *Life Sci* 66:411–423
10. Chan PT, Fong WP, Cheung YL, Huang Y, Ho WK, Chen ZY (1999) Jasmine green tea epicatechins are hypolipidemic in hamsters (*Mesocricetus auratus*) fed a high fat diet. *J Nutr* 129:1094–1101
11. Bursill C, Roach PD, Bottema CD, Pal S (2001) Green tea upregulates the low-density lipoprotein receptor through the sterol-regulated element binding protein in HepG2 liver cells. *J Agric Food Chem* 49:5639–5645
12. Bursill CA, Roach PD (2006) Modulation of cholesterol metabolism by the green tea polyphenol (–)-epigallocatechin gallate in cultured human liver (HepG2) cells. *J Agric Food Chem* 54:1621–1626
13. Kuhn DJ, Burns AC, Kazi A, Dou QP (2004) Direct inhibition of the ubiquitin–proteasome pathway by ester bond-containing green tea polyphenols is associated with increased expression of sterol regulatory element-binding protein 2 and LDL receptor. *Biochim Biophys Acta* 1682:1–10
14. Chisaka T, Matsuda H, Kubomura Y, Mochizuki M, Yamahara J, Fujimura H (1988) The effect of crude drugs on experimental hypercholesterolemia: mode of action of (–)-epigallocatechin gallate in tea leaves. *Chem Pharm Bull (Tokyo)* 36:227–233
15. Ikeda I, Imasato Y, Sasaki E, Nakayama M, Nagao H, Takeo T, Yayabe F, Sugano M (1992) Tea catechins decrease micellar solubility and intestinal absorption of cholesterol in rats. *Biochim Biophys Acta* 1127:141–146
16. Bursill CA, Abbey M, Roach PD (2007) A green tea extract lowers plasma cholesterol by inhibiting cholesterol synthesis and upregulating the LDL receptor in the cholesterol-fed rabbit. *Atherosclerosis* 193:86–93
17. Huang MT, Ho CT, Wang ZY, Ferraro T, Finnegan-Olive T, Lou YR, Mitchell JM, Laskin JD, Newmark H et al (1992) Inhibitory effect of topical application of a green tea polyphenol fraction on tumor initiation and promotion in mouse skin. *Carcinogenesis* 13:947–954
18. Clifton PM, Chang L, Mackinnon AM (1988) Development of an automated Lowry protein assay for the Cobas-Bio centrifugal analyser. *Anal Biochem* 172:165–168
19. Wolthers BG, Walrecht HT, van der Molen JC, Nagel GT, Van Doormaal JJ, Wijnandts PN (1991) Use of determinations of 7-lathosterol (5 alpha-cholest-7-en-3 beta-ol) and other cholesterol precursors in serum in the study and treatment of disturbances of sterol metabolism, particularly cerebrotendinous xanthomatosis. *J Lipid Res* 32:603–612
20. Kempen HJ, Glatz JF, Gevers Leuven JA, van der Voort HA, Katan MB, (1988) Serum lathosterol concentration is an indicator of whole-body cholesterol synthesis in humans. *J Lipid Res* 29:1149–1155
21. Tilvis RS, Miettinen TA (1986) Serum plant sterols and their relation to cholesterol absorption. *Am J Clin Nutr* 43:92–97
22. Roach PD, Zollinger M, Noel SP (1987) Detection of the low density lipoprotein (LDL) receptor on nitrocellulose paper with colloidal gold–LDL conjugates. *J Lipid Res* 28:1515–1521
23. Roach PD, Noel SP (1985) Solubilization of the 17 alpha-ethinyl estradiol-stimulated low density lipoprotein receptor of male rat liver. *J Lipid Res* 26:713–720
24. Roach PD, Kerry NL, Whiting MJ, Nestel PJ (1993) Coordinate changes in the low density lipoprotein receptor activity of liver and mononuclear cells in the rabbit. *Atherosclerosis* 101:157–164
25. Grundy SM (1991) George Lyman Duff memorial lecture. Multifactorial etiology of hypercholesterolemia. Implications for prevention of coronary heart disease. *Arterioscler Thromb* 11:1619–1635
26. Albertini R, Moratti R, De Luca G (2002) Oxidation of low-density lipoprotein in atherosclerosis from basic biochemistry to clinical studies. *Curr Mol Med* 2:579–592
27. Steinberg D (1997) Low density lipoprotein oxidation and its pathobiological significance. *J Biol Chem* 272:20963–20966
28. Ohashi R, Mu H, Wang X, Yao Q, Chen C (2005) Reverse cholesterol transport and cholesterol efflux in atherosclerosis. *QJM* 98:845–856
29. Randomised trial of cholesterol lowering in 4,444 patients with coronary heart disease: the Scandinavian simvastatin survival study (4S) (1994) *Lancet* 344:1383–1389
30. MRC/BHF heart protection study of cholesterol lowering with simvastatin in 20,536 high-risk individuals: a randomised placebo-controlled trial (2002) *Lancet* 360:7–22
31. Roach PD BS, Hirata F, Abbey M, Szanto A, Simons LA, Nestel PJ (1993) The low-density lipoprotein receptor and cholesterol synthesis are affected differently by dietary cholesterol in the rat. *Biochim Biophys Acta* 1170(2):165–172
32. Wang S, Noh SK, Koo SI (2006) Epigallocatechin gallate and caffeine differentially inhibit the intestinal absorption of cholesterol and fat in ovariectomized rats. *J Nutr* 136(11):2791–2796
33. Cornelis MC, El-Sohehy A (2007) Coffee, caffeine, and coronary heart disease. *Curr Opin Lipidol* 18(1):13–9



## Effects of Cigarette Smoke on Cell Viability, Linoleic Acid Metabolism and Cholesterol Synthesis, in THP-1 Cells

Silvia Ghezzi · Patrizia Risé · Stefania Ceruti ·  
Claudio Galli

Received: 12 February 2007 / Accepted: 24 April 2007 / Published online: 6 June 2007  
© AOCS 2007

**Abstract** Cigarette smoke (CS) contains thousands of substances, mainly free radicals that have as a target the polyunsaturated fatty acids (PUFA). Long chain PUFA are produced through elongation and desaturation reactions from their precursors; the desaturation reactions are catalyzed by different enzymes: the conversion of 18:2n-6 (linoleic acid, LA) to 18:3n-6 by  $\Delta 6$  desaturase, while that of 20:3n-6 to 20:4n-6 by  $\Delta 5$  desaturase. The aim of this work is to evaluate the effect of serum exposed to cigarette smoke (SE-FBS) on (1) cell viability and proliferation, (2) [1- $^{14}$ C] LA conversion and desaturase activities in THP-1 cells, a monocytic cell line. In THP-1, CS inhibits cell proliferation dose-dependently, by producing a modification in the cell cycle with a reduced number of cells in synthesis and mitosis phases at higher concentrations. CS also decreases [1- $^{14}$ C] LA conversion to its derivatives in a concentration-dependent manner, inhibiting the activities of  $\Delta 6$  and mainly  $\Delta 5$  desaturase. In addition, CS does not modify the incorporation of LA into various lipid classes but it reduces cholesterol synthesis from radiolabelled acetate, and increases free fatty acid, TG and CE levels. In conclusion, CS affects lipid metabolism, inhibiting LA conversion and desaturase activities. CS also shifts the “de novo” lipid synthesis from free cholesterol to TG and CE, where LA is preferentially esterified.

**Keywords** Polyunsaturated fatty acids · Linoleic acid · Cholesterol · Human desaturases · Cigarette smoke

### Introduction

Cigarette smoke (CS) contains an extremely high number of products of various chemical nature, in both gas and tar phases, mainly free radicals ( $10^{15}$  free radicals/g of tar phase) [1], and it indirectly increases the production of reactive oxygen species, by activation of inflammatory cells [2]. Chronic cigarette smoke exposure is therefore associated with oxidative stress due to the increased free radical burden, followed by alteration of various oxidative stress indexes [3]. When free radicals are produced in excess or they are not efficiently removed, cellular damage (peroxidation of membrane lipids or oxidation of proteins and damage to DNA) occurs [4]. Lipids are among the compounds susceptible to free radical mediated alterations, and more specifically the polyunsaturated fatty acids (PUFA) are major targets of peroxidative processes and sources of lipid-derived radicals [4].

PUFA, especially the long chain PUFA (LC-PUFA) are endowed with biologically “essential” features, due to their basic contribution to membrane structures and cell functions. In addition, while the levels of the LC-PUFA of the n-3 series, e.g., docosahexaenoic acid (22:6n-3, DHA), in cells and tissues are largely dependent upon dietary intakes, PUFA of the n-6 series, i.e., arachidonic acid (20:4n-6, AA), is produced to a significant extent, by the endogenous conversion of linoleic acid (18:2n-6, LA), a relevant component of dietary fats. The conversion of LA and alpha linolenic acid (18:3n-3,  $\alpha$ -LNA) to their longer chain derivatives in both the n-6 and the n-3 pathways proceed through elongation and especially desaturation reactions. These are catalyzed by different enzymes, namely the  $\Delta 6$  desaturase on 18C and 24C, and the  $\Delta 5$  desaturase on 20C fatty acids.

The activity of human desaturases ( $\Delta 9$ ,  $\Delta 6$  and  $\Delta 5$ ) is modulated by different factors: it is inhibited by the meta-

S. Ghezzi · P. Risé (✉) · S. Ceruti · C. Galli  
Department of Pharmacological Sciences,  
University of Milan, via Balzaretti 9,  
20133 Milan, Italy  
e-mail: patrizia.rise@unimi.it

bolic products of desaturases [5] and by cholesterol rich diets [6]. In addition, the activity of  $\Delta 6$  desaturase is enhanced by low EFA intake, while diets rich in LA and in  $\alpha$ -LNA inhibit both  $\Delta 5$  and  $\Delta 6$  desaturase activities [6, 7]. These enzymes are also modulated by hormones (activated by insulin and reduced by adrenalin, glucagon, and steroids) [8] and by different classes of xenobiotics: peroxisome proliferators [9], calcium antagonists and some phenolic compounds [10], oxysterols [11], and statins [12, 13].

In addition, various studies have shown the effects of toxic compounds, i.e., CS on PUFA metabolism and/or their levels. In vitro CS negatively affects, in a concentration-dependent manner, LC-PUFA production. In mammary gland cells there is a decrease of DHA and EPA levels from  $\alpha$ -LNA, and of the 20:5/20:4n-3 ratio [14, 15].

In-vivo levels of LC-PUFA of the n-3 series, namely DHA, together with those of AA, were shown to be reduced, in milk from smoking- in comparison to non-smoking-mothers [16]; in addition, DHA is reduced in blood lipids of infants born to smoking mothers [17]. Finally CS decreases the 20:4/20:3n-6 ratio in plasma of subjects who smoke [18].

The rather limited data on the detailed effects of CS on n-6 PUFA metabolism indicate that this is an area that needs to be explored, especially since n-6 FA are certainly the major PUFA components of our diets in the form of LA, and also because the endogenous pools of AA, a key FA in the modulation of several functions in various cell types, appear to be largely dependent on its formation from LA [19]. In fact, LA and AA, in the body, are incorporated in different lipids (triglycerides, cholesterol esters and phospholipids).

On the basis of the above considerations, the purpose of this work was to evaluate the cell viability and proliferation after exposure to CS, and to study the detailed effects of CS exposed serum on labelled LA conversion and on desaturase activities. Finally, the effects of CS exposed serum on the synthesis of cholesterol from labelled acetate were also assessed. All these parameters were evaluated in THP-1 cells, a monocytic cell line that effectively is able to convert LA to its longer derivatives, while incorporating the labelled FAs mainly in the PL fraction [12]. This last feature will facilitate the detection of alterations in the fate of n-6 FA incorporation into different lipid pools following cell exposure to CS.

## Materials and Methods

### Materials and Reagents

The materials for cell cultures (RPMI 1640 medium, fetal bovine serum (FBS), penicillin, and streptomycin) were from Sigma (Sigma Aldrich S.r.l., Milan, Italy). Solvents

and TLC (thin layer chromatography) plates were from E. Merck (Darmstadt, Germany). The radiolabelled compounds [ $1\text{-}^{14}\text{C}$ ] LA (specific activity 55 mCi/mmol), [ $1\text{-}^{14}\text{C}$ ] acetic acid sodium salt (specific activity 58 mCi/mmol), and [ $6\text{-}^3\text{H}$ ] thymidine (specific activity 27 Ci/mmol), were from Amersham (Amersham Pharmacia Biotech, Little Chalfont, England). Simvastatin in lactone form (Merck, Sharp & Dohme Research Laboratories, Woolbridge, NJ) was dissolved in 0.1 M NaOH to give the active, open  $\beta$ -hydroxy acid form.

### Cell Culture

THP-1 cells, a human monocytic cell line [20], were grown in RPMI medium containing 10% FBS, 100  $\mu\text{g}/\text{ml}$  penicillin, 100 IU/ml streptomycin, and 2 mM l-glutamine.

### Smoking Machine

To expose cells to CS, a popular brand of Italian cigarettes was used, MS with filter. A device was developed to allow a controlled incorporation of CS, in appropriate and reproducible conditions, into the FBS, through aspiration by a pump under controlled vacuum, to obtain smoke exposed FBS (SE-FBS) [15, 21]. Specifically, smoke from two cigarettes was bubbled through 5 ml FBS for 5 min at 8 puffs/min. 100  $\mu\text{l}$  of SE-FBS correspond to 0.04 cigarettes (4% of one cigarette).

### Experimental Design

At the time of the experiments, cells were centrifuged at  $200\times g$  for 10 min, and the pellet obtained was resuspended in RPMI medium without FBS; the concentration of the cells was adjusted to  $10^6$  cells/ml. Cells were then incubated with different aliquots of SE-FBS (12.5–25–37.5–50  $\mu\text{l}$  corresponding to 0.005–0.01–0.015–0.02 cigarettes). At 24 h the appropriate labelled substrate ([ $1\text{-}^{14}\text{C}$ ] LA 0.1  $\mu\text{Ci}/10^6$  cells or [ $1\text{-}^{14}\text{C}$ ] acetic acid sodium salt 1  $\mu\text{Ci}/10^6$  cells) was also added for the additional 24 h. At the end of the incubation (48 h), cells were centrifuged, resuspended in a given volume of PBS, 50  $\mu\text{l}$  of which were counted with a cell counter, and the total lipids extracted according to Folch et al. [22]. Aliquots of total lipid extracts were counted in a  $\beta$ -counter in order to determine the radioactivity recovered in the samples.

### Time Course

Cells were incubated with different amounts of SE-FBS (25 and 50  $\mu\text{l}$  corresponding to 0.01 and 0.02 cigarettes respectively) for different time periods (4–8–16–24–48 h). [ $1\text{-}^{14}\text{C}$ ] LA (0.1  $\mu\text{Ci}/10^6$  cells) was added at the start of the

experiment for the 4–8–16 and 24 h, and after 24 h of incubation for the 48 h.

#### Polyphenol Assay

To standardize the procedure of SE-FBS preparation, the levels of polyphenols, after their extraction from SE-FBS [23], were measured as described by Visioli et al. [24]. Briefly, 50  $\mu\text{l}$  of folin and ciocalteu's phenol reagent (Sigma Aldrich S.r.l.) were added to increasing amounts of SE-FBS. After 3 min of incubation, 100  $\mu\text{l}$  saturated  $\text{Na}_2\text{CO}_3$  and distilled water were added to each sample (final volume 2.5 ml). Samples were analyzed spectrophotometrically at 725 nm after 1 h of incubation in the dark at room temperature.

#### TBARS Assay

TBARS levels, markers of the lipid peroxide production, were evaluated as described by Balla et al. [25]. Briefly, 400  $\mu\text{l}$  of total lipids, for each sample, were added to 600  $\mu\text{l}$  thiobarbituric acid reagent. After heating at 100 °C for 15 min, the samples were cooled at room temperature and were centrifuged at 10,000 $\times g$  for 10 min. The clear supernatants were analyzed spectrophotometrically at 532 nm.

#### Cell Proliferation

Cell proliferation was evaluated by the incorporation of [6- $^3\text{H}$ ] thymidine (1  $\mu\text{Ci}/10^6$  cells) into nucleic acids, after exposure to different amounts of SE-FBS (25–50–75–100  $\mu\text{l}$  corresponding to 0.01–0.02–0.03–0.04 cigarettes). At the end of the experiment aliquots of cell suspensions were counted in a  $\beta$ -counter in order to determine the radioactivity recovered in the samples.

#### Evaluation of Apoptosis

The percentage of apoptotic cells was evaluated as described by Abbracchio et al. [26]. Briefly, after exposure to SE-FBS, cells were centrifuged at 200 $\times g$  for 10 min and the pellet obtained was gently resuspended in 1 ml hypotonic fluorochrome solution (propidium iodide, PI 50  $\mu\text{g}/\text{ml}$  in 0.1% sodium citrate plus 0.1% Triton X-100; Sigma). Cells were analyzed after a minimum of 30 min of incubation in the dark at room temperature, and apoptosis was detected in individual cells using a flow cytometer (equipped with a single 488 nm argon laser; Becton Dickinson, San Josè, CA) by reduced fluorescence of PI in apoptotic nuclei.

#### Analysis of Labelled Fatty Acids by HPLC

LC-PUFA production from the precursor [1- $^{14}\text{C}$ ] LA was evaluated as radioactivity associated with different fatty

acid methyl esters and assessed by HPLC coupled with an on-line radiodetector (Flow Scintillation Analyzer 500TR Series, PerkinElmer), as previously described [12].

#### Separation of Lipid Classes

The incorporation of [1- $^{14}\text{C}$ ] LA and [1- $^{14}\text{C}$ ] acetic acid sodium salt in the various lipid classes (phospholipids PL, diglycerides DAG, free fatty acids FFA, triglycerides TG, and cholesterol esters CE) was evaluated after separation by a monodimensional thin layer chromatography (TLC, hexane/diethylether/acetic acid 70/30/1.5 by vol). To detect free cholesterol (Cho) and monoglycerides (MG) a different solvent system was used (chloroform/methanol 98/2 by vol). Lipids were visualized on plates by exposure to iodine vapours; spots were scraped off and the radioactivity was detected, after addition of 1 ml methanol/water (1:1 by vol) and 10 ml of scintillation fluid, in a  $\beta$ -counter.

#### Statistical Analysis

Significance of differences, when comparing control and treated cells, was assessed by the use of Student's *t*-test.

## Results

#### Standardization of the Method for the Preparation of SE-FBS

To validate the procedure for the preparation of SE-FBS, the levels of polyphenols, transferred from CS to serum, are evaluated. In fact, in control conditions (FBS not exposed to CS), polyphenols are detectable only in traces, whereas, when 5 ml FBS is exposed to one or two cigarettes (Fig. 1), there is a significant increase, with respect to control, of polyphenol levels of about  $46 \pm 1\%$  and  $89 \pm 4\%$ , respectively. There is a dose related accumulation of polyphenols, since their levels in the two cigarettes SE-FBS are double than those in the one cigarette SE-FBS, with a 1.99 ratio.

TBARS levels, a marker of oxidation, are also determined; a positive correlation between increasing amounts (corresponding to 200–300–400–500  $\mu\text{g}$  of total lipids) of SE-FBS and TBARS levels is found ( $R^2 = 0.997$ ) (Fig. 2).

#### Cell Viability and Proliferation

To evaluate the effects of CS on cell viability and proliferation, two different methods are used. As shown in Fig. 3, the incorporation of [6- $^3\text{H}$ ] thymidine in THP-1 cells, treated with different concentration of SE-FBS, decreases

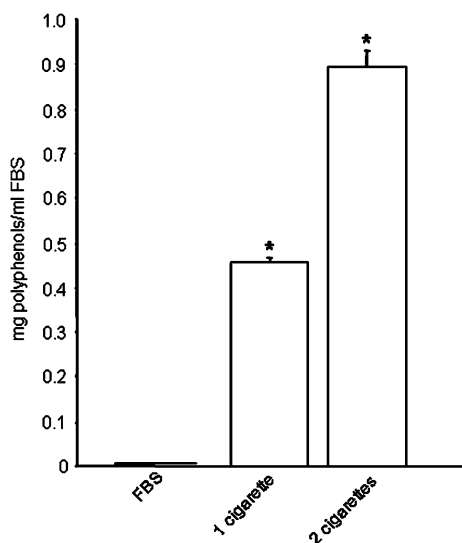


**Fig. 1** Polyphenol levels in serum not exposed or in serum (5 ml) exposed to one or two cigarettes. The results are expressed as mg of polyphenols for ml of serum and represent means  $\pm$  SE of three independent experiments. Differences are significantly different from FBS at \*  $p \leq 0.001$

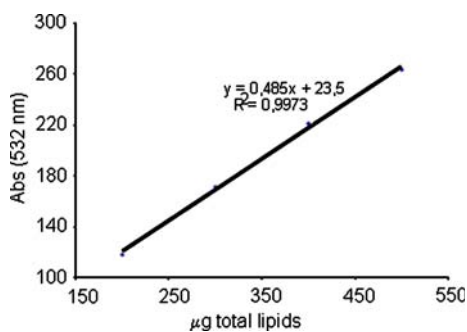


**Fig. 2** TBARS levels in increasing amounts of serum (from 120 to 300  $\mu$ l, corresponding to a range of 200–500  $\mu$ g of total lipids) exposed to cigarette smoke, prepared bubbling two cigarettes in 5 ml of FBS. Results are expressed as absorbance at 532 nm

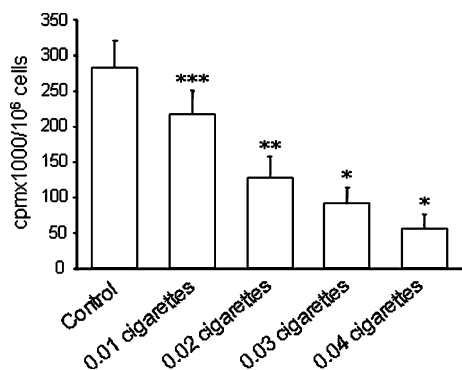


**Fig. 3** [<sup>3</sup>H] thymidine incorporation in THP-1 cells after treatment with serum exposed to cigarette smoke (0.01–0.02–0.03–0.04 cigarettes). The results are expressed as cpm of [<sup>3</sup>H] thymidine  $\times$  1,000 for 10<sup>6</sup> cells and represent mean  $\pm$  SE of three independent experiments. Differences are significantly different from control at \*  $p \leq 0.001$ ; \*\*  $p \leq 0.005$ ; \*\*\*  $p \leq 0.05$

in a dose-dependent manner, with a significant reduction already at the lowest concentration of SE-FBS (0.01 cigarettes) used, from  $283.27 \pm 21.50$  to  $217.78 \pm 18.91$  cpm  $\times$  1,000/10<sup>6</sup> cells ( $-23\%$  with respect to control). At the highest concentration used (0.04 cigarettes) there is a decrease of 80% with respect to control. Figure 4 shows a representative experiment in which the apoptotic and necrotic processes are detected: there is a significant increase of apoptosis and necrosis (M<sub>1</sub> and M<sub>2</sub> segments, respectively) only at the highest concentrations used, from 6.13% in control cells to 8.73 and 19.16% with 0.020 and 0.040 cigarettes, respectively. In addition, when the same data are analyzed in a linear scale, there is a decrease of the number of cells in synthesis (S phase) and mitosis (G<sub>2</sub>–M phase) at the highest concentration used (0.04 cigarettes), of about 40% with respect to control (not shown).

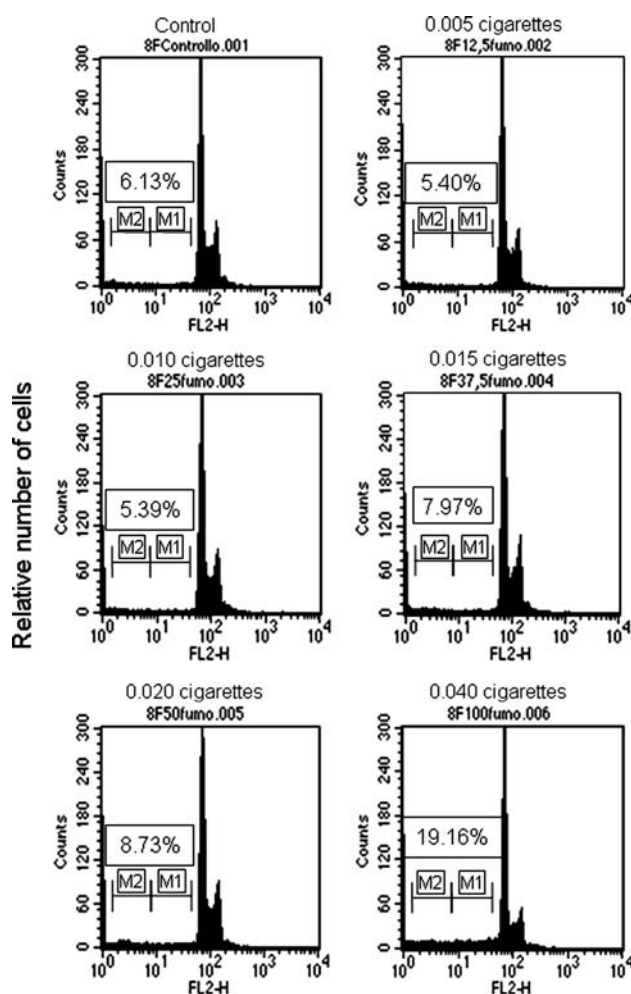


**Fig. 4** Detection of apoptotic (M<sub>1</sub>) and necrotic (M<sub>2</sub>) processes in THP-1 cells treated with serum exposed to cigarette smoke (0.005–0.010–0.015–0.020–0.040 cigarettes) for 48 h. The results are expressed as relative number of cells. The percentages represent the apoptotic plus necrotic processes of a representative experiment

## LA Conversion

The total conversion of [ $^{14}\text{C}$ ] LA (calculated as the sum of the percentages of the radioactivity associated to its derivatives, 18:3, 20:3, 20:4 and 22:4n-6) is  $47.56 \pm 1.66\%$  in control cells. After treatment with CS, LA total conversion decreases in a dose-dependent manner and the reduction is already significant ( $-28\%$  with respect to control) with 0.01 cigarettes. At the highest SE-FBS concentration, the LA total conversion is reduced to  $22.54 \pm 2.43\%$  (Fig. 5).

With increasing concentrations of SE-FBS, the activities of both  $\Delta 5$  and  $\Delta 6$  desaturases (expressed as product/precursor ratios) decrease in a dose-dependent manner, although the effect is more pronounced on the  $\Delta 5$  desaturase, as shown in Fig. 6.  $\Delta 6$  desaturation, expressed as the 18:3/18:2n-6 ratio, is significantly decreased, from  $0.045 \pm 0.002$  in control cells to  $0.029 \pm 0.003$  and  $0.013 \pm 0.003$  with 0.01 and 0.02 cigarettes respectively (Fig. 6, panel A).  $\Delta 5$  desaturation (20:4/20:3n-6 ratio) significantly decreases already with the lowest SE-FBS concentration used (0.005 cigarettes), from  $0.94 \pm 0.06$  in control cells to  $0.63 \pm 0.04$ ; with the highest concentration of SE-FBS  $\Delta 5$  desaturation decreases to  $0.19 \pm 0.03$  (Fig. 6, panel B).

Table 1 shows the radioactivity associated to the LA metabolites. There is a significant reduction of 18:3, 20:4 and 22:4n-6 starting from 0.010 cigarettes. The percentage of 18:3 decreases from  $2.51 \pm 0.15\%$  in control cells to  $0.86 \pm 0.15\%$  at the highest concentration used (0.020 cigarettes). For 20:4 there is a reduction from  $17.79 \pm 2.01\%$  in controls to  $2.50 \pm 0.58\%$  with 0.020 cigarettes, and for 22:4 from  $1.55 \pm 0.33\%$  to  $0.19 \pm 0.09\%$ .

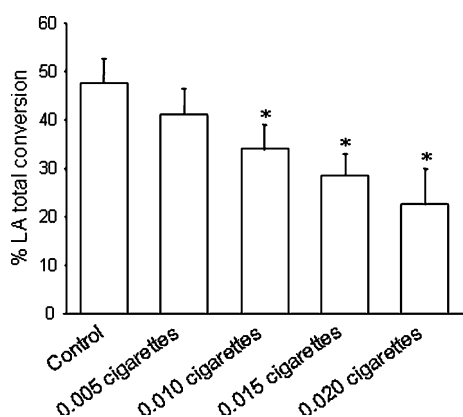


**Fig. 5** [ $^{14}\text{C}$ ] linoleic acid (LA) total conversion in THP-1 cells treated with serum exposed to cigarette smoke (0.005–0.010–0.015–0.020 cigarettes) for 48 h. The results are expressed as percentage of total LA conversion (calculated as the sum of the percentages of the radioactivity associated to its derivatives, 18:3, 20:3, 20:4 and 22:4n-6) and represent mean  $\pm$  SE of seven independent experiments. Differences are significantly different from control at \*  $p < 0.001$

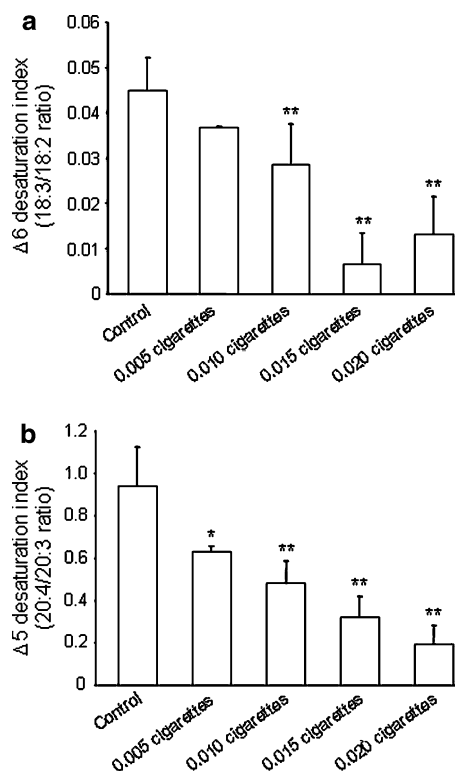


**Fig. 6**  $\Delta 5$  and  $\Delta 6$  desaturation indexes in THP-1 cells treated with serum exposed to cigarette smoke (0.005–0.010–0.015–0.020 cigarettes) for 48 h. The results are expressed as product/precursor ratio (20:4/20:3 ratio for  $\Delta 5$  desaturase and 18:3/18:2 ratio for  $\Delta 6$  desaturase) and represent the mean  $\pm$  SE of seven independent experiments. Differences are significantly different from control at \*  $p < 0.05$ ; \*\*  $p < 0.001$

The relative percentage of the radioactivity associated to different lipid classes, after [ $^{14}\text{C}$ ] LA incubation, is not affected by SE-FBS, with about 75% of radioactivity recovered in PL and 20% in TG (Table 2).

## Time Course

The total conversion of [ $^{14}\text{C}$ ] LA increases, in control cells, from  $21.66 \pm 3.83\%$  at 4 h to  $45.75 \pm 0.90\%$  at 48 h (Fig. 7). LA conversion increases also in SE-FBS treated cells over time: from  $15.15 \pm 0.87\%$  at 4 h to  $33.20 \pm 4.48\%$  at 48 h with 0.01 cigarettes, and from  $12.93 \pm 0.04\%$  at 4 h to  $20.96 \pm 7.40\%$  at 48 h with 0.02 cigarettes. Otherwise the percentages of conversion with 0.02 cigarettes are lower than those of controls and of samples exposed to 0.01 cigarettes, at any time considered.

## Cholesterol Synthesis

SE-FBS significantly decreases the incorporation of radiolabelled acetate in free cholesterol (Table 3), from

**Table 1** Relative percentage of the radioactivity associated to linoleic acid metabolites, in THP-1 cells treated with increasing concentrations of serum exposed to cigarette smoke, after [1-<sup>14</sup>C] linoleic acid incubation

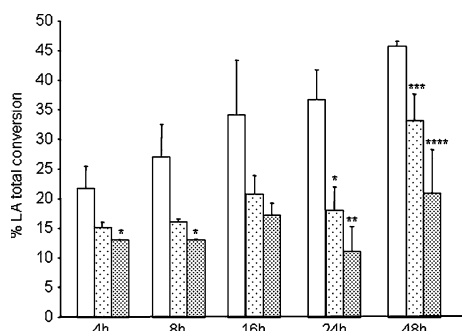
	Control	0.005 C	0.01 C	0.015 C	0.02 C
18:3	2.51 ± 0.15	2.14 ± 0.04	1.84 ± 0.16***	0.43 ± 0.43***	0.86 ± 0.15****
20:4	17.79 ± 2.01	14.56 ± 2.29	8.35 ± 1.16****	6.77 ± 2.49*	2.50 ± 0.58****
20:3	21.62 ± 0.56	23.03 ± 2.55	20.24 ± 0.96	20.65 ± 1.29	15.23 ± 0.88****
22:4	1.55 ± 0.33	1.46 ± 0.55	0.61 ± 0.16**	0.50 ± 0.50	0.19 ± 0.09****

Values are the mean ± SD ( $n = 7$ ). C cigarettes. Differences are significantly different from control at: \*  $p < 0.05$ , \*\*  $p < 0.01$ , \*\*\*  $p < 0.005$ , \*\*\*\*  $p < 0.001$

**Table 2** Relative percentage of the radioactivity associated to different lipid classes, in THP-1 cells treated with increasing concentrations of serum exposed to cigarette smoke, after [1-<sup>14</sup>C] linoleic acid incubation

Lipid classes	Control	0.01 cigarettes	0.02 cigarettes
PL	77.34 ± 4.18	75.88 ± 3.56	73.07 ± 3.22
DAG	2.02 ± 0.22	2.00 ± 0.33	1.64 ± 0.28
FFA	0.29 ± 0.04	0.31 ± 0.02	0.32 ± 0.06
TG	19.78 ± 4.09	21.28 ± 3.39	24.14 ± 2.96
CE	0.57 ± 0.08	0.53 ± 0.14	0.84 ± 0.22

Values are the mean ± SD ( $n = 3$ ). PL phospholipids, DAG diglycerides, FFA free fatty acids, TG triglycerides, CE cholesterol esters.

**Fig. 7** [1-<sup>14</sup>C] linoleic acid (LA) total conversion in THP-1 cells treated with serum exposed to cigarette smoke (0.010–0.020 cigarettes) for different time periods (4–8–16–24–48 h). The results are expressed as percentage of total LA conversion and represent mean ± SE of three independent experiments. Differences are significantly different from control at \*  $p < 0.05$ ; \*\*  $p < 0.03$ ; \*\*\*  $p < 0.01$ ; \*\*\*\*  $p < 0.001$  (open bar) control; (sparsely dotted bar) 0.010 cigarettes; (dotted bar) 0.020 cigarettes

10.66 ± 0.70% in control cells to 6.21 ± 0.09% and 4.00 ± 0.00% with 0.01 and 0.02 cigarettes, respectively. On the contrary, in FFA the incorporation of acetate increases from 0.59 ± 0.15% in control cells to 0.84 ± 0.35% with 0.01 cigarettes, and to 1.06 ± 0.04% with 0.02 cigarettes. In addition, there is an increase of acetate incorporation in TG and CE, although not significant.

**Table 3** Relative percentage of radioactivity associated to different lipid classes, after treatment of THP-1 cells with different concentrations of serum exposed to cigarette smoke, after incubation with [1-<sup>14</sup>C] acetic acid sodium salt. Also the radioactivity for mg of total lipids is shown

Lipid classes	Control	0.01 cigarettes	0.02 cigarettes
cpm/mg TL × 1000	11,996	11,867	10,791
% Recovered radioactivity			
CE	0.84 ± 0.22	1.11 ± 0.20	2.08 ± 0.97
TG	6.05 ± 0.51	12.02 ± 4.40	18.61 ± 8.12
FFA	0.59 ± 0.15	0.84 ± 0.35	1.06 ± 0.04*
MG	0.75 ± 0.11	1.05 ± 0.09	0.80 ± 0.00
Cho	10.66 ± 0.70	6.21 ± 0.09*	4.00 ± 0.00*
DAG	1.55 ± 0.14	1.83 ± 0.29	1.79 ± 0.00
PL	79.57 ± 0.16	76.95 ± 5.23	69.81 ± 10.98

Values are the mean ± SD ( $n = 3$ ). TL total lipids; CE cholesterol esters; TG triglycerides, FFA free fatty acids, MG monoglycerides, Cho cholesterol, DAG diglycerides, PL phospholipids. Differences are significantly different from control at \*  $p \leq 0.05$

## Discussion

In order to expose THP-1 cells to CS the method of Bernhard et al. [21], modified by Marangoni et al. [15], was used. This method allows one to prepare an FBS containing the CS constituents similar in concentration and distribution to the in vivo situation [21]. The procedure was also standardized in our laboratory measuring the concentration of phenol derivatives and peroxidation products, that have been reported in CS [27], in relation to the number of cigarettes used.

In our experimental model, CS has a dose-dependent effect on the inhibition of cell proliferation: CS modifies the cell cycle with a significant reduction of the number of cells in synthesis and mitosis phases only at the concentration of 0.04 cigarettes. For this reason we have used (as the highest) the concentration of 0.02 cigarettes to evaluate the effects on LA conversion and on desaturation steps; at this concentration in fact, cell proliferation is inhibited, but apoptotic and necrotic processes are not observed.

CS inhibits the total conversion of LA (calculated as the sum of the percentages of the radioactivity associated to its derivatives, 18:3, 20:3, 20:4 and 22:4n–6) to its derivatives in a concentration-dependent manner; both  $\Delta 5$  and  $\Delta 6$  desaturations are also decreased. The inhibition of LA conversion by CS occurs starting from 4 h when the highest concentration is used, whereas the use of 0.01 cigarette inhibits LA conversion starting from 24 h of incubation. Our data are in accordance with those of Marangoni et al. [15] who have investigated the effects of CS on the n–3 FA pathway and reported that the incubation of mammary gland cells with SE-FBS determined a significant reduction of DHA production from  $\alpha$ -LNA and also a decrease of the 20:5/20:4n–3 ratio (an index of  $\Delta 5$  desaturase activity), in a dose-dependent manner [14, 15].

In addition, the decreased LA conversion and AA production that we have reported could explain the inhibition or reduction of eicosanoid synthesis observed both in vitro and in vivo in certain studies [28, 29].

In vivo studies concerning the effects of CS on PUFA metabolism are scarce. Pawlosky et al. [18] have evaluated the metabolism of deuterated LA in smoking and non-smoking subjects: in smokers there was a decrease (–37%) of the 20:3n–6 conversion to 20:4, with a reduction in the  $\Delta 5$  desaturation. Simon et al. [30] have also found a positive correlation between smoking and the levels of 20:3n–6 in PL, and negative correlations between smoking and arachidonic acid levels in PL and CE. It would appear therefore that in smokers the  $\Delta 5$  desaturation step is mainly affected in vivo but in vitro also the  $\Delta 6$  desaturation step is reduced.

$\Delta 5$  and  $\Delta 6$  desaturases are microsomal enzymes; they contain a N-terminal domain that is orthologous to the microsomal cytochrome *b*<sub>5</sub> [31], and it has been proposed that the cytochrome *b*<sub>5</sub> domain allows cytochrome *b*<sub>5</sub> reductase to transfer electrons to the catalytic domain of the desaturase and thereby eliminate the need for cytochrome *b*<sub>5</sub> protein per se [32]. It has been demonstrated that the content of cytochrome *b*<sub>5</sub> and the activity of its reductase were significantly reduced in animal (ferrets and mice) liver microsomes after exposure to tobacco smoke [33, 34]. This can explain the reduction of both  $\Delta 5$  and  $\Delta 6$  desaturations and consequently the decreased conversion of LA to its long chain derivatives, after CS exposure.

Our results show also that the relative percentage of the radioactivity associated to different lipid classes, after [1-<sup>14</sup>C] LA incubation, after exposure to different CS concentrations, is not significantly modified. This is somewhat predictable, since in THP–1 cells, at difference from hepatocytes, mainly characterized by metabolic functions, the endogenous FA pool is typically structural, and therefore accumulation of FA in storage lipids represents a minor pathway possibly less affected by CS [35].

Furthermore, CS increases significantly the FFA, and also TG and CE levels, while concomitantly reducing the conversion of acetate to cholesterol, in THP–1 cells. This is in accordance with the in vivo studies that have shown higher TG levels in plasma of smokers when compared to non-smokers [36, 37]. In addition, Maehira et al. [38] demonstrated a decreased activity of rat aortic cholesteryl ester hydrolases with a consequent increase in the CE content, after CS exposure. A shift of biosynthetic processes from acetate, in particular from the new cholesterol synthesis to the production of FFA and their final incorporation in TG and CE could be hypothesized.

Concerning the CS components responsible for the inhibition of LC-PUFA metabolism, Marangoni et al. [15] have found that cigarette smoke itself, and serum or buffer exposed to CS, contain mainly acetaldehyde, nicotine, limonene and phenol derivatives (2-methyl-phenol, 4-methyl-phenol and 2-methoxy-phenol) as typical components, and therefore the treatment of cells with a CS exposed serum reflects the effect of CS that occurs in smoking subjects. We have found that nicotine alone does not affect the LA metabolism (data not shown), which, therefore, appear to be affected by other CS components.

In conclusion, in THP–1 cells, CS inhibits the conversion of LA, the major PUFA in our diets, and the 18:3/18:2n–6 and 20:4/20:3n–6 product/precursor ratios, as an index of modified  $\Delta 6$  and  $\Delta 5$  activities. This is not directly related to a major cellular damage induced by CS at the concentration used (i.e., inhibition of cell viability and proliferation), as shown by our data. Therefore we hypothesize that the effect of CS on LA conversion is due to an inhibition of the desaturases possibly related to changes in their expression, a task for future studies.

## References

1. Church D, Pryor W (1985) Free-radical chemistry of cigarette smoke and its toxicological implications. *Environ Health Perspect* 64:111–126
2. Do B, Garewal H, Clements N, Peng Y, Habib M (1996) Exhaled ethane and antioxidant vitamin supplements in active smokers. *Chest* 110:159–164
3. Halliwell B (1993) Cigarette smoking and health: a radical view. *J R Soc Health* 113:91–96
4. Reddy R, Yao J (2003) Environmental factors and membrane polyunsaturated fatty acids in schizophrenia. *Prostaglandins Leukot Essent Fatty Acids* 69:385–391
5. Brenner RR (1989) Factors influencing fatty acid chain elongation and desaturation. In: Vergroessen AJ, Crawford M (edn) *The role of fats in human nutrition*, 2nd eds. Academic, London, pp 45–79
6. Melin T, Nilsson A (1997) Delta-6-desaturase and delta-5-desaturase in human HepG2 cells are both fatty acid interconversion rate limiting and are up regulated under essential fatty acid deficient conditions. *Prostaglandins Leukot Essent Fatty Acids* 56(6):437–442

7. Peluffo RO, Nervi AM, Brenner RR (1976) Linoleic acid desaturation activity of liver microsomes of essential fatty acid deficient and sufficient rats. *Biochim Biophys Acta* 441(1):25–31
8. Brenner RR (2003) Hormonal modulation of delta 6 and delta 5 desaturases: case of diabetes. *Prostaglandins Leukot Essent Fatty Acids* 68(2):151–162
9. Kawashima Y, Musoh K, Kozuka H (1990) Peroxisome proliferators enhance linoleic acid metabolism in rat liver. *J Biol Chem* 265(16):9170–9175
10. Risé P, Ghezzi S, Levati MG, Mirtini R, Colombo C, Galli C (2003) Pharmacological modulation of fatty acid desaturation and of cholesterol biosynthesis in THP-1 cells. *Lipids* 38(8):841–846
11. Risé P, Camera M, Caruso D, Ghezzi S, Visioli F, Galli C (2004) Synthesis of long-chain polyunsaturated fatty acids is inhibited in vivo in hypercholesterolemic rabbits and in vitro by oxysterols. *Prostaglandins Leukot Essent Fatty Acids* 71:79–86
12. Risé P, Colombo C, Galli C (1997) Effects of simvastatin on the metabolism of polyunsaturated fatty acids and on glycerolipid, cholesterol, and de novo lipid synthesis in THP-1 cells. *J Lipid Res* 38:1299–1307
13. Risé P, Ghezzi S, Galli C (2003) Relative potencies of statins in reducing cholesterol synthesis and enhancing linoleic acid metabolism. *Eur J Pharmacol* 467:73–75
14. Risé P, Marangoni F, Galli C (2002) Regulation of PUFA metabolism: pharmacological and toxicological aspects. *Prostaglandins Leukot Essent Fatty Acids* 67(2–3):85–89
15. Marangoni F, Colombo C, De Angelis L, Gambaro V, Agostoni C, Giovannini M, Galli C (2004) Cigarette smoke negatively and dose-dependently affects the biosynthetic pathway of the n-3 polyunsaturated fatty acid series in human mammary epithelial cells. *Lipids* 39:633–637
16. Agostoni C, Marangoni F, Giovannini M, Riva E, Galli C (1998) Long-chain polyunsaturated fatty acids, infant formula, and breast feeding. *Lancet* 352:1703–1704
17. Agostoni C, Galli C, Riva E, Colombo C, Giovannini M, Marangoni F (2005) Reduced docosahexaenoic acid synthesis may contribute to growth restriction in infants born to mothers who smoke. *J Pediatr* 147(6):854–856
18. Pawlosky R, Hibbeln J, Wegher B, Sebring N, Salem Jr N (1999) The effects of cigarette smoking on the metabolism of essential fatty acids. *Lipids* 34 (supplement)
19. Das UN (2006) Essential fatty acids: biochemistry, physiology and pathology. *Biotechnol J* 1(4):420–439
20. Tsuchiya S, Yamabe M, Yamaguchi Y, Kobayashi Y, Konno T, Toda K (1980) Establishment and characterization of a human acute monocytic leukemia cell line (THP-1). *Int J Cancer* 26:171–176
21. Bernhard D, Huck CW, Jakschitz T, Pfister G, Henderson B, Bonn GK, Wick G (2004) Development and evaluation of an in vitro model for the analysis of cigarette smoke effects on cultured cells and tissues. *J Pharmacol Toxicol Methods* 50:45–51
22. Folch J, Lees M, Sloane Stanley GH (1957) A simple method for the isolation and purification of total lipids from animal tissue. *J Biol Chem* 226:497–509
23. Caruso D, Visioli F, Patelli R, Galli C, Galli G (2001) Urinary excretion of olive oil phenols and their metabolites in humans. *Metabolism* 50(12):1426–1428
24. Visioli F, Vinceri FF, Galli C (1995) Waste waters' from olive oil production are rich in natural antioxidants. *Experientia* 51:32–34
25. Balla G, Jacob HS, Eaton JW, Belcher JD, Vercellotti GM (1991) Hemin: a possible physiological mediator of low density lipoprotein oxidation and endothelial injury. *Arterioscler Thromb* 11(6):1700–1711
26. Abbracchio MP, Ceruti S, Barbieri D, Franceschi C, Malorni W, Biondo L, Burnstock G, Cattabeni F (1995) A novel action for adenosine : apoptosis of astroglial cells in rat brain primary cultures. *Biochem Biophys Res Commun* 213:908–915
27. Van der Vaart H, Postma DS, Timens W, Ten Hacken NHT (2004) Acute effects of cigarette smoke on inflammation and oxidative stress: a review. *Thorax* 59:713–721
28. Sugano N, Shimada K, Ito K, Murai S (1998) Nicotine inhibits the production of inflammatory mediators in U937 cells through modulation of nuclear factor-kappaB activation. *Biochem Biophys Res Comm* 252:25–28
29. Laviolette M, Chang J, Newcombe DS (1981) Human alveolar macrophages: a lesion in arachidonic acid metabolism in cigarette smokers. *Am Rev Respir Dis* 124:397–401
30. Simon JA, Fong J, Bernert JT Jr, Browner WS (1996) Relation of smoking and alcohol consumption to serum fatty acids. *Am J Epidemiol* 144:325–334
31. Napier JA, Michaelson LV, Sayanova O (2003) The role of cytochrome *b*<sub>5</sub> fusion desaturases in the synthesis of polyunsaturated fatty acids. *Prostaglandins Leukot Essent Fatty Acids* 68:135–143
32. Cho HP, Nakamura M, Clarke SD (1999) Cloning, expression, and fatty acid regulation of the human Δ-5 desaturase. *J Biol Chem* 274(52):37335–37339
33. Sindhu RK, Rasmussen RE, Yamamoto R, Fujita I, Kikkawa Y (1995) Depression of hepatic cytochrome P450 monooxygenases after chronic environmental tobacco smoke exposure of young ferrets. *Toxicol Lett* 76:227–238
34. Villard P, Seree EM, Re J, De Meo M, Barra Y, Attolini L, Dumenil G, Catalin J, Durand A, Lacarelle B (1998) Effects of tobacco smoke on the gene expression of the Cyp1a, Cyp2b, Cyp2e, Cyp3a subfamilies in mouse liver and lung: relation to single strand breaks of DNA. *Toxicol Appl Pharmacol* 148:195–204
35. Risé P, Ghezzi S, Priori I, Galli C (2005) Differential modulation by simvastatin of the metabolic pathways in the n-9, n-6, and n-3 fatty acid series in human monocytic and hepatocytic cell lines. *Biochem Pharmacol* 69:1095–1100
36. Gokkusu C, Ademoglu E, Tamer S, Alkan G (2001) Oxidant-antioxidant profiles of platelet rich plasma in smokers. *Addict Biol* 6(4):325–330
37. Whig J, Singh CB, Soni GL, Bansal AK (1992) Serum lipids & lipoprotein profiles of cigarette smokers & passive smokers. *Indian J Med Res* 96:282–287
38. Maehira F, Zaha F, Miyagi I, Tanahara A, Noho A (2000) Effects of passive smoking on the regulation of rat aortic cholesteryl ester hydrolases by signal transduction. *Lipids* 35(5):503–511



# Cytochrome P450-Dependent Metabolism of Vitamin E Isoforms is a Critical Determinant of Their Tissue Concentrations in Rats

Chisato Abe · Tomono Uchida · Moeka Ohta ·  
Tomio Ichikawa · Kanae Yamashita · Saiko Ikeda

Received: 10 January 2007 / Accepted: 10 April 2007 / Published online: 23 May 2007  
© AOCS 2007

**Abstract** The aim of this study was to clarify the contribution of cytochrome P450 (CYP)-dependent metabolism of vitamin E isoforms to their tissue concentrations. We studied the effect of ketoconazole, a potent inhibitor of CYP-dependent vitamin E metabolism in cultured cells, on vitamin E concentration in rats. Vitamin E-deficient rats fed a vitamin E-free diet for 4 weeks were administered by oral gavage a vitamin E-free emulsion, an emulsion containing  $\alpha$ -tocopherol,  $\gamma$ -tocopherol or a tocotrienol mixture with or without ketoconazole.  $\alpha$ -Tocopherol was detected in the serum and various tissues of the vitamin E-deficient rats, but  $\gamma$ -tocopherol,  $\alpha$ - and  $\gamma$ -tocotrienol were not detected. Ketoconazole decreased urinary excretion of 2,5,7,8-tetramethyl-2(2'-carboxyethyl)-6-hydroxychroman after  $\alpha$ -tocopherol or a tocotrienol mixture administration, and that of 2,7,8-trimethyl-2(2'-carboxyethyl)-6-hydroxychroman ( $\gamma$ -CEHC) after  $\gamma$ -tocopherol or a tocotrienol mixture administration. The  $\gamma$ -tocopherol,  $\alpha$ - and  $\gamma$ -tocotrienol concentrations in the serum and various tissues at 24 h after their administration were elevated by ketoconazole, while the  $\alpha$ -tocopherol concentration was not affected. The  $\gamma$ -tocopherol or  $\gamma$ -tocotrienol concentration in the jejunum at 3 h after each administration was also elevated by ketoconazole. In addition, significant amount of  $\gamma$ -CEHC was in the jejunum at 3 h after  $\gamma$ -tocopherol or

$\gamma$ -tocotrienol administration, and ketoconazole inhibited  $\gamma$ -tocopherol metabolism to  $\gamma$ -CEHC in the jejunum. These results showed that CYP-dependent metabolism of  $\gamma$ -tocopherol and tocotrienol is a critical determinant of their concentrations in the serum and tissues. The data also suggest that some amount of dietary vitamin E isoform is metabolized by a CYP-mediated pathway in the intestine during absorption.

**Keywords** Cytochrome P450 · Ketoconazole · Rats · Tocopherol · Tocotrienol · Vitamin E

## Abbreviations

$\alpha$ -CEHC	2,5,7,8-Tetramethyl-2(2'-carboxyethyl)-6-hydroxychroman
$\gamma$ -CEHC	2,7,8-Trimethyl-2(2'-carboxyethyl)-6-hydroxychroman
CYP	Cytochrome P450
$\alpha$ -TTP	$\alpha$ -Tocopherol transfer protein

## Introduction

Vitamin E is a potent fat-soluble antioxidant that inhibits lipid peroxidation in biological membranes. In nature, compounds with vitamin E activity are  $\alpha$ -,  $\beta$ -,  $\gamma$ - or  $\delta$ -tocopherol and  $\alpha$ -,  $\beta$ -,  $\gamma$ - or  $\delta$ -tocotrienol. Dietary vitamin E isoforms are absorbed in the intestine and secreted with triacylglycerol-rich chylomicron into lymph and blood [1, 2]. After lipolysis of chylomicron triacylglycerol by lipoprotein lipase, vitamin E isoforms are transported to the liver [3].  $\alpha$ -Tocopherol transfer protein ( $\alpha$ -TTP) in the liver catalyzes  $\alpha$ -tocopherol secretion by a non-Golgi-mediated

C. Abe · T. Uchida · M. Ohta · T. Ichikawa ·  
S. Ikeda (✉)  
Department of Nutritional Sciences,  
Nagoya University of Arts and Sciences, 57 Takenoyama,  
Iwasaki, Nissin 470-0196, Japan  
e-mail: saiko@nuas.ac.jp

K. Yamashita  
Department of Food and Nutrition,  
Sugiyama Jogakuen University, Nagoya 464-8662, Japan

pathway, and  $\alpha$ -tocopherol is incorporated into VLDL and subsequently transported to the various tissues by lipoproteins [4, 5]. The other isoforms of vitamin E such as  $\gamma$ -tocopherol and tocotrienol are metabolized and excreted because their affinity for  $\alpha$ -TTP is much lower than that of  $\alpha$ -tocopherol [6]. Therefore, the  $\gamma$ -tocopherol and tocotrienol levels in the serum and tissues are extremely low. The importance of  $\alpha$ -TTP for the vitamin E distribution is also shown by the extremely low level of  $\alpha$ -tocopherol in plasma of the patients who have ataxia with vitamin E deficiency due to mutations in the  $\alpha$ -TTP gene [7] and in plasma and various tissues of  $\alpha$ -TTP-knockout mice [8, 9].

Vitamin E isoforms are known to undergo metabolism to phytyl chain-shortened metabolites, such as 2,5,7,8-tetramethyl-2(2'-carboxyethyl)-6-hydroxychroman ( $\alpha$ -CEHC) and 2,7,8-trimethyl-2(2'-carboxyethyl)-6-hydroxychroman ( $\gamma$ -CEHC), excreted into urine in human [10–12] and rats [13–15]. Pathway of the metabolism involves  $\omega$ -hydroxylation of phytyl chain and the following  $\beta$ -oxidation [16, 17], and the rate-limiting step is  $\omega$ -hydroxylation by cytochrome P450 (CYP) 4F [17, 18]. Ketoconazole, an imidazole antifungal agent, is known as a potent inhibitor of human CYP3A [19], and also inhibits the CYP4F-dependent vitamin E metabolism in cultured cells [20, 21]. Parker et al. [20] reported that ketoconazole inhibited the production of  $\gamma$ - and  $\delta$ -tocopherol metabolites in HepG2 cells, human hepatoblastoma, and that of  $\alpha$ - and  $\gamma$ -tocopherol metabolites in rat primary hepatocytes. You et al. [21] also reported that  $\delta$ -tocotrienol metabolite production was inhibited by ketoconazole in A549 cells, human lung epithelial cells. However, it is not known whether vitamin E metabolism affects tissue concentrations of vitamin E isoforms in vivo because their low affinity for  $\alpha$ -TTP is a critical role for their concentrations in the tissues. In this study, we examined the contribution of CYP-dependent metabolism of vitamin E isoforms to their concentrations in rat tissues using ketoconazole.

## Experimental Procedures

### Materials

RRR- $\alpha$ -Tocopherol, RRR- $\gamma$ -tocopherol and a tocotrienol mixture extracted from natural source were used for oral administration. The tocotrienol mixture composition was 339 mg/g  $\alpha$ -tocotrienol, 40 mg/g  $\beta$ -tocotrienol, 471 mg/g  $\gamma$ -tocotrienol, 110 mg/g  $\delta$ -tocotrienol and 1 mg/g RRR- $\delta$ -tocopherol.  $\alpha$ -,  $\beta$ - and  $\gamma$ -tocopherol were not detected in the mixture. Vitamin E,  $\alpha$ - and  $\gamma$ -CEHC were generously donated by Eisai Food and Chemical (Tokyo, Japan). Ketoconazole was purchased from Sigma (Tokyo, Japan). It was dissolved in ethanol and used for oral administration.

### Animals and Diets

Male Wistar rats (6 weeks old) were purchased from Japan SLC (Shizuoka, Japan) and maintained at 23 °C with a 12-h light cycle (lights on from 08:00 to 20:00 h). Before the start of the Experiments 1 and 2, rats were fed a vitamin E-free diet for 4 weeks to deplete tissue  $\alpha$ -tocopherol stores because it is difficult to be elevate the other isoform concentrations in  $\alpha$ -tocopherol-rich tissues. The composition of the vitamin E-free diet was as follows; 200 g casein/kg, 3 g L-cystine/kg, 35 g mineral mixture (AIN93-MX)/kg [22], 10 g vitamin mixture (vitamin E-free AIN93-VX)/kg [22], 2.5 g choline/kg, 70 g vitamin E-stripped corn oil/kg, 50 g cellulose powder/kg, 100 g sucrose/kg, 529.5 g corn starch/kg. This study was approved by the Laboratory Animal Care Committee of Nagoya University of Arts and Sciences, and all procedures were performed in accordance with the Animal Experimentation Guidelines of Nagoya University of Arts and Sciences.

### Experiment 1

Rats were administered an oral gavage of 1 ml of vitamin E-free emulsion (control group,  $n = 5$ ), vitamin E-free emulsion containing 50 mg ketoconazole/kg body weight (KCZ group,  $n = 5$ ), 10 mg of  $\alpha$ -tocopherol ( $\alpha$ T group,  $n = 5$ ), 10 mg of  $\alpha$ -tocopherol and 50 mg ketoconazole/kg body weight ( $\alpha$ T + KCZ group,  $n = 5$ ), 10 mg of  $\gamma$ -tocopherol ( $\gamma$ T group,  $n = 5$ ), 10 mg of  $\gamma$ -tocopherol and 50 mg ketoconazole/kg body weight ( $\gamma$ T + KCZ group,  $n = 7$ ), 29.5 mg of tocotrienol mixture (T3 group,  $n = 5$ ), or 29.5 mg of tocotrienol mixture and 50 mg ketoconazole/kg body weight (T3 + KCZ group,  $n = 5$ ). All the emulsions also contained 200 mg of sodium taurocholate and 200 mg of triolein. The rats had access to food until the oral administration and were deprived of food after the administration.

Twenty four hours after the oral administration, the rats were killed by decapitation, and the serum, liver, adrenal gland, spleen, lung, kidney, heart, thymus, soleus muscle, perirenal adipose tissue, epididymal fat, skin, brain and aorta were removed and stored at  $-80$  °C. The upper one-third section ( $\sim 25$  cm) of the small intestine between the stomach and cecum was taken and the upper 5 cm was cut off as the duodenum. The remaining section was sampled as jejunum and washed twice with 10 ml of saline using a syringe. The fluid was removed from jejunum with paper and stored at  $-80$  °C. For the last 12 h, the urine was collected in a test tube kept cool with dry ice as soon as the rats urinated on a plastic tray under each wire screen-bottomed cage. The urine was stored at  $-80$  °C under nitrogen until used for the determination of  $\alpha$ -CEHC and  $\gamma$ -CEHC concentrations.

## Experiment 2

Rats were administered an oral gavage of 1 ml of emulsion containing 10 mg of  $\alpha$ -tocopherol ( $\alpha$ T group,  $n = 18$ ), 10 mg of  $\alpha$ -tocopherol and 50 mg ketoconazole/kg body weight ( $\alpha$ T + KCZ group,  $n = 18$ ), 10 mg of  $\gamma$ -tocopherol ( $\gamma$ T group,  $n = 18$ ), 10 mg of  $\gamma$ -tocopherol and 50 mg ketoconazole/kg body weight ( $\gamma$ T + KCZ group,  $n = 18$ ), 29.5 mg of tocotrienol mixture (T3 group,  $n = 18$ ), or 29.5 mg of tocotrienol mixture and 50 mg ketoconazole/kg body wt (T3 + KCZ group,  $n = 18$ ). All emulsion also contained 200 mg of sodium taurocholate and 200 mg of triolein. The rats were deprived of food for 12 h until oral administration of the emulsion. At 0.5, 1 or 3 h after the oral administration, six rats of each group were anesthetized with diethyl ether, and the blood was drawn from the heart using a heparinized needle and syringe. The jejunum and liver were sampled and handled as described for Experiment 1.

## Experiment 3

Male Wistar rats (10 weeks old) were fed a commercial diet (CE-2, Clea Japan, Tokyo, Japan) for 5 days and deprived of food for the last 12 h. The rats were administered an oral gavage of 1 ml of emulsion containing 10 mg of  $\gamma$ -tocopherol ( $\gamma$ T group,  $n = 4$ ), 10 mg of  $\gamma$ -tocopherol and 50 mg ketoconazole/kg body weight ( $\gamma$ T + KCZ group,  $n = 4$ ), 29.5 mg of tocotrienol mixture (T3 group,  $n = 4$ ) or 29.5 mg of tocotrienol mixture and 50 mg ketoconazole/kg body wt (T3 + KCZ group,  $n = 4$ ). All emulsions also contained 200 mg of sodium taurocholate and 200 mg of triolein. At 3 h after each administration, the rats were anesthetized with diethyl ether, and the blood was drawn from the heart using a heparinized needle and syringe. The jejunum and liver were sampled and handled as described for Experiment 1.

## Vitamin E Concentration

Tissues were homogenized in distilled water. The tissue homogenate (0.5 ml) was put in a test tube, and 0.5 ml of ethanol containing 60 g/l pyrogallol and 0.45  $\mu$ g of 2,2,5,7,8-pentamethyl-6-chroman as an internal standard were added. Then, 0.1 ml of 600 g/l potassium hydroxide was added and saponified at 70 °C for 30 min. After the addition of 2.25 ml of 20 g/l sodium chloride, tocopherols and tocotrienols were extracted with 0.5 ml of hexane containing 10% (v/v) ethyl acetate. Serum (75  $\mu$ l) was put in a test tube, and 90 ng of 2,2,5,7,8-pentamethyl-6-chroman as an internal standard was added. After the addition of 0.5 ml of water and 1.0 ml of ethanol, vitamin E was extracted with 5 ml of hexane. Vitamin E concentration

was determined by HPLC [23]. The instrumentation used for HPLC was a Shimadzu LC-10AD (Shimadzu, Kyoto, Japan) with a Shimadzu RF-10AXL fluorescence detector (excitation 298 nm, emission 325 nm). The analytical column used was a Wakosil 5SIL (4.6  $\times$  250 mm, Wako Pure Chemical Industries, Osaka, Japan). The mobile phase was hexane containing 1% (v/v) dioxane and 0.2% (v/v) isopropyl alcohol with a flow rate of 1 ml/min.

## $\alpha$ - and $\gamma$ -CEHC Concentrations

Both conjugated and unconjugated  $\alpha$ - and  $\gamma$ -CEHC in the urine and jejunum were methylated and extracted by the method of Kiyose et al. [24], and the concentration was determined using HPLC with an electrochemical detector. One milliliter of the urine diluted with distilled water, or the jejunum homogenate with distilled water was added to 0.1 ml of 500 g/l ascorbic acid and 1 ml of 0.54 mmol/l EDTA. The sample was methylated in 3 mol/l methanolic hydrochloric acid at 60 °C for 1 h under nitrogen, and the methylated vitamin E metabolite was extracted with hexane. The hexane was evaporated by nitrogen, and the residue was dissolved in 200  $\mu$ l of 45% (v/v) acetonitrile containing 50 mmol/l sodium perchlorate; 10  $\mu$ l of this solution was subjected to HPLC. Instrumentation used for HPLC was a Shimadzu LC-10Ai with a Coulochem III electrochemical detector (MC Medical, Osaka, Japan) and an ODS-3 column (250 mm  $\times$  2.1 mm, GL Science, Tokyo, Japan). The mobile phase was 45% (v/v) acetonitrile containing 50 mmol/l sodium perchlorate, pH 3.6, and the flow rate was 0.2 ml/min. For coulometric detection, the analytical and guard cells were set to +0.4 and +0.45 V, respectively.

## Statistical Analysis

Data are presented as mean values  $\pm$  SEM,  $n = 5$  or 7 in Experiment 1,  $n = 6$  in Experiment 2, and  $n = 4$  in Experiment 3. They were analyzed by two-way ANOVA with Tukey's post-hoc test (Graph Pad Prism for Windows version 4.0, GraphPad Software Inc, CA, USA). When variances among groups were unequal, the data were logarithmically transformed before statistical analysis by two-way ANOVA. Differences were regarded as significant at  $P$ -value  $< 0.05$ .

## Results

### Experiment 1

Neither vitamin E ( $P \geq 0.05$ ) nor ketoconazole ( $P \geq 0.05$ ) administration affected the body and relative liver weights

(Table 1). Urinary excretion of  $\alpha$ -CEHC in the  $\alpha$ T + KCZ group was 5% ( $P < 0.05$ ) that in the  $\alpha$ T group. The  $\gamma$ -CEHC excretion in the  $\gamma$ T + KCZ was 17% ( $P < 0.05$ ) that in the  $\gamma$ T group. The  $\alpha$ - and  $\gamma$ -CEHC excretion in the T3 + KCZ group was 27% ( $P < 0.05$ ) and 57% ( $P < 0.05$ ) those in the T3 group, respectively.

The  $\alpha$ -tocopherol concentrations in the serum, liver, jejunum, kidney, adrenal gland, lung, heart, spleen, thymus, aorta and muscle of the  $\alpha$ T and  $\alpha$ T + KCZ groups did not differ, although those of the  $\alpha$ T group were higher ( $P < 0.05$ ) than those of the control group (Table 2).  $\gamma$ -Tocopherol,  $\alpha$ - and  $\gamma$ -tocotrienol were not detected in the serum and tissues of the control and KCZ groups. The  $\gamma$ -tocopherol concentration in the serum, liver, jejunum, kidney, adrenal gland, lung, heart, spleen, thymus, brain and muscle of the  $\gamma$ T + KCZ group was higher ( $P < 0.05$ ) than that of the  $\gamma$ T group (Table 3). The  $\alpha$ -tocotrienol concentration in the heart, thymus and muscle of the T3 group was higher ( $P < 0.05$ ) than the  $\gamma$ -tocopherol concentration in those tissues of the  $\gamma$ T group. The  $\alpha$ -tocotrienol concentration in the serum, liver, jejunum, kidney, adrenal gland, lung, spleen and brain of the T3 + KCZ group was higher ( $P < 0.05$ ) than that of the T3 group. The  $\gamma$ -tocotrienol concentration in the jejunum, heart and muscle of the T3 group and the  $\gamma$ -tocopherol concentrations of the  $\gamma$ T group did not differ ( $P \geq 0.05$ ), while the  $\gamma$ -tocotrienol concentration in the tissues of the T3 group was lower ( $P < 0.05$ ) than the  $\alpha$ -tocotrienol concentration. The  $\gamma$ -tocotrienol concentration in the liver, jejunum, kidney, adrenal gland, lung, heart, spleen, thymus and muscle of the T3 + KCZ group was higher ( $P < 0.05$ ) than that of the T3 group.

## Experiment 2

Jejunum  $\alpha$ -tocopherol concentrations of the  $\alpha$ T and  $\alpha$ T + KCZ groups at 0.5, 1 and 3 h did not differ ( $P \geq 0.05$ ) (Fig. 1A). The  $\alpha$ -tocopherol concentrations in the plasma (Fig. 1B) and liver (Fig. 1C) of the  $\alpha$ T and  $\alpha$ T + KCZ groups were elevated ( $P < 0.05$ ) at 3 h. Ketoconazole did not affect ( $P \geq 0.05$ ) the  $\alpha$ -tocopherol concentrations in the jejunum, plasma and liver. The jejunum  $\gamma$ -tocopherol concentration of the  $\gamma$ T group was lowered ( $P < 0.05$ ) at 3 h, but the  $\gamma$ -tocopherol concentration of the  $\gamma$ T + KCZ group was not changed ( $P \geq 0.05$ ) for 3 h (Fig. 1D). The  $\gamma$ -tocopherol concentration of the  $\gamma$ T + KCZ group at 3 h was 464% that of the  $\gamma$ T group. The  $\gamma$ -tocopherol concentration in the plasma (Fig. 1E) and liver (Fig. 1F) was not affected ( $P < 0.05$ ) by ketoconazole. Ketoconazole did not significantly change ( $P \geq 0.05$ ) the  $\alpha$ -tocotrienol concentration in the jejunum (Fig. 2A), plasma (Fig. 2B) and liver (Fig. 2C), but elevated ( $P < 0.05$ ) the  $\gamma$ -tocotrienol concentration in the jejunum

**Table 1** Body and relative liver weights,  $\alpha$ - and  $\gamma$ -CEHC excretion into urine of rats administered a vitamin E-free emulsion (control), an emulsion containing ketoconazole (KCZ),  $\alpha$ -tocopherol ( $\alpha$ T),  $\alpha$ -tocopherol with ketoconazole ( $\alpha$ T + KCZ),  $\gamma$ -tocopherol ( $\gamma$ T),  $\gamma$ -tocopherol with ketoconazole ( $\gamma$ T + KCZ), tocotrienol mixture (T3), or tocotrienol mixture with ketoconazole (T3 + KCZ), at 24 h after each administration in Experiment 1

	Control				KCZ				$\alpha$ T				$\alpha$ T + KCZ				$\gamma$ T				$\gamma$ T + KCZ				T3				T3 + KCZ				P-value			
	Vitamin E		KCZ		Vitamin E		KCZ		Vitamin E		KCZ		Vitamin E		KCZ		Vitamin E		KCZ		Vitamin E		KCZ		Vitamin E		KCZ		Vitamin E		KCZ		Vitamin E		KCZ	
Body weight (g)	333	± 6	341	± 2	337	± 1	334	± 2	338	± 2	338	± 2	329	± 3	334	± 3	336	± 3	NS	NS	NS	NS	NS	NS	NS	NS	NS	NS	NS	NS	NS	NS	NS	NS	NS	
Relative liver weight (g/kg body weight)	25.1	± 0.9	25.3	± 1.4	24.4	± 0.3	25.3	± 0.5	23.8	± 0.2	24.3	± 1.1	25.7	± 0.5	24.3	± 0.9	25.3	± 0.9	NS	NS	NS	NS	NS	NS	NS	NS	NS	NS	NS	NS	NS	NS	NS	NS	NS	
$\alpha$ -CEHC excretion (nmol/12 h)	ND	ND	ND	ND	119	± 35 <sup>b,c</sup>	6	± 4 <sup>a</sup>	ND	ND	ND	ND	150	± 25 <sup>c</sup>	40	± 11 <sup>ab</sup>	40	± 11 <sup>ab</sup>	NS	<0.001	NS	<0.001	NS	<0.001	NS	<0.001	NS	<0.001	NS	<0.001	NS	<0.001	NS	<0.001	NS	
$\gamma$ -CEHC excretion (nmol/12 h)	ND	ND	ND	ND	ND	ND	ND	1787	± 83 <sup>c</sup>	303	± 30 <sup>a</sup>	2033	± 383 <sup>c</sup>	1147	± 116 <sup>b</sup>	1147	± 116 <sup>b</sup>	<0.001	<0.001	<0.001	<0.001	<0.001	<0.001	<0.001	<0.001	<0.001	<0.001	<0.001	<0.001	<0.001	<0.001	<0.001	<0.001	<0.001	<0.001	

Values are mean  $\pm$  SEM,  $n = 5$  or 7. Mean values in a row with superscripts without a common letter differ,  $P < 0.05$

NS not significant  $P \geq 0.05$ , ND not detected

**Table 2**  $\alpha$ -Tocopherol concentration in serum ( $\mu\text{mol/l}$ ) and tissues ( $\text{nmol/g}$ ) of rats administered a vitamin E-free emulsion (control), an emulsion containing ketoconazole (KCZ),  $\alpha$ -tocopherol ( $\alpha\text{T}$ ) or  $\alpha$ -tocopherol with ketoconazole ( $\alpha\text{T} + \text{KCZ}$ ), at 24 h after each administration in Experiment 1

	Control	KCZ	$\alpha\text{T}$	$\alpha\text{T} + \text{KCZ}$	P-value		
					$\alpha\text{T}$	KCZ	$\alpha\text{T} \times \text{KCZ}$
Serum	2.8 $\pm$ 0.5 <sup>a</sup>	3.6 $\pm$ 0.2 <sup>a</sup>	35.4 $\pm$ 6.3 <sup>b</sup>	44.2 $\pm$ 6.2 <sup>b</sup>	<0.001	NS	NS
Liver	11.6 $\pm$ 0.5 <sup>a</sup>	14.8 $\pm$ 1.5 <sup>a</sup>	333 $\pm$ 42 <sup>b</sup>	459 $\pm$ 56 <sup>b</sup>	<0.001	NS	NS
Jejunum	7.8 $\pm$ 1.0 <sup>a</sup>	7.9 $\pm$ 1.4 <sup>a</sup>	118 $\pm$ 16 <sup>b</sup>	108 $\pm$ 16 <sup>b</sup>	<0.001	NS	NS
Kidney	12.6 $\pm$ 0.7 <sup>a</sup>	13.1 $\pm$ 2.0 <sup>a</sup>	26.5 $\pm$ 0.6 <sup>b</sup>	28.0 $\pm$ 1.1 <sup>b</sup>	<0.001	NS	NS
Adrenal gland	104 $\pm$ 15 <sup>a</sup>	123 $\pm$ 5 <sup>a</sup>	522 $\pm$ 23 <sup>b</sup>	552 $\pm$ 19 <sup>b</sup>	<0.001	NS	NS
Lung	9.5 $\pm$ 0.7 <sup>a</sup>	12.4 $\pm$ 0.4 <sup>b</sup>	52.1 $\pm$ 3.2 <sup>c</sup>	60.0 $\pm$ 5.4 <sup>c</sup>	<0.001	<0.05	NS
Heart	20.1 $\pm$ 1.2 <sup>a</sup>	18.2 $\pm$ 1.8 <sup>a</sup>	39.8 $\pm$ 1.6 <sup>b</sup>	42.1 $\pm$ 2.1 <sup>b</sup>	<0.001	NS	NS
Spleen	20.3 $\pm$ 0.7 <sup>a</sup>	21.2 $\pm$ 1.3 <sup>a</sup>	125 $\pm$ 7 <sup>b</sup>	130 $\pm$ 6 <sup>b</sup>	<0.001	NS	NS
Thymus	7.1 $\pm$ 0.5 <sup>a</sup>	7.4 $\pm$ 1.0 <sup>a</sup>	19.5 $\pm$ 1.8 <sup>b</sup>	17.5 $\pm$ 1.6 <sup>b</sup>	<0.001	NS	NS
Brain	28.5 $\pm$ 1.9 <sup>a,b</sup>	26.5 $\pm$ 0.8 <sup>a</sup>	30.0 $\pm$ 0.4 <sup>a,b</sup>	31.8 $\pm$ 1.1 <sup>b</sup>	<0.05	NS	NS
Aorta	7.5 $\pm$ 1.1 <sup>a</sup>	7.1 $\pm$ 1.7 <sup>a</sup>	16.6 $\pm$ 2.3 <sup>b</sup>	13.7 $\pm$ 1.5 <sup>b</sup>	<0.001	NS	NS
Muscle	12.7 $\pm$ 1.0 <sup>a</sup>	12.8 $\pm$ 1.2 <sup>a</sup>	16.5 $\pm$ 0.5 <sup>b</sup>	17.3 $\pm$ 0.8 <sup>b</sup>	<0.001	NS	NS

Values are mean  $\pm$  SEM,  $n = 5$ . Mean values in a row with superscripts without a common letter differ,  $P < 0.05$

NS not significant  $P \geq 0.05$

**Table 3**  $\gamma$ -Tocopherol concentration in the serum ( $\mu\text{mol/l}$ ) and tissues ( $\text{nmol/g}$ ) of rats administered  $\gamma$ -tocopherol ( $\gamma\text{T}$ ) or  $\gamma$ -tocopherol with ketoconazole ( $\gamma\text{T} + \text{KCZ}$ ) and  $\alpha$ - and  $\gamma$ -tocotrienol concentrations of rats administered tocotrienol mixture (T3) or tocotrienol mixture with ketoconazole (T3 + KCZ), at 24 h after each administration in Experiment 1

	$\gamma$ -Tocopherol		$\alpha$ -Tocotrienol		$\gamma$ -Tocotrienol		P-value		
	$\gamma\text{T}$	$\gamma\text{T} + \text{KCZ}$	T3	T3 + KCZ	T3	T3 + KCZ	Vitamin E	KCZ	Vitamin E $\times$ KCZ
Serum	3.9 $\pm$ 0.9 <sup>b</sup>	49.8 $\pm$ 4.0 <sup>d</sup>	3.4 $\pm$ 0.8 <sup>b</sup>	13.7 $\pm$ 1.8 <sup>c</sup>	ND	0.9 $\pm$ 0.4 <sup>a</sup>	<0.001	<0.001	<0.05
Liver	32.6 $\pm$ 3.5 <sup>b,c</sup>	189 $\pm$ 24 <sup>e</sup>	20.5 $\pm$ 1.6 <sup>b</sup>	100 $\pm$ 24 <sup>d,e</sup>	2.0 $\pm$ 0.3 <sup>a</sup>	72.0 $\pm$ 28.1 <sup>c,d</sup>	<0.001	<0.001	<0.01
Jejunum	30.5 $\pm$ 3.5 <sup>a,b</sup>	141 $\pm$ 21 <sup>c</sup>	48.6 $\pm$ 10.7 <sup>b</sup>	192 $\pm$ 32 <sup>c</sup>	18.3 $\pm$ 5.4 <sup>a</sup>	181 $\pm$ 42 <sup>c</sup>	<0.05	<0.001	<0.05
Kidney	6.5 $\pm$ 0.4 <sup>b</sup>	23.2 $\pm$ 1.7 <sup>c</sup>	11.4 $\pm$ 0.8 <sup>b</sup>	34.0 $\pm$ 5.4 <sup>c</sup>	0.9 $\pm$ 0.04 <sup>a</sup>	8.4 $\pm$ 1.9 <sup>b</sup>	<0.001	<0.001	<0.05
Adrenal gland	206 $\pm$ 25 <sup>c</sup>	574 $\pm$ 35 <sup>d</sup>	162 $\pm$ 32 <sup>c</sup>	453 $\pm$ 50 <sup>d</sup>	11.1 $\pm$ 1.9 <sup>a</sup>	82.8 $\pm$ 17.2 <sup>b</sup>	<0.001	<0.001	<0.05
Lung	13.6 $\pm$ 1.5 <sup>b</sup>	56.2 $\pm$ 4.0 <sup>c</sup>	22.6 $\pm$ 3.2 <sup>b</sup>	98.1 $\pm$ 10.2 <sup>c</sup>	1.0 $\pm$ 0.1 <sup>a</sup>	30.0 $\pm$ 14.2 <sup>b</sup>	<0.001	<0.001	<0.001
Heart	11.0 $\pm$ 1.1 <sup>a</sup>	28.8 $\pm$ 1.4 <sup>b</sup>	42.1 $\pm$ 4.0 <sup>b,c</sup>	71.0 $\pm$ 11.1 <sup>c</sup>	10.9 $\pm$ 1.1 <sup>a</sup>	37.5 $\pm$ 7.8 <sup>b</sup>	<0.001	<0.001	NS
Spleen	51.5 $\pm$ 4.6 <sup>c</sup>	151 $\pm$ 8 <sup>d</sup>	21.8 $\pm$ 2.4 <sup>b</sup>	73.6 $\pm$ 5.6 <sup>c</sup>	2.2 $\pm$ 0.2 <sup>a</sup>	16.0 $\pm$ 2.2 <sup>b</sup>	<0.001	<0.001	<0.001
Thymus	5.2 $\pm$ 0.7 <sup>b</sup>	12.6 $\pm$ 1.1 <sup>c</sup>	8.7 $\pm$ 0.9 <sup>c</sup>	12.9 $\pm$ 1.8 <sup>c</sup>	1.9 $\pm$ 0.2 <sup>a</sup>	5.3 $\pm$ 0.6 <sup>b</sup>	<0.001	<0.001	<0.05
Brain	0.8 $\pm$ 0.1 <sup>a</sup>	3.0 $\pm$ 0.2 <sup>b</sup>	1.1 $\pm$ 0.1 <sup>a</sup>	2.4 $\pm$ 0.4 <sup>b</sup>	ND	ND	NS	<0.001	<0.05
Muscle	2.2 $\pm$ 0.2 <sup>a</sup>	5.3 $\pm$ 0.4 <sup>b,c</sup>	7.2 $\pm$ 0.5 <sup>b,c</sup>	10.9 $\pm$ 2.1 <sup>c</sup>	2.0 $\pm$ 0.2 <sup>a</sup>	5.1 $\pm$ 0.9 <sup>b</sup>	<0.001	<0.001	NS

Values are mean  $\pm$  SEM,  $n = 5$  or 7. Mean values in a row with superscripts without a common letter differ,  $P < 0.05$

NS not significant  $P \geq 0.05$ , ND not detected

(Fig. 2D) and liver (Fig. 2F). The  $\gamma$ -tocotrienol concentration in the jejunum of the T3 + KCZ group at 3 h was 355% ( $P < 0.05$ ) that of the T3 group, and the concentration in the liver was 469% ( $P < 0.05$ ).

### Experiment 3

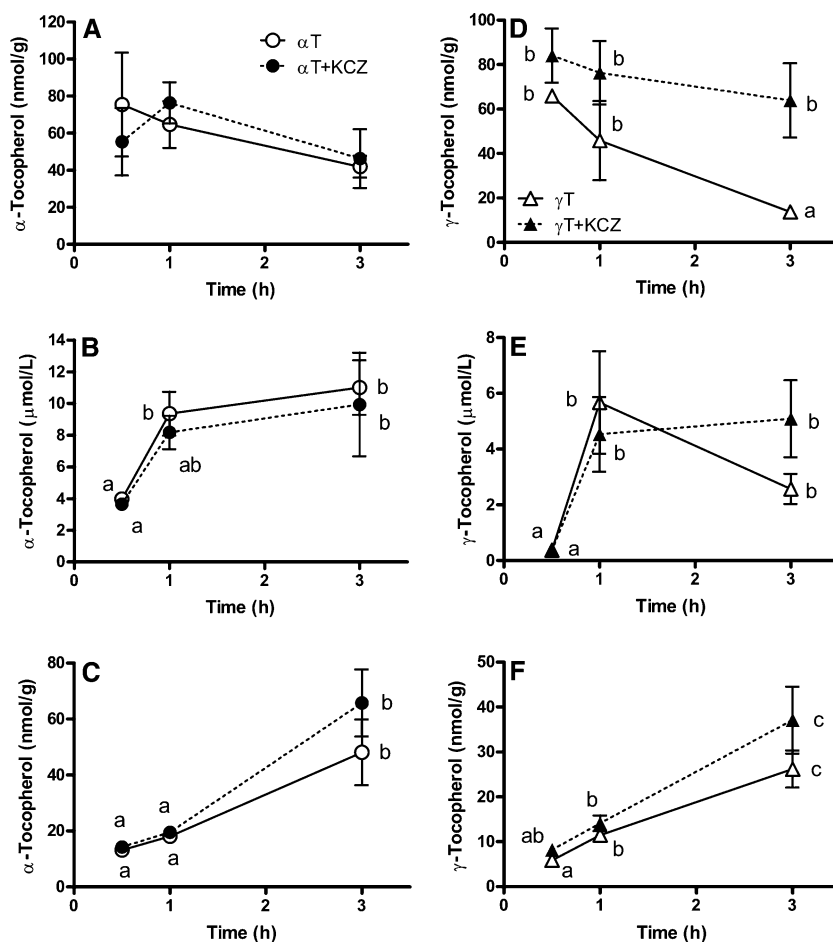
A small amount of  $\alpha$ -CEHC was detected in the jejunum of the T3 and T3 + KCZ groups, but the concentrations were not different from that of the rats without vitamin E administration (data not shown). However, the jejunum

$\gamma$ -CEHC concentration of the  $\gamma\text{T} + \text{KCZ}$  was markedly lower ( $P < 0.05$ ) than that of the  $\gamma\text{T}$  group (Fig. 3). The  $\gamma$ -CEHC concentration of the T3 + KCZ group tended to be lower than that of the T3 group.

### Discussion

Ketoconazole has been known as a potent inhibitor of human CYP3A [19] but it also inhibits various CYP isoforms because the nitrogen atom of the imidazole ring of

**Fig. 1**  $\alpha$ -Tocopherol concentration in jejunum (A), plasma (B) and liver (C) of rats administered  $\alpha$ -tocopherol ( $\alpha T$ ) or with ketoconazole ( $\alpha T + KCZ$ ), and  $\gamma$ -tocopherol concentration in jejunum (D), plasma (E) and liver (F) of rats administered  $\gamma$ -tocopherol ( $\gamma T$ ) or with ketoconazole ( $\gamma T + KCZ$ ) in Experiment 2. Values are mean  $\pm$  SEM,  $n = 6$ . Time effect was detected ( $P < 0.05$ ) in panels B–F, and KCZ effect was also detected ( $P < 0.05$ ) in panel D by two-way ANOVA. Mean values in a panel with *superscripts* without a common letter differ,  $P < 0.05$



ketoconazole can bond heme iron of CYP isoforms. In fact, ketoconazole inhibits rat CYP1A, 2A, 2C, 2E and 3A [25, 26]. In addition, ketoconazole may inhibit CYP4F because of the potent inhibition of CYP4F-dependent vitamin E metabolism by ketoconazole in cultured cells [20, 21]. In order to clarify the contribution of CYP4F-dependent metabolism of vitamin E isoforms to their tissue concentrations, the effect of ketoconazole on tocopherol and tocotrienol concentrations in various tissues of rats was studied. We used vitamin E-deficient rats fed a vitamin E-free diet for 4 weeks in Experiments 1 and 2, because the other isoform concentrations were difficult to be elevated in the  $\alpha$ -tocopherol-rich tissues. The plasma pyruvate kinase activity, a marker for vitamin E deficiency, was not changed by the deficiency for 4 weeks (unpublished data), but the  $\alpha$ -tocopherol concentration in the plasma and liver was 16 and 20% those at the start of the experiment [27].

Ketoconazole decreased urinary excretion of  $\alpha$ -CEHC after administration of  $\alpha$ -tocopherol or a tocotrienol mixture, and that of  $\gamma$ -CEHC after administration of  $\gamma$ -tocopherol or a tocotrienol mixture (Table 1). Thus, the metabolism of vitamin E isoforms to their metabolites was clearly inhibited by ketoconazole in rats. The decrease of

urinary metabolite excretion by ketoconazole was accompanied by the marked elevation of the  $\gamma$ -tocopherol,  $\alpha$ - and  $\gamma$ -tocotrienol concentrations in the serum and various tissues (Table 3). These results show that CYP-dependent metabolism regulates the  $\gamma$ -tocopherol and tocotrienol concentrations in the tissues. The affinity of  $\gamma$ -tocopherol and  $\alpha$ -tocotrienol for  $\alpha$ -TTP is 9 and 12% that of  $\alpha$ -tocopherol, respectively [6]. Therefore, the regulation of vitamin E metabolism influences the tissue concentrations even though their affinity for  $\alpha$ -TTP is very low. In contrast, the  $\alpha$ -tocopherol concentration in the serum and various tissues was not affected by ketoconazole (Table 3), while the urinary  $\alpha$ -CEHC excretion was markedly inhibited by ketoconazole (Table 2). The reason of the different effect of ketoconazole on the  $\alpha$ -tocopherol and the other isoform concentrations is unclear. The  $\alpha$ -tocopherol concentration in the tissues after  $\alpha$ -tocopherol administration may be too high to be further elevated by ketoconazole.

We recently showed that Triton WR1339, an inhibitor of lipoprotein lipase, prevented vitamin E transport to the liver and subsequent transport to the various tissues [3]. The large amount of vitamin E associated with chylomicrons accumulated in the serum at 6 h after oral adminis-

**Fig. 2**  $\alpha$ -Tocotrienol concentration in jejunum (A), plasma (B) and liver (C) and  $\gamma$ -tocotrienol concentration in jejunum (D), plasma (E) and liver (F) of rats administered a tocotrienol mixture (T3) or with ketoconazole (T3 + KCZ) in Experiment 2. Values are mean  $\pm$  SEM,  $n = 6$ . Time effect was detected ( $P < 0.05$ ) in all panels, and KCZ effect was also detected ( $P < 0.05$ ) in panels D and F by two-way ANOVA. Mean values in a panel with *superscripts* without a common *letter* differ,  $P < 0.05$ . Neither  $\alpha$ - nor  $\gamma$ -tocotrienol was detected in the liver of the T3 and T3 + KCZ groups at 0.5 h

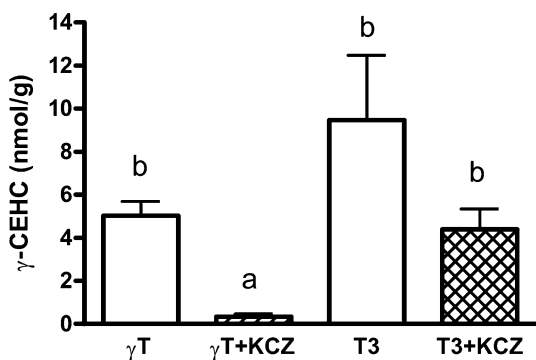
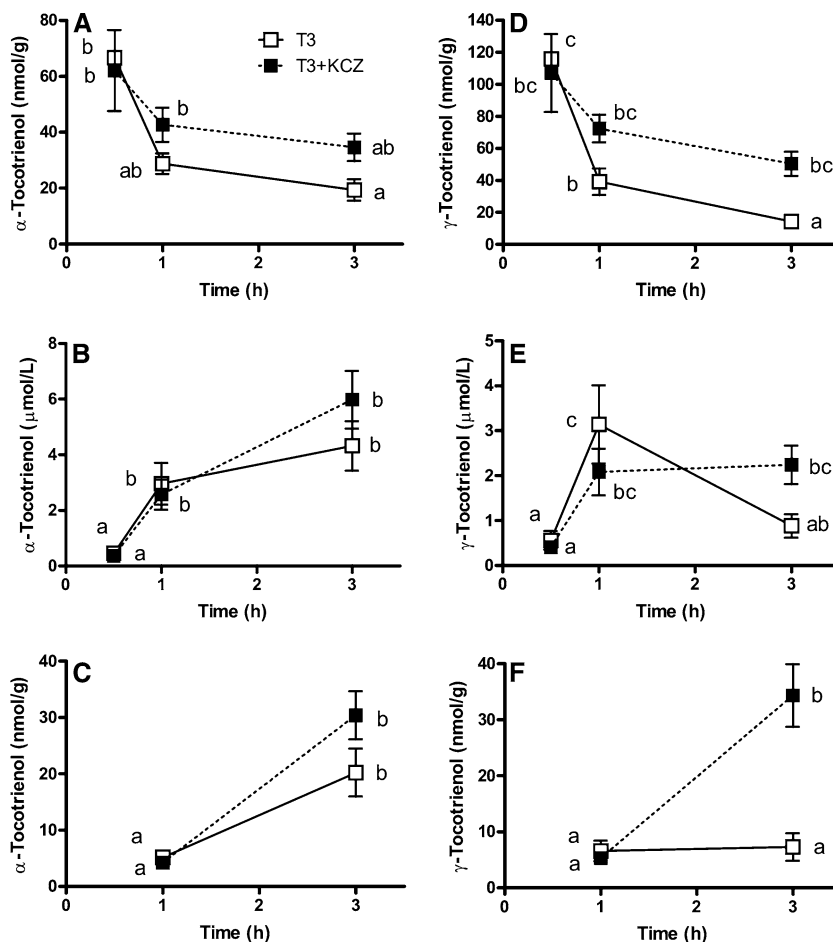


**Fig. 3** Jejunum  $\gamma$ -CEHC concentration at 3 h after oral administration of  $\gamma$ -tocopherol ( $\gamma$ T),  $\gamma$ -tocopherol with ketoconazole ( $\gamma$ T + KCZ), a tocotrienol mixture (T3), or a tocotrienol mixture with ketoconazole (T3 + KCZ) in Experiment 3. Values are mean  $\pm$  SEM,  $n = 4$ . There were effects of vitamin E isoform ( $P < 0.05$ ), ketoconazole ( $P < 0.05$ ) and their interaction ( $P < 0.05$ ) by two-way ANOVA. Mean values with *superscripts* without a common *letter* differ,  $P < 0.05$

tration of vitamin E with Triton, but there was a marked difference between each isoform concentration. The serum vitamin E isoform concentrations after each isoform

administration with Triton were as follows:  $\alpha$ -tocopherol, 102.3  $\mu$ mol/l;  $\gamma$ -tocopherol, 74.3  $\mu$ mol/l;  $\alpha$ -tocotrienol, 45.8  $\mu$ mol/l;  $\gamma$ -tocotrienol, 11.1  $\mu$ mol/l. In addition, rat CYP4F (CYP4F1, 4F4, 4F5 and 4F6) mRNA was detected in the jejunum (unpublished data). These results propose the hypothesis that some amount of vitamin E isoforms is metabolized in the intestine during their absorption. In order to see this hypothesis, the effect of ketoconazole on the vitamin E isoform concentrations in the jejunum, plasma and liver (Experiment 2), and the  $\gamma$ -CEHC concentration in the jejunum (Experiment 3) for 3 h after each administration was studied. The jejunum  $\alpha$ -tocopherol concentration was not affected by ketoconazole administration (Fig. 1A), but the  $\gamma$ -tocopherol (Fig. 1D) and  $\gamma$ -tocotrienol (Fig. 2D) concentrations 1 h after each administration tended to be elevated by ketoconazole administration, and those at 3 h were significantly elevated. The elevation of the jejunum  $\gamma$ -tocotrienol concentration by ketoconazole may be caused by the inhibition of its metabolism in the liver and the excretion through the bile, because the liver is a major tissue that metabolizes vitamin E isoforms, and the  $\gamma$ -tocotrienol concentration in the liver was markedly elevated by ketoconazole (Fig. 2F). Then,

we determined the  $\gamma$ -CEHC concentration in the jejunum (Experiment 3). A significant amount of  $\gamma$ -CEHC was detected in the jejunum 3 h after oral administration of  $\gamma$ -tocopherol or a tocotrienol mixture, and ketoconazole inhibited  $\gamma$ -tocopherol metabolism to  $\gamma$ -CEHC in the jejunum (Fig. 3). These results suggest that a certain amount of dietary vitamin E isoform is metabolized to its metabolite by CYP-dependent pathway in the intestine during absorption. Sontag et al. recently showed that the maximal specific activity ( $V_{\max}$ ) of human CYP4F2 for  $\gamma$ -tocopherol,  $\alpha$ - and  $\gamma$ -tocotrienol was much higher than that for  $\alpha$ -tocopherol in a kinetic study using human microsomes or insect microsomes expressing human CYP4F2 [28]. The affinity of  $\alpha$ - and  $\gamma$ -tocotrienol for the enzyme (apparent  $K_m$  value) was higher than those of  $\alpha$ - and  $\gamma$ -tocopherol. Thus,  $\gamma$ -tocopherol and  $\gamma$ -tocotrienol may be effectively metabolized to  $\gamma$ -CEHC in the intestine, while  $\alpha$ -tocopherol may be poorly metabolized.

The present study showed that CYP-dependent metabolism of vitamin E isoforms is a critical determinant of their tissue concentrations. This study also showed that  $\gamma$ -tocopherol and  $\gamma$ -tocotrienol are metabolized to  $\gamma$ -CEHC in the jejunum, and suggests that a certain amount of vitamin E isoform is metabolized by CYP-dependent metabolism in the intestine during absorption. Therefore, not only the discrimination of vitamin E isoforms by  $\alpha$ -TTP in the liver but also their metabolism by CYP-dependent pathway in the liver and intestine may regulate the tissue concentrations of vitamin E isoforms.

**Acknowledgments** This study was supported in part by Grant-in Aid for Scientific Research 15680018 from Japan Society for the Promotion of Science, Japan. The authors are grateful to Eisai Food & Chemical for their contribution of vitamin E isoforms and their metabolites, and to Hiroaki Oda for his assistance with animal experimentation.

## References

- Traber MG, Sies H (1996) Vitamin E in humans: demand and delivery. *Annu Rev Nutr* 16:321–347
- Kayden HJ, Traber MG (1993) Absorption, lipoprotein transport, and regulation of plasma concentrations of vitamin E in humans. *J Lipid Res* 34:343–358
- Abe C, Ikeda S, Uchida T, Yamashita K, Ichikawa T (2007) Triton WR1339, an Inhibitor of lipoprotein lipase, decreases vitamin E concentration in some tissues of rats by inhibiting its transport to liver. *J Nutr* 137:345–350
- Traber MG, Arai H (1999) Molecular mechanisms of vitamin E transport. *Annu Rev Nutr* 19:343–355
- Traber MG, Burton GW, Hamilton RL (2004) Vitamin E trafficking. *Ann NY Acad Sci* 1031:1–12
- Hosomi A, Arita M, Sato Y, Kiyose C, Ueda T, Igarashi O, Arai H, Inoue K (1997) Affinity for  $\alpha$ -tocopherol transfer protein as a determinant of the biological activities of vitamin E analogs. *FEBS Lett* 409:105–108
- Ouahchi K, Arita M, Kayden H, Hentati F, Ben Hamida M, Sokol R, Arai H, Inoue K, Mandel JL, Koenig M (1995) Ataxia with isolated vitamin E deficiency is caused by mutations in the  $\alpha$ -tocopherol transfer protein. *Nat Genet* 9:141–145
- Leonard SW, Terasawa Y, Farese Jr RV, Traber MG (2002) Incorporation of deuterated RRR- or all-*rac*- $\alpha$ -tocopherol in plasma and tissues of  $\alpha$ -tocopherol transfer protein-null mice. *Am J Clin Nutr* 75:555–560
- Traber MG, Siddens LK, Leonard SW, Schock B, Gohil K, Krueger SK, Cross CE, Williams DE (2005)  $\alpha$ -Tocopherol modulates Cyp3a expression, increases  $\gamma$ -CEHC production, and limits tissue  $\gamma$ -tocopherol accumulation in mice fed high  $\gamma$ -tocopherol diets. *Free Radic Biol Med* 38:773–785
- Schultz M, Leist M, Petrzika M, Gassmann B, Brigelius-Flohé R (1995) Novel urinary metabolite of  $\alpha$ -tocopherol, 2,5,7,8-tetramethyl-2-(2'-carboxyethyl)-6-hydroxychroman, as an indicator of an adequate vitamin E supply? *Am J Clin Nutr* 62:1527S–1534S
- Swanson JE, Ben RN, Burton GW, Parker RS (1999) Urinary excretion of 2,7,8-trimethyl-2-( $\beta$ -carboxyethyl)-6-hydroxychroman is a major route of elimination of  $\gamma$ -tocopherol in humans. *J Lipid Res* 40:665–671
- Lodge JK, Ridlington J, Leonard S, Vaule H, Traber MG (2001)  $\alpha$ - and  $\gamma$ -Tocotrienols are metabolized to carboxyethyl-hydroxychroman derivatives and excreted in human urine. *Lipids* 36:43–48
- Chiku S, Hamamura K, Nakamura T (1984) Novel urinary metabolite of  $\alpha$ -tocopherol in rats. *J Lipid Res* 25:40–48
- Hattori A, Fukushima T, Imai K (2000) Occurrence and determination of a natriuretic hormone, 2,7,8-trimethyl-2-( $\beta$ -carboxyethyl)-6-hydroxychroman, in rat plasma, urine, and bile. *Anal Biochem* 281:209–215
- Saito H, Kiyose C, Yoshimura H, Ueda T, Kondo K, Igarashi O (2003)  $\gamma$ -Tocotrienol, a vitamin E homolog, is a natriuretic hormone precursor. *J Lipid Res* 44:1530–1535
- Birringer M, Pfluger P, Kluth D, Landes N, Brigelius-Flohé R (2002) Identities and differences in the metabolism of tocotrienols and tocopherols in HepG2 Cells. *J Nutr* 132:3113–3118
- Parker RS, Sontag TJ, Swanson JE, McCormick C (2004) Discovery, characterization, and significance of the cytochrome P450  $\omega$ -hydroxylase pathway of vitamin E catabolism. *Ann NY Acad Sci* 1031:13–21
- Sontag TJ, Parker RS (2002) Cytochrome P450  $\omega$ -hydroxylase pathway of tocopherol catabolism: novel mechanism of regulation of vitamin E status. *J Biol Chem* 277:25290–25296
- Sheets JJ, Mason JJ (1984) Ketoconazole: a potent inhibitor of cytochrome P-450-dependent drug metabolism in rat liver. *Drug Metab Dispos* 12:603–606
- Parker RS, Sontag TJ, Swanson JE (2000) Cytochrome P450A-dependent metabolism of tocopherols and inhibition by sesamin. *Biochem Biophys Res Commun* 277:531–534
- You C.-S, Sontag TJ, Swanson JE, Parker RS (2005) Long-chain carboxychromanols are the major metabolites of tocopherols and tocotrienols in A549 lung epithelial cells but not HepG2 cells. *J Nutr* 135:227–232
- Reeves PG, Nielsen FH, Fahey GC Jr (1993) AIN-93 Purified diets for laboratory rodents: final report of the American Institute of Nutrition ad hoc writing committee on the reformulation of the AIN-76A rodent diet. *J Nutr* 123:1939–1951
- Ueda T, Igarashi O (1987) New solvent system for extraction of tocopherols from biological specimens for HPLC determination and the evaluation of 2,2,5,7,8-pentamethyl-6-chromanol as an internal standard. *J Micronutr Anal* 3:185–198
- Kiyose C, Saito H, Kaneko K, Hamamura K, Tomioka M, Ueda T, Igarashi O (2001)  $\alpha$ -Tocopherol affects the urinary and biliary



- excretion of 2,7,8-trimethyl-2(2'-carboxyethyl)-6-hydroxychroman,  $\gamma$ -tocopherol metabolite, in rats. *Lipids* 36:467–472
25. Eagling VA, Tjia JF, Back DJ (1998) Differential selectivity of cytochrome P450 inhibitors against probe substrates in human and rat liver microsomes. *Br J Clin Pharmacol* 45:107–114
26. Kobayashi K, Urashima K, Shimada N, Chiba K (2003) Selectivities of human cytochrome P450 inhibitors toward rat P450 isoforms: study with cDNA-expressed systems of the rat. *Drug Metab Dispos* 31:833–836
27. Abe C, Ikeda S, Yamashita K (2005) Dietary sesame seeds elevate  $\alpha$ -tocopherol concentration in rat brain. *J Nutr Sci Vitaminol* 51:223–230
28. Sontag TJ, Parker RS (2007) Comparative influence of major structural features of tocopherols and tocotrienols on kinetics of their  $\omega$ -oxidation by cellular and microsomal tocopherol- $\omega$ -hydroxylase. *J Lipid Res*. Epub ahead of print

# Polar and Neutral Lipid Composition in the Pelagic Tunicate *Pyrosoma atlanticum*

Patrick Mayzaud · Marc Boutoute ·  
Renzo Perissinotto · Peter Nichols

Received: 6 February 2007 / Accepted: 17 April 2007 / Published online: 2 June 2007  
© AOCS 2007

**Abstract** Structure and functioning of colonial pyrosomes are largely undescribed and their lipid characteristics have received limited attention. The aim of this paper is to fill this gap on one of the dominant species *Pyrosoma atlanticum*. Lipid content is tightly coupled to size and weight. Lipid composition shows a large dominance of structural polar lipids. Neutral lipids were dominated by sterols with low levels of acylglycerols and free fatty acids. Phospholipids show a dominance of PC with intermediate percentages of PE and DPG. Other constituents (PS, PI, LPC, sphingolipids) were present at lower levels. Fatty acid composition of DAG and TAG showed a dominance of saturated acids (16:0, 14:0), DHA and intermediate levels of MUFA. Phospholipids were dominated by DHA with values exceeding 30% of total FA in all categories except for PI, where lower percentages occurred. Saturated acids were second in abundance with MUFA showing intermediate concentrations. Sterols were dominated by 24-methylcholesta-5,22E-dien-3 $\beta$ -ol with more than 22% of the total sterol. Cholesterol (cholest-5-en-3 $\beta$ -ol) represented only 12 % of the total while 24-methylcholesta-

5,24(28)E-dien-3 $\beta$ -ol accounted for 11% of the total sterols. The low levels of triacylglycerols and free fatty acids, coupled with high concentrations of glycolipids and phytoplankton-derived degraded chloropigments, is evidence of a direct link with the digestive activity and substantiate the idea of a high physiological turnover as an alternative to large lipid accumulation. The fatty acid and sterol profiles are consistent with a diverse phytoplankton diet, and a strong contribution of phospholipid classes to energy needs, including locomotion.

## Introduction

Pyrosomas are a small group of holoplanktonic tunicates, currently including only 8 described species and 3 genera [1]. They are restricted to the warmer open ocean waters, between approximately 50°N and 50°S in all oceans [2]. Our knowledge of the lipid composition in tunicates remains fragmentary and detailed reports encompass essentially benthic tunicates, e.g. ascidians [3, 4] as well as salps, doliolids and appendicularians [5–8]. Knowledge of the lipid composition of *Pyrosoma* is limited to total fatty acid composition of *Pyrosoma atlanticum* reported by Culkin and Morris [9] and Jeffs et al. [10]. Both studies observed that the concentration of total lipids is generally low and dominated by structural lipids.

Neither of the two studies on *P. atlanticum* considered the lipid composition in terms of lipid classes and their related fatty acid structure. During the last leg of the ANTARES-4 cruise to the south Indian and the Southern oceans, substantial numbers of *P. atlanticum* colonies were observed in the region north of the Subtropical Front. As examination of biomarker lipid profiles from different lipid

P. Mayzaud (✉) · M. Boutoute  
Université Pierre et Marie Curie,  
Observatoire Océanologique,  
UMR-CNRS 7093, LOV, BP. 28,  
06230 Villefranche sur mer, France  
e-mail: mayzaud@obs-vlfr.fr

R. Perissinotto  
School of Biological and Conservation Sciences,  
G. Campbell Building, University of KwaZulu-Natal,  
Howard College Campus, Durban 4041, South Africa

P. Nichols  
CSIRO, Marine and Atmospheric Research,  
Castray Esplanade, Hobart, TAS 7001, Australia

classes may provide more detailed information pertinent to life cycle adaptation and food web research than is obtained from total fatty acid profiles, the availability of a sufficient number of samples prompted an investigation of the lipid constitution with special emphasis on the polar structural lipids.

## Materials and Methods

### Sampling

All samples were taken during the ANTARES-4 cruise of the research vessel *Marion Dufresne*, during the period 5 January–23 February 1999. The operational area was restricted between approximately 43–46°S and 61–65 °E, in the Indian sector of the Southern Ocean and the region of the Agulhas Front (for details see map in Perissinotto et al., 16). Colonies of *P. atlanticum* were collected only in the Agulhas Front region, north of the Subtropical Convergence, during the period 2–16 February at stations G4 (44°21'03S; 62°33'37E). Specimens were collected using a 160 cm-diameter Omori Net (1,000 µm mesh, towed obliquely from 200 m to the surface). Specimens were sorted out immediately, briefly rinsed with distilled water, blotted dry on sharkskin filter paper and deep frozen in liquid nitrogen. Samples were kept at –80 °C until return to the laboratory within 3 months.

### Size, Weight Measurements and Lipid Extraction

Entire specimens were placed frozen on crushed ice and brought to 0 °C. Size (total length = TL) and fresh weight (WW) were measured prior to lipid extraction according to the method of Bligh and Dyer [11]. The Bligh and Dyer method when used as published may not fully extract neutral lipids. This problem can be overcome using the same solvent ratios (i.e. one phase), and a longer extraction time. All lipid extracts were placed under nitrogen at –70 °C until analysis. Individual dry weight (DW) was recorded on sub-samples of 6 colonies dried at 70 °C for six days to obtain the dry weight/wet weight ratio.

### Lipid Analyses

Lipid classes were quantified after chromatographic separation coupled with FID detection on an Iatroscan MK V TH 10. Total lipid extracts were applied to SIII chromarods using a SAS A4100 autospotter set up to deliver 1 µl of chloroform extract on each rod. Analyses were done in triplicate. Neutral lipids were separated using a double development procedure with the following solvent systems: n-hexane: benzene: formic acid 80:20:1 (by volume)

followed by n-hexane:diethyl ether:formic acid 97:3:1.5 (v/v). Phospholipids were separated with chloroform: methanol: NH<sub>4</sub> 50:50:5 (v/v). Separation of glycolipids was achieved with chloroform/ethyl acetate/acetone/methanol/ acetic acid/water (60/12/15/16/3/3). Calibration was achieved using commercial standards (Tripalmitin, 1,2 di-palmitoyl-rac-glycerol, stearic acid, cholesterol, 3-sn-phosphatidyl-L-serine from bovine brain, L- $\alpha$ -phosphatidyl inositol from bovine liver, sphingomyelin from bovine brain and  $\alpha$ -lysophosphatidylcholine from egg yolk were obtained from Sigma; MGDG and DGDG from spinach were obtained from Larodan; L- $\alpha$ -Lecithin from egg yolk, L-phosphatidyl- ethanolamine from egg and cardiolipin from bovine heart were obtained from Avanti Polar Lipids).

Separation of neutral and polar lipids was achieved on a preparative scale by column chromatography on silica gel (Supelcosil A, Supelco). The neutral lipid fraction was eluted with six column volumes of chloroform, the acetone mobile compounds were eluted with four volumes of acetone and the phospholipids were eluted with six volumes of methanol. Each fraction collected was further separated by thin-layer chromatography (TLC) on pre-coated silica gel plates (Analtech, Uniplate) and developed with hexane : diethyl ether : acetic acid, 170:30:2 (v/v) for neutral lipids, or chloroform : methanol : aqueous ammonia 70:30:4 (v/v) for glycolipids, and chloroform: methanol: aqueous ammonia 50: 50: 5 (v/v) for polar lipids. All operations took place under nitrogen. Lipid classes were visualized using dichlorofluorescein and identification was achieved by comparison with standard mixtures. Acetone fraction was further separated on HPTLC using the same solvent system as TLC, but with specific detection of glycolipids made with Bial's Orcinol reagents (Alltech). No attempt was made to separate possible plasmalogen phospholipids.

Each band from TLC was scraped off and submitted to methylation. Fatty acid methyl esters (FAME) of total lipids were prepared with 7% boron trifluoride in methanol [12]. FAME were purified on TLC and recovered in hexane. Gas chromatography (GC) of all esters was carried out on a 30 m length x 0.32 mm internal diameter quartz capillary column coated with Famewax (Restek) in a Perkin-Elmer XL Autolab GC equipped with a flame ionization detector (FID). The column was operated isothermally at 185 °C for FAME. Helium was used as carrier gas at 7 psig. Injector and detector were maintained at 250 °C. Individual components were identified by comparing retention time data with those obtained from authentic (Nu-Check prep) and laboratory standards (capelin : menhaden oils 50:50). In addition to the examination of FAME as recovered, a part of all FAME samples was completely hydrogenated and the products examined qualitatively and quantitatively by GC. The level of accuracy is  $\pm 5\%$  for major components, 1 to 9% for intermediate components

and up to  $\pm 30\%$  for minor components. Additional GLC analysis was carried out on a 30 m length  $\times$  0.25 mm internal diameter non polar DB1 column (J&W Scientific) to resolve the co-elution of 20:1 and 18:5 fatty acids on Fawemawax.

Analysis of sterols was conducted on an aliquot of the separated sterol fraction after conversion to TMSi (trimethylsilyl) ethers using *N,O*-bis-(trimethylsilyl)-trifluoroacetamide (BSFA, 50  $\mu$ l) at 60 °C for 1 h. GC and GC-MS analysis of sterols was achieved as described in Jeffs et al. [10].

### Statistical Treatment

Allometric relationships between dry weight (DW) and length (TL) for the different colonies ( $DW = a * TL^b$ ) were computed after log–log transformation and model I regression [13]. Bivariate analyses were made with Statgraphics XV. Cluster analysis was based on Bray-Curtis distance and farthest neighbour clustering (see: 15).

Correspondence analysis [14] was performed on a reduced data matrix of fatty acids transformed to relative frequencies and scaled so that each row (or column) could be viewed as a row (or column) of conditional probability distribution. Distances between profiles were computed with  $\chi^2$  metrics. This distance gives symmetry to the two sets of data so that each factorial axis associated to the cluster of variables (fatty acids) corresponds to a factorial axis of the cluster of observations (phospholipids). Thus, it was possible to represent simultaneously descriptors and observations on the plane defined by the factorial axes. Details on the method and means of interpretation are given in Mayzaud et al. [16]. Computation of multivariate tests was made using the SPAD 5.5 software [17].

Six replicates were used to compute all means and standard deviations.

## Results

### Size, Weight and Lipid Relationships

The size of the colonies of pyrosomes collected during the ANTARES 4 cruise ranged from 13 to 25 cm. The corresponding wet and dry weight varied from 22 to 64 g and from 1.1 to 3.6 g respectively, with water content exceeding 90%. Lipid content on a dry weight basis was generally low and ranged from 5 to 7%.

The weight (DW) relationships with size or lipid content were established using specimens of different size. The assumption is that the increase in length and weight should reflect a fair degree of integration of the number and metabolism of the different individual zooids constitutive

of the colony. The log-linear regressions between size and weight (Fig. 1) were highly significant and resulted in an overall regression equation of:

$$\log DW = -1.804 + 1.69 \log TL \quad (R^2 = 0.906, F = 38.36, p = 0.003),$$

The relationship between DW and total lipids was also highly significant and is presented in Fig. 1. The resulting log linear regression is:

$$\log Lip_{tot} = 1.898 + 0.839 \log DW \quad (R^2 = 0.968, F = 120, p = 0.001).$$

A relatively low value for the allometric exponent  $b$  was observed, suggesting a slow rate of lipid accumulation with increasing weight.

### Lipid Class Composition

A detailed composition of the lipids from *Pyrosoma atlanticum* is presented in Table 1. Total lipid concentrations (% dry weight) ranged from 4.9 to 6.9 % with a mean value of  $5.7 \pm 0.7$  %. Neutral lipids were dominated by sterols with a mean value exceeding 8% of the total lipids, while low percentages of triacylglycerols (TAG), diacylglycerols (DAG) and free fatty acids were recorded. Polar lipids (% total lipids) were dominated by phosphatidyl-choline (PC) followed by phosphatidylethanol-

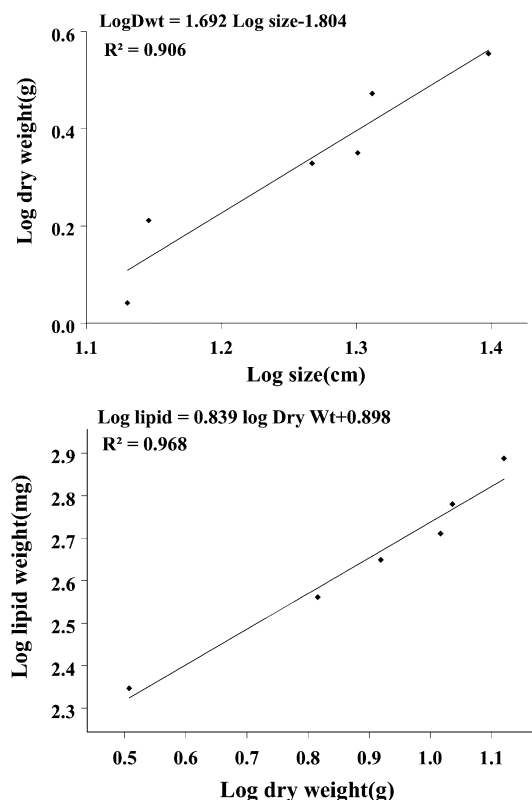


**Fig. 1** log–log regressions between dry weight and length and between lipid content and dry weight for *Pyrosoma atlanticum*

**Table 1** Lipid content and composition in lipid classes of *Pyrosoma atlanticum*

<i>Pyrosoma atlanticum</i>	<i>n</i> = 6
Total lipids (% dry weight)	5.70 ± 0.67
Lipid classes (% total lipids)	
Phosphatidylcholine	45.7 ± 2.57
Phosphatidylethanolamine	13.9 ± 1.70
Diphosphatidylglycerol	6.41 ± 1.90
Phosphatidylserine + inositol	2.92 ± 1.07
Lysophosphatidyl choline	2.63 ± 0.64
Sphingolipids	2.12 ± 0.17
Glycolipid # 1 MGDG	4.33 ± 1.56
Glycolipid # 2 DGDG like	4.18 ± 1.43
Diacylglycerols	2.28 ± 0.69
Triacylglycerols	3.52 ± 0.80
Free fatty acids	3.92 ± 0.98
Sterols	8.13 ± 0.60

Values expressed as mean ± standard deviation

amine (PE), diphosphatidylglycerol (DPG) with lower levels of phosphatidylserine+inositol (PS+PI), sphingomyelin and lysophosphatidylcholine (LPC). The lack of significant relationships between total lipids or lipid class per unit weight and either size or dry weight may be related to the small number of data points ( $n = 6$ ), or to the lack of direct interactions between body mass and lipid metabolism.

Two glycolipids fractions were found in concentrations exceeding 4% which can be attributed to the filter-feeding mode of the colonies. Their identification on HPTLC using Bial's Orcinol reagents, a sugar specific stain, showed that one fraction displayed the same  $R_f$  as commercial MGDG, while the second one run slightly faster than DGDG with the solvent system used. The high concentration of ingested chloropigments (from 0.3 to 1.6  $\mu\text{g colony}^{-1}$ , see Perissinotto et al., 18), suggests that the second fraction also originated from ingested phytoplankton. As discussed below, the high level of saturation of this later fraction (96% saturated acids) could explain the difference in migration as it is more saturated than the higher plant standard. This would agree with the possibility of a partial post ingestion modification.

#### Fatty Acid Composition of the Total and Neutral Lipids

The relative composition of the total fatty acids and the main neutral lipid classes is presented in Table 2. Fatty acid composition of the total lipids was driven by the abundance of polar lipids. Docosahexaenoic acid (DHA, 22:6n-3) dominated largely with more than 36% of the total fatty acids. Saturated acids were second in abun-

dance (> 30%) with palmitic (16:0) and myristic (14:0) as major components. Monounsaturated fatty acids (MUFA) showed intermediate percentages (12%), with 18:1n-9, 16:1n-7 and 18:1n-7 as major contributors. Among PUFAs other than DHA, eicosapentaenoic acid (EPA 20:5n-3) was the dominant pentaene, 18:2n-6, 18:3n-3 and 18:4n-3 dominated their respective group. DAG and TAG showed a dominance of saturated acids with 16:0 and 14:0, followed by 22:6n-3 with respective percentages of 18.6% and 21.9% of total fatty acids. Both the DAG and TAG fractions showed relatively high levels of 18:4n-3 (12.5 and 10.5%) and intermediate levels of MUFA with the same characteristic fatty acids. The two acylglycerols showed similar fatty acid composition, the only difference being the larger proportion of myristic acid (14:0) in DAG. The free fatty acid fraction was considered because of the high probability that it originates from digestive hydrolysis. Indeed, DHA showed the highest percentages with values ranging from 32 to 64% of the total fatty acids (mean 44.5%) despite the similar concentrations of free fatty acid contained in each specimen analyzed (3 to 4.5 % of total lipids). Stearic and myristic acids were the dominant saturated acids with respective ranges of 2 to 15% and 0.6 to 10%. EPA ranged from 3 to 12%, while oleic acid was the major MUFA with values ranging between 3.8 and 6.8%. Other MUFA and PUFA included 18:1n-7, 16:1n-7, 18:2n-6, 18:4n-3 and 20:4n-6 with percentages close to 2%. Odd branched chain acids (iso and anteiso) exhibited moderately high values in all neutral fractions, with percentages of iso15:0, anteiso15:0 and iso17:0 exceeding 1%.

#### Fatty Acid Fraction of the Glycolipids

The fatty acid composition of the two glycolipid fractions will only be summarized because of the unusual variability between replicates. The partial composition presented in Table 3, showed a large dominance of the saturated acids with 16:0 and 20:0 as main contributors for MGDG and DGDG respectively. DHA was second in importance but with values ranging from 2.8 to 20.4% for MGDG and from 1.1 to 25.9% for DGDG. Hence, the percent variability in fatty acid composition of MGDG, based on six replicates, is 13% for the saturated acids, 35% for the monoenes, 82% for 20:5 and 86% for 22:6. An increasing trend which agrees with the hypothesis of selective loss of polyunsaturated acids. The second fraction (DGDG-like) showed 40% variability for the saturated acids, 90% for the monoenes, and 120% for most unsaturated categories. Since the glycolipids originated from the phytoplankton chloroplast membranes, such extreme variance can only originate from different degree of digestive degradation.

**Table 2** Fatty acid composition (% total fatty acids) of *Pyrosoma atlanticum* total lipids and neutral lipid fractions

Fatty acid	Total lipids		Free fatty acids		TAG		DAG	
	Mean %	Sd	Mean %	Sd	Mean %	Sd	Mean %	Sd
14:0	6.93	0.27	5.55	4.81	8.72	2.74	15.05	4.47
Iso15:0	0.32	0.02	1.38	1.88	0.79	0.17	1.55	0.28
Aiso15:0	0.45	0.02	1.10	1.48	0.95	0.13	1.22	0.08
15:0	1.40	0.06	1.18	0.87	1.82	0.16	2.12	0.19
Iso16:0	0.30	0.02	0.37	0.36	0.87	0.16	0.61	0.25
Iso17:0	1.01	0.10	1.47	1.85	1.57	0.45	1.22	0.11
Aiso17:0	0.45	0.11	0.61	0.92	0.49	0.18	0.51	0.05
16:0	16.48	0.25	10.03	7.01	16.62	0.48	16.97	0.78
17:0*	0.77	0.07	0.88	1.00	0.85	0.02	0.83	0.23
Iso18:0	0.38	0.03	0.80	1.01	0.71	0.06	0.38	0.10
18:0	1.19	0.04	1.65	2.07	1.55	0.23	1.83	0.58
20:0	0.19	0.02	0.19	0.16	0.14	0.01	0.05	0.04
22:0	0.06	0.02	0.13	0.03	0.01	0.02	0.05	0.02
<b>Σ saturates</b>	<b>30.40</b>	<b>0.48</b>	<b>25.89</b>	<b>19.34</b>	<b>36.22</b>	<b>2.82</b>	<b>43.17</b>	<b>5.09</b>
16:1n-7	2.51	0.07	1.99	1.42	4.23	0.55	3.56	0.11
16:1n-5	0.29	0.03	0.26	0.21	0.90	0.39	0.87	0.06
17:1	0.49	0.03	0.56	0.23	0.67	0.08	1.15	0.55
18:1n-9	6.78	0.19	5.00	1.57	5.60	0.40	3.44	0.31
18:1n-7	1.70	0.12	2.22	1.51	2.53	0.08	1.47	0.36
18:1n-5	0.09	0.02	0.25	0.30	0.21	0.07	0.20	0.08
20:1n-11	0.18	0.05	0.03	0.02	–	–	–	–
20:1n-9	0.14	0.03	0.14	0.00	0.13	0.01	0.03	0.05
20:1n-7	0.75	0.05	0.45	0.33	0.49	0.02	0.46	0.14
20:1n-5	0.03	0.02	0.12	0.11	0.23	0.04	0.05	0.03
24:1	0.05	0.02	0.06	0.04	0.02	0.01	0.07	0.04
<b>Σ monoenes</b>	<b>12.45</b>	<b>0.12</b>	<b>11.08</b>	<b>4.04</b>	<b>15.38</b>	<b>1.07</b>	<b>11.30</b>	<b>0.80</b>
18:2n-9	0.05	0.01	0.20	0.27	0.13	0.11	0.17	0.03
18:2n-6	2.34	0.08	1.82	0.49	3.39	0.26	2.72	0.24
20:2n-6	0.13	0.01	0.19	0.11	0.18	0.01	0.16	0.13
<b>Σ Dienes</b>	<b>2.74</b>	<b>0.06</b>	<b>2.67</b>	<b>1.03</b>	<b>4.67</b>	<b>0.38</b>	<b>3.81</b>	<b>0.33</b>
18:3n-6	0.11	0.01	0.12	0.04	0.20	0.07	0.22	0.03
18:3n-3	1.01	0.02	0.49	0.19	1.76	0.10	2.04	0.21
20:3n-6	0.09	0.01	0.18	0.10	0.09	0.06	0.07	0.02
20:3n-3	0.10	0.03	0.05	0.02	0.08	0.01	0.06	0.01
<b>Σ Trienes</b>	<b>1.35</b>	<b>0.05</b>	<b>0.91</b>	<b>0.20</b>	<b>2.16</b>	<b>0.05</b>	<b>2.49</b>	<b>0.32</b>
16:4n-3	0.18	0.03	0.18	0.13	0.58	0.02	0.76	0.25
16:4n-1	–	–	0.06	0.05	0.13	0.01	0.14	0.02
18:4n-3	3.95	0.14	2.42	0.33	10.53	0.92	12.51	1.02
20:4n-6	2.10	0.01	2.77	1.83	0.82	0.09	0.42	0.05
20:4n-3	0.27	0.01	0.46	0.41	0.34	0.01	0.31	0.06
<b>Σ Tetraenes</b>	<b>6.56</b>	<b>0.16</b>	<b>6.06</b>	<b>1.59</b>	<b>12.40</b>	<b>0.83</b>	<b>14.14</b>	<b>1.07</b>
18:5n-3	0.29	0.03	0.04	0.03	0.89	0.11	1.15	0.27
20:5n-3	7.18	0.25	7.20	4.67	4.67	0.18	4.17	0.38
21:5n-3	0.33	0.01	0.47	0.25	0.51	0.10	0.55	0.16
22:5n-6	0.19	0.01	0.47	0.26	0.35	0.03	0.04	0.03
22:5n-3	0.75	0.02	0.72	0.61	0.78	0.06	0.52	0.04
<b>Σ Pentaenes</b>	<b>8.74</b>	<b>0.25</b>	<b>8.91</b>	<b>5.33</b>	<b>7.20</b>	<b>0.25</b>	<b>6.43</b>	<b>0.67</b>

**Table 2** continued

Fatty acid	Total lipids		Free fatty acids		TAG		DAG	
	Mean %	Sd	Mean %	Sd	Mean %	Sd	Mean %	Sd
22:6n-3	36.66	0.44	44.47	17.32	21.96	1.06	18.67	2.05

Sd standard deviation, *n* = 6, –not detected, TAG triacylglycerols, DAG diacylglycerols, \* include phytanic acid

### Fatty Acid Composition of the Total Phospholipids and Phospholipid Classes

Total phospholipids (PL<sub>T</sub>), like all phospholipid classes, were dominated by DHA with percentages exceeding 30% of the total fatty acids (Table 3), except for PI where lower percentages were recorded (23.6%). The saturated acids were second in abundance with palmitic acid and, to a minor extent myristic acid as the main constituents. PS showed a slightly different pattern with 16:0, 18:0 and 15:0 as the dominant saturates. MUFA showed intermediate concentrations with percentages ranging between 12 and 18% in total phospholipids, PC, PE, LPC, DPG and values higher than 20% in PS and PI (Table 3). Oleic (18:1n-9), palmitoleic (16:1n-7) and vaccenic (18:1n-7) acids were the main components, except in PS where 20:1n-7 accounted for 4.2% of the total fatty acids. Pentaenes repre-

sented the fourth largest group in abundance, with EPA as the main component with values exceeding 15% in PE, ranging from 7.5 to 9% in PC, DPG and PI. Lower EPA values were recorded in PC and LPC with percentages of 5–6%. Three other PUFA were present in smaller but significant concentrations: 18:4n-3 with values above 3% in PL<sub>T</sub>, PC, DPG, LPC and below 1% in the other polar lipids classes; 20:4n-6 with values above 4% in PE, PI and below 1.2% in PC, LPC; 18:3n-3 with percentages around 1% in all phospholipid classes.

Contrary to the pattern observed with neutral lipids, odd and even branch chain acids (iso15:0, iso16:0, iso18:0, anteiso15:0 and anteiso17:0) exhibited low concentrations with values below 0.5% of total fatty acid. Iso17:0 showed higher percentages with values ranging from 0.5 to 1.1, with maxima in PI and LPC.

### Sterol Composition

As indicated earlier, sterols made a large fraction of the total lipid. A total of 21 sterols were identified in *P. atlanticum* (Table 4). The sterol composition was dominated by 24-methylcholesta-5,22E-dien-3 $\beta$ -ol with more than 22% of the total sterol. Cholesterol (cholest-5-en-3 $\beta$ -ol), which usually dominates in most animal tissues, represented only 12% of the total while 24-methylcholesta-5,24(28)-dien-3 $\beta$ -ol (24-methylenecholesterol) accounted for 11% of the total sterols. Additional important constituents ranging from 5 to 9% included: 5 $\alpha$ -cholest-22Z-en-3 $\beta$ -ol (cis-22-dehydrocholestanol), 24-ethylcholest-5-en-3 $\beta$ -ol (24-ethylcholesterol), cholesta-5,22Z-dien-3 $\beta$ -ol (cis-22-dehydrocholesterol) and 5 $\alpha$ -cholestan-3 $\beta$ -ol (cholestanol). This composition contrasts with the large dominance of cholesterol classically reported for crustaceans [27] and suggests a large influence of ingested phytoplankton as suggested by the high chlorophyll content recorded in these specimens Table 5.

### Discussion

Pyrosomas are important tunicates that play a major role in food webs of many oceanic areas [19]. Yet, they are among the least investigated of all invertebrates, with very little information on their lipid structure. Their lipid class

**Table 3** Partial fatty acid composition limited to the major components (% total fatty acids) of *Pyrosoma atlanticum* glycolipid fractions

Fatty acid	MGDG		DGDG like	
	Mean %	Sd	Mean %	Sd
14:0	1.03	0.38	4.39	5.24
16:0	31.54	3.17	10.40	8.34
18:0	8.41	1.74	1.83	1.05
20:0	4.97	1.96	34.45	30.90
22:0	2.68	0.69	10.18	9.12
<b><math>\Sigma</math> saturates</b>	<b>79.20</b>	<b>10.22</b>	<b>69.19</b>	<b>29.032</b>
16:1n-7	1.06	0.21	1.99	1.94
18:1n-9	1.36	0.82	5.08	4.61
<b><math>\Sigma</math> monoenes</b>	<b>6.15</b>	<b>2.15</b>	<b>9.82</b>	<b>8.81</b>
18:2n-6	0.54	0.25	1.46	1.20
<b><math>\Sigma</math> Dienes</b>	<b>1.17</b>	<b>0.24</b>	<b>2.00</b>	<b>2.10</b>
20:3n-3	1.52	0.63	0.04	0.07
<b><math>\Sigma</math> Trienes</b>	<b>2.20</b>	<b>0.28</b>	<b>0.57</b>	<b>0.60</b>
18:4n-3	0.94	0.37	1.19	1.19
<b><math>\Sigma</math> Tetraenes</b>	<b>1.69</b>	<b>0.77</b>	<b>2.21</b>	<b>2.47</b>
20:5n-3	0.97	0.79	3.47	2.51
<b><math>\Sigma</math> Pentaenes</b>	<b>1.34</b>	<b>1.20</b>	<b>4.18</b>	<b>3.12</b>
22:6n-3	8.25	6.96	12.03	12.71

Sd standard deviation, MGDG monogalactosyl diglycerides, DGDG digalactosyl diglycerides

**Table 4** Fatty acid composition (% total fatty acids) of *Pyrosoma atlanticum* total phospholipids (PL) and phospholipid fractions

Fatty acid	Total PL		PC		PE		DPG		PS		PI		LPC	
	Mean	Sd	Mean	Sd	Mean	Sd	Mean	Sd	Mean	Sd	Mean	Sd	Mean	Sd
14:0	6.37	0.15	7.69	0.94	1.69	0.67	6.88	0.05	0.87	0.09	0.78	0.35	0.92	0.14
Iso15:0	0.27	0.03	0.31	0.02	0.17	0.02	0.26	0.02	0.19	0.04	0.23	0.07	0.21	0.07
Aiso15:0	0.38	0.06	0.38	0.01	0.63	0.39	0.29	0.01	0.31	0.08	0.90	0.10	0.25	0.06
15:0	1.35	0.04	1.68	0.09	0.59	0.10	1.54	0.03	6.26	1.81	1.27	0.52	0.81	0.10
Iso16:0	0.29	0.06	0.36	0.02	0.16	0.10	0.33	0.02	0.41	0.05	0.35	0.11	0.21	0.05
Iso17:0	0.78	0.11	0.54	0.02	0.69	0.08	0.60	0.02	0.90	0.07	1.10	0.11	1.10	0.08
Aiso17:0	0.37	0.17	0.19	0.01	0.54	0.24	0.17	0.02	0.58	0.09	0.63	0.11	0.43	0.01
16:0	16.21	0.78	15.47	0.19	15.44	0.45	16.85	0.05	11.60	0.07	15.01	0.41	19.19	1.93
17:0*	0.74	0.07	0.59	0.03	0.74	0.04	0.52	0.06	1.53	0.18	1.28	0.08	1.49	0.15
Iso18:0	0.53	0.05	0.39	0.09	0.22	0.03	0.53	0.08	0.78	0.14	0.96	0.22	0.93	0.03
18:0	0.99	0.04	1.06	0.08	0.99	0.20	1.02	0.09	4.73	0.21	4.76	0.03	6.95	0.99
19:0	0.17	0.01	0.14	0.01	0.10	0.03	0.11	0.03	0.76	0.16	1.11	0.36	0.74	0.47
20:0	0.16	0.05	0.12	0.05	0.02	0.01	0.34	0.02	1.19	0.26	0.75	0.04	0.66	0.14
22:0	0.10	0.07	0.02	0.01	0.20	0.01	0.11	0.04	–	–	0.19	0.008	0.06	0.01
<b>Σ saturates</b>	<b>28.77</b>	<b>0.85</b>	<b>29.07</b>	<b>1.10</b>	<b>22.24</b>	<b>1.21</b>	<b>30.60</b>	<b>0.08</b>	<b>30.21</b>	<b>1.56</b>	<b>29.32</b>	<b>1.48</b>	<b>33.96</b>	<b>3.08</b>
16:1n-7	2.65	0.02	2.80	0.10	2.40	0.24	3.84	0.10	0.67	0.02	2.09	0.03	1.71	0.06
16:1n-5	0.36	0.09	0.48	0.07	0.27	0.10	0.55	0.03	0.28	0.12	0.35	0.06	0.39	0.03
17:1	0.48	0.02	0.52	0.02	0.74	0.07	0.63	0.03	0.80	0.05	1.49	0.11	0.72	0.06
18:1n-9	6.49	0.21	5.03	0.17	10.13	0.41	8.92	0.97	10.50	0.98	13.29	0.24	7.59	0.90
18:1n-7	1.96	0.12	2.11	0.25	2.45	0.48	1.87	0.65	3.54	0.34	4.05	0.26	2.48	0.08
18:1n-5	0.08	0.04	0.11	0.04	0.09	0.06	0.17	0.04	0.54	0.13	0.46	0.06	–	–
20:1n-11	0.19	0.03	0.18	0.05	–	–	0.19	0.12	–	–	–	–	–	–
20:1n-9	0.34	0.11	0.13	0.01	0.10	0.02	0.23	0.11	1.20	0.06	–	–	–	–
20:1n-7	0.80	0.03	0.97	0.08	0.15	0.04	1.62	0.16	4.22	1.25	1.62	0.45	2.49	0.34
<b>Σ monoenes</b>	<b>13.64</b>	<b>0.20</b>	<b>12.45</b>	<b>0.12</b>	<b>16.54</b>	<b>0.18</b>	<b>18.18</b>	<b>0.65</b>	<b>23.64</b>	<b>1.11</b>	<b>24.91</b>	<b>1.96</b>	<b>15.46</b>	<b>1.03</b>
18:2n-6	2.28	0.11	2.34	0.14	1.70	0.09	2.61	0.03	1.81	0.15	2.54	0.22	2.08	0.05
20:2n-6	0.24	0.05	0.16	0.03	0.04	0.02	0.14	0.10	0.23	0.02	0.50	0.23	–	–
<b>Σ Dienes</b>	<b>2.56</b>	<b>0.11</b>	<b>2.57</b>	<b>0.13</b>	<b>1.79</b>	<b>0.04</b>	<b>2.81</b>	<b>0.09</b>	<b>2.04</b>	<b>0.13</b>	<b>3.05</b>	<b>0.36</b>	<b>2.08</b>	<b>0.05</b>
18:3n-6	0.11	0.01	0.20	0.04	0.02	0.01	0.20	0.01	–	–	–	–	–	–
18:3n-3	0.98	0.06	1.17	0.10	0.60	0.08	0.88	0.05	0.62	0.06	0.70	0.069	0.80	0.13
20:3n-9	0.07	0.03	0.05	0.00	0.03	0.01	–	–	–	–	–	–	–	–
20:3n-6	0.11	0.02	0.12	0.01	0.05	0.03	0.29	0.09	0.04	0.01	0.54	0.41	–	–
20:3n-3	0.07	0.00	0.07	0.03	0.02	0.02	0.01	0.01	0.05	0.04	–	–	–	–
<b>Σ Trienes</b>	<b>1.35</b>	<b>0.11</b>	<b>1.60</b>	<b>0.10</b>	<b>0.73</b>	<b>0.06</b>	<b>1.39</b>	<b>0.06</b>	<b>0.71</b>	<b>0.07</b>	<b>1.27</b>	<b>0.44</b>	<b>0.80</b>	<b>0.13</b>
18:4n-3	3.86	0.33	5.43	0.36	0.95	0.09	3.30	0.05	1.70	0.39	1.75	0.08	3.73	0.19
20:4n-6	2.16	0.07	1.19	0.08	5.92	0.29	2.85	0.38	2.10	0.04	4.54	0.37	0.78	0.16
20:4n-3	0.27	0.01	0.36	0.01	0.13	0.02	0.25	0.00	0.25	0.02	0.24	0.11	0.33	0.01
<b>Σ Tetraenes</b>	<b>6.36</b>	<b>0.28</b>	<b>7.36</b>	<b>0.41</b>	<b>7.14</b>	<b>0.30</b>	<b>6.44</b>	<b>0.35</b>	<b>4.31</b>	<b>0.53</b>	<b>6.52</b>	<b>0.41</b>	<b>4.84</b>	<b>0.36</b>
18:5n-3	0.36	0.04	0.31	0.09	0.11	0.02	–	–	–	–	–	–	–	–
20:5n-3	7.44	0.26	5.74	0.26	15.91	0.48	8.38	0.06	4.68	0.32	10.10	0.37	4.33	0.74
21:5n-3	0.32	0.01	0.40	0.02	0.10	0.02	0.25	0.02	0.51	0.18	0.11	0.03	0.46	0.01
22:5n-6	0.18	0.04	0.15	0.02	0.21	0.02	0.11	0.04	0.52	0.16	0.77	0.38	–	–
22:5n-3	0.76	0.04	0.73	0.06	0.43	0.09	0.55	0.03	0.60	0.04	0.33	0.05	0.61	0.19
<b>Σ Pentaenes</b>	<b>9.07</b>	<b>0.18</b>	<b>7.33</b>	<b>0.14</b>	<b>16.77</b>	<b>0.52</b>	<b>9.29</b>	<b>0.04</b>	<b>6.32</b>	<b>0.38</b>	<b>11.31</b>	<b>0.10</b>	<b>5.40</b>	<b>0.92</b>
22:6n-3	38.24	0.33	39.62	0.67	34.80	0.70	31.29	0.35	32.77	0.94	23.62	2.45	37.46	2.66

Sd standard deviation,  $n = 3$ , – not detected, PC phosphatidylcholine, PE phosphatidylethanolamine, DPG diphosphatidylglycerol, PS phosphatidylserine, PI phosphatidylinositol, LPC lysophosphatidylcholine, \* include phytanic acid



**Table 5** Sterol composition of *Pyrosoma atlanticum* as % of total sterols

Stérol	%
24-norcholesta-5,22E-dien-3 $\beta$ -ol	1.9
24-nor-5 $\alpha$ -cholest-22E-en-3 $\beta$ -ol	0.2
cholesta-5,22Z-dien-3 $\beta$ -ol	6.7
27-nor-24-methylcholesta-5,22E-dien-3 $\beta$ -ol	
5 $\alpha$ -cholest-22Z-en-3 $\beta$ -ol	0.4
cholesta-5,22E-dien-3 $\beta$ -ol	8.3
5 $\alpha$ -cholesta-22E-en-3 $\beta$ -ol	2.2
cholest-5-en-3 $\beta$ -ol	11.7
5 $\alpha$ -cholestan-3 $\beta$ -ol	5.6
24-methylcholesta-5,22E-dien-3 $\beta$ -ol	22.7
24-methyl-5 $\alpha$ -cholest-22E-en-3 $\beta$ -ol	
5 $\alpha$ -cholest-7-en-3 $\beta$ -ol	3.1
24-methylcholesta-5,24(28)-dien-3 $\beta$ -ol	11.1
24-methyl-5 $\alpha$ -cholest-24(28)-en-3 $\beta$ -ol	3.2
24-methylcholest-5-en-3 $\beta$ -ol	
24-methyl-5 $\alpha$ -cholestan-3 $\beta$ -ol	0.4
23,24-dimethylcholesta-5,22E-dien-3 $\beta$ -ol	1.4
24-ethylcholesta-5,22E-dien-3 $\beta$ -ol	3.9
24-ethyl-5 $\alpha$ -cholest-22E-en-3 $\beta$ -ol	0.8
24-ethylcholest-5-en-3 $\beta$ -ol	8.3
24-ethylcholesta-5,24(28)E-dien-3 $\beta$ -ol	0.7
24-ethyl-5 $\alpha$ -cholestan-3 $\beta$ -ol	1.2
24-ethyl-5 $\alpha$ -cholest-24(28)Z-en-3 $\beta$ -ol	0.6
Others	5.4
Total	99.9

\* C<sub>24</sub> stereochemistry not determined in this study, hence only systematic names rather than trivial names are given

composition is unknown, but the dominance of phospholipids is in agreement with data on other subtropical pelagic tunicates [6,7,10]. The low levels of triacylglycerols and free fatty acids, coupled with high concentrations of glycolipids, is also in agreement with the observation made by Deibel et al. [6] on a different pelagic tunicate, the larvacean *Oikopleura vanhoeffeni*. The concentration of glycolipids is likely related to the high levels of chloropigments (present as degradation products) recorded in *Pyrosoma atlanticum* [18] and substantiates the idea of a high physiological turnover as an alternative to large lipid accumulation. Indeed, pyrosomas are known to graze on a wide range of microplanktonic taxa, ranging from sub-micronic particles to large diatoms, and in warm oligotrophic waters are facing relatively continuous food supply. The presence of a pool of free fatty acids coupled with two phytoplankton glycolipid fractions seems indicative of such feeding activity and digestive processes [18]. The presence of phospholipids in excess of 70% of the total lipids seems a general feature of gelatinous pelagic

organisms and indicative of investment in cell membranes as reported for ctenophores [20, 21], larvaceans [6] and chaetognaths [22, 23]. In terms of polar lipid constituents, *P. atlanticum* follows the pattern described for most marine zooplankters, with PC as the main component followed by PE and DPG [24].

A comparison of the total fatty acid pattern among samples collected at different locations in the subtropical Atlantic Ocean by Culkin and Morris [9], the Pacific Ocean by Jeffs et al. [10] and the Indian Ocean in the present study shows a relatively similar composition, with very high levels of DHA, palmitic, oleic and myristic acids and EPA as main descriptors. Lower percentages of myristic, palmitic and palmitoleic acids associated with higher levels of DHA were observed in the present study, compared to the data of Culkin and Morris [9]. The variation in the fatty acid profiles may be attributed to differences in the diet of animals, temperature or to the analytical procedures. A cluster analysis of all data on *P. atlanticum* and other pelagic tunicates, such as *Salpa cylindrica* and *Dolioletta gegenbauri*, separated the older data from the more recent ones (Fig. 2), irrespective of the taxonomic group considered. Interestingly, the pelagic tunicate *Dolioletta gegenbauri* was clearly separated from *P. atlanticum* for both recent studies, based on higher levels of myristic, palmitoleic and arachidic acids and lower percentages of palmitic and oleic acids. The differences between the two taxa are likely related to the differences in phospholipid levels and composition. Higher percentages of polar lipids in *Pyrosoma* is translated in the total lipid fraction into lower myristic, palmitoleic and arachidic acids, which accounts for lower percentages than in neutral lipids.

The analysis of lipids in marine animals can often provide valuable insights into the trophic interactions between primary consumers and their food supply (see review by Dalsgaard et al., 25). Because tunicates are known to retain particles from less than 1  $\mu$ m in diameter to phytoplankton cells larger than 10  $\mu$ m size range [26], the presence of fatty acid markers of bacteria and phytoplankton in the neutral fractions (TAG, FFA and DAG) is consistent with a very diverse diet. In our study, diatom markers (16:1n-7; 16:4 PUFA, 20:5n-3) were recorded but in small proportion, illustrating either a small contribution to the total ingestion or a very high turnover rate. Prymnesiophytes and dinoflagellates markers (C<sub>18</sub> PUFA including 18:5n-3, 22:6n-3) dominated suggesting a large contribution of these two groups to the diet of *P. atlanticum*. Contribution of bacterial markers (iso and anteiso acids, 18:1n-7) was also present with relatively high percentages of iso 17:0 and 18:1n-7. An alternate approach was developed in Perissinotto et al. [18], using multivariate discriminant analysis, which coupled all data published on phytoplankton fatty acids and the pattern of both TAG and FFA

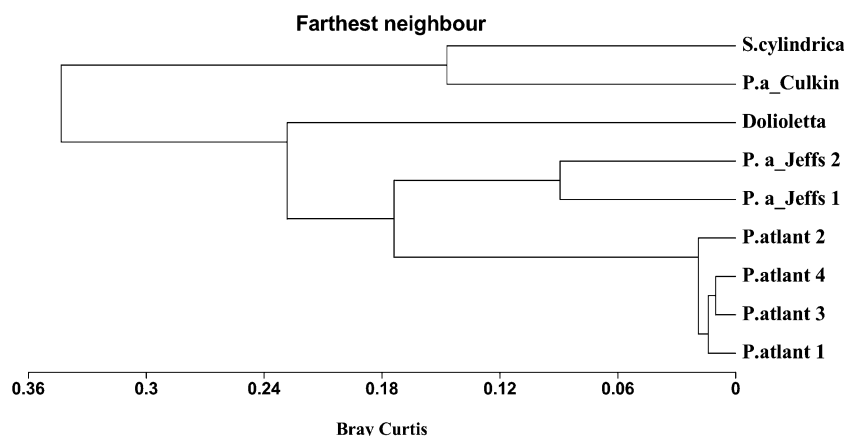


**Fig. 2** Cluster analysis of all published total fatty acid profiles for pelagic tunicates based on computed Bray-Curtis distance ( $x$  axis non dimensional). Symbols: P. atlant # = *Pyrosoma atlanticum* from the present study; P.a\_Jeffs # = *Pyrosoma atlanticum* from Jeffs et al.

(2004); P.a\_Culkin = *Pyrosoma atlanticum* from Culkin and Morris (1970); Doliioletta = *Doliioletta gengenbauri* from Pond and Sargent (1998); S. cylindrica = *Salpa cylindrica* from Culkin and Morris (1970)

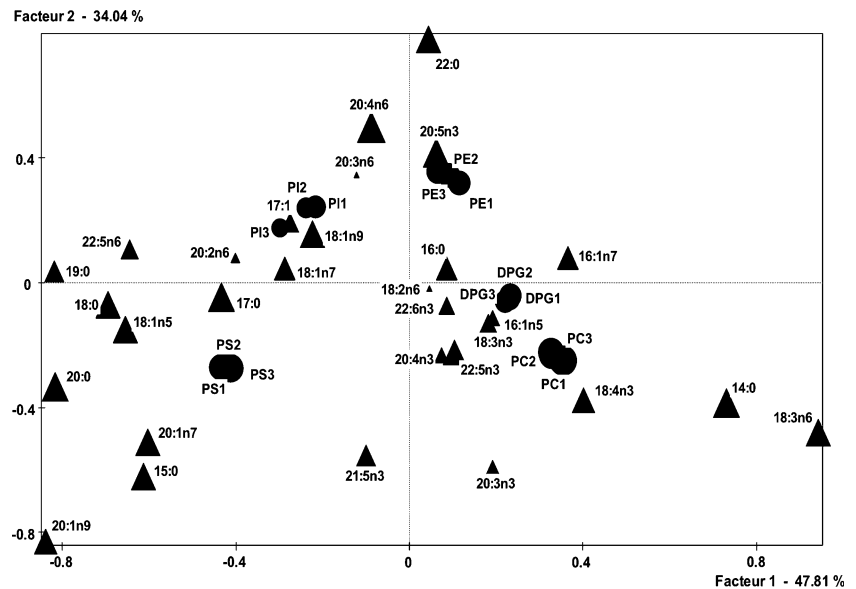
acids recorded for the present samples. Results confirmed that both dinoflagellates and prymnesiophytes are dominant constituents in the ingested material. One question always open with colonial organisms is whether or not ingested chlorophyll has passed the plasma membrane of each individual. The actual process of ingestion and digestion is a complicated one and no direct microscopic observation could be made during this study. However, as shown by Perissinotto et al. [18], most chloropigments were in the form of pheopigments (80 to 90%) with a high rate of degradation into non-fluorescent compounds. Such a process only occurs during gut transit and strongly support the hypothesis that the phytoplankton cells were taken up by individual zooids and digested.

Information on sterol composition is scarce and the present data can only be compared with those of Jeffs et al. [10] for samples of *Pyrosoma atlanticum* and Makar'eva et al. [27] for samples of *Pyrosoma giganteum*. The patterns of sterols recorded for *P. atlanticum* show both similarities and differences. Both profiles show dominance of 24-methylcholesta-5,22E-dien-3(-ol, cholesterol, *cis*-22-dehydrocholesterol and similar levels of 24-ethylcholesta-5,22E-dien-3(-ol, 24-ethylcholest-5-ene-3(-ol and 24-norhydrocholesterol. However, our specimens from the Indian Ocean exhibit higher percentages of 24-methylene cholesterol and *cis*-22-dehydrocholestanol. They also lack in some of the major sterols observed off the New Zealand coast, e.g. 24-methylcholesterol and dinosterol. The differences are likely related to the heterogeneity of particles ingested at the two sites, which may differ substantially in their phytoplankton and microheterotroph-derived sterols. We have no knowledge of the sterol metabolism of tunicates, but the low level of cholesterol observed in *P. atlanticum* may suggest that the ability to convert phytosterols to cholesterol, reported for many crustaceans

[28] may not be as effective in *P. atlanticum*. Copepods, euphausiids, ostracods, phyllosomes and other invertebrates, such as siphonophores and ctenophores, show a large dominance of cholesterol in contrast to tunicates (ascidians and pyrosomes), which contain mostly algal-derived sterols (10, present study). In terms of trophic linkage sterol markers of diatoms (22-dehydrocholesterol, cholesterol, 24-methylenecholesterol), prymnesiophytes and dinoflagellates (24-methylcholesta-5,22E-dien-3(-ol, 24-ethylcholesta-5,22E-dien-3(-ol, 24-ethylcholest-5-ene-3(-ol, 24-methylenecholesterol) are present but as indicated by Volkman [29], many sterols are widely distributed and assignment to a specific algal class remains difficult. The lack of dinosterol in our samples may seem contradictory with the trophic link described earlier, but a number of dinoflagellate species do not contain dinosterol [30,31]. Hence, it may be that species of dinoflagellates lacking dinosterol dominated this component of its diet. In oligotrophic waters, such as those studied in this paper, the sterol composition would tend to support a diet dominated by dinoflagellates and prymnesiophytes [29].

Our knowledge of the phospholipid composition of pelagic marine organisms is, to a large extent, limited to a description of the main classes in crustaceans: i.e., copepods, euphausiids, decapods [24–34], and cnidaria (see review by Joseph, 35). Reports of fatty acid composition is generally limited to benthic ascidians and total polar lipid fraction [4], thus preventing meaningful taxonomic comparisons. Differences between fatty acid composition of the phospholipid constituents seem directly related to the specificity in the pathways of synthesis involved. In this study, a comparison of the various profiles was achieved using a factorial correspondence analysis (FCA). The first three factorial axes accounted for more than 90% of the total variance and projection of both fatty acid descriptors

**Fig. 3** *Pyrosoma atlanticum*. Correspondence analysis of the fatty acid structure of the main phospholipid classes. Projection in the factorial plane defined by axes 1 and 2. Filled triangles illustrate fatty acid descriptors and filled circles illustrate polar lipid fractions. PC phosphatidylcholine; PE phosphatidylethanolamine; PI phosphatidylinositol; PS phosphatidylserine and DPG diphosphoglycerols. Size of symbols is representative of significance on the plane of projection



and phospholipid constituents, on the plane defined by the first two axes (Fig. 3), discriminated between two groups. The first axis separated PC, PE, DPG on the one hand and PS, PI on the other, whereas it opposed PC to PE and PS to PI on the second axis. This is consistent with the concept of main interrelated synthetic routes via CDP-choline and CDP-ethanolamine leading to PC and PE and secondary transformations from PS to produce PE, and from CDP-diacylglycerol to produce PI [36]. In terms of fatty acid profiles, differences in PC were linked with 18:4n-3, 18:3n-3, 20:3n-3, 18:3n-6 and 14:0, while differences in PE were associated with EPA, arachidonic acid and 22:0. Discrimination between PI and PS were related respectively to arachidonic acid, 17:1, oleic and *cis* vaccenic acids and to 20:1n-7, 21:5n-3, 20:1n-9, 20:0 and 15:0.

The fatty acid composition of all polar lipid classes of *P. atlanticum* also shared several common features: a high degree of unsaturation with more than 35% of EPA and DHA; a relatively constant percentage of DHA; and similar levels of saturated acids, although with different constituents. Phospholipids containing high levels of DHA are often associated with the need for high energy processes. They have been proposed to be required as conformational co-factors for the functional assemblage of membrane proteins, ion pumps and/or complexes of the mitochondrial electron transport chain [37, 38]. In the specific case of *P. atlanticum*, locomotion is slow as a consequence of a slow continuous jet emerging from the cloacal aperture of the colony. The jet is produced by the ciliary activity of each individual zooid, which is under nervous control [2]. We have no knowledge of the energy needed and the complex ion and electron transport processes involved in this motion, but data agree with the hypothesis of a strong

contribution of all phospholipid classes. Within the membrane bilayer system, PC, PE and DPG are often associated with both passive and active transport, while PS and PI are linked to nervous stimulation and PI hydrolysis is associated to the production of intracellular messengers. Such a view is consistent with the processes controlling locomotion and the regulation of buoyancy, which utilizes sulphate exclusion [2].

In summary, new results for the lipid class and component fatty acid and sterol distributions of the gelatinous pelagic tunicate *P. atlanticum* collected from the Indian Ocean sector of the Southern Ocean have been obtained. The profiles are consistent with a high physiological turnover, diverse phytoplankton diet, and strong contribution of phospholipid classes to energy needs, including locomotion.

**Acknowledgements** We thank the French CNRS, the French Polar Institute (IPEV), the South African NRF and the University of KwaZulu-Natal (Durban, South Africa) for providing funds for this study. Finally, we like to thank the captain, officers and crew of the “RV *Marion-Dufresne*” for their assistance and cooperation during the ANTARES-4 voyage.

## References

1. vanSoest RWM (1981) A monograph of the order Pyrosomatida (Tunicata, Thaliacea). *J Plankton Res* 3:603–631
2. Bone Q (1998) Locomotion, locomotor muscles and buoyancy. In: Bone Q (ed) *The biology of pelagic tunicates*. Oxford University Press, Oxford, pp 35–53
3. Slantchev K, Yalçın F, Ersöz T, Nechev J, Cahs I, Stefanov K, Popov F (2002) Composition of lipophilic extracts of two tunicates. *Styela sp.* and *Phallusia sp.* from the eastern Mediterranean. *Z Naturforsch* 57:534–540

4. Veracaoundin I, Barnathan G, Gaydou EM, Aknin M (2003) Phospholipid FA from Indian Ocean Tunicates *Eudistoma bituminis* and *Cystodytes violatinctus*. *Lipids* 38:85–88
5. Reinhardt SB, Van Vleet ES (1986) Lipid composition of twenty two species of Antarctic midwater zooplankton and fish. *Mar Biol* 91:149–159
6. Deibel D, Cavaletto JF, Riehl M, Gardner WS (1992) Lipid and lipid class content of the pelagic tunicate *Oikopleura vanhoeffeni*. *Mar Ecol Prog Ser* 88:297–302
7. Pond DW, Sargent JR (1998) Lipid composition of the pelagic tunicate *Doiloleta gegenbauri* (Tunicata, Thaliacea). *J Plankton Res* 20:169–174
8. Phleger CF, Nelson MM, Mooney B, Nichols PD (2000) Lipids of Antarctic salps and their commensal hyperiid amphipods. *Polar Biol* 23:329–337
9. Culkin F, Morris RJ (1970) The fatty acid composition of two marine filter-feeders in relation to a phytoplankton diet. *Deep Sea Res* 17:861–865
10. Jeffs AG, Nichols PD, Mooney BD, Philipps KL, Phleger CF (2004) Identifying potential prey of the pelagic larvae of the spiny lobster  *Jasus edwardsii* using signature lipids. *Comp Biochem Physiol* 137B:487–507
11. Bligh EG, Dyer WJ (1959). A rapid method of total lipid extraction and purification. *Canadian Journal of Biochemistry and Physiol* 37:911–917
12. Morrison WR, Smith LM (1964) Preparation of fatty acid methyl esters and dimethylacetals from lipids with boron fluoride-methanol. *J Lipid Res* 5:600–608
13. Sokal RR, Rohlf FJ (1981) *Biometry*. Freeman and Co, New York
14. Gower JC (1987) Introduction to ordination techniques. In: Legendre P, Legendre L (eds) *Development in numerical ecology*. NATO ASI series G14, pp. 3–64
15. Pielou EC (1984) *The interpretation of ecological data*. Wiley-Interscience, New York
16. Mayzaud P, Chanut JP, Ackman RG (1989) Seasonal changes of the biochemical composition of marine particulate matter with special reference to fatty acid and sterols. *Mar Ecol Prog Ser* 56:189–204
17. Lebart L, Morineau A, Piron M (1995) *Statistique exploratoire multidimensionnelle*. Dunod, Paris
18. Perissinotto R, Mayzaud P, Nichols PD, Labat J-P (2007) Grazing of *Pyrosoma atlanticum* (Tunicata, Thaliacea) in the south Indian Ocean. *Mar Ecol Prog Ser* 330:1–11
19. Drits AV, Arashkevich EG, Semenova TN (1992) *Pyrosoma atlanticum* (Tunicata, Thaliacea): grazing impact on phytoplankton standing stock and role in organic carbon flux. *J Plankton Res* 14:799–809
20. Lee RF (1974) Lipids of zooplankton from Bute Inlet, British Columbia. *J Fish Res Bd Can* 31:1577–1582
21. Morris RJ, McCartney MJ, Schulze-Rönnecke A (1983) *Bolinopsis infundibulum* biochemical composition in relation to diet. *J Exp Mar Biol Ecol* 67:149–157
22. Lee RF (1975) Lipids of Arctic zooplankton. *Comp Biochem Physiol* 51B:263–266
23. Falk-Petersen S, Sargent JR, Tande KS (1987) Lipid composition of zooplankton in relation to the sub-arctic food web. *Polar Biol* 8:115–120
24. Hagen W (1988) On the significance of lipids in Antarctic zooplankton. *Berichte zur Polarforschung* 49:1–129 (*Can Trans Fish Aquat; Sci.*, 5458)
25. Dalsgaard J, St John M, Kattner G, Müller-Navarra D, Hagen W (2003) Fatty acid trophic markers in the pelagic marine environment: a review. *Adv Mar Biol* 46:225–340
26. Harbison GR, McAlister VL (1979) The filter-feeding rates and particle retention efficiencies of three species of Cyclosalpa (Tunicata, Thaliacea). *Limnol Oceanogr* 24:875–892
27. Makar'eva TN, Grebnev BB, Dmitrenok AS, Stonik VA (1993) Sterol composition of *Pyrosoma giganteum*. *Chem Natural Compounds* 28:517–518
28. Teshima S (1972) Sterol metabolism. *Mem Fac Fish Kagoshima University* 21:69–147
29. Volkman JK (1986) A review of sterol markers for marine and terrigenous organic matter. *Org Geochem* 9:83–99
30. Mansour MP, Volkman JK, Jackson AE, Blackburn SI (1999) The fatty acid and sterol composition of five marine dinoflagellates. *J Phycol* 35:710–720
31. Piretti MV, Pagliuca G, Boni L, Pistocchi R, Diamante M, Gazzoti T (1997) Investigation of 4-methyl sterols from cultured dinoflagellate algal strains. *J Phycol* 33:61–67
32. Mayzaud P, Albessard E, Cuzin-Roudy J (1998). Changes in lipid composition of the Antarctic krill *Euphausia superba* in the Indian sector of the Antarctic Ocean. Distribution among organs and sexual maturity stage. *Mar Ecol Prog Ser* 173:149–162
33. Mayzaud P, Albessard E, Virtue P, Boutoute M (2000) Environmental constraints on the lipid structure and metabolism of euphausiids: the case of *Euphausia superba* and *Meganocyctiphanes norvegica*. *Can J Fish Aquat Sci* 57:91–103
34. Mayzaud P, Boutoute M, Alonzo F (2003) Lipid composition of the euphausiids *Euphausia vallentini* and *Thysanoessa macrura* during the summer in the Indian sector of the Southern ocean. *Antarctic Sci* 15:463–475
35. Joseph JD (1979) Lipid composition of marine and estuarine invertebrates: porifera and cnidaria. *Prog Lipid Res* 18:1–30
36. Lehninger AL, Nelson DL, Cox MM (1993) *Principles of biochemistry*. Worth Publishers, New York
37. Infante JP, Kirwan RC, Brenna JT (1987) High levels of docosahexaenoic acid (22:6n-3)-containing phospholipids in high frequency contraction muscles of hummingbirds and rattlesnakes. *Comp Biochem Physiol* 130B:291–298
38. Zachowcki A (1993) Phospholipids in animal eukaryotic membranes: transverse asymmetry and movement. *Biochem J* 294:1–14

# Uniform Fatty Acid Mobilization from Anatomically Distinct Fat Depots in the Sable (*Martes zibellina*)

Petteri Nieminen · Anne-Mari Mustonen

Received: 27 March 2007 / Accepted: 30 March 2007 / Published online: 2 June 2007  
© AOCS 2007

**Abstract** The mobilization of fatty acids (FA) is a selective process in humans, rodents and the few previously studied carnivores. The FA composition of and mobilization from different fat depots reflect the functions of adipose tissues, e.g. in energy storage or insulation. Sixteen farm-raised sables (*Martes zibellina*), a terrestrial mustelid, were assigned into a fed control group or fasted for 4 days. The FA composition of the sable was relatively similar to other previously studied mustelids. The masses of the different fat depots decreased by 28–55% during fasting. The subcutaneous (sc) and intraabdominal (iab) fats had a uniform FA composition and the sable could mobilize both sc and iab FA. 18:3n-3, 18:4n-3 and 16:1n-7 were effectively mobilized, while long-chain saturated (SFA) and monounsaturated FA (MUFA) increased in proportion. Relative mobilization (RM) correlated inversely with the FA chain length and  $\Delta 9$ -desaturation increased RM of several MUFA compared to SFA. The results reinforce the hypothesis that the terrestrial sable can utilize sc and iab fat depots as energy reserves during nutritional scarcity. The natural history of the species is an important determinant of the FA composition and RM between anatomically different fat depots.

**Keywords** Fasting · Fatty acids · *Martes zibellina* · Sable · White adipose tissue

## Abbreviations

ANOVA Analysis of variance  
BM Body mass

BMI	Body mass index
DBI	Double bond index
$\Delta 9$ -DI	$\Delta 9$ -Desaturation index
EDTA	Ethylenediaminetetraacetic acid
FA	Fatty acid
FAME	Fatty acid methyl ester
FFA	Free fatty acid
FID	Flame ionization detector
iab	Intraabdominal
mes	Mesenteric
MUFA	Monounsaturated fatty acid
om	Omental
PG	Prostaglandin
PUFA	Polyunsaturated fatty acid
RM	Relative mobilization
rp	Retroperitoneal
sc	Subcutaneous
SFA	Saturated fatty acid
TACL	Total average chain length
UFA	Unsaturated fatty acid
VLCFA	Very-long-chain fatty acid
WAT	White adipose tissue

## Introduction

White adipose tissue (WAT) is presently considered to be an active organ and not just an inert energy store. WAT is endocrinologically active [1–2], it regulates the immune response [3] and reflects the long-term nutritional history of the individual [4]. In laboratory rats (*Rattus norvegicus*) the release of fatty acids (FA) from WAT reserves is selective and influenced by the carbon chain length and the

P. Nieminen (✉) · A.-M. Mustonen  
Faculty of Biosciences, University of Joensuu,  
P.O. Box 111, 80101 Joensuu, Finland  
e-mail: pniemine@cc.joensuu.fi

degree of unsaturation [5]. FA are mobilized more effectively if they have short carbon chains, are unsaturated and if their double bonds are located close to the terminal methyl group of the chain. In rats [6], American minks (*Mustela vison*) [7], raccoon dogs (*Nyctereutes procyonoides*) [8] and emperor penguins (*Aptenodytes forsteri*) [9], longer-chain saturated (SFA) and monounsaturated FA (MUFA) have relatively low mobilization rates. Also in the American marten (*Martes americana*), 20:0, 20:1n-11, 20:1n-9 and 22:1n-11 are poorly mobilized [10]. The differences in mobilization efficiency are independent of recent FA intake and probably caused by the structure of FA [11].

Many mammals inhabiting the boreal climate experience autumnal fattening followed by wintertime food scarcity and energy catabolism (for the sable *M. zibellina*, see [12]). This type of seasonal body mass (BM) fluctuation is considered nonpathological, while the human weight cycling caused by repeated dieting and weight gain is a health risk due to an increased incidence of e.g. cardiovascular diseases [13]. The sable is a terrestrial mustelid inhabiting Palearctic coniferous forests [14]. It is mostly carnivorous but feeds also on seeds and berries [15, 16]. At temperatures below  $-30^{\circ}\text{C}$ , the sable can stay in the den for several days [17]. As a consequence, the species probably experiences short-term food deprivation in its natural habitat. During a 4-day fasting period the farmed sable uses both subcutaneous (sc) and intraabdominal (iab) fat depots as metabolic energy [18]. Of these fat tissues, the relative loss of mass is the highest for retroperitoneal (rp) fat. In addition, the species utilizes body proteins during fasting indicated by e.g. increased plasma levels of urea and essential amino acids. It also experiences hepatic dysfunction evidenced by elevated plasma transaminase activities and liver triacylglycerol content. It can be hypothesized that the sable would exhibit active mobilization of diverse FA during fasting and there also exists the possibility of specialized roles of anatomically distinct WAT in the use of FA.

The specific aims of this study were (1) to determine the FA composition of sable plasma, liver and regional WAT depots after a balanced long-term feeding of the same diet, (2) to study the effects of food deprivation on the FA profiles of these tissues, (3) to determine the possible selectivity in mobilization of different FA and WAT depots during food deprivation and (4) to investigate the structural basis of this selectivity. Previous data on the physiology of the sable are scarce and basic information on the fat metabolism of the species can be useful not only in comparative physiology but also due to the status of the sable as a fur-producing species.

## Experimental Procedures

For these experiments 16 male sables born in spring 2004 were randomly divided into two experimental groups. The animals were housed singly in standard cages ( $85 \times 30 \times 46$  cm) with wooden nest boxes ( $24 \times 32 \times 35$  cm) suspended above ground in an unheated shed at a commercial fur farm in Himanka, Finland ( $64^{\circ}9'N$ ,  $23^{\circ}42'E$ ). Before the experiment the animals were fed for several months with a standard fur animal feed ( $200\text{--}220$  g or  $1,500\text{--}1,600$  kJ animal $^{-1}$  day $^{-1}$ ; slaughterhouse offal 35%, Baltic herring 24%, barley 14%, cooked cereal 5%, protein concentrate 4%, fox fat 4%, meat and feather flour 3%, mashed potatoes 2%; metabolizable energy 7,400 kJ kg fresh weight $^{-1}$ ; protein 13.6%, fat 9.8%, carbohydrates 13.9%; Himangan kala ja minkki Oy, Himanka). The FA composition of the diet is depicted in Table 1. The fasting experiment was conducted between October 29–November 1, 2004. Half of the animals were put to a total 4-day fast, while the other half was fed using the diet and procedure described above. The duration of the fast was determined to be safe for mustelids of this body size [7, 10, 18–21], yet long enough to detect the specific effects of fasting on the various FA in diverse WAT depots.

**Table 1** The proportions of the most abundant fatty acids ( $\geq 1$  mol%) in the diet of the sables (mean  $\pm$  SE;  $n = 5$ )

Fatty acid	mol% in diet
14:0	1.9 $\pm$ 0.1
16:0	21.0 $\pm$ 0.8
18:0	6.8 $\pm$ 0.3
$\Sigma$ :SFA	31.2 $\pm$ 0.9
16:1n-7	5.0 $\pm$ 0.2
18:1n-9	30.4 $\pm$ 1.0
18:1n-7	2.5 $\pm$ 0.1
20:1n-9	1.0 $\pm$ 0.1
$\Sigma$ :MUFA	41.8 $\pm$ 1.2
18:2n-6	16.4 $\pm$ 2.1
20:2n-6	1.6 $\pm$ 0.8
18:3n-3	2.0 $\pm$ 0.2
18:4n-1	1.6 $\pm$ 0.9
22:6n-3	1.7 $\pm$ 0.1
$\Sigma$ :PUFA	27.1 $\pm$ 1.7
n-6 PUFA	18.9 $\pm$ 1.6
n-3 PUFA	6.3 $\pm$ 0.3
n-3/n-6 PUFA ratio	0.3 $\pm$ <0.1
UFA/SFA ratio	2.2 $\pm$ <0.1

Also minor fatty acids not listed in the table are included in the sums SFA saturated fatty acid, MUFA monounsaturated fatty acid, PUFA polyunsaturated fatty acid, UFA unsaturated fatty acid

The fed group was fasted overnight before the sampling to avoid e.g. lipemic plasma caused by the eating of food remnants. The overnight fast was considered relatively short to allow sampling from the fed group during phase I of fasting. Water was available for both experimental groups ad lib. The experiment was approved by the Animal Care and Use Committee of the University of Joensuu and complied with current EU laws.

Body mass were recorded on the first day of the experiment and at sampling. Body lengths from the tip of the nose to the anus were also determined at sampling. Body mass indices (BMI) indicating body adiposity of the sable [18] were calculated with the formula  $BMI = BM \text{ (kg)} [\text{body length}^3 \text{ (m)}]^{-1}$ . The animals were anaesthetized with intramuscular ketamine (5 mg kg<sup>-1</sup>) and xylazine (2 mg kg<sup>-1</sup>). Blood samples were obtained sterilely by cardiac punctures and the animals were euthanized with an intracardial injection of a mixture of embutramide (60 mg kg<sup>-1</sup>), mebezonium (15 mg kg<sup>-1</sup>) and tetracaine hydrochloride (1.5 mg kg<sup>-1</sup>). Blood samples were placed into test tubes containing EDTA to prevent clotting, centrifuged for 15 min at 4,000g, after which the plasma was removed. The livers were dissected and the WAT samples collected as follows: sc scapular, sc rump, sc ventral, iab omental (om), iab mesenteric (mes) and iab rp. The sc samples were collected from the middle of each anatomical region and the mass of the sc depots was determined as a whole. The iab depots were dissected and weighed separately. The rp depot represents all WAT at the dorsal side of the abdominal cavity around the kidneys and the great blood vessels, while om fat and mes fat represent the whole of the omentum and mesentery, respectively. All samples were frozen immediately in Eppendorf vials with liquid nitrogen and stored at -80°C. The carcasses were frozen at -20 °C, thawed later and the remaining WAT were dissected and weighed.

The plasma free FA (FFA) concentrations were measured with the NEFA Non Esterified Fatty Acids reagents (Randox Laboratories Ltd, Crumlin, UK) using the Technicon RA-XT<sup>TM</sup> analyzer (Swords, Ireland). For the FA analyses, subsamples of WAT, liver and plasma were transmethylated according to Christie [22] by heating with 1% methanolic H<sub>2</sub>SO<sub>4</sub> under nitrogen atmosphere. The formed FA methyl esters (FAME) were extracted with hexane. The dried and concentrated FAME were analyzed by a gas-liquid chromatograph equipped with two injectors and flame ionization and mass detectors (GC-FID and GC-MS, 6890N network GC system with autosampler, FID detector and 5973 mass selective detector, Agilent Technologies Inc, Palo Alto, CA, USA). The GC-FID and GC-MS lines were both equipped with a DB-wax capillary column (30 m, ID 0.25 mm, film 0.25 µm, J&W Scientific, Folsom, CA, USA). The injection volume was 2 µl, and the

split ratio 1:20. The injectors were set at 250 °C, and the FID and mass interphases were at 250 and 200 °C. Helium was used as a carrier gas (1.8 and 1.0 ml min<sup>-1</sup> for FID and mass detecting lines). The initial oven temperature of 180 °C was held for 8 min, and then programmed to rise by 3 °C min<sup>-1</sup> to a final temperature of 210 °C, which was maintained for 25 min. The peaks were reintegrated manually and the mass spectra extracted using the Agilent ChemStation software (Agilent Technologies Inc). The FAME were identified based on the retention time, mass spectrum and comparisons with authentic (Sigma, St. Louis, MO, USA) and natural standards of a known composition and published reference spectra (WW Christie <http://www.lipidlibrary.co.uk/masspec.html>). Quantifications were based on FID responses. The peak areas of the FID chromatograms were converted to mol% by using the theoretical response factors [23] and calibrations with quantitative authentic standards. The FA were marked by using the abbreviations: [carbon number]:[number of double bonds] n-[position of the first double bond calculated from the methyl end]. If not stated otherwise, polyunsaturated FA (PUFA) were methylene-interrupted.

The double bond index (DBI) and the total average chain length (TACL) indicating the mean number of double bonds or carbon atoms per molecule were calculated according to standard formulae [24].  $\Delta 9$ -Desaturation index ( $\Delta 9$ -DI), the ratio of the most important potentially endogenous  $\Delta 9$ -MUFA to the corresponding SFA, was calculated as  $[(\text{mol}\% \text{ 14:1n-5}) + (\text{mol}\% \text{ 16:1n-7}) + (\text{mol}\% \text{ 16:1n-9}) + (\text{mol}\% \text{ 18:1n-9}) + (\text{mol}\% \text{ 18:1n-7})]:[(\text{mol}\% \text{ 14:0}) + (\text{mol}\% \text{ 16:0}) + (\text{mol}\% \text{ 18:0})]$ . The very-long-chain FA (VLCFA) were calculated as the sum of all FA with a chain length  $\geq 24$  carbons (i.e. 24:0 + 24:1n-9; ref. 25). Relative mobilization (RM) was calculated by the formula:  $[\text{mol}\% \text{ in the fed animals} - \text{mol}\% \text{ in the fasted animals}]:[\text{mol}\% \text{ in the fed animals}]$  [10]. The FA composition and RM were also determined for the total pooled sc (scapular, rump and ventral combined) and total pooled iab (om, mes and rp combined) fat depots.

Multiple comparisons were performed with the one-way analysis of variance (ANOVA) followed by the Duncan's post hoc test. The normality of distribution and the homogeneity of variances were determined with the Kolmogorov-Smirnov test and the Levene test. Comparisons between the two study groups were performed with the Student's *t* test for independent samples. In case of non-parametric data (normality of distribution and homogeneity of variances not attained after standard transformations), the Mann-Whitney *U* test was used. Significant differences in the time series (BM) were analyzed with the *t*-test for related samples. Correlations were calculated using the Spearman correlation coefficient ( $r_s$ ). The *P* value less than 0.05 was considered to be statistically significant. The re-

sults are presented as the mean  $\pm$  SE. FA with proportions  $> 0.1\%$  are presented in the tables, but also FA with trace amounts were included in the sums and used in the calculation of indices.

## Results

The initial BM of the fed ( $1.20 \pm 0.04$  kg) and the fasted sables ( $1.17 \pm 0.05$  kg) did not differ between the experimental groups, while the BM of the fasted animals was lower after the 4-day food deprivation period ( $1.14 \pm 0.03$  vs.  $0.98 \pm 0.03$  kg). Decreases in the absolute and relative masses of the specific fat depots due to fasting were as follows: total sc fat: fed  $59.0 \pm 7.1$  vs. fasted  $27.6 \pm 6.6$  g; difference 53%;  $P < 0.05$ ; om fat:  $9.2 \pm 1.0$  vs.  $6.3 \pm 1.6$  g; 32%; NS; mes fat:  $8.5 \pm 0.8$  vs.  $6.1 \pm 1.4$  g; 28%; NS; rp fat:  $13.8 \pm 2.4$  vs.  $6.2 \pm 1.4$  g; 55%;  $P < 0.05$  and total iab fat:  $33.5 \pm 4.2$  vs.  $19.6 \pm 4.6$  g; 41%;  $P < 0.05$ . The body fat% was significantly higher in the fed animals than in the fasted group ( $8.0 \pm 0.8$  vs.  $4.7 \pm 1.0\%$ ).

The concentrations of plasma FFA were higher in the fasted animals ( $0.6 \pm 0.18$  vs.  $2.6 \pm 0.57$  mmol  $l^{-1}$ ,  $P < 0.05$ ). The most abundant FA (proportion  $> 1\%$ ) in sable plasma were 16:0, 18:0, 18:1n-9, 18:1n-7, 18:2n-6, 20:4n-6, 20:5n-3, 22:5n-3 and 22:6n-3 (Table 2). Fasting caused decreases in the proportions of 15:0, 17:0, 18:0, 16:1n-9, 18:2n-6, total dienes and trienes, n-6 PUFA and total PUFA in plasma, while the proportions of 14:0, 16:0, total SFA, 14:1n-9, 20:1n-11, 20:1n-9, 22:1n-11, total MUFA and total n-3 PUFA as well as the n-3/n-6 PUFA ratios increased. The ratio of unsaturated FA (UFA) to SFA decreased in plasma. In liver, the most obvious decreases induced by fasting were in 17:0, 18:0, 22:0, 24:0, 20:4n-6, 22:4n-6, total n-6 PUFA and total PUFA, while the proportions of 12:0, 14:0, 14:1n-5, 18:1n-9, 20:1n-11, 20:1n-9 and total MUFA increased. The DBI and TACL decreased in liver due to food deprivation. In plasma and liver the proportions of 16:0, 18:0, 20:4n-6, 20:5n-3 and 22:6n-3 were higher than in the WAT, while the proportions of several MUFA, especially 16:1n-7 and 18:1n-9, were lower. The most abundant FA with decreased proportions in WAT due to fasting were 16:1n-7, 18:3n-3 and 18:4n-3, while the percentages of 14:0, 20:0, 22:0, 24:0, 20:1n-11, 20:1n-9, 22:1n-11 and 24:1n-9 increased (Tables 2, 3, 4). The n-3/n-6 PUFA ratio decreased in the pooled sc and iab fat depots as well as in the mes and rp fats. The sum of VLCFA increased in the pooled sc and iab fat depots.

Most FA increased in proportion in the WAT during fasting (Fig. 1). 20:0, 22:1n-11, 20:1n-11, 20:1n-9 and 22:5n-3 were mostly preserved, while 18:3n-3, 18:4n-3, 16:1n-7, 17:1n-8, 15:0 and 16:0 had high RM values. There were no differences in RM of FA between the different

WAT. RM of SFA correlated negatively with the chain length when all trunk WAT were analyzed as a whole ( $r_s = -0.127$ ,  $P < 0.01$ ; Fig. 2a). The same was observed in n-5 ( $r_s = -0.191$ ,  $P < 0.01$ ), n-7 ( $r_s = -0.285$ ,  $P < 0.01$ ) and n-9 MUFA ( $r_s = -0.366$ ,  $P < 0.01$ ; Fig. 2b). The influence of chain length on RM of PUFA was tested by comparing PUFA with the same degree of unsaturation and position of the first double bond but a different chain length. The difference was significant in five out of eight pairs in the way that the PUFA with the longer chain length had a lower RM value (Fig. 2c). When SFA and corresponding MUFA were compared, RM increased significantly with  $\Delta 9$ -desaturation in three out of seven pairs (Fig. 2d). The influence of unsaturation on RM of PUFA was studied by comparing PUFA with the same chain length and position of the first double bond but with a different double bond number. The difference was significant in one out of eight pairs in the way that the PUFA with the higher number of double bonds had a higher RM rate. The influence of positional isomerism on RM of MUFA was tested by comparing MUFA of the same chain length but different position of the double bond. The difference was statistically significant in 4 out of 11 pairs in the way that the MUFA with the double bond closer to the methyl end of the molecule had a lower (three cases) or a higher RM value (one case). When comparing PUFA with the same chain length and unsaturation but with a different position of the first double bond, the difference was statistically significant in one out of seven pairs in the way that the PUFA with the first double bond closer to the methyl end had a lower RM rate.

## Discussion

The FA composition of the tissues of the farmed sable was quite similar to another mustelid, the farmed American mink [7, 26–27] with 16:0, 18:0, 18:1n-9 and 18:2n-6 as the most abundant FA. The sc and iab WAT depots of the sable contained less total MUFA (46 vs. 52–55%) but higher proportions of total PUFA (20 vs. 10%) compared to the mink due to e.g. the high percentage of 18:2n-6 (16 vs. 7–8%). The FA profile of the sable was also very similar to the closely related farmed American marten [10], which had slightly more SFA, especially 14:0 and 20:0 in its fat tissues, while the percentages of MUFA, especially 18:1n-9, were higher in the sable. As the FA composition of the diets probably varied between the studies, the observed differences between the species could have been caused by different FA intake. The most abundant FA in the WAT of the farmed sable were also mostly the same as recorded previously for the wild raccoon dog, European brown bear (*Ursus arctos arctos*) and gray wolf (*Canis lupus*; 28).



**Table 2** Effects of fasting on the composition of the most abundant fatty acids (mol%) in total sc and iab fat tissues, plasma and livers of the sables (mean  $\pm$  SE)

Fatty acid	Total sc fat		Total iab fat		Plasma		Liver	
	Fed	Fasted	Fed	Fasted	Fed	Fasted	Fed	Fasted
12:0	0.7 $\pm$ <0.1 <sup>a</sup>	0.8 $\pm$ <0.1 <sup>*b</sup>	0.7 $\pm$ <0.1 <sup>a</sup>	0.7 $\pm$ <0.1 <sup>a</sup>	0.3 $\pm$ 0.1	0.3 $\pm$ 0.1	0.9 $\pm$ 0.2	3.1 $\pm$ 0.5*
14:0	5.1 $\pm$ 0.2 <sup>a</sup>	6.1 $\pm$ 0.3 <sup>*b</sup>	5.0 $\pm$ 0.3 <sup>a</sup>	5.3 $\pm$ 0.4 <sup>a</sup>	0.6 $\pm$ 0.1	0.9 $\pm$ 0.1*	1.3 $\pm$ 0.2	3.4 $\pm$ 0.7*
16:0	20.5 $\pm$ 0.2	19.6 $\pm$ 0.5	20.8 $\pm$ 0.3	19.7 $\pm$ 0.7	22.9 $\pm$ 0.4	27.0 $\pm$ 0.6*	25.6 $\pm$ 0.5	27.0 $\pm$ 0.6
17:0	0.3 $\pm$ <0.1	0.3 $\pm$ <0.1	0.3 $\pm$ <0.1	0.3 $\pm$ <0.1	0.4 $\pm$ <0.1	0.3 $\pm$ <0.1*	0.4 $\pm$ <0.1	0.3 $\pm$ <0.1*
18:0	6.3 $\pm$ 0.2	6.5 $\pm$ 0.2	6.7 $\pm$ 0.2	7.8 $\pm$ 0.4*	12.7 $\pm$ 0.3	11.0 $\pm$ 0.2*	14.3 $\pm$ 0.9	8.6 $\pm$ 1.6*
$\Sigma$ :0	33.9 $\pm$ 0.3	33.3 $\pm$ 1.4	34.5 $\pm$ 0.4	35.1 $\pm$ 0.6	38.3 $\pm$ 0.4	40.9 $\pm$ 0.6*	43.8 $\pm$ 0.6	43.6 $\pm$ 0.5
14:1n-5	0.2 $\pm$ <0.1	0.3 $\pm$ <0.1	0.2 $\pm$ <0.1	0.2 $\pm$ <0.1	0.1 $\pm$ <0.1	0.1 $\pm$ <0.1	0.1 $\pm$ <0.1	0.2 $\pm$ <0.1*
16:1n-9	0.6 $\pm$ <0.1	0.6 $\pm$ <0.1*	0.6 $\pm$ <0.1	0.6 $\pm$ <0.1	0.3 $\pm$ <0.1	0.2 $\pm$ <0.1*	0.4 $\pm$ <0.1	0.5 $\pm$ <0.1
16:1n-7	4.4 $\pm$ 0.3 <sup>b</sup>	3.8 $\pm$ 0.2 <sup>ab</sup>	3.9 $\pm$ 0.2 <sup>b</sup>	3.1 $\pm$ 0.3 <sup>*a</sup>	0.9 $\pm$ 0.1	1.0 $\pm$ 0.1	1.6 $\pm$ 0.2	2.7 $\pm$ 0.5
18:1n-9	35.9 $\pm$ 0.3	35.4 $\pm$ 0.2	35.6 $\pm$ 0.3	34.6 $\pm$ 1.0	13.8 $\pm$ 0.3	15.2 $\pm$ 0.6	12.2 $\pm$ 0.6	16.1 $\pm$ 1.6*
18:1n-7	2.6 $\pm$ <0.1	2.6 $\pm$ <0.1	2.6 $\pm$ <0.1	2.7 $\pm$ 0.1	1.8 $\pm$ <0.1	1.9 $\pm$ 0.1	2.3 $\pm$ 0.1	2.4 $\pm$ 0.1
24:1n-9	0.1 $\pm$ <0.1	0.1 $\pm$ <0.1*	0.1 $\pm$ <0.1	0.2 $\pm$ <0.1*	0.5 $\pm$ <0.1	0.6 $\pm$ <0.1	0.3 $\pm$ <0.1	0.2 $\pm$ <0.1
$\Sigma$ :1	46.1 $\pm$ 0.4	43.8 $\pm$ 1.8	45.6 $\pm$ 0.3	44.4 $\pm$ 1.1	18.2 $\pm$ 0.4	20.1 $\pm$ 0.7*	17.7 $\pm$ 0.6	23.4 $\pm$ 2.2*
$\Delta$ 9-DI	1.4 $\pm$ <0.1	1.3 $\pm$ <0.1	1.3 $\pm$ <0.1	1.3 $\pm$ <0.1	0.5 $\pm$ <0.1	0.5 $\pm$ <0.1	0.4 $\pm$ <0.1	0.6 $\pm$ 0.1*
18:2n-6	15.8 $\pm$ 0.2	15.8 $\pm$ 0.1	16.0 $\pm$ 0.2	16.2 $\pm$ 0.4	22.5 $\pm$ 1.0	15.3 $\pm$ 0.5*	15.4 $\pm$ 0.4	16.5 $\pm$ 0.5
20:2n-6	0.3 $\pm$ <0.1	0.3 $\pm$ <0.1	0.3 $\pm$ <0.1	0.3 $\pm$ <0.1	0.1 $\pm$ <0.1	0.2 $\pm$ <0.1	0.3 $\pm$ <0.1	0.2 $\pm$ <0.1
18:3n-6	0.1 $\pm$ <0.1	0.1 $\pm$ <0.1*	0.1 $\pm$ <0.1	0.1 $\pm$ <0.1*	0.6 $\pm$ <0.1	0.2 $\pm$ <0.1*	0.5 $\pm$ <0.1	0.3 $\pm$ <0.1*
18:3n-3	1.2 $\pm$ <0.1 <sup>c</sup>	1.0 $\pm$ <0.1 <sup>*b</sup>	1.2 $\pm$ <0.1 <sup>c</sup>	0.9 $\pm$ 0.1 <sup>*a</sup>	0.5 $\pm$ <0.1	0.4 $\pm$ <0.1	0.6 $\pm$ 0.1	0.8 $\pm$ 0.1
18:4n-3	0.1 $\pm$ <0.1	0.1 $\pm$ <0.1*	0.1 $\pm$ <0.1	0.1 $\pm$ <0.1*	0.1 $\pm$ <0.1	0.1 $\pm$ <0.1	0.1 $\pm$ <0.1	0.2 $\pm$ <0.1
20:3n-6	0.1 $\pm$ <0.1	0.2 $\pm$ <0.1	0.1 $\pm$ <0.1	0.2 $\pm$ <0.1	0.9 $\pm$ 0.1	0.4 $\pm$ <0.1*	0.8 $\pm$ 0.1	0.3 $\pm$ <0.1*
20:4n-6	0.2 $\pm$ <0.1	0.2 $\pm$ <0.1	0.2 $\pm$ <0.1	0.6 $\pm$ 0.3	7.4 $\pm$ 0.4	8.1 $\pm$ 0.2	6.1 $\pm$ 0.5	3.4 $\pm$ 0.7*
22:4n-6	0.1 $\pm$ <0.1	0.1 $\pm$ <0.1	0.1 $\pm$ <0.1	0.2 $\pm$ <0.1	0.2 $\pm$ <0.1	0.2 $\pm$ <0.1	0.2 $\pm$ <0.1	0.1 $\pm$ <0.1*
20:5n-3	0.2 $\pm$ <0.1	0.1 $\pm$ <0.1*	0.2 $\pm$ <0.1	0.2 $\pm$ <0.1	2.3 $\pm$ 0.1	2.2 $\pm$ 0.2	1.5 $\pm$ 0.1	1.1 $\pm$ 0.1*
22:5n-3	0.3 $\pm$ <0.1	0.3 $\pm$ <0.1	0.3 $\pm$ <0.1	0.3 $\pm$ 0.1	1.2 $\pm$ 0.1	1.2 $\pm$ 0.1	1.3 $\pm$ 0.1	0.9 $\pm$ 0.1
22:6n-3	0.9 $\pm$ <0.1	0.9 $\pm$ 0.1	0.8 $\pm$ <0.1	0.8 $\pm$ 0.2	7.1 $\pm$ 0.4	10.0 $\pm$ 0.7*	10.8 $\pm$ 0.4	8.6 $\pm$ 1.5
$\Sigma$ :PUFA	20.0 $\pm$ 0.2	20.3 $\pm$ 0.7	19.9 $\pm$ 0.3	20.5 $\pm$ 0.9	43.5 $\pm$ 0.6	39.1 $\pm$ 0.7*	38.5 $\pm$ 1.0	33.0 $\pm$ 1.8*
$\Sigma$ :n-6 PUFA	16.8 $\pm$ 0.2	18.0 $\pm$ 1.3	16.9 $\pm$ 0.2	17.7 $\pm$ 0.7	32.0 $\pm$ 1.0	24.8 $\pm$ 0.6*	23.7 $\pm$ 0.5	21.0 $\pm$ 0.4*
$\Sigma$ :n-3 PUFA	3.0 $\pm$ 0.1	3.4 $\pm$ 0.7	2.7 $\pm$ 0.1	2.6 $\pm$ 0.3	11.4 $\pm$ 0.5	14.1 $\pm$ 0.7*	14.6 $\pm$ 0.5	11.8 $\pm$ 1.5
n-3/n-6 PUFA	0.2 $\pm$ <0.1 <sup>c</sup>	0.2 $\pm$ <0.1 <sup>*b</sup>	0.2 $\pm$ <0.1 <sup>bc</sup>	0.1 $\pm$ 0.1 <sup>*a</sup>	0.4 $\pm$ <0.1	0.6 $\pm$ <0.1*	0.6 $\pm$ <0.1	0.6 $\pm$ <0.1
$\Sigma$ :VLCFA	0.1 $\pm$ <0.1	0.2 $\pm$ <0.1*	0.1 $\pm$ <0.1	0.2 $\pm$ <0.1*	0.7 $\pm$ <0.1	0.7 $\pm$ <0.1	0.4 $\pm$ <0.1	0.3 $\pm$ 0.1
UFA/SFA	2.0 $\pm$ <0.1	2.5 $\pm$ 0.6	1.9 $\pm$ <0.1	1.9 $\pm$ <0.1	1.6 $\pm$ <0.1	1.5 $\pm$ <0.1*	1.3 $\pm$ <0.1	1.3 $\pm$ <0.1
DBI	0.9 $\pm$ <0.1	0.9 $\pm$ <0.1	0.9 $\pm$ <0.1	0.9 $\pm$ <0.1	1.6 $\pm$ <0.1	1.7 $\pm$ <0.1	1.6 $\pm$ <0.1	1.4 $\pm$ <0.1*
TACL	17.3 $\pm$ <0.1	17.3 $\pm$ <0.1	17.3 $\pm$ <0.1	17.4 $\pm$ 0.1	17.9 $\pm$ <0.1	18.0 $\pm$ <0.1	18.0 $\pm$ 0.1	17.4 $\pm$ 0.2*

sc subcutaneous, iab intraabdominal,  $\Delta$ 9-DI  $\Delta$ 9-desaturation index, PUFA polyunsaturated fatty acid, VLCFA very-long-chain fatty acid (chain length  $\geq$  24 C), UFA unsaturated fatty acid, SFA saturated fatty acid, DBI double bond index, TACL total average chain length. Also minor fatty acids not listed in the table are included in the sums

\* Significant difference between the fed and the fasted animals (*t* test, Mann–Whitney *U* test,  $P < 0.05$ ), means with no common letter indicate that the values of sc and iab fats differ at  $P < 0.05$  (one-way ANOVA)

The FA composition of the trunk WAT was very uniform in the sable and no clear differences could be detected in the FA proportions between the sc and iab fats. This is quite different from the related American mink, which has significantly lower proportions of total SFA but higher percentages of total MUFA in its sc fats compared to the iab depots [7]. In addition, the DBI and  $\Delta$ 9-DI are higher in the sc depots of the mink, which results from the high

proportions of longer-chain SFA in the iab fats. These FA have high melting points and could thus be at risk of solidification during swimming if they were concentrated in the sc depots of the mink. As a terrestrial species with good insulation against cold air, the sable does not seem to require similar FA gradients as a thermal adaptation. While it has been established that an unsaturation gradient exists also between the trunk fats and the body appendages in the

**Table 3** Effects of fasting on the composition of the most abundant saturated and monounsaturated fatty acids (mol%) in adipose tissues of the sables (mean  $\pm$  SE)

Fatty acid	Scapular sc fat		Rump sc fat		Ventral sc fat		Mesenteric fat		Omental fat		Retropitoneal fat	
	Fed	Fasted	Fed	Fasted	Fed	Fasted	Fed	Fasted	Fed	Fasted	Fed	Fasted
12:0	0.7 $\pm$ 0.1	0.7 $\pm$ 0.1	0.6 $\pm$ <0.1	0.8 $\pm$ 0.1	0.7 $\pm$ <0.1	0.8 $\pm$ <0.1*	0.6 $\pm$ <0.1	0.6 $\pm$ 0.1	0.8 $\pm$ 0.1	0.8 $\pm$ 0.1	0.6 $\pm$ <0.1	0.6 $\pm$ <0.1
14:0	5.4 $\pm$ 0.6	5.8 $\pm$ 0.5	4.8 $\pm$ 0.2	5.8 $\pm$ 0.5	5.0 $\pm$ 0.4	6.7 $\pm$ 0.6*	4.3 $\pm$ 0.2	4.4 $\pm$ 0.7	6.4 $\pm$ 0.4	6.4 $\pm$ 0.4	6.8 $\pm$ 0.4	4.1 $\pm$ 0.1
16:0	20.8 $\pm$ 0.3	19.6 $\pm$ 0.9	20.3 $\pm$ 0.3	19.2 $\pm$ 1.0	20.5 $\pm$ 0.4	20.2 $\pm$ 0.7	20.2 $\pm$ 0.5	19.6 $\pm$ 1.2	22.3 $\pm$ 0.4	21.4 $\pm$ 1.3	20.0 $\pm$ 0.4	18.1 $\pm$ 1.1
18:0	6.1 $\pm$ 0.5	6.8 $\pm$ 0.3	6.3 $\pm$ 0.3	6.6 $\pm$ 0.5	6.4 $\pm$ 0.3	6.3 $\pm$ 0.2	7.2 $\pm$ 0.3	8.6 $\pm$ 0.8	5.7 $\pm$ 0.3	6.3 $\pm$ 0.4	7.3 $\pm$ 0.2	8.4 $\pm$ 0.6
$\Sigma$ :0	34.3 $\pm$ 0.4	34.4 $\pm$ 0.8	33.3 $\pm$ 0.4	33.9 $\pm$ 0.8	34.0 $\pm$ 0.6	31.5 $\pm$ 4.2	33.7 $\pm$ 0.5	34.9 $\pm$ 1.2	36.6 $\pm$ 0.5	36.7 $\pm$ 1.0	33.4 $\pm$ 0.3	33.7 $\pm$ 0.7
14:1n-5	0.3 $\pm$ 0.1	0.2 $\pm$ <0.1	0.2 $\pm$ <0.1	0.3 $\pm$ <0.1	0.2 $\pm$ <0.1	0.3 $\pm$ <0.1*	0.2 $\pm$ <0.1	0.2 $\pm$ <0.1	0.3 $\pm$ <0.1	0.3 $\pm$ <0.1	0.2 $\pm$ <0.1	0.2 $\pm$ <0.1
16:1n-9	0.6 $\pm$ <0.1	0.6 $\pm$ <0.1	0.6 $\pm$ <0.1	0.7 $\pm$ <0.1	0.6 $\pm$ <0.1	0.6 $\pm$ <0.1	0.6 $\pm$ <0.1	0.6 $\pm$ 0.1	0.6 $\pm$ <0.1	0.6 $\pm$ <0.1	0.6 $\pm$ <0.1	0.7 $\pm$ <0.1
16:1n-7	4.6 $\pm$ 0.6	3.4 $\pm$ 0.3	4.4 $\pm$ 0.4	3.9 $\pm$ 0.4	4.1 $\pm$ 0.3	4.1 $\pm$ 0.3	3.5 $\pm$ 0.3	2.6 $\pm$ 0.4	4.8 $\pm$ 0.4	4.2 $\pm$ 0.5	3.5 $\pm$ 0.2	2.5 $\pm$ 0.4
18:1n-9	35.4 $\pm$ 0.5	35.7 $\pm$ 0.4	36.2 $\pm$ 0.4	35.7 $\pm$ 0.5	36.0 $\pm$ 0.5	34.9 $\pm$ 0.4	36.2 $\pm$ 0.4	33.7 $\pm$ 2.8	34.2 $\pm$ 0.5	34.3 $\pm$ 0.5	36.4 $\pm$ 0.3	35.7 $\pm$ 0.8
18:1n-7	2.5 $\pm$ 0.1	2.6 $\pm$ 0.1	2.6 $\pm$ <0.1	2.6 $\pm$ 0.2	2.6 $\pm$ <0.1	2.6 $\pm$ 0.1	2.6 $\pm$ 0.1	2.8 $\pm$ 0.1	2.5 $\pm$ 0.1	2.5 $\pm$ 0.1	2.6 $\pm$ <0.1	2.8 $\pm$ 0.1
20:1n-11	0.2 $\pm$ <0.1	0.3 $\pm$ <0.1*	0.3 $\pm$ <0.1	0.3 $\pm$ <0.1*	0.3 $\pm$ <0.1	0.3 $\pm$ <0.1	0.3 $\pm$ <0.1	0.4 $\pm$ 0.1	0.2 $\pm$ <0.1	0.3 $\pm$ 0.1	0.3 $\pm$ <0.1	0.4 $\pm$ 0.1
20:1n-9	1.0 $\pm$ 0.1	1.4 $\pm$ 0.1*	1.1 $\pm$ 0.1	1.4 $\pm$ 0.2	1.1 $\pm$ 0.1	1.2 $\pm$ 0.1	1.2 $\pm$ 0.1	1.2 $\pm$ 0.2	0.9 $\pm$ 0.1	1.2 $\pm$ 0.2	1.2 $\pm$ 0.1	1.7 $\pm$ 0.3
24:1n-9	0.1 $\pm$ <0.1	0.1 $\pm$ <0.1*	0.1 $\pm$ <0.1	0.1 $\pm$ <0.1	0.1 $\pm$ <0.1	0.1 $\pm$ <0.1	0.1 $\pm$ <0.1	0.2 $\pm$ <0.1*	0.1 $\pm$ <0.1	0.1 $\pm$ <0.1*	0.1 $\pm$ <0.1	0.2 $\pm$ <0.1*
$\Sigma$ :1	45.8 $\pm$ 0.5	45.6 $\pm$ 0.4	46.6 $\pm$ 0.7	46.2 $\pm$ 0.6	46.0 $\pm$ 0.7	39.7 $\pm$ 5.4	45.9 $\pm$ 0.5	43.0 $\pm$ 3.2	44.8 $\pm$ 0.5	44.7 $\pm$ 0.4	46.0 $\pm$ 0.4	45.5 $\pm$ 0.8
$\Delta$ 9-DI	1.4 $\pm$ <0.1	1.3 $\pm$ <0.1	1.4 $\pm$ <0.1	1.4 $\pm$ <0.1	1.4 $\pm$ <0.1	1.3 $\pm$ <0.1	1.4 $\pm$ <0.1	1.3 $\pm$ 0.1	1.2 $\pm$ <0.1	1.2 $\pm$ <0.1	1.4 $\pm$ <0.1	1.3 $\pm$ <0.1

sc subcutaneous,  $\Delta$ 9-DI  $\Delta$ 9-desaturation index. Also minor fatty acids not listed in the table are included in the sums

\* Significant difference between the fed and the fasted animals (*t* test, Mann–Whitney *U* test, *P* < 0.05)

**Table 4** Effects of fasting on the composition of the most abundant polyunsaturated fatty acids (mol%) in adipose tissues of the sables (mean  $\pm$  SE)

Fatty acid	Scapular sc fat		Rump sc fat		Ventral sc fat		Mesenteric fat		Omental fat		Retropitoneal fat	
	Fed	Fasted	Fed	Fasted	Fed	Fasted	Fed	Fasted	Fed	Fasted	Fed	Fasted
18:2n-6	15.7 $\pm$ 0.4	16.0 $\pm$ 0.2	15.9 $\pm$ 0.3	15.9 $\pm$ 0.3	15.5 $\pm$ 0.3	17.4 $\pm$ 0.9	16.5 $\pm$ 0.2	17.4 $\pm$ 0.9	14.9 $\pm$ 0.3	15.1 $\pm$ 0.4	16.7 $\pm$ 0.2	16.3 $\pm$ 0.4
18:3n-3	1.2 $\pm$ 0.1	1.0 $\pm$ 0.1*	1.2 $\pm$ 0.1	1.0 $\pm$ 0.1*	1.0 $\pm$ 0.1*	0.8 $\pm$ 0.1*	1.2 $\pm$ 0.1	0.8 $\pm$ 0.1*	1.2 $\pm$ 0.1	1.0 $\pm$ 0.1	1.2 $\pm$ 0.1	0.8 $\pm$ 0.1*
18:4n-3	0.1 $\pm$ <0.1	0.1 $\pm$ <0.1	0.2 $\pm$ <0.1	0.1 $\pm$ <0.1	0.1 $\pm$ <0.1	0.1 $\pm$ <0.1*	0.1 $\pm$ <0.1	0.1 $\pm$ <0.1*	0.2 $\pm$ <0.1	0.1 $\pm$ <0.1	0.1 $\pm$ <0.1	0.1 $\pm$ <0.1*
20:4n-6	0.2 $\pm$ <0.1	0.2 $\pm$ <0.1	0.3 $\pm$ 0.1	0.3 $\pm$ 0.1	0.2 $\pm$ <0.1	0.2 $\pm$ <0.1	0.2 $\pm$ <0.1	1.1 $\pm$ 0.9	0.2 $\pm$ <0.1	0.2 $\pm$ <0.1	0.2 $\pm$ <0.1	0.6 $\pm$ 0.4
22:4n-6	0.1 $\pm$ <0.1	0.2 $\pm$ <0.1	0.1 $\pm$ <0.1	0.2 $\pm$ <0.1	0.1 $\pm$ <0.1	0.1 $\pm$ <0.1	0.1 $\pm$ <0.1	0.2 $\pm$ <0.1	0.1 $\pm$ <0.1	0.1 $\pm$ <0.1	0.1 $\pm$ <0.1	0.2 $\pm$ <0.1
20:5n-3	0.2 $\pm$ <0.1	0.1 $\pm$ <0.1*	0.1 $\pm$ <0.1	0.1 $\pm$ <0.1	0.1 $\pm$ <0.1	0.1 $\pm$ <0.1	0.1 $\pm$ <0.1	0.3 $\pm$ 0.3	0.2 $\pm$ <0.1	0.1 $\pm$ <0.1*	0.1 $\pm$ <0.1	0.1 $\pm$ 0.1
22:5n-3	0.3 $\pm$ <0.1	0.3 $\pm$ <0.1	0.3 $\pm$ <0.1	0.3 $\pm$ 0.1	0.3 $\pm$ <0.1	0.3 $\pm$ <0.1	0.3 $\pm$ <0.1	0.3 $\pm$ 0.1	0.2 $\pm$ <0.1	0.3 $\pm$ <0.1	0.3 $\pm$ <0.1	0.5 $\pm$ 0.2
22:6n-3	0.9 $\pm$ 0.1	0.9 $\pm$ 0.1	0.9 $\pm$ 0.1	0.9 $\pm$ 0.1	0.8 $\pm$ 0.1	0.8 $\pm$ 0.1	0.8 $\pm$ 0.1	0.8 $\pm$ 0.1	0.7 $\pm$ 0.1	0.7 $\pm$ 0.1	0.8 $\pm$ 0.1	1.0 $\pm$ 0.4
$\Sigma$ :PUFA	19.9 $\pm$ 0.5	20.0 $\pm$ 0.4	20.1 $\pm$ 0.4	19.9 $\pm$ 0.1	20.0 $\pm$ 0.3	21.2 $\pm$ 1.9	20.4 $\pm$ 0.3	22.1 $\pm$ 2.3	18.6 $\pm$ 0.4	18.5 $\pm$ 0.6	20.6 $\pm$ 0.3	20.8 $\pm$ 1.1
$\Sigma$ :n-6 PUFA	16.7 $\pm$ 0.4	17.0 $\pm$ 0.3	16.9 $\pm$ 0.3	16.9 $\pm$ 0.4	16.9 $\pm$ 0.2	20.2 $\pm$ 3.8	17.5 $\pm$ 0.2	19.3 $\pm$ 1.9	15.7 $\pm$ 0.3	15.9 $\pm$ 0.5	17.6 $\pm$ 0.2	17.9 $\pm$ 0.5
$\Sigma$ :n-3 PUFA	3.0 $\pm$ 0.1	2.8 $\pm$ 0.2	3.0 $\pm$ 0.2	2.7 $\pm$ 0.2	3.0 $\pm$ 0.1	4.8 $\pm$ 2.1	2.8 $\pm$ 0.1	2.6 $\pm$ 0.5	2.7 $\pm$ 0.1	2.4 $\pm$ 0.1	2.7 $\pm$ 0.1	2.8 $\pm$ 0.6
n-3/n-6 PUFA	0.2 $\pm$ <0.1	0.2 $\pm$ <0.1	0.2 $\pm$ <0.1	0.2 $\pm$ <0.1	0.2 $\pm$ <0.1	0.2 $\pm$ <0.1	0.2 $\pm$ <0.1	0.1 $\pm$ <0.1*	0.2 $\pm$ <0.1	0.2 $\pm$ <0.1	0.2 $\pm$ <0.1	0.1 $\pm$ <0.1*
$\Sigma$ :VLCFA	0.1 $\pm$ <0.1	0.2 $\pm$ <0.1	0.1 $\pm$ <0.1	0.2 $\pm$ <0.1	0.1 $\pm$ <0.1	0.1 $\pm$ <0.1	0.1 $\pm$ <0.1	0.3 $\pm$ 0.1	0.1 $\pm$ <0.1	0.1 $\pm$ <0.1	0.1 $\pm$ <0.1	0.2 $\pm$ 0.1
UFA/SFA	1.9 $\pm$ <0.1	1.9 $\pm$ 0.1	2.0 $\pm$ <0.1	2.0 $\pm$ 0.1	2.0 $\pm$ 0.1	3.7 $\pm$ 1.9	2.0 $\pm$ <0.1	1.9 $\pm$ 0.1	1.7 $\pm$ <0.1	1.7 $\pm$ 0.1	2.0 $\pm$ <0.1	2.0 $\pm$ 0.1
DBI	0.9 $\pm$ <0.1	0.9 $\pm$ <0.1	1.0 $\pm$ <0.1	0.9 $\pm$ <0.1	0.9 $\pm$ <0.1	0.9 $\pm$ <0.1	0.9 $\pm$ <0.1	1.0 $\pm$ 0.1	0.9 $\pm$ <0.1	0.9 $\pm$ <0.1	0.9 $\pm$ <0.1	1.0 $\pm$ 0.1
TACL	17.3 $\pm$ 0.1	17.3 $\pm$ <0.1	17.3 $\pm$ <0.1	17.3 $\pm$ 0.1	17.2 $\pm$ <0.1	17.4 $\pm$ 0.1	17.4 $\pm$ <0.1	17.4 $\pm$ 0.1	17.2 $\pm$ <0.1	17.2 $\pm$ 0.1	17.4 $\pm$ <0.1	17.5 $\pm$ 0.1

sc subcutaneous, PUFA polyunsaturated fatty acid, VLCFA very-long-chain fatty acid (chain length  $\geq$  24 C), UFA unsaturated fatty acid, SFA saturated fatty acid, DBI double bond index, TACL total average chain length. Also minor fatty acids not listed in the table are included in the sums

\* Significant difference between the fed and the fasted animals (*t* test, Mann–Whitney *U* test, *P* < 0.05)

**Fig. 1** In vivo relative mobilization of the most abundant fatty acids in the white adipose tissues of the sables fasted for 4 days, all trunk adipose tissues analyzed as a whole (mean + SE). *Positive values* indicate that the proportion of a fatty acid has decreased in the fasted animals compared to the fed control group, *negative values* signify that the proportion of a fatty acid has increased compared to the fed group. The *asterisk* indicates that the proportion (mol%) of a fatty acid in the fasted group is significantly different from the corresponding value of the fed animals

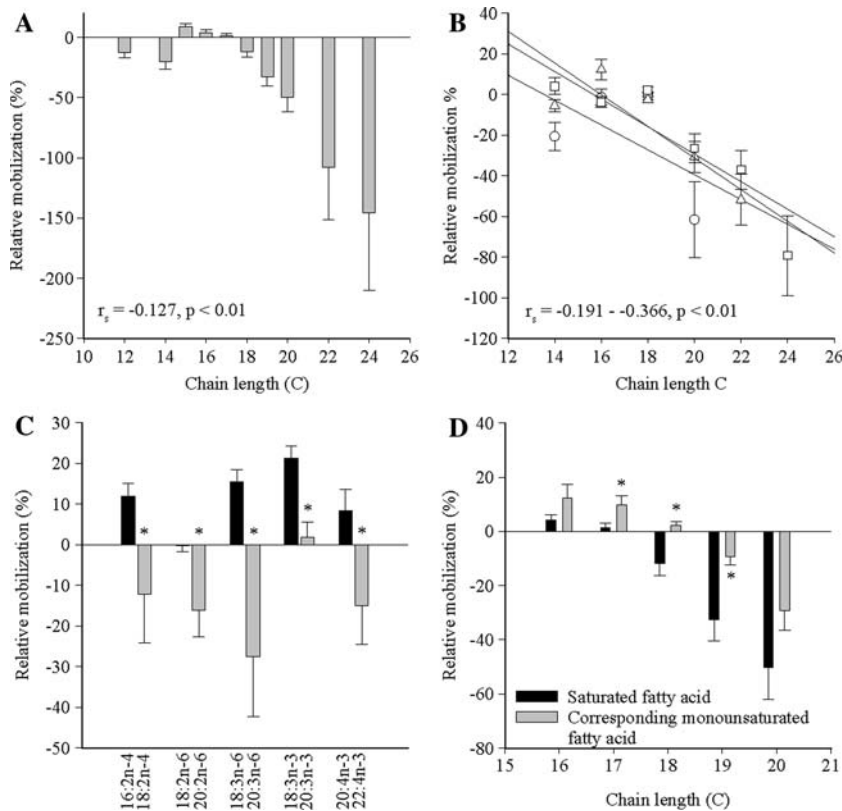
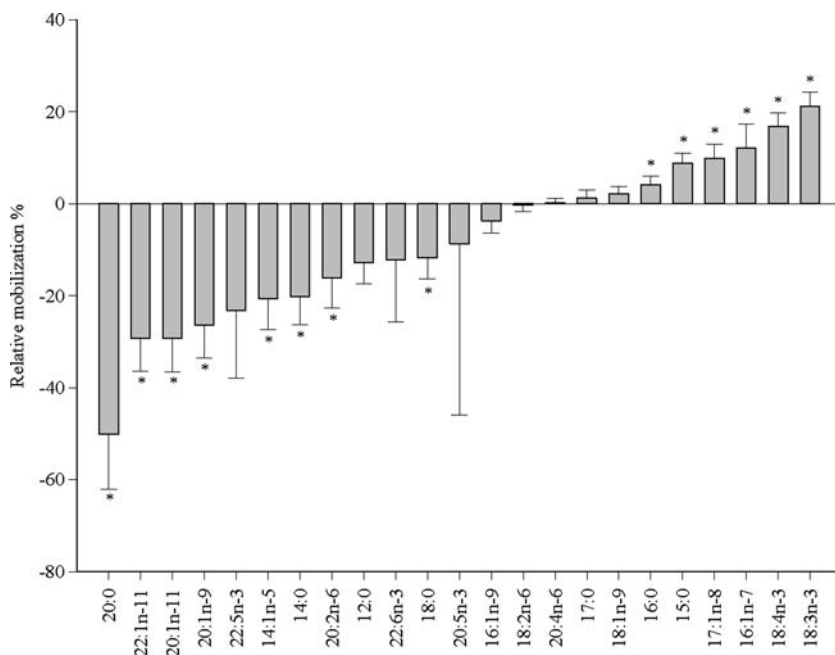


**Fig. 2** Effects of fatty acid structure on relative mobilization in the sables after 4 days of fasting, all trunk adipose tissues analyzed as a whole. *Positive values* indicate that the proportion of a fatty acid has decreased in the fasted animals compared to the fed control group, *negative values* signify that the proportion of a fatty acid has increased compared to the fed group. **a** Relative mobilization of saturated fatty acids (SFA) of different carbon chain lengths (mean + SE). **b** Correlation between relative mobilization and fatty acid chain length of monounsaturated fatty acids (MUFA), cir-

cles = n-5 MUFA, triangles = n-7 MUFA, squares = n-9 MUFA (mean ± SE). **c** Effect of fatty acid chain length on relative mobilization of selected polyunsaturated fatty acids (PUFA), \*significant difference in relative mobilization between PUFA with the same degree of unsaturation but different chain length (*t* test,  $P < 0.05$ ; mean + SE). **d** The influence of  $\Delta 9$ -desaturation on relative mobilization of selected fatty acids, \*significant difference in relative mobilization between SFA and corresponding MUFA (*t* test,  $P < 0.05$ ; mean + SE)

sable [29], it is more modest than in the American mink [7]. The terrestrial American marten also exhibits an indistinct FA gradient with a lower percentage of 18:0 and a higher proportion of 16:1n-7 in the sc fat compared to the iab depots but no differences in the total SFA, MUFA or fluidity indices, thus bearing close similarity to the sable [10].

Several changes in the relative proportions of minor FA were recorded in the fasted sables. Many of these statistically significant effects can be physiologically quite irrelevant by themselves, while the sum of these effects, e.g. changes in the n-3/n-6 PUFA balance can be important. Preferential hydrolysis of particular PUFA can have significant health effects (discussed later) or reveal details about the structural basis of FA mobilization, which has previously been shown to be selective in e.g. rats [6], American marten and mink [7, 10] and raccoon dogs [8]. According to Raclot et al. [11], the site of fat depot has no major influence on the mobilization of FA in rats and the same was established also for the American marten [10] and the sable. In contrast, the semiaquatic American mink mobilizes FA more efficiently from its iab depots compared to the sc fats probably as an adaptation to preserve fluidity in the sc depots for aquatic predation [7].

The shorter and more unsaturated FA of triacylglycerol molecules are supposedly distributed more peripherally in the lipid droplet at the water-lipid interface [30]. As a result, they could be more easily accessible to hormone-sensitive lipases and hydrolyzed during food deprivation leading to an increase in the relative amount of less polar FA in the WAT depots. This was observed also in the sables as chain length correlated negatively with RM in SFA, most MUFA and several PUFA. This seems to be a general feature of FA mobilization in mammals, as the same has been observed in rats [6], American marten and mink [7, 10] and raccoon dogs [8]. In these species, especially 20:0, 20:1n-11, 20:1n-9, 22:1n-11 and 24:1n-9 are poorly mobilized and similar phenomena were observed in the WAT of the fasted sables. Only the ventral sc fat diverged slightly from this by the relative preservation of especially 12:0, 14:0 and 14:1n-5. In addition, the proportion of 12:0 in liver increased over three-fold after 4 d of fasting. The increase in the percentages of 12:0 and 14:0 could have been caused e.g. by chain-shortening of longer FA. These mechanisms would decrease the undesirable fasting-induced changes in the fluidity by preserving those SFA that have relatively low melting points, especially in the ventral sc depot, which would be in the closest contact with snow in winter. In rats, for FA of the same carbon chain length, mobilization usually increases with the number of double bonds [6]. Similar results could be obtained from the sables, as the RM of MUFA was higher than that of the corresponding SFA in several cases. In

PUFA, there were no significant changes in RM with increasing unsaturation. These data were also quite similar to previous studies on the American marten [10].

The principle of competitive inhibition in the metabolism of PUFA in mammals suggests that n-3 PUFA are preferred over n-6 PUFA in the rate-limiting steps of desaturation reactions [31]. The more intensive RM of n-3 PUFA from the fat depots of the sable could be observed in the decrease of the n-3/n-6 PUFA ratio in the sc and iab fats. Opposite to this, the n-3/n-6 PUFA ratio and the proportion of n-3 PUFA increased in plasma as n-3 PUFA were released into the circulation to be utilized for metabolic energy. An exception was the unchanged WAT proportion of 22:6n-3, which is very important for biological membranes [32]. In fact, some of the observed decreases in the proportions of various n-3 PUFA could be due to their metabolic conversion into 22:6n-3. As a result, the relative abundance of circulating 22:6n-3 increased to be distributed to various tissues. Similar effects of fasting on n-3 and n-6 PUFA have been previously detected in the rat [30] and several carnivores [7–8, 10]. The fasted sables also had decreased proportions of 18:2n-6 in plasma, while in the other studied tissues the percentages of this important precursor of longer-chain n-6 PUFA were stable. The observed decrease could be due to altered lipoprotein profile in plasma due to fasting. It is also possible that 18:2n-6 could have been transferred into various tissues to be used in biosynthesis pathways causing the relative decrease in the plasma percentages.

It has been previously established that the lymphocyte count of the sable decreases during fasting indicating immunosuppression [18]. Important molecular regulators of the immune function derive from particular long-chain PUFA. 18:2n-6 is first metabolized into 18:3n-6, which is further converted into long-chain n-6 PUFA [31]. Of these, 20:3n-6 is the precursor of 1-series prostaglandins (PG), while 20:4n-6 and 22:4n-6 are transformed into 2- and 4-series PG. 18:3n-3 is converted via 18:4n-3 and 20:4n-3 into 20:5n-3, which is the precursor of 3-series PG, especially PGE<sub>3</sub> and leukotrienes. The decreases in 18:3n-3 and 18:4n-3 observed in the sc and iab fats of this study can be due to the conversion of these PUFA into 20:5n-3 to be used in PG synthesis. Yet also the percentages of longer-chain PUFA eventually decreased, as the 20:5n-3 proportion of WAT and the 20:4n-6 and 22:4n-6 percentages of liver decreased during fasting. This could indicate transformation of these PUFA into PGE<sub>3</sub> and 2- and 4-series PG. PGE<sub>3</sub> is especially important as it has beneficial health effects in humans, such as inhibition of lung cancer cell proliferation [33]. Increased proportions of n-6 PUFA predispose to cardiac diseases [34], while the proportions very-long-chain n-3 PUFA correlate inversely with the incidence of myocardial infarction [35]. These phenomena

could be among the causes of adverse health effects observed during prolonged food deprivation in various mammalian species experiencing preferential hydrolysis of n-3 PUFA.

The FA composition showed a high similarity between the sc and iab WAT in the terrestrial sable. The species was able to mobilize all its major sc and iab fat depots while preserving particular PUFA, such as 20:4n-6 and 22:6n-3, required for e.g. eicosanoid production and membrane stability. This was similar to another terrestrial mustelid, the American marten [10] but different from the semi-aquatic American mink, which displays a clear FA gradient of unsaturation between its sc and iab trunk fats and mobilizes FA from its iab depots more efficiently as an adaptation to aquatic predation [7]. The mechanisms of selective FA mobilization in the sable are most probably dictated by the structure of FA molecules. FA chain length and  $\Delta 9$ -desaturation seem to exert the strongest influence on the RM in the species.

**Acknowledgments** This study was financially supported by the Academy of Finland, by the Otto A. Malm's Donation Fund and by the Helve Foundation. We sincerely thank Tommi Paakkonen for assistance and Eero Joensuu and his personnel for providing us with the experimental animals.

## References

- Zhang Y, Proenca R, Maffei M, Barone M, Leopold L, Friedman JM (1994) Positional cloning of the mouse obese gene and its human homologue. *Nature* 372:425–432
- Scherer PE, Williams S, Fogliano M, Baldini G, Lodish HF (1995) A novel serum protein similar to C1q, produced exclusively in adipocytes. *J Biol Chem* 270:26746–26749
- MacQueen HA, Pond CM (1998) Immunofluorescent localisation of tumour necrosis factor- $\alpha$  receptors on the popliteal lymph node and the surrounding adipose tissue following a simulated immune challenge. *J Anat* 192:223–231
- Pond CM, Mattacks CA, Gilmour I, Johnston MA, Pillinger CT, Prestrud P (1995) Chemical and carbon isotopic composition of fatty acids in adipose tissue as indicators of dietary history in wild arctic foxes (*Alopex lagopus*) on Svalbard. *J Zool* 236:611–623
- Raclot T (2003) Selective mobilization of fatty acids from adipose tissue triacylglycerols. *Prog Lipid Res* 42:257–288
- Raclot T, Groscolas R (1995) Selective mobilization of adipose tissue fatty acids during energy depletion in the rat. *J Lipid Res* 36:2164–2173
- Nieminen P, Käkälä R, Pyykönen T, Mustonen A-M (2006) Selective fatty acid mobilization in the American mink (*Mustela vison*) during food deprivation. *Comp Biochem Physiol* 145B:81–93
- Mustonen A-M, Käkälä R, Käkälä A, Pyykönen T, Aho J, Nieminen P (2007) Lipid metabolism in the adipose tissues of a carnivore, the raccoon dog, during prolonged fasting. *Exp Biol Med* 232:58–69
- Groscolas R (1990) Metabolic adaptations to fasting in emperor and king penguins. In: Davis LS, Darby JT (eds) *Penguin biology*. Academic, San Diego, pp 269–296
- Nieminen P, Rouvinen-Watt K, Collins D, Grant J, Mustonen A-M (2006) Fatty acid profiles and relative mobilization during fasting in adipose tissue depots of the American marten (*Martes americana*). *Lipids* 41:231–240
- Raclot T, Mioskowski E, Bach AC, Groscolas R (1995) Selectivity of fatty acid mobilization: a general metabolic feature of adipose tissue. *Am J Physiol* 269:R1060–R1067
- Miyoshi K, Higashi S (2005) Home range and habitat use by the sable *Martes zibellina brachyura* in a Japanese cool-temperate mixed forest. *Ecol Res* 20:95–101
- Hamm P, Shekelle RB, Stamler J (1989) Large fluctuations in body weight during young adulthood and twenty-five-year risk of coronary death in men. *Am J Epidemiol* 129:312–318
- Anderson E (1970) Quaternary evolution of the genus *Martes* (Carnivora, Mustelidae). *Acta Zool Fenn* 130:1–132
- Brzeziński M (1994) Summer diet of the sable *Martes zibellina* in the Middle Yenisei taiga, Siberia. *Acta Theriol* 39:103–107
- Buskirk SW, Ma Y, Jiang Z (1996) Diets of, and prey selection by, sables (*Martes zibellina*) in Northern China. *J Mammal* 77:725–730
- Bakeyev NN, Sinitsyn AA (1994) Status and conservation of sables in the Commonwealth of Independent States. In: Buskirk SW, Harestad AS, Raphael MG, Powell RA (eds) *Martens, sables, and fishers, biology and conservation*. Cornell University Press, Ithaca, pp 246–254
- Mustonen A-M, Puukka M, Saarela S, Paakkonen T, Aho J, Nieminen P (2006) Adaptations to fasting in a terrestrial mustelid, the sable (*Martes zibellina*). *Comp Biochem Physiol* 144A:444–450
- Harlow HJ, Buskirk SW (1991) Comparative plasma and urine chemistry of fasting white-tailed prairie dogs (*Cynomys leucurus*) and American martens (*Martes americana*): representative fat- and lean-bodied animals. *Physiol Zool* 64:1262–1278
- Mustonen A-M, Pyykönen T, Paakkonen T, Ryökkynen A, Asikainen J, Aho J, Mononen J, Nieminen P (2005) Adaptations to fasting in the American mink (*Mustela vison*): carbohydrate and lipid metabolism. *Comp Biochem Physiol* 140A:195–202
- Mustonen A-M, Puukka M, Pyykönen T, Nieminen P (2005) Adaptations to fasting in the American mink (*Mustela vison*): nitrogen metabolism. *J Comp Physiol B* 175:357–363
- Christie WW (1993) Preparation of ester derivatives of fatty acids for chromatographic analysis. In: Christie WW (ed) *Advances in lipid methodology—two*. Oily Press, Dundee, pp 69–111
- Ackman RG (1992) Application of gas-liquid chromatography to lipid separation and analysis: qualitative and quantitative analysis. In: Chow CK (ed) *Fatty acids in foods and their health implications*. Marcel Dekker, New York, pp 47–63
- Kates M (1986) *Techniques of lipidology: isolation, analysis and identification of lipids*, 2nd edn. Elsevier, Amsterdam
- Käkälä R (1996) Fatty acid composition in subspecies of ringed seal (*Phoca hispida*) and several semiaquatic mammals: site-specific and dietary differences. PhD Thesis, University of Joensuu, Joensuu
- Walker BL, Lishchenko VF (1966) Fatty acid composition of normal mink tissues. *Can J Biochem* 44:179–185
- Rouvinen K, Kiiskinen T (1989) Influence of dietary fat source on the body fat composition of mink (*Mustela vison*) and blue fox (*Alopex lagopus*). *Acta Agric Scand* 39:279–288
- Käkälä R, Hyvärinen H (1996) Site-specific fatty acid composition in adipose tissues of several northern aquatic and terrestrial mammals. *Comp Biochem Physiol* 115B:501–514
- Mustonen A-M, Nieminen P (2006) Fatty acid composition in the central and peripheral adipose tissues of the sable (*Martes zibellina*). *J Therm Biol* 31:617–625

30. Raclot T, Groscolas R (1993) Differential mobilization of white adipose tissue fatty acids according to chain length, unsaturation, and positional isomerism. *J Lipid Res* 34:1515–1526
31. Ackman RG, Cunnane SC (1992) Long-chain polyunsaturated fatty acids: sources, biochemistry and nutritional/clinical applications. In: Padley FB (ed) *Advances in applied lipid research*, vol 1. JAI Press, London, pp 161–215
32. Kim H-Y, Bigelow J, Kevala JH (2004) Substrate preference in phosphatidylserine biosynthesis for docosahexaenoic acid containing species. *Biochemistry* 43:1030–1036
33. Yang P, Chan D, Felix E, Cartwright C, Menter DG, Madden T, Klein RD, Fischer SM, Newman RA (2004) Formation and antiproliferative effect of prostaglandin E<sub>3</sub> from eicosapentaenoic acid in human lung cancer cells. *J Lipid Res* 45:1030–1039
34. Kark JD, Kaufmann NA, Binka F, Goldberger N, Berry EM (2003) Adipose tissue n-6 fatty acids and acute myocardial infarction in a population consuming a diet high in polyunsaturated fatty acids. *Am J Clin Nutr* 77:796–802
35. Pedersen JI, Ringstad J, Almendingen K, Haugen TS, Stensvold I, Thelle DS (2000) Adipose tissue fatty acids and risk of myocardial infarction—a case-control study. *Eur J Clin Nutr* 54:618–625

# Cholesterol Oxidation is Increased and PUFA Decreased by Frozen Storage and Grilling of Atlantic Hake Fillets (*Merluccius hubbsi*)

Tatiana Saldanha · Neura Bragagnolo

Received: 30 October 2006 / Accepted: 30 March 2007 / Published online: 11 May 2007  
© AOCS 2007

**Abstract** Fresh fillets of Atlantic hake were stored at  $-18^{\circ}\text{C}$  for 120 days and changes in lipid composition and the formation of cholesterol oxidation products (COP) during storage and subsequent grilling were evaluated. Fresh hake showed low COP levels ( $8.0\ \mu\text{g/g}$ , dry basis); however, a significant increase in COP ( $P < 0.02$ ) and a concomitant decrease in the cholesterol and polyunsaturated fatty acids content during frozen storage and after grilling were observed. The main cholesterol oxides present in the analyzed samples were: 19-Hydroxycholesterol, 24(*S*)-hydroxycholesterol, 22(*S*)-hydroxycholesterol, 25-hydroxycholesterol, 25(*R*)-hydroxycholesterol and 7-Ketocholesterol. The oxides which were more influenced by the thermal treatment were 24(*S*)-OH and 25(*R*)-OH; however, after 120 days of storage 7-ketocholesterol was the main product formed. Frozen storage and subsequent grilling under domestic conditions are important factors in damage of cholesterol and unsaturated fatty acids levels, with consequent production of cholesterol oxides, although the mechanism of the formation of these compounds by the different processes is probably different.

**Keywords** Cholesterol · Cholesterol oxides · Storage · Heat treatment · Fatty acids

## Abbreviations

COP	Cholesterol oxidation products
FA	Fatty acids
SFA	Saturated fatty acids
MUFA	Monounsaturated fatty acids

PUFA	Polyunsaturated fatty acids
EPA	Eicosapentaenoic fatty acid
DHA	Docosahexaenoic fatty acid
19-OH	19-Hydroxycholesterol
24( <i>S</i> )-OH	24( <i>S</i> )-hydroxycholesterol
22( <i>S</i> )-OH	22( <i>S</i> )-hydroxycholesterol
25-OH	25-Hydroxycholesterol
25( <i>R</i> )-OH	25( <i>R</i> )-hydroxycholesterol
20 $\alpha$ -OH	20 $\alpha$ -Hydroxycholesterol
22( <i>R</i> )-OH	22( <i>R</i> )-hydroxycholesterol
7-keto	7-Ketocholesterol
$\beta$ -EP	5,6 $\beta$ -Epoxicholesterol
$\alpha$ -EP	5,6 $\alpha$ -Epoxicholesterol
7 $\beta$ -OH	7 $\beta$ -Hydroxycholesterol
7 $\alpha$ -OH	7 $\alpha$ -Hydroxycholesterol

## Introduction

Atlantic hake or Merluza is a member of the same family as the cod, a species economically important in South America, for normal consumption and for the processing industry. Fish is one of the main sources of animal protein available in the tropics and has been widely accepted as a good source of  $\omega$ -3 polyunsaturated fatty acids (PUFA) such as eicosapentaenoic (EPA) and docosahexaenoic (DHA) acids. These acids appear to play a key role in neural development, functioning of the cardiovascular and immune systems [1], besides the prevention of some types of cancer, including colon, breast and prostate [2], brain aging and Alzheimer disease [3].

However, fish also show significant cholesterol contents. These two types of compounds,  $\omega$ -3 PUFA and cholesterol, are lipids susceptible to oxidation [4]. Cholesterol can

T. Saldanha · N. Bragagnolo (✉)  
Department of Food Science, Faculty of Food Engineering,  
State University of Campinas, 13083-862 Campinas, SP, Brazil  
e-mail: neura@fea.unicamp.br



undergo oxidation to form a large amount of COP after heating at elevated temperatures for a certain period of time [5]. The triacylglycerols accelerate decomposition of cholesterol and the oxidized cholesterols are generated during peroxidation of these compounds by heating [6]. Another study [7] suggested that cholesterol in the raw materials of processed marine fish foods was oxidized in conjunction with the oxidation of polyunsaturated triacylglycerols during heat-processing and subsequent storage in air. Thus, the levels of COP in processed seafood were much higher than other food products [8].

Storage under frozen conditions has long been known as a technology for extending the shelf life of food products; however, fish and fish products can undergo undesirable changes during frozen storage and deterioration may limit the storage time [9]. Lipid deterioration is the main cause of the low shelf life of fatty fish due to progressive oxidation and enzymatic hydrolysis of unsaturated fatty acids in fish [10].

It has been reported that the intake an excess of COP may be linked to a series of physiological dysfunctions, including atherogenesis, cytotoxicity, mutagenicity, angiotoxicity, atherogenicity, carcinogenesis and cell membrane damage [11, 12]. The levels of cholesterol oxides found in various processed marine products raise some questions about the potential safety of these products, which are normally considered beneficial for the health [13]. There have been some studies [4, 7, 8, 14, 15] on the effect of heating on the formation of cholesterol oxides in complex food systems such as processed marine foods. However, studies on the effect of the frozen storage and cholesterol oxidation in fish samples have not been found.

The objective of this study was to verify the effect of grilling and domestic freezing on the formation of cholesterol oxides and alteration in the fatty acid composition in hake samples. Hake fish is commonly consumed in Brazil and the grilling and freezing reproduced the traditional way of cooking and storing them.

## Materials and Methods

### Sample Handling

Three kilogram of fresh Atlantic hake fillets were obtained from a local store in Sao Paulo, Brazil, and separated into five lots. One of them was analyzed on the day of the acquisition of the fish, corresponding to zero time. The other samples were packed in polyethylene film, stored at  $-18\text{ }^{\circ}\text{C}$  in a domestic freezer, and removed for analysis after 30, 60, 90 and 120 days. The hake fillets were thawed and cut lengthwise, one half being grilled and the other analyzed raw. The samples were grilled at  $175\text{ }^{\circ}\text{C}$  for

2 min on each side, until reaching an internal temperature of  $75 \pm 1\text{ }^{\circ}\text{C}$ . The temperature was monitored by contact, using a digital calibrated thermometer (Traceable Long-Stem, Friendswood, TX, USA). The samples were ground and homogenized in a multi-processor to obtain a homogeneous mass. Convenient aliquots were taken for the analyses, which were carried out in triplicate, and the experiment was carried out in duplicate.

### Methods

Moisture was measured as described by the AOAC [16]. The lipids were extracted and determined according to Bligh and Dyer [17]. The fatty acids composition of the hake samples was determined after methyl esterification according to Joseph and Ackman [18], followed by gas chromatography using a gas chromatograph (Varian 3400CX, Walnut Creek, CA, USA), equipped with a split injector (1:50), fused silica CP-SIL 88 capillary column  $100\text{ m} \times 0.25\text{-mm i.d.}$ ,  $0.20\text{-}\mu\text{m}$  film thickness (Chrom-pack, Middelburg, The Netherlands), flame ionization detector and workstation. The oven program was: initial temperature,  $120\text{ }^{\circ}\text{C}$  (8 min); a heating rate of  $15\text{ }^{\circ}\text{C}/\text{min}$  to a temperature of  $160\text{ }^{\circ}\text{C}$  (0 min); then a heating rate of  $4\text{ }^{\circ}\text{C}/\text{min}$  to  $195\text{ }^{\circ}\text{C}$  (12 min); and then a heating rate of  $10\text{ }^{\circ}\text{C}/\text{min}$  to a final temperature of  $230\text{ }^{\circ}\text{C}$  (25 min); injector and detector temperature  $280\text{ }^{\circ}\text{C}$ . The carrier gas was hydrogen at a flow rate  $1\text{ mL}/\text{min}$ , and nitrogen was used as the make-up gas as  $30\text{ mL}/\text{min}$ . Identification was done by comparison of the retention times of methyl ester standards (Supelco<sup>TM</sup> FAME Mix 18919-1AMP, Bellefonte, PA, USA) with those of the samples and quantification by internal standard using nonadecanoic methyl ester (Sigma, St. Louis, MO USA). The amounts obtained in  $\text{g}/100\text{ g}$  of oil were calculated according to Carpenter et al. [19].

Cholesterol and cholesterol oxides were extracted by direct saponification according to Saldanha et al. [20], and analyzed by high performance liquid chromatography. A liquid chromatograph (Shimadzu, Kyoto, Japan) equipped with UV-visible (SPD-10 AV<sub>VP</sub>) and refractive index (RID-10AV<sub>VP</sub>) detectors, rheodyne injector ( $20\text{-}\mu\text{L}$  loop), tertiary solvent delivery system (LC-10<sub>VP</sub>), oven heated column at  $32\text{ }^{\circ}\text{C}$  (CTO-10<sub>VP</sub>) and software (CLASS LC-10) was used. The analytical column used was a Nova Pack CN HP  $300\text{ mm} \times 3.9\text{-mm}$  column,  $4\text{ }\mu\text{m}$  (Waters, Milford, MA, USA), preceded by a Hypersil BDS CN  $7.5\text{ mm} \times 4.6\text{ mm}$ ,  $4\text{-}\mu\text{m}$  pre column (Alltech, Deerfield, IL, USA). The mobile-phase was *n*-hexane: 2-propanol (97:3, v/v) at a flow rate of  $1\text{ mL}/\text{min}$  and an analysis time of 30 min. Cholesterol, 5,6 $\beta$ -Epoxicholesterol ( $\beta$ -EP) and 5,6 $\alpha$ -Epoxicholesterol ( $\alpha$ -EP) were detected using a refractive index detector, and the other oxides were detected using the UV detector at 210 nm.

Identification was carried out by comparing the retention times of cholesterol, 19-Hydroxycholesterol (19-OH), 20 $\alpha$ -Hydroxycholesterol (20 $\alpha$ -OH), 22(*S*)-hydroxycholesterol (22(*S*)-OH), 22(*R*)-hydroxycholesterol (22(*R*)-OH), 25-Hydroxycholesterol (25-OH), 7-Ketocholesterol (7-keto), 7 $\beta$ -Hydroxycholesterol (7 $\beta$ -OH),  $\beta$ -EP,  $\alpha$ -EP (Sigma Chemical Company, St. Louis, MO, USA), 24(*S*)-hydroxycholesterol (24(*S*)-OH), 25(*R*)-hydroxycholesterol (25(*R*)-OH) and 7 $\alpha$ -hydroxycholesterol (7 $\alpha$ -OH) standards (Steraloids, Wilton, NH, USA) with the retention time of the samples. Quantification was done by external standardization, with a concentration range from 0.3 to 70  $\mu$ g/mL for the oxides and from 0.2 to 1.8 mg/mL for cholesterol. The quantification limits were 0.1  $\mu$ g/g for 19-OH and 20 $\alpha$ -OH; 0.18  $\mu$ g/g for 22(*R*)-OH, 24(*S*)-OH, 25(*R*)-OH and 25-OH; 0.2  $\mu$ g/g for 22(*S*)-OH, 7 $\beta$ -OH and 7 $\alpha$ -OH; 0.03  $\mu$ g/g for 7-keto; 0.02  $\mu$ g/g for cholesterol; and 0.5  $\mu$ g/g for  $\beta$ -EP and  $\alpha$ -EP. HPLC–APCI–MS was used to confirm the identity of cholesterol and cholesterol oxides in the fish samples [20].

A one-way analysis of variance (ANOVA) was applied to the data. The means of the different storage periods and preparation forms (raw and grilled) were compared using the Tukey multiple comparisons test, with  $P < 0.02$ . Software used was Origin 5.0 for Windows.

## Results and Discussion

### Moisture, Total Lipids and Cholesterol Contents

Moisture, fat and cholesterol contents in raw and grilled hake during storage time are presented in Table 1. The lipids and cholesterol were calculated on a dry weight basis.

The moisture levels ranged from  $81.8 \pm 0.2$  to  $70.3 \pm 0.3$  g/100 g in raw and grilled samples, during the storage time. Similar levels were determined by Méndez and González [21] in raw Atlantic hake (81.2 and 81.6 g/100 g) caught in March and September. Grilling affected the moisture contents significantly ( $P < 0.02$ ) as well as freezing after 60, 90 and 120 days of storage.

The lipid contents varied from  $12.6 \pm 0.6$  to  $7.9 \pm 0.7$  g/100 g in raw and grilled hake, over the storage time. After 120 days of storage a significant increase ( $P < 0.02$ ) in the lipid was observed in raw fillets. In refrigerated and frozen conditions, the published results [22–26] indicate that the extractability of the lipids may be affected by the changes in the protein–lipid complexes in the fish tissues during storage, which results in a more complete extraction by solvents and the proportion of fat increases. Thus, the changes observed in this experiment may be related to the weakening of the lipid–protein bonds that in turn facilitate the fat extraction from thawed hake. On the other hand,

**Table 1** Moisture (g/100 g), total lipid (g/100 g, dry basis) and cholesterol (mg/100 g, dry basis) levels in raw and grilled Atlantic hake during 120 days of storage

	Zero time		30 Days		60 Days		90 Days		120 Days	
	Raw	Grilled	Raw	Grilled	Raw	Grilled	Raw	Grilled	Raw	Grilled
Moisture	$81.80 \pm 0.2^A$	$73.30 \pm 0.5^a$	$80.90 \pm 0.9^{AB}$	$72.70 \pm 0.6^{ab}$	$80.10 \pm 0.9^B$	$71.90 \pm 0.4^b$	$79.50 \pm 1.0^{BC}$	$70.90 \pm 0.7^{bc}$	$78.80 \pm 0.3^C$	$70.30 \pm 0.3^c$
Total lipids	$9.40 \pm 0.2^D$	$7.90 \pm 0.7^d$	$10.70 \pm 0.7^C$	$9.20 \pm 0.5^c$	$11.40 \pm 1.0^{BC}$	$10.00 \pm 0.8^b$	$11.80 \pm 0.4^{AB}$	$10.50 \pm 0.5^b$	$12.60 \pm 0.6^A$	$11.40 \pm 0.4^a$
Cholesterol	$277.70 \pm 0.9^A$	$232.20 \pm 2.2^a$	$266.90 \pm 2.5^B$	$217.40 \pm 0.3^b$	$230.50 \pm 2.9^C$	$185.20 \pm 1.5^c$	$221.30 \pm 1.4^C$	$168.00 \pm 1.7^d$	$196.60 \pm 3.9^P$	$152.30 \pm 5.7^c$

Values are mean  $\pm$  standard deviation of the six analysis (two lots analyzed in triplicates). Values bearing different letters (capital letters) are significantly different ( $P < 0.02$ ) at the storage time in the raw samples. Values bearing different letters (small letters) are significantly different ( $P < 0.02$ ) at the storage time in the grilled samples. All the raw and grilled samples are significantly differences

**Table 2** Fatty acids composition (g/100 g of oil) in raw and grilled Atlantic hake during 120 days of storage

	Zero time		30 Days		60 Days		90 Days		120 Days	
	Raw	Grilled	Raw	Grilled	Raw	Grilled	Raw	Grilled	Raw	Grilled
	Lauric C12:0	0.64 ± 0.01 <sup>A</sup>	0.53 ± 0.02 <sup>a</sup>	0.61 ± 0.03 <sup>A</sup>	0.52 ± 0.02 <sup>a</sup>	0.60 ± 0.02 <sup>A</sup>	0.51 ± 0.02 <sup>a</sup>	0.59 ± 0.01 <sup>A</sup>	0.51 ± 0.01 <sup>a</sup>	0.58 ± 0.03 <sup>A</sup>
Myristic 14:0	4.20 ± 0.2 <sup>A</sup>	3.86 ± 0.2 <sup>a</sup>	4.17 ± 0.1 <sup>A</sup>	3.75 ± 0.2 <sup>b</sup>	4.18 ± 0.1 <sup>A</sup>	3.69 ± 0.2 <sup>b</sup>	4.16 ± 0.3 <sup>A</sup>	3.93 ± 0.2 <sup>a</sup>	4.15 ± 0.1 <sup>A</sup>	3.86 ± 0.2 <sup>a</sup>
Pentadecylic 15:0	0.95 ± 0.03 <sup>A</sup>	0.77 ± 0.1 <sup>ab</sup>	0.92 ± 0.04 <sup>A</sup>	0.75 ± 0.03 <sup>b</sup>	0.89 ± 0.01 <sup>A</sup>	0.72 ± 0.1 <sup>b</sup>	0.95 ± 0.05 <sup>A</sup>	0.81 ± 0.05 <sup>a</sup>	0.92 ± 0.02 <sup>A</sup>	0.83 ± 0.01 <sup>a</sup>
Palmitic 16:0	13.98 ± 0.4 <sup>A</sup>	13.25 ± 0.4 <sup>a</sup>	13.89 ± 0.2 <sup>B</sup>	13.04 ± 0.4 <sup>b</sup>	13.81 ± 0.3 <sup>B</sup>	13.00 ± 0.2 <sup>b</sup>	13.89 ± 0.4 <sup>B</sup>	13.15 ± 0.2 <sup>a</sup>	13.85 ± 0.5 <sup>B</sup>	13.00 ± 0.3 <sup>b</sup>
Margaric 17:0	0.24 ± 0.05 <sup>A</sup>	0.19 ± 0.03 <sup>a</sup>	0.22 ± 0.01 <sup>A</sup>	0.16 ± 0.05 <sup>a</sup>	0.23 ± 0.02 <sup>A</sup>	0.17 ± 0.02 <sup>a</sup>	0.27 ± 0.01 <sup>A</sup>	0.22 ± 0.01 <sup>a</sup>	0.25 ± 0.03 <sup>A</sup>	0.19 ± 0.01 <sup>a</sup>
Stearic 18:0	1.86 ± 0.6 <sup>A</sup>	1.67 ± 0.2 <sup>a</sup>	1.83 ± 0.2 <sup>A</sup>	1.61 ± 0.3 <sup>a</sup>	1.84 ± 0.01 <sup>A</sup>	1.59 ± 0.3 <sup>ab</sup>	1.75 ± 0.2 <sup>AB</sup>	1.55 ± 0.3 <sup>b</sup>	1.88 ± 0.2 <sup>A</sup>	1.62 ± 0.1 <sup>a</sup>
Arachidic 20:0	0.59 ± 0.02 <sup>A</sup>	0.46 ± 0.03 <sup>a</sup>	0.55 ± 0.01 <sup>AB</sup>	0.45 ± 0.01 <sup>a</sup>	0.56 ± 0.05 <sup>AB</sup>	0.44 ± 0.02 <sup>a</sup>	0.57 ± 0.01 <sup>A</sup>	0.45 ± 0.01 <sup>a</sup>	0.51 ± 0.01 <sup>B</sup>	0.45 ± 0.01 <sup>a</sup>
Behenic 22:0	0.71 ± 0.05 <sup>A</sup>	0.62 ± 0.01 <sup>a</sup>	0.69 ± 0.02 <sup>A</sup>	0.57 ± 0.02 <sup>a</sup>	0.70 ± 0.01 <sup>A</sup>	0.59 ± 0.01 <sup>a</sup>	0.68 ± 0.02 <sup>A</sup>	0.61 ± 0.02 <sup>a</sup>	0.69 ± 0.03 <sup>A</sup>	0.63 ± 0.01 <sup>a</sup>
Lignoceric 24:0	0.67 ± 0.08 <sup>A</sup>	0.58 ± 0.02 <sup>a</sup>	0.64 ± 0.01 <sup>A</sup>	0.55 ± 0.01 <sup>a</sup>	0.66 ± 0.02 <sup>A</sup>	0.52 ± 0.02 <sup>a</sup>	0.66 ± 0.01 <sup>A</sup>	0.56 ± 0.01 <sup>a</sup>	0.60 ± 0.02 <sup>A</sup>	0.54 ± 0.02 <sup>a</sup>
Myristoleic 14:1 ω9	0.35 ± 0.01 <sup>A</sup>	0.29 ± 0.02 <sup>a</sup>	0.32 ± 0.01 <sup>A</sup>	0.26 ± 0.03 <sup>b</sup>	0.29 ± 0.01 <sup>AB</sup>	0.21 ± 0.01 <sup>c</sup>	0.27 ± 0.02 <sup>B</sup>	0.20 ± 0.05 <sup>c</sup>	0.25 ± 0.04 <sup>B</sup>	0.18 ± 0.01 <sup>d</sup>
Palmitoleic 16:1 ω7	8.95 ± 0.8 <sup>A</sup>	7.79 ± 0.6 <sup>a</sup>	8.31 ± 0.7 <sup>B</sup>	7.45 ± 0.6 <sup>b</sup>	7.97 ± 0.8 <sup>C</sup>	6.60 ± 0.6 <sup>c</sup>	7.20 ± 0.5 <sup>D</sup>	6.27 ± 0.5 <sup>d</sup>	6.86 ± 0.3 <sup>E</sup>	5.96 ± 0.7 <sup>e</sup>
Margaroleic 17:1 ω7	2.33 ± 0.4 <sup>A</sup>	1.95 ± 0.1 <sup>a</sup>	2.17 ± 0.4 <sup>AB</sup>	1.56 ± 0.4 <sup>b</sup>	2.04 ± 0.6 <sup>B</sup>	1.35 ± 0.2 <sup>c</sup>	1.72 ± 0.1 <sup>BC</sup>	1.19 ± 0.02 <sup>d</sup>	1.55 ± 0.5 <sup>C</sup>	1.04 ± 0.05 <sup>e</sup>
Oleic 18:1 ω9	15.85 ± 1 <sup>A</sup>	14.52 ± 1 <sup>a</sup>	14.96 ± 0.9 <sup>B</sup>	13.87 ± 0.5 <sup>b</sup>	14.24 ± 0.8 <sup>C</sup>	12.93 ± 0.7 <sup>c</sup>	13.82 ± 1 <sup>D</sup>	12.42 ± 0.9 <sup>d</sup>	12.97 ± 0.8 <sup>E</sup>	12.00 ± 1 <sup>e</sup>
Gadoleic 20:1 ω11	0.55 ± 0.02 <sup>A</sup>	0.48 ± 0.03 <sup>a</sup>	0.47 ± 0.01 <sup>AB</sup>	0.36 ± 0.01 <sup>ab</sup>	0.39 ± 0.02 <sup>B</sup>	0.23 ± 0.02 <sup>bc</sup>	0.35 ± 0.02 <sup>BC</sup>	0.20 ± 0.01 <sup>e</sup>	0.24 ± 0.05 <sup>BC</sup>	0.16 ± 0.00 <sup>c</sup>
Erucic 22:1 ω9	0.47 ± 0.01 <sup>A</sup>	0.34 ± 0.05 <sup>a</sup>	0.36 ± 0.02 <sup>B</sup>	0.29 ± 0.01 <sup>ab</sup>	0.30 ± 0.01 <sup>BC</sup>	0.21 ± 0.03 <sup>bc</sup>	0.25 ± 0.01 <sup>C</sup>	0.18 ± 0.02 <sup>cd</sup>	0.22 ± 0.01 <sup>C</sup>	0.15 ± 0.00 <sup>d</sup>
Nervonic 24:1 ω6	0.61 ± 0.02 <sup>A</sup>	0.54 ± 0.02 <sup>a</sup>	0.57 ± 0.02 <sup>AB</sup>	0.42 ± 0.01 <sup>b</sup>	0.50 ± 0.01 <sup>B</sup>	0.39 ± 0.01 <sup>B</sup>	0.42 ± 0.01 <sup>BC</sup>	0.35 ± 0.01 <sup>bc</sup>	0.40 ± 0.01 <sup>C</sup>	0.30 ± 0.01 <sup>c</sup>
Linoleic C18:2 ω6	0.60 ± 0.00 <sup>A</sup>	0.51 ± 0.00 <sup>a</sup>	0.55 ± 0.00 <sup>A</sup>	0.43 ± 0.00 <sup>b</sup>	0.44 ± 0.00 <sup>B</sup>	0.31 ± 0.00 <sup>c</sup>	0.35 ± 0.00 <sup>C</sup>	0.29 ± 0.00 <sup>c</sup>	0.23 ± 0.00 <sup>D</sup>	0.15 ± 0.00 <sup>d</sup>
Linoleic 18:3 ω3	0.28 ± 0.00 <sup>A</sup>	0.20 ± 0.00 <sup>a</sup>	0.24 ± 0.00 <sup>A</sup>	0.14 ± 0.00 <sup>ab</sup>	0.19 ± 0.00 <sup>AB</sup>	0.10 ± 0.00 <sup>b</sup>	0.13 ± 0.00 <sup>BC</sup>	0.08 ± 0.00 <sup>b</sup>	0.10 ± 0.00 <sup>C</sup>	0.07 ± 0.00 <sup>b</sup>
γ-linoleic 18:3 ω6	1.54 ± 0.3 <sup>A</sup>	1.35 ± 0.1 <sup>a</sup>	1.39 ± 0.4 <sup>B</sup>	1.14 ± 0.1 <sup>b</sup>	1.28 ± 0.3 <sup>C</sup>	1.02 ± 0.2 <sup>c</sup>	1.15 ± 0.4 <sup>D</sup>	0.90 ± 0.1 <sup>d</sup>	1.00 ± 0.2 <sup>E</sup>	0.79 ± 0.1 <sup>e</sup>
Arachidonic 20:4 ω6	2.50 ± 0.05 <sup>A</sup>	2.33 ± 0.01 <sup>a</sup>	2.21 ± 0.02 <sup>B</sup>	2.00 ± 0.01 <sup>b</sup>	1.93 ± 0.02 <sup>C</sup>	1.64 ± 0.02 <sup>c</sup>	1.54 ± 0.05 <sup>D</sup>	1.38 ± 0.01 <sup>d</sup>	1.32 ± 0.02 <sup>E</sup>	1.09 ± 0.01 <sup>e</sup>
EPA 20:5 ω3	6.17 ± 0.3 <sup>A</sup>	4.92 ± 0.3 <sup>a</sup>	5.74 ± 0.1 <sup>B</sup>	4.35 ± 0.5 <sup>b</sup>	5.12 ± 0.3 <sup>C</sup>	3.89 ± 0.3 <sup>c</sup>	4.75 ± 0.6 <sup>D</sup>	3.26 ± 0.2 <sup>d</sup>	3.97 ± 0.1 <sup>E</sup>	2.43 ± 0.1 <sup>e</sup>
DHA C22:6 ω3	18.86 ± 0.8 <sup>A</sup>	16.45 ± 0.7 <sup>a</sup>	16.62 ± 0.5 <sup>B</sup>	14.54 ± 0.6 <sup>b</sup>	14.98 ± 0.4 <sup>C</sup>	13.29 ± 0.8 <sup>c</sup>	13.74 ± 0.7 <sup>D</sup>	11.69 ± 0.3 <sup>d</sup>	11.89 ± 0.1 <sup>E</sup>	9.95 ± 0.2 <sup>e</sup>
Elaidic 18:1 tr ω9	0.29 ± 0.00 <sup>A</sup>	0.36 ± 0.00 <sup>a</sup>	0.25 ± 0.00 <sup>AB</sup>	0.30 ± 0.00 <sup>ab</sup>	0.18 ± 0.00 <sup>B</sup>	0.25 ± 0.01 <sup>b</sup>	0.13 ± 0.05 <sup>BC</sup>	0.20 ± 0.01 <sup>bc</sup>	0.11 ± 0.01 <sup>C</sup>	0.17 ± 0.03 <sup>c</sup>
Linolelaidic 18:2 tr ω6	0.36 ± 0.02 <sup>A</sup>	0.45 ± 0.01 <sup>a</sup>	0.30 ± 0.03 <sup>A</sup>	0.38 ± 0.01 <sup>ab</sup>	0.26 ± 0.03 <sup>AB</sup>	0.37 ± 0.01 <sup>ab</sup>	0.23 ± 0.02 <sup>B</sup>	0.30 ± 0.02 <sup>bc</sup>	0.18 ± 0.02 <sup>B</sup>	0.26 ± 0.01 <sup>c</sup>
Σ SFA	23.84	21.93	23.52	21.40	23.47	21.23	23.52	21.69	23.43	21.62
Σ MUFA	29.21	25.51	27.16	24.21	25.73	21.92	24.03	20.81	22.49	19.79
Σ PUFA	29.87	25.76	26.75	22.60	23.94	20.25	21.18	17.60	18.51	14.48
Σ FA	82.92	73.20	77.43	68.21	73.14	63.40	68.74	60.10	64.43	55.89
Σ ω6	5.25	4.73	4.72	3.99	4.15	3.36	3.46	2.92	2.95	2.33
Σ ω3	25.31	21.57	22.60	19.03	20.29	17.28	18.62	15.03	15.96	12.45
ω3/ω6	4.82	4.56	4.78	4.76	4.88	5.14	5.38	5.14	5.41	5.34
Σ trans	0.65	0.81	0.55	0.68	0.44	0.62	0.36	0.50	0.29	0.43
PUFA/SFA	1.25	1.17	1.13	1.05	1.02	0.95	0.90	0.81	0.79	0.67

Values are means ± standard deviation of the six analysis (two lots analyzed in triplicates). All the raw and grilled samples are significantly different ( $P < 0.02$ ). Values bearing and different letters (capital letters) have significant differences ( $P < 0.02$ ) at differing storage times in the raw samples. Values bearing different letters (small letters) have significant differences ( $P < 0.02$ ) at various storage times in the grilled samples

after grilling, significant ( $P < 0.02$ ) losses of the lipid contents were observed, from 9.5 to 16%. Although fish do not have adipose tissue, the fat excess is stored as peripheral triacylglycerols in muscle, a fact that may favour fat loss when a high grilling temperature is used to cook the fish [27].

The cholesterol content in fresh hake was  $277 \pm 1$  mg/100 g, and the levels were significantly lower ( $P < 0.02$ ) during frozen storage and after grilling. The loss of cholesterol by heating is extremely rapid when the heating temperature is above 175 °C [28]. Other studies [4, 29] showed a decrease in the cholesterol levels after heat treatment in fish samples. Some cholesterol contained in foods is subjected to oxidizing conditions during processing, preparation and storage [6]; thus, the changes in cholesterol content during this experiment could probably be attributed to the oxidative process.

### Fatty Acid Composition

The fatty acids composition and the effects of grilling and frozen storage on the individual fatty acids of Atlantic hake are presented in Table 2, expressed in g/100 g of oil.

In the total fatty acids (FA) determined in raw samples 29% corresponded to saturated fatty acids (SFA), of which palmitic acid was present in the highest amounts. Another 35% were monounsaturated fatty acids (MUFA), with oleic acid as the most abundant one. The percentage of polyunsaturated (PUFA) was 36%, consisting mostly of DHA and EPA fatty acids. These findings are in agreement with those obtained by other studies in hake samples [21, 29]. A significant ( $P < 0.02$ ) decrease was observed in the PUFA and *trans* fatty acids contents after 120 days of storage. Oxidative reactions occur in the lipid fraction of frozen foods, and tend to increase with higher oxygen permeability of the packing material and higher fat content in the muscle [30, 31]. These oxidative reactions are initiated in the highly susceptible membrane-bound phospholipids, and this process particularly affects unsaturated lipids [32]. In this study, the hake fillets were only stored in plastic film and under similar domestic conditions; moreover, the samples presented high contents of unsaturated fat, factors that can accelerate the oxidative peroxidation in hake samples, causing the important losses in the unsaturated fatty acids content. Another factor to be considered is the presence of the lipolytic enzymes that remain active in the uncooked fish during frozen storage at  $-18$  °C [33].

After grilling a significant decrease ( $P < 0.02$ ) was observed in the total amount of FA, mainly of MUFA and PUFA in all the analyzed times. The losses were between 12 and 13% in FA; 11 and 15% in MUFA, and from 14 to 22% in PUFA contents. As already observed, PUFA

are more susceptible to thermal oxidation than their MUFA analogues, especially at elevated temperatures. During the grilling process, fish are subjected to heating and atmospheric oxygen and these two factors can accelerate the oxidative deterioration of fish fat, and lipid oxidation in grilled hake should also be considered. Therefore, the loss of PUFA from grilling suggests the formation of hydroperoxides to some extent in the grilled samples [34]. In contrast, the content of *trans* fatty acids increased from between 24 and 48% after heat treatment, although Candela et al. [29] observed that the *trans* fatty acids were not uniformly affected by cooking in hake samples.

Eicosapentaenoic and DHA fatty acids are typical of fish fat, and these products have an essential role in human diet to prevent diseases. Fresh hake showed the highest levels of these  $\omega$ -3 fatty acids,  $6.2 \pm 0.3$  and  $18.9 \pm 0.8$  g/100 g for EPA and DHA, respectively. Grilling produced a significant reduction in these values, namely between 20 and 39% for EPA; 11 and 16% for DHA. These results are in agreement with other studies [7, 34], that reported a decrease in the EPA and DHA levels in fish samples during grilling. However, other authors observed that the heat treatment of the raw fish species did not cause a significant decrease in the EPA + DHA contents [35]. Candela et al. [36] observed that the changes in the EPA and DHA contents after cooking were related to the initial amount in the raw fish and therefore to the species, in addition, this change may be due to differences in cooking methods [35].

After 120 days of storage, a significant decrease ( $P < 0.02$ ) in EPA and DHA contents was observed, around 36% in raw hake samples. The losses of these compounds after grilling and during frozen storage probably have been related to the autoxidation of lipids.

The  $\omega$ 3/ $\omega$ 6 ratio was not uniformly modified in hake samples. During freezing this ratio remained constant after 30 and 60 days; however, an increase in the  $\omega$ 3/ $\omega$ 6 ratio after 90 and 120 days of storage was observed. No significant changes were observed in the  $\omega$ 3/ $\omega$ 6 ratio after grilling, only an increase at 60 days of storage. The ratio of PUFA/SFA was significantly reduced during frozen storage and after grilling in all evaluated samples.

### Cholesterol Oxides

Cholesterol oxides determined in hake samples (dry basis) are presented in Table 3. Six COP (Fig. 1) were determined in hake samples: 24(*S*)-OH, 22(*S*)-OH, 25(*R*)-OH, 25-OH, 19-OH and 7-keto, although twelve products were researched. The most oxides were originated from the cholesterol side chain, and only two oxides (19-OH and 7-keto) were originated from the main chain. In fish foods,

**Table 3** Cholesterol oxides levels ( $\mu\text{g/g}$ , dry basis) in raw and grilled Atlantic hake during 120 days of storage

	Zero time		30 Days		60 Days		90 Days		120 Days	
	Raw	Grilled	Raw	Grilled	Raw	Grilled	Raw	Grilled	Raw	Grilled
	19-OH	2.10 $\pm$ 0.1 <sup>E</sup>	3.70 $\pm$ 0.3 <sup>e</sup>	3.90 $\pm$ 0.4 <sup>D</sup>	7.80 $\pm$ 0.7 <sup>d</sup>	6.10 $\pm$ 0.5 <sup>C</sup>	10.90 $\pm$ 1.0 <sup>c</sup>	11.70 $\pm$ 0.6 <sup>B</sup>	16.30 $\pm$ 1.3 <sup>b</sup>	15.20 $\pm$ 0.9 <sup>A</sup>
24(S)-OH	0.20 $\pm$ 0.03 <sup>E</sup>	0.90 $\pm$ 0.1 <sup>e</sup>	1.40 $\pm$ 0.6 <sup>D</sup>	3.80 $\pm$ 0.3 <sup>d</sup>	4.30 $\pm$ 0.7 <sup>C</sup>	7.10 $\pm$ 0.5 <sup>c</sup>	5.60 $\pm$ 0.6 <sup>B</sup>	8.30 $\pm$ 0.2 <sup>b</sup>	7.90 $\pm$ 0.5 <sup>A</sup>	11.70 $\pm$ 0.3 <sup>a</sup>
22(S)-OH	0.90 $\pm$ 0.05 <sup>E</sup>	1.60 $\pm$ 0.7 <sup>e</sup>	1.20 $\pm$ 0.08 <sup>D</sup>	3.80 $\pm$ 0.1 <sup>d</sup>	3.30 $\pm$ 0.4 <sup>C</sup>	6.90 $\pm$ 0.3 <sup>c</sup>	4.10 $\pm$ 0.6 <sup>B</sup>	7.90 $\pm$ 0.2 <sup>b</sup>	6.20 $\pm$ 0.5 <sup>A</sup>	9.50 $\pm$ 0.6 <sup>a</sup>
25-OH	4.10 $\pm$ 0.2 <sup>E</sup>	10.50 $\pm$ 1.0 <sup>e</sup>	9.20 $\pm$ 0.3 <sup>D</sup>	16.40 $\pm$ 0.9 <sup>d</sup>	13.70 $\pm$ 1.1 <sup>C</sup>	20.50 $\pm$ 0.9 <sup>c</sup>	16.60 $\pm$ 0.7 <sup>B</sup>	26.40 $\pm$ 0.6 <sup>b</sup>	23.80 $\pm$ 1.3 <sup>A</sup>	35.20 $\pm$ 1.4 <sup>a</sup>
25(R)-OH	0.70 $\pm$ 0.01 <sup>E</sup>	1.20 $\pm$ 0.3 <sup>e</sup>	1.40 $\pm$ 0.2 <sup>D</sup>	6.10 $\pm$ 0.6 <sup>d</sup>	5.20 $\pm$ 0.7 <sup>C</sup>	12.70 $\pm$ 0.4 <sup>c</sup>	9.90 $\pm$ 0.8 <sup>B</sup>	16.40 $\pm$ 0.5 <sup>b</sup>	15.80 $\pm$ 1.6 <sup>A</sup>	29.40 $\pm$ 1.0 <sup>a</sup>
7-Keto	–	0.60 $\pm$ 0.1 <sup>e</sup>	1.40 $\pm$ 0.4 <sup>D</sup>	3.70 $\pm$ 0.1 <sup>d</sup>	2.60 $\pm$ 0.5 <sup>C</sup>	5.20 $\pm$ 0.3 <sup>c</sup>	6.50 $\pm$ 0.7 <sup>B</sup>	11.40 $\pm$ 0.6 <sup>b</sup>	9.20 $\pm$ 1.0 <sup>A</sup>	16.70 $\pm$ 0.9 <sup>a</sup>
TOTAL	8.00 $\pm$ 0.1	18.50 $\pm$ 0.4	18.50 $\pm$ 0.3	41.60 $\pm$ 0.5	35.20 $\pm$ 0.6	63.30 $\pm$ 0.5	54.40 $\pm$ 0.6	86.70 $\pm$ 0.5	78.10 $\pm$ 2	122.30 $\pm$ 1.4

Values are means  $\pm$  standard deviation of the six analysis (two lots analyzed in triplicates). All the raw and grilled samples are significantly different ( $P < 0.02$ ). Values bearing different letters (capital letters) have significant differences ( $P < 0.02$ ) at different storage times in the raw samples. Values bearing different letters (small letters) have significant differences ( $P < 0.02$ ) at different storage times in the grilled samples

the B-ring oxidation products such as: 7-keto, 7 $\beta$ -OH, 7 $\alpha$ -OH, 5,6 $\alpha$ -EP and 5,6 $\beta$ -EP were dominant in the total of COP [4, 7, 8, 14, 15, 34]. Normally, 25-OH was the only side chain COP found in seafood products [15], even so under the chromatographic conditions used in the present study it was possible to separate and to identify a large number of the oxides originating from the lateral chain oxidation, normally not determined in food products.

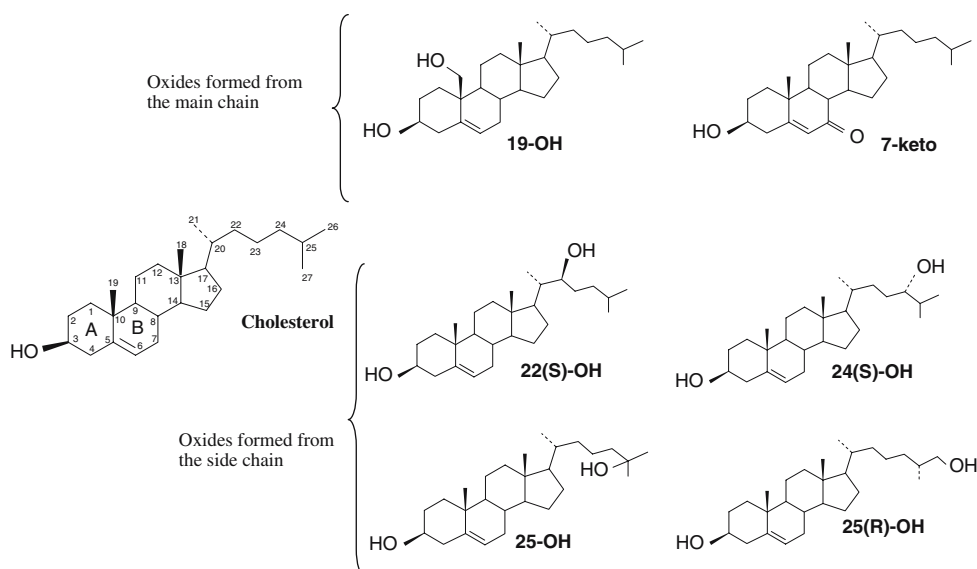
Quantitatively, the most abundant oxides were 25-OH (4.1–23.8  $\mu\text{g/g}$ ) and 19-OH (2.1–15.2  $\mu\text{g/g}$ ) in raw and grilled samples. 7-keto, the major oxide found in food systems and considered an indicator of oxidation was not observed in fresh hake, only in the defrosted or grilled samples. Probably, this oxide had been formed by oxidative processes during frozen storage and after thermal treatment. It is likely that when different fats coexist, cholesterol is oxidized even when it is not heated. The presence of oxidized cholesterol in the nonheated or moderately heated processed marine products suggested that the degree of unsaturation of food fats may influence the production of these oxides [8].

The total COP contents increased significantly ( $P < 0.02$ ) after grilling, with rises between 57 and 131%, being his difference higher in zero time. In relation to the individual oxides 24(S)-OH and 25(R)-OH had more pronounced increases, with 350 and 335%. According to Osada et al. [8] the autoxidation of cholesterol may occur in a short time when subjected to temperatures above 120 °C. Moreover, the PUFA in seafood are oxidized during processing such as a heating at high temperatures during which peroxy radicals or singlet oxygen are formed. These radicals interact with cholesterol and promote oxidation of sterols [37]. According to Al-Saghir et al. [38] the higher degree of unsaturation, the higher the lipid oxidative process, and the more COP are formed. In another study, the levels of 7-keto were significantly higher when heating more unsaturated oils [28]. Considering the amounts of PUFA found in the fresh hake and the temperature of grilling, the increase in oxide formation after thermal treatment can be understood.

During frozen storage, the oxide contents exhibited a gradual and significant increase ( $P < 0.02$ ) in the evaluated samples. Among the COP, the 7-keto formation was the highest, followed by 22(S)-OH and 24(S)-OH. After 120 days of storage, the increase in the total of oxides in raw hake was 876%, demonstrating that the frozen storage in domestic conditions increases significantly the susceptibility to oxidation. According to the results obtained, it can be considered that the frozen storage brings about more oxide formation than the grilling.

Observing the degree of formation of the cholesterol oxides it can be concluded that the temperature employed is an important factor in the production of these

**Fig. 1** Chemical structures of cholesterol and cholesterol oxides found in raw and grilled Atlantic hake



compounds, although the mechanisms of formation by thermal treatment and frozen storage are probably different. In agreement, Kim and Nawar [39] suggested that in the cholesterol oxidative process, these reactions and interactions may be significantly influenced by the reaction conditions, e.g., temperature, type and concentration of the components.

## Conclusions

In this study it was evident that frozen storage at  $-18^{\circ}\text{C}$  and subsequent grilling are the important factors in the changes in the lipid profile and consequent rise of the cholesterol oxides in hake samples. Frozen storage had a greater effect on the production of oxides than grilling, and the mechanisms of formation for thermal treatment and frozen storage are probably different. Due to the complexity of the food itself, it is difficult to study cholesterol oxidation in real food systems. Therefore, more systematic research on cooking methods and prolonged storage under domestic conditions and its consequences for lipidic composition, with emphasis on cholesterol oxide production in fish samples is necessary.

**Acknowledgments** The authors thank the Sao Paulo State (FAPESP) and the National Brazilian Research Foundations (CAPES and CNPq) for financial support.

## References

- Lauritzen L, Hansen HS, Jorgensen MH, Michaelsen KF (2001) The essentially of long chain n-3 fatty acids in relation to development and function and brain and retina. *Progr Lipid Res* 40:1–94
- Marchioli R, Barzi F, Bomba E, Chieffo C, Di Gregorio D, Di Mascio R, Franzosi MG, Geraci E, Levantesi G, Maggioni AP, Mantini L, Marfisi RM, Mastrogiuseppe G, Mininni N, Nicolosi GL, Santini M, Schweiger C, Tavazzi L, Tognoni G, Tucci C, Valagussa F (2002) Early protection against sudden death by n-3 polyunsaturated fatty acids after myocardial infarction: time course analysis of the results of GISSI-prevenzione. *Circulation* 105:1897–1903
- Kyle DJ (1999) Low serum docosahexaenoic acid is a significant risk factor for Alzheimer's dementia. *Lipids* 34S:245
- Echarte M, Zulet MA, Astiasarán I (2001) Oxidation process affecting fatty acids and cholesterol in fried and roasted salmon. *J Agric Food Chem* 49:5662–5667
- Tai CY, Chen YC, Chen BH (2000) Analysis, formation and inhibition of cholesterol products in foods: an overview: part II. *J Food Drug Anal* 8:1–15
- Kim SK, Nawar WW (1993) Parameters influencing cholesterol oxidation. *Lipids* 28:917–922
- Ohshima T, Shozen K, Ushio H, Koizumi C (1996) Effects of grilling on formation of cholesterol oxides in seafood products rich in polyunsaturated fatty acids. *LWT-Food Sci Tech* 29:94–99
- Osada K, Kodama T, Cui L, Yamada K, Sugano M (1993) Levels and formation of oxidized cholesterols in processed marine foods. *J Agric Food Chem* 41:1893–1898
- Tokur B, Ozkütük S, Atici E, Ozyurt G, Ozyurt CE (2006) Chemical and sensory quality changes of fish fingers made from Mirror Carp (*Cyprinus carpio* L, 1758) during frozen storage ( $-18^{\circ}\text{C}$ ). *Food Chem*. 99:335–341
- Srikar LN, Hiremath JG (1972) Fish preservation-I. Studies on changes during frozen storage of oil sardine. *J Food Sci Tech* 9:191–193
- Gallina T. T, Caboni M. F (1992) Cholesterol oxides: biological behaviour and analytical determination. *Ital. J Food Sci* 4:223–228
- Schroepfer GJ (2000) Oxysterols: modulators of cholesterol metabolism and other processes. *Physiol Rev* 80:361–554
- Savage GP, Dutta PC, Rodriguez-Estrada MT (2002) Cholesterol oxides: their occurrence and methods to prevent their generation in foods. *Asia Pac J Clin Nut* 11:72–78
- Ohshima T, Li N, Koizumi C (1993) Oxidative decomposition of cholesterol in fish products. *JAOCS* 70:595–600

15. Ohshima T (2002) Formation and content of cholesterol oxidation products in seafood and seafood products, in cholesterol and phyto-sterol oxidation products in foods and biological samples: analysis, occurrence and biological effects. In: Guardiola F, Dutta P, Codony R, Savage GP (eds) AOAC Press, New York, pp 187–203
16. AOAC (2002) Moisture Content. 950.46. Official methods of analysis (17th ed) Gaithersburg, Maryland: Association of Official Analytical Chemists
17. Bligh E, Dyer W (1959) A rapid method of total lipid extraction and purification. *Can J Biochem Phys* 37:911–917
18. Joseph JD, Ackman RG (1992) Capillary column gas chromatographic method for analysis of encapsulated fish oil and fish oil ethyl esters: collaborative study. *JAOAC Intern* 75:488–506
19. Carpenter DE, Ngeh-Ngwainbi J, Lee S (1993) Lipid analysis. In: Sullivan DM, Carpenter DE (eds) Methods of analysis for nutritional labeling. AOAC International, Arlington, pp 85–101
20. Saldanha T, Sawaya ACF, Eberlin MN, Bragagnolo N (2006) HPLC separation and determination of 12 cholesterol oxidation products in fish: comparative study of RI, UV and APCI-MS detectors. *J Agric Food Chem* 54:4107–4113
21. Méndez E, González RM (1997) Seasonal changes in the chemical and lipid composition of fillets of the Southwest Atlantic hake (*Merluccius hubbsi*). *Food Chem* 59:213–217
22. Jiménez-Colmenero F (1979) In: *Elaboración y Conservación al Estado Congelado de Pastas de Jurel (Trachurus trachurus)* PhD Thesis, Universidad Complutense de Madrid. Facultad de Ciencias Químicas
23. Béltran A, Moral A (1990) Gas chromatographic estimation of oxidative deterioration in sardine during frozen storage. *LWT Food Sci Tech* 23:499–504
24. Béltran A, Moral A (1991) Changes in fatty acid composition of fresh and frozen sardines (*Sardina pilchardus* W.) during smoking. *Food Chem* 42:99–109
25. García-Arias MT, Álvarez-Pontes E, García-Linares MC, García-Fernández MC, Sánchez-Muniz FJ (2003) Grilling of sardines fillets. Effects of frozen and thawed modality on their protein quality. *LWT Food Sci Tech* 36:763–769
26. Wood G, Hintz L, Salwin H (1968) Chemical alterations in fish tissue during storage at a low temperatures. *JAOAC* 52:904–910
27. Sargent JR (1997) Fish oils and human diet. *Brit J Nut* 78:S 5–13
28. Xu Z, Zhang T, Prinyawiwatkul W, Golber S (2005) Capabilities of different cooking oils in prevention of cholesterol oxidation during heating. *JAOCS* 82:243–248
29. Candela M, Astiasáran I, Bello J (1997) Effects of frying and warmholding on fatty acids and cholesterol of sole (*Solea solea*), codfish (*Gadus morrhua*) and hake (*Merluccius merluccius*). *Food Chem* 58:227–231
30. Brewer MS, Wu SY (1993) Display, packaging and meat block location effects on colour and lipid oxidation of frozen lean ground beef. *J Food Sci* 58:1219–1223
31. Farouk MM, Swan JE (1998) Effect of muscle condition before freezing and simulated chemical changes during frozen storage on the pH and colour of beef. *Meat Sci* 50:245–256
32. Conchillo A, Ansorena D, Astiasáran I (2005) Intensity of lipid oxidation and formation of cholesterol oxidation products during frozen storage of raw and cooked chicken. *J Sci Food Agric* 85:141–146
33. Mai J, Kinsella JE (1979) Changes in lipid composition of cooked mince carp (*Cyprinus carpio*) During frozen storage. *J Food Sci* 44:1619–1624
34. Shozen K, Ohshima T, Ushio H, Koizumi C (1995) Formation of cholesterol oxides in marine fish products induced by grilling. *Fish Sci* 61:817–821
35. Gladyshev MI, Sushchik NN, Guabanenko GA, Dermichieva SM, Kalachova GS (2006) Effect of way of cooking on content of essential polyunsaturated fatty acids in muscle tissue of hump-back salmon (*Oncorhynchus gorbuscha*). *Food Chem* 96:446–451
36. Candela M, Astiasáran I, Bello J (1998) Deep-fat frying modifies high-fat fish lipid fraction. *J Agric Food Chem* 46:2793–2796
37. Ansari GAS, Smith LL (1979) High-performance liquid chromatography of cholesterol autoxidation products. *J Chromatogr* 175:307–315
38. Al-Saghir S, Thurner K, Wagner KH, Frisch G, Luf W, Razzazi-Fazeli E, Elmadfa I (2004) Effects of different cooking procedures on lipid quality and cholesterol oxidation of farmed salmon fish (*Salmo salar*). *J Agric Food Chem* 52:5290–5296
39. Kim SK, Nawar WW (1991) Oxidative interactions of cholesterol with triacylglycerols. *JAOCS* 68:931–934

# Classification of Adipose Tissue Species using Raman Spectroscopy

J. Renwick Beattie · Steven E. J. Bell ·  
Claus Borggaard · Anna M. Fearon ·  
Bruce W. Moss

Received: 30 October 2006 / Accepted: 21 March 2007 / Published online: 8 May 2007  
© AOCS 2007

**Abstract** In this study multivariate analysis of Raman spectra has been used to classify adipose tissue from four different species (chicken, beef, lamb and pork). The adipose samples were dissected from the carcass and their spectra recorded without further preparation. 102 samples were used to create and compare a range of statistical models, which were then tested on 153 independent samples. Of the classical multivariate methods employed, Partial Least Squares Discriminant Analysis (PLSDA) performed best with 99.6% correct classification of species in the test set compared with 96.7% for Principal Component Linear Discrimination Analysis (PCLDA). Kohonen and Feed-forward artificial neural networks compared well with the PLSDA, giving 98.4 and 99.2% correct classification, respectively.

**Keywords** Raman spectroscopy · Gas chromatography · Classification · Speciation · Adipose · Fat · Oil · Lipid · Fatty acid · Triglyceride · FAME

## Abbreviations

PCA Principal components analysis  
PLSDA Partial least squares discriminant analysis

LDA Linear discriminant analysis  
GC Gas chromatography  
FAME Fatty acid methyl ester  
PUFA Polyunsaturated fatty acid  
MUFA Monounsaturated fatty acid  
ANN Artificial neural network

## Introduction

The adulteration of foodstuffs is a major problem for the specialist food markets. Many foods can become contaminated through careless handling, or through unintentional or deliberate intervention. Many expensive products are adulterated with cheaper alternatives to increase profit margins, or expensive ingredients are replaced with a cheaper alternative. In some cases this action simply reduces the quality of the product, but such practices may even have moral and ethical implications. Many religions and cultures ban the consumption of various foodstuffs, and it is of particular interest to these religious groupings to prevent the inadvertent consumption of the prohibited substance. A rapid, non-destructive technique for classifying the species from which a fat originates would allow more extensive testing of samples than more laborious traditional methods (e.g. chromatography or “wet chemistry”). Traditional methods are necessarily confined to smaller sample sets for reasons of practicality.

The potential of Raman spectroscopy for the analysis of fats and oils has been recognised for some decades [1–3]. The main advantages of the technique are that no sample preparation is required (allowing in situ or on-line studies) and that it can be applied to any physical state including liquids, gels, amorphous solids and crystals. However, until

J. R. Beattie · S. E. J. Bell (✉)  
School of Chemistry and Chemical Engineering,  
Queen’s University, Belfast BT9 5AG, Northern Ireland  
e-mail: S.Bell@QUB.ac.uk

C. Borggaard  
Danish Meat Research Institute, 2 Magleggaardsvej,  
P.O. Box 57, 4000 Roskilde, Denmark

A. M. Fearon · B. W. Moss  
School of Agriculture and Food Science, Queen’s University,  
Belfast BT9 5AG, Northern Ireland



recently, adoption of Raman methods for routine analysis of fats and oils has been hindered by the high cost and complexity of the instrumentation required. This situation is now changing rapidly; a number of technological advances such as holographic notch filters for rejection of elastically-scattered light and the availability of long wavelength (750–1,064 nm) excitation lasers (which reduce background fluorescence problems) are making the technique more accessible than ever before and the introduction of simple-to-use commercial instruments means that it is straightforward for non-specialists to record good quality Raman data.

Since technical problems no longer dominate the field there are clear opportunities for routine analysis by Raman spectroscopy. Indeed, it has already been successfully used to determine important composition/physical structure parameters relevant to the analysis of animal fats. These include: *cis/trans* geometrical isomer ratio [4], molar unsaturation (C = C per molecule) [4], mass unsaturation (C = C per unit mass, molal, degree of unsaturation) [2, 5], conjugated double bond content [6], chain length [7], lipolysis [8], fatty acid composition [9, 10], crystal structure [11] and adulteration [12].

Due to the high information content of the Raman signal it is typically necessary to reduce the number of variables to a more manageable number. Multivariate statistics [13] are capable of simultaneously analysing multiple variables and combining interrelated variables such as the pattern of Raman bands that match particular components of a sample. Principal component analysis (PCA) is a nondirected, non-supervised method of data reduction, which determines the main sources of variation within the spectra, allowing transformation of several related data points into a single number. Projection to latent structures discriminant analysis (PLSDA) differs from PCA in that each source of variation is not ranked in relation to the overall variation, but according to how it accounts for variation between data subsets (groups). This has the consequence that PLSDA typically refines the discrimination by ignoring data variations that do not contribute to group separation, reducing any disruptive influence these sources may have. An alternative to multivariate statistics that has become popular in recent years is the use of non-linear algorithms based on the structure of animal brains. These artificial neural networks (ANN) are structured with an input that connects with hidden calculation 'neurons' that convert the input into an output. ANNs are capable of forming pathways between any 'neurons' in adjacent layers allowing complex non-linear connections to be made. As with animal brains these ANNs have to be trained first using training data in order to learn how to transform the data from the raw input into a reference value.

This paper is part of series investigating the application of Raman spectroscopy to the analysis of fatty acid based

fats and oils, from models systems to complex 'real life' samples [7, 9, 10, 14, 15]. The aim of this paper is to investigate the extent to which the species of an adipose tissue sample can be classified from its Raman spectrum.

## Experimental

The samples used in this investigation were subcutaneous adipose tissue dissected from above the longissimus dorsi muscle in the position of the 12th rib for beef, lamb and pork, and from above the breast for chicken. In order to obtain a wide range of variation within each species the samples were obtained from a number of commercial and experimental sources and included a wide variety of breeds and feeding regimes. Spectra were accumulated at ambient temperature (19–21 °C) from each side (towards the skin and inner) of the samples and were stored and processed separately, giving 2 spectra for each animal. A total of 255 spectra were recorded (84 pork, 82 beef, 53 lamb and 36 chicken). Samples were obtained from a number of research sources and were all dissected within 48 h of slaughter.

### Gas Chromatography

Fatty acid composition was determined on a subset of 74 of the samples following lipid extraction, preparation of fatty acid methyl esters and analysis by gas chromatography, as described previously [10]. The total combined abundance of PUFAs was determined by summing the relative abundances of all the polyunsaturated fatty acids including those only detected in pork and chicken (half of the samples).

### Raman Spectroscopy

Raman measurements were carried out using a home-built system previously described [9] with line-focused 785 nm excitation (typically 100–120 mW at the sample). The Raman signal was recorded from 270 to 1,900  $\text{cm}^{-1}$ , the region containing the C–C, C = C, C–O and C = O stretches and the C–H bends. The spectra were processed as described previously [9] using a standard 14-point linear baseline subtraction.

The classification of the spectra using a number of statistical routines was compared for PCA, PLSDA, Feed forward networks and Kohonen Maps. The data were normalised about the carbonyl stretching band at ca. 1,745  $\text{cm}^{-1}$  and mean centred prior to analysis. The data was split into a training (102 samples) and an independent test (153) set (replicates of any sample were retained in the same set). Comparison of the different methods was by the

percentage of the test-set samples which were classified as belonging to the correct species of origin for each sample. PLSDA and the PCA data reduction steps were carried out using Simca-P 8.0 (Umetrics, Umeå, Sweden), while Linear Discriminant Analysis (LDA) of the PCA-reduced Raman data was performed in SPSS V13.0. Feed forward networks and Kohonen maps were calculated using a beta version of a neural network package Antbrain, developed by CB.

## Results and Discussion

In our previous papers we investigated the effect of altering either chemical composition or physical state on the experimental and calculated Raman spectra of model FAMES [7, 14, 15]. We also investigated the use of Raman spectra to predict the fatty acid composition of clarified butterfat and adipose tissue [9, 10]. In this paper, an expanded adipose tissue data set was employed. The samples were again studied at ambient temperature where the physical state depends on the fatty acid composition, positional isomerisation and any inherent matrix ordering/disordering effects, which vary between species and to a lesser extent between individual animals of the same species. Since it was previously found that the variation in physical state caused by chemical differences between the samples enhanced the information content of the Raman spectrum of fatty acid lipids, use of ambient temperature measurements should maximise the spectral difference between species [10]. Figure 1 shows the average Raman spectrum of adipose tissue from each of the species used in this experiment and it is clear that the samples exhibited mixed phases, the spectra exhibit sharp solid phase bands (e.g. 1,060 and 1,130  $\text{cm}^{-1}$ ) superimposed on broad liquid phase bands (e.g. 1,090  $\text{cm}^{-1}$ ). Comparison with the spectra previously published on a smaller set of samples (20 for each species) shows that the expanded dataset retains the superficial similarities and differences observed in that set. The assignments of the major bands have been given previously [10].

## Classification

Much of the early work on Raman spectroscopic analysis of fatty acids concentrated on the bulk properties, and in particular unsaturation [2, 4, 16]. The average bulk properties of the adipose tissue of the four species investigated here were calculated from the GC profile of the fat extracted from a subset of samples [10] and are shown in Table 1. It is immediately apparent that the species differences between these average bulk parameters are small. For example,

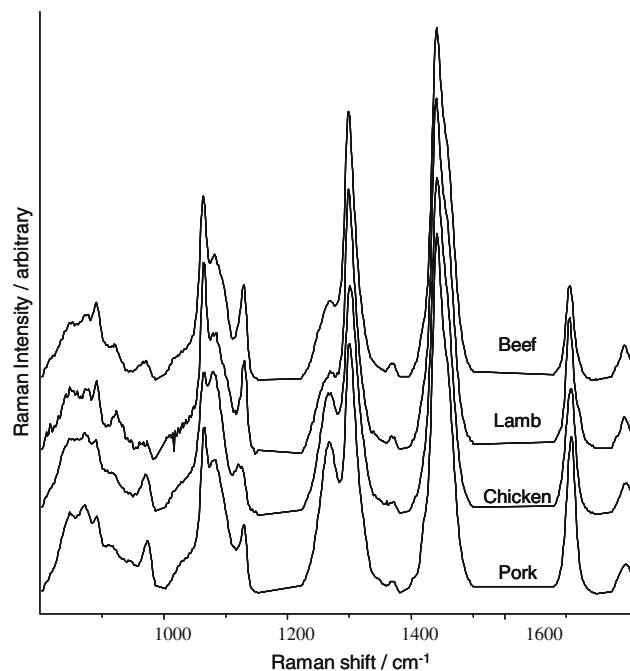


**Fig. 1** Average Raman spectra for the four species investigated in this study (beef, lamb, chicken and pork), recorded using 785-nm excitation

**Table 1** The average chemical subunit content for each of the species, derived from the subset used for GC analysis

Parameter (per chain)	Species	Average	Standard deviation
Total number of carbons (No. of C)	Pork	17.573	0.053
	Chicken	17.383	0.024
	Lamb	17.095	0.056
	Beef	17.046	0.074
Total number of saturated methylenes No. $\text{CH}_2$	Lamb	13.999	0.122
	Beef	13.902	0.090
	Chicken	13.577	0.033
Total number of unsaturated bonds No. $\text{C}=\text{C}$	Pork	1.030	0.076
	Chicken	0.903	0.020
	Beef	0.572	0.038
<i>trans:cis</i> Ratio (%)	Lamb	0.548	0.059
	Beef	13.341	7.818
	Lamb	6.080	2.019
	Chicken	0.872	0.096
	Pork	0.089	0.049

For each chemical subunit the samples are arranged in descending order

although there are detectable differences between pork and chicken adipose tissue (pork has a higher average chain length and higher average number of double bonds per molecule) there is a marginal difference in the main bulk

chemical properties of the lamb and beef adipose samples, apart from a slightly higher proportion of *trans* fatty acids in the beef within this subset of samples analysed by GC. At the simplest level, these changes in bulk composition are reflected in the average Raman spectra from each of the species (Fig. 1). Unsaturation gives rise to bands around  $1,270\text{ cm}^{-1}$  ( $=\text{C}-\text{H}$  bend) and  $1,660\text{ cm}^{-1}$  ( $\text{C}=\text{C}$  stretch)  $\text{cm}^{-1}$  and the spectrum of pork adipose tissue shows the largest bands at these positions, followed by chicken and then beef and lamb, which are both very similar, reflecting the expected composition of the four species. The largest difference between the beef and lamb spectra is the small shoulder at  $1,670\text{ cm}^{-1}$  on the  $1,660\text{ cm}^{-1}$  band of the lamb spectra, which corresponds to *trans* isomers. This indicates that the *trans* content of lamb in the expanded dataset for the Raman (Fig. 1) contains significantly more *trans* than the smaller GC subset (Table 1), illustrating the problem of depending on simple univariate measurements for discriminating species. In practice, we have found that it is not possible to reliably classify the species (75% correct classification) of a given sample on the basis of simple measurements of those band intensities that correspond to bulk properties. This can be attributed to the overlap in the values of various parameters between some species since the composition of each species is affected by many other factors including age, breed, feed, sex and climatic conditions [17–20].

Using the GC-calculated bulk properties simultaneously as input into PLSDA gives 93% correct classification (full cross validation), with 10% of the beef and lamb samples misclassified as each other. This is significantly better than the 75% correct classification rate obtained by using the classical spectroscopic method of a single band ratio. In Fig. 2, the score plot for the two most significant components from the PLSDA analysis of the bulk values, shows

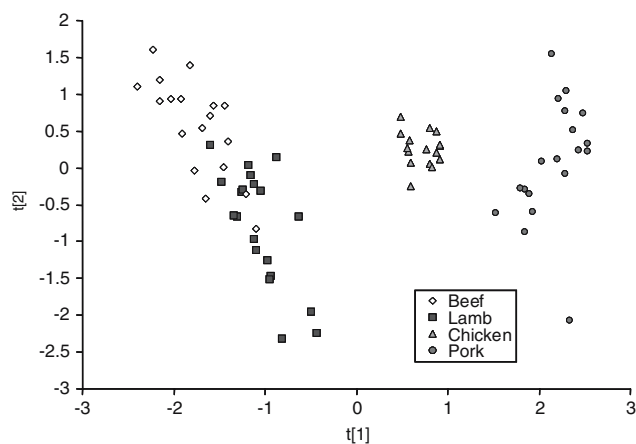


**Fig. 2** Score plot obtained from PLSDA of the bulk values of the adipose tissue, as calculated from fatty acid composition. The two ruminant species are not well separated by the major components, but they are isolated from the non-ruminant species

that the chicken and pork are well separated from each other and from the beef and lamb samples. Subsequent components improve the separation of the beef and lamb (data not shown). However, the beef and lamb do overlap considerably, accounting for the classification errors. Using the full fatty acid composition data obtained from the GC to classify the species was 100% successful when using all the fatty acids recorded, even if, for some of the species, they were below the cut off limit for detection on the GC instrument. This clearly demonstrates that a method capable of providing information on the detailed chemical composition of a lipid has the potential to classify the species of an adipose tissue sample.

Since we have previously demonstrated that multivariate analysis of Raman spectra can be used to quantify the relative abundances of various fatty acids in adipose tissue [10], it might be expected a similar level of differentiation between adipose tissue taken from different animal species could be achieved by using multivariate data analysis rather than the simple gross measurements of the intensities of the small number of well-known bands that correlate with bulk properties described above.

Multivariate data reduction combined with discriminant analysis was indeed found to be capable of accounting for the subtle differences between the species. PCA data reduction on the adipose Raman data set followed by LDA allowed 97.6% correct classification of the samples in LDA, while using the PLSDA method further improved the correct classification rate to 99.61% (Fig. 3), i.e. only one sample incorrectly assigned. The improvement given by the PLSDA method is expected since the data reduction step is designed to determine the variation that gives rise to the maximum group separation, in contrast the PCA reduction prior to LDA is based on variation without respect to the grouping of the samples. The PLSDA method used 80 % of the total variation within the dataset to explain the difference between the groups, which explains why the Raman spectrum is such a powerful discriminatory tool. By using simple manual measurements of the intensities of the characteristic marker bands we would reduce 1,152 variables (the number of data points in each spectrum) to around 10—thus using only ca. 1% of the information. However, by using multivariate data reduction fewer than 10 variables (factors) can retain 80% of the information contained in the original data with its 1,152 variables.

The data were then run on a Kohonen map, with PCA preprocessing at unit variance. The underlying structure of Kohonen maps is a grid of vectors (ca. average spectrum) that accounts for all the spectral variation observed, with incremental changes between each cell. The location of a sample within a particular square indicates it is most similar to that vector, and its distance from the centre relates

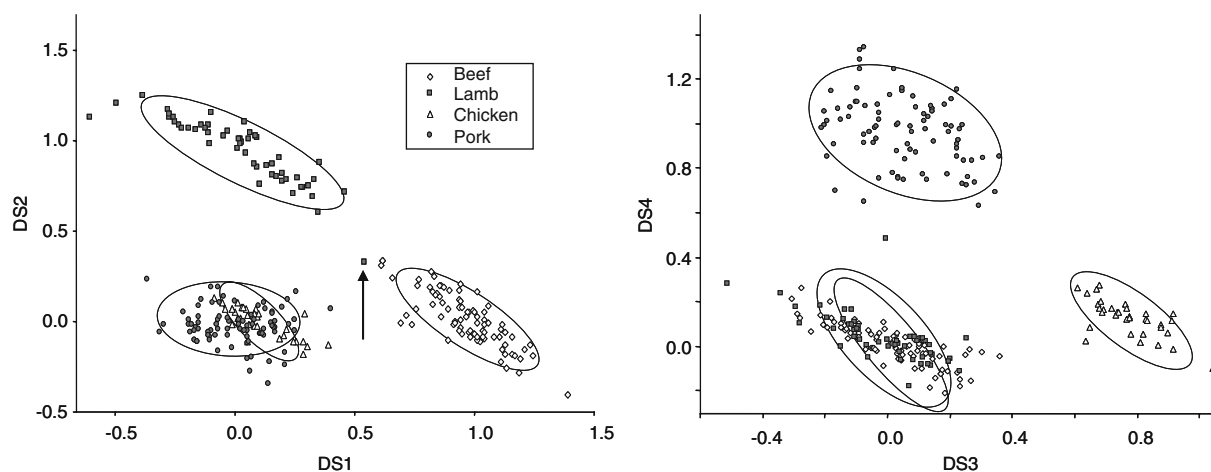


**Fig. 3** Discriminant score (calculated from a function of the eight components shown in Fig. 6) plots showing how the calculated discriminant score separates out the test set samples. 95% confidence intervals are shown, incorrectly classified samples are marked with an *arrow*

how similar it is to the vector for that square. This means that similar spectra group closely together, while dissimilar spectra will be well separated in the grid. The Kohonen map (Fig. 4) marginally improved the separation of PCA preprocessed spectra compared to LDA, but was not as successful as the PLSDA, since 1.6% of the samples (3 beef, 1 lamb) were incorrectly classified. The samples were also run on a feed forward network, using PCA preprocessing (scaled to unit variance) to obtain a regression to predict species. The feed forward network yielded a stan-

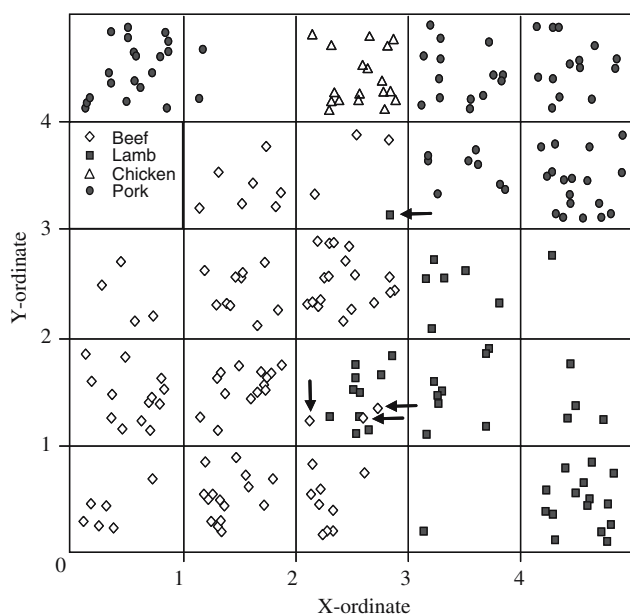


**Fig. 4** Kohonen map showing the separation of subcutaneous adipose tissue into different species (beef, lamb, chicken and pork), using the Raman spectra of intact adipose tissue, recorded at 19–21 °C. Key has been placed in empty cell for convenient reference. Misclassified spectra are indicated by *arrows*

dard error of prediction of just 0.027 (Fig. 5). Only two (0.8%) of the samples were incorrectly classified (less than 0.5 from the mean for the species), which is only one sample more than using the PLSDA method.

Figure 6 shows the loadings used by the PLSDA method to reduce the spectral data to the scores that were used in the discriminant analysis and the plot of those resultant scores in Fig. 3. The first two PLSDA components are the most important and are shown as a score plot in Fig. 7, in the figure there is a clear difference between the ruminant (beef and lamb) from the non-ruminant (chicken and pork) samples in the first component. Comparison of the Raman bands used in the relevant loading plot (Fig. 6, loading 1) with their assignments [10] show that the bands accounting for this divide are unsaturated (positive peaks, more intense

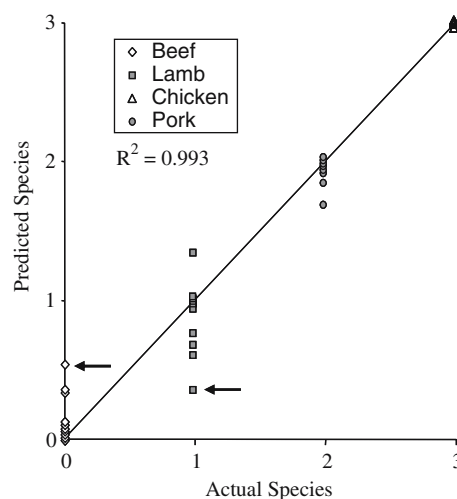


**Fig. 5** Feed forward network prediction of species using the Raman spectra of intact subcutaneous adipose tissue recorded at 19–21 °C. Incorrectly assigned samples marked with a *black arrow*

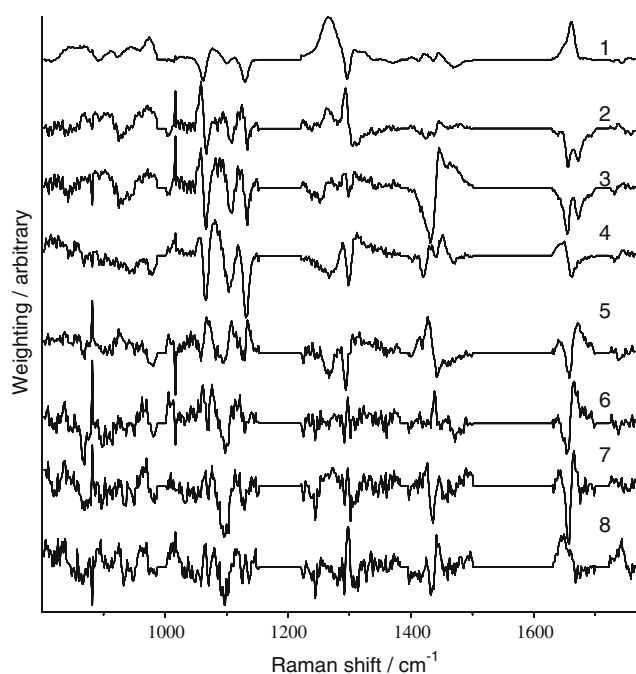


**Fig. 6** PLSDA loadings for the significant components used to reduce the Raman variables to a discriminant function allowing classification of the species of origin from a Raman spectrum of adipose tissue. The numbering refers to the order of significance of each loading from 1 for the most significant to 8, the least significant

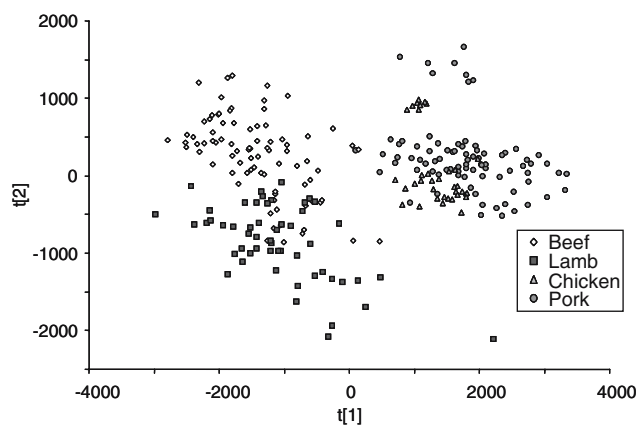


**Fig. 7** Score plot of the two major components obtained from PLSDA of the Raman data. There is a clear separation of ruminant (beef and lamb) from non-ruminant (pork and chicken), but further components are required to separate each of these groups

in spectra of non-ruminant samples) against saturated (negative peaks, more intense in ruminant samples). This result agrees with the data presented in Table 1.

Component 2 partially separates lamb from the beef (Fig. 7) and the loadings appear to be a complex array of subtle physical changes in the Raman spectrum (Fig. 6, loading 2), with conformation-sensitive bands showing shifts in intensity such as the *trans/gauche* sensitive C–C

stretching modes between 1,060 and 1,130  $\text{cm}^{-1}$ , the  $\text{CH}_2$  twisting mode 1,293/1,305  $\text{cm}^{-1}$  and the olefinic conformation band at 1,655  $\text{cm}^{-1}$ . Also contributing is a negative component related to *trans* isomers of the olefinic bonds, which typically are implicated in the overall physical properties of fatty acid mixtures, even when in low abundance.

The higher numbered components are a complex mixture of other subtle physical interactions (conformation of the fatty acid chain and changes in chain packing) and chemical changes. For example the third loading is similar to the second but contains a significant contribution from the  $\text{CH}_2$  scissoring region (1,400–1,500  $\text{cm}^{-1}$ ), which is highly sensitive to the packing of the fatty acid chains and the extent of intermolecular order (as opposed to the intramolecular order reflected in the C–C stretching and  $\text{CH}_2$  twist regions mentioned above). The second and third components are superficially similar but there are a number of subtle, though significant, differences. This is explained by the fact that the inter- and intra-molecular properties of fatty acid chains are influenced by the same environmental parameters (hence broadly the same pattern of changes), but they react to the environment independently of each other (accounting for the subtle differences).

Interpreting each loading is beyond the scope of this investigation; however the overall understanding is that the discrimination is based on not just the chemical differences in the fatty acid composition of the different species, but also the complex physical variations that are a result of interactions between these various fatty acids.

Raman spectroscopy has many advantages in the analysis of food lipids in that it requires no sample preparation and yet has excellent prediction ability even for the species of origin (for example, where the fatty acids that show significant variation between lamb and beef fat are present at <2.3%) or the abundance of minor fatty acids [10]. It is also simple to adapt the method to a range of applications giving a range of levels of information, especially in combination with appropriate statistical methods capable of maximising the use of the information contained within the Raman spectrum. For example, here we have demonstrated that the spectrum that has been recorded can be used to accurately determine the species of the sample (this is most effective in conjunction with PLSDA) while previous studies showed that the level of unsaturation [7], the solid fat content [9], or the abundance of individual fatty acids [10] (in conjunction with PLS) can also be determined from Raman spectra. Another major advantage is the level of diagnostic capability arising from the well-understood relationship between the Raman spectrum and factors (chemical and physical) that influence it.

This study has clearly demonstrated that the combination of Raman spectroscopy with multivariate and neural

network analytical methods allows the species of an adipose tissue sample to be assigned according to its Raman signal with greater than 99% accuracy. It was found that classical univariate methods of using the Raman signal were unable to give a satisfactory classification as the differences between some of the species were very subtle and univariate methods only retain <1% of the spectral information. The type of multivariate analysis or neural network made little difference to the classification rate, though PLSDA and feed-forward networks performed slightly better than LDA and Kohonen networks, both employing PCA preprocessing.

## References

1. Tu AT (1982) Raman spectroscopy in biology: principles and applications. Wiley, New York
2. Sadeghi-Jorabchi H, Hendra PJ, Wilson RH, Belton PS (1990) Determination of the total unsaturation in oils and fats by Fourier transform Raman spectroscopy. *JAOCS* 67:483–486
3. Larsson K (1973) Conformation dependent features in the Raman spectra of simple lipids. *Chem Phys Lipids* 10:165
4. Bailey GF, Horvat RJ (1972) Raman spectroscopy analysis of the *cis/trans* isomer composition of edible vegetable oils. *JAOCS* 49:494–498
5. Afseth NK, Wold JP, Segtnan VH (2006) The potential of Raman spectroscopy for characterisation of the fatty acid unsaturation of salmon. *Anal Chim Acta* 572:85–92
6. Chmielarz B, Bajdor K, Labudzinska A, Klukowskamajewska Z (1995) Studies on the double-bond positional isomerization process in linseed oil by UV, IR and Raman-Spectroscopy. *J Mol Struct* 348:313–316
7. Beattie JR, Bell SEJ, Moss BW (2004) A critical evaluation of Raman spectroscopy for the analysis of lipids: fatty acid methyl esters. *Lipids* 39:407–419
8. Weldon MK, Morris MD (2000) Surface-enhanced Raman spectroscopic investigation of bacterial lipolysis in a skin pore phantom. *Appl Spectrosc* 54:20–23
9. Beattie JR, Bell SEJ, Borggaard C, Fearon AM, Moss BW (2004) Multivariate prediction of clarified butter composition using Raman spectroscopy. *Lipids* 39:897–906
10. Beattie JR, Bell SEJ, Borggaard C, Fearon A, Moss BW (2006) Prediction of adipose tissue composition using Raman spectroscopy: average properties and individual fatty acids. *Lipids* 41:287–294
11. Sprunt JC, Jayasooriya UA, Wilson RH (2000) A simultaneous FT-Raman-DSC (SRD) study of polymorphism in *sn*-1,3-distearoyl-2-oleoylglycerol (SOS). *Phys Chem Chem Phys* 2:4299–4305
12. Heise HM, Damm U, Lampen P, Davies AN, McIntyre PS (2005) Spectral variable selection for partial least squares calibration applied to authentication and quantification of extra virgin olive oils using Fourier transform Raman spectroscopy. *Appl Spectrosc* 59:1286–1294
13. Williams P, Norris K (2001) Near-Infrared technology in the agricultural and food industries. AACC Press, St Paul, p 312
14. Oakes RE, Beattie JR, Moss B, Bell SEJ (2002) Conformations, vibrational frequencies and Raman intensities of short chain fatty acid methyl esters using DFT with 6–31 G(d) and Sadlej pVTZ basis sets. *J Mol Struct* 586:91–110
15. Oakes RE, Beattie JR, Moss BW, Bell SEJ (2003) DFT studies of long-chain fatty acids: theoretical justification for determining chain length and unsaturation from experimental Raman Spectra. *J Mol Struct-Theochem* 626:27–45
16. Sadeghi-Jorabchi H, Wilson RH, Belton PS, Edwards-Webb JD, Coxon DT (1991) Quantitative analysis of oils and fats by Fourier transform Raman Spectroscopy. *Spectrochim Acta* 47A:1449–1458
17. Enser M, Hallett KG, Hewett B, Fursey GAJ, Wood JD, Harrington G (1998) Fatty acid content and composition of UK beef and lamb muscle in relation to production system and implications for human nutrition. *Meat Sci* 49:329–341
18. Raes K, De Smet S, Demeyer D (2004) Effect of dietary fatty acids on incorporation of long chain polyunsaturated fatty acids and conjugated linoleic acid in lamb, beef and pork meat: a review. *Anim Feed Sci Technol* 113:199–221
19. Wachira AM, Sinclair LA, Wilkinson RG, Enser M, Wood JD, Fisher AV (2002) Effects of dietary fat source and breed on the carcass composition, n-3 polyunsaturated fatty acid and conjugated linoleic acid content of sheep meat and adipose tissue. *Br J Nutr* 88:697–709
20. Warren HE, Enser M, Hallett K, Wood JD, Dhanoa MS, Scollan ND (2004) Effect of age on the fatty acid classes of beef muscle. In: *Proceedings of the British Society of Animal Science*, p 83

## Arachidonic Acid but not Eicosapentaenoic Acid (EPA) and Oleic Acid Activates NF- $\kappa$ B and Elevates ICAM-1 Expression in Caco-2 Cells

Julian D. Ramakers · Ronald P. Mensink · Gert Schaart · Jochum Plat

Received: 28 November 2006 / Accepted: 28 April 2007 / Published online: 3 July 2007  
© AOCS 2007

**Abstract** In patients with inflammatory bowel disease (IBD), intestinal activation of the transcription factor NF- $\kappa$ B as well as intercellular adhesion molecule (ICAM)-1 expression, which is involved in recruiting leukocytes to the site of inflammation is increased. Moreover, colonic arachidonic acid (ARA) proportions are increased and oleic acid (OA) proportions are decreased. Fish oils are protective in IBD patients however, a side-by-side comparison between effects of fish oils, ARA and OA has not been made. We therefore, compared effects of eicosapentaenoic acid (EPA) versus ARA and OA on ICAM-1 expression in Caco-2 enterocytes. To validate our model we showed that dexamethasone, sulfasalazine and PPAR $\alpha$  (GW7647) or PPAR $\gamma$  (troglitazone) agonists significantly lowered ICAM-1 expression. ICAM-1 expression of non-stimulated and cytokine stimulated Caco-2 cells cultured for 22 days with ARA was significant higher as compared to EPA and OA. Furthermore, ARA increased NF- $\kappa$ B activation in a reporter cell-line as compared to EPA. Antibody array analysis of multiple inflammatory proteins particularly showed an increased monocyte chemotactic protein (MCP)-1 and angiogenin production and a de-

creased interleukin (IL)-6 and IL-10 production by ARA as compared to EPA. Our results showed that ARA but not EPA and OA activates NF- $\kappa$ B and elevates ICAM-1 expression in Caco-2 enterocytes. It suggests that replacement of ARA by EPA or OA in the colon mucosa might have beneficial effects for IBD patients. Finally, we suggest that the pro-inflammatory effects of ARA versus EPA and OA are not related to PPAR $\gamma$  activation and/or eicosanoid formation.

**Keywords** Intestinal inflammation · Caco-2 cells · Prostaglandins · Peroxisome proliferator-activated receptor (PPAR)

### Abbreviations

ARA	Arachidonic acid
CD	Crohn's disease
COX	Cyclooxygenase
EPA	Eicosapentaenoic acid
GRO	Growth regulated protein
IBD	Inflammatory bowel disease
ICAM	Intercellular adhesion molecule
IFN	Interferon
IL	Interleukin
MCP	Monocyte chemotactic protein
MIP	Macrophage inflammatory protein
MUFA	Monounsaturated fatty acid
NF- $\kappa$ B	Nuclear factor-kappa B
OA	Oleic acid
PGE <sub>2</sub>	Prostaglandin E <sub>2</sub>
PPAR	Peroxisome proliferator-activated receptor
PUFA	Polyunsaturated fatty acid
UC	Ulcerative colitis

J. D. Ramakers (✉) · R. P. Mensink · J. Plat  
Department of Human Biology,  
Nutrition and Toxicology Research Institute  
Maastricht (NUTRIM), Maastricht University,  
P.O. Box 616, 6200 MD Maastricht, The Netherlands  
e-mail: j.ramakers@hb.unimaas.nl

G. Schaart  
Movement Sciences,  
Nutrition and Toxicology Research Institute  
Maastricht (NUTRIM), Maastricht University,  
Maastricht, The Netherlands

## Introduction

Epidemiological studies have shown a low incidence of inflammatory bowel disease (IBD) in Eskimo's as compared to West-European populations [1] and increasing incidences of IBD in Japan [2]. These findings suggest that an increased dietary intake of n-6 polyunsaturated fatty acids (PUFA) and a lower intake of n-3 PUFAs contribute to the development of IBD. Thus, n-3 fish oil PUFAs may have anti-inflammatory effects as compared to n-6 PUFA [3]. Indeed, elevated proportions of the n-6 PUFA arachidonic acid (ARA) in colon mucosa of both ulcerative colitis (UC) and Crohn's disease (CD) patients as compared to those of control subjects have been shown [4–7]. Although the proportion of the n-3 PUFA eicosapentaenoic acid (EPA) in the mucosa was in most studies not statistically different between IBD patients and healthy controls, one study reported a tendency towards lower EPA proportions in IBD patients [4]. In contrast to EPA, the proportion of the fish oil PUFA docosahexaenoic acid (DHA) was elevated in colonic mucosa of IBD patients as compared to control subjects [4, 5, 7]. Interestingly, the proportion of the n-9 monounsaturated fatty acid (MUFA) oleic acid (OA) was lower in colon mucosa of IBD patients [4, 7]. Because of these observations, and because EPA is a more important precursor of eicosanoids than DHA [8], we decided to compare the effects of EPA versus ARA and OA in an in vitro model of intestinal inflammation. OA is already the most abundant fatty acid present both in our diet [9] as well as in colon mucosa [4]. Therefore, and because of differences in ability to compete with ARA for incorporation in tissue phospholipids [10, 11], it is probably easier to lower mucosal ARA levels by increasing fish oil intake than by increasing OA intake. Indeed, by increasing their intake of fish oil, ARA in the colon mucosa of IBD patients was replaced by EPA and DHA [12], which was associated with significantly reduced corticosteroid requirements [12] and lower relapse rates [13]. It should be noted however, that not all intervention studies using fish oils were that positive, although the overall conclusion is that fish oil supplementation shows at least minor protective effects [14].

The intercellular adhesion molecule (ICAM)-1 plays an important role in the pathology of IBD. In IBD patients intestinal ICAM-1 expression [15] and plasma levels of soluble ICAM-1 (sICAM) are increased [16], and IBD is associated with polymorphisms in the gene encoding for ICAM-1 [17]. Moreover, animal models [18, 19] and a human intervention study [20] have shown that ICAM-1 blocking inhibited intestinal inflammation. The transcription factor NF- $\kappa$ B is a key regulator of the inflammatory response and activation of NF- $\kappa$ B seems to play a critical role in the initiation and perpetuation of intestinal inflam-

mation in IBD [21, 22]. NF- $\kappa$ B activity in the colon is increased during active episodes in IBD patients and certain anti-inflammatory drugs commonly used for IBD appear to inhibit NF- $\kappa$ B [23–27]. In animal models, NF- $\kappa$ B blockade abolished experimental colitis [28, 29]. A side-by-side comparison of the n-3 PUFA EPA, the n-6 PUFA ARA and the n-9 MUFA OA on ICAM-1 expression and NF- $\kappa$ B activation of intestinal cells has, as far as we are aware of, never been performed. Therefore the aim of the present study was to compare the effects of EPA, ARA and OA on ICAM-1 expression and NF- $\kappa$ B activation in the human intestinal epithelial Caco-2 cell line in vitro.

## Materials and Methods

### Reagents

Bovine serum albumin (BSA; endotoxin and fatty acid-free), sulfasalazine, dexamethasone, GW7647, oleic acid (OA), arachidonic acid (ARA), eicosapentaenoic acid (EPA) and indomethacin were obtained from Sigma Chemical Company (St Louis, MO). Troglitazone was purchased from Biomol (Plymouth Meeting, PA). Recombinant human IL-1 $\beta$  and interferon (IFN) $\gamma$  were purchased from Roche Molecular Biochemicals (Mannheim, Germany). DMEM, trypsin, penicillin streptomycin (PS), sodium pyruvate (SP) and non-essential amino acids (NEAA) were obtained from Invitrogen Corporation (Paisley, UK). Fetal calf serum (FCS; South-American) was obtained from Greiner Bio-one (Frickenhausen, Germany).

### Intestinal Cell Cultures

The human cell line Caco-2 was purchased from the American Tissue Type Collection (ATTC). Caco-2 cells were cultured in DMEM supplemented with 10% heat-inactivated FCS and 1% penicillin streptomycin (PS), 1% sodium pyruvate (SP) and 1% non-essential amino acids (NEAA). Cells were cultured at 37 °C in a 5% CO<sub>2</sub> humidified atmosphere, refreshed every second day and separated by trypsin–0.03% EDTA, when they had reached 70–90% confluence. To evaluate the immune-modulating effects of different interventions, Caco-2 cells were plated in six well tissue culture plates at an initial density of  $0.5 \times 10^6$  cells/mL in a total volume of 1.5 mL. Medium was replaced every other day for 24 days. After 24 days Caco-2 wells were fully differentiated into small intestinal enterocytes [30]. First, effects of immune-suppressive pharmacological compounds (sulfasalazine, dexamethasone and troglitazone) were tested to validate the model. Although these pharmacologic compounds have known



immune-suppressive effects, effects on ICAM-1 expression in Caco-2 cells have—as far as we know—not been reported before. Therefore, after Caco-2 cells were fully differentiated, medium was replaced by medium containing the compound of interest in combination with an inflammation-inducing cocktail consisting of the cytokines IFN $\gamma$  (100 U/mL) and IL-1 $\beta$  (50 U/mL). The compounds of interest were pre-incubated 30 min (sulfasalazine) or 2 h (dexamethasone, troglitazone or GW7647) before stimulation with the cytokine cocktail. After 16 h of cytokine stimulation, cells were used to determine cell surface ICAM-1 protein expression.

### Fatty Acid Experiments

The effects of various fatty acids were evaluated using the same Caco-2 cell model. For this, various fatty acids were added at indicated concentrations 2 days after plating the cells and again for the following 22 days each time when the medium was refreshed. We used OA as a control n-9 MUFA because this is the most abundant fatty acid in the diet [9]. We further compared the effects of the n-6 PUFA ARA versus the n-3 PUFA EPA. We have explicitly chosen to use EPA instead of DHA since the proportion DHA in the colon mucosa of IBD patients was already higher as compared to control subjects [4, 5, 7]. In addition, EPA is most likely a more important eicosanoid precursor [8]. The fatty acids were dissolved in ethanol up to a final ethanol concentration in the medium of maximal 0.5% (v/v). To prevent cytotoxicity of the fatty acids the FA were bound to albumin, by pre-incubating the fatty acids dissolved in ethanol for 30 min at 37 °C in full culture medium together with 10% FCS, which also contained 0.1% BSA. Caco-2 cells were cultured with respectively 160  $\mu$ M OA [C18:1(n-9)] versus 130  $\mu$ M ARA [C20:4(n-6)] plus 30  $\mu$ M OA (in total 160  $\mu$ M fatty acids) or 6  $\mu$ M EPA [C20:5(n-3)] plus 154  $\mu$ M OA (in total also 160  $\mu$ M fatty acids). By this approach the total molarity of fatty acids supplied was similar in all experiments, while supplying different amounts of the fatty acid of interest (i.e., 130  $\mu$ M ARA or 6  $\mu$ M EPA). These relatively low concentrations of OA (160  $\mu$ M), ARA (130  $\mu$ M) and EPA (6  $\mu$ M) were chosen because they are four times higher than normally present in culture medium of Caco-2 cells containing 10% FCS. We have deliberately chosen for this low EPA concentration since the EPA concentration is very low in FCS. However, the EPA concentration used is—as for all fatty acids used in these experiments—already four times higher than normally present in culture medium. We cultured the cells for 22 days with these relatively low concentrations of fatty acids to simulate a realistic long-term in vivo change in dietary fatty acid intake. After 22 days culture with fatty acids, medium was replaced by medium enriched

with the different fatty acids plus the cytokine cocktail [IFN $\gamma$  (100 U/mL) and IL-1 $\beta$  (50 U/mL)]. After 16 h stimulation, ICAM-1 expression on living cells was measured and culture medium was collected to determine inflammatory protein expression profiles. To evaluate the effects of the fatty acids on NF- $\kappa$ B activity and the role of cyclooxygenase (COX)-enzymes, the experiments with the fatty acids ARA and EPA were repeated but now in our NF- $\kappa$ B reporter Caco-2 cell line with and without indomethacin (20  $\mu$ M) added 2 h before and during cytokine stimulation. Prostaglandin PGE $_2$  levels in the supernatant were quantitated using a PGE $_2$  Biotrak enzyme-immunoassay (EIA) system (Amersham Biosciences Ltd, Buckinghamshire, UK) according to the high sensitivity enzyme immunoassay protocol 2.

### Flow Cytometry Analysis of ICAM-1

In order to quantify cell surface ICAM-1 protein expression on living Caco-2 cells, we developed a flow cytometry assay. After 16 h of stimulation, the cells were washed three times with PBS and detached with trypsin–0.03% EDTA. Next, medium was added and cell suspensions were centrifuged for 5 min at 1,200 rpm at room temperature, followed by resuspending the pellets in 500  $\mu$ L PBS-1% BSA. Cells were counted and diluted to 10 $^6$  cells/mL in PBS-1% BSA. Recombinant-phycoerythrin (R-PE)-conjugated mouse-anti-human CD-54 monoclonal antibody (anti-ICAM-1) or isotype-matched control antibody (Becton Dickinson Biosciences, San Diego, CA; 20  $\mu$ L/10 $^6$  cells) was added and incubated for 30 min on ice in the dark. Next, cell suspensions were centrifuged for 5 min at 1,500 rpm and pellets were resuspended in 500  $\mu$ L PBS-1% BSA. The amount of fluorescence of 10,000 living cells was counted and analyzed with the FACSsort and CellQuest analysis software (Becton Dickinson, Franklin Lakes, NJ).

### Stable Transfection of NF- $\kappa$ B in Caco-2 Cells

For evaluating the effects of the various interventions on transcriptional activity of NF- $\kappa$ B, a stable NF- $\kappa$ B reporter Caco-2 cell line was created. The 6 $\kappa$ B-TK-luciferase (NF- $\kappa$ B reporter) plasmid and neomycin resistance plasmid were both kindly provided by Dr. R.C. Langen (Department of Pulmonology, Maastricht University, The Netherlands). Cells were transfected using Lipofectamine 2000 (Invitrogen Corporation, Paisley, UK) according the manufacturers' instructions. Positive clones were selected by culturing with geneticin (1 mg/mL). To determine luciferase activity, non-stimulated and 3 h cytokine (100 U/mL IFN $\gamma$  and 50 U/mL IL-1 $\beta$ ) stimulated cells were lysed in luciferase lysis buffer (Promega, Madison, WI) and stored at –80 °C. Luciferase (Promega) activity was measured

according to the manufacturers' instructions and expressed relative to total protein (Bio-rad assay; Bio-rad, Hercules, CA).

#### Peroxisome Proliferator-Activated Receptor (PPAR) $\gamma$ and PPAR $\alpha$ mRNA Expression of Differentiated Caco-2 Cells

Total RNA was extracted from differentiated Caco-2 cells with Trizol according to the manufacturers' instructions (Gibco BRL, Gaithersburg, MD). Next, cDNA was made as described [31], and mRNA expression of PPAR $\gamma$  and PPAR $\alpha$  was determined using commercially available Taqman gene expression assays (Applied Biosystems, Foster city, CA). Data were normalized against  $\beta$ -actin as housekeeping gene.

#### Fatty Acid Composition of Caco-2 Cells

Fatty acid incorporation into the Caco-2 cells was evaluated using extraction and analysis procedures as previously described [32]. Briefly, total lipids were extracted from 500  $\mu$ L cell suspension in PBS-1% BSA according to the method of Bligh and Dyer [33]. Aminopropyl-bonded silica columns (Varian, Harbor City, CA) were used to separate phospholipids from the total lipid extract [34]. The phospholipids were then saponified, and the resultant fatty acids were methylated into their corresponding fatty acid methyl esters (FAMES) [35]. Fatty acids were separated on an Autosystem (Perkin-Elmer, Norwalk, CT) gas chromatograph that was fitted with a silica-gel column (Cp-sil 88 for FAME, 50 m  $\times$  0.25 mm, 0.2- $\mu$ m film thickness; Chrompack, Middelburg, The Netherlands) with helium gas (130 kPa) as the carrier gas. Both the injection and detection temperatures were set at 300  $^{\circ}$ C. The starting temperature of the column was 160  $^{\circ}$ C. Ten min after injection, the temperature was increased up to 190  $^{\circ}$ C at a rate of 2.5  $^{\circ}$ C/min. After 20 min at 190  $^{\circ}$ C, the temperature was increased up to 230  $^{\circ}$ C at a rate of 4  $^{\circ}$ C/min. The final temperature of 230  $^{\circ}$ C was maintained for 10 min. Data were analyzed by using CHROMCARD software (version 1.21; CE Instruments, Milan, Italy). The fatty acid compositions of the Caco-2 cells are expressed in relative amounts (% of total fatty acids identified; w/w).

#### Inflammatory Protein Expression Profiles Using an Antibody Array

Protein expression patterns of multiple cytokines, chemokines and growth factors, were detected simultaneously in Caco-2 cell culture media with the human cytokine antibody array III (Ray Biotech Inc., Norcross, GA) according to the manufacturers' instructions. First, duplicates of cell

culture media of Caco-2 cells cultured with ARA and EPA after cytokine stimulation were pooled. One millilitre of the pooled samples was added to the array membranes. After incubating and washing, the protein-bound membrane was incubated with a cocktail of biotin-labeled antibodies, followed by the addition of horseradish peroxidase-conjugated streptavidin. Array spot intensity was detected by using a LAS-3000 Lite Image reader (Raytest GmbH, Straubenhart, Germany) based on chemiluminescence imaging. Intensity of the spots was quantified in arbitrary units (a.u.) by densitometry using Aida software version 3.50 (Raytest GmbH), thereby correcting for background staining of the gel. Comparison of protein expression profiles was possible after normalization of each spot on an array using the positive controls, provided by the manufacturer. The sensitivity of the array is not the same for the various proteins. Differences in heights of bars from different proteins do therefore not necessarily represent differences in concentrations. The cytokines used for stimulation (IFN $\gamma$  and IL-1 $\beta$ ) were excluded from analysis.

#### Detection of ICAM-1 on Caco-2 Frozen Sections

To determine the localization of ICAM-1 in our in vitro Caco-2 cell model, Caco-2 cells were cultured and differentiated into small intestinal enterocyte on collagen-coated polyfluoroethylene transwell membrane inserts with a 0.4  $\mu$ m membrane pore size (Corning Costar, Cambridge, MA). Differentiated Caco-2 cells were stimulated with IFN $\gamma$  (100 U/mL) and IL-1 $\beta$  (50 U/mL) for 16 h, embedded in Tissue-Tek (Sakura Finetek, Zoeterwoude, The Netherlands) and rapidly frozen in 2-propanol (Fluka, Zwijndrecht, The Netherlands), dry-ice-cooled and stored at -80  $^{\circ}$ C. Serial cryosections (10  $\mu$ m) were obtained using a Leica CM3050 cryostat (Leica Microsystems GmbH, Wetzlar, Germany) and thaw mounted on uncoated glass slides. Before processing or storage at -80  $^{\circ}$ C, the samples were air dried overnight. To detect ICAM-1 the sections were incubated 30 min in the dark at room temperature with recombinant-phycoerythrin (R-PE)-conjugated mouse-anti-human CD-54 monoclonal antibody or isotype-matched control antibody (Becton Dickinson Biosciences, San Diego, CA) 1:50 diluted in PBS-1% BSA. To detect cytokeratin (CK)-19 the sections were simultaneously incubated with a monoclonal antibody directed to CK-19, kindly obtained from Dr. E.B. Lane (University Dundee, Dundee, UK) 1:10 diluted. Then the sections were washed three times for 5 min in PBS. After that the secondary antibody goat anti-mouse IgG1 (ALEXA555) (Molecular Probes Europe, Leiden, The Netherlands) (1:500) against anti-CD54 (to evade fast quenching of the PE-label) and goat anti-mouse IgG2b (FITC) (Southern Biotech, Sanbio BV, Uden, The Netherlands) (1:50) against CK-19 diluted

in PBS-1% BSA was added to the sections and incubated for 30 min. Again the sections were washed three times for 5 min with PBS. Finally, sections were mounted in Mowiol-TRIS pH 8.5 (Calbiochem, Omnilabo International, Etten-Leur, The Netherlands) containing 0.5 g/mL 4–6-diamino-2-phenylindole (DAPI; Molecular Probes Europe) to stain the nuclei. All sections were examined using a Nikon E800 fluorescence microscope (Uvikon, Bunnik, The Netherlands) coupled to a Basler A101C progressive scan colour CCD camera. By just a simple shift in filters, images were grabbed in fluorescence using the ALEXA excitation filter (540–580 nm), the FITC excitation filter (465–495 nm) and DAPI UV excitation filter (340–380 nm) in the red, green and blue channel, respectively. The images acquired were merged to examine the cellular localisation and level of expression of ICAM-1.

### Statistical Analysis

Data were expressed as means and standard deviations (SD) for the non-stimulated condition, the cytokine stimulated condition and cytokine stimulated–non-stimulated (called net stimulated) condition. To determine statistical significance unpaired *t*-tests (comparison between two

interventions) or ANOVA (comparison between three interventions) with a Bonferonni post-hoc test when differences between interventions were significantly different, were performed. First non-stimulated values between interventions were tested to examine differences in basal values. Then, net stimulated values between interventions were tested to examine differences in cytokine-induced changes. Furthermore cytokines stimulated values were tested to examine differences in “end” values. All statistical analyses were performed using SPSS 11 for Mac Os X (SPSS, Chicago, IL). *P*-values of less than 0.05 were considered statistically significant.

## Results

### Model Validation

Stimulation with IL-1 $\beta$  and IFN $\gamma$  increased cell-surface ICAM-1 protein expression on Caco-2 cells, which resulted in a net stimulated ICAM-1 expression of about 50 a.u. (Fig. 1, panels a and b). After pre-treatment of the cells for 2 h with dexamethasone, a corticosteroid with known therapeutic effects in IBD patients, the cytokine stimulated

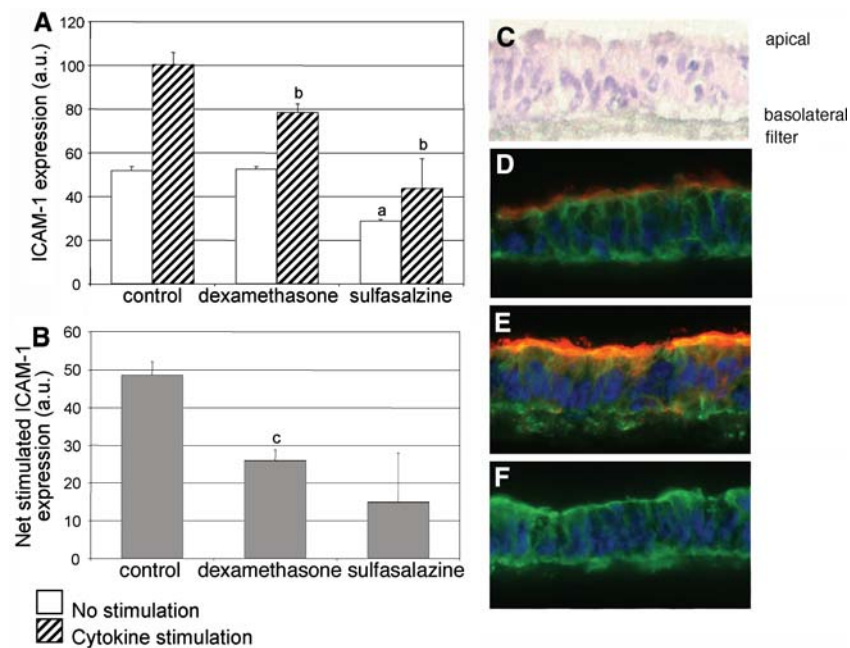


**Fig. 1** Model validation. **a** ICAM-1 expression (in arbitrary units a.u.) on living control Caco-2 cells and after 2 h pre-treatment with 1  $\mu$ M dexamethasone or 30 min 5 mM sulfasalazine with and without cytokine stimulation for 16 h (100 U/mL IFN $\gamma$  and 50 U/mL IL-1 $\beta$ ) and **b** net stimulated (stimulated–non-stimulated) ICAM-1 expression. Results represent means  $\pm$  SD; *n* = 2. Representative representation of two independent experiments. <sup>a</sup>*P* < 0.05 versus control non-stimulated, <sup>b</sup>*P* < 0.05 versus control cytokine stimulated,

<sup>c</sup>*P* < 0.05 versus control net stimulated. (**c–f**) Immunohistochemistry of ICAM-1 (red) on frozen sections of Caco-2 cells on a transwell showed increased apical expression after cytokine stimulation (100 U/mL IFN $\gamma$  and 50 U/mL IL-1 $\beta$ ). **c** Hematoxylin staining **d** Non-stimulated Caco-2 cells **e** Apical cytokine stimulated Caco-2 cells **f** Isotype control staining of ICAM-1. Red staining ICAM-1, green staining cytoskeleton (cytokeratin-19), blue staining nucleus. Magnification 40X

ICAM-1 expression was significantly decreased as compared to control ( $P = 0.044$ ). Also the net stimulated ICAM-1 expression (25 a.u.) was significantly reduced as compared to control ( $P = 0.019$ ). Next, we examined the effect of another frequently used therapeutic drug for IBD patients, sulfasalazine. Effects of sulfasalazine were comparable to those observed for dexamethasone. However, also ICAM-1 expression without cytokine stimulation ( $P = 0.004$ ) (Fig. 1, panel a) was lowered. Altogether, these results show that in our cell model ICAM-1 expression is related to the clinical outcomes of drugs proven to treat IBD and could therefore be used as the main outcome parameter in the following experiments. To further validate characteristics of our in vitro model, we also localized the site of ICAM-1 expression on the Caco-2 cells by means of immunohistochemistry on frozen sections. As shown in Fig. 1 (panels c–f), ICAM-1 was expressed on the apical (lumen) side of the polarized Caco-2 cells. Besides a low constitutive expression (panel d), there was a clear increase after stimulation with the cytokine cocktail (panel e). This localisation is in line with the apical ICAM-1 expression, as found in intestinal biopsies from IBD patients [36].

#### Effects of PPAR Agonists on ICAM-1 Expression and NF- $\kappa$ B Activation

Since PPARs are known modulators of inflammation and fatty acids are natural ligands for PPARs, we first examined PPAR expression in our differentiated Caco-2 cells. We found that PPAR $\alpha$  and PPAR $\gamma$  mRNA are expressed in equal amounts (data not shown). Next we examined the effects of the PPAR $\gamma$  agonist troglitazone [a thiazolidin-

edione (TZD)] and the PPAR $\alpha$  agonist GW7647 on ICAM-1 expression. Although both troglitazone and GW7647 significantly lowered the cytokine stimulated ICAM-1 expression as compared to control ( $P < 0.001$  and  $P = 0.009$ , respectively), only troglitazone significantly ( $P = 0.008$ ) reduced the net stimulated ICAM-1 expression (Fig. 2, panels a and b). Troglitazone and GW7647 were used at a concentration where they are selective for their receptor subtypes [37, 38]. It is known that PPARs suppress inflammation by inhibiting the transcription factor NF- $\kappa$ B, which is a key regulator of inflammation [39]. Therefore, we also examined effects of troglitazone on NF- $\kappa$ B transactivation in our Caco-2 NF- $\kappa$ B reporter cell line. These results showed that the cytokine cocktail induced after already 3 h a more than 200% increase in NF- $\kappa$ B transactivation. This increase of NF- $\kappa$ B transactivation was significantly ( $P = 0.008$ ) lower after 2 h pre-treatment with the PPAR $\gamma$  agonist troglitazone (Fig. 2, panels c and d). Moreover, the inhibitory effect of pre-treatment with the PPAR $\gamma$  agonist troglitazone on cytokine induced NF- $\kappa$ B transactivation was significantly ( $P = 0.001$ ) larger as compared to pre-treatment with the PPAR $\alpha$  agonist GW7647 (data not shown).

#### Fatty Acid Incorporation in Phospholipids

Table 1 shows that the fatty acids kept for 22 days in the culture medium were incorporated into the phospholipid fraction (% of total fatty acids) of the Caco-2 cells. Fatty acid incorporation into phospholipids showed the same pattern as the fatty acid composition of total lipids (data not shown), although changes in the total lipids were more

**Fig. 2** a, b ICAM-1 expression (in arbitrary units a.u.) on living control Caco-2 cells and after pre-treatment with PPAR agonists (2 h; PPAR $\gamma$  troglitazone 100  $\mu$ M and PPAR $\alpha$  GW7647 1  $\mu$ M) and c, d NF- $\kappa$ B transactivation measured by luciferase activity (in RLU/mg) in a NF- $\kappa$ B reporter Caco-2 cell-line of control cells and after troglitazone pre-treatment with and without cytokine stimulation for 3 h (100 U/mL IFN $\gamma$  and 50 U/mL IL-1 $\beta$ ) and net stimulated (stimulated–non-stimulated). Results represent means  $\pm$  SD;  $n = 2$ . Representative representation of two independent experiments. <sup>b</sup> $P < 0.05$  versus control cytokine stimulated, <sup>c</sup> $P < 0.05$  versus control net stimulated

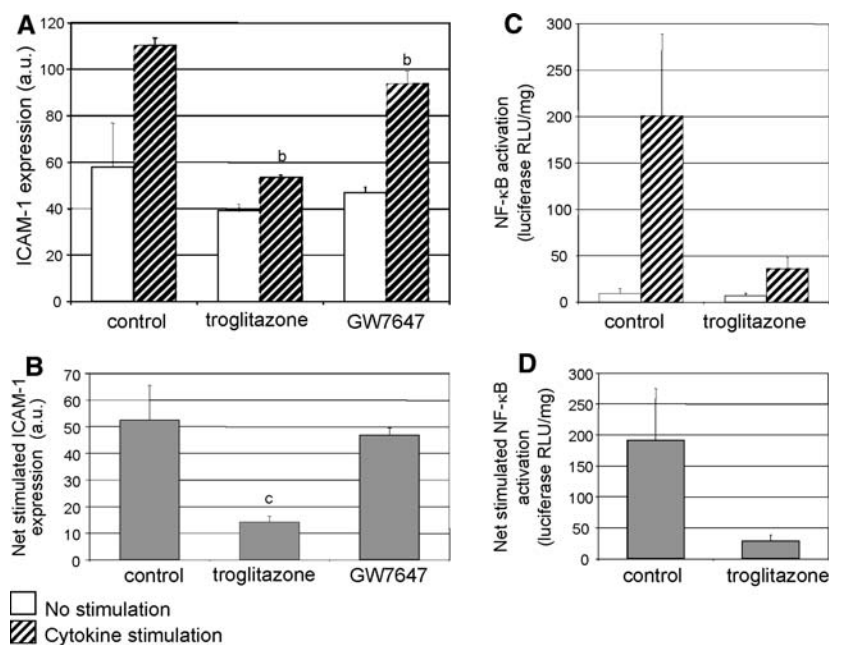


**Table 1** Fatty acid composition in phospholipids of Caco-2 cells without (–) and with (+) cytokine stimulation (IL-1 $\beta$  and IFN $\gamma$ ) supplemented with different fatty acids (% of total fatty acids)

Fatty acids	OA (160 $\mu$ M)		ARA + OA (130 + 30 $\mu$ M)		EPA + OA (6 + 154 $\mu$ M)	
	–	+	–	+	–	+
16:0 (PA)	16.0	16.1	18.7	19.5	16.3	15.8
18:0 (SA)	5.9	6.1	9.6	10.5	6.7	6.5
18:1 trans	3.0	3.1	6.1	5.7	2.7	2.7
18:1 (n-7)	3.4	3.4	2.6	2.5	3.3	3.3
18:1 (n-9) (OA)	47.1	46.3	14.4	13.8	45.2	45.0
18:2 (n-6) (LA)	1.7	1.7	1.1	1.1	1.7	1.6
20:1 (n-9)	2.1	2.1	0.3	0.3	1.7	1.7
20:4 (n-6) (ARA)	9.3	9.4	29.3	28.9	8.9	8.9
20:5 (n-3) (EPA)	0.4	0.4	0.0	0.0	2.1	2.2
22:1 (n-9)	0.8	0.8	1.5	1.3	0.8	0.8
24:1 (n-9)	2.0	2.1	0.9	1.0	2.0	2.1
22:4 (n-6)	0.4	0.4	7.7	7.8	0.3	0.3
22:5 (n-3)	0.5	0.5	0.4	0.4	1.3	1.3
22:6 (n-3) (DHA)	1.1	1.1	0.6	0.6	0.7	0.6
$\Sigma$	93.7	93.5	93.2	93.4	93.7	92.8
$\Sigma$ SAFA	21.9	22.2	28.3	30.0	23.0	22.3
$\Sigma$ MUFA	58.4	57.8	25.8	24.6	55.7	55.6
$\Sigma$ PUFA	12.3	12.4	38.5	38.2	14.3	14.3
$\Sigma$ n-3	2.0	2.0	1.0	1.0	4.1	4.1
$\Sigma$ n-6	11.4	11.5	38.1	37.8	10.9	10.8
$\Sigma$ n-9	52.0	51.3	17.1	16.4	49.7	49.6

Data are representative for two independent experiments and the data are derived from pooled samples

ARA arachidonic acid, EPA eicosapentaenoic acid, LA linoleic acid, MUFA monounsaturated fatty acids, OA oleic acid, PA palmitic acid, PUFA polyunsaturated fatty acids, SA stearic acid, SAFA saturated fatty acids,  $\Sigma$  sum, – non-stimulated, + cytokine stimulated

pronounced. Moreover, the fatty acid profiles of phospholipids (Table 1) and total lipids (data not shown) were similar in non-stimulated and stimulated Caco-2 cells. Cells cultured with ARA showed in particular an increase in the proportion of long chain n-6 PUFAs (mainly ARA) and a decrease in n-9 MUFAs (mainly OA) as compared with cells cultured with only OA. The cells cultured with EPA showed an increase in the proportion of n-3 fatty acids (mainly EPA) whereas the proportions of n-9 MUFAs and n-6 PUFAs did not change much as compared with cells cultured with only OA.

#### Effects of Fatty Acids on ICAM-1 Expression and NF- $\kappa$ B Activation

ICAM-1 expression was analyzed on living cells. FACS analysis did not show significant changes in cell populations cultured with the various fatty acids, suggesting no significant cell death. As shown in Fig. 3 (panel a), ARA significantly elevated ICAM-1 expression as compared to OA or EPA (non-stimulated  $P < 0.001$  ARA versus OA and ARA versus EPA, and stimulated  $P = 0.010$  ARA versus OA, and  $P = 0.013$  ARA versus EPA). Interestingly, stimulated and non-stimulated ICAM-1 expression on cells cultured with EPA did not significantly differ from those cultured with OA (Fig. 3, panel a). Despite these

clear differences in non-stimulated and stimulated ICAM-1 expression between ARA and EPA or OA, the net stimulated ICAM-1 expression did not differ between the groups (ANOVA  $P = 0.134$ ). Since dietary interventions aiming at lowering mucosal ARA content are most likely more successful by dietary EPA enrichments than by OA enrichment—because OA is the most abundant fatty acid present in our diet [9], making higher intakes not realistic—in further experiments we have focused on effects of ARA versus EPA. First, we examined the effects on NF- $\kappa$ B activation in the stable NF- $\kappa$ B reporter Caco-2 cell line (Fig. 4). NF- $\kappa$ B transactivation in stimulated Caco-2 cells cultured with ARA was significantly increased as compared to that in stimulated cells cultured with EPA (Fig. 4, panels a and b) (stimulated  $P = 0.017$  and net stimulated  $P = 0.001$ ). To evaluate whether the effects were related to the production of different families of eicosanoids we measured PGE<sub>2</sub> production and examined the effects of the different fatty acids in the presence of the cyclooxygenase (COX)-inhibitor indomethacin. As expected, PGE<sub>2</sub> production by Caco-2 cells cultured with ARA was significantly higher than by cells cultured with EPA (data not shown). Stimulation of the cells with the cytokine cocktail did however, not influence PGE<sub>2</sub> production. Since cytokine stimulation enhanced NF- $\kappa$ B activation, this suggests that PGE<sub>2</sub> is not directly involved in NF- $\kappa$ B activation.

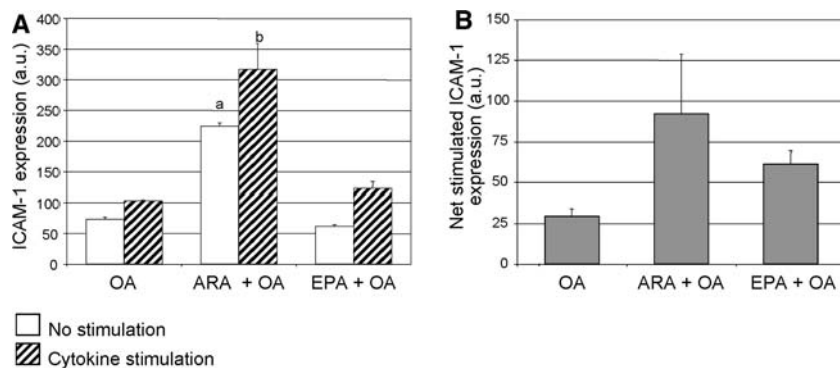


**Fig. 3 a–b** ICAM-1 expression (in arbitrary units a.u.) on living Caco-2 cells cultured for 22 days with 160  $\mu$ M oleic acid (OA) or 130  $\mu$ M arachidonic acid (ARA) plus 30  $\mu$ M OA or 6  $\mu$ M eicosapentaenoic acid (EPA) plus 154  $\mu$ M OA with and without cytokine stimulation for 16 h (100 U/mL IFN $\gamma$  and 50 U/mL IL-1 $\beta$ ) and net stimulated (stimulated–non-stimulated). Results represent

means  $\pm$  SD;  $n = 2$ . Representative representation of two independent experiments. ANOVA between groups, non-stimulated  $P < 0.001$ , stimulated  $P = 0.006$  and net stimulated  $P = 0.134$ . <sup>a</sup>Bonferroni  $P < 0.05$  versus OA and EPA non-stimulated, <sup>b</sup>Bonferroni  $P < 0.05$  versus OA and EPA cytokine stimulated

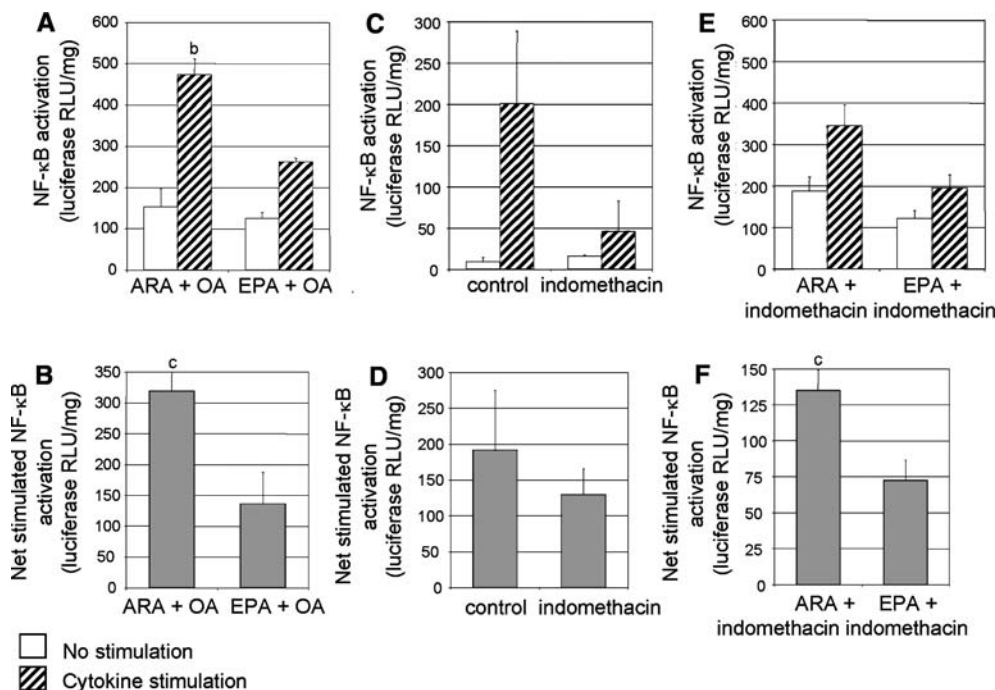


**Fig. 4** NF- $\kappa$ B transactivation with and without cytokine stimulation for 3 h (100 U/mL IFN $\gamma$  and 50 U/mL IL-1 $\beta$ ) (a, c, e) and net stimulated (stimulated–non-stimulated) (b, d, f) in a NF- $\kappa$ B reporter Caco-2 cell line measured by luciferase activity (in RLU/mg). a–b Reporter Caco-2 cells cultured for 22 days with 130  $\mu$ M arachidonic acid (ARA) plus 30  $\mu$ M oleic acid (OA) or 6  $\mu$ M eicosapentaenoic acid (EPA) plus 154  $\mu$ M OA. c–d Control reporter Caco-2 cells and

after 2 h pre-treatment with the COX-inhibitor indomethacin (20  $\mu$ M). e–f Reporter Caco-2 cells cultured for 22 days with 130  $\mu$ M arachidonic acid (ARA) plus 30  $\mu$ M OA or 6  $\mu$ M eicosapentaenoic acid (EPA) plus 154  $\mu$ M OA and 2 h pre-treatment with the COX-inhibitor indomethacin (20  $\mu$ M). Results represent means  $\pm$  SD;  $n = 2$ . <sup>b</sup> $P < 0.05$  versus EPA cytokine stimulated, <sup>c</sup> $P < 0.05$  versus EPA or EPA + indomethacin net stimulated

Indomethacin decreased PGE $_2$  production of Caco-2 cells by approximately 70% (data not shown), but had no effect on NF- $\kappa$ B transactivation (Fig. 4, panels c and d) as compared to untreated Caco-2 cells. Also ICAM-1 expression was not affected (data not shown). However, as shown in Fig. 4, the effects of ARA versus EPA in the

presence of indomethacin treatment (panel e) showed an identical pattern as observed without indomethacin (panel a). Also in the presence of indomethacin the net cytokine stimulated NF- $\kappa$ B transactivation was significantly higher after ARA as compared to EPA ( $P = 0.047$ ) (Fig. 4, panel f). This indicates that the increased basal PGE $_2$  production

by ARA cannot explain the different effects of ARA and EPA on NF- $\kappa$ B activation.

### Effects of Fatty Acids on Inflammatory Proteins Expression Profiles

Finally, to explore the effects of ARA and EPA on a broader scale, we evaluated protein expression profiles consisting of various inflammatory mediators by using antibody arrays. Figure 5 shows that ARA treatment particularly increased expression of monocyte chemotactic protein (MCP)-1 and angiogenin, while EPA treatment increased IL-10, IL-6, macrophage inflammatory protein (MIP)-1 $\delta$ , and growth regulated protein (GRO) expression.

### Discussion

ICAM-1 seems important in the pathology of IBD [15]. Whether fish oils, which have been shown to protect against relapses in IBD patients on remission [13], have effects on ICAM-1 expression, is however, unknown. In addition, a direct side-by-side comparison of fish oils with ARA, which is postulated to have pro-inflammatory effects [40] and is elevated in the colon mucosa of IBD patients [4, 7], has never been made. The transcription factor NF- $\kappa$ B is important in regulating intestinal inflammation and is elevated in IBD patients [21, 22, 26]. We have now shown that the n-3 PUFA EPA, as compared to the n-6 PUFA

ARA, clearly reduced cytokine stimulated NF- $\kappa$ B activation and ICAM-1 expression in enterocytes in vitro. Moreover, effects of OA on ICAM-1 expression were comparable to those of EPA. Because EPA and OA resulted in comparable changes in the proportions of ARA in the phospholipids of the enterocytes, the reported effects may be ascribed to the increased ARA proportion in the ARA cultured cells. Thus, decreasing cellular ARA levels seems to be a crucial step. Since OA is already the most abundant fatty acid present in our diet [9] and in the colon mucosa [4], decreasing mucosal ARA levels may be easier by increasing fish oil intake than by increasing OA intake. Moreover, EPA does compete with ARA for incorporation into tissue phospholipids [10, 11].

Our data showed that replacing ARA for EPA or OA decreased ICAM-1 expression and NF- $\kappa$ B activation in Caco-2 enterocytes. In line with our observations in enterocytes, n-6 PUFAs also increased NF- $\kappa$ B activation as compared to n-3 PUFAs in monocytes [41] and macrophages [42]. Also, earlier in vitro studies have demonstrated that fish oils reduced cytokine stimulated ICAM-1 expression in endothelial cells [43] and monocytes [44] as compared to conditions without addition of fatty acids. Moreover, in vivo ICAM-1 expression (surface and mRNA) on peritoneal macrophages was reduced in mice fed fish oils compared to that in mice fed coconut oil [45]. In humans, dietary fish oil supplementation lowered expression of ICAM-1 on ex vivo stimulated monocytes as compared to no supplementation [46]. However, our study

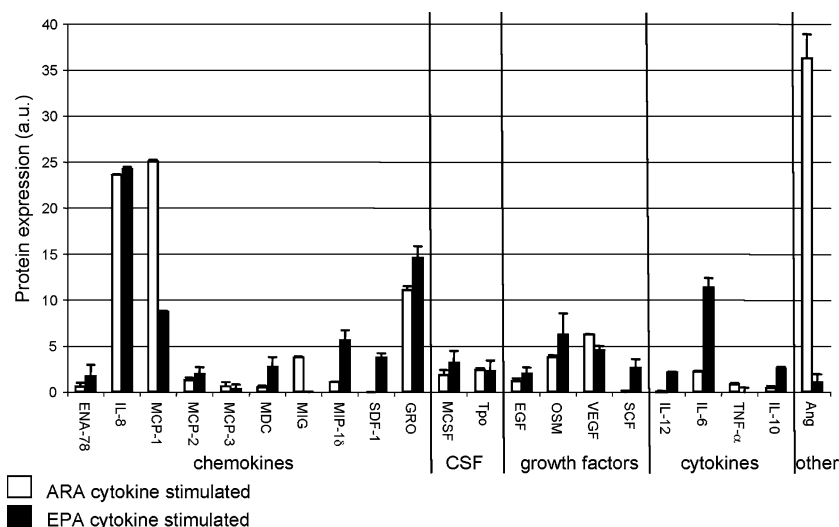


**Fig. 5** Protein expression profile in the culture medium of Caco-2 cells cultured for 22 days with 130  $\mu$ M arachidonic acid (ARA) plus 30  $\mu$ M oleic acid (OA) or 6  $\mu$ M eicosapentaenoic acid (EPA) plus 154  $\mu$ M OA after 16 h cytokine stimulation (100 U/mL IFN $\gamma$  and 50 U/mL IL-1 $\beta$ ) measured with an antibody array. Results are represented as mean  $\pm$  SD;  $n = 2$ . CSF colony stimulating factor, ENA epithelial-derived neutrophil activating protein, MCP monocyte

chemotactic protein, MDC, macrophage derived chemokine, MIG monokine induced by gamma interferon, MIP macrophage inflammatory protein, SDF stromal cell-derived factor, GRO growth regulated protein, MCSF Macrophage colony stimulating factor, Tpo thrombopoietin, EGF epidermal growth factor, OSM oncostatin M, VEGF Vascular endothelial growth factor, SCF stem cell factor, IL interleukin, TNF tumor necrosis factor, Ang angiogenin

is the first that examined effects of EPA versus ARA on ICAM-1 expression and NF- $\kappa$ B activation in enterocytes. We however, realize that, although enterocytes play an important role in intestinal inflammation, immune modulating effects of fatty acids in CD patients will be influenced not only by enterocytes, but also the interaction with other intestinal immune and non-immune cells is important. Therefore, in future experiments effects on other cell types, e.g. isolated from mucosal biopsies of CD patients should be evaluated. Moreover, to validate if the effects of EPA versus ARA are also applicable in the pathogenesis or even the treatment of CD patients, these effects should be confirmed in appropriate animal models of IBD.

We used an approach of supplying different amounts of the fatty acids of interest (i.e., 130  $\mu$ M ARA or 6  $\mu$ M EPA), while the total molarity of fatty acids supplied was similar in all experiments by adding OA. These different concentrations of ARA and EPA were deliberately chosen because they were both four times the amount, in which the cells grow normally (i.e., the fatty acid composition of culture medium with 10% FCS). Since the EPA concentration is very low in FCS, we have deliberately chosen for a low EPA concentration. Higher concentrations of EPA would be interesting to examine, however, are difficult to be achieved with dietary interventions in vivo. Using isomolaric total concentrations of fatty acids is essential, because an increase in total fat can be immune suppressive [47]. Therefore, we used OA as a reference fatty acid to make total fatty acid concentrations between experimental fatty acid conditions iso-molaric, i.e. OA was exchanged for ARA or EPA. In addition, we evaluated the condition of OA only. The results of this latter condition showed that decreasing ARA levels in the mucosa seems to be more important than increasing EPA levels.

Regarding the pathways underlying the anti-inflammatory effect of fish oils, several suggestions have been made. As compared to n-6 PUFAs, n-3 PUFAs may have different effects on (I) signal transduction pathways, and (II) the types and levels of eicosanoids synthesized [40]. Regarding the first mechanism, our finding that EPA lowered NF- $\kappa$ B activation and ICAM-1 expression as compared to ARA indeed showed that EPA and ARA differently affected the NF- $\kappa$ B signal transduction pathway. In this respect, two peroxisome proliferators-activated receptors (PPARs), PPAR $\alpha$  and PPAR $\gamma$ , seem relevant, since fatty acids are natural ligands for these PPARs. Both PPARs seem to have anti-inflammatory effects by inhibiting NF- $\kappa$ B activation [48, 49]. In our in vitro model, the PPAR $\gamma$  agonist troglitazone inhibited NF- $\kappa$ B activation, and cytokine and net stimulated ICAM-1 expression, while the PPAR $\alpha$  agonist GW7647 only inhibited cytokine-stimulated ICAM-1 expression. This suggests that both PPAR $\gamma$  and PPAR $\alpha$  have anti-inflammatory effects on enterocytes, in which

effects of PPAR $\gamma$  seem more pronounced. This is in agreement with the finding that PPAR $\gamma$  agonists but not a PPAR $\alpha$  agonist inhibited IL-8 expression of Caco-2 cells and HT-29 cells [50]. Differences between fatty acids in activation of PPARs might explain the activation of NF- $\kappa$ B by ARA and not by EPA in our Caco-2 cells. However, our findings are not supported by the PPAR $\gamma$  binding affinities of EPA and ARA, which are about the same [51], while we used much lower EPA concentrations than ARA concentrations. Secondly, not only EPA but also OA lowered intestinal ICAM-1 expression while OA is a poor PPAR $\gamma$  ligand [51]. Therefore, although PPAR $\gamma$  activation certainly protects against inflammation, our results do not suggest that the protective effects of EPA and OA as compared to ARA on intestinal inflammation are PPAR $\gamma$ -mediated. Therefore, there should be another explanation why effects of OA and EPA were comparable but different from those of ARA.

The mechanism underlying a second possible explanation relates to the incorporation of fatty acids into cell membrane phospholipids and eicosanoids synthesis. Eicosanoids can modulate the intensity and duration of the inflammatory response. [8, 40] Replacement of ARA by EPA in the culture medium of the cells resulted in a decrease in the proportion of ARA in cell membranes and an increase in the EPA proportion and as expected the PGE<sub>2</sub> production of Caco-2 cells cultured with EPA was also lower than PGE<sub>2</sub> production of cells cultured with ARA. However, PGE<sub>2</sub> production was not different between non-stimulated and stimulated cells, while stimulation resulted in an abundant elevation of NF- $\kappa$ B activation. To our opinion this rules out the role of PGE<sub>2</sub> in the NF- $\kappa$ B activation of ARA and EPA. Moreover, although in our experiments indomethacin—a blocker of COX—indeed inhibited PGE<sub>2</sub> production, it did not lower NF- $\kappa$ B activation. This is in line with findings of De Catherina et al. [43] showing that in endothelial cells the effects of DHA on VCAM-1 expression could not be inhibited by indomethacin, although prostacyclin production was completely suppressed. Therefore, we fully agree that in an in vivo situation pro-inflammatory effects of ARA are probably mediated by eicosanoids synthesized from ARA, however, these effects are not derived from a direct eicosanoid mediated activation of NF- $\kappa$ B as shown in our model.

Finally, we evaluated inflammatory protein signatures of Caco-2 cell culture medium after 22 days treatment with EPA versus ARA. Since these signatures were analyzed in pooled material we cannot draw conclusions based on statistical analysis. However, this array was intended to generate hypotheses about differences in immune modulating effect of ARA versus EPA based on the protein expression profiles. These profiles indicate, that both fatty



acids induced specific changes in various inflammation mediators. Most of these proteins, but not all, are regulated by NF- $\kappa$ B. For example, IL-6 protein expression was higher after EPA as compared to ARA, whereas NF- $\kappa$ B activation was higher after ARA. It should however, be considered that although highly important, NF- $\kappa$ B is not the only transcription factor involved in the regulation of IL-6 and other inflammatory proteins. Thus, expression of individual proteins cannot be predicted by the level of NF- $\kappa$ B activation solely. In addition, we found clear differences between EPA and ARA, i.e., that some proteins were expressed higher after EPA (IL-6, IL-10, MIP-1 $\delta$  and GRO), while others were higher expressed after ARA (MCP-1, and angiogenin). The precise role of these individual proteins in the process of intestinal inflammation is not clear. However, the increased MCP-1 expression after ARA treatment is in line with the finding that MCP-1 expression is upregulated in the mucosa of IBD patients and correlates with disease activity [52]. The increased expression of the Th2 cytokine IL-10 after EPA treatment fits with the anti-inflammatory role for IL-10 in IBD pathology. In this respect, IL-10 knockout mice develop chronic intestinal inflammation and delivery of recombinant IL-10 to the intestinal mucosa by the bacterium *L. lactis* attenuated mucosal inflammation in two mouse models [53]. In humans, a pilot study using these bacteria showed also promising effects [54].

In conclusion, we have shown that ARA but not EPA and OA activates NF- $\kappa$ B and elevates ICAM-1 expression in Caco-2 enterocytes and we hypothesize that the effects are not related to PPAR $\gamma$  activation or eicosanoid formation.

**Acknowledgments** The authors thank Hasibe Aydeniz (Department of Human Biology, Maastricht University, The Netherlands) for analyzing the fatty acid composition of the Caco-2 cells, Maurice Konings (Department of Human Biology) for analyzing PPAR $\gamma$  and PPAR $\alpha$  mRNA expression in Caco-2 cells and Martine Hulsbosch (Department of Human Biology) for PGE<sub>2</sub> measurements.

## References

- Kromann N, Green A (1980) Epidemiological studies in the Upernavik district, Greenland. Incidence of some chronic diseases 1950–1974. *Acta Med Scand* 208:401–406
- Shoda R, Matsueda K, Yamato S, Umeda N (1996) Epidemiologic analysis of Crohn disease in Japan: increased dietary intake of n-6 polyunsaturated fatty acids and animal protein relates to the increased incidence of Crohn disease in Japan. *Am J Clin Nutr* 63:741–745
- Belluzzi A (2002) n-3 Fatty acids for the treatment of inflammatory bowel diseases. *Proc Nutr Soc* 61:391–395
- Nishida T, Miwa H, Shigematsu A, Yamamoto M, Fujishima M (1987) Increased arachidonic acid composition of phospholipids in colonic mucosa from patients with active ulcerative colitis. *Gut* 28:1002–1007
- Buhner S, Nagel E, Korber J, Vogelsang H, Linn T, Pichlmayr R (1994) Ileal and colonic fatty acid profiles in patients with active Crohn's disease. *Gut* 35:1424–1428
- Pacheco S, Hillier K, Smith C (1987) Increased arachidonic acid levels in phospholipids of human colonic mucosa in inflammatory bowel disease. *Clin Sci (Lond)* 73:361–364
- Fernandez-Banares F, Esteve-Comas M, Mane J, Navarro E, Bertran X, Cabre E, Bartoli R, Boix J, Pastor C, Gassull MA (1997) Changes in mucosal fatty acid profile in inflammatory bowel disease and in experimental colitis: a common response to bowel inflammation. *Clin Nutr* 16:177–183
- Calder PC (2006) n-3 Polyunsaturated fatty acids, inflammation, and inflammatory diseases. *Am J Clin Nutr* 83:1505S–1519S
- Hulshof KFAM, Jansen-van der Vliet M, Westenbrink S, Doest ID (2004) De inneming van vetzuren en vetzuurclusters (voedselconsumptiepeiling 1997–1998). TNO Voeding, Zeist
- Li B, Birdwell C, Whelan J (1994) Antithetic relationship of dietary arachidonic acid and eicosapentaenoic acid on eicosanoid production in vivo. *J Lipid Res* 35:1869–1877
- Zhou L, Nilsson A (2001) Sources of eicosanoid precursor fatty acid pools in tissues. *J Lipid Res* 42:1521–1542
- Hawthorne AB, Daneshmend TK, Hawkey CJ, Belluzzi A, Everitt SJ, Holmes GK, Malkinson C, Shaheen MZ, Willars JE (1992) Treatment of ulcerative colitis with fish oil supplementation: a prospective 12 month randomised controlled trial. *Gut* 33:922–928
- Belluzzi A, Brignola C, Campieri M, Pera A, Boschi S, Miglioli M (1996) Effect of an enteric-coated fish-oil preparation on relapses in Crohn's disease. *N Engl J Med* 334:1557–1560
- MacLean CH, Mojica WA, Newberry SJ, Pencharz J, Garland RH, Tu W, Hilton LG, Gralnek IM, Rhodes S, Khanna P et al. (2005) Systematic review of the effects of n-3 fatty acids in inflammatory bowel disease. *Am J Clin Nutr* 82:611–619
- Bernstein CN, Sargent M, Gallatin WM (1998) Beta2 integrin/ICAM expression in Crohn's disease. *Clin Immunol Immunopathol* 86:147–160
- Goke M, Hoffmann JC, Evers J, Kruger H, Manns MP (1997) Elevated serum concentrations of soluble selectin and immunoglobulin type adhesion molecules in patients with inflammatory bowel disease. *J Gastroenterol* 32:480–486
- Matsuzawa J, Sugimura K, Matsuda Y, Takazoe M, Ishizuka K, Mochizuki T, Seki SS, Yoneyama O, Bannai H, Suzuki K, et al. (2003) Association between K469E allele of intercellular adhesion molecule 1 gene and inflammatory bowel disease in a Japanese population. *Gut* 52:75–78
- Hamamoto N, Maemura K, Hirata I, Murano M, Sasaki S, Katsu K (1999) Inhibition of dextran sulphate sodium (DSS)-induced colitis in mice by intracolonic administered antibodies against adhesion molecules (endothelial leucocyte adhesion molecule-1 (ELAM-1) or intercellular adhesion molecule-1 (ICAM-1)). *Clin Exp Immunol* 117:462–468
- Rijcken E, Kriegelstein CF, Anthoni C, Laukoetter MG, Mennigen R, Spiegel HU, Senninger N, Bennett CF, Schuermann G (2002) ICAM-1 and VCAM-1 antisense oligonucleotides attenuate in vivo leucocyte adherence and inflammation in rat inflammatory bowel disease. *Gut* 51:529–535
- van Deventer SJ, Tami JA, Wedel MK (2004) A randomised, controlled, double blind, escalating dose study of alicaforsen enema in active ulcerative colitis. *Gut* 53:1646–1651
- Schreiber S (2005) The complicated path to true causes of disease: role of nuclear factor kappaB in inflammatory bowel disease. *Gut* 54:444–445
- Neurath MF, Becker C, Barbulescu K (1998) Role of NF-kappaB in immune and inflammatory responses in the gut. *Gut* 43:856–860
- Auphan N, DiDonato JA, Rosette C, Helmberg A, Karin M (1995) Immunosuppression by glucocorticoids: inhibition of

- NF-kappa B activity through induction of I kappa B synthesis. *Science* 270:286–290
24. Gan HT, Chen YQ, Ouyang Q (2005) Sulfasalazine inhibits activation of nuclear factor-kappaB in patients with ulcerative colitis. *J Gastroenterol Hepatol* 20:1016–1024
  25. Bantel H, Berg C, Vieth M, Stolte M, Kruijs W, Schulze-Osthoff K (2000) Mesalazine inhibits activation of transcription factor NF-kappaB in inflamed mucosa of patients with ulcerative colitis. *Am J Gastroenterol* 95:3452–3457
  26. Rogler G, Brand K, Vogl D, Page S, Hofmeister R, Andus T, Knuechel R, Baeuerle PA, Scholmerich J, Gross V (1998) Nuclear factor kappaB is activated in macrophages and epithelial cells of inflamed intestinal mucosa. *Gastroenterology* 115:357–369
  27. Schreiber S, Nikolaus S, Hampe J (1998) Activation of nuclear factor kappa B in inflammatory bowel disease. *Gut* 42:477–484
  28. De Vry CG, Prasad S, Komuves L, Lorenzana C, Parham C, Le T, Adda S, Hoffman J, Kahoud N, Garlapati R, et al. (2007) Non-viral delivery of nuclear factor-kappaB decoy ameliorates murine inflammatory bowel disease and restores tissue homeostasis. *Gut* 56:524–533
  29. Neurath MF, Pettersson S, Meyer zum Buschenfelde KH, Strober W (1996) Local administration of antisense phosphorothioate oligonucleotides to the p65 subunit of NF-kappa B abrogates established experimental colitis in mice. *Nat Med* 2:998–1004
  30. Hidalgo JJ, Raub TJ, Borchardt RT (1989) Characterization of the human colon carcinoma cell line (Caco-2) as a model system for intestinal epithelial permeability. *Gastroenterology* 96:736–749
  31. Thijssen MA, Malpuech-Brugere C, Gregoire S, Chardigny JM, Sebedio JL, Mensink RP (2005) Effects of specific CLA isomers on plasma fatty acid profile and expression of desaturases in humans. *Lipids* 40:137–145
  32. Wensing AG, Mensink RP, Hornstra G (1999) Effects of dietary n-3 polyunsaturated fatty acids from plant and marine origin on platelet aggregation in healthy elderly subjects. *Br J Nutr* 82:183–191
  33. Bligh EG, Dyer WJ (1959) A rapid method of total lipid extraction and purification. *Can J Biochem Physiol* 37:911–917
  34. Kaluzny MA, Duncan LA, Merritt MV, Epps DE (1985) Rapid separation of lipid classes in high yield and purity using bonded phase columns. *J Lipid Res* 26:135–140
  35. Morrison WR, Smith LM (1964) Preparation Of fatty acid methyl esters and dimethylacetals from lipids with boron fluoride-methanol. *J Lipid Res* 5:600–608
  36. Parkos CA, Colgan SP, Diamond MS, Nusrat A, Liang TW, Springer TA, Madara JL (1996) Expression and polarization of intercellular adhesion molecule-1 on human intestinal epithelia: consequences for CD11b/CD18-mediated interactions with neutrophils. *Mol Med* 2:489–505
  37. Willson TM, Brown PJ, Sternbach DD, Henke BR (2000) The PPARs: from orphan receptors to drug discovery. *J Med Chem* 43:527–550
  38. Brown PJ, Stuart LW, Hurley KP, Lewis MC, Winegar DA, Wilson JG, Wilkison WO, Ittoop OR, Willson TM (2001) Identification of a subtype selective human PPARalpha agonist through parallel-array synthesis. *Bioorg Med Chem Lett* 11:1225–1227
  39. Delerive P, Fruchart JC, Staels B (2001) Peroxisome proliferator-activated receptors in inflammation control. *J Endocrinol* 169:453–459
  40. Teitelbaum J, Walker W (2001) Review: the role of omega 3 fatty acids in intestinal inflammation. *J Nutr Biochem* 12:21–32
  41. Camandola S, Leonarduzzi G, Musso T, Varesio L, Carini R, Scavazza A, Chiarpotto E, Baeuerle PA, Poli G (1996) Nuclear factor kB is activated by arachidonic acid but not by eicosapentaenoic acid. *Biochem Biophys Res Commun* 229:643–647
  42. Novak TE, Babcock TA, Jho DH, Helton WS, Espat NJ (2003) NF-kappa B inhibition by omega -3 fatty acids modulates LPS-stimulated macrophage TNF-alpha transcription. *Am J Physiol Lung Cell Mol Physiol* 284:L84–89
  43. De Caterina R, Cybulsky MI, Clinton SK, Gimbrone MA Jr, Libby P (1994) The omega-3 fatty acid docosahexaenoate reduces cytokine-induced expression of proatherogenic and proinflammatory proteins in human endothelial cells. *Arterioscler Thromb* 14:1829–1836
  44. Hughes DA, Southon S, Pinder AC (1996) (n-3) Polyunsaturated fatty acids modulate the expression of functionally associated molecules on human monocytes in vitro. *J Nutr* 126:603–610
  45. Miles EA, Wallace FA, Calder PC (2000) Dietary fish oil reduces intercellular adhesion molecule 1 and scavenger receptor expression on murine macrophages. *Atherosclerosis* 152:43–50
  46. Hughes DA, Pinder AC, Piper Z, Johnson IT, Lund EK (1996) Fish oil supplementation inhibits the expression of major histocompatibility complex class II molecules and adhesion molecules on human monocytes. *Am J Clin Nutr* 63:267–272
  47. Luyer MD, Buurman WA, Hadfoune M, Jacobs JA, Konstantinov SR, Dejong CH, Greve JW (2004) Pretreatment with high-fat enteral nutrition reduces endotoxin and tumor necrosis factor-alpha and preserves gut barrier function early after hemorrhagic shock. *Shock* 21:65–71
  48. Ricote M, Li AC, Willson TM, Kelly CJ, Glass CK (1998) The peroxisome proliferator-activated receptor-gamma is a negative regulator of macrophage activation. *Nature* 391:79–82
  49. Poynter ME, Daynes RA (1998) Peroxisome proliferator-activated receptor alpha activation modulates cellular redox status, represses nuclear factor-kappaB signaling, and reduces inflammatory cytokine production in aging. *J Biol Chem* 273:32833–32841
  50. Su CG, Wen X, Bailey ST, Jiang W, Rangwala SM, Keilbaugh SA, Flanagan A, Murthy S, Lazar MA, Wu GD (1999) A novel therapy for colitis utilizing PPAR-gamma ligands to inhibit the epithelial inflammatory response. *J Clin Invest* 104:383–389
  51. Xu HE, Lambert MH, Montana VG, Parks DJ, Blanchard SG, Brown PJ, Sternbach DD, Lehmann JM, Wisely GB, Willson TM, et al. (1999) Molecular recognition of fatty acids by peroxisome proliferator-activated receptors. *Mol Cell* 3:397–403
  52. Herfarth H, Goke M, Hellerbrand C, Muhlbauer M, Vogl D, Scholmerich J, Rogler G (2003) Polymorphism of monocyte chemoattractant protein 1 in Crohn's disease. *Int J Colorectal Dis* 18:401–405
  53. Stokkers PC, Hommes DW (2004) New cytokine therapeutics for inflammatory bowel disease. *Cytokine* 28:167–173
  54. Braat H, Rottiers P, Huyghebaert N, Zelinkova Z, Remaut E, Remon JP, Deventer vS, Neiryck S, Peppelenbosch M, Steidler L et al. (2005) Interleukin-10 producing *Lactococcus lactis* for the treatment of Crohn's disease. *Gastroenterology* 128:A104

## The Effects of Omega-3 Polyunsaturated Fatty Acids on TNF- $\alpha$ and IL-10 Secretion by Murine Peritoneal Cells In Vitro

Ingibjorg H. Skuladottir · Dagbjort H. Petursdottir ·  
Ingibjorg Hardardottir

Received: 26 January 2007 / Accepted: 29 May 2007 / Published online: 29 June 2007  
© AOCs 2007

**Abstract** Omega-3 polyunsaturated fatty acids (PUFA) affect immune response, partly by affecting cytokine secretion. Omega-3 PUFA decrease tumor necrosis factor (TNF)- $\alpha$  secretion by RAW 264.7 macrophages but increase TNF- $\alpha$  secretion by primary elicited peritoneal macrophages in vitro. In this study, the effects of omega-3 and omega-6 PUFA on lipopolysaccharide induced TNF- $\alpha$  and interleukin (IL)-10 secretion by murine primary resident and elicited peritoneal macrophages and by RAW 264.7 macrophages, were examined in vitro using an enzyme-linked immunosorbent assay. In addition, the effects of dietary omega-3 PUFA on the number of cells secreting these cytokines were examined with enzyme-linked immunospot assay. All cell types secreted more TNF- $\alpha$  but similar amounts of IL-10 when incubated with the omega-3 PUFA, eicosapentaenoic acid or docosahexaenoic acid, compared with that when incubated with the omega-6 PUFA, linoleic acid or arachidonic acid. Dietary fish oil did not affect the number of TNF- $\alpha$  secreting resident peritoneal macrophages but decreased the number of macrophages secreting IL-10 ex vivo. These results show that dietary omega-3 PUFA and omega-3 PUFA added to cells in vitro increase TNF- $\alpha$  secretion by resident peritoneal macrophages, probably by a direct effect on the cells. In contrast, omega-3 PUFA did not affect IL-10 secretion by the cells but decreased the number of cells secreting IL-10 ex vivo, possibly by affecting cell recruitment, maturation or proliferation.

**Keywords** Omega-3 fatty acids · Macrophages · TNF- $\alpha$  · IL-10

### Introduction

Dietary omega-3 polyunsaturated fatty acids (PUFA) have immunomodulatory effects that are thought to be anti-inflammatory based on human clinical and epidemiological studies, as well as murine models [7, 9, 14, 21]. The anti-inflammatory effects of omega-3 PUFA may partly be explained by their effects on lymphocytes, as omega-3 PUFA suppress T-cell proliferation and pro-inflammatory cytokine secretion [1, 13, 18, 19, 32]. In contrast to the anti-inflammatory effects of omega-3 PUFA on T-lymphocytes, results from our laboratory and others indicate that dietary omega-3 PUFA may have pro-inflammatory effects on cytokine secretion by resident peritoneal macrophages, as they increase lipopolysaccharide (LPS) induced tumor necrosis factor (TNF)- $\alpha$  secretion and decrease interleukin (IL)-10 secretion by these cells ex vivo [5, 6, 8, 10, 15, 24, 27, 38]. Dietary omega-3 PUFA also increase LPS induced TNF- $\alpha$  secretion by splenic macrophages and increase their IL-10 secretion [26]. The effects of dietary omega-3 PUFA on TNF- $\alpha$  secretion by murine elicited peritoneal macrophages varies, with some studies showing an increase in TNF- $\alpha$  secretion [31, 37], others showing no change [16, 33, 35, 37], and still others showing a decrease in TNF- $\alpha$  secretion [4, 29, 36, 40] compared with that by elicited peritoneal macrophages from animals fed a diet rich in omega-6 PUFA.

In contrast to the numerous studies examining the effects of dietary omega-3 PUFA on cytokine secretion by resident peritoneal macrophages ex vivo, to our knowledge no studies have examined the effects of omega-3 PUFA on

I. H. Skuladottir · D. H. Petursdottir · I. Hardardottir (✉)  
Department of Biochemistry and Molecular Biology,  
Faculty of Medicine, University of Iceland,  
Vatnsmyrarvegur 16, 101 Reykjavik, Iceland  
e-mail: ih@hi.is

TNF- $\alpha$  and IL-10 secretion by murine primary resident peritoneal macrophages *in vitro*. Two studies have examined the effects of omega-3 PUFA on TNF- $\alpha$  secretion by primary elicited peritoneal macrophages, showing increased TNF- $\alpha$  secretion by elicited peritoneal macrophages when incubated with omega-3 PUFA compared with that by cells incubated without fatty acids or incubated with omega-6 PUFA [17, 34]. In contrast, results from studies using a murine peritoneal macrophage cell line, RAW 264.7, show that omega-3 PUFA decrease TNF- $\alpha$  secretion compared with that by cells incubated with omega-6 PUFA or control media [22, 25].

The objective of this study was to determine the effects of omega-3 PUFA on TNF- $\alpha$  and IL-10 secretion by murine primary resident and elicited peritoneal macrophages, and the macrophage cell line, RAW 264.7, *in vitro* and to examine the effects of dietary fish oil on the number of TNF- $\alpha$  and IL-10 secreting cells in the peritoneum of mice.

## Experimental Procedure

### Animals and Diets

All experimental procedures using laboratory animals complied with the National Research Council's Guide for the Care and Use of Laboratory Animals. Female BalbC mice (18–20 g) (Bomholtgaard, Copenhagen, Denmark) received standard diet (Special Diets Services, Witham, UK), water *ad libitum*, and were housed at 25 °C with a 12-h light:dark cycle. For feeding experiments, mice were randomly divided into two groups of ten mice each and housed five per cage at 25 °C with a 12-h light:dark cycle. Experimental diets were designed according to the American Institute of Nutrition (AIN)-93 guidelines [28] with modification in fat content. The experimental diets were based on a nutritionally complete diet made for the addition of 200 g/kg of fat (ICN Pharmaceuticals, Aurora, OH, USA). The fish oil diet contained 180 g/kg menhaden fish oil and 20 g/kg corn oil (ICN Pharmaceuticals, Asse-Rellegem, Belgium). The corn oil diet contained 200 g/kg corn oil. The fatty acid composition of the diets was analyzed as described previously [27] and is shown in Table 1. The antioxidant *tert*-butylhydroquinone (t-BHQ) (ICN Bio-medicals, Aurora, OH, USA) (1.2 mmol/L) was added to the oils to prevent their deterioration [12]. Diets were prepared in bulk and daily portions packed in zip lock bags, flushed with nitrogen, sealed and stored at –20 °C. Water and food were provided *ad libitum*. The mice were fed the experimental diets for 6 weeks. Mice were anesthetized with isoflurane (Abbot Scandinavia, Solna, Sweden) and euthanized by cervical dislocation. For induction of elicited peritoneal macrophages, mice were injected intra-perito-

**Table 1** Selected fatty acid composition (g/100 g) of the diets

Fatty acid	Corn oil diet <sup>b</sup>	Fish oil diet <sup>c</sup>
16:0	11.0	19.3
18:0	2.3	3.9
18:1 n-9	28.5	16.2
18:2 n-6	57.1	8.5
18:3 n-3	1.2	1.4
18:4 n-3	–	3.0
20:5 n-3	–	14.1
22:5 n-3	–	2.6
22:6 n-3	–	10.5
(n-3)/(n-6) <sup>a</sup>	0.02	3.4

<sup>a</sup> (n-3)/(n-6):  $\Sigma$ 18:3; 18:4; 20:4; 20:5; 21:5; 22:5; 22:6/ $\Sigma$ 18:2; 18:3; 20:4

<sup>b</sup> Corn oil diet contained 200 g/kg corn oil

<sup>c</sup> Fish oil diet contained 180 g/kg menhaden fish oil and 20 g/kg corn oil

neally with 0.8 mL of 3% thioglycolate (TG) broth (Difco, Becton Dickinson, Microbiology Systems, Sparks, MD, USA) 72 h before collection of cells.

### Preparation of Fatty Acids for Incubation

Fatty acids (Sigma, Steinheim, Germany) were dissolved in ethanol, flushed with nitrogen and stored at –20 °C. Fatty acids were incubated at 3:1 mole ratio with bovine serum albumin (BSA) (Sigma, Steinheim, Germany) at 37 °C for 16 h. The fatty acid–BSA complexes were stored in the presence of nitrogen for maximum of 7 days at 4 °C. The maximum final concentration of ethanol in the cultures was 0.05%.

### Isolation, Culturing and Activation of Resident and Elicited Peritoneal Macrophages

Resident and elicited peritoneal macrophages were collected in cold phosphate-buffered saline (PBS) without calcium or magnesium. Cells were washed with PBS and resuspended in Dulbecco's Modified Eagle Medium (DMEM) with Gluta-MAX-I, penicillin (100 U/mL), and streptomycin (100  $\mu$ g/mL), all from Gibco, Paisley, UK. Cells were counted in 0.4% Trypan Blue (Sigma, Steinheim, Germany) on a hemocytometer and  $1 \times 10^6$  cells/mL plated on a 48-well flat-bottomed multidish and incubated at 37 °C in 5% CO<sub>2</sub> atmosphere. Cells were cultured in DMEM with 10% fetal bovine serum (FBS) (Gibco, Paisley, UK) with or without 10–50  $\mu$ M concentration of linoleic acid (LA), arachidonic acid (AA), eicosapentaenoic acid (EPA), or docosahexaenoic acid (DHA), for 4–24 h. BSA and ethanol, in a concentration equal to that used for cells cultured with fatty

acids, was added to cells cultured without fatty acids. Fatty acids were replaced by fresh media and the cells stimulated with LPS (2  $\mu\text{g}/\text{mL}$ ) (*Escherichia coli* 055:B5, Fluka Chemie CmbH, Buchs, Switzerland) for 6–12 h.

#### Murine Macrophage Cell Line, RAW 264.7

The RAW 264.7 cell line was obtained from American Type Culture Collection (ATCC) (Manassas, VA, USA). Cells were maintained in DMEM with 10% FBS (ATCC, Manassas, VA, USA), penicillin (100 U/mL), and streptomycin (100  $\mu\text{g}/\text{mL}$ ) at 37 °C in 5% CO<sub>2</sub> atmosphere. Cells were counted, plated, and cultured as described above except that cells were allowed to adhere to culture plates for 2 h before incubation with fatty acids. All experiments were performed at passages 6–11.

#### TNF- $\alpha$ and IL-10 Determination

After centrifugation, supernatants were collected and stored at -70 °C. TNF- $\alpha$  and IL-10 were measured by enzyme-linked immunosorbent assay using DuoSet (R&D Systems, Minneapolis, MN, USA).

#### Determination of the Number of TNF- $\alpha$ and IL-10 Secreting Cells and Mean TNF- $\alpha$ and IL-10 Secretion per Cell

Numbers of TNF- $\alpha$  and IL-10 secreting cells and the mean TNF- $\alpha$  and IL-10 secretion per cell were evaluated by enzyme-linked immunospot (ELISPOT) assay (R&D systems, Minneapolis MN, USA). Cells were collected from the peritoneum of mice fed diets containing fish oil or corn oil and counted on a hemocytometer. Then,  $0.63 \times 10^4$  cells/well were incubated on a polyvinylidene difluoride microplate (Millipore, Moisheim, France) coated with anti-mouse TNF- $\alpha$  and  $2.5 \times 10^5$  cells/well on a plate coated with anti-mouse IL-10. Cells were cultured with or without LPS (2  $\mu\text{g}/\text{mL}$ ) for 24 h, the plates washed and incubated with biotinylated anti-mouse TNF- $\alpha$  or IL-10 overnight. After incubation with streptavidin-AP, spots were developed using 5-bromo-4-chloro-3-indolyl phosphate/nitro blue tetrazolium as chromogen (R&D Systems, Minneapolis, MN, USA). The number of TNF- $\alpha$  and IL-10 secreting cells per 1,000 cells and mean TNF- $\alpha$  and IL-10 secretion per cell (determined as area per spot) were automatically evaluated using a computer-assisted video image analyzer (KS ELISPOT, Version 4.8; Zeiss, Jena, Germany).

#### Statistical Analysis

Differences between treatments in vitro were analyzed using one-way analysis of variance, followed by Bonfer-

roni post hoc test. Differences between dietary groups were analyzed using unpaired *t*-test,  $P < 0.05$ , two-tailed. The statistical analysis was performed in Statsdirect (Version 2.5.4, Cheshire, UK).

## Results

### The Effects of Omega-3 PUFA on TNF- $\alpha$ and IL-10 Secretion by Resident Peritoneal Macrophages In Vitro

Resident peritoneal macrophages cultured with 50  $\mu\text{M}$  concentration of EPA or DHA, for 12 h, secreted 60 and 75% more TNF- $\alpha$  than macrophages cultured without fatty acids and 30 and 40% more than macrophages cultured with omega-6 fatty acids (Fig. 1). Resident peritoneal macrophages incubated with EPA for 8 h secreted similar amounts of TNF- $\alpha$  as resident peritoneal macrophages incubated with AA, whereas macrophages incubated with EPA for 12, 20, or 24 h secreted more TNF- $\alpha$  than macrophages incubated with AA for the same length of time (Fig. 2). Resident peritoneal macrophages incubated with 10 or 25  $\mu\text{M}$  of EPA secreted similar amounts of TNF- $\alpha$  ( $146 \pm 1$  and  $135 \pm 6$  pg/mL, respectively) as resident peritoneal macrophages incubated with 10 or 25  $\mu\text{M}$  of AA ( $136 \pm 1$  and  $122 \pm 2$  pg/mL, respectively). There was no difference in IL-10 secretion by resident peritoneal macrophages incubated without fatty acids or with 50  $\mu\text{M}$  concentration of the fatty acids LA, AA, EPA, or DHA (Table 2).

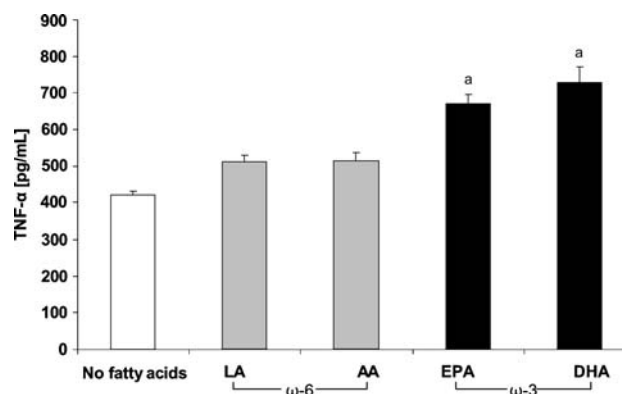


**Fig. 1** The effects of omega-6 and omega-3 polyunsaturated fatty acids on tumor necrosis factor (TNF)- $\alpha$  secretion by resident peritoneal macrophages. Resident peritoneal macrophages were incubated with or without linoleic acid (LA), arachidonic acid (AA), eicosapentaenoic acid (EPA), or docosahexaenoic acid (DHA) (50  $\mu\text{M}$ ) for 12 h. The fatty acids were removed and the cells stimulated with lipopolysaccharide (LPS) (*E. coli* 055:B5) (2  $\mu\text{g}/\text{mL}$ ) for 12 h. TNF- $\alpha$  was measured by enzyme-linked immunosorbent assay (ELISA). Values are means + standard error of the mean (SEM),  $n = 8$ –9. The results are pooled from three separate experiments. **a** Different from *No fatty acids* and *Omega-6 fatty acids* ( $P < 0.05$ )

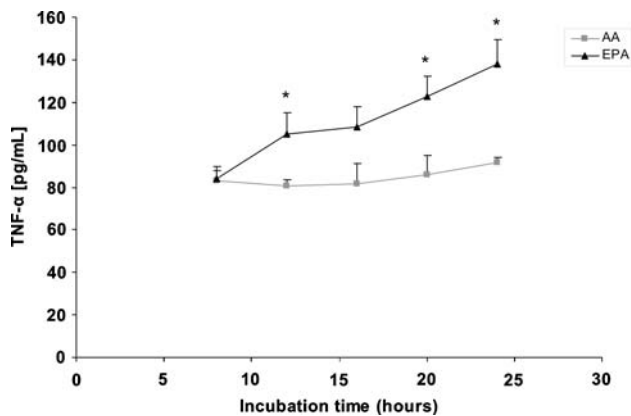


**Fig. 2** Time course of the effects of EPA and AA on TNF- $\alpha$  secretion by resident peritoneal macrophages. Resident peritoneal macrophages were incubated with AA or EPA (50  $\mu$ M) for 8, 12, 16, 20, and 24 h. The fatty acids were removed and the cells stimulated with LPS (*E. coli* 055:B5) (2  $\mu$ g/mL) for 12 h. TNF- $\alpha$  was measured by ELISA. Values are means  $\pm$  SEM,  $n = 7$ –10, except for the 16-h time point,  $n = 4$ . The results are pooled from three separate experiments. The abbreviations used are the same as for Fig. 1. \* Different from the mean for cells incubated with AA at each time point,  $P < 0.05$

#### The Effects of Dietary Fish Oil on the Number of Resident Peritoneal Cells Secreting TNF- $\alpha$ and IL-10 Ex Vivo and Mean TNF- $\alpha$ and IL-10 Secretion per Cell

The effects of dietary fish oil on the number of cells secreting TNF- $\alpha$  and IL-10 were examined ex vivo. Dietary fish oil did not affect the number of resident peritoneal macrophages secreting TNF- $\alpha$  when stimulated with LPS ex vivo (Fig. 3a). In contrast, dietary fish oil decreased the number of resident peritoneal macrophages secreting IL-10 ex vivo (Fig. 3b) compared with the number of IL-10 secreting resident peritoneal macrophages from mice fed the corn oil-rich diet. The mean TNF- $\alpha$  secretion per cell (determined by ELISPOT as the area per spot) from the peritoneum of mice fed the fish oil diet ( $3,409 \pm 239$ ) was higher than the mean TNF- $\alpha$  secretion per cell from the peritoneum of mice fed the corn oil diet ( $2,352 \pm 230$ ,

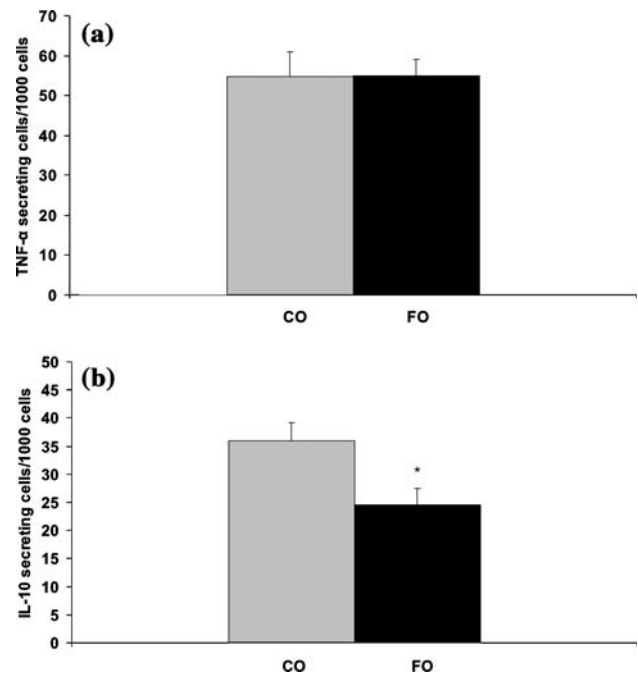


**Fig. 3** The effects of dietary fish oil on the number of resident peritoneal cells secreting TNF- $\alpha$  or interleukin (IL)-10. BalbC mice were fed diets containing fish oil or corn oil for 6 weeks and resident peritoneal macrophages collected. Numbers of TNF- $\alpha$  (a) and IL-10 (b) secreting cells were determined by enzyme-linked immunospot (ELISPOT) assay. Values are means  $\pm$  SEM,  $n = 8$ –10. The abbreviations used are the same as for Fig. 1. \* $P < 0.05$

$P < 0.05$ ). There was no difference in the mean IL-10 secretion per cell from the peritoneum of mice fed the different diets ( $1,940 \pm 87$  vs.  $1,744 \pm 89$ , for the fish oil and the corn oil diets, respectively).

#### The Effects of Omega-3 PUFA on TNF- $\alpha$ and IL-10 Secretion by Thioglycolate-Elicited Peritoneal Macrophages In Vitro

Thioglycolate-elicited peritoneal macrophages incubated with 50  $\mu$ M concentration of EPA or DHA for 20 h se-

**Table 2** IL-10 secretion (pg/mL) by murine resident peritoneal macrophages, elicited peritoneal macrophages, and the RAW 264.7 cell line

	Treatment				
	No fatty acids	LA 50 $\mu$ M	AA 50 $\mu$ M	EPA 50 $\mu$ M	DHA 50 $\mu$ M
Resident peritoneal cells <sup>a</sup>	489 $\pm$ 16	511 $\pm$ 23	487 $\pm$ 22	460 $\pm$ 18	509 $\pm$ 18
Elicited peritoneal cells <sup>b</sup>	212 $\pm$ 35	164 $\pm$ 39	188 $\pm$ 44	208 $\pm$ 38	209 $\pm$ 33
RAW 264.7 cell line <sup>c</sup>	5,050 $\pm$ 392	4,690 $\pm$ 460	4,120 $\pm$ 640	4,910 $\pm$ 240	6,570 $\pm$ 307 <sup>d</sup>

Values are mean  $\pm$  SEM

<sup>a</sup> Incubated with the fatty acids for 12 h,  $n = 8$ –9

<sup>b</sup> Incubated with the fatty acids for 20 h,  $n = 5$ –6

<sup>c</sup> Incubated with the fatty acids for 20 h,  $n = 3$ , representative of three separate experiments

<sup>d</sup> Different from all other treatments,  $P < 0.05$

creted 90 and 175% more TNF- $\alpha$  than macrophages incubated without fatty acids, 120 and 235% more TNF- $\alpha$  than macrophages incubated with LA and 80 and 170% more TNF- $\alpha$  than macrophages incubated with AA (Fig. 4). Elicited peritoneal macrophages incubated with DHA secreted 50% more TNF- $\alpha$  than elicited peritoneal macrophages incubated with EPA (Fig. 4). There was no difference in IL-10 secretion by elicited peritoneal macrophages incubated without fatty acids or with LA, AA, EPA, or DHA (Table 2).

#### The Effects of Omega-3 PUFA on TNF- $\alpha$ and IL-10 Secretion by the Macrophage Cell Line, RAW 264.7, In Vitro

RAW 264.7 macrophages cultured with 50  $\mu$ M concentration of EPA for 20 h secreted 50 and 70% more TNF- $\alpha$  after stimulation with LPS than macrophages cultured without fatty acids or with LA (Fig. 5). RAW 264.7 macrophages cultured with DHA secreted 60–95% more TNF- $\alpha$  than RAW 264.7 macrophages cultured without fatty acids or with LA or AA (Fig. 5). There was no difference in IL-10 secretion by RAW 264.7 macrophages cultured without fatty acids or with LA, AA, or EPA (Table 2). However, RAW 264.7 macrophages incubated with DHA secreted 30% more IL-10 than macrophages incubated without fatty acids (Table 2).

## Discussion

The results from the present study show that omega-3 PUFA increase TNF- $\alpha$  secretion by primary resident and

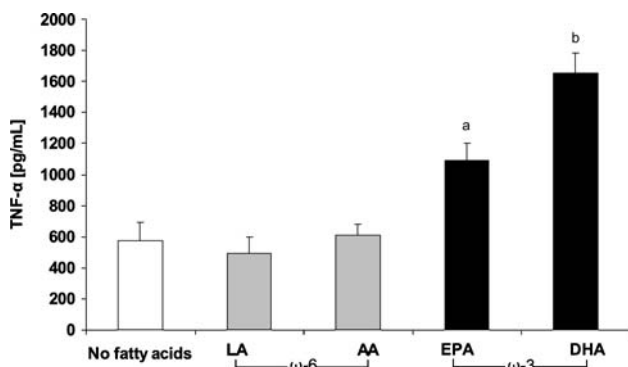


**Fig. 4** The effects of omega-6 and omega-3 PUFA on TNF- $\alpha$  secretion by thioglycolate-elicited peritoneal macrophages. Thioglycolate-elicited peritoneal macrophages were incubated with or without LA, AA, EPA, or DHA (50  $\mu$ M) for 20 h. The fatty acids were removed and the cells stimulated with LPS (*E. coli* 055:B5) (2  $\mu$ g/mL) for 12 h. TNF- $\alpha$  was measured by ELISA. Values are means + SEM,  $n = 5-6$ . Results are pooled from two separate experiments. **a** Different from *No fatty acids* and *Omega-6* fatty acids, **b** Different from *EPA* ( $P < 0.05$ ). The abbreviations used are the same as for Fig. 1

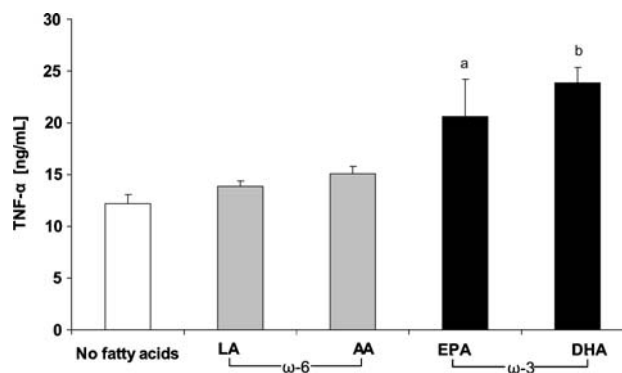


**Fig. 5** The effects of omega-6 and omega-3 PUFA on TNF- $\alpha$  secretion by the murine peritoneal macrophage cell line, RAW 264.7. RAW 264.7 macrophages were incubated with or without LA, AA, EPA, or DHA (50  $\mu$ M) for 20 h. The fatty acids were removed and the cells stimulated with LPS (*E. coli* 055:B5) (2  $\mu$ g/mL) for 12 h. TNF- $\alpha$  was measured by ELISA. Values are means + SEM,  $n = 2-3$ . The results are representative of three separate experiments. **a** Different from *No fatty acids* and *LA*, **b** Different from *No fatty acids* and *Omega-6* fatty acids ( $P < 0.05$ ). The abbreviations used are the same as for Fig. 1

elicited peritoneal macrophages as well as the cell line, RAW 264.7. In addition, dietary omega-3 PUFA increased TNF- $\alpha$  secretion per cell ex vivo, as determined by ELISPOT assay, in the present study. These results are in accordance with results from several studies showing that dietary omega-3 PUFA increase TNF- $\alpha$  secretion by these cells ex vivo [5, 6, 8, 10, 15, 24, 27, 38]. That omega-3 PUFA have the same effects on TNF- $\alpha$  secretion by resident peritoneal macrophages in vitro as dietary fish oil has ex vivo indicates that the effects of omega-3 PUFA on TNF- $\alpha$  secretion may be due to incorporation of omega-3 PUFA into cell membranes and their effects on lipid mediator production or intracellular signaling molecules. It has previously been shown that the increase in TNF- $\alpha$  secretion by resident peritoneal macrophages from mice fed fish oil is partly explained by a decrease in prostaglandin (PG) E<sub>2</sub> production by these cells [16, 27]. Other mechanisms at work have not been identified but increased activation of extracellular receptor-activated kinases 1/2 and increased binding of early growth response-1 (Egr-1) to the TNF- $\alpha$  promoter have been shown to contribute to the increased LPS induced TNF- $\alpha$  secretion by macrophages treated with ethanol [30]. Reduced activation of mitogen-activated protein kinase (P44/P42) [23], AP-1 transcription factor [3], and transcription factor nuclear factor (NF)  $\kappa$ B [20, 25] have been proposed to mediate omega-3 PUFA induced decrease in TNF- $\alpha$  secretion by the murine macrophage cell line, RAW 264.7 whereas reduced LPS binding, suppression of CD14 upregulation [11], reduced nuclear p65 levels, and increased I $\kappa$ B $\alpha$  expression have been proposed to mediate omega-3 PUFA

induced decrease in TNF- $\alpha$  secretion by the human macrophage cell line, THP-1 [39].

In contrast to omega-3 PUFA increasing TNF- $\alpha$  secretion by primary resident peritoneal cells they had no effect on IL-10 secretion by these cells in vitro. In addition, there was no effect of dietary omega-3 PUFA on the average IL-10 secretion per cell ex vivo. On the other hand, there was a decrease in the number of cells from the peritoneum of mice fed the fish oil diet secreting IL-10 compared with that from the peritoneum of mice fed the corn oil diet. These results are in accordance with results from our previous study showing decreased IL-10 in the medium from peritoneal macrophages from mice fed fish oil compared to that in the medium from macrophages from mice fed corn oil. Thus, the decrease in IL-10 secretion by resident peritoneal macrophages from mice fed fish oil seen in a previous study [27] is explained by a decrease in the number of cells, secreting IL-10 upon stimulation with LPS ex vivo. The effect of dietary fish oil to decrease the number of IL-10 secreting cells in the peritoneum of mice may perhaps be brought about by an effect on cell recruitment to the peritoneum or by an effect on maturation or proliferation of peritoneal cells.

Although, to our knowledge, the present study is the first to examine the effects of omega-3 PUFA on TNF- $\alpha$  and IL-10 secretion by resident peritoneal macrophages in vitro, others have studied their effects on primary elicited peritoneal macrophages. Our results showing increased TNF- $\alpha$  secretion by elicited peritoneal macrophages incubated with omega-3 PUFA compared with that by cells incubated with omega-6 PUFA are in agreement with results from these other studies [17, 34].

The results from the present study showing increased TNF- $\alpha$  secretion by RAW 264.7 macrophages incubated with omega-3 PUFA compared with that when incubated without fatty acids or with omega-6 PUFA are in disagreement with results from previous studies [2, 22, 25]. In these studies, RAW 264.7 macrophages incubated with EPA or with Omegaven, a fatty acid emulsion consisting of various fatty acids, including EPA and DHA, secreted less TNF- $\alpha$  than cells incubated without EPA [22] or with Lipovenos, an omega-6 PUFA emulsion [25], respectively. In the latter study the cells were incubated with Omegaven for only 4 h and stimulated with LPS for 3 h. However, longer incubation and stimulation times do not seem to explain the different results obtained in the present study, because when we incubated the RAW 264.7 cells with omega-3 or omega-6 PUFA for 4 h and stimulated them for 6 h, cells incubated with omega-3 PUFA still secreted more TNF- $\alpha$  than cells incubated without fatty acids or with LA (results not shown). Neither is the difference in  $\alpha$ -tocopherol concentration in incubations in the two studies likely to explain the different results, as the  $\alpha$ -tocopherol

concentration in cultures with Omegaven [25] is below that shown to decrease TNF- $\alpha$  secretion by RAW 264.7 cells [39]. Whether the different source of omega-3 PUFA, inclusion of serum in the cultures, or different passages of the RAW 264.7 cells explain the differences in results between the present study and the one by Novak et al. [25] remains to be examined. Lo et al. [22] used a higher concentration of EPA than we used in the present study and a cytotoxicity assay with L929 cells to measure TNF- $\alpha$  but how these differences between the study by Lo et al. [22] and the present study can explain the contrasting results is difficult to envisage.

In summary, results from the present study show that omega-3 PUFA increase TNF- $\alpha$  secretion by primary resident and elicited peritoneal macrophages and the RAW 264.7 cell line but have little effect on IL-10 secretion by these cells. In addition, omega-3 PUFA have the same effect on TNF- $\alpha$  secretion by resident peritoneal macrophages in vitro as dietary fish oil has on TNF- $\alpha$  secretion by these cells stimulated ex vivo. Thus, omega-3 PUFA may be incorporated into the cell membrane and from there affect lipid mediator production or intracellular signaling and thereby TNF- $\alpha$  secretion. In contrast, the effects of dietary omega-3 PUFA on IL-10 secretion by resident peritoneal macrophages ex vivo is not mimicked by incubating these cells with omega-3 PUFA in vitro. These effects are probably due to an effect of dietary fish oil on the cell population in the peritoneum of mice in vivo, possibly brought about by an effect on cell recruitment, maturation, or proliferation. Although omega-3 PUFA may have an anti-inflammatory effect on lymphocytes, the results from the present study indicate that omega-3 PUFA have pro-inflammatory effects on macrophages. These effects may be important in maintaining the innate immune response.

**Acknowledgments** This study was supported by a grant from the Icelandic Research Fund, Graduate Education Fund (IHS), and The University of Iceland Research Fund.

## References

1. Arrington JL, Chapkin RS, Switzer KC, Morris JS, McMurray DN (2001) Dietary n-3 polyunsaturated fatty acids modulate purified murine T-cell subset activation. *Clin Exp Immunol* 125:499–507
2. Babcock TA, Helton WS, Hong D, Espat NJ (2002) Omega-3 fatty acid lipid emulsion reduces LPS-stimulated macrophage TNF-alpha production. *Surg Infect (Larchmt)* Summer 3(2):145–149
3. Babcock TA, Kurland A, Helton WS, Rahman A (2003) Inhibition of activator protein-1 transcription factor activation by [omega]-3 fatty acid modulation of mitogen-activated protein kinase signaling kinases. *JPEN* 27(3):176–180
4. Bhattacharya A, Sun D, Rahman M, Fernandes G (2007) Different ratios of eicosapentaenoic and docosahexaenoic omega-3



- fatty acids in commercial fish oils differentially alter pro-inflammatory cytokines in peritoneal macrophages from C57BL/6 female mice. *J Nutr Biochem* 18:23–30
5. Blok WL, Vogels MT, Curfs HJ, Eling WM, Buurman WA, van der Meer MWM (1992) Dietary fish oil supplementation in experimental gram-negative infection and in cerebral malaria in mice. *J Infect Dis* 165:898–903
  6. Bonatto SJ, Folador A, Aikawa J, Yamazaki RK, Pizzato N, Oliveira HH, Vecchi R, Curi R, Calder PC, Fernandes LC (2004) Lifelong exposure to dietary fish oil alters macrophage responses in Walker 256 tumor-bearing rats. *Cell Immunol* 231:56–62
  7. Calder PC (2006) n-3 Polyunsaturated fatty acids, inflammation, and inflammatory diseases. *Am J Clin Nutr* 83(Suppl):1505S–1519S
  8. Carrick JB, Schnellmann RG, Moore JN (1994) Dietary source of omega-3 fatty acids affects endotoxin-induced peritoneal macrophage tumor necrosis factor and eicosanoid synthesis. *Shock* 2:421–426
  9. Cathcart ES, Mortensen RF, Leslie CA, Conte JM, Gonnerman WA (1987) A fish oil diet inhibits amyloid P component (AP) acute phase responses in arthritis susceptible mice. *J Immunol* 139:89–91
  10. Chang HR, Arsenijevic D, Pechere JC, Piguat PF, Mensi N, Girardier L, Dulloo AG (1992) Dietary supplementation with fish oil enhances in vivo synthesis of tumor necrosis factor. *Immunol Lett* 54:13–18
  11. Chu AJ, Walton MA, Prasad JK, Seto A (1999) Blockade by polyunsaturated n-3 fatty acids of endotoxin-induced monocytic tissue factor activation is mediated by the depressed receptor expression in THP-1 cells. *Surg Res* 87:217–224
  12. Fritsche KL, Johnston PV (1988) Rapid autoxidation of fish oil in diets without added antioxidants. *J Nutr* 118:425–426
  13. Fritsche KL, Byrge M, Feng C (1999) Dietary omega-3 polyunsaturated fatty acids from fish oil reduce interleukin-12 and interferon-gamma production in mice. *Immunol Lett* 65:167–173
  14. Geusens P, Wouters C, Nijs J, Jiang Y, Dequeker J (1994) Long-term effect of omega-3 fatty acid supplementation in active rheumatoid arthritis. A 12-month, double-blind, controlled study. *Arthritis Rheum* 37:824–829
  15. Hardardottir I, Kinsella JE (1991) Tumor necrosis factor production by murine resident peritoneal macrophages is enhanced by dietary n-3 polyunsaturated fatty acids. *Biochim Biophys Acta* 1095:187–195
  16. Hardardottir I, Kinsella JE (1992) Increasing the dietary (n-3) to (n-6) polyunsaturated fatty acid ratio increases tumor necrosis factor production by murine resident peritoneal macrophages without an effect on elicited peritoneal macrophages. *J Nutr* 122:1942–1951
  17. Hubbard NE, Lim D, Somers SD, Erickson KL (1993) Effects of in vitro exposure to arachidonic acid on TNF-alpha production by murine peritoneal macrophages. *J Leukoc Biol* 54:105–110
  18. Jolly CA, Jiang YH, Chapkin RS, McMurray DN (1997) Dietary (n-3) polyunsaturated fatty acids suppress murine lymphoproliferation, interleukin-2 secretion, and the formation of diacylglycerol and ceramide. *J Nutr* 127:37–43
  19. Jolly CA, McMurray DN, Chapkin RS (1998) Effect of dietary n-3 fatty acids on interleukin-2 and interleukin-2 receptor alpha expression in activated murine lymphocytes. *Prostaglandins Leukot Essent Fatty Acids* 58:289–293
  20. Komatsu W, Ishihara K, Murata M, Saito H, Shinohara K (2003) Docosahexaenoic acid suppresses nitric oxide production and inducible nitric oxide synthase expression in interferon-gamma plus lipopolysaccharide-stimulated murine macrophages by inhibiting the oxidative stress. *Free Radic Biol Med* 34(8):1006–1016
  21. Kremer JM (1991) Clinical studies of omega-3 fatty acid supplementation in patients who have rheumatoid arthritis. *Rheum Dis Clin North Am* 17:391–402
  22. Lo CJ, Chiu KC, Fu M, Lo R, Helton S (1999) Fish oil decreases macrophage tumor necrosis factor gene transcription by altering the NF kappa B activity. *J Surg Res* 82:216–221
  23. Lo CJ, Chiu KC, Fu M, Chu A, Helton S (2000) Fish oil modulates macrophage P44/P42 mitogen-activated protein kinase activity induced by lipopolysaccharide. *JPEN* 24(3):159–166
  24. Lokesh BR, Sayers TJ, Kinsella JE (1990) IL-1 and tumor necrosis factor synthesis by mouse peritoneal macrophages is enhanced by dietary n-3 polyunsaturated fatty acids. *Immunol Lett* 23:281–286
  25. Novak TE, Babcock TA, Jho DH, Helton WS, Espat NJ (2003) NF-kappa B inhibition by omega-3 fatty acids modulates LPS-stimulated macrophage TNF-alpha transcription. *Am J Physiol Lung Cell Mol Physiol* 284:L84–L89
  26. Petursdottir DH, Hardardottir I (2007) Dietary fish oil increases the number of splenic macrophages secreting TNF-alpha and IL-10 but decreases the secretion of these cytokines by splenic T cells of mice. *J Nutr* 137:665–670
  27. Petursdottir DH, Olafsdottir I, Hardardottir I (2002) Dietary fish oil increases tumor necrosis factor secretion but decreases interleukin-10 secretion by murine peritoneal macrophages. *J Nutr* 132:3740–3743
  28. Reeves PG, Nielsen FH, Fahey GC Jr (1993) AIN-93 purified diets for laboratory rodents: final report of the American Institute of Nutrition ad hoc writing committee on the reformulation of the AIN-76A rodent diet. *J Nutr* 23:1939–1951
  29. Renier G, Skamene E, DeSanctis J, Radzioch D (1993) Dietary n-3 polyunsaturated fatty acids prevent the development of atherosclerotic lesions in mice. Modulation of macrophage secretory activities. *Arterioscler Thromb Vasc Biol* 13:1515–1524
  30. Shi L, Kishore R, McMullen MR, Nagy LE (2002) Chronic ethanol increases lipopolysaccharide-stimulated Egr-1 expression in RAW 264.7 macrophages. *J Biol Chem* 277(17):14777–14785
  31. Somers SD, Erickson KL (1994) Alteration of tumor necrosis factor-alpha production by macrophages from mice fed diets high in eicosapentaenoic and docosahexaenoic fatty acids. *Cell Immunol* 153:287–297
  32. Switzer KC, McMurray DN, Morris JS, Chapkin RS (2003) (n-3) Polyunsaturated fatty acids promote activation-induced cell death in murine T lymphocytes. *J Nutr* 133:496–503
  33. Tappia PS, Grimble RF (1994) Complex modulation of cytokine induction by endotoxin and tumour necrosis factor from peritoneal macrophages of rats by diets containing fats of different saturated, monounsaturated and polyunsaturated fatty acid composition. *Clin Sci (Lond)* 87:173–178
  34. Tappia PS, Man WJ, Grimble RF (1995) Influence of unsaturated fatty acids on the production of tumour necrosis factor and interleukin-6 by rat peritoneal macrophages. *Mol Cell Biochem* 143:89–98
  35. Turek JJ, Schoenlein IA, Bottoms GD (1991) The effect of dietary n-3 and n-6 fatty acids on tumor necrosis factor-alpha production and leucine aminopeptidase levels in rat peritoneal macrophages. *Prostaglandins Leukot Essent Fatty Acids* 43:141–149
  36. Wallace FA, Miles EA, Calder PC (1999) The effect of dietary fat on cytokine production by murine macrophages in different activation states. *Lipids* 34(Suppl):S145
  37. Watanabe S, Hayashi H, Onozaki K, Okuyama H (1991) Effect of dietary alpha-linolenate/linoleate balance on lipopolysaccharide-induced tumor necrosis factor production in mouse macrophages. *Life Sci* 48:2013–2020

38. Watanabe S, Onozaki K, Yamamoto S, Okuyama H (1993) Regulation by dietary essential fatty acid balance of tumor necrosis factor production in mouse macrophages. *J Leukoc Biol* 53:151–156
39. Weldon SM, Mullen AC, Loscher CE, Hurley LA, Roche HM (2007) Docosahexaenoic acid induces an anti-inflammatory profile in lipopolysaccharide-stimulated human THP-1 macrophages more effectively than eicosapentaenoic acid. *J Nutr Biochem* 18:250–258
40. Yaqoob P, Calder P (1995) Effects of dietary lipid manipulation upon inflammatory mediator production by murine macrophages. *Cell Immunol* 163:120–128

## Conjugated Linoleic Acids Can Change Phagocytosis of Human Monocytes/Macrophages by Reduction in Cox-2 Expression

Ewa Stachowska · Magdalena Bańkiewicz-Masiuk ·  
Violetta Dziezdziejko · Grażyna Adler · Joanna Bober ·  
Bogusław Machaliński · Dariusz Chlubek

Received: 18 January 2007 / Accepted: 30 April 2007 / Published online: 15 June 2007  
© AOCS 2007

**Abstract** Prostaglandin E<sub>2</sub> produced endogenously (by cyclooxygenases) can regulate macrophage phagocytosis. Cyclooxygenase activity reduction (mainly through inhibition of inducible Cox-2) can induce PGE<sub>2</sub> synthesis depression and can activate the phagocytosis process. There are no reports in the literature explaining whether conjugated linoleic acid dienes (*trans*-10, *cis*-12 CLA and *cis*-9, *trans*-11 CLA) modify the phagocytic activity of human macrophages. For the purpose of this study, monocytes were isolated from venous blood, incubated for 7 days with 30 μM CLAs, and then (in some experiments) LPS (1 μg/mL) was added to the medium. Subsequently, monocyte/macrophage phagocytosis, NF-κB transcription factor activity, Cox-2 and PPARγ mRNA expression (and the amounts of Cox-2 and PPARγ proteins) and PGE<sub>2</sub> synthesis were determined. Both CLA isomers increased macrophage phagocytosis through inhibition of Cox-2 expression (might by inactivation the NF-κB pathway). The inhibition of mRNA Cox-2 expression contributed

(particularly with respect to *trans*-10, *cis*-12 CLA) to a decrease in protein Cox-2 synthesis and to reduction of prostaglandin E<sub>2</sub> content in the cell. The inhibition of PGE<sub>2</sub> synthesis (by CLA treatment) enhanced the phagocytosis process in macrophages.

**Keywords** Conjugated linoleic acid · Monocytes/macrophages · Phagocytosis · NF-κB · Prostaglandin E<sub>2</sub>

### Abbreviations

CLA	Conjugated linoleic acid
Cox	Cyclooxygenase
LPS	Lipopolysaccharide
NF-κB	Nuclear factor κB
PPAR	Peroxisome proliferator activated receptors
PGE <sub>2</sub>	Prostaglandin E <sub>2</sub>

### Introduction

Introduction of a specific diet may be highly important for the treatment of diseases with an inflammatory background, cancer or atherosclerosis [1]. Dietary fatty acids may change the activity of immune system cells through modification of the biological membranes composition [2], the effect on eicosanoid synthesis [3, 4] and gene expression regulation by, for example, PPAR family receptors [5]. Conjugated linoleic acid dienes (CLAs) are fatty acids which can modulate the function of immune system cells in human [6, 7] and animal bodies [8, 9]. Conjugated linoleic acids are positional and geometric isomers of linoleic acid with the presence of conjugated double bonds [10, 11]. In the human body, CLAs originate from two sources: from

E. Stachowska (✉) · V. Dziezdziejko · D. Chlubek  
Department of Biochemistry,  
Pomeranian Medical University, Szczecin, Poland  
e-mail: ewast@sci.pam.szczecin.pl

M. Bańkiewicz-Masiuk · B. Machaliński  
Department of General Pathology,  
Pomeranian Medical University, Szczecin, Poland

G. Adler  
Department of Clinical Biochemistry  
and Laboratory Diagnostics,  
Pomeranian Medical University, Szczecin, Poland

J. Bober  
Department of Medical Chemistry,  
Pomeranian Medical University, Szczecin, Poland

food and from the conversion of other *trans* isomers of fatty acids [12]. Their content in human plasma depends on the dietary habits and rises upon diet supplementation with these fatty acids. Conjugated linoleic acids are transported to the tissues with plasma lipoproteins. The activity of intravascular lipoprotein lipase (LPL) leads to CLA uptake and their inclusion in the cellular metabolic pool, where CLAs serve as energetic material or may be built into membrane phospholipids [13].

Conjugated linoleic acids are considered to have anti-inflammatory [14], anti-atherogenic [9, 15, 16, 17], anti-diabetogenic [18, 19] and anti-adipogenic properties [20, 21].

Immune response may be triggered by bacterial infection. The presence of a microorganism in the body, stimulates the cells to activate the  $\kappa$ B transcription factor, to express pro-inflammatory enzymes, and to start the phagocytosis process. Many factors with immunomodulatory properties may enhance the phagocytosis process in macrophages. They also include fatty acids forming the phospholipids of cellular membranes [22]. Differences in fatty acid composition of the cellular membrane phospholipids in peripheral blood mononuclear cells (PMBC) correlate with differences in phagocytic activity of these cells [22, 23].

The transcription factor NF- $\kappa$ B is one of the key regulators of inflammation; the activated NF- $\kappa$ B can mediate the induction of more than 160 genes which have a crucial role in atherogenesis [24, 25]. The  $\kappa$ B sequence is located within the genes important for the processes of proliferation and apoptosis, participating in inflammatory processes [25]. NF- $\kappa$ B is a family of five transcription factors: p65 (rel A), c-Rel, Rel-B, p50 (NF- $\kappa$ B 1) and p52 (NF- $\kappa$ B2) [24, 26, 27, 28]. These proteins form homodimers or heterodimers, of which p65p50 is the most abundant [24]. In the cytoplasm, the inactive NF- $\kappa$ B complex remains bound to the inhibitor—I $\kappa$ Bs family proteins (I $\kappa$ B $\alpha$ , I $\kappa$ B $\beta$ , I $\kappa$ B $\epsilon$ , I $\kappa$ B $\gamma$ ); their function is to block the translocation of the active NF- $\kappa$ B complex into the cell nucleus [29, 30, 31]. NF- $\kappa$ B activation is mediated by the I $\kappa$ B kinase complex containing two catalytic subunits (IKK 1 and IKK 2) and a regulatory subunit; NF- $\kappa$ B essential modulator (NEMO). Upon stimulation, the IKK complex phosphorylates I $\kappa$ B inducing its degradation. NF- $\kappa$ B is then free to translocate to the nucleus, where it facilitates the transcription of genes with a promoter sequence present in the gene enhancer region GGGGACTTTCC [24]. NF- $\kappa$ B, through its participation in the stimulation of Cox-2 expression, has also an effect on prostanoid synthesis in cells [32].

PPAR $\gamma$  is a receptor that may play an important role in regulating inflammatory and immune responses through

modulation of the monocyte and macrophage activity [23]. The PPAR $\gamma$  are a subfamily of nuclear hormone receptors activated by dietary as well as endogenous fatty acids and their derivatives [33]. PPAR $\gamma$  agonists such as 15-deoxy- $\Delta$ -12, 14-prostaglandin J<sub>2</sub> or thiazolidinediones reduce acute inflammation [33], although in primary human monocytes they induce Cox-2 expression and PGE<sub>2</sub> secretion [34].

The expression of Cox-2 in macrophage cells may be regulated by a negative feedback loop mediated through PPAR $\gamma$  by interfering with the NF- $\kappa$ B pathway (by a PGD<sub>2</sub> metabolites) [35]. Conjugated linoleic acids increased PPAR $\gamma$  expression in macrophages [15] and in other cell types [36, 37]. The *trans*-10, *cis*-12 CLA isomer may be a direct ligand and activator of PPAR $\gamma$  [38].

Arachidonic acid metabolites—prostanoids are endogenous mediators of inflammation. Prostaglandin E<sub>2</sub> (PGE<sub>2</sub>) which is a product of two cyclooxygenase isoforms—Cox-1 and Cox-2, plays an important role in this process [39]. Cox-1 is a constitutive enzyme with constant low activity whereas Cox-2 is inducible and its amount in the cell rapidly increases in inflammation [39]. Lipopolysaccharide (LPS) present in the bacterial wall is a strong Cox-2 activator in monocyte cells [40]. Cox-2 expression following LPS administration takes place via the NF- $\kappa$ B pathway [40]. An important source of PGE<sub>2</sub> in the place of inflammation are monocytes/macrophages [40]. PGE<sub>2</sub> synthesis (mediated by Cox-2 expression) dramatically increases in inflammation. The endogenously produced PGE<sub>2</sub> can regulate macrophage phagocytosis PGE<sub>2</sub> synthesis inhibition enhances phagocytosis while PGE<sub>2</sub> synthesis activation inhibits this process [41].

So far, few studies have been published to explain whether CLA isomers may modify immune functions of monocytes/macrophages. In the pioneering study by Kang [42] the *trans*-10, *cis*-12 CLA isomer was shown not to modify phagocytic capacity of cultivated polymorphonuclear cells (PMN cells). Nevertheless, PMN cell phagocytosis increased when the supernatant of peripheral blood mononuclear cells (PMBC) incubated with *trans*-10, *cis*-12 CLA was added to PMN cells [42]. The next study by Kang (published when this study was being edited) demonstrated that the *trans*-10, *cis*-12 CLA isomer might activate phagocytosis in (pig) PMBC through a PPAR $\gamma$ -dependent mechanism [23].

The objective of this study is to explain whether phagocytic capacity may be regulated in monocytes/macrophages incubated with CLAs through modifications of Cox-2 activity and of PGE<sub>2</sub> synthesis. Particular attention was paid in the study to the function of the Cox-2 and NF- $\kappa$ B transcription factor in phagocytosis.

## Experimental Procedure

### Reagents

Cell culture media and reagents were supplied by Gibco (Gibco, UK) and Sigma (Sigma-Aldrich Poland), indomethacin, Bradford reagent and lipopolysaccharide (*E. coli*) were supplied by Sigma-Aldrich, Poland. N-2-cyclohexyloxy-4-nitrophenyl-methanesulfonamide (NS 398) was supplied by Cayman Chemical (USA).

Lymphocyte separation medium was supplied by PAP Laboratories, Austria. Conjugated linoleic acids (*cis*-9, *trans*-11 CLA; *trans*-10, *cis*-12 CLA) were supplied by Nu-CheK Prep (98% purity) (USA). Phagotest was supplied by Opregen Pharma (Germany). All reagents and solvents for the PGE<sub>2</sub> extraction were supplied by Aldrich (Sigma-Aldrich, Poland). ELISA commercial kits for PGE<sub>2</sub> concentration measurements were supplied by R&D (R&D Systems, UK). The NF- $\kappa$ B p65/Rel A Transcription Factor Assay ELISA kit and Nuclear Extract Isolation Kit were supplied by Active Motif (Belgium). C<sub>18</sub> reverse phase columns were supplied by JT Baker, (USA) and the solid phase extraction–Vacuum Manifold system for PGE<sub>2</sub> extraction were supplied by Supelco (Supelco, Poland).

The mRNA isolation kit was supplied by Qiagen (USA). Reagents for real-time PCR: i.e. 5 $\times$  First Strand Buffer, oligo (dT) and DTT, were supplied by Sigma-Aldrich, deoxy-NTPs were supplied by Promega (USA) and SUPERScript II reverse transcriptase was supplied by Invitrogen (USA).

The monoclonal anti-Cox-2, and anti-PPAR $\gamma$  antibodies were supplied by Santa Cruz Biotechnology (USA). The anti- $\beta$ -actin monoclonal antibody was supplied by Sigma-Aldrich (Sigma-Aldrich, Poland).

### Preparation of Monocytes from Peripheral Blood Mononuclear Cells (PBMC)

Monocytes were isolated from peripheral blood of 55 healthy donors, Caucasian whites (31 males, 24 females), aged 20–25 years. Because age-related increase in Cox-2 expression in mononuclear cells was observed in humans [43], donors older than 25 years old and donors with a history of hypertension or diabetes were excluded from the study. Ten patients were ex-smokers and the remaining ones had never smoked. An average standard of living was found for all patients and there were no cases of malnutrition. Patients were fully informed as to the study objectives and benefits and provided their written consent prior to enrolment.

Cells obtained from 25, 15, 6, 9 and 3 donors were used for phagocytic activity quantification, PGE<sub>2</sub> concentration, measurement NF- $\kappa$ B activation determination, real-time

PCR and the Western blot analysis, respectively. In each single experiment (e.g. phagocytosis measurement), the cells obtained from one donor were cultured with BSA or separate CLA isomers. Blood sampling was performed in accordance with the principles outlined in the Declaration of Helsinki (Cardiovascular Research 1997; 35:2–3). First peripheral blood mononuclear cells (PBMCs) were isolated from anti-coagulated blood by lymphocyte separation media density gradient as described [44]. The cells were cultured at a density of  $3 \times 10^6$  cells/well in plastic culture dishes. Monocytes were isolated from lymphocytes by adherence to plates (2 h at 37 °C, 5% CO<sub>2</sub>) as described [44]. Then, the adherent cells were incubated in the RPMI 1640 medium supplemented with 10% autologous serum, penicillin (100 U/mL) and streptomycin (100 mg/mL) at 37 °C in 5% CO<sub>2</sub>. The cells were cultured with CLAs: *cis*-9, *trans*-11 C18:2; *trans*-10 or *cis*-12 C18:2, at final concentrations of 30  $\mu$ M in the medium for 7 days. The incubation time and fatty acid concentration were selected on the basis of the results obtained in preliminary experiments. Fatty acids were complexed to 1 mM fatty acid-free bovine albumin (1 mM BSA: 4 mM fatty acids) and added to medium as proposed [36, 45]. The medium was changed every 2 days for 7 days. The cells (after 7 days of incubation in the medium with autologous serum) were characterised by morphological criteria such as CD 14 and CD 68 antigen expression (BD Pharmingen, USA) The percentage of CD 14 and CD 68 cells was assessed by flow-cytometry (FACScan) using CellQuest software as previously described [46]. The resulting cells may be described as “monocyte-derived macrophages” [47] with CD 14 and CD 68 antigens expression.

Cells (after 7 days of incubation with BSA or CLAs) were scraped from the wells and their viability was assessed by trypan blue exclusion as described [44]. Cells whose viability exceeded 90% were used for the experiments.

### Quantification of Phagocytic Activity of Monocytes

Phagocytosis was measured using the PHAGOTEST kit. Before the measurement, the cells were incubated for 4 h at 37 °C with opsonised fluorescein isothiocyanate-labelled *E. coli* (20  $\mu$ L), in compliance with the manufacturer's instruction. The reaction was stopped by the addition of ice-cold quenching solution (100  $\mu$ L). At the completion of phagocytosis, monocytes/macrophages were fixed, and DNA was stained according to the manufacturer's instructions. Cell preparations were then analysed by flow cytometry in a flow cytometer (FACSCalibur, Becton Dickinson). Fluorescence data were collected on  $10 \times 10^4$  cells and analysed using the CELLQUEST software. The percentage of cells engaging in phagocytosis was

determined. In some experiments, the cells (cultured for 7 days with RPMI+10% autologous serum) were pretreated with the Cox inhibitor indomethacin (10  $\mu$ M) or NS 386 (4  $\mu$ M) for 30 min and then challenged with opsonised fluorescein isothiocyanate-labelled *E. coli* (20  $\mu$ L), as described above.

#### Measurement of NF- $\kappa$ B Activation

NF- $\kappa$ B activation was measured in nuclear extract with the NF- $\kappa$ B p65/Rel A Transcription Factor Assay kit. The active p65/Rel A was measured in cells cultivated with CLAs for 7 days. Subsequently, the cells were incubated with LPS (1  $\mu$ g/mL, 4 h at 37 °C in 5% CO<sub>2</sub>). To some cells LPS was not added.

The cells were briefly washed with ice-cold PBS, scraped into tubes and centrifuged. The pellet was lysed with the complete lysis buffer containing dithiothreitol and protease inhibitor cocktail of the Nuclear Extract Isolation Kit. After centrifugation at 5,000g and 4 °C for 20 min, protein concentration in the supernatant (whole cell extract) was determined with the Bradford-based assay. To determine the NF- $\kappa$ B activation with an ELISA-based kit, an oligonucleotide containing the NF- $\kappa$ B consensus binding site (5'-GGGACTTTCC-3') specific for the active form of NF- $\kappa$ B was immobilized on a 96-well plate and the well was filled with 10  $\mu$ g of the nuclear extract. After the incubation and washing, the primary antibody against the active form of NF- $\kappa$ B was added followed by the secondary antibody conjugated with horseradish peroxidase, to achieve a sensitive readout by spectrophotometry at 450 nm.

The experiments were performed in duplicate and the results were expressed as OD<sub>450 nm</sub> [48].

#### Measurement of PGE<sub>2</sub> Concentration

After 7-day incubation with fatty acids, the cells were exposed to a medium containing *E. coli* LPS (1  $\mu$ g/mL) according producer instruction. In some experiments, cells incubated for 7 days with RPMI with 10% autologous serum were pretreated for 30 min before LPS administration with indomethacin (10  $\mu$ M) or NS 386 (4  $\mu$ M) (stimulated cells). In other experiments, the cells were cultured for 7 days with BSA or CLAs, whereas LPS was not administered to them (at the end non-stimulated cells). After incubation, the supernatant was collected and PGE<sub>2</sub> in the supernatant was measured by enzyme immunoassay. The cells were scraped, washed twice with ice-cold PBSs (centrifuged at 2,000g for 10 min.), and protein concentration in the pellet was determined with a Bradford-based assay. For PGE<sub>2</sub> extraction, typical C<sub>18</sub> reverse phase columns (JT Backer, USA) and the solid phase extract

Vacuum Manifold system (Supelco, Poland) were used according to the R&D assay procedure.

#### PCR Reaction with the Analysis of Real-Time Product Quantity Increase (Real-Time PCR)

The Qiagen kit was used for isolation of m RNA from cells. In order to confirm enzymatic activity regulation, the quantitative expression analysis was performed by real time PCR using GAPDH as the reference gene, as described in details [49]. For the cDNA synthesis, 1  $\mu$ g of total RNA was reverse transcribed at 42 °C for 50 min in a total volume of 40  $\mu$ l of reaction buffer containing 5 $\times$ First Strand Buffer, oligo (dT), DTT, deoxy-NTPs, and 200 units of SUPERScript II reverse transcriptase. cDNA was subjected to real-time PCR in a reaction mixture containing the QuantiTect SYBR Green PCR (Qiagen) mix and primers. The sequences of primers used in this study:

Cox-2	Forward primer: 5'- ATGAGATTGTGGGAAAATTGCT-3'
	Reverse primer: 5'-GATCATCTCTGCCTGAGTATC-3'
PPAR $\gamma$	Forward primer: 5'-ATGACAGCGACTTGCCAA-3'
	Reverse primer: 5'-TCAATGGGCTTCACATTC-3'
GAPDH	Forward primer: 5'-GCCAGCCGAGCCACATC-3'
	Reverse primer: 5'-GCGCCAATACGACCAAA-3'

All real-time PCR reactions were performed on the DNA Engine Option II (MJ Research). The thermal profile included initial denaturation for 15 min at 95 °C, followed by 40 amplification cycles of denaturation for 30 s at 72 °C. Following the PCR amplification, melting curve analysis was performed with a temperature profile slope of 1 °C/s from 35 °C to 95 °C. A negative control without cDNA template was run with every assay to ensure overall specificity. The expression rates were calculated as described [49, 50].

#### Western Blot for Cox-2 Analysis

The cells were harvested in the lysis buffer at pH 6.8, as described [44]. The cellular debris was removed (14,000g for 15 min) and protein concentration was determined by the Bradford assay. Equal amounts of lysates were subjected to SDS-PAGE (7% polyacrylamide) and transblotted onto nitro-cellulose membrane. Membranes were incubated for 12 h/4 °C with antibodies directed against Cox-2 (1/1,000), PPAR $\gamma$  (1/600),  $\beta$ -actin (Sigma-Aldrich, Poland) was used as a control of protein loading [19]. The blots were incubated with peroxidase-conjugated secondary antibody (1/5,000) for 1 h at room temperature. The bands

were visualized by enhanced chemiluminescence (Amersham Pharmacia Biotech, USA) [51].

### Statistical Analysis

All results are expressed as mean values  $\pm$  standard deviation (SD). Before statistical analysis, normality of distribution was tested by the Shapiro–Wilk test. As the distribution in most cases deviated from normal, non-parametric tests were used. For related samples, the significance was first checked with Friedmann's ANOVA and then significant results were subjected to the Wilcoxon matched-pair test. The software used was Statistica 6.1 (Statsoft, Poland).

## Results

### CLAs Modified the Phagocytic Activity of Monocytes/Macrophages

Significant changes in the phagocytic activity were observed ( $P < 0.0001$ ; Friedmann's ANOVA test). Both conjugated linoleic acids enhanced the percent of cells engaging in phagocytosis. The *trans*-10, *cis*-12 C18:2 isomer increased this process by 61% ( $P < 0.001$ ; Wilcoxon matched-pair test) as compared to control, and the *cis*-9, *trans*-11 C18:2 isomer increased phagocytosis by 73% ( $P < 0.001$ ; Wilcoxon matched-pair test) (Fig. 1a). The phagocytic capacity was induced by the addition of cyclooxygenase inhibitors indomethacin ( $P < 0.05$ ; Wilcoxon matched-pair test) and NS 386 ( $P < 0.05$ ; Wilcoxon matched-pair test) to the cells (Fig. 1b).

### CLAs Reduced the Amount of Active Form of NF- $\kappa$ B Transcription Factor

In this study, we investigated the effect of on NF- $\kappa$ B activity using the immunoenzymatic method in which the primary antibodies used to detect NF- $\kappa$ B recognise an epitope on p65/Rel A that is only accessible when NF- $\kappa$ B is activated and bound to its target DNA. As compared to control BSA, both conjugated linoleic acid dienes, reduced the activation of the p65/Rel A subunit of the NF- $\kappa$ B complex ( $P < 0.03$  for both CLA isomers; Wilcoxon matched-pair test) (Fig. 2). In LPS-stimulated cells, low activity of the p65/Rel A subunit was noted, without any visible effect of fatty acids.

### CLAs Decreased PGE<sub>2</sub> Synthesis

In non-LPS-stimulated cells incubated with CLAs, PGE<sub>2</sub> synthesis was low, without any significant effect of fatty

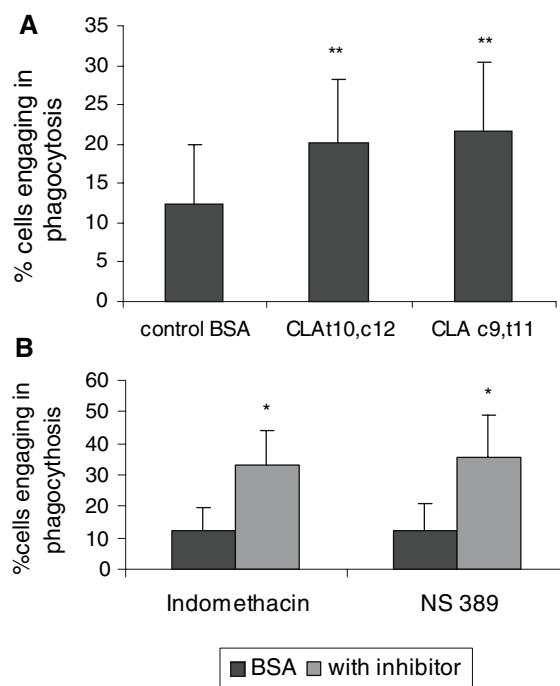


**Fig. 1** **a** Effect of conjugated linoleic acid on monocyte/macrophage phagocytic activity. Monocytes were incubated for 7 days with the 30  $\mu$ M *trans*-10, *cis*-12 CLA and *cis*-9, *trans*-11 CLA. Data were expressed as a percentage of cells engaging in phagocytosis and shown as the mean  $\pm$  SD (represented by vertical bars) in 16 separate experiments.  $**P < 0.001$  significant difference versus the corresponding control. **b** The effect of Cox inhibitors: indomethacin and NS 386 on the phagocytic activity. Cells were cultured for 7 days with BSA (control) or with Cox inhibitor indomethacin (10  $\mu$ M) or specific Cox-2 inhibitor NS 386 (4  $\mu$ M). The data were expressed as percentage of cells engaging in phagocytosis and shown as the mean  $\pm$  SD in five separate experiments (indomethacine) or four separate experiments (NS 386).  $*P < 0.05$  significant difference versus the corresponding control

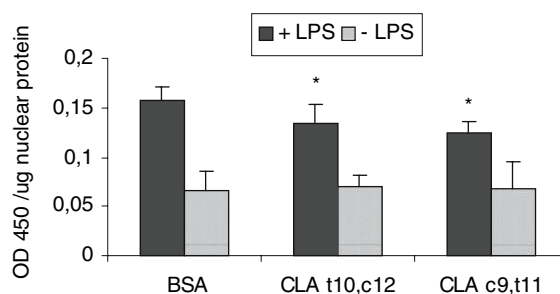


**Fig. 2** Influence of conjugated linoleic acid dienes on NF- $\kappa$ B pathway activation. Monocytes were cultivated for 7 days in a medium containing 30  $\mu$ M fatty acids, then LPS (1  $\mu$ g/mL) was added or cells were cultured without LPS administration. A nuclear cell extract was obtained and NF- $\kappa$ B activation was measured using an ELISA-based kit. The data were expressed as OD<sub>450 nm</sub> and shown as the mean  $\pm$  SD (represented by vertical bars) in six separate experiments.  $*P < 0.05$  significant difference versus the corresponding control

acids on PGE<sub>2</sub> concentration in the culture. In LPS-stimulated cells, the synthesis of PGE<sub>2</sub> was enhanced (as compared to non-stimulated cells), and in cells incubated with CLAs, the PGE<sub>2</sub> production was reduced (Fig. 3). The changes in PGE<sub>2</sub> concentrations depending on the CLA isomer were statistically significant ( $P < 0.03$ , Friedmann's ANOVA test). Both CLA isomers significantly reduced PGE<sub>2</sub> production compared to the BSA control ( $P < 0.01$ ) (Fig. 3).

Both types of Cox inhibitors reduced PGE<sub>2</sub> synthesis. As compared to control, the NS 386 reduced PGE<sub>2</sub> concentration with this same intensity as indomethacin (near 80%) (Fig. 3).

#### Effect of CLAs on Relative mRNA and Protein Concentration of Cox-2 and PPAR $\gamma$ Expression and Enzyme Protein Synthesis

The *trans*-10, *cis*-12 isomer reduced Cox-2 mRNA expression in macrophages after 7 days of incubation. A strong trend towards mRNA expression reduction is manifested in cells incubated with the *cis*-9, *trans*-11 isomer (Fig. 4). The semi-quantitative measurement of Cox-2 protein contents (Western-blot method) showed both CLA isomers to limit the amount of this enzyme in the cell (Fig. 5).

In the cells incubated with both CLA isomers, a strong trend towards PPAR $\gamma$  mRNA expression increase was

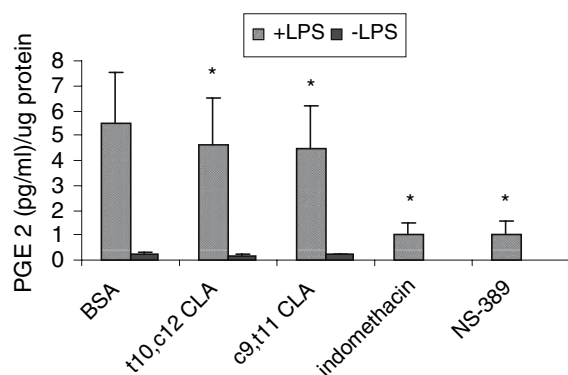


**Fig. 3** The effect of conjugated linoleic acid and Cox inhibitors, indomethacin and NS 386, on the PGE<sub>2</sub> synthesis. Monocytes were cultivated for 7 days in a medium containing 30  $\mu$ M CLA. After incubation, some cells were stimulated by addition of 1  $\mu$ g/mL LPS for 4 h. The data were expressed and shown as mean PGE<sub>2</sub> (pg/ml  $\mu$ g protein)  $\pm$  SD in six separate experiments (cells stimulated) or nine experiments (cells unstimulated by LPS). In the experiments with Cox-2 inhibitors, the cells were incubated for 7 days with BSA (control) and with Cox inhibitor indomethacin (10  $\mu$ M), or NS 386 (4  $\mu$ M). After incubation the cells were stimulated by administration of 1  $\mu$ g/mL LPS for 4 h. The data were expressed and shown as mean PGE<sub>2</sub> (pg/ml  $\mu$ g protein)  $\pm$  SD in five separate experiments (indomethacin) or four separate experiments (NS 386). \* $P < 0.05$  significant difference of the mean versus the corresponding control

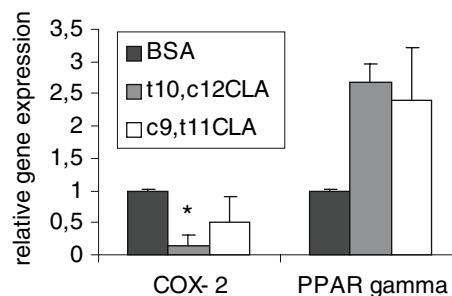


**Fig. 4** Effect of CLAs on the expression of Cox-2 and PPAR $\gamma$  genes verified by the quantitative real-time PCR. Data expressed as the relative gene expression ratio. The mean values  $\pm$  SD,  $n = 3$  done in triplicates are shown; \* $P < 0.05$  significant difference versus the corresponding control

noted (Fig. 4). The presence of PPAR $\gamma$  protein in these cells was confirmed by immunoelectrophoresis (Fig. 6).

#### Discussion

So far, only few studies have been published on the role of CLAs in modulating the phagocytic response of the cell [23, 42]. The study by Kang (published when this study was being edited) presenting the role of CLA—*trans*-10, *cis*-12 CLA in modifying the phagocytic capacity of peripheral blood polymorphonuclear cells (PMBC)—throws some light on this issue [23]. The study by Kang focused on investigation of changes in phagocytic capability through an effect on TNF- $\alpha$  synthesis via the PPAR $\gamma$ -dependent pathway [23]. On the other hand, this study investigates the potential participation of the Cox-2 and  $\kappa$ B transcription factor in this process. We were prompted to undertake the studies on the basis of the results indicating that phagocytosis in macrophages correlates with PGE<sub>2</sub> concentration

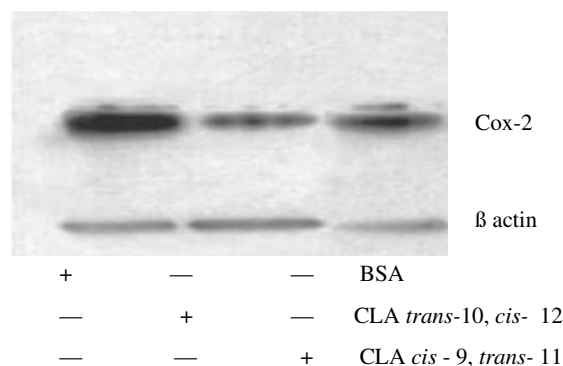


**Fig. 5** Role of conjugated linoleic acid in Cox-2 protein induction. The cells were incubated for 7 days in a medium containing 30  $\mu$ M CLA or BSA. Cox-2 proteins were determined by the Western analysis. Blots are representative of three independent experiments performed with different cell cultures



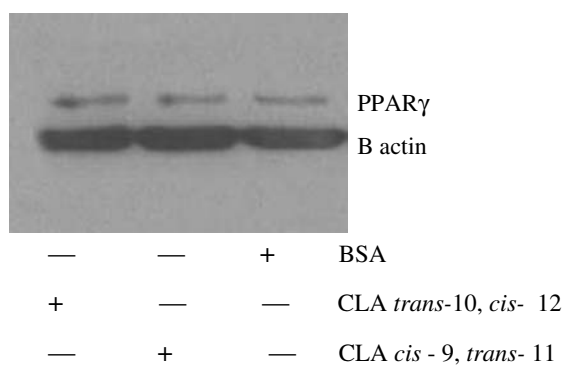


**Fig. 6** Role of conjugated linoleic acid in PPAR $\gamma$  protein induction. The cells were incubated for 7 days in a medium containing 30  $\mu$ M CLA or BSA. PPAR $\gamma$  proteins were determined by the Western analysis. Blots are representative of three independent experiments performed with different cell cultures

[41]. PGE $_2$  in macrophages is for the most part a product of Cox-2 [41], and NF- $\kappa$ B is the transcription factor regulating Cox-2 expression [32]. Because CLA isomers reduce PGE $_2$  release mainly through limiting Cox-2 expression [52], a decision was made to investigate whether CLAs may have an effect on phagocytic capacity of macrophages through an effect on expression of this enzyme.

As demonstrated by our observations, the *trans*-10, *cis*-12 CLA isomer reduced Cox-2 mRNA expression in macrophages, whereas the other isomer definitely reduced Cox-2 expression (although statistically significant results were not obtained in this case). Both isomers seem to contribute to limiting the Cox-2 protein quantities in cells. Similar results were obtained in lung cells incubated with CLA isomers [53]. Considerable (80%) inhibition of Cox-2 expression was noted in the presence of the *trans*-10, *cis*-12 CLA isomer. This inhibition was much lower in the presence of the *cis*-9, *trans*-11 CLA isomer. Proportionally to changes in Cox-2 expression, also PGE $_2$  synthesis was reduced in the cells. A similar tendency was noted in *in vivo* studies in mice receiving feed supplemented with CLAs. In these animals, a 30% reduction in Cox-2 mRNA expression and PGE $_2$  synthesis reduction was noted in the presence of the *trans*-10, *cis*-12 CLA isomer. The authors associate this phenomenon (Cox-2 mRNA reduction and PGE $_2$  synthesis lowering) with inhibition of the NF- $\kappa$ B pathway caused by CLA [53]. Also in cancer cells (canine mammary cells) and control cells (healthy cells) incubated with CLAs, both isomers inhibited Cox-2 protein expression. On the other hand, the *trans*-10, *cis*-12 isomer was a more potent repressor of Cox-2 synthesis in cancer cells [54].

Pronounced differences in intensity of phagocytosis in these studies were shown between control macrophages (incubated with BSA) and macrophages incubated with CLAs following the addition of an inflammatory factor

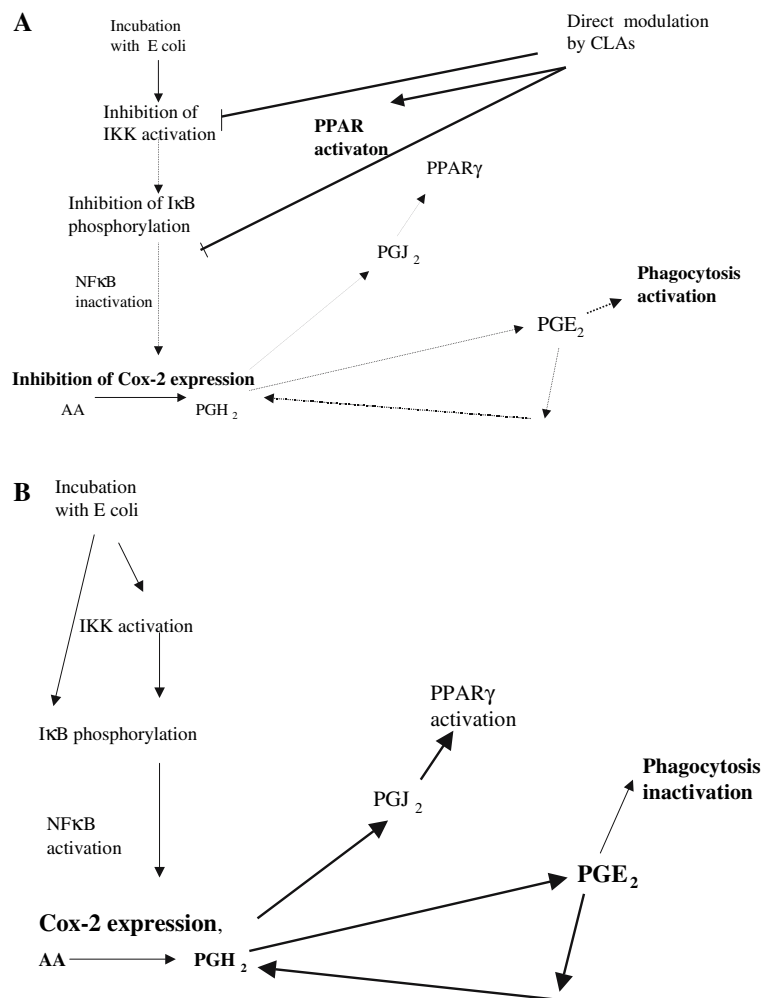
(LPS). When the cells were cultivated with BSA (control cells) the addition of bacteria (LPS) to the culture caused activation of the  $\kappa$ B transcription factor (NF- $\kappa$ B), which triggered Cox-2 expression. The increase in the amount of Cox-2 elevated the synthesis of PGE $_2$  in the cells. The increased amount of PGE $_2$  contributes to the inhibition of phagocytosis through the activation of PGE $_2$  receptors subtypes EP2 and EP4, and leads to an increase in cAMP concentration in the cell which additionally causes rebound activation of Cox-2 [41].

On the other hand, in cells incubated with CLAs both isomers activated phagocytosis. How can CLAs change this process? They might contribute to an inhibition of PGE $_2$  synthesis by reduction of mRNA Cox-2 expression and its activity. This may be evidenced by the reduced PGE $_2$  synthesis and concomitant activation of phagocytosis following the administration of NS 389—a selective Cox-2 inhibitor. NS 389 limited PGE $_2$  synthesis to the same extent as indomethacin, which implies that the factor primarily responsible for PGE $_2$  synthesis in the cell was Cox-2. The phenomenon of limiting Cox-2 expression by CLAs was also noted in murine macrophages (RAW 264.7), where the addition of *cis*-9, *trans*-11 CLA led to a reduction in Cox-2 expression (inhibition of Cox-2 promoter expression) and diminished PGE $_2$  synthesis [15].

In this study, Cox-2 expression reduction might take place through limitation of NF- $\kappa$ B activation—both CLA isomers inhibited activation of this transcription factor. This is not an isolated phenomenon—a reduction of the NF- $\kappa$ B pathway by fatty acids was reported previously, and it was shown that and other fatty acids may directly inhibit NF- $\kappa$ B [55, 56]. The mechanism which links with NF- $\kappa$ B inactivation, consists in the reduction of I $\kappa$ B kinase activity (leading to the inhibition of NF- $\kappa$ B phosphorylation). In these circumstances, dissociation of the NF- $\kappa$ B complex from its inhibitor, *i.e.* I $\kappa$ B, is decreased [57, 58]. Additionally, CLAs, like the other fatty acids (DHA and oleic acid) are likely to directly inhibit NF- $\kappa$ B activation through the effect on inactive NF- $\kappa$ B complex [55]. The inhibition of Cox-2 expression triggers a reduction in PGE $_2$  synthesis in the cell. A low amount of PGE $_2$  in the cells increased phagocytosis (Fig. 1). A similar phenomenon was observed in *in vivo* and *in vitro* studies conducted on mouse skin cells (in HR-1 hairless mouse skin). In these cells, the *cis*-9 *trans*-11 isomer inhibited the NF- $\kappa$ B dependent Cox-2 expression through blockade of activity of the IKK kinase [59] (Fig. 7).

The phenomenon of NF- $\kappa$ B inactivation in the presence of CLAs may also be associated with the expression and probable activation [38] of nuclear PPAR $\gamma$ . PPAR $\gamma$  are receptors which may interfere with NF- $\kappa$ B [25, 60]. The direct mechanism associating PPAR expression with NF- $\kappa$ B inactivation may be PPAR-forced reduction in I $\kappa$ B

**Fig. 7** Modulation of phagocytosis by CLAs, AA arachidonic acid, *IκB* inhibitor of *IκB*, *IKK* *IκB* kinase, *PPAR* $\gamma$  peroxysome proliferator-activated receptor  $\gamma$



kinase activity, inhibiting NF- $\kappa$ B/*IκB* complex dissociation and thus inhibiting NF- $\kappa$ B activation [25].

We concluded that CLA isomers increased macrophage phagocytosis through inhibition of Cox-2 expression what contributed to reduction of prostaglandin E<sub>2</sub> content in the cell. The inhibition of PGE<sub>2</sub> synthesis (by CLA treatment) enhanced the phagocytosis process in macrophages.

**Acknowledgments** Supported by grant no. 3PO5B 11723 from the State Committee for Scientific Research, Poland. M. Bańkiewicz-Masiuk is a scholarship holder of the Foundation for Polish Science.

## References

- Paoletti R, Poli A, Cignarella A (2006) The emerging link between nutrition, inflammation and atherosclerosis. *Expert Rev Cardiovasc Ther* 4:385–393
- de Pablo MA, Alvarez de Cienfuegos G (2000) Modulatory effects of dietary lipids on immune system functions. *Immunol Cell Biol* 78:31–39
- Fritsche K (2006) Fatty acids as modulators of the immune response. *Annu Rev Nutr* 26:45–73
- Calder PC (2006) n-3 polyunsaturated fatty acids, inflammation, and inflammatory diseases. *Am J Clin Nutr* 83:1505S–1519S
- Sampath H, Ntambi JM (2004) Polyunsaturated fatty acid regulation of gene expression. *Nutr Rev* 62:333–339
- Ramakers JD, Plat J, Sebedio JL, Mensink RP (2005) Effects of the individual isomers *cis*-9, *trans*-11 vs. *trans*-10, *cis*-12 of conjugated linoleic acid (CLA) on inflammation parameters in moderately overweight subjects with LDL-phenotype B. *Lipids* 40:909–918
- Schleser S, Ringseis R, Eder K (2005) Conjugated linoleic acids have no effect on TNF alpha-induced adhesion molecule expression, U937 monocyte adhesion, and chemokine release in human aortic endothelial cells. *Atherosclerosis* 186:337–344
- Zhang H, Guo Y, Yuan J (2005) Conjugated linoleic acid enhanced the immune function in broiler chicks. *Br J Nutr* 94:746–752
- Toomey S, Harhen B, Roche HM, Fitzgerald D, Belton O (2006) Profound resolution of early atherosclerosis with conjugated linoleic acid. *Atherosclerosis* 187:40–49
- Torres-Duarte AP, Vanderhoek JY (2003) Conjugated linoleic acid exhibits stimulatory and inhibitory effects on prostanoid production in human endothelial cells and platelets. *Biochim Biophys Acta* 1640:69–76
- Banni S, Petroni A, Blasevich M, Carta G, Cordeddu L, Murru E, Melis MP, Mahon A, Belury MA (2004) Conjugated linoleic

- acids (CLA) as precursors of a distinct family of PUFA. *Lipids* 39:1143–1146
12. Turpeinen AM, Mutanen M, Aro A, Salminen I, Basu S, Palmquist DL, Griinari JM (2002) Bioconversion of vaccenic acid to conjugated linoleic acid in humans. *Am J Clin Nutr* 76:504–510
  13. Burdge GC, Lupoli B, Russell JJ, Tricon S, Kew S, Banerjee T, Shingfield KJ, Beever DE, Grimble RF, Williams CM, Yaqoob P, Calder PC (2004) Incorporation of *cis*-9, *trans*-11 or *trans*-10, *cis*-12 conjugated linoleic acid into plasma and cellular lipids in healthy men. *J Lipid Res* 45:736–741
  14. Zulet MA, Marti A, Parra MD, Martinez JA (2005) Inflammation and conjugated linoleic acid: mechanisms of action and implications for human health. *J Physiol Biochem* 61:483–494
  15. Yu Y, Correll PH, Van den Heuvel JP (2002) Conjugated linoleic acid decreases production of pro-inflammatory products in macrophages: evidence for a PPAR gamma-dependent mechanism. *Biochim Biophys Acta* 1581:89–99
  16. Ecker J, Langmann T, Moehle C, Schmitz G (2007) Isomer specific effects of conjugated linoleic acid on macrophage ABCG1 transcription by a SREBP-1c dependent mechanism. *Biochem Biophys Res Commun* 352:805–811
  17. Llaverias G, Lacasa D, Vinals M, Vazquez-Carrera M, Sanchez RM, Laguna JC, Alegret M (2004) Reduction of intracellular cholesterol accumulation in THP-1 macrophages by a combination of rosiglitazone and atorvastatin. *Biochem Pharmacol* 68:155–163
  18. Houseknecht KL, Vanden Heuvel JP, Moya-Camarena SY, Portocarrero CP, Peck LW, Nickel KP, Belury MA (1998) Dietary conjugated linoleic acid normalizes impaired glucose tolerance in the Zucker diabetic fatty fa/fa rat. *Biochem Biophys Res Commun* 244:678–682
  19. Taylor CG, Zahradka P (2004) Dietary conjugated linoleic acid and insulin sensitivity and resistance in rodent models. *Am J Clin Nutr* 79:1164S–1168S
  20. Wang YW, Jones PJ (2004) Conjugated linoleic acid and obesity control: efficacy and mechanisms. *Int J Obes Relat Metab Disord* 28:941–955
  21. Pariza MW, Park Y, Cook ME (1999) Conjugated linoleic acid and the control of cancer and obesity. *Toxicol Sci* 52:107–110
  22. Kew S, Banerjee T, Minihane AM, Finnegan YE, Williams CM, Calder PC (2003) Relation between the fatty acid composition of peripheral blood mononuclear cells and measures of immune cell function in healthy, free-living subjects aged 25–72 y. *Am J Clin Nutr* 77:1278–1286
  23. Kang JH, Lee GS, Jeung EB, Yang MP (2007) *Trans*-10, *cis*-12-conjugated linoleic acid increases phagocytosis of porcine peripheral blood polymorphonuclear cells in vitro. *Br J Nutr* 97:117–125
  24. Kanters E, Pasparakis M, Gijbels MJ, Vergouwe MN, Partouns-Hendriks I, Fijneman RJ, Clausen BE, Forster I, Kockx MM, Rajewsky K, Kraal G, Hofker MH, de Winther MP (2003) Inhibition of NF-kappaB activation in macrophages increases atherosclerosis in LDL receptor-deficient mice. *J Clin Invest* 112:1176–1185
  25. Collins T, Cybulsky MI (2001) NF-kappaB: pivotal mediator or innocent bystander in atherogenesis? *J Clin Invest* 107:255–264
  26. Bureau F, Vanderplassen A, Jaspard F, Minner F, Pastoret PP, Merville MP, Bours V, Lekeux P (2002) Constitutive nuclear factor-kappaB activity preserves homeostasis of quiescent mature lymphocytes and granulocytes by controlling the expression of distinct Bcl-2 family proteins. *Blood* 99:3683–3691
  27. Jeremias I, Kupatt C, Baumann B, Herr I, Wirth T, Debatin KM (1998) Inhibition of nuclear factor kappaB activation attenuates apoptosis resistance in lymphoid cells. *Blood* 91:4624–4631
  28. Piret B, Piette J (1996) Topoisomerase poisons activate the transcription factor NF-kappaB in ACH-2 and CEM cells. *Nucleic Acids Res* 24:4242–4248
  29. Schoonbroodt S, Piette J (2000) Oxidative stress interference with the nuclear factor-kappa B activation pathways. *Biochem Pharmacol* 60:1075–1083
  30. Bours V, Bentires-Alj M, Hellin AC, Viatour P, Robe P, Delhalle S, Benoit V, Merville MP (2000) Nuclear factor-kappa B, cancer, and apoptosis. *Biochem Pharmacol* 60:1085–1089
  31. Webster GA, Perkins ND (1999) Transcriptional cross talk between NF-kappaB and p53. *Mol Cell Biol* 19:3485–3495
  32. Poligone B, Baldwin AS (2001) Positive and negative regulation of NF-kappaB by COX-2: roles of different prostaglandins. *J Biol Chem* 276:38658–38664
  33. Zhao GP, Zhou ZG, Lei WZ, Yu YY, Zheng XL, Gao HK (2005) Anti-inflammatory effects of polyunsaturated fatty acids in THP-1 cells. *Biochem Biophys Res Commun* 336:909–917
  34. Pontsler AV, St Hilaire A, Marathe GK, Zimmerman GA, McIntyre TM (2002) Cyclooxygenase-2 is induced in monocytes by peroxisome proliferator activated receptor gamma and oxidized alkyl phospholipids from oxidized low density lipoprotein. *J Biol Chem* 277:13029–13036
  35. Inoue H, Tanabe T, Umesono K (2000) Feedback control of cyclooxygenase-2 expression through PPARgamma. *J Biol Chem* 275:28028–28032
  36. Evans M, Geigerman C, Cook J, Curtis L, Kuebler B, McIntosh M (2000) Conjugated linoleic acid suppresses triglyceride accumulation and induces apoptosis in 3T3-L1 preadipocytes. *Lipids* 35:899–910
  37. Meadus WJ, MacInnis R, Dugan ME (2002) Prolonged dietary treatment with conjugated linoleic acid stimulates porcine muscle peroxisome proliferator activated receptor gamma and glutamine-fructose aminotransferase gene expression in vivo. *J Mol Endocrinol* 28:79–86
  38. Belury MA, Moya-Camarena SY, Lu M, Shi L, Leesnitzer LM, Blanchard SG (2002) Conjugated linoleic acid is an activator and ligand for peroxisome proliferator-activated receptor-gamma (PPAR $\gamma$ ). *Nutr Res* 22:817–824
  39. Tilley SL, Coffman TM, Koller BH (2001) Mixed messages: modulation of inflammation and immune responses by prostaglandins and thromboxanes. *J Clin Invest* 108:15–23
  40. Takashiba S, Van Dyke TE, Amar S, Murayama Y, Soskolne AW, Shapira L (1999) Differentiation of monocytes to macrophages primes cells for lipopolysaccharide stimulation via accumulation of cytoplasmic nuclear factor kappaB. *Infect Immun* 67:5573–5578
  41. Aronoff DM, Canetti C, Petrs-Golden M (2004) Prostaglandin E<sub>2</sub> inhibits alveolar macrophage phagocytosis through an E-prostanoid 2 receptor-mediated increase in intracellular cyclic AMP. *Immunol* 173:559–565
  42. Kang JH, Kim JH, Chung CS, Lee CY, Yang MP (2004) Immuno-enhancing effects of conjugated linoleic acid on phagocytosis activity of porcine peripheral blood phagocytes. *J Vet Clin* 21:336–342
  43. Kang KB, Van Der Zyp A, Iannazzo L, Majewski H (2006) Age-related changes in monocyte and platelet cyclooxygenase expression in healthy male humans and rats. *Transl Res* 148:289–94
  44. Eligini S, Colli S, Basso F, Sironi L, Tremoli E (1999) Oxidized low density lipoprotein suppresses expression of inducible cyclooxygenase in human macrophages. *Arterioscler Thromb Vasc Biol* 19:1719–1725
  45. Evans M, Park Y, Patiza M, Curtis L, Kuebler B, McIntosh M (2001) *Trans*-10, *cis*-12 conjugated linoleic acid reduces triglyceride content while differentially affecting peroxisome

- proliferator activated receptor gamma2 and aP2 expression in 3T3-L1 preadipocytes. *Lipids* 36:1223–1232
46. Umino T, Skold CM, Pirruccello SJ, Spurzem JR, Rennard SI (1999) Two-colour flow-cytometric analysis of pulmonary alveolar macrophages from smokers. *Eur Respir J* 13:894–899
  47. Marx N, Sukhova G, Murphy C, Libby P, Plutzky J (1998) Macrophages in human atheroma contain PPARgamma: differentiation-dependent peroxisomal proliferator-activated receptor gamma (PPARGamma) expression and reduction of MMP-9 activity through PPARgamma activation in mononuclear phagocytes in vitro. *Am J Pathol* 153:17–23
  48. Zapolska-Downar D, Siennicka A, Kaczmarczyk M, Kolodziej B, Naruszewicz M (2004) Butyrate inhibits cytokine-induced VCAM-1 and ICAM-1 expression in cultured endothelial cells: the role of NF-kappaB and PPARalpha. *J Nutr Biochem* 15:220–228
  49. Dembinska-Kiec A, Polus A, Kiec-Wilk B, Grzybowska J, Mikolajczyk M, Hartwich J, Razny U, Szumilas K, Banas A, Bodzioch M, Stachura J, Dyduch G, Laidler P, Zagajewski J, Langman T, Schmitz G (2005) Proangiogenic activity of beta-carotene is coupled with the activation of endothelial cell chemotaxis. *Biochim Biophys Acta* 1740:222–239
  50. Pfaffl MW (2001) A new mathematical model for relative quantification in real-time RT-PCR. *Nucleic Acids Res* 29:e45
  51. Eligini S, Stella Barbieri S, Cavalca V, Camera M, Brambilla M, De Franceschi M, Tremoli E, Colli S (2005) Diversity and similarity in signaling events leading to rapid Cox-2 induction by tumor necrosis factor-alpha and phorbol ester in human endothelial cells. *Cardiovasc Res* 65:683–693
  52. Li G, Dong B, Butz DE, Park Y, Pariza MW, Cook ME (2006) NF-kappaB independent inhibition of lipopolysaccharide-induced cyclooxygenase by a conjugated linoleic acid cognate, conjugated nonadecadienoic acid. *Biochim Biophys Acta* 1761:969–72
  53. Li G, Barnes D, Butz D, Bjorling D, Cook ME (2005) 10t, 12c-conjugated linoleic acid inhibits lipopolysaccharide-induced cyclooxygenase expression in vitro and in vivo. *J Lipid Res* 46:2134–42
  54. Wang LS, Huang YW, Liu S, Chang HL, Ye W, Shu S, Sugimoto Y, Funk JA, Smeaks DD, Hill LN, Lin YC (2006) Conjugated linoleic acid (CLA) modulates prostaglandin E2 (PGE2) signaling in canine mammary cells. *Anticancer Res* 26:889–98
  55. De Caterina R, Spiecker M, Solaini G, Basta G, Bosetti F, Libby P, Liao J (1999) The inhibition of endothelial activation by unsaturated fatty acids. *Lipids* 34:S191–S204
  56. Cheng WL, Lii CK, Chen HW, Lin TH, Liu KL (2004) Contribution of conjugated linoleic acid to the suppression of inflammatory responses through the regulation of the NF-kappaB pathway. *J Agric Food Chem* 52:71–78
  57. Inoue H, Tanabe T, Umesono K (2000) Feedback control of cyclooxygenase-2 expression through PPARgamma. *J Biol Chem* 275:28028–28032
  58. Fukushima M (1992) Biological activities and mechanisms of action of PGJ<sub>2</sub> and related compounds: an update. *Prostaglandins Leukot Essent Fatty Acids* 47:1–12
  59. Hwang DM, Kundu JK, Shin JW, Lee JC, Lee HJ, Surh YJ (2007) *cis*-9, *trans*-11-conjugated linoleic acid down-regulates phorbol ester-induced NF-kappaB activation and subsequent COX-2 expression in hairless mouse skin by targeting IkappaB kinase and PI3K-Akt. *Carcinogenesis* 28:363–371
  60. Zambon A, Gervois P, Pauletto P, Fruchart JC, Staels B (2006) Modulation of hepatic inflammatory risk markers of cardiovascular diseases by PPAR-alpha activators: clinical and experimental evidence. *Arterioscler Thromb Vasc Biol* 26:977–986

# Moderate Dietary Intake of Myristic and Alpha-Linolenic Acids Increases Lecithin-Cholesterol Acyltransferase Activity in Humans

Carole Vaysse-Boué · Henry Dabadie · Evelyne Peuchant ·  
Pascale Le Ruyet · François Mendy · Henry Gin · Nicole Combe

Received: 19 October 2006 / Accepted: 30 April 2007 / Published online: 13 June 2007  
© AOCS 2007

**Abstract** Cholesterol removal from tissues into HDL depends on the activity of lecithin-cholesterol acyltransferase (LCAT; E.C. 2.3.1.43) that is associated with lower cardiovascular diseases risk. HDL cholesterol concentration and LCAT activity can be modulated by dietary fatty acids. Original data with substrate models have shown a positive effect of myristic acid (MA) on the esterification rate of cholesterol. The purpose of this study was to examine the effect of moderate intakes of MA associated with recommended intake of alpha-linolenic acid (ALA) on LCAT activity in humans. Two experimental diets were tested for 3 months each. Diet 1-MA 1.2% of total energy (TE) and ALA 0.9% TE, diet 2-MA 1.8% and ALA 0.9% TE; a control diet (MA 1.2% and ALA 0.4% TE) was given 3 months before diet 1 and diet 2. The endogenous activity of LCAT was determined at completion of each diet. Compared with the control diet ( $13.2 \pm 3.1 \mu\text{mol CE}/(\text{L}\cdot\text{h})$ ), LCAT activity increased significantly ( $P < 0.001$ )

with diet 1 ( $24.2 \pm 3.6 \mu\text{mol CE}/(\text{L}\cdot\text{h})$ ) and diet 2 ( $33.3 \pm 7.4 \mu\text{mol CE}/(\text{L}\cdot\text{h})$ ); the increase observed with diet 2 was significantly ( $P < 0.001$ ) greater than that due to diet 1. These results suggest that ALA (from rapeseed oil, mainly in *sn*-2 position) and MA (from dairy fat, mainly in *sn*-2 position) favor LCAT activity, by respective increases of 83 and 38%. When they are supplied together, a complementary effect was observed (average increase of 152%). Moreover, these observations were associated with a decrease of the ratio of total to HDL-cholesterol. In conclusion, our results suggest that moderate supply of MA (1.8% TE) associated with the recommended intake of ALA (0.9% TE) contributes to improve LCAT activity.

**Keywords** Myristic acid · Alpha-linolenic acid · *sn*-2 position · Physiological intakes · Human study · Plasma lipid profile · LCAT activity

## Abbreviations

ACAT	Acyl-CoA:cholesterol acyltransferase
ALA	$\alpha$ -Linolenic acid
CE	Cholesteryl esters
LA	Linoleic acid
LCAT	Lecithin-cholesterol acyltransferase
MA	Myristic acid
PC	Phosphatidyl-choline
TE	Total energy

## Introduction

Lecithin-cholesterol acyltransferase (LCAT; E.C. 2.3.1.43) is an enzyme synthesized by the liver that in the blood

C. Vaysse-Boué · N. Combe (✉)  
ITERG, Département de Nutrition, c/o Université Bordeaux 1,  
Avenue des Facultés, 33405 Talence Cedex, France  
e-mail: n.combe@istab.u-bordeaux1.fr

H. Dabadie · H. Gin  
Service de Nutrition, Hôpital Haut-Lévêque,  
33600 Pessac, France

E. Peuchant  
Laboratoire de Biochimie, Hôpital Saint-André,  
33000 Bordeaux, France

P. Le Ruyet  
Lactalis Recherche & Développement,  
35240 Retiers, France

F. Mendy  
CNIEL, 75000 Paris, France

preferentially binds to HDL. Alterations in LCAT activity have been associated with changes in HDL cholesterol concentrations [1, 2]. The protective role of HDL is usually attributed to its ability to transport excess cholesterol from peripheral tissues back to the liver in a process termed reverse cholesterol transport. This reverse transport by HDL is intimately connected with the actions of LCAT, that converts cholesterol into long-chain cholesteryl esters (CE) on HDL and promotes cholesterol movement from tissues into HDL. Lecithin-cholesterol acyltransferase utilizes the *sn*-2 fatty acid of a phosphatidyl-choline (PC) molecule to convert cholesterol to CE, resulting in a shift from the particle surface to the core of HDL. The LCAT activity level depends on several factors that include dietary fatty acid composition, molecular species composition of plasma PC and specificity of LCAT towards various PC species [3]. Concerning dietary fatty acids, data from Thornburg et al. [4] have shown in monkeys that the diet composition has only small effects on the absolute amount of circulating enzyme. On the other hand, the composition of PC molecular species in circulating HDL is significantly altered by dietary fat intake. Positional specificity (>90% *sn*-2) of human LCAT has been well documented [5]. Nevertheless, when the *sn*-2 chain is very long (C20, C22), there is increased utilization of the *sn*-1 acyl chain [6, 7]. Other data indicate that the phospholipid environment in which LCAT contacts and binds its substrate may be important in determining the apparent affinity of the enzyme for any one substrate molecular species [8, 9]. Original data from Pownall et al. [8] have determined how molecular structure of PC independently regulate cholesteryl ester formation via LCAT action. Concerning dietary myristic acid (MA, 14:0), Loison et al. [10] have recently reported in hamsters a positive correlation between plasma HDL concentration and the amount of MA in the diet.

Data from two meta-analyses have shown that the SFA 12:0–16:0 [11–13], particular 14:0 [13], are far more HDL cholesterol increasing than MUFA or PUFA. Moreover, Tholstrup et al. [12] observed in humans the plasma HDL-cholesterol level was 8% higher with a diet providing 16% total energy (TE) as MA compared with a diet providing 16% TE as palmitic acid (respectively,  $1.10 \pm 0.06$  vs.  $1.01 \pm 0.05$  mmol;  $P < 0.006$ ). A recent study [14] has observed in humans an increase in HDL cholesterol concentrations by increasing SFA intake (from 8.4 to 11% TE), while plasma apo A-I concentration and LCAT activity both decreased ( $P < 0.02$ ). On the other hand, in hypertriglyceridemic patients, a high-fat diet significantly increased HDL cholesterol and LCAT, while a subsequent low-fat diet decreased HDL cholesterol and LCAT [15]. Recently, Wood et al. [16] showed that a carbohydrate restriction diet (i.e. 10% carbohydrate, 65% fat, and 25%

protein) resulted at the same time in increasing the HDL cholesterol concentration by 12% and LCAT activity by 55%, in overweight and slightly obese men.

In a previous study, we observed that intakes of MA (1.2 or 1.8% TE) and ALA (0.9% TE), both mainly provided in the *sn*-2 position of dietary triacylglycerols were associated with favourable lipoprotein and n-3 PUFA profiles [17]. These results are probably related to the protective effect of the *sn*-2 position on triacylglycerols towards fatty acid  $\beta$ -oxidation, improving the bioavailability of the fatty acid located in the *sn* position [18]. The aim of the present study was to evaluate the influence of long term moderate intakes of MA (1.2 or 1.8% TE) from dairy fat (mainly in the *sn*-2 position) associated with the recommended intake of ALA (0.9% TE) from rapeseed oil (mainly in the *sn*-2 position) on plasma LCAT activity, measured within the context of available substrate (endogenous substrate) and cofactors, due to importance of the phospholipid environment on LCAT activity.

## Materials and Methods

### Subjects

Thirty-two male monks of a Benedictine monastery (Randol Abbey) located in the center of France were enrolled for a 1 year interventional study. Twenty-nine of them were followed till the end of the study. They were between 25 and 85 years old (average, 57 years), weighed between 53 and 99 kg (average, 71 kg), and their body mass index (BMI) ranged from 28 to 18 kg/m<sup>2</sup> (average, 23 kg/m<sup>2</sup>). None of them were known to have dyslipidemia (according to NCEP ATP III) before the study and none of them were taking any lipid-lowering drug or medication affecting lipid metabolism. Most of them had a moderate amount of physical activity (e.g. working in the fields, regular walking). Physical activity and lifestyle were kept unchanged during the study. Anthropometric measurements and blood pressure were obtained for each subject at the baseline and at the end of the two dietary periods. The protocol and aim of the study were fully explained to the subjects and their written consent was taken. The research protocol was approved by the hospital ethics committee.

### Diets

The study design was described in details previously [17]. Briefly, it was the following. The study lasted 12 months, with four periods of 3 months: P<sub>3</sub>, P<sub>6</sub>, P<sub>9</sub> and P<sub>12</sub>. Twenty-nine monks consumed successively control diet (i.e. controlled fat intake of habitual diet) (P<sub>3</sub>), diet 1 (P<sub>6</sub>), control diet (P<sub>9</sub>) and finally diet 2 (P<sub>12</sub>). Control diet provided 32%

TE from fat (11% SFA, 1.2% MA), 13% MUFA and 8% PUFA, of which 5.5% LA and 0.4% ALA). Both interventional diets provided the same intake levels of SFA (11–12% TE), oleic acid (11% TE), linoleic acid (LA; 4.5% TE) and ALA (0.9% TE), but MA intakes were different in diet 1 (1.2% TE) and diet 2 (1.8% TE) (Table 1).

### Plasma Lipid Analysis

Fasting blood samples were obtained from all twenty-nine subjects at a baseline visit before the initiation of each interventional period and at the end of the two 3 months nutritional interventions. Total lipids were extracted from plasma with 5 ml hexane/isopropanol (3:2; v/v). Total cholesterol, HDL-cholesterol and triacylglycerols were analyzed enzymatically (17). LDL-cholesterol was calculated using the Friedewald equation. The apo A-I and apo B were measured using a turbidimetry method kLE LX 20.

### Plasma LCAT Activity

LCAT activity was assayed by conversion of [<sup>3</sup>H] unesterified cholesterol to [<sup>3</sup>H] esterified cholesterol, according to the method of Glomset and Wright [19]. Substrate for LCAT was prepared by incubating [<sup>3</sup>H] unesterified cholesterol–albumin suspension with heat inactivated normal human plasma (55 °C for 30 min) at 4 °C for overnight. For each determination, test plasma (75 µl) was added to 100 µl of labelled heat-treated plasma and mercaptoethanol

(0.15%, v/v) and incubated at 37 °C for 1 h. The reaction was stopped by addition of methanol and lipids were extracted three times with hexane. After evaporation of the organic solvent under nitrogen, free cholesterol and cholesterol esters were separated by thin layer chromatography developed in a hexane/diethyl ether/acetic acid (90:10:1; v/v/v). The cholesterol ester spot was visualized by exposure to iodine, transferred into liquid scintillant for measurement of radioactivity in a scintillation counter. The cholesterol-esterifying activity was expressed as micromoles of cholesterol esterified per hour per liter of plasma.

### Statistical Analysis

The Wilcoxon signed ranks test was used for comparisons of plasma lipid as described previously [17]. The LCAT activity differences in dependent variables between two experimental periods were analyzed by the Wilcoxon signed ranks test. Differences were considered significant at  $P < 0.05$ . The effect of ALA has been assessed by comparing data from baseline (control diet) and diet 1. Association ALA/MA has been analyzed by comparing data from baseline to diet 2 (Table 2).

## Results

### Plasma Lipids, Lipoproteins and Apo-Proteins (Table 2)

In comparison with the control values ( $P_3$ ) found before starting diet 1, lower concentrations of total cholesterol ( $P < 0.0001$ ), LDL-cholesterol ( $P < 0.001$ ), HDL-cholesterol ( $P < 0.05$ ) and triacylglycerols ( $P < 0.05$ ) were obtained after diet 1 ( $P_6$ ). The ratio of total to HDL-cholesterol decreased ( $P < 0.05$ ) and the ratio of apo A-I:apo B tended to increase. Compared to the previous control diet ( $P_9$ ), diet 2 was associated with a decreased concentration of triacylglycerols ( $P < 0.05$ ) and an increased HDL-cholesterol concentration ( $P < 0.05$ ); the ratio of total to HDL-cholesterol decreased ( $P < 0.05$ ). These differences were not significant by comparing with data from the first period of control diet ( $P_3$ ).

### Plasma LCAT Activity (Table 2)

In order to compare the effect of different intake levels of MA and ALA on the endogenous activity of LCAT, the cholesterol esterification rate was assessed in whole plasma at the end of each feeding period. Significant differences ( $P < 0.001$ ) in plasma LCAT activity (µmol CE formed/(L.h)) were observed between the four dietary periods. Compared to control diet (1.2% TE as MA; 0.4% TE as

**Table 1** Nutrient daily intake in control and experimental diets

	Control diet	Diet 1	Diet 2
Energy (kcal)	2,100	2,100	2,200
Fat [g (%)]	73.3 (32.0)	77.4 (33.0)	85.6 (36.0)
Saturated fat [g (%)]	24.8 (11.0)	24.4 (11.0)	29.0 (12.0)
14:0	2.9 (1.2)	2.9 (1.2)	4.0 (1.8)
16:0	12.8 (5.5)	12.9 (5.5)	13.7 (5.6)
18:0	5.7 (2.4)	5.2 (2.4)	5.4 (2.2)
Monounsaturated fat [g (%)]	30.0 (13.0)	32.3 (14.0)	35.5 (15.0)
18:1n-9	22.6 (9.7)	26.3 (11.3)	28.3 (11.6)
Polyunsaturated fat [g (%)]	19.4 (8.0)	17.4 (8.0)	17.9 (8.0)
18:2n-6	12.8 (5.5)	10.7 (4.6)	10.9 (4.5)
18:3n-3	0.8 (0.4)	2.1 (0.9)	2.1 (0.9)
20:5n-3	0.21	0.21	0.21
22:6n-3	0.54	0.54	0.54
22:6n-3/20:5n-3 ratio	2.57	2.57	2.57
18:2/18:3 ratio	15.2	5.1	5.2
Cholesterol (mg)	254.0	251.0	333.0
Carbohydrate [g (%)]	271.6 (53.0)	271.6 (52.0)	269.0 (50.0)
Protein [g (%)]	76.0 (15.0)	76.0 (15.0)	77.4 (14.0)

**Table 2** Plasma lipids, lipoproteins concentrations and LCAT activity after the two interventional diets

	Unit	Control diet (P <sub>3</sub> )	Diet 1 (P <sub>6</sub> )	Control diet (P <sub>9</sub> )	Diet 2 (P <sub>12</sub> )
Total cholesterol	mmol/L	5.38 ± 0.91	4.91 <sup>d</sup> ± 0.91	5.12 ± 0.75	5.12 ± 0.72
LDL-cholesterol		3.57 ± 0.70	3.23 <sup>c</sup> ± 0.72	3.39 ± 0.59	3.39 ± 0.57
HDL-cholesterol		1.42 ± 0.39	1.34 <sup>a</sup> ± 0.36	1.29 ± 0.28	1.37 <sup>a</sup> ± 0.28
Triglycerides		0.82 ± 0.33	0.77 <sup>a</sup> ± 0.36	0.95 ± 0.42	0.88 <sup>a</sup> ± 0.38
Total cholesterol/HDL-C		3.99 ± 1.01	3.81 <sup>a</sup> ± 0.97	4.12 ± 0.93	3.92 <sup>a</sup> ± 0.94
Apo A-I	mg/dl	163 ± 30	160 ± 26	153 ± 21	163 ± 27
Apo B		100 ± 18	95 ± 21	93 ± 17	95 ± 15
Apo A-I/Apo B		1.68 ± 0.40	1.78 ± 0.45	1.70 ± 0.38	1.76 ± 0.38
LCAT activity	μmol/h/L plasma	13.2 ± 3.1	24.2 <sup>c</sup> ± 3.6	20.7 ± 7.5	33.3 <sup>c,c</sup> ± 7.4

Results are mean ± SEM of 29 monks in each group. Values for diet 1 and diet 2 with different lowercase superscript letters are significantly different from previous control diet (P<sub>6</sub> vs. P<sub>3</sub>, P<sub>12</sub> vs. P<sub>9</sub>); values with different uppercase superscript letters are significantly different from diet 1 P values: *a* < 0.05; *b* < 0.005; *c* < 0.001; *d* < 0.0001

ALA), both experimental diets contributed to increase LCAT activity values, by 83% with diet 1 that provided more ALA (0.9% TE), and by 152% with diet 2 that provided more ALA (0.9% TE) and more MA (1.8% TE). At the end of the 2nd period of control diet (P<sub>9</sub>), LCAT activity rate remained higher than that observed after the 1st control period (P<sub>3</sub>), i.e. 20.7 ± 7.5 versus 13.2 ± 3.1 μmol CE/(L.h). Thus, compared to the 2nd control period, diet 2 led to an increase in LCAT activity lower than that compared to the 1st period (61% vs. 152%).

## Discussion

Current evidence suggests that HDL facilitates reverse cholesterol transport, a process by which LCAT allows the removal of cholesterol from tissues and its transport to the liver to be eliminated [5]. There is a positive relation between HDL cholesterol concentration and LCAT activity in plasma; these two parameters can be modulated by dietary fatty acids. Lecithin-cholesterol acyltransferase is synthesized by the liver, the molecular mechanism that regulates the plasma LCAT concentrations is not well understood. The LCAT activity level seems to depend in part on the mass of the enzyme in plasma, and in part on the substrate and cofactors available to the enzyme. However, about the mass of the enzyme, a recent study has shown that LCAT production by Hep G2 cells was unaffected by palmitic acid and shorter saturated fatty acids [20], while the increase in HDL cholesterol concentrations by dietary SFA is well documented. Thus regulation of LCAT at the gene level seems not significant in vivo. Rather, LCAT activity appears to be regulated in plasma by the surface properties of its lipoprotein substrates.

The modulation of LCAT activity in vivo depends, most likely, on changes in substrate composition and structure, in

the various natural HDL subclasses that are chemically and physically heterogeneous particles, and on the presence of activators or inhibitors. For these reasons, in order to compare LCAT activity at completion of the different experimental diets, we preferred using the method with endogenous substrate that provides real environment of the enzyme in vivo action, with important factors, as apoproteins. For instance, apoA-I appears the best activator of LCAT, but apoE, apoA-IV, and apoC-I are good activators of LCAT to the extent that, in the absence of apoA-I in vivo, they may promote significant cholesterol esterification in plasma [5]. Moreover, the relative order of activation of LCAT by apoA-I and apoC-I depends on the phospholipid vesicle quality, i.e., apoC-I appears to be a more effective activator of LCAT than apoA-I with dimyristoyl PC model vesicles, while it is the opposite with palmitoyl, palmitoyl-PC. Besides, LCAT presents a molecular and interfacial selectivity for different PCs. It seems that in general, mixed chain PC particles are the preferred substrates of LCAT, followed by disaturated PCs of increasing chain length, and by long chain polyunsaturated-PC particles.

From the results of Pownall et al. [8], it can be concluded that the LCAT binding site for the acyl donor recognizes the phosphate glycerol backbone, has some selectivity for a basic head group, but not excluding other glycerophospholipid head groups, and favors the binding of shorter, saturated, less bulky chains. Based on these observations made on models in vitro [8], the objective of the present study was to ascertain whether MA favors LCAT activity in vivo.

Previous results [17] obtained from these subjects fed the same dietary protocol have shown that intakes of MA (1.2% TE) and ALA (0.9% TE), both mainly in the *sn*-2 position of dietary triacylglycerols, were associated with favourable lipid and n-3 PUFA profiles; moreover the red blood cell membrane fluidity increased (*P* < 0.001).



The aim of the present study was to evaluate the influence of moderate intakes of MA (1.2 or 1.8% TE) associated with the recommended intake of ALA (0.9% TE), both mainly supplied through the *sn*-2 position, on the plasma LCAT activity. We determined LCAT activity according to the method of Glomset and Wright [19], with endogenous substrate that provides a measure of enzyme activity within the context of available substrate and cofactors (endogenous LCAT activity).

#### Comparison of Diet 1 versus Control Diet

The diets were very similar, except for their fatty acid composition. Compared to the control diet, the major change in diet 1 concerned the increase in ALA supply (0.9% TE vs. 0.4% TE), from rapeseed oil in the two diets. MA content in diet 1 was the same as in the control diet (1.2% TE) and had the same origin (dairy products). Diet 1 led to an increase in LCAT activity that suggests this improvement was due to the increase in ALA supply, at the recommended value, mainly through the *sn*-2 position of dietary triacylglycerols. This effect was associated with a decrease in the ratio of total to HDL-cholesterol. ALA impact on LCAT was confirmed in the next period. After diet 1, a lower ALA intake level in control diet led to a lower LCAT activity rate. At the same time, the ratio of total to HDL-cholesterol increased. However, the baseline value ( $P_3$ ) was not restored.

#### Comparison of Diet 2 versus Diet 1

Results on ALA bioavailability at the end of both control periods ( $P_3$  and  $P_9$ ), assessed through the ALA percentage in fasting plasma CE showed equivalence ( $0.65 \pm 0.27\%$  and  $0.65 \pm 0.28\%$  of total fatty acids, respectively) [17]. So, diet 2 was compared to diet 1. Diet 2 provided the same total SFA intake as the control diet and diet 1 (11–12% TE). However, in diet 2, MA supply was higher than in control diet and diet 1 (1.8% TE vs. 1.2% TE). Diet 2 provided the same intake of ALA as did diet 1 (0.9% TE), that was more than two times higher ALA intake than the control diet did (0.4% TE). Compared to the baseline (control diet), diet 2 led to a greater increase in LCAT activity than diet 1 (152 vs. 83%). This effect probably resulted from the increase in MA intake. This effect of MA, is already known but at levels much greater than 1.2 and 1.8% of TE [12, 13].

Thus, in vitro rates of cholesterol esterification found in this study show that LCAT activity increases in response to an increase in ALA or MA intake. Moreover, an increased intake in both ALA and MA caused a more pronounced increase in LCAT activity suggesting a complementary effect of ALA and MA on LCAT activity.

In response to experimental diets, fatty acid compositions of plasma phospholipids and CE were modified [17]. Diet 1 was associated with an increase in ALA, EPA, and DHA levels in phospholipids and CE. Diet 2 was associated with an increase in ALA in phospholipids and CE [17]. Our results agree with those reported by Babin et al. [21] showing that, in preterm infants, ALA levels in CE can be considered as representative of ALA dietary intakes, mainly supplied via the *sn*-2 position of dietary triacylglycerols, whereas LA levels in CE appears as a poor marker of LA intakes. The authors found the ALA percentage in CE was very significantly correlated with the ALA intake level ( $r = 0.70$ ;  $P = 0.0001$ ), whereas the LA percentage in CE was not correlated with the LA intake level ( $r = 0.17$ ;  $P = 0.31$ ).

Thornburg et al. [4] proposed that in addition to direct effects on composition of phospholipids, as observed in our study, changes in the HDL PC molecular species might occur. On the other hand, Dorfman et al. [3] have found that LCAT endogenous and exogenous activities did not differ in response to saturated relative to polyunsaturated fat in hamsters. This may be due to lower levels of apo A-I and/or other factors such as a post-translational modification of LCAT protein, or different levels of other factors that may alter enzyme activity such as apo A-II, an inhibitor of LCAT activity, emphasizing the role of LCAT environment on enzymatic reactivity. Our results suggest that ALA and MA do not act on the same level towards LCAT. Thus, ALA, because of its incorporation within “substrate” phospholipids of LCAT could improve LCAT affinity for its substrate. On the other hand, MA would act upstream, by modulating the LCAT protein amount in plasma.

Our results on the LCAT endogenous activity contrast with those found by Bérard et al. [14]. The authors compared a diet providing 11% TE as SFA with a diet that supplied a lower SFA content (8.4% TE), compensated by a higher carbohydrate content (+8%). The diet enriched in SFA led to an increase in HDL cholesterol, while plasma apo A-I concentration and the activity of LCAT both decreased. These discrepancies with our results might be explained by the method applied for assessing LCAT activity, i.e. using exogenous substrate (proteoliposome models) or endogenous substrate (plasma lipoproteins). Recently, Wood et al. [16], using an endogenous substrate method, showed increased LCAT activity and HDL cholesterol concentration, resulting from a carbohydrate restriction diet at the expense of fat. These various observations are in accordance with several mechanistic studies which have shown the importance of the phospholipid environment on LCAT activity.

In conclusion, this current study suggests there would seem to be a complementary effect between MA and ALA

in the *sn*-2 position of dietary triacylglycerols, within the framework of combined physiological intakes, that exerts a positive impact on the metabolism of plasma HDL.

**Acknowledgments** The authors are indebted to the Benedictine monks of Randol (France). They would like to thank Laurence Fonseca and Sabrina Serrano (ITERG) for technical assistance. Supported by a grant from CERIN: Centre de Recherche et d'Information Nutritionnelles, Paris (France), CNIEL Paris (France) and Lactalis Recherche et Développement, Retiers (France).

## References

- Brousseau ME, Santamarina-Fojo S, Vaisman BL, Applebaum-Bowden D, Bérard AM, Talley GD, Brewer HB Jr, Hoeg JM (1997) Overexpression of human lecithin-cholesterol acyltransferase in cholesterol-fed rabbits: LDL metabolism and HDL metabolism are affected in a gene dose-dependent manner. *J Lipid Res* 38:2537–2547
- Mehlum A, Staels B, Duverger N, Tailleux A, Castro G, Fievet C, Luc G, Fruchart JC, Olivecrona G, Skretting G, Auwerx J, Prydz H (1995) Tissue-specific expression of the human gene for lecithin-cholesterol acyltransferase in transgenic mice alters blood lipids, lipoproteins and lipases towards a less atherogenic profile. *Eur J Biochem* 230:567–575
- Dorfman SE, Wang S, Vega-López S, Jauhiainen M, Lichtenstein AH (2005) Dietary fatty acids and cholesterol differentially modulate HDL cholesterol metabolism in golden-Syrian hamsters. *J Nutr* 135:492–498
- Thornburg JT, Parks JS, Rudel LL (1995) Dietary fatty acid modification of HDM phospholipid molecular species alters lecithin-cholesterol acyltransferase reactivity in cynomolgus monkeys. *J Lipid Res* 36:277–289
- Jonas A (2000) Lecithin-cholesterol acyltransferase. *Biochem Biophys Acta* 1529:245–256
- Subbaiah PV, Liu M, Bolan PJ, Paltauf F (1992) Altered positional specificity of human plasma lecithin-cholesterol acyltransferase in the presence of *sn*-2 arachidonoyl phosphatidylcholines. Mechanism of formation of saturated cholesteryl esters. *Biochim Biophys Acta* 1128:83–92
- Subbaiah PV, Sowa JM, Davidson MH (2004) Evidence for altered positional specificity of LCAT in vivo: Studies with docosahexaenoic acid feeding in humans. *J Lipid Res* 45:2245–2251
- Pownall HJ, Pao Q, Massey JB (1985) Acyl chain and headgroup specificity of human plasma lecithin-cholesterol acyltransferase: separation of matrix and molecular specificities. *J Biol Chem* 260:2146–2152
- Jonas A (1986) Synthetic substrates of lecithin-cholesterol acyltransferase. *J Lipid Res* 27:689–698
- Loison C, Mendy F, Sérougne C, Lutton C (2002) Dietary myristic acid modifies the HDL-cholesterol concentration and liver scavenger receptor BI expression in the hamster. *Br J Nutr* 87:1–13
- Temme EMH, Mensink RP, Hornstra G (1996) Comparison of the effects of diets enriched in lauric, palmitic, or oleic acids on serum lipids and lipoproteins in healthy women and men. *Am J Clin Nutr* 63:897–903
- Tholstrup T, Marckmann P, Jespersen J, Vessby B, Jart A, Sandstrom B (1994) Effect on blood lipids, coagulation, and fibrinolysis of a fat high in myristic acid and a fat high in palmitic acid. *Am J Clin Nutr* 60:919–925
- Zock P, de Vries J, Katan M (1994) Impact of myristic acid versus palmitic acid on plasma lipids and lipoprotein levels in healthy women and men. *Arterioscler Thromb* 14:567–575
- Bérard AM, Dabadie H, Palos-Pinto A, Dumon MF, Darmon M (2004) Reduction of dietary saturated fatty acids correlates with increased plasma lecithin-cholesterol acyltransferase activity in humans. *Eur J Clin Nutr* 58:881–887
- Pieke B, Von Eckardstein A, Gulbahce E, Chirazi A, Schulte H, Assmann G, Wahrburg U (2000) Treatment of hypertriglyceridemia by two diets rich either in unsaturated fatty acids or in carbohydrates: effects on lipoprotein subclasses, lipolytic enzymes, lipid transfer proteins, insulin and leptin. *Int J Obes Relat Metab Disord* 24:1286–1296
- Wood RJ, Volek JS, Liu Y, Shachter NS, Contois JH, Fernandez ML (2006) Carbohydrate restriction alters lipoprotein metabolism by modifying VLDL, LDL, and HDL subfraction distribution and size in overweight men. *J Nutr* 136:384–389
- Dabadie H, Motta C, Peuchant E, LeRuyet P, Mendy F (2006) Variations in daily intakes of myristic and alpha-linolenic acids in *sn*-2 position modify lipid profile and red blood cell membrane fluidity. *Br J Nutr* 96:283–289
- Wang S, Koo SI (1993) Plasma clearance and hepatic utilization of stearic, myristic and hepatic utilization of stearic, myristic, and linoleic introduced via chylomicrons in rats. *Lipids* 28:697–708
- Glomset JA, Wright JL (1964) Some properties of a cholesterol esterifying enzyme in human plasma. *Biochim Biophys Acta* 89:266–276
- Fungwe TV, Kudchodkar BJ, Lacko AG, Dory L (1998) Fatty acids modulate lecithin-cholesterol acyltransferase secretion independently of effects on triglyceride secretion in primary rat hepatocytes. *J Nutr* 128:1270–1275
- Babin F, Rodriguez A, Sarda P, Vandeputte B, Mendy F, Descomps B (2000) Alpha linolenic acid in cholesterol esters: a marker of alpha-linolenic acid intake in newborns. *Eur J Clin Nutr* 54:840–843

# Supplemental Conjugated Linoleic Acid Consumption Does Not Influence Milk Macronutrient Contents in all Healthy Lactating Women

Samuel A. Mosley · Alam M. Shahin · Janet Williams · Mark A. McGuire · Michelle K. McGuire

Received: 21 December 2006 / Accepted: 7 June 2007 / Published online: 4 July 2007  
© AOCS 2007

**Abstract** The term “conjugated linoleic acid” (CLA) refers to a group of positional and geometric isomers that are derived from linoleic acid and are found primarily in meat and milk products from ruminant animals. Due to the array of putative benefits associated with various forms of CLA, there has been recent interest in supplementing human diets with these fatty acids especially when weight loss is desired. However, in many animal models, CLA has been shown to decrease milk fat production. There is some concern, therefore, that maternal CLA supplementation during lactation might inadvertently decrease nutrient supply to the nursing infant. However, there is only limited research on the effect of CLA consumption on milk fat content in women. Based on previously published work from our laboratory, we hypothesized that CLA supplementation would reduce the milk fat percentage in lactating women in a dose-dependent manner. Breastfeeding women ( $n = 12$ ) were assigned randomly to treatments of 4 g/day safflower oil (SFO), 2 g/day CLA plus

2 g/day SFO, or 4 g/day CLA in a double blind,  $3 \times 3$  Latin square design. Conjugated linoleic acid supplements contained approximately equal amounts of *cis*9,*trans*11–18:2 and *trans*10,*cis*12–18:2; the two most common isoforms of CLA. Milk was collected by complete breast expression on the last day (day 5) of each intervention period and analyzed for macronutrient and fatty acid composition. On day 4 of each intervention period, infant milk consumption was estimated by 24 h weighing of the infant. Washout periods were 9 days in length. We observed a dose-dependent increase in the concentrations of *cis*9,*trans*11–18:2 and *trans*10,*cis*12–18:2 in the milk fat. However, we detected neither a change in overall macronutrient composition nor infant milk consumption. These data do not support those obtained from animal models or our previous human work suggesting that consumption of CLA mixtures necessarily reduces milk fat. It is possible that either (1) the interpretation of our previously published data should be reevaluated, and/or (2) there are important intra- and inter-species differences in this regard.

S. A. Mosley · M. A. McGuire  
Department of Animal and Veterinary Sciences,  
University of Idaho, Moscow, ID 83843-2330, USA

A. M. Shahin · J. Williams · M. K. McGuire (✉)  
Department of Food Science and Human Nutrition,  
Washington State University,  
Pullman, WA 99164-6376, USA  
e-mail: smcguire@wsu.edu

*Present Address:*

A. M. Shahin  
Texas A & M University, College Station,  
TX 77843-2476, USA

*Present Address:*

J. Williams  
Department of Animal and Veterinary Sciences,  
University of Idaho, Moscow, ID 83843-2330, USA

**Keywords** Breastfeeding · Lactation · Conjugated linoleic acid · Milk fat · Human milk · Dietary supplement

## Abbreviations

BMI Body mass index  
CLA Conjugated linoleic acid  
SFO Safflower oil

## Introduction and Hypotheses

The term “conjugated linoleic acid” (CLA) refers to a group of positional and geometric isomers of linoleic acid

(18:2n-6) derived in the human diet primarily from meat and milk products from ruminant animals [1]. Interest in various CLA isomers has grown substantially in the past decade, primarily due to the finding that the *cis*9,*trans*11–18:2 isomer inhibits mammary cancer in animal models and cell culture systems [2–5]. In fact, the National Research Council in 1996 stated that CLA (or forms, thereof) is the only fatty acid shown unequivocally to inhibit carcinogenesis in experimental animals [6]. In addition to having anticarcinogenic properties, investigators using mixed isomers of CLA have reported antiatherosclerotic properties, effects on glucose tolerance, alterations in growth or body composition, and milk fat depression [7–12]. Some studies also suggest adverse effects of CLA on health such as those relating to decreasing HDL cholesterol, Lp(a), and endothelial function [13–15]. It is now generally accepted that different isomers of CLA have a wide variety of biological effects; some being potentially health-promoting and others being detrimental [16].

Aside from the potential to influence human health, there is also much interest in understanding the potential effects of CLA isomers in animal agriculture. For example, studies suggest that the *trans*10,*cis*12–18:2 (but not *cis*9,*trans*11–18:2) isomer of CLA is a potent inhibitor of milk fat synthesis in cows and mice [11, 17]. As such, consumption or infusion of commercially-produced CLA (mixed isomers) imparts milk fat depressing effects in cows and rats [18, 19]. These commercially available CLA mixtures often contain equal amounts of *trans*10,*cis*12 and *cis*9,*trans*11–18:2 isomers as well as other minor isomeric forms [20, 21].

Because of the myriad possible benefits of CLAs (e.g., their anticarcinogenic and antiadipogenic effects), there has been much interest in supplementing human diets with these fatty acids. Indeed, CLA supplements are readily available for purchase at many pharmacies and “health food” stores. However, one concern with consumption of CLA mixture preparations is the possibility that it might reduce milk fat in lactating women, ultimately causing reduced nutrient supply to the nursing infant. Unfortunately, studies of the effects of CLA in lactating women are limited and unclear. For example, work from our laboratory suggests a decreased milk fat percentage when women consume a commercially available CLA mixture as compared to an olive oil placebo [12]. However, data from other studies suggest that increased CLA intake from naturally CLA-enriched cheese (in which the predominant CLA isomer was *cis*9,*trans*11–18:2) does not alter milk fat percentage [22–24]. Thus, there exists limited but not completely convincing evidence that some, but not all, forms of CLA might decrease milk fat in women. Clearly, in order to understand the health implications of CLA supplementation in this important segment of the population, more research is required.

As such, the objective of this work was to further investigate the impact of consumption of mixed isomers of CLA on milk composition in lactating women. Specifically, we hypothesized that intake of commercially-available CLA supplements would reduce milk fat percentage in a dose-dependent manner. It is noteworthy that this study was specifically designed as an experimentally similar follow-up experiment to that done by us previously [12].

## Materials and Methods

### Subjects

Healthy, non-pregnant, lactating women ( $n = 12$ ) were recruited from the Moscow, ID and Pullman, WA area. Inclusion criteria were the following: (1) 6–10 months postpartum, (2) breastfeeding at least four times per day, and (3) feeding supplemental foods to their infants. It is noteworthy that, because our hypothesis predicted that our treatment would result in milk fat depression, we did not enroll women who were exclusively breastfeeding their infants. However, we systematically emphasized the importance of continuing to feed their infants on-demand during the duration of the study. These eligibility criteria were required by our Institutional Review Board.

Upon enrollment, subjects completed a questionnaire providing general information concerning maternal and infant health, and baseline measures of height and weight from subjects and their infants were recorded (Table 1). Maternal adiposity was estimated using dual-energy X-ray absorptiometry (DEXA, Hologic QDR 4500 Acclaim Series), and body mass index (BMI) was calculated (Table 1). A urine-based pregnancy test was administered to subjects to confirm non-pregnant status before each DEXA scan. The Washington State University Institutional Review

**Table 1** Demographic and anthropometric variables of women ( $n = 12$ ) and their infants at the time of enrollment

Variable	Mean $\pm$ SEM
<b>Maternal</b>	
Age (year)	28.1 $\pm$ 1.2
Weight (kg)	72.5 $\pm$ 3.8
Height (cm)	165.9 $\pm$ 1.5
BMI (kg/m <sup>2</sup> )	26.3 $\pm$ 1.3
Body fat (%)	33.5 $\pm$ 1.2
Parity (#)	1.8 $\pm$ 0.2
<b>Infant</b>	
Age (week)	31.6 $\pm$ 1.3
Weight (kg)	9.0 $\pm$ 0.9
Length (cm)	68.7 $\pm$ 0.7

Board approved all procedures used in this study, and informed consent was obtained from all subjects.

### Experimental Design and Dietary Treatment

Subjects were assigned randomly to a treatment sequence in a  $3 \times 3$  Latin square design. In this way, each subject received each treatment and carry-over effects were controlled for. This study was conducted as a double-blind trial in which neither subjects nor investigators knew of the treatment sequence until the study was completed. Intervention periods were 5 days in length, with intervening 9 day washout periods.

During intervention periods, subjects ingested supplements containing safflower oil (SFO; Cognis Corp., LaGrange, IL, USA) and/or CLA (Tonalin<sup>®</sup> SG1000C; Cognis Corp., LaGrange, IL, USA) such that there were three treatments: 4 g/day SFO (considered the placebo or control period), 2 g/day SFO and 2 g/day CLA (considered the 2 g CLA period), and 4 g/day CLA (considered the 4 g CLA period). The SFO contained predominantly linoleic acid (18:2n-6), while *cis*9,*trans*11–18:2 and *trans*10,*cis*12–18:2 were the major fatty acids in the CLA supplements (Table 2). Subjects consumed approximately 1,263 and 2,527 mg/day CLA from the supplements during the 2 g/day and 4 g/day CLA interventions, respectively (Table 2). Subjects were asked to consume the supplements between 0700 and 0800 hours each day of each intervention period.

### Milk Collection

Milk samples were collected on the day immediately preceding the first intervention period, on the final day of each

**Table 2** Major fatty acid composition (% of total lipid) of safflower oil (SFO) and conjugated linoleic acid (CLA) capsules used in this study and total intake (mg/day) of these fatty acids during intervention periods from these capsules

Fatty acid	Individual capsules		Daily intake from capsules		
	SFO (% of total lipid)	CLA	SFO (mg/day)	2 g CLA	4 g CLA
16:0	6.45	1.85	258.0	166.1	74.2
18:0	2.37	2.57	94.9	99.0	103.0
<i>cis</i> 9–18:1	12.23	11.09	489.1	466.4	443.7
<i>cis</i> 9, <i>cis</i> 12–18:2	72.05	0.53	2,882.0	1,451.6	21.1
<i>cis</i> 9, <i>trans</i> 11–18:2	ND	31.42	ND	628.7	1257.4
<i>trans</i> 10, <i>cis</i> 12–18:2	ND	31.70	ND	634.3	1268.5

During intervention periods, subjects ingested 4 g/day SFO (control period), 2 g/day SFO and 2 g/day CLA (2 g CLA period), or 4 g/day CLA (4 g CLA period)

ND not detectable

washout period, and on day 5 of each intervention period between 1300 and 1500 hours by complete breast expression using an electric breast pump provided by us (model SMR-B-R, Ameda-Egnell Inc., Cary, IL, USA) or one owned by the subject and with which she was comfortable. To decrease variability due to between-breast differences, breast fullness, and changes in milk composition over a breastfeeding bout, milk was always obtained from the same breast, at least 2 h after the previous feeding, and until milk flow ceased. Milk was stored at  $-80^{\circ}\text{C}$  until further analysis. Infant milk consumption was estimated on day 4 of each intervention period by weighing the infant before and after each nursing for a 24 h period.

### Milk Analysis

Milk lipids were extracted by a modified Folch procedure using chloroform:methanol (2:1), and percent lipid was determined gravimetrically for all milk samples prior to the methylation procedure [25]. Extracted lipids from day 0 and 5 of each period were methylated using base catalyzed transesterification [26]. The fatty acid methyl esters (FAME) were analyzed on a gas chromatograph (Hewlett-Packard 6890 Series with auto injector) fitted with a flame ionization detector and a  $100\text{ m} \times 0.25\text{ mm}$ , with  $0.2\text{ }\mu\text{m}$  film, capillary column (SP-2560; Supelco, Bellefonte, PA, USA). The identities of fatty acid peaks were established by comparing retention times to a mixture of 19 FAME (NuChek, Elysian, MN, USA) and a CLA mixture reference standard (Matreya, Pleasant Gap, PA, USA).

Protein and lactose concentrations of milk were measured spectrophotometrically using the Bio-Rad<sup>®</sup> Protein Assay kit (Bio-Rad Laboratories; Hercules, CA, USA) and the lactose assay procedure described by Polberger and Lönnerdal, respectively [27]. Cholesterol content of milk samples was determined using a modified procedure of Fletouris et al. [28].

### Statistical Analysis

Mean and variance estimates for maternal and infant descriptive statistics were generated using the “univariate procedure” of SAS (SAS v 9.1, Cary, NC, USA). Milk composition, milk yield, and fatty acid data were analyzed as a  $3 \times 3$  Latin square using the “mixed procedure” of SAS. Sources of variation in the model included effects due to subject, period (reflecting order of treatment), treatment (placebo vs. 2 g CLA vs. 4 g CLA) and residual error. To help control for subject variability, pretreatment milk composition values from samples collected on the day immediately preceding the first intervention period or on the last day of the preceding washout period for the second

and third intervention periods were used as covariates in the statistical analysis.

To investigate the possible interaction between maternal body composition and treatment on milk composition, subjects were also separated into high (% body fat > 34% or BMI > 27 kg/m<sup>2</sup>) and low (% body fat < 33% or BMI < 25 kg/m<sup>2</sup>) body fat or BMI, and this variable was initially tested statistically. However, body fat designation was eventually removed from the model due to lack of interactive or main effect. Similarly, there was no effect of order of treatment (entered in the model as “period”), although this variable was retained in all final models. Interactions were considered significant at  $P \leq 0.10$ , and main effects and individual differences at  $P \leq 0.05$ .

## Results

### Effect of Treatment on Infant Milk Consumption and Milk Composition

Milk consumption and composition data in each treatment period are provided in Table 3. Although infant milk consumption on day 4 of each intervention period was variable, ranging from 605 to 707 g/day, there was no overall effect of dietary intervention nor were their individual differences between treatments. Similarly, on day 5 of each intervention period mean milk fat percentages were similar regardless of treatment and ranged from 4.2 to 4.8% (wt:wt; SEM = 0.5%). Likewise, regardless of dose, CLA supplementation did not affect milk protein, lactose, or cholesterol content on day 5.

### Milk Fatty Acid Composition

There were few alterations in the composition of fatty acids in milk fat (Table 4). However, *cis9,trans11–18:2* was

**Table 3** Estimated infant milk consumption (day 4) and milk composition (day 5) from women ( $n = 12$ ) consuming the placebo (safflower oil) or conjugated linoleic acid (CLA) supplements; data represent means and pooled SEM

Variable	Placebo	2 g CLA	4 g CLA	SEM
Milk consumption (g/day)	605	674	707	70.2
Milk composition				
Fat (%)	4.5	4.8	4.2	0.5
Protein (mg/ml)	8.4	8.8	8.7	0.5
Lactose (mg/ml)	60.3	60.8	63.8	1.8
Cholesterol (mg/dl)	14.8	15.7	13.8	1.1

During intervention periods, subjects ingested 4 g/day SFO (control period), 2 g/day SFO and 2 g/day CLA (2 g CLA period), or 4 g/day CLA (4 g CLA period)

increased ( $P < 0.02$ ) when subjects consumed 2 g/day CLA compared with they consumed the placebo (SFO). There was also a tendency ( $P = 0.11$ ) for *cis9,trans11–18:2* to be further increased when subjects consumed 4 g/day CLA compared with 2 g/day CLA. Similarly, *trans10,cis12–18:2* in milk fat increased ( $P < 0.03$ ) when subjects consumed 2 g/day CLA compared to they consumed the placebo. Again, there was a tendency ( $P = 0.09$ ) for 4 g/day CLA to further increase *trans10,cis12–18:2* compared with 2 g/day CLA. There were no other observed differences in fatty acid composition of milk due to treatment.

## Discussion

Results from the study presented here lead us to reject our a priori hypothesis that consumption of a supplement containing mixed CLA isomers necessarily results in milk fat depression in women; let alone in a dose-dependent manner. Clearly, these results present us and others studying the putative physiologic effects of CLA with a series of intellectual and logistic challenges. For example, were there important differences in subjects, experimental design, laboratory procedures, or statistical analysis between our previous study [12] and the one reported here that might explain these disparate and unexpected findings? Or are there factors of which we are unaware that might

**Table 4** Milk fatty acid profiles (mean and pooled SEM; % of total fatty acids) from women consuming the placebo (safflower oil) or conjugated linoleic acid (CLA)

Fatty acid	Placebo	2 g CLA	4 g CLA	SEM
8:0	0.18	0.19	0.21	0.01
10:0	1.34	1.40	1.43	0.05
12:0	5.49	5.59	5.84	0.41
14:0	6.58	6.30	6.53	0.45
14:1	0.22	0.21	0.21	0.02
15:0	0.36	0.36	0.34	0.02
16:0	22.26	21.69	21.51	0.53
16:1	2.39	2.21	2.42	0.13
18:0	8.17	8.53	8.29	0.38
18:1	32.58	33.99	33.01	0.86
<i>cis9,cis12–18:2</i>	16.68	15.47	15.18	0.73
<i>cis9,trans11–18:2</i>	0.49 <sup>a</sup>	0.90 <sup>b</sup>	1.15 <sup>b</sup>	0.11
<i>trans10,cis12–18:2</i>	0.10 <sup>a</sup>	0.42 <sup>b</sup>	0.63 <sup>b</sup>	0.09
18:3n-6	0.11	0.11	0.11	0.01
18:3n-3	1.33	1.08	1.24	0.14

During intervention periods, subjects ingested 4 g/day SFO (control period), 2 g/day SFO and 2 g/day CLA (2 g CLA period), or 4 g/day CLA (4 g CLA period)

<sup>a,b</sup> Means within a row not sharing common superscripts differ ( $P < 0.05$ )

interact with CLA consumption to influence its effect on milk fat content in women? As such, the remainder of this manuscript will discuss these issues and venture a conclusion as to why the findings are so clearly different than what we had hypothesized. Further, we discuss what might be investigated in the future to tease out the apparently complex and variable physiologic effects of CLA and other biologically active fatty acids on milk fat in humans.

First, we must examine the issue of whether differences in subject characteristics and/or experimental design might have possibly resulted in disparate findings between previously published work and that presented here. Compared to the women studied by Masters et al. [12] some of whom were still exclusively breastfeeding their infants; the subjects in the current study were approximately 2 months later in lactation, producing approximately 200 g/day more milk, and producing milk with substantially higher (~50%) milk fat. These differences were due largely to the as previously discussed, ethical considerations requiring that we study only women nursing older infants being fed significant amounts of supplementary foods. It is certainly possible that these factors (time postpartum, milk output, overall milk fat content, and infant feeding practices) might independently and/or interactively modulate the potential for CLA to influence milk fat. For example, the milk fat-depressing effects of CLA might only be experienced by women during the first months of lactation, or those producing milk of lower milk fat. Future studies might be designed to test these possibilities.

There were also slight differences in BMI between the two studies. Masters et al. [12] reported a mean BMI of 23.4 kg/m<sup>2</sup> compared with 26.3 kg/m<sup>2</sup> in the current study (% body fat was not measured by Masters et al. [12]). Consequently, it is possible that higher body fat content attenuates the potential negative effect of CLA on milk fat in humans. Interestingly, body fat content has been repeatedly shown to be related to milk fat in humans, although the mechanisms driving this association are unclear [29, 30]. Previous work from our group, in fact, has suggested the possibility of an interaction between body fat percentage and intake of other *trans* fatty acids on total milk fat in humans [21]. In that study, data indicated that women with lower body fat (<30% body fat) consuming high levels of *trans* fatty acids produced milk with lower ( $P < 0.05$ ) milk fat percentage when compared to when they consumed low levels of *trans* fatty acids. In contrast, milk fat of women with higher body fat (>30% body fat) was not responsive to *trans* fatty acid intake. It is noteworthy that the average body fat content of the women enrolled in the present study was 33.5%, a level that may have been high enough to counteract the potential milk fat depressing effects of the CLA isomers studied (both of which are *trans* fatty acids). We have also observed

*trans*10,*cis*12–18:2 induced milk fat depression in food-restricted (lean), but not ad libitum-fed, lactating rats (Mosley et al, unpublished data). However, we statistically tested for an interaction between treatment and body fat percent on milk fat in the present study and found no such association. Nonetheless, we believe that there might exist a physiologic interaction between body composition and CLA consumption on milk fat, and future studies should be designed such that the variation in body fat content of subjects is large enough to test this interaction more directly.

There are also several differences in experimental design between our previous study [12] and that presented here that might help to explain the disparate findings. As previously discussed, in the present study we were only allowed to study women who were feeding significant amounts of supplementary and complementary food to their breastfeeding infants; the past study allowed the enrollment of exclusively-breastfeeding women in earlier lactation. It is possible that, in later lactation and/or at a higher milk production level, the mammary gland is able to compensate for any milk-fat depressing effects that may occur due to CLA consumption. As such, it is quite possible that different recommendations concerning consumption of mixed CLA supplements should be made to lactating women depending upon their particular stage of lactation and milk production level. This would fit well with the current nutritional sciences and public health concept of “personalized diet prescriptions” [31]. Clearly, a one-size-fits-all approach to the study of nutrition and health including the effects of CLA is likely not optimal.

Another potentially important difference between our previous and present work is the choice of material used in the “placebo” supplement. The major fatty acid in the placebo (olive oil) used by Masters et al. [12] was oleic acid (18:1), whereas linoleic acid (18:2n-6) was the predominant fatty acid in the SFO placebos used here. Interestingly, we did not originally consider this a significant change in design. Instead, we simply made this change because in fact the CLA found in our supplements is chemically derived from SFO, and we felt that this “placebo” more closely mirrored our treatment capsules. However, we had no reason to believe prior to the initiation of the present study that using a different “placebo” would alter our results. Nonetheless, it is possible that the placebo used by Masters et al. [12] actually induced an increase in milk fat percentage, thus importantly changing the possible interpretation of the results reported for that study. Clearly, the only way to test this hypothesis is to conduct an additional intervention study designed to examine the effect of olive oil on milk fat; in this case it would be our recommendation that the placebo used be void of any fatty

acids or other known or potentially biologically active compounds.

Other possible differences between the previous and present studies include CLA dosages, duration of treatment and washout periods, number of subjects, and sampling schedules. In our previous work, subjects consumed 560 and 547 mg/day of *trans*10,*cis*12–18:2 and *cis*9,*trans*11–18:2, respectively. Because the study reported here was designed as a follow-up to the previous one, our lower dose (2 g CLA) provided similar amounts of CLA isomers (634 and 629 mg/day of *trans*10,*cis*12–18:2 and *cis*9,*trans*11–18:2, respectively). Thus, we do not believe that our dosage was insufficient. Further, both studies employed similar treatment durations (5 days), and the present study actually had longer washout periods (9 vs. 7 days, respectively). In addition, compared to our previous work, the present study had more women ( $n = 10$  vs. 12, respectively) and used the more powerful Latin square design instead of a simple cross-over, suggesting that statistical power was actually enhanced in this study. In addition, we used the exact same milk sampling schedules and procedures in both studies. We do not believe, therefore, that any of these factors were responsible for differences in study results.

Another issue that is always a concern when interpreting data collected in a human intervention trials is compliance. Indeed, there is no intervention if there is no compliance. In both studies, we relied on milk fatty acid values as our indicator of compliance as this measure is a sensitive gauge of dietary intake especially for minor fatty acids such as the CLA isomers. Our biochemical data suggest a high level of subject compliance both in the present study and in that conducted previously by us. In the study reported here, consumption of mixed isomers of CLA resulted in increased concentrations of *cis*9,*trans*11–18:2 and *trans*10,*cis*12–18:2 isomers of CLA in milk lipid in a dose-dependent fashion. Masters et al. [12] reported similar increases in the concentrations of *trans*10,*cis*12–18:2 and *cis*9,*trans*12–18:2 in milk. This suggests that, although these studies differ in their findings of a potential milk fat lowering effect of CLA mixtures, consumption of CLA mixtures resulted in somewhat similar effects on milk fatty acid profiles. These data again suggest that there may be a yet undescribed modulating factor that can either attenuate or enhance the potential milk-fat depressing effects of CLA in some women.

Thus, although the results obtained from the present study do not support our initial hypotheses, they raise important questions for future study. For example, were the conclusions made by Masters et al. [12] that CLA supplementation causes milk fat depression misinterpretations of the data, because the real effect was actually a milk fat-enhancing one of olive oil? Additionally, is there an interaction between maternal body fat content and CLA

intake on milk fat percentage? Clearly, because commercially-available CLA supplements are widely available for promotion of weight loss (something that is highly desirable in many postpartum women), understanding their effects on milk fat content in both lean and overweight lactating women is of both public health and scientific importance.

**Acknowledgments** The authors would like to sincerely thank the women and children who participated in this study. This research was supported in part by USDA NRI # 2000–01188, Washington State Dairy Products Commission, Center of Biomedical Research Excellence (COBRE) Grant # P20 RR15587, and Cognis Corp., LaGrange, IL, USA

## References

1. Pariza MW, Park Y, Cook ME (2000) Mechanisms of action of conjugated linoleic acid: evidence and speculation. *Proc Soc Exp Biol Med* 223:8–13
2. Ip C, Chin SF, Scimeca JA, Pariza MW (1991) Mammary cancer prevention by conjugated dienoic derivative of linoleic acid. *Cancer Res* 51:6118–6124
3. Ip C, Singh M, Thompson HJ, Scimeca JA (1994) Conjugated linoleic acid suppresses mammary carcinogenesis and proliferative activity of the mammary gland in the rat. *Cancer Res* 54:1212–1215
4. Shultz TD, Chew BP, Seaman WR, Lueddecke LO (1992) Inhibitory effect of conjugated dienoic derivatives of linoleic acid and  $\beta$ -carotene on the in vitro growth of human cancer cells. *Cancer Lett* 63:125–133
5. Cesano A, Visonneau S, Scimeca JA, Kritchevsky D, Santoli D (1998) Opposite effects of linoleic acid and conjugated linoleic acid on human prostate cancer in SCID mice. *Anticancer Res* 18:833–838
6. National Research Council (1996) *Carcinogens and anticarcinogens in the human diet*. National Academy Press, Washington
7. Lee KN, Kritchevsky D, Pariza MW (1994) Conjugated linoleic acid and atherosclerosis in rabbits. *Atherosclerosis* 108:19–25
8. Houseknecht KL, Vanden Heuvel JP, Moya-Camarena SY, Portocarrero CP, Peck LW, Nickel KP, Belury MA (1998) Dietary conjugated linoleic acid normalizes impaired glucose tolerance in the Zucker diabetic fatty *falfa* rat. *Biochem Biophys Res Commun* 244:678–682
9. Chin SF, Storkson JM, Albright KJ, Cook ME, Pariza MW (1994) Conjugated linoleic acid is a growth factor for rats as shown by enhanced weight gain and improved feed efficiency. *J Nutr* 124:2344–2349
10. Belury MA, Kempa-Steczko A (1997) Conjugated linoleic acid modulates hepatic lipid composition in mice. *Lipids* 32:199–204
11. Baumgard LH, Corl BA, Dwyer DA, Saebo A, Bauman DE (2000) Identification of the conjugated linoleic acid isomer that inhibits milk fat synthesis. *Am J Physiol* 278:R179–R184
12. Masters N, McGuire MA, Beerman KA, Dasgupta N, McGuire MK (2002) Maternal supplementation with CLA decreases milk fat in humans. *Lipids* 37:133–138
13. Taylor JS, Williams SR, Rhys R, James P, Frenneaux MP (2006) Conjugated linoleic acid impairs endothelial function. *Arterioscler Thromb Vasc Biol* 26:307–312
14. Nakanishi T, Oikawa D, Koutoku T, Hirakawa H, Kido Y, Tachibana T, Furuse M (2004) Gamma-linolenic acid prevents conjugated linoleic acid-induced fatty liver in mice. *Nutrition* 20:390–393



15. Javadi M, Beynen AC, Hovenier R, Lankhorst A, Lemmens AG, Terpstra AH, Geelen MJ (2004) Prolonged feeding of mice with conjugated linoleic acid increases hepatic fatty acid synthesis relative to oxidation. *J Nutr Biochem* 15:680–687
16. McGuire MA, McGuire MK (2000) Conjugated linoleic acid (CLA): a ruminant fatty acid with beneficial effects on human health. *Proc Am Soc Anim Sci* 1999
17. Loor JJ, Lin X, Herbein JH (2003) Effects of dietary *cis*9, *trans*11–18:2, *trans*10, *cis*12–18:2, or vaccenic acid (*trans*11–18:1) during lactation on body composition, tissue fatty acid profiles, and litter growth in mice. *Br J Nutr* 90:1039–1048
18. Chouinard PY, Corneau L, Barbano DM, Metzger LE, Bauman DE (1999) Conjugated linoleic acids alter milk fatty acid composition and inhibit milk fat secretion in dairy cows. *J Nutr* 129:1579–1584
19. Ringseis R, Saal D, Müller A, Steinhart H, Eder K (2004) Dietary conjugated linoleic acids lower the triacylglycerol concentration in the milk of lactating rats and impair the growth and increase the mortality of their suckling pups. *J Nutr* 134:3327–3334
20. Sehat N, Kramer J, Mossoba MM, Yurawecz MP, Roach JAG, Eulitz K, Morehouse KM, Ku Y (1998) Identification of conjugated linoleic acid isomers in cheese by gas chromatography, silver ion high performance liquid chromatography and mass reconstructed ion profiles. Comparison of chromatographic elution sequences. *Lipids* 33:963–971
21. Yurawecz MP, Sehat N, Mossoba MM, Roach JAG, Kramer JKG, Ku Y (1999) Variations in isomer distribution in commercially available conjugated linoleic acid. *Fett/Lipid* 101:277–282
22. Ritzenthaler KL, McGuire MK, McGuire MA, Shultz TD, Koepf AE, Luedecke LO, Hanson TW, Dasgupta N, Chew BP (2005) Consumption of conjugated linoleic acid (CLA) from CLA-enriched cheese does not alter milk fat or immunity in lactating women. *J Nutr* 135:422–430
23. Park Y, McGuire MK, Behr R, McGuire MA, Evans MA, Schultz TD (1999) High-fat dairy product consumption increases  $\Delta^9c,11t-18:2$  (rumenic acid) and total lipid concentrations of human milk. *Lipids* 34:543–549
24. Anderson NK, Beerman KA, McGuire MA, Dasgupta N, Griinari JM, Williams J, McGuire MK (2005) Dietary fat type influences total milk fat content in lean women. *J Nutr* 135:416–421
25. Clark RM, Ferris AM, Fey M, Brown PB, Hundricser KE, Jensen RG (1982) Changes in the lipids of human milk from 2–16 weeks postpartum. *J Pediatr Gastroenterol Nutr* 1:311–315
26. Christie WW (1982) A simple procedure for rapid transmethylation of glycerolipids and cholesteryl esters. *J Lipid Res* 23:1072–1075
27. Polberger S, Lönnnerdal B (1993) Simple and rapid macronutrient analysis of human milk for individualized fortification: basis for improved nutritional management of very-low-birth-weight infants? *J Pediatr Gastroenterol Nutr* 17:283–290
28. Fletouris DJ, Botsoglou NA, Psomas IE, Mantis AI (1998) Rapid determination of cholesterol in milk and milk products by direct saponification and capillary gas chromatography. *J Dairy Sci* 81:2833–2840
29. Barbosa L, Butte NF, Villalpando S, Wong WW, Smith EO (1997) Maternal energy balance and lactation performance of Mesoamericans as a function of body mass index. *Am J Clin Nutr* 66:575–583
30. Prentice AM, Goldberg GR, Prentice A (1994) Body mass index and lactation performance. *Eur J Clin Nutr* 48:S78–S86
31. Watkins SM, Hammock BD, Newman JW, German JB (2001) Individual metabolism should guide agriculture toward foods for improved health and nutrition. *Am J Clin Nutr* 74:283–286

# Generation of ENU-Induced Mouse Mutants with Hypocholesterolemia: Novel Tools for Dissecting Plasma Lipoprotein Homeostasis

Bernhard Aigner · Birgit Rathkolb · Manuela Mohr ·  
Martina Klempt · Martin Hrabé de Angelis ·  
Eckhard Wolf

Received: 3 April 2007 / Accepted: 10 May 2007 / Published online: 7 June 2007  
© AOCS 2007

**Abstract** Pathologic plasma lipoprotein cholesterol levels play a key role in the development and pathogenesis of human atherosclerotic cardiovascular diseases. Plasma cholesterol homeostasis is regulated by genetic predispositions and environmental factors. Animal models showing aberrant plasma cholesterol levels are used for the identification and analysis of novel causative genes. Here, we searched for inherited hypocholesterolemia phenotypes in randomly mutant mice which may contribute to the detection of disease protective alleles. In the Munich ENU mouse mutagenesis project, clinical chemistry blood analysis was carried out on more than 15,500 G1 offspring and 230 G3 pedigrees of chemically mutagenized inbred C3H mice to detect dominant and recessive mutations leading to a decreased plasma total cholesterol level. We identified 66 animals consistently showing hypocholesterolemia. Transmission of the altered phenotype to the subsequent generations led to the successful establishment of 14 independent hypocholesterolemic lines. Line-specific differences were detected by clinical chemistry analysis of plasma HDL cholesterol, LDL cholesterol and triglycerides. Thus, we successfully established a novel panel of ENU-derived mutant mouse lines for their use in the identification of alleles selectively influencing the plasma

cholesterol homeostasis. Such findings may be subsequently used for humans and other species.

**Keywords** Cholesterol · Ethylnitrosourea · HDL · LDL · Phenotype-driven screen

## Introduction

Animal models are used to examine the causes as well as the pathogenesis and potential therapeutic strategies for multifactorial and polygenic human diseases. Development of atherosclerotic cardiovascular disease is influenced by dyslipidemia including increased values of the normal proportion of low density lipoprotein cholesterol (LDL-C) and high density lipoprotein cholesterol (HDL-C). Beneath a subset of rare monogenic forms, pathologic cholesterol levels often occur as a polygenic and multifactorial disorder [1–4]. Humans show predominantly LDL-C and are sensitive to diet-induced elevations of LDL-C. In contrast, mice exhibit high amounts of HDL-C and a low LDL-C level [5, 6]. Therefore, instead of acting as model to enlighten the pathogenesis of human cardiovascular diseases, mice are the animal model of choice to search for additional alleles influencing the plasma lipoprotein cholesterol homeostasis.

Phenotype-driven strategies for the genome-wide search of causative loci are carried out by examining the genetic polymorphisms which result in different plasma lipoprotein phenotypes of the already existing mouse strains as well as by the generation of novel mutant lines harbouring altered plasma lipoprotein levels. Mapping of genetic determinants of plasma cholesterol levels in independent and combined crosses of inbred mouse strains has been used to establish a mouse map of quantitative trait loci (QTL) controlling

B. Aigner (✉) · B. Rathkolb · M. Mohr ·  
M. Klempt · E. Wolf  
Institute of Molecular Animal Breeding and Biotechnology,  
Ludwig-Maximilians-University Munich, Hackerstr. 27,  
85764 Oberschleißheim, Germany  
e-mail: b.aigner@gen.vetmed.uni-muenchen.de

M. Hrabé de Angelis  
Institute of Experimental Genetics,  
GSF Research Center for Environment and Health,  
85764 Neuherberg, Germany

HDL-C levels. Confirmation of most QTL in different crosses indicated the saturation of the mouse QTL map. The high degree of concordance between mouse and human QTL suggested that the underlying genes may be the same. Narrowing the genomic regions and further molecular genetic analyses will reveal the responsible polymorphisms both in mice and humans [7, 8]. In addition, genetic polymorphisms of heterogeneous stock mice influencing the total cholesterol level were examined by high-resolution whole-genome association studies of quantitative traits [9].

Random mutagenesis of the mouse genome and subsequent phenotypic analysis of the animals for defined alterations are carried out in various mouse mutagenesis programs using the chemical ethylnitrosourea (ENU) [10]. Specific pathologic states have been identified by appropriate routine procedures allowing the screening of large numbers of mice for a broad spectrum of parameters [11, 12]. In the Munich ENU mouse mutagenesis project, a screening profile of clinical chemistry blood parameters was established for the analysis of offspring of chemically mutagenized inbred C3H mice in order to detect phenotypic variants with defects of diverse organ systems or changes in metabolic pathways. Breeding of the affected mice and screening of the offspring confirmed the transmission of the altered phenotype to the subsequent generations, thereby revealing a mutation as cause for the aberrant phenotype [13, 14]. Mutant lines from the Munich ENU project with the causative mutation already identified are successfully used in different areas of biomedical research (e.g., [15, 16]).

We recently described the establishment of nine ENU-induced mutant lines with heritable hypercholesterolemia [17]. Here we report the generation and phenotypic description of mutant lines exhibiting primary hypocholesterolemia. These lines increase the panel of novel mouse mutants available for dissecting the genetic control of plasma cholesterol homeostasis.

## Experimental Procedure

### Mutagenesis and Breeding of Mice

The experiments were carried out on the inbred C3HeB/FeJ (C3H) genetic background as described [17]. Ten-week-old male mice (=generation G0) were injected intraperitoneally with ENU ( $3 \times 90$  mg/kg in weekly intervals).

The screen for dominant mutations was performed on G1 animals, which were derived from the mating of the mutagenized G0 males to wildtype C3H females. Inheritance of the observed abnormal phenotype was tested on G2 mice which were derived from the mating of the

affected G1 mouse exhibiting the altered phenotype and wildtype mice.

The screen for recessive mutations was carried out on G3 mice produced in a two-step breeding scheme from G1 mice. G1 males, which were excluded to exhibit dominant mutations by phenotypic analysis, were mated to wildtype females for the production of G2 animals. Subsequently, 6–8 G2 females were backcrossed to the G1 male to produce the G3 mice of the pedigree. The analysis of the inheritance of an observed abnormal phenotype in G3 mice was done on G5 mice. Therefore, the affected G3 mouse presumably harbouring a homozygous recessive mutation was mated to a wildtype mouse for the production of the presumably heterozygous mutant G4 mice with an inconspicuous phenotype. Subsequently, the G5 mice derived from the mating of G4 mice to each other were tested for the abnormal phenotype. Alternatively, G5 mice derived from the backcross of a G4 mouse to the affected G3 animal were examined.

After the identification of the causative mutation, the internal names of the established lines will be replaced according to the official nomenclature. Mouse husbandry was done under a continuously controlled specific pathogen-free (SPF) hygiene standard according to the FELASA protocols (<http://www.felasa.org>) [18]. Standard rodent diet (Altromin, Lage, Germany) and water were provided ad libitum. All animal experiments were carried out under the approval of the responsible animal welfare authority (Regierung von Oberbayern).

### Clinical Chemistry Analysis

Blood samples from 3-month-old G1 and G3 mice fasted overnight were obtained by puncture of the retroorbital sinus under ether anesthesia. Physiologic parameter values were determined in male and female C3H controls. Plasma from Li-heparin treated blood was analyzed using an Olympus AU400 autoanalyzer (Olympus, Hamburg, Germany) and the adapted reagents (Olympus). Calibration and quality control were performed according to the manufacturer's protocols. Total cholesterol, HDL-C and LDL-C were examined by enzymatic colorimetry tests using the reagents OSR6116, OSR6187 and OSR6183 (Olympus) with the linear measurement ranges of 25–700 mg/dl, 2–180 mg/dl and 10–400 mg/dl, respectively, for human samples.

In addition, the primary clinical chemistry screen included the following plasma parameters: substrates—creatinine, glucose, total protein, triglycerides, urea, uric acid; electrolytes—calcium, chloride, inorganic phosphorus, potassium, sodium; enzymes—alanine aminotransferase, alkaline phosphatase, aspartate aminotransferase, creatine kinase.

## Statistical Analysis

The statistical analysis of the data was carried out using the software program Microsoft Excel 2000 (Microsoft, Redmond, WA). Values are presented as means and standard deviations unless stated otherwise. Statistical significance (defined as  $P < 0.05$ ) was evaluated using Student's *t* test.

## Results

### Plasma Total Cholesterol in C3H Control Mice

Plasma total cholesterol was determined in 3-month-old inbred C3H mice after overnight fasting of the animals [17]. Four hundred and seventy male animals showed a range of 78–171 mg/dl (mean  $\pm$  standard deviation  $132 \pm 15$  mg/dl), whereas 407 females showed a range of 56–180 mg/dl ( $109 \pm 17$  mg/dl). The 95% range of the values (100–161 mg/dl in males and 76–141 mg/dl in females) corresponded to the data range including two standard deviations above and below the mean, which indicated the Gaussian distribution of the data. The values within this range were defined to be physiologic thereby eliminating outlier data [5]. Thus, hypocholesterolemia was defined in our analysis for male and female mice showing values below the cut-off levels of 100 and 75 mg/dl, respectively, in two measurements within a 3-week interval (Fig. 1).

### ENU-Induced Phenotypic Variants Showing Decreased Plasma Total Cholesterol

In the Munich ENU mouse mutagenesis project, more than 15,500 3-month-old G1 offspring of ENU-treated mice were screened for dominant mutations. About 60% of the mice screened for dominant mutations were male animals. Thirty-six male and 12 female mice showed decreased

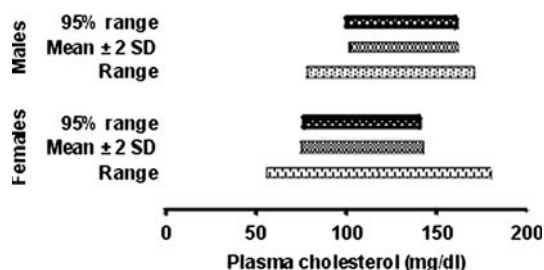


**Fig. 1** Physiologic range of plasma total cholesterol (mg/dl) in 3-month-old C3H wildtype mice. The mean values are 132 mg/dl in males ( $n = 470$ ) and 109 mg/dl in females ( $n = 407$ ). 100 and 75 mg/dl were chosen as cut-off level in males and females, respectively, to detect hypocholesterolemia

plasma total cholesterol levels which were confirmed in a second sample taken 3 weeks later. The means of the two samples ranged between 64 and 98 mg/dl in the male phenotypic variants and between 44 and 70 mg/dl in the female phenotypic variants. For revealing recessive mutations, over 6,500 3-month-old G3 offspring were examined from more than 230 different pedigrees of ENU-treated animals. Eight male and ten female mice exhibited decreased plasma total cholesterol levels, with means of the two measurements ranging between 79 and 95 mg/dl and between 11 and 75 mg/dl, respectively (Table 1).

### Transmission of Hypocholesterolemia to the Subsequent Generations

The analysis of the inheritance of the hypocholesterolemic phenotype was carried out on G2 offspring from the mating of 25 G1 phenotypic variants to wildtype mice in the screen for dominant mutations and on G4 intercross or G4  $\times$  G3 backcross offspring after breeding 9 G3 phenotypic variants to wildtype mice in the screen for recessive mutations. When no offspring were generated, the phenotypic variants were mated to another wildtype animal. Sperm was cryo-conserved from most of the male phenotypic variants where no confirmation cross was set up (Table 1). Twenty of the 34 phenotypic variants (59%) mated produced no or negative offspring. The female phenotypic variant exhibiting 11 mg/dl plasma total cholesterol in both measurements also produced no offspring (Table 2). The observed illness and/or sterility in the phenotypic variants with no offspring may be due to pleiotropic effects of the mutations, to negative consequences of the decreased cholesterol levels on the reproductive system of the affected mice and/or to the appearance of additional detrimental mutations.

Fourteen of the 34 mated mice showing hypocholesterolemia (41%) produced phenotypic mutant offspring. Heritable hypocholesterolemia was diagnosed when plasma total cholesterol values below the cut-off level (male 100 mg/dl; female 75 mg/dl) were detected in offspring of the phenotypic variants in two measurements performed in a 3-weeks interval. Additional successful production of phenotypic mutant offspring was done with three animals (one G3 male, one G1 female and one G3 female) exhibiting plasma cholesterol levels in the first measurement above the cut-off level. Thus, in total 17 hypocholesterolemic mutants were obtained. However, the three female G3 mutants were derived from the same ENU-mutagenized G0 founder (Table 2).

The majority of the hypocholesterolemic founder mice showed no obvious deviations in the additional clinical chemistry plasma parameters measured (see “[Experimental Procedure](#)”) and also appeared normal in the general

**Table 1** Screen and analysis of the inheritance for hypocholesterolemia in ENU-mutagenized mice

	Dominant screen (G1) <sup>a</sup>	Recessive screen (G3)	Total
Animals examined	>15,500	ND	
Pedigrees examined	ND	>230	
Variants <sup>b</sup> : <i>n</i> (m/f)	48 (36/12)	18 (8/10)	66 (44/22)
Variants mated: <i>n</i> (m/f)	25 (17/8)	9 (1/8)	34 (18/16)
Mutants <sup>c</sup> : <i>n</i> (m/f)	13 (8/5)	4 (1/3 <sup>d</sup> )	17 (9/8)

*m/f* Males/females, *ND* not determined

<sup>a</sup> 60% of the G1 mice screened for dominant mutations were male animals

<sup>b</sup> G1/G3 offspring of ENU-treated mice showing hypocholesterolemia (male ≤ 100 mg/dl, female ≤ 75 mg/dl) in two measurements of a 3-weeks interval

<sup>c</sup> The numbers of the mutants include three mice (one G3 male, one G1 female and one G3 female) which did not appear as mated variants because their plasma cholesterol level of the first measurement was above the cut-off level. Offspring were produced by mating the G1 phenotypic variants to wildtype mice (screen for dominant mutations) and from G4 intercross or G4 × G3 backcross approaches after breeding the G3 phenotypic variants to wildtype mice (screen for recessive mutations). Heritable hypocholesterolemia was diagnosed when offspring of the phenotypic variants occurred showing cholesterol levels below the cut-off level (male 100 mg/dl, female 75 mg/dl) in two measurements of a 3-weeks interval

<sup>d</sup> The three female G3 mutants were derived from the same ENU-mutagenized G0 founder

clinical examination. Thus, most lines harbour mutations in genes which do not cause hypocholesterolemia secondary to preceding alterations in other metabolic pathways, but primarily and selectively influence the plasma cholesterol homeostasis.

Breeding of the 17 confirmed mutants resulted in the successful establishment of 12 hypocholesterolemic lines harbouring dominant mutations (lines CHOLD01–D12) and three hypocholesterolemic lines harbouring recessive mutations (lines CHOLR01A, CHOLR01B, CHOLR02). Two additionally established lines from one G1 founder and one G3 founder were not preserved and, therefore, lost. The G3 founder mutants of the two lines CHOLR01A and CHOLR01B were derived from the same ENU-mutagenized G0 founder, therefore, both lines may have the same causative mutation. This may be tested by breeding heterozygous mutants between the lines.

Mutant offspring showing hypocholesterolemia below the cut-off level (male 100 mg/dl; female 75 mg/dl) were produced by mating heterozygous mutants to wildtype animals in the lines CHOLD01–D12 and by breeding heterozygous mutant mice in the lines CHOLR01–R02. The male and female phenotypic mutants of the 15 lines (Table 3) showed mean plasma total cholesterol levels between 62 and 95 mg/dl and between 53 and 68 mg/dl,

**Table 2** Transmission of hypocholesterolemia to the offspring of the male (*n* = 18) and female (*n* = 16) phenotypic variants mated

Plasma cholesterol (mg/dl)	Male variants		Female variants	
	Negative <sup>a</sup>	Mutants	Negative <sup>a</sup>	Mutants <sup>b</sup>
100	D			
95	D	D(R <sup>c</sup> )		
90	DDDDR			
85	D	DDD		
80	DD			(D <sup>c</sup> )
75		DDD	R	(R <sup>c</sup> )
70			D	DD
65		D	RRR	DRR
60			D	
55			D	
50				D
45			DR	
40				
35				
<30			R	
<i>n</i>	10	8 (+1)	10	6 (+2)

The phenotypic variants are classified according to their mean plasma total cholesterol level (mg/dl) of the two measurements. Animals within a range of 5 mg/dl plasma cholesterol were grouped

*D* phenotypic variants derived from the screen for dominant mutations, *R* phenotypic variants derived from the screen for recessive mutations

<sup>a</sup> Variants producing no offspring are included

<sup>b</sup> The three female G3 mutants (R) were derived from the same ENU-mutagenized G0 founder

<sup>c</sup> The three mutants exhibiting plasma cholesterol levels in the first measurement above the cut-off level are shown additionally in parentheses

respectively. In the lines CHOLD01–D12 harbouring dominant mutations, no homozygous mutant animals were produced to date.

Viable knock-out mice have been established as low-cholesterol and high-desmosterol model with the reduction of the liver and brain cholesterol levels by more than 90% and virtually undetectable plasma cholesterol levels with the consequence of exhibiting a relatively mild phenotype [19, 20]. Compared to these almost “cholesterol-free” mice [19], our lines showed “intermediate” levels of hypocholesterolemia.

The phenotypic penetrance of the decreased total cholesterol levels in the 15 lines was analyzed by defining 100% phenotypic penetrance in the case of the appearance of 50 and 25% hypocholesterolemic offspring after mating phenotypic mutants to wildtype mice in the lines with dominant mutations and after crossing heterozygous phenotypic mutant mice in the lines with recessive mutations, respectively. Without taking into account the sampling

**Table 3** Phenotypic penetrance and extent of hypocholesterolemia in the 15 preserved mutant lines

Line <sup>a</sup>	mg/dl <sup>b</sup>	Offspring tested <sup>c</sup> : <i>n</i> (m/f)	Hypocholesterolemia <sup>d</sup> (m/f)				Established generations
			<i>n</i>	% Penetrance	Range (mg/dl)	Mean (mg/dl)	
CHOLD01	64	47 (28/19)	22 (15/7)	94 (100/74)	59–90/44–65	75/56	4
CHOLD02	65	63 (33/30)	31 (20/11)	98 (100/73)	55–100/49–75	78/64	4
CHOLD03	66	65 (30/35)	29 (13/16)	89 (87/91)	70–100/54–75	85/65	5
CHOLD04	67	48 (26/22)	22 (13/9)	92 (100/82)	67–100/48–74	81/63	4
CHOLD05	72	142 (75/67)	56 (35/21)	79 (93/63)	66–99/52–74	89/68	4
CHOLD06	72	72 (38/34)	17 (6/11)	47 (32/65)	60–99/29–75	81/63	6
CHOLD07	74	63 (29/34)	24 (13/11)	76 (90/65)	56–96/51–75	83/64	4
CHOLD08	75	35 (20/15)	16 (11/5)	91 (100/67)	82–100/44–68	93/62	3
CHOLD09	81	77 (47/30)	28 (17/11)	73 (72/73)	59–98/37–68	78/59	3
CHOLD10	81	34 (19/15)	18 (10/8)	100 (100/100)	69–89/48–60	75/53	3
CHOLD11	84	14 (6/8)	7 (5/2)	100 (100/50)	78–91/60–66	86/63	2
CHOLD12	91	68 (27/41)	8 (4/4)	24 (30/20)	89–100/60–72	95/66	3
CHOLR01A	65	44 (21/23)	13 (9/4)	100 (100/70)	22–97/25–76	68/60	6
CHOLR01B	68	51 (25/26)	19 (11/8)	100 (100/100)	17–90/20–74	62/53	8
CHOLR02	79	35 (18/17)	10 (7/3)	100 (100/71)	66–96/45–69	82/60	7

*m/f* Males/females

<sup>a</sup> CHOL, line showing hypocholesterolemia; D01–D12, dominant mutation; R01–R02, recessive mutation. The G3 founder mutants of the lines CHOLR01A and CHOLR01B were derived from the same ENU-mutagenized G0 founder. The established lines from the G1 founder mutant 10039669f and the G3 founder 10136667f were not preserved

<sup>b</sup> The mutant lines are listed according to the mean plasma total cholesterol level (mg/dl) of both measurements of the founder G1/G3 mutant of the line. For the founders of the lines D06, R01B and R02, the values of the second measurement are shown as the first measurement was above the cut-off level

<sup>c</sup> Offspring after mating heterozygous mutants to wildtype mice in the lines with dominant mutations and offspring of heterozygous mutant mice in the lines with recessive mutations

<sup>d</sup> Hypocholesterolemia in the offspring was defined by the appearance of total cholesterol levels below the cut-off level (male 100 mg/dl, female 75 mg/dl) in two subsequent measurements. 100% phenotypic penetrance is defined in our breeding scheme by the appearance of 50 and 25% hypocholesterolemic offspring in the lines harbouring a dominant and recessive mutation, respectively

variation, a high phenotypic penetrance of hypocholesterolemia was observed in 13 of the 15 lines which facilitates the effective subsequent phenotypic and molecular genetic analyses. The two lines CHOLD06 and CHOLD12 showed a low phenotypic penetrance. Both males and females showed a similar degree of the phenotypic penetrance within the lines. All mutant lines except of CHOLD11 were bred for multiple generations without losing their mutant phenotype. In all 15 preserved lines, the numbers of animals exhibiting plasma cholesterol levels below the cut-off level were significantly ( $\chi^2$ -test,  $P < 0.001$ ) higher than the expected 2.5% of the C3H mouse population (Table 3).

#### Additional Clinical Chemical Analysis of the Mutant Lines

For the detailed analysis of the hypocholesterolemic alteration, HDL-C and LDL-C levels were measured in the phenotypic mutants of ten selected lines. The proportions of HDL-C and LDL-C to the plasma total cholesterol levels were determined in the male and female phenotypic

mutants and compared to sex-matched littermate controls. The physiologic ranges greatly varied between the lines and/or analyses (mean value  $\pm$  standard deviation of HDL-C 78  $\pm$  3% to 95% in males and 77  $\pm$  7% to 96  $\pm$  4% in females; LDL-C 7  $\pm$  0.2% to 13  $\pm$  2% in males and 9  $\pm$  0.4% to 14% in females). Compared to the control values, the phenotypic mutants showed line- and/or sex-specific HDL-C and LDL-C values where the expected complementary shifts of the HDL-C and LDL-C proportions appeared in most of the 18 separate analyses (data not shown). The detection of the HDL-C values was carried out with reagents for human samples and included immunoinhibition steps (Olympus) which may result in species-specific inaccuracies and overestimation of the HDL-C values. In addition, some of the LDL-C measurements fell below the linear measurable range. In most cases the examination of additional mutants has to be carried out to obtain significant results. This may be done best after the causative mutation is discovered.

In humans, low HDL-C appears as a typical symptom of diabetic dyslipidemia together with hypertriglyceridemia

[21–23]. Therefore, the plasma parameters triglyceride and glucose were determined in the phenotypic mutants. The mean values of the phenotypic mutants within the litters were compared to the mean values of the sex-matched littermate controls. In most lines, the phenotypic mutants of both sexes showed lower mean triglyceride values in the majority of the litters examined. Abnormal lipid metabolism may affect the blood cholesterol levels in these lines. However, in line CHOLD07 the phenotypic mutants of both sexes showed higher triglyceride values. None of the mutant lines displayed significant elevations in plasma glucose which eliminates the possibility that the hypocholesterolemia phenotypes result as a consequence of diabetic dyslipidemia (data not shown).

## Discussion

High-throughput screening of a large number of randomly mutant mice for hypocholesterolemia resulted in the establishment of 14 independent lines harbouring dominant or recessive mutations in genes involved in the control of cholesterol levels. Most of the mutant lines showed selectively decreased plasma total cholesterol levels without obvious disturbances in any of the other metabolic pathways investigated, suggesting that the affected genes play a specific role for the regulation of cholesterol homeostasis.

In humans, primary hypolipoproteinemia is increasingly diagnosed in the course of population screening for high plasma cholesterol. Individuals with primary low plasma cholesterol levels normally do not seem to have any disadvantage unless the decrease is profound, e.g., as in abetalipoproteinemia. Indeed, their relative freedom from cardiovascular disease may lead to longevity. However, the discovery of the crucial role of cholesterol in human embryogenesis and the identification of several inherited rare disorders of cholesterol biosynthesis showed that hypocholesterolemia may have mild to severe consequences for human development and health [24]. Existence of mouse models enabled the detailed analysis of the pathophysiology of these disorders [25, 26]. Secondary symptomatic hypolipoproteinemia occurs more often due to acquired diseases such as malignancies or malabsorption [1]. In addition, hypocholesterolemia is discussed as a factor of predisposition for certain diseases [27]. Thus, our established panel of hypocholesterolemic lines may be used not primarily in the analysis of human hypocholesterolemic alterations but contribute to the detection of alleles protecting from atherosclerotic cardiovascular disease.

From more than 15,500 G1 offspring and G3 mice from over 230 pedigrees examined in the clinical chemistry

screen of the Munich ENU mouse mutagenesis program [13, 14], more than half of all mutants found with plasma substrate abnormalities in our screen showed an abnormal total cholesterol level (Rathkolb et al. unpublished results). This confirms the involvement of a large number of genes in the homeostasis of the blood cholesterol level.

Our previous screen for hypercholesterolemia resulted in the establishment of nine ENU-induced mutant lines. Breeding of almost ten phenotypic variants was necessary to establish one mutant line with hypercholesterolemia in this project. Three of the nine lines showed a low phenotypic penetrance of the mutation. In eight lines, the hypercholesterolemic mutants showed no other gross abnormalities indicating that the lines most likely harbour mutations in genes which primarily and selectively influence the plasma cholesterol homeostasis [17].

Compared to the breeding approaches for the establishment of ENU-derived mutant lines exhibiting hypercholesterolemia, transmission of hypocholesterolemia from the phenotypic variants to the offspring was successful in more than every third mating and, therefore, more efficient. Cryo-conserved sperm from the not yet mated phenotypic male G1/G3 variants may be used for the production of additional hypocholesterolemic lines. The penetrance of the mutant phenotype usually was high. As tendency, it increased with the age of the mice (not shown). The high phenotypic penetrance may be due to the correct choice of the cut-off level to define hypocholesterolemia. Our studies indicate that low plasma cholesterol phenotypes are more reproducible than high cholesterol phenotypes.

Extensive variations in the plasma cholesterol concentrations have been found in different genetic backgrounds (<http://www.jax.org/phenome>; <http://www.eumorphia.org>) [28]. Therefore, generation and subsequent analysis of hybrids and/or congeneric strains will give rise to variations in the appearance of hypocholesterolemia. In addition to our screen in the Munich ENU mouse mutagenesis project, the appearance of dislipidemic lines was reported in another ENU project. The lines were produced on a different genetic background (BALB/c × C3H) where additional mutations may occur to cause hypocholesterolemia [29].

Prerequisite for the selection of candidate genes is the determination of the chromosomal position of the causative mutation in every mouse line by linkage analysis. Therefore, two backcross generations are produced using a second inbred strain, and the subsequent offspring are phenotypically classified into mutant and non-mutant animals. Using a genome-wide polymorphic marker set, linkage analysis of the DNA samples will then reveal the chromosomal position of the mutation.

In this study we describe the successful establishment of 14 independent hypocholesterolemic lines in the Munich ENU mouse mutagenesis project. Due to the triggering of

random mutations by ENU, new genes and/or alleles not yet known to be involved in the plasma cholesterol metabolism may be discovered by molecular genetic analysis of our mouse mutants. In summary, we successfully established a novel panel of ENU-derived mutant mouse lines for their subsequent use in the identification of alleles influencing the plasma cholesterol homeostasis in humans and other species.

**Acknowledgments** This work was supported by the German Human Genome Project (DHGP) and the National Genome Research Network (NGFN) (MHdA, EW).

## References

- Greiling H, Gressner AM (1995) Lehrbuch der Klinischen Chemie und Pathobiochemie. Schattauer, Stuttgart
- Rader DJ, Cohen J, Hobbs HH (2003) Monogenic hypercholesterolemia: new insights in pathogenesis and treatment. *J Clin Invest* 111:1795–1803
- Dastani Z, Engert JC, Genest J, Marcil M (2006) Genetics of high-density lipoproteins. *Curr Opin Cardiol* 21:329–335
- Watkins H, Farrall M (2006) Genetic susceptibility to coronary artery disease: from promise to progress. *Nat Rev Genet* 7:163–173
- Loeb WF, Quimby FW (1999) The clinical chemistry of laboratory animals. Taylor & Francis, Philadelphia
- Dietschy JM, Turley SD (2002) Control of cholesterol turnover in the mouse. *J Biol Chem* 277:3801–3804
- Wang X, Paigen B (2005) Genetics of variation in HDL cholesterol in humans and mice. *Circ Res* 96:27–42
- Wittenburg H, Lyons MA, Li R, Kurtz U, Wang X, Mossner J, Churchill GA, Carey MC, Paigen B (2006) QTL mapping for genetic determinants of lipoprotein cholesterol levels in independent and combined crosses of inbred mouse strains. *J Lipid Res* 47:1780–1790
- Valdar W, Solberg LC, Gauguier D, Burnett S, Klenerman P, Cookson WO, Taylor MS, Rawlins JN, Mott R, Flint J (2006) Genome-wide genetic association of complex traits in heterogeneous stock mice. *Nat Genet* 38:879–887
- Beckers J, Hrabe de Angelis M (2002) Large-scale mutational analysis for the annotation of the mouse genome. *Curr Opin Chem Biol* 6:17–23
- Hrabe de Angelis M, Flaswinkel H, Fuchs H, Rathkolb B, Soewarto D, Marschall S, Heffner S, Pargent W, Wuensch K, Jung M, Reis A, Richter T, Alessandrini F, Jakob T, Fuchs E, Kolb H, Kremmer E, Schaeble K, Rollinski B, Roscher A, Peters C, Meitinger T, Strom T, Steckler T, Holsboer F, Klopstock T, Gekeler F, Schindewolf C, Jung T, Avraham K, Behrendt H, Ring J, Zimmer A, Schughart K, Pfeffer K, Wolf E, Balling R (2000) Genome-wide, large-scale production of mutant mice by ENU mutagenesis. *Nat Genet* 25:444–447
- Nolan PM, Peters J, Strivens M, Rogers D, Hagan J, Spurr N, Gray IC, Vizer L, Brooker D, Whitehill E, Washbourne R, Hough T, Greenaway S, Hewitt M, Liu X, McCormack S, Pickford K, Selley R, Wells C, Tymowska-Lalanne Z, Roby P, Glenister P, Thornton C, Thaug C, Stevenson JA, Arkell R, Mburu P, Hardisty R, Kiernan A, Erven A, Steel KP, Voegelings S, Guenet JL, Nickols C, Sadri R, Nasse M, Isaacs A, Davies K, Browne M, Fisher EM, Martin J, Rastan S, Brown SD, Hunter J (2000) A systematic, genome-wide, phenotype-driven mutagenesis programme for gene function studies in the mouse. *Nat Genet* 25:440–443
- Rathkolb B, Decker T, Fuchs E, Soewarto D, Fella C, Heffner S, Pargent W, Wanke R, Balling R, Hrabe de Angelis M, Kolb HJ, Wolf E (2000) The clinical-chemical screen in the Munich ENU Mouse Mutagenesis Project: screening for clinically relevant phenotypes. *Mamm Genome* 11:543–546
- Rathkolb B, Fuchs E, Kolb HJ, Renner-Muller I, Krebs O, Balling R, Hrabe de Angelis M, Wolf E (2000) Large-scale *N*-ethyl-*N*-nitrosourea mutagenesis of mice—from phenotypes to genes. *Exp Physiol* 85:635–644
- Vreugde S, Erven A, Kros CJ, Marcotti W, Fuchs H, Kurima K, Wilcox ER, Friedman TB, Griffith AJ, Balling R, Hrabe de Angelis M, Avraham KB, Steel KP (2002) Beethoven, a mouse model for dominant, progressive hearing loss DFNA36. *Nat Genet* 30:257–258
- Hafezparast M, Klocke R, Ruhrberg C, Marquardt A, Ahmad-Annuar A, Bowen S, Lalli G, Witherden AS, Hummerich H, Nicholson S, Morgan PJ, Oozageer R, Priestley JV, Averill S, King VR, Ball S, Peters J, Toda T, Yamamoto A, Hiraoka Y, Augustin M, Korthaus D, Wattler S, Wabnitz P, Dickneite C, Lampel S, Boehme F, Peraus G, Popp A, Rudelius M, Schlegel J, Fuchs H, Hrabe de Angelis M, Schiavo G, Shima DT, Russ AP, Stumm G, Martin JE, Fisher EM (2003) Mutations in dynein link motor neuron degeneration to defects in retrograde transport. *Science* 300:808–812
- Mohr M, Klempt M, Rathkolb B, Hrabe de Angelis M, Wolf E, Aigner B (2004) Hypercholesterolemia in ENU-induced mouse mutants. *J Lipid Res* 45:2132–2137
- Nicklas W, Baneux P, Boot R, Decelle T, Deeny AA, Fumanelli M, Illgen-Wilcke B (2002) Recommendations for the health monitoring of rodent and rabbit colonies in breeding and experimental units. *Lab Anim* 36:20–42
- Wechsler A, Brafman A, Shafir M, Heverin M, Gottlieb H, Damari G, Gozlan-Kelner S, Spivak I, Moshkin O, Fridman E, Becker Y, Skaliter R, Einat P, Faerman A, Bjorkhem I, Feinstein E (2003) Generation of viable cholesterol-free mice. *Science* 302:2087
- Brown AJ (2004) Of cholesterol-free mice and men. *Curr Opin Lipidol* 15:373–375
- Taskinen MR (2003) Diabetic dyslipidaemia: from basic research to clinical practice. *Diabetologia* 46:733–749
- Rohrer L, Hersberger M, von Eckardstein A (2004) High density lipoproteins in the intersection of diabetes mellitus, inflammation and cardiovascular disease. *Curr Opin Lipidol* 15:269–278
- Semenkovich CF (2006) Insulin resistance and atherosclerosis. *J Clin Invest* 116:1813–1822
- Waterham HR (2002) Inherited disorders of cholesterol biosynthesis. *Clin Genet* 61:393–403
- Nwokoro NA, Wassif CA, Porter FD (2001) Genetic disorders of cholesterol biosynthesis in mice and humans. *Mol Genet Metab* 74:105–119
- Herman GE (2003) Disorders of cholesterol biosynthesis: prototypic metabolic malformation syndromes. *Hum Mol Genet* 12:R75–R88
- Perez-Guzman C, Vargas MH (2006) Hypocholesterolemia: a major risk factor for developing pulmonary tuberculosis? *Med Hypotheses* 66:1227–1230
- Paigen K, Eppig JT (2000) A mouse phenome project. *Mamm Genome* 11:715–717
- Hough TA, Nolan PM, Tsipouri V, Toye AA, Gray IC, Goldsworthy M, Moir L, Cox RD, Clements S, Glenister PH, Wood J, Selley RL, Strivens MA, Vizer L, McCormack SL, Peters J, Fisher EM, Spurr N, Rastan S, Martin JE, Brown SD, Hunter AJ (2002) Novel phenotypes identified by plasma biochemical screening in the mouse. *Mamm Genome* 13:595–602



## Seasonal Variations of Lipid Content and Composition in *Perna viridis*

Duo Li · Yonghua Zhang · Andrew J. Sinclair

Received: 13 February 2006 / Accepted: 11 May 2007 / Published online: 19 June 2007  
© AOCS 2007

**Abstract** The total lipid content, composition of main lipid classes, composition of sterols and composition of fatty acids in the main glycerolipids of *Perna viridis* were analyzed through four seasons using TLC-FID and GLC. Mussel samples were collected during different seasons between 2003 and 2004 from Shengsi Island, Zhejiang Province, China and stored frozen prior to freeze-drying and lipid extraction. Ten grams of dried mussel powder of each season were analyzed. Total lipid content ranged from 14.5 g/100 g in spring month to 7.8 g/100 g dried mussel powder in autumn month. The predominant lipid in spring month was triacylglycerol (TAG), however, in the other three seasons the phospholipids (PL) was the main lipid class. The most abundant fatty acid in TAG, PL and phosphatidylcholine (PC) was 16:0, with the summer samples having the highest proportion (24–30% of total fatty acid) and winter the lowest (14–22%). In phosphatidylethanolamine (PE), the spring samples had the highest proportions of 16:0. The predominant polyunsaturated fatty acids (PUFA) were 22:6n-3 and 20:5n-3 in TAG, PL, PE and PC (25–40%). The proportions of 22:6n-3 and 20:5n-3 were higher in spring than in other seasons in PL and PE. There were nine sterols identified, with cholesterol being the predominant sterol, and other main ones were desmosterol/brassicasterol and 24-methylenecholesterol. Proportions of other fatty acids in different lipid fractions and the sterol compositions as well also varied seasonally.

There were subject to the seasonal variations. Differences in lipid content and composition, fatty acid composition in different lipid fractions may be caused by multiple factors such as lifecycle, sex, variation of plankton in different seasons and temperature, which could influence physiological activities and metabolism.

**Keywords** Chinese mussel (*Perna viridis*) · Lipid content · Sterol · Fatty acid · Polyunsaturated fatty acids · Triacylglycerol · Phosphatidylethanolamine · Phosphatidylcholine

### Abbreviations

PL	Phospholipids
TAG	Triacylglycerol
SE	Sterol ester
PC	Phosphatidylcholine
PE	Phosphatidylethanolamine
NZGLM	New Zealand Green Lipped Mussel ( <i>Perna canaliculus</i> )
TBM	Tasmanian Blue Mussel ( <i>Mytilus edulis</i> )
TMSi	Trimethylsilyl
BSTFA	<i>N, O</i> -bis-trimethylsilyl-trifluoroacetamide
FFA	Free fatty acid
PUFA	Polyunsaturated fatty acid
MUFA	Monounsaturated fatty acid
SFA	Saturated fatty acid

D. Li (✉) · Y. Zhang  
Department of Food Science and Nutrition,  
Zhejiang University, Hangzhou, China 310029  
e-mail: duoli@zju.edu.cn

A. J. Sinclair  
School of Applied Sciences, RMIT University,  
Melbourne, Australia

### Introduction

Mussels are easily cultured shellfish, which are cultivated worldwide. Mussels are widely distributed in China, and they

have been consumed for thousands of years. It is a significant source of long chain PUFA, especially n-3 PUFA, in China.

Qing et al. [1] analyzed lipid content and fatty acid composition of soft body, digestive gland and gonad in *Perna viridis*, and samples were cultured and collected in spring in Guangdong, China. The lipid content was significantly higher in the digestive gland than the soft body and gonad. Fatty acid composition was not significantly different between the three tissues, with the predominant fatty acid being 16:0, other main fatty acids were 20:5n-3, 16:1 and 22:6n-3.

Total lipid and phospholipid (PL) content in *Mytilus edulis* (Linne), samples were collected in Qingdao China, varied from the highest in March (spring) to the lowest in December (winter) and September (autumn), respectively. Major fatty acids in PL were 16:0, 20:5n-3 and 22:6n-3 [2].

Murphy et al. [3] examined the total lipid content, sterol and fatty acid compositions in the New Zealand Green Lipped Mussel (*Perna canaliculus*, NZGLM) and Tasmanian Blue Mussel (*Mytilus edulis*, TBM) (both species of mussels were collected in October, late spring). The predominant lipid was PL in both NZGLM and TBM. Cholesterol was the major sterol. The main fatty acids were 16:0, 20:5n-3 and 22:6n-3 in both species. In a later study by this group, there were no significant differences in the fatty acid and sterol proportions between different sample treatments (frozen and freeze-dried) in NZGLM from three sites in New Zealand [4].

Seasonal variation in fatty acid compositions in other bivalve species have also been reported in boreal freshwater fish species [5], wild marine shrimp [6], sea bream [7], horse-mackerel [8].

Phospholipids play an important role in ion transport, receptors and cell biosynthesis, while triacylglycerol (TAG) mainly serves as energy storage. To our knowledge, there is no data on the seasonal difference with respect to lipids and fatty acids in *P. viridis*. The aim of the present study was to investigate the seasonal variations of lipid content and compositions, and fatty acid compositions of *P. viridis*. The data may provide useful information for food industries and mussel aquaculture.

## Materials and Methods

### Sampling

About 20 kg (equivalent to 1,110 mussels for summer and autumn, 1,350 for winter and spring) of *P. viridis* were collected each season from Shengsi Island, Zhejiang Province, China, during 2003–2004 (Summer, July 28, 2003; Autumn, October 22, 2003; Winter, January 7, 2004; Spring, March 27, 2004), and stored at  $-80^{\circ}\text{C}$ . In the

middle of April 2004, shells of the mussels from the four seasons ( $n = 4,920$ ) were removed and the fleshy portion was cut into small pieces, which were then vacuum freeze-dried. The mean moisture content was 71.8%. Lipid extraction and analysis were performed in triplicate - analyses for the seasonal samplings originating from a single pooled tissue sample of the month of the season.

### Lipids Analysis

The lipids of *P. viridis* powders were extracted with chloroform:methanol (2:1, by vol.) containing 10 mg/l of butylated-hydroxytoluene (BHT, Sigma Chemical Co, St Louis, USA) [9]. Total lipid contents were determined by gravimetric analysis. Lipid compositions were analyzed by using an IATROSCAN TLC-FID Analyzer (IATRON Laboratories Inc., Japan) [10].

### Fatty Acid Compositions of Triacylglycerol and Phospholipid

TAG and PL fractions of *P. viridis* extract were separated by laboratory-prepared silica gel 60G (Merck, Darmstadt, Germany) thin-layer chromatography using the solvent system of petroleum ether:diethyl ether:acetic acid (85:15:2, by vol). The methyl esters of the fatty acids (FAME) of the TAG and PL fractions were prepared by using  $\text{H}_2\text{SO}_4$  in methanol (5%, vol/vol). The FAME was separated by Shimadzu GC 17A (Shimadzu Corporation, Japan) fitted with FID and a 60 m  $\times$  0.32 mm (I.D.) fused silica column bonded phase column (BPX70, SGE, Melbourne, Australia). Fatty acids were identified by comparison with standard mixtures of fatty acid methyl esters and the results were calculated using response factors derived from chromatograph of standards of known composition (Nu-Chek-Prep, Elysian, MN, USA) [11].

### Fatty Acid Compositions of Phosphatidylethanolamine and Phosphatidylcholine

Phosphatidylethanolamine (PE) and phosphatidylcholine (PC) fractions of *P. viridis* extract were separated by using a commercial silica gel 60 (Merck, Darmstadt, Germany) thin-layer chromatography plate using a solvent system of chloroform:methanol:acetic acid:water (100:75:7:4, by vol.), into distinct narrow bands capable of being visualized under UV light after spraying the plate with dichlorofluorescein. FAME preparation and determination were the same as above.

### Sterol Compositions

*Perna viridis* lipid extracts were treated with 5% of potassium hydroxide in methanol (wt/vol) for 3 h at  $80^{\circ}\text{C}$ .

The sterols were then extracted into hexane:chloroform (4:1, by vol, 3 × 1.5 ml). Then the sample was dried under nitrogen, and treated with *N*, *O*-bis-trimethylsilyl-trifluoroacetamide (BSTFA, 50 µl, 40 °C, 30 min) to convert the sterols to corresponding trimethylsilyl (TMSi) ethers. The sample was dissolved using chloroform after it was dried under nitrogen. The analyses were performed using a Shimadzu GC 17A (Shimadzu Corporation, Japan) fitted with an FID and a 50 m × 0.32 mm BPX5 5% Phenyl Polysilphenylen–Siloxane capillary column with 0.25 µm thick film thickness (SGE, Australia). Sterols were identified by comparison with mixtures of sterols from the New Zealand Green Lipped mussel, which had been previously identified by GC-MS [3].

## Results

### Total Lipid Content

The lipid content of *P. viridis* (g/100 g frozen dried sample) was significantly higher in spring than in the other three seasons (Table 1). There were five lipid sub-classes identified, sterol ester (SE), TAG, free fatty acids, sterols and PL. The predominant lipid in spring was TAG, however, in the other three seasons it was PL. All individual lipids showed a significant variation across the four seasons (Table 2).

### Fatty Acid Compositions of Triacylglycerol and Phospholipid

The most abundant fatty acid was 16:0, and the content varied throughout the seasons in both TAG and PL fractions, with summer having the highest and winter the lowest. The other three main fatty acids were 16:1, 22:6n-3 and 20:5n-3 in the TAG fraction and 22:6n-3 and 20:5n-3 in the PL fraction. In TAG fraction, there was a decreasing for 22:6n-3 proportion from summer to autumn to spring to winter, for 20:5n-3 proportion winter was higher than other three seasons, for 16:1 from spring to winter to autumn to summer. In PL fraction, there was a decreasing for 22:6n-3 proportion from spring to winter to summer to autumn, and also for 20:5n-3 proportion from spring to winter to autumn

**Table 1** Total Lipid content in *P. viridis* (g/100g dried mussel)

<i>P. viridis</i>	Lipid content
Spring (March)	14.49 ± 0.78
Summer (July)	8.39 ± 0.59
Autumn (October)	7.85 ± 1.08
Winter (January)	9.26 ± 1.07

All samples were analyzed in triplicate from a pooled sample from the particular season

**Table 2** Lipid class content of *P. viridis* (% of total lipid)

Lipids	<i>P. viridis</i>			
	Spring	Summer	Autumn	Winter
SE	8.23 ± 0.98	6.49 ± 0.12	10.32 ± 0.10	20.46 ± 0.26
TAG	44.68 ± 1.81	33.59 ± 1.08	24.59 ± 0.57	18.46 ± 0.51
FFA	2.53 ± 0.27	3.58 ± 0.10	2.62 ± 0.22	2.58 ± 0.06
Sterols	4.34 ± 0.40	8.56 ± 0.31	8.97 ± 0.22	6.63 ± 0.57
PL	40.22 ± 1.54	47.78 ± 1.19	53.50 ± 0.63	51.87 ± 0.95

All samples were analyzed in triplicate from a pooled sample from the particular season

SE sterol esters, TAG triacylglycerols, FFA free fatty acids, PL phospholipids

to summer. All fatty acids showed significant variations between seasons, except for 20:1n-9 in TAG, and 15:0, 20:3n-6 and 22:5n-3 in PL fraction (Tables 3, 4).

### Fatty Acid Compositions of Phosphatidylethanolamine and Phosphatidylcholine

The most predominant fatty acid in PE was 18:0 and in PC it was 16:0. The other two main fatty acids were 22:6n-3 and 20:5n-3 in both PE and PC fractions. The proportions of these fatty acids varied between the seasons (Tables 5, 6). The seasonal change of the 20:5n-3 proportion in PE and PC was similar, with spring having the highest, followed by winter, autumn, and summer contained the lowest proportion. The 22:6n-3 proportion in the PE fraction showed a decrease from spring to winter to summer to autumn, in PC from summer to winter to autumn to spring.

### Sterol Compositions

The predominant sterol was cholesterol, with autumn having the highest and spring the lowest proportion. Another main sterol was the peak containing both desmosterol and brassicasterol (desmosterol and brassicasterol have similar structures and they were not separated by the method used in the present study, but this peak did not show significant variations between the seasons. Other sterols in order from the highest proportion were 24-methylenecholesterol, *trans*-22-dehydrocholesterol, 24-methylcholesterol, 24-norhydrocholesterol, β-sitosterol and ocellasterol. Except for *trans*-22-dehydrocholesterol, the other sterols showed significant variations between seasons (Table 7).

## Discussion

The aim of the present study was to evaluate the composition of lipids, sterols and fatty acids in different lipid

**Table 3** TAG fatty acid composition of *P. viridis* (% of total TAG fatty acid)

Fatty acid	<i>P. viridis</i>			
	Spring	Summer	Autumn	Winter
14:0	7.61 ± 0.08	4.16 ± 0.05	3.21 ± 0.14	7.66 ± 0.04
14:1	0.17 ± 0.00	0.06 ± 0.00	0.07 ± 0.00	0.10 ± 0.01
15:0	0.57 ± 0.01	0.77 ± 0.02	0.81 ± 0.02	0.44 ± 0.01
15:1	0.12 ± 0.00	0.18 ± 0.01	0.20 ± 0.01	0.45 ± 0.04
16:0	18.67 ± 0.27	23.97 ± 0.17	23.25 ± 0.16	14.22 ± 0.02
16:1	16.16 ± 0.23	7.69 ± 0.31	9.22 ± 0.29	12.97 ± 0.10
17:0	0.53 ± 0.02	1.01 ± 0.02	1.28 ± 0.03	0.45 ± 0.01
17:1	2.71 ± 0.10	1.85 ± 0.10	0.84 ± 0.06	4.95 ± 0.08
18:0	2.07 ± 0.09	3.49 ± 0.02	3.94 ± 0.05	1.60 ± 0.02
18:1n-9	5.84 ± 0.08	2.32 ± 0.09	3.39 ± 0.07	4.71 ± 0.05
18:1n-7	2.40 ± 0.05	2.33 ± 0.05	3.38 ± 0.08	1.89 ± 0.02
18:2n-6	1.98 ± 0.00	3.51 ± 0.02	2.44 ± 0.00	2.07 ± 0.01
18:3n-6	0.42 ± 0.02	0.26 ± 0.01	0.27 ± 0.08	0.28 ± 0.01
18:3n-3	1.61 ± 0.02	2.53 ± 0.01	3.40 ± 0.04	2.62 ± 0.09
20:0	0.26 ± 0.00	0.29 ± 0.04	0.09 ± 0.02	0.27 ± 0.01
18:4n-3	5.89 ± 0.14	5.76 ± 0.13	3.21 ± 0.04	10.41 ± 0.01
20:1n-9	1.89 ± 0.46	1.64 ± 0.07	2.24 ± 0.01	1.77 ± 0.01
20:1n-7	0.84 ± 0.00	0.92 ± 0.01	1.53 ± 0.01	0.75 ± 0.03
20:1n-5	1.48 ± 0.02	0.34 ± 0.01	0.89 ± 0.03	0.55 ± 0.01
20:2n-6	0.41 ± 0.00	1.45 ± 0.03	0.88 ± 0.01	0.46 ± 0.01
20:3n-6	0.28 ± 0.01	0.26 ± 0.01	0.22 ± 0.00	0.19 ± 0.01
20:4n-6	0.41 ± 0.01	0.78 ± 0.01	1.51 ± 0.02	0.49 ± 0.00
20:3n-3	0.14 ± 0.01	0.16 ± 0.00	0.21 ± 0.01	0.14 ± 0.00
20:5n-3	12.17 ± 0.39	12.31 ± 0.35	12.97 ± 0.30	17.21 ± 0.08
22:2trans*	0.85 ± 0.01	0.65 ± 0.05	1.48 ± 0.02	0.65 ± 0.01
22:2n-6	0.19 ± 0.06	0.47 ± 0.07	0.46 ± 0.05	0.17 ± 0.00
22:3n-6	0.99 ± 0.11	0.81 ± 0.01	0.79 ± 0.02	1.42 ± 0.01
24:0	0.28 ± 0.06	0.35 ± 0.01	0.71 ± 0.08	0.23 ± 0.01
22:5n-3	0.67 ± 0.10	0.81 ± 0.06	1.14 ± 0.06	0.48 ± 0.02
22:6n-3	11.91 ± 0.55	18.63 ± 0.02	15.48 ± 0.38	9.83 ± 0.05
Total SFA	30.00 ± 0.40	34.04 ± 0.18	33.30 ± 0.19	24.87 ± 0.07
Total MUFA	31.61 ± 0.59	17.33 ± 0.32	21.75 ± 0.42	28.15 ± 0.03
Total n-6	5.53 ± 0.18	8.19 ± 0.05	8.06 ± 0.13	5.72 ± 0.01
Total n-3	32.40 ± 0.99	40.19 ± 0.33	36.41 ± 0.73	40.70 ± 0.11
Total PUFA	37.93 ± 1.01	48.38 ± 0.30	44.46 ± 0.61	46.42 ± 0.10
n-6:n-3	0.17 ± 0.01	0.20 ± 0.00	0.22 ± 0.01	0.14 ± 0.00

All samples were analyzed in triplicate from a pooled sample from the particular season

\* The identify of this fatty acid is only tentative due to lack of a standard and GC-MS result

fractions of *P. viridis* sampled in four season months. From our knowledge, this is the first study that compares the different season's fatty acid compositions of the different lipid class in *P. viridis*. The data will provide useful information for food industries and mussel aquaculture.

## Lipids

Previous studies showed that accumulation and depletion of stored reserves of Mollusca are dependent mainly on the environmental influences on metabolic activities, and the

quantity and nutritional value of the food supply [12–14]. In the present study, the total lipid content was higher in spring than in the other seasons. This result is in agreement with the findings in *Mytilus edulis* (Linne) [2], which found that the highest lipid content was in March (spring). Total lipid contents of *P. viridis* in summer, autumn and winter in the present study (freeze dried powder) are consistent with the previous studies in freeze-dried NZGLM [4]. They collected samples from three different locations in March (autumn in New Zealand) and reported a total lipid content of 8.4 g/100 g freeze dried powder. In order to have suf-

**Table 4** PL fatty acid composition of *P. viridis* (% of total PL fatty acid)

Fatty acid	<i>P. viridis</i>			
	Spring	Summer	Autumn	Winter
14:0	3.10 ± 0.04	2.82 ± 0.10	1.29 ± 0.03	1.77 ± 0.38
15:0	0.64 ± 0.05	0.66 ± 0.01	0.70 ± 0.02	0.67 ± 0.14
15:1	0.25 ± 0.03	0.19 ± 0.01	0.26 ± 0.01	0.42 ± 0.01
16:0	23.05 ± 0.30	23.85 ± 0.40	22.68 ± 0.86	20.59 ± 0.22
16:1	3.68 ± 0.09	3.22 ± 0.08	3.38 ± 0.16	4.03 ± 0.09
17:1	1.68 ± 0.04	1.73 ± 0.03	1.77 ± 0.22	1.17 ± 0.03
18:0	5.94 ± 0.33	9.06 ± 0.38	5.94 ± 0.14	5.15 ± 0.36
18:1n-9	1.83 ± 0.13	0.89 ± 0.02	0.89 ± 0.04	1.26 ± 0.02
18:1n-7	2.26 ± 0.06	1.40 ± 0.07	1.67 ± 0.04	1.69 ± 0.03
18:2n-6	0.94 ± 0.03	1.59 ± 0.03	1.29 ± 0.01	1.06 ± 0.01
18:3n-6	0.39 ± 0.03	0.22 ± 0.04	0.26 ± 0.04	0.17 ± 0.00
18:3n-3	0.67 ± 0.01	0.90 ± 0.03	1.67 ± 0.02	1.05 ± 0.03
18:4n-3	1.36 ± 0.03	1.19 ± 0.11	1.02 ± 0.06	2.14 ± 0.10
20:1n-11	0.58 ± 0.03	3.08 ± 0.49	3.55 ± 0.28	1.85 ± 0.13
20:1n-9	4.11 ± 0.12	3.84 ± 0.27	3.66 ± 0.05	3.67 ± 0.05
20:1n-7	0.88 ± 0.04	0.88 ± 0.01	0.94 ± 0.05	0.82 ± 0.02
20:1n-5	2.45 ± 0.07	3.93 ± 0.10	5.12 ± 0.27	3.36 ± 0.03
20:2n-6	0.38 ± 0.01	0.85 ± 0.02	0.49 ± 0.02	0.39 ± 0.02
20:3n-6	0.27 ± 0.09	0.18 ± 0.01	0.21 ± 0.01	0.22 ± 0.01
20:4n-6	1.90 ± 0.00	2.68 ± 0.06	4.81 ± 0.12	4.72 ± 0.06
22:0	0.16 ± 0.01	0.21 ± 0.02	0.11 ± 0.02	0.12 ± 0.03
20:5n-3	18.28 ± 0.20	11.24 ± 0.72	14.13 ± 0.57	16.16 ± 0.41
22:2trans*	2.92 ± 0.08	4.24 ± 0.11	4.17 ± 0.06	4.44 ± 0.02
22:2n-6	0.70 ± 0.06	1.40 ± 0.02	1.10 ± 0.15	1.29 ± 0.13
22:3n-6	0.66 ± 0.03	0.48 ± 0.00	0.53 ± 0.07	0.67 ± 0.11
22:4n-6	0.40 ± 0.05	0.28 ± 0.03	0.47 ± 0.01	0.60 ± 0.05
24:0	0.95 ± 0.03	0.89 ± 0.05	1.25 ± 0.10	1.15 ± 0.08
22:5n-3	1.54 ± 0.27	1.24 ± 0.08	1.61 ± 0.18	1.37 ± 0.07
22:6n-3	18.04 ± 0.22	16.86 ± 0.12	15.00 ± 0.24	17.99 ± 0.18
Total SFA	33.84 ± 0.11	37.47 ± 0.08	31.98 ± 0.63	29.45 ± 0.71
Total MUFA	17.72 ± 0.34	19.16 ± 0.41	21.24 ± 0.92	18.27 ± 0.17
Total n-6	8.56 ± 0.22	11.93 ± 0.21	13.33 ± 0.18	13.57 ± 0.29
Total n-3	39.89 ± 0.60	31.43 ± 0.66	33.45 ± 0.65	38.71 ± 0.64
Total PUFA	48.45 ± 0.43	43.37 ± 0.46	46.78 ± 0.48	52.28 ± 0.55
n-6:n-3	0.21 ± 0.01	0.38 ± 0.01	0.40 ± 0.01	0.35 ± 0.01

All samples were analyzed in triplicate from a pooled sample from the particular season

\* The identify of this fatty acid is only tentative due to the lack of a standard and GC-MS result

ficient reserves for spawning, mussels store more energy as lipids before spawning [15]. We collected the spring sample in March, which was before spawning, and this had higher lipid content than the other three seasons. This result is agreement with studies in NZGLM [14] and in Chinese mussel *Mytilus edulis* (Linne) [2], and in other marine invertebrates such as *Silurus asotus* [16], *Ostrea edulis* (L) [17] and *Haliotis rubra* [18].

In spring, the predominant lipid was TAG, whereas in summer, autumn and winter months the main lipid was PL. This can be attributed to the fact that TAG is mainly used as energy, whereas PL is mainly a component of the cell

structures. The calculated PL content, based on total lipid × PL proportion revealed that in spring there was the highest PL content (6.0 g/100 g compared with values of 4.0, 4.2 and 4.8 g/100 g for summer, autumn and winter respectively). Similar calculations showed that the TAG content in spring was 6.5 g/100 g compared with 2.9, 1.9 and 1.7 g/100 g in summer, autumn and winter [19], respectively. After the spawning period, energy requirements are reduced, especially in the winter. In the colder seasons, mussels enter a winter dormancy period, where many of their metabolic processes are slowed or shut down. During this time, they grow very slowly, energy (lipid)

**Table 5** PE fatty acid composition of *P. viridis* (% of total PE fatty acid)

Fatty acid	<i>P. viridis</i>			
	Spring	Summer	Autumn	Winter
14:0	0.43 ± 0.05	0.54 ± 0.14	0.15 ± 0.02	0.61 ± 0.08
15:0	0.37 ± 0.09	0.25 ± 0.07	0.17 ± 0.03	0.22 ± 0.01
16:0	6.04 ± 0.22	3.56 ± 0.15	3.77 ± 0.29	5.37 ± 0.28
16:1	0.84 ± 0.04	1.35 ± 0.20	1.32 ± 0.14	1.58 ± 0.14
17:0	3.51 ± 0.11	2.84 ± 0.05	2.53 ± 0.18	2.87 ± 0.34
17:1	1.73 ± 0.07	4.71 ± 0.25	3.07 ± 0.17	3.65 ± 0.15
18:0	29.33 ± 1.25	28.00 ± 0.61	24.80 ± 3.04	25.81 ± 3.17
18:1n-9	0.67 ± 0.02	0.74 ± 0.21	0.68 ± 0.05	0.44 ± 0.08
18:1n-7	1.56 ± 0.04	0.93 ± 0.14	1.04 ± 0.02	1.00 ± 0.16
18:4n-3	0.73 ± 0.21	5.64 ± 0.41	5.43 ± 0.91	0.79 ± 0.06
20:1n-9	2.83 ± 0.72	5.59 ± 0.34	3.96 ± 0.08	1.39 ± 0.34
20:1n-7	0.70 ± 0.17	1.24 ± 0.05	1.42 ± 0.70	0.58 ± 0.07
20:1n-5	9.04 ± 0.27	10.42 ± 0.27	11.39 ± 0.48	10.00 ± 0.34
20:2n-6	0.26 ± 0.03	1.28 ± 0.09	0.50 ± 0.04	0.24 ± 0.03
20:4n-6	1.71 ± 0.06	3.51 ± 0.31	6.77 ± 0.44	5.17 ± 0.48
20:5n-3	19.78 ± 0.43	10.74 ± 0.46	13.40 ± 0.64	14.55 ± 0.89
22:2trans*	3.48 ± 0.05	4.63 ± 0.15	5.93 ± 0.78	4.40 ± 0.28
22:2n-6	1.16 ± 0.09	2.48 ± 0.30	1.80 ± 0.10	2.31 ± 0.15
22:3n-6	0.32 ± 0.00	0.37 ± 0.05	0.27 ± 0.02	0.45 ± 0.01
22:4n-6	0.32 ± 0.00	0.46 ± 0.06	0.73 ± 0.03	1.12 ± 0.10
24:0	0.79 ± 0.01	0.71 ± 0.10	1.18 ± 0.16	1.37 ± 0.08
22:5n-3	1.34 ± 0.20	1.05 ± 0.01	1.39 ± 0.07	1.74 ± 0.16
22:6n-3	12.45 ± 0.14	7.79 ± 0.41	7.22 ± 0.55	12.41 ± 0.81
Total SFA	40.47 ± 1.11	35.91 ± 0.58	32.60 ± 3.53	36.26 ± 3.74
Total MUFA	17.38 ± 0.68	24.98 ± 0.69	22.90 ± 0.74	18.64 ± 0.65
Total n-6	7.25 ± 0.15	12.73 ± 0.23	16.01 ± 1.37	13.69 ± 1.03
Total n-3	34.29 ± 0.57	25.22 ± 0.85	27.44 ± 1.93	29.49 ± 1.88
Total PUFA	41.54 ± 0.72	37.95 ± 1.03	43.45 ± 3.29	43.18 ± 2.90
n-6:n-3	0.21 ± 0.00	0.50 ± 0.01	0.58 ± 0.01	0.46 ± 0.01

All samples were analyzed in triplicate from a pooled sample from the particular season

\* The identify of this fatty acid is only tentative due to the lack of a standard and GC-MS result

requirement is very low, because the TAG stores have been depleted this leads to a relatively increased PL proportion.

Phosphatidylethanolamine and PC make up more than 80% of PL, and are relatively rich in n-3 PUFA, especially 20:5n-3 and 22:6n-3, which play an important role in ion, receptors and cell biosynthesis [20]. The *P. viridis* contained a high proportion of PUFA, which accounted for 30–50% of total fatty acid in different lipid fractions. The 22:6n-3 and 20:5n-3 were the predominant PUFA in all lipid fractions. The 22:6n-3 and 20:5n-3 were also the predominant PUFA reported in total lipid of fresh NZGLM and TBM [3], in total lipid of frozen and freeze-dried NZGLM [4], and in PL in *Mytilus edulis* [2]. As similarly reported by Lin et al. [2] in *Mytilus edulis* (Linne), 20:5n-3 proportion in PL in *P. viridis* was significantly higher in spring than in other three seasons, and lowest in summer. The 20:5n-3 proportion in PC and PE fractions showed the same trend with PL in the present study. However, 22:6n-3

was higher in summer than in other three seasons in PC. The proportion of PUFA was higher for PL and PC in winter, for TAG in summer and for PE in autumn, whereas SFA were higher in summer than in other three seasons in TAG, PL and PC. Previous studies in fish and shellfish have reported that PUFA content varies inversely with the water temperature [21–23], while SFA content changes positively with the water temperature [13, 24], and that the increased PUFA at colder temperature was mainly due to a higher proportion of n-3 PUFA [24–26], it has been suggested that an increase in membrane PUFA and a decrease in SFA when the temperature falls could contribute to the maintenance of cell membrane fluidity, as PUFA has a lower melting point than do SFA. It has also been suggested that increased unsaturated fatty acids (PUFA and MUFA) of non-membrane lipids such as TAG in the flesh would also be expected to help maintain body flexibility for movement at reduced temperatures [24]. Fatty acids in

**Table 6** PC fatty acid composition of *P. viridis* (% of total PC fatty acid)

Fatty acid	<i>P. viridis</i>			
	Spring	Summer	Autumn	Winter
14:0	3.32 ± 0.06	3.62 ± 0.04	1.64 ± 0.06	2.91 ± 0.03
15:0	0.79 ± 0.01	1.20 ± 0.01	1.12 ± 0.03	1.02 ± 0.02
15:1	0.12 ± 0.00	0.18 ± 0.00	0.21 ± 0.00	0.21 ± 0.05
16:0	28.22 ± 0.19	29.95 ± 0.10	24.42 ± 0.60	22.02 ± 0.40
16:1	4.30 ± 0.09	4.05 ± 0.03	3.49 ± 0.07	4.52 ± 0.07
17:0	1.15 ± 0.02	1.38 ± 0.01	1.70 ± 0.05	1.12 ± 0.06
17:1	1.04 ± 0.01	0.66 ± 0.01	0.83 ± 0.02	1.13 ± 0.10
18:0	4.77 ± 0.15	5.08 ± 0.35	6.10 ± 0.18	4.12 ± 0.65
18:1n-9	2.11 ± 0.01	1.05 ± 0.01	1.30 ± 0.02	1.26 ± 0.02
18:1n-7	3.25 ± 0.02	1.97 ± 0.03	2.83 ± 0.03	2.48 ± 0.03
18:2n-6	1.14 ± 0.01	2.38 ± 0.02	2.01 ± 0.01	1.47 ± 0.02
18:3n-6	0.29 ± 0.00	0.11 ± 0.01	0.11 ± 0.00	0.14 ± 0.02
18:3n-3	0.73 ± 0.01	1.13 ± 0.01	2.17 ± 0.02	1.28 ± 0.04
20:0	0.29 ± 0.01	0.10 ± 0.00	0.08 ± 0.01	0.13 ± 0.03
18:4n-3	1.78 ± 0.01	1.90 ± 0.03	1.59 ± 0.05	2.61 ± 0.14
20:1n-11	0.27 ± 0.01	0.81 ± 0.04	1.79 ± 0.05	0.79 ± 0.04
20:1n-9	2.04 ± 0.02	1.22 ± 0.01	1.49 ± 0.05	1.68 ± 0.05
20:1n-7	0.73 ± 0.01	0.48 ± 0.00	0.85 ± 0.02	0.79 ± 0.02
20:1n-5	0.86 ± 0.01	0.48 ± 0.03	0.97 ± 0.01	1.07 ± 0.05
20:2n-6	0.38 ± 0.00	0.63 ± 0.00	0.55 ± 0.01	0.48 ± 0.01
20:3n-6	0.17 ± 0.00	0.19 ± 0.03	0.13 ± 0.00	0.17 ± 0.00
20:4n-6	0.97 ± 0.01	1.62 ± 0.01	3.27 ± 0.02	2.59 ± 0.01
20:5n-3	20.00 ± 0.23	13.30 ± 0.10	15.84 ± 0.44	17.72 ± 0.59
22:2trans*	1.66 ± 0.17	1.00 ± 0.05	1.89 ± 0.14	3.51 ± 0.30
22:2n-6	0.26 ± 0.03	0.52 ± 0.01	0.54 ± 0.02	0.70 ± 0.04
22:3n-6	0.61 ± 0.02	0.57 ± 0.00	0.57 ± 0.02	0.86 ± 0.05
22:4n-6	0.13 ± 0.00	0.16 ± 0.01	0.32 ± 0.00	0.36 ± 0.00
24:0	0.46 ± 0.04	0.34 ± 0.00	0.83 ± 0.05	0.71 ± 0.03
22:5n-3	0.99 ± 0.03	1.23 ± 0.01	1.82 ± 0.05	1.48 ± 0.11
22:6n-3	17.17 ± 0.30	22.70 ± 0.12	19.54 ± 0.61	20.64 ± 0.41
Total SFA	39.00 ± 0.37	41.66 ± 0.26	35.89 ± 0.84	32.05 ± 1.07
Total MUFA	14.72 ± 0.16	10.89 ± 0.07	13.76 ± 0.24	13.93 ± 0.14
Total n-6	5.61 ± 0.18	7.19 ± 0.08	9.39 ± 0.15	10.28 ± 0.22
Total n-3	40.66 ± 0.51	40.26 ± 0.13	40.96 ± 1.15	43.74 ± 1.29
Total PUFA	46.28 ± 0.42	47.45 ± 0.19	50.35 ± 1.08	54.03 ± 1.21
n-6:n-3	0.14 ± 0.01	0.18 ± 0.00	0.23 ± 0.01	0.24 ± 0.01

All samples were analyzed in triplicate from a pooled sample from the particular season

\* The identify of this fatty acid is only tentative due to the lack of a standard and GC-MS result

seafood vary depending on several biological and environmental factors, such as taxonomy, diet of the animals, seasonal changes in water temperature, and the latitude at which they were harvested [24, 27]. It has been documented that seasonal fatty acids changes could also be related to the reproductive cycles [28]

#### CE Versus Sterols

Invertebrates have been reported to contain a wide range of sterols [29]. There were 9 sterols identified in the present

study, however, the 17 had been identified previously in both the frozen NZGLM and TBM when the authors used GC-MS to identify the sterols, and 14 were identified from frozen and freeze-dried NZGLM [3]. Our results are consistent with the previous studies [3, 4], in that cholesterol and desmosterol/brassicasterol were the main sterols present, followed by 24-methylenecholesterol, and that their quantities varied seasonally.  $\beta$ -sitosterol, a predominant phytosterol, was only present in minor amounts (2–5% of total sterol) in *P. viridis*. Plankton is the predominant diet of mussels, which contains various sterols, and they can be

**Table 7** Sterol Composition of *P. viridis* (% of total sterols)

Sterols*	<i>P. viridis</i>			
	Spring	Summer	Autumn	Winter
24-Nordehydrocholesterol	5.89 ± 0.40	2.25 ± 0.33	4.63 ± 0.78	5.40 ± 0.53
Occlasterol	2.50 ± 0.22	2.19 ± 0.40	1.20 ± 0.19	1.46 ± 0.02
<i>trans</i> -22-Dehydrocholesterol	7.07 ± 0.17	6.03 ± 0.78	6.84 ± 1.09	6.75 ± 0.26
Cholesterol	26.64 ± 0.20	31.57 ± 1.64	36.89 ± 5.87	35.08 ± 1.67
Desmosterol/Brassicasterol**	31.68 ± 0.10	28.76 ± 0.99	28.76 ± 4.66	31.99 ± 0.25
24-Methylcholesterol	7.86 ± 0.08	3.82 ± 0.14	2.04 ± 0.48	5.52 ± 0.06
24-Methylenecholesterol	15.37 ± 0.28	20.84 ± 1.98	9.02 ± 1.44	11.21 ± 1.08
$\beta$ -Sitosterol	2.99 ± 0.07	4.53 ± 0.17	2.39 ± 0.39	2.60 ± 0.40

All samples were analyzed in triplicate from a pooled sample from the particular season

\* Sterols were identified by comparison with mixtures of sterols from the New Zealand Green Lipped mussel, which had been previously identified by GC-MS (2)

\*\* Desmosterol and brassicasterol have a similar structure and they were not separated under these chromatography conditions

incorporated into mussel tissues, and some sterols such as cholesterol can be synthesized from plankton cholesterol precursors [16].

In conclusions, the composition of lipid and sterol, composition of fatty acids in TAG, PL, PE and PC, and total lipid content varied seasonally.

## References

- Qing N, Lin YG, Zhen Q (1999) Compositions of fatty acids in 3 species of maricultured bivalves. *Trop Oceanol* 18:79–82
- Lin H, Jiang J, Xue CH, Zhang B, Xu JC (2003) Seasonal changes in phospholipids of mussel (*Mytilus edulis* Linne). *J Sci Food Agric* 83:133–135
- Murphy K, Mooney BD, Nichols PD, Sinclair AJ (2002) Lipid, fatty acid and sterol composition of New Zealand Green Lipped Mussel (*Perna Canaliculus*) and Tasmanian Blue Mussel (*Mytilus edulis*). *Lipids* 37:587–595
- Murphy KJ, Mann NJ, Sinclair AJ (2003) Fatty acid and sterol composition of frozen and freeze-dried New Zealand Green Lipped Mussel (*Perna canaliculus*) from three sites in New Zealand. *Asia Pac J Clin Nutr* 12:50–60
- Agren J, Muje P, Hanninen O, Herranen J, Penttila I (1987) Seasonal variations of lipid fatty acids of boreal freshwater fish species. *Comp Biochem Physiol B* 88:905–909
- Yanar Y, Çelik M (2005) Note: seasonal variations of fatty acid composition in wild marine shrimps (*Penaeus semisulcatus* De Haan, 1844 and *Metapenaeus monoceros* Fabricius, 1789) from the Eastern. *Food Sci Tech Int* 11:391–395
- Özyurt G, Polat A, Özkütük S (2005) Seasonal changes in the fatty acids of gilthead sea bream (*Sparus aurata*) and white sea bream (*Diplodus sargus*) captured in Iskenderun Bay, eastern Mediterranean coast of Turkey. *Eur Food Res Technol* 220:120–124
- Bandarra NM, Batista I, Nunes ML, Empis JM (2001) Seasonal variation in the chemical composition of horse-mackerel (*Trachurus trachurus*). *Eur Food Res Technol* 212:535–539
- Folch J, Lees M, Sloane-Stanley GH (1957) A simple method for the insolation and purification of total lipids from animal tissues. *J Biol Chem* 226:497–509
- Li D, Zhang YH (2003) Application of IATROSCAN TLC-FID Analyzer on analysis of lipids in crab with seasonal variation. *J Chin Inst Food Sci Tech* S227–S231
- Li D, Ng A, Mann NJ, Sinclair AJ (1998) Contribution of meat fat to dietary arachidonic acid. *Lipids* 33:437–440
- Pieters H, Klutymans JH, Zandee DI, Cadee GC (1980) Tissue composition and reproduction of *Mytilus edulis* dependent upon food availability. *Neth J Sea Res* 14:349–361
- Pazos AJ, Sánchez JL, Román G, Pérez-Parallé ML, Abad M (2003) Seasonal changes in lipid classes and fatty acid composition in the digestive gland of *Pecten maximus*. *Comp Biochem Physiol* 134B:367–380
- Su XQ, Antonas KN, Li D (2004) Comparison of n-3 polyunsaturated fatty acid contents of wild and cultured Australian abalone. *Int J Food Sci Nutr* 55:149–154
- Pieters H, Klutymans JH, Zurburg W, Zandee DI (1979) The influence of seasonal changes on energy metabolism in *Mytilus edulis* (L.). 1. Growth rate and biochemical composition in relation to environmental parameters and spawning. In: Naylor E, Hartnoll RG (eds) *Cyclic phenomena in marine plants and animals*. Pergamon Press, Oxford pp 285–292
- McLean CH, Bulling KR (2005) Differences in lipid profile of New Zealand marine species over four seasons. *J Food Lipids* 12:313–326
- Shirai N, Suzuki H, Toukairin S, Wada S (2001) Spawning and season affect lipid content and fatty acid composition of ovary and liver in Japanese catfish (*Silurus asotus*). *Comp Biochem Physiol B Biochem Mol Biol* 129:185–195
- Labarta U, Fernandez-Reiriz MJ, Perez-Camacho A (1999) Dynamics of fatty acids in the larval development, metamorphosis and post-metamorphosis of *Ostrea edulis* (L.). *Comp Biochem Physiol* 123:249–254
- Su XQ, Antonas KN, Li D (2002) Comparison of n-3 polyunsaturated fatty acid and total lipid content of spawning and nonspawning Australian blacklip abalone. *Asia Pac J Clin Nutr* 11:S308
- Hazel JR, Williams EE (1990) The role of alterations in membrane lipid composition in enabling physiological adaptation of organisms to their physical environment. *Prog Lipid Res* 29:167–227
- Piretti MV, Zuppa F, Paglinca G, Taioli F (1988) Investigation of the seasonal variations of fatty acid. Constituents in selected tissue of the bivalve mollusc, *Scapharca inaequalvi* (Bruguiere). *Comp Biochem Physiol* 89B:183–187



22. Chu FLE, Greaves J (1991) Metabolism of palmitic, linoleic, and linolenic acids in adult oysters. *Crassostrea virginica* Mar Biol 110:229–236
23. Ingemansson T, Olsson NU, Kaufmann P (1993) Lipid composition of light and dark muscle of rainbow trout (*Oncorhynchus mykiss*) after thermal acclimation: a multivariate approach. *Aquaculture* 113:153–165
24. Dunstan GA, Olley J, Ratkowsky DA (1999) Major environmental and biological factors influencing the fatty acid composition of seafood from Indo-Pacific to Antarctic waters. *Recent Res Devel Lipids Res* 3:63–86
25. Sargent JR (1976) The structure, metabolism and function of lipids in marine organisms. In: Malins DC, Sargent JR (eds) *Biochemical and biophysical perspectives in marine biology*, vol 3, Academic, New York, pp 149–212
26. Bell MV, Henderson RJ, Sargent JR (1986) The role of polyunsaturated fatty acids in fishes. *Comp Biochem Physiol* 83B:711–719
27. Linehan LG, O'Connor TP, Burnell G (1999) Seasonal variation in the chemical composition and fatty acid profile of Pacific oysters (*Crassostrea gigas*). *Food Chem* 64:2111–2214
28. Soudant P, Ryckeghem K Van, Marty Y, Moal J, Samain JF, Sorgeloos P (1999) Comparison of polar lipid class and fatty acid composition between a reproductive cycle in nature and a standard hatchery conditioning of the pacific oyster *Crassostrea gigas*. *Comp Biochem Physiol* B123:209–222
29. Gordon DT (1982) Sterols in Mollusks and Crustacea of the Pacific Northwest. *AOCS* 59:536–545

# Effects of In Ovo Administration of DHEA on Lipid Metabolism and Hepatic Lipogenetic Genes Expression in Broiler Chickens During Embryonic Development

Sumei Zhao · Haitian Ma · Sixiang Zou · Weihua Chen

Received: 2 February 2007 / Accepted: 12 April 2007 / Published online: 16 June 2007  
© AOCS 2007

**Abstract** In order to study the mechanism of DHEA (Dehydroepiandrosterone) in reducing fat in broiler chickens during embryonic development, fertilized eggs were administrated with DHEA before incubation and its effect on lipid metabolism and expression of hepatic lipogenetic genes was investigated. The mRNA levels of acetyl CoA carboxylase (ACC), fatty acid synthase (FAS), malic enzyme (ME), apolipoprotein B100 (apoB100) and sterol regulator element binding protein-1c (SREBP-1c) were determined using real time quantitative PCR. Samples of livers were collected from the chickens on days 9, 14, and 19 of embryonic development as well as at hatching. Blood samples were extracted on days 14, 19 of incubation and at hatching. The results showed that DHEA decreased the concentration of triacylglycerol in the blood and the content in liver, and the mRNA levels of ACC, FAS, ME, SREBP-1c and apoB. This suggested that DHEA decreased the expression of hepatic lipogenetic genes and suppressed triglycerols transport, by which it reduced the deposition of fat in adipose tissue in broiler chickens during embryonic development and hatching.

**Keywords** Lipid metabolism · mRNA · Liver · Broiler · DHEA

## Introduction

In the last few decades, the aim of poultry production in many countries has been to increase the growth rates, but excessive fat deposition in the abdomen has been neglected. Fatness needs to be controlled, due to its negative effect on productivity. In meat-type chickens, excessive adipose tissue reduces both feed efficiency during rearing and the yield of lean meat after processing. In avian species, the liver is the main site of de novo fatty acid synthesis and accounts for 95% in young chicks [1, 2]. In consequence, most of the endogenous body lipids are of hepatic origin [3] and the development of adipose tissue depends on the availability of plasma triglycerides that are hydrolyzed prior to their utilization by adipocytes. Triglycerides are supplied specifically to adipocytes by specific lipoprotein classes: very low density lipoproteins (VLDL) transport de novo synthesized hepatic lipids [4, 5]. Thus a higher rate of triglyceride synthesis and transport from the liver is responsible for the higher weight of abdominal fat in chickens.

According to previous studies, differences in the degree of obesity are due to various steps of lipid metabolism, among which liver fatty acid metabolism has been considered as the main source of variability [6–9]. These results prompted researches into gene expression in the liver, especially those genes involved in fatty acid synthesis and secretion [10–11]. Accordingly, the present study focused on the expression of lipogenetic genes in liver. Acetyl-CoA carboxylase (ACC), the rate-limiting enzyme in fatty acid synthesis, catalyzes the carboxylation of acetyl-CoA to malonyl-CoA [12]. Fatty acid synthase (FAS) is a key enzyme in fatty acid synthesis that catalyzes the synthesis of long-chain fatty acid through the condensation of acetyl-CoA and malonyl-CoA in a

S. Zhao · H. Ma · S. Zou (✉) · W. Chen  
Key Laboratory of Animal Physiology and Biochemistry,  
The Ministry of Agriculture, Nanjing Agricultural University,  
Nanjing 210095, People's Republic of China  
e-mail: sixiangzou@njau.edu.cn

complex seven-step reaction [13]. Malic enzyme catalyzes the oxidative decarboxylation of malate to pyruvate and CO<sub>2</sub> simultaneously generating NADPH from NADP<sup>+</sup>. In the avian liver, most of the NADPH used by fatty acid for catalyzing the synthesis of palmitate is generated by the malic enzyme [14]. The availability of apoB plays a major role in determining the capacity of hepatocytes to assemble and secrete VLDL [15, 16]. SREBP (Sterol response element binding protein) is among many potential regulators. These transcription factors of the leucine zipper family have been described as regulators of biosynthesis of cholesterol and fatty acids in the liver [17]. SREBP-1c is preferentially involved in the activation of genes that control the synthesis of fatty acid [18, 19]. The gene for SREBP-1c is highly expressed in the liver. Moreover, different studies have shown that SREBPs can directly stimulate the transcription of genes encoding ACC [20–22], FAS enzymes [23], making them good candidates as common regulators of the lipogenetic genes. Therefore, expression of these hepatic lipogenetic genes plays a pivotal role in the process of de novo TG synthesis.

Dehydroepiandrosterone (DHEA, 3 $\beta$ -hydroxy-5-androsten-17-one)-a naturally occurring steroid, is secreted from the adrenal gland as a sulfate ester, which is interconvertible with free DHEA in vivo. DHEA is not a hormone but it is a very important prohormone [24], which exerts various physiological activities through intermediate products when administered to rats and mice. The studies from others have revealed that DHEA has various functions on the regulating of lipid metabolism, which includes decreasing the metabolic efficiency in mammalian species [25, 26], regulating the synthesis of fat, decreasing the number of adipocytes [27–29]. In rodents, long term DHEA treatment resulted in suppression of body weight gain without changes in food intake. During DHEA treatment, liver size is increased with decreasing hepatic lipogenesis [25, 30].

DHEA has a fat-reducing function. However, the mechanism of this physiological role of DHEA has not yet been fully clarified [31, 32]. Moreover, most of previous studies were focused on rodents with only a few studies on chickens and they indicated that DHEA did not significantly suppress body weight of chickens and liver size [33]. No detailed information was available about the effect of DHEA on lipid metabolism in broiler chickens during embryonic development. The fertilized egg would be an appropriate substance in studying the mechanism of DHEA in the regulation of fatty metabolism because the embryo is enclosed in an eggshell, and is hardly influenced by external factors [34].

The objective of the present study was to explore the effect of DHEA on lipid metabolism and hepatic lipogenetic

genes expression in broiler chickens during embryonic development which may help to identify the possible mechanism of DHEA in decreasing the deposition of fat in adipose tissue.

## Material and Methods

### Animal Experiment

Fertilized eggs of laying hens (Arbor Acres) used in this study were obtained from Jiangsu Wuxi Chicken Breeding Company (Wuxi, China). All eggs were numbered and weighed individually prior to the beginning of incubation. Afterwards, eggs were fumigated (80 g potassium permanganate in 130 ml 40% formaldehyde solution per m<sup>3</sup> for 20 min) and randomly divided into two groups. In the control group (CON group), the eggs were injected with 50  $\mu$ L DMSO, while in DHEA group, the eggs were injected with 50 mg DHEA (Sigma, USA) per kg eggs weight diluted in 50  $\mu$ L DMSO. All treatments were performed just prior to putting the eggs into the incubator. 50  $\mu$ L of solution were added to the air sac. Prior to injection, the blunt end of the egg was sterilized with 70% ethanol. A single hole was created with a dental drill bit without penetrating the chorio-allantoic membrane. Each solution was injected into the blunt end of the egg to a depth of 5.0 mm after drilling the shell. Micropipettes were used for injections (Sealpette, Jencons, Finland). After injection, the holes were immediately sealed with melted paraffin wax. They were placed into an electric forced-draft incubator at 37.5  $\pm$  0.5  $^{\circ}$ C and 60% relative humidity and turned every 2 h. All eggs were incubated in the same incubator. All eggs were candled before incubation and only unchipped and unbroken eggs were used in the experiment. All experimental procedures were performed according to the Guide for Animal Care and Use of Laboratory Animals in the Institutional Animal Care and Use Committee of Nanjing Agricultural University. The experimental protocol was approved by the Departmental Animal Ethics Committee of Nanjing Agricultural University.

Eggs were opened on days 9, 14, 19 of incubation. Samples of liver were collected, weighed and numbered at E9, E14, E19 and at hatching. All liver tissue samples were snap frozen in liquid nitrogen and stored at  $-80^{\circ}$ C prior to homogenization. Blood samples were collected from the blood vessel at E14d and the heart at E19d with a heparinized syringe. The blood was collected from the jugular vein at hatching. The blood samples were centrifuged at 4  $^{\circ}$ C, 9,000  $\times$  g for 4 min, and the serum was gathered and kept in a  $-40^{\circ}$ C freezer. The start of incubation was called day 1 (E1d) and after hatching called day 1 (H1).

## Measurement of Lipid Parameters

Total liver lipid content was determined on homogenized liver samples using a mixture of chloroform and methanol (2:1 v/v) according to the method of Folch et al. [35]. The levels of hepatic and serum triglyceride (TG) and total cholesterol (TC) content were determined using commercial kits (GPO-PAP and CHOD-PAP) purchased from the Nanjing Jiancheng Bioengineering Institute (NJBI). TG and TC levels in homogenates of liver and serum were evaluated following the manufacturer's protocols. The optic density of the samples was measured using a spectrophotometer three times at a wavelength of 546 nm. Total TG in liver and serum and TC in serum were calculated through absorption of the tested sample divided by standard sample and multiplied by TG and TC content in standard sample.

## RNA Extraction

Total RNAs were extracted from the liver using TRIZOL reagent (Takara, Japan) according to the manufacturer's protocols. Total RNA concentration was then quantified by measuring the optic density at 260 nm in a photometer (Eppendorf Biophotometer). Ratios of absorption (260/280 nm) of all preparations were between 1.8 and 2.0. Aliquots of RNA samples were subjected to electrophoresis through a 1.4% agarose formaldehyde gel to verify their integrity.

## Real-Time Quantitative RT-PCR

Reverse transcription was performed using the RNA (2 µg) described above in a final volume of 25 µL containing 10 units of MMLV reverse transcriptase (Promega, Belgium), 1 mM dNTP mixture (Promega, Belgium), 40 units of

recombinant RNasin ribonuclease inhibitor (Promega, Belgium) and 0.5 µg of oligo (dT) 18 (Promega, Belgium) in sterilized water and buffer supplied by the manufacturer. After incubation at 42 °C for 60 min, the mixture was heat treated at 95 °C for 5 min. An aliquot of cDNA samples was mixed with 25 µl SYBR<sup>®</sup> Green PCR Master Mix (Takara, Japan), in the presence of 10 pmol of each forward and reverse primer for acetyl CoA carboxylase (ACC), fatty acid synthase (FAS), malic enzyme (ME), apolipoprotein B100 (apoB100) and sterol regulator element binding protein-1c (SREBP-1c) (Table 1), and then subjected to PCR under standard conditions (40 cycles). As an internal control, the same RT products were also subjected to PCR in the presence of a second pair of primers specific to chicken  $\beta$ -actin RNA. Mixtures were incubated in an ABI Prism 7300 Sequence Detection System (Applied Biosystems) programmed to conduct one cycle (95 °C for 10 s) and 40 cycles (95 °C for 5 s and 60 °C for 31 s) or one cycle (95 °C for 10 min) and 40 cycles (95 °C for 15 s and 62 °C for 1 min). Results (fold changes) were expressed as  $2^{-\Delta\Delta Ct}$  with  $\Delta\Delta Ct = (Ct_{ij} - Ct_{\beta\text{-actin } j}) - (Ct_{i1} - Ct_{\beta\text{-actin } 1})$ , where  $Ct_{ij}$  and  $Ct_{\beta\text{-actin } j}$  are the  $Ct$  for gene  $i$  and for  $\beta$ -actin in a pool or a sample (named  $j$ ) and where  $Ct_{i1}$  and  $Ct_{\beta\text{-actin } 1}$  are the  $Ct$  in pool 1 or sample 1, expressed as the standard. All primers used were designed by Primes Premier 5 and synthesized by Shanghai Saibaisheng Biological Company (Shanghai, China).

## Statistical Analysis

The results were expressed as mean  $\pm$  SE and differences were considered significant when  $P < 0.05$  tested by two-way analysis of variance (ANOVA) (with treatments and developmental stages as the main effects) and the pair  $t$ -test with Statistical Packages for Social Science 12.0 and Excel 2003 in Microsoft.

**Table 1** Oligonucleotide PCR primers

Gene	Genbank accession number	Primers sequence (5'–3')	Orientation	Product size (bp)
$\beta$ -actin	L08165	TGCGTGACATCAAGGAGAAG	Forward	300
		TGCCAGGGTACATTGTGGTA	Reverse	
ACC	J03541	CACTTCGAGGCGAAAACTC	Forward	447
		GGAGCAAATCCATGACCACT	Reverse	
FAS	J04485	TGAAGGACCTTATCGCATTGC	Forward	195
		GCATGGGAAGCATTGTTGT	Reverse	
ME	AF408407	AGCATTACGGTTTAGCATTTCCGG	Forward	239
		CAGGTAGGCACTCATAAGGTTC	Reverse	
SREBP	AY029224	GTCGGCGATCCTGAGGAA	Forward	104
		CTCTTCTGCACGGCCATCTT	Reverse	
ApoB100	M18421	CACGCCTCACACAGACCAAGTA	Forward	407
		CCAGTCAAACGGCACATCTA	Reverse	

## Results

### Effect of In Ovo Administration of DHEA on Body weights and Liver Weights at Embryonic Stages and Hatching

The effect of in ovo administration of DHEA on body weight, absolute and relative liver weights at embryonic stages and hatching was shown in Table 2. In both groups, body weights sharply increased with developmental stage ( $p < 0.05$ ). Body weight in the CON group was slightly higher than that in the DHEA group throughout the whole embryonic development ( $p > 0.05$ ). Daily gain in the CON group slightly exceeded that of the DHEA group throughout the whole embryonic development ( $p > 0.05$ ).

In both groups, absolute liver weights increased greatly with developmental stage and the values of the control were a little higher than those of in ovo administration of DHEA. But the difference was not significant ( $p > 0.05$ ). In both groups, relative liver weights (g liver/g embryo weight) in the CON group was insignificantly higher than that in the DHEA group during the whole embryonic development ( $p > 0.05$ ).

### Effect of In Ovo Administration of DHEA on Plasma and Liver Lipid Metabolism Parameters at Embryonic Stages and Hatching

The effect of in ovo administration of DHEA on total blood TG, TC and hepatic TG content of broiler during embryonic development and at hatching were shown in Table 3. In both groups, the TG content in the liver (mmol/g liver) greatly increased with developmental stages ( $p < 0.05$ ). The TG content in the liver (mmol/g) was similar between CON and DHEA groups at E9d. However, the TG content in CON group was significantly higher than that in DHEA group at E14d, E19d as well as at hatching ( $p < 0.05$ ).

The blood TG (mmol/L) contents in both groups gradually decreased with developmental stages ( $p > 0.05$ ). The TG content in the CON group was significantly higher than that in the DHEA group throughout the whole embryonic development ( $p < 0.05$ ).

The blood TC content remained relatively the same in the two groups during the embryonic development. However, the plasma TC content in the DHEA group was significantly higher than that in the CON group at hatching ( $p < 0.05$ ).

**Table 2** Effect of in ovo administration of DHEA on body weight, liver weight and lipid parameters during embryonic development

	E9	E14	E19	H1
Body weight (g)				
CON	2.12 ± 0.25 <sup>a</sup>	12.55 ± 1.59 <sup>b</sup>	29.36 ± 3.25 <sup>c</sup>	40.69 ± 2.97 <sup>c</sup>
DHEA	2.01 ± 0.23 <sup>A</sup>	12.46 ± 1.54 <sup>B</sup>	29.27 ± 4.35 <sup>C</sup>	39.31 ± 3.15 <sup>C</sup>
Absolute liver weight (g)				
CON	0.04 ± 0.01 <sup>a</sup>	0.22 ± 0.04 <sup>b</sup>	0.52 ± 0.11 <sup>c</sup>	0.87 ± 0.12 <sup>d</sup>
DHEA	0.04 ± 0.01 <sup>A</sup>	0.20 ± 0.05 <sup>B</sup>	0.50 ± 0.10 <sup>C</sup>	0.80 ± 0.11 <sup>D</sup>
Relative liver weight (%)				
CON	1.78 ± 0.23 <sup>a</sup>	1.80 ± 0.21 <sup>a</sup>	1.77 ± 0.27 <sup>a</sup>	2.19 ± 0.31 <sup>a</sup>
DHEA	1.75 ± 0.27 <sup>A</sup>	1.56 ± 0.28 <sup>A</sup>	1.70 ± 0.28 <sup>A</sup>	1.99 ± 0.31 <sup>A</sup>
Daily gain (g/d)				
CON		2.09 ± 0.27 <sup>a</sup>	3.36 ± 0.76 <sup>b</sup>	2.28 ± 0.23 <sup>b</sup>
DHEA		2.08 ± 0.25 <sup>A</sup>	3.32 ± 0.71 <sup>B</sup>	2.11 ± 0.31 <sup>B</sup>

Means ± SE without a common letter differ significantly between age groups (small letter for CON group and capital letter for DHEA treatment).

\* Treatment differences at the same age ( $P < 0.05$ ) ( $n = 10$ )

**Table 3** Effect of in ovo administration of DHEA on lipid parameters during embryonic development

	E9	E14	E19	H1
Hepatic TG (mmol/g liver)				
CON	4.45 ± 0.51 <sup>a</sup>	19.43 ± 1.55 <sup>b*</sup>	22.25 ± 1.52 <sup>b*</sup>	25.54 ± 1.21 <sup>b*</sup>
DHEA	4.01 ± 0.43 <sup>A</sup>	12.62 ± 1.22 <sup>B</sup>	19.33 ± 1.43 <sup>B</sup>	21.74 ± 1.44 <sup>B</sup>
Plasma TG (mmol/L)				
CON		5.11 ± 0.55 <sup>a*</sup>	2.93 ± 0.35 <sup>b</sup>	2.25 ± 0.55 <sup>c*</sup>
DHEA		3.60 ± 0.41 <sup>A</sup>	2.31 ± 0.28 <sup>B</sup>	1.40 ± 0.43 <sup>C</sup>
Plasma TC (mmol/L)				
CON		3.05 ± 1.36 <sup>b</sup>	7.04 ± 2.74 <sup>c</sup>	7.35 ± 2.07 <sup>c*</sup>
DHEA		4.58 ± 2.17 <sup>B</sup>	6.45 ± 3.66 <sup>C</sup>	9.96 ± 2.89 <sup>C</sup>

Means ± SE without common letter differ significantly between age groups (small letter for CON group and capital letter for DHEA treatment).

\* Treatment differences at the same age ( $P < 0.05$ ) ( $n = 10$ )

### Effect of In Ovo Administration of DHEA on Hepatic ACC Gene Expression During Embryonic Development and at Hatching

The effect of in ovo administration of DHEA on ACC gene expression during embryonic development and at hatching was investigated in this study and the results were shown in Fig 1. mRNA level of ACC increased with embryonic development proceeding, but it decreased significantly at hatching in both groups ( $p < 0.05$ ). Expression level of the ACC gene in CON group was significantly lower than that in DHEA group during embryonic 19 days ( $p < 0.05$ ). However, ACC gene expression in CON group was four fold higher than that in DHEA group at hatching.

### Effect of In Ovo Administration of DHEA on Hepatic FAS Gene Expression During Embryonic Development and at Hatching

We then studied the effect of in ovo administration of DHEA on FAS gene expression during embryonic development. The result showed that FAS gene expression levels were nearly the same in both groups during embryonic development (Fig 2). FAS gene expression of CON was 18-fold higher than that in DHEA group at hatching and this difference was significant ( $p < 0.05$ ). FAS gene expression exhibited an increase in the CON group during embryonic development and at hatching. However, FAS gene expression decreased sharply in DHEA group at hatching ( $p < 0.05$ ).

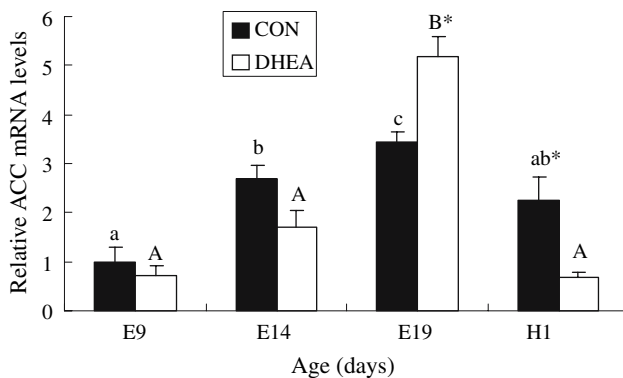


**Fig. 1** Effect of in ovo administration of DHEA on hepatic ACC gene expression during embryonic development and at hatching. RNA molecules extracted from liver of different stages of embryonic development or hatching were reverse transcribed to cDNA and analyzed by quantitative RT-PCR. For comparison between different samples, the ACC transcript level of each sample was normalized for the beta-actin level and expressed as a multiple of ACC level of E9. Each column represented the mean and standard error of results obtained with 6 experiments. Black bars, control group (CON); Blank bars, DHEA group (DHEA); Asterisks indicate the differences between CON and DHEA group are significant ( $P < 0.05$ )

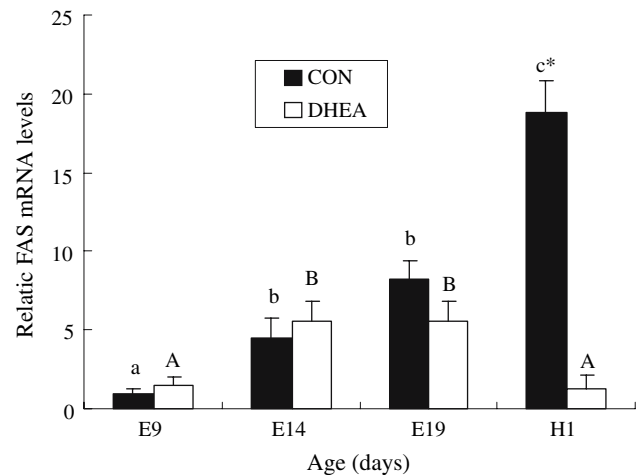


**Fig. 2** The effect of in ovo administration of DHEA on hepatic FAS gene expression during embryonic development and at hatching—RNA molecules were extracted from the liver at different stages of embryonic development or at hatching and were reverse transcribed to cDNA and analyzed by quantitative RT-PCR. For comparison between different samples, the FAS transcript level of each sample was normalized for the beta-actin level and expressed as a multiple of the FAS level of E9. Each column represented the mean and standard error of results obtained with six experiments. Black bars, control group (CON); Blank bars, DHEA group (DHEA); Asterisks indicate the differences between CON and DHEA group are significant ( $P < 0.05$ )

### Effect of In Ovo Administration of DHEA on Hepatic SREBP-1c Gene Expression During Embryonic Development and at Hatching

The result of in ovo administration of DHEA on hepatic SREBP-1c gene expression during embryonic development and at hatching was shown in Fig. 3. SREBP-1c gene expression levels were the same in the DHEA group as in the CON group during the embryonic development. At hatching, SREBP-1c transcript level in the CON group was three-fold higher than that in the DHEA group. The difference was significant ( $p < 0.05$ ). SREBP-1c gene expression exhibited increasing with embryonic development in two groups. However, the expression level of SREBP-1c in the CON group increased more than that in the DHEA group.

### The Effect of in Ovo Administration of DHEA on Hepatic ME Gene Expression During Embryonic Development and at Hatching

In this study, we also investigate the effect of in ovo administration of DHEA on ME gene expression during embryonic development and at hatching. The result was shown in Fig. 4. The transcript level of ME in CON group was significantly higher than that in DHEA group from embryonic development of 14 days to hatching ( $p < 0.05$ ).

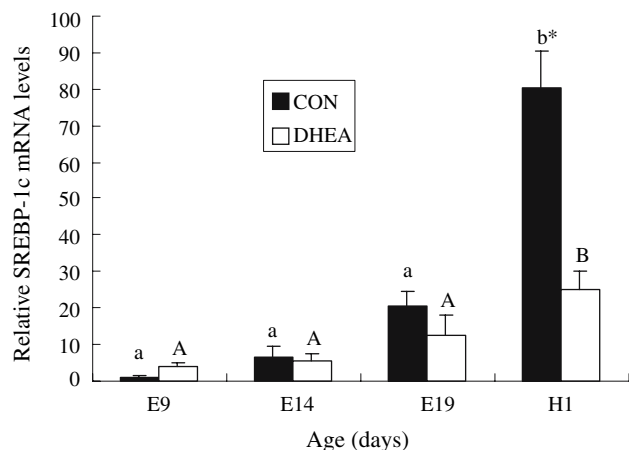


**Fig. 3** The effect of in ovo administration of DHEA on hepatic *SREBP-1c* gene expression during embryonic development and at hatching. RNA molecules extracted from liver of different stages of embryonic development or hatching were reverse transcribed to cDNA and analyzed by quantitative RT-PCR. For comparison between different samples, the *SREBP-1c* transcript level of each sample was normalized for the beta-actin level and expressed as a multiple of *SREBP-1c* level of E9. Each column represented the mean and standard error of results obtained with six experiments. *Black bars*, control group (CON); *Blank bars*, DHEA group (DHEA); *Asterisks* indicate that the differences between CON and DHEA groups are significant ( $P < 0.05$ )

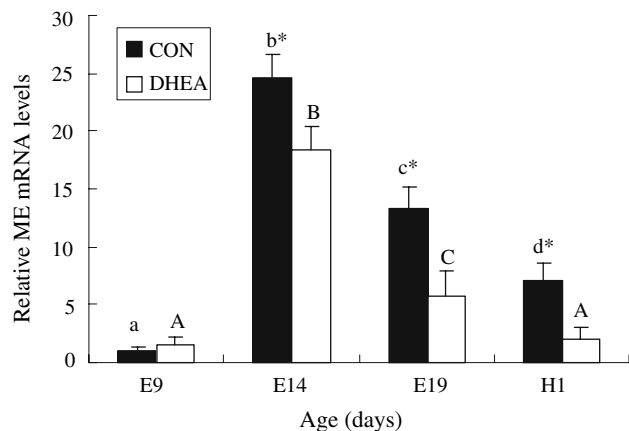


**Fig. 4** The effect of in ovo administration of DHEA on hepatic *ME* gene expression during embryonic development and at hatching. RNA molecules extracted from liver of different stages of embryonic development or hatching were reverse transcribed to cDNA and analyzed by quantitative RT-PCR. For comparison between different samples, the *ME* transcript level of each sample was normalized for the beta-actin level and expressed as a multiple of *ME* level of E9. Each column represented the mean and standard error of results obtained with 6 experiments. *Black bars*, control group (CON); *Blank bars*, DHEA group (DHEA); *Asterisks* indicate the differences between CON and DHEA group are significant ( $P < 0.05$ )

Moreover, the CON to DHEA ratio of expression level increased with embryonic development. The expression level of *ME* decreased from E14 days to hatching.

### Effect of In Ovo Administration of DHEA on Hepatic *ApoB* Gene Expression During Embryonic Development and at Hatching

Finally, we studied the effect of in ovo administration of DHEA on *apoB* gene expression during embryonic development and at hatching, and the result was shown in Fig. 5. The expression level of the hepatic *apoB* gene significantly increased through the course of embryonic development ( $p < 0.05$ ). Measured by RT-PCR, the mRNA level of *apoB* in the CON group was significantly higher than that in DHEA treatment throughout all the stages of embryonic development ( $p < 0.05$ ).

### Discussion

Long term DHEA treatment results in suppression of body weight gain in rodents [36, 37]. However, no significant effect of in ovo administration of DHEA on body weight, body weight gain and absolute liver weight was observed in this experiment. In contrast to its effects on rats and mice, DHEA did not significantly depress body weight of chickens [33]. Rats fed with DHEA had a slower growth rate compared with rats fed with a control diet, whereas rats treated with DHEA i.p. had growth rates identical to those of controls. The liver weights of rats administrated DHEA p.o. or i.p. increased significantly compared to those of control rats [39]. In lean rats, DHEA treatment did not decrease liver weight [38]. Liver weights of DHEA treated rats were higher than those of control rats [39]. Administration of DHEA to rats results in lowered body weight, higher liver weights and DNA, RNA, and/or protein content, but lowered lipid and glycogen levels [40]. These data indicate that the effect of DHEA on body weight gain, food intake, and hepatic and peripheral adiposity are dependent on the species of animal, the adrenal status, the DHEA dose and the age of embryonic development at which measurements were made [41, 42].

DHEA has a fat-reducing effect, however, this effect may be exerted by different mechanisms [31]. It has been shown in this study that in ovo administration of DHEA to fertilized eggs before incubation reduced plasma and liver TG content. This result agreed with other studies in rodents. For example, the study by Mikheil and Leila [43] indicated that dehydroepiandrosterone influences on lipid metabolism - reduces the levels of TC, TG, LDL, VLDL. Mohan. PF and Cleary. MP [39, 40] suggested DHEA treatment reduced hepatic lipids in rats and under some circumstances, altered a number of serum factors including glucose, insulin, cholesterol, and triacylglycerol. Therefore, DHEA may reduce the adipose tissue by reducing the TG content in adipose tissue.

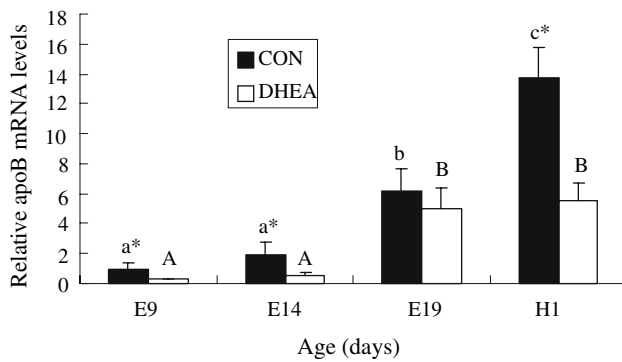


**Fig. 5** The effect of in ovo administration of DHEA on hepatic *apoB* gene expression during embryonic development and at hatching. RNA molecules extracted from liver of different stages of embryonic development or hatching were reverse transcribed to cDNA and analyzed by quantitative RT-PCR. For comparison between different samples, the *apoB* transcript level of each sample was normalized for the beta-actin level and expressed as a multiple of the *apoB* level of E9. Each column represented the mean and standard error of results obtained with six experiments. Black bars, control group (CON); Blank bars, DHEA group (DHEA); Asterisks indicate the differences between CON and DHEA group are significant ( $P < 0.05$ )

Other studies also indicated that DHEA treatment altered the activity levels of a lot of enzymes in the liver that are involved in lipid metabolism [40]. This could be one of the mechanisms of DHEA for decreasing the fat level of the animal. For example, Valentine et al. [33] reported that liver cytosolic malic enzyme activity were depressed in chickens treated with DHEA compared with that in untreated animals. This study showed that the expression level of the hepatic *ME* gene in DHEA group was lower than that in the CON group. The relative abundances of malic enzyme mRNAs were associated with malic enzyme activity and liver total lipid concentration [44]. The activity of the hepatic malic enzyme is positively correlated with the rate of fatty acid synthesis, the percentage of body fat, and the percentage of abdominal fat in chicks. Meanwhile, Casazza et al. [45] hypothesized that DHEA inhibited fat synthesis by diminishing the availability of NADPH, but no data gave support to the hypothesis that administration of DHEA resulted in decreased cytoplasmic NADPH in the liver of rats. In the avian liver, most of the NADPH used by fatty acid synthase to catalyze the synthesis of palmitate is generated by the malic enzyme [14]. Therefore, DHEA reduced hepatic *ME* gene expression so as to decrease the hepatic fatty acid synthesis and de novo TG synthesis.

In our published study, we suggested that expression of the key gene (*FAS*) in the liver was responsible for de novo synthesis of fatty acid prior to hatching and at hatching [46]. The rate of hepatic lipogenesis was decreased by approximately 70% in DHEA-treated mice [47]. Noteworthy, the fat-reducing effect of DHEA seems to be more evident at the level of visceral adipose tissue [31, 41].

Moreover, this study showed that DHEA significantly depressed the *FAS* gene expression at hatching. This means that DHEA decreased *FAS* gene expression to reducing fat especially at hatching.

In avian species, the development of adipose tissue depends on the availability of plasma triglycerides that are hydrolyzed prior to their uptake by adipocytes. They are specifically transported to adipocytes by specific lipoprotein classes: very low density lipoproteins (VLDL) transport de novo synthesized hepatic lipids [4, 5]. *ApoB* participated in the assembly of VLDL. This study showed DHEA decreased the *apoB* gene expression, which suggested that DHEA depressed the assembly of VLDL, resulting in the suppression of the transportation of hepatic TG to various tissues.

As one of potential regulators, *SREBP-1c* can directly stimulate the transcription of genes encoding *ACC* [20–22], *FAS* [23] enzymes. In this study, DHEA decreased the expression of both *SREBP-1c* and *FAS* genes throughout the whole embryonic development. However, DHEA significantly reduced the expression of all three genes, *SREBP-1c*, *ACC* and *FAS* at hatching. Our previous studies indicated that embryonic liver synthesized fatty acid prior to hatching or at hatching [46]. This suggested that by decreasing the expression of transcriptional regulator, DHEA altered the expression levels of various downstream genes that are involved in the synthesis of TG.

In conclusion, this study analyzed the effect of in ovo administration of DHEA on blood lipid metabolism and hepatic lipogenic genes expression in broiler chicken during embryonic development. The result indicated that DHEA significantly decreased liver weight, blood TG content, hepatic TG content and the expression levels of hepatic *ACC*, *FAS*, *ME*, *SREBP-1c* and *apoB* genes in broiler chicken during embryonic development. All of these affected genes are involved in the metabolism of fat tissue. A higher rate of triglyceride synthesis and secretion from the liver would be responsible for the higher abdominal fat weight in chickens. Over all, our data suggested that DHEA decreased the synthesis of TG in liver and its transport in circulation, which is probably the mechanism of DHEA in reducing the accumulation of fat in chicken.

**Acknowledgments** This work was supported by National Basic Research Program (Project No. 2004CB117505). We are grateful to Ms. Pasha Apontes for editing the manuscript.

## References

- Leveille GA (1969) In vitro hepatic lipogenesis in the hen and chick. *Comp Biochem Physiol* 28:431–435
- Pearce J (1977) Some differences between avian and mammalian biochemistry. *Int J Biochem* 8:269–275



3. O'Hea EK, Leveille GA (1969) Lipogenesis in isolated adipose tissue of domestic chick (*Gallus domesticus*). *Comp Biochem Physiol* 26:111–120
4. Noyan M, Lossow WJ, Brot N, Chaikoff IL (1964) Pathway and form of absorption of palmitic acid in the chicken. *J Lipid Res* 5:538–541
5. Bensadoun A, Rothfeld A (1972) The form of absorption of lipids in the chicken *Gallus domesticus*. *Proc Soc Exp Biol Med* 141:814–817
6. Saadoun A, Leclercq B (1983) Comparison of in vivo fatty acid synthesis of the genetically lean and fat chickens. *Comp Biochem Physiol B* 75:641–644
7. Hermier D, Chapman MJ (1985) Lipoprotein plasmatiques et engraissement: description d'un modele chez le poulet domestique *Gallus domesticus*. *Reprod Nutr Dev* 25:235–241
8. Leclercq B, Hermier D, Guy G (1990) Metabolism of very low density lipoproteins in genetically lean or fat lines of chicken. *Reprod Nutr Dev* 30:701–715
9. Legrand P, Hermier D (1992) Hepatic delta 9 desaturation and plasma VLDL level in genetically lean and fat chickens. *Int J Obes Relat Metab Disord* 16:289–294
10. Douaire M, Le Fur N, el Khadir-Mounier C, Langlois P, Flamant F, Mallard J (1992) Identifying genes involved in the variability of genetic fatness in the growing chicken. *Poult Sci* 71:1911–1920
11. Daval S, Lagarrigue S, Douaire M (2000) Messenger RNA levels and transcription rates of hepatic lipogenesis genes in genetically lean and fat chickens. *Genet Sel Evol* 32:521–531
12. McGarry JD, Takabayashi Y, Foster DW (1978) The role of malonyl-CoA in the coordination of fatty acid synthesis and oxidation in isolated rat hepatocytes. *J Biol Chem* 253:8294–8300
13. Back DW, Goldman MJ, Fisch JE, Ochs RS, Goodridge AG (1986) The fatty acid synthase gene in avian liver: two mRNA are expressed and regulated in parallel by feeding, primarily at the level of transcription. *J Biol Chem* 261:4190–4197
14. Hillgartner FB, Salati LM, Goodridge AG (1995) Physiological and molecular mechanisms involved in nutritional regulation of fatty acid synthesis. *Physiol Rev* 75:47–76
15. Davis RA, Boogaerts JR, Borchardt RA, Malone-McNeal M, Archambault-Schexnayder J (1985) Intrahepatic assembly of very low density lipoproteins. *J Biol Chem* 260:14137–14144
16. Boren J, Wettesten M, Rustaeus S, Anderson M, Olofsson SO (1993) The assembly and secretion of apoB-100-containing lipoproteins. *Biochem Soc Trans* 21:487–493
17. Brown MS, Goldstein JL (1997) The SREBP pathway: regulation of cholesterol metabolism by proteolysis of a membrane-bound transcription factor. *Cell* 89:331–340
18. Shimano H, Horton JD, Hammer RE, Shimomura I, Brown MS, Goldstein JL (1996) Overproduction of cholesterol and fatty acids causes massive liver enlargement in transgenic mice expressing truncated SREBP-1a. *J Clin Invest* 98:1575–1584
19. Shimano H, Shimomura I, Hammer RE, Herz J, Goldstein JL, Brown MS, et al (1997) Elevated levels of SREBP-2 and cholesterol synthesis in livers of mice homozygous for a targeted disruption of the SREBP-1 gene. *J Clin Invest* 100:2115–2124
20. Magana MM, Lin SS, Dooley KA, Osborne TF (1997) Sterol regulation of acetyl coenzyme A carboxylase promoter requires two interdependent binding sites for sterol regulatory element binding proteins. *J Lipid Res* 38:1630–1638
21. Yin L, Zhuang Y, Hillgartner FB (2002) Sterol regulatory element-binding protein-1 interacts with the nuclear thyroid hormone receptor to enhance acetyl-CoA carboxylase- $\alpha$  transcription in hepatocytes. *J Biol Chem* 277:19554–19565
22. Zhuang Y, Yin L, Hillgartner FB (2003) SREBP-1 integrates the actions of thyroid hormone, insulin, cAMP, and medium chain fatty acids on ACC  $\alpha$  transcription in hepatocytes. *J Lipid Res* 44:356–368
23. Magana MM, Koo SH, Towle HC, Osborne TF (2000) Different sterol regulatory element-binding protein-1 isoforms utilize distinct co-regulatory factors to activate the promoter for fatty acid synthase. *J Biol Chem* 275:4726–4733
24. Labrie F, Luu-The V, Belanger A, Lin SX, Simard J, Pelletier G (2005) Is dehydroepiandrosterone a hormone? *J Endocrinol* 187:169–196
25. Yen TT, Allen JA, Pearson DV, Acton J, Greenberg MM (1977) Prevention of obesity in mice by dehydroepiandrosterone. *Lipids* 12:409–413
26. Tagliaferro A, Davis JR, Truchon S, Van Hamont N (1986) Effect of dehydroepiandrosterone acetate on metabolism, body weight and composition of male and female rats. *J Nutr* 116:1977–1983
27. Araghi-Niknam M, Ardestani SK, Molitor Inerra P, Eskelson Cd, Watson RR (1998) Dehydroepiandrosterone (DHEA) sulfate prevents reduction in tissue vitamin E and increased lipid peroxidation due to murine retrovirus infection of aged mice. *Proc Soc Exp Biol Med* 218:210–217
28. Barrou Z, Charru P, Lidy C (1997) Dehydroepiandrosterone (DHEA) and aging. *Arch Gerontol Geriatr* 4:233–241
29. Khalil A, Lehoux JG, Wagner RJ, Lesur O, Crux S, Dupont E, Jay-Gerin JP, Wallach J, Fulop T (1998) Dehydroepiandrosterone against copper-induced lipid peroxidation in the rat. *Free Radic Biol Med* 22:1289–1294
30. Cleary MP, Billheimer J, Finan A, Sartin JL, Schwartz AG (1984) Metabolic consequences of dehydroepiandrosterone in lean and obese adult Zucker rats. *Horm Metab Res* 16(Suppl 1):43–46
31. De Pergola G (2000) The adipose tissue metabolism: role of testosterone and Dehydroepiandrosterone. *Int J Obes Relat Metab Disord* 24(Suppl 2):S59–63
32. Berdanier CD, McIntosh MK (1989) Further studies on the effects of dehydroepiandrosterone on hepatic metabolism in BHE rats. *Proc Soc Exp Biol Med* 192:242–247
33. Valentine B, Nancy K, Monica B, Daniela B, Umberto M, Henry L (1993) Comparative studies of effects of Dehydroepiandrosterone on rat and chicken liver. *Comp Biochem Physiol* 105B:643–647
34. Sato Momoka, Tachibana Tetsuya, Furuse Mitsuhiro (2006a) Heat production and lipid metabolism in broiler and layer chickens during embryonic development. *Comp Biochem Physiol Part A* 143:382–388
35. Folch J, Lee M, Slane-Stanley GH (1957) A simple method for the isolation and purification of total lipids from animal tissues. *J Biochem* 226:497–509
36. Cleary MP (1991) The antiobesity effect of dehydroepiandrosterone in rats. *Proc Soc Exp Biol Med* 196:8–16
37. Cleary MP, Zisk JF (1986) Anti-obesity effect of two different levels of dehydroepiandrosterone in lean and obese middle-aged female Zucker rats. *Int J Obes* 10:193–204
38. Shepherd A, Cleary MP (1984) Metabolic alterations after dehydroepiandrosterone treatment in Zucker rats. *Am J Physiol* 246:E123–128
39. Mohan PF, Cleary MP (1988) Effect of short-term DHEA administration on liver metabolism of lean and obese rats. *Am J Physiol* 255:E1–8
40. Margot P, Cleary MP (1990) Effect of dehydroepiandrosterone treatment on liver metabolism in rats. *Int J Biochem* 22:205–210
41. McIntosh MK, Berdanier CD (1988) Strain differences in the dose-response curves of adrenalectomized, starved-refed rats to dehydroepiandrosterone (DHEA). *Proc Soc Exp Biol Med* 187:216–222
42. Henry MH, Burke WH (1999) The effects of in ovo administration of testosterone or an antiandrogen on growth of chick

- embryos and embryonic muscle characteristics. *Poul Sci* 78:1006–1013
43. vili Mikheil S, Leila B (2005) Hyperandrogenia and lipid metabolism. *Ann Biomed Res Edu* 5:39–41
44. Morris SM Jr, Winberry LK, Fisch JE, Back DW, Goodridge AG (1984) Developmental and nutritional regulation of the messenger RNAs for fatty acid synthase, malic enzyme and albumin in the livers of embryonic and newly-hatched chicks. *Mol Cell Biochem* 64:63–68
45. Casazza JP, Schaffer WT, Veech RL (1986) The effect of DHEA on liver metabolites. *J Nutr* 116:304–310
46. S. Zhao, Ma H, Zou S, Chen W, Zhao R (2007) Hepatic lipogenesis gene expression in broiler chicken with different fat deposition during embryonic development. *J Vet Med.A* 54:1–6
47. Marrero M, Prough RA, Frenkel RA, Milewich L (1990) Dehydroepiandrosterone feeding and protein phosphorylation, phosphatases, and lipogenic enzymes in mouse liver. *Proc Soc Exp Biol Med* 193:110–117

# New Sphingolipids with a Previously Unreported 9-Methyl-C<sub>20</sub>-sphingosine Moiety from a Marine Algal Endophytic Fungus *Aspergillus niger* EN-13

Yi Zhang · Song Wang · Xiao-Ming Li ·  
Chuan-Ming Cui · Chao Feng · Bin-Gui Wang

Received: 4 February 2007 / Accepted: 27 May 2007 / Published online: 29 June 2007  
© AOCS 2007

**Abstract** Asperamides A (**1**) and B (**2**), a sphingolipid and their corresponding glycosphingolipid possessing a hitherto unreported 9-methyl-C<sub>20</sub>-sphingosine moiety, were characterized from the culture extract of *Aspergillus niger* EN-13, an endophytic fungus isolated from marine brown alga *Colpomenia sinuosa*. The structures were elucidated by spectroscopic and chemical methods as (2*S*,2'*R*,3*R*,3'*E*,4*E*,8*E*)-*N*-(2'-hydroxy-3'-hexadecenoyl)-9-methyl-4,8-icosadien-1,3-diol (**1**) and 1-*O*-β-D-glucopyranosyl-(2*S*,2'*R*,3*R*,3'*E*,4*E*,8*E*)-*N*-(2'-hydroxy-3'-hexadecenoyl)-9-methyl-4,8-icosadien-1,3-diol (**2**). In the antifungal assay, asperamide A (**1**) displayed moderate activity against *Candida albicans*.

**Keywords** Marine alga · *Colpomenia sinuosa* · Endophytic fungus · *Aspergillus niger* · Sphingolipid · Glycosphingolipid · Asperamide A · Asperamide B

## Abbreviations

CC Column chromatography  
COSY Correlation spectroscopy

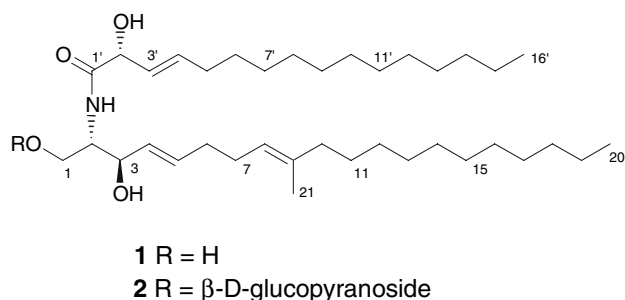
DEPT Distortionless enhancement by polarization transfer  
GC-MS Gas chromatography-mass spectrometry  
HMBC Heteronuclear multiple bond correlation  
HMQC Heteronuclear multiple quantum correlation  
HR High resolution  
LCB Long chain base

## Introduction

Sphingolipids are commonly distributed among some of the bacteria and almost all eukaryotic organisms, such as fungi, sponges, higher plants, and mammals. They play an important role in recognition of pathogens, signal transduction, cell differentiation, and apoptosis of cancer cells. Many sphingolipids have been found to exhibit antihepatotoxic, antitumor, antifungal, antiviral, neuritogenic, and immunoregulatory activities [1–4] and have drawn more and more interest from chemical and medicinal researchers. Since the 1990s, marine derived fungi have been recognized as a rich source of novel bioactive metabolites because their environments differ from those of terrestrial fungi [5]. In the course of our investigation of the bioactive secondary metabolites of *Aspergillus niger* EN-13, an endophytic fungus isolated from marine brown alga *Colpomenia sinuosa*, two new sphingolipids (namely, asperamides A (**1**) and B (**2**), Scheme 1) with a previously unreported 9-methyl-C<sub>20</sub>-sphingosine moiety were characterized. This paper describes the isolation, structural determination, and antifungal activity of asperamides A (**1**) and B (**2**).

Y. Zhang · S. Wang · X.-M. Li · C.-M. Cui ·  
C. Feng · B.-G. Wang (✉)  
Key Laboratory of Experimental Marine Biology,  
Institute of Oceanology, Chinese Academy of Sciences,  
Qingdao 266071, People's Republic of China  
e-mail: wangbg@ms.qdio.ac.cn

Y. Zhang · S. Wang · C.-M. Cui · C. Feng  
Graduate School of the Chinese Academy of Sciences,  
Beijing 100039, People's Republic of China



**Scheme 1** Chemical structures of **1** and **2**

## Experimental Procedures

### Chromatographic and Instrumental Methods

Melting points were measured using a SGW X-4 micro-melting point apparatus and uncorrected. Optical rotations were obtained on a JASCO P-1020 digital polarimeter. IR spectra were taken on a NICOLET 510P FT-IR spectrometer in KBr discs. NMR spectra were recorded on a Bruker Avance 500 MHz spectrometer (500 MHz for  $^1\text{H}$  and 125 MHz for  $^{13}\text{C}$ ) using TMS as internal standard and chemical shifts were recorded as  $\delta$  values. Mass spectra were measured on VG AutoSpec 3000 mass spectrometer. GC-MS analysis was performed on an Agilent 6890-5973 GC-MS apparatus.

### Materials

Silica gel (200–300 mesh and GF-254) for column chromatography (CC) and preparative thin-layer chromatography were the products of the Qingdao Haiyang Chemical Group Co., Qingdao, China. RP-18 reverse-phase silica gel was the product of the Merck Corporation. Sephadex LH-20 was purchased from the Pharmacia Corporation. Amphotericin B was produced by the Sigma Corporation.

### Microorganism

The fungal strain *Aspergillus niger* EN-13 was isolated from the inner tissue of surface-sterilized fresh brown alga *Colpomenia sinuosa* (Roth) Derbeset Solier that was collected in May of 2004 along the Qingdao coastline of Shandong Province, People's Republic of China, according to a method we recently reported [6]. The taxonomic identification as *A. niger* was performed based on fungal morphology (both macroscopic and microscopic) by one of the authors (Y.Z.) and a voucher strain was deposited in the China Center for Type Culture Collection (depository number: CCTCC AF 206004).

### Fermentation

A small spoon of spores growing on malt agar slant was inoculated onto a malt agar plate and cultured at 28 °C for 7 days. Then a piece (size: 4 cm<sup>2</sup>) of mycelium was inoculated into 1,000-ml Erlenmeyer flasks containing 300 ml of a culture medium composed of glucose 2%, peptone 0.5%, malt extract 0.3%, yeast extract 0.3%, artificial sea salt 2.44%. The pH was adjusted to 7.4 before autoclaving. Static fermentation was carried out at 25 °C for 30 days.

### Extraction and Isolation

The culture broth (30 l) was filtrated and separated into mycelia and supernatant. Air-dried mycelia were smashed and extracted with 3 l of MeOH to give a MeOH-soluble extract. The supernatant was concentrated under reduced pressure to about 4 l, and then extracted three times with EtOAc to give an EtOAc-soluble extract. Since the two extracts displayed similar TLC and HPLC profiles, they were combined and evaporated under reduced pressure, resulting in a total extract (42.0 g). This extract was subjected to a silica gel CC eluting stepwise from  $\text{CHCl}_3$  to MeOH to give 14 fractions. Fraction VIII (3.0 g) was subsequently subjected to a silica gel CC eluted with  $\text{CHCl}_3/\text{MeOH}$  (30:1, by vol) to give six sub-fractions. Sub-fr. II (157 mg) was further separated with consecutive CC on silica gel eluted with  $\text{CHCl}_3/\text{MeOH}$  (40:1, by vol) and RP-18 (MeOH) to provide compound **1** (88 mg). Fraction XIV (960 mg) was subjected to a silica gel CC eluted with  $\text{CHCl}_3/\text{MeOH}$  (8:1, by vol) to give three subfractions. Sub-fr. II (220 mg) was successively purified by CC on RP-18 (MeOH) and Sephadex LH-20 (MeOH) to yield compound **2** (80 mg).

#### (2S,2'R,3R,3'E,4E,8E)-N-(2'-Hydroxy-3'-Hexadecenoyl)-9-Methyl-4,8-Icosadien-1,3-Diol (**1**)

White amorphous powder; m.p. 64–66 °C;  $[\alpha] -5.6^\circ$  ( $c = 0.60$ ,  $\text{CHCl}_3$ ). IR (KBr)  $\gamma_{\text{max}}$  3,377, 3,274, 2,921, 2,851, 1,630, 1,538, 1,467, 722  $\text{cm}^{-1}$ ;  $^1\text{H}$  and  $^{13}\text{C}$ -NMR data see Table 1; EIMS (70 eV)  $m/z$  (rel. int.) 592  $[\text{M} + \text{H}]^+$  (1), 574  $[\text{M} + \text{H} - \text{H}_2\text{O}]^+$  (26), 340 (20), 323 (28), 253 (44), 125 (22), 111 (50), 97 (65), 83 (94), 69 (87), 60 (100); positive FABMS  $m/z$  592  $[\text{M} + \text{H}]^+$ , 574  $[\text{M} + \text{H} - \text{H}_2\text{O}]^+$ . HRESIMS  $m/z$  592.5314 (calcd. for  $\text{C}_{37}\text{H}_{70}\text{NO}_4$ , 592.5304).

#### 1-O- $\beta$ -D-Glucopyranosyl-(2S,2'R,3R,3'E,4E,8E)-N-(2'-Hydroxy-3'-Hexadecenoyl)-9-Methyl-4,8-Icosadien-1,3-Diol (**2**)

White amorphous powder; m.p. 184–186 °C;  $[\alpha] -1.2^\circ$  ( $c = 0.36$ , MeOH). IR (KBr)  $\gamma_{\text{max}}$  3,418, 2,921, 2,851,

1,640, 1,541, 1,466, 1,080, 718  $\text{cm}^{-1}$ ;  $^1\text{H}$ - and  $^{13}\text{C}$ -NMR data see Table 1; EIMS (70 eV)  $m/z$  (rel. int.) 323 (5), 253 (17), 163 (8), 125 (16), 111 (44), 97 (72), 83 (73), 69 (100), 60(94); ESIMS (70 eV)  $m/z$  (rel. int.) 754  $[\text{M} + \text{H}]^+$ , 736  $[\text{M} + \text{H} - \text{H}_2\text{O}]^+$ ; HRESIMS  $m/z$  754.5843 (calcd. for  $\text{C}_{43}\text{H}_{80}\text{NO}_9$ , 754.5833).

### Methanolysis of 1

Compound 1 (11 mg) was refluxed with 3.0 ml of 0.9 N HCl in 80% aq. methanol for 16 h [7]. The reaction mixture was immediately cooled and extracted with *n*-hexane. The *n*-hexane layer was concentrated to give the fatty acid

**Table 1**  $^{13}\text{C}$  and  $^1\text{H}$ -NMR data of compounds 1 and 2

Atom no.	Compound 1 <sup>a</sup>		Compound 2 <sup>b</sup>	
	$^{13}\text{C}$ (DEPT)	$^1\text{H}$ ( <i>J</i> in Hz)	$^{13}\text{C}$ (DEPT)	$^1\text{H}$ ( <i>J</i> in Hz)
1	62.1 (CH <sub>2</sub> )	3.95 ( <i>dd</i> , 11.3, 3.4) 3.73 ( <i>dd</i> , 11.3, 3.0)	69.7 (CH <sub>2</sub> )	4.17 ( <i>dd</i> , 10.2, 5.4) 3.73 ( <i>dd</i> , 10.2, 3.2)
2	54.5 (CH)	3.89 ( <i>m</i> )	54.6 (CH)	3.99 ( <i>m</i> )
3	74.3 (CH)	4.31 ( <i>dd</i> , 7.7, 3.8)	72.9 (CH)	4.14 ( <i>dd</i> , 7.1, 5.5)
4	128.7 (CH)	5.53 ( <i>dd</i> , 15.3, 6.4)	131.0 (CH)	5.48 ( <i>dd</i> , 15.3, 7.4)
5	134.0 (CH)	5.80 ( <i>dt</i> , 15.3, 6.3)	134.5 (CH)	5.73 ( <i>dt</i> , 15.3, 6.6)
6	32.5 (CH <sub>2</sub> )	2.09 ( <i>m</i> )	33.8 (CH <sub>2</sub> )	2.10 ( <i>m</i> )
7	27.5 (CH <sub>2</sub> )	2.08 ( <i>m</i> )	28.6 (CH <sub>2</sub> )	2.07 ( <i>m</i> )
8	123.0 (CH)	5.09 ( <i>t</i> , 6.6)	124.9 (CH)	5.16 ( <i>t</i> , 5.7)
9	136.4 (C)		136.7 (C)	
10	39.7 (CH <sub>2</sub> )	1.95 ( <i>t</i> , 7.7)	40.8 (CH <sub>2</sub> )	1.99 ( <i>t</i> , 7.3)
11	28.0 (CH <sub>2</sub> )	1.36 ( <i>m</i> )	29.1 (CH <sub>2</sub> )	1.41 ( <i>m</i> )
12–17	29.7–29.2 (CH <sub>2</sub> )	1.31–1.25 ( <i>br s</i> )	30.8–30.4 (CH <sub>2</sub> )	1.36–1.31 ( <i>br s</i> )
18	31.9 (CH <sub>2</sub> )	1.31–1.25 ( <i>br s</i> )	33.1 (CH <sub>2</sub> )	1.36–1.31 ( <i>br s</i> )
19	22.7 (CH <sub>2</sub> )	1.31–1.25 ( <i>br s</i> )	23.8 (CH <sub>2</sub> )	1.36–1.31 ( <i>br s</i> )
20	14.1 (CH <sub>3</sub> )	0.88 ( <i>t</i> , 7.0)	14.5 (CH <sub>3</sub> )	0.92 ( <i>t</i> , 7.0)
21	16.0 (CH <sub>3</sub> )	1.58 ( <i>s</i> )	16.2 (CH <sub>3</sub> )	1.62 ( <i>s</i> )
NH		7.03 ( <i>br s</i> )		7.75 ( <i>d</i> , 9.3)
1'	173.0 (C)		175.4 (C)	
2'	73.2 (CH)	4.54 ( <i>d</i> , 7.1)	74.1 (CH)	4.46 ( <i>d</i> , 5.8)
3'	127.1 (CH)	5.55 ( <i>dd</i> , 15.2, 7.1)	129.0 (CH)	5.51 ( <i>dd</i> , 15.3, 6.0)
4'	136.3 (CH)	5.90 ( <i>dt</i> , 15.2, 7.7)	134.7 (CH)	5.85 ( <i>dt</i> , 15.3, 7.7)
5'	32.3 (CH <sub>2</sub> )	2.06 ( <i>m</i> )	33.4 (CH <sub>2</sub> )	2.03 ( <i>m</i> )
6'	28.9 (CH <sub>2</sub> )	1.38 ( <i>m</i> )	30.2 (CH <sub>2</sub> )	1.42 ( <i>m</i> )
7'–13'	29.7–29.2 (CH <sub>2</sub> )	1.31–1.25 ( <i>br s</i> )	30.8–30.4 (CH <sub>2</sub> )	1.36–1.31 ( <i>br s</i> )
14'	31.9 (CH <sub>2</sub> )	1.31–1.25 ( <i>br s</i> )	33.1 (CH <sub>2</sub> )	1.36–1.31 ( <i>br s</i> )
15'	22.7 (CH <sub>2</sub> )	1.31–1.25 ( <i>br s</i> )	23.8 (CH <sub>2</sub> )	1.36–1.31 ( <i>br s</i> )
16'	14.1 (CH <sub>3</sub> )	0.88 ( <i>t</i> , 7.0)	14.5 (CH <sub>3</sub> )	0.92 ( <i>t</i> , 7.0)
Glucosyl moiety				
1''			104.7 (CH)	4.29 ( <i>d</i> , 7.7)
2''			75.0 (CH)	3.22 ( <i>t</i> , 8.1)
3''			77.9 (CH)	3.37 ( <i>t</i> , 8.8)
4''			71.6 (CH)	3.30 ( <i>m</i> )
5''			78.0 (CH)	3.30 ( <i>m</i> )
6''			62.7 (CH <sub>2</sub> )	3.89 ( <i>br d</i> , 11.7) 3.69 ( <i>dd</i> , 11.7, 4.3)

Data assignments were made by DEPT, COSY, HMQC, and HMBC analysis

<sup>a</sup> Measured in  $\text{CDCl}_3$

<sup>b</sup> Measured in  $\text{CD}_3\text{OD}$

methyl ester **1a**, which could be identified as methyl 2-hydroxy-3-hexadecenoate through GC-MS showing the molecular ion peak at  $m/z$  284 and fragment ion peaks at  $m/z$  253  $[M - OMe]^+$ , 235  $[M - OMe - H_2O]^+$ , and  $m/z$  85  $[M - OMe - C_{12}H_{25}]^+$ . The aqueous MeOH layer was neutralized with saturated  $Na_2CO_3$ , concentrated to dryness, and extracted with EtOAc. The EtOAc phase was filtered, concentrated, and purified by CC over silica gel eluted with petroleum ether/acetone (5:1) to give a long-chain base (LCB, **1b**), which showed a pseudo-molecular ion peak at 340  $[M + H]^+$  in the EI spectrum.

### Methanolysis of **2**

Following the same method as that of **1**, compound **2** was also methanolized and analyzed by GC-MS, showing the same result as those of **1**.

### Antifungal Assay

The antifungal assay against *Candida albicans* (ATCC 10231) was performed by use of a modified Well Diffusion method that was referenced to the National Committee for Clinical Laboratory Standards (NCCLS) [8, 9]. Sabouraud dextrose agar plates were swabbed with the respective broth culture of *C. albicans* (diluted to 0.5 McFarland Standard with saline) and kept for 15 min for absorption to take place. Wells were made in agar plates using the broad end of a sterile Pasteur pipette (6 mm in diameter), and 20  $\mu$ l of 1 mg  $ml^{-1}$  sample dissolved in 5% aqueous DMSO was added to each well. Twenty micro liter of 0.1 mg  $ml^{-1}$  amphotericin B in 5% aqueous DMSO were used as positive control. The plates were incubated at 37 °C for 48 h and the diameters of the inhibition zones were measured in millimeter after the incubation period.

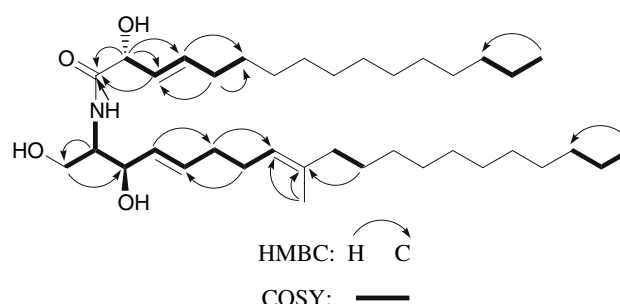
## Results and Discussion

The culture broth extract of *A. niger* was separated by CC on silica gel, RP-18, and Sephadex LH-20 to give compounds **1** and **2**. Their structures were elucidated as follows.

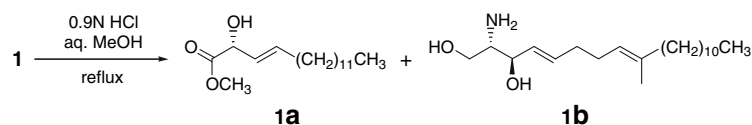
Compound **1** was obtained as white amorphous powder. The positive HRESI-MS spectrum exhibited a molecular ion peak at  $m/z$  592.5314  $[M + H]^+$  which suggested the molecular formula as  $C_{37}H_{69}NO_4$  (calcd. for  $C_{37}H_{70}NO_4$  592.5304). Its IR spectrum exhibited the absorption bands for secondary amide at 3,274 (spike) and 1,630  $cm^{-1}$  and for hydroxyl groups at 3,377 (broad)  $cm^{-1}$ . In the  $^{13}C$  and  $^1H$ -NMR spectra (Table 1), the tertiary carbon signal resonated at  $\delta_C$  173.0 was assigned to an amide carbon, while

five methine signals presented at  $\delta_C$  123.0 ( $\delta_H$  5.09), 127.1 ( $\delta_H$  5.55), 128.7 ( $\delta_H$  5.53), 134.0 ( $\delta_H$  5.80), and 136.3 ( $\delta_H$  5.90), and one quaternary carbon at  $\delta_C$  136.4 indicated the presence of three double bonds. The signals resonated at  $\delta_C$  14.1 ( $CH_3 \times 2$ ) and  $\delta_H$  0.88 (6H, *t*,  $J = 7.0$  Hz) indicated the presence of two terminal methyls. Additionally, the  $^{13}C$  and  $^1H$ -NMR spectra showed resonances for a hydroxymethyl at  $\delta_C$  62.1 ( $\delta_H$  3.95 and 3.73), two hydroxymethines at  $\delta_C$  73.2 ( $\delta_H$  4.54) and 74.3 ( $\delta_H$  4.31), a methine bonded to nitrogen at  $\delta_C$  54.5 ( $\delta_H$  3.89), and resonances for aliphatic chains among  $\delta_C$  28–32 ( $\delta_H$  1.25–1.31). The above spectral data and literature precedents enabled the structure of **1** to be established as (2*S*,2'*R*,3*R*,3'*E*,4*E*,8*E*)-*N*-(2'-hydroxy-3'-hexadecenoyl)-9-methyl-4,8-icosadien-1,3-diol. This conclusion could be further confirmed as follows. The methine proton at  $\delta_H$  3.89 (H-2) exhibited correlations in the COSY spectrum (Scheme 2) with the amide proton ( $\delta_H$  7.03, NH), the hydroxymethyl ( $\delta_H$  3.95 and 3.73, H-1a and H-1b), and the hydroxymethine ( $\delta_H$  4.31, H-3). The latter displayed further COSY correlation with an olefinic methine at  $\delta_H$  5.53 (H-4). In the HMBC spectrum (Scheme 2), the protons at  $\delta_H$  3.89 (H-2) and  $\delta_H$  3.73 (H-1b) exhibited correlations with the hydroxymethyl ( $\delta_C$  62.1, C-1) and the hydroxymethine ( $\delta_C$  74.3, C-3), respectively. The hydroxymethine at  $\delta_H$  4.54 (H-2') displayed correlations in the HMBC spectrum with the carbonyl at  $\delta_C$  173.0 and the olefinic methines at  $\delta_C$  127.1 (C-3') and 136.3 (C-4'). The above COSY and HMBC correlations indicated the presence of a 1,3-dihydroxy-4-en- unit in the sphingosine moiety and a 2-hydroxy-3-en- fatty acid moiety in **1**.

Acidic methanolysis of **1** (Scheme 3) produced a long chain fatty acid methyl ester **1a**, which was identified as methyl 2-hydroxy-3-hexadecenoate by GC-MS analysis as evidenced by a molecular ion peak at  $m/z$  284 and three characteristic fragment ion peaks at  $m/z$  253  $[M - OMe]^+$ , 235  $[M - OMe - H_2O]^+$ , and 85  $[M - OMe - C_{12}H_{25}]^+$ . The remained long chain base (LCB, **1b**) was suggested to be a  $C_{21}$  sphingosine as supported by a pseudo-molecular ion peak at 340  $[M + H]^+$  (attributed to  $C_{21}H_{42}NO_2$ ) in its EI spectrum. These two segments were also confirmed by the



**Scheme 2** Key HMBC and  $^1H$ - $^1H$  COSY correlations of **1**

**Scheme 3** Methanolysis of **1**

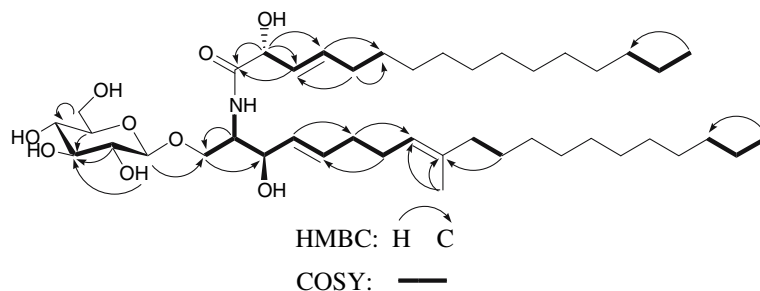
fragment ion peaks at  $m/z$  253 ( $C_{16}H_{29}O_2$ ), 323 ( $C_{21}H_{39}O_2$ ), and 338 ( $C_{21}H_{40}NO_2$ ) in the EI spectrum of **1**. The double bonds at the positions C-3' and C-4 were determined to be *trans*-type by the coupling constants ( $J_{3', 4'} = 15.2$  Hz and  $J_{4, 5} = 15.3$  Hz), while the double bond at C-8 was also identified as *trans*-type due to the chemical shift of C-9 methyl at  $\delta_C$  16.0 (C-21) in the  $^{13}C$ -NMR spectrum [10], and this was confirmed by the comparison with the chemical shift of the C-9 methyl ( $\delta_C$  15.9) of (2*S*,3*R*,4*E*,8*E*)-1-( $\beta$ -D-glucopyranosyl)-3-hydroxy-2-[(*R*)-2'-hydroxyheptadecanoyl]amino-9-methyl-4,8-octadecadiene [7]. Associated with the correlations observed in the HMBC and  $^1H$ - $^1H$  COSY (Scheme 2), the linear structure of the long chain fatty acid and the LCB were elucidated as 2-hydroxy-3*E*-hexadecenoic acid and (4*E*,8*E*)-2-amino-1,3-dihydroxy-9-methyl-4,8-dien-icosane, respectively.

The absolute stereochemistry for sphingolipids is commonly characterized by the comparison of the NMR data with related literature reports [1, 7, 11, 12]. For **1**, the configurations at C-2, C-2', and C-3 were determined based on the proton chemical shifts and coupling constants at  $\delta_H$  3.95 (*dd*, 11.4, 3.4, H-1a),  $\delta_H$  3.73 (*dd*, 11.3, 3.0, H-1b),  $\delta_H$  3.89 (*m*, H-2),  $\delta_H$  4.54 (*d*, 7.1, H-2'), and  $\delta_H$  4.31 (*dd*, 7.7, 3.8, H-3), which were identical to those of the previously reported for (2*S*,2'*R*,3*R*,3'*E*,4*E*,8*E*)-*N*-(2'-hydroxy-3'-octadecenoyl)-9-methyl-4,8-octadecadiene-1,3-diol (**3**), a sphingolipid previously isolated from *Penicillium funiculosum* (13). Meanwhile, the specific optical rotation of **1** ( $[\alpha]_D^{20} - 5.6$ ) was also in agreement with that of **3** ( $[\alpha]_D^{25} - 8.2$ ) [13]. Accordingly, the structure of **1** was established as (2*S*,2'*R*,3*R*,3'*E*,4*E*,8*E*)-*N*-(2'-hydroxy-3'-hexadecenoyl)-9-methyl-4,8-icosadien-1,3-diol, which was named as asperamide A.

Compound **2** was also obtained as a white amorphous powder and its formula was determined as  $C_{43}H_{79}NO_9$  by the HRESIMS at  $m/z$  754.5843  $[M + H]^+$  (calcd. for

$C_{43}H_{80}NO_9$  754.5833). Its IR spectrum was very similar to that of **1** except for the absorptive band at  $1,080\text{ cm}^{-1}$  attributed to C–O–C group. The  $^1H$  and  $^{13}C$ -NMR spectra (Table 1) were very similar to those of **1** while showing additional signals due to the sugar moiety including an anomeric proton at  $\delta_H$  4.29 (*d*,  $J = 7.7$  Hz), four protons geminal to the hydroxyl group between  $\delta_H$  3.22–3.37 and hydroxymethyl protons at  $\delta_H$  3.69 and 3.89 in the  $^1H$ -NMR spectrum as well as the presence of six additional oxygenated carbons at  $\delta_C$  104.7 (CH), 78.0 (CH), 77.9 (CH), 75.0 (CH), 71.6 (CH), and 62.7 (CH<sub>2</sub>) in the  $^{13}C$ -NMR spectrum. These data suggested that **2** was a  $\beta$ -D-glucopyranoside of **1**. The attachment of the glucose moiety at C-1 was proved by the significant downfield chemical shift ( $\Delta$  7.6 ppm) of the hydroxymethyl carbon at  $\delta_C$  69.7 (C-1) in the  $^{13}C$ -NMR spectrum and confirmed by the additional correlation between the anomeric proton ( $\delta_H$  4.29, H-1") and the hydroxymethyl carbon ( $\delta_C$  69.7, C-1) in the HMBC spectrum (Scheme 4). The coupling constant for the anomeric proton (7.7 Hz) indicated the  $\beta$ -configuration for the glucosyl moiety. Methanolysis of **2** also produced the same main product, methyl 2-hydroxy-3-hexadecenoate as that of **1**. The absolute configuration of the core structure at chiral centers 2, 3, and 2' was also determined as 2*S*, 3*R*, and 2'*R* with the same method as **1** by comparison with the reported  $^1H$  and  $^{13}C$ -NMR chemical shifts of two glycosphingolipids Pen II (the glucoside of **3**) [13] and cerebroside C [14]. Therefore, the structure of **2** was determined as 1-*O*- $\beta$ -D-glucopyranosyl-(2*S*,2'*R*,3*R*,3'*E*,4*E*,8*E*)-*N*-(2'-hydroxy-3'-hexadecenoyl)-9-methyl-4,8-icosadien-1,3-diol, which was named as asperamide B.

A literature survey revealed that sphingolipids containing a 9-methyl- $C_{18}$ -sphingosine moiety have been very commonly and frequently reported, both for natural occurring and synthetic ones [4, 15], while those possessing a 9-methyl- $C_{20}$ -sphingosine moiety have not been reported so far. To the best of our knowledge, compounds **1**

**Scheme 4** Key HMBC and  $^1H$ - $^1H$  COSY correlations of **2**

and **2** represent the first example of sphingolipids consist of a 9-methyl-C<sub>20</sub>-sphingosine moiety. They are also most likely the first new sphingolipids discovered in marine algal-derived fungi.

In the antifungal assay, compound **1** exhibited moderate activity against *Candida albicans*, with a faint while obvious inhibition zone ( $\varphi$  12 mm), compared to the clear inhibition zone ( $\varphi$  12 mm) of the positive control Amphotericin B.

**Acknowledgments** This work was financially supported by the National Natural Science Foundation of China (No. 30530080) and by the Department of Science and Technology of Shandong Province (2006GG2205023). We wish to acknowledge H.-M. Zhong at Qingdao Science and Technology University for his help of the work. The authors are grateful to B.-M. Xia and L.-P. Ding at the Institute of Oceanology, Chinese Academy of Sciences for identifying the algal material. The program Bairen Jihua from the Chinese Academy of Sciences (awarded to B.-G. W.) is also gratefully acknowledged. We would also like to acknowledge the editors and anonymous referees for the critical comments and suggestions to our manuscript.

## References

- Chen JH, Cui GY, Liu JY, Tan RX (2003) Pinelloside, an antimicrobial cerebroside from *Pinellia ternate*. *Phytochemistry* 64:903–906
- Mukhtar N, Iqbal K, Anis I, Malik A (2002) Sphingolipids from *Conyza canadensis*. *Phytochemistry* 61:1005–1008
- Brodesser S, Sawatzki P, Kolter T (2003) Bioorganic chemistry of ceramide. *Eur J Org Chem* 2003:2021–2034
- Tan RX, Chen JH (2003) The cerebrosides. *Nat Prod Rep* 20:509–534
- Bugni TS, Ireland CM (2004) Marine-derived Fungi: a chemically and biologically diverse group of microorganisms. *Nat Prod Rep* 21:143–163
- Wang S, Li XM, Teuscher F, Li DL, Diesel A, Ebel R, Proksch P, Wang BG (2006) Chaetopyranin, a benzaldehyde derivative, and other related metabolites from *Chaetomium globosum*, an endophytic fungus derived from the marine red alga *Polysiphonia urceolata*. *J Nat Prod* 69:1622–1625
- Gao JM, Hu J, Dong ZJ, Liu JK (2001) New glycosphingolipid containing an unusual sphingoid base from the Basidiomycete *Polyporus ellisii*. *Lipids* 36:521–527
- Juliani HR, Biurrun F, Koroch AR, Oliva MM, Demo MS, Trippi VS, Zygadlo JA (2002) Chemical constituents and antimicrobial activity of the essential oil of *Lantana xenica*. *Planta Med* 68:762–764
- Al-Burtamani SKS, Fatope MO, Marwah RG, Onifade AK, Al-Saidi SH (2005) Chemical composition, antibacterial and antifungal activities of the essential oil of *Haplophyllum tuberculatum* from Oman. *J Ethnopharmacol* 96:107–112
- Genshiro K, Yonosuke I, Keisuk T (1994) Fruiting of *Schizophyllum Commune* induced by certain ceramides and cerebrosides from *Penicillium funiculosum*. *Agric Biol Chem* 59:144–147
- Gao JM, Hu J, Dong ZJ, Liu JK (2001) A new ceramide from the Basidiomycete *Russula cyanoxantha*. *Lipids* 36:175–180
- Chen X, Wu YL, Chen D (2002) Structure determination and synthesis of a new cerebroside isolated from the traditional Chinese Medicine *Typhonium giganteum* Engl. *Tetrahedron Lett* 43:3529–3532
- Mori K, Uenishi K (1996) Synthesis of sphingosine relatives. Part 17. Synthesis of (2*S*,2'*R*,3*R*,3'*E*,4*E*,8*E*)-1-*O*-( $\beta$ -D-Glucopyranosyl)-*N*-(2'-hydroxy-3'-octadecenoyl)-9-Methyl-4,8-Sphingadine (Pen II), the major cerebroside isolated from *Penicillium funiculosum* as the fruiting-inducer against *Schizophyllum commune*. *Liebigs Annalen der Chemie*, pp 1–6
- Keusgen M, Yu CM, Curtis JM, Brewer D, Ayer SW (1996) A cerebroside from the marine fungus *Microsphaeropsis olivacea* (Bonord.) hönn. *Biochem Syst Ecol* 24:465–468
- Xie F, Guo SX (2002) Progress in the research on structures and activities of fungi derived sphingolipids. *Chin Pharm J* 37:481–484



# Liquid Chromatography–Mass Spectrometric Analysis of Lipids Present in Human Meibomian Gland Secretions

Igor A. Butovich · Eduardo Uchiyama ·  
Mario A. Di Pascuale · James P. McCulley

Received: 23 April 2007 / Accepted: 27 May 2007 / Published online: 29 June 2007  
© AOCS 2007

**Abstract** The purpose of the study was to qualitatively characterize the major lipid species present in human meibomian gland secretions (MGS) by means of high-performance liquid chromatography with atmospheric pressure ionization mass spectrometric detection of the analytes (NP HPLC-MS). Two different NP HPLC-MS methods have been developed to analyze lipid species that were expected to be present in MGS. The first method was optimized for the analysis of relatively nonpolar lipids [wax esters (WE), di- and triacyl glycerols (DAG and TAG), cholesterol (Chl) and its esters (Chl-E), and ceramides (Cer)], while the second method was designed to separate and detect phospholipids. The major lipid species in MGS were found to be WE, Chl-E, and TAG. A minor amount of free Chl (less than 0.5% of the Chl-E fraction) was detected in MGS. No appreciable amounts of DAG and Cer were found in MGS. The second NP HPLC-MS method, capable of analyzing model mixtures of authentic phospholipids (e.g. phosphatidylglycerol, phosphatidylethanolamine, phosphatidic acid, phosphatidylinositol, phosphatidylserine, phosphatidylcholine, and sphingomyelin) in submicrogram/mL concentrations, showed little or no presence of these species in the MGS samples. These observations suggest that MGS are a major source of the nonpolar lipids of the WE and Chl-E families for the tear film lipid layer (TFLL), but not of the previously reported phospholipid components of the TFLL.

**Keywords** Lipids · HPLC · Mass spectrometry · Tear film lipid layer · Human meibomian gland

## Abbreviations

APCI	Atmospheric pressure chemical ionization
API	Atmospheric pressure ionization
Cer	Ceramide
Chl	Cholesterol
Chl-E	Cholesteryl ester
Chl-O	Cholesteryl oleate
DA	Diarachidoylglycerol
DAG	Diacyl glycerol
DES	Dry eye syndrome
ESI	Electrospray ionization
GC	Gas chromatography
HP	<i>n</i> -Hexane/propan-2-ol (95:5, by vol) solvent mixture
HPA	<i>n</i> -Hexane/propan-2-ol/acetic acid (95:5:0.1, by vol) solvent mixture
HPLC	High-performance liquid chromatography
IS-CID	Ion source collision induced dissociation
MGS	Meibomian gland secretions
MS	Mass spectrometry
NMR	Nuclear magnetic resonance spectroscopy
NP-HPLC	Normal-phase HPLC
C <sub>16:0</sub> /C <sub>18:1</sub> -PA	1-Palmitoyl-2-oleoyl-phosphatidic acid
C <sub>16:0</sub> /C <sub>18:1</sub> -PC	1-Palmitoyl-2-oleoyl-phosphatidylcholine
C <sub>16:0</sub> /C <sub>16:0</sub> -PE	1,2-Dipalmitoyl-phosphatidylethanolamine
C <sub>16:0</sub> /C <sub>18:1</sub> -PG	1-Palmitoyl-2-oleoyl-phosphatidylglycerol
C <sub>18:0</sub> /C <sub>20:4</sub> -PI	1-Stearoyl-2-arachidonoyl-phosphatidylinositol

I. A. Butovich (✉) · E. Uchiyama ·  
M. A. D. Pascuale · J. P. McCulley  
Department of Ophthalmology,  
University of Texas Southwestern Medical Center at Dallas,  
5323 Harry Hines Boulevard, Dallas, TX 75390-9057, USA  
e-mail: igor.butovich@utsouthwestern.edu

PL	Phospholipid(s)
C <sub>18:0</sub> /C <sub>18:1</sub> -PS	1-Stearoyl-2-oleoyl-phosphatidylserine
RT	Retention time (min)
C <sub>18:0</sub> -SM	C <sub>18:0</sub> -sphingomyelin
SS	Stearyl stearate
TAG	Triacyl glycerol
TFLL	Tear film lipid layer
TP	Tripalmitoylglycerol
WE	Wax ester

## Introduction

Lipids that are produced by human meibomian glands (MG) are an integral part of the tear film lipid layer (TFLL) which covers the ocular surface [1–4] and, among other functions, protects it from losing water due to excessive evaporation [3–6]. It is postulated that the lipids form the outermost part of the TFLL [1, 2]. The amount of produced lipid material and its composition largely determine the quality of the TFLL. Changes in lipid profiles of MGS were correlated with the development of dry eye syndrome (DES) [7–9] which is a wide-spread condition that severely deteriorates the quality of life of millions of people [10] and impairs vision [11, 12]. Therefore, qualitative and quantitative characterization of the lipids in MGS could provide vital information about the mechanisms that are central to the development of DES.

Previously, the major classes of MG lipids produced by different mammals have been characterized by thin layer chromatography (TLC, [13, 14]), gas chromatography (GC) [13, 15, 16], high-performance liquid chromatography (HPLC) with UV detection of the analytes [17–19], and <sup>31</sup>P nuclear magnetic resonance (<sup>31</sup>P-NMR) [20]. Most of the earlier research work has been done with animal models (e.g., steer [17, 21], hamster [15], and rabbit [20, 22]). Detected lipids represented a wide range of nonpolar lipids [sterol and wax esters (WEs), tri- and diacylglycerols, free cholesterol, and fatty acids) and a range of more polar lipids including primarily phospholipids. Limited information is available for human samples [13, 18, 19].

Though useful, many of the above techniques have their shortcomings and are not well-suited for analyzing small samples. The TLC-based experiments lack resolving power and specificity, which may lead to misidentification of the analytes. These methods are also prone to problems with sample degradation due to prolonged exposure to air, acids, and bases. GC, on the other hand, is a very sensitive and reproducible method, but it requires that samples be derivatized in order to become volatile. This typically involves partial hydrolysis and transesterification and/or silylation of complex higher molecular weight lipids,

e.g., wax esters (WE) and cholesteryl esters (Chl-E) [7, 13]. Reportedly, GC separation of the corresponding derivatives of the hydrolysis products took several hours and was conducted at high temperatures [13], which could compromise the analytes by inadvertent isomerization and/or decomposition of labile molecules. The higher molecular weight analytes (above C<sub>30</sub> equivalent chain length) were not successfully detected by this method [13]. The product yields and sample recovery during the derivatization procedures are also an issue. Another serious problem that arises from these types of experiments is that it is very difficult, if not impossible, to determine which combination of the resulting hydrolysis products existed in the precursor compounds. Therefore, no full precursor structures have been typically reported, only the corresponding hydrolysis products—fatty acids and alcohols in case of Chl-E and WE [7, 13, 23].

Currently, one of the more promising analytical approaches appears to be HPLC with atmospheric pressure ionization mass spectrometric (API MS) detection of the analytes [24, 25]. The HPLC-MS method combines the resolving power of modern HPLC columns with the high sensitivity and selectivity of the MS detectors. Importantly, API MS also provides critical information on the molecular masses of the analytes, which can be used to identify individual compounds in complex mixtures.

Therefore, the goal of this study was to determine which lipid classes were present in the individual intact samples of human MGS collected from normal subjects, using the HPLC technique combined with API MS detection of the lipids<sup>1</sup>. Compared with previously used procedures, this approach minimized inevitable losses and/or alterations of the analytes that were described above.

## Materials and Methods

The following equipment, reagents, and supplies were used in this study: acetic acid, *n*-hexane, methanol, propan-2-ol, HPLC grade water, and ammonium formate were purchased from Aldrich (Milwaukee, WI, USA) and/or from Burdick & Jackson (Muskegon, MI, USA) through VWR (West Chester, PA, USA). Lipid standards of highest purity available were products of Avanti Polar Lipids, Inc. (Alabaster, AL, USA) and Sigma Chemical Co. (St Louis, MO, USA). A Lichrosphere Si-60 silica gel column (3.2 mm × 150 mm, 5 μm) was a product of Supelco (Bellefonte, PA, USA). A Lichrosphere Diol HPLC column (3.2 mm × 150 mm, 5 μm) was obtained from Phenome-

<sup>1</sup> The results of this study were presented in part at 2006 ARVO Annual Meeting (Butovich et al, *IOVS* 2006;47:ARVO E-Abstract 5605).

nex (Torrance, CA, USA). A Waters Alliance 2695 HPLC Separations Module was purchased from Waters Corp. (Milford, MA, USA). An LCQ Deca XP Max MS<sup>n</sup> spectrometer equipped with an atmospheric pressure chemical ionization (APCI) ion source and an electrospray ionization (ESI) ion source was a product of Thermo Electron Corp. (San Jose, CA, USA).

#### Collection of the MGS

Meibomian gland secretions samples were collected from eight normal young volunteers (four male and four female, average age  $31 \pm 3$  years, with no signs and histories of ocular diseases, who underwent standard clinical tests for DES [26–31]). The samples were analyzed individually 2–4 times each. The study was approved by the Institutional Review Board. Informed consents were obtained from all participating subjects. The research was conducted in accordance with the principles of the Declaration of Helsinki. The samples were collected as follows. A clean, dry, pre-weighed glass vial was filled with ~1 mL of GC/MS-grade chloroform. The MGS were expressed by squeezing each of a subject's four eyelids using a plastic conformer and a cotton swab. The lipid samples were collected directly from the MG orifices with a polished platinum spatula. Care was taken to avoid scrubbing the eyelids. The secretions that had been expressed from the glands immediately solidified at room temperature to assume a waxy texture (Fig. 1). The sample was transferred into the vial with chloroform. The sample solution in chloroform was brought to dryness at room temperature under a stream of dry nitrogen and the vial with the sample was re-weighed to determine the weight of the dry lipid material. Depending on the donors, the dry sample weights were between 0.1 and 1 mg. The standard error of weighing was  $\leq 5\%$  for each of the samples. The average weight of the samples collected from eight individual subjects was 0.43 mg. The samples were stored in a nitrogen atmosphere at  $-80^\circ\text{C}$ . Under such conditions, dry samples were

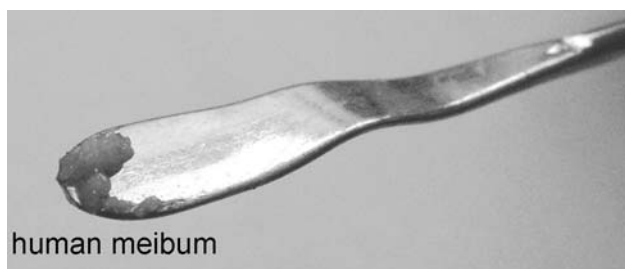


**Fig. 1** A sample of human meibomian gland secretions at room temperature

stable for at least 2 months without apparent deterioration of the major lipid components.

#### HPLC-MS Analysis of Lipids

Considering that MGS were reported to be a complex mixture of nonpolar lipids and phospholipids [1, 2, 7–9, 13–23], two different API techniques were used—APCI, which is optimal for analyzing nonpolar to moderately polar compounds, and ESI, which is better suited for the analysis of complex molecules of moderately polar to polar nature. The choice of lipid standards was based on previously reported groups of lipids determined in mammalian and human MGS [1, 2, 7–9, 13–23]. Two different standard lipid mixtures were prepared. The first model mixture was composed of nonpolar to moderately polar lipids and included cholesteryl oleate (Chl-O, molecular mass 650.6), stearyl stearate (SS, 536.6), tripalmitoylglycerol (TP, 806.7), 1,2- and 1,3-diarachidoylglycerols (DA, 680.6), free cholesterol (Chl, 386.7), and C<sub>18</sub>- and C<sub>24</sub>-ceramides (Cer, 565.5 and 649.6, respectively). The second model mixture was composed of standard phospholipids (PLs): 1-palmitoyl-2-oleoyl-phosphatidylglycerol (C<sub>16:0</sub>/C<sub>18:1</sub>-PG, 748.5), 1,2-dipalmitoyl-phosphatidylethanolamine (C<sub>16:0</sub>/C<sub>16:0</sub>-PE, 691.5), 1-palmitoyl-2-oleoyl-phosphatidic acid (C<sub>16:0</sub>/C<sub>18:1</sub>-PA, 674.5), 1-stearoyl-2-arachidonoyl-phosphatidylinositol (C<sub>18:0</sub>/C<sub>20:4</sub>-PI, 886.6), 1-stearoyl-2-oleoyl-phosphatidylserine (C<sub>18:0</sub>/C<sub>18:1</sub>-PS, 789.6), 1-palmitoyl-2-oleoyl-phosphatidylcholine (C<sub>16:0</sub>/C<sub>18:1</sub>-PC, 760.6), and C<sub>18:0</sub>-sphingomyelin (C<sub>18:0</sub>-SM, 731.6).

#### Standard Nonpolar Lipids

Authentic nonpolar lipid standards were analyzed by normal phase (NP) HPLC-MS. A Lichrosphere Diol (3.2 mm  $\times$  150 mm, 5  $\mu\text{m}$ ) HPLC column was used. The samples were dissolved in a *n*-hexane/propan-2-ol/acetic acid (949:50:1, by vol) solvent mixture (HPA). Lipids were isocratically eluted from the column with the HPA solvent mixture at 30  $^\circ\text{C}$  and a flow rate of 0.3 mL/min. The solvent composition was chosen to ensure complete solubility of all the analyzed lipid samples in the indicated concentration ranges, as well as their effective separation and ionization under the tested conditions. In preliminary experiments, the samples (~10–20  $\mu\text{g}$  of total lipid/mL) were dissolved either in chloroform/methanol (2:1, by vol) mixture, or in the mobile phase. There were no differences in the results obtained with either approach. Because of: (1) known ability of chloroform to decompose releasing hydrochloric acid and phosgene, which are capable of deteriorating lipid samples, and (2) poorer miscibility of this relatively polar mixture with our mobile phase, which could change the retention times of the most nonpolar

compounds if injected in large volumes, we chose to dissolve samples in *n*-hexane/propan-2-ol mixtures. Between 1 and 10  $\mu\text{L}$  of the sample solutions were injected. The entire flow of the effluent was directed into an APCI ion source and analyzed either in the positive, or the negative ion modes. High-purity nitrogen was utilized as sheath gas. The following MS settings were used: sheath gas flow of 25 arbitrary units; auxiliary/sweep gas 5; vaporizer temperature 375  $^{\circ}\text{C}$ ; capillary temperature 300  $^{\circ}\text{C}$ ; capillary voltage 12 V (for positive ion mode experiments) and  $-15$  V (for the negative ion mode). The discharge current was set to be 5  $\mu\text{A}$ . The full MS spectra were typically collected between  $m/z$  values of 200 and 1,000 for the entire period of the experiment.

### Standard Phospholipids

The samples of standard PLs and their mixtures were analyzed by NP HPLC-MS using a Lichrosphere Si-60 (3.2 mm  $\times$  150 mm, 5  $\mu\text{m}$ ) HPLC column. HPLC separation of the polar lipids (mainly, PL) was performed using gradient elution of the lipids by *n*-hexane/propan-2-ol/5 mM aqueous ammonium formate mixtures at 30  $^{\circ}\text{C}$  according to the protocol presented in Table 1. The entire flow of the effluent was directed to the ESI ion source and analyzed either in the positive, or the negative ion modes. A mixture of standard PLs ( $\sim 1$   $\mu\text{g}/\text{mL}$  each) was dissolved in a *n*-hexane/propan-2-ol (95:5, by vol) solvent mixture (HP). No acetic acid was added to this solvent to avoid possible hydrolysis/isomerization of the compounds. Between 0.5 and 10  $\mu\text{L}$  of the sample solutions were injected. The following MS settings were used: sheath gas flow of 25 arbitrary units; auxiliary/sweep gas 0; capillary temperature 300  $^{\circ}\text{C}$ ; spray voltage 3 kV; capillary voltage 6 V (for positive ion mode experiments) and  $-21$  V (for the negative ion mode). The full MS spectra were typically collected between  $m/z$  values of 150–200 and 1,000 for the entire period of the experiment.

**Table 1** Gradient NP HPLC analysis of phospholipids on a Lichrosphere Si-60 column

Step	Time (min)	Flow (mL/min)	Propan-2-ol (%)	5 mM $\text{NH}_4^+\text{COO}^-$ in water (%)	<i>n</i> -Hexane (%)
1	0	0.5	40	2	58
2	5	0.5	40	2	58
3	25	0.5	40	5	55
4	40	0.5	40	5	55
5	41	1	40	5	55
6	60	1	40	5	55
7	61	0.5	40	2	58
8	70	0.5	40	2	58

For the compounds of phosphatidylcholine (PC) and sphingomyelin (SM) families, additional MS experiments were carried out that took advantage of the presence of a unique common positively charged phosphocholine fragment  $(\text{HO})_2\text{P}(\text{O})\text{O}-(\text{CH}_2)_2-\text{N}^+(\text{CH}_3)_3$  (theoretical molecular mass and  $m/z$  184.1) in both the PL families. The lipid components of the HPLC effluent were subjected to the ion source collision induced dissociation (IS-CID) at energy of 90 V and analyzed in the positive ion mode using the settings described above. When phosphocholine-containing lipids were present in the lipid mixture, a prominent fragmentation product with  $m/z$  value of 184.1 was invariably observed. This product ion was used as an analytical ion for detecting PC and/or SM in human MGS and model lipid mixtures.

### Meibomian Gland Secretions

Individual samples of MGS were dissolved in chloroform to bring the final concentration of their stock solutions to 500  $\mu\text{g}$  total lipid/mL. The working solutions of the analytes were made by dissolving the chloroformic stock solutions with the HP solvent. For nonpolar lipids analyses, the samples were diluted to 25  $\mu\text{g}/\text{mL}$  as the signals of the nonpolar lipids were strong. The injection volume was between 1 and 5  $\mu\text{L}$ . For routine lipid analyses in the negative ion mode, the optimal working sample concentration was found to be 100  $\mu\text{g}/\text{mL}$ , while the sample volume varied between 1 and 15  $\mu\text{L}$ . In an attempt to detect the very minor (phospholipid) components of MGS (see below), the stock sample solutions in chloroform were concentrated to  $\sim 3$  mg dry weight/mL, and the injected without diluting with the HPLC mobile phase. The injection volume was increased up to 20  $\mu\text{L}$ . The samples were analyzed exactly as described above for nonpolar lipids and phospholipids.

## Results

To analyze sub-milligram amounts of complex lipid mixtures that constitute human MGS, we needed to develop HPLC-MS protocols that would, firstly, provide adequate separation of the lipids of various classes, and, secondly, ensure sufficient sensitivity of the analyses. Considering wide diversity of the lipid species reported to be present in mammalian and human MGS [1, 2, 7–9, 13–23], we developed and tested two separate HPLC-MS protocols designed to analyze, correspondingly, (a) nonpolar lipids, and (b) relatively polar phospholipids. To maximize sensitivity of the MS analyses, nonpolar lipids were analyzed using APCI-MS detection of the analytes, while phospholipids were analyzed mostly using the ESI technique.

## HPLC-MS Analyses of Standard Nonpolar Lipids

A typical total ion chromatogram (TIC) of a nonpolar lipid mixture taken in the positive ion mode is presented in Figs. 2 and 3. The test mixture was composed of Chl-O, SS, TP, 1,2- and 1,3-DA, Chl, and C<sub>24</sub>- and C<sub>18</sub>-Cer, all of which were used in equimolar ratio. The effluent was monitored in the positive ion mode. There were six HPLC peaks detected in the positive ion mode (peaks I–VI, Fig. 2a), and only two in the negative ion mode (peaks VII and VIII, Fig. 3a).

The MS spectrum of peak I (Fig. 2a) showed the presence of the following major ions with *m/z* values of 369.6, 537.7, and 551.6. The reconstructed chromatograms of those ions revealed three coeluting peaks each with RT of ~3.1 min (Figs. 2b–d). In a separate experiment, it was observed that individually injected Chl-O, SS, and TP each had retention times (RT) of about 3.1 min (data not shown). These compounds coeluted regardless of the solvent composition or the HPLC column. Upon NP HPLC-MS analysis, Chl-O (and other Chl-Es) produced a characteristic fragment with an *m/z* value of 369.4 (Chl–H<sub>2</sub>O + H<sup>+</sup>; theoretical *m/z* 369.4) through a neutral loss of oleic acid (molecular weight 282.3). SS was detected as an intense ion with *m/z* 537.7 ([M + H]<sup>+</sup>; theoretical *m/z* 537.6), while TP was seen as a signal *m/z* 807.8 ([M + H]<sup>+</sup>; theoretical *m/z* 807.7) and a major fragment *m/z* 551.6 ([M – 256 + H]<sup>+</sup>). The later was formed from the precursor ion *m/z* 807.7 through an apparent neutral loss of palmitic acid (molecular weight 256.2). Therefore, peak I was identified as a mixture of coeluting Chl-O, SS, and TP.

High-performance liquid chromatography peaks II and III (Fig. 2a) produced identical signals *m/z* 663.6 (major) and 369.5 (minor). Fragment *m/z* 663.6 with all likelihood was identified as a product of DA dehydration ([M–H<sub>2</sub>O + H]<sup>+</sup>, theoretical mass 663.6), while ion *m/z* 369.5 was a product of neutral loss of arachidic acid residue (molecular weight 312.3). Because (a) the tested compound was a mixture of two positional isomers of DA (1,2- and 1,3-DA), and (b) 1,2- and 1,3-diacyl glycerols (DAG) are known to rapidly undergo spontaneous positional isomerization [32, 33] via acyl-migration, their order of elution remained unknown.

High-performance liquid chromatography peak IV of the nonpolar lipid mixture coeluted with individual Chl and gave one major signal with *m/z* 369.3, similar to the one observed in HPLC peak I. Therefore, both Chl and Chl-O produced identical characteristic fragments, which could be used to identify Chl-containing lipids in complex mixtures. Due to the substantial differences in the RT values between Chl-O (RT 3.1 min) and free Chl (RT 6.0 min), one can

easily discriminate between these two species if their RTs are known.

Peaks V and VI were C<sub>24</sub>- and C<sub>18</sub>-Cer (Fig. 2a). When injected individually, the longer-chain C<sub>24</sub>-Cer eluted faster than its C<sub>18</sub>-counterpart (RT 10.0 and 11.1 min, respectively). C<sub>24</sub>-Cer produced two characteristic peaks *m/z* 650.6 ([M + H]<sup>+</sup>) and 632.5 ([M–H<sub>2</sub>O + H]<sup>+</sup>), while C<sub>18</sub>-Cer gave ions *m/z* 566.4 ([M + H]<sup>+</sup>) and 548.5 ([M–H<sub>2</sub>O + H]<sup>+</sup>).

Interestingly, under the conditions of the NP HPLC-MS analysis in the HPA solvent mixture, all the tested nonpolar compounds, and their fragments, were easily detected as proton adducts. This finding simplified and streamlined the MS analyses of complex lipid mixtures compared to other published procedures that implemented alkaline cations to promote formation of their adducts with certain lipids [34].

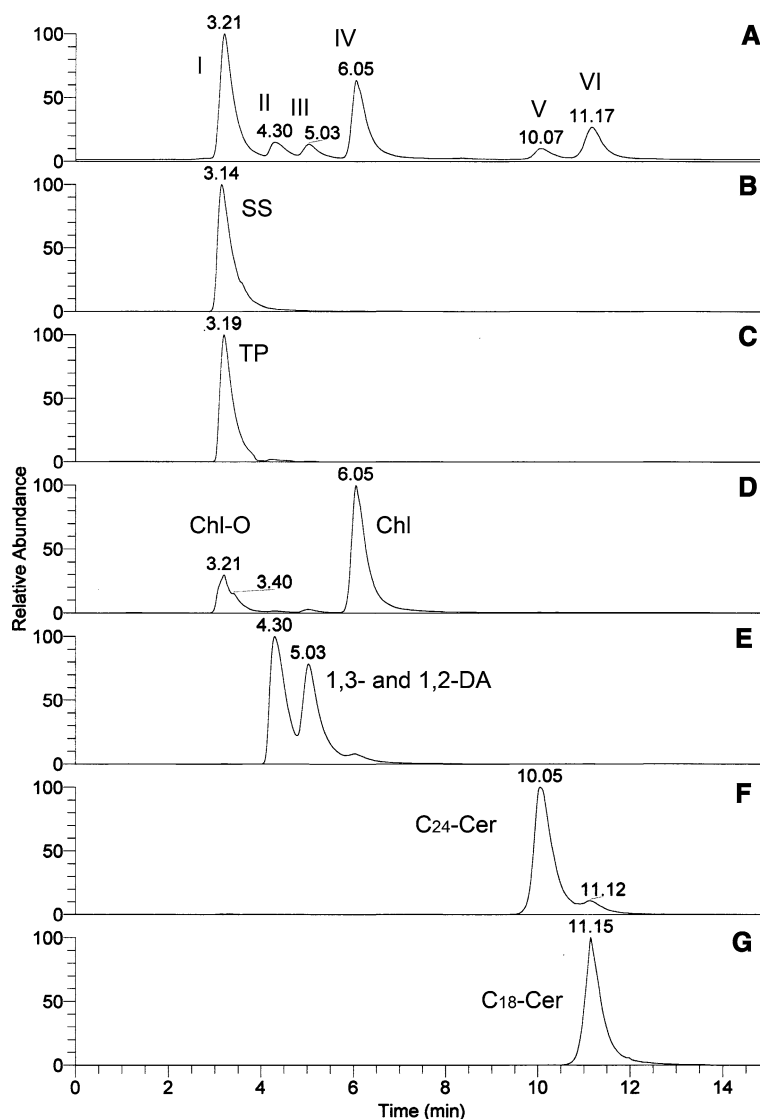
When the mixture of nonpolar lipids was analyzed in the negative ion mode, there were only two HPLC peaks detected with RT of 10.1 and 11.2 min (Fig. 3a–c). Their representative MS spectra (Fig. 3d and e) were indicative of, respectively, C<sub>24</sub>- and C<sub>18</sub>-Cer. Peak VII produced two ions *m/z* 648.7 (C<sub>24</sub>-Cer, [M–H]<sup>–</sup>, theoretical *m/z* 648.6) and 708.3 ([M + CH<sub>3</sub>COO]<sup>–</sup>, theoretical *m/z* 708.6). Peak VIII was identified as C<sub>18</sub>-Cer with *m/z* 564.6 ([M–H]<sup>–</sup>, theoretical *m/z* 564.5) and 624.2 ([M + CH<sub>3</sub>COO]<sup>–</sup>, theoretical *m/z* 624.6). No other tested standard nonpolar lipids produced detectable ions in the negative ion mode.

## NP HPLC-MS Analyses of Standard Phospholipids

Phospholipid analysis was carried out in the negative ion mode, where all of the tested compounds were easily detectable either as anions (M–H)<sup>–</sup> due to the presence of phosphoric acid residues in their structures, or as formic acid adducts [M + HCOO]<sup>–</sup>. A good separation of various PL was achieved using the protocol presented in Table 1 (Fig. 4). The RT values of C<sub>16:0</sub>/C<sub>18:1</sub>-PG, C<sub>16:0</sub>/C<sub>16:0</sub>-PE, C<sub>18:0</sub>/C<sub>20:4</sub>-PI, C<sub>16:0</sub>/C<sub>18:1</sub>-PA, C<sub>18:0</sub>/C<sub>18:1</sub>-PS, C<sub>16:0</sub>/C<sub>18:1</sub>-PC, and C<sub>18:0</sub>-SM detected were, respectively, 20.5, 25.6, 29.8, 31.4, 35.0, 38.1, and 39.4 min. Their characteristic ions that were used as analytical ions are presented in the legend to Fig. 4. The sensitivity of the analysis was sufficient for detecting ≤5 ng of each of the PL per injection. Comparable sensitivity was achieved in the positive ion mode, where most of the lipids were visible either as their molecular ions (M<sup>+</sup>, C<sub>16:0</sub>/C<sub>18:1</sub>-PC, and C<sub>18:0</sub>-SM), or their proton, sodium, and/or ammonium adducts (all the lipids, data not shown).

In a IS-CID experiment conducted in the positive ion mode, authentic C<sub>16:0</sub>/C<sub>18:1</sub>-PC released a phosphocholine ion with *m/z* 184.1. A reconstructed chromatogram of the ion is shown in Fig. 5a. Simultaneously, two precursor

**Fig. 2** Normal phase HPLC analysis of nonpolar lipid standards with APCI-MS detection in the positive ion mode. Panel **a** A TIC of a nonpolar lipid mixture composed of the proton adducts of SS (peak I), TP (peak I), Chl-O (peak I), 1,2- and 1,3-DA (peaks 2 and 3), Chl (peak 4), C<sub>18</sub>- and C<sub>24</sub>-Cer (peaks 5 and 6). Panels **b–g** Reconstructed ion chromatograms of SS (RT 3.1 min;  $m/z$  537.7,  $[M + H]^+$ ), TP (RT 3.2 min;  $m/z$  551.6,  $[M + H - \text{palmitic acid}]^+$ ), Chl-O (RT 3.2 min;  $m/z$  369.4,  $[M + H - \text{oleic acid}]^+$ ), and Chl (RT 6.1 min;  $m/z$  369.4,  $[M + H - H_2O]^+$ ), 1,2- and 1,3-DA (RT 4.3 and 5.0 min;  $m/z$  663.6,  $[M + H - H_2O]^+$ ), C<sub>24</sub>-Cer (RT 10.1 min;  $m/z$  650.5,  $[M + H]^+$ ) and C<sub>18</sub>-Cer (RT 11.2 min;  $m/z$  548.5,  $[M + H - H_2O]^+$ ). Conditions of the analysis: Lichrosphere Diol HPLC column; isocratic elution with HPA solvent mixture; flow rate 0.3 mL/min; column temperature 30 °C



ions with  $m/z$  760.6 and 782.6 ( $M^+$  and  $[M - H + Na]^+$ ) were detected (Figs. 5b and c). Their retention times were identical to that of the phosphocholine ion. Using this method, the detection limit for determining C<sub>16:0</sub>/C<sub>18:1</sub>-PC was at least 0.2 ng or less per injected sample. Similar sensitivity of the analysis was achieved for C<sub>18:0</sub>-SM (data not shown). A few important observations were made as to how C<sub>16:0</sub>/C<sub>18:1</sub>-PC and C<sub>18:0</sub>-SM fragmented. Under the conditions of IS-CID at 90V, C<sub>16:0</sub>/C<sub>18:1</sub>-PC produced ( $M$ )<sup>+</sup> and ( $M - H + Na$ )<sup>+</sup> ions along with the phosphocholine ion  $m/z$  184.1 (see Fig. 5). The relative intensities of these signals were, correspondingly, 1:3:1.5. A similar pattern was observed for C<sub>18:0</sub>-SM (data not shown). Therefore, in such experiments, the phosphocholine ion was a prominent feature of the spectra for both the compounds—C<sub>16:0</sub>/C<sub>18:1</sub>-PC and C<sub>18:0</sub>-SM.

#### NP HPLC-MS Analysis of the MGS

Under the implemented conditions of isocratic NP HPLC-MS analysis in the positive ion mode, all of the tested individual samples of normal human MGS produced qualitatively similar results. The samples collected from the different individuals were remarkably similar to each other. There were no differences in the relative intensities of the major MS peaks seen in both the positive and the negative ion modes, with the exception OA ( $m/z$  283,  $[M + H]^+$ ), which fluctuated from sample to sample. Therefore, with the exception of OA, the chromatograms and mass spectra discussed below are representative of all samples studied (see below).

Analyzed in the positive ion mode using the APCI/MS technique, human MGS produced only one noticeable HPLC peak of nonpolar lipids with RT of 3.1 min

**Fig. 3** Normal phase HPLC analysis of nonpolar lipid standards with ESI-MS detection in the negative ion mode. Panel **a** A TIC of a nonpolar lipid mixture composed of SS, TP, Chl-O, 1,2- and 1,3-DA, Chl, C<sub>18</sub>- and C<sub>24</sub>-Cer. Panels **b** and **c**. Reconstructed ion chromatograms of, respectively, C<sub>24</sub>-Cer (peak VII; RT 10.1 min;  $m/z$  648.7, [M-H]<sup>-</sup>) and C<sub>18</sub>-Cer (peak VIII; RT 11.2 min;  $m/z$  564.6, [M-H]<sup>-</sup>). Other components of the mixture are not visible in the negative ion mode as they do not produce negative ions under the implemented conditions of APCI-MS analysis. Panels **d** and **e** Mass spectra of, respectively, C<sub>24</sub>-Cer (peak RT 10.1 min) and C<sub>18</sub>-Cer (peak RT 11.2 min). Note formation of acetic acid adducts of the compounds in addition to deprotonated species. Conditions of the analysis: Lichrosphere Diol HPLC column; isocratic elution with HPA solvent mixture; flow rate 0.3 mL/min; column temperature 30 °C

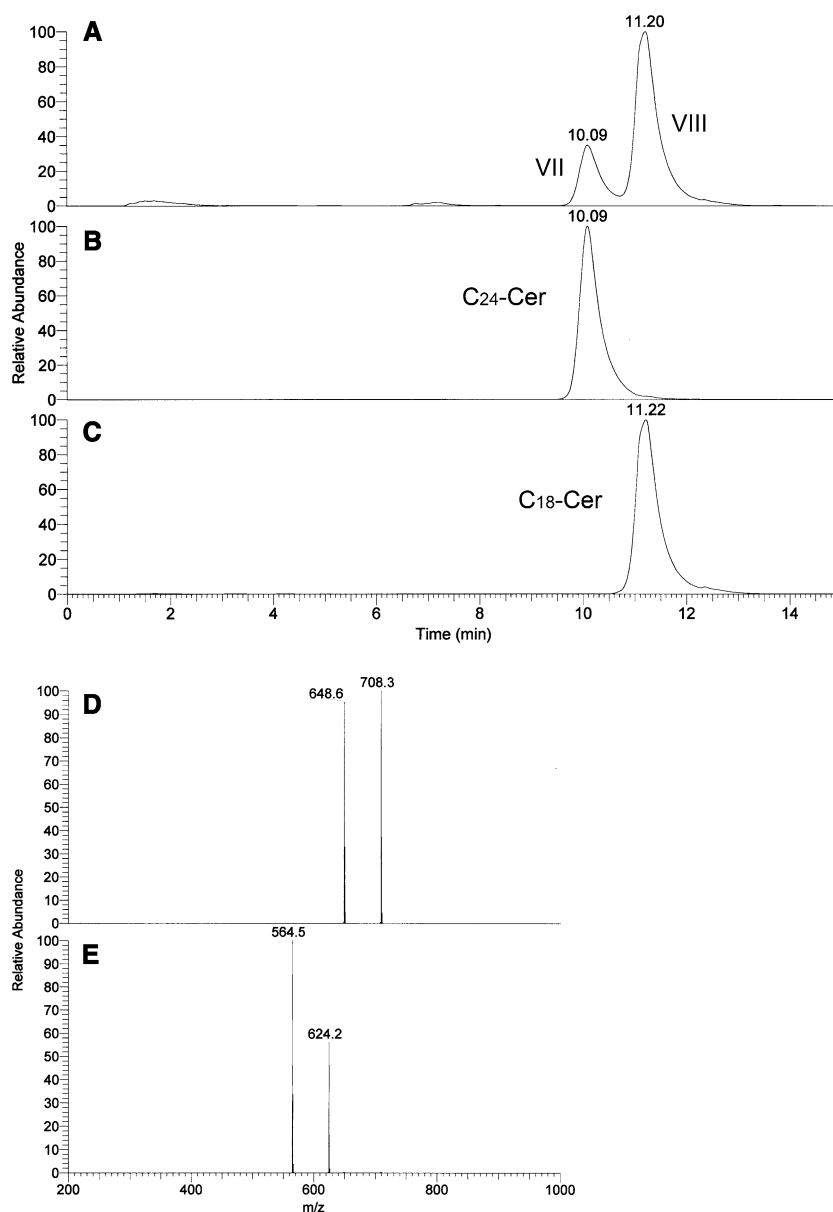


(Fig. 6a). The MS spectrum of this peak is presented in Fig. 6b. NP HPLC separation of the standard mixture of nonpolar lipids (Fig. 2) revealed that three distinctive classes of nonpolar lipids—Chl-O (a cholesteryl ester), SS (a WE) and TP (a triacylglycerol)—co-eluted as one peak with a very similar RT of 3.2 min. A strong peak with RT 3.1 min and a small NP HPLC peak of free Chl (RT 6.0 min) were detected in a reconstructed chromatogram of the same sample of MGS after extraction of ion  $m/z$  369.3 (Fig. 6c). The major component with  $m/z$  369.4 coeluted with Chl-O, and, therefore, was tentatively identified as a cholesteryl ester(s). The intensity of the second HPLC peak with  $m/z$  369.3 did not exceed 0.5% of that of the major peak. Its RT and  $m/z$  value were identical to those of free Chl, and, therefore, the compound was tentatively identi-

fied as free Chl. No major components in the MGS that would coelute with lipids of either the DAG or Cer families were detected in the samples. Relative abundances of the major ions detected in the analyzed samples in the HPLC peaks of nonpolar compounds (RT between 3 and 4 min) are presented in Fig. 7.

When the MGS were analyzed in the positive ion mode using NP HPLC-ESI/MS on a Lichrosphere Si-60 column for the expected presence of PLs, several minor HPLC peaks with RTs similar to standard PLs were detected (not shown). The peaks were too small to be reproducibly detected and analyzed. To answer a question whether these compounds were phosphocholine-containing lipids, the samples were analyzed in a IS-CID HPLC-ESI/MS experiment as described above for standard C<sub>16:0</sub>/C<sub>18:1</sub>-PC

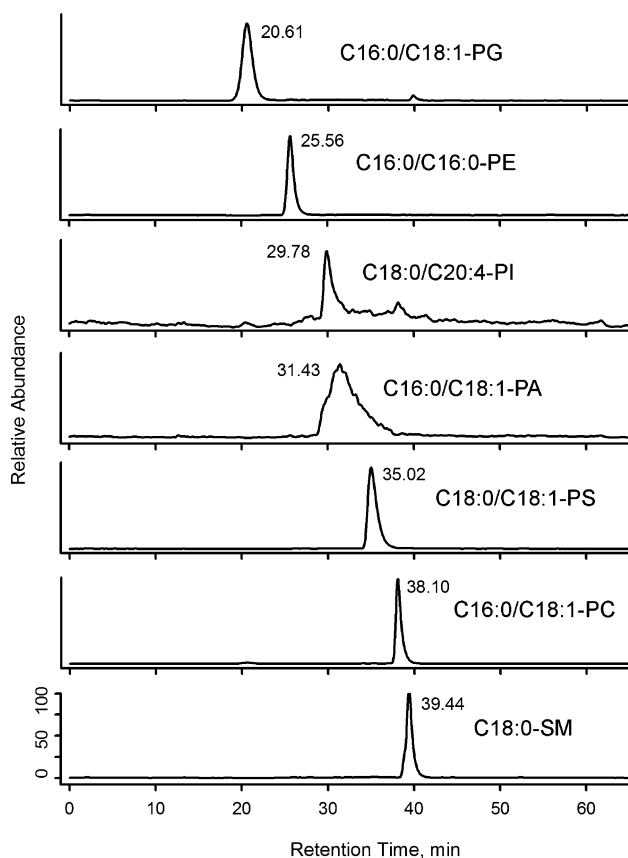


**Fig. 4** Normal phase HPLC analysis of polar lipid standards with ESI-MS detection in the negative ion mode. Reconstructed ion chromatograms of, respectively, C<sub>16:0</sub>/C<sub>18:1</sub>-PG (RT 20.5 min; *m/z* 747.8; [M–H]<sup>−</sup>), C<sub>16:0</sub>/C<sub>16:0</sub>-PE (RT 25.6 min; *m/z* 690.6; [M–H]<sup>−</sup>), C<sub>18:0</sub>/C<sub>20:4</sub>-PI (RT 29.9 min, *m/z* 885.6, [M–H]<sup>−</sup>), C<sub>16:0</sub>/C<sub>18:1</sub>-PA (RT 31.4 min; *m/z* 673.7, [M–H]<sup>−</sup>), C<sub>18:0</sub>/C<sub>18:1</sub>-PS (RT 35.0 min; *m/z* 788.5; [M–H]<sup>−</sup>), C<sub>16:0</sub>/C<sub>18:1</sub>-PC (RT 38.1 min; *m/z* 804.8, [M + HCOO]<sup>−</sup>), and C<sub>18:0</sub>-SM (RT 39.4 min; *m/z* 775.6, [M + HCOO]<sup>−</sup>). Conditions of the analysis: Lichrosphere Si-60 HPLC column; gradient elution with a solvent mixture as described in Table 1; column temperature 30 °C

and C<sub>18:0</sub>-SM. However, no detectable HPLC peak was observed when the effluent was monitored at *m/z* 183–185 (Figs. 8a and b). At the same time, if a sample of MGS was pre-mixed with an internal standard (C<sub>16:0</sub>/C<sub>18:1</sub>-PC) to form a mixture of 2.4 mg/mL MGS and 1 μg/mL C<sub>16:0</sub>/C<sub>18:1</sub>-PC (the mass ratio of C<sub>16:0</sub>/C<sub>18:1</sub>-PC to MGS 1:2,400), the ion with *m/z* value of 184.1 was clearly visible (Figs. 8c and d) and eluted with the RT identical to that of authentic C<sub>16:0</sub>/C<sub>18:1</sub>-PC (Fig. 5). The practical limit of detection of the phosphocholine ion was found to be about ≤0.2 ng C<sub>16:0</sub>/C<sub>18:1</sub>-PC/mL (Fig. 5).

A single major HPLC peak was detected in the negative ion mode (Fig. 9a). The peak was composed of a series of apparently related compounds with the most prominent components possessing *m/z* values of 729.8, 757.9, 775.4, 803.3, and 831.3 (Fig. 9b). Its RT (about 1.6 min) was

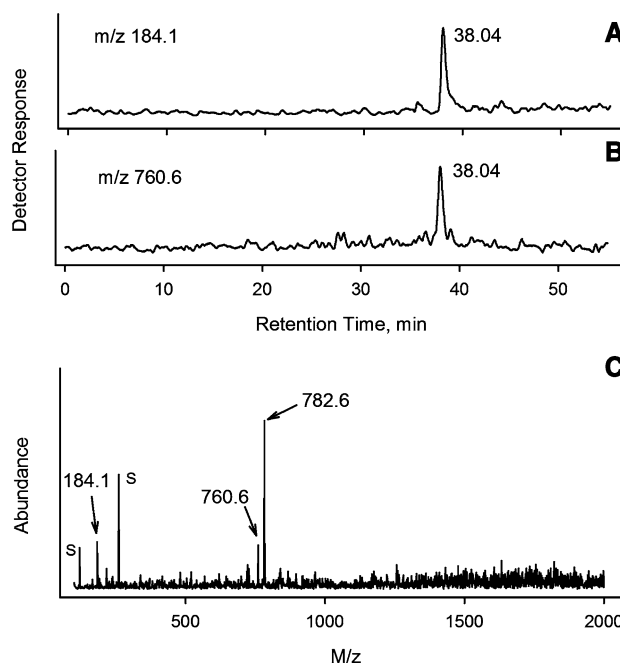


**Fig. 5** Detection of phosphatidylcholine using IS-CID of the precursor(s). Panel a A reconstructed ion chromatogram of ion with *m/z* 184.1 generated from authentic C<sub>16:0</sub>/C<sub>18:1</sub>-PC (0.1 μg/mL). Panel b A reconstructed ion chromatogram of ion with *m/z* 760.6 generated from authentic C<sub>16:0</sub>/C<sub>18:1</sub>-PC (0.1 μg/mL). Panel c ESI-MS spectrum of the peak with RT 38.0 min. Conditions of the analysis: ESI-MS analysis in the positive ion mode. Injection volume 2 μL (=200 pg C<sub>16:0</sub>/C<sub>18:1</sub>-PC). Sample subjected to IS-CID at energy of 90 V. S—solvent ions/impurities present throughout the gradient

much shorter than those of standard phospholipids (20–40 min, Fig. 4) tested in identical conditions. When analyzed on a Lichrosphere Diol HPLC column in the HPA solvent mixture, the compounds with *m/z* values of 729.8, 757.9, 775.4, 803.3, and 831.3 had RTs of 4.0–4.5 min and eluted between WEs (RT 3.2–3.6 min) and DAGs (RT 4.5–6.0 min) (data not shown), and, therefore, belong to the family of nonpolar lipids. Finally, no discernible PL ions were detected above the noise level in the expected PL elution region (RT between 20 and 40 min, Figs. 9a and c).

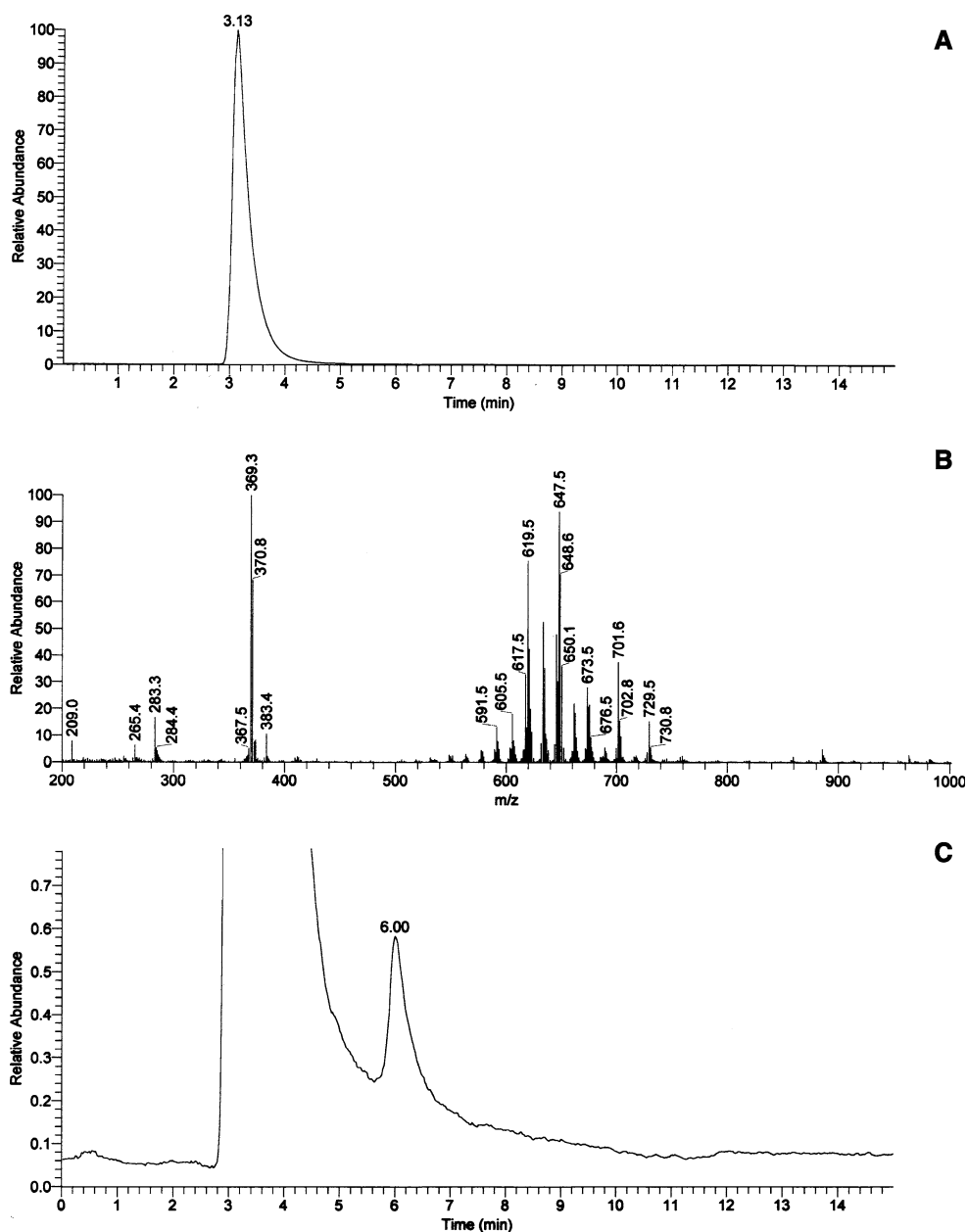
## Discussion

Evaluation of the lipid composition of human MGS is a challenging task because of the difficulties associated with collecting the samples from human subjects, small amount of the gathered secretions (an average sample of collected human MGS was ~0.4 mg), and the complex nature of the lipid mixtures.

To overcome these difficulties, we decided to implement a more sensitive method of HPLC analysis with API (in its



**Fig. 6** NP HPLC analyses of nonpolar lipids present in human MGS with APCI-MS detection in the positive ion mode. Panel **a** A TIC of a mixture of human MGS; Panel **b** Mass spectrum of the peak with RT 3.1 min; Panel **c** Reconstructed ion chromatograms of ion  $m/z$  369.3 (RT 3.1 and 6.0 min; Chl-E and Chl, respectively). Conditions of the analysis: Lichrosphere Diol HPLC column; isocratic elution with HPA solvent mixture; flow rate 0.3 mL/min; column temperature 30 °C



APCI and ESI forms) MS detection of the analytes. A series of different, but apparently homologues compounds was detected in the positive ion mode (Fig. 6). Inasmuch as (1) the MS analysis of the major MGS components produced ions that were characteristic of a mixture of WE with general formula  $C_nH_{2n-2}O_2$  (Fig. 6b); (2) none of them coeluted with standard DAG (Figs. 2 and 6a); and (3) no major ions with  $m/z$  values of 800 and above, which would be indicative of TAG species, were detected in MGS, (Fig. 6b), we concluded that the nonpolar component of MGS was composed mostly of WE, Chl-E, small amounts of Chl itself (Fig. 6c) and, possibly, TAGs [note a group of low intensity ions with  $m/z$  values of 850–890 (Fig. 6b)]. Coelution of WE and Chl-E under the conditions of NP-

HPLC is a well-known problem, which theoretically could have been resolved by using alumina HPLC method proposed by Moreau et al. [35], if not for the poor compatibility of their solvent mixture with mass-spectrometric detectors. Therefore, we are currently conducting a detailed MS/MS analysis of the detected nonpolar species, the results of which will be reported separately.

API MS is undoubtedly the de facto standard method of analyzing phospholipids [24, 25]. The method has also been previously used to evaluate the composition of the nonpolar lipids of the MGS [36, 37]. To our surprise, human subjects did not show a noticeable presence of any of the typical PL species (Figs. 6, 8, 9) in their MGS. At the same time, mixtures of various lipid standards could be

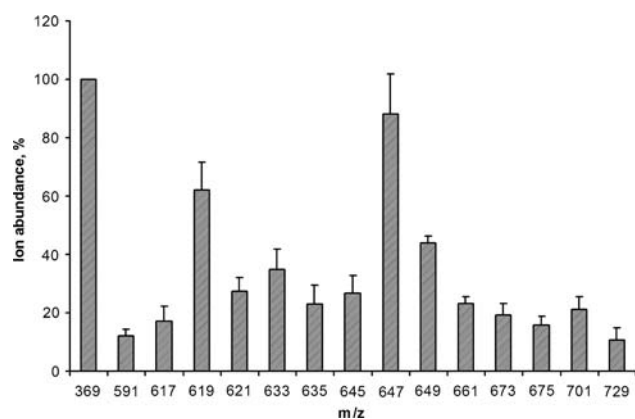


**Fig. 7** Relative abundances of the major ions detected in human meibomian gland secretions in the positive ion mode HPLC-MS experiments. The data obtained for eight individual study samples were taken from Fig. 6 (Panel b) and presented as mean values  $\pm$  standard errors. The most prominent signal  $m/z$  369 ( $[\text{Chl}-\text{H}_2\text{O} + \text{H}]^+$ ) was used as a reference point and assumed to be 100% for each of the samples

routinely and reliably analyzed at  $\leq 1$   $\mu\text{g}/\text{mL}$  levels with the injected volumes being 0.5–10  $\mu\text{L}$ , thus giving a sensitivity level of the analysis of 1 ng per injection and below (Figs. 2, 3, 4, 5). Considering that, firstly, the previously reported presence of PLs in the MGS was around 5% (w/w), of which PC and SM, depending on the publication, amounted to up to 50% of the entire phospholipid pool; and, secondly, that the concentrations of the MGS solutions used in our PL experiments were 0.1–3 mg/mL, the PC and SM species should have been readily visible at even lower (PC + SM)/total lipids ratios. The sensitivity of our current

HPLC-MS approach was such that tested PLs could be detected in complex mixtures if present in mass ratios of 1:2,400 (0.04%, w/w) or less (Fig. 8). The absolute sensitivity for the  $\text{C}_{16:0}/\text{C}_{18:1}$ -PC analysis was shown to be at least an order of magnitude better than that exceeding 0.1  $\mu\text{g}/\text{mL}$ , or 0.2 ng per injection (Fig. 5). Pre-separation of the lipid classes in the HPLC columns before the MS detection/analysis of the MGS samples should have helped in avoiding mass spectrometric interference from non-polar lipids and eliminating any chances of PL ion suppression by nonpolar lipids [9, 34].

Minor compounds with HPLC mobilities comparable to those of  $\text{C}_{16:0}/\text{C}_{18:1}$ -PC and  $\text{C}_{18:0}$ -SM were shown not to have phosphocholine in their structures, as their fragmentation did not produce the phosphocholine ion  $m/z$  184.1 (Fig. 8). Therefore, HPLC-ESI/MS analysis produced no evidences of the presence of typical PLs—PC and SM—in individual normal human MGS, while showing the presence of a set of compounds, whose elucidation is currently underway.

The apparent absence of the phosphocholine product ion in the MS spectra of human normal MGS secretions was surprising as MGs are holocrine glands and their secretions were expected to contain some PLs originating from, at least, cell membranes. On the contrary, our experiments clearly demonstrated that phosphocholine-containing phospholipids were not nearly as dominant PL species in MGS as had been reported before. If PLs were present in our normal MGS samples, their mass ratio to other (non-polar) lipids must have been well below 1:2,400, or two orders of magnitude lower than previously thought. Such

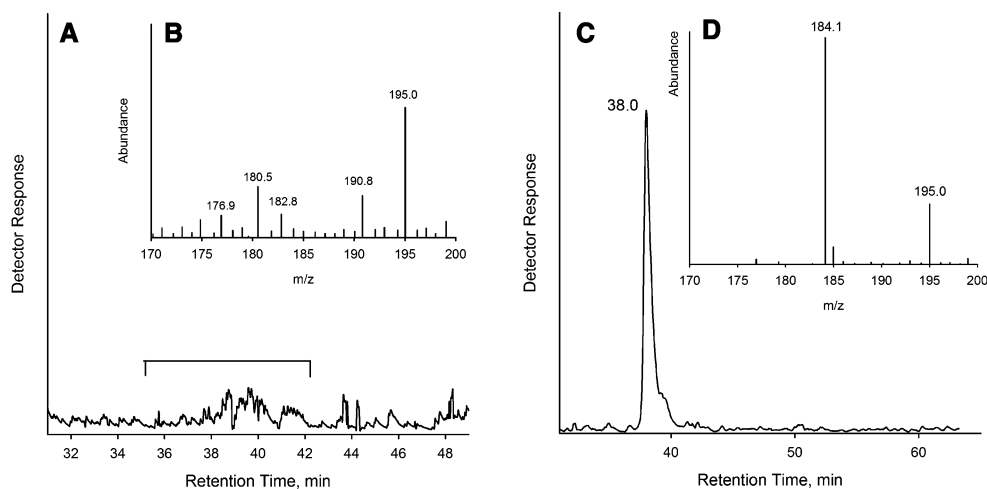


**Fig. 8** NP HPLC-ESI/MS analysis of polar lipids present in human MGS in a collision-induced dissociation experiment in the positive ion mode. Panel a A reconstructed ion chromatogram of ion with  $m/z$  184 generated from human MGS (3 mg/mL) subjected to IS-CID at energy of 90 V. Panel b Partial mass spectrum of the elution region

35–42 min. Panel c A reconstructed ion chromatogram of ion with  $m/z$  184 generated in a HPLC-ESI MS experiment with human MGS (2.4 mg/mL) mixed with 1  $\mu\text{g}/\text{mL}$   $\text{C}_{16:0}/\text{C}_{18:1}$ -PC and subjected to IS-CID at energy of 90 V; Panel d Partial mass spectrum of the elution peak with RT 38 min

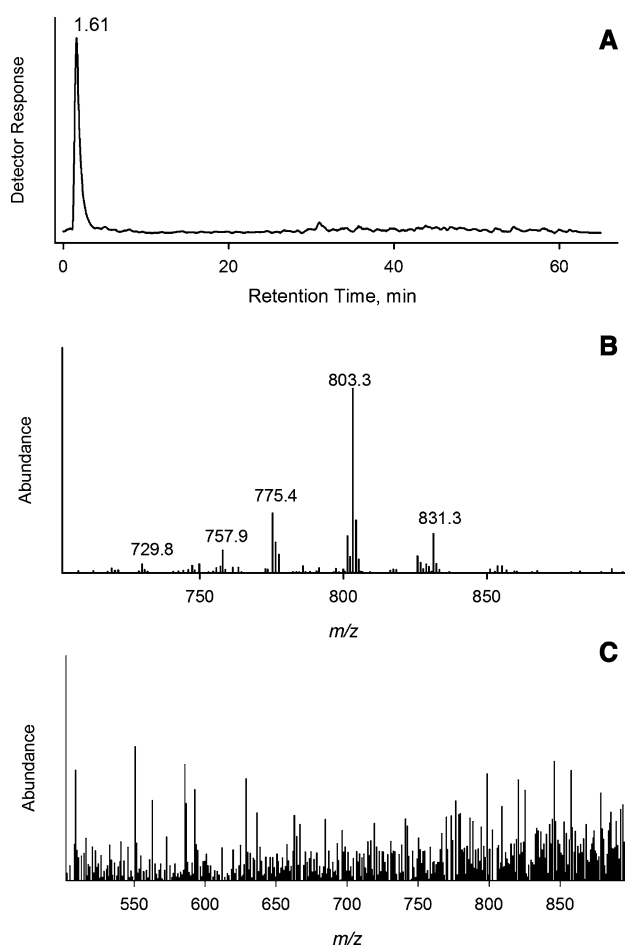


**Fig. 9** Normal phase HPLC analyses of human MGS with ESI-MS detection in the negative ion mode. Panel **a** A TIC of a mixture of human MGS; Panel **b** Mass spectrum of the peak with RT 1.6 min; Panel **c** MS spectrum of the PL fraction (RTs between 20 and 42 min). Note the absence of clearly identifiable signals of PLs. Conditions of the analysis: Lichrosphere Si-60 HPLC column; gradient elution with a solvent mixture as described in Table 1; column temperature 30 °C

the low mass ratio could be indicative of a high prevalence of nonpolar lipids biosynthesis over the production of polar ones in MGs, or high a rate of phospholipid re-absorption/degradation ones the cells filled with large quantities of nonpolar lipids get released from the glands.

The discrepancy between the current findings and the much higher presence of, for example, PE, PC, and SM in MGS reported in the earlier studies [18, 19] could possibly be explained by a range of factors. Those could include, among others, (1) inadvertent contamination of those samples by cell debris originating from various epithelial and MG cells, and, possibly, with lipids produced by corneal epithelial cell, conjunctiva, and/or lacrimal glands; and (2) misidentification of the HPLC elution peaks. Complicating the previous analyses of human MGS was

the choice of the HPLC detection method: in the earlier experiments with human MGS, unmodified lipids were detected by using UV absorbance monitoring at 220 nm [18, 19]. This particular approach was not the best choice as the UV method of detection of lipids lacks sensitivity and specificity as most of the lipids do not have any specific UV chromophores and are virtually transparent at  $\geq 220$  nm. Identification of the analytes was based solely on comparison of their RTs with those of chemical standards [18, 19], which are prone to fluctuate and overlap. Our current techniques of collecting MGS samples and of their HPLC-MS analyses minimized the chances of the above problems and allowed positive identification of various compounds and/or their groups in complex mixtures. Considering that the RTs of some of the minor unidentified compounds detected in our experiments were close to those of  $C_{16:0}/C_{18:1}$ -PC and  $C_{18:0}$ -SM, PC, and SM species reported earlier [18, 19] could, in fact, have been the same unknown compounds that coeluted with the PL standards in our experiments.

With the exception of the  $^{31}\text{P}$ -NMR studies performed on homogenized tarsal plates of rabbits [20], little is known about MGS phospholipids as individual intact species. Their role in formation of TFLL and in the mechanisms underlying human DES remains to be detailed. Some animal species which have been reported to have PLs in their meibum (e.g., steer [17, 21], hamster [15], and rabbit [20, 22]) are not considered to be an ideal model of human DES [38, 39]. Importantly, it was shown by cauterization and subsequent gluing of the MG orifices that much of the lipids that form TFLL in rabbits are supplied by sources other than MG. Those sources were proposed to include ocular surface structures, Harder's gland, and sebaceous glands in the caruncle [39]. Pertinent to this discussion is an observation that large quantities of Chl-E and free Chl could be produced and excreted by corneal epithelial cells, possibly through the high-density lipoprotein-mediated reverse cholesterol transport mechanism ([40] and references cited therein). Therefore, we cannot rule out a priori a possibility that in humans lipids are supplied to the TFLL not only by MG, but by other sources too.

In conclusion, NP HPLC analysis with API detection of the analytes has proven to be an effective tool for evaluating the lipid composition of the human MGS collected from individual subjects. Our results suggest that MGs are a major source of nonpolar lipids of remarkably consistent composition (Fig. 7) for the TFLL, but not of more polar components of phospholipid and ceramide nature.

**Acknowledgment** The project was supported by NIH grants EY012430 and EY016664 and an unrestricted grant from the Research to Prevent Blindness, Inc. (New York, NY, USA). The authors would like to thank Joel D. Aronowicz, MD for his help in collecting samples of human MGS.

## References

- McCulley JP, Shine W (1997) A compositional based model for the tear film lipid layer. *Trans Am Ophthalmol Soc* 95:79–88; discussion 88–93
- McCulley JP, Shine WE (1998) Tear film structure and dry eye. *Contactologia* 20:45–149
- Tsubota K, Yamada M (1992) Tear evaporation from the ocular surface. *Invest Ophthalmol Vis Sci* 33:2942–2950
- Ohashi Y, Gogru M, Tsubota K (2006) Laboratory findings in tear fluid analysis. *Clin Chim Acta* 369:17–28
- Mathers WD (1993) Ocular evaporation in meibomian gland dysfunction and dry eye. *Ophthalmology* 100:347–351
- Mathers WD (2004) Evaporation from the ocular surface. *Exp Eye Res* 78:389–394
- Shine WE, McCulley JP (2000) Association of meibum oleic acid with meibomian seborrhea. *Cornea* 19:72–74
- Sullivan BD, Evans JE, Cermak JM, Krenzer KM, Dana MR, Sullivan DA (2002) Complete androgen insensitivity syndrome: effect on human meibomian gland secretions. *Arch Ophthalmol* 120:1689–1699
- Ham BM, Jacob JT, Cole RB (2005) MALDI-TOF MS of phosphorylated lipids in biological fluids using immobilized metal affinity chromatography and solid ionic-crystal matrix. *Anal Chem* 77:4439–4447
- Schaumberg DA, Sullivan DA, Dana MR (2002) Epidemiology of dry eye syndrome. *Adv Exp Med Biol* 506(part B): 989–998
- Goto E, Yagi Y, Matsumoto Y, Tsubota K (2002) Impaired functional visual acuity of dry eye patients. *Am J Ophthalmol* 133:181–186
- Goto E, Yagi Y, Kaido M, Matsumoto Y, Konomi K, Tsubota K (2003) Improved functional visual acuity after punctual occlusion in dry eye patients. *Am J Ophthalmol* 135:704–705
- Tiffany JM (1978) Individual variations in human meibomian lipid composition. *Exp Eye Res* 27:289–300
- Nicolaides N, Santos EC, Smith RE, Jester JV (1989) Meibomian gland dysfunction. III. Meibomian gland lipids. *Invest Ophthalmol Vis Sci* 30:946–951
- Harvey DJ (1989) Identification by gas chromatography/mass spectrometry of long-chain fatty acids and alcohols from hamster meibomian glands using picolinyl and nicotinate derivatives. *Biomed Chromatogr* 3:251–254
- Shine WE, McCulley JP (1991) The role of cholesterol in chronic blepharitis. *Invest Ophthalmol Vis Sci* 32:2272–2280
- McFadden WH, Bradford DC, Eglinton G, Hajlbrahim SK, Nicolaides N (1979) Application of combined liquid chromatography/mass spectrometry (LC/MS): analysis of petroporphyrins and meibomian gland waxes. *J Chromatogr Sci* 17:518–522
- Shine WE, McCulley JP (2003) Polar lipid in human meibomian gland secretions. *Curr Eye Res* 26:89–94
- Shine WE, McCulley JP (2004) Meibomianitis: Polar lipid abnormalities. *Cornea* 23:781–783
- Greiner JV, Glonek T, Korb DR, Leahy CD (1996) Meibomian gland phospholipids. *Cur Eye Res* 15:371–375
- Nicolaides N, Santos EC (1985) The di- and triesters of the lipids of steer and human meibomian glands. *Lipids* 20:454–467
- Tiffany JM (1979) The meibomian lipids of the rabbit. I. Overall composition. *Exp Eye Res* 29:195–202
- Shine WE, McCulley JP (1993) Role of wax ester fatty alcohols in chronic blepharitis. *Invest Ophthalmol Vis Sci* 34:3515–3521
- Sommer U, Herscovitz H, Welty FK, Costello CE (2006) LC-MS-based method for the qualitative and quantitative analysis of complex lipid mixtures. *J Lipid Res* 47:804–814
- Murphy RC (2002) Mass spectrometry of phospholipids: tables of molecular and product ions. Illuminati Press, Los Angeles
- Mathers WD, Shields WJ, Sachdev M, Petroll WM, Jester JV (1991) Meibomian gland morphology and tear osmolarity: changes with Accutane therapy. *Cornea* 10:286–290
- Macri A, Pflugfelder S (2000) Correlation of the Schirmer I and fluorescein clearance tests with the severity of corneal epithelial and eyelid disease. *Arch Ophthalmol* 118:1632–1638
- McCulley JP, Sciallis GF (1977) Meibomian keratoconjunctivitis. *Am J Ophthalmol* 84:788–793
- Prydal JI, Artal P, Woon H, Campbell FW (1992) Study of human precorneal tear film thickness and structure using laser interferometry. *Invest Ophthalmol Vis Sci* 33:2006–2011
- King-Smith PE, Fink BA, Fogt N, Nichols KK, Hill RM, Wilson GS (2000) The thickness of the human precorneal tear film: evidence from reflection spectra. *Invest. Ophthalmol Vis Sci* 41:3348–3359
- Doane MG, Lee ME (1998) Tear film interferometry as a diagnostic tool for evaluating normal and dry-eye tear film. *Adv Exp Med Biol* 438:297–303
- Stimmel BF, King CG (1934) Preparation and properties of  $\beta$ -monoglycerides. *J Am Chem Soc* 56:1724–1725
- Doerschuk AP (1952) Acyl migrations in partially acylated, polyhydroxylic systems. *J Am Chem Soc* 74:4202–4203
- Ham BM, Cole RB, Jacob JT (2006) Identification and comparison of the polar phospholipids in normal and dry eye rabbit tears by MALDI-TOF mass spectrometry. *Invest Ophthalmol Vis Sci* 47:3330–3338
- Moreau RA, Kohout K, Singh V (2002) Temperature-enhanced alumina HPLC method for the analysis of wax esters, sterol esters, and methyl esters. *Lipids* 37:1201–1204
- Sullivan BD, Evans JE, Krenzer KL, Dana MR, Sullivan DA (2000) Impact of antiandrogen treatment on the fatty acid profile of neutral lipids in human meibomian gland secretions. *J Clin Endocrinol Metabol* 85:4866–4873
- Krenzer KL, Dana MR, Ullman MD, Cermak JM, Tolls DB, Evans JE, Sullivan DA (2000) Effect of androgen deficiency on the human meibomian gland and ocular surface. *J Clin Endocrinol Metabol* 85:4874–4882
- Barabino S, Reza Dana M (2004) Animal models of dry eye: a critical assessment of opportunities and limitations. *Invest Ophthalmol Vis Sci* 45:1641–1646
- Greiner JV, Glonek T, Korb DR, Hearn SL, Whalen AC, Esway JE, Leahy CD (1998) Effect of meibomian gland occlusion on tear film layer thickness. In: Sullivan DA, Dartt DA, Meneray MA (eds) *Lacrimal gland, tear film, and dry eye syndromes 2*. Plenum Press, New York, London
- Cenedella RJ, Fleschner CR (1989) Cholesterol biosynthesis by the cornea. Comparison of rates of sterol synthesis with accumulation during early development. *J Lipid Res* 30:1079–1084

## Cholesterol Oxidation is Increased and PUFA Decreased by Frozen Storage and Grilling of Atlantic Hake Fillets (*Merluccius hubbsi*)

Tatiana Saldanha · Neura Bragagnolo

Published online: 5 July 2007  
© AOCs 2007

### Erratum to: Lipids

DOI 10.1007/s11745-007-3062-4

The original version of this article unfortunately contained several mistakes in Table 2.

Linoleic C18:2  $\omega$ 6 has to be changed to Linoleic 18:2  $\omega$ 6  
Linoleic 18:3  $\omega$ 3 has to be changed to Linolenic 18:3  
 $\omega$ 3 and  
 $\gamma$ -linoleic 18:3  $\omega$ 6 has to be changed to  $\gamma$ -Linolenic  
18:3  $\omega$ 6

Enclosed please find the correct version of Table 2.

---

The online version of the original article can be found under  
doi:10.1007/s11745-007-3062-4.

---

T. Saldanha · N. Bragagnolo (✉)  
Department of Food Science, Faculty of Food Engineering,  
State University of Campinas, 13083-862 Campinas,  
SP, Brazil  
e-mail: neura@fea.unicamp.br

**Table 2** Fatty acids composition (g/100 g of oil) in raw and grilled Atlantic hake during 120 days of storage

	Zero time		30 Days		60 Days		90 Days		120 Days	
	Raw	Grilled	Raw	Grilled	Raw	Grilled	Raw	Grilled	Raw	Grilled
	Lauric C12:0	0.64 ± 0.01 <sup>A</sup>	0.53 ± 0.02 <sup>a</sup>	0.61 ± 0.03 <sup>A</sup>	0.52 ± 0.02 <sup>a</sup>	0.60 ± 0.02 <sup>A</sup>	0.51 ± 0.02 <sup>a</sup>	0.59 ± 0.01 <sup>A</sup>	0.51 ± 0.01 <sup>a</sup>	0.58 ± 0.03 <sup>A</sup>
Myristic 14:0	4.20 ± 0.2 <sup>A</sup>	3.86 ± 0.2 <sup>a</sup>	4.17 ± 0.1 <sup>A</sup>	3.75 ± 0.2 <sup>b</sup>	4.18 ± 0.1 <sup>A</sup>	3.69 ± 0.2 <sup>b</sup>	4.16 ± 0.3 <sup>A</sup>	3.93 ± 0.2 <sup>a</sup>	4.15 ± 0.1 <sup>A</sup>	3.86 ± 0.2 <sup>a</sup>
Pentadecic 15:0	0.95 ± 0.03 <sup>A</sup>	0.77 ± 0.1 <sup>ab</sup>	0.92 ± 0.04 <sup>A</sup>	0.75 ± 0.03 <sup>b</sup>	0.89 ± 0.01 <sup>A</sup>	0.72 ± 0.1 <sup>b</sup>	0.95 ± 0.05 <sup>A</sup>	0.81 ± 0.05 <sup>a</sup>	0.92 ± 0.02 <sup>A</sup>	0.83 ± 0.01 <sup>a</sup>
Palmitic 16:0	13.98 ± 0.4 <sup>A</sup>	13.25 ± 0.4 <sup>a</sup>	13.89 ± 0.2 <sup>B</sup>	13.04 ± 0.4 <sup>b</sup>	13.81 ± 0.3 <sup>B</sup>	13.00 ± 0.2 <sup>b</sup>	13.89 ± 0.4 <sup>B</sup>	13.15 ± 0.2 <sup>a</sup>	13.85 ± 0.5 <sup>B</sup>	13.00 ± 0.3 <sup>b</sup>
Margaric 17:0	0.24 ± 0.05 <sup>A</sup>	0.19 ± 0.03 <sup>a</sup>	0.22 ± 0.01 <sup>A</sup>	0.16 ± 0.05 <sup>a</sup>	0.23 ± 0.02 <sup>A</sup>	0.17 ± 0.02 <sup>a</sup>	0.27 ± 0.01 <sup>A</sup>	0.22 ± 0.01 <sup>a</sup>	0.25 ± 0.03 <sup>A</sup>	0.19 ± 0.01 <sup>a</sup>
Stearic 18:0	1.86 ± 0.6 <sup>A</sup>	1.67 ± 0.2 <sup>a</sup>	1.83 ± 0.2 <sup>A</sup>	1.61 ± 0.3 <sup>a</sup>	1.84 ± 0.01 <sup>A</sup>	1.59 ± 0.3 <sup>ab</sup>	1.75 ± 0.2 <sup>AB</sup>	1.55 ± 0.3 <sup>b</sup>	1.88 ± 0.2 <sup>A</sup>	1.62 ± 0.1 <sup>a</sup>
Arachidic 20:0	0.59 ± 0.02 <sup>A</sup>	0.46 ± 0.03 <sup>a</sup>	0.55 ± 0.01 <sup>AB</sup>	0.45 ± 0.01 <sup>a</sup>	0.56 ± 0.05 <sup>AB</sup>	0.44 ± 0.02 <sup>a</sup>	0.57 ± 0.01 <sup>A</sup>	0.45 ± 0.01 <sup>A</sup>	0.51 ± 0.01 <sup>B</sup>	0.45 ± 0.01 <sup>A</sup>
Behenic 22:0	0.71 ± 0.05 <sup>A</sup>	0.62 ± 0.01 <sup>a</sup>	0.69 ± 0.02 <sup>a</sup>	0.57 ± 0.02 <sup>a</sup>	0.70 ± 0.01 <sup>A</sup>	0.59 ± 0.01 <sup>a</sup>	0.68 ± 0.02 <sup>A</sup>	0.61 ± 0.02 <sup>a</sup>	0.69 ± 0.03 <sup>A</sup>	0.63 ± 0.01 <sup>a</sup>
Lignoceric 24:0	0.67 ± 0.08 <sup>A</sup>	0.58 ± 0.02 <sup>a</sup>	0.64 ± 0.01 <sup>A</sup>	0.55 ± 0.01 <sup>a</sup>	0.66 ± 0.02 <sup>A</sup>	0.52 ± 0.02 <sup>a</sup>	0.66 ± 0.01 <sup>A</sup>	0.56 ± 0.01 <sup>a</sup>	0.60 ± 0.02 <sup>A</sup>	0.54 ± 0.02 <sup>a</sup>
Myristoleic 14:1 <i>ω</i> 9	0.35 ± 0.01 <sup>A</sup>	0.29 ± 0.02 <sup>a</sup>	0.32 ± 0.01 <sup>A</sup>	0.26 ± 0.03 <sup>b</sup>	0.29 ± 0.01 <sup>AB</sup>	0.21 ± 0.01 <sup>c</sup>	0.27 ± 0.02 <sup>B</sup>	0.20 ± 0.05 <sup>c</sup>	0.25 ± 0.04 <sup>B</sup>	0.18 ± 0.01 <sup>d</sup>
Palmitoleic 16:1 <i>ω</i> 7	8.95 ± 0.8 <sup>A</sup>	7.79 ± 0.6 <sup>a</sup>	8.31 ± 0.7 <sup>B</sup>	7.45 ± 0.6 <sup>b</sup>	7.97 ± 0.8 <sup>C</sup>	6.60 ± 0.6 <sup>c</sup>	7.20 ± 0.5 <sup>D</sup>	6.27 ± 0.5 <sup>d</sup>	6.86 ± 0.3 <sup>E</sup>	5.96 ± 0.7 <sup>e</sup>
Margaroleic 17:1 <i>ω</i> 7	2.33 ± 0.4 <sup>A</sup>	1.95 ± 0.1 <sup>a</sup>	2.17 ± 0.4 <sup>AB</sup>	1.56 ± 0.4 <sup>b</sup>	2.04 ± 0.6 <sup>B</sup>	1.35 ± 0.2 <sup>c</sup>	1.72 ± 0.1 <sup>BC</sup>	1.19 ± 0.02 <sup>d</sup>	1.55 ± 0.5 <sup>C</sup>	1.04 ± 0.05 <sup>e</sup>
Oleic 18:1 <i>ω</i> 9	15.85 ± 1 <sup>A</sup>	14.52 ± 1 <sup>a</sup>	14.96 ± 0.9 <sup>B</sup>	13.87 ± 0.5 <sup>b</sup>	14.24 ± 0.8 <sup>C</sup>	12.93 ± 0.7 <sup>c</sup>	13.82 ± 1 <sup>D</sup>	12.42 ± 0.9 <sup>d</sup>	12.97 ± 0.8 <sup>E</sup>	12.00 ± 1 <sup>e</sup>
Gadoleic 20:1 <i>ω</i> 11	0.55 ± 0.02 <sup>A</sup>	0.48 ± 0.03 <sup>a</sup>	0.47 ± 0.01 <sup>AB</sup>	0.36 ± 0.01 <sup>ab</sup>	0.39 ± 0.02 <sup>B</sup>	0.23 ± 0.02 <sup>bc</sup>	0.35 ± 0.02 <sup>BC</sup>	0.20 ± 0.01 <sup>c</sup>	0.24 ± 0.05 <sup>BC</sup>	0.16 ± 0.00 <sup>e</sup>
Erucic 22:1 <i>ω</i> 9	0.47 ± 0.01 <sup>A</sup>	0.34 ± 0.05 <sup>a</sup>	0.36 ± 0.02 <sup>B</sup>	0.29 ± 0.01 <sup>ab</sup>	0.30 ± 0.01 <sup>BC</sup>	0.21 ± 0.03 <sup>bc</sup>	0.25 ± 0.01 <sup>C</sup>	0.18 ± 0.02 <sup>cd</sup>	0.22 ± 0.01 <sup>C</sup>	0.15 ± 0.00 <sup>d</sup>
Nervonic 24:1 <i>ω</i> 6	0.61 ± 0.02 <sup>A</sup>	0.54 ± 0.02 <sup>a</sup>	0.57 ± 0.02 <sup>AB</sup>	0.42 ± 0.01 <sup>b</sup>	0.50 ± 0.01 <sup>B</sup>	0.39 ± 0.01 <sup>b</sup>	0.42 ± 0.01 <sup>BC</sup>	0.35 ± 0.01 <sup>bc</sup>	0.40 ± 0.01 <sup>c</sup>	0.30 ± 0.01 <sup>c</sup>
Linoleic 18:2 <i>ω</i> 6	0.60 ± 0.00 <sup>A</sup>	0.51 ± 0.00 <sup>a</sup>	0.55 ± 0.00 <sup>A</sup>	0.43 ± 0.00 <sup>b</sup>	0.44 ± 0.00 <sup>B</sup>	0.31 ± 0.00 <sup>c</sup>	0.35 ± 0.00 <sup>C</sup>	0.29 ± 0.00 <sup>c</sup>	0.23 ± 0.00 <sup>D</sup>	0.15 ± 0.00 <sup>d</sup>
Linolenic 18:3 <i>ω</i> 3	0.28 ± 0.00 <sup>A</sup>	0.20 ± 0.00 <sup>a</sup>	0.24 ± 0.00 <sup>A</sup>	0.14 ± 0.00 <sup>ab</sup>	0.19 ± 0.00 <sup>AB</sup>	0.10 ± 0.00 <sup>b</sup>	0.13 ± 0.00 <sup>BC</sup>	0.08 ± 0.00 <sup>b</sup>	0.10 ± 0.00 <sup>C</sup>	0.07 ± 0.00 <sup>b</sup>
$\gamma$ -Linolenic 18:3 <i>ω</i> 6	1.54 ± 0.3 <sup>A</sup>	1.35 ± 0.1 <sup>a</sup>	1.39 ± 0.4 <sup>B</sup>	1.14 ± 0.1 <sup>b</sup>	1.28 ± 0.3 <sup>c</sup>	1.02 ± 0.2 <sup>c</sup>	1.15 ± 0.4 <sup>D</sup>	0.90 ± 0.1 <sup>d</sup>	1.00 ± 0.2 <sup>E</sup>	0.79 ± 0.1 <sup>e</sup>
Arachidonic 20:4 <i>ω</i> 6	2.50 ± 0.05 <sup>A</sup>	2.33 ± 0.01 <sup>a</sup>	2.21 ± 0.02 <sup>B</sup>	2.00 ± 0.01 <sup>b</sup>	1.93 ± 0.02 <sup>C</sup>	1.64 ± 0.02 <sup>c</sup>	1.54 ± 0.05 <sup>D</sup>	1.38 ± 0.01 <sup>d</sup>	1.32 ± 0.02 <sup>E</sup>	1.09 ± 0.01 <sup>e</sup>
EPA 20:5 <i>ω</i> 3	6.17 ± 0.3 <sup>A</sup>	4.92 ± 0.3 <sup>a</sup>	5.74 ± 0.1 <sup>B</sup>	4.35 ± 0.5 <sup>b</sup>	5.12 ± 0.3 <sup>C</sup>	3.89 ± 0.3 <sup>c</sup>	4.75 ± 0.6 <sup>D</sup>	3.26 ± 0.2 <sup>d</sup>	3.97 ± 0.1 <sup>E</sup>	2.43 ± 0.1 <sup>e</sup>
DHA C22:6 <i>ω</i> 3	18.86 ± 0.8 <sup>A</sup>	16.45 ± 0.7 <sup>a</sup>	16.62 ± 0.5 <sup>B</sup>	14.54 ± 0.6 <sup>b</sup>	14.98 ± 0.4 <sup>C</sup>	13.29 ± 0.8 <sup>c</sup>	13.74 ± 0.7 <sup>D</sup>	11.69 ± 0.3 <sup>d</sup>	11.89 ± 0.1 <sup>E</sup>	9.95 ± 0.2 <sup>e</sup>
Elaidic 18:1 tr <i>ω</i> 9	0.29 ± 0.00 <sup>A</sup>	0.36 ± 0.00 <sup>a</sup>	0.25 ± 0.00 <sup>AB</sup>	0.30 ± 0.00 <sup>ab</sup>	0.18 ± 0.00 <sup>B</sup>	0.25 ± 0.01 <sup>b</sup>	0.13 ± 0.05 <sup>BC</sup>	0.20 ± 0.01 <sup>bc</sup>	0.11 ± 0.01 <sup>C</sup>	0.17 ± 0.03 <sup>c</sup>
Linolelaidic 18:2 tr <i>ω</i> 6	0.36 ± 0.02 <sup>A</sup>	0.45 ± 0.01 <sup>a</sup>	0.30 ± 0.03 <sup>A</sup>	0.38 ± 0.01 <sup>ab</sup>	0.26 ± 0.03 <sup>AB</sup>	0.37 ± 0.01 <sup>ab</sup>	0.23 ± 0.02 <sup>B</sup>	0.30 ± 0.02 <sup>bc</sup>	0.18 ± 0.02 <sup>B</sup>	0.26 ± 0.01 <sup>c</sup>
$\Sigma$ SFA	23.84	21.93	23.52	21.40	23.47	21.23	23.52	21.69	23.43	21.62
$\Sigma$ MUFA	29.21	25.51	27.16	24.21	25.73	21.92	24.03	20.81	22.49	19.79
$\Sigma$ PUFA	29.87	25.76	26.75	22.60	23.94	20.25	21.18	17.60	18.51	14.48
$\Sigma$ FA	82.92	73.20	77.43	68.21	73.14	63.40	68.74	60.10	64.43	55.89
$\Sigma$ <i>ω</i> 6	5.25	4.73	4.72	3.99	4.15	3.36	3.46	2.92	2.95	2.33
$\Sigma$ <i>ω</i> 3	25.31	21.57	22.60	19.03	20.29	17.28	18.62	15.03	15.96	12.45
<i>ω</i> 3/ <i>ω</i> 6	4.82	4.56	4.78	4.76	4.88	5.14	5.38	5.14	5.41	5.34
$\Sigma$ <i>trans</i>	0.65	0.81	0.55	0.68	0.44	0.62	0.36	0.50	0.29	0.43
PUFA/SFA	1.25	1.17	1.13	1.05	1.02	0.95	0.90	0.81	0.79	0.67

Values are means ± standard deviation of the six analysis (two lots analyzed in triplicates). All the raw and grilled samples are significantly different ( $P < 0.02$ ). Values bearing and different letters (capital letters) have significant differences ( $P < 0.02$ ) at differing storage times in the raw samples. Values bearing different letters (small letters) have significant differences ( $P < 0.02$ ) at various storage times in the grilled samples

## Selective COX-2 Inhibitors, Eicosanoid Synthesis and Clinical Outcomes: A Case Study of System Failure

M. J. James · R. J. Cook-Johnson · L. G. Cleland

Received: 10 December 2006 / Accepted: 2 April 2007 / Published online: 2 June 2007  
© AOCs 2007

**Abstract** Elucidation of differences between the active sites of COX-1 and COX-2 allowed the targeted design of the selective COX-2 inhibitors known as coxibs. They were marketed as non-steroidal anti-inflammatory drugs (NSAIDs) that had improved upper gastrointestinal (GI) safety compared with older non-selective NSAIDs such as diclofenac and naproxen. Two GI safety studies conducted with arthritis patients demonstrated that in terms of upper GI safety, celecoxib was not superior to diclofenac (CLASS study) but rofecoxib was superior to naproxen (VIGOR study). However, the VIGOR study revealed also that rofecoxib had increased cardiovascular (CV) risk compared with naproxen. This clinical outcome was supported by the existence of plausible eicosanoid-based biological mechanisms whereby selective COX-2 inhibition could increase CV risk. Nevertheless, the existence of CV risk with rofecoxib was successfully discounted by its pharmaceutical company owner, Merck & Co, with the assistance of specialist opinion leaders and rofecoxib achieved widespread clinical use for 4–5 years. Rofecoxib was withdrawn from the market when several clinical trials in colorectal cancer and post-operative pain revealed increased CV risk with not only rofecoxib, but also coxibs. The commercial success of rofecoxib provides a case-study of failure of the medical journal literature to guide drug usage. Attention to ethical issues may have provided a more useful guide for prescribers.

**Keywords** COX-2 · Rofecoxib · Vioxx · Eicosanoids · Ethics

### Introduction

Cyclooxygenase (COX) is the target for the traditional non-steroidal anti-inflammatory drugs (NSAID), examples of which include indomethacin, naproxen, ibuprofen and diclofenac [1]. These drugs are effective in providing symptomatic relief from inflammation most likely because the COX product prostaglandin E<sub>2</sub> (PGE<sub>2</sub>) is involved in vasodilation, extravasation of fluid, and hyperalgesia in inflammatory foci. However, PGE<sub>2</sub> also has a protective role in the stomach where it is involved in maintenance of the protective mucosal barrier [2]. Therefore, NSAID use for symptomatic treatment of inflammation is associated with gastropathies and these can be sufficiently severe to result in hospitalization and death [3].

The discovery of two COX isotypes and the further discovery that COX-2 was involved in production of PGE<sub>2</sub> in inflammatory sites whereas COX-1 was involved in maintenance of gastric mucosal protection, provided a face-value rationale for development of selective COX-2 inhibitors as anti-inflammatory agents with reduced upper GI adverse effects compared with traditional NSAID [2].

### Cyclooxygenase Isotypes and Selective Inhibitors

Both COX isotypes have long hydrophobic substrate binding channels with the channel being slightly larger in COX-2 than COX-1. Molecular modelling indicates the presence of a hydrophobic pocket that branches from the main substrate binding channel. However, access to the pocket is restricted

M. J. James (✉) · R. J. Cook-Johnson ·  
L. G. Cleland  
Rheumatology Unit, Royal Adelaide Hospital,  
North Terrace, Adelaide, SA 5000, Australia  
e-mail: mjames@mail.rah.sa.gov.au

in COX-1 due to the presence at position 523 of a bulky isoleucine whereas in COX-2 this position is occupied by a valine [4]. This structural difference allowed the development of coxibs, a class of selective COX-2 inhibitors that exploit selective access to the side pocket in COX-2 [5]. However, some traditional NSAID also have selectivity for COX-2 inhibition when examined *in vitro*. There is a continuum of selectivities among traditional NSAIDs and coxibs ranging from COX-1 selective to COX-2 selective. For example, indomethacin is COX-1 selective, diclofenac and celecoxib are modestly COX-2 selective and each have similar selectivities for COX-2, whereas rofecoxib is highly COX-2 selective [6].

### Eicosanoid Synthesis: In Vitro Studies

Selective COX-2 inhibitors were developed with the goal of inhibiting PGE<sub>2</sub> synthesis in areas of inflammation but not in the stomach. However, this goal did not recognise that PGE<sub>2</sub> is not the immediate product of COX-1 or COX-2. Both COX-1 and COX-2 catalyse the same reaction, which with arachidonic acid as substrate, is the production of PGH<sub>2</sub>. PGH<sub>2</sub> is the common substrate for a number of prostaglandin synthases and thromboxane synthase (Fig. 1).

Inspection of Fig. 1 suggests that inhibition of COX-1 or COX-2 or both isotypes should decrease synthesis of all PGH<sub>2</sub> metabolites. However, selective COX-2 inhibition results in selective inhibition of PGE<sub>2</sub> rather than TXA<sub>2</sub> in monocytes [7] and selective inhibition of PGI<sub>2</sub> rather than TXA<sub>2</sub> in endothelial cells [8, 9]. This phenomenon is probably linked to the observations that early after monocyte or endothelial cell stimulation, only TXA<sub>2</sub> is produced whereas with increasing time to allow for induction of COX-2, there is an increase in monocyte PGE<sub>2</sub> or endothelial PGI<sub>2</sub> with little or no further increase in TXA<sub>2</sub> synthesis [7–11] (Fig. 2).

A possible explanation for all of these findings lies in the different  $K_m$  values of the synthase enzymes. TX synthase has a 17-fold lower  $K_m$  than PGE synthase [11] and indirect studies infer a similar situation for TX synthase versus PGI synthase [8]. Thus, in the early phase of endothelial cell stimulation when only constitutive COX-1 is present, the PGH<sub>2</sub> concentration is sufficient for TXA<sub>2</sub> synthesis but

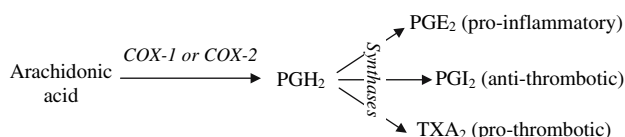


**Fig. 1** Metabolism of arachidonic acid by cyclooxygenases

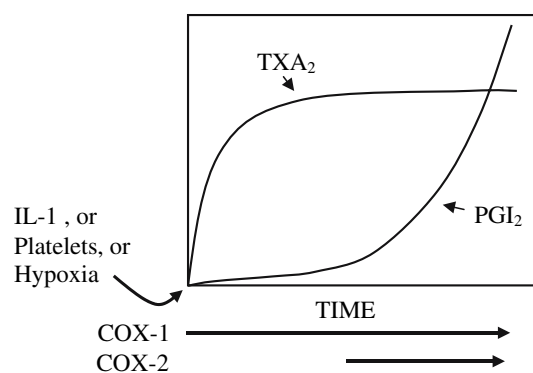


**Fig. 2** Depiction of changes in COX isotype expression and eicosanoid synthesis in stimulated endothelial cells [8, 9]

not substantive PGI<sub>2</sub> synthesis. With time there is induction of COX-2, which substantially increases PGH<sub>2</sub> concentration leading to PGI<sub>2</sub> synthesis. However, due to the lower  $K_m$  of TX synthase compared with that of PGI synthase, there is little if any further increase in TXA<sub>2</sub> synthesis due to saturation of TX synthase with substrate. Conversely, selective inhibition of COX-2 would decrease PGI<sub>2</sub> synthesis with little or no effect on TXA<sub>2</sub> synthesis, as has been observed in endothelial cells stimulated with IL-1 $\beta$  or platelets or hypoxia [8–10].

These findings from *in vitro* studies suggest that endothelial COX-2 has a protective anti-thrombotic role in response to stress.

### Eicosanoid Synthesis: In Vivo Studies

Although it is not possible to directly measure endothelial PGI<sub>2</sub> synthesis *in vivo*, human studies support the importance of COX-2 for PGI<sub>2</sub> synthesis. The selective COX-2 inhibitors, celecoxib and rofecoxib, decreased the urinary content of PGI<sub>2</sub> metabolites while having little or no effect on platelet TXA<sub>2</sub> synthesis in healthy volunteers [12, 13]. Whether or not the source of the PGI<sub>2</sub> metabolites in urine was the endothelium is not known. Also, whether or not COX-2 is present in unstimulated healthy endothelium is not known although it is clearly present in atherosclerotic vessels [14–16]. While laminar flow has been shown to up-regulate endothelial COX-2 *in vitro* [17], COX-2 is generally found in low levels or not detected in non-atherosclerotic endothelium [14].

Studies on COX-2 in the heart indicate that myocardial up-regulation of COX-2 is an important protective response to injury caused by anthracyclines or oxidative stress [18, 19]. Also, myocardial COX-2 upregulation and consequent PGI<sub>2</sub> production is a critical event in the protective effect of ischemic pre-conditioning [20].



Collectively, the studies on eicosanoid synthesis *in vitro* and *in vivo* suggest that COX-2 upregulation provides a cardioprotective response in stressed myocardium and an anti-thrombotic response in blood vessels. It is noteworthy that selective COX-2 inhibition has the opposite action of low dose aspirin in suppressing endothelial prostacyclin synthesis but not platelet thromboxane synthesis [21] (Fig. 3).

### Clinical Effects of Selective COX-2 Inhibitors

The first two coxibs approved for clinical use were celecoxib and rofecoxib, marketed as Celebrex and Vioxx, respectively. They both relieved the signs and symptoms of inflammation with efficacy similar to that of the conventional NSAIDs [5]. However, in order to claim that they had superior upper GI safety over the traditional NSAIDs, the regulatory authorities required clinical trials, in which measurement of upper GI safety was the primary aim. The most important measure of upper GI safety is that of ulcer complications, i.e. bleeds, perforations, obstructions. These events cause morbidity and hospitalisation and are potentially life-threatening. A less important measure is that of symptomatic ulcers because they are not life-threatening and are readily treated with medication that can be curative.

CLASS was a combination of two upper GI safety studies in osteoarthritis and rheumatoid arthritis where participants were allocated either to celecoxib or one of two conventional NSAIDs, diclofenac or ibuprofen. Low-dose aspirin, widely used as an anti-thrombotic agent, was allowed as indicated. Outcomes at 6 months of treatment were published and these showed a statistically significant advantage of celecoxib over the combined NSAID groups for the composite measure of ulcer complications + symptomatic ulcers; however there was no advantage of celecoxib for ulcer complications alone [22]. The

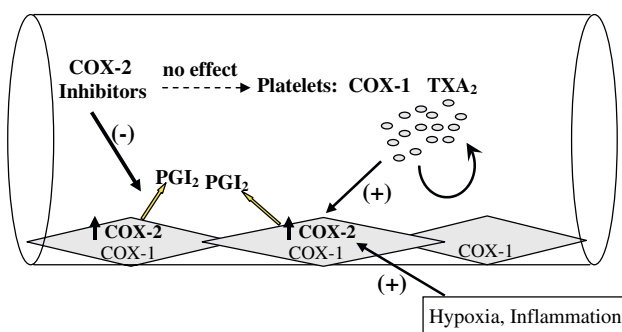


**Fig. 3** Scheme depicting endothelial and platelet COX isotypes, eicosanoid synthesis, and the effect of COX-2 inhibitors (Reproduced by permission of Lippincott Williams & Wilkins)

submission of these data to the FDA by GD Searle & Co indicated that the actual duration of the two safety studies was in fact 12 and 15 months. These were the durations required to reach the pre-specified end-point of at least 20 ulcer complications in each study or a maximum of 45 ulcer complications in both studies combined. The FDA analysis shows that at actual study completion, celecoxib was not superior to the combined NSAID groups for either of the upper GI safety measure [23]. It was revealed that the complete 12–15 month trial data for CLASS were available when the 6-month analysis was published. The FDA review also concluded that there was no evidence of cardiovascular risk with celecoxib from the CLASS study.

The adenoma prevention with celecoxib (APC) study examined colorectal cancer prevention with celecoxib versus placebo in participants with adenomatous colorectal polyps. While there was a decreased incidence of colorectal adenomas with celecoxib, there was statistically significant dose-related increase in thrombotic cardiovascular events with celecoxib [24].

As for celecoxib, rofecoxib also was examined for upper GI safety and later for colorectal cancer prevention. The upper GI safety study known as VIGOR allocated rheumatoid arthritis patients to either rofecoxib or the conventional NSAID, naproxen. Aspirin use or a requirement for aspirin use was an exclusion criterion. Unlike CLASS, VIGOR demonstrated superiority to the NSAID comparator, naproxen, for both upper GI safety measures, i.e. ulcer complications alone and the combined measure of ulcer complications + symptomatic ulcers [25, 26]. However, there was a four fold increase in myocardial infarction with rofecoxib [25, 26]. The FDA review showed that the increase in the combined thrombotic cardiovascular events with rofecoxib matched its upper GI benefits and therefore, the FDA review concluded that rofecoxib offered no overall safety advantage over naproxen [25]. By contrast, the New England Journal Medicine (NEJM) publication of the VIGOR trial concluded with no supporting evidence that the increased myocardial infarction with rofecoxib did not exist and that the results were due to a cardioprotective effect of naproxen. The overall conclusion was that VIGOR was a success in demonstrating upper GI safety [26].

A further study with rofecoxib, APPROVE, like the APC study with celecoxib, had the aim of examining colorectal cancer prevention. Patients with a history of colorectal adenomas were randomly allocated to rofecoxib or placebo. The trial was stopped early due to an approximate 5-fold increased risk of myocardial infarction and an approximate two fold increased risk of combined adverse cardiovascular events [27].

A randomised controlled trial of oral valdecoxib and its intravenous pro-drug, parecoxib, for analgesia in patients having coronary artery bypass surgery also showed an

approximate four fold increased risk of combined cardiovascular events [28].

Thus, evidence from these randomised controlled trials suggests that increased cardiovascular risk is a class effect with coxibs. Meta-analysis of database and case-control studies suggests that there is increased cardiovascular risk with many NSAIDs, although not with naproxen [29]. In that analysis, the highest relative risk was 1.40 and that occurred with diclofenac, which is also the most COX-2 selective of the traditional NSAIDs [6, 29].

### Marketing of the Coxibs and Maintenance of Uncertainty

The results of the CLASS and VIGOR trials were published in 2000. The respective publications declared celecoxib and rofecoxib to have superior upper GI safety to the comparator NSAIDs [22, 26]. However, the FDA reviews showed this was not true for celecoxib at the pre-planned time of study completion and showed that, when the increased cardiovascular events with rofecoxib were considered, it had no overall safety advantage [23, 25]. Notwithstanding the FDA analyses both drugs achieved “blockbuster” status in the marketplace [30].

It is accepted that most researchers and clinicians do not examine the FDA website for reviews of pharmaceutical company submissions. However, it is difficult to understand why there was an uncritical acceptance of the conclusions of the medical journal publications of CLASS and VIGOR. As discussed below it is difficult also to understand how the interpretations of data published in these prestigious journals survived disinterested critical review.

Even though only the 6-month data from CLASS were originally published [22], it was clear that celecoxib was not superior to the combined NSAID comparator group for the incidence of complicated upper GI events, which clinically is the more important outcome measure [31]. In the publication of the VIGOR results, it was clear that there was a 4-fold increase in myocardial infarction in the rofecoxib group [26]. Although this publication concluded that this result was due to a protective effect of naproxen, no evidence was presented for such an effect. In addition, it was soon followed by publication of the analyses of a large Medicaid database that concluded naproxen did not have a protective effect and that rofecoxib was associated with an increase in cardiovascular risk [32, 33].

Despite this published information, Vioxx exceeded US\$2 billion in sales per year for 2001–03 [34]. The principle that there should be caution with the prescribing of new drugs due to limited information about their effectiveness, long-term safety, and whether they offer an overall advantage over existing medications did not seem

to be applied [35]. A possible explanation is that clinicians were persuaded by consistently positive marketing messages. In the year after the launch of Vioxx, spending on direct to consumer advertising in the US for Vioxx exceeded the advertising expenditure for Pepsi and Budweiser [36]. Also, the US congressional hearings into the relationships between the FDA and the pharmaceutical industry revealed that Merck’s instructions to their sales representatives were designed to dampen any physician concerns about cardiovascular risk. If clinicians enquired about this risk, the sales representative handed them a “Cardiovascular Card”, which contained no data from the VIGOR study and in addition, claimed that Vioxx was actually 8–11 times safer than anti-inflammatory drugs like naproxen. When an FDA advisory committee recommended that clinicians should be informed of the cardiovascular results from the VIGOR study, the sales staff were specifically instructed not to initiate discussion with clinicians on the FDA Advisory recommendation [37].

Thus, one reason for the sustained blockbuster status of Vioxx and Celebrex is that clinician concerns were allayed by pharmaceutical company sales and marketing practices. However, this does not necessarily explain why there was not an appropriate response at the academic level to the medical journal literature. The reviewers of the NEJM submission on the VIGOR study should have insisted that the conclusion that naproxen had a cardioprotective effect was without merit [26]. They should also have insisted that the manuscript conclude that the study showed no overall safety advantage of Vioxx, when both serious upper GI events and cardiovascular events were taken into consideration.

Shortly after publication of the NEJM article on the VIGOR study, a pooled analysis of cardiovascular risk using data from Merck trials with rofecoxib was published in *Circulation* [38]. The study concluded there was no cardiovascular risk with rofecoxib relative to placebo and non-naproxen NSAIDs. However, the studies varied in duration from only 4 weeks to 15 months, five of the seven authors were Merck employees, and the manuscript was accepted one day after submission. None of these factors alone necessarily determines how one should assess the merits of a publication. However, one should be mindful that this publication served to reinforce the notion that naproxen was cardioprotective and that rofecoxib only appeared to increase CV risk against this comparator. At the very least, this apparently unrefereed publication in *Circulation* helped sustain uncertainty about CV risk with rofecoxib during the ensuing years until its withdrawal from the market.

Thus there was a second reason for the maintenance of Vioxx sales, i.e. there was a failure in academic and therapeutic medicine to deal with this uncertainty. Recourse to

the principles used by Research Ethics Committees/Institutional Review Boards (REC/IRB) would have provided a straightforward remedy. These committees deal routinely with such prominent uncertainty by simply informing the research participants of its existence. Thus, if presented with a clinical trial involving Vioxx, it is likely that the REC/IRB would have insisted that the cardiovascular results of the VIGOR study were communicated in the Informed Consent document. This is a simple way of dealing with uncertainty and it accords with the principle of patient or research participant autonomy, also expressed as respect for persons. This consideration, which is embraced in the institutional research environment was lacking in the therapeutic/marketing environment.

### Summary and Conclusions

An examination of this sequence of events shows inappropriate acts of omission, commission and lack of integration. The aims of VIGOR were to examine safety. However, the report in the NEJM [26] overemphasized upper GI safety and greatly downplayed CV safety to an extent which was an act of omission and to an extent that should not have been accepted by the reviewers or the journal. The subsequent FDA review of VIGOR was exemplary in concluding that, when the increase in adverse CV events is considered “This risk reduction in relevant GI events did not translate into an overall safety benefit of rofecoxib over naproxen.” and that “Information regarding cardiovascular thrombotic events should be added to the VIOXX label.” [25]. However, there was a delay of nearly two years in adding a CV warning to the prescribing information [37, 39]. Labelling delay notwithstanding, it is not clear that the label warning had a substantial influence on prescribing in the face of more than \$100 million per year spent on direct-to-consumer advertising and a sales force directed to use an information card for prescribers, the “cardiovascular card” that deliberately omitted mention of cardiovascular risk [36, 37, 39].

The omission by Merck of accurate information on cardiovascular risk in its advertising and sales force packages may or may not be illegal. This issue is currently playing out in the legal actions underway in the US jurisdiction. However, this omission was certainly unethical. It was a disregard for people’s right to information that was material in their decision making as to whether to take or to prescribe Vioxx. It was a disregard for the ethical principle of respect for a person’s autonomy. The omission of balanced discussion of CV risk in the NEJM publication of VIGOR is perplexing. Whether the reviewers of the article and the journal would have treated committed inaccuracies

more diligently than they treated this act of omission is unknown.

This sequence of events raises the question of who should have taken responsibility for integration of this information into a risk and benefit evaluation. While several individuals published concerns about CV risk with coxibs [33, 40, 41] the medical journal literature collectively served to promote efficacy but perpetuate uncertainty about CV risk. The interested pharmaceutical company downplayed or omitted mention of CV risk. However, the regulator, i.e. the FDA, dispassionately assessed Vioxx as having no net health benefit. It has been argued that the FDA should have acted quicker on the labelling change and that they should have mandated a CV safety study [39]. Their obligations in the regulation of Vioxx has been considered by the US Congress [37, 42].

As a postscript, it is worth noting that although the coxibs attracted premium pricing due to their claims of superior upper GI safety compared with traditional less-selective NSAIDs, the NSAID gastropathy epidemic had essentially finished before the introduction of coxibs. This is well illustrated by the following epidemiological study that used databases on >5,500 rheumatoid arthritis (RA) patients in the US and Canada. It showed that hospitalizations for NSAID-related gastropathies increased from 0.6% of this RA population in 1981 to a peak of 1.5% in 1992 whereafter it declined back to 0.5% in 2000 *with the main decline occurring before the introduction of the selective COX-2 inhibitors, celecoxib and rofecoxib* [3]. The decline was due to movement away from the most gastrotoxic NSAIDs and to moderation of doses. If this result had been reported during the development phase of the selective COX-2 inhibitors, the business projections may have been less enthusiastic.

### References

1. Moncada S, Ferreira SH, Vane JR (1975) Inhibition of prostaglandin biosynthesis as the mechanism of analgesia of aspirin-like drugs in the dog knee joint. *Eur J Pharmacol* 31:250–260
2. Vane JR, Bakhle YS, Botting RM (1998) Cyclooxygenases 1 and 2. *Annu Rev Pharmacol Toxicol* 38:97–120
3. Fries JF, Murtagh KN, Bennett M, Zatarain E, Lingala B, Bruce B (2004) The rise and decline of nonsteroidal antiinflammatory drug-associated gastropathy in rheumatoid arthritis. *Arthritis Rheum* 50:2433–2440
4. Kurumbail RG, Stevens AM, Gierse JK, McDonald JJ, Stegeman RA, Pak JY, Gildehaus D, Miyashiro JM, Penning TD, Seibert K, Isakson PC, Stallings WC (1996) Structural basis for selective inhibition of cyclooxygenase-2 by anti-inflammatory agents. *Nature* 384:644–648
5. Hawkey CJ (1999) COX-2 inhibitors. *Lancet* 353:307–314
6. Warner TD, Giuliano F, Vojnovic I, Bukasa A, Mitchell JA, Vane JR (1999) Nonsteroid drug selectivities for cyclo-oxygenase-1

- rather than cyclo-oxygenase-2 are associated with human gastrointestinal toxicity: a full in vitro analysis. *Proc Natl Acad Sci USA* 96:7563–7568
7. Demasi M, Cleland LG, Cook-Johnson RJ, Caughey GE, James MJ (2003) Effects of hypoxia on monocyte inflammatory mediator production: dissociation between changes in cyclooxygenase-2 expression and eicosanoid synthesis. *J Biol Chem* 278:38607–38616
  8. Caughey GE, Cleland LG, Penglis PS, Gamble JR, James MJ (2001) Roles of cyclooxygenase (COX) -1 and -2 in prostanoid production by human endothelial cells: selective upregulation of prostacyclin synthesis by COX-2. *J Immunol* 167:2831–2838
  9. Cook-Johnson RJ, Demasi M, Cleland LG, Gamble JR, Saint DA, James MJ (2006) Endothelial cell COX-2 expression and activity in hypoxia: transcriptional control mechanisms. *BBA-Cell Mol Biol Lipids* 1761:1443–1449
  10. Caughey GE, Cleland LG, Gamble JR, James MJ (2001) Up-regulation of endothelial cyclooxygenase-2 and prostanoid synthesis by platelets: role of thromboxane A<sub>2</sub>. *J Biol Chem* 276:37839–37845
  11. Penglis PS, Cleland LG, Demasi M, Caughey GE, James MJ (2000) Differential regulation of prostaglandin E<sub>2</sub> and thromboxane A<sub>2</sub> production in human monocytes: implications for the use of cyclooxygenase inhibitors. *J Immunol* 165:1605–1611
  12. Catella-Lawson F, McAdam B, Morrison BW, Kapoor S, Kujubu D, Antes L, Lasseter KC, Quan H, Gertz BJ, Fitzgerald GA (1999) Effects of specific inhibition of cyclooxygenase-2 on sodium balance, hemodynamics, and vasoactive eicosanoids. *J Pharmacol Exp Ther* 289:735–741
  13. McAdam BF, Catella-Lawson F, Mardini IA, Kapoor S, Lawson JA, Fitzgerald GA (1999) Systemic biosynthesis of prostacyclin by cyclooxygenase (COX)-2: the human pharmacology of a selective inhibitor of COX-2. *Proc Natl Acad Sci USA* 96:272–277
  14. Stemme V, Swedenborg J, Claesson H-E, Hansson GK (2000) Expression of cyclo-oxygenase-2 in human atherosclerotic carotid arteries. *Eur J Vasc Endovasc Surg* 20:146–152
  15. Belton O, Byrne D, Kearney D, Leahy A, Fitzgerald DJ (2000) Cyclooxygenase-1 and -2-dependent prostacyclin formation in patients with atherosclerosis. *Circulation* 102:840–845
  16. Baker CS, Hall RJ, Evans TJ, Pomerance A, Maclouf J, Creminon C, Yacoub MH, Polak JM (1999) Cyclooxygenase-2 is widely expressed in atherosclerotic lesions affecting native and transplanted human coronary arteries and colocalizes with inducible nitric oxide synthase and nitrotyrosine particularly in macrophages. *Arterioscler Thromb Vasc Biol* 19:646–655
  17. Topper JN, Cai J, Falb D, Gimbrone MA (1996) Identification of vascular endothelial genes differentially responsive to fluid mechanical stimuli: cyclooxygenase-2, manganese superoxide dismutase, and endothelial nitric oxide synthase are selectively up-regulated by steady laminar shear stress. *Proc Natl Acad Sci USA* 93:10417–10422
  18. Dowd NP, Scully M, Adderley SR, Cunningham AJ, Fitzgerald DJ (2001) Inhibition of cyclooxygenase-2 aggravates doxorubicin-mediated cardiac injury in vivo. *J Clin Invest* 108:585–590
  19. Adderley SR, Fitzgerald DJ (1999) Oxidative damage of cardiomyocytes is limited by extracellular regulated kinases 1/2-mediated induction of cyclooxygenase-2. *J Biol Chem* 274:5038–5046
  20. Bolli R, Shinmura K, Tang XL, Kodani E, Xuan YT, Guo Y, Dawn B (2002) Discovery of a new function of cyclooxygenase (COX)-2: COX-2 is a cardioprotective protein that alleviates ischemia/reperfusion injury and mediates the late phase of preconditioning. *Cardiovasc Res* 55:506–519
  21. Patrono C, Garcia Rodriguez LA, Landolfi R, Baigent C (2005) Low-dose aspirin for the prevention of atherothrombosis. *N Engl J Med* 353:2373–2383
  22. Silverstein FE, Faich G, Goldstein JL, Simon LS, Pincus T, Whelton A, Makuch R, Eisen G, Agrawal NM, Stenson WF, Burr AM, Zhao WW, Kent JD, Lefkowitz JB, Verburg KM, Geis GS (2000) Gastrointestinal toxicity with celecoxib vs. nonsteroidal anti-inflammatory drugs for osteoarthritis and rheumatoid arthritis: the CLASS study: a randomized controlled trial. Celecoxib long-term arthritis safety study. *JAMA* 284:1247–1255
  23. US Food and Drug Authority (accessed April 2007) FDA Advisory Committee briefing document. NDA 20–998/S-009. Celebrex capsules (Celecoxib). Medical Officer Review. [http://www.fda.gov/ohrms/dockets/ac/01/briefing/3677b1\\_03\\_med.doc](http://www.fda.gov/ohrms/dockets/ac/01/briefing/3677b1_03_med.doc)
  24. Bertagnolli MM, Eagle CJ, Zauber AG, Redston M, Solomon SD, Kim K, Tang J, Rosenstein RB, Wittes J, Corle D, Hess TM, Woloj GM, Boisserie F, Anderson WF, Viner JL, Bagheri D, Burn J, Chung DC, Dewar T, Foley TR, Hoffman N, Macrae F, Pruitt RE, Saltzman JR, Salzberg B, Sylwestrowicz T, Gordon GB, Hawk ET (2006) Celecoxib for the prevention of sporadic colorectal adenomas. *N Engl J Med* 355:873–884
  25. US Food and Drug Authority (accessed April 2007) FDA Advisory Committee briefing document. NDA 21–042, s007. VIOXX gastrointestinal safety. [http://www.fda.gov/ohrms/dockets/ac/01/briefing/3677b2\\_03\\_med.pdf](http://www.fda.gov/ohrms/dockets/ac/01/briefing/3677b2_03_med.pdf)
  26. Bombardier C, Laine L, Reicin A, Shapiro D, Burgos-Vargas R, Davis B, Day R, Ferraz MB, Hawkey CJ, Hochberg MC, Kvien TK, Schnitzer TJ, Weaver A (2000) Comparison of upper gastrointestinal toxicity of rofecoxib and naproxen in patients with rheumatoid arthritis. *N Engl J Med* 343:1520–1528
  27. Bresalier RS, Sandler RS, Quan H, Bolognese JA, Oxenius B, Horgan K, Lines C, Riddell R, Morton D, Lanasa A, Konstam MA, Baron JA (2005) Cardiovascular events associated with rofecoxib in a colorectal adenoma chemoprevention trial. *N Engl J Med* 352:1092–1102
  28. Nussmeier NA, Whelton AA, Brown MT, Langford RM, Hoelt A, Parlow JL, Boyce SW, Verburg KM (2005) Complications of the COX-2 inhibitors parecoxib and valdecoxib after cardiac surgery. *N Engl J Med* 352:1081–1091
  29. McGettigan P, Henry D (2006) Cardiovascular risk and inhibition of cyclooxygenase: a systematic review of the observational studies of selective and nonselective inhibitors of cyclooxygenase 2. *JAMA* 296:1633–1644
  30. Couzin J (2004) Drug safety: withdrawal of vioxx casts a shadow over COX-2 inhibitors. *Science* 306:384–385
  31. Juni P, Rutjes AWS, Dieppe PA (2002) Are selective COX-2 inhibitors superior to traditional non-steroidal anti-inflammatory drugs? *Br Med J* 324:1287–1288
  32. Ray WA, Stein CM, Hall K, Daugherty JR, Griffin MR (2002) Non-steroidal anti-inflammatory drugs and risk of serious coronary heart disease: an observational cohort study. *Lancet* 359:118–123
  33. Ray WA, Stein CM, Daugherty JR, Hall K, Arbogast PG, Griffin MR (2002) COX-2 selective non-steroidal anti-inflammatory drugs and risk of serious coronary heart disease. *Lancet* 360:1071–1073
  34. Merck & Co (accessed April 2007) Annual Report. 2001–04. <http://phx.corporate-ir.net/phoenix.zhtml?c=73184&p=irol-reportsannual>
  35. Lexchin J (2002) Should doctors be prescribing new drugs? *Int J Risk Safety Med* 15:213–222
  36. National Institute for Health Care Management (accessed April 2007) Prescription Drugs and Mass Media Advertising, 2000. <http://www.nihcm.org/finalweb/DTCbrief2001.pdf>
  37. Waxman HA (accessed April 2007) Statement of Rep. Henry A. Waxman for the hearing “The role of FDA and pharmaceutical

- companies in ensuring the safety of approved drugs, like Vioxx.’’  
<http://democrats.reform.house.gov/Documents/20050505113149-41995.pdf>
38. Konstam MA, Weir MR, Reicin A, Shapiro D, Sperling RS, Barr E, Gertz BJ (2001) Cardiovascular thrombotic events in controlled, clinical trials of rofecoxib. *Circulation* 104:2280–2288
  39. Topol EJ (2004) Failing the public health-rofecoxib, Merck, and the FDA. *N Engl J Med* 351:1707–1709
  40. Mukherjee D, Nissen SE, Topol EJ (2001) Risk of cardiovascular events associated with selective COX-2 inhibitors. *JAMA* 286:954–959
  41. Cleland LG, James MJ, Stamp LK, Penglis PS (2001) COX-2 inhibition and thrombotic tendency: a need for surveillance. *Med J Aust* 175:214–217
  42. Graham DJ (accessed April 2007) Testimony of Dr David Graham, US Senate Committee on Finance. <http://www.senate.gov/~finance/hearings/testimony/2004test/111804dgtest.pdf>

## The Diversity of Health Effects of Individual *trans* Fatty Acid Isomers

Sarah K. Gebauer · Tricia L. Psota ·  
Penny M. Kris-Etherton

Received: 6 February 2007 / Accepted: 27 June 2007 / Published online: 11 August 2007  
© AOCs 2007

**Abstract** There are multiple adverse effects of *trans* fatty acids (TFA) that are produced by partial hydrogenation (i.e., manufactured TFA), on CVD, blood lipids, inflammation, oxidative stress, endothelial health, body weight, insulin sensitivity, and cancer. It is not yet clear how specific TFA isomers vary in their biological activity and mechanisms of action. There is evidence of health benefits on some of the endpoints that have been studied for some animal TFA isomers, such as conjugated linoleic acid; however, these are not a major TFA source in the diet. Future research will bring clarity to our understanding of the biological effects of the individual TFA isomers. At this point, it is not possible to plan diets that emphasize individual TFA from animal sources at levels that would be expected to have significant health effects. Due to the multiple adverse effects of manufactured TFA, numerous agencies and governing bodies recommend limiting TFA in the diet and reducing TFA in the food supply. These initiatives and regulations, along with potential TFA alternatives, are presented herein.

**Keywords** *trans* Fatty acid isomers ·  
C18:1 *trans* fatty acids · C18:2 *trans* fatty acids ·  
Vaccenic acid · Elaidic acid · Conjugated linoleic acid ·  
Hydrogenation · Ruminant fat · Cardiovascular disease

### Introduction

Recent research has made evident the numerous adverse effects of *trans* fatty acids (TFA) as a group, and specifically those produced by partial hydrogenation on CVD, blood lipids, inflammation, oxidative stress, endothelial health, body weight, insulin sensitivity, and cancer. While it is clear that TFA intake from partially hydrogenated fats is associated with multiple harmful outcomes, it is not yet clear how specific TFA isomers vary in their biological activity and mechanisms of action. Evidence suggests that TFA from different sources, as well as individual isomers within these subgroups, elicit differential biological effects, both favorable and adverse. In this paper, we will review the current literature regarding the effects of TFA on various endpoints, while noting differences observed among various TFA isomers. In addition, we will address the regulatory issues related to TFA, initiatives to reduce TFA in the food supply, potential TFA alternatives, and looming challenges to food manufacturers and consumers, which were all discussed at a recent American Heart Association conference [1].

### Sources of TFA Isomers

There are two major sources of TFA, those that come from ruminant animals and those that are industrially produced. The concentration of TFA in meat and milk from ruminants (i.e., cattle, sheep, goats, etc.) ranges from 3 to 8% of total fat. The majority of TFA is found in partially hydrogenated vegetable oils (which contain 10–40% as TFA) [2]. The C18:1t isomers comprise approximately 80–90% of total TFA in foods [3]. Other TFA isomers include C16:1t, C18:2t, C18:3t, and long chain polyunsaturated TFA [4].

S. K. Gebauer · T. L. Psota · P. M. Kris-Etherton (✉)  
Department of Nutritional Sciences,  
The Pennsylvania State University,  
S126 Henderson Building, University Park,  
PA 16802, USA  
e-mail: pmk3@psu.edu

Elaidic acid (C18:1 $\Delta$ 9t) typically is the major isomer in industrial sources of TFA. However, there are many isomers of TFA in hydrogenated vegetable oils and C18:1 $\Delta$ 10t also can be a major component. The *trans* isomer of vaccenic acid (C18:1 $\Delta$ 11t), a precursor for conjugated linoleic acid (CLA), is the major TFA isomer in ruminant fat, and also is found in industrial TFA in lesser amounts [4]. CLA are a group of positional and geometric conjugated isomers of linoleic acid. The two predominant isomers, with known bioactive properties, are *cis*-9, *trans*-11 (c9t11), and *trans*-10, *cis*-12 (t10c12) [5]. There has been recent interest in CLA due to the beneficial effects on health outcomes observed in animal studies; however, more research is needed in humans [6–8]. Thus, individual isomers of TFA can elicit differential effects on various endpoints. It is hypothesized that ruminant TFAs, or certain TFA isomers from ruminant sources, may confer some health benefits; however, a strong database is lacking. Table 1 shows the common name, chemical name, and sources of major *trans* isomers.

### Health Effects of TFA

This section reviews the effects of TFA, as a group, on various disease endpoints. Furthermore, individual effects of CLA on these endpoints are summarized.

#### Cardiovascular Disease

Epidemiologic studies have consistently shown an association between intake of TFA and risk of CHD. Research

suggests that there is a stronger association with intake of TFA and CHD risk than that with intake of saturated fatty acids (SFA) [9]. In the Seven Countries Study, countries with high TFA intake, such as Northern European countries, had higher CHD mortality rates, while countries with low TFA intake, such as Mediterranean countries and Japan, had lower CHD mortality rates [10]. In this study, average intake of elaidic acid (C18:1t) was strongly associated with 25-year mortality from CHD ( $r = 0.78$ ;  $P < 0.001$ ). In the Nurses' Health Study, the relative risk (RR) of CHD across increasing quintiles of TFA intake was 1.5 (95% CI 1.12–2.00;  $P = 0.001$ ). This risk was higher for individuals whose margarine consumption did not change over the previous 10 years (RR = 1.67; 95% CI 1.05–2.66;  $P = 0.002$ ) [11]. The positive association between TFA intake and risk of CHD was accounted for by partially hydrogenated vegetable oil, while there was a nonsignificant inverse association with TFA from ruminant sources and CHD risk. In the Zutphen Elderly Study, a 2% increase in baseline total TFA intake resulted in a 29% increase in risk of 10-year incidence of CHD (RR = 1.29; 95% CI 1.09–1.52) [12]. There was no significant difference in RR for CHD between ruminant and industrially produced sources of 18:1 *trans* isomers. An analysis by Oomen et al. [12] used pooled data from four prospective cohort studies to indicate that an increase of 2% energy in TFA intake is associated with a RR of 1.25 (95% CI 1.11–1.40). Thus, removal of 2% of energy from TFA from the diet can significantly reduce CHD risk. In the Cardiovascular Health Study, red blood cell membrane levels of total TFA, a biomarker of total TFA intake, was associated with a modest increase in the risk of primary cardiac arrest [13]. However, after adjustment for EPA and DHA, this relationship was no longer significant. The C18:2t isomers, but not C18:1t isomers (C18:1 $\Delta$ 9t, C18:1 $\Delta$ 10t, C18:1 $\Delta$ 11t), were significantly associated with primary cardiac arrest, even after adjustment for EPA and DHA (OR = 3.05; 95% CI 1.71–5.44). Fatty acid analysis of plasma phospholipids showed that higher levels of plasma phospholipids C18:2t were associated with higher risk of fatal ischemic heart disease (IHD) (OR = 1.68; 95% CI 1.21–2.33) [14]. In contrast, higher levels of C18:1t, above the 20th percentile, were associated with a lower risk (OR = 0.34; 95% CI 0.18–0.63). Similarly, higher levels of C18:2t were associated with a higher risk of sudden cardiac death (SCD) (OR = 2.34; 95% CI 1.27–4.31), while higher levels of C18:1t were associated with a lower risk (OR = 0.18; 95% CI 0.06–0.54). The correlations for individual C18:2t and C18:1t isomers were not reported. There were no significant associations with plasma phospholipids levels of C16:1t and fatal IHD [14]. The results suggest that C18:2t isomers may be responsible for the increased risk for primary cardiac arrest, fatal IHD, and SCD in this study.

**Table 1** Major *trans* fatty acid isomers

Common name	Chemical name of common isomers	Major source
Palmitoleic acid	C16:1	Ruminant meat and milk
Elaidic acid	C18:1 $\Delta$ 9t <sup>a</sup>	Partially hydrogenated oils
Vaccenic acid <sup>b</sup>	C18:1 $\Delta$ 11t <sup>a</sup>	Ruminant meat and milk
Linolelaidic acid	C18:2-t9t12	Partially hydrogenated oils
Conjugated linoleic acid (CLA)	C18:2-c9t11 <sup>c</sup> C18:2-t10c12	Ruminant meat and milk

<sup>a</sup> C18:1t isomers comprise approximately 80–90% of total TFA in foods [3]

<sup>b</sup> Vaccenic acid constitutes 40–70% of total *trans* 18:1 [127]

<sup>c</sup> Predominant isomer of CLA (90%) [128]

However, it is important to note that C18:1t isomers comprise approximately 80–90% of total TFA in foods [3].

Results from studies investigating the association of TFA from ruminant sources and CHD risk have indicated no association or a potential beneficial association [11, 15, 16]. However, a recent review points out that most comparisons of sources of TFA in these studies are based on relative intake data from quintiles of intake [17]. When absolute amounts of TFA (0–2.5 g/day) were calculated and compared from these studies, there were no significant differences in risk of CHD for different sources of TFA [4]. Based on the analysis by Oomen et al., it was estimated that 2.5 g of TFA would be associated with a 15% increase in CHD risk. At intakes greater than 3 g/day, total TFA and industrially produced TFA were associated with an increased risk of CHD. Intakes of ruminant TFA were below this amount, thus conclusions could not be drawn about higher intakes of ruminant TFA.

### Blood Lipids

Randomized controlled trials consistently have shown that TFA increase LDL-cholesterol (LDL-C) similar to SFA, and decrease HDL-cholesterol (HDL-C) compared with SFA, resulting in a dose-dependent relationship between TFA intake and the ratio of LDL-C:HDL-C and TC:HDL-C that is stronger than that for SFA since SFA also increase HDL-C [18]. Results from a meta-analysis of clinical studies demonstrate that the replacement of carbohydrate with TFA causes an increase in the ratio of TC:HDL-C and that this effect is almost twice the magnitude of replacing a mixture of SFA for carbohydrate [19]. In the Nurses' Health Study, higher levels of total TFA in red blood cells were associated with increased LDL-C, HDL-C, and ratios of LDL-C:HDL-C. Furthermore, individuals who consumed the most TFA had a 3.3 times higher risk for developing CHD compared to those who consumed the least amount of TFA [20]. Lichtenstein et al. demonstrated that increases in TFA result in a dose-dependent increase in LDL-C and decrease in HDL-C. Six experimental diets that provided 30% energy from total fat were evaluated. Two-thirds of the fat was provided by either soybean oil (<0.5 g TFA per 100 g of fat), semi-liquid margarine (<0.5 g per 100 g), soft margarine (7.4 g per 100 g), shortening (9.9 g per 100 g), stick margarine (20.1 g per 100 g), or butter (1.25 g per 100 g). Compared with the butter diet, the vegetable fat diets elicited the following reductions in TC, LDL-C, and HDL-C: (1) soybean oil diet: 10, 12, and 3%, respectively; (2) the semi-liquid margarine diet: 10, 11, and 4%, respectively; and (3) the stick margarine diet: 3, 5, and 6%, respectively. The stick margarine diet

increased the TC:HDL-C ratio by 40%; the other vegetable fats decreased it. The diets containing the fats with the least TFA, the soybean oil and semi-liquid margarine diets, had the most beneficial effects on lipids/lipoproteins [21].

In addition to the effects on LDL-C and HDL-C, TFA increase triglycerides and Lp(a), when substituted for SFA [18]. It has been estimated that reducing TFA intake by 2% of energy would result in a decrease in triglyceride levels of approximately 3 mg/dl [22]. Furthermore, increasing amounts of TFA resulted in an increase in small dense LDL particles in a dose-dependent manner, when compared with a diet rich in SFA [23]. As reviewed by Ascherio [22], an estimated reduction in TFA intake of 2% of calories would result in a 7% reduction in CHD mortality due to the effects on the ratio of LDL-C:HDL-C. Compared to the estimates from epidemiologic studies, this lower estimate indicates that the adverse effects of TFA are more extensive than only their effects on blood lipids.

Intervention studies that demonstrate the specific effects of individual TFA isomers on blood lipids are lacking. In a randomized, parallel intervention study in 42 healthy young men, a vaccenic acid-rich diet (3.6 g/day of vaccenic acid) lowered TC and HDL-C by 6 and 9%, respectively ( $P \leq 0.05$ ), when compared with a control diet [24]. However, it was concluded that differences may have been due to higher MUFA and lower SFA in the vaccenic acid-rich diet rather than due to vaccenic acid alone. More research is needed to determine the effects of individual isomers on clinical endpoints.

All mechanisms by which TFA elicit their numerous effects remain unclear; however, it is clear that TFA affect lipid metabolism through multiple pathways. As recently reviewed by Mozaffarian et al. [25], TFA have been shown to increase rates of apolipoprotein (apo) A-I catabolism, decrease rates of LDL apoB-100 catabolism, decrease LDL-C particle size, and increase activity of cholesteryl ester transfer protein in humans; and increase secretion and cellular accumulation of free cholesterol and cholesterol esters in HepG2 cells. In vitro studies also have shown that TFA decrease HDL via inhibition of lecithin:cholesterol acyltransferase (LCAT) activity [26].

Results from studies investigating the effects of CLA supplementation on lipids and lipoproteins have been mixed [27–33]. Differential effects of t10c12 and c9t11 isomers have been reported in some studies [34, 35]. One study found that purified t10c12 CLA and a mixture of t10c12 and c9t11 CLA isomers (3.4 g/day) significantly decreased HDL-C by 4 and 2%, respectively, compared with placebo ( $P < 0.01$ ,  $P < 0.05$ ) [34]. In another study, t10c12 isomers (0.63, 1.26, and 2.52 g/day) increased the ratios of LDL-C:HDL-C and TC:HDL-C from baseline. In contrast, c9t11 isomers (doses of 0.59, 1.19, and 2.38 g/day)



decreased LDL-C:HDL-C and TC:HDL-C. There was no significant effect of dose of CLA isomers [35]. A recent study in moderately overweight subjects with LDL phenotype B compared the effects of a drinkable dairy product enriched with c9t11 or t10c12 (3 g/day, 3 weeks) on the lipid and lipoprotein profile [36]. There were no significant differences in the proportions of plasma small dense LDL or serum concentrations of LDL-C, HDL-C, and TG after either the c9t11 or t10c12-enriched products, compared to control product that was not enriched with CLA. The TRANSFACT study is a randomized, controlled, crossover trial specifically designed to compare the effects of industrial and natural sources of TFA on lipids and lipoproteins [37]. In this study, two specifically designed test fats (milk fat enriched in TFA and partially hydrogenated vegetable oil balanced in SFA) provide approximately 5.4% of energy from TFA in healthy individuals. Results from this study are expected soon.

### Inflammation and Oxidative Stress

Inflammation is an independent risk factor for CVD. Epidemiologic studies have suggested that TFA may have an adverse effect on inflammatory markers. In the Nurses' Health Study, TFA intake, assessed by semiquantitative food-frequency questionnaires, was positively associated with tumor necrosis factor receptor (TNFR) levels in healthy women ( $P$  for trend < 0.001), and was also associated with levels of C-reactive protein (CRP) and IL-6 in women with higher BMI ( $P = 0.03$ ) [38]. Regression analysis from a cross-sectional study of the Nurses' Health Study found that TFA intake was positively related to plasma levels of TNFR2 ( $P = 0.002$ ) and CRP ( $P = 0.009$ ), independent of BMI [39]. In patients with established heart disease, red blood cell membrane levels of TFA were positively associated with IL-1, IL-6, IL-10, and TNF $\alpha$  ( $P < 0.05$ ) [40]. In two of these studies, the association was due to C18:1t and C18:2t isomers, while no association was observed with C16t isomers [38, 39]. Results from RCTs have indicated a pro-inflammatory effect of TFA, which is consistent with epidemiologic data [41, 42]. A study by Han et al. [41] found that TNF $\alpha$  and IL-6 were 58 and 36% higher, respectively, after a stick margarine diet (6.7% energy from TFA) versus a soybean oil diet (0.6% energy from TFA). In a study by Baer et al. [42], a diet rich in TFA (8% energy enrichment from TFA) resulted in significantly higher levels of CRP versus a carbohydrate diet (8.5% of energy from fat replaced by digestible carbohydrate) ( $P < 0.05$ ).

There are mixed results from studies investigating the effects of CLA on inflammation. In randomized controlled trials, mixtures of c9t11, t10c12 CLA (3.4, 4.2 g/day)

caused a significant increase in CRP in healthy individuals and in those with metabolic syndrome [43, 44] and had no effect on TNF $\alpha$  and TNF $\alpha$  receptors in healthy individuals [43]. In a recent study, supplementation of 6.4 g/day of CLA for 12 weeks resulted in significant increases in CRP, IL-6, and white blood cells [45]. In contrast, in a study in subjects with type 2 diabetes, there was no effect of a CLA mixture (3 g/day) on CRP or IL-6 [46]. Furthermore, supplementation of either 3 g/day of c9 t11 CLA or t10 c12 CLA for 13 weeks in individuals with a high risk of CHD did not significantly affect LPS induced production of IL-6, IL-8, and TNF $\alpha$  by peripheral blood mononuclear cells, and whole blood as well as plasma CRP concentrations [47]. Studies in mice demonstrate that t10c12 CLA leads to induction of TNF $\alpha$  and IL-6 gene expression without affecting serum levels [48]. Mechanistically, t10c12 CLA was found to directly induce secretion of TNF $\alpha$  and IL-6 in adipocytes via nuclear factor kappaB and promote macrophage infiltration into adipose tissue [48].

### Endothelial Function

In addition to pro-inflammatory effects, evidence suggests that TFA also could impair endothelial function, and that these effects could be more substantial than those of SFA. Observational studies have shown that TFA intake is associated with higher levels of VCAM, ICAM, and E-selectin ( $P < 0.01$ ) [39]. In a randomized controlled trial, there was a 5.6% increase in E-selectin levels when TFA replaced 8% of energy for SFA [42]. In another study, flow mediated dilation was 29% lower on a TFA diet (9.2% energy from TFA) compared with a SFA diet [49]. Both epidemiologic and controlled trials indicate that TFA impair endothelial function more than SFA. Furthermore, endothelium-dependent vasodilation has been shown to be related to the fatty acid composition of serum lipids in healthy individuals [50].

There is little information about the effects of CLA on endothelial function. Treatment of human aortic endothelial cells with CLA did not alter cytokine-induced expression of VCAM, ICAM, and E-selectin [51]. In contrast, in another experiment, cytokine-induced monocyte adhesion to endothelial cells was inhibited dose-dependently by t10c12 CLA isomer [52]. Addition of the isomer in amounts of 6, 12.5, 25, 50  $\mu$ M resulted in inhibition of TNF $\alpha$ -induced monocyte adhesion by 30, 42, 50, 58%, respectively. In a recent study in 40 overweight men, a CLA mixture (4.5 g/day) reduced FMD by 1.3%, thus impairing endothelial function [53]. More clinical studies are needed to further examine the effect of CLA on markers of endothelial health.

## Body Weight and Body Fatness

Numerous animal and cell culture studies have found that CLA reduces body weight and fat deposition [54]. In a study in young, growing mice fed 1% CLA, there was a 60% decrease in body fat [55]. Most animal and cell studies have used mixtures of CLA isomers, although studies in which the ratio of specific isomers was varied indicate that the t10c12 isomer is responsible for the effects on body weight and body composition [54, 56]. Overall, clinical studies have shown no significant effect of CLA on body weight in humans [8, 54]. In a review of eight studies evaluating the effect of CLA on body composition in humans, there were no significant effects of the CLA group (CLA doses ranging from 0.70 to 6.8 g/day; t10c12 doses ranging from 0.35 to 2.0 g/day) compared to the control group for BMI, body weight, and lean body mass [57]. There was a significant effect on body fat (ranging from -3.7 to -22.2%) in the CLA group versus the control group in two of the studies [33, 58]; however, both of these studies included an exercise component, which may have influenced the results. Furthermore, there was no association with the dose of t10c12 isomer and the observed effect. In contrast, after supplementation with a CLA mixture in subjects with type 2 diabetes (8 g/day) for 8 weeks, t10c12 was inversely correlated with body weight changes ( $r = -0.43$ ;  $P < 0.05$ ) [59]. This study suggests that CLA supplementation at higher doses may promote weight loss in individuals with type 2 diabetes, although further research is needed. Two recent long-term studies in humans found that CLA supplementation of 3.4 g/day for 6 months [60] and 12 months [61] reduced body fat mass in overweight and overweight/obese individuals, respectively. However, in a recent study, CLA supplementation (3.4 g/day) for 1 year did not prevent weight or fat mass regain in moderately obese individuals [62].

## Insulin Sensitivity and Glucose Metabolism

In the Nurses' Health Study, dietary TFA was associated with an increased risk of developing type 2 diabetes [63]. For a 2% increase in energy from TFA, there was a 39% increase in risk (95% 1.15–1.67;  $P < 0.001$ ). In the Health Professionals Follow-Up Study, there was not a significant association with TFA at lower intakes (median intake 1.3% of energy from TFA) and diabetes risk [64]. This prompted the question of whether TFA affects insulin resistance, a major cause of type 2 diabetes. In controlled feeding studies in healthy individuals, there was no significant difference in insulin sensitivity, measured by frequently sampled intravenous glucose tolerance test, when comparing a TFA diet (5% total energy) to a monounsaturated

fat diet (MUFA; 5% total energy from oleic acid) [65] and a TFA diet (9% total energy) to a SFA diet (9% of energy as palmitic acid) [66]. In a study in hypercholesterolemic overweight adults comparing diets varying in TFA amount (3–7% total energy), insulin sensitivity, measured indirectly by fasting insulin levels, could not be attributed to the different fatty acid profiles of the various diets [67, 68]. A study in insulin resistant individuals with type 2 diabetes found that a high *trans* MUFA diet (20% total energy) resulted in a 59% higher postprandial insulin response ( $P < 0.05$ ) to a standardized meal compared to a *cis* MUFA diet (20% total energy), although this response was not significantly different than the response to a SFA diet [69].

Results from animal and human studies have suggested an adverse effect of CLA on insulin sensitivity, as reviewed by Wang and Jones [54]. CLA mixtures containing 0.7–2.0 g of the t10c12 isomer did not cause significant changes in plasma insulin levels [57]. In a RCT in obese insulin resistant men, individuals were given supplements (3.4 g) of a CLA mixture (50:50 c9t11 CLA, t10c12 CLA), purified t10c12 CLA, or placebo (olive oil) for 12 weeks [34]. Compared to placebo, insulin resistance, measured directly by euglycemic clamp, was increased by 19% after t10c12 CLA supplementation ( $P < 0.01$ ). In addition, this isomer significantly increased urinary F2-isoprostanes, a marker of oxidative stress ( $P < 0.0001$ ) [44]. The effect of the CLA mixture on insulin sensitivity was not significantly different from the placebo; however, it significantly increased fasting glucose concentrations and decreased HDL-C [34]. A subsequent study investigated the effect of a purified c9t11 CLA preparation in obese insulin resistant men and found that insulin sensitivity was decreased by 15% compared to placebo ( $P < 0.05$ ) [70]. These results recently were confirmed in a RCT in which CLA supplementation (50:50 c9t11 CLA, t10c12 CLA; 3 g/day) or placebo was given to individuals with type 2 diabetes for 8 weeks [46]. Compared to baseline, the CLA supplement resulted in an increase in fasting glucose concentrations by 6% ( $P < 0.05$ ), reduced insulin sensitivity by homeostasis model assessment ( $\Delta = 0.54$ ;  $P < 0.05$ ) and reduced oral glucose insulin sensitivity ( $\Delta = -11.24$ ;  $P \leq 0.05$ ). Other studies have found no significant changes in glycemia [27], glucose [31, 34, 35, 71], or insulin levels [27, 35, 53] after intake of CLA isomer mixtures.

Overall, the data suggest that TFA do not have a significant effect on insulin sensitivity in healthy normal weight individuals and overweight individuals with elevated cholesterol. In subjects with type 2 diabetes, high TFA intake could increase insulin resistance; however, more studies with larger numbers of participants are needed. The results of clinical studies with CLA isomers indicate that CLA has an adverse effect on insulin sensitivity in insulin resistant men.

## Cancer

Some epidemiologic studies have found that TFA intake is associated with increased risk of colorectal cancer [72] and prostate cancer [73]. Studies with CLA in cells and animals have suggested an anticarcinogenic property of CLA for various forms of cancer, including breast, gastrointestinal, colon, and prostate cancer, as summarized in a recent review [6]. In addition, some studies have found an anticarcinogenic effect of *trans*-vaccenic acid as a precursor to c9, t11 CLA [74, 75]. However, there is limited clinical research investigating the effect of CLA on cancer development in humans. Clinical studies have shown no clear association between dietary CLA, adipose or serum levels of CLA, and reduced risk for breast cancer [76–79]. There has been one human study that has suggested that intake of high-fat dairy foods and CLA reduces the risk for colorectal cancer [80]. In this prospective study, women who consumed  $\geq 4$  servings per day of high-fat dairy foods had a RR of 0.59 compared with women who consumed less than one serving per day of high-fat dairy (95% CI 0.44–0.79). The RR for CLA intake when comparing the highest and lowest quartiles of intake was 0.71 (95% CI 0.55–0.91). Although there are some data suggesting a beneficial association of CLA intake on cancer risk, intervention studies evaluating the effects of CLA supplementation on cancer risk are lacking.

## Position Statements, Regulations, and Initiatives on TFA

As reviewed above, substantial epidemiologic data demonstrate adverse effects of TFA on CVD risk, as well as other chronic diseases. Although a large-scale randomized trial to assess the effects of TFA on chronic disease risk has not been done and cannot be done, due to ethical considerations, clinical data also demonstrate the adverse effects of TFA on chronic disease risk factors and the pathogenesis of chronic disease. Therefore, numerous expert committees have made evidence-based statements that recommend limiting dietary TFA intake:

- Institute of Medicine, 2002—TFA consumption should be as low as possible [81].
- 2005 Dietary Guidelines Advisory Committee (DGAC), 2005—TFA consumption by all population groups should be kept as low as possible, which is about 1% of energy intake or less [82].
- 2005 Dietary Guidelines for Americans, 2005—keep TFA consumption as low as possible [83].
- WHO/FAO report, Diet, Nutrition, and Chronic Disease, 2003—the population nutrient intake goal for TFA is less than 1% energy from TFA [84].

- International Society for the Study of Fatty Acids and Lipids (ISSFAL), 1999—the maximum level of TFA should be 1% of energy [85].
- Nutrition and Diet for Healthy Lifestyles in Europe, EURODIET, 2000—a population goal of less than 2% energy from TFA [86].
- UK Ministry of Agriculture, 1998—less than 2% of energy [87].
- Netherlands Health Council, 2006—less than 1% of energy intake should be from TFA [88].
- National Cholesterol Education Program, 2001—intakes of TFA should be kept low [89].
- American Heart Association (AHA), 2006—less than 1% of energy as TFA [90].
- American Diabetes Association, 2007—intake of TFA should be minimized [91].

In addition to position statements by various agencies, governing bodies have mandated regulations regarding TFA in the food supply. In 2003, the Danish Government stated that industrially produced TFA, those from partially hydrogenated oils, should be limited to 2% of the total amount of fat or oil in a food [92]. The Danish government chose to use government regulations so that the responsibility was with the food industries unlike food labeling where the responsibility lies with the consumers. Following the Danish example, Health Canada's Trans Fat Task Force issued recommendations for regulating TFA in the food supply to the Minister of Health in June 2006 [93]. In *TRANSforming the Food Supply*, the task force recommended that: (1) TFA be limited to 2% of total fat content in all vegetable oils and soft, spreadable margarines to be sold or used in food preparation and (2) TFA be limited to 5% of total fat content in all other foods purchased by a retail or food service establishment for consumer sale or in food preparation, with the exception of food products for which the fat originates exclusively from ruminant meat or dairy products [93]. More recently, the New York City Board of Health placed a ban on TFA in foods, which was greatly opposed by the restaurant industry [94]. According to the ban, restaurants will have to eliminate oils, shortenings, and margarines used for frying and spreads with  $\geq 0.5$  g of TFA per serving by July 2007 [95]. Other USA cities, such as Boston, Chicago, and Los Angeles, have proposed similar bans on TFA in restaurant foods [96–98].

In contrast to Denmark and Canada, some countries, such as the Netherlands, have opted against government regulations, yet have made significant progress in reducing TFA in the food supply. The effort in the Netherlands was initiated by the food industry and continued via the Product Board for Margarine, Fats, and Oils (MVO), which represents all trade and production companies in

the Dutch edible oils and fats chain. MVO set up a Task Force for Responsible Fatty Acid Composition to campaign for the reduction of partially hydrogenated oils and SFA by using liquid frying oils in place of hard frying oils in restaurants [99]. Although this was not a government rule, 45% of all Dutch fast-food restaurants switched to using liquid frying oils containing less than 5% TFA, the goal set by the task force, within one year [99].

Although the Australian government is currently not regulating TFA in the food supply, it has issued a statement of support for the recently established National Collaboration on Trans Fats, consisting of the National Heart Foundation of Australia, the Dietitians Association of Australia, the Australian Food and Grocery Council and Food Standards Australia New Zealand. The National Collaboration on Trans Fat will propose initiatives aimed at reducing the amount of TFA in food sold in Australia [100].

An initiative set forth to reduce the amount of TFA in foods in the USA resulted from the settlement of a class action lawsuit against McDonald's. In March 2006, the American Heart Association received \$7 million to be used for: "(1) public education regarding TFA; (2) encouraging substitution of partially hydrogenated oils by the food industry; (3) holding conferences on health issues associated with TFA and the substitution of partially hydrogenated oils; and (4) other activities regarding the impact of TFA on public health" [101]. The strategic plan of the AHA TFA initiative focuses on consumer research, consumer education, industry conferences, NYC restaurants, and advocacy.

Given the considerable amount of evidence that TFA have adverse effects on cardiovascular health, along with other disease states, some have advocated government regulation in the USA. Currently, partially hydrogenated vegetable oils are allowed in USA food products under the category of GRAS, "generally regarded as safe". As pointed out by Willett [102], this contradicts current evidence which was considered strong enough to warrant the FDA to rule that the TFA content of foods be included on the Nutrition Facts Panel. In accordance with this, the Center for Science in the Public Interest submitted a petition to the FDA to remove TFA from partially hydrogenated vegetable oils from the GRAS category. If partially hydrogenated vegetable oils were removed from the GRAS category, less TFA would potentially be in the food supply and therefore the responsibility for lowering dietary TFA intake would be shared by consumers and the food industry. Removing all TFA from the food supply would be challenging due to the process of deodorization that is used to remove volatile components prior to human consumption. This process results in the production of

small amounts of TFA; however, not using this process results in oils that are less stable [103].

### TFA on the Food Label

Currently, the listing of TFA on the food label is the only federal regulation regarding TFA in the USA. As a result of an FDA ruling in 2003, the Nutrition Facts Panel includes the TFA content of most food products, effective 1 January 2006. According to the rule, TFA are defined as "all unsaturated FAs that contain one or more isolated double bonds in *trans* configuration" [104]. Since only TFA with non-conjugated double bonds are included in the FDA definition of TFA, CLA is excluded from the food label. However, other TFA of ruminant origin, such as *trans*-vaccenic acid, would be accounted for under the TFA definition.

If the TFA content of a product is greater than or equal to 0.5 g per serving, it must be stated on the Nutrition Facts Panel as a separate line item. If the TFA content of a product is less than 0.5 g per serving, it is expressed as 0 g TFA [104]. Therefore, it is important to educate consumers such that they are aware that if a product lists zero TFA it is not necessarily *trans* free. Additionally, a %Daily Value (%DV) is not listed as is done for other cholesterol-raising nutrients (i.e., SFA and dietary cholesterol) since there is no reference value from which a %DV can be set for TFA.

The FDA acknowledges the need for resolving some issues about the TFA information presented on food labels [105]. Therefore, the FDA issued an advance notice of proposed rule making (ANPR) the same day the food label ruling was issued. The goal of the ANPR is to elicit comments regarding: (1) definitions for nutrient content claims for TFA "free" and "reduced"; (2) limits on TFA amounts, in conjunction with SFA, for nutrient content claims, health claims, and disclosure and disqualifying levels; (3) a daily value; and (4) a footnote or disclosure statement for enhancing consumer understanding of cholesterol-raising lipids [105]. With consumers being held responsible for making healthy food decisions, specifically when choosing foods low in cholesterol-raising nutrients, extensive nutrition education on TFA will be necessary.

### Potential Challenges to Food Manufacturers

The primary challenge faced by food manufacturers relative to decreasing the TFA content of foods is the quality of the oils and fats available for food applications [106]. When considering TFA alternatives, food manufacturers are concerned with the functional characteristics of the finished products and how the products will be received by

the consumer [107]. When decreasing the TFA content of food products, the SFA content may increase and the shelf life of the finished product may decrease. Oils that are not hydrogenated are less stable and are more susceptible to oxidation than hydrogenated oils. Therefore, antioxidants may need to be added to these oils to overcome these challenges. Another concern of the food industry is the supply of TFA alternatives. If a restaurant is going to switch to a new TFA-free fat, it must be assured that there will be a consistent and adequate supply of the product. Furthermore, the production costs of TFA alternatives are greater than conventional hydrogenated oils [106, 108]. Therefore, suppliers of TFA alternatives want to assure a steady demand for their products to justify investing in the production of TFA alternatives. Suppliers also need to update equipment and technologies for producing new TFA alternatives [107].

### TFA Alternatives

TFA alternatives are being sought by the food industry due to the regulation of TFA in foods in some countries and the FDA-required food labeling in the USA. Food manufacturers are producing naturally stable oils that require little or no hydrogenation such as cottonseed, corn, high-oleic canola, high-oleic safflower, mid- and high-oleic sunflower, low-linolenic soybean oils and tropical oils (palm oil, palm kernel oil, and coconut oil) [107]. Food manufacturers consider tropical oils adequate replacements for partially hydrogenated oils in baked goods due to their high content of SFA and higher melting points [108]. As with fully hydrogenated vegetable oils, the use of tropical oils increases the SFA content of these products.

A variety of technologies are already being implemented while others are being developed and refined to reduce or eliminate TFA in food products [107, 108]. Interesterification rearranges the FA within triglycerides to yield customized melting characteristics. Another method for reducing TFA in food products is altering the hydrogenation process to yield partially hydrogenated fats lower in TFA. This is accomplished by using metal catalysts that prevent the formation of *trans* isomers [109–111] or promote the formation of *cis* isomers [109] and by changing the time and temperature of the hydrogenation process [107]. Numerous plant breeding and genetic engineering technologies are being used to manipulate the FA composition of oil seeds to increase oxidative stability during deep-fat frying and to extend shelf life by decreasing the amount of relatively unstable fatty acids (i.e., linolenic) or increasing the amount of relatively stable fatty acids (i.e., oleic) [107, 108].

While the AHA applauds efforts to reduce the consumption of TFA in restaurants, it cautions against the use of other “unhealthy oil products”. Therefore, the AHA recommends providing guidance to eateries on which oils to use and how to incorporate them and TFA-free shortenings into their menu and food preparation processes [112]. When restaurants use these TFA alternatives, it is important that the entire FA profile of them be considered. When available, healthy fats should be substituted for fats that contain TFA. Although there are some SFA with neutral effects on blood cholesterol, if TFA are simply replaced by cholesterol-raising SFA, the health effects might be negated, in part or almost completely.

### TFA in the Food Supply

A recent analysis (November 2004–September 2005) of popular foods (fries and chicken nuggets) from fast food chains, specifically McDonald’s and KFC, indicates that the TFA content of one large serving varies greatly between countries (<1 g/serving to 24 g/serving) and even within countries (<1 g/serving to 5 g/serving) [113]. However, the frying oil used in the food industry in the majority of European countries contains ~10% TFA, with foods from both chains in Denmark containing less than 1 g TFA. In contrast, the oils in the USA and Peru contain 23 and 24% TFA, respectively. Another analysis indicates that since the imposition of the Danish government rule, much fewer food products in Danish eateries contain more than 2% TFA when compared to an investigation of food samples in the same categories (baked products, potato products, and microwave popcorn) prior to the ruling [92].

A reduction in the TFA in food products may translate to a decrease in cardiovascular events [114]. Data from Costa Rica indicate that prior to industrial modifications that reduce TFA in foods (1994–1999), TFA intake in the highest quintile (median = 2.02 g/100 g) was associated with an increased risk of MI (OR = 4.76; 95% CI 2.24–10.11). However after industrial modification (2000–2003), TFA intake (median = 1.4 g/100 g) was not associated with an increased risk (OR = 1.15; 95% CI 0.80–1.64). The lack of association during the later years may be due to the lower TFA intake; mean TFA intakes were 4.1 and 2.9 g/day during 1994–1999 and 2000–2003, respectively. While associations between TFA intake and CVD biomarkers and events exist in populations with higher intakes of TFA (~4 g/day), none exist at lower intakes (~2 g/day) [114]. Therefore, reducing TFA in the food supply as low as possible will most likely translate to an overall decrease in the population intake and CVD risk.

Due to government regulations and the increasing awareness of the detrimental effects of manufactured TFA

on health, numerous chain eateries are eliminating or reducing TFA in their products. Fast food outlets in Denmark and the Netherlands have been very successful at maintaining the quality of their food products while considerably reducing the TFA content of them [92, 99]. Furthermore, the amount of SFA has slightly decreased with a concomitant increase in MUFA (18:1c) and PUFA (18:2Δ6c) [99]. Many common chain eateries in the USA, such as KFC, Wendy's, Taco Bell, and Starbucks, are following suit [115–119]. Other chain outlets are expected to change in the foreseeable future in the USA [99].

### Potential Challenges to Consumers

While the food industry is facing food production challenges, consumers are confronted with many decisions regarding their food choices for health. A new online resource to help consumers with these challenges is the AHA's Face the Fats website. Since the TFA content of foods with less than 500 mg of TFA per serving is listed as 0 g, consumers may unknowingly consume an unhealthy amount of TFA, especially if >1 serving is eaten. For this reason, recommendations should be made to read the ingredient list on the Nutrition Facts Panel, paying special attention to partially hydrogenated oils.

Consumers continue to struggle to understand the different kinds of fats, how they affect health, and how to incorporate fats into the diet [120–122]. Consumers should be advised to choose foods based on their overall nutrient profile including the amounts of all cholesterol-raising nutrients (SFA, TFA, and dietary cholesterol) they contain. Consumers are advised to consider both fully hydrogenated oils and partially hydrogenated oils listed in the ingredient lists of products. When vegetable oils are fully hydrogenated, stearic acid is the primary SFA produced [107], which has neutral effects on lipids and lipoproteins [123, 124]. The amount of SFA on the Nutrition Facts Panel will include stearic acid along with all other individual SFA. Therefore, checking the ingredient label for fully hydrogenated oils will indicate whether stearic acid is in the product. Since CLA is not included in the FDA definition of TFA, consumers should be aware that foods from animal sources may contain CLA. Thus, consumers are advised to refer to the food ingredient list to determine whether a food contains TFA from partially hydrogenated oils, stearic acid from fully hydrogenated oils, and CLA from meat and dairy products (i.e., milk). Reading and understanding the ingredient lists of foods presents another potential challenge to consumers whom already find it difficult to read and comprehend food labels and to understand how different kinds of fats effect one's health [120–122]. Furthermore, the production

costs of TFA alternatives are typically greater than those of partially hydrogenated oils. If this cost is defrayed by more expensive products, consumers will have to choose between cost and health [107].

### Effects of Substituting Stearic Acid for TFA

As reviewed by Kris-Etherton et al. [124], if a male (consuming 2,666 kcal/day) substituted stearic acid for 1% of energy from TFA (recommended upper intake level by 2005 DGAC and WHO/FAO report), it would result in stearic acid intakes of 11.2 g/day (8.2 g from usual diet plus 3 g from TFA substitution), or 3.7% of calories. If the required amount of stearic acid for substitution were double the intake of TFA, then stearic acid intake would be 14.2 g/day, or 4.7% of calories. At the upper end of TFA intake [3], which is 3.2% of calories, if a one-to-one substitution of stearic acid for TFA occurred, daily stearic acid intake would be 17 g, or 6% of calories. If the required amount of stearic acid for substitution were double the amount of TFA at this upper level of intake, then stearic acid intake would be 26 g/day, or 9% of calories. This higher level of intake is unlikely since multiple fats are proposed as substitutes for TFA [43]. To date, research suggests no adverse effects of stearic acid [123], although there is a suggestion that very high intakes (beyond what is expected with current intake practices and anticipated outcomes) may be associated with adverse consequences [125]. Research is needed to determine the consequences of substituting various FA, especially stearic acid and inter-esterified stearic acid, which are leading candidates for TFA substitutes for solid fat applications in the diet.

### Conclusions

There are many TFA isomers that have unique biological effects. Notwithstanding, the industrially produced TFA clearly have adverse health effects. Although there is evidence of health benefits of the animal TFA isomers on some of the endpoints that have been studied, these are not a major TFA source in the diet. Future research will bring clarity to our understanding of the biological effects of the TFA family. At this point, it is not possible to plan diets that emphasize individual TFA from animal sources at levels that would be expected to have significant health effects. Moreover, since TFA from animal sources accompany SFA, a message to emphasize is that increasing a single ruminant TFA in the diet is not appropriate because it will increase SFA. Thus, according to the American Heart Association, the best message for consumers presently is to limit TFA, SFA, and dietary cholesterol by following a

healthy overall dietary pattern that emphasizes fruits, vegetables, whole-grain foods, fat free and low fat dairy products, lean meats, poultry and fish twice a week. Following this dietary pattern will limit TFA and SFA intake and is consistent with current dietary recommendations made by many organizations worldwide.

## References

- Eckel R, Borra S, Lichtenstein A, Yin-Piazza S (2007) Understanding the complexity of trans fatty acid reduction in the American diet. *Circulation* 115:2231–2246
- Kodali D (2005) *Trans* fats—chemistry, occurrence, functional need in foods and potential solutions. In: Kodali D, List G (eds) *Trans fat alternatives*. AOCS Press, Champaign
- Allison DB, Egan SK, Barraj LM, Caughman C, Infante M, Heimbach JT (1999) Estimated intakes of *trans* fatty and other fatty acids in the US population. *J Am Diet Assoc* 99:166–174; quiz 175–166
- Weggemans RM, Rudrum M, Trautwein EA (2004) Intake of ruminant versus industrial *trans* fatty acids and risk of coronary heart disease—what is the evidence? *Eur J Lipid Sci Technol*, 106:390–397
- Rainer L, Heiss CJ (2004) Conjugated linoleic acid: health implications and effects on body composition. *J Am Diet Assoc* 104:963–968, quiz 1032
- Bhattacharya A, Banu J, Rahman M, Causey J, Fernandes G (2006) Biological effects of conjugated linoleic acids in health and disease. *J Nutr Biochem* 17:789–810
- Tricon S, Burdge GC, Williams CM, Calder PC, Yaqoob P (2005) The effects of conjugated linoleic acid on human health-related outcomes. *Proc Nutr Soc* 64:171–182
- Salas-Salvado J, Marquez-Sandoval F, Bullo M (2006) Conjugated linoleic acid intake in humans: a systematic review focusing on its effect on body composition, glucose, and lipid metabolism. *Crit Rev Food Sci Nutr* 46:479–488
- Hu FB, Stampfer MJ, Manson JE, Rimm E, Colditz GA, Rosner BA, Hennekens CH, Willett WC (1997) Dietary fat intake and the risk of coronary heart disease in women. *N Engl J Med* 337:1491–1499
- Kromhout D, Menotti A, Bloemberg B, Aravanis C, Blackburn H, Buzina R, Dontas AS, Fidanza F, Giampaoli S, Jansen A et al (1995) Dietary saturated and *trans* fatty acids and cholesterol and 25-year mortality from coronary heart disease: the Seven Countries study. *Prev Med* 24:308–315
- Willett WC, Stampfer MJ, Manson JE, Colditz GA, Speizer FE, Rosner BA, Sampson LA, Hennekens CH (1993) Intake of *trans* fatty acids and risk of coronary heart disease among women. *Lancet* 341:581–585
- Oomen CM, Ocke MC, Feskens EJ, van Erp-Baart MA, Kok FJ, Kromhout D (2001) Association between *trans* fatty acid intake and 10-year risk of coronary heart disease in the Zutphen Elderly Study: a prospective population-based study. *Lancet* 357:746–751
- Lemaitre RN, King IB, Raghunathan TE, Pearce RM, Weinmann S, Knopp RH, Copass MK, Cobb LA, Siscovick DS (2002) Cell membrane *trans*-fatty acids and the risk of primary cardiac arrest. *Circulation* 105:697–701
- Lemaitre RN, King IB, Mozaffarian D, Sotoodehnia N, Rea TD, Kuller LH, Tracy RP, Siscovick DS (2006) Plasma phospholipid *trans* fatty acids, fatal ischemic heart disease, and sudden cardiac death in older adults: the cardiovascular health study. *Circulation* 114:209–215
- Ascherio A, Hennekens CH, Buring JE, Master C, Stampfer MJ, Willett WC (1994) *Trans*-fatty acids intake and risk of myocardial infarction. *Circulation* 89:94–101
- Pietinen P, Ascherio A, Korhonen P, Hartman AM, Willett WC, Albanes D, Virtamo J (1997) Intake of fatty acids and risk of coronary heart disease in a cohort of Finnish men. The Alpha-Tocopherol, Beta-Carotene Cancer Prevention Study. *Am J Epidemiol* 145:876–887
- Jakobsen MU, Bysted A, Andersen NL, Heitmann BL, Hartkopp HB, Leth T, Overvad K, Dyerberg J (2006) Intake of ruminant *trans* fatty acids and risk of coronary heart disease—an overview. *Atheroscler Suppl* 7:9–11
- Ascherio A (2006) *Trans* fatty acids and blood lipids. *Atheroscler Suppl* 7:25–27
- Mensink RP, Zock PL, Kester AD, Katan MB (2003) Effects of dietary fatty acids and carbohydrates on the ratio of serum total to HDL cholesterol and on serum lipids and apolipoproteins: a meta-analysis of 60 controlled trials. *Am J Clin Nutr* 77:1146–1155
- Sun Q (2006) New evidence links *trans* fats to increased heart disease risk. American Heart Association
- Lichtenstein A, Ausman L, Jalbert S, Schaefer E (1999) Effects of different forms of dietary hydrogenated fats on serum lipoprotein cholesterol levels. *N Engl J Med* 25:1930–1940
- Ascherio A, Katan MB, Zock PL, Stampfer MJ, Willett WC (1999) *Trans* fatty acids and coronary heart disease. *N Engl J Med* 340:1994–1998
- Mauger JF, Lichtenstein AH, Ausman LM, Jalbert SM, Jauhainen M, Ehnholm C, Lamarche B (2003) Effect of different forms of dietary hydrogenated fats on LDL particle size. *Am J Clin Nutr* 78:370–375
- Tholstrup T, Raff M, Basu S, Nonboe P, Sejrnsen K, Straarup EM (2006) Effects of butter high in ruminant *trans* and monounsaturated fatty acids on lipoproteins, incorporation of fatty acids into lipid classes, plasma C-reactive protein, oxidative stress, hemostatic variables, and insulin in healthy young men. *Am J Clin Nutr* 83:237–243
- Mozaffarian D, Katan MB, Ascherio A, Stampfer MJ, Willett WC (2006) *Trans* fatty acids and cardiovascular disease. *N Engl J Med* 354:1601–1613
- Subbaiah PV, Subramanian VS, Liu M (1998) *Trans* unsaturated fatty acids inhibit lecithin: cholesterol acyltransferase and alter its positional specificity. *J Lipid Res* 39:1438–1447
- Smedman A, Vessby B (2001) Conjugated linoleic acid supplementation in humans—metabolic effects. *Lipids* 36:773–781
- Mougiou V, Matsakas A, Petridou A, Ring S, Sagredos A, Melissopoulou A, Tsigilis N, Nikolaidis M (2001) Effect of supplementation with conjugated linoleic acid on human serum lipids and body fat. *J Nutr Biochem* 12:585–594
- Benito P, Nelson GJ, Kelley DS, Bartolini G, Schmidt PC, Simon V (2001) The effect of conjugated linoleic acid on plasma lipoproteins and tissue fatty acid composition in humans. *Lipids* 36:229–236
- Noone EJ, Roche HM, Nugent AP, Gibney MJ (2002) The effect of dietary supplementation using isomeric blends of conjugated linoleic acid on lipid metabolism in healthy human subjects. *Br J Nutr* 88:243–251
- Riserus U, Berglund L, Vessby B (2001) Conjugated linoleic acid (CLA) reduced abdominal adipose tissue in obese middle-aged men with signs of the metabolic syndrome: a randomised controlled trial. *Int J Obes Relat Metab Disord* 25:1129–1135
- Petridou A, Mougiou V, Sagredos A (2003) Supplementation with CLA: isomer incorporation into serum lipids and effect on body fat of women. *Lipids* 38:805–811
- Blankson H, Stakkestad JA, Fagertun H, Thom E, Wadstein J, Gudmundsen O (2000) Conjugated linoleic acid reduces body

- fat mass in overweight and obese humans. *J Nutr* 130:2943–2948
34. Riserus U, Arner P, Brismar K, Vessby B (2002) Treatment with dietary *trans*10*cis*12 conjugated linoleic acid causes isomer-specific insulin resistance in obese men with the metabolic syndrome. *Diabetes Care* 25:1516–1521
  35. Tricon S, Burdge GC, Kew S, Banerjee T, Russell JJ, Jones EL, Grimble RF, Williams CM, Yaqoob P, Calder PC (2004) Opposing effects of *cis*-9,*trans*-11 and *trans*-10,*cis*-12 conjugated linoleic acid on blood lipids in healthy humans. *Am J Clin Nutr* 80:614–620
  36. Naumann E, Carpentier YA, Saebo A, Lassel TS, Chardigny JM, Sebedio JL, Mensink RP, (2006) *Cis*-9, *trans*-11 and *trans*-10, *cis*-12 conjugated linoleic acid (CLA) do not affect the plasma lipoprotein profile in moderately overweight subjects with LDL phenotype B. *Atherosclerosis* 188:167–174
  37. Chardigny JM, Malpuech-Brugere C, Dionisi F, Bauman DE, German B, Mensink RP, Combe N, Chaumont P, Barbano DM, Enjalbert F, Bezelgues JB, Cristiani I, Moulin J, Boirie Y, Golay PA, Giuffrida F, Sebedio JL, Destaillets F (2006) Rationale and design of the TRANSFACT project phase I: a study to assess the effect of the two different dietary sources of *trans* fatty acids on cardiovascular risk factors in humans. *Contemp Clin Trials* 27:364–373
  38. Mozaffarian D, Pischon T, Hankinson SE, Rifai N, Joshipura K, Willett WC, Rimm EB (2004) Dietary intake of *trans* fatty acids and systemic inflammation in women. *Am J Clin Nutr* 79:606–612
  39. Lopez-Garcia E, Schulze MB, Meigs JB, Manson JE, Rifai N, Stampfer MJ, Willett WC, Hu FB (2005) Consumption of *trans* fatty acids is related to plasma biomarkers of inflammation and endothelial dysfunction. *J Nutr* 135:562–566
  40. Mozaffarian D, Rimm EB, King IB, Lawler RL, McDonald GB, Levy WC (2004) *Trans* fatty acids and systemic inflammation in heart failure. *Am J Clin Nutr* 80:1521–1525
  41. Han SN, Leka LS, Lichtenstein AH, Ausman LM, Schaefer EJ, Meydani SN (2002) Effect of hydrogenated and saturated, relative to polyunsaturated, fat on immune and inflammatory responses of adults with moderate hypercholesterolemia. *J Lipid Res* 43:445–452
  42. Baer DJ, Judd JT, Clevidence BA, Tracy RP (2004) Dietary fatty acids affect plasma markers of inflammation in healthy men fed controlled diets: a randomized crossover study. *Am J Clin Nutr* 79:969–973
  43. Smedman A, Basu S, Jovinge S, Fredrikson GN, Vessby B (2005) Conjugated linoleic acid increased C-reactive protein in human subjects. *Br J Nutr* 94:791–795
  44. Riserus U, Basu S, Jovinge S, Fredrikson GN, Arnlov J, Vessby B (2002) Supplementation with conjugated linoleic acid causes isomer-dependent oxidative stress and elevated C-reactive protein: a potential link to fatty acid-induced insulin resistance. *Circulation* 106:1925–1929
  45. Steck SE, Chalecki AM, Miller P, Conway J, Austin GL, Hardin JW, Albright CD, Thuillier P, (2007) Conjugated linoleic acid supplementation for twelve weeks increases lean body mass in obese humans. *J Nutr* 137:1188–1193
  46. Moloney F, Yeow TP, Mullen A, Nolan JJ, Roche HM (2004) Conjugated linoleic acid supplementation, insulin sensitivity, and lipoprotein metabolism in patients with type 2 diabetes mellitus. *Am J Clin Nutr* 80:887–895
  47. Ramakers JD, Plat J, Sebedio JL, Mensink RP (2005) Effects of the individual isomers *cis*-9,*trans*-11 vs. *trans*-10,*cis*-12 of conjugated linoleic acid (CLA) on inflammation parameters in moderately overweight subjects with LDL-phenotype B. *Lipids* 40:909–918
  48. Poirier H, Shapiro JS, Kim RJ, Lazar MA (2006) Nutritional supplementation with *trans*-10, *cis*-12-conjugated linoleic acid induces inflammation of white adipose tissue. *Diabetes* 55:1634–1641
  49. de Roos NM, Bots ML, Katan MB (2001) Replacement of dietary saturated fatty acids by *trans* fatty acids lowers serum HDL cholesterol and impairs endothelial function in healthy men and women. *Arterioscler Thromb Vasc Biol* 21:1233–1237
  50. Sarabi M, Vessby B, Millgard J, Lind L (2001) Endothelium-dependent vasodilation is related to the fatty acid composition of serum lipids in healthy subjects. *Atherosclerosis* 156:349–355
  51. Schleser S, Ringseis R, Eder K (2006) Conjugated linoleic acids have no effect on TNF alpha-induced adhesion molecule expression, U937 monocyte adhesion, and chemokine release in human aortic endothelial cells. *Atherosclerosis* 186:337–344
  52. Sneddon AA, McLeod E, Wahle KW, Arthur JR (2006) Cytokine-induced monocyte adhesion to endothelial cells involves platelet-activating factor: suppression by conjugated linoleic acid. *Biochim Biophys Acta* 1761:793–801
  53. Taylor JS, Williams SR, Rhys R, James P, Frenneaux MP (2006) Conjugated linoleic acid impairs endothelial function. *Arterioscler Thromb Vasc Biol* 26:307–312
  54. Wang YW, Jones PJ (2004) Conjugated linoleic acid and obesity control: efficacy and mechanisms. *Int J Obes Relat Metab Disord* 28:941–955
  55. Terpstra AH, Beynen AC, Everts H, Kocsis S, Katan MB, Zock PL (2002) The decrease in body fat in mice fed conjugated linoleic acid is due to increases in energy expenditure and energy loss in the excreta. *J Nutr* 132:940–945
  56. Pariza MW, Park Y, Cook ME (1999) Conjugated linoleic acid and the control of cancer and obesity. *Toxicol Sci* 52:107–110
  57. Terpstra AH (2004) Effect of conjugated linoleic acid on body composition and plasma lipids in humans: an overview of the literature. *Am J Clin Nutr* 79:352–361
  58. Thom E, Wadstein J, Gudmundsen O (2001) Conjugated linoleic acid reduces body fat in healthy exercising humans. *J Int Med Res* 29:392–396
  59. Belury MA, Mahon A, Banni S (2003) The conjugated linoleic acid (CLA) isomer, t10c12-CLA, is inversely associated with changes in body weight and serum leptin in subjects with type 2 diabetes mellitus. *J Nutr* 133:257S–260S
  60. Gaullier JM, Halse J, Hoivik HO, Hoye K, Syvertsen C, Nurminen M, Hassfeld C, Einerhand A, O'Shea M, Gudmundsen O (2007) Six months supplementation with conjugated linoleic acid induces regional-specific fat mass decreases in overweight and obese. *Br J Nutr* 97:550–560
  61. Gaullier JM, Halse J, Hoye K, Kristiansen K, Fagertun H, Vik H, Gudmundsen O (2005) Supplementation with conjugated linoleic acid for 24 months is well tolerated by and reduces body fat mass in healthy, overweight humans. *J Nutr* 135:778–784
  62. Larsen TM, Toubro S, Gudmundsen O, Astrup A (2006) Conjugated linoleic acid supplementation for 1 y does not prevent weight or body fat regain. *Am J Clin Nutr* 83:606–612
  63. Salmeron J, Hu FB, Manson JE, Stampfer MJ, Colditz GA, Rimm EB, Willett WC (2001) Dietary fat intake and risk of type 2 diabetes in women. *Am J Clin Nutr* 73:1019–1026
  64. van Dam RM, Willett WC, Rimm EB, Stampfer MJ, Hu FB (2002) Dietary fat and meat intake in relation to risk of type 2 diabetes in men. *Diabetes Care* 25:417–424
  65. Louheranta AM, Turpeinen AK, Vidgren HM, Schwab US, Uusitupa MI (1999) A high-*trans* fatty acid diet and insulin sensitivity in young healthy women. *Metabolism* 48:870–875
  66. Lovejoy JC, Smith SR, Champagne CM, Most MM, Lefevre M, DeLany JP, Denkins YM, Rood JC, Veldhuis J, Bray GA (2002) Effects of diets enriched in saturated (palmitic), monounsaturated



- rated (oleic), or *trans* (elaidic) fatty acids on insulin sensitivity and substrate oxidation in healthy adults. *Diabetes Care* 25:1283–1288
67. Lichtenstein AH, Erkkila AT, Lamarche B, Schwab US, Jalbert SM, Ausman LM (2003) Influence of hydrogenated fat and butter on CVD risk factors: remnant-like particles, glucose and insulin, blood pressure and C-reactive protein. *Atherosclerosis* 171:97–107
  68. Riserus U (2006) *Trans* fatty acids and insulin resistance. *Atheroscler Suppl* 7:37–39
  69. Christiansen E, Schnider S, Palmvig B, Tauber-Lassen E, Pedersen O (1997) Intake of a diet high in *trans* monounsaturated fatty acids or saturated fatty acids. Effects on postprandial insulinemia and glycemia in obese patients with NIDDM. *Diabetes Care* 20:881–887
  70. Riserus U, Vessby B, Arnlov J, Basu S (2004) Effects of *cis*-9,*trans*-11 conjugated linoleic acid supplementation on insulin sensitivity, lipid peroxidation, and proinflammatory markers in obese men. *Am J Clin Nutr* 80:279–283
  71. Taylor CG, Zahradka P (2004) Dietary conjugated linoleic acid and insulin sensitivity and resistance in rodent models. *Am J Clin Nutr* 79:1164S–1168S
  72. Astorg P (2005) Dietary fatty acids and colorectal and prostate cancers: epidemiological studies. *Bull Cancer* 92:670–684
  73. King IB, Kristal AR, Schaffer S, Thornquist M, Goodman GE (2005) Serum *trans*-fatty acids are associated with risk of prostate cancer in beta-carotene and retinol efficacy trial. *Cancer Epidemiol Biomarkers Prev* 14:988–992
  74. Banni S, Angioni E, Murru E, Carta G, Melis MP, Bauman D, Dong Y, Ip C (2001) Vaccenic acid feeding increases tissue levels of conjugated linoleic acid and suppresses development of premalignant lesions in rat mammary gland. *Nutr Cancer* 41:91–97
  75. Lock AL, Corl BA, Barbano DM, Bauman DE, Ip C (2004) The anticarcinogenic effect of *trans*-11 18:1 is dependent on its conversion to *cis*-9, *trans*-11 CLA by delta9-desaturase in rats. *J Nutr* 134:2698–2704
  76. Voorrips LE, Brants HA, Kardinaal AF, Hiddink GJ, van den Brandt PA, Goldbohm RA (2002) Intake of conjugated linoleic acid, fat, and other fatty acids in relation to postmenopausal breast cancer: the Netherlands Cohort Study on diet and cancer. *Am J Clin Nutr* 76:873–882
  77. Chajes V, Lavillonniere F, Ferrari P, Jourdan ML, Pinault M, Maillard V, Sebedio JL, Bougnoux P (2002) Conjugated linoleic acid content in breast adipose tissue is not associated with the relative risk of breast cancer in a population of French patients. *Cancer Epidemiol Biomarkers Prev* 11:672–673
  78. Aro A, Mannisto S, Salminen I, Ovaskainen ML, Kataja V, Uusitupa M (2000) Inverse association between dietary and serum conjugated linoleic acid and risk of breast cancer in postmenopausal women. *Nutr Cancer* 38:151–157
  79. McCann SE, Ip C, Ip MM, McGuire MK, Muti P, Edge SB, Trevisan M, Freudenheim JL (2004) Dietary intake of conjugated linoleic acids and risk of premenopausal and postmenopausal breast cancer, Western New York Exposures and Breast Cancer Study (WEB Study). *Cancer Epidemiol Biomarkers Prev* 13:1480–1484
  80. Larsson SC, Bergkvist L, Wolk A (2005) High-fat dairy food and conjugated linoleic acid intakes in relation to colorectal cancer incidence in the Swedish Mammography Cohort. *Am J Clin Nutr* 82:894–900
  81. IOM (2002) Dietary reference intakes: energy, carbohydrates, fiber, fat, fatty acids, cholesterol, protein, and amino acids. National Academies Press, Washington, DC
  82. Committee DGA (2005) Dietary Guidelines Advisory Committee Report 2005. <http://www.health.gov/dietaryguidelines/dga2005/report/> (accessed 6 September 2005)
  83. USDHHS, USDA (2005) Dietary guidelines for Americans, 2005, 6th edn. Government Printing Office, Washington, DC
  84. Joint WHO/FAO Expert Consultation (2003) Diet, nutrition, and the prevention of chronic diseases, 916, 89–90. Geneva, WHO. WHO Technical Report Series
  85. ISSFAL (2007) ISSFAL—fatty acids, lipids and health studies: adequate intakes. <http://www.issfal.org.uk/adequate-intakes.html> (accessed 7 January 2007)
  86. EURODIET (2000) Nutrition & diet for healthy lifestyles in Europe. Science & Policy Implications, in 1–17, Crete
  87. Krawczyk T (2001) Fat in dietary guidelines around the world. *INFORM* 12, 132–138
  88. Netherlands H.C.o.t. (2006) Guidelines for a healthy diet 2006. Publication no. 2006/21, in The Hague: Health Council of the Netherlands
  89. Executive Summary of The Third Report of The National Cholesterol Education Program (NCEP) (2001) Expert panel on detection, evaluation, and treatment of high blood cholesterol in adults (Adult Treatment Panel III). *JAMA* 285:2486–2497
  90. Lichtenstein AH, Appel LJ, Brands M, Carnethon M, Daniels S, Franch HA, Franklin B, Kris-Etherton P, Harris WS, Howard B, Karanja N, Lefevre M, Rudel L, Sacks F, Van Horn L, Winston M, Yllie-Rosett J (2006) Diet and lifestyle recommendations revision 2006: a scientific statement from the American Heart Association Nutrition Committee. *Circulation* 114:82–96
  91. American Diabetes Association (2007) Nutrition recommendations and interventions for diabetes. *Diabetes Care* 30(Suppl): S48–S65
  92. Leth T, Jensen HG, Mikkelsen AA, Bysted A (2006) The effect of the regulation on *trans* fatty acid content in Danish food. *Atheroscler Suppl* 7:53–56
  93. Canada H (2006) TRANSforming the food supply: Report of the Trans Fat Task Force submitted to the Minister of Health
  94. Lueck TJ, Severson K. New York bans most *trans* fats in restaurants. *The New York Times*, 6 December 2006
  95. DOHMH (2006) Notice of the adoption of an Amendment (81.08) to Article 81 of the New York City Health Code. New York City, 5 December 2006
  96. Smith S (2006) City looks at banning *trans* fats in eateries. *The Boston Globe*, 20 December 2006
  97. Tufts University. *Trans* fat ban: watch saturated fats and calories too. <http://www.physorg.com/news86011604.html> (accessed 6 February 2007)
  98. Barboza T (2007) LA restaurants to phase out *trans* fat. *Los Angeles Times*, 30 January 2007
  99. Katan MB (2006) Regulation of *trans* fats: the gap, the Polder, and McDonald's French fries. *Atheroscler Suppl* 7:63–66
  100. Ageing. A.G.D.o.H.a., Government supports initiatives to reduce *trans* fats in food. <http://www.health.gov.au/internet/ministers/publishing.nsf/Content/health-mediarel-yr2006-cp-pyn069.htm> (accessed 6 February 2007)
  101. AHA. The pulse of the Western States affiliate: AHA receives rest of \$7 million settlement payment from McDonald's for *trans* fat initiative. <http://www.americanheart.org/presenter.jhtml?identifier=3039369#ahamcdo> (accessed 31 January 2007)
  102. Willett WC (2006) The scientific basis for TFA regulations—is it sufficient? Comments from the USA. *Atheroscler Suppl* 7:69–71
  103. Chaiyasit W, Elias RJ, McClements DJ, Decker EA (2007) Role of physical structures in bulk oils on lipid oxidation. *Crit Rev Food Sci Nutr* 47:299–317

104. DHHS/FDA (2003) Food labeling: *trans* fatty acids in nutrition labeling; nutrient content claims, and health claims: final rule. Fed Regist 68:41433–41506
105. Moss J (2006) Labeling of *trans* fatty acid content in food, regulations and limits—the FDA view. *Atheroscler Suppl* 7:57–59
106. Nielsen K (2006) Is the quality and cost of food affected if industrially produced *trans* fatty acids are removed?. *Atheroscler Suppl* 7:61–62
107. Kodali DR, List GR (2005) *trans* Fat alternatives. AOCS Press, Champaign
108. Tarrago-Trani MT, Phillips KM, Lemar LE, Holden JM (2006) New and existing oils and fats used in products with reduced *trans*-fatty acid content. *J Am Diet Assoc* 106:867–880
109. Wright AJ, Wong A, Diosady LL (2003) Ni catalyst promotion of a *Cis*-selective Pd catalyst for canola oil hydrogenation. *Food Res Int* 36:1069–1072
110. Mondal K, Lalani S (2000) A second order model for the catalytic-transfer hydrogenation of edible oils. *J Am Oil Chem Soc* 77:1–8
111. Bunge Oils Inc, ELITE Bakery Shortenings & Margarines. <http://www.bungefoods.com/ShortOilMarg.htm> (accessed 5 January 2007)
112. AHA, American Heart Association Media Statement: Position on New York City DOHMH's revised regulation of *trans* fats. <http://www.americanheart.org> (accessed 6 February 2007)
113. Stender S, Dyerberg J, Astrup A (2006) High levels of industrially produced *trans* fat in popular fast foods. *N Engl J Med* 354:1650–1652
114. Colon-Ramos U, Baylin A, Campos H (2006) The relation between *trans* fatty acid levels and increased risk of myocardial infarction does not hold at lower levels of *trans* fatty acids in the Costa Rican food supply. *J Nutr* 136:2887–2892
115. Corporation K, KFC announces switch to zero *trans* fat cooking oil following two-year test for same great taste. <http://www.kfc.com/about/pressreleases/103006.asp> (accessed 7 January 2007)
116. consumeraffairs.com, Wendy's cuts *trans* fats in fries and chicken. [http://www.consumeraffairs.com/news04/2006/06/wendys\\_transfat.html](http://www.consumeraffairs.com/news04/2006/06/wendys_transfat.html) (accessed 7 January 2007)
117. Press A, Taco Bell to cut artery-clogging *trans* fats: all Mexican fast food restaurants to switch to healthier canola oil by April. <http://www.msnbc.msn.com/id/15748882/> (accessed 7 January 2007)
118. Jargon J, Starbucks cuts *trans* fat from Chicago products. <http://www.chicagobusiness.com/cgi-bin/news.pl?id=23281> (accessed 7 January 2007)
119. Woodward C, Starbucks bans *trans* fat-laden pastries at half its US stores. <http://www.mercurynews.com/mld/mercurynews/business/16372823.htm> (accessed 7 January 2007)
120. Foundation I.F.I.C., How consumers feel about food and nutrition messages. <http://www.ific.org/research/newconvres.cfm> (accessed 7 January 2007)
121. Foundation I.F.I.C., Questions and answers about *trans* fats. <http://www.ific.org/publications/qa/transqa.cfm> (accessed 7 January 2007)
122. Foundation I.F.I.C., Fitting dietary fat into a healthful diet—a consumer point of view. <http://www.ific.org/research/fatsres.cfm> (accessed 7 January 2007)
123. Thijssen MA, Mensink RP (2005) Small differences in the effects of stearic acid, oleic acid, and linoleic acid on the serum lipoprotein profile of humans. *Am J Clin Nutr* 82:510–516
124. Kris-Etherton PM, Griel AE, Psota TL, Gebauer SK, Zhang J, Etherton TD (2005) Dietary stearic acid and risk of cardiovascular disease: intake, sources, digestion, and absorption. *Lipids* 40:1193–1200
125. Sundram K, Karupaiah T, Hayes K (2007) Stearic acid-rich interesterified fat and *trans*-rich fat raise the LDL/HDL ratio and plasma glucose relative to palm olein in humans. *Nutr Metab (Lond)* 4:3
126. Meijer GW, Weststrate JA (1997) Interesterification of fats in margarine: effect on blood lipids, blood enzymes, and hemostasis parameters. *Eur J Clin Nutr* 51:527–534
127. Kraft J, Hanske L, Mockel P, Zimmermann S, Hartl A, Kramer JK, Jahreis G (2006) The conversion efficiency of *trans*-11 and *trans*-12 18:1 by Delta9-desaturation differs in rats. *J Nutr* 136:1209–1214
128. Molzentgen J (2000) Occurrence and biochemical characteristics of natural bioactive substances in bovine milk lipids. *Br J Nutr* 84(Suppl 1):S47–S53

# Prenatal Fatty Acid Status and Immune Development: The Pathways and the Evidence

Susan L. Prescott · Janet A. Dunstan

Received: 10 October 2006 / Accepted: 22 January 2007 / Published online: 13 March 2007  
© AOCS 2007

**Abstract** This review explores the effects of dietary long chain polyunsaturated fatty acids (LCPUFA) on various aspects of early immune development and their potential role in the development or the prevention of immune disease. Modern diets have become increasingly rich in n-6 LCPUFA and relatively n-3 LCPUFA deficient. These potentially “pro-inflammatory” dietary changes have clear implications for the immature and developing fetal immune system. It is now well known that immunological abnormalities precede the development of allergic disease and are frequently evident at birth or in the first months of life. This has led to the hypothesis that potential effects of LCPUFA could be greatest in very early life before immune responses and clinical phenotype are established. Here we summarise the evidence that patterns of LCPUFA exposure in pregnancy can influence aspects of fetal immune in ways that are consistent with the immunological properties of these nutrients in adults. Specifically, human studies have shown that higher levels of n-3 LCPUFA are associated with reduction in neonatal oxidative stress, reduced production of inflammatory leukotienne B4 (LTB4) and altered T cell function. Inverse correlations between n-3 LCPUFA levels and neonatal T cell cytokine production, are consistent with adult studies showing reduction in T cell cytokine production with fish oil supplementation. At this stage the relevance of these effects in the prevention of

disease is unclear. Although there have been no effects of postnatal fish oil supplementation (from 6 months of age) on allergy prevention, preliminary studies suggest possible merits in pregnancy and there are ongoing pregnancy intervention studies to address this more definitively.

**Keywords** n-3 PUFA · Fatty acid · Cord blood · Immune function · Neonate · Allergy prevention · T cells · Antigen presenting cells

## Introduction

There is intensifying interest in the role of early life events and exposures in the aetiology and prevention of disease. Diet and nutrition in pregnancy have a fundamental influence on fetal development, and there is growing focus on the role of key dietary nutrients in subsequent health or disease. This review explores the effects of dietary long chain polyunsaturated fatty acids (LCPUFA) on early immune development and their potential role in the development or the prevention of immune disease.

This early critical period of development is of great interest for a number of reasons. Firstly, developing systems are more susceptible to influence while they are immature. Exposures during pregnancy when the immune system is less mature have been shown to significantly alter subsequent immune programming in both animals [1] and humans [2]. So far, this has mainly been studied in terms of microbial exposure, but it is likely that other environmental exposures, such as diet, could also have an effect. Secondly, immune diseases such as (such as atopic dermatitis and food allergy)

---

S. L. Prescott (✉) · J. A. Dunstan  
School of Paediatrics and Child Health,  
University of Western Australia,  
Princess Margaret Hospital for Children,  
GPO Box D184, Perth 6840 WA, Australia  
e-mail: susanp@ichr.uwa.edu.au

manifest very early in infancy, often within months of birth. This indicates that the events that lead to immune dysregulation are initiated very early in development, and further highlights the potential influence of antenatal exposures. The exponential rise in both allergic and autoimmune mediated immune diseases [3] provides compelling evidence for a role in relatively recent environmental changes in this epidemic. Although the reasons are not clear, a number of hypotheses have been presented. Broadly speaking, these models propose that modern environments are either “more inflammatory” or that there has been a relative “loss of protective factors” which normally inhibit development of inflammatory responses. While reduced microbial exposure is one of the most prominent theories to explain the rise in immune dysregulation [4], environmental changes have clearly been multi-factorial and there have also been persuasive arguments that suggest that dietary changes in the last 30–40 years may play a role [5–7].

### The Basis for Interest in Fatty Acids in Early Immune Development

The extensive immunomodulatory properties of LCPUFA are well recognised in adults and animal models, as reviewed elsewhere [8, 9], and mediate these effects through a number of potential mechanisms. Less is known about these effects in immature and developing systems. In addition to influences on production of eicosanoids, n-3 PUFAs can regulate T cell function directly through effects on cell membrane fluidity and consequent cell signalling and gene transcription (reviewed in [10, 11]). It has been logical to investigate how these effects influence early immune development.

Changing patterns of dietary LCPUFA intake are clearly relevant in pregnancy for the developing foetus. There has been a progressive decline in the intake of dietary anti-inflammatory omega 3 (n-3) PUFA in Western diets, and a corresponding increase in “pro-inflammatory” omega 6 (n-6) PUFA [5]. This has resulted in considerably higher ratios of n-6:n-3 LCPUFA (20–30:1) compared to the ratio in more traditional diets (1–2:1) [12]. These dietary changes are also reflected in the changing content of breast milk, which has similarly shown falling n-3 PUFA content and increasing n-6 PUFA levels over the last 20 years [13]. This, coupled with previously inadequate supplementation of milk formulae, has led to falling intake of anti-inflammatory n-3 PUFA during early life during the critical period of immune maturation.

Epidemiological and experimental data provide a plausible link between these dietary changes and the rise in allergic immune diseases (reviewed in [5, 6]). Although difficult to prove, these associations are supported by the well-described difference in the immune effects of n-3 and n-6 LCPUFA in vivo and in vitro.

Early population studies suggested that the risk of asthma may be higher in children with higher n-6:n-3 diets; either in association with low consumption of fish [14, 15], or high consumption of n-6 rich vegetable oils [16]. Several subsequent studies have also shown protective effects of fish oil. A well-known Australian study showed that children who regularly consumed oily fish were significantly less likely to develop asthma (odds ratio 0.26) [17]. Two more recent birth cohort studies have also reported that lower dietary n-6:n-3 intake (i.e. higher fish intake) reduced the risk of developing asthma [18, 19]. However, this has not been confirmed by all studies, and at least one large study found that higher fish intake was associated with a significantly higher prevalence of asthma (odds ratio: 1.117) [20]. In general, because of the limitations of these population-based studies, there has been a growing focus on well-controlled intervention studies (below).

Based on these observations and the limitations of population-based studies, we undertook the first human intervention study using high dose fish oil in pregnancy to investigate the effects of n-3 LCPUFA on early immune development [21]. We gave fish oil (3.7 g n-3 PUFA/ day) or a placebo supplements to allergic women ( $n = 98$ ) for the final 20 weeks of pregnancy [21–23]. Fish oil supplementation achieved significantly higher proportions of n-3 PUFAs in neonatal erythrocyte membranes compared to the control group ( $P < 0.001$ ) [21, 22]. Here, we review the effects on various aspects of immune function, where possible including relevant findings (from observational and animal studies) by other groups.

### Potential Pathways of Effect During Early Immune Programming

Inappropriate immune responses to environmental (allergens) or endogenous (self) antigens underpin most forms of immune disease. This review will focus principally on the events that occur during the initiation of exogenous environmental antigen responses. Although there is debate about when immune programming first occurs [24] it is clear that this occurs in the neonatal period, if not before. For this reason, the

capacity for LCPUFA to influence immune function during this period is of central interest.

A complex series of events occur during the programming of antigen-specific immune responses (as illustrated in Fig. 1). This typically begins in local tissues where antigen (allergen) proteins are first encountered by surveying antigen presenting cells (APC), such as tissue dendritic cells (DC), which ingest the proteins and digest them into small peptides. These are expressed on the cell surface with MHC class II receptors to effector T cells, after migration to the regional lymph nodes. The local tissue conditions play an important part in determining the maturation and activity of APC. This in turn has a significant effect on down-stream T cell programming (below). Local inflammation has a direct effect on increasing the expression of Class II, cytokines (such as interleukin [IL]-12) and co-stimulatory molecules on APC, which all act to promote an effector response. In contrast, the absence of inflammation is more likely to lead to T cell apoptosis, anergy and tolerance. Once activated, the pattern of APC cytokine production also determines the pattern of T helper cell differentiation. Type 1 (Th1) T cells develop under the influence of IL-12, whereas T cell producing Type 2 (Th2) cytokine responses develop in the relative absence of IL-12 (or the presence of pro-Th2 factors such as prostaglandin [25]). These differences in T cell cytokine production determine the pattern of B-cell antibody production; with Th2 cytokines (IL-4, IL-5 and IL-13) promoting IgE production and allergic inflammation whereas Th1 cytokines (IFN $\gamma$ ) largely inhibit this in favour of low level IgG production (Fig. 1). Tissue factors are again important in determining whether these immune responses result in clinically relevant disease (such as

asthma, allergic rhinitis or atopic dermatitis) although this is still not well understood. More recently there has been growing recognition of the role of specialised “regulatory” cells in immune programming and subsequent immune regulation. This encompasses a broad range of cells that regulate effector T cell responses through direct cell contact and/or production of regulatory cytokines such as IL-10 and TGF  $\beta$  (Fig. 1).

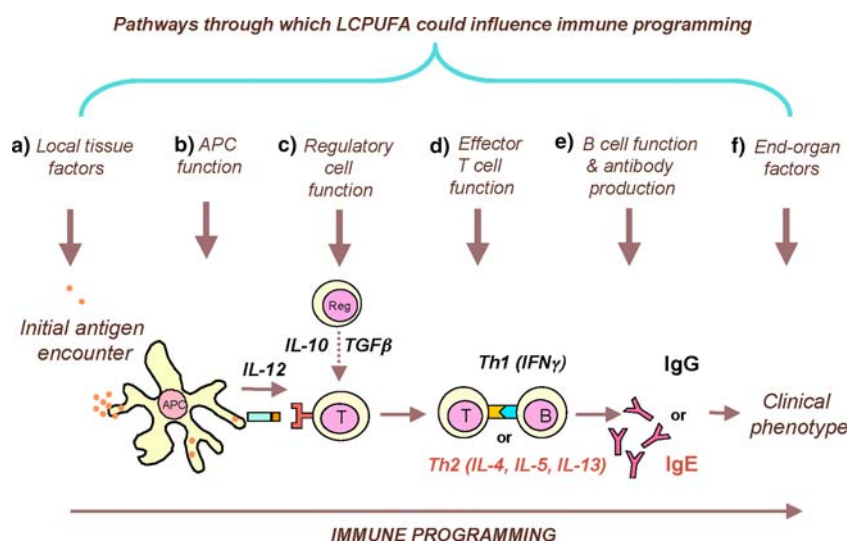
Variations in LCPUFA composition of neonatal cell membranes have the potential to influence immune programming at many levels during this complex process. Here we examine the evidence for effects on cells and mediators involved in each stage of the process described above and shown on Fig. 1.

#### Effects on Local Tissue Inflammation in Neonates

Firstly, we speculated that alterations in neonatal LCPUFA may influence local inflammatory responses through effects on the production of lipid derived inflammatory mediators by local tissue neutrophils (Fig. 2). As discussed elsewhere [26], these fatty acids are the major substrate for the production of eicosanoid mediators including prostaglandin and leukotrienes. Higher levels of n-6 LCPUFA (arachidonic acid [AA] 20:4n-6) lead to preferential production of the pro-inflammatory 2-series prostaglandins (such as PGE2) and the four series leukotrienes (LTB4) [27, 28]. In contrast eicosanoids (PGE3 and LTB5) produced from n-3 PUFA (eicosapentanoic acid [EPA] 20:5n-3 and docosahexaenoic acid [DHA] 22:6n-3) are far less potent than oxidative derivatives of n-6 PUFA [29].

Using fresh neonatal neutrophils isolated from cord blood samples from our pregnancy intervention study

**Fig. 1** Potential avenues of influence of LCPUFA on immune development



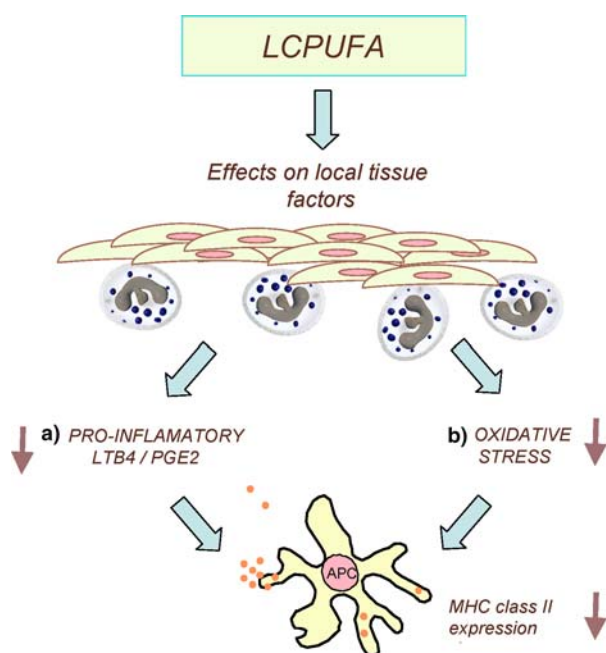


**Fig. 2** Potential influences on APC during initial antigen presentation

[21, 22], we tested the hypothesis that maternal fish oil supplementation would alter the pattern of neonatal LTB4 and LTB5 production. The characteristics of this cohort are well described elsewhere [21, 22]. Neutrophil samples were available from 30 neonates whose mothers had received a daily dose of 4 g of fish oil (containing 3.7 g n-3 LCPUFA as 56% DHA and 27% EPA) and 34 neonates whose mothers received the same amount of olive oil for the final 18–20 weeks of pregnancy. Following stimulation with calcium ionophore, production of proinflammatory LTB4 was significantly lower in the fish oil group ( $P = 0.03$ ). There was also a trend for higher LTB5 production (with 10–30 times less inflammatory potential than LTB4 [30]) in the fish oil group, although this was not statistically significant. This confirms that the maternal diet can have effects on the propensity of neonatal neutrophils to generate inflammatory products. To date, effects on neonatal prostaglandins have not been assessed in this context, but we speculate that this may be also altered in a similar pattern, with a relative shift from PGE2 to PGE3 with maternal fish oil supplementation.

Secondly, we examined the effects of maternal fish oil supplementation on neonatal oxidative stress. Excessive oxidative stress may play a role in inflammation and tissue damage. It has been demonstrated that changes in the oxidative status can influence APC during T cell programming by altering cytokine production. Improved oxidative balance can promote

pro-Th1 signalling by APC, by enhancing IL-12 production in mice [31] and humans [32]. In contrast, adverse oxidative balance (oxidative stress and reduced glutathione) promotes CD4 T cell Th2 differentiation [31] and the downstream production of IL-4 and IL-5 which contribute to allergic inflammation. We therefore assessed the effects of fish oil supplementation on oxidative stress in our pregnancy intervention study, using F<sub>2</sub>-isoprostanes as a robust measure of lipid peroxidation. Maternal fish oil supplementation resulted in significantly lowered plasma ( $P < 0.0001$ ) F<sub>2</sub>-isoprostanes [33]. Of note, although HLA-DR expression on APC was not different between the groups, there was a significant relationship between F<sub>2</sub>-isoprostanes and APC (monocyte) MHC Class II (HLA-DR) expression ( $P = 0.007$ ), although HLA-DR expression was not different between the groups. In multiple regression analysis, 28.8% of the variance in plasma F<sub>2</sub>-isoprostanes was explained by positive relationships with n-6 AA membrane levels and HLA-DR expression and a negative relationship with n-3 EPA. This shows that maternal supplementation with fish oil can attenuate neonatal lipid peroxidation, and suggests potential effects on APC function.

Thus, as shown schematically on Fig. 2, neonatal LCPUFA status has the potential to influence both the oxidative balance and the production of inflammatory mediators in local tissues. This is relevant to immune programming as variations in the local tissue milieu have the potential to influence APC function during initially antigen encounter (as discussed above) with potential implications for subsequent patterns of immune function. While we acknowledge that it is difficult to extrapolate relationships observed in cord blood to local tissues, it is not ethically possible to do more invasive studies in humans.

#### Effects on Neonatal APC

APC function is impaired in the neonatal period [34, 35], and appear to lack the capacity to deliver important Th1 polarising signals to T-cells [35–37]. This may contribute to an increased susceptibility to infection and tolerance induction, and a propensity for the induction of Th2 responses in early life. In the context of disease propensity, a number of investigators have highlighted important differences in APC function between atopic and non-atopic adults [38–40]. However, it is not clear whether altered APC function antedates sensitisation and the onset of allergic disease, or whether functional differences arise secondary to allergic inflammation. This issue can only be addressed

by examining APC function in early life, prior to allergic sensitisation.

Effects of n-3 LCPUFA on mature APC are well documented. Increasing the content of n-3 PUFAs in cell membranes reduces the capacity of APC to present antigen to T cells by inhibiting the upregulation of MHC class II receptors, cytokine production and expression of co-stimulatory molecules [41, 42]. The first studies to explore this in neonates used animal models, and showed that DHA inhibited the IFN $\gamma$ -induced MHC class II expression on neonatal murine APC [43]. In our own studies we examined the effects of maternal fish oil supplementation in pregnancy on various aspects of APC function including Class II expression (HLR-DR), cytokine production (IL-12 and IL-6) and nitric oxide production, but did not see any differences between the neonates in the fish oil compared with the olive oil placebo group. These findings do not support our hypothesis that n-3 LCPUFA supplementation may modify neonatal APC function. This is possibly because most aspects of neonatal APC function are already reduced in the neonatal period. While it could be argued that the olive oil placebo could also have had immunomodulatory effects, there were no differences in oleic acid levels between the groups.

#### Effects on Regulatory Pathways

This is another potential pathway through which LCPUFA could mediate effects on immune function. Because the role of specialised regulatory T cells has only been recognised recently there are still no studies examining the effects of LCPUFA on these pathways. However, there are a number of potential pathways through which LCPUFA could logically exert an immune effect through actions on these cells. Firstly, because recent studies have shown that PGE2 induces T regulatory cell function (and FOXP3 gene expression) [44] it is possible that LCPUFA could have an effect through altering PGE2 associated pathways. However, if this is the case it might be expected that n-3 LCPUFA (which inhibit PGE2 production) may also inhibit T regulatory function, which would not explain the immunomodulatory effects of these fatty acids. Alternatively, LCPUFA could have effects through microbial recognition molecules (Toll-like receptors [TLR]) that are found on both T regulatory cells and APC, and are important for activation of these cells. One recent study [41] has shown that the immunomodulatory actions of n-3 LCPUFA are mediated through TLR pathways on APC. It is possible, but not yet known if these effects are also relevant on other TLR expressing cells, such as T regulatory cells.

#### Effects on Neonatal Effector T Cell Function

Effects of modifying LCPUFA composition on T cell function have been extensively studied in adults. Many studies have demonstrated that dietary n-3 PUFA supplementation in both humans [27, 45–47] and rodents [48–50] significantly reduces lymphocyte proliferation to mitogens. In vitro studies in which peripheral blood mononuclear cells (PBMC) were incubated with fatty acids, have also generally shown a decrease in T cell responses to mitogens [51–53]. To our knowledge, there are only two studies to examine these in human neonates, including our own intervention study (above) [21, 23] and an observational study which examined the relationship between cord blood fatty acid levels and immune function in a Boston cohort [54].

In our own study, we looked (a) at the effects of maternal supplementation on circulating (in vivo) T cell cytokine levels in cord blood, (b) the effects on in vitro T cell responses to specific stimuli, and (c) the relationship between fatty acid levels and T cell cytokine responses (in vivo and in vitro). Firstly, we noted that there were significantly (65%) lower circulating Th2 IL-13 cytokine responses ( $P < 0.05$ ) in the fish oil group [23]. There were no differences in the levels of other cytokine levels (including Th1 IFN $\gamma$  which was only present at very low levels). Secondly, we noted consistent trends for lower neonatal cytokine responses to all allergens tested. There was a consistent trend for all cytokines studied (IL-5, IL-13, IL-10, IFN- $\gamma$ ) to be lower in the fish oil group (although this was statistically significant only for IL-10 responses to cat allergen) [21]. Thirdly, there were statistically significant inverse relationships between the n-3 PUFA content of neonatal erythrocytes and cytokine responses [21]. Although these relationships were most evident for IFN- $\gamma$  and IL-10 responses, the same trends were seen for most other Th2 cytokines. Conversely, there were significant positive relationships between the n-6 PUFA content of neonatal erythrocytes and the cytokine responses [21]. There was also an inverse relationship between the circulating IL-13 and the DHA content of neonatal erythrocytes [23].

The Boston observation study also examined the relationship between LCPUFA levels in cell membranes and in vitro immune responses. Consistent with our findings, they found that n-3 EPA levels were associated with reduced lymphoproliferation ( $n = 192$ ) and reduced IFN $\gamma$  cytokine production ( $n = 167$ ) [54]. They also noted that n-6 levels (linoleic acid) were associated with higher Th2 IL-13 responses (to house dust mite and cockroach). However in contrast to our

findings, they noted that higher n-6 (arachidonic acid) was associated with reduced lymphoproliferation and cytokines responses [54]. This significance of these contrasting effects is not clear, but the findings collectively suggest that LCPUFA in pregnancy has effects on neonatal immune function.

We also have (as yet unpublished) preliminary data that demonstrate the intracellular effects of maternal fish oil supplementation on neonatal T cells. Isolated T cells from the fish oil group showed differential expression of protein kinase C (PKC) isoenzymes compared with the control group, specifically with lower expression of PKC-alpha ( $P < 0.05$ ) and higher expression of PKC-zeta ( $P < 0.05$ ). The significance of this in relation to functional effects on T cell cytokine production are yet to be determined.

Monounsaturated fatty acid (MUFA), oleic acid (18n-1), is also recognised to have anti-inflammatory properties although these are generally thought to be less potent than n-3 PUFA effects. In our study, described above [21], we report a significant inverse association between oleic acid and allergen-specific (IL-5, IL-10, IL-13, IFN $\gamma$ ) cytokine responses (Table 1). Mitogen or bacterial lipopolysaccharide stimulated responses were not associated with oleic acid levels. In a previous study in adults, olive oil supplementation had little effect [55] however in animals, high-level oleic acid supplementation results in inhibition of lymphoproliferation, IL-2 responses, NK cell function and expression of IL-2 receptors and adhesion molecules [56]. To our knowledge, no previous studies have examined oleic acid and neonatal immune response or allergen specific responses in adults. The effect of oleic acid (Table 1)

was still evident after adjusting for PUFA levels which may indicate a selective effect of MUFA on low level T cell responses.

In summary, we (and others) have shown that LCPUFA status (and therefore maternal diet) can influence neonatal T cell function. Monounsaturated fatty acids found in dietary olive oil may also play a role in the regulation of T cell responses and further studies are required.

#### Effects on Infant B Cell Function and Subsequent Immunoglobulin Production

To our knowledge there have not been any studies to directly assess the relationship between neonatal LCPUFA status and B cell function directly. However, there are several logical pathways of influence. Firstly, variations in PGE<sub>2</sub> production could have direct effect on B cell maturation as PGE<sub>2</sub> is known to synergise with IL-4 to promote immunoglobulin IgE-isotype switching in B cells [57]. Secondly, the documented effects on neonatal T cell cytokine production are likely to have secondary effects on B cell function during T-B cell interaction (Fig. 1). We saw indirect evidence of B cell effects in our study, with a trend for reduced allergen-specific IgE production in the fish oil group at 12 months of age [21]. Specifically, children in the fish oil group were three times less likely to have egg-specific IgE (a positive skin prick test to egg) at 1 year of age (OR 0.34; 95% CI, 0.11–1.02;  $P = 0.055$ ). Further studies are needed to determine the clinical significance of this.

**Table 1** Association (regression coefficient) between neonatal erythrocyte membrane oleic acid (18:1n-9) and cytokine responses to OVA, cat and PHA

Cytokine	Stimulant	Regression coefficient	(95% CI)	Adjusted regression coefficient <sup>a</sup>	(95% CI)
IFN $\gamma$	OVA	-0.62	(-1.0, -0.19)*	-0.52	(-1.0, 0.03)*
	CAT	-0.58	(-0.99, 0.18)**	-0.50	(-0.9, 0.1)**
	PHA	-0.26	(-0.6, 0.1)	-0.30	(-0.7, 0.07)
IL-5	OVA	-0.34	(-0.6, -0.9)*	-0.31	(-0.6, -0.05)*
	CAT	-0.32	(-0.5, -0.07)*	-0.33	(-0.6, -0.06)*
	PHA	0.03	(-0.2, 0.32)	0.04	(-0.2, 0.3)
IL-13	OVA	-0.40	(-0.7, -0.15)**	-0.40	(-0.6, -0.12)**
	CAT	-0.20	(-0.5, 0.01)	-0.24	(-0.51, 0.04)
	PHA	0.17	(-0.04, 0.38)	0.15	(-0.08, 0.4)
IL-10	OVA	-0.32	(-0.5, -0.1)***	-0.36	(-0.6, -0.12)***
	CAT	-0.23	(-0.4, -0.04)***	-0.35	(-0.5, -0.14)***
	PHA	-0.06	(-0.3, 0.14)	-0.05	(-0.3, 0.19)

Results of simple and multiple regression analyses ( $n = 83$ ) with cytokine levels and neonatal erythrocyte oleic acid (18:1n-9).  $P < 0.05$  considered significant (shaded)

<sup>a</sup> Adjusted for sex, parity, method of delivery, total n-3 PUFA and total n-6 PUFA

Indicates significance \*  $P < 0.05$ , \*\*  $P < 0.01$ , \*\*\*  $P < 0.005$



### Relationship Between Early LCPUFA Status and Subsequent Inflammatory Disease (Allergy and Asthma)

At this stage there is only very limited data on the relationship between neonatal LCPUFA status and subsequent risk of allergic disease. Existing data derived from both observational and intervention studies are limited (largely because of small sample sizes) and not definitive at this stage.

#### Observational Studies

A number of early observational studies suggested a link between cord blood n-6:n-3 ratios and allergy risk [58, 59]. However, all of these studies were too small (less than 60 subjects) to look at clinical outcomes definitively. They also only examined cord blood LCPUFA in relation to family allergy [58] or very early outcomes [60], which are also not definitive. At the time of this review there has only been one published study to address this in a large enough population with long-term follow up [61]. This UK-based observational study ( $n = 1238$ ) examined the relationship between cord blood LCPUFA and clinical allergy outcomes at 3.5 years of age [61]. Although they found that a higher cord blood n3:n6 ratio was associated with an increased risk of eczema ( $P = 0.04$ ) and late-onset wheeze ( $P = 0.019$ ), none of these relationships was significant after adjusting for multiple comparisons [61]. They concluded that LCPUFA is unlikely to be a major determinant of allergy and asthma risk.

#### Intervention Studies

Although we examined the effects of maternal fish oil supplementation on clinical outcomes in our intervention study, the findings cannot be viewed definitely because the study was designed to assess immune function rather than clinical effects (which would have required a larger population size). At this stage there are no other published intervention studies in pregnancy that have addressed this. However, there are several larger studies in progress (in Europe and Australia) which are specifically designed to assess this and the results are awaited with great interest. In our study [21], we did note that infants in the fish oil group were consistently less likely to develop clinical features including food allergy, recurrent wheeze, persistent cough, diagnosed asthma, angioedema, or anaphylaxis, compared to the control group [21]. Although there was no difference in the frequency of atopic dermatitis

at 1 year of age, infants in the fish oil group had significantly less severe disease (OR 0.09; 95% CI, 0.01–0.94;  $P = 0.045$ ). As noted previously, sensitisation to egg was also less common in the fish oil group. Although it is not possible to make conclusions from this, this study has provided justification for the larger, long-term studies.

The only other study to examine the role of fish oil supplementation in allergy prevention was initiated in the postnatal period. The Childhood Asthma Prevention Study (CAPS) was a randomised controlled trial which separately assessed the preventive effects (a) house dust mite avoidance and (b) increasing consumption of n-3 fatty acids. They recruited pregnant women ( $n = 616$ ) whose unborn children were to be deemed to be at risk of developing asthma (affected parents). Those assigned to the dietary intervention were randomised to receive a daily supplement of tuna fish oil (500 mg oil/day) along with margarines and cooking oils rich in n-3 fatty acids; the control group received a placebo supplement plus polyunsaturated margarines and cooking oils. This intervention commenced at 6 months of age or at weaning (which ever occurred first). The children were assessed clinically at 18 months [62], 3 years [63] and 5 years [64] of age. Although the initial findings were encouraging, with a reduction in respiratory symptoms such as reduced wheeze at 18 months [62], and reduced coughing (atopic infants only) in the “active” diet group at 3 years [63], there was no reduction in the development of asthma at this age. Furthermore, despite confirmed effects on LCPUFA status during the intervention [62], at 5 years of age there was no reduction in the prevalence of asthma, wheezing, atopic dermatitis, or allergic sensitisation in children who had received n-3 PUFA enriched diets [64]. They concluded that fish oil supplementation at this age had no place in preventing sensitisation, asthma or other allergic disease [64].

It is probable that if LCPUFA have clinical relevant effects, that these are more likely at a younger age before immune responses and clinical phenotype is established. We and others have shown that immunological abnormalities precede the development of allergic disease and are frequently evident at birth or in the first months of life [65–68]. This may also explain why intervention studies in later childhood to reduce symptoms in established asthma have only shown weakly beneficial effects [69] or had no effect [70]. As indicated previously, there are currently a number of other studies (still on going) that will assess the effects of earlier supplementation (from birth or in pregnancy) with higher doses of n-3 PUFA.

## Summary and Conclusions

There is now evidence that the patterns of LCPUFA exposure in pregnancy can influence aspects of fetal immune function in ways that are consistent with the immunological properties of these nutrients in more mature individuals. Namely, we and others have seen that higher levels of n-3 LCPUFA are associated with reduction in neonatal oxidative stress, reduced production of inflammatory leukotrienes (LTB<sub>4</sub>) and altered T cell function. Although we did not see any significant differences in neonatal APC function with maternal fish oil supplementation, we did see LCPUFA associated variations in APC MHC class II expression. This could be consistent with animal studies demonstrating reduced neonatal APC class II expression with n-3 LCPUFA supplementation *in vitro*. The inverse correlations between n-3 LCPUFA levels and neonatal T cell cytokine production, are also consistent with adult studies showing reduction in T cell cytokine production with fish oil supplementation. We have also provided preliminary evidence that maternal fish oil supplementation alters intracellular signalling pathways in neonatal T cells. These findings clearly illustrate that LCPUFA can influence perinatal immune programming at a number of different stages in this complex process (as summarised on Fig. 1). There is still a need to explore the potential effects of LCPUFA in regulatory pathways.

At this stage the relevance of these effects in the prevention of disease is unclear. Although there have been no effects of postnatal fish oil supplementation (from 6 months of age) for allergy prevention, preliminary studies suggest possible merits in pregnancy and there are ongoing studies to address this more definitively. There is also a need to examine the role of early LCPUFA status in the risk and modulation of autoimmune disease, although prevention studies are more difficult because these conditions occur at much lower prevalence than allergic disease.

In one intervention study the use of cod liver oil during the first year of life was associated with lower risk of childhood-onset type 1 diabetes [71]. This is also of growing interest given the parallel rise in autoimmunity and the reported benefits of n-3 LCPUFA in established autoimmune inflammation.

In conclusion, epidemiologic associations and biological properties of LCPUFA have provided a compelling case for investigating the effects of these dietary nutrients on immune development. Although we have now provided evidence of the immunomodulatory effects in this early period, it is still not clear what role dietary changes have in the rising rates of immune

diseases. While this issue may remain difficult to determine, the results of ongoing larger intervention studies will be of great importance in determining the role of fish oil supplementation in pregnancy on disease prevention.

**Acknowledgement** Janet Dunstan is funded by the Child Health Research Foundation of Western Australia

## References

- Blumer N, Herz U, Wegmann M, Renz H (2005) Prenatal lipopolysaccharide-exposure prevents allergic sensitisation and airway inflammation, but not airway responsiveness in a murine model of experimental asthma. *Clin Exp Allergy* 35:397–402
- Ege MJ, Bieli C, Frei R, van Strien RT, Riedler J, Ublagger E, Schram-Bijkerk D, Brunekreef B, van Hage M, Scheynius A, Pershagen G, Benz MR, Lauener R, von Mutius E, Braun-Fahrlander CT. The Parsifal Study (2006) Prenatal farm exposure is related to the expression of receptors of the innate immunity and to atopic sensitisation in school-age children. *J Allergy Clin Immunol* 117(4):817–823
- Bach JF (2002) The effect of infections on susceptibility to autoimmune and allergic diseases. *N Engl J Med* 347(12):911–920
- Wills-Karp M, Luyimbazi J, Xu X, Schofield B, Neben TY, Karp CL, Donaldson DD (1998) Interleukin-13: central mediator of allergic asthma. *Science* 282(5397):2258–2261
- Weiss S (1997) Diet as a risk factor for asthma. In: Holgate S (ed) CIBA foundation symposium. Wiley, New York pp 244–257
- Black P, Sharpe S (1997) Dietary fat and asthma: is there a connection? *Eur Respir J* 10:6–12
- Herz U, Petschow B (2005) Perinatal events affecting the onset of allergic diseases. *Curr Drug Targets Inflamm Allergy* 4(5):523–529
- Calder PC (2003) N-3 polyunsaturated fatty acids and inflammation: from molecular biology to the clinic. *Lipids* 38(4):343–352
- Stulnig TM (2003) Immunomodulation by polyunsaturated fatty acids: mechanisms and effects. *Int Arch Allergy Immunol* 132(4):310–321
- Calder PC, Yaqoob P, Thies F, Wallace FA, Miles EA (2002) Fatty acids and lymphocyte functions. *Br J Nutr* 87(Suppl1):S31–S48
- Stulnig TM, Zeyda M (2004) Immunomodulation by polyunsaturated fatty acids: impact on T-cell signaling. *Lipids* 39(12):1171–1175
- Simopoulos AP (1999) Essential fatty acids in health and chronic disease. *Am J Clin Nutr* 70(3Suppl):560S–569S
- Makrides M, Simmer K, Neumann M, Gibson R (1995) Changes in the polyunsaturated fatty acids of breast milk from mothers of full-term infants over 30 wk of lactation. *Am J Clin Nutr* 61(6):1231–1233
- Peat J, Salome C, Woolcock A (1992) Factors associated with bronchial hyper-responsiveness in Australian adults and children. *Eur Respir J* 5:921–929
- Poysa L, Korppi M, Remes K, Juntunen-Backman K (1991) Atopy in childhood and diet in infancy. A nine-year follow-up study. I. Clinical manifestations. *Allergy Proc* 12(2):107–111
- Dunder T, Kuikka L, Turtinen J, Rasanen L, Uhari M (2001) Diet, serum fatty acids, and atopic diseases in childhood. *Allergy* 56(5):425–428

17. Hodge L, Salome C, Peat J, Haby M, Xuan W, Woolcock A (1996) Consumption of oily fish and childhood asthma risk. *Med J Aust* 164:137–140
18. Oddy WH, de Klerk NH, Kendall GE, Mihrshahi S, Peat JK (2004) Ratio of omega-6 to omega-3 fatty acids and childhood asthma. *J Asthma* 41(3):319–326
19. Salam MT, Li YF, Langholz B, Gilliland FD (2005) Maternal fish consumption during pregnancy and risk of early childhood asthma. *J Asthma* 42(6):513–518
20. Takemura Y, Sakurai Y, Honjo S, Tokimatsu A, Gibo M, Hara T, Kusakari A, Kugai N (2002) The relationship between fish intake and the prevalence of asthma: the Tokorozawa childhood asthma and pollinosis study. *Prev Med* 34(2):221–225
21. Dunstan J, Mori TA, Barden A, Beilin LJ, Taylor A, Holt PG, Prescott SL (2003) Fish oil supplementation in pregnancy modifies neonatal allergen-specific immune responses and clinical outcomes in infants at high risk of atopy: a randomised controlled trial. *J Allergy Clin Immunol* 112:1178–1184
22. Dunstan JA, Mori TA, Barden A, Beilin LJ, Holt PG, Calder PC, Taylor AL, Prescott SL (2004) Effects of n-3 polyunsaturated fatty acid supplementation in pregnancy on maternal and fetal erythrocyte fatty acid composition. *Eur J Clin Nutr* 58(3):429–437
23. Dunstan JA, Mori TA, Barden A, Beilin LJ, Taylor AL, Holt PG, Prescott SL (2003) Maternal fish oil supplementation in pregnancy reduces interleukin-13 levels in cord blood of infants at high risk of atopy. *Clin Exp Allergy* 33(4):442–448
24. Prescott SL (2006) Maternal allergen exposure as a risk factor for childhood asthma. *Curr Asthma Allergy Rep* 6(1):75–80
25. Snijdwint F, Kalinski P, Wieringa E, Bos J, Kapsenberg M (1993) Prostaglandin E2 differentially modulates cytokine secretion profiles of human T-helper lymphocytes. *J Immunol* 150:5321–5329
26. Harizi H, Gualde N (2005) The impact of eicosanoids on the crosstalk between innate and adaptive immunity: the key roles of dendritic cells. *Tissue Antigens* 65(6):507–514
27. Meydani SN, Dinarello CA (1993) Influence of dietary fatty acids on cytokine production and its clinical implications. *Nutr Clin Pract* 8(2):65–72
28. Caughey GE, Mantzioris E, Gibson RA, Cleland LG, James MJ (1996) The effect on human tumor necrosis factor alpha and interleukin 1 beta production of diets enriched in n-3 fatty acids from vegetable oil or fish oil. *Am J Clin Nutr* 63(1):116–122
29. von Schacky C (1987) Prophylaxis of atherosclerosis with marine omega-3 fatty acids. A comprehensive strategy. *Ann Intern Med* 107(6):890–899
30. Strasser T, Fischer S, Weber PC (1985) Leukotriene B5 is formed in human neutrophils after dietary supplementation with icosapentaenoic acid. *Proc Natl Acad Sci USA* 82(5):1540–1543
31. Murata Y, Shimamura T, Hamuro J (2002) The polarization of T(h)1/T(h)2 balance is dependent on the intracellular thiol redox status of macrophages due to the distinctive cytokine production. *Int Immunol* 14(2):201–212
32. Utsugi M, Dobashi K, Ishizuka T, Endou K, Hamuro J, Murata Y, Nakazawa T, Mori M (2003) c-Jun N-terminal kinase negatively regulates lipopolysaccharide-induced IL-12 production in human macrophages: role of mitogen-activated protein kinase in glutathione redox regulation of IL-12 production. *J Immunol* 171(2):628–635
33. Barden A, Mori TA, Dunstan JA, Taylor AL, Thornton CA, Croft KD, Beilin LJ, Prescott SL (2004) Fish oil supplementation in pregnancy lowers F2 Isoprostanes in neonatal at high risk of atopy. *Free Radical Res* 38(3):233–239
34. Ridge J, Fuchs E, Matzinger P (1996) Neonatal tolerance revisited: turning on newborn T cells with dendritic cells. *Science* 271:1723–1726
35. Trivedi HN, HayGlass KT, Gangur V, Allardice JG, Embree JE, Plummer FA (1997) Analysis of neonatal T cell and antigen presenting cell functions. *Hum Immunol* 57(2):69–79
36. Taylor S, Bryson Y (1985) Impaired production of gamma-interferon by newborn cells in vitro is due to a functionally immature macrophage. *J Immunol* 134(3):1493–1497
37. Delespesse G, Yang LP, Shu U, Byun DG, Demeure CE, Ohshima Y, Wu CY, Sarfati M (1996) Role of interleukin-12 in the maturation of naive human CD4 T cells. *Ann N Y Acad Sci* 795:196–201
38. Hammad H, Charbonnier AS, Duez C, Jacquet A, Stewart GA, Tonnel AB, Pestel J (2001) Th2 polarization by Der p 1-pulsed monocyte-derived dendritic cells is due to the allergic status of the donors. *Blood* 98(4):1135–1141
39. Reider N, Reider D, Ebner S, Holzmann S, Herold M, Fritsch P, Romani N (2002) Dendritic cells contribute to the development of atopy by an insufficiency in IL-12 production. *J Allergy Clin Immunol* 109(1):89–95
40. Charbonnier AS, Hammad H, Gosset P, Stewart GA, Alkan S, Tonnel AB, Pestel J (2003) Der p 1-pulsed myeloid and plasmacytoid dendritic cells from house dust mite-sensitized allergic patients dysregulate the T cell response. *J Leukoc Biol* 73(1):91–99
41. Weatherill AR, Lee JY, Zhao L, Lemay DG, Youn HS, Hwang DH (2005) Saturated and polyunsaturated fatty acids reciprocally modulate dendritic cell functions mediated through TLR4. *J Immunol* 174(9):5390–5397
42. Hughes DA, Pinder AC (1996) Influence of n-3 polyunsaturated fatty acids (PUFA) on the antigen-presenting function of human monocytes. *Biochem Soc Trans* 24(3):389S
43. Khair-el-Din TA, Sicher SC, Vazquez MA, Wright WJ, Lu CY (1995) Docosahexaenoic acid, a major constituent of fetal serum and fish oil diets, inhibits IFN gamma-induced Ia-expression by murine macrophages in vitro. *J Immunol* 154(3):1296–1306
44. Baratelli F, Lin Y, Zhu L, Yang SC, Heuze-Vourc'h N, Zeng G, Reckamp K, Dohadwala M, Sharma S, Dubinett SM (2005) Prostaglandin E2 induces FOXP3 gene expression and T regulatory cell function in human CD4+ T cells. *J Immunol* 175(3):1483–1490
45. Endres S, Meydani SN, Ghorbani R, Schindler R, Dinarello CA (1993) Dietary supplementation with n-3 fatty acids suppresses interleukin-2 production and mononuclear cell proliferation. *J Leukoc Biol* 54(6):599–603
46. Thies F, Nebe-von-Caron G, Powell JR, Yaqoob P, News-holme EA, Calder PC (2001) Dietary supplementation with gamma-linolenic acid or fish oil decreases T lymphocyte proliferation in healthy older humans. *J Nutr* 131(7):1918–1927
47. Kelley DS, Branch LB, Love JE, Taylor PC, Rivera YM, Iacono JM (1991) Dietary alpha-linolenic acid and immunocompetence in humans. *Am J Clin Nutr* 53(1):40–46
48. Alexander NJ, Smythe NL (1988) Dietary fat modulation of in vitro lymphocyte function. *Ann Nutr Metab* 32(4):192–199
49. Kumar GS, Das UN (1994) Effect of prostaglandins and their precursors on the proliferation of human lymphocytes and their secretion of tumor necrosis factor and various interleukins. *Prostaglandins Leukot Essent Fatty Acids* 50(6):331–334

50. Jolly CA, Jiang YH, Chapkin RS, McMurray DN (1997) Dietary (n-3) polyunsaturated fatty acids suppress murine lymphoproliferation, interleukin-2 secretion, and the formation of diacylglycerol and ceramide. *J Nutr* 127(1):37–43
51. Soyland E, Nenseter MS, Braathen L, Drevon CA (1993) Very long chain n-3 and n-6 polyunsaturated fatty acids inhibit proliferation of human T-lymphocytes in vitro. *Eur J Clin Invest* 23(2):112–121
52. Khalfoun B, Lacord M, Bardos P, Lebranchu Y (1996) Effects of docosahexaenoic and eicosapentaenoic acids on in vitro-induced human lymphoproliferative responses. *Transplant Proc* 28(5):2913–2914
53. Purasiri P, McKechnie A, Heys SD, Eremin O (1997) Modulation in vitro of human natural cytotoxicity, lymphocyte proliferative response to mitogens and cytokine production by essential fatty acids. *Immunology* 92(2):166–172
54. Gold DR, Willwerth BM, Tantisira KG, Finn P, Schaub B, Perkins D, Tzianabos A, Ly NP, Schroeter C, Gibbons F, Campos H, Oken E, Gillman MW, Palmer LJ, Ryan J, Weiss ST (2006) Associations of cord blood fatty acids with lymphocyte proliferation, IL-13, and IFN- $\gamma$ . *J Allergy Clin Immunol* 117(4):931–938
55. Yaqoob P, Knapper JA, Webb DH, Williams CM, News-holme EA, Calder PC (1998) Effect of olive oil on immune function in middle-aged men. *Am J Clin Nutr* 67:129–135
56. Yaqoob P (1998) Monounsaturated fats and immune function. *Proc Nutr Soc* 57:511–520
57. Roper RL, Brown DM, Phipps RP (1995) Prostaglandin E2 promotes B lymphocyte Ig isotype switching to IgE. *J Immunol* 154(1):162–170
58. Beck M, Zelczak G, Lentze MJ (2000) Abnormal fatty acid composition in umbilical cord blood of infants at high risk of atopic disease. *Acta Paediatr* 89(3):279–284
59. Galli E, Picardo M, Chini L, Passi S, Moschese V, Terminali O, Paone F, Fraioli G, Rossi P (1994) Analysis of polyunsaturated fatty acids in newborn sera: a screening tool for atopic disease? *Br J Dermatol* 130(6):752–756
60. Yu G, Bjorksten B (1998) Serum levels of phospholipid fatty acids in mothers and their babies in relation to allergic disease. *Eur J Pediatr* 157(4):298–303
61. Newson RB, Shaheen SO, Henderson AJ, Emmett PM, Sherriff A, Calder PC (2004) Umbilical cord and maternal blood red cell fatty acids and early childhood wheezing and eczema. *J Allergy Clin Immunol* 114(3):531–537
62. Mihrshahi S, Peat JK, Marks GB, Mellis CM, Tovey ER, Webb K, Britton WJ, Leeder SR (2003) Eighteen-month outcomes of house dust mite avoidance and dietary fatty acid modification in the Childhood Asthma Prevention Study (CAPS). *J Allergy Clin Immunol* 111(1):162–168
63. Peat JK, Mihrshahi S, Kemp AS, Marks GB, Tovey ER, Webb K, Mellis CM, Leeder SR (2004) Three-year outcomes of dietary fatty acid modification and house dust mite reduction in the Childhood Asthma Prevention Study. *J Allergy Clin Immunol* 114(4):807–813
64. Marks GB, Mihrshahi S, Kemp A, Tovey ER, Webb K, Almqvist C, Ampon RD, Crisafulli D, Belousova E, Mellis CM, Peat JK, Leeder SR (2006) Prevention of asthma during the first 5 years of life: a randomised controlled trial. *J Allergy Clin Immunol* ePub ahead of print
65. Prescott S, Macaubas C, Smallacombe T, Holt B, Sly P, Loh R, Holt P (1999) Development of allergen-specific T-cell memory in atopic and normal children. *Lancet* 353(9148):196–200
66. Borres MP, Bjorksten B (2004) Peripheral blood eosinophils and IL-4 in infancy in relation to the appearance of allergic disease during the first 6 years of life. *Pediatr Allergy Immunol* 15(3):216–220
67. van der Velden VH, Laan MP, Baert MR, de Waal Malefyt R, Neijens HJ, Savelkoul HF (2001) Selective development of a strong Th2 cytokine profile in high-risk children who develop atopy: risk factors and regulatory role of IFN- $\gamma$ , IL-4 and IL-10. *Clin Exp Allergy* 31(7):997–1006
68. Martinez F, Stern D, Wright A, Holberg C, Taussig L, Halonen M (1995) Association of interleukin-2 and interferon- $\gamma$  production by blood mononuclear cells in infancy with parental allergy skin tests and with subsequent development of atopy. *J Allergy Clin Immunol* 96:652–660
69. Nagakura T, Matsuda S, Shichijyo K, Sugimoto H, Hata K (2000) Dietary supplementation with fish oil rich in omega-3 polyunsaturated fatty acids in children with bronchial asthma. [In Process Citation]. *Eur Respir J* 16(5):861–865
70. Hodge L, Salome CM, Hughes JM, Liu-Brennan D, Rimmer J, Allman M, Pang D, Armour C, Woolcock AJ (1998) Effect of dietary intake of omega-3 and omega-6 fatty acids on severity of asthma in children. *Eur Respir J* 11(2):361–365
71. Stene LC, Joner G (2003) Use of cod liver oil during the first year of life is associated with lower risk of childhood-onset type 1 diabetes: a large, population-based, case-control study. *Am J Clin Nutr* 78(6):1128–1134

# Membrane Fatty Acids as Pacemakers of Animal Metabolism

A. J. Hulbert

Received: 31 January 2007 / Accepted: 30 March 2007 / Published online: 27 April 2007  
© AOCs 2007

**Abstract** The recent discovery that the fatty acid composition of tissue phospholipids varies in a systematic manner among species has led to the proposal that membrane fatty acid composition is an important determinant of the metabolic rate characteristic for each species. Endotherms (mammals and birds) have a basal metabolic rate (BMR) that is several times that of ectotherms and have more polyunsaturated membranes. In both birds and mammals, as species size increases there is a decrease in mass-specific BMR and a decrease in membrane polyunsaturation. Membrane-associated processes are significant components of BMR and important membrane proteins operate at much faster rates in species with high BMR than in those with low BMR. A series of “species-crossover” experiments show that the rate of this molecular activity is largely due to the nature of the membrane bilayer surrounding these membrane proteins such that polyunsaturated membranes are associated with fast membrane-associated processes. It is suggested that this influence is due to the physical properties that such polyunsaturated membranes possess. This has been called the membrane pacemaker theory of metabolism and provides a framework to understand factors such as the influence of diet on metabolism. It is noted that in the rat membrane fatty acid composition is a regulated parameter being more influenced by the balance between n-3 and n-6 polyunsaturates in the diet than it is by general diet content of saturated, monounsaturated and total polyunsaturated fats.

**Keywords** Ectothermy · Endothermy · Metabolic rate · Mitochondria · Na<sup>+</sup>, K<sup>+</sup>-ATPase

## Introduction

The idea that “for many problems there is an animal on which it can be most conveniently studied” has been called ‘The August Krogh Principle’ after its first clear exponent [1] and nowadays this idea, also described by the concept of ‘model species’, permeates much biological investigation. There are many examples of such species. The most obvious modern ones being *Caenorhabditis elegans*, *Drosophila melanogaster*, *Mus musculus* and *Rattus norvegicus*. As well as being a Nobel laureate, August Krogh was one of the originators of zoo-physiology (now known as comparative physiology and biochemistry) and provided considerable insight into how living systems work by studying a wide range of different animal species [2]. Besides examining the biology of particular individual species, much insight was obtained by looking at the differences between species. Such a comparative perspective has recently yielded considerable insight into the influence of membrane lipid composition on the rate of animal metabolism. Specifically, it has become apparent that the fatty acid composition of membrane bilayers varies in a systematic manner among species. Furthermore, this variation is an important determinant of the pace of membrane-associated processes and, in turn, the metabolic rate of cells, tissues and consequently the whole organism. The concept that the fatty acid composition of membranes is an important determinant of the metabolic rate characteristic for each species has been called the “membrane pacemaker” theory of metabolism [3, 4] and is the subject matter of this contribution.

A. J. Hulbert (✉)  
Metabolic Research Centre and School of Biological Sciences,  
University of Wollongong, Wollongong  
NSW 2522, Australia  
e-mail: hulbert@uow.edu.au

## Metabolic Rates of Different Animals

When comparing the rate of metabolism among species, it is normal to use the metabolic rate measured under a set of standard conditions. In endotherms (mammals and birds), this is normally the basal metabolic rate (BMR), which is the rate of metabolism of a fasting adult, during a state of rest in a thermoneutral environment. The BMR does not include the cost of growing, moving, thermoregulating or processing a meal and thus represents the minimal ‘cost of living’ for an endotherm. In ectotherms (i.e. most other animal species apart from mammals and birds), because body temperature is determined by environmental temperature, the temperature of measurement (and thus body temperature) needs to be also specified. For ectotherms this minimal ‘cost of living’ is called the standard metabolic rate (SMR—however, for convenience I will use BMR for both endotherms and ectotherms in the remainder of this contribution). When the BMR of endotherms is compared to the SMR of similar-sized ectotherms at the same body temperature, it is observed the minimal ‘‘cost of living’’ is much (7–10 times) greater in endotherms than in ectotherms [5, 6].

Within each of these groups, it was observed long ago that as the species increase in size the speed of their metabolism per unit mass decreases. Larger species obviously require more energy to live than smaller species, but metabolic rate does not increase in direct proportion to body mass. This is largely because of geometrical constraints. For every doubling of size, the surface area of an object increases by only 59% and not 100% (i.e. surface area is related to  $\text{mass}^{0.67}$ ). Basal metabolism similarly scales allometrically with body mass of a species and depending on the study is reported to increase by only 59–69% with every doubling of body mass, i.e. BMR is proportional to  $\text{mass}^{0.67-0.76}$  [7, 8]. The constraints on metabolic rate imposed by surface limitations are made especially obvious by the calculation that if a mouse-sized mammal increased in size to that of a horse without a change in its mass-specific BMR, then this horse-sized mouse would need a surface temperature of  $\sim 100^\circ\text{C}$  to rid itself of its resting heat production [5]. If mammals of different sizes are to maintain essentially the same body temperature, then metabolic rate must be modulated accordingly. The mass-specific BMR of a 10-g shrew is approximately 100-times that of 3,800-kg elephant, and approximately 30-times that of a 70-kg human. In mammals, for every doubling of body mass there is 15–20% decrease in mass-specific BMR (i.e. mass-specific BMR is proportional to  $\text{mass}^{-0.24}$ – $\text{mass}^{-0.33}$ ). The same modulation of BMR with changes in body size is also observed in birds, which evolved endothermy independently to mammals.

Although part of these substantial differences in BMR between (1) endotherms and ectotherms, and (2) between species that differ in body size can be explained by differences in the size of important internal organs and tissues, much of the explanation is related to systematic differences in the rate of cellular metabolism (see reference [4] for a more detailed discussion). It is the purpose of this presentation to briefly examine the evidence that the evolutionary modulator of cellular metabolic rate of different species is the fatty acid composition of cellular membranes.

## Membrane-Associated Processes Are Important Components of BMR

An interesting finding over the last couple of decades has been that, while the relative contribution of various cellular processes differs between cell types, membrane-associated processes are significant components of the resting metabolism of all cells. The data is most complete for rats, in which it has been estimated (when both the size and metabolic activity of various tissues have been collated) that of the oxygen consumed by a rat during BMR, 15% is non-mitochondrial oxygen consumption, 20% is consumption by mitochondria associated with proton leak (i.e. not due to ATP production) and 65% is used for mitochondrial ATP production. The main processes that consume energy in the form of ATP are (1) activity of the  $\text{Na}^+$  pump ( $\sim 25\%$  of total oxygen consumed during BMR), (2) protein synthesis ( $\sim 18\%$ ), (3)  $\text{Ca}^{2+}$  pump activity ( $\sim 5\%$ ), (4) muscle contraction ( $\sim 5\%$ ), (5) gluconeogenesis ( $\sim 7\%$ ) and (6) all remaining processes ( $\sim 5\%$ ) [9]. Thus the maintenance of two trans-membrane ion gradients (namely, the  $\text{Na}^+$  gradient across the plasmalemma, and the  $\text{H}^+$  gradient across the inner mitochondrial membrane) are together responsible for almost half of the energy consumption associated with BMR in mammals [9].

Another interesting finding has been that although overall cellular metabolic rate decreases in a systematic manner with increasing body mass in mammals, the relative contribution of various subcellular processes remains relatively constant. For example, when the respiration rate of isolated hepatocytes from eight mammalian species, ranging in size from mice to horses, were compared, the relative contribution of mitochondrial ATP production, mitochondrial proton leak and non-mitochondrial oxygen consumption to total hepatocyte respiration did not change with body mass even though total hepatocyte respiration decreased by 13% for every doubling of body mass (i.e. it was proportional to  $\text{mass}^{-0.20}$ ) [10]. The relative contribution of these processes to hepatocyte respiration is essentially the same in a mammal and a reptile (of the same size

and body temperature) even though there is a fourfold difference in the total respiration rate of hepatocytes from these species [11]. Similarly, it is estimated that the activity of the  $\text{Na}^+$  pump is a relatively constant proportion of tissue metabolic rate of liver and kidney even though tissue respiration varies significantly, both in mammals ranging in size from mice to cattle [12] and in a comparison of endotherms and ectotherms of the same size and body temperature [13]. The conclusion from these and other studies is that metabolism appears to be a series of linked processes, and that when BMR varies between species all subcellular processes that constitute metabolic activity seem to vary in unison (see [4]).

The maintenance of key ion gradients across membranes is a significant energetic cost of living. Two have been particularly studied in a variety of species. They are (1) the plasmalemmal  $\text{Na}^+$  gradient and (2) the  $\text{H}^+$  gradient across the mitochondrial inner membrane. Both of these gradients can be regarded as a means of storing energy for maintaining other functions. For example, the trans-plasmalemmal  $\text{Na}^+$  gradient is the source of energy for action potentials in excitable tissues, as well as the source of energy for cellular volume regulation, cellular pH regulation and cellular homeostasis for other ions and the active uptake of other molecules. The relative energy requirements for its maintenance varies between cell types, varying from about 60% of total cellular metabolic in nerves and kidney tubule epithelial cells to about 10% of total metabolic rate of liver cells [14], averaging out at about 25% of the BMR of the whole animal [9]. The homeostatic maintenance of a low intracellular  $\text{Na}^+$  concentration is due to a steady state where the extrusion of  $\text{Na}^+$  from the cell (by the membrane-associated  $\text{Na}^+$ ,  $\text{K}^+$ -ATPase) equals the sum of “leaks” of  $\text{Na}^+$  into the cell. Cells of endotherms and ectotherms maintain essentially the same intracellular  $\text{Na}^+$  concentration but the cells of endothermic vertebrates (mammals and birds) are several times leakier to  $\text{Na}^+$  than are the cells of the ectothermic vertebrates (reptiles, amphibian, fish) and the cellular oxygen consumption devoted to providing ATP for operating the  $\text{Na}^+$  pump are consequently much greater in the endotherms [13, 15]. The greater extrusion of  $\text{Na}^+$  from the endotherm cells is not associated with a greater pump concentration per cell but is instead associated with a faster turnover rate for each individual  $\text{Na}^+$  pump in the endotherm cell compared to the ectotherm. For example, when measured *in vitro* at 37 °C, the molecular activity of the  $\text{Na}^+$ ,  $\text{K}^+$ -ATPase isolated from kidney cells of the rat is about 8,000  $\text{ATP min}^{-1}$  compared to about 2,000  $\text{ATP min}^{-1}$  for kidney  $\text{Na}^+$ ,  $\text{K}^+$ -ATPase from the similar-sized toad [16]. Essentially the same differences were also observed for the brain from these two species that differ dramatically in their BMR. Just as the plasma membrane is

leakier in cells of endotherms compared to those of ectotherms, so is the mitochondrial inner membrane of endotherms leakier to protons compared to similar-sized ectotherms [11, 17].

### Membrane Pacemaker Theory of Metabolism

Early analysis of the underlying basis of this variation in the speed of metabolism among species (described above) dismissed species-variation in chemical composition of cells as an explanation (see p. 191 of ref. 7). However, variation in the fatty acid composition of cellular membranes was not considered in that analysis. The first indication that different membrane fatty acid composition might be associated with the variation in metabolic rate among animal species comes from the observation, by Gudbjarnason and colleagues, of a strong positive relationship between the docosahexaenoic acid (DHA) content of cardiac phospholipids and the heart rate of mammals ranging in size from mice to whales [18]. As resting heart rate of a species is a correlate of its mass-specific BMR this was the first demonstration that mammals with fast BMR differed in their membrane composition to those with a slower BMR. It was later realised that this relationship was not restricted to cardiac phospholipids but was also observed in the phospholipids from several other important metabolic tissues, notably liver, kidney, and skeletal muscle [19]. In most tissues, the phospholipids (and thus membrane bilayers) of small mammals have a high DHA content compared to larger mammal species [19, 20]. This is not true for brain phospholipids which have a high DHA content irrespective of the size of the mammal species. Possible reasons for this will be discussed later.

The association of a high DHA content of membranes with a fast BMR is not restricted to mammals of different body size but seems to be a more general phenomenon. It is also observed in birds where the DHA content of phospholipids also decreases with increasing body size, in skeletal muscle [21], heart [22] as well as in other tissues such as liver and kidney but not brain (Hulbert, unpublished observations). It is also observed in the comparison of liver and kidney phospholipids from similar-sized mammals and reptiles with their substantial difference in BMR [23].

The DHA content of tissue phospholipids decreases with increasing body size in mammals and birds, however there is no change in the total content of all unsaturated fatty acids (UFA) in tissue phospholipids with body size [20, 21]. This lack of change in total UFA with body size is due compensatory changes in other fatty acid classes. For example, in phospholipids from both skeletal muscle and kidney of mammals there is an increase in monounsatu-

rated fatty acids (MUFA) with body size, while in heart phospholipids of mammals there is an increase in the omega-6 polyunsaturated fatty acids (n-6 PUFA) with body size [20]. The differences described above for the fatty acid composition of total tissue phospholipids appear to be general for subcellular membranes as they have also been observed liver mitochondria from mammals [24] and birds [25] and reptiles [11, 17] as well as for microsomes from mammals and birds (e.g. [26]). As an example of the general trends of changes membrane fatty acid composition with body size, the data for skeletal muscle phospholipids in mammals and birds is shown in Fig. 1.

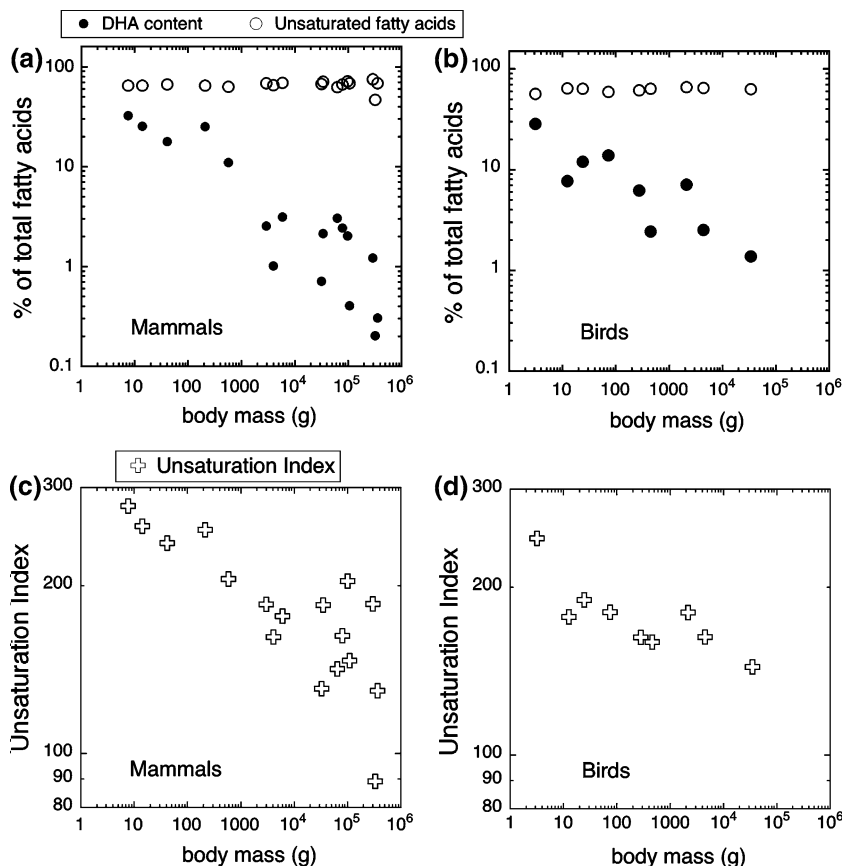
The general conclusion that emerges from these studies is that although there is essentially no difference in the percentage of UFA in cellular membranes of species that dramatically differ in their BMR, it is consistently observed that species with high BMR have a significantly greater density of double-bonded carbons ( $-C=C-$ ) in their cellular membrane bilayers than those species with lower BMR.

In the 1990s, the observation of a consistent pattern of membrane fatty acid composition associated with BMR in both the ectotherm–endotherm comparison and the comparison of different-sized mammals led to a hypothesis, described as the “membrane pacemaker” theory of

metabolism [3, 4]. It can be summarised by the following postulates:

1. Variation in BMR among species is associated with differences in both the size of metabolically active tissues and in the cellular metabolic rate of these tissues.
2. Membrane-associated processes are significant and substantial components of the resting metabolic rate of cells.
3. When BMR varies among species, all activities that make up this metabolic rate seem to vary in unison.
4. Species with high mass-specific BMR have membranes that have a higher degree of polyunsaturation than species with low BMR.
5. That DHA is an important (but not the sole) contributor to this high degree of membrane polyunsaturation.
6. That highly polyunsaturated membranes have physical properties that result in a faster molecular activity of membrane proteins.
7. Which, in turn, results in higher rates of membrane-associated activities, a faster rate of cellular metabolism, a faster rate of tissue metabolism and consequently a high BMR of the whole organism.

**Fig. 1** The relationship between body size of species and fatty acid composition of skeletal muscle phospholipids from mammals (graphs a, c) and birds (graphs b, d). Top two graphs (a, b) show total unsaturated fatty acids and docosahexaenoic acid (DHA) content as a percent of total fatty acids. Bottom two graphs show Unsaturation Index (= total number of double bonds per 100 fatty acids). Data for mammals are from reference [20] while those for birds are from reference [21]





As the initial development of the membrane pacemaker theory of metabolism was based on ectotherm–endotherm comparisons as well as studies of different-sized mammals, it was tested by examining of whether the same correlations observed in mammals were also present in the other vertebrate class that independently evolved endothermy; the birds. The results of the comparison of bird species ranging from 14-g zebra finches to 34-kg emus showed essentially the same body size trends as previously observed in mammals (e.g. 21, 25–27).

### Membranes Lipids and Molecular Activity of Membrane Proteins

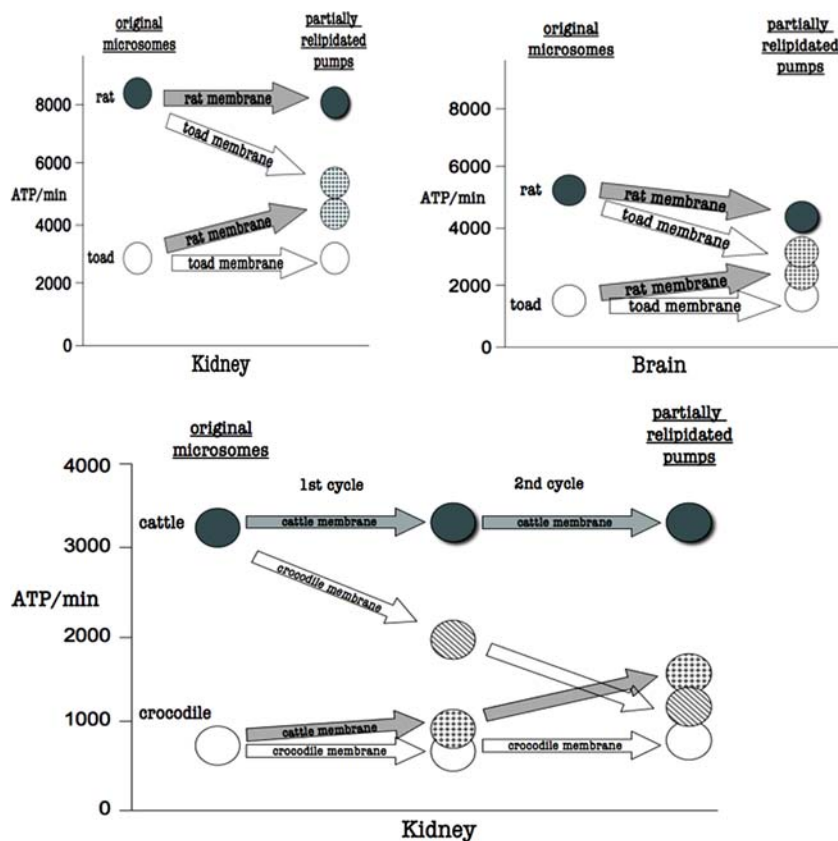
One of the main problems associated with these species-comparisons is that while they show correlations between membrane composition and metabolic rate, they do not, of course, demonstrate a ‘cause and effect’ relationship. In order, to experimentally test whether species-differences in membrane composition result in different activity of membrane proteins, a series of ‘species-crossover’ studies have been performed [28, 29]. The results of these studies are summarised in Fig. 2 and show, by partial delipidation–relipidation of the membrane-bound  $\text{Na}^+$ ,  $\text{K}^+$ -ATPase, that the composition of the surrounding

membrane bilayer is an important determinant of the molecular activity of the sodium pump. Such experimental manipulations (e.g. [28, 29]) support the proposal that the correlation observed between membrane fatty acid composition and the molecular activity of the  $\text{Na}^+$ ,  $\text{K}^+$ -ATPase (e.g. [30]) is one of cause and effect.

Although similar correlations between membrane composition and the molecular activity of some mitochondrial proteins from different species have been reported [31], they have not yet been tested by similar ‘species-crossover’ experiments. However, studies of cold acclimation in fish suggest a cause and effect relationship between membrane fatty acid composition and activity of membrane proteins. Mitochondrial membrane lipids extracted from cold-acclimated goldfish produce a greater reactivation of delipidated succinic dehydrogenase than do those from warm-acclimated goldfish [32]. Similarly, cold-acclimated trout increase their erythrocyte membrane polyunsaturation and sodium pump activity while the sodium pump number remains unchanged [33].

What is it about a highly polyunsaturated bilayer that results in enhanced activity of proteins in that membrane? It appears that the physical properties of such membrane lipids are important in this regard. Although there is no rotation around the *cis* double bonds of unsaturated fatty acid chains (and the double bonds themselves are rigid),

**Fig. 2** The effect of partial delipidation (by mild detergent treatment) followed by partial relipidation on the molecular activity (ATP/min) of microsomal  $\text{Na}^+$ ,  $\text{K}^+$ -ATPase. Relipidation was either with membrane lipids from the same or the other species. The results of these partial ‘species-crossover’ experiments show that the source of the surrounding membrane lipids have a strong influence on the molecular activity of the membrane protein. The results for the rat–toad experiment are from reference [28], those for the cattle–crocodile experiment are from reference [29]



there are extremely low potential barriers to rotation around the carbon-carbon *single* bonds that occur on either side of the doubled bonded carbon units in fatty acid chains. This makes highly unsaturated PUFA molecules such as DHA very physically active and flexible molecules [34–36]. For an excellent illustration of the relative movement of DHA compared a saturated fatty acid, the reader is referred to Dr. Scott Fellers web-site (<http://persweb.wabash.edu/facstaff/fellers/>, see the bottom of the “lipid animations” page) where he has an animation of 0.5 nanoseconds (i.e. 1/100 millionth the duration of an action potential) in the life of a DHA-containing phosphatidylcholine molecule.

A rapidly moving polyunsaturated chain will exert lateral pressure on its neighbouring molecules within a membrane bilayer. When both (1) the molecular activity of  $\text{Na}^+$ ,  $\text{K}^+$ -ATPase was measured in microsomes from different sources, and (2) the lateral pressure was measured in monolayers of phospholipids from the same sources, there were strong correlations between this physical property of the membrane lipids and the molecular activity of the individual  $\text{Na}^+$ ,  $\text{K}^+$ -ATPase molecules [37]. The greater the lateral pressure in the membrane the greater the activity of the membrane-bound enzyme (Fig. 3). In this study, kidney and brain were used as the source of microsomes because of their very high tissue density of sodium pumps. Membrane fatty acid composition was also measured and it was

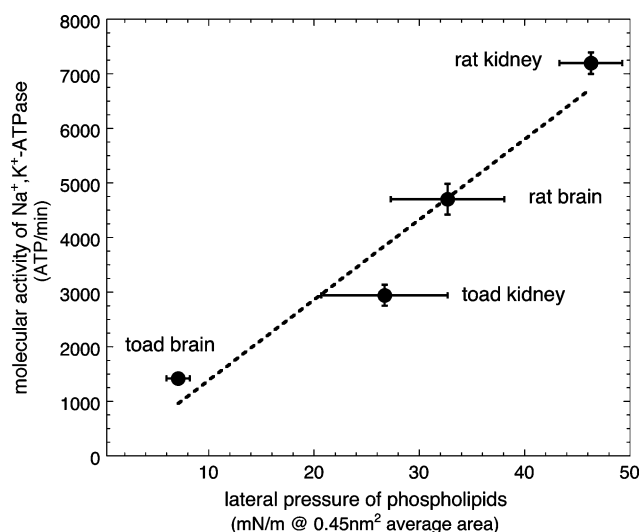


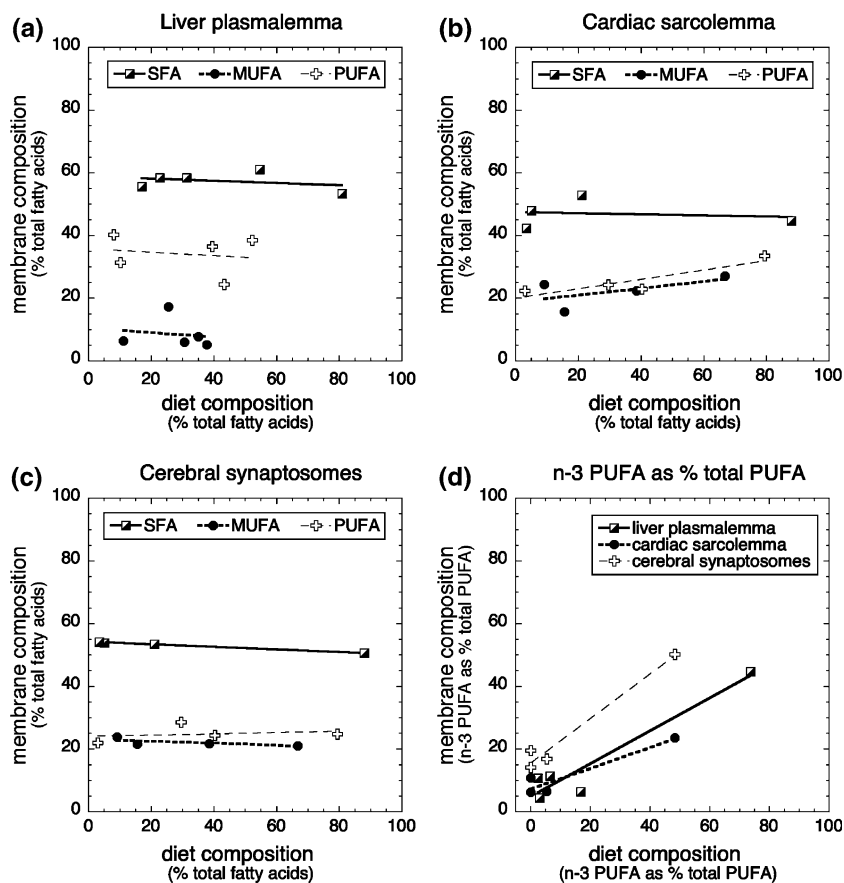
**Fig. 3** The relationship between the molecular activity (ATP/min) of microsomal  $\text{Na}^+$ ,  $\text{K}^+$ -ATPase and the lateral surface pressure exerted by the surrounding membrane lipids. The lateral surface pressure was measured on monolayers of phospholipids extracted from the same microsomal preparation used for molecular activity measurements. Data are from reference [37]. Each data point is the average of six preparations and *error bars* represent  $\pm$ SEM. The lateral pressure is that is that measured when the average area occupied by each phospholipid molecule is 0.45 nm<sup>2</sup>. All measurements were made at 37 °C

observed that the molecular activity of  $\text{Na}^+$ ,  $\text{K}^+$ -ATPase was more strongly correlated with the lateral pressure exerted by the membrane lipids than it was with any individual aspect of membrane fatty acid composition. It should be noted that although both kidney and brain are good sources of sodium pumps they have very different and distinctive fatty acid compositions of their phospholipids. Kidney phospholipids are very high in n-6 PUFA but very low in n-3 PUFA, while n-3 PUFA dominate in the brain.

It is appropriate to now return to possible reasons why the brain does not show the same body size trends in membrane fatty acid composition that exist in other tissues. While in the human, the concentration of PUFA (especially DHA) in brain is much higher than observed in other tissues, this is not the case for smaller species. For example in the mouse, DHA is equally common in membranes of all tissues [20]. To understand this tissue difference we need to appreciate that the first mammals were the size of mice. It was necessary to decrease mass-specific BMR (and its associated heat production) as some mammal species increased in body size over evolutionary time, in order for different-sized mammals to maintain essentially the same body temperature (as discussed earlier). The membrane pacemaker theory suggests that this was achieved by decreasing the degree of polyunsaturation of membrane lipids, which in turn resulted in a lower mass-specific BMR by slowing the activity of membrane proteins of larger mammals. Obviously, slowing the speed of membrane processes in nervous tissue such as the brain would likely be disadvantageous as it would presumably decrease the speed of behavioural response. We have suggested elsewhere [3] that this is likely the primary reason why brain phospholipids retain their high degree of polyunsaturation irrespective of the size of the species.

So far, in this contribution I have used the fatty acid composition of tissue phospholipids as a description of membrane fatty acid composition. Of course, this is a simplification of membrane composition. Polyunsaturated fatty acids are not randomly distributed within membranes, especially in the plasmalemma. Firstly, the external and cytoplasmic leaflets of the plasmalemma differ in the phospholipids headgroup composition, cholesterol content as well as fatty acid composition and this non-symmetric composition results in a transbilayer fluidity gradient regulated by unsaturated fatty acids [38, 39]. Secondly, the plasmalemma also contains lateral domains (lipid rafts/caveolae as well as non-raft domains) which differ in their lipid composition and protein distribution (for reviews see 40–42). For example, the  $\text{Na}^+$ ,  $\text{K}^+$ -ATPase appears to be distributed primarily in the non-raft domains of the plasmalemma, at least in some cells [43, 44] and  $\text{Na}^+$ ,  $\text{K}^+$ -ATPase activity is influenced by the transbilayer

**Fig. 4** The relationship between fatty acid composition of diet and the fatty acid composition of three different membranes in the rat. *Graph (a)* is for liver plasmalemma, *graph (b)* is for cardiac sarcolemma, and *graph (c)* is for cerebral synaptosomes. All *three graphs* show the data for percentage of saturated fatty acids (SFA), percentage of monounsaturated fatty acids (MUFA) and percentage of polyunsaturated fatty acids (PUFA). *Graph (d)* shows the relationship between dietary balance of n-3 PUFA and n-6 PUFA (expressed as percentage of total PUFA that are n-3 PUFA) and the membrane composition of all three membranes. Data sources are given in reference [61]



fluidity gradient [45–48]. Both space constraints and limited knowledge of the situation in a range of species limit consideration of this important aspect here.

### Influence of Diet on Membrane Composition and Metabolic Rate

A role for membrane polyunsaturation in the determination of metabolic rate may explain a number of observations. For example, fish-eating seals have a much higher BMR than is predicted from their body mass [49], and fish-eating seabirds also have relatively high BMR [50]. Termite-eating mammal species have a lower than predicted BMR [51]. It is tempting to speculate that the high n-3 PUFA content of fish and the low PUFA/high MUFA content of ants and termites are responsible for these BMR deviations. Other evidence that the type of fats in the diet influence metabolic rate are that the metabolic rate of rats are elevated when they are fed diets enriched with either n-6 PUFA [52] or n-3 PUFA [53]. Other studies also show that increased PUFA content of the diet increases metabolic rate of rats [54], baboons [55] and chickens [56]. Human studies have demonstrated similar enhancement of metabolic rate with elevated dietary PUFA (e.g. 57, 58).

Dietary polyunsaturated fats have also been shown to influence the pattern of and metabolic rate during torpor (hibernation) in some mammals and in such cases the influence of dietary polyunsaturates is almost certainly mediated by effects on membrane composition. In the chipmunk (*Eutamias amoenus*), mitochondrial membrane composition changes of ~20% have been recorded following manipulation of the polyunsaturated fat content of the diet [59] and increased unsaturation of dietary fats results in both extended length of torpor periods and a lower body temperature during torpor as well as a lower metabolic rate at these very low body temperatures [60].

The effects on metabolic rate are often not as large as the changes in dietary PUFA content and this is likely related to the degree of change in membrane composition following dietary changes. Membrane fatty acid composition is a regulated variable and is influenced by diet to only a limited extent. As is illustrated in Fig. 4, substantial changes in the percent content of SFA, MUFA and PUFA in the diet have a very limited influence on the total percent content of these fatty acid in membranes of the rat. Because animals can synthesise both SFA and MUFA from non-lipid sources but are incapable of de novo synthesis of either n-6 and n-3 PUFA (and are unable to interconvert these two types of PUFA), both n-6 and n-3 PUFA are

essential dietary components. As can be seen from Fig. 4, membrane composition however is much more responsive to the balance between n-6 and n-3 PUFA in the diet. Recent experiments have shown that this is also the case in the membranes of human cheek mucosal cells (Hulbert, unpublished results). The influence of diet on membrane composition (especially the balance between n-6 and n-3 PUFA) is an emerging factor that has important implications for metabolism and disease [61].

**Acknowledgments** I would like express my sincere gratitude to my colleagues (notably Dr Paul Else, Dr. Martin Brand, Dr. Patrice Couture, Dr. Ben Wu and Dr. Nigel Turner) who over the years have made significant and substantial input to ideas presented here. Much of the work by AJH cited in this contribution has been supported by grants from the Australian Research Council.

## References

- Krebs HA (1975) The August Krogh principle: "For many problems there is an animal on which it can be most conveniently studied". *J Exp Zool* 194:221–226
- Schmidt-Nielsen B (1995) August and Marie Krogh. Lives in science. Oxford, New York
- Hulbert AJ, Else PL (1999) Membranes as possible pacemakers of metabolism. *J Theor Biol* 199:257–274
- Hulbert AJ, Else PL (2000) Mechanisms underlying the cost of living in animals. *Annu Rev Physiol* 62:207–235
- Hemmingsen AM (1960) Energy metabolism as related to body size and respiratory surfaces and its evolution. *Rept Steno Meml Hosp Nord Insulin Lab* 9:1–110
- Hulbert AJ (1980) The evolution of energy metabolism in mammals. In: Schmidt-Nielsen K, Bolis L, Taylor CR (Eds) *Comparative physiology: primitive mammals*. Cambridge University Press, Cambridge, pp 129–139
- Kleiber M (1961) *The fire of life*. Wiley, New York
- White CR, Seymour RS (2003) Mammalian basal metabolic rate is proportional to body mass<sup>2/3</sup>. *Proc Natl Acad Sci USA* 100:4046–4049
- Rolfe DF, Brown GC (1997) Cellular energy utilization and molecular origin of standard metabolic rate in mammals. *Physiol Rev* 77:731–58
- Porter RK, Brand MD (1995) Causes of differences in respiration rate of hepatocytes from mammals of different body mass. *Am J Physiol* 269:R1213–24
- Brand MD, Couture P, Else PL, Withers KW, Hulbert AJ (1991) Evolution of energy metabolism: proton permeability of the inner membrane of liver mitochondria is greater in a mammal than in a reptile. *Biochem J* 275:81–86
- Couture P, Hulbert AJ (1995) On the relationship between body mass, tissue metabolic rate and sodium pump activity in mammalian liver and kidney. *Am J Physiol* 268:R641–R650
- Else PL, Hulbert AJ (1987) The evolution of mammalian endothermic metabolism: "leaky membranes" as a source of heat. *Am J Physiol* 253:R1–R7
- Clausen TC, Hardeveld CV, Everts ME (1991) Significance of cation transport in control of energy metabolism and thermogenesis. *Physiol Rev* 71:733–775
- Hulbert AJ, Else PL (1990) The cellular basis of endothermic metabolism: a role for "leaky" membranes?. *News Physiol Sci* 5:25–28
- Else PL, Windmill DJ, Markus V (1996) Molecular activity of sodium pumps in endotherms and ectotherms. *Am J Physiol* 271:R1287–R1294
- Brookes PS, Buckingham JA, Tenreiro AM, Hulbert AJ, Brand MD (1998) The proton permeability of the inner membrane of liver mitochondria from ectothermic and endothermic vertebrates and from obese rats: correlations with standard metabolic rate and phospholipid composition. *Comp Biochem Physiol B* 119:325–334
- Gudbjarnason S, Doell B, Oskardottir G, Hallgrimsson J (1978) Modification of cardiac phospholipids and catecholamine stress tolerance. In: de Duve C, Hayaishi O (eds) *Tocopherol oxygen and biomembranes*. Elsevier, Amsterdam, pp 297–310
- Couture P, Hulbert AJ (1995) Membrane fatty acid composition of tissues is related to body mass of mammals. *J Memb Biol* 148:27–39
- Hulbert AJ, Rana T, Couture P (2002). The acyl composition of mammalian phospholipids: an allometric analysis. *Comp Biochem Physiol B* 132:515–527
- Hulbert AJ, Faulks SC, Buttemer WA, Else PL (2002) Acyl composition of muscle membranes varies with body size in birds. *J Exp Biol* 205:3561–3569
- Szabo A, Febel H, Mezes M, Balogh K, Horn P, Romvari R (2006) Body size related adaptations of the avian myocardial phospholipid fatty acyl chain composition. *Comp Biochem Physiol B* 144:496–502
- Hulbert AJ, Else PL (1989) The evolution of endothermic metabolism: mitochondrial activity and changes in cellular composition. *Am J Physiol* 256:R1200–08
- Porter RK, Hulbert AJ, Brand MD (1996) Allometry of mitochondrial proton leak: influence of membrane surface area and fatty acid composition. *Am J Physiol* 271:R1550–R1560
- Brand MD, Turner N, Ocloo A, Else PL, Hulbert AJ (2003) Proton conductance and fatty acyl composition of liver mitochondria correlates with body mass in birds. *Biochem J* 376:741–748
- Turner N, Haga KL, Hulbert AJ, Else PL (2005) Relationship between body size, Na<sup>+</sup>-K<sup>+</sup>-ATPase activity, and membrane lipid composition in mammal and bird kidney. *Am J Physiol* 288:R301–R310
- Else PL, Brand MD, Turner N, Hulbert AJ (2004) Respiration rate of hepatocytes varies with body size in birds. *J Exp Biol* 207:2305–2311
- Else PL, Wu BJ (1999) What role for membranes in determining the higher sodium pump molecular activity of mammals compared to ectotherms. *J Comp Physiol B* 169:296–302
- Wu BJ, Hulbert AJ, Storlien LH, Else PL (2004) Membrane lipids and sodium pumps of cattle and crocodiles: an experimental test of the membrane pacemaker theory of metabolism. *Am J Physiol* 287:R633–R641
- Turner N, Else PL, Hulbert AJ (2003) Docosahexaenoic acid content of membranes determines molecular activity of the sodium pump: implications for diseases states and metabolism. *Naturwissenschaften* 90:521–523
- Hulbert AJ, Turner N, Hinde J, Else PL, Guderley H (2006) How might you compare mitochondria from different tissues and different species?. *J Comp Physiol B* 176:93–105
- Hazel JR (1972) The effect of temperature acclimation upon succinic dehydrogenase activity from the epaxial muscle of the common goldfish (*Carassius auratus* L.) II. Lipid reactivation of the salable enzyme. *Comp Biochem Physiol B* 43:863–82
- Raynard RS, Cossins AR (1991) Homeoviscous adaptation and thermal compensation of sodium pump of trout erythrocytes. *Am J Physiol* 260:R916–24
- Feller SE, Gawrisch K, MacKerell AD Jr (2002) Polyunsaturated fatty acids in lipid bilayers: intrinsic and environmental contri-

- butions to their unique physical properties. *J Am Chem Soc* 124:318–326
35. Mitchell DC, Gawrisch K, Litman BJ, Salem N Jr (1998) Why is docosahexenoic acid essential for nervous system function?. *Biochem Soc Trans* 26:365–370
  36. Stillwell W, Wassall SR (2003) Docosahexaenoic acid: membrane properties of a unique fatty acid. *Chem Phys Lipids* 126:1–27
  37. Wu BJ, Else PL, Storlien LH, Hulbert AJ (2001) Molecular activity of Na<sup>+</sup>/K<sup>+</sup>-ATPase from different sources is related to the packing of membrane lipids. *J Exp Biol* 204:4271–4280
  38. Sweet WD, Schroeder F (1988) Polyunsaturated fatty acids alter sterol transbilayer domains in LM fibroblast plasma membrane. *FEBS Lett* 229:188–192
  39. Kier AB, Sweet WD, Cowlen MS, Schroeder F (1986) Regulation of transbilayer distribution of a fluorescent sterol in tumor cell plasma membranes. *Biochim Biophys Acta* 861:287–301
  40. Schroeder F, Atshaves BP, Gallegos AM, McIntosh AL, Liu JC, Kier AB, Huang H, Ball JM (2005) Lipid rafts and caveolae organization. In: Frank PG, Lisanti MP (eds) *Advances in molecular and cell biology*. Elsevier, Amsterdam, pp 3–36
  41. Pike LJ, Han X, Chung K-N, Gross RW (2002) Lipid rafts are enriched in arachidonic acid and plasmenylethanolamine and their composition is independent of caveolin-1 expression: a quantitative electrospray ionization/mass spectrometric analysis. *Biochemistry* 41:2075–2088
  42. Pike LJ (2003) Lipid rafts: bringing order to chaos. *J Lipid Res* 44:655–667
  43. Atshaves BP, Gallegos A, McIntosh AL, Kier AB, Schroeder F (2003) Sterol carrier protein-2 selectively alters lipid composition and cholesterol dynamics of caveolae/lipid raft vs non-raft domains in L-cell fibroblast plasma membranes. *Biochemistry* 42:14583–14598
  44. Gallegos AM, Storey SM, Kier AB, Schroeder F, Ball JM (2006) Structure and cholesterol dynamics of caveolae/raft and non-raft plasma membrane domains. *Biochemistry* 45:12100–12116
  45. Sweet WD, Schroeder F (1986) Charged anaesthetics alter LM-fibroblast plasma-membrane enzymes by selective fluidization of inner or outer membrane leaflets. *Biochem J* 239:301–310
  46. Sweet WD, Schroeder F (1986) Plasma membrane lipid composition modulates action of anesthetics. *Biochim Biophys Acta* 861:53–61
  47. Schroeder F, Sweet WD (1988) The role of membrane lipid and structure asymmetry on transport systems. In: Jorgensen PL, Verna R (eds) *Advances in biotechnology of membrane ion transport*. Serono Symposia, New York, pp 183–195
  48. Sweet WD, Schroeder F (1988) Lipid domains and enzyme activity. In: Aloia RC, Cirtain CC, Gordon LM (eds) *Advances in membrane fluidity: lipid domains and the relationship to membrane function*, Alan R. Liss Inc., New York, pp 17–42
  49. Hurley JA, Costa DP (2001) Standard metabolic rate at the surface and during trained submersions in adult California sea (*Zalophus californicus*). *J Exp Biol* 204:3273–3281
  50. Ellis HI (1984) Energetics of free-ranging seabirds. In: Whittow GC, Rahn H (eds) *Seabird energetics*. Plenum, New York, pp 203–234
  51. McNab BK (1986) The influence of food habits on the energetics of eutherian mammals. *Ecol Monogr* 56:1–19
  52. Shimomura Y, Tamura T, Suzuki M (1990) Less body fat accumulation in rats fed a safflower oil diet than rats fed a beef tallow diet. *J Nutr* 120:1291–1296
  53. Pan DA, Storlien LH (1993) Effect of dietary lipid profile on the metabolism of omega-3 fatty acids: Implications for obesity prevention. In: Drevon CA, Baksass I, Krokkan HE (eds) *Omega-3 fatty acids: metabolism and biological effects*. Birkhauser Verlag, Basel pp 97–106
  54. Takeuchi H, Matsuo T, Tokuyama K, Shimomura Y, Suzuki M (1995) Diet-induced thermogenesis is lower in rats fed a lard diet than those fed a high oleic acid safflower oil diet, a safflower oil diet, or a linseed oil diet. *J Nutr* 125:920–925
  55. Savage N, Goldstone BW (1965) Effect of different dietary fats on oxygen consumption and serum lipid levels in the baboon (*Papio ursinus*). *Brit J Nutr* 19:459–467
  56. Newman RE, Bryden WL, Fleck E, Ashes JR, Buttemer WA, Storlien LH, Downing JA (2002) Dietary n-3 and n-6 fatty acids alter avian metabolism: metabolism and abdominal fat deposition. *Brit J Nutr* 88:11–18
  57. Jones PJH, Schoeller DA (1988) Polyunsaturated:saturated ratio of diet fat influences energy substrate utilization in the human. *Metabolism* 37:145–151
  58. Van Marken Lichtenbelt WD, Mensink RP, Westerterp KR (1997) The effect of fat composition of the diet on energy metabolism *Zeitschrift fur Ernahrungswissenschaft* 36:303–305
  59. Geiser F (1990) Influence of polyunsaturated and saturated dietary lipids on adipose tissue, brain and mitochondrial membrane fatty acid composition of a mammalian hibernator. *Biochim Biophys Acta* 1046:159–166
  60. Geiser F, McAllan BM, Kenagy GJ (1994). The degree of dietary fatty-acid unsaturation affects torpor patterns and lipid-composition of a hibernator. *J Comp Physiol B* 164:299–305
  61. Hulbert AJ, Turner N, Storlien LH, Else PL (2005) Dietary fats and membrane function: implications for metabolism and disease. *Biol Rev* 80:155–169

## Dietary Lipids Impacts on Healthy Ageing

Harumi Okuyama · Kazuyo Yamada ·  
Daisuke Miyazawa · Yuko Yasui · Naoki Ohara

Received: 14 December 2006 / Accepted: 28 April 2007 / Published online: 2 June 2007  
© AOCs 2007

**Abstract** Healthy ageing is gaining attention in the lipid nutrition field. As *in vivo* biomarkers of healthy ageing, we have evaluated the survival, learning/memory performance, and physical potencies in rodents fed a diet supplemented with high-linoleic acid (LNA,  $\omega 6$ ) safflower oil or high- $\alpha$ -linolenic acid (ALA,  $\omega 3$ ) perilla oil for long periods. The results suggested that perilla oil with a low  $\omega 6/\omega 3$  ratio is beneficial for healthy ageing. In order to address this issue further, we determined the survival of stroke-prone SHR (SHRSP) rats fed a conventional rodent diet supplemented with 10% fat or oil. Survival was longer with  $\omega 3$ -rich oils compared with  $\omega 6$ -rich oils. However, some kinds of vegetable oils and hydrogenated oils shortened the survival of SHRSP rats to an unusual degree (ca. 40% compared with that of  $\omega 6$ -rich oil) that could not be accounted for by the fatty acid and phytosterol composition of the oils. The observed decrease in platelet counts was associated with pathological changes in the kidney and other organs. Dihydro-vitamin K1 is proposed as a likely candidate as a stroke-stimulating factor in hydrogenated oils. Thus, factors other than fatty acids ( $\omega 6/\omega 3$  balance) and phytosterols must be taken into account when fats and oils are evaluated in relation to healthy ageing.

**Keywords** Fatty acid · Oil · Fat · Longevity · Carcinogenesis · Anti-nutritional factor · Survival · Vitamin K · Canola · Perilla

### Abbreviations

ALA  $\alpha$ -Linolenic acid  
ARA Arachidonic acid  
CHD Coronary heart disease  
EPA Eicosapentaenoic acid (icosapentaenoic acid)  
LNA Linoleic acid

### Introduction

Caloric restriction is known to prolong the survival of rodents, and genes related to longevity have been identified [1]. However, the causes of death are variable among individuals and no simple *in vitro* markers seem to suffice as criteria for healthy ageing. In lipid nutrition, short-term and long-term dietary manipulations often result in different effects; hence long-term effects need to be evaluated when fats and oils are evaluated for their preventive effects on chronic diseases and healthy ageing.

One of difficulties in this field is that it takes  $\geq 3$  years using conventional rat strains to determine the survival times of groups fed different fats or oils. The SHRSP rat strain dies of cerebral bleeding at high frequencies particularly when salt is given, and its mean survival time is relatively short. Taking advantage of the relatively short survival of this strain, we began to estimate mean survival times of SHRSP rats fed a conventional diet supplemented with 10% fat or oil. In this review, we present an overview of the beneficial effects of oils with low  $\omega 6/\omega 3$  ratios

H. Okuyama (✉) · K. Yamada · D. Miyazawa · Y. Yasui  
Laboratory of Preventive Nutraceutical Sciences,  
Kinjo Gakuin University College of Pharmacy,  
2-1723 Omori, Moriyamaku, Nagoya 463-8521, Japan  
e-mail: okuyamah@kinjo-u.ac.jp

N. Ohara  
Hatano Research Institute, Food and Drug Safety Center,  
Kanagawa, Japan

observed mainly in conventional rats and mice [2, 3], and on the anti-nutritional factors in some vegetable oils that have mainly been observed in SHRSP rats.

### Beneficial Effects of High-ALA Perilla Oil on Healthy Ageing of Rodents: An Overview

ALA-rich perilla oil or LNA-rich safflower oil was fed to a conventional strain of rats from weaning, mated at 11 weeks of age, and the survival was estimated for male rats ( $F_0$ ). The mean survival time of the perilla oil group was longer by about 10% compared with the safflower oil group. The male offspring ( $F_1$ ) were fed the same diet as the dams' and a brightness-discrimination learning task was imposed when their ages reached 80% of the mean survival time of the male  $F_0$  rats. The correct response ratio and memory retention were superior in the ALA-rich diet group compared with LNA-rich diet group [2]. Not only ALA-rich oil, but also fish oil diets enriched with DHA (docosahexaenoic acid,  $\omega_3$ ) lead to superior learning performance in a passive avoidance test compared with safflower oil in SHRSP rats treated with the test diets for 14 weeks [3]. Similarly in conventional male mice (ICR, Crj:CD-1), performance in the spatial learning test (Morris water-maze) was superior in the perilla oil group compared to the safflower oil group [4]. In senescence-accelerated mice (SAM P8), however, perilla oil was reported to improve learning performance in ageing but slightly shorten the survival compared with safflower oil [5]. The behavioral changes induced by dietary  $\omega_6$  and  $\omega_3$  fatty acids were associated with changes in lipid compositions, microscopic appearance (synaptic vesicle density) [6] and gene expression in the brain.

Except in the case of mutant mice (SAM), in which the site of the mutation(s) has not been identified, dietary oils with relatively low  $\omega_6/\omega_3$  ratios (e.g., perilla oil, flaxseed oil, and fish oil) were beneficial for the healthy ageing of rodents as measured by behaviors and survival rates.

### Factors that Shorten the Survival of SHRSP Rats

Perilla oil with a  $\omega_6/\omega_3$  ratio of 1/4, as well as fish oil, prolonged the survival of SHRSP rats by about 10% compared with safflower oil ( $\omega_6/\omega_3$  ratio of 20) and soybean oil ( $\omega_6/\omega_3$  ratio of ~10), suggesting that low  $\omega_6/\omega_3$  ratios of dietary oils are beneficial in this animal model as well. Canola oil (from double-low rapeseeds) with a relatively low  $\omega_6/\omega_3$  ratio (2.5) was expected to be beneficial for this rat strain, but unexpectedly it shortened the survival by ~40% with water, and by 10–20% with

1% NaCl as drinking water as compared with soybean oil [7, 8]. In these experiments, a test diet was prepared by mixing a standard diet containing 4% lipids and a fat or oil at a 9:1 ratio, and fed to male SHRSP rats from weaning at 4 weeks of age and survival was followed. The survival-shortening activity of canola oil was significant when it was diluted with soybean oil at a ratio of 1:3 (dose-dependency). Fish oil prolonged the survival in the absence of NaCl-loading but EPA (eicosapentaenoic acid ethyl ester,  $\omega_3$ ) shortened the survival with 1% NaCl-loading [9], possibly due to a decreased production of PGE<sub>2</sub> that is essential for the proper functioning of the kidney.

### The Presumed Factors Other than Fatty Acids

Soybean oil was relatively safe in this model as described above but partially hydrogenated soybean oil shortened the survival by >30% compared with soybean oil [10]. Ratnayake et al. [11, 12] added olive oil and corn oil to the group of oils with survival-shortening activity in SHRSP rats. Free fatty acid fractions from canola oil and hydrogenated soybean oil exhibited no or decreased survival-shortening activity despite little change in phytosterol composition [8], hence the presence in these oils of minor components that stimulate the onset of stroke and shorten survival was presumed.

### Phytosterols Proposed as a Part of Survival-Shortening Factor

Phytosterol was proposed as the survival-shortening factor by Ratnayake's group [12]. This proposal was based on the observations that the phytosterol contents of several vegetable oils were negatively associated with survival times, and that the addition of crystallized phytosterol shortened the survival although the amount of added phytosterol was two times greater than that of canola oil. Olive oil was exceptional in that its phytosterol content was the lowest but survival-shortening activity was the highest among the oils examined [12]. However, our data led to the proposal that factors other than phytosterols should be considered because, (a) phytosterol compositions were very similar but survival rates were much different between the high oleic type and high-linoleic type of safflower oil, and between soybean oil and hydrogenated soybean oil [13], (b) addition of five times more phytosterol was reported to be necessary to reproduce the activity of canola oil [14], and (c) a mixture of phytosterols with different structures is unlikely to crystallize and the presence of other minor components in this crystal (aggregates?) cannot be excluded.

## Pathological Changes Observed in the Tissues of SHRSP Rats Fed Canola Oil Compared With Soybean Oil

Pathological changes were observed in the kidney, bone marrow, brain and other tissues. The decreases in platelet counts, which were observed not only in rats but also in piglets fed canola oil [15, 16], were associated with kidney lesions, a decreased number of megakaryocytes in the bone marrow, and an increased number of megakaryocytes in the spleen, possibly through decreased erythropoietin [17]. The activity was partially separated using a CO<sub>2</sub>-supercritical liquid extraction method; a low-pressure extract exhibited essentially no survival-shortening activity while the residual oil fraction had high activity [17].

### Microarray Analysis of Gene Expression in SHRSP Rat Tissues

Significant differences in gene expression were detected in the tissues of the canola oil and soybean oil groups. Genes for some isoforms of K<sup>+</sup> channels were over-expressed while those for a few other K<sup>+</sup> channels were under-expressed in the liver of canola-oil group. Two to three vitamin K-related genes were over-expressed in the testis and adrenal of the canola-oil group (Table 1), suggesting that the putative factors affected vitamin K-related reactions.

### Dihydro-vitamin K1 as a Potential Stroke-Stimulating Factor in the Hydrogenated Soybean Oil

Vitamin K1 (phylloquinone) contents are relatively high in vegetable oils such as soybean oil (210 µg/100 g) and canola oil (120 µg/100 g). One of the 4 isoprenyl units of the side chain of vitamin K1 is unsaturated but is converted in many tissues of mammals into vitamin K2 (menaquinone 4) with 4 unsaturated isoprenyl units (Fig. 1). When vegetable oils are partially hydrogenated, the dihydro-form of K1 (dihydro-K1) is formed [18], which cannot be converted to K2 by animals [19, 20]. The physiological activities of K1 and K2 differ; dihydro-K1 is partially active in reducing the formation of PIVKA (protein induced by vitamin K absence) but is essentially inactive in restoring the formation of under-carboxylated osteocalcin in humans [19]. Thus, dihydro-K1 in the hydrogenated soybean and canola oils is a likely factor that accelerates bleeding tendencies, stimulates the onset of stroke and shortens the survival in SHRSP rats. Because dihydro-K1 is not a major component in common vegetable oils, the presence of substances with properties similar to those of dihydro-K1 is suspected in canola and other vegetable oils. Canola and hydrogenated soybean oil elicited common physiological effects on SHRSP rats including lesions in

**Table 1** Vitamin K-related genes differentially expressed in SHRSP rats fed a diet supplemented with canola oil or soybean oil—results of DNA microarray analysis

Tissues	Genes supposed to be related with vitamin K	Can/Soy <sup>a</sup>
Liver	Bone gamma-carboxyglutamic acid (Gla) protein (osteocalcin)	0.40
	Protein C	0.21
Adrenal	<i>Rattus norvegicus</i> Matrix Gla protein (Mgp), mRNA.	1.52
	Similar to Protein:NP_032623 matrix gamma-carboxyglutamate (gla) protein	1.45
Testis	<i>Rattus norvegicus</i> Matrix Gla protein (Mgp), mRNA.	2.37
	Similar to Protein:NP_032623 matrix gamma-carboxyglutamate (gla) protein	2.04
	Similar to Translation of nuc:S78744_1 protein S = activated protein C cofactor [rats, liver, mRNA, 3315 nt]; activated protein C cofactor (?)	1.67

<sup>a</sup> Ratio of gene expressed in canola oil group to that in soybean oil group

the kidney and testis, decreased platelet counts, accelerated onset of stroke and shortened survival [10, 17 and unpublished observations].

### Inter-Esterified Oils between Animal Fats and High-ALA Vegetable Oils as Alternatives of Hydrogenated Vegetable Oils (*trans*-Fatty Acids)

Partial hydrogenation of vegetable oils produces isomers of *cis* and *trans*-fatty acids as well as dihydro-K1 described above. The *trans*-fatty acids have been recognized as a risk factor for coronary heart disease (CHD), although the relative risk from an increased intake of *trans*-fatty acid is relatively small (( 1.5) [21] and not always statistically significant [22]. However, partially-hydrogenated canola

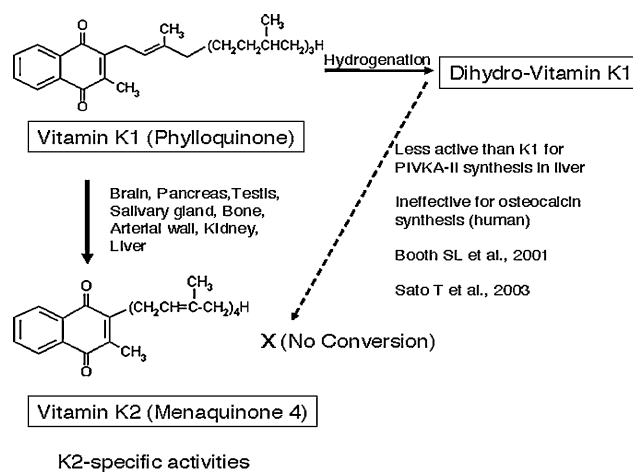


**Fig. 1** Vitamin Ks and their physiological activities



and soybean oil are not safe in animal experiments; they shorten the survival of SHRSP rats compared with diets containing butter, lard and an oil prepared by inter-esterification between lard and perilla oil [23, 24]. Animal fats are safer than many kinds of vegetable oils with anti-nutritional activities as described further below.

### Cancer-Promoting Activities of Some Vegetable Oils

Another aspect to be considered is the cancer-promoting activity of some kinds of vegetable oils. We understand that an enhanced activity of the arachidonate (ARA) cascade and associated persistent inflammation are major causes for many types of cancers, and therefore oils with high  $\omega 6/\omega 3$  ratios promote and those with low ratios (perilla oil, flaxseed oil, fish oil) suppress carcinogenesis; oleate ( $\omega 9$ )-rich oils are generally weaker than LNA ( $\omega 6$ )-rich oils in promoting carcinogenesis [25]. Additional evidence that support these concepts is that many kinds of drugs that inhibit the LNA-ARA cascade suppress carcinogenesis, and that knockouts of genes related to the production of ARA-metabolites (eicosanoids) and their receptors are effective in suppressing carcinogenesis in mice.

However, the cancer-promoting activities of oils are not simply accounted for by their fatty acid compositions. For example, the relative activities of olive oil, high-LNA safflower oil and perilla oil were 4:2:1 in promoting colon carcinogenesis in rats [26]. Palm oil (palm-olein) with a fatty acid composition similar to that of olive oil was as active as high-LNA safflower oil in promoting colon carcinogenesis [27] while high-oleic safflower oil did not promote colon carcinogenesis in rats [28].

In clinical studies, the level of intake and the plasma concentration of ALA were positively associated with prostate cancer [29]. This is not consistent with the observation that the incidence of prostate cancer is higher but the intake and plasma level of ALA are lower in the USA as compared with those in Japan. Moreover, high-ALA perilla oil suppressed carcinogenesis in the prostate compared with animal fats in rats [30]. All these observations suggest that there are agents other than fatty acids present in some vegetable oils, which are associated with carcinogenesis [31].

The presumed anti-nutritional factors in some vegetable oils should not be overlooked and efforts to identify them need to be promoted.

### Conclusion

The consequences of long-term feeding must be evaluated in estimating the effects of fats and oils on healthy ageing.

Oils with relatively low  $\omega 6/\omega 3$  ratios (perilla oil, flaxseed oil, fish oil) are suggested to be beneficial for healthy ageing. The importance of putative anti-nutritional factors other than fatty acids (triacylglycerol) and phytosterols, e.g., dihydro-vitamin K1, is noted. Such factors appear to be associated with bleeding tendencies and cancer promotion, and hence with unhealthy ageing.

**Acknowledgments** This work was supported in part by a grant for the promotion of sciences in private universities from the Ministry of Education, Culture, Sports, Science and Technology, Japan.

### References

1. Sinclair DA (2005) Toward a unified theory of caloric restriction and longevity regulation. *Mech Ageing Dev* 12:987–1002
2. Yamamoto N, Okaniwa Y, Mori S, Nomura M, Okuyama H (1991) Effects of a high-linoleate and a high- $\alpha$ -linolenate diet on the learning ability of aged rats. *J Gerontol* 46:B17–22
3. Minami M, Kimura S, Endo T, Hamaue N, Hirafuji M, Monma Y, Togashi H, Yoshioka M, Saito H, Watanabe S, Kobayashi T, Okuyama H (1997) Effects of dietary docosahexaenoic acid on survival time and stroke-related behavior in stroke-prone spontaneously hypertensive rats. *Gen Pharmacol* 29:401–407
4. Nakashima Y, Yuasa S, Fukamizu Y, Okuyama H, Ohara T, Kameyama T, Nabeshima T (1993) Effect of a high linoleate and a high  $\alpha$ -linolenate diet on general behavior and drug sensitivity in mice. *J Lipid Res* 34:239–247
5. Umezawa M, Ohta A, Tojo H, Yagi H, Hosokawa M, Takeda T (1995) Dietary alpha-linolenate/linoleate balance influences learning and memory in the senescence-accelerated mouse (SAM). *Brain Res* 669:225–233
6. Yoshida S, Yasuda A, Kawazato H, Sakai K, Shimada T, Takeshita M, Yuasa S, Kobayashi T, Watanabe S, Okuyama H (1997) Synaptic vesicle ultrastructural changes in the rat hippocampus induced by a combination of alpha-linolenate deficiency and a learning task. *J Neurochem* 68:1261–1268
7. Huang M-Z, Naito Y, Watanabe S, Kobayashi T, Kanai H, Nagai H, Okuyama H (1996) Effect of rapeseed and dietary oils on the mean survival time of stroke-prone spontaneously hypertensive rats. *Biol Pharm Bull* 19:554–557
8. Miyazaki M, Huang M-Z, Takemura N, Watanabe S, Okuyama H (1998) Free fatty acid fractions from some vegetable oils exhibit reduced survival time-shortening activity in stroke-prone spontaneously hypertensive rats. *Lipids* 33:655–661
9. Yasugi T, Tojihara T, Fujioka T, Kato S, Saito E, Mitsui E, Ito T, Ueno T, Kanno H, Yamada T (1990) Eicosapentaenoic acid and apoplexy. Influence of EPA loading on SHRSP. *Ann NY Acad Sci* 598:324–338
10. Miyazaki M, Huang M-Z, Watanabe S, Kobayashi T, Okuyama H (1998) Early mortality effect of partially hydrogenated vegetable oils in stroke-prone spontaneously hypertensive rats (SHRSP). *Nutr Res* 18:1049–1056
11. Ratnayake WM, Plouffe L, Hollywood R, L'Abbe MR, Hidiroglou N, Sarwar G, Mueller R (2000) Influence of sources of dietary oils on the life span of stroke-prone spontaneously hypertensive rats. *Lipids* 35:409–420
12. Ratnayake WMN, L'Abbe MR, Muller R, Hayward S, Plouffe L, Hollywood R, Trick K (2000) Vegetable oils high in phytosterols make erythrocytes less deformable and shorten the life span of stroke-prone spontaneously hypertensive rats. *J Nutr* 130:1166–1178

13. Tatematsu K, Fuma S, Nagase T, Ichikawa Y, Fujii Y, Okuyama H (2004) Factors other than phytosterols in some vegetable oils affect the survival of SHRSP rats. *Food Chem Toxicol* 42:1443–1451
14. Ogawa H, Yamamoto K, Kamisako K, Meguro T (2003) Phytosterol additives increase blood pressure and promote stroke onset in salt-loaded stroke-prone spontaneously hypertensive rats. *Clin Exp Pharmacol Physiol* 30:919–924
15. Innis SM, Dyer RA (1999) Dietary canola oil alters hematological indices and blood lipids in neonatal piglets fed formula. *J Nutr* 129:1261–1268
16. Naito Y, Yoshida H, Nagata T, Tanaka A, Ono H, Ohara N (2000) Dietary intake of rapeseed oil or soybean oil as the only fat nutrient in spontaneously hypertensive rats and Wistar Kyoto rats—blood pressure and pathophysiology. *Toxicology* 146:197–208
17. Ohara N, Naito Y, Nagata T, Tatematsu K, Fuma SY, Tachibana S, Okuyama H (2006) Exploration for unknown substances in rapeseed oil that shorten survival time of stroke-prone spontaneously hypertensive rats. Effects of super critical gas extraction fractions. *Food Chem Toxicol* 44:952–963
18. Booth SL, Pennington JAT, Sadowski JA (1996) Dihydro-vitamin K<sub>1</sub>: primary food source and estimated dietary intakes in the American diet. *Lipids* 31:715–720
19. Booth SL, Lichtenstein AH, O'Brien-Morse M, McKeown NM, Wood RJ, Saltzman E, Gundberg CM (2001) Effects of a hydrogenated form of vitamin K on bone formation and resorption. *Am J Clin Nutr* 74:783–790
20. Sato T, Ozaki R, Kamo S, Hara Y, Konishi S, Isobe Y, Saitoh S, Harada H (2003) The biological activity and tissue distribution of 2',3'-dihydrophyloquinone in rats. *Biochim Biophys Acta* 1622:145–150
21. Oh K, Hu FB, Manson JE, Stampfer MJ, Willett WC (2005) Dietary fat intake and risk of coronary heart disease in women. *Am J Epidemiol* 161:672–679
22. Ascherio A, Rimm EB, Giovannucci EL, Spiegelman D, Stampfer M, Willett WC (1996) Dietary fat and risk of coronary heart disease in men: cohort follow up study in the United States. *BMJ* 313:84–90
23. Tatematsu K, Hirose N, Ichikawa Y, Fujii Y, Takami A, Okuyama H (2004) Nutritional evaluation of an inter-esterified perilla oil and lard in comparison with butter and margarine based on the survival of stroke-prone spontaneously hypertensive (SHRSP) rats. *J Health Sci* 50:108–111
24. Tatematsu K, Fuma S, Satoh J, Ichikawa Y, Fujii Y, Okuyama H (2004) Dietary canola oil and soybean oil fed to SHRSP rat dams differently affect the growth and survival of their male pups. *J Nutr* 134:1347–1352
25. Okuyama H, Kobayashi T, Watanabe S (1996) Dietary fatty acids—the N-6/N-3 balance and chronic elderly diseases. Excess linoleic acid and relative N-3 deficiency syndrome seen in Japan. *Prog Lipid Res* 35:409–457
26. Onogi N, Okuno M, Komaki C, Moriwaki H, Kawamori T, Tanaka T, Mori H, Muto Y (1996) Suppressing effect of perilla oil on azoxymethane-induced foci of colonic aberrant crypts in rats. *Carcinogenesis* 17:1291–1296
27. Narisawa T, Takahashi M, Kotanagi H, Kusaka Y, Yamazaki H, Koyama H (1991) Inhibitory effect of dietary perilla oil rich in n-3 polyunsaturated fatty acid  $\alpha$ -linolenic acid on colon carcinogenesis in rats. *J Cancer Res* 82:1089–1096
28. Takeshita M, Ueda H, Shirabe K, Higuchi Y, Yoshida S (1997) Lack of promotion of colon carcinogenesis by high-oleic safflower oil. *Cancer* 79:1487–1493
29. Godley PA, Campbell MK, Gallgher P, Martinson FE, Mohler JL, Sandler RS (1996) Biomarkers of essential fatty acid consumption and risk of prostatic carcinoma. *Cancer Epidemiol Biomarkers Prev* 5:889–895
30. Mori T, Imaida K, Tamano S, Sano M, Takahashi S, Asamoto M, Takeshita M, Ueda H, Shirai T (2001) Beef tallow, but not perilla or corn oil, promotion of rat prostate and intestinal carcinogenesis by 3,2'-dimethyl-4-aminobiphenyl. *Jpn J Cancer Res* 92:1026–1033
31. Shields PG, Xu GX, Blot WJ, Fraumeni JF Jr, Trivers GE, Pellizzari ED, Qu YH, Gao YT, Harris CC (1995) Mutagens from heated Chinese and US cooking oils. *J Natl Cancer Inst* 87:836–841

# Oleoyl-Estrone Treatment to Late Pregnant and Mid-Lactating Rats Affects the Expression of Lipid Metabolism Genes

Beatriz García-Peláez · Ruth Vilà · Xavier Remesar

Received: 20 April 2007 / Accepted: 29 May 2007 / Published online: 11 July 2007  
© AOCs 2007

**Abstract** The purpose of this study was to determine whether OE treatment affects the expression of genes related to lipid metabolism under two physiological conditions: late pregnancy and mid-lactation, both characterized by lipid mobilization. Samples of periovarian and retroperitoneal adipose tissue from 21-day pregnant or 15-day lactating dams were used. The expression of LPL, FATP1, FABP4, HSL, ACC1, FAS, PEPCK, GLUT4, PDK4, SREBP1c, adiponutrin and leptin, were compared with their expression in virgin rats. In pregnant rats, FABP4, HSL, PEPCK and PDK4 were over expressed in the periovarian site compared to virgin rats, whereas adiponutrin, FAS, GLUT4 and SREBP1c were underexpressed; the retroperitoneal fat depot showed a similar pattern but ACC1 and leptin were also underexpressed. OE treatment caused a generalized decrease in gene expression in both adipose depots. In lactating dams, the gene expression profile at the periovarian depot was similar to that observed in pregnant rats. OE treatment mimicked the trend observed in pregnant rats, although the intensity of the gene expression changes was lower. After OE treatment, the retroperitoneal adipose depot showed a completely different pattern since the values were close to those of virgin rats. These results corroborate that OE effects in adipose tissue, lowering lipids and depressing their metabolism, already described under

other physiological situations, can be also found in late pregnancy and lactation.

**Keywords** Oleoyl-estrone · Gene expression · White adipose tissue · Late pregnancy · Mid-lactation

## Abbreviations

ACC1	Acetyl coA carboxylase 1
ARBP	Acidic ribosomal binding protein
FABP4	Fatty acid binding protein 4
FAS	Fatty acid synthetase
FATP1	Fatty acid transport protein 1
GLUT4	Glucose transporter 4
HSL	Hormone sensitive lipase
LPL	Lipoprotein lipase
OE	Oleoyl-estrone
PDK4	Pyruvate dehydrogenase kinase 4
PEPCK	Phospho enol pyruvate carboxy kinase
SREBP1c	Sterol regulatory element binding protein 1c
WAT	White adipose tissue

## Introduction

Oleoyl-estrone is synthesized from estrone by adipose cells [1] and released into the bloodstream. Treatment with OE leads to a decrease in food intake that is initially paralleled by a decrease in body weight. The experimental use of OE in rats cause a significant decrease in body fat, with no alteration in protein content [2, 3] consequently, it has been considered a lipostatic signal that can help regulate body fat mass [4] through the selective reduction at specific sites [5]. The mechanism of the action of OE remains yet to be

B. García-Peláez · R. Vilà · X. Remesar (✉)  
Departament de Nutrició i Bromatologia,  
Facultat de Biologia, Universitat de Barcelona,  
Av. Diagonal, 645, 08028 Barcelona, Spain  
e-mail: xremesar@ub.edu

R. Vilà · X. Remesar  
Ciber Fisiopatología Obesidad y Nutrición (CB06/03)  
Instituto de Salud Carlos III, Madrid, Spain

fully elucidated; however, the involvement of specific receptors other than classical oestrogen receptors has been postulated [6].

The administration of OE during the reproductive cycle provokes a pattern of body fat reduction similar to that of virgin rats [7]. Oleoyl-estrone effects can be detected both in the dam and her litter. In spite of their differential traits, physiological adaptation to pregnancy or lactation share huge metabolic pressure of energy demands that necessarily affect their lipid reserves [8, 9].

The changes elicited by OE treatment on adipose tissue are in part due to apoptosis [10], despite the lack of uniformity in the OE response in different adipose tissue sites. Induction of apoptosis coexists with changes in adipose tissue lipid metabolism [10].

The objective of the present study was to determine how OE treatment affects the expression of lipid metabolism related genes under the conditions of intense energy demands of late pregnant rats and mid-lactating dams.

## Materials and Methods

### Animals

Female virgin Wistar rats (Harlan-Interfauna, Sant Feliu de Codines, Spain) were used. A group ( $n = 6$ ) of intact animals was sacrificed and used as reference (virgin rats). The remaining stock ( $n = 24$ ) was mated with adult males until impregnation (detected by the presence of spermatozoa in daily vaginal smears). The day of impregnation was considered as day 0. The litters were limited to 10 pups immediately after delivery to limit the variability that may be derived from litter size. Animals were kept under standard conditions (12 h light cycle, 22 °C and 65% humidity) and had free access to standard chow pellet (Panlab, Barcelona, Spain) (digestible energy, 13.26 MJ kg<sup>-1</sup>) and water. All procedures were in accordance with the guidelines for the use of experimental animals established by the European Union, Spain and Catalonia, and were specifically approved by the Animal Handling and Ethics Committee of the University of Barcelona.

From days 11–21 of pregnancy, a group of six animals were given a daily intragastric gavage of 0.2 mL sunflower oil containing 10 μmol oleoyl-estrone kg<sup>-1</sup> of body weight (OED, Barcelona, Spain) (treated group). The control group ( $n = 6$ ) received a daily intragastric gavage of 0.2 mL sunflower oil during the same period (non-treated group). The remaining pregnant rats ( $n = 12$ ) were allowed to deliver normally and were randomly divided into two groups of six dams each: those in the first group received a

daily intragastric gavage (from day 1 to day 15 after delivery) of 10 μmol oleoyl-estrone kg<sup>-1</sup> (treated group); and the second group received only the vehicle (non-treated group). Each pregnant rat or dam plus its litter were placed in individual cages. Daily consumption of food and body weight, both of pregnant rats and lactating dams and of their respective offspring were measured. Pregnant rats were killed by decapitation on day 21, and lactating dams on day 15 after delivery.

### Tissue Samples

Periovarian and retroperitoneal WAT were dissected, immediately frozen in liquid nitrogen and stored at -80 °C until processed. DNA content was measured in WAT samples using a standard fluorimetric method with 3,5-diaminobenzoic acid (Sigma, MO, USA) using bovine thymus DNA as a standard [5]. Since all mammal cell nuclei contain the same amount of DNA (about 6 pg cell<sup>-1</sup>), we estimated the approximate number of cells in a given WAT depot by dividing its DNA content by the mean DNA content of a cell. The mean mass of the cells in a given WAT site was determined by dividing the weight of the tissue by the number of cells it contained [5].

### RNA Isolation

Total RNA was extracted from adipose tissue using the Tripure isolation reagent (Roche, Mannheim, Germany). RNA concentration and quality were measured by spectrophotometric analysis at 260 and 280 nm using a Nanodrop spectrophotometer (Wilmington DE, USA), RNA integrity was assessed by agarose gel electrophoresis.

### Real-Time PCR

The selected targets for Real-Time PCR were: LPL, FATP1, FABP4, HSL, ACC1, FAS, PEPCK, GLUT4, PDK4, SREBP1c, adiponutrin, leptin; ARBP was used as control gene.

Specific mRNA levels were determined by semi-quantitative real-time PCR. To disrupt the potential formation of secondary structures, 2 μg total RNA and 40 μg oligo dT primers (Roche) in 10 μL were incubated for 5 min at 70 °C and then chilled on ice. Complementary cDNA was synthesized by adding: 200 U MMLV RT (Promega, Madison WI, USA), 25 U RNAsin (Promega), 0.5 mM dNTPs (GeneCraft, Lüdinghausen, Germany) and MMLV RT buffer. Twenty-five μL of reaction mixture was incubated at 42 °C for 60 min with the cDNA product used for the subsequent PCR amplification with specific primers.

The PCR mixture (10  $\mu$ L final volume) contained ca. 8 ng cDNA, Power SYBR Green PCR Mastermix (Applied Biosystems), and 300 nM of forward and reverse primers. Taq Man primers and the probe for LPL (assay ID: Rn 00561482\_ml) were assay-on-demand (AoD) selected gene expression products (Applied Biosystems). The PCR mixture (10  $\mu$ L initial volume) contained 8 ng cDNA and 1X iQ Supermix (Bio-Rad, Hercules CA, USA), with a final concentration of 250 nM for the probe and 900 nM for each primer. The thermal conditions were: initial denaturation of cDNA (10 min at 95 °C); amplification of target cDNA (denaturation 15 s at 95 °C and 40 cycles of amplification for 1 min at 60 °C). A melting curve analysis was performed in the SYBR assay to identify the product and discard the presence of dimmers.

The real-time assay was performed using a 7900 HT instrument (Applied Biosystems, Foster City CA, USA). The expression of rat FAS, FATP1, FABP4, HSL, ACC1, PEPCK, GLUT4, PDK4, SREBP1c, adiponutrin, leptin and ARBP mRNA was analyzed using SYBR Green (Sigma, St Louis MO, USA), and LPL, using Taq Man methodology (Gene Link, Hawthorne NY, USA). The signals corresponding to ARBP mRNA were used to normalize the changes in mRNA levels for each gene.

Primers from genes analyzed by SYBR Green were designed (Primer 3 program) to be exon spanning to avoid amplification of genomic DNA. PCR products were resolved on 2% agarose gel to confirm the amplification length. Primer sequences are shown in Table 1.

#### Data Analysis

Results were calculated using the “comparative Ct method of quantification” ( $\Delta\Delta$  Ct). Each target gene was analyzed separately and normalized to the expression of the internal standard ARBP. The normalization accounts for the possible variability in RNA quantity and integrity and the different efficiency of the reverse transcription process. To determine the quantity of the target gene-specific transcripts present in treated and untreated samples, their respective Ct values were first normalized by subtracting the Ct values obtained from the Ct value of the ARBP gene ( $\Delta$  Ct = Ct target – Ct ARBP). The concentration of the gene-specific mRNA in treated and untreated samples relative to the virgin group was calculated by subtracting the normalized Ct values of the treated/untreated samples from the Ct values of the virgin group ( $\Delta\Delta$  Ct =  $\Delta$  Ct treated/untreated –  $\Delta$  Ct virgin). The relative concentration was determined by  $2^{-\Delta\Delta$  Ct} method (arbitrary units) [11]. Differences were calculated considering the virgin samples as a reference control. Statistical differences were calculated among the three groups.

**Table 1** Forward and reverse primer sequences for PCR amplification and the length of the PCR product

FAS	5'-CTTGGGTGCCGATTACAACC-3' 5'-GCCCTCCCGTACTACTACTC-3' (163 bp)
ACC1	5'-AGGAAGATGGTGTCCCGCTCTG-3' 5'-GGGGAGATGTGCTGGGTCAT-3' (145 bp)
Adiponutrin	5'-GTGTGCCCGAATGACCATGT-3' 5'-GCCTTGGGGTTTGTGGAGAG-3' (112 bp)
PEPCK	5'-CCCCCTGTCTACGAAGCTC-3' 5'-ACCTTGCCCTTATGCTCTGC-3' (99 bp)
GLUT4	5'-CTTGATGACGGTGGCTCTGC-3' 5'-CACAATGAACCAGGGGATGG-3' (127 bp)
PDK4	5'-GTCAGGCTATGGGACAGATGC-3' 5'-TTGGGGATACACCAGTCATCAGC-3' (137 bp)
SREBP1c	5'-AAACCAGCCTCCCCAGAGC-3' 5'-CCAGTCCCCATCCACGAAGA-3' (153 bp)
FABP4	5'-CCTTTGTGGGGACCTGGAAA-3' 5'-TGACCGGATGACGACCAAGT-3' (152 bp)
HSL	5'-CCCATAAGACCCCATTCCTG-3' 5'-CTGCCTCAGACACACTCCTG-3' (93 bp)
FATP	1 5'-GTGCGACAGATTGGCGAGTT-3' 5'-GCGTGAGGATACGGCTGTTG-3' (106 bp)
Leptin	5'-CGGTTCCCTGTGGCTTTGGTC-3' 5'-CCGACTGCGTGTGTGAAATG-3' (130 bp)
ARBP	5'-GAGCCAGCGAAGCCACACT-3' 5'-GATCAGCCCGAAGGAGAAGG-3' (62 bp)

#### Statistical Methods

Values for the real-time PCR analyses are expressed as the mean ( $\pm$ SEM). Data were evaluated using the unpaired Student's *t* test with Prism 4.0 software (GraphPad Software, San Diego CA, USA). Table 2 data have been analysed with an unpaired Student's *t* test and data are the mean ( $\pm$  SEM) of six animals. In both analyses, differences in *P*-values < 0.05 were considered statistically significant.

#### Results

Table 2 shows the body and adipose tissue depot weights of virgin, 21-day pregnant and 15-day lactating rats. Food intake was decreased in OE-treated groups both in pregnancy and lactation. OE-treatment decreased body weight in both pregnant and lactating versus non-treated dams; this is largely due to the marked loss of weight of white adipose tissue in the periovarian and retroperitoneal sites. In pregnant rats, these decreases were mainly the consequences of the loss of cells, which was not observed in lactating dams. In the latter, the periovarian depot showed a

**Table 2** Weight of 21-day pregnant and 15-day lactating dams before and after OE-treatment

	Virgin rats	21-day pregnant		15-day lactating	
		Non-treated	OE-treated	Non-treated	OE-treated
<b>Animal Weight</b>					
Initial (g)	220 ± 3.15	232 ± 2.75	249 ± 7.54	226 ± 7.61	233 ± 2.31
Beginning of treatment (g)		268 ± 3.52	275 ± 9.23	258 ± 11.4	262 ± 5.18
End of treatment (g)		360 ± 8.18	308 ± 12.7*	300 ± 9.73	273 ± 3.02*
<b>Food intake during</b>					
Treatment (g)		242 ± 16.2	143 ± 13.9*	605 ± 48.0	467 ± 15.2*
<b>Tissue</b>					
Periovarian WAT weight (g)	3.60 ± 0.26	7.44 ± 1.61+	3.58 ± 0.71*	3.51 ± 0.57	1.66 ± 0.11+*
Mean cell mass (ng)	11.9 ± 0.95	16.2 ± 3.85	14.1 ± 1.45	9.41 ± 0.84	7.02 ± 1.50
Cell number (×10 <sup>6</sup> )	269 ± 52.2	559 ± 128	243 ± 26.5*	371 ± 50.9	239 ± 43.6
Retroperitoneal WAT weight (g)	1.93 ± 0.22	4.69 ± 0.78+	2.05 ± 0.21*	1.63 ± 0.36	1.57 ± 0.23
Mean cell mass (ng)	11.2 ± 0.76	22.1 ± 2.11+	21.2 ± 2.73+	11.9 ± 1.19	8.70 ± 2.33
Cell number (×10 <sup>6</sup> )	177 ± 24.6	212 ± 34.5	99.4 ± 7.13+*	131 ± 22.9	187 ± 33.9

Changes in cell mass and in cell number were calculated from the DNA content and the tissue weight. The results are the mean (± SEM) of six animals. Statistical differences (unpaired Student's *t* test): + = *P* < 0.05 versus virgin rats; \* = *P* < 0.05 versus Non-treated group

diminution in cell numbers while retroperitoneal WAT site increased the number of cells.

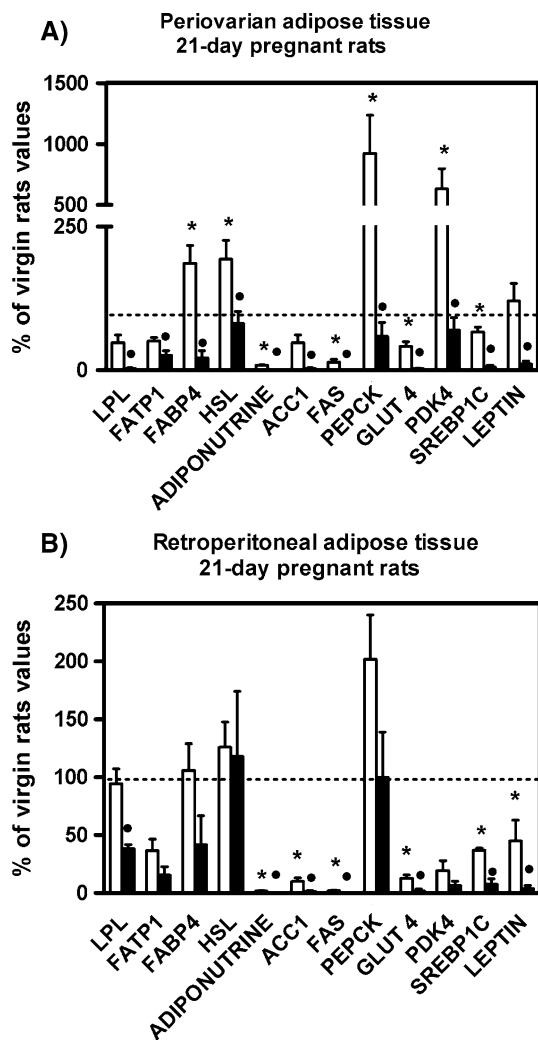
Figure 1 presents the effects of OE on the expression of different genes involved in lipid metabolism in two WAT locations of late pregnant rats. The dotted line represents the expression of these genes in virgin rats as it is used as a reference for intact rats. The effect of OE-treatment versus non-treated animals is also shown. In the periovarian site, OE induced a significant overexpression of FABP4, HSL, PEPCK and PDK4, and adiponutrin. FAS, GLUT4 and SREBP1c were underexpressed compared with virgin controls. OE treatment caused a generalized, significant decrease in the expression of all the genes analyzed. The gene expression pattern in retroperitoneal WAT was similar to that of the periovarian; in general terms, OE-treatment tended to lower gene expression.

Figure 2 shows the effect of OE-treatment on the expression of the same genes in mid-lactating rats compared with virgin controls. In lactating dams there was a general trend to under expression in periovarian WAT. The differences became statistically significant for FABP4, adiponutrin, ACC1, FAS, GLUT4, SREBP1c and leptin. In general, the effects of OE treatment were less marked than those observed in late pregnancy. Gene expression was significantly decreased for FABP4, HSL, PEPCK, PDK4, SREBP1c and leptin. The pattern of expression of retroperitoneal WAT was again different, since PEPCK was significantly over expressed in comparison with virgin controls, whereas practically all the other genes studied were under expressed; in comparison with the other tissues analysed retroperitoneal WAT gene expression tended to increase under OE treatment. The final expression levels

for most of these genes were in the same range of those of virgin rats. Nevertheless, the degree of over expression versus virgin controls was slightly lower in the retroperitoneal than in the periovarian WAT site; OE-treatment induced changes brought the expression of most of the studied genes closer to those of virgin controls.

## Discussion

In the last third of pregnancy, the net lipolytic situation [12] may be the compounded consequence of increased expression of lipolytic (i.e., HSL) and decreased lipogenic enzymes (FAS, ACC1), thus shifting the equilibrium towards triacylglycerol mobilization. In previous studies [13], late pregnancy induced a decrease LPL and an increase HSL expression and activity in rat retroperitoneal adipose tissue. Our data reinforce these findings, although the main changes were only observed in periovarian WAT. In pregnant women, decreased GLUT4 expression has been reported [14], and can be linked to a decline in glucose uptake and further utilization during pregnancy. Thus, the increases in the PEPCK and PDK4 (a key regulatory component of the pyruvate dehydrogenase complex), the main control enzymes of the amino acid hydrocarbon skeleton catabolic pathway, imply the utilization of amino acids as fuel; as a consequence, there is an important *N* outflow that is compatible with the protein catabolic phase described in the last third of pregnancy [15]. In addition, the fatty acids released from triacylglycerols by lipases in WAT may be eventually used for the synthesis of triacylgly-



**Fig. 1** The effects of OE treatment on the expressions of different genes in periovarian (a) and retroperitoneal (b) adipose tissue of late pregnant rats are shown. Bars represent the expression of the genes as percentage of the expression found in virgin rats. White bars non-treated rats. Black bars OE-treated rats. The horizontal dotted line represents the 100% values for each individual gene, i.e., the virgin rats' expression. The data are the mean ( $\pm$ SEM) of six different animals. Statistical differences Student's *t* test. \**P* < 0.05 versus virgin rats. •*P* < 0.05 versus non-treated rats

cerols in the mammary gland, after their uptake by the liver and incorporation into Very Low Density Lipoproteins responsible for the late pregnancy hypertriglyceridemia [16].

The differences between the expression patterns found in these two WAT sites may be just a manifestation of their intrinsic metabolic differences since WAT site distribution deeply affects their handling of lipids, their sensitivity to hormones and their signalling protein patterns and effectiveness [17]. In late pregnancy, the low lipolytic capacity in the retroperitoneal WAT could indicate lower triacylglycerol degradation than periovarian WAT and thus

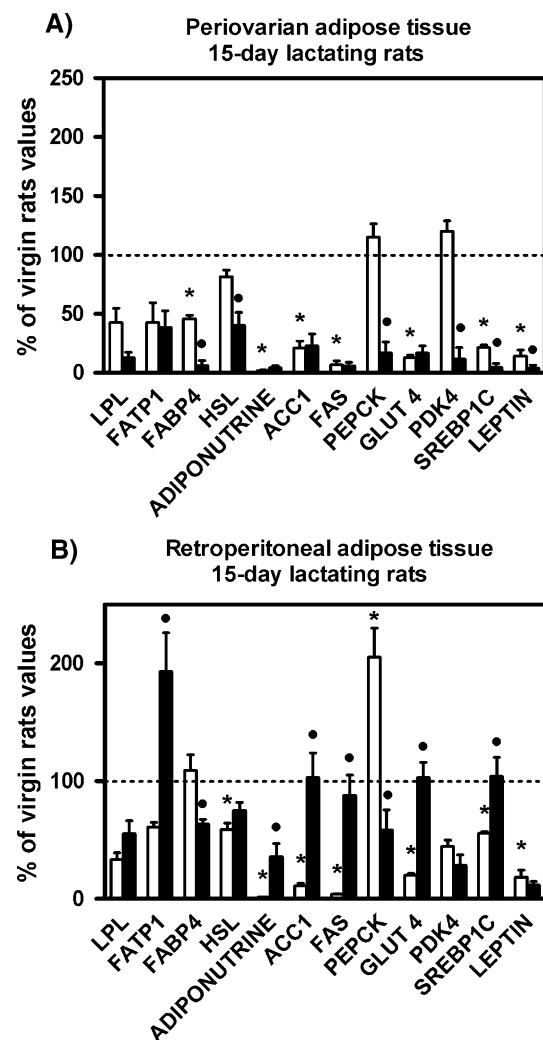


**Fig. 2** Effects of OE treatment on the expressions of different genes in periovarian (a) and retroperitoneal (b) adipose tissue of mid-lactating dams. Bars represent the expression of the genes as percentage of the expression in virgin rats. White bars non-treated rats. Black bars OE-treated rats. The horizontal dotted line represents the 100% values for each individual gene, i.e., the virgin rats' expression. The data are the mean ( $\pm$  SEM) of six different animals. Statistical differences: Student's *t* test. \**P* < 0.05 versus virgin rats. •*P* < 0.05 versus non-treated rats

coincide with the described storage role, ready to use, in the lactation period [18].

OE treatment induces a net reduction in the expression of key lipid metabolism enzymes in adipose tissue, especially in the periovarian site. This process is partly mediated by apoptosis [10], which justifies the changes in cellularity observed. The decreases in the expression of the lipogenic enzymes (ACC1 and FAS), and a decreased synthesis, as shown by the low SREBP1c expression [19], may contribute to the net lipolytic balance. This imbalance leads to the observed decrease in adipose tissue mass, which in turn results in lowered expression of leptin, as

indicator of fat store size [20]. The overall low gene expression levels caused by OE treatment in both tissue depots, confirms the importance of OE in the regulation of WAT lipid handling.

In mid-lactation, the high metabolic pressure exerted on the dam's own metabolism to produce the milk needed to rear the pups [9], results in a transient mobilization of subcutaneous adipose tissue lipids [21]. In consequence, the weights of individual adipose depots are close to those of virgin rats, but lower than those found in late-pregnant rats. It seems logical to assume that this may be a consequence of the low levels of expression of enzymes or transcription factors related to lipid synthesis and transport, such as ACC1, FAS, FABP4 and SREBP1c in the periovarian site. The decrease of leptin expression during lactation reflects the reduction of adipose mass [22]. The retroperitoneal pattern of expression differs from the periovarian in the potential decrease in lipolytic activity (HSL), which is accompanied by a parallel increase in the utilization of amino acid hydrocarbon skeleton mainly for glycerogenesis, as indicated by the PEPCK increase. Since the rate of fatty acids release from adipose tissue depends on the balance between lipolysis and re-esterification [23], we can postulate that in this adipose tissue depot, the shift is less lipolytic than in the periovarian, in spite of the low lipogenesis rate; this may help explain the lack of significant changes in the adipose tissue mass versus virgin rats.

The effects of OE treatment in lactation again result in marked differences between the adipose locations studied. In the periovarian depot, OE treatment tended to either maintain or decrease lipid metabolism gene expression, whereas in the retroperitoneal WAT, OE in general increased lipid metabolism and lipid content gene expression. This may be explained by the similarity in weight and cell number of this site in relation with non-treated dams. Thus, we can safely assume that retroperitoneal WAT is more sensitive to OE than periovarian. The results agree with OE inducing the recovery of normal metabolic parameters at the peak of lactation when the maximal metabolic pressure has been achieved [24]; from then on, lipids from adipose tissue use for milk production will sharply decrease [25]. The differential trend shown by these two adipose sites suggests that OE action on WAT is susceptible of adaptation to particular metabolic physiological situations.

The different metabolic and hormonal status that the physiological conditions studied represent, together with the specific hormonal or paracrine status of each adipose depot markedly influences gene expression. The effects of OE-treatment modify the expression of the genes analysed, both in pregnancy or lactation and in both tissue locations; the retroperitoneal adipose tissue of lactating rats being the most sensitive to OE-treatment. In any case, further studies

are necessary to determine the differential mechanism of action of OE in the adipose tissue locations.

**Acknowledgments** Thanks are given to the Language Advisory Service of the University of Barcelona for revision of the manuscript. This work was partially funded by Fondo de Investigaciones Sanitarias (PI052179) from Spanish Government.

## References

- Esteve M, Savall P, Virgili J, Fernández-López JA, Remesar X, Alemany M (2001) Modulation by leptin, insulin and corticosterone of oleoyl-estrone synthesis in cultured 3T3L1 cells. *Biosci Rep* 21:755–763
- Sanchis D, Balada F, Grasa MM, Virgili J, Peinado J, Monserrat C, Fernández-López JA, Remesar X, Alemany M (1996) Oleoyl-estrone induces the loss of body fat in rats. *Int J Obes* 20:588–594
- Grasa MM, Cabot C, Esteve M, Yubero P, Masanés RM, Blay MT, Vilà R, López-Martí J, Fernández-López JA, Remesar X, Alemany M (2001) Daily oral oleoyl-estrone gavage induces a dose-dependent loss of fat in Wistar rats. *Obes Res* 9:202–209
- Fernández-Real JM, Sanchis D, Ricart W, Casamitjana R, Balada F, Remesar X, Alemany M (1999) Plasma oestrone-fatty acid ester levels are correlated with body fat mass in humans. *Clin Endocrinol* 50:253–260
- Remesar X, Fernández-López JA, Blay MT, Savall P, Salas A, Díaz-Silva M, Esteve M, Grasa MM, Alemany M (2002) Effect of oleoyl-estrone on adipose tissue composition in male rats. *Int J Obes* 26:1092–1102
- Cabot C, Grasa MM, Masanés RM, de Matteis R, Cinti S, Fernández-López JA, Remesar X, Alemany M (2001) Oleoyl-estrone does not have direct estrogenic effects on rats. *Life Sci* 69:749–761
- García-Peláez B, Vilà R, Remesar X (2007) The administration of oleoyl-estrone to lactating dams induces selective changes in the normal growth pattern of their pups. *Horm Metab Res* (in press)
- López-Luna P, Muñoz T, Herrera E (1986) Body fat in pregnant rats at mid- and late gestation. *Life Sci* 39:1389–1393
- Vernon RG, Pond CM (1997) Adaptations of maternal adipose tissue to lactation. *J Mammary Gland Biol Neoplasia* 2:231–241
- Salas A, Remesar X, Esteve M (2007) Oleoyl-estrone treatment activates apoptotic mechanisms in white adipose tissue. *Life Sci* 80:293–298
- Livak KJ, Schmittgen TD (2001) Analysis of relative gene expression data using real-time quantitative PCR and the  $2^{-\Delta\Delta Ct}$  method. *Methods* 25:402–408
- Chaves JM, Herrera E (1978) In vitro glycerol metabolism in adipose tissue from fasted pregnant rats. *Biochem Biophys Res Commun* 85:1299–1306
- Martín-Hidalgo A, Holm C, Belfrage P, Schotz MC, Herrera E (1994) Lipoprotein lipase and hormone-sensitive lipase activity and mRNA in rat adipose tissue during pregnancy. *Am J Physiol* 226:E930–E935
- Okuno S, Akazawa S, Yasuhi I, Kawasaki E, Matsumoto K, Yamasaki H, Matsuo H, Yamaguchi Y, Nagataki S (1995) Decreased expression of the GLUT4 glucose transporter protein in adipose tissue during pregnancy. *Horm Metab Res* 27:231–234
- Naismith DJ, Morgan BLG (1976) The biphasic nature of protein metabolism during pregnancy in the rat. *Br J Nutr* 36:563–566
- Knopp RH, Bonet B, Lasuncion MA, Montelongo A, Herrera E (1992) Lipoprotein metabolism in pregnancy. In: Herrera E,



- Knopp RH (eds) Perinatal biochemistry. CRC, Boca Raton, pp 19–51
17. Wajchenberg BL (2000) Subcutaneous and visceral adipose tissue: their relation to metabolic syndrome. *Endocr Rev* 21:697–738
  18. Pujol E, Proenza AM, Lladó I, Roca P (2005) Pregnancy effects on rat adipose tissue lipolytic capacity are dependent on anatomical location. *Cell Physiol Biochem* 16:229–236
  19. Jump DB, Botolin D, Wang Y, Xu J, Christian B, Demeure O (2005) Fatty acid regulation of hepatic gene transcription. *J Nutr* 135:2503–2506
  20. Frühbeck G, Gómez-Ambrosi J, Muruzábal FJ, Burrell MA (2001) The adipocyte: a model for integration of endocrine and metabolic signalling in energy metabolism regulation. *Am J Physiol* 280:E827–E847
  21. Remesar X, Arola L, Palou A, Alemany M (1981) Body and organ size and composition during the breeding cycle of the rat (*Rattus norvegicus*). *Lab Animal Sci* 31:67–70
  22. Terada Y, Yamakawa K, Sugaya A, Toyoda N (1998) Serum leptin levels do not rise during pregnancy in age-matched rats. *Biochem Biophys Res Commun* 253:841–844
  23. Hanson RW, Reshef L (2003) Glycerogenesis revisited. *Biochimie* 85:1199–1205
  24. Vernon RG, Flint DJ (1984) Adipose tissue: metabolic adaptations during lactation. *Symp Zool Soc London* 51:119–145
  25. Moore BJ, Inokuchi T, Horwitz BA, Stern J (1989) Maternal brown fat metabolism returns to control level by four weeks post-weaning in rats. *J Nutr* 119:1992–1998

# Consumption of *c9,t11*–18:2 or *t10,c12*–18:2 Enriched Dietary Supplements Does Not Influence Milk Macronutrients in Healthy, Lactating Women

Afroza Hasin · J. Mikko Griinari · Janet E. Williams ·  
Alam M. Shahin · Mark A. McGuire · Michelle K. McGuire

Received: 15 February 2007 / Accepted: 8 June 2007 / Published online: 11 August 2007  
© AOCs 2007

**Abstract** Substantial research suggests that the *t10,c12*–18:2, but not the *c9,t11*–18:2, isomer of conjugated linoleic acid (CLA) reduces milk fat synthesis in lactating bovine and rodent species. Because fat is the major energy-yielding component in human milk, we were interested in whether this is true for women as well. Thus, the effects of *c9,t11*–18:2 and *t10,c12*–18:2 on milk fat were examined in breast-feeding women ( $n = 12$ ) in a double-blind, placebo-controlled, crossover study with latin-square design. The study was divided into six periods: baseline (3 days), three intervention periods (5 days each), and two washout periods (9 days each). During each intervention period,

women consumed 750 mg/day of a supplement containing predominantly *c9,t11*–18:2, *t10,c12*–18:2, or 18:1 (olive oil placebo). Milk was collected by complete breast expression on the final day of each period. Infant milk consumption was estimated by 24 h weighing on the penultimate day of each intervention and washout period, and maternal adiposity (% body fat) was determined at baseline using dual energy X-ray absorptiometry. Milk *c9,t11*–18:2 and *t10,c12*–18:2 concentrations were greater ( $P < 0.05$ ) during the corresponding CLA treatment periods as compared to the placebo period, providing strong evidence of subject compliance. Both CLA isomers were transferred into milk fat at relatively high efficiency; average transfer efficiency was estimated to be 23.3%. Compared to the placebo treatment, milk fat content was not reduced during either CLA treatment. Data indicate that body fatness did not modify any putative effect of isomeric CLA consumption on milk fat concentration. The evidence from this study suggests that the sensitivity of lactating women's mammary tissue to an anti-lipogenic effect of the *t10,c12*–18:2 isoform of CLA may be less than previously hypothesized.

A. Hasin · J. E. Williams · A. M. Shahin · M. K. McGuire (✉)  
Department of Food Science and Human Nutrition,  
Washington State University,  
Pullman, WA 99164-6376, USA  
e-mail: smcguire@wsu.edu

J. M. Griinari  
Department of Animal Science,  
University of Helsinki, Helsinki, Finland

M. A. McGuire  
Department of Animal and Veterinary Science,  
University of Idaho, Moscow, ID 83844-2330, USA

*Present Address:*  
J. E. Williams  
Department of Animal and Veterinary Science,  
University of Idaho, Moscow, ID 83844-2330, USA

*Present Address:*  
A. M. Shahin  
Texas A & M University, College Station,  
TX 77843-2476, USA

**Keywords** Milk fat · Lactation · Human · Conjugated linoleic acid · CLA · *c9,t11*–18:2 · *t10,c12*–18:2

## Abbreviations

BMI	Body mass index
CLA	Conjugated linoleic acid
DEXA	Dual energy X-ray absorptiometry
FAME	Fatty acid methyl ester
NEFA	Non-esterified fatty acid
GC	Gas chromatograph
LBF	Low body fat
HBF	High body fat

## Introduction

Human milk provides optimal nutrition to the breast-fed infant. Although fat is the most variable component in milk, it consistently represents over 50% of the energy content of human milk [1]. Consequently, fat content is the primary determinant of the energy density of milk. To illustrate this basic concept, a longitudinal study [2] designed to document total nutrient intakes and growth patterns of breast and formula-fed infants during the first 12 months of life found that the energy density of milk and milk fat concentration are almost perfectly correlated ( $r = 0.99$ ).

Milk lipids are generally thought to be comprised of those coming directly from the maternal diet (~30%), de novo synthesis within the mammary gland (~10%), and synthesis in or mobilization from other tissues (~60%) [3]. Data are scarce regarding the relationship between the components of maternal diet and milk fat concentration in well-nourished women, and the few studies that have been conducted in this area involve small number of subjects, making it difficult to draw firm conclusions. Data suggest, however, that neither excess maternal intake of macronutrients nor moderate macro or micronutrient deficiency appreciably alters milk macronutrient composition (including total fat) [3, 4]. However, there appears to be a somewhat consistent positive relationship between maternal body fat and milk fat [2, 5], although the physiological mechanism by which these two factors are associated is not established.

Nonetheless, most research on this subject generally suggests that maternal diet does not influence milk fat percentages in women. It has been demonstrated, however, that certain forms of conjugated linoleic acids (CLA), and more specifically the *t10,c12-18:2* isomer of conjugated linoleic acid (CLA), is a potent inhibitor of milk fat synthesis in other mammals. In fact, CLA-induced milk fat reduction has been observed in bovine, ovine, and murine species [6–8]. Similarly, we have reported that consumption of a preparation consisting mainly of two CLA isomers (*c9,t11-* and *t10,c12-18:2*) reduced milk fat concentration by 23% in a group of well-nourished women [9], although more recent work from our group does not appear to support this [10]. A reduction in milk fat percentage was also observed in lactating women consuming large amounts of a *trans* fatty acid-containing margarine in comparison to when they consumed diets containing large amounts of a low *trans* fatty acid margarine [11]. In this study, *trans* fatty acid-induced milk fat reduction was observed only in the group of women with body fat percentages <30% in contrast to women with body fat percentages  $\geq 30\%$ . These data suggest that body fatness may modulate the effect of biologically active fatty acids on milk fat content.

The study reported here was designed to determine whether either of the two most common CLA isomers (*c9,t11-* and *t10,c12-18:2*) can independently result in a reduction in milk fat in women. The possible interaction between body fatness and CLA intake on milk fat was also examined. The following hypotheses were tested: (1) maternal supplementation with *t10,c12-18:2* - but not *c9,t10-18:2*-decreases the concentration of fat in human milk, and (2) high maternal body fat attenuates CLA-induced milk fat reduction.

## Experimental Procedures

### Subjects

Lactating women ( $n = 12$ ) between 2 and 24 months postpartum were recruited from the Pullman, WA-Moscow, ID area. Inclusion criteria of subjects included the following: at least 21 years of age, free from known chronic illness (e.g., heart disease, diabetes), and breast feeding their infants at least four times daily. Subjects who were pregnant or smoked were excluded, as well as those who reported that they were ill at any time during the study. All study procedures were approved by the Washington State University Institutional Review Board, and all participants provided written consent for themselves and their infants prior to enrollment.

### Study Design and Dietary Intervention

This 36 days study was designed as a randomized, double-blind, placebo-controlled, latin-square trial (a pair of replicated  $3 \times 3$  latin-squares, balanced for potential carry-over effects), consisting of a baseline period (3 days), three treatment periods (5 days each), and two washout periods (9 days each). During the baseline period, all subjects completed an initial questionnaire regarding maternal and infant health and demographic information; anthropometric measurements were also obtained at this time. Maternal and infant weights were measured using electronic scales (Seca Alpha, Model 770, Hamburg, Germany ( $\pm 0.1$  kg) and Seca Model 727, Hamburg, Germany ( $\pm 1.0$  g), respectively). Maternal height and infant length were measured using a wooden height board (Seca Measure-All<sup>TM</sup>, Hamburg, Germany ( $\pm 0.1$  cm)).

During each treatment period, subjects consumed either a placebo (750 g each; olive oil) or CLA supplement daily (750 mg each; *c9,t11-18:2* or *t10,c12-18:2*; Natural, Ltd., Hovdebygd, Norway) between 0700 and 0900 hours. No capsules were consumed during the washout periods. The

**Table 1** Predominant fatty acid composition of conjugated linoleic acid (CLA; *c*9,*t*11–18:2 and *t*10,*c*12–18:2) and placebo supplements

Fatty acid	Supplement type		
	<i>c</i> 9, <i>t</i> 11–18:2 <sup>a</sup>	<i>t</i> 10, <i>c</i> 12–18:2 <sup>a</sup>	Placebo <sup>b</sup>
	(mg/capsule)		
16:0	–	–	62.2
18:0	–	–	24.6
18:1n-9	43.2	12.4	551.3
18:2n-6	1.7	–	50.5
<i>c</i> 9, <i>t</i> 11–18:2	595.1	79.2	–
<i>t</i> 10, <i>c</i> 12–18:2	58.5	630.5	–
<i>c</i> 9, <i>c</i> 11–18:2	4.6	–	–
<i>c</i> 10, <i>c</i> 12–18:2	2.0	5.9	–
<i>t</i> 9, <i>t</i> 11 + <i>t</i> 10, <i>t</i> 12–18:2	15.9	16.9	–

<sup>a</sup> CLA supplements consisted primarily of free fatty acids

<sup>b</sup> Olive oil supplements consisted primarily of triacylglycerides

predominant fatty acid profiles of the CLA supplements and placebo capsules are summarized in Table 1.

#### Determination of Maternal Dietary Intake

During day 4 and 5 of each intervention period, subjects were asked to weigh and record all foods and drinks consumed (excluding supplements). Selected data from dietary records were analyzed using a computerized dietary assessment program (Food Processor<sup>®</sup>, version 7.5; ESHA Research, Salem, OR, USA). The program was modified by us to include CLA contents of various foods [12, 13].

#### Determination of Body Fat

It is noteworthy that women were neither included nor excluded due to any criterion related to maternal body composition. However, because our previous work with *trans* fatty acids suggested an interaction between their consumption and body fatness on milk fat, we hypothesized that maternal body fat would interact with *t*10,*c*12–18:2 consumption to influence milk fat. We therefore measured maternal body fat as part of our study protocol. During the baseline period, maternal adiposity (% body fat) was determined using dual-energy X-ray absorptiometry (DEXA; Hologic QDR<sup>®</sup> 4500 Acclaim<sup>™</sup> Series, Bedford, MA, USA). A urine-based pregnancy test was performed (SureStep<sup>™</sup>, no. 6008; Applied Biotech, Inc., San Diego, CA, USA) to confirm non-pregnant status of each woman prior to her DEXA scan. In order to investigate the possible interaction between treatment and maternal body composition, each subject was also classified as being in a low

body fat (<30% body fat, LBF; *n* = 6) or high body fat (≥ 30% body fat, HBF; *n* = 5) group. This cut-off was used, because there was a natural separation of women into two groups at this level. It should be noted that we were unable to obtain DEXA data for one subject.

#### Collection of Milk Samples

On the final day of each intervention (day 5) and washout (day 9) period, milk samples were collected between 1700–1900 hours by complete breast expression using an electric breast pump (Model SMR-B-R, Ameda-Egnell, Inc., Cary, IL, USA). Subjects collected samples from the same breast throughout the entire study and were asked to pump 2–3 h after a previous complete breast expression, while nursing the infant on the other breast until the milk flow stopped. Milk samples were initially stored in polypropylene containers in subjects' refrigerators and transported within 2 h of collection to the laboratory where they were then stored at –70 °C.

#### Estimation of Infant Milk Consumption

Infant milk consumption was estimated by weighing the infant before and after each feeding session on day 4 of each intervention period using an electronic infant scale (Seca Model 727, Hamburg, Germany (±1.0 g)). Neither clothes nor diapers were changed between these weighings. The initial weight was subtracted from the final weight at each feeding session to determine milk consumption by the infant at that particular feeding, and values from all feeding sessions within a 24 h period were used to estimate total daily milk consumption by the infant.

#### Determination of Milk Fat Concentration and Fatty Acid Analysis

Milk lipid was extracted using a modified procedure by Ingalls et al. [14]. Briefly, milk (1 mL) was extracted using 4 mL chloroform:methanol (2:1, v/v; J. T. Baker, Phillipsburg, NJ, USA). After vigorous vortexing (2 min), samples were centrifuged at 2,500 rpm (12 min), and the chloroform layer was filtered through an anhydrous Na<sub>2</sub>SO<sub>4</sub> Pasteur pipette column. For quantitative analysis of total milk lipid, the extraction procedure was repeated and completed with a final column rinse of 200 µL chloroform:methanol (2:1, v/v). Samples were dried under nitrogen in a heated water bath and weighed. The intra and interassay coefficients of variation were 1.46 and 2.78%, respectively.

After extraction of milk fat, fatty acid methyl esters (FAME) were prepared using a method described by Christie [15]. With 2 mg lipid, 300 µg of methylheptacosanoate (C21:0; Matreya, Pleasant Gap, PA, USA) was added as an internal standard and dried under nitrogen. After adding 1 mL of diethyl ether, 20 µL methyl acetate, and 40 µL sodium methoxide (0.5 M), samples were agitated briefly to ensure thorough mixing and incubated for 15–20 min. Thirty µL of 50% oxalic acid in ether was added to stop the reaction, and the solution centrifuged for 2–5 min at 1,500 rpm to precipitate the sodium oxalate. The solvent was evaporated under nitrogen, and 1 mL hexane was added and filtered through a Pasteur pipette column filled with glass wool and silica gel. After drying completely under nitrogen, 100 µL hexane was added.

Samples were analyzed on a gas chromatograph (Hewlett-Packard 6890, Agilent Technologies, Wilmington, DE, USA) equipped with a capillary column (SP<sup>TM</sup>-2560; 100 m, 0.25 mm id with 0.2 µm film thickness; Supelco, Inc., Bellefonte, PA, USA) and helium as the carrier gas. Samples were injected in the splitless mode at an injection temperature of 255 °C. The identities of fatty acid peaks were established by comparing retention times to a mixture of 19 FAME (NuChek, Elysian, MN, USA) and a CLA mixture reference standard (Matreya, Pleasant Gap, PA, USA). Other fatty acids were not quantified in this study.

#### Determination of Milk Protein and Lactose Concentrations

Milk protein was analyzed using a modified spectrophotometric procedure for human milk described by Polberger and Lönnerdal [16]. Bovine serum albumin was used as a standard (Protein Assay Kit II, Bio-Rad, Hercules, CA, USA); samples were thawed at room temperature, diluted (1:20), and combined with 3 mL dye reagent. Absorbance was determined spectrophotometrically (595 nm) after a 5 min incubation. The intra and interassay coefficients of variation were 1.2 and 2.3%, respectively. Milk lactose was also analyzed spectrophotometrically as described by Polberger and Lönnerdal [16]. The β-galactosidase enzyme (Sigma Diagnostics<sup>®</sup>, St Louis, MO, USA) was used to cleave lactose into glucose and galactose, and milk glucose values were then used to calculate milk lactose concentration. The intra and interassay coefficients of variation were 1.44 and 2.45%, respectively.

#### Statistical Analyses

Data were analyzed as a latin-square design using standard ANOVA procedures (SAS Institute Inc., version 8.1; Cary,

NC, USA). Data analyses found no carry-over effects from one intervention period to the next. Thus, only data from the intervention periods (not washout periods) were considered in further analyses. Initial statistical models included body fat group (LBF or HBF), treatment (c9,t11–18:2, t10,c12–18:2, or placebo), and the treatment × body fat group interaction. Comparisons between means were made using Tukey-Kramer adjustments. Main effects and simple comparisons were considered significant at  $P < 0.05$ , and interactions were considered significant at  $P \leq 0.10$ .

## Results

### Subjects

All subjects ( $n = 12$ ) completed the study, and except for one woman who was not able to participate in the DEXA scan, data collection was complete for these subjects. Selected demographic information and anthropometric measurements of the participating women and their infants are shown in Table 2. On average, subjects were 31 week postpartum with mean body weight and height of 69.7 kg and 165.3 cm, respectively. There was no statistical effect of body fat group on any of these variables except percent (%) body fat and body mass index (BMI); by design LBF

**Table 2** Demographic characteristics and anthropometric measurements of participating women and infants

Maternal	
Age (years)	28.4 ± 1.6
Time postpartum (week)	31.0 ± 5.0
Parity (no. of children)	2.0 ± 0.5
Weight (kg)	69.7 ± 5.0
Height (cm)	165.3 ± 2.1
Body fat (%) <sup>a</sup>	
Low body fat (LBF) group	23.7 ± 1.7
High body fat (HBF) group	37.9 ± 1.7
Body mass index (BMI; kg/m <sup>2</sup> ) <sup>b</sup>	
Low body fat (LBF) group	22.1 ± 1.2
High body fat (HBF) group	28.7 ± 2.2
Infant	
Height (cm)	69.3 ± 2.3
Weight (kg)	8.0 ± 0.5

Values represent mean ± SEM;  $n = 12$  unless data were divided into body fat groups in which case data from one woman were excluded  
LBF < 30% body fat ( $n = 6$ )

HBF ≥ 30% body fat ( $n = 5$ )

<sup>a</sup> Effect of body fat group ( $P < 0.0001$ )

<sup>b</sup> Effect of body fat group ( $P < 0.05$ )

women had less body fat and lower BMI values than HBF women ( $P < 0.0005$  and  $P < 0.05$ , respectively).

### Dietary Intake

Information regarding dietary intake of subjects during each intervention period is presented in Table 3. There was an interaction ( $P = 0.05$ ) between treatment and body fat group on total energy intake, such that compared to LBF women, the HBF women consumed more energy during the placebo period but not the CLA treatment periods. There was neither an interactive nor independent effect of body fat group on the intakes of any of the nutrient groups. Intake of polyunsaturated fatty acids was higher during the  $c9,t11-18:2$  period compared to  $t10,c12-18:2$  and placebo periods. Dietary intakes (excluding supplements) of  $c9,t11-18:2$  were similar across the treatments (data not shown) averaging  $133 \pm 10.3$  mg/day.

### Milk Composition and Infant Milk Consumption

Information regarding the effect of treatment on milk fat, protein, and lactose concentrations is shown in Table 4.

**Table 3** Daily maternal intakes of energy-yielding nutrients estimated by 2 days dietary records during each intervention period

Variable	Dietary treatment			SEM
	$c9,t11-18:2$	$t10,c12-18:2$	Placebo <sup>1</sup>	
Energy (kJ) <sup>2</sup>				
Low body fat (LBF) group 3	8,773.8 <sup>bc</sup>	9,054.2 <sup>ac</sup>	7,991.4 <sup>bc</sup>	398.7
High body fat (HBF) group 4	9,778.0 <sup>ac</sup>	9,602.3 <sup>ac</sup>	11,367.9 <sup>a</sup>	398.7
Protein (g)	91.4	97.1	93.9	5.8
Carbohydrate (g)	282.8	290.2	322.0	14.4
Fat (g)	86.4	81.3	82.5	5.1
Saturated fat (g)	29.7	30.8	29.2	1.9
Monounsaturated fat (g)	28.5	24.6	24.0	2.3
Polyunsaturated fat (g) <sup>3</sup>	14.5 <sup>b</sup>	11.1 <sup>a</sup>	11.6 <sup>a</sup>	1.0

Values represent means;  $n = 12$  unless data were divided into body fat groups in which case data from one woman were excluded; values do not include nutrients supplied by supplements

LBF < 30% body fat ( $n = 6$ )

HBF  $\geq$  30% body fat ( $n = 5$ )

<sup>abc</sup> Values not sharing a common superscript are different ( $P \leq 0.05$ )

<sup>1</sup> Olive oil

<sup>2</sup> Treatment  $\times$  body fat group interaction ( $P = 0.05$ )

<sup>3</sup> Effect of treatment ( $P < 0.05$ )

**Table 4** Milk fat, protein, and lactose concentrations, and daily milk consumption by infants during each intervention period

Variable	Dietary treatment			SEM
	$c9,t11-18:2$	$t10,c12-18:2$	Placebo <sup>a</sup>	
Milk fat (%)	4.2	5.4	5.1	0.6
Milk protein (mg/mL)	8.0	8.4	8.2	0.4
Lactose (mg/mL)	59.8	58.8	59.3	1.2
Daily milk consumption (g/day)	734	756	716	80

Values represent means;  $n = 12$

<sup>a</sup> Olive oil

Neither a significant interaction between treatment and body fat group nor an independent effect of treatment or body fat was found for any of these variables. Similarly, there was neither an interaction nor independent effect of treatment or body fat group on infant milk consumption. No significant correlations were found between infant milk consumption and milk fat, milk lactose, or maternal body fat.

### Milk Fatty Acids

Predominant milk fatty acid profiles during each intervention period are presented in Table 5. Four of the fatty acids investigated revealed treatment by body fat interactions ( $P \leq 0.10$ ); these were 14:1, 15:0, 16:1 and 17:0. High body fat (HBF) women, but not LBF women, had higher concentrations of 14:1, 15:0 and 17:0 in their milk during the  $t10,c12-18:2$  period compared to the placebo ( $P < 0.05$ ). Low body fat (LBF) women, but not HBF women, had higher levels of 16:1 in their milk during the  $c9,t11-18:2$  period compared to  $t10,c12-18:2$  period ( $P < 0.05$ ). High body fat women had higher levels of 16:1 during both the  $c9,t11-18:2$  and  $t10,c12-18:2$  periods compared to the placebo ( $P < 0.05$ ). No independent effect of body fat was found for any fatty acid.

As expected, an independent effect of treatment was found for concentrations of both  $c9,t11-18:2$  and  $t10,c12-18:2$ . The concentration of  $t10,c12-18:2$  was higher during the  $t10,c12-18:2$  period compared to the  $c9,t11-18:2$  and placebo periods. Milk  $c9,t11-18:2$  concentration was higher during the  $c9,t11-18:2$  period compared to the other two periods.

### Discussion

The fundamental objective of this study was to determine whether either of the two most common CLA isomers

**Table 5** Effect of dietary treatment on major fatty acid content (mg/g lipid) in human milk

Fatty acid	Dietary treatment			SEM
	<i>c</i> 9, <i>t</i> 11–18:2	<i>t</i> 10, <i>c</i> 12–18:2	Placebo <sup>1</sup>	
12:0	20.8	21.0	17.6	2.6
14:0	43.5	46.6	38.3	3.7
14:1 <sup>2</sup>				
Low body fat (LBF) group	1.65 <sup>bc</sup>	1.35 <sup>ab</sup>	1.63 <sup>bd</sup>	0.12
High body fat (HBF) group	1.24 <sup>ab</sup>	1.59 <sup>bc</sup>	1.01 <sup>a</sup>	0.12
15:0 <sup>2</sup>				
Low body fat (LBF) group	3.00 <sup>b</sup>	2.50 <sup>bc</sup>	3.02 <sup>b</sup>	0.20
High body fat (HBF) group	2.15 <sup>ac</sup>	2.60 <sup>bc</sup>	1.73 <sup>a</sup>	0.20
16:0	160.6	159.6	139.4	8.7
16:1 <sup>2</sup>				
Low body fat (LBF) group	23.7 <sup>c</sup>	18.3 <sup>b</sup>	20.9 <sup>bc</sup>	1.2
High body fat (HBF) group	18.5 <sup>b</sup>	18.8 <sup>b</sup>	13.9 <sup>a</sup>	1.2
17:0 <sup>2</sup>				
Low body fat (LBF) group	2.87 <sup>b</sup>	2.32 <sup>ab</sup>	2.62 <sup>ab</sup>	0.16
High body fat (HBF) group	2.56 <sup>ab</sup>	2.83 <sup>b</sup>	1.96 <sup>a</sup>	0.16
18:0	53.00	56.14	49.77	2.90
18:1n9	251.4	248.2	214.2	14.1
<i>t</i> 9–18:1	1.11	4.62	3.20	1.23
<i>t</i> 10–18:1	9.43	12.37	5.72	2.10
<i>t</i> 11–18:1	6.70	9.87	11.42	2.84
<i>t</i> 12–18:1	8.20	6.90	5.14	1.57
18:2n-6	121.5	115.8	107.1	9.0
18:3n-3	9.13	9.44	9.52	0.90
20:4n-6	4.07	3.86	3.39	0.24
<i>c</i> 9, <i>t</i> 11–18:2 <sup>3</sup>	7.55 <sup>b</sup>	3.96 <sup>a</sup>	2.98 <sup>a</sup>	0.34
<i>t</i> 10, <i>c</i> 12–18:2 <sup>3</sup>	0.38 <sup>a</sup>	3.57 <sup>b</sup>	0.15 <sup>a</sup>	0.17
22:0	3.03	2.82	2.56	0.20

Values represent means;  $n = 12$  unless data were divided into body fat groups in which case data from one woman were excluded

LBF < 30% body fat ( $n = 6$ )

HBF  $\geq$  30% body fat ( $n = 5$ )

<sup>abcd</sup> Values within a row not sharing a common superscript are different ( $P \leq 0.05$ )

<sup>1</sup> Olive oil

<sup>2</sup> Treatment  $\times$  body fat group interaction ( $P < 0.1$ )

<sup>3</sup> Effect of treatment ( $P < 0.05$ )

(*c*9,*t*11- or *t*10,*c*12–18:2) can independently result in a reduction in milk fat in women. The possible modulatory role of body fatness on CLA-induced milk fat response was also examined. Like our previous work [9], the current

study used a relatively powerful latin-square design balanced for carry-over effects in which each study subject served as her own control. However, in contrast to our previous work [9] the results from the current study did not suggest a reduction in milk fat in women supplemented with CLA regardless of the isomer consumed. Further, stratifying the study population into high and low body fat groups did not show a modulating effect of maternal body composition on CLA-induced milk fat depression. These data have therefore led us to reject both of our initial hypotheses, at least as they apply to healthy, lactating women of average body fat content like those who participated in this study.

Daily infant milk consumption and concentrations of milk fat, protein, and lactose were all within normal ranges, suggesting the subjects included in the study were representatives of a population of healthy, well-nourished lactating women [17–19]. However, milk fat percentage during the placebo period (5.1%) was somewhat higher than average milk fat concentration (3.0–4.1%) typically observed by others [2, 4] as well as our laboratory [9]. The physiologic and molecular regulators of milk fat in human milk are not well understood, but it is possible that CLA might only cause milk fat depression in women who inherently produce milk of lower fat content. Future studies might be designed to specifically enroll two groups of women: those whose milk fat is generally low (e.g., <3.5%) and those whose milk fat is generally high (e.g., >4%). This approach would require investigators to obtain several samples of appropriately collected milk from women prior to determining subject eligibility.

Of particular interest to us at the present time is the considerable variability of mean milk fat concentrations across studies completed by our own research group especially that of Masters et al. [9] as very similar collection methods were used in all of them. As previously described, body fatness is known to be positively associated with milk fat concentration [2, 5]. It is possible that differences in maternal adiposity among studies might contribute to differences we have seen in average milk fat concentrations in these studies. Although there were no appreciable differences in body fatness based on BMI values between the present study and that reported by Masters et al. [9], maternal body fat was not measured via DEXA in the previous study. Because BMI is not a particularly accurate measure of adiposity during the postpartum period, it is possible that maternal adiposity was in fact different between these investigations. Time postpartum, parity, and estimated dietary fat intakes were also similar between these studies.

Another possible factor that may have contributed to the difference in average milk fat concentrations between these two studies might be the relative fullness of the breast at

the time the milk was sampled. Hartmann et al. [4] have shown that the lactating human mammary gland is at its minimum “volume” (i.e., lowest fullness) in the evening in contrast to maximum “volume” (highest fullness) upon the first feeding bout in the morning. Accordingly, Hartmann et al. [4] concluded that minimum milk fat content will consequently occur at the highest mammary fullness, and maximum milk fat content will occur at the lowest mammary fullness. Thus, controlling for breast fullness is essential in studies of milk fat regulation. The effect of breast fullness at the time of milk sampling on milk fat concentration is, however, an unlikely explanation for the difference in milk fat observed in these two studies. This is because the women were advised similarly in both studies to collect the milk sample 2–3 h after a previous complete breast expression and to make sure that the breast was as empty as possible prior to cessation of milk collection. In summary, it is not evident to us why the average fat percentage was so much higher in the current study compared to that reported by Masters et al. [9] who studied the effect of CLA (mixture) supplementation on human milk fat. Indeed, understanding the physiologic mechanisms driving the relatively high inter-individual variation in human milk fat remains a fertile area of study and is deserving of more rigorous investigation.

It is also noteworthy that average milk volume was higher in the current study compared to that reported by Masters et al. [9] (735 g/day vs. 420 g/day, respectively). The reason for higher estimated milk volume in the present study could theoretically be due in part to more complete expression of milk; however, this would have consequently resulted in a relatively lower milk fat concentration which was not what we observed. Moreover, we had no qualitative indication of difficulty with milk pumping procedures in either study, and therefore the reason underlying this discrepancy remains unsolved.

Although comparable doses of  $t10,c12-18:2$  and  $c9,t11-18:2$  were used as treatments in the current study and that by Masters et al. [9], the total amount of CLA consumed was approximately 50% less in the current study. Thus, another explanation for the disparate findings of an effect (or lack thereof) of CLA on milk fat is that neither isomer supplied alone at this level produces a reduction in milk fat, but a combination of the two doses is required. Nonetheless, there is evidence both from lactating mice and cows that  $t10,c12-18:2$  inhibits milk fat synthesis, whereas the  $c9,t11-18:2$  form of CLA does not [9, 20]. In fact, the relationship between the dose of postruminally infused  $t10,c12-18:2$  and milk fat reduction is very close in lactating cows over a wide dose range [21]. Similarly, Chouinard et al. [22] conducted a postruminal infusion study using a mixture of  $c9,t11-18:2$  and  $t10,c12-18:2$  (7.2 and 7.1 g/day, respectively) and found a reduction in milk

fat that was comparable to the reduction that is produced by  $t10,c12-18:2$  alone [21] suggesting that the effect of  $c9,t11-18:2$  present in the mixture was neutral with respect to an effect on milk fat.

Indeed, correlating the postruminally infused dose of  $t10,c12-18:2$  and secretion of this isomer in milk fat using data from seven studies in lactating cows produces a nearly linear relationship, where the slope term indicates the efficiency of transfer from the intestine to milk [21]. These data suggest that the transfer of  $t10,c12-18:2$  in lactating cows is linear across a wide dose range averaging approximately 22%. Similarly, others have reported that the transfer efficiency of  $t10,c12-18:2$  is typically lower than that of other CLA isomers not involved in milk fat regulation [22, 23]. These observations point toward a relatively low transfer efficiency being a characteristic of CLA isomers that exert anti-lipogenic effects. Interestingly, a reduced transfer efficiency has been observed for another milk fat inhibiting CLA ( $c10,t12-18:2$ ) also tested in postruminally-infused lactating cows [24].

For comparison, we have estimated the transfer efficiencies of the two CLA isomers examined in the current study and that of Masters et al. [9]. These calculations suggest that within each of these studies the transfer efficiencies of the two isomers were relatively similar. However, the transfer efficiency of CLA isomers in the current study was markedly higher than that of the previous study (23.3 vs. 6.4%). Interestingly, this relatively high transfer efficiency would seem to indicate that the dose and delivery of the CLA isomers, especially  $t10,c12-18:2$  form, to the mammary gland should have been sufficient to exert its anti-lipogenic effect if the sensitivity of the human secretory tissue were comparable to that observed in the lactating cow. Furthermore, because the appearance of  $t10,c12-18:2$  in milk fat expressed as a proportion of total milk fat fatty acids correlated closely with the reduction in milk fat synthesis in cows [21], one would have expected that the concentration of this fatty acid in milk fat might be used to predict milk fat reduction in lactating women as well. An alternative explanation of these data is that, compared to our previous study, the women in the present experiment may have been inherently more able to incorporate dietary fatty acids into their milk fat. Several possibilities may account for this difference (e.g., alterations in lipoprotein lipase activity), and these may have resulted in a reduced responsiveness to CLA's capacity to inhibit the uptake of preformed fatty acids into mammary epithelial cells or reduce the synthesis of de novo fatty acids within the alveolar cells. Of course, this alternative explanation remains speculative and would require further experimentation in a larger number of more heterogeneous women.



It is perplexing that the enrichment of  $\text{t}10,\text{c}12\text{--}18:2$  in milk fat in the current study (3.57 mg/g of lipid) was comparable to that reported by Masters et al. [9], yet we found no evidence of milk fat depression. In fact, if one were to use this level of  $\text{t}10,\text{c}12\text{--}18:2$  enrichment in milk fat to estimate milk fat depression in the bovine, one would predict a milk fat reduction of over 40% [22]. Because we found no reduction in milk fat in the current study, these data suggest that the women enrolled in this trial were less sensitive to the anti-lipogenic effect of CLA than are lactating cows. Species differences in sensitivity to the anti-lipogenic effect of CLA have been observed previously. For example, when mice were supplemented with relatively pure  $\text{t}10,\text{c}12\text{--}18:2$  (10 g/kg of diet), its concentration in milk fat increased to 30 mg/g of lipid, but this enrichment was associated with only 25% decrease in milk fat percentage [8]. In lactating cows, milk fat reaches its nadir (50%) already when its concentration of  $\text{t}10,\text{c}12\text{--}18:2$  is 5 mg/g of lipid [22]. We speculate that these species differences may be largely due to the fact that human milk fat is thought to be synthesized primarily from preformed fatty acids, whereas de novo fatty acids produced in the mammary alveolar cells contribute a much larger percentage of the lipid in milk from other animals such as the cow.

In conclusion, the results from this study suggest that dietary supplementation with either  $\text{c}9,\text{t}11\text{--}18:2$  or  $\text{t}10,\text{c}12\text{--}18:2$  (750 mg/day) does not reduce milk fat in healthy, breast-feeding women. These data do not support our initial hypothesis and are contrary to our previous findings [9]. There is no simple explanation for the discrepant responses between the two studies, although the total CLA doses varied and average fat content of the milk produced by the women in the present study was higher than in previous studies. It is also possible that other minor fatty acids present in the previously used CLA mixture [9] were responsible for its milk fat lowering effect, although data from a more recent dose-response study conducted in our laboratory do not support this hypothesis [10]. Nonetheless, evidence from this study points toward the possibility that the sensitivity of the lactating woman's mammary tissue to the milk fat depressing effect of the  $\text{t}10,\text{c}12$  isoform of CLA may be less than previously thought.

**Acknowledgments** The authors would like to sincerely thank the women and children who participated in this study. This research was supported in part by USDA NRI # 2000-01188, Washington State Dairy Products Commission, Center of Biomedical Research Excellence (COBRE) Grant # P20 RR15587, and Cognis Corp., LaGrange, IL, USA.

## References

- Picciano MF (2001) Nutrient composition of human milk. *Pediatr Clin North Am* 48:53–67
- Nommsen LA, Lovelady CA, Heinig MJ, Lönnerdahl BL, Dewey KG (1991) Determinants of energy, protein, lipid, and lactose concentrations in human milk during the first 12 months of lactation: the DARLING study. *Am J Clin Nutr* 53:457–465
- Hachey DL, Thomas MR, Emken EA, Garza C, Brown-Booth L, Adlof RO, Klein PD (1987) Human lactation: maternal transfer of dietary triglycerides labelled with stable isotope. *J Lipid Res* 28:185–1192
- Hartmann PE, Sherriff JL, Mitoulas LR (1998) Homeostatic mechanisms that regulate lactation during energetic stress. *J Nutr* 128:394S–399S
- Villalpando S, del Prado M (1999) Interrelation among dietary energy and fat intakes, maternal body fatness, and milk total lipid in humans. *J Mammary Gland Biol Neoplasia* 4:285–295
- Bauman DE, Corl BA, Peterson DG (2003) The biology of conjugated linoleic acids in ruminants. In: Sebedio JL, Christie WW, Adlof RO (eds) *Advances in conjugated linoleic acid research*, vol 2. AOCS, Champaign, pp 146–173
- Lock A, Teles BM, Perfield JW 2nd, Bauman DE, Sinclair LA (2006) A conjugated linoleic acid supplement containing *trans*-10, *cis*-12 reduces milk fat synthesis in lactating sheep. *J Dairy Sci* 89:1525–1532
- Loor JJ, Herbein JH (2003) Effects of dietary *cis*-9, *trans*-11–18:2, *trans*-10, *cis*-12–18:2, or vaccenic acid (*trans*-11 18:1) during lactation on body composition, tissue fatty acid profiles, and litter growth in mice. *Br J Nutr* 90:1039–1048
- Masters N, McGuire MA, Beerman K, Dasgupta N, McGuire MK (2002) Maternal supplementation with CLA decreases milk fat in humans. *Lipids* 37:133–138
- Mosley SA, Shahin AM, Williams JE, McGuire MA, McGuire MK (2007) Supplemental conjugated linoleic acid consumption does not influence milk macronutrient contents in all healthy lactating women. (in press) doi:10.1007/s11745-007-3087-8
- Anderson NK, Beerman KA, McGuire MA, Dasgupta N, Griinari JM, Williams J, McGuire MK (2005) Dietary fat type influences total milk fat content in lean women. *J Nutr* 135:416–421
- Park Y, McGuire MK, Behr R, McGuire MA, Evans A, Shultz TD (1999) High fat dairy product consumption increases  $\Delta 9\text{c},11\text{t}\text{--}18:2$  (rumenic acid) and total lipid concentrations of human milk. *Lipids* 34:543–549
- Ritzenthaler KL, McGuire MK, Falen R, Shultz TD, Dasgupta N, McGuire MA (2001) Estimation of conjugated linoleic acid intake by written dietary assessment methodologies underestimates actual intake evaluated by food duplicate methodology. *J Nutr* 131:1548–1554
- Ingalls ST, Xu Y, Hoppel CL (1995) Determination of plasma non-esterified fatty acids and triglyceride fatty acids by gas chromatography of their methyl esters after isolation by column chromatography on silica gel. *J Chromatogr B Biomed Appl* 666:1–12
- Christie WW (1982) A simple procedure for rapid transmethylation of glycerolipids and cholesteryl esters. *J Lipid Res* 23:1072–1075
- Polberger S, Lönnerdal B (1993) Simple and rapid macronutrient analysis of human milk for individualized fortification: basis for improved nutritional management of very-low-birth-weight infants? *J Pediatr Gastroenterol Nutr* 17:283–290
- Allen JC, Keller PR, Archer P, Neville MC (1991) Studies in human lactation: milk composition and daily secretion rates of macronutrients in the first year of lactation. *Am J Clin Nutr* 54:69–80
- Jensen RG, Thompson MP (1995) *The handbook of milk composition*. Academic, San Diego
- Michaelsen KF, Skafte L, Badsberg JH, Jörgensen M (1990) Variation in macronutrients in human bank milk: influencing factors and implications for human milk banking. *J Pediatr Gastroenterol Nutr* 11:229–239

20. Baumgard LH, Corl BA, Dwyer DA, Sæbø A, Bauman DE (2000) Identification of the conjugated linoleic acid isomer that inhibits milk fat synthesis. *Am J Physiol Regul Integr Comp Physiol* 278:R179–R184
21. de Veth MJ, Griinari JM, Pfeiffer AM, Bauman DE (2004) Effect of CLA on milk fat synthesis in dairy cows: comparison of inhibition by methyl esters and free fatty acids, and relationships among studies. *Lipids* 39:365–372
22. Chouinard PY, Corneau L, Sæbø A, Bauman DE (1999) Milk yield and composition during abomasal infusion of conjugated linoleic acids in dairy cows. *J Dairy Sci* 82:2737–2745
23. Perfield JW, Sæbø A, Bauman DE (2004) Use of conjugated linoleic acid (CLA) enrichments to examine the effects of *trans*-8, *cis*-10 CLA, and *cis*-11, *trans*-13 CLA on milk-fat synthesis. *J Dairy Sci* 87:1196–1202
24. Sæbø A, Sæbø PC, Griinari JM, Shingfield KJ (2005) Effect of abomasal infusions of geometric isomers of 10,12 CLA conjugated linoleic acid on milk fat synthesis in dairy cows. *Lipids* 40:823–832

# Supplementation with Commercial Mixtures of Conjugated Linoleic Acid in Association with Vitamin E and the Process of Lipid Autoxidation in Rats

Lilia Ferreira Santos-Zago · Adriana Prais Botelho · Admar Costa de Oliveira

Received: 6 February 2007 / Accepted: 29 May 2007 / Published online: 31 July 2007  
© AOCS 2007

**Abstract** CLA has been studied for its beneficial effects on health. However, the possibility of adverse effects, such as increased oxidative stress, must also be considered. The present work aims to assess the effect of CLA supplementation on the process of lipid autoxidation, both in the presence and in absence of an antioxidant. The investigation consisted in a biological assay with 60 rats divided into six groups: C (control), CE (control + vitamin E), AE (AdvantEdge<sup>®</sup>CLA), AEE (AdvantEdge<sup>®</sup>CLA + Vitamin E), CO (CLA One<sup>®</sup>) and COE (CLA One<sup>®</sup> + vitamin E). The CLA amount was 2% of feed consumption. Animals were supplemented for 42 days. As indicators of lipid autoxidation, peroxide (IP), malondialdehyde (MDA), 8-iso-PGF<sub>2</sub><sub>α</sub> isoprostane and catalase were determined. Hepatic IP results indicated that CLA increased oxidation: values for CLA-supplemented groups, particularly group CO (84.38 ± 10.97 mequiv/kg), were higher than those of the control group (54.75 ± 9.70 mequiv/kg). In contrast, serum MDA results showed that CLA reduces oxidation both for group AE (1.8 ± 0.67 mg of MDA/l) and for group CO (2.43 ± 0.61 mg of MDA/l) as compared to the control group (3.85 ± 0.24 mg of MDA/l). Serum catalase indicated a reduction of oxidation: groups AE and CO displayed 4734.23 ± 1078.93 kU/l and 5916.06 ± 2490.71 kU/l, respectively. These values are significantly lower than those of the control group. An increase in 8-iso-PGF<sub>2</sub><sub>α</sub> in urine was observed, particularly in group AE (95.13 ± 20.26 pg/ml) as compared to the control group (69.46 ± 16.65 pg/ml). It was concluded that the influence

of CLA on lipid autoxidation is dependent on supplement type, supplement dosage and chosen indicator, including its tissue and determination methodology.

## Introduction

Conjugated linoleic acids (CLA), a group of position and geometrical isomers with conjugated double bonds of the octadecadienoic acid (C18:2), is found in small amounts in a large variety of foods, and it is estimated that there are 56 possible isomers [1, 2].

Interest for conjugated linoleic acid (CLA) arose in 1979 when researchers found antimutagenic and anticarcinogenic substances, among them CLA, in grilled meats [3, 4]. Subsequently, numerous works demonstrated other beneficial health effects of CLA, including body composition change, reduction of arteriosclerosis, prevention and treatment of type 2 diabetes mellitus, enhancement of bone mineralization, immune system modulation, and an anti-thrombogenic effect [1]. Adverse effects of CLA supplementation have also been studied, particularly regarding increased susceptibility to lipid autoxidation [5–8]. CLA can be synthesized by ruminants by the biohydrogenation of unsaturated fatty acids by bacteria present in the rumen, in such a way that the predominant isomer is *cis*-9, *trans*-11 [9, 10]. The *cis*-9, *trans*-11 CLA isomer can be produced in mammary glands by the delta 9 desaturase path. The *trans*-10, *cis*-12 isomer is also believed to be one of the isomers synthesized in the rumen of polygastric animals [11]. Thus, significant concentrations of CLA, especially *cis*-9, *trans*-11 CLA, can be found in meats, milk, and their products [12].

L. F. Santos-Zago (✉) · A. P. Botelho · A. C. de Oliveira  
Laboratory of Lipids, Department of Food and Nutrition,  
College of Food Engineering, State University of Campinas,  
P.O. Box 6121, Campinas, SP 13083-862, Brazil  
e-mail: lzago@fea.unicamp.br

Numerous commercial mixtures of CLA and its isomers have been studied for their physiological effects. The *cis*-9, *trans*-11 and the *trans*-10, *cis*-12 isomers have distinct biological activities. The *trans*-10, *cis*-12 isomer is more closely related to lipid and glucose metabolism and body fat reduction [13], whereas the *cis*-9, *trans*-11 isomer is associated to antioxidant and anticarcinogenic effects [14, 15].

Although CLA physiological effects have been widely studied, some of them are not completely elucidated, and further investigation is needed, particularly concerning biological lipid oxidation [6, 7, 16].

With the aim of investigating the influence of CLA on the lipid oxidation process, many compounds with specific chemical structures that lend themselves to determination by various methods are used as biological indicators. They may result from autoxidation or from the action of enzymes (cyclooxygenases and lipoxygenases). Quantification of primary and secondary autoxidation products, such as peroxides and malondialdehyde, respectively, or products of enzymatic oxidation such as 8-isoPGF<sub>2 $\alpha$</sub>  isoprostane, has been used to assess the degree of oxidative stress in biological systems subjected to CLA supplementation [6–8]. The determination of the activity of antioxidant enzymatic systems such as catalase is also used as a parameter to evaluate biologic lipid oxidation in CLA assays [5]. In view of a possible pro-oxidant action of CLA resulting from the fact that it is a conjugated diene, there is a hypothesis that its supplementation in association with the antioxidant protection provided by vitamin E could minimize the deleterious action of CLA on the process of biological lipid oxidation. Thus, the objective of the present study is to assess the effects of conjugated linoleic acid supplementation, both in the presence and in the absence of vitamin E, on the process of lipid autoxidation in healthy growing Wistar rats.

## Materials and Methods

### Supplements

Supplements used were linoleic acid 60% Sigma (code L 1376), the conjugated linoleic acid commercial mixtures 75% AdvantEdge<sup>®</sup> CLA (EAS<sup>™</sup>, Golden, CO, USA) and 75% CLA One<sup>®</sup> Free Fatty Acid Oil 1CLA1-FFBL-KG (Pharmanutrients, Gurnee, IL, USA), and DL- $\alpha$ -tocopherol acetate Ephynal<sup>®</sup> (Roche Brazil). Fatty acid composition of the linoleic acid supplement 60% Sigma (code L 1376) and the commercial conjugated linoleic acid mixtures 75% AdvantEdge<sup>®</sup>, CLA (EAS<sup>™</sup>), and 75% CLA One<sup>®</sup> Free Fatty Acid Oil 1CLA1-FFBL-KG (Pharmanutrients), expressed in g/100 g of fatty acids, can be seen in Table 1.

### Animals and Diets

For biological assays, albino male healthy recently weaned Wistar rats were used, aged 21–23 days, with a mean weight of  $59.7 \pm 5.84$  g, from the Multidisciplinary Center for Biological Investigation, State University of Campinas. Animals remained in individual growth cages for 38 days, and in individual metabolic cages for 4 days for urine collection. They received water and feed ad libitum; temperature and humidity were kept in the ranges of  $22 \pm 1$  °C and 60–70%, respectively, and the light/dark cycle was of 12 h. This work has been approved by the Animal Experiment Ethics Commission (CEEA - IB/UNICAMP, Protocol no. 564–1). Diet was powdered AIN93G, prepared according to the American Society for Nutrition [17], with a protein concentration of 12% [18]. The diet protein concentration was changed to 12% because this is a work on dietetic manipulation, and a diet with the original protein concentration would make it more difficult to observe the differences in animal growth that might result from CLA supplementation (Table 2).

### Experimental Design

The biological assay experimental protocol was as follows. Sixty rats remained in an adaptation period for 7 days, receiving the respective diets and drinking water ad libitum. After this period, animals were randomly divided into six groups of ten animals each in order to achieve body weight homogeneity within and across groups. Experimental groups were divided as follows: group C (control) received 60% linoleic acid; group CE received linoleic acid + DL- $\alpha$ -tocopherol acetate; group AE received AdvantEdge<sup>®</sup> CLA, group AEE received AdvantEdge<sup>®</sup> CLA + DL- $\alpha$ -tocopherol acetate; group CO received CLA One<sup>®</sup> Free Fatty Acid Oil; and group COE received CLA One<sup>®</sup> Free Fatty Acid Oil + DL- $\alpha$ -tocopherol acetate. Supplement dosage was 2% of daily feed consumption, and DL-alpha-tocopherol acetate dosage was 30 mg/day. Animals were supplemented daily for 6 weeks. Body weight and food consumption were determined every 2 days. The following determinations were done: hepatic peroxide index (primary lipid autoxidation products), serum and hepatic malondialdehyde (secondary lipid autoxidation products), plasma and urine 8-iso-PGF<sub>2 $\alpha$</sub>  isoprostane, and serum catalase activity. As described above, in the last four assay days animals remained in metabolic cages for urine collection. Lipid oxidation indicators were determined for eight animals of each group, because that was the number of available metabolic cages. For blood determinations, six samples were used, as two were discarded due to hemolysis.

**Table 1** Fatty acid composition of linoleic acid and commercial conjugated linoleic acid mixtures (g/100 g of fatty acids)

Fatty acids	Linoleic acid 60% sigma (code L 1376)	Conjugated linoleic acid 75% advantEdge® CLA (EAS™)	CLA one® free fatty acid oil 75% 1CLA1-FFBL-KG (Pharmanutrients)
C8:0	–	0.02	0.06
C10:1	–	0.01	–
C12:0	–	0.01	–
C14:0	0.13	–	–
C16:0 iso	0.02	–	–
C16:0	2.89	2.15	3.86
C16:1 <i>cis</i> -9	0.17	0.01	–
C17:0	0.04	0.03	–
C17:1	0.07	0.01	–
C18:0	0.80	2.96	1.91
C18:1 <i>cis</i> -9	25.90	13.23	16.86
C18:1 <i>cis</i> -11	2.06	1.04	0.94
C18:2 <i>cis</i> -9, <i>cis</i> -12	59.64	0.75	0.93
C18:2 <i>cis</i> -9, <i>trans</i> -11 CLA	0.09	40.12	36.81
C18:2 <i>trans</i> -10, <i>cis</i> -12 CLA	0.08	39.15	36.27
C18:2 <i>cis</i> -11 <i>trans</i> -13 CLA	–	–	1.44
C18:2 <i>trans</i> -11 <i>cis</i> -15	0.82	0.21	0.47
C18:3	–	0.06	0.13
C20:0	1.01	–	–
C20:1	–	0.06	0.13
C20:2	6.18	0.01	–
C20:3	–	0.04	–
C20:4	0.01	–	–
C20:5	0.01	0.02	0.03
C22:0	–	0.04	0.07
Total	100.00	100.00	100.00

CLA conjugated linoleic acid

## Supplementation

Animals were supplemented by orogastric intubation with 1 mL disposable syringes and gavage needles. The amount of supplement was calculated every other day on the basis of the average feed consumption of each group, so that supplementation followed normal feed ingestion. The amount of supplement varied from 0.25 to 0.49 mL and was calculated with help of the density. Supplements were aspirated with the syringe and kept away from light till the moment of administration. For the groups receiving DL- $\alpha$ -tocopherol acetate, this product was aspirated into the syringe before linoleic acid and conjugated linoleic acid supplements, and administered with the same syringe. Rats were removed group by group from the experiment room, placed in plastic boxes, and taken to the supplementation room. This procedure was done daily during daytime and always at the same time, since rodent have nocturnal habits.

## Determination of Fatty Acid Profiles of Linoleic Acid and Conjugated Linoleic Acid Mixtures

Methylation followed the Christie method [19]. About 50 g of each sample were weighed in conic bottom graduated

**Table 2** Mean values  $\pm$  standard deviation ( $n = 10$ ) of feed consumption, weight gain and feed efficiency of experimental and control groups over the 6-week intervention period

Groups	Consumption (g)	Weight gain (g)	Feed efficiency
C	631.2 $\pm$ 48.7 <sup>a,b</sup>	192.5 $\pm$ 27.2 <sup>a</sup>	0.30 $\pm$ 0.02 <sup>a,b</sup>
CE	589.6 $\pm$ 41.0 <sup>b</sup>	166.3 $\pm$ 14.2 <sup>b</sup>	0.28 $\pm$ 0.01 <sup>b</sup>
AE	645.7 $\pm$ 27.6 <sup>a</sup>	203.5 $\pm$ 17.9 <sup>a</sup>	0.31 $\pm$ 0.01 <sup>a</sup>
AEE	641.9 $\pm$ 55.4 <sup>a,b</sup>	194.6 $\pm$ 27.2 <sup>a</sup>	0.30 $\pm$ 0.02 <sup>a,b</sup>
CO	621.9 $\pm$ 30.9 <sup>a,b</sup>	187.0 $\pm$ 10.4 <sup>a,b</sup>	0.30 $\pm$ 0.01 <sup>a,b</sup>
COE	633.3 $\pm$ 53.8 <sup>a,b</sup>	195.2 $\pm$ 22.7 <sup>a</sup>	0.31 $\pm$ 0.01 <sup>a</sup>

Values not sharing similar letter in the same column are different ( $P \leq 0.05$ ) in the Tukey test

extraction tubes. Then 2 mL of 1% methanolic sulphuric acid were added. Tubes were capped and shaken in an electric agitator for 1 min. Tubes remained in water bath for 2 h; 5 mL of sodium chloride 5% were added, followed by 1 min shaking, 5 mL of hexane were added, and tubes were again shaken for 30 s. The supernatant (hexane and methyl ester) was transferred to another extraction tube, to which 4 mL of 5% potassium bicarbonate were added. Tubes were shaken in an electric agitator for 1 min, and phase separation occurred rapidly. The new supernatant was transferred to another extraction tube containing 1 g of sodium sulphate. The hexane was evaporated with help of a nitrogen flux under water bath at 40 °C. Finally, 2 mL of hexane were added, and the solution was transferred to a chromatography vial, labeled, and stored at –20 °C. Fatty acid profile was determined by gas chromatography with a capillary silica column CP SIL 88 (0.25 mm × 0.2 µm × 100 m) and a fire ionization detector (FID). A temperature gradient with initial temperature of 70 °C was used for 4 min, followed by an increase at the rate of 13 °C/min until 175 °C; after 27 min the temperature was raised again at the rate of 4 °C/min, to 240 °C where it remained for 4 min, totaling 70 min for the whole run. Injector and detector temperatures were 250 and 300 °C, respectively. Injection was in split mode with a ratio of 50:1. The carrier gas was hydrogen with a flux of 1.8 mL/min, and pressure of 36.3 psi at the column head [20]. Results were expressed in percentage of total fatty acids. The standard adopted was CRM-164 (Commission of the European Communities, Community Bureau of Reference, Brussels, Belgium), which has certified values for 11 fatty acids; they were used to establish the correction factor for each certified fatty acid in order to transform the peak expressed in percentage of area into mass (mg/g total fatty acids).

#### Collection of Serum and Plasma from Blood and Urine of Animals for Determination of Lipid Autoxidation Indices

Blood from the animals was collected under anaesthesia (sodium pentobarbital, Hypnol 3%, 46 mg/kg), by cardiac puncture after a 12-h fast at the end of each experiment. Blood samples were collected with 10 mL syringes and gently poured, without the needle, down the walls of polyethylene tubes, without anticlotter for serum, and with anticlotter for plasma. Tubes remained in a water bath at 37 °C for 30 min, and centrifuged at 3,000 rpm for 10 min. After that, supernatant serum and plasma were separated with a pipette, and stored in polypropylene microtubes in an Ultra Low Freezer at –80 °C until analysis. Urine was collected in 25 mL graduated cylinders with 1 mL of 20% sulfuric acid, kept for a period of 24 h, filtered, and stored at –80 °C until analysis.

#### Peroxide Index (Primary Lipid Autoxidation Products)

For the determination of the peroxide index, lipids were previously extracted from the liver of each rat by the method of Bligh and Dyer [21] with some modifications due to sample peculiarities. About 1 g of sample was homogenized in 5 mL of chloroform, 10 mL of methanol, and 4 mL of water, followed by continual rotary agitation for 30 min. After this, 5 mL of chloroform and 5 mL of 1.5% sodium sulphate aqueous solution were added, and the sample was vigorously and continually shaken for 2 min. After dilution and complete separation of phases, the upper methanol layer containing water and non-lipid compounds was aspirated, and the lower chloroform layer containing total lipids was filtered in quantitative paper filter to obtain a clear solution. Immediately after lipid extraction, peroxide index determination was performed according to the official AOAC method [22], which is based on the oxidation of iodine in the presence of potassium iodide by the peroxide present in the sample, assuming that all oxidizing substances in the sample are peroxides. For the computation of the peroxide index, the amount of lipids present in the chloroform solution resulting from the lipid extraction procedure of Bligh and Dyer [21] was used.

#### Malondialdehyde, MDA (Secondary Lipid Autoxidation Products)

Determination of thiobarbituric acid reactive substances was done for the serum and liver of each animal using about 1.5 mL and 0.2 g of samples, respectively, in triplicate. The method chosen for this analysis was proposed by Sinnhuber; Yu [23], and its basic principle is the formation of a pink-red pigment composed of two molecules of thiobarbituric acid and one molecule of malondialdehyde (MDA). Its absorbance was read in visible light with a wavelength of 535 nm, using a 1% solution of 2-thiobarbituric acid for calibration; results were expressed in mg malondialdehyde per kg of sample.

#### Determination of 8-iso-PGF<sub>2α</sub> Isoprostane

Determination of 8-iso-PGF<sub>2α</sub> isoprostane in plasma and urine of the rats was done by enzyme immunoassay using a commercial kit from Cayman Chemical, catalog number 516351. The method is based in the competition between 8-iso-PGF<sub>2α</sub> isoprostane and conjugated 8-iso-PGF<sub>2α</sub> isoprostane-acetylcholinesterase (marker) by a limited number of binding sites for the specific antiserum of 8-iso-PGF<sub>2α</sub> isoprostane. Results were expressed in pg/mL of sample.

## Catalase Activity Determination

For the catalase activity determination, the methodology described by Góth [24] was used. It consists in the determination of serum catalase by the reaction with hydrogen peroxide. Determination was performed as follows: 0.2 mL of serum were incubated in a substrate solution composed of hydrogen peroxide (65  $\mu$ mol) in phosphate buffer (60 mmol/L, pH 7.4), for 1 min at 37 °C. After the incubation period, the reaction was interrupted by adding 1.0 mL of ammonium molybdate (32.4 mmol/L). Absorbance of the yellow complex formed between ammonium molybdate and hydrogen peroxide was read at 405 nm. Results were expressed in kU/L, considering that one unit of catalase decomposes, in the conditions described above, 1 mmol of hydrogen peroxide per minute.

## Statistical Analysis

Results are expressed as mean  $\pm$  SD. Data were analysed statistically by ANOVA using Statistical Analysis System [25] to test the effect of CLA mixtures and the interaction between CLA mixtures and vitamin E. The effect of supplementation time on food consumption and growth was also examined. The Tukey test was used to test the differences among groups. Differences were considered significant at  $P < 0.05$ .

## Results

With regard to feed consumption, weight gain and food efficiency, Table 1 shows that differences were found only between groups CE and AE ( $P \leq 0.05$ ). Figure 1 represents the weight gain curve and feed consumption of the rats during the period of CLA supplementation, and shows that growth was normal.

With regard to effects of CLA on lipid autoxidation, it can be said that results obtained are in agreement with the literature, i.e., there is no consensus about the real effect of this supplement on the oxidation process of biological lipids: many of the results point to the investigation of antioxidant properties, and others to the investigation of a possible pro oxidant effect of CLA. In Table 3, the results of all lipid oxidation indicators determined in this experiment are described. There was a difference in hepatic peroxide index (IP) only between groups C and CO. Group CO did exhibit a higher IP value than group C ( $P \leq 0.05$ ), which might suggest that the CLA One<sup>®</sup> supplement had a more discernible influence on the process of biological lipid oxidation as compared with the AdvantEdge<sup>®</sup> CLA supplement, since the group of rats receiving the latter displayed a mean peroxide value similar to the control

group, and smaller than group CO. Serum malondialdehyde average values were significantly smaller in groups receiving CLA supplementation, both for CLA One<sup>®</sup> and AdvantEdge<sup>®</sup> CLA ( $P \leq 0.05$ ). Hepatic MDA values did not differ between control group ( $13.50 \pm 3.23$  mg/kg of sample) and groups receiving supplementation: AE ( $12.51 \pm 2.41$  mg/kg of sample) and CO ( $14.26 \pm 0.71$  mg/kg of sample). However, group AEE, which received CLA supplementation associated with vitamin E, exhibited significantly lower values ( $P \leq 0.05$ ). Regarding the 8-iso-PGF<sub>2 $\alpha$</sub>  isoprostane results, differences in plasma values were observed only between groups AE and COE ( $P \leq 0.05$ ). 8-iso-PGF<sub>2 $\alpha$</sub>  isoprostane values in urine for group AE were significantly higher, whereas for group CO values were significantly lower than those of the controls ( $P \leq 0.05$ ). Such results suggest that effects on the lipid autoxidation process can be different as a result of the characteristics of each supplement. Supplements used in the present research contained 79.27 and 73.08% CLA for the brands AdvantEdge<sup>®</sup> CLA e CLA One<sup>®</sup>, respectively, and the proportion between the predominant isomers *cis*-9, *trans*-11 and *trans*-10, *cis*-12 was approximately 1:1. The mean values expressing catalase activity were significantly lower ( $P \leq 0.05$ ) in the groups receiving CLA, with the exception of group CO. These findings suggest the possibility of an antioxidant effect of CLA, as this enzyme plays a major role in protecting the organism against damage of oxidative stress by means of the degradation of peroxides, which result from lipid oxidation.

## Discussion

Regarding feed consumption and weight gain of the rats during the supplementation period, it can be said that, even though differences between some of the groups were observed at certain moments, growth was normal. Feed consumption changes seen in the graph are a consequence of supplement amount correction. The administered concentration of CLA followed the feed consumption, i.e., as consumption rose, supplement quantity was raised, leading to a drop in feed consumption, because CLA, as a lipid, produced greater satiety in the rats. This occurred cyclically throughout the assay, but it is important to note that these oscillations did not compromise animal growth, as seen in the body weight curves (Fig. 1).

Regarding results on the influence of CLA on biological lipid oxidation, a point to be discussed is that PI results of a preliminary assay in our laboratory [26] represent a fairly strong indication of an increase of this indicator in groups receiving CLA supplementation, and those results were higher than in the present assay. The main objective of the previous assay was to standardize CLA supplementation

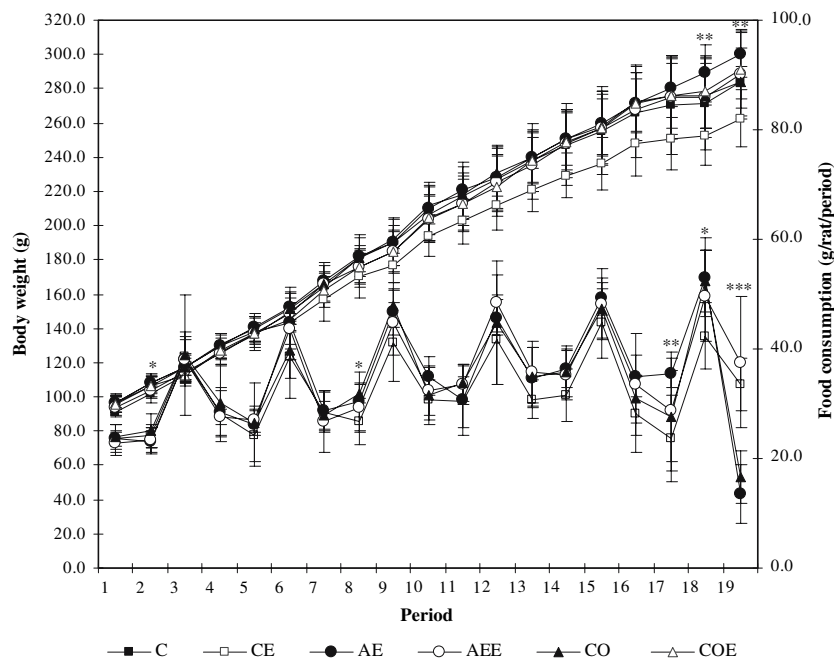


**Fig. 1** Body weight (g) and food consumption (g/rat/period) in control and experimental groups ( $n = 10$ ). *Upper lines* represent mean weight values (g); *lower lines* represent mean food consumption (g) in a period of two days. C control group, CE control group with vitamin E, AE group supplemented with AdvantEdge® CLA, AEE group supplemented with AdvantEdge® CLA + vitamin E, CO group supplemented with one® CLA, COE group supplemented with One®

CLA + vitamin E. \*statistical difference between group CO and group C, and \*\* statistical difference between group CE and groups AE and COE for body weight according to Tukey test ( $P \leq 0.05$ ); statistical difference between group CE and groups C and CO, \*\*statistical difference between AE and groups C and CE and \*\*\*statistical difference between groups C, AE and CO, and groups CE, AEE and COE for food consumption according to Tukey test ( $P \leq 0.05$ )

**Table 3** Mean values  $\pm$  standard deviation of the hepatic peroxide index ( $n = 8$ ), serum ( $n = 6$ ) and hepatic ( $n = 8$ ) malondialdehyde (MDA), plasma and urine 8-iso-PGF<sub>2 $\alpha$</sub>  isoprostane ( $n = 6$ ) and serum catalase activity ( $n = 6$ ) in control and experimental groups

Groups	Peroxide index <sup>1</sup> mequiv/kg	MDA mg MDA/kg		8-iso-PGF <sub>2<math>\alpha</math></sub> isoprostane pg/ml		Serum catalase kU/l
		Serum	Liver <sup>1</sup>	Plasma	Urine	
C	54.75 $\pm$ 9.70 <sup>a</sup>	3.85 $\pm$ 0.24 <sup>a</sup>	13.50 $\pm$ 3.23 <sup>a</sup>	13.84 $\pm$ 3.55 <sup>ab</sup>	69.46 $\pm$ 16.65 <sup>a</sup>	10496.52 $\pm$ 5121.84 <sup>a</sup>
CE	67.39 $\pm$ 11.26 <sup>ab</sup>	2.43 $\pm$ 1.32 <sup>b</sup>	11.89 $\pm$ 3.96 <sup>a</sup>	15.29 $\pm$ 7.14 <sup>ab</sup>	24.37 $\pm$ 4.54 <sup>b</sup>	3827.68 $\pm$ 1131.79 <sup>b</sup>
AE	53.66 $\pm$ 13.55 <sup>ab</sup>	1.80 $\pm$ 0.67 <sup>b</sup>	12.51 $\pm$ 2.41 <sup>a</sup>	18.86 $\pm$ 3.41 <sup>a</sup>	95.13 $\pm$ 20.26 <sup>c</sup>	4734.23 $\pm$ 1078.93 <sup>b</sup>
AEE	76.16 $\pm$ 36.47 <sup>ab</sup>	1.64 $\pm$ 0.71 <sup>b</sup>	6.73 $\pm$ 3.45 <sup>b</sup>	13.54 $\pm$ 2.84 <sup>ab</sup>	73.03 $\pm$ 9.15 <sup>a</sup>	3228.14 $\pm$ 1567.98 <sup>b</sup>
CO	84.38 $\pm$ 10.97 <sup>b</sup>	2.43 $\pm$ 0.61 <sup>b</sup>	14.26 $\pm$ 0.71 <sup>a</sup>	13.72 $\pm$ 2.34 <sup>ab</sup>	54.50 $\pm$ 13.81 <sup>d</sup>	5916.06 $\pm$ 2490.71 <sup>ab</sup>
COE	72.03 $\pm$ 14.12 <sup>ab</sup>	2.17 $\pm$ 0.42 <sup>b</sup>	13.46 $\pm$ 2.12 <sup>a</sup>	10.17 $\pm$ 1.62 <sup>b</sup>	49.88 $\pm$ 5.51 <sup>d</sup>	3645.86 $\pm$ 2178.95 <sup>b</sup>

Values not sharing similar letters in the same column are different ( $P \leq 0.05$ ) in the Tukey test

<sup>1</sup> Values expressed in dry basis

C control group, CE control group with vitamin E, AE group supplemented with AdvantEdge® CLA, AEE group supplemented with AdvantEdge® CLA + vitamin E, CO group supplemented with One® CLA, COE group supplemented with One® CLA + vitamin E

conditions. Growing male Wistar rats were supplemented for 21 days with *commercial conjugated linoleic acid mixture 75% AdvantEdge® CLA (EAS<sup>TM</sup>)* in the concentrations of 1, 2 and 4% of the daily feed consumption, having linoleic acid as a control. The concentration adopted for the present assay—2% of feed consumption—was chosen on the basis of results and operational conditions of

supplementation in the preliminary assay. As discussed above, the PI concentration in the present assay was higher. This observation might be explained by the duration of supplementation, which was greater in the present assay, coupled to the fact that peroxides are primary products of lipid oxidation, i.e., as supplementation time increases peroxide concentration diminishes due to their cleavage



into secondary products. This hypothesis can be confirmed by the results of malondialdehyde (MDA) shown in Table 3. Although there was no significant difference ( $P > 0.05$ ) between control groups and those receiving CLA without vitamin E (hepatic values), mean serum and hepatic values of malondialdehyde (MDA), a representative of secondary lipid oxidation, are higher in the present assay, in which supplementation ran for a period twice as long as the previous assay [26]. Results reported above are in agreement with works regarded as crucial for the reinvestigation of CLA effects on the lipid autoxidation process. Studies such as those by Cantwell et al. [5], Basu et al. [6] and Yamasaki et al. [7], which aimed at assessing the effect of CLA on lipid autoxidation, clearly point to the need for reinvestigating the antioxidant properties and the possible pro-oxidant effect of CLA.

The IP and MDA results of the present work are different from those reported by some research teams that studied antioxidant and pro-oxidant properties of CLA. The previously mentioned works [5–7] found MDA results that led to the conclusion that CLA acts as a pro-oxidizing agent. In a more recent work on the effect of CLA on low-density lipoprotein oxidation, Flintoff-Dye and Omaye [27] demonstrated that the four isomers under study (*cis*-9, *trans*-11; *trans*-10, *cis*-12; *trans*-9, *trans*-11; and *cis*-9, *cis*-11) promoted a significant increase in TBARS concentration in the samples.

Regarding 8-iso-PGF<sub>2α</sub> isoprostane, a product of non-enzymatic lipid oxidation and, according to the literature, the most specific biological indicator for the assessment of oxidative stress, results showed that when it was determined in the urine, AE supplement increased oxidation, whereas CO reduced it. Since the identification in the 1990s of series F prostaglandins, particularly 8-iso-PGF<sub>2α</sub> isoprostane, as fairly specific indicators of lipid autoxidation [28], many studies aimed at assessing oxidative stress by its determination in different experimental models, including humans. Works evaluating the influence of CLA on oxidative stress using series F prostaglandin determinations as indicators have been published only recently and are still scarce. Basu et al. [29], supplementing humans with abdominal obesity with CLA for one month, found urinary values of 8-iso-PGF<sub>2α</sub> isoprostane significantly higher than the group receiving placebo, and these values returned to basal levels after conclusion of CLA supplementation. In 2000, Basu et al. [6] categorically stated that CLA induces lipid peroxidation in humans after finding a significant increase of 8-iso-PGF<sub>2α</sub> isoprostane in urine, about four times higher than the basal amount, after supplementation with 4.2 g of CLA for 12 weeks.

There is an ongoing debate about the action of a specific CLA isomer in promoting a certain physiological effect, such as the case of total body fat reduction, one of the most

widely studied effects of CLA, and promoted mainly by the *trans*-10, *cis*-12 [30] isomer. There is no information, about which isomer is responsible for influencing lipid autoxidation in the studies of CLA and oxidative stress. It is believed that this influence is promoted by both predominant isomers, *cis*-9, *trans*-11 and *trans*-10, *cis*-12 [27]. In order to investigate whether the process of biological lipid oxidation is influenced by a specific isomer, Riséus et al. [31] supplemented men bearing metabolic syndrome with six capsules of 3.4 g per day of CLA isomer mixture, and the isolated isomer *trans*-10, *cis*-12 for a period of 12 weeks. The authors found urine values of 8-iso-PGF<sub>2α</sub> isoprostane 25 times higher in men receiving supplementation with a mixture of CLA than in the control group. This led to the conclusion that biological lipid oxidation is influenced by CLA, and that pure *trans*-10, *cis*-12 isomer had a more potent influence on the oxidation process. Similar results are reported in the work of Smedman et al. [32], which aimed at understanding the mechanism, by which CLA influences the oxidation process, and whether this influence is promoted by a specific CLA isomer. In a double-blind randomized study, Riséus et al. [8] supplemented obese men for a period of 12 weeks with 3 g/day of CLA mixture containing predominantly the *cis*-9, *trans*-11 isomer. Urine concentration of 8-iso-PGF<sub>2α</sub> isoprostane was 50% higher after supplementation with the CLA isomer, indicating that lipid oxidation is increased not only by isomer *trans*-10, *cis*-12 but by *cis*-9, *trans*-11 as well. Although this was not the only isomer in the mixture, it corresponded to 83% of it. Flintoff-Dye and Omaye [27] assessed the antioxidant and pro-oxidant properties of the CLA isomers *cis*-9, *trans*-11 and *trans*-10, *cis*-12 by means of the determination of LDL in human blood samples. Results indicated that both isomers influenced the lipid oxidation process in a similar way. Based on the phenomenon of hormesis, that characterizes the change in effect according to the dosage [33], the authors point out that CLA acts in a paradoxical way, in that it initially acts as a pro-oxidant (in low concentrations), then as an antioxidant (in intermediate concentrations), and finally as pro-oxidant again (in high concentrations), but they go on to conclude that, in general, CLA is a pro-oxidant agent because of the increase of oxidative stress observed in low concentrations, when an antioxidant effect would be expected.

The lower catalase activity would indicate smaller peroxide production, which in turn would indicate a lower degree of oxidative stress. In a work by Cantwell et al. [5] aiming at assessing the effect of CLA on the enzymatic system of antioxidant defense in hepatic cells of rats, it was demonstrated that CLA promoted a significant reduction of catalase activity when hepatocytes were exposed to a higher concentration (20 ppm). These results led to the conclusion that CLA could act as an antioxidant; however,

the authors point to the need of investigating long-term exposure to CLA. Catalase (EC 1.11.1.6, CAT), a tetrameric heme protein, is present in most aerobic cells, and is predominantly found in peroxisome, a cell organelle where oxidation of long-chain and very-long-chain fatty acids takes place. Peroxisome beta-oxidation results in the production of hydrogen peroxide ( $H_2O_2$ ), a catalase substrate.

The above discussion of the results can be supported by the influence of CLA on the expression of transcription factors, such as peroxisome proliferator activated receptors (PPAR), particularly PPAR  $\alpha$  and PPAR  $\gamma$ . Research works seeking to understand the action of CLA as activator or inhibitor of these nuclear receptors are somewhat conflicting, since both activation [34, 35] and inhibition [36, 37] are reported. Interpreting results of the present work on the assumption that CLA acts as a PPAR  $\alpha$  ligand, as shown by Moya-Camarena et al. [34], does not seem consistent, since the increase of PPAR  $\alpha$  expression would cause an increase in mitochondrial and peroxisome oxidation of fatty acids, and consequently an increase in  $H_2O_2$  production, leading to increased catalase activity, and this was not observed in the present research. On the other hand, looking at the same results considering the findings of Kang et al. [36] and Granlund et al. [37], who demonstrated that CLA inhibits PPAR  $\gamma$  expression, it can be said that the results of the present work are consistent. This seems to be confirmed by the work of Girnun et al. [38], which suggests that the increase in PPAR  $\gamma$  expression can increase catalase activity. Assuming that this relation is inversely proportional, a possible PPAR  $\gamma$  inhibition by CLA could lead to a decrease in catalase activity, as observed in the present research.

A further objective of this study was to assess the possibility of associating CLA administration to an antioxidant protection by means of a concomitant supplementation with DL- $\alpha$ -tocopherol acetate. It is widely accepted that supplementation with antioxidants, particularly  $\alpha$ -tocopherol, reduces oxidative stress [39], although there is some controversy. In recent years the scientific community has developed a new outlook about antioxidant supplementation, as a result of some evidence of adverse effects involving increased susceptibility to some diseases such as cancer and cardiovascular diseases. As a matter of fact, concerning cardiovascular diseases, the Dietary Guidelines of the American Heart Association say that there is no positive support for using antioxidant supplements in order to reduce the risk of cardiovascular diseases [40, 41].

There are practically no studies of CLA administered concomitantly with antioxidant protection, perhaps because there is a controversy surrounding its antioxidant properties [42, 43]. Results obtained in the present study showed that CLA supplementation concomitant with vitamin E did not

significantly reduce lipid oxidation ( $P > 0.05$ ). The group receiving supplementation of CLA One<sup>®</sup> + DL  $\alpha$ -tocopherol acetate (group COE) did not display values different from the group receiving CLA mixture only (group CO) in any of the parameters under study. However, the group receiving AdvantEdge<sup>®</sup> CLA +DL- $\alpha$ -tocopherol acetate (group AEE) had lower values ( $P \leq 0.05$ ) for hepatic TBARS and urinary 8-iso-PGF<sub>2 $\alpha$</sub>  isoprostane. It is widely known in the scientific community that vitamin E is one of the most potent antioxidants; however, factors such antioxidant dosage and bioavailability, and degree of exposure of the organism to oxidative stress must be taken into account. In a review by McCall and Frei [39], the real action of antioxidant compounds, including vitamin E, in the reduction of damage caused by oxidative stress was discussed. After considering the population, supplementation duration and dosage, lipid oxidation indicators and their determination methods, and the endpoints determined in the reviewed studies, the authors reported that vitamin E can protect the organism against lipid oxidation, but only in very high concentrations, far beyond the daily recommended values. The authors were led to conclude that further research is needed in order to clarify many doubts still surrounding the efficiency of antioxidant vitamin supplementation for oxidative stress prevention. From results of the present study, some hypotheses can be discussed in order to understand the low efficiency of vitamin E supplementation on most of the determined indicators, in addition to a possible inefficiency of antioxidant supplementation in some situations:

#### Supplement Dosage

The amount of DL- $\alpha$ -tocopherol acetate used in this work was 30 mg/day, a relatively high amount compared to values recommended by AIN93G [17], namely, 75 mg/kg of diet. According to this recommendation, the daily consumption of vitamin E through diet for the rats in the present experiment would be in the range of 1.5–3 mg (taking into account the feed consumption variation during the experimental period: 20–40 g/day). It should be pointed out that the amount of DL- $\alpha$ -tocopherol acetate used in the assay was chosen on the basis of previous works of this laboratory. In view of the above, it is plausible that the amount of supplement might have been excessive, preventing the detection of any difference that might exist among groups, since there is a debate about the inefficiency of even the adverse result of excessive supplementation. This hypothesis is based on the concept of the previously mentioned phenomenon of hormesis, which has already been documented for many compounds, including vitamins [33].

## Exposure to Oxidative Stress

It is important to point out that one of the objectives of the present research, based on the chemical structure of CLA, was to gather information to clarify the supposition that this supplement has a pro-oxidative effect. Thus, rats would be exposed to a pro-oxidative agent, and from this, protection of vitamin E against this agent would be assessed, since it can increase oxidative stability of unsaturated fatty acids with conjugated double bonds [44]. However, although the issue is still unresolved, there is a hypothesis that CLA acts as an antioxidant agent [42, 43], which would explain the results, as the rats would not have been so exposed to oxidative stress. Such a hypothesis would also lend some support to the conclusion that, if CLA really has an antioxidant effect, this effect is not enhanced by the presence of vitamin E.

## Conclusions

After examining the results of IP, MDA and 8-iso-PGF<sub>2α</sub> isoprostane, we conclude that the influence of conjugated linoleic acid on lipid oxidation, as measured by these indicators, depends on the CLA supplement type. Mean values expressing serum catalase were significantly lower in CLA supplemented groups, with or without vitamin E, than in the control group, suggesting antioxidative activity. The efficiency of vitamin E supplementation, particularly for the control group for the indicators catalase and 8-iso-PGF<sub>2α</sub> isoprostane, should be highlighted. Thus, the results of lipid autoxidation indicators are uncertain, but did warrant the conclusion that supplementation with conjugated linoleic acid influenced the process of biological lipid oxidation in different ways, and the influence is dependent on supplement type and the autoxidation indicator used, including its tissue and determination method.

**Acknowledgments** To Fundação de Amparo à Pesquisa do Estado de São Paulo – FAPESP (Process 2003/07648-4); to the Conselho Nacional de Desenvolvimento Científico e Tecnológico - CNPq (Process 133874/2003-6) for the financial support, and to researcher BOTELHO, A.P, respectively; and to Dr. Elisangela Faria of the Laboratory of Natural Products, Institute of Biology, State University of Campinas for technical assistance.

## References

- Salas-Salvadó J, Marquez-Sandoval F, Bulló M (2006) Conjugated linoleic acid intake in humans: a systematic review focusing on its effects on body composition, glucose, and lipid metabolism. *Crit Rev Food Sci Nutr* 46:479–488
- Yurawecz MP, Sehat N, Mossoba MM, Roach JAG, Kramer JKG, Ku Y (1999) Variations in isomer distribution in commercially available conjugated linoleic acid. *Fett/Lipid* 101:277–282
- Pariza MW, Ashoor SH, Chu FS, Lund DB (1979) Effects of temperature and time on mutagen formation in pan-fried hamburger. *Cancer Lett* 7:63
- Pariza MW, Hargraves WA (1985) A beef-derived mutagenesis modulator inhibits initiation of mouse epidermal tumors by 7,12-dimethylbenz[*a*]anthracene. *Carcinogenesis* 6:591
- Cantwell H, Devery R, O'shea M, Stanton C (1999) The effect of conjugated linoleic acid on the antioxidant enzyme defense system in rat hepatocytes. *Lipids* 34:833–839
- Basu S, Smedman A, Vessby B (2000) Conjugated linoleic acid induces lipid peroxidation in humans. *FEBS Lett* 468:33–36
- Yamasaki M, Mansho K, Mishima H, Kimura G, Sasaki M, Kasai M, Tachibana H, Yamada K (2000) Effect of dietary conjugated linoleic acid on lipid peroxidation and histological change in rat liver tissues. *J Agr Food Chem* 48:6367–6371
- Riséus U, Vessby B, Årnlöv J, Basu S (2004) Effects of *cis*-9, *trans*-11 conjugated linoleic acid supplementation on insulin sensitivity, lipid peroxidation, and proinflammatory markers in obese men. *Am J Clin Nutr* 80:279–283
- Parodi PW (1977) Conjugated octadecadienoic acids of milk fat. *J Dairy Sci* 60:1550–1553
- Oustrowska E, Walker GP, Doyle PT, Dunshea FR (2004) Milk conjugated linoleic and *trans*-vaccenic acids are highest in Spring in grazing cows. *Asia Pac J Clin Nutr* 13(Suppl):S53
- Bauman DE, Baumgard LH, Corl BA, Griinari JM (1999) Biosynthesis of conjugated linoleic acid in ruminants, *Proc Am Soc Anim Sci* Available at: <http://www.asas.org/jas/symposia/proceedings/0937.pdf>
- Corl BA, Baumgard LH, Dwyer DA, Griinari JM, Philips BS, Bauman DE (2001) The role of delta-9-desaturase in the production of *cis*-9, *trans*-11. *J Nutr Biochem* 12:622–630
- Park Y, Storkson JM, Ntambi JM, Cook ME, Sih CJ, Pariza MW (1999) Evidence that the *trans*-10, *cis*-12 isomer of conjugated linoleic acid induces body composition changes in mice. *Lipids* 34:235–241
- Park HS, Cho HY, Ha YL, Park JHY (2004) Dietary conjugated linoleic acid increases the mRNA ratio of Bax/Bcl-2 in the colonic mucosa of rats. *J Nutr Biochem* 15:229–235
- Tanmahasamut P, Liu J, Hendry LB, Sidell N (2004) Conjugated linoleic acid blocks estrogen signaling in human breast cancer cells. *J Nutr* 134:674–680
- Munday JS, Thompson KG, James KA (1999) Dietary conjugated linoleic acids promote fatty streak formation in the C57BL/6 mouse atherosclerosis model. *Br J Nutr* 81:251–255
- Reeves PG, Nielsen FH, Fahey GC Jr (1993) AIN-93 Purified diets for laboratory rodents: final report of the American Institute of Nutrition Ad Hoc Writing Committee on the Reformulation of the AIN-76A rodent diet. *J Nutr* 123:1939–1951
- Goena M, Mazo F, Fernández-González L, Tosar A, Fruhbeck G, Santidrián S (1989) Effect of the raw legume *Vicia erviltha* on muscle and liver protein metabolism in growing rats. *Rev Esp Fisiol* 45:55–60 Supplement
- Christie WW (1982) A simple procedure for rapid transmethylation of glycerolipids and cholesterol esters. *J Lipid Res* 23:1072–1074
- Sehat N, Kramer JK, Mossoba MM, Yurawecz MP, Roach JAG, Eulitz K, Morehouse KM, Ku Y (1998) Identification of conjugated linoleic acid isomers in cheese by gas chromatography, silver ion high performance liquid chromatography and mass spectral reconstructed ion profiles. Comparison of chromatographic elution sequences. *Lipids* 33:963–971
- Bligh EG, Dyer WJ (1959) A rapid method of total lipid extraction and purification. *Can J Biochem Physiol* 37:911–917

22. Association Of Official Analytical Chemists, AOAC (1995) Official methods of analysis 16 ed. Cunnif P(ed) Virginia: AOAC International v 1
23. Sinnhuber RO, Yu TC (1958) 2-Thiobarbituric acid method for the measurement of rancidity in fishery products. II. The quantitative determination of malonaldehyde. *Food Technol* 12:9–12
24. Góth L (1991) A simple method for determination of serum catalase activity and revision of reference range. *Clin Chim Acta* 196:143–152
25. SAS Institute Project for Windows: User's Guide: statistics. Version 8.0. Cary, SAS inst, 2003
26. Santos-Zago LF, Botelho AP, Reis SMPM, Oliveira AC (2005) Effect of conjugated linoleic acid on lipid autoxidation in wistar. *Anais do 3 Simpósio em Ciência de Alimentos, Florianópolis v3*
27. Flintoff-Dye NL, Omaye ST (2005) Antioxidant effects of conjugated linoleic acid isomers in isolated human low-density lipoproteins. *Nutr Res* 25:1–12
28. Roberts LJ, Morrow JD (2000) Measurement of F<sub>2</sub>-isoprostanes as an index of oxidative stress in vivo. *Free Radic Biol Med* 28:505–513
29. Basu S, Risérus U, Turpeinen A, Vessby B (2000) Conjugated linoleic acid induces lipid peroxidation in men with abdominal obesity. *Clin Sci* 99:511–516
30. Park Y, Storkson JM, Albright KJ, Liu W, Pariza MW (1999) Evidence that the *trans*-10, *cis*-12 isomer of conjugated linoleic acid induces body composition changes in mice. *Lipids* 34:235–241
31. Risérus U, Basu S, Jovinge S, Fredrikson GN, Årnlöv J, Vessby B (2002) Supplementation with conjugated linoleic acid causes isomer-dependent oxidative stress and elevated C-reactive protein—a potential link to fatty acid-induced insulin resistance. *Circulation* 106:1925–1929
32. Smedman A, Vessby B, Basu S (2004) Isomer-specific effects of conjugated linoleic acid on lipid peroxidation in humans: regulation by  $\alpha$ -tocopherol and cyclo-oxygenase-2 inhibitor. *Clin Sci* 106:67–73
33. Calbrese EJ, Baldwin LA (1999) Chemical hormesis: its historical foundations as a biological hypothesis. *Toxicol Pathol* 27:195–216
34. Moya-Camarena SY, Heuvel JPV, Blanchard SG, Leesnitzer LA, Belury MA (1999) Conjugated linoleic acid is a potent naturally occurring ligand and activator of PPAR $\alpha$ . *J Lipid Res* 40:1426–1433
35. Belury MA, Moya-Camarena SY, Lu M, Shi L, Leesnitzer LM, Blanchard SG (2002) Conjugated linoleic acid is na activator and ligand for peroxisome proliferator-activated receptor-gamma (PPAR $\gamma$ ). *Nutr Res* 22:817–824
36. Kang K, Liu W, Albright KJ, Park Y, Pariza MW (2003) *trans*-10, *cis*-12 CLA inhibits differentiation of 3T3-L1 adipocytes and decreases PPAR $\gamma$  expression. *Biochem Biophys Res Co* 303:795–799
37. Granlund L, Juvenet LK, Pedersen JI, Nebb HI (2003) *trans*10, *cis*12-conjugated linoleic acid prevents triacylglycerol accumulation in adipocytes by acting as a PPAR $\gamma$  modulator. *J Lipid Res* 44:1441–1452
38. Girmum GD, Domann FE, Moore SA, Robbins MEC (2002) Identification of a functional peroxisome proliferators-activated receptor response element in the rat catalase promoter. *Mol Endocrinol* 16:2793–2801
39. Mccall M, Frei B (1999) Can antioxidant vitamins materially reduce oxidative damage in humans? *Free Radic Biol Med* 26:1034–1053
40. Williams KJ, Fisher EA (2005) Oxidation, lipoproteins and atherosclerosis which is wrong, the antioxidants or the theory? *Curr Opin Clin Nutr* 8:139–146
41. Kris-Etherton PM, Lichtenstein AH, Howard BV (2004) Antioxidant vitamin supplements and cardiovascular disease. *Circulation* 110:637–641
42. Ha YL, Grimm NK, Pariza MW (1987) Anticarcinogens from fried ground beef: heat-altered derivatives of linoleic acid. *Carcinogenesis* 8:1881–1887
43. Ha YL, Storkson J, Pariza M (1990) Inhibition of benzo(a)pyrene-induced mouse forestomach neoplasia by conjugated linoleic acid. *Cancer Res* 50:1097–1101
44. Tsuzuki T, Igarashi M, Iwata T, Ymauchi-Sato Y, Yamamoto T, Ogita K, Suzuki T, Miyazawa T (2004) Oxidation rate of conjugated linoleic acid and conjugated linolenic acid is slowed by triacylglycerol esterification and  $\alpha$ -tocopherol. *Lipids* 39:475–480

# The Effects of Simultaneous Administration of Dietary Conjugated Linoleic Acid and Telmisartan on Cardiovascular Risks in Rats

Mohammad M. Abdullah · Zuyuan Xu ·  
Grant N. Pierce · Mohammed H. Moghadasian

Received: 20 April 2007 / Accepted: 2 July 2007 / Published online: 7 August 2007  
© AOCs 2007

**Abstract** Dietary conjugated linoleic acid (CLA) and the antihypertensive drug, telmisartan, have both been shown to modify cardiovascular risks. The effects of a combination of these two agents have, however, not been investigated. This 20 week study sought to assess the therapeutic potential of a CLA/telmisartan co-administration in rats fed a high-fructose high-fat diet. Thirty-three male Sprague–Dawley rats were randomly assigned to five experimental groups, including control, losartan, telmisartan, CLA, and CLA + telmisartan-treated animals. Body weight, blood pressure, and blood levels of lipids, glucose, insulin, and inflammatory markers were measured. Co-administration of CLA and telmisartan resulted in significant ( $P < 0.05$ ) reductions in body weight, visceral fat, serum total cholesterol, triglycerides, glucose, plasma insulin concentra-

tions, and systolic blood pressure compared with those in the control group. Moreover, plasma levels of IL1- $\alpha$  and IFN- $\gamma$  were reduced and levels of IL1- $\beta$ , IL-4, IL-6, and IL-10, plus TNF- $\alpha$  were increased in the co-therapy group, compared with controls. In conclusion, this study suggests that a combination of CLA with telmisartan may modify several risk factors of cardiovascular disease commonly seen in metabolic syndrome. This combination of nutraceuticals and pharmaceuticals may be a safe and cost-effective strategy in a number of high-risk subjects. Future studies will further document clinical benefits of such combination therapy.

**Keywords** Cardiovascular disease · Metabolic syndrome · Obesity · Diabetes · Conjugated linoleic acid · Telmisartan · Peroxisome proliferator-activated receptor · Fatty acid · Angiotensin II receptor blocker

M. M. Abdullah · M. H. Moghadasian  
Department of Human Nutritional Sciences,  
The University of Manitoba and St. Boniface General Hospital  
Research Centre, Winnipeg, MB, Canada

M. H. Moghadasian  
Department of Pathology, The University of Manitoba and St.  
Boniface General Hospital Research Centre, Winnipeg,  
MB, Canada

M. M. Abdullah · Z. Xu · G. N. Pierce · M. H. Moghadasian  
The Canadian Centre for Agri-Food Research in Health and  
Medicine (CCARM), The University of Manitoba and St.  
Boniface General Hospital Research Centre, Winnipeg,  
MB, Canada

M. H. Moghadasian (✉)  
Pathology Research Laboratory, St. Boniface General Hospital  
Research Centre, 351 Tache Ave, Winnipeg, MB,  
Canada R2H 2A6  
e-mail: mmoghadasian@sbr.ca

## Abbreviations

ARB	Angiotensin II receptor blocker
AUC	Area under the curve
CLA	Conjugated linoleic acid
CVD	Cardiovascular disease
DBP	Diastolic blood pressure
FA	Fatty acid
HDL	High-density lipoprotein
HFHF	High-fructose high-fat
IL	Interleukin
INF	Interferon
ip	Intraperitoneally
LDL	Low-density lipoprotein
LPS	Lipopolysaccharide
MetS	Metabolic syndrome
OGTT	Oral glucose tolerance test
PPAR	Peroxisome proliferator-activated receptor

SBP	Systolic blood pressure
SEM	Standard error of the mean
SFO	Safflower oil
TC	Total cholesterol
TG	Triglyceride
TNF	Tumor necrosis factor
UCP	Uncoupling protein

## Introduction

Cardiovascular diseases (CVD) continue to be a major global epidemic and leading cause of morbidity and mortality. In addition to the conventional risk factors, such as hypercholesterolemia and hypertension, recent studies highlight the importance of other metabolic abnormalities, including obesity and type 2 diabetes on the worldwide heart-related mortality. Over the past few decades the incidence of these metabolic disorders has increased dramatically. Metabolic syndrome (MetS) is a cluster of central obesity, insulin resistance, hypertension, atherogenic dyslipidemia, and a pro-inflammatory state [1] that is now a subject of great scientific interest. Although the specific causes of the MetS are not completely recognized, an inappropriate lifestyle, including poor dietary habits, is believed to play a major role. In this regard, several studies suggest beneficial effects of dietary interventions along with daily life modifications in patients with MetS [2].

Primarily found in ruminant meat and dairy products, conjugated linoleic acid (CLA) is a mixture of positional and geometric isomers of linoleic acid (LA; 18:2n-6) that may generate cardiovascular health-promoting properties. CLA isomers have been widely known to have antiobesity, antidiabetic, anti-atherogenic, and anti-inflammatory [3–6] properties in animal models and human subjects. One potential mechanism for such effects may lie in CLA's ability to induce dose-dependent activation of the transcription factors peroxisome proliferator-activated receptor (PPAR)- $\alpha$  and  $\gamma$  subtypes [7, 8] that control the gene expression of several key enzymes of glucose and lipid metabolism. Similarly, telmisartan (Micardis), an angiotensin II receptor blocker (ARB), has been shown to serve as a partial agonist for PPAR- $\gamma$  [9]. Treatment with telmisartan reduced body-weight gain and decreased serum glucose, insulin, and triglyceride (TG) levels in rats fed high-carbohydrate high-fat diets [9]. Furthermore, telmisartan has been reported to reduce levels of glucose and insulin to normal values over eight weeks of treatment in patients with MetS [10].

On the basis of the current state of our knowledge and available lines of evidence, we sought to investigate

long-term benefits of a combination of dietary CLA with telmisartan against several known risk factors for vascular diseases in a wild-type rat model consuming a high-fructose high-fat (HFHF) diet over twenty weeks.

## Experimental Procedure

### Animals and Diets

Thirty-three, five-week-old male Sprague–Dawley (SD) rats were obtained from the Central Animal Care at the University of Manitoba (Winnipeg, MB, Canada) and housed in stainless-steel cages at an ambient temperature of 22–24°C and 12:12 h light–dark cycle. A HFHF diet, containing 60% fructose and 10% lard (TD.03293.PWD; Harlan Teklad, WI, USA) was used as “base diet”. The composition of this diet is summarized in Table 1. This diet was further supplemented with either 1.0% (w/w) safflower oil (SFO), or 1.0% (w/w) CLA. After 10 days of adaptation, the rats were randomly assigned to one of five treatment groups:

1. control group ( $n = 7$ ) fed SFO-supplemented diet;
2. losartan-treated group ( $n = 5$ ) fed SFO-supplemented diet and received losartan in drinking water at 5 mg kg<sup>-1</sup> body weight per day;
3. telmisartan-treated group ( $n = 7$ ) fed SFO-supplemented diet and received telmisartan in drinking water at 5 mg kg<sup>-1</sup> body weight per day;
4. CLA-treated group ( $n = 7$ ) fed CLA-supplemented diet; and
5. CLA + telmisartan-treated group ( $n = 7$ ) fed CLA-supplemented diet and received telmisartan in drinking water at 5 mg kg<sup>-1</sup> body weight per day.

The animals in these five experimental groups had comparable mean body weight and serum total cholesterol (TC) levels at baseline. CLA (Bioriginal Food and Science,

**Table 1** Composition of the high-fructose high-fat diet (TD.03293.PWD)

Ingredient	Diet (g kg <sup>-1</sup> )	Percentage
Casein	207.0	20.7
DL-Methionine	3.0	0.3
Fructose	600.0	60
Lard	100.0	10
Cellulose	42.0	4.2
Calcium carbonate (CaCO <sub>3</sub> )	3.0	0.3
Mineral mix, AIN-76	35.0	3.5
Vitamin mix, Teklad	10.0	1.0
Total	1000	100

SK, Canada) was composed of a 75% mixture of the *c9*, *t11* and *t10*, *c12* isomers in a 50:50 ratio, and 8.1% of other isomers. Telmisartan and losartan were received from St. Boniface General Hospital Pharmacy (Winnipeg, MB, Canada) and administered as previously reported [9]. To ensure accurate delivery of drug doses, drug concentrations were adjusted in the drinking water each week based on the average body weight and water consumption in each group, as previously described [9, 11]. Similar to telmisartan, losartan is an ARB commonly used to treat essential hypertension. However, unlike telmisartan, losartan does not seem to be partial agonist of PPAR- $\gamma$  [9] and was, therefore, used in this study as a “control drug” for telmisartan. Similarly, SFO, which is void of CLA was used as “control oil” for CLA and also to provide n-6 essential fatty acids (FA) for the control group. Table 2 summarizes the diet/drug treatment protocols. Daily food intake was estimated from the amount of food which disappeared from the animals’ cages. Animals’ body weights were recorded weekly whereas food and water intake were measured each day. Blood samples were obtained in a non-fed state by jugular venipuncture under light anesthesia (induced by 1–2% isoflurane) at baseline, week 4, and week 8 of the study. Sera were used for biochemical assays as described in following sections. The experiment lasted 20 weeks, during which time all animals looked healthy and active. On the morning of its last day on the treatment (week 20), each rat was intraperitoneally (ip) injected with 400  $\mu\text{g}$  of bacterial lipopolysaccharide (LPS; Sigma–Aldrich, ON, Canada) and 100 IU heparin (LEO Pharma, ON, Canada) 2 h and 10 min before sacrifice, respectively. A final blood sample was collected, after euthanization by  $\text{CO}_2$ , through cardiac puncture, and a complete autopsy was performed. The study was approved by the Animal Care Committee on the Use of Animals in Research at the University of Manitoba.

**Table 2** Summary of experimental groups and the diet/drug treatment protocols

Group	Diet/drug protocol
Control ( $n = 7$ )	Control diet [(high-fructose high-fat) <sup>a</sup> + 1.0% (w/w) safflower oil]
Losartan-treated ( $n = 5$ )	Control diet + 5.0 mg $\text{kg}^{-1}$ body weight per day losartan in drinking water
Telmisartan-treated ( $n = 7$ )	Control diet + 5.0 mg $\text{kg}^{-1}$ body weight per day telmisartan in drinking water
CLA-treated ( $n = 7$ )	High-fructose high-fat diet + 1.0% (w/w) CLA <sup>b</sup>
CLA + telmisartan-treated ( $n = 7$ )	High-fructose high-fat diet + 1.0% CLA + 5.0 mg $\text{kg}^{-1}$ body weight per day telmisartan in drinking water

<sup>a</sup> Contains 60% fructose and 10% lard

<sup>b</sup> Composed of 75% mixture of *c9*, *t11* and *t10*, *c12* in a 50:50 ratio

## Lipid Profiles

Serum TG, TC, and HDL-cholesterol concentrations were measured at baseline, week 4, and week 8 of the study using standard enzymatic methods (Diagnostic Chemicals, PEI, Canada) as previously reported [12–14]. A standard precipitation method [14] was used to prepare the HDL fraction. Serum LDL-cholesterol concentrations were calculated according to the Friedewald formula [15].

## Glucose and Insulin

Serum glucose levels were determined at baseline, week 4, and week 8 using a commercially available glucose-oxidase kit (Wako Chemicals, VA, USA; [16]). Plasma insulin levels were quantified at week 20 using ultra sensitive ELISA kit (Crystal Chem, IL, USA), as previously described [17].

## Blood Pressure

Systolic blood pressure (SBP) was recorded at weeks 12–14 using the standard tail-cuff method in conscious animals as previously reported [18]. Five readings were obtained from each rat and averaged after the highest and the lowest values were excluded as previously described [19]. Diastolic blood pressure (DBP) was then calculated using the equation  $\text{DBP} = [(3\text{MAP}) - \text{SBP}]/2$ , where MAP represents the mean arterial pressure [20].

## Glucose Tolerance Testing

Oral glucose tolerance test (OGTT) was carried out at the end of the study in conscious rats after administration of 100 mg/100 g body weight glucose (Sigma–Aldrich) by gastric gavage in an overnight-fasting state [9]. Immediately before, and 30, 60, and 120 min after oral administration of glucose, whole-blood glucose levels were recorded by use of a conventional blood-glucose meter (LifeScan, CA, USA), as previously reported [21]. Total area under the curve of glucose (AUC<sub>glu</sub>) response during the OGTT was calculated by the linear trapezoidal rule [22].

## Cytokine Profiles

Plasma samples from the final blood collection (week 20) of each experimental group were pooled and assayed by rat cytokine array techniques (RayBiotech, GA, USA), as previously described [23].

## Statistical Analysis

All values are expressed as mean  $\pm$  standard error of the mean (SEM) unless otherwise stated. Data were analyzed using SPSS 11.5 statistical software for Windows (SPSS, IL, USA). SBP, DBP, food, and water intake, AUCglu, and insulin data were statistically evaluated by one-way ANOVA followed by the Tukey test for comparisons across multiple groups. The differences among all dietary groups and time points (diet  $\times$  time interaction) for body weight, TG, TC, HDL-cholesterol and LDL-cholesterol, glucose, and the OGTT data were analyzed by repeated measures of ANOVA. To compare the effects of each treatment at a given time point, a separate one-way ANOVA was performed followed by Tukey multiple comparison tests. The level of statistical significance was set at  $P < 0.05$ .

## Results

### Body Weight

Rats in all the experimental groups gained weight throughout the study period. The extent of weight gain was, however, significantly lower in the CLA + telmisartan-treated rats than in the other groups. Starting at week 8, rats receiving CLA + telmisartan showed a significantly lower mean body weight relative to the control ( $P < 0.01$ ) or CLA-treated ( $P < 0.05$ ) groups. However, the differences in body weight between the two groups of combination therapy and telmisartan were not statistically significant. The diet/drug combination therapy group progressively gained less body weight throughout the study period. Figure 1 demonstrates body-weight gain among the experimental groups over the course of the study. Figure 1 also demonstrates that treatment with CLA, telmisartan, or losartan did not result in statistically significant differences in body-weight gain compared with controls.

### Amount of Visceral Fat

Figure 2 shows representative photographs of visceral adipose tissue among the experimental groups. The CLA + telmisartan-treated rats exhibited a remarkable diminution in the visceral fat pad size relative to other groups.

### Food and Water Intake

Calculated average daily food and water intake are shown in Figs. 3a and 3b, respectively. Average daily food consumption was similar ( $29.0 \pm 1.5$  g day<sup>-1</sup>) among the

different experimental groups. Similarly, average water intake ( $42.3 \pm 2.2$  mL day<sup>-1</sup>) was comparable in all five experimental groups.

## Serum Lipids

Compared with the baseline data the HFHF diet notably raised serum TG levels in all of the experimental groups by week 4 of the study (Table 3), at which time only the CLA + telmisartan-treated rats exhibited significantly lower ( $P < 0.01$ ) TG concentrations, compared with controls ( $1.0 \pm 0.2$  vs.  $2.3 \pm 0.2$  mmol L<sup>-1</sup>). At week 8, administration of telmisartan treatment was associated with a 90% reduction ( $P < 0.05$ ) in serum TG levels whereas CLA alone resulted in a non-significant 31% reduction compared with controls. The combination of CLA and telmisartan resulted in greater reductions in serum TG concentrations compared with the effects of each agent alone. At week 8, the CLA + telmisartan-treated group had significantly lower serum TG levels as compared with the control, losartan, or CLA-treated rats. Serum levels of TC were comparable in all of the experimental groups by week 4 of the study. However, a non-significant trend of reduced TC levels was observed in telmisartan, CLA, and CLA + telmisartan-treated rats compared with either control or losartan-treated rats. It should be mentioned that both TG and TC levels were comparable between the telmisartan and CLA + telmisartan groups. At week 8, only CLA + telmisartan-treated rats exhibited a significant ( $P < 0.05$ ) reduction of 48% in TC levels relative to the control or losartan-treated animals (Table 3). Serum HDL-cholesterol levels were slightly higher in the control and losartan-treated rats relative to those in other groups

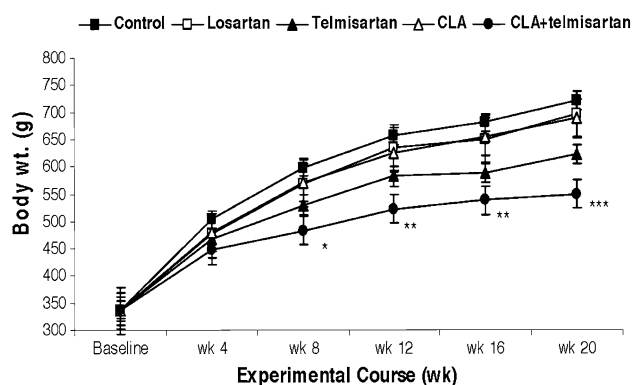


**Fig. 1** Patterns of body-weight gain among the experimental groups during the course of the study. Values are mean  $\pm$  SEM,  $n = 7$ , for all experimental groups except the losartan-treated group ( $n = 5$ ). \* $P < 0.01$  versus control and  $P < 0.05$  versus CLA, \*\* $P < 0.01$  versus control and  $P < 0.05$  versus losartan, \*\*\* $P < 0.01$  versus control, CLA, or losartan. body-weight gain was comparable among CLA, telmisartan, losartan, and control groups



**Fig. 2** Representative photographs taken from the experimental animals at autopsy (week 20 of study). Animals from CLA + telmisartan group (e) show diminished visceral fat pad size compared with other groups (a–d) a control, b losartan, c telmisartan, d CLA, e CLA + telmisartan. Arrows indicate abdominal adipose tissue

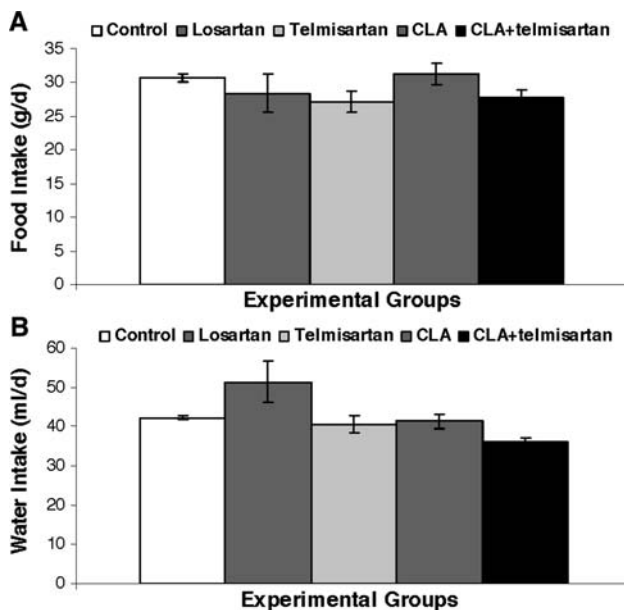
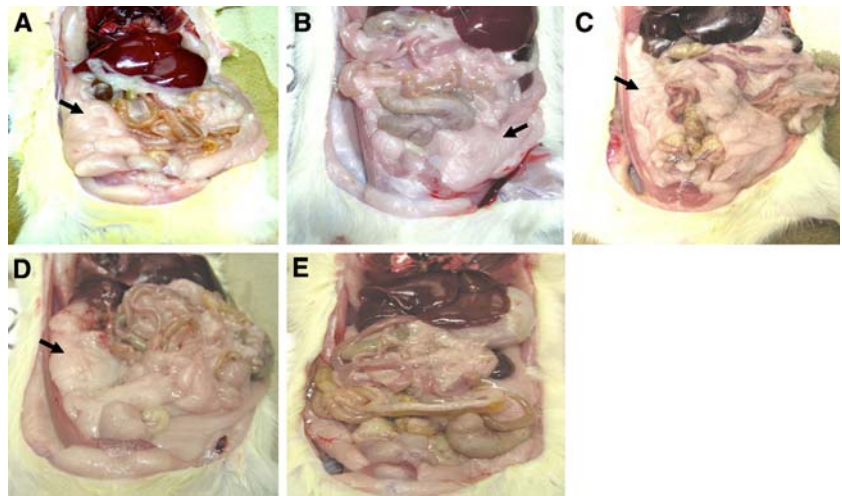


**Fig. 3** Average daily food (a) and water (b) consumption by the experimental rats throughout the study period. Values are mean  $\pm$  SEM,  $n = 7$ , for all experimental groups except the losartan-treated group ( $n = 5$ )

throughout the study period (Table 3). This may reflect the higher levels of TC in these two groups of rats. Similarly, the levels of serum LDL-cholesterol were not significantly different among the experimental groups (Table 3). The CLA + telmisartan-treated rats, however, did show 22 and 13% less LDL-cholesterol levels at week 4 and week 8, respectively, compared with the controls.

#### Serum Glucose

Serum glucose levels of the rats at different times in the study are summarized in Table 3. Introduction of the HFHF diet did not significantly raise serum glucose levels

in the control group over 8 weeks of the experiment. At week 4, only losartan-treated rats showed a significant reduction of approximately 40% ( $P < 0.05$ ) in serum glucose levels, compared with those in the CLA-treated group, but not to the controls. At week 8, the losartan, telmisartan, and CLA + telmisartan-treated rats showed significantly ( $P < 0.05$ ) lower serum glucose concentrations (39, 23, and 30%, respectively) relative to the controls. Glucose levels in the CLA-treated animals and in the control group remained comparable throughout the study period. Similarly, both telmisartan and CLA + telmisartan groups had comparable serum glucose levels.

#### Systolic and Diastolic Blood Pressure

Administration of either losartan or telmisartan caused significant reductions in SBP. Losartan-treated rats exhibited significantly lower SBP as compared with the control group ( $113.0 \pm 4.0$  vs.  $138.0 \pm 8.0$  mmHg,  $P < 0.001$ ). The telmisartan-treated rats also showed a significant reduction in their SBP as compared with the controls ( $103.0 \pm 7.0$  vs.  $138.0 \pm 8.0$  mmHg,  $P < 0.001$ ). Similarly, the CLA + telmisartan-treated rats exhibited a significant reduction in SBP relative to the controls ( $121.0 \pm 13.0$  vs.  $138.0 \pm 8.0$  mmHg,  $P < 0.05$ ) however, the extent of reductions in SBP in the combination therapy group was lower than that in the telmisartan intervention group ( $121.0 \pm 13.0$  vs.  $103.0 \pm 7.0$  mmHg,  $P < 0.01$ ). The CLA-treated rats and the control group had comparable SBP. Animals on all the different diets showed comparable DBP. Data on SBP and DBP are summarized in Table 3.

#### Plasma Insulin

The co-administration of CLA and telmisartan resulted in significantly lower plasma insulin levels, as compared with

**Table 3** Effects of diets on serum levels of triglycerides (TG), total cholesterol (TC), high-density lipoprotein (HDL), low-density lipoprotein (LDL), and glucose, plus the total areas under the curve for

Experimental groups/variables	Control (n = 7)	Losartan (n = 5)	Telmisartan (n = 7)	CLA (n = 7)	CLA + telmisartan (n = 7)
Serum TG (mmol L <sup>-1</sup> )					
Week 0	0.8 ± 0.1	0.7 ± 0.0	0.9 ± 0.1	0.7 ± 0.1	0.8 ± 0.0
Week 4	2.3 ± 0.2	1.3 ± 0.1	1.9 ± 0.4	2.0 ± 0.2	1.0 ± 0.2*
Week 8	3.8 ± 0.3	3.0 ± 0.8	2.0 ± 0.4**	2.9 ± 0.5	1.1 ± 0.1***
Serum TC (mmol L <sup>-1</sup> )					
Week 0	1.5 ± 0.1	1.7 ± 0.2	1.5 ± 0.1	1.5 ± 0.1	1.5 ± 0.1
Week 4	1.9 ± 0.2	2.0 ± 0.3	1.6 ± 0.2	1.7 ± 0.1	1.4 ± 0.1
Week 8	2.4 ± 0.1	2.4 ± 0.3	2.1 ± 0.2	2.1 ± 0.2	1.6 ± 0.2*
Serum HDL-cholesterol (mmol L <sup>-1</sup> )					
Week 0	0.3 ± 0.0	0.3 ± 0.0	0.3 ± 0.0	0.2 ± 0.0	0.3 ± 0.0
Week 4	0.5 ± 0.0	0.5 ± 0.1	0.5 ± 0.0	0.4 ± 0.0	0.4 ± 0.0
Week 8	0.6 ± 0.0	0.6 ± 0.1	0.5 ± 0.1	0.5 ± 0.1	0.5 ± 0.0
Serum LDL-cholesterol (mmol L <sup>-1</sup> )					
Week 0	1.0 ± 0.0	1.2 ± 0.1	1.0 ± 0.0	1.1 ± 0.0	1.0 ± 0.1
Week 4	1.0 ± 0.0	1.2 ± 0.1	0.7 ± 0.0	0.9 ± 0.0	0.8 ± 0.0
Week 8	1.1 ± 0.0	1.2 ± 0.0	1.1 ± 0.0	1.0 ± 0.0	0.9 ± 0.1
Serum glucose (mmol L <sup>-1</sup> )					
Week 0	8.0 ± 0.4	7.8 ± 0.8	8.1 ± 0.4	7.7 ± 0.2	7.8 ± 0.2
Week 4	8.9 ± 0.3	7.0 ± 0.3*	7.7 ± 0.8	9.7 ± 0.4	8.0 ± 0.5
Week 8	8.6 ± 0.2	6.2 ± 0.6**	7.0 ± 0.4***	7.3 ± 0.3	6.6 ± 0.2**
AUCglu (mmol L <sup>-1</sup> 2 h <sup>-1</sup> )					
Week 20	15.7 ± 0.5	16.1 ± 1.4	14.8 ± 0.7	14.3 ± 0.5	12.8 ± 0.3*
SBP (mmHg)					
Week 12–14	138.0 ± 3.7	113.0 ± 3.5*	103.0 ± 2.5**	128.0 ± 3.3	121.0 ± 4.8***
DBP (mmHg)					
Week 12–14	98.7 ± 3.1	92.0 ± 4.6	84.6 ± 2.7	98.9 ± 1.0	91.6 ± 5.5
Plasma insulin (ng mL <sup>-1</sup> )					
Week 20	2.3 ± 0.2	2.2 ± 0.4	1.6 ± 0.2	1.6 ± 0.1	1.2 ± 0.1*

Values are mean ± SEM

TG: \*  $P < 0.01$  versus control, \*\*  $P < 0.05$  versus control, \*\*\*  $P < 0.001$  versus control or  $P < 0.05$  versus losartan and CLA

TC: \*  $P < 0.05$  versus control and losartan

Glucose: \*  $P < 0.05$  versus CLA, \*\*  $P < 0.01$  versus control, \*\*\*  $P < 0.05$  versus control

AUCglu: \*  $P < 0.05$  versus control and losartan

SBP: \*  $P < 0.001$  versus control, \*\*  $P < 0.001$  versus control or CLA and  $P < 0.01$  versus CLA + telmisartan, \*\*\*  $P < 0.05$  versus control

Insulin: \*  $P < 0.01$  versus control and  $P < 0.05$  versus losartan

the controls ( $P < 0.01$ ) or with the losartan-treated ( $P < 0.05$ ) rats at week 20 (Table 3).

#### OGTT and AUCglu

The CLA + telmisartan-treated rats showed significantly lower ( $P < 0.05$ ) whole-blood glucose concentrations at 0 time-point of OGTT, as compared with the control or CLA-treated rats. No statistically significant differences, however, were observed among the experimental groups 30, 60

and 120 min after OGTT (Fig. 4). AUCglu values were significantly lower ( $P < 0.05$ ) in the diet/drug co-therapy compared with values in the control or losartan-treated rats (Table 3).

#### Plasma Cytokines

The levels of various cytokines and the calculated differences between the control values and those from each treatment group are presented in Table 4. Plasma IL1- $\alpha$

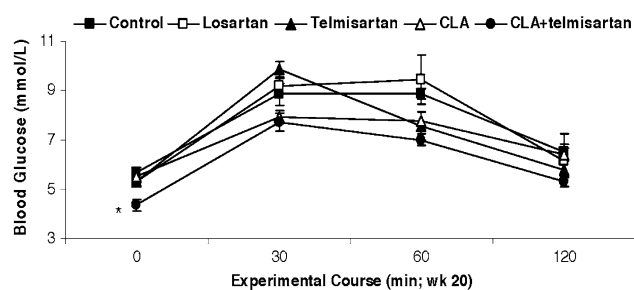


**Fig. 4** Levels of whole-blood glucose during the oral glucose tolerance test (OGTT) at week 20 of the study. Glucose solution of 100 mg/100 g body weight was administered to each rat by gastric gavage. Values are mean  $\pm$  SEM,  $n = 7$  for all experimental groups except for losartan-treated group ( $n = 5$ ). \* $P < 0.05$  versus control or CLA-treated groups

levels were slightly higher in the telmisartan and CLA-treated rats but lower in the CLA + telmisartan-treated rats. Plasma IL1- $\beta$  levels were 35, 73, and 28% higher in the telmisartan, CLA, and CLA + telmisartan-treated rats, respectively, compared with controls. IL-6 levels were 50% higher in the telmisartan-treated rats and 36% higher in the CLA + telmisartan-treated rats, compared with controls. IFN- $\gamma$  levels were higher in the losartan and telmisartan-treated groups by 33 and 24%, respectively, compared with controls. The levels of IL-4 and IL-10 were higher in CLA-treated groups by 87 and 94%, respectively, and in the CLA + telmisartan-treated rats by 55 and 75%, respectively, relative to the controls. The levels of pro-inflammatory cytokine TNF- $\alpha$  were remarkably higher in all treated groups (108% in losartan, 239% in telmisartan, 249% in CLA, and 188% in CLA + telmisartan) relative to the controls.

## Discussion

Patients with MetS are at higher risk of CVD and diabetes and have increased CVD-related mortality [1, 24].

Globally, there has been growing interest in therapeutic approaches that can target the multiple risk factors within MetS simultaneously. This can be achieved through combination therapies or administration of multi-functional agents. Owing to its antihypertensive and antiglycemic properties, telmisartan can be one such agent [9, 25]. Another agent could be dietary CLA, which has been reported to improve glucose, lipid, and energy metabolism, probably through activation of PPAR- $\alpha$  and PPAR- $\gamma$  [7, 8, 26]. Although evidence of the effectiveness of such individual drug or dietary agent against cardiovascular risk is strong, the outcome of their combination has yet to be reported. Herein we report the effects of co-administration of CLA and telmisartan on a number of well-known cardiovascular risk factors in a rat model.

One of the most interesting findings of this study is the efficacy of CLA/telmisartan co-therapy in reducing the amount of abdominal fat and, thereby, maintaining lean body weight. In agreement with previous studies [27, 28], we observed no significant effect of dietary CLA alone on body-weight gain. Similarly, telmisartan alone did not significantly reduce body-weight gain in the rats. However, co-administration of CLA and telmisartan markedly attenuated the rats' body-weight gain throughout the treatment period. The autopsy inspection revealed that the reduction in body weight in the co-therapy group was mainly due to reduction in the amount of visceral fat. While the mechanisms responsible for such dramatic effect remain to be established, the effects on uncoupling proteins (UCPs), that are involved in the regulation of energy synthesis and expenditure, might be a possibility. With this regard, previous studies [29] reported an association between reduced body weight, an increase in UCP-2, and to a lesser extent UCP-3, mRNA levels in skeletal muscles of *c9*, *t11*-CLA-fed rats. Similarly, Ryder et al. reported that CLA (*c9*, *t11* and 50:50) intake upregulated UCP-2 mRNA abundance in muscle and adipose tissue in ZDF rats

**Table 4** Effects of diets on pooled plasma cytokine profiles at week 20

Analytes	Control	Losartan	Telmisartan	CLA	CLA + telmisartan
IL1- $\alpha$	659	646 (−2.0%)	844 (+28%)	821(+25%)	548 (−20%)
IL1- $\beta$	830	939 (+13%)	1124 (+35%)	1435 (+73%)	1059 (+28%)
IL-4	469	488 (+4%)	536 (+14%)	879 (+87%)	726 (+55%)
IL-6	529	583 (+10%)	794 (+50%)	537 (+15%)	722 (+36%)
IL-10	537	676 (+26%)	750 (+40%)	1040 (+94%)	938 (+75%)
IFN- $\gamma$	976	1294 (+33%)	1208 (+24%)	987 (+1%)	917 (−6%)
TNF- $\alpha$	1628	3385 (+108%)	5515 (+239%)	5680 (+249%)	4694 (+188%)

<sup>a</sup> Values are optical density with background subtraction

<sup>b</sup> Rats were injected with LPS (400  $\mu$ g per rat, ip) 2 h before sacrifice; plasma cytokine levels were analyzed in pooled samples

IL, interleukin; IFN, interferon; TNF, tumor necrosis factor

Numbers in brackets indicate the extent of changes relative to control values: − decreases, + increases

on high-fat diets [30]. Furthermore, one recent study has shown the ability of telmisartan to increase UCP-1 mRNA expression in brown adipose tissue in diet-induced obese mice [31]. Therefore, it is reasonable to speculate that the CLA/telmisartan co-administration might generate additive effects, and increased activities and/or expression of various UCPs. Data from this study and previous reports suggest investigation of such additive effects for CLA/telmisartan co-therapy in an appropriate model.

In humans, several studies have shown that increased visceral fat is an independent risk factor for metabolic disorders including atherosclerosis [32]. Several guidelines, therefore, have been developed to target the body mass index (BMI) at an acceptable range. Various strategies including lifestyle modifications, therapeutic approaches, and surgical procedures have been introduced for prevention of central obesity. With this regard, data from animal experiments suggest that dietary CLA may reduce energy intake [33] or increase energy expenditure [34], reduce fat cell size [27], alter preadipocyte differentiation [35], increase apoptosis of adipocytes [36], inhibit lipogenesis [37], and increase FA oxidation [38]. Similarly, one recent study has reported reductions in visceral fat and adipocyte size in rats treated with telmisartan [11]. In the current study the substantial reductions in the amount of visceral fat were associated with a significant reduction in serum TG levels in the combination therapy group, as compared with controls. Increased levels of serum TG are also an independent risk factor for atherosclerosis [39, 40]. Previous studies reported that both telmisartan and CLA, individually, reduce plasma TG levels in experimental animals [9, 41]. Our study further shows that the combination of these two agents seems to generate an additive or synergistic effect, as the extent of reductions of TG levels in the combination therapy group was greater than that in other groups of rats. It has been shown that CLA activates PPAR- $\alpha$ , and that hepatic PPAR- $\alpha$  activation is involved in regulation of energy balance, lipid homeostasis, and body-weight gain [42, 43]. The mechanisms underlying body weight and lipid-lowering effects of the CLA/telmisartan co-therapy might, therefore, be related, at least in part, to an increase in extent of PPARs activation.

The effects of CLA on glucose metabolism have not been entirely defined. Some studies have indicated that CLA improves insulin sensitivity in Zucker *fa/fa* rats [19, 44], while others have reported that CLA induces insulin resistance in C57BL/6J mice [33, 35]. Choi et al. [29] showed that a mixture of *c9*, *t11* and *t10*, *c12* CLA markedly reduces serum glucose and enhances glucose tolerance and insulin metabolism in SD rats. In another study, telmisartan treatment was associated with a 12% reduction in serum glucose levels in SD rats on a high-calorie diet [9]. In our current work we observed that a

combination of CLA and telmisartan reduces serum glucose levels by 30% over four weeks. This effect on glucose metabolism was associated with reduced plasma insulin concentrations in the combination group, compared with controls. These changes in glucose metabolism might be a result of reduced visceral fat, serum TG levels, and consequent alterations in FA metabolism.

Hypertension is a well-known independent risk factor for CVD [45]. Limited studies have shown anti-hypertensive effects of CLA in some rat models [46, 47]. On the other hand, telmisartan is widely known as a potent anti-hypertensive drug [48]. The current study not only failed to show a significant anti-hypertensive activity for CLA, but also suggested that CLA may partially mask telmisartan's antihypertensive effects. The extent of reductions in SBP of the combination group was lower than that of telmisartan-treated animals. At the moment, the reasons for this effect of dietary CLA are not clear. Despite changes in SBP, DPB remained comparable among all the experimental groups.

It is well-established that diabetes and atherosclerosis are generally associated with a pro-inflammatory state [49]. Several lipid-lowering or anti-hypertensive drugs have been shown to reduce the levels of pro-inflammatory mediators. Dietary CLA has been shown to reduce production of TNF- $\alpha$  both in human subjects and animal models [50]. Our study failed to reproduce similar effects. Levels of TNF- $\alpha$  increased substantially in all treatment groups compared with controls. One of the major sources of TNF- $\alpha$  production is adipose tissue. It is interesting that in the current study the plasma levels of TNF- $\alpha$  seem to be independent of the amount visceral fat. Plasma levels of TNF- $\alpha$  were comparable among the CLA/telmisartan co-therapy group (which had little or no visceral fat) and the other experimental groups (which had noticeable amounts of visceral fat). On the other hand, plasma levels of anti-atherogenic cytokines, such as IL-10, were notably increased in the CLA- and CLA+ telmisartan-treated rats relative to the controls. Many studies have reported an anti-atherogenic effect for IL-10 in both experimental animals and humans [51, 52]. At the same time, CLA/telmisartan co-therapy was not able to reduce the levels of pro-atherogenic cytokines IL-1 $\beta$  and IL-6. The importance of these observations in the context of reductions in body weight and abdominal fat, improvements in serum lipid profiles, blood pressure, and glucose metabolism warrants further investigation.

In conclusion, optimal therapeutic strategies that simultaneously reduce several cardiovascular risk factors in conditions such as MetS are in great demand. Such strategies could be achieved by combination of pharmaceuticals; several disadvantages, including undesirable drug–drug interactions, low cost-effectiveness, and low patient compliance, may limit this approach, however. In

contrast, these limiting factors may be reduced by a combination of pharmaceutical and nutraceutical means. Herein we report that a combination of dietary CLA and the anti-hypertensive drug telmisartan significantly reduced body weight, abdominal fat, serum TG and TC levels, and SBP, with improvements in glucose metabolism and a mixed response in several pro and anti-inflammatory markers. At present, the mechanisms involved in the generation of such effects remain to be completely defined. Nevertheless, our observations suggest that this combination may be an attractive strategy for further consideration in prevention/treatment of some of the abnormalities associated with MetS. In particular, the observed dramatic effect of the combination therapy on the amount of abdominal fat warrants extra investigation of the effectiveness of such intervention against the ever-escalating prevalence of obesity and its associated disorders. Although this approach seems safe and inexpensive, whether such a combination therapy results in clinical benefits has yet to be addressed. The animal model used in this study was not appropriate for testing the effects of this diet/drug combination on the development of atherosclerotic lesions. This can be potentially fruitful for future research before making suggestions of clinical benefits of such therapy for patients with CVD.

**Acknowledgments** The research program of M.H.M is supported by grants from the Natural Engineering and Science Research Council of Canada (NSERC), the Canadian Foundation for Innovation (CFI), the Heart and Stroke Foundation of Canada, and Manitoba Health Research Council. CLA was a generous gift from Bioriginal Food and Science Corporation (Saskatoon, Canada). Assistance of Dr Pram Tappia in the blood-pressure measurements is greatly appreciated. The authors are also grateful to Dr Miyoung Suh, Dr Evelyn Fitz, and Rgia Othman for their significant contribution. M.M.A is a recipient of Kuwait University's Scholarship for Grad. Studies, State of Kuwait.

## References

- Moller DE, Kaufman KD (2005) Metabolic syndrome: a clinical and molecular perspective. *Annu Rev Med* 56:45–62
- Aude YW, Mego P, Mehta JL (2004) Metabolic syndrome: dietary interventions. *Curr Opin Cardiol* 19:473–479
- Wang YW, Jones PJ (2004) Conjugated linoleic acid and obesity control: efficacy and mechanisms. *Int J Obes Relat Metab Disord* 28(8):941–955. Review
- Houseknecht KL, Vanden Heuvel JP, Moya-Camarena SY, Portocarrero CP, Peck LW, Nickel KP, Belury MA (1998) Dietary conjugated linoleic acid normalizes impaired glucose tolerance in the Zucker diabetic fatty fa/fa rat. *Biochem Biophys Res Commun* 244(3):678–682
- Kritchevsky D, Tepper SA, Wright S, Tso P, Czarnecki SK (2000) Influence of conjugated linoleic acid (CLA) on establishment and progression of atherosclerosis in rabbits. *J Am Coll Nutr* 19(4):472S–477S
- Zulet MA, Marti A, Parra MD, Martinez JA (2005) Inflammation and conjugated linoleic acid: mechanisms of action and implications for human health. *J Physiol Biochem* 61(3):483–94. Review
- Moya-Camarena SY, Van den Heuvel JP, Blanchard SG, Leesnitzer LA, Belury MA (1999) Conjugated linoleic acid is a potent naturally occurring ligand and activator of PPAR- $\alpha$ . *J Lipid Res* 40:1426–1433
- Moya-Camarena SY, Van den Heuvel JP, Belury MA (1999) Conjugated linoleic acid activates peroxisome proliferator-activated receptor alpha and beta subtypes but does not induce hepatic peroxisome proliferation in Sprague-Dawley rats. *Biochim Biophys Acta* 1436:331–342
- Benson SC, Pershadsingh HA, Ho CI, Chittiboyina A, Desai P, Pravenec M, Qi N, Wang J, Avery MA, Kurtz TW (2004) Identification of telmisartan as a unique angiotensin II receptor antagonist with selective PPAR- $\gamma$ -modulating activity. *Hypertension* 43:993–1002
- Pershadsingh HA, Kurtz TW (2004) Insulin-sensitizing effects of telmisartan: implications for treating insulin-resistant hypertension and cardiovascular disease. *Diabetes Care* 27:1015
- Sugimoto K, Qi NR, Kazdova L, Pravenec M, Ogihara T, Kurtz TW (2006) Telmisartan but not valsartan increases caloric expenditure and protects against weight gain and hepatic steatosis. *Hypertension* 47:1003–1009
- Moghadasian MH, McManus BM, Godin DV, Rodrigues B, Frohlich JJ (1999) Proatherogenic and antiatherogenic effects of probucol and phytosterols in apolipoprotein E-deficient mice: possible mechanisms of action. *Circulation* 99:1733–1739
- Moghadasian MH (2006) Dietary phytosterols reduce probucol-induced atherogenesis in apo E-KO mice. *Atherosclerosis* 188:28–34
- Moghadasian MH, McManus BM, Nguyen LB, Shefer S, Nadji M, Godin DV, Green TJ, Hill J, Yang Y, Scudamore CH, Frohlich JJ (2001) Pathophysiology of apolipoprotein E deficiency in mice: relevance to apo E-related disorders in humans. *FASEB J* 15:2623–2630
- Friedewald WT, Levy RI, Fredrickson DS (1972) Estimation of the concentration of low-density lipoprotein cholesterol in plasma, without use of the preparative ultracentrifuge. *Clin Chem* 18:499–502
- Stark AH, Timar B, Madar Z (2000) Adaptation of Sprague Dawley rats to long-term feeding of high fat or high fructose diets. *Eur J Nutr* 39:229–234
- Bhattacharya A, Rahman MM, Sun D, Lawrence R, Mejia W, McCarter R, O'Shea M, Fernandes G (2005) The combination of dietary conjugated linoleic acid and treadmill exercise lowers gain in body fat mass and enhances lean body mass in high fat-fed male Balb/C mice. *J Nutr* 135:1124–1130
- Donnelly R, Ho H, Reaven GM (1995) Effects of low sodium diet and unilateral nephrectomy on the development of carbohydrate-induced hypertension. *Blood Press* 4:164–169
- Naga K, Inoue N, Wang YM, Yanagita T (2003) Conjugated linoleic acid enhances plasma adiponectin level and alleviates hyperinsulinemia and hypertension in Zucker diabetic fatty (fa/fa) rats. *Biochem Biophys Res Commun* 310:562–566
- Fortuno MA, Ravassa S, Etayo JC, Diez J (1998) Overexpression of Bax protein and enhanced apoptosis in the left ventricle of spontaneously hypertensive rats: effects of AT1 blockade with losartan. *Hypertension* 32(2):280–286
- Schlenker EH, Shi Y, Wipf J, Martin DS, Kost CK Jr (2004) Fructose feeding and intermittent hypoxia affect ventilatory responsiveness to hypoxia and hypercapnia in rats. *J Appl Physiol* 97(4):1387–1394
- Purves RD (1992) Optimum numerical integration methods for estimation of area-under-the-curve (AUC) and area-under-the-moment-curve (AUMC). *J Pharmacokinet Biopharm* 20(3):211–226

23. Watanabe M, Guo W, Zou S, Sugiyu S, Dubner R, Ren K (2005) Antibody array analysis of peripheral and blood cytokine levels in rats after masseter inflammation. *Neurosci Lett* 382:128–133
24. Lakka HM, Laaksonen DE, Lakka TA, Niskanen LK, Kumpusalo E, Tuomilehto J, Salonen JT (2002) The metabolic syndrome and total and cardiovascular disease mortality in middle-aged men. *JAMA* 288:2709–2716
25. Kurtz TW (2005) Treating the metabolic syndrome: telmisartan as a peroxisome proliferator-activated receptor-gamma activator. *Acta Diabetol* 42(Suppl 1):S9–16
26. Yu Y, Correll PH, Van den Heuvel JP (2002) Conjugated linoleic acid decreases production of pro-inflammatory products in macrophages: evidence for a PPAR gamma-dependent mechanism. *Biochim Biophys Acta* 1581:89–99
27. Azain MJ, Hausman DB, Sisk MB, Flatt WP, Jewell DE (2000) Dietary conjugated linoleic acid reduces rat adipose tissue cell size rather than cell number. *J Nutr* 130:1548–1554
28. Yamasaki M, Mansho K, Mishima H, Kimura G, Sasaki M, Kasai M, Tachibana H, Yamada K (2000) Effect of dietary conjugated linoleic acid on lipid peroxidation and histological change in rat liver tissues. *J Agric Food Chem* 48:6367–6371
29. Choi JS, Jung MH, Park HS, Song J (2004) Effect of conjugated linoleic acid isomers on insulin resistance and mRNA levels of genes regulating energy metabolism in high-fat-fed rats. *Nutrition* 20:1008–1017
30. Ryder JW, Portocarrero CP, Song XM, Cui L, Yu M, Combatsiaris T, Galuska D, Bauman DE, Barbano DM, Charron MJ, Zierath JR, Houseknecht KL (2001) Isomer-specific antidiabetic properties of conjugated linoleic acid. Improved glucose tolerance, skeletal muscle insulin action, and UCP-2 gene expression. *Diabetes* 50:1149–1157
31. Araki K, Masaki T, Katsuragi I, Tanaka K, Kakuma T, Yoshimatsu H (2006) Telmisartan prevents obesity and increases the expression of uncoupling protein 1 in diet-induced obese mice. *Hypertension* 48:51–57
32. Pi-Sunyer FX (2004) The epidemiology of central fat distribution in relation to disease. *Nutr Rev* 62:S120–126
33. West DB, Delany JP, Camet PM, Blohm F, Truett AA, Scimeca J (1998) Effects of conjugated linoleic acid on body fat and energy metabolism in the mouse. *Am J Physiol* 275:R667–672
34. West DB, Blohm FY, Truett AA, DeLany JP (2000) Conjugated linoleic acid persistently increases total energy expenditure in AKR/J mice without increasing uncoupling protein gene expression. *J Nutr* 130:2471–2477
35. Evans M, Geigerman C, Cook J, Curtis L, Kuebler B, McIntosh M (2000) Conjugated linoleic acid suppresses triglyceride accumulation and induces apoptosis in 3T3-L1 preadipocytes. *Lipids* 35:899–910
36. Tsuboyama-Kasaoka N, Takahashi M, Tanemura K, Kim HJ, Tange T, Okuyama H, Kasai M, Ikemoto S, Ezaki O (2000) Conjugated linoleic acid supplementation reduces adipose tissue by apoptosis and develops lipodystrophy in mice. *Diabetes* 49:1534–1542
37. Park Y, Storkson JM, Albright KJ, Liu W, Pariza MW (1999) Evidence that the trans-10, cis-12 isomer of conjugated linoleic acid induces body composition changes in mice. *Lipids* 34:235–2341
38. Sergiel JP, Chardigny JM, Sebedio JL, Berdeaux O, Juaneda P, Loreau O, Pasquis B, Noel JP (2001) Beta-oxidation of conjugated linoleic acid isomers and linoleic acid in rats. *Lipids* 36:1327–1329
39. He Y, Lam TH, Li LS, He SF, Liang BQ (2004) Triglyceride and coronary heart disease mortality in a 24-year follow-up study in Xi'an, China. *Ann Epidemiol* 14:1–7
40. Austin MA (1997) Triacylglycerol and coronary heart disease. *Proc Nutr Soc* 56:667–670
41. Li YQ, Ji H, Zhang YH, Ding DY, Ye XL (2006) Metabolic effects of telmisartan in spontaneously hypertensive rats. *Naunyn Schmiedeberg Arch Pharmacol* 373:264–2670
42. Fruchart JC (2001) Peroxisome proliferator-activated receptor-alpha activation and high-density lipoprotein metabolism. *Am J Cardiol* 88:24N–29N
43. Fruchart JC, Staels B, Duriez P (2001) PPARs, metabolic disease and atherosclerosis. *Pharmacol Res* 44:345–352
44. Henriksen EJ, Teachey MK, Taylor ZC, Jacob S, Ptock A, Kramer K, Hasselwander O (2003) Isomer-specific actions of conjugated linoleic acid on muscle glucose transport in the obese Zucker rat. *Am J Physiol* 285:E98–E105
45. Wilson PW (1997) An epidemiologic perspective of systemic hypertension, ischemic heart disease, and heart failure. *Am J Cardiol* 80:3J–8J
46. Nagao K, Inoue N, Wang YM, Hirata J, Shimada Y, Nagao T, Matsui T, Yanagita T (2003) The 10*trans*, 12*cis* isomer of conjugated linoleic acid suppresses the development of hypertension in Otsuka Long-Evans Tokushima fatty rats. *Biochem Biophys Res Commun* 306:134–138
47. Inoue N, Nagao K, Hirata J, Wang YM, Yanagita T (2004) Conjugated linoleic acid prevents the development of essential hypertension in spontaneously hypertensive rats. *Biochem Biophys Res Commun* 323:679–684
48. Sharpe M, Jarvis B, Goa KL (2001) Telmisartan: a review of its use in hypertension. *Drugs* 61:1501–1529
49. Haffner SM (2006) The metabolic syndrome: inflammation, diabetes mellitus, and cardiovascular disease. *Am J Cardiol* 97:3A–11A
50. O'Shea M, Bassaganya-Riera J, Mohede IC (2004) Immunomodulatory properties of conjugated linoleic acid. *Am J Clin Nutr* 79:1199S–1206S
51. Fichtlscherer S, Breuer S, Heeschen C, Dimmeler S, Zeiher AM (2004) Interleukin-10 serum levels and systemic endothelial vasoreactivity in patients with coronary artery disease. *J Am Coll Cardiol* 44:44–49
52. Pinderski Oslund LJ, Hedrick CC, Olvera T, Hagenbaugh A, Territo M, Berliner JA, Fyfe AI (1999) Interleukin-10 blocks atherosclerotic events in vitro and in vivo. *Arterioscler Thromb Vasc Biol* 19:2847–2853

# Dietary Counseling and Probiotic Supplementation During Pregnancy Modify Placental Phospholipid Fatty Acids

Niina Kaplas · Erika Isolauri · Anna-Maija Lampi ·  
Tiina Ojala · Kirsi Laitinen

Received: 3 January 2007 / Accepted: 29 June 2007 / Published online: 24 July 2007  
© AOCs 2007

**Abstract** It has previously been shown that maternal nutrition affects the fetal environment, with consequences for the infant's health. From early pregnancy onwards participants here received a combination of dietary counseling and probiotics (*Lactobacillus* GG and *Bifidobacterium lactis* Bb12;  $n = 10$ ), dietary counseling with placebo ( $n = 12$ ), or placebo alone ( $n = 8$ ). The major differences in placental fatty acids were attributable to a higher concentration of n-3 polyunsaturated fatty acids in both intervention arms than in controls. Further, dietary counseling with probiotics resulted in higher concentrations of

linoleic (18:2n-6) and dihomo- $\gamma$ -linolenic acids (20:3n-6) compared with dietary counseling with placebo or controls.

**Keywords** Diet · Placenta · Polyunsaturated fatty acids · Probiotics

## Abbreviations

AA	Arachidonic acid
DHA	Docosahexaenoic acid
DHGA	Dihomo- $\gamma$ -linolenic acid
EPA	Eicosapentaenoic acid
LA	Linoleic acid
MUFA	Monounsaturated fatty acid
PUFA	Polyunsaturated fatty acid
SFA	Saturated fatty acid

**Electronic supplementary material** The online version of this article (doi:10.1007/s11745-007-3094-9) contains supplementary material, which is available to authorized users.

N. Kaplas · K. Laitinen (✉)  
Functional Foods Forum, University of Turku,  
20014 Turku, Finland  
e-mail: kirsi.laitinen@utu.fi

K. Laitinen  
Department of Biochemistry and Food Chemistry,  
University of Turku, Turku, Finland

E. Isolauri  
Department of Paediatrics,  
University of Turku, Turku, Finland

E. Isolauri · T. Ojala · K. Laitinen  
Department of Paediatrics,  
Turku University Central Hospital, Turku, Finland

A.-M. Lampi  
Department of Applied Chemistry and Microbiology,  
University of Helsinki, Helsinki, Finland

## Introduction

The placenta regulates the nutritional, immunological, and endocrine environment of the fetus [1]. The importance of fatty acids, known to exert immunomodulatory effects via eicosanoid production [2], may culminate during pregnancy, their complex metabolism ranging from their deposition in maternal tissues in early pregnancy to their release during late pregnancy to supply fetal demands [3].

Earlier attempts to modify the pregnant mother's diet and thereby the nutritional and immunological environment of the fetus have focused on supplementation with long-chain polyunsaturated fatty acids (PUFA), fish oil [6], and probiotic bacteria [7]. Their synergistic effects [6, 7] imply the need to consider the overall diet.

Consequently, we chose dietary counseling together with probiotic supplementation to investigate whether

placental and umbilical cord serum phospholipid fatty acids and thus the fetal environment can be modified.

## Methods

### Subjects and Study Design

Placenta and umbilical cord serum samples were collected shortly after delivery from 30 healthy women participating in an ongoing mother–infant follow-up study, in order of enrolment [8]. Written informed consent was obtained from the participants and the study was approved by the Ethical Committee of the Hospital District of South-West Finland.

At the first visit, at 13.8 (SD 1.4) weeks of gestation, the recruited women were randomly assigned to three study groups. The dietary counseling groups received capsules of probiotics (diet/probiotics) containing *Lactobacillus rhamnosus GG* (ATCC 53103; Valio, Helsinki, Finland) and *Bifidobacterium lactis Bb12* (Chr. Hansen, Hørsholm, Denmark)  $10^9$  cfu day<sup>-1</sup> each, with demonstrated anti-inflammatory effects in young infants [9], or placebo (microcrystalline cellulose; diet/placebo), randomization proceeding in double-blind manner, while the control group received placebo (control/placebo) in single-blind manner.

Dietary counseling aimed at a dietary intake complying with that currently recommended [10], monounsaturated fatty acids (MUFA) contributing 10–15%, PUFA 5–10%, and saturated fatty acids (SFA) 10% or less of energy intake. Dietary counseling, supported with provision of conventional food products with favorable fat composition to be consumed at home, resulted in changes in dietary intake attributable to a higher intake of unsaturated and a lower intake of SFA, as reported in detail elsewhere [8]. Information regarding the course of pregnancy and infants' birth weights and heights was obtained from hospital records. The pre-pregnancy body-mass index was calculated using measured height and self-reported pre-pregnancy weight. Total gestational weight gain was calculated by subtracting the pre-pregnancy weight from that recorded at prenatal visit or delivery hospital within 1 week before delivery.

### Fatty Acid Analysis

To test the preservation of fatty acids during sampling and processing, one placenta was sampled 0.5, 1, 2, 4, 6, 12, and 24 h after delivery and analyzed for fatty acid concentrations. When stored at +4°C, the concentrations of PUFA remained relatively unchanged until 24 h after delivery, with a minor decrease at 12 h (data not shown).

To confirm the preservation of fatty acids placentas were sampled within 6 h and immediately frozen at -70°C. The blood samples were taken from the umbilical vessels directly after severing, and the serum was separated and frozen at -70°C.

Approximately 0.3 g placentas and 500 µL umbilical cord serum were used for analysis in duplicate. Placenta samples were homogenized on ice for 5 min using an Ultra-Turrax T8-homogenizer (IKA Werke, Staufen, Germany). The lipids in the placenta and cord serum samples were extracted with chloroform–methanol, 2:1 (v/v) [11] with dipentadecanoyl phosphatidylcholine (Larodan Fine Chemicals, Malmö, Sweden) as internal standard. Phospholipids were separated [12] using Sep-Pak Silica cartridges (100 mg; Waters, Milford, MA, USA). Fatty acid methyl esters were prepared by incubation in 1 mol L<sup>-1</sup> boron trifluoride in methanol at +100°C for 60 min and analyzed by gas chromatography [13]. Fatty acid contents were calculated from the respective methyl esters.

### Statistical Analysis

Results presented are the medians and interquartile ranges of the concentrations (mg g<sup>-1</sup> wet weight for placenta and mg mL<sup>-1</sup> for serum) and proportions (% w/w) of the fatty acids detected. Statistical differences among the three groups were analyzed by use of the Kruskal–Wallis test, and when significant, differences between two groups by use of the Mann–Whitney *U* test. Associations of the fatty acids in the placenta and the umbilical cord serum were assessed by Spearman's rank correlation test. SPSS for Windows (version 13.0; SPSS, Chicago, IL, USA) was used for statistical analyses.

## Results

The three study groups were comparable in terms of clinical characteristics (Table 1); the women were healthy and had no metabolic disorders. The pregnancies were uncomplicated and all infants were delivered at term.

The study groups differed in respect of placental fatty acids (Table 2). Evaluation in quantitative terms (mg g<sup>-1</sup>) showed dietary counseling to result in an increase in concentrations of the sum of n-3 PUFA and eicosatetraenoic acid (20:4n-3) in comparison of the diet/probiotics or diet/placebo groups with control/placebo. Assessment of proportional change in fatty acids showed higher proportion of dihomo- $\gamma$ -linolenic acid (20:3n-6, DHGA) in both intervention groups compared with control/placebo.

Comparison of the diet/probiotics group with the diet/placebo group showed administration of probiotics to affect placental fatty acids. The concentrations and propor-



**Table 1** Clinical characteristics of the women and their infants

	Diet/probiotics ( <i>n</i> = 10)		Diet/placebo ( <i>n</i> = 12)		Control/placebo ( <i>n</i> = 8)	
<b>Women</b>						
Age (years)	29	25–34	31	28–36	33	27–34
BMI before pregnancy (kg m <sup>-2</sup> )	22	20–23	25	23–29	23	22–25
Total weight gain during pregnancy (kg)	17	14–20	14	11–16	15	9–17
Duration of gestation (week)	40	39–41	39	39–41	40	39–42
<b>Infants</b>						
Birth weight (g)	3,800	3,470–4,150	3,790	3,470–3,940	3,600	3,160–3,810
Birth length (cm)	52	51–52	52	50–53	51	49–53

Values are medians with interquartile ranges. Differences amongst the groups not significant by Kruskal–Wallis test

tions of precursor fatty acids for eicosapentaenoic acid (20:5n-3, EPA) and arachidonic acid (20:4n-6, AA), 20:4n-3 and DHGA, respectively (Fig. 1), and the concentration of linoleic acid (18:2n-6, LA), were highest in the women receiving probiotics. For the proportion of DHGA and the concentration of 20:4n-3, the effect of combined dietary and probiotic intervention (diet/probiotics) was greater than that of dietary intervention alone (diet/placebo group), and changes in the proportion of AA and the concentrations of LA and DHGA could be attributed to probiotics.

Neither dietary counseling nor probiotic intervention caused changes in umbilical cord serum phospholipid fatty acids, except that the proportion of DHGA was higher with combined dietary counseling and probiotic intervention (diet/probiotics group) compared with control/placebo (Table 3; Electronic supplementary material). All PUFA in placenta and umbilical cord serum phospholipids were positively correlated ( $P < 0.05$ ; data not shown).

## Discussion

We showed here that placental phospholipid fatty acid content and composition may be modified by combined dietary and probiotic intervention. In view of the well documented role early nutrition plays in later life, culminating in early materno–fetal communication and transfer of fatty acids [14], health benefits may be expected.

The concentrations of PUFA in the placenta were comparable with those previously determined [15]. Nonetheless, dietary counseling resulted in increased dietary intakes of PUFA during pregnancy [8], reflected in higher concentrations of PUFA in placental phospholipids, but not in umbilical cord serum phospholipids, although placenta and cord blood fatty acids were correlated. The characteristics of umbilical cord blood, reflecting both the arterial and venal blood of the fetus, may confound the direct effect of maternal diet on cord blood composition, the association being nevertheless generally detected when comparing

dietary and serum fatty acid compositions [16]. Further, quantification of fatty acids as concentrations resulted in detection of differences amongst the study groups in respect of additional fatty acids, DHA and LA, not revealed by proportional profiles.

Although transfer of fatty acids across the placenta is partly determined by concentration gradient, the placenta has been shown to take up certain fatty acids selectively [17]. This was also reflected here, because the proportion of PUFA was greater in placental than in cord blood phospholipids, the difference being seen particularly in AA, the accumulation of which in placental phospholipids has previously been shown [18]. Fatty acids incorporated into phospholipids may be utilized in intrinsic placental fatty acid metabolism [19] to synthesize either longer-chain derivatives or inflammatory modulators. Importantly, they also serve as a reservoir to satisfy fetal demands for growth and development [19].

Beyond the effect of modification of maternal dietary lipid composition, also previously observed when comparing the placental fatty acids of vegetarian, omnivore, and diabetic mothers [20], administration of probiotics was seen here to modify placental phospholipid fatty acids. The mechanisms involved are poorly understood, but experimental evidence points to interplay between fatty acids and probiotics. First, one interaction may arise from effects of fatty acids on bacterial cell membranes [21] and hence on probiotic adherence and the intestinal epithelial cell innate immune response [22]. Second, probiotics and fatty acids may exert their systemic effects via similar signaling pathways, including soluble CD14 [23–25], or by control of proinflammatory cytokines [26]. Finally, the observed differences may result from the properties of probiotics in regulating desaturases involved in the metabolism of fatty acids to their longer-chain derivatives. It has been shown in rats that a range of probiotics affects the activity of liver  $\Delta 6$ -desaturase [27]. Clinical evidence is scarce regarding the interplay between probiotics and fatty acids, but in one study administration of formula supplemented with probi-

**Table 2** Placental phospholipid fatty acids (% of total fatty acids and mg g<sup>-1</sup>) in the three intervention groups

Fatty acid	Diet/probiotics ( <i>n</i> = 10)		Diet/placebo ( <i>n</i> = 12)		Control/placebo ( <i>n</i> = 8)	
% of total fatty acids						
n-3 PUFA						
18:3n-3	0.07	0.06–0.10	0.08	0.06–0.09	0.07	0.05–0.08
20:4n-3 <sup>b</sup>	0.16 <sup>c, d</sup>	0.14–0.20	0.10	0.09–0.15	0.09	0.07–0.10
20:5n-3	0.27	0.17–0.39	0.20	0.18–0.31	0.21	0.16–0.26
22:5n-3	0.98	0.88–1.05	1.03	0.89–1.08	0.99	0.87–1.06
22:6n-3	5.42	5.19–6.17	5.56	4.79–6.29	4.89	4.46–5.52
Sum of n-3 PUFA	6.92	6.54–7.87	6.92	6.25–7.70	6.26	5.59–6.88
n-6 PUFA						
18:2n-6	9.93	9.56–10.96	9.55	8.75–10.24	9.07	8.39–10.14
20:2n-6	0.63	0.58–0.67	0.60	0.50–0.70	0.62	0.59–0.72
20:3n-6 <sup>b</sup>	6.94 <sup>c, d</sup>	6.07–7.61	6.08 <sup>c</sup>	5.48–6.48	5.54	4.71–5.64
20:4n-6 <sup>a</sup>	19.5 <sup>c, e</sup>	18.2–20.9	21.5	20.0–22.5	22.0	20.5–22.7
Sum of n-6 PUFA	37.4	36.0–38.1	37.4	36.9–38.1	36.4	35.7–38.4
n-6/n-3 ratio	5.4	4.6–5.9	5.5	4.8–6.0	5.7	5.2–6.8
Sum of SFA	42.2	41.6–42.5	42.0	41.3–42.7	42.3	41.9–43.5
Sum of MUFA	13.5	12.6–14.1	13.6	13.0–13.8	14.2	13.4–15.4
Sum of PUFA	44.7	43.7–45.1	44.4	43.7–45.4	43.0	42.0–44.3
mg g <sup>-1</sup>						
n-3 PUFA						
18:3n-3	0.004	0.004–0.006	0.005	0.004–0.005	0.004	0.003–0.004
20:4n-3 <sup>b</sup>	0.010 <sup>c, d</sup>	0.008–0.013	0.006 <sup>c</sup>	0.005–0.009	0.005	0.004–0.005
20:5 n-3	0.016	0.012–0.022	0.012	0.010–0.020	0.011	0.010–0.013
22:5n-3	0.060	0.055–0.068	0.062	0.055–0.066	0.055	0.046–0.057
22:6n-3 <sup>a</sup>	0.36 <sup>c</sup>	0.31–0.41	0.36	0.29–0.39	0.27	0.25–0.30
Sum of n-3 PUFA <sup>a</sup>	0.45 <sup>d</sup>	0.40–0.51	0.45 <sup>c</sup>	0.37–0.48	0.34	0.31–0.38
n-6 PUFA						
18:2n-6 <sup>a</sup>	0.66 <sup>c, e</sup>	0.59–0.69	0.58	0.54–0.64	0.48	0.45–0.62
20:2n-6	0.041	0.036–0.043	0.038	0.032–0.042	0.035	0.030–0.045
20:3n-6 <sup>a</sup>	0.43 <sup>c, d</sup>	0.37–0.50	0.37	0.32–0.40	0.29	0.24–0.38
20:4n-6	1.21	1.11–1.39	1.26	1.18–1.43	1.15	1.06–1.50
Sum of n-6 PUFA	2.43	2.19–2.51	2.28	2.07–2.37	1.92	1.83–2.59
Sum of SFA	2.76	2.42–2.86	2.51	2.43–2.66	2.35	2.12–2.80
Sum of MUFA	0.85	0.77–0.98	0.81	0.80–0.83	0.76	0.71–0.90
Sum of PUFA	2.91	2.58–2.99	2.71	2.57–2.81	2.28	2.14–2.95

Values are medians with interquartile ranges

<sup>a</sup> Significant difference amongst the three study groups *P* < 0.05

<sup>b</sup> *P* < 0.01 by Kruskal–Wallis test

<sup>c</sup> Significantly different from diet/placebo *P* < 0.05

<sup>d</sup> From control/placebo *P* < 0.01

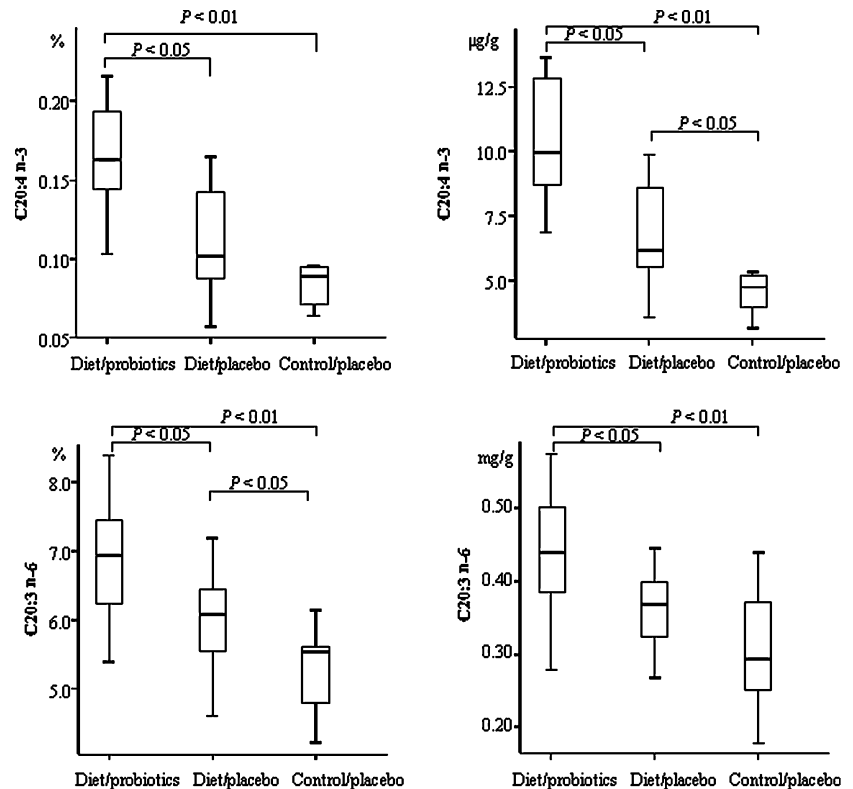
<sup>e</sup> *P* < 0.05 by Mann–Whitney *U* test

otics resulted in changes in the fatty acid composition of infants' serum phospholipids [28].

Dietary counseling and administration of probiotics during pregnancy were shown here to affect lipid metabolism, highlighting the synergistic effects of fatty acids and probiotics. This approach may initiate a cascade of events,

the effects being clinically manifested in health benefits at an early age, including promotion of neurological development [29] and alleviation of a range of immunoinflammatory disorders, for example allergic and cardiovascular diseases [30], not to mention the reduced maternal risk of pregnancy-related complications [31].

**Fig. 1** The proportions (%) and concentrations (mg g<sup>-1</sup>) of eicosatetraenoic acid (20:4n-3) and dihomo- $\gamma$ -linolenic acid (20:3n-6), the precursors of EPA and AA, in the placentas of the three study groups. The columns represent median and interquartile range, and the error bars range



**Acknowledgments** The authors thank the women who participated in this study, Satu Leinonen and Tanja Achrenius for laboratory assistance, and Robert MacGilleon for revision of the English text. Financial support from the Sigrid Jusélius Foundation, the Social Insurance Institution of Finland, and the Academy of Finland is gratefully acknowledged.

## References

- Murphy VE, Smith R, Giles WB, Clifton VL (2006) Endocrine regulation of human fetal growth: the role of the mother, placenta, and fetus. *Endocr Rev* 27:141–169
- Calder PC (2006) n-3 Polyunsaturated fatty acids, inflammation, and inflammatory diseases. *Am J Clin Nutr* 83:1505S–1519S
- Herrera E, Amusquivar E, López-Soldado I, Ortega H (2006) Maternal lipid metabolism and placental lipid transfer. *Horm Res* 65(Suppl 3):59–64
- Szajewska H, Horvath A, Koletzko B (2006) Effect of n-3 long-chain polyunsaturated fatty acid supplementation of women with low-risk pregnancies on pregnancy outcomes and growth measures at birth: a meta-analysis of randomized controlled trials. *Am J Clin Nutr* 83:1337–1344
- Kalliomäki M, Salminen S, Arvilommi H, Kero P, Koskinen P, Isolauri E (2001) Probiotics in primary prevention of atopic disease: a randomised placebo-controlled trial. *Lancet* 357:1076–1079
- Laitinen K, Kalliomäki M, Poussa T, Lagström H, Isolauri E (2005) Evaluation of diet and growth in children with and without atopic eczema: follow-up study from birth to 4 years *Br J Nutr* 94:565–574
- Kankaanpää PE, Salminen SJ, Isolauri E, Lee YK (2001) The influence of polyunsaturated fatty acids on probiotic growth and adhesion. *FEMS Microbiol Lett* 194:149–153
- Piirainen T, Isolauri E, Lagström H, Laitinen K (2006) Impact of nutrition counseling on nutrient intake during pregnancy: a prospective cohort study. *Br J Nutr* 96:1095–1104
- Rautava S, Kalliomäki M, Isolauri E (2005) New therapeutic strategy for combating the increasing burden of allergic disease: probiotics—a nutrition, allergy, mucosal immunology and intestinal microbiota (nami) research group report. *J Allergy Clin Immunol* 116:31–37
- Becker W, Lyhne N, Pedersen AN, Aro A, Fogelhom M, Phorsdottir I, Alexander J, Anderssen SA, Meltzer HM, Pedersen JI (2004) Nordic nutrition recommendations 2004—integrating nutrition and physical activity. *Scand J Nutr* 48:178–187
- Folch J, Lees M, Sloane Stanley GH (1957) A simple method for the isolation and purification of total lipids from animal tissues. *J Biol Chem* 226:497–509
- Hamilton JG, Comai K (1988) Rapid separation of neutral lipids, free fatty acids and polar lipids using prepacked silica Sep-Pak columns. *Lipids* 23:1146–1149
- Laiho K, Lampi A, Hamalainen M, Moilanen E, Piironen V, Arvola T, Syrjanen S, Isolauri E (2003) Breast milk fatty acids, eicosanoids, and cytokines in mothers with and without allergic disease. *Pediatr Res* 53:642–647
- Haggarty P (2002) Placental regulation of fatty acid delivery and its effect on fetal growth—a review. *Placenta* 23(Suppl A):S28–S38
- Klingler M, Demmelmair H, Larqué E, Koletzko B (2003) Analysis of FA contents in individual lipid fractions from human placental tissue. *Lipids* 38:561–566
- Nikkari T, Räsänen L, Viikari J, Akerblom HK, Vuori I, Pyörälä K, Uhari M, Dahl M, Lähde P, Pesonen E, Suoninen P (1983)

- Serum fatty acids in 8-year-old Finnish boys: correlations with qualitative dietary data and other serum lipids. *Am J Clin Nutr* 37:848–854
17. Larqué E, Demmelmair H, Berger B, Hasbargen U, Koletzko B (2003) In vivo investigation of the placental transfer of (13)C-labeled fatty acids in humans. *J Lipid Res* 44:49–55
  18. Kuhn DC, Crawford M (1986) Placental essential fatty acid transport and prostaglandin synthesis. *Prog Lipid Res* 25:345–353
  19. Coleman RA, Haynes EB (1987) Synthesis and release of fatty acids by human trophoblast cells in culture. *J Lipid Res* 28:1335–1341
  20. Lakin V, Haggarty P, Abramovich DR, Ashton J, Moffat CF, McNeill G, Danielian PJ, Grubb D (1998) Dietary intake and tissue concentration of fatty acids in omnivore, vegetarian and diabetic pregnancy. *Prostaglandins Leukot Essent Fatty Acids* 59:209–220
  21. Kankaanpää P, Yang B, Kallio H, Isolauri E, Salminen S (2004) Effects of polyunsaturated fatty acids in growth medium on lipid composition and on physicochemical surface properties of lactobacilli. *Appl Environ Microbiol* 70:129–136
  22. Walker WA (2000) Role of nutrients and bacterial colonization in the development of intestinal host defense. *J Pediatr Gastroenterol Nutr* 30(Suppl 2):2–7
  23. Laitinen K, Hoppu U, Hämäläinen M, Linderborg K, Moilanen E, Isolauri E (2006) Breast milk fatty acids may link innate and adaptive immune regulation: analysis of soluble CD14, prostaglandin E2, and fatty acids. *Pediatr Res* 59:723–727
  24. Yu B, Hailman E, Wright SD (1997) Lipopolysaccharide binding protein and soluble CD14 catalyze exchange of phospholipids. *J Clin Invest* 99:315–324
  25. Goldblum SE, Brann TW, Ding X, Pugin J, Tobias PS (1994) Lipopolysaccharide (LPS)-binding protein and soluble CD14 function as accessory molecules for LPS-induced changes in endothelial barrier function, in vitro. *J Clin Invest* 93:692–702
  26. Calder PC (2005) Polyunsaturated fatty acids and inflammation. *Biochem Soc Trans* 33:423–427
  27. Fukushima M, Yamada A, Endo T, Nakano M (1999) Effects of a mixture of organisms, *Lactobacillus acidophilus* or *Streptococcus faecalis* on delta6-desaturase activity in the livers of rats fed a fat and cholesterol-enriched diet. *Nutrition* 15:373–378
  28. Kankaanpää PE, Yang B, Kallio HP, Isolauri E, Salminen SJ (2002) Influence of probiotic supplemented infant formula on composition of plasma lipids in atopic infants. *J Nutr Biochem* 13:364–369
  29. Yavin E (2006) Versatile roles of docosahexaenoic acid in the prenatal brain: from pro- and anti-oxidant features to regulation of gene expression. *Prostaglandins Leukot Essent Fatty Acids* 75:203–211
  30. Buckley AJ, Jaquiere AL, Harding JE (2005) Nutritional programming of adult disease. *Cell Tissue Res* 322:73–79
  31. Solomon CG, Carroll JS, Okamura K, Graves SW, Seely EW (1999) Higher cholesterol and insulin levels in pregnancy are associated with increased risk for pregnancy-induced hypertension. *Am J Hypertens* 12:276–282

## Effect of Sterol Carrier Protein-2 Expression on Sphingolipid Distribution in Plasma Membrane Lipid Rafts/Caveolae

Barbara P. Atshaves · John R. Jefferson · Avery L. McIntosh · Adalberto Gallegos · Bonnie M. McCann · Kerstin K. Landrock · Ann B. Kier · Friedhelm Schroeder

Received: 16 May 2007 / Accepted: 24 June 2007 / Published online: 7 August 2007  
© AOCs 2007

**Abstract** Although sphingolipids are highly important signaling molecules enriched in lipid rafts/caveolae, relatively little is known regarding factors such as sphingolipid binding proteins that may regulate the distribution of sphingolipids to lipid rafts/caveolae of living cells. Since early work demonstrated that sterol carrier protein-2 (SCP-2) enhanced glycosphingolipid transfer from membranes *in vitro*, the effect of SCP-2 expression on sphingolipid distribution to lipid rafts/caveolae in living cells was examined. Using a non-detergent affinity chromatography method to isolate lipid rafts/caveolae and non-rafts from purified L-cell plasma membranes, it was shown that lipid rafts/caveolae were highly enriched in multiple sphingolipid species including ceramides, acidic glycosphingolipids (ganglioside GM1); neutral glycosphingolipids (monohexosides, dihexosides, globosides), and sphingomyelin as compared to non-raft domains. SCP-2 overexpression further enriched the content of total sphingolipids and select sphingolipid species in the lipid rafts/caveolae domains. Analysis of fluorescence binding and displacement data revealed that purified human

recombinant SCP-2 exhibited high binding affinity (nanomolar range) for all sphingolipid classes tested. The binding affinity decreased in the following order: ceramides > acidic glycosphingolipid (ganglioside GM1) > neutral glycosphingolipid (monohexosides, hexosides, globosides) > sphingomyelin. Enrichment of individual sphingolipid classes to lipid rafts/caveolae versus non-rafts in SCP-2 expressing plasma membranes followed closely with those classes most strongly bound to SCP-2 (ceramides, GM1 > the neutral glycosphingolipids (monohexosides, dihexosides, and globosides) > sphingomyelin). Taken together these data suggested that SCP-2 acts to selectively regulate sphingolipid distribution to lipid rafts/caveolae in living cells.

### Abbreviations

SCP-2	Sterol carrier protein-2
L-FABP	Liver fatty acid binding protein
PITP	Phosphatidylinositol transfer protein
ConA	Concanavalin A
NBD-sphingomyelin	6-((N-(7-nitrobenz-2-oxa-1,3-diazol-4-yl)amino)-hexanoyl)sphingosyl-phosphocholine
SM	Sphingomyelin
Cer	Ceramide
Glo	Globosides
GlcCer	Glucosylceramide
GalCer	Galactosylceramide
LacCer	Lactosylceramide
GSL	Glycosphingolipid

B. P. Atshaves · A. L. McIntosh · B. M. McCann · K. K. Landrock · F. Schroeder (✉)  
Department of Physiology and Pharmacology,  
Texas A&M University, TVMC, College Station,  
TX 77843-4466, USA  
e-mail: fschroeder@cvm.tamu.edu

J. R. Jefferson  
Department of Chemistry, Luther College,  
Decorah, IA 52101-1045, USA

A. Gallegos · A. B. Kier  
Department of Pathobiology,  
Texas A&M University, TVMC,  
College Station, TX 77843-4467, USA

## Introduction

Although the existence of transbilayer and lateral cholesterol-rich lipid domains in both model and plasma membranes was identified and characterized several decades ago [1], functional interest in these domains essentially lagged until the discovery that plasma membrane lipid rafts/caveolae were especially rich in signaling proteins [2, 3] and lipids involved in signaling lipids such as sphingolipids (sphingomyelin, gangliosides, ceramide), phosphatidylinositols, and diacylglycerol [4–8]. This was evidenced by the appearance of several thousand papers in the past decade correlating a growing diversity of activities to the lipid substrates of signaling proteins in lipid rafts/caveolae. The importance of lipid rafts/caveolae to these signaling protein functions is shown by the fact that disruption of cholesterol-rich microdomains inhibits activity [2].

It must be noted, however, that the above compositional studies of lipid rafts were performed with lipid rafts isolated from detergent and high pH bicarbonate buffer preparations, despite growing concerns that such preparations may not equate with lipid rafts/caveolae and not reflect the biological nature of intact cells [9–11]. These issues were recently alleviated in part by studies with lipid rafts/caveolae isolated without detergents or high pH carbonate buffers confirming that plasma membrane lipid rafts/caveolae domains are enriched in signaling proteins [12] as well as at least two lipids involved in signaling, i.e., sphingomyelin and less so phosphatidylinositol [13, 14]. However, while these studies suggest that intact lipid rafts/caveolae are required for organizing signaling lipid substrates and signaling proteins in close proximity, it is not completely clear which signaling sphingolipid species, other than sphingomyelin, are enriched in lipid rafts/caveolae, especially lipid rafts/caveolae isolated without detergents or high pH carbonate buffers. Furthermore, despite the significance of lipid rafts/caveolae in lipid mediated cellular signaling, relatively little is known regarding mechanism(s) whereby the level of lipid substrates such as sphingolipids in lipid rafts/caveolae are regulated and replenished. Since sphingolipids are synthesized in the endoplasmic reticulum and/or Golgi apparatus, both vesicular and non-vesicular pathways for preferential transport to plasma membrane lipid rafts/caveolae have been proposed [15–17]. In recent years, much attention has focused on vesicular pathways while, with the exception of the glycolipid transfer protein [18], almost nothing is known regarding the role(s) of proteins involved in regulating molecular sphingolipid transport and distribution of sphingolipid species (sphingomyelin, ceramide, neutral glycosphingolipids (monohexosides, dihexosides, globosides), and acidic glycosphingolipids

(ganglioside GM1)) to lipid rafts/caveolae. One candidate protein, caveolin-1, was shown to cross-link with photoactivatable gangliosides in the plasma membrane caveolae-suggesting that caveolin-1 is either a close neighbor of gangliosides, binds gangliosides, and/or possibly may be involved in ganglioside transport/targeting to caveolae [19]. A number of studies suggest sterol carrier protein-2 (SCP-2) as an additional candidate protein: (1) early *in vitro* studies with SCP-2 containing pH 5.1 supernatants from the liver showed that these supernatants markedly enhanced the transfer of sphingomyelin as well as neutral (globoside) and acidic (ganglioside) glycosphingolipids from model membranes to high density lipoproteins (HDL) or biological membranes [20, 21]. However, while SCP-2 is present in the pH 5.1 supernatant, this supernatant is also the starting fraction for purification of several other lipid transfer proteins including PITP, L-FABP, and others [22]. Furthermore, PITP itself has been shown to bind/transfer sphingomyelin [23, 24], (2) immunofluorescence confocal microscopy and immunogold electron microscopy show significant portions of SCP-2 are localized in the cytoplasm [25, 26], (3) immunoprecipitation, double immunofluorescence fluorescence resonance energy transfer (FRET) confocal microscopy, double immunogold electron microscopy, coimmunoprecipitation, yeast two hybrid, and plasma membrane fractionation into lipid rafts and non-raft domains show that SCP-2 directly interacts with caveolin-1 in plasma membrane lipid rafts, but SCP-2 is not associated with non-rafts [26, 27].

The purpose of the present investigation was to determine: (1) sphingolipid class distribution in lipid rafts/caveolae isolated by affinity chromatography without the use of detergents or high pH carbonate, (2) effect of SCP-2 expression on sphingolipid distribution to lipid rafts/caveolae vs non-rafts, and (3) lipid raft/caveolae sphingolipid class distribution correlation with SCP-2 affinity for these sphingolipid classes.

## Materials and Methods

### Materials

Lipid standards were from Matreya Inc., (Pleasant Gap, PA, USA) and Calbiochem (La Jolla, CA, USA). Concanavalin A (Con A) sepharose resin was purchased from Pharmacia (Piscataway, NJ, USA). Silica Gel G and Silica Gel 60 thin layer chromatography (TLC) plates were from Analtech (Newark, DE, USA) and EM Industries, Inc. (Darmstadt, Germany), respectively. NBD-sphingomyelin was purchased from molecular probes (Eugene, OR, USA). Sphingomyelin, galactosylceramide, ceramide, and ganglioside

GM1 were purchased from Avanti (Alabaster, AL, USA). Cerebrosides, lactosylceramide, glucosylceramides, and globosides were purchased from Matreya Inc. (Pleasant Gap, PA, USA). Rabbit polyclonal antisera to recombinant human SCP-2 was prepared as described previously [28]. Rabbit polyclonal anti-sera to caveolin-1 was purchased from BD Transduction Laboratories (Palo Alto, CA, USA). Rabbit anti-Na, K-ATPase was purchased from Novus Biologicals (Littleton, CO, USA). All reagents and solvents used were of the highest grade available and were cell culture tested.

#### L-Cell Culture

Murine L-cells were grown to confluence at 37 °C and 5% CO<sub>2</sub> in Higuchi medium, supplemented with 10% fetal bovine serum (Hyclone, Logan, UT, USA) as described earlier [29]. Control L-cells and L-cells transfected with the 15-kDa pro-SCP-2 cDNA were prepared as described earlier [30]. Western blot analysis performed on the SCP-2 expression cells revealed that levels of SCP-2 (0.036% cytosol protein) were in the physiological range found in animal tissues [31]. In untransfected and control/mock transfected cells, levels of these proteins were below the level of detection.

#### Isolation of Lipid Rafts/Caveolae and Non-Raft Enriched Fraction from L-Cell Fibroblasts

Plasma membranes were isolated from cultured L-cells as described earlier [14, 32, 33]. A non-detergent affinity chromatography method using concanavalin-A (ConA) sepharose 4B was then employed to isolate lipid rafts/caveolae and non-raft domains from the purified plasma membranes as described earlier [9, 14, 33, 34]. The basis for the isolation method ensued from the specificity of ConA for carbohydrates: (1) simple sugars and oligosaccharides that have D-manno or D-glucopyranoside configuration with unmodified hydroxyl groups at C-3, C-4, and C-6 of the  $\alpha$ (anomer, which is preferred over the  $\beta$  anomer) [35], (2) glycopeptides with a core structure of Man $\alpha$ 1  $\rightarrow$  3[Man $\alpha$ 1  $\rightarrow$  6]Man $\beta$ 1  $\rightarrow$  4GlcNAc $\beta$ 1  $\rightarrow$  4GlcNAc  $\rightarrow$  Asn [35]. Such carbohydrate receptor structures are present in several lipid raft/caveolae components such as SR-B1 [36] and glucosylceramide found in L-cells [37].

#### Sphingolipid Analysis of Lipid Rafts/Caveolae and Non-Raft Domains

Sphingolipids were extracted with chloroform/methanol/water/pyridine (60:30:6:1) and insoluble particulates were removed by filtration [37]. Pooled extracts were evaporated

to dryness under N<sub>2</sub>. Lipids were saponified using methanol in NaOH for 2 h at 37 °C followed by neutralization with acetic acid. The solvent was evaporated under N<sub>2</sub>, and the lipids were dissolved in MeOH/H<sub>2</sub>O/CHCl<sub>3</sub>, 94:96:6 (v/v/v). The organic phase was then desalted with a Waters Sep-Pak C18 column (Milford, MA, USA), pre-equilibrated with CHCl<sub>3</sub>/CH<sub>3</sub>OH (1:1). After the sample was loaded, the columns were washed twice with H<sub>2</sub>O, then eluted first with methanol followed by chloroform/methanol (1:1 v/v). The eluting fractions were pooled and the sphingolipids thus obtained were dried with N<sub>2</sub> and pumped under vacuum. The residue was dissolved in a minimum volume chloroform/methanol (1:1 v/v) and resolved along with appropriate lipid standards on Silica G60 TLC plates developed in chloroform/methanol/15 mM CaCl<sub>2</sub> (aq) (65:35:8). Lipids were visualized with the fluorescent dye primulin under UV irradiation [37] and analyzed by scanning densitometry using Scion image analysis software. Lipid content was quantitated by comparison to standard curves developed on each TLC plate and normalized to the total protein content to give units of nmol lipid/mg protein. Total protein was determined on the samples before extraction by Bradford reagent (Sigma, St Louis, MO, USA) with BSA used as the standard.

#### Western Blot Analysis of Lipid Rafts/Caveolae and Non-Raft Domains

The relative enrichment of plasma membrane protein markers (caveolin-1 and Na, K-ATPase) and the distribution of SCP-2 in the lipid rafts/caveolae and non-raft domains eluted from the ConA affinity column was determined by western blotting. Aliquots of each fraction were separated by SDS-PAGE and analyzed as follows: Samples (10  $\mu$ g) were run on tricine gels (12%) and transferred to nitrocellulose membranes. The blots were blocked in 3% gelatin in TBST (10 mM Tris-HCL, pH 8, 100 mM NaCl, 0.05% Tween-20) for 1 h at room temperature, then washed 2 $\times$  with TBST. The blots were incubated overnight at room temperature with the respective polyclonal rabbit primary antibodies at dilutions of 1:500 (anti-SCP-2 and anti-caveolin-1) or 1:1,000 (anti-Na, K-ATPase) in 1% gelatin in TBST. After several washes with TBST, the blots were incubated for 2 h at room temperature with the appropriate secondary antibody (alkaline-phosphatase conjugates of goat anti-rabbit IgG) diluted 1:4,500 in 1% gelatin TBST. The blot was washed 3 $\times$  with TBST and bands of interest were visualized by development with Sigma Fast 5-bromo-4-chloro-3-indolyl phosphate/nitro blue tetrazolium tablets (Sigma, St Louis, MO, USA) according to the manufacturer's protocol. Images of each blot were acquired using a single-chip CCD (charge couple device) video camera and a computer

workstation (IS-500 system from Alpha Innotech, San Leandro, CA, USA). Densitometric analysis of image files was then performed (mean 8 bit gray scale density) using NIH Image, available by anonymous FTP from zippy.nimh.nih.gov, to obtain relative levels of respective protein detected in each fraction expressed as integrated density values.

#### Analysis of Ganglioside GM1 Levels in Lipid Rafts/Caveolae and Non-Raft Plasma Membrane Domains

GM1 levels in each fraction were determined as described elsewhere [38]. Briefly, samples were spotted onto nitrocellulose membrane blots and washed with PBS. The blots were blocked in 3% (w/v) BSA in PBS and incubated with cholera toxin B (1 µg/ml) for 30 min at 4 °C. Membranes were washed and incubated with rabbit anti-cholera toxin B for 1 h, followed by incubation with alkaline phosphatase-conjugated swine anti-rabbit Ig for an additional 30 min. Sigma Fast 5-bromo-4chloro-3-indolyl phosphate/nitro blue tetrazolium tablets (Sigma, St Louis, MO, USA) were used to visualize spots. GM1 levels were quantitated by densitometric analysis as for protein analysis described above.

#### NBD-Sphingomyelin Binding to SCP-2

Recombinant human SCP-2 was isolated as described earlier [39]. The binding of SCP-2 protein to NBD-sphingomyelin was determined as described previously for other NBD-labeled lipids [40]. The NBD-sphingomyelin was excited at 480 nm and fluorescence emission spectra recorded from 490 to 600 nm at 25 °C on a PC1 photon counting spectrofluorometer (ISS Instruments, Champaign, IL, USA). Excitation and emission bandwidths (4 and 8 nm, respectively) were kept to a minimum to reduce photobleaching. The sample absorbance for NBD-labeled probes was kept below 0.1 to avoid the inner filter effect. Light scatter was reduced by the use of dilute samples and appropriate low fluorescence cutoff filters in the emission paths. Fluorescence emission was corrected for blank (without SCP-2 present) and background fluorescence.

SCP-2 binding affinity ( $K_d$ ) for NBD-sphingomyelin was calculated as described in [41, 42] using the following equation:  $1/(1 - F/F_{max}) = C_L/(F/F_{max}) \times (1/K_d - (nE_0)/K_d)$  where  $F$  and  $F_{max}$  are corrected measured and maximal fluorescence intensity of the ligand, respectively,  $C_L$  is the total ligand concentration, and  $E_0$  is the protein concentration. A plot of  $1/(1 - F/F_{max})$  versus  $C_L/(F/F_{max})$  yielded a linear function with a slope of  $(1/K_d)$  and an ordinate intercept of  $(nE_0)/K_d$  where  $n$  equals the number of binding sites. In order to determine the number of binding sites to a higher degree of accuracy, a reverse titration experiment

was performed in which increasing amounts of SCP-2 (100–795 nM) were added to a fixed concentration of NBD-sphingomyelin (220 nM) as described in [43]. The data were fit to equation  $Y = F_{max}X/(B + X)$  where  $X$  is the protein concentration,  $F_{max}$  is the maximal bound fluorescence intensity, and  $B$  is a fitting parameter. In order to convert the fluorescent intensities into ligand bound concentrations,  $F_{max}$  was divided by the fixed concentration of NBD-sphingomyelin. Fluorescent intensities from the previous titrations (non-reverse) were then converted to ligand bound concentrations and plotted as  $L_B/P_T$  versus  $L_F$  where  $L_B$  is bound NBD-sphingomyelin,  $P_T$  is total protein concentration, and  $L_F$  is the free NBD-sphingomyelin in solution. The data was fitted to equation  $Y = nL_F/(K_d + L_F)$  by non-linear regression to give the binding site saturation curve where  $n$  is the number of binding sites and  $K_d$  is the dissociation constant.

#### Displacement of SCP-2-Bound NBD-Sphingomyelin by Sphingolipids

The relative affinity of SCP-2 for non-fluorescent sphingolipids was determined by displacement of SCP-2 bound NBD-sphingomyelin basically as described earlier for other fluorescent lipids [44]. All NBD-sphingomyelin displacement studies were performed below the critical micelle concentration for each non-fluorescent sphingolipid ligand. The decrease in maximum fluorescence intensity of NBD-sphingomyelin at 540 nm was plotted versus the displacing ligand concentrations. From the plot, the  $I_{50}$  value was determined, and the equation,  $K_i = [I_{50}]/(1 + [L]/K_d)$ , was used to calculate the dissociation constant ( $K_i$ ) for each lipid examined where  $[L]$  was the NBD-sphingomyelin concentration used in the experiment, and  $K_d$  was the dissociation constant for NBD-sphingomyelin and SCP-2 binding ( $375 \pm 34$  nM). Measurements were corrected for the blank (ligand or protein only) and photobleaching as described above.

#### Determination of DHE Sterol Transfer in Lipid Rafts/Caveolae and Non-Raft Domains Isolated from L-Cell Fibroblast Plasma Membranes

Dehydroergosterol (DHE, a naturally fluorescent sterol) was incorporated into caveolae/lipid raft and non-raft domains as previously described [32]. The DHE sterol transfer between the isolated membrane fractions was measured over approximately 4 h according to a fluorescence polarization exchange assay previously described by our laboratory [32, 45]. Isolated lipid rafts/caveolae and non-raft membranes were resuspended in filtered (0.2 µm) buffer (2 ml, 10 mM PIPES, pH 7.4) and placed in thermostated ( $37 \pm 0.3$  °C) quartz cuvettes with temperature maintained



through use of a water heating bath (Fisher Scientific, Pittsburgh, PA, USA). The steady-state fluorescence polarization of DHE in the membrane fractions was measured on a PC1 spectrofluorometer with photon-counting electronics (ISS Instruments, Inc., Champaign, IL, USA) in the T-format with the emission monochromator set at 375 nm, with 16 nm spectral slit widths and KV-389 emission filters from Schott Glass Technologies, Inc., Duryea, PA, USA. Samples were stirred continuously with a magnetic stir bar below the level of the light beam. Residual light scatter from membranes contributing to polarization measurements was corrected by converting polarization to anisotropy according to  $r = 2P/(3-P)$  followed by subtraction of residual fluorescence anisotropy of both donor and acceptor membranes from all experimental data. To avoid inner filter artifacts, the absorbance of sample solutions at the excitation wavelength was maintained  $<0.15$  absorbance units. Kinetic parameters including initial rate of sterol transfer and the exchangeable sterol fraction were determined as described in [14].

#### Statistics

All values were expressed as the mean  $\pm$  SEM with  $n$  and  $p$  indicated in “Results”. Statistical analysis was performed using analysis of variance (ANOVA) combined with the Newman-Keuls multiple comparisons test (GraphPad Prism, San Diego, CA, USA) or Student’s  $t$  test. Values with  $P < 0.05$  were considered statistically significant.

## Results

### Total Sphingolipid (TSL) Content of Lipid Rafts/Caveolae and Non-raft Domains: Effect of SCP-2 Expression

Although several sphingolipid classes are enriched in lipid rafts/caveolae isolated by methods using detergents and/or high pH carbonate buffer, such methods are increasingly thought to themselves affect the distribution of lipids as well as proteins into lipid rafts/caveolae [46]. Therefore, a detergent-free, high pH carbonate buffer-free, ConA affinity chromatography method was used to simultaneously isolate lipid rafts/caveolae and non-raft domains from plasma membranes purified from L-cell fibroblasts as described in “Methods”. To confirm that the ConA adherent and non-adherent fractions isolated from control and SCP-2 expressing plasma membranes indeed represented lipid rafts/caveolae and non-raft enriched fractions, western blotting for marker proteins was performed to determine the presence of caveolin-1 (a lipid rafts/caveolae protein marker) and Na, K-ATPase (a non-raft protein marker). While

the transferrin receptor (also known as CD71) is an excellent protein marker for non-rafts in endothelial cells as well as other cells [47, 48], in the present work transferrin was not detectable (data not shown). However, when the non-adherent fraction isolated from control cells was tested for another non-raft protein marker Na, K-ATPase, a 3.2-fold enrichment was observed as compared to the ConA adherent fraction (Fig. 1b). To distinguish whether the ConA adherent fraction was enriched in lipid raft protein markers, western blotting was performed with the known lipid raft protein marker caveolin-1. The ConA adherent fraction isolated from control cells contained fivefold more caveolin-1 as compared to the non-adherent fraction (Fig. 1a, closed bar vs. hatched bar). In SCP-2 expressing cells, a similar pattern of lipid raft protein markers was observed, i.e., enrichment of caveolin-1 in the ConA adherent fraction. However, while Na, K-ATPase was enriched in the non-raft fraction isolated from SCP-2 cells (compared to the lipid raft fraction), a comparison between non-rafts isolated from control and SCP-2 expressing cells showed a 5.4-fold increase in Na, K-ATPase content in SCP-2 expressing cells (Fig. 1b). Concomitantly, levels of Na, K-ATPase in the lipid rafts/caveolae were increased 3.2-fold as compared to lipid rafts/caveolae isolated from control cells (Fig. 1b). In

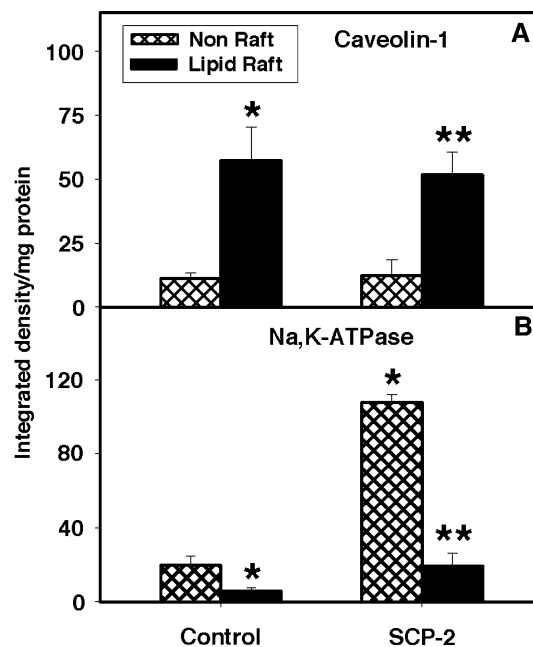


**Fig. 1** Distribution of plasma membrane protein markers in lipid rafts/caveolae and non-raft fractions. Quantitative analysis of protein expression was performed to determine relative expression levels of caveolin-1 (Panel A) and Na, K-ATPase (Panel B) in lipid rafts/caveolae (closed bar) and non-raft (hatched bar) fractions isolated from control and SCP-2 expressing cells. Values represent mean  $\pm$  SEM ( $n = 3-4$ ). \* $P < 0.05$  versus non-raft fractions isolated from control cells; \*\* $P < 0.004$  versus non-rafts isolated from SCP-2 expressing cells

summary, western blotting of protein markers confirmed that ConA adherent fractions and non-adherent fractions were enriched in lipid rafts/caveolae and non-rafts, respectively, and expression of SCP-2 significantly increased the relative content of Na, K-ATPase in non-rafts and lipid rafts/caveolae as compared to control cells.

Next, lipids from lipid rafts/caveolae and non-raft domains were extracted, total sphingolipid mass was quantitated as described in “Methods”. Total sphingolipids were defined as the sum of ceramides, globosides, dihexosides, monohexosides, sphingomyelin, and ganglioside GM1 present in each fraction. Lipid rafts/caveolae isolated from control (i.e., mock transfected) L-cells contained significant levels of total sphingolipid ( $369 \pm 35$  nmol/mg protein) (Fig. 2). In control cells, the total sphingolipid content in lipid rafts/caveolae was higher than in non-rafts, however, this trend did not achieve statistical significance (Fig. 2). In contrast, SCP-2 expression significantly increased the lipid rafts/caveolae total sphingolipid mass/mg protein when compared to non-rafts isolated from SCP-2 overexpression cells or to lipid rafts/caveolae isolated from control cells (Fig. 2), suggesting that SCP-2 acts to selectively regulate sphingolipid distribution to lipid rafts/caveolae. In order to determine whether these results correlated with expression levels of SCP-2 in the isolated membrane fractions, western blot analysis was performed on plasma membranes, caveolae, and non-caveolae fractions isolated from control and SCP-2 expressing cells. In the plasma membranes isolated from control cells there was little to no SCP-2 present (Fig. 3a, lane 1). In contrast, SCP-2 was observed in plasma membranes (Fig. 3a, lane 2)

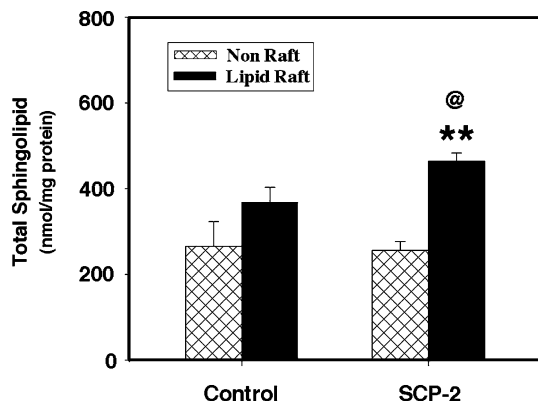


**Fig. 2** Total sphingolipid content of lipid rafts/caveolae and non-rafts isolated from plasma membranes from control and SCP-2 expressing cells. Total sphingolipids were extracted, quantitated, and expressed in units of nmol TSL/mg protein. Values represent mean  $\pm$  SEM ( $n = 7-11$ ).  $**P < 0.003$  versus non-raft fractions isolated from SCP-2 expressing cells; @ indicates  $P < 0.03$  versus lipid rafts/caveolae fractions isolated from control cells. TSL total sphingolipids

and lipid rafts/caveolae fractions (Fig. 3a, lane 4) isolated from SCP-2 overexpressing cells, with little to no SCP-2 observed in fractions isolated from non-caveolae (Fig. 3a, lane 3). Quantitative analysis showed that levels of SCP-2 in the caveolae fraction were increased 15-fold as compared to the non-caveolae fraction. In summary, these data show that: (1) in control cells total sphingolipid mass was only slightly higher in lipid rafts/caveolae than in non-rafts, and (2) SCP-2 overexpression significantly increased the total sphingolipid mass in lipid rafts/caveolae, but not non-rafts.

#### Mass Distribution of Sphingolipid Classes in Lipid Rafts/Caveolae and Non-Raft Domains: Effect of SCP-2 Expression

To determine if the lipid rafts/caveolae were enriched in select sphingolipid classes, total sphingolipids were resolved by thin layer chromatography, visualized, and quantitated as described in “Methods”. For the non-glycosylated sphingolipid classes, including sphingomyelin and ceramide, the mass of sphingomyelin, but not ceramide, in control cells was several fold higher in the lipid raft/caveolae fractions as compared to non-rafts (Table 1). SCP-2 overexpression abolished the difference in sphin-

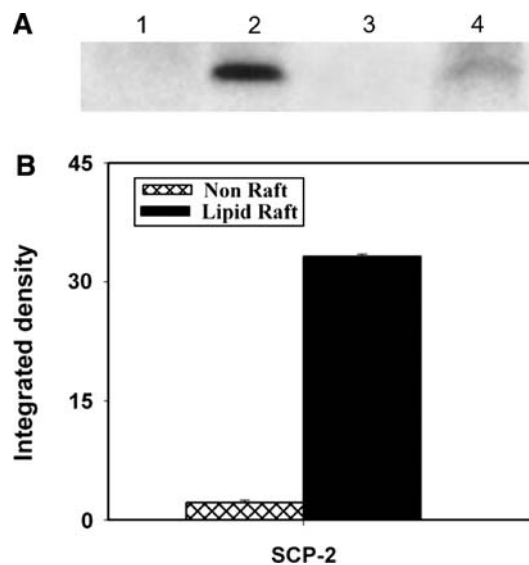


**Fig. 3** Distribution of SCP-2 in plasma membrane, non-raft, and lipid rafts/caveolae fractions from control and SCP-2 expressing cells (Panel A). Western blot analysis was performed to determine expression levels of SCP-2 in L-cell plasma membranes (lane 1) and in plasma membranes (lane 2), non-rafts (lane 3), and lipid rafts/caveolae (lane 4) isolated from SCP-2 expressing cells (Panel B). Relative expression levels of SCP-2 in non-raft (hatched bar) and lipid rafts/caveolae (closed bar) fractions isolated from SCP-2 expressing cells were determined as described in “Methods”

gomyelin mass between lipid rafts/caveolae and non-rafts, while concomitantly increasing the mass of ceramide in lipid rafts/caveolae versus non-rafts (Table 1).

In control cells the mass of neutral glycosphingolipids, including monohexosides (glucosylceramide), dihexosides (lactosylceramide) and tetrahexosides (globosides) in lipid rafts/caveolae as well as non-rafts was lower than that of sphingomyelin and ceramide within these fractions (Table 1). Furthermore, the content of these neutral glycosphingolipids was markedly different in lipid rafts/caveolae as compared to non-raft domains. The content of monohexosides and globosides was 7 and 6.4-fold higher in the lipid raft/caveolae fraction as compared to the non-raft fraction of plasma membranes from control L-cells (Table 1). While the content of dihexosides also appeared greater in lipid rafts/caveolae, this difference did not achieve statistical significance. The SCP-2 overexpression markedly increased the content of monohexosides and globosides in both lipid rafts/caveolae and non-rafts (Table 1). Overall, neutral sphingolipids were enriched in lipid rafts/caveolae as compared to non-raft domains and SCP-2 overexpression significantly enriched the content of neutral sphingolipids, especially globosides and monohexosides to higher levels in lipid rafts/caveolae than in non-rafts.

Levels of the ganglioside GM1 in lipid rafts/caveolae of control L-cells were 4.1-fold higher than in non-raft domains (Table 1). Likewise, the GM1 content in lipid rafts/caveolae isolated from SCP-2 expressing cells was increased fourfold higher when compared to levels in non-rafts (Table 1). However, much like sphingomyelin, levels of GM1 were decreased 2.3-fold in the lipid rafts/caveolae isolated from SCP-2 expressing cells versus control cell lipid rafts/caveolae. Taken together, these data indicate that while lipid rafts/caveolae are enriched in sphingolipids such as sphingomyelin, GM1, and hexosides, these effects can be potentiated by SCP-2 expression.

#### Effect of SCP-2 Expression on the % Distribution of Sphingolipid Classes in Lipid Rafts/Caveolae and Non-raft Domains

When the sphingolipid mass data was expressed as % distribution, differences were also observed in lipid rafts/caveolae as compared to non-raft domains (Table 2). In control cells, the % distribution of sphingolipids in lipid rafts/caveolae was in the following order: ceramides > sphingomyelin > dihexosides > globosides > monohexosides > GM1 with the relative ratios being 19:18:6:5:3:1. The order of sphingolipid species % distribution was the same in non-rafts but the ratios were significantly different 106:25:13:2.8:1.6:1 due to the two and threefold lower percent sphingomyelin and GM1, respectively, in the non-raft fraction (Table 2).

SCP-2 overexpression significantly altered the % distribution of sphingolipids in both lipid rafts/caveolae and non-raft domains. The % distribution of sphingolipids in lipid rafts/caveolae in SCP-2 expressing cells was in the order: ceramides >> sphingomyelin > globosides > monohexosides, dihexosides > gangliosides with the relative ratios being 80:23:16:10:9.8:1. This order was the same in non-rafts, but the ratios were differed significantly (170:100:30:17:14:1). Overall, with the exception of sphingomyelin the overexpression of SCP-2 tended to reduce the difference in sphingolipid class % distribution between lipid rafts/caveolae and non-rafts. Furthermore, SCP-2 expression increased the proportion of ceramides in the lipid rafts/caveolae fraction while decreasing the % GM1 (2.9-fold), % sphingomyelin (2.2-fold) and % dihexosides (1.6-fold) (Table 2). Thus, the % distribution of sphingolipid classes differed significantly between lipid rafts/caveolae and non-rafts. Additionally, a comparison of % distribution of sphingolipids in the non-raft fractions isolated from control and SCP-2 expressing cells revealed that levels of sphingomyelin, monohexosides, and

**Table 1** Effect of SCP-2 expression on mass distribution of sphingolipid classes in lipid rafts/caveolae and non-rafts isolated from plasma membranes of L-cell fibroblasts

Sphingolipid class	Control		SCP-2 overexpressor	
	nmol/mg protein			
	Non-raft	Lipid raft/caveolae	Non-raft	Lipid raft/caveolae
Sphingomyelin	44 ± 9	130 ± 21*	77 ± 12	76 ± 5 <sup>#</sup>
Ceramides	189 ± 55	138 ± 27	132 ± 16	266 ± 16* <sup>#</sup>
Neutral glycosphingolipids				
Monohexosides	3 ± 1	21 ± 3*	12 ± 3 <sup>#</sup>	34 ± 5* <sup>#</sup>
Dihexosides	25 ± 9	40 ± 7	11 ± 1	32 ± 4*
Globosides	5 ± 1	32 ± 4*	24 ± 4 <sup>#</sup>	53 ± 5* <sup>#</sup>
Acidic glycosphingolipid				
Ganglioside GM1	1.8 ± 0.4	7.5 ± 0.4*	0.8 ± 0.6	3.2 ± 0.7* <sup>#</sup>

Values represent the mean ± SEM (*n* = 7–12)

\* *P* < 0.04 versus non-raft in the same cells

<sup>#</sup> *P* < 0.05 versus the same fraction in control cells

**Table 2** Effect of SCP-2 expression on % distribution of individual sphingolipid classes among total sphingolipids

Sphingolipid Class	Control		SCP-2 overexpressor	
	(%)			
	Non-raft	Lipid raft/caveolae	Non-raft	Lipid raft/caveolae
Sphingomyelin	17 ± 2	35 ± 5*	30 ± 5 <sup>#</sup>	16 ± 1* <sup>#</sup>
Ceramides	71 ± 20	38 ± 7*	51 ± 6	56 ± 3 <sup>#</sup>
Neutral glycosphingolipids				
Monohexosides	1.1 ± 0.3	6 ± 1*	5 ± 1 <sup>#</sup>	7 ± 1
Dihexosides	9 ± 3	11 ± 2	4.3 ± 0.4	6.9 ± 0.9* <sup>#</sup>
Globosides	1.9 ± 0.4	9 ± 1*	9 ± 1 <sup>#</sup>	11 ± 1
Acidic glycosphingolipid				
Ganglioside GM1	0.67 ± 0.08	2.0 ± 0.1*	0.3 ± 0.02 <sup>#</sup>	0.7 ± 0.1* <sup>#</sup>

Values represent the mean ± SEM ( $n = 7$ – $12$ )

\*  $P < 0.04$  versus non-raft in the same cells

<sup>#</sup>  $P < 0.05$  versus the same fraction in control cells

globosides were increased up to fivefold while levels of ceramides, dihexosides, and GM1 were decreased in non-rafts isolated from SCP-2 expressing cells. These results indicate that SCP-2 expression differentially alters the % distribution of select sphingolipid classes in both lipid rafts/caveolae and non-raft fractions—consistent with selective targeting and/or increased sphingolipid metabolism.

#### Interaction of SCP-2 with Sphingomyelin

Since SCP-2 overexpression clearly altered the mass and % distribution of sphingolipid classes in lipid rafts/caveolae versus non-rafts, it was important to demonstrate whether this was associated with direct binding of these lipids—something which had heretofore not been demonstrated (see “Introduction”). Therefore, the ability of SCP-2 to directly bind representative non-glycosylated sphingolipids (sphingomyelin, ceramide), neutral glycosphingolipids (monohexosides, dihexosides, globosides), and acid sphingolipid (GM1) classes was determined.

The SCP-2 binding of sphingomyelin was examined by use of a fluorescent sphingomyelin derivative (i.e., NBD-sphingomyelin). Although NBD-sphingomyelin in aqueous buffer fluoresces maximally near 540 nm, emission intensity was much less without SCP-2 present (data not shown). Plotting the maximal intensity of NBD-sphingomyelin emission at 543 nm versus increasing NBD-sphingomyelin concentration yielded a monophasic saturation binding curve (Fig. 4a). The double reciprocal of this binding curve was linear, consistent with the presence of a single binding site (Fig. 4a, inset). A reverse titration experiment in which increasing amounts of SCP-2 were added to a fixed concentration of NBD-sphingomyelin provided maximal fluorescence of completely bound NBD-sphingomyelin and allowed determination of the number of binding sites to a higher degree of accuracy (Fig. 4b). A plot of bound versus free NBD-sphingomyelin yielded a binding site saturation curve (Fig. 4b) where  $B_{\max} = 1.4 \pm 0.2$ , indicative of a single binding site for NBD-sphingomyelin,

and a dissociation constant ( $K_d$ ) for NBD-sphingomyelin binding to SCP-2 equal to  $375 \pm 34$  nM.

In order to resolve whether the NBD chemical moiety attached to sphingomyelin might itself impact the binding of sphingomyelin to SCP-2, SCP-2 bound NBD-sphingomyelin was displaced with increasing unlabeled sphingomyelin. When a complex of NBD-sphingomyelin and SCP-2 was incubated with increasing amounts of non-fluorescent sphingomyelin, the maximal fluorescence emission intensity of NBD-sphingomyelin was decreased in monophasic fashion—consistent with displacement of fluorescent NBD-sphingomyelin by non-fluorescent sphingomyelin at a single binding site (not shown). The concentration at which sphingomyelin displaced 50% of SCP-2 bound NBD-sphingomyelin intensity (i.e.,  $K_i$ ) was  $173 \pm 6$  nM (Table 3). Thus, the  $K_i$  for NBD-sphingomyelin displacement by sphingomyelin was about twofold lower than the  $K_d$  for NBD-sphingomyelin direct binding. In summary, SCP-2 exhibited high affinity in the nM range for sphingomyelin. This affinity was not an artifact due to the presence of the NBD chemical moiety in NBD-sphingomyelin since the  $K_d$  for binding NBD-sphingomyelin was within a factor of two of the  $K_i$  for displacement with non-fluorescent sphingomyelin.

#### Effect of the Phosphocholine Moiety of Sphingomyelin on Binding to SCP-2

Since ceramide is both the precursor of sphingomyelin and a product of sphingolipid degradation, the binding of ceramide to SCP-2 was also examined. Incubation of a SCP-2/NBD-sphingomyelin complex with increasing concentrations of ceramide resulted in displacement of NBD-sphingomyelin with a monophasic displacement curve (Fig. 4c). Analysis of multiple displacement curves yielded a  $K_i = 5 \pm 1$  nM (Table 3)—the highest affinity of SCP-2 for any sphingolipid class examined. By comparing the structures of ceramide and sphingomyelin it was clear that the absence the phosphocholine group increased SCP-2's

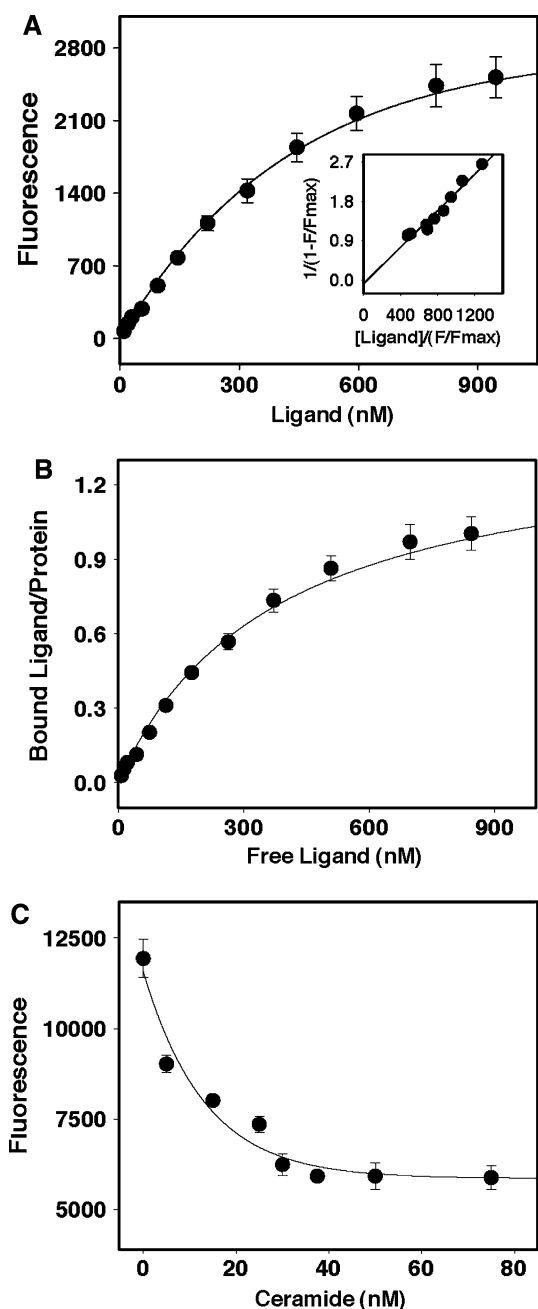


**Fig. 4** Ligand binding and displacement studies (*Panel A*). Titration of SCP-2 with NBD-sphingomyelin was followed by an increase in fluorescence, (excitation 480 nm, emission 540 nm). The data was fit to a simple, single binding site model as described in “Methods”. *Inset*, linear plot of  $1/(1 - F/F_{max})$  versus  $[ligand]/(F/F_{max})$  for titration of SCP-2 with NBD-sphingomyelin (*Panel B*). The binding site saturation curve was determined as described in “Methods” (*Panel C*). SCP-2 was preincubated with NBD-sphingomyelin, followed by addition of increasing concentration of displacing ligand ceramide. The fluorescence intensity decay in the presence of competitive non-fluorescent sphingomyelin was measured to determine  $K_i$  as described in “Methods”

**Table 3** Competitive inhibition of NBD-sphingomyelin binding to SCP-2 by non-fluorescent ligands

Ligand	$K_i$ (nM)
Sphingomyelin and precursor ceramide	
Sphingomyelin	173 ± 6
Ceramide	5 ± 1
Neutral glycosphingolipids	
Glucosylceramide (monohexoside)	101 ± 16
Galactosylceramide (monohexoside)	110 ± 10
Lactosylceramide (dihexoside)	116 ± 9
Globosides (tetrahexoside)	121 ± 2
Acidic glycosphingolipids	
Ganglioside GM1	43 ± 6

Values represent mean ± SE,  $n = 3$

Displacement assays were performed as described in “Methods”

Inhibition constants ( $K_i$ ) were calculated from a non-linear fit to an exponential decay curve of NBD-sphingomyelin fluorescence versus the competitor concentration

$K_i$  was equal to the ligand concentration at  $F_{max}/2$

affinity for this sphingolipid nearly 35-fold (Table 3). These data indicated that SCP-2 had significantly higher affinity for ceramide, both a precursor and metabolite of sphingomyelin and other sphingolipids.

#### Binding of Neutral Glycosphingolipids to SCP-2

Ceramide is metabolized not only to sphingomyelin, but is also glycosylated to form neutral sphingolipids including monohexosides (e.g., glucosylceramide, galactosylceramide), dihexosides (e.g., lactosylceramide), and tetrahexosides (e.g., globosides). Therefore, the effect of linking neutral sugars to ceramide on binding to SCP-2 was examined using the NBD-sphingomyelin displacement assay. Increasing concentrations of monohexosides such as glucosylceramide and galactosylceramide both resulted in displacement of SCP-2 bound NBD-sphingomyelin, yielding  $K_i$ s of  $101 ± 16$  and  $110 ± 10$  nM, respectively (Table 3). Covalently linking additional sugars as in lactosylceramide (a dihexoside) and globosides (tetrahexosides) also resulted in displacement of SCP-2 bound sphingomyelin, but these more complex neutral glycosphingolipids did not significantly further alter the  $K_i$ s which were  $116 ± 9$  and  $121 ± 2$  nM for lactosylceramide and globosides, respectively (Table 3). Thus, monoglycosylation of ceramide to form neutral glycosphingolipids decreased the binding affinity to SCP-2 more than 20-fold as compared to ceramide itself (Table 3). However, the presence of more extended sugar chains did not further

reduce binding affinity of the neutral glycosphingolipids to SCP-2.

#### Binding of Acidic Glycosphingolipid to SCP-2

In addition to sphingomyelin and neutral glycosphingolipids, ceramide can also be metabolized to form acidic glycosphingolipids by linking an acid sugar such as sialic acid. Gangliosides, such as GM1 represent typical acidic glycosphingolipids. The effect of linking an acidic sugar to the glycosphingolipids on binding affinity to SCP-2 was therefore examined using the NBD-sphingomyelin displacement assay. As observed with the neutral glycosphingolipids, increasing concentrations of the acidic glycosphingolipid ganglioside GM1 also displaced SCP-2 bound NBD-sphingomyelin, yielding a  $K_i$  of  $43 \pm 6$  nM for ganglioside GM1 (Table 3). Thus, covalently linking an acidic sugar to the glycosphingolipid enhanced the affinity of SCP-2 for the branched-chain GM1 nearly threefold as compared to neutral sphingolipids for SCP-2 (Table 3). Overall, these data indicated that SCP-2 exhibited the following order of affinities for sphingolipids:ceramides, GM1 > the neutral glycosphingolipids (monohexosides, dihexosides, and globosides) > sphingomyelin.

#### Spontaneous Sterol Transfer from Lipid Rafts/Caveolae Isolated from Plasma Membranes Purified from Control and SCP-2 Expressing Cells

Since SCP-2 was shown to selectively regulate sphingolipid distribution to lipid rafts/caveolae in living cells (as described above), the possibility that cholesterol dynamics were also affected was next examined using a sterol transfer polarization assay as described in “Methods”. Spontaneous sterol (DHE) transfer from purified lipid raft/caveolae donors (containing DHE) to lipid raft/caveolae acceptor (containing cholesterol but no DHE) was determined and compared to DHE transfer from lipid raft/caveolae donor/acceptor pairs isolated from SCP-2 expressing cells. When the DHE polarization changes during sterol transfer were kinetically analyzed, two kinetic domains were resolved in lipid rafts/caveolae: (1) a rapidly exchangeable sterol domain with  $t_{1/2}$  on the order of minutes, and (2) a slowly exchangeable sterol domain with  $t_{1/2}$  on the order of days. In control cells, the initial rate of molecular sterol transfer from lipid rafts/caveolae donors to acceptors was  $0.339 \pm 0.021$  pmole/min, twofold faster than that observed with domains isolated from SCP-2 expressing cells ( $0.166 \pm 0.024$  pmol/min, Fig. 5a). Concomitantly, the size of the rapidly exchangeable sterol domain was decreased from  $0.230 \pm 0.017$  to  $0.109 \pm 0.013$  in domains isolated from SCP-2 expressing cells (Fig. 5b). Thus, SCP-2 expression significantly altered the spontaneous sterol

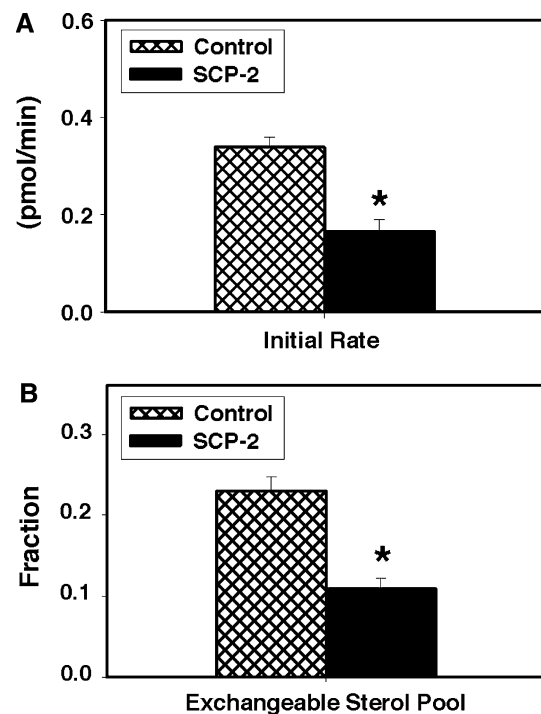


**Fig. 5** Kinetic analysis of sterol transfer between lipid rafts/caveolae isolated from plasma membranes purified from control and SCP-2 expressing cells. Fluorescence polarization for DHE sterol transfer from lipid rafts/caveolae donors to acceptors was analyzed as described in “Methods”. The initial rate (Panel A) of sterol transfer and the fraction of sterol available for rapid exchange (Panel B) was determined by kinetic analysis of exchange curves as described in [14]. Values represent mean  $\pm$  SEM ( $n = 4$ ). \* $P < 0.002$  versus lipid raft/caveolae fractions isolated from control cells

dynamics in lipid rafts/caveolae to decrease the initial rate of sterol transfer and exchangeable sterol pool size.

#### Discussion

Despite the importance of sphingolipids to cell signaling at the plasma membrane, relatively little is known regarding factors that regulate sphingolipid distribution to plasma membrane lipid rafts/caveolae. While lipid rafts/caveolae are rich in cholesterol [14], these microdomains are also thought to be enriched in sphingolipids such as sphingomyelin, ceramide, and gangliosides [4–8, 49] and enzymes involved in sphingolipid signaling [2], conclusions based largely on work with lipid rafts/caveolae isolated by use of detergents or high pH carbonate buffer. However, increasingly there are growing concerns that methods using detergent or high pH carbonate buffer to isolate lipid rafts/caveolae (often starting from whole cell homogenates rather than purified plasma membranes) may not reflect the biological nature of lipid rafts/caveolae in intact cells [9–11]. To avoid these concerns, the current investigation determined the sphingolipid distribution of lipid rafts/

caveolae and non-rafts isolated from purified plasma membranes by affinity chromatography without the use of detergents or high pH carbonate buffer [9, 14, 33, 34]. Extending earlier work with whole cells [37], we examined for the first time: (1) the potential role of SCP-2 in regulating the distribution of individual sphingolipid classes to lipid rafts/caveolae and non-raft domains of plasma membranes from living cells, and (2) whether SCP-2 binds specific sphingolipid classes with high affinity.

First, it was shown that lipid rafts/caveolae isolated without the use of detergents or high pH carbonate buffers were enriched in sphingolipids. Not only sphingomyelin, but also monohexosides, globosides, and the ganglioside GM1 were highly enriched in plasma membrane lipid rafts/caveolae as compared to non-rafts isolated from control L-cells. The content of dihexoside also tended to be higher, but these trends did not achieve statistical significance. Quantitative and qualitative comparison of sphingolipid analyses shown herein versus sphingolipid analyses for lipid rafts/caveolae isolated by use of detergents or high pH carbonate buffers [4, 50] revealed important differences: (1) sphingomyelin and gangliosides were less highly enriched in lipid rafts/caveolae isolated without detergents or high pH carbonate buffer, (2) globosides were enriched only in lipid rafts/caveolae isolated without detergents, (3) ceramides and dihexosides were much less highly enriched in lipid rafts/caveolae isolated without detergents [4, 50], and (4) monohexosides were highly enriched in lipid rafts/caveolae isolated without, but not with, detergents [50]. Thus, while lipid rafts/caveolae isolated without the use of detergents or high pH carbonate buffer share some features with lipid rafts/caveolae isolated by the latter, important quantitative as well as qualitative differences exist.

Second, SCP-2 overexpression in L-cell fibroblasts significantly altered the mass content and % distribution of sphingolipids in lipid rafts/caveolae isolated from purified plasma membranes. As shown herein, the lipid rafts/caveolae isolated from purified plasma membranes derived from SCP-2 expressing cells contained close to twofold more total sphingolipid than the non-raft domains, reflecting significant increase in the mass content of ceramides (twofold), the neutral glycosphingolipids monohexosides (2.8-fold), dihexosides (2.9-fold), globosides (2.2-fold), and the acidic glycosphingolipid GM1 (fourfold). In contrast, SCP-2 expression had less effect on the mass distribution of sphingomyelin—consistent with the fluorescence binding data showing that SCP-2 exhibited the least binding affinity for sphingomyelin as compared to other sphingolipids. In keeping with this trend, those sphingolipids most strongly targeted to lipid raft/caveolae fractions (ceramides, GM1, and the neutral glycosphingolipids (monohexosides, dihexosides, and globosides)) were bound with highest affinity by SCP2.

The biological significance of altered sphingolipid composition to plasma membrane structure and function can be realized from in vitro studies using model membranes [51] and isolated plasma membranes from SCP-2 overexpressing cells [45]. These and other studies [14] showed a strong interaction between sphingomyelin and cholesterol such that membranes high in sphingolipid exhibited reduced size of exchangeable cholesterol domains in membranes, reduced spontaneous cholesterol efflux, and reduced ability of SCP-2 to potentiate cholesterol efflux therefrom [52, 53]. Furthermore, SCP-2 induced alteration of sphingolipid composition and content in lipid rafts/caveolae may also potentially enhance or disrupt signaling and/or vesicular transport activities in the cell since extensive studies have shown distinct roles for several sphingolipid species in these cellular processes [15, 54]. For example, increased levels of ceramides disrupt the organization of cholesterol in lipid rafts and thereby alter cholesterol efflux [15]. SCP-2 overexpression increased the level of ceramide in lipid rafts/caveolae and, as shown earlier, reduced HDL-mediated cholesterol efflux [52]. In the present work, the functional consequence of increased ceramide levels on cholesterol dynamics within lipid raft/caveolae was shown by measuring sterol transfer between lipid rafts derived from control or SCP-2 expressing cells. Analysis of kinetic parameters revealed that the initial rate of molecular sterol transfer from lipid rafts/caveolae donors to acceptors was twofold slower in the presence of increased SCP-2 and ceramides. The size of the exchangeable sterol pool was also two-fold smaller, suggesting SCP-2 significantly altered the spontaneous sterol dynamics in lipid rafts/caveolae by way of ceramide disruption of lipid rafts [55]. Overall, the molecular basis for the reduced cholesterol dynamics in sphingolipid-enriched lipid rafts may be related to the increased rigidity (reduced fluidity) of these domains [33]. The importance of membrane sphingolipids to biological activity is also reflected in the ability of certain viral and bacterial molecules to gain entry into the cell via binding to specific sphingolipids in lipid rafts/caveolae. Cholera toxin from *Vibrio cholera* and *Escherichia coli* bind to the ganglioside GM1 [56] while Shiga toxin from *Shigella dysenteriae* binds to globosides [57]. As seen herein, the mass of GM1, a specific ganglioside involved in signaling [14], as well as globosides, were significantly increased in lipid rafts as compared to non-raft fractions, whereas the effect of SCP-2 expression was to increase mass content of globosides and decrease GM1 as compared to lipid rafts isolated from control cells. Other signal transduction pathways mediated by sphingolipids and potentially regulated by SCP-2 expression include: Ca<sup>2+</sup> flux (dihexosides, globosides, GM1); differentiation (gangliosides); proliferation (gangliosides, dihexosides); cAMP accumulation (globosides), phosphorylation (dihexosides, gangliosides); and PLC signaling (GM1) [15].

Third, the ability of SCP-2 to alter sphingolipid distribution and targeting was correlated with its binding affinity for sphingolipids. The SCP-2 had a single binding site and bound sphingomyelin with affinity near 173 nM. All sphingolipids tested readily displaced SCP-2 bound NBD-sphingomyelin with  $K_i$ s in the nanomolar range of 5–121 nM. The relative order of displacement was: ceramide ( $K_i = 5$  nM) > acidic glycosphingolipid (ganglioside GM1,  $K_i = 43$  nM) > neutral glycosphingolipids ( $K_i$ s = 101–121 nM). Comparison with the effects of SCP-2 expression on altering the distribution of sphingolipid classes to lipid rafts/caveolae suggested that SCP-2 was most effective in mediating enrichment of sphingolipid classes in lipid rafts/caveolae for the sphingolipid class that was bound most tightly by SCP-2 (ceramide). The SCP-2 had the opposite effect on distribution to lipid rafts/caveolae of the sphingolipid class which it bound most weakly (sphingomyelin). Taken together, these findings suggest two potential mechanisms whereby SCP-2 may play a role in regulating distribution of sphingolipids to lipid rafts: (1) SCP-2 may directly transfer bound sphingolipid species to lipid rafts. Model membrane studies demonstrated that SCP-2 interacts directly with negatively charged membranes through its N-terminal amphipathic  $\alpha$ -helical domain to facilitate transfer of bound ligand [58, 59], (2) as a secondary effect SCP-2 may also influence sphingolipid distribution to lipid rafts by regulating vesicular transport. This possibility is supported by the fact that SCP-2 has high affinity for not only for sphingolipids involved in vesicular trafficking, but also for other ligands that regulate vesicle budding at the Golgi i.e., phosphatidylinositol [26] and fatty acyl CoA [60]. Interestingly, while sphingomyelin, along with cholesterol, is known to be enriched in plasma membrane lipid rafts/caveolae, in the present work sphingomyelin was also found in the non-raft fractions which may include lipids and proteins involved in non-caveolar endocytic pathways, i.e., macropinocytosis, clathrin-mediated, clathrin-independent, and caveolae-independent. Recently, by using a fluorescent analog of sphingomyelin, Pagano showed that sphingomyelin was internalized from the plasma membrane equally by clathrin-dependent and independent pathways [61], suggesting participation in both pathways. In SCP-2 expressing cells levels of sphingomyelin increased almost twofold in non-rafts as compared to non-rafts isolated from control cells. However, since SCP-2 was nearly absent from the non-raft fraction (Fig. 3a) and exhibited the least preference for binding to sphingomyelin (Table 3), it remains unclear whether increased targeting of sphingomyelin to non-rafts in SCP-2 expressing cells is SCP-2 mediated or facilitated by another protein enriched in the non-raft fraction. In conclusion, for the first time it was shown that SCP-2 exhibited high affinity for select sphingolipid classes and

that SCP-2 overexpression significantly altered both the mass and % distribution of sphingolipid classes in lipid rafts/caveolae. Taken together, these findings suggest that SCP-2 is a potential candidate for regulating sphingolipid distribution to lipid rafts/caveolae in the cell.

**Acknowledgments** This work was supported in part by the USPHS, NIH grants GM31651 (FS and ABK) and DK70965 (BPA). The technical assistance of Ms. Meredith Dixon was much appreciated.

## References

- Schroeder F (1984) Fluorescent sterols: probe molecules of membrane structure and function (Review). *Prog Lipid Res* 23:97–113
- Anderson R (1998) The caveolae membrane system. *Ann Rev Biochem* 67:199–225
- Feron O (2005) The caveolin interaction with endothelial nitric oxide synthase (eNOS). In: Lisanti MP, Frank PG (eds) *Caveolae and lipid rafts: roles in signal transduction and the pathogenesis of human disease*, vol 36. Elsevier, San Diego, pp 91–108
- Brown DA, Rose JK (1992) Sorting of GPI anchored proteins to glycolipid-enriched membrane subdomains during transport to the apical cell surface. *Cell* 68:533–544
- Liu P, Anderson RGW (1995) Compartmentalized production of ceramide at the cell surface. *J Biol Chem* 270:27179–27185
- Pike LJ, Casey L (1996) Localization and turnover of phosphatidylinositol 4,5-bisphosphate in caveolin-enriched membrane domains. *J Bio Chem* 26453–26456
- Wang XQ, Sun P, Paller AS (2002) Ganglioside induces caveolin-1 redistribution and interaction with the epidermal growth factor receptor. *J Biol Chem* 277:47028–47034
- Ortegren U, Karlsson M, Blazic N, Blomqvist M, Nysrom FH, Gustavsson J, Fredman P, Stralfors P (2004) Lipids and glycosphingolipids in caveolae and surrounding plasma membrane of primary rat adipocytes. *Eur J Biochem* 271:2028–2036
- Gallegos AM, Storey SM, Kier AB, Schroeder F, Ball JM (2006) Structure and cholesterol dynamics of caveolae/raft and non-raft plasma membrane domains. *Biochem* 45:12100–12116
- Skwarek M (2004) Recent controversy surrounding lipid rafts. *Arch Immunol Ther Exp* 52:427–431
- Schuck S, Honsho M, Ekroos K, Shevchenko A, Simons K (2003) Resistance of cell membranes to different detergents. *Proc Natl Acad Sci USA* 100:5795–5800
- Foster LJ, de Hoog CL, Mann M (2003) Unbiased quantitative proteomics of lipid rafts reveals high specificity for signaling factors. *Proc Natl Acad Sci USA* 100:5813–5818
- Pike LJ, Han X, Chung KN, Gross RW (2002) Lipid rafts are enriched in arachidonic acid and plasmenylethanolamine and their composition is independent of caveolin-1 expression: a quantitative electrospray ionization/mass spectrometric analysis. *Biochemistry* 41:2075–2088
- Atshaves BP, Gallegos A, McIntosh AL, Kier AB, Schroeder F (2003) Sterol carrier protein-2 selectively alters lipid composition and cholesterol dynamics of caveolae/lipid raft versus non-raft domains in L-cell fibroblast plasma membranes. *Biochemistry* 42:14583–14598
- Kasahara K, Sanai Y (2006) Functional roles of glycosphingolipids in signal transduction via lipid rafts. *Glycoconj J* 17:153–162
- Hannun YA, Obeid LM (2002) The ceramide-centric universe of lipid-mediated cell regulation: stress encounters of the lipid kind. *J Biol Chem* 277:25847–25850



17. Merrill AH Jr (2002) De novo sphingolipid biosynthesis: a necessary, but dangerous, pathway. *J Biol Chem* 277:25843–25846
18. Brown RE (1998) Sphingolipid organization in biomembranes: what physical studies of model membranes reveal. *J Cell Sci* 111:1–9
19. Pitto M, Brunner J, Ferraretto A, Ravasi D, Palestini P, Masserini M (2000) Use of a photoactivatable GM1 ganglioside analogue to assess lipid distribution in caveolae bilayer. *Glycoconj J* 17:215–222
20. Bloj B, Zilversmit DB (1981) Accelerated transfer of neutral glycosphingolipids and ganglioside GM1 by a purified lipid transfer protein. *J Biol Chem* 256:5988–5991
21. Fong TH, Wang SM, Lin HS (1996) Immunocytochemical demonstration of a lipid droplet specific capsule in cultured Leydig cells of golden hamsters. *J Cell Biochem* 63:366–373
22. DiCorleto PE, Warach JB, Zilversmit DB (1979) Purification and characterization of two phospholipid exchange proteins from bovine heart. *J Biol Chem* 254:7795–7802
23. Cockcroft S (1998) Phosphatidylinositol transfer proteins: a requirement in signal transduction and vesicle traffic. *Bioessays* 20:423–432
24. Cockcroft S (1999) Mammalian phosphatidylinositol transfer protein: emerging roles in signal transduction and vesicular traffic. *Chem Phys Lipids* 98:23–33
25. Schroeder F, Zhou M, Swaggerty CL, Atshaves BP, Petrescu AD, Storey S, Martin GG, Huang H, Helmkamp GM, Ball JM (2003) Sterol carrier protein-2 functions in phosphatidylinositol transfer and signaling. *Biochemistry* 42:3189–3202
26. Zhou M, Parr RD, Petrescu AD, Payne HR, Atshaves BP, Kier AB, Ball JA, Schroeder F (2004) Sterol carrier protein-2 directly interacts with caveolin-1 in vitro and in vivo. *Biochem* 43:7288–7306
27. Parr RD, Martin GG, Hostetler HA, Schroeder ME, Mir KD, Kier AB, Ball JM, Schroeder F (2007) A new N-terminal recognition domain in caveolin-1 interacts with sterol carrier protein-2 (SCP-2). *Biochemistry (revision pending)*
28. Atshaves BP, Petrescu A, Starodub O, Roths J, Kier AB, Schroeder F (1999) Expression and intracellular processing of the 58 kDa sterol carrier protein 2/3-oxoacyl-CoA thiolase in transfected mouse L-cell fibroblasts. *J Lipid Res* 40:610–622
29. Atshaves BP, Storey SM, Schroeder F (2003) Sterol carrier protein-2/sterol carrier protein-x expression differentially alters fatty acid metabolism in L-cell fibroblasts. *J Lipid Res* 44:1751–1762
30. Moncecchi DM, Murphy EJ, Prows DR, Schroeder F (1996) Sterol carrier protein-2 expression in mouse L-cell fibroblasts alters cholesterol uptake. *Biochim Biophys Acta* 1302:110–116
31. Gallegos AM, Atshaves BP, Storey SM, Starodub O, Petrescu AD, Huang H, McIntosh A, Martin G, Chao H, Kier AB, Schroeder F (2001) Gene structure, intracellular localization, and functional roles of sterol carrier protein-2. *Prog Lipid Res* 40:498–563
32. Gallegos AM, Atshaves BP, Storey S, McIntosh A, Petrescu AD, Schroeder F (2001) Sterol carrier protein-2 expression alters plasma membrane lipid distribution and cholesterol dynamics. *Biochemistry* 40:6493–6506
33. Gallegos AM, McIntosh AL, Atshaves BP, Schroeder F (2004) Structure and cholesterol domain dynamics of an enriched caveolae/raft isolate. *Biochem J* 382:451–461
34. Schroeder F, Fontaine RN, Kinden DA (1982) LM fibroblast plasma membrane subfractionation by affinity chromatography on ConA-sepharose. *Biochim Biophys Acta* 690:231–242
35. Baenziger JU, Fiete D (1979) Structural determinants of concanavalin A specificity for oligosaccharides. *J Biol Chem* 254:2400–2407
36. Babbitt J, Trigatti B, Rigotti A, Smart EJ, Anderson RGW, Xu S, Krieger M (1997) Murine SR-BI, a high density lipoprotein receptor that mediates selective lipid uptake, is *N*-glycosylated and fatty acylated and colocalizes with plasma membrane caveolae. *J Biol Chem* 272:13242–13249
37. Milis DG, Moore MK, Atshaves BP, Schroeder F, Jefferson JR (2006) Sterol carrier protein-2 expression alters sphingolipid metabolism in transfected mouse L-cell fibroblasts. *Mol Cell Biochem* 283:57–66
38. van der Luit AH, Budde M, Ruurs P, Verheij M, van Blitterswijk WJ (2002) Alkyl-lysophospholipid accumulates in lipid rafts and induces apoptosis via raft-dependent endocytosis and inhibition of phosphatidylcholine synthesis. *J Biol Chem* 277:39541–39547
39. Yamamoto R, Kallen CB, Babalola GO, Rennert H, Billheimer JT, Strauss JFI (1991) Cloning and expression of a cDNA encoding human sterol carrier protein 2. *Proc Natl Acad Sci* 88:463–467
40. Frolov A, Petrescu A, Atshaves BP, So PTC, Gratton E, Serrero G, Schroeder F (2000) High density lipoprotein mediated cholesterol uptake and targeting to lipid droplets in intact L-cell fibroblasts. *J Biol Chem* 275:12769–12780
41. Nemezc G, Hubbell T, Jefferson JR, Lowe JB, Schroeder F (1991) Interaction of fatty acids with recombinant rat intestinal and liver fatty acid-binding proteins. *Arch Biochem Biophys* 286:300–309
42. Gutfreund H (1972) Ligand binding. In: Gutfreund H (ed) *Enzymes: physical principles*. Wiley, New York, pp 68–94
43. Schroeder F, Myers-Payne SC, Billheimer JT, Wood WG (1995) Probing the ligand binding sites of fatty acid and sterol carrier proteins: effects of ethanol. *Biochemistry* 34:11919–11927
44. Frolov A, Miller K, Billheimer JT, Cho TC, Schroeder F (1997) Lipid specificity and location of the sterol carrier protein-2 fatty acid binding site: a fluorescence displacement and energy transfer study. *Lipids* 32:1201–1209
45. Frolov A, Woodford JK, Murphy EJ, Billheimer JT, Schroeder F (1996) Spontaneous and protein-mediated sterol transfer between intracellular membranes. *J Biol Chem* 271:16075–16083
46. Schroeder F, Atshaves BP, Gallegos AM, McIntosh AL, Liu JC, Kier AB, Huang H, Ball JM (2005) Lipid rafts and caveolae organization. In: Frank PG, Lisanti MP (eds) *Advances in molecular and cell biology*, vol 36. Elsevier, Amsterdam, pp 3–36
47. Ehehalt R, Keller P, Haass C, Thiele C, Simons K (2003) Amyloidogenic processing of the Alzheimer  $\beta$ -amyloid precursor protein depends on lipid rafts. *J Cell Biol* 160:113–123
48. Damjanovich S, Matyus L, Damjanovich L, Bene L, Jenei A, Matko J, Gaspar R, Szollosi J (2007) Does mosaicism of the plasma membrane at molecular and higher hierarchical levels in human lymphocytes carry information on the immediate history of cells? *Immunol Lett* 82:93–99
49. Fridricksson EK, Shipkova PA, Sheets ED, Holowka D, Baird B, McLafferty FW (1999) Quantitative analysis of phospholipids in functionally important membrane domains from RBL-2H3 mast cells using tandem high-resolution mass spectrometry. *Biochemistry* 38:8056–8063
50. Tietz P, Jefferson JR, Pagano R, LaRusso NF (2005) Membrane microdomains in hepatocytes: potential target areas for proteins involved in canalicular bile secretion. *J Lipid Res* 46:1426–1432
51. Schroeder F, Frolov AA, Murphy EJ, Atshaves BP, Jefferson JR, Pu L, Wood WG, Foxworth WB, Kier AB (1996) Recent advances in membrane cholesterol domain dynamics and intracellular cholesterol trafficking. *Proc Soc Exp Biol Med* 213:150–177
52. Atshaves BP, Starodub O, McIntosh AL, Roths JB, Kier AB, Schroeder F (2000) Sterol carrier protein-2 alters HDL-mediated cholesterol efflux. *J Biol Chem* 275:36852–36861
53. Frolov AA, Woodford JK, Murphy EJ, Billheimer JT, Schroeder F (1996) Fibroblast membrane sterol kinetic domains: modulation

- by sterol carrier protein 2 and liver fatty acid binding protein. *J Lipid Res* 37:1862–1874
54. Smith DC, Lord JM, Roberts LM, Johannes L (2004) Glycosphingolipids as toxin receptors. *Semin Cell Dev Biol* 15:397–408
  55. Yu C, Alterman M, Dobrowsky RT (2005) Ceramide displaces cholesterol from lipid rafts and decreases the association of the cholesterol binding protein caveolin-1. *J Lipid Res* 46:1678–1691
  56. Griffiths SL, Finkelstein RA, Critchley DR (1986) Characterization of the receptor for cholera toxin and *Escherichia coli* heat-labile toxin in rabbit intestinal brush borders. *Biochem J* 238:313–322
  57. Lingwood CA, Law H, Richardson S, Petric M, Brunton JL, De Grandis S, Karmali M (1987) Glycolipid binding of purified and recombinant *Escherichia coli* produced verotoxin in vitro. *J Biol Chem* 262:8834–8839
  58. Huang H, Ball JA, Billheimer JT, Schroeder F (1999) The sterol carrier protein-2 amino terminus: a membrane interaction domain. *Biochemistry* 38:13231–13243
  59. Huang H, Ball JA, Billheimer JT, Schroeder F (1999) Interaction of the N-terminus of sterol carrier protein-2 with membranes: role of membrane curvature. *Biochem J* 344:593–603
  60. Frolov A, Cho TH, Billheimer JT, Schroeder F (1996) Sterol carrier protein-2, a new fatty acyl coenzyme A-binding protein. *J Biol Chem* 271:31878–31884
  61. Puri V, Watanabe R, Singh RD, Dominguez M, Brown JC, Wheatley CL, Marks DL, Pagano RE (2001) Clathrin-dependent and independent internalization of plasma membrane sphingolipids initiates two Golgi targeting pathways. *J Cell Biol* 154:535–547

# Fatty Acid Supplied as Triglyceride Regulates SRE-Mediated Gene Expression as Efficiently as Free Fatty Acids

Narumon Densupsoontorn · Tilla S. Worgall ·  
Toru Seo · Hiroko Hamai · Richard J. Deckelbaum

Received: 14 December 2006 / Accepted: 26 June 2007 / Published online: 7 August 2007  
© AOCs 2007

**Abstract** Sterol regulatory element binding proteins (SREBPs) are key transcription proteins that bind to sterol regulatory elements (SRE) of genes essential for cellular cholesterol and fatty acid homeostasis. Polyunsaturated fatty acids (PUFA) strongly inhibit SREBP processing at post-transcriptional levels. We questioned if delivering PUFA as part of a triglyceride (TG) molecule would have similar effects and efficiency as free non-esterified PUFA. CHO cells stably transfected with an SRE-promoter linked to the luciferase reporter gene were incubated for 8–24 h with linoleic acid (LA) complexed to BSA (molar ratios 0.5–4:1), VLDL-sized trilinolein emulsions (TL, 25–200 µg/ml), and chylomicron-sized soy oil emulsions in the presence and absence of apoE. Effects of LA and TL on decreasing SRE-luciferase activity were similar and dose and time dependent. Both TL and LA significantly and rapidly ( $\leq 2$ –12 h) reduced SRE-mediated gene expression by up to 75%. At equal fatty acid concentrations, SRE inhibition by TL was as effective as LA. ApoE addition increased inhibition by TL. Inhibition of gene expression was highly correlated to cell TG accumulation. We conclude that TG like fatty acids are rapid and efficient modulators of SRE-mediated gene expression.

**Keywords** SRE-mediated gene expression · SREBP · Trilinolein · Linoleic acid · De novo triglyceride synthesis

## Abbreviations

ACCoA	Acetyl CoA carboxylase
apoE	Apolipoprotein E
CHO	Chinese hamster ovarian
HSPG	Heparan sulfate proteoglycans
LA	Linoleic acid
LCT	Long chain triglyceride
LRP	Low-density lipoprotein receptor related-protein
mSREBP	Mature form of SREBP
OA	Oleic acid
SRE	Sterol regulatory element
SREBP	Sterol regulatory element binding protein
TG	Triglyceride
TGRP	Triglyceride-rich particle
TL	Trilinolein

## Introduction

Dietary fatty acids function in several roles such as a source of energy and provision of essential fatty acids [1]. They also regulate transcription of lipogenic and glycolytic genes [2–9], and this regulation, in part, is related to sterol regulatory element binding protein (SREBP) processing and binding to sterol regulatory elements (SRE) [10–14]. SRE are located in the promoter region of genes encoding key regulatory enzymes involved in fatty acid and triglyceride (TG) metabolism (i.e., responsive to SREBP-1a, SREBP-1c), and cholesterol synthesis (responsive to SREBP2) [15, 16]. In conditions of cellular sterol depletion, the mature forms of SREBP (mSREBP), the active transcription factors, are generated after a two-step prote-

N. Densupsoontorn · T. S. Worgall · T. Seo ·  
H. Hamai · R. J. Deckelbaum (✉)  
Institute of Human Nutrition and Department of Pediatrics,  
College of Physicians and Surgeons, Columbia University,  
630 W. 168th St., PH1512, New York, NY 10032, USA  
e-mail: rjd20@columbia.edu

olytic process. mSREBP translocate to the nucleus to bind to the SRE in the promoter regions of key genes of lipid metabolism [15]. Increasing cell sterols leads to suppression of gene transcription of SRE-promoter containing genes [17].

In addition to sterols [18, 19], unsaturated fatty acids regulate SRE-mediated gene expression [10–13, 20]. For example, mono- and polyunsaturated fatty acids down-regulate SRE-dependent HMG-CoA synthase gene transcription in vitro [10]. Moreover, suppression of SRE-dependent gene expression increases with the number of fatty acid carbons and double bonds [10].

A large fraction of dietary and endogenous fatty acids are delivered to tissues as part of a TG molecule. A number of studies have provided evidence that substantial amounts of triglyceride-rich particles (TGRP) can be taken up by tissues without substantial intravascular lipolysis [21]. Compared to free fatty acids, TG can undergo different pathways of intracellular metabolism [22, 23]. Thus, we questioned whether the regulation of SRE-dependent gene expression by fatty acid delivered as TG is different from free fatty acid. To address this, we used lipid emulsions as model TGRP and compared the effects of chylomicron-sized soy oil based TGRP, VLDL-sized trilinolein based TGRP, and linoleic acid (LA) complexed to albumin. Our findings indicate that polyunsaturated TG like polyunsaturated free fatty acid are also very efficient at down-regulating SRE-dependent gene expression.

## Experimental Procedures

### Materials

Linoleic acid and oleic acid (OA) were purchased from Sigma-Aldrich, Inc. (St Louis, MO). Trilinolein was purchased from Nu-Chek Prep, Inc. (Elysian, MN). Egg yolk phosphatidylcholine was obtained from Avanti Polar-Lipids, Inc. (Alabaster, AL). [9,10 <sup>3</sup>H (N)]—oleic acid and [9,10 <sup>3</sup>H (N)]—triolein were purchased from PerkinElmer Life and Analytical Science, Inc. (Shelton, CT). Purified recombinant apolipoproteinE<sub>3</sub> (apoE) produced in *E. coli* was provided by Biotechnology General (Rehovot, Israel). TRIZol and SREBP-1a primer were obtained from Invitrogen (Carlsbad, CA).

### Lipid Emulsions

Phospholipid-stabilized commercial emulsions of n-6 soy oil TG (LCT) provided by B. Braun Melsungen AG (Melsungen, Germany) contained 20 g TG/100 ml, and 2.5 g glycerol/100 ml, emulsified by 1.2 g/100 ml of egg

yolk lecithin. These TGRP contained ~54% of their triglyceride fatty acids as LA; their detailed composition has been published elsewhere [24]. Laboratory-made VLDL-sized trilinolein lipid emulsions were prepared using egg yolk phosphatidylcholine /trilinolein (1:4, by weight). The mixture was dried under N<sub>2</sub> gas and then desiccated under vacuum overnight. A vial containing the dried lipid mixture was vortexed with 8 ml of 150 mM NaCl and 0.24 mM disodium EDTA, after adding 0.8 g of sucrose (10%), pH 8.4, at 60 °C. The lipid mixture was then sonicated using a Branson Sonifier model 450 (Branson Scientific, Melville, NY) for 1 h at 40–42 °C, 140 W under nitrogen gas. Buffer solution was added every 10 min during sonication to keep the original volume. Following sonication, emulsion TGRP were dialyzed in buffer for 24 h to remove sucrose. Dialyzed TGRP were overlaid with buffer in a centrifuge tube (Beckman Coulter, Inc., Fullerton, CA) and centrifuged for 20 min at 40,000 rpm, 4 °C, in a Beckman SW 40 Ti rotor (Beckman, Fullerton, CA) to remove dense excess phospholipid-rich liposomes with trapped sucrose. The infranatant was transferred into another centrifuge tube and then overlaid with buffer and centrifuged for 18 h at 28,000 rpm 4 °C in the same rotor. The resulting top cream layer consisting of VLDL-sized emulsion particles and these were analyzed for the amounts of TG and PL by an enzymatic calorimetric assay using a triglycerides/glycerol blanked kit (Roche Diagnostics Corporation, Indianapolis, IN) and a phospholipid kit (Wako Chemicals USA, Inc., Richmond, VA) The triglyceride:phospholipid mass ratio was 5.0 ± 1.0:1 similar to that of VLDL-sized particles. Lipid emulsions contained <0.1% of total glycerols as free fatty acids.

For experiments to follow the cellular uptake and conversion of emulsion TG to free fatty acid, TL emulsions were radiolabeled with <sup>3</sup>H-triolein by incorporating <sup>3</sup>H-triolein with the dried lipid mixture. Following incubations the amount in TG versus free fatty acid was determined after Dole's extraction of cell lipids [25].

### Free Fatty Acids

Free fatty acids were dissolved in 100% ethanol and complexed to BSA as previously described [26]. Equal amounts of ethanol (<0.1% of medium volume) were added under control conditions and had no effects on reporter gene expression as described [10].

### Cells

Chinese hamster ovarian cells (CHO) were stably transfected with an SRE-promoter of HMG-CoA synthase linked to a luciferase reporter gene and luciferase activity

was measured as previously detailed [10]. The pSyn SRE plasmid contains a generic TATA and three SRE elements (–325 to –225) of the hamster HMG-CoA synthase promoter fused into the luciferase pGL2 Basic vector (Promega, Madison, WI). All incubations were carried out in serum-free Dulbecco's modified Eagle's media under conditions detailed in the figure legends.

#### Isolation of RNA and Real-Time Quantitative PCR

Total RNA was isolated from CHO cells with TRIzol and one microgram of isolated RNA was reverse-transcribed using iScript cDNA Synthesis kit (Bio-Rad Laboratories, Hercules, CA). The resulting cDNA was diluted 1:10 and quantitated for ACCoA and SREBP-mRNA levels using Mx3005P™ real-time PCR (Stratagene, La Jolla, CA) using  $\beta$ -actin as a reference gene. The sequences of primers were as follows: ACCoA, 5' primer 5'-ATGTGTGGAAGTCGATGTGC-3' and 3' primer, 5'-TTGCCAATTGTGATTCGGTA-3'; SREBP-1a, 5' primer, 5'-GCGCCATGGAGG-AGCTGCCCTTCG-3', and 3' primer, 5'-GTCAGTCTTGGTTGTTGATG-3';  $\beta$ -actin, 5' primer, 5'-CACCAGGGCGTGAT-GGTGGG-3', and 3' primer, 5'-GATGCCTCTCTTGCTCTGGGC-3' [27]. Real-time PCR analyses were carried out in duplicates and were repeated at least two times for consistency.

#### Statistical Analyses

The data were expressed as means  $\pm$  SEM. One-way analysis of variance (ANOVA) was performed to determine statistical significance at  $P \leq 0.05$ . A Bonferroni test was used for the post hoc multiple comparisons. All statistical analyses were performed with the use of SPSS software (version 11.5; SPSS Inc, Chicago, IL).

## Results

We first assessed the effect of soy oil based TGRP on SRE-mediated gene expression (Fig. 1a). Because these n-6 TGRP contain 53.9 and 23.8% of LA and OA, respectively, as their major fatty acid components, we next compared the effects of these two free fatty acids on SRE-mediated gene expression. Linoleate had significantly greater effect down-regulating SRE-mediated gene transcription than oleate (Fig. 1b) indicating that an increased number of double bond fatty acids resulted in more suppression of SRE-mediated gene expression. Thus, we chose to carry out most experiments comparing effects of LA with trilinolein (TL).

To determine whether TL would act as rapidly as LA in suppressing SRE expression, CHO cells were incubated with LA or TL for 2–24 h. Figure 2 shows that the inhib-

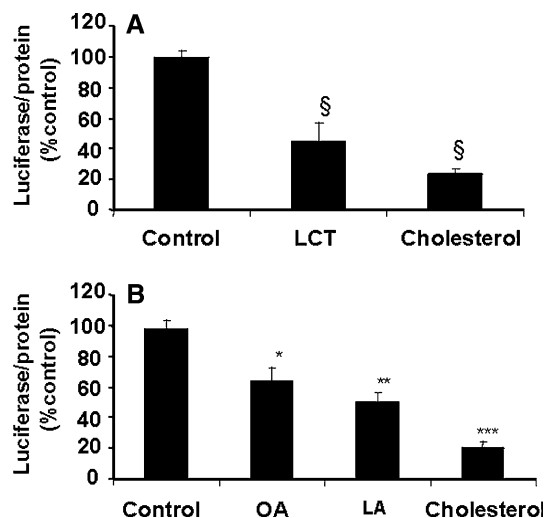


**Fig. 1** Effects of a soy oil TGRP (*LCT*), oleate, and linoleate on SRE expression in CHO cells. After 12 h of up-regulation in lipid-free medium, CHO cells stably transfected with an SRE-promoter reporter gene were incubated for 12 h with control medium alone (containing 1% BSA), medium containing *LCT* emulsion (200  $\mu$ g/ml) or cholesterol (10  $\mu$ g/ml with 1  $\mu$ g/ml of 25-OH cholesterol) (a), or medium supplemented with OA (C18:1n-9) (0.3 mM), LA (C18:2n-6) (0.3 mM), or cholesterol (10  $\mu$ g/ml with 1  $\mu$ g/ml of 25-OH cholesterol) (b). Luciferase activity and cell protein were measured. Data are expressed as percent of control (mean  $\pm$  SEM) from three experiments each performed in triplicate. § $P < 0.001$ ; \* $P < 0.05$ ; \*\* $P < 0.01$ ; \*\*\* $P < 0.001$  compared to control

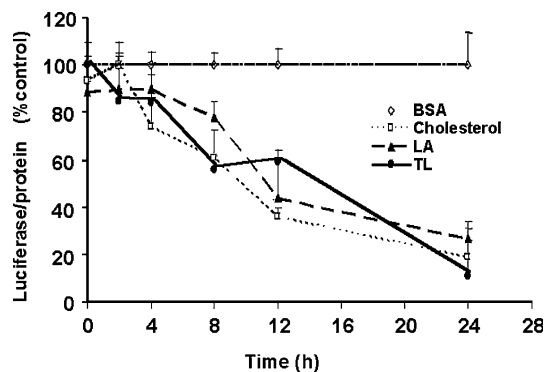


**Fig. 2** Time-dependent effects of sterols, LA and TL on SRE expression in CHO cells. After 12 h of up-regulation, CHO cells stably transfected with an SRE-promoter reporter gene were incubated in control medium alone (*open diamonds*), medium supplemented with sterol (10  $\mu$ g/ml of cholesterol with 1  $\mu$ g/ml of 25-OH cholesterol) (*open squares*), medium containing LA (0.3 mM) (*filled triangles*), and medium supplemented with TL emulsion (200  $\mu$ g/ml) (*filled circles*) for 2, 4, 8, 12, and 24 h. Luciferase activity normalized to cell protein was measured. Data are expressed as percent of control (mean  $\pm$  SEM) from three experiments each performed in triplicate

itory effects of cholesterol, LA and TL on SRE-mediated gene expression were similar, although in this experiment molar amounts of TL fatty acid exceeded that of LA.

Although effects were maximal after 24 h of incubation, cell protein values decreased slightly with trilinolein emulsions at 24 h. Therefore, further experiments were performed within 12 h incubation periods. At this time point, as we have reported previously for free fatty acids [10], TG emulsions had no cell toxic effects.

Using emulsions with radiolabeled  $^3\text{H}$ -triolein we observed that after a 4-h incubation the amount of new TG in cells was  $4.6 \pm 0.5$  mg/mg cell protein ( $n = 3$ ), similar to our previous reported results. Cell TG decreased after removal of TG from the media at a rate of  $-0.20$  mg TG/mg cell protein/h. Also at 4 h, of total recovered counts 49% were found as FA increasing to 59% with a further 4 h incubation without lipids. These latter results show that emulsions were both taken up by cells, and efficiently converted to FA intracellularly.

To assess whether the regulation of SRE-dependent gene expression by free fatty acid versus TG was different or similar, we performed experiments with similar molar concentrations of LA as fatty acid and TG. Figure 3 indicates that the effect of FFA levels on suppression of gene expression occurs in a graded, concentration-dependent manner for both LA, and TL TGRP. At equal estimated FA concentrations (0.15, 0.45 and 0.6 mM), SRE inhibition by TL was equal as or more effective as LA.

To determine if decreases in SRE expression as measured by luciferase reported gene activity reflected changes in regulation of genes dependent on SREBP processing, we assayed expression of acetyl CoA carboxylase (ACCoA) in cells after incubation with LA and TL emulsions after a 4-h

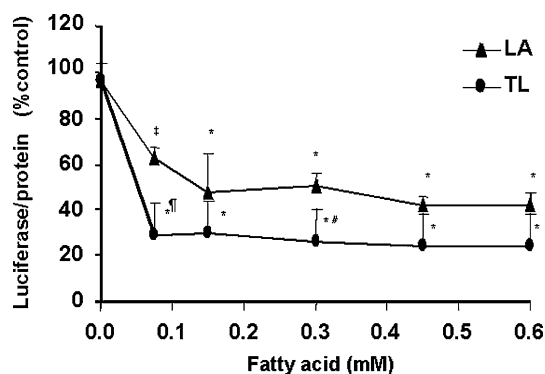


**Fig. 3** Effects of increasing concentrations of LA and TL emulsion on SRE expression in CHO cells. Following 12 h up-regulation, CHO cells stably transfected with an SRE-promoter reporter gene were incubated in control medium alone (containing 1% BSA) and medium containing LA (filled triangles) at the following concentrations: 0.075, 0.15, 0.3, 0.45, and 0.6 mM, and medium supplemented with TL emulsion (filled circles) at 25, 50, 100, 150, and 200  $\mu\text{g}/\text{ml}$  to achieve equal concentrations of fatty acid as LA, respectively. Luciferase activity normalized to cell protein was measured. Data are expressed as percentages of control (mean  $\pm$  SEM) from three experiments each performed in duplicate.  $^\ddagger P < 0.01$ ;  $*P < 0.001$  compared to control;  $^\# P < 0.05$ ;  $^* P < 0.01$  compared to LA

incubation and a 12-h lipid free chase. ACCoA mRNA expression normalized by  $\beta$ -actin decreased by 65.6 and 51.3% for TL (200 mg/ml) and LA (0.3 mM), respectively, when compared to control incubations with albumin alone ( $n = 2$ ). Thus, decreases in SRE-luciferase activity were quite similar to levels of inhibition of expression of an SREBP1-regulated target gene, ACCoA.

Apolipoprotein E (apoE) plays a role as a ligand for lipoprotein uptake via receptor-related pathways, i.e., LDL receptor, LRP pathways [24, 28, 29]. In addition, apoE mediates TGRP uptake via non-receptor mechanisms such as cell surface proteoglycans [30–33]. ApoE added to TL-derived TGRP led to enhanced suppression of SRE-mediated gene expression (Fig. 4). In separate experiments adding lipid-free apoE alone without TGRP at similar concentration as used in incubation with the TRGP, there was no suppression of SRE-mediated gene expression (data not shown).

We questioned whether inhibition of SRE-mediated gene expression could be correlated to increased intracellular TG mass as a result of incubation with either LA or TGRP. Figure 5 depicts a close correlation between suppression of SRE-mediated gene expression and increases in cell TG mass ( $R^2 = 0.6733$ ), likely because higher cell TG provides a higher level of intracellular fatty acid release.

We examined whether changes in SREBP-1a mRNA levels (the SREBP isoform mainly found in cultured cells) contributed to regulation of SRE-mediated gene by TL or LA. Figure 6 shows that there were no significant differences in SREBP-1a mRNA levels of CHO cells incubated with cholesterol, LA, TL, or TL plus apoE. Thus, effects of TG on SRE-mediated gene expression, like those of free fatty acid, are mainly post-transcriptional.

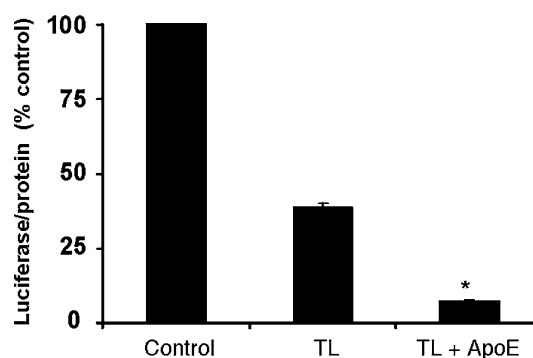


**Fig. 4** Effect of apolipoproteinE-mediated TGRP uptake on suppression of gene expression. CHO cells stably transfected with an SRE-promoter reporter gene were incubated with TL or TL plus 5% apoE (weight/weight) for 12 h. Then luciferase and protein were assayed. Suppression of SRE expression shown by luciferase activity were compared to control incubations (1% fatty acid-free BSA). Data are expressed as mean  $\pm$  SEM from three experiments each performed in triplicate ( $*P < 0.05$ )

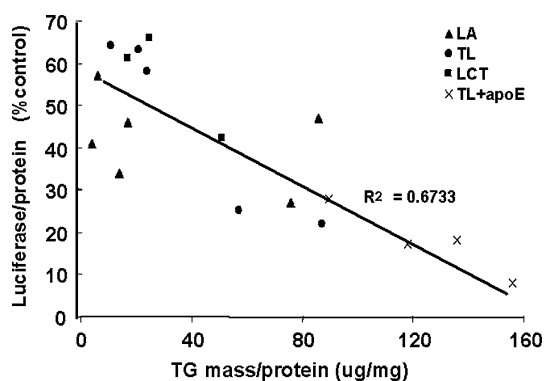


**Fig. 5** Correlation between inhibition of SRE-mediated gene expression and cell TG mass. CHO cells stably transfected with an SRE-promoter reporter gene were incubated with a range of concentrations of LA, TL, LCT, and TL in the presence of 5% apoE for 12 h. Luciferase activity, TG, and cell protein were assayed and SRE-mediated gene expression shown by luciferase activity was compared to net TG mass increases calculated by the TG mass differences from control cells not incubated with fatty acid or TG ( $R^2 = 0.6733$ )

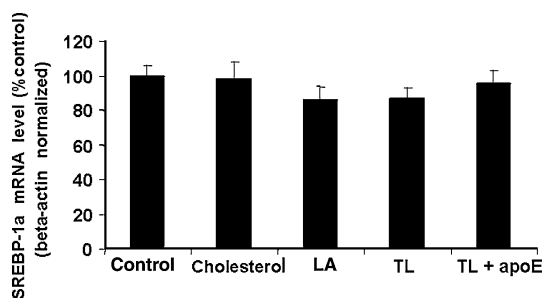


**Fig. 6** Effects of linoleic acid, trilinolein, and cholesterol on SREBP-1a mRNA expression in CHO cells. Sterol-depleted CHO cells were incubated with cholesterol/25-OH cholesterol (10, 1  $\mu\text{g}/\text{ml}$ , respectively), LA (0.0375–0.6 mM), TL (12.5–200  $\mu\text{g}/\text{ml}$ ), in the presence or absence of apoE (5%, weight/weight) for 12 h. At the end of experiments, total RNA were isolated to determine SREBP-1a levels using real-time PCR as described in “Experimental Procedures”. Data were normalized by  $\beta$ -actin and expressed as percentages relative to control performed in duplicates. There were no significant differences between each group

## Discussion

Previous studies delineating effects of fatty acids on regulating SREBP processing have used albumin-bound fatty acids for in vitro analyses or dietary feeding of n-3 fatty acid enriched diets. Substantial amounts of dietary fatty acids are delivered to cells and tissues as part of a TG molecule. It remains an open question as to whether fatty acid-mediated decrease of SREBP processing requires delivery as a free fatty acid molecule cell, or whether intracellular delivery via TGRP can be equally effective. Studies of others have shown that in some tissues delivering free fatty acid versus TG has different effects on a number of parameters related to intracellular lipid metabolic endpoints such as energy

utilization [22, 34]. Our studies, using an in vitro cell culture approach, show that delivery of fatty acids as TG is equally or even more efficient at decreasing SRE-mediated gene expression than delivery of free fatty acid. Moreover, these effects are related to the amount of newly accumulating TG, either from uptake of free fatty acid or TG itself within cells. The effects of both TG and free fatty acids are posttranscriptional in that they do not affect expression of SREBP-1a mRNA, the relevant form of SREBP-1 in cell culture models.

Our current studies largely focused on LA complexed to albumin and trilinolein particles since, in previous studies, we showed that saturated fatty acids have little or no effect on SREBP processing, and in the current study, LA was more inhibitory than the previously reported effect of OA [10]. Our current studies show that uptake of both fatty acid and TG is rapid. This is in keeping with our previous studies where we showed rapid and efficient uptake by cultured cells with of model TGRP in the presence or absence of apoE, at concentrations similar to those used herein, [34, 35]. Moreover, under cell culture conditions used for our current studies, little or no lipolysis of TG takes place in cell media indicating that the effects we observed are not associated with hydrolysis of particle TG before uptake into cells [35, 36].

There are some limitations to our studies. Although in the incubation media we attempted to deliver equal amounts of LA as free fatty acid or TGRP, we could not precisely assess actual cellular uptake of LA or TGRP. Thus, we cannot determine if our results truly reflect exactly equal concentrations of LA delivered intracellularly. This would have been difficult to assess since internalized fatty acid and TG both shunt rapidly towards oxidation to  $\text{CO}_2$  and other intracellular pathways. Still, our experiments using radiolabeled TG showed not only substantial uptake of TGRP-TG by cells but also very efficient cellular catabolism to fatty acid. (Likely, both cell uptakes of TG and cell FA levels were underestimated as we did not measure their conversion to  $\text{CO}_2$ ). Usually, uptake of free fatty acids is studied over time periods of a few minutes [37] while studies on SRE-mediated gene expression need to be carried out over time periods of hours. Still we do not believe that this is a serious confounder in that even when delivered as TG, LA released intracellularly from TGRP led to effects of similar magnitude as that of LA complexed to albumin. It is also possible that apoE has distinct effects on SRE processing and SRE-mediated gene expression separate from effects on increasing TGRP cellular uptake [24, 31, 35]. However, in experiments where we added lipid free apoE in incubation with LA, we found no independent effects of exogenous apoE on SRE-mediated gene expression. Thus, we conclude the effects of apoE are linked to increasing intracellular delivery of TGRP.

The close correlation of inhibition of SRE-mediated gene expression with net accumulation of cell TG is of interest. Unsaturated fatty acids are most effective in decreasing SREBP in the presence of high TG mass. These findings raise the possibility that, early after uptake of free fatty acid or TG most TG fatty acid and fatty acid themselves are utilized for oxidation and only with ongoing continuous delivery of fatty acids or their metabolites to specific intracellular targets SREBP processing is affected. Likely, hydrolysis of intracellular TG provide a continuing intracellular source for fatty acids to inhibit SREBP processing. At this point, while speculative, it is possible that before acting intracellularly, free fatty acids must first be repackaged into intracellular TG followed by release of fatty acids to decrease the generation of mSREBP. This would result in less activation of genes involved in de novo fatty acid synthesis (such as fatty acid synthase) and result in decreased endogenous TG production (Fig. 7). Another open question is whether it is free fatty acids themselves or their metabolites that are active in suppressing and SREBP-mediated gene expression. While it is possible that the TG molecule itself might affect SREBP processing between the endoplasmic reticulum and the Golgi, we do not believe this to be likely since long chain TG molecules, such as TL, are generally regarded as an “inert” storage form for biologically active fatty acids. Because of the molecular

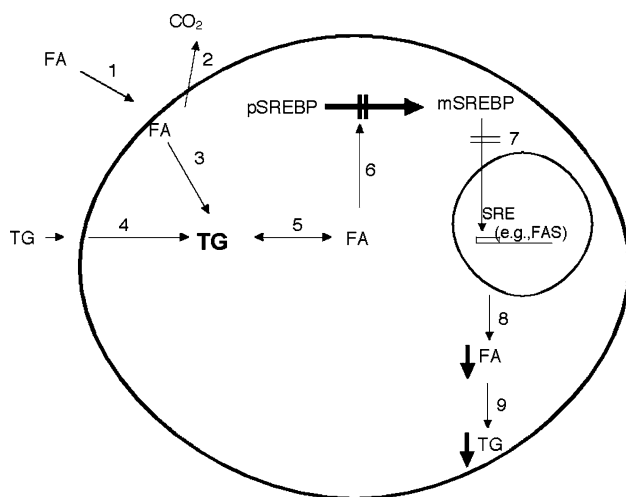


**Fig. 7** TG and FA as interactive partners in SREBP processing and suppression of SRE-mediated gene expression. As an example, SRE dependent expression of fatty acid synthase (FAS) is shown. Exogenous FA moves into the intracellular compartment (step 1), then it is either oxidized resulting in CO<sub>2</sub> production (step 2) or re-esterified to TG (step 3). Cell TG can also accumulate for exogenous TG (step 4) to be part of the TG pool. After hydrolyzing TG from the intracellular pool (step 5), released FA suppress SREBP processing (step 6) from its precursor form (pSREBP) to its mature form (mSREBP). As a result, SRE-dependent gene activity is decreased (step 7). With decreased FA synthesis (step 8), decreased de novo TG synthesis and deposition also occur (step 9)

properties of the very apolar TG, it is unlikely to be a direct effector. TG would need to break free from its aggregation state and require a protein for transport through an aqueous phase. In contrast, FA has molecular properties (and intracellular protein transporters) that allow its rapid diffusion anywhere in the cell.

Studies in human and animal models with intravenous TG emulsions have shown that provision of exogenous TG depresses de novo TG synthesis in liver and other tissues [38, 39]. During lipid-free intravascular nutrition support, increased endogenous TG synthesis and accumulation in liver has been documented [38]. Our findings are consistent with a mechanism whereby intracellular delivery of TG suppress de novo fatty acid synthesis by inhibition of SREBP-activated genes such as fatty acid synthase [12, 40] and as shown herein, ACCoA. To conclude, delivering exogenous fatty acid as part of a TG molecule is equally effective as free fatty acids in suppressing SRE-mediated gene expression and expression of genes involved in fatty acid and TG syntheses. Since normal humans have triglyceridemia post-prandially for many hours of a day, it is likely that direct delivery of triglyceride-rich particles to cells does have physiologically modulating effects on SRE-mediated gene expression.

**Acknowledgments** This study was supported by the National Institute of Health Grant HL40404. Narumon Densupsoontorn was supported by the Faculty of Medicine Siriraj Hospital, Mahidol University, Bangkok, Thailand. We thank Fannie Keyserman and Inge Hansen for their excellent, skillful technical assistance. None of the authors has any conflicts of interest relating to any data reported in this paper.

## References

1. Uauy R, Trean M, Hoffman DR (1989) Essential fatty acid metabolism and requirements during development. *Semin Perinatol* 13:118–130
2. Jump DB, Clarke SD, Thelen A, Liimatta M (1994) Coordinate regulation of glycolytic and lipogenic gene expression by polyunsaturated fatty acids. *J Lipid Res* 35:1076–1084
3. Katsurada A, Iritani N, Fukuda H, Noguchi T, Tanaka T (1987) Influence of diet on the transcriptional and post-transcriptional regulation of malic enzyme induction in the rat liver. *Eur J Biochem* 168:487–491
4. Blake WL, Clarke SD (1990) Suppression of rat hepatic fatty acid synthase and S14 gene transcription by dietary polyunsaturated fat. *J Nutr* 120:1727–1729
5. Katsurada A, Iritani N, Fukuda H, Matsumura Y, Nishimoto N, Noguchi T, Tanaka T (1990) Effects of nutrients and hormones on transcriptional and post-transcriptional regulation of acetyl-CoA carboxylase in rat liver. *Eur J Biochem* 190:435–441
6. Ntambi JM (1992) Dietary regulation of stearoyl-CoA desaturase 1 gene expression in mouse liver. *J Biol Chem* 267:10925–10930
7. Liimatta M, Towle HC, Clarke S, Jump DB (1994) Dietary polyunsaturated fatty acids interfere with the insulin/glucose activation of L-type pyruvate kinase gene transcription. *Mol Endocrinol* 8:1147–1153



8. Clarke SD (2000) Polyunsaturated fatty acid regulation of gene transcription: a mechanism to improve energy balance and insulin resistance. *Br J Nutr* 83(Suppl 1):S59–S66
9. Clarke SD, Gasperikova D, Nelson C, Lapillonne A, Heird WC (2002) Fatty acid regulation of gene expression: a genomic explanation for the benefits of the Mediterranean diet. *Ann NY Acad Sci* 967:283–298
10. Worgall TS, Sturley SL, Seo T, Osborne TF, Deckelbaum RJ (1998) Polyunsaturated fatty acids decrease expression of promoters with sterol regulatory elements by decreasing levels of mature sterol regulatory element-binding protein. *J Biol Chem* 273:25537–25540
11. Mater MK, Thelen AP, Pan DA, Jump DB (1999) Sterol response element-binding protein 1c (SREBP1c) is involved in the polyunsaturated fatty acid suppression of hepatic S14 gene transcription. *J Biol Chem* 274:32725–32732
12. Yahagi N, Shimano H, Hasty AH, Amemiya-Kudo M, Okazaki H, Tamura Y, Iizuka Y, Shionoiri F, Ohashi K, Osuga J, Harada K, Gotoda T, Nagai R, Ishibashi S, Yamada N (1999) A crucial role of sterol regulatory element-binding protein-1 in the regulation of lipogenic gene expression by polyunsaturated fatty acids. *J Biol Chem* 274:35840–35844
13. Xu J, Nakamura MT, Cho HP, Clarke SD (1999) Sterol regulatory element binding protein-1 expression is suppressed by dietary polyunsaturated fatty acids. A mechanism for the coordinate suppression of lipogenic genes by polyunsaturated fats. *J Biol Chem* 274:23577–23583
14. Jump DB (2002) Dietary polyunsaturated fatty acids and regulation of gene transcription. *Curr Opin Lipidol* 13:155–164
15. Horton JD, Shimomura I (1999) Sterol regulatory element-binding proteins: activators of cholesterol and fatty acid biosynthesis. *Curr Opin Lipidol* 10:143–150
16. Horton JD, Goldstein JL, Brown MS (2002) SREBPs: activators of the complete program of cholesterol and fatty acid synthesis in the liver. *J Clin Invest* 109:1125–1131
17. Brown MS, Goldstein JL (1997) The SREBP pathway: regulation of cholesterol metabolism by proteolysis of a membrane-bound transcription factor. *Cell* 89:331–340
18. Horton JD, Shah NA, Warrington JA, Anderson NN, Park SW, Brown MS, Goldstein JL (2003) Combined analysis of oligonucleotide microarray data from transgenic and knockout mice identifies direct SREBP target genes. *Proc Natl Acad Sci USA* 100:12027–12032
19. Sudhof TC, Russell DW, Brown MS, Goldstein JL (1987) 42 bp element from LDL receptor gene confers end-product repression by sterols when inserted into viral TK promoter. *Cell* 48:1061–1069
20. Jump DB (2004) Fatty acid regulation of gene transcription. *Crit Rev Clin Lab Sci* 41:41–78
21. Hultin M, Carneheim C, Rosenqvist K, Olivecrona T (1995) Intravenous lipid emulsions: removal mechanisms as compared to chylomicrons. *J Lipid Res* 36:2174–2184
22. Listenberger LL, Han X, Lewis SE, Cases S, Farese RV Jr., Ory DS, Schaffer JE (2003) Triglyceride accumulation protects against fatty acid-induced lipotoxicity. *Proc Natl Acad Sci USA* 100:3077–3082
23. Augustus AS, Kako Y, Yagyu H, Goldberg IJ (2003) Routes of FA delivery to cardiac muscle: modulation of lipoprotein lipolysis alters uptake of TG-derived FA. *Am J Physiol Endocrinol Metab* 284:E331–339
24. Qi K, Seo T, Al-Haideri M, Worgall TS, Vogel T, Carpentier YA, Deckelbaum RJ (2002) Omega-3 triglycerides modify blood clearance and tissue targeting pathways of lipid emulsions. *Biochemistry* 41:3119–3127
25. Dole VP (1956) A relation between non-esterified fatty acids in plasma and the metabolism of glucose. *J Clin Invest* 35:150–154
26. Rumsey SC, Galeano NF, Lipschitz B, Deckelbaum RJ (1995) Oleate and other long chain fatty acids stimulate low density lipoprotein receptor activity by enhancing acyl coenzyme A:cholesterol acyltransferase activity and altering intracellular regulatory cholesterol pools in cultured cells. *J Biol Chem* 270:10008–10016
27. Shimomura I, Bashmakov Y, Shimano H, Horton JD, Goldstein JL, Brown MS (1997) Cholesterol feeding reduces nuclear forms of sterol regulatory element binding proteins in hamster liver. *Proc Natl Acad Sci USA* 94:12354–12359
28. Mahley RW (1988) Apolipoprotein E: cholesterol transport protein with expanding role in cell biology. *Science* 240:622–630
29. Kowal RC, Herz J, Goldstein JL, Esser V, Brown MS (1989) Low density lipoprotein receptor-related protein mediates uptake of cholesteryl esters derived from apoprotein E-enriched lipoproteins. *Proc Natl Acad Sci USA* 86:5810–5814
30. Hussain MM, Mahley RW, Boyles JK, Fainaru M, Brecht WJ, Lindquist PA (1989) Chylomicron–chylomicron remnant clearance by liver and bone marrow in rabbits. Factors that modify tissue-specific uptake. *J Biol Chem* 264:9571–9582
31. Al-Haideri M, Goldberg IJ, Galeano NF, Gleeson A, Vogel T, Gorecki M, Sturley SL, Deckelbaum RJ (1997) Heparan sulfate proteoglycan-mediated uptake of apolipoprotein E-triglyceride-rich lipoprotein particles: a major pathway at physiological particle concentrations. *Biochemistry* 36:12766–12772
32. Obunike JC, Pillarisetti S, Paka L, Kako Y, Butteri MJ, Ho YY, Wagner WD, Yamada N, Mazzone T, Deckelbaum RJ, Goldberg IJ (2000) The heparin-binding proteins apolipoprotein E and lipoprotein lipase enhance cellular proteoglycan production. *Arterioscler Thromb Vasc Biol* 20:111–118
33. Ji ZS, Pitas RE, Mahley RW (1998) Differential cellular accumulation/retention of apolipoprotein E mediated by cell surface heparan sulfate proteoglycans. Apolipoproteins E3 and E2 greater than e4. *J Biol Chem* 273:13452–13460
34. Schwiigelshohn B, Presley JF, Gorecki M, Vogel T, Carpentier YA, Maxfield FR, Deckelbaum RJ (1995) Effects of apoprotein E on intracellular metabolism of model triglyceride-rich particles are distinct from effects on cell particle uptake. *J Biol Chem* 270:1761–1769
35. Ho YY, Al-Haideri M, Mazzone T, Vogel T, Presley JF, Sturley SL, Deckelbaum RJ (2000) Endogenously expressed apolipoprotein E has different effects on cell lipid metabolism as compared to exogenous apolipoprotein E carried on triglyceride-rich particles. *Biochemistry* 39:4746–4754
36. Granot E, Schwiigelshohn B, Tabas I, Gorecki M, Vogel T, Carpentier YA, Deckelbaum RJ (1994) Effects of particle size on cell uptake of model triglyceride-rich particles with and without apoprotein E. *Biochemistry* 33:15190–15197
37. Stump DD, Fan X, Berk PD (2001) Oleic acid uptake and binding by rat adipocytes define dual pathways for cellular fatty acid uptake. *J Lipid Res* 42:509–520
38. Hall RI, Grant JP, Ross LH, Coleman RA, Bozovic MG, Quarfordt SH (1984) Pathogenesis of hepatic steatosis in the parenterally fed rat. *J Clin Invest* 74:1658–1668
39. Carpentier YA, Nordenstrom J, Robin A, Kinney JM (1981) Glycerol turnover and kinetics of exogenous fat in surgical patients. *Acta Chir Scand Suppl* 507:226–237
40. Jump DB, Clarke SD (1999) Regulation of gene expression by dietary fat. *Annu Rev Nutr* 19:63–90

# Effects of Dietary Cholesterol on Tissue Ceramides and Oxidation Products of Apolipoprotein B-100 in ApoE-Deficient Mice

Ikuyo Ichi · Yuka Takashima · Noriko Adachi ·  
Kayoko Nakahara · Chiaki Kamikawa ·  
Mariko Harada-Shiba · Shosuke Kojo

Received: 1 March 2007 / Accepted: 20 April 2007 / Published online: 24 July 2007  
© AOCs 2007

**Abstract** Oxidized LDL (oxLDL) has been shown to activate the sphingomyelinase pathway producing ceramide in vascular smooth muscle cells. Therefore ceramide, which is a biologically active lipid causing apoptosis in a variety of cells, may be involved in the apoptotic action of oxLDL. In this study, we examined whether cholesterol enriched diets affected ceramide metabolism and oxidation product of LDL, represented by degradation of apolipoprotein B-100 (apoB) in apoE-deficient (apoE<sup>-/-</sup>) mice. ApoE<sup>-/-</sup> and wild type mice were fed a standard (AIN-76) diet or 1% cholesterol-enriched diet for 8 weeks. Tissue ceramide levels were analyzed using electrospray tandem mass spectrometry (LC-MS/MS). Ceramide levels in the plasma and the liver of apoE<sup>-/-</sup> mice were intrinsically higher than those of the wild type. In apoE<sup>-/-</sup> mice, dietary cholesterol significantly increased several ceramides and degradation products of apoB in plasma compared to those fed the control diet. Dietary cholesterol did not affect tissue ceramide levels in the wild type mice. Based on these results, plasma ceramides possibly correlate with the increase in LDL oxidation and are a risk factor for atherosclerosis.

**Keywords** Ceramide · Cholesterol ·  
Apolipoprotein B-100 · Oxidation · LC-MS/MS

## Abbreviations

ApoB	apolipoprotein B-100
ApoE <sup>-/-</sup>	apoE deficient
IMT	Intima-media thickness of the carotid artery
LDL	Low-density lipoprotein
oxLDL	oxidized LDL
SDS-PAGE	Sodium dodecyl sulfate polyacrylamide gel electrophoresis
SM	Sphingomyelin
SMase	Sphingomyelinase
SPT	Serine palmitoyl-CoA transferase
TG	Triglyceride

## Introduction

Ceramide has been implicated in regulating cell-cycle arrest, apoptosis, and cell senescence [1–3] and is reported to serve as an intracellular second messenger [4]. Therefore, ceramide has attracted much attention as a new lipid mediator. Ceramide consists of a fatty acid of C16–C26 chain length bound to the amino group of sphingosine. Ceramide is generated by sphingomyelin (SM) hydrolysis by sphingomyelinase (SMase) or by de novo synthesis starting from serine-palmitoyl transferase (SPT) [5]. A significant positive correlation was observed between plasma levels of SM and the severity of coronary heart disease [6], and plasma SM levels increased in human familial hyperlipidemias [7]. Recent studies have demonstrated correlations between sphingomyelin and atherogenic risk factors of plasma in humans [8] and inhibitions of de novo SM and ceramide biosynthesis reduced atherosclerotic lesion in apoE-deficient (apoE<sup>-/-</sup>) mice [9, 10].

I. Ichi · Y. Takashima · N. Adachi · K. Nakahara ·  
C. Kamikawa · S. Kojo (✉)  
Department of Food Science and Nutrition,  
Nara Women's University, Nara 630-8506, Japan  
e-mail: kojo@cc.nara-wu.ac.jp

M. Harada-Shiba  
Department of Bioscience,  
National Cardiovascular Center Research Institute,  
Osaka 565-8565, Japan

We recently showed that ceramide concentrations in human plasma had a significantly positive correlation with lipid markers that associated with atherosclerosis [11]. Plasma ceramide concentration increased drastically at a high level of LDL cholesterol (more than 170 mg/dL). Therefore, an increase in ceramide may be a risk factor for atherosclerosis, like LDL cholesterol.

Oxidative modification of LDL is an important factor in the development of atherosclerosis [12]. Although LDL is composed of lipids, protein, and sugar chains, studies on the oxidation of LDL have mainly focused on lipid peroxidation [13]. The protein part of LDL, apolipoprotein B-100 (apoB), is also reactive to radical oxidation and it undergoes fragmentation and conjugation [14, 15]. Among the plasma proteins, apoB is unusually reactive to radical reactions compared to albumin and transferrin and even comparable to vitamin E, a typical radical scavenger [14]. Thus, both fragmented and conjugated apoB proteins are present in normal human serum and these oxidation reaction products of LDL tend to increase with age [15]. In addition, we reported that B-ox, namely the sum of fragmented and conjugated apoB proteins determined by an immunoblot assay, showed a significant positive correlation with IMT (intima-media thickness of the carotid artery) and LDL cholesterol, and a negative correlation with HDL cholesterol, and vitamin C [15]. These reports suggest that B-ox is a reliable mechanism-based indicator of atherosclerosis.

Proteolytic degradation of apoB has been shown to cause aggregation and fusion of LDL [16]. Aggregated LDL in atherosclerotic lesions is proposed as representing a central process in atherosclerosis [17] and is enriched with ceramide [18]. Furthermore, LDL treated with SMase induces foam cell formation in vitro [18, 19]. Based on these reports, a correlation between ceramide and oxLDL is suggested.

Dietary cholesterol raises LDL cholesterol levels and a very high intake of cholesterol causes atherosclerosis. The activity of SPT, which catalyzes the first step in ceramide synthesis, is augmented in the aorta of rabbits fed high cholesterol diets [20]. Treatment of mice with myriocin, a specific inhibitor of SPT, lowered plasma cholesterol levels of ceramide in a dose-dependent manner. Therefore, high cholesterol diets may affect ceramide synthesis. The apoE<sup>-/-</sup> mice exhibit high levels of plasma cholesterol as a result of impaired clearance of cholesterol-enriched lipoproteins [21]. Therefore, apoE<sup>-/-</sup> mice are more sensitive to dietary cholesterol. In the present study, we examine the effect of high cholesterol diets on the ceramide levels in plasma, liver, and adipose tissues of apoE<sup>-/-</sup> mice in comparison with wild-type mice. We also demonstrate that dietary cholesterol results in enhancement of oxidation of apoB, namely degradation of apoB, in apoE<sup>-/-</sup> mice.

## Experimental Procedures

### Materials

All solvents were purchased from Wako Pure Chemicals Co. (Osaka, Japan). All other reagents were obtained from Funakoshi Co. (Tokyo, Japan). A commercially available diagnostic kit for cholesterol and triglyceride (TG) were purchased from Wako Pure Chem. Co. (Osaka, Japan). Silica gel 60 TLC plates were purchased from Merck (Darmstadt, Germany). A Vectastain ABC-PO (goat IgG) kit was purchased from Vector Lab. Inc. (Burlingame, CA, USA). Anti-human lipoprotein B goat IgG was purchased from Sigma Chem. Co. (St. Louis, MO, USA). Polyvinylidene difluoride (PVDF) membrane filters were purchased from Millipore (Tokyo, Japan). Electrophoresis reagents were purchased from Nacalai Tesque Inc. (Kyoto, Japan).

### Animals and Diets

This study was approved by the Animal Care Committee of Nara Women's University. Eight-week-old male apoE<sup>-/-</sup> mice on C57BL/6J background mice were purchased from Jackson Laboratories (Bar Harbor, Me., USA). Eight-week-old male C57BL/6J mice were also obtained from Japan SLC Co. (Hamamatsu, Shizuoka, Japan). The animals were housed in a room at 24 ± 2 °C, with a 12/12 h light–dark cycle. A standard diet was formulated according to the AIN-76 formula. The control group was fed a standard diet, and the cholesterol group was fed a standard diet supplemented with 1% cholesterol. Mice were randomized into the two groups. Mice were fed these experimental diets ad libitum for 8 weeks. All mice were starved for 6 h before killing.

### Analytical Method

Mice were anesthetized with Nembutal, and blood samples were collected by right-ventricle puncture using a syringe containing sodium heparin as an anticoagulant. After perfusion, the liver and adipose tissues were dissected out. Blood was centrifuged to separate the plasma.

Plasma cholesterol and TG were measured using a commercially available diagnostic kit. Liver cholesterol concentration was analyzed by gas–liquid chromatography (GC-2014, Shimadzu, Kyoto, Japan) using 5 $\alpha$ -cholestane as an internal standard [22]. Liver TG was analyzed as described by Fletcher et al. [23]. Vitamin C was measured according to a specific and sensitive method involving chemical derivatization and HPLC [24].

## Ceramide Analysis

Lipid of each tissue was extracted according to the method of Folch et al. [25]. Lipid in the liver and the adipose tissues was dissolved in chloroform to perform silica gel 60 TLC (Merck, Darmstadt, Germany). TLC separation was performed as previously described [26].

Quantitative measurement of ceramide species was made using a triple-quadrupole mass spectrometer (Finnigan MAT TSQ 7000). ESI-MS/MS was performed as previously described [11, 26]. HPLC was conducted with a  $\mu$ -Bondasphere column (5  $\mu$ C18 100A Waters). Elution was performed at a flow rate of 0.2 ml/min with a mixture of 5 mM ammonium formate, methanol, and tetrahydrofuran at a volume ratio of 1:2:7. The mobile phase stream was connected to the ionspray interface of an ESI-MS/MS system. Standards and cellular ceramide extracts were stored at  $-20^{\circ}\text{C}$ . Mass analysis was performed in the positive mode in a heated capillary tube at  $250^{\circ}\text{C}$  with an electrospray potential of 4.5 kV, a sheath gas pressure of 70 psi, and a collision gas pressure of 1.6–2.0 mtorr. Under optimized conditions, monitoring ions were ceramide molecular species  $(\text{M}+\text{H})^{+}$  for the product ion at  $m/z$  264 of the sphingoid base. Standards and samples were injected with 5  $\mu\text{l}$  of 5 pmol C8:0-ceramide as an internal standard for ESI-MS/MS. The quantity of each ceramide was calibrated from each ceramide/C8:0-ceramide ratio, assuming that the calibration curve of ceramides bearing C16–24 acyl chains was similar to that of C16:0-ceramide as previously described [11, 26]. Each sample was analyzed in duplicate.

## Western Blot Analysis

For electrophoresis, the sample was applied to 4% sodium dodecyl sulfate polyacrylamide gel electrophoresis (SDS-PAGE), and immunoblot analysis was performed, both as described previously [14, 15]. Proteins separated on the gel were electrophoretically transferred to PVDF membrane

filters and immunoblotting analyses of apoB were performed as previously described [14, 15].

Anti-mouse apoB antiserum was prepared by immunizing mouse LDL to a rabbit. Chemiluminescence was analyzed with ATTO Densitograph Software Library (CS Analyzer Ver2.0).

## Statistical Analysis

The data were expressed as mean  $\pm$  SE. Differences between group means were considered significant at  $P < 0.05$  using Fisher's protected least significant difference test (PLSD).

## Results

### Effect of Dietary Cholesterol on Body Weight and Lipids

The body weight of the apoE<sup>-/-</sup> control group was higher than those of the other groups (Table 1). Liver weight of apoE<sup>-/-</sup> mice was higher than that of the wild type control group. The weight of total white adipose tissue of the apoE<sup>-/-</sup> control group was higher than those of the wild control group and the apoE<sup>-/-</sup> cholesterol group. No differences were observed in daily food consumption among these four groups (data not shown).

Plasma cholesterol of apoE<sup>-/-</sup> mice fed a control diet was about 6.7 times higher than that of the wild type mice fed a control diet (Table 2). In the cholesterol group, plasma cholesterol of the apoE<sup>-/-</sup> mice was also about six times higher than that of the wild type mice. However, the liver cholesterol in the apoE<sup>-/-</sup> mice was not different from that of the wild type mice. Cholesterol levels of plasma and the liver in both the wild type and the apoE<sup>-/-</sup> mice fed cholesterol were higher than those in mice fed a diet without cholesterol. No difference was observed among all groups in plasma TG. However, the liver TG of the wild type control group was lower than that of the other groups.

**Table 1** Effect of dietary cholesterol on weights of body, liver, and white adipose tissue (WAT) of wild type and apoE<sup>-/-</sup> mice

	Wild control	Wild cholesterol	ApoE <sup>-/-</sup> control	ApoE <sup>-/-</sup> cholesterol
Body weight (g)	32.3 $\pm$ 0.9 <sup>a</sup>	33.8 $\pm$ 1.3 <sup>a</sup>	38.1 $\pm$ 1.3 <sup>b</sup>	35.1 $\pm$ 1.0 <sup>a</sup>
Liver weight (g)	1.30 $\pm$ 0.09 <sup>a</sup>	1.67 $\pm$ 0.12 <sup>ac</sup>	1.84 $\pm$ 0.11 <sup>bc</sup>	1.84 $\pm$ 0.18 <sup>bc</sup>
Epididymal WAT weight (g)	0.68 $\pm$ 0.11 <sup>a</sup>	1.12 $\pm$ 0.15 <sup>b</sup>	1.33 $\pm$ 0.13 <sup>b</sup>	0.76 $\pm$ 0.11 <sup>a</sup>
Perirenal WAT weight (g)	0.39 $\pm$ 0.07 <sup>a</sup>	0.47 $\pm$ 0.07 <sup>ac</sup>	0.68 $\pm$ 0.08 <sup>b</sup>	0.38 $\pm$ 0.08 <sup>a</sup>
Mesenteric WAT weight (g)	0.38 $\pm$ 0.06 <sup>a</sup>	0.50 $\pm$ 0.08 <sup>ac</sup>	0.63 $\pm$ 0.06 <sup>bc</sup>	0.33 $\pm$ 0.05 <sup>a</sup>
Total WAT weight (g)	1.49 $\pm$ 0.21 <sup>a</sup>	2.08 $\pm$ 0.30 <sup>ac</sup>	2.64 $\pm$ 0.27 <sup>bc</sup>	1.44 $\pm$ 0.22 <sup>a</sup>

The values were mean  $\pm$  SE for eight C57BL/6J and ten apoE<sup>-/-</sup> mice. Differences between group means were considered significant at  $P < 0.05$  using Fisher's protected least significant difference test (PLSD). Values with different superscript letters show significant difference at  $P < 0.05$

**Table 2** Effect of dietary cholesterol on plasma and liver lipids of wild type and apoE<sup>-/-</sup> mice

	Wild control	Wild cholesterol	ApoE <sup>-/-</sup> control	ApoE <sup>-/-</sup> cholesterol
Plasma cholesterol (mg/dL)	77.4 ± 12.7 <sup>a</sup>	140 ± 11 <sup>a</sup>	517 ± 46 <sup>b</sup>	873 ± 64 <sup>c</sup>
Plasma triacylglycerol (mg/dL)	30.4 ± 1.9	28.6 ± 2.0	42.4 ± 6.3	46.6 ± 13.4
Liver cholesterol (mg/g)	3.36 ± 0.44 <sup>a</sup>	14.3 ± 1.9 <sup>b</sup>	5.76 ± 0.48 <sup>a</sup>	15.2 ± 1.4 <sup>b</sup>
Liver triacylglycerol (mg/g)	44.2 ± 8.8 <sup>a</sup>	115 ± 30 <sup>b</sup>	179 ± 25 <sup>b</sup>	119 ± 21 <sup>b</sup>

The values were mean ± SE for eight C57BL/6J and ten apoE<sup>-/-</sup> mice. Differences between group means were considered significant at  $P < 0.05$  using Fisher's protected least significant difference test (PLSD). Values with different superscript letters show significant difference at  $P < 0.05$

### Effect of Dietary Cholesterol on Ceramide

Table 3 shows the distribution of ceramide species in plasma. A major ceramide in plasma was C24:0 in both wild type and apoE<sup>-/-</sup> mice. The plasma level of total ceramide of the apoE<sup>-/-</sup> mice fed a control diet was about six times higher than that of the wild type mice fed a control diet. In the cholesterol group, the plasma level of total ceramide in the apoE<sup>-/-</sup> mice was also about 5.1 times higher than that of the wild type mice. In apoE<sup>-/-</sup> mice, the plasma level of total ceramide of the cholesterol group tended to be higher than that of the control group ( $p = 0.08$ ), while C16:0, C24:1, and C24:2 of the cholesterol group were significantly higher than those of the control group. In the wild type mice, dietary cholesterol did not affect plasma levels of ceramide.

Table 4 shows the distribution of ceramide species in the liver. The major ceramide of the liver was also C24:0 in the wild type and the apoE<sup>-/-</sup> mice. In the liver, the total ceramide of the apoE<sup>-/-</sup> mice fed a control diet was about 1.5 times higher than that of the wild type mice fed a control diet. In the cholesterol group, the total ceramide of apoE<sup>-/-</sup> mice was not different from that of the wild type mice. Thus, the difference in total ceramide level between

wild type and apoE<sup>-/-</sup> mice in the liver was less than that in plasma. In addition, dietary cholesterol did not affect ceramide levels of the liver in either the wild type or the apoE<sup>-/-</sup> mice.

Table 5 shows the distribution of ceramide species in the mesenteric white adipose tissue. Major ceramides of white adipose tissue were C24:0, C16:0, and C24:1. The ratio of C16:0 and C18:0 in adipose tissues was higher than that in plasma and the liver. In the wild type mice and the apoE<sup>-/-</sup> mice fed cholesterol, the content of C16:0 of the adipose tissue was similar to that of C24:0. In the adipose tissue, the total ceramide of the wild type was not different from that of the apoE<sup>-/-</sup> mice. In addition, dietary cholesterol did not affect ceramides of the adipose tissue in either wild type or apoE<sup>-/-</sup> mice.

### Effect of Dietary Cholesterol on Cross-Linked and Fragmented apoB

The band, which was larger than the band of apoB (512 kDa) was assumed to be a cross-linking product as previously reported [15] and the band, which was smaller than the band of apoB was assumed to be a fragmented product. However, neither cross-linking nor fragmentation

**Table 3** Effect of dietary cholesterol on ceramide concentration (nmol/ml) in the plasma

	Wild control	Wild cholesterol	ApoE <sup>-/-</sup> control	ApoE <sup>-/-</sup> cholesterol
C16:0	0.75 ± 0.13 <sup>a</sup>	1.20 ± 0.18 <sup>a</sup>	4.11 ± 0.32 <sup>b</sup>	5.71 ± 0.42 <sup>c</sup>
C18:0	0.07 ± 0.01 <sup>a</sup>	0.10 ± 0.02 <sup>a</sup>	0.75 ± 0.11 <sup>b</sup>	0.85 ± 0.1 <sup>b</sup>
C22:0	3.05 ± 0.83 <sup>a</sup>	4.12 ± 0.80 <sup>a</sup>	25.5 ± 3.8 <sup>b</sup>	24.5 ± 3.3 <sup>b</sup>
C24:0	6.16 ± 1.54 <sup>a</sup>	9.04 ± 1.46 <sup>a</sup>	34.3 ± 2.8 <sup>b</sup>	41.5 ± 4.6 <sup>b</sup>
C24:1	3.36 ± 0.77 <sup>a</sup>	4.70 ± 0.98 <sup>a</sup>	15.3 ± 1.4 <sup>b</sup>	20.2 ± 2.2 <sup>c</sup>
C24:2	0.14 ± 0.03 <sup>a</sup>	0.22 ± 0.04 <sup>a</sup>	2.03 ± 0.38 <sup>b</sup>	5.01 ± 0.67 <sup>c</sup>
Total	13.4 ± 3.3 <sup>a</sup>	19.1 ± 3.3 <sup>a</sup>	80.6 ± 6.8 <sup>b</sup>	97.8 ± 11.0 <sup>b</sup>

The values were mean ± SE for eight C57BL/6J and ten apoE<sup>-/-</sup> mice. Differences between group means were considered significant at  $P < 0.05$  using Fisher's protected least significant difference test (PLSD). Values with different superscript letters show significant difference at  $P < 0.05$

**Table 4** Effect of dietary cholesterol on ceramide concentration (nmol/g tissue) in the liver

	Wild control	Wild cholesterol	ApoE <sup>-/-</sup> control	ApoE <sup>-/-</sup> cholesterol
C16:0	19.6 ± 3.0 <sup>a</sup>	22.3 ± 2.6 <sup>ab</sup>	28.5 ± 2.4 <sup>b</sup>	27.5 ± 3.2 <sup>b</sup>
C18:0	2.52 ± 0.5 <sup>a</sup>	2.16 ± 0.29 <sup>ab</sup>	3.90 ± 0.33 <sup>ac</sup>	4.36 ± 0.93 <sup>c</sup>
C22:0	38.4 ± 4.1 <sup>a</sup>	47.1 ± 5.1 <sup>a</sup>	80.6 ± 6.3 <sup>b</sup>	50.0 ± 4.9 <sup>ac</sup>
C24:0	75.0 ± 10.1 <sup>a</sup>	88.9 ± 6.5 <sup>ab</sup>	99.6 ± 7.4 <sup>b</sup>	97.7 ± 8.7 <sup>b</sup>
C24:1	50.3 ± 8.2	61.8 ± 5.5	63.1 ± 5.9	71.6 ± 6.3
C24:2	4.62 ± 0.84 <sup>a</sup>	5.57 ± 0.58 <sup>a</sup>	5.80 ± 0.74 <sup>a</sup>	9.59 ± 1.12 <sup>b</sup>
Total	190 ± 19 <sup>a</sup>	228 ± 17 <sup>ab</sup>	281 ± 19 <sup>b</sup>	261 ± 23 <sup>b</sup>

The values were mean ± SE for eight C57BL/6J and ten apoE<sup>-/-</sup> mice. Differences between group means were considered significant at  $P < 0.05$  using Fisher's protected least significant difference test (PLSD). Values with different superscript letters show significant difference at  $P < 0.05$

**Table 5** Effect of dietary cholesterol on ceramide concentration (nmol/g tissue) in the mesenteric white adipose tissues

	Wild control	Wild cholesterol	ApoE <sup>-/-</sup> control	ApoE <sup>-/-</sup> cholesterol
C16:0	51.4 ± 4.7	52.7 ± 15.0	43.8 ± 10.0	55.9 ± 9.3
C18:0	16.9 ± 3.5	19.7 ± 5.2	10.8 ± 1.8	19.9 ± 4.4
C22:0	21.1 ± 2.9	17.3 ± 3.2	15.4 ± 2.8	16.9 ± 2.9
C24:0	63.0 ± 10.4	53.3 ± 11.1	49.6 ± 11.1	56.5 ± 11.7
C24:1	53.8 ± 9.0	47.6 ± 9.2	40.1 ± 8.4	49.6 ± 9.8
C24:2	8.40 ± 1.41	7.68 ± 1.69	6.09 ± 1.05	10.2 ± 2.2
Total	215 ± 30	198 ± 45	159 ± 34	209 ± 38

The values were mean ± SE for eight C57BL/6J and ten apoE<sup>-/-</sup> mice. Differences between group means were considered significant at  $P < 0.05$  using Fisher's protected least significant difference test (PLSD). Values with different superscript letters show significant difference at  $P < 0.05$

of apoB-48 (250 kDa) were detected (Fig. 1a). Western blot analysis of plasma revealed that apoB-100 with molecular weight of 512 kDa in the apoE<sup>-/-</sup> cholesterol group was lower than that in the apoE<sup>-/-</sup> control group (Fig. 1a, b). Though cross-linking of apoB-100 was not detected in apoE<sup>-/-</sup> mice, fragmentation of apoB-100 in the apoE<sup>-/-</sup> cholesterol group was 2.5 times higher than that in the apoE<sup>-/-</sup> control group (Fig. 1c). In the wild type mice, neither cross-linked nor fragmented apoB proteins were discernible (data not shown).

The amount of the aortic area covered with plaques was significantly greater in the apoE<sup>-/-</sup> mice fed cholesterol compared to the apoE<sup>-/-</sup> mice fed a control diet, as is well established (data not shown).

#### Effect of Dietary Cholesterol on Vitamin C

In plasma, vitamin C of apoE<sup>-/-</sup> mice was higher than that of wild type mice (Table 6). Vitamin C of both wild type and the apoE<sup>-/-</sup> mice fed a cholesterol diet was higher than for mice fed a control diet.

#### Discussion

Sphingolipids such as ceramide and sphingosine-1-phosphate are bioactive lipid mediators [27]. The importance of sphingolipids as mediators in cardiovascular pathophysiology has recently been reported [28]. In addition, it was shown that SPT activity was higher in apoE<sup>-/-</sup> mice compared with C57BL/6J mice [9]. In this study, it was shown that the total ceramide level in plasma and the liver of the apoE<sup>-/-</sup> control group was higher than that of the wild control group. Therefore, decreasing ceramide levels in plasma and the liver may be beneficial for prevention of atherogenesis.

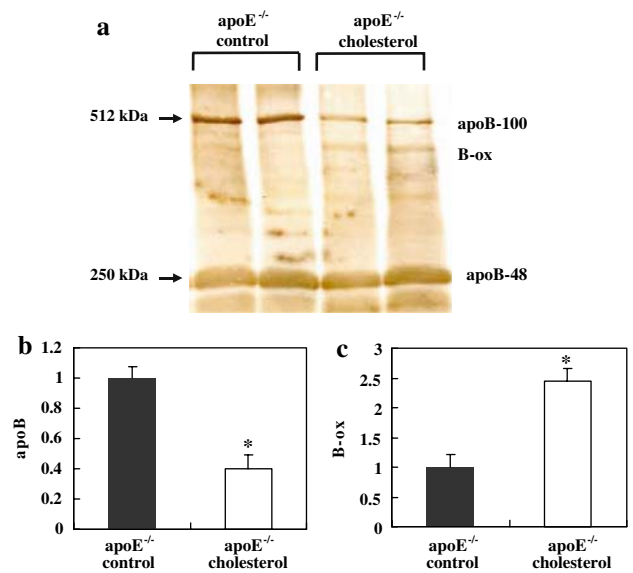


**Fig. 1** ApoB and fragmented apoB-100 proteins in plasma of apoE<sup>-/-</sup> mice fed a standard diet and supplemented with 1% cholesterol. Plasma was loaded on 4% SDS-PAGE gel and Western blot analysis was performed (a). Densitometry of apoB (b) and fragmented apoB (c) in plasma of apoE<sup>-/-</sup> mice. The values were means ± SE for 4–5 apoE<sup>-/-</sup> mice and asterisks indicated significant differences from the corresponding the apoE<sup>-/-</sup> control group

**Table 6** Effect of dietary cholesterol on plasma Vitamin C concentration (nmol/mL) of wild type and apoE<sup>-/-</sup> mice

	Wild control	Wild cholesterol	ApoE <sup>-/-</sup> control	ApoE <sup>-/-</sup> cholesterol
Vitamin C	69.6 ± 8.5 <sup>a</sup>	96.3 ± 3.5 <sup>b</sup>	115 ± 6 <sup>b</sup>	146 ± 5 <sup>c</sup>

The values were mean ± SE for five C57BL/6J and six apoE<sup>-/-</sup> mice. Differences between group means were considered significant at  $P < 0.05$  using Fisher's protected least significant difference test (PLSD). Values with different superscript letters show significant differences at  $P < 0.05$

In the present study, we investigated the effects of dietary cholesterol on ceramide and oxidative products of apoB in apoE<sup>-/-</sup> mice, of which the plasma and aorta responded sufficiently to cholesterol-enriched diets. Our recent study demonstrated that the correlation coefficient between plasma cholesterol and total ceramide in human subjects was particularly high among lipid markers associated with atherosclerosis [11]. Treatment with myriocin, which is a potent and specific SPT inhibitor and is known to have an immunosuppressive activity [29], significantly lowered plasma cholesterol levels of apoE<sup>-/-</sup> mice in a dose-dependent manner [30]. In this study, we demonstrated that a cholesterol-enriched diet did not affect ceramide levels of the tissues in the wild type mice. However, in apoE<sup>-/-</sup> mice, the plasma levels of several ceramides in the cholesterol group were significantly

higher than those in the control group and the plasma level of total ceramides in the cholesterol group also tended to be higher than for mice fed a control diet. This result indicated a correlation between increased cholesterol intake and the elevation of the plasma levels of ceramide.

In the liver, the total ceramides of apoE<sup>-/-</sup> mice were higher than those of the wild control group. However, the difference of ceramides levels between the wild type and the apoE<sup>-/-</sup> mice in the liver was not so large as that in plasma. In plasma, the difference of total ceramides between the wild type and the apoE<sup>-/-</sup> mice coincided with the change of cholesterol. Furthermore, the cholesterol-enriched diet did not cause a significant increase in liver ceramide levels. Therefore, a relationship between cholesterol accumulation and ceramide metabolism change in the liver was not supported.

It is well known that a fat-enriched diet is an important factor in the development of atherosclerosis. Overnutrition leads to hypertrophy of adipocytes, and high-fat diets promote obesity [31]. The islet obese fa/fa Zucker diabetic fatty rats exhibit an increase in de novo synthesis of [<sup>3</sup>H]-ceramide from [<sup>3</sup>H]-palmitate [32]. Based on these reports, a correlation between ceramide and deposition of visceral fat is suggested. In this study, although the weight of total white adipose tissues in the apoE<sup>-/-</sup> control group was higher than in the other groups, ceramide levels in the white adipose tissue of the apoE<sup>-/-</sup> control group were not higher than those of other groups. Therefore, it is suggested that fat accumulation in the white adipose tissue did not increase ceramide content.

Oxidative modification of LDL and its recognition by macrophages have been suggested as being an initial event of atherosclerosis [17]. In this study, we analyzed the oxidation profile of apoB, namely the sum of fragmented and conjugated apoB proteins determined by an immunoblot assay. We reported that these oxidation products of apoB-100, termed B-ox are a reliable indicator of atherosclerosis [15]. In human plasma, the conjugated apoB-100 was higher than the fragmented apoB-100. However, conjugated apoB-100 was not detected clearly in apoE<sup>-/-</sup> mice. In addition, in plasma of apoE<sup>-/-</sup> mice it was reported that the major apoB is apoB-48 and the minor apoB is apoB-100 [33]. In this study, conjugated and fragmented apoB-48 were not detected in apoE<sup>-/-</sup> mice. It is necessary to examine the difference of apoB-100 oxidation between human and mice and the difference of oxidation between apoB-100 and apoB-48.

Our previous studies demonstrated that the reactivity of apoB toward radicals is extremely high and even comparable to vitamin E [14]. Hence degraded apoB fragments were present in normal human plasma and tended to increase with aging [15]. In this study, the apoE<sup>-/-</sup> chole-

sterol group, which demonstrated a significant increase in the size of lesions as is well established [33], also exhibited decreased apoB and increased fragmented apoB proteins compared to the control group. These results demonstrated that the cholesterol diet increased the development of atherosclerotic lesions and promoted oxidation of apoB in the apoE<sup>-/-</sup> mice. We reported that cross-linked and fragmented apoB-100 is a reliable index of atherosclerosis and oxidative stress [15]. Therefore, it is suggested that fragmentation of apoB is also a reliable indicator of atherosclerosis in apoE<sup>-/-</sup> mice as well as humans.

OxLDL have been shown to induce apoptosis of culture cells [34, 35]. Ceramides also have been shown to cause apoptosis in a variety of cells. Apoptosis of endothelial cells is widely implicated in the early stage of atherosclerosis. It was reported that oxLDL was involved in the formation of various sphingolipid mediators [36] and activated the generation of ceramide in endothelial cells [37]. Our results also demonstrated that apoE<sup>-/-</sup> mice, which showed increased size of lesions, exhibited higher ceramide levels and fragmented apoB in plasma. Based on these results, a correlation between increased oxLDL and ceramide is suggested. However, oxLDL-induced activation of the SMase-ceramide pathway has not yet been fully studied and is still controversial. Further studies are needed to clarify the relationship between LDL oxidation and ceramide metabolism.

Vitamin C is a potent water-soluble antioxidant that scavenges reactive oxygen species [38, 39]. Sublethal lipopolysaccharide, which is associated with oxidative stress, temporarily increased liver vitamin C in the mouse [40]. In addition, the deficiency of glutathione, which plays various important roles in the protection against oxidant stress [41], increased hepatic ascorbate synthesis in mice [42]. These studies indicate that vitamin C synthesis is enhanced by oxidative stress in mice. In this study, plasma vitamin C in apoE<sup>-/-</sup> mice was higher than that in the wild type mice. It is suggested that apoE<sup>-/-</sup> mice at this young age increased vitamin C production compared to the wild type mice to prevent increased oxidative stress. In addition, plasma vitamin C in the wild type and apoE<sup>-/-</sup> mice fed a cholesterol diet was higher than in those fed a control diet. The increase of B-ox in the apoE<sup>-/-</sup> mice fed a cholesterol diet suggested enhanced stress, which resulted in the elevation of plasma vitamin C just like in the mice under enhanced oxidative stress as described above [40, 42].

In conclusion, this study demonstrated that dietary cholesterol increased ceramide levels and products of oxidized LDL in plasma of the apoE<sup>-/-</sup> mice. In addition, we propose that ceramides, the toxicities of which are much higher than that of cholesterol, are a new risk factor for atherosclerosis.

**Acknowledgments** This work was supported by the Ministry of Education, Culture, Sports, Science, and Technology of Japan, and the Uehara Memorial Foundation.

## Reference

- Hannun YA, Obeid LM (2002) The ceramide-centric universe of lipid-mediated cell regulation: stress encounters of the lipid kind. *J Biol Chem* 277:25847–25850
- Merrill AH (2002) De novo sphingolipid biosynthesis: a necessary, but dangerous, pathway. *J Biol Chem* 277:25843–25846
- Olivera A, Spiegel S (2001) Sphingosine kinase: a mediator of vital cellular functions. *Prostaglandins Other Lipid Mediat* 64:123–134
- Kolesnick R (1992) Ceramide: a novel second messenger. *Trends Cell Biol* 2:232–236
- Merrill AH, Jones DD (1990) An update of the enzymology and regulation of sphingomyelin metabolism. *Biochim Biophys Acta* 1044:1–12
- Jiang XC, Paulre F, Pearson TA, Reed RG, Francis CK, Lin M, Berglund L, Tall AR (2000) Plasma sphingomyelin level as a risk factor for coronary artery disease. *Arterioscler Thromb Vasc Biol* 20:2614–2618
- Noel C, Marcel YL, Davignon J (1972) plasma phospholipids in the different types of primary hyperlipoproteinemia. *J Lab Clin Med* 79:611–612
- Nelson JC, Jiang XC, Tabas I, Tall A, Shea S (2006) Plasma sphingomyelin and subclinical atherosclerosis: findings from the multi-ethnic study of atherosclerosis. *Am J Epidemiol* 163:903–912
- Park TS, Panek RL, Mueller SB, Hanselman JC, Rosebury WS, Robertson AW, Kindt EK, Homan R, Karathanasis SK, Reckter MD (2004) Inhibition of sphingomyelin synthesis reduces atherogenesis in apolipoprotein E-knockout mice. *Circulation* 110:3465–3471
- Hojjati MR, Li Z, Zhou H, Tang S, Huan C, Ooi E, Lu S, Jiang XC (2005) Effect of myriocin on plasma sphingolipid metabolism and atherosclerosis in ApoE-deficient mice. *J Biol Chem* 280:10284–10289
- Ichi I, Nakahara K, Miyashita Y, Hidaka A, Kutsukake S, Inoue K, Maruyama T, Miwa Y, Harada-Shiba M, Tsushima M, Kojo S (2006) Association of ceramides in human plasma with risk factors of atherosclerosis. *Lipids* 41:859–863
- Steinberg D, Parthasarathy S, Carew TE, Khoo JC, Witztum JL (1989) Beyond cholesterol: modifications of low density lipoprotein that increase its atherogenicity. *N Engl J Med* 320:915–924
- Witztum JL, Steinberg D (1991) Role of oxidized low density lipoprotein in atherogenesis. *J Clin Invest* 88:1785–1792
- Hashimoto R, Narita S, Yamada Y, Tanaka K, Kojo S (2000) Unusually high reactivity of apolipoprotein B-100 among proteins to radical reactions induced in human plasma. *Biochem Biophys Acta* 1483:236–240
- Hashimoto R, Matsukawa N, Nariyama Y, Ogiri Y, Hamagawa E, Tanaka K, Usui Y, Nakano S, Maruyama T, Kyotani S, Tsushima M, Kojo S (2002) Evaluation of apolipoprotein B-100 fragmentation and cross-link in the serum as an index of atherosclerosis. *Biochim Biophys Acta* 1584:123–128
- Pentikainen MO, Lehtonen EMP, Kovanen PT (1996) Aggregation and fusion of modified low density lipoprotein. *J Lipid Res* 37:2638–2649
- Ross R (1993) The pathogenesis of atherosclerosis: a perspective for 1990s. *Nature* 362:801–809
- Schissel SL, Tweedie-Hardman J, Rapp JH, Graham G, Williams KJ, Tabas I (1996) Rabbit aorta and human atherosclerotic lesions hydrolyze the sphingomyelin of retained low-density lipoprotein. *J Clin Invest* 98:1455–1464
- Xu XX, Tabas I (1991) Sphingomyelinase enhances low density lipoprotein uptake and ability to induce cholesteryl ester accumulation in macrophages. *J Biol Chem* 266:24849–24858
- Williams RD, Sgoutas DS, Zaatari GS (1986) Enzymology of long-chain base synthesis by aorta: induction of serine palmitoyltransferase activity in rabbit aorta during atherogenesis. *J Lipid Res* 27:763–770
- Zhang SH, Reddick RL, Piedrahita JA, Maeda N (1992) Spontaneous hypercholesterolemia and arterial lesions in mice lacking apolipoprotein E. *Science* 258:468–471
- Ikedo I, Tanaka K, Sugano M, Vahouny GV, Gallo LL (1988) Discrimination between cholesterol and sitosterol for absorption in rats. *J Lipid Res* 29:1583–1591
- Fletcher MJ (1968) A colorimetric method for estimation of serum triglycerides. *Clin Chim Acta* 22:393–397
- Kishida E, Nishimoto Y, Kojo S (1992) Specific determination of ascorbic acid with chemical derivatization and high-performance liquid chromatography. *Anal Chem* 64:1505–1507
- Folch J, Ascoli I, Lees M, Meath JA, LeBaron N (1966) Preparation of lipid extracts from brain tissues. *J Biol Chem* 191:833–841
- Yamada Y, Kajiwaru K, Yano M, Kishida E, Masuzawa Y, Kojo S (2001) Increase of ceramides and its inhibition by catalase during chemically induced apoptosis of HL-60 cells determined by electrospray ionization tandem mass spectrometry. *Biochim Biophys Acta* 1532:115–120
- Huwiler A, Kolter T, Pfeilschifter J, Sandhoff K (2000) Physiology and pathophysiology of sphingolipid metabolism and signaling. *Biochim Biophys Acta* 1485:63–99
- Levade T, Auge N, Veldman RJ, Cu villier O, Negre-Salvayre A, Salvayre R (2001) Sphingolipid mediators in cardiovascular cell biology and pathology. *Circ Res* 89:957–968
- Miyake Y, Kozutsumi Y, Nakamura S, Fujita T, Kawasaki T (1995) Serine palmitoyltransferase is the primary target of a sphingosine-like immunosuppressant, ISP-1/myriocin. *Biochem Biophys Res Commun* 211:396–403
- Park TS, Panek RL, Reckter MD, Mueller SB, Rosebury WS, Robertson A, Hanselman JC, Kindt E, Homan R, Karathanasis SK (2006) Modulation of lipoprotein metabolism by inhibition of sphingomyelin synthesis in ApoE knockout mice. *Atherosclerosis* 189:264–272
- Golay A, Bobbioni E (1997) The role of dietary fat in obesity. *Int J Obes Relat Metab Disord* 21:2–11
- Shimabukuro M, Higa M, Zhou YT, Wang MY, Newgard CB, Unger RH (1998) Lipoapoptosis in beta-cells of obese prediabetic fa/fa rats. Role of serine palmitoyl transferase overexpression. *J Biol Chem* 273:32487–32490
- Ishibashi S, Herz J, Maeda N, Goldstein JL, Brown MS (1994) The two-receptor model of lipoprotein clearance: tests of the hypothesis in “knockout” mice lacking the low density lipoprotein receptor, apolipoprotein E, or both proteins. *Proc Natl Acad Sci USA* 91: 4431–4435
- Escargueil I, Nègre-Salvayre A, Pieraggi MT, Salvayre R (1992) Oxidized low density lipoproteins elicit DNA fragmentation of cultured lymphoblastoid cells. *FEBS Lett* 305:155–159
- Harada-Shiba M, Kinoshita M, Kamido H, Shimokado K (1998) Oxidized low density lipoprotein induces apoptosis in cultured human umbilical vein endothelial cells by common and unique mechanisms. *J Biol Chem* 273:9681–9687
- Chatterjee S (1998) Sphingolipids in atherosclerosis and vascular biology. *Arterioscler Thromb Vasc Biol* 18:1523–1533
- Auge N, Andrieu N, Negre-Salvayre A, Thiers JC, Levade T, Salvayre R (1996) The sphingomyelin-ceramide signaling pathway is involved in oxidized low density lipoprotein-induced cell proliferation. *J Biol Chem* 271:19251–19255



38. Frei B, England L, Ames BN (1989) Ascorbate is an outstanding antioxidant in human blood plasma. *Proc Natl Acad Sci USA* 86:6377–6381
39. Kojo S (2004) Vitamin C, basic metabolism and its function as an index of oxidative stress. *Curr Med Chem* 11:1041–1064
40. Kuo SM, Tan CH, Dragan M, Wilson JX (2005) Endotoxin increases ascorbate recycling and concentration in mouse liver. *J Nutr* 135:2411–2416
41. Rahman I, MacNee W (2000) Oxidative stress and regulation of glutathione synthesis in lung inflammation. *Eur Respir J* 16:16534–16554
42. Martensson J, Meister A (1992) Glutathione deficiency increases hepatic ascorbic acid synthesis in adult mice. *Proc Natl Acad Sci USA* 89:11566–11568

## Effect of Dietary Cholesterol and Fat on Cell Cholesterol Transfer to Postprandial Plasma in Hyperlipidemic Men

Wayne H. F. Sutherland · Sylvia A. de Jong · Robert J. Walker

Received: 4 March 2007 / Accepted: 11 July 2007 / Published online: 7 August 2007  
© AOCs 2007

**Abstract** Postprandial chylomicrons are potent ultimate acceptors of cell membrane cholesterol and are believed to accelerate reverse cholesterol transport (RCT). We compared the effects of meals rich in polyunsaturated fat (PUFA) and either high (605 mg) or low (151 mg) in cholesterol and a meal rich in dairy fat (DF) in the form of cream on net in vitro transport of red blood cell (RBC) membrane cholesterol to 4 and 6 h postprandial plasma in eight normotriglyceridemic (NTG-H) and eight hypertriglyceridemic (HTG-H) men with mild to moderate hypercholesterolemia. In HTG-H men, cell cholesterol accumulation in 6-h postprandial plasma was significantly ( $P = 0.02$ ) less after the PUFA-HC meal compared with the other meals. The significant ( $P < 0.001$ ) increase in cell plus endogenous cholesterol accumulation in the triglyceride-rich lipoprotein (TRL) fraction of 4 h postprandial plasma incubated with RBC was significantly ( $P = 0.007$ ) higher after the PUFA-HC meal compared with DF meal in HTG-H men. In NTG-H men, cholesterol accumulation in plasma and plasma lipoproteins in the presence and absence of RBC was not significantly affected by the type of meal ingested. These data suggest that addition of large amounts of cholesterol to a PUFA meal may impair diffusion-mediated transport of cell membrane cholesterol to postprandial plasma and that replacing DF with PUFA in a meal increases postprandial lipemia and may potentially increase cholesterol accumulation in atherogenic postprandial TRL in HTG-H men.

**Keywords** Postprandial lipemia · Reverse cholesterol transport · Dietary cholesterol · Polyunsaturated fat · Dairy fat · Hyperlipidemia

### Abbreviations

apoB	Apolipoprotein B
ABCA1	ATP binding cassette A1
ABCG1	ATP binding cassette G1
CE	Cholesteryl esters
CETP	Cholesteryl ester transfer protein
DF	Dairy fat
HDL	High density lipoprotein
HTG-H	Hypertriglyceridemic and hypercholesterolemic
LCAT	Lecithin:cholesterol acyltransferase
LDL	Low density lipoprotein
MUFA	Monounsaturated fatty acids
NTG-H	Normotriglyceridemic and hypercholesterolemic
PUFA-HC	Polyunsaturated fatty acid-high cholesterol
PUFA-LC	Polyunsaturated fatty acid-low cholesterol
RBC	Red blood cells
RCT	Reverse cholesterol transport
SAFA	Saturated fatty acids
SRB1	Scavenger receptor B1
TG	Triglycerides
TC	Total cholesterol
TRL	Triglyceride-rich lipoproteins
UC	Unesterified cholesterol
VLDL	Very low density lipoproteins

W. H. F. Sutherland (✉) · S. A. de Jong · R. J. Walker  
Department of Medical and Surgical Sciences,  
Dunedin School of Medicine, University of Otago,  
P.O. Box 913, Dunedin 9054, New Zealand  
e-mail: wayne.sutherland@stonebow.otago.ac.nz

### Introduction

Reverse cholesterol transport (RCT) moves cholesterol from peripheral cells via the blood to the liver where

cholesterol can be metabolised and excreted from the body. Efflux of cell cholesterol to acceptors in plasma occurs by several mechanisms including passive, aqueous diffusion and pathways mediated by scavenger receptor B1 (SR-B1) and ATP-binding cassette transporters ABCA1 and ABCG1 [1, 2]. Recent evidence suggests that a large proportion of the cholesterol efflux from fibroblasts and cholesterol-enriched macrophages to human serum may be mediated by aqueous diffusion and independently of ABCA-1 and SR-B1 [3]. The diffusion-mediated cell cholesterol flux is bidirectional and relies on a concentration gradient in unesterified cholesterol (UC) between cell membranes and extracellular acceptors of cholesterol. High density lipoprotein (HDL) or its apolipoproteins are the main initial plasma acceptors of cell cholesterol and esterification of cholesterol by the associated lecithin:cholesterol acyltransferase (LCAT) enzyme maintains the UC concentration gradient for diffusion-mediated cell cholesterol efflux. Cholesteryl esters (CE) formed by LCAT activity are transferred by cholesteryl ester transfer protein (CETP) activity to apolipoprotein B (apoB)-containing lipoproteins for transport to the liver [4]. Red blood cells (RBC) are thought to efflux membrane cholesterol solely by aqueous diffusion [5]. They do not synthesize cholesterol and do not have intracellular membranes.

Postprandial lipemia and especially chylomicrons, increases net loss of cell cholesterol from cultured fibroblasts [6] and isolated red blood cells (RBC) [7] to postprandial plasma isolated from healthy subjects after a fatty meal. Chylomicrons are potent acceptors of cholesterol from cell membranes and from endogenous lipoproteins LDL and HDL via LCAT and CETP [7, 8]. Lipolytic remnants of chylomicrons are thought to transport this accepted cholesterol to the liver [5–8]. The cholesterol content and type of fat in a meal influence postprandial lipemia. Meals highly enriched in cholesterol (210–710 mg) increase large triglyceride-rich lipoprotein triglycerides in postprandial plasma of normolipidemic subjects [9]. In addition, there is evidence that postprandial lipemia is lower after ingestion of dairy fat (DF) compared with polyunsaturated fats (PUFA) [10, 11]. Hyperlipidemia may also influence cell cholesterol transport after a fatty meal. In baboons, dietary hypercholesterolemia inhibits normal stimulation of postprandial cholesterol metabolism and movement of cholesterol from RBC to postprandial plasma after a meal rich in saturated fat (SAFA) and cholesterol [12]. On the other hand, the efflux of radiolabelled cholesterol from cultured cells to postprandial plasma is increased in patients with type IIB hyperlipidemia after a fatty meal rich in PUFA and monounsaturated fat (MUFA) and low in cholesterol [13]. Few studies have compared the effect of meals rich in PUFA and high or low in cholesterol and meals rich in DF or PUFA on net transport of cell cholesterol to postprandial plasma in individuals with

mild to moderate hyperlipidemia. The type of fat and the cholesterol content of meals is relevant to dietary advice aimed at lipid lowering in hyperlipidemic individuals [14]. The aim of the present study was to compare the effect of meals rich in PUFA and low and high in cholesterol and meals rich in PUFA or DF, on in vitro transport of cholesterol from RBC to postprandial plasma and amounts of total, cell-derived and endogenous cholesterol that accumulate in plasma lipoproteins in men with mild to moderate hypercholesterolemia with or without hypertriglyceridemia.

## Subjects and Methods

### Subjects

We recruited 16 men ages 39–67 years with plasma cholesterol concentrations  $>5.2$  mmol/l and  $<7.9$  mmol/l and fasting plasma triglyceride (TG) concentrations  $<3$  mmol/l. These exclusion criteria were aimed at excluding men with severe familial hyperlipidemia and at including men with common forms of hyperlipidemia in the study population. Participants were recruited from respondents to notices placed in Dunedin Public Hospital and from hyperlipidemic individuals on a register maintained by the Human Nutrition Department, University of Otago. Men who expressed an interest in participating in the study were screened and those with plasma lipids in the appropriate range and who were non-smokers, had no history of serious illness and were not receiving medications were accepted into the study. None of the men was following a lipid-lowering diet. Subjects were divided into a hypertriglyceridemic group (HTG-H; plasma TG  $> 1.7$  mmol/l) or a normotriglyceridemic group (NTG-H; plasma TG  $\leq 1.7$  mmol/l). This cut-off point for plasma TG concentration has been used previously to identify the hypertriglyceridemic component of the metabolic syndrome [15]. The HTG-H men ( $n = 8$ ) had a mean age of  $51 \pm 6$  years and a mean BMI of  $28.5 \pm 5.0$  kg/m<sup>2</sup>. The NTG-H men had a mean age of  $54 \pm 7$  years and a mean BMI of  $25.1 \pm 2.7$  kg/m<sup>2</sup>. The study was approved by the Lower South Regional Ethics Committee and all participants gave written and informed consent before participation in the study.

### Study Design

The study had a single-blind, randomized, crossover design. Men were randomized to one of 6 sequences of the three test meals using random number tables. The last digit of a designated series of random numbers (ignoring digits 0, 8 and 9) was used to assign participants to a meal sequence. There was at least a week between each of the

meals. After an overnight fast, blood was taken in the early morning immediately before and at 4 and 6 h after the meals.

### Meals

The meals were given as milkshakes and contained safflower oil (90 g) or cream (238 g), trim milk (70–200 ml), egg white (30 g), yoghurt (10 g), and tinned apricots without syrup (50 g). Egg yolk (12 g) and soy lecithin (12 g) were added to the polyunsaturated fat-low cholesterol (PUFA-LC) milkshake. Egg yolk (48 g) was also added to the polyunsaturated fat-high cholesterol (PUFA-HC) milkshake. Soy lecithin was added to account for the extra egg yolk phospholipid in the PUFA-HC meal. Soy lecithin (12 g) and a small quantity of extra cream fat (3 g) were added to the milkshake rich in DF to give an equivalent fat intake compared with the other meals. All milkshakes contained chocolate flavoring (15 g, 92% sugar). The macronutrient composition of the meals is shown in Table 1. The men consumed the milkshakes within 15 min and ingested a volume of milkshake to give 40 g fat/m<sup>2</sup> body surface area. Participants were instructed to refrain from eating or drinking beverages excepting water during the postprandial period after the meals and were also instructed to maintain their usual diet during the non-intervention days of the study.

### Transport of RBC Cholesterol to Plasma

Transport of cell membrane cholesterol from autologous RBC to plasma in vitro was measured essentially as described previously [7]. Briefly, blood was collected in tubes containing dipotassium EDTA and the tubes were placed in an ice-bath immediately after collection. The blood was spun at 223g for 10 min at 4 °C. The plasma supernatant was collected and kept briefly at 4 °C leaving one third of the plasma trapped within packed RBCs. Packed cells (8 ml) were transferred into a plastic tube using a Gilson pipette with a wide-bore plastic tip. Plasma (1 ml) was added to the packed cells to give a twofold excess of RBCs to plasma. The remaining plasma was divided into two aliquots. One aliquot of plasma and the mixture of RBCs and plasma were incubated at 37 °C for 18 h without shaking. The other aliquot of plasma was maintained at 4 °C. At the end of the incubation period, the RBC-plasma mixture was centrifuged at 1,500g for 30 min at 4 °C and the plasma was harvested. Aliquots (2 ml) of this plasma and plasma incubated at 37 °C or maintained at 4 °C were adjusted to  $d = 1.006$  g/ml and ultracentrifuged in a Beckman type 50.3 Ti rotor for 18 h at 400,000 rpm

**Table 1** Composition of the meals

Nutrient	Meals		
	PUFA-LC	PUFA-HC	DF
Fat (g)	102	102	102
SAFA (g)	10	12	56
PUFA (g)	60	59	7
Carbohydrate (g)	33	33	34
Protein (g)	13	18	13
Energy (kJ)	4,574	4,657	4,590
Cholesterol (mg)	151	605	325
Fat (%E)	84	82	84
Carbohydrate (%E)	11	11	12
Protein (%E)	5	6	5

*PUFA-LC* polyunsaturated fat-low cholesterol, *PUFA-HC* polyunsaturated fat-high cholesterol, *DF* dairy fat, *SAFA* saturated fat, *E* energy

and 10 °C. The  $d < 1.006$  g/ml fraction containing very low density lipoproteins (VLDL) and chylomicrons, and the  $d > 1.006$  g/ml fraction were collected quantitatively by tube-slicing. HDL was isolated in the supernatant after precipitation of apoB-containing lipoproteins with dextran sulfate and magnesium chloride [16]. Cholesterol and TG in plasma and plasma fractions were measured enzymatically using an autoanalyzer (Abbott, ABA-100) and commercial kits and calibrators (Roche, Boehringer Mannheim). Plasma UC was measured by an automated colorimetric method using a reagent with a composition as described previously [17] plus methanol (58 ml/l) and Preciset cholesterol standards (Roche, Boehringer Mannheim). Cholesterol in the LDL fraction was calculated by subtracting HDL cholesterol (HDL-C) from cholesterol in the  $d > 1.006$  g/ml fraction. Cell cholesterol accumulation in plasma and total cholesterol accumulation (cell + endogenous) in plasma lipoprotein fractions was calculated as the difference between levels in plasma incubated at 37 °C in the presence of RBCs and plasma maintained at 4 °C. Cholesterol accumulation in lipoprotein fractions attributable to cell cholesterol was estimated as the difference between levels in plasma incubated at 37 °C with and without RBC. Endogenous cholesterol metabolism in plasma and plasma lipoproteins was estimated by the difference between cholesterol concentrations in plasma incubated at 37 °C or maintained at 4 °C.

### Statistics

Values are given as mean  $\pm$  SD unless stated otherwise. Repeated measures ANOVA with meals and time after meals as within-subject factors was used to analyse the data

**Table 2** Lipid and lipoprotein concentrations in control plasma during the meals

Lipids (mmol/l)	Time (h)	NTG-H ( <i>n</i> = 8)			HTG-H ( <i>n</i> = 8)		
		PUFA-LC	PUFA-HC	DF	PUFA-LC	PUFA-HC	DF
TG <sup>a</sup>	0	1.26 ± 0.37	1.20 ± 0.22	1.28 ± 0.41	2.13 ± 0.51	2.21 ± 0.49	2.14 ± 0.57
	4	2.21 ± 1.13	2.15 ± 0.80	2.05 ± 0.83	3.72 ± 0.80	4.53 ± 1.31 <sup>f</sup>	3.47 ± 1.29 <sup>f</sup>
	6	1.66 ± 0.96	1.41 ± 0.62	1.81 ± 0.95	3.21 ± 0.58	3.23 ± 0.97	3.10 ± 1.28
TRL-TG <sup>a</sup>	0	0.62 ± 0.30	0.57 ± 0.17	0.62 ± 0.33	1.33 ± 0.42	1.40 ± 0.41	1.28 ± 0.50
	4	1.51 ± 0.98	1.42 ± 0.71	1.27 ± 0.70	2.71 ± 0.63	3.35 ± 1.12 <sup>f</sup>	2.43 ± 1.11 <sup>f</sup>
	6	1.01 ± 0.76	0.78 ± 0.58	1.05 ± 0.74	2.26 ± 0.45	2.25 ± 0.75	2.10 ± 1.11
TC	0	6.03 ± 0.78	6.21 ± 0.81	6.15 ± 0.90	6.43 ± 0.90	6.52 ± 0.82	6.29 ± 0.79
	4	5.87 ± 0.73	6.17 ± 0.78	6.05 ± 0.83	6.49 ± 0.84	6.67 ± 0.83	6.31 ± 0.80
	6	5.84 ± 0.80	6.10 ± 0.74	6.11 ± 0.81	6.40 ± 0.84	6.54 ± 0.87	6.38 ± 0.85
UC <sup>b</sup>	0	1.43 ± 0.18	1.49 ± 0.26	1.43 ± 0.19	1.53 ± 0.20	1.58 ± 0.23	1.54 ± 0.23
	4	1.43 ± 0.16	1.52 ± 0.22	1.48 ± 0.18	1.60 ± 0.19	1.72 ± 0.18	1.60 ± 0.23
	6	1.43 ± 0.16	1.51 ± 0.23	1.47 ± 0.20	1.57 ± 0.19	1.66 ± 0.20	1.63 ± 0.25
CE <sup>c</sup>	0	4.60 ± 0.63	4.72 ± 0.61	4.72 ± 0.74	4.90 ± 0.72	4.94 ± 0.60	4.76 ± 0.59
	4	4.44 ± 0.63	4.65 ± 0.58	4.56 ± 0.70	4.89 ± 0.68	4.95 ± 0.68	4.70 ± 0.61
	6	4.41 ± 0.68	4.59 ± 0.54	4.63 ± 0.64	4.82 ± 0.67	4.89 ± 0.69	4.75 ± 0.65
TRL-C <sup>d</sup>	0	0.34 ± 0.21	0.33 ± 0.14	0.33 ± 0.16	0.65 ± 0.25	0.68 ± 0.24	0.67 ± 0.20
	4	0.45 ± 0.29	0.40 ± 0.21	0.40 ± 0.19	0.89 ± 0.23	0.92 ± 0.35	0.78 ± 0.36
	6	0.41 ± 0.32	0.33 ± 0.24	0.42 ± 0.26	0.90 ± 0.23	0.90 ± 0.41	0.80 ± 0.41
LDL-C <sup>e</sup>	0	4.41 ± 0.76	4.55 ± 0.87	4.52 ± 0.87	4.68 ± 0.98	4.74 ± 0.75	4.54 ± 0.90
	4	4.17 ± 0.70	4.43 ± 0.80	4.36 ± 0.83	4.53 ± 0.88	4.67 ± 0.73	4.44 ± 0.86
	6	4.16 ± 0.83	4.40 ± 0.78	4.38 ± 0.81	4.44 ± 0.91	4.58 ± 0.73	4.46 ± 0.92
HDL-C	0	1.28 ± 0.18	1.33 ± 0.17	1.31 ± 0.20	1.11 ± 0.22	1.10 ± 0.21	1.08 ± 0.22
	4	1.25 ± 0.20	1.33 ± 0.16	1.29 ± 0.22	1.08 ± 0.25	1.08 ± 0.22	1.08 ± 0.23
	6	1.27 ± 0.20	1.37 ± 0.20	1.31 ± 0.24	1.06 ± 0.23	1.08 ± 0.22	1.12 ± 0.25

Values are mean ± SD. Meal abbreviations are shown in Table 1

NTG-H normotriglyceridemic-hypercholesterolemic men, HTG-H hypertriglyceridemic-hypercholesterolemic men, TG triglycerides, TRL-TG triglyceride rich lipoprotein triglycerides, TC total cholesterol, UC unesterified cholesterol, CE cholesteryl esters, TRL-C triglyceride rich lipoprotein cholesterol, LDL-C low density lipoprotein cholesterol, HDL-C high density lipoprotein cholesterol

<sup>a</sup> Significant time effect. 4 h > 0 h: NTG-H and HTG-H, *P* < 0.01. 6 h > 0 h: HTG-H, *P* < 0.01

<sup>b</sup> Significant time effect. 4 h > 0 h: HTG-H, *P* < 0.001. 6 h > 0 h: HTG-H, *P* = 0.002

<sup>c</sup> Significant time effect. 6 h < 0 h: NTG-H, *P* = 0.01

<sup>d</sup> Significant time effect. 4 h < 0 h: NTG-H, *P* = 0.03; HTG-H, *P* = 0.006. 6 h > 0 h: HTG-H, *P* = 0.008

<sup>e</sup> Significant time effect. 4 h < 0 h, NTG-H and HTG-H, *P* = 0.02. 6 h < 0 h: NTG-H and HTG-H, *P* = 0.005

<sup>f</sup> Significant meal × time interactions in repeated measures ANOVA at *P* < 0.01

(SPSS 11.0). Sequence of meals was also included as a between subjects factor. Since there were no significant effects of meal sequence detected, the simplified models without a meal sequence term are reported. The relatively long period between the meals was designed to minimise any effect of meal sequence and carry-over on the data. Student's *t* test was used to compare unpaired data and the paired *t* test was used to compare paired data. Pearson's product-moment correlation coefficients were used to test for relationships between variables. Two-tailed tests of significance were used and a value of *P* < 0.05 was considered to be statistically significant.

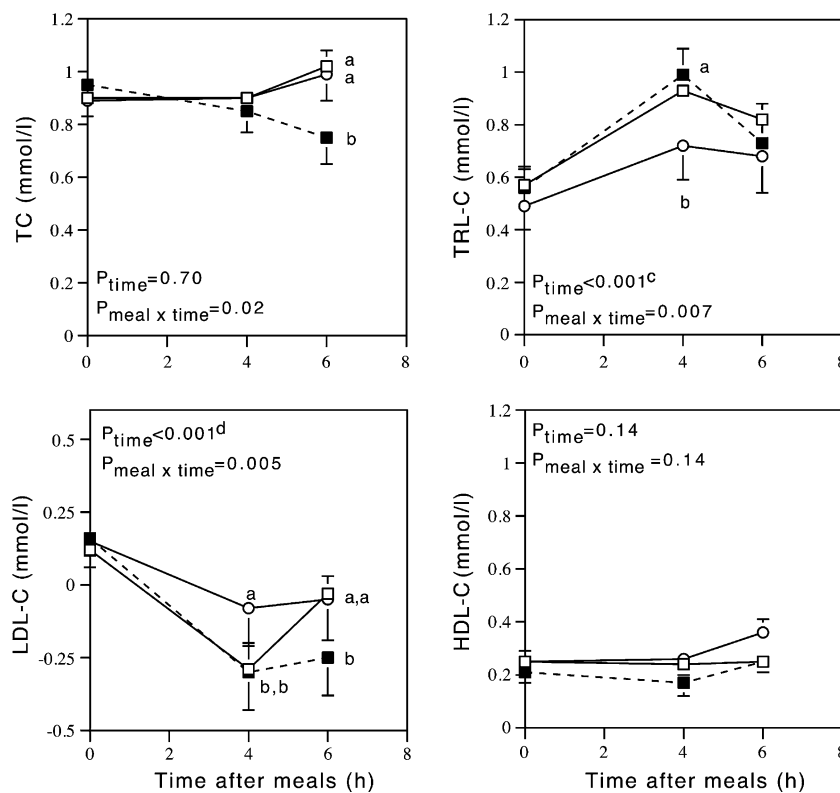
## Results

Table 2 shows plasma lipids and lipoprotein concentrations in the NTG-H and HTG-H men during the meals. In HTG-H men, the response of plasma TG was significantly (*P* = 0.008) different among the meals with a significant and 74% larger increase during 4 h after the PUFA-HC meal compared with the DF meal. Plasma TRL-TG concentrations paralleled these changes during the meals. In NTG-H men, postprandial changes in plasma lipids and lipoprotein lipids were not significantly different among the meals. Ultracentrifuge recovery in the separation of

TRL from LDL + HDL was  $96 \pm 2\%$  ( $n = 48$ ) in fasted plasma,  $97 \pm 3\%$  ( $n = 48$ ) in 4 h postprandial plasma, and  $98 \pm 2\%$  ( $n = 48$ ) in 6 h postprandial plasma. All data were corrected for ultracentrifuge recovery.

Figures 1 and 2 show cholesterol accumulation in plasma and plasma lipoprotein fractions calculated as the difference between values in plasma incubated with RBC at 37 °C and plasma maintained at 4 °C, in HTG-H and NTG-H men, respectively during the meals. The cholesterol accumulation in plasma indicates the amount of cholesterol that has been lost from RBC. The cholesterol accumulation in plasma lipoproteins includes both cell-derived and endogenous cholesterol. In HTG-H men (Fig. 1), the loss of RBC cholesterol to plasma tended to decrease during the PUFA-HC meal and tended to increase during the other meals and these trends were significantly ( $P = 0.02$ ) different at 6 h after the meals. The accumulation of cholesterol in the TRL fraction of 4 h ( $P < 0.001$ ) and 6 h ( $P = 0.02$ ) postprandial plasma incubated with RBC was significantly higher than baseline after all the

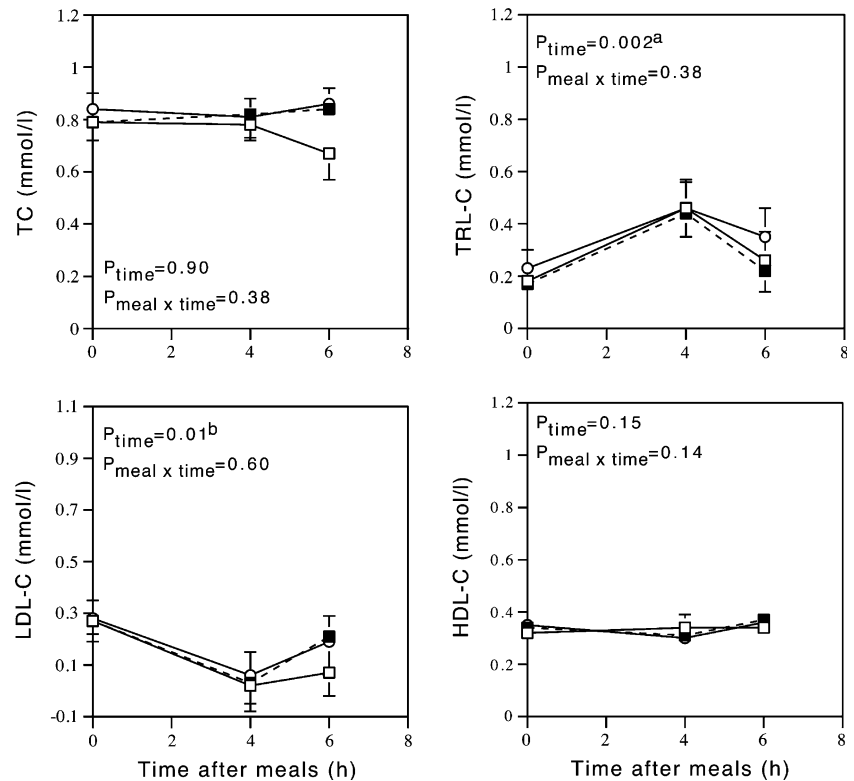
meals and was significantly ( $P = 0.007$ ) higher in 4 h postprandial plasma after the PUFA-HC meal compared with the DF meal. This increased accumulation of cholesterol in TRL was also higher during the PUFA-LC compared with DF meal but not significantly ( $P = 0.12$ ). During all the meals, the cholesterol content of the LDL fraction decreased significantly in postprandial plasma incubated with RBC. This depletion of cholesterol in the LDL fraction was significantly greater in 4 h postprandial plasma after both PUFA-LC and PUFA-HC meals compared with the DF meal and in 6 h postprandial plasma after the PUFA-HC meal compared with the other two meals. The cholesterol content of the HDL fraction did not vary significantly during incubation of RBC with plasma obtained during the meals. In NTG-H men (Fig. 2), the accumulation of cholesterol in the TRL fraction of plasma incubated with RBC was significantly ( $P = 0.005$ ) higher in 4 h postprandial and was not significantly different in 6 h postprandial plasma compared with fasting plasma. The corresponding accumulation of cholesterol in the LDL



**Fig. 1** The effect of meals rich in polyunsaturated fat and low (squares) or high (filled squares) in cholesterol or rich in dairy fat (circle) on accumulation of cholesterol in plasma and plasma lipoproteins calculated as differences in plasma cholesterol and lipoprotein cholesterol between plasma incubated at 37 °C with red blood cells and plasma maintained at 4 °C, in men with mild to moderate hypercholesterolemia and hypertriglyceridemia. The

cholesterol accumulation in plasma indicates the amount of cholesterol that has been lost from RBC. The cholesterol accumulation in plasma lipoproteins includes both cell-derived and endogenous cholesterol. Values are mean  $\pm$  SEM,  $n = 8$ . <sup>a,b</sup>Different symbols indicate significantly ( $P < 0.05$ ) different meal  $\times$  time interactions between meals in repeated measures ANOVA. <sup>c</sup>4 h  $>$  0 h,  $P < 0.001$ ; 6 h  $>$  0 h,  $P = 0.02$ . <sup>d</sup>4 h  $<$  0 h,  $P = 0.002$ ; 6 h  $<$  0 h,  $P = 0.005$

**Fig. 2** The effect of meals rich in polyunsaturated fat and low (*squares*) or high (*filled squares*) in cholesterol or rich in dairy fat (*circles*) on accumulation of cholesterol in plasma and plasma lipoproteins calculated as differences in plasma cholesterol and lipoprotein cholesterol between plasma incubated at 37 °C with red blood cells and plasma maintained at 4 °C, in normotriglyceridemic men with mild to moderate hypercholesterolemia. The cholesterol accumulation in plasma indicates the amount of cholesterol that has been lost from RBC. The cholesterol accumulation in plasma lipoproteins includes both cell-derived and endogenous cholesterol. Values are mean  $\pm$  SEM,  $n = 8$ .  
<sup>a</sup>4 h > 0 h,  $P = 0.005$ .  
<sup>b</sup>4 h < 0 h,  $P = 0.01$

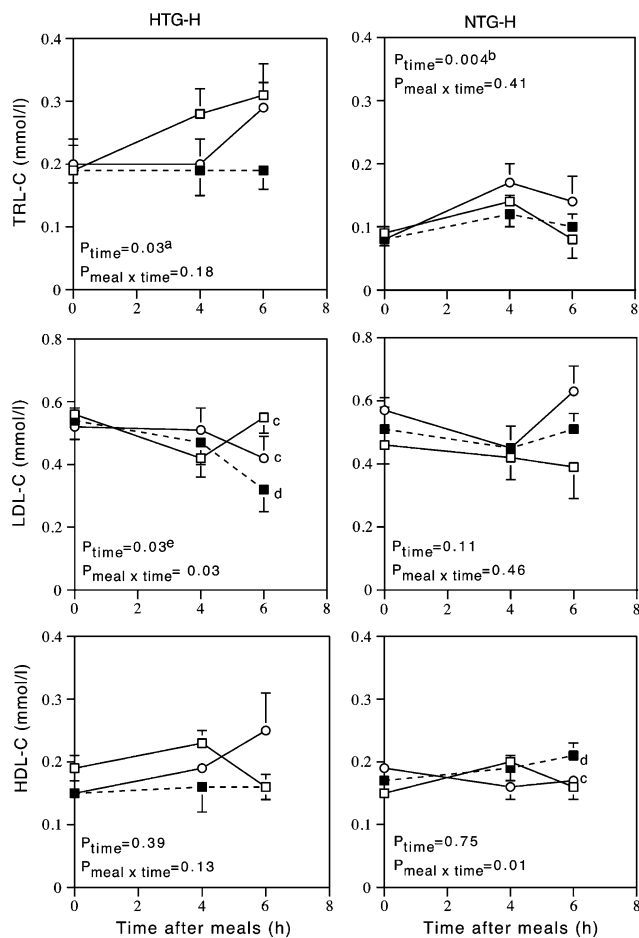


fraction of 4 h postprandial plasma was significantly ( $P = 0.01$ ) reduced after all the meals and these changes were not significantly different among the meals. Cholesterol accumulation in the HDL fraction and cell cholesterol accumulation in plasma during incubation of postprandial plasma with RBC did not change significantly from baseline during the meals. At baseline (first visit), cholesterol accumulation was significantly higher ( $P < 0.001$ ) in the TRL fraction and significantly lower in the LDL ( $P = 0.006$ ) and HDL ( $P = 0.01$ ) fractions in HTG-H compared with NTG-H men.

Figure 3 shows the distribution of effluxed cell cholesterol calculated as the difference between plasma incubated at 37 °C with and without RBC, among plasma lipoprotein fractions in HTG-H and NTG-H men during the meals. In HTG-H men, cell cholesterol content of the TRL fraction increased significantly 6 h after the meals mainly due to increases during the PUFA-LC and DF meals. Cell cholesterol content of the TRL fraction remained unchanged during the PUFA-HC meal but this response was not significantly different from the corresponding response during the other meals. Cell cholesterol content of the LDL fraction decreased significantly during the meals with a significantly larger decrease between baseline and 6 h after the PUFA-HC meal compared with the other meals. In NTG-H men, cell cholesterol content of the TRL fraction increased significantly between baseline and 4 h after the

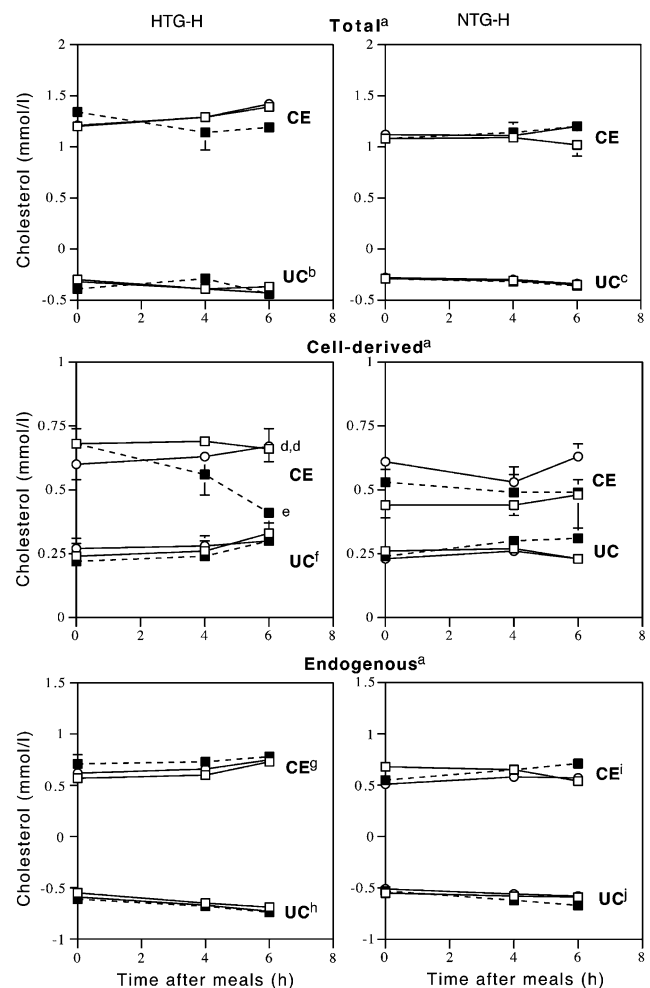
meals and this response was not significantly different among the meals. Cell cholesterol content in the HDL fraction of these men tended to increase during the PUFA-HC meal and tended to decrease during the DF meal and these trends were significantly different. At baseline (first visit), cell cholesterol accumulation in the TRL fraction of plasma incubated with RBC was significantly ( $P = 0.03$ ) higher in HTG-H men compared with NTG-H men. This difference remained significant during the meals.

Figure 4 shows the response of total, cell-derived and endogenous CE and UC in plasma incubated with or without RBC during the meals. In HTG men the total (cell-derived + endogenous) and endogenous plasma UC decreased significantly while the cell-derived plasma UC increased significantly during the meals without significant differences in response among the meals. Cell-derived plasma CE decreased significantly ( $P = 0.002$ ) between baseline and 6 h after the PUFA-HC meal and this change was marginally significantly different compared with the corresponding changes during the other meals ( $P_{\text{meal} \times \text{time}} = 0.05$ ). Endogenous plasma CE increased significantly at 6 h after the meals. In NTG-H men, total and endogenous plasma UC decreased significantly during the meals. The significant meal  $\times$  time interaction in the increase in endogenous CE content of plasma incubated at 37 °C was due to the significantly ( $P = 0.001$ ) higher value at baseline before the PUFA-LC meal compared with the other meals.



**Fig. 3** The effect of meals rich in polyunsaturated fat and low (squares) or high (filled squares) in cholesterol or rich in dairy fat (circles) on cell-derived cholesterol in plasma lipoproteins calculated as differences in plasma cholesterol and lipoprotein cholesterol between plasma incubated at 37 °C with and without red blood cells, in hypertriglyceridemic (HTG-H) and normotriglyceridemic (NTG-H) men with mild to moderate hypercholesterolemia. Values are mean  $\pm$  SEM,  $n = 8$ . <sup>a</sup>6 h > 0 h,  $P = 0.03$ . <sup>b</sup>4 h > 0 h,  $P = 0.003$ . <sup>c,d</sup>Different symbols indicate significantly ( $P < 0.05$ ) different meal  $\times$  time interactions between meals in repeated measures ANOVA. <sup>e</sup>4 h < 0 h,  $P = 0.04$ ; 6 h < 0 h,  $P = 0.03$

Figure 5 shows the changes in endogenous cholesterol in plasma lipoprotein fractions during incubation of plasma at 37 °C. In HTG-H men, accumulation of cholesterol in the TRL fraction was significantly increased from baseline at 4 and 6 h after the meals. In HTG-H and NTG-H men, cholesterol accumulation was significantly lower than baseline in the LDL fraction at 4 and 6 h and in the HDL fraction at 4 h after the meals. In NTG-H men, cholesterol in the TRL fraction increased significantly 4 h and was not significantly different from baseline 6 h after the meals. These changes were not significantly different among the meals. At baseline (first visit), endogenous cholesterol accumulation was significantly higher in the TRL fraction ( $P = 0.001$ ) and was significantly lower in the LDL



**Fig. 4** The effect of meals rich in polyunsaturated fat and low (squares) or high (filled squares) in cholesterol or rich in dairy fat (circles) on total, cell-derived and endogenous cholesterol esters (CE) and unesterified cholesterol (UC) in plasma incubated with and without red blood cells (RBC), in hypertriglyceridemic (HTG-H) and normotriglyceridemic (NTG-H) men with mild to moderate hypercholesterolemia. Values are mean  $\pm$  SEM,  $n = 8$ . <sup>a</sup>Total = difference between plasma incubated at 37 °C with RBC and plasma maintained at 4 °C; *Cell derived* = difference between plasma incubated at 37 °C with and without RBC; *Endogenous* = difference between plasma incubated at 37 °C and maintained at 4 °C. <sup>b,c</sup>Significant time effect. 6 h < 0 h,  $P = 0.001$ . <sup>d,e</sup>Different symbols indicate marginally significantly ( $P = 0.05$ ) different meal  $\times$  time interactions between meals in repeated measures ANOVA. <sup>f</sup>Significant time effect. 6 h > 0 h,  $P = 0.007$ . <sup>g</sup>Significant time effect. 6 h > 0 h,  $P = 0.008$ . <sup>h</sup>Significant time effect. 4 h < 0 h,  $P = 0.003$  and 6 h < 0 h,  $P < 0.001$ . <sup>i</sup>Significantly different ( $P < 0.01$ ) meal  $\times$  time interaction between PUFA-LC meal and other meals in repeated measures ANOVA. <sup>j</sup>Significant time effect. 4 h < 0 h,  $P = 0.02$  and 6 h < 0 h,  $P < 0.001$

( $P = 0.001$ ) and HDL fractions ( $P < 0.001$ ) in HTG-H compared with NTG-H men. These differences remained significant during the meals.

In the total study population, the amount of cell cholesterol that accumulated in plasma was correlated



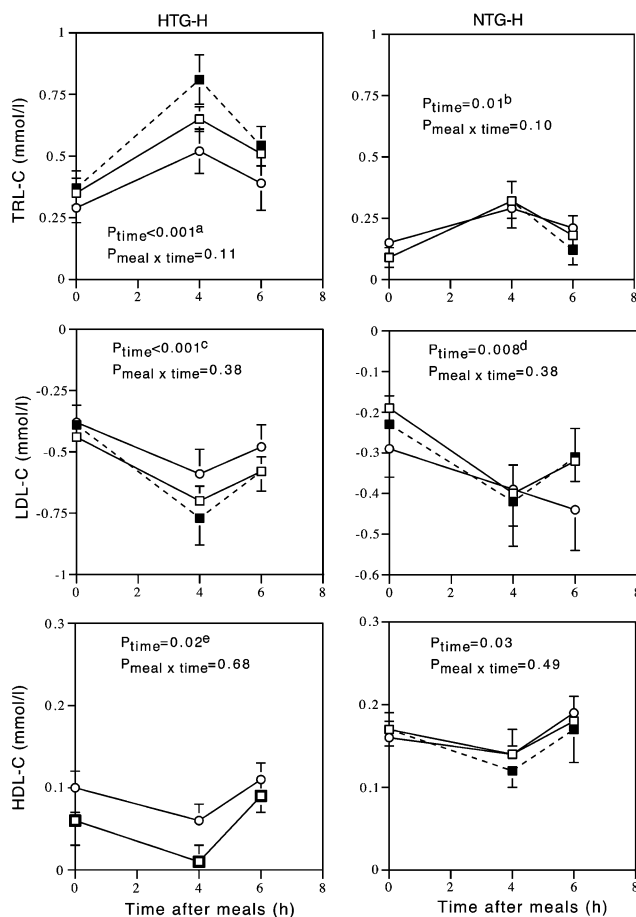


**Fig. 5** The effect of meals rich in polyunsaturated fat and low (squares) or high (filled squares) in cholesterol or rich in dairy fat (circles) on differences in lipoprotein cholesterol concentrations between plasma incubated at 37 °C and plasma maintained at 4 °C, in hypertriglyceridemic (HTG-H) and normotriglyceridemic (NTG-H) men with mild to moderate hypercholesterolemia. Values are mean  $\pm$  SEM,  $n = 8$ . <sup>a</sup>4 h > 0 h,  $P < 0.001$  and 6 h > 0 h,  $P = 0.03$ . <sup>b</sup>4 h > 0 h,  $P = 0.009$ . <sup>c</sup>4 h < 0 h,  $P = 0.001$  and 6 h < 0 h,  $P = 0.01$ . <sup>d</sup>4 h < 0 h,  $P = 0.01$  and 6 h < 0 h,  $P = 0.02$ . <sup>e</sup>4 h < 0 h,  $P = 0.03$

significantly ( $r = 0.702$ – $0.913$ ,  $P \leq 0.002$ ) with the increase in plasma CE during incubation of RBC with fasted and postprandial plasma after all the meals. Also, the 4 h increases in total cholesterol accumulation in the plasma TRL fraction of plasma incubated with RBC were correlated significantly with the corresponding increases in plasma TG during the meals (PUFA-LC,  $r = 0.836$ ; PUFA-HC,  $r = 0.826$ ; DF,  $r = 0.750$ , all  $P \leq 0.001$ ). In HTG-H men, the 6 h decrease in cell cholesterol accumulation in the LDL fraction during the PUFA-HC meal was correlated significantly ( $r = 0.762$ ,  $P = 0.03$ ,  $n = 8$ ) with the corresponding decrease in CE derived from the esterification of cell cholesterol in plasma. At baseline (first visit), cell cholesterol accumulation in fasted and postprandial plasma was not correlated significantly or at marginal significance

with corresponding plasma concentrations of lipids and lipoproteins (data not shown).

## Discussion

This study has shown that addition of large amounts of cholesterol to a PUFA-rich meal decreases the accumulation of RBC cholesterol in postprandial plasma and LDL in vitro in HTG-H men. The magnitude of postprandial lipemia and the accumulation of cell plus endogenous cholesterol in the 4 h postprandial plasma TRL fraction were markedly higher during the PUFA-HC meal compared with the DF meal in these men. In NTG-H men, the type of meal did not differentially affect cell and total cholesterol accumulation in plasma and plasma lipoproteins. Our data suggest that the quantity of cholesterol and type of fat in the meal may influence transport of cell cholesterol to postprandial plasma, postprandial lipemia and the capacity of the postprandial TRL fraction to accumulate cholesterol in men with mild combined hyperlipidemia.

A previous study in normolipidemic subjects has reported that postprandial plasma isolated 4 h after a fatty meal accumulates 28% more cholesterol than fasted plasma during incubation with RBC [7]. However, our study in hyperlipidemic men has shown that while there was substantial net transport of RBC cholesterol to fasted plasma in vitro, this did not increase appreciably when cells were incubated with postprandial plasma obtained 4 h after a fatty meal (Figs. 1, 2). It is possible this failure of postprandial lipemia to accelerate cell cholesterol transport may be due to a hyperlipidemia-induced attenuation of cell cholesterol esterification in plasma. The quantity of cholesterol esterified did not increase appreciably (Fig. 4) and was closely correlated with the amount of RBC cholesterol transported to 4 h postprandial plasma during incubation with RBC. A close relationship between cholesterol esterification and net transport of RBC to plasma in vitro has been documented previously in normolipidemic subjects [7]. Also, the amount of plasma CE increased in line with the increase in RBC cholesterol transport to 4 h postprandial plasma [7]. Efficient esterification of UC by LCAT is essential for net transfer of RBC cholesterol to plasma. Previous studies have reported that inhibition of plasma LCAT activity [7] or absence of LCAT [18] increases influx of UC from plasma to cells preventing net loss of cell cholesterol to plasma in vitro. In baboons with diet-induced hypercholesterolemia, plasma cholesterol esterification is inhibited and movement of RBC cholesterol to postprandial plasma in vitro is reversed after a fatty meal [12]. On the other hand, increased plasma cholesterol esterification and efflux of radiolabelled cholesterol from cultured cells to dilute postprandial plasma from patients

with type IIB hyperlipidemia after a fatty meal has been reported previously [13]. However, the efflux of radiolabelled cholesterol does not measure net transport of cholesterol mass from cells. Other differences such as types of cells, between experimental models may also contribute to the differences in cell cholesterol transport to postprandial plasma among the studies.

The decrease in total cholesterol accumulation in 6 h postprandial plasma and its LDL fraction during incubation with RBC (Fig. 1) was mainly due to the corresponding decrease in cell cholesterol accumulation in LDL (Fig. 3), in HTG-H men after the PUFA-HC meal compared with other meals. Failure of cell cholesterol to accumulate in TRL also tended to contribute to this decrease in RBC cholesterol transport to plasma. These decreases in cell cholesterol accumulation in plasma and lipoproteins may be due to attenuated esterification of cell cholesterol in plasma and/or impaired ability of postprandial LDL to accept cell cholesterol transferred from HDL via LCAT and CETP. The decrease in cell cholesterol accumulation in plasma LDL was correlated with the concomitant decrease in cell-cholesterol derived CE in plasma. Impaired cell cholesterol esterification and transfer of CE to TRL might also contribute to the failure of cell cholesterol to accumulate in postprandial TRL during the PUFA-HC meal. The ability of postprandial LDL to bind CE transferred from HDL via LCAT and CETP may also be impaired in HTG-H men. A previous study has reported that fasting LDL has impaired ability to accept CE from HDL and has low affinity for the CETP protein in patients with combined hyperlipidemia [19]. Abnormal chemical composition including increased CE content and structure appear to underlie this defect in LDL [19]. Postprandial lipemia is known to alter the composition and properties of LDL [9, 20]. Also, there is evidence that the presence of chylomicrons in plasma impairs the ability of LDL and HDL to accept cell cholesterol *in vitro* [7, 8]. Thus, in the present study, it is conceivable that the particularly high level of postprandial lipemia following the PUFA-HC meal in HTG-H men may have altered the composition and properties of postprandial LDL including the ability to bind CE. This high level of postprandial lipemia may be due to the combined effect of high cholesterol content of the meal, abnormalities of TG metabolism, and efficient absorption of PUFA from the gut. A previous study has reported that ingestion of large amounts of cholesterol (700 mg) in a meal rich in PUFA and MUFA increases peak postprandial concentrations of large TRL-TG in normolipidemic men [9]. This effect of ingested cholesterol may be enhanced by inefficient clearance of postprandial TRL in hypertriglyceridemic subjects. There is evidence that PUFAs are more efficiently absorbed from the gut compared with long-chain saturated fatty acids in bovine fat [21].

Incorporation of cholesterol from cells and endogenous lipoproteins into TRL has been postulated as the initial step in a pathway that may enhance delivery of this cholesterol to the liver during the postprandial state [6–8]. Postprandial plasma TRL are potent acceptors of cholesterol from both cells and endogenous lipoproteins via LCAT and CETP [6–8]. In HTG-H men in the present study, the type of fat in the meal affected the total quantity of cholesterol (cell-derived + endogenous) that accumulated in the TRL fraction of postprandial plasma incubated with RBC. This cholesterol accumulation in plasma TRL was higher 4 h after meals rich in PUFA compared with DF. Higher levels of postprandial lipemia appeared to be mainly responsible for this increased accumulation of cholesterol in postprandial TRL after the PUFA-rich meals. The 4 h increase in TRL cholesterol in postprandial plasma incubated with RBC was correlated closely with the concomitant increase in plasma TRL-TG concentrations. The larger increase in total cholesterol accumulation in 4 h postprandial TRL after PUFA-rich meals appeared to be mainly due to increased transfer of cholesterol from endogenous lipoproteins via LCAT and CETP into postprandial TRL. The increase in cholesterol accumulation in the TRL fraction of plasma incubated at 37 °C essentially paralleled and accounted for most of the corresponding increase in total cholesterol accumulation in the TRL fraction of plasma incubated with RBC during the meals in HTG-H men (Figs. 1, 5). Plasma LDL supplied most of the endogenous CE that was transferred into postprandial TRL as indicated by the enhanced decrease in LDL cholesterol in postprandial plasma incubated at 37 °C. This finding is in keeping with previous studies indicating that LDL is a major donor of CE to postprandial TRL [8, 22].

Efficient hepatic clearance of TRL remnant lipoproteins from the circulation may accelerate the transport of cholesterol from cells and from LDL to the liver during postprandial lipemia [6, 8, 23]. However, when clearance is delayed increased levels of cholesterol-enriched, proatherogenic TRL remnant lipoproteins [24] may increase risk of atherosclerotic disease [25, 26]. In subjects with combined hyperlipidemia, transfer of CE from HDL to TRL is enhanced during fasting and postprandial lipemia [13, 27], clearance of postprandial TRL after a fatty meal is impaired [28] and risk of coronary artery disease is abnormally high. In the current study, accumulation of both cell-derived and endogenous cholesterol in TRL was higher and there was evidence that clearance of postprandial TRL was impaired in HTG-H men compared with NTG-H men. Accelerated transfer of CE into TRL may contribute to this higher accumulation of cholesterol in TRL and lower cholesterol accumulation in HDL in fasting and postprandial plasma from HTG-H men. Plasma TG

concentrations 6 h after the meals were clearly higher than fasted values in HTG-H men suggesting impaired clearance of postprandial TRL particles. Thus, enhanced accumulation of cholesterol from cells and endogenous lipoproteins in postprandial TRL after meals rich in PUFA compared with DF may not accelerate RCT and may increase the atherogenic potential of TRL remnant lipoproteins in these men. On the other hand, replacing DF with PUFA in the diet induces a chronic decrease in plasma LDL-C concentration that decreases risk of coronary artery disease.

In NTG-H men, the cholesterol content and type of fat in the meal did not influence appreciably postprandial lipemia and cholesterol accumulation in plasma and plasma lipoproteins during incubation with RBC. This finding may be due to relatively efficient TRL metabolism leading to lower plasma TRL concentrations and to the absence of LDL particles with abnormalities induced by hypertriglyceridemia.

This study has limitations. The number of subjects studied was small and all the participants were men. Thus care must be exercised in the extrapolation of the findings to other populations of hyperlipidemic individuals. Also, the fat composition of the habitual diet of the participants was not determined. The type of fat in the habitual diet influences the postprandial response of plasma lipoprotein lipid levels to ingested fat [29]. On the other hand, impaired TG metabolism in HTG-H men has a more potent impact on postprandial response of lipoproteins to fatty meals. The calculation of cell cholesterol accumulation in plasma lipoprotein fractions as the difference in lipoprotein cholesterol levels between plasma incubated with and without RBC, assumes that endogenous cholesterol metabolism in plasma is the same in the presence and absence of RBC. Any changes in plasma endogenous cholesterol metabolism in the presence of RBC could contribute to the differences in calculated cell cholesterol accumulation in plasma lipoprotein fractions among the meals in HTG-H men.

In conclusion, our data indicate that the effect of meals varying in cholesterol content and type of dietary fat on transport of cell membrane cholesterol to plasma, postprandial lipemia, and accumulation of cell and endogenous cholesterol in plasma TRL, is influenced importantly by fasting plasma TG levels in men with mild to moderate hypercholesterolemia. In HTG-H men, addition of large amounts of cholesterol to PUFA rich meals leads to postprandial plasma with impaired ability to support net transport of cell membrane cholesterol to plasma and its LDL fraction. In these men, postprandial lipemia is higher after meals rich in PUFA compared with DF increasing the capacity for cholesterol accumulation in potentially atherogenic CE-enriched TRL remnant lipoproteins. Whether

impaired diffusion-mediated cell membrane cholesterol transport influences cholesterol content of atherosclerotic lesions remains to be determined.

**Acknowledgments** The authors are grateful to the participants in the study. We are also grateful to Wendy Aitken in the Department of Human Nutrition for help in recruiting subjects. This study was supported by a Laurensen Award from the Otago Medical School Research Foundation.

## References

1. Yancey PG, Bortnick AE, Kellner-Weibel G, de la Llera-Moya M, Phillips MC, Rothblat GH (2003) Importance of different pathways of cellular cholesterol efflux. *Arterioscler Thromb Vasc Biol* 23:712–719
2. Cavelier C, Lorenzi I, Rohrer L, von Eckardstein A (2006) Lipid efflux by the ATP-binding cassette transporters ABCA1 and ABCG1. *Biochim Biophys Acta* 1761:655–666
3. Duong MN, Collins HL, Jin W, Zanotti I, Favari E, Rothblat GH (2006) Relative contributions of ABCA1 and SR-B1 to cholesterol efflux to serum from fibroblasts and macrophages. *Arterioscler Thromb Vasc Biol* 26:541–547
4. Schwartz CC, VandenBroek JM, Cooper PS (2004) Lipoprotein cholesteryl ester production, transfer, and output in vivo in humans. *J Lipid Res* 45:1594–1607
5. Fielding CJ, Fielding PE (1995) Molecular physiology of reverse cholesterol transport. *J Lipid Res* 36:211–228
6. Castro GR, Fielding CJ (1985) Effects of postprandial lipemia on plasma cholesterol metabolism. *J Clin Invest* 75:874–882
7. Chung BH, Franklin F, Cho BHS, Segrest JP, Hart K, Darnell BE (1998) Potencies of lipoproteins in fasting and postprandial plasma to accept additional cholesterol molecules released from cell membranes. *Arterioscler Thromb Vasc Biol* 18:1217–1230
8. Chung BH, Liang P, Doran S, Simon Cho BH, Franklin F (2004) Postprandial chylomicrons: potent vehicles for transporting cholesterol from endogenous LDL + HDL and cell membranes to the liver via LCAT and CETP. *J Lipid Res* 45:1242–1255
9. Dubois C, Armand M, Mekki N, Portugal H, Pauli A-M, Bernard P-M, Lafont H, Lairon D (1994) Effects of increasing amounts of dietary cholesterol on postprandial lipemia and lipoproteins in human subjects. *J Lipid Res* 35:1993–2007
10. Mekki N, Charbonnier M, Borel P, Leonardi J, Juhel C, Portugal H, Lairon D (2002) Butter differs from olive oil and sunflower oil in its effects on postprandial lipemia and triacylglycerol-rich lipoproteins after single mixed meals in healthy young men. *J Nutr* 132:3642–3649
11. Tholstrup T, Sandström B, Bysted A, Holmer G (2001) Effect of 6 dietary fatty acids on the postprandial lipid profile, plasma fatty acids, lipoprotein lipase and cholesterol ester transfer activities in healthy young men. *Am J Clin Nutr* 73:198–208
12. Fielding PE, Jackson EM, Fielding CJ (1989) Chronic fat and cholesterol inhibit the normal postprandial stimulation of plasma cholesterol metabolism. *J Lipid Res* 30:1211–1217
13. Guerin M, Egger P, Soudant C, Le Goff W, van Tol A, Dupuis R, Chapman MJ (2002) Cholesteryl ester flux from HDL to VLDL-1 is preferentially enhanced in type IIB subjects in the postprandial state. *J Lipid Res* 43:1652–1660
14. Knopp RH, Retzlaff BM, Walden CE, Dowdy AA, Tsunehara CH, Austin MA, Nguyen T (1997) A double-blind, randomized, controlled trial of the effects of two eggs per day in moderately hypercholesterolemic and combined hyperlipidemic subjects taught the NCEP step I diet. *J Am Coll Nutr* 16:551–561

15. National Institutes of Health: Executive Summary (2001) In: Third report of the national cholesterol education program expert panel on detection, evaluation, and treatment of high blood cholesterol in adults (Adult Treatment Panel III). Washington, DC, US Govt. Printing Office, 2001 (NIH publ. no. 01–3670)
16. Warnick GR, Benderson JA, Albers JJ (1982) Dextran-sulphate-Mg<sup>2+</sup> precipitation procedure for quantification of high density lipoprotein cholesterol. *Clin Chem* 28:1379–1388
17. Albers JJ, Chen CH, Adolphson JL (1981) Lecithin: cholesterol acyltransferase (LCAT) mass; its relationship to LCAT activity and cholesterol esterification rate. *J Lipid Res* 22:1206–1213
18. Czarnecka H, Yokoyama S (1996) Regulation of cellular cholesterol efflux by lecithin:cholesterol acyltransferase reaction through nonspecific lipid exchange. *J Biol Chem* 271:2023–2028
19. Guérin M, Bruckert E, Dolphin PJ, Chapman MJ (1996) Absence of cholesteryl ester transfer protein-mediated cholesteryl ester mass transfer from high-density lipoprotein to low-density lipoprotein particles is a major feature of combined hyperlipidaemia. *Eur J Clin Invest* 26:485–494
20. Karpe F, Tornvall P, Olivercrona T, Steiner G, Carlson LA, Hamsten A (1993) Composition of human low density lipoprotein: effects of postprandial triglyceride-rich lipoproteins, lipoprotein lipase, hepatic lipase and cholesteryl ester transfer protein. *Atherosclerosis* 98:33–49
21. Braaco U (1994) Effect of triglyceride structure on fat absorption. *Am J Clin Nutr* 60(suppl):1002S–1009S
22. Lassel TS, Guerin M, Auboiron S, Guy-Grand B, Chapman MJ (1999) Evidence for a cholesteryl ester donor activity of LDL particles during alimentary lipemia in normolipidemic subjects. *Atherosclerosis* 147:41–48
23. Chung B-H, Simon Cho BH, Liang P, Doran S, Osterlund L, Oster RA, Darnell B, Franklin F (2004) Contribution of postprandial lipemia to the dietary fat-mediated changes in endogenous lipoprotein-cholesterol concentrations in humans. *Am J Clin Nutr* 80:1145–1158
24. Havel RJ (2000) Remnant lipoproteins as therapeutic targets. *Curr Opin Lipidol* 11:615–620
25. Patsch JR, Miesenböck G, Hofpfenweiler T, Muhlberger V, Knapp E, Dunn JK, Gotto AM Jr, Patsch W (1992) Relation of triglyceride metabolism and coronary artery disease in normolipidemic men with and without coronary artery disease: studies in post-prandial state. *Arterioscler Thromb* 12:1336–1345
26. Weintraub MS, Grosskopf I, Rassin T, Miller H, Charach G, Rotmensch HH, Liron M, Rubenstein A, Iaina A (1996) Clearance of chylomicron remnants in normolipidemic patients with coronary artery disease: case control study over three years. *BMJ* 312:936–939
27. Guérin M, Lassel TS, Le Goff W, Farnier M, Chapman MJ (2000) Action of atorvastatin in combined hyperlipidemia: preferential reduction of cholesteryl ester transfer from HDL to VLDL1 particles. *Arterioscler Thromb Vasc Biol* 20:189–197
28. Castro Cabezas M, de Bruin TWA, Jansen H, Kock LAW, Kortland W, Erkelens DW (1993) Impaired chylomicron remnant clearance in familial combined hyperlipidemia. *Arterioscler Thromb* 13:804–814
29. Bergeron N, Havel RJ (1995) Influence of diets-rich in saturated fat and omega-6 polyunsaturated fatty acids on the postprandial response of apolipoproteins B-48, B-100, E, and lipids in triglyceride-rich lipoproteins. *Arterioscler Thromb Vasc Biol* 15:2111–2121

## Linoleic Acid Decreases Leptin and Adiponectin Secretion from Primary Rat Adipocytes in the Presence of Insulin

P. Pérez-Matute · J. A. Martínez · A. Martí ·  
M. J. Moreno-Aliaga

Received: 12 September 2006 / Accepted: 18 June 2007 / Published online: 24 July 2007  
© AOCs 2007

**Abstract** Obesity rates have dramatically increased over the last few decades and, at the same time, major changes in the type of fatty acid intake have occurred. Linoleic acid, an n-6 polyunsaturated fatty acid, is an essential fatty acid occurring in high amounts in several western diets. A potential role of this fatty acid on obesity has been suggested. Controversial effects of linoleic acid on insulin sensitivity have also been reported. Thus, the aim of this study was to examine the direct effects of linoleic acid on leptin and adiponectin production, two adipokines known to influence weight gain and insulin sensitivity. Because insulin-stimulated glucose metabolism is an important regulator of leptin production, the effects of linoleic acid on adipocyte metabolism were also examined. For this purpose, isolated rat adipocytes were incubated with linoleic acid (1–200  $\mu\text{M}$ ) in the absence or presence of insulin. Linoleic acid (1–200  $\mu\text{M}$ ) significantly decreased insulin-stimulated leptin secretion and expression ( $P < 0.05$ ), however, no changes in basal leptin production were observed. Linoleic acid also induced a significant decrease (~20%) in adiponectin secretion ( $P < 0.05$ ), but only in the presence of insulin and at the highest concentration tested (200  $\mu\text{M}$ ). This fatty acid did not modify either glucose uptake or lactate production and the percentage of glucose metabolized to lactate was not changed either. Together, these results suggest that linoleic acid seems to interfere with other insulin signalling pathway different from those

controlling glucose uptake and metabolism, but involved in the regulation of leptin and adiponectin production.

**Keywords** Linoleic acid · Insulin · Glucose metabolism · Adipocytes · Leptin · Adiponectin · Obesity · Insulin resistance

### Abbreviations

n-6 PUFA n-6 Polyunsaturated fatty acids

### Introduction

While the debate continues on whether dietary fat is the primary determinant of excessive body fat, the evidence is compelling for the greater importance of types of fat, rather than the total amount of fat, as a risk for chronic disease [1]. Thus, several studies have suggested that the type of fat ingested may be an important determinant in the development of obesity and other associated diseases such as insulin resistance, type 2 diabetes and cardiovascular diseases [2, 3]. In this sense, it has been demonstrated that saturated fat intake induces obesity and insulin resistance [4, 5] meanwhile diets rich in fish oils (n-3 PUFAs) seem to prevent the development of these diseases [6, 7]. Furthermore, body fat accumulation is greater in rats fed a beef tallow diet (rich in saturated fatty acids) than in rats fed on diets enriched with other types of fatty acids such as n-3 fatty acids [8] or n-6 PUFAs [9–11].

Concerning the intake of n-6 and n-3 polyunsaturated fatty acids (PUFAs), a striking rise in the linoleic acid/ $\alpha$  linolenic acid ratio has been observed during the last decades, which is likely related to an increase in linoleic acid

P. Pérez-Matute · J. A. Martínez · A. Martí ·  
M. J. Moreno-Aliaga (✉)  
Department of Physiology and Nutrition,  
University of Navarra, 31008 Pamplona,  
Navarra, Spain  
e-mail: mjmoreno@unav.es

intake [12]. Linoleic acid (18:2n-6), is an essential fatty acid occurring in several edible vegetable oils such as corn, soy and safflower oil [13]. In fact, several western dietary patterns such as the North American diet are typically high in linoleic acid [1], and it has been suggested that the consumption of this fatty acid could also contribute to the onset of obesity and other related disorders such as insulin resistance. Thus, several trials have demonstrated that high n-6 linoleic acid consumption might aggravate insulin resistance in humans [14]. In fact, a positive correlation has been observed between linoleic acid concentration in muscle membrane phospholipids and insulin resistance [15], suggesting that rather than being beneficial, high n-6 PUFA diets may have some long-term side effects within the cluster of hyperinsulinemia, atherosclerosis and tumorigenesis [14]. In contrast, Vessby [16] observed that insulin resistance and disorders characterized by insulin resistance are associated with a specific fatty acid pattern of the serum lipids with reduced levels of linoleic acid.

Leptin and adiponectin are hormones secreted by white adipose tissue with important metabolic effects. In fact, leptin is involved in the regulation of body weight, body fat storage and insulin sensitivity [17]. Plasma adiponectin levels are positively associated with whole-body insulin sensitivity and are decreased in obesity [18]. A number of studies have demonstrated that insulin stimulates leptin gene expression and secretion by increasing the adipocyte glucose utilization [19]. Several studies have also suggested a role of insulin in the regulation of adiponectin secretion although data were conflicting [20, 21].

Several *in vivo* studies have observed that feeding rats with linoleic acid-enriched diets (high-safflower oils) induced an increase in body fat stores and also in the gene expression and circulating levels of leptin [8, 22]. To our knowledge, there are no data available regarding the potential actions of linoleic acid on adiponectin secretion by cultured adipocytes.

For this reason, the aim of the present study was to investigate the *in vitro* effects of linoleic acid on leptin and adiponectin production from primary rat adipocytes cultured in a collagen matrix for 96 h. The effects of linoleic acid on insulin-stimulated glucose utilization and lactate production were also studied on our adipocyte culture model.

## Methods

### Materials

Media (Dulbecco's modified Eagle's medium, DMEM), minimal essential medium amino acids, penicillin/strepto-

mycin, fetal bovine serum (FBS), and nystatin were purchased from Gibco-Invitrogen Life Technologies (Carlsbad, CA, USA; Grand Island, NY, USA). Bovine serum albumin fraction V, 4-(2-hydroxyethyl)-1-piperazineethansulfonic acid (HEPES), insulin, and linoleic acid were purchased from Sigma Chemical Co. (St Louis, MO, USA). Collagen (Vitrogen 100) was obtained from Cohesion Technologies (Palo Alto, CA, USA). Type I collagenase was purchased from Worthington Biochemical Corporation (Lakewood, NJ, USA).

### Animals

Male Wistar rats (250–280 g) obtained from the Applied Pharmacobiology Center (CIFA, Spain) were used to provide adipocytes isolated from the epididymal fat depot. These animals were housed in cages in temperature-controlled rooms ( $22 \pm 2^\circ\text{C}$ ) with a 12-h light–dark cycle. All experimental procedures were performed according to National and Institutional Guidelines for Animal Care and Use and approved by the Ethical Committee for Animal Care and Use at the University of Navarra, Spain. Animals were euthanized and epididymal adipose tissue was quickly removed.

### Adipocyte Isolation and Culture

Adipocytes were isolated from epididymal fat depots as previously described [23]. Epididymal fat was minced and digested in HEPES buffer (pH 7.4; containing 5 mM D-glucose, 2% BSA, 135 mM NaCl, 2.2 mM  $\text{CaCl}_2 \cdot 2\text{H}_2\text{O}$ , 1.25 mM  $\text{MgSO}_4 \cdot 7\text{H}_2\text{O}$ , 0.45 mM  $\text{KH}_2\text{PO}_4$ , 2.17 mM  $\text{Na}_2\text{HPO}_4$ , and 10 mM HEPES) with type I collagenase (1.25 mg/ml per 0.5 g tissue) at  $37^\circ\text{C}$  with gentle shaking for 30 min. The resulting cell suspension was diluted in HEPES-phosphate buffer and the isolated adipocytes were then separated from the undigested tissue by filtration through a  $400\ \mu\text{m}$  nylon mesh and washed three times. Isolated adipocytes were then resuspended in DMEM supplemented with 1% FBS and incubated for 40 min at  $37^\circ\text{C}$ . The isolated adipocytes (150  $\mu\text{l}$  of 2:1 ratio of packed cells to medium) were then plated on 500  $\mu\text{l}$  of a collagen matrix (Vitrogen 100, Cohesion Technologies, Palo Alto, CA) in 6-well culture plates. After 50 min of incubation at  $37^\circ\text{C}$ , the culture media containing 0 or 1.6 nM insulin and the different concentrations (0, 1, 10, 50, 100, and 200  $\mu\text{M}$ ) of the assayed linoleic acid were added and the cells were maintained in an incubator at  $37^\circ\text{C}$  in 5%  $\text{CO}_2$  for up to 96 h. Aliquots (300  $\mu\text{l}$ ) of the media were collected at 24, 48, 72, and 96 h, and replaced with fresh medium containing the appropriate concentration of insulin and linoleic acid.

## Assays

Leptin concentrations in the medium were determined after 96 h of culture using a radioimmunoassay for rat leptin (Linco Research, St Charles, MO, USA). Adiponectin concentrations were analyzed using a mouse/rat adiponectin Elisa kit (B-Bridge International Inc., USA). Glucose and lactate concentrations in the media were measured by an autoanalyzer (Cobas Roche Diagnostic, Basel, Switzerland) [24].

## Analysis of mRNA

Leptin mRNA levels were determined by northern blotting [23]. The leptin cDNA probe was a 388 bp fragment of mouse leptin cDNA, which was kindly provided by Dr. Charles Mobbs (Mount Sinai School of Medicine, NY, USA). The 18S ribosomal probe was obtained from Ambion (Ambion, Austin, TX, USA). RNA was extracted according to the Gibco Life Technologies procedure using Trizol (Life Technologies Inc., Grand Island, NY, USA). The UV absorbance and integrity gels were used to estimate RNA. Leptin and 18S cDNA probes were labeled by random priming (Rediprime kit, Amersham, Buckinghamshire, UK) in the presence of  $^{32}\text{P}$  dCTP (3,000 Ci/mmol, Amersham, UK). Unincorporated nucleotides were removed using NucTrap probe purification columns (Stratagene, La Jolla, CA, USA). For each tissue sample, 7  $\mu\text{g}$  of total RNA were fractionated by electrophoresis on a denaturing 1% agarose gel containing 2.2 M formaldehyde and 1 $\times$  MOPS running buffer. One microliter of a 50  $\mu\text{g}/\text{ml}$  ethidium bromide (Gibco BRL, Gaithersburg, MD, USA) stock solution was added in order to check RNA integrity and even loading. After electrophoresis, RNA was transferred to nylon membrane (Duralon-UV, Stratagene, La Jolla, CA, USA) by overnight capillary transfer and UV cross-linked (Stratalinker 1800, Stratagene, La Jolla, CA, USA). Blots were then hybridized for 1 h at 68  $^{\circ}\text{C}$  in presence of labeled cDNA probe ( $2 \times 10^6$  cpm/ml Express Hyb solution, Clontech, Palo Alto, CA, USA and  $1 \times 10^6$  cpm/ml with the 18S cDNA probe). After washing at high stringency, blots were exposed to X-ray films with an intensifying screen at  $-80^{\circ}\text{C}$ . The expression level of 18S ribosomal RNA was used as an internal control to correct minor variation in total RNA amount.

## Intensity Light Scattering

This technique was used in order to test if linoleic acid is in the free form or the micellar form in our cell culture system when added at concentrations above 100  $\mu\text{M}$ . Several previous studies stated that linoleic acid has a critical micelle

concentration (CMC) of 150  $\mu\text{M}$  at pH 9 (in borate buffer at 20  $^{\circ}\text{C}$ ) and less than 100  $\mu\text{M}$  at pH 6.3 and 8 [25, 26]. In addition, it was observed that CMC at pH 7.4 and 37  $^{\circ}\text{C}$  was 75  $\mu\text{M}$  (Murphy E. J, personal communication). The scattered intensity was measured at a right angle with respect to the source (820 nm diode laser) with a photon correlation spectrometer Dyna-Pro MS/X. The temperature in the cell was set at 37  $^{\circ}\text{C}$ . Prior to each measurement, the sample was passed through 0.45  $\mu\text{m}$  nylon syringe filters. We did not detect the sharp increase in the scattered intensity typical of micellization within the range 0–500  $\mu\text{M}$  of linoleic acid. This led us to conclude that, under our experimental conditions (DMEM-1% FBS, pH = 7.4, 37  $^{\circ}\text{C}$ ), the linoleic acid must be in its monomer form, and that the critical micellar concentration (CMC) is higher than 500  $\mu\text{M}$  (data not shown). The differences between our data and the aforementioned studies could be due to the presence of FBS in our system, which could minimize the impact of micelles and perhaps reduce their formation.

## Statistical Analysis

Glucose utilization was assessed by measuring the concentration of glucose in the media at 96 h and subtracting the value from the initial glucose concentration. Lactate production was calculated as the increase of media lactate at 96 h. The amount of carbon released as lactate per amount of carbon taken up as glucose over 96 h was calculated as  $\Delta[\text{lactate}]/\Delta[\text{glucose}]$  where  $\Delta$  is the difference, and was expressed as a percentage. In order to check if our data followed a normal distribution, two different methods (Kolmogorov–Smirnov and the Shapiro–Wilk tests) were used (SPSS/Windows version 11.0, SPSS Inc., Chicago, USA). The experimental results from each adipocyte suspension prepared from a single animal were analyzed in relation to a control well from the same suspension. For this reason, the statistical analysis of the data was performed by repeated measures ANOVA followed by a Dunnett's post-test (GraphPad Prism, GraphPad Software Inc., San Diego, CA, USA). Results were also analyzed and expressed as the percentage of the control. Differences were set as statistically significant at  $P < 0.05$ .

## Results

### Effects of Linoleic Acid on Leptin Expression and Secretion

Incubation of adipocytes over 96 h with linoleic acid (1–200  $\mu\text{M}$ ) did not modify basal leptin secretion as compared with control cells (Fig. 1a). As expected, insulin at 1.6 nM increased ( $P < 0.01$ ) leptin secretion by  $\sim 80\%$

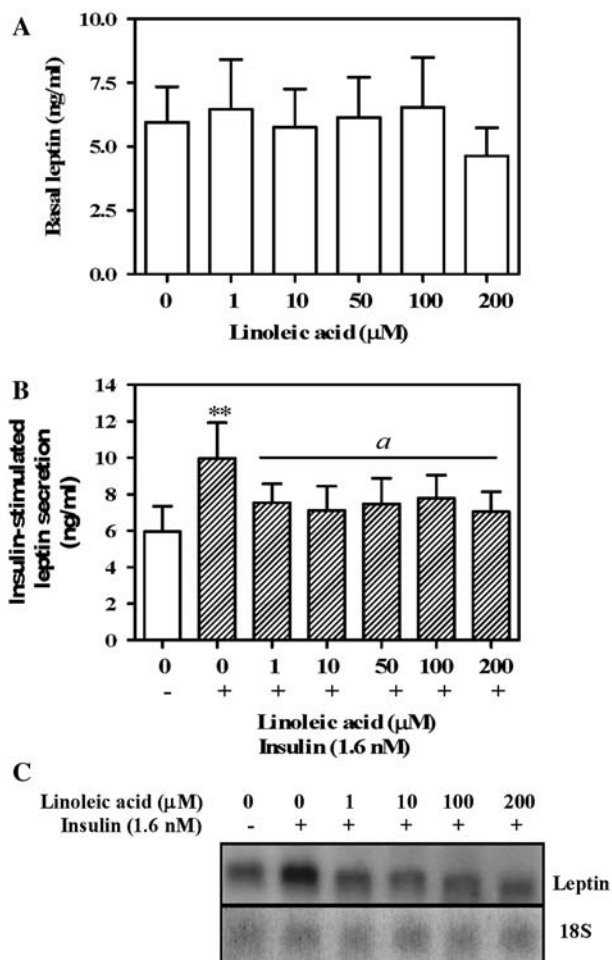


**Fig. 1** Effects of linoleic acid (1–200 μM) on basal (a) and insulin-stimulated (b) leptin secretion by isolated rat adipocytes over 96 h in culture ( $n = 6$ , mean  $\pm$  SE)  $**P < 0.01$  versus control (cells without linoleic and insulin treatment) and  $^aP < 0.05$  versus cells incubated with insulin alone. Effects of linoleic acid (1–200 μM) on insulin-stimulated leptin mRNA expression, as assessed by northern blots (c). The expression level of 18S ribosomal RNA was determined and used as an internal control to correct minor variation in total RNA amount. Results are representative of at least two independent experiments

( $5.94 \pm 1.39$  vs.  $9.96 \pm 1.95$  ng/ml). Linoleic acid in the presence of insulin significantly decreased ( $P < 0.05$ ) leptin secretion by 15 to  $\sim 25\%$  at all concentrations tested (1–200 μM) (Fig. 1b). The patterns of linoleic acid's effects on leptin gene expression at 96 h of treatment were similar to those observed for leptin secretion; insulin-stimulated leptin gene expression was decreased by treatment with all concentrations of linoleic acid (Fig. 1c).

#### Effects of Linoleic Acid on Adiponectin Secretion

Linoleic acid at the concentration of 200 μM induced a significant decrease ( $P < 0.05$ ) by  $\sim 20\%$  in adiponectin secretion in presence of 1.6 nM insulin ( $277.7 \pm 99.4$  vs.

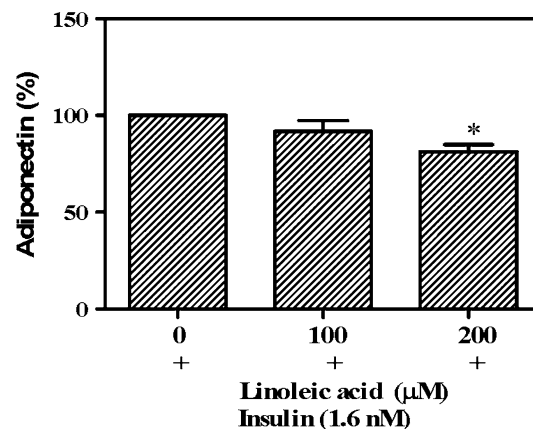


**Fig. 2** Effects of linoleic acid (100 and 200 μM) on adiponectin secretion by isolated rat adipocytes in presence of 1.6 nM insulin. ( $n = 3$ , mean  $\pm$  SE, expressed as percentage of the cells incubated with insulin alone).  $*P < 0.05$  versus insulin treated cells

$226.6 \pm 86.2$  ng/ml) (Fig. 2), while no significant changes were observed in adiponectin secretion in the absence of insulin (data not shown).

#### Effects of Linoleic Acid on Glucose Utilization and Metabolism

Linoleic acid did not affect glucose utilization and metabolism. Thus, this fatty acid did not modify either glucose uptake or lactate production in the presence of insulin at any of the concentrations tested (Fig. 3a, b). Thus, although a small decrease in glucose uptake was observed after treatment with 200 μM of linoleic acid ( $\sim 10\%$ ), it did not reach statistical significance. Furthermore, the proportion of glucose carbon metabolized to and released as lactate over 96 h was not affected by linoleic acid in presence of insulin at any of the assayed concentrations (Fig. 3c).

#### Discussion

Several in vivo studies have observed that a high fat diet rich in linoleic acid (safflower oil diet) induced a significant increase in epididymal and perirenal adipose tissues and also in leptin gene expression in comparison with a low-fat diet (as expected), while other high-fat diets rich in gamma-linolenic acid or in omega-3 fatty acids failed to do so [22, 27]. These observations suggest that although the adiposity is lower in all these diets rich in polyunsaturated fatty acids (linoleic acid, gamma linolenic acid or n-3 fatty acids) compared to the saturated fat rich diets as previously reported [8–11], the magnitude of their effects on adiposity vary.



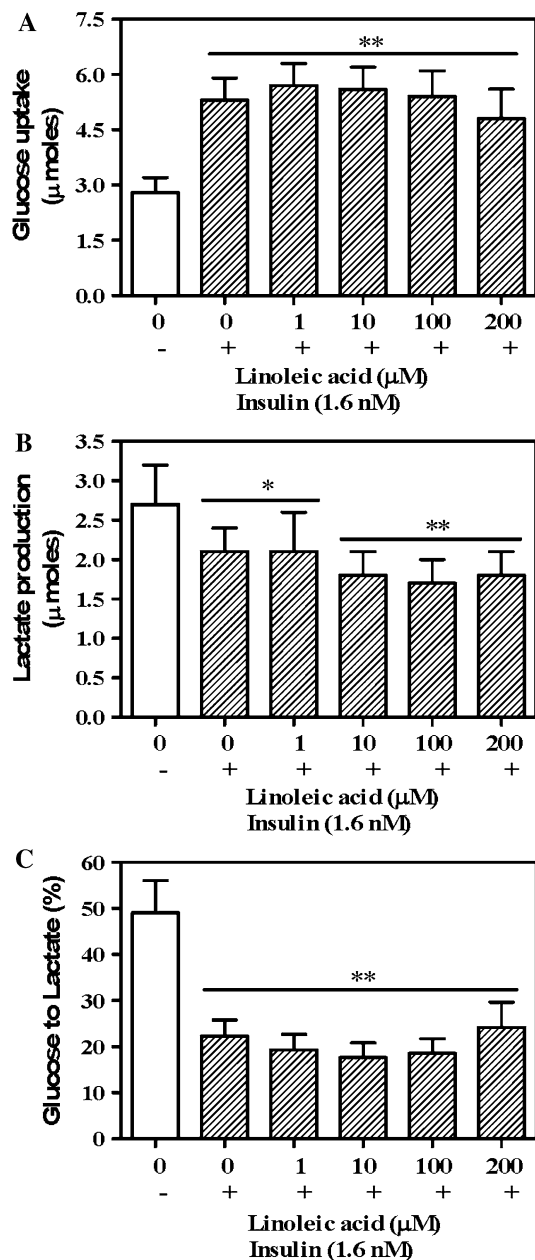


**Fig. 3** Effects of linoleic acid (1–200 μM) on glucose uptake (a) lactate production (b) and the percentage of glucose carbon released as lactate (c) by isolated adipocytes over 96 h in culture. ( $n = 5$ , mean  $\pm$  SE) \* $P < 0.05$ ; \*\* $P < 0.01$  versus control (cells without linoleic acid and insulin treatment)

In the current study, we examined the direct effects of linoleic acid on leptin gene expression and secretion in primary cultured rat adipocytes, and observed that linoleic acid (1–200 μM) did not show any significant effect on basal leptin secretion and gene expression. Kang and Pariza [28] also observed a lack of effect of linoleic acid on basal leptin secretion in 3T3-L1 adipocytes and a study from Hutley et al. [29] also supports our results as they demonstrated minimal leptin gene expression changes in

human fat cell precursors after linoleic acid treatment (100 μM). These data suggest that the increased leptin mRNA levels observed in the aforementioned in vivo studies [22, 27] seem not to be due to a direct action of the fatty acid on leptin gene, but could be secondary to the increase observed in the white adipose tissue fat pads. Interestingly, the lack of effects on basal leptin secretion has been also described for other 18 carbons chain fatty acids such as oleic acid and  $\gamma$ -linoleic acid, as reported in the study of Cammisotto et al. [30]. However, a recent study by our group demonstrated that CLA (a group of positional and geometric isomers of linoleic acid) inhibited basal leptin production in primary cultured rat adipocytes [31]. Furthermore, several in vivo studies have showed that diets supplemented with CLA reduced body fat mass and also decreased circulating concentrations and adipose mRNA levels of leptin in rodents [32–35]. Therefore, the different actions observed on basal leptin production between linoleic acid and its isomers (CLA) suggest that the positional and geometric differences between the acids contribute specifically to their actions on leptin production.

On the other hand, both arachidonic acid (20:4n-6) and palmitic acid (16:0) have been reported to inhibit basal leptin secretion and expression in rat adipocytes [23, 30, 36] similarly to what was observed for CLA. In contrast, eicosapentaenoic acid (20:5n-3) (10–200 μM) showed a significant stimulatory effect on leptin production by cultured rat adipocytes [37].

Our present data also showed that the well-known stimulatory effect of insulin on leptin gene expression and secretion was prevented by linoleic acid at all concentrations tested (1–200 μM). Levy et al. [38] published that basal and insulin-stimulated leptin secretion are regulated by independent mechanisms. These observations could indicate that linoleic acid interfered only with the mechanisms involved in the stimulation of leptin production by insulin and not with those involved in basal leptin secretion. It has been demonstrated [19, 39, 40] that insulin-stimulated glucose metabolism rather than insulin per se is a major determinant of leptin production in both rodents and humans. Thus, inhibitors of glucose uptake and metabolism inhibit insulin-stimulated leptin secretion in proportion to their metabolic effects [19]. Takahashi and Ide [22] observed a down-regulation of the glucose transporter 4 (insulin-dependent glucose transporter-4) mRNA levels in white adipose tissue after feeding animals with a high safflower oil diet, suggesting a decrease in the insulin-stimulated glucose uptake by the adipocytes. In addition, Hutley et al. [29] also observed a significant decrease in insulin-stimulated glucose uptake after 100 μM linoleic acid treatment in human preadipocytes. These results suggest that the inhibitory actions of linoleic acid on insulin-stimulated leptin secretion could be secondary,

at least in part, to a decrease in glucose uptake. However, in the present study we did not find significant changes in insulin-stimulated glucose utilization. Previous reports showed that leptin secretion is inversely related to the proportion of glucose that is metabolized to lactate [19, 23, 41, 42]. In fact, the inhibitory actions of CLA and the n-6 arachidonic acid on insulin-stimulated leptin production were correlated with the increase observed in the anaerobic metabolism of glucose to lactate [23, 31]. However, in the present study, neither lactate production nor the percentage of glucose that was anaerobically metabolized to lactate were affected by incubation with linoleic acid, suggesting that other mechanisms are involved in the inhibitory actions of linoleic acid on insulin-stimulated leptin production. Thus, the current data suggest that linoleic acid and its isomers act on the adipocyte metabolism in a different way. Furthermore, although both linoleic and arachidonic acid are n-6 fatty acids, their actions on glucose metabolism and leptin production seem to be different.

Circulating adiponectin concentrations are reduced in obese individuals and negatively correlated with increasing adiposity in humans and animals [18, 43–45]. However, there are no studies on the potential direct effects of linoleic acid on adiponectin production by cultured adipocytes. Thus, in the present study, we demonstrated for the first time that linoleic acid had no effects on basal adiponectin secretion (as observed with leptin) but it inhibited adiponectin secretion in the presence of insulin at the highest concentration tested (200  $\mu\text{M}$ ). Again, the results herein described are in contrast to those observed with the CLA, which inhibited basal adiponectin secretion (50–200  $\mu\text{M}$ ) but, on the other hand, it did not affect the adiponectin secretion in the presence of insulin [31]. Furthermore, the inhibitory action of linoleic acid on adiponectin secretion in the presence of insulin were less potent than that observed on insulin-stimulated leptin secretion, which was detected from the lowest concentration of linoleic acid tested (1  $\mu\text{M}$ ), suggesting that linoleic acid specially interfered with the mechanisms involved in the regulation of leptin production by insulin.

The biological actions of insulin in the adipose tissue are mediated by high-affinity cell-surface receptors with intrinsic tyrosine kinase activity [46]. Binding of insulin to its transmembrane receptor leads to the activation of two major signalling cascades, the Akt and the Erk pathways, which mediate most metabolic and transcriptional effects of insulin in adipocytes [47]. Gao et al. [48] observed in their study that linoleic acid (300  $\mu\text{M}$ ) induced insulin resistance in 3T3-L1 adipocytes by decreasing insulin-stimulated glucose uptake and also inducing a serine phosphorylation in IRS-1 [48]. However, the lack of effects of linoleic acid on insulin-stimulated glucose uptake observed in the present study could suggest that this fatty acid

did not interfere with the Akt pathway which is responsible for the glucose uptake. On the contrary, linoleic acid might interfere with the Erk pathway, which has also been involved in the regulation of leptin and adiponectin production [47, 49].

In summary, our data showed a direct inhibitory effect of linoleic acid on leptin and, to a lower extent, on adiponectin production in the presence of insulin. These linoleic acid actions do not seem to be related to alterations in adipocyte glucose uptake and metabolism. The inhibition of leptin and adiponectin production by linoleic acid could also contribute to a decrease in whole-body insulin sensitivity, as suggested by previous studies in humans.

**Acknowledgments** This work was supported in part by the Government of Navarra (Department of Education and Culture) and Línea Especial de Investigación “Nutrición, Obesidad y Salud” (University of Navarra). P. Pérez-Matute was supported by a doctoral grant from “Instituto Danone” (Spain) and Asociación de Amigos de la Universidad de Navarra. We thank Dr. Peter. J. Havel, Kimber Stanhope (Department of Nutrition, University of California, Davis, CA, USA) and Dr. Gustavo González-Gaitano (Department of Physical Chemistry, University of Navarra, Pamplona, Spain) for their scientific advice. The expert technical assistance of A. Lorente and V. Ciáurriz is gratefully acknowledged.

## References

1. Khor GL (2004) Dietary fat quality: a nutritional epidemiologist's view. *Asia Pac J Clin Nutr* 13:S22
2. Bray GA, Lovejoy JC, Smith SR, DeLany JP, Lefevre M, Hwang D, Ryan DH, York DA (2002) The influence of different fats and fatty acids on obesity, insulin resistance and inflammation. *J Nutr* 132:2488–2491
3. Riccardi G, Giacco R, Rivellese AA (2004) Dietary fat, insulin sensitivity and the metabolic syndrome. *Clin Nutr* 23:447–456
4. Kraegen EW, Clark PW, Jenkins AB, Daley EA, Chisholm DJ, Storlien LH (1991) Development of muscle insulin resistance after liver insulin resistance in high-fat fed rats. *Diabetes* 40:1397–1403
5. Oakes ND, Cooney GJ, Camilleri S, Chisholm DJ, Kraegen EW (1997) Mechanisms of liver and muscle insulin resistance induced by chronic high-fat feeding. *Diabetes* 46:1768–1774
6. Roche HM, Gibney MJ (2000) Effect of long-chain n-3 polyunsaturated fatty acids on fasting and postprandial triacylglycerol metabolism. *Am J Clin Nutr* 71:232S–237S
7. Storlien LH, Kraegen EW, Chisholm DJ, Ford GL, Bruce DG, Pascoe WS (1987) Fish oil prevents insulin resistance induced by high-fat feeding in rats. *Science* 237:885–888
8. Cha MC, Jones PJ (1998) Dietary fat type and energy restriction interactively influence plasma leptin concentration in rats. *J Lipid Res* 39:1655–1660
9. Shimomura Y, Tamura T, Suzuki M (1990) Less body fat accumulation in rats fed a safflower oil diet than in rats fed a beef tallow diet. *J Nutr* 120:1291–1296
10. Dulloo AG, Mensi N, Seydoux J, Girardier L (1995) Differential effects of high-fat diets varying in fatty acid composition on the efficiency of lean and fat tissue deposition during weight recovery after low food intake. *Metabolism* 44:273–279
11. Matsuo T, Takeuchi H, Suzuki H, Suzuki M (2002) Body fat accumulation is greater in rats fed a beef tallow diet than in rats

- fed a safflower or soybean oil diet. *Asia Pac J Clin Nutr* 11:302–308
12. Ailhaud G, Massiera F, Weill P, Legrand P, Alessandri JM, Guesnet P (2006) Temporal changes in dietary fats: role of n-6 polyunsaturated fatty acids in excessive adipose tissue development and relationship to obesity. *Prog Lipid Res* 45:203–236
  13. Rodriguez-Cruz M, Tovar AR, del Prado M, Torres N (2005) Molecular mechanisms of action and health benefits of polyunsaturated fatty acids. *Rev Invest Clin* 57:457–472
  14. Yam D, Eliraz A, Berry EM (1996) Diet and disease—the Israeli paradox: possible dangers of a high omega-6 polyunsaturated fatty acid diet. *Isr J Med Sci* 32:1134–1143
  15. Simopoulos AP (1994) Is insulin resistance influenced by dietary linoleic acid and trans fatty acids? *Free Radic Biol Med* 17:367–372
  16. Vessby B (2000) Dietary fat and insulin action in humans. *Br J Nutr* 83(Suppl 1):S91–S96
  17. Marti A, Berraondo B, Martinez JA (1999) Leptin: physiological actions. *J Physiol Biochem* 55:43–49
  18. Stefan N, Bunt JC, Salbe AD, Funahashi T, Matsuzawa Y, Tataranni PA (2002) Plasma adiponectin concentrations in children: relationships with obesity and insulinemia. *J Clin Endocrinol Metab* 87:4652–4656
  19. Mueller WM, Gregoire FM, Stanhope KL, Mobbs CV, Mizuno TM, Warden CH, Stern JS, Havel PJ (1998) Evidence that glucose metabolism regulates leptin secretion from cultured rat adipocytes. *Endocrinology* 139:551–558
  20. Fasshauer M, Klein J, Neumann S, Eszlinger M, Paschke R (2002) Hormonal regulation of adiponectin gene expression in 3T3-L1 adipocytes. *Biochem Biophys Res Commun* 290:1084–1089
  21. Halleux CM, Takahashi M, Delporte ML, Detry R, Funahashi T, Matsuzawa Y, Brichard SM (2001) Secretion of adiponectin and regulation of apM1 gene expression in human visceral adipose tissue. *Biochem Biophys Res Commun* 288:1102–1107
  22. Takahashi Y, Ide T (2000) Dietary n-3 fatty acids affect mRNA level of brown adipose tissue uncoupling protein 1, and white adipose tissue leptin and glucose transporter 4 in the rat. *Br J Nutr* 84:175–184
  23. Perez-Matute P, Marti A, Martinez JA, Moreno-Aliaga MJ (2003) Effects of arachidonic acid on leptin secretion and expression in primary cultured rat adipocytes. *J Physiol Biochem* 59:201–208
  24. Moreno-Aliaga MJ, Martinez JA, Stanhope KL, Fernandez-Otero MP, Havel PJ (2002) Effects of treading, a beta3-adrenergic agonist, on leptin secretion, glucose and lipid metabolism in isolated rat adipocytes. *Int J Obes Relat Metab Disord* 26:912–919
  25. Lagocki JW, Emken EA, Law JH, Kezdy FJ (1976) Kinetic analysis of the action of soybean lipoxygenase on linoleic acid. *J Biol Chem* 251:6001–6006
  26. Lopez-Nicolas JM, Bru R, Sanchez-Ferrer A, Garcia-Carmona F (1995) Use of “soluble lipids” for biochemical processes: linoleic acid-cyclodextrin inclusion complexes in aqueous solutions. *Biochem J* 308(Pt 1):151–154
  27. Takahashi Y, Ide T, Fujita H (2000) Dietary gamma-linolenic acid in the form of borage oil causes less body fat accumulation accompanying an increase in uncoupling protein 1 mRNA level in brown adipose tissue. *Comp Biochem Physiol B* 127:213–222
  28. Kang K, Pariza MW (2001) *trans*-10,*cis*-12-conjugated linoleic acid reduces leptin secretion from 3T3-L1 adipocytes. *Biochem Biophys Res Commun* 287:377–382
  29. Hutley LJ, Newell FM, Joyner JM, Suchting SJ, Herington AC, Cameron DP, Prins JB (2003) Effects of rosiglitazone and linoleic acid on human preadipocyte differentiation. *Eur J Clin Invest* 33:574–581
  30. Cammisotto PG, Gelinas Y, Deshaies Y, Bukowiecki LJ (2003) Regulation of leptin secretion from white adipocytes by free fatty acids. *Am J Physiol Endocrinol Metab* 285:E521–E526
  31. Perez-Matute P, Marti A, Martínez JA, Fernandez-Otero MP, Stanhope KL, Havel PJ, Moreno-Aliaga MJ (2007) Conjugated linoleic acid inhibits glucose metabolism, leptin and adiponectin secretion in primary cultured rat adipocytes. *Mol Cell Endocrinol* 268:50–58
  32. Yamasaki M, Ikeda A, Oji M, Tanaka Y, Hirao A, Kasai M, Iwata T, Tachibana H, Yamada K (2003) Modulation of body fat and serum leptin levels by dietary conjugated linoleic acid in Sprague–Dawley rats fed various fat-level diets. *Nutrition* 19(1):30–35
  33. Wang YW, Jones PJ (2004) Conjugated linoleic acid and obesity control: efficacy and mechanisms. *Int J Obes Relat Metab Disord* 28(8):941–955
  34. Ohashi A, Matsushita Y, Kimura K, Miyashita K, Saito M (2004) Conjugated linoleic acid deteriorates insulin resistance in obese/diabetic mice in association with decreased production of adiponectin and leptin. *J Nutr Sci Vitaminol (Tokyo)* 50:416–421
  35. Poirier H, Rouault C, Clement L, Niot I, Monnot MC, Guerre-Millo M, Besnard P (2005) Hyperinsulinaemia triggered by dietary conjugated linoleic acid is associated with a decrease in leptin and adiponectin plasma levels and pancreatic beta cell hyperplasia in the mouse. *Diabetologia* 48:1059–1065
  36. Shintani M, Nishimura H, Yonemitsu S, Masuzaki H, Ogawa Y, Hosoda K, Inoue G, Yoshimasa Y, Nakao K (2000) Downregulation of leptin by free fatty acids in rat adipocytes: effects of triacsin C, palmitate, and 2-bromopalmitate. *Metabolism* 49:326–330
  37. Perez-Matute P, Marti A, Martinez JA, Fernandez-Otero MP, Stanhope KL, Havel PJ, Moreno-Aliaga MJ (2005) Eicosapentaenoic fatty acid increases leptin secretion from primary cultured rat adipocytes: role of glucose metabolism. *Am J Physiol Regul Integr Comp Physiol* 288:R1682–R1688
  38. Levy JR, Gyarmati J, Lesko JM, Adler RA, Stevens W (2000) Dual regulation of leptin secretion: intracellular energy and calcium dependence of regulated pathway. *Am J Physiol Endocrinol Metab* 278:E892–E901
  39. Moreno-Aliaga MJ, Stanhope KL, Havel PJ (2001) Transcriptional regulation of the leptin promoter by insulin-stimulated glucose metabolism in 3t3-l1 adipocytes. *Biochem Biophys Res Commun* 283:544–548
  40. Wellhoener P, Fruehwald-Schultes B, Kern W, Dantz D, Kerner W, Born J, Fehm HL, Peters A (2000) Glucose metabolism rather than insulin is a main determinant of leptin secretion in humans. *J Clin Endocrinol Metab* 85:1267–1271
  41. Mueller WM, Stanhope KL, Gregoire F, Evans JL, Havel PJ (2000) Effects of metformin and vanadium on leptin secretion from cultured rat adipocytes. *Obes Res* 8:530–539
  42. Havel PJ (2000) Role of adipose tissue in body-weight regulation: mechanisms regulating leptin production and energy balance. *Proc Nutr Soc* 59:359–371
  43. Havel PJ (2004) Update on adipocyte hormones: regulation of energy balance and carbohydrate/lipid metabolism. *Diabetes* 53(Suppl 1):S143–S151
  44. Cnop M, Havel PJ, Utzschneider KM, Carr DB, Sinha MK, Boyko EJ, Retzlaff BM, Knopp RH, Brunzell JD, Kahn SE (2003) Relationship of adiponectin to body fat distribution, insulin sensitivity and plasma lipoproteins: evidence for independent roles of age and sex. *Diabetologia* 46:459–469
  45. Hotta K, Funahashi T, Bodkin NL, Ortmeier HK, Arita Y, Hansen BC, Matsuzawa Y (2001) Circulating concentrations of the adipocyte protein adiponectin are decreased in parallel with reduced insulin sensitivity during the progression to type 2 diabetes in rhesus monkeys. *Diabetes* 50:1126–1133

46. Cheatham B, Kahn CR (1995) Insulin action and the insulin signaling network. *Endocr Rev* 16:117–142
47. Laviola L, Perrini S, Cignarelli A, Giorgino F (2006) Insulin signalling in human adipose tissue. *Arch Physiol Biochem* 112:82–88
48. Gao Z, Zhang X, Zuberi A, Hwang D, Quon MJ, Lefevre M, Ye J (2004) Inhibition of insulin sensitivity by free fatty acids requires activation of multiple serine kinases in 3T3-L1 adipocytes. *Mol Endocrinol* 18:2024–2034
49. Bradley RL, Cheatham B (1999) Regulation of ob gene expression and leptin secretion by insulin and dexamethasone in rat adipocytes. *Diabetes* 48:272–278

## Dietary Virgin Olive Oil Reduces Oxidative Stress and Cellular Damage in Rat Brain Slices Subjected to Hypoxia–Reoxygenation

J. A. González-Correa · J. Muñoz-Marín ·  
M. M. Arrebola · A. Guerrero · F. Narbona ·  
J. A. López-Villodres · J. P. De La Cruz

Received: 28 March 2007 / Accepted: 2 July 2007 / Published online: 7 August 2007  
© AOCS 2007

**Abstract** We investigated how virgin olive oil (VOO) affected platelet and hypoxic brain damage in rats. Rats were given VOO orally for 30 days at 0.25 or 0.5 mL kg<sup>-1</sup> per day (doses A and B, respectively). Platelet aggregation, thromboxane B<sub>2</sub>, 6-keto-PGF<sub>1α</sub>, and nitrites + nitrates were measured, and hypoxic damage was evaluated in a hypoxia–reoxygenation assay with fresh brain slices. Oxidative stress, prostaglandin E<sub>2</sub>, nitric oxide pathway activity and lactate dehydrogenase (LDH) activity were also measured. Dose A inhibited platelet aggregation by 36% and thromboxane B<sub>2</sub> by 19%; inhibition by dose B was 47 and 23%, respectively. Virgin olive oil inhibited the reoxygenation-induced increase in lipid peroxidation (57% in control rats vs. 2.5% (*P* < 0.05) in treated rats), and reduced the decrease in glutathione concentration from 67 to 24% (dose A) and 41% (dose B). Brain prostaglandin E<sub>2</sub> after reoxygenation was 306% higher in control animals, but the increases in treated rats were only 53% (dose A) and 45% (dose B). The increases in nitric oxide production (213% in controls) and activity of the inducible isoform of nitric oxide synthase (175% in controls) were both smaller in animals given VOO

(dose A 84%; dose B 12%). Lactate dehydrogenase activity was reduced by 17% (dose A) and 42% (dose B). In conclusion, VOO modified processes related to thrombogenesis and brain ischemia. It reduced oxidative stress and modulated the inducible isoform of nitric oxide synthase, diminishing platelet aggregation and protecting the brain from the effects of hypoxia–reoxygenation.

**Keywords** Olive oil · Platelets · Oxidative stress · Nitric oxide · Brain

### Abbreviations

cNOS	Constitutive isoform of nitric oxide synthase
GSH	Reduced glutathione
GSSG	Oxidized glutathione
GSHpx	Glutathione peroxidase
GSHtf	Glutathione transferase
iNOS	Inducible isoform of nitric oxide synthase
LDH	Lactate dehydrogenase
NO	Nitric oxide
NOS	Nitric oxide synthase
NO <sub>2</sub> <sup>-</sup> + NO <sub>3</sub> <sup>-</sup>	Plasma nitrite + nitrate
PGE <sub>2</sub>	Prostaglandin E <sub>2</sub>
TxB <sub>2</sub>	Thromboxane B <sub>2</sub>
TBARS	Thiobarbituric acid reactive substances
VOO	Virgin olive oil

This study was partially supported by a grant from the Ministerio de Ciencia y Tecnología, Spain (AGL-04-7935-C03-02).

J. A. González-Correa · J. Muñoz-Marín ·  
A. Guerrero · F. Narbona · J. A. López-Villodres ·  
J. P. De La Cruz (✉)

Laboratorio de Investigaciones Antitrombóticas e Isquemia Tisular (LIAIT), Department of Pharmacology, School of Medicine, University of Málaga, Campus de Teatinos s/n, 29071 Málaga, Spain  
e-mail: jpcruz@uma.es

M. M. Arrebola  
Clinical Laboratory, Hospital Universitario Carlos Haya,  
Málaga, Spain

### Introduction

Scientific evidence from several sources has accumulated on the beneficial effects of the Mediterranean diet in

preventing cardiovascular disease [1–3] and cancer [4], and in reducing overall mortality [4, 5]. The nutritional guidelines of several international scientific organizations now recommend a healthy diet compatible with the main characteristics of the “Mediterranean diet model” [6, 7] to prevent cardiovascular disease, obesity, diabetes, cancer, and other conditions related to oxidation processes [8, 9]. The benefits of the Mediterranean diet have been attributed, in part, to the antioxidant effect of some of its components. A key component of this diet is olive oil, which contains monounsaturated fatty acids and polyphenols, compounds with a clear antioxidant effect [10].

In humans several factors are involved in the process of brain ischemia. A key event, in which platelet and endothelial functions play a major role, is the formation of an arterial thrombus. Another key factor is the activation of biochemical pathways such as oxidative stress and the nitric oxide pathway, which lead to irreversible neuronal damage [11, 12].

Because of its importance in the Mediterranean diet, olive oil may be a key element in the prevention of cardiovascular disease; we therefore wished to examine its effect on these biochemical pathways. The objective of this study was to investigate, in rats, how virgin olive oil (VOO) consumed as part of the diet affected basic mechanisms of brain ischemia, i.e. platelet and endothelial functions and biochemical pathways that are activated at a tissue level during this process.

## Experimental Procedures

### Materials

Lactate dehydrogenase reagent kits were obtained from Biosystem (Barcelona, Spain). L-[<sup>3</sup>H]Arginine, thromboxane B<sub>2</sub>, 6-keto-prostaglandin F<sub>1α</sub> and prostaglandin E<sub>2</sub> enzyme immunoassay kits were from Amersham International (Little Chalfont, Buckinghamshire, UK). The nitrite/nitrate ELISA kit was obtained from Cayman Chemical (Ann Arbor, MI, USA). All other reagents were from Sigma Chemical (St Louis, MO, USA). Olive oil used was VOO of the Hojiblanca variety and was purchased from local department stores. The composition of the VOO oil administered to rats is shown in Table 1.

### Study Design

The experimental animals ( $n = 45$ , 15 rats per group) were 2-month-old adult male Wistar rats (body weight 200–250 g). All rats were used in accordance with current Spanish legislation for animal care, use, and housing (RD 223/1998, based on European Directive 86/609/CEE). The

**Table 1** Main composition of the virgin olive oil administered to rats

Fatty acids	%
C16:0	14.7
C16:1	1.8
C17:0	0.09
C17:1	0.2
C18:0	2.1
C18:1	69.5
C18:2	10.0
C20:0	0.4
C18:3	0.7
C20:1	0.3
C22:0	0.1
C24:0	0.06
Total	100
Minor components	
Alpha-tocopherol (mg kg <sup>-1</sup> )	176
<i>ortho</i> -Diphenols (mmol kg <sup>-1</sup> )	0.19
Cholesterol (mg kg <sup>-1</sup> )	0.002
β-Sitosterol (mg kg <sup>-1</sup> )	1.4

recommendations in the Guide for the Care and Use of Laboratory Animals (NIH publication No. 86–23, revised 1985) were followed, and, where applicable, Spanish Law on the Protection of Animals. The study protocol was approved by the University of Malaga Ethics Committee for the Use of Animals. The rats were allocated randomly to three groups of 15 animals each:

control-group animals treated with daily saline p.o., studied for 30 days;

animals treated with 0.25 mL kg<sup>-1</sup> per day p.o. VOO for 30 days; and

animals treated with 0.5 mL kg<sup>-1</sup> per day p.o. VOO for 30 days.

Chow and water were self-administered ad libitum. Either saline or VOO were administered from 9:00 to 10:00 a.m. The last dose was administered 2 h before the animal was killed. We initiated treatment at a rate of two rats per day in order to process two rats per day at the end of the treatment period. The doses of VOO were chosen according to previously published data [13] by interpolation of the dose used in this study in healthy humans (25 mL day<sup>-1</sup>).

### Sample Processing

At the end of day 30 all animals from all groups were anesthetized with pentobarbital sodium (40 mg kg<sup>-1</sup> i.p.). A medial laparotomy was made to withdraw blood from the vena cava; 3% sodium citrate at a proportion of 1:10 was used as anticoagulant. The rats were decapitated with a

guillotine and the thoracic and abdominal aorta and brain were removed. Part of the blood was centrifuged at 2,000g for 10 min at 4°C, and the supernatant (plasma) was frozen at –80°C until the experiment.

#### In-vitro Model of Rat Brain Hypoxia–Reoxygenation

We used a previously described in-vitro method of hypoxia–reoxygenation in brain slices [14]. The cortex and midbrain were coronally cut into 1 mm slices with a vibrating microtome (Capdem Instruments, San Francisco, CA, USA). The slices were placed in buffer (composition mmol L<sup>-1</sup>: 100 NaCl, 0.05 KCl, 24 NaHCO<sub>3</sub>, 0.55 KH<sub>2</sub>PO<sub>4</sub>, 0.005 CaCl<sub>2</sub>, 2 MgSO<sub>4</sub>, 9.8 glucose, pH 7.4) and perfused with a mixture of 95% O<sub>2</sub> and 5% CO<sub>2</sub>. After 30 min to reach equilibrium the slices were placed in fresh buffer of the same composition except that the concentration of CaCl<sub>2</sub> was 3 mmol L<sup>-1</sup>, that of MgSO<sub>4</sub> was 0.001 mmol L<sup>-1</sup>, and no glucose was included. This solution was perfused with a mixture of 95% N<sub>2</sub> and 5% CO<sub>2</sub> for 20 min (hypoxia). The slices were then placed in fresh buffer containing glucose and the solution was perfused with a mixture of 95% O<sub>2</sub> and 5% CO<sub>2</sub> (reoxygenation).

Brain slices (two per analytical test) were analyzed:

1. after 30 min of incubation and before N<sub>2</sub> perfusion;
2. after 20 min of perfusion with N<sub>2</sub>; and
3. after 180 min of reoxygenation.

For all studies the tissues were quickly frozen in liquid nitrogen and stored at –80°C until the day of the experiment, which was conducted no longer than 7 days after freezing.

#### Analytical Techniques

All techniques were run in a single-blind manner, i.e. the persons who did the assays were unaware of the origin and nature of the samples. Some measurements (plasma glucose levels and the basic plasma lipid profile) were done automatically at the Analytical Laboratory, Hospital Universitario Carlos Haya, Málaga, Spain.

#### Platelet Aggregometry

Platelet aggregation in whole blood was tested at 37°C by the electrical impedance method (Chrono-Log aggregometer; Izasa, Madrid, Spain). Collagen (10 µg mL<sup>-1</sup>) was used as the inducing agent. All measurements were performed within 1 h of obtaining the blood. Maximum change in impedance after 10 min of induction was recorded as maximum intensity of platelet aggregation.

#### Platelet Thromboxane B<sub>2</sub> (TxB<sub>2</sub>)

After 10 min aggregation was complete; then 100 µmol L<sup>-1</sup> indomethacin was added and the blood sample was centrifuged at 10,000g for 5 min, and the supernatant was frozen at –80°C until quantification of thromboxane B<sub>2</sub> (stable thromboxane A<sub>2</sub> metabolite) with a commercial immunoenzyme assay kit. The entire process was performed within 1 h of obtaining the blood, and TxB<sub>2</sub> was measured within one week after freezing the samples. Automated cell counts (Cell Counter Baker 8000; Menarini, Barcelona, Spain) were obtained in whole blood before platelet aggregation started.

#### Vascular 6-Keto-Prostaglandin F<sub>1α</sub>

An aortic ring was incubated at 37°C in buffer containing (mmol L<sup>-1</sup>): 100 NaCl, 4 KCl, 25 NaHCO<sub>3</sub>, 2.1 Na<sub>2</sub>SO<sub>4</sub>, 20 sodium citrate, 2.7 glucose, and 50 Tris (pH 8.3), and calcium ionophore A23187 (1 µmol L<sup>-1</sup>) was added. Five minutes later the sample was dried and weighed, and the supernatant was frozen at –80°C until the assay. Production of 6-keto-prostaglandin F<sub>1α</sub> (stable metabolite of prostacyclin) was quantified with a commercial immunoenzyme assay kit.

#### Plasma Nitrite + Nitrate (NO<sub>2</sub><sup>-</sup> + NO<sub>3</sub><sup>-</sup>)

As an indirect indicator of overall nitric oxide (NO) production in each animal, we determined plasma nitrite + nitrate levels. Blood was centrifuged at 10,000g for 10 min, and the supernatant was filtered through Ultrafree MC microcentrifuge filters to remove hemoglobin released by cell lysis. The nitrite + nitrate level was measured with a commercial kit.

#### Lipid Peroxidation

To quantify lipid peroxidation we measured thiobarbituric acid-reactive substances (TBARS) [11] in cell membrane-enriched fractions [15]. Absorbance was determined spectrophotometrically at 532 nm (Perkin–Elmer, USA, C-532001 spectrophotometer). The results were expressed as µmol TBARS mg<sup>-1</sup> protein; the latter was determined by the method of Bradford et al. [16].

#### Glutathione Levels

Total glutathione was measured spectrofluorimetrically [17]. Brain tissue was homogenized in 0.1 mol L<sup>-1</sup> sodium phosphate buffer (pH 8.0) with 25% phosphoric acid in the proportion 1:20, then centrifuged at 13,000g for 15 min at

4°C to obtain the supernatant. Cuvettes were prepared for spectrofluorimetry with sodium phosphate buffer, the supernatant for each sample, and *o*-phthaldehyde. To determine the proportions of oxidized and reduced glutathione we incubated the supernatant from each sample with 4-vinylpyridine, then proceeded as for as total glutathione.

#### *Enzyme Activity Related to Glutathione*

Glutathione peroxidase (GSHpx) and glutathione transferase (GSHtf) were determined by spectrophotometric kinetics [18, 19]. Tissue samples were diluted with 0.1 mol L<sup>-1</sup> phosphate-buffered saline (pH 7.0) and 25% phosphoric acid. The mixture was homogenized and centrifuged at 13,000g for 15 min at 4°C. The supernatant was used to determine protein concentration after neutralization with 0.1 mol L<sup>-1</sup> NaOH, and to determine enzyme activity as described below.

#### *Glutathione Peroxidase*

A volume equivalent to 25 µg protein was taken from each supernatant and 0.1 mol L<sup>-1</sup> phosphate-buffered saline was added to a volume of 880 µL, together with 53 µL glutathione reductase, 133 µL GSH, 100 µL nicotinamide-adenine dinucleotide phosphate (NADPH), and 100 µL tertbutyl-hydroperoxide. The preparation was read at 340 nm and the decrease in absorbance was recorded every 30 s for 5 min.

#### *Glutathione Transferase*

One hundred microliters of GSH was added to the volumes of sample and buffer indicated above for glutathione peroxidase, and the test was conducted in the same way.

#### *Lactate Dehydrogenase (LDH) Assay*

Tissue damage was measured by examining the LDH efflux [20]. The enzyme activity was measured spectrophotometrically at 340 nm by recording oxidation of NADH in the presence of pyruvate.

#### *Brain Nitrite + Nitrate Concentration*

One milliliter of the perfusion buffer was used to determine nitrite + nitrate using the same method as in plasma.

#### *Nitric Oxide Synthase Activity (NOS)*

Samples were homogenized (1:5 w/v) in buffer containing 10 mmol L<sup>-1</sup> HEPES, 320 mmol L<sup>-1</sup> sucrose, 1 mmol L<sup>-1</sup>

EDTA, 1 mmol L<sup>-1</sup> DL-dithiothreitol (DTT), 10 µg mL<sup>-1</sup> leupeptin, and 2 µg mL<sup>-1</sup> aprotinin, at 0°C. The homogenates were centrifuged at 12,000g for 20 min at 4°C, and the supernatant was used to measure NOS synthase. Enzymatic reactions were tested at room temperature for 30 min with a mixture of 40 µL supernatant and 100 µL 40 mmol L<sup>-1</sup> potassium phosphate buffer (pH 7.0) consisting of 4.8 mmol L<sup>-1</sup> *dl*-valine, 1 mmol L<sup>-1</sup> NADPH, 1 mmol L<sup>-1</sup> MgCl<sub>2</sub>, 2 mmol L<sup>-1</sup> CaCl<sub>2</sub>, 20 µmol L<sup>-1</sup> L-arginine and 1.25 µL mL<sup>-1</sup> L-[<sup>3</sup>H]arginine (59 Ci per mole, Amersham Life Science). For each assay three parallel samples were run:

1. a sample prepared as described above;
2. a sample that included 1 mmol L<sup>-1</sup> <sup>14</sup>N-methyl-L-arginine (non-specific activity); and
3. a sample without calcium salts but containing 1 mmol L<sup>-1</sup> EDTA and 1 mmol L<sup>-1</sup> ethyleneglycol-tetraacetic acid (EGTA).

In all cases the reaction was stopped by adding cold buffer consisting of 0.2 mmol L<sup>-1</sup> EDTA. The samples were assayed with 50W-XA Dowex resin columns (Na<sup>+</sup> form). One hundred microliters of supernatant was added to 5 mL scintillation fluid, and counts per minute (cpm) were recorded.

#### *Quantification of Prostaglandin E<sub>2</sub> (PGE<sub>2</sub>)*

The samples were homogenized (1:10 w/v) in 15% methanol with 0.1 mol L<sup>-1</sup> phosphate-buffered saline (pH 7.5), then centrifuged at 37,000g for 15 min at 4°C. The supernatant was run through a C<sub>18</sub> column (Bio-Rad Laboratories, Hercules, CA, USA). Prostaglandins were eluted with methyl formate. The samples were then dried under a nitrogen current and reconstituted with phosphate-buffered saline. The concentration of PGE<sub>2</sub> was measured with a commercial enzyme immunoassay (Amersham International).

#### *Statistical Methods*

The data in the text, tables, and figures are expressed as the mean ± standard error of the mean for 15 animals or measurements. All statistical analysis was performed with the Statistical Program for Social Sciences v. 12.0 (SPSS, Chicago, IL, USA). One-way analysis of variance followed by Bonferroni transformation and paired Student's *t* test were used, and differences were considered significant when *P* < 0.05.



## Results

### Basic Parameters

After 1 month of treatment with VOO there were no statistically significant differences between groups in basic zoometric parameters, blood glucose levels, and plasma lipid profiles (Table 2).

### Platelet and Endothelium Biomarkers

Collagen-induced platelet aggregation was inhibited by VOO at 0.25 (36.1% inhibition with respect to the control group) and 0.5 (47.3% inhibition) mL kg<sup>-1</sup> per day p.o. Platelet production of thromboxane B<sub>2</sub> was significantly inhibited by VOO at 0.25 (19.5% inhibition) and 0.5 mL kg<sup>-1</sup> per day (26.3% inhibition) with respect to the control group. Aortic 6-keto-PGF<sub>1α</sub> did not change significantly after treatment with VOO. The thromboxane/prostacyclin ratio was significantly reduced after both 0.25 (19.0%) and 0.5 (33.2%) mL kg<sup>-1</sup> per day p.o. Plasma nitrite + nitrate concentration did not change after 30 days of treatment with VOO (Table 3).

### Biochemical Changes in Rat Brain Slices after Hypoxia–Reoxygenation

After 20 min of hypoxia the differences for all parameters were not statistically significant in comparison to pre-hypoxic values. The results obtained after reoxygenation will therefore be reported below. In brain slices subjected to hypoxia–reoxygenation there was an increase in TBARS production, which rose by 57.8 ± 7.0% after 180 min of reoxygenation in comparison with the pre-hypoxia value. Reduced glutathione levels decreased by 67.2 ± 5.7%. The percentage of oxidized glutathione increased by

31.5 ± 3.5%, and GSHpx activity increased by 7.6 ± 0.4%, whereas GSHtf activity decreased by 31.1 ± 3.1%. Brain PGE<sub>2</sub> production was 3.06-fold the pre-hypoxic values. Nitrite + nitrate concentration increased by 213 ± 45%, cNOS activity decreased by 77.1 ± 8.3%, and iNOS activity increased by 175 ± 19%. Efflux of LDH into the incubation medium increased by 96.8 ± 9% after 180 min of reoxygenation (Fig. 1; Table 4).

### Effects of Virgin Olive Oil in the Brain Hypoxia–Reoxygenation Model

None of the parameters measured in pre-hypoxic brain slices (baseline values) differed significantly between rats that were given VOO and untreated animals. The increase in TBARS concentration after reoxygenation was almost completely abolished in rats treated with VOO; with respect to reoxygenated slices from untreated rats the increases were 2.7% after dose A, and 2.5% after dose B (Table 4). The reduction in reduced glutathione after reoxygenation was significantly smaller in rats given VOO (41% after 0.25 mL kg<sup>-1</sup> per day and 24% after 0.5 mL kg<sup>-1</sup> per day) than in untreated rats (Table 4). The increase in the percentage of oxidized glutathione after reoxygenation was similar in rats given VOO and in untreated animals (*P* > 0.05 with respect to the control group) (Table 4). The increase in GSHpx activity did not differ significantly with respect to untreated rats, and the reduction in GSHtf was not modified (Table 4). The increase in NO production in brain slices after reoxygenation in rats treated with VOO at 0.5 mL kg<sup>-1</sup> per day p.o. was significantly lower (84 ± 9% with respect to pre-hypoxic values) than in the control group. Moreover, the reduction in cNOS activity observed in untreated rats was smaller in VOO-treated rats (53 ± 6% after 0.25 and 50 ± 5% after 0.5 mL kg<sup>-1</sup> per day, respectively), and the increase in

**Table 2** Mean values ± SEM of basic zoometric and plasma lipid parameters in control rats and animals treated with virgin olive oil at 0.25 or 0.5 mL kg<sup>-1</sup> per day p.o. during 30 days

	Virgin olive oil (mL kg <sup>-1</sup> per day p.o. for 30 days)		
	0	0.25	0.5
Baseline body weight (g)	223 ± 6.5	221 ± 5.7	223 ± 6.0
Increase in body weight (g) <sup>a</sup>	71.9 ± 4.3	70.1 ± 3.8	79.7 ± 5.1
Rate of chow ingestion (g day <sup>-1</sup> )	39.7 ± 0.7	38.3 ± 1.2	38.4 ± 1.2
Glucose (mmol L <sup>-1</sup> )	5.4 ± 0.3	5.5 ± 0.2	5.3 ± 0.2
Total cholesterol (mmol L <sup>-1</sup> )	1.5 ± 0.06	1.4 ± 0.08	1.4 ± 0.07
HDL-cholesterol (mmol L <sup>-1</sup> )	0.7 ± 0.04	0.7 ± 0.03	0.9 ± 0.06
Triacylglycerols (mmol L <sup>-1</sup> )	1.8 ± 0.2	1.9 ± 0.2	2.0 ± 0.2
Ratio total cholesterol/HDL-cholesterol	2.0 ± 0.2	2.0 ± 0.3	1.6 ± 0.2

<sup>a</sup> Difference between body weight after 30 days of treatment and initial body weight

*n* = 15 rats per group

**Table 3** Mean values  $\pm$  SEM for platelet and endothelium biomarkers in control rats and animals treated with virgin olive oil at 0.25 or 0.5 mL kg<sup>-1</sup> per day p.o. during 30 days

	Virgin olive oil (mL kg <sup>-1</sup> per day p.o. for 30 days)		
	0	0.25	0.5
$I_{\max}$ (ohms)	11.5 $\pm$ 0.7	7.4 $\pm$ 0.3***	6.1 $\pm$ 0.9***
TxB <sub>2</sub> (nmol per 10 <sup>9</sup> platelets)	266 $\pm$ 5.1	214 $\pm$ 2.9**	196 $\pm$ 2.9**
6-keto-PGF <sub>1<math>\alpha</math></sub> (ng mg <sup>-1</sup> aorta)	153 $\pm$ 6.8	150 $\pm$ 3.3	168 $\pm$ 12.4
TxB <sub>2</sub> /6-keto-PGF <sub>1<math>\alpha</math></sub> ratio	1.72 $\pm$ 0.2	1.40 $\pm$ 0.1*	1.1 $\pm$ 0.1**
NO <sub>2</sub> <sup>-</sup> + NO <sub>3</sub> <sup>-</sup> ( $\mu$ mol L <sup>-1</sup> )	9.7 $\pm$ 0.8	9.8 $\pm$ 1.6	10.2 $\pm$ 1.8

$n = 15$  rats per group

$I_{\max}$  maximum intensity of collagen-induced platelet aggregation in whole blood

\*  $P < 0.05$ ; \*\*  $P < 0.001$ ; \*\*\*  $P < 0.0001$  with respect to the control group

iNOS activity was also smaller in VOO-treated rats (12.6  $\pm$  1.8% and 13.1  $\pm$  1.5%, respectively) (Table 4). The increase in prostaglandin  $E_2$  concentration was smaller in VOO-treated animals (50.8 and 52.3% lower, respectively, than in control rats) (Table 4). The efflux of LDH was significantly inhibited in VOO-treated animals in comparison with the control group. After reoxygenation, LDH values were lower by 17.5 and 42.5% in rats treated with 0.25 and 0.5 mL kg<sup>-1</sup> per day, respectively, than in brain slices from untreated rats (Fig. 1).

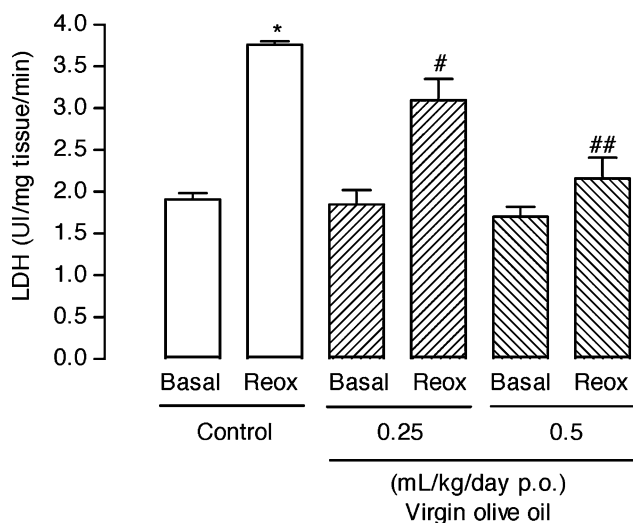


**Fig. 1** Lactate dehydrogenase (LDH) efflux in rat brain slices subjected to hypoxia followed by 180 min of reoxygenation (Reox). \* $P < 0.05$  in comparison with the baseline value in the control group. # $P < 0.05$ ; ## $P < 0.001$ , with respect to reoxygenated slices in the control group ( $n = 15$  rats per group)

## Discussion

Our results show that the daily oral administration of VOO in healthy rats modified platelet and endothelial biomarkers and acted on some of the biochemical pathways involved in brain damage. The findings of earlier research, however, are ambiguous, ranging from a clear antiaggregant effect in humans [21] and rabbits [10] to the absence of effect in humans both in vitro [22] and ex vivo [23]. Some studies have even reported that a diet enriched with unsaturated fat (mainly linoleic acid) stimulated platelet aggregation [24]. In healthy human volunteers who consumed a diet enriched with VOO, an antiaggregant effect was seen after 8 weeks, but the effect was significantly blunted after 16 weeks [21]. All earlier studies used higher doses of VOO than those used in our experiments. Animals treated with VOO showed not only inhibited platelet aggregation, but also reduced production of thromboxane, an agent that favors aggregation and vasoconstriction. At least one study in humans also reported a reduction in thromboxane production [25].

Inhibition of cyclooxygenase activity after administration of monounsaturated and/or polyunsaturated fatty acids is well documented in several models [26–29]. This effect was responsible for the beneficial effect of VOO on the thromboxane/prostacyclin ratio, an important factor in the prevention of thrombosis. The weak effect of VOO on endothelial pathways of platelet inhibition (prostacyclin and NO) may reflect the fact that our experimental animals were healthy at the start of our experiments. Treatment with VOO also reportedly had a weak effect on biochemical parameters in non-stimulated human endothelial cells [30]. The administration of VOO to healthy rats thus had an inhibitory effect on platelet function and led to a favorable change in the thromboxane/prostacyclin ratio.

Our findings in the model of brain hypoxia–reoxygenation showed that in rats treated with VOO, brain cell death caused by hypoxia–reoxygenation, measured as LDH efflux, was 42.5% lower than in untreated rats. Virgin olive oil thus modified all three of the pathways of cerebral cytoprotection we investigated. It curtailed the increase in lipid peroxides in brain tissue, limited the reduction in glutathione stores, and inhibited the overproduction of prostaglandin  $E_2$  and NO, mainly by inhibiting iNOS activity.

The antioxidant effect of VOO in the brain of healthy rabbits has been reported previously [31]. Some components of virgin olive oil, specifically polyphenols and vitamin E, have clear antioxidant effects in some cells and tissues [32–34]. Although TBARS determination is a non-definitive and inexact representation of lipid peroxidation in comparison with other methods, the percentage differences between groups represents the qualitative changes in

**Table 4** Main parameters measured in rat brain slices before (pre-hypoxia) and after hypoxia followed by 180 min of reoxygenation

	Virgin olive oil (mL kg <sup>-1</sup> per day p.o. for 30 days)		
	0 (A) Pre-hypoxia (B) 180 min reoxygenation	0.25 (180 min reoxygenation)	0.5 (180 min reoxygenation)
TBARS (nmol mg <sup>-1</sup> protein)	A) 0.4 ± 0.02 B) 0.6 ± 0.09*	0.4 ± 0.02**	0.3 ± 0.03**
GSH (μmol g <sup>-1</sup> tissue)	A) 23.6 ± 1.1 B) 13.7 ± 0.5*	15.3 ± 0.6	19.7 ± 1.2**
% GSSG with respect to GSH + GSSG	A) 9.8 ± 0.9 B) 11.6 ± 1.8	11.2 ± 0.9	13.5 ± 1.4
GSHpx (μmol min <sup>-1</sup> )	A) 5.3 ± 0.2 B) 5.7 ± 0.1	5.7 ± 0.3	5.4 ± 0.3
GSHtf (μmol min <sup>-1</sup> )	A) 2.7 ± 0.2 B) 1.9 ± 0.2*	1.8 ± 0.2	2.2 ± 0.3
NO <sub>2</sub> <sup>-</sup> + NO <sub>3</sub> <sup>-</sup> (nmol mg <sup>-1</sup> protein)	A) 2.5 ± 0.4 B) 7.7 ± 0.4*	7.3 ± 0.3	2.7 ± 0.2**
cNOS (pmol (mg protein) <sup>-1</sup> min <sup>-1</sup> )	A) 257 ± 22 B) 54.7 ± 5.7*	126 ± 12**	123 ± 18**
iNOS (pmol mg <sup>-1</sup> protein min <sup>-1</sup> )	A) 187 ± 20 B) 516 ± 66*	214 ± 33**	171 ± 17**
PGE <sub>2</sub> (pg mg <sup>-1</sup> tissue)	A) 12.1 ± 2.5 B) 36.9 ± 1.5*	18.2 ± 2.4**	17.6 ± 2.5**

TBARS, thiobarbituric acid-reactive substances; GSH, reduced glutathione; GSSG, oxidized glutathione; GSHpx, glutathione peroxidase; GSHtf, glutathione transferase; NO<sub>2</sub><sup>-</sup> + NO<sub>3</sub><sup>-</sup>, nitrites + nitrates; cNOS, constitutive nitric oxide synthase; iNOS, inducible nitric oxide synthase; PGE<sub>2</sub>, prostaglandin E<sub>2</sub>

*n* = 15 rats per group

\* *P* < 0.05 with respect to pre-hypoxia values; \*\* *P* < 0.05 with respect to reoxygenated control slices

this parameter. Researchers who have investigated the effect of different types of oil and their components on the glutathione system mostly concur that changes in this system are not dependent on the fatty acid composition of the oil, but rather on non-glyceride components, especially vitamin E and polyphenols [27, 35–38]. We found no reports of this effect in the model of brain ischemia–reperfusion we used.

In ischemia or in neuronal degeneration processes, prostaglandin synthesis is known to result from stimulation of inducible cyclooxygenase (cyclooxygenase-2) [39]. However, there is evidence that type-1 cyclooxygenase is induced under certain circumstances, for example global cerebral ischemia [40], *N*-methylaspartate-induced excitotoxicity [41], traumatic brain injury [42], and activated microglia associated with amyloid plaques [43]. This is consistent with the marked increase in prostaglandin E<sub>2</sub> production after reoxygenation in our experimental model. Accordingly, despite the clear effect of VOO on the accumulation of prostaglandin E<sub>2</sub> in reoxygenated slices, our findings do not suggest which cyclooxygenase isoform was affected by VOO in our experimental model.

The effect of VOO on NO accumulation suggests that the components of this oil may affect iNOS activity or the inflammatory mediators that stimulate this enzyme [30]. Vitamin E has been found to inhibit the expression and synthesis of iNOS [44], and polyphenols have been shown to significantly reduce peroxynitrite formation in humans [32, 45]. In addition, cell culture experiments have shown that these phenols increase the overall production of NO [34]. However, the free radical-scavenging capacity of these phenols has been shown to prevent the formation of peroxynitrite [30, 32, 34]. Thus the effect of VOO on the expression and formation of iNOS, and its antioxidant effect and ability to prevent peroxynitrite formation, might account for the decrease in iNOS activity in brain tissues from animals treated with VOO and then subjected to hypoxia–reoxygenation.

Because VOO polyphenols are the components most likely to be responsible for the antioxidant effect of this Mediterranean fat, it is important to know whether they are detectable in the rat brain after oral intake. We have found no published studies that investigated polyphenols, although D'Angelo et al. [46] measured hydroxytyrosol in

the rat brain 1 h after a single intravenous injection of 1.5 mg of this antioxidant from VOO per kg body weight, and found the brain tissue to contain 0.31% of the maximum plasma concentration. Schaffer et al. [47] recently showed that a hydroxytyrosol extract prepared from olive mill wastewater (45.5% hydroxytyrosol) reduced neuronal damage induced by ferrous salts or sodium nitroprusside as oxidative inducers.

This study has two main limitations—lack of a negative control group (i.e. refined olive oil) and the poor polyphenol content of the VOO used. In preliminary unreported experiments we are confirming the absence of effect on the variables determined in this study when refined olive oil is administered to rats; moreover, a similar amount of the polyphenol mixture measured in the VOO used has a similar effect on brain oxidative status in healthy rats.

Some criticism [48] has been raised about recommending VOO consumption to protect against cardiovascular diseases because it is presumed to increase the risk of becoming overweight. In our experimental model a greater increase in the body weight was observed for rats treated with 0.5 mL kg<sup>-1</sup> day<sup>-1</sup> than in the control group (0.91% with respect to control group), which was not statistically significant. Bes-Rastrollo et al. [49] demonstrated that a consumption during a mean of 28.5 months of 0.15 mL kg<sup>-1</sup> day<sup>-1</sup> by an apparently healthy population increased the body weight by 1.14%, concluding that even consumption of a large amount of olive oil is not associated with greater weight gain.

In conclusion, administration of VOO modulates a series of biochemical phenomena that play a key role in the process of thrombogenesis and brain ischemia. These effects of VOO are the result of its ability to reduce oxidative stress and, possibly, regulate inducible enzyme pathways; these biochemical effects make VOO a potentially ideal candidate for prophylactic treatment against thrombogenesis and brain ischemia, either alone or as an adjuvant to medication.

Despite the absence of cohort studies of stroke prevention in people who consume a Mediterranean type diet [29], the beneficial effects of this diet on cardiovascular risk factors [50] may well be valid for cerebrovascular ischemic processes also [51, 52]. Our experimental study supports a possible role of VOO in the prevention of ischemic stroke. Further studies including clinical trials in humans will be needed to test the ability of virgin VOO to prevent ischemic stroke.

**Acknowledgments** We thank A. Pino Blanes for its excellent technical assistance and K. Shashok for translating parts of the manuscript into English.

## References

- Barzi F, Woodward M, Marfisi RM, Tavazzi L, Valagussa F, Marchioli R, GISSI-Prevenzione Investigators (2003) Mediterranean diet and all-causes mortality after myocardial infarction: results from the GISSI-Prevenzione trial. *Eur J Clin Nutr* 57:604–611
- de Lorgril M, Salen P, Martin JL, Mamelle N, Monjaud I, Touboul P, Delaye J (1996) Effect of a mediterranean type diet on the rate of cardiovascular complications in patients with coronary artery disease. *J Am Coll Cardiol* 28:1103–1108
- Keys A (1980) Seven countries: a multivariate analysis of diet and coronary heart disease. Harvard University Press, Boston
- Knoops KT, Groot de LC, Fidanza F, Alberti-Fidanza A, Kromhout D, van Staveren WA (2006) Comparison of three different dietary scores in relation to 10-year mortality in elderly European subjects: the HALE project. *Eur J Clin Nutr* 60:746–755
- Trichopoulou A, Orfanos P, Norat T, Bueno-de-Mesquita B, Ocke MC, Peeters PH, van der Schouw YT, Boeing H, Hoffmann K et al (2005) Modified mediterranean diet and survival: EPIC-elderly prospective cohort study. *BMJ* 330:991–998
- Krauss RM, Eckel RH, Howard B, Appel LJ, Daniels SR, Deckelbaum RJ, Erdman JW Jr, Kris-Etherton P, Goldberg IJ, et al. (2000) AHA dietary guidelines: revision 2000: a statement for healthcare professionals from the nutrition committee of the American heart association. *Stroke* 31:2751–2766
- World Health Organization Study Group (2003) Diet, nutrition, and the prevention of chronic diseases. Geneva, Switzerland. World Health Organization; Technical Report Series 916
- McCord JM, Edeas MA (2005) SOD, oxidative stress and human pathologies: a brief history and a future vision. *Biomed Pharmacother* 59:139–142
- Violi F, Cangemi R (2005) Antioxidants and cardiovascular disease. *Curr Opin Investig Drugs* 6:895–900
- Visioli F, Poli A, Gall C (2002) Antioxidant and other biological activities of phenols from olives and olive oil. *Med Res Rev* 22:65–75
- Alexandrova ML, Bochev PG (2005) Oxidative stress during the chronic phase after stroke. *Free Radic Biol Med* 39:297–316
- Guix FX, Uribealago I, Coma M, Munoz FJ (2005) The physiology and pathophysiology of nitric oxide in the brain. *Prog Neurobiol* 76:126–152
- Weinbrenner T, Fito M, Farre Albaladejo M, Saez GT, Rijken P, Tormos C, Coolen S, De La Torre R, Covas MI (2004) Bioavailability of phenolic compounds from olive oil and oxidative/antioxidant status at postprandial state in healthy humans. *Drugs Exp Clin Res* 30:207–212
- De La Cruz JP, Villalobos MA, Sedeno G, Sanchez De La Cuesta F (1998) Effect of propofol on oxidative stress in an in vitro model of anoxia-reoxygenation in the rat brain. *Brain Res* 800:136–144
- Bossman HB, Hemsworth BD (1969) Structure and function of nervous system. Academic, London, pp 1–24
- Bradford MM (1976) A rapid and sensitive method for the quantitation of microgram quantities of protein utilizing the principle of protein-dye binding. *Anal Biochem* 72:248–254
- Hissin PJ, Hill R (1976) A fluorimetric method of determination of oxidized and reduced glutathione in tissues. *Anal Biochem* 74:214–226
- Flohé L, Gunzler WA (1985) Assays of glutathione peroxidase. *Meth Enzymol* 105:114–121
- Warholm M, Guthenberg C, von Bahr C, Mannervik B (1985) Glutathione transferases from human liver. *Meth Enzymol* 113:449–503

20. Lobner D (2000) Comparison of the LDH and MTT assays for quantifying cell death: validity for neuronal apoptosis? *J Neurosci Meth* 96:147–152
21. Kelly CM, Smith RD, Williams CM (2001) Dietary monounsaturated fatty acids and haemostasis. *Proc Nutr Soc* 60:161–170
22. Freese R, Mutanen M, Valsta LM, Salminen I (1994) Comparison of the effects of two diets rich in monounsaturated fatty acids differing in their linoleic/alpha-linolenic acid ratio on platelet aggregation. *Thromb Haemost* 71:73–77
23. Vicario IM, Malkova D, Lund EK, Johnson IT (1998) Olive oil supplementation in healthy adults: effects in cell membrane fatty acid composition and platelet function. *Ann Nutr Metab* 42:160–169
24. Turpeinen AM, Pajari AM, Freese R, Sauer R, Mutanen M (1998) Replacement of dietary saturated by unsaturated fatty acids: effects of platelet protein kinase C activity, urinary content of 2,3-dinor-TXB2 and in vitro platelet aggregation in healthy man. *Thromb Haemost* 80:649–655
25. Visioli F, Caruso D, Grande S, Bosisio R, Villa M, Galli G, Sirtori C, Galli C (2005) *Eur J Nutr* 44:121–127
26. Bartoli R, Fernandez-Banares F, Navarro E, Castella E, Mane J, Alvarez M, Pastor C, Cabre E, Gassull MA (2000) Effect of olive oil on early and late events of colon carcinogenesis in rats: modulation of arachidonic acid metabolism and local prostaglandin E(2) synthesis. *Gut* 46:191–199
27. De La Cruz JP, Villalobos MA, Carmona JA, Martín-Romero M, Sánchez de la Cuesta F (2000) Antithrombotic potential of olive oil administration in rabbits with elevated cholesterol. *Thromb Res* 100:305–315
28. Moreno JJ (2003) Effect of olive oil minor components on oxidative stress and arachidonic acid mobilization and metabolism by macrophages RAW 264.7. *Free Radic Biol Med* 35:1073–1081
29. Nieto N, Torres MI, Ríos A, Gil A (2002) Dietary polyunsaturated fatty acids improve histological and biochemical alterations in rats with experimental ulcerative colitis. *J Nutr* 132:11–19
30. Perona JS, Cabello-Moruno R, Ruiz-Gutierrez V (2006) The role of virgin olive oil components in the modulation of endothelial function. *J Nutr Biochem* 14:429–445
31. De La Cruz JP, Quintero L, Villalobos MA, Sánchez de la Cuesta F (2000) Lipid peroxidation and glutathione system in hyperlipemic rabbits: influence of olive oil administration. *Biochim Biophys Acta* 1485:36–44
32. De La Puerta R, Domínguez ME, Ruíz V, Flavill JA, Houlst JRS (2001) Effects of virgin olive oil on scavenging of reactive nitrogen species and upon nitregeric neurotransmission. *Life Sci* 69:1213–1222
33. Villalobos MA, De La Cruz JP, Carrasco T, Smith-Agreda JM, Sanchez de la Cuesta F (1994) Effects of alpha-tocopherol on lipid peroxidation and mitochondrial reduction of tetraphenyl tetrazolium in the rat brain. *Brain Res Bull* 33:313–318
34. Visioli F, Bellomo G, Galli C (1998) Free radical-scavenging properties of olive oil polyphenols. *Biochem Biophys Res Commun* 247:60–64
35. De La Cruz JP, Martín-Romero M, Carmona JA, Villalobos MA, Sanchez de la Cuesta F (1997) Effect of evening primrose oil on platelet aggregation in rabbits fed an atherogenic diet. *Thromb Res* 87:141–149
36. Hünkar T, Aktan F, Ceylan A, Karasu Ç (2002) Effects of cod liver oil on tissue antioxidant pathways in normal and streptozotocin-diabetic rats. *Cell Biochem Funct* 20:297–302
37. López-Torres M, Thiele JJ, Sindo Y, Han D, Packer L (1998) Topical application of *n*-tocopherol modulates the antioxidant network and diminishes ultraviolet-induced oxidative damage in murine skin. *Br J Dermatol* 138:207–215
38. Ochoa-Herrera JJ, Huertas JR, Quiles JL, Mataix J (2001) Dietary oils high in oleic acid, but with different non-glyceride contents, have different effects on lipid profiles and peroxidation in rabbit hepatic mitochondria. *J Nutr Biochem* 12:357–364
39. ÓBannon MK (1999) cyclooxygenase-2 and Alzheimer's disease: potential roles in inflammation and neurodegeneration. *Expert Opin Investig Drugs* 8:1521–1536
40. Candelario-Jalil E, Gonzalez-Falcon A, Garcia-Cabrera M, Alvarez D, Al-Dalain S, Martinez G, Leon OS, Springer JE (2003) Assessment of the relative contribution of COX-1 and COX-2 isoforms to ischemia-induced oxidative damage and neurodegeneration following transient global cerebral ischemia. *J Neurochem* 86:545–555
41. Pepicelli O, Fedele E, Berardi M, Raiteri M, Levi G, Greco A, Ajmone-Cat MA, Minghetti L (2005) Cyclo-oxygenase-1 and -2 differently contribute to prostaglandin E2 synthesis and lipid peroxidation after in vivo activation of *N*-methyl-D-aspartate receptors in rat hippocampus. *J Neurochem* 93:1561–1567
42. Schwab JM, Beschorner R, Meyermann R, Gozalan F, Schluesener HJ (2002) Persistent accumulation of cyclooxygenase-1-expressing microglial cells and macrophages and transient upregulation by endothelium in human brain injury. *J Neurosurg* 96:892–899
43. Yermakova AV, Rollins J, Callahan LM, Rogers J, O'Banion MK (1999) Cyclooxygenase-1 in human Alzheimer and control brain: quantitative analysis of expression by microglia and CA3 hippocampal neurons. *J Neuropathol Exp Neurol* 58:1135–1146
44. Fang YZ, Yang S, Wu G (2002) Free radicals, antioxidants, and nutrition. *Nutrition* 18:872–879
45. Deiana M, Aruoma OI, Bianchi ML, Spencer JP, Kaur H, Halliwell B, Aeschbach R, Banni S, Dessi MA, Corongiu FP (1999) Inhibition of peroxynitrite dependent DNA base modification and tyrosine nitration by the extra virgin olive oil-derived antioxidant hydroxytyrosol. *Free Radic Biol Med* 26:762–769
46. D'Angelo S, Manna C, Migliardi V, Mazzoni O, Morrica P, Capasso G, Pontoni G, Galletti P, Zappia V (2001) Pharmacokinetics and metabolism of hydroxytyrosol, a natural antioxidant from olive oil. *Drug Metab Dispos* 29:1492–1498
47. Schaffer S, Podstawa M, Visioli F, Bogani P, Müller WE, Eckert GP (2007) Hydroxytyrosol-rich olive mill wastewater protects brain cells in vitro and ex vivo. *J Agric Food Chem* 55:5043–5049
48. Martínez-González MA (2006) The SUN cohort study (Seguimiento University of Navarra). *Public Health Nutr* 9:127–131
49. Ferro-Luzzi A, James WPT, Kafatos A (2002) The high-fat Greek diet: a recipe for all? *Eur J Clin Nutr* 56:796–809
50. Bes-Rastrollo M, Sanchez-Villegas A, De La Fuente C, De Irala J, Martínez JA, Martínez-González MA (2006) 41:249–256
51. Covas MI (2007) Olive oil and the cardiovascular system. *Pharmacol Res* 55:175–186
52. Martínez-González MA, Sánchez-Villegas A, De Irala J, Martí A, Martínez JA (2002) Mediterranean diet and stroke: objectives and design of the SUN Project. *Nutr Neurosci* 5:65–73

## *Ricinus communis* Contains an Acyl-CoA Synthetase that Preferentially Activates Ricinoleate to Its CoA Thioester

Xiaohua He · Grace Q. Chen · Sung T. Kang · Thomas A. McKeon

Received: 23 March 2007 / Accepted: 10 June 2007 / Published online: 7 August 2007  
© AOCs 2007

**Abstract** As part of our effort to identify enzymes that are critical for producing large amounts of ricinoleate in castor oil, we have isolated three cDNAs encoding acyl-CoA synthetase (ACS) in the castor plant. Analysis of the cDNA sequences reveals that two of them, designated RcACS 2 and RcACS 4, contain complete coding regions corresponding to 694 and 690 amino acids, respectively. The third cDNA, RcACS 1, encodes a truncated gene sequence. The RcACS 2 and RcACS 4 share 77% identity at the amino acid sequence level. Complementation tests showed that both RcACS 2 and RcACS 4 successfully restored growth of a yeast mutant strain (YB525) deficient in ACS. Lysates from yeast cells expressing RcACS 2 and 4 were enzymatically active when using  $^{14}\text{C}$ -labeled oleic acid as a substrate. A cell fractionation study indicates that RcACS 2 and 4 are mainly associated with membranes. Substrate specificity assays indicate that the RcACS 2 preferentially activates ricinoleate, while the RcACS 4 has a preference for nonhydroxy fatty acids.

**Keywords** Acyl-CoA synthetase · Complementation test · Real-time PCR · *Ricinus communis* · *Saccharomyces cerevisiae* · Substrate specificity

### Abbreviations

ACS	acyl-CoA synthetase
AtLACS 6	acyl-CoA synthetase from <i>Arabidopsis thaliana</i>
BSA	Bovine serum albumin
FAH	Fatty acyl hydroxylase
RACE	Rapid amplification of cDNA ends
RcACS	acyl-CoA synthetase from <i>Ricinus communis</i>
RT-PCR	Reverse transcription-polymerase chain reaction
SD	Standard deviation
SDM	Synthetic defined media
U	Uracil

### Introduction

The castor plant (*Ricinus communis*) produces a seed oil of unique composition, with up to 90% of the fatty acid content as ricinoleate (12-hydroxy oleate). As a result of the hydroxy group, the oil has physical and chemical properties that make it desirable for numerous industrial uses, such as lubricants, coatings, plastics and cosmetics [1]. However, production of castor oil is seriously hindered by the presence of the highly toxic protein ricin, its homologue *Ricinus communis* agglutinin, and potent allergens in the seeds. Because of the potential for expanded use of castor oil in industrial and biodiesel applications, it is of great interest to develop a safe domestic source of castor oil. One logical approach is to genetically modify a commodity oilseed to produce castor oil. The feasibility of altering the oil composition of oilseeds has been amply demonstrated [2–4], but the results have been disappointing in most cases. The

X. He · G. Q. Chen · T. A. McKeon (✉)  
Western Regional Research Center, USDA,  
800 Buchanan St, Albany, CA 94710, USA  
e-mail: tmckeon@pw.usda.gov

S. T. Kang  
Department of Food Science and Technology,  
Seoul National University of Technology,  
Seoul, South Korea

enzyme responsible for synthesis of ricinoleate in castor plant is the oleoyl-12-hydroxylase (FAH), and it was cloned previously [5]. To date, oilseeds transformed to express FAH produce less than 20% hydroxy fatty acid content in oil [6], much less than the 90% present in castor oil. It has been hypothesized that excessive accumulation of ricinoleate in lipid disrupts membrane integrity and impairs normal plant growth and development. Plants appear to have “editing” mechanisms that exclude unusual fatty acids from the membrane [7]. However, the castor plant has evolved the enzymes needed to produce and incorporate ricinoleate into storage lipids at a high level [8]. Thus, we initiated an approach to identify additional enzyme components in castor that enable it to produce oil with 90% ricinoleate [9].

We have previously cloned a diacylglycerol acyltransferase type 1 gene from the castor plant (RcDGAT), and demonstrated that the gene product has a twofold preference for acylation of diricinolein substrate versus other diacylglycerols in the final step of oil biosynthesis [10]. We believe that this RcDGAT is one of the necessary components for high accumulation of ricinoleate in transgenic plants. Based on our previous work [9], additional enzymes are also required for high ricinoleate production in castor. Since acyl-CoA is the acyl donor for DGAT activity and the acyl-CoA synthetase (ACS) plays a central role in the metabolism of free fatty acids in plants and their incorporation into storage lipids in seed, we hypothesized that ACS may be involved in enhancing ricinoleate incorporation into TAG. Multiple isoforms of ACS have been isolated from many organisms, these isoforms differ in fatty acid preference, subcellular location and regulation [11–13]. In this paper, we report the isolation of ACS genes from castor plants, complementation of these ACS genes in a yeast mutant strain deficient in ACS and studies of their enzymatic specificity.

## Experimental Procedures

### Cloning of ACS cDNAs from *R. communis*

Degenerate primers were designed based on the nucleic acid sequences of conserved regions of known ACS sequences. The primers are for ACS 1: 5'-ACTGGTGAYCCNAARGGAGT-3' and 5'-TCWGTWAGACCRTATCCTTG-3'; ACS 2: 5'-GACTACAAATGGATGAC-3' and 5'-TCCCCTTGGTAGAAHCCAA-3'; ACS 4: 5'-GAAGGMTAYGGAATGAC-3' and 5'-TTGAARATGTTCTTYTCC-3'. Reverse transcription (RT)-PCR was performed following the Gibco BRL SuperScript First-Strand Synthesis System for RT-PCR instruction (Grand Island, NY) using these primers and a mixture of RNA samples

extracted from different castor tissues including leaf, stem, root and germinating seeds according to the method of Gu et al. [14]. The sequences of the PCR products obtained were used to generate gene-specific primers for 3'- and 5'-RACE (rapid amplification of cDNA ends) [15]. Finally, primers for end-to-end amplification were designed to obtain the complete genes from the RACE-ready cDNA template following the manufacturer's instruction (Invitrogen, Carlsbad, CA). The full-length cDNAs were then cloned into a pCR4-TOPO vector using TOPO TA Cloning Kit for Sequencing (Invitrogen) and completely sequenced in both directions using ABI3100 DNA analyzer and ABI PRISM Big Dye Terminators v3.1 Cycle Sequencing Kit (Applied Biosystems, Foster City, CA).

### Cloning of Castor ACS Genes in Yeast Cells

The coding regions of ACS genes were reamplified using new primers: 5'-AGAAATGGACATGGATTCAGCTCAACG-3' and 5'-CAGTTTCGGGGAGGGATCGGAC-3' for RcACS 2; 5'-GACAATGGAATCAACAACAGCTCAACG-3' and 5'-ATCCAAGGTAGCAGTCTCAGC-3' for RcACS 4, and cloned into a yeast expression vector, pYES2.1/V5-His-TOPO (Invitrogen). The translation stop sites were removed to fuse the genes in frame with the V5 epitope and polyhistidine tag for detection and purification of the proteins. The recombinant vectors were first transformed into competent *E. coli*. Plasmid DNA from the bacterial colonies was then transformed into yeast YB525 cells, kindly provided by Professor J.I. Gordon, Washington University, St Louis [16] that had been made competent for chemical transformation using the S.c. EasyComp kit (Invitrogen).

### Expression of ACS in Yeast Cells

Yeast YB525 cells containing the expression constructs were selected on Synthetic Defined Media (SDM)-uracil (U) plates consisting of 0.17% yeast nitrogen base, 0.5% ammonium sulfate, 2% dextrose, 0.08% complete supplement minus uracil, and 1.7% agar (BIO 101 Systems 4813-075, Q-Biogene, Irvine, CA). Overnight cultures from single colonies grown in SDM-U liquid medium were induced to express transgenes from the Gal1 promoter of the vector by adding galactose to a concentration of 2% (w/v). Yeast cells were harvested after growing 12–18 h in induction medium at 30 °C. Microsomes were isolated from the harvested yeast cells as described by Urban et al. [17] and resuspended in 0.1M Tris-HCl, pH 7.0, containing 20% glycerol and used as enzyme sources for the ACS assay. To test the constructs for their ability to complement the phenotype of yeast strain YB525, aliquots of each culture containing these constructs were plated on SDM-U

plates with galactose plus 500  $\mu\text{M}$  myristic acid and 25  $\mu\text{M}$  cerulenin and incubated at 30  $^{\circ}\text{C}$  for 2–3 days.

#### Western Blot Analysis

Yeast cells were resuspended in breaking buffer (50 mM sodium phosphate, pH 7.4, 1 mM EDTA, 5% glycerol and 1 mM PMSF) to obtain an  $\text{OD}_{600}$  of 50 and lysed by adding an equal volume of acid-washed glass beads (0.4–0.6 mm size from Sigma-Aldrich, St Louis, MO) and beating for 4 min at 4  $^{\circ}\text{C}$  on a Mini-BeadBeater-8 (Biospec Products, Bartlesville, OK). The lysate collected was centrifuged at 10,000g for 10 min to remove cell debris. The supernatant used as total protein fraction (T) was centrifuged again at 100,000g for 1 h to obtain a water soluble fraction (S) and a membrane fraction (P). Protein samples (10  $\mu\text{g}$ ) from each fraction were separated by SDS-PAGE and electrotransferred to PVDF membranes. The membranes were incubated with the anti-V5 antibodies (Invitrogen) at 1:5,000 dilution and horseradish peroxidase-conjugated goat-anti-mouse secondary antibodies (Roche, Indianapolis, IN) at 1:1,000 dilution. Horseradish peroxidase activity was visualized by chemiluminescence using the ECL kit (Amersham, Arlington Heights, IL).

#### Assay for ACS Activity

The *in vitro* ACS assays were performed as in Shockey et al. [18] with minor modification. The reaction mixture (100  $\mu\text{L}$ ) consisted of 100 mM bis-tris-propane (pH 7.6), 10 mM  $\text{MgCl}_2$ , 5 mM ATP, 1 mM CoA, 2.5 mM dithiothreitol, 0.1% bovine serum albumin (BSA), 20  $\mu\text{M}$  1- $^{14}\text{C}$  fatty acid (specific activity 49–56  $\text{mCi mmol}^{-1}$ , from American Radiolabeled Chemicals, St Louis, except 1- $^{14}\text{C}$  laurate and 11- and 12-hydroxy laurates from Cypex Ltd., Dundee, Scotland) and 20  $\mu\text{g}$  yeast microsomal protein. The reaction was incubated at 25  $^{\circ}\text{C}$  for 20 min and stopped by addition of 100  $\mu\text{L}$  of 10% (v/v) acetic acid in isopropanol and extracted twice with 900  $\mu\text{L}$  of hexane saturated with 50% (v/v) isopropanol.

Enzyme activity was determined by measuring the counts in the aqueous phase using a liquid scintillation counter (Packard Instrument Company, Downers Grove, IL). Each assay was performed in duplicate and all experiments were repeated 3 times.

#### RNA Extraction and Real-time PCR

RNA samples were extracted from germinating seeds (3 days after imbibition), developing seeds (33 days after pollination), and cotyledons, roots, hypocotyls, leaves at 16 days after imbibition using method of Gu et al. [14]. The first-strand cDNA was synthesized using 5  $\mu\text{g}$  of total RNA as template and oligo (dT) as primer following the Gibco BRL SuperScript First-Strand Synthesis System for RT-PCR instruction (Grand Island, NY). Real-time PCR mixture (25  $\mu\text{L}$ ) contained one tenth of the first-strand cDNA, 1x iQ SYBR Green I Supermix (Bio-Rad, Hercules, CA) and 300 nM forward and reverse primers. The Bio-Rad iCycler iQ-system was used for all PCRs. The PCR protocol applied consisted of an initial denaturation step of 95  $^{\circ}\text{C}$  for 3 min, followed by 40 repeats of 95  $^{\circ}\text{C}$  for 10 s and 55  $^{\circ}\text{C}$  for 30 s. A melt-curve protocol immediately followed the amplification with 95  $^{\circ}\text{C}$  for 1 min and 50  $^{\circ}\text{C}$  for 1 min, followed by 80 repeats of heating for 10 s, starting at 50  $^{\circ}\text{C}$  with 0.5  $^{\circ}\text{C}$  increments. PCR product specificity was confirmed by melting-curve analysis and electrophoresis on 4% agarose gel. The information for the optimized primer pairs is listed in Table 1.

#### Real-time Quantitative PCR Data Analysis

The method of Pfaffl [19] was applied to calculate comparative expression levels between samples. Castor actin gene (a house keeping gene) was used as an internal reference to normalize the relative amount of mRNAs for all samples. For each tissue, triplicate sets of PCR including the target genes, actin gene and negative controls (reaction without cDNA template) were performed. The SYBR fluorescence was analyzed by iQ iCycler software and the  $C_T$

**Table 1** Primer sequences, size of amplification products, and PCR efficiencies

Gene name	Forward primer reverse primer	Amplicon size (bp)	PCR efficiency
RcACS 1	TAGTAGCATATTCTTGGGAGG TCACACTCTCAAGTAGCC	195	102
RcACS 2	GACTACGGGAGAGGTTATTTAATG TTACACGCCCAACAAAGC	210	106.2
RcACS 4	TCGCCTGACATAATGGACTTTC ACTTCTCTCGTCTGGACACC	281	101.9
Actin	GAATCCACGAGACTACATACAAC TTATGAAGGTTATGCTCTC	176	95.4



value for each gene was reported. The average  $C_7$  value for RcACS4 in seed samples was calibrated as one copy number. The PCR experiments were repeated to ensure similar results were obtained.

## Results and Discussion

### Cloning of cDNAs Coding for Acyl-CoA Synthetases in *R. communis*

Highly conserved regions of ACS genes were identified by sequence comparison of known ACSs. Degenerate primers were generated based on corresponding DNA sequences of these conserved regions. Three cDNA fragments were obtained by RT-PCR using these primers and RNA samples extracted from castor. The sizes were 563 bp for RcACS 1, 1,665 bp for RcACS 2 and 326 bp for RcACS 4, respectively. Based on the sequences of these fragments, gene-specific primers for 3′- and 5′-RACE were designed and amplification of full-length cDNAs for RcACS 1, 2, and 4 were attempted. Sequence analysis indicated that the cDNAs for RcACS 2 (GenBank accession number DQ300358) and RcACS 4 (DG300359) were 2,545 bp and 2,367 bp long with 202 bp and 47 bp 5′-untranslated regions, and 258 bp and 247 bp 3′-untranslated regions, respectively. Both cDNAs contained sequences encoding full-length enzymes of 694 and 690 amino acids. For RcACS 1 (DQ300357), the cDNA obtained was 2,215 bp long and BLAST similarity search results suggested that the coding sequence at the 5′ end is truncated. The deduced amino acid sequences of RcACS 2 and RcACS 4 share 77% identity (Fig. 1). The most notable motif identified by ScanProsite Results Viewer (<http://us.expasy.org/prosite/>) in both proteins is the AMP-binding domain signature: ICYTSGTTGTPK and GYGMTE, which is highly conserved in members of the AMP-binding protein (AMPBP) superfamily [20]. When aligned with all nine LACS isoforms in *Arabidopsis* [18], RcACS 2 is most closely related to AtLACS 6, a well-characterized peroxisomal ACS (data not shown). The amino acid sequences of RcACS 2 and AtLACS 6 are 79% identical (Fig. 1).

### Functional Expression of Castor ACS Genes in Yeast

To determine whether these cloned RcACS cDNAs encode active acyl-CoA synthetases and to further characterize their activity, we cloned RcACS 2 and 4 into the pYES2.1/V5-His-TOPO vector and transformed them into *S. cerevisiae*, YB525 strain. This strain contains insertional disruptions in two of its fatty acid activation (FAA) genes, FAA1 and FAA2, encoding acyl-CoA synthetases that account for 99% of total cellular myristoyl-CoA and

palmitoyl-CoA synthetase activities [16, 21]. It is not viable in media containing cerulenin, because cerulenin specifically inhibits the fatty acid synthetase complex, which catalyzes de novo synthesis of long chain acyl-CoAs. Growth of YB525 on media containing cerulenin and fatty acids such as myristate, palmitate or oleate can be restored by introducing an active ACS into cells, as the ACS activates the imported fatty acids to form acyl-CoAs.

Yeast YB525 colonies bearing constructs expressing RcACS 2 or RcACS 4 were selected from SDM-U plates containing 2% galactose, 500  $\mu$ M myristate, plus 25  $\mu$ M cerulenin and grown in aliquid medium. The ability of RcACS 2 and 4 to complement the YB525 mutant phenotype was evident based on colony vigor. To identify the gene products of RcACS 2 and 4 in yeast cells, cell-free lysates were prepared from cells induced with galactose for different time periods and examined by western blot analysis. The size of the RcACS 2 and 4 detected was very close to the predicted molecular weight of these proteins (77 kDa, plus 5 kDa from V5 epitope and the polyhistidine tag) (Fig. 2a) and the highest levels of RcACS 2 and RcACS 4 were detected after induction for 18 and 12 h, respectively (data not shown). The lysates from cells at these stages were used as enzyme sources for ACS activity assays. Lysates with RcACS 2 and 4 were enzymatically active, compared to lysate from cells with an empty pYES vector (Fig. 3). The western blot of proteins from cell fractionation indicates that RcACS 2 and 4 are highly enriched in membrane fractions (Fig. 2b), which is consistent with previous observations [22, 23]. Therefore, membrane fractions (microsomes) were used as the enzyme source in further characterization studies.

### Fatty Acid Substrate Specificities of RcACS 2 and RcACS 4

One of the ACS functions is to make fatty acids available for TAG biosynthesis by activating free fatty acids to acyl-CoA thioesters. Castor seed contains 90% ricinoleate in its oil, and we thought it possible that castor possesses a distinct ACS enzyme, which could preferentially catalyze the formation of ricinoleoyl-CoA to be used for synthesis of TAG. We thus measured acyl-CoA synthetase enzyme activity by in vitro assay using microsomes prepared from YB525 cells expressing RcACS 2 and 4. Eight different fatty acids were included in substrate specificity assays. As reported for ACS from other organisms [18, 24], both RcACS 2 and 4 utilized a range of substrates. Overall, the enzymatic activity was relatively higher when using microsomes expressing RcACS 2 versus RcACS 4 for the fatty acids tested (Fig. 4), although the RcACS 2 expressed in microsomes detected by western blot was repeatedly less abundant than RcACS 4 (Fig. 2b). This observation sug-

**Fig. 1** Alignments of deduced amino acid sequences of acyl-CoA synthetases in *Ricinus communis* (RcACS) and *Arabidopsis thaliana* (AtLACS 6). Alignments were generated by using the Clustal W program, version 1.83, which is freely available at <http://www.ebi.ac.uk/clustalw/>. The GenBank accession numbers for AtLACS 6, RcACS 2 and RcACS 4 are AB030317.2, DQ300358 and DQ300359. The identical residues among the three proteins are labeled with an asterisk under them. The putative AMP-binding domain signature is shaded in gray

Table showing amino acid sequence alignments for AtLACS6, RcACS2, and RcACS4. The sequences are aligned in columns with residue numbers on the right. Asterisks indicate identical residues. A putative AMP-binding domain signature is shaded in gray in the original image.

gests that the RcACS 2 is more active than the RcACS 4. The most remarkable result observed from the comparison of enzyme activity with the eight fatty acids was the strong preference of RcACS 2 for ricinoleate, the unusual fatty acid found in castor oil. The activity of RcACS 2 using ricinoleate is over 60% higher than that using other fatty acids. The RcACS 2 also shows slight preference for the hydroxy-laurate fatty acids versus laurate. In contrast, RcACS 4 has low activity toward hydroxy fatty acids, and does not have obvious specificity as the activation rates for all the non-hydroxy fatty acid substrates are fairly similar.

**Expression of RcACS in Castor Plants**

To examine the expression pattern of RcACS genes in castor plants, real-time PCR was performed using an equal amount of total RNA from germinating seeds (G.seeds),

developing seeds (D. seeds), cotyledons, roots, hypocotyls and young leaves. The three ACS genes isolated from castor plant were analyzed using optimized primer pairs (Table 1). The actin gene was used as the internal control to ensure the amount of RNA used is equal. To compare the relative amount of target in different samples, the average  $C_T$  value for RcACS 4 in seed sample was arbitrarily chosen to be calibrated as one copy number because it has the lowest expression level. The results from real-time PCR assay indicate that the three RcACS genes are expressed in all tissues tested, but the expression patterns vary greatly (Fig. 5). The most distinctive result is the high accumulation of RcACS2 in germinating seeds. Based on the sequence similarity of RcACS 2 to the peroxisomal ACS, AtLACS 6 (Fig. 1) and the presence of a moderately rare type 1 peroxisomal targeting sequence [25] at the extreme C-terminus, RcACS 2 is likely to be a peroxisomal

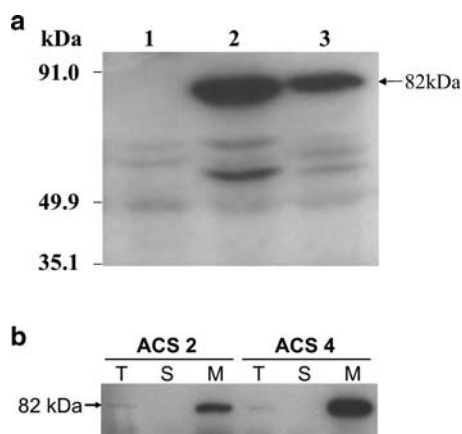


**Fig. 2** Expression of RcACS 2 and 4 in yeast cells. **a** Western blot of cell-free lysate proteins (50 µg/lane) extracted from yeast YB525 cells transformed with pYES2.1 empty vector (lane 1), RcACS 4 (lane 2) and RcACS 2 (lane 3). Overnight cultures were harvested after 12 (RcACS4) and 18 (RcACS2) hours induction with 2% galactose. The blot was probed with anti-V5 antibodies. **b** Western blot of proteins (10 µg/lane) extracted from different fractions of yeast YB525 cells transformed with RcACS2 and RcACS4. Overnight cultures were harvested after 12 (with RcACS4 cells) and 18 (with RcACS2 cells) hours induction with 2% galactose. Proteins from cell-free lysate (T), soluble (S) and membrane (M) fractions were separated on a SDS-PAGE and transferred to a PVDF membrane. The membrane was then probed with anti-V5 antibodies

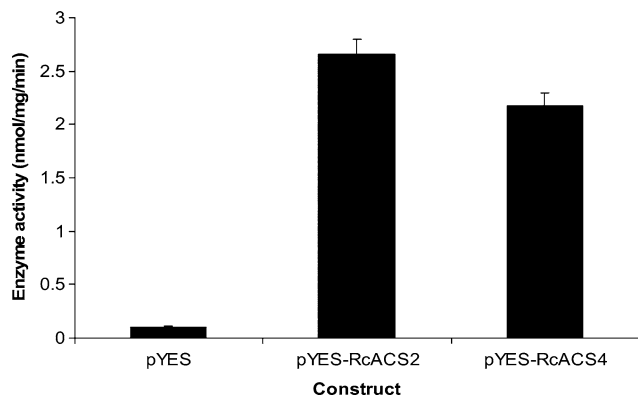


**Fig. 3** ACS enzyme activities in cell-free lysates of yeast YB525. Yeast cells carrying the indicated plasmids were harvested after galactose induction. Cell-free extracts were prepared by beating cells with glass beads and used as enzyme sources in ACS enzyme assays. 1- $^{14}\text{C}$  oleic acid was used as a substrate. Enzyme activities were measured based on the  $^{14}\text{C}$  label incorporated into the acyl-CoA fraction (aqueous-soluble counts) per assay. Values are means of triplicate with standard deviation (SD)

ACS isoform. The high expression of RcACS 2 in germinating seeds indicates that the plant has a strong demand for the enzyme at this stage, when peroxisomal ACSs are actively involved in  $\beta$ -oxidation. The castor seeds contain 90% ricinoleate, and large amounts of fatty acids (mostly ricinoleate) are released from the oil bodies upon germination. These fatty acids require activation to acyl-CoA by

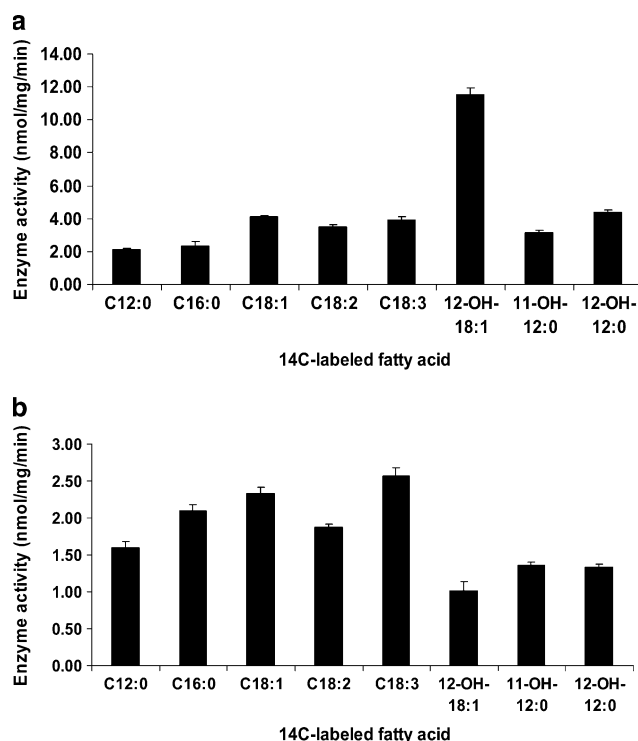


**Fig. 4** Substrate specificity of RcACS 2 (**a**) and RcACS 4 (**b**) using eight different fatty acid substrates. Batches of microsomes (with 20 µg of total microsomal protein) extracted from cells expressing RcACS 2 or RcACS 4 were used as enzyme sources and incubated with 20 µM 1- $^{14}\text{C}$  fatty acids for 20 min at 25 °C. Assays were then terminated by adding equal volume of 10% acetic acid in isopropanol. Enzyme activities were measured based on the  $^{14}\text{C}$  label incorporated into the acyl-CoA fraction (aqueous-soluble counts) per assay. Values are means of triplicate with SD

ACS for degradation through  $\beta$ -oxidation. The RcACS 2 has the ability to efficiently activate ricinoleate and provide the seedling with adequate metabolic energy. The expression patterns of the RcACS genes measured by real-time PCR indicate that none of these genes is seed specific or upregulated in developing seeds. It is possible that additional ACS genes may exist for fatty acyl-CoA metabolism in developing seeds, although all three appear to be present in developing seeds.

One of the major challenges in plant lipid biochemistry is understanding how plants such as castor can produce a seed oil containing high levels of a single FA, especially one with a polar substituent, like ricinoleate. We have previously inferred that, besides the hydroxylase required for ricinoleate biosynthesis, other enzymes involved in castor oil biosynthesis are necessary to produce high levels of ricinoleate [26, 27]. The ACSs catalyze many important steps in numerous pathways involving fatty acid and lipid metabolism, and an *in vitro* study on the ACS activity present in developing castor seeds showed that ricinoleate is an efficient substrate at low concentrations [28], therefore,

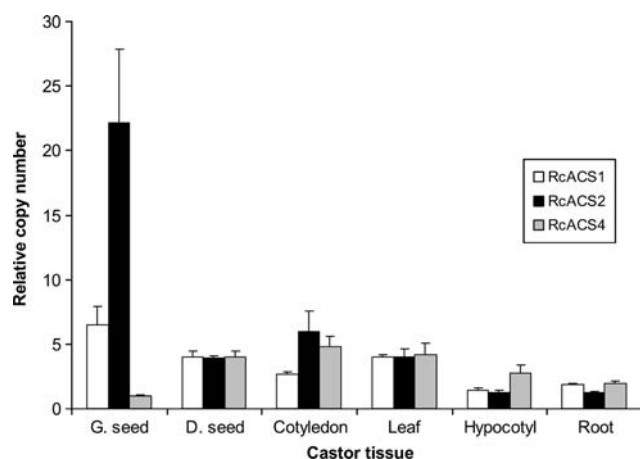


**Fig. 5** Expression of RcACS genes in the castor plant. Aliquots of total RNA were analyzed for expression of each gene in different tissues by real-time PCR using gene-specific primer pairs. The average  $C_T$  value for RcACS 4 in seed was calibrated as one copy number and used to calculate the relative amounts of other genes. Values are means of triplicate with SD

the ACS enzymes are logical choices for contributing to high ricinoleate incorporation in castor oil. ACS genes have been cloned from several plant species [11, 18] and most ACS enzymes display highest levels of activity with the fatty acids that make up the common structural and storage lipids in the plant. In this study, we were particularly interested in the substrate specificities of RcACSs because one of the reasons for high accumulation of ricinoleate in castor seeds could be that one of the ACSs in castor can efficiently activate ricinoleate to ricinoleoyl-CoA for TAG synthesis. We found that both RcACS 2 and 4 were active in microsomal fraction from yeast cells. The RcACS 2 was distinguishable from RcACS 4 on the basis of fatty acid incorporation, using hydroxy fatty acids preferentially, while the RcACS 4 uses the more non-polar fatty acids. The greatest activity observed in the series of assays was the RcACS 2 acylation of CoASH with ricinoleate. Since our long-term goal is to understand the specific role of ACS and create new oilseed species with high ricinoleate content in oil, RcACS 2 could be an attractive target for manipulation of ricinoleate incorporation in oilseeds.

**Acknowledgments** This work was supported in part by ARS CRIS Project 5325-21000-006-00D, ARS Research Associate Program, and a cooperative agreement with Dow Chemical Company (Midland, MI). We thank Professor J.I. Gordon for kindly providing us the yeast YB525 strain.

## References

- Caupin HJ (1997) Products from castor oil: past, present, and future, in lipid technologies and applications. Gunstone FD, Padley FB (eds) Marcel Dekker, New York, pp 787–795
- Voelker TA, Hayes TR, Cranmer AM, Turner JC, Davies HM (1996) Genetic engineering of a quantitative trait: metabolic and genetic parameters influencing the accumulation of laurate in rapeseed. *Plant J* 9:229–241
- Eccleston VS, Ohlrogge JB (1998) Expression of lauroyl-acyl carrier protein thioesterase in *Brassica napus* seeds induces pathways for both fatty acid oxidation and biosynthesis and implies a set point for triacylglycerol accumulation. *Plant Cell* 10:613–622
- Knutzon DS, Hayes TR, Wyrick A, Xiong H, Davies HM, Voelker TA (1999) Lysophosphatidic acid acyltransferase from coconut endosperm mediates the insertion of laurate at the sn-2 position of triacylglycerols in lauric rapeseed oil and can increase total laurate levels. *Plant Physiol* 120:739–746
- Van de Loo FJ, Broun P, Turner S, Somerville C (1995) An oleate 12-hydroxylase from *Ricinus communis* L. Is a fatty acyl desaturase homolog. *Proc Natl Acad Sci USA* 92:6743–6747
- Broun P, Somerville C (1997) Accumulation of ricinoleic, lesquerolic, and densipolic acids in seeds of transgenic *Arabidopsis* plants that express a fatty acyl hydroxylase cDNA from castor bean. *Plant Physiol* 113:933–942
- Millar AA, Smith MA, Kunst L (2000) All fatty acids are not equal: discrimination in plant membrane lipids. *Trends Plant Sci* 5:95–101
- Bafor M, Smith MA, Jonsson L, Stobart K, Stymne S (1991) Ricinoleic acid biosynthesis and triacylglycerol assembly in microsomal preparations from developing castor bean (*Ricinus communis*) endosperm. *Biochem J* 280:507–514
- Lin JT, Woodruff CL, Lagouche OJ, McKeon TA, Stafford AE, Goodrich-Tanrikulu M, Singleton JA, Haney CA (1998) Biosynthesis of triacylglycerols containing ricinoleate in castor microsomes using 1-acyl-2-oleoyl-sn-glycero-3-phosphocholine as the substrate of oleoyl-12-hydroxylase. *Lipids* 33:59–69
- He H, Turner C, Chen GQ, Lin JT, McKeon TA (2004) Cloning and characterization of a cDNA encoding diacylglycerol acyltransferase from castor bean. *Lipids* 39:311–318
- Fulda M, Heinz E, Wolter FP (1997) *Brassica napus* cDNA encoding fatty acyl-CoA synthetase. *Plant Mol Biol* 33:911–922
- Schnurr JA, Shockey JM, de Boer GJ, Browse JA (2002) Fatty acid export from the chloroplast. Molecular characterization of a major plastidial acyl-coenzyme A synthetase from *Arabidopsis*. *Plant Physiol* 129:1700–1709
- Van Horn CG, Cavignola JM, Li LO, Wang SL, Granger DA, Coleman RA (2005) Characterization of recombinant long-chain acyl-CoA synthetase isoforms 3 and 6: identification of a novel variant of isoform 6. *Biochemistry* 44:1635–1642
- Gu YQ, Yang C, Thara VK, Zhou J, Martin GB (2000) Pti4 is induced by ethylene and salicylic acid, and its product is phosphorylated by the pto kinase. *Plant Cell* 12:771–785
- Schaefer BC (1995) Revolutions in rapid amplification of cDNA ends: new strategies for polymerase chain reaction cloning of full-length cDNA ends. *Anal Biochem* 227:255–273
- Knoll LJ, Johnson DR, Gordon JI (1995) Complementation of *Saccharomyces cerevisiae* strains containing fatty acid activation gene (FAA) deletions with a mammalian acyl-CoA synthetase. *J Biol Chem* 270:10861–10867
- Urban P, Werck-Reichhart D, Teutsch HG, Durst F, Regnier S, Kazmaier M, Pompon D (1994) Characterization of recombinant plant cinnamate 4-hydroxylase produced in yeast. Kinetic and spectral properties of the major plant P450 of the phenylpropanoid pathway. *Eur J Biochem* 222:843–850
- Shockey JM, Fulda MS, Browse JA (2002) *Arabidopsis* contains nine long-chain acyl-coenzyme A synthetase genes that participate in fatty acid and glycerolipid metabolism. *Plant Physiol* 129:1710–1722

19. Pfaffl MW (2001) A new mathematical model for relative quantification in real-time RT-PCR. *Nucleic Acids Res* 29:2002–2007
20. Black PN, DiRusso CC, Metzger AK, Heimert TL (1992) Cloning, sequencing, and expression of the *fadD* gene of *Escherichia coli* encoding acyl coenzyme A synthetase. *J Biol Chem* 267:25513–25520
21. Fargeman NJ, Black PN, Zhao XD, Knudsen J, DiRusso CC (2001) The acyl-CoA synthetases encoded within FAA1 and FAA4 in *Saccharomyces cerevisiae* function as components of the fatty acid transport system linking import, activation, and intracellular utilization. *J Biol Chem* 276:37051–37059
22. Schmelter T, Trigatti BL, Gerber GE, Mangroo D (2004) Biochemical demonstration of the involvement of fatty acyl-CoA synthetase in fatty acid translocation across the plasma membrane. *J Biol Chem* 279:24163–24170
23. Hayashi H, Bellis LD, Hayashi Y, Nito K, Lato A, Hayashi M, Hara-Nishimura I, Nishimura M (2002) Molecular characterization of an *Arabidopsis* acyl-coenzyme A synthetase localized on glyoxysomal membranes. *Plant Physiol* 130:2019–2026
24. Jiang DW, Englund PT (2001) Four *Trypanosoma brucei* fatty acyl-coa synthetases: fatty acid specificity of the recombinant proteins. *Biochem J* 358:757–761
25. Reumann S, Ma C, Lemke S, Babujee L (2004) Araperox. a database of putative *arabidopsis* proteins from plant peroxisomes. *Plant Physiol* 136:2587–2608
26. Lu CF, Fulda M, Wallis JG, Browse J (2006) A high-throughput screen for genes from castor that boost hydroxy fatty acid accumulation in seed oils of transgenic *Arabidopsis*. *Plant J* 45:847–856
27. McKeon TA, Lin JT (2002) Biosynthesis of ricinoleic acid for castor oil production, in lipid biotechnology. Kuo TM, Gardner HW (eds) Marcel Dekker, New York, pp 129–139
28. Ichihara K, Yamane K, Hirano E (1997) Acyl-CoA synthetase in oilseeds: fatty acid structural requirements for activity and selectivity. *Plant Cell Physiol* 38(6):717–724

# Methodology for the In Vivo Measurement of the $\Delta^9$ -Desaturation of Myristic, Palmitic, and Stearic Acids in Lactating Dairy Cattle

Erin E. Mosley · Mark A. McGuire

Received: 2 January 2007 / Accepted: 7 June 2007 / Published online: 6 July 2007  
© AOCS 2007

**Abstract** There is limited methodology available to quantitatively assess the activity of the  $\Delta^9$ -desaturase enzyme in vivo without chemically inhibiting the enzyme or using radioactively labeled substrates. The objective of these experiments was to develop methodology to determine the incorporation and desaturation of  $^{13}\text{C}$ -labeled fatty acids into milk lipids. In a preliminary experiment, 3.7 g  $[1-^{13}\text{C}]$ myristic acid ( $[1-^{13}\text{C}]14:0$ ), 19.5 g  $[1-^{13}\text{C}]$  palmitic acid ( $[1-^{13}\text{C}]16:0$ ), 20.0 g  $[1-^{13}\text{C}]$ stearic acid ( $[1-^{13}\text{C}]18:0$ ) were combined and infused into the duodenum of a cow over 24 h. In a following experiment, 5.0 g  $[1-^{13}\text{C}]14:0$ , 40.0 g  $[1-^{13}\text{C}]16:0$ , and 50.0 g  $[1-^{13}\text{C}]18:0$  were infused into the abomasums of separate cows as a bolus over 20 min or continuously over 24 h. Milk fat was extracted using chloroform:methanol. Fatty acids were methylated, and fatty acid methyl esters (FAME) were converted to dimethyl disulfide derivatives (DMDS). The FAME and DMDS were analyzed by gas chromatography mass spectrometry. In the preliminary experiment,  $^{13}\text{C}$  enrichment in 14:0 but not 16:0 or 18:0 was observed. When dosage amounts were increased in the following experiment, peak enrichments from the bolus infusion were observed at 8 h. Enrichments for continuous infusion peaked at 16 h for 14:0 and 18:0, and at 24 h for 16:0. The  $\Delta^9$ -desaturase products of these fatty acids were estimated to be 90% of *cis*-9 14:1, 50% of *cis*-9 16:1, and 59% of *cis*-9 18:1. This study demonstrates that  $^{13}\text{C}$ -labeled fatty

acids may be utilized in vivo to measure the activity of the  $\Delta^9$ -desaturase enzyme.

## Abbreviations

CE	Cholesterol ester
CLA	Conjugated linoleic acid
DM	Dry matter
DMDS	Dimethyl disulfide
E	Enrichment
FAME	Fatty acid methyl ester
MDG	Mono and diacylglycerols
MUFA	Monounsaturated fatty acids
$[1-^{13}\text{C}]14:0$	$[1-^{13}\text{C}]$ myristic acid
NEFA	Non-esterified fatty acids
$[1-^{13}\text{C}]16:0$	$[1-^{13}\text{C}]$ palmitic acid
PL	Phospholipid
PUFA	Polyunsaturated fatty acids
SFA	Saturated fatty acids
$[1-^{13}\text{C}]18:0$	$[1-^{13}\text{C}]$ stearic acid
TTR	Tracer to tracee ratio
TG	Triacylglycerol
VA	Vaccenic acid

## Introduction

Impact of the ruminant diet on the fatty acid profile of milk fat and total fat production is an active area of research. Academic and industry recommendations for “ideal” milk fatty acids [1] included changing the fatty acid profile from the typical 5% polyunsaturated fatty acids (PUFA)

E. E. Mosley · M. A. McGuire (✉)  
Department of Animal and Veterinary Science,  
University of Idaho, PO Box 442330,  
Moscow, ID 83844-2330, USA  
e-mail: mmcguire@uidaho.edu

including n-3 fatty acids, 70% saturated fatty acids (SFA), and 25% monounsaturated fatty acids (MUFA) to 10% PUFA, up to 8% SFA with the remainder (>80%) being MUFA. Some reasons for altering the fatty acid profile are to benefit consumer health by decreasing the content of saturated and *trans* fatty acids, and increasing the content of mono and polyunsaturated fatty acids, which are generally considered healthier for the consumer [2]. Included in the mono and polyunsaturated groups of fatty acids are the products of the  $\Delta^9$ -desaturase enzyme, *cis*-9 mono and diunsaturated fatty acids, such as *cis*-9, *trans*-11 18:2 (conjugated linoleic acid; CLA).

One mechanism for specifically altering the *cis*-9 monounsaturated and *cis*-9, *trans*-11 CLA content of milk fat is via the  $\Delta^9$ -desaturase enzyme. The  $\Delta^9$ -desaturase enzyme is present in many tissues within the cow and is very active in the mammary gland inserting a double bond at carbon 9 into saturated fatty acids [3]. The  $\Delta^9$ -desaturase enzyme is important in maintaining liquidity of the milk fat globule [4]. This enzyme uses myristic (14:0), palmitic (16:0) and stearic acid (18:0) as substrates for its actions creating myristoleic (14:1), palmitoleic (16:1) and oleic (18:1) acid, respectively [5]. Additionally, *cis*-9, *trans*-11 CLA can be made from *trans*-vaccenic acid (*trans*-11 18:1; VA) by the action of the  $\Delta^9$ -desaturase in the mammary gland [6, 7]. The substrate product pairs of this enzyme represent approximately 75% of the total fatty acids in milk fat [8]. Thus, the  $\Delta^9$ -desaturase enzyme is a very important determinant for the fatty acid content of milk fat.

One approach that has been explored in the research of the  $\Delta^9$ -desaturase enzyme is to genetically modify ruminant animals to increase the expression of the  $\Delta^9$ -desaturase enzyme gene [9]. However, the use of genetically modified dairy cattle for milk production may not be well received by the consumer. Additionally, its implementation into large commercial production settings may be impractical. On the other hand, understanding the regulation of the  $\Delta^9$ -desaturase enzyme may lead to new management strategies that would result in altered milk fatty acid profile.

Understanding and controlling the activity of the  $\Delta^9$ -desaturase enzyme could lead to increased MUFA content resulting in an improved milk fatty acid profile. The use of *in vivo* measurements of the enzyme's activity in response to various dietary manipulations would provide information on the impact of diet and regulation of the enzyme. A long term goal would be to alter the  $\Delta^9$ -desaturase enzyme activity using nutrients provided in the diet. The first step in this process is to develop an *in vivo* assay of  $\Delta^9$ -desaturase enzyme activity. The objective of these preliminary studies was to determine the methodology necessary to use  $^{13}\text{C}$ -labeled fatty acid substrates to measure the activity of the  $\Delta^9$ -desaturase enzyme *in vivo* in lactating dairy cattle.

While the experiments described only utilized one cow per fatty acid per infusion treatment, the data yielded have provided valuable information in the implementation of this methodology. For example, these data provided the methodology necessary to demonstrate the conversion of [ $^{13}\text{C}$ ]vaccenic acid to *cis*-9, *trans*-11 CLA *in vivo* in lactating dairy cattle and women by our lab [6, 10]. Without the data from each of these cows, we would be limited in our attempts to develop new and innovative techniques.

## Materials and Methods

The University of Idaho Animal Care and Use Committee preapproved all of the procedures involving cows. All cows were housed in tie-stalls and had *ad libitum* access to feed and water. Dietary dry matter (DM) was ~64% and the ingredients were alfalfa silage, barley silage, whole cottonseed, alfalfa hay, and a concentrate pellet. The diet contained 18.1% crude protein, 26.8% neutral detergent fiber, 20.4% acid detergent fiber, and 6.1% ether extract on a DM basis.

In the preliminary experiment, one multiparous Holstein cow received 3.7 g [ $^{13}\text{C}$ ]myristic acid ([ $^{13}\text{C}$ ]14:0), 19.5 g [ $^{13}\text{C}$ ]palmitic acid ([ $^{13}\text{C}$ ]16:0), and 20.0 g [ $^{13}\text{C}$ ]stearic acid ([ $^{13}\text{C}$ ]18:0) delivered in a semi-continuous manner every 3 h over a 24 h period via a duodenal cannula. The cow was milked every 6 h for 36 h prior to the infusion, and every 6 h for 60 h after the initial infusion. At 60 h post infusion, the cow was returned to the milking herd, and milk samples were taken in the parlor every 12 h for 24 h. Blood samples were taken via a jugular catheter at each milking and infusion time. This frequent collection of milk and blood served as the template for determining adequate  $^{13}\text{C}$  labeled fatty acid dosage and sample times in the subsequent experiment.

Three primiparous ruminally cannulated Holstein cows (~150 days in milk, consumed (mean  $\pm$  SE) 18.3  $\pm$  0.8 kg DM, and produced 35.1  $\pm$  0.8 kg of milk per day with 3.5  $\pm$  0.1% fat) each received infusions of different  $^{13}\text{C}$ -labeled fatty acids. Infusion lines were passed through the rumen cannula and secured in the abomasum with a rubber flange. The fatty acids were delivered as a bolus infusion over 20 min or continuous infusion over 24 h. Infusion periods were separated by a 7-day washout period. The free fatty acids (5.0 g of [ $^{13}\text{C}$ ]myristic acid, 40.0 g of [ $^{13}\text{C}$ ]palmitic acid, or 50.0 g of [ $^{13}\text{C}$ ]stearic acid (Isotec, Miamisburg, OH, USA)) were converted to potassium salts and combined with 5 or 15 L of water for the bolus or continuous infusion, respectively. For the bolus infusion period, the cows were milked every 6 h for 24 h prior to the infusion, and every 4 h for 48 h after the

infusion began. At 48 h post infusion, the cows were returned to the milking herd, and milk samples were taken in the parlor every 12 h for 24 h. Prior to each machine milking and every 2 h for 48 h after the infusion began, additional milk samples were taken by hand. Blood samples were taken via a jugular catheter at each hand milking and at times 0.25, 0.5, 0.75, 1, 1.5, 2.5, 3, 3.5, 5, and 7 h after initiation of infusion. Fecal samples were also taken at each hand milking time. For the continuous infusion period, milk and fecal samples were taken as in the bolus period. Blood samples were taken at the hand milking times. Heparinized blood samples (10,000 U/L) were centrifuged for 20 min at  $1,000\times g$  at 4 °C, and the plasma was collected. All plasma, milk, and fecal samples were stored at -20 °C.

Milk and plasma lipids were processed as previously described by Mosley et al. [10]. Freeze-dried ground fecal samples were methylated in a two-step procedure using methanolic-HCl and sodium methoxide [11]. The fatty acid methyl esters (FAME) (<1 mg) of milk, plasma lipid fractions (triacylglycerols (TG), cholesterol esters (CE), mono and diacylglycerols (MDG), phospholipids (PL), and non-esterified fatty acids (NEFA)), and feces were converted to dimethyl disulfide (DMDS) derivatives, and the FAME and DMDS derivatives were analyzed by GC and GC-MS as previously described [6].

#### Data Analysis

For saturated fatty acids, the tracer to tracee ratio (TTR) was calculated from the mass abundance of the molecular ion ( $M$ ) and  $M + 1$  fragments using the equation  $TTR = (M + 1)/M$ . For monounsaturated fatty acids, the TTR was calculated from analysis of the DMDS of FAME. The DMDS derivatives produce distinctive spectral fragments that are indicative of the double bond position when analyzed by mass spectrometry. The TTR was calculated from the mass abundance of the  $^{12}C$  and  $^{13}C$  fragments (mass fragments 217 and 218) using the equation  $TTR = ^{13}C/^{12}C$ . In order to account for the natural levels of  $^{13}C$ , the mean TTR of samples taken before the infusion was subtracted from the TTR of all samples. Therefore, enrichment ( $E$ ) of the fatty acid with  $^{13}C$  at each sample period was calculated as  $(TTR - \text{mean } TTR_{\text{prior to infusion}}) \times 100$ . The calculated  $E$  was adjusted for spectrum skew [12].

Data from the enrichment of milk fatty acids in the bolus and continuous infusions were used to calculate an estimate of the desaturation of the  $^{13}C$ -labeled saturated fatty acids. Trend lines were fit to the observed data from each cow. Area under each curve was calculated and used to determine the percent of the substrate fatty acid desaturated, as previously described [6]. Statistical analyses were not performed on data from either experiment because there

was only one observation per time per treatment per fatty acid. Therefore, the data will only be described.

#### Results

Milk production parameters were not affected by the duodenal or abomasal infusion of  $^{13}C$ -labeled fatty acids. For the preliminary experiment (Fig. 1), average enrichment pre-infusion was 0% for 14:0, 16:0, 18:0, and the  $\Delta^9$ -desaturase products of these fatty acids (data not shown) in milk fat. Enrichment was only detected in 14:0 and 16:0 in milk fat. Enrichment values did not increase for 18:0 or any of the  $\Delta^9$ -desaturase products of these fatty acids in milk fat due to inadequate dosage of the  $^{13}C$ -labeled fatty acids. Similar results were observed when plasma lipid was analyzed (Fig. 1).

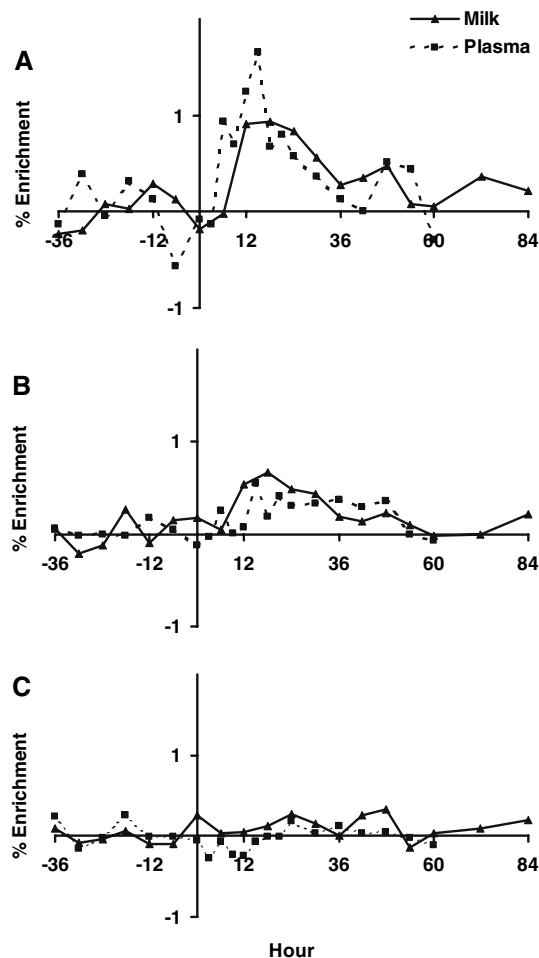


**Fig. 1** Enrichment of  $^{13}C$  in **a** myristic, **b** palmitic, and **c** stearic acid of milk and plasma from one lactating cow receiving a semi-continuous duodenal dose of 3.7 g  $[1-^{13}C]$ myristic acid, 19.5 g  $[1-^{13}C]$ palmitic acid, and 20.0 g  $[1-^{13}C]$ stearic acid. Infusions started at hour zero



In the subsequent experiment, in milk fat the  $^{13}\text{C}$  enrichments from the bolus infusion peaked at 8 h and then declined until not detected after 24 h (Fig. 2). Enrichments for the 24 h continuous infusion reached a plateau from about 12–30 h after initiation of the infusion and then declined. Enrichment was detected in  $\Delta^9$ -desaturase products for both bolus and continuous infusions, with enrichment patterns similar to the saturated substrate. Milk samples taken by hand prior to machine milking for both bolus and continuous abomasal infusions of fatty acids yielded data similar to that from milk fat obtained during machine milking (data not shown). Using area under the curve analysis and FAME data (Table 1), the percent of the product originating from the substrate for the bolus and continuous infusions, respectively, was calculated as 90 and 92% for myristoleic, 51 and 56% for palmitoleic, and

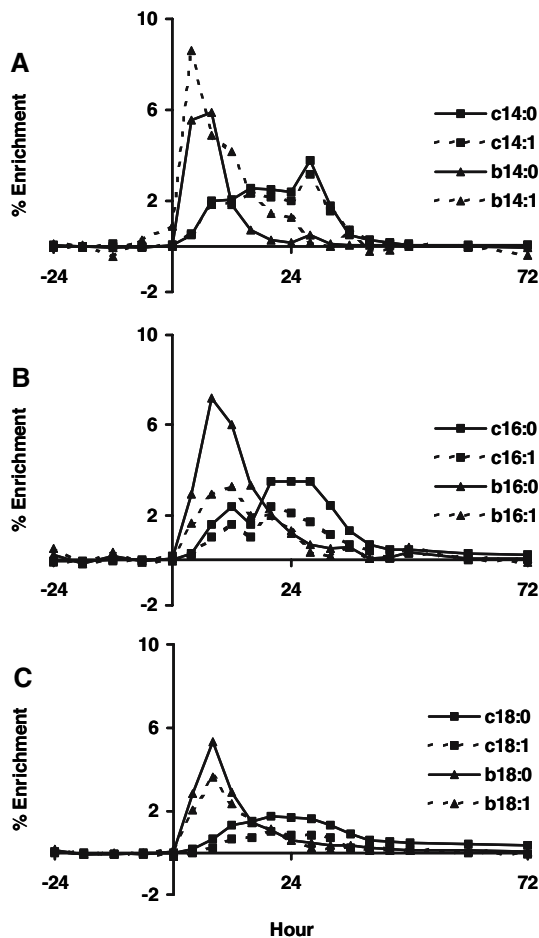


**Fig. 2** Enrichment of  $^{13}\text{C}$  in myristic acid (14:0; A), myristoleic acid (14:1; A), palmitic acid (16:0; B), palmitoleic acid (16:1; B), stearic acid (18:0; C) and oleic acid (18:1; C) of milk during either a bolus (b) or continuous (c) abomasal infusion of (a) 5 g [ $^{13}\text{C}$ ]myristic acid, (b) 40 g [ $^{13}\text{C}$ ]palmitic acid, or (c) 50 g [ $^{13}\text{C}$ ]stearic acid. Bolus infusions were delivered within 20 min while continuous infusions were delivered over 24 h. Infusions started at hour zero. Each panel represents data from a single cow

**Table 1** Fatty acid composition of milk fat

Fatty acid	Infusion		
	Preliminary	Bolus	Continuous
	g/100 g fatty acids		
4:0	3.3 ± 0.12	2.8 ± 0.2	2.6 ± 0.2
6:0	2.3 ± 0.11	1.5 ± 0.2	1.6 ± 0.2
8:0	1.1 ± 0.06	0.8 ± 0.2	0.9 ± 0.2
10:0	2.3 ± 0.16	1.6 ± 0.5	1.9 ± 0.5
12:0	2.4 ± 0.16	1.7 ± 0.5	2.2 ± 0.6
13:0	0.1 ± 0.01	0.1 ± 0.01	0.1 ± 0.02
14:0	9.2 ± 0.42	7.4 ± 1.2	8.6 ± 1.2
<i>cis</i> -9 14:1	0.7 ± 0.06	0.5 ± 0.1	0.6 ± 0.1
15:0	0.7 ± 0.02	0.7 ± 0.1	0.8 ± 0.1
16:0	29.5 ± 0.68	26.4 ± 1.2	26.9 ± 1.6
17:0	1.0 ± 0.07	1.2 ± 0.2	1.2 ± 0.1
<i>cis</i> -9 16:1	0.5 ± 0.02	0.7 ± 0.1	0.6 ± 0.1
18:0	16.2 ± 0.69	14.9 ± 1.9	13.3 ± 1.02
<i>trans</i> -18:1 <sup>a</sup>	4.2 ± 0.21	3.0 ± 0.3	2.8 ± 0.2
<i>cis</i> -9 18:1	18.4 ± 0.85	27.8 ± 2.2	26.8 ± 3.3
<i>cis</i> -18:1 <sup>b</sup>	2.4 ± 0.19	1.6 ± 0.1	1.5 ± 0.1
<i>cis</i> -9, <i>cis</i> -12 18:2	2.6 ± 0.45	2.9 ± 0.3	2.7 ± 0.3
<i>cis</i> -9, <i>trans</i> -11 18:2	0.3 ± 0.02	0.4 ± 0.04	0.4 ± 0.1
<i>cis</i> -9, <i>cis</i> -12, <i>cis</i> -15 18:3	0.3 ± 0.03	0.4 ± 0.04	0.4 ± 0.1
20:0	0.1 ± 0.01	0.1 ± 0.03	0.1 ± 0.01
Others	2.3 ± 0.09	3.7 ± 0.2	3.8 ± 0.2

Values represent a mean of all samples taken in each experimental infusion period. Data for preliminary infusion are mean ± SD from 20 measurements taken from one cow. Data for bolus and continuous infusions are mean ± SD from 33 measurements taken from each of three cows during each infusion

<sup>a</sup> *trans*-18:1 sum of all *trans*-18:1 isomers

<sup>b</sup> *cis*-18:1 sum of all *cis*-18:1 isomers excluding *cis*-9

74 and 43% for oleic acid, resulting in 5.2 and 7.0% of myristic acid, 2.6 and 2.5% of palmitic acid, and 60.3 and 48.7% of stearic acid being desaturated by the  $\Delta^9$ -desaturase enzyme.

Furthermore,  $^{13}\text{C}$  enrichment was observed in 14:0, 16:0, and 18:0 in the TG, CE, NEFA, and PL of plasma in the bolus infusion. Between 1.5 and 3 h post-infusion, maximal enrichments for TG, CE, NEFA, PL, and total plasma 14:0 were 81.1, 2.6, 3.8, 15.4, and 33.5%, respectively. Between 2 and 3 h post-infusion, maximal enrichments for TG, CE, NEFA, PL, and total plasma 16:0 were 92.6, 5.2, 5.2, 1.4, and 9.0%, respectively. Maximal enrichments for TG, CE, NEFA, PL, and total plasma 18:0 were also detected between 2 and 3 h post-infusion (26.5, 9.1, 7.5, 0.4, and 3.3%, respectively). Maximal enrichments detected in the continuous infusions occurred at later times than was observed in the bolus period. For example,

maximal enrichment of TG, CE, NEFA, PL, and total plasma 14:0 occurred between 8 and 24 h post-infusion (13.4, 2.2, 1.2, 3.0, and 5.1%, respectively), between 20 and 24 h post-infusion for 16:0 (6.2, 0.3, 0.5, 1.8, and 1.8%, respectively), and again between 8 and 24 h post-infusion for 18:0 (2.4, 2.0, 0.2, 0.6, and 0.9%, respectively). However, enrichment was not observed in the MDG fractions for either the bolus or continuous infusions. Unlike the enrichment of the infused saturated fatty acids in plasma lipid fractions, the  $\Delta^9$ -desaturase products of these fatty acids were not enriched at any time with  $^{13}\text{C}$  in any plasma lipid fraction (data not shown).

In fecal samples (Fig. 3),  $^{13}\text{C}$  enrichments from the bolus infusion were maximal from 8 to 10 h and then declined until not detected after about 20 h. The  $^{13}\text{C}$  enrichments from the continuous infusion reached a plateau from about 16 to 30 h and then began to decline. No enrichment was detected for any of the  $\Delta^9$ -desaturase products of these fatty acids in fecal lipid during either the bolus or continuous infusions (data not shown). The ratio of the area under the bolus and continuous enrichment curves was 0.43, 0.56, and 0.57 for myristic, palmitic, and stearic acids, respectively.

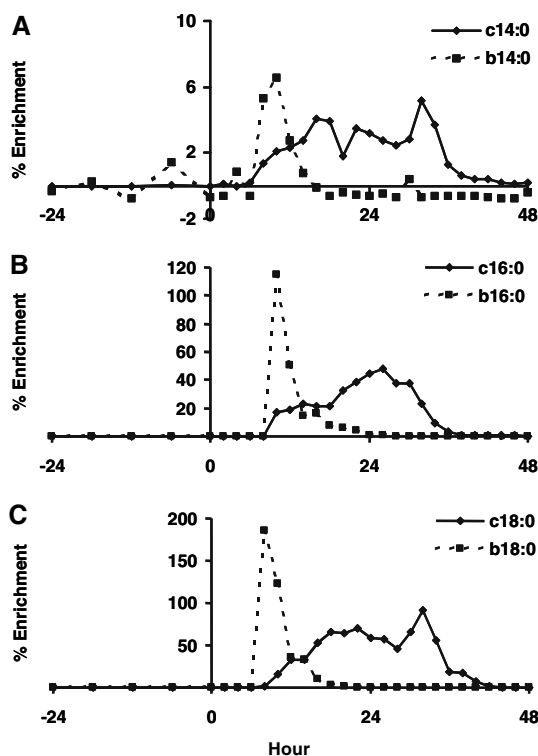


**Fig. 3** Enrichment of  $^{13}\text{C}$  in myristic acid (14:0; A), palmitic acid (16:0; B), and stearic acid (18:0; C) of feces during either a bolus (b) or continuous (c) abomasal infusion of (a) 5 g [ $^{13}\text{C}$ ]myristic acid, (b) 40 g [ $^{13}\text{C}$ ]palmitic acid, or (c) 50 g [ $^{13}\text{C}$ ]stearic acid. Bolus infusions were delivered within 20 min while continuous infusions were delivered over 24 h. Infusions started at hour zero. Each panel represents data from a single cow

## Discussion

Industry and academic recommendations for altering the profile of milk fatty acids included decreasing SFA and increasing unsaturated fatty acids, MUFA and PUFA [1]. While the recommendations may be dated, there is still strong desire to enrich milk with MUFA while reducing SFA [13]. For example, conversion of SFA to MUFA in milk fat would be beneficial to the human consumer by reducing their risk of coronary heart disease [14]. Understanding and controlling the activity of the  $\Delta^9$ -desaturase enzyme would lead to increased MUFA, thereby improving the milk fatty acid profile.

The  $\Delta^9$ -desaturase enzyme is present in many tissues within the cow and inserts a double bond at carbon 9 into saturated fatty acids [3]. The enzyme in bovine tissues occurs primarily in mammary [15] and adipose tissue [16, 17] while rates of desaturation in liver are quite low [18]. Variability in desaturase activity between tissues may be explained somewhat by dietary [19] and breed differences [20]. Our data agree that the majority of *cis*-9 desaturation of fatty acids occurs primarily in the mammary gland within 24 h of absorption. However, the lack of detection of  $^{13}\text{C}$  in the plasma of  $\Delta^9$ -desaturase products indicates that tissues other than the mammary gland do not contribute to their synthesis. However, the lower activity of the  $\Delta^9$ -desaturase enzyme in tissues other than mammary and the rate of turnover of individual fatty acids between lipid pools may simply be beyond the detection limits of the assay. It may be possible to detect these changes using continuous infusions longer than 24 h with higher doses of the  $^{13}\text{C}$  tracer.

It is also interesting to note the differences in maximal enrichment detected in the various plasma lipid fractions. In our initial experiment, we only measured total plasma enrichment (Fig. 1). It was evident that the enrichments achieved in milk fatty acids were not possible unless lipid classes within the total plasma had enrichment that exceeded that which was measured in milk. For example, we labeled only a small lipid pool in the plasma and larger unlabeled lipid pools essentially diluted the total enrichment values. This is supported by our second experiment where the TG pool contained the greatest maximal enrichment regardless of infusion type. As we would not be able to attain enrichments in the final pool (milk fatty acids) that was greater than our starting material (the plasma lipid pool utilized by the mammary gland to extract fatty acids), our data indicate that the TG pool is the primary pool utilized for delivering preformed fatty acids to the mammary gland. More research is needed for further analysis of fatty acid transfer between the various plasma lipid classes and the mammary gland. This type of data could be used to determine the actual contribution of each

plasma lipid class to the fatty acids extracted for milk fat synthesis by the mammary gland.

This study utilized  $^{13}\text{C}$ -labeled fatty acids to develop an *in vivo* assay of  $\Delta^9$ -desaturase enzyme activity in lactating dairy cattle. Typically, enzyme assays utilize a radiolabeled substrate and microsomal preparations from collected tissue in an *in vitro* system [16, 21]. The conditions used to isolate microsomal protein for *in vitro* assays and the detection limits associated with these methods may inhibit one's ability to quantitatively determine the conversion of substrate to product as it relates to *in vivo* metabolism. For example, *in vitro* estimates of mammary desaturation of 18:0 are only ~31% [21] while *in vivo* calculations provide an estimate of ~52% [22]. The development of an *in vivo* assay (i.e., utilizing metabolic tracer methodology coupled with measurements of gene expression changes) may prove useful when quantitatively determining treatment effects on the  $\Delta^9$ -desaturase enzyme while examining all of the fatty acid substrates simultaneously. Similar concepts for the *in vitro* assay are used for the *in vivo* assay, without using a radioactive fatty acid and with minimal disruption of the physiological state of the animal. The stably labeled fatty acid is used as a metabolic tracer, preferably with a dose that does not alter the fatty acid pools within the animal. Additionally, the stable tracer may be detected in the blood and milk. This labeling of two pools allows for identification of desaturation occurring in the mammary gland versus the rest of the body tissues. A drawback of this method is that liver, adipose, and other tissues cannot be distinguished from each other.

Reports of alterations in the synthesis of  $\Delta^9$ -desaturase enzyme products generally focus on relative changes in some ratio of the milk fat concentrations of the product to substrate, also referred to as the desaturase index. The desaturase index does not provide a quantitative measurement of  $\Delta^9$ -desaturase enzyme activity, it only serves as a proxy measurement. In order to estimate the actual enzyme activity, one approach is to assume that 100% of myristoleic acid is derived from the  $\Delta^9$ -desaturase enzyme and then chemically inhibit the enzyme, again assuming 100% efficiency [7]. Alternatively, estimates of  $\Delta^9$ -desaturase enzyme activity may be based on the duodenal flow of the  $\Delta^9$ -desaturase substrates and milk fat composition of the products and substrates [23] or arterio-venous differences in the  $\Delta^9$ -desaturase enzyme products and substrates [22].

Our data show that ~90% of myristoleic and ~50% of palmitoleic acids are synthesized by the  $\Delta^9$ -desaturase enzyme. We are unaware of any *in vivo* estimates for the synthesis of myristoleic or palmitoleic acids in the lactating bovine. Previously, the desaturation of stearic to oleic acid was calculated to be 52% based on arterio-venous differences [22]. Our data show that during a continuous infusion, ~49% of the stearic acid pool is desaturated, yielding

~43% of the oleic acid in the milk fat. However, during the bolus infusion, the conversion was increased to ~60%, yielding ~74% of the oleic acid. It is likely that the 50 g bolus dose of [1- $^{13}\text{C}$ ]18:0 increased the typical quantity of stearic acid available to be absorbed from the intestine. This is supported by differences in the label recovered in the feces. In all instances, approximately two times more label was recovered in the feces during the continuous infusions. The  $^{13}\text{C}$  enrichment of stearic acid in milk was most affected. One possible explanation is the preferential use of specific fatty acids for various metabolic functions. Another consideration would be differences in the digestibilities of the various fatty acids, as shorter chain fatty acids are considered more digestible [24]. We did not evaluate these types of factors, however, it is an area for future investigations utilizing  $^{13}\text{C}$ -labeled fatty acid methodology. Despite these effects due to type of infusion, the methodology does yield similar results when compared to other data, as demonstrated in our infusion of [1- $^{13}\text{C}$ ]vacenic acid in lactating dairy cows [6].

The  $^{13}\text{C}$  enrichment detected is dependent on the dose of  $^{13}\text{C}$ -labeled fatty acid. In the preliminary experiment, the dose of  $^{13}\text{C}$ -labeled fatty acids delivered was underestimated because the dose was initially calculated based on the daily output of each fatty acid in milk. The  $^{13}\text{C}$  enrichment was only detected in 16:0 and 18:0 when the dose was about 12% of the milk output of both substrate and product (Table 2). The 14:0 dose was acceptable in both experiments. However, the higher dose used in experiment 2 was needed to detect the  $^{13}\text{C}$  enrichment in desaturase products. The comparison of bolus versus continuous administration of the  $^{13}\text{C}$ -labeled fatty acids also showed a relationship between dose, maximum enrichment detected, and route of administration. While both types of infusion provide information about the utilization of the  $^{13}\text{C}$ -labeled fatty acids *in vivo*, the bolus infusion resulted in greater  $^{13}\text{C}$  enrichment values for the same mass of fatty acids delivered continuously over 24 h. Because of the expense of  $^{13}\text{C}$ -labeled fatty acids and the analytical

**Table 2** Dose of  $^{13}\text{C}$ -labeled fatty acids based on milk fatty acid output

Fatty acid	Preliminary experiment			Bolus versus continuous experiment		
	Dose (g)	Output (g)	%	Dose (g)	Output (g)	%
14:0 + <i>cis</i> -9 14:1	3.7	120	3.1	5.0	98	5.1
16:0 + <i>cis</i> -9 16:1	19.5	370	5.4	40.0	321	12.5
18:0 + <i>cis</i> -9 18:1	20.0	420	4.8	50.0	476	10.5

%, dose as a percent of output

techniques utilized, the ability to maximize  $^{13}\text{C}$  enrichment with minimal input is desirable.

This study demonstrates that  $^{13}\text{C}$ -labeled fatty acids may be utilized in vivo to measure the activity of the  $\Delta^9$ -desaturase enzyme. Doses of the  $^{13}\text{C}$ -labeled fatty acids are dependent on the production level of the animal and preliminary measurements of milk fat would be warranted for determination of an appropriate dosage level. This methodology will provide a powerful tool in assessing dietary impacts on  $\Delta^9$ -desaturase enzyme activity. In the future, this in vivo assay of enzyme activity may be coupled with other techniques such as gene expression analyses in order to provide more insight on the impact of treatments on the  $\Delta^9$ -desaturase enzyme.

**Acknowledgments** Supported in part by the United Dairymen of Idaho, the Idaho Agricultural Experiment station, NIH-BRIN, National Research Initiative Competitive Grant nos. 2003-35206-13669 and 2006-35206-16819 from the USDA Cooperative State Research, Education, and Extension Service, and NIH-NRRI grant P20 RR15587.

## References

- O'Donnell JA (1989) Milk fat technologies and markets: a summary of the Wisconsin milk marketing board 1988 roundtable. *J Dairy Sci* 72:3109–3115
- Hu FB, Manson JE, Willett WC (2001) Types of dietary fat and risk of coronary heart disease: a critical review. *J Am Coll Nutr* 20:5–19
- Christie WW (1981) The effects of diet and other factors on the lipid composition of ruminant tissues and milk. In: *Lipid metabolism in ruminant animals*. Pergamon Press, Oxford, pp 193–226
- Timmen H, Patton S (1988) Milk fat globules: fatty acid composition, size and in vivo regulation of fat liquidity. *Lipids* 23:685–689
- Ntambi JM (1999) Regulation of stearoyl-CoA desaturase by polyunsaturated fatty acids and cholesterol. *J Lipid Res* 40:1549–1558
- Mosley EE, Shafii B, Moate PJ, McGuire MA (2006a) Conjugated linoleic acid (*cis*-9, *trans*-11 CLA) is synthesized directly from vaccenic acid in lactating dairy cattle. *J Nutr* 136:570–575
- Griinari JM, Corl BA, Lacy SH, Chouinard PY, Nurmela KVV, Bauman DE (2000) Conjugated linoleic acid is synthesized endogenously in lactating dairy cows by  $\Delta^9$ -desaturase. *J Nutr* 130:2285–2291
- Jensen RG (2002) The composition of bovine milk lipids: January 1995 to December 2000. *J Dairy Sci* 85:295–350
- Reh WA, Maga EA, Collette NMB, Moyer A, Conrad-Brink JS, Taylor SJ, DePeters EJ, Oppenheim S., Rowe JD, BonDurant RH, Anderson GB, Murray JD (2004) Hot topic: using a stearoyl-CoA desaturase transgene to alter milk fatty acid composition. *J Dairy Sci* 87:3510–3514
- Mosley EE, McGuire MK, Williams JE, McGuire MA (2006b) *cis*-9, *trans*-11 conjugated linoleic acid is synthesized from vaccenic acid in lactating women. *J Nutr* 136:2297–2301
- Kramer JK, Fellner V, Dugan MER, Sauer FD, Mossoba MM, Yurawecz MP (1997) Evaluating acid and base catalysts in the methylation of milk and rumen fatty acids with special emphasis on conjugated dienes and total *trans* fatty acids. *Lipids* 32:1219–1228
- Wolfe RR (1992) Radioactive and stable isotope tracers in biomedicine, principles and practice of kinetic analysis. Wiley, New York
- Hillbrick G, Augustin MA (2002) Milkfat characteristics and functionality: opportunities for improvement. *Aust J Dairy Technol* 57:45–51
- German JB, Dillard CJ (2004) Saturated fats: what dietary intake? *Am J Clin Nutr* 80:550–559
- McDonald TM, Kinsella JE (1973) Stearyl-CoA desaturase of bovine mammary microsomes. *Arch Biochem Biophys* 156:223–231
- St John LC, Lunt DK, Smith SB (1991) Fatty acid elongation and desaturation enzyme activities of bovine liver and subcutaneous adipose tissue microsomes. *J Anim Sci* 69:1064–1073
- Yang A, Larsen TW, Smith SB, Tume RK (1999)  $\Delta^9$ -desaturase activity in bovine subcutaneous adipose tissue of different fatty acid composition. *Lipids* 34:971–978
- Bell AW (1981) Lipid metabolism in liver and selected tissues and in the whole body of ruminant animals. In: *Lipid metabolism in ruminant animals*. Pergamon Press, Oxford, pp 363–410
- Chang JHP, Lunt DK, Smith SB (1992) Fatty acid composition and fatty acid elongase and stearoyl-CoA desaturase activities in tissues of steers fed high oleate sunflower seed. *J Nutr* 122:2074–2080
- Siebert BD, Pitchford WS, Kruk ZA, Kuchel H, Deland MPB, Bottema CDK (2003) Differences in  $\Delta^9$ -desaturase activity between Jersey and Limousin-sired cattle. *Lipids* 38:539–543
- Kinsella JE (1972) Stearyl CoA as a precursor of oleic acid and glycerolipids in mammary microsomes from lactating bovine: possible regulatory step in milk triglyceride synthesis. *Lipids* 7:349–355
- Enjalbert F, Nicot M, Bayourthe C, Moncoulon R (1998) Duodenal infusions of palmitic, stearic or oleic acids differently affect mammary gland metabolism of fatty acids in lactating dairy cows. *J Nutr* 128:1525–1532
- Piperova LS, Sampugna J, Teter BB, Kalscheur KF, Yurawecz MP, Ku Y, Morehouse KM, Erdman RA (2002) Duodenal and milk *trans* octadecenoic acid and conjugated linoleic acid (CLA) isomers indicate that postabsorptive synthesis is the predominant source of *cis*-9-containing CLA in lactating dairy cows. *J Nutr* 132:1235–1241
- Steele W, Moore JH (1968) The digestibility coefficients of myristic, palmitic, and stearic acids in the diet of sheep. *J Dairy Res* 35:371–376

# Highly Efficient Enzymatic Synthesis of 2-Monoacylglycerides and Structured Lipids and their Production on a Technical Scale

Jan Pfeffer · Andreas Freund · Rachid Bel-Rhlid ·  
Carl-Erik Hansen · Matthias Reuss · Rolf D. Schmid ·  
Steffen C. Maurer

Received: 23 March 2007 / Accepted: 27 May 2007 / Published online: 11 July 2007  
© AOCs 2007

**Abstract** We report here a two-step process for the high-yield enzymatic synthesis of 2-monoacylglycerides (2-MAG) of saturated as well as unsaturated fatty acids with different chain lengths. The process consists of two steps: first the unselective esterification of fatty acids and glycerol leading to a triacylglyceride followed by an *sn*1,3-selective alcoholysis reaction yielding 2-monoacylglycerides. Remarkably, both steps can be catalyzed by lipase B from *Candida antarctica* (CalB). The whole process including esterification and alcoholysis was scaled up in a miniplant to a total volume of 10 l. With this volume, a two-step process catalyzed by CalB for the synthesis of 1,3-oleoyl-2-palmitoylglycerol (OPO) using tripalmitate as starting material was established. On a laboratory scale, we obtained gram quantities of the synthesized 2-monoacylglycerides of polyunsaturated fatty acids such as arachidonic-, docosahexaenoic- and eicosapentaenoic acids and up to 96.4% of the theoretically possible yield with 95% purity. On a technical scale (>100 g of product, >5 l of reaction volume), 97% yield was reached in the esterification and 73% in the alcoholysis and a new promising process for the enzymatic synthesis of OPO was established.

**Keywords** 2-Monoacylglycerides · Lipase · Miniplant technology · OPO · Polyunsaturated fatty acids (PUFA) · Up scaling

## Introduction

Arachidonic acid (ARA or C20:4n-6), docosahexaenoic acid (DHA or C22:6n-3) and eicosapentaenoic acid (EPA or C20:5n-3) are polyunsaturated fatty acids (PUFA) involved in a wide range of biologically relevant functions and have strong effects on human health [1, 2]. ARA is an essential fatty acid in human nutrition and a major component of human milk and necessary for the cognitive development of infants. ARA is also a precursor of biologically active prostaglandins and leukotrienes, involved in inflammatory processes [3–5]. DHA is important for the development of the central nervous system [3]. EPA shows significant effects in preventing heart diseases and lowering blood cholesterol levels and thus reduces the risk of arteriosclerosis [6, 7]. The fatty acid distribution on the glycerol backbone influences the adsorption and tissue uptake of glycerides [8, 9]. Generally speaking, 2-monoacylglycerides (2-MAG) are most readily absorbed through the intestinal mucosa and are also the most rapidly absorbed among PUFA derivatives. 2-MAG have very good emulsifying properties and are physiologically essential molecules involved in lipid absorption. In vertebrates, 2-MAG and not glycerol is preferentially utilised for triacylglycerol and phosphatidylcholine biosynthesis [10]. Up to now, these molecules only have limited industrial applications because of difficulties in their synthesis. The chemical synthesis takes several steps, a costly purification and often results in very low yields [11]. Enzymatic synthesis of 2-MAG usually depends on two types of li-

---

J. Pfeffer · R. D. Schmid · S. C. Maurer (✉)  
Institute of Technical Biochemistry,  
University of Stuttgart,  
Allmandring 31, 70569 Stuttgart, Germany  
e-mail: steffen.maurer@itb.uni-stuttgart.de

A. Freund · M. Reuss  
Institute of Biochemical Engineering,  
University of Stuttgart,  
Allmandring 31, 70569 Stuttgart, Germany

R. Bel-Rhlid · C.-E. Hansen  
Nestlé Research Center, Lausanne, Nestec Ltd.,  
Vers-Chez-Les-Blanc, 1000 Lausanne 26, Switzerland

pase: an unspecific enzyme for the esterification and an *sn*1,3-specific lipase for the alcoholysis (usually ethanololysis) reaction to the 2-MAG.

The type of fatty acid in the 1,3-position of triglycerides [12] also influences the intestinal adsorption as 2-MAG after the TAG are regiospecifically hydrolyzed in mouth, stomach and small intestine. Symmetrically structured triglycerides incorporate the same fatty acids in *sn*1 and *sn*3 position (ABA type). ABA with medium chain fatty acid groups (C<sub>6</sub>–C<sub>10</sub>) in the outer positions and a PUFA in the middle position have excellent dietary and absorption characteristics. Additionally the PUFA residue is protected against oxidation by the two saturated fatty acid residues protecting the more oxidizable PUFA in the middle position from oxygen (sterical reasons). Several experiments by Endo and colleagues proved that 1,2-dipalmitoyl-3-PUFA-glycerol is oxidised much more readily than 1,3-dipalmitoyl-2-PUFA-glycerol [13, 14]. The medium-chain fatty acids are easily hydrolyzed in the gastrointestinal tract by the pancreatic lipase. The resulting 2-MAG are readily absorbed and used either as a high-energy resource or for several health-protecting actions [8, 15, 16].

Fish oil, especially tuna and salmon oils, are well-known and inexpensive natural sources of PUFAs. A large variety of health products are made of or contain fish oil-derived compounds, e.g., the encapsulation of these oils in gelatine is of interest as a health food supplement for the prevention and treatment of cardiovascular diseases, neurodegenerative disorders and cancer [9, 17].

1,3-Oleoyl-2-palmitoylglycerol (OPO) is an important ABA-type TAG in infant nutrition. Human milk fats contain palmitic acid predominantly in the *sn*2-position of TAG. Often infant formulas contain palmitic acid in *sn*1,3-positions, which leads to the formation of calcium soaps after their release. These soaps are only poorly absorbed by the intestine, which results in indigestion and loss of calcium [18].

We have developed a two-step process leading to 2-monoacylglycerides which is enzymatically catalyzed by lipases. Lipases [triacylglycerol-hydrolases (EC 3.1.1.3)] catalyze the hydrolysis of triacylglycerols at the interface between water and the hydrophobic substrate. Besides the hydrolysis of triacylglycerols, lipases also catalyze the enantio- and regioselective hydrolysis or synthesis of a wide range of natural and unnatural esters [19, 20]. Especially lipases from microorganisms have received a lot of interest because they are useful catalysts for many industrial applications [21, 22] such as ester synthesis, optical resolution [23–25], transesterification or washing processes [26]. In the process described here the same lipase was used for both steps - the esterification as well as the following alcoholysis: Lipase B from *Candida antarctica* (CalB) [27]. CalB reveals high enantioselectivity against secondary alcohols and, due

to its extraordinary stability in organic solvents and at high temperature, has become one of the most frequently used enzymes in industrial applications [28]. For hydrolysis or transesterification of TAG, CalB is classified as an *sn*1,3-specific lipase. On the other side it is known that in esterification, CalB forms homogeneous TAG (AAA type). Starting from this knowledge, our strategy was first to synthesize a homogeneous TAG of PUFAs followed by the conversion to the desired 2-MAG. In the present work we synthesized the 2-MAG of three different PUFA: ARA, DHA and EPA all in gram quantities and high purities. We also showed that 2-MAG of short and medium chain length can be synthesized by the same method.

After this process was successfully established on a laboratory scale it was transferred and scaled up to a miniplant (total reaction volume up to 10 l). A miniplant is a minimized production line involving all processing steps regarding different parameters such as temperature, pH value and mass transfer.

For the synthesis of OPO, a CalB-driven two-step miniplant process was established. Starting with tripalmitate, the substrate was first converted to the corresponding 2-monopalmitate in an alcoholysis reaction followed by an esterification with oleic acid. Again only CalB was used as the biocatalyst.

## Materials and Methods

### Lipases and Chemicals

Lipase CalB (Novozym 435) was from Novozymes (Bagsvaerd, Denmark). The lipase gene was derived from *Candida antarctica* and transferred to the host organism *Aspergillus oryzae* in which the lipase was expressed. The purified lipase was immobilized on a macroporous acrylic resin. All lipases were purchased from Fluka. Immobilized CalB was removed after the reaction by filtration, washed three times, dried in a desiccator and afterwards could be used again. All chemicals except the PUFAs and solvents used were of analytical reagent grade and purchased from normal suppliers (Sigma, Fluka and Riedel de Haën). PUFAs were supplied by Nu-Chek Prep (Elysian, USA). References of MAG, DAG and TAG for GC/MS analysis were also supplied by Nu-Chek Prep.

### Esterification Reaction

Purified 2-MAG (100 mg, obtained from alcoholysis reactions) or glycerol and fatty acids (molar ratio 1:3) [29] were dissolved in 20 ml *n*-hexane. The water, generated during the reaction was removed by addition of 200 mg activated molecular sieve (pore diameter 3 Å, bead

diameter ~2 mm, UOP Type 3A, Fluka, Buchs, Switzerland). The mixture was stirred magnetically (level 10 on a RCTbasic, IKA Labortechnik, Staufen, Germany) and incubated at 50 °C. The reaction was started by adding 100 mg immobilized lipase (CalB). After 24 h the reaction was stopped by removing the lipase (Fig. 1) as described above.

### Alcoholysis Reaction of Triglycerides

The homogeneous TAG of PUFA or other TAG (100 mg) were mixed with pure ethanol (molar ratio TAG:ethanol is 1:4) and emulsified for 30 min at 25 °C. The reaction was started by adding CalB (100 mg) and stopped after 4–5 h by filtration of the catalyst (Fig. 1). The reaction process was monitored using TLC.

### Reactions on a Technical Scale (Reaction Volume: 8 l)

The miniplant was built by the Institute of Biochemical Engineering (IBVT, University of Stuttgart, Germany) within a Bosch-Rexroth frame (UTZ Ratio Technik, Korb, Germany). Process control equipment and software were supplied by National Instruments Germany GmbH, München and National Instruments (Labview®, Austin, TX, USA), respectively. The enzyme reactions were performed in a 10 l glass-vessel (Type BDAV, HWS Labortechnik, Mainz, Germany). The reaction mixture was stirred by air-driven stirrers (Gebr. Buddeberg GmbH, Mannheim, Germany). The temperature was controlled by a thermostat (F33, Julabo, Seelbach, Germany) [30].

The reactions in the miniplant were performed as batch processes under a nitrogen atmosphere. The amounts of

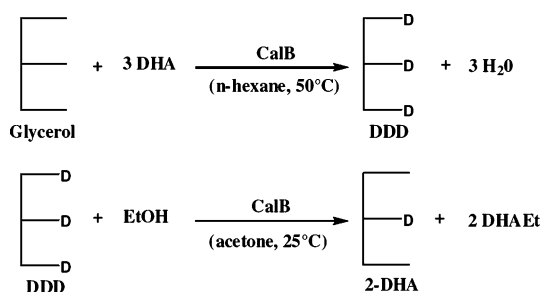


**Fig. 1** Two-step synthesis of 2-monoglyceride of DHA catalyzed by CalB. The process consists of two steps. First esterification of glycerol and free fatty acids leads to homogeneous TAG and water. TAGs are further converted in an alcoholysis reaction to the corresponding 2-MAGs and ethyl esters. The ethyl esters are removed in the following purification step in a two-phase (acetonitrile/water and *n*-hexane) system via a separatory funnel. Both steps are catalyzed by CalB which acts unspecific in the esterification and *sn*1,3-specific in the following alcoholysis. Synthesis of the 2-MAGs of AA and EPA was achieved according to the same scheme (D, DHA: Docosahexaenoic acid; DHAEt: DHA ethyl ester)

chemicals and lipase were calculated to the working volume of the miniplant which was 8 litres.

Because of the high price of highly purified PUFA, erucic acid (EA or C22:1n-9), a cheaper, long-chain unsaturated fatty acid was used as a model substrate for the esterification with glycerol. 8 l *n*-hexane, 304 g erucic acid, 37 g glycerol, 60 g immobilized CalB and 500 g molecular sieves (pore diameter 3 Å, beads diameter ~2 mm, UOP Type 3A, Fluka, Buchs, Switzerland) were applied.

In the alcoholysis reaction tripalmitate was converted to 2-monopalmitate. TAG and ethanol were emulsified in a molar ratio of 1:10 and then the vessel was filled up with acetone to the working volume (8 l acetone, 283 g tripalmitate, 161 g ethanol and 60 g immobilized CalB).

This product was afterwards esterified with oleic acid leading to OPO (8 l *n*-hexane, 84 g 2-monopalmitate, 260 g oleic acid, 60 g immobilized CalB and 500 g molecular sieves; Fig. 2).

### Purification of 2-Monoacylglycerides and Triglycerides

For purification of 2-MAG of PUFA, the solvent was evaporated and the concentrate was dissolved in acetonitrile/water (95:5 v/v, 10-fold volume compared to the concentrate) and washed three times with the same volume of hexane for ethyl ester removal [31]. The pure 2-MAG are found in the acetonitrile/water phase.

2-Monopalmitate was purified via crystallization. After filtering off the catalyst, the excess solvent was evaporated and the residue was dissolved in *n*-hexane:methyl-*tert*-butylether (MTBE) (70:30 v/v, 10-fold volume compared to the concentrate) and stored for 1 h at –25 °C. After this period, the white crystals formed were collected by filtration at –25 °C. The supernatant containing ethyl esters, fatty acids, and a small amount of diglycerides was

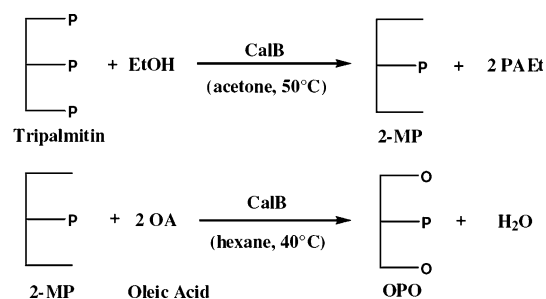


**Fig. 2** Two-step synthesis of OPO catalyzed by CalB. Starting substrate for OPO synthesis is tripalmitate, which is converted to 2-monopalmitate in an alcoholysis reaction and afterwards purified by crystallization. The following reaction consisted of esterification of 2-monopalmitate with oleic acid to OPO, which was purified via a silica-gel column. Both steps were catalyzed by CalB (PAEt: Palmitic acid ethyl ester)

discarded. The 2-MP was recrystallized until the TLC plate showed only one band of 2-MP. The purity of 2-MP was confirmed by GC/MS analysis.

For purification of TAG, the solvent was evaporated and the TAG purified by silica gel column chromatography eluted with *n*-hexane/methyl-*tert*-butylether (MTBE) (70:30 v/v). The TAG are eluted first followed by ethyl ester, fatty acids, di- and finally monoacylglycerides.

### TLC Analysis

For rapid analysis during the process, thin-layer-chromatography (TLC) was performed using aluminium sheets with silica gel (Merck KGaA, Darmstadt, Germany) as the stationary phase; *n*-hexane/MTBE (70:30 v/v) was the mobile phase. TLCs were developed in a staining solution (10 g cer(IV)-sulphate, 2 g molybdato-phosphoric acid, 10 ml concentrate sulphuric acid, 100 ml water) for 30 s and afterwards dried with a heat gun. The spots were identified using the corresponding references.

### GC/MS Analysis

For GC/MS analysis, samples were derivatized with 1% of trimethylchlorosilane in *N,O*-bis(trimethylsilyl)trifluoroacetamide. The derivatization reagent converts all hydroxyl- and carboxyl groups to the corresponding trimethylsilyl ethers and -esters. After addition of the derivatization solution, samples were incubated for 30 min at 60 °C.

Products were identified on a Shimadzu GC/MS-QP2010 (Shimadzu Corporation, Kyoto, Japan) equipped with a 30 m FS-Supreme-5 column (5% diphenyl polysiloxane/95% dimethyl polysiloxane, internal diameter 0.25 mm, film thickness 0.25 µm) using helium as the carrier gas at a linear velocity of 30 cm s<sup>-1</sup>. Analysis of mono-, di- and triglycerides was performed using the following program: 200 °C followed by heating (8 °C/min) to 360 °C. Using the GC/MS software GC/MS-solution® (Shimadzu Corporation, Kyoto, Japan) the amounts of substrate and products as well as the yield were calculated. For product identification the respective references were measured on the GC/MS and the reaction products compared in terms of retention time and mass spectra.

## Results

### Synthesis of PUFA 2-Monoacylglycerides

So far, direct esterification of PUFA and glycerol or an adequate interesterification leading to 2-MAG of PUFA has been impossible because there is no *sn*-2 specific lipase known. Therefore we developed a two-step process

including esterification of glycerol and PUFA leading to TAG followed by ethanolysis resulting in the desired 2-MAG (Fig. 1). The potential of CalB for synthesis of triglycerides in an unspecific manner has already been described [29]. A glycerol:PUFA ratio of 1:3 was found to be the optimum for the reaction. Excess of glycerol or fatty acids is inappropriate because of the production of large amounts of MAG and diacylglycerols (DAG) decreasing the yield of TAG.

For the *sn*1,3-specific alcoholysis, several lipases classified as *sn*1,3-specific were tested: *Candida antarctica* B lipase (CalB), *Penicillium camembertii* lipase, *Pseudomonas fluorescens* lipase, *Rhizomucor mihei* lipase, *Rhizopus javanicus* lipase and *Rhizopus oryzae* lipase [32]. Only CalB was able to convert all three TAG of PUFA to the desired 2-MAG. The lipase of *Rhizopus oryzae* was able to convert the TAG of ARA to the 2-MAG, but failed in the case of TAG of DHA (DDD) and EPA (EEE). For most lipases, the substrates seem to be too sterically demanding for their substrate-binding-site and therefore cannot be converted. Interestingly CalB, which acts in the first reaction as an unspecific catalyst is able to convert the substrates regioselectively to 2-MAG.

The alcoholysis reaction was very fast (Fig. 3). After 240 min the reaction was completed and almost no TAG was detected by TLC anymore. The reaction rate was constant from the beginning till the end of the reaction after 240 min. No DAG or free fatty acids were detectable. Fatty acid ethyl ester was able to be completely removed by liquid-liquid extraction. No isomerization of MAG was observed. TLC-analysis revealed a single spot of 2-MAG.

No acyl migration was observed when the alcoholysis reaction was performed in a temperature range from 25 to 30 °C. Temperatures higher than 40 °C led to increasing acyl migration and partial deacylation to glycerol.

The 2-MAG of the three model PUFA (ARA, DHA, EPA) were synthesized in gram quantity with purities higher than 85% and yields up to 96% (Table 1).

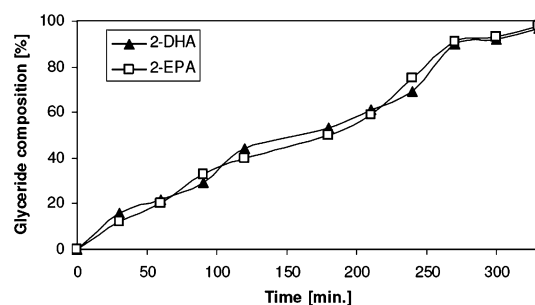


**Fig. 3** Product formation during the alcoholysis reaction of DDD and EEE. The reaction is catalyzed by CalB and the product formation proceeded continuously until 240 min where the amount of product reached its final plateau



**Table 1** Mass, purity and yields of PUFA-2-monoacylglycerides performed in lab scale

2-Monoacylglyceride of	Isolated yields (g)	Purity (%)	Yield (%)
Arachidonic acid (ARA)	1,4	86	84
Docosahexaenoic acid (DHA)	1,2	86	72
Eicosapentaenoic acid (EPA)	1,6	95	96

**Table 2** Mass, purity and yields of products from miniplant reactions

Reaction	Isolated yield (g)	Purity (%)	Yield (%)
Esterification of glycerol with erucic acid (TAG Synthesis)	352	95	97
Alcoholysis of tripalmitate (synthesis of 2-MP)	84	77	73
Esterification of 2-MP with oleic acid (OPO Synthesis)	198	95	90

The same process was proven to be usable for the synthesis of 2-MAG of short and middle-chain fatty acids such as caprylic- (C8), palmitic- (C16) and oleic- (C18:1) acid. The corresponding 2-MAG were not purified as these studies were only performed to explore the range of 2-MAG accessible by the technology described herein. So the substrate spectra of the 1,3-specific alcoholysis reaction with CalB covers all chain lengths from short to long and saturated or polyunsaturated.

### Synthesis of Triglycerides in the Miniplant

For upscaling, erucic acid was chosen as a cheap substrate since it is available in large quantities with high purity. The CalB-catalyzed esterification yielded 352 g of triglyceride of erucic acid corresponding to 97% of the theoretically possible yield (Table 2). The glycerol:fatty acid ratio of 1:3 led to a highly efficient esterification and less than 5% of by-products like mono- and diglycerides.

### Synthesis of OPO in the Miniplant

OPO was synthesized in the miniplant starting with tripalmitate as substrate. In the first step, tripalmitate was converted to 2-monopalmitate (2-MP) in an alcoholysis reaction, followed by esterification of 2-MP with oleic acid to OPO (Fig. 2). The yield of 2-MP was 73% corresponding to 84 g (77% purity). The esterification led to 198 g of OPO (yield 90%) with a purity of 95% (Table 2).

During the alcoholysis reaction no acyl migration was detectable.

In general, immobilized CalB could be reused after filtration, washing and drying at least three times without any loss of activity.

### Discussion

In our study we showed that it is possible within a two-step process to synthesize several 2-MAG without limitations regarding chain-length and saturation degree with just one biocatalyst. The reactions were successfully scaled up to 8 l scale and also a two-step process for the synthesis of OPO was established.

The easiest and most effective route towards 2-MAG would be the application of an *sn2*-specific lipase which would allow to synthesize these desired molecules in a one-step reaction. With such an outstanding catalyst it would be possible to perform a direct esterification of glycerol and fatty acids (glycerolysis) leading to 2-MAG or to perform an interesterification reaction between two homogeneous triglycerides leading to an ABA type TAG. Such an enzyme would be an outstanding innovation in the field of enzyme technology. Up to now only very few lipases like Lipase A from *Candida antarctica* (CalA) [33] have been described to show significant preference for position *sn2* of glycerides. For other enzymes this characteristic is discussed, as, for example, the lipases from *Vernonia anthelmintica* [34] or *Candida parapsilosis* [35, 36]. Recently the expression of CalA in *E. coli* on a microtiter plate scale has been described allowing directed evolution of this lipase [37]. So the prerequisites for a possible tailoring of CalA towards an *sn2*-specific lipase via directed evolution are fulfilled.

The results of the esterification and alcoholysis reactions showed that CalB displays either an unspecific or a very strict *sn1,3*-specific behaviour depending on the reaction conditions. We also observed that, after complete conversion of TAG to 2-MAG, the catalyst starts to hydrolyze the 2-MAG leading to glycerol and ethyl esters. So the reaction has to be stopped by removing the lipase directly after the TAG are converted quantitatively. These results indicate that CalB is not a “classical” or “totally” *sn1,3*-specific lipase because it is also able to convert 2-MAG. 2-MAG are not hydrolyzed at all by highly *sn1,3*-specific lipases, e.g., the *Rhizomucor mihei* lipase. It is probable that the addition of ethanol converts CalB from an unspecific to a more 1,3-regiospecific enzyme. A possible reason for this behaviour might be decreased flexibility of the tertiary structure of CalB caused by ethanol, hindering the substrate from accessing the catalytic binding pocket with the acyl group in the middle position [31]. This increased rigidity should also be favoured by decreasing the reaction temperature to 25 °C. Thus CalB should be classified as an

unspecific lipase which can be tailored by reaction engineering to a more *sn*1,3-specific enzyme. The most important advantage over all other *sn*1,3-specific lipases tested in our work is the ability of CalB to convert the sterically demanding TAG of PUFAs which do not fit into the substrate binding pockets of other lipases (e.g., the *Rhizopus* lipases).

Reduced acyl migration has been reported when lowering the water content of the reaction mixture or adjusting the water activity [38]. In the reactions described here the water content was adjusted to a low level by addition of molecular sieve. Even though in other processes the water activity is exactly adjusted [39] we did not detect any effect of acyl migration in our miniplant reactions. Accordingly the temperature was the most determinant parameter for acyl migration.

In a first attempt the alcoholysis reaction in the miniplant was performed in pure ethanol as solvent and co-substrate, which ended in very weak product formation and low yield. Ethanol inhibits the lipase activity: after a certain amount of time the reaction stopped although most of tripalmitate was not converted. After filtration of the lipase and removing the ethanol, the enzyme was active again. This indicates a kind of inhibitory complex that is formed between the enzyme and ethanol. Still the alcoholysis reaction in pure ethanol worked fine on a small scale. This may be due to significantly higher lipase concentration on a small scale compared to technical scale. Consequently, the amount of ethanol was decreased in the miniplant reactions. In this case no inhibition of the lipase was detectable.

Inhibition of the alcoholysis reaction by ethanol in the miniplant was surprising. It is even more surprising that the reaction performed well in an acetone/ethanol mixture since this kind of mixture has been said to inactivate lipases [40, 41]. The results presented here show that high-yield production of 2-monopalmitate in acetone is possible. As acetone is regarded as food-safe, the process is suitable for the production of nutrition-related materials.

The purification, taking advantage of the high solubility of 2-MAG in acetonitrile/water (95:5 v/v), while more hydrophobic by-products are more soluble in *n*-hexane, allowed an easy and fast purification of the 2-MAG of PUFA. Monoacylglycerides and ethyl esters could be clearly separated. Usually the purification of 2-MAG is performed via crystallization as in the case of 2-MP. This is unsuitable in the case of PUFA because of their very deep freezing point. A possible alternative that also has been tested is the purification via a silica gel column treated with boric acid. In that case, large amounts of organic solvents were necessary and significant acyl migration was detected (up to 40%).

Yield and purity of OPO synthesized in the miniplant with CalB was slightly lower than in a similar process

catalyzed by *Rhizopus* (*Rhizopus delemar*, *Rhizopus oryzae* and *Rhizomucor mihei*) lipases [39]. In the alcoholysis reaction a yield of 85% with a purity >95% was described. Still this process was performed on a laboratory scale whereas in our case we reached a technical scale (>100 g of product) indicating further upscaling for industrial production is possible. Processes for OPO synthesis have been described using two different lipases with distinct regioselectivity for the ethanolysis and esterification reaction [42]. The use of only one enzyme as suggested in our work will facilitate industrial applications.

The potential of our approach is further underlined by comparison of the results to the latest literature on 2-MAG synthesis. A lab-scale process for the enzymatic synthesis (by ethanolysis) of 2-MAG described by Shimada and colleagues yielded only 28–29 mol% of 2-MAG content [43]. Yang and colleagues described a CalB-driven glycerolysis process yielding 2-MAG of PUFA [44]. Still the yield in the stirred tank just reached 70% and unfortunately they had to work with a multiphase-system.

With respect to process development and further upscaling, the use of only one lipase for the unspecific esterification and the *sn*1,3-selective alcoholysis is a big advantage of the process described here. Reusability of immobilized CalB in the batch processes indicates that establishment of continuous production processes is possible. Thus new promising applications of this outstanding biocatalyst might arise.

**Acknowledgments** We thank the Nestlé Company for the financial support of our work.

## References

- Biscione F, Pignalberi C, Totteri A, Messina F, Altamura G (2007) Cardiovascular effects of omega-3 free fatty acids. *Curr Vasc Pharmacol* 5:163–172
- Gill I, Valivety R (1997) Polyunsaturated fatty acids .1. Occurrence, biological activities and applications. *Trends Biotechnol* 15:401–409
- Innis SM (1991) Essential fatty-acids in growth and development. *Prog Lipid Res* 30:39–103
- Koletzko B, Schmidt E, Bremer HJ, Haug M, Harzer G (1989) Effects of dietary long-chain poly-unsaturated fatty-acids on the essential fatty-acid status of premature-infants. *Eur J Pediatr* 148:669–675
- Koletzko B, Decsi T, Demmelmair H (1996) Arachidonic acid supply and metabolism in human infants born at full term. *Lipids* 31:79–83
- Weylandt KH, Kang JX, Leaf A (1996) Polyunsaturated fatty acids exert antiarrhythmic actions as free acids rather than in phospholipids. *Lipids* 31:977–982
- Simopoulos AP (1991) Omega-3-fatty-acids in health and disease and in growth and development. *Am J Clin Nutr* 54:438–463
- Christensen MS, Hoy CE, Becker CC, Redgrave TG (1995) Intestinal-absorption and lymphatic transport of eicosapentaenoic (Epa), docosahexaenoic (Dha), and decanoic acids—dependence

- on intramolecular triacylglycerol structure. *Am J Clin Nutr* 61:56–61
9. Sadou H, Leger CL, Descomps B, Barjon JN, Monnier L, Depaulet AC (1995) Differential incorporation of fish-oil eicosapentaenoate and docosahexaenoate into lipids of lipoprotein fractions as related to their glyceryl esterification—a short-term (Postprandial) and long-term study in healthy humans. *Am J Clin Nutr* 62:1193–1200
  10. Oxley A, Jutfelt F, Sundell K, Olsen RE (2007) Sn-2-monoacylglycerol, not glycerol, is preferentially utilised for triacylglycerol and phosphatidylcholine biosynthesis in Atlantic salmon (*Salmo salar* L.) intestine. *Comp Biochem Physiol B Biochem Mol Biol* 146:115–123
  11. Yamane T (1999) Monoacylglycerols. *Encyclopedia of bioprocess technology: fermentation, biocatalysis and bioseparation* 4:1810–1818
  12. Mutsuda M, Michel KP, Zhang X, Montgomery BL, Golden SS (2003) Biochemical properties of CikA, an unusual phytochrome-like histidine protein kinase that resets the circadian clock in *Synechococcus elongatus* PCC 7942. *J Biol Chem* 278:19102–10
  13. Endo Y, Hoshizaki S, Fujimoto K (1997) Oxidation of synthetic triacylglycerols containing eicosapentaenoic and docosahexaenoic acids: effect of oxidation system and triacylglycerol structure. *J Am Oil Chem Soc* 74:1041–1045
  14. Endo Y, Hoshizaki S, Fujimoto K (1997) Autoxidation of synthetic isomers of triacylglycerol containing eicosapentaenoic acid. *J Am Oil Chem Soc* 74:543–548
  15. Babayan VK (1987) Medium chain triglycerides and structured lipids. *Lipids* 22:417–420
  16. Mascioli EA, Bistrrian BR, Babayan VK, Blackburn GL (1987) Medium chain triglycerides and structured lipids as unique nonglucose energy-sources in hyperalimentation. *Lipids* 22:421–423
  17. Davis TA, Gao L, Yin HY, Morrow JD, Porter NA (2006) In vivo and in vitro lipid peroxidation of arachidonate esters: the effect of fish oil omega-3 lipids on product distribution. *J Am Oil Chem Soc* 128:14897–14904
  18. Lien EL, Boyle FG, Yuhas R, Tomarelli RM, Quinlan P (1997) The effect of triglyceride positional distribution on fatty acid absorption in rats. *J Pediatr Gastroenterol Nutr* 25:167–174
  19. Okumura S, Iwai M, Tsujisaka Y (1979) Synthesis of various kinds of esters by four microbial lipases. *Biochim Biophys Acta* 575:156–165
  20. Nakano H, Kitahata S, Tominaga Y, Takenishi S (1991) Esterification of glycosides with glycerol and trimethylolpropane moieties by *Candida cylindracea* lipase. *Agric Biol Chem* 55:2083–2089
  21. Björkling F, Godtfredsen SE, Kirk O (1991) The future impact of industrial lipases. *Trends Biotechnol* 9:360–363
  22. Schmid RD, Verger R (1998) Lipases, interfacial enzymes with attractive applications. *Agnew Chem Int Ed Engl* 37:1608–1633
  23. Ghanem A (2006) Trends in lipase-catalyzed asymmetric access to enantiomerically pure/enriched compounds. *Tetrahedron* 63:1721–1754
  24. Kirchner G, Scollar MP, Klivanov AM (1985) Resolution of racemic mixtures via lipase catalysis in organic solvents. *J Am Chem Soc* 107:7072–7076
  25. Langrand G, Secchi M, Buono G, Baratti J, Triantaphylides C (1985) Lipase-catalyzed ester formation in organic solvents. An easy preparative resolution of alpha-substituted cyclohexanols. *Tetrahedron Lett* 26:1857–1860
  26. Kojima Y, Yokoe M, Mase T (1994) Purification and characterization of an alkaline lipase from *Pseudomonas fluorescens* AK102. *Biosci Biotechnol Biochem* 58:1564–1568
  27. Hoegh I, Patkar S, Halkier T, Hansen M.T (1995) Two lipases from *Candida antarctica*: cloning and expression in *Aspergillus oryzae*. *Can J Bot* 73:869–875
  28. Anderson EM, Larsson KM, Kirk O (1998) One biocatalyst—many applications: the use of *Candida antarctica* lipase B—lipase in organic synthesis. *Biocat Biotransform* 16:181–204
  29. Medina AR, Cerdán LE, Giménez AG, Páez BC, González MJ, Grima EM (1999) Lipase-catalyzed esterification of glycerol and polyunsaturated fatty acids from fish and microalgae oils. *J Biotechnol* 70:379–391
  30. Berendsen WR, Gendrot G, Freund A, Reuss M (2006) A kinetic study of lipase-catalyzed reversible kinetic resolution involving verification at miniplant-scale. *Biotechnol Bioeng* 95:883–892
  31. Irimescu R, Iwasaki Y, Hou CT (2002) Study of TAG ethanolysis to 2-MAG by immobilized *Candida antarctica* lipase and synthesis of symmetrically structured TAG. *J Am Oil Chem Soc* 79:879–883
  32. Bornscheuer UT, Kazlauskas RJ (1999) Hydrolases in organic synthesis
  33. Rogalska E, Cudrey C, Ferrato F, Verger R (1993) Stereoselective hydrolysis of triglycerides by animal and microbial lipases. *Chirality* 5:24–30
  34. Olney CE, Jensen RG, Sampugna J, Quinn JG (1968) Purification and Specificity of a Lipase from *Vernonia anthelmintica* Seed. *Lipids* 3:498–502
  35. Brunel L, Neugnot V, Landucci L, Boze WN, Moulin G, Bigey F, Dubreucq E (2004) High-level expression of *Candida parapsilosis* lipase/acyltransferase in *Pichia pastoris*. *J Biotechnol* 111:41–50
  36. Neugnot V, Moulin G, Dubreucq E, Bigey F (2002) The lipase/acyltransferase from *Candida parapsilosis*: molecular cloning and characterization of purified recombinant enzymes. *Eur J Biochem* 269:1734–1745
  37. Pfeiffer J, Rusnak M, Hansen CE, Rhlid RB, Schmid RD, Maurer SC (2007) Functional expression of Lipase A from *Candida antarctica* in *Escherichia coli*—a prerequisite for high-throughout screening and directed evolution. *J Mol Cat: B Enzymatic* 45:62–67
  38. Goderis HL, Fouwe BL, van Cauwenbergh SM, Tobback PP (1986) Measurements and control of water content of organic solvents. *Anal Chem* 58:1561–1563
  39. Schmid U, Bornscheuer UT, Soumanou MM, McNeill GP, Schmid RD (1999) Highly selective synthesis of 1,3-oleoyl-2-palmitoylglycerol by lipase catalysis. *Biotechnol Bioeng* 64:678–684
  40. Heinsman NWJT, Valente AM, Smienk HGF, van der Padt A, Franssen MCR, de Groot A, van't Riet K (2001) The effect of ethanol on the kinetics of lipase-mediated enantioselective esterification of 4-methyloctanoic acid and the hydrolysis of its ethyl ester. *Biotechnol Bioeng* 76:193–199
  41. Yamane T (1987) A comparison of assay on hydrolytic activity of lipase with and without surfactants. *J Jpn Oil Chem Soc* 36:402–408
  42. Chen ML, Vali SR, Lin JY, Ju YH (2004) Synthesis of the structured lipid 1,3-dioleoyl-2-palmitoylglycerol from palm oil. *J Am Oil Chem Soc* 81:525–532
  43. Shimada Y, Ogawa J, Watanabe Y, Nagao T, Kawashima A, Kobayashi T, Shimizu S (2003) Regiospecific analysis by ethanolysis of oil with immobilized *Candida antarctica* lipase. *Lipids* 38:1281–1286
  44. Yang T, Rebsdorf M, Engelrud U, Xu X (2005) Enzymatic production of monoacylglycerols containing polyunsaturated fatty acids through an efficient glycerolysis system. *J Agric Food Chem* 53:1475–1481

2-methoxyethyl, and C<sub>2</sub>–C<sub>4</sub> *n*-alkyl esters from TAG, phospholipids, methyl esters, and intact lipids. It involved transesterification under base-catalyzed conditions using potassium alkoxides, which were prepared by proton exchange between potassium *tert*-butoxide and the corresponding primary alcohols. Mild reaction conditions allowed complete derivatization, i.e., picolinyl ester from TAG and phospholipids, 2 min at room temperature [9]; and 2-methoxyethyl and *n*-alkyl esters from TAG, 15 min at 40 °C [10]. Dubois et al. [11] reported complete derivatization of methyl esters to picolinyl esters in 45 min at 45 °C. Because 9-anthrylmethyl esters are also esters of a primary alcohol, this methodology is applicable to their synthesis.

This paper proposes a one-step method for rapid preparation of fatty acid 9-anthrylmethyl esters using base-catalyzed transesterification. The aim of the present study is to reveal properties of the new method and to assess its utility in fatty acid analysis of TAG in the ranges 0.1–5 µg or 0.1–5 nmol. For this purpose, some standard and natural TAG were subjected to this method, and the products were analyzed by reversed-phase HPLC with fluorescence detection. Fish oils TAG, containing a wide variety of fatty acids, were used as the natural TAG samples.

## Materials and Methods

### Reagents

Potassium *tert*-butoxide (1.0 mol L<sup>-1</sup> solution in tetrahydrofuran (THF)) and 9-anthracenemethanol (98%) were purchased from Aldrich Chemicals (Milwaukee, WI, USA) and Acros Organics (Geel, Belgium), respectively. THF anhydrous (99.5%, stabilized with BHT, Kanto Chemical, Tokyo, Japan) was distilled once and stored in the dark in the presence of molecular sieves 4A (powder, Nacalai Tesque, Kyoto, Japan). Dichloromethane anhydrous (99.5%) and cyclohexane (99.5%) were products of Kanto Chemical, and the former was dried over molecular sieves 4A.

Standard TAG used were tripalmitoylglycerol (16:0-TAG; Extrasynthèse, Genay, France), trionadecanoylglycerol (19:0-TAG; Sigma Chemical, St Louis, MO, USA), trilinoleoylglycerol (18:2-TAG; Sigma Chemical) and tridocosahexaenoylglycerol (22:6-TAG; Nu-Chek-Prep, Elysian, MN, USA). The 22:6-TAG was purified by thin-layer chromatography on silica gel 60G (Merck, Darmstadt, Germany) with hexane/diethyl ether (90:10, *v/v*) for development. The other standards were used without purification. Fish oils TAG, bonito head oil TAG and cod liver/mackerel oil TAG, were isolated from industrial oils by column chromatography on silica gel 60 (Merck) with hexane/diethyl ether (95:5 and 90:10, *v/v*) for elution [1].

### General Procedure for Synthesis of 9-Anthrylmethyl Esters

9-Anthracenemethanol (60 mg) and potassium *tert*-butoxide in THF (1.0 mol L<sup>-1</sup>, 20 µL) were taken in a screw-capped glass vial (0.6 mL-volume). Anhydrous THF (200 µL) was added to the vial and vigorously mixed with a vortex mixer to produce a saturated solution of potassium 9-anthracenemethoxide. The mixture was dried over 40 mg of anhydrous calcium sulfate for 1 h at room temperature. The supernatant was used as potassium 9-anthracenemethoxide reagent within one day.

TAG (0.1–5 µg) and 19:0-TAG (100 pmol = 93.4 ng) as an internal standard were dissolved in 10 µL of anhydrous dichloromethane in a screw-capped 0.6 mL-volume glass vial. The potassium 9-anthracenemethoxide reagent (10 µL) was added to the solution, and vigorously mixed with a vortex mixer for 10 s. After the mixture was left to stand for 10 min in the dark at room temperature, 2 µL of acetic acid/dichloromethane (1:10, *v/v*) was added to stop the reaction. After removing the solvents in a stream of nitrogen, resulting fatty acid 9-anthrylmethyl esters were taken up from the residue into 160 µL of cyclohexane, and 10 µL of the solution was subjected to reversed-phase HPLC.

### HPLC

Reversed-phase HPLC was done with a Hitachi L-6200 pump (Hitachi, Tokyo, Japan), a Shimadzu RF-10A<sub>XL</sub> fluorescence detector (Shimadzu, Kyoto, Japan) and a Shimadzu C-R6A integrator. A column of Supersphere 100 RP-18e (25 cm × 4 mm i.d., 4 µm particles, Merck) was used with HPLC-grade acetonitrile, ethanol and hexane as mobile phase at a flow rate of 1.0 mL min<sup>-1</sup>. A linear gradient of acetonitrile to acetonitrile/ethanol/hexane (30:40:30, *v/v/v*) was generated over 20 min. The column temperature was held at 10 °C with a Shimadzu CTO-10AS<sub>VP</sub> column oven. Peaks were detected at the excitation and emission wavelengths of 365 and 412 nm, respectively. Flow cell temperature of the detector was set at 20 °C.

## Results and Discussion

### Formation of Fatty Acid 9-Anthrylmethyl Esters

Figure 1 shows HPLC profiles of the reaction products formed from standard and fish oils TAG by the present method. Formation of fatty acid 9-anthrylmethyl esters was checked by comparison of the chromatographic behavior of

the products with those of standard esters. As the standards, authentic free fatty acids were converted to 9-anthrylmethyl esters by using ADAM reagent [8]. In the HPLC of the products formed from a mixture of 16:0, 19:0, 18:2, and 22:6-TAG, four peaks appeared in the chromatogram (Fig. 1a). Elution times of these peaks corresponded to those of the standard 16:0, 19:0, 18:2 and 22:6 esters. It is apparent that 9-anthrylmethyl esters are synthesized from TAG by the one-step method.

A blank test of the present method, including the reversed-phase HPLC, was carried out by using 100 pmol of 19:0-TAG internal standard (Fig. 1b). At earlier elution times, many unidentified large peaks appeared, whereas there was practically no peak after 8 min except for one peak of 19:0 ester. Under the HPLC conditions used in this study, all of the identified peaks eluted after 8 min (Figs. 1c, d). The 9-anthrylmethyl esters produced by the present method can be directly subjected to reversed-phase HPLC without purification.

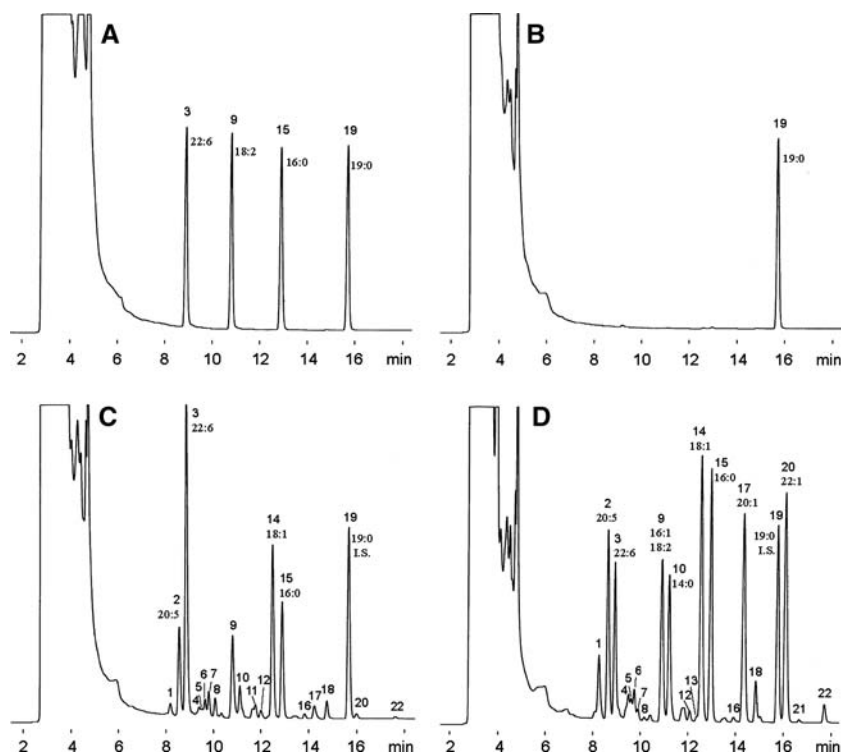
#### Yield of 9-Anthrylmethyl Esters

Time-course changes of formation of fatty acid 9-anthrylmethyl esters were investigated by using an equimolar mixture of 16:0, 19:0, 18:2, and 22:6-TAG (each 100 pmol) at room temperature (20–22 °C) (Fig. 2). Peak

areas of the 9-anthrylmethyl esters rapidly increased, reached maxima at 2–5 min, and then tended to somewhat decrease (10 and 20 min). During the first 10 min, the 22:6 ester was found to change in a manner somewhat different from those of the other esters. The 22:6 ester reached maximum faster (2 min) and the maximum level was higher. The transesterification of 22:6-TAG seems to proceed at a higher rate. In contrast, after longer reaction time (10–20 min), the four fatty acid esters had changed very little. The changes were parallel to each other. Differences in the peak areas of the four esters were less than 4% at both 10 and 20 min.

In order to determine theoretical yield of the 9-anthrylmethyl esters, 18.75 pmol of standard 16:0 ester, corresponding to 100% yield of this ester, was injected for reversed-phase HPLC. The peak area was  $15.8 \times 10^4$  units (mean of triplicate determinations). Theoretical yields calculated for the above four esters were 83–92% (2 min), 85–91% (5 min), 82–85% (10 min), and 80–83% (20 min). This result shows that the conversion of TAG to fatty acid 9-anthrylmethyl esters is not complete. Lower yields were observed for reactions with no or insufficient dryness of the potassium 9-anthracenemethoxide reagent and solvents with desiccants (data not shown). It is probable that the incomplete conversion resulted from hydrolysis (saponification) of TAG and 9-anthrylmethyl esters caused by moisture remaining in the reaction system.

**Fig. 1** HPLC profiles of fatty acid 9-anthrylmethyl esters produced from standard and fish oils TAG. **a** Mixture of 16:0, 19:0, 18:2, and 22:6-TAG (each 100 pmol); **b** 19:0-TAG (100 pmol) used as an internal standard; **c** bonito head oil TAG (0.5 µg) mixed with 19:0-TAG (100 pmol); and **d** cod liver/mackerel oil TAG (1 µg) mixed with 19:0-TAG (100 pmol). The numbered peaks were identified by using standard esters as follows: 1, 18:4n-3 + 18:4n-1; 2, 20:5n-3; 3, 22:6n-3; 4, 18:3n-3 + 18:3n-6 + 16:2 + 12:0; 5, 20:4n-3; 6, 22:5n-3; 7, 20:4n-6; 8, 22:5n-6; 9, 16:1 + 18:2n-6 + 20:3 + 22:4n-6; 10, 14:0; 11, 17:1n-8; 12, 15:0; 13, 20:2n-6; 14, 18:1; 15, 16:0; 16, 17:0; 17, 20:1; 18, 18:0; 19, 19:0; 20, 22:1; 21, 20:0; and 22, 24:1



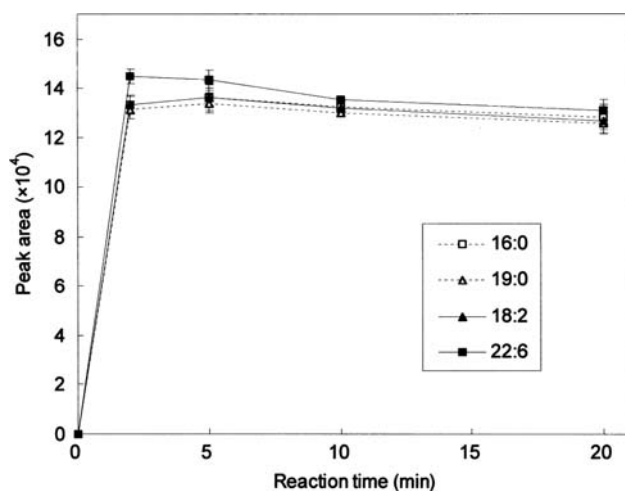


**Fig. 2** Time-course change of formation of fatty acid 9-anthrylmethyl esters from TAG. A mixture of 16:0, 19:0, 18:2, and 22:6-TAG (each 100 pmol) was converted to the 9-anthrylmethyl esters at room temperature (20–22 °C). Peak areas were obtained by HPLC under the conditions described in the text. Data represent mean  $\pm$  standard deviation of triplicate reactions

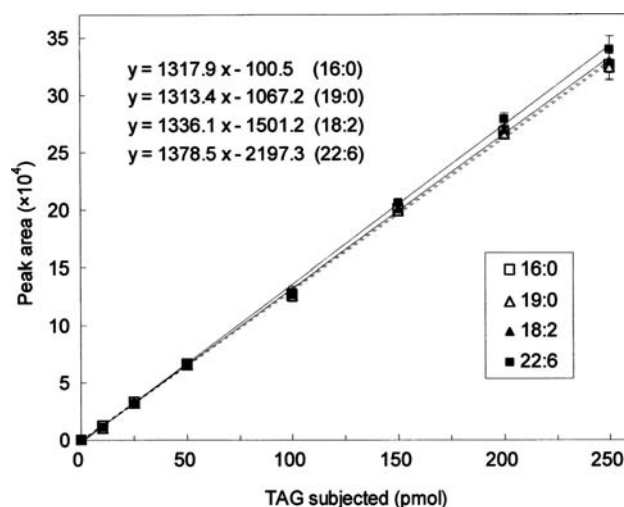


**Fig. 3** Plots of the amounts of 9-anthrylmethyl esters versus TAG subjected to the synthesis. An equimolar mixture of 16:0, 19:0, 18:2, and 22:6-TAG was subjected to the reactions conducted for 10 min at room temperature (20–22 °C). Peak areas were obtained by HPLC under the conditions described in the text. Data represent mean  $\pm$  standard deviation of triplicate reactions

### Standard Curves

Detection limits of the fatty acid 9-anthrylmethyl esters were determined by using the above 10-min reaction products. The esters corresponding to each 91.5 fmol of the 22:6, 18:2, 16:0, and 19:0-TAG were injected for reversed-phase HPLC. Detection limits ( $S/N = 3$ ) were all 26 fmol as the standard monoacid TAG. Calculated from the yields of 9-anthrylmethyl esters (82–85%), detection limits of the esters were about 65 fmol ( $S/N = 3$ ).

The amount of fatty acid 9-anthrylmethyl esters as a function of the amount of starting TAG was also checked by using equimolar mixtures of standard TAG (Fig. 3). The reactions were conducted at room temperature for 10 min. Excellent linear relationships were observed for all TAG standards ranging from 10 to 250 pmol. The correlation coefficients of individual fatty acids were more than 0.999. The present method appears to be usable for fatty acid analysis of a mixture of 10–250 pmol of TAG molecular species. The slopes of the plots were not identical among the four standards. However, differences in the slopes were calculated to be less than 5%.

### Fatty Acid Analysis of Fish Oils TAG

The present method was applied to fatty acid analysis of bonito head oil and cod liver/mackerel oil TAG (Figs. 1c, d). Peak components were identified by comparing the elution times with those of authentic fatty acid esters. Table 1 shows the compositions of fatty acid 9-

anthrylmethyl esters produced from 0.1 to 5  $\mu$ g of the fish oils TAG. In both fish oils, almost consistent compositions were observed in the analyses of 0.5–5  $\mu$ g of TAG. For example, major fatty acids in the bonito head oil TAG, 22:6n-3, 18:1 and 16:0, were found at concentrations of 31.2–31.8, 17.5–18.1, and 11.3–11.9 mol%, respectively. The 20:5n-3 ester was 8.5–8.6 mol%. In the cod liver/mackerel oil TAG, major fatty acids were found at 14.3–14.5 mol% (18:1), 12.3–12.7 mol% (16:0), 11.8–12.2 mol% (20:1), and 12.8–13.3 mol% (22:1). The 20:5n-3 and 22:6n-3 esters were 9.3–9.4 and 7.7–8.0 mol%, respectively. In the analyses of 0.1 and 0.2  $\mu$ g of TAG, minor fatty acids could not be determined. However, major fatty acids showed the percentages not very different from those observed in the analyses of 0.5–5  $\mu$ g of TAG.

Table 1 also shows the compositions obtained by other methodologies. One of them was determined by HPLC of 9-anthrylmethyl esters prepared by ordinary multi-step methodology, where 10 mg of the TAG were saponified by the method of Christie [1] and a portion of resulting free fatty acids (50  $\mu$ g) were converted to 9-anthrylmethyl esters in a methanolic solution of ADAM reagent [8]. The other one was determined by gas-liquid chromatography (GLC) of fatty acid methyl esters (FAME) prepared by transmethylation of 2 mg of TAG using sodium methoxide in methanol [1]. The compositions of fatty acid 9-anthrylmethyl esters prepared by the present one-step method were similar to those determined by the ADAM-HPLC and FAME-GLC methods. This result indicates that fatty acid composition of fish oil TAG determined by way of the present one-step synthesis is comparable to those

**Table 1** Fatty acid compositions of fish oils TAG, obtained by the present and other methods (Mol%, mean  $\pm$  standard deviation)

Fatty acid	Present one-step method ( $n = 3$ )						ADAM <sup>a</sup> ( $n = 3$ )	FAME <sup>b</sup> ( $n = 3$ )
	0.1 $\mu$ g	0.2 $\mu$ g	0.5 $\mu$ g	1.0 $\mu$ g	2.5 $\mu$ g	5.0 $\mu$ g		
<b>Bonito head oil TAG</b>								
18:4n-3 <sup>c</sup>	0.8 $\pm$ 0.6	0.8 $\pm$ 0.6	1.2 $\pm$ 0.1	1.2 $\pm$ 0.1	1.3 $\pm$ 0.1	1.3 $\pm$ 0.1	1.2 $\pm$ 0.0	1.2 $\pm$ 0.0
20:5n-3	8.8 $\pm$ 0.4	8.3 $\pm$ 0.0	8.5 $\pm$ 0.1	8.6 $\pm$ 0.0	8.6 $\pm$ 0.0	8.6 $\pm$ 0.0	8.5 $\pm$ 0.1	8.3 $\pm$ 0.0
22:6n-3	31.4 $\pm$ 1.3	30.5 $\pm$ 0.4	31.6 $\pm$ 0.9	31.8 $\pm$ 0.2	31.4 $\pm$ 0.1	31.2 $\pm$ 0.1	31.0 $\pm$ 0.2	30.1 $\pm$ 0.1
18:3n-3 + 16:2 <sup>d</sup>	ND	0.2 $\pm$ 0.1	0.9 $\pm$ 0.0	1.2 $\pm$ 0.2	1.3 $\pm$ 0.0	1.3 $\pm$ 0.0	1.0 $\pm$ 0.2	2.8 $\pm$ 0.0 <sup>i</sup>
20:4n-3	ND	Tr	0.5 $\pm$ 0.0	0.6 $\pm$ 0.0	0.7 $\pm$ 0.0	0.6 $\pm$ 0.1	0.7 $\pm$ 0.0	0.6 $\pm$ 0.0
22:5n-3	0.9 $\pm$ 0.2	0.9 $\pm$ 0.0	1.4 $\pm$ 0.0	1.6 $\pm$ 0.1	1.7 $\pm$ 0.0	1.7 $\pm$ 0.0	1.6 $\pm$ 0.0	1.5 $\pm$ 0.0
20:4n-6	2.0 $\pm$ 0.1	2.0 $\pm$ 0.0	2.2 $\pm$ 0.0	2.3 $\pm$ 0.1	2.5 $\pm$ 0.0	2.5 $\pm$ 0.0	2.4 $\pm$ 0.0	2.1 $\pm$ 0.0
22:5n-6	1.5 $\pm$ 0.0	1.4 $\pm$ 0.0	1.5 $\pm$ 0.1	1.6 $\pm$ 0.1	1.8 $\pm$ 0.0	1.8 $\pm$ 0.0	1.7 $\pm$ 0.0	1.5 $\pm$ 0.0
16:1 + 18:2n-6 <sup>e</sup>	9.9 $\pm$ 0.7	10.5 $\pm$ 0.4	9.8 $\pm$ 0.1	9.6 $\pm$ 0.0	9.4 $\pm$ 0.0	9.4 $\pm$ 0.0	9.6 $\pm$ 0.1	9.6 $\pm$ 0.1
14:0	3.7 $\pm$ 0.8	4.5 $\pm$ 0.3	3.8 $\pm$ 0.1	3.7 $\pm$ 0.0	3.6 $\pm$ 0.1	3.7 $\pm$ 0.0	3.7 $\pm$ 0.0	3.2 $\pm$ 0.1
17:1n-8	0.9 $\pm$ 0.3	1.4 $\pm$ 0.1	1.4 $\pm$ 0.0	1.4 $\pm$ 0.0	1.4 $\pm$ 0.0	1.4 $\pm$ 0.0	1.3 $\pm$ 0.0	1.1 $\pm$ 0.0
15:0	0.2 $\pm$ 0.3	0.9 $\pm$ 0.1	0.8 $\pm$ 0.0	0.8 $\pm$ 0.0	0.8 $\pm$ 0.0	0.8 $\pm$ 0.0	0.8 $\pm$ 0.0	0.7 $\pm$ 0.0
20:2n-6	ND	ND	0.2 $\pm$ 0.0	NR	NR	NR	0.1 $\pm$ 0.1	0.2 $\pm$ 0.0
18:1	19.9 $\pm$ 1.0	19.0 $\pm$ 0.6	18.1 $\pm$ 0.4	17.8 $\pm$ 0.1 <sup>g</sup>	17.6 $\pm$ 0.1 <sup>g</sup>	17.5 $\pm$ 0.1 <sup>g</sup>	17.8 $\pm$ 0.2	18.9 $\pm$ 0.0
16:0	14.0 $\pm$ 0.5	13.2 $\pm$ 0.3	11.9 $\pm$ 0.2	11.6 $\pm$ 0.1	11.3 $\pm$ 0.0	11.3 $\pm$ 0.0	11.8 $\pm$ 0.2	12.2 $\pm$ 0.1
17:0	Tr	0.5 $\pm$ 0.0	0.5 $\pm$ 0.0	0.5 $\pm$ 0.0	0.5 $\pm$ 0.0	0.5 $\pm$ 0.0	0.5 $\pm$ 0.0	0.5 $\pm$ 0.0
20:1	1.7 $\pm$ 0.1	1.6 $\pm$ 0.1	1.7 $\pm$ 0.0	1.7 $\pm$ 0.0	1.7 $\pm$ 0.0	1.7 $\pm$ 0.0	1.7 $\pm$ 0.0	1.5 $\pm$ 0.1
18:0	2.4 $\pm$ 0.2	2.1 $\pm$ 0.2	1.7 $\pm$ 0.0	1.8 $\pm$ 0.0	1.8 $\pm$ 0.0	1.8 $\pm$ 0.0	1.7 $\pm$ 0.1	1.7 $\pm$ 0.0
22:1	Tr	0.7 $\pm$ 0.0	0.6 $\pm$ 0.0	0.6 $\pm$ 0.0	0.6 $\pm$ 0.0	0.6 $\pm$ 0.0	0.6 $\pm$ 0.0	0.4 $\pm$ 0.0
20:0	ND	ND	Tr	Tr	0.1 $\pm$ 0.0	0.1 $\pm$ 0.0	0.0 $\pm$ 0.0	0.0 $\pm$ 0.0
24:1	ND	ND	0.2 $\pm$ 0.0	0.2 $\pm$ 0.0	0.2 $\pm$ 0.0	0.2 $\pm$ 0.0	0.2 $\pm$ 0.0	0.2 $\pm$ 0.1
Others	2.0 $\pm$ 0.2	1.5 $\pm$ 0.5	1.4 $\pm$ 0.2	1.6 $\pm$ 0.2	1.9 $\pm$ 0.0	1.9 $\pm$ 0.0	2.2 $\pm$ 0.1	1.7 $\pm$ 0.1
Amount (nmol) <sup>f</sup>	0.28 $\pm$ 0.01	0.57 $\pm$ 0.03	1.51 $\pm$ 0.02	3.11 $\pm$ 0.01	7.79 $\pm$ 0.05	15.14 $\pm$ 0.08	–	–
<b>Cod liver/mackerel oil TAG</b>								
18:4n-3 <sup>c</sup>	3.7 $\pm$ 0.4	4.0 $\pm$ 0.1	3.6 $\pm$ 0.0	3.6 $\pm$ 0.1	3.7 $\pm$ 0.2	3.7 $\pm$ 0.1	3.5 $\pm$ 0.1	3.3 $\pm$ 0.0
20:5n-3	9.9 $\pm$ 0.2	9.7 $\pm$ 0.2	9.3 $\pm$ 0.2	9.4 $\pm$ 0.0	9.4 $\pm$ 0.0	9.3 $\pm$ 0.0	9.2 $\pm$ 0.1	8.9 $\pm$ 0.1
22:6n-3	6.9 $\pm$ 0.3	7.2 $\pm$ 0.4	7.7 $\pm$ 0.2	7.9 $\pm$ 0.1	8.0 $\pm$ 0.0	7.9 $\pm$ 0.0	7.4 $\pm$ 0.0	7.2 $\pm$ 0.1
18:3n-3 + 16:2 <sup>d</sup>	0.2 $\pm$ 0.2	0.7 $\pm$ 0.4	1.6 $\pm$ 0.1	1.7 $\pm$ 0.0	1.8 $\pm$ 0.1	1.8 $\pm$ 0.1	1.8 $\pm$ 0.0	2.7 $\pm$ 0.0 <sup>i</sup>
20:4n-3	Tr	0.2 $\pm$ 0.3	0.8 $\pm$ 0.0	0.8 $\pm$ 0.1	0.9 $\pm$ 0.0	0.9 $\pm$ 0.1	0.9 $\pm$ 0.0	0.8 $\pm$ 0.0
22:5n-3	0.6 $\pm$ 0.0	0.7 $\pm$ 0.2	1.4 $\pm$ 0.0	1.4 $\pm$ 0.1	1.5 $\pm$ 0.0	1.5 $\pm$ 0.0	1.4 $\pm$ 0.0	1.2 $\pm$ 0.0
20:4n-6	Tr	Tr	0.5 $\pm$ 0.0	0.5 $\pm$ 0.0	0.5 $\pm$ 0.0	0.6 $\pm$ 0.0	0.5 $\pm$ 0.0	0.3 $\pm$ 0.0
22:5n-6	ND	ND	0.1 $\pm$ 0.1	0.1 $\pm$ 0.0	0.2 $\pm$ 0.0	0.2 $\pm$ 0.0	0.1 $\pm$ 0.0	Tr
16:1 + 18:2n-6 <sup>e</sup>	9.7 $\pm$ 0.2	9.5 $\pm$ 0.1	8.9 $\pm$ 0.0	8.8 $\pm$ 0.0	8.7 $\pm$ 0.0	8.6 $\pm$ 0.0	8.8 $\pm$ 0.1	8.8 $\pm$ 0.1
14:0	8.8 $\pm$ 0.2	8.3 $\pm$ 0.1	7.7 $\pm$ 0.0	7.6 $\pm$ 0.0	7.8 $\pm$ 0.2	7.7 $\pm$ 0.1	7.6 $\pm$ 0.0	7.6 $\pm$ 0.1
17:1n-8	ND	Tr	1.2 $\pm$ 0.1 <sup>h</sup>	1.2 $\pm$ 0.0 <sup>h</sup>	1.2 $\pm$ 0.0 <sup>h</sup>	1.2 $\pm$ 0.1 <sup>h</sup>	0.5 $\pm$ 0.0	0.7 $\pm$ 0.0
15:0	0.1 $\pm$ 0.2	0.5 $\pm$ 0.0	0.5 $\pm$ 0.0	0.5 $\pm$ 0.0	0.5 $\pm$ 0.0	0.5 $\pm$ 0.0	0.5 $\pm$ 0.0	0.5 $\pm$ 0.0
20:2n-6	ND	ND	0.1 $\pm$ 0.0	NR	NR	NR	0.2 $\pm$ 0.0	0.2 $\pm$ 0.0
18:1	15.5 $\pm$ 0.1	15.0 $\pm$ 0.2	14.4 $\pm$ 0.1	14.5 $\pm$ 0.1 <sup>g</sup>	14.3 $\pm$ 0.1 <sup>g</sup>	14.3 $\pm$ 0.0 <sup>g</sup>	14.2 $\pm$ 0.1	14.5 $\pm$ 0.1
16:0	14.2 $\pm$ 0.1	13.8 $\pm$ 0.2	12.7 $\pm$ 0.0	12.6 $\pm$ 0.0	12.4 $\pm$ 0.1	12.3 $\pm$ 0.0	12.5 $\pm$ 0.1	13.1 $\pm$ 0.1
17:0	ND	ND	0.2 $\pm$ 0.0	0.2 $\pm$ 0.0	0.3 $\pm$ 0.0	0.3 $\pm$ 0.0	0.2 $\pm$ 0.0	0.2 $\pm$ 0.0
20:1	12.9 $\pm$ 0.1	12.8 $\pm$ 0.1	12.2 $\pm$ 0.0	12.1 $\pm$ 0.1	11.9 $\pm$ 0.1	11.8 $\pm$ 0.0	12.0 $\pm$ 0.1	11.7 $\pm$ 0.1
18:0	2.3 $\pm$ 0.2	2.1 $\pm$ 0.1	2.1 $\pm$ 0.0	2.0 $\pm$ 0.0	2.0 $\pm$ 0.0	2.0 $\pm$ 0.0	2.0 $\pm$ 0.0	1.9 $\pm$ 0.0
22:1	14.2 $\pm$ 0.2	14.2 $\pm$ 0.2	13.3 $\pm$ 0.0	13.1 $\pm$ 0.1	12.9 $\pm$ 0.1	12.8 $\pm$ 0.0	12.9 $\pm$ 0.1	12.9 $\pm$ 0.1
20:0	ND	ND	0.1 $\pm$ 0.0	0.1 $\pm$ 0.0	0.1 $\pm$ 0.0	0.1 $\pm$ 0.0	0.1 $\pm$ 0.0	0.1 $\pm$ 0.0

**Table 1** continued

Fatty acid	Present one-step method ( <i>n</i> = 3)						ADAM <sup>a</sup> ( <i>n</i> = 3)	FAME <sup>b</sup> ( <i>n</i> = 3)
	0.1 µg	0.2 µg	0.5 µg	1.0 µg	2.5 µg	5.0 µg		
24:1	0.2 ± 0.3	0.9 ± 0.0	0.9 ± 0.0	1.0 ± 0.0	1.0 ± 0.0	1.0 ± 0.0	0.9 ± 0.0	0.7 ± 0.0
Others	0.8 ± 0.8	0.4 ± 0.5	0.8 ± 0.3	0.9 ± 0.1	1.1 ± 0.1	1.4 ± 0.0	2.7 ± 0.1	2.6 ± 0.1
Amount (nmol) <sup>f</sup>	0.28 ± 0.00	0.57 ± 0.01	1.48 ± 0.01	3.00 ± 0.02	7.69 ± 0.04	15.27 ± 0.04	–	–

ND, not detected; Tr, trace amount; NR, not resolved

<sup>a</sup> HPLC of the 9-anthrylmethyl esters prepared by hydrolysis of the TAG and esterification with ADAM reagent <sup>b</sup>GLC of the fatty acid methyl esters prepared by transmethylation of the TAG

<sup>c–e</sup> Including 18:4n-1<sup>c</sup>; 18:3n-6 and 12:0<sup>d</sup>; and 20:3 and 22:4n-6<sup>e</sup>

<sup>f</sup> Amount of total fatty acids calculated from peak area ratios to internal standard (100 pmol of 19:0-TAG = 300 pmol of 19:0 acid)

<sup>g, h</sup> Including 20:2n-6<sup>g</sup> and unidentified fatty acid<sup>h</sup> not resolved from the peaks

<sup>i</sup> Including branched-chain fatty acids inseparable from 16:2 by the GLC

determined by ordinary methods. It is apparent that fatty acid analysis of 0.5–5 µg or less of TAG can be carried out by using the one-step transesterification.

#### Advantages of the Present One-Step Method

The present method is based on the methodology developed for rapid preparation of fatty acid picolinyl esters [9, 11], C<sub>2</sub>–C<sub>4</sub> *n*-alkyl esters and 2-methoxyethyl esters [10]. However, some improvements were also required. Differing from the preceding cases, 9-anthracenemethanol is a solid alcohol. Because of its limited solubility, the concentration of the potassium 9-anthracenemethoxide reagent is much lower than those of the previous alkoxides. Moisture in the solid 9-anthracenemethanol was removed by adding anhydrous calcium sulfate after preparation of the reagent. The transesterification was stopped by adding acetic acid in accordance with methods for transmethylation [1]. The reagent was precipitated by exchanging the solvent (mixture of dichloromethane and THF) for a non-polar solvent (cyclohexane), and 9-anthrylmethyl esters were taken up in the cyclohexane. Repeated injections of this solution did not have negative effect on the reversed-phase HPLC.

In the present study, the new method was revealed to be usable for synthesis of fatty acid 9-anthrylmethyl esters from TAG. It was also revealed that the resulting 9-anthrylmethyl esters are usable for fatty acid analysis of 0.1–5 µg of natural TAG including those from fish oils. The esters can be synthesized in 10 min, and subjected to HPLC after a few min. Compared with multi-step methodology taking about 1.5 h for preliminary hydrolysis, the present method seems to be great improvement of the derivatization time. Precision of fatty acid analysis also seems to be improved, because of much less use of reagents, solvents, apparatuses, and their handling. The

present method is the most rapid and convenient synthesis of 9-anthrylmethyl esters from TAG, and very effective to facilitate fatty acid analysis of small amount of natural TAG.

#### References

- Christie WW (2003) Lipid analysis, 3rd edn. The Oily Press, Bridgwater, pp. 106–108, 205–215, 273
- Mukherjee PS, Kernes HT (1996) Ultraviolet and fluorescence derivatization reagents for carboxylic acids suitable for high performance liquid chromatography: a review. *Biomed Chromatogr* 10:193–204
- Yasaka Y, Tanaka M (1994) Labeling of free carboxyl groups. *J Chromatogr* 659B:139–155
- Ohkuma Y, Kai M, Nohta H (1994) Fluorogenic reactions for biomedical chromatography. *J Chromatogr* 659B:85–107
- Terasaki M, Itabashi Y, Suzuki T, Nishimura K (2002) An improved method for determining the composition of FFA in red tide flagellates by RP-HPLC with fluorescence detection. *J Am Oil Chem Soc* 79:1181–1186
- Nishimura K, Suzuki T, Monchilova S, Miyashita K, Katsura E, Itabashi Y (2005) Analysis of conjugated linoleic acids as 9-anthrylmethyl esters by reversed-phase high-performance liquid chromatography with fluorescence detection. *J Chromatogr Sci* 43:494–499
- Quilliam MA, Gago-Martínez A, Rodríguez-Vázquez JA (1998) Improved method for preparation and use of 9-anthryldiazomethane for derivatization of hydroxycarboxylic acids. Application to diarrhetic shellfish poisoning toxins. *J Chromatogr* 807A:229–239
- Nimura N, Kinoshita T (1980) Fluorescent labeling of fatty acids with 9-anthryldiazomethane (ADAM) for high performance liquid chromatography. *Anal Lett* 13:191–202
- Destaillets F, Angers P (2002) One-step methodology for the synthesis of FA picolinyl esters from intact lipids. *J Am Oil Chem Soc* 79:253–256
- Destaillets F, Angers P (2002) Base-catalyzed derivatization methodology for FA analysis. Application to milk fat and celery seed lipid TAG. *Lipids* 37:527–532
- Dubois N, Barthelemy C, Bergé J-P (2006) Convenient preparation of picolinyl derivatives from fatty acid esters. *Eur J Lipid Sci Technol* 108:28–32



# Important Differences Exist in the Dose–Response Relationship between Diet and Immune Cell Fatty Acids in Humans and Rodents

Kevin Fritsche

Received: 21 February 2007 / Accepted: 16 July 2007 / Published online: 23 August 2007  
© AOCS 2007

**Abstract** Omega-3 polyunsaturated fatty acids (n-3 PUFA) are noted for their ability to diminish inflammatory and immune responses in vitro and in a variety of animal-based models of autoimmunity and inflammation. Yet, recent systematic reviews suggest that the evidence for these fatty acids having beneficial effects on inflammation or autoimmunity in humans is equivocal. A possible explanation for these disappointing and somewhat paradoxical findings emerged from the analyses described in this review. The available data on the changes in immune cell fatty acid profiles in mice, rats and humans, fed various forms and amounts of n-3 PUFA are summarized and displayed graphically. The dose–response curves generated provide new insights into the relationship between dietary n-3 PUFA and immune cell fatty acid profiles. The author suggests that the poor predictive value of most in vitro as well as many animal trials may, in part, be a consequence of the frequent adoption of experimental conditions that create differences in immune cell fatty acid profiles that far exceed what is possible in free-living humans through dietary intervention. Recommendations for improving the preclinical value of future in vitro and animal-based studies with n-3 PUFA are provided.

**Keywords** Fatty acid metabolism · Metabolism, n-3 fatty acids · Nutrition, immunology · Physiology, arachidonic acid · Specific lipids, fish oil · Specific lipids, n-3 fatty acids · Specific lipids

## Abbreviations

AA	Arachidonic acid
DHA	Docosahexaenoic acid
DPA	Docosapentaenoic acid
en%	Energy percent
EPA	Eicosapentaenoic acid
HUFA	Highly unsaturated fatty acids
ALA	Alpha-linolenic acid
M $\phi$	Macrophages
PBMC	Peripheral blood mononuclear cells
PUFA	Polyunsaturated fatty acids
n-3	omega-3
n-6	omega-6
SDA	Stearidonic acid

## Introduction

The ability of certain fatty acids to influence the immune system and the function of its various cellular components has been recognized for nearly 30 years [1]. Most of the research on this topic has focused on polyunsaturated fatty acids (PUFA). There are two major families of PUFA, the omega-6 (n-6) and the omega-3 (n-3). These fatty acids cannot be synthesized *de novo* in animals, thus they must be provided in the diet. Evidence for the essentiality of these PUFA is unequivocal [2]. In most Western societies dietary intake of n-6 PUFA greatly exceeds that of PUFA from the n-3 family [3, 4]. This imbalance between n-6 and n-3 PUFA intake has been blamed for the high rate of numerous chronic diseases, including inflammatory and autoimmune diseases [5, 6].

The principle mechanism underlying this diet-disease paradigm is thought to be the accumulation of tissue

K. Fritsche  
University of Missouri, Columbia, MO, USA

K. Fritsche (✉)  
110 Animal Science Center, 920 East Campus Drive, Columbia,  
MO 65211-0001, USA  
e-mail: fritschek@missouri.edu

arachidonic acid (AA), an n-6 PUFA, at the expense of unsaturated fatty acids of the n-3 family, particularly docosahexaenoic acid (DHA). AA serves as a precursor to cellular biosynthesis of eicosanoids, a large family of lipid mediators, many of which have pro-inflammatory and immuno-regulatory activity [7]. Lipid mediators derived from n-3 PUFA, however, tend to have biological activities that differ from those derived from AA [8]. Referred to as “resolvins” and “protectins”, some n-3 PUFA-derived mediators have been shown to promote resolution of inflammation and to protect cells from oxidant-induced cell death [9, 10].

The amount and type of fat people consume affects the balance between n-6 and n-3 PUFA in their tissues. Specifically, as diet n-3 PUFA intake increases, tissue AA declines and n-3 PUFA accumulate. Measuring cellular fatty acids is a relatively simple and reliable means to discern exposure to n-3 PUFA, whether through diet or experimental *in vitro* manipulation. More than a decade ago a leading researcher in the field developed a series of equations for predicting this diet-tissue PUFA relationship, first in rats [11], then in humans [12]. These equations are based on fatty acid profiles of circulating lipids (i.e., triglycerides and phospholipids) and may be particularly useful in predicting short-term PUFA intake in free-living humans. However, the dose–response relationship between dietary PUFA and immune cell fatty acid profiles has not previously been examined in a comprehensive manner. Thus, the primary objective of this review is to describe the quantitative relationship between diet and immune cell PUFA content and compare and contrast this relationship in humans, rats, and mice. Such analyses should address the question of whether rodent and human immune cells respond to dietary n-3 PUFA in a quantitatively similar manner.

## The Evidence

What is described in this review is a cross-study meta-regression dose–response analyses of the effect of dietary n-3 highly unsaturated fatty acids (HUFA, fatty acids with greater than three double bonds) on the arachidonic acid (AA) content of human, murine, and rat immune cells. Studies that met the following criteria were included in the analyses: (1) dietary n-3 HUFA (i.e., EPA and/or DHA) or AA intake was a dependent variable in the study design; (2) the fatty acid profile of an identifiable immune cell population was reported; (3) data were published and identified in PUBMED (National Library of Medicine, Bethesda, MD, USA) through December of 2006.

To accomplish the primary objective of this review, fatty acid intake in human and animal-based studies must

be expressed in a way that allows for direct comparison. In most human trials, n-3 PUFA intake is most often expressed as grams consumed per day, or occasionally, on a body weight basis (i.e., mg/kg/day). In contrast, most animal studies provide information about total fat content and the relative amount of various individual fatty acids (i.e., g/100 g of total fatty acids) in the fat/diet. Information about food intake is rarely provided and difficult to measure accurately in rodent studies. Expressing n-3 PUFA intake as a percentage of energy (en%) in the diet obviates the need to measure food intake in rodent studies and allows for meaningful comparisons between human and animal-based studies in this field. Therefore, in this review, dietary n-3 PUFA will be expressed as a percentage of energy (en%) consumed (humans) or provided by the diet (rodents).

The data in Tables 1 and 2 are organized according to species and/or dominant immune cell type/source. This review focuses on diet-induced changes to immune cell highly unsaturated fatty acids (i.e., those with four or more double bonds; HUFA). HUFA are much more potent modulators of inflammation and immune cell function than their 18-carbon PUFA precursors (i.e., linoleic and  $\alpha$ -linolenic acids, n-6 and n-3 PUFA, respectively). Since mice and rats are the most frequently used animal models for studying the impact of dietary fats on the immune response, the data in these tables are derived from these two rodent species as well as from humans. Fatty acid data from other animal species exist, but were not included in these tables because of the limited nature of these data sets and space considerations. To simplify comparisons and clarify trends across studies most of the fatty acid data presented in Tables 1 and 2 have been rounded off to the nearest whole integer. In situations where meaningful information may have been lost by such rounding off, values were reported to the nearest single decimal.

The spleen and peritoneal cavity have been the source of immune cells most frequently used in rodent studies. In contrast, the peripheral blood has been the sole source of immune cells in human studies. Generally, immune organ or whole blood leukocyte preparations are fractionated via density gradient centrifugation prior to analyses. With blood samples this procedure separates the erythrocytes and polymorphonuclear cells (e.g., neutrophils) from peripheral blood mononuclear cells (PBMC). PBMC consist of T- and B-lymphocytes primarily, and lesser numbers of natural killer cells and monocytes.

## Marine n-3 HUFA and Lymphocyte HUFA Content

Baseline fatty acid profiles are remarkably similar between rodent splenocytes and human peripheral blood

mononuclear cells (PBMC). For example, these lymphocyte-rich immune cell preparations are rich in arachidonic acid (AA, 20:4n-6). AA typically accounts for 19 to 23% of total fatty acids in these cells. Furthermore, these immune cells generally contain 2–3% n-3 HUFA, primarily docosahexaenoic acid (DHA, 22:6n-3). The presence of other n-3 HUFA, such as eicosapentaenoic acid (EPA, 20:5n-3) and docosapentaenoic acid (DPA, 22:5n-3), in immune cells is more variable and typically is lower than DHA content. The impact of varying dietary n-3 PUFA on the HUFA content of lymphocyte-rich immune cell preparations from human blood and rodent spleens is summarized in Table 1. Data from human subjects are provided first, followed by data from mice, and finally rats. On some occasions the researcher did not isolate immune cells (i.e., splenocytes) prior to conducting fatty acid analysis of the spleen. The spleen is rich in erythrocytes, thus these data reflect a combination of lymphocyte and erythrocyte fatty acid profiles. However, the presence of erythrocytes did not seem to significantly affect the ability to detect diet-induced changes in fatty acid profiles. In fact, diet-induced changes in erythrocyte and PBMC appear to be quite similar in magnitude [13]. Furthermore, omitting the data from studies using whole spleen (1 of 6 rat studies; 3 of 7 mouse studies) did not significantly change the shape of the rodent lymphocyte fatty acid profile curves.

As n-3 HUFA content of the diet increases, lymphocyte AA content declines in a curvilinear fashion (Fig. 1). The data displayed in this figure are derived from 17 of the 18 studies in Table 1. One study (i.e., Jenski) was omitted from Fig. 1, because the initial AA content of the mouse splenocytes was inexplicably low (i.e., 4%). Also, the absence of DHA in the splenocytes of control mice reported in this study suggests that the authors may have experienced some technical problems with their fatty acid analyses. Note that in human studies n-3 HUFA in the diet never exceeded three percent of total energy (i.e., 3 en%) intake, while intake in most of the rodent studies was considerably higher. Importantly, these data suggest that at lower levels of n-3 HUFA intake, rodent lymphocytes appear to be much more responsive than human to the effects of n-3 HUFA on lymphocyte AA content. This rodent-only response is best described by a two-phase exponential decay curve ( $R^2 = 0.95$ ) and is depicted in Fig. 1 by the line with alternating dots and dashes.

One possible explanation for this differential responsiveness is that human diets routinely contain some n-3 and n-6 HUFA, while experimental rodent diets are typically devoid of all HUFA. Thus, it may be that a small amount of n-3 HUFA has a greater impact on immune cell AA when incorporated into a diet devoid of n-3 and n-6 HUFA (as was the situation in all rodent studies), than when some n-3 PUFA are already present in the diet, as was the case with

most free-living human subjects. A second, alternative, explanation for this differential responsiveness between rodents and humans may relate to immune cell source, in other words peripheral blood lymphocytes maybe less responsive than tissue lymphocytes to dietary n-3 HUFA. Surprisingly, not a single study exists for which fatty acid data are reported for immune cells isolated from blood and a tissue in the same animal or human subject following n-3 PUFA intake. A third possible explanation relates to the differential predominance of T- versus B-lymphocytes in PBMC and rodent spleen, respectively. Evidence from one study suggests that diet-induced changes in fatty acid profiles of various immune cell subtypes found in the blood may not be similar [14]. Their data indicate that high-dose fish oil supplementation failed to reduce human monocyte AA content, but led to a 10, 20, and over 40% reduction in neutrophils, B-cells, and T-cells, respectively. Finally, it is possible that human immune cells are simply more resistant to n-3 HUFA-mediated changes in AA content compared to rodent immune cells.

Lymphocyte EPA content in free-living human subjects and in the rodents fed low n-3 PUFA “control” diets is generally quite low (e.g., typically undetectable to less than 1% of total fatty acids). Because of these very low and variable initial levels, expressing diet-induced changes in EPA content as a “fold-change” or “percent change” is problematic, and is best avoided. The actual amount of EPA in the cell is likely to have more biological relevance than the fold-change. Therefore, data for EPA and other N-3 HUFA in tables and figures are presented simply as a percentage of total cellular fatty acids.

Providing a source of pre-formed EPA in the diet results in its rapid accumulation in human and rodent lymphocytes (Table 1). The relationship between dietary EPA and lymphocyte EPA appears to be curvilinear for EPA intake ranging from 0 to over 4 en% in the diet (Fig. 2). This relationship is best represented by the following equation:  $Y = 0.27 + 4.28X - 0.453X^2$  ( $R^2 = 0.89$ ). Note that EPA accumulation in human lymphocytes never exceeded 4% of total lymphocyte fatty acids. In contrast, it appears that rodent lymphocytes can accumulate considerably more EPA (e.g., up to 12% of total fatty acids). However, one possible explanation of this observation is that dietary EPA intake was considerably lower in the human studies compared to the rodent studies. For example, three of four doses of EPA provided in the human trials were less than 1 en% EPA, with the highest intake less than 2 en%. In contrast, the majority of studies with rodent lymphocytes provided EPA at levels exceeding 2 en% of the diet.

Following EPA consumption, its elongation product, DPA generally increased in the lymphocyte enriched immune cell preparations (Table 1). These changes as well as the relative content of lymphocyte DPA were greater in

**Table 1** Summary of data demonstrating the effect of dietary polyunsaturated fatty acids (PUFA) to alter arachidonic acid (AA), eicosapentaenoic acid (EPA), docosapentaenoic acid (DPA), and docosahexaenoic acid (DHA) content of human versus rodent lymphocyte-rich immune cells/tissues

Tissue/cell type <sup>a</sup>	Species	n-3 source <sup>b</sup>	n-3 intake <sup>c</sup>	Duration (weeks)	%AA <sup>d</sup> 20:4(n-6)	%EPA <sup>d</sup> 20:5(n-3)	%DPA <sup>d</sup> 22:5(n-3)	%DHA <sup>d</sup> 22:6(n-3)	Comments	Citation
PBMC	Human	Tuna oil	0.15 en% 0.33 en% (1 EPA: 4 DHA)	4	23 → 22 23 → 22	0.4 → 0.5 0.4 → 0.6	NR	2 → 3 2 → 3	Subjects were breast-feeding women, 4 week post-partum ( <i>n</i> = 12–15/ treatment group)	[54]
PBMC	Human (healthy males)	FO capsules (corn oil)	0.6 en% 1.2 en% 1.8 en% (4 g EPA/day) (4 EPA: 1 DHA)	12	19 → 16 17 → 15 18 → 15	0.5 → 1.4 0.4 → 2.2 0.6 → 2.9	2.5 → 3.6 2.0 → 3.8 2.2 → 4.4	2.5 → 2.3 2.2 → 2.2 2.1 → 2.3	Older subjects (~60 year old) tended to incorporate more EPA compared to young subjects (~25 year old) reported here	[55]
PBMC	Human (healthy males, 21–44 year old)	FO capsules (palm and hi oleic sunflower oil)	0.9 en% (3 EPA: 1 DHA)	12	(a) 17 → 16 (-5%)	0.7 → 1.6	NR	2.3 → 2.2	Data are reported as pre- and post-trt means within each group of subjects. ( <i>n</i> = 8–10)	[25]
PBMC	Human	borage oil <i>echium oil</i> FO capsules <i>ALA-spread</i>	(b) 0.8 en% GLA (c) 0.4 en% SDA (1 g/day) (a) 0.8 en% (b) 0.4 en% (2 EPA: 3 DHA) (c) 4.5 en% ALA (d) 2.2 en% ALA (5 g/day)	25	(b) 21 → 20 (c) 21 → 20 (a) 19 → 15 (-21%) (b) 19 → 16 (-16%) (c) 18 → 15 (-17%) (d) 19 → 16 (-16%)	0.9 → 0.9 0.4 → 0.9 0.6 → 1.1 0.5 → 0.6 0.6 → 0.8 0.5 → 0.5	3 → 3 3 → 3 3 → 3 4 → 4	3.0 → 2.4 1.8 → 3 2.6 → 3.3 2.9 → 2.7 2.5 → 2.0 3.2 → 2.3	<i>n</i> = 29–31 pre treatment group. Data from week 12 was similar to week 25 values shown here. Basal intake of ALA, AA, EPA, DHA was 1.5, 0.2, 0.2, 0.3 g/day	[20]
PBMC	Human (Crohn's patients)	MaxEPA™	1.2 en% (2 EPA: 1 DHA)	(a) 8 (b) 16 (c) 24	19 → 15 (-21%) 18 → 16 (-11%) 21 → 18 (-14%)	0.5 → 2 0.8 → 2 0.7 → 3	2 → 4 2 → 3 3 → 4	3 → 5 3 → 5 2 → 3.5	Kinetics indicate that changes in PBMC are mostly complete within first 8 week, only EPA seems to accumulate through the study; Plasma PL reflected similar changes, but could not reliably predict changes in PBMC	[56]
(a) T-cells (b) B-cells	Human	MaxEPA	2.7 en% (2 EPA: 1 DHA)	12	(a) 16 → 12 (-25%) (b) 11 → 8 (-27%)	1 → 3 1 → 3	NR	4 → 4 2 → 4	Data from 2 week stowed similar changes in fatty acids	[14]

Table 1 continued

Tissue/cell type <sup>a</sup>	Species	n-3 source <sup>b</sup>	n-3 intake <sup>c</sup>	Duration (weeks)	%AA <sup>d</sup> 20:4(n-6)	%EPA <sup>d</sup> 20:5(n-3)	%DPA <sup>d</sup> 22:5(n-3)	%DHA <sup>d</sup> 22:6(n-3)	Comments	Citation
PBMC	Human	DHA only (LA)	2.7 en% (6 g DHA/day)	12	20 → 11 (-45%)	NR	NR	2 → 7	DHA was incorporated into foods in place of LA; small study (n = 7)	[57]
Spleen	Mouse	n-3 ethyl esters (olive oil)	(a) 0.3 en% EPA (b) 0.7 en% DHA (c) 0.8 en% ALA	1.5	15 → 11 (-27%) 15 → 8 (-47%) 15 → 13 (-13%)	0 → 4 0 → 1 0 → 2	0.3 → 4 0.3 → 1 0.3 → 3	2 → 7 2 → 9 2 → 6	Similar reduction in ex vivo PG and leukotriene production regardless of n-3 source	[37]
Splenocytes	Mouse	MaxEPA (olive oil: SAF mix)	2 en% 4 8 12 en% (4 EPA: 3 DHA)	4	21 → 13 (-38%) 21 → 10 (-52%) 21 → 8 (-62%) 21 → 7 (-67%)	0.1 → 4 0.1 → 7 0.1 → 8.5 0.1 → 9	2 → 4 2 → 5 2 → 5 2 → 5	5 → 12 5 → 12 5 → 13 5 → 13	Curvilinear dose response suggests that changes in DPA and DHA saturate at lower n-3 PUFA intake than AA and EPA	[58]
Splenocytes	Mouse	MFO (corn oil) <i>linseed oil</i>	4 en% (3 EPA: 1 DHA) 11 en% ALA	10	19 → 12 (-37%) 19 → 13 (-32%)	0.1 → 12 0.1 → 4	0.8 → 8 0.8 → 5	3 → 11 3 → 6	Ex vivo PG production was reduce 70–80% with either n-3 source. Source differentially affected NK activity	[59]
Splenocytes	Mouse	MFO (hydrogenated coconut oil)	4 en% (3 EPA: 2 DHA)	34	23 → 8 (-65%)	0 → 8	0 → 4	4 → 9	Balb/c mice were 9 months old at start and 18 months at end of study	[60]
Splenocytes	Mouse	MFO (corn oil)	1 en% 2 en% 4 en% (3 EPA: 2 DHA)	3	4 → 2 (-50%) 4 → 3.5 4 → 3.6	0 → 3 0 → 4 0 → 4	0 → 1 0 → 3 0 → 2	0 → 3 0 → 6 0 → 6	Unclear how many mice were used or the # of samples that were analyzed for fatty acids; no statistical analyses were reported	[61]
Spleen	Mouse	EPA-EE	4 en% EPA only	4	20 → 7 (-65%)	0 → 7	1 → 7	3 → 3	Similar results with C3H and C57 strains of mice	[16]
Spleen	Mouse	MFO (SAF)	6 en% (2 EPA: 1 DHA)	4	19 → 8 (-58%)	0 → 9	0 → 6	6 → 11		[62]
Splenocytes	Rat	MaxEPA (corn oil) <i>linseed oil</i>	1 en% (3 EPA: 2 DHA) 2 en% ALA	6	19 → 11 (-42%) 19 → 15 (-21%)	0.5 → 3 0.5 → 1	1 → 2 1 → 1	2 → 2 2 → 2	Detailed info on PL subclass content and fatty acid profiles as well as PG and leukotriene biosynthesis in vitro	[63]

Table 1 continued

Tissue/cell type <sup>a</sup>	Species	n-3 source <sup>b</sup>	n-3 intake <sup>c</sup>	Duration (weeks)	%AA <sup>d</sup> 20:4(n-6)	%EPA <sup>d</sup> 20:5(n-3)	%DPA <sup>d</sup> 22:5(n-3)	%DHA <sup>d</sup> 22:6(n-3)	Comments	Citation
Splenocytes	Rat	EPA-sTG	2 en% (3 EPA; 1 DHA)	6	18 → 14 (-22%)	0.3 → 2	1 → 2	3 → 5	Position of n-3 HUFA within structured TG did not significantly affect diet-induced changes in lymphocyte fatty acid profiles	[20]
		DHA-sTG (mix of palm, canola, soy oils)	1.5 en% DHA		18 → 13 (-26%)	0.3 → 0.5	1 → 1	3 → 6		
Splenocytes	Rat (5 strains)	MaxEPA (olive oil)	5.5 en% (3 EPA; 2 DHA)	4	19 → 9 (-53%)	0 → 11	0.9 → 5	1 → 5	These data suggest that diet is a more important determinant of membrane fatty acid composition than genetics	[39]
			2 en%	23 → 10 (-57%)	0 → 10	0.4 → 5	2 → 5			
			13 en%	22 → 9 (-59%)	0 → 11	0.4 → 5	1 → 5			
			20 en% (ALA only)	21 → 10 (-52%)	0 → 10	0.5 → 5	1 → 5			
			9 en% ALA	21 → 10 (-52%)	0 → 10	0.5 → 5	2 → 6			
Splenocytes	Rat	<i>linseed oil</i> <i>Linseed oil</i> (sunflower oil)	1 en%	6	19–23 to 12–16 (-30%)	0 to 3–5	0.4–1 to 4	1–2 to 1–2	Data should be viewed with caution due to the complete absence of detectable DHA in these lymphocyte samples	[64]
			2 en%	12 → 14	NR	NR	NR			
			13 en%	12 → 7 (-40%)						
			20 en% (ALA only)	12 → 8 (-33%)						
Splenocytes	Rat (male, Lewis)	MFO (coconut oil) olive oil safflower oil primrose oil	7 en% (2 EPA; 1 DHA)	10	10 → 2 (-80%)	2 → 4	NR	1 → 3	Data for PL fraction similar to that shown here for total lipids	[65]
				10 → 7 (-30%)	2 → 1		1 → 1			
				10 → 5 (-50%)	2 → 1		1 → 1			
				10 → 6 (-40%)	2 → 1		1 → 2			
Spleen	BB rat Diabetes-prone	MFO <i>Flaxseed oil</i>	3.5 en% (2 EPA; 1 DHA)	3	15 → 8 (-50%)	0.8 → 5	3 → 4	3.5 → 5.4	Ratio of IFN $\gamma$ /IL-10 mRNA in GALT reduced by MFO, ALA had opposite impact; no effect in pancreas or on insulinitis	[66]
			8 en% ALA		15 → 9 (-40%)	0.8 → 1	3 → 3	3.5 → 2		

en% % of energy, ALA  $\alpha$ -linolenic acid, MFO menhaden fish oil, M $\phi$  macrophages, NR not reported, PBMC peripheral blood mononuclear cell, PL phospholipids, PG prostaglandin, SAF safflower oil

<sup>a</sup> All M $\phi$  were from the peritoneum, unless indicated otherwise

<sup>b</sup> Fat source in parentheses designates the placebo/control oil/fatty acid; data from plant sources of (n-3) PUFA are shown in italics

<sup>c</sup> Energy % (en%) calculations for humans are based on a 2,000 kcal/day intake

<sup>d</sup> Fatty acid data are presented as the value before and after or without and with dietary treatment with n-3 PUFA, expressed as a % of total fatty acids present. For AA only, the relative change, pre- versus post-treatment, is indicated as a percentage within the parenthesis. Most values have been rounded off to the nearest integer

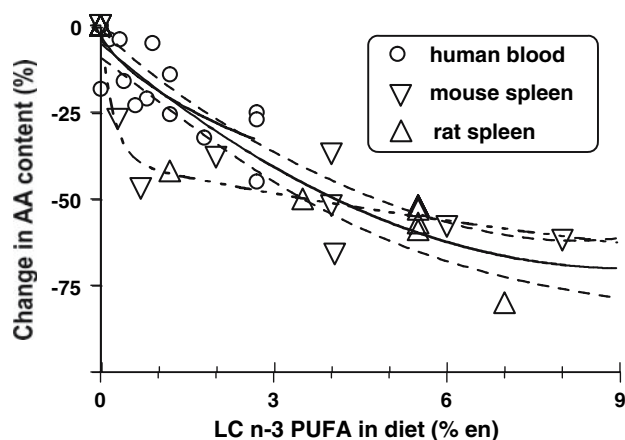


**Fig. 1** Cross-study meta-regression dose–response analyses of the effect of dietary n-3 highly unsaturated fatty acids (HUFA) on the arachidonic acid (AA) content of human, murine, and rat lymphocytes. Studies that met the following criteria were included in the analyses: (1) dietary n-3 HUFA (i.e., EPA and/or DHA) intake was a dependent variable in the study design; (2) the fatty acid profile of an identifiable immune cell population was reported; (3) data were published and identified in PUBMED (National Library of Medicine, Bethesda, MD, USA) through December of 2006. N-3 PUFA intake is expressed as a percentage of total energy consumed (i.e., en%). In most studies, daily caloric intake was not reported. Thus, the following assumptions were made: (1) human subjects consumed 2,000 kcal/day; (2) rodents consumed the same calories across diet treatment groups. AA data are expressed as a percent change from basal or “control” (i.e., lowest n-3 PUFA treatment group). Best-fit lines/curves and the 95% confidence limits (dotted lines) were generated using Prism software (v. 4.0b, GraphPad, San Diego, CA, USA). The equation for the AA curve in this figure is as follows:  $y = -4.87 + -14.2x + 0.776x^2$ ,  $r^2 = 0.85$ . At lower levels of n-3 HUFA intake, rodent lymphocytes appear to be much more responsive than human to the effects of diet n-3 HUFA on lymphocyte AA content. This rodent-only response is best described by a two-phase exponential decay curve ( $R^2 = 0.95$ ) and is depicted in Fig. 1 by the line with alternating dots and dashes

rodent lymphocyte preparations compared to those from human subjects. To date direct evidence that DPA affects immune cell function is lacking. Yet, it is present in immune tissues in significant amounts particularly when EPA is provided in the diet. Recent findings of the potent anti-inflammatory activities of EPA- and DHA-derived metabolites suggest that DPA might also be metabolized to biologically active agents. Investigating the potential function of DPA in these and other cells where it is found in significant quantities seems warranted.

Only two studies investigated the impact of EPA by itself on immune cells DPA and DHA content. In one study [15], mice were fed a diet containing 0.3 en% EPA, as an ethyl ester, for 10 days prior to immune cell isolation and analyses. EPA, DPA and DHA content of murine splenocytes increased significantly. In contrast to these findings, Fujikawa et al. [16] reported that feeding mice 4 en% EPA

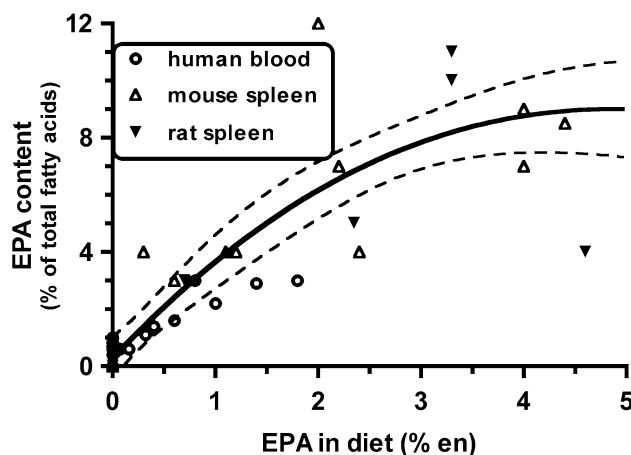


**Fig. 2** Cross-study meta-regression dose–response analyses of the effect of dietary eicosapentaenoic acid (EPA) on the EPA content of human, murine, and rat lymphocytes. Refer to the legend in Fig. 1 for criteria for study inclusion and a description of how the data in the figure were analyzed. EPA data are expressed as a percentage of total fatty acids (i.e., g/100 g) present in the cells. The relationship between dietary EPA and lymphocyte EPA appears to be curvilinear for EPA intake ranging from 0 to over 4 en% in the diet. The best-fit equation for the EPA curve depicted is as follows:  $y = 0.27 + 4.28x + -0.453x^2$ ,  $r^2 = 0.89$ . Note that EPA accumulation in human lymphocytes never exceeded 4% of total lymphocyte fatty acids. In contrast, it appears that rodent lymphocytes can accumulate considerably more EPA (e.g., up to 12% of total fatty acids)

as the sole n-3 PUFA in the diet increased splenocyte EPA and DPA, but left DHA content unchanged. Feeding mice only DHA (0.7 en%) greatly enriches splenocyte DHA, but is much less effective than a smaller amount of dietary EPA at elevating immune cell EPA and DPA.

The relationship between dietary DHA on lymphocyte DHA content is shown in Fig. 3. Consuming more DHA results in an increase in immune cell DHA content, but the effects in rats and humans were not as pronounced as those frequently noted for immune cell EPA or DPA. This may be due, in part, to the relatively higher initial DHA content of these cells. Rat splenocytes and human PBMC typically contained between 2 and 3% DHA. This is true even when rats are fed diets devoid of n-3 PUFA. In human trials, DHA intake prior to supplementation was rarely measured. However, it is estimated that n-3 HUFA intake by individuals in Western societies is approximately 200 mg/day (i.e., 0.1 en%) [4, 17].

The data in Fig. 3 illustrates how DHA content of lymphocytes-rich cell preparations from both rats and humans modestly increased in a linear fashion as DHA in the diet increases. This relationship is represented by the following equation:  $Y = 2.2 + 1.43X$  ( $r^2 = 0.75$ ). In contrast, the response in mice is quite different to that observed in rats and people. This relationship is curvilinear with the best-fit line and 95% confidence intervals depicted on

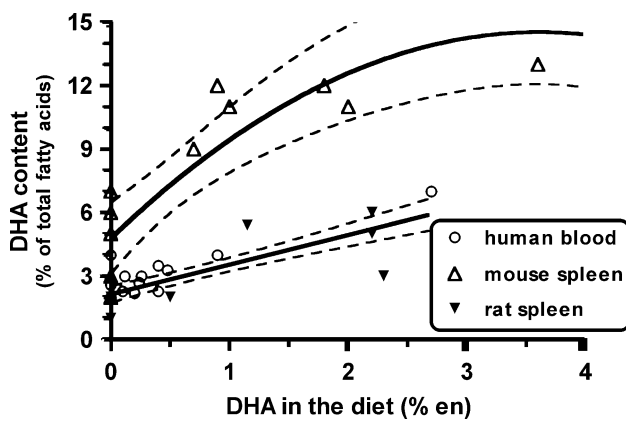


**Fig. 3** Cross-study meta-regression dose–response analyses of the effect of dietary docosahexaenoic acid (DHA) on the DHA content of human, murine, and rat lymphocytes. Refer to the legend in Fig. 1 for criteria for study inclusion and a description of how the data in the figure were analyzed. DHA data are expressed as a percentage of total fatty acids (i.e., g/100 g) present in the cells. The best-fit equation for the diet-lymphocyte DHA response in humans and rats was linear with a best-fit equation represented as follows:  $y = 2.2 + 1.43x$  ( $r^2 = 0.75$ ). In contrast, the diet-lymphocyte DHA response in mice was curvi-linear, with the best-fit equation as follows:  $y = 5.13 + 5.1x + -0.7x^2$ ,  $r^2 = 0.80$

Fig. 3. This best-fit line is represented by a second order polynomial equation (i.e.,  $Y = 5.13 + 5.1X + -0.7X^2$ ;  $R^2 = 0.80$ ).

Interestingly, the initial DHA content of murine lymphocytes averages more than twofold greater than lymphocytes from rats or human subjects. DHA content of murine lymphocytes appears to plateau at  $\sim 12\%$  of total fatty acids, while only occasionally reaching 6% of the total fatty acids in rat or human lymphocytes. This differential response of murine immune cells to become more enriched with DHA relative to rats and humans is evident even at comparable levels of DHA in the diet. These data are consistent with the observations of Hulbert et al. [18] They reported that DHA content of phospholipids from various tissues (i.e., heart, liver, kidney and skeletal muscle) is significantly and inversely correlated with body mass. For example, DHA content of kidney microsomes in mice and rats was reported to vary by  $\sim 6$ -fold (i.e., 29 vs. 5% of total fatty acids). This large difference in membrane DHA content appeared to have a genetic basis, since both rodent species were being fed the same diet in this study [19].

#### Plant-based n-3 PUFA Affect Lymphocyte HUFA

Current estimates suggest that the average U.S. citizen consumes 0.6 en% n-3 PUFA and that  $>90\%$  of this is in the form of alpha-linolenic acid (ALA, 18:3n-3) from plant

sources, such as soybean and canola oils [17]. Direct comparisons between plant-based sources of n-3 PUFA with preformed EPA and DHA to affect immune cell HUFA content were conducted in humans and rodent studies. The data in Table 1 suggest that mice are more capable of converting ALA into n-3 HUFA than rats or humans. In humans, ALA is approximately one-tenth as effective as n-3 HUFA at lowering AA and raising EPA, but fails to elevate DHA content of PBMC [20]. This species difference may be a consequence of the higher desaturase activity in rodents compared with humans [21]. Another contributing factor to this observed difference is that the rodents in these studies were “young” relative to the human subjects. It is well known that desaturase activity declines substantially with age [22]. Another factor that may contribute to the relative inefficient conversion of ALA to HUFA in humans is the presence of HUFA in the typical human diet. Dietary HUFA are quite effective at depressing hepatic desaturase activity [23].

A novel plant-based n-3 PUFA, stearidonic acid (SDA; 18:4n-3) may be considerably more effective than ALA at enriching tissue n-3 HUFA [24]. When healthy male subjects consumed 0.4 en% of SDA (i.e., 1 g/day) from Echium oil there was a modest increase in both EPA and DHA content of PBMC, from 0.4 to 0.9% and 1.8 to 3% of total fatty acids, respectively [25]. SDA had no impact on PBMC AA content. Studies in which the impact of both ALA- and SDA-rich oils are directly compared relative to modulation of immune cell HUFA profiles do not exist presently. Although limited in scope, these data suggest that SDA is more effective than ALA at affecting immune cell HUFA content.

#### Monocyte/M $\phi$

In addition to lymphocytes, monocyte/M $\phi$  are the other immune cell type for which considerable data exist regarding the impact of dietary PUFA on their fatty acid composition. Monocytes/M $\phi$  are part of the innate immune system [26]. These cells are responsible for engulfing bacterial pathogens, dead cells and processing and presenting foreign antigens to T- and B-lymphocytes. By producing pro- and anti-inflammatory eicosanoids and cytokines, these cells play a central role in initiating and resolving inflammation and tissue injury [27].

In rodent models the peritoneum has served as the primary source of M $\phi$ , which typically make up approximately 50% of the resident cells. After collection, in vitro adherence followed by vigorous washing is frequently employed to increase the purity of this cell preparation (e.g., typically  $\sim 90\%$  M $\phi$ ). Also, it is common for researchers to inject a sterile inflammatory agent (e.g., thioglycolate broth,



proteose peptone, or glycogen) into the peritoneum of rodents prior to cell collection. These agents greatly enhance immune cell yield by tenfold or more. Another benefit of eliciting immune cells is the increase in homogeneity within the immune cell population harvested. For example, when cells are collected within the first 12–24 h post-elicitation, neutrophils make up greater than 85% of the total cells. [28] In contrast, M $\phi$  are the predominant cell type present when collection occurs 3–4 days later.

These “elicited” M $\phi$  are derived primarily from blood monocytes that migrate to the inflammatory site (i.e., peritoneum). In fact, it is widely thought that tissue M $\phi$  are primarily derived from peripheral blood monocytes [29]. This relationship, as well as functional similarities between monocytes and tissue M $\phi$ , served as the primary justification for grouping these immune cell populations together in Table 2. Elicited M $\phi$  differ from resident peritoneal M $\phi$  in several important ways, including: cytokine and eicosanoid production [30–32]. Therefore, fatty acid data for resident and elicited M $\phi$  were presented separately. Interestingly, the fatty acid data suggest that these two immune cell populations also differ in responsiveness to dietary HUFA treatment.

#### Marine n-3 PUFA and Monocyte/M $\phi$ HUFA

AA and DHA content of monocyte/M $\phi$ -rich cell preparations tended to be much more variable than lymphocyte-rich immune cell preparations. For example, AA content of M $\phi$  from mice and rats fed control diets across the 10 studies included in Table 2 ranged from 8 to 28% of total fatty acids. Rodent M $\phi$  DHA content varied from 0 to 7% of total fatty acids in these same studies. Some of the factors that may have contributed to this variability in basal HUFA, include: genetic/species differences, differences in dietary PUFA content of background/control diets, differences in cell purity, and differences in analytical procedures used by the various investigators. Whatever the underlying cause(s), this variation makes direct comparisons between studies problematic. Thus, diet-induced changes in fatty acid AA and DHA content are described in the context of fold-change as well as in terms of actual percentage of total fatty acids. However, caution should be exercised in the interpretation of these data. For example, it is unclear whether a doubling of immune cell DHA from an initial low value (e.g., from 0.5 up to 1%) is functionally equivalent to the same fold increase in cells containing substantially more initial DHA (e.g., from 3 up to 6%). Additionally, it is uncertain whether a 50% decline in AA will have the same physiologic consequence if cells start out with vastly different initial AA content.

Similar to lymphocyte-rich immune cell populations, the inclusion of n-3 HUFA in the diet of rodents, as well as human subjects, can have a significant effect on the AA content of monocytes/M $\phi$ . As n-3 HUFA intake increases, M $\phi$  AA levels decline in a curvilinear fashion (Fig. 4). The decline appears to plateau at reduction in AA content of ~50% of the original content, once n-3 HUFA intake reaches 3 en%. The best-fit line and 95% confidence intervals is depicted on the figure and are represented by a one-phase exponential decay equation:  $Y = 50.9 \exp(-1.1X) + -50.1$  ( $R^2 = 0.72$ ). The data from human subjects suggest that peripheral blood monocytes may be less responsive to n-3 HUFA-mediated changes in AA content than rodent M $\phi$ . However, the human monocyte data are too limited to analyze separately.

The dose–response relationships between EPA intake and monocyte/M $\phi$  EPA accumulation is illustrated in Fig. 5. EPA accumulation in human monocytes and elicited rodent peritoneal M $\phi$  increases in a curvilinear fashion with increasing dietary EPA. This relationship is represented by the following equation:  $Y = 0.29 + 2.58X + -0.436X^2$  ( $R^2 = 0.86$ ). Accumulation of EPA in monocyte/M $\phi$  plateaus at ~4% of total fatty acids, which is only half as much observed in lymphocyte-rich cell preparations. In contrast to human monocytes and elicited peritoneal M $\phi$ , the relationship between dietary EPA and EPA content of resident peritoneal M $\phi$  is linear (i.e.,  $Y = 0.4 + 3.3X$ ;  $r^2 = 0.89$ ). Interestingly, resident M $\phi$  from the peritoneum of rodents accumulate more EPA than human monocytes and elicited M $\phi$  rodents at each level of dietary EPA intake. Yet, only a single research group directly compared the response of resident and elicited M $\phi$  to diet n-3 PUFA treatment [33]. Those data, however, follow the same general pattern illustrated in Fig. 5 in that the dose–response relationship between EPA intake and cellular EPA is steeper in resident than elicited M $\phi$ .

DHA content of monocyte/M $\phi$  increases in a linear fashion in response to increasing DHA intake (Fig. 6). However, these data are quite variable (i.e.,  $Y = 3.8 + 1.7X$ ;  $r^2 = 0.42$ ). The “fit” was only slightly improved when non-linear functions were used to represent these data. Unlike lymphocytes, a “species effect” in the dose–response relationship between dietary DHA and DHA in the monocyte/M $\phi$ -rich populations is not readily apparent. Yet, human blood monocytes seem relatively resistant to the accumulation of DHA. Figure 6 shows that DHA content of rodent M $\phi$ , elicited and resident alike, exceed that found in human monocytes at every level of dietary DHA intake. Surprisingly, direct evidence that blood monocytes and tissue M $\phi$  are differentially responsive under identical experimental conditions (i.e., same subject on the same dietary treatment) is lacking.

**Table 2** Summary of data demonstrating the effect of dietary polyunsaturated fatty acids (PUFA) to alter arachidonic acid (AA), eicosapentaenoic acid (EPA), docosapentaenoic acid (DPA), and docosahexaenoic acid (DHA) content of human versus rodent innate immune cells/tissues

Tissue/cell type <sup>a</sup>	Species	n-3 source <sup>b</sup>	n-3 intake <sup>c</sup>	Duration (weeks)	%AA <sup>d</sup> 20:4(n-6)	%EPA <sup>d</sup> 20:5(n-3)	%DPA <sup>d</sup> 22:5(n-3)	%DHA <sup>d</sup> 22:6(n-3)	Comments	Citation
Monocytes	Human	EPA + DHA ethyl esters	1 en% (3 EPA; 2 DHA)	12	19 → 15 (-20%)	0.2 → 1.7	1 → 3	2 → 3.5	Fatty acid data deduced from figures; data from 18 week washout indicated rapid drop in EPA, slower response with DHA	[13]
Monocytes	Human	Cod liver-oil	2.7 en% (3 EPA; 2 DHA)	6	23 → 15 (-35%)	0.04 → 2	NR	0.7 → 2	Individual values ( <i>n</i> = 9) for AA and EPA illustrate variation in responsiveness	[67]
Monocytes	Human	MaxEPA <sup>TM</sup>	2.7 en% (2 EPA; 1 DHA)	12	13 → 12 (-8%)	1 → 3	NR	4 → 4	Most change (>90%) occurred within 2 week	[14]
Resident Mφ	Mouse	Sardine oil (SAF mix)	0.26 en% 0.54 en% 2.8 en% (2 EPA; 1 DHA)	2	8 → 7 (-13%) 8 → 5 (-38%) 8 → 4 (-50%)	0.1 → 1 0.1 → 2 0.1 → 5	0.1 → 3 0.1 → 3 0.1 → 4	1 → 4 1 → 5 1 → 7	50% reduction in <i>in vitro</i> Mφ cytotoxicity maxed out at middle dose of n-3 PUFA	[33]
Resident Mφ	Mouse	Fish oil (mix of oils) tri-ALA	0.4 en% 1 en% 3 en% (2 EPA; 1 DHA) 0.5 en% 1.1 en% 2.8 en% ALA	2	9 → 5 (-45%) 9 → 5 9 → 4 9 → 9 9 → 7 9 → 6	0 → 2 0 → 3 0 → 5 0 → 0.1 0 → 0.5 0 → 1	0.1 → 3 0.1 → 3 0.1 → 4 0.1 → 1 0.1 → 2 0.1 → 2	1 → 5 1 → 6 1 → 7 1 → 3 1 → 3 1 → 4	LA content of all diets was kept constant at ~3 en%. Data are from PL fraction only	[34]
Resident Mφ	Mouse	Fish oil (corn oil)	2 en% (3 EPA; 2 DHA)	9	24 → 12 (-50%)	0 → 4	NR	6 → 10	Most of the changes in fatty acids occurred within the 1st week according to kinetic data	[42]
Resident Mφ	Mouse	AA ethyl ester (mix of oils and triglycerides)	1.3 en% 3.7 en% (AA only)	2	11 → 19 (+68%) 11 → 18 (+57%)	NR	NR	1 → 1 1 → 1		[36]

Table 2 continued

Tissue/cell type <sup>a</sup>	Species	n-3 source <sup>b</sup>	n-3 intake <sup>c</sup>	Duration (weeks)	%AA <sup>d</sup> 20:4(n-6)	%EPA <sup>d</sup> 20:5(n-3)	%DPA <sup>d</sup> 22:5(n-3)	%DHA <sup>d</sup> 22:6(n-3)	Comments	Citation
Resident M $\phi$	Rat	MaxEPA (corn oil) <i>linseed oil</i>	(a) 1.2 en% (2 EPA: 1 DHA) (b) 2 en% ALA	6	(a) 15 $\rightarrow$ 9 (-40%) (b) 15 $\rightarrow$ 10 (-33%)	0.5 $\rightarrow$ 4 0.5 $\rightarrow$ 1	2 $\rightarrow$ 4 2 $\rightarrow$ 3	2 $\rightarrow$ 4 2 $\rightarrow$ 2	Detailed info on PL (PC, PE, PL, PS) content and fatty acid profiles as well as PGE, TXB, LTB biosynthesis in vitro	[35]
Resident M $\phi$	Rat	Sardine oil (rapeseed/ peanut oils; 1:1)	2.4 en% (3 EPA: 1 DHA)	16	28 $\rightarrow$ 13 (-54%)	0.2 $\rightarrow$ 8	NR	7 $\rightarrow$ 11	No n-3 effect on adherence or phagocytosis	[68]
Elicited M $\phi$	Mouse	Sardine oil (SAF mix)	0.26 en%	2	11 $\rightarrow$ 10 (-9%)	1 $\rightarrow$ 1	0.5 $\rightarrow$ 2	3 $\rightarrow$ 3	50% reduction in in vitro M $\phi$ cytotoxicity maxed out at middle dose of n-3 PUFA	[33]
Elicited M $\phi$	Mouse	Sardine oil (SAF)	0.3 en%	2	15 $\rightarrow$ 12 (-20%)	0 $\rightarrow$ 0.5	0.5 $\rightarrow$ 2	2 $\rightarrow$ 4	Dose response was quite similar in the liver PL. LT production was reduced ~35% at median dose with no additional effect of more n-3 PUFA	[69]
Elicited M $\phi$	Mouse	MFO (sunflower oil)	4 en% (1 EPA: 1 DHA)	6	12 $\rightarrow$ 6 (-50%)	0.4 $\rightarrow$ 5	0.5 $\rightarrow$ 5	1 $\rightarrow$ 4	Cells were collected 4 days post-Listeria challenge and were nearly equal numbers of M $\phi$ and lymphocytes	[48]
Elicited M $\phi$	Mouse	MFO (SAF)	4 en% (3 EPA: 2 DHA)	4	13 $\rightarrow$ 7 (-45%)	0 $\rightarrow$ 4	NR	1 $\rightarrow$ 6		[70]
Elicited M $\phi$	Mouse	MFO (SAF)	6 en% (3 EPA: 2 DHA)	4	15 $\rightarrow$ 6 (-60%)	0 $\rightarrow$ 4	0 $\rightarrow$ 7	0 $\rightarrow$ 4	Study also included a borage oil and coconut oil-fed groups	[62]
Neutrophils	Human	(a) EPA capsules (b) DHA capsules	(a) 2 en% EPA (b) 2 en% DHA	4	(a) 14 $\rightarrow$ 13 (-7%) (b) 16 $\rightarrow$ 12 (-20%)	1 $\rightarrow$ 3 1 $\rightarrow$ 2	1 $\rightarrow$ 3 1 $\rightarrow$ 2	3 $\rightarrow$ 3 3 $\rightarrow$ 5	EPA group also consumed 0.7 g/day DHA;	[38]
Neutrophils	Human	MaxEPA	2.7 en% (2 EPA: 1 DHA)	12	11 $\rightarrow$ 10 (-9%)	1 $\rightarrow$ 3	NR	2 $\rightarrow$ 3	DHA group also consumed 0.8 g/day EPA	[14]
									Most change (>90%) occurred within 2 week	

Table 2 continued

Tissue/cell type <sup>a</sup>	Species	n-3 source <sup>b</sup>	n-3 intake <sup>c</sup>	Duration (weeks)	%AA <sup>d</sup> 20:4(n-6)	%EPA <sup>d</sup> 20:5(n-3)	%DPA <sup>d</sup> 22:5(n-3)	%DHA <sup>d</sup> 22:6(n-3)	Comments	Citation
Neutrophils	Human	Echium oil	1.9 en% ALA + 0.8 en% SDA	4	9 → 9	0.1 → 0.5	0.6 → 1.2	0.7 → 0.9	Treatment reduced plasma (71) by 25% in subjects with hypertriglyceridemia	[40]
Elicited PMN (30 min post-zymosan i.p.)	Mouse	Ethyl ester of DHA (~10 en% LA in all diets)	0.8 en% 1.7 en% 7.4 en% (DHA only)	2	28 → 18 (-36%) 28 → 12 (-57%) 28 → 8 (-71%)	0 → 0 0 → 0.3 0 → 1.5	0 → 1 0 → 2 0 → 2	2 → 9 2 → 12 2 → 15	Reduction of in vivo PGE max at 0.8 en%; for PGI and LTE max at 1.7 en% DHA. Fatty acid data converted from nmoles/mouse to %	[37]
Elicited PMN	Mouse	Sardine oil (safflower oil)	3 en% (2 EPA; 1 DHA)	3	13 → 6 (-45%)	0 → 4	0 → 2	2 → 7	Frequency of consumption of high n-3 HUFA diet was purposely varied from 1 day/week to daily	[46]
Elicited PMN	Rat	MaxEPA (olive oil; MaxEPA @ 1:1)	6 en% (3 EPA; 2 DHA)	3	19 → 12 (-30%)	5 → 14	NR	1.5 → 3	"Control" diet contained 3 en% n-3 HUFA	[71]
Elicited PMN	Rat (5 strains)	MaxEPA (olive oil)	5.5 en% (3 EPA; 2 DHA)	4	21 → 14 (-33%) 27 → 13 (-52%) 25 → 13 (-48%) 23 → 14 (-39%) 25 → 15 (-40%)	0 → 14 0 → 14 0 → 16 0 → 12 0 → 13	0.3 → 2 0.2 → 3 0.1 → 3 0.1 → 2 0.1 → 2	1 → 2 1 → 3 1 → 3 1 → 3 1 → 2	These data suggest that diet is a more important determinant of membrane fatty acid composition than genetics	[39]
		linseed oil	9 en% ALA		21 → 27 to 14 → 21 (-25%)	0 to 4 → 6	0.2 to 1 → 2	1 to 2 → 3		

en% % of energy, ALA  $\alpha$ -linolenic acid, MFO menhaden fish oil, M $\phi$  macrophages, NR not reported, PBMC peripheral blood mononuclear cell, PL phospholipids, PG prostaglandin, SAF safflower oil

<sup>a</sup> All M $\phi$  were from the peritoneum, unless indicated otherwise

<sup>b</sup> Fat source in parentheses designates the placebo/control oil/fatty acid; data from plant sources of (n-3) PUFA are shown in italics

<sup>c</sup> Energy % (en%) calculations for humans are based on a 2,000 kcal/day intake

<sup>d</sup> Fatty acid data are presented as the value before and after or without and with dietary treatment with n-3 PUFA, expressed as a % of total fatty acids present. For AA only, the relative change, pre- versus post-treatment, is indicated as a percentage within the parenthesis. Most values have been rounded off to the nearest integer

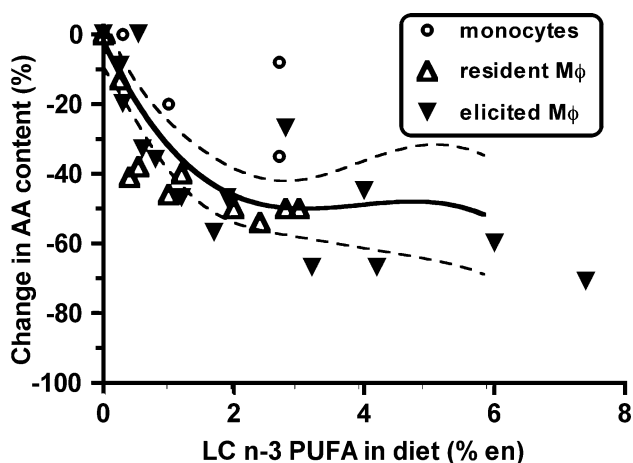


**Fig. 4** Cross-study meta-regression dose–response analyses of the effect of dietary n-3 highly unsaturated fatty acids (HUFA) on the arachidonic acid (AA) content of human, murine, and rat monocytes/macrophages (M $\phi$ ). Refer to the legend in Fig. 1 for criteria for study inclusion and a description of how the data in the figure were analyzed. The best-fit line and 95% confidence intervals is depicted on the figure and are represented by a one-phase exponential decay equation:  $Y = 50.9 \exp(-1.1X) + -50.1$  ( $R^2 = 0.72$ ). The data from human subjects suggest that peripheral blood monocytes may be less responsive to n-3 HUFA-mediated changes in AA content than rodent M $\phi$ . However, the human monocyte data are too limited to analyze separately

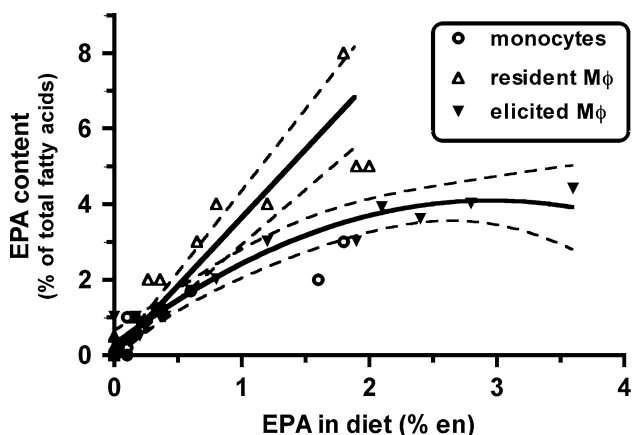


**Fig. 5** Cross-study meta-regression dose–response analyses of the effect of dietary eicosapentaenoic acid (EPA) on the EPA content of human monocytes, as well as resident and elicited peritoneal macrophages (M $\phi$ ) from mice and rats. Refer to the legend in Figs. 1 and 2 for criteria for study inclusion and a description of how the data in the figure were analyzed and presented. The equation for the EPA curve for human monocytes and elicited peritoneal M $\phi$  from rodents was:  $y = 0.29 + 2.58x + -0.436x^2$ ,  $r^2 = 0.86$ ; while the best-fit for EPA in resident peritoneal M $\phi$  (is linear:  $y = 0.4 + 3.3x$ ;  $r^2 = 0.89$ )

#### Plant-based n-3 PUFA Affect Monocyte/M $\phi$ HUFA

As with lymphocytes, dietary ALA appears to be considerable less effective at reducing AA and elevating n-3 HUFA in M $\phi$ . For example, Whelan et al. [34] conducted a carefully designed experiment to directly compare the potency of n-3 HUFA from fish oil to the shorter-chain

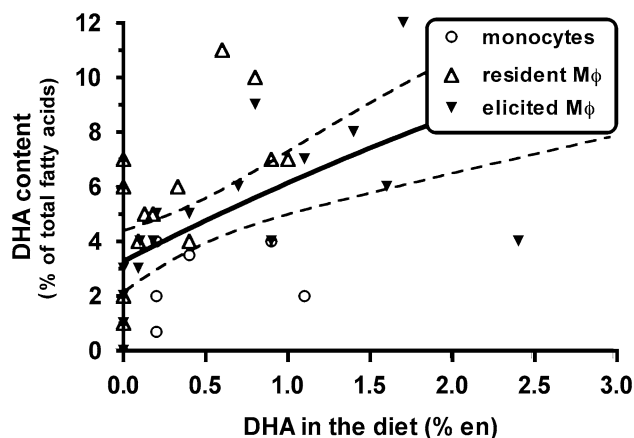


**Fig. 6** Cross-study meta-regression dose–response analyses of the effect of dietary docosahexaenoic acid (DHA) on the DHA content of human monocytes, as well as resident and elicited peritoneal macrophages (M $\phi$ ) from mice and rats. Refer to the legend in Figs. 1 and 3 for criteria for study inclusion and a description of how the data in the figure were analyzed and presented. The equation for DHA is:  $y = 3.8 + 1.7x$ ,  $r^2 = 0.42$ . The “fit” for the DHA data is not significantly improved when non-linear functions are used (data not shown). Human blood monocytes seem relatively resistant to the accumulation of DHA. Furthermore, DHA content of rodent M $\phi$ , elicited and resident alike, exceed that found in human monocytes at every level of dietary DHA intake

length precursor n-3 PUFA (i.e., ALA) at three different levels in the diet (i.e., ~0.5, 1 and 3 en%). They formulated experimental diets to contain similar amounts of total fat, but variable levels of n-3 HUFA from fish oil or a manufactured tri-ALA. Their data indicate that consuming a diet with 3 en% ALA for two weeks was nearly as effective as 0.4 en% n-3 HUFA at lowering resident murine M $\phi$  AA and elevating EPA, DPA, and DHA content. Brouard et al. [35] reported that 2 en% ALA from linseed oil was nearly as effective as 1.2 en% n-3 HUFA from fish oil at lowering AA and elevating DPA content in rat resident peritoneal M $\phi$ . Yet, this plant-derived n-3 PUFA was much less effective at elevating EPA and did not change DHA content of these immune cells.

There is only a single report describing the impact of dietary AA on immune cell fatty acid profiles [36]. As expected, the addition of preformed AA to the diet (i.e., 1.3 or 3.7 en%) enhanced resident murine M $\phi$  AA content by 57 and 68%, respectively, but had no effect on DHA levels (data on EPA and DPA were not reported). In contrast, when LA intake of mice was increased from ~4 to 8% of total calories, neither hepatic lipids or resident peritoneal macrophage phospholipid AA content were significantly increased.

#### Neutrophils

Neutrophils are the predominant leukocyte in human blood and play a central role in early “innate” host

defense against bacterial infection. Yet, the data on diet-induced changes of their PUFA content are limited to three studies with human neutrophils, one study comparing five different rat strains, and a possibly a single mouse study (Table 2). There is some uncertainty about the identification of the immune cells analyzed by Lokesh et al. [37]. These researchers indicated that they were working with macrophages, yet the cells isolated were from the peritoneum of mice 30 min following the injection of an inflammatory agent (i.e., zymosan). The predominate immune cell that would have been recovered under these circumstances would have been neutrophils, not macrophages. Therefore, this study has been included in this section of the Table 2.

Overall, the data in this section of Table 2 indicate that neutrophil HUFA content can be affected by dietary n-3 PUFA. In fact, the amount of EPA that rat neutrophils incorporated in response to n-3 HUFA intake was striking (i.e., from undetectable levels to greater than 12% of total fatty acids). This response in rats contrasts sharply with the more modest accumulation of EPA observed in human neutrophils, that was never reported to exceed 3% of total fatty acids. Accumulation of DPA and DHA in neutrophils following n-3 HUFA supplementation was similar among rats and humans; was considerably lower than that seen with EPA.

Kew et al. [38] directly compared the impact of EPA to DHA on human neutrophil fatty acid profiles and function. They found that consumption of 2 en% EPA for 4 weeks resulted in only a modest increase in EPA and DPA, but with little detectable change in either AA or DHA. In contrast, intake of a similar amount of DHA decreased AA by 20% and increased DHA content from 3 to 5% of total fatty acids, while EPA and DPA were also modestly increased. These data suggest that DHA-enriched oils may be more effective at changing the fatty acid profiles of some human immune cells compared to EPA-rich oils.

Cleland et al. [39] directly compared the impact of a fish oil source of n-3 PUFA (i.e., MaxEPA) with a plant-based source (i.e., linseed oil) on the fatty acid profiles of neutrophils from five different strains of rats. They demonstrated that compared to 5.5 en% n-3 HUFA, 9 en% ALA resulted in more modest reductions in AA and increases in EPA in these immune cells. However, DPA and DHA accumulation was modest and similar between the fish oil-derived and plant derived sources of n-3 PUFA. Surette et al. [40] reported that ALA and SDA from Echium oil, a novel plant source of n-3 PUFA, were able to modestly affect human blood neutrophils fatty acid profiles. After 4 weeks of consuming 1.9 en% ALA along with 0.8 en% SDA, neutrophil EPA increased from 0.1 to 0.5% and DPA doubled (i.e., 0.6–1.2%), while AA and DHA levels were not significantly affected.

In contrast to these studies with dietary n-3 PUFA, intake of LA over a broad range failed to alter AA content of human neutrophils or plasma lipids [41]. Yet, in rats increasing dietary LA over a range of 0.3–7 en% was associated with a modest increase in the AA content in elicited peritoneal macrophages [41].

## Kinetics

Data from time course studies with mice [42] and humans [43] suggest that diet-induced changes in immune cell fatty acid profiles occur rapidly (i.e., within a few weeks). This time frame is quite similar to that observed with other tissues, such as heart, liver and kidney [44]. In recognition of the rapid response of tissues to n-3 HUFA, many researchers using animal models feed experimental diets for 4 weeks or less. This appears to be sufficient to alter rodent immune cell fatty acid composition, and in most cases, *in vitro* functions. In contrast, most human studies use fatty acid treatment periods extending several months, and in one case, a year. Presumably, extended treatments are done to increase the likelihood of observing treatment effects at more modest doses of n-3 PUFA. The data suggest that HUFA incorporate into cell membranes in proportion to their availability (i.e., concentration in the plasma or extracellular milieu), with the length of time they are exposed being much less important. For example, changes in fatty acid profiles for human PBMC were similar at 3 versus 6 months of dietary n-3 PUFA supplementation [45]. Extended treatment periods make subject recruitment more difficult, reduces overall subject compliance, increases dropout rates, and is more costly. For example, the impact of fish oil supplementation on HUFA content of PBMC from 31 Crohn's patients appeared to peak at 8 week, then declined as the supplementation period extended to 16 and 24 week. All of these outcomes would detract from, rather than, strengthen a clinical trial. Clinicians should reconsider the need for using extended treatment periods in clinical trials with fatty acids, unless there are clear and compelling reasons for doing so.

In an interesting and clinically-relevant approach to study kinetics and dose-response, Broughton and Morgan [46] investigated the impact of periodicity of n-3 HUFA intake on tissue fatty acid composition and eicosanoid biosynthesis. For this study, mice were offered diets enriched with EPA (~2 en%) and DHA (~1 en%) for one or more days per week. As the number of days mice consumed the fish oil-containing diet increased there was a frequency-dependent reduction in immune cell AA; elevations in EPA, DPA and DHA. Changes in eicosanoid biosynthesis were statistically different only when the n-3 PUFA enriched diet was consumed at least on an every

other day basis, while tissue fatty acid changes differed with n-3 PUFA intake occurring as infrequently as once every 5 days. This study is intriguing because the experimental feeding approach closely mimics the pattern of n-3 HUFA intake that occur with free-living individuals whom might occasionally consume cold-water, fatty fish (e.g., tuna, salmon, herring) or fish oil supplements.

## Discussion and Recommendations

The major objective of this review was to provide readers with a better understanding of the dose–response relationship between diet and subsequent immune cell HUFA content. Inclusion of n-3 HUFA in the diet of humans and laboratory rodents produces a predictable pattern of changes in immune cell fatty acid profiles: AA content diminishes, while n-3 HUFA accumulate. It is clear from these data that preformed n-3 HUFA are significantly more effective at inducing these changes compared to plant sources of n-3 PUFA (e.g., alpha-LNA). Furthermore, consumption of preformed AA does appear to elevate immune cell AA. Unfortunately, the diet AA data are too limited to draw conclusions about dose–response relationships, differential responsiveness among types of immune cells or across species. This is particularly unfortunate since human diets routinely contain AA and understanding the impact of this fatty acid on the accumulation of n-3 HUFA as well as the reduction of immune cell AA may be central to improving the outcome of ongoing human n-3 PUFA clinical trials.

Clear identification of the immune cell population under study was an important consideration in the presentation and interpretation of these data. While the functional differences between various types of immune cell are well recognized, potential biochemical distinctions are less well defined. Collectively the data presented in this review suggest that the nature of the immune cell population under study affect both the initial, as well as diet-induced changes in, fatty acid content. However, changes in PUFA or HUFA intake do not appear to significantly affect immune cell subset distribution in humans or rodents [47, 48]. Therefore, it seems reasonable to conclude that changes in fatty acid profiles within a given study noted in this review are not a consequence of diet-induced shifts in immune cell distribution. While n-3 PUFA intake induces similar patterns of change in fatty acid profiles among the various immune cell populations examined, significant differences existed for individual HUFA. Though limited (i.e.,  $n = 8$  subjects), data from a single study suggest that human B-cells may contain lower amounts of AA and DHA, than T-cells. The relative proportion of T- and B-cells in human blood [i.e., 6:1] is quite different than that found in the

rodent spleen, which contains one T-cell for every three B-cells. At the present time it is unclear to what extent tissue of origin or species of origin may be contributing to some of the differences observed in humans and mice regarding their response to dietary n-3 PUFA exposure. Furthermore, it is possible that differences in cellular activities for tissue versus blood-borne immune cells may contribute to some of the differences in HUFA incorporation noted in this review. What is needed to resolve this issue are data from blood and tissue immune cells obtained from the same experimental subjects following consumption of diets enriched with n-3 PUFA. Such studies would help discern the independent contribution of cell source on dietary n-3 PUFA-driven changes to immune cell HUFA content.

Importantly, while humans and rodents share similar patterns of changes in immune cell HUFA content, they do not appear to be equally responsive to dietary n-3 HUFA. N-3 HUFA do not appear to lower AA, nor enrich n-3 HUFA, in human blood monocytes as much as in tissue  $M\phi$  from either rats or mice. These data may also be interpreted to mean that responsiveness to n-3 PUFA enrichment for circulating immune cells is not the same for tissue immune cells within the same lineage. For example, cells of the monocytic lineage differ in responsiveness as follows: resident  $M\phi >$  elicited  $M\phi >$  blood monocytes. The absence of fatty acid data from blood monocytes and tissue  $M\phi$  from the same human subjects or animals after n-3 PUFA supplementation makes it impossible to distinguish between these two equally plausible explanations. For lymphocytes, there is solid evidence for differential responsiveness to diet n-3 HUFA between species. For example, the reduction in AA content in response to low doses of n-3 HUFA intake (i.e., 0–1 en%) appears to be much greater in rodents than humans. Furthermore, murine lymphocytes start out with, and accumulate more, DHA than human or rat lymphocytes in response to n-3 PUFA intake. The underlying mechanism(s) for, and biological significance of, such differences in immune cell responsiveness to n-3 PUFA are unclear at this time, but warrant further study.

The data presented in this review may help explain, in part, the paradox of equivocal results from human clinical trials with n-3 PUFA to treat inflammatory and immune-mediated diseases [49]. In contrast, there have been many positive outcomes reported for animal(rodent)-based models of such diseases. First, as noted in this review, the relative amount of n-3 PUFA provided to animals in most “immune-focused” studies far exceed what is achievable in free-living humans. This difference in n-3 PUFA intake results in changes in HUFA profiles in rodents immune cells that surpass those achieved in humans. Though unproven, it is widely presumed that changes in immune cell membrane phospholipids fatty acid content are both

**Table 3** Recommendations for improving the preclinical value of animal- and cell culture-based experiments with n-3 PUFA

## Animal-based n-3 PUFA/HUFA diet studies:

Good: Design experimental diets to provide a level of n-3 PUFA intake that is achievable in humans (e.g., ~1 en% or less)

Better: Only provide an amount and form of dietary n-3 PUFA in animal diets that reproduces the changes in fatty acid HUFA content previously reported in humans

Best: Provide a source of pre-formed AA in the control and n-3 PUFA treatment diets

## Cell culture (in vitro) studies:

Good: Introduce fatty acids in a physiological context (i.e., complexed to albumin)

Better: Check fatty acid profiles of cells prior to treatment. It is not uncommon for cells maintained in culture for prolonged periods of time to be depleted of HUFA. Normalization of cell HUFA levels in cell lines will avoid problems associated with essential fatty acid deficiency. The goal of this normalization process should be to reproduce the fatty acid profile found in freshly isolated primary cells prior to in vitro HUFA treatment

Better: Avoid using HUFA concentrations in vitro that exceed those typically observed in vivo (i.e., 10  $\mu$ M)

Better: Extend fatty acid treatment beyond 24 h to model in vivo exposure via diet and to avoid acute treatment artifacts (e.g., membrane disruption, triacylglyceride accumulation)

Best: Use treatment conditions that mimic the quantity and quality of fatty acid changes noted in these same cells following dietary n-3 PUFA supplementation. One way to accomplish this outcome is to use of mixtures of various fatty acids, rather than just adding one single fatty acid

necessary and sufficient to affect immune cell function (e.g., eicosanoid production, cytokine biosynthesis, receptor function, and cell signaling). Therefore, if health benefits associated with dietary n-3 PUFA require changes in immune cell function, then the poor outcome of most clinical trials might have been predicted on this basis alone. Another, important and often overlooked, difference between most animal-based studies and human clinical trials is that in the former test subjects are provided high n-3 diets BEFORE and during the disease development. In human clinical trials published to date, subject selection is based on the individual already suffering clinical signs of the “disease” for which n-3 PUFA are supposed to treat.

One way to look at these findings is that for animal-based studies to have greater preclinical value, diets should be designed to include only enough n-3 PUFA to reproduce the changes in immune cell HUFA noted in human clinical trials. However, it is not known if changes in immune cell HUFA content simply correlate with or are necessary for changes in immune cell function and subsequent in vivo inflammation and immune responses.

Another factor that may be contributing to the greater frequency of positive outcomes in rodent-based studies of n-3 PUFA is the fatty acid composition of “control” diets. Most rodent studies of n-3 PUFA bioactivity use vegetable oil (e.g., corn and soybean oils) as the fat source in the diet of the control group animals. These fats contain high levels (i.e., 50%) of linoleic acid (18:2n-6) and no preformed AA or n-3 HUFA. Yet, intake of AA and n-3 HUFA for non-vegetarian individuals is common. The inclusion of small amounts of AA and n-3 HUFA to match current average daily intake in humans to “control” as well as “experimental” rodent diets may significantly improve how well rodent studies extrapolate to human n-3 PUFA

supplementation trials. Similarly, investigators using in vitro fatty acid treatment to explore mechanism by which n-3 PUFA affect immune cell function may wish to establish treatment modalities that mimic the pattern and amount of fatty acid changes described here in Tables 1 and 2. The author’s experience is that it is all too easy to induce changes in cellular fatty acid profiles in vitro that far exceed what can be achieved by dietary intervention.

Finally, the recent generation of a line of transgenic mice (i.e., *fat-1* mice), that are capable of synthesizing n-3 PUFA from endogenous n-6 PUFA, has created many new opportunities to study the biological effects of these essential nutrients [50]. Compared to wild-type mice, *fat-1* mice are protected from dextran sulfate-induced colitis and show diminished growth of implanted B16 melanoma cells [51, 52]. Tissues of *fat-1* mice possess lower n-6 and higher n-3 HUFA compared to their wild-type littermates. These differences occur in the absence of any dietary manipulation. It appears that the changes in n-3 and n-6 HUFA content of some tissues of *fat-1* mice mimic the sort of changes that occur upon feeding wild-type mice diets rich in n-3 PUFA. However, no data on immune cells from these mice have been published to date. Generation of *fat-1* mice, as well as the recently developed *fat-1* pigs [53], provide researchers with a powerful tool to study underlying mechanisms potentially responsible for some of the health benefits associated with increased dietary intake of n-3 PUFA. Yet, results from studies with these novel transgenic animals should be viewed with caution until it is clear that this genetic modification accurately models diet-induced changes in tissue fatty acid profiles and function.

There is nearly universal agreement that current intake levels for n-3 PUFA by most individuals in the USA and other westernized societies are less than optimal. In the



past few years many countries have adopted dietary guidelines that call for increasing intake of n-3 PUFA. Yet, the evidence that such a change will have the expected beneficial outcomes remains equivocal. It remains unclear what form, how often, and how much n-3 PUFA individuals need to consume to obtain a health benefit. On what basis should dietitians and other health professionals advise people on this issue? Evidence from randomized clinical trials (RCT) is the gold standard in clinical medicine. Yet, RCT are very expensive and in many ways impractical for establishing dietary guidelines. Current recommendations for n-3 PUFA are based largely on epidemiological evidence. Thanks largely to advances in micro-encapsulation new food products enriched with n-3 PUFA are entering the marketplace at a rapid pace. Widespread distribution and consumption of such products will undermine the reliability of existing nutrient databases to accurately estimate n-3 PUFA intake patterns in free-living human subjects. The net effect of this could be an undermining of the reliability of epidemiological studies for setting future guidelines for optimal n-3 PUFA intake. Animal-based and in vitro experimental approaches for investigating the health benefits of n-3 PUFA can make significant contributions to this field. However, modest changes in experimental design could substantially enhance the preclinical value of such studies relative to understanding how and when n-3 PUFA may affect human health (Table 3).

**Acknowledgments** The author is grateful to Dr. Jay Whelan (University of Tennessee) for his inspiration and advice regarding this manuscript.

## References

- Meade CJ, Mertin J (1978) Fatty acids and immunity. *Adv Lipid Res* 16:127–165
- Innis SM (2000) Essential fatty acids in infant nutrition: lessons and limitations from animal studies in relation to studies on infant fatty acid requirements. *Am J Clin Nutr* 71:238S–244S
- Kris-Etherton PM, Taylor DS, Yu-Poth S, Huth P, Moriarty K, Fishell V, Hargrove RL, Zhao G, Etherton TD (2000) Polyunsaturated fatty acids in the food chain in the United States. *Am J Clin Nutr* 71:179S–188S
- Meyer BJ, Mann NJ, Lewis JL, Milligan GC, Sinclair AJ, Howe PR (2003) Dietary intakes and food sources of omega-6 and omega-3 polyunsaturated fatty acids. *Lipids* 38:391–398
- Simopoulos AP (2002) Omega-3 fatty acids in inflammation and autoimmune diseases. *J Am Coll Nutr* 21:495–505
- Lands WE (2005) Dietary fat and health: the evidence and the politics of prevention: careful use of dietary fats can improve life and prevent disease. *Ann N Y Acad Sci* 1055:179–192
- Bates EJ (1995) Eicosanoids, fatty acids and neutrophils: their relevance to the pathophysiology of disease. *Prostaglandins Leukot Essent Fatty Acids* 53:75–86
- Miles EA, Aston L, Calder PC (2003) In vitro effects of eicosanoids derived from different 20-carbon fatty acids on T helper type 1 and T helper type 2 cytokine production in human whole-blood cultures. *Clin Exp Allergy* 33:624–632
- Serhan CN, Arita M, Hong S, Gotlinger K (2004) Resolvins, docosatrienes, and neuroprotectins, novel omega-3-derived mediators, and their endogenous aspirin-triggered epimers. *Lipids* 39:1125–1132
- Serhan CN (2005) Novel eicosanoid and docosanoid mediators: resolvins, docosatrienes, and neuroprotectins. *Curr Opin Clin Nutr Metab Care* 8:115–121
- Lands WE, Morris A, Libelt B (1990) Quantitative effects of dietary polyunsaturated fats on the composition of fatty acids in rat tissues. *Lipids* 25:505–516
- Lands WE, Libelt B, Morris A, Kramer NC, Prewitt TE, Bowen P, Schmeisser D, Davidson MH, Burns JH (1992) Maintenance of lower proportions of (n-6) eicosanoid precursors in phospholipids of human plasma in response to added dietary (n-3) fatty acids. *Biochim Biophys Acta* 1180:147–162
- Marangoni F, Angeli MT, Colli S, Eligini S, Tremoli E, Sirtori CR, Galli C (1993) Changes of n-3 and n-6 fatty acids in plasma and circulating cells of normal subjects, after prolonged administration of 20:5 (EPA) and 22:6 (DHA) ethyl esters and prolonged washout. *Biochim Biophys Acta* 1210:55–62
- Gibney MJ, Hunter B (1993) The effects of short- and long-term supplementation with fish oil on the incorporation of n-3 polyunsaturated fatty acids into cells of the immune system in healthy volunteers. *Eur J Clin Nutr* 47:255–259
- Lokesh BR, German B, Kinsella JE (1988) Differential effects of docosahexaenoic acid and eicosapentaenoic acid on suppression of lipoxygenase pathway in peritoneal macrophages. *Biochim Biophys Acta* 958:99–107
- Fujikawa M, Yamashita N, Yamazaki K, Sugiyama E, Suzuki H, Hamazaki T (1992) Eicosapentaenoic acid inhibits antigen-presenting cell function of murine splenocytes. *Immunology* 75:330–335
- Trumbo P, Schlicker S, Yates AA, Poos M (2002) Dietary reference intakes for energy, carbohydrate, fiber, fat, fatty acids, cholesterol, protein and amino acids. *J Am Diet Assoc* 102:1621–1630
- Hulbert AJ, Rana T, Couture P (2002) The acyl composition of mammalian phospholipids: an allometric analysis. *Comp Biochem Physiol B Biochem Mol Biol* 132:515–527
- Turner N, Haga KL, Hulbert AJ, Else PL (2005) Relationship between body size, Na<sup>+</sup>-K<sup>+</sup>-ATPase activity, and membrane lipid composition in mammal and bird kidney. *Am J Physiol Regul Integr Comp Physiol* 288:R301–R310
- Kew S, Banerjee T, Minihane AM, Finnegan YE, Williams CM, Calder PC (2003) Relation between the fatty acid composition of peripheral blood mononuclear cells and measures of immune cell function in healthy, free-living subjects aged 25–72 y. *Am J Clin Nutr* 77:1278–1286
- Nakamura MT, Nara TY (2003) Essential fatty acid synthesis and its regulation in mammals. *Prostaglandins Leukot Essent Fatty Acids* 68:145–150
- Brenner RR (1987) Biosynthesis and interconversion of the essential fatty acids. In: Willis AL (eds) *CRC handbook of eicosanoids: prostaglandins and related lipids*, 1 edn. CRC, Boca Raton, pp 99–117
- Cho HP, Nakamura MT, Clarke SD (1999) Cloning, expression, and nutritional regulation of the mammalian delta-6 desaturase. *J Biol Chem* 274:471–477
- Ursin VM (2003) Modification of plant lipids for human health: development of functional land-based omega-3 fatty acids. *J Nutr* 133:4271–4274
- Miles EA, Banerjee T, Dooper MM, M'Rabet L, Graus YM, Calder PC (2004) The influence of different combinations of

- gamma-linolenic acid, stearidonic acid and EPA on immune function in healthy young male subjects. *Br J Nutr* 91:893–903
26. Liu H, Pope RM (2004) Phagocytes: mechanisms of inflammation and tissue destruction. *Rheum Dis Clin North Am* 30:19–39
  27. Fujiwara N, Kobayashi K (2005) Macrophages in inflammation. *Curr Drug Targets Inflamm Allergy* 4:281–286
  28. Fritsche KL, McGuire SO (1996) The adverse effects of an in vivo inflammatory challenge on the vitamin E status of rats is accentuated by fish oil feeding. *J Nutr Biochem* 7:623–631
  29. Gordon S, Taylor PR (2005) Monocyte and macrophage heterogeneity. *Nat Rev Immunol* 5:953–964
  30. Abe M, Takahashi H, Gouya T, Nagata N, Shigematsu N (1990) Enhanced superoxide anion generation but reduced leukotriene B<sub>4</sub> productivity in thioglycollate-elicited peritoneal macrophages. *Prostaglandins Leukot Essent Fatty Acids* 40:109–115
  31. Hardardottir I, Whelan J, Surette ME, Broughton KS, GuoPing L, Larsen EC, Kinsella JE (1993) The effects of dietary n-3 polyunsaturated fatty acids and cyclic AMP-elevating agents on tumor necrosis factor production by murine-resident and thioglycollate-elicited peritoneal macrophages. *J Nutr Biochem* 4:534–542
  32. Whelan J, Golemboski KA, Broughton KS, Kinsella JE, Dieter RR (1997) Characterization of leukotriene production in vivo and in vitro in resident and elicited peritoneal macrophages in chickens and mice. *Prostaglandins Leukot Essent Fatty Acids* 56:41–49
  33. Black JM, Kinsella JE (1993) Dietary n-3 fatty acids alter murine peritoneal macrophage cytotoxicity. *Ann Nutr Metab* 37:110–120
  34. Whelan J, Broughton KS, Kinsella JE (1991) The comparative effects of dietary alpha-linolenic acid and fish oil on 4- and 5-series leukotriene formation in vivo. *Lipids* 26:119–126
  35. Brouard C, Pascaud M (1993) Modulation of rat and human lymphocyte function by n-6 and n-3 polyunsaturated fatty acids and acetylsalicylic acid. *Ann Nutr Metab* 37:146–159
  36. Whelan J, Broughton KS, Surette ME, Kinsella JE (1992) Dietary arachidonic and linoleic acids: comparative effects on tissue lipids. *Lipids* 27:85–88
  37. Lokesh BR, Black JM, German JB, Kinsella JE (1988) Docosahexaenoic acid and other dietary polyunsaturated fatty acids suppress leukotriene synthesis by mouse peritoneal macrophages. *Lipids* 23:968–972
  38. Kew S, Mesa MD, Tricon S, Buckley R, Minihane AM, Yaqoob P (2004) Effects of oils rich in eicosapentaenoic and docosahexaenoic acids on immune cell composition and function in healthy humans. *Am J Clin Nutr* 79:674–681
  39. Cleland LG, Gibson RA, Hawkes JS, James MJ (1990) Comparison of cell membrane phospholipid fatty acids in five rat strains fed four test diets. *Lipids* 25:559–564
  40. Surette ME, Edens M, Chilton FH, Trampusch KM (2004) Dietary echium oil increases plasma and neutrophil long-chain (n-3) fatty acids and lowers serum triacylglycerols in hypertriglyceridemic humans. *J Nutr* 134:1406–1411
  41. James MJ, Gibson RA, D'Angelo M, Neumann MA, Cleland LG (1993) Simple relationships exist between dietary linoleate and the n-6 fatty acids of human neutrophils and plasma. *Am J Clin Nutr* 58:497–500
  42. Leslie CA, Gonnerman WA, Ullman MD, Hayes KC, Franzblau C, Cathcart ES (1985) Dietary fish oil modulated macrophage fatty acids and decreases arthritis susceptibility in mice. *J Exp Med* 162:1336–1349
  43. Trebble TM, Arden NK, Wootton SA, Calder PC, Mullee MA, Fine DR, Stroud MA (2004) Fish oil and antioxidants alter the composition and function of circulating mononuclear cells in Crohn disease. *Am J Clin Nutr* 80:1137–1144
  44. Huang YS, Mills DE, Ward RP, Horrobin DF, Simmons VA (1989) Effect of essential fatty acid depletion on tissue phospholipid fatty acids in spontaneously hypertensive and normotensive rats. *Lipids* 24:565–571
  45. Kew S, Banerjee T, Minihane AM, Finnegan YE, Muggli R, Albers R, Williams CM, Calder PC (2003) Lack of effect of foods enriched with plant- or marine-derived n-3 fatty acids on human immune function. *Am J Clin Nutr* 77:1287–1295
  46. Broughton KS, Morgan LJ (1994) Frequency of (n-3) polyunsaturated fatty acid consumption induces alterations in tissue lipid composition and eicosanoid synthesis in CD-1 mice. *J Nutr* 124:1104–1111
  47. Wallace FA, Miles EA, Calder PC (2003) Comparison of the effects of linseed oil and different doses of fish oil on mononuclear cell function in healthy human subjects. *Br J Nutr* 89:679–689
  48. Huang SC, Fritsche KL (1992) Alteration in mouse splenic phospholipid fatty acid composition and lymphoid cell populations by dietary fat. *Lipids* 27:25–32
  49. Fritsche K (2006) Fatty acids as modulators of the immune response. *Annu Rev Nutr* 26:45–73
  50. Kang JX, Wang J, Wu L, Kang ZB (2004) Transgenic mice: *fat-1* mice convert n-6 to n-3 fatty acids. *Nature* 427:504
  51. Xia S, Lu Y, Wang J, He C, Hong S, Serhan CN, Kang JX (2006) Melanoma growth is reduced in *fat-1* transgenic mice: impact of omega-6/omega-3 essential fatty acids. *Proc Natl Acad Sci U S A* 103:12499–12504
  52. Hudert CA, Weylandt KH, Lu Y, Wang J, Hong S, Dignass A, Serhan CN, Kang JX (2006) Transgenic mice rich in endogenous omega-3 fatty acids are protected from colitis. *Proc Natl Acad Sci U S A* 103:11276–11281
  53. Lai L, Kang JX, Li R, Wang J, Witt WT, Yong HY, Hao Y, Wax DM, Murphy CN, et al. (2006) Generation of cloned transgenic pigs rich in omega-3 fatty acids. *Nat Biotechnol* 24:435–436
  54. Hawkes JS, Bryan DL, Makrides M, Neumann MA, Gibson RA (2002) A randomized trial of supplementation with docosahexaenoic acid-rich tuna oil and its effects on the human milk cytokines interleukin 1 beta, interleukin 6, and tumor necrosis factor alpha. *Am J Clin Nutr* 75:754–760
  55. Rees D, Miles EA, Banerjee T, Wells SJ, Roynette CE, Wahle KW, Calder PC (2006) Dose-related effects of eicosapentaenoic acid on innate immune function in healthy humans: a comparison of young and older men. *Am J Clin Nutr* 83:331–342
  56. Trebble TM, Arden NK, Wootton SA, Mullee MA, Calder PC, Burdge GC, Fine DR, Stroud MA (2004) Peripheral blood mononuclear cell fatty acid composition and inflammatory mediator production in adult Crohn's disease. *Clin Nutr* 23:647–655
  57. Kelley DS, Taylor PC, Nelson GJ, Schmidt PC, Ferretti A, Erickson KL, Yu R, Chandra RK, Mackey BE (1999) Docosahexaenoic acid ingestion inhibits natural killer cell activity and production of inflammatory mediators in young healthy men. *Lipids* 34:317–324
  58. Hinds A, Sanders TAB (1993) The effect of increasing levels of dietary fish oil rich in eicosapentaenoic and docosahexaenoic acids on lymphocyte phospholipid fatty acid composition and cell-mediated immunity in the mouse. *Br J Nutr* 69:423–429
  59. Fritsche KL, Johnston PV (1990) Effect of dietary alpha-linolenic acid on growth, metastasis, fatty acid profile and prostaglandin production of two murine mammary adenocarcinomas. *J Nutr* 120:1601–1609
  60. VanMeter AR, Ehringer WD, Stillwell W, Blumenthal EJ, Jenks LJ (1994) Aged lymphocyte proliferation following incorporation and retention of dietary omega-3 fatty acids. *Mech Ageing Dev* 75:95–114
  61. Jenks LJ, Bowker GM, Johnson MA, Ehringer WD, Fetterhoff T, Stillwell W (1995) Docosahexaenoic acid-induced alteration of

- Thy-1 and CD8 expression on murine splenocytes. *Biochim Biophys Acta* 1236:39–50
62. Chapkin RS, Somers SD, Schumacher L, Erickson KL (1988) Fatty acid composition of macrophage phospholipids in mice fed fish or borage oil. *Lipids* 23:380–383
  63. Brouard C, Pascaud M (1990) Effects of moderate dietary supplementations with n-3 fatty acids on macrophage and lymphocyte phospholipids and macrophage eicosanoid synthesis in the rat. *Biochim Biophys Acta* 1047:19–28
  64. Jeffery NM, Sanderson P, Sherrington EJ, Newsholme EA, Calder PC (1996) The ratio of n-6 to n-3 polyunsaturated fatty acids in the rat diet alters serum lipid levels and lymphocyte functions. *Lipids* 31:737–745
  65. Yaqoob P, Newsholme EA, Calder PC (1995) Influence of cell culture conditions in diet-induced changes in lymphocyte fatty acid composition. *Biochim Biophys Acta* 1255:333–340
  66. Kleemann R, Scott FW, Worz-Pagenstert U, Nimal Ratnayake WM, Kolb H (1998) Impact of dietary fat on Th1/Th2 cytokine gene expression in the pancreas and gut of diabetes-prone BB rats. *J Autoimmun* 11:97–103
  67. Fisher M, Levine PH, Weiner BH, Johnson MH, Doyle EM, Ellis PA, Hoogasian JJ (1990) Dietary n-3 fatty acid supplementation reduces superoxide production and chemiluminescence in a monocyte-enriched preparation of leukocytes. *Am J Clin Nutr* 51:804–808
  68. Mitjavila MT, Rodriguez MC, Saiz MP, Lloret S, Moreno JJ (1996) Effect of degree of unsaturation in dietary fatty acids on arachidonic acid mobilization by peritoneal macrophages. *Lipids* 31:661–666
  69. Broughton KS, Whelan J, Hardardottir I, Kinsella JE (1991) Effect of increasing the dietary (n-3) to (n-6) polyunsaturated fatty acid ratio on murine liver and peritoneal cell fatty acids and eicosanoid formation. *J Nutr* 121:155–164
  70. Somers SD, Chapkin RS, Erickson KL (1989) Alteration of in vitro murine peritoneal macrophage function by dietary enrichment with eicosapentaenoic and docosahexaenoic acids in menhaden fish oil. *Cell Immunol* 123:201–211
  71. James MJ, Cleland LG, Gibson RA, Hawkes JS (1991) Interaction between fish and vegetable oils in relation to rat leukocyte leukotriene production. *J Nutr* 121:631–637

# Oxygenation of 1-Docosahexaenoyl Lysophosphatidylcholine by Lipoxygenases; Conjugated Hydroperoxydiene and Dihydroxytriene Derivatives

Long Shuang Huang · Mee Ree Kim ·  
Dai-Eun Sok

Received: 17 May 2007 / Accepted: 7 August 2007 / Published online: 19 September 2007  
© AOCs 2007

**Abstract** Oxygenation of 1-docosahexaenoyl lysophosphatidylcholine (docosahexaenoyl-lysoPC) by soybean lipoxygenase-1 (LOX-1) or porcine leukocyte LOX was examined. The oxidized products were identified to be hydroperoxydocosahexaenoyl-lysoPC by UV and LC/MS spectrometric analyses. In SP-HPLC and chiral phase-HPLC analyses, the products from the oxygenation of docosahexaenoyl-lysoPC by soybean LOX-1 and porcine leukocyte LOX were found to contain hydroperoxide group mainly at C-17 and C-14, respectively with the *S* form as a major enantiomer. Next, the sequential exposure of docosahexaenoyl-lysoPC to soybean LOX-1 and porcine leukocyte LOX led to the formation of conjugated triene derivatives possessing a maximal absorption at 271 nm with shoulders at 262 and 281 nm. Based on MS-MS analysis, the conjugated triene derivatives were identified to be 10,17- or 16,17-dihydroxydocosahexaenoyl-lysoPC analogues, suggesting that the diols were produced mainly from hydrolysis of 16,17(*S*)-epoxide intermediate. In kinetic studies, docosahexaenoyl-lysoPC was more favorable than docosahexaenoic acid as substrate for soybean LOX-1 or leukocyte LOX. Taken together, it is proposed that docosahexaenoyl-lysoPC can be oxygenated as substrates for some lipoxygenases to form conjugated diene and/or triene derivatives.

**Keywords** Docosahexaenoyl-lysoPC · Leukocyte lipoxygenase · Soybean lipoxygenase-1 · Oxygenation · 17(*S*)-hydroperoxydocosahexaenoyl-lysoPC

## Abbreviations

lysoPC	Lysophosphatidylcholine
LOX	Lipoxygenase
HDHA	Hydroxydocosahexaenoic acid
HPDHA	Hydroperoxydocosahexaenoic acid
SP	Straight-phase
RP	Reverse phase

## Introduction

Lipoxygenase (linoleate:oxygen oxidoreductase, EC 1.13.11.12) belongs to a diverse family of nonheme ferroproteins that catalyze the regio- and stereospecific oxygenation of free polyunsaturated fatty acids [1–3]. Lipoxygenases (LOXs) are designated as 5-, 12-, and 15-LOX on the basis of their positional selectivity in lipoxygenation of arachidonic acid, are known to form various bioactive substances from polyunsaturated fatty acids [2–4]. Generally, free polyunsaturated fatty acids are preferred as substrates for LOXs [1, 2–4]. Nonetheless, there have been reports [5–14] that certain plant LOXs can oxidize phospholipids [5–7] or triglycerides [8]. Additionally, mammalian LOXs such as reticulocyte LOX (15-LOX) or leukocyte-type LOX (12-LOX) oxygenate complex substrates such as phospholipids or biomembranes [9–14]. Besides, endothelial cell lipoxygenase can oxidize phospholipids in low density lipoprotein [15]. Recently, linoleoyl-lysoPC and linoleoyl-lysoPA, water-soluble,

L. S. Huang · D.-E. Sok (✉)  
College of Pharmacy, Chungnam National University,  
Yuseong-ku, Taejon 305–764, Korea  
e-mail: daesok@cnu.ac.kr

M. R. Kim  
Department of Food and Nutrition,  
Chungnam National University, Yuseong-ku,  
Taejon, Korea

were found to be readily oxidized by C12- or C15- specific LOXs such as soybean LOX-1, reticulocyte LOX or leukocyte LOX [16, 17], although potato 5-LOX did not oxygenate lysophospholipids. From these, it is suggested that lysophospholipids, containing a polyunsaturated fatty acyl chain, may correspond to endogenous substrates for position-specific lipoxygenases.

Meanwhile, recent data [18–20] indicate that docosahexaenoic acid is oxygenated by soybean or leukocyte lipoxygenase to form various oxygenated docosahexaenoic acid derivatives, monohydroperoxy and dihydroxy acids, some of which are known to be anti-inflammatory mediators. In this regard, it is supposed that docosahexaenoyl-lysophosphatidylcholine, favorable in the membrane transport [21, 22], may be also oxygenated by certain lipoxygenases to produce oxidized docosahexaenoic acid derivatives.

Here, it is demonstrated that 1-docosahexaenoyl lysophosphatidylcholine is more favorable than docosahexaenoic acid as substrate of soybean LOX-1 or leukocyte-type LOX. In addition, leukocyte-type LOX converts 17(*S*)-hydroperoxydocosahexaenoyl-lysoPC to conjugated dihydroxytriene derivative.

## Experimental Procedures

### Materials

Didocosahexaenoyl phosphatidylcholine (DDPC, 99%) was obtained from Avanti Polar Lipid (Alabaster, AL, USA). Soybean lipoxygenase (lipoxidase Type I-B, 187,400 Sigma units/mg protein), phospholipase A<sub>2</sub> (honey bee venom), sodium borohydride and docosahexaenoic acid were purchased from Sigma-Aldrich Corp (St. Louis, MO, USA). Leukocyte 12-lipoxygenase (porcine leukocyte, 1625 units/ml), 17(*S*, *R*)-hydroxydocosahexaenoic acid and 14 (*S*, *R*)- hydroxydocosahexaenoic acid were from Cayman Chemical Co. (Ann Arbor, MI, USA). HPLC solvents were of HPLC grade, and other chemicals were of analytical grade. Separately, 14(*S*)-HDHA and 17(*S*)-HDHA were prepared by the incubation of DHA with soybean LOX and leukocyte LOX, respectively as reported previously [13, 18]. 10(*S*),17(*S*)-dihydroxydocosahexa-4*Z*,7*Z*,11*E*,13*Z*,15*E*,19*Z*-enoic acid was prepared by incubating soybean LOX-1 with DHA as described before [19]. 1-Docosahexaenoyl lysophosphatidylcholine (docosahexaenoyl-lysoPC) was prepared from PLA<sub>2</sub>-catalyzed hydrolysis of didocosahexaenoyl phosphatidylcholine as described previously with a slight modification [16, 23]; DDPC (2.5 mg), dissolved in chloroform, was dried under N<sub>2</sub>, and then rapidly dispersed in 15 ml of 10 mM borax buffer, pH 8.5 containing 100 mM CaCl<sub>2</sub>. The hydrolysis

was started by adding PLA<sub>2</sub> (200 units), and allowed to continue under N<sub>2</sub> for 1 h at room temperature.

### Assay of LOX Activities in Oxygenation of Docosahexaenoic Acid Derivatives

Activities of various LOXs were monitored by measuring the increase in absorbance at 234 nm due to the formation of hydroperoxide ( $\epsilon_{234} = 28,000 \text{ M}^{-1} \text{ cm}^{-1}$ ) at 25 °C as described before [1, 24, 25]. One unit is defined as the amount of LOXs that can produce one nanomole of conjugated diene per min. The reaction mixture (500  $\mu\text{l}$ ) includes porcine leukocyte LOX (1 unit/ml) in 100 mM phosphate buffer (pH 7.5) containing 5 mM EDTA and 0.03% Tween 20, and the reaction was started by including each docosahexaenoic acid derivative (100  $\mu\text{M}$ ) into the above mixture. Separately, soybean LOX-1 (2.5 units/ml) was incubated with each docosahexaenoic acid derivative (100  $\mu\text{M}$ ) in 50 mM borax buffer (pH 9.0) at 25 °C.

### Determination of Kinetic Values in LOX-Catalyzed Oxygenation of a Docosahexaenoic Acid Derivative

Leukocyte LOX (1 units/ml) or soybean LOX-1 (2.5 units/ml) was incubated with a docosahexaenoic acid derivative of various concentrations as described above. The values of kinetic parameters were obtained according to Lineweaver Burke plot analyses as described previously [17, 24]. The catalytic efficiency of the substrate is defined as the relative value of  $V_m/K_m$ .

### LC/ESI-MS Analysis for Identification of Hydroperoxydocosahexaenoyl-LysoPC

Oxygenation of docosahexaenoyl-lysoPC was started by adding soybean LOX-1 (10 units/ml) to 150  $\mu\text{l}$  of 50 mM borax buffer (pH 9.0) containing docosahexaenoyl-lysoPC (100  $\mu\text{M}$ ), or including leukocyte LOX (1.5 units/ml) in 150  $\mu\text{l}$  of 50 mM phosphate buffer (pH 7.4) containing docosahexaenoyl-lysoPC (100  $\mu\text{M}$ ). After 10 min incubation at room temperature, the reaction products were subjected to LC/ESI-MS analysis, which was performed using a MSDI spectrometer (HP 1100 series LC/MSD, Hewlett Packard, USA) equipped with ZORBAX Eclipse XDB C<sub>18</sub> column (5  $\mu\text{m}$ , 50  $\times$  4.6 mm, Agilent Technologies, USA). The oxidized docosahexaenoyl-lysoPC was eluted (1 ml/min) with an isocratic solvent system of 45% solvent B (formic acid/acetonitrile/H<sub>2</sub>O; 0.1:80:20) in solvent A (methanol/H<sub>2</sub>O; 10:90), and the eluate was monitored at 234 nm [16].

### Determination of Position Specificity in LOX-Catalyzed Oxygenation of Docosahexaenoyl-LysoPC

Docosahexaenoyl-lysoPC (400  $\mu\text{M}$ ) was incubated with soybean LOX-1 (10 units/ml) or leukocyte LOX (30 units/ml) in 6 ml of the respective incubation buffer as described above. After 30 min incubation, the reaction products were subjected to  $\text{NaBH}_4$  reduction, and then subjected to hydrolysis in alkaline solution (1 M NaOH) at room temperature for 1 h under  $\text{N}_2$ . Finally, the lipid was extracted as described previously [15], and analyzed by SP-HPLC system equipped with silica gel column (10  $\mu\text{m}$ , 300  $\times$  7.8 mm, Phenomenex, USA), which was eluted (1 ml/min) with *n*-hexane/isopropyl alcohol/acetic acid (100:3:0.1) for HDHA from soybean LOX-1 - induced oxidation of docosahexaenoyl-lysoPC, or with *n*-hexane/isopropyl alcohol/acetic acid (100:2:0.1) for HDHA from leukocyte LOX-induced oxidation of docosahexaenoyl-lysoPC. The identification of each HDHA was performed by coinjection with each standard, 17(*S,R*)-HDHA or 14(*S,R*)-HDHA [17].

### Determination of Stereo-Selectivity in LOX-Catalyzed Oxygenation of Docosahexaenoyl-LysoPC

17-HDHA or 14-HDHA, obtained by SP-HPLC as described above, was subjected to analysis by chiral phase HPLC with a Chiralcel OD-H column (250  $\times$  4.6 mm, 5  $\mu\text{m}$ , Daicel Chemical Industries, LTD, Japan), which was eluted with the solvent system of *n*-hexane / isopropyl alcohol / trifluoroacetic acid (950:50:1). Identification of *S* and *R* enantiomers of 17-HDHA or 14-HDHA was performed by coinjection with each (*S*) HDHE standard. Under the condition used, two enantiomers of 17(*S,R*)-HDHA or 14(*S,R*)-HDHA were completely separated from each other. The flow rate of was 0.5 ml per min, and the effluent was monitored at 234 nm [17].

### Identification of Docosatriene Derivatives Generated from Oxygenation of Docosahexaenoyl-LysoPC

Docosahexaenoyl-lysoPC (100  $\mu\text{M}$ ) was incubated with soybean LOX-1 (100 units/ml) in 40 ml of 5 mM borax buffer (pH 9.0) at 4  $^\circ\text{C}$  for 1 h. Then, the reaction mixture, after pH adjustment to pH 7.0, was further incubated with leukocyte LOX (30 units/ml) for 1 h at 4  $^\circ\text{C}$ . The mixture was partially purified using a  $\text{C}_{18}$  extraction column (1  $\times$  3 cm), which was eluted with methanol. The products from the eluate, after  $\text{NaBH}_4$  reduction and alkaline hydrolysis, were again partially purified using  $\text{C}_{18}$

extraction column (1  $\times$  3 cm). The sample was diluted in methanol, and loaded onto a  $\text{C}_{18}$  column (3  $\mu\text{m}$ , 100  $\times$  3 mm, Waters, Island) connected to  $\text{C}_{18}$  pre-column (3  $\mu\text{m}$ , 20  $\times$  3 mm, Waters, Island), which was eluted (0.3 ml/min) with a gradient solvent system of solvent B (methanol/acetate; 100:0.1) in solvent A ( $\text{H}_2\text{O}$ /acetate; 100:0.1); 40% to 95% from 0 to 30 min. ESI-MS/MS was carried out on a 4000 QTrap quadrupole tandem mass spectrometer equipped with a turbo electrospray ion source (Applied Biosystems, CA, USA). The heated nebulizer at 500  $^\circ\text{C}$  was used with a curtain gas 20 psi, nitrogen collision gas (CAD) set to medium, GS1 50 psi and GS2 50 psi. The entrance potential was set to 10 V for all transitions. The data were collected in the negative ion mode from 100 to 400  $m/z$ . Parent ions (selected parent ion,  $m/z$  359) were detected on full-scan mode on Q1 quadrupole, and selected parent/daughter ion pairs for 10,17-dihydroxydocosahexaenoic acid and 16,17-dihydroxydocosahexaenoic acid were  $m/z$  359/153 and  $m/z$  359/231, respectively [26–28].

## Results

### LOX-Catalyzed Conversion of Docosahexaenoyl-LysoPC to Hydroperoxydocosahexaenoyl-LysoPC

When soybean LOX-1 was incubated with docosahexaenoyl-lysoPC, a time-dependent increase of absorption at 236 nm was observed (data not shown), consistent with the formation of conjugated dienes. Likewise, a similar change in the UV spectrum was also observed in the incubation of docosahexaenoyl-lysoPC with leukocyte LOX. Thus, docosahexaenoyl-lysoPC was effectively oxygenated by soybean LOX-1 and leukocyte LOX. In an attempt to isolate the oxygenation product, the products from the exposure of docosahexaenoyl-lysoPC to soybean LOX-1 were partially purified using  $\text{C}_{18}$  extraction column, and then subjected to RP-HPLC, which was monitored at 234 nm. Figure 1a shows that a peak with a retention time of 8.2 min appeared as a predominant product. When the compound from the major peak was analyzed by LC/ESI-MS (Fig. 1b), it was found to possess the mass spectrum characteristic of hydroperoxydocosahexaenoyl-lysoPC; molecular ions at  $m/z$  600.2 ( $[\text{M} + \text{H}]^+$ ),  $m/z$  622.2 ( $[\text{M} + \text{Na}]^+$ ) and  $m/z$  638.2 ( $[\text{M} + \text{K}]^+$ ). Thus, hydroperoxydocosahexaenoyl-lysoPC appeared as a major oxygenation product during soybean LOX-1-catalyzed oxygenation of docosahexaenoyl-lysoPC. The same result was also obtained when the products from leukocyte LOX-catalyzed oxygenation of docosahexaenoyl-lysoPC were subjected to UV spectrometry and LC/ESI-MS analysis (data not shown).

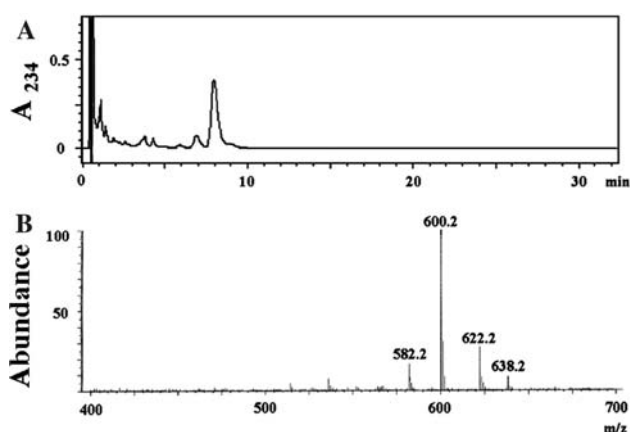


**Fig. 1** LC/ESI-MS analysis of products from oxygenation of docosahexaenoyl-lysoPC by soybean LOX-1. **a** The product, obtained from 10 min incubation of docosahexaenoyl-lysoPC (100  $\mu$ M) with soybean LOX-1 (10 units/ml) in 150  $\mu$ l of borax buffer (50 mM, pH 9.0), was injected into ZORBAX Eclipse XDB C<sub>18</sub> column (5  $\mu$ m, 50  $\times$  4.6 mm), which was eluted (1 ml/min) with isocratic solvent system of 45% solvent A (acetate/acetonitrile/H<sub>2</sub>O; 0.5:80:20) in solvent B (methanol/H<sub>2</sub>O; 10:90) as described in Experimental Procedures. The products were monitored by UV detection at 234 nm. **b** Representative mass spectrum of peroxy derivative of docosahexaenoyl-lysoPC. The mass spectrum of the major peak (retention time, 8.2 min) in Fig. 2a was obtained by ESI-MS analysis system using positive-ion scan mode as described in Experimental Procedures

#### Determination of Position- and Stereo-Selectivity in Oxygenation of Docosahexaenoyl-LysoPC

To establish the oxygenation position in oxygenation of docosahexaenoyl-lysoPC, the product from soybean LOX-1-catalyzed oxygenation of docosahexaenoyl-lysoPC was subjected to NaBH<sub>4</sub> reduction, followed by alkaline hydrolysis, to afford hydroxydocosahexaenoic acid (HDHA), which was further purified by SP-HPLC. When the purified HDHA was coinjected with each standard HDHA, it was

found that the predominant peak (retention time, 18.6 min) migrated with 17-HDHA (Fig. 2a, solid line arrow). Next, when the oxygenation position in leukocyte LOX-catalyzed oxygenation of docosahexaenoyl-lysoPC was determined (Fig. 2b), the major product (elution time, 20.0 min) was found to migrate with 14-HDHA (dotted line). Taken together, docosahexaenoyl-lysoPC is oxygenated mainly at C-14 by leukocyte 12-lipoxygenase, and at C-17 by soybean 15-lipoxygenase. In related studies, the stereo-specificity in the oxygenation of docosahexaenoyl-lysoPC was analyzed by chiral phase HPLC. When 17-HDHA, obtained as described in Fig 2a, was subjected to chiral phase HPLC analysis, the major part of 17-HDHA (retention time, 15.5 min) was found to migrate with 17(*S*)-HDHA (Fig. 3a). Separately, most of 14-HDHA (retention time, 14.1 min), obtained as described in Fig 2b, was found to migrate with 14(*S*)-HDHA (Fig. 3b). Thus, it is commonly observed that both LOXs express a stereo-specificity toward the *S* form enantiomer in oxygenation of docosahexaenoyl-lysoPC.

#### Conversion of 17(*S*)-Hydroperoxydocosahexaenoyl-LysoPC to Dihydroxydocosahexaenoyl-LysoPC

Previously, 17(*S*)-hydroperoxydocosahexaenoic acid (HPDHA) was shown to be converted to 10,17(*S*)-dihydroxydocosahexaenoic acid isomers via 16,17(*S*)-epoxide intermediate in leukocytes [29, 30]. In this relation, docosahexaenoyl-lysoPC was first exposed to soybean LOX-1 in a borax buffer (pH 9.0) to maximally produce 17(*S*)-hydroperoxydocosahexaenoyl-lysoPC, and then the mixture was further incubated with porcine leukocyte LOX at pH 7. As exhibited in Fig. 4a, the sequential exposure of docosahexaenoyl-lysoPC to soybean LOX-1 and leukocyte LOX resulted in the appearance of a particular UV spectrum,

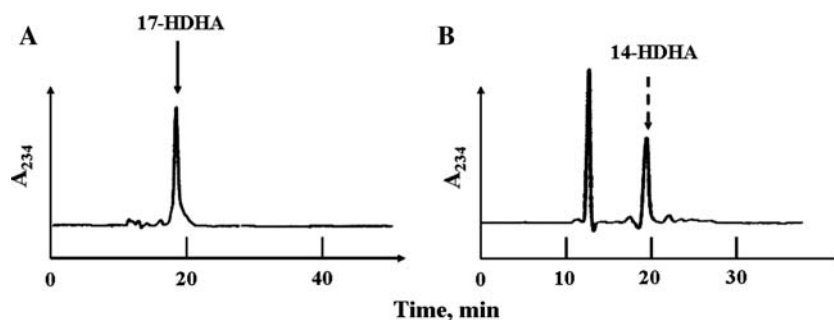


**Fig. 2** SP-HPLC determination of oxygenation position in lipoxygenase-catalyzed oxygenation of docosahexaenoyl-lysoPC. Docosahexaenoyl-lysoPC was incubated with each LOX for 30 min, and after NaBH<sub>4</sub> reduction and alkaline hydrolysis, the final products were analyzed by SP-HPLC, equipped with silica gel column (300  $\times$  7.6 mm), which was eluted (1 ml/min) with *n*-hexane/

isopropyl alcohol/acetic acid (100:3:0.05) for 17-HDHA, and *n*-hexane/isopropyl alcohol/acetic acid (100:2:0.05) for 14-HDHA. **a** Incubation of docosahexaenoyl-lysoPC with soybean LOX-1 at pH 9.0. **b** Incubation of docosahexaenoyl-lysoPC with leukocyte LOX at pH 7.4. And the major products were co-injected with standard compounds, 17-HDHA (solid arrow) and 14-HDHA (dotted arrow)

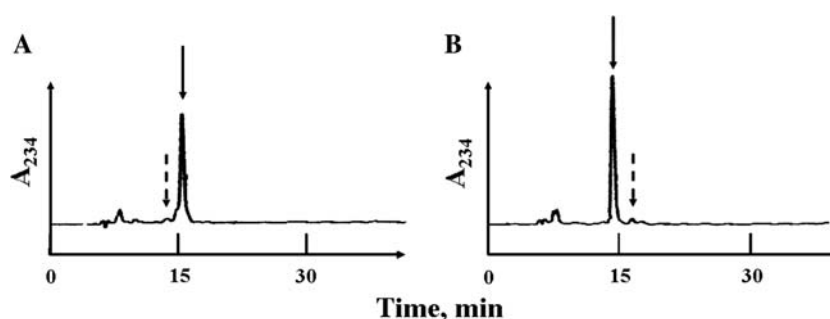
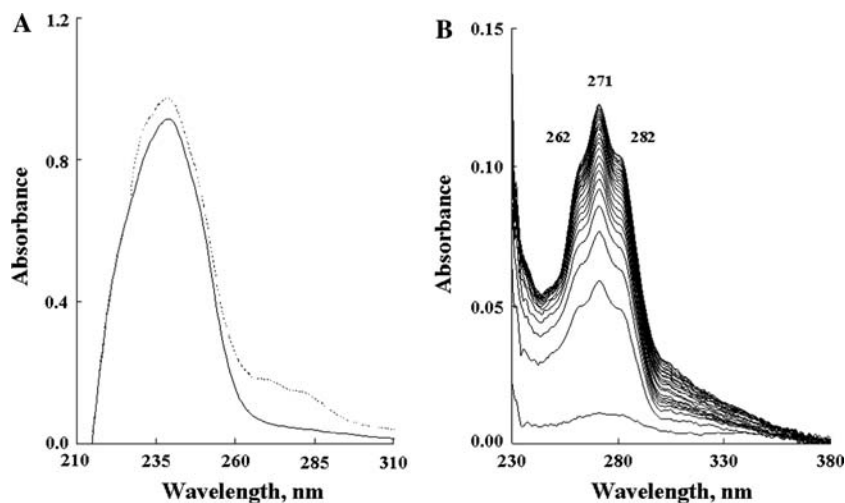


**Fig. 3** Chiral-phase HPLC of HDHA derived from oxygenation of docosahexaenoyl-lysoPC by lipoxygenases. 17-HDHA and 14-HDHA, prepared as described in Fig. 3, were analyzed by chiral phase HPLC, equipped with chiralcel OD-H column, which was eluted with the solvent system of n-hexane/isopropyl alcohol/trifluoroacetic acid (950:50:1). The flow rate was 0.5 ml per min and the effluent was

monitored at 234 nm. **a** 17-HDHA derived from exposure of docosahexaenoyl-lysoPC to soybean LOX-1. **b** 14-HDHA derived from exposure of docosahexaenoyl-lysoPC to leukocyte LOX. Under condition used, (*S,R*) HDHA was separated into two peaks (*dotted and solid arrows*). The *arrow* indicates the coinjection with (*S*) isomer (*solid line*) or (*R*) isomer (*dotted line*) of 14-HDHA or 17-HDHA

**Fig. 4** Changes of UV spectra during sequential exposure of docosahexaenoyl-lysoPC to soybean LOX-1 and leukocyte LOX. **a** Docosahexaenoyl-lysoPC (100  $\mu$ M) was incubated with soybean LOX-1 (20 units/ml) in 5 mM borax buffer (pH 9) for 1 h at 4  $^{\circ}$ C, and then the mixture, after pH adjusted to pH 7.0, was further incubated with leukocyte LOX (30 units/ml) at r.t. for 30 min. **b** The UV spectral change in differential spectrometry was scanned with the cycle time of 1 min



characteristic of conjugated triene structure [31]. In the differential spectrophotometry (Fig. 4b), the compound was found to exhibit the UV spectrum with a maximum absorption at 271 nm and shoulders at 262 nm and 281 nm, quite similar to the observation after the incubation of DHA with leukocyte cells [30]. Thus, docosahexaenoyl-lysoPC is oxygenated by soybean LOX-1 to produce 17(*S*)-hydroperoxydocosahexaenoyl-lysoPC, which is in turn converted to conjugated triene derivatives by leukocyte LOX. Meanwhile, the further oxygenation of 17(*S*)-hydroperoxydocosahexaenoyl-lysoPC by soybean LOX-1 was negligible. In the next experiment to identify the products with conjugated triene structure, the oxidized products, after separation on a  $C_{18}$  extraction column, were subjected to  $\text{NaBH}_4$  reduction and alkaline hydrolysis to afford dihydroxydocosahexaenoic acids. Then, the final products, after partial purification on  $C_{18}$  column, were subjected to LC/MS-MS analyses employing selected parent ion

monitoring at  $m/z$  359, corresponding to  $[\text{M}-\text{H}]^-$  of dihydroxydocosahexaenoic acid, and selected parent/daughter ion pairs monitoring at  $m/z$  359/153. As demonstrated in Fig. 5a, b, it was found that three peaks, peak I (16.2 min), peak II (16.7 min) and peak III (17.0 min), showed the ions characteristic of the compound corresponding to 10,17(*S*)-dihydroxydocosahexaenoic acid [18, 19, 20]; a representative MS-MS spectrum (Fig 6a) showed several prominent fragment ions at  $m/z$  359.1 (M-H), 341.0 (M-H- $\text{H}_2\text{O}$ ), 323.4 (M-H- $2\text{H}_2\text{O}$ ), 315.0 (M-H- $\text{CO}_2$ ), and 297.2 (M-H- $\text{H}_2\text{O}-\text{CO}_2$ ). Supportive diagnostic ions demonstrating the presence of the 10 and 17 alcohol-containing carbon positions include the ions at  $m/z$  205.9, 261.0 and 289.0 (Fig 6a), in addition to the characteristic ion at  $m/z$  153.0 (Figs. 5b and 6a) as reported previously [18]. Separately, Fig. 5a, c demonstrated that two peaks, peak IV (17.8 min) and peak V (19.0 min), possessed the ions characteristic of 16,17(*S*)-dihydroxydocosahexaenoic acid [18]; its MS-MS (Fig. 6b) showed



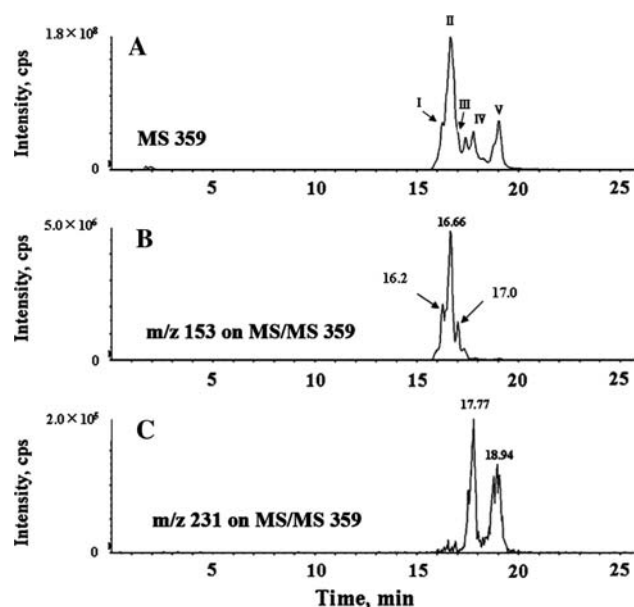


**Fig. 5** LC-MS/MS chromatography of products with conjugated triene structure. Docosahexaenoyl-lysoPC was sequentially exposed to soybean LOX-1 and leukocyte LOX as described in Fig. 4, and the final products, after  $\text{NaBH}_4$  reduction and alkaline hydrolysis, were subjected to analysis of LC-MS/MS system as described in Materials and Methods. **a** Selected ion monitoring at  $m/z$  359 (parent ion) for dihydroxydocosahexaenoic acid derivative-containing products. **b** Selected ion monitoring at  $m/z$  153 in  $\text{MS}^2$  359 for 10,17-dihydroxydocosahexaenoic acid isomers: peak I, 16.2 min; peak II, 16.7 min; peak III, 17.0 min. **c** Selected ion monitoring at  $m/z$  231 in  $\text{MS}^2$  359 for 16,17-dihydroxydocosahexaenoic acid isomers: peak IV, 17.8 min; peak V, 19.0 min

several prominent fragment ions at  $m/z$  359.2 (M-H), 341.2 (M-H- $\text{H}_2\text{O}$ ), 323.4 (M-H- $2\text{H}_2\text{O}$ ), 315.1 (M-H- $\text{CO}_2$ ), 297.1 (M-H- $\text{H}_2\text{O}-\text{CO}_2$ ) and 279.3 (M-H- $2\text{H}_2\text{O}-\text{CO}_2$ ). Supportive diagnostic ions demonstrating the presence of the 16 and 17 alcohol-containing carbon positions include ions at  $m/z$  261.2 and 289.3 (Fig. 6b), in addition to the characteristic ion at  $m/z$  231.1 (Figs. 5c and 6b). Taken together, at least three isomers of 10,17(*S*)-dihydroxydocosahexaenoic acid derivative and two isomers of 16,17(*S*)-dihydroxydocosahexaenoic acid derivative were generated from the sequential exposure of docosahexaenoyl-lysoPC to soybean LOX-1 and leukocyte LOX. Noteworthy, peaks I and III appeared reproducibly as isomers of a similar amount in repeated experiments, where the rapid hydrolysis of the oxidized products was performed. However, the amount of peak II (retention time, 16.7 min), comigrating with 10(*S*),17(*S*)-dihydroxydocosahexa-4*Z*,7*Z*,11*E*,13*Z*,15*E*,19*Z*-enoic acid in RP- HPLC, decreased greatly when the partial purification of oxidized lipids on C18 column was omitted (data not shown), excluding the possibility that peak II was produced during the sequential exposure of docosahexaenoyl-lysoPC to lipoxygenases.

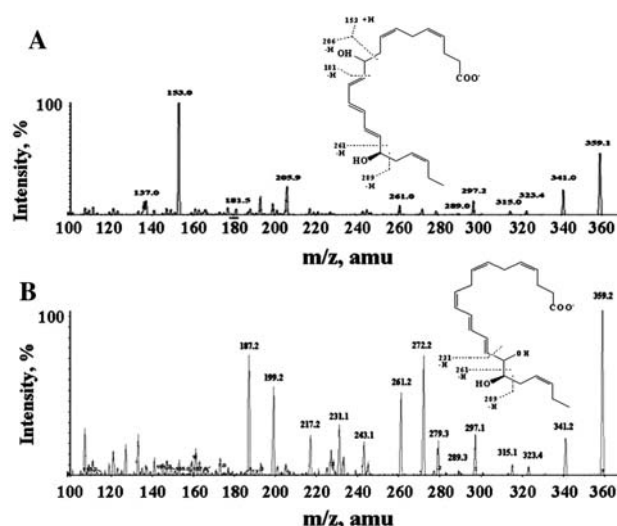


**Fig. 6** MS/MS spectrum of products with conjugated triene structure **a**, Representative MS/MS spectrum of the product from peak I, II or III in Fig. 5a. **b**, Representative MS/MS spectrum of the product from peak IV or V in Fig. 5a

#### Determination of Kinetic Values in LOX-Catalyzed Oxygenation of DHA Derivatives

Subsequently, LOX-catalyzed oxygenation of DHA derivatives was examined kinetically. As demonstrated in Fig. 7, the oxygenation of DHA derivative by each LOX followed classical Michaelis–Menten kinetics. From Lineweaver Burk plot analysis, the  $K_m$  and  $V_m$  values were estimated to be 2.2  $\mu\text{M}$  and 104.2 units/ $\mu\text{g}$  protein, respectively in oxygenation of docosahexaenoyl-lysoPC by soybean LOX-1, and 16.8  $\mu\text{M}$  and 178.0 units/ $\mu\text{g}$  protein, respectively in oxygenation of DHA by the enzyme (Table 1). Thus, the catalytic efficiency ( $V_m/K_m$ ) of docosahexaenoyl-lysoPC as substrate of soybean LOX-1 was about 4-fold greater than that of DHA. Next, in the oxygenation by leukocyte LOX (Table 2), the  $K_m$  and  $V_m$  values were estimated to be 3.4  $\mu\text{M}$  and 77.2 units/mg protein, respectively for docosahexaenoyl-lysoPC, and 17.6  $\mu\text{M}$  and 35.9 units/mg protein, respectively for DHA. Thus, the catalytic efficiency of docosahexaenoyl-lysoPC for leukocyte LOX was approximately 10-fold greater than that of docosahexaenoic acid. Nonetheless, docosahexaenoyl-lysoPC was not significantly oxygenated by potato LOX.

#### Discussion

Recently, lysophospholipids such as linoleoyl-lysoPC or linoleoyl-lysoPA were observed to be efficient substrates for lipoxygenases such as soybean LOX-1, leukocyte LOX or reticulocyte LOX [16, 17]. The present study

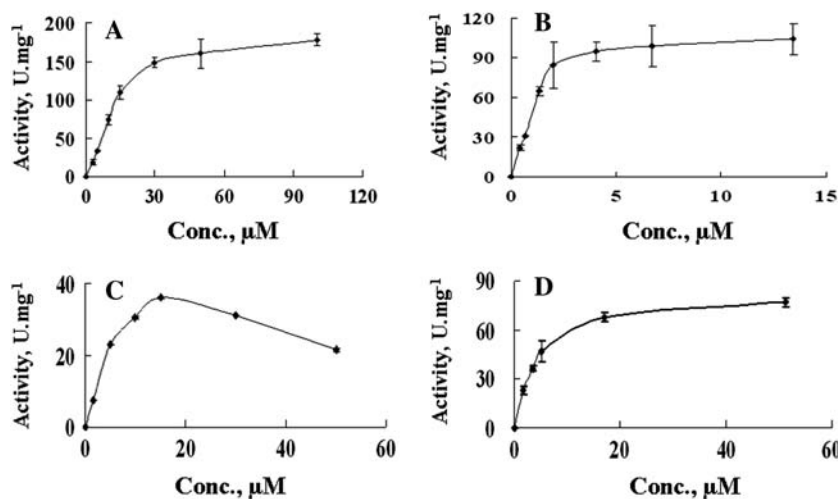


**Fig. 7** Effect of substrate concentration on LOX-catalyzed oxygenation of docosahexaenoyl-lysoPC and docosahexaenoic acid. Soybean LOX-1 (2.5 units/ml) was incubated with docosahexaenoic acid (A) or docosahexaenoyl-lysoPC (B) of various concentrations in borax buffer (50 mM, pH 9.0). Separately, leukocyte LOX (1 unit/ml) was

incubated with docosahexaenoic acid (C) or docosahexaenoyl-lysoPC (D) of various concentrations in 100 mM phosphate buffer (pH 7.5) containing 5 mM EDTA and 0.03% Tween 20. Data were expressed as mean  $\pm$  SD of results from at least three independent experiments

**Table 1** Kinetic values in oxygenation of docosahexaenoic acid derivatives by soybean LOX-1

	Km ( $\mu$ M)	Vm (units/ $\mu$ g)	Vm/Km (units/ $\mu$ g/ $\mu$ M)
Docosahexaenoic acid	16.8 $\pm$ 1.4	178.0 $\pm$ 7.4	10.3 $\pm$ 1.3
Docosahexaenoyl-lysoPC	2.2 $\pm$ 0.6	104.2 $\pm$ 5.2	42.4 $\pm$ 7.2
Didocosahexaenoyl-PC	1072 $\pm$ 184	7.8 $\pm$ 0.3	0.007 $\pm$ 0.001

Soybean LOX-1 (2.5 units/ml) was incubated with docosahexaenoyl-lysoPC, didocosahexaenoyl-lysoPC or docosahexaenoic acid of various concentrations in 500  $\mu$ l of 50 mM borax buffer (pH 9.0) at 25  $^{\circ}$ C. Kinetic values were obtained from Lineweaver Burke plot. Values were expressed as mean  $\pm$  SD of results from at least three independent experiments

**Table 2** Kinetic values in oxygenation of docosahexaenoyl-lysoPC or docosahexaenoic acid by leukocyte LOX

	Km ( $\mu$ M)	Vm (units/mg)	Vm/Km (units/mg/ $\mu$ M)
Docosahexaenoic acid	17.6 $\pm$ 1.7	35.9 $\pm$ 0.5	2.1 $\pm$ 0.9
Docosahexaenoyl-lysoPC	3.4 $\pm$ 1.8	77.2 $\pm$ 2.8	22.7 $\pm$ 0.8

Porcine leukocyte LOX (2 units/ml) was incubated with each substrate (docosahexaenoyl-lysoPC or docosahexaenoic acid) of various concentrations in 500  $\mu$ l of 100 mM phosphate buffer (pH 7.4) containing 5 mM EDTA and 0.03% Tween 20 at 25  $^{\circ}$ C

demonstrates that docosahexaenoyl-lysoPC is also oxygenated efficiently by soybean LOX-1 or leukocyte LOX. The higher catalytic efficiency of docosahexaenoyl-lysoPC, compared to DHA, may suggest that carboxyl group is not required for the interaction of substrates with lipooxygenases such as soybean LOX-1 or leukocyte LOX. Meanwhile, the lower catalytic efficiency (Vm/Km) of DHA, compared to docosahexaenoyl-lysoPC, may be ascribed to the negative charge property adopted by the free fatty acid, as suggested from its higher Km value. Alternatively, the difference of catalytic efficiency between

DHA and docosahexaenoyl-lysoPC may be accounted for by the difference of the micellar concentration [31, 32]. However, this possibility is not supported by present findings that the Km values of docosahexaenoyl-lysoPC and DHA are much below their critical micellar concentrations (>50  $\mu$ M). In this context, it is suggested that monomeric form of docosahexaenoyl-lysoPC is directly recognized by LOX as substrate, consistent with previous reports [15, 33]. It is well known that DHA is oxygenated by porcine leukocyte 12-LOX and soybean 15-LOX to produce 14(S)-HPDHA and 17(S)-HPDHA, respectively

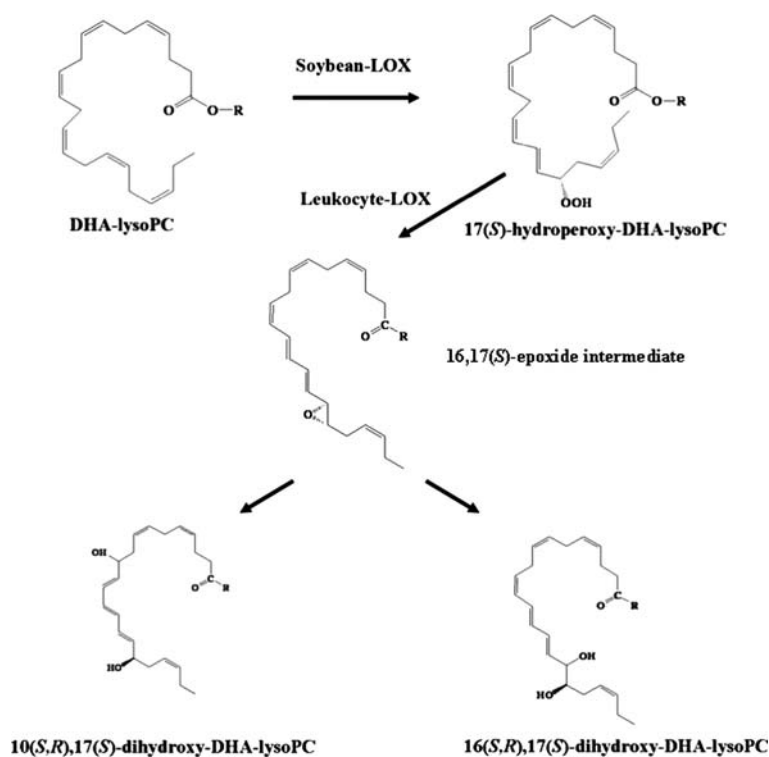
[13, 28]. Such a stereo- and positional specificity was also reproduced in oxygenation of docosahexaenoyl-lysoPC. Thus, the stereo- and positional specificity of soybean LOX or leukocyte LOX was not altered by the esterification of docosahexaenoic acid [34, 35].

Recent studies have shown that 17(*S*)-HPDHA, which is generated from lipoxygenation of DHA, is further converted to 10,17(*S*)-dihydroxydocosahexaenoic acid isomers via 16,17(*S*)-epoxide intermediate in cellular systems [29, 30, 36]. The same pathway may apply to leukocyte LOX-catalyzed conversion of 17(*S*)-hydroperoxydocosahexaenoyl-lysoPC to dihydroxydocosahexaenoyl-lysoPC as suggested from gradual UV spectral change indicative of the conversion of conjugated diene to conjugated triene structure. Moreover, LC/MS-MS analysis indicates that the final oxidized products with conjugated triene include at least three isomers of 10,17(*S*)-dihydroxydocosahexaenoic acid derivative and two isomers of 16,17(*S*)-dihydroxydocosahexaenoic acid derivative. Concerning the mechanism for the formation of dihydroxydocosahexaenoic acid derivatives, there can be two possibilities; one is the epoxide intermediate pathway, and the other dioxygenation pathway. According to the former, 17(*S*)-hydroperoxydocosahexaenoyl-lysoPC may be converted by leukocyte LOX to dihydroxydocosahexaenoyl-lysoPC via 16,17-epoxide intermediate, consistent with the mechanism established for the conversion of DHA to 10,17(*S*)- and 16,17(*S*)-dihydroxyhexaenoic acids in leukocytes [29, 30]. This is strongly supported by present findings that in

addition to two isomers (peaks I and III) of 10,17(*S*)-dihydroxydocosahexaenoic acid derivative, two isomers (peaks IV and V) of 16,17(*S*)-dihydroxydocosahexaenoic acid derivative appeared as isomeric products of a similar quantity (Fig. 5), resulting from non-enzymatic hydrolysis of 16,17(*S*) epoxide intermediate. In this regard, the compounds from peaks I and III are proposed to contain double bond geometry configuration of 11*E*,13*E*,15*E* as described in Fig. 8. Meanwhile, it is not likely that peak II, comigrating with 10(*S*),17(*S*)-dihydroxydocosahexa-4*Z*,7*Z*,11*E*,13*Z*,15*E*,19*Z*-enoic acid [19], was derived from double oxygenation of docosahexaenoyl-lysoPC by lipoxygenases, since dihydroperoxydocosahexaenoyl-lysoPC was not detected in LC/MS monitoring at *m/z* 632 (*M* + *H* + 2*O*) [data not shown]. Furthermore, a significant amount of conjugated triene product was not produced after the exposure of docosahexaenoyl-lysoPC to excess soybean LOX-1, in contrast to soybean LOX-catalyzed conversion of DHA to 10(*S*),17(*S*)-dihydroxydocosahexa-4*Z*,7*Z*,11*E*,13*Z*,15*E*,19*Z*-enoic acid [19, 37]. Although peak II appeared as a major product in the present condition used, the height of peak II decreased to a great extent when the isolation of lipids on C18 column was omitted, implying that the peak II might be caused by the delayed process of lipid isolation.

A previous report indicates that docosahexaenoyl-lysoPC exists in human plasma [38] to a low level ( $\sim 1 \mu\text{M}$ ). However, the plasma level of docosahexaenoyl-lysoPC is close to its *K<sub>m</sub>* value for leukocyte LOX. Moreover,

**Fig. 8** Proposed pathway for enzymatic formation of dihydroxydocosahexaenoyl-lysoPC isomers from docosahexaenoyl-lysoPC. R, glycerophosphorylcholine moiety



docosahexaenoyl-lysoPC is oxygenated more readily than docosahexaenoic acid as substrate for leukocyte LOX. In addition, lysophosphatidylcholine was proposed as being a preferred physiological transporter of polyunsaturated fatty acids such as docosahexaenoic acid [21, 22]. In this regard, docosahexaenoyl-lysoPC may be preferentially utilized by certain lipoxygenases *in vivo*, which needs further study.

Taken all together, the current data demonstrate that docosahexaenoyl-lysoPC can be efficiently oxygenated by soybean and leukocyte lipoxygenases. In addition, 17(*S*)-hydroperoxydocosahexaenoyl-lysoPC can be further metabolized to an epoxide of the leukotriene A type, which is hydrolyzed to produce lysoPC derivatives containing dihydroxydocosahexaenoic acid.

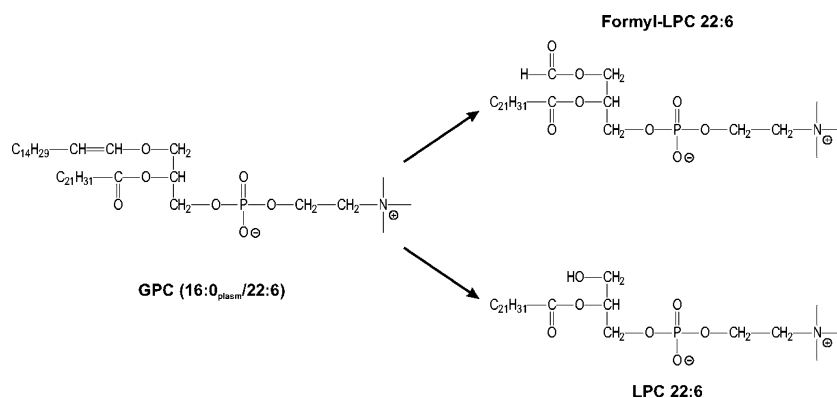
**Acknowledgments** This work was financially supported by the Korean Research Foundation grant funded by Korean Government (KRF-2007-211-E00010), South Korea.

## References

- Christopher J, Axelrod B (1971) On the different positional specificities of peroxidation of linoleate shown by two isozymes of soybean lipoxygenase. *Biochem Biophys Res Commun* 44:731–736
- Smith WL, Lands WE (1972) Oxygenation of polyunsaturated fatty acids during prostaglandin biosynthesis by sheep vesicular gland. *Biochemistry* 11:3276–3285
- Yamamoto S (1992) Mammalian lipoxygenases: molecular structures and functions. *Biochim Biophys Acta* 1128:117–131
- Mass RL, Brash A, Oates JA (1982) In: Samuelsson B, Padetti R (eds) *Leukotrienes and Other Lipoxygenase Products*. Raven press, New York, pp 29–44
- Maccarrone M, van Aarle PG, Veldink GA, Vliegenthart JF (1994) *In vitro* oxygenation of soybean biomembranes by lipoxygenase-2. *Biochim Biophys Acta* 1190:164–169
- Kondo Y, Kawai Y, Hayashi T, Ohnishi M, Miyazawa T, Itoh S, Mizutani J (1993) Lipoxygenase in soybean seedlings catalyzes the oxygenation of phospholipid and such activity changes after treatment with fungal elicitor. *Biochim Biophys Acta* 1170:301–306
- Pérez-Gilabert M, Veldink GA, Vliegenthart JF (1998) Oxidation of dilinoleoyl phosphatidylcholine by lipoxygenase 1 from soybeans. *Arch Biochem Biophys* 354:18–23
- Feussner I, Wasternack C, Kindl H, Kuhn H (1995) Lipoxygenase-catalyzed oxygenation of storage lipids is implicated in lipid mobilization during germination. *Proc Natl Acad Sci USA* 92:11849–11853
- Kuhn H, Belkner J, Wiesner R, Brash AR (1990) Oxygenation of biological membranes by the pure reticulocyte lipoxygenase. *J Biol Chem* 265:18351–18361
- Kuhn H, Brash AR (1990) Occurrence of lipoxygenase products in membranes of rabbit reticulocytes. Evidence for a role of the reticulocyte lipoxygenase in the maturation of red cells. *Biol Chem* 265:1454–1458
- Takahashi Y, Glasgow WC, Suzuki H, Taketani Y, Yamamoto S, Anton M, Kuhn H, Brash AR (1993) Investigation of the oxygenation of phospholipids by the porcine leukocyte and human platelet arachidonate 12-lipoxygenases. *Eur J Biochem* 218:165–171
- Conrad DJ, Kuhn H, Mulkins M, Highland E, Sigal E (1992) Specific inflammatory cytokines regulate the expression of human monocyte 15-lipoxygenase. *Proc Natl Acad Sci USA* 89:217–221
- Hada T, Ueda N, Takahashi Y, Yamamoto S (1991) Catalytic properties of human platelet 12-lipoxygenase as compared with the enzymes of other origins. *Biochim Biophys Acta* 1083:89–93
- Jung G, Yang DC, Nakao A (1985) Oxygenation of phosphatidylcholine by human polymorphonuclear leukocyte 15-lipoxygenase. *Biochem Biophys Res Commun* 130:559–566
- Kuhn H, Belkner J, Suzuki H, Yamamoto S (1994) Oxidative modification of human lipoproteins by lipoxygenases of different positional specificities. *J Lipid Res* 10:1749–1759
- Huang LS, Kim MR, Sok DE (2006) Linoleoyl lysophosphatidylcholine is an efficient substrate for soybean lipoxygenase-1. *Arch Biochem Biophys* 455:119–126
- Huang LS, Kim MR, Jeong TS, Sok DE (2007) Linoleoyl lysophosphatidic acid and linoleoyl lysophosphatidylcholine are efficient substrates for mammalian lipoxygenases. *Biochim Biophys Acta* 1770:1062–1070
- Hong S, Gronert K, Devchand PR, Moussignac RL, Serhan CN (2003) Novel docosatrienes and 17*S*-resolvins generated from docosahexaenoic acid in murine brain, human blood, and glial cells. Autocoids in Anti-Inflammation. *J Biol Chem* 278:14677–14687
- Butovich IA (2006) A one-step method of 10,17-dihydro(pero)xydocosahexa-4*Z*,7*Z*,11*E*,13*Z*,15*E*,19*Z*-enoic acid synthesis by soybean lipoxygenase. *J Lipid Res* 47:854–863
- Mukherjee PK, Marcheselli VL, Serhan CN, Bazan NG (2004) Neuroprotectin D1: a docosahexaenoic acid-derived docosatriene protects human retinal pigment epithelial cells from oxidative stress. *Proc Natl Acad Sci USA* 101:8491–8496
- Lagarde M, Bernoud N, Brossard N, Lemaitre-Delaunay D, Thies F, Croset M, Lecerf J (2001) Lysophosphatidylcholine as a preferred carrier form of docosahexaenoic acid to the brain. *J Mol Neurosci* 16:201–204
- Thies F, Delachambre MC, Bentejac M, Lagarde M, Lecerf J (1992) Unsaturated fatty acids esterified in 2-acyl-l-lysophosphatidylcholine bound to albumin are more efficiently taken up by the young rat brain than the unesterified form. *J Neurochem* 59:1110–1116
- Roberts MF, Deems RA, Dennis EA (1977) Dual role of interfacial phospholipid in phospholipase A<sub>2</sub> catalysis. *Proc Natl Acad Sci USA* 74:1950–1954
- Egmond MR, Brunori M, Fasella PM (1976) The steady-state kinetics of the oxygenation of linoleic acid catalysed by soybean lipoxygenase. *Eur J Biochem* 61:93–100
- Bild GS, Ramadoss CS, Axelrod B (1977) Multiple dioxygenation by lipoxygenase of lipids containing all-*cis*-1, 4, 7-octatriene moieties. *Arch Biochem Biophys* 184:36–41
- Yoon HR, Kim H, Cho SH (2003) Quantitative analysis of acyl-lysophosphatidic acid in plasma using negative ionization tandem mass spectrometry. *J Chromatogr B Analyt Technol Biomed Life Sci* 788:85–92
- Hong S, Lu Y, Yang R, Gotlinger KH, Petasis NA, Serhan CN (2007) Resolvin D1, protectin D1, and related docosahexaenoic acid-derived products: analysis via electrospray/low energy tandem mass spectrometry based on spectra and fragmentation mechanisms. *J Am Soc Mass Spectrom* 18:128–144
- Butovich IA, Lukyanova SM, Bachmann C (2006) Dihydroxydocosahexaenoic acids of the neuroprotectin D family: synthesis, structure, and inhibition of human 5-lipoxygenase. *J Lipid Res* 47:2462–2474
- Bannenberg GL, Chiang N, Ariel A, Arita M, Tjonahen E, Gotlinger KH, Hong S, Serhan CN (2005) Molecular circuits of

- resolution: formation and actions of resolvins and protectins. *J Immunol* 174:4345–4355
30. Serhan CN, Gotlinger K, Hong S, Lu Y, Siegelman J, Baer T, Yang R, Colgan SP, Petasis NA (2006) Anti-inflammatory actions of neuroprotectin D1/protectin D1 and its natural stereoisomers: assignments of dihydroxy-containing docosatrienes. *J Immunol* 176:1848–1859
  31. Li Z, Mintzer E, Bittman R (2004) The critical micelle concentrations of lysophosphatidic acid and sphingosylphosphorylcholine. *Chem Phys Lipids* 130:197–201
  32. Kumar VV, Baumann WJ (1991) Lanthanide-induced phosphorus-31 NMR downfield chemical shifts of lysophosphatidylcholines are sensitive to lysophospholipid critical micelle concentration. *Biophys J* 59:103–107
  33. Began G, Sudharshan E, Appu Rao AG (1999) Change in the positional specificity of lipoxygenase 1 due to insertion of fatty acids into phosphatidylcholine deoxycholate mixed micelles. *Biochemistry* 38:13920–13927
  34. Burger F, Krieg P, Marks F, Furstemberger G (2000) Positional- and stereo-selectivity of fatty acid oxygenation catalysed by mouse 12(S)-lipoxygenase isoenzymes. *Biochem J* 348:329–335
  35. Hamberg M (1971) Steric analysis of hydroperoxides formed by lipoxygenase oxygenation of linoleic acid. *Anal Biochem* 43:515–526
  36. Sun YP, Oh SF, Uddin J, Yang R, Gotlinger K, Campbell E, Colgan SP, Petasis NA, Serhan CN (2007) Resolvin D1 and its aspirin-triggered 17R epimer. Stereochemical assignments, anti-inflammatory properties, and enzymatic inactivation. *J Biol Chem* 282:9323–9334
  37. Butovich IA (2005) On the structure and synthesis of neuroprotectin D1, a novel anti-inflammatory compound of the docosahexaenoic acid family. *J Lipid Res* 46:2311–2314
  38. Croset M, Brossard N, Polette A, Lagarde M (2000) Characterization of plasma unsaturated lysophosphatidylcholines in human and rat. *Biochem J* 345:61–67

**Fig. 1** Oxidation of 1-*O*-hexadec-1'-enyl-2-docosahexaenoyl-*sn*-glycero-3-phosphocholine (GPC 16:0<sub>plasm</sub>/22:6) to 1-hydroxy-2-docosahexaenoyl-*sn*-glycero-3-phosphocholine (LPC 22:6) and formyl-LPC 22:6. For further mechanistic details concerning oxidation of the docosahexaenoyl residue see [5]



plasmalogens under the influence of Cu(II)/H<sub>2</sub>O<sub>2</sub> or the free radical initiator AAPH (2,2'-azobis-2-methyl-propanimidamide, dihydrochloride) [5, 6]. Whereas the first oxidant induced primarily oxidation at carbon-5 of the arachidonoyl residue [6], the second oxidant gave a more complex mixture of products [5].

In the present paper we investigated the organic extracts of spermatozoa from cattle and roe deer because they are known to possess large amounts of plasmalogens [3]. Matrix-assisted laser desorption and ionization time-of-flight mass spectrometry (MALDI-TOF MS) [7] with post source decay (PSD) fragmentation [8] was used for lipid analysis as a fast and reliable method. This method was already successfully used for the investigation of oxidation products from PCs [9] under the influence of HOCl as well as for the analysis of oxidatively modified human lipoproteins [10].

We will show that along with 1-hydroxy-2-docosahexaenoyl-*sn*-glycero-3-phosphocholine (LPC 22:6), formyl-LPC 22:6 is an additional important oxidation product of plasmalogens under conditions that promote lipid oxidation. Particularly formyl-LPC 22:6 may serve as a selective marker of plasmalogen oxidation.

In addition to lipids from animal spermatozoa, selected experiments were also performed with purified phospholipids in order to check whether the results obtained under both conditions agree with each other.

## Materials and Methods

### Chemicals

All phospholipid standards used as reference compounds were obtained from Avanti Polar Lipids (Alabama, USA) as solutions in CHCl<sub>3</sub> and used without further purification. All further chemicals for sample preparation, MALDI-TOF MS (2,5-dihydroxybenzoic acid, DHB) as well as all solvents (chloroform and methanol) were obtained in highest commercially available purity from Fluka Feinchemikalien

GmbH (part of Sigma-Aldrich Chemie GmbH, Taufkirchen, Germany) and used as supplied. Phospholipase A<sub>2</sub> from hog pancreas was also obtained from Fluka. Percoll (L 6143) was purchased from Biochrom (Berlin, Germany).

### Semen Samples and Processing

Bull semen was obtained from different fertile animals at a breeding station (Rinderbesamung Berlin-Brandenburg GmbH, Besamungsbullenstation Schmergow, Germany). One ml portions of each ejaculate were centrifuged at room temperature (12,000×g, 2 min) and the seminal plasma was removed by pipette. The sperm cell sediment was carefully re-suspended with 1 ml 0.9% NaCl and the supernatant discarded after centrifugation (12,000×g, 2 min).

After the second washing step in 0.9% NaCl the cell concentrations in the remaining pellets were adjusted with 0.9% NaCl to about 4 × 10<sup>8</sup> spermatozoa/ml. Those samples were stored for 24 h at 16 °C without further protective agents or frozen at -20 °C until use for lipid extraction. Lipid extraction (according to a modified Bligh and Dyer method [11]) was performed in the following way: 0.3 ml of the thawed cell suspension (i.e., about 1.2 × 10<sup>8</sup> spermatozoa) were diluted with 0.5 ml 0.9% NaCl solution. Afterwards, 3 ml of a CHCl<sub>3</sub>/CH<sub>3</sub>OH (1:2 v/v) mixture were added and the sample was vigorously vortexed for 1 min and incubated for 30 min at RT. One ml CHCl<sub>3</sub> was added and the sample again vortexed for 1 min. After addition of 1 ml acetic acid (40 mM) and vortexing, the sample was centrifuged (10 min, 1,000×g, 4 °C) and the organic layer was removed and used for all further experimental procedures. Roe deer spermatozoa were obtained by electroejaculation at the field station of the Leibniz Institute for Zoo and Wildlife Research, and washed and extracted in the same way. Unprotected storage of semen was performed at 5 °C. Spermatozoa from cattle and roe deer were cryopreserved by slow freezing in commercial media (Minitüb, Landshut, Germany)

containing egg yolk. After thawing sperm cells were centrifuged (20 min, 600×g, 25 °C) through a Percoll gradient [45, 70, 90% in Hepes-buffered NaCl solution (HBS)] to remove the cryoextender (particularly the egg yolk). The resulting sperm pellets were washed again with 5 ml HBS (10 min, 500×g, 25 °C) and the pellet was re-suspended in HBS with a sperm number of about  $1 \times 10^7$  cells in 800  $\mu$ l for lipid extraction.

#### Autoxidation of Phospholipids

Oxidation of 1-*O*-octadecyl-1'-enyl-2-docosa-hexaenoyl-*sn*-glycero-3-phosphocholine and 1-palmitoyl-2-docosa-hexaenoyl-*sn*-glycero-3-phosphocholine was performed as described [12]. Briefly, 0.1 mg of the corresponding phospholipid dissolved in 100  $\mu$ l of chloroform was transferred to a small glass test tube and evaporated under a stream of nitrogen. The lipid residue was allowed to autoxidize while being exposed to air for 24 h. This simple approach was considered to be sufficient as no quantitative data analysis was planned.

#### Artificial Modifications of Phospholipids Extracted From Spermatozoa

Commercially available PLs and PLs extracted from spermatozoa were digested by the enzyme phospholipase A<sub>2</sub> to obtain the corresponding lysophospholipids (LPLs) [13]. Briefly, aliquots of the organic extracts of spermatozoa (see above) were evaporated to dryness. Lipid vesicles were prepared by dissolving the resulting PL film in 50 mM phosphate buffer, pH 7.4 and vortexing vigorously for 30 s. Vesicles were treated with 0.5 mg/ml phospholipase A<sub>2</sub> (ca. 100 U/ml) for 2 h at 37 °C. No further efforts were made to determine the exact PLA<sub>2</sub> activity as the only aim was the complete digestion of the PLs of spermatozoa. PLs were subsequently extracted in the same way as described above.

In order to prove the sensitivity of alkenyl-acyl species to acid treatment, a flask with the dried lipids obtained from roe deer spermatozoa was exposed to HCl fumes for 10 min by keeping the inverted flask over an open bottle of concentrated HCl [14].

#### MALDI-TOF Mass Spectrometry

Total spermatozoa extracts and individual autoxidized PLs were investigated by MALDI-TOF MS using 0.5 mol/l 2,5-dihydroxybenzoic acid (DHB) in methanol as matrix [15]. A recent investigation has shown that this isomer of

dihydroxybenzoic acid is most suitable as MALDI matrix [16]. All MALDI-TOF mass spectra were acquired on a Bruker Autoflex mass spectrometer (Bruker Daltonics, Bremen, Germany). The system utilizes a pulsed nitrogen laser, emitting at 337 nm. The extraction voltage was 20 kV and gated matrix suppression was applied to prevent the saturation of the detector by matrix ions [17]. One hundred and twenty-eight single laser shots were averaged for each mass spectrum to minimize shot-to-shot deviations. The laser strength was kept about ten percent above threshold to obtain optimum signal-to-noise (S/N) ratio. In order to enhance the spectral resolution all spectra were acquired in the reflector mode using delayed extraction conditions. A more detailed methodological description of MALDI-TOF MS is given in [7, 18].

In the PSD (post source decay) experiments, the precursor ions of interest were isolated using a timed ion selector. The laser intensities for PSD spectra were maintained the same as in the (reference) reflector mode spectra for the first segment spectrum but were gradually enhanced for all further segment spectra. Further information how to record PSD spectra is available in [19]. The fragment ions were refocused onto the detector by stepping the voltage applied to the reflectron in appropriate increments. This was done automatically by using the "FAST" (fragment analysis and structural TOF) subroutine of the Flex Control Program delivered by Bruker Daltonics [20]. As peaks in PSD spectra are broadened in comparison to standard mass spectra, not even the first decimals are given in that case [19].

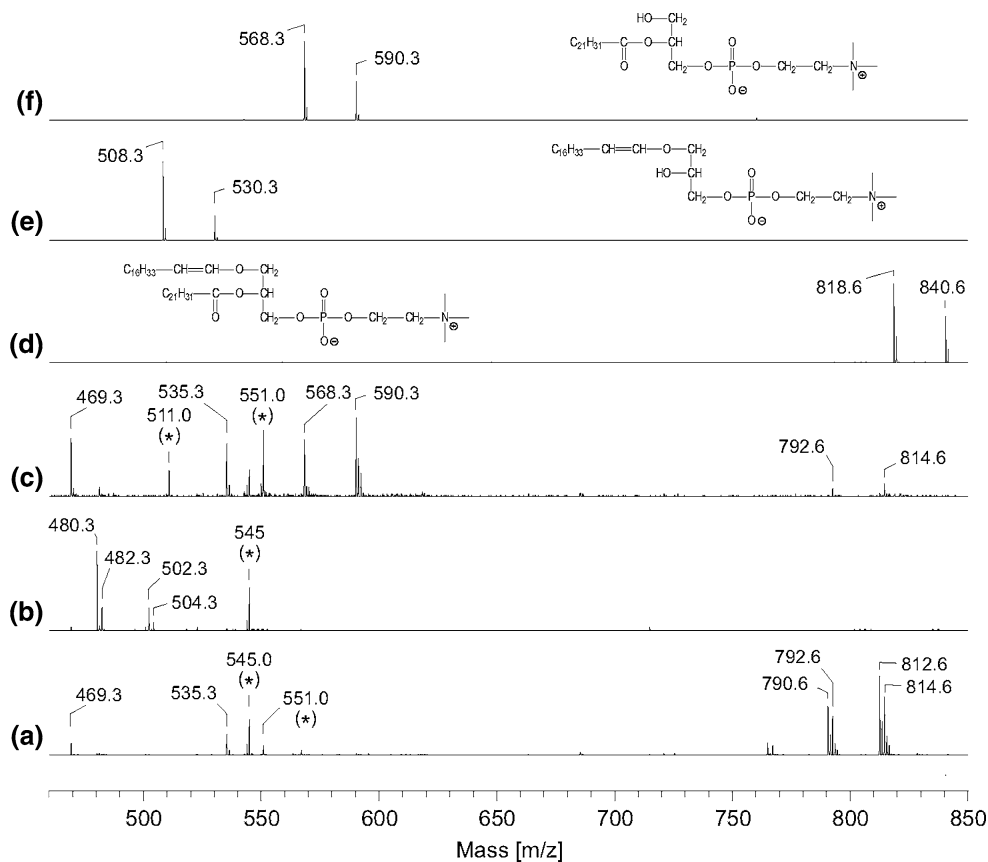
#### Results and Discussion

Although a MALDI-TOF mass spectrometric characterization of bull spermatozoa lipid extracts was already performed [21], corresponding data on the lipid composition of roe deer spermatozoa are not yet available. Therefore, the method how the PL analysis may be performed by MALDI-TOF MS in combination with chemical modifications of the organic spermatozoa extracts shall be shortly introduced.

In Fig. 2 selected positive ion MALDI-TOF mass spectra of an organic extract of roe deer (a–c) and of a selected reference plasmalogen (d–f) are shown. Trace (2a) represents the native roe deer extract, whereas (2b) was recorded subsequent to PLA<sub>2</sub> digestion and (2c) subsequent to exposition to HCl fumes. PLA<sub>2</sub> cleaves the fatty acyl residue in *sn*-2 position selectively and HCl affects the vinyl ether linkage in *sn*-1 position. Therefore, the combination of both modifications provides important structural information.

The peaks at  $m/z = 790.6$  and  $812.6$  (2a) can be assigned to the H<sup>+</sup> and Na<sup>+</sup> adducts of 1-*O*-hexadec-1'-en-

**Fig. 2** Positive ion MALDI-TOF mass spectra of an organic extract of roe deer (a–c) and one commercially available plasmalogen 1-*O*-1'-(*Z*)-octadecenyl-2-docosahexaenoyl-*sn*-glycero-3-phosphocholine (d–f). Spectra were recorded from the native samples (a, d) and subsequent to phospholipase A<sub>2</sub> digestion (b, e) or exposition to HCl fumes (c, f). Peaks are labeled according to their *m/z* values and peaks stemming from the applied DHB matrix (0.5 mol/l in CH<sub>3</sub>OH) are marked with asterisks [16]. Please note that the contribution of matrix signals is more pronounced in the spermatozoa extracts because these are much less concentrated and contain higher amounts of salts than the commercially available plasmalogen sample



yl-2-docosahexaenoyl-*sn*-glycero-3-phosphocholine (GPC 16:0<sub>plasm</sub>/22:6), whereas the peaks at *m/z* = 792.6 and 814.6 are stemming from 1-*O*-hexadec-1'-enyl-2-docosapentaenoyl-*sn*-glycero-3-phosphocholine (GPC 16:0<sub>plasm</sub>/22:5) and the corresponding alkyl ether, 1-*O*-palmityl-2-docosahexaenoyl-*sn*-glycero-3-phosphocholine (GPC 16:0<sub>alkyl</sub>/22:6). The reasons leading to these assignments will be outlined below in more detail. This composition is similar to that of bull [21] and boar [22] spermatozoa. It is well known that the content of ether-linked PLs and particularly plasmalogens is characteristic of bull and boar spermatozoa [21]. In contrast, spermatozoa from man consist nearly exclusively of regular PCs but with high contents of highly unsaturated fatty acyl residues [13]. As the contribution of further PLs in spermatozoa is relatively low and PCs are most sensitively detected in mixtures under MALDI conditions [17], PCs will be exclusively discussed in this paper.

Of course, the peak assignment given above is based exclusively on the *m/z* value and, therefore, rather ambiguous. The most simple and traditional method of confirming peak assignments is to alter the compound of interest chemically in a defined way and to check whether the observed changes are in agreement with the putative compound [21]. Subsequent to the digestion of the roe deer spermatozoa lipid extract with the enzyme PLA<sub>2</sub> (2b) that cleaves the acyl residue in *sn*-2 position selectively, it is

evident that the peaks in the original extract are replaced completely by the corresponding lyso compounds at *m/z* = 480.3 and 482.3 (H<sup>+</sup> adducts) as well as 502.3 and 504.3 (Na<sup>+</sup> adducts). This is in agreement with the previous assumption of the alkenyl (about 75%) and the alkyl ether (about 25%) but does not allow clear conclusions about the acyl residues in *sn*-2 position. However, this information can also be easily obtained. Subsequent to HCl-induced hydrolysis (2c), there are significant amounts of LPC 22:6 (*m/z* = 568.3 and 590.3), but only relatively small amounts of LPC 22:5 (*m/z* = 570.3 and 592.3). Please note that there are still small peaks at *m/z* = 792.6 and 814.6. These signals represent the corresponding alkyl ether that is—in contrast to the plasmalogens—not affected by the HCl fumes. It was not the primary aim of this paper to investigate the lipid composition of roe deer spermatozoa in more detail but it is evident from these data that ether-linked PLs (1-*O*-hexadecyl-2-docosahexaenoyl-*sn*-glycero-3-phosphocholine (GPC 16:0<sub>alkyl</sub>/22:6) and particularly plasmalogens (1-*O*-hexadec-1'-enyl-2-docosahexaenoyl-*sn*-glycero-3-phosphocholine (GPC 16:0<sub>plasm</sub>/22:6) and 1-*O*-hexadec-1'-enyl-2-docosapentaenoyl-*sn*-glycero-3-phosphocholine (GPC 16:0<sub>plasm</sub>/22:5) are their most abundant constituents. Please also note that the peaks at *m/z* = 551.0, 545.0 and 511.0 are stemming from the applied DHB matrix [16].



The reliability of the applied method can be easily verified by using a commercially available plasmalogen species and treating this compound in the same way as the spermatozoa extract: 1-*O*-1'-(*Z*)-octadecenyl-2-docosahexaenoyl-*sn*-glycero-3-phosphocholine was used because the most relevant plasmalogen of spermatozoa (with a hexadecenyl instead a octadecenyl residue) is not commercially available. The only difference between this reference compound and the plasmalogen of spermatozoa is one bismethylene group and, therefore, all masses differ for 28 Da. Accordingly, the pure plasmalogen gives two peaks at  $m/z = 818.6$  and  $840.6$  (2d), after cleavage of the docosahexaenoyl residue by PLA<sub>2</sub> digestion at  $m/z = 508.3$  and  $530.3$  (2e) and after cleavage of the alkenyl ether by HCl treatment at  $m/z = 568.3$  and  $590.3$  (2f). This is in perfect agreement with the data obtained with the spermatozoa extract. Please note that the much higher contribution of matrix peaks [8] in the spermatozoa extracts (marked with asterisks) is a clear indication of the lower lipid concentration in the case of the spermatozoa. Finally, spermatozoa extracts also give signals at  $m/z = 469.3$  and  $535.3$  (2c). Unfortunately, the origin of these peaks could not be clarified so far. However, it is most likely that these compounds represent PLs as they disappear completely subsequent to digestion with PLA<sub>2</sub> (cf. 2b).

All MALDI-TOF mass spectrometers equipped with a reflector detector are basically capable of recording MS/MS spectra and this technique is called post source decay (PSD). PSD enables the identification of significant fragment ions that may help to confirm the identity of putative lipids, but has also the disadvantage that higher sample amounts in comparison to conventional MALDI-TOF MS are required [20].

The post source decay mass spectra of the most prominent peaks of spermatozoa extracts are shown in Fig. 3. The quality of the PSD spectra derived from the precursor ions with  $m/z = 812.6$  (3a) and  $814.6$  (3b) is rather poor. Nevertheless both spectra are, besides the mass shift of 2 Da, virtually identical and confirm the proposed structures. The only difference is one fragment ion at  $m/z = 279$  that is exclusively derived from the plasmalogen but not from the ether lipid.

Unfortunately, it is very difficult to obtain information on acyl compositions of PCs by PSD because PCs are under conditions of MALDI-TOF MS only detectable as positive but not as negative ions [7]. In contrast, the negative ion PSD mass spectra would be most useful to obtain information about the released fatty acids. Nevertheless, the PSD spectra clearly confirm the presence of PC species [23].

One aim of this paper is the evaluation of the lipid composition of spermatozoa and the generation of

characteristic lipid oxidation products in dependence of storage conditions. In Fig. 4 characteristic positive ion MALDI-TOF mass spectra of organic extracts of cattle (4a, c) and roe deer spermatozoa (4b, d) are shown. Fresh ejaculates were cryopreserved and lipids were extracted after thawing and washing (4a, 4b). Fresh ejaculates were washed and stored in physiological NaCl solution (without any preserving agent) for 24 h at 16 °C (c) or 5 °C (d) before lipid extraction. Both data sets (4a, b and 4c, d) differ significantly as the cryomedium contains a significant amount of egg yolk PC ( $m/z = 782.6$ , for instance, is attributable to the Na<sup>+</sup> adduct of PC 16:0/18:1) that—even after centrifugation through a Percoll gradient—sticks to the spermatozoa membrane [24] and cannot be simply removed from the spermatozoa extracts by the washing process. Although the egg yolk PC interferes with the spermatozoa membrane lipids, it is obvious that the preserved spermatozoa do not give significant signals in the low mass region (the peak at  $m/z = 551.0$  in trace 4a and 4b is a matrix peak [17]).

Compared to cryopreservation, unprotected storage of spermatozoa from both ruminants leads to plasmalogen oxidation (4c, 4d). The LPC content is most pronounced in the roe deer sample after storage at 5 °C (4d). In addition to LPC 22:6 at  $m/z = 568.4$  and  $590.4$  there are also intense signals of formyl-LPC 22:6 ( $m/z = 596.4$  and  $618.4$ ), but only very small signals indicating a cleavage of the double bonds along the docosahexaenoyl residue. Although a variety of such oxidation products was previously detected [5], their generation obviously does not play any major role in ruminantia spermatozoa. Additionally, the LPC 22:6 and formyl-LPC 22:6 ratio indicates that the generation of the latter species is slightly preferred under these conditions (cf. the intensities of the signals at  $m/z = 590.4$  and  $618.4$ ). Accompanying investigations of isolated plasmalogen and PC species gave very similar results and will be discussed below in more detail. Please note that the peaks at  $m/z = 531.4$  and  $553.4$  are not caused by oxidation but by the cleavage of the quaternary amine group of LPC 22:6 [23].

Further confirmation of peak assignments was obtained by PSD mass spectrometry. In Fig. 5 two typical PSD spectra of putative LPC 22:6 (5a) and formyl-LPC 22:6 (5b) are shown. The Na<sup>+</sup> adducts ( $m/z = 590.4$  and  $618.4$ ) were exclusively chosen as parent ions because Na<sup>+</sup> adducts give a more intense fragmentation pattern than the corresponding H<sup>+</sup> adducts [23]. The structural assignments of all observed fragments are also provided in Fig. 5. It is obvious that all detected fragment ions agree perfectly with the previous peak assignments and, accordingly, LPC 22:6 as well as formyl LPC 22:6 can be assumed as the prime products of plasmalogen oxidation.

Spermatozoa are known to contain different types of phospholipases [25] that might be released if the

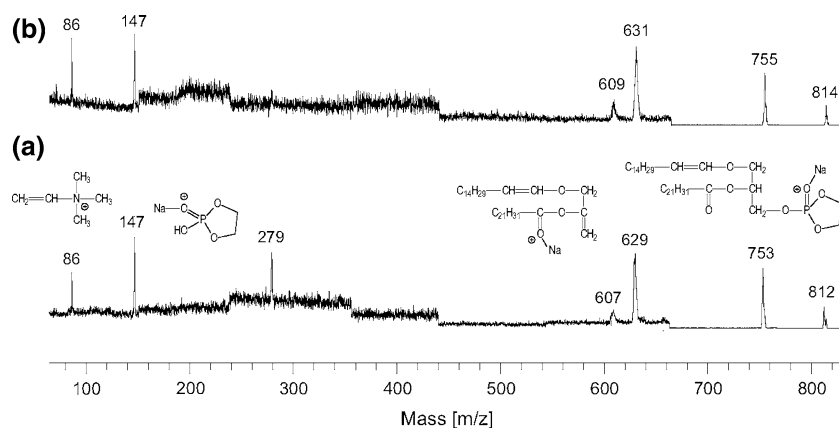
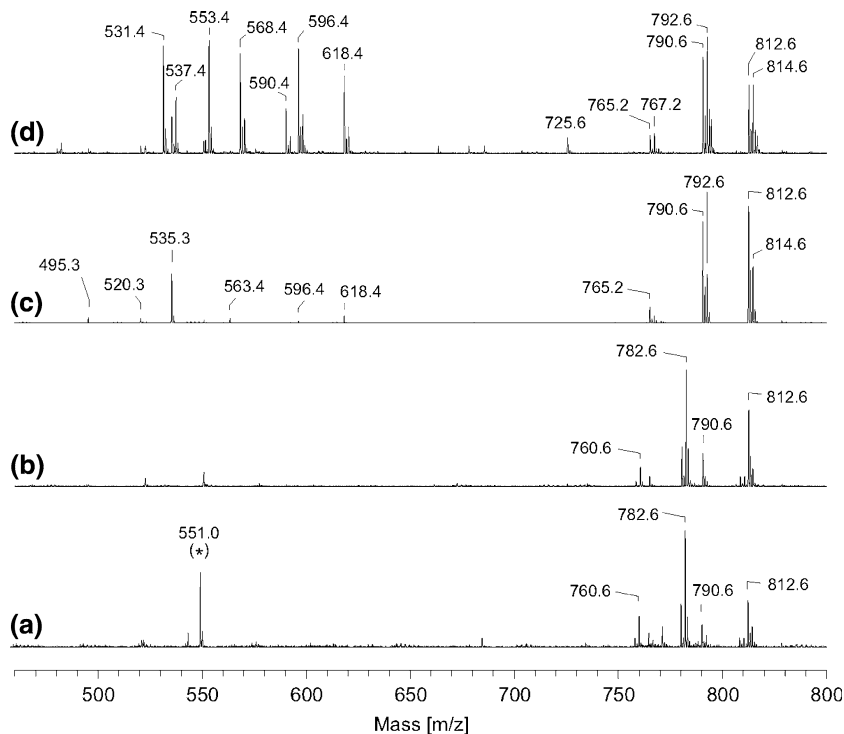


**Fig. 3** Post source decay (PSD) MALDI-TOF fragment ion mass spectra of the spermatozoa lipids with  $m/z = 812.6$  (a) and  $814.6$  (b) as parent ions. The same sample as shown in trace 1a was used. The derived fragment ions were refocused onto the detector by stepping the applied reflector voltage in appropriate increments. This is done automatically by using the “FAST” (“fragment analysis and structural TOF”) subroutine of the Flex Analysis Program provided by

Bruker Daltonics. Please note that the reflector voltage was gradually increased from higher to lower masses. Therefore, in the same order the noise level increases. Structural assignments of the observed fragments are also provided (according to data given in [23]). Please note that under the applied PSD conditions no cleavage of C–C bonds occurs [20]

**Fig. 4** Positive ion MALDI-TOF mass spectra of organic extracts (obtained according to Bligh and Dyer) of spermatozoa from cattle (a, c) and roe deer (b, d). Samples shown in a and b were cryopreserved [21]. Samples in c and d were stored in NaCl solution for 24 h at 16 and 5 °C, respectively. All samples were mixed 1:1 (v/v) with a 0.5 mol/l DHB solution in CH<sub>3</sub>OH. Peaks marked with asterisks are caused by the DHB matrix. A more detailed methodological description of MALDI-TOF MS is available in [8] and typical matrix peak patterns are discussed in [16]



spermatozoa membrane gets damaged upon storage. We cannot rule out the contribution of phospholipases completely. However, formyl-LPC 22:6 may be only generated in the presence of oxygen. As the formyl-LPC 22:6 peaks possess a higher intensity than the LPC 22:6 peaks, we suggest the dominating role of oxidation processes but only a minor contribution of phospholipases.

In order to exclude that PCs (e.g., from the applied media or the spermatozoa) potentially interfere with the

observed oxidation products, one selected PC (1-palmitoyl-2-docosahexaenoyl-*sn*-glycero-3-phosphocholine, PDPC) was also investigated by positive ion MALDI-TOF MS prior (6a) and subsequent to air oxidation (6b). These results were compared with 1-*O*-1'-(*Z*)-octadecenyl-2-docosahexaenoyl-*sn*-glycero-3-phosphocholine prior (6c) and subsequent to air oxidation (6d). It is obvious from (6a) that pure PDPC does not provide any other peaks than the H<sup>+</sup> and the Na<sup>+</sup> adducts at  $m/z = 806.6$  and  $828.6$ , respectively.

**Fig. 5** PSD MALDI-TOF mass spectra of  $m/z = 590.4$  (a) and 618.4 (b) as parent ions. Structural assignments of the observed fragments are also provided. Please note that it was not the aim of this paper to assign details of fragment ion structures. Therefore, the positions of charges and ions were only made by comparison with reference data [23]

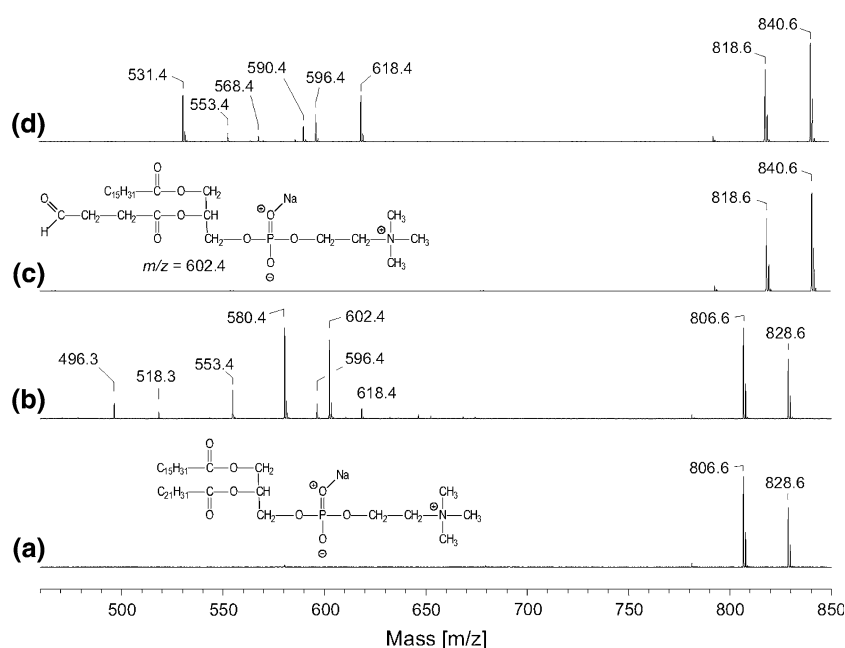
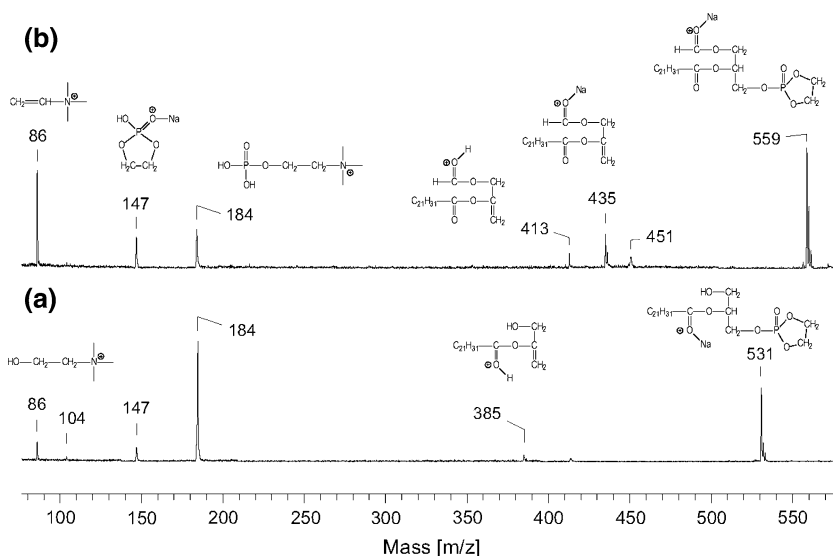


**Fig. 6** Positive ion MALDI-TOF mass spectra of 1-palmitoyl-2-docosahexaenoyl-*sn*-glycero-3-phosphocholine (PDPC) (a) and subsequent to air oxidation (b). Traces (c) and (d) correspond to pure 1-*O*-1'-(*Z*)-octadecenyl-2-docosahexaenoyl-*sn*-glycero-3-phosphocholine (c) and after exposition to air (d). 2,5-dihydroxybenzoic acid (DHB) was used as matrix and all samples (1 mg/ml) were mixed 1:1

(v/v) with a 0.5 mol/l DHB solution in CH<sub>3</sub>OH. Details on methodology and phospholipid oxidation are provided in “Materials and Methods”. The given structures correspond to intact PDPC and the corresponding oxidation product. For means of clarity the corresponding Na<sup>+</sup> adducts (but not the H<sup>+</sup> adducts) are exclusively shown

However, subsequent to air oxidation (6b), many peaks with lower masses are obvious. These peaks can be assigned to LPC 16:0 ( $m/z = 496.3$  and 518.3) that indicates the cleavage of the complete docosahexaenoyl residue and an oxidation product that corresponds to the cleavage of the double bond next to the ester linkage under generation of an aldehyde (cf. structure in the Fig) [7]. The two peaks with highest intensities ( $m/z = 580.4$  and 602.4)

can be easily assigned to the corresponding aldehyde, whereas the minor peaks at  $m/z = 596.4$  and 618.4 are assumed to correspond to the organic acid resulting from the oxidation of the initially generated aldehyde. There are no products indicating an oxidative cleavage along the docosahexaenoyl residue in other positions than the position next to the ester linkage. In contrast, the artificial oxidation of the plasmalogen (6d) gives nearly exclusively

LPC 22:6 and formyl-LPC 22:6. Therefore, in both cases the preferred oxidation site is the double bond next to the glycerol backbone and the number of the remaining olefinic residues along the acyl chain is less important.

From these results we conclude that (a) formyl-LPC 22:6 is an intrinsic marker of spermatozoa lipid oxidation and (b) this compound as well as LPC 22:6 can be easily determined by MALDI-TOF MS without the need of major sample workup. Both markers may be of high relevance for the determination of oxidative damages induced by the storage of spermatozoa (Fig. 6).

**Acknowledgments** This work was supported by the German Research Council (DFG Schi 476/5-1, Mu 1520/2-1) and the Federal Ministry of Education and Research (Grant BMBF 0313836).

## References

- Brites P, Waterham HR, Wanders RJ (2004) Functions and biosynthesis of plasmalogens in health and disease. *Biochim Biophys Acta* 1636:219–231. doi:10.1016/j.bbalip.2003.12.010
- Nagan N, Zoeller RA (2001) Plasmalogens: biosynthesis and functions. *Prog Lipid Res* 40:199–229. doi:10.1016/S0163-7827(01)00003-0
- Lenzi A, Picardo M, Gandini L, Dondero F (1996) Lipids of the sperm plasma membrane: from polyunsaturated fatty acids considered as markers of sperm function to possible scavenger therapy. *Hum Reprod Update* 2:246–256. doi:10.1093/humupd/2.3.246
- Thompson DH, Inerowicz HD, Grove J, Sarna T (2003) Structural characterization of plasmenylcholine photooxidation products. *Photochem Photobiol* 78:323–330. doi:10.1562/00318655(2003)078 < 0323:SCOPPP > 2.0.CO;2
- Zemski Berry KA, Murphy RC (2005) Free radical oxidation of plasmalogen glycerophosphocholine containing esterified docosahexaenoic acid: structure determination by mass spectrometry. *Antioxid Redox Signal* 7:157–169. doi:10.1089/ars.2005.7.157
- Khaselev N, Murphy RC (2000) Peroxidation of arachidonate containing plasmenyl glycerophosphocholine: facile oxidation of esterified arachidonate at carbon-5. *Free Radic Biol Med* 29:620–632. doi:10.1016/S0891-5849(00)00361-0
- Schiller J, Süß R, Arnhold J, Fuchs B, Leßig J, Müller M, Petković M, Spalteholz H, Zschörnig O, Arnold K (2004) Matrix-assisted laser desorption and ionization time-of-flight (MALDI-TOF) mass spectrometry in lipid and phospholipid research. *Prog Lipid Res* 43:449–488. doi:10.1016/j.plipres.2004.08.001
- Schiller J, Süß R, Fuchs B, Müller M, Zschörnig O, Arnold K (2007) MALDI-TOF MS in lipidomics. *Front Biosci* 12:2568–2579. doi:10.2741/2255
- Arnhold J, Osipov AN, Spalteholz H, Panasenko OM, Schiller J. (2001) Effects of hypochlorous acid on unsaturated phosphatidylcholines. *Free Radic Biol Med* 31:1111–1119. doi:10.1016/S0891-5849(01)00695-5
- Schiller J, Zschörnig O, Petković M, Müller M, Arnhold J, Arnold K (2001) Lipid analysis of human HDL and LDL by MALDI-TOF mass spectrometry and <sup>31</sup>P-NMR. *J Lipid Res* 42:1501–1508
- Bligh EG, Dyer WJ (1959) A rapid method of total lipid extraction and purification. *Can J Biochem Physiol* 3:911–917
- Watson AD, Leitinger N, Navab M, Faull KF, Hörkkö S, Witztum JL, Palinski W, Schwenke D, Salomon RG, Sha W, Subbanagounder G, Fogelman AM, Berliner JA (1997) Structural identification by mass spectrometry of oxidized phospholipids in minimally oxidized low density lipoprotein that induce monocyte/endothelial interactions and evidence for their presence in vivo. *J Biol Chem* 272:13597–13607. doi:10.1074/jbc.272.21.13597
- Schiller J, Arnhold J, Glander HJ, Arnold K (2000) Lipid analysis of human spermatozoa and seminal plasma by MALDI-TOF mass spectrometry and NMR spectroscopy—effects of freezing and thawing. *Chem Phys Lipids* 106:145–156. doi:10.1016/S0009-3084(00)00148-1
- Wright LC, Nouri-Sorkhabi MH, May GL, Danckwerts LS, Kuchel PW, Sorrell TC (1997) Changes in cellular and plasma membrane phospholipid composition after lipopolysaccharide stimulation of human neutrophils, studied by <sup>31</sup>P NMR. *Eur J Biochem* 243:328–335. doi:10.1111/j.1432-1033.1997.0328a.x
- Schiller J, Arnhold J, Benard S, Müller M, Reichl S, Arnold K (1999) Lipid analysis by matrix-assisted laser desorption and ionization mass spectrometry: a methodological approach. *Anal Biochem* 267:46–56. doi:10.1006/abio.1998.3001
- Schiller J, Süß R, Fuchs B, Müller M, Petković M, Zschörnig O, Waschipyk H (2007) The suitability of different DHB isomers as matrices for the MALDI-TOF MS analysis of phospholipids: which isomer for what purpose? *Eur Biophys J* 36:517–527. doi:10.1007/s00249-006-0090-6
- Petković M, Schiller J, Müller M, Benard S, Reichl S, Arnold K, Arnhold J (2001) Detection of individual phospholipids in lipid mixtures by matrix-assisted laser desorption/ionization time-of-flight mass spectrometry: phosphatidylcholine prevents the detection of further species. *Anal Biochem* 289:202–216. doi:10.1006/abio.2000.4926
- Schiller J, Arnold K (2000) Mass spectrometry in structural biology. In: Meyers RA (ed) *Encyclopedia of analytical chemistry*. Wiley, Chichester
- Hillenkamp F, Peter-Katalinić J (2007) MALDI MS—a practical guide to instrumentation, methods and applications. Wiley-VCH, Weinheim
- Fuchs B, Schober C, Richter G, Süß R, Schiller J (2007) MALDI-TOF MS of phosphatidylethanolamines: different adducts cause different post source decay (PSD) fragment ion spectra. *J Biochem Biophys Methods* 70:689–692. doi:10.1016/j.jbbm.2007.03.001
- Schiller J, Müller K, Süß R, Arnhold J, Gey C, Herrmann A, Leßig J, Arnold K, Müller P (2003) Analysis of the lipid composition of bull spermatozoa by MALDI-TOF mass spectrometry—a cautionary note. *Chem Phys Lipids* 126:85–94. doi:10.1016/S0009-3084(03)00097-5
- Leßig J, Gey C, Süß R, Schiller J, Glander HJ, Arnhold J (2004) Analysis of the lipid composition of human and boar spermatozoa by MALDI-TOF mass spectrometry, thin layer chromatography and <sup>31</sup>P NMR spectroscopy. *Comp Biochem Physiol B* 137:265–277. doi:10.1016/j.cbpc.2003.12.001
- Al-Saad KA, Siems WF, Hill HH, Zabrouskov V, Knowles NR (2003) Structural analysis of phosphatidylcholines by post-source decay matrix-assisted laser desorption/ionization time-of-flight mass spectrometry. *J Am Soc Mass Spectrom* 14:373–382. doi:10.1016/S1044-0305(03)00068-0
- Cerolini S, Maldjian A, Pizzi F, Gliozzi TM (2001) Changes in sperm quality and lipid composition during cryopreservation of boar semen. *Reproduction* 121:395–401. doi:10.1530/rep.0.1210395
- Roldan ERS, Shi QX (2007) Sperm phospholipases and acrosomal exocytosis. *Front Biosci* 12:89–104. doi:10.2741/2050

targets can be achieved using effective statins or combination therapy [11]. However, the net benefit in CVD risk reduction is around 50%. If we aspire to a better result we may also need to address other lipid risk factors, such as HDL-C [12] or TAGs.

To assess whether baseline fasting TAG levels independently predict subsequent CVD events in patients with established coronary heart disease (CHD) we carried out a post hoc analysis of the GREek Atorvastatin and coronary-heart-disease evaluation (GREACE) study [13]. We also investigated whether the extent of statin-induced reduction in TAG levels is related to a decrease in CVD events both in the entire study population and in the subgroup of patients with CHD and metabolic syndrome (MetS).

## Study Population: Methods

### Study Design, Patients and Methods

The entire duration of the GREACE study, including the recruitment period, was 4 years (January 1998–February 2002); the mean follow-up period was 3 years. The design of the GREACE study and its main findings has been previously reported [13–19]. Briefly, GREACE included 1,600 men (78%) and women (22%) with established CHD, aged <75 years (mean 58.3 years). Their serum LDL-C concentration was >100 mg/dL (2.6 mmol/L) and serum TAG levels <400 mg/dL (4.5 mmol/L). Patients with recent acute coronary syndromes were not excluded. All patients attended the Atherosclerosis or the Metabolic Syndrome Units of the University Hospital, Thessaloniki, and if eligible were randomized either into the structured care group, followed up by the University Clinic, or into the usual care group followed up by heart specialists or general practitioners of the patient's choice outside the hospital. In the structured care group, the starting dose of atorvastatin was 10 mg/day. With evaluations every 6 weeks the dose of atorvastatin was titrated up to 80 mg/day for patients not reaching the National Cholesterol Education Program Adult Treatment Panel III (NCEP ATP III) LDL-C goal (<100 mg/dL; 2.6 mmol/L) at lower dosages. Those in the structure care ( $n = 800$ ) received a mean dose of 24 mg of atorvastatin a day, and 95% of them reached the LDL-C target [13]. In the usual care group ( $n = 800$ ) only 12% of subjects were on statin treatment and only 3% were at LDL-C target [13]. Usual care consisted of lifestyle changes plus necessary drug treatment, including lipid lowering agents; atorvastatin was not excluded. All patients were followed for a mean of 3 years. Other secondary prevention treatments were similar in both treatment groups [13].

All recorded endpoints were based on hospital records. Two independent committees, one for each initial

GREACE patient group, recorded and validated endpoints. Each committee was blinded to the results of the other group. The analyses include all CVD events (excluding non-cardiac mortality), vascular events [excluding congestive heart failure (CHF)], and hard vascular endpoints [CVD death, non-fatal myocardial infarction (MI), and stroke]. Standardized criteria for endpoints were used in all treatment groups.

In the present post hoc analysis we performed three different analyses:

1. using the initial study design (structured vs. usual care-intention to treat analysis),
2. statin treated ( $n = 869$ ) vs. not statin treated subjects ( $n = 731$ ), irrespective of their initial allocation to structured or usual care groups (treatment based analysis),
3. dividing subjects into those with ( $n = 365$ ) or without MetS ( $n = 504$ ) on a statin vs. those with ( $n = 347$ ) or without MetS ( $n = 384$ ) not treated with a statin, irrespective of their initial allocation to structured or usual care groups (subgroup analysis).

The aim of this post hoc analysis was to evaluate the effect of statin-related TAG reduction on overall and vascular events both in the whole study population and in those with/without MetS. We also assessed whether baseline TAG levels predicted the risk of an event. CVD events included CVD death, cardiac morbidity (non-fatal MI, revascularisation, UA, and CHF) and stroke. Vascular events included non-fatal MI, revascularisation, UA and stroke. Hard vascular endpoints included CVD death, non-fatal MI, and stroke.

### Definition of MetS

Participants having three or more of the following criteria (according to the American Heart Association/National Heart, Lung, and Blood Institute statement [20]), were defined as having MetS:

1. Abdominal obesity: waist circumference (WC)  $\geq 102$  cm in men and  $\geq 88$  cm in women.
2. Hypertriglyceridaemia: fasting TAGs  $\geq 150$  mg/dL (1.7 mmol/L).
3. Low HDL-C <40 mg/dL (1.0 mmol/L) in men and <50 mg/dL (1.3 mmol/L) in women.
4. Raised blood pressure:  $\geq 130/\geq 85$  mmHg or use of antihypertensive medication.
5. Raised fasting plasma venous glucose:  $\geq 100$  mg/dL (5.6 mmol/L) or treatment for diabetes.

This definition is practically identical with that of the NCEP ATP III [8] but with a lower fasting glucose

threshold [100 mg/dL (5.6 mmol/L) instead of 110 mg/dL (6.1 mmol/L)].

## Assessments

After fasting overnight, total cholesterol, HDL-C and TAG were assessed using an Olympus AU 560 autoanalyser (Olympus Diagnostica GmbH, Clare, Ireland). LDL-C was calculated by the Friedewald formula [LDL-C mg/dL = total cholesterol in mg/dL – (TAG mg/dL/5 + HDL-C mg/dL)]. The non-HDL-C value was obtained by subtracting the HDL-C value from that of total cholesterol. Biochemical parameters in all patients were assessed at baseline, at the sixth treatment week and every 6 months thereafter.

## Statistical Analyses

On-study lipid values were compared with those at baseline, using analysis of variance (ANOVA) to assess differences over time within and between treatment groups. A univariate analysis was initially performed, including 25 predictors of CHD-related events. Then, after the removal of 6 predictors with a  $P > 0.10$ , the remaining 19 were used. To calculate the hazards ratio (HR) and 95% confidence interval (CI) for all vascular events during the entire duration of the study we used a multivariate Cox Predictive Model. This involved a time-dependent backward stepwise logistic regression using the mean TAG levels during the entire duration of the study as a continuous variable and 18 more predictors of vascular events as categorical variables (0–1). All univariate or multivariate analyses were performed at each 20% stepwise reduction in TAG levels. The SPSS 11.01 software package (SPSS, Inc., Chicago, IL) was used for all statistical analyses. A two-tailed  $P < 0.05$  was considered significant. We tested another possible model of stepwise regression. We calculated the change in variables (including TAGs) up to the 6th treatment month and then correlated this change with the time-dependent event rate in the two groups thereafter (two and a half year period). This analysis showed that correlations were similar with the method finally used (mean values and changes during the entire duration of the study; described above). The six-month method was not considered appropriate, because it would not include sharp changes in variables (during the remaining two and a half year period) due to drug discontinuation or drug addition. The benefit with every 20% reduction in TAGs (which are the last predictor used in the backward stepwise logistic regression analysis) was calculated after the extraction of the harm

or benefit induced by the rest of the CVD risk factors used in the multivariate model.

## Results (Tables 1, 2, 3)

### Overall GREACE Population

#### *Structured vs. Usual Care (Intention to Treat Analysis)*

TAG levels at baseline, after adjustment for body mass index (BMI) had a positive correlation with plasma glucose levels ( $r = 0.55$ ,  $P < 0.0001$ ) and smoking ( $r = 0.31$ ,  $P = 0.01$ ) and a negative one with HDL-C levels ( $r = -0.52$ ,  $P = 0.0002$ ). In the usual care group, baseline TAG levels were an independent predictor of overall vascular events (HR 1.20, 95% CI 1.06–1.59,  $P = 0.04$ ), after adjusting for LDL-C, HDL-C as well as the use of beta-blockers and angiotensin-converting enzyme inhibitors (ACE-I). The effect of atorvastatin treatment on plasma TAGs was dose-related. In subjects receiving 10–20 mg/d ( $n = 688$ ) the mean reduction in TAG levels was 29% and for those on 40–80 mg/d ( $n = 112$ ) the mean reduction was 35% ( $P < 0.0001$ ). The response to atorvastatin treatment was also related to the TAG baseline value (the higher the baseline value, the greater the reduction). In the structured care group subjects ( $n = 448$ ) with baseline TAG value  $> 150$  mg/dL (1.7 mmol/L) the mean reduction was 35%, while in those ( $n = 352$ ) with TAGs  $< 150$  mg/dL (1.7 mmol/L) at baseline the mean reduction was 24% ( $P < 0.0001$ ). The relationship of TAG level change during the study with clinical outcome (CVD events, vascular events, hard vascular endpoints) after stepwise regression analysis is shown in Table 2.

#### *Statin vs. No Statin Treatment (Treatment Based Analysis)*

We separated patients into those on a statin ( $n = 869$ ) and to those not on a statin ( $n = 731$ ) regardless of their initial allocation to structured or usual care. In those not on a statin, baseline TAG levels were an independent predictor of overall vascular events (HR 1.26, 95% CI 1.04–1.62,  $P = 0.03$ ), after adjusting for LDL-C, HDL-C as well as the use of beta-blockers and ACE-I. In the statin treated patients baseline TAG levels were not predictive of vascular events. The low percentage of women included in the study (22%) did not allow separate calculations of risk and relative risk reductions by gender. Stepwise regression analysis showed an association of TAG level change during the study with clinical outcome (CVD events, vascular events, hard vascular endpoints) (Table 3).

**Table 1** Characteristics of patients with and without the metabolic syndrome (MetS) receiving or not receiving statin treatment at the end of the study (changes from baseline in parenthesis)

	MetS (+)/statin (+) Group A (% change vs. baseline)	MetS (+)/statin (-) Group B (% change vs. baseline)	P value Group B	MetS (-)/statin (+) Group C (% change vs. baseline)	MetS (-)/statin (-) Group D (% change vs. baseline)	P value Group C vs. Group D
N	365	347	-	504	384	-
Dyslipidaemia (%)	8	99	<0.0001	10	97	<0.0001
Arterial hypertension** (%)	48	47	NS	30	27	NS
Diabetes mellitus (%)	44	45	NS	2	3	<0.0001
BMI (kg/m <sup>2</sup> )	28 ± 3 (-3%)	28 ± 4 (-1%)	NS	25 ± 4 (4%)	24 ± 3 (4%)	NS
SBP (mmHg)	124 ± 10 (-6%)*	125 ± 11 (-7%)*	NS	123 ± 9 (-2%)	124 ± 10 (-2%)	NS
DBP (mmHg)	74 ± 69 (-11%)*	75 ± 5 (-10%)*	NS	74 ± 7 (-2%)	74 ± 6 (1%)	NS
FPG (mg/dL)	131 ± 15 (-10%)*	131 ± 16 (-13%)*	NS	89 ± 4 (-4%)*	89 ± 6 (-6%)*	NS
TC (mg/dL)	162 ± 11 (-35%)*	253 ± 31 (2%)	<0.0001	161 ± 12 (-36%)*	249 ± 39 (-3%)	<0.0001
LDL-C (mg/dL)	101 ± 4 (-43%)*	175 ± 29 (-3%)	<0.0001	104 ± 5 (43%)*	180 ± 28 (-2%)	<0.0001
TAG (mg/dL)	108 ± 21 (-32%)*	160 ± 36 (-2%)	<0.0001	92 ± 16 (-30%)*	130 ± 19 (-3%)	<0.0001
HDL-C (mg/dL)	40 ± 5 (8%)*	36 ± 5 (0%)	0.003	45 ± 4 (7%)*	43 ± 6 (0%)	0.04
Non-HDL-C (mg/dL)	121 ± 10 (-44%)*	217 ± 26 (0%)	<0.0001	120 ± 9 (44%)*	207 ± 28 (-4%)	<0.0001
Statin treatment (%)	100	0		100	0	
Aspirin or other antiplatelets (%)	89	86	NS	88	87	NS
Beta blockers (%)	85	84	NS	86	84	NS
ACEIs or ARBs (%)	55	54	NS	54	52	NS
Diuretics (%)	11	10	NS	12	10	NS
Hypoglycaemic drugs (%)	44	45	NS	2	3	NS

BMI body mass index, SBP systolic blood pressure, DBP diastolic blood pressure, FPG fasting plasma glucose, TC total cholesterol, LDL-C low density lipoprotein cholesterol, TAG triacylglycerols, HDL-C high density lipoprotein cholesterol, ACEIs angiotensin converting enzyme inhibitors, ARBs angiotensin receptor blockers

To convert data from mg/dL to mmol/L divide total, LDL, HDL, and non-HDL cholesterol values by 38.7, triacylglycerols by 88.6 and FPG levels by 18.2

Data are mean ± 1 SD, unless otherwise indicated

\*  $P < 0.05$  vs. baseline, arterial hypertension, \*\* patients with either high blood pressure or on antihypertensive drugs

**Table 2** Multivariate Cox Predictive Model for all cardiovascular related events (cardiovascular disease (CVD) events (CVD deaths, non fatal myocardial infarction (MI), unstable angina, revascularisation, congestive heart failure, and stroke) involving backwardstepwise logistic regression ( $P > 0.10$  in univariate analysis to remove) in subjects with CHD in the structured care group ( $n = 800$ ) vs. those in the usual care group ( $n = 800$ ). Intension to treat analysis

Variables	Multivariate Cox Predictive Model for all adverse clinical events <sup>a</sup>	
	HR (95% CI)	P value
Age (years)	1.08 (1.05–1.12)	0.001
On treatment LDL-C <100 mg/dL <sup>b</sup>	0.64 (0.45–0.84)	<0.0001
On treatment HDL-C >40 mg/dL <sup>b</sup>	0.86 (0.75–0.95)	0.003
Use of beta-blockers during the study	0.71 (0.56–0.88)	<0.0001
Use of ACE inhibitors during the study	0.85 (0.71–0.97)	0.02
TAGs (with every 20% reduction)	0.88 (0.75–0.95)	0.007

<sup>a</sup> Eighteen univariate predictors of all vascular events all with  $P < 0.10$  (the above plus: gender male, gender female, current smoking, family history of premature coronary artery disease, arterial hypertension, diabetes mellitus, prior revascularisation, acute coronary syndrome, and prior myocardial infarction) were initially entered

<sup>b</sup> On treatment values were considered as the mean values of LDL-C and HDL-C during the entire study

CHD coronary artery disease, HR hazards ratio, CI confidence interval, LDL-C low density lipoprotein cholesterol, HDL-C high density lipoprotein cholesterol, ACE angiotensin converting enzyme inhibitors, TAGs triacylglycerols

**Table 3** Multivariate Cox Predictive Model for all cardiovascular related events (cardiovascular disease (CVD) events (CVD deaths, non fatal myocardial infarction (MI), unstable angina, revascularisation, congestive heart failure, and stroke) involving backwardstepwise logistic regression ( $P > 0.10$  in univariate analysis to remove) in subjects with CHD in a statin ( $n = 869$ ) vs. those not taking a statin ( $n = 731$ ) regardless of their initially assigned groups. Treatment based analysis

Variables	Multivariate Cox Predictive Model for all adverse clinical events <sup>a</sup>	
	HR (95% CI)	P value
Age (years)	1.09 (1.06–1.14)	0.006
On treatment LDL-C <100 mg/dL <sup>b</sup>	0.67 (0.55–0.84)	<0.0001
On treatment HDL-C >40 mg/dL <sup>b</sup>	0.86 (0.73–0.94)	0.003
Use of beta-blockers during the study	0.71 (0.58–0.85)	<0.0001
Use of ACE inhibitors during the study	0.84 (0.70–0.93)	0.004
TAGs (with every 20% reduction)	0.92 (0.81–0.97)	0.02

<sup>a</sup> Eighteen univariate predictors of all vascular events all with  $P < 0.10$  (the above plus: gender male, gender female, current smoking, family history of premature coronary artery disease, arterial hypertension, diabetes mellitus, prior revascularisation, acute coronary syndrome, and prior myocardial infarction) were initially entered

<sup>b</sup> On treatment values were considered as the mean values of LDL-C and HDL-C during the entire study

CHD coronary artery disease, HR hazards ratio, CI confidence interval, LDL-C low density lipoprotein cholesterol, HDL-C high density lipoprotein cholesterol, ACE angiotensin converting enzyme inhibitors, TAGs triacylglycerols

### Statin vs. No Statin Treatment in CHD Subjects with MetS [MetS (+)] or without Mets [MetS (–)] (Subgroup Analysis)

#### Treatment Groups and Predictive Value of Baseline TAGs

Group A consisted of 365 CHD patients MetS (+) who were on statins (mainly atorvastatin,  $n = 323$ ), Group B included 347 patients with CHD MetS (+) not on statin treatment, Group C included 504 CHD patients MetS (–) on a statin (mainly atorvastatin,  $n = 457$ ) and Group D included 384 CHD patients MetS (–) not on statins. In

groups A and C (all patients were on statin treatment), baseline TAG levels were not predictive of subsequent vascular events. In Group B (statin untreated), TAG levels were an independent predictor of overall vascular events (HR 1.32, 95% CI 1.06–1.59,  $P = 0.02$ ), after adjusting for LDL-C, HDL-C as well as the use of beta-blockers and ACE-I. After adjusting for glucose levels the predictive value of TAG levels for recurrent vascular events remained significant (HR 1.21, 95% CI 1.02–1.74,  $P = 0.04$ ). In Group D (statin untreated) high TAG levels ( $> 150$  mg/dL, 1.7 mmol/L) were predictive of CVD risk to a similar degree as in group B, but after adjusting for glucose levels



this predictive value was no longer significant (HR 1.17, 95% CI 0.89–1.86,  $P = 0.09$ ). The patient characteristics at the end of the study and their change from baseline are shown in Table 1.

### Effect of Statins on Lipid Profile

All patients in groups A [CHD MetS (+)] and C [CHD MetS (–)] were on statins. Of them, 90% were on atorvastatin (mean dose 23 mg/day), and the rest on different statins at various doses. Statin-treated patients experienced a reduction in LDL-C levels by 43% ( $P < 0.0001$ ). They had lower LDL-C levels than patients not receiving statin treatment in Groups B [CHD MetS (+)] and D [CHD MetS (–)] ( $P < 0.0001$ ) (Table 1), and most of them (92%) were at the NCEP ATP III LDL-C target ( $<100$  mg/dL; 2.6 mmol/L). In Groups A and C, TAGs were reduced by 32 and 30%, respectively,  $P < 0.0001$  vs. baseline and vs. Groups B and D for both comparisons, Table 1). Non-HDL-C was reduced by 44% in both Groups A and C ( $P < 0.0001$  vs. baseline and Groups B and D, for both comparisons, Table 1). The mean increase in HDL-C levels in Groups A and C was 8 and 7%, respectively ( $P < 0.005$  vs. baseline and vs. Groups B and D, for both comparisons, Table 1).

### Vascular Events in the Overall Population and MetS Patient Subgroups

During the (mean) 3-year follow-up there were 287 CVD events (including the fatal ones but excluding non-cardiac mortality). These were related to CVD mortality, non-fatal MI, UA, revascularisation, CHF and stroke. Of those there were 254 vascular events (excluding CHF), and after excluding revascularisation and UA (considered to be softer vascular endpoints) there were 156 hard vascular endpoints (CVD death, non-fatal MI and stroke). Five patients died from non-CVD causes.

### Overall Population According to Statin Treatment

In the untreated group ( $n = 731$ ) there were 180 (24.6%) CVD events (CVD mortality, non-fatal MI, UA, revascularisation, CHF, and stroke), while those on a statin ( $n = 869$ ) had 107 CVD events (12.3%,  $RR = 0.51$ , 95% CI 0.30–0.73,  $P < 0.0001$ ). In regard to vascular events (cardiac mortality, non-fatal MI, UA, revascularisation and stroke) in the respective groups there were 167 (22.8%) events vs. 94 (10.8%,  $RR = 0.48$ , 95% CI 0.26–0.75,  $P < 0.0001$ ). Finally, in regard to hard vascular endpoints

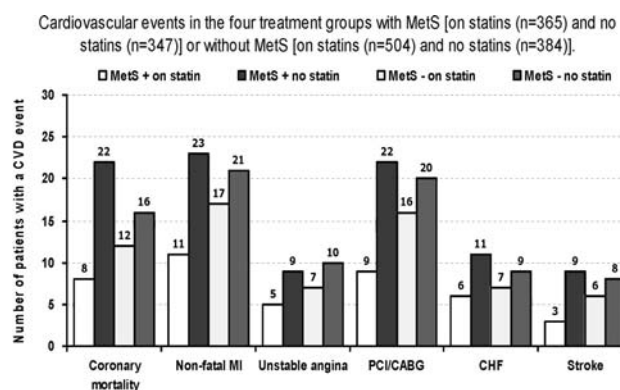


**Fig. 1** Number of patients with a recurrent cardiovascular disease (CVD) event (CVD deaths, non-fatal myocardial infarction (MI), unstable angina, revascularisation, congestive heart failure, and stroke panel A), vascular event (CVD deaths, non-fatal MI, unstable angina, revascularisation, and stroke panel B), and hard vascular endpoint (CVD deaths, non-fatal MI, and stroke panel C) in the treatment groups with or without the metabolic syndrome (MetS) on statin or without statin treatment

(cardiac mortality, non-fatal MI, and stroke) in the respective groups there were 99 (13.5) events vs. 56 (6.4%,  $RR = 0.47$ , 95% CI 0.24–0.78,  $P < 0.0001$ ) (Fig. 1).

### Subgroup Analysis According to Presence of MetS and Statin Treatment

In the subgroup analysis (Fig. 1) there were 42 (11.5%) CVD events in 365 patients with CHD + MetS on statins (Group A) and 96 (27.7%) in 347 patients with CHD + MetS but not on statin treatment (Group B); [risk ratio ( $RR$ ) = 0.42, 95% CI 0.20–0.62,  $P < 0.0001$ ]. In Group C ( $n = 504$ ), 65 CVD events were recorded (12.9%), while in Group D ( $n = 384$ ), 84 CVD related events (21.8%) occurred; ( $RR = 0.58$ , 95% CI 0.37–0.82,  $P < 0.0001$ ). The difference in vascular event rate between Groups A and C was not significant (11.5 vs. 12.9%,  $P = 0.1$ ), whereas the difference between Groups B and D was significant (27.7 vs. 21.8%,  $P = 0.002$ ). In regard to vascular events there was also a significant difference between groups A and B (36 vs. 54 events,  $RR = 0.41$ , 95% CI 0.18–0.79,  $P < 0.0001$ ). When only hard vascular endpoints were taken into consideration differences were very significant (22 vs. 54 events,  $RR = 0.40$ , 95% CI 0.18–0.88,  $P = 0.0005$ ). The time course of CVD events, vascular events, and hard vascular endpoints in the two MetS groups is shown in Fig. 2. Differences in CVD events ( $RR = 0.52$ , 95% CI 0.38–0.89,  $P = 0.001$ ), vascular events ( $RR = 0.53$ , 95% CI 0.36–0.91,  $P = 0.0016$ ) and hard vascular endpoints ( $RR = 0.54$ , 95% CI 0.41–0.92,  $P = 0.014$ ) were also significant between Groups C and D (Fig. 1), but at a lower level. The age ( $\pm$ SD) of subjects in

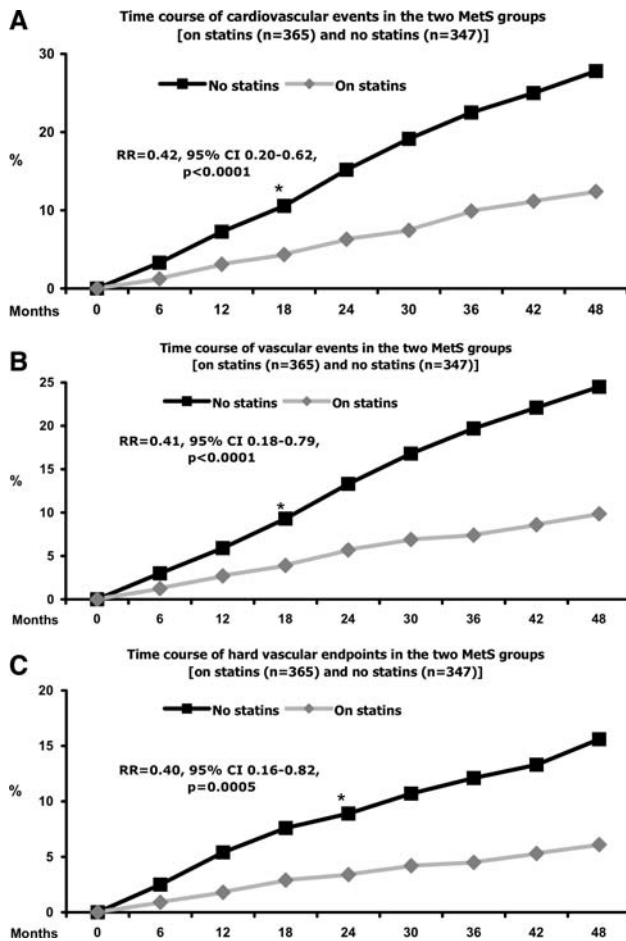


**Fig. 2** Change over time (up to 48 months) in cardiovascular disease (CVD) events (CVD deaths, non-fatal myocardial infarction (MI), unstable angina, revascularisation, congestive heart failure, and stroke panel A), vascular events (CVD deaths, non-fatal MI, unstable angina, revascularisation, and stroke panel B), and in hard vascular endpoints (CVD deaths, non-fatal MI, and stroke panel C) in the treatment groups with the metabolic syndrome on statin or without statin treatment. *MetS*, metabolic syndrome; *RR*, relative risk; *CI*, confidence interval. Asterisk time at which difference became statistically significant ( $P < 0.05$ )

Groups A, B, C, and D were  $59 \pm 8$ ,  $58 \pm 7$ ,  $59 \pm 6$ ,  $58 \pm 9$ , respectively ( $P = \text{NS}$ ). Percentage of smokers was very low (approximately 4%) and these were similarly distributed in the four treatment groups ( $P = \text{NS}$ ).

#### Relation Between TAG Levels Changes and Clinical Outcome in the Overall Population and MetS Patient Subgroups

The contribution of TAG level reduction (with each 20% decrease) to CVD risk reduction in the entire study population and subgroups in univariate and multivariate analysis is reported below. In the structured vs. usual care groups, univariate analysis of CVD events showed a HR of 0.74,

95% CI 0.52–0.86,  $P < 0.0001$ , while in multivariate analysis the HR was 0.88, 95% CI 0.75–0.95,  $P = 0.007$  (Table 2). In the patients treated with a statin vs. untreated patients univariate analysis of CVD events showed a HR of 0.76, 95% CI 0.55–0.88,  $P < 0.0001$ , while in multivariate analysis the HR was 0.92, 95% CI 0.81–0.97,  $P = 0.02$  (Table 3). In MetS patients on a statin vs. those with MetS not on a statin, univariate analysis of CVD events showed a HR of 0.71, 95% CI 0.53–0.87,  $P < 0.0001$ , while in multivariate analysis the HR was 0.85, 95% CI 0.65–0.94,  $P = 0.005$  (Table 4, part A). When only vascular events were taken into consideration univariate analysis of CVD events showed a HR of 0.74, 95% CI 0.48–0.86,  $P < 0.0001$ , while in multivariate analysis the HR was 0.82, 95% CI 0.57–0.96,  $P = 0.03$  (Table 4, part B), and when only hard vascular endpoints were considered univariate analysis of CVD events showed a HR of 0.78, 95% CI 0.51–0.95,  $P = 0.002$ , while in multivariate analysis the HR was 0.84, 95% CI 0.53–1.07,  $P = 0.08$  (Table 4, part C)

#### Discussion

This post hoc analysis of the GREACE study showed that fasting TAG levels predict vascular events among statin untreated patients with CHD. Patients who also had MetS were at a greater risk. Statin treatment (mainly with atorvastatin) resulted in a significant reduction in TAG levels and was related to a decrease in subsequent vascular events. This effect was independent of established risk factors, LDL-C, HDL-C or secondary prevention treatments. Patients with MetS experienced an even greater benefit from statin-induced TAG level reduction. In the present analysis of GREACE, all three pairs of patient groups compared [structured vs. usual care, treated with a statin vs. untreated, MetS (+) on a statin vs. MetS (+) not on a statin] received similar lifestyle advice and drug treatment for other CVD risk factors (e.g. diabetes, hypertension). Thus, the fall in TAG levels should mainly be attributed to statin treatment.

Our findings are in agreement with those of a study involving patients with premature CHD and controls, where fasting plasma TAG levels  $\geq 200$  mg/dL (2.3 mmol/L) were significantly associated with CHD even after adjusting for HDL-C and other risk factors [21]. Furthermore, the investigators found that the risk of premature CHD increased with high TAGs at all levels of HDL-C, even when HDL levels exceeded 40 mg/dL (1.0 mmol/L) [21].

In the present study the extent of TAG reduction after statin treatment was greater at higher the baseline TAG levels and the greater the statin-induced LDL-C reduction (or the higher the dose of the statin used), the greater was

**Table 4** Multivariate Cox Predictive Model for all cardiovascular related events involving backward stepwise logistic regression ( $P > 0.10$  in univariate analysis to remove) in subjects with CHD

+ metabolic syndrome (MetS) on statin (365) and CHD + MetS not on statin treatment (347). Subgroup analysis

Variables	Multivariate Cox Predictive Model for all adverse clinical events <sup>a</sup>	
	HR (95% CI)	<i>P</i> value
<b>A. Cardiovascular disease (CVD) events (CVD deaths, non fatal myocardial infarction (MI), unstable angina, revascularisation, congestive heart failure, and stroke)</b>		
Age (years)	1.14 (1.06–1.19)	<0.0001
On treatment LDL-C <100 mg/dL; 2.6 mmol/L <sup>b</sup>	0.70 (0.50–0.87)	<0.0001
On treatment HDL-C >40 mg/dL; 1.0 mmol/L <sup>b</sup>	0.84 (0.73–0.95)	0.001
Use of beta-blockers during study	0.86 (0.74–0.98)	0.02
Use of ACE inhibitors during study	0.80 (0.61–0.93)	0.0008
TAGs (with every 20% reduction)	0.85 (0.65–0.94)	0.005
<b>B. Vascular events (CVD deaths, non fatal MI, unstable angina, revascularisation, and stroke)</b>		
Age (years)	1.12 (1.04–1.17)	0.0003
On treatment LDL-C <100 mg/dL; 2.6 mmol/L <sup>b</sup>	0.67 (0.51–0.84)	<0.0001
On treatment HDL-C >40 mg/dL; 1.0 mmol/L <sup>b</sup>	0.86 (0.74–0.97)	0.0009
Use of beta-blockers during study	0.83 (0.69–0.92)	0.0002
Use of ACE inhibitors during study	0.81 (0.63–0.94)	0.001
TAGs (with every 20% reduction)	0.82 (0.57–0.96)	0.03
<b>C. Hard vascular endpoints events (CVD deaths, non fatal MI, and stroke)</b>		
Age (years)	1.15 (1.09–1.21)	0.001
On treatment LDL-C <100 mg/dL; 2.6 mmol/L <sup>b</sup>	0.69 (0.52–0.86)	<0.0001
On treatment HDL-C >40 mg/dL; 1.0 mmol/L <sup>b</sup>	0.88 (0.64–0.99)	0.04
Use of beta-blockers during study	0.86 (0.70–0.98)	0.03
Use of ACE inhibitors during study	0.79 (0.53–0.95)	0.01
TAGs (with every 20% reduction)	0.84 (0.53–1.07)	0.08

<sup>a</sup> Eighteen univariate predictors of all vascular events all with  $P < 0.10$  (the above plus: gender male, gender female, current smoking, family history of premature coronary artery disease, arterial hypertension, diabetes mellitus, prior revascularisation, acute coronary syndrome, and prior myocardial infarction) were initially entered

<sup>b</sup> On treatment values were considered as the mean values of LDL-C and HDL-C during the entire study

CHD coronary artery disease, HR hazards ratio, CI confidence interval, LDL-C low density lipoprotein cholesterol, HDL-C high density lipoprotein cholesterol, ACE angiotensin converting enzyme inhibitors, TAGs triacylglycerols

the reduction in TAG levels. A similar relationship has been previously reported [22].

The statin-related TAG level reduction and associated decline in subsequent vascular events, independently of established CHD risk factors (including LDL-C and HDL-C) is reported for the first time. Endpoint trials focused on LDL-C reduction and in post hoc analyses investigated the joint effect of high LDL-C and TAGs as well as low HDL-C [23–26]. Investigators proposed that the higher CVD risk associated with elevated TAGs is due to the concomitant low HDL-C, a more established risk factor. For example, in two previous studies, the risk associated with TAGs  $\geq 200$  mg/dL (2.3 mmol/L) was dependent on low HDL-C levels or on an elevated LDL-C/HDL-C ratio [2, 26]. Nevertheless, a recent prospective study in a population with prevalent MetS showed that plasma TAGs is an independent predictor of CVD in men, but the risk increment did not reach significance in women [27].

Furthermore, in a meta-analysis of 17 population-based prospective studies of 46,413 men and 10,864 women, adjusting for HDL-C and other risk factors, there were increases of 16 and 42% in CVD endpoints in men and women, respectively, for every 100 mg/dL (1.1 mmol/L) increase in TAG level [4].

The Scandinavian Simvastatin Survival Study (4S) meta-analyses [23, 24], the joint meta-analysis of 4S and Air Force/Texas Coronary Atherosclerosis Prevention study (AFCAPS) [25], and the meta-analysis of Helsinki Heart Study (a fibrate trial) [26] showed that subjects with the lipid triad (elevated LDL-C, low HDL-C and increased TAGs) benefitted, both in primary and secondary CHD prevention, more than those with an isolated LDL-C increase. Nevertheless, 4S and AFCAPS did not assess the effect of statin-induced TAG reduction, after adjusting for LDL-C and HDL-C, on clinical outcome. The relatively “normal” baseline TAG levels and small reductions

achieved with the statins and doses used might be the reason for a lack of positive findings. In contrast, GREACE [13] had both higher baseline TAG levels and substantial reductions during treatment in most patients.

TAG-rich remnant-like lipoprotein (RLP) particles are atherogenic and predictive of CHD, [28]. However, RLP levels do not provide additional information about CHD incidence over and above TAG levels [28]. Therefore, their measurement may not provide valuable information if fasting TAGs are available [28]. The exact prognostic value of postprandial hypertriglyceridaemia remains to be established [29].

Atorvastatin lowers cholesterol content in all LDL subfractions (including small dense LDL particles), non-HDL particles, RLP lipoproteins, fasting and postprandial TAGs and TAGs in different very low-density lipoprotein (VLDL) classes [28–33]. Moreover, atorvastatin increases cholesterol in large HDL particles and significantly decreases the density of LDL particles resulting in a shift from small, dense LDL to more buoyant and less atherogenic particles [33–35]. This shift was mainly attributed to the significant (>30%, similar to that in our analysis) decrease in TAG levels in patients after atorvastatin treatment [34, 36]. Thus, the significant LDL-C reduction as well as a shift of LDL particles to a less atherogenic pattern might have contributed to the significant risk reduction we observed in statin-treated patients (mainly on atorvastatin). The NCEP ATP III [8] accepted small dense LDL as an emerging CVD risk factor [37]. However, the contribution of increasing LDL particle diameter in reducing CHD events is not yet widely acknowledged despite some supporting evidence from fibrate studies [26, 38]. After the Fenofibrate Intervention and Endpoint Lowering in Diabetes (FIELD) trial [39], it seems that targeting TAGs with a fibrate without a simultaneous substantial reduction in LDL-C and no increase in HDL-C does not result in clinical benefit. The contribution of other non-lipid effects of statins remains to be established [40, 41].

We also investigated MetS (+)/(-) subjects with elevated TAG levels because these patients are at a greater risk for recurrent CVD events even after adjusting for traditional risk factors [42]. Moreover, CHD MetS (+) patients are categorised by the NCEP ATP III 2004 update [43], as a very high risk group that need an even lower LDL-C target that those with stable CHD without MetS or diabetes.

### Study Limitations

The relatively small number of patients included in GREACE ( $n = 1,600$ ) and the small number of hard vascular

endpoints (CVD death, non-fatal MI, and stroke) does not allow a clear cut definition of the effect of TAG level reduction on the incidence of these events although there was a strong trend in this direction. The low percentage of women included in the study (22%) did not allow separate calculations of risk and risk reductions by gender but all analyses were adjusted for gender. The present study incurs all the limitations of a post hoc analysis.

### Conclusions

Fasting TAG levels predict CVD events in statin untreated CHD patients, especially in those MetS (+). The statin-induced reduction in TAG levels resulted in a significant decrease in risk of CVD and vascular events, which was independent of traditional risk factors, LDL-C, HDL-C or secondary prevention treatments. MetS (+) patients experienced an even greater benefit from statin-induced TAG level reduction. These findings suggest that statins that achieve a substantial reduction in TAG levels might provide an additional clinical benefit, especially in MetS (+) subjects.

**Conflict of Interest** This study was conducted independently; no company or institution supported it financially. Some of the authors have attended conferences, given lectures and participated in advisory boards or other trials sponsored by various pharmaceutical companies.

### References

1. Castelli WP (1986) The triglyceride issue: a view from Framingham. *Am Heart J* 112:432–437
2. Assmann G, Schulte H (1992) Role of triglycerides in coronary artery disease: lessons from the Prospective Cardiovascular Munster Study. *Am J Cardiol* 70:10H–13H
3. Criqui MH, Heiss G, Cohn R, Cowan LD, Suchindran CM, Bangdiwala S, Kritchevsky S, Jacobs DR Jr, O'Grady HK, Davis CE (1993) Plasma triglyceride level and mortality from coronary heart disease. *N Engl J Med* 328:1220–1225
4. Hokanson JE, Austin MA (1996) Plasma triglyceride level is a risk factor for cardiovascular disease independent of high-density lipoprotein cholesterol level: a meta-analysis of population-based prospective studies. *J Cardiovasc Risk* 3:213–219
5. Ninomiya JK, L'Italien G, Criqui MH, Whyte JL, Gamst A, Chen RS (2004) Association of the metabolic syndrome with history of myocardial infarction and stroke in the third national health and nutrition examination survey. *Circulation* 109:42–46
6. Sacks FM, for the Expert Group on HDL Cholesterol (2002) The role of high-density lipoprotein (HDL) cholesterol in the prevention and treatment of coronary heart disease: expert group recommendations. *Am J Cardiol* 90:139–143
7. The UK HDL-C consensus group (2004) Role of fibrates in reducing coronary risk: a UK consensus. *Curr Med Res Opin* 20:241–247
8. Expert Panel on Detection, Evaluation, Treatment of High Blood Cholesterol in Adults (2001) Executive summary of the third

- report of the national cholesterol education program (NCEP) expert panel on detection, evaluation, and treatment of high blood cholesterol in adults (adult treatment panel III). *JAMA* 285:2486–2497
9. Smith SC Jr, Allen J, Blair SN, Bonow RO, Brass LM, Fonarow GC, Grundy SM, Hiratzka L, Jones D, Krumholz HM, Mosca L, Pasternak RC, Pearson T, Pfeffer MA, Taubert KA (2006) AHA/ACC guidelines for secondary prevention of patients with coronary and other atherosclerotic vascular disease: 2006 update: endorsed by the National Heart, Lung and Blood Institute. *Circulation* 113:2363–2372
  10. British Cardiac Society., British Hypertension Society., Diabetes UK., HEART UK., Primary Care Cardiovascular Society., Stroke Association. (2005) JBS 2: Joint British Societies' guidelines on prevention of cardiovascular disease in clinical practice. *Heart* 91(Suppl 5):v1–v52
  11. Daskalopoulou SS, Mikhailidis DP (2006) Reaching goal in hypercholesterolaemia: dual inhibition of cholesterol synthesis and absorption with simvastatin plus ezetimibe. *Curr Med Res Opin* 22:511–528
  12. Athyros VG, Mikhailidis DP, Kakafika AI, Karagiannis A, Hatzitolios A, Tziomalos K, Ganotakis ES, Liberopoulos EN, Elisaf M (2007) Identifying and attaining LDL-C goals: mission accomplished? Next target: new therapeutic options to raise HDL-C levels. *Curr Drug Targets* 8:483–488
  13. Athyros VG, Papageorgiou AA, Mercouris BR, Athyros VV, Symeonidis AN, Basayannis EO, Demitriadis DS, Kontopoulos AG (2002) Treatment with atorvastatin to the National Cholesterol Educational Program goals versus usual care in secondary coronary heart disease prevention. The GREek Atorvastatin and coronary-heart-disease evaluation (GREACE) study. *Curr Med Res Opin* 18:220–228
  14. Athyros VG, Mikhailidis DP, Papageorgiou AA, Bouloukos VI, Pehlivanidis AN, Symeonidis AN, Kakafika AI, Daskalopoulou SS, Elisaf M (2005) Effect of statins and aspirin alone and in combination on clinical outcome in dyslipidaemic patients with coronary heart disease. A subgroup analysis of the GREACE study. *Platelets* 16:65–71
  15. Athyros VG, Mikhailidis DP, Papageorgiou AA, Symeonidis AN, Daskalopoulou SS, Kakafika AI, Pehlivanidis AN, Bouloukos VI, Langer A, GREACE Study Collaborative Group (2004) Relationship between LDL-C and non-HDL-C levels and clinical outcome in the GREek Atorvastatin and coronary-heart-disease evaluation (GREACE) study. *Curr Med Res Opin* 20:1385–1392
  16. Athyros VG, Mikhailidis DP, Papageorgiou AA, Bouloukos VI, Pehlivanidis AN, Symeonidis AN, Elisaf M, GREACE Study Collaborative Group (2004) Effect of statins and ACE inhibitors alone and in combination on clinical outcome in patients with coronary heart disease. *J Hum Hypertens* 18:781–788
  17. Athyros VG, Mikhailidis DP, Papageorgiou AA, Symeonidis AN, Pehlivanidis AN, Bouloukos VI, Elisaf M (2004) The effect of statins versus untreated dyslipidemia on renal function in patients with coronary heart disease: a subgroup analysis of the Greek atorvastatin and coronary heart disease evaluation (GREACE) study. *J Clin Pathol* 57:728–734
  18. Athyros VG, Elisaf M, Papageorgiou AA, Symeonidis AN, Pehlivanidis AN, Bouloukos VI, Milionis HJ, Mikhailidis DP, GREACE Study Collaborative Group (2004) Effect of statins versus untreated dyslipidemia on serum uric acid levels in patients with coronary heart disease: a subgroup analysis of the GREek Atorvastatin and coronary-heart-disease evaluation (GREACE) study. *Am J Kidney Dis* 43:589–599
  19. Liberopoulos EN, Mikhailidis DP, Athyros VG, Elisaf M (2006) The effect of cholesterol lowering treatment on renal function. *Am J Kidney Dis* 47:561
  20. Grundy SM, Cleeman JI, Daniels SR, Donato KA, Eckel RH, Franklin BA, Gordon DJ, Krauss RM, Savage PJ, Smith SC Jr, Spertus JA, Costa F, American Heart Association, National Heart, Lung, and Blood Institute (2005) Diagnosis and management of the metabolic syndrome: an American Heart Association/National Heart, Lung, and Blood Institute Scientific Statement. *Circulation* 112:2735–2752
  21. Hopkins PN, Wu LL, Hunt SC, Brinton EA (2005) Plasma triglycerides and type III hyperlipidemia are independently associated with premature familial coronary artery disease. *J Am Coll Cardiol* 45:1003–1012
  22. Stein EA, Lane M, Laskarzewski P (1998) Comparison of statins in hypertriglyceridemia. *Am J Cardiol* 81(4A):66B–69B
  23. Ballantyne CM, Olsson AG, Cook TJ, Mercuri MF, Pedersen TR, Kjekshus J (2001) Influence of low high-density lipoprotein cholesterol and elevated triglyceride on coronary heart disease events and response to simvastatin therapy in 4S. *Circulation* 104:3046–3051
  24. Pyorala K, Ballantyne CM, Gumbiner B, Lee MW, Shah A, Davies MJ, Mitchel YB, Pedersen TR, Kjekshus J, Scandinavian Simvastatin Survival Study (4S) (2004) Reduction of cardiovascular events by simvastatin in nondiabetic coronary heart disease patients with and without the metabolic syndrome. Subgroup analyses of the Scandinavian Simvastatin Survival Study (4S). *Diabetes Care* 27:1735–1740
  25. Girmen CJ, Rhodes T, Mercuri M, Pyorala K, Kjekshus J, Pedersen TR, Beere PA, Gotto AM, Clearfield M, 4S Group, the AFCAPS/TexCAPS Research Group (2004) The metabolic syndrome and risk of major coronary events in the Scandinavian Simvastatin Survival Study (4S) and the Air Force/Texas coronary atherosclerosis prevention study (AFCAPS/TexCAPS). *Am J Cardiol* 93:136–141
  26. Manninen V, Tenkanen L, Koskinen P, Huttunen JK, Manttari M, Heinonen OP, Frick MH (1992) Joint effects of serum triglyceride and LDL cholesterol and HDL cholesterol concentrations on coronary heart disease risk in the Helsinki heart study. Implications for treatment. *Circulation* 85:37–45
  27. Onat A, Sari I, Yazici M, Can G, Hergenc G, Avci GS (2006) Plasma triglycerides, an independent predictor of cardiovascular disease in men: a prospective study based on a population with prevalent metabolic syndrome. *Int J Cardiol* 108:89–95
  28. Imke C, Rodriguez BL, Grove JS, McNamara JR, Waslien C, Katz AR, Willcox B, Yano K, Curb JD (2005) Are remnant-like particles independent predictors of coronary heart disease incidence? The Honolulu heart study. *Arterioscler Thromb Vasc Biol* 25:1718–1722
  29. Kolovou GD, Anagnostopoulou KK, Daskalopoulou SS, Mikhailidis DP, Cokkinos DV (2005) Clinical relevance of postprandial lipaemia. *Curr Med Chem* 12:1931–1945
  30. Athyros VG, Papageorgiou AA, Symeonidis AN, Elisaf M (2003) Non-high density lipoprotein cholesterol and coronary events during long-term statin treatment. *Atherosclerosis* 168:397–398
  31. Stein DT, Devaraj S, Balis D, Adams-Huet B, Jialal I (2001) Effect of statin therapy on remnant lipoprotein cholesterol levels in patients with combined hyperlipidemia. *Arterioscler Thromb Vasc Biol* 21:2026–2031
  32. Schaefer EJ, McNamara JR, Tayler T, Daly JA, Gleason JA, Seman LJ, Ferrari A, Rubenstein JJ (2002) Effects of atorvastatin on fasting and postprandial lipoprotein subclasses in coronary disease patients versus control subjects. *Am J Cardiol* 90:689–696
  33. Schaefer EJ, McNamara JR, Tayler T, Daly JA, Gleason JL, Seman LJ, Ferrari A, Rubenstein JJ (2004) Comparisons of effects of statins (atorvastatin, fluvastatin, lovastatin, pravastatin, and simvastatin) on fasting and postprandial lipoproteins in

- patients with coronary heart disease versus control subjects. *Am J Cardiol* 93:31–39
34. Pontrelli L, Parris W, Adeli K, Cheung RC (2002) Atorvastatin treatment beneficially alters the lipoprotein profile and increases low-density lipoprotein particle diameter in patients with combined dyslipidemia and impaired fasting glucose/type 2 diabetes. *Metabolism* 51:334–342
  35. Guerin M, Lassel TS, Le Goff W, Farnier M, Chapman MJ (2000) Action of atorvastatin in combined hyperlipidemia: preferential reduction of cholesteryl ester transfer from HDL to VLDL1 particles. *Arterioscler Thromb Vasc Biol* 20:189–197
  36. Kontopoulos AG, Athyros VG, Papageorgiou AA, Hatzikonstantinou HA, Mayroudi MC, Boudoulas H (1996) Effects of simvastatin and ciprofibrate alone and in combination on lipid profile, plasma fibrinogen and low density lipoprotein particle structure and distribution in patients with familial combined hyperlipidaemia and coronary artery disease. *Coron Artery Dis* 7:843–850
  37. Gazi IF, Tsimihodimos V, Tselepis AD, Elisaf M, Mikhailidis DP (2007) Clinical importance and therapeutic modulation of small dense low-density lipoprotein particles. *Expert Opin Biol Ther* 7:53–72
  38. Rubins HB, Robins SJ, Collins D, Fye CL, Anderson JW, Elam MB, Faas FH, Linares E, Schaefer EJ, Schectman G, Wilt TJ, Wittes J (1999) Gemfibrozil for the secondary prevention of coronary heart disease in men with low levels of high-density lipoprotein cholesterol: veterans affairs high-density lipoprotein cholesterol intervention trial study group. *N Engl J Med* 341:410–418
  39. Keech A, Simes RJ, Barter P, Best J, Scott R, Taskinen MR, Forder P, Pillai A, Davis T, Glasziou P, Drury P, Kesaniemi YA, Sullivan D, Hunt D, Colman P, d’Emden M, Whiting M, Ehnholm C, Laakso M, FIELD study investigators (2005) Effects of long-term fenofibrate therapy on cardiovascular events in 9795 people with type 2 diabetes mellitus (the FIELD study): randomised controlled trial. *Lancet* 366:1849–1861
  40. Athyros VG, Papageorgiou AA, Athyrou VV, Demetriadis DS, Kontopoulos AG (2002) Atorvastatin and micronized fenofibrate alone and in combination in type 2 diabetes with combined hyperlipidemia. *Diabetes Care* 25:1198–1202
  41. Tsiara S, Elisaf M, Mikhailidis DP (2003) Early vascular benefits of statin therapy. *Curr Med Res Opin* 19:540–556
  42. Gami AS, Witt BJ, Howard DE, Erwin PJ, Gami LA, Somers VK, Montori VM (2007) Metabolic syndrome and risk of incident cardiovascular events and death: a systematic review and meta-analysis of longitudinal studies. *J Am Coll Cardiol* 49:403–414
  43. Grundy SM, Cleeman JI, Merz CN, Brewer HB Jr, Clark LT, Hunninghake DB, Pasternak RC, Smith SC Jr, Stone NJ, National Heart, Lung, Blood Institute; American College of Cardiology Foundation; American Heart Association (2004) Implications of recent clinical trials for the National Cholesterol Education Program Adult Treatment Panel III guidelines. *Circulation* 110:227–239

Despite the growing body of evidence that DHA is important to health, the American diet is generally low in this nutrient. On average, Americans consume less than 100 mg of DHA per day [10, 11] despite recommendations for intakes of 200–300 mg DHA per day for pregnant and nursing women and 0.65–2 g per day of total long-chain omega-3 fatty acids DHA + eicosapentaenoic acid (EPA) for cardiovascular health [4, 12, 13]. The primary sources of dietary DHA are fish and marine foods. However, with recent concerns over oceanic contamination in some fish species and fish oils, and with US government warnings to reduce intake of some predatory species of fish, other, more sustainable sources of DHA are helping to meet a growing demand for this nutrient [14, 15]. Algae are the primary producers of DHA in the food chain, and two algal oil sources of DHA are available for fortification of infant formulas and foods, and for dietary supplements for adults including pregnant women.

One such algal DHA source, DHASCO<sup>1</sup>-T oil, is a triglyceride produced in a controlled, closed fermentation process by the microalga *Cryptocodinium cohnii*. This oil contains approximately 40% DHA by weight and no appreciable amount of any other polyunsaturated fatty acids (PUFA). This oil has been studied extensively in clinical trials in adults, children, and infants [16–35] and is now used commercially as a source of DHA for infant formula in the US and around the world. These studies consistently show increases in plasma and erythrocyte levels of DHA when infants receive formulas fortified with DHASCO-T oil and when adults and children were supplemented with DHASCO-T oil capsules. This algal oil has been widely tested for safety [36–41], and the US FDA has affirmed DHASCO-T as Generally Recognized As Safe (GRAS) for use in infant formula when combined with a fungal-derived arachidonic acid, ARASCO<sup>2</sup> (20:4n-6, ARA) oil [42].

Another algal DHA product, DHASCO-S, is a triglyceride produced by the microalga *Schizochytrium* sp. This oil also contains approximately 40% DHA as well as other PUFA including about 15% of the omega-6 fatty acid, docosapentaenoic acid (22:5n-6, DPAn-6) and 2.5% eicosapentaenoic acid (20:5n-3, EPA). The algae producing this oil have been used as an animal feed supplement in applications to enhance the level of DHA in eggs [43]. DHASCO-S oil has been used in a number of clinical studies [44–46], and the safety of the oil and the originating

algae have been confirmed [47–50]. This oil is affirmed as GRAS by US FDA for use in food fortification at levels up to 1.5 g DHA per day [51]. Both DHASCO-T and DHASCO-S oils have excellent organoleptic qualities, making them useful for food fortification applications.

Comparison of DHA levels following supplementation across clinical trials suggests that the DHASCO-T and DHASCO-S capsules deliver similar amounts of DHA to plasma, but different dosages and dosing schedules employed in these studies have made direct comparison between studies difficult. Moreover, previous studies suggested that DHASCO-T and DHASCO-S may have different effects on ARA and DPAn-6 levels in plasma, and others have suggested that DPAn-6 may interfere with DHA accretion. The present paper reports results from a clinical study undertaken to assess the bioequivalence, as well as the accretion kinetics and dose response, of DHA from the two algal-oil sources discussed above. The study directly compares DHASCO-T and DHASCO-S capsules at several DHA doses to each other as well as to an algal-oil fortified food, thus addressing the efficacy of fortified foods as vehicles for delivering dietary algal DHA. Bioequivalence of the algal DHA oils were assessed by comparing levels of the active ingredient, DHA, in plasma following 2- and 4-week supplementation of healthy adults.

## Subjects and Methods

### Experimental Procedures

#### Design

This study was an 8-arm, parallel group, randomized, clinical study designed to compare plasma phospholipid (PL) and erythrocyte DHA accretion after supplementation with either DHASCO-T or DHASCO-S algal DHA oil capsules over a range of DHA doses in a placebo-controlled, double-masked fashion, and to compare the capsules with an algal fortified snack bar (not masked). The study population included men and women in stable good health between the ages of 18 and 70 who resided in the greater Baltimore region. Pregnant women or adults consuming long-chain omega-3 supplements or whose intake of DHA exceeded 200 mg per day from their regular diet were excluded from the study. Dietary evaluation employed a validated seven-item food frequency questionnaire [52], which queried for intake of DHA/EPA-containing foods and calculated intakes based upon EPA and DHA contents reported in the USDA Nutrient Database for Standard Reference (release 14, 2002). One hundred and eleven subjects were screened for the study. The first 96 subjects who met the entrance criteria were

<sup>1</sup> DHASCO (DHA Single Cell Oil) is a registered trademark of Martek Biosciences Corporation of Columbia, MD, USA. DHASCO is contained in products marketed under the Martek trademarks of Neuromins, DHA Gold, Gold Circle Farms, Martek DHA, *life'sDHA* and in products sold by licensees under other trademarks.

<sup>2</sup> ARASCO (ARA Single Cell Oil) is a registered trademark of Martek Biosciences Corporation of Columbia, MD, USA.

randomly assigned to one of the eight treatment groups and received study supplements daily for 28 days. The treatments, outlined in Table 1, included placebo oil, and 200, 600, or 1,000 mg DHA doses from DHASCO-T or DHASCO-S algal oil capsules, or DHASCO-S-fortified snack bars. Study subjects were asked to maintain their normal diets, alcohol, and exercise levels throughout the study. Long-chain omega-3 intake from the subjects' background diet was monitored pre- and post-study by a validated food-frequency questionnaire. All adverse experiences were recorded and evaluated medically throughout the study period. Fasting blood samples for fatty acid analyses were collected by venipuncture at baseline, and after 14 and 28 days of supplementation. This study was conducted in compliance with Good Clinical Practices and conformed to the tenets of the Declaration of Helsinki. The protocol was approved by The New England Institutional Review Board (40 Washington Street, Suite 130, Wellesley, MA 02481, USA).

### Supplements

The study supplements were gelatin capsules containing 500 mg of DHASCO-T or DHASCO-S algal oil (Martek Biosciences Corporation, Columbia, MD, USA) or corn/soy placebo oil. The DHASCO-T and DHASCO-S capsules contained 201.5 and 194.2 mg DHA per capsule, respectively, and, as required for a bioequivalence study, were within 5% of each other for DHA content. The fatty acid composition of the algal oils and placebo oil are shown in Table 2. Subjects consumed 1, 3 or 5 capsules per day to achieve the desired doses of 200, 600, or 1,000 mg

**Table 1** Treatments administered

Group	DHA dose (mg per day)	Oil	Product form	# Capsules or bars per day
1	200	DHASCO-T	Capsules	1
2	200	DHASCO-S	Capsules	1
3	600	DHASCO-T	Capsules	3
4	600	DHASCO-S	Capsules	3
5	465	DHASCO-S	Snack bars	1
6	1,000	DHASCO-T	Capsules	5
7	1,000	DHASCO-S	Capsules	5
8	0	Corn/soy placebo	Capsules	1, 3, or 5

Subjects were instructed to consume 1, 3, or 5 capsules per day to achieve the desired DHA dose in the algal oil capsule groups. Within the placebo group, one third of the subjects were randomly assigned to receive one capsule per day, another one third to receive three capsules per day, and the remaining subjects to receive five capsules per day, to facilitate blinding and to ensure comparable fat intake with each of the DHA capsule treatment groups. Placebo subgroups were combined within a single placebo group for all analyses

DHA (Table 1). Since subjects in the placebo group were also randomly assigned to 1, 3, or 5 placebo capsules per day and all capsules were identical in appearance, the study was double masked, and placebo controlled for all capsule groups. A final supplementation group was assigned to receive 50 g chocolate-coated coconut snack bars containing 465 mg DHA from DHASCO-S oil. Bars were composed of 33 g carbohydrate, 2 g protein, 12 g fat, and 5 g water per bar.

### Fatty Acid Analyses

Blood for fatty acid analyses was collected into Vacutainer tubes containing EDTA and separated into plasma and erythrocytes by centrifugation. Erythrocytes were washed twice with isotonic saline. Both the plasma and erythrocytes were purged with N<sub>2</sub> and stored at -80°C until analysis. Plasma and erythrocyte lipids were extracted using the method of Folch [53] or the method of Bligh and

**Table 2** Fatty acid composition of supplements (g per 100 g fatty acid)

Fatty acid	Placebo oil	DHASCO-T	DHASCO-S
8:0	<0.1	0.92	<0.1
10:0	<0.1	1.02	<0.1
12:0	<0.1	2.80	0.25
14:0	<0.1	12.74	7.71
14:1	<0.1	0.13	<0.1
16:0	10.88	13.42	12.13
16:1	0.10	1.40	0.35
18:0	2.81	<0.1	0.73
18:1n-9	25.11	21.86	0.40
18:1n-7	1.12	0.16	0.37
18:2n-6	54.28	1.27	0.47
18:3n-3	2.97	<0.1	0.1
18:3n-6	0.36	<0.1	<0.1
18:4n-3	<0.1	<0.1	0.4
20:0	0.40	<0.1	<0.1
20:1n-9	0.61	<0.1	<0.1
20:4n-6	<0.1	<0.1	1.06
20:4n-5	<0.1	<0.1	0.22
20:4n-3	<0.1	<0.1	0.98
20:5n-3	<0.1	<0.1	2.54
22:0	0.31	0.24	<0.1
22:4n-6	<0.1	<0.1	0.41
22:5n-6	<0.1	<0.1	16.36
22:5n-3	<0.1	0.21	0.43
22:6n-3	<0.1	42.34	40.33
24:0	0.16	0.12	0.22
Others	0.89	0.33	0.38
DHA (mg per capsule)	0	201.5	194.2



Dyer [54], respectively. The phospholipid fraction as well as the other lipid subfractions (sterol esters, triglycerides, unesterified fatty acids) of plasma were isolated by thin-layer chromatography (TLC) on silica gel plates developed in a 60:40:3 ratio solution (v/v/v) of hexane:ether:acetic acid. Internal standard (23:0 fatty acid) was added to each of the plasma lipid subfractions and total erythrocyte lipids. Lipids were saponified with 0.5 mol L<sup>-1</sup> NaOH in methanol, and the resulting fatty acids were methylated using 14% BF<sub>3</sub> in methanol and then extracted with hexane. The fatty acid methyl esters were separated by capillary column gas chromatography on an Agilent Series 6890 System equipped with a 30 m FAMEWAX (Restek, State College, PA, USA) column using a 48:1 split flow ratio with helium as a carrier gas and a programmed temperature gradient (130–250°C). Fatty acid methyl esters were identified by flame ionization detection and comparison of retention times to a mixed fatty acid methyl ester standard from NuChek Prep (Elysian, MN, USA). Fatty acids were quantified by comparison to the 23:0 internal standard. Individual fatty acid levels are reported as grams per 100 g total fatty acids or as an estimated concentration (μg mL<sup>-1</sup>).

#### Statistical Methods

The primary objective of this study was to establish the bioequivalence of DHA from DHASCO-T and DHASCO-S oil by comparing levels of the active ingredient DHA in plasma PL following dosing over a range of 200–1,000 mg DHA per day over a period of 4-week. A secondary objective was to assess the bioavailability of DHA from DHASCO-S in nutritional bars and its bioequivalence compared to soft gelatin capsules. The bioequivalence analysis was conducted in compliance with FDA standards for the statistical analysis of bioequivalence studies as described in the 1992 guidance [55]. Per this guidance, bioequivalence is established if the 90% confidence intervals for the geometric mean ratios of plasma levels of the active ingredient fall within the limits of 80–125%. Since baseline DHA and possibly subject weight was expected to be a significant covariate of interest, the geometric mean ratio was computed by fitting the following model:

$$\log \left( \frac{\text{week 4 DHA}}{\text{baseline DHA}} \right) = \text{treatment} \log(\text{baseline DHA}) \log(\text{weight})$$

where treatment is a class variable with levels designating each of the treatment groups.

Geometric mean percent changes and their standard errors were calculated for each treatment level by back

transforming the log scale LSMeans. Back transformations were done as follows:

$$\text{Geometric mean percent change} = 100 \times (e^{\log \text{ scale LSMean}} - 1)$$

$$\text{SE} = 100 \times (\log \text{ scale SE}) \times e^{\log \text{ scale LSMean}}$$

Geometric mean ratios were calculated between DHASCO-T and DHASCO-S treatments at each dose level (200, 600, and 1,000 mg). The geometric mean ratio and its confidence interval were calculated as follows:

$$\text{Geometric mean ratio} = 100 \times e^{(\log \text{ scale DHASCO-S LSMean} - \log \text{ scale DHASCO-T LSMean})}$$

$$\text{Lower bound} = 100 \times e^{\log \text{ lower bound}}$$

$$\text{Upper bound} = 100 \times e^{\log \text{ upper bound}}$$

where log lower bound and log upper bound are the respective boundaries for the 90% confidence interval for: log scale DHASCO-S LSMean – log scale DHASCO-T LSMean.

A step-down dose response testing scheme using a linear contrast in ANCOVA was implemented in order to assess the dose response relationship of DHASCO-T and DHASCO-S supplementation groups on plasma PL DHA levels. For this analysis, subjects were grouped together according to their dosage. Subjects receiving snack bars were not included in the analysis. The ANCOVA was performed on the change from baseline in plasma PL DHA levels and included main effect of dose and covariates baseline DHA and weight. The step-down trend testing scheme begins with testing a linear contrast up to and including the 1,000 mg dose group. If this contrast was found to be statistically significant, another linear contrast was tested with all dose groups up to and including the 600 mg dose. Testing continued in this same manner until a linear contrast had found to be non-significant or all linear contrasts had been tested. Since this was a closed testing scheme, no adjustments for multiplicity were used. All tests were performed to a 0.05 level of significance.

All analyses were performed on an intent-to-treat basis and included all subjects. As was contemplated in both the protocol and the statistical analysis plan, placebo subgroups receiving 1, 3, or 5 placebo capsules daily were combined into a single placebo group for analyses since there were no differences between the subgroups in DHA levels or in the main fatty acids found in placebo oil (LA or oleic acid) in either plasma PL or erythrocytes before or after supplementation. Statistics were performed using

SAS Version 8.2 (Cary, NC, USA) or MiniTab Software, version 13.32 (MiniTab, State College, PA, USA).

## Results

### Compliance and Baseline Demographics

This study compared DHA bioequivalence between two different algal DHA oil capsules, containing DHASCO-T or DHASCO-S oils, and also compared the bioavailability of these algal oil capsules to an algal-oil fortified snack bar. All 96 subjects completed the study along with all assessments. Mean compliance with study supplements over the 4-week study period, based on returned capsule or bar counts, was greater than 95% in all groups. All individuals, with one exception in the placebo group, consumed greater than 80% of their study supplements, the a priori lower limit for compliance as defined in the protocol. Subject weights and DHA intake from the background diet were stable throughout the study, and there were only minor changes in alcohol intake and exercise recorded in a few subjects. No subjects were excluded from the analyses based on these lifestyle changes. All analyses included all subjects on an intent-to-treat basis. The baseline demographic characteristics of the study groups are shown in Table 3. There were no statistically significant differences in weight, height, BMI, age, gender, race, or DHA intake at baseline between the study groups. Mean baseline dietary DHA intakes were less than 100 mg per day in each group, which is typical for American adults [10].

### Changes in DHA Fatty Acid Levels

Mean DHA levels in plasma PLs and erythrocytes at baseline and following supplementation for 2- or 4-week with DHASCO-T or DHASCO-S capsules, placebo capsules or DHASCO-S nutrition bars are shown in Fig. 1. Supplementation with both the DHASCO-T and DHASCO-S capsules resulted in similar rapid, dose-dependent increases in plasma PL DHA levels, with the majority of the increase occurring within the first 2 weeks of supplementation (Fig. 1a). Post-supplementation plasma DHA levels in the DHASCO-T and DHASCO-S capsule groups at each dose level were nearly identical. The DHA levels in the DHASCO-T and DHASCO-S capsule supplementation groups were compared at each dose level using the Student's *t* test. There were no differences between the groups at any time point at any dose level. Post-supplementation plasma DHA levels in the DHASCO-S bar group receiving 465 mg DHA per day were similar to those in the

**Table 3** Baseline demographics means ( $\pm$ SD) or counts were compared by ANOVA or Chi square analyses

Demographic	DHASCO-T		DHASCO-S					
	Placebo	Capsules	Capsules		Bar			
	Capsules ( <i>n</i> = 12)	200 mg DHA ( <i>n</i> = 12)	600 mg DHA ( <i>n</i> = 12)	1,000 mg DHA ( <i>n</i> = 12)	200 mg DHA ( <i>n</i> = 12)	600 mg DHA ( <i>n</i> = 12)	1,000 mg DHA ( <i>n</i> = 12)	465 mg DHA ( <i>n</i> = 12)
Age	40.2 (14.65)	30.8 (9.40)	41.1 (9.07)	42.2 (14.42)	35.9 (11.34)	36.9 (11.48)	41.0 (11.40)	37.4 (10.44)
Weight (lb)	170.9 (39.24)	161.7 (42.22)	185.4 (35.37)	171.8 (23.73)	162.0 (30.69)	159.6 (38.32)	177.6 (33.94)	160.1 (23.51)
Height (in)	65.8 (4.37)	66.3 (3.29)	69.7 (4.85)	69.5 (3.05)	66.5 (4.87)	66.4 (3.08)	67.2 (3.99)	67.9 (5.16)
BMI	27.2 (3.64)	25.5 (5.38)	26.6 (4.04)	24.8 (2.99)	25.7 (4.89)	25.0 (4.14)	27.2 (2.53)	24.2 (2.23)
Race (% white)	92	92	92	92	75	92	83	92
Gender (M/F)	4/8	4/8	8/4	8/4	3/9	3/9	6/6	5/7
DHA daily intake (mg per day)	82.5 (31.95)	93.1 (52.96)	91.8 (45.50)	95.1 (57.52)	77.3 (34.25)	99.6 (34.85)	83.3 (53.31)	75.2 (35.61)

There were no significant differences in baseline demographic characteristics between any of the study groups

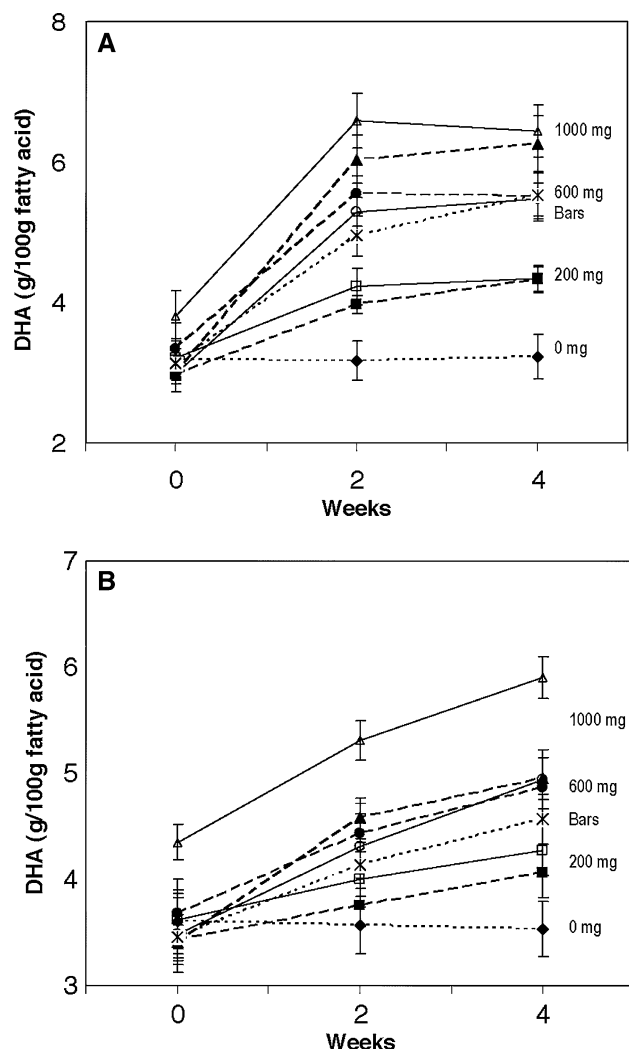


**Fig. 1** DHA levels in plasma phospholipids. Mean ( $\pm$ SEM) DHA levels (g per 100g fatty acid) in plasma phospholipids (a) and erythrocytes (b) following supplementation with placebo (diamonds) or 200 mg (squares), 600 mg (circles), or 1,000 mg (triangles) of DHA per day from DHASCO-T oil (solid lines, solid symbols) or DHASCO-S oil (dashed lines, open symbols) or with snack bars (asterisks) for 2- and 4-week in plasma PL (a) and erythrocyte lipids (b). The DHA levels and concentrations in plasma PL and erythrocytes in the DHASCO-T and DHASCO-S capsule supplementation groups were compared at each dose level using the Student's *t* test. There were no differences between the groups at any time point at any dose level

DHASCO-T or DHASCO-S capsule groups receiving 600 mg DHA per day. There were no changes in plasma DHA levels in the placebo group over the 4-week supplementation period.

DHA levels also increased in a dose-dependent manner in erythrocyte lipids in all of the DHASCO-T and DHASCO-S capsule groups, as well as in the DHASCO-S bar group (Fig. 1b). In contrast to the plasma, the erythrocyte DHA levels rose more slowly and steadily throughout the 4-week treatment period in both the

DHASCO-T and DHASCO-S treatment groups. The erythrocyte DHA levels in the placebo group remained constant with time. The 1,000 mg DHASCO-T group had relatively high baseline erythrocyte DHA levels, but this was not statistically higher than the other groups. Nonetheless, the DHA levels in both the DHASCO-T and DHASCO-S 1,000 mg DHA treatment groups appeared to increase in a parallel fashion.

The mean change from baseline DHA levels as proportions of fatty acids and absolute DHA concentrations in plasma PLs and erythrocytes at the 4-week timepoint are shown in Fig. 2. The DHASCO-T and DHASCO-S oils resulted in very similar increases in DHA levels and concentrations with each of the DHASCO-T and DHASCO-S dose groups with no effect of the placebo. By visual inspection of Fig. 2, the nutritional bars (450 mg DHA per bar) resulted in increases in the DHA levels and concentrations in plasma PLs and erythrocytes similar to the 600-mg DHA doses from DHASCO-T and DHASCO-S capsules, suggesting similar or somewhat elevated DHA accretion with the bars. The DHA response in plasma PLs was highly dependent on baseline DHA levels ( $p < 0.001$ ), but there was no effect of age, race, weight, or gender on the DHA response (data not shown).

#### DHA Bioequivalence Assessments

Because DHASCO-T has been studied more extensively in clinical settings, it served as the reference compound and DHASCO-S as the comparator in this bioequivalence study. To assess bioequivalence of the two oils, the geometric LS mean ratio of the DHASCO-S to DHASCO-T 4-week change in DHA levels was calculated at each dose level. This ratio is expressed as a percent (100% represents unity). The 90% confidence intervals of the ratios must fall within 20% of unity (80–125% on a geometric scale) for the oils to be considered bioequivalent [55]. Figure 3 shows that the confidence intervals of the ratios of the DHASCO-S to DHASCO-T products at each DHA dose for both DHA levels and absolute concentrations in plasma PLs and erythrocytes fell within the 80–125% limits, thus establishing bioequivalence per FDA standards between the two products at all dose levels. A formal bioequivalence assessment was not conducted on the bar group because the doses were not within 5% of the capsule mid-dose level. However, the nutritional bars appeared to result in similar increases in the DHA levels in plasma PLs and erythrocytes as the 600 mg DHA doses from DHASCO-T and DHASCO-S capsules (Fig. 2), and therefore, DHASCO-S oil formulated into snack bars appears to deliver equivalent amounts of DHA on a per DHA consumed basis as DHASCO-S gelatin capsules.

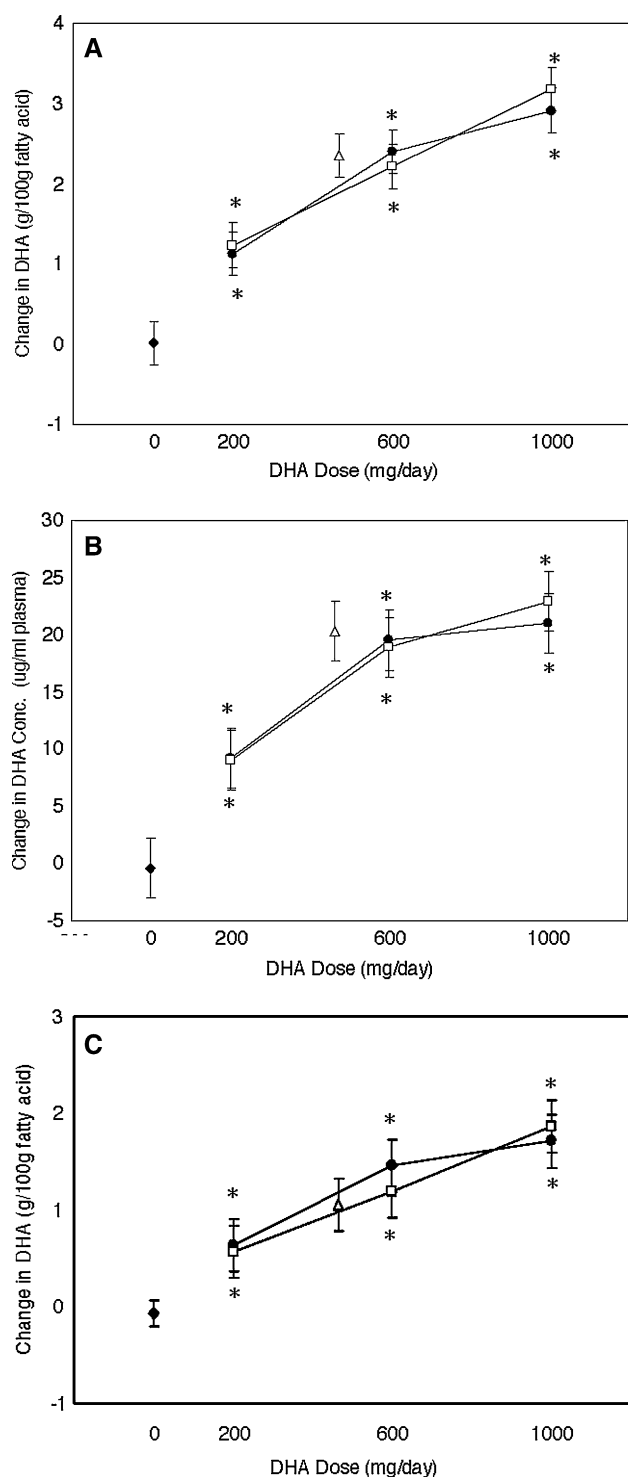


**Fig. 2** Change in DHA levels and concentrations. LS Mean change ( $\pm$ SEM) in plasma PL DHA levels (a), in plasma PL DHA absolute concentrations (b) and in erythrocyte DHA levels (c) following 4-week of supplementation with placebo (filled diamonds), DHASCO-T (filled circles) or DHASCO-S (open squares) oil capsules or DHASCO-S fortified snack bars (open triangles). Capsule groups were compared to the placebo group using the step down trend test. \* $p < 0.05$  compared to placebo. Bar groups were not included in this analysis

### DHA Dose–Response Assessment

The DHA dose–response relationship of the two oils was explored using a step down trend test. Since the two oils resulted in equivalent DHA responses, the results from both oils at each dose level were initially combined for this dose response assessment. Mean DHA levels (95% CIs) in plasma PLs for the combined 200, 600, and 1,000 mg DHA doses increased by 1.17 (0.52, 1.82), 2.28 (1.63, 2.93) and 3.03 (2.38, 3.67) g per 100 g fatty acid, respectively ( $p < 0.001$  for each dose in comparison with placebo), indicating a dose–response relationship. Similar statistically significant dose-dependent increases in plasma PL and erythrocyte DHA levels and concentrations were observed when analyzed by the step down trend test for individual supplementation groups of DHASCO-T and DHASCO-S (Fig. 2). A general linear model analyzing the two oils separately further indicated that there was an effect of dose, confirming a dose response, and no interactions between dose and compound or dose by dose, indicating that the dose responses are linear and parallel for each compound for plasma PL DHA levels. In a regression model, with baseline DHA levels used as a covariate, the equation for the 4-week change in plasma PL DHA levels for the combined DHASCO-T and DHASCO-S oils group was:

$$\Delta \text{DHA levels} = 2.171 + 0.003 (\text{DHA dose}) - 0.535 (\text{baseline DHA level})$$

where DHA levels are expressed in g per 100 g fatty acids and DHA dose in mg per day ( $n = 72$ ,  $R^2 = 0.586$ ,  $p < 0.001$ ). This regression equation indicates that for every 100 mg of dietary DHA from either DHASCO-T or DHASCO-S oil supplements, plasma PL DHA levels increase by 0.3 g per 100 g fatty acid in the dose range studied.

### Effects on DHA Levels in Other Plasma Lipid Subfractions

We chose the mid-dose level to explore the effects of supplementation on the various lipid subfractions. Figure 4 shows the change from baseline in DHA levels in the various lipid subfractions of plasma after 4-week of supplementation with either DHASCO-T or DHASCO-S oil capsules at the 600 mg DHA dose level. Baseline DHA levels were 2.78 and 2.84 g per 100 g fatty acids in phospholipids, 0.40 and 0.51 g per 100 g in triglycerides, 0.45 and 0.46 g per 100 g in sterol esters, 0.62 and 0.58 g per 100 g as unesterified fatty acids, and 1.52 and 1.66 g per 100 g in whole plasma for DHASCO-T and DHASCO-S supplementation groups, respectively. Both oil supplements

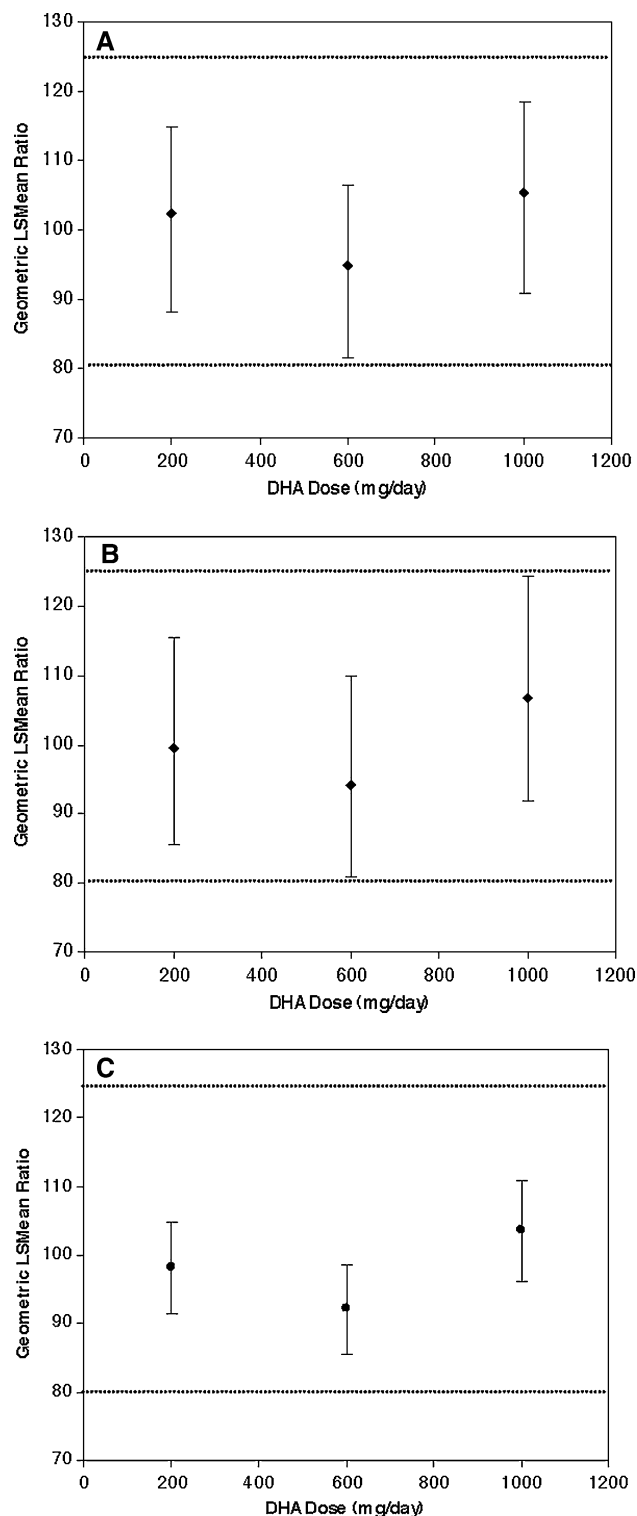


**Fig. 3** DHA bioequivalence assessment. Graphs show ratios in percent of the LSmean change in DHA levels or concentrations of DHASCO-S to DHASCO-T ( $\pm 90\%$  confidence intervals). Ratios of plasma PL DHA levels measured in g per 100g fatty acids (a), of plasma PL absolute DHA concentrations as measured in  $\mu\text{g mL}^{-1}$  (b) and of erythrocyte levels as measured in g per 100 g fatty acids (c). Dotted lines show the limits of bioequivalence. The 90% confidence intervals of all the ratios fell within the 80–125% limits to establish bioequivalence

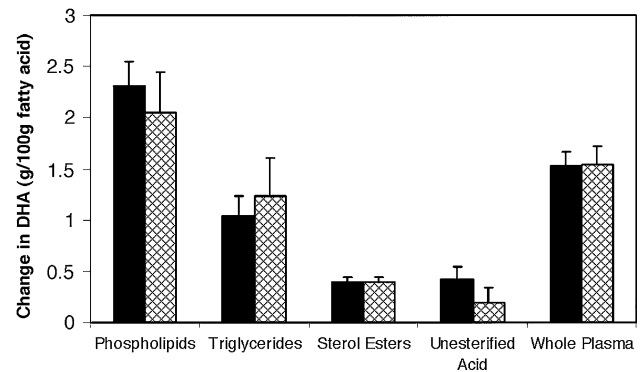


**Fig. 4** Changes in DHA Levels in plasma. Mean  $\pm$  SEM of the 4-week change in DHA levels in the various lipid subfractions of plasma following supplementation with DHASCO-T (solid bars) or DHASCO-S (hatched bars) at the 600 mg DHA dose level. There were no differences in the DHA responses between the supplementation groups when compared by Student's *t* tests

resulted in increases at the 4-week timepoint in DHA levels in each plasma fraction. There were no differences between the DHA responses of the DHASCO-T or DHASCO-S groups for any of the lipid fractions, indicating that the two oils resulted in the same magnitude of increase and the same distribution of DHA among the lipid fractions in plasma. Since unesterified fatty acids may be the bioactive form of fatty acids in plasma, we measured actual concentrations of unesterified DHA in whole plasma. The mean unesterified DHA concentration in plasma following supplementation with either oil ( $n = 24$ ) increased from 0.85 to 1.35  $\mu\text{mol L}^{-1}$  at this 600 mg DHA dose level.

#### Effects on ARA Levels

Baseline mean ARA levels in all groups ranged between 11.8 and 13.2 g per 100 g fatty acid in plasma PLs. The effects of DHASCO-T and DHASCO-S capsule and snack bar supplementation on the change in plasma PL ARA levels at the 4-week timepoint are presented in Fig. 5a. This figure shows a typical smooth dose-dependent reduction in ARA levels following DHASCO-T supplementation, with significant reductions in ARA at both the 600 and 1,000 mg doses relative to placebo (stepdown trend test). However, DHASCO-S supplementation resulted in a nonlinear ARA response with no significant reductions in ARA levels at any dose. The ARA levels between the oils deviated most at the 1,000 mg dose where the DHASCO-S nearly maintained ARA levels, whereas the DHASCO-T oil resulted in a significant reduction in ARA levels. This finding was corroborated by regression analysis showing a significant inverse correlation ( $r = -0.20$ ,  $p = 0.036$ ) between change in DHA levels and change in ARA levels when the DHA was provided by

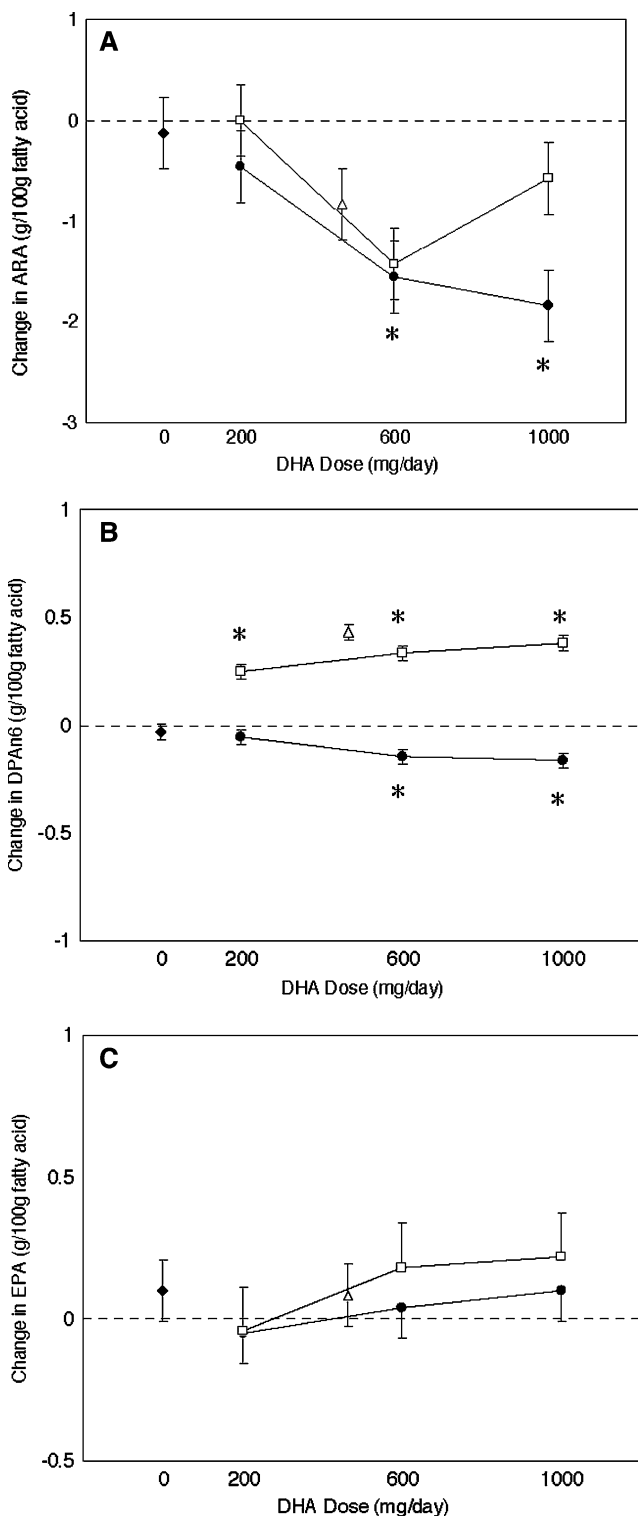


**Fig. 5** Changes in other fatty acids. Four-week change in plasma PL ARA (a), DPAn-6 (b) and EPA (c) levels following supplementation with placebo (filled diamonds), DHASCO-T (filled circles) or DHASCO-S (open squares) oil capsules or DHASCO-S fortified snack bars (open triangles). Mean  $\pm$  SEM. Capsule groups were compared to the placebo group using the step down trend test. \* $p < 0.05$  compared to control. Bar groups were not included in this analysis

DHASCO-T capsules, but no such relationship ( $r = 0.11$ ,  $p = 0.187$ ) when DHA was provided by DHASCO-S capsules. The dose–response relationships between the oils and the resulting plasma ARA levels were further explored in post hoc analyses with general linear regression models using dose as a continuous variable. This analysis indicated a significant main effect of compound, i.e., differences between the DHASCO-T and DHASCO-S effect on plasma PLs ARA levels. Therefore, the dose response was further explored for each compound separately. These analyses confirmed a significant linear dose effect for DHASCO-T and a curvilinear (quadratic) dose effect for DHASCO-S<sup>3</sup>. Regression equations describing the dose effect of DHA supplementation from DHASCO-T on 4-week change in plasma PL ARA levels indicate that ARA levels decrease approximately 0.20 g per 100 g fatty acid for each 100 mg DHA dose from DHASCO-T.

#### Effects on DPAn-6 Levels

Baseline DPAn-6 levels in all groups ranged between 0.3 and 0.4 g per 100 g fatty acid in plasma PLs. The effects of DHASCO-T and DHASCO-S capsule and snack bar supplementation on the change in plasma PL DPAn-6 levels at the 4-week timepoint are presented in Fig. 5b. DHASCO-T oil led to a modest decrease in DPAn-6 levels, which was statistically significant at both the 600 and 1,000 mg dose groups (step down trend test) whereas DHASCO-S oil led to an increase in DPAn-6 levels at all three dose levels compared to placebo. The DHASCO-S nutritional bars led to an increase in plasma PL DPAn-6 levels of a similar magnitude to the mid-dose DHASCO-S capsules. These results are corroborated by regression analysis showing a highly significant reduction in DPAn-6 with DHASCO-T supplementation ( $r = -0.53$ ,  $p < 0.001$ ) and a highly significant increase in DPAn-6 ( $r = 0.62$ ,  $p < 0.001$ ) following supplementation with DHASCO-S, after adjustment for dose.

The efficiencies of DPAn-6 and DHA accretion following dietary administration of the respective fatty acids were evaluated by comparing actual concentrations in whole plasma following supplementation with the mid-dose of DHASCO-S oil capsules, which contains both fatty acids. The mid-dose DHASCO-S capsule group received 600 mg of DHA and 240 mg of DPAn-6 daily, which resulted in increases of 46.4 and 7.6  $\mu$ g of DHA and

<sup>3</sup> DHASCO-T ARA regression equation is: change in plasma PL ARA levels =  $4.087 - 0.002$  (DHA dose in mg per day)  $- 0.333$  (baseline ARA levels).  $n = 84$ ,  $R^2 = 0.420$ ,  $p < 0.001$ . The DHASCO-S ARA regression equation is: change in plasma PL ARA levels =  $3.971 - 0.005$  (DHA Dose) +  $0.000004$  (DHA Dose) (DHA Dose)  $- 0.296$  (Baseline ARA levels).  $n = 84$ ,  $R^2 = 0.224$ ,  $p = 0.01$ .

DPAn-6, respectively, per mL whole plasma. This suggests that DHA accumulates more efficiently in plasma ( $7.7 \mu\text{g mL}^{-1}$  plasma per 100 mg in the diet) than does dietary DPAn-6, which accumulates at  $3.2 \mu\text{g mL}^{-1}$  plasma per 100 mg dietary DPAn-6.

#### Effects on EPA and other Fatty Acids

Baseline mean EPA levels in plasma PLs ranged between 0.6 and 0.8% of fatty acids. The change in the plasma PL DHA levels are shown in Fig. 5c. EPA levels tended to modestly increase in a dose-dependent manner in both the DHASCO-T and DHASCO-S groups, with the DHASCO-S oil tending to have larger increases, but none of the differences was statistically different from placebo. Tables 4 and 5 available on line (Supplementary Material; doi: [10.1007/s11745-007-3098-5](https://doi.org/10.1007/s11745-007-3098-5)) show all fatty acid levels in plasma PLs and erythrocytes in each group at the 4-week timepoint. In addition to the aforementioned effects on PUFA, DHASCO-T and DHASCO-S oils result in significant dose-dependent reductions in DPAn-3 in plasma PLs and erythrocytes and in 22:4n-6 levels in plasma PLs. There was no effect of either algal oil on total saturated or monounsaturated fatty acid levels in either plasma PLs or erythrocytes (Tables 4 and 5, available through the journal online; doi: [10.1007/s11745-007-3098-5](https://doi.org/10.1007/s11745-007-3098-5)).

#### Safety

In compliance with good clinical practices, safety was assessed in this study by monitoring adverse events throughout the study. There were no deaths or serious or clinically significant adverse events (AEs) reported for any subject during the supplementation period. No subject discontinued supplementation due to an AE. All AEs were evaluated by the Investigator as being “Mild” to “Moderate” in severity. Only eructation was significantly associated with supplementation. Eructation was reported mainly by subjects receiving DHASCO-T 200 mg (50%), 600 mg (58%), and 1,000 mg (33%). Only one subject (1,000 mg) in the DHASCO-S groups reported eructation. A statistically significant difference was observed in the incidence of eructation between DHASCO-T 200 and 600 mg groups when compared to placebo. No other significant differences were noted.

#### Discussion

Previous studies have shown that both the DHASCO-T and DHASCO-S oils result in increases in plasma levels of DHA in humans. However, this was the first study to

compare the bioequivalence of these two different algal DHA sources. Bioequivalence was determined by assessing the levels as well the concentrations of the bioactive ingredient DHA in plasma and erythrocytes following 4-week of supplementation. The results of this study clearly establish that DHASCO-T and DHASCO-S oils are bioequivalent sources of DHA, per FDA standards, whether reported as proportions of fatty acids or as absolute concentrations of DHA in plasma or erythrocytes. This is also the first study to demonstrate that a DHA-rich oil, specifically DHASCO-S oil, incorporated into a fortified food, results in similar or somewhat enhanced amounts of DHA in blood as does supplementation with the encapsulated oil, indicating that DHASCO-S fortified foods are an appropriate vehicle for DHA supplementation. The observed trend toward enhanced bioavailability of DHA from food bars is consistent with previously reported greater bioavailability of LCPUFA from food rather than from capsules [56]. Those authors posited that the larger lipid bolus associated with food versus capsules activated lipid absorption. On the other hand, we conducted a clinical study demonstrating that the DHA in DHASCO-T oil capsules is equally bioavailable as the DHA in cooked salmon, a natural food source of this nutrient (Arterburn L manuscript submitted). Together, our results demonstrate that algal oil capsules, algal oil fortified foods or natural food sources of DHA are all equivalent sources of DHA with respect to raising blood levels of this nutrient. These sources all represent predominantly triglyceride forms of DHA. Others have found that DHA presented in capsules as an ethyl ester fish oil extract is not as bioavailable as DHA derived from fish, suggesting that triglycerides are the preferred DHA form with respect to bioavailability [56]. In this study, plasma PL levels of DHA increase at a rate of approximately 0.3 g per 100 g fatty acids for every 100 mg DHA administered over the daily dose range of 200–1,000 mg DHA. DHA accretion in plasma is highly inversely dependent on baseline DHA levels but is independent of age, weight, gender, or race.

The standard format for bioequivalence studies with pharmaceuticals is a pharmacokinetic crossover design following acute administration [57]. However, DHA washout times are on the order of weeks, so a crossover study is not appropriate [58]. Moreover, a more relevant measure for a nutrient such as DHA is to assess equilibrium plasma levels of DHA following subchronic rather than acute administration of the supplement, thus more closely mimicking a natural intake pattern. This type of assessment will not detect small differences in rate of uptake post-prandially, but rather assesses the more relevant measure of total accretion over time, which would reflect differences, if they exist, in the overall bioavailability, metabolism, and disposition of the DHA in the body. Plasma DHA levels are

known to equilibrate within approximately 2–3 weeks of daily supplementation [59]. Subjects in this study were supplemented for 4-week, ensuring measurement at an equilibrium state. The study therefore indicates that over time, these two algal oils result in equivalent plasma PL and erythrocyte equilibrium levels of DHA. Moreover, the study indicates that the DHA from DHASCO-T and DHASCO-S oils in plasma accumulates in and is distributed equivalently among the other plasma lipid subclasses, including sterol esters, triglycerides and unesterified fatty acid fractions, as well as in whole plasma. DHA as an unesterified fatty acid increased from 0.85 to 1.35  $\mu\text{mol L}^{-1}$  in whole plasma at the 600 mg DHA dose level. These concentrations may help determine physiologically relevant concentrations of DHA for designing and interpreting cell culture experiments.

The study included 2 weeks and 4-week assessments of blood DHA levels after supplementation, allowing assessment of the kinetics of uptake in blood. The results confirm earlier assessments that DHA levels in plasma PLs rapidly increase and reach new equilibrium levels after about 2 weeks of supplementation, irrespective of dose, and then remain at the new equilibrium level during the remaining course of supplementation [59]. Erythrocytes levels on the other hand continued to rise during the entire 4-week supplementation period, indicating that they had not yet reached an equilibrium status. Others have also reported slower equilibration of erythrocytes DHA levels in blood, which is not unexpected given their 120 days lifespan in the blood [59].

The DHA dose response was linear over the dose range studied. At higher doses of DHA, however, blood levels of this nutrient begin to saturate [59]. The range of doses used in this study (200–1,000 mg DHA per day, equivalent to approximately 3–14 mg  $\text{kg}^{-1}$  body weight per day for a 70-kg adult) encompasses doses to reflect levels in fortified foods, supplements and infant formulas. The high dose (1,000 mg DHA per day) is similar to DHA doses obtained by infants receiving fortified infant formulas in which DHA levels typically range between 0.1 and 0.35% of fat. This study therefore establishes bioequivalence of the DHASCO-T and DHASCO-S oils over a range of doses typical of intakes for infants and adults, and suggests that the oils may be interchangeable on a DHA basis for these applications.

The DHA contents of these two algal triglyceride oils are similar at ~40% of fatty acids. However, the overall fatty acid profiles of the DHASCO-S and DHASCO-T oils differ markedly. In particular, DHASCO-S contains a number of other long-chain PUFAs, including EPA at ~2.5% and DPAn-6 at ~15% of total fatty acids, whereas DHASCO-T oil has no appreciable amounts of any LC-PUFA other than DHA. It was unclear how other PUFA might affect the accretion of DHA from these oils. Both

DPAn-6 and DHA are 22-carbon PUFA that differ by one double bond at the omega-3 position, and it was possible that DPAn-6 may be accreted at the expense of DHA. However, this study clearly demonstrated that DPAn-6 had no effect on DHA accretion in either plasma or erythrocytes. Since plasma PLs are the primary carrier of lipids to tissues, tissue DHA levels are unlikely to be affected by the DPAn-6 present in the DHASCO-S oil either. Indeed, Lim et al. [60] have shown that co-administration of DPAn-6 with DHA does not interfere with DHA incorporation into brain tissue. To confirm this, a preclinical study to specifically address the question of whether accretion of DHA into multiple tissues is equivalent between both oils is being conducted in a piglet model.

An interesting and novel finding in this study is that while the oils were equivalent with respect to DHA bio-availability and accretion, they had markedly different effects on ARA levels. DHA supplementation, possibly through down regulation of  $\Delta 6$  desaturase and/or direct competition for acyl-CoA-mediated incorporation in phospholipids [61, 62], typically reduces ARA levels in plasma and tissues in a dose-dependent fashion, as was observed with the DHASCO-T supplementation in this study [59]. However, while the DHASCO-S oil at the low and mid-dose level resulted in the expected reduction in ARA levels, similar in magnitude to that observed with DHASCO-T oil, at the high dose it nearly maintained ARA levels in plasma, resulting in a curvilinear response on ARA levels in plasma. We hypothesize that the DPAn-6 contributes to maintaining ARA levels through a retro-conversion process of DPAn-6 to ARA, analogous to the DHA retroconversion to EPA [19, 59]. The curvilinear response represents a balance between the effect of DHA on reducing ARA levels, which predominates at the lower doses, and the DPAn-6 retroconversion to ARA, which predominates at the high dose, resulting in what appears to be a threshold effect of DPAn-6 occurring at the mid-dose level, which delivered 600 mg DHA + 240 mg DPAn-6. Since conducting this study, we have observed other ARA curvilinear responses of DHASCO-S oil in both animals and humans (L. Arterburn and A. Ryan, unpublished results).

The two algal oils also had differential effects on DPAn-6 plasma levels. As expected, DHASCO-T resulted in reduced levels of DPAn-6, whereas DHASCO-S resulted in elevated levels of DPAn-6 in plasma PLs. DPAn-6 levels increased at all doses of the DHASCO-S oil, but there was no apparent dose-response effect, suggesting that at higher doses of dietary DPAn-6, the fatty acid is converted to other fats, such as ARA, or simply  $\beta$ -oxidized for energy. Our study further indicated that the DHA accretion rate in whole plasma (approximately 8  $\mu\text{g}$  per 100 mg dietary DHA) was over twice the accretion rate of DPAn-6



(approximately 3  $\mu\text{g}$  per 100 mg DPAn-6) when the two fatty acids are administered in combination in the DHASCO-S oil. DPAn-6 accretion would be the net result of the DHA pressure to reduce this n-6 fatty acid and the tendency of the dietary DPAn-6 to accumulate as DPAn-6 or to be converted to other fatty acids, including ARA. The net result is that there is real but less pronounced accumulation of DPAn-6 following administration of DHASCO-S oil, whereas typically DHA oils significantly reduce the accumulation of DPAn-6.

The DHASCO-T and DHASCO-S oils had similar but small effects on EPA levels in plasma PLs, with a modest tendency to increase EPA levels, but not significantly so at the doses tested. The small increases in EPA levels are likely caused by the EPA present in the DHASCO-S, as well as retroconversion from DHA from the two oils.

Algal oils are produced in closed, tightly controlled fermentation facilities under Good Manufacturing Practices for foods, and unlike marine food sources, these oils are never in contact with oceanic contaminants. These oils, therefore, represent excellent and sustainable sources of bioavailable DHA.

## Conclusions

The algal oil sources of DHA, DHASCO-S, and DHASCO-T, provided in capsules or a fortified food, represent safe and equally bioavailable sources of DHA for humans. The DHASCO-S oil, at the highest dose is associated with maintenance of long-chain n-6 fatty acids in plasma, and therefore may be suitable for applications in which maintenance of ARA is beneficial.

**Acknowledgments** We would like to acknowledge Lynne Jones for technical assistance with the study and Matt Hudson for performing statistical analyses. L. Arterburn designed the study, analyzed data, and wrote the manuscript. J. Hoffman conducted the safety assessment and assisted with writing the manuscript. Eileen Bailey-Hall and G. Chung performed the fatty acid analyses. D. McCarthy monitored the conduct of the study. H. Oken was the principal investigator who oversaw the conduct of the study. J. Hamersley was the study coordinator who ran the study. D. Rom oversaw the statistical analyses of the data. Financial Disclosure: James P. Hoffman, Eileen Bailey-Hall, Gloria Chung, and Deanna McCarthy are employed by Martek Biosciences Corporation. Linda M. Arterburn was an employee of Martek Biosciences Corporation during the time this study was conducted and the manuscript was prepared. Harry Oken is currently a consultant to Martek Biosciences Corporation, but had no financial interest in the company at the time that the study was conducted. Dror Rom is a consulting statistician to Martek Biosciences Corporation.

## References

- McCann JC, Ames BN (2005) Is docosahexaenoic acid, an n-3 long-chain polyunsaturated fatty acid, required for development of normal brain function? An overview of evidence from cognitive and behavioral tests in humans and animals. *Am J Clin Nutr* 82(2):281–295
- Morale SE et al (2005) Duration of long-chain polyunsaturated fatty acids availability in the diet and visual acuity. *Early Hum Dev* 81(2):197–203
- Fleith M, Clandinin MT (2005) Dietary PUFA for preterm and term infants: review of Clinical Studies. *Crit Rev Food Sci Nutr* 45:205–229
- Brenna JT (2005) Meeting report: European consensus conference on recommendations for long chain polyunsaturated consumption for pregnant and lactating women (PERILIP). *ISSFAL Newslett* 12(3):4–6
- Helland IB et al (2003) Maternal supplementation with very-long-chain n-3 fatty acids during pregnancy and lactation augments children's IQ at 4 years of age. *Pediatrics* 111(1):e39–e44
- Holub DJ, Holub BJ (2004) Omega-3 fatty acids from fish oils and cardiovascular disease. *Mol Cell Biochem* 263(1–2):217–225
- Mori TA, Woodman RJ (2006) The independent effects of eicosapentaenoic acid and docosahexaenoic acid on cardiovascular risk factors in humans. *Curr Opin Clin Nutr Metab Care* 9(2):95–104
- Maclean CH et al (2005) Effects of omega-3 fatty acids on cognitive function with aging, dementia, and neurological diseases. *Evid Rep Technol Assess (Summ)* 114:1–3
- SanGiovanni JP, Chew EY (2005) The role of omega-3 long-chain polyunsaturated fatty acids in health and disease of the retina. *Prog Retin Eye Res* 24(1):87–138
- Ervin RB, Wright JD, Wang CY, Kennedy-Stephenson, J (2004) Dietary intake of fats and fatty acids for the United States population: 1999–2000. *Adv Data* 8(348):1–6 (Hyattsville, Maryland: National Center or Health Statistics): p. DHHS Publication No. (PHS) 2005-1250 04-0565
- Wang C, C.M., Lichtenstein A, Balk E, Kupelnick B, DeVine D, Lawrence A, Lau J (2004) Effects of Omega-3 Fatty Acids on Cardiovascular Disease. *Evid Rep Technol Assess No. 94* (Prepared by Tufts-New England Medical Center Evidence-based Practice Center, under Contract No. 290–02–0022). AHRQ Publication No. 04-E009-2. Rockville, MD: Agency for Healthcare Research and Quality
- Simopoulos AP, Leaf A, Salem N Jr (2000) Workshop statement on the essentiality of and recommended dietary intakes for omega-6 and omega-3 fatty acids. *Prostaglandins Leukot Essent Fatty Acids* 63(3):119–121
- Kris-Etherton PM, Harris WS, Appel LJ (2003) Omega-3 fatty acids and cardiovascular disease: new recommendations from the American Heart Association. *Arterioscler Thromb Vasc Biol* 23(2):151–152
- FDA (2001) An important message for pregnant women and women of childbearing age who may become pregnant about the risks of mercury in fish. Center for Food Safety and Applied Nutrition, Washington DC, p 3
- Environmental Protection Agency (2003) National advice on mercury in fish caught by family and friends: for women who are pregnant or may become pregnant, nursing mothers, and young children. EPA. p 3
- Agren JJ et al (1996) Fish diet, fish oil and docosahexaenoic acid rich oil lower fasting and postprandial plasma lipid levels. *Eur J Clin Nutr* 50(11):765–71
- Conquer JA et al (2000) Effect of DHA supplementation on DHA status and sperm motility in asthenozoospermic males [In Process Citation]. *Lipids* 35(2):149–54
- Conquer JA, Holub BJ (1998) Effect of supplementation with different doses of DHA on the levels of circulating DHA as non-esterified fatty acid in subjects of Asian Indian background. *J Lipid Res* 39(2):286–292

19. Conquer JA, Holub BJ (1997) Dietary docosahexaenoic acid as a source of eicosapentaenoic acid in vegetarians and omnivores. *Lipids* 32(3):341–345
20. Davidson MH et al (1997) Effects of docosahexaenoic acid on serum lipoproteins in patients with combined hyperlipidemia: a randomized, double-blind, placebo-controlled trial. *J Am Coll Nutr* 16(3):236–243
21. Nelson GJ et al (1997) The effect of dietary docosahexaenoic acid on plasma lipoproteins and tissue fatty acid composition in humans. *Lipids* 32(11):1137–1146
22. Innis SM, Hansen JW (1996) Plasma fatty acid responses, metabolic effects, and safety of microalgal and fungal oils rich in arachidonic and docosahexaenoic acids in healthy adults. *Am J Clin Nutr* 64(2):159–167
23. Makrides M, Neumann MA, Gibson RA (1996) Effect of maternal docosahexaenoic acid (DHA) supplementation on breast milk composition. *Eur J Clin Nutr* 50(6):352–357
24. Stark KD, Holub BJ (2004) Differential eicosapentaenoic acid elevations and altered cardiovascular disease risk factor responses after supplementation with docosahexaenoic acid in postmenopausal women receiving and not receiving hormone replacement therapy. *Am J Clin Nutr* 79(5):765–773
25. Marangell LB et al (2003) A double-blind, placebo-controlled study of the omega-3 fatty acid docosahexaenoic acid in the treatment of major depression. *Am J Psychiatry* 160(5):996–998
26. Lloyd-Still JD et al (2006) Bioavailability and safety of a high dose of docosahexaenoic acid triacylglycerol of algal origin in cystic fibrosis patients: a randomized, controlled study. *Nutrition* 22(1):36–46
27. Engler MM et al (2004) Docosahexaenoic acid restores endothelial function in children with hyperlipidemia: results from the EARLY study. *Int J Clin Pharmacol Ther* 42(12):672–679
28. Jensen CL et al (2005) Effects of maternal docosahexaenoic acid intake on visual function and neurodevelopment in breastfed term infants. *Am J Clin Nutr* 82(1):125–132
29. Voigt RG et al (2001) A randomized, double-blind, placebo-controlled trial of docosahexaenoic acid supplementation in children with attention-deficit/hyperactivity disorder. *J Pediatr* 139(2):189–196
30. Birch DG (2005) A randomized placebo-controlled clinical trial of docosahexaenoic acid (DHA) supplementation for X-linked retinitis pigmentosa. *Ret Degener Dis Exp Ther* 28S(8):S52–S54
31. Hoffman DR et al (2004) Maturation of visual acuity is accelerated in breast-fed term infants fed baby food containing DHA-enriched egg yolk. *J Nutr* 134(9):2307–2313
32. Hoffman DR et al (2004) Maturation of visual acuity is accelerated in breast-fed term infants fed baby food containing DHA-enriched egg yolk. *J Nutr* 134:2307–2313
33. Hoffman D et al (2003) Visual function in breast-fed term infants weaned to formula with or without long-chain polyunsaturates at 4 to 6 months: a randomized clinical trial. *J Pediatr* 142(6):669–677
34. Hoffman DR et al (2002) Post-weaning supply of docosahexaenoic acid (DHA) improves visual maturation in breast-fed term infants. *Exp Biol*
35. Clandinin MT et al (2005) Growth and development of preterm infants fed infant formulas containing docosahexaenoic acid and arachidonic acid. *J Pediatr* 146(4):461–468
36. Boswell K et al (1996) Preclinical evaluation of single-cell oils that are highly enriched with arachidonic acid and docosahexaenoic acid. *Food Chem Toxicol* 34(7):585–93
37. Arterburn LM et al (2000) A combined subchronic (90-day) toxicity and neurotoxicity study of a single-cell source of docosahexaenoic acid triglyceride (DHASCO oil). *Food Chem Toxicol* 38(1):35–49
38. Arterburn LM et al (2000) A developmental safety study in rats using DHA- and ARA-rich single cell oils. *Food Chem Toxicol* 38(9):763–771
39. Arterburn LM et al (2000) In vitro genotoxicity testing of ARASCO and DHASCO oils. *Food Chem Toxicol* 38:971–6
40. Wibert GJ et al (1997) Evaluation of single cell sources of docosahexaenoic acid and arachidonic acid: a 4-week oral safety study in rats. *Food Chem Toxicol* 35(10–11):967–974
41. Burns RA et al (1999) Evaluation of single-cell sources of docosahexaenoic acid and arachidonic acid: 3-month rat oral safety study with an in utero phase. *Food Chem Toxicol* 37(1):23–36
42. FDA (2001) Agency response letter GRAS notice No. GRN 000041, in US. Food and Drug Administration, Department of Health and Human Services. <http://www.cfsan.fda.gov/~rdb/opa-g041.html>
43. Van Elswyk ME (1997) Comparison of n-3 fatty acid sources in laying hen rations for improvement of whole egg nutritional quality: a review. *Br J Nutr* 78(1):S61–S69
44. Sanders TAB, Miller GJ (2002) Assessment of the safety of DHA GOLD oil, an algal source of docosahexaenoic acid in human subjects. Martek Internal Files
45. Sanders TA et al (2006) Influence of an algal triacylglycerol containing docosahexaenoic acid (22:6n-3) and docosapentaenoic acid (22:5n-6) on cardiovascular risk factors in healthy men and women. *Br J Nutr* 95(3):525–531
46. Maki KVE, M E, McCarthy D, Hess SP, Veith PE, Bell MV, Subbaiah PV, Davidson MH (2005) Lipid responses to a dietary docosahexaenoic acid supplement in men and women with low levels of high density lipoprotein cholesterol. *J Am Coll Nutr* 24(2005):189–199
47. Hammond BG et al (2001) Safety assessment of DHA-rich microalgae from *schizochytrium* sp. Part III. Single generation rat reproduction study. *Regul Toxicol Pharmacol* 33(3):356–362
48. Hammond BG et al (2001) Safety assessment of DHA-rich microalgae from *schizochytrium* sp. Part II. Developmental toxicity evaluation in rats and rabbits. *Regul Toxicol Pharmacol* 33(2):205–217
49. Hammond BG et al (2001) Safety assessment of DHA-rich microalgae from *schizochytrium* sp Part I. Subchronic rat feeding study. *Regul Toxicol Pharmacol* 33(2):192–204
50. Hammond BG et al (2002) Safety assessment of DHA-rich microalgae from *schizochytrium* sp. Part IV. Mutagenicity studies. *Regul Toxicol Pharmacol* 35(2 Pt 1):255–265
51. FDA, Agency response letter Gras Notification No. GRN000137, in US (2004) Food and Drug Administration, Department of Health and Human Services. <http://www.cfsan.fda.gov/~rdb/opa-g137.html>
52. Benisek D et al (2002) Validation of a simple food frequency questionnaire as an indicator of long chain omega-3 intake (abstr). Inform 2002. Abstracts of the 93rd Annual AOCs Meeting and Expo, Montreal, Quebec, Canada, p S96
53. Folch J, Lees M, Sloane Stanley G (1957) A simple method for the isolation and purification of total lipids from animal tissues. *J Biol Chem* 226(1):497–509
54. Bligh EG, Dyer WJ (1954) A rapid method of total lipid extraction and purification. *Can J Biochem Physiol* 37:911–917
55. FDA (1992) Guidance for industry: statistical procedures for bioequivalence studies using a standard two-treatment cross-over design. US Department of Health and Human Services, Drug Information Branch, Center for Drug Evaluation and Research
56. Visioli F et al (2003) Dietary intake of fish versus formulations leads to higher plasma concentrations of n-3 fatty acids. *Lipids* 38(4):415–418
57. FDA (2002) Guidance for industry: bioavailability and bioequivalence studies for orally administered drug products—

- general considerations. US Department of Health and Human Services, Center for Drug Evaluation and Research
58. Marangoni F et al (1993) Changes of n-3 and n-6 fatty acids in plasma and circulating cells of normal subjects, after prolonged administration of 20:5 (EPA) and 22:6 (DHA) ethyl esters and prolonged washout. *Biochim Biophys Acta* 1210(1):55–62
  59. Arterburn L, Hall EB, Oken H (2006) Distribution, interconversion, and dose response of n-3 fatty acids in humans 1–4. *Am J Clin Nutr* 83(6S):1467S–1476S
  60. Lim SY, Hoshiba J, Salem N Jr (2005) An extraordinary degree of structural specificity is required in neural phospholipids for optimal brain function: n-6 docosapentaenoic acid substitution for docosahexaenoic acid leads to a loss in spatial task performance. *J Neurochem* 10:1–10
  61. Gronn M et al (1992) Effects of dietary purified eicosapentaenoic acid (20:5(n-3)) and docosahexaenoic acid (22:6(n-3)) on fatty acid desaturation and oxidation in isolated rat liver cells. *Biochim Biophys Acta* 1125(1):35–43
  62. Vidgren HM et al (1997) Incorporation of n-3 fatty acids into plasma lipid fractions, and erythrocyte membranes and platelets during dietary supplementation with fish, fish oil, and docosahexaenoic acid-rich oil among healthy young men. *Lipids* 32(7):697–705

methods to reduce body fat within their breeding programs. Considerable research efforts have been expended to study the factors that are associated with fat deposition and the methods needed to reduce it, and several beneficial solutions to address this complex problem have been identified [3–5].

Dehydroepiandrosterone (DHEA, 3 $\beta$ -hydroxy-5-androsterone-17-one) is a steroidal compound that is secreted by the mammalian adrenal cortex gland [6, 7]. It is known to be associated with various physiological actions, including antiobesity, antidiabetic and anticarcinogenic effects, when administered to rats and mice [8]. Many reports [9, 10] have described its effect on lipid metabolism. It has been shown to decrease serum TG levels in hyperlipidemic rats, and it also affects the peroxisomal  $\beta$ -oxidation pathway directly in mice hepatocytes [10–12]. Even though some research has been conducted on the regulation of DHEA on lipid metabolism in rats and mice, there has been a paucity of data generated on the effects of DHEA on lipid metabolism in broiler chickens. Our previous study (unpublished results) demonstrated that DHEA decreased abdominal lipid deposition and increased the rate of lipid catabolism by regulating serum metabolic hormones and parameters in broiler chickens.

The liver is the primary site of fatty acid synthesis in poultry [4]. Most of the body's endogenous lipids are of hepatic origin [13]. The liver shows a marked total fat content change, and TG, HL, and NEFA are primarily involved in hepatic lipid metabolism procedures [14, 15]. Many studies have shown that, among the different lipid metabolic pathway steps that can give rise to variations in the relative degree of obesity, liver fatty acid metabolism has been evidenced as the main source of variability [16, 17]. These results have prompted a focus on gene expression in the liver, particularly those genes that are involved in fatty acid synthesis and secretion [18, 19], including SREBP-1c, ACC, PPAR $\alpha$ , CPTI and ACOX1. In contrast to the large number of studies on these liver metabolic parameters and lipogenic gene mRNA expression variances induced by DHEA in mice, rats and humans [20, 21], little is known about the effect of DHEA on hepatic lipid metabolism in poultry, and especially in broiler chickens.

Therefore, the aim of the current study was to elucidate the effects of DHEA on abdominal lipid deposition, hepatic lipid metabolism parameters, and lipogenic gene mRNA expression in broiler chickens

## Experimental Procedures

### Animals and Housing

Seventy-two commercial broiler chickens (1-day age, 38 g, Nanjing Jiachang commercial broiler chicken company)

were housed from day 1 to 42 and included starter (day 1–21) and finishing (day 21–42) phases. Starter phase broiler chickens were housed in lighted coops (24-h day), with constant temperature ( $20 \pm 3$  °C) and humidity ( $50 \pm 3\%$ ); finishing phase broilers were kept on the ground with natural lighting. Nutrient levels of the diets (Table 1) were based on NRC (1994) recommendations [22]. Animal care and use above was approved by the Institutional Animal Care and Use Committee of Nanjing Agricultural University.

### Treatment and Diets

All broiler chickens were randomly divided into three equal groups (24 per group), and each group was assigned

**Table 1** Ingredients and nutrient composition of diets

Ingredient (%)	Starter (0–21 days)	Finisher (21–42 days)
Corn	52.6	57.4
Soybean meal	31.1	27
Wheat bran	2.0	4
Fish meal <sup>a</sup>	6.0	3
Rapeseed oil <sup>b</sup>	5.0	5
NaCl	0.3	0.3
Calcium phosphate	1.0	1.5
Limestone	1.2	1.2
DL-Methionine	0.3	0.1
Vitamin-mineral premix <sup>c</sup>	0.5	0.5
Nutrition composition		
Calculated		
ME (Mcal/kg)	3.10	3.14
CP (%)	22.52	19.74
Lys (%)	1.19	1.08
Met + cysteine (%)	0.93	0.71
Ca (%)	1.00	0.90
Total P (%)	0.80	0.76
Available P (%)	0.47	0.39
Analyzed		
CP (%)	22.44	19.66
Ca (%)	1.03	0.94
Total P (%)	0.84	0.79

Nutrient level of the diets was based on NRC recommendations

<sup>a</sup> Crude protein content is 62.5% and ME is 2.79 Mcal/kg

<sup>b</sup> Metabolizable energy is 8.8 Mcal/kg

<sup>c</sup> Supplied per kilogram of diet: vitamin A (retinyl acetate) 1,500 IU, cholecalciferol 200 IU, vitamin E (DL- $\alpha$ -tocopheryl acetate) 10 IU, riboflavin 3.5 mg, pantothenic acid 10 mg, niacin 30 mg, cobalamin 10  $\mu$ g, choline chloride 1,000 mg, biotin 0.15 mg, folic acid 0.5 mg, thiamine 1.5 mg, pyridoxine 3.0 mg, Fe 80 mg, Zn 40 mg, Mn 60 mg, I 0.18 mg, Cu 8 mg, Se 0.15 mg

to 1 of 3 treatments. Birds in each group were kept in three pens (8 broilers each). All birds were offered a similar basal diet, with the addition of DHEA (Changzhou Jiaerke Pharmaceuticals Group Corp) at levels of 0 (control), 5 or 20 mg/kg. All birds had free access to feed and drinking water. Chickens were weighed individually at 42 days to determine final body weight. At the end of the experiment, food was withheld for 12 h before slaughter. After the birds were slaughtered, gender was identified, abdominal fat and liver were collected, blotted dry and weighed. The same part of the liver was cut into slices and rapidly frozen in liquid nitrogen, and stored at  $-80\text{ }^{\circ}\text{C}$  until RNA isolation. The liver blocks were isolated immediately for electron micrograph and the rest of them were stored at  $-40\text{ }^{\circ}\text{C}$  for the subsequent analysis of hepatic lipid parameters.

#### Determination of Hepatic Lipid Parameters Assay

A portion of the liver was homogenized, and the lipids were extracted with a mixture of chloroform-methanol (2:1 v/v) according to the method of Folch et al. [23]. TG content in the supernatant was determined by enzymatic/colorimetric GPO-PAP kit (Dongou, China) following the manufacturer's protocols. The optic density of the samples was measured using spectrophotometer in triplicate at a wavelength of 546 nm. Hepatic lipase (HL) and non-esterified fatty acid (NEFA) content was determined by using commercial kits from Nanjing Jianchen Biotechnology Institution. Approximately 100 mg of liver was homogenized on ice with 1 mL of physiological saline. An aliquot of these homogenates was used for protein determination according to the method described by Markwell et al. [24] and the remainder was centrifuged at  $1,000\times g$  for 10 min at  $4\text{ }^{\circ}\text{C}$ . Clear supernatants were used for the assay. HL and NEFA concentrations were directly proportional to the colour intensity and were determined by measurement of absorbance at 550 and 440 nm, respectively. One unit of HL enzyme activity represents 1 mg tissue protein releasing 1  $\mu\text{mol}$  of fatty acid per hour.

#### Electron Micrograph Preparations

Electron microscopy was conducted as described by Ikeda et al. [25]. Liver blocks were fixed in 2% glutaraldehyde in 0.1 M sodium phosphate (pH 7.4), post-fixed in 2%  $\text{OsO}_4$  in the same buffer, dehydrated and embedded in epoxy resin. Ultrathin sections were double stained with uranyl acetate followed by lead citrate and observed with a H-7650 transmission electron microscope (HITACHI Company, Japan).

#### Total RNA Isolation

Total RNAs were extracted from the liver by TRIZOL Reagent Kit (Sigma). The RNA concentration was then quantified by measuring the absorbance at 260 nm in a photometer (Eppendorf Biophotometer). Ratios of absorption (260/280 nm) of all preparations were between 1.8 and 2.0. Aliquots of RNA samples were subjected to electrophoresis through a 1.4% agarose-formaldehyde gel to verify their integrity. The RNA concentrations were adjusted to 1  $\mu\text{g}/\mu\text{l}$  by measuring the OD value, and stored at  $-80\text{ }^{\circ}\text{C}$ .

#### Oligonucleotide Primers Sequences

These primers were designed by premier 5.0 software (Premier Biosoft International, Palo Alto, CA, USA) and the positions are referred to chicken for SREBP-1c, ACC, PPAR $\alpha$ , CPTI, ACOX1 and 18s (Table 2). The primers synthesized by Shanghai Saibaisheng Biological Company were designed to flank known or putative introns, preventing amplification of any contaminating genomic DNA.

#### Semi-Quantitative RT-PCR

Two microgram of total RNA was reverse transcribed by incubation at  $37\text{ }^{\circ}\text{C}$  for 1 h in a 25  $\mu\text{l}$  mixture consisting of 100 U M-MLV reverse transcriptase (Promega, USA), 8 U RNase inhibitor (Promega, USA), 21  $\mu\text{mol/L}$  random primers (6 bp), 50 mmol/L Tris-HCl (pH 8.3), 3 mmol/L  $\text{MgCl}_2$ , 75 mmol/L KCl, 10 mmol/L DDT and 0.8 mmol/L each dNTP (Promega, USA). The reaction was terminated by heating at  $95\text{ }^{\circ}\text{C}$  for 5 min and quickly cooling on ice. Two microlitre of RT reaction mix was used for PCR in a final volume of 25  $\mu\text{l}$  containing 2.5  $\mu\text{l}$  of  $10\times$  PCR buffer, 2  $\mu\text{l}$  of each 2.5 mM dNTP mixture, 1 unit of Ex Taq DNA polymerase (Takara, Japan), 10 pmol of each forward and reverse primer. The condition of PCR amplification was as follows: one cycle at  $97\text{ }^{\circ}\text{C}$  for 5 min, 25–30 cycles at  $95\text{ }^{\circ}\text{C}$  for 30 s,  $50\text{--}60\text{ }^{\circ}\text{C}$  for 30 s and  $72\text{ }^{\circ}\text{C}$  for 1 min, and a final extension cycle at  $72\text{ }^{\circ}\text{C}$  for 10 min. The PCR products from each reaction were sent to Haojia Biotech, Ltd China for sequencing to verify the specificity. The reported sequences exactly matched those published in GenBank. PCR-amplified fragments were run beside molecular weight markers on 2% agarose gels stained with ethidium bromide. Gels were photographed with a digital camera and the net intensities of individual bands were measured using Kodak Digital Science 1D software (Eastman Kodak Company Rochester, NY, USA). The semi-quantitative measurement of gene expression was normalized to 18s.

**Table 2** Oligonucleotide PCR primers

Gene	Genbank accession number	Primers sequence (5'–3')	Orientation	Product size (bp)
18s	AF173612	CGGACATCTAAGGGCATCA	Forward	535
		AAGACGGACCAGAGCGAAA	reverse	
SREBP	AY029224	GAGGAAGGCCATCGAGTACA	Forward	392
		GGAAGACAAAGGCACAGAGG	reverse	
ACC	J03541	CACTTCGAGGCGAAAACTC	Forward	447
		GGAGCAAATCCATGACCACT	reverse	
PPAR $\alpha$	AF163809	TGGACGAATGCCAAGGTC	Forward	813
		GATTCCTGCAGTAAAGGGTG	reverse	
CPTI	AY675193	CAATGCGGTACTCCCTGAAA	Forward	337
		CATTATTGGTCCACGCCCTC	reverse	
ACOX1	NM001006205	TGCTGGTATTGAGGAATGTCG	Forward	387
		CTCAGATGCTCGACAAGGT	reverse	

### Statistical Analysis

The results were analyzed using GLM procedure of SAS software 9.0 (SAS Institute Inc., 2006). Independent variables included treatment, gender, and treatment  $\times$  gender interactions. Means and standard deviations were calculated and the mean differences were separated with the least significant difference procedure at the significance level of 95%.

## Results

### Body Weight and Liver Weight with Body Conversion Ratio

As shown in Table 3, body weight was significantly lower in female broiler chickens fed 5 and 20 mg DHEA/kg, and the same result was apparent in male broiler chickens fed 20 mg DHEA/kg, as compared to the control groups. During the experimental period, male broiler chickens fed 5 or 20 mg DHEA/kg and female broiler chickens fed 20 mg DHEA/kg had a significantly lower abdominal fat content when expressed as a percentage of body weight than did the control groups. In contrast, the relative liver weight was significantly higher than the control liver weight for both male and female broiler chickens.

### Hepatic Lipid Metabolic Parameters

The level of TG was significantly lower in female broiler chickens fed 5 or 20 mg DHEA/kg than those fed 0 (control), while in male broiler chickens, only those fed 20 mg DHEA/kg were lower. In contrast, male broiler chickens fed with 20 mg DHEA/kg resulted in a

pronounced higher level of HL as compared to the control group. However, no significant difference in HL was observed among female birds administered 0, 5, or 20 mg DHEA/kg. The concentration of NEFA was significantly higher in males and females at 20 mg DHEA/kg than at the control level (Table 4).

### Hepatic Lipid Metabolic Gene mRNA Expression

No significant differences were observed in both SREBP-1c (Fig. 1) and ACC (Fig. 2) mRNA expression in broiler livers treated with DHEA, except for a decline in the expression of ACC in females fed 5 mg DHEA/kg. As shown in Figs. 3 and 4, PPAR $\alpha$  and CPTI mRNA expression showed a trend toward enhancement as the treatment concentration of DHEA increased, in the absence of a gender difference, and the mRNA expression of both genes was higher in female as compared to male broilers. Similarly, this tendency toward increased mRNA expression was also indicated for ACOX1 gene (Fig. 5) in both male and female broilers. However, the peak expression of ACOX1 in male broilers was found at a treatment level of 5 mg DHEA/kg.

### Morphological Observations

The induction of hepatic peroxisome proliferation was examined by electron microscopy (Fig. 6). Normal broiler liver morphology (a limited number of peroxisomes with a visible core) is illustrated for male and female broiler chickens, respectively, in Fig. 6a, c (control groups). In contrast, numerous peroxisomes without a prominent core were evident in broilers fed 5 or 20 DHEA/kg (Fig. 6b, d,

**Table 3** Effect of DHEA on body weight gain, liver weight and abdominal fat weight

	DHEA (mg/kg), male broiler chickens			DHEA (mg/kg), female broiler chickens		
	0	5	20	0	5	20
SBWT (g)	2080.7 ± 58.3	1923.1 ± 53.3	1916.3 ± 54.6*	1900.8 ± 61.8	1679.2 ± 39.3*	1611.8 ± 54.7*
PDLI (%)	2.05 ± 0.04	2.32 ± 0.05*	2.39 ± 0.07*	2.06 ± 0.09	2.27 ± 0.10	2.47 ± 0.05*
PDAT (%)	1.63 ± 0.13	1.38 ± 0.58*	1.34 ± 0.06*	1.94 ± 0.10	1.80 ± 0.13	1.54 ± 0.07*

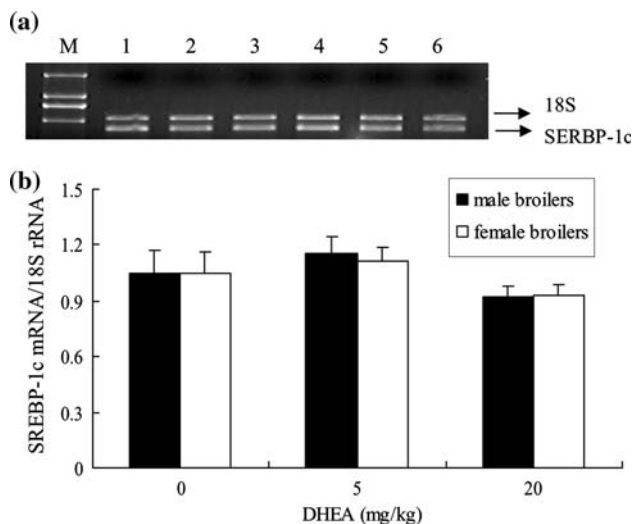
Values are means ± SEM. Each DHEA treated group represent 12 chickens at the age of 42 days

SBWT weight just prior to slaughter, PDLI liver weight/SBWT, PDAT abdominal fat weight/SBWT, \*  $P < 0.05$ , compared with the value of 0 mg of DHEA/kg group

**Table 4** Effect of dehydroepiandrosterone (DHEA) on liver homogenates concentrations of triglycerides (TG), hepatic lipase (HL), non-esterified fatty acid (NEFA)

	DHEA (mg/kg), male broiler chickens			DHEA (mg/kg), female broiler chickens		
	0	5	20	0	5	20
TG (mmol/g liver)	3.01 ± 0.21	2.73 ± 0.08	2.37 ± 0.18*	3.13 ± 0.21	2.54 ± 0.14*	2.62 ± 0.12*
HL (U/mg prot)	0.31 ± 0.01	0.29 ± 0.03	0.41 ± 0.05*	0.47 ± 0.04	0.41 ± 0.06	0.44 ± 0.05
NEFA (μmol/g prot)	81.57 ± 12.78	126.31 ± 16.82	147.30 ± 15.48*	106.28 ± 11.08	121.85 ± 14.74	168.32 ± 23.30*

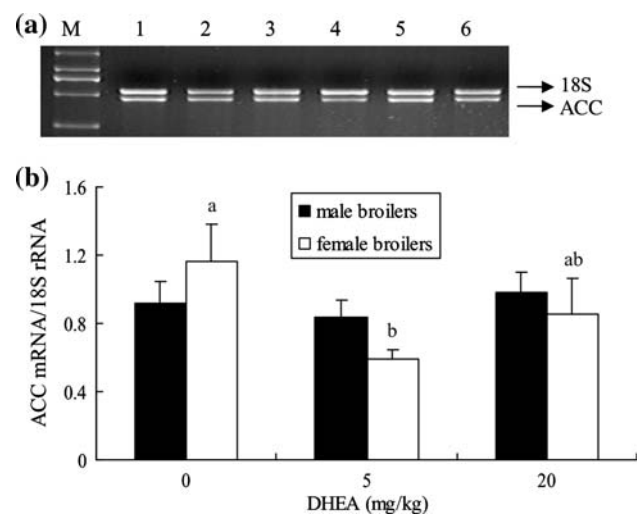
Values are mean ± SEM. Each DHEA treated group represent 12 chickens at the age of 42 days. \*  $P < 0.05$ , compared with the value of 0 mg of DHEA/kg group

**Fig. 1** Effect of DHEA on SREBP-1c mRNA expression in broiler livers

respectively). The increase in the number of peroxisomes was the same in male and female birds.

## Discussion

The present study reports the effect of 5 and 20 mg/kg DHEA on body weight, abdominal fat weight, and the

**Fig. 2** Effect of DHEA on ACC mRNA expression in broiler livers

relative weight of livers in poultry. The results demonstrated that broiler chickens fed a DHEA-containing diet for 42 days had reduced body weight and abdominal fat weight as compared to a non-DHEA control group, regardless of gender difference. In contrast, liver weight as a percentage of body weight was significantly increased in these same birds treated with DHEA. The above results are in agreement with the results of Gansler et al [26], who reported that DHEA given chronically to lean or obese Zucker rats resulted in decreased body weight. The results

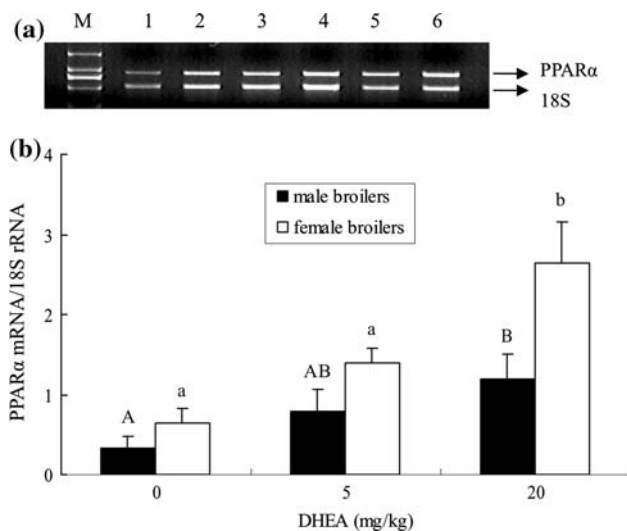


**Fig. 3** Effect of DHEA on PPAR $\alpha$  mRNA expression in broiler livers

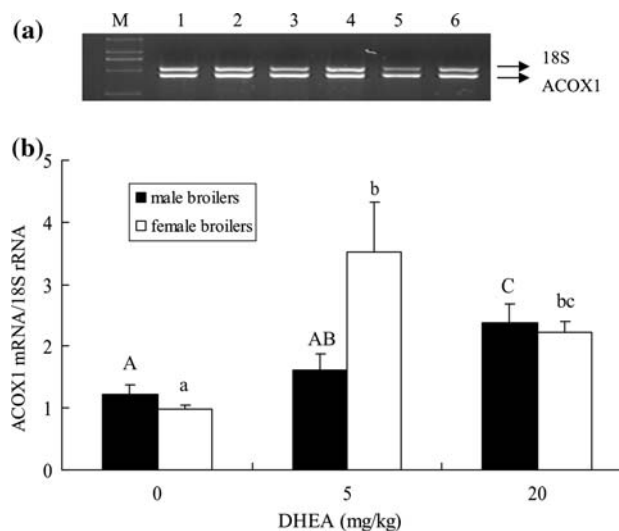


**Fig. 5** Effect of DHEA on ACOXI mRNA expression in broiler livers

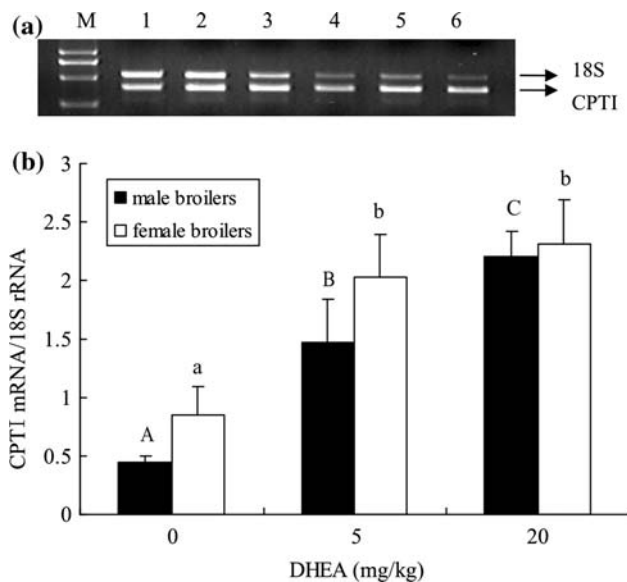


**Fig. 4** Effect of DHEA on CPTI mRNA expression in broiler livers

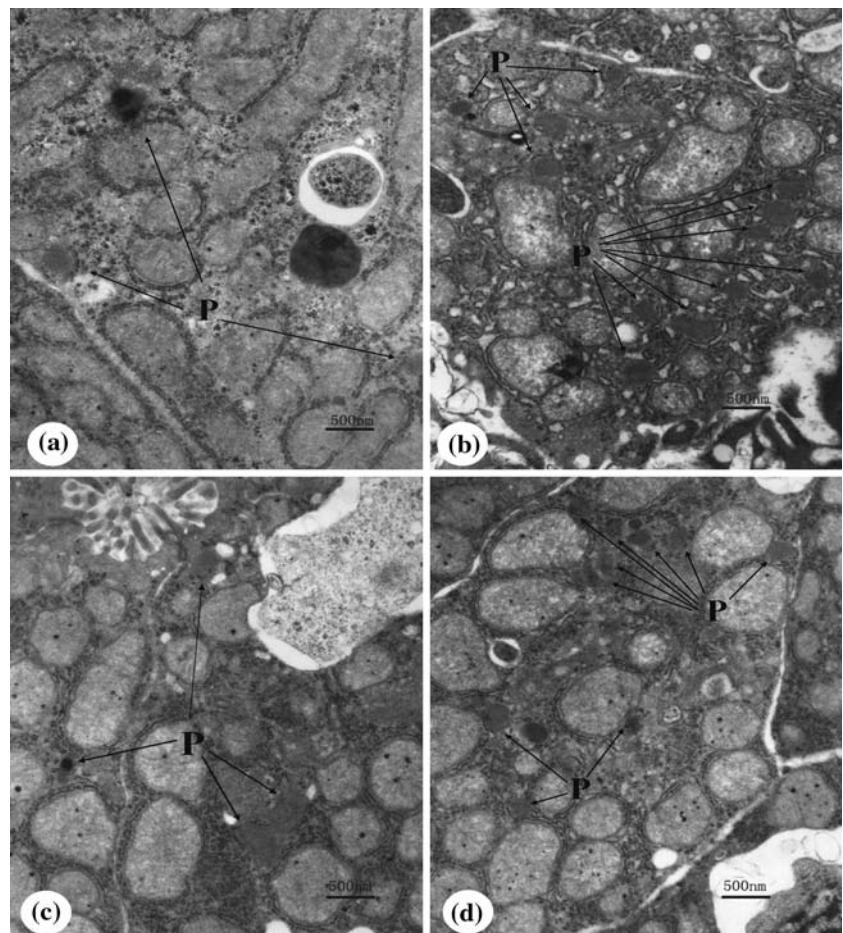
obtained here are also similar to a report [9], which showed that relative liver weight was enhanced in growing rats fed with DHEA. According to recent research [8], it is possible that DHEA activates hepatic mitochondria through the action of liver proteins, which enhance RNA transcription and subsequent protein synthesis, resulting in a higher relative liver weight than is evident in control-fed birds. However, the results of this study are in disagreement with those of Bobyleva et al. [27], which showed that DHEA did not significantly decrease body and liver weight in chickens. This discrepancy may be explained by the different breed and age of chickens used in the two studies. Furthermore, other results from our laboratory (unpublished data) have shown that supplementation of DHEA decreases

body weight and weight gain without having any adverse effect on feed intake. All chickens fed DHEA exhibited decreased abdominal fat weight with only a slight difference in breast and leg muscle weight, in accordance with previous studies that have found that DHEA administration reduces abdominal fat accumulation in both rats [28] and elderly women and men [29]. It is important to note that DHEA may decrease overall abdominal fat content without influencing feed intake or carcass composition.

The liver is the primary site of fatty acid synthesis in poultry [4]. Previous studies [30] have demonstrated that DHEA can induce a classic peroxisome proliferator-activated response via a procedure involving characteristic variances in hepatic peroxisome morphology and activation of gene transcription involving several PPAR $\alpha$  target genes, such as LPL, ACS and ACO [20]. Our morphological observations of hepatic peroxisomes illustrate that the liver from broilers fed with 5 or 20 mg DHEA/kg have some proliferation of hepatic peroxisomes without core and an increased number of peroxisomes, both in male and female birds. These findings were in accordance with previous reports [9] that state that rats treated with DHEA demonstrate a characteristic peroxisome multiplication. It is reasonable to suggest that DHEA, as a typical peroxisome proliferator, elicits all of these characteristic responses in broiler chickens. In the present study, supplementation of 5 or 20 mg DHEA/kg in male and female broilers improved the liver NEFA level. In contrast, the liver TG level declined in both male and female broilers. From the above findings, it is reasonable to speculate that DHEA directly stimulated the  $\beta$ -oxidation pathway in hepatocytes, catalyzed the conversion of TG to glycerol and fatty acids, and increased the hepatic uptake of the released



**Fig. 6** Electron micrographs of the liver peroxisome proliferation induced by DHEA from broilers. Ultrathin sections observed with magnification  $\times 10,000$ . **a, c** male and female control, **b, d** male and female DHEA-treated. *P* denote peroxisomes



NEFF [14, 15]. Another possible mechanism of action is that the dramatic activation of peroxisomal  $\beta$ -oxidation, which is associated with a more moderate induction of mitochondrial  $\beta$ -oxidation, results in less acyl-CoA esters being available to be utilized for triglyceride synthesis in birds treated with DHEA, leading to a decreased concentration of liver TG [20]. In addition to the above liver lipid metabolic parameters, HL is another important lipid metabolic enzyme produced primarily by the liver [31]. This study demonstrated a pronounced increase in HL activity after administration of 20 mg DHEA/kg in male broilers. In association with the increased HL activity, there were decreases in HDL-C in our previous study (results unpublished), consistent with the function of HL activity to catalyze the hydrolysis of triacylglycerols and phospholipids, mediate the removal of lipoproteins from plasma, and result in decreased lipid synthesis [31, 32].

As shown in Fig. 3, DHEA treatment caused a significant up-regulation of PPAR $\alpha$  expression in broilers liver tissue, which is in keeping with a recent study in Wistar rats [20], where significantly increased expression of PPAR $\alpha$  in liver tissue was observed. Together with the decreased abdominal fat effect caused by DHEA, one

possible explanation for this is that DHEA improved the activity of peroxisome proliferators activated receptor  $\alpha$  (PPAR $\alpha$ ). Activation of PPAR $\alpha$  induces transcriptional up-regulation of fatty acid transport proteins that facilitate fatty acid entry into cells and the enzymes involved in the  $\beta$ -oxidation of fatty acids, resulting in decreased expression of fatty acid synthesis [20]. Furthermore, although no obvious variance difference in SREBP-1c expression was found across treatments, a down-regulation tendency in gene expression was indicated for broilers treated with 20 mg DHEA/kg. A recent study [33] demonstrated that SREBP-1c activity and lipid synthesis in the liver was controlled by PPAR $\alpha$  through an increase in stearoyl-CoA desaturase activity. Our result, demonstrating enhanced SREBP-1c expression, in some way, was in agreement with that conclusion [33]. Moreover, different studies have shown that SREBP-1c can directly stimulate the transcription of genes encoding ACC [34, 35], making it a good candidate as a common regulator of the lipogenic genes expressed in the fat chicken lines. However, no significant variance in ACC expression was observed in the male broilers. Therefore, the non-significance of the expression analysis results for the SREBP-1c and ACC

genes indicates that neither of these two genes was directly responsible for the effect of DHEA on lipid synthesis at the DNA level. However, a weak expression of ACC was found in female broilers fed 5 mg DHEA/kg, which may have been the result of a combined effect of estrogen and DHEA. However, elucidation of the precise mechanism involved in the modification of ACC needs further investigation.

Similarly to the results for PPAR $\alpha$ , an increased tendency toward mRNA expression was also indicated for the ACOX1 gene in both male and female broilers, which is the first-step enzyme in peroxisomal  $\beta$ -oxidation [36]. Although its peak expression in females was shown at the treatment level of 5 mg DHEA/kg, the results are in accordance with a study conducted with turkeys, whereby the ACOX1 mRNA was highly expressed in the abdominal fat pad and in the liver [37], suggesting a strong peroxisomal FA  $\beta$ -oxidation capacity. The ACOX1 enzyme is the rate-limiting enzyme for peroxisomal FA  $\beta$ -oxidation. Its expression is regulated by PPAR $\alpha$  [38]. In the current study, it was demonstrated that a higher expression of ACOX1 was evident at a higher concentration of PPAR $\alpha$ , which verified the early reports that PPAR $\alpha$  increased the expression of ACOX1 in poultry livers [39, 40]. Our observation in broilers is similar to that seen in turkeys [37], mice [41], and humans [42], indicating that a considerable capacity for peroxisomal FA  $\beta$ -oxidation in liver is available in broiler chickens treated with DHEA.

Another interesting observation in this study was that the expression of CPTI was increased by DHEA, and that this was accompanied by an increased expression of PPAR $\alpha$ . CPTI catalyzes the formation of long-chain acyl-carnitine from activated fatty acids and free carnitine, thus committing fatty acids to oxidation [37]. By virtue of its inhibition by malonyl-coenzyme (CoA), CPTI controls the rate of  $\beta$ -oxidation and regulates the deposition or oxidation of fatty acids [43]. An increase in DHEA resulted in increased PPAR $\alpha$  expression in liver, which increased the rate of  $\beta$ -oxidation in liver cells and decelerated the transportation of acetyl-CoA from the mitochondria to the cytosol [44]. The rate of synthesis of malonyl-CoA decreases with a decline in the concentration of cytosolic acetyl-CoA [45]. By virtue of the decreased cellular synthesis of malonyl-CoA, the activity of CPTI in liver increases [46] and results in a higher rate of  $\beta$ -oxidation of fatty acids [47, 48], thus decreasing the abdominal fat content.

In conclusion, the present study confirms that the administration of DHEA in poultry accelerates liver catabolic processes through the regulation of the hepatic lipid metabolic pathways and the expression of the relevant genes involved.

**Acknowledgments** This work was supported by the National Natural Science Foundation of China (NO.30600439) and the National Key Basic Research Development Program of China, 973 Program (NO. 2004CB117505). We are also grateful to Dr. Dongmin Liu Assistant Professor, Human Nutrition, Food and Exercise, Virginia Polytechnic Institute and State University, Blacksburg, VA and Dr. William W. Riley, Research Director in Feed and Grow International CO, Ltd., for their critical reading of the manuscript.

## References

- Mallard J, Douaire M (1988) Strategies of selection for leanness in meat production. In: Leanness in domestic birds: genetic, metabolic and hormonal aspects, Butterworth-Heinemann, Oxford
- Wu GQ, Deng XM, Li JY, Li JY, Yang N (2006) A potential molecular marker for selection against abdominal fatness in chickens. *Poult Sci* 85:1896–1899
- Wang Q, Li H, Li N, Leng L, Wang Y, Tang Z (2006) Identification of single nucleotide polymorphism of adipocyte fatty acid-binding protein gene and its association with fatness traits in the chicken. *Poult Sci* 85:429–434
- Xu ZR, Wang MQ, Mao HX, Zhan XA, Hu CH (2003) Effects of L-carnitine on growth performance, carcass composition, and metabolism of lipids in male broilers. *Poult Sci* 82:408–413
- Szabo A, Febel H, Mezes M, Horn P, Balogh K, Romvari R (2005) Differential utilization of hepatic and myocardial fatty acids during forced molt of laying hens. *Poult Sci* 84:106–112
- Orentreich N, Brind JL, Vogelmann JH, Andres R, Baldwin H (1992) Long-term longitudinal measurements of plasma dehydroepiandrosterone sulfate in normal men. *J Clin Endocrinol Metab* 75:1002–1004
- Parker CR (1999) Dehydroepiandrosterone and dehydroepiandrosterone sulfate production in the human adrenal during development and aging. *Steroids* 64:640–647
- Arlt W (2004) Dehydroepiandrosterone replacement therapy. *J Semin Reprod Med* 22:379–388
- Yamada J, Sakuma M, Ikeda T, Fukuda K, Suga T (1991) Characteristics of dehydroepiandrosterone as a peroxisome proliferators. *Biochim Biophys Acta* 1092:233–243
- Sakuma M, Yamada J, Suga T (1993) Induction of peroxisomal  $\beta$ -oxidation by structural analogues of dehydroepiandrosterone in cultured rat hepatocytes: structure–activity relationships. *Biochim Biophys Acta* 1169:66–72
- Suga T, Tamura H, Watanabe T, Yamada J (1996) Induction of peroxisomal enzymes by dehydroepiandrosterone metabolic activation by sulfate conjugation. *N Y Acad Sci* 804:284–296
- Waxman DJ (1996) Role of metabolism in the activation of dehydroepiandrosterone as a peroxisome proliferator. *J Endocrinol* 150:129–147
- O’Hea EK, Leveille GA (1969) Lipogenesis in isolated adipose tissue of domestic chick (*Gallus domesticus*). *Comp Biochem Physiol* 26:111–120
- Frenkel B, Mayorek N, Hertz R, Bar-Tana J (1988) The hypochylomicronemic effect of beta, beta’-methyl-substituted hexadecanedioic acid (MEDICA 16) is mediated by a decrease in apolipoprotein C-III. *J Biol Chem* 263:8491–8497
- Frenkel B, Bisbara-Shieban J, Bar-Tana J (1994) The effect of beta, beta-tetramethylhexadecanedioic acid (MEDICA 16) on plasma very-low-density lipoprotein metabolism in rats: role of apolipoprotein C-III. *Biochem J* 298:409–414
- Leclercq B, Hermier D, Guy G (1990) Metabolism of very low density lipoproteins in genetically lean or fat lines of chicken. *Reprod Nutr Dev* 30:701–715

17. Legrand P, Hermier D (1992) Hepatic delta 9 desaturation and plasma VLDL level in genetically lean and fat chickens. *Int J Obes Relat Metab Disord* 16:289–294
18. Douaire M, Le Fur N, el Khadir-Mounier C, Langlois P, Flamant F, Mallard J (1992) Identifying genes involved in fatness genetic variability in the growing chicken. *Poultry Sci* 71:1911–1920
19. Daval S, Lagarrigue S, Douaire M (2000) Messenger RNA levels and transcription rates of hepatic lipogenesis genes in genetically lean and fat chickens. *Genet Sel Evol* 32:521–531
20. Schoonjans K, Staels B, Auwerx J (1996) Role of the peroxisome proliferator-activated receptor (PPAR) in mediating the effects of fibrates and fatty acids on gene expression. *J Lipid Res* 37:907–925
21. Kochan Z, Karbowska J (2004) Dehydroepiandrosterone upregulates resistin gene expression in white adipose tissue. *Mol Cell Endocrinol* 218:57–64
22. Yang CM, Chen AG, Hong QH, Liu JX, Liu JS (2006) Effects of cysteamine on growth performance, digestive enzyme activities, and metabolic hormones in broilers. *Poult Sci* 85:1912–1916
23. Folch J, Lee M, Slane-Stanley GH (1957) A simple method for the isolation and purification of total lipids from animal tissues. *J Biol Chem* 226:497–509
24. Markwell MAK, Haas SM, Bieber LL, Tolbert NE (1978) A modification of the Lowry procedure to simplify protein determination in membrane and lipoprotein samples. *Anal Biochem* 87:206–210
25. Ikeda T, Ida-Enomoto M, Mori I, Fukuda K, Iwabuchi H, Komai T, Suga T (1988) Induction of peroxisome proliferation in rat liver by dietary treatment with 2,2,4,4,6,8,8-heptamethylnonane. *Xenobiotica* 18:1271–1280
26. Gansler TS, Muller S, Cleary MP (1985) Chronic administration of dehydroepiandrosterone reduces pancreatic  $\beta$ -cell hyperplasia and hyperinsulinemia in genetically obese Zucker rats. *Proc Soc Exp Biol Med* 180:155–162
27. Bobyleva V, Kneer N, Bellei M, Battelli D, Muscatello U, Lardy H (1993) Comparative studies of effects of dehydroepiandrosterone on rat and chicken liver. *Comp Biochem Physiol B* 105:643–647
28. Cleary MP, Zisk JF (1986) Anti-obesity effect of two different levels of dehydroepiandrosterone in lean and obese middle-aged female Zucker rats. *Int J Obes* 10:193–204
29. Villareal DT, Holloszy JO (2004) Effect of DHEA on abdominal fat and insulin action in elderly women and men: a randomized controlled trial. *JAMA* 292:2243–2248
30. Prough RA, Webb SJ, Wu HQ, Lapenson DP, Waxman DJ (1994) Induction of microsomal and peroxisomal enzymes by dehydroepiandrosterone and its reduced metabolite in rat. *Cancer Res* 54:2878–2886
31. Kinnunen PKJ, Virtanen JA, Vainio P (1983) Lipoprotein lipase and hepatic endothelial lipase: their roles in plasma lipoprotein metabolism. *Atheroscler Rev* 11:65–105
32. Herbst KL, Amory JK, Brunzell JD, Chansky HA, Bremner WJ (2003) Testosterone administration to men increases hepatic lipase activity and decreases HDL and LDL size in 3 wk. *Am J Physiol Endocrinol Metab* 284:E1112–E1118
33. Knight BL, Hebbachi A, Huaton D, Brown AM, Wiggins D, Patel DD, Gibbons GF (2005) A role for PPAR $\alpha$  in the control of SREBP activity and lipid synthesis in the liver. *Biochem J* 389:413–421
34. Yin L, Zhang Y, Hillgartner FB (2002) Sterol regulatory element-binding protein-1 interacts with the nuclear thyroid hormone receptor to enhance acetyl-CoA carboxylase- $\alpha$  transcription in hepatocytes. *J Biol Chem* 277:19554–19565
35. Zhang Y, Yin L, Hillgartner FB (2003) SREBP-1 integrates the actions of thyroid hormone, insulin, cAMP, and medium chain fatty acids on ACC $\alpha$  transcription in hepatocytes. *J Lipid Res* 44:356–368
36. Ishii H, Ishii S, Suga T, Kazama M (1985) Developmental changes in the activities of peroxisomal and mitochondrial  $\beta$ -oxidation in chicken liver. *Arch Biochem Biophys* 237:151–159
37. Ding ST, Li YC, Nestor KE, Velleman SG, Mersmann HJ (2003) Expression of turkey transcription factors and acyl-coenzyme oxidase in different tissues and genetic populations. *Poult Sci* 82:17–24
38. Bell AR, Savory R, Horley NJ, Choudhury AI, Dickins M, Gray TJ, Salter AM, Bell DR (1998) Molecular basis of non-responsiveness to peroxisome proliferators: the guinea-pig PPAR $\alpha$  is functional and mediates peroxisome proliferator-induced hypolipidaemia. *Biochem J* 332:689–693
39. Dreyer C, Krey G, Keeler H, Givel F, Helftenbein G, Wahli W (1992) Control of the peroxisomal beta-oxidation pathway by a novel family of nuclear hormone receptors. *Cell* 68:879–887
40. Zhang B, Marcus SL, Sajjadi FG, Alvares K, Reddy JK (1992) Identification of a peroxisome proliferator-responsive element upstream of the gene encoding rat peroxisomal enoyl-CoA hydratase/3-hydroxyacyl-CoA dehydrogenase. *Proc Natl Acad Sci* 89:7541–7545
41. Issemann I, Green S (1990) Activation of a member of the steroid hormone receptor superfamily by peroxisome proliferators. *Nature* 347:645–650
42. Schmidt A, Endo N, Rutledge SJ, Vogel R, Shinar D, Rodan GA (1992) Identification of a new member of the steroid hormone receptor superfamily that is activated by a peroxisome proliferator and fatty acids. *Mol Endocrinol* 6:1634–1641
43. Zammit VA (1999) Carnitine acyltransferases: functional significance of subcellular distribution and membrane topology. *Prog Lipid Res* 38:199–224
44. Schoonjans K, Staels B, Auwerx J (1996) The peroxisome proliferator activated receptors (PPARs) and their effects on lipid metabolism and adipocyte differentiation. *Biochim Biophys Acta* 1302:93–109
45. Dyck JR, Barr AJ, Barr RL, Kolattukudy PE, Lopaschuk GD (1998) Characterization of cardiac malonyl-CoA decarboxylase and its putative role in regulating fatty acid oxidation. *Am J Physiol* 275:2122–2129
46. Velasco G, Gomez del Pulgar T, Carling D, Guzman M (1998) Evidence that the AMP-activated protein kinase stimulates rat liver carnitine palmitoyltransferase I by phosphorylating cytoskeletal components. *FEBS Lett* 439:317–320
47. Winder WW, Hardie DG (1996) Inactivation of acetyl-CoA carboxylase and activation of AMP-activated protein kinase in muscle during exercise. *Am J Physiol* 270:E299–E304
48. Velasco G, Geelen MJ, Guzman M (1997) Control of hepatic fatty acid oxidation by 5 P-AMP-activated protein kinase involves a malonyl-CoA-dependent and a malonyl CoA-independent mechanism. *Arch Biochem Biophys* 337:169–175

physiological processes in these animals therefore changes in the lipid composition reflect changes in the ecology, nutrition, and health of corals. For example, coral bleaching is accompanied by significant variations in total lipid content and proportions of the main lipid classes in coral colonies [5–7]. The composition of lipids depends both on the currently prevailing food source of corals and the light regimes [8, 9] and varies during the annual cycle [10]. Also the lipid content of tumorous coral tissue is characterized by a reduced level of stored lipids [11].

The composition of fatty acids (FAs) is the primary common characteristic of lipids; therefore important aspects of coral life, with lipids involved, can be investigated by the analysis of coral FAs. FAs can serve as markers for a type of symbiotic zooxanthellae [12]; and they indicate the lipid exchange between symbionts and their coral host [13]. FA is most probably indicative of external food sources such as zoo- and phytoplankton in polytrophic feeding of corals [14].

FAs have been used for the biochemical classification of several groups of marine biota, such as bacteria, fungi, microalgae, plankton, macrophytic algae, and sea grasses [15–18]. Some combinations of FAs were supposed to be the distinguishing features of several taxonomic groups of reef-building corals [19, 20]; however, some investigators are inclined to conclude that FAs are not really useful for the biochemical classification of these cnidarians [3, 19]. On the one hand, this negative conclusion was due to a close resemblance of FA qualitative profiles of different coral species and the perceptible intraspecific variations of some FA contents exceeding the interspecific variations [21], on the other hand, a shortage of comparable FA data on numerous allied coral species was an obstacle to the fruitful advance of chemotaxonomy of corals. Recently, a principal components analysis (PCA) of FA composition was successfully applied to the chemotaxonomy of 32 soft coral species, and a clear division of soft coral specimens according to their orders (Gorgonacea, Alcyonacea, Antipatharia) was consequently attained [22]. Therefore, the application of PCA (or similar statistical methods) for the FA composition of sufficiently large species groups can be useful for the chemotaxonomic studies of another vast coral group—that of reef-building corals.

Studies of lipids in reef-building corals have not so far been systematic and data on FA contents of total lipids of the corals is limited [2, 3, 20, 23]. In the current study we both determined and compared the FA composition of 16 species of reef-building corals from Vietnam. We then supplemented this new data with the results of our earlier research on the subject [20] and sought to determine from this: (1) what taxonomic groups of reef-building corals can be distinguished through the use of FA data statistical processing; (2) what FAs are essential for this process; and

(3) what are the possible reasons of the differences in FA composition of the distinguished coral groups.

## Experimental Procedures

Sixteen species of scleractinian corals were collected by SCUBA divers in the South China Sea (Vietnam), firstly in the Nha Trang Bay in March–June 2004 at 2–4 m depths and, secondly, by the Mun Island (8°45'N, 106°38'E) in May 2005 at 1.5–2 m depths. The colonies were carefully cleaned of all non-coral debris. Three different colonies were used for a FA analysis. The corals were identified by the use of the taxonomic scheme of Wells [24].

The corals collected were placed into tanks under water at the site of collection and transported to the laboratory within half an hour. The coral samples were crushed into 1–3 mm pieces and total lipids were extracted by intensive homogenization in a chloroform/methanol (1:2, by vol.) mixture (30 ml for 10 g of coral weight). The obtained homogenate was filtered and the residue was repeatedly extracted (6 h, 4 °C) in a chloroform/methanol (2:1, by vol.) mixture (2 × 30 ml). The extracts were then mixed and separated into layers by adding 35 ml of water and 30 ml of chloroform. The lower layer was evaporated and the total lipids obtained were redissolved in chloroform and stored at –18 °C.

Fatty acid methyl esters (FAMES) were obtained by a sequential treatment of the total lipids with 1% sodium methylate/methanol and 5% HCl/methanol according to Carreau and Dubacq [25] and purified by preparative silica gel thin-layer chromatography (TLC) using the precoated silica gel plates Sorbfil PTLC-AF-V (Sorbfil, Krasnodar, Russia) developed in benzene. *N*-acylpyrrolidide derivatives of FAs were prepared according to Andersson [26] by direct treatment of the FAMES with pyrrolidine/acetic acid (10:1, by vol.) in a capped vial (1 h, 100 °C) followed by ethereal extraction from the acidified solution and purification by preparative TLC developed in ethyl acetate.

A gas chromatography (GC) analysis of FAMES was carried out on a Shimadzu GC-17A chromatograph (Shimadzu, Kyoto, Japan) with a flame ionization detector on a SUPELCOWAX 10 (Supelco, Bellefonte, PA) capillary column (bonded polyethylene glycol 20 M; 30 m × 0.25 mm i.d.) at 210 °C. Helium was used as the carrier gas at a linear velocity 30 cm/s (split ratio was 1:30). FAMES were identified by a comparison with authentic standards (a mixture of PUFA methyl esters No. 3 from menhaden oil was purchased from Supelco, Bellefonte, PA) and with the use of a table of equivalent chain-lengths (ECL) [27]. The structures of FAs were confirmed by gas chromatography–mass spectrometry (GC–MS) of their methyl esters and *N*-acylpyrrolidide derivatives. GC–MS of

FAMES was performed with a Shimadzu GCMS-QP5050A instrument (Shimadzu, Kyoto, Japan). The ionization of samples was undertaken by electron impact at 70 eV. Helium was used as the carrier gas at a linear velocity 30 cm/s (split ratio was 1:10) A Supelco MDN-5S (Bellefonte, PA) capillary column (bonded and crosslinked (5% phenyl)methylpolysiloxane; 30 m × 0.25 mm i.d.) was used at 160 °C with a 2 °C/min ramp to 240 °C held for 20 min. The injector and detector temperatures were 250 °C. GC–MS of *N*-acylpyrrolidides was performed on the same instrument, the injector and detector temperatures being 300 °C and 270 °C, respectively, the column temperature was 210 °C with a 3 °C/min ramp to 270 °C that was held for 40 min. GCSolution and GCMSSolution software (Shimadzu, Kyoto, Japan) were used for GC and GC–MS analysis. The percentage compositions of FAs were estimated by use of the GCSolution program, which integrated the GC chromatogram. All the data were the mean values of the results of the analyses of the FA composition of the three different colonies.

All variables (square root of ten PUFA contents) measured for the 35 specimens studied were included in multidimensional scale analyses (two dimensions used). The analyses were performed using the software STATISTICA 5.1 (StatSoft, Inc., USA).

## Results

Tables 1, 2, 3 show the data on distribution of fatty acids (FAs) in total lipids of 16 scleractinian species belonging to six families (Acroporidae, Pocilloporidae, Poritidae, Faviidae, Pectiniidae, and Fungiidae). Saturated 16:0 and 18:0 acids were predominant in all species. Other principal FAs were 14:0, 16:1(n-7), 18:1(n-9), 18:3(n-6), 18:4(n-3), 20:3(n-6), 20:4(n-6), 20:4(n-3), 20:5(n-3), 22:4(n-6), 22:5(n-3), and 22:6(n-3). The content of some ordinary even-chain acids, such as 18:1(n-7), 18:2(n-6), 20:1(n-7), 20:2(n-6), and 22:2(n-6), did not exceed the value of 2%. Except for *Sandalolitha robusta* (Fungiidae), odd-chain and methyl-branched FAs were detected in small amounts (0.2–1.4% of the total).

Saturated, mono-, di-, tri-, and tetraenoic very-long-chain FAs with 24 carbon atoms were identified in the Poritidae species. The mass spectra of methyl esters of 24:0, 24:1, two 24:2 isomers, 24:3, and 24:4 acids gave molecular ion peaks ( $M^+$ ) at  $m/z$  382,  $m/z$  380,  $m/z$  378,  $m/z$  376, and  $m/z$  374, respectively, confirming the presence of a corresponding number of double bonds and a  $C_{24}$  chain in the original FAs. Additionally, a strong characteristic peak at  $m/z$  348 ( $[M-MeOH]^+$ ) in mass spectra of 24:1 and a base peak at  $m/z$  79 with a peak at  $m/z$  108 characteristic of (n-3) polyunsaturated FAMES in mass-spectra of 24:4 were

observed. The first isomer of 24:2 was identified as methylene-interrupted 24:2(n-6) acid and a strong peak at  $m/z$  150 was particularly abundant in the mass spectra of its methyl ester [28]. The second isomer was nonmethylene-interrupted 24:2(5,9) acid. A combination of abundant ions at  $m/z$  81, 109, and 141 in its mass spectra was very characteristic of the 5,9-dienoic FAMES. The same characteristic peaks observed in the mass spectra of tetracosatrienoic acid methyl ester (24:3) indicated the presence of 5,9-dienoic fragment in the fatty chain.

The mass spectrum of the *N*-acylpyrrolidide derivative of 24:1(n-9) gave a molecular ion peak at  $m/z$  419 ( $M^+$ ) and diagnostic fragments at  $m/z$  280 and  $m/z$  292. Molecular ion peaks at  $m/z$  417 ( $M^+$ ), fragments at  $m/z$  140, 152, 194, 206, and at  $m/z$  280, 292, 320, 332 were found in the mass spectra of the *N*-acylpyrrolidide derivative of 24:2(5,9) and 24:2(n-6), respectively. The mass spectrum of the derivative of 24:3(5,9,17) gave a molecular ion peak at  $m/z$  415 ( $M^+$ ) and fragment peaks at  $m/z$  140, 152, 194, 206, 304, and 316. Also, the spectra from 5,9-unsaturated FA derivatives exhibited an intensive peak at  $m/z$  180. The mass spectrum of the *N*-acylpyrrolidide derivative of 24:4(n-3) showed a molecular ion peak at  $m/z$  413 ( $M^+$ ) and fragments at  $m/z$  238, 250, 278, 290, 318, 330, 358, and 370, indicating that the double bonds were localized at 12, 15, 18, and 21 carbon atoms of the original FA [26].

The ECL values on a SUPELCOWAX 10 column were 24.17, 24.42, 24.60, 25.03, and 25.36 for 24:1(n-9), 24:2(5,9), 24:2(n-6), 24:3(5,9,17), and 24:4(n-3), respectively. Each of these  $C_{24}$  acids amounted to no more than 0.3% of total FAs but they were absent in the other families investigated.

Unsaturated acids were about 50% of total FAs for all coral families studied. The highest levels of 18:1(n-7) and 16:1(n-7) were found in *S. robusta*. The contents of 20:4(n-6) and 20:5(n-3) ranged from 1.7 to 16.5% for the Acroporidae species, but the highest concentrations of 20:4(n-6) and 20:5(n-3) among all species studied were registered for *Acropora formosa* (14.7%) and *Acropora cerealis* (16.5%), respectively. The Pocilloporidae species were characterized by the highest average level of 20:3(n-6), 20:4(n-3), and 22:6(n-3), especially in comparison to the family Acroporidae. The average contents of principal PU-FAs in the Poritidae species were similar to that in the Pocilloporidae species, except for oleic acid (18:1(n-9)) and dihomo- $\gamma$ -linolenic acid (20:3(n-6)) whose highest concentration were 19.0% for *Porites lobata* and 3.1% for *Seriatopora hystrix*, respectively. Among all the species investigated, the most noticeable amount of 18:1(n-9) was recorded in *Echinophyllia orpheensis* (Pectiniidae). The average content of octadecatetraenoic acid (18:4(n-3)) was similar for all coral species investigated, but this acid was absent in *S. robusta*.

**Table 1** Fatty acid composition (% of total FAs) of Acroporidae

Fatty acids	<i>Acropora cerealis</i>	<i>Acropora formosa</i>	<i>Acropora gemmifera</i>	<i>Acropora palifera</i>	<i>Acropora</i> sp.	<i>Acropora nobilis</i>
12:0	0.5 ± 0.2	0.2 ± 0.0	0.6 ± 0.4	0.7 ± 0.2	0.2 ± 0.1	0.1 ± 0.1
14:0	3.2 ± 0.1	2.9 ± 0.4	3.6 ± 0.1	2.3 ± 0.1	4.4 ± 0.2	5.9 ± 0.3
14:1	0.2 ± 0.1	0.2 ± 0.1	0.3 ± 0.1	0.2 ± 0.1	0.1 ± 0.0	0.2 ± 0.1
i-15:0	0.2 ± 0.0	0.2 ± 0.0	–	–	0.3 ± 0.1	0.4 ± 0.0
15:0	0.1 ± 0.0	0.2 ± 0.0	0.2 ± 0.0	0.1 ± 0.0	0.1 ± 0.0	0.3 ± 0.1
15:1	0.3 ± 0.2	0.3 ± 0.1	0.1 ± 0.0	–	0.1 ± 0.0	0.1 ± 0.0
16:0	25.3 ± 1.1	22.8 ± 3.0	30.8 ± 0.6	42.2 ± 2.8	51.2 ± 1.5	39.9 ± 0.9
16:1(n-7)	2.3 ± 0.2	3.1 ± 0.9	2.9 ± 0.1	1.9 ± 0.0	1.9 ± 0.3	4.1 ± 0.4
i-17:0	–	–	–	–	–	0.1 ± 0.1
ai-17:0	0.1 ± 0.0	0.1 ± 0.0	0.1 ± 0.0	0.1 ± 0.0	0.4 ± 0.2	0.3 ± 0.1
16:2	0.1 ± 0.0	0.2 ± 0.0	0.1 ± 0.0	–	0.1 ± 0.1	0.1 ± 0.0
17:0	0.1 ± 0.0	0.1 ± 0.0	0.1 ± 0.0	0.1 ± 0.0	0.2 ± 0.1	0.2 ± 0.1
17:1	0.4 ± 0.1	0.4 ± 0.1	0.4 ± 0.1	0.2 ± 0.1	0.1 ± 0.0	0.1 ± 0.0
18:0	13.0 ± 0.2	11.4 ± 0.6	9.3 ± 1.2	20.4 ± 0.7	8.9 ± 0.6	8.4 ± 0.5
18:1(n-9)	2.9 ± 0.4	3.5 ± 1.7	5.8 ± 5.7	3.3 ± 0.8	6.0 ± 1.6	6.8 ± 1.5
18:1(n-7)	0.5 ± 0.0	0.6 ± 0.1	0.4 ± 0.1	0.6 ± 0.1	0.4 ± 0.1	0.9 ± 0.2
18:2	0.1 ± 0.0	0.2 ± 0.1	0.1 ± 0.0	0.2 ± 0.0	0.3 ± 0.1	0.5 ± 0.1
18:2(n-6)	0.9 ± 0.1	1.0 ± 0.4	1.2 ± 0.5	0.6 ± 0.1	1.4 ± 0.4	1.6 ± 0.4
19:0	0.4 ± 0.1	0.4 ± 0.0	0.3 ± 0.1	0.3 ± 0.1	0.2 ± 0.1	0.2 ± 0.0
18:3(n-6)	3.6 ± 0.1	5.1 ± 0.8	4.2 ± 0.7	2.6 ± 0.4	6.8 ± 0.6	8.0 ± 0.7
18:3(n-3)	0.1 ± 0.0	–	–	–	–	0.1 ± 0.0
18:4(n-3)	1.4 ± 0.1	1.8 ± 0.4	1.2 ± 0.1	1.0 ± 0.1	1.6 ± 0.2	2.7 ± 0.4
20:0	1.0 ± 0.1	0.8 ± 0.1	1.0 ± 0.4	0.8 ± 0.1	1.0 ± 0.2	0.9 ± 0.3
20:1(n-9)	2.2 ± 0.0	1.8 ± 0.1	1.5 ± 0.4	1.1 ± 0.0	1.7 ± 0.1	2.3 ± 0.3
20:1(n-7)	0.3 ± 0.0	0.5 ± 0.2	0.3 ± 0.1	0.5 ± 0.1	0.1 ± 0.0	0.2 ± 0.0
20:2(n-6)	0.6 ± 0.1	0.4 ± 0.0	0.4 ± 0.1	0.3 ± 0.1	0.1 ± 0.1	0.4 ± 0.2
20:3	–	–	0.7 ± 0.1	0.4 ± 0.1	0.4 ± 0.1	–
20:3(n-6)	0.9 ± 0.1	0.9 ± 0.0	1.1 ± 0.3	0.4 ± 0.0	1.1 ± 0.2	1.3 ± 0.3
20:4(n-6)	6.7 ± 0.4	14.7 ± 2.1	10.4 ± 0.8	1.8 ± 0.2	2.0 ± 0.3	2.3 ± 0.3
20:4(n-3)	0.1 ± 0.1	0.2 ± 0.1	0.3 ± 0.1	0.1 ± 0.1	0.2 ± 0.1	0.3 ± 0.1
20:5(n-3)	16.5 ± 0.4	9.5 ± 1.3	10.3 ± 0.7	9.9 ± 2.1	1.7 ± 0.3	3.0 ± 0.5
22:0	0.3 ± 0.1	0.2 ± 0.0	–	0.2 ± 0.0	0.1 ± 0.0	–
22:1	0.2 ± 0.1	0.1 ± 0.0	0.2 ± 0.1	0.2 ± 0.1	0.2 ± 0.1	0.2 ± 0.1
22:2(n-6)	0.4 ± 0.4	0.3 ± 0.1	1.0 ± 0.2	0.1 ± 0.1	–	–
22:4(n-6)	5.5 ± 0.6	7.2 ± 1.2	4.1 ± 1.1	2.6 ± 0.6	1.1 ± 0.2	1.3 ± 0.3
22:5(n-3)	3.9 ± 0.1	3.1 ± 0.6	2.6 ± 0.6	1.7 ± 0.1	0.7 ± 0.1	1.2 ± 0.3
22:6(n-3)	6.3 ± 0.4	6.2 ± 0.1	4.9 ± 1.0	3.3 ± 0.4	4.1 ± 0.3	4.2 ± 0.4
Saturated	44.1 ± 0.4	39.1 ± 2.8	45.6 ± 0.9	66.9 ± 3.2	67.1 ± 2.7	56.6 ± 1.1
Monoenoic	8.9 ± 0.6	10.2 ± 2.3	12.5 ± 5.1	7.9 ± 1.3	10.3 ± 0.8	14.6 ± 1.7
Dienoic	1.9 ± 0.3	1.9 ± 0.4	2.1 ± 1.0	1.0 ± 0.4	1.9 ± 0.7	2.5 ± 0.6
Trienoic	4.5 ± 0.1	6.0 ± 0.8	5.7 ± 1.5	3.2 ± 0.7	8.3 ± 0.9	9.5 ± 0.6
Tetraenoic	13.6 ± 0.8	23.7 ± 3.7	15.9 ± 2.0	5.4 ± 0.8	4.8 ± 0.7	6.6 ± 0.8
Pentaenoic	20.4 ± 0.5	12.5 ± 2.0	12.9 ± 1.3	11.6 ± 2.2	2.4 ± 0.4	4.2 ± 0.4
Hexaenoic	6.3 ± 0.4	6.2 ± 0.1	4.9 ± 1.0	3.3 ± 0.4	4.1 ± 0.3	4.2 ± 0.4
n-6	18.4 ± 0.5	29.4 ± 2.3	21.8 ± 1.8	8.3 ± 0.6	12.4 ± 1.1	14.9 ± 1.3
n-3	28.2 ± 0.9	20.6 ± 2.5	19.2 ± 2.3	15.8 ± 1.8	8.3 ± 0.9	11.6 ± 1.4
n-6/n-3	0.7	1.4	1.1	0.5	1.5	1.3

Values are mean ± SD (*n* = 3)

**Table 2** Fatty acid composition (% of total FAs) of Pocilloporidae, Pectiniidae, and Fungiidae

Fatty acids	Pocilloporidae			Pectiniidae	Fungiidae
	<i>Stylophora pistillata</i>	<i>Pocillopora damicornis</i>	<i>Seriatopora hystrix</i>	<i>Echinophyllia orpheensis</i>	<i>Sandalolitha robusta</i>
12:0	0.2 ± 0.1	0.2 ± 0.0	0.1 ± 0.0	0.1 ± 0.0	0.1 ± 0.1
14:0	5.3 ± 1.4	3.6 ± 0.2	5.9 ± 0.6	1.5 ± 0.2	4.6 ± 0.2
14:1	0.2 ± 0.1	0.2 ± 0.0	0.2 ± 0.0	0.2 ± 0.0	0.9 ± 0.2
i-15:0	–	0.1 ± 0.0	–	–	0.4 ± 0.1
15:0	0.1 ± 0.0	0.1 ± 0.0	0.1 ± 0.0	0.1 ± 0.0	0.6 ± 0.2
15:1					
16:0	39.9 ± 4.0	36.8 ± 1.0	42.9 ± 2.5	40.0 ± 1.2	35.5 ± 1.1
16:1(n-7)	3.8 ± 0.5	2.2 ± 0.1	3.9 ± 0.0	2.2 ± 0.2	4.8 ± 0.5
i-17:0	–	–	–	–	0.6 ± 0.1
Ai-17:0	0.3 ± 0.2	0.1 ± 0.0	–	0.4 ± 0.1	0.3 ± 0.0
16:2	0.2 ± 0.1	–	0.1 ± 0.0	0.2 ± 0.0	1.3 ± 0.2
17:0	0.1 ± 0.0	0.1 ± 0.0	0.2 ± 0.0	–	0.9 ± 0.2
17:1	0.1 ± 0.0	0.2 ± 0.0	0.1 ± 0.0	–	0.4 ± 0.2
18:0	7.9 ± 0.5	14.5 ± 1.2	10.8 ± 0.4	5.7 ± 0.4	14.2 ± 0.7
18:1(n-9)	7.2 ± 1.7	4.8 ± 0.5	5.3 ± 0.1	20.3 ± 0.8	8.0 ± 0.5
18:1(n-7)	1.3 ± 0.1	0.7 ± 0.1	1.1 ± 0.1	0.7 ± 0.2	3.5 ± 0.2
18:2	0.1 ± 0.0	–	0.2 ± 0.0	0.6 ± 0.2	0.4 ± 0.1
18:2(n-6)	0.6 ± 0.1	1.3 ± 0.1	0.5 ± 0.0	1.0 ± 0.3	1.4 ± 0.2
19:0	–	0.1 ± 0.0	–	–	0.5 ± 0.1
18:3(n-6)	0.9 ± 0.1	2.3 ± 0.1	1.5 ± 0.1	2.4 ± 0.2	1.2 ± 0.3
18:3(n-3)	0.2 ± 0.1	0.2 ± 0.0	0.1 ± 0.0	–	0.1 ± 0.0
18:4(n-3)	1.8 ± 0.1	2.1 ± 0.1	1.2 ± 0.0	1.1 ± 0.2	0.1 ± 0.0
20:0	0.6 ± 0.1	1.6 ± 0.2	0.5 ± 0.1	0.3 ± 0.1	1.1 ± 0.3
20:1(n-9)	1.0 ± 0.5	1.5 ± 0.1	0.4 ± 0.1	1.7 ± 0.2	1.4 ± 0.2
20:1(n-7)	0.1 ± 0.0	–	–	0.2 ± 0.0	0.5 ± 0.1
20:2(n-6)	0.4 ± 0.1	0.4 ± 0.0	0.2 ± 0.0	0.5 ± 0.1	0.7 ± 0.2
20:3	0.1 ± 0.0	0.3 ± 0.2	–	–	0.2 ± 0.1
20:3(n-6)	2.9 ± 0.3	2.4 ± 0.0	3.1 ± 0.4	0.7 ± 0.2	0.6 ± 0.2
20:4(n-6)	5.1 ± 0.2	3.9 ± 0.0	3.5 ± 0.5	3.4 ± 0.3	4.2 ± 0.3
20:4(n-3)	1.8 ± 0.5	0.8 ± 0.1	1.0 ± 0.1	0.3 ± 0.0	–
20:5(n-3)	1.8 ± 0.1	3.0 ± 0.3	1.8 ± 0.2	1.7 ± 0.2	1.6 ± 0.1
22:0	–	0.3 ± 0.1	–	–	0.2 ± 0.1
22:1	–	–	–	0.3 ± 0.2	0.5 ± 0.2
22:2(n-6)	0.4 ± 0.0	0.6 ± 0.3	–	–	0.3 ± 0.1
22:4(n-6)	1.9 ± 0.1	2.6 ± 0.1	1.2 ± 0.1	1.7 ± 0.2	1.4 ± 0.2
22:5(n-3)	1.1 ± 0.3	0.7 ± 0.1	1.1 ± 0.3	2.3 ± 0.3	0.7 ± 0.2
22:6(n-3)	13.2 ± 2.1	12.3 ± 0.1	13.3 ± 2.2	9.2 ± 0.4	2.6 ± 0.2
Saturated	54.5 ± 5.2	57.2 ± 0.6	60.7 ± 3.4	48.1 ± 0.9	58.6 ± 2.0
Monoenoic	13.4 ± 1.6	9.4 ± 0.2	10.8 ± 0.5	25.4 ± 1.1	20.0 ± 0.7
Dienoic	1.4 ± 0.2	2.3 ± 0.4	0.9 ± 0.2	2.2 ± 0.3	4.0 ± 0.2
Trienoic	4.0 ± 0.2	5.1 ± 0.3	4.6 ± 0.5	3.1 ± 0.3	2.1 ± 0.3
Tetraenoic	10.5 ± 0.8	9.4 ± 0.2	6.8 ± 0.4	6.4 ± 0.7	5.6 ± 0.4
Pentaenoic	2.9 ± 0.2	3.7 ± 0.4	2.9 ± 0.5	4.0 ± 0.3	2.4 ± 0.3
Hexaenoic	13.2 ± 2.1	12.3 ± 0.1	13.3 ± 2.2	9.2 ± 0.4	2.6 ± 0.2
n-6	11.8 ± 0.8	13.5 ± 0.6	9.8 ± 0.1	9.6 ± 0.5	9.8 ± 0.7
n-3	19.7 ± 2.8	19.0 ± 0.4	18.4 ± 2.9	14.5 ± 0.9	4.9 ± 0.4
n-6/n-3	0.6	0.7	0.5	0.7	2.0

Values are mean ± SD (*n* = 3)

**Table 3** Fatty acids composition (% of total FAs) of Poritidae and Faviidae

Fatty acids	Poritidae			Faviidae	
	<i>Porites cylindrica</i>	<i>Porites nigrescens</i>	<i>Porites lobata</i>	<i>Favia</i> sp. I	<i>Favia</i> sp. II
12:0	0.3 ± 0.0	0.1 ± 0.0	0.2 ± 0.0	0.2 ± 0.0	0.1 ± 0.0
14:0	2.3 ± 0.2	1.5 ± 0.0	2.3 ± 0.2	4.9 ± 0.4	5.0 ± 0.4
14:1	0.2 ± 0.1	0.1 ± 0.0	–	–	–
i-15:0	–	–	0.2 ± 0.0	–	0.2 ± 0.0
15:0	0.1 ± 0.0	0.2 ± 0.1	0.5 ± 0.1	–	–
16:0	36.3 ± 10.0	40.8 ± 2.8	35.4 ± 3.4	40.4 ± 2.4	38.7 ± 2.9
16:1(n-7)	1.6 ± 0.1	1.5 ± 0.1	2.8 ± 0.5	3.7 ± 0.3	4.3 ± 0.6
ai-17:0	0.1 ± 0.0	0.2 ± 0.1	0.2 ± 0.0	0.3 ± 0.1	0.2 ± 0.1
16:2	0.1 ± 0.0	0.1 ± 0.0	0.2 ± 0.1	0.1 ± 0.0	0.3 ± 0.0
17:0	0.1 ± 0.0	0.1 ± 0.0	0.3 ± 0.0	–	–
17:1	0.2 ± 0.1	0.2 ± 0.1	0.3 ± 0.0	–	–
18:0	9.8 ± 0.7	12.7 ± 0.4	7.9 ± 0.7	4.5 ± 0.7	5.2 ± 0.4
18:1(n-9)	15.1 ± 1.3	9.4 ± 0.1	19.0 ± 1.2	7.6 ± 0.4	9.1 ± 0.9
18:1(n-7)	0.6 ± 0.1	0.5 ± 0.0	1.4 ± 0.2	1.1 ± 0.2	1.1 ± 0.2
18:2	0.2 ± 0.0	0.2 ± 0.0	0.2 ± 0.0	1.1 ± 0.3	0.6 ± 0.1
18:2(n-6)	1.1 ± 0.1	0.6 ± 0.1	1.5 ± 0.2	1.6 ± 0.2	3.0 ± 0.2
19:0	0.1 ± 0.0	0.1 ± 0.0	0.2 ± 0.0	–	–
18:3(n-6)	1.6 ± 0.4	0.6 ± 0.0	1.3 ± 0.2	10.6 ± 0.8	9.9 ± 0.6
18:3(n-3)	0.1 ± 0.0	–	0.1 ± 0.0	–	–
18:4(n-3)	1.7 ± 0.7	1.6 ± 0.1	0.6 ± 0.1	1.2 ± 0.2	1.1 ± 0.1
20:0	0.5 ± 0.1	0.5 ± 0.0	0.4 ± 0.1	0.4 ± 0.0	0.6 ± 0.1
20:1(n-9)	1.1 ± 0.1	1.3 ± 0.3	1.2 ± 0.3	0.4 ± 0.1	0.5 ± 0.0
20:1(n-7)	0.5 ± 0.4	0.4 ± 0.1	–	–	–
20:2(n-6)	1.1 ± 0.1	0.7 ± 0.3	0.9 ± 0.2	0.1 ± 0.0	0.3 ± 0.0
20:3	0.1 ± 0.0	0.6 ± 0.6	–	0.1 ± 0.0	–
20:3(n-6)	0.4 ± 0.1	0.2 ± 0.0	0.6 ± 0.1	1.9 ± 0.3	2.1 ± 0.2
20:4(n-6)	6.1 ± 1.6	3.2 ± 0.2	7.0 ± 1.4	4.6 ± 0.2	3.7 ± 0.3
20:4(n-3)	0.2 ± 0.0	0.2 ± 0.0	0.2 ± 0.0	0.2 ± 0.0	0.2 ± 0.1
20:5(n-3)	4.1 ± 1.1	4.8 ± 0.7	2.0 ± 0.2	0.8 ± 0.2	1.0 ± 0.2
22:0	0.3 ± 0.1	0.3 ± 0.1	–	0.1 ± 0.0	–
22:1	0.1 ± 0.0	0.2 ± 0.1	–	–	0.2 ± 0.0
22:2(n-6)	0.1 ± 0.0	0.3 ± 0.0	–	0.1 ± 0.0	–
22:4(n-6)	3.1 ± 1.1	3.2 ± 0.9	4.2 ± 0.6	2.1 ± 0.4	2.0 ± 0.4
22:5(n-3)	1.3 ± 0.4	1.5 ± 0.4	2.1 ± 0.5	6.7 ± 0.5	6.2 ± 0.6
22:6(n-3)	8.7 ± 2.9	11.6 ± 0.5	5.5 ± 0.4	3.6 ± 0.4	2.9 ± 0.3
24:0	0.1 ± 0.0	0.2 ± 0.0	0.2 ± 0.0	–	–
24:1(n-9)	0.1 ± 0.0	0.1 ± 0.0	0.1 ± 0.0	–	–
24:2(n-6)	–	0.1 ± 0.0	0.1 ± 0.0	–	–
24:2(5,9)	0.1 ± 0.0	0.1 ± 0.0	0.2 ± 0.0	–	–
24:3(5,9,17)	0.1 ± 0.0	0.3 ± 0.1	0.2 ± 0.0	–	–
24:4(n-3)	0.1 ± 0.0	0.2 ± 0.1	0.2 ± 0.1	–	–
Saturated	48.7 ± 10.8	56.8 ± 2.9	47.7 ± 4.0	50.9 ± 2.8	50.0 ± 3.4
Monoenoic	19.3 ± 2.1	13.5 ± 0.1	24.6 ± 1.5	12.8 ± 0.9	15.2 ± 1.1
Dienoic	2.8 ± 0.3	1.9 ± 0.6	2.7 ± 0.7	3.0 ± 0.7	4.2 ± 0.8
Trienoic	2.3 ± 0.5	1.7 ± 0.6	2.1 ± 0.5	12.6 ± 1.0	12.0 ± 0.8
Tetraenoic	11.2 ± 3.5	8.3 ± 1.2	12.1 ± 3.2	8.1 ± 0.6	7.0 ± 0.7
Pentaenoic	5.4 ± 1.5	6.3 ± 1.1	4.2 ± 1.4	7.6 ± 0.6	7.2 ± 0.7
Hexaenoic	9.9 ± 2.9	11.6 ± 0.5	5.5 ± 0.4	3.6 ± 0.4	2.9 ± 0.3



**Table 3** continued

Fatty acids	Poritidae			Faviidae	
	<i>Porites cylindrica</i>	<i>Porites nigrescens</i>	<i>Porites lobata</i>	<i>Favia</i> sp. I	<i>Favia</i> sp. II
n-6	13.4 ± 3.5	8.6 ± 1.7	15.6 ± 3.4	21.0 ± 2.3	21.0 ± 2.2
n-3	17.3 ± 5.1	19.8 ± 0.6	10.6 ± 0.8	12.6 ± 1.1	11.4 ± 1.5
n-6/n-3	0.8	0.4	1.5	1.7	1.8

Values are mean ± SD ( $n = 3$ )

In general, the qualitative FA composition of the sixteen coral species investigated was similar enough and typical for other Scleractinia [3, 20]. To uncover differences in a quantitative FA composition, our data on PUFA content for the 16 specimens investigated were supplemented with that on the 19 reef-building coral specimens (the Acroporidae, Pocilloporidae, Poritidae, Dendrophylliidae, and Milleporidae families) studied previously by the same analytical protocol [20] (Table 4).

Figure 1 illustrates a comparison of the average contents of ten principal PUFAs for six reef-building coral families. Each family may be associated with characteristic FAs such as 18:3(n-6), 20:5(n-3), 22:4(n-6), and 22:5(n-3) for Acroporidae; 20:3(n-6), 20:4(n-3), and 22:6(n-3) for Pocilloporidae; 20:4(n-6) and 22:6(n-3) for Poritidae. The Faviidae species showed an enlarged percentage of 18:3(n-6) and 22:5(n-3) acids. The Dendrophylliidae, represented by *Tubastrea*, are mostly azooxanthellate corals [29]. Dominant among the fatty acids of the (n-3) series in the Dendrophylliidae were 20:5(n-3) and 22:5(n-3), while the proportion of DHA, the main PUFA in hermatypic corals, did not exceed 1%. The major PUFAs for Milleporidae (class Hydrozoa) were DHA and 22:5(n-6) (the sum was about 48% of total FAs) [20], though scleractinian corals have this last acid only in traces.

Five of the (n-6) series principal C<sub>18–22</sub> PUFAs (18:3(n-6), 20:3(n-6), 20:4(n-6), 22:4(n-6), 22:5(n-6)) and five of (n-3) series ones (18:4(n-3), 20:4(n-3), 20:5(n-3), 22:5(n-3), 22:6(n-3)) were selected as marker variables for further chemotaxonomic investigation of reef-building corals and subjected to multidimensional scale analysis (MSA).

Figure 2 shows the results of the MSA performed on data for the 35 specimens of 26 reef-building coral species belong to eight families. Curved lines were manually drawn to determine the boundaries of the regions for each family. Three coral families (Milleporidae, Dendrophylliidae, and Faviidae) were clearly separated in the non-overlapping regions of the two-dimensional space formed by axis 1 and axis 2. The central domain consisted of slightly-overlapping regions of the next three coral families (Acroporidae, Poritidae, and Pocilloporidae) (Fig. 2). Single species of Pectiniidae, as well Fungiidae, fell into the central domain. The separation of each family

is generated in both axis 1 and axis 2. At the family level, Milleporidae, Pocilloporidae and Dendrophylliidae separated from Acroporidae and Poritidae in axis 1. The families Milleporidae and Faviidae separated from other families in axis 2. Axis 1 serves as a discriminant between Acroporidae species, and axis 2 as that for Pocilloporidae species. The Acroporidae region was quite diffusive, and it could be conveniently divided into two groups whose separation was mainly caused by variations in 20:5(n-3) and 20:4(n-6) contents. Application of factor analysis to the same variables lead to a result (plots not shown) similar to that obtained by MSA (but with a longer distance between the non-scleractinian Milleporidae and other scleractinian corals). Axis 1 was most influenced by the main variable 22:4(n-6) followed by 20:3(n-6), 20:5(n-3), and 20:4(n-3). Axis 2 was mainly defined by 22:5(n-6) and 22:6(n-3) acids; 18:4(n-3), 22:5(n-3), 20:4(n-6); while the 20:5(n-3) acids were significant but had lower loading factors. Together both axes explained 68% of the total data variance.

## Discussion

Current data available on the FA composition of reef-building corals are very limited. Lipids and FAs of several wide-distributed species of the families Acroporidae, Pocilloporidae, and Poritidae have been described [3, 20] but the FA profiles of Faviidae, Fungiidae, and Pectiniidae species are practically unknown. The FA compositions of *Acropora cerealis*, *A. formosa*, *A. gemmifera*, *A. palifera*, *A. nobilis*, *S. hystrix*, *Porites nigrescens*, *P. lobata*, *Favia* spp., *E. orpheensis*, and *S. robusta* from Vietnam were determined in the present study for the first time, but the FAs of *Stylophora pistillata* and *Pocillopora damicornis* from the Seychelles and Vietnam had previously been investigated in our laboratory [20], and the lipid composition was described for *Porites cylindrica* from Okinawa [3].

In *S. pistillata* and *P. damicornis*, the concentrations of the main PUFAs determined earlier [20] were very close to that obtained in this present study (Table 2) except for 18:3(n-6) and 20:3(n-6) acids (the latter is biosynthesized

**Table 4** Reef-building coral specimens, which were used for comparison and multidimensional scaling analysis (MSA) of their fatty acid composition

Number	Family	Species name	Region	Collection place
1	Acroporidae	<i>Acropora nasuta</i> [20]	Vietnam	The Tyam Island
2		<i>Acropora nasuta</i> [20]	Vietnam	The Thoty Island
3		<i>Acropora millepora</i> [20]	Vietnam	The Tyam Island
4		<i>Acropora millepora</i> [20]	Vietnam	The Thoty Island
5		<i>Acropora florida</i> [20]	Vietnam	The Thoty Island
6		<i>Acropora cerealis</i>	Vietnam	The Mun Island
7		<i>Acropora formosa</i>	Vietnam	The Mun Island
8		<i>Acropora gemmifera</i>	Vietnam	The Mun Island
9		<i>Acropora palifera</i>	Vietnam	The Mun Island
10		<i>Acropora</i> sp.	Vietnam	The Nha Trang Bay
11		<i>Acropora nobilis</i>	Vietnam	The Nha Trang Bay
12	Pocilloporidae	<i>Seriatopora caliendrum</i> [20]	Seychelles	The Aldabra Island
13		<i>Seriatopora hystrix</i>	Vietnam	The Mun Island
14		<i>Stylophora pistillata</i> [20]	Seychelles	The Coetivy Island
15		<i>Stylophora pistillata</i> [20]	Vietnam	The Tyam Island
16		<i>Stylophora pistillata</i> [20]	Vietnam	The Thoty Island
17		<i>Stylophora pistillata</i>	Vietnam	The Mun Island
18		<i>Pocillopora damicornis</i> [20]	Vietnam	The Thoty Island
19		<i>Pocillopora damicornis</i> [20]	Vietnam	The Thoty Island
20		<i>Pocillopora damicornis</i>	Vietnam	The Mun Island
21		<i>Pocillopora verrucosa</i> [20]	Vietnam	The Thoty Island
22	Pectiniidae	<i>Echinophyllia orpheensis</i>	Vietnam	The Nha Trang Bay
23	Fungiidae	<i>Sandalolitha robusta</i>	Vietnam	The Nha Trang Bay
24	Poritidae	<i>Goniopora</i> sp. I [20]	Vietnam	The Tyam Island
25		<i>Goniopora</i> sp. II [20]	Vietnam	The Tyam Island
26		<i>Porites cylindrica</i>	Vietnam	The Mun Island
27		<i>Porites nigrescens</i>	Vietnam	The Mun Island
28		<i>Porites lobata</i>	Vietnam	The Nha Trang Bay
29	Faviidae	<i>Favia</i> sp. I	Vietnam	The Nha Trang Bay
30		<i>Favia</i> sp. II	Vietnam	The Nha Trang Bay
31	Dendrophylliidae	<i>Tubastrea coccinea</i> [20]	Seychelles	The Aldabra Island
32		<i>Tubastrea micrantha</i> [20]	Seychelles	The Aldabra Island
33	Milleporidae	<i>Millepora</i> sp. [20]	Vietnam	The Thoty Island
34		<i>Millepora platyphylla</i> [20]	Seychelles	The Aldabra Island
35		<i>Millepora dichotoma</i> [20]	Seychelles	The Aldabra Island

by a C<sub>2</sub>-elongation of 18:3(n-6)). Previously, the abrupt depth-dependent increase of 18:3(n-6) level in *S. pistillata* was interpreted as being due to an increase in the number of zooxanthellae in deep-water corals [20]. Then, Zhukova and Titlyanov [12] confirmed that 18:3(n-6) acids are the main (n-6) series PUFAs in pure zooxanthellae isolated from *S. pistillata* and *P. damicornis*. It may therefore be presumed that one of the possible reasons for the variations in 18:3(n-6) content in *S. pistillata* and *P. damicornis* could be due to seasonal changes in the symbiotic algal population.

In the case of *P. cylindrica*, any direct comparison of our data with previous results was not possible because

analytical protocols were different, but the total FA profiles obtained in both studies were similar, except for docosahexaenoic acid (22:6(n-3), DHA). The concentrations of DHA in *P. cylindrica* from Okinawa were 0.8 and 0.9% for neutral and polar lipid fractions, respectively [3], contrary to the value of 8.7% that was detected for total lipids of *P. cylindrica* from Vietnam (Table 3). The reason for this difference is not clear but the last value conforms to the high levels of DHA (5.3–15.7% of total FAs) in five other Poritidae species from Vietnam, which were examined in our present and previous [20] studies.

The detection of a number of C<sub>24</sub> FAs, found only in the *Porites* species, seems very interesting, because the total

FA profiles (except for 18:1(n-9)) of the Poritidae and Pocilloporidae species investigated were quite similar. If C<sub>24</sub> FAs mentioned could be identified in other species of the family Poritidae, it may be an important chemotaxonomic sign of this family or the genus *Porites*. It has been shown that the subclass Hexacorallia, including the order Scleractinia, lacks marker tetracosapolyenoic 24:5(n-6) and 24:6(n-3) acids [30]. Our investigation confirmed the absence of the marker group of C<sub>24</sub> PUFAs with 5 and 6 double bonds in the scleractinian species, but another group of 24:0–24:4 acids was found in the genus *Porites*. It is clear that these two FA groups have completely different biosynthetic and biological origins. A biosynthetic sequence, including elongation and desaturation, from 20:4(n-6) and 20:5(n-3) acids to 24:5(n-6) and 24:6(n-3) acids, respectively, is supported by Vysotskii and Svetahev [31]. Contrary to this, most probably, the way for synthesis of the C<sub>24</sub> FAs in the genus *Porites* may be either a desaturation of 24:0 acids or an elongation of C<sub>22</sub> monoenoic (n-9) and polyunsaturated (n-6) acids. A Δ<sup>5,9</sup> non-methylene-interrupted double bond group presented in two of the five C<sub>24</sub> FAs from *Porites* is very typical of sponges [32]. It may be supposed that these FAs can originate from some sponges that infect corals but we did not find in the *Porites* samples the other main sponge markers, C<sub>26</sub> Δ<sup>5,9</sup> PUFAs (26:2Δ<sup>5,9</sup> and 26:3Δ<sup>5,9</sup>,19) that are very characteristic of Demospongia [32]. Whatever the case, we should consider the group of C<sub>24</sub> FAs as a signature of the *Porites* species if we are to precisely detect these FAs in all other Poritidae species collected at different times and places.

The highest level of *cis*-vaccenic acid 18:1(n-7) (3.6% of total FAs) and the sum of odd-chain and methyl-branched FAs (3.9% of total FAs) (Table 2) that are regarded as biomarkers of bacteria [33] were found in *S. robusta* (Fungiidae). It indicated the presence of an advanced bacterial community in this coral species compared to other species investigated.

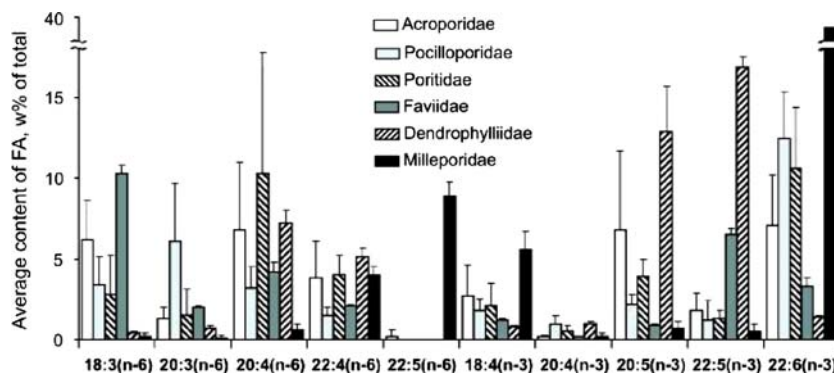
To uncover differences in a quantitative FA composition of reef-building corals, we combined and compared our

data on the FA content for the 16 specimens obtained with those on the 19 reef-building specimens (belong to families Acroporidae, Pocilloporidae, Poritidae, Dendrophylliidae, and Milleporidae) studied previously [20]. The most interesting family-specific differences were observed in the content of polyunsaturated FAs (Fig. 1, ref. “Results”).

The availability of the family-specific sets of FAs (Fig. 1) pointed to a possibility of applying these FAs to the chemotaxonomy of reef-building coral based on an appropriate multivariate statistical method. In the example of soft corals, it has been recently shown that selected PUFAs are more suitable for the determination of significant distinctions between coral species than the total FA matrix [21, 22]. In the present study, the contents of five PUFAs of the (n-6) series and five PUFAs of (n-3) series mentioned above (Fig. 1) were used as the variables. According to general concept, PUFAs of (n-6) and (n-3) series are biosynthesized by chain-elongation and the desaturation of the corresponding (n-6) and (n-3) shorter-chain unsaturated FAs. Thus, in the case of reef-building corals, (n-6) series PUFAs that are selected for a statistical analysis may be presented as the links of the (n-6) pathway: 18:3(n-6)–20:3(n-6)–20:4(n-6)–22:4(n-6)–22:5(n-6). Correspondently, selected (n-3) series PUFAs form the (n-3) pathway: 18:4(n-3)–20:4(n-3)–20:5(n-3)–22:5(n-3)–22:6(n-3). These two parallel pathways were performed by the same sequential enzymatic actions: C<sub>2</sub>-elongation, Δ<sup>5</sup> desaturation, C<sub>2</sub>-elongation, and Δ<sup>4</sup> desaturation, but direct investigations of this process in coral hosts and zooxanthellae have not been published. There is strong evidence that the last enzymatic step is more complex and includes an elongation of PUFAs from C<sub>22</sub> to C<sub>24</sub> followed by Δ<sup>6</sup>-desaturation and degradation to Δ<sup>4</sup> C<sub>22</sub> PUFAs via β-oxidation [34]. However, the key tetracosapolyenoic acids 24:6(n-3) and 24:5(n-6) have not been found in Hexacorallia, and the absence of these acids are the central chemotaxonomic distinction between Hexacorallia (stony corals) and Octocorallia (soft corals) [31].

Multivariate analyses such as principal components analysis, factor analysis, and multidimensional scaling

**Fig. 1** Average content of principal fatty acids (% of total FAs) in families Acroporidae, Pocilloporidae, Poritidae, Faviidae, Dendrophylliidae, and Milleporidae, which are indicated in Table 4



analysis (MSA), were performed on the selected variables (data of coral PUFA contents). The most obvious plot was obtained by MSA (Fig. 2), furthermore, the using of other FA sets or total FA matrix have led to less clear plots. The MSA data plot shows (Fig. 2) that all representative reef-building coral families, which have essential phylogenetic and morphological distinctions [29] can be separated on the basis of their FA composition, and the select PUFAs may serve as chemotaxonomic markers of reef-building corals at the family level.

No significant differences were observed at species or genus level. In spite of the fact that *E. orpheensis* (Pectiniidae; point 22; Fig. 2) and *S. robusta* (Fungiidae; point 23; Fig. 2) fell into the Poritidae and Acroporidae regions, respectively (Fig. 2), the single species data is not enough to come to any conclusion about relationships between the families Pectiniidae and Poritidae, as well as Fungiidae and Acroporidae.

The established division (Fig. 2) was caused by the difference in content of individual PUFAs, mainly with 22 carbon atoms such as 22:4(n-6), 22:5(n-6), and 22:6(n-3) (Fig. 1). These marker PUFAs have not only different biosynthetic origins (mentioned above) but also different biological sources. Corals are polytrophic organisms, i.e., they simultaneously derive nutrients through a variety of mechanisms from different trophic sources, which include

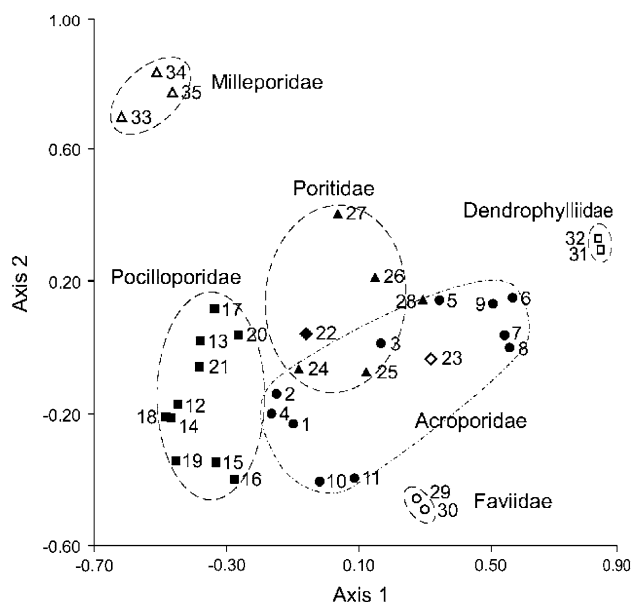


**Fig. 2** Multidimensional scale analysis performed using the ten variables (square root of ten PUFA contents) measured in all the 35 reef-building coral specimens. Specimens are numbered as in Table 4. Curved lines were arbitrarily drawn to delimit regions for each family. Filled circles Acroporidae, Filled squares Pocilloporidae, Filled triangles Poritidae, Open circles Faviidae, Open squares Dendrophylliidae, Open triangles Milleporidae, Filled rhombi Pectiniidae, Open rhombi Fungiidae

the uptake of both particulate living and dead organic matter (POM) and the absorption of dissolved organic material. The POM supply is highly diverse in quantity and quality and comprises of different classes of plankton and organic detritus [35–37]. In zooxanthellate species, the phototrophic supply is delivered by endosymbiotic dinoflagellates [38]. All of these energy and food sources make a significant contribution to the total FAs of corals. Also, environmental conditions such as light intensity and water temperature induce seasonal changes in the coral lipids [10, 39]. The simultaneous influence of these factors leads inevitably to the dispersion of the FA content in coral samples [3], being the probable cause of the absence of chemotaxonomic differences at species and genus levels (Fig. 2).

The phototrophic supply is the most important carbon source for hermatypic corals. In some corals more than 90% of photosynthate may be released by the symbiont to its host cell [40]. Coral lipids and their FAs are mainly derived from carbon photosynthetically fixed by symbiotic dinoflagellates [2]. The active transport of saturated FAs from symbiotic dinoflagellates to the host is documented [2, 41]. As for unsaturated FAs, some studies suggest symbiotic dinoflagellates support only one PUFA [42], others suggest three PUFAs [39] or a diverse variety of PUFAs [13, 43]. The possibility of the translocation of total PUFAs of symbiotic dinoflagellates to the host is very probable, since hermatypic coral is able to digest up to 6% of its own symbiotic dinoflagellates per day and consume their lipids and proteins [44].

It is supposed that every coral taxonomic group contains dinoflagellates of its own type that is characterized by specific FA composition [12, 43]. The specific intracellular symbiotic dinoflagellates of “L” (large) type with a high content of exclusive 22:5(n-6) acid was found in hydrocoral species *Millepora intricata* [12, 45]. Other symbiotic dinoflagellates of “B” (brown) and “G” (green) types were found in scleractinian species *P. damicornis*, *S. hystrix*, and *S. pistillata* and characterized by the absence of 22:5(n-6) acid and a significant level of DHA [12].

Three coral groups examined such as hydroid coral Milleporidae, azooxanthellate Dendrophylliidae, and other zooxanthellate families have the most taxonomic and biological distinctions. The C<sub>22</sub> PUFA profiles of these three coral family groups were similar to the C<sub>22</sub> PUFA composition of their symbiotic dinoflagellates. Hydroid coral Milleporidae had extremely high levels of 22:5(n-6) acid (up to 10%) [20] but other hermatypic coral families (except of Dendrophylliidae) showed an absence of 22:5(n-6) acid and a noticeable concentration of DHA (about 10%) (Fig. 1). Correspondingly, the lowest level of DHA (1.4%) (Fig. 2) was found in Dendrophylliidae [20], which lack symbiotic dinoflagellates. Generally, corals without

zooxanthellae have low contents of polyenoic C<sub>18</sub> and 20:3(n-6) acids but high levels of characteristic 22:5(n-3) acid [20, 43].

Thus, the difference in FA composition of the symbiotic dinoflagellates may be one of the probable reasons for the difference in C<sub>22</sub> PUFA content of reef-building coral families; the latter mainly determine the chemotaxonomic separation of the coral families (Fig. 2).

In hermatypic corals, the algal population in a host should be viewed as a dynamic, and perhaps non-equilibrium, system [46]. The zooxanthellae community consists of several *Symbiodinium* phylotypes, which may have different FA compositions. The diversity of zooxanthellae in an individual coral taxonomic group depends on environment factors such as solar irradiance and water temperature [47]. In the coral host, the absorption and accumulation of zooxanthellate FAs are probably selective for some PUFAs. For example, there have been numerous unsuccessful attempts to detect in coral colonies any appreciable amount of 18:5(n-3) acid that is regarded as a marker for coral intracellular symbiotic [12] and free-living plankton [15] dinoflagellates. Therefore, additional studies of zooxanthellate FA diversity and transport will be useful for determining the limits and prospects of application of FAs for chemotaxonomic analysis of reef-building corals.

**Acknowledgments** Information and data offered by the following are gratefully acknowledged: Nikolay Latyshev, Nikolay Naumenko, and Vasily Svetashev. This work was supported by the project N21 “Chemical and biological studies of coral reefs of Vietnam and marine natural products” and the grant 07-03-90001-Viet of the Russian Foundation of Basic Research.

## References

- Stimson JS (1987) Location, quantity and rate of change in quantity of lipids in tissue of Hawaiian hermatypic corals. *Bull Mar Sci* 41:889–904
- Harland AD, Navarro JC, Davies PS, Fixter LM (1993) Lipids of some Caribbean and Red Sea corals—total lipid, wax esters, triglycerides and fatty acids. *Mar Biol* 117:113–117
- Yamashiro H, Oku H, Higa H, Chinen I, Sakai K (1999) Composition of lipids, fatty acids and sterols in Okinawan corals. *Comp Biochem Physiol B* 122:397–407
- Batthey JF, Patton JS (1984) A reevaluation of the role of glycerol in carbon translocation in zooxanthellae-coelenterate symbiosis. *Mar Biol* 79:27–38
- Grottoli AG, Rodrigues LJ, Juarez C (2004) Lipids and stable carbon isotopes in two species of Hawaiian corals, *Porites compressa* and *Montipora verrucosa*, following a bleaching event. *Mar Biol* 145:621–631
- Yamashiro H, Oku H, Onaga K (2005) Effect of bleaching on lipid content and composition of Okinawan corals. *Fish Sci* 71:448–453
- Bachok Z et al (2006) Characterization of fatty acid composition of healthy and bleached corals from Okinawa, Japan. *Coral Reefs* 25:545–554
- Meyers PA (1979) Polyunsaturated fatty acids in coral: indicators of nutritional sources. *Mar Biol Lett* 1:69–75
- Saunders SM, Radford B, Bourke SA, Thiele Z, Bech T, Mardon J (2005) A rapid method for determining lipid fraction ratios of hard corals under varying sediment and light regimes. *Environ Chem* 2:331–336
- Oku H, Yamashiro H, Onaga K, Sakai K, Iwasaki H (2003) Seasonal changes in the content and composition of lipids in the coral *Goniastrea aspera*. *Coral Reefs* 22:83–85
- Yamashiro H, Oku H, Onaga K, Iwasaki H, Takara K (2001) Coral tumors store reduced level of lipids. *J Exp Mar Biol Ecol* 265:171–179
- Zhukova NV, Titlyanov EA (2003) Fatty acid variations in symbiotic dinoflagellates from Okinawan corals. *Phytochemistry* 62:191–195
- Papina M, Meziane T, van Woesik R (2003) Symbiotic zooxanthellae provide the host-coral *Montipora digitata* with polyunsaturated fatty acids. *Comp Biochem Physiol B* 135:533–537
- Widdig A, Schlichter D (2001) Phytoplankton: a significant trophic source for soft corals? *Helgol Mar Res* 55:198–211
- Dalsgaard J, John MS, Kattner G, Muller-Navarra D, Hagen W (2003) Fatty acid trophic markers in the pelagic marine environment. *Adv Mar Biol* 46:225–340
- Dunstan GA, Brown MR, Volkman JK (2005) Cryptophyceae and Rhodophyceae; chemotaxonomy, phylogeny, and application. *Phytochemistry* 66:2557–2570
- Volkman JK, Barrett SM, Blackburn SI, Mansour MP, Sikes EL, Gelin F (1998) Microalgal biomarkers: a review of recent research developments. *Org Geochem* 29:1163–1179
- Khotimchenko SV (2003) Lipids of marine macrophytic algae and grasses: structure, distribution, analysis. *Dal'nauka, Vladivostok*
- Latypov YY, Latyshev NA, Khotimchenko SV (1988) The fatty acid composition and the systematic position of reef-building corals. *Proc 6th Int Coral Reef Symp* 1:235
- Latyshev NA, Naumenko NV, Svetashev VI, Latypov YY (1991) Fatty acids of reef-building corals. *Mar Ecol Prog Ser* 76:295–301
- Imbs AB, Luu HV, Pham LQ (2007) Intra- and interspecific variability of fatty acid composition of the soft corals. *Russ J Mar Biol* 33:70–73
- Luu VH, Doan LP, Pham QL, Imbs AB (2005) Fatty acids as chemotaxonomy of Vietnamese coral. *Vietnamese J Sci Technol* 43:92–100
- Al Lihaihi SS, Al Sofyani AA, Niaz GR (1998) Chemical composition of corals in Saudi Red Sea Coast. *Oceanol Acta* 21:495–501
- Wells JW (1956) Scleractinia. In: Moore RC (ed) *Treatise on invertebrates. Paleontology Coelenterata*. University of Kansas Press, Kansas, pp 328–440
- Carreau JP, Dubacq JP (1979) Adaptation of macro-scale method to the micro-scale for fatty acid methyl transesterification of biological lipid extracts. *J Chromatogr* 151:384–390
- Andersson BA (1978) Mass spectrometry of fatty acid pyrrolidides. *Prog Chem Fats other Lipids* 16:279–308
- Christie WW (1988) Equivalent chain lengths of methyl ester derivatives of fatty acids on gas chromatography—a reappraisal. *J Chromatogr* 447:305–314
- Takagi T, Kaneniwa M, Itabashi Y (1986) Fatty acids in Crinoidea and Ophiuroidea: occurrence of all-*cis*-6,9,12,15,18,21-tetracosahexaenoic acid. *Lipids* 21:430–433
- Veron JEN (2000) *Corals of the world*. Australian Institute of Marine Science, Townsville
- Svetashev VI, Vysotsky MV (1998) Fatty acids of *Heliopora coerulea* and chemotaxonomic significance of tetracosapolyenoic acids in coelenterates. *Comp Biochem Physiol B* 119:73–75

- Vysotskii MV, Svetashev VI (1991) Identification, isolation and characterization of tetracosapolyenoic acids in lipids of marine coelenterates. *Biochim Biophys Acta* 1083:161–165
- Rodkina SA (2005) Fatty acids and other lipids of marine sponges. *Russ J Mar Biol* 31:387–397
- Kaneda T (1991) Iso-fatty and anteiso-fatty acids in bacteria—biosynthesis, function, and taxonomic significance. *Microbiol Rev* 55:288–302
- Sprecher H (2000) Metabolism of highly unsaturated n-3 and n-6 fatty acids. *Biochem Biophys Acta* 1486:219–231
- Sorokin YI (1993) Coral reef ecology. Springer, Heidelberg
- Ayukai T (1995) Retention of phytoplankton and planktonic microbes on coral reefs within the Great Barrier Reef, Australia. *Coral Reefs* 14:141–147
- Fabricius KE, Dommissie M (2000) Depletion of suspended particulate matter over coastal reef communities dominated by zooxanthellate soft corals. *Mar Ecol Prog Ser* 196:157–167
- Muscatine L, Weis V (1992) Productivity of zooxanthellae and biochemical cycles. In: Falkowski PG, Woodhead AD (eds) Primary productivity and biogeochemical cycles in the sea. Environmental Science Research, Plenum, New York, pp 257–271
- Al Moghrabi S, Allemand D, Couret JM, Jaubert J (1995) Fatty acids of the scleractinian coral *Galaxea fascicularis*—effect of light and feeding. *J Comp Physiol B* 165:183–192
- Muscatine L (1990) The role of symbiotic algae in carbon and energy flux in reef corals. In: Dubinsky Z (ed) Coral reefs. Elsevier, Amsterdam, pp 75–87
- Ward S (1995) Two patterns of energy allocation for growth, reproduction and lipid storage in the scleractinian coral *Pocillopora damicornis*. *Coral Reefs* 17:87–90
- Harland AD, Fixter LM, Davies PS, Anderson RA (1991) Distribution of lipids between the zooxanthellae and animal compartment in the symbiotic sea anemone *Anemonia viridi*-wax esters, triglycerides and fatty acids. *Mar Biol* 110:13–19
- Bishop DG, Kenrick JR (1980) Fatty acid composition of symbiotic zooxanthellae in relation to their hosts. *Lipids* 15:799–804
- Titlyanov EA, Titlyanova TV, Leletkin VA, Tsukahara J, van Woesik R, Yamazato K (1996) Degradation of zooxanthellae and regulation of their density in hermatypic corals. *Mar Ecol Prog Ser* 139:167–178
- Titlyanov EA, Titlyanova TV, Amat A, Yamazato K (2001) Morphophysiological variations of symbiotic dinoflagellates in hermatypic corals from a fringing reef at Sesoko Island. *Galaxea J Jpn Coral Reef Soc* 3:51–63
- Kinzie RA (1999) Sex, symbiosis and coral reef communities. *Am Zool* 39:80–91
- Fabricius KE, Mieog JC, Colin PL, Idip D, van Oppen MJH (2004) Identity and diversity of coral endosymbionts (zooxanthellae) from three Palauan reefs with contrasting bleaching, temperature and shading histories. *Mol Ecol* 13:2445–2458

fatty acids are of pharmacological interest, since they are very good topoisomerase I inhibitors (IC<sub>50</sub> 0.9–1.3 μM) [11], display cytotoxicity, and more recently we have shown that they inhibit the enoyl-ACP reductase (Fab I) enzyme of *Plasmodium falciparum* (malarial parasite) with an IC<sub>50</sub> of 0.35 μM [12]. Therefore, fatty acids containing both an α-methoxy functionality and a Δ<sup>5,9</sup> double bond in a single acyl chain could be of considerable interest, not only as fatty acids with a unique and novel biosynthetic origin, but also as worthwhile marine natural products for pharmacological studies.

In this work is reported, for the first time, a novel series of α-methoxylated Δ<sup>5,9</sup> fatty acids with an interesting biosynthetic origin, and the complex phospholipid fatty acid composition of the Caribbean sponge *Erylus goffrilleri* (class Demospongiae, order Astrophorida, family Geodiidae) is also described.

## Materials and Methods

### General Experimental Procedures

Fatty acid methyl esters, pyrrolidides, and dimethyl disulfide derivatives were analyzed by direct ionization using GC–MS (Hewlett-Packard 5972A MS) at 70 eV equipped with a 30 m × 0.25 mm special performance capillary column (HP-5MS) of polymethylsiloxane cross-linked with a 5% phenyl methylpolysiloxane. The temperature program was as follows: 130 °C for 1 min, increased at a rate of 3 °C/min to 270 °C, and maintained for 30 min at 270 °C. IR spectra were recorded on a Nicolet 600 FT-IR spectrophotometer.

### Sponge Collection

The sponge *Erylus goffrilleri* (class Demospongiae, order Astrophorida, family Geodiidae, genus *Erylus*) (Weidenmayer 1977) was collected from Mona Island (near Cabo Norte), Puerto Rico in 13 July 2006 at 80 feet depth by scuba. The sponge was freeze-dried and stored at –20 °C until extraction. A voucher specimen (IM06-80) is stored at the Chemistry Department of the University of Puerto Rico, Río Piedras campus.

### Extraction and Isolation of Phospholipids

The sponge (17.7 g) was carefully cleaned and cut into small pieces. Extraction with 2 × 200 mL of CHCl<sub>3</sub>/MeOH (1:1) yielded the total lipids (5.4 g). The neutral

lipids, glycolipids, and phospholipids (3.1 g) were separated by column chromatography on Si gel (60–200 mesh) using the procedure of Privett et al. [13]. The phospholipid classes were qualitatively identified by thin-layer chromatography using Si gel H plates and CHCl<sub>3</sub>/MeOH/NH<sub>4</sub>OH (65:35:5) as developing solvent. The main phospholipids identified were phosphatidylethanolamine (PE), phosphatidylglycerol (PG), and phosphatidylserine (PS).

### Preparation and Isolation of Fatty Acid Derivatives

The fatty acyl components of the phospholipids (0.18 g) were obtained as their methyl esters by reaction of the phospholipids with methanolic HCl followed by column chromatography on Si gel eluting with hexane/ether (9:1). The methyl esters were hydrogenated in 10 mL methanol with catalytic amounts of Pd/C (10%). The double-bonds and methyl-branching positions in these compounds were determined by pyrrolidide and dimethyl disulfide derivatization following preparation procedures previously described [6, 9]. Mass spectral data for the novel methyl esters, and its derivatives, are presented below.

### All Fatty Acid Methyl Esters

IR (neat)  $\nu_{\max}$  2,925, 2,854, 1,743, 1,463, 1,436, 1,377, 1,260, 1,196, 1,170, 1,021, 800, 722 cm<sup>-1</sup>

### Methyl (5Z,9Z)-2-methoxy-5,9-hexadecadienoate

ECL = 16.76; GC–MS  $m/z$  (relative intensity) [M–32]<sup>+</sup> 264 (1), 237 (2), 225 (1), 205 (2), 193 (1), 185 (4), 171 (2), 166 (5), 147 (2), 139 (8), 135 (5), 134 (2), 133 (3), 129 (7), 125 (7), 123 (8), 111 (19), 107 (9), 104 (20), 103 (2), 97 (27), 95 (19), 91 (7), 87 (41), 85 (12), 81 (35), 79 (25), 69 (59), 67 (38), 59 (25), 57 (40), 55 (100).

### Methyl (5Z,9Z)-2-methoxy-5,9-octadecadienoate

ECL = 18.71, GC–MS  $m/z$  (relative intensity) M<sup>+</sup> 324 (2), 292 (6), 265 (11), 233 (11), 225 (0.1), 211 (0.1), 193 (2), 185 (0.1), 179 (6), 171 (3), 166 (6), 165 (7), 155 (1), 153 (2), 147 (4), 143 (1), 139 (36), 138 (12), 134 (6), 133 (6), 129 (1), 123 (6), 112 (5), 111 (39), 109 (12), 107 (21), 104 (100), 97 (18), 95 (22), 91 (15), 87 (6), 81 (59), 80 (30), 79 (83), 69 (31), 67 (62), 59 (17), 57 (26), 55 (70).

## Methyl (5Z,9Z)-2-methoxy-5,9-nonadecadienoate

ECL = 19.70, GC–MS  $m/z$  (relative intensity)  $[M-32]^+$  306 (1), 279 (2), 247 (3), 225 (1), 211 (1), 193 (1), 185 (1), 179 (2), 171 (2), 167 (1), 166 (3), 165 (3), 147 (2), 143 (3), 139 (13), 134 (2), 133 (3), 129 (3), 123 (6), 112 (5), 111 (21), 107 (10), 104 (37), 103 (3), 95 (23), 91 (9), 87 (17), 85 (29), 81 (40), 80 (14), 79 (34), 69 (46), 67 (46), 59 (16), 57 (83), 55 (100).

## Methyl (5Z,9Z)-2-methoxy-5,9-eicosadienoate

ECL = 20.70, GC–MS  $m/z$  (relative intensity)  $M^+$  352 (1), 320 (3), 293 (4), 261 (5), 254 (4), 234 (3), 225 (1), 193 (2), 181 (2), 171 (3), 166 (3), 147 (5), 139 (24), 135 (7), 134 (4), 133 (6), 129 (8), 123 (6), 112 (6), 111 (32), 107 (17), 104 (77), 103 (6), 97 (24), 95 (23), 91 (10), 87 (17), 85 (37), 81 (52), 80 (24), 79 (65), 69 (48), 67 (53), 59 (18), 57 (100).

## Methyl (5Z,9Z)-2-methoxy-15-methyl-5,9-hexadecadienoate

ECL = 17.32, GC–MS  $m/z$  (relative intensity)  $M^+$  310 (1), 278 (4), 251 (5), 219 (4), 197 (5), 193 (2), 192 (4), 185 (4), 179 (4), 171 (3), 166 (5), 165 (7), 153 (4), 147 (5), 143 (6), 139 (26), 135 (8), 134 (6), 133 (7), 129 (5), 123 (10), 112 (6), 111 (33), 107 (20), 104 (87), 103 (8), 95 (30), 91 (18), 87 (21), 81 (62), 80 (26), 79 (79), 69 (51), 67 (63), 59 (24), 57 (43), 55 (100).

## Methyl (9Z)-2-methoxy-15-methyl-9-hexadecenoate

ECL = 17.55, GC–MS  $m/z$  (relative intensity)  $M^+$  312 (1), 280 (5), 257 (1), 256 (1), 253 (24), 227 (0.1), 221 (3), 220 (4), 195 (1), 185 (1), 179 (2), 168 (1), 165 (3), 153 (2), 149 (4), 147 (2), 143 (5), 139 (4), 136 (7), 135 (11), 129 (4), 123 (14), 117 (5), 112 (3), 111 (16), 107 (10), 104 (31), 103 (3), 95 (55), 91 (12), 87 (17), 83 (46), 81 (64), 80 (21), 79 (34), 71 (61), 69 (66), 67 (75), 59 (17), 57 (44), 55 (100).

## Methyl 2-methoxy-15-methyl-9,10-bis(methylthio)hexadecanoate

GC–MS  $m/z$  (relative intensity)  $M^+$  406 (10), 359 (1), 247  $[C_{12}H_{23}SO_3]^+$  (73), 215 (2), 199 (3), 187 (5), 167 (12), 159  $[C_9H_{19}S]^+$  (29), 155 (20), 135 (5), 127 (16), 111 (17), 109 (14), 104 (9), 95 (24), 93 (15), 87 (46), 81 (30), 71 (94), 69 (89), 67 (40), 61 (40), 59 (15), 57 (88), 55 (100).

## Results and Discussion

The phospholipid composition of *E. goffrilleri* was typical of other sponges that have been previously analyzed [10]. It mainly consisted of phosphatidylethanolamine (PE), phosphatidylserine (PS), and phosphatidylglycerol (PG). The phospholipids were characterized by thin-layer chromatography (TLC) comparisons with authentic standards. Other minor phospholipids in the mixture were not characterized.

The fatty acids of the phospholipids were obtained by transesterification of the whole phospholipid mixture with HCl/MeOH as previously described [6]. *Erylus goffrilleri* presented a rather complex phospholipid fatty acid composition of around 70 identifiable fatty acids (Table 1). The presence of methyl-branched fatty acids was particularly noteworthy in the sponge suggesting the presence of a considerable number of bacterial symbionts. For example, the typical *isol anteiso*  $C_{15}$ – $C_{17}$  fatty acids of marine bacteria accounted for almost 21% of the total fatty acid composition. Other common bacterial fatty acids such as the 10-methylhexadecanoic acid (10-Me-16:0) and the 11-methyloctadecanoic acid (11-Me-18:0) were also particularly abundant in *E. goffrilleri* accounting for almost 13% of the total fatty acid composition. Another interesting characteristic of the fatty acids from *E. goffrilleri* was the presence of a considerable number of very-long chain  $\Delta 5,9$  fatty acids, but those between 26 and 29 carbons predominated. Most of the  $\Delta 5,9$  fatty acids were also *isol anteiso* methyl-branched, a not surprising fact since these so-called “demospongiac acids” are known to originate from bacterial *isol anteiso*  $C_{15}$ – $C_{17}$  fatty acids [10]. An *isol anteiso* pair of  $C_{21:2}$   $\Delta 5,9$  fatty acids was also present in *E. goffrilleri*, compounds which seem to be characteristic of the genus *Erylus* since these same fatty acids were characterized for the first time in the Caribbean sponge *Erylus formosus* [14]. Characterization of all of these fatty acids was possible by means of GC–MS of their corresponding methyl esters and pyrrolidide derivatives, which allowed the determination of the exact location of the methyl-branching in the acyl chain [15]. Monounsaturations in the acyl chains were best determined by preparing the corresponding dimethyl disulfide derivatives as previously described followed by mass spectrometry [16]. Catalytic hydrogenation ( $H_2/PtO_2$ ) of the whole fatty acid methyl ester mixture was also useful in elucidating the presence of unusual substitutions in the acyl chain as well as conversion of the unknowns to known standards. Comparison of GC retention times of the most interesting fatty acid methyl esters with our library of marine fatty acids also confirmed our mass spectral structural assignments [3].

The most interesting and novel series of fatty acids in *E. goffrilleri* were seven  $\alpha$ -methoxylated fatty acids present



**Table 1** Identified phospholipid fatty acids from *Erylus gofrilleri*

Fatty acids	Relative abundance (wt%)
Tridecanoic (13:0)	0.2
12-Methyltridecanoic ( <i>i</i> -14:0)	0.6
Tetradecanoic (n-14:0)	2.7
3-Methyltetradecanoic (3-Me-14:0)	0.6
13-Methyltetradecanoic ( <i>i</i> -15:0)	7.4
12-Methyltetradecanoic ( <i>ai</i> -15:0)	7.0
9-Pentadecenoic (15:1n-6)	0.5
Pentadecanoic (n-15:0)	3.3
3-Methylpentadecanoic (3-Me-15:0)	1.0
14-Methylpentadecanoic ( <i>i</i> -16:0)	2.8
13-Methylpentadecanoic ( <i>ai</i> -16:0)	0.4
( <i>Z</i> )-9-Hexadecenoic (16:1n-7)	1.8
( <i>Z</i> )-11-Hexadecenoic (16:1n-5)	0.6
Hexadecanoic (n-16:0)	7.5
( <i>Z</i> )-15-Methyl-9-hexadecenoic ( <i>i</i> -17:1n-7)	4.8
10-Methylhexadecanoic (10-Me-16:0)	6.5
15-Methylhexadecanoic ( <i>i</i> -17:0)	4.3
14-Methylhexadecanoic ( <i>ai</i> -17:0)	2.4
(5 <i>Z</i> ,9 <i>Z</i> )-2-Methoxy-5,9-hexadecadienoic (2-OMe-16:2) <sup>a</sup>	0.3
( <i>Z</i> )-9-Heptadecenoic (17:1n-8)	2.1
( <i>Z</i> )-11-Heptadecenoic (17:1n-6)	1.3
Heptadecanoic (n-17:0)	2.3
(5 <i>Z</i> ,9 <i>Z</i> )-2-Methoxy-15-methyl-5,9-hexadecadienoic (2-OMe- <i>i</i> -17:2) <sup>a</sup>	0.2
Methylheptadecanoic ( <i>br</i> -18:0)	0.7
(5 <i>Z</i> ,9 <i>Z</i> )-5,9-Octadecadienoic (18:2n-9)	0.3
(9 <i>Z</i> )-2-Methoxy-15-methyl-9-hexadecenoic (2-OMe- <i>i</i> -17:1) <sup>a</sup>	0.4
( <i>Z</i> )-9-Octadecenoic (18:1n-9)	0.7
( <i>Z</i> )-11-Octadecenoic (18:1n-7)	2.1
2-Methoxy-14-methylhexadecanoic (2-OMe- <i>ai</i> -17:0)	0.1
Octadecanoic (n-18:0)	4.5
Methyl-6-octadecenoic ( <i>br</i> -19:1n-12)	1.4
(5 <i>Z</i> ,9 <i>Z</i> )-17-Methyl-5,9-octadecadienoic ( <i>i</i> -19:2n-9)	0.4
11-Methyloctadecanoic (11-Me-18:0)	6.2
Methylnonadecanoic ( <i>br</i> -20:0)	0.5
17-Methyloctadecanoic ( <i>i</i> -19:0)	0.9
16-Methyloctadecanoic ( <i>ai</i> -19:0)	0.7
(5 <i>Z</i> ,9 <i>Z</i> )-2-Methoxy-5,9-octadecadienoic (2-OMe-18:2) <sup>a</sup>	0.2
11-Nonadecenoic (19:1n-8)	2.1
Nonadecanoic (n-19:0)	0.2
5,8,11,14-Eicosatetraenoic (20:4n-6)	0.7
18-Methylnonadecanoic ( <i>i</i> -20:0)	0.2
17-Methylnonadecanoic ( <i>ai</i> -20:0)	0.6

**Table 1** continued

Fatty acids	Relative abundance (wt%)
(5 <i>Z</i> ,9 <i>Z</i> )-2-Methoxy-5,9-nonadecadienoic (2-OMe-19:2) <sup>a</sup>	0.2
11-Eicosenoic (20:1n-9)	0.2
Eicosanoic (n-20:0)	0.2
(5 <i>Z</i> ,9 <i>Z</i> )-19-Methyl-5,9-eicosadienoic ( <i>i</i> -21:2n-11)	0.8
(5 <i>Z</i> ,9 <i>Z</i> )-18-Methyl-5,9-eicosadienoic ( <i>ai</i> -21:2n-11)	0.1
Methyleicosanoic ( <i>br</i> -21:0)	0.2
(5 <i>Z</i> ,9 <i>Z</i> )-5,9-Heneicosadienoic (21:2n-11)	0.1
19-Methyleicosanoic ( <i>i</i> -21:0)	0.1
18-Methyleicosanoic ( <i>ai</i> -21:0)	0.3
(5 <i>Z</i> ,9 <i>Z</i> )-2-Methoxy-5,9-eicosadienoic (2-OMe-20:2) <sup>a</sup>	0.3
Docosanoic (n-22:0)	0.2
16-Methyldocosanoic (16-Me-22:0)	0.3
21-Methyldocosanoic ( <i>i</i> -23:0)	0.6
20-Methyldocosanoic ( <i>ai</i> -23:0)	1.1
Tricosanoic (n-23:0)	0.1
Methyltricosanoic ( <i>br</i> -24:0)	0.1
Tetracosanoic (n-24:0)	0.2
Methyltetracosanoic ( <i>br</i> -25:0)	1.3
(5 <i>Z</i> ,9 <i>Z</i> )-24-Methyl-5,9-pentacosadienoic ( <i>i</i> -26:2n-16)	1.4
(5 <i>Z</i> ,9 <i>Z</i> )-23-Methyl-5,9-pentacosadienoic ( <i>ai</i> -26:2n-16)	0.4
(5 <i>Z</i> ,9 <i>Z</i> )-5,9-Hexacosadienoic (n-26:2n-17)	0.8
(5 <i>Z</i> ,9 <i>Z</i> )-25-Methyl-5,9-hexacosadienoic ( <i>i</i> -27:2n-17)	1.8
(5 <i>Z</i> ,9 <i>Z</i> )-24-Methyl-5,9-hexacosadienoic ( <i>ai</i> -27:2n-17)	2.9
(5 <i>Z</i> ,9 <i>Z</i> )-5,9-Heptacosadienoic (n-27:2n-18)	0.4
(5 <i>Z</i> ,9 <i>Z</i> )-26-Methyl-5,9-heptacosadienoic ( <i>i</i> -28:2n-17)	0.4
(5 <i>Z</i> ,9 <i>Z</i> )-25-Methyl-5,9-heptacosadienoic ( <i>ai</i> -28:2n-17)	0.4
(5 <i>Z</i> ,9 <i>Z</i> )-5,9-Octacosadienoic (n-28:2n-19)	0.9
(5 <i>Z</i> ,9 <i>Z</i> )-5,9-Nonacosadienoic (n-29:2n-20)	0.9

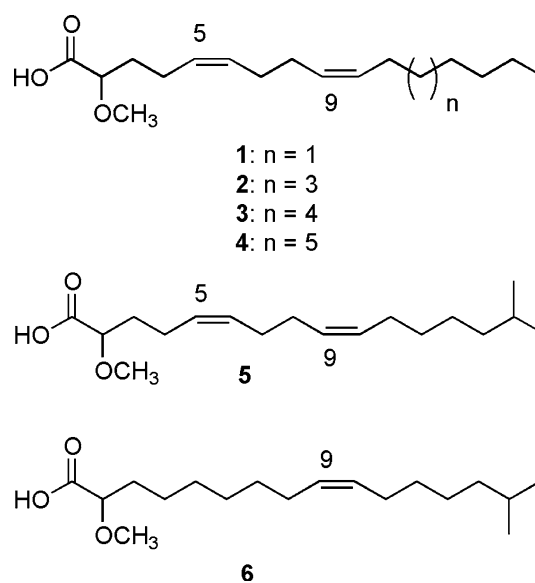
<sup>a</sup> Unprecedented in nature

in less than 1.5% of the total fatty acid composition. Due to their presence in such small amounts in a complex fatty acid mixture, isolation of the individual fatty acids was practically impossible, and therefore, their characterization had to rely mainly in the GC-MS of the different derivatives. Four of these methoxylated fatty acids were a series of C<sub>16</sub>–C<sub>20</sub> normal-chain  $\alpha$ -methoxylated  $\Delta$ 5,9 fatty acids, identified as the acids (5*Z*,9*Z*)-2-methoxy-5,9-hexadecadienoic acid (**1**), (5*Z*,9*Z*)-2-methoxy-5,9-octadecadienoic

acid (**2**), (5*Z*,9*Z*)-2-methoxy-5,9-nonadecadienoic acid (**3**), and (5*Z*,9*Z*)-2-methoxy-5,9-eicosadienoic acid (**4**). The characterization of the methyl esters of **1–4** was complicated by the fact that, as we will see from the equivalent chain length (ECL) values, they co-eluted in GC with the corresponding one carbon longer non-methoxylated saturated *anteiso* fatty acid methyl esters. For example, methyl (5*Z*,9*Z*)-2-methoxy-5,9-octadecadienoate (ECL = 18.71) co-elutes in GC with methyl 16-methyloctadecanoate (*ai*-19:0), which presents the same ECL value. The methyl esters of **1–4** presented in their mass spectra a series of diagnostic peaks that allowed their full characterization (Fig. 1). All methyl esters presented a prominent and characteristic McLafferty rearrangement peak at  $m/z$  104 and a strong  $M^+$ -CO<sub>2</sub>CH<sub>3</sub> fragment due to  $\alpha$ -cleavage to the carbonyl. Revealing the presence of the  $\Delta$ 5,9 diunsaturation was a fragment at  $m/z$  171 (due to allylic cleavage between carbons 7 and 8) which readily loses a molecule of methanol to yield a more abundant and characteristic fragmentation at  $m/z$  139 (Scheme 1). The  $m/z$  139 fragment loses again another molecule of methanol (there are two methoxy substituents at this side of the molecule) to finally yield the fragmentation at  $m/z$  107. In addition, the  $\Delta$ 9 double bond in **1–4** was also confirmed by a second but less abundant allylic fragmentation between carbons 11 and 12 in the molecule, which resulted in a smaller fragment at  $m/z$  225. This fragment either loses the molecule of methanol to yield a  $m/z$  193 peak or a methoxy carbonyl fragment to afford another fragment at  $m/z$  166. Further loss of either a methoxy carbonyl fragment from the  $m/z$  193 peak or a methanol molecule from the  $m/z$  166 peak results in the same fragmentation observed at  $m/z$  134 (Scheme 1). Further confirmation of the  $\alpha$ -methoxy functionality and the linear chain present in **1–4** was obtained by catalytic hydrogenation of the whole fatty acid methyl ester mixture, which afforded the known methyl esters methyl 2-methoxyhexadecanoate, methyl 2-methoxyoctadecanoate, methyl 2-methoxynonadecanoate, and methyl 2-methoxyeicosanoate. The presence of the saturated analogs of **1–4** was confirmed by their mass spectra and comparison of their GC retention times with those of our library of saturated 2-methoxylated fatty acids previously isolated from other sponges. Fourier transform infrared (FT-IR) of the whole fatty acid mixture failed to yield an absorption between 900 and 1,000 cm<sup>-1</sup>, thus indicating the absence of *trans* double bonds in our fatty acid methyl ester mixture and favoring the *cis* assignment for all of the double bonds in the identified fatty acids.

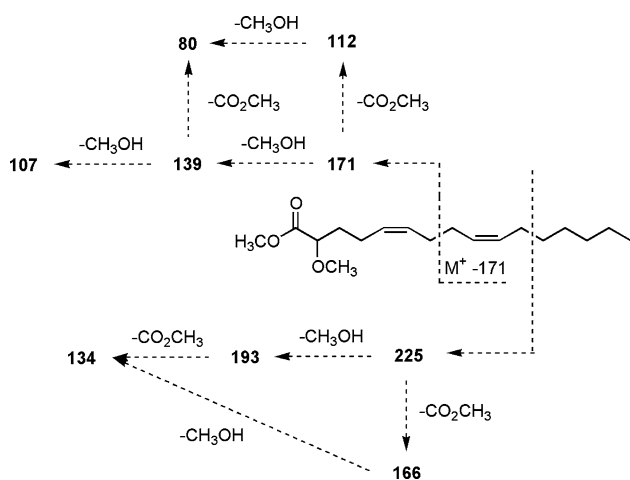
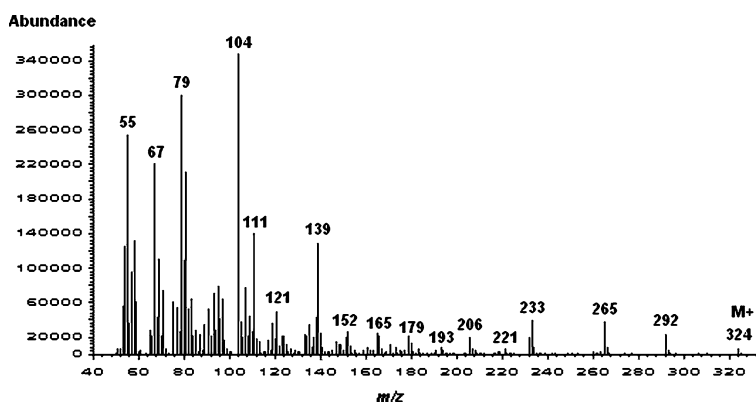
Another set of interesting  $\alpha$ -methoxylated fatty acids in *E. goffrilleri* were three methyl-branched 2-methoxylated fatty acids. One of these, namely the 2-methoxy-14-methylhexadecanoic acid (2-OMe-*ai*-17:0) was previously described by us from an *Agelas* sponge [17]. However, two

of these  $\alpha$ -methoxylated methyl-branched fatty acids have not been described before in the literature. They were characterized as the (5*Z*,9*Z*)-2-methoxy-15-methyl-5,9-hexadecadienoic acid (**5**) and as the (9*Z*)-2-methoxy-15-methyl-9-hexadecenoic acid (**6**). The methyl ester of **5** ( $M^+$  = 310) presented the same mass spectral characteristics as the methyl esters of the acids **1–4** that we described above. However, its GC retention time was different from the other  $\alpha$ -methoxylated  $\Delta$ 5,9 methyl esters inasmuch as it displayed an ECL value of 17.32, thus implying methyl-branching in the acyl chain. A normal chain  $\alpha$ -methoxylated C<sub>17:2</sub> $\Delta$ 5,9 methyl ester would have been predicted to elute in GC with an ECL value of 17.70. Catalytic hydrogenation provided the means by which the *iso*-terminal methyl-branching was elucidated inasmuch as **5** was converted into the methyl 2-methoxy-15-methylhexadecanoate (2-OMe-*i*-17:0).



The second methyl-branched  $\alpha$ -methoxylated fatty acid in *E. goffrilleri* presented an ECL value of 17.55 and in its mass spectrum a molecular ion ( $M^+$ ) at  $m/z$  312, as well as a McLafferty rearrangement at  $m/z$  104; this indicates that **6** is a 2-methoxylated monounsaturated fatty acid. Upon catalytic hydrogenation the methyl ester of **6** was also converted into the 2-OMe-*i*-17:0, thus confirming the presence of the *iso* terminal methyl-branching. Dimethyl disulfide derivatization was key in elucidating the double bond position [16]. For example, methyl 2-methoxy-15-methyl-9,10-bis(methylthio)-hexadecanoate presented the key fragmentation ions at  $m/z$  247 [C<sub>12</sub>H<sub>23</sub>SO<sub>3</sub>]<sup>+</sup> and at  $m/z$  159 [C<sub>9</sub>H<sub>19</sub>S]<sup>+</sup>, which indicates a double bond at C-9. Therefore, the experimental data supports the (9*Z*)-2-methoxy-15-methyl-9-hexadecenoic acid (**6**) as the unknown in *E. goffrilleri*. Most of the previously identified 2-methoxylated monounsaturated fatty acids in sponges

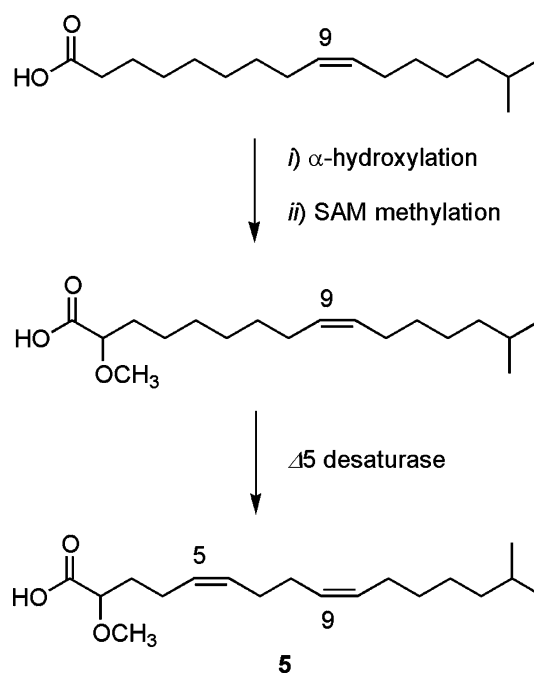
**Fig. 1** Electron impact mass spectrum (70 eV) for methyl (5*Z*, 9*Z*)-2-methoxy-5,9-octadecadienoate



**Scheme 1** Characteristic allylic mass spectral fragmentations (70 eV) for the 2-methoxylated  $\Delta$ 5,9 fatty acid methyl esters

contained a  $\Delta$ 6 double bond [3], but the monounsaturated acid **6** in *E. goffrilleri* is different inasmuch as it has a  $\Delta$ 9 double bond. This indicates that  $\Delta$ 9 desaturases are important in the biosynthesis of fatty acids in *E. goffrilleri*.

The identified *iso*-methoxylated fatty acids **5** and **6** in *E. goffrilleri* are of interest since they could have originated from the acid *i*-17:1 $\Delta$ 9, which was also present in the sponge in a 4.8% relative abundance (Table 1). This tends to indicate that the fatty acid biosynthetic pathway *i*-17:1 $\Delta$ 9  $\rightarrow$  2-OMe-*i*-17:1 $\Delta$ 9  $\rightarrow$  2-OMe-*i*-17:2 $\Delta$ 5,9 might be operative in *E. goffrilleri*, or most likely, by a symbiotic microorganism within the sponge (Scheme 2). This is in contrast to the dual desaturation mechanism responsible for the biosynthesis of the very long-chain  $\Delta$ 5,9 fatty acids in sponges, i.e., sponge cells are capable of utilizing either a  $\Delta$ 5 desaturase or a  $\Delta$ 9 desaturase first, followed by the introduction of the other missing desaturations, either the  $\Delta$ 9 or  $\Delta$ 5 double bonds, respectively [10]. In animals the first double bond is normally introduced at C-9, with the second and subsequent ones inserted between the first bond and the carboxyl end [10]. Our proposed biosynthetic sequence for the 2-OMe-*i*-17:2 $\Delta$ 5,9 acid thus suggests that



**Scheme 2** Proposed biosynthetic origin for the (5*Z*,9*Z*)-2-methoxy-15-methyl-5,9-hexadecadienoic acid (**5**) in *E. goffrilleri*. The three fatty acids shown were identified in the sponge

the acid might be originating from a symbiotic microorganism within *E. goffrilleri* and not from a fatty acid biosynthesis within sponge cells. In fact, we have recently identified the 2-methoxypentadecanoic acid in a *Virgibacillus marismortui* isolated from Lake Pomorie in Bulgaria, which indicates that bacteria can be the primary source of this type of fatty acids (N. Carballeira and K. Stefanov, unpublished data).

In addition to the interesting biosynthetic proposals arising from our *E. goffrilleri* work, our results, besides presenting the complex phospholipid fatty acid composition of *E. goffrilleri* for the first time, also expand our present knowledge of possible 2-OMe- $\Delta$ 5,9 fatty acids to be found in sponges [3]. A few  $\alpha$ -methoxylated diunsaturated fatty acids were first reported from the sponge

*Higginsia tethyoides* [7], but the only reported example of a 2-OMe- $\Delta$ 5,9 fatty acid was the identification of the (5Z,9Z)-2-methoxy-5,9-hexacosadienoic acid in the sponge *Topsentia roquensis* [9]. The identification of the novel 2-OMe- $\Delta$ 5,9 fatty acids described in this work present new structural templates for further biological studies and the evaluation of these  $\alpha$ -methoxylated fatty acids as novel enzyme inhibitors.

**Acknowledgments** This work was supported by a grant from the SCORE program of the National Institutes of Health (grant no. S06GM08102). D. Oyola and J. Vicente thank the NIH-MARC program for undergraduate fellowships.

## References

1. Carballeira NM (2006) Marine methoxylated fatty acids have biomedical potential. *Inform* 17:121–123
2. Carballeira NM, Ortiz D, Parang K, Sardari S (2004) Total synthesis and in vitro-antifungal activity of ( $\pm$ )-2-methoxytetradecanoic acid. *Arch Pharm* 337:152–155
3. Carballeira NM (2002) New advances in the chemistry of methoxylated lipids. *Prog Lipid Res* 41:437–456
4. Carballeira NM, Cruz H, Orellano EA, González FA (2003) The first total synthesis of the marine fatty acid ( $\pm$ )-2-methoxy-13-methyltetradecanoic acid: a cytotoxic fatty acid to leukemia cells. *Chem Phys Lipids* 126:149–153
5. Lee S, Shim SH, Kim JS, Shin KH, Kang SS (2005) Aldose reductase inhibitors from the fruiting bodies of *Ganoderma applanatum*. *Biol Pharm Bull* 28:1103–1105
6. Carballeira NM, Pagán M (2001) New methoxylated fatty acids from the Caribbean sponge *Callyspongia fallax*. *J Nat Prod* 64:620–623
7. Ayanoglu E, Popov S, Kornprobst JM, Aboud-Bichara A, Djerassi C (1983) Phospholipid studies of marine organisms: V. New  $\alpha$ -methoxy acids from *Higginsia tethyoides*. *Lipids* 18:830–836
8. Carballeira NM, Colón R, Emiliano A (1998) Identification of 2-methoxyhexadecanoic acid in *Amphimedon compressa*. *J Nat Prod* 61:675–676
9. Carballeira NM, Negrón V, Reyes ED (1992) Novel naturally occurring  $\alpha$ -methoxy acids from the phospholipids of Caribbean sponges. *Tetrahedron* 48:1053–1058
10. Djerassi C, Lam W-K (1991) Sponge phospholipids. *Acc Chem Res* 24:69–75
11. Nemoto T, Yoshino G, Ojika M, Sakagami Y (1997) Amphimic acids and related long-chain fatty acids as DNA topoisomerase I inhibitors from an Australian sponge, *Amphimedon* sp.; Isolation, structure, synthesis, and biological evaluation. *Tetrahedron* 53:16699–16710
12. Tasdemir D, Topaloglu B, Perozzo R, Brun R, O'Neill R, Carballeira NM, Zhang X, Tonge PJ, Linden A, Rüedi P (2007) Marine natural products from the Turkish sponge *Agelas oroides* that inhibit the enoyl reductases from *Plasmodium falciparum*, *Mycobacterium tuberculosis* and *Escherichia coli*. *Bioorg Med Chem* (in press)
13. Privett OS, Dougherty KA, Erdahl WL, Stolyhwo A (1973) Lipid composition of developing soybeans. *J Am Oil Chem Soc* 50:516–520
14. Carballeira NM, Negrón V (1991) Identification and characterization of two new methylicosadienoic acids from *Erylus formosus*. *J Nat Prod* 54:305–309
15. Andersson BA (1978) Mass spectrometry of fatty acid pyrrolidides. *Prog Chem Fats Lipids* 16:279–308
16. Christie WW (1998) Gas chromatography–mass spectrometry methods for structural analysis of fatty acids. *Lipids* 33:343–353
17. Carballeira NM, Cruz H, Ayala NL (2002) Total synthesis of 2-methoxy-14-methylpentadecanoic acid and the novel 2-methoxy-14-methylhexadecanoic acid identified in the sponge *Agelas dispar*. *Lipids* 37:1033–1037

TLC	Thin-layer chromatography
TLOOH	Trilinoleoylglycerol hydroperoxide
UVA	Ultraviolet A

## Introduction

Cholesterol is an essential class of lipids constituting bio-membranes. Cholesterol hydroperoxides (Chol-OOHs) are formed as primary products when cholesterol is peroxidized by reactive oxygen species. Chol-OOHs are known to be more resistant to glutathione peroxidase-dependent elimination than fatty acid hydroperoxides and their esterified form [1, 2]. Accordingly, Chol-OOHs seem to accumulate for a long time in biological fluid and tissues resulting in diverse effects on the body. It has been reported that exposure of experimental animals to chronic alcohol induces an imbalance of oxysterol metabolism by non-enzymatically produced cholesterol oxidation products including Chol-OOHs in skeletal muscle [3, 4] and liver [5]. Oxysterols derived from Chol-OOHs have been shown to participate in cell dysfunction as a result of oxidized plasma low-density lipoprotein (LDL) [6]. It has, on the other hand, been suggested Chol-OOH levels in rat skin increase with aging [7, 8]. Chol-OOHs are potential biomarkers of human oxidative stress, as indicated by the fact that Chol-OOHs have been clearly detected in the liver of alcoholic fatty liver patients [9], in human erythrocyte membranes [10], and in human skin after exposure to sunlight [11].

Chromatographic techniques such as HPLC combined with chemiluminescence (CL) detection are frequently applied to the quantitative analysis of Chol-OOHs in biological samples [4, 5, 7–11]. However, complicated and time-consuming pretreatment seems to be required for the preparation of Chol-OOHs from a variety of lipid classes. Furthermore, Adachi et al. [12] recently indicated that quantitative values of phosphatidylcholine hydroperoxide (PCOOH) obtained by HPLC with the CL detection technique are variable depending on the type of column used for the analysis. This implies that quantification of lipid hydroperoxides (LOOHs) using HPLC with CL should be performed carefully, with investigation of specificity. In contrast, gas chromatography–electron ionization–mass spectrometry (GC–EI–MS) with selected-ion monitoring (SIM) is a highly reliable method, because characteristic ions can be selected for monitoring specific compounds. In general, analysis of LOOHs by GC–EI–MS requires reduction of LOOHs to their hydroxyl derivatives as a pretreatment procedure, because LOOHs are thermally decomposed during GC–EI–MS analysis [13]. Thus

convenient pretreatment including separation and reduction procedures is desired for analysis of Chol-OOHs by GC–EI–MS/SIM.

We have already developed thin-layer chromatography (TLC) blotting with diphenyl-1-pyrenylphosphine (DPPP) reagent for simultaneous separation and reduction of LOOHs [14, 15]. We also succeeded in use of this technique for pretreatment in GC–MS/SIM analysis of cholesteryl ester hydroperoxide isomers in oxidized plasma LDL [16]. Here our objective was to develop a simple and sensitive method of analyzing peroxidized cholesterol, especially Chol-OOHs, using a combination of TLC blotting with DPPP reagent and GC–MS/SIM analysis.

## Experimental Procedures

### Chemicals and Reagents

Cholesterol was purchased from Kanto Chemical (Tokyo, Japan).  $\beta$ -Sitosterol was obtained from Tama Biochemical (Tokyo, Japan). Cholest-5-en-3 $\beta$ ,7 $\beta$ -diol (7 $\beta$ -hydroxycholesterol; Chol 7 $\beta$ -OH), cholest-5-en-3 $\beta$ ,25-diol (25-hydroxycholesterol), cholest-5-en-3 $\beta$ -ol-7-one (7-ketocholesterol), 5 $\alpha$ ,6 $\alpha$ -epoxycholestan-3 $\beta$ -ol (cholesterol 5 $\alpha$ ,6 $\alpha$ -epoxide), and 5 $\beta$ ,6 $\beta$ -epoxycholestan-3 $\beta$ -ol (cholesterol 5 $\beta$ ,6 $\beta$ -epoxide) were obtained from Sigma Chemical (St Louis, MO, USA). Cholestan-3 $\beta$ ,5 $\alpha$ ,6 $\beta$ -triol (cholestanetriol) and cholest-5-en-3 $\beta$ ,7 $\alpha$ -diol (7 $\alpha$ -hydroxycholesterol; Chol 7 $\alpha$ -OH) were purchased from Steraloids (Wilton, NH, USA). Trilinoleoylglycerol hydroperoxide (TLOOH) and linoleic acid hydroperoxide (LAOOH) were prepared from methylene blue-sensitized photooxidation products of trilinolein and linoleic acid, respectively, using preparative TLC, in accordance with a method described previously [17, 18]. PCOOH and phosphatidylethanolamine hydroperoxide (PEOOH) were prepared from methylene blue-sensitized photooxidation products of egg yolk PC and PE, respectively, and isolated using reversed phase-column chromatography [19]. All compounds were checked for purity by TLC. DPPP was purchased from Dojindo Laboratories (Kumamoto, Japan). Polyvinylidenedifluoride (PVDF) membranes, polytrifluoroethylene (PTFE) membranes, and glass fiber filters were obtained from ATTO (Tokyo, Japan). 2,4-Dimethylvaleronitrile (AMVN) and 2,2'-azobis(2-amidinopropane) dihydrochloride (AAPH) were products of Wako Pure Chemical Industries (Osaka, Japan). Hematoporphyrin was purchased from Sigma. *N,O*-Bis(trimethylsilyl)trifluoroacetamide in acetonitrile solution was obtained from Tokyo Kasei Kogyo (Tokyo, Japan). All other reagents and solvents were of guaranteed reagent grade from Kanto Chemical.

### Preparation of Peroxidized Cholesterol and Purification of Standard Chol-OOHs and $\beta$ -Sitosterol Hydroperoxide

Peroxidized cholesterol was prepared by azo radical-induced peroxidation of cholesterol or hematoporphyrin-sensitized photooxidation as follows. Cholesterol ( $0.1 \text{ mol L}^{-1}$ ; final concentration) was oxidized with AMVN ( $0.01 \text{ mol L}^{-1}$ ; final concentration) in 1:1 (*v/v*) hexane–isopropanol as solvent, at  $4^\circ\text{C}$  for 72 h. Photosensitized oxidation of cholesterol was based on the report by Kulig and Smith [20]. Briefly, cholesterol ( $8.3 \text{ mmol L}^{-1}$ , final concentration) was dissolved in 2:1 (*v/v*) chloroform–methanol containing *tert*-butyl hydroxytoluene ( $0.5 \text{ mmol L}^{-1}$ ). Hematoporphyrin ( $0.1 \text{ mmol L}^{-1}$ , final concentration) was then added and the solution was photo-irradiated with a tungsten projection lamp (300 W) at  $4^\circ\text{C}$  for 24 h. The hydroperoxide concentration of each solution was quantified using the potassium iodine method [21]. For preparation of  $\beta$ -sitosterol hydroperoxide (St-OOH),  $\beta$ -sitosterol was subjected to hematoporphyrin-sensitized photooxidation by the same procedure as used for cholesterol. St-OOH was purified from the photoirradiated solution using preparative TLC on silica gel F<sub>254</sub>, 0.25 mm thickness, 20 cm  $\times$  20 cm (Merck, Germany) with 93:7 (*v/v*) hexane–isopropanol as mobile phase. The band that newly emerged was scraped off and extracted. This extract was dissolved in 2:1 (*v/v*) chloroform–methanol. Chol-OOH for the TLC blot analysis of the standard LOOH mixture was separately prepared by methylene blue-sensitized photooxidation as follows. Cholesterol ( $65 \text{ mmol L}^{-1}$ ) was dissolved in 2:1 (*v/v*) chloroform–methanol containing methylene blue ( $0.1 \text{ mmol L}^{-1}$ ) and photoirradiated with a tungsten projection lamp (300 W) at  $4^\circ\text{C}$  for 6 h. Chol-OOH was isolated by preparative TLC using the same procedure as for St-OOH.

### Preparation of Peroxidized Human Low-Density Lipoprotein

Blood plasma was obtained from heparinized blood samples by centrifugation for 10 min at  $4^\circ\text{C}$ . Low-density lipoprotein (LDL) was obtained by density-gradient centrifugation, as described elsewhere [22]. Briefly, plasma obtained from male volunteers was adjusted to  $d = 1.21$  with KBr and overlaid with saline ( $d = 1.008$ ), and centrifugation was performed at 600,000 g for 40 min at  $4^\circ\text{C}$ . Then the LDL fraction was collected. Protein content was adjusted to  $1.2 \text{ mg protein mL}^{-1}$  phosphate-buffered saline (PBS). Oxidation of LDL was initiated by addition of AAPH ( $1 \text{ mmol L}^{-1}$ ) to 1 mL LDL solution. After incubation at  $37^\circ\text{C}$  for 6 h, total lipids were extracted according to the method of Bligh and Dyer [23]. Extracted lipids were dissolved in 20  $\mu\text{L}$  chloroform and subjected to DPPP-TLC blotting and GC–MS/SIM analysis.

### Cell Culture and UVA Treatment

A human keratinocyte cell line, HaCaT, kindly donated by Dr K. Takahata of Okayama University, was seeded in 60 mm dishes at a density of  $5 \times 10^5$  cells per dish and cultured for 2 days in Dulbecco's modified Eagle's medium (DMEM, SIGMA) with 10% fetal bovine serum (FBS; EQUITEC-BIO, TX, USA) at  $37^\circ\text{C}$  in a 5%  $\text{CO}_2$ /95% air mixed humidified incubator. Before irradiation the media were replaced with HBSS containing  $1 \mu\text{mol L}^{-1}$  hematoporphyrin; photo-irradiation was then performed with a UVA projection lamp (Black-light blue fluorescent lamp; Matsushita Electric Works, Osaka, Japan; 320–400 nm) at an intensity of  $2.5 \text{ J cm}^{-2}$  (700  $\mu\text{W}$ , 60 min) on an ice bath. Control cells were also kept in the dark for 60 min on an ice bath. After the UVA irradiation, cells were harvested by trypsinization. The suspension with exfoliated cells in DMEM was then centrifuged at 200g for 3 min at  $4^\circ\text{C}$  and the supernatant was removed. The pellet obtained was washed with HBSS three times and dispersed in HBSS. Total lipids in the pellet were extracted according to the method of Bligh and Dyer [23]. The lipid extract was dissolved in 20  $\mu\text{L}$  chloroform and subjected to DPPP-TLC blotting and GC–MS/SIM analysis.

### Animal Experiment

Male Hos; HR-1 hairless mice, 8 weeks old, were purchased from SLC Japan, (Hamamatsu, Japan) and maintained under standard experimental conditions ( $25^\circ\text{C}$ , 60% humidity; light and dark cycle every 12 h) according to the Guidelines for Animal Experimentation of Tokushima University. Mice were anesthetized with sodium pentobarbital ( $50 \text{ mg kg}^{-1}$ ) and exposed to irradiation with the UVA projection lamp for 8 h in a state where half of their back skin was covered with a cloth of UVA-fault permeability. The amount of UVA delivered to the skin was adjusted to  $47 \text{ J cm}^{-2}$ . After irradiation the mice were again anesthetized with sodium pentobarbital and part of dorsal skin, 1.0 cm  $\times$  3.0 cm, was obtained, avoiding contamination with hypodermic fats, and stored at  $-80^\circ\text{C}$  until analysis (no more than 5 days). Skin which had not been irradiated was also prepared and stored by the same procedure. Nine volumes of  $10 \text{ mmol L}^{-1}$  PBS was added to the dorsal skin preparation and the mixture was homogenized with a Polytron homogenizer (Kinematica AG, Littau/Luzern, Switzerland). The cholesterol content of the skin homogenate was quantified using a Cholesterol/Cholesteryl Ester Quantitation Kit (Bio Vision, CA, USA). The total lipids were extracted from the homogenates by the method of Bligh and Dyer [23] after addition of St-OOH as internal standard. Extracted lipids were dissolved in 20  $\mu\text{L}$  chloroform and subjected to DPPP-TLC blotting and GC–EI–MS/SIM analysis.

## DPPP-TLC Blotting for the Preparation of Chol-OOH Derivatives from Extracted Lipids

DPPP-TLC blotting was performed for extracted lipids to isolate Chol-OOHs as reduced hydroxyl derivatives from large amounts of non-oxidized lipids, in accordance with the method of Terao et al. [14]. First, peroxidized cholesterol solution or lipid extracted from a biological sample was applied to a TLC plate (silica gel F<sub>254</sub>, 0.25 mm thickness; Merck) and developed with 93:7 (v/v) hexane–isopropanol as mobile phase. The TLC plate was then blotted on to a PVDF membrane as follows. The plate was dried and then dipped in 0.01% (w/v) DPPP-containing blotting solvent (isopropanol–0.2% aqueous CaCl<sub>2</sub>–methanol, 40:20:7, v/v) for 30 s, after which it was placed on a glass fiber filter. Then the plate was covered with a PVDF membrane, a PTFE membrane, and finally a glass fiber filter, in layers. This TLC-blotting sandwich was pressed evenly for 90 s at 180°C using a TLC thermal blotter AC-5970 (ATTO, Tokyo, Japan) at a press level of 8. After blotting, the spot whose *R<sub>F</sub>* value corresponded to standard Chol-OOHs was cut out and immersed in 600 μL 1:1 (v/v) chloroform–methanol, with shaking for 1 min, to extract reduced Chol-OHs. The solvent was then removed with nitrogen gas. The residue was mixed with 50 μL *N,O*-bis(trimethylsilyl)trifluoroacetamide in acetonitrile solution and incubated at 60°C for 5 min for preparation of trimethylsilyloxy derivatives.

### GC–EI–MS/SIM Analysis

GC–EI–MS analysis was performed with an AQP5050 mass spectrometer (Shimadzu, Kyoto, Japan) equipped with an SPB-1 fused silica capillary column (30 m × 0.25 mm i.d., 10 μm film thickness; Supelco, Bellefonte, PA, USA). Splitless injection of 1 μL was performed with helium, flow rate 1.0 mL min<sup>-1</sup>, as carrier gas. The injection temperature was 260°C and the column oven was held at 150°C for 5 min before being elevated at 10° min<sup>-1</sup> to 280°C and then at 5° min<sup>-1</sup> to 300°C, which was held for 10 min. Full-scan mass spectra were obtained by electron-impact ionization, electron energy 70 eV, over the mass range *m/z* 50 to 600. SIM was performed with a dwell time of 200 ms.

## Results and Discussion

### GC–EI–MS Analysis of Oxysterol Standards

A mixture of Chol 7 $\alpha$ -OH, Chol 7 $\beta$ -OH, cholesterol 5 $\alpha$ ,6 $\alpha$ -epoxide, cholesterol 5 $\beta$ ,6 $\beta$ -epoxide, cholestanetriol, 7-ketocholesterol, and 25-hydroxycholesterol was analyzed by GC–EI–MS after derivatization to trimethylsilyloxy derivatives (Fig. 1). These oxysterol derivatives were

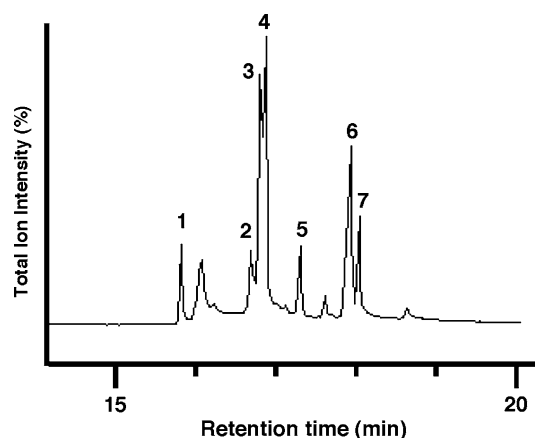


**Fig. 1** GC–EI–MS analysis of standard oxysterols. A total ion mass chromatogram of the standard mixture was obtained using the total ion current mode. The identities of the peaks were: 1, 7 $\alpha$ -hydroxycholesterol; 2, cholesterol 5 $\beta$ ,6 $\beta$ -epoxide; 3, 7 $\beta$ -hydroxycholesterol; 4, cholesterol 5 $\alpha$ ,6 $\alpha$ -epoxide; 5, cholestanetriol; 6, 7-ketocholesterol; 7, 25-hydroxycholesterol

separated incompletely from one another in the total-ion chromatogram. Therefore, SIM using a specific fragment ion for each oxysterol should be used for analysis of peroxidized cholesterol in biological samples. Table 1 shows the retention time of each oxysterol and its characteristic fragment ion in the chromatogram. The fragment ion derived from the elimination of trimethylsilyanol from the molecular ion,  $[M - \text{HOSi}(\text{CH}_3)_3]^+$ , was detected remarkably well for all the oxysterol derivatives except cholestanetriol. In addition, Table 1 shows the detection limit and response factor for each oxysterol derivative in the SIM chromatogram, using  $[M - \text{HOSi}(\text{CH}_3)_3]^+$ . The response factor is an area ratio of the fragment ion from each oxysterol derivative to that from the derivative of Chol 7 $\alpha$ -OH in the SIM chromatogram. The detection limit for each Chol-OH derivative was calculated from their response factors to be 20–60 fmol. Thus, analysis of peroxidized cholesterol using the GC–EI–MS/SIM technique seems to be either superior to or comparable with that with the HPLC–CL technique in sensitivity. Thus, we applied GC–EI–MS/SIM using  $[M - \text{HOSi}(\text{CH}_3)_3]^+$  as the selected ion as a method for analyzing peroxidized cholesterol in biological samples.

### Reduction of Chol-OOHs by DPPP-TLC Blotting and GC–EI–MS Analysis

Figure 2 illustrates results from DPPP-TLC blot analysis of LOOH standards including Chol-OOH in which each LOOH emerged as a fluorescent spot in two different solvent systems. The fluorescence derived from diphenyl-1-pyrenylphosphine oxide, which is formed by oxidation of DPPP with reduction of Chol-OOHs, could be visualized at

**Table 1** Characteristics of oxysterols in GC–EI–MS analysis

Compound number	Compound name	Major ion ( <i>m/z</i> )	[M – HOSi(CH <sub>3</sub> ) <sub>3</sub> ] <sup>+</sup> ( <i>m/z</i> )	Retention time (min)	Response factor	Detection limit (fmol)
	Cholesterol	368	368	15.95	–	–
1	7 $\alpha$ -Hydroxycholesterol	456	456	15.85	1.00	60
2	Cholesterol 5 $\beta$ ,6 $\beta$ -epoxide	384, 474	384	16.70	1.65	35
3	7 $\beta$ -Hydroxycholesterol	456	456	16.78	1.16	50
4	Cholesterol 5 $\alpha$ ,6 $\alpha$ -epoxide	384, 474	384	16.89	5.93	10
5	Cholestanetriol	456, 403	546	17.33	0.42	140
6	7-Ketcholesterol	382, 472	382	17.95	0.91	60
7	25-Hydroxycholesterol	456, 271	456	18.04	2.53	20

a concentration higher than 50 pmol and this spot migrated with an  $R_F$  value close to that of the spot of Chol-OHs (data not shown). Kriska and Girotti [24] indicated that Chol 7 $\alpha$ -OH was clearly separated from its hydroperoxide on the TLC plate. However, our TLC analysis is unlikely to distinguish Chol-OOH mixtures from respective Chol-OHs in biological samples. Thus, we decided to focus on the sum of Chol-OOH and Chol-OH, i.e. Chol-(O)OH, without distinguishing Chol-OOH from Chol-OH in peroxidized cholesterol, as heat-labile Chol-OOH should be reduced to its Chol-OH for GC–EI–MS analysis. Figure 3 shows the result of the GC–EI–MS analysis for the spot of Chol-OOH of peroxidized cholesterol after DPPP-TLC blotting and trimethylsilyloxylation. Peaks I and II, which originated from the spot of the blotting membrane, because of the

products of the azo radical-induced oxidation of cholesterol, appeared at the same retention times as the peaks for the Chol 7 $\alpha$ -OH and Chol 7 $\beta$ -OH standards in the chromatogram. In general, reducing agents such as NaBH<sub>4</sub> are used for reduction of hydroperoxyl groups in a GC–EI–MS analysis of lipid hydroperoxides. Here it was found that the hydroperoxyl group of peroxidized cholesterol was reduced effectively to its hydroxyl group by DPPP in the process of TLC blotting, as in previous reports for PCOOH [14, 15] and cholesteryl ester hydroperoxides [14, 16]. It was therefore concluded that peaks I and II are trimethylsilyloxy derivatives of  $\alpha$ -hydroperoxycholest-5-en-3 $\beta$ -ol (cholesterol 7 $\alpha$ -hydroperoxide; Chol 7 $\alpha$ -OOH) and 7 $\beta$ -hydroperoxycholest-5-en-3 $\beta$ -ol (cholesterol 7 $\beta$ -hydroperoxide; Chol 7 $\beta$ -OOH), respectively. Thus, we succeeded in reduction of Chol-OOHs to Chol-OHs and blotting of Chol-OHs to the membranes simultaneously. On the other hand, peak III appeared at a different retention time from Chol 7 $\alpha$ -OOH and Chol 7 $\beta$ -OOH in the case of peroxidized cholesterol prepared by hematoporphyrin-sensitized photooxidation. Photosensitized oxidation of cholesterol is known to yield Chol 5 $\alpha$ -hydroperoxycholest-6-en-3 $\beta$ -ol (Cholesterol 5 $\alpha$ -hydroperoxide; Chol 5 $\alpha$ -OOH) as a singlet molecular oxygen (<sup>1</sup>O<sub>2</sub>) oxygenation-specific product [25, 26]. It is therefore confirmed that peak III is derived from Chol 5 $\alpha$ -OOH. From these results, it can be concluded that DPPP-TLC blotting is a helpful pretreatment method in GC–EI–MS/SIM analysis of Chol-OOH isomers as trimethylsilyloxy derivatives. Taken together, we propose a method of GC–EI–MS with DPPP-TLC blotting for analysis of Chol-OOHs from biological samples, as shown in Scheme 1. First, cholesterol peroxidation products are separated from cholesterol and other lipids by the use of TLC analysis. Next, the TLC plate is blotted on to a PVDF membrane together with reduction of Chol-OOHs to Chol-OHs. The membrane corresponding to the region of Chol-OOHs is cut out and extracted with a mixture of chloroform and methanol. After trimethylsilylation, trimethylsilyloxy derivatives are

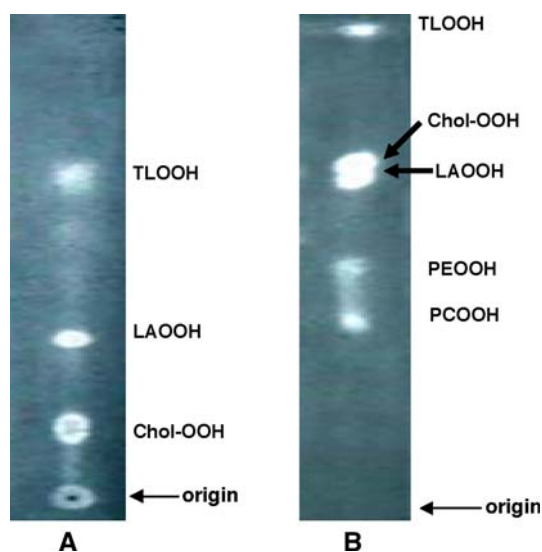
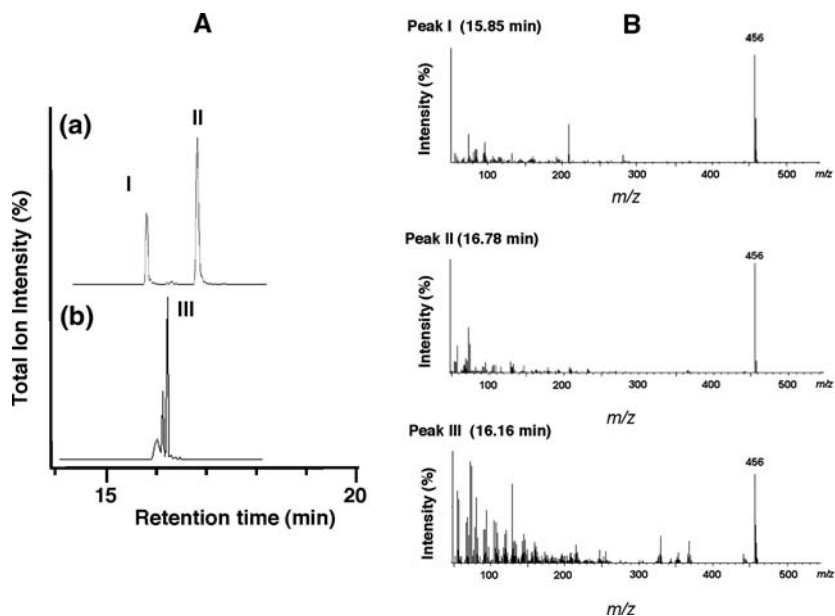


**Fig. 2** Results from DPPP-TLC blot analysis of a mixture of TLOOH, LAOOH, Chol-OOH, PCOOH, and PEOOH standards, 500 pmol each, on a TLC plate. The lanes show the results obtained by use of the mobile phases (a) hexane–diethyl ether–acetic acid, 70:30:1 (v/v) and (b) chloroform–methanol–water, 65:25:4 (v/v)



**Fig. 3** Results from GC–EI–MS analysis of peroxidized cholesterol after DPPP–TLC blotting. **A** Total-ion current mass chromatogram of the cholesterol peroxidation products, obtained using the total ion collection mode. (a) Cholesterol peroxidation products prepared by azo radical oxidation. (b) Cholesterol peroxidation products prepared by hematoporphyrin-sensitized photooxidation. **B** Mass spectrum of each peak shown in Fig. 3A. The peaks were identified as the trimethylsilyloxy derivative of Chol 7 $\alpha$ -OOH (I), Chol 7 $\beta$ -OOH (II), and Chol 5 $\alpha$ -OOH (III)



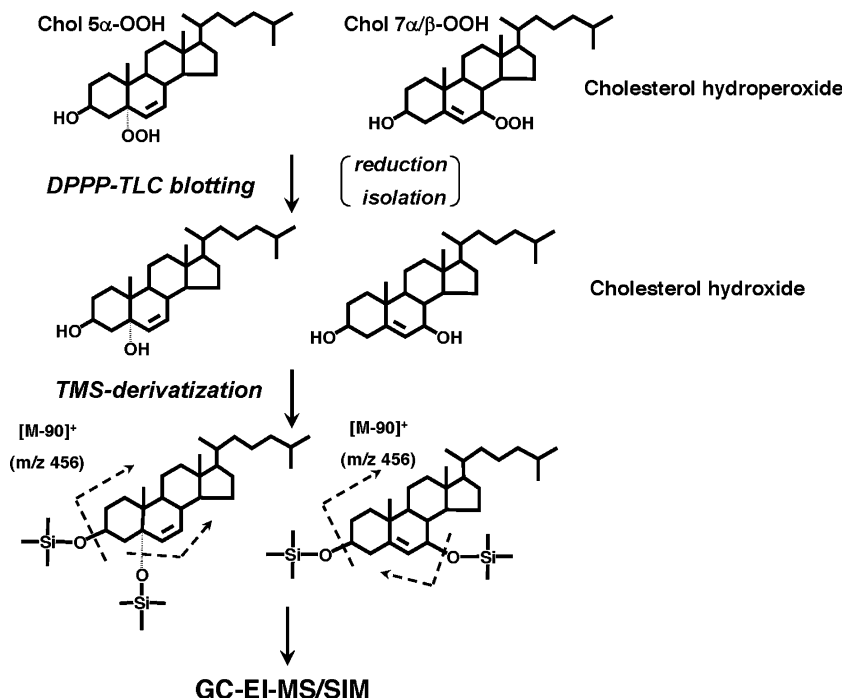
analyzed by GC–EI–MS/SIM. The recovery of standard Chol-OOHs by DPPP–TLC blotting was found to be 86%. It is likely that the combination of DPPP–TLC blotting and GC–EI–MS/SIM overcomes the problem of complicated and time-consuming pretreatment including reduction of hydroperoxyl groups and separation of cholesterol peroxidation products from extracted lipids. Furthermore, conversion of the reactive Chol-OOH to the stable Chol-OH during the blotting process is helpful in preventing the

formation of their decomposition products as artifacts during the analytical process.

#### Analysis and Quantification of Peroxidized Cholesterol in Biological Samples

We first used DPPP–TLC blotting as pretreatment for GC–EI–MS/SIM analysis of peroxidized cholesterol in human plasma LDL, because it has been suggested that

**Scheme 1** Flow chart for analysis of cholesterol hydroperoxides, as trimethylsilyloxy derivatives, by DPPP–TLC blotting and GC–EI–MS/SIM



peroxidation of LDL is involved in the initial stages of atherosclerosis. It has been already confirmed that peroxidized cholesterol was present in the oxidized LDL [6]. Trimethylsilyloxy derivatives of Chol 7 $\alpha$ -(O)OH and Chol 7 $\beta$ -(O)OH, radical mediated oxidation-specific products, were detected in the LDL after azo-radical oxidation, although no derivatives were found in intact human LDL (Fig. 4). Second, we applied this technique to analysis of peroxidized cholesterol from photoirradiated cultured cells. HaCaT cells were exposed to UVA irradiation in the presence of hematoporphyrin as photosensitizer and then peroxidized cholesterol in the lipid extract was detected using this technique. Compared with the non-irradiated cells, trimethylsilyloxy derivatives of Chol 5 $\alpha$ -(O)OH, in addition to those of Chol 7 $\alpha$ -(O)OH and Chol 7 $\beta$ -(O)OH, were readily detected in the UVA-exposed cells Fig. 5. Chol 5 $\alpha$ -OOH is a  $^1\text{O}_2$  oxygenation-specific oxidation product of cholesterol, as mentioned above, and detection of Chol 5 $\alpha$ -OOH has been used as evidence of the participation of  $^1\text{O}_2$  in the reaction mechanism of oxidative damage to biological samples [27]. That the peak corresponding to Chol 5 $\alpha$ -(O)OH was observed in the chromatogram of peroxidized cholesterol from the UVA-exposed cells implies that hematoporphyrin acts as a type II photosensitizer, which generates  $^1\text{O}_2$  by energy transfer from its excited state, in cultured cell systems.

Finally, the technique was used for quantification of peroxidized cholesterol present in mouse skin by use of an internal standard. We selected  $\beta$ -sitosterol, a major plant sterol, and prepared its hydroperoxide (St-OOH) by the method of hematoporphyrin-sensitized photooxidation. Figure 6 shows the chromatogram and mass spectrum

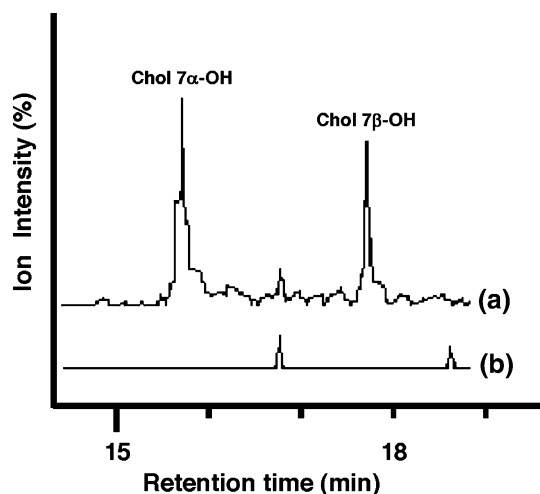


**Fig. 4** Results from GC–EI–MS/SIM analysis of peroxidized cholesterol from human LDL after DPPP–TLC blotting. SIM chromatogram of peroxidized cholesterol from (a) LDL after azo radical-induced peroxidation, and (b) control LDL. The chromatograms were obtained in SIM mode using the specific fragment ion  $m/z$  456

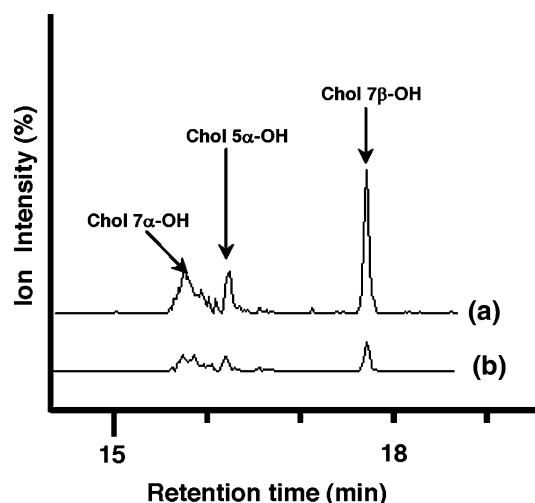


**Fig. 5** Results from GC–EI–MS/SIM analysis of peroxidized cholesterol from human keratinocyte cells after DPPP–TLC blotting. SIM chromatogram of peroxidized cholesterol from (a) UVA-irradiated cells, and (b) non-irradiated control cells. The chromatograms were obtained in SIM mode using the specific fragment ion  $m/z$  456

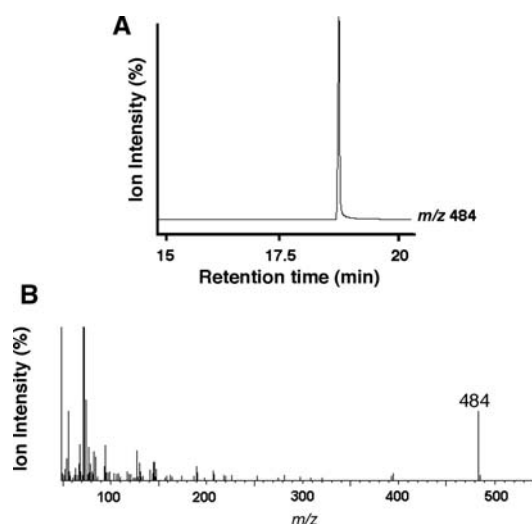


**Fig. 6** Results from GC–EI–MS/SIM analysis of peroxidized  $\beta$ -sitosterol after DPPP–TLC blotting.  $\beta$ -Sitosterol hydroperoxide was prepared by hematoporphyrin-sensitized photooxidation of  $\beta$ -sitosterol and subjected to GC–EI–MS/SIM analysis after DPPP–TLC blotting. (a) SIM chromatogram for specific fragment ion  $m/z$  484; (b) mass spectrum of the peak that appeared

obtained from the trimethylsilyloxy derivative of St-OOH isolated from the reaction mixture by DPPP–TLC blotting. A characteristic fragment ion for the derivative,  $[\text{M} - \text{HOSi}(\text{CH}_3)_3]^+$ , appeared at  $m/z$  484 in the GC peak corresponding to St-OOH. This ion was therefore used for SIM of the internal standard for the determination of Chol-(O)OHs. We tried to determine the amount of Chol-(O)OHs accumulated in hairless mouse skin as trimethylsilyloxy derivatives. The skin was removed from the

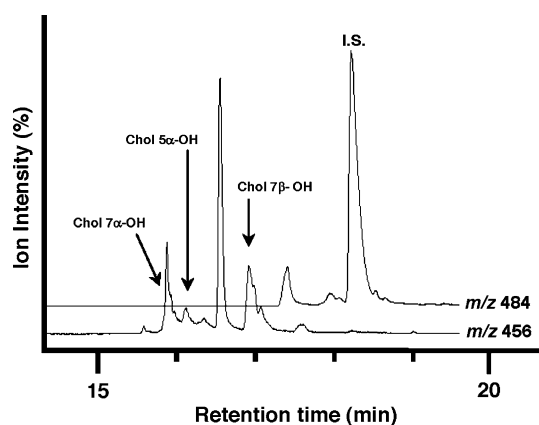


**Fig. 7** Results from GC–EI–MS/SIM analysis of peroxidized cholesterol obtained from the skin tissue of hairless mice after DPPP–TLC blotting. Total lipids were extracted from the skin tissue and subjected to GC–EI–MS/SIM after DPPP–TLC blotting. SIM chromatograms were obtained by use of the specific fragment ions  $m/z$  456 and  $m/z$  484 from peroxidized cholesterol and the internal standard, respectively

animal's back with or without irradiation of UVA and analyzed by DPPP–TLC blotting and GC–EI–MS/SIM after addition of St–OOH to the skin homogenate and extraction of total lipids. Figure 7 shows the SIM chromatogram of peroxidized cholesterol in mouse skin. The peaks were identified as the trimethylsilyloxy derivatives of Chol 7 $\alpha$ –(O)OH, Chol 5 $\alpha$ –(O)OH, and Chol 7 $\beta$ –(O)OH, respectively, by comparison with chromatograms obtained from the respective standards (Figs. 1 and 3). The amount of Chol 7 $\alpha$ –(O)OH and Chol 7 $\beta$ –(O)OH was determined from the standard calibration plots for Chol–OOHs obtained from cholesterol peroxidation products prepared by azo radical initiation (correlation coefficient = XX). The amount of Chol 5 $\alpha$ –(O)OH was indirectly measured by use of the response factor for Chol 5 $\alpha$ –OH (=1.2), which was obtained from the difference between the peak area of each Chol–OH from hematoporphyrin-sensitized photooxidation and that of Chol–7 $\alpha$ OH spiked Chol–OHs.

It was found that isomeric Chol–(O)OHs accumulated in considerable amounts in non-irradiated skin (Table 2). It is therefore likely that hairless mouse skin was subject to substantial oxidative stress under normal conditions, because Chol–(O)OHs, in particular Chol 7–(O)OH, are used as suitable oxidative stress markers in the skin [8, 11]. It was also clarified that  $^1\text{O}_2$  participated in the peroxidation of cholesterol in mouse skin even under normal conditions. Interestingly, *not* Chol 7 $\alpha/\beta$ –(O)OH *but* Chol 5 $\alpha$ –(O)OH level increased substantially after UVA-irradiation of the skin. Chol 5 $\alpha$ –OOH is capable of giving Chol 7 $\alpha$ –OOH by rearrangement of the hydroperoxyl group [20]. We confirmed this rearrangement was unlikely to occur during the sample processing, because the ratio of Chol 5 $\alpha$ –(O)OH in

**Table 2** Determination of peroxidized cholesterol in the skin of hairless mice with and without UVA irradiation

	Non-irradiation	UVA irradiation
Chol 7 $\alpha$ –(O)OH		
$\mu\text{mol mol}^{-1}$ cholesterol	11.1 $\pm$ 5.9	16.0 $\pm$ 12.4
$\text{nmol g}^{-1}$ wet tissue	0.38 $\pm$ 0.24	0.56 $\pm$ 0.55
Chol 5 $\alpha$ –(O)OH		
$\mu\text{mol mol}^{-1}$ cholesterol	4.3 $\pm$ 3.0	6.1 $\pm$ 2.8*
$\text{nmol g}^{-1}$ wet tissue	0.14 $\pm$ 0.11	0.20 $\pm$ 0.11
Chol 7 $\beta$ –(O)OH		
$\mu\text{mol mol}^{-1}$ cholesterol	13.5 $\pm$ 9.7	17.7 $\pm$ 12.3
$\text{nmol g}^{-1}$ wet tissue	0.47 $\pm$ 0.38	0.62 $\pm$ 0.50

Total lipids were extracted from skin tissue and subjected to DPPP–TLC blotting and GC–EI–MS/SIM analysis with the specific fragment ion  $m/z$  456

Data are expressed as the average value  $\pm$  SD ( $n = 10$ )

Chol 5 $\alpha$ –(O)OH was determined by using its response factor (1.20)

\* Significantly different from the corresponding non-irradiated sample,  $P < 0.05$  (paired  $t$ -test)

the total Chol–OOHs was not changed by incubation of the skin homogenate for 1 h at 37°C after spiking with Chol–OOHs (data not shown). However, there is a possibility that some Chol 5 $\alpha$ –OOH was converted to Chol 7 $\alpha$ –OOH during UVA irradiation. In any case, the contribution of  $^1\text{O}_2$  to peroxidation of cholesterol was found to be enhanced when the skin was exposed to UVA irradiation. Coproporphyrin produced from *Propionibacterium acnes* has been implicated as a photosensitizer in human skin [29]. It was recently suggested that proteins of the extracellular matrix [28] and 3-hydroxypyridine chromophore [30] are endogenous photosensitizers present in human skin cells. Yamazaki et al. [31] have demonstrated that Chol 5 $\alpha$ –OOH accumulated in the skin when rats were administered pheophorbide, a type II photosensitizer, and exposed to visible light. Nevertheless, our results indicate that an unknown type II photosensitizer, which is capable of generating  $^1\text{O}_2$  on exposure to UVA, is located in mouse skin.

In conclusion, the combination of DPPP–TLC blotting and GC–EI–MS/SIM is effective for quantitative analysis of peroxidized cholesterol, particularly Chol–(O)OHs, with high sensitivity and simplicity. This technique is useful for detecting participation of  $^1\text{O}_2$  in oxidative damage occurring in tissues and fluids, although it is difficult to distinguish Chol–OOHs from their reduced Chol–OHs. We are now using this technique to evaluate the role of  $^1\text{O}_2$  in photoirradiation-induced oxidative stress in experimental animals.

**Acknowledgments** This study was partly supported by the program of the twenty-first century Center of Excellence “Human nutritional science on stress control” and a grant-in aid for scientific research of

the Ministry of Education, Culture, Sports, Science and Technology, Japan.

## References

1. Thomas JP, Maiorino M, Ursini F, Girotti AW (1990) Protective action of phospholipid hydroperoxide glutathione peroxidase against membrane-damaging lipid peroxidation. *J Biol Chem* 265:454–461
2. Thomas JP, Girotti AW (1988) Photooxidation of cell membranes in the presence of hematoporphyrin derivative: reactivity of phospholipid and cholesterol hydroperoxides with glutathione peroxidase. *Biochim Biophys Acta* 962:297–307
3. Fujita T, Adachi J, Ueno Y, Peters TJ, Preedy VR (2002) Chronic ethanol feeding increases 7-hydroperoxycholesterol and oxysterols in rat skeletal muscle. *Metabolism* 51:737–742
4. Adachi J, Asano M, Ueno Y, Reilly M, Mantle D, Peters TJ, Preedy VR (2000) 7 $\alpha$ - and 7 $\beta$ -hydroperoxycholest-5-en-3 $\beta$ -ol in muscle as indices of oxidative stress: response to ethanol dosage in rats. *Alcohol Clin Exp Res* 24:675–681
5. Ariyoshi K, Adachi J, Asano M, Ueno Y, Rajendram R (2002) Effect of chronic ethanol feeding on oxysterols in rat liver. *Free Radic Res* 36:661–666
6. Steffen Y, Wiswedel I, Peter D, Schewe T, Sies H (2006) Cytotoxicity of myeloperoxidase/nitrite-oxidized low-density lipoprotein toward endothelial cells is due to a high 7 beta-hydroxycholesterol to 7-ketocholesterol ratio. *Free Radic Biol Med* 41:1139–1150
7. Ozawa N, Yamazaki S, Chiba K, Aoyama H, Tomisawa H, Tateishi M, Watabe T (1991) Occurrence of cholesterol 7 alpha- and 7 beta-hydroperoxides in rat skin as aging marker. *Biochem Biophys Res Commun* 178:242–247
8. Yamazaki S, Ozawa N, Hiratsuka A, Watabe T (1999) Cholesterol 7-hydroperoxides in rat skin as a marker for lipid peroxidation. *Biochem Pharmacol* 58:1415–1423
9. Asano M, Adachi J, Ueno Y (1999) Cholesterol-derived hydroperoxides in alcoholic liver disease. *Lipids* 34:557–561
10. Adachi J, Asano M, Naito T, Ueno Y, Tatsuno Y (1998) Chemiluminescent determination of cholesterol hydroperoxides in human erythrocyte membrane. *Lipids* 33:1235–1240
11. Yamazaki S, Ozawa N, Hiratsuka A, Watabe T (1999) Increases in cholesterol 7-hydroperoxides in lipids of human skin by sunlight exposure. *Free Radic Biol Med* 26:1126–1133
12. Adachi J, Yoshioka N, Funae R, Nagasaki Y, Naito T, Ueno Y (2004) Phosphatidylcholine hydroperoxide levels in human plasma are lower than previously reported. *Lipids* 39:891–896
13. Yoshida Y, Niki E (2004) Detection of lipid peroxidation in vivo: total hydroxyoctadecadienoic acid and 7-hydroxycholesterol as oxidative stress marker. *Free Radic Res* 38:787–794
14. Terao J, Miyoshi S, Miyamoto S (2001) Thin-layer chromatography blotting for the fluorescence detection of phospholipid hydroperoxides and cholesteryl ester hydroperoxides. *J Chromatogr B Biomed Sci Appl* 765:199–203
15. Miyamoto S, Dupas C, Murota K, Terao J (2003) Phospholipid hydroperoxides are detoxified by phospholipase A2 and GSH peroxidase in rat gastric mucosa. *Lipids* 38:641–649
16. Kawai Y, Miyoshi M, Moon JH, Terao J (2007) Detection of cholesteryl ester hydroperoxide isomers using gas chromatography–mass spectrometry combined with thin-layer chromatography blotting. *Anal Biochem* 360:130–137
17. Terao J, Matsushita S (1981) Analysis of photosensitized oxidation products of unsaturated triglycerides and vegetable oils by gas chromatography–mass spectrometry. *Agric Biol Chem* 43:601–608
18. Terao J, Shibata SS, Matsushita S (1988) Selective quantification of arachidonic acid hydroperoxides and their hydroxyl derivatives in reverse-phase high performance liquid chromatography. *Anal Biochem* 169:415–423
19. Terao J, Asano I, Matsushita S (1985) Preparation of hydroperoxy and hydroxy derivatives of rat liver phosphatidylcholine and phosphatidylethanolamine. *Lipids* 20:312–317
20. Kulig MJ, Smith LL (1973) Sterol metabolism. XXV. Cholesterol oxidation by singlet molecular oxygen. *J Org Chem* 38: 3639–3643
21. Cramer GL, Miller JF Jr, Pendleton RB, Lands WE (1991) Iodometric measurement of lipid hydroperoxides in human plasma. *Anal Biochem* 193:204–211
22. Murota K, Hotta A, Ido H, Kawai Y, Moon JH, Sekido K, Hayashi H, Inakuma T, Terao J (2007) Antioxidant capacity of albumin-bound quercetin metabolites after onion consumption in humans. *J Med Invest* (in press)
23. Bligh EG, Dyer WJ (1959) A rapid method of total lipid extraction and purification. *Can J Biochem Physiol* 37:911–917
24. Kriska T, Girotti AW (2005) A thin-layer chromatographic method for determining the enzymatic activity of peroxidases catalyzing the two-electron reduction of lipid hydroperoxides. *J Chromatogr B* 827:58–64
25. Girotti AW, Korytowski W (2000) Cholesterol as a singlet oxygen detector in biological systems. *Methods Enzymol* 319:85–100
26. Girotti AW (2001) Photosensitized oxidation of membrane lipids: reaction pathways, cytotoxic effects and cytoprotective mechanism. *J Photochem Photobiol B* 63:103–113
27. Yamazaki S, Ozawa N, Hiratsuka A, Watabe T (1999) Photogeneration of 3 $\beta$ -hydroxy-5 $\alpha$ -cholest-6-ene-5-hydroperoxide in rat skin: evidence for occurrence of singlet oxygen in vivo. *Free Radic Biol Med* 27:301–308
28. Arakane K, Ryu A, Hayashi C, Masunaga T, Shinmoto K, Mashiko S, Nagano T, Hirobe M (1996) Singlet oxygen generation from coproporphyrin in propionibacterium acnes on irradiation. *Biochem Biophys Res Commun* 223:578–582
29. Wondrak GT, Roberts MJ, Cervantes-Laurean D, Jacobson MK, Jacobson EL (2003) Proteins of the extracellular matrix are sensitizers of photo-oxidative stress in human skin cells. *J Invest Dermatol* 121:578–586
30. Wondrak GT, Roberts MJ, Jacobson MK, Jacobson EL (2004) 3-Hydroxypyridine chromophores are endogenous sensitizer of photooxidative stress in human skin cells. *J Biol Chem* 279:30009–30020
31. Yamazaki S, Ozawa N, Hiratsuka A, Watanabe T (1999) Quantitative determination of cholesterol 5 $\alpha$ -, 7 $\alpha$ -, and 7 $\beta$ -hydroperoxides in rat skin. *Free Radic Biol Med* 27:110–118

the latest and simplest in vivo method that addresses the capability of an organism to produce highly unsaturated fatty acids (HUFA). In the present note on methodology, information and computations required to carry out the whole-body fatty acid balance method are presented.

## Description of the Method

For the execution of the whole-body fatty acid balance method a feeding trial is a fundamental necessity. The basic concept on which the method is based on is the quantification of the initial and final fatty acid composition of the whole-body and the quantification of the net intake of dietary fatty acids, based on a feeding trial.

The feeding trial must be of a sufficient duration to guarantee an adequate weight gain in order to enable an accurate quantification of fatty acid elongation and desaturation. Moreover, as the present method is fundamentally a mass balance analysis, by increasing the difference between the factors, it is possible to increase the sensitivity of the measurement. It is crucial that the feed intake is measured accurately. The total collection of faeces or a corresponding digestibility estimation using an appropriate dietary marker is essential for the quantification of the net intake of fatty acids.

The type of diet used for the whole-body fatty acid balance method is unimportant given that its proximate and fatty acid compositions are known. However, for the quantification of elongase and desaturase activities a diet containing minimal amounts of these enzyme products (i.e. HUFA) is desired. Considering the method is based mainly on a mass balance analysis of individual fatty acids, a high intake of HUFA can mask the appearance of newly elongated and/or desaturated fatty acids [5].

The analyses required for the subsequent computations of the whole-body fatty acid balance method are: the initial and final body weight, initial and final quantitative fatty acid composition of the whole body, the total feed intake, the quantitative fatty acid composition of the diet and the fatty acid digestibility or the quantitative fatty acid composition of the total faeces produced during the experiment.

The computation of the whole-body fatty acid balance method is best dealt with in four steps.

The first step is to determine the partitioning of the dietary fatty acids amongst excretion, accumulation, appearance or disappearance, as described previously by Cunnane and Anderson [4].

The individual fatty acid amounts in diet, faeces, initial and final carcass need to be expressed in mg per animal. After calculating the individual fatty acid (FA) intake ( $= \text{g of feed intake} \times \text{mg of FA per g of feed}$ ), excretion ( $= \text{mg of FA intake} \times \text{FA digestibility}$ ; or  $= \text{g of faeces} \times \text{mg of FA per g of faeces}$ ) and accumulation ( $= \text{mg of FA in final carcass} - \text{mg of FA in initial carcass}$ ) it is possible to estimate the fatty acid appearance or disappearance ( $= \text{FA accumulation} - \text{FA intake} - \text{FA excretion}$ ) (Fig. 1).

A disappearance of fatty acids may involve their elongation and desaturation to longer chain fatty acids or utilization of their carbon skeleton through  $\beta$ -oxidation for energy production. For purposes of this communication the metabolic pathway of  $\alpha$ -linolenic acid (18:3n-3) is presented. The metabolic pathways of other fatty acids are simpler and can therefore be deduced accordingly.

The common 18:3n-3 metabolic pathway can be subdivided into three categories: chain-shortening and oxidation (Ox), elongation towards dead end products (DE) and the normal elongation/desaturation pathway (NED). The fatty acids involved in the 18:3n-3 DE pathway are 20:3n-3 and 22:3n-3. While those involved in the 18:3n-3 NED pathway include 18:4n-3, 20:4n-3, 20:5n-3, 22:5n-3 and 22:6n-3. The production 22:6n-3 involves a further elongation of 22:5n-3 to 24:5n-3, a  $\Delta$ -6 desaturation of 24:5n-3 to 24:6n-3 and a chain-shortening reaction from 24:6n-3 to 22:6n-3 [2]. However, 24:5n-3 and 24:6n-3 are seldom present in detectable amounts and therefore, the passage from 22:5n-3 to 22:6n-3 is in the present computation considered as a sole elongase,  $\Delta$ -6 desaturase and chain-shortening reaction.

The second step of the method involves the computation of the 18:3n-3 balance. The amount of fatty acids represented in the 18:3n-3 metabolic pathway needs to be converted from mg to mmol of appeared/disappeared FA per animal.

**Fig. 1** Schematic representation of the mass balance analysis of the individual fatty acid intake and accumulation. The first step in the whole-body fatty acid balance method

<b>Final fatty acid body content</b> - <b>Initial fatty acid body content</b> = 		<b>Fatty acid intake</b> - <b>Fatty acid excretion</b> = 	
<b>Fatty acid accumulation</b>	-	<b>Fatty acid net intake</b>	= <b>Fatty acid appearance/disappearance</b>

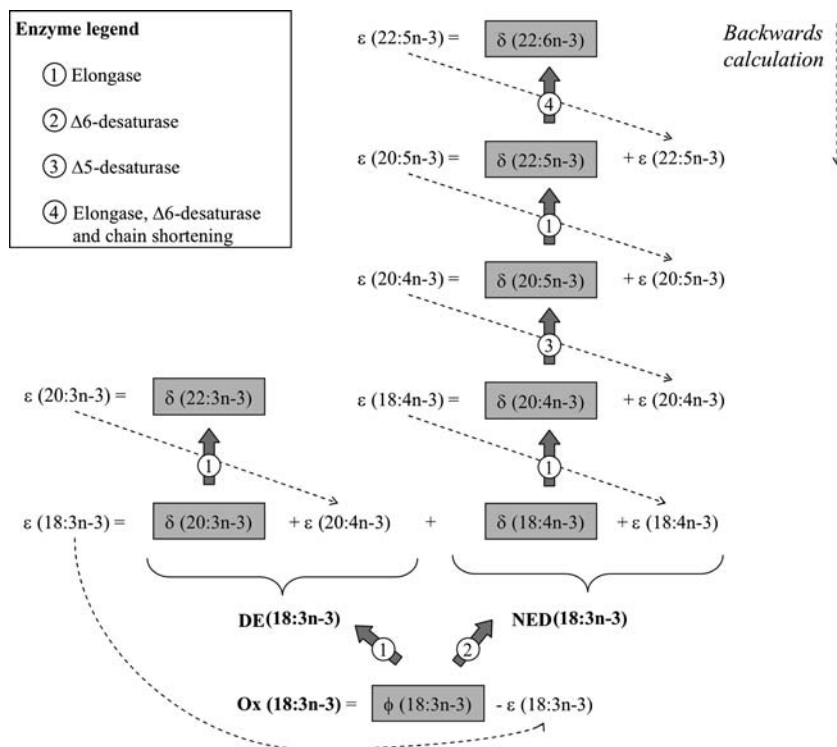


**Fig. 2** Schematic representation of the computation involved in the whole-body fatty acid balance method. Shaded figures [ $\delta$  values i.e.  $\delta(22:6n-3)$ ,  $\delta(22:5n-3)$ , etc.] represent the results obtained following the first step of the method (mmol of the specified FA appeared/disappeared), while the  $\phi$  value (for 18:3n-3 only) represents the total number of mmol of 18:3n-3 disappeared (given that no appearance is possible in vertebrates). Via a backwards calculation, starting from the end of the two pathways it is possible to calculate the  $\epsilon$  values,

which represent the mmol of specified FA converted to longer or more unsaturated homologues. Successively, it is possible to quantify the fate of  $\alpha$ -linolenic acid (18:3n-3) as (i) chain shortening and oxidation (Ox), (ii) elongation towards a dead end product (DE) or (iii) elongation and desaturation along the normal pathway (NED). Ultimately, it is possible to estimate the elongase,  $\Delta$ -5 and  $\Delta$ -6 desaturase activities

The number of mmol of longer chain fatty acids that appeared is subtracted from the number of mmol of the previous fatty acid in the fatty acid elongation/desaturation pathway. A diagram depicting the backwards calculation along the fatty acid metabolic pathways is provided (Fig. 2). The mathematical model used for the whole-body fatty acid balance computation for n-3 fatty acids is described by the following equations (Eqs. 1, 2, 3, 4, 5, 6) [where:  $\epsilon$  = mmol of specified FA converted (elongated or desaturated);  $\delta$  = mmol of the specified FA appeared/disappeared per animal; if  $\delta$  is a negative number (FA disappeared = oxidized), then  $\delta = 0$  for the following computation]:

NED pathway:

$$\epsilon(22:5n-3) = \delta(22:6n-3) \tag{1}$$

$$\epsilon(20:5n-3) = \delta(22:5n-3) + \epsilon(22:5n-3) \tag{2}$$

$$\epsilon(20:4n-3) = \delta(20:5n-3) + \epsilon(20:5n-3) \tag{3}$$

$$\epsilon(18:4n-3) = \delta(20:4n-3) + \epsilon(20:4n-3) \tag{4}$$

DE pathway:

$$\epsilon(20:3n-3) = \delta(22:3n-3) \tag{5}$$

Total 18:3n-3 balance:

$$\epsilon(18:3n-3) = \delta(20:3n-3) + \epsilon(20:3n-3) + \delta(18:4n-3) + \epsilon(18:4n-3) \tag{6}$$

The estimation of the fate (elongation, desaturation or oxidation) of each fatty acid can therefore be computed accordingly to its specific metabolic pathway; for example 18:2n-6, 18:3n-6, 20:3n-6, 20:4n-6, 22:4n-6 or 18:1n-9, 18:2n-9, 20:2n-9, 20:3n-9, and pathways involving the  $\Delta$ -9 desaturase enzyme such as 16:0, 16:1n-7, 18:1n-7 can be evaluated as well.

At this point (the third step of the method) it is possible to quantify the amount of 18:3n-3 used in  $\beta$ -oxidation or elongated and desaturated (Fig. 2). The total 18:3n-3 balance can therefore be delineated by the following equations (Eqs. 7, 8, 9, 10, 11, 12) [where: DE(18:3n-3) = total 18:3n-3 elongated to dead end products; NED(18:3n-3) = total 18:3n-3 converted through the normal elongation/desaturation pathway; Ox(18:3n-3) = total 18:3n-3 oxidized;  $\phi$  (18:3n-3) = total number of mmol of 18:3n-3 disappeared]:

$$\text{DE}(18:3n-3) = \delta(20:3n-3) + \varepsilon(20:3n-3) \quad (7)$$

$$\text{NED}(18:3n-3) = \delta(18:4n-3) + \varepsilon(18:4n-3) \quad (8)$$

$$\text{Ox}(18:3n-3) = \phi(18:3n-3) - \text{DE}(18:3n-3) - \text{NED}(18:3n-3) \quad (9)$$

The fate of 18:3n-3 can be further reported as a percentage relative to its total net intake (NI; calculated from the first step of the method; NI = FA intake – FA excretion and converted into mmol)

$$\begin{aligned} \text{\% of 18:3n-3 elongated to dead end products} \\ = \text{DE}(18:3n-3) \times \text{NI}(18:3n-3)^{-1} \times 100 \end{aligned} \quad (10)$$

$$\begin{aligned} \text{\% of 18:3n-3 elongated and desaturated} \\ = \text{NED}(18:3n-3) \times \text{NI}(18:3n-3)^{-1} \times 100 \end{aligned} \quad (11)$$

$$\begin{aligned} \text{\% of 18:3n-3 oxidized} \\ = \text{Ox}(18:3n-3) \times \text{NI}(18:3n-3)^{-1} \times 100 \end{aligned} \quad (12)$$

Ultimately, it is possible to estimate the total elongase,  $\Delta$ -5 and  $\Delta$ -6 desaturase activities with the fourth and final step of the method. The enzyme activity is expressed as mmol of products per gram of body weight (average body weight) per day with the following equations (Eqs. 13–16):

$$\begin{aligned} \text{Gram of BW day}^{-1} \\ = (\text{initial body weight} + \text{final body weight}) \\ \times 2^{-1} \times \text{no. of days}^{-1} \end{aligned}$$

$$\begin{aligned} \Delta\text{-6 desaturase} = [\delta(18:4n-3) + \varepsilon(18:4n-3) + \delta(22:6n-3)] \\ (\text{gram of BW day}^{-1})^{-1} \end{aligned} \quad (14)$$

$$\begin{aligned} \Delta\text{-5 desaturase} = [\delta(20:5n-3) + \varepsilon(20:5n-3)] \\ (\text{gram of BW day}^{-1})^{-1} \end{aligned} \quad (15)$$

$$\begin{aligned} \text{Elongase} = [\delta(20:3n-3) + \varepsilon(20:3n-3) + \varepsilon(18:4n-3) \\ + \varepsilon(20:5n-3) + \varepsilon(22:5n-3)](\text{gram of BW day}^{-1})^{-1} \end{aligned} \quad (16)$$

## Computation example

The following example is reported to further clarify the steps in the calculations for the execution of the presented method. The example is based on data reported previously [5] on the freshwater fish Murray cod (*Maccullochella peelii peelii*) fed a semi purified diet containing linseed oil as the principal lipid source for 112 days. The sample preparation is of paramount importance for the proper functioning of the method. To properly quantify the fatty acid content of the whole body, the entire specimen (or pooled specimens) needs to be chopped and subsequently finely minced to obtain a representative and homogenous sample. Admittedly, this is a limit of the method and it can be difficult for large animals or animals with tough tissues. With fish samples, we find the repeated utilization of a heavy duty meat mincer, with a reduction of the die size after each pass, well suited for homogenization. Lipid extraction should then be performed on a relatively large sample, on as many replicates as possible to improve the accuracy of the quantification and accordingly to standardized reliable protocols [7]. A second, equally important aspect is to implement a proper chromatographic quantitative procedure, as the simple, commonly adopted evaluation of fatty acids as a percentage value is not informative enough and can not be utilised. The use of a suitable internal standard and the correction by theoretical relative FID response factors of the resulting peak areas are essential for accurate FA quantification [8].

In Table 1, the results obtained from the calculation of the first step of the whole-body fatty acid balance method are reported. Subsequently, following the second step of the whole-body fatty acid balance method it is possible to calculate the  $\varepsilon$  values (Fig. 2) along the NED and DE pathways:

(Eq. 1):

$$\varepsilon(22:5n-3) = \delta(22:6n-3) = 12.8(\text{mmol per fish})$$

(Eq. 2):

$$\begin{aligned} \varepsilon(20:5n-3) = \delta(22:5n-3) + \varepsilon(22:5n-3) \\ = 123.2 + 12.8 = 136.0(\text{mmol per fish}) \end{aligned}$$

(Eq. 3):

$$\begin{aligned} \varepsilon(20:4n-3) = \delta(20:5n-3) + \varepsilon(20:5n-3) = -111.4 + 136.0 \\ = 24.6(\text{mmol per fish}) \end{aligned}$$

**Table 1** The first step of the whole-body fatty acid balance method; data is relative to the n-3 fatty acid balance during a 112-day period on Murray cod fed a linseed oil based diet [5]

	18:3n-3	18:4n-3	20:3n-3	22:3n-3	20:4n-3	20:5n-3	22:5n-3	22:6n-3
mg FA per fish								
Intake	4561.8	18.7	ND	ND	ND	46.2	10.4	72.3
Excretion	72.1	ND	ND	ND	ND	2.3	ND	4.7
Initial body content	17.5	21.7	1.7	ND	12.8	82.3	51.8	153.8
Final body content	2377.8	284.2	75.2	ND	137.4	92.5	102.9	225.7
Accumulation	2360.3	262.5	73.6	ND	124.6	10.2	51.1	71.9
Appearance/disappearance								
	18:3n-3	18:4n-3	20:3n-3	22:3n-3	20:4n-3	20:5n-3	22:5n-3	22:6n-3
mg FA per fish								
	-2129.4	243.8	73.6	ND	124.6	-33.7	40.7	4.2
	$\phi(18:3n-3)$	$\delta(18:4n-3)$	$\delta(20:3n-3)$	$\delta(20:3n-3)$	$\delta(20:4n-3)$	$\delta(20:5n-3)$	$\delta(22:5n-3)$	$\delta(22:6n-3)$
mmol FA per fish								
	7646.0	881.6	240.0	ND	409.3	-111.4	123.2	12.8

In the last row,  $\delta$  values represent the mmol of the specified FA appeared or disappeared (if value is positive or negative, respectively), while the  $\phi$  value (for 18:3n-3 only) represents the total number of mmol of 18:3n-3 disappeared

ND not detected

(Eq. 4):

$$\begin{aligned}\varepsilon(18:4n-3) &= \delta(20:4n-3) + \varepsilon(20:4n-3) = 409.3 + 24.6 \\ &= 433.9(\text{mmol per fish})\end{aligned}$$

(Eq. 5):

$$\varepsilon(20:3n-3) = \delta(22:3n-3) = 0(\text{mmol per fish})$$

Once the individual  $\varepsilon$  values which represent the mmol of specified FA converted to longer or more unsaturated homologues have been calculated, it is possible to calculate the total amount of 18:3n-3 elongated and desaturated through both of the pathways:

(Eq. 6):

$$\begin{aligned}\varepsilon(18:3n-3) &= \delta(20:3n-3) + \varepsilon(20:3n-3) + \delta(18:4n-3) \\ &+ \varepsilon(18:4n-3) = 240.0 + 0 + 881.6 + 433.9 \\ &= 1555.5(\text{mmol per fish})\end{aligned}$$

Through the third step of the method, it is possible to quantify the amount of 18:3n-3 used in  $\beta$ -oxidation or elongated and desaturated (Fig. 2).

(Eq. 7):

$$\begin{aligned}\text{DE}(18:3n-3) &= \delta(20:3n-3) + \varepsilon(20:3n-3) \\ &= 240 + 0 = 240(\text{mmol per fish})\end{aligned}$$

(Eq. 8):

$$\begin{aligned}\text{NED}(18:3n-3) &= \delta(18:4n-3) + \varepsilon(18:4n-3) \\ &= 881.6 + 433.9 = 1315.5(\text{mmol per fish})\end{aligned}$$

(Eq. 9):

$$\begin{aligned}\text{Ox}(18:3n-3) &= \phi(18:3n-3) - \text{DE}(18:3n-3) \\ &- \text{NED}(18:3n-3) = 7646.0 - 240 - 1315.5 \\ &= 6090.5(\text{mmol per fish})\end{aligned}$$

At this stage, with Eqs. 10, 11 and 12, the fate (DE, NED or Ox) of 18:3n-3 can be additionally reported as a percentage relative to its total net intake; in this example 1.5, 8.2 and 37.8%, respectively.

Ultimately, with the fourth and final step, through Eqs. 13, 14, 15, 16 it is possible to estimate the total elongase,  $\Delta$ -5 and  $\Delta$ -6 desaturase activities expressed as mmol of product per gram of body weight per day. In the example reported the initial fish weight was 21.3, final fish weight was 74.6 and the experimental period was 112 days, therefore (Eq. 13) the grams of BW day<sup>-1</sup> equates to 5,370.

(Eq. 14):

$$\begin{aligned}\Delta\text{-6 desaturase} &= [\delta(18:4n-3) + \varepsilon(18:4n-3) + \delta(22:6n-3)] \\ &(\text{gram of BW day}^{-1})^{-1} = (881.6 + 433.9 + 12.8) \\ &\times (5370)^{-1} = 0.24735(\text{mmol g}^{-1}\text{day}^{-1})\end{aligned}$$



(Eq. 15):

$$\begin{aligned}\Delta-5 \text{ desaturase} &= [\delta(20:5n-3) + \varepsilon(20:5n-3)] \\ (\text{gram of BW day}^{-1})^{-1} &= (-111.4 + 136.0) \times (5370)^{-1} \\ &= 0.00458(\text{mmol g}^{-1}\text{day}^{-1})\end{aligned}$$

(Eq. 16):

$$\begin{aligned}\text{Elongase} &= [\delta(20:3n-3) + \varepsilon(20:3n-3) + \varepsilon(18:4n-3) \\ &+ \varepsilon(20:5n-3) + \varepsilon(22:5n-3)](\text{gram of BW day}^{-1})^{-1} \\ &= (240.0 + 0 + 433.9 + 136.0 + 12.8) \times (5370)^{-1} \\ &= 0.15319(\text{mmol g}^{-1}\text{day}^{-1}).\end{aligned}$$

As previously reported [5], fish were housed in three replicate tanks (30 fish per tank) with four fish culled per tank and analyzed individually in duplicate. The analytical variability recorded was relatively low. For example, the average coefficient of variability ( $\text{st.dev} \times 100 \times \text{mean}^{-1}$ ) of DHA in the whole body within the replicates was 1.43%. However, the biological variability recorded between the four individuals was greater (8.43%), with the highest variability recorded in fish from the same tank ranging from 23 to 28 mg of DHA per g of lipid. Although this information is useful in understanding the analytical and biological variability within individual specimen, the actual replicate has to be considered the tank, hence  $N = 3$ , from a statistical viewpoint. If we were to focus our attention on the total  $\Delta$ -6 desaturase activity (Eq. 14) evidenced using the whole body fatty acid balance method, we recorded for the three tanks the values 0.20068, 0.26297 and 0.27840  $\text{mmol g}^{-1} \text{day}^{-1}$ . Clearly this is to be considered as a broad indication for the estimation of appropriate sample size when fish are used. Understandably, the specific variability of an individual sample would need to be taken into consideration if the method was to be applied to a different animal.

## Discussion

A variety of methods have been developed for measuring elongase and desaturase activity. The methodology presented here employs an in vivo approach which provides a reliable estimation of an organism's overall capacity to metabolize fatty acids. To date, to the best of the authors' knowledge, this method has been applied only twice [5, 6], but not presented in detail. With respect to the quantification of elongase and desaturase activity, the results obtained in these studies are highly consistent and in general agreement within the highly variable range of results obtained using ex vivo counterparts. For example,

the  $\Delta$ -6 desaturase activity reported on 18:3n-3 in the above mentioned separate studies and measured with the whole-body fatty acid balance method in juvenile fresh-water finfish Murray cod (*Maccullochella peelii peelii*) were  $0.147 \pm 0.006 \text{ mmol g}^{-1} \text{day}^{-1}$  and  $0.247 \pm 0.012 \text{ mmol g}^{-1} \text{day}^{-1}$  in fish fed semi purified diets containing only a blend of vegetable oils [6] and linseed oil [5] as the dietary lipid source. The differences in enzyme activity were ascribable to the difference in the percentage of 18:3n-3 in the diets, which were 25.7 and 55.4%, respectively.

Unfortunately, to date, it has not been possible to directly compare the results obtained by the utilization of the presented method with results from different ex vivo methods because they are generally reported as pmol per hour per gram of protein of the isolated cells, and not relative to the entire organism. Moreover, the two methods have not been implemented on a single species, and therefore a hypothetical comparison would be misleading.

Admittedly, there are certain limitations that can restrict accuracy and applicability of the proposed method. One variable that the whole-body fatty acid balance method does not take into consideration is the allowance of eicosanoid production. However, it is acceptable that the conversion of 20:4n-6 and 20:5n-3 is minimal, having little impact on the total balance of fatty acids [4]. A second variable not taken into consideration is the possible chain-shortening and oxidation of fatty acids previously elongated and desaturated [9]; for example if a given amount of 18:3n-3 is desaturated to 18:4n-3 and successively oxidized it will be considered as an oxidation process of 18:3n-3. However, although oxidation of longer and more unsaturated chain fatty acids is occurring to a lesser extent than their precursor [9], this is a possible occurrence, and hence a limit, also for other methods such as ex vivo approaches that employ whole cells and their incubation with labeled fatty acids. If for example [ $1\text{-}^{14}\text{C}$ ] labeled 18:3n-3 is utilised, the radioactive acid-soluble fatty acid oxidation products determined to quantify  $\beta$ -oxidation activity can derive from [ $1\text{-}^{14}\text{C}$ ] 18:3n-3 directly oxidized but also from [ $1\text{-}^{14}\text{C}$ ] 18:3n-3 previously desaturated to [ $1\text{-}^{14}\text{C}$ ] 18:4n-3 and successively oxidized.

In consideration that the method provides an accurate mass balance analysis it can quantify an animal's capability in depositing HUFA. We can therefore conclude that the whole-body fatty acid balance method is a simple, relatively inexpensive, routine laboratory technique and its utilization on different species will be instrumental in expanding our understanding of animal lipid metabolism.

**Acknowledgements** Giovanni Turchini's contribution to this study was made whilst holding a Post Doctoral Fellowship from the Australian Research Council and this support is gratefully acknowledged.

## References

1. Nakamura MT, Nara TY (2004) Structure, function, and dietary regulation of delta-6, delta-5, and delta-9 desaturases. *Annu Rev Nutr* 24:345–376
2. Sprecher H, Luthria DL, Mohammed BS, Baykousheva SP (1995) Reevaluation of the pathways for the biosynthesis of polyunsaturated fatty acids. *J Lipid Res* 36:2471–2477
3. Brown JE (2005) A critical review of methods used to estimate linoleic acid  $\Delta$  6-desaturation ex vivo and in vivo. *Eur J Lipid Sci Technol* 107:119–134
4. Cunnane SC, Anderson MJ (1997) The majority of dietary linoleate in growing rats is  $\beta$ -oxidized or stored in visceral fat. *J Nutr* 127:146–152
5. Turchini GM, Francis DS, De Silva SS (2006) Fatty acid metabolism in the freshwater fish Murray cod (*Maccullochella peellii peellii*) deduced by the whole-body fatty acid balance method. *Comp Biochem Phys B* 144:110–118
6. Francis DS, Turchini GM, Jones PL, De Silva SS (2007) Dietary lipid source modulates in vivo fatty acid metabolism in the freshwater fish, Murray cod (*Maccullochella peellii peellii*). *J Agric Food Chem* 55:1582–1591
7. Christie WW (2003) Lipid analysis. Isolation, separation, identification and structural analysis of lipids, 3rd edn. The Oily Press, P. J. Barnes and Associates, Bridgewater, pp 416
8. Ackman RG (2002) The gas chromatograph in practical analyses of common and uncommon fatty acids for the 21st century. *Anal Chim Acta* 465:175–192
9. Cunnane SC (2001) Application of new methods and analytical approaches to research on polyunsaturated fatty acid homeostasis. *Lipids* 36:975–979

4-methyl-1,2,4-triazoline-3,5-dione (MTAD) adducts for definitive identification of double bond positions. In addition, silver ion high-performance liquid chromatography (HPLC) has proved very useful for the separation of geometrical and positional isomers both on analytical and preparative scales.

In this review, we have been pragmatic and highly selective in describing those methods that appear to us to be most useful for isolation and analysis of CLA and CLA isomers, as opposed to an exhaustive discussion of the literature. There is inevitably an element of subjectivity in our approach. Most analysts will employ GC for routine analysis of CLA and this may be supplemented with mass spectrometry for definitive identifications. Silver ion high-performance liquid chromatography is an invaluable alternative or complementary procedure. However, CLA levels in tissues of foodstuffs may be too low to be directly amenable to such analyses. Then, pre-concentration methods may have to be applied. Detailed protocols for many of the methods described here are available in earlier reviews [3, 5].

### Preparation of Methyl Ester Derivatives of Lipids Containing CLA

The first step before chromatographic analysis of lipids containing CLA is preparation of the methyl ester derivatives. It is well established that acid-catalysed transesterification of lipids can bring about isomerization of *cis,trans*- to the *trans,trans*-forms with some loss of CLA, so that base-catalysed methods are most suitable for the purpose [6]. Sodium methoxide in anhydrous methanol is the preferred reagent for glycerolipids. Free fatty acids cannot be esterified by this means, and while trimethylsilyl-diazomethane is occasionally recommended, there is ample evidence that it can lead to artefact formation. However, free fatty acids can be methylated by acid-catalysed procedures if the reaction time is kept short. For example, boron trifluoride–methanol or sulfuric acid (1% v/v)–methanol reagents can be employed provided that scrupulous attention is paid to detail [5]; in particular, freshly prepared reagent should be used and the reaction time kept to the minimum. For example, free fatty acids are fully and safely methylated with boron trifluoride–methanol in 10 min at ambient temperature (or with sulfuric acid–methanol (1%) at 50 °C for up to 1 h). Methods of preparing methyl esters have been reviewed exhaustively elsewhere [7].

### Gas Chromatographic Analysis

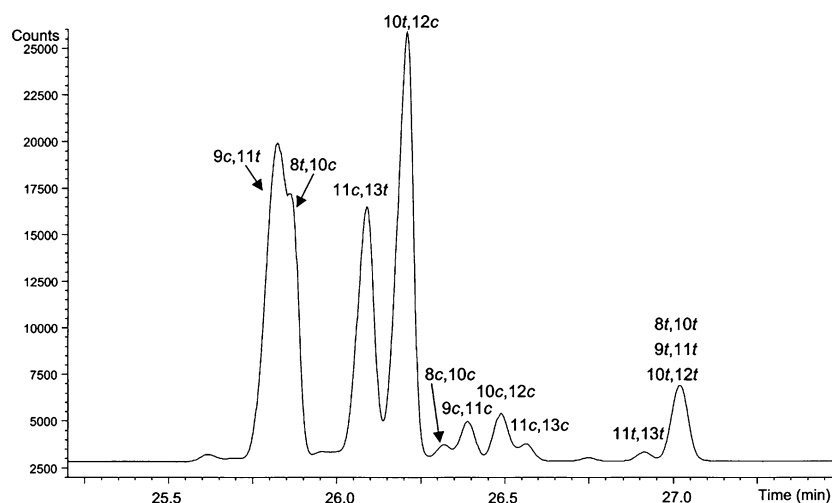
Gas chromatography is by far the most widely used method for the analysis of the total CLA content of samples and for

the composition of individual isomers. Coupled to mass spectrometry for identification purposes, it is an extremely useful tool. It is recognized that long (50 or 100 m) polar columns coated with 100% cyanopropyl polysiloxane (e.g., CP-Sil 88<sup>TM</sup>, SP2380<sup>TM</sup> and SP 2560<sup>TM</sup>) give optimum resolution of CLA isomers. Under optimal conditions, methyl esters of CLA isomers elute just after 18:3(n-3) and 20:1 isomers and before 20:2(n-6), although under some conditions 20:1 isomers can interfere with the analysis of CLA. On a 100 m CP-Sil 88<sup>TM</sup> column, the following conditions have been used successfully for total cheese fatty acid methyl esters (FAMES); holding the temperature at 75 °C for 2 min, temperature programming at 5 °C/min to 180 °C, holding at 180 °C for 33 min, then at 4 °C/min to 225 °C and finally holding at 225 °C for 44 min [8]. Under these conditions the CLA isomers eluted between 49 and 53 min. The low starting temperature enabled short-chain fatty acids to be separated, but a higher starting temperature (150–175°C) can be used for most other tissue samples. If the total CLA content is all that is required, a column of medium polarity (CP-Wax 58<sup>TM</sup>) and moderate length (25 m) can be used, the CLA region emerging after 18:3(n-3), and before all C<sub>20</sub> and C<sub>21</sub> FAMES.

The distribution of CLA isomers in commercial preparations has been examined by GC of the methyl esters [with identification by GC–MS of the DMOX derivatives (see below)] [9]. Typical commercial CLA mixtures contain mainly *cis,trans/trans,cis* isomers and less *cis,cis* and *trans,trans* isomers (Fig. 1). The *trans,cis* CLA isomers elute before the *cis,cis* and finally the *trans,trans* isomers emerge. Usually only one of the *cis,trans/trans,cis* forms (e.g., 9*c*,11*t*-18:2 but not 9*t*,11*c*-18:2) of each positional isomer occurs. The main isomers are 9*c*11*t*- and 10*t*12*c*-18:2 in roughly equal amounts, and 8*t*10*c*- and 11*c*13*t*-18:2 may be either absent or present to varying degrees. The 8*t*10*c*-18:2 isomer is sometimes totally masked by the 9*c*11*t*-18:2 isomer but can be seen as a definite later-eluting shoulder or even as a split peak when the proportion of the two isomers is similar. The 11*c*13*t*-18:2 isomer emerges next and may not be totally resolved from the 10*t*12*c*-18:2 isomer. Trace amounts of 10*c*,12*t*- and 9*t*,11*c*-18:2 isomers are sometimes apparent, occurring between the 9*c*,11*t*-/8*t*,10*c*- and 11*c*,13*t*-18:2 peaks. Low levels of *cis,cis* isomers are reasonably well resolved (elution order 8,10- < 9,11- < 10,12- < 11,13-18:2) occurring just after the 10*t*,12*c*-18:2 peak. Within the *trans,trans* isomers the 11,13-18:2 isomer elutes ahead of the other (8,10-, 9,11- and 10,12-18:2) poorly resolved isomers.

Similarly, GC (and GC–MS of DMOX derivatives) has been utilized for characterizing CLA in a variety of natural samples. The materials may be analysed without pre-treatment or after concentration of total CLA by RP–HPLC (see below) or, for the most detailed examination as has

**Fig. 1** Partial gas chromatogram of a commercial CLA methyl ester mixture, separated on a CP-Sil 88 capillary column (100 m × 0.25 mm id × 0.2 μm film thickness; Chrompack UK Ltd, London, UK) with flame-ionization detection. The oven temperature was held at 160 °C for 3 min, then was programmed at 2 °C/min to 220 °C and held at 220 °C for 20 min. Hydrogen was the carrier gas at a constant flow rate of 1 ml/min and a split ratio of 50:1 was used



been applied to cheese, after fractionation of the CLA by silver-ion HPLC (discussed below). In the latter case it is interesting that a short non-polar (30 m HP5MS) column can be used for CLA analysis. It would appear that optimum resolution by GC may not be essential if pre-fractionation by silver ion HPLC is carried out.

Natural samples for CLA analysis often contain more isomers than commercial CLA and the proportion of isomers within each sample type is different, affecting peak resolution. Invariably the 9*c*,11*t*-18:2 isomer is the major peak representing 80–90% of total CLA isomers. The isomer distribution in cheese contains all the isomers found in other foods (Fig. 2) [10, 11]. The *cis,trans/trans,cis*, *cis,cis* and *trans,trans* groups all contain positional isomers ranging from 7,9- to 12,14-18:2. Within the *cis,trans/trans,cis* isomers, in contrast to most commercial CLA, all possible geometrical isomers have been detected with the exception of 8*c*,10*t*- and 12*t*,14*c*-18:2. Retention times increase with increasing distance of the *cis* double bond from the ester moiety, and for isomers that have the same *cis* double bond, with the exception of the 10*t*,12*c*-/12*c*,14*t*-18:2 pair, the isomer with the *trans* double bond nearest the ester moiety elutes first. In cheese, none of the *cis,trans/trans,cis* isomers elute as pure peaks; 7*t*,9*c*-, 8*t*,10*c*- and 9*c*,11*t*-18:2 overlap, as do 9*t*,11*c*- and 10*c*,12*t*-18:2, and 10*t*,12*c*- and 12*c*,14*t*-18:2, and 11*t*,13*c*-18:2 overlaps with the first *cis,cis* peak (Fig. 2). Within the *cis,cis* isomers, presumably due to the wide range in the relative amounts of the different positional isomers, only two peaks are apparent, the first comprising the 7,9- to 9,11-18:2 isomers, the second the 10,12- to 12,14-18:2 isomers. The 12*t*,14*t*-18:2 isomer elutes first followed by the 11*t*,13*t*-18:2 isomer and then the major *trans,trans* peak, comprising 7*t*,9*t*-10*t*,12*t*-18:2.

A CLA standard mixture for is essential for identifying CLA isomers in natural samples by GC. A commercial CLA mixture is useful but it does not contain all the

isomers found in natural samples. Other standard mixtures can be prepared. Preparations of mixtures containing all 16 possible isomers ranging from 8,10- to 11,13-18:2, obtained by isomerization of commercial CLA with either iodine or *p*-toluenesulfonic acid as catalyst [12], or with additional 7*t*,9*c*- and 12*c*,14*t*-18:2 isomers using a procedure involving sigmatropic rearrangements and selenium-catalysed geometrical isomerization [13], are useful as standards to assist identifications. All 32 possible isomers from 6,8- to 13,15-18:2 have been synthesised and the relative retention times determined on a 100 m CP-Sil 88™ [14] (Table 1).

Several peaks (e.g., 21:0) that are not CLA isomers may occur in the CLA region of the gas chromatogram of natural CLA samples, and in samples extracted from tissue derived from animals fed commercial CLA. The 21:0 is often at similar concentrations to the minor CLA isomers and can elute anywhere between 11*c*,13*t*- (as in Fig. 2) and 10*c*,12*c*-18:2 depending on the GC conditions [15]. Care has to be taken to avoid misidentifications, and use of columns differing in polarity can remove some dubiety. Mass spectrometry can eliminate all doubts [8].

### Silver Ion High-Performance Liquid Chromatography

Silver-ion high-performance liquid chromatography (Ag-HPLC) complements gas chromatographic analysis of samples containing CLA, and has the additional advantage of being a micro-preparative technique. Retention in Ag-HPLC is due primarily to the formation of transient complexes between the Ag<sup>+</sup> ions in the HPLC column and unsaturation (pi electrons) in the sample molecules. In general, the more unsaturation (double bonds), the more strongly the molecule is retained, though conjugated double bonds are an exception. Double bond configuration is

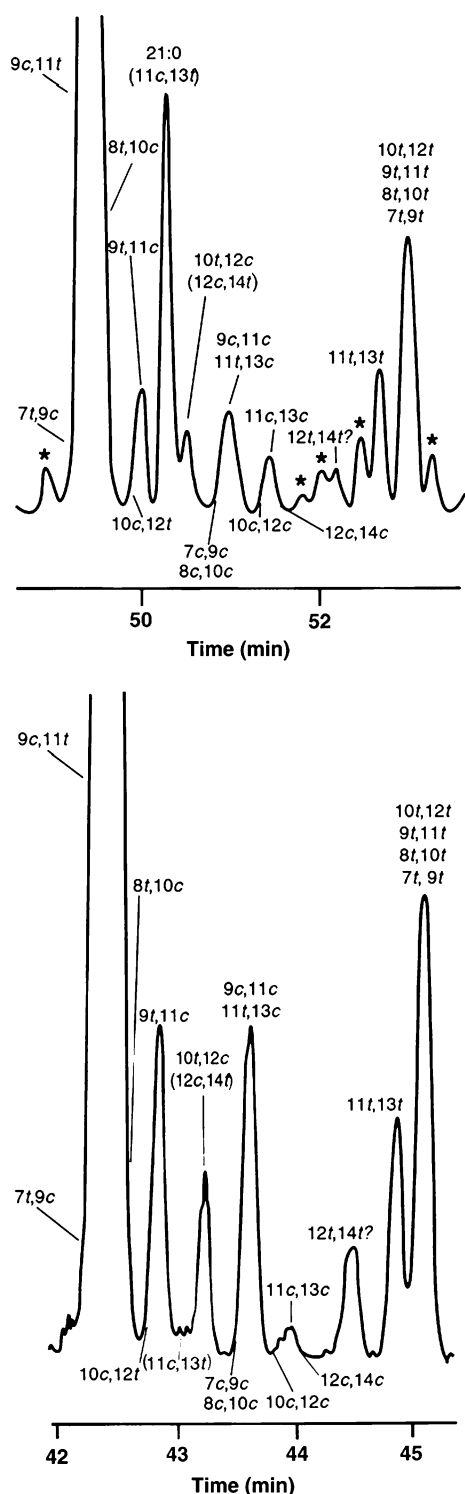


**Fig. 2** Comparison of partial gas chromatograms of the CLA methyl ester region from cheese total fatty acid methyl esters with flame-ionization detection (*top*) and the same region with high-resolution selected-ion recording (*SIR*) at  $m/z$  294.2559 (molecular weight of CLA methyl ester) (*bottom*). Separations were performed using a CP-Sil 88 capillary column (100 m  $\times$  0.25 mm id  $\times$  0.2  $\mu$ m film thickness; Chrompack Inc., Raritan, NJ) using hydrogen as carrier gas. For gas chromatography, the oven temperature was held at 75 °C for 2 min, programmed at 5 °C/min to 180 °C, held at 180 °C for 33 min, programmed at 4 °C/min to 225 °C, and finally held at 225 °C for 43.8 min. For GC–MS, the oven temperature was held at 75 °C for 2 min, programmed at 5 °C/min to 170 °C, held at 170 °C for 40 min, programmed at 5 °C/min to 220 °C, and finally held at 220 °C for 20 min. Peaks indicated by an asterisk were not found in the SIR chromatogram and are not CLA isomers. CLA isomers in brackets were detected at low levels. Redrawn from Roach et al. [8] with permission of the authors and *Lipids*. Some identities have been annotated using information from Delmonte et al. [14] and Sehat et al. [11]

**Table 1** Relative retention times (RRT) of CLA methyl ester isomers on a 100 m CP-Sil 88<sup>TM</sup> column

Isomer	RRT	Isomer	RRT
7c9t	1.083	9c11c	1.137
8c10t	1.085	10c12c	1.145
6c8t	1.086	13c15t	1.147
6t8c	1.086	12t14c	1.149
7t9c	1.091	11c13c	1.151
9c11t	1.091	12c14c	1.159
8t10c	1.097	13t15c	1.166
10c12t	1.104	13c15c	1.166
9t11c	1.109	12t14t	1.171
11c13t	1.114	11t13t	1.184
12c14t	1.118	13t15t	1.184
10t12c	1.122	9t11t	1.191
6c8c	1.128	8t10t	1.191
8c10c	1.131	10t12t	1.192
7c9c	1.131	6t8t	1.192
11t13c	1.136	7t9t	1.193

RRT relative to  $\gamma$ -linolenic acid methyl ester (GLA) calculated using  $(RT_{\text{isomer}} - RT_{\text{solvent}}) / (RT_{\text{GLA}} - RT_{\text{solvent}})$ . Oven temperature programme: 75 °C for 2 min, then 5 °C/min to 175 °C, holding at 175 °C for 33 min, then at 5 °C/min to 225 °C and finally holding at 225 °C for 8 min. Adapted from Delmonte et al. [14]

also important, with *cis* double bonds retained more strongly than *trans*. Ag-HPLC utilizing columns packed with 5–10  $\mu$ m Nucleosil SA<sup>TM</sup> or a similar material, with phenylsulfonic acid groups bonded to a silica substrate, in which the sulfonic acid protons have been exchanged with Ag<sup>+</sup> ions, is an especially useful technique for the separation and isolation of *cis* and *trans* geometrical and

positional isomers of CLA as FAMES and, to a lesser extent, as free fatty acids (FFAs) and triacylglycerols (TAGs). The technique has been reviewed in relation to lipids in general [16, 17] and CLA specifically [18].

One of the most popular Ag-HPLC columns is the ChromSpher Lipids<sup>TM</sup> column (Cat. No. 28313; 4.6 mm ID  $\times$  250 mm stainless steel; 5  $\mu$ m particle size), which can be purchased from Varian-Chrompack International, Middelburg, The Netherlands. Many analysts recommend

the employment of two such columns connected in series to improve sample capacity and to provide the required peak-to-peak resolutions, but up to six columns in series have been used for enhanced separations [12]. Typical isocratic flow rates of 1.0–2.0 ml/min and compositions of 0.1–1.0% acetonitrile in hexane in the mobile phase, maintained at a constant temperature of  $\sim 23$  °C, are adjusted to maintain pump head pressures at  $\leq 2,500$  psi and to maintain total sample elution times of 35 min or less. Void volumes are approximately 1.0 ml per column.

In a solvent system of acetonitrile in hexane, the acetonitrile competes with the  $\text{Ag}^+$  ions for the unsaturated sites of the sample molecules. The more acetonitrile in the solvent, the faster the sample elutes from the column. With dioenoic fatty acids, the greater the distance between the double bonds (up to three methylene groups at least), the more strongly they are retained. Thus, fatty acids with conjugated double bonds elute before those with methylene-interrupted double bonds, and the expected elution order (*trans,trans*-, then *cis,trans/trans,cis*-, then *cis,cis*-) is observed. These arguments also apply to the three fatty acid molecules attached to a glycerol backbone of TAG (ABA, AAB, ABC, etc.), but the location is also important. Fatty acids on the 1(3)-positions of the TAG molecule (the “A” in ABA) shield that in the 2-position (the “B”) from the  $\text{Ag}^+$  ions. So, while oleic acid (O; 9*c*-18:1) is retained more strongly than stearic acid (S; 18:0), for TAGs composed of two O and one S fatty acids, the elution order is SOS before SSO.

### Separation as Methyl Esters

Ag-HPLC analysis of CLA isomers as methyl esters (or other ester derivatives [11, 19, 20]) continues to be the single largest application for this technology, an excellent example of which is illustrated in Fig. 3. Utilizing three Ag-HPLC columns connected in series and an isocratic solvent system of 0.1% acetonitrile in hexane, Eulitz and co-workers [12] were able to separate the very difficult 9*c*,11*t*- and 9*t*,11*c*-18:2 isomer pair as FAMES, and, by utilizing two elution systems, others were able to determine the relative retention orders of all 32 *cis/trans* 6,8- to 13,15-CLA isomers [21]. Two to six columns connected in series were required to separate such isomer pairs as 8*t*,10*c*- from 7*t*,9*c*- and 11*c*,13*t*- from 9*t*,13*c*-18:2. In comparison, analysis of this mixture by GC utilizing a 100 m, highly polar capillary column could separate the *cis/cis*, the *cis/trans* and *trans/cis* (incomplete separation) and *trans/trans* 11,13-18:2 isomers, but could not resolve *trans/trans* 8,10-, 9,11- or 10,12-18:2. Propionitrile or butyronitrile in heptane may give a more stable performance as mobile phases (although these solvents are more much toxic than acetonitrile) [22].

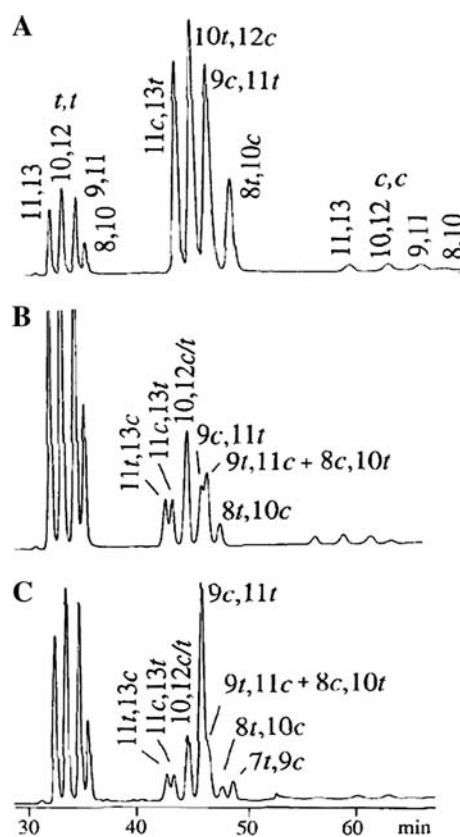


**Fig. 3** Partial Ag-HPLC profile of (A) the methyl esters of a commercial CLA isomer mixture, (B) of the  $\text{I}_2$ -isomerized product of (A) and (C) of the  $\text{I}_2$ -isomerized product of (A) co-injected with cheese total lipid FAME. Three Chromspher Lipids™ columns in series with a mobile phase of 0.1% acetonitrile in hexane (1 ml/min) and detection by UV spectroscopy at 234 nm (with the permission of the authors and AOCS Press, and redrawn from the original) [12]

In the analysis of CLA in tissue samples by such methods, especially at low concentrations, it has been recommended that the results should be confirmed by GC and/or GC-MS to eliminate errors due to false positives [22].

Ag-HPLC ( $4.6 \times 250$  mm columns) may also be used for the semi-preparative isolation of CLA esters. Two Ag-HPLC columns connected in series were also used to isolate milligram quantities of CLA isomers from a mixture of 78.8% 9*t*,11*t*-18:2/21.2% 9*c*,11*t*-18:2 (both 17,17,18,18- $d_4$ ) (Fig. 4) [23]. Resolution of the two CLA isomers, which decreased with increasing weights of samples injected, was maintained at  $>95\%$  of baseline by decreasing the percentage of acetonitrile in the isocratic hexane/acetonitrile solvent system. Purities of the isolated fractions were found to be  $>96\%$  by GC analysis. A 10 mg sample was fractionated within 35 min using a solvent system of 1.0 ml/min of 0.15% acetonitrile in hexane. One could continue to compensate for losses in peak-to-peak resolution with increased sample sizes by

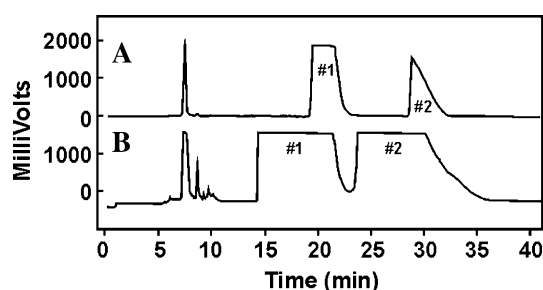


**Fig. 4** Fractionation of a CLA sample by dual column Ag-HPLC. Sample sizes: 5 mg (A) and 10 mg (B). Flow rate: 1.0 ml/min 0.15% acetonitrile in hexane. UV detection at 215 and 212 nm, respectively. Peak #1 = 9-*trans*,11-*trans*-18:2; #2 = 9-*cis*,11-*trans*-18:2 (Published with the permission of Elsevier Ltd. and redrawn from the original) [23]

decreasing the percentage of acetonitrile in the solvent; but a 15 mg sample of the CLA isomer mixture (1.0 ml/min 0.1% acetonitrile in hexane) required some 80 min to elute. Two 10 mg samples could actually be fractionated within 70 min ( $2 \times 35$  min), less time than that required to separate one 15 mg sample.

#### Separation of Free Fatty Acids

More limited work has been done with the underivatized fatty acids. Using a single Chromspher Lipids™ Ag-HPLC column and isocratic solvent systems of hexane, acetonitrile (0.0–0.025%) and acetic acid (3.0–2.5%) and with UV detection at 234 nm, Cross and co-workers [24] fractionated a mixture of CLA isomers (8*t*,10*c*-, 9*c*,11*t*-, 10*t*,12*c*- and 11*c*-13*t*-18:2) in free fatty acid form. The resulting pattern was similar to that obtained with CLA FAME with acetonitrile in hexane as solvent (see Fig. 3). The FA composition of the isolated fractions, determined after conversion to FAME (BF<sub>3</sub>/methanol) and analysis by GC, were also identical to that obtained for CLA as FAME. The same group [25] utilized Ag-HPLC and a similar solvent system to fractionate mixtures of CLA isomers obtained from commercial mixtures and from biological samples. The most abundant isomers, *cis/trans* 10,12-18:2 and *cis/trans* 9,11-18:2, were separated better as free acids on a single column than in the methyl ester form. However, a diminution in retention over time of the Ag-HPLC columns was noted, possibly as a result of a loss of silver ions because of the acetic acid in the mobile phase [25].

#### Separation of Triacylglycerols

By utilizing Ag-HPLC, successful analysis of seed oils high in conjugated dienoic or trienoic fatty acids has been

achieved. Thus, Joh and co-workers [26] used a Nucleosil™ 5SA column (4.6 × 250 mm) saturated with silver ions and a complex gradient system of dichloromethane/dichloroethane/acetone/acetonitrile (1 ml/min) to separate TAGs from the Chinese melon [*Momordica charantia*; 57.1 mol% conjugated triene, primarily  $\alpha$ -eleostearic (9*c*,11*t*,13*t*-18:3)]. Ag-HPLC (1.5 ml/min of 1.0% acetonitrile in hexane) was also utilized to fractionate a commercially available CLA-enriched TAG formulation (G-80; Loders Crokiaan B.V., The Netherlands), as illustrated in Fig. 5 [27]. The elution patterns were achieved with either three (Fig. 5 Inset A) or four (Fig. 5 and Inset B) Ag-HPLC columns connected in series. A minimum of three columns in series were required to achieve ca. 50% separation (Fig. 5 Inset A) of peaks #3 and #4, but no fractionation of the major TAG peak (peak #4) was noted. Utilizing four Ag-HPLC columns connected in series resulted in a pattern of four distinct minor and one major peak (Fig. 5). The fractions were collected (the major peak was divided into three fractions, 2A1, 2A2 and 2A3), converted to FAMES and analysed by GC. Peak #1 = mono-CLA/2 misc FAs, peak #2 = di-CLA/mono-saturated FA, peak #3 = di-CLA/9*c*-18:1, peak #4 = Tri-CLA, and peak #5 = di-CLA/mono *cis/cis* CLA isomer. (In this instance, the term “CLA” is used for both the 9,11- and the 10,12-isomers, and *cis/cis*

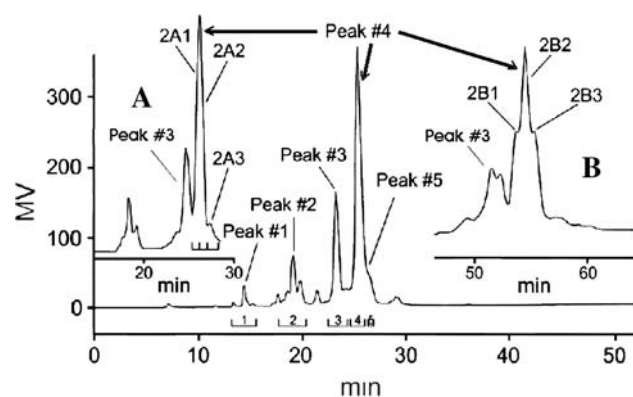


**Fig. 5** Analysis of a commercial triacylglycerol formulation containing CLA by four-column Ag-HPLC [27]. Sample size: 100  $\mu$ g. Flow rate 1.5 ml/min, 1.0% acetonitrile in hexane. UV detection at 206 nm. Peak #1 = mono-CLA with two miscellaneous fatty acids, peak #2 = di-CLA/mono-saturated fatty acid, peak #3 = di-CLA/mono 9*c*-18:1 and peak #4 = Tri-CLA; peak #5 = Tri-CLA. Inset A three-column Ag-HPLC. Sample size, 50  $\mu$ g; flow rate 2.0 ml/min, 0.6% acetonitrile in hexane. Fraction 2A1 = 54/37%:10*t*,12*c*-18:2/9*c*,11*t*-18:2; fraction 2A2 = 36/56%:10*t*,12*c*-18:2/9*c*,11*t*-18:2; fraction 2A3 = 75/11%; di-9*c*,11*t*-18:2/mono-*cis/cis*-CLA (where *cis/cis* refers to 9*c*,11*c*- and 10*c*,12*c*-18:2). Inset B four-column Ag-HPLC. Sample size, 50  $\mu$ g; flow rate 1.5 ml/min, 0.7% acetonitrile in hexane. Note: The two major peaks in Insets A and B are peaks #3 and #4 of the main chromatogram and illustrate changes in separation due to changes in the number of columns used or in solvent composition. (Published with permission of Elsevier Ltd. and redrawn from the original)

refers to 9*c*,11*c*- and 10*c*,12*c*-18:2). At 0.6% acetonitrile (1.5 ml/min), the desired peak could not be eluted within 120 min. At 0.7% acetonitrile (1.5 ml/min), the peak #4 eluted at 55 min and was partially fractionated into three peaks (Fig. 5 Inset B; <10% resolution; 1:2:1 ratio). Fractionation of the individual TAG isomers was improved, but at a cost of increased elution time. Solvent flow rates and compositions could be adjusted to yield total TAG elution patterns within 30–35 min and to maintain a system pressure < 2,500 psi. Comparable methods could no doubt be used for other lipid classes after conversion to suitable non-polar derivatives.

### Concentration of Natural CLA Isomers for Further Analysis

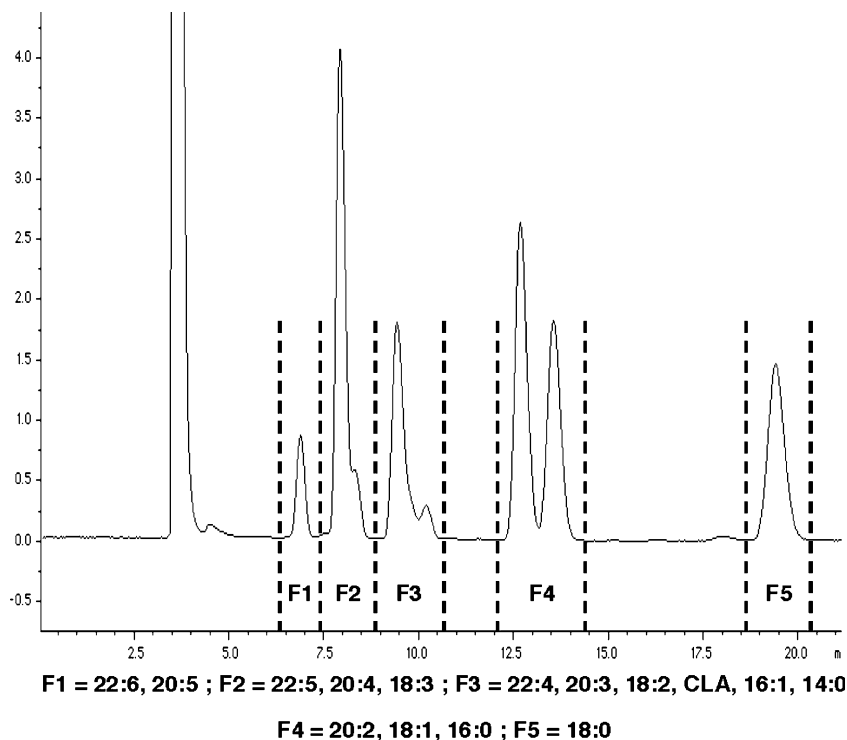
In order to have sufficient material for analysis with tissue samples containing CLA at low levels, a pre-concentration step may be required. This can be accomplished either by subjecting the methyl esters to reversed-phase HPLC or Ag chromatography or at times by using the two techniques sequentially [28].

In reversed-phase chromatography, CLA isomers elute close to linoleate and can be collected preparatively by collecting a single broad C<sub>18</sub> diene fraction. Many analysts add water to the mobile phase or use acetonitrile–water gradients. However, acetonitrile alone is preferable either at a constant flow rate or with a flow gradient, as there is

no sacrifice of resolution and it is easier to recover the required esters by evaporation of the mobile phase. Most columns of the octadecylsilyl (ODS) type can be used for methyl esters of fatty acids [28], and base-stabilized ODS columns are of value for use with DMOX derivatives and picolinyl esters (but not free fatty acids) [29]. Evaporative light-scattering detection with a stream splitter can be used, or UV detection at 206 nm (isolated double bonds) or 230 nm (conjugated double bonds specifically), to collect appropriate fractions. Keeping the column at a constant temperature aids the reproducibility of the separation but is not essential for adequate resolution. On a standard analytical column (4.6 mm diameter), about 1 mg of sample can be separated in micro-preparative mode, but up to 20 mg can be chromatographed on a preparative column (10 mm diameter), as illustrated in Fig. 6 [5].

Ag thin-layer chromatography (TLC) and HPLC methods are available to obtain a concentrate of CLA as well as for analysis (see below), but they are needlessly complex for many purposes. A simple small-scale solid-phase extraction method adapted from a published procedure can be recommended in which an adsorbent with bonded phenylsulfonate groups is utilized in the silver ion form [30]. This can be applied to any methyl ester preparation, and to the C<sub>18</sub> diene fraction isolated by reversed-phase HPLC as above, as the CLA isomers tend to elute with the monoene fraction rather than with the methylene-interrupted dienes in this instance.

**Fig. 6** Reversed-phase HPLC separation of fatty acid methyl esters including CLA. A Nucleosil C<sub>18</sub> column (250 × 10 mm ID; 5 μm particles) was used with acetonitrile as mobile phase, and UV detection at 234 nm. Methyl esters (20 mg) in acetone were injected, with acetonitrile as mobile phase and a flow rate of 4 ml/min. The fraction corresponding to the C<sub>18</sub> dienes may also contain some 14:0, 16:1 and certain polyunsaturated fatty acids [28]





## Reversed-Phase HPLC With Second Derivative UV Detection

Conjugated dienes exhibit a distinct UV absorbance in the region of 230–235 nm, while isolated double bonds absorb at 206–210 nm. As the latter tend to be present in most tissues at relatively high levels, they can still interfere with the analysis of CLA isomers in tissues. Murru et al. [31] solved the problem by taking the differential of the first derivative spectrum and calculating a second derivative with two distinct peaks with minima at 234 and 242 nm. As the Beer–Lambert law is unaffected by differentiation, this technique enabled sensitive and accurate estimation of the conjugated diene content of fatty acids. In combination with reversed-phase HPLC, this is a powerful technique both for isolation and estimation of CLA and especially of CLA metabolites formed by elongation and desaturation of CLA in animal tissues, e.g., 9*c*,11*t*-18:2, 6*c*,9*c*,11*t*-18:3, 8*c*,11*c*,13*t*-20:3, and 5*c*,8*c*,11*c*,13*t*-20:4, together with the corresponding fatty acids formed by chain elongation and desaturation of 10*t*,12*c*-18:2. The 18:2 and 20:3 isomers tend to elute together, as do 18:3 and 20:4, but subsequent separation of these by GC is straightforward.

## Gas Chromatography–Mass Spectrometry

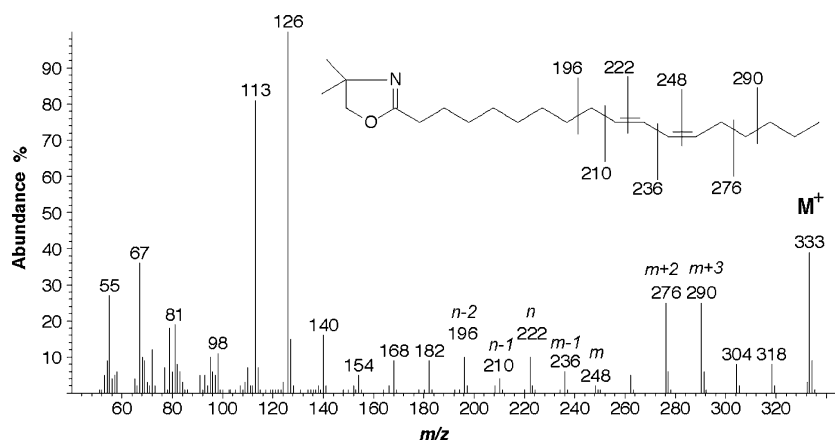
Although GC with appropriate standards will allow some tentative identification of CLA isomers to be made, GC–MS is essential for structural confirmation and for detecting overlapping isomers. The EI mass spectra of the methyl esters of CLA isomers are qualitatively indistinguishable from one another and from methyl linoleate. Although there may be some differences in the relative intensities of some ions, these are of limited value in the analysis of CLA mixtures. However, they are useful for distinguishing CLA peaks from other fatty acids that elute in the same region of the chromatogram. In order to distinguish between different CLA positional isomers, specific derivatives of either the carboxyl group or the conjugated diene system have been formed. The most useful derivatives of the carboxyl group for determining the structure of unsaturated fatty acids contain nitrogen atoms [29]. Following ionization, radical-site-induced cleavage occurs at every carbon in the chain, and by applying simple rules to the resultant mass spectrum, the structures of unknown fatty acids can usually be deduced from first principles without having to refer to the mass spectra of standard compounds. DMOX derivatives afford the most informative mass spectra for distinguishing CLA isomers and have the added advantage that the chromatographic resolution is comparable to methyl esters at only slightly higher column temperatures [29].

DMOX derivatives are easily prepared by reacting the free fatty acids or esters/intact lipids with an excess of 2-amino-2-methyl-1-propanol at 190°C for 6 and 18 h, respectively, followed by addition of water, extraction of the derivatives with diethyl ether/isohexane (1:1) and washing the extract with water [5]. The products should be dried and stored over anhydrous sodium sulfate to prevent ring opening. Although no adverse effects of using high temperatures for derivatizing CLA have been reported, other milder preparation procedures are available [32].

The mass spectra of DMOX derivatives of CLA contain an intense ion at  $m/z = 113$  corresponding to a McLafferty rearrangement ion and a molecular ion at  $m/z = 333$  (confirming a diunsaturated  $C_{18}$  structure) [33]. There is a series of ions between  $m/z = 318$  ( $[M-15]^+$  ion) and  $m/z = 126$ , each corresponding to chain fragments with one less carbon. In a saturated part of the chain, the difference between adjacent ions is 14 amu, corresponding to loss of a methylene group, but the pattern is altered when a double bond is encountered. If a double bond occurs between carbons at positions  $n$  and  $n + 1$  carbons (counting from the carboxyl end of the molecule) then there is a gap of 12 amu between ions containing  $n-1$  and  $n$  carbons. Thus in 10,12-18:2 the double bonds at  $\Delta 10$  and  $\Delta 12$  give rise to gaps of 12 amu between  $m/z$  values corresponding to C-9 ( $m/z = 210$ ) and C-10 ( $m/z = 222$ ), and C-11 ( $m/z = 236$ ) and C-12 ( $m/z = 248$ ) fragments, respectively (Fig. 7). Another characteristic feature is the presence of two intense ions (at  $m/z = 276$  and 290 for 10,12-18:2) containing  $m + 2$  (where  $m$  denotes the first carbon of the distal double bond, i.e., due to cleavage allylic to the distal double bond) and  $m + 3$  carbons. The allylic ion containing  $n-2$  carbons ( $m/z = 196$ ) (where  $n$  denotes the first carbon of the proximal double bond) is also often abundant. The same patterns hold for the published mass spectra of the DMOX derivatives of isomers from 6,8-18:2 to 13,15-18:2 except that the  $m + 2$  ion predominates over the  $m + 3$  ion as the diene system moves towards the extremities of the molecule, i.e., for 6,8-18:2 to 8,10-18:2 and 13,15-18:2.

Conjugated dienes react with  $\alpha,\beta$ -unsaturated carbonyl compounds to form six-membered ring adducts by a cycloaddition reaction known as the Diels–Alder reaction. CLA (as the methyl esters) readily react with the dienophile, MTAD thus fixing the position of the double bond, and the resultant adducts give informative mass spectra [34, 35]. The reaction is carried out by simply briefly mixing CLA with a solution of MTAD in dichloromethane at 0°C and stopping the reaction with 1,3-hexadiene. The adducts are analysed on a non-polar column (30 m DB5-MS<sup>TM</sup>) at high temperatures (160 °C for 3 min then programmed at 5 °C/min to 350 °C). There is a strong molecular ion at  $m/z = 407$  and an  $[M-CH_3O]^+$  ion at  $m/z = 376$ . Cleavages alpha to the ring give rise to two intense  $[M-R_1]^+$  and

**Fig. 7** Gas chromatography-electron-impact mass spectrum of the 4,4-dimethyloxazoline (DMOX) derivative of *trans*-10, *cis*-12-18:2 from a commercial CLA mixture



$[M-R_2]^+$  ions (where  $R_1$  corresponds to the alkyl moiety and  $R_2$  the methyl ester part of the chain), readily allowing the original position of the diene system to be deduced. Loss of methanol from  $[M-R_1]^+$  produces another prominent ion ( $[M-R_1-CH_3OH]^+$ ). Thus, for 9,11-18:2 and 10,12-18:2 the  $[M-R_1]^+$ ,  $[M-R_2]^+$  and  $[M-R_1-CH_3OH]^+$  ions occur at  $m/z = 322$ , 250 and 290 and  $m/z = 336$ , 236 and 304, respectively (Fig. 8).

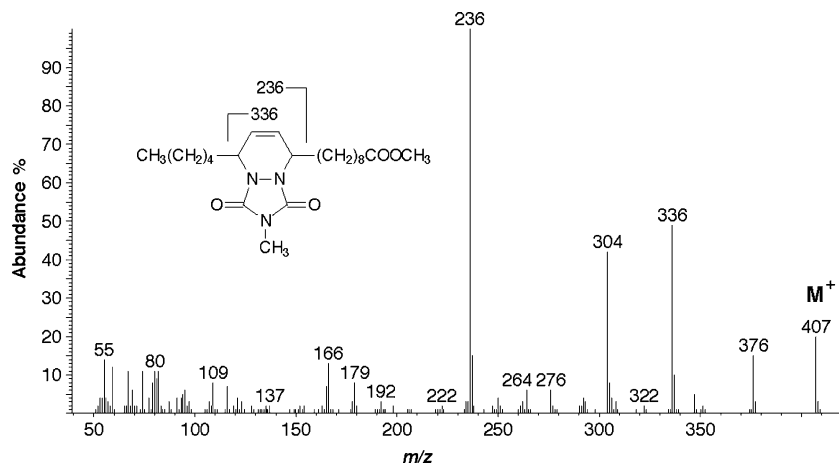
MTAD adducts are especially useful for commercial CLA preparations, particularly for determining 8,10-18:2 which is difficult to separate from 9,11-18:2 by GC as methyl ester or DMOX derivatives [34]. Adducts of isomer mixtures occur as a single chromatographic peak (there is a small degree of separation within the peak) and individual isomers are identified by using reconstructed ion chromatograms (RICs) of the  $[M-R_1]^+$  and  $[M-R_2]^+$  ions. It is possible to estimate the different positional isomers semi-quantitatively using the summation of the areas of the  $[M-R_1]^+$  and  $[M-R_2]^+$  ions, although because of the lack of chromatographic resolution it can be difficult to be certain about the presence of isomers at very low levels. For isomers ranging from 7,9- to 11,13-18:2 good agreement with  $^{13}C$  NMR spectroscopy was obtained

for a highly isomerized CLA mixture, although NMR had the advantage that geometrical isomers could be distinguished [36]. In the GC-MS approach, geometrical isomers are not distinguished, the ions representing a particular positional isomer being derived from the sum of the geometrical isomers. However, it may be possible to utilize the claim that *cis,trans/trans,cis* and *trans,trans* isomers give MTAD adducts of different stereochemistry (*trans* and *cis* isomers of the chains about the ring, respectively) that can be resolved by GC-MS [35].

Tissue or food samples containing CLA at natural or slightly elevated levels do not appear to have been analysed as the MTAD adducts by GC-MS. Such an approach is likely to be problematic, partly because of the relatively low abundance of isomers compared to the major 9*c*11*t*-18:2 isomer and partly because it has been observed that MTAD may react with methylene-interrupted unsaturated fatty acids if conditions are too harsh [34].

Because CLA isomers in both commercial and natural CLA invariably overlap by GC there has been use of reconstructed ion chromatograms of specific ions to aid identification of CLA isomers in the form of DMOX derivatives. Roach and colleagues [37] have highlighted

**Fig. 8** Gas chromatography-electron-impact mass spectrum of the 4-methyl-1,2,4-triazoline-3,5-dione (MTAD) adduct of 10,12-18:2 methyl ester from a commercial CLA mixture



seven diagnostic ions per isomer, giving a total of 28 ions (56 ions were highlighted but some occurred more than once) for isomers ranging from 6,8- to 13,15-18:2, which are useful for identifying positional isomers (Table 2). The two pairs of ions (containing  $n-1$  and  $n$  and  $m-1$  and  $m$  carbons) each differing by 12 amu due to fragmentation around the double bonds can be used, but the allylic cleavage ion containing  $m+2$  carbons and that with  $m+3$  carbons are often more useful, especially for detecting isomers at trace levels, because of their greater intensity. However, the  $m/z$  values for the latter ions are not specific to any one positional isomer and therefore, some degree of chromatographic separation, which is often the case, is useful. Indeed, after locating an isomer using the latter ions, signal contributions from adjacent peaks can be subtracted so that a representative mass spectrum of the isomer can be obtained to confirm its identity. As an example, the RIC for the allylic cleavage ion ( $m/z = 234$ ) clearly showed the presence of two 7,9-18:2 *cis,trans/trans,cis* isomers at the leading edge of the major 9 $c$ ,11 $t$ -18:2 peak (allylic ion  $m/z = 262$ ) in a variety of materials [38]. The 7 $t$ ,9 $c$ -18:2 isomer, found to be the second major isomer at about 7% of the total CLA, had previously gone unnoticed because it was masked by the major 9 $c$ ,11 $t$ -18:2 peak. In addition, a rapid, specific and sensitive high-resolution GC-MS method using selected ion recording (SIR) of the molecular ion of CLA methyl ester ( $m/z$  294.2559) was developed to unambiguously differentiate CLA isomers from non-CLA peaks in total cheese FAMES [8] (Fig. 2).

DMOX derivatives, picolinyl esters and MTAD adducts have all been used, often in a complementary manner, to analyse the metabolites formed by elongation and desaturation of CLA following suitable fractionation by HPLC [4]. For example, the metabolites isolated from rats fed a commercial CLA containing a mixture of isomers were

examined as the DMOX derivatives. The structures of 8,11,13-20:3 (derived from 9,11-18:2), and 8,12,14-20:3 and 5,8,12,14-20:4 (derived from 10,12-18:2) acids were readily determined by using the “12 amu rule”. For example, the molecular ion for the DMOX derivative of 8,12,14-20:3 was at  $m/z = 359$  and gaps of 12 amu between  $m/z$  182 and 194, 236 and 248, and 262 and 274 located the double bonds at C-8, C-12 and C-14, respectively. The base peak at  $m/z = 222$  was due to cleavage between C-10 and C-11, i.e., at the centre of the *bis*-methylene-interrupted double bond system. However, the complete structure of a 5,8,11,13-20:4 acid (derived from 9,11-18:2) could not be elucidated from the mass spectrum of the DMOX derivative. The positions of all double bonds were determined from the mass spectrum of the picolinyl ester only after deuteration of the double bonds, gaps of 15 amu locating the positions of methylene groups containing a deuterium atom. Additionally, the position of the conjugated system was confirmed from the mass spectrum of the MTAD adduct of the methyl ester. The molecular ion was at  $m/z = 431$  and the  $[M-R_2]^+$  ion at  $m/z = 250$  corresponded to a hexyl chain attached to the ring, thus confirming an 11,13 conjugated double bond system. The intensity of the  $[M-R_1]^+$  ion ( $m/z = 346$ ) was particularly weak.

A powerful tandem mass spectrometry (MS/MS) technique using acetonitrile chemical ionization was developed for determining double bond position and geometry in CLA isomers from natural samples [39]. The acetonitrile generated a (1-methyleneimino)-1-ethenyl cation which reacted with the CLA isomers, as the methyl esters, to form a  $[M+54]^+$  ion which upon collisionally activated dissociation produced two ions as a result of carbon-carbon cleavage at positions vinylic to either side of the conjugated diene system. The two ions were characteristic of the

**Table 2** Diagnostic ions for DMOX derivatives of CLA positional isomers ranging from 6,8-18:2 to 13,15-18:2

Isomer	$n-2$ ion ( $m/z$ )	$n-1$ ion ( $m/z$ )	$n$ ion ( $m/z$ )	$m-1$ ion ( $m/z$ )	$m$ ion ( $m/z$ )	$m+2$ ion ( $m/z$ )	$m+3$ ion ( $m/z$ )
6, 8 <sup>a</sup>	140	154	166	180	192	220	234
7, 9 <sup>b</sup>	154	168	180	194	206	234	248
8, 10 <sup>c</sup>	168	182	194	208	220	248	262
9, 11	182	196	208	222	234	262	276
10, 12	196	210	222	236	248	276	290
11, 13	210	224	236	250	262	290	304
12, 14	224	238	250	264	276	304	318
13, 15	238	252	264	278	290	318	332

The molecular ion is  $m/z = 333$

Adapted from Roach et al. [37]

<sup>a</sup>  $m/z$  154 is weak and  $m/z = 220$  is more abundant than  $m/z = 234$

<sup>b</sup>  $m/z$  154 is weak and  $m/z = 234$  is more abundant than  $m/z = 248$

<sup>c</sup>  $m/z$  248 is more abundant than  $m/z = 262$

position of the double bonds, one ( $\alpha$ ) containing the ester group, the other ( $\omega$ ) the terminal methyl group. The ion resulting from vinylic cleavage to a *trans* double bond was more abundant than that from a *cis* double bond. Therefore, the ratio of the abundance of  $\alpha$  to that of  $\omega$  was highest ( $>4.8$ ) for a *cis,trans* arrangement, lowest ( $<0.5$ ) for *trans,cis* and intermediate (0.7–3.2) for *cis,cis* and *trans,trans*, thus allowing differentiation of the geometrical isomers (with pure standards at least). When used in conjunction with GC retention time data the majority of CLA isomers in milk samples were identified

### Distinguishing *cis* and *trans* Double Bonds

While infrared spectroscopy methods are especially useful for confirming the presence of *trans* double bonds in fatty acids, they do not help to locate the specific position in the fatty acid chain. For this purpose, there is no alternative to using chemical degradative techniques. The first step is to obtain a pure single component either by reversed-phase or silver ion chromatography (or by a combination of both). The CLA isomer must then be subjected to partial hydrogenation with hydrazine to yield a mixture of *cis* and *trans* monoenes, which can be easily separated by silver ion chromatography and identified either by chemical oxidative procedures or by GC–MS. Procedures of this kind have been used to identify natural CLA isomers [40] and for the elongation products of CLA [4]. Mass spectrometry with acetonitrile-covalent adduct chemical ionization can also be helpful though not necessarily definitive [39].

### Nuclear Magnetic Resonance Spectroscopy

$^{13}\text{C}$ -NMR spectroscopy has proven to be the single most comprehensive method for the identification and quantification of all the positional (7,9- to 11,13-18:2) and geometrical isomers (*cis,trans*-, *trans,cis*-, *cis,cis*- and *trans,trans*-) present in commercial CLA preparations [36]. This is arguably the most comprehensive analytical procedure for CLA, but unfortunately the methodology requires substantial amounts of sample and is not likely to be applicable to tissue extracts at natural levels.

**Acknowledgments** This work has been funded in part by the Scottish Executive Environment and Rural Affairs Department.

### References

1. Yurawecz MP, Mossoba MM, Kramer JKG, Pariza MW, Nelson GJ (eds) (1999) Advances in conjugated linoleic acid research, vol 1. AOCS Press, Champaign
2. Sebedio JL, Christie WW, Adlof RO (eds) (2003) Advances in conjugated linoleic acid research. vol 2, AOCS Press, Champaign
3. Yurawecz MP, Kramer JKG, Gudmundsen O, Pariza MW, Banni S (eds) (2006) Advances in conjugated linoleic acid research, vol 3. AOCS Press, Champaign
4. Sébédio JL, Juanéda P, Dobson G, Ramilison I, Martin JC, Chardigny JM, Christie WW (1997) Metabolites of conjugated isomers of linoleic acid (CLA) in the rat. *Biochim Biophys Acta* 1345:5–10
5. Christie WW, Sébédio JL, Juanéda P (2001) A practical guide to the analysis of conjugated linoleic acid (CLA). *INFORM* 12, 147–152. Available online at <http://www.lipidlibrary.co.uk/>
6. Shantha NC, Decker EA, Hennig B (1993) Comparison of methylation methods for the quantitation of conjugated linoleic acid isomers. *J Assoc Off Anal Chem* 76:644–649
7. Christie WW (1993) Preparation of ester derivatives of fatty acids for chromatographic analysis. In: Christie WW (ed) *Advances in lipid methodology two*. Oily Press, Dundee, pp 69–111
8. Roach JAG, Yurawecz MP, Kramer JKG, Mossoba MM, Eulitz K, Ku Y (2000) Gas chromatography–high resolution selected-ion mass spectrometric identification of trace 21:0 and 20:2 fatty acids eluting with conjugated linoleic acid isomers. *Lipids* 35:797–802
9. Yurawecz MP, Sehat N, Mossoba MM, Roach JAG, Kramer JKG, Ku Y (1999) Variations in isomer distribution in commercially available conjugated linoleic acid. *Fett/Lipid* 101:277–282
10. Lavillonniere F, Martin JC, Bougnoux P, Sébédio J-L (1998) Analysis of conjugated linoleic acid isomers and content in French cheeses. *J Am Oil Chem Soc* 75:343–352
11. Sehat N, Kramer JKG, Mossoba MM, Yurawecz MP, Roach JAG, Eulitz K, Morehouse KM, Ku Y (1998) Identification of conjugated linoleic acid isomers in cheese by gas chromatography, silver ion high performance liquid chromatography and mass spectral reconstructed ion profiles. Comparison of chromatographic elution sequences. *Lipids* 33:963–971
12. Eulitz K, Yurawecz MP, Sehat N, Fritsche J, Roach JAG, Mossoba MM, Kramer JKG, Adlof RO, Ku Y (1999) Preparation and confirmation of the eight geometrical *cis/trans* conjugated linoleic acid isomers 8,10- through 11,13-18:2. *Lipids* 34:873–877
13. Destailats F, Angers P (2003) Directed sequential synthesis of conjugated linoleic acid isomers from  $\Delta^{7,9}$  and  $\Delta^{12,14}$ . *Eur J Lipid Sci Technol* 105:3–8
14. Delmonte P, Roach JAG, Mossoba MM, Losi G, Yurawecz MP (2004) Synthesis, isolation, and GC analysis of all the 6,8- to 13,15-*cis/trans* conjugated linoleic acid isomers. *Lipids* 39:185–191
15. Cruz-Hernandez C, Deng Z, Zhou J, Hill AR, Yurawecz MP, Delmonte P, Mossoba MM, Dugan MER, Kramer JKG (2004) Methods for the analysis of conjugated linoleic acids and *trans*-18:1 isomers in dairy fats by using a combination of gas chromatography, silver-ion thin-layer chromatography/gas chromatography, and silver-ion liquid chromatography. *J AOAC Int* 87:545–561
16. Nikolova-Damyanova B (1992) Silver ion chromatography and lipids. In: Christie WW (ed) *Advances in lipid methodology-one*. Oily Press, Dundee, pp 181–237
17. Nikolova-Damyanova B (2003) Lipid analysis by silver ion chromatography. In: Adlof RO (ed) *Advances in lipid methodology-five*. Oily Press, Bridgwater, pp 43–123
18. Adlof RO (2003) Application of silver ion chromatography to the separation of conjugated linoleic acid isomers. In: Christie W, Sébédio J, Adlof RO (eds) *Advances in conjugated linoleic acid research*, vol 2. AOCS Press, Champaign, pp 37–55

19. Yurawecz MP, Morehouse KM (2001) Silver-ion HPLC of conjugated linoleic acid isomers. *Eur J Lipid Sci Technol* 103:609–613
20. Nikolova-Damyanova B, Momchilova S, Christie WW (2000) Silver ion high-performance liquid chromatographic separation of conjugated linoleic acid isomers, and other fatty acids, after conversion to *p*-methoxyphenacyl derivatives. *J High Resolut Chromatogr* 23:348–352
21. Delmonte P, Kataoka A, Corl BA, Bauman DE, Yurawecz MP (2005) Relative retention order of all isomers of *cis/trans* conjugated linoleic acid FAME from the 6,8- to 13,15-positions using silver ion HPLC with two elution systems. *Lipids* 40:509–514
22. Müller A, Düsterloh K, Ringseis R, Eder K, Steinhart H (2006) Development of an alternate eluent system for Ag<sup>+</sup>-HPLC analysis of conjugated linoleic acid isomers. *J Sep Sci* 29:358–365
23. Adlof RO (2004) Separation of conjugated linoleic acid methyl esters by silver-ion high performance liquid chromatography in semi-preparative mode. *J Chromatogr A* 1033:369–371
24. Cross RF, Ostrowska E, Muralitharan M, Dunshea FR (2000) Mixed mode retention and the use of competing acid for the Ag<sup>+</sup>-HPLC analysis of underivatized conjugated linoleic acids. *J High Resolut Chromatogr* 23:317–323
25. Ostrowska E, Dunshea FR, Muralitharan M, Cross RF (2000) Comparison of silver-ion high-performance liquid chromatographic quantification of free and methylated conjugated linoleic acids. *Lipids* 35:1147–1153
26. Joh Y-G, Kim S-J (1998) Analysis of molecular species of triacylglycerols from vegetable oils containing fatty acids with non-methylene-interrupted double bonds, by HPLC in the silver-ion mode. *J Jpn Oil Chem Soc* 47:927–936
27. Adlof RO, Menzel A, Dorovska-Taran V (2002) Analysis of CLA-enriched triacylglycerol mixtures by silver-ion HPLC. *J Chromatogr A* 953:293–297
28. Juanéda P, Sébédio JL (1999) Combined silver-ion and reversed-phase high-performance liquid chromatography for the separation and identification of C<sub>20</sub> metabolites of conjugated linoleic acid isomers in rat liver lipids. *J Chromatogr B* 724:213–219
29. Christie WW (1998) Gas chromatography–mass spectrometry methods for structural analysis of fatty acids. *Lipids* 33:343–353
30. Christie WW (1989) Silver ion chromatography using solid-phase extraction columns packed with a bonded-sulfonic acid phase. *J Lipid Res* 30:1471–1473
31. Murru E, Angioni E, Carta G, Melis MP, Spada S, Banni S (2003) Reversed-phase HPLC analysis of conjugated linoleic acid and its metabolites. In: Sébédio JL, Christie WW, Adlof RO (eds) *Advances in conjugated linoleic acid research*, vol 2. AOCS Press, Champaign, pp 94–100
32. Kuklev DV, Smith WL (2003) A procedure for preparing oxazolines of highly unsaturated fatty acids to determine double bond positions by mass spectrometry. *J Lipid Res* 44:1060–1066
33. Spitzer V, Marx F, Pfeilsticker K (1994) Electron impact mass spectra of the oxazoline derivatives of some conjugated diene and triene C<sub>18</sub> fatty acids. *J Am Oil Chem Soc* 71:873–876
34. Dobson G (1998) Identification of conjugated fatty acids by GC–MS of 4-methyl-1,2,4-triazoline-3,5-dione adducts. *J Am Oil Chem Soc* 75:137–142
35. Reaney MJT, Liu Y-D, Taylor WG (2001) Gas chromatographic analysis of Diels–Alder adducts of geometrical and positional isomers of conjugated linoleic acid. *J Am Oil Chem Soc* 78:1083–1086
36. Davis AL, McNeill GP, Caswell DC (1999) Analysis of conjugated linoleic acid isomers by <sup>13</sup>C NMR spectroscopy. *Chem Phys Lipids* 97:155–165
37. Roach JAG, Mossoba MM, Yurawecz MP, Kramer JKG (2002) Chromatographic separation and identification of conjugated linoleic acid isomers. *Anal Chim Acta* 465:207–222
38. Yurawecz MP, Roach JAG, Sehat N, Mossoba MM, Kramer JKG, Fritsche J, Steinhart H, Ku Y (1998) A new conjugated linoleic acid isomer, 7 *trans*, 9 *cis*-octadecadienoic acid, in cow milk, cheese, beef and human milk and adipose tissue. *Lipids* 33:803–809
39. Michaud AL, Yurawecz MP, Delmonte P, Corl BA, Bauman DE, Brenna JT (2003) Identification and characterization of conjugated fatty acid methyl esters of mixed double bond geometry by acetonitrile chemical ionization tandem mass spectrometry. *Anal Chem* 75:4925–4930
40. Christie WW (1973) The structure of bile phosphatidylcholines. *Biochim Biophys Acta* 316:204–211

in food from ruminants, milk and meat mainly, as a result of rumen biohydrogenation and endogenous conversion from vaccenic acid. To date, numerous animal studies indicate that CLA may influence diverse physiologic functions and promote health with regard to cancer, atherosclerosis, bone formation, growth modulation and immunity, and lately there is a growing focus on the physiological role of CLA in humans [1]. The major CLA isomers with known physiologic activities are 9-*cis*,11-*trans* linoleic acid, also called rumenic acid and 10-*trans*,12-*cis* linoleic acid, a predominant isomer in CLA commercial forms.

In the search for a possible anticarcinogenic mechanism, CLA has been tested for its antioxidant effects using model systems. In this context, antioxidative properties [2–6], no effect or even prooxidant activity [7, 8] has been reported. Likewise, studies on the oxidative stability of CLA and its non-conjugated counterpart, LA (linoleic acid), are also contradictory, showing either higher susceptibility of CLA [9–12], similar behavior of CLA and LA [13] or lower oxidative stability of CLA than that of LA [14] in model systems including free fatty acids, methyl esters, ethyl esters and triacylglycerols. The great variety of oxidation conditions (temperature, oxygen availability, light–dark, etc.) and, above all, the diversity of methods applied, normally evaluating only partial aspects of lipid oxidation, may have contributed to the differences in the results obtained.

The mechanism of autoxidation of methylene-interrupted fatty acid double bonds is well-established and involves a catalytic process which proceeds via a free radical mechanism [15]. The initiation step consists on alkyl radical formation ( $R^{\cdot}$ ) in the carbon adjacent to the double bond and the propagation step on addition of oxygen to form alkylperoxyl radicals ( $ROO^{\cdot}$ ), hence the oxygen consumed is primarily converted to hydroperoxides ( $ROOH$ ). However, Yurawecz, Eulitz and co-workers [13, 16] have suggested that the same mechanism is not likely to occur in CLA because high energy is a prior requirement for separating double bonds from conjugation, which could explain that formation of other compounds may be favored. On the basis of the reaction products detected by gas liquid chromatography–mass spectrometry (GLC–MS), these authors reported that CLA underwent 1,2 and 1,4 cycloadditions with oxygen, which gave rise to dioxetane structures, and endoperoxides leading to furan fatty acids, respectively. Other reactions such as dimerization and polymerization, although not evaluated, were not ruled out by those authors. In contrast to these assumptions, Hämäläinen et al. supported that hydroperoxides are one type of primary oxidation products formed during autoxidation of CLA [17, 18]. The controversy over this issue warrants further investigations on the oxidation mechanisms of CLA.

The objective of this study was to gain more insight into the oxidation kinetics of CLA. Samples of 9-*cis*,12-*cis*, 9-*cis*,11-*trans*, and 10-*trans*,12-*cis* linoleic acid methyl esters, oleic acid methyl ester,  $\alpha$ -linolenic acid methyl ester and selected mixtures were used. Experiments were conducted at 30 °C in the dark and loss of substrate was determined by gas liquid chromatography (GLC) along the oxidation process. Additionally, a different analytical approach was used here for the first time to monitor oxidation of conjugated fatty acid methyl esters throughout the entire process, which provided a good measurement of compounds formed during early and advanced oxidation stages concomitantly [19, 20]. It consisted on a simple and direct analysis by high-performance size-exclusion chromatography (HPSEC), run in just 15 min and without any previous treatment of the sample.

## Experimental Procedure

### Samples

Methyl esters of oleic acid (O), 9-*cis*,12-*cis*-linoleic acid (L) and  $\alpha$ -linolenic acid (Ln) (99% purity) and methyl esters of 9-*cis*,11-*trans*-linoleic acid (CL1) and 10-*trans*,12-*cis*-linoleic acid (CL2) (90% purity) were purchased from Nu-Chek Prep. Inc. (Elysian, MN, USA). Mixtures of CL1 and CL2 (CLM), of L and CL1 (LCL1), and of L and CL2 (LCL2) were prepared with a 1:1 ratio.

### Oxidation Conditions

One gram-samples were placed in glass tubes of 1.3-cm inner diameter (surface-to-volume ratio of  $1.33 \text{ cm}^{-1}$ ) and heated in an oven at 30 °C. Experiments were carried out in duplicate.

### Analytical Methods

- Determination of remaining substrate by GLC.* Fatty acid methyl esters were separated by GLC using a CP-Sil 88 fused-silica capillary column (100 m  $\times$  0.25 mm i.d.  $\times$  0.2  $\mu\text{m}$  film thickness, Chrompack, Middelburg, Netherlands) on a Perkin–Elmer chromatograph (Model Clarus, Beaconsfield, UK) equipped with a flame ionization detector. The column was held at 100 °C for 1 min after injection, temperature-programmed at 7 °C/min to 170 °C, held there for 55 min, then temperature programmed at 10 °C/min to 230 °C and held there for 23 min. Helium was the carrier gas with a column inlet pressure set at

214 KPa and a splitless injection system. Injection volume was 1.0  $\mu\text{L}$  (50 mg/mL). The areas of the O, L, Ln, CL1 and CL2 peaks were calculated as mg/g of sample using nonadecanoic acid (C19:0) methyl ester as internal standard.

- (b) *Quantitation of oxidized monomers, dimers and polymers by HPSEC.* Samples (20 mg) were dissolved in diisopropyl ether (50 mg/mL) for direct analysis by HPSEC, using a Rheodyne 7725i injector with 10- $\mu\text{L}$  sample loop, a Waters 510 pump and a Waters 2414 refractive index detector (Waters, Milford, MA, USA). The separation was performed on two 100- and 500- $\text{\AA}$  Ultrastaygel columns ( $25 \times 0.77$  cm i.d.) packed with porous, highly cross linked styrene-divinylbenzene copolymers (film thickness: 10  $\mu\text{m}$ ) (Hewlett-Packard, Avondale, PA, USA) connected in series, with tetrahydrofuran (1 mL/min) as the mobile phase [21]. The groups of compounds separated in methyl ester samples were unoxidized compounds (Unox) oxidized monomers (OxMon), dimers (Dim) and polymers (Pol). In certain samples, separation of Pol in trimers and higher oligomers could be achieved.

## Results

Figure 1 shows the time course of the remaining substrates during the oxidation period up to levels around 50% residual amounts. Results correspond to means from duplicate experiments and showed coefficients of variation lower than 8% for samples with substrate loss higher than 9%. As expected, O remained practically unchanged and Ln, the most unsaturated compound tested, degraded fastest (Fig. 1a). As to conjugated samples (CL1, CL2, CL1 in mixture CLM, CL2 in mixture CLM), no differences were observed between conjugated linoleic (CL) isomers, and their loss rate was slower than that of L samples. Results obtained in 1:1 mixtures of L and CL1 or CL2 (Fig. 1b) showed that the rate of substrate loss for L and CL samples was practically reversed in mixtures, that is, CL disappeared more rapidly than L in mixtures. As an illustrative example, about 50% unoxidized substrate was left at 33 days in the case of L versus 23 days in the case of CL in mixtures, while such a loss occurred at 22 days in the case of L and 34 days in the case of CL when assayed separately.

Data obtained were used to calculate oxidation rate constants for CL samples alone or in mixtures with L samples, following kinetic considerations applied by Minemoto and co-workers [22]. The entire autoxidation process can be expressed by the following autocatalytic-type equation:

$$dY/dt = -kY(1 - Y) \quad (1)$$

where  $Y$  is the fraction of unoxidized remaining substrate,  $t$  is the time and  $k$  is the rate constant. Integration of Eq. (1) under the condition of  $Y = Y_0$  at  $t = 0$  gives:

$$\ln[(1 - Y)/Y] = kt + \ln[(1 - Y_0)/Y_0] \quad (2)$$

Figure 2 shows the plots of  $\ln[(1 - Y)/Y]$  versus  $t$  for CL1 and CL2 alone and in mixtures with L, which lie on a straight line that allowed us to evaluate the rate constant  $k$ . Values of  $k$  for CL1 and CL2 alone were 1.24 and  $1.21 \times 10^4 \text{ s}^{-1}$ , respectively, while in mixtures with L (LCL1 And LC2),  $k$  increased to 2.01 and  $2.03 \times 10^4 \text{ s}^{-1}$ , respectively.

The time course of formation of OxMon, Dim and Pol quantitated by HPSEC for all compounds tested is shown in Fig. 3. Through this analytical approach, a complete picture of the oxidative state can be attained. The basis of the technique is separation by molecular weight or size, and groups of oxidation compounds elute in decreasing order of molecular weight, i.e., Pol, Dim and OxMon. Results are means from duplicate experiments and showed coefficients of variation lower than 4%. Presence of OxMon, Dim or Pol was not detected in starting samples. As in Fig. 1, no appreciable differences were found between CL isomers (CL1 and CL2) and the 1:1 mixture of both (CLM). Even though CL samples started to oxidize later than did L samples, in agreement with results obtained for remaining substrates (Fig. 1), the first group of compounds formed were polymerization products. Pol continued to increase throughout all the oxidation period without any significant parallel increase of OxMon, and up to levels markedly higher than those found in L samples. In the mixtures of non-conjugated and conjugated linoleic acid methyl esters, the most outstanding results were the marked decrease in formation of OxMon as compared to the level expected to come from L contribution, as well as the notable increase of Pol as compared to the level expected to come from CL contribution. These results are consistent and complementary with data on substrate loss.

Figure 4 illustrates the differences in the oxidation profiles obtained in HPSEC chromatograms corresponding to samples oxidized for 30 days. It is clearly observed that OxMon and Dim were the most abundant oxidation compounds in L and Ln. In contrast, an unusual profile is shown by CL samples, polymers being practically the only compounds present. This is also clearly shown by overlapping HPSEC chromatograms of L (dotted line) and CL (solid line) samples with the same level of total oxidation (Fig. 5). Between Dim and OxMon peaks in L and Ln samples (Fig. 4), some compounds with intermediate molecular weight often elute, coming from  $\beta$ -scission of

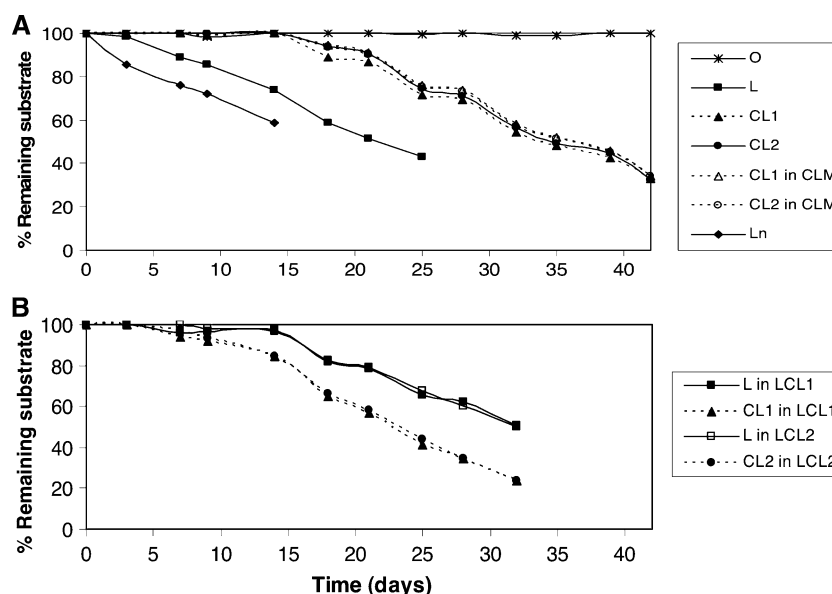


**Fig. 1** Remaining amounts of methyl esters during oxidation at 30 °C in the dark. **(a)** methyl oleate (*O*); methyl 9-*cis*,12-*cis* linoleate (*L*); methyl 9-*cis*,12-*cis*,15-*cis* linolenate (*Ln*); methyl 9-*cis*,11-*trans* linoleate (*CL1*); methyl 10-*trans*,12-*cis* linoleate (*CL2*); methyl 9-*cis*,11-*trans* linoleate in a 1:1 mixture of methyl 9-*cis*,11-*trans* and methyl 10-*trans*,12-*cis* linoleate (*CL1 in CLM*); methyl 10-*trans*,12-*cis* linoleate in a 1:1 mixture of methyl 9-*cis*,11-*trans* linoleate and methyl 10-*trans*,12-*cis* linoleate (*CL2 en CLM*). **(b)** methyl 9-*cis*,12-

*cis* linoleate in a 1:1 mixture of methyl 9-*cis*,12-*cis* linoleate and 9-*cis*,11-*trans* (*L in LCL1*); methyl 9-*cis*,11-*trans* linoleate in a 1:1 mixture of methyl 9-*cis*,12-*cis* linoleate and 9-*cis*,11-*trans* (*CL1 in LCL1*); methyl 9-*cis*,12-*cis* linoleate in a 1:1 mixture of methyl 9-*cis*,11-*trans* and methyl 10-*trans*,12-*cis* (*L in LCL2*) and methyl 10-*trans*,12-*cis* linoleate in a 1:1 mixture of methyl 9-*cis*,12-*cis* linoleate and 10-*trans*,12-*cis* (*CL2 in LCL2*)

the alkoxy radical derived from hydroperoxides, which is the main mechanism for volatile formation.

To illustrate the large degree of polymerization (DP) found in CL samples, Fig. 6 represents the contribution of polymers with DP higher than three in samples of CLM and Ln. Even though Ln possesses three double bonds and higher polymerization degree is therefore expected as compared to CL, the abundance of larger polymers was by

far higher in CLM, and even from the beginning of the oxidation process.

## Discussion

From the results obtained through evaluation of substrate loss (Fig. 1), it can be deduced that oxidation was more rapid in non-conjugated than in conjugated linoleic moieties. As to the similar loss substrate rate for CL isomers, results agree with those reported by Jiang and Kamal-Eldin in experiments under quite different oxidation conditions, i.e., photooxidation using methylene blue as a sensitizer [10]. Results obtained in 1:1 mixtures of L and CL1 or CL2 provided interesting information on the possible interaction between oxidative pathways of non-conjugated and conjugated linoleic acid moieties. The increase in oxidation rate for CL samples in mixtures with L (LCL1 and LC2) as compared to CL1 and CL2 alone (Fig. 2) could be due to the potential free radical scavenging properties of CL [5, 23, 24], and specifically to the reaction of furan fatty acids derived from CL oxidation with hydroperoxide radicals coming from L oxidation, thus producing a dioxoene compound which has been unequivocally detected by GLC-MS [13, 25, 26].

Application of HPSEC added essential information on oxidation kinetics since formation of different groups of

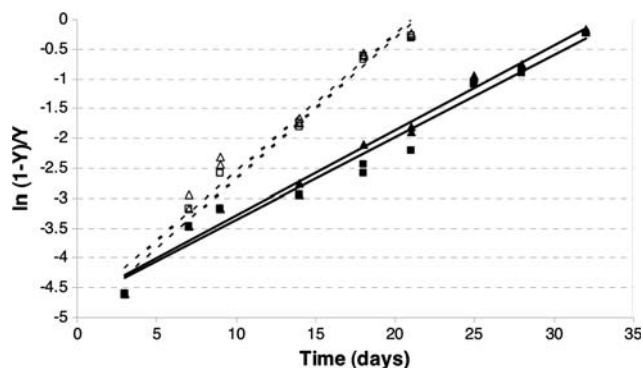


**Fig. 2** Applicability of equation  $\ln[(1 - Y)/Y] = kt + \ln[(1 - Y_0)/Y_0]$  to changes in the fraction of unoxidized, remaining methyl esters: CL1 (filled triangles), CL2 (filled squares), CL1 in LCL1 (void triangles), CL2 in LCL2 (void squares). *Y* fraction of remaining methyl esters; *t* time; *k* rate constant; *Y* = *Y*<sub>0</sub> at *t* = 0. Other abbreviations as in Fig. 1



**Fig. 3** Time-course of formation of oxidized monomers (*filled diamonds*), dimers (*filled squares*) and polymers (*filled triangles*) in samples of O, L, Ln, CL1, CL2, CLM, LCL1 and LCL2 during oxidation at 30 °C in the dark. Abbreviations as in Fig. 1

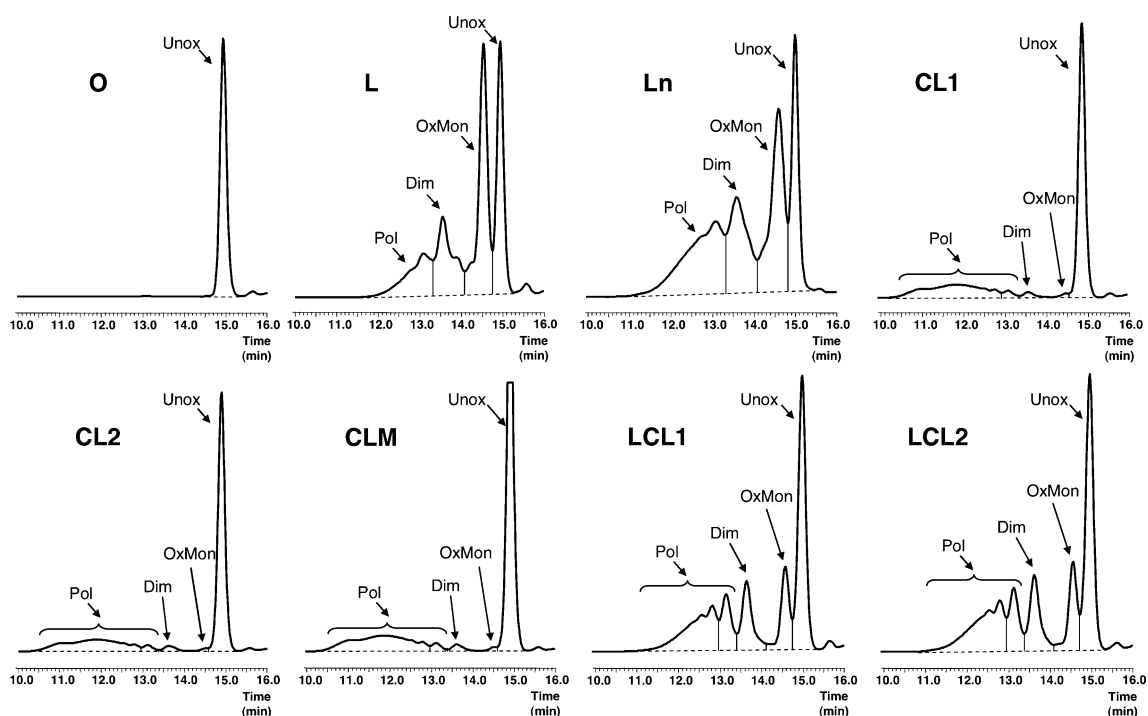
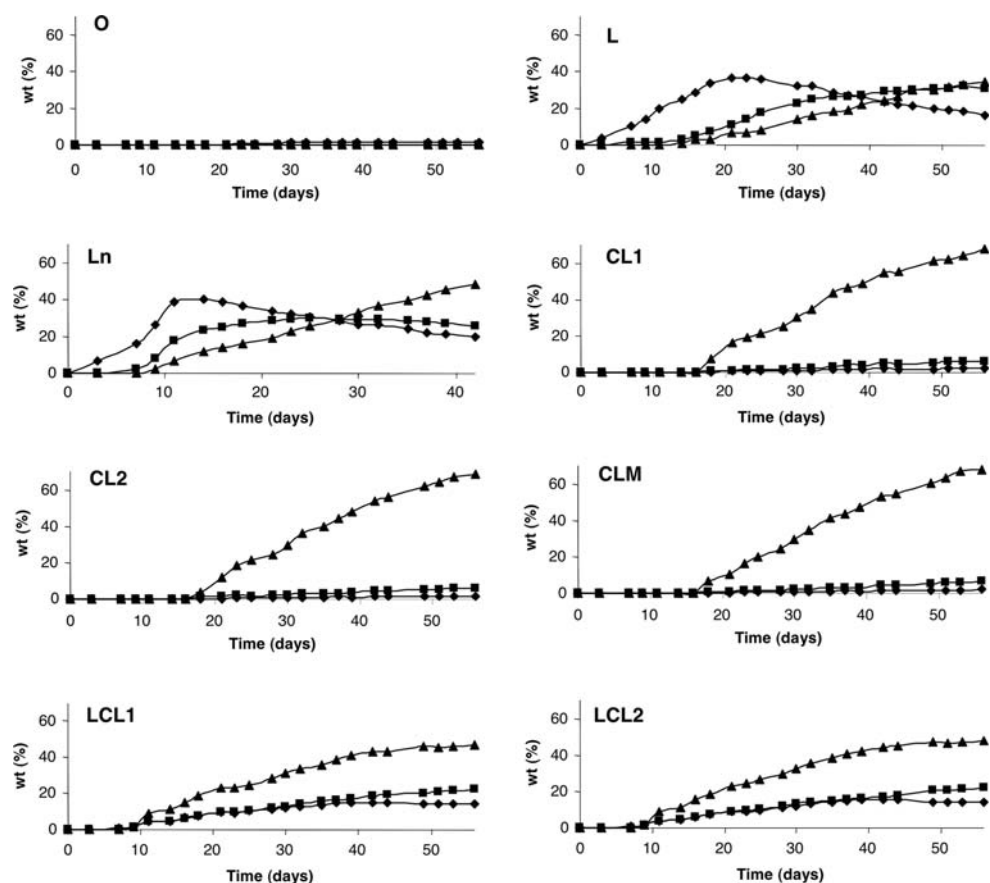


**Fig. 4** Elution profiles by HPSEC of O, L, Ln, CL1, CL2, CLM, LCL1 and LCL2 after 30 days at 30 °C in the dark. *Unox* unoxidized compounds; *OxMon* oxidized monomers; *Dim* dimers and *Pol* polymers. Other abbreviations as in Fig. 1

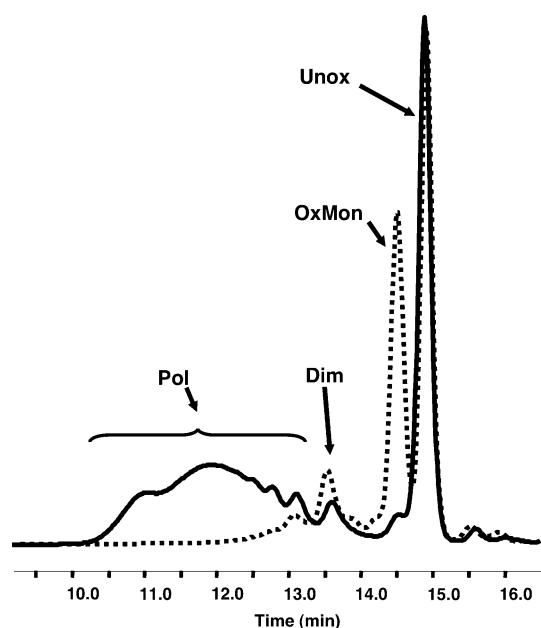


**Fig. 5** Elution profiles by HPSEC of L (dotted line) and CLM (solid line) samples containing the same level of total oxidation compounds. *Unox* unoxidized compounds; *OxMon* oxidized monomers; *Dim* dimers and *Pol* polymers. Other abbreviations as in Fig. 1

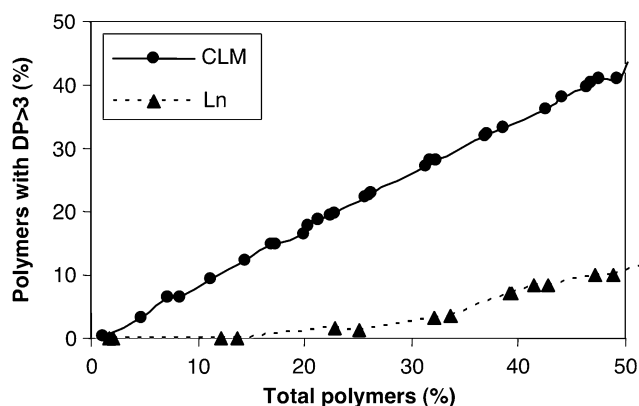


**Fig. 6** Plot of polymers with degree of polymerization (DP) over three versus total polymers in Ln (filled triangles) and CLM (filled circles) samples. Other abbreviations as in Fig. 1

oxidation compounds could be followed from the beginning and along the oxidation period. The method offers the advantage that differences in molecular weight between unoxidized and oxidized monomeric molecules of monoacid methyl esters are sufficient as to be eluted at distinct retention times [19, 20]. However, when analyzing triacylglycerols, fats or oils, a preliminary step to separate the non-oxidized fraction is essential, as described previously [21]. Oxidized monomers comprise the primary oxidation products, i.e., hydroperoxides, and once oxidation proceeds, include also secondary monomeric oxidation compounds, with oxygenated functions such as hydroxy-, keto- or epoxy-. In the same analysis, compounds typical of

advanced oxidation stages, i.e., dimers (two molecules) and polymers (more than two molecules), are concomitantly quantitated. Applications of methodologies based on HPSEC for quantitation of oxidation compounds have been reviewed recently [27, 28].

In Fig. 3, the typical oxidation profile can be observed for L and Ln, that is, initial formation of OxMon, mainly comprised of hydroperoxides during early oxidation, and further acceleration of oxidation denoted by a significant rise in Dim and Pol [19, 29]. As expected, the accumulation of sufficient amounts of OxMon led to the formation of Dim and, likewise, Pol did not build up until a notable increase of Dim had occurred. Also expected was the higher polymerization rate in Ln samples as compared to L samples as a result of increased degree of unsaturation. However, CL samples showed a very different oxidation pattern, not described so far in the literature. Thus, formation of typical primary oxidation products, i.e., hydroperoxides (included in the OxMon peak), seemed to be negligible in CL samples. Furthermore, Dim formation was rare and the starting point of oxidation for these samples was characterized by the appearance of polymers.

Interestingly, a study carried out back in the late 1940s reported that autoxidation of CLA methyl esters proceeded three times slower and eight to ten times the amount of peroxides was formed than in the autoxidation of methyl linoleate [30]. In addition, recent studies have indicated that peroxide values and TBARS did not increase in oxidized CLA at the levels expected from the increase in absorbed oxygen and loss of substrate found [31, 32].

Polymerization reactions in substrates with conjugated double bonds under conditions of oxidation at low temperatures are practically unknown. To our knowledge, only one recent study has published any results on polymer formation in relation to oxidative stability of CLA [31]. The authors found that the main oxidation products of bitter melon oil–triacylglycerols (61.6% conjugated linolenic acids) and CLA containing oil–triacylglycerols (69.5% conjugated linoleic acids) at 50 °C were dimers and polymers, whereas hydroperoxides were the main products in the oxidation of perilla oil–triacylglycerols (54.5% non-conjugated linolenic acid) and soybean oil–triacylglycerols (56.1% non-conjugated linoleic acid). In this context, Brimberg and Kamal-Eldin carried out a kinetic evaluation of rate data on CLA oxidation taken from literature and suggested that oligomeric peroxides can be formed in the very beginning of the oxidation in substrates with conjugated double bonds [33].

In this study, the early retention time at which polymers started to elute in CL samples, with unusually high molecular weight or size (Figs. 4, 5) in addition to the substantial contribution of such compounds to the total polymer fraction (Fig. 6) indicate that formation of very

complex molecules is favored even under the mild oxidation conditions used, i.e., 30 °C in the dark. This is of extraordinary importance since such structures are unknown and even the implication of high molecular size compounds due to steric configuration or cyclization should not be disregarded.

Overall, the results obtained in this study show that different oxidation pathways could be involved in conjugated and non-conjugated fatty acids, the latter showing an oxidation pattern where polymers were the main group of compounds formed. One of the most important conclusions of this work is that validity of a single index to evaluate partial aspects of oxidation needs to be questioned. Thus, a misleading picture of the development of oxidation of CLA can be obtained when the methods applied are based only on evaluation of hydroperoxides (peroxide value) or monomeric oxidation products (thio-barbituric acid reactive substances or carbonyl compounds). Otherwise, indirect methods such as loss of substrate and oxygen consumption provide useful information but, above all, from the results obtained in this study, it appears that polymer quantitation can be an appropriate measurement to follow-up oxidation of CLA. Finally, the results obtained support further studies aimed at examining the interaction of non-conjugated and conjugated fatty acids, and triacylglycerols containing them, in mixtures at compositions closer to those found in nutritional supplements and foods. Experiments are underway in our laboratory to determine differences in oxidative stability between linoleic acid-rich oils and conjugated linoleic acid-rich oils.

**Acknowledgments** This work was supported by the Ministerio de Educación y Ciencia (Research Project AGL2005-04760-C02-01/ALI) and Comunidad Autónoma de Madrid (Research Project S-0505/AGR-0153).

## References

1. Yurawecz MP, Kramer JKG, Gudmundsen O, Pariza MW, Banni S (2006) Advances in conjugated linoleic acid research, vol 3. AOCS Press, Champaign
2. Ha YL, Grimm NK, Pariza MW (1987) Anticarcinogens from fried ground beef: heat-altered derivatives of linoleic acid. *Carcinogenesis* 8:1881–1887
3. Ha YL, Storkson J, Pariza MW (1990) Inhibition of benzo(a)pyrene-induced mouse forestomach neoplasia by conjugated dienoic derivatives of linoleic acid. *Cancer Res* 50:1097–1101
4. Ip C, Chin SF, Scimeca JA, Pariza MW (1991) Mammary cancer prevention by conjugated dienoic derivative of linoleic acid. *Cancer Res* 51:6118–6124
5. Yu L (2001) Free radical scavenging properties of conjugated linoleic acid. *J Agric Food Chem* 49:3452–3456
6. Park Y, Ha YL, Pariza MW (2007)  $\pi$ -complex formation of conjugated linoleic acid with iron. *J Agric Food Chem* 100: 972–976
7. Van den Berg JJM, Cook NE, Tribble DL (1995) Reinvestigation of the antioxidant properties of conjugated linoleic acid. *Lipids* 30:599–605
8. Chen ZY, Chan PT, Kwan KY, Zhang A (1997) Reassessment of the antioxidant activity of conjugated linoleic acids. *J Am Oil Chem Soc* 73:749–753
9. Zhang A, Chen ZY (1997) Oxidative stability of conjugated linoleic acids relative to other polyunsaturated fatty acids. *J Am Oil Chem Soc* 74:1611–1613
10. Jiang J, Kamal-Eldin A (1998) Comparing methylene blue-photosensitized oxidation methyl-conjugated linoleate and methyl linoleate. *J Agric Food Chem* 46:923–927
11. Yang L, Leung LK, Huang Y, Chen ZY (2000) Oxidative stability of conjugated linoleic acid isomers. *J Agric Food Chem* 48:3072–3076
12. Chen JF, Tai CY, Chen YC, Chen BH (2001) Effects of conjugated linoleic acid on the degradation and oxidation stability of model lipids during heating and illumination. *Food Chem* 72:199–206
13. Yurawecz MP, Delmonte P, Vogel T, Kramer JKG (2003) Oxidation of conjugated linoleic acid: initiators and simultaneous reactions: theory and practice. In: Sébédio JL, Christie WW, Adlof R (eds) *Advances in CLA research*, vol 2. AOCS Press, Champaign
14. Suzuki R, Nakao K, Kobayashi M, Miyashita K (2001) Oxidative stability of conjugated polyunsaturated fatty acids and their esters in bulk phase. *J Oleo Sci* 50:491–495
15. Frankel EN (2005) *Lipid oxidation*. The Oily Press, Dundee
16. Eulitz K, Yurawecz MP, Ku Y (1999) The oxidation of conjugated linoleic acid. In: Yurawecz MP, Mossoba MM, Kramer JKG, Pariza MW, Nelson GJ (eds) *Advances in CLA research*, vol 1. AOCS Press, Champaign
17. Hämäläinen TI, Sundberg S, Mäkinen M, Kaltia S, Hase T, Hopia A (2001) Hydroperoxide formation during autoxidation of conjugated linoleic acid methyl ester. *Eur J Lipid Sci Technol* 103:588–593
18. Hämäläinen TI, Sundberg S, Hase T, Hopia A (2002) Stereochemistry of the hydroperoxides formed during autoxidation of CLA methyl ester in the presence of alpha-tocopherol. *Lipids* 37:533–540
19. Márquez-Ruiz G, Martín-Polvillo M, Dobarganes MC (1996) Quantitation of oxidized triglyceride monomers and dimers as an useful measurement for early and advanced stages of oxidation. *Grasas y Aceites* 47:48–53
20. Márquez-Ruiz G, Holgado F, García-Martínez MC, Dobarganes MC (2007) A direct and fast method to monitor lipid oxidation progress in model fatty acid methyl esters by high-performance size-exclusion chromatography. *J Chromatogr A* 1167:122–127
21. Márquez-Ruiz G, Jorge N, Martín-Polvillo M, Dobarganes MC (1996) Rapid, quantitative determination of polar compounds in fats and oils by solid-phase extraction and exclusion chromatography using monostearin as internal standard. *J Chromatogr A* 749:55–60
22. Minemoto Y, Adachi S, Shimada Y, Nagao T, Iwata T, Yamauchi-Sato Y, Yamamoto T, Kometani T, Matsuno R (2003) Oxidation kinetics for *cis*-9, *trans*-11 and *trans*-10, *cis*-12 isomers of CLA. *J Am Oil Chem Soc* 80:675–678
23. Leung YH, Liu RH (2000) *Trans*-10, *cis*-12 conjugated linoleic acid isomer exhibits stronger oxyradical scavenging capacity than *cis*-9, *trans*-11-conjugated linoleic acid isomer. *J Agric Food Chem* 48:5469–5475
24. Yin JJ, Yu L, Yurawecz MP, Roach JAG, Mossoba MM, Yu L, Kramer JKG (2006) Antioxidative activity of conjugated linoleic acid determined by ESR. In: Yurawecz MP, Kramer JKG, Gudmundsen O, Pariza MW, Banni S (eds) *Advances in conjugated linoleic acid research*, vol 3. AOCS Press, Champaign

25. Okada Y, Okajima H, Konishi H, Terauchi M, Ishii K, Liu IM, Watanabe H (1990) Antioxidant effect of naturally occurring furan fatty acids on oxidation of linoleic acid in aqueous dispersion. *J Am Oil Chem Soc* 67:858–862
26. Batna A, Spiteller G (1994) Oxidation of furan fatty acids by soybean lipoxygenase-1 in the presence of linoleic acid. *Chem Phys Lipids* 70:179–185
27. Márquez-Ruiz G, Dobarganes MC (2005) Analysis of non-volatile lipid oxidation products by high-performance size-exclusion chromatography. In: Kamal-Eldin A, Pokorny J (eds) *Analysis of lipid oxidation*. AOCS Press, Champaign
28. Márquez-Ruiz G, Dobarganes MC (2006) High-performance size-exclusion chromatography for lipid analysis in organic media. In: Mossoba MM, Kramer JKG, Brenna JT, McDonald RE (eds) *Lipid analysis and lipidomics. New techniques and applications*. AOCS Press, Champaign
29. Márquez-Ruiz G, Martín-Polvillo M, Dobarganes MC (2003) Effect of temperature and addition of alpha-tocopherol on the oxidation of trilinolein model systems. *Lipids* 38:233–240
30. Allen RR, Jackson A, Kummerow FA (1949) Factors which affect the stability of highly unsaturated fatty acids. I Difference in the oxidation of conjugated and nonconjugated linoleic acid. *J Am Oil Chem Soc* 26:395–399
31. Suzuki R, Abe M, Miyashita K (2004) Comparative study of the autoxidation of TAG containing conjugated and non conjugated C<sub>18</sub> PUFA. *J Am Oil Chem Soc* 81:563–569
32. Tsuzuki T, Igarashi M, Iwata T, Yamauchi-Sato Y, Yamamoto T, Ogita K, Suzuki T, Miyazawa T (2004) Oxidation rate of conjugated linoleic acid is slowed by triacylglycerol esterification and  $\alpha$ -tocopherol. *Lipids* 39:475–480
33. Brimberg UI, Kamal-Eldin A (2003) On the kinetics of the autoxidation of fats: substrates with conjugated double bonds. *Eur J Lipid Sci Technol* 105:17–22

## Introduction

In recent years, conjugated linoleic acid isomers have received much attention due their potential beneficial properties to human health [1–3]. CLA has been implicated in the prevention of carcinogenesis, atherogenesis, obesity and enhancement of the immune function in animal models; however, in human studies inconsistent effects have been reported [4–7]. Of the two physiologically important isomers, *cis*-9,*trans*-11 CLA is the most prevalent accounting for up to 80–90% of total CLA in ruminant products, whereas *trans*-10,*cis*-12 CLA comprises 3–5% of total CLA [8]. The main dietary source of CLA in food is ruminant meat, milk and their products [9, 10].

It is well known that *cis*-9,*trans*-11 CLA is formed from two sources, one originates from ruminal biohydrogenation of linoleic acid to stearic acid in the rumen by *Butyrivibrio fibrisolvens* and other bacteria [11, 12]. The second source is the endogenous conversion of *trans*-11 18:1 by  $\Delta^9$ -desaturase in the mammary gland of dairy cows and ruminant adipose tissue [10, 13]. VA is a common intermediate produced during ruminal biohydrogenation of linolenic acid (18:3n-3) and linoleic acid (18:2n-6) [14, 15]. Griinari et al. [10] demonstrated that endogenous synthesis of *cis*-9,*trans*-11 CLA from VA represents the primary source in milk fat of lactating cows. More recently, Mosley et al. [16] confirmed using  $^{13}\text{C}$ -labeled VA that endogenous conversion of dietary VA to *cis*-9,*trans*-11 CLA in the mammary gland catalyzed by  $\Delta^9$ -desaturase occurred. The authors [16] found that approximately 80% of milk fat *cis*-9,*trans*-11 CLA originated from VA. In the course of endogenous synthesis of *cis*-9,*trans*-11 CLA, VA and  $\Delta^9$ -desaturase are the two primary prerequisites. Daniel et al. [17] demonstrated that the  $\Delta^9$ -desaturase is active in sheep adipose tissues, and its mRNA is well expressed. The genetic basis for the individual variation in milk fat content of *cis*-9,*trans*-11 CLA and the  $\Delta^9$ -desaturase index remains to be identified.

Furthermore, numerous investigations have demonstrated that diet has a substantial effect on the content of VA and *cis*-9,*trans*-11 CLA both in milk and intramuscular fat [1, 9, 13, 19]. When comparing pasture and concentrate diets there are several differences that relate to milk and intramuscular fat *cis*-9,*trans*-11 CLA [9]. Most research investigating the biohydrogenation of dietary fatty acids to VA, the desaturation of VA to *cis*-9,*trans*-11 CLA and the endogenous synthesis of *cis*-9,*trans*-11 CLA has focused on milk fat [1, 9]. However, there is a lack of information about the pathway of VA and *cis*-9,*trans*-11 CLA from the rumen, via duodenal digesta and blood transport into the muscle and subcutaneous fat.

A large study was carried out by Nuernberg et al. [19] to investigate the effect of feeding pasture versus concentrate

to two different cattle breeds (German Holstein and German Simmental bulls) on meat quality and fatty acid composition of intramuscular fat of bulls. The diet effects of pasture feeding on carcass- and meat quality, total fatty acid composition, fatty acid composition of polar and neutral lipids, CLA and *trans*-18:1 isomers in muscles and subcutaneous fat had been published previously [20–22]. However, the experiment results of diet effects on fatty acid concentrations in the rumen, duodenal digesta and blood have not been published until now. The objective of this paper was to compare the VA and *cis*-9,*trans*-11 CLA concentrations in the rumen and different tissues in beef cattle fed different diets, and to determine the relationships between VA and *cis*-9,*trans*-11 CLA concentrations in different tissues.

## Experimental Procedures

### Materials

Sixty-four bulls (5–6 months old) were randomly assigned to two dietary treatments (concentrate vs. grass-based) in the experiment. For indoor housing the concentrate group consisted of 16 German Simmental (GS) and 17 German Holstein (GH) bulls. The animals were fed semi ad libitum maize silage, concentrate, hay, straw and a mixture of minerals and vitamins up to 620 kg live weight. The pelleted concentrate for the indoor concentrate group was a mixture of winter barley, molasses, and soybean meal (Vollkraft-Mischfutterwerk, Güstrow, Germany). The other animals, (15 GS and 16 GH bulls) were kept on pasture during the summer period. During the following winter period and 3 months before finishing these bulls were kept in a stable and were fed wilted silage, hay, a pelleted concentrate diet and a mixture of minerals and vitamins up to 620 kg live weight. The pelleted concentrate for the pasture group was a mixture of 76% sugar beet pulp (molasses), 12% barley, and 10% coarsely cracked linseed (Vollkraft Mischfutterwerk, Güstrow, Germany). This is termed a grass based feeding. The details of chemical and fatty acid composition of the diet were previously described by Nuernberg et al. [19].

All bulls were slaughtered as they reached 620 kg live weight in the abattoir of the Research Institute for the Biology of Farm Animals in Dummerstorf, Germany. The slaughter and dressing procedures were in accordance with EU specifications. The carcasses were chilled (4 °C) before muscle samples were removed. The blood, rumen content, duodenal digesta (1 m after pylorus), heart and liver tissue samples were taken immediately after slaughter. Samples of longissimus muscle (at the sixth rib of the left carcass side), subcutaneous fat and semitendinosus muscles (left

carcass side) were taken 24 h after slaughter. Rumen content and digesta samples were prepared on the slaughter day. All tissue samples were stored frozen at  $-70\text{ }^{\circ}\text{C}$  until lipid extraction was carried out.

## Methods

### *Extraction and Methylation of Lipids*

**Plasma and Erythrocytes** For plasma and erythrocytes preparation EDTA blood was centrifuged at  $2,750\times g$  at  $4\text{ }^{\circ}\text{C}$  for 10 min into plasma and erythrocytes. Approximately 2 g plasma samples were taken for lipid extraction. Erythrocyte samples were washed two times by 0.9% sodium chloride solution, and then a 2 g sample was added to 5 ml methanol (cold, shaking by vortex). Waiting for 10 min, and then 10 ml chloroform was added to extract total lipids. After filtration the solution was dried under gentle nitrogen stream at room temperature. To obtain the phospholipid fraction (PL) of the isolated erythrocytes lipids were separated by thin layer chromatography on pre-coated silica gel 60 plates using the solvent mixture *n*-hexane/diethyl ether/acetic acid (70:30:2, vol/vol/vol). PL fraction was viewed under ultraviolet light after spraying with 2,7-dichlorofluoresceine (0.1% in ethanol, wt/vol). The PL bands were scraped off and eluted with chloroform/methanol (2:1, vol/vol), decanted after 1 h and eluted once more with chloroform/methanol (2:1, vol/vol). After combining both extracts, the solvent was removed under nitrogen at room temperature. The phospholipids were treated with 0.5 M methanolic sodium methylate for 20 min at room temperature. Methylation of fatty acids was performed with borontrifluoride/methanol (14% wt/vol) for 20 min at room temperature. The fatty acid methyl ester (FAME) formed was extracted with *n*-hexane, then evaporate using a rotary evaporator and dried under a gentle nitrogen stream at room temperature. The FAME was dissolved in *n*-heptane for gas chromatography analysis (GC).

**Tissue Samples** For tissue samples (muscle approximately 2g, subcutaneous fat 1 g, heart 2 g, liver 2 g), total lipids were extracted with chloroform/methanol (2:1, vol/vol) by homogenisation (Ultra Turrax,  $3 \times 15\text{ s}$ , 12,000 revolutions per minute) at room temperature according to Folch et al. [23]. The details of methylation were described previously [24].

**Rumen and Duodenal Digesta** Approximately 60 g of rumen content (representative mix of whole rumen content)

and 60 g duodenal digesta were freeze-dried, and then 1.2 g freeze-dried rumen or 1.2 g freeze-dried duodenal digesta content were taken for lipid extraction (duplicates). For extraction and direct fatty acid methylation of the rumen and digesta, a modified method from Sukhija and Palmquist [25] was used. The samples were treated with 3.5 ml toluene (containing 19:0 methyl ester as internal standard) and 4 ml of 5% methanolic HCl. The mixture was shaken in a water bath at  $60\text{ }^{\circ}\text{C}$  for 2 h. After cooling, methyl esters of total fatty acids were extracted with 3.5 ml toluene in the presence of 8.75 ml 6%  $\text{K}_2\text{CO}_3$  solution and stirred with a vortex stirrer. After centrifugation (1,200g for 5 min at  $4\text{ }^{\circ}\text{C}$ ) the toluene phase was separated and 1 g  $\text{Na}_2\text{SO}_4$  and activated charcoal were added and stored overnight until the organic phase was colourless. After filtration, an aliquot of the toluene extract was taken and analysed by GC.

### *Gas Chromatography (GC) Analysis*

An aliquot of this FAME extract was used for the gas chromatographic analyses of total fatty acids. The fatty acid composition of the samples was determined by GC on a CP SIL 88,  $100\text{ m} \times 0.25\text{ mm} \times 0.25\text{ }\mu\text{m}$  capillary column (Chrompack-Varian, USA) installed in a Perkin Elmer gas chromatograph Autosys XL with a flame ionisation detector and split injection. The initial oven temperature was  $120\text{ }^{\circ}\text{C}$ , held for 5 min, subsequently increased to  $170\text{ }^{\circ}\text{C}$  at a rate of  $2\text{ }^{\circ}\text{C min}^{-1}$ , held for 15 min, then to  $200\text{ }^{\circ}\text{C}$  at  $5\text{ }^{\circ}\text{C min}^{-1}$ , held for 5 min, then to  $235\text{ }^{\circ}\text{C}$  at  $2\text{ }^{\circ}\text{C min}^{-1}$  and held for 10 min. Hydrogen was used as the carrier gas at a flow rate of  $1\text{ ml min}^{-1}$ . The split ratio was 1:20; the injector was set at  $260\text{ }^{\circ}\text{C}$  and the detector at  $280\text{ }^{\circ}\text{C}$ . A reference standard mix added with *trans*-11 18:1 methyl ester, *cis*-9,*trans*-11 CLA methyl ester, 22:5n-3 methyl ester, *cis*-11 18:1 methyl ester, 18:4n-3 methyl ester and 22:4n-6 methyl ester was used for calibration and correction factors for individual fatty acids. The proportion and concentrations were calculated using the internal standard method of Turbochrom workstation software. 19:0 methyl ester was used as internal standard. The *cis*-9, *trans*-11 CLA concentrations includes the isomers *trans*-7,*cis*-9 CLA and *trans*-8,*cis*-10 CLA, because the separation of these CLA isomers is not possible by GC under these conditions [26]. The calculation for the index of  $\Delta^9$ -desaturase activity was calculated according to Malau-Aduli et al. [27]  $\Delta^9$ -Desaturase index =  $100 \times [(14:1 + 16:1 + 18:1)/(14:1 + 16:1 + 18:1 + 14:0 + 16:0 + 18:0)]$ .

**Reagents** FAMES were purchased from Sigma-Aldrich (Deisenhofen, Germany) and Matreya (Pleasant Gap, PA,

USA). The TLC plates coated with 0.25 mm silica gel (20 × 20 cm) were obtained from Merck (Darmstadt, Germany). FAMES were identified by means of purified standards (“Sigma-FAME mixture”, Sigma Aldrich Deisenhofen, Germany). Fatty acid methyl esters of *trans*-11 18:1, *cis*-11 18:1, 22:5n-3, 22:4n-6, *cis*-9,*trans*-11 18:2 were purchased from Matreya (Pleasant Gap, USA). All solvents used were HPLC grade from Lab-Scan (Dublin, Ireland). The 0.5 M methanolic sodium methylate were purchased from Fluka (Switzerland) and borontrifluoride/methanol (14% wt/vol) from Sigma-Aldrich (Deisenhofen, Germany).

**Statistical analysis.** All data were analysed by the least-squares method using the GLM procedures with fixed factors feeding and breed (SAS<sup>®</sup> Systems, Release 8.2, SAS Institute Inc., Cary, NC). All tables contain the least squares means (LSM) and the standard error (SE) of the LSM. All statistical tests of LSM were performed for a significance level of  $P \leq 0.05$ . Relationships between *cis*-9,*trans*-11 CLA and TVA in different tissues were examined by regression analysis using REG procedure (SAS<sup>®</sup> Systems).

## Results

The total fatty acid composition of longissimus and semitendinosus muscles, subcutaneous fat, liver and heart in German Holstein and German Simmental bulls fed different diets have been previously published [19–22].

Pasture-fed beef generally had lower intramuscular fat contents compared to concentrate-fed beef; therefore, when CLA proportions of the beef were calculated, the differences were less pronounced between pasture- and concentrate-fed beef [19]. Consequently, the results in the

present paper base on concentrations (mg/100 g fresh tissue or mg/100 g dry matter). The concentrations of *cis*-9,*trans*-11 CLA, VA and  $\Delta^9$ -desaturase index in rumen and duodenal digesta of German Holstein and German Simmental bulls are presented in Table 1. The diet had no effect on *cis*-9,*trans*-11 CLA concentration in both rumen and duodenal digesta. There was a significant interaction between diet and breed for the VA concentration in the rumen. Grazing of German Holstein bulls decreased the VA content but in grass-fed German Simmental bulls the VA concentration was higher compared with concentrate-fed bulls. However, compared with concentrate feeding, pasture feeding significantly increased the VA concentration in duodenal digesta (Table 1).

The *cis*-9,*trans*-11 CLA and VA concentration in plasma and erythrocyte phospholipids of German Holstein and German Simmental bulls is shown in Table 2. The results demonstrated that diet significantly affected the VA and *cis*-9,*trans*-11 CLA contents. The level of VA and *cis*-9,*trans*-11 CLA in plasma and erythrocyte PL was much lower ( $P < 0.05$ ) by concentrate feeding compared to pasture feeding of both breeds. The concentrations of *cis*-9,*trans*-11 CLA and VA in German Simmental bulls were more than two times higher with pasture feeding as compared with concentrate feeding. In contrast, the differences of *cis*-9,*trans*-11 CLA and VA contents in plasma and erythrocyte PL of German Holstein bulls were much smaller between both diets (Table 2).

The concentrations of *cis*-9,*trans*-11 CLA and VA (mg/100 g tissue) and  $\Delta^9$ -desaturase index in longissimus muscle, semitendinosus muscle and subcutaneous fat of German Holstein and German Simmental bulls are given in Table 3. There was a breed effect on the deposition of *cis*-9,*trans*-11 CLA in longissimus muscle, and the *cis*-9,*trans*-11 CLA concentration in muscle of German Holstein bulls

**Table 1** Concentration of *cis*-9,*trans*-11 CLA, VA and in rumen content (mg/100 g DM) and duodenal digesta (mg/g DM) of German Holstein and German Simmental bulls

	German Holstein				German Simmental				Significance <sup>a</sup> ( $P < 0.05$ )
	Concentrate <i>N</i> = 17		Pasture <i>N</i> = 16		Concentrate <i>N</i> = 16		Pasture <i>N</i> = 15		
	LSM	SE	LSM	SE	LSM	SE	LSM	SE	
Rumen (mg/100 g DM <sup>b</sup> )									
<i>cis</i> -9, <i>trans</i> -11 CLA	2.25	0.64	0.86	1.38	2.60	0.72	1.93	1.07	
VA	87.32	9.86	53.40	14.90	42.07	10.18	58.58	10.54	D*B
Duodenal digesta (mg/g DM)									
<i>cis</i> -9, <i>trans</i> -11 CLA	0.06	0.01	0.07	0.01	0.07	0.01	0.09	0.01	
VA	0.25	0.05	0.31	0.05	0.23	0.06	0.42	0.06	D

<sup>a</sup> D Significant influence of diet; B significant influence of breed; D\*B significant influence of interaction D\*B

<sup>b</sup> DM dry matter

**Table 2** Concentration of *cis-9,trans-11* CLA, VA in plasma ( $\mu\text{g/g}$ ) and erythrocyte phospholipids ( $\mu\text{g/g}$ ) of German Holstein and German Simmental bulls

	German Holstein				German Simmental				Significance <sup>a</sup> ( $P < 0.05$ )
	Concentrate <i>N</i> = 17		Pasture <i>N</i> = 16		Concentrate <i>N</i> = 16		Pasture <i>N</i> = 15		
	LSM	SE	LSM	SE	LSM	SE	LSM	SE	
Plasma ( $\mu\text{g/g}$ )									
<i>cis-9,trans-11</i> CLA	2.12	0.20	2.57	0.18	1.40	0.19	3.11	0.22	D, D*B
VA	12.54	1.44	16.61	1.30	9.87	1.34	23.78	1.56	D, D*B
Erythrocytes pl ( $\mu\text{g/g}$ )									
<i>cis-9,trans-11</i> CLA	1.94	0.22	1.78	0.25	1.46	0.22	3.17	0.22	D, D*B
VA	1.04	0.15	1.30	0.17	0.77	0.15	2.28	0.15	D, B, D*B

<sup>a</sup> For footnotes see Table 1**Table 3** Concentration of *cis-9,trans-11* CLA, VA (mg/100 g fresh tissue) and  $\Delta^9$ -desaturase index in longissimus muscle, semitendinosus muscle and subcutaneous fat of German Holstein and German Simmental bulls

	German Holstein				German Simmental				Significance ( $P < 0.05$ )
	Concentrate <i>N</i> = 17		Pasture <i>N</i> = 16		Concentrate <i>N</i> = 16		Pasture <i>N</i> = 15		
	LSM	SE	LSM	SE	LSM	SE	LSM	SE	
Longissimus muscle									
<i>cis-9,trans-11</i> CLA	17.12	1.72	17.34	1.77	13.32	1.77	11.51	1.83	B
VA	70.84	8.23	83.73	9.57	86.24	9.57	76.69	8.95	
$\Delta^9$ -desaturase index	50.87	0.66	46.06	0.68	48.64	0.68	44.92	0.70	D, B
Semitendinosus muscle									
<i>cis-9,trans-11</i> CLA	4.91	0.63	4.23	0.65	4.85	0.65	3.19	0.67	
VA	18.66	2.77	11.50	2.86	13.69	2.86	9.02	2.95	
$\Delta^9$ -desaturase index	53.47	0.65	48.61	0.67	50.72	0.67	47.11	0.69	D, B
Subcutaneous fat									
<i>cis-9,trans-11</i> CLA	423.09	23.88	397.23	24.62	354.40	26.32	375.69	25.43	
VA	1187.63	91.81	1739.09	94.64	917.94	91.17	1320.01	97.74	D, D*B
$\Delta^9$ -desaturase index	55.57	0.82	48.42	0.85	54.55	0.91	45.78	0.88	D, B

<sup>a</sup> For footnotes see Table 1

was significantly higher than that in German Simmental bulls. Furthermore, diet did not affect the deposition of *cis-9,trans-11* CLA in semitendinosus muscle and subcutaneous fat. Between the different tissues longissimus muscle, semitendinosus muscle and subcutaneous fat) *cis-9,trans-11* CLA accumulation in subcutaneous fat was the highest, up to 397.2 mg/100 g tissue in German Holstein bulls and 375.7 mg/100 g tissue in German Simmental bulls by pasture feeding (Table 3). The VA concentrations in subcutaneous fat were significantly higher with pasture compared to concentrate feeding.

The concentration of *cis-9,trans-11* CLA, VA (mg/100 g tissue) and  $\Delta^9$ -desaturase index (calculated) in

splanchnic tissue of liver and heart of German Holstein and German Simmental bulls is shown in Table 4. In contrast to the muscle and subcutaneous tissue, pasture feeding significantly increased CLA deposition in liver and heart tissue compared with concentrate feeding. The *cis-9,trans-11* CLA concentrations in heart tissue of German Simmental bulls was higher than that in German Holstein bulls, indicating breed difference. The accumulation of VA by pasture feeding was also enhanced significantly both in heart and liver tissue of German Holstein and German Simmental bulls. A diet effect on  $\Delta^9$ -desaturase index was detected, showing that the index was higher feeding concentrate relative to pasture, except in the heart of German



**Table 4** Concentration of *cis*-9,*trans*-11 CLA, VA (mg/100 g fresh tissue) and  $\Delta^9$ -desaturase index in liver and heart tissue of German Holstein and German Simmental bulls

	German Holstein				German Simmental				Significance ( $P < 0.05$ )
	Concentrate <i>N</i> = 17		Pasture <i>N</i> = 16		Concentrate <i>N</i> = 16		Pasture <i>N</i> = 15		
	LSM	SE	LSM	SE	LSM	SE	LSM	SE	
<b>Liver</b>									
<i>cis</i> -9, <i>trans</i> -11 CLA	10.46	1.00	14.02	1.03	6.98	1.03	15.94	1.07	D, D*B
VA	27.79	1.85	36.26	1.90	28.03	1.90	50.20	1.97	D, B, D*B
$\Delta^9$ -Desaturase index	24.20	0.63	21.36	0.65	24.40	0.65	22.55	0.67	D
<b>Heart</b>									
<i>cis</i> -9, <i>trans</i> -11 CLA	2.90	0.23	5.26	0.24	3.17	0.24	6.54	0.25	D, B, D*B
VA	19.94	1.50	25.52	1.55	23.85	1.55	36.41	1.60	D, B, D*B
$\Delta^9$ -Desaturase index	35.55	0.65	33.06	0.67	34.90	0.67	34.45	0.69	D

<sup>a</sup> For footnotes see Table 1

Simmental bulls. The relationships between the concentration of *cis*-9,*trans*-11 CLA and VA in ruminal content, duodenal digesta, plasma, erythrocytes, longissimus muscle, semitendinosus muscle, subcutaneous fat, liver and

heart are presented in Fig. 1. There was linear trend between the concentration of VA and *cis*-9,*trans*-11 CLA and this correlation was shown to vary from rumen to different tissues. The R-Square values of linear equation

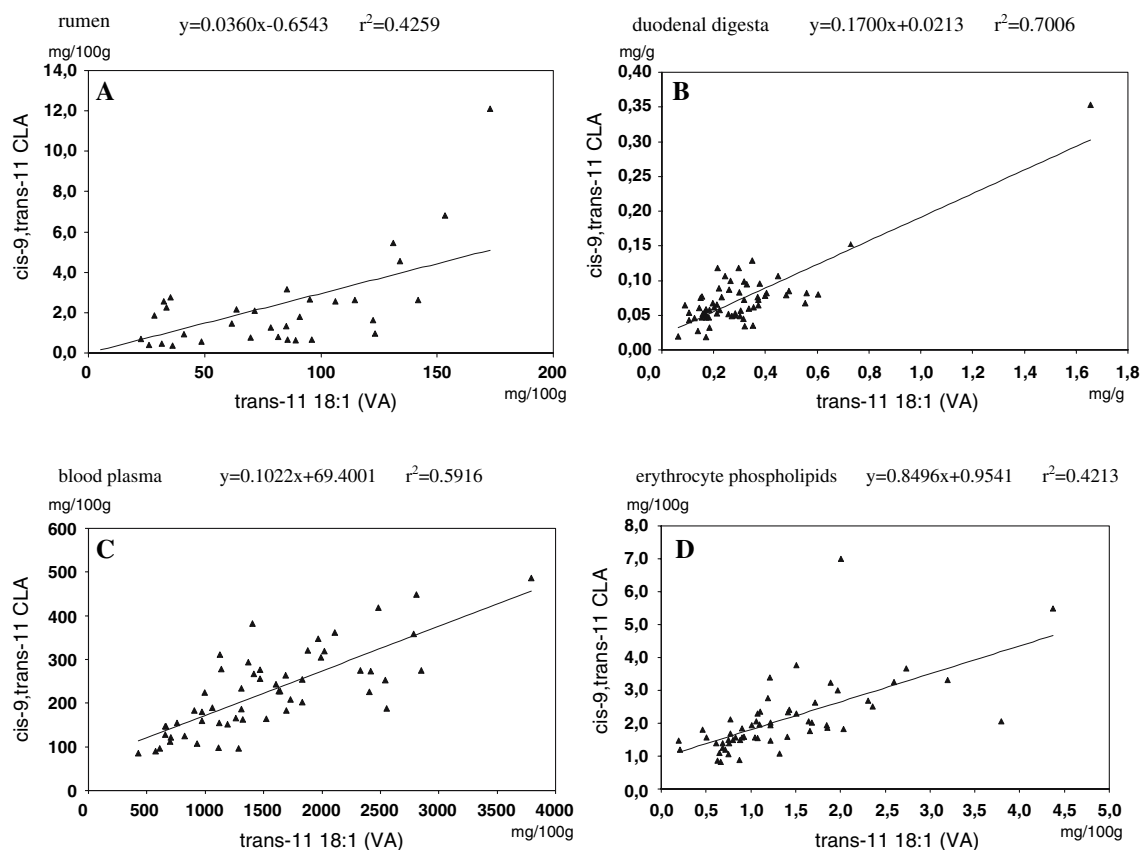


**Fig. 1** Relationship between VA and *cis*-9,*trans*-11 CLA in **a** rumen content, **b** duodenal digesta, **c** plasma, **d** erythrocyte phospholipids, **e** longissimus muscle, **f** semitendinosus muscle, **g** subcutaneous fat, **h**

liver and **i** heart in German Holstein and German Simmental bulls fed different diets

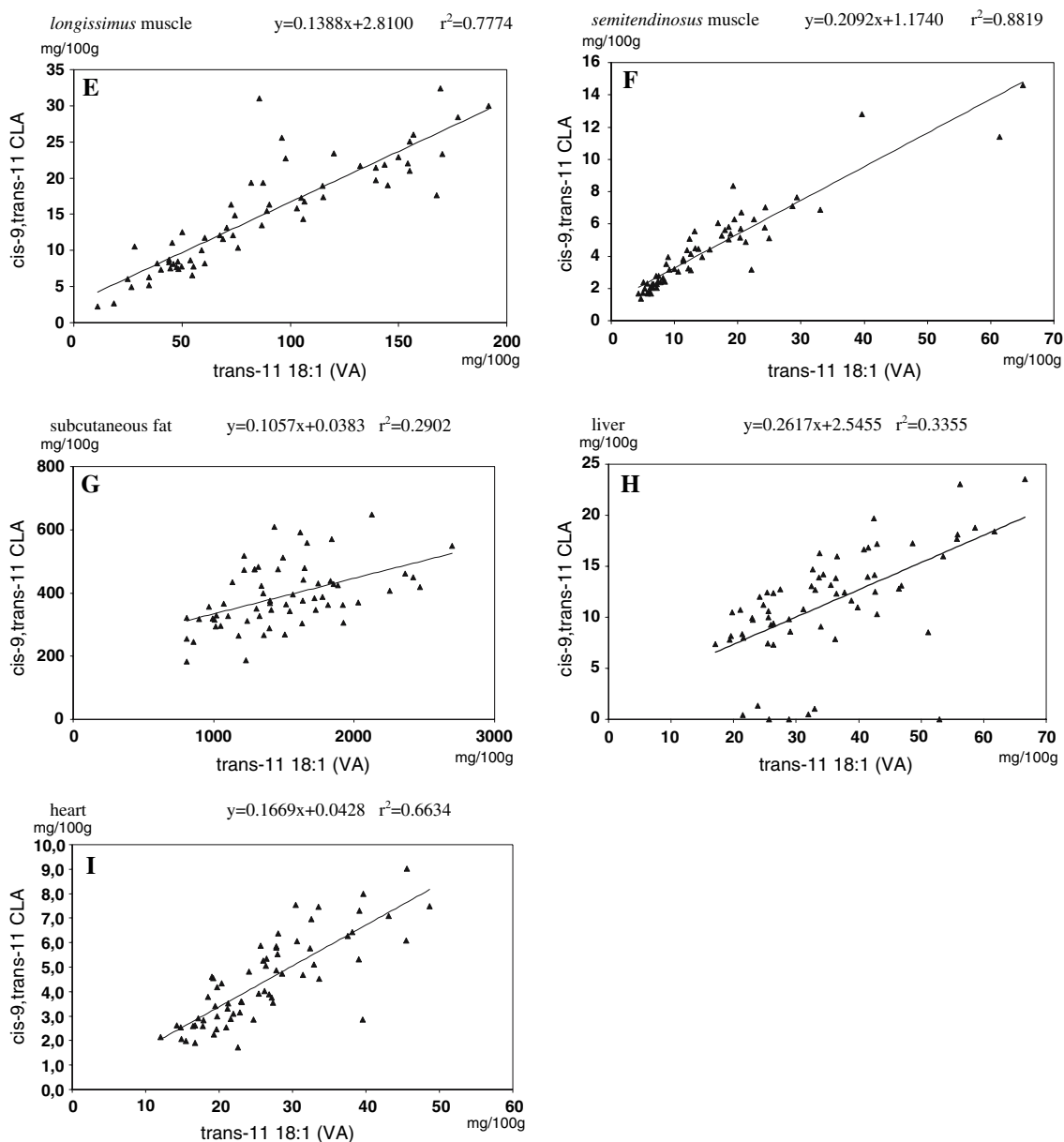


Fig. 1 continued

between *cis-9,trans-11* CLA and VA in rumen content, duodenal digesta content, plasma, erythrocyte phospholipids, *longissimus* muscle, *semitendinosus* muscle, subcutaneous fat, liver and in heart lipids were 0.43, 0.70, 0.59, 0.42, 0.78, 0.88, 0.29, 0.34 and 0.66, respectively (Fig. 1).

## Discussion

The majority of research examining the biohydrogenation of dietary fatty acids to VA, the desaturation of VA to *cis-9,trans-11* CLA, the absorption and the de novo synthesis

of *cis-9,trans-11* CLA has been focused on milk fat [1, 8, 10, 13–16]. Only a few papers reported the pathway of a *cis-9,trans-11* CLA and VA from the formation in the rumen, via duodenal digesta, and blood transport into the different muscle tissues [4, 8]. The present paper discusses the concentration of the two compounds VA and *cis-9,trans-11* CLA in the rumen, duodenal digesta, plasma, erythrocyte phospholipids and different tissues of beef at one sampling point (after slaughter) under two different feeding conditions. Increasing *cis-9,trans-11* CLA content in meat and milk from ruminants depends on the understanding of the sequential processes involved in the biohydrogenation of dietary unsaturated fatty acids in the

rumen. This process could be modified to increase *cis*-9,*trans*-11 CLA and VA output from the rumen by manipulating the ruminant diet [1, 4, 8]. In the rumen, *cis*-9,*trans*-11 CLA is formed from isomerization of dietary 18:2n-6 during the first step of the biohydrogenation process [28]. Once the *cis*-9,*trans*-11 CLA is formed, biohydrogenation of the *cis*-9 bond occurs by microbial reductase (group A microorganisms) to form VA. The extent, to which VA is hydrogenated to stearic acid (18:0; group B microorganisms) depends on the conditions in the rumen [28–30]. Dietary 18:3n-3 also undergoes biohydrogenation by being first isomerized to a conjugated triene (*cis*-9,*trans*-11,*cis*-15 18:3), followed by reductions of double bonds at carbons 9, 15, and 11 to yield *trans*-11, *cis*-15 18:2, VA, and 18:0, respectively [14, 30]. The lipids in the pasture diet are high in 18:3n-3, and the biohydrogenation by rumen micro-organisms does not include *cis*-9,*trans*-11 CLA as an intermediate [28]. VA is formed during the biohydrogenation of 18:3n-3 and 18:2n-6 to 18:0, and therefore VA is a common intermediate in the metabolic pathway of both PUFAs [28]. In the present study, feeding pasture-based diets to German Holstein and German Simmental bulls resulted in significantly higher VA concentrations in duodenal digesta, plasma, erythrocyte PL compared to concentrate-fed animals. Furthermore, these accumulations of VA by pasture feeding compared to concentrate feeding bulls were also measured in liver and heart tissues, and subcutaneous fat. The significantly higher VA concentrations in the rumen and duodenal digesta on a pasture diet indicates, that ruminal biohydrogenation of the predominant fatty acid in pasture diets, 18:3n-3, led to the production of high amounts of VA in the rumen and duodenal digesta. However, the *cis*-9,*trans*-11 CLA concentrations in the rumen and duodenal digesta were not affected by the diet. Very recently, Fukuda et al. [31, 32] found two new strains of *Butyrivibrio fibrosolvens*. One strain (MDT-10) does not have a great ability to hydrogenate 18:2n-6 to VA, and the other strain (MDT-5) rapidly isomerizes 18:2n-6 and 18:3n-3 to *cis*-9,*trans*-11 CLA and to *cis*-9,*trans*-11,*cis*-15 18:3. The authors assumed that the introduction of MDT-10 to the rumen might increase the amount of absorbed VA and therefore increase the conversion of VA to *cis*-9,*trans*-11 CLA in tissues [31, 32]. Harfoot and Hazlewood [28] have shown that *cis*-9,*trans*-11 CLA is rapidly metabolized, while VA accumulates during biohydrogenation of PUFA in the rumen. Piperova et al. [33] confirmed these results and demonstrated that the ratio of total *trans* 18:1 to *cis*-9,*trans*-11 CLA was high, approximately 60:1, in the duodenal flow of cows fed low and high levels of forage. It is known that pasture feeding resulted in significantly higher concentrations of *cis*-9,*trans*-11 CLA in milk and intramuscular fat [1, 13, 20, 34, 35]. With pasture feeding,

the duodenal flow of VA is higher, compared with low forage-containing diets, in which lipids are higher in linoleic acid [33, 36, 37]. Furthermore, Piperova et al. [33] and Sackmann et al. [37] demonstrated that the duodenal output of *trans* 18:1 fatty acids was high in *trans*-10 18:1 in diets with low forage contents. Under these conditions, shifts in the ruminal biohydrogenation pathway have occurred resulting in *trans*-10 18:1 replacing VA as predominant *trans* 18:1 fatty acids isomer leaving the rumen [33, 36, 38]. Finally, the amount of duodenal *trans*-10,*cis*-12 CLA isomer was significantly increased in cows fed diets with a low forage content [33].

Plasma is the transportation system of nutritional ingredients, and erythrocyte phospholipid fatty acids status reflects the overall long-term (erythrocytes 120 days half-time) lipid metabolism influenced by diet and rumen microbial activity. For blood lipids, phospholipids and cholesterol esters are the main components and account for over 95% of the total lipids in the plasma of ruminant animals. However, triglycerides and free fatty acids only represent < 5% and 1% of total plasma lipids, respectively [36]. PUFA that escape ruminal biohydrogenation are preferentially esterified to the plasma cholesterol esters and phospholipids [39]. The current study demonstrated that pasture feeding significantly increased the concentrations of *cis*-9,*trans*-11 CLA and VA both in the plasma and erythrocyte PL compared to concentrate feeding, with one exception *cis*-9,*trans*-11 CLA in erythrocyte PL of German Holstein bulls. The *cis*-9,*trans*-11 CLA and VA concentration was significantly higher (up to two times) on pasture in comparison with concentrate feeding, in German Simmental bulls. Loo et al. [40] investigated the rumen, blood and milk of Holstein cows fed diets with a high ratio of concentrate to forage (grass, hay) (65:35) supplemented with fish oil, linseed oil or sunflower oil. The authors also observed that significantly higher *cis*-9,*trans*-11 CLA contents in blood plasma with linseed oil supplements (high in 18:3n-3) compared with sunflower or fish oil supplements. However, the highest VA contents were detected in the blood plasma with fish oil compared with the other supplements. It is well known that a major proportion of the *cis*-9,*trans*-11 CLA found in ruminant tissues is formed through the activity of  $\Delta^9$ -desaturase on VA [12, 30]. Kinetic studies of rumen biohydrogenation of 18:2n-6 acid to 18:0 have shown that *cis*-9,*trans*-11 CLA is a transient intermediate in the rumen, whereas VA is the intermediate that accumulates under these certain dietary conditions [30, 41, 42]. Furthermore, dietary addition of plant oils containing 18:3n-3 also increases the *cis*-9,*trans*-11 CLA content of ruminant fat, and intermediates in its pathway of biohydrogenation include VA but not *cis*-9,*trans*-11 CLA [10, 41]. Griinari's results [10] demonstrated that an estimated 64% of the CLA in milk fat was of

endogenous origin, and endogenous synthesis of CLA from *trans*-11 18:1 represented the primary source of CLA in the milk fat of lactating cows [13]. Kay et al. [13] reported the first study to examine the importance of endogenous synthesis of *cis*-9,*trans*-11 CLA in the milk fat of pasture-fed cows. The authors confirmed these results and showed that approximately 90% of *cis*-9,*trans*-11 CLA was produced endogenously. Several investigations confirmed that pasture feeding to dairy cows doubles the *cis*-9,*trans*-11 CLA content of milk fat [41]. Kraft et al. [34] and Collomb et al. [35] showed differences between the individual CLA isomer distributions in milk lipids of cows fed diets with concentrates rations in PUFA indoors and grazing cows in the Alps (Switzerland). For intramuscular fat, Dannenberger et al. [21] concluded that pasture feeding affected the distribution of individual CLA isomers in the muscle lipids. No related investigations for milk fat have been reported to establish the importance of endogenous synthesis of *cis*-9,*trans*-11 CLA in the intramuscular fat of ruminant tissues. It could be assumed that the contribution from endogenous synthesis is similar to that reported for milk because VA and  $\Delta^9$ -desaturase are necessary requirements.

Martin et al. [43] and Ward et al. [44] showed that mammary gland and adipose tissue of ruminants have substantial  $\Delta^9$ -desaturase activity. A linear relationship between VA and *cis*-9,*trans*-11 CLA has been observed for milk fat in a number of studies and across a wide range of diets reviewed by Griinari and Bauman [41]. This relationship has also been observed over a wide range of TVA concentrations, indicating a high capacity for endogenous synthesis of *cis*-9,*trans*-11 CLA [41]. Madron et al. [45] and Enser et al. [46] observed a linear relationship between the concentration of *cis*-9,*trans*-11 CLA and VA in muscle adipose tissue in beef. The extent, to which  $\Delta^9$ -desaturase is responsible for *cis*-9,*trans*-11 CLA production in the muscle adipose tissue showed no differences in the index of  $\Delta^9$ -desaturase activity in muscle fat among diet treatments. Meanwhile, Ntambi [47] showed that there was a repressive effect of long-chain PUFA on the activity of the  $\Delta^9$ -desaturase. The results of our study confirmed that there was a correlation between *cis*-9,*trans*-11 CLA and VA concentrations in the rumen, duodenal digesta, blood and in the different tissues (Fig. 1). Piperova et al. [33] assumed that tissue level of *cis*-9,*trans*-11 CLA may not be a simple reflection of the proportions of these compound that escaped rumen biohydrogenation. The major source of tissue *cis*-9,*trans*-11 CLA should be the post absorptive synthesis via  $\Delta^9$ -desaturation of TVA produced during rumen biohydrogenation of dietary PUFA. However, in our experiment, pasture feeding led to different accumulation rates of *cis*-9,*trans*-11 CLA in the tissues. Although pasture feeding significantly increased the *cis*-9,*trans*-11 CLA concentrations in liver and heart, diet had no effect on the

*cis*-9,*trans*-11 CLA concentrations in the muscles and subcutaneous fat. The  $\Delta^9$ -desaturase index was significantly lower in all investigated tissues and gave no additional information about the cause for the different accumulation rates of *cis*-9,*trans*-11 CLA in the different tissues. Smith et al. [48] concluded that  $\Delta^9$ -desaturase index was not an indicator of absolute enzyme activity. Further research is needed to investigate the reasons of different accumulation of *cis*-9,*trans*-11 CLA in the beef tissues by pasture feeding and include the absolute enzyme activity measurement of  $\Delta^9$ -desaturase. Very recently J.M. Griinari and K. Shingfield (2006, private communication) established that the *cis*-9,*trans*-11 CLA accumulation in ruminant lipids can be increased up to ten fold by feeding diets that enhance the production of VA in the rumen. The focus should be on ruminal formation of VA rather than *cis*-9,*trans*-11 CLA. It suggests that the most effective methods to enhance *cis*-9,*trans*-11 CLA concentration in ruminant products is to feed supplements containing VA or manipulate rumen biohydrogenation to increase the formation of VA. So, understanding the mechanism involved in the biosynthesis of *cis*-9,*trans*-11 CLA and other CLA isomers will allow scientists to design feeding strategies for enhancing the CLA concentration in ruminant products.

**Acknowledgments** We thank B. Jentz and H. Rooch of the Department of Muscle Biology and Growth, who conducted the sample preparation and GC measurements. Funding: The research was supported by grants from the European Commission (Research Project QLRT-CT-2000-31423), the Agricultural Ministry of China (Grant No. 26/2005–2006 “Adipogenesis”) and the National Natural Science Foundation of China (Project No. 30371040).

## References

1. Lock AL, Bauman DE (2004) Modifying milk fat composition of dairy cows to enhance fatty acids beneficial to human health, review. *Lipids* 39:1197–1206
2. Tricon S, Burdge GC, Kew S, Banerjee T, Russell JJ, Grimble RF, Williams CM, Calder PC, Yaqoob P (2004) Effects of *cis*-9,*trans*-11 and *trans*-10,*cis*-12 conjugated linoleic acid on immune cell function in healthy humans. *Am J Clin Nutr* 80:1626–1633
3. Kelley DS, Erickson KL (2003) Modulation of body composition and immune cell functions by conjugated linoleic acid in humans and animal models: benefits vs. risks, review. *Lipids* 38:377–386
4. Lock AL, Corl BA, Barbano DM, Bauman DE, Ip C (2004) The anticarcinogenic effect of *trans*-11 18:1 is dependent on its conversion to *cis*-9, *trans*-11 CLA by delta9-desaturase in rats. *J Nutr* 134:2698–2704
5. Attar-Bashi NM, Weisinger RS, Begg DP, Li D, Sinclair AJ (2007) Failure of conjugated linoleic acid supplementation to enhance biosynthesis of docosahexaenoic acid from alpha-linolenic acid in healthy human volunteers. *Prostaglandins Leukot Essent Fatty acids* 76:121–130
6. Tricon S, Yaqoob P (2006) Conjugated linoleic acid and human health: a critical evaluation of the evidence. *Curr Opin Clin Nutr Metab Care* 9:105–110

7. Badinga L, Greene ES (2006) Physiological properties of conjugated linoleic acid and implications for human health. *Nutr Clin Pract* 21:367–373
8. Nuernberg K, Nuernberg G, Ender K, Lorenz S, Winkler K, Rickert R, Steinhart H (2002) *N*-3 fatty acids and conjugated linoleic acids of longissimus muscle in beef cattle. *Eur J Lipid Sci Technol* 104:463–471
9. Scollan ND, Hocquette J, Nuernberg K, Dannenberger D, Richardson RI, Moloney A (2006) Innovations in beef production systems that enhance the nutritional and health value of beef lipids and their relationship with meat quality, review. *Meat Sci* 74:17–33
10. Griinari JM, Corl BA, Lacy SH, Chouinard PY, Nurmela KV, Bauman DE (2000) Conjugated linoleic acid is synthesized endogenously in lactating dairy cows by delta(9)-desaturase. *J Nutr* 130:2285–2291
11. Kepler CR, Hirons KP, McNeill JJ, Tove SB (1966) Intermediates and products of the biohydrogenation of linoleic acid by *Butyrivibrio fibrisolvens*. *J Biol Chem* 241:1350–1354
12. Jenkins TC (1993) Lipid metabolism in the rumen, review. *J Dairy Sci* 76:3851–3863
13. Kay JK, Mackle TR, Auldist MJ, Thomson NA, Bauman DE (2004) Endogenous Synthesis of *cis*-9, *trans*-11 conjugated linoleic acid in dairy cows fed fresh pasture. *J Dairy Sci* 87:369–378
14. Destailats F, Trottier JP, Galvez JM, Angers P (2005) Analysis of alpha-linolenic acid biohydrogenation intermediates in milk fat with emphasis on conjugated linolenic acids. *J Dairy Sci* 88:3231–3239
15. Bessa RJB, Santos-Silva J, Ribeiro JMR, Portugal AV (2000) Reticulo-rumen biohydrogenation and the enrichment of ruminant edible products with linoleic acid conjugated isomers. *Livest Prod Sci* 63:201–211
16. Mosley EE, Shafii B, Moate PJ, McGuire MA (2006) *Cis*-9, *trans*-11 conjugated linoleic acid is synthesized directly from vaccenic acid in lactating dairy cattle. *J Nutr* 136:570–575
17. Daniel ZC, Wynn RJ, Salter AM, Buttery PJ (2004) Differing effects of forage and concentrate diets on the oleic acid and conjugated linoleic acid content of sheep tissues: the role of stearoyl-coA desaturase. *J Anim Sci* 82:747–758
18. Kelsey JA, Corl BA, Collier RJ, Bauman DE (2003) The effect of breed, parity, and stage of lactation on conjugated linoleic acid (CLA) in milk fat from dairy cows. *J Dairy Sci* 86:2588–2597
19. Nuernberg K, Dannenberger D, Nuernberg G, Ender K, Voigt J, Scollan ND, Wood JD, Nute GR, Richardson RI (2005) Effect of a grass-based and a concentrate feeding system on meat quality characteristics and fatty acid composition of longissimus muscle in different cattle breeds. *Livest Prod Sci* 94:137–147
20. Dannenberger D, Nuernberg G, Scollan ND, Schabbel W, Steinhart H, Ender K, Nuernberg K (2004) Effect of diet on the deposition of *n*-3 fatty acids, conjugated linoleic and C18:1*trans* fatty acid isomers in muscle lipids of German Holstein bulls. *J Agric Food Chem* 52:6607–6615
21. Dannenberger D, Nuernberg K, Nuernberg G, Scollan ND, Steinhart H, Ender K (2005) Effect of pasture vs. concentrate diet on CLA isomer distribution in different tissue lipids of beef cattle. *Lipids* 40:589–598
22. Dannenberger D, Nuernberg K, Nuernberg G, Ender K (2006) Carcass- and meat quality of pasture vs. concentrate fed German Simmental and German Holstein bulls. *Arch Tierz* 49:315–328
23. Folch J, Lees M, Stanley SGH (1957) A simple method for the isolation and purification of total lipids from animal tissues. *J Biol Chem* 226:497–509
24. Nuernberg K, Nuernberg G, Ender K, Lorenz S, Winkler K, Rickert R, Steinhart H (2002) *N*-3 fatty acids and conjugated linoleic acids of longissimus muscle in beef cattle. *Eur J Lipid Sci Technol* 104:463–471
25. Sukhija PS, Palmquist DL (1988) Rapid method for determination of total fatty acid content and composition of feedstuffs and feces. *J Agric Food Chem* 36:1202–1206
26. Fritsche J, Fritsche S, Solomon MB, Mossoba MM, Yurawecz MP, Morehouse K, Ku Y (2000) Quantitative determination of conjugated linoleic acid isomers in beef fat. *Eur J Lipid Sci Technol* 102:667–672
27. Malau-Aduli AEO, Siebert BD, Bottema CDK, Pitchford WS (1997) A comparison of fatty acid composition of triacylglycerols in adipose tissue from Limousin and Jersey cattle. *Aust J Agric Res* 48:715–722
28. Harfoot CG, Hazlewood GP (1988) The rumen microbial ecosystem. In: Hobson PN (ed) *Lipid metabolism in the rumen*, Elsevier, London, pp 285–322
29. Wilde PF, Dawson RMC (1966) The biohydrogenation of alpha-linolenic acid and oleic acid by rumen microorganisms. *Biochem J* 98:469–475
30. Song MK, Kenelly JK (2003) Biosynthesis of conjugated linoleic acid and its incorporation into ruminant's products. *Asian-Aust J Anim Sci* 16:306–314
31. Fukuda S, Suzuki Y, Murai M, Asanuma N, Hino T (2006) Isolation of a novel strain of *Butyrivibrio fibrisolvens* that isomerizes linoleic acid to conjugated linoleic acid without hydrogenation, and its utilization as a probiotic for animals. *J Appl Microbiol* 100:787–794
32. Fukuda S, Suzuki Y, Murai M, Asanuma N, Hino T (2006) Augmentation of vaccenate production and suppression of vaccenate biohydrogenation in cultures of mixed ruminal microbes. *J Dairy Sci* 89:1043–1051
33. Piperova LS, Sampugna J, Teter BB, Kalscheur KF, Yurawecz MP, Ku Y., Morehouse KM, Erdman RA (2002) Duodenal and milk *trans* octadecenoic acid and conjugated linoleic acid (CLA) isomers indicate that post absorptive synthesis is the predominant source of *cis*-9 containing CLA in lactating dairy cows. *J Nutr* 132:1235–1241
34. Kraft J, Collomb M, Möckel P, Sieber R, Jahreis G. (2003) Differences in CLA isomer distribution of cow's milk lipids. *Lipids* 38:657–664
35. Collomb M, Sieber R, Bütikofer U (2004) CLA isomers in milk fat from cows fed diets with high levels of unsaturated fatty acids. *Lipids* 39:355–364
36. Lake SL, Weston TR, Scholljegerdes EJ, Murrieta CM, Alexander BM, Rule DC, Moss GE, Hess BW (2007) Effects of postpartum dietary fat and body condition score at parturition on plasma, adipose tissue, and milk fatty acid composition of lactating beef cows. *J Anim Sci* 85:717–730
37. Sackmann JR, Duckett SK, Gillis MH, Realini CE, Parks AH, Egelston RB (2003) Effects of forage and sunflower oil on ruminal biohydrogenation of fatty acids and conjugated linoleic acid formation in beef steers fed finishing diets. *J Anim Sci* 81:3174–3181
38. Shingfield KJ, Reynolds CK, Hervas G, Griinari JM, Grandison AS, Beever DE (2006) Examination of the persistency of milk fatty acid composition responses to fish oil and sunflower oil in the diet of dairy cows. *J Dairy Sci* 89:714–732
39. Christie WW (1981) *Lipid metabolism in ruminant animals*. Pergamon, New York
40. Loor JJ, Ferlay A, Ollier A, Ueda K, Doreau M, Chilliard Y (2005) High-concentrate diets and polyunsaturated oils alter *Trans* and conjugated isomers in bovine rumen, blood, and milk. *J Dairy Sci* 88:3986–3999
41. Griinari JM, Bauman DE (1999) Biosynthesis of conjugated linoleic acid and its incorporation into meat and milk in ruminants. In: Yurawecz MP, Mossoba MM, Kramer JKG, Pariza MW, Nelson G (eds) *Advances in conjugated linoleic acid research*. AOCS Press, Champaign, vol 1, pp 180–200

42. Keeney M (1970) Physiology of digestion and metabolism in the ruminant. In: Phillipson AT (eds) *Lipid metabolism in the rumen*. Oriel Press, Newcastle upon Tyne, pp 489–503
43. Martin GS, Lunt DK, Britain KG, Smith SB (1999) Postnatal development of stearoyl coenzyme A desaturase gene expression and adiposity in bovine subcutaneous adipose tissue. *J Anim Sci* 77:630–636
44. Ward RJ, Travers MT, Richards SE, Vernon RG, Salter AM, Buttery PJ, Barber MC (1998) Stearoyl-coA desaturase mRNA is transcribed from a single gene in the ovine genome. *Biochim Biophys Acta* 1391:145–156
45. Madron MS, Peterson DG, Dwyer DA, Corl BA, Baumgard LH, Beermann DH, Bauman DE (2002) Effect of extruded full-fat soybeans on conjugated linoleic acid content of intramuscular, intermuscular, and subcutaneous fat in beef steers. *J Anim Sci* 80:1135–1143
46. Enser M, Scollan ND, Choi NJ, Kurt E, Hallett K, Wood JD (1999) Effect of dietary lipid on the content of conjugated linoleic acid (CLA) in beef muscle. *Anim Sci* 69:143–146
47. Ntambi JM (1999) Regulation of stearoyl-coA desaturase by polyunsaturated fatty acids and cholesterol. *J Lipid Res* 40:1549–1558
48. Smith SB, Hively TS, Cortese GM, Han JJ, Chung KY, Castenada P, Gilbert CD, Adams VL, Mersmann HJ (2002) Conjugated linoleic acid depresses the  $\Delta^9$ -desaturase index and stearoyl coenzyme A desaturase enzyme activity in porcine subcutaneous adipose tissue. *J Anim Sci* 80:2110–2115

It is clear that bypassing the rumen increases n-3 FA in plasma and muscle, hence a key element to using feedstuffs containing n-3 FA is to protect it in the rumen from biohydrogenation. The concentration of 18:3n-3 increases in the blood when emulsions of flaxseed oil are infused into the abomasum, the true stomach of ruminants, [11, 12] or into the duodenum, [13]. There is evidence that the 18:3n-3 levels of neutral lipid in the muscle of cattle and sheep can be increased if more 18:3n-3 is made available for absorption from the small intestine [14–16]. Protecting n-3 FA by encapsulating them in a matrix of formaldehyde-treated protein increases n-3 FA levels in the muscle [17]. Although this method is believed to provide protection for polyunsaturated FA (PUFA) from microbial hydrogenation [12, 18], the use of formaldehyde lowers its consumer acceptance. In addition, there are conflicting results with respect to the effectiveness of this process [19, 20]. Several other approaches have been tested for protecting n-3 FA from microbial hydrogenation in the rumen that do not use formaldehyde, but these have had little success [20–24]. More recently, a method using a whey protein isolate gel appears promising [25, 26], but this approach may be impractical.

Therefore, the primary objective of this study was to find a practical, simple, and consumer-acceptable method to protect the 18:3n-3 in flaxseed from hydrogenation by rumen microbes. Condensed tannin has the ability to bind with plant proteins in the rumen, with enzymes secreted by rumen bacteria, and with rumen bacteria, but do this without altering absorption in the entire gastrointestinal tract [27, 28]. Hence, we rationalized that tannins might help protect 18:3n-3 in flaxseed from hydrogenation by rumen microbes. Furthermore, we rationalized that adding the protein casein to ground flaxseed before treating it with condensed tannin may help encase the 18:3n-3 in flaxseed in a protective coating. Therefore, the specific objectives were to: (1) determine if treating ground flaxseed with tannin with or without casein would result in less disappearance of 18:3n-3 during fermentations in vitro with cattle rumen fluid, and (2) determine if treating ground flaxseed with condensed tannin could increase the level of 18:3n-3 and other n-3 FA in the blood of cattle consuming forage or grain-based diets.

## Experimental Procedures

### Flaxseed Treatment with Tannin

Ground flaxseed was treated with condensed tannin (quebracho tannin), or condensed tannin plus either low (45 g/227 g flaxseed) or high (90.8 g/227 g flaxseed) amounts of casein. Ground flaxseed was treated with condensed tannin

by mixing 45.4 g of quebracho tannin syrup (34% DM; Tannin Corp., Peabody, MA) with 28.3 g of warm tap water then thoroughly mixing this solution with 227 g of ground flaxseed before drying in a forced air oven at 50 °C. For flaxseed containing casein, either 45.4 g of casein (Sigma-Aldrich, St. Louis, MO) or 90.8 g of casein was mixed with 227 g of ground flaxseed to which a solution containing 45.4 g of quebracho tannin syrup in 125 g of warm tap water was added and thoroughly mixed. The flaxseed-tannin-casein mixtures were dried as described above for the flaxseed-tannin mixture.

### Fermentation In Vitro

Fermentation of untreated and treated flaxseed with bovine rumen fluid was done at 39 °C and the reduction in 18:3n-3 assessed at 24 h. Each flask contained 250 mg of ground alfalfa-grass hay, 250 mg of untreated ground flaxseed or one of three treated flaxseeds, 40 ml of buffer solution, and 10 ml of strained rumen fluid. Rumen fluid was obtained from two ruminally fistulated beef cows and kept separate in pre-warmed insulated containers until it was used in the trial within 30 min after collection. The cows were fed alfalfa hay ad libitum for a month before ruminal digesta was collected for the trial. The rumen fluid was flooded with CO<sub>2</sub> while it was put into the flasks and again after the addition of the feedstuffs. Flasks were agitated at 1, 12 and 18 h. Microbial activity in the 0 time samples as well as 24 h fermentations was stopped by pouring the contents of each flask into a plastic bag then quickly freezing it as a thin (ca. 0.5 cm) layer. The buffer solution was distilled water and 0.68 mM CaCl<sub>2</sub>, 2 mM MgSO<sub>4</sub>, 73 mM KH<sub>2</sub>PO<sub>4</sub>, 142 mM Na<sub>2</sub>CO<sub>3</sub>, 8.6 mM NaCl, 7.9 mM Na<sub>2</sub>SO<sub>3</sub>, and 8.3 mM NH<sub>2</sub>CONH<sub>2</sub>. Each combination of flaxseed treatments was replicated twice with rumen fluid from one cow used in one replicate set and rumen fluid from the second cow used in the other.

### Calculations for the Fermentation Reaction

The percent change in the 18:3n-3 level at 24 h was determined relative to the initial levels at time 0. Percent change was used because initial amount of this FA varied somewhat as a function of whether or not the flaxseed was or was not treated with tannin. The Mixed Model Procedure of SAS [29] was used for data analysis, and tests were conducted to assure that data were normally distributed. The rumen-fluid donor cow was the random factor in all statistical analyses. The variance-covariance structure was examined and the variance components option was used. Means were considered different at an  $\alpha$  of 0.05.

## Assessment of Tannin-Treated Flaxseed In Vivo

Ten yearling Angus steers (castrated males) with a mean body weight of 392 kg (SD = 21 kg) were used in a trial with a factorial design with flaxseed treatment (none or tannin-treated) and time of blood collection (pre- or post-prandial) as the two factors. Separate analyses were conducted for each type of basal diet, which were either grain or forage. Five of the steers were given a grain-based diet during the whole trial and were given tannin-treated ground flaxseed for 15 days followed by collection of blood into heparinized tubes. These cattle were then fed non-treated ground flaxseed for 15 days before blood was collected. The other five steers on the forage-based diet followed the same treatment regimen as steers on the grain-based diet.

The steers were fed at 6 am and 6 pm, and on average had a daily intake of 7.8 or 8.8 kg of the grain or forage basal rations, respectively, plus 907 g of either ground flaxseed or 980 g of tannin-treated ground flaxseed (half of each fed per feeding). More tannin-treated flaxseed was fed to adjust for the additional weight of the tannin so that cattle received the same amount of flaxseed. Ground flaxseed was treated with quebracho tannin by mixing the flaxseed meal with tannin and water at a rate of 5:1:0.625 (w/w/w) then drying in a forced-air oven at 50 °C. Both grain and forage rations were formulated to meet or exceed the nutrient requirements of the growing steers [30].

The feed and nutritional composition of the two basal diets is described in Table 1 along with their composition of 18-carbon FA. Liquid molasses was added to the grain mixture to help maintain its integrity when fed, improve its palatability, and reduce feed dust. The alfalfa hay cubes in the forage-based diet were about 4 cm<sup>3</sup> in size and composed of coarsely chopped alfalfa hay. The same amount of liquid molasses and mineral-vitamin mixture was added to the forage ration.

Plasma neutral and phospholipid n-3 FA levels were evaluated with respect to flaxseed treatment and time of blood collection (post-prandial, 10-30 to 11 am or pre-prandial, 5-30 to 6 pm) using the Mixed Model Procedure of SAS [29]. Separate analyses were done for animals on the two basal diets since their daily intake of 18:3n-3 from the basal diets was 14 g for the forage-fed steers versus 8 g for the grain-fed steers. Animals were the random factor for both analyses. The variance-covariance structures were examined and the variance components option was used for both analyses. Means were considered different at an  $\alpha$  of 0.05.

## Plasma Total Lipid Extraction and Fatty Acid Analysis

Plasma lipids were then extracted by transferring a 200  $\mu$ l aliquot of plasma into a tube containing 5 ml of chloroform-

**Table 1** Ingredients and nutrient composition of the grain and forage basal diets consumed by yearling beef steers

	Grain	Forage
Ingredient (% as fed)		
Rolled corn	58	–
Cracked peas	6	–
Soybean meal	3	–
Sugar beet pulp pellets	25	50
Alfalfa cubes	–	42
Liquid molasses	7	7
Mineral-vitamin mixture <sup>a</sup>	0.7	0.7
Composition (% of DM)		
Nitrogen	1.59	2.09
IVDMD	79	77
Fatty acids		
18:0	0.08	0.04
18:1n-9	1.12	0.18
18:2n-6	2.61	0.38
18:3n-3	0.10	0.16

<sup>a</sup> Mineral-vitamin mixture = dicalcium phosphate, trace mineral salt, limestone, and vitamin A, D, and E

methanol (2:1, v/v) followed by mixing it by vortexing [31]. The addition of 1 ml of 0.9% KCl to these tubes resulted in two phases, which were thoroughly mixed and then separated overnight in a –20 °C freezer. The upper phase was removed, and the lipid-containing lower phase was rinsed with 1 ml of theoretical upper phase, consisting of chloroform-methanol-water (3:48:47, v/v), to remove any aqueous soluble contaminants [31]. The upper phase was discarded and the neutral lipids and phospholipids separated using solid-phase extraction with silicic acid [10]. The neutral lipids were eluted with chloroform and the phospholipids eluted with methanol. The respective solvents were removed via evaporation under a stream of nitrogen and the lipids redissolved in *n*-hexane:2-propanol (3:2 v/v). This lipid extract was stored at –80 °C until analysis.

A portion of each lipid fraction was used to determine fatty acid composition of the plasma neutral lipids and phospholipids. The *n*-hexane:2-propanol was removed by evaporation under a stream of nitrogen and 2 ml of 0.5 M KOH dissolved in anhydrous methanol was added to make fatty acid methyl esters (FAME) via a base-catalyzed transesterification [32]. The FAME were extracted from the methanol using 2 ml of *n*-hexane and the *n*-hexane phase containing the FAME was removed. The lower phase was reextracted two more times with 3 ml of *n*-hexane, and these washes were combined with the original aliquot. Individual FA were separated by GLC using an SP-2330 column (0.32 mm i.d.  $\times$  30 m length) and a Trace GLC (ThermoElectron, Austin, TX) equipped with dual auto-samplers and dual FID. FA were quantified using a



standard curve from commercially purchased standards (Nu-Chek-Prep, Elysian, MN) and 17:0 was used as the internal standard.

#### Fatty Acid Analysis of Feed for Cattle Trial and In Vitro Residue

Dietary ingredients were analyzed for fatty acids via direct transesterification with methanolic-HCl [33, 34]. In vitro fermentation samples were lyophilized (Freezemobile 25 SL, The Virtis Co., Gardiner, NY), ground with a mortar and pestle, and analyzed for fatty acids [35]. Briefly, 200 mg was subjected to direct saponification in 4.0 ml of ethanol containing 1 ml of 33% (w/v) KOH. Direct saponification was done in 16 × 25 mm tubes with Teflon-lined screw-caps at 85 °C for 1 h with vortex-mixing every 1 min. Tubes were cooled, and 1.0 ml of 12 M HCl and 3.0 ml of hexane were added to each tube and mixed by vortexing. The hexane layer was transferred to a clean tube and dried under a stream of N<sub>2</sub> gas. Fatty acid methyl esters were prepared by incubating the dried hexane layer with 4.0 ml of 0.5 M HCl in methanol that contained 1 mg of tridecanoic acid (Sigma, St. Louis, MO) as the internal standard for 1 h at 85 °C. Separation of fatty acid methyl esters was achieved by GLC (Model CP-3800, Varian Inc., Palo Alto, CA) equipped with a 100 m capillary column (SP-2560, Supelco, Bellefonte, PA). Identification of peaks was accomplished using purified standards (Sigma-Aldrich, St. Louis, MO; Nu-Chek Prep, Elysian, MN).

## Results

### In Vitro Fermentation Trial

The percent change in level of 18:3n-3 at 24 h were similar ( $P = 0.73$ ) among the three tannin treatments, indicating that adding either of the two amounts of casein to the flaxseed-tannin mixture did not reduce hydrogenation (Fig. 1). However, across the 24-h period, treating the ground flaxseed with condensed tannin reduced ( $P = 0.01$ ) hydrogenation of 18:3n-3 to only 13% compared to a loss of 43% in the untreated flaxseed.

### Assessment of Tannin-Treated Flaxseed In Vivo

With respect to neutral lipids in blood plasma, when the basal diet was either forage or grain, ingesting tannin-treated flaxseed did not raise plasma 18:3n-3 levels over those observed when the cattle consumed normal ground flaxseed ( $P \geq 0.10$ ; Fig. 2). Levels of 20:5n-3 were not

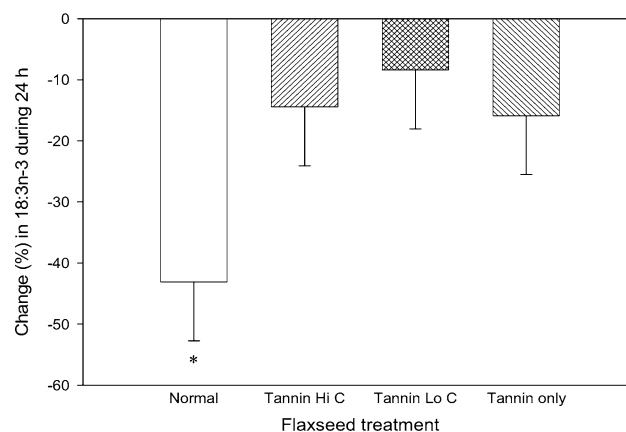


**Fig. 1** Least square means and standard errors (*T*-bars) for % change in 18:3n-3 during the 24 h period of fermentations in vitro of normal ground flaxseed (*Normal*), ground flaxseed mixed with a high amount of casein then treated with condensed tannin (*Tannin Hi C*), ground flaxseed mixed with a low amount of casein then treated with condensed tannin (*Tannin Lo C*), or ground flaxseed treated with only condensed tannin (*Tannin only*). The asterisk indicates significance from control  $P < 0.05$

raised by ingestion of treated flaxseed regardless of basal diet ( $P \geq 0.17$ ) nor were total n-3 levels (18:3n-3 and 20:5n-3) for either basal diet ( $P \geq 0.07$ ).

The level of plasma neutral lipid 18:3n-3 was similar at both blood collection times for forage-fed steers ( $P = 0.38$ ), but 18:3n-3 level was slightly higher (4.8%) at the pre-prandial collection time for the grain-fed steers ( $P = 0.04$ ). Neutral lipid 20:5n-3 level did not differ as a function of time of blood collection for either the forage- or grain-fed steers ( $P \geq 0.50$ ).

The ingestion of tannin-treated flaxseed increased blood plasma phospholipid 18:3n-3 by 11.2% ( $P = 0.03$ ) for the grain-fed steers but not for their forage-fed cohorts ( $P = 0.20$ ; Fig. 2). Levels of 22:5n-3 and 22:6n-3 were higher for the grain-fed steers when they ate the non-treated flaxseed ( $P \leq 0.02$ ), but levels of 22:5n-3 and 22:6n-3 were not affected by the type of flaxseed ingested for the forage-fed steers ( $P \geq 0.09$ ). Total plasma n-3 FA concentrations were not influenced by type of flaxseed ingested regardless of basal diet ( $P = 0.90$ ).

Forage-fed steers had slightly higher levels of phospholipid 22:5n-3 at the post-prandial time of blood collection ( $P = 0.02$ ), but levels of phospholipids 22:6n-3 were higher at the pre-prandial time of blood collection for both basal diets ( $P < 0.01$ ). Levels of phospholipids 18:3n-3 were not influenced by time of collection ( $P \geq 0.67$ ).

## Discussion

There are a number of treatment methods that have been used to treat flaxseed in order to reduce biohydrogenation.

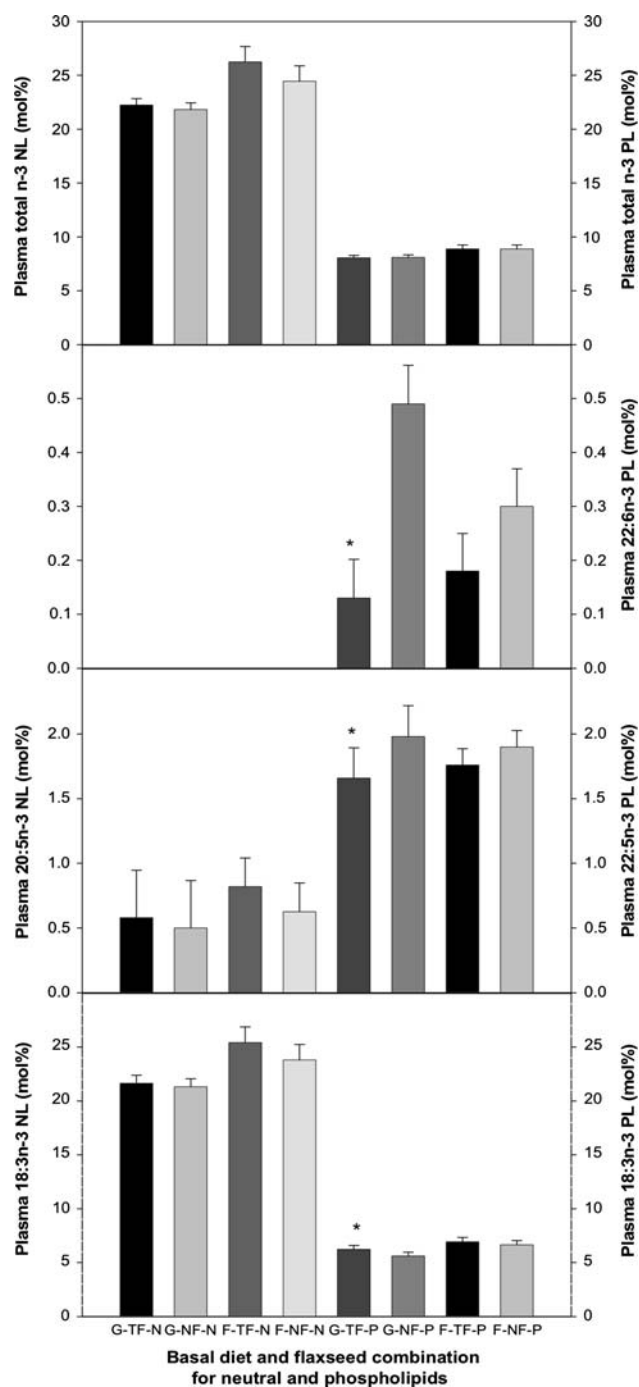


**Fig. 2** Least square means and standard errors (*T*-bars) for mol% of 18:3n-3, 20:5n-3 and total n-3 (18:3n-3 and 20:5n-3 combined) in neutral (*N* or *NL*), and for mol% of 18:3n-3, 22:5n-3, 22:6n-3 and total n-3 (18:3n-3, 22:5n-3, and 22:6n-3 combined) in phospholipid (*P* or *PL*) in blood plasma of yearling Angus steers consuming either a grain-based diet (*G*) or a forage-based diet (*F*) and either tannin-treated ground flaxseed (*TF*) or non-treated ground flaxseed (*NF*). The three sets of four bars on the left side of the figure represent neutral lipid levels and the four sets of four bars on the right side of the figure represent phospholipid levels. The *asterisk* indicates significance from control  $P < 0.05$

For instance, in lactating cows consuming a complex of a 1:1 (w/w) mixture of soybean and flaxseed oils mixed with a whey protein isolate gel, their mean 18:3n-3 level (g/100 g lipid) in the plasma triacylglycerol fraction was 4.9-fold higher than the same lactating cows consuming a 1:1 (w/w) mixture of soybean and flaxseed oils with their basal diet [25]. However, the practicality of this method is questionable. Additional treatment regimens include protecting 18:3n-3 by encapsulation of the n-3 containing feed in a matrix of formaldehyde-treated proteins [17]. Although this is likely the only practical method that may provide some protection for polyunsaturated FA (PUFA) from rumen microbial hydrogenation [15, 18], using formaldehyde in a production setting would undoubtedly meet with limited consumer acceptance. Thus, it is important to derive a useful method for protecting n-3 FA containing oil seeds from the n-3 FA reducing effects of ruminal biohydrogenation.

Although we found a significant protection in our fermentation experiment, a similar positive effect was not seen in vivo. Tannin-treated flaxseed did not increase 18:3n-3 or total n-3 FA levels in plasma neutral lipids from forage-fed or grain-fed steers. Because the rumen pH of cattle on a diet dominated by grains is acidic ( $\text{pH} \leq 5.5$ ), this ruminal environment was expected to reduce the effectiveness of condensed tannin as a protection treatment [36], however we did not expect a similar result with forage-fed cattle.

It is important to note that the seed coat of flaxseed may also provide a small amount of protection for 18:3n-3 from rumen microbes. However, beef muscle had more phospholipid 18:3n-3, 20:5n-3, and 22:5n-3 and more neutral lipid 18:3n-3 when cattle were fed ground versus whole flaxseed [10], suggesting that the seed coat is not an important factor in protecting 18:3n-3 from hydrogenation. Yet, when whole flaxseeds were fed to yearling steers, plasma 18:3n-3 content (weight % of total fatty acid methyl esters) increased 2.6-fold compared to that for steers not consuming flaxseed [13]. However, in the same experiment when flaxseed oil was continuously infused into the proximal duodenum of yearling steers, thus bypassing the rumen microbes, plasma 18:3n-3 content increased 5.7-fold compared to that of control steers [13]. Thus, it is important to get more 18:3n-3 into the duodenum and this indicates the potential for increasing plasma 18:3n-3 if a highly rumen-protective treatment can be found for flaxseed.

We observed in our in vitro trial that treating flaxseed with condensed tannin significantly reduced hydrogenation, with a loss of only 13% of the 18:3n-3 over 24 h versus a 43% loss for the untreated flaxseed. Despite this significant reduction we observed no increase in 18:3n-3 in plasma neutral lipid when cattle were fed tannin-treated flaxseed. There are several explanations for this disparity.

First, that absorption of fatty acids is influenced by the intestinal wall. However, since both post-ruminal infusions of flaxseed oil and flaxseed oil in a gel with a whey protein isolate have raised blood plasma levels of 18:3n-3, we doubt that fatty acid absorption through the intestinal wall accounts for this disparity. Second, ingestion and rumination in the in vivo trial versus lack of this chewing action in the in vitro trial may have allowed for greater hydrogenation of 18:3n-3 in the treated flaxseed for the in vivo trial. Third, the ratio of n-3 fatty acids to ruminal fluid differed between the fermentations in vitro and the feeding regimen in vivo. When fish oil is incubated for 24-h in vitro with sheep rumen fluid, only 10–15% of the n-3 FA were hydrogenated (when the ratio of fish oil to rumen fluid exceeded 5 mg/ml) [37]. They concluded that sheep rumen microbes showed a great capacity to hydrogenate 20:5n-3 and 22:6n-3 in fish oil when the concentration of oil was less than 1 mg per ml of rumen fluid. The ratio of flaxseed oil to rumen fluid in our in vitro trial was about 9 mg per ml of rumen fluid. We expect that the ratio in vivo was much lower. Recently, others have argued that unrealistically high levels of oil should be avoided in fermentations in vitro relative to the amount of substrate used [38]. They suggested that FA in the tested oil or oilseed should be about 3% of substrate DM. Perhaps, the higher ratio of treated flaxseed (and condensed tannin) to rumen fluid in the fermentations in vitro permitted a much greater suppression of microbial hydrogenation than in vivo with its lower level of tannin in the total ruminal mix. However, greatly increasing the amount of tannin-treated flaxseed fed to cattle is probably not a viable option given the cost of flaxseed and tannin, but it may be useful to evaluate other types of condensed tannin since they affect rumen microbes differently [39].

In summary, results from our cattle trial indicate that treating ground flaxseed with quebracho tannin is probably not an effective method for reducing hydrogenation of 18:3n-3 by ruminal microbes in cattle. A method that protects most if not all of the 18:3n-3 in flaxseed must be identified before beef with much higher levels of 18:3n-3 and its long chain derivatives can be produced.

**Acknowledgments** We thank Clay Erickson and Curtis Klein for assistance with cattle management and feeding, and Faye Kroh and Becky Wald for feed nutritional analysis and assistance with fatty acid analysis of feed and fermentation residue. This work was supported, in part, by the intramural research program of the ARA, by the Healthy Beef Initiative, and by NIH grant #1P20 RR17699 (EJM).

## References

1. Simopoulos AP (1999) Essential FA in health and chronic diseases. *Am J Clin Nutr* 70(Suppl):560S–569S
2. Kris-Etherton PM, Harris WS, Appel LJ (2003) Omega-3 fatty acids and cardiovascular disease: new recommendations from the American Heart Association. *Arterioscler Thromb Vasc Biol* 23:151–152
3. Economic Research Service, Fishery Products—Per Capita Consumption. <http://www.ers.usda.gov/Data/FoodConsumption/spreadsheets/mtfish.xls>. Accessed Dec 2006
4. Myers RA, Worm B (2003) Rapid worldwide depletion of predatory fish communities. *Nature* 423:280–283
5. Naylor R, Burke M (2005) Aquaculture and ocean resources: raising tigers of the sea. *Annu Rev Environ Resour* 30:185–218
6. Economic Research Service, Total Red Meat—Per Capita Consumption. <http://www.ers.usda.gov/Data/FoodConsumption/spreadsheets/mtredsuxls#total!a1>. Accessed Dec 2006
7. Rule DC, Broughton KS, Shellito SM, Maiorano G (2002) Comparison of muscle fatty acid profiles and cholesterol concentrations of bison, beef cattle, elk, and chicken. *J Anim Sci* 80:1202–1211
8. Scollan ND, Dhanoa MS, Choi NJ, Maeng WJ, Enser M, Wood JD (2001) Biohydrogenation and digestion of long chain fatty acids in steers fed on different sources of lipid. *J Agric Sci* 136:345–355
9. Kronberg SL, Barceló-Coblijn G, Shin J, Lee K, Murphy EJ (2006) Bovine muscle n-3 fatty acid content is increased with flaxseed feeding. *Lipids* 41:1059–1069
10. Maddock TD, Bauer ML, Koch KB, Anderson VL, Maddock RJ, Barceló-Coblijn G, Murphy EJ, Lardy GP (2006) Effect of processing flax in beef feedlot diets on performance, carcass characteristics, and trained sensory panel ratings. *J Anim Sci* 84:1544–1551
11. Moore JH, Noble RC, Steele W (1969) The incorporation of linolenic and linoleic acids into the plasma lipids of sheep given intra-abomasal infusions of linseed oil, maize oil or linoleic acid. *Br J Nutr* 23:141–152
12. Scott TW, Cook LJ, Mills SC (1971) Protection of dietary polyunsaturated fatty acids against microbial hydrogenation in ruminants. *J Amer Oil Chem Soc* 48:358–364
13. Scislawski V, Bauchart D, Gruffat D, Laplaud PM, Durand D (2005) Effects of dietary n-6 or n-3 polyunsaturated fatty acids protected or not protected against ruminal hydrogenation on plasma lipids and their susceptibility to peroxidation in fattening steers. *J Anim Sci* 83:2162–2174
14. Ogilvie BM, McClymont GL (1961) Effect of duodenal administration of highly unsaturated fatty acids on composition of ruminant depot fat. *Nature* 190:725–726
15. Scott TW, Ashes JR (1993) Dietary lipids for ruminants: protection, utilization and effects on remodelling of skeletal muscle phospholipids. *Aust J Agric Res* 44:495–508
16. Scollan ND, Enser M, Gulati SK, Richardson I, Wood JD (2003) Effects of including a ruminally protected lipid supplement in the diet on the fatty acid composition of beef muscle. *Brit J Nutr* 90:709–716
17. Ashes JR, Siebert BD, Gulati SK, Cuthbertson AZ, Scott TW (1992) Incorporation of n-3 fatty acids of fish oil into tissue and serum lipids of ruminants. *Lipids* 27:629–631
18. Ashes JR, Gulati SK, Cook LJ, Scott TW, Donnelly JB (1979) Assessing the biological effectiveness of protected lipid supplements for ruminants. *J Am Oil Chem Soc* 56:522–527
19. Petit HV, Dewhurst RJ, Scollan ND, Proulx JG, Khalid M, Haresign W, Twagiramungu H, Mann GE (2002) Milk production and composition, ovarian function, and prostaglandin secretion of dairy cows fed omega-3 fats. *J Dairy Sci* 85:889–899
20. Sinclair LA, Cooper SL, Huntington JA, Wilkinson RG, Hallett KG, Enser M, Wood JD (2005) In vitro biohydrogenation of n-3 polyunsaturated fatty acids protected against ruminal microbial metabolism. *Anim Feed Sci Tech* 123–124:579–596

21. Van Nevel C, Demeyer DI (1995) Lipolysis and biohydrogenation of soybean oil in the rumen in vitro: inhibition by antimicrobials. *J Dairy Sci* 78:2797–2806
22. Van Nevel CJ, Demeyer DI (1996) Effect of pH on biohydrogenation of polyunsaturated fatty acids and their Ca-salts by rumen microorganisms in vitro. *Arch Anim Nutr* 49:151–157
23. Petit HV, Tremblay GF, Tremblay E, Nadeau P (2002) Ruminant biohydrogenation of fatty acids, protein degradability, and dry matter digestibility of flaxseed treated with different sugar and heat combinations. *Can J Anim Sci* 82:241–250
24. Gonthier C, Mustafa AF, Berthiaume R, Petit HV, Martineau R, Ouellet DR (2004) Effects of feeding micronized and extruded flaxseed on ruminal fermentation and nutrient utilization by dairy cows. *J Dairy Sci* 87:1854–1863
25. Heguy JM, Juchem SO, DePeters EJ, Rosenberg M, Santos JEP, Taylor SJ (2006) Whey protein gel composites of soybean and linseed oils as a dietary method to modify the unsaturated fatty acid composition of milk lipids. *Anim Feed Sci Tech* 131:370–388
26. Carroll SM, DePeters EJ, Rosenberg M (2006) Efficacy of a novel whey protein gel complex to increase the unsaturated fatty acid composition of bovine milk fat. *J Dairy Sci* 89:640–650
27. Jones GA, McAllister TA, Muir AD, Cheng J (1994) Effects of sainfoin (*Onobrychis viciifolia* Scop.) condensed tannins on growth and proteolysis by four strains of ruminal bacteria. *Appl Environ Microbiol* 60:1374–1378
28. McSweeney CS, Palmer B, McNeill DM, Krause DO (2001) Microbial interactions with tannins: nutritional consequences for ruminants. *Anim Feed Sci Tech* 91:83–93
29. SAS (1996) SAS systems for mixed models. SAS Institute, Inc., Cary
30. NRC (2000) Nutrient requirements of beef cattle. 7th edn. Natl Acad Press, Washington
31. Folch J, Lees M, Sloane Stanley GH (1957) A simple method for the isolation and purification of total lipids from animal tissues. *J Biol Chem* 226:497–509
32. Brockerhoff H (1975) Determination of the positional distribution of fatty acids in glycerolipids. *Meth Enzymol* 35:315–325
33. Whitney MB, Hess BW, Kaltenbach JE, Harlow HJ, Rule DC (1999) Direct transesterification of lipids from feedstuffs and ruminal bacteria. *Can J Anim Sci* 79:247–249
34. Kucuk O, Hess BW, Ludden PA, Rule DC (2001) Effect of forage:concentrate ratio on ruminal digestion and duodenal flow of fatty acids in ewes. *J Anim Sci* 79:2233–2240
35. Lake SL, Scholljegerdes EJ, Weston TR, Rule DC, Hess BW (2006) Postpartum supplemental fat, but not maternal body condition score at parturition, affects plasma and adipose tissue fatty acid profiles of suckling beef calves. *J Anim Sci* 84:811–1819
36. Waghorn GC, Ulyatt MJ, John A, Fisher MT (1987) The effect of condensed tannins on the site of digestion of amino acids and other nutrients in sheep fed *Lotus corniculatus* L. *Brit J Nutr* 57:115–126
37. Gulati SK, Ashes JR, Scott TW (1999) Hydrogenation of eicosapentaenoic and docosahexaenoic acids and their incorporation into milk fat. *Anim Feed Sci Tech* 79:57–64
38. Jouany JP, Lassalas B, Doreau M, Glasser F (2007) Dynamic features of the rumen metabolism of linoleic acid, linolenic acid and linseed oil measured in vitro. *Lipids* 42:351–360
39. Aerts RJ, McNabb WC, Molan A, Brand A, Barry TN, Peters JS (1999) Condensed tannin from *Lotus corniculatus* and *Lotus pedunculatus* exert different effects on the in vitro rumen degradation of ribulose-1,5-bisphosphate carboxylase/oxygenase (Rubisco) protein. *J Sci Food Agric* 79:79–85

effects. Studies were conducted to investigate the growth inhibitory effects of low dose treatment of simvastatin, lovastatin, mevastatin and pravastatin alone or in combination with  $\gamma$ -tocotrienol on neoplastic +SA mouse mammary epithelial cells. Additional studies were also conducted to determine the intracellular signaling mechanisms involved in mediating the inhibitory effects of combined  $\gamma$ -tocotrienol and statin treatment on EGF-dependent mitogenesis.

## Experimental Procedures

### Reagents and Chemicals

All materials were purchased from Sigma Chemical Company (St Louis, MO, USA), unless otherwise stated. Simvastatin, lovastatin, mevastatin and pravastatin (sodium salt) were purchased from EMD Biosciences (La Jolla, CA, USA). Purified  $\gamma$ -tocotrienol was provided as a gift by Dr. Abdul Gapor (Malaysian Palm Oil Board, Kuala Lumpur, Malaysia). Antibodies for phospho-Akt (Ser473), phospho-p44/42 MAPK, phospho-p54/46 JNK, and phospho-p38 were purchased from Cell Signaling Technology (Beverly, MA, USA). Goat anti-rabbit secondary antibody was purchased from PerkinElmer Biosciences (Boston, MA, USA). Mouse anti-actin and peroxidase goat anti-mouse antibodies were purchased from Calbiochem (San Diego, CA, USA).

### Cell Line and Culture Conditions

Cell culture and experimental procedures have been previously described in detail [11, 13, 16–18]. Briefly, neoplastic mouse +SA mammary epithelial cells were grown and maintained in serum-free defined control media consisting of Dulbecco's modified Eagle's medium (DMEM)/F12 containing 5 mg/mL bovine serum albumin (BSA), 10  $\mu$ g/mL transferrin, 100 U/mL soybean trypsin inhibitor, 100 U/mL penicillin, 0.1 mg/mL streptomycin, 10 ng/mL EGF, and 10  $\mu$ g/mL insulin. Cells were maintained in a humidified incubator at 37 °C in an atmosphere of 95% air and 5% CO<sub>2</sub>.

### Experimental Treatments

In all experiments, the highly lipophilic  $\gamma$ -tocotrienol was first conjugated with bovine serum albumin (BSA) to form an aqueous stock solution as described previously [11, 19]. Simvastatin, lovastatin or mevastatin exist in their inactive lactone forms and must be activated prior to addition to

treatment media. To activate, these statins were first dissolved in a 70% ethanol solution containing 0.1 N NaOH and then incubated at 50 °C for 1 h. This process converts statins to their corresponding open-ring hydroxy-derivative (active form). This alkaline statin solution was then neutralized by the addition of an equal volume of 70% ethanol solution containing 0.1 N HCl to form a stock solution that was then used to prepare treatment media. Activated statins were freshly prepared daily. Pravastatin does not require activation because it contains an active open ring structure and was directly dissolved in 70% ethanol to form a stock solution. All media was adjusted so that the final ethanol concentration was same in all the groups within a given experiment and never exceeded 0.05%, and all cells were fed fresh control or treatment media everyday.

### Growth and Cytotoxicity Studies

Neoplastic +SA mammary epithelial cells were initially plated at a density of  $5 \times 10^4$  cells/well (6 wells/group) in serum-free defined control media in 24-well culture plates and allowed to attach overnight. Cells were then divided into different treatment groups and fed control or treatment media everyday. In growth studies, +SA cells were treated with individual statins (0–100  $\mu$ M) or  $\gamma$ -tocotrienol (0–4  $\mu$ M) for 4 days and then viable cell number was determined. In cytotoxicity studies, cells were plated in 24-well plates as described above, but maintained on serum-free defined control media for 3 days. Afterwards, cells were divided into different treatment groups, and fresh treatment media was added to their corresponding wells. After a 24 h treatment exposure period, viable cell number in each treatment groups was assayed.

### Measurement of Viable Cell Number

Viable +SA cell number was determined using the 3-(4,5-dimethylthiazol-2-yl)-2,5-diphenyl tetrazolium bromide (MTT) colorimetric assay as described previously [11, 18]. The optical density of each sample was measured at 570 nm on a microplate reader (SpectraCount, Packard BioScience Company, Meriden, CT, USA). The number of cells/well was calculated against a standard curve prepared by plating various concentrations of cells, as determined by hemocytometry, at the start of each experiment [11, 18].

### Electrophoresis and Western Blot Analysis

For Western blot analysis, +SA cells were plated at a density of  $1 \times 10^6$  cells/100 mm culture plate and grown in

serum-free defined control or treatment media. After a 4 day treatment period, cells were isolated with trypsin, washed, and whole cell lysates were then prepared as previously described [18, 19]. Protein concentration in each sample was determined using the Bio-Rad protein assay kit (Bio-Rad, Hercules, CA, USA). Equal amounts (30 µg/lane) of each sample were subjected to electrophoresis through 10% SDS-polyacrylamide minigels. Proteins were then transblotted (30 V for 12–16 h at 4 °C) to PVDF membranes (Dupont, Boston, MA, USA) according to the method of Towbin [20]. The membranes were then blocked with 2% BSA in 10 mM Tris-HCl containing 50 mM NaCl and 0.1% Tween 20, pH 7.4 (TBST) and then, incubated with specific primary antibodies against phospho-Akt, phospho-p44/42 MAPK, phospho-p54/46 JNK, and phospho-p38, diluted 1:5,000 in TBST/2% BSA for 2 h. Membranes were washed five times with TBST and then incubated with horseradish peroxidase-conjugated goat anti-rabbit antibody diluted 1:5,000 in TBST/2% BSA for 1 h followed by rinsing with TBST. Chemiluminescence (Pierce, Rockford, IL, USA) was used to visualize the antibody bound proteins. The visualization of actin was used to confirm that there was equal sample loading in each lane. Images of protein bands on the film were acquired and the densitometric analysis was performed with Metamorph Analysis software (Universal Imaging Corp.)

#### Treatment Synergism and Statistical Analysis

The level of interaction between individual statins and  $\gamma$ -tocotrienol was determined by isobologram and combination-index (CI) methods [21]. Data obtained from antiproliferative studies were used to perform these analyses. Isobologram is a graphical depiction of the pharmacological interaction of a two-drug combination and is constructed at a certain level of growth inhibition. In these studies,  $IC_{50}$  (dose resulting in 50% cell growth inhibition) values for  $\gamma$ -tocotrienol, statins and their combination were used.  $IC_{50}$  values were determined by non-linear regression curve fit analysis using GraphPad Prism 4. The straight line in each isobologram was formed by plotting  $IC_{50}$  doses of  $\gamma$ -tocotrienol and individual statins on the  $x$ - and  $y$ -axes, respectively. The data point in each isobologram corresponds to  $IC_{50}$  dose of  $\gamma$ -tocotrienol and individual statins given in combination. If a data point is on or near the line, this represents an additive treatment effect, whereas a data point that lies below or above the line indicates synergism or antagonism, respectively.

The combination index (CI) method is a quantitative representation of pharmacological interaction between two drugs. CI value of 1 indicates an additive effect, whereas a

CI < 1 or >1 indicates synergism or antagonism, respectively. The CI values were calculated at 50% cell growth inhibition, as:

$$CI = [S_C/S + T_C/T]$$

$S$  and  $T$  are the concentrations of statin and  $\gamma$ -tocotrienol, respectively, that induce a 50% cell growth inhibition;  $S_C$  and  $T_C$  are the concentrations of statin and  $\gamma$ -tocotrienol in combination that also inhibit cell growth by 50%.

The Dose Reduction Index (DRI) value represents the fold decrease in the dose of each individual agent possible if the two drugs are given in combination, as opposed to alone, to achieve a particular cell growth inhibition. DRI values for statins ( $DRI_S$ ) and  $\gamma$ -tocotrienol ( $DRI_T$ ) were calculated as:

$$DRI_S = S/S_C \text{ and } DRI_T = T/T_C$$

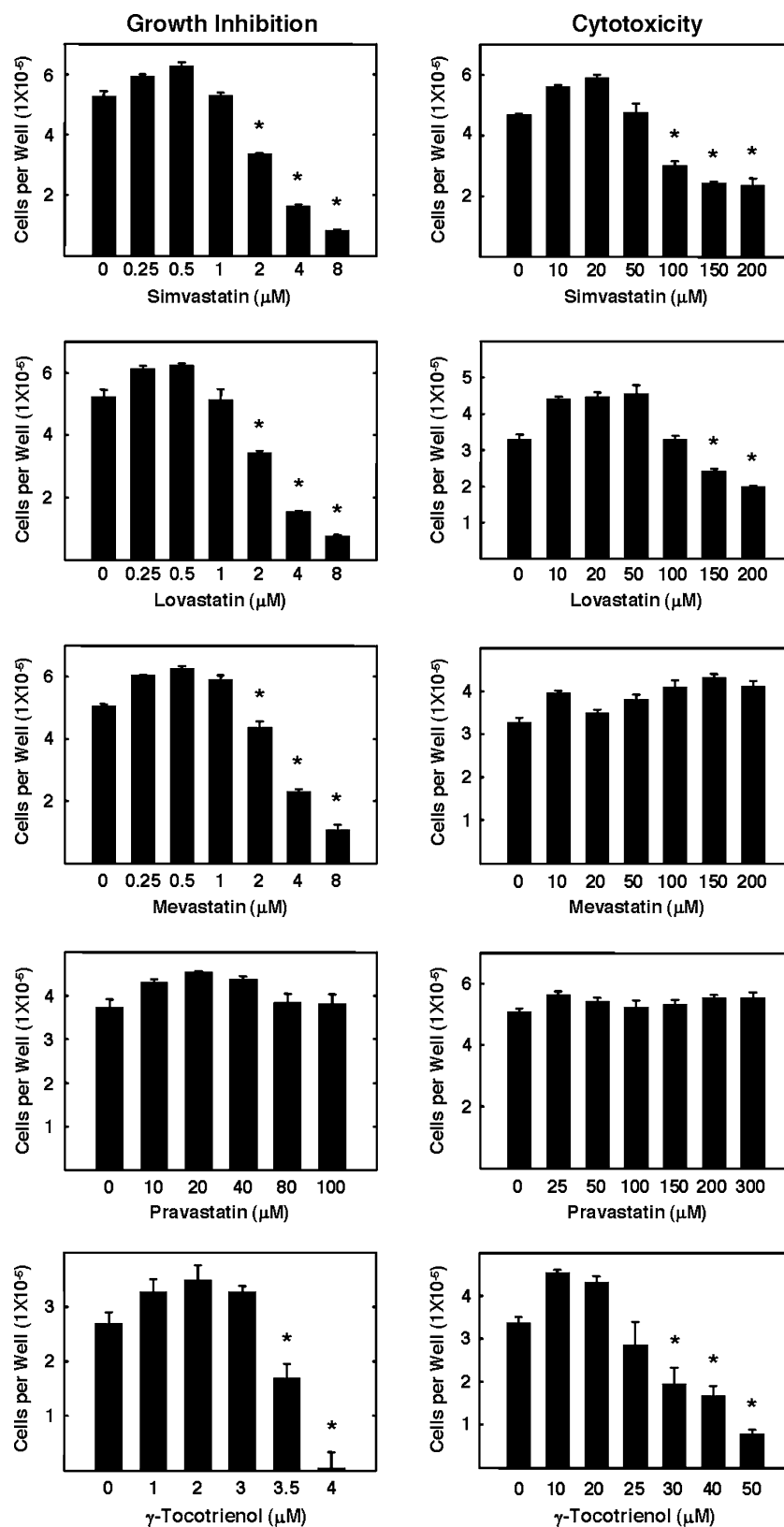
Differences among the various treatment groups in cell growth and viability studies were determined by analysis of variance (ANOVA) followed by Dunnett's  $t$ -test. A difference of  $P < 0.05$  was considered to be significant as compared to vehicle-treated controls.

## Results

### Growth and Cytotoxic Effects of $\gamma$ -Tocotrienol and Individual Statins

The effects of various doses of different statins and  $\gamma$ -tocotrienol on neoplastic +SA mammary epithelial cell proliferation over a 4 day culture period are shown in Fig. 1 (Left). Treatment with 0–8 µM simvastatin, lovastatin, mevastatin or 3–4 µM  $\gamma$ -tocotrienol significantly inhibited +SA cell growth in a dose-responsive manner, as compared to cells in the vehicle-treated control group (Fig. 1, Left). In contrast, similar treatment with 10–100 µM pravastatin had no inhibitory effect on +SA cell growth (Fig. 1, Left). The  $IC_{50}$  values for simvastatin, lovastatin, mevastatin and  $\gamma$ -tocotrienol were 1.97, 1.99, 2.7 and 3.52 µM, respectively. The cytotoxic effects of acute 24 h treatment exposure to various doses of  $\gamma$ -tocotrienol and individual statins and on +SA cell viability are shown in Fig. 1 (Right). Acute treatment with 0–50 µM of simvastatin, lovastatin, and mevastatin or 0–25 µM  $\gamma$ -tocotrienol had no effect on +SA viable cell number (Fig. 1, Right). However, similar treatment with 100–200 µM simvastatin, lovastatin or 30–50 µM  $\gamma$ -tocotrienol significantly reduced +SA viable cell number as compared to vehicle-treated controls (Fig. 1, Right). Acute 24 h treatment with 0–200 µM mevastatin or 0–300 µM pravastatin had no effect on neoplastic +SA mammary epithelial cell viability (Fig. 1, Right).

**Fig. 1** Antiproliferative (*Left*) and cytotoxic (*Right*) effects of individual statins and  $\gamma$ -tocotrienol on neoplastic +SA mammary epithelial cells in vitro. In growth studies (*Left*), cells were plated at a density of  $5 \times 10^4$  cells/well (6 wells/group) in 24-well culture plates and exposed to treatment media for a 4 day period. Afterwards, viable cell number was determined using MTT colorimetric assay. In cytotoxic studies (*Right*), cells were again plated at a density of  $5 \times 10^4$  cells/well and maintained on serum-free defined control media for 3 days. Afterwards, cells were divided into different treatment groups and media was replaced with their respective treatment media. After an acute 24 h treatment exposure, viable cell number was determined using the MTT assay. Vertical bars indicate the mean cell count  $\pm$  SEM in each treatment group. \* $P < 0.05$  as compared with vehicle-treated controls



## Growth and Cytotoxic Effects of Combined Treatment of Individual Statins with $\gamma$ -Tocotrienol

The effects of combined treatment of subeffective doses of  $\gamma$ -tocotrienol with subeffective doses of individual statins on neoplastic +SA mammary epithelial cell proliferation over a 4 day culture period are shown in Fig. 2. Treatment with 0.25–2.0  $\mu$ M  $\gamma$ -tocotrienol, 0.25  $\mu$ M simvastatin, lovastatin, mevastatin, or 10  $\mu$ M pravastatin had no effect on +SA cell growth (Fig. 2). However, combined treatment of 0.25  $\mu$ M simvastatin, lovastatin or mevastatin with 0.25–2.0  $\mu$ M  $\gamma$ -tocotrienol induced a significant inhibition of +SA cell growth in a dose-responsive manner, as compared to cells in the vehicle treated control group (Fig. 2). Similarly, combined treatment of 10  $\mu$ M pravastatin with 0.5–2.0  $\mu$ M  $\gamma$ -tocotrienol was also found to significantly inhibit +SA cell growth (Fig. 2).

In other studies, treatment with a subeffective dose of  $\gamma$ -tocotrienol (1.0  $\mu$ M) in combination with a range of subeffective doses of individual statins (0.25–1.0  $\mu$ M simvastatin, lovastatin, mevastatin or 5–15  $\mu$ M pravastatin) also resulted in a significant dose-responsive inhibition in +SA cell growth as compared to vehicle-treated controls (Fig. 3). Acute 24 h treatment of 0.25–2.0  $\mu$ M of  $\gamma$ -tocotrienol in combination with 0.25 or 10  $\mu$ M of individual statins had no effect on neoplastic +SA mammary epithelial cell viability (Fig. 4).

## Synergistic Antiproliferative Effects of Combined Treatment of $\gamma$ -Tocotrienol and Statins

Photomicrographs of treatment effects on the morphology of neoplastic +SA mammary epithelial cells grown in culture are shown in Fig. 5a. Exposure to 0.25  $\mu$ M simvastatin, 0.25  $\mu$ M or 1.0  $\mu$ M  $\gamma$ -tocotrienol alone had no effect on +SA cell growth or morphology throughout the 4 day treatment period. However, combined treatment of 0.25  $\mu$ M simvastatin with 0.25 or 1.0  $\mu$ M  $\gamma$ -tocotrienol resulted in a large suppression in +SA cell proliferation and a change from a flat squamosal morphology to a rounded metaplastic morphology (Fig. 5a). Isobologram analysis of combined treatment effects of  $\gamma$ -tocotrienol and individual statins are shown in Fig. 5b. Results showed that the growth inhibitory effect of combined treatment of subeffective doses of simvastatin, lovastatin, or mevastatin in combination with subeffective doses of  $\gamma$ -tocotrienol was synergistic because the data point in each isobologram was well below the line defining an additive effect (Fig. 5b). It was not possible to conduct isobologram analysis for the combined treatment of pravastatin and  $\gamma$ -tocotrienol because the  $IC_{50}$  value for pravastatin could not be determined with the doses tested in this study.

Table 1 shows a summary of isobologram analysis of combination treatment effects of  $\gamma$ -tocotrienol and individual statins. CI values for all the combinations tested were less than 1, indicating a high level of synergism that

**Fig. 2** Effects of range of subeffective doses of  $\gamma$ -tocotrienol when given alone or in combination with a subeffective dose of individual statins, on the growth of neoplastic +SA mammary epithelial cell growth. Cells were initially plated at a density of  $5 \times 10^4$  cells/well (6 wells/group) in 24-well culture plates and exposed to treatments for a 4 day period. Afterwards, viable cell number was determined using MTT colorimetric assay. Vertical bars indicate the mean cell count  $\pm$  SEM in each treatment group. \* $P < 0.05$  as compared with vehicle-treated controls

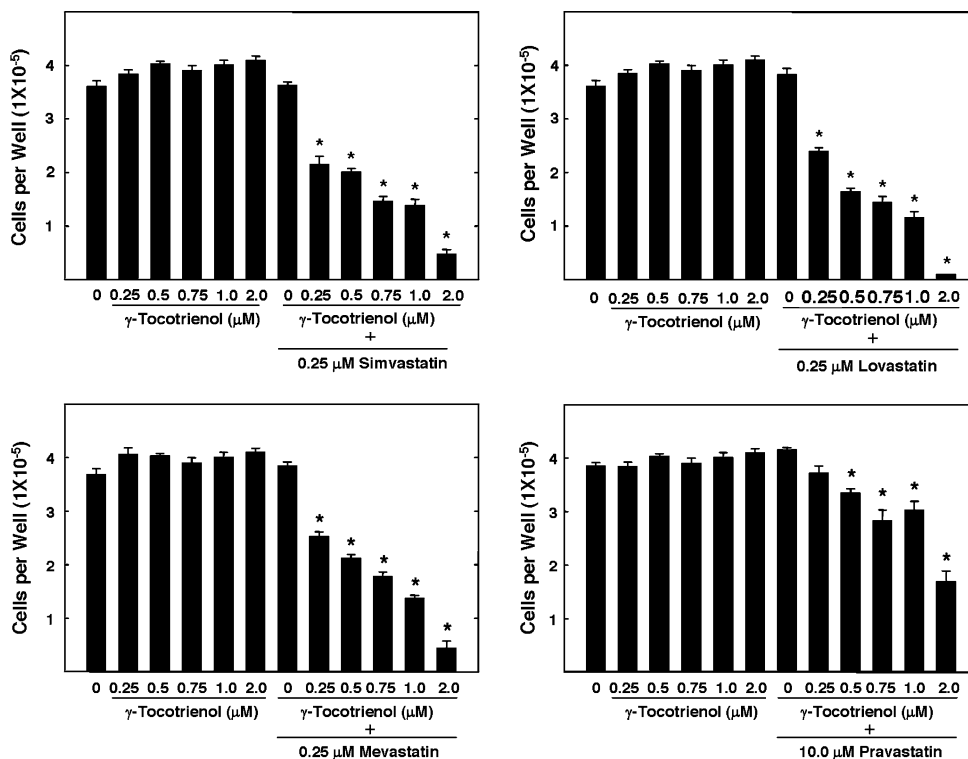




**Fig. 3** Effects of 1  $\mu\text{M}$  (subeffective dose)  $\gamma$ -tocotrienol when given alone or in combination with a range of subeffective doses of individual statins on the growth of neoplastic +SA mammary epithelial cell growth. Cells were plated at a density of  $5 \times 10^4$  cells/well (6 wells/group) in 24-well culture plates and treated for 4 days. Afterwards, viable cell number was determined by MTT assay. Vertical bars indicate the mean cell count  $\pm$  SEM in each treatment group.  $*P < 0.05$ , as compared with vehicle-treated controls

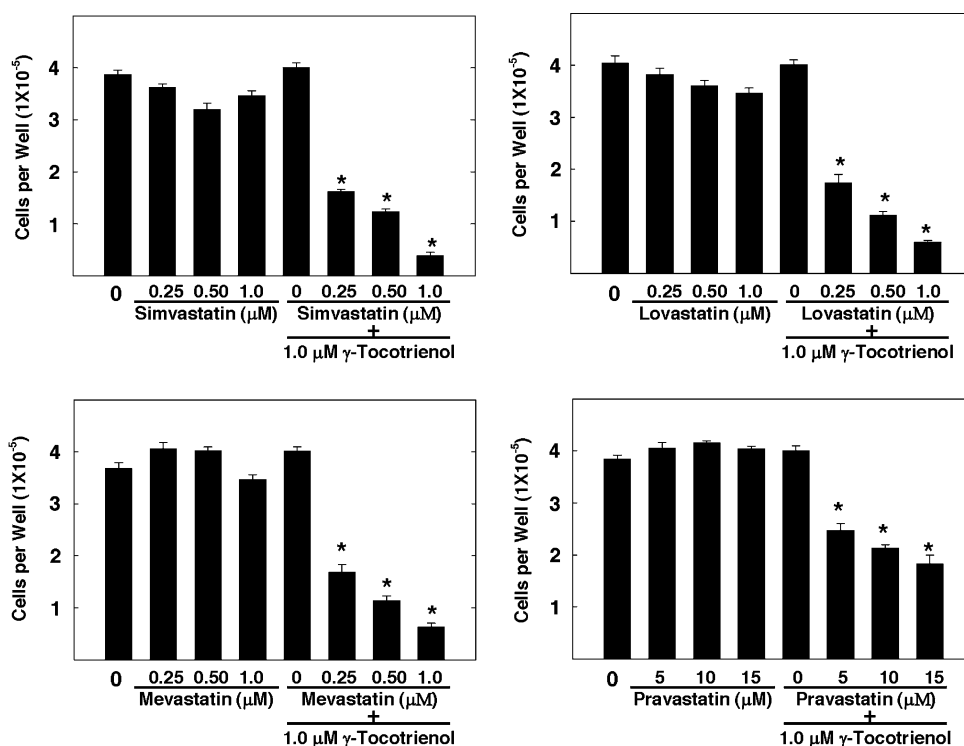
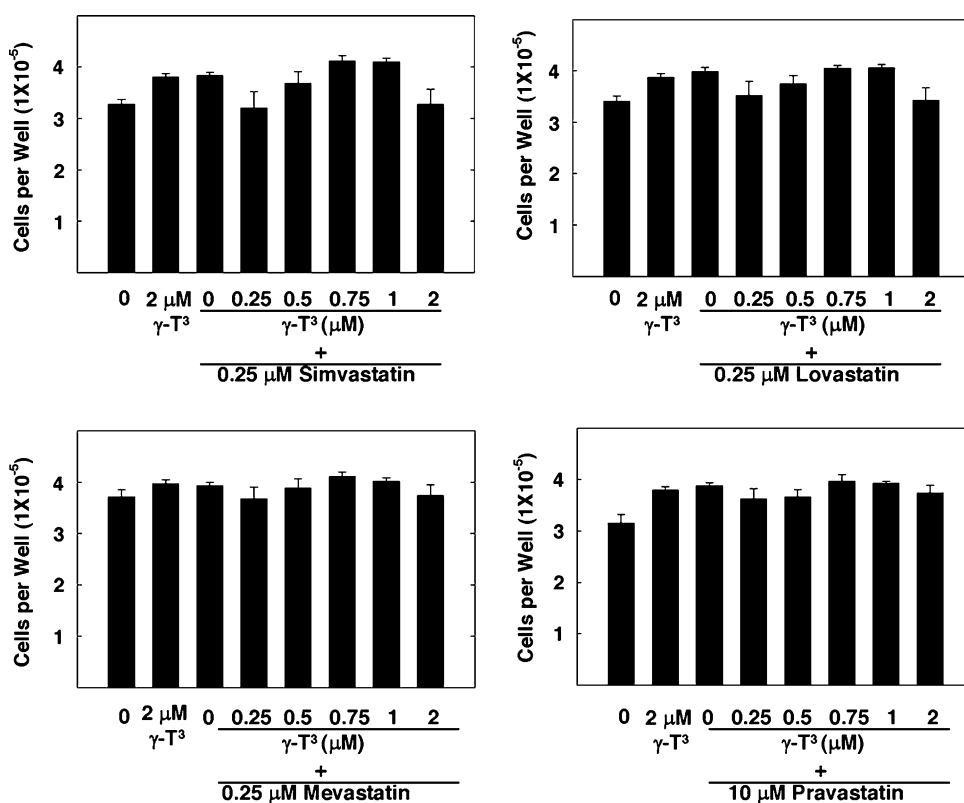


**Fig. 4** Effects of acute 24 h treatment exposure to low doses of  $\gamma$ -tocotrienol ( $\gamma$ -T<sup>3</sup>) and individual statins given alone and in combination on neoplastic +SA mammary epithelial cell viability. Cells were plated at a density of  $5 \times 10^4$  cells/well and maintained on serum-free defined control media for 3 days. Afterwards, control media in different treatment groups was replaced by their respective treatment media. After 24 h, viable cell count was determined using the MTT assay. Vertical bars indicate the mean cell count  $\pm$  SEM in each treatment group.  $*P < 0.05$ , as compared with vehicle-treated controls



resulted from combined treatment (Table 1). The dose reduction index (DRI) confirmed a high level of synergism that resulted from combined treatment. Specifically, the  $\text{IC}_{50}$  dose of simvastatin, lovastatin or mevastatin alone

could be reduced 8 to 11-fold and still produce the same antiproliferative effects if combined with  $\gamma$ -tocotrienol. Likewise, the  $\text{IC}_{50}$  dose of  $\gamma$ -tocotrienol given alone could be reduced 5 to 7-fold and still produce the same

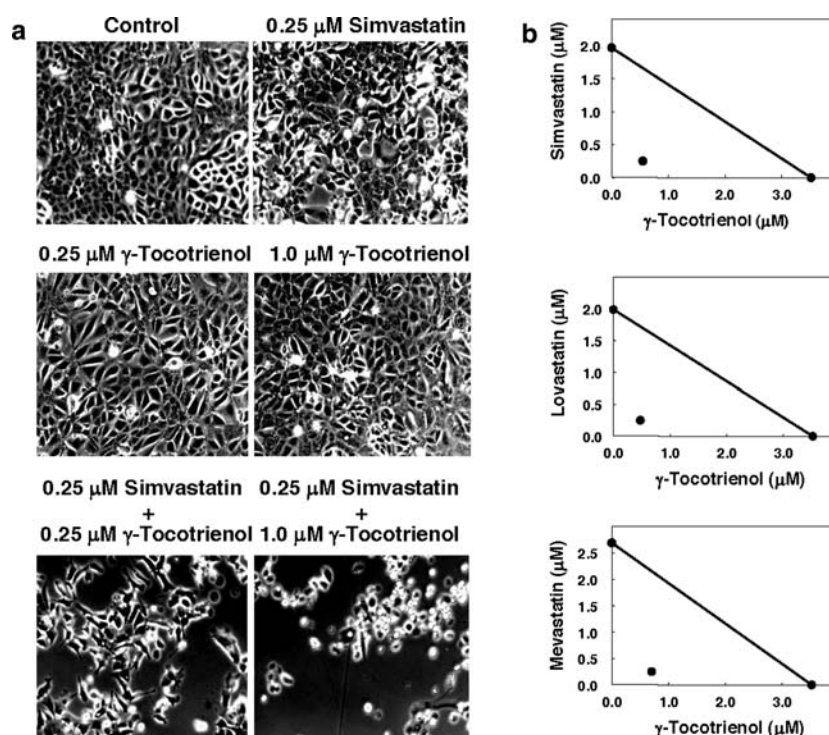


**Fig. 5** **a** Photomicrographs of neoplastic +SA mammary epithelial cells in the different treatment groups after a 4 day incubation period. Magnification in each photomicrograph was 100 $\times$ . **b** Isobolograms of  $\gamma$ -tocotrienol and individual statin antiproliferative effects on neoplastic +SA mammary epithelial cells. Individual  $\text{IC}_{50}$  doses (dose that resulted in a 50% inhibition in cell growth over a 4 day period as compared to vehicle-treated controls) for  $\gamma$ -tocotrienol and individual statins were plotted on the  $x$ - and  $y$ -axes, respectively. The *solid line*

connecting these points represents the drug doses of each compound to induce the same relative growth inhibition when used in combination if the interaction between these compounds is additive. The *data point* on each isobologram represents the actual doses of  $\gamma$ -tocotrienol and individual statins which when used in combination result in 50% growth inhibition. Since all data points were positioned well below the line on each isobologram, these results indicate a strong synergistic antiproliferative effect

**Table 1** CI and DRI values for combined treatment of individual statins and  $\gamma$ -tocotrienol that resulted in a 50% inhibition of +SA cell growth

Combinations	Combination index (CI)	Dose reduction index (DRI)	
		Statin	$\gamma$ -tocotrienol
Simvastatin + $\gamma$ -tocotrienol	0.28	7.88	6.41
Lovastatin + $\gamma$ -tocotrienol	0.26	7.96	7.43
Mevastatin + $\gamma$ -tocotrienol	0.29	10.8	5.01

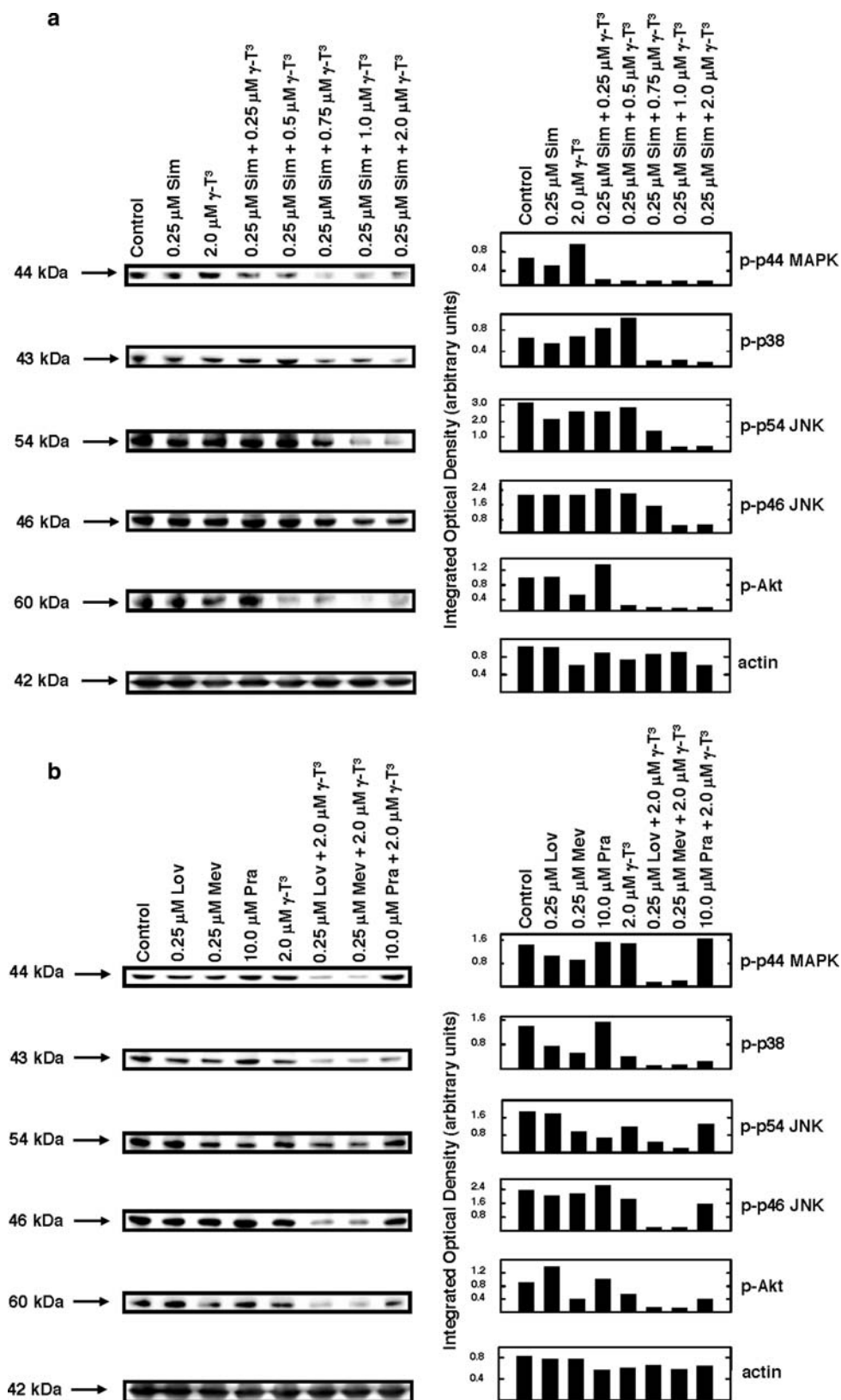
antiproliferative effect if combined with individual statins (Table 1). DRI values for the combination of pravastatin with  $\gamma$ -tocotrienol were not calculated because the  $\text{IC}_{50}$  value for pravastatin could not be determined with the doses tested in this study.

#### Treatment Effect on MAPK, JNK, p38 and Akt Activation

Figure 6 shows Western blot and scanning densitometric analysis of treatment effects on levels of phosphorylated

(activated) p44 MAPK, p38, p54/46 JNK and Akt, intracellular proteins involved in mediating EGF-dependent mitogenesis in neoplastic +SA mammary epithelial cells. Treatment with subeffective doses of simvastatin (0.25  $\mu\text{M}$ ) or  $\gamma$ -tocotrienol (2.0  $\mu\text{M}$ ) alone had little or no effect, whereas combined treatment of 0.25  $\mu\text{M}$  simvastatin with 0.25–2.0  $\mu\text{M}$   $\gamma$ -tocotrienol resulted in a large relative decrease in intracellular levels of these activated mitogenic signaling proteins as compared to vehicle-treated controls (Fig. 6a). In other studies, treatment with 0.25  $\mu\text{M}$  lovastatin, 0.25  $\mu\text{M}$  mevastatin or 10  $\mu\text{M}$  pravastatin alone had little or no effect on phosphorylated p44-MAPK, p38, p54/46 JNK or Akt, whereas combined treatment of 2.0  $\mu\text{M}$   $\gamma$ -tocotrienol with either 0.25  $\mu\text{M}$  lovastatin or mevastatin also caused in a relative large decrease in phosphorylated p44 MAPK, p38, p54/46 JNK and Akt, as compared to vehicle-treated controls (Fig. 6b). Combined treatment of 0.25  $\mu\text{M}$   $\gamma$ -tocotrienol with 10.0  $\mu\text{M}$  pravastatin had little or no effect on the relative levels of phosphorylated p44 MAPK, p54/46 JNK or Akt, while causing a relatively large decrease in intracellular levels of phospho-p38. (Fig. 6b). None of the treatments

**Fig. 6** Western blot and scanning densitometric analysis of  $\gamma$ -tocotrienol and statin treatment effects when given alone or in combination on the relative levels of phosphorylated intracellular signaling proteins (p-p44 MAPK, p-p38, p-p54/46 JNK and p-Akt) associated with EGF-dependent mitogenic signaling after a 4 day incubation period. **a** Neoplastic +SA mammary epithelial cells were initially plated at a density of  $1 \times 10^6$  cells/100 mm culture dish and treated with control or treatment media containing either 0.25  $\mu$ M simvastatin (Sim) alone or in combination with 0–2  $\mu$ M  $\gamma$ -tocotrienol ( $\gamma$ -T<sup>3</sup>). **b** +SA cells were plated in the same manner as described above in (a) and then exposed to control or treatment media containing 0.25  $\mu$ M lovastatin (Lov), 0.25  $\mu$ M mevastatin (Mev) or 10  $\mu$ M pravastatin (Pra) alone or in combination with 2  $\mu$ M  $\gamma$ -tocotrienol ( $\gamma$ -T<sup>3</sup>). Cells were fed fresh treatment media everyday throughout the 4 day incubation period. Afterwards, whole cell lysates were prepared for subsequent separation by polyacrylamide gel electrophoresis (30  $\mu$ g/lane), followed by Western blot analysis. Scanning densitometric analysis was performed for each blot and shown as bar graphs adjacent to corresponding Western blots. Vertical bars in the graphs indicate the integrated optical density of bands visualized in each lane



were found to induce any change in phospho-p42 MAPK levels as compared to vehicle-treated controls (data not shown).

## Discussion

These results demonstrate that  $\gamma$ -tocotrienol synergistically enhances the antiproliferative effects of statins on the highly malignant +SA mammary epithelial cells in vitro. Combined treatment of subeffective doses of simvastatin, lovastatin, mevastatin or pravastatin with subeffective doses (0.25–2.0  $\mu$ M) of  $\gamma$ -tocotrienol resulted in nearly an 2 to 11-fold reduction in the dose of statin required to obtain the same growth inhibitory effects as statin treatment alone. Furthermore, this synergistic growth inhibitory effect of combined treatment of  $\gamma$ -tocotrienol with individual statins was found to be cytostatic, not cytotoxic. Additional studies showed that the synergistic antiproliferative effects of combined treatment was associated with a suppression in multiple EGF-dependent mitogenic signaling pathways, including a relatively large reduction in the levels of phosphorylated (activated) p44MAPK, p38, p54/46JNK, and Akt.

Previous studies have shown that individual statins display growth inhibitory effects against different types of cancer cell lines [7, 22–26]. The present study confirms and extends these previous findings by demonstrating that treatment with 2–8  $\mu$ M simvastatin, lovastatin or mevastatin treatment alone significantly inhibited, whereas treatment with 10–100  $\mu$ M pravastatin had no effect neoplastic +SA mammary epithelial cell growth. Although the exact reason why pravastatin displays less potent anticancer activity [27, 28] than other statins is presently unknown, it may be related to the fact that pravastatin is much less lipophilic than the other statins and this physical characteristic may restrict drug uptake and/or accumulation into tumor cells. Additional studies are required to determine if this hypothesis is correct. It is also possible that the greater bioactivity of other statins may be due to actions independent of their HMGCoA reductase inhibition. The closed beta-lactone ring form of these statins has been shown to inhibit proteasome degradation of cyclin-dependent kinase inhibitors, p21 and p27, resulting in cell cycle arrest [29, 30]. Results also showed that treatment with growth inhibitory doses (2–8  $\mu$ M) of simvastatin, lovastatin, or mevastatin was not found to be cytotoxic to +SA mammary tumor cells. These statins were found to induce cytotoxicity and reduce viable +SA cell number only when used at very high, clinically irrelevant doses (100–200  $\mu$ M).

While treatment with 2–8  $\mu$ M simvastatin, lovastatin or mevastatin alone was found to significantly inhibit +SA

mammary tumor cell growth, it should be pointed out that an oral dose of 25 mg/kg or higher would be required to achieve the same levels of these statins in the blood of humans. However, use of treatment doses of 25 mg/kg or higher in humans is associated with severe adverse side effects, particularly myotoxicity [10]. As a result, the use of these statins as monotherapy in the prevention or treatment of cancer has been limited in order to avoid potential detrimental effects that would have a negative impact on the health and well-being of the patient.

In order to avoid unwanted adverse side effects associated with high dose statin use, several studies have taken the approach to combine low doses of statins with other anticancer agents [31–37]. Previous reports from this laboratory have demonstrated that low doses of  $\gamma$ -tocotrienol, a member of the vitamin E family of compounds, displays potent antiproliferative and apoptotic effects against the neoplastic +SA mammary epithelial cells [11, 13, 17]. Results showed that combined treatment with a subeffective dose (0.25  $\mu$ M) of simvastatin, lovastatin or mevastatin with subeffective doses (0.25–2.0  $\mu$ M) of  $\gamma$ -tocotrienol resulted in a synergistic inhibition of +SA cell growth. Furthermore, although treatment with high doses (10–100  $\mu$ M) of pravastatin alone had no growth inhibitory effects against +SA cells, combined treatment of 10  $\mu$ M pravastatin with subeffective doses of  $\gamma$ -tocotrienol resulted in a significant dose-responsive inhibition in +SA cell proliferation. However, these data again demonstrate that pravastatin is a much less potent anticancer agent either alone or in combination with  $\gamma$ -tocotrienol, as compared to the other statins tested. In addition, it is interesting to note that none of these low dose combinations of  $\gamma$ -tocotrienol and individual statins were found to be cytotoxic. These findings may have very important clinical implications in that combined low dose statin and  $\gamma$ -tocotrienol treatment may be effective in the treatment of breast cancer without the risk of severe myotoxicity that is associated with high dose statin use.

Additional studies showed that when given alone, subeffective doses of  $\gamma$ -tocotrienol and individual statins had no effect on EGF-dependent mitogenic signaling in neoplastic +SA mammary epithelial cells. However, when these subeffective doses of  $\gamma$ -tocotrienol and simvastatin, lovastatin or mevastatin were used in combination, a marked suppression in the relative intracellular levels of phosphorylated (activated) p44 MAPK, p54/46 JNK, p38 and Akt was observed. In contrast, combined treatment of  $\gamma$ -tocotrienol and pravastatin resulted only in a large suppression of phosphorylated p38 and had no significant effect on the relative intracellular levels of phosphorylated (activated) p44 MAPK, p54/46 JNK, and Akt. These results may explain, at least in part, why pravastatin is less potent than the other statins tested in combination with

$\gamma$ -tocotrienol in suppressing mammary tumor cell growth. These findings are consistent with previous findings that showed that tocotrienols inhibit MAPK and Akt activation in +SA mammary tumor cells [17, 38] and statin treatment inhibits the activation of MAPK, JNK, p38 and Akt in SKBr3 breast cancer cells [7]. However, other studies showed that statin treatment increased the activation of JNK, and induced apoptosis in MCF-7 and MD-MB 231 cells [24]. Differences between these results and those obtained in the present study may be due to the possibility that combined treatment with subeffective doses may modulate intracellular signaling pathway differently than high dose statin treatment alone. Additional studies are required to further characterize and differentiate the exact mechanisms involved in mediating the inhibitory effects of  $\gamma$ -tocotrienol and individual statins on specific intracellular signaling pathways, particularly the MAPK, PI3K/Akt, and JNK mitogenic cascades.

Studies have shown that statins and  $\gamma$ -tocotrienol both inhibit HMGCoA reductase activity and subsequent mevalonate synthesis through independent mechanisms. It has been established that  $\gamma$ -tocotrienol induces a down-regulation in HMGCoA reductase levels through a post-transcriptional acceleration in degradation [15], whereas statins act directly to inhibit HMGCoA reductase enzymatic activity [39]. Since cells treated with statins often display a compensatory up-regulation in HMGCoA reductase expression [40], it is possible that combined treatment with  $\gamma$ -tocotrienol counteracts this compensatory response and prevents the restoration of mevalonate synthesis. Since mevalonate is an upstream intermediate in the synthesis of reactive farnesyl residues, synergistic suppression of HMGCoA reductase activity by the combined treatment of statins and  $\gamma$ -tocotrienol might ultimately prevent the farnesylation and anchoring of Ras to the interior of the cell membrane [41, 42]. Once Ras is anchored to the cell membrane, it is able to interact with activated membrane bound receptors, such as the EGF-receptor, and initiate activation of the MAPK and Akt mitogenic signaling pathways [41–44]. Therefore, the synergistic antiproliferative effects of combined statin and  $\gamma$ -tocotrienol treatment may result from their independent actions to inhibit HMGCoA reductase activity, mevalonate synthesis, and subsequent farnesylation of second messengers involved in mediating EGF-dependent mitogenic signaling. Further studies are needed to determine if the synergistic anticancer effects of statins and  $\gamma$ -tocotrienol are due solely through the inhibition of mevalonate synthesis or also include other mechanisms. Studies have shown that  $\gamma$ -tocotrienol can directly inhibit EGF-receptor activation and mitogenic signaling [13].

In summary, these findings demonstrate the synergistic antiproliferative effects of combined low dose treatment of

$\gamma$ -tocotrienol and individual statins against mammary tumor cells. These findings strongly suggest that combined  $\gamma$ -tocotrienol and statin therapy may provide significant health benefits in the prevention and/or treatment of breast cancer in women, while at the same time avoiding myotoxicity that is associated with high dose statin treatment.

**Acknowledgments** This work was performed at the College of Pharmacy, University of Louisiana at Monroe, Monroe, LA, USA and supported in part by National Institutes of Health Grant CA 86833. The authors would like to thank the Malaysian Palm Oil Board and Carotech Bhd. for their support in generously providing  $\gamma$ -tocotrienol for use in these studies.

## References

- Graaf MR, Richel DJ, van Noorden CJ, Guchelaar HJ (2004) Effects of statins and farnesyltransferase inhibitors on the development and progression of cancer. *Cancer Treat Rev* 30:609–641
- Habenicht AJ, Glomset JA, Ross R (1980) Relation of cholesterol and mevalonic acid to the cell cycle in smooth muscle and Swiss 3T3 cells stimulated to divide by platelet-derived growth factor. *J Biol Chem* 255:5134–5140
- Fairbanks KP, Witte LD, Goodman DS (1984) Relationship between mevalonate and mitogenesis in human fibroblasts stimulated with platelet-derived growth factor. *J Biol Chem* 259:1546–1551
- Kaneko I, Hazama-Shimada Y, Endo A (1978) Inhibitory effects on lipid metabolism in cultured cells of ML-236B, a potent inhibitor of 3-hydroxy-3-methylglutaryl-coenzyme-A reductase. *Eur J Biochem* 87:313–321
- Quesney-Huneus V, Galick HA, Siperstein MD, Erickson SK, Spencer TA, Nelson JA (1983) The dual role of mevalonate in the cell cycle. *J Biol Chem* 258:378–385
- Maltse WA, Defendini R, Green RA, Sheridan KM, Donley DK (1985) Suppression of murine neuroblastoma growth in vivo by mevinolin, a competitive inhibitor of 3-hydroxy-3-methylglutaryl-coenzyme A reductase. *J Clin Invest* 76:1748–1754
- Campbell MJ, Esserman LJ, Zhou Y, Shoemaker M, Lobo M, Borman E, Baehner F, Kumar AS, Adduci K, Marx C, Petricoin EF, Liotta LA, Winters M, Benz S, Benz CC (2006) Breast cancer growth prevention by statins. *Cancer Res* 66:8707–8714
- Seeger H, Wallwiener D, Mueck AO (2003) Statins can inhibit proliferation of human breast cancer cells in vitro. *Exp Clin Endocrinol Diabetes* 111:47–48
- Shibata MA, Ito Y, Morimoto J, Otsuki Y (2004) Lovastatin inhibits tumor growth and lung metastasis in mouse mammary carcinoma model: a p53-independent mitochondrial-mediated apoptotic mechanism. *Carcinogenesis* 25:1887–1898
- Thibault A, Samid D, Tompkins AC, Figg WD, Cooper MR, Hohl RJ, Trepel J, Liang B, Patronas N, Venzon DJ, Reed E, Myers CE (1996) Phase I study of lovastatin, an inhibitor of the mevalonate pathway, in patients with cancer. *Clin Cancer Res* 2:483–491
- McIntyre BS, Briski KP, Gapor A, Sylvester PW (2000) Anti-proliferative and apoptotic effects of tocopherols and tocotrienols on preneoplastic and neoplastic mouse mammary epithelial cells. *Proc Soc Exp Biol Med* 224:292–301
- Shah S, Sylvester PW (2004) Tocotrienol-induced caspase-8 activation is unrelated to death receptor apoptotic signaling in neoplastic mammary epithelial cells. *Exp Biol Med (Maywood)* 229:745–755

13. Samant GV, Sylvester PW (2006) gamma-Tocotrienol inhibits ErbB3-dependent PI3K/Akt mitogenic signalling in neoplastic mammary epithelial cells. *Cell Prolif* 39:563–574
14. McIntyre BS, Briski KP, Tirmenstein MA, Fariss MW, Gapor A, Sylvester PW (2000) Antiproliferative and apoptotic effects of tocopherols and tocotrienols on normal mouse mammary epithelial cells. *Lipids* 35:171–180
15. Parker RA, Pearce BC, Clark RW, Gordon DA, Wright JJ (1993) Tocotrienols regulate cholesterol production in mammalian cells by post-transcriptional suppression of 3-hydroxy-3-methylglutaryl-coenzyme A reductase. *J Biol Chem* 268:11230–11238
16. Danielson KG, Anderson LW, Hosick HL (1980) Selection and characterization in culture of mammary tumor cells with distinctive growth properties in vivo. *Cancer Res* 40:1812–1819
17. Shah SJ, Sylvester PW (2005) Gamma-tocotrienol inhibits neoplastic mammary epithelial cell proliferation by decreasing Akt and nuclear factor kappaB activity. *Exp Biol Med* (Maywood) 230:235–241
18. Shah S, Gapor A, Sylvester PW (2003) Role of caspase-8 activation in mediating vitamin E-induced apoptosis in murine mammary cancer cells. *Nutr Cancer* 45:236–246
19. Sylvester PW, Birkenfeld HP, Hosick HL, Briski KP (1994) Fatty acid modulation of epidermal growth factor-induced mouse mammary epithelial cell proliferation in vitro. *Exp Cell Res* 214:145–153
20. Towbin H, Staehelin T, Gordon J (1979) Electrophoretic transfer of proteins from polyacrylamide gels to nitrocellulose sheets: procedure and some applications. *Proc Natl Acad Sci USA* 76:4350–4354
21. Chou TC, Tan QH, Sirotnak FM (1993) Quantitation of the synergistic interaction of edatrexate and cisplatin in vitro. *Cancer Chemother Pharmacol* 31:259–264
22. Ajith TA, Harikumar KB, Thasna H, Sabu MC, Babitha NV (2006) Proapoptotic and antitumor activities of the HMG-CoA reductase inhibitor, lovastatin, against Dalton's lymphoma ascites tumor in mice. *Clin Chim Acta* 366:322–328
23. Cerezo-Guisado MI, Alvarez-Barrientos A, Argent R, Garcia-Marin LJ, Bragado MJ, Lorenzo MJ (2007) c-Jun N-terminal protein kinase signalling pathway mediates lovastatin-induced rat brain neuroblast apoptosis. *Biochim Biophys Acta* 1771:164–176
24. Koyuturk M, Ersoz M, Altioek N (2006) Simvastatin induces apoptosis in human breast cancer cells: p53 and estrogen receptor independent pathway requiring signalling through JNK. *Cancer Lett*. doi:10.1016/j.canlet.2006.10.009
25. Marcelli M, Cunningham GR, Haidacher SJ, Padayatty SJ, Sturgis L, Kagan C, Denner L (1998) Caspase-7 is activated during lovastatin-induced apoptosis of the prostate cancer cell line LNCaP. *Cancer Res* 58:76–83
26. Shellman YG, Ribble D, Miller L, Gendall J, Vanbuskirk K, Kelly D, Norris DA, Dellavalle RP (2005) Lovastatin-induced apoptosis in human melanoma cell lines. *Melanoma Res* 15:83–89
27. Mueck AO, Seeger H, Wallwiener D (2003) Effect of statins combined with estradiol on the proliferation of human receptor-positive and receptor-negative breast cancer cells. *Menopause* 10:332–336
28. van Vliet AK, Negre-Aminou P, van Thiel GC, Bolhuis PA, Cohen LH (1996) Action of lovastatin, simvastatin, and pravastatin on sterol synthesis and their antiproliferative effect in cultured myoblasts from human striated muscle. *Biochem Pharmacol* 52:1387–1392
29. Rao S, Porter DC, Chen X, Herliczek T, Lowe M, Keyomarsi K (1999) Lovastatin-mediated G1 arrest is through inhibition of the proteasome, independent of hydroxymethyl glutaryl-CoA reductase. *Proc Natl Acad Sci USA* 96:7797–7802
30. Efuet ET, Keyomarsi K (2006) Farnesyl and geranylgeranyl transferase inhibitors induce G1 arrest by targeting the proteasome. *Cancer Res* 66:1040–1051
31. Bocci G, Fioravanti A, Orlandi P, Bernardini N, Collecchi P, Del Tacca M, Danesi R (2005) Fluvastatin synergistically enhances the antiproliferative effect of gemcitabine in human pancreatic cancer MIAPaCa-2 cells. *Br J Cancer* 93:319–330
32. Duncan RE, El-Sohehy A, Archer MC (2005) Regulation of HMG-CoA reductase in MCF-7 cells by genistein, EPA, and DHA, alone and in combination with mevastatin. *Cancer Lett* 224:221–228
33. Kozar K, Kaminski R, Legat M, Kopec M, Nowis D, Skierski JS, Koronkiewicz M, Jakobisiak M, Golab J (2004) Cerivastatin demonstrates enhanced antitumor activity against human breast cancer cell lines when used in combination with doxorubicin or cisplatin. *Int J Oncol* 24:1149–1157
34. Mantha AJ, Hanson JE, Goss G, Lagarde AE, Lorimer IA, Dimitroulakos J (2005) Targeting the mevalonate pathway inhibits the function of the epidermal growth factor receptor. *Clin Cancer Res* 11:2398–2407
35. Mantha AJ, McFee KE, Niknejad N, Goss G, Lorimer IA, Dimitroulakos J (2003) Epidermal growth factor receptor-targeted therapy potentiates lovastatin-induced apoptosis in head and neck squamous cell carcinoma cells. *J Cancer Res Clin Oncol* 129:631–641
36. Soma MR, Pagliarini P, Butti G, Paoletti R, Paoletti P, Fumagalli R (1992) Simvastatin, an inhibitor of cholesterol biosynthesis, shows a synergistic effect with *N,N'*-bis(2-chloroethyl)-*N*-nitrosourea and beta-interferon on human glioma cells. *Cancer Res* 52:4348–4355
37. McAnally JA, Gupta J, Sodhani S, Bravo L, Mo H (2007) Tocotrienols potentiate lovastatin-mediated growth suppression in vitro and in vivo. *Exp Biol Med* (Maywood) 232:523–531
38. Sylvester PW, Nachnani A, Shah S, Briski KP (2002) Role of GTP-binding proteins in reversing the antiproliferative effects of tocotrienols in preneoplastic mammary epithelial cells. *Asia Pac J Clin Nutr* 11(suppl 7):S452–S459
39. Istvan ES, Deisenhofer J (2001) Structural mechanism for statin inhibition of HMG-CoA reductase. *Science* 292:1160–1164
40. Brown MS, Faust JR, Goldstein JL, Kaneko I, Endo A (1978) Induction of 3-hydroxy-3-methylglutaryl coenzyme A reductase activity in human fibroblasts incubated with compactin (ML-236B), a competitive inhibitor of the reductase. *J Biol Chem* 253:1121–1128
41. Bassa BV, Roh DD, Vaziri ND, Kirschenbaum MA, Kamanna VS (1999) Effect of inhibition of cholesterol synthetic pathway on the activation of Ras and MAP kinase in mesangial cells. *Biochim Biophys Acta* 1449:137–149
42. Casey PJ, Solski PA, Der CJ, Buss JE (1989) p21ras is modified by a farnesyl isoprenoid. *Proc Natl Acad Sci USA* 86:8323–8327
43. Nakagawa H, Mutoh T, Kumano T, Kuriyama M (1998) HMG-CoA reductase inhibitor-induced L6 myoblast cell death: involvement of the phosphatidylinositol 3-kinase pathway. *FEBS Lett* 438:289–292
44. Rodriguez-Viciana P, Warne PH, Dhand R, Vanhaesebroeck B, Gout I, Fry MJ, Waterfield MD, Downward J (1994) Phosphatidylinositol-3-OH kinase as a direct target of Ras. *Nature* 370:527–532

recommended daily intake of phytosterols to lower elevated LDL-cholesterol is 2 g/day, which results on average in a 10% reduction in LDL-cholesterol [2]. Higher intakes (>2.5 g/day) offer little additional benefit; intakes below 2 g/day result in a lower, although still significant LDL-cholesterol lowering effect [3].

In healthy individuals, 30–60% of the dietary cholesterol is absorbed, whereas, despite their almost identical structure, less than 2% of the phytosterols are absorbed. Consequently, the total phytosterol level in plasma of healthy individuals is less than 25  $\mu\text{mol/l}$  (<1 mg/dl) [4], representing less than 0.4% of the total plasma sterol level. Phytosterol concentrations in endothelial tissues of healthy subjects are mostly unknown, and hence in vitro studies are hampered by this lack in knowledge. However, it is plausible that the phytosterol concentrations in endothelial tissues should be considerably lower than recently reported in an atheromatous plaque study with patients undergoing carotid endarterectomy (1–4 mg/100 g of tissue) [5]. Despite the low absorption of phytosterols, elevated phytosterol levels have been associated with an increased risk for coronary artery disease (CAD) in hypercholesterolemic subjects and in families with a family history of CAD [6–8]. These studies have given rise to certain concerns whether an increased dietary intake of phytosterols results in an increased risk for CAD. Whether phytosterols are indeed a CAD risk factor is speculative and needs further clarification, since other studies do not show an association between elevated plasma phytosterol levels and an increased risk for CAD [9, 10].

Uncontrolled influx of oxLDL-cholesterol into macrophages via scavenger receptors is generally recognised as one of the hallmarks of the atherogenic process. Without proper defence cholesterol accumulates in macrophages, ultimately leading to atherogenic lipid-laden foam cells. Phytosterols are likewise taken up by macrophages [11, 12], and with increasing dietary intake may well accumulate in macrophages.

Kinetic data elucidating how phytosterols are handled by macrophages are still lacking. Isolating arterial macrophages from human tissue in sufficient amounts to study influx and efflux of phytosterols is technically challenging and as an alternative, an immortalised cell line may be used. The human THP-1 monocytic cell line is one of these established in vitro models frequently used for studying lipid metabolism. After phorbol-ester treatment THP-1 cells exhibit a more differentiated macrophage morphology and function, compared to other available monocytic cell lines [13]. Therefore, we studied whether phytosterols preferentially accumulate in human macrophages by monitoring the influx and efflux of sterols using differentiated THP-1 cells as a cellular model with lipoproteins as a carrier system.

## Materials and Methods

### Materials

THP-1 monocytes were obtained from the European Collection of Cell Cultures (Salisbury, UK). Amplex Red Cholesterol Assay Kit, foetal bovine serum (FBS) and RPMI 1640 medium were obtained from Invitrogen (Paisley, UK). 9-*cis*-retinoic acid, 22(*R*)-hydroxycholesterol, anti- $\beta$ -actin antibody, cholesterol, methyl- $\beta$ -cyclodextrin (M $\beta$ CD, average molecular weight 1,338 g/mol), phorbol-12-myristate-13-acetate (PMA), sitostanol and  $\beta$ -sitosterol were obtained from Sigma (Schnellendorf, Germany). Campesterol was obtained from Steraloids (Newport, RI, USA). ATPLite-M kit was obtained from Packard BioScience (Groningen, The Netherlands). Apolipoprotein (Apo) A-I, LDL and high-density lipoprotein (HDL) were obtained from Calbiochem (La Jolla, CA, USA). [ $1\alpha,2\alpha(n)^3\text{H}$ ]-cholesterol [specific activity (SA) 1.55 TBq/mmol, purity 99%] was obtained from Amersham International (Buckinghamshire, UK). [ $3\alpha\text{-}^3\text{H}$ ]-campesterol (SA 666 GBq/mmol, purity 97%), [ $22,23(n)^3\text{H}$ ]-sitosterol (SA 814 GBq/mmol, purity 93%) and [ $5,6(n)^3\text{H}$ ]-sitostanol (SA 1.63 TBq/mmol, purity 95%) were a kind gift of Dr. D. J. Sanders (Unilever, Bedfordshire, UK). A Bio-Rad Protein DC kit was obtained from Bio-Rad Laboratories (Richmond, CA, USA). 8-Bromo-cAMP (8-Br-cAMP) was obtained from Tocris (Ellisville, MO, USA). Complete protease inhibitors were obtained from Roche (Mannheim, Germany). Cy5-conjugated goat-anti-mouse antibody, ECL Kit, Hyperfilm ECL and Sepharose NAP-10 column were obtained from Amersham Biosciences (Uppsala, Sweden). Peroxidase-conjugated swine-anti-rabbit antibody was obtained from DAKO (Glostrup, Denmark). Anti-ABCA1 antibody was obtained from Novus Biologicals (Littleton, CO, USA). Immobilin-P nitrocellulose membranes were obtained from Millipore (Bedford, MA, USA).

### Cell Culture

THP-1 monocytes (passage 24–30) were grown in suspension in RPMI medium with 10% v/v FBS and antibiotics at 37 °C in 5% CO<sub>2</sub>. Monocyte-derived THP-1 macrophages were obtained by incubating cells for 48 h with 50 ng/ml PMA in a culture medium. PMA was absent during kinetic experiments.

### Incorporation of Sterols in M $\beta$ CD

Radiolabelled sterols (500 nM) were mixed with 2.5 mM unlabelled sterols, either campesterol, cholesterol, sitostanol

or  $\beta$ -sitosterol in chloroform. The organic solvent was evaporated under a gentle stream of nitrogen and 10 mM M $\beta$ CD in RPMI was added to the dry film of sterols. After 24 h of rotation at 37 °C, non-dissolved sterols were removed by 0.22  $\mu$ m filtration. The recovery of cholesterol, campesterol,  $\beta$ -sitosterol and sitostanol, either labelled or unlabelled, was on average 44, 18, 12 and 9.0%, respectively. The sterol containing M $\beta$ CD solution was diluted with RPMI to a final concentration of 2.5 mM M $\beta$ CD. Lower sterol concentrations were obtained by diluting in 2.5 mM sterol-free M $\beta$ CD.

### Incorporation of Sterols in oxLDL

Lipoproteins were commercially obtained or isolated from normolipemic human plasma by density ultracentrifugation. Isolated LDL ( $\rho$  1.006–1.063 g/ml) and HDL ( $\rho$  1.063–1.21 g/ml) were stored in PBS pH 7.2, 10  $\mu$ M EDTA and 10  $\mu$ M ascorbic acid at 4 °C. oxLDL was initially obtained by incubating LDL with 100  $\mu$ M CuSO<sub>4</sub> for 2 h at 37 °C, but in later experiments CuSO<sub>4</sub> was excluded, since the incorporation procedure also led to oxidation. The extent of oxidation was assessed by measuring thiobarbituric acid-reactive substances, mainly malondialdehyde (MDA). Organic solvent, containing radiolabelled sterol (400 pmol/mg LDL protein), was evaporated under a gentle stream of nitrogen and LDL (1 mg protein/ml) was added. After gentle rotation with glass beads for 24 h at 37 °C, non-incorporated radiolabelled sterols were removed by passage through a Sepharose NAP-10 column pre-equilibrated with RPMI, followed by filtration. Protein content of lipoproteins was determined and labelled oxLDL was diluted to 75  $\mu$ g protein/ml in RPMI.

### Influx Experiments

THP-1 cells were washed with serum-free RPMI and loaded with radiolabelled sterols using either M $\beta$ CD (in serum-free RPMI) or oxLDL (in RPMI with 1% FBS) as donor vehicle. At indicated time-points, cells were washed with PBS, lysed in 1% v/v Triton X-100 (TX-100) and total cell-associated radioactivity was measured on a TriCarb<sup>®</sup> 2300TR (Packard Bioscience, Groningen, The Netherlands). Total sterol influx was normalised for variation in protein content per well and in the case of oxLDL, for variation in radiolabelled sterol content.

### Efflux Experiments

THP-1 cells were incubated for 18–24 h with sterol-loaded oxLDL (75  $\mu$ g protein/ml) in the presence of 1% v/v FBS.

In some experiments, 100  $\mu$ M 8-Br-cAMP was present. THP-1 cells were washed with serum-free RPMI and either HDL (0–160  $\mu$ g protein/ml) or ApoA-I (100  $\mu$ g protein/ml) was added. At indicated time-points an aliquot of the efflux medium was removed, centrifuged (1,000g for 2 min) and radioactivity was determined. Total cell-associated radioactivity was measured after cell lysis in 1% v/v TX-100. Sterol efflux of radiolabelled sterols from cells to efflux medium or as cell-associated sterol was determined as a fraction of the total radioactivity in cells at time  $t = 0$  h. The presence of FBS in the medium improved cell viability, but caused some efflux to bovine HDL. Therefore, values were corrected for non-specific release to the medium alone. Total cellular cholesterol and cholesteryl ester were determined by the Amplex Red Cholesterol Assay Kit.

### ABCA1 Western Blotting

THP-1 cells were washed and scraped in PBS and lysed in 10 mM Tris-HCl, pH 7.3, 1 mM MgCl<sub>2</sub>, and 0.5% Nonidet P-40 containing protease inhibitors. Post-nuclear supernatants from cell lysates were prepared by centrifugation (3,000g for 10 min at 4 °C). Protein samples (40  $\mu$ g) were reduced with 2-mercaptoethanol in gel loading buffer, and separated by electrophoresis on a 4–12% Tris glycine polyacrylamide gel (Cambrex, Rockland, USA) and transferred to an Immobilon-P membrane using a semi-dry blotting apparatus (Ancos, Hojby, Denmark). Immunoblotting was performed using an anti-ABCA1 antibody (1:1,000) and a peroxidase-conjugated swine-anti-rabbit secondary antibody (1:1,000) and detection was done using an ECL kit followed by exposure to Hyperfilm ECL. Equal loading was confirmed after reprobing the membrane with an anti- $\beta$ -actin antibody (1:1,000) and Cy5-conjugated goat-anti-mouse secondary antibody (1:1,000) for detection. Induction of ABCA1 was verified by treating cells with 64  $\mu$ M 22(R)-hydroxycholesterol and 1  $\mu$ M 9-*cis*-retinoic acid. The relative intensities of the bands were determined by densitometry using TotalLab TL100 analysis software (Nonlinear Dynamics, Newcastle upon Tyne, UK).

### Data analysis

Retention of radiolabelled sterols in cells was described by Eq. 1:  $[\text{}^3\text{H}]_t/[\text{}^3\text{H}]_0 = C_1e^{-kt} + C_2$ . The release to medium of radiolabelled sterol was described by Eq. 2:  $1 - [\text{}^3\text{H}]_t/[\text{}^3\text{H}]_0$ , where  $t$  = incubation time (h);  $[\text{}^3\text{H}]_t$  = the amount of radioactivity in pmol/well after  $t$  hour and corrected for non-specific release of sterols to lipoprotein free



medium alone;  $[^3\text{H}]_0$  = the initial loading in pmol/well at time = 0 h and  $e$  = natural logarithm. Retention of radio-labelled sterols in cells starts at  $C_1$  (=span + plateau as fraction of  $[^3\text{H}]_0$ ) and decays to  $C_2$  (=plateau as fraction of  $[^3\text{H}]_0$ ) with a rate constant  $k$  (per h) [14].  $t_{1/2} = \ln 2/k$ . (Non-) linear regression and statistical analysis was performed using GraphPad Prism version 4.00 for Windows (GraphPad Software, San Diego, CA). Direct comparisons between two groups were performed using the Student's  $t$  test; data from more than two groups were analysed using one-way or two-way ANOVA. Data are presented as mean  $\pm$  SEM.

## Results

### Influx of Sterols into THP-1 Cells

$M\beta\text{CD}$  was used to deliver defined amounts of sterols in the micromolar range to THP-1 cells. Without cyclodextrin, the solubility of the sterols was less than 1 nM. With cyclodextrin, the solubility of the sterols increased, ranging from  $276 \pm 25 \mu\text{M}$  ( $n = 12$ ) for cholesterol to  $56 \pm 6 \mu\text{M}$  ( $n = 5$ ) for sitostanol. Intermediate values were obtained for campesterol ( $113 \pm 11 \mu\text{M}$ ,  $n = 5$ ) and  $\beta$ -sitosterol ( $75 \pm 6 \mu\text{M}$ ,  $n = 12$ ). The influx of sterols into THP-1 cells could not be saturated within the applied concentration range. So the initial influx rate of each sterol was determined when the rate approached first-order kinetics at  $t = 30$  min. No significant differences were observed in the initial influx rate between cholesterol, campesterol,  $\beta$ -sitosterol and sitostanol ( $4.0 \pm 0.2$ ,  $4.0 \pm 0.5$ ,  $3.7 \pm 0.3$  and  $3.6 \pm 0.3$  pmol/min per

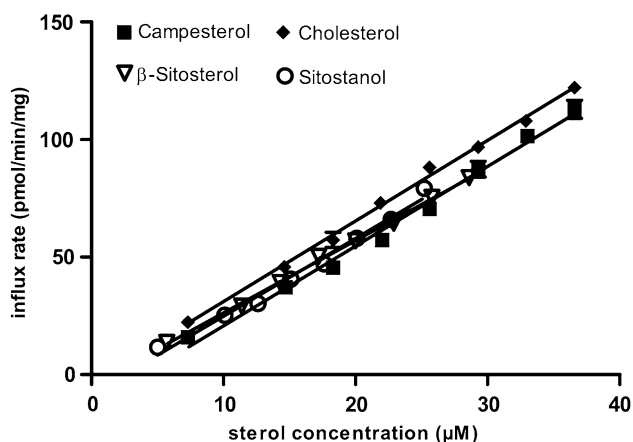


**Fig. 1** Sterol influx of  $M\beta\text{CD}$  delivered sterols by THP-1 cells. Cells were incubated with increasing concentrations of sterols either, campesterol, cholesterol,  $\beta$ -sitosterol or sitostanol. After 30 min, cells were harvested and the influx rate in pmol/min per mg cellular protein was determined. The initial uptake rate is defined as the slope of the linear phase of sterol influx. Values are mean  $\pm$  SEM of a representative experiment ( $n = 2$  wells)

mg cellular protein, respectively,  $n = 3$  experiments) (Fig. 1).

To determine whether the influx of sterols via endocytosis of oxLDL displayed differences for the various sterols, sterol-loaded oxLDL ( $33 \pm 5$  nmol MDA equivalents/mg protein,  $n = 9$ ) was added to the THP-1 cells. The ranking of incorporation of sterols into oxLDL was comparable to that obtained with  $M\beta\text{CD}$ , but lower quantities were incorporated ( $88 \pm 27$ ,  $78 \pm 25$ ,  $78 \pm 18$  or  $44 \pm 14$  pmol/mg oxLDL protein for cholesterol, campesterol,  $\beta$ -sitosterol and sitostanol, respectively,  $n = 3$ ). As shown in Table 1, all sterols were taken up equally well at all time-points tested, when the sterol influx was normalised for the observed variations in incorporation in oxLDL.

The amount of cholesterol and cholesteryl ester in THP-1 cells after PMA stimulation was typically 20- $\mu\text{g}$  cholesterol/mg cellular protein with less than 2- $\mu\text{g}$  cholesteryl ester/mg cellular protein. Exposure to sterol-loaded cyclodextrin for 30 min decreased the cellular cholesterol and cholesteryl ester mass by approximately 25 and 40%, respectively. No significant differences in cellular ATP content, a marker for cell viability, was observed when THP-1 cells were incubated with sterol-loaded cyclodextrin compared to RPMI alone (data not shown). Exposure to sterol-loaded oxLDL for 18 h increased the cellular cholesterol mass by 150% and the cholesteryl ester mass by at least 500%.

### Efflux of Sterols from THP-1 Cells to HDL

In the next step towards mimicking the in vivo situation, THP-1 cells were preloaded with  $[^3\text{H}]$ -sterol-loaded oxLDL, washed and the efflux to HDL was monitored over time. The sterol efflux from THP-1 cells approached, but did not reach a steady state as observed in the efflux medium (Fig. 2a) or in cell extracts (Fig. 2b). As shown in Table 2, the rate constant of campesterol efflux did not significantly differ from that of cholesterol. However the rate constants of both  $\beta$ -sitosterol efflux ( $P < 0.05$ ) as well as sitostanol efflux ( $P < 0.001$ ) were significantly different from that of cholesterol. Comparable results were obtained when interpreting data from cell extracts ( $P < 0.01$  and  $P < 0.05$  for  $\beta$ -sitosterol and sitostanol, respectively). The sum of sterols in both fractions was approximately 1, indicating that all sterols were distributed over both compartments.

### $\beta$ -Sitosterol Efflux from THP-1 Cells to HDL or ApoA-I

To initiate elucidation of the underlying mechanism, the efflux to HDL versus ApoA-I alone was monitored in the

**Table 1** Total influx of oxLDL delivered sterols into THP-1 cells

Time (h)	Total sterol influx (corrected pmol/mg protein)			
	Cholesterol	Campesterol	$\beta$ -Sitosterol	Sitostanol
2	1.37 $\pm$ 0.02	1.18 $\pm$ 0.09	1.58 $\pm$ 0.41	1.55 $\pm$ 0.02
4	1.97 $\pm$ 0.13	1.72 $\pm$ 0.13	2.28 $\pm$ 0.28	2.16 $\pm$ 0.54
8	3.49 $\pm$ 0.32	3.21 $\pm$ 0.19	3.67 $\pm$ 0.29	3.51 $\pm$ 0.18

Total influx of oxLDL delivered sterols into THP-1 cells. Cells were incubated with sterol-loaded oxLDL as described in the methodology. At the indicated time-points, cells were harvested and the influx of [ $^3$ H]-sterols per milligram cellular protein was determined. The total sterol influx was normalised for variations in incorporation of sterols into oxLDL. Values are means  $\pm$  SEM of three experiments ( $n = 8$  wells, except at  $t = 8$  h,  $n = 5$  wells)

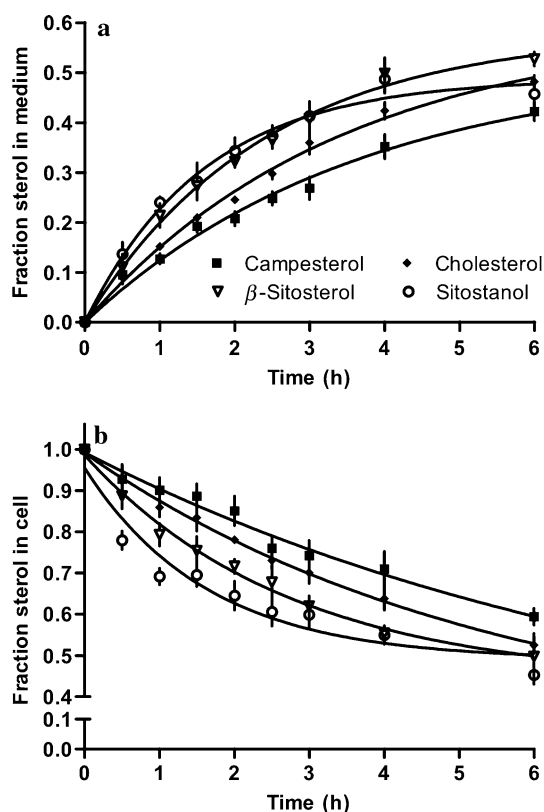


**Fig. 2** Sterol efflux from THP-1 cells to HDL. Cells were incubated with labelled oxLDL with either cholesterol, campesterol,  $\beta$ -sitosterol or sitostanol, washed and HDL was added. At indicated time-points radioactivity in the medium was determined (a) or cells were lysed and cell-associated [ $^3$ H]-sterols per milligram cellular protein was determined (b). Fractional sterol efflux was calculated relatively to the [ $^3$ H]-sterol content in cells at  $t = 0$  h. All values are mean  $\pm$  SEM of two experiments ( $n = 5$  wells)

presence of 8-Br-cAMP. THP-1 cells expressed ABCA1 protein, which was modestly increased after 8-Br-cAMP treatment (1.4-fold) and strongly increased after 9-*cis*-retinoic acid/22(*R*)-hydroxycholesterol treatment (2.4-fold, Fig. 3a). As depicted in Fig. 3b, the efflux of  $\beta$ -sitosterol and cholesterol to ApoA-I was significantly lower than efflux to HDL ( $P < 0.0001$ ). The efflux of cholesterol to

HDL could not be increased to levels observed for  $\beta$ -sitosterol when 8-Br-cAMP was added. The presence of 8-Br-cAMP resulted in a modest, but significant increase in  $\beta$ -sitosterol efflux to ApoA-I ( $P < 0.05$ ). The efflux of  $\beta$ -sitosterol to ApoA-I tended to be higher than that of cholesterol in the presence of 8-Br-cAMP ( $P = 0.086$ ). Fractional release of  $\beta$ -sitosterol and cholesterol to the medium alone was comparable (approximately 0.05), irrespective of the treatment.

## Discussion

Isolating macrophages in sufficient numbers from human arterial tissue to study the influx and efflux of phytosterols *ex vivo* is technically challenging and alternatively, immortalised cells, such as monocyte-derived THP-1 macrophages may be used. THP-1 cells are frequently used for studying macrophage specific processes and therefore this study was undertaken to examine for the first time the handling of phytosterols by macrophages with lipoproteins as the main carrier system. The rationale was to determine whether free phytosterols, which comprise approximately 30% of total phytosterol content in normal human LDL [15], preferentially accumulate in arterial macrophages and may thus affect atherogenesis.

Miettinen et al. [5] observed that the concentration of  $\beta$ -sitosterol and campesterol in atherosclerotic plaque of patients undergoing carotid endarterectomy was 0.72–2.7 and 0.72–4.1 mg per 100 g of tissue, respectively, emphasizing the need for an *in vitro* carrier system capable of delivering high concentrations (in the micromolar range) of plant sterols. M $\beta$ CD, a cyclic oligosaccharide, was initially used as a carrier system because of its particle-like structure, but moreover, for its ability to deliver relative high concentrations of metabolic active sterols to cells [16]. Our data show that the initial influx rate of phytosterols from M $\beta$ CD to THP-1 cells did not differ significantly from that of cholesterol. The cyclodextrin molecules were, however, not saturated with phytosterols

**Table 2** Rate constants of sterol efflux by THP-1 cells

Sterol	$k$ (per h)	$t_{1/2}$ (h)	$C_1$ (fraction of total at $t = 0$ )	$C_2$ (fraction of total at $t = 0$ )
Cholesterol	$0.29 \pm 0.03$	$2.4 \pm 0.3$	$0.59 \pm 0.03$	$0.40 \pm 0.04$
Campesterol	$0.23 \pm 0.05$	$3.0 \pm 0.8$	$0.54 \pm 0.06$	$0.45 \pm 0.06$
$\beta$ -Sitosterol	$0.41 \pm 0.04^*$	$1.7 \pm 0.2$	$0.58 \pm 0.02$	$0.42 \pm 0.02$
Sitostanol	$0.62 \pm 0.08^{**}$	$1.1 \pm 0.2$	$0.49 \pm 0.02$	$0.51 \pm 0.02$

THP-1 cells were incubated with sterol-loaded oxLDL and the sterol transfer to HDL in the medium was monitored as described in “Materials and Methods” (Eq. 2). Retention of radiolabelled sterols in cells starts at  $C_1$  (=span + plateau as fraction of  $[^3\text{H}]_0$ ) and decays to  $C_2$  (=plateau as fraction of  $[^3\text{H}]_0$ ) with a rate constant  $k$  [14].  $t_{1/2} = \ln 2/k$ . All values are mean  $\pm$  SEM of two experiments ( $n = 5$  wells)

\* Statistically significant from cholesterol,  $P < 0.05$ ; \*\*  $P < 0.001$

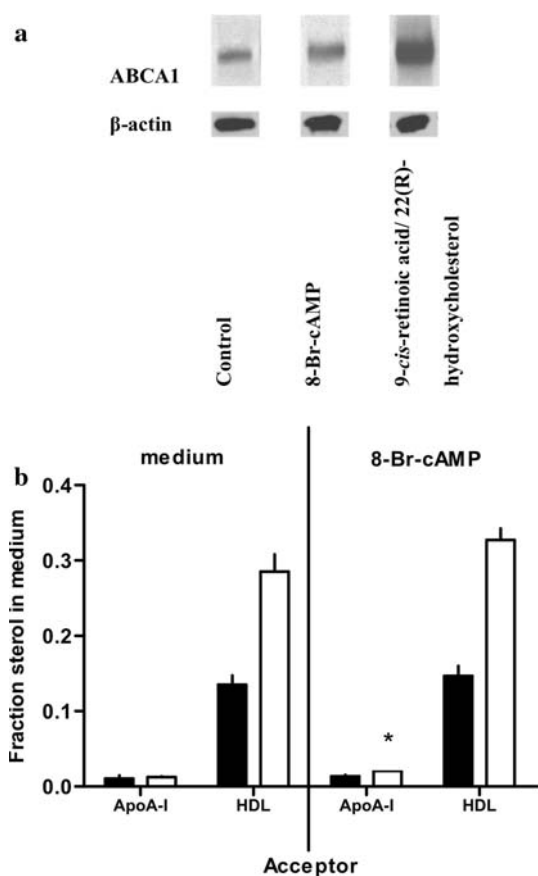


**Fig. 3** Sterol efflux from THP-1 cells to HDL or ApoA-I. The presence of ABCA1 protein was verified in THP-1 cells after incubation with 8-Br-cAMP or 9-*cis*-retinoic acid/22(*R*)-hydroxycholesterol as described in “Materials and Methods” (a). Cells were incubated with labelled oxLDL with or without 8-Br-cAMP, washed and HDL or ApoA-I was added (b). At  $t = 3$  h fractional efflux to medium of  $[^3\text{H}]$ -cholesterol (closed bars) versus  $[^3\text{H}]$ - $\beta$ -sitosterol (open bars) was calculated relatively to the  $[^3\text{H}]$ -sterol content in cells at  $t = 0$  h. All values are mean  $\pm$  SEM of three experiments ( $n = 9$  wells), except for ApoA-I ( $n = 4$  wells). \* Statistically significant from efflux to ApoA-I in medium alone,  $P < 0.05$

due to low affinity. Consequently, the influx of phytosterols from cyclodextrin concomitantly occurred with the efflux of cellular cholesterol to cyclodextrin. As a result of this

efflux, the influx of sterols from cyclodextrin might be hampered and hence, a more physiological carrier system, like LDL is preferred.

Receptor-mediated endocytosis of modified LDL, like oxLDL, has been implicated in the pathogenesis of atherosclerosis, since it leads to the development of foam cells, an early step in atherogenesis. To determine whether sterol influx via receptor-mediated endocytosis of oxLDL was different for the various sterols, oxLDL was loaded with sterols and added to THP-1 cells. The observed ranking in affinity of oxLDL for sterols (cholesterol > campesterol >  $\beta$ -sitosterol > sitostanol) was interesting, since it correlates with the degree of similarity of phytosterols with cholesterol. Addition of one methyl group at C24 of the side chain (campesterol) was the smallest alteration and resulted in the highest affinity. Addition of an ethyl group at the same C24 position ( $\beta$ -sitosterol) resulted in an intermediate alteration and concomitantly a lower affinity. Addition of an ethyl group at C24 and saturation of the delta-5 double bond (sitostanol) was the biggest alteration and consequently resulted in the lowest affinity for oxLDL.

Several scavenger receptors mediate internalisation of the entire oxLDL particle, including scavenger receptors of class A and cluster determinant 36 (CD36) [17]. Whether these receptors exhibit sterol specificity during internalisation of the oxLDL particle is unknown, but our data do not indicate such a relationship, since no differences in cholesterol versus phytosterol influx were observed. The data are in line with results of an earlier mouse study [12]. It is possible that in our model, oxLDL simply facilitates diffusion of phytosterols from particle to cell, and that the particle itself is not internalised. If so, our data suggest that influx of phytosterols into cells, either mediated via passive diffusion or receptor-facilitated internalisation, does not differ from that of cholesterol.

In a next step towards mimicking the *in vivo* situation, THP-1 cells were incubated with oxLDL and then with HDL. HDL is considered to be the primary cholesterol carrier in reverse cholesterol transport; a process of

removing excess cholesterol from the periphery into the liver and bile, followed by excretion in stool. Our efflux data show that  $\beta$ -sitosterol and sitostanol were more efficiently transferred to HDL than campesterol and cholesterol, with the highest efficiency found for sitostanol. These data could indicate that the more a phytosterol differs structurally from cholesterol, the more efficiently it is removed from a peripheral cell and excreted from the body. It is again coincidental that the ranking in affinity of phytosterols for the applied carrier systems roughly correlates with their efflux efficiency to HDL, underscoring how physical properties of sterols can vary significantly, despite modest differences in molecular structure. A portion of the sterols was not exchanged (indicated by the plateau C2), presumably because they were excluded from efflux due to esterification by acyl-CoA:cholesterol *O*-acyltransferase (ACAT) type 1 and storage in lipid droplets during the pre-loading period with oxLDL. Nevertheless, for cholesterol the observed  $t_{1/2}$  was within the range of values found for other cell types (1–3 h) [14, 18]. Whether the differences in the sterol efflux were caused by different kinetics in tritium exchange due to different labelling positions is unknown and may be worth exploring in a subsequent study.

Since esterification and storage of esters in lipid droplets result in a decline of the intracellular sterol pool available for efflux, one could speculate that modest substrates for ACAT-1, like phytosterols, are more efficiently transferred to HDL than cholesterol. Although ACAT inhibition did decrease the fraction of cholesterol retained in THP-1 cells, levels as low as for  $\beta$ -sitosterol were not reached (data not shown). Another important step in sterol efflux is the hydrolysis of steryl esters by cellular cholesterol esterase. It might be that  $\beta$ -sitosterol and sitostanol, when esterified in the cell, are efficiently hydrolysed and thus rapidly available for efflux. However, a preferred hydrolysis of esterified  $\beta$ -sitosterol by cholesterol esterase is unlikely due to a reported twofold lower cholesterol esterase activity for  $\beta$ -sitosterol as compared to cholesterol [19]. A lower cholesterol esterase activity might also be expected for sitostanol, the hydrogenated form of  $\beta$ -sitosterol.

Several transporters, next to passive diffusion, may be responsible for the preferential efflux of  $\beta$ -sitosterol and sitostanol in our model, including ABCA1 [20]. ABCA1 was detected and inducible in our THP-1 model. In our experiments, the presence of 8-Br-cAMP modestly increased ABCA1 protein mass as reported earlier for human fibroblasts [21]. However, whether cAMP analogues indeed increase ABCA1 expression is still open for debate, since other groups did not observe any effect of cAMP analogues on human ABCA1 expression [22, 23].

Despite an excess of ApoA-I and the presence of ABCA1, the efflux to ApoA-I was relatively modest, even for cholesterol, indicating that the ABCA1–ApoA-I

pathway may not be responsible for the observed effects in our model. However, the small but statistically significant increase of  $\beta$ -sitosterol efflux to ApoA-I is noteworthy, since it might indicate that certain phytosterols are preferentially transported via this pathway. This observation is intriguing, since it might indicate a discriminatory role of ACAT1 in macrophages. Similarly to cholesterol, plant sterols are esterified by ACAT-1, but with lower efficiency [24], and secreted via chylomicrons into lymph. Since ABCA1 and ACAT-1 use the same pool of free sterols as substrate [25], a poor ACAT-1 substrate like  $\beta$ -sitosterol, might be more available for the alternative ABCA1–ApoA-I pathway than, e.g., cholesterol. Similarly to ABCA1, the CD36 and LIMPII analogous-1 receptor (CLA-1) may also not play an important role in our model. Results from earlier studies have shown that PMA stimulation reduces CLA-1 mRNA expression in THP-1 cells [26] and oxLDL incubation reduces expression of SR-BI, the mouse homologue of CLA-1, in mouse macrophages [27]. Therefore the role of another ABC protein, ABCG1, might be more relevant. ABCG1 is responsible for the transfer of cholesterol to HDL [28] and THP1 cells express ABCG1 mRNA [29]. Whether this transporter is indeed responsible for the observed preferential efflux of phytosterols requires further investigation.

Nguyen et al. [11] isolated monocytes from healthy individuals and determined their sterol concentration. A total of 3.8% was of phytosterol origin, including  $\beta$ -sitosterol (56%), campesterol (30%) and sitostanol (14%). Surprisingly, more  $\beta$ -sitosterol than campesterol was found in monocytes, despite a higher concentration of campesterol in plasma. Our data support the view that macrophages transfer  $\beta$ -sitosterol more efficiently than campesterol, and as a consequence might contain more of the latter. A possible explanation for this difference could be that phytosterol efflux in monocytes is different from that of macrophages. The preferential efflux of  $\beta$ -sitosterol and sitostanol to HDL is in agreement with the observation that phytosterols tend to accumulate in HDL of healthy individuals [15] and patients suffering from sitosterolemia [30], an autosomal recessive disorder characterised by an elevated plasma and tissue concentrations of phytosterols [4].

In conclusion, the present in vitro results indicate that (1) THP-1 cells absorb phytosterols at a level similar to that of cholesterol and (2)  $\beta$ -sitosterol and sitostanol are transferred to HDL more efficiently than cholesterol. Consequently, one could speculate that arterial macrophages in vivo also transfer phytosterols efficiently to HDL and that this transfer is increased as the molecular structure deviates more from cholesterol. Whether our in vitro results can be extrapolated to an in vivo situation requires more analysis. Suitable animal models or other

macrophage models should therefore be selected to test and study this hypothesis and the current results could be used as guideline for future work.

**Acknowledgments** We thank Dr. R. Diks, Dr. Y. Lin and Dr. I. Demonty for critically reading this manuscript.

## References

- Moreau RA, Whitaker BD, Hicks KB (2002) Phytosterols, phytostanols, and their conjugates in foods: structural diversity, quantitative analysis, and health-promoting uses. *Prog Lipid Res* 41:457–500
- NCEP (2002) Third report of the National Cholesterol Education Program (NCEP) expert panel on detection, evaluation, and treatment of high blood cholesterol in adults (Adult Treatment Panel III) final report. *Circulation* 106:3143–3421
- Katan MB, Grundy SM, Jones P, Law M, Miettinen T, Paoletti R (2003) Efficacy and safety of plant stanols and sterols in the management of blood cholesterol levels. *Mayo Clin Proc* 78:965–978
- Salen G, Shefer S, Lien NY, Ness GC, Tint GS, Shore V (1992) Sitosterolemia. *J Lipid Res* 33:945–955
- Miettinen TA, Railo M, Lepantalo M, Gylling H (2005) Plant sterols in serum and in atherosclerotic plaques of patients undergoing carotid endarterectomy. *J Am Coll Cardiol* 45:1794–1801
- Glueck CJ, Speirs J, Tracy T, Streicher P, Illig E, Vandegrift J (1991) Relationships of serum plant sterols (phytosterols) and cholesterol in 595 hypercholesterolemic subjects, and familial aggregation of phytosterols, cholesterol, and premature coronary heart-disease in hyperphytosterolemic probands and their 1st-degree relatives. *Metabolism* 40:842–848
- Sudhop T, Gottwald BM, von Bergmann K (2002) Serum plant sterols as a potential risk factor for coronary heart disease. *Metabolism* 51:1519–1521
- Assmann G, Cullen P, Erbey J, Ramey DR, Kannenberg F, Schulte H (2006) Plasma sitosterol elevations are associated with an increased incidence of coronary events in men: results of a nested case-control analysis of the Prospective Cardiovascular Munster (PROCAM) study. *Nutr Metab Cardiovasc Dis* 16:13–21
- Wilund KR, Yu LQ, Xu F, Vega GL, Grundy SM, Cohen JC, Hobbs HH (2004) No association between plasma levels of plant sterols and atherosclerosis in mice and men. *Arterioscler Thromb Vasc Biol* 24:2326–2332
- Pinedo S, Vissers MN, von Bergmann K, Elharchaoui K, Lutjohann D, Luben R, Wareham NJ, Kastelein JJP, Khaw KT, Boekholdt SM (2007) Plasma levels of plant sterols and the risk of coronary artery disease: the prospective EPIC-Norfolk population study. *J Lipid Res* 48:139–144
- Nguyen LB, Salen G, Shefer S, Tint GS, Ruiz F (2001) Macrophage 3-hydroxy-3-methylglutaryl coenzyme A reductase activity in sitosterolemia: effects of increased cellular cholesterol and sitosterol concentrations. *Metabolism* 50:1224–1229
- Sato Y, Nishikawa K, Aikawa K, Mimura K, Murakamimurofushi K, Arai H, Inoue K (1995) Side-chain structure is critical for the transport of sterols from lysosomes to cytoplasm. *Biochim Biophys Acta* 1257:38–46
- Auwerx J (1991) The human leukemia-cell line, Thp-1—a multifaceted model for the study of monocyte-macrophage differentiation. *Experientia* 47:22–31
- Johnson WJ, Bamberger MJ, Latta RA, Rapp PE, Phillips MC, Rothblat GH (1986) The bidirectional flux of cholesterol between cells and lipoproteins—effects of phospholipid depletion of high-density-lipoprotein. *J Biol Chem* 261:5766–5776
- Tilvis RS, Miettinen TA (1986) Serum plant sterols and their relation to cholesterol absorption. *Am J Clin Nutr* 43:92–97
- Christian AE, Haynes MP, Phillips MC, Rothblat GH (1997) Use of cyclodextrins for manipulating cellular cholesterol content. *J Lipid Res* 38:2264–2272
- Kunjathoor VV, Febbraio M, Podrez EA, Moore KJ, Andersson L, Koehn S, Rhee JS, Silverstein R, Hoff HF, Freeman MW (2002) Scavenger receptors class A-I/II and CD36 are the principal receptors responsible for the uptake of modified low density lipoprotein leading to lipid loading in macrophages. *J Biol Chem* 277:49982–49988
- Gillotte-Taylor K, Nickel M, Johnson WJ, Francone OL, Holvoet P, Lund-Katz S, Rothblatt GH, Phillips MC (2002) Effects of enrichment of fibroblasts with unesterified cholesterol on the efflux of cellular lipids to apolipoprotein A-I. *J Biol Chem* 277:11811–11820
- Ikeda I, Tanaka K, Sugano M, Vahouny GV, Gallo LL (1988) Inhibition of cholesterol absorption in rats by plant sterols. *J Lipid Res* 29:1573–1582
- Oram JF (2002) ATP-binding cassette transporter A1 and cholesterol trafficking. *Curr Opin Lipidol* 13:373–381
- Lawn RM, Wade DP, Garvin MR, Wang XB, Schwartz K, Porter JG, Seilhamer JJ, Vaughan AM, Oram JF (1999) The Tangier disease gene product ABC1 controls the cellular apolipoprotein-mediated lipid removal pathway. *J Clin Invest* 104:R25–R31
- Denis M, Bissonnette R, Haïdar B, Krimbou L, Bouvier M, Genest J (2003) Expression, regulation, and activity of ABCA1 in human cell lines. *Mol Genet Metab* 78:265–274
- Kiss RS, Maric J, Marcel YL (2005) Lipid efflux in human and mouse macrophagic cells: evidence for differential regulation of phospholipid and cholesterol efflux. *J Lipid Res* 46:1877–1887
- Temel RE, Gebre AK, Parks JS, Rudel LL (2003) Compared with Acyl-CoA:cholesterol *O*-acyltransferase (ACAT) 1 and lecithin:cholesterol acyltransferase, ACAT2 displays the greatest capacity to differentiate cholesterol from sitosterol. *J Biol Chem* 278:47594–47601
- Sugimoto K, Tsujita M, Wu CA, Suzuki K, Yokoyama S (2004) An inhibitor of acylCoA: cholesterol acyltransferase increases expression of ATP-binding cassette transporter A1 and thereby enhances the ApoA-I-mediated release of cholesterol from macrophages. *Biochim Biophys Acta* 1636:69–76
- Murao K, Terpstra V, Green SR, Kondratenko N, Steinberg D, Quehenberger O (1997) Characterization of CLA-1, a human homologue of rodent scavenger receptor BI, as a receptor for high density lipoprotein and apoptotic thymocytes. *J Biol Chem* 272:17551–17557
- Han JH, Nicholson AC, Zhou XY, Feng JW, Gotto AM, Hajjar DP (2001) Oxidized low density lipoprotein decreases macrophage expression of scavenger receptor B-I. *J Biol Chem* 276:16567–16572
- Wang N, Lan DB, Chen WG, Matsuura F, Tall AR (2004) ATP-binding cassette transporters G1 and G4 mediate cellular cholesterol efflux to high-density lipoproteins. *Proc Natl Acad Sci USA* 101:9774–9779
- Wong J, Quinn CM, Brown AJ (2004) Statins inhibit synthesis of an oxysterol ligand for the liver X receptor in human macrophages with consequences for cholesterol flux. *Arterioscler Thromb Vasc Biol* 24:2365–2371
- Robins SJ, Fasulo JM (1997) High density lipoproteins, but not other lipoproteins, provide a vehicle for sterol transport to bile. *J Clin Invest* 99:380–384

integrity of red blood cells which is affected in the hypercholesterolemic situation is effectively countered by dietary curcumin and capsaicin [5, 6]. The antioxidant potential of spice principles—curcumin and capsaicin has been experimentally documented in *in vitro* systems and in a few *in vivo* studies [1]. We have also recently reported the beneficial influences of dietary curcumin, capsaicin and their combination on the susceptibility of low-density lipoprotein (LDL) to oxidation and that the protective effect of the combination of curcumin and capsaicin on LDL oxidation was greater than that of the individual compounds [7]. We have also observed that while both dietary curcumin and capsaicin moderately lowered carrageenan-induced paw inflammation, these spice principles in combination were more effective [7].

The present animal study examined the hypolipidemic influence of dietary curcumin and capsaicin individually and in combination in induced hypercholesterolemic rats especially to verify if there is any additive or synergistic effect of these two bioactive compounds. Information on the possibility of an additive or synergistic effect of two hypolipidemic agents would be most relevant in the context of their possible use in the management of cardiovascular diseases. The study also examined their influence on antioxidant molecules and a few antioxidant enzymes in blood and liver in hypercholesterolemic condition.

## Experimental Procedures

### Chemicals and Reagents

The spice active principles—curcumin and capsaicin were procured from M/s Fluka Chemie, Switzerland. All other chemicals used were of analytical grade obtained from M/s Sigma Chemical Co., St Louis, USA and the solvents were distilled before use.

### Animal Treatment

Animal experiments were carried out taking appropriate measures to minimize pain or discomfort in accordance with the guidelines laid down by the NIH (USA) regarding the care and use of animals for experimental procedures and with due clearance from the Institute's Animal Ethics Committee. Female Wistar rats (eight per group) weighing 110–120 g and housed in individual stainless steel cages were maintained on various experimental diets *ad libitum* for 8 week. The basal diet consisted of: casein 21%, cane sugar 10%, corn starch 54%, NRC vitamin mixture 1%, Bernhardt–Tommarrelli modified NRC salt mixture 4%, and refined peanut oil 10%. The hypercholesterolemic diet

consisted of 0.5% cholesterol and 0.125% bile salts at the expense of an equivalent amount of corn starch in the basal diet, and also hydrogenated vegetable fat was used in place of refined peanut oil at 10% level in this diet. The spice principles were incorporated into the basal diet/hypercholesterolemic diet, replacing an equivalent amount of corn starch to give the various experimental diets containing: curcumin (0.2%), capsaicin (0.015%) and curcumin (0.2%) + capsaicin (0.015%). At the end of the experimental period, overnight fasted animals were sacrificed under light ether anesthesia. Blood was collected by heart puncture and serum separated by centrifugation. The liver was quickly excised, weighed and stored frozen till lipid extraction.

### Lipid Profile

Total lipids were extracted according to Folch et al. [8] and estimated gravimetrically. Cholesterol [9], triglycerides [10] and phospholipids [11] were determined in the lipid extracts of serum and liver by using standard procedures. Serum cholesterol and triglyceride associated with HDL fraction were determined after precipitation of apolipoprotein-B containing lipoproteins with heparin-manganese reagent according to the method of Warnick and Albers [12]. LDL–VLDL precipitate was extracted with chloroform:methanol (2:1, v/v) and used for cholesterol and triglyceride determination.

### Lipid Peroxides

Serum lipid peroxides were estimated by the fluorimetric measurement of the thiobarbituric acid complex by the method of Yagi [13]. The fluorimetric measurement was carried out at an excitation wavelength of 515 nm and an emission wavelength of 553 nm and compared with the standards prepared by reacting 0.5 nmol 1,1,3,3-tetraethoxy-propane with TBA reagent. Lipid peroxide in liver tissue was determined by the method described by Ohkawa et al. [14] involving photometric measurement of thiobarbituric acid complex extracted into butanol. Absorbance of the butanol extract was measured at 532 nm and compared with that of standard tetraethoxypropane, treated similarly.

### Antioxidant Molecules

Total thiols in serum and liver were measured spectrophotometrically by using Ellman's reagent according to Sedlock and Lindsay [15]. Glutathione in serum and liver was estimated by using Ellman's reagent according to

Beutler et al. [16]. Ascorbic acid was estimated spectrophotometrically by measuring the 2,4-dinitrophenylhydrazine derivative of dehydroascorbic acid according to Omaye et al. [17].  $\alpha$ -Tocopherol in liver and serum was determined by the HPLC method described by Zaspel and Csallany [18] using an ODS column (C-18) and an UV-visible detector (295 nm) and a solvent system acetonitrile–methanol (1:1).

#### Antioxidant Enzymes

Glutathione reductase activity was assayed in serum and liver homogenate by measuring the oxidation of NADPH at 340 nm by oxidized glutathione as described by Carlberg and Mannervik [19]. Glutathione-S-transferase activity was assayed by measuring the CDNB–GSH conjugate formed using 1-chloro-2,4-dinitrobenzene as the substrate as described by Warholm et al. [20]. Glutathione peroxidase activity in serum and liver homogenate was determined by following NADPH oxidation in a coupled reduction system consisting of hydrogen peroxide and oxidized glutathione as described by Flohe and Gunzler [21]. Catalase activity in serum and liver homogenate was assayed according to the method of Aebi [22] by following the decomposition of hydrogen peroxide at 240 nm.

#### Statistical Analysis

Results are expressed as means  $\pm$  SEM and comparisons between groups were made by means of one-way ANOVA for basal diet groups and another one-way ANOVA for high cholesterol diet groups [23]. Comparisons among

different groups were made applying the Dunnett test. Differences were considered significant when  $P < 0.05$ .

## Results

### Serum Lipid Profile

High cholesterol feeding for 8 weeks resulted in a significant increase in blood total cholesterol concentration and this increase was observed mainly in the LDL/VLDL-associated fraction (Table 1). The increase in total blood cholesterol was as much as sixfold. Dietary curcumin, capsaicin or their combination significantly countered the extent of hypercholesterolemia. Blood total cholesterol was 20, 22 and 21.5% lower in these respective animal groups compared to their corresponding control. The reduction in blood cholesterol brought about by dietary spice principles was predominantly in the LDL/VLDL-cholesterol fraction. The HDL-cholesterol fraction essentially remained unchanged as a result of treatment with spice principles. While the effect of curcumin and capsaicin on blood cholesterol was quantitatively almost equal at their dietary levels used here, the combination of the two spice principles—curcumin and capsaicin did not have any additive effect on blood cholesterol level. Neither of the two dietary spice principles had any effect on blood cholesterol level in normal rats.

Serum total triglyceride concentration was significantly lower in high cholesterol treatment when compared to the normal-control (Table 1). This decrease was about 33%, and was due to a specific decrease in the LDL/VLDL-associated fraction (38%). There was no change in the concentration of triglyceride associated with HDL as a

**Table 1** Influence of dietary curcumin and capsaicin on serum lipid profile

Animal group	Cholesterol			Triglycerides			Phospholipids
	Total	LDL + VLDL	HDL	Total	LDL + VLDL	HDL	
Control	55.6 $\pm$ 2.00	34.9 $\pm$ 1.42	20.7 $\pm$ 1.74	112.3 $\pm$ 2.76	96.4 $\pm$ 3.41	16.0 $\pm$ 1.06	118.5 $\pm$ 4.50
Curcumin	55.2 $\pm$ 3.55	33.1 $\pm$ 1.50	22.1 $\pm$ 1.48	101.3 $\pm$ 5.52	85.0 $\pm$ 5.67	16.2 $\pm$ 0.29	108.0 $\pm$ 3.81
Capsaicin	57.8 $\pm$ 2.11	32.6 $\pm$ 2.39	25.2 $\pm$ 1.56	91.2 $\pm$ 8.01**	76.7 $\pm$ 4.94**	14.5 $\pm$ 0.47	108.8 $\pm$ 3.72
Curcumin + capsaicin	57.3 $\pm$ 3.33	36.7 $\pm$ 2.31	20.6 $\pm$ 0.99	98.0 $\pm$ 4.50**	82.7 $\pm$ 4.60**	15.3 $\pm$ 0.31	111.5 $\pm$ 1.77
HCD control	398.0 $\pm$ 20.8	377.9 $\pm$ 22.0	20.1 $\pm$ 0.77	75.7 $\pm$ 3.46	59.5 $\pm$ 3.64	16.2 $\pm$ 0.85	159.6 $\pm$ 5.83
HCD curcumin	317.8 $\pm$ 13.7**	298.2 $\pm$ 14.7**	19.6 $\pm$ 0.49	71.4 $\pm$ 4.50	55.7 $\pm$ 3.84	15.8 $\pm$ 1.49	228.8 $\pm$ 5.54*
HCD capsaicin	309.2 $\pm$ 15.9**	289.0 $\pm$ 11.7**	20.2 $\pm$ 1.06	65.7 $\pm$ 5.23	52.1 $\pm$ 2.66	13.6 $\pm$ 0.96	185.4 $\pm$ 6.27*
HCD curcumin + capsaicin	312.6 $\pm$ 19.7**	291.7 $\pm$ 24.1**	20.9 $\pm$ 0.54	85.9 $\pm$ 2.70	69.0 $\pm$ 2.32	16.9 $\pm$ 0.63	201.6 $\pm$ 7.61*

Values expressed as mg/dl are the mean  $\pm$  SEM of eight rats in each group

LDL low-density lipoprotein, HDL high-density lipoprotein, VLDL very low-density lipoprotein, HCD high cholesterol diet

\* Significant increase compared to corresponding control ( $P < 0.05$ ), \*\* significant decrease compared to corresponding control ( $P < 0.05$ )

result of high cholesterol feeding. Dietary spice principles—curcumin, capsaicin or their combination did not alter the blood triglyceride concentration in these induced hypercholesterolemic animals. On the other hand, there was a statistically significant decrease in total triglycerides and LDL/VLDL-associated triglycerides in normal rats as a result of dietary capsaicin and dietary curcumin + capsaicin. The decreases in blood total triglyceride concentration brought about in the normal rats belonging to the two respective diet groups were 19 and 13%, which was mainly from the LDL/VLDL-associated fraction.

While the dietary spice principles did not affect the blood phospholipid concentration in normal rats, higher phospholipid content resulted in hypercholesterolemic rats by feeding these spice principles (Table 1). A hypercholesterolemic diet brought about a 32% increase in blood phospholipid concentration compared to normal control. The increases in phospholipid concentration seen in hypercholesterolemic rats in the diet groups—curcumin, capsaicin, and curcumin + capsaicin were 43, 16 and 26%, respectively, compared to HCD-control. No particular additive effect is seen when the two spice principles—curcumin and capsaicin were given in combination.

#### Liver Lipid Profile

The hepatic cholesterol concentration was significantly lowered as a result of dietary spice principles in normal rats (Table 2). This decrease was 20, 27 and 23% in curcumin fed, capsaicin fed and curcumin + capsaicin fed animals, respectively. Liver cholesterol was not influenced by the two spice compounds or their combination in hypercholesterolemic animals. The liver triglyceride level was significantly lowered in both normal and hypercholesterolemic rats maintained on a capsaicin diet, the decrease

brought about being 51 and 29%, respectively. Hepatic phospholipid concentration remained unaffected by dietary spice principles in both normal and hypercholesterolemic rats. The dietary capsaicin treatment lowered total lipids in the liver by 15% in hypercholesterolemic rats and by 26% in normal rats. Hepatic total lipid content was also lower in the normal—curcumin + capsaicin group, which was about 20%.

#### Antioxidant Molecules in Blood

Among the various antioxidant molecules, serum ascorbic acid concentration was not influenced by the dietary spice principles in normal rats, while it was significantly enhanced in hypercholesterolemic animals (Table 3). The extent of the increase in serum ascorbic acid produced by dietary curcumin, capsaicin and their combination was 64, 34 and 44%, respectively. Thus, the effect of curcumin seen on serum ascorbic acid was more than that produced by capsaicin, and there was no additive effect by their combination. On the other hand, serum  $\alpha$ -tocopherol concentration was significantly lowered in hypercholesterolemic animals by dietary curcumin, capsaicin, and their combination, the effect being 72, 71.5 and 35%, respectively (Table 3). Thus, the combination of the two spice principles produced a lower decrease in the concentration of this antioxidant vitamin than the two individual spice principles. Serum  $\alpha$ -tocopherol was not influenced by any of the spice principles in normal animals. Serum  $\alpha$ -tocopherol was about three times higher in the hypercholesterolemic animals (1.698 vs 0.57  $\mu$ g/dl).

Total thiol content in serum was lower as a result of treatment with spice principles in both normal and hypercholesterolemic animals, the effect being more in the latter (Table 3). The decreases in serum total thiol concentration

**Table 2** Influence of dietary curcumin and capsaicin on hepatic lipid profile

Animal group	Total lipids	Cholesterol	Triglycerides	Phospholipids
Control	65.6 $\pm$ 0.82	5.73 $\pm$ 0.19	27.8 $\pm$ 0.95	27.5 $\pm$ 0.30
Curcumin	62.0 $\pm$ 0.63	4.58 $\pm$ 0.15**	24.4 $\pm$ 0.78	26.8 $\pm$ 0.42
Capsaicin	48.4 $\pm$ 2.56**	4.18 $\pm$ 0.11**	13.7 $\pm$ 0.95**	24.6 $\pm$ 0.33
Curcumin + capsaicin	52.6 $\pm$ 3.55**	4.43 $\pm$ 0.19**	23.7 $\pm$ 2.53	26.6 $\pm$ 0.38
HCD control	203.4 $\pm$ 5.96	59.3 $\pm$ 0.68	54.7 $\pm$ 2.97	22.8 $\pm$ 0.04
HCD curcumin	199.5 $\pm$ 2.54	64.6 $\pm$ 1.60	47.3 $\pm$ 2.60	21.4 $\pm$ 0.04
HCD capsaicin	172.6 $\pm$ 8.84**	53.4 $\pm$ 2.65	39.1 $\pm$ 2.57**	22.9 $\pm$ 0.77
HCD curcumin + capsaicin	206.3 $\pm$ 3.52	58.6 $\pm$ 0.79	46.6 $\pm$ 2.38	21.9 $\pm$ 0.07

Values expressed as mg/g liver are mean  $\pm$  SEM of eight rats in each group

HCD high cholesterol diet

\*\* Significant decrease compared to corresponding control ( $P < 0.05$ )



were 20, 19 and 18% by dietary curcumin, capsaicin and curcumin + capsaicin, respectively, in normal rats. The decreases in serum total thiol concentration produced in hypercholesterolemic animals by these respective diet groups were 14, 38 and 33%. Significant decreases in serum glutathione concentration were also observed as a result of feeding animals with these spice principles, more so in hypercholesterolemic animals. The decreases in serum glutathione concentration seen in hypercholesterolemic rats maintained on curcumin, capsaicin, and their combination were 23, 56 and 41%, respectively. Blood lipid peroxide content was lower in the hypercholesterolemic rats as a result of feeding either curcumin and capsaicin or their combination (Table 3). The extent of reduction in lipid peroxide was 13, 17 and 41% in the respective diet groups. Dietary spice principles did not have any influence on the blood lipid peroxide value in the case of normal rats.

#### Antioxidant Molecules in the Liver

Ascorbic acid concentration in the liver was favourably influenced by dietary curcumin, capsaicin and their combination in normal rats (Table 4). The extent of the increase in hepatic ascorbic acid was 21, 14 and 11% in the respective diet groups. These dietary spice principles did not show any beneficial effect on liver ascorbic acid levels in hypercholesterolemic rats. On the other hand, there were marginal decreases in hepatic ascorbic acid of hypercholesterolemic rats in the dietary curcumin, capsaicin and curcumin + capsaicin groups. The decreases were of the order of 23, 16 and 27% in the respective diet groups.

Hepatic total thiols were higher as a result of dietary spice principles—curcumin, capsaicin or curcumin + capsaicin in normal rats (Table 4). The increase in total thiols was 11, 26 and 39% in the respective diet groups as compared to control. Thus, the combination of curcumin

**Table 3** Influence of dietary curcumin and capsaicin on serum antioxidant molecules and lipid peroxides

Animal group	Total thiols (mmol/dl)	Glutathione ( $\mu\text{g/dl}$ )	Ascorbic acid (mg/dl)	$\alpha$ -Tocopherol ( $\mu\text{g/dl}$ )	Lipid peroxides ( $\mu\text{mol/dl}$ )
Control	14.71 $\pm$ 0.52	0.221 $\pm$ 0.019	0.277 $\pm$ 0.010	0.570 $\pm$ 0.019	88.0 $\pm$ 5.13
Curcumin	11.76 $\pm$ 0.46**	0.173 $\pm$ 0.013**	0.266 $\pm$ 0.014	0.527 $\pm$ 0.009	89.2 $\pm$ 3.15
Capsaicin	11.91 $\pm$ 0.36**	0.208 $\pm$ 0.009	0.258 $\pm$ 0.017	0.499 $\pm$ 0.023	100.7 $\pm$ 6.08
Curcumin + Capsaicin	12.08 $\pm$ 0.84**	0.170 $\pm$ 0.017**	0.300 $\pm$ 0.022	0.607 $\pm$ 0.013	102.1 $\pm$ 7.19
HCD Control	33.66 $\pm$ 1.14	0.391 $\pm$ 0.031	0.250 $\pm$ 0.015	1.698 $\pm$ 0.057	86.3 $\pm$ 3.22
HCD Curcumin	28.90 $\pm$ 1.53**	0.302 $\pm$ 0.025**	0.409 $\pm$ 0.040*	0.472 $\pm$ 0.081**	75.1 $\pm$ 3.02**
HCD Capsaicin	20.97 $\pm$ 0.43**	0.170 $\pm$ 0.016**	0.334 $\pm$ 0.023*	0.483 $\pm$ 0.049**	71.9 $\pm$ 3.53**
HCD Curcumin + Capsaicin	22.42 $\pm$ 0.55**	0.230 $\pm$ 0.026**	0.360 $\pm$ 0.012*	1.096 $\pm$ 0.080**	50.6 $\pm$ 5.15**

Values are expressed as the mean  $\pm$  SEM of eight rats in each group

HCD high cholesterol diet

\* Significant increase compared to corresponding control ( $P < 0.05$ ), \*\* significant decrease compared to corresponding control ( $P < 0.05$ )

**Table 4** Influence of dietary curcumin and capsaicin on liver antioxidant molecules and lipid peroxides

Animal group	Total thiols (mmol/mg protein)	Glutathione ( $\mu\text{g/mg protein}$ )	Ascorbic acid ( $\mu\text{g/mg protein}$ )	Lipid peroxides (nmol/mg protein)
Control	0.512 $\pm$ 0.015	0.336 $\pm$ 0.030	0.269 $\pm$ 0.008	8.078 $\pm$ 0.329
Curcumin	0.567 $\pm$ 0.016*	0.432 $\pm$ 0.034*	0.326 $\pm$ 0.007*	5.389 $\pm$ 0.519**
Capsaicin	0.647 $\pm$ 0.033*	0.482 $\pm$ 0.022*	0.306 $\pm$ 0.009*	7.027 $\pm$ 0.231**
Curcumin + capsaicin	0.713 $\pm$ 0.019*	0.430 $\pm$ 0.016*	0.299 $\pm$ 0.005*	6.668 $\pm$ 0.439**
HCD control	0.957 $\pm$ 0.024	0.528 $\pm$ 0.022	0.411 $\pm$ 0.007	3.959 $\pm$ 0.179
HCD curcumin	0.870 $\pm$ 0.032	0.512 $\pm$ 0.011	0.318 $\pm$ 0.011**	3.157 $\pm$ 0.179**
HCD capsaicin	0.892 $\pm$ 0.017	0.550 $\pm$ 0.029	0.345 $\pm$ 0.012**	2.896 $\pm$ 0.294**
HCD curcumin + capsaicin	0.925 $\pm$ 0.009	0.724 $\pm$ 0.031*	0.302 $\pm$ 0.008**	2.714 $\pm$ 0.248**

Values are expressed as mean  $\pm$  SEM of eight rats in each group

HCD high cholesterol diet

\* Significant increase compared to corresponding control ( $P < 0.05$ ), \*\* significant decrease compared to corresponding control ( $P < 0.05$ )

and capsaicin produced an effect higher than the two individual compounds. Total thiols were 87% higher in high cholesterol treatment as compared to their normal counterpart. The spice principles did not have any influence on the same in hypercholesterolemic rats. Hepatic glutathione content was higher in normal rats under the influence of dietary curcumin, capsaicin or the combination of these two (Table 4). Dietary curcumin, capsaicin and curcumin + capsaicin produced an increase in hepatic glutathione of 29, 43 and 28%, respectively. Hypercholesterolemic rats displayed a higher hepatic glutathione content (0.528  $\mu\text{g}/\text{mg}$  protein in the HCD-control compared to 0.336  $\mu\text{g}/\text{mg}$  protein in the normal-control). Unlike in normal rats, only the combination of curcumin and capsaicin produced an enhancing effect on hepatic glutathione in hypercholesterolemic animals, the effect being 37%. Hepatic lipid peroxides were lowered by dietary spice compounds both in normal and hypercholesterolemic situation (Table 4), the decrease produced being 33, 13 and 17% by dietary curcumin, capsaicin and their combination, respectively, in normal rats, while in hypercholesterolemic rats, the decrease was by 20, 27 and 31% by the respective diet groups.

#### Antioxidant Enzymes in Serum

Activities of serum glutathione reductase and catalase were higher in hypercholesterolemic animals when compared to their normal counterparts (Table 5). Activity of glutathione reductase was significantly enhanced by dietary curcumin, capsaicin and curcumin + capsaicin in normal rats. The increase in the enzyme activity produced by these diet groups was 41, 82 and 44%, respectively. However, in the hypercholesterolemic animals, there was no similar

beneficial influence of these spice principles. Dietary curcumin, capsaicin and their combination produced beneficial increases in the activity of glutathione peroxidase in hypercholesterolemic rats (Table 5). The enzyme activity was 23, 23 and 18% higher in these diet groups. However, the same spice compounds negatively influenced the activity of glutathione peroxidase in normal rats, the extent of decrease being 15, 20 and 47% in the respective groups. This negative effect was much higher in the spice combination group compared to that of individual spice compounds.

Glutathione transferase activity was much higher as a result of dietary curcumin, capsaicin, and curcumin + capsaicin in normal rats (Table 5). The increase in the enzyme activity was 41, 35 and 32% in the respective groups. The enzyme activity was similarly higher (by 25%) as a result of curcumin feeding in hypercholesterolemic animals. Dietary capsaicin or the spice principles combination had no influence on the enzyme activity in hypercholesterolemic rats. Serum catalase activity was similarly beneficially influenced by dietary curcumin, capsaicin and curcumin + capsaicin in normal rats (Table 5). The increase in catalase activity was 43, 30 and 22% in the respective groups. Catalase activity was similarly higher (by 16%) only in the curcumin-fed group of hypercholesterolemic animals. Dietary capsaicin or the spice principles combination had no influence on this enzyme activity in hypercholesterolemic rats.

#### Antioxidant Enzymes in Liver

Activities of all the hepatic antioxidant enzymes examined here—glutathione reductase, glutathione peroxidase, glutathione transferase and catalase were lower in

**Table 5** Influence of dietary curcumin and capsaicin on serum antioxidant enzymes

Animal group	GSH reductase (mmol/min per ml)	GSH peroxidase (mmol/min per ml)	GSH transferase (mmol/min per dl)	Catalase (mmol/min per dl)
Control	25.4 $\pm$ 0.42	1.130 $\pm$ 0.015	1.970 $\pm$ 0.096	14.75 $\pm$ 1.03
Curcumin	35.9 $\pm$ 1.74*	0.964 $\pm$ 0.015**	2.781 $\pm$ 0.078*	21.13 $\pm$ 1.80*
Capsaicin	46.3 $\pm$ 1.98*	0.905 $\pm$ 0.038**	2.661 $\pm$ 0.212*	19.13 $\pm$ 1.54*
Curcumin + capsaicin	36.5 $\pm$ 1.74*	0.600 $\pm$ 0.070**	2.607 $\pm$ 0.168*	18.00 $\pm$ 0.48*
HCD control	34.6 $\pm$ 3.06	1.246 $\pm$ 0.070	2.126 $\pm$ 0.126	22.25 $\pm$ 0.65
HCD curcumin	33.3 $\pm$ 2.88	1.535 $\pm$ 0.060*	2.649 $\pm$ 0.216*	25.88 $\pm$ 1.04*
HCD capsaicin	32.4 $\pm$ 3.24	1.538 $\pm$ 0.015*	2.084 $\pm$ 0.102	20.38 $\pm$ 1.21
HCD curcumin + capsaicin	33.6 $\pm$ 1.80	1.473 $\pm$ 0.063*	2.126 $\pm$ 0.150	18.75 $\pm$ 1.80

Values are expressed as the mean  $\pm$  SEM of eight rats in each group

HCD high cholesterol diet

\* Significant increase compared to the corresponding control ( $P < 0.05$ ), \*\* significant decrease compared to the corresponding control ( $P < 0.05$ )

hypercholesterolemic animals when compared to their normal counterparts (Table 6). Dietary curcumin, capsaicin and their combination significantly enhanced the activity of glutathione reductase in the liver of normal rats. The increases in this enzyme activity were 28, 24 and 34%, respectively, as a result of feeding curcumin, capsaicin or their combination. Dietary curcumin also enhanced hepatic glutathione reductase activity in hypercholesterolemic animals (by 24%). Hepatic glutathione peroxidase activity was unaffected by dietary spice principles in both normal and hypercholesterolemic animals. Whereas, dietary spice principles had no effect on hepatic glutathione transferase activity in normal rats, the same was increased by curcumin in hypercholesterolemic animals (by 17%). Hepatic catalase activity was unaffected by dietary spice principles in normal rats, which however was negatively influenced in all the three experimental groups of hypercholesterolemic rats (Table 6), the observed decreases being 32, 47 and 50%, respectively, in curcumin, capsaicin and curcumin + capsaicin groups.

## Discussion

In this study, spice compounds were fed to animals at levels corresponding to about ten times the average dietary intake of the corresponding spices among the Indian population [24]. The food intake was essentially similar in various spice principles fed groups and corresponding control group. Similarly, the gain in body weight during the 8-week spice treatment was comparable to corresponding controls [final weight (g) ranged from  $178.1 \pm 5.7$  to  $197.5 \pm 6.6$  in normal rats and from  $190.5 \pm 5.8$  to  $206.4 \pm 6.5$  in hypercholesterolemic animals] indicating

that dietary spices did not negatively affect the feed intake and body weight gain.

This animal study has shown that dietary curcumin, capsaicin and their combination significantly countered hypercholesterolemia brought about by high cholesterol feeding, and the effect was to a similar extent in all the three experimental groups and that the combination of the two spice compounds did not have any additive effect in this respect. The reduction in blood cholesterol brought about by dietary spice principles was mainly in the LDL–VLDL fraction.

Subba Rao et al. have reported lowering of serum and liver cholesterol levels in rats fed curcumin at 0.1–0.5% in the hypercholesterolemic diet, the anti-hypercholesterolemic effect being attended by an increase in the fecal excretion of bile acids and cholesterol [25]. The anti-hypercholesterolemic effect of curcumin has been evidenced at even a 0.05% dietary level and at as early as 4 week feeding [26]. The anti-hypercholesterolemic efficacy of dietary curcumin has been recently demonstrated in rats fed an atherogenic high cholesterol diet, which also resulted in countering the changes in the membrane lipid profile in the erythrocytes [5]. The hypocholesterolemic and hypotriglyceridemic action of dietary curcumin (0.5%) has also been demonstrated in streptozotocin-induced diabetic rats [27].

Reduction in serum cholesterol levels in rats on a normal 10% fat diet incorporated with 1.5, 3 and 15 mg% capsaicin [28], and lowered liver cholesterol in induced hypercholesterolemic rats by dietary 15 mg% capsaicin have been reported [29]. Fecal excretion of cholesterol and bile acids was enhanced in animals fed capsaicin in these studies. In a subchronic toxicity study in rats administered 50 mg/kg per day of capsaicin for 60 days, plasma

**Table 6** Influence of dietary curcumin and capsaicin on liver antioxidant enzymes

Animal group	GSH reductase ( $\mu\text{mol}/\text{min}$ per mg protein)	GSH peroxidase ( $\text{mmol}/\text{min}$ per mg protein)	GSH transferase ( $\text{mmol}/\text{min}$ per mg protein)	Catalase ( $\text{mmol}/\text{min}$ per mg protein)
Control	$29.6 \pm 1.53$	$1.250 \pm 0.075$	$1.025 \pm 0.069$	$11.64 \pm 0.54$
Curcumin	$37.8 \pm 1.10^*$	$1.341 \pm 0.052$	$0.988 \pm 0.047$	$10.32 \pm 0.66$
Capsaicin	$36.6 \pm 1.58^*$	$1.152 \pm 0.052$	$0.910 \pm 0.049$	$10.08 \pm 0.78$
Curcumin + capsaicin	$39.7 \pm 2.84^*$	$1.300 \pm 0.051$	$1.038 \pm 0.043$	$11.82 \pm 0.48$
HCD control	$22.5 \pm 2.46$	$1.061 \pm 0.088$	$0.693 \pm 0.020$	$8.10 \pm 0.42$
HCD curcumin	$28.0 \pm 2.28^*$	$0.953 \pm 0.050$	$0.809 \pm 0.033^*$	$5.52 \pm 0.60^{**}$
HCD capsaicin	$22.8 \pm 1.20$	$0.976 \pm 0.019$	$0.746 \pm 0.028$	$4.32 \pm 0.48^{**}$
HCD curcumin + capsaicin	$19.2 \pm 1.55$	$0.937 \pm 0.018$	$0.730 \pm 0.043$	$4.08 \pm 0.78^{**}$

Values are expressed as the mean  $\pm$  SEM of eight rats in each group

HCD high cholesterol diet

\* Significant increase compared to corresponding control ( $P < 0.05$ ), \*\* significant decrease compared to corresponding control ( $P < 0.05$ )

cholesterol levels were significantly reduced along with triglycerides and phospholipids [30]. Negulesco et al. [31] have observed that administration of 8 mg capsaicin/day for 35 days to rabbits on a 0.5% cholesterol diet produced a beneficial lowering of plasma cholesterol and triglycerides. Young turkeys on a 2–3 mg capsaicin/kg feed for 9 days along with 0.5% cholesterol had lower total serum cholesterol than controls [32]. Recently, the anti-hypercholesterolemic efficacy of dietary capsaicin has been shown in rats fed an atherogenic high cholesterol diet which resulted in countering of the changes in the membrane lipid profile in the erythrocytes [5].

Hepatic cholesterol concentration was significantly lowered in the present investigation as a result of dietary spice principles in normal rats, while the same was not influenced in hypercholesterolemic animals. Liver triglyceride levels were significantly lowered in both normal and hypercholesterolemic rats maintained on a capsaicin diet. Thus, no particular additive effect is seen when the two spice compounds—curcumin and capsaicin were given in combination with regard to blood and the liver lipid profile.

Among the various antioxidant molecules in serum, ascorbic acid and  $\alpha$ -tocopherol concentrations were significantly affected in hypercholesterolemic animals by dietary spice principles but not in normal rats. Serum ascorbic acid level was significantly enhanced by dietary spices in hypercholesterolemic animals while  $\alpha$ -tocopherol concentration was significantly lowered. The effect of curcumin on serum ascorbic acid was higher than that produced by capsaicin, and there was no additive effect in the case of their combination. Serum  $\alpha$ -tocopherol was about three times higher in the hypercholesterolemic animals, and this could probably explain the control of oxidative stress in the hypercholesterolemic situation where the lipid peroxide level in blood was essentially the same as found in normal animals.

Blood lipid peroxide content was lower in the hypercholesterolemic rats as a result of feeding curcumin, capsaicin or their combination; the lowering of blood lipid peroxides was cumulative when curcumin and capsaicin were fed in combination. The increase in blood ascorbic acid concentration in these three diet groups may have contributed to the observed reduced lipid peroxide level. Hepatic antioxidants—thiols, glutathione and ascorbic acid were elevated in hypercholesterolemic rats with concurrent low titres of lipid peroxides. All the three dietary spice principle groups brought about further depletion in hepatic lipid peroxides. Ascorbic acid concentration in liver was favourably influenced by dietary curcumin, capsaicin and their combination in normal rats while the increase in ascorbic acid was countered by dietary spice principles in hypercholesterolemic rats. With respect to hepatic glutathione content, only the combination of curcumin and

capsaicin produced an enhancing effect in hypercholesterolemic animals. Similarly, the combination of curcumin and capsaicin produced an effect higher than the two individual compounds in increasing the total thiol content in liver of normal rats.

There are several reports on the antioxidant effects of curcumin and capsaicin with regard to the modulation of lipid peroxide level and antioxidant status. Curcumin has been reported to exert a protective effect against nicotine-induced lung toxicity by modulating the extent of lipid peroxidation and augmenting the antioxidant defense system [33]. The enhanced circulatory lipid peroxides in nicotine-treated rats which was accompanied by a significant decrease in the levels of ascorbic acid, vitamin E, reduced glutathione, glutathione peroxidase, superoxide dismutase, and catalase was significantly countered by the administration of curcumin (80 mg/kg given simultaneously for 22 weeks) which significantly lowered the lipid peroxidation and enhanced the antioxidant status. Dietary supplementation of curcumin (2%) to mice for 30 days has been reported to have significantly increased the activities of glutathione peroxidase, glutathione reductase and catalase in liver [34]. Curcumin has been reported to have a protective role in alcohol and  $\delta$ -PUFA induced oxidative stress in Wistar rats [35]. The liver TBARS and antioxidants such as ascorbic acid,  $\alpha$ -tocopherol, reduced glutathione, and antioxidant enzymes were altered significantly in alcohol and  $\delta$ -PUFA groups, while administration of curcumin abrogated this effect by effectively modulating the antioxidant status. In vivo antioxidative effects of curcumin have been reported in trichloroethylene-induced oxidative stress in mouse liver [36]. Increases in the contents of peroxisome and TBARS and decreases in glutathione content of mouse liver by the trichloroethylene administration were suppressed by the pre-administration of curcumin. Iron-induced liver lipid peroxidation was 29% lower in turmeric-fed (1% in diet) Wistar rats [37]. The activities of antioxidant enzymes were higher in liver homogenates of rats fed the turmeric-containing diet in comparison with the controls, suggesting that dietary turmeric lowers lipid peroxidation by enhancing the activities of antioxidant enzymes. Wistar rats administered capsaicin (3 mg/kg) for three consecutive days showed a reduction in oxidative stress in the liver and other tissues suggesting that capsaicin can be a potent antioxidant [38].

In the present study, activities of glutathione reductase, glutathione transferase and catalase in the serum were significantly enhanced by dietary curcumin, capsaicin and curcumin + capsaicin in normal rats. Dietary curcumin, capsaicin and their combination produced beneficial increases in the activity of glutathione peroxidase in hypercholesterolemic rats. Glutathione transferase and catalase activities were higher as a result of curcumin

feeding in hypercholesterolemic animals. Dietary curcumin, capsaicin and their combination significantly enhanced the activity of glutathione reductase in the liver of normal rats. Dietary curcumin also enhanced hepatic glutathione reductase and glutathione transferase activities in hypercholesterolemic animals.

Activities of hepatic antioxidant enzymes—glutathione transferase, glutathione reductase and catalase were significantly depleted under hypercholesterolemia. Cholesterol feeding has been reported to decrease the level of TBARS, SOD and catalase [39]. The decrease in hepatic glutathione transferase activity in rats fed high cholesterol diet suggests a deficiency in defense against electrophilic compounds. Dietary spice principles were effective in reducing the oxidant stress, which was indicated by one or more of the following: (1) enhancing one or more of antioxidant molecules in the circulation, (2) enhancing one or more antioxidant molecules in the liver, (3) increasing the activities of antioxidant enzymes in blood, or (4) countering the depleted hepatic antioxidant enzymes—glutathione reductase, glutathione-*S*-transferase and catalase. Induction of glutathione transferase activity by curcumin has been reported in mice and rats [40, 41]. Similar to the observation in the current study, cholesterol feeding has been reported to decrease liver glutathione peroxidase in rats but controversial results exist in studies involving lipid peroxidation [42].

Dietary curcumin and capsaicin or their combination in the present study have demonstrated a significant stimulation of hepatic glutathione reductase activity in normal rats, while curcumin had a similar effect even in hypercholesterolemic animals. Earlier studies showed that curcumin causes an increase in glutathione transferase activity in rodent liver which may contribute to its anti-cancer and anti-inflammatory activities [43]. Glutathione peroxidase activity towards cumene hydroperoxide in liver homogenate was also found to be increased in a dose-dependent manner by curcumin. Induction of enzymes (glutathione transferase and glutathione peroxidase) involved in the detoxification of the electrophilic products of lipid peroxidation may contribute to the anti-inflammatory and anti-cancer activities of curcumin.

Thus, the present study has shown the absence of any additive effect of the combination of two hypocholesterolemic spice compounds—curcumin and capsaicin on blood cholesterol in experimentally induced hypercholesterolemic rats. The dietary spice compounds were effective in reducing the oxidant stress, which was indicated by countering of the changes in antioxidant molecules and activity of antioxidant enzymes in blood and liver. Although generally the beneficial effect of dietary curcumin and capsaicin was not additive when given in combination with respect to their hypolipidemic influence or antioxidant effect in hypercholesterolemic situation, the effect of the

combination of curcumin and capsaicin was certainly more pronounced than their individual effects in a few instances. We have also recently observed that the combination of dietary curcumin and capsaicin produced a higher protective effect on LDL oxidation and also lowered carrageenan-induced paw inflammation more effectively than their individual influences [7].

**Acknowledgments** H. Manjunatha is grateful to Council of Scientific and Industrial Research, New Delhi for the award of research fellowship.

## References

1. Srinivasan K (2005) Role of spices beyond food flavouring: nutraceuticals with multiple health effects. *Food Rev Int* 21:167–188
2. Srinivasan K, Sambaiah K, Chandrasekhara N (2004) Spices as beneficial hypolipidemic food adjuncts: a review. *Food Rev Int* 20:187–220
3. Joe B, Vijayakumar M, Lokesh BR (2004) Biological properties of curcumin: cellular and molecular mechanisms of action. *Crit Rev Food Sci Nutr* 44:97–111
4. Govindarajan VS, Satyanarayana MN (1991) Capsicum—production, technology, chemistry, & quality. Part-V: impact on physiology, pharmacology, nutrition, and metabolism; structure, pungency, pain and desensitization sequences. *Crit Rev Food Sci Nutr* 29:435–474
5. Kempaiah RK, Srinivasan K (2002) Integrity of erythrocytes of hypercholesterolemic rats during spices treatment. *Mol Cell Biochem* 236:155–161
6. Kempaiah RK, Srinivasan K (2005) Influence of dietary spices on the fluidity of erythrocytes in hypercholesterolemic rats. *Br J Nutr* 93:81–91
7. Manjunatha H, Srinivasan K (2006) Protective effect of curcumin, capsaicin and their combination on induced oxidation of low-density lipoprotein, iron-induced hepatotoxicity and carrageenan-induced inflammation in experimental rats. *FEBS J* 273:4528–4537
8. Folch J, Lees M, Sloane-Stanley GH (1957) A simple method for the isolation and purification of total lipids from animal tissues. *J Biol Chem* 226:497–509
9. Searcy RL, Bergquist LM (1960) A new color reaction for the quantitation of serum cholesterol. *Clin Chim Acta* 5:192–197
10. Fletcher MJ (1968) A colorimetric method for estimating serum triglycerides. *Clin Chim Acta* 22:393–397
11. Charles J, Stewart M (1980) Colorimetric determination of phospholipids with ammonium ferrioxalate. *Anal Biochem* 104:10–14
12. Warnick GR, Albers JJ (1978) A comprehensive evaluation of heparin-manganese procedure for estimating HDL-cholesterol. *J Lipid Res* 19:65–76
13. Yagi K (1984) Assay of lipid peroxides in blood plasma or serum. *Methods Enzymol* 105:328–331
14. Ohkawa H, Ohishi N, Yagi K (1979) Assay for lipid peroxides in animal tissue by thiobarbituric acid reaction. *Anal Biochem* 95:351–358
15. Sedlock J, Lindsay RH (1968) Estimation of total, protein bound and nonprotein sulfhydryl groups in tissues with Ellman's reagent. *Anal Biochem* 25:192–205
16. Beutler E, Duron O, Kelly BM (1963) Improved method for the determination of blood glutathione. *J Lab Clin Med* 61:882–888

17. Omaye ST, Turnbull JD, Sauberlich HE (1973) Selected methods for the determination of ascorbic acid in animal cells, tissues and fluids. *Methods Enzymol* 62:3–11
18. Zaspel BJ, Csallany AS (1983) Determination of  $\alpha$ -tocopherol in tissues and plasma by HPLC. *Anal Biochem* 130:146–150
19. Carlberg I, Mannervik B (1985) Glutathione reductase. *Methods Enzymol* 113:484–490
20. Warholm M, Guthenberg C, Bahr CV, Mannervik B (1985) Glutathione transferase from human liver. *Methods Enzymol* 113:499–504
21. Flohe L, Gunzler WA (1984) Assays of glutathione peroxidase. *Methods Enzymol* 105:114–121
22. Aebi H (1984) Catalase in vitro. *Methods Enzymol* 105:121–126
23. Dowdy S, Wearden S (1983) *Statistics for research*. Wiley, New York
24. Thimmayamma BVS, Rao P, Radhaiah G (1983) Use of spices and condiments in the dietaries of urban and rural families. *Indian J Nutr Diet* 20:153–162
25. SubbaRao D, Chandrasekhara N, Satyanarayana MN, Srinivasan M (1970) Effect of curcumin on serum and liver cholesterol levels in the rat. *J Nutr* 100:1307–1316
26. Patil TN, Srinivasan M (1971) Hypocholesterolemic effect of curcumin in induced hyper-cholesterolemic rats. *Indian J Exp Biol* 9:167–169
27. Babu PS, Srinivasan K (1997) Hypolipidemic action of curcumin, coloring principle of turmeric (*Curcuma longa*) in streptozotocin induced diabetic rats. *Mol Cell Biochem* 166:169–175
28. Sambaiah K, Satyanarayana MN, Rao MVL (1978) Effect of red pepper (chilli) and capsaicin on fat absorption and liver fat in rats. *Nutr Rep Int* 18:521–529
29. Sambaiah K, Satyanarayana MN (1980) Hypocholesterolemic effect of red pepper and capsaicin. *Indian J Exp Biol* 18:898–899
30. Monsereenusorn S (1983) Subchronic toxicity studies of capsaicin and capsicum in rats. *Res Commun Chem Pathol Pharmacol* 41:95–100
31. Negulesco JA, Noel SA, Newman HA, Naber EC, Bhat HB, Witiak DT (1987) Effect of pure capsaicinoids (capsaicin and dihydrocapsaicin) on plasma lipids and lipoprotein concentrations of turme y pou lts. *Atherosclerosis* 64:85–90
32. Ki P, Negulesco JA, Murnane M (1982) Decreased total serum myocardial and aortic cholesterol levels following capsaicin treatment. *IRCS Med Sci* 10:446–447
33. Kalpana C, Menon VP (2004) Modulatory effects of curcumin on lipid peroxidation and antioxidant status during nicotine-induced toxicity. *Pol J Pharmacol* 56:581–586
34. Iqbal M, Sharma SD, Okazaki Y, Fujisawa M, Okada S (2003) Dietary supplementation of curcumin enhances antioxidant and phase II metabolizing enzymes in ddY male mice: possible role in protection against chemical carcinogenesis and toxicity. *Pharmacol Toxicol* 92:33–38
35. Rickman R, Aruna K, Varma PS, Rajasekaran KN, Menon VP (2004) Comparative effects of curcumin and an analog of curcumin on alcohol and PUFA induced oxidative stress. *J Pharm Pharm Sci* 7:274–283
36. Watanabe S, Fukui T (2000) Suppressive effect of curcumin on trichloroethylene-induced oxidative stress. *J Nutr Sci Vitaminol* 46:230–234
37. Reddy AC, Lokesh BR (1994) Effect of dietary turmeric (*Curcuma longa*) on iron-induced lipid peroxidation in the rat liver. *Food Chem Toxicol* 32:279–283
38. Lee CY, Kim M, Yoon SW, Lee CH (2003) Short-term control of capsaicin on blood and oxidative stress of rats in vivo. *Phytother Res* 17:454–458
39. Lu YF, Chiang CF (2001) Effect of dietary cholesterol and fat levels on lipid peroxidation and the activities of the antioxidant enzymes in rats. *Int J Vitam Nutr Res* 71:339–346
40. Susan M, Rao MNA (1992) Induction of glutathione-S-transferase activity by curcumin in mice. *Arz Forsch Drug Res* 42:962–963
41. Yokota H, Hashimoto H, Motoya M, Yuosa A (1988) Enhancement of UDP-glucuronyl transferase, UDP-glucuronyl dehydrogenase and GSH-transferase activity in rat liver by dietary administration of eugenol. *Biochem Pharmacol* 37:799–802
42. Mahfouz MM, Kummrow FA (2000) Cholesterol rich diets have different effects on lipid peroxidation, cholesterol oxides and antioxidant enzymes in rats and rabbits. *J Nutr Biochem* 11:293–302
43. Piper JT, Singhal SS, Salameh MS, Torman RT, Awasthi YC, Awasthi S (1998) Mechanisms of anticarcinogenic properties of curcumin: the effect of curcumin on glutathione linked detoxification enzymes in rat liver. *Int J Biochem Cell Biol* 30:445–456

adaptations induced by hormonal changes and the production of inflammatory cytokines to fight the infection and/or facilitate tissue repair. The acute phase response is characterized by the hepatic synthesis of several acute phase proteins but also by profound alterations in plasma lipid and lipoprotein metabolism [1–3]. In man, plasma concentration of total cholesterol (TC), LDL-cholesterol and HDL-cholesterol decreases within the first 48 h following infectious or non-infectious insults with variable changes in plasma triglyceride (TG) levels [4, 5]. The extent of alterations in the concentration of plasma lipids notably depends on the type and severity of the insult [4]. The reduction of cholesterol-rich lipoproteins may result from reduced secretion, increased catabolism and from increased sequestration of lipoproteins in extra-vascular compartments. A negative correlation has been reported between TC as well as HDL-cholesterol levels and clinical outcome in critically ill and septic patients [4, 6, 7].

The composition of plasma lipoproteins has been mainly studied in conditions of sepsis with severe inflammation and substantial changes have been documented in LDL and HDL [8–11]. Alterations in lipoprotein lipid and apolipoprotein composition may enhance pro-inflammatory and pro-atherogenic properties of LDL and convert HDL from anti- into pro-inflammatory particles with reduced antioxidant functions [9, 12].

Major surgical injury also induces a severe acute phase response with postoperative decreases of plasma (as well as LDL and HDL) cholesterol concentration as reported after cardiac surgery [5, 7, 13, 14]. In contrast to sepsis, which is a very heterogeneous condition, cardiac surgery with cardiopulmonary bypass follows strict routine procedures and represents a fairly standardized insult. In addition to surgical trauma, contact of blood cells and plasma components with artificial membranes of the extracorporeal circuit, and ischemia–reperfusion are responsible for the severe systemic inflammation observed after cardiac surgery with cardiopulmonary bypass [15–17]. Since the composition of plasma lipoproteins has not been investigated in depth after surgery, we questioned whether the acute phase response induced by major cardiac surgery would affect plasma LDL and HDL composition differently as compared to previous observations in severely septic patients. Further, since such operations are associated to substantial oxidative stress and reduced plasma levels of vitamin E (alpha-tocopherol) [18], lipoprotein fractions were also used to determine whether decreased levels of vitamin E are due to a decreased number of lipoprotein carriers or to a reduced content of alpha-tocopherol. Improved knowledge on compositional changes occurring in plasma LDL and HDL after surgery may be important to better define strategies preventing pro-inflammatory changes.

## Materials and Methods

### Study Group Selection

The study group included 21 ASA 3 (American Society of Anesthesiologists class 3) patients undergoing elective cardiac surgery (coronary artery bypass or mitral valve replacement) with cardiopulmonary bypass. Clinical characteristics of the patients are shown in Table 1.

Major exclusion criteria were: patients on steroids or with body mass index  $>30 \text{ kg/m}^2$ , plasma creatinine concentration  $>1.5 \text{ mg/dl}$ , altered liver function tests, or diabetes mellitus. None of the patients received corticosteroids in the perioperative period. Patients were not on statin treatment before surgery, except for three of them in whose statins were not reinitiated during the immediate postoperative period of the study protocol. The patients were allowed nothing per os from the evening before the operation until day 1 post-surgery. The study was approved by the Ethical Committee of Erasme Hospital (Université Libre de Bruxelles, Brussels, Belgium) and all participating patients received complete information and signed a written consent form.

### Anesthesia and Cardiopulmonary Bypass

Anesthesia was induced and maintained with a target-controlled infusion of remifentanyl and propofol with cisatracurium. All patients received a full-dose of aprotinin ( $2 \times 10^6 \text{ KIU}$  at induction, followed by  $5 \times 10^5 \text{ KIU/h}$  until the end of surgery and  $1 \times 10^6 \text{ KIU}$  in the cardiopulmonary bypass). Cardiopulmonary bypass was performed under mild systemic hypothermia ( $>35^\circ\text{C}$ ). After cross-clamping of the ascending aorta, antegrade cold hyperkalemic cardioplegia was induced, followed by intermittent retrograde cold hyperkalemic cardioplegia whenever necessary. Mean aortic cross-clamp and cardiopulmonary bypass time as well as data on blood transfusion are shown in Table 1.

### Study Protocol

In order to ensure that measurements of lipoprotein composition are made during the acute phase response (and the resulting changes in plasma lipids), measurements of inflammatory proteins, of selected apolipoproteins, and of plasma lipid parameters were performed before surgery and on postoperative day 2 in the first six patients. Assessment of antioxidant status, of vitamin E and of PON was also performed in these patients. In addition, alpha-tocopherol content was analyzed in platelets, white blood

**Table 1** Patients clinical characteristics

Variable	Patients ( <i>n</i> = 21)
Mean age (range)	69 ± 3 (42–83)
Gender (M:F)	19:2
CABG:mitral valve replacement	15:6
CPB (min)	108 ± 5
Aortic clamping (min)	83 ± 4
Patients requiring blood products	8
Number of patients transfused PRBC (mean units of PRBC transfused)	6 (3 ± 1)
Number of patients transfused FFP (mean units FFP transfused)	5 (4 ± 1)
Number of patients transfused platelets (mean units platelets transfused)	3 (2 ± 1)

CABG Coronary artery bypass graft, CPB cardiopulmonary bypass, PRBC packed red blood cells, FFP fresh frozen plasma

cells and red blood cells isolated from fresh blood samples [19]. In the 15 following patients, plasma lipoprotein fractions were isolated and analysed, before surgery and on postoperative day 2, for their content in lipid components, apolipoproteins, alpha-tocopherol as well as hydroperoxides. Preoperative concentrations of the different biological variables did not significantly differ from values recently measured in a control population from the same region of comparable age and gender with no known coronary heart disease [20, 21].

### Blood Sampling

Blood samples were drawn at the time of anesthesia induction (baseline) and again on day 2 post-surgery. Blood was collected in tubes with EDTA (1 mg/mL) for plasma separation and without EDTA for serum separation. Plasma and serum were immediately separated by low speed centrifugation at 3,500g (4 °C; 15 min) in a J2.21 centrifuge (Beckman Instruments, Fullerton, CA, USA).

### Separation of Lipoproteins

Plasma LDL and HDL fractions were isolated by sequential ultracentrifugation [22] in a L8–55 ultracentrifuge using a 50–4Ti rotor (Beckman, Palo Alto, CA, USA). Plasma density was adjusted by addition of solid KBr at density ranges 1.019–1.063 g/ml and 1.063–1.210 g/ml for separation of LDL and HDL, respectively. Plasma was centrifuged at 227,000g (5 °C) during 20 h for LDL and 40 h for HDL. LDL and HDL fractions were then either kept at 4°C for immediate lipid and protein measurements or at –70 °C for vitamin E analysis performed within

2 weeks. EDTA and salts present in the LDL and HDL fractions were removed by filtration on PD10 Sephadex columns (Amersham Pharmacia, Uppsala, Sweden) prior to hydroperoxide measurements by the FOX-2 method [23] or to evaluation of LDL resistance to *ex vivo* oxidation according to Esterbauer et al. [24].

### Analytical Measurements

TC and TG were measured in plasma, LDL and HDL fractions using enzymatic kits CHOD-PAP (Roche Diagnostics GmbH, Mannheim, Germany) and Triglycerides Glycerol blanked (Roche Diagnostics GmbH), respectively. Free Cholesterol (FC) and phospholipid concentrations were determined using enzymatic kits CHOD-PAP (Sopachem, Brussels, Belgium) and PAP 150 (Biomérieux, Lyon, France), respectively. Cholesteryl ester (CE) concentration was calculated by subtracting FC from TC.

Alpha-tocopherol was analysed in plasma and lipoprotein fractions by reverse-phase HPLC (Merck-Hitachi Ltd, Tokyo, Japan) using a Lichrospher column 100 RP 18 (5 µm; 125 × 4 mm, L × ID) with a mobile phase of methanol:water (95/5, w/w) at a flow rate of 1.5 ml/min; alpha-tocopherol was monitored by a UV detector at 292 nm [25]. In cells, alpha-tocopherol concentration was expressed relative to cell phospholipid content.

Plasma total antioxidant status (TAOS) was determined by the capacity to inhibit the peroxidase-mediated formation of the ATBS (2,2'-azinobis-3-ethylbenzothiazoline-6-sulfonic acid) radical [26]. In parallel, paraoxonase (PON) activity was determined spectrophotometrically at 270 nm by measuring the hydrolysis of phenyl acetate [27].

Total protein concentration was determined in plasma fractions using bovine serum/globulin solution as standard [28]. Apolipoproteins (apo) B and A1, as well as serum amyloid A (SAA) were measured in plasma and lipoprotein fractions by ELISA using rabbit polyclonal antibodies for apo A1, B or SAA, respectively [29].

CRP level was determined in plasma using high sensitive CRP immuno-turbidimetric method [30].

### Calculation of LDL and HDL Particle Size

Assuming a spherical configuration, LDL and HDL radii were determined by calculating both particle core volume and surface area. Calculations of core volume were based on the molar content of CE and TG per particle; values of 1.068 and 1.556 nm<sup>3</sup> were used for the molecular volume of CE and TG, respectively [31]. Total particle radius was obtained by adding surface monolayer thickness (2.02 nm) to core radius [32]. Calculations of surface area were based



on the molar content of phospholipids and FC per particle; values of 0.310 and 0.685 nm<sup>2</sup> were used for the molecular surface area of phospholipids and FC, respectively [31].

### Statistical Analysis

All results are expressed as mean values  $\pm$  SEM. Statistical significance of differences between pre- and postoperative values was assessed by the paired Student's *t*-test.

## Results

### Measurements of Selected Plasma Proteins, Apolipoproteins, Lipids and Antioxidants

Pre- and postoperative measurements of plasma parameters in the first six subjects are shown in Table 2 (statistical significance of tabulated results refers to the paired difference in pre- and postoperative absolute values, whilst in the text it often refers to the paired difference in percent changes relative to preoperative baseline values). Total protein concentration decreased by 15.7  $\pm$  3.4% on postoperative day 2 ( $P < 0.025$ ). In contrast, CRP concentration increased from 0.41  $\pm$  0.18 mg/dl (preoperative) to 13.90  $\pm$  3.90 mg/dl ( $P < 0.005$ ) and SAA concentration from 0.22  $\pm$  0.06 to 25.40  $\pm$  5.77 mg/dl ( $P < 0.005$ ) on postoperative day 2. Plasma concentration of apoB and apoA1 decreased by, respectively, 41.3  $\pm$  6.0% ( $P < 0.01$ ) and 31.2  $\pm$  1.1% ( $P < 0.0001$ ) post-surgery. This decrease of plasma apoB and apoA1 was

**Table 2** Plasma concentration of selected proteins, apolipoproteins, lipids and antioxidant measurements

Biological variables	Preoperative (n = 6)	Postoperative (n = 6)
Protein (g/l)	67.3 $\pm$ 2.0	56.0 $\pm$ 2.5 <sup>a</sup>
CRP (mg/dl)	0.41 $\pm$ 0.18	13.90 $\pm$ 3.90 <sup>c</sup>
SAA (mg/dl)	0.22 $\pm$ 0.06	25.40 $\pm$ 5.77 <sup>c</sup>
ApoB (mg/dl)	94.8 $\pm$ 17.3	54.5 $\pm$ 10.1 <sup>a</sup>
ApoA1 (mg/dl)	183.8 $\pm$ 14.8	126.4 $\pm$ 10.0 <sup>d</sup>
TC (mmol/l)	5.17 $\pm$ 0.43	3.31 $\pm$ 0.31 <sup>b</sup>
TG (mmol/l)	1.42 $\pm$ 0.34	0.97 $\pm$ 0.17
$\alpha$ -Tocopherol ( $\mu$ mol/l)	33.76 $\pm$ 3.43	22.30 $\pm$ 3.44 <sup>b</sup>
PON ( $\mu$ mol/min ml)	84.5 $\pm$ 7.3	66.8 $\pm$ 7.6 <sup>c</sup>
TAOS (%)	19.0 $\pm$ 3.9	3.2 $\pm$ 2.8 <sup>a</sup>

CRP C-reactive protein, SAA serum amyloid A, apoB apolipoprotein B, apoA1 apolipoprotein A1, TC total cholesterol, TG triglycerides, PON paraoxonase, TAOS total antioxidant status

Values are expressed as mean  $\pm$  SEM. *P* values were calculated by paired Student *t* test. <sup>a</sup> $P < 0.05$ , <sup>b</sup> $P < 0.01$ , <sup>c</sup> $P < 0.005$ , <sup>d</sup> $P < 0.001$ , <sup>e</sup> $P < 0.0001$  versus preoperative value

more marked than that of total plasma proteins. Indeed, apoB/total protein ratio decreased by 30.6  $\pm$  6.6% ( $P < 0.01$ ) on postoperative day 2 [from 14.5  $\pm$  2.8 to 9.8  $\pm$  1.7 mg/g ( $P < 0.05$ )]. Similarly, apoA1/total protein ratio decreased by 17.8  $\pm$  3.2% ( $P < 0.005$ ) post-surgery [from 28.0  $\pm$  2.7 to 22.9  $\pm$  2.2 mg/g ( $P < 0.05$ )].

Plasma concentration of TC and TG decreased by, respectively, 35.5  $\pm$  4.3% ( $P < 0.001$ ) and 23.7  $\pm$  9.5% ( $P < 0.06$ ) from initial values. Plasma alpha-tocopherol concentration decreased by 34.9  $\pm$  5.6% postoperatively ( $P < 0.005$ ). Of interest, alpha-tocopherol/TC ratio was not significantly modified after surgery ( $P > 0.25$ ). Postoperative alpha-tocopherol content in red blood cells and platelets (expressed in relation to phospholipid content) remained unchanged on postoperative day 2 ( $P > 0.4$ ). However, alpha-tocopherol content in white blood cells, (also expressed relative to phospholipid content), decreased by 20.5  $\pm$  6.1% ( $P < 0.03$ ) on postoperative day 2 (Table 3).

A dramatic fall in plasma TAOS was observed postoperatively, from 19.0  $\pm$  3.9 to 3.2  $\pm$  2.8% ( $P < 0.01$ ). Similarly, serum PON activity was decreased by 21.7  $\pm$  2.4% ( $P < 0.0001$ ) after surgery.

### Measurements of LDL and HDL Parameters

In 15 other subjects, plasma CRP concentrations increased from 0.41  $\pm$  0.14 mg/dl (preoperative) to a postoperative value of 12.04  $\pm$  1.95 mg/dl ( $P < 0.001$ ), these changes being comparable to those found in the first six patients ( $P > 0.6$ ). Results of pre- and postoperative measurements of LDL and HDL parameters are given in Tables 4 and 5.

### Apolipoproteins

LDL apoB concentration was decreased by 45.5  $\pm$  5.7% ( $P < 0.0001$ ) on postoperative day 2. This reflects a substantial reduction in the number of circulating LDL particles after cardiac surgery.

Likewise, HDL apoA1 concentration decreased by 21.8  $\pm$  6.5% ( $P < 0.005$ ) on postoperative day 2. This may

**Table 3** Alpha-tocopherol content in blood cells ( $\mu$ mol/mmol PL)

Biological variables	Preoperative (n = 5)	Postoperative (n = 5)
Red blood cells	8.03 $\pm$ 0.91	8.22 $\pm$ 1.06
White blood cells	17.27 $\pm$ 1.89	13.50 $\pm$ 1.45 <sup>a</sup>
Platelets	17.04 $\pm$ 2.20	16.39 $\pm$ 1.75

Values are expressed as mean  $\pm$  SEM. *P* values were calculated by paired Student *t* test. <sup>a</sup> $P < 0.03$  versus preoperative value

PL Phospholipids

**Table 4** LDL and HDL absolute values

Biological variables	Preoperative (n = 15)	Postoperative (n = 15)
LDL-apoB (mg/dl)	71.5 ± 9.5	43.2 ± 8.7 <sup>c</sup>
HDL-apoAI (mg/dl)	142.4 ± 12.3	108.5 ± 11.2 <sup>c</sup>
HDL-apoSAA (mg/dl)	0.5 ± 0.2	39.2 ± 17.2 <sup>a</sup>
LDL-TC (mmol/l)	2.67 ± 0.15	1.52 ± 0.17 <sup>e</sup>
LDL-CE (mmol/l)	1.98 ± 0.11	1.09 ± 0.13 <sup>e</sup>
LDL-FC (mmol/l)	0.69 ± 0.04	0.43 ± 0.04 <sup>e</sup>
HDL-TC (mmol/l)	0.97 ± 0.10	0.79 ± 0.07 <sup>b</sup>
HDL-CE (mmol/l)	0.78 ± 0.08	0.60 ± 0.05 <sup>c</sup>
HDL-FC (mmol/l)	0.19 ± 0.02	0.19 ± 0.02
LDL-TG (mmol/l)	0.20 ± 0.02	0.19 ± 0.02
HDL-TG (mmol/l)	0.08 ± 0.01	0.07 ± 0.01
LDL-PL (mmol/l)	0.80 ± 0.04	0.50 ± 0.05 <sup>e</sup>
HDL-PL (mmol/l)	0.77 ± 0.06	0.73 ± 0.05
LDL-hydroperoxides (μmol/l)	14.1 ± 4.3	15.5 ± 4.4
HDL-hydroperoxides (μmol/l)	10.5 ± 2.0	13.8 ± 4.6
LDL-α-tocopherol (μmol/l)	11.3 ± 0.7	6.6 ± 0.6 <sup>e</sup>
HDL-α-tocopherol (μmol/l)	8.3 ± 1.0	6.3 ± 0.6 <sup>d</sup>

Values are expressed as mean ± SEM. *P* values were calculated by the paired Student *t* test. <sup>a</sup>*P* < 0.05, <sup>b</sup>*P* < 0.01, <sup>c</sup>*P* < 0.005, <sup>d</sup>*P* < 0.001, <sup>e</sup>*P* < 0.0001 versus preoperative value

*apoB* Apolipoprotein B, *apoAI* apolipoprotein A1, *TC* total cholesterol, *FC* free cholesterol, *TG* triglycerides, *PL* phospholipids

correspond to a decrease in the number of HDL particles if an unchanged mean number of apoA1 molecules per HDL particle is assumed. The HDL apoSAA concentration increased markedly post-surgery, from 0.5 ± 0.2 to 39.2 ± 17.2 mg/dl (*P* < 0.05).

### Cholesterol

CE concentration in the LDL fraction decreased from 1.98 ± 0.11 to 1.09 ± 0.13 mmol/l (*P* < 0.0001), corresponding to a decrease of 45.9 ± 4.4% (*P* < 0.0001) from initial values. This fall in LDL-CE was comparable to the decrease in LDL-apoB. FC concentration in the LDL fraction decreased by 38.1 ± 4.5% (*P* < 0.0001) on postoperative day 2. The FC/CE and FC/apoB molar ratios in LDL increased by, respectively, 16.9 ± 4.4% (*P* < 0.002) and 21.6 ± 9.5% (*P* < 0.05) after cardiac surgery.

Comparable postoperative changes of CE and FC content were observed in the HDL fraction. HDL-CE decreased from 0.78 ± 0.08 to 0.60 ± 0.05 mmol/l (*P* < 0.005), i.e., by 18.9 ± 6.6% (*P* < 0.02) from preoperative values. In contrast, FC concentration in the HDL fraction remained unchanged after surgery (*P* > 0.8). Thus, the FC/CE ratio in the HDL fraction increased by 36.3 ± 8.3% (*P* < 0.001) post-surgery. HDL CE/apoA1

ratio was not significantly modified post-surgery (*P* > 0.31), while FC/apoA1 increased by 42.9 ± 7.1% compared to preoperative values (*P* < 0.0001).

### Triglycerides

In sharp contrast to cholesterol, TG concentration in the LDL fraction remained unchanged post-surgery (*P* > 0.6). Hence, the TG/CE ratio in LDL increased by 101.5 ± 18.9% (*P* < 0.0001) on postoperative day 2. Similarly, TG/apoB ratio in LDL increased by 112.9 ± 26.2% (*P* < 0.001) after surgery.

Likewise, TG concentration in the HDL fraction was not significantly modified after surgery (*P* > 0.5). TG/CE and TG/apoA1 ratios in the HDL fraction, however, increased by 31.3 ± 16.9% (*P* = 0.08) and 34.3 ± 15.2% (*P* < 0.05), respectively. Thus, TG content relative to either CE or apoA1 tended to be or increased in HDL but to a lesser extent than in LDL fraction.

### Phospholipids

Phospholipid concentration in the LDL fraction decreased by 37.6 ± 4.5% (*P* < 0.0001) on postoperative day 2. In contrast, phospholipid/apoB ratio in LDL increased by 22.5 ± 8.6% (*P* < 0.025) post-surgery.

Phospholipid concentration in the HDL fraction was not significantly modified after surgery (*P* > 0.9). Hence, phospholipid/apoA1 ratio increased by 30.2 ± 6.1% (*P* < 0.001) on postoperative day 2 compared to preoperative values.

In fair agreement with current knowledge [32], FC/phospholipid molar ratio was, before surgery, about four times higher in LDL (0.86 ± 0.02 mmol/mmol) than in HDL (0.23 ± 0.01 mmol/mmol). This ratio was unaffected by surgery in LDL but increased by 17.6 ± 7.4% (*P* < 0.05) in HDL.

### Calculation of LDL and HDL Particle Size

Before surgery, LDL particle radius calculated from the sum of core lipid molecule volumes averaged 9.98 ± 0.29 nm, in fair agreement with current knowledge [32] and also with LDL radius calculation from surface area molecules (including one apoB molecule), which averaged 9.60 ± 0.34 nm. After surgery, unchanged CE and increased TG content (+113%) per LDL particle imply an increase in the size of LDL particles. Consistently, FC/apoB and phospholipid/apoB ratios increased by 21.6 ± 9.5 and 22.5 ± 8.6%, respectively (*P* < 0.05) after surgery;

**Table 5** LDL and HDL ratios

Biological variables	Preoperative ( <i>n</i> = 15)	Postoperative ( <i>n</i> = 15)
LDL-CE/apoB (mmol/g)	3.30 ± 0.33	3.46 ± 0.46
LDL-FC/apoB (mmol/g)	1.18 ± 0.14	1.46 ± 0.21 <sup>a</sup>
LDL-FC/CE (mmol/mmol)	0.35 ± 0.01	0.41 ± 0.02 <sup>c</sup>
HDL-CE/apoA1 (mmol/g)	0.59 ± 0.06	0.62 ± 0.07
HDL-FC/apoA1 (mmol/g)	0.14 ± 0.01	0.20 ± 0.02 <sup>d</sup>
HDL-FC/CE (mmol/mmol)	0.23 ± 0.01	0.31 ± 0.02 <sup>d</sup>
LDL-TG/apoB (mmol/g)	0.34 ± 0.04	0.75 ± 0.12 <sup>d</sup>
LDL-TG/CE (mmol/mmol)	0.10 ± 0.01	0.20 ± 0.02 <sup>c</sup>
HDL-TG/apoA1 (mmol/g)	0.06 ± 0.01	0.08 ± 0.01
HDL-TG/CE (mmol/mmol)	0.11 ± 0.01	0.14 ± 0.02
LDL-PL/apoB (mmol/g)	1.36 ± 0.16	1.71 ± 0.24 <sup>b</sup>
LDL-PL/CE (mmol/mmol)	0.41 ± 0.01	0.48 ± 0.02 <sup>d</sup>
LDL-FC/PL (mmol/mmol)	0.86 ± 0.02	0.86 ± 0.02
HDL-PL/apoA1 (mmol/g)	0.57 ± 0.05	0.75 ± 0.08 <sup>d</sup>
HDL-PL/CE (mmol/mmol)	0.98 ± 0.06	1.18 ± 0.06 <sup>a</sup>
HDL-FC/PL (mmol/mmol)	0.23 ± 0.01	0.26 ± 0.01 <sup>a</sup>
LDL-hydroperoxides/TC (μmol/mmol)	6.40 ± 2.45	17.27 ± 7.17
LDL-hydroperoxides/apoB (μmol/g)	22.45 ± 7.98	55.58 ± 16.32 <sup>b</sup>
HDL-hydroperoxides/TC (μmol/mmol)	10.87 ± 1.70	16.50 ± 3.94
HDL-hydroperoxides/apoA1 (μmol/g)	8.26 ± 1.51	15.03 ± 4.85
LDL-α-tocopherol/TC (μmol/mmol)	4.32 ± 0.25	4.59 ± 0.27
LDL-α-tocopherol/apoB (μmol/g)	18.99 ± 2.05	22.62 ± 2.97
LDL-α-tocopherol/FC+PL (μmol/mmol)	7.69 ± 0.44	7.27 ± 0.34
HDL-α-tocopherol/TC (μmol/mmol)	8.63 ± 0.37	7.94 ± 0.30 <sup>a</sup>
HDL-α-tocopherol/apoA1 (μmol/g)	6.21 ± 0.67	6.41 ± 0.72
HDL-α-tocopherol/FC+PL (μmol/mmol)	8.61 ± 0.40	6.74 ± 0.26 <sup>d</sup>

Values are expressed as mean ± SEM. *P* values were calculated by the paired Student *t* test. <sup>a</sup>*P* < 0.05, <sup>b</sup>*P* < 0.025, <sup>c</sup>*P* < 0.01, <sup>d</sup>*P* < 0.001, <sup>e</sup>*P* < 0.0001 versus preoperative value  
*CE* Cholesteryl ester, *FC* free cholesterol, *TG* triglycerides, *PL* phospholipids, *apoB* apolipoprotein B, *apoA1* apolipoprotein A1

comparable changes were found for LDL-FC/CE (+16.9 ± 4.4%) and LDL phospholipid/CE ratios (+18.0 ± 3.9%) after surgery. These ratios suggest a postoperative increase of surface area and of particle radius by 14 ± 5% (*P* < 0.03) and 6 ± 2% (*P* < 0.03), respectively.

Before surgery, the HDL core volume corresponded to a core radius of 2.56 ± 0.09 nm and a total particle radius of 4.58 ± 0.09 nm, in fair agreement with current knowledge [32, 33]. Calculations from the sum of surface components (assuming a mean of 3 apoA1 molecules per HDL particle) correspond to a core radius of 3.02 ± 0.05 nm, in fair agreement with the HDL calculated core radius from core volume. The unchanged CE content and increased TG content in postoperative HDL particles imply an increase in core lipid molecules and volume. Accordingly, both FC/apoA1 and phospholipid/apoA1 ratios increased in HDL post-surgery, with a mean increase of, respectively, 42.9 ± 7.1% (*P* < 0.001) and 30.2 ± 6.1% (*P* < 0.001). Comparable percentages were obtained for HDL-FC/CE (36.3 ± 8.3%) and HDL-phospholipid/CE ratios (23.6 ± 6.7%). This suggests an increase of HDL area by 31 ± 6% (*P* < 0.001) and of HDL radius by 14 ± 3% (*P* < 0.001) after cardiac surgery. Note that calculations of

HDL size are underestimates since the molecular volume of apoSAA is not taken into account.

#### Hydroperoxides

The hydroperoxide concentration in the LDL fraction was not significantly modified after surgery (*P* > 0.3). However, hydroperoxide/apoB and hydroperoxide/TC ratios increased by, respectively, 189.1 ± 83.0 and 191.3 ± 89.2% on postoperative day 2 (*P* < 0.05).

Similarly, the hydroperoxide concentration in the HDL fraction was not significantly modified (*P* > 0.5) post-surgery but, when expressed relative to TC content, the hydroperoxide/TC ratio in HDL increased by 62.4 ± 29.3% (*P* < 0.03) after surgery.

#### Alpha-tocopherol

In the LDL fraction, alpha-tocopherol concentration decreased by 41.0 ± 3.9% (*P* < 0.0001) on postoperative day 2. However, alpha-tocopherol content relative to apoB

or TC content in the LDL fraction was not decreased by surgery. Similarly, the alpha-tocopherol/FC+phospholipid ratio was not modified after surgery.

In the HDL fraction, alpha-tocopherol concentration had decreased by  $21.6 \pm 4.4\%$  ( $P < 0.001$ ) on postoperative day 2. Alpha-tocopherol content relative to apoA1 or TC content was not or little affected after surgery. In contrast, the alpha-tocopherol/FC+phospholipid ratio had decreased by  $20.5 \pm 2.9\%$  ( $P < 0.001$ ) after surgery.

Notice that alpha-tocopherol/TC ratio was two times higher ( $P < 0.001$ ) in HDL versus LDL in pre- and post-operative conditions.

### LDL Peroxidation

LDL resistance towards oxidative stress, reflected by the lag phase preceding the generation of conjugated dienes from LDL exposed to  $\text{CuSO}_4$ , did not significantly decrease after surgery ( $73 \pm 3$  vs.  $71 \pm 3$  min; NS). The propagation slope decreased slightly after surgery (by  $10.4 \pm 4.0\%$ ;  $P < 0.025$ ). This coincided with a trend towards a lower maximal value for the generation of conjugated dienes, with a postoperative/preoperative ratio for dienes averaging  $91.8 \pm 4.5\%$  ( $P < 0.09$ ).

### Discussion

The present study was aimed at characterizing changes in plasma lipoprotein composition induced by cardiac surgery with cardiopulmonary bypass, notably in comparison to alterations reported in sepsis. Indeed, most current data on LDL and HDL alterations occurring in acute phase reactions comes from observations in patients with severe septic conditions [8, 9].

Analyses of plasma lipid parameters are in agreement with prior observations on the effect of surgical stress, i.e., decreased levels of TC, TG and alpha-tocopherol [5, 14, 34, 35]. An important decrease of apoB and apoA1 level was also observed in the present study that largely exceeded the reduction of total plasma protein concentration. The marked increase of SAA levels paralleled and even exceeded that of CRP. Reduced TAOS indicates decreased antioxidant defenses and/or consumption of antioxidant scavengers in response to oxidative stress as previously described after cardiac surgery with cardiopulmonary bypass [36]. Furthermore, the activity of the antioxidant enzyme PON, largely associated to HDL particles, was decreased post-surgery; this may substantially reduce protection against LDL oxidation [12]. Such alterations in antioxidant parameters have also been described in sepsis [37–39]. In this study, alpha-tocopherol content in blood

cells was analysed to evaluate whether the decreased antioxidant defenses and more specifically whether the marked reduction in circulating alpha-tocopherol level are associated to impaired alpha-tocopherol delivery to cells. Indeed, apart from one study reporting unchanged alpha-tocopherol content in erythrocytes after surgery [40], no data is currently available on alpha-tocopherol content in blood cells of surgical or septic patients. Since blood cell counts are modified after surgery, alpha-tocopherol content was expressed relative to cell phospholipid concentration, which to our knowledge, is not affected by the operative procedure. Alpha-tocopherol content was unchanged in erythrocytes and platelets on postoperative 2, but was decreased in leukocytes. This may reflect increased consumption by white blood cells or an impaired alpha-tocopherol uptake, or both; after surgery, another possibility is that, leukocytes released in great number in the circulation after surgery have a lower alpha-tocopherol content.

Analyses of lipoprotein fractions in 15 subjects characterize the effect of cardiac surgery on changes in the number, composition, and size of circulating particles.

LDL-cholesterol markedly decreased ( $-45\%$ ) after surgery. Such a decrease in LDL cholesterol is commonly observed after surgery [5, 14, 34] and in other types of acute phase reactions, including sepsis [11, 41, 42] and acute myocardial infarct [43]. In the later condition, however, cholesterol production and secretion appear not to be reduced but are rather augmented [44]. If this was also the case in the surgical acute phase, the lower LDL-cholesterol level would largely result from increased particle disposal (endocytosis via LDL B, E and scavenger receptors, and possible margination of LDL particles outside the plasma compartment).

ApoB concentration in the LDL fraction also substantially decreased ( $-46\%$ ) after cardiac surgery. Since LDL particles contain one single apoB molecule, this change reflects a proportional reduction of the number of circulating LDL particles. Lipid content per LDL particle was reflected by the concentration of each component relative to LDL-apoB (Fig. 1). CE content per LDL particle remained unchanged after cardiac surgery, while TG content was increased ( $+113\%$ ) together with surface components FC ( $+22\%$ ) and phospholipids ( $+23\%$ ). Such increase of both core and surface lipid components strongly suggests an increased LDL particle size postoperatively. This is in sharp contrast with changes observed during sepsis where the decrease in LDL number is associated with the appearance of small sized and denser LDL particles, in which an increased TG content is largely compensated for by a reduced CE content [45, 46]. Such small dense LDL particles are more sensitive to peroxidative damage, are more cytotoxic, and have an increased

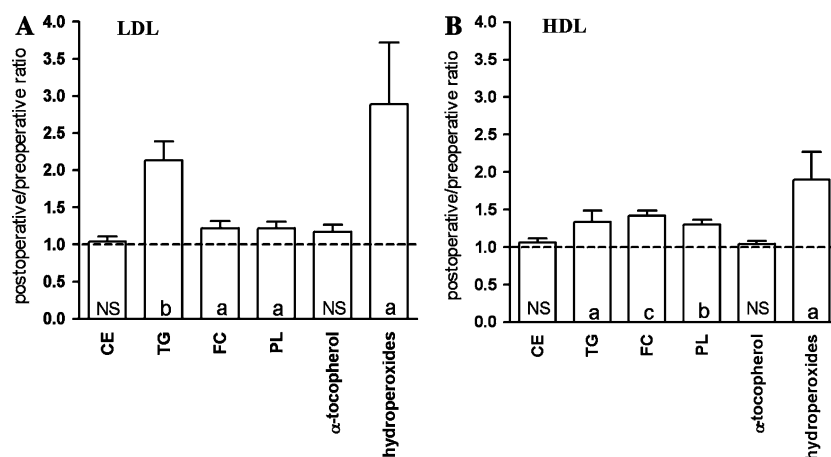


**Fig. 1** Postoperative changes in LDL (A) and HDL (B) composition. LDL and HDL lipid components are expressed relative to LDL-apoB and HDL-apoA1, respectively. The figure shows an unchanged cholesteryl ester (CE) content in LDL and HDL particles, an increased triglyceride (TG) content (particularly in LDL) together with an increase in surface components [free cholesterol (FC) and

phospholipids (PL)]; in spite of unchanged alpha-tocopherol content, LDL and HDL showed increased hydroperoxide content. Values are expressed as mean  $\pm$  SEM. *P* values were calculated by paired Student *t* test. <sup>a</sup>*P* < 0.05, <sup>b</sup>*P* < 0.01, <sup>c</sup>*P* < 0.005, <sup>d</sup>*P* < 0.001, <sup>e</sup>*P* < 0.0001 versus preoperative value

atherogenic potential [47]. Of interest, alpha-tocopherol content per LDL particle remained unchanged after surgery and no difference of susceptibility to peroxidation was observed between pre- and postoperative circulating LDL particles when subjected *ex vivo* to copper oxidative stress. Still, as reported in sepsis [47], an increased hydroperoxide content was measured in circulating LDL particles after cardiac surgery, suggesting that the (unchanged) alpha-tocopherol content in postoperative LDL particles could not completely prevent the oxidative stress associated to cardiac surgery with cardiopulmonary bypass. From current data it is difficult to speculate whether these changes in LDL composition and size can modulate properties of LDL and influence (in one or another direction) the inflammatory response.

In contrast to LDL particles, which are characterized by the presence of one single apoB molecule, HDL particles contain 2 to 4 apoA1 molecules in physiological conditions [33]. In addition, HDL apolipoprotein composition is substantially modified during the acute phase reaction, notably by a massive increase of SAA [48, 49]. While high SAA concentrations had previously been suggested to displace apoA1 from HDL particles, apoA1 decrease during acute phase response seems to result mainly from an increased catabolic rate, which parallels that of HDL particles [50]. If one assumes that the mean number of apoA1 molecules in HDL is not appreciably modified by cardiac surgery, the number of circulating HDL particles would decrease by 20% on postoperative day 2. Such a decrease in HDL particles is lower than that observed for LDL and it is not as marked as in patients with sepsis [42, 51]. Of interest,

HDL-CE decreased by  $18.9 \pm 6.6\%$  (*P* < 0.02) postoperatively so that HDL-CE/apoA1 ratio remained virtually unchanged (Fig. 1). As indicated by the increased HDL-TG/apoA1 (+34%) and HDL-TG/CE (+31%) ratios, TG content in HDL particles increased after surgery, but to a lesser extent than in LDL particles. Such an increase in LDL- and HDL-TG content on postoperative day 2 contrasts with a lower plasma TG concentration. Lower plasma TG concentrations do not usually induce cholesteryl ester transfer protein-mediated exchanges of core lipids between TG-rich and CE-rich lipoproteins [52, 53]. Hence, TG enrichment in LDL and HDL may result from reduced hepatic lipase activity as reported in conditions of sepsis and inflammation [41]. The increase of core lipid molecules in postoperative HDL is associated to an increase of surface components, as indicated by increased FC/apoA1 and phospholipid/apoA1 ratios (Fig. 1). All together these changes and the presence of SAA molecules in HDL surface indicate an increased particle size after cardiac surgery. Changes in the balance between HDL surface lipid components were also observed after surgery with a higher FC relative to phospholipid content. This is in agreement with observations in septic patients where reduced lecithin:cholesterol acyltransferase activity is associated with an increased FC content in HDL particles [54, 55]. Finally, the alpha-tocopherol level decreased in the HDL fraction after cardiac surgery in close relation to the reduced number of circulating HDL particles. The hydroperoxide content in HDL increased after surgery but to a lesser extent than in LDL particles. The global reduction of alpha-tocopherol transport by LDL and

HDL may affect alpha-tocopherol delivery to cells and organs in a condition (ischemia–reperfusion) characterized by oxidative stress.

There are some limitations that need to be addressed regarding this study. First, it does not allow one to distinguish between the impact of surgical trauma, that of cardiopulmonary bypass and that of anesthesia on the inflammatory response and more particularly on the changes in plasma lipoproteins and oxidative stress. Second, measurements reflect changes in circulating LDL and HDL particles, but more profound alterations may occur in those lipoproteins that marginate outside the plasma compartment. Third, measurements were performed at two time points, i.e., before (=baseline) and at 48 h after surgery, the latter corresponding to the peak of the inflammatory response but not to the peak of systemic oxidative stress, which takes place during surgery (after reperfusion) and in the immediate postoperative period [56]. Finally, since the measured postoperative alterations of lipoprotein composition probably last over a limited period of time, their impact on the functional properties of circulating plasma lipoproteins remains to be determined.

In summary, the present study indicates that the acute phase response that occurs after major cardiac surgery induces profound alterations not only in the concentration but also in the composition of circulating LDL and HDL particles. Several of these surgery-induced alterations in the lipid composition of LDL and HDL particles differ from changes previously observed in sepsis. Thus acute phase reactions caused by different conditions may affect the properties of plasma lipoproteins differently and should be considered specifically. Although the increase in LDL and HDL particle size probably limits the pro-inflammatory risk, additional experiments are required to fully determine the impact of postoperative modifications on the roles and function of circulating lipoproteins. Reduced levels of circulating lipoproteins post-surgery may also affect the delivery to cells and tissues of substrates such as alpha-tocopherol.

**Acknowledgments** Part of this study was presented in abstract form at the conference of the New York Academy of Science “vitamin E and Health”, Boston (2004) [57]. The authors gratefully thank Dr. R.J. Deckelbaum (Institute of Human Nutrition, Columbia University, New York, USA) for helpful discussions and advice.

## References

- Gabay C, Kushner I (1999) Acute-phase proteins and other systemic responses to inflammation. *N Engl J Med* 340:448–54
- Carpentier YA, Scruel O (2002) Changes in the concentration and composition of plasma lipoproteins during the acute phase response. *Curr Opin Clin Nutr Metab Care* 5:153–8
- Feingold KR, Staprans I, Memon RA, Moser AH, Shigenaga JK, Doerfler W, Dinarello CA, Grunfeld C (1992) Endotoxin rapidly induces changes in lipid metabolism that produce hypertriglyceridemia: low doses stimulate hepatic triglyceride production while high doses inhibit clearance. *J Lipid Res* 33:1765–76
- Fraunberger P, Schaefer S, Werdan K, Walli AK, Seidel D (1999) Reduction of circulating cholesterol and apolipoprotein levels during sepsis. *Clin Chem Lab Med* 37:357–62
- Akgun S, Ertel NH, Mosenthal A, Oser W (1998) Postsurgical reduction of serum lipoproteins: interleukin-6 and the acute-phase response. *J Lab Clin Med* 131:103–8
- Chien JY, Jerng JS, Yu CJ, Yang PC (2005) Low serum level of high-density lipoprotein cholesterol is a poor prognostic factor for severe sepsis. *Crit Care Med* 33:1688–93
- Gordon BR, Parker TS, Levine DM, Saal SD, Wang JC, Sloan BJ, Barie PS, Rubin AL, (2001) Relationship of hypolipidemia to cytokine concentrations and outcomes in critically ill surgical patients. *Crit Care Med* 29:1563–8
- Hudgins LC, Parker TS, Levine DM, Gordon BR, Saal SD, Jiang XC, Seidman CE, Tremaroli JD, Lai J, Rubin AL (2003) A single intravenous dose of endotoxin rapidly alters serum lipoproteins and lipid transfer proteins in normal volunteers. *J Lipid Res* 44:1489–98
- Khovidhunkit W, Kim MS, Memon RA, Shigenaga JK, Moser AH, Feingold KR, Grunfeld C (2004) Effects of infection and inflammation on lipid and lipoprotein metabolism: mechanisms and consequences to the host. *J Lipid Res* 45:1169–96
- Kitchens RL, Thompson PA, Munford RS, O’Keefe GE (2003) Acute inflammation and infection maintain circulating phospholipid levels and enhance lipopolysaccharide binding to plasma lipoproteins. *J Lipid Res* 44:2339–48
- Hardardottir I., Grunfeld C, Feingold KR (1994) Effects of endotoxin and cytokines on lipid metabolism. *Curr Opin Lipidol* 5:207–15
- Van Lenten BJ, Hama SY, de Beer FC, Stafforini DM, McIntyre TM, Prescott SM, La Du BN, Fogelman AM, Navab M (1995) Anti-inflammatory HDL becomes pro-inflammatory during the acute phase response. Loss of protective effect of HDL against LDL oxidation in aortic wall cell cocultures. *J Clin Invest* 96:2758–67
- Stephens CJ, Graham RM, Yadava OP, Leong LL, Sturm MJ, Taylor RR (1992) Plasma platelet activating factor degradation and serum lipids after coronary bypass surgery. *Cardiovasc Res* 26:25–31
- Cunningham MJ, Boucher TM, McCabe CH, Horowitz GL, Pasternak RC (1987) Changes in total cholesterol and high-density lipoprotein cholesterol in men after coronary artery bypass grafting. *Am J Cardiol* 60:1393–4
- Levy JH, Tanaka KA (2003) Inflammatory response to cardiopulmonary bypass. *Ann Thorac Surg* 75:S715–20
- Larmann J, Theilmeier G (2004) Inflammatory response to cardiac surgery: cardiopulmonary bypass versus non-cardiopulmonary bypass surgery. *Best Pract Res Clin Anaesthesiol* 18:425–38
- Goudeau JJ, Clermont G, Guillery O, Lemaire-Ewing S, Musat A, Vernet M, Vergely C, Guiguet M, Rochette L, Girard C (2007) In high-risk patients, combination of antiinflammatory procedures during cardiopulmonary bypass can reduce incidences of inflammation and oxidative stress. *J Cardiovasc Pharmacol* 49:39–45
- Coghlan JG, Flitter WD, Clutton SM, Ilsley CD, Rees A, Slater TF (1993) Lipid peroxidation and changes in vitamin E levels during coronary artery bypass grafting. *J Thorac Cardiovasc Surg* 106:268–74
- Pouliot M, Fiset ME, Masse M, Naccache PH, Borgeat P (2002) Adenosine up-regulates cyclooxygenase-2 in human

- granulocytes: impact on the balance of eicosanoid generation. *J Immunol* 169:5279–86
20. Sharrett AR, Ballantyne CM, Coady SA, Heiss G, Sorlie PD, Catellier D, Patsch W (2001) Coronary heart disease prediction from lipoprotein cholesterol levels, triglycerides, lipoprotein(a), apolipoproteins A-I and B, and HDL density subfractions: the Atherosclerosis Risk in Communities (ARIC) study. *Circulation* 104:1108–13
  21. Nzuzi Tembo N, Bazelmans C, Dufourny G, Levèque A, Nève J, Carpentier YA (2006) Comparison of cardiovascular risk factors between different ethnic groups living in the region of Brussels. 28th ESPEN Congress, Istanbul (Turkey) Abstract
  22. Havel RJ, Eder HA, Bragdon JH (1955) The distribution and chemical composition of ultracentrifugally separated lipoproteins in human serum. *J Clin Invest* 34:1345–53
  23. Jiang ZY, Hunt JV, Wolff SP (1992) Ferrous ion oxidation in the presence of xylenol orange for detection of lipid hydroperoxide in low density lipoprotein. *Anal Biochem* 202:384–9
  24. Esterbauer H, Dieber-Rotheneder M, Striegl G, Waeg G (1991) Role of vitamin E in preventing the oxidation of low-density lipoprotein. *Am J Clin Nutr* 53:314S–321S
  25. Traber MG, Kayden HJ (1989) Preferential incorporation of alpha-tocopherol vs gamma-tocopherol in human lipoproteins. *Am J Clin Nutr* 49:517–26
  26. Wong WM, Stephens JW, Acharya J, Hurel SJ, Humphries SE, Talmud PJ (2004) The APOA4 T347S variant is associated with reduced plasma TAOS in subjects with diabetes mellitus and cardiovascular disease. *J Lipid Res* 45:1565–71
  27. Eckerson HW, Wyte CM, La Du BN (1983) The human serum paraoxonase/arylesterase polymorphism. *Am J Hum Genet* 35:1126–38
  28. Lowry OH, Rosebrough NJ, Farr AL, Randall RJ (1951) Protein measurement with the Folin phenol reagent. *J Biol Chem* 193:265–75
  29. Dubois DY, Cantraine F, Malmendier CL (1987) Comparison of different sandwich enzyme immunoassays for the quantitation of human apolipoproteins A-I and A-II. *J Immunol Methods* 96:115–20
  30. Cotton F, Thiry P, Hsain AB, Boeynaems JM (2001) Analyzer transfer of a broad range high-sensitivity C-reactive protein immunoassay. *Clin Lab* 47:405–9
  31. Pruzanski W, Stefanski E, de Beer FC, de Beer MC, Ravandi A, Kuksis A (2000) Comparative analysis of lipid composition of normal and acute-phase high density lipoproteins. *J Lipid Res* 41:1035–47
  32. Gotto AM Jr, Pownall HJ, Havel RJ (1986) Introduction to the plasma lipoproteins. *Methods Enzymol* 128:3–41
  33. Eisenberg S (1984) High density lipoprotein metabolism. *J Lipid Res* 25:1017–58
  34. Malmendier CL, Amerijckx JP, Bihain BE, Fischer ML (1985) Changes in apolipoprotein and lipids in patients after surgery. *Biomed Pharmacother* 39:192–5
  35. Cavarocchi NC, England MD, O'Brien JF, Solis E, Russo P, Schaff HV, Orszulak TA, Pluth JR, Kaye MP (1986) Superoxide generation during cardiopulmonary bypass: is there a role for vitamin E? *J Surg Res* 40:519–27
  36. McColl AJ, Keeble T, Hadjiniakou L, Cohen A, Aitkenhead H, Glenville B, Richmond W (1998) Plasma antioxidants: evidence for a protective role against reactive oxygen species following cardiac surgery. *Ann Clin Biochem* 35(Pt 5):616–23
  37. Goode HF, Cowley HC, Walker BE, Howdle PD, Webster NR (1995) Decreased antioxidant status and increased lipid peroxidation in patients with septic shock and secondary organ dysfunction. *Crit Care Med* 23:646–51
  38. Wu A, Hinds CJ, Thiemermann C (2004) High-density lipoproteins in sepsis and septic shock: metabolism, actions, and therapeutic applications. *Shock* 21:210–21
  39. Chuang CC, Shiesh SC, Chi CH, Tu YF, Hor LI, Shieh CC, Chen MF (2006) Serum total antioxidant capacity reflects severity of illness in patients with severe sepsis. *Crit Care* 10:R36
  40. Ballmer PE, Reinhart WH, Jordan P, Buhler E, Moser UK, Gey KF (1994) Depletion of plasma vitamin C but not of vitamin E in response to cardiac operations. *J Thorac Cardiovasc Surg* 108:311–20
  41. Sammalkorpi K, Valtonen V, Kerttula Y, Nikkila E, Taskinen MR (1988) Changes in serum lipoprotein pattern induced by acute infections. *Metabolism* 37:859–65
  42. van Leeuwen HJ, Heezius EC, Dallinga GM, van Strijp JA, Verhoef J, van Kessel KP (2003) Lipoprotein metabolism in patients with severe sepsis. *Crit Care Med* 31:1359–66
  43. Rosenson RS (1993) Myocardial injury: the acute phase response and lipoprotein metabolism. *J Am Coll Cardiol* 22:933–40
  44. Pfohl M, Schreiber I, Liebich HM, Haring HU, Hoffmeister HM (1999) Upregulation of cholesterol synthesis after acute myocardial infarction—is cholesterol a positive acute phase reactant? *Atherosclerosis* 142:389–93
  45. Feingold KR, Krauss RM, Pang M, Doerrler W, Jensen P, Grunfeld C (1993) The hypertriglyceridemia of acquired immunodeficiency syndrome is associated with an increased prevalence of low density lipoprotein subclass pattern B. *J Clin Endocrinol Metab* 76:1423–7
  46. Grunfeld C, Pang M, Doerrler W, Shigenaga JK, Jensen P, Feingold KR (1992) Lipids, lipoproteins, triglyceride clearance, and cytokines in human immunodeficiency virus infection and the acquired immunodeficiency syndrome. *J Clin Endocrinol Metab* 74:1045–52
  47. Memon RA, Staprans I, Noor M, Holleran WM, Uchida Y, Moser AH, Feingold KR, Grunfeld C (2000) Infection and inflammation induce LDL oxidation in vivo. *Arterioscler Thromb Vasc Biol* 20:1536–42
  48. Coetzee GA, Strachan AF, van der Westhuyzen DR, Hoppe HC, Jeenah MS, de Beer FC (1986) Serum amyloid A-containing human high density lipoprotein 3. Density, size, and apolipoprotein composition. *J Biol Chem* 261:9644–51
  49. Clifton PM, Mackinnon AM, Barter PJ (1985) Effects of serum amyloid A protein (SAA) on composition, size, and density of high density lipoproteins in subjects with myocardial infarction. *J Lipid Res* 26:1389–98
  50. Hosoi H, Webb NR, Glick JM, Tietge UJ, Purdom MS, de Beer FC, Rader DJ (1999) Expression of serum amyloid A protein in the absence of the acute phase response does not reduce HDL cholesterol or apoA-I levels in human apoA-I transgenic mice. *J Lipid Res* 40:648–53
  51. Gordon BR, Parker TS, Levine DM, Saal SD, Wang JC, Sloan BJ, Barie PS, Rubin AL (1996) Low lipid concentrations in critical illness: implications for preventing and treating endotoxemia. *Crit Care Med* 24:584–9
  52. Eisenberg S, Gavish D, Oschry Y, Fainaru M, Deckelbaum RJ (1984) Abnormalities in very low, low and high density lipoproteins in hypertriglyceridemia. Reversal toward normal with bezafibrate treatment. *J Clin Invest* 74:470–82
  53. Deckelbaum RJ, Granot E, Oschry Y, Rose L, Eisenberg S (1984) Plasma triglyceride determines structure-composition in low and high density lipoproteins. *Arteriosclerosis* 4:225–31
  54. Ly H, Francone OL, Fielding CJ, Shigenaga JK, Moser AH, Grunfeld C, Feingold KR (1995) Endotoxin and TNF lead to reduced plasma LCAT activity and decreased hepatic LCAT mRNA levels in Syrian hamsters. *J Lipid Res* 36:1254–63

55. Khovidhunkit W, Shigenaga JK, Moser AH, Feingold KR, Grunfeld C (2001) Cholesterol efflux by acute-phase high density lipoprotein: role of lecithin: cholesterol acyltransferase. *J Lipid Res* 42:967–75
56. Christen S, Finckh B, Lykkesfeldt J, Gessler P, Frese-Schaper M, Nielsen P, Schmid ER, Schmitt B (2005) Oxidative stress precedes peak systemic inflammatory response in pediatric patients undergoing cardiopulmonary bypass operation. *Free Radic Biol Med* 38:1323–32
57. Hacquebard M, Ducart A, Schmartz D, Tembo N, Carpentier YA (2004) Tocopherol in lipoproteins and blood cells after cardiac surgery. *Ann N Y Acad Sci* 1031:432–4



[13]. The diet of the wild raccoon dog contains a large variety of FA and the FA composition of its WAT depots is homogeneous without significant vertical gradients [14]. As the raccoon dog is an omnivore [15], the obtained results can have biomedical value. Previously, the *in vivo* FA mobilization from regional WAT depots of captive raccoon dogs was shown to be selective [10]. Fasting stimulated the mobilization of shorter-chain saturated (SFA), monounsaturated (MUFA) and polyunsaturated FA (PUFA). There were also site-specific differences in fractional mobilization and the omental adipose tissue was the most divergent. The selectivity of FA accumulation remains uninvestigated in the species.

The FA composition of WAT, i.e., the FA signature, can be used to monitor the long-term dietary habits of humans and foraging ecology of predators. In humans, an important aspect is to estimate the supply and reserves of essential PUFA and the balance between n-3 and n-6 PUFA [16]. In ecophysiological studies, FA accumulated in the fat depots reflect the diet of predators [17]. It is important to understand the selective changes in the FA composition of WAT and plasma caused by seasonal weight regulation of wild mammals or by weight cycling of humans to interpret the obtained FA profiles correctly.

Selective mobilization of FA from WAT during energy depletion and selective incorporation of FA into WAT during energy storage have been scarcely examined in wild mammals. It can be hypothesized that the selectivity of FA release observed in captivity [4, 10] would be present also in wild animals. Using repeated sampling of free-ranging raccoon dogs the present study investigated (1) the effects of wintertime nutritional scarcity and summertime abundance on the WAT and plasma FA signatures and the selectivity of seasonal FA mobilization and incorporation, (2) the basis of this selectivity at the molecular level and (3) whether the molecular background of FA release and incorporation observed in laboratory animals and humans can be demonstrated in wild mammals living in their natural habitat. The present study significantly adds to our knowledge of lipid metabolism in the raccoon dog because it reflects the real world situation of seasonal FA metabolism in the wild.

## Experimental Procedures

The study area was located in Eastern Finland (62°33.094'N; 29°9.409'E). It has a boreal, continental climate with an average annual ambient temperature of +2.0°C and precipitation of 600 mm. The summers are relatively warm (mean and max in July +15.8 and +32.0°C) but the winters cold (mean and min in January -11.9 and -42.2°C). The permanent snow cover usually lasts from

mid-late November to late April with an average max snow depth of 63 cm. Potential food items for the raccoon dog include small mammals, frogs, insects, carcasses, fish, plant material, birds and eggs [18].

Seven wild raccoon dogs (four males and three females) were captured in autumn 2004 and fasted overnight before sampling. They were anaesthetized with intramuscular (im) ketamine (5 mg kg<sup>-1</sup>) and xylazine (2 mg kg<sup>-1</sup>). A blood sample was taken from a superficial vein of the hind leg with sterile needles and syringes with EDTA as an anti-coagulant. The complete blood count was determined with the Vet abc Animal Blood Counter (ABX Hematologie, Montpellier, France) calibrated to the canine hematologic profile. Plasma was removed after centrifugation of whole blood at 1,500g and stored at -80 °C. A 3-cm incision was cut caudal from the umbilicus and 1–2 g of ventral subcutaneous (sc) fat was removed. The WAT samples were immediately frozen in liquid nitrogen and stored at -80 °C. The skin was sutured with 3-0 resorbable madras knots. A single dose of im benzylpenicillin-procaine was used for antibiotic prophylaxis.

The animals were fitted with radio transmitter collars (Biotrack Ltd, Wareham, UK) to enable recapture. Body mass (BM) and body length were determined and body mass indices (BMI) correlating with the fat % calculated using the formula: BM (kg)/[body length<sup>3</sup> (m)] [19]. The animals were released at the capture sites, located with a portable radio receiver (AR8000, AOR Ltd, Tokyo, Japan) and a hand-held antenna in spring 2005, recaptured, sedated and sampled. Two raccoon dogs were shot by hunters and one lost its radio tag. Also two new females were captured, sampled and released. Four of these animals were recaptured in autumn 2005, two were shot by hunters. Also three new individuals (two males and one female) entered the study. Two of these animals were recaptured in spring 2006. One was killed by a dog, one was killed by a car, one died of scabies and one could not be located. The captured animals were sedated and sampled and the radio tags were removed. The sex, age, radio-tracking periods and sampling procedure of each individual are presented in Fig. 1. The Animal Care and Use Committee of the University of Joensuu approved all the procedures of the study.

For the FA analysis, subsamples of WAT and plasma were transmethylated [20] by heating with 1% (v/v) H<sub>2</sub>SO<sub>4</sub> in methanol under nitrogen atmosphere. The formed FA methyl esters (FAME) were extracted with hexane in two steps. The dried and concentrated FAME were analyzed with a gas-liquid chromatograph equipped with two injectors and flame ionization and mass detectors (GC-FID and GC-MS, 6890N network GC system with autosampler, FID detector and 5973 mass selective detector, Agilent Technologies Inc., Palo Alto, CA, USA) as described previously [10, 21]. The peak areas of the FID chromatograms were

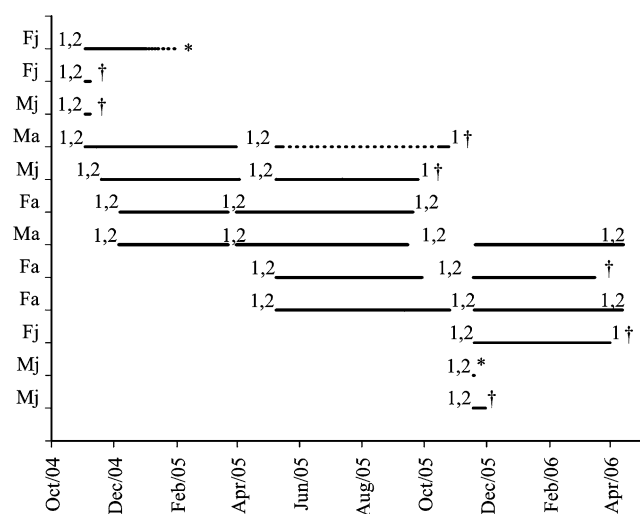


**Fig. 1** The sex, age, sampling and periods of radio-tracking of the observed raccoon dogs between autumn 2004–spring 2006. *M* male, *F* female, *j* juvenile at first capture, *a* adult at first capture, *dagger* animal died from a natural cause or by human action, *asterisk* animal was lost, *1* white adipose tissue sampling, *2* blood sampling. *Dotted lines* indicate lost animals or dysfunctional radio collars

converted to mol% by using the theoretical response factors [22] and calibrations with quantitative authentic standards. The FA were marked by using the abbreviations: [carbon number]:[number of double bonds] n-[position of the first double bond calculated from the methyl end]. The double bond index (DBI) and the total average chain length (TACL) indicating the mean numbers of double bonds or carbon atoms per molecule were calculated according to standard formulae [23]. The  $\Delta 9$ -desaturation index ( $\Delta 9$ -DI), the ratio of the most important potentially endogenous  $\Delta 9$ -MUFA to the corresponding SFA, was calculated as  $[(\text{mol}\% \text{ 14:1n-5}) + (\text{mol}\% \text{ 16:1n-7}) + (\text{mol}\% \text{ 16:1n-9}) + (\text{mol}\% \text{ 18:1n-9}) + (\text{mol}\% \text{ 18:1n-7})] / [(\text{mol}\% \text{ 14:0}) + (\text{mol}\% \text{ 16:0}) + (\text{mol}\% \text{ 18:0})]$  [14]. Very-long-chain FA (VLCFA) were calculated as the sum of FA with a chain length of 24.

Relative changes in the proportions of FA in WAT during winter were calculated by the formula  $[\text{mol}\% \text{ in spring} - \text{mol}\% \text{ in autumn}] / [\text{mol}\% \text{ in autumn}] \times 100$  and during summer by the formula  $[\text{mol}\% \text{ in autumn} - \text{mol}\% \text{ in spring}] / [\text{mol}\% \text{ in spring}] \times 100$ . Relative changes were calculated only for the individuals that could be recaptured during two consecutive seasons (autumn–spring  $n = 7$ ; spring–autumn  $n = 6$ ), while the seasonal FA profiles of WAT and plasma consisted of all sampled individuals (WAT autumn  $n = 16$ , WAT spring  $n = 9$ , plasma autumn  $n = 14$ , plasma spring  $n = 8$ ). The numbers of WAT and plasma samples were dissimilar within a season, as some animals were killed and in some of these cases a WAT sample of good quality could still be obtained from a fresh carcass, while the blood had already clotted. The WAT FA

profile of one individual differed from the other raccoon dogs as this animal fed on freshwater fish discarded by fishermen on ice in winter 2005–2006 instead of fasting like the rest of the animals. For this reason, its vernal FA percentages were not included in the statistical analyses or in the means. The plasma total cholesterol (Chol), low-density lipoprotein (LDL) and high-density lipoprotein (HDL) Chol, triacylglycerols (TAG), glucose, creatinine, alanine aminotransferase (ALT), aspartate aminotransferase (AST), total protein, urea, ammonia, uric acid, bilirubin and creatine kinase were determined as described previously [10].

Differences in the BM and BMI in the time series were determined with the repeated measures analysis of variance using the SPSS program (SPSS Inc., Chicago, IL, USA). Comparisons between the two seasons were performed with the Student's *t*-test or the Mann–Whitney *U*-test for parametric and nonparametric data, respectively. Bivariate correlations were calculated with the Spearman correlation coefficient ( $r_s$ ). A *P* value less than 0.05 was considered statistically significant. The results are presented as mean  $\pm$  SE. To analyze the relationships in the FA composition of WAT and plasma during the two seasons, the data were also subjected to the multivariate principal component analysis (PCA) using the SIRIUS 6.5 software package (Pattern Recognition Systems AS, Bergen, Norway [24]). The data were standardized and the relative positions of the samples and variables were plotted using two new coordinates, the principal components PC1 and PC2, describing the largest and the second largest variance among the samples.

## Results

The raccoon dogs lost 3.4 kg (42%) of BM in winter and gained 5.1 kg (125%) in summer (Table 1). The seasonal changes in BMI for winter and summer were  $-35$  and  $+88\%$ , respectively. The hemoglobin, hematocrit, monocyte %, eosinophil %, plasma TAG, HDL-Chol, urea and ammonia concentrations and urea:creatinine ratios were higher in autumn than in spring. The percentages of 14:0, 16:0, total SFA, 16:1n-7, 18:3n-3 and total n-3 PUFA decreased in WAT in winter, while the proportions of 18:1n-9, 20:1n-11, 20:1n-9, total MUFA, 22:4n-6 and 22:5n-3 increased (Tables 2, 3, 4). In plasma, the proportions of *i*18:0, 18:2n-4 and 20:5n-3 decreased, while those of *i*15:0, 20:0, 20:1n-9, 24:1n-9 and 22:5n-6 increased. Opposite changes were observed in the FA profiles from spring to autumn. According to PCA, 16–18C SFA and MUFA were mostly responsible for the seasonal differences in the WAT FA composition. The differences between the autumnal and vernal plasma FA profiles were

minor and the FA that separated the seasons were 16–18C SFA, 18:1n-9 and n-6 PUFA.

The FA with the highest relative mobilization from WAT in winter included 20:5n-3, 18:3n-3, 16:1n-7, 15:1n-6, 14:1n-5, 20:4n-3 and 18:4n-3 (–47 to –80%), while preservation was the highest for 22:1n-11, 20:0, 22:4n-6, 20:1n-9, 22:1n-9, 22:1n-7, 22:0 and 20:1n-11 (201–607%; Fig. 2). In summer, 20:5n-3, 18:4n-3, 20:4n-3, 18:3n-3, 16:1n-7, 14:1n-5 and 22:6n-3 increased (139–734%) and 20:0, 22:4n-6, 22:0, 20:1n-11, 19:0, 20:1n-9 and 20:1n-7 decreased the most in proportion (–47 to –72%) in WAT. One female raccoon dog did not fast, unlike the rest of the animals in winter. In this individual, 20:5n-3, 20:4n-3, 18:4n-3, 16:1n-5, 18:3n-6 and 20:4n-6 increased in proportion in winter, while they were mobilized in the other animals. Moreover, this individual preserved more 22:5n-6, 20:1n-5, 22:1n-7, 20:1n-7, 20:1n-11, 17:1n-br, 22:5n-3 and 20:3n-6 than the other raccoon dogs.

Wintertime preservation of FA in WAT correlated positively with the FA chain length of SFA ( $r_s = 0.766$ ,  $P < 0.001$ ; Fig. 3) and n-5, n-7 and n-9 MUFA ( $r_s = 0.640$ – $0.824$ ,  $P < 0.001$ ; subset of data in Fig. 4). The influence of chain length on the preservation of PUFA was investigated by comparing PUFA with the same degree of unsaturation and position of the first double bond from the methyl end but with different chain lengths. In five out of eight pairs the PUFA with the longer chain length was more preserved during wintering (subset of data in Fig. 5). When SFA and the corresponding MUFA were compared, mobilization was higher in MUFA in five out of six cases (subset of data in Fig. 6). The influence of unsaturation on the mobilization of PUFA was investigated by comparing PUFA with the same chain length and position of the first double bond but with different double bond numbers. The difference was significant in six out of nine pairs in the way that the PUFA with the higher number of double bonds had a higher mobilization rate in five cases and a lower mobilization rate in one case (subset of data in Fig. 7). The influence of positional isomerism on the preservation of MUFA was investigated by comparing MUFA of the same chain length but of a different position of the double bond. The preservation of 14, 15, 16, 18 and 20C MUFA correlated positively with the position of the double bond ( $r_s = 0.525$ – $0.869$ ,  $P < 0.05$ ; subset of data in Fig. 8). When comparing PUFA with the same chain length and unsaturation but with a different position of the first double bond, the difference was significant in six out of eight pairs in the way that the PUFA with the first double bond closer to the methyl end had a lower (one case) or a higher mobilization rate (five cases; subset of data in Fig. 9).

**Table 1** The effects of season on the body mass, body mass index, complete blood count and plasma clinical chemistry of the wild raccoon dogs (mean  $\pm$  SE)

	Autumn	Spring
BM (kg)		
Adults	8.6 $\pm$ 0.49*	4.3 $\pm$ 0.19*
Juveniles	6.2 $\pm$ 0.31*	
BM change (%)	125 $\pm$ 14*	–42 $\pm$ 6*
BMI [kg (m <sup>3</sup> ) <sup>–1</sup> ]		
Adults	30.4 $\pm$ 1.99*	17.2 $\pm$ 0.67*
Juveniles	25.5 $\pm$ 0.98*	
BMI change (%)	88 $\pm$ 18*	–35 $\pm$ 5*
WBC [10 <sup>3</sup> (mm <sup>3</sup> ) <sup>–1</sup> ]	14.0 $\pm$ 0.79	13.1 $\pm$ 1.41
RBC [10 <sup>6</sup> (mm <sup>3</sup> ) <sup>–1</sup> ]	5.9 $\pm$ 0.15	5.3 $\pm$ 0.28
HGB (g l <sup>–1</sup> )	120 $\pm$ 4*	103 $\pm$ 5*
HCT (%)	36.4 $\pm$ 1.13*	31.6 $\pm$ 1.41*
PLT [10 <sup>3</sup> (mm <sup>3</sup> ) <sup>–1</sup> ]	456 $\pm$ 46	455 $\pm$ 50
MCV ( $\mu$ m <sup>3</sup> )	61.9 $\pm$ 1.22	59.6 $\pm$ 1.30
MCH (pg)	20.3 $\pm$ 0.43	19.4 $\pm$ 0.58
MCHC (g dl <sup>–1</sup> )	32.8 $\pm$ 0.36	32.6 $\pm$ 0.52
RDW (%)	16.3 $\pm$ 0.26	16.5 $\pm$ 0.39
MPV ( $\mu$ m <sup>3</sup> )	8.4 $\pm$ 0.31	9.3 $\pm$ 0.29
LYM (%)	9.0 $\pm$ 0.98	7.5 $\pm$ 0.58
MON (%)	3.0 $\pm$ 0.24*	1.9 $\pm$ 0.22*
GRA (%)	88.0 $\pm$ 1.19	90.6 $\pm$ 0.76
EOS (%)	8.4 $\pm$ 1.36*	3.7 $\pm$ 1.51*
Glucose (mmol l <sup>–1</sup> )	6.9 $\pm$ 0.59	6.4 $\pm$ 0.62
Triacylglycerols (mmol l <sup>–1</sup> )	0.6 $\pm$ 0.10*	0.4 $\pm$ 0.04*
Total cholesterol (mmol l <sup>–1</sup> )	4.3 $\pm$ 0.35	3.6 $\pm$ 0.25
LDL-cholesterol (mmol l <sup>–1</sup> )	0.4 $\pm$ 0.06	0.3 $\pm$ 0.03
HDL-cholesterol (mmol l <sup>–1</sup> )	3.2 $\pm$ 0.27*	2.3 $\pm$ 0.20*
Bilirubin ( $\mu$ mol l <sup>–1</sup> )	4.3 $\pm$ 0.75	3.6 $\pm$ 0.92
ALT (U l <sup>–1</sup> )	91 $\pm$ 15	64 $\pm$ 14
AST (U l <sup>–1</sup> )	71 $\pm$ 11	43 $\pm$ 14
CK (U l <sup>–1</sup> )	424 $\pm$ 110	230 $\pm$ 76
Urea (mmol l <sup>–1</sup> )	9.3 $\pm$ 1.88*	4.0 $\pm$ 0.54*
Ammonia ( $\mu$ mol l <sup>–1</sup> )	867 $\pm$ 44*	743 $\pm$ 37*
Uric acid ( $\mu$ mol l <sup>–1</sup> )	23.1 $\pm$ 3.53	19.0 $\pm$ 3.18
Total protein (g l <sup>–1</sup> )	67 $\pm$ 2	69 $\pm$ 3
Creatinine ( $\mu$ mol l <sup>–1</sup> )	76 $\pm$ 10	75 $\pm$ 5
Urea:creatinine ratio	150 $\pm$ 33*	55 $\pm$ 9*

BM body mass, BMI body mass index, WBC white blood cell count, RBC red blood cell count, HGB hemoglobin, HCT hematocrit, PLT platelet count, MCV mean corpuscular volume, MCH mean corpuscular hemoglobin, MCHC mean corpuscular hemoglobin concentration, RDW red cell distribution width, MPV mean platelet volume, LYM lymphocyte, MON monocyte, GRA granulocyte, EOS eosinophil, LDL low-density lipoprotein, HDL high-density lipoprotein, ALT alanine aminotransferase, AST aspartate aminotransferase, CK creatine kinase

\* Significant difference between the seasons ( $P < 0.05$ )

**Table 2** The effects of season on the white adipose tissue and plasma compositions of saturated fatty acids (mol%) in the wild raccoon dogs (mean  $\pm$  SE)

Fatty acid	White adipose tissue		Plasma	
	Autumn	Spring	Autumn	Spring
12:0	0.4 $\pm$ 0.04	0.3 $\pm$ 0.02	0.1 $\pm$ 0.03	0.2 $\pm$ 0.11
<i>i</i> 14:0	0.05 $\pm$ 0.002	0.05 $\pm$ 0.005	0.05 $\pm$ 0.005	0.08 $\pm$ 0.012
14:0	4.3 $\pm$ 0.24*	3.5 $\pm$ 0.21*	0.5 $\pm$ 0.05	0.4 $\pm$ 0.03
<i>i</i> 15:0	0.3 $\pm$ 0.03	0.3 $\pm$ 0.07	0.5 $\pm$ 0.11*	0.9 $\pm$ 0.21*
<i>ai</i> 15:0	0.12 $\pm$ 0.005	0.14 $\pm$ 0.018	0.08 $\pm$ 0.005	0.10 $\pm$ 0.008
15:0	0.4 $\pm$ 0.02*	0.3 $\pm$ 0.03*	0.3 $\pm$ 0.02	0.3 $\pm$ 0.02
<i>i</i> 16:0	0.2 $\pm$ 0.01	0.2 $\pm$ 0.02	0.2 $\pm$ 0.02	0.2 $\pm$ 0.01
16:0	20.4 $\pm$ 0.47*	14.8 $\pm$ 0.49*	15.6 $\pm$ 0.38	16.8 $\pm$ 0.45
<i>i</i> 17:0	0.3 $\pm$ 0.03	0.4 $\pm$ 0.07	0.5 $\pm$ 0.04	0.6 $\pm$ 0.09
<i>ai</i> 17:0	0.5 $\pm$ 0.03	0.5 $\pm$ 0.05	0.4 $\pm$ 0.03	0.3 $\pm$ 0.04
17:0	0.7 $\pm$ 0.06	0.6 $\pm$ 0.07	0.9 $\pm$ 0.08	0.7 $\pm$ 0.09
<i>i</i> 18:0	0.13 $\pm$ 0.008*	0.19 $\pm$ 0.022*	0.15 $\pm$ 0.013*	0.09 $\pm$ 0.012*
18:0	10.9 $\pm$ 0.80	13.7 $\pm$ 1.10	19.0 $\pm$ 0.62	17.9 $\pm$ 0.51
19:0	0.1 $\pm$ 0.01*	0.2 $\pm$ 0.03*	0.2 $\pm$ 0.02	0.2 $\pm$ 0.01
20:0	0.21 $\pm$ 0.009*	0.67 $\pm$ 0.067*	0.18 $\pm$ 0.010*	0.24 $\pm$ 0.013*
22:0	0.05 $\pm$ 0.003*	0.12 $\pm$ 0.013*	0.12 $\pm$ 0.009	0.16 $\pm$ 0.020
24:0	0.04 $\pm$ 0.002*	0.08 $\pm$ 0.012*	0.28 $\pm$ 0.013	0.31 $\pm$ 0.015
$\Sigma$ :0	38.9 $\pm$ 0.76*	35.9 $\pm$ 0.81*	39.0 $\pm$ 0.60	39.3 $\pm$ 0.33

*i* iso, *ai* anteiso\* Significant difference between the seasons ( $P < 0.05$ )**Table 3** The effects of season on the white adipose tissue and plasma compositions of monounsaturated fatty acids (mol%) in the wild raccoon dogs (mean  $\pm$  SE)

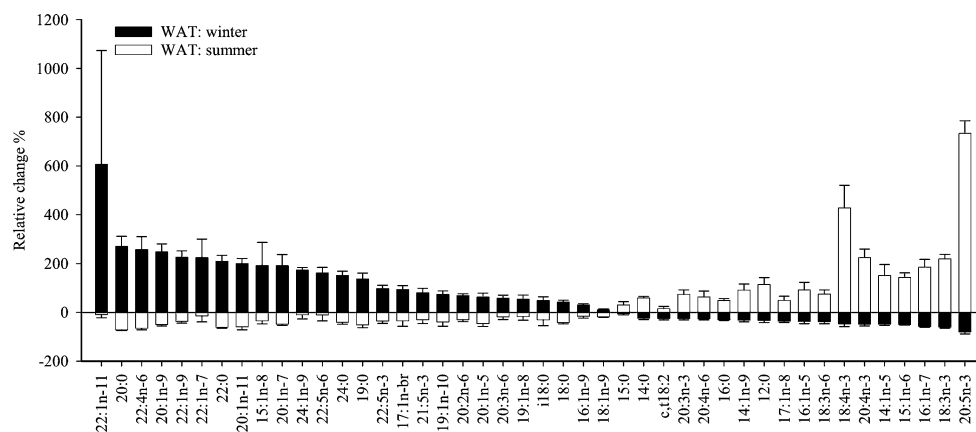
Fatty acid	White adipose tissue		Plasma	
	Autumn	Spring	Autumn	Spring
14:1n-9	0.03 $\pm$ 0.002*	0.02 $\pm$ 0.002*	0.06 $\pm$ 0.008	0.07 $\pm$ 0.007
14:1n-7	0.03 $\pm$ 0.003	0.04 $\pm$ 0.004	0.11 $\pm$ 0.012	0.08 $\pm$ 0.011
14:1n-5	0.4 $\pm$ 0.03*	0.3 $\pm$ 0.02*	0.1 $\pm$ <0.01	0.1 $\pm$ <0.01
15:1n-8	0.03 $\pm$ 0.004	0.05 $\pm$ 0.011	0.05 $\pm$ 0.009	0.05 $\pm$ 0.005
15:1n-6	0.03 $\pm$ 0.002*	0.01 $\pm$ 0.001*	0.03 $\pm$ 0.002*	0.05 $\pm$ 0.007*
16:1n-9	0.5 $\pm$ 0.04	0.5 $\pm$ 0.04	0.3 $\pm$ 0.04	0.3 $\pm$ 0.02
16:1n-7	5.9 $\pm$ 0.30*	2.7 $\pm$ 0.30*	1.0 $\pm$ 0.06	0.9 $\pm$ 0.05
16:1n-5	0.12 $\pm$ 0.010*	0.08 $\pm$ 0.007*	0.09 $\pm$ 0.011	0.09 $\pm$ 0.010
17:1n-br	0.1 $\pm$ 0.01*	0.2 $\pm$ 0.05*	0.2 $\pm$ 0.03	0.2 $\pm$ 0.01
17:1n-8	0.6 $\pm$ 0.02*	0.3 $\pm$ 0.03*	0.2 $\pm$ 0.02	0.2 $\pm$ 0.04
18:1n-9	34.1 $\pm$ 0.70*	38.5 $\pm$ 1.15*	10.5 $\pm$ 1.17	12.0 $\pm$ 1.34
18:1n-7	2.6 $\pm$ 0.07	2.6 $\pm$ 0.07	2.7 $\pm$ 0.17	2.5 $\pm$ 0.22
18:1n-5	0.2 $\pm$ 0.01	0.2 $\pm$ 0.02	0.1 $\pm$ 0.02	0.1 $\pm$ 0.01
19:1n-10	0.2 $\pm$ 0.01*	0.3 $\pm$ 0.04*	0.1 $\pm$ 0.01	0.1 $\pm$ 0.01
19:1n-8	0.08 $\pm$ 0.004*	0.11 $\pm$ 0.008*	0.09 $\pm$ 0.005	0.09 $\pm$ 0.007
20:1n-11	0.3 $\pm$ 0.03*	1.2 $\pm$ 0.19*	0.1 $\pm$ 0.02	0.1 $\pm$ 0.02
20:1n-9	0.43 $\pm$ 0.032*	1.41 $\pm$ 0.164*	0.16 $\pm$ 0.013*	0.20 $\pm$ 0.015*
20:1n-7	0.05 $\pm$ 0.004*	0.13 $\pm$ 0.012*	0.08 $\pm$ 0.012	0.06 $\pm$ 0.007
20:1n-5	0.02 $\pm$ 0.002*	0.05 $\pm$ 0.007*	0.03 $\pm$ 0.005	0.03 $\pm$ 0.007
22:1n-11	0.07 $\pm$ 0.016*	0.30 $\pm$ 0.120*	0.03 $\pm$ 0.011	0.03 $\pm$ 0.012
22:1n-9	0.04 $\pm$ 0.003*	0.11 $\pm$ 0.018*	0.06 $\pm$ 0.007	0.05 $\pm$ 0.007
22:1n-7	0.01 $\pm$ 0.001*	0.02 $\pm$ 0.005*	0.04 $\pm$ 0.008	0.03 $\pm$ 0.005
24:1n-9	0.03 $\pm$ 0.004*	0.08 $\pm$ 0.017*	0.40 $\pm$ 0.034*	0.63 $\pm$ 0.057*
$\Sigma$ :1	45.9 $\pm$ 0.56*	49.3 $\pm$ 0.90*	16.7 $\pm$ 1.04	17.9 $\pm$ 1.13
$\Delta$ 9-DI	1.2 $\pm$ 0.03*	1.4 $\pm$ 0.05*	0.4 $\pm$ 0.03	0.5 $\pm$ 0.04

*br* branched-chain,  $\Delta$ 9-DI  $\Delta$ 9-desaturation index\* Significant difference between the seasons ( $P < 0.05$ )

**Table 4** The effects of season on the white adipose tissue and plasma compositions of polyunsaturated fatty acids (mol%) in the wild raccoon dogs (mean  $\pm$  SE)

Fatty acid	White adipose tissue		Plasma	
	Autumn	Spring	Autumn	Spring
16:2n-4	0.04 $\pm$ 0.005	0.07 $\pm$ 0.029	0.17 $\pm$ 0.019	0.21 $\pm$ 0.049
18:2n-7	0.2 $\pm$ 0.03	0.1 $\pm$ 0.02	0.1 $\pm$ 0.02	0.1 $\pm$ 0.03
18:2n-6	7.2 $\pm$ 0.29	7.5 $\pm$ 0.33	14.3 $\pm$ 1.51	15.8 $\pm$ 0.92
18:2n-4	0.2 $\pm$ 0.02	0.2 $\pm$ 0.06	0.2 $\pm$ 0.02*	0.1 $\pm$ 0.02*
18:3n-6	0.07 $\pm$ 0.004*	0.04 $\pm$ 0.004*	0.14 $\pm$ 0.009*	0.09 $\pm$ 0.011*
18:3n-3	2.5 $\pm$ 0.15*	0.9 $\pm$ 0.05*	0.9 $\pm$ 0.14	0.9 $\pm$ 0.35
<i>c,t</i> 18:2	0.3 $\pm$ 0.02*	0.2 $\pm$ 0.02*	0.1 $\pm$ 0.02	0.1 $\pm$ 0.02
18:4n-3	0.11 $\pm$ 0.016*	0.05 $\pm$ 0.018*	0.08 $\pm$ 0.012	0.07 $\pm$ 0.009
18:4n-1	0.03 $\pm$ 0.003	0.03 $\pm$ 0.006	0.08 $\pm$ 0.011	0.09 $\pm$ 0.029
20:2n-6	0.3 $\pm$ 0.03*	0.6 $\pm$ 0.06*	0.3 $\pm$ 0.06	0.3 $\pm$ 0.01
20:3n-6	0.2 $\pm$ 0.01*	0.3 $\pm$ 0.04*	0.7 $\pm$ 0.07	0.8 $\pm$ 0.06
20:4n-6	1.1 $\pm$ 0.11*	0.8 $\pm$ 0.08*	18.0 $\pm$ 1.06	16.0 $\pm$ 1.27
20:3n-3	0.2 $\pm$ 0.01	0.1 $\pm$ 0.01	0.1 $\pm$ 0.02	0.1 $\pm$ 0.01
20:4n-3	0.15 $\pm$ 0.018*	0.08 $\pm$ 0.009*	0.13 $\pm$ 0.023	0.09 $\pm$ 0.011
20:5n-3	0.5 $\pm$ 0.05*	0.1 $\pm$ 0.03*	2.8 $\pm$ 0.41*	1.3 $\pm$ 0.32*
21:5n-3	0.04 $\pm$ 0.004*	0.09 $\pm$ 0.015*	0.07 $\pm$ 0.022	0.09 $\pm$ 0.025
22:4n-6	0.4 $\pm$ 0.04*	1.2 $\pm$ 0.17*	1.2 $\pm$ 0.10	1.2 $\pm$ 0.14
22:5n-6	0.1 $\pm$ 0.01*	0.2 $\pm$ 0.03*	0.2 $\pm$ 0.04*	0.4 $\pm$ 0.06*
22:4n-3	0.02 $\pm$ 0.002	0.03 $\pm$ 0.004	0.04 $\pm$ 0.009	0.03 $\pm$ 0.010
22:5n-3	0.7 $\pm$ 0.06*	1.4 $\pm$ 0.19*	2.0 $\pm$ 0.18	1.7 $\pm$ 0.23
22:6n-3	0.8 $\pm$ 0.11	0.7 $\pm$ 0.14	2.5 $\pm$ 0.32	3.3 $\pm$ 0.69
$\Sigma$ :PUFA	15.2 $\pm$ 0.73	14.8 $\pm$ 0.70	44.3 $\pm$ 1.32	42.8 $\pm$ 1.06
$\Sigma$ :n-6 PUFA	9.4 $\pm$ 0.44	10.6 $\pm$ 0.45	34.9 $\pm$ 1.39	34.6 $\pm$ 0.94
$\Sigma$ :n-3 PUFA	5.0 $\pm$ 0.38*	3.5 $\pm$ 0.29*	8.7 $\pm$ 0.80	7.6 $\pm$ 0.80
n-3/n-6 PUFA	0.53 $\pm$ 0.028*	0.32 $\pm$ 0.021*	0.26 $\pm$ 0.028	0.22 $\pm$ 0.025
$\Sigma$ :VLCFA	0.07 $\pm$ 0.005*	0.17 $\pm$ 0.027*	0.68 $\pm$ 0.037*	0.94 $\pm$ 0.061*
UFA/SFA	1.6 $\pm$ 0.05*	1.8 $\pm$ 0.07*	1.6 $\pm$ 0.04	1.5 $\pm$ 0.02
DBI	0.9 $\pm$ 0.03	0.9 $\pm$ 0.02	1.7 $\pm$ 0.05	1.6 $\pm$ 0.06
TACL	17.4 $\pm$ 0.02*	17.7 $\pm$ 0.03*	18.3 $\pm$ 0.05	18.3 $\pm$ 0.06

*c* cis, *t* trans, PUFA polyunsaturated fatty acid, VLCFA very-long-chain fatty acid ( $\geq 24$ C), UFA unsaturated fatty acid, SFA saturated fatty acid, DBI double bond index, TACL total average chain length  
\* Significant difference between the seasons ( $P < 0.05$ )

**Fig. 2** The relative changes (%) in the proportions of white adipose tissue (WAT) fatty acids (FA) of the wild raccoon dogs during winter and summer (mean  $\pm$  SE). + values indicate that a FA increased in proportion during winter or summer and – values signify a decrease in proportion. All winter and summer means differ significantly from each other ( $P < 0.05$ ), *br* branched-chain, *i* iso, *c* cis, *t* trans

In summer, the incorporation of FA into WAT correlated inversely with the FA chain length of SFA ( $r_s = -0.818$ ,  $P < 0.001$ ; Fig. 3) and n-5 and n-7 MUFA

( $r_s = -0.700$  to  $-0.845$ ,  $P < 0.001$ ; Fig. 4). In PUFA pairs the difference was significant in five out of eight cases in the way that the PUFA with the longer chain length was

**Fig. 3** The correlations between the relative seasonal change (%) and the chain length (C) of saturated fatty acids (FA) of the wild raccoon dogs during winter (a) and summer (b). + values indicate that a FA increased in proportion during winter or summer and – values signify a decrease in proportion

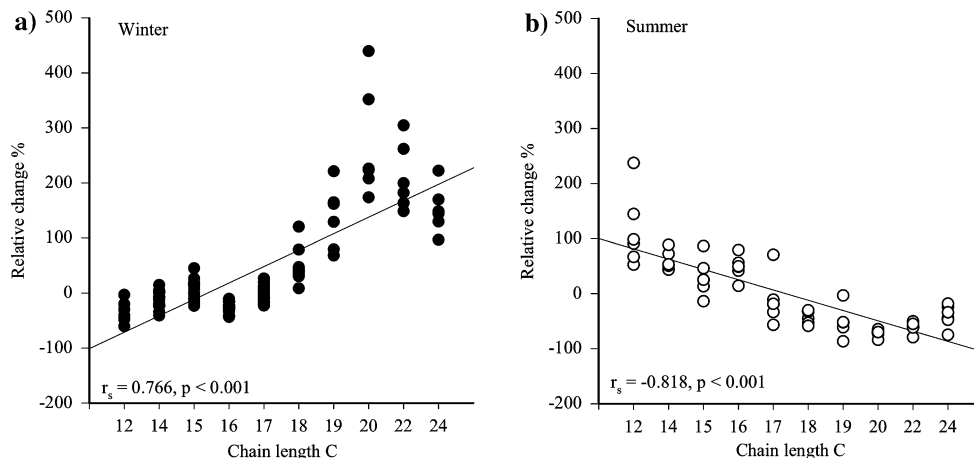
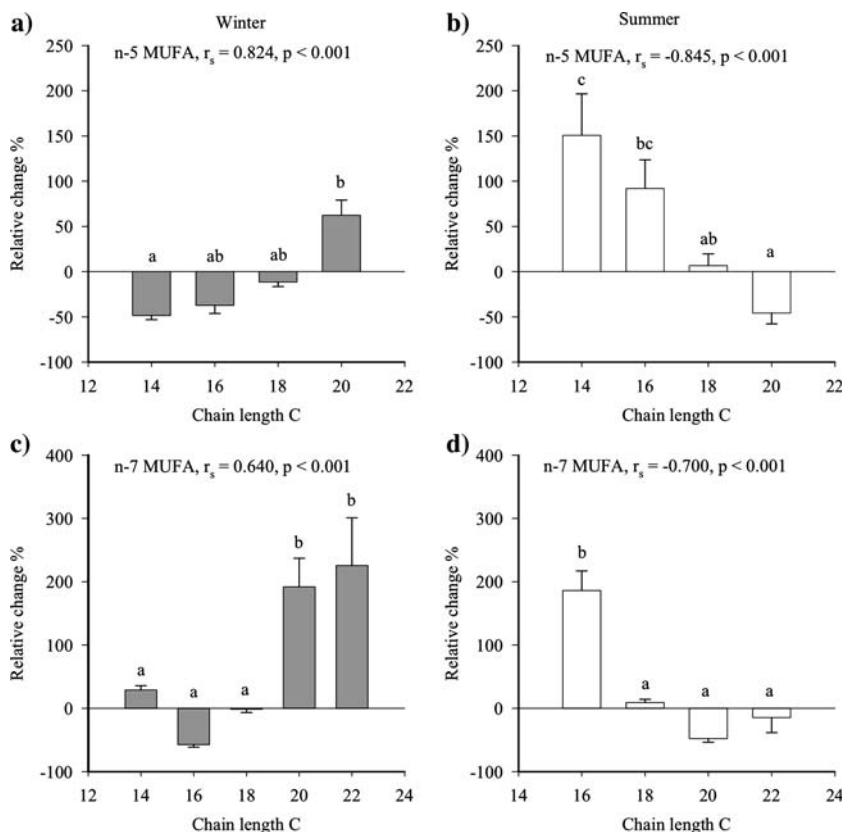


**Fig. 4** The effect of chain length (C) on the relative seasonal change (%) in the proportions of white adipose tissue n-5 and n-7 monounsaturated fatty acids (FA) of the wild raccoon dogs during winter (a, c) and summer (b, d; mean + SE). + values indicate that a FA increased in proportion during winter or summer and – values signify a decrease in proportion. Dissimilar letters signify statistically significant differences between the means ( $P < 0.05$ )



less accumulated in summer (subset of data in Fig. 5). When SFA and the corresponding MUFA were compared, incorporation was higher in MUFA in four out of six cases (subset of data in Fig. 6). In seven out of nine PUFA pairs the PUFA with the higher number of double bonds had higher (six cases) or lower accumulation (one case; subset of data in Fig. 7). The incorporation of 15–16C MUFA correlated negatively with the position of the double bond from the methyl end ( $r_s = -0.564$  to  $-0.869$ ,  $P < 0.05$ ; Fig. 8). When comparing PUFA pairs the difference was significant in five out of eight cases in the way that the PUFA with the first double bond closer to the methyl end

had higher (four cases) or lower accumulation (one case; subset of data in Fig. 9).

## Discussion

### Selective Mobilization of FA from the sc Adipose Tissue

Selective mobilization of FA from WAT was previously investigated, e.g., in humans fasted for 14–20 h [8] and in laboratory rodents fasted for 1–10 days [4]. Little data exist

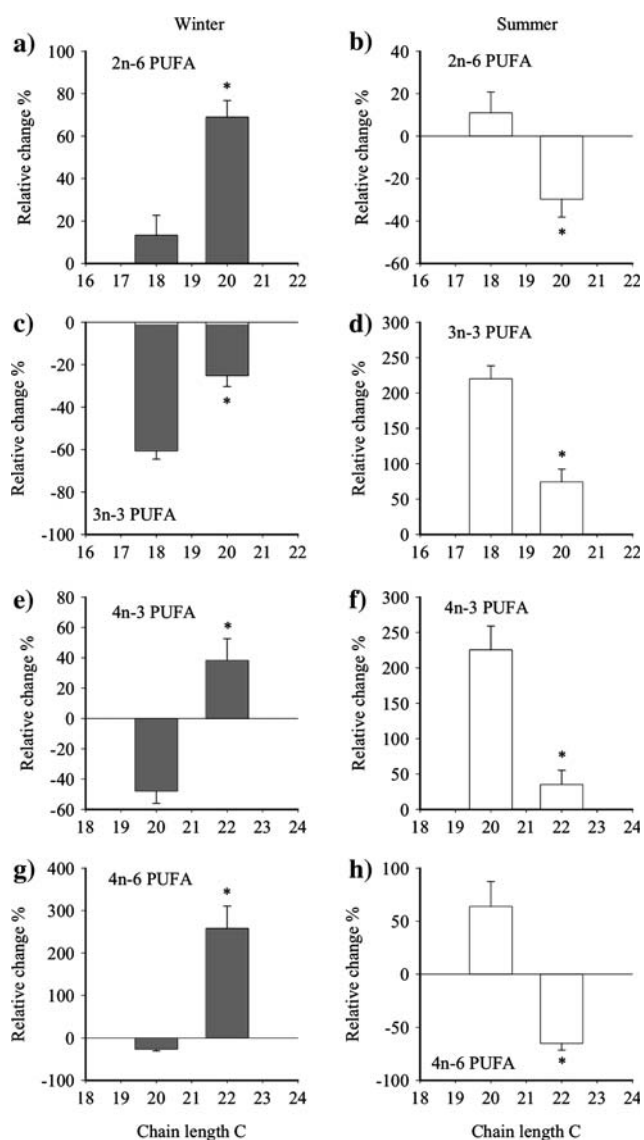


**Fig. 5** The effect of chain length ( $C$ ) on the relative seasonal change (%) in the proportions of representative white adipose tissue polyunsaturated fatty acids ( $FA$ ) of the wild raccoon dogs during winter (**a, c, e, g**) and summer (**b, d, f, h**; mean  $\pm$  SE). + values indicate that a  $FA$  increased in proportion during winter or summer and – values signify a decrease in proportion. Asterisks signify statistically significant differences between the means ( $P < 0.05$ )

from wild animals with a long fast as a natural part of their seasonal weight cycling. The  $FA$  mobilization from the sc adipose tissue of the spontaneously fasting emperor penguin (*Aptenodytes forsteri*) was studied in this respect yielding results with high similarity to captive mammals [25]. The present study explored the selective  $FA$  mobilization in the wild raccoon dog. The sc adipose tissue samples were obtained from the same individuals before and after wintering and the results could be compared to previous data from the same species in captivity [10]. Although the average BM of the animals decreased by 42%, the fat stores

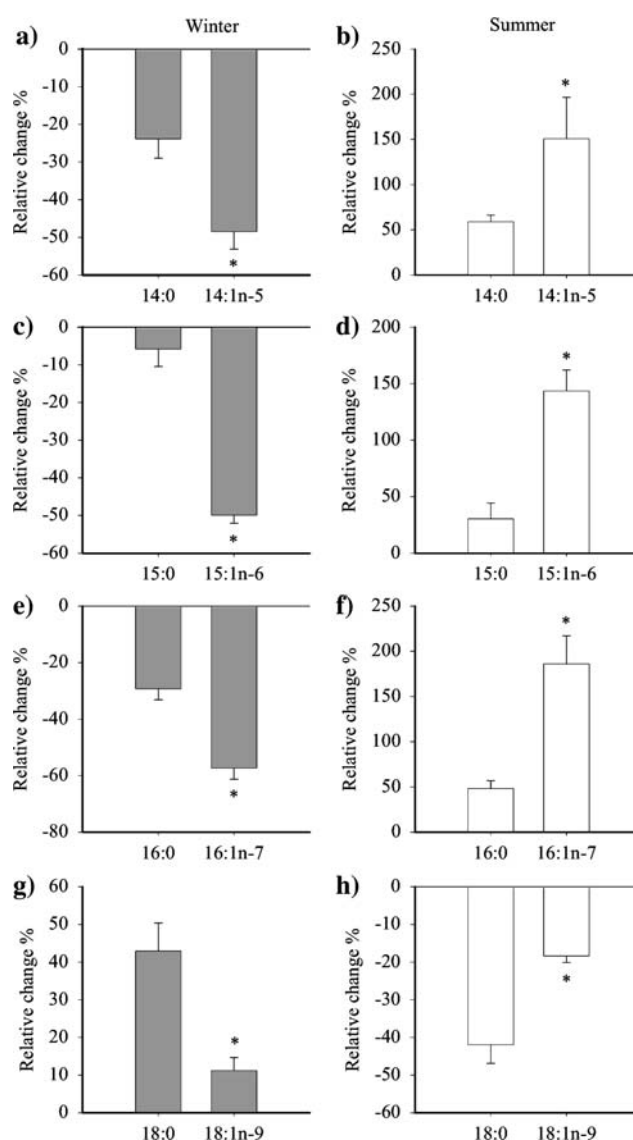


**Fig. 6** The effect of  $\Delta 9$ -desaturation on the relative seasonal change (%) in the proportions of representative white adipose tissue fatty acids ( $FA$ ) of the wild raccoon dogs during winter (**a, c, e, g**) and summer (**b, d, f, h**; mean  $\pm$  SE). + values indicate that a  $FA$  increased in proportion during winter or summer and – values signify a decrease in proportion. Asterisks signify statistically significant differences between the means ( $P < 0.05$ )

were large enough to provide metabolic energy during wintering without the need to stimulate proteolysis [13]. The negative energy balance did not cause deleterious health effects, such as liver or kidney dysfunction, in the animals.

The mobilization of  $FA$  decreases with the chain length for a given degree of unsaturation in laboratory rodents [4]. Similar to captive raccoon dogs [10], the wild raccoon dogs had an inverse correlation between the  $FA$  chain length and the mobilization of SFA, n-5, n-7 and n-9 MUFA and particular n-3 and n-6 PUFA. The observed low mobilization

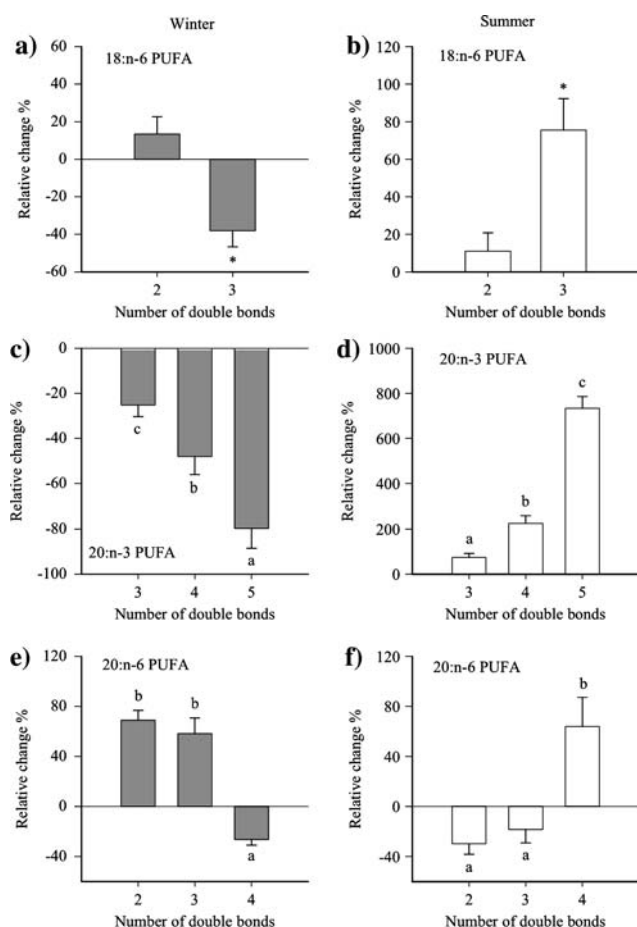


**Fig. 7** The effect of double bond number on the relative seasonal change (%) in the proportions of representative white adipose tissue polyunsaturated fatty acids (FA) of the wild raccoon dogs during winter (a, c, e) and summer (b, d, f; mean + SE). + values indicate that a FA increased in proportion during winter or summer and – values signify a decrease in proportion. Asterisks and dissimilar letters signify statistically significant differences between the means ( $P < 0.05$ )

rate of 20–24C SFA and MUFA was previously documented in fasting rats [4] and emperor penguins [25]. 12–16C SFA and 14–16C MUFA were among the most mobilized FA in the farmed [10] and wild raccoon dogs, while 15:1n-8 and 16:1n-9 were less utilized. It is possible that the raccoon dogs had to prevent the solidification of the sc fat layer by chain-shortening of 18:1n-9 and 17:1n-8 leading to increased proportions of 16:1n-9 and 15:1n-8. In laboratory rats, rabbits and humans the mobilization of FA increases with unsaturation for a given chain length [4, 7, 8]. In the wild raccoon dogs, too, FA mobilization increased with  $\Delta 9$ -desaturation and with double bond number in n-3 and n-6 PUFA. The effect of unsaturation on mobilization efficiency was more prominent in the wild raccoon dogs than in captive animals [10].

It has been suggested that TAG are distributed in the lipid droplet according to their polarity. As the shorter and more

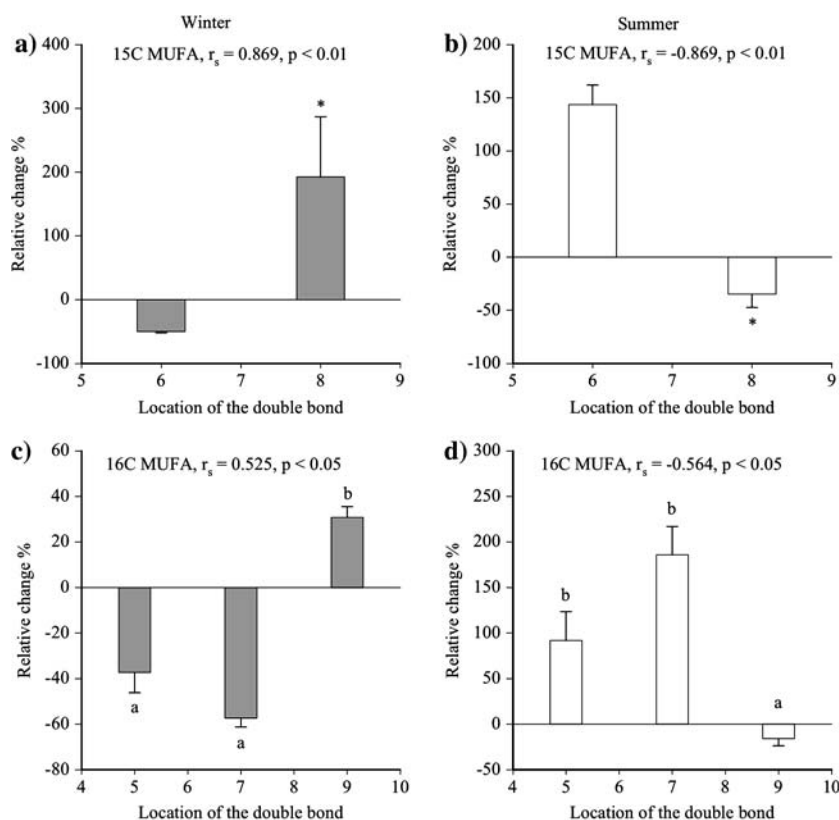
unsaturated FA are more polar, TAG containing them are located at the periphery of the lipid droplet. Thus they are more accessible to hydrolysis by hormone-sensitive lipase (HSL) at the lipid–water interface resulting in the preservation of the longer-chain FA [9, 26]. The preference of HSL to hydrolyze shorter-chain [27] and unsaturated FA (UFA) [28] could partly explain their depletion from WAT during wintering. Moreover, the reuptake of the more polar FA to WAT is weaker than that of the less polar FA during lipolysis [29], short SFA can be more readily oxidized than longer SFA [30] and peroxisomal  $\beta$ -oxidation increases with unsaturation [31]. On the other hand, the positional distribution of FA in TAG cannot explain the preferential mobilization of the more polar FA [32]. In the wild raccoon dogs, the highly unsaturated 22:4n-6, 22:5n-3, 22:5n-6 and 22:6n-3 were less mobilized than most other PUFA possibly as a result of their long carbon chains, resistance to HSL [33], their significance in membrane phospholipids and, in the case of 22:4n-6, in the synthesis of 4-series prostaglandins [2].

In laboratory rats, the mobilization of UFA increases when the double bonds are located closer to the methyl end of the FA chain [4]. The same was observed for most MUFA and for several n-3 and n-6 PUFA pairs in the wild raccoon dogs, while the effect was less pronounced in captive animals [10]. It has been demonstrated in several species that fasting decreases the proportions of particular n-3 PUFA in adipose tissue [4, 10, 21, 34]. In addition to the wild raccoon dog, the proportion of 18:3n-3 in the reindeer (*Rangifer tarandus tarandus*) adipose tissue also decreases during nutritional scarcity in winter [35]. This is in accordance with the principle of competitive inhibition, which states that in the rate-limiting steps of PUFA desaturation n-3 substrates are favored over n-6 ones [2]. In the scarcity of dietary n-3 PUFA the shorter-chain n-3 PUFA could be metabolized to produce the biologically most important member of the n-3 family, 22:6n-3, the WAT and plasma percentages of which were preserved during wintering.

In the rat, n-3 PUFA are mobilized in vitro in the following order: 20:5n-3 > 18:4n-3 > 22:6n-3 > 22:5n-3 [36], similar to the wild raccoon dog. 20:5n-3 is preferred over 22:5n-3 and 22:6n-3 by HSL [33] and it functions as the precursor for 3-series prostaglandins [2], which may be associated with its depletion during fasting. During lipolysis, the selective reuptake to WAT is weak for PUFA with 16–20C and 4–5 double bonds [37], i.e., the highly mobilized FA 20:5n-3, 20:4n-3 and 18:4n-3 in the present study. Moreover, the dietarily essential 18:3n-3 is a preferred substrate for  $\beta$ -oxidation and a precursor of longer-chain, more unsaturated n-3 PUFA [38]. The preferential mobilization of n-3 PUFA causes a decrease in the n-3/n-6 PUFA ratio, which affects the quality of eicosanoids produced. When 1-, 2- and 4-series prostaglandins (derived



**Fig. 8** The effect of the location of the double bond from the methyl end on the relative seasonal change (%) in the proportions of white adipose tissue 15–16C monounsaturated fatty acids (FA) of the wild raccoon dogs during winter (a, c) and summer (b, d; mean + SE). + values indicate that a FA increased in proportion during winter or summer and – values signify a decrease in proportion. Asterisks and dissimilar letters signify statistically significant differences between the means ( $P < 0.05$ )



from cyclooxygenated n-6 PUFA) increase their proportion at the expense of 3-series prostaglandins (derived from cyclooxygenated 20:5n-3) and comparable cascades occur in other eicosanoids; platelet aggregation, vascular tonus and blood pressure can change in an undesirable direction [2]. Therefore fasting or weight cycling may cause adverse health effects.

In contrast to the other raccoon dogs of the present study, one female was very active throughout the winter feeding on freshwater fish discarded by local fishermen on the ice in February–March. This individual had increased proportions of 16:1n-5 and particular n-3 and n-6 PUFA in WAT, unlike the other animals. Moreover, it preserved more 20–22C MUFA, 22:5n-3 and particular n-6 PUFA. The different FA composition was presumably caused by the intake of freshwater fish containing, e.g., high proportions of n-3 and n-6 PUFA [39, 40]. While the other raccoon dogs fasted in winter dens and utilized the most readily mobilizable FA, especially n-3 PUFA, this individual was able to restore these FA continuously from dietary sources.

#### Selective Incorporation of FA into the sc Adipose Tissue

The uptake of dietary FA into adipocytes occurs in several steps: (1) absorption, (2) incorporation into chylomicron

TAG, (3) hydrolysis of TAG by adipose tissue lipoprotein lipase (LPL), (4) uptake of FA into adipocytes and their esterification. The steps of FA accumulation have been previously investigated in laboratory animals and humans [36, 41–48] but rarely in seasonal mammals. In the captive alpine marmot (*Marmota marmota*) the FA composition of the sc and gonadal WAT did not change in spite of hibernation and the subsequent refeeding period with fat accumulation [49]. Wild Belding's ground squirrels (*Spermophilus beldingi*), on the other hand, accumulated 16:1n-7 and 18:1n-9 during the fattening period between summer and autumn with a simultaneous decrease in the proportion of 18:3n-3 in the sc and intraabdominal adipose tissues [50].

In contrast to studies on FA mobilization yielding similar results in diverse animal species and time periods of fasting [4, 8, 10, 25], data on FA incorporation into WAT have failed to provide comprehensive principles of FA storage in relation to their structure. It is known that while FA deposition depends on the composition of dietary FA, selectivity will influence the eventual profile of deposited FA in WAT [43, 44, 46–48]. Moreover, the in vivo accumulation of particular n-3 PUFA is inversely related to their in vitro mobilization in the rat [36]. Yet there is a lack of data on the selective accumulation of FA into WAT of wild mammals. The present study had certain advantages over previous work on laboratory rodents and humans: (1)

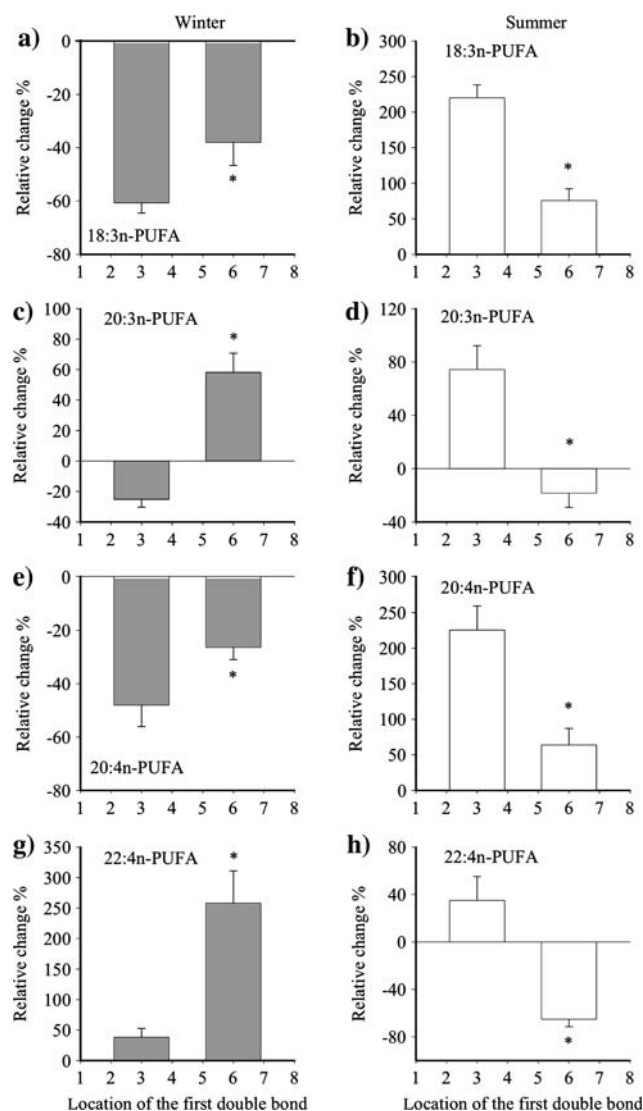


**Fig. 9** The effect of the location of the first double bond from the methyl end on the relative seasonal change (%) in the proportions of representative white adipose tissue polyunsaturated fatty acids (FA) of the wild raccoon dogs during winter (a, c, e, g) and summer (b, d, f, h; mean + SE). + values indicate that a FA increased in proportion during winter or summer and – values signify a decrease in proportion. Asterisks signify statistically significant differences between the means ( $P < 0.05$ )

it was conducted on free-ranging animals feeding on their natural diet, (2) the period of body fat accumulation lasted for 6–7 months with an 88% increase in the body fat content (BMI), (3) the vernal and autumnal FA profiles were determined from the same individuals and (4) 61 FA could be identified and their accumulation analyzed in relation to the FA structure.

The incorporation of FA into WAT was higher for shorter-chain SFA, n-5 and n-7 MUFA and PUFA in the wild raccoon dog, which may be due to a variety of factors, such as the preferential hydrolysis of shorter FA by LPL

[51, 52]. In contrast, longer FA were incorporated more efficiently than 10:0 and 12:0 in the rat [44]. According to Lin et al. [46], MUFA and PUFA accumulated more efficiently than SFA in the rabbit and the data from the wild raccoon dog support these findings. The incorporation into WAT was higher for several MUFA compared to the corresponding SFA and the accumulation of several PUFA increased with the insertion of an additional double bond. However, previous studies have shown decreased LPL hydrolysis with increased unsaturation [53]. For this reason, there may be also other mechanisms explaining the effect of the double bond number on the accumulation of FA into WAT of the wild raccoon dog.

15–16C MUFA accumulated more readily into WAT of the wild raccoon dogs when their double bond was located closer to the methyl end of the chain. Also particular n-3 PUFA had a higher accumulation efficiency than the corresponding n-6 PUFA. Our results are similar to those of Lin et al. [54] who showed in cattle (*Bos taurus*) that the in vitro incorporation of 18:3n-3 into adipocytes can be higher than that of 18:2n-6. In contrast, n-6 PUFA were stored more efficiently than n-3 PUFA in humans [48] and the deposition index of 18:2n-6 was higher than that of 18:3n-3 in rabbits [46]. According to previous studies [36, 45], n-3 PUFA are incorporated into WAT in the following order: 22:5n-3 > 22:6n-3 > 18:4n-3 > 20:5n-3, opposite to their relative mobilization. The wild raccoon dogs did not follow this rule during the summertime fat accumulation.

It is possible that the short-term storage of n-3 PUFA in WAT could have been weak [48] also in the raccoon dogs. Yet the animals were able to reverse the wintertime losses of the efficiently utilized n-3 PUFA in summer. In contrast, during short-term weight cycling of rats (24-h of fasting + 72-h of ad lib refeeding, four cycles), 18:3n-3 was selectively depleted from adipose tissue despite the adequate supply of this PUFA from the diet [55]. As the raccoon dogs mobilized 20:5n-3 and 18:4n-3 efficiently in winter, the relative increases in their proportions were high during the food abundance in summer. The long time period for fat accumulation could have masked the regulatory mechanisms responsible for the short-term control of fat storage. It is understandable that in a species with a lifespan often exceeding 1 year, the wintertime losses of particular FA have to be replenished in summer in order to return to the same physiological status as in the preceding autumn.

In conclusion, (1) the wild raccoon dog utilized preferentially 18–20C n-3 PUFA, 14–17C MUFA and 12–16C SFA as energy sources during wintertime nutritional scarcity. In summer, the same FA were selectively incorporated into WAT. (2) Mobilization was enhanced by short carbon chain length and unsaturation. In addition, n-3 PUFA were

preferred over n-6 PUFA. The same molecular determinants correlated with the incorporation of FA into WAT reversing the wintertime losses of the efficiently mobilized FA. (3) The molecular background for FA mobilization was the same in nature as observed previously in laboratory experiments, while the control of the long-term FA storage in wild mammals could be different from the short-term regulation of FA incorporation observed in laboratory animals and humans.

**Acknowledgments** This study was financially supported by the Academy of Finland, the Alfred Kordelin Foundation and the Finnish Game Management Fund. The technical help of Rauni Kojo, Tommi Paakkonen and Kasper Heikkilä is greatly acknowledged.

## References

- Beltowski J (2003) Adiponectin and resistin—new hormones of white adipose tissue. *Med Sci Monitor* 9:RA55–RA61
- Ackman RG, Cunnane SC (1992) Long-chain polyunsaturated fatty acids: sources, biochemistry and nutritional/clinical applications. In: Padley FB (ed) *Advances in applied lipid research*, vol 1. JAI, London
- Pond CM, Mattacks CA (1998) In vivo evidence for the involvement of the adipose tissue surrounding lymph nodes in immune responses. *Immunol Lett* 63:159–167
- Raclot T, Groscolas R (1995) Selective mobilization of adipose tissue fatty acids during energy depletion in the rat. *J Lipid Res* 36:2164–2173
- Spitzer JJ, Nakamura H, Gold M, Altschuler H, Lieberman M (1966) Correlation between release of individual free fatty acids and fatty acid composition of adipose tissue. *Proc Soc Exp Biol Med* 122:1276–1279
- Hunter JD, Buchanan H, Nye ER (1970) The mobilization of free fatty acids in relation to adipose tissue triglyceride fatty acids in the rat. *J Lipid Res* 11:259–265
- Connor WE, Lin DS, Colvis C (1996) Differential mobilization of fatty acids from adipose tissue. *J Lipid Res* 37:290–298
- Halliwell KJ, Fielding BA, Samra JS, Humphreys SM, Frayn KN (1996) Release of individual fatty acids from human adipose tissue in vivo after an overnight fast. *J Lipid Res* 37:1842–1848
- Raclot T, Groscolas R (1993) Differential mobilization of white adipose tissue fatty acids according to chain length, unsaturation, and positional isomerism. *J Lipid Res* 34:1515–1526
- Mustonen A-M, Käkälä R, Käkälä A, Pyykönen T, Aho J, Nieminen P (2007) Lipid metabolism in the adipose tissues of a carnivore, the raccoon dog, during prolonged fasting. *Exp Biol Med* 232:58–69
- Asikainen J, Mustonen A-M, Hyvärinen H, Nieminen P (2004) Seasonal physiology of the wild raccoon dog (*Nyctereutes procyonoides*). *Zool Sci* 21:385–391
- Viro P (1983) The raccoon dog (in Finnish). In: Koivisto I (ed) *Animals in Finland 1*. Weilin+Göös, Espoo
- Mustonen A-M, Nieminen P, Puukka M, Asikainen J, Saarela S, Karonen S-L, Kukkonen JVK, Hyvärinen H (2004) Physiological adaptations of the raccoon dog (*Nyctereutes procyonoides*) to seasonal fasting-fat and nitrogen metabolism and influence of continuous melatonin treatment. *J Comp Physiol B* 174:1–12
- Käkälä R, Hyvärinen H (1996) Site-specific fatty acid composition in adipose tissues of several northern aquatic and terrestrial mammals. *Comp Biochem Physiol B* 115:501–514
- Siivonen L (1972) The raccoon dog (in Finnish). In: Siivonen L (ed) *Mammals in Finland II*. Otava, Keuruu
- Wijendran V, Hayes KC (2004) Dietary n-6 and n-3 fatty acid balance and cardiovascular health. *Annu Rev Nutr* 24:597–615
- Iverson SJ, Frost KJ, Lowry LF (1997) Fatty acid signatures reveal fine scale structure of foraging distribution of harbor seals and their prey in Prince William Sound, Alaska. *Mar Ecol Prog Ser* 151:255–271
- Kauhala K (1992) Ecological characteristics of the raccoon dog in Finland. Ph.D. dissertation. University of Helsinki, Helsinki
- Nieminen P, Saarela S, Pyykönen T, Asikainen J, Mononen J, Mustonen A-M (2004) Endocrine response to fasting in the overwintering captive raccoon dog (*Nyctereutes procyonoides*). *J Exp Zool A* 301:919–929
- Christie WW (1993) Preparation of ester derivatives of fatty acids for chromatographic analysis. In: Christie WW (ed) *Advances in lipid methodology—two*. Oily, Dundee
- Nieminen P, Käkälä R, Pyykönen T, Mustonen A-M (2006) Selective fatty acid mobilization in the American mink (*Mustela vison*) during food deprivation. *Comp Biochem Physiol B* 145:81–93
- Ackman RG (1992) Application of gas-liquid chromatography to lipid separation and analysis: qualitative and quantitative analysis. In: Chow CK (ed) *Fatty acids in foods and their health implications*. Marcel Dekker, NY
- Kates M (1986) *Techniques of lipidology: isolation, analysis and identification of lipids*, 2nd edn. Elsevier, Amsterdam
- Kvalheim OM, Karstang TV (1987) A general-purpose program for multivariate data analysis. *Chemometr Intell Lab* 2:235–237
- Groscolas R (1990) Metabolic adaptations to fasting in emperor and king penguins. In: Davis LS, Darby JT (eds) *Penguin biology*. Academic, San Diego
- Raclot T (1997) Selective mobilization of fatty acids from white fat cells: evidence for a relationship to the polarity of triacylglycerols. *Biochem J* 322:483–489
- Raclot T, Holm C, Langin D (2001) A role for hormone-sensitive lipase in the selective mobilization of adipose tissue fatty acids. *Biochim Biophys Acta* 1532:88–96
- Hazel JR, Sidell BD (2004) The substrate specificity of hormone-sensitive lipase from adipose tissue of the Antarctic fish *Trematomus newnesi*. *J Exp Biol* 207:897–903
- Raclot T, Oudart H (2000) Net release of individual fatty acids from white adipose tissue during lipolysis in vitro: evidence for selective fatty acid re-uptake. *Biochem J* 348:129–136
- Leyton J, Drury PJ, Crawford MA (1987) Differential oxidation of saturated and unsaturated fatty acids in vivo in the rat. *Br J Nutr* 57:383–393
- Hovik R, Osmundsen H (1987) Peroxisomal  $\beta$ -oxidation of long-chain fatty acids possessing different extents of unsaturation. *Biochem J* 247:531–535
- Raclot T, Leray C, Bach AC, Groscolas R (1995) The selective mobilization of fatty acids is not based on their positional distribution in white-fat-cell triacylglycerols. *Biochem J* 311:911–916
- Raclot T, Holm C, Langin D (2001) Fatty acid specificity of hormone-sensitive lipase: implication in the selective hydrolysis of triacylglycerols. *J Lipid Res* 42:2049–2057
- Nieminen P, Rouvinen-Watt K, Collins D, Grant J, Mustonen A-M (2006) Fatty acid profiles and relative mobilization during fasting in adipose tissue depots of the American marten (*Martes americana*). *Lipids* 41:231–240
- Soppela P, Nieminen M (2002) Effect of moderate wintertime undernutrition on fatty acid composition of adipose tissues of reindeer (*Rangifer tarandus tarandus* L.). *Comp Biochem Physiol A* 132:403–409

36. Raclot T, Groscolas R (1994) Individual fish-oil n-3 polyunsaturated fatty acid deposition and mobilization rates for adipose tissue of rats in a nutritional steady state. *Am J Clin Nutr* 60:72–78
37. Raclot T (2003) Selective mobilization of fatty acids from adipose tissue triacylglycerols. *Prog Lipid Res* 42:257–288
38. Sinclair AJ, Attar-Bashi NM, Li D (2002) What is the role of  $\alpha$ -linolenic acid for mammals? *Lipids* 37:1113–1123
39. Ågren J, Muje P, Hänninen O, Herranen J, Penttilä I (1987) Seasonal variations of lipid fatty acids of boreal freshwater fish species. *Comp Biochem Physiol B* 88:905–909
40. Żmijewski T, Kujawa R, Jankowska B, Kwiatkowska A, Marnicz A (2006) Slaughter yield, proximate and fatty acid composition and sensory properties of rapfen (*Aspius aspius* L) with tissue of bream (*Abramis brama* L) and pike (*Esox lucius* L). *J Food Compos Anal* 19:176–181
41. Bernard A, Carlier H (1991) Absorption and intestinal catabolism of fatty acids in the rat: effect of chain length and unsaturation. *Exp Physiol* 76:445–455
42. Herzberg GR, Skinner C (1997) Differential accumulation and release of long-chain n-3 fatty acids from liver, muscle, and adipose tissue triacylglycerols. *Can J Physiol Pharmacol* 75:945–951
43. Leaf DA, Connor WE, Barstad L, Sexton G (1995) Incorporation of dietary n-3 fatty acids into the fatty acids of human adipose tissue and plasma lipid classes. *Am J Clin Nutr* 62:68–73
44. Lhuillery C, Mebarki S, Lecourtier M-J, Demarne Y (1988) Influence of different dietary fats on the incorporation of exogenous fatty acids into rat adipose glycerides. *J Nutr* 118:1447–1454
45. Lin DS, Connor WE (1990) Are the n-3 fatty acids from dietary fish oil deposited in the triglyceride stores of adipose tissue? *Am J Clin Nutr* 51:535–539
46. Lin DS, Connor WE, Spenler CW (1993) Are dietary saturated, monounsaturated, and polyunsaturated fatty acids deposited to the same extent in adipose tissue of rabbits? *Am J Clin Nutr* 58:174–179
47. Perona JS, Portillo MP, Macarulla MT, Tueros AI, Ruiz-Gutiérrez V (2000) Influence of different dietary fats on triacylglycerol deposition in rat adipose tissue. *Br J Nutr* 84:765–774
48. Summers LKM, Barnes SC, Fielding BA, Beysen C, Ilic V, Humphreys SM, Frayn KN (2000) Uptake of individual fatty acids into adipose tissue in relation to their presence in the diet. *Am J Clin Nutr* 71:1470–1477
49. Cochet N, Georges B, Meister R, Florant GL, Barré H (1999) White adipose tissue fatty acids of alpine marmots during their yearly cycle. *Lipids* 34:275–281
50. Frank CL (1991) Adaptations for hibernation in the depot fats of a ground squirrel (*Spermophilus beldingi*). *Can J Zool* 69:2707–2711
51. Melin T, Qi C, Bengtsson-Olivecrona G, Åkesson B, Nilsson A (1991) Hydrolysis of chylomicron polyenoic fatty acid esters with lipoprotein lipase and hepatic lipase. *Biochim Biophys Acta* 1075:259–266
52. Wang C-S, Bass H, Whitmer R, McConathy WJ (1993) Effects of albumin and apolipoprotein C-II on the acyl-chain specificity of lipoprotein lipase catalysis. *J Lipid Res* 34:2091–2098
53. Sato K, Suzuki K, Akiba Y (1998) Species differences in substrate specificity of lipoprotein lipase purified from chickens and rats. *Comp Biochem Physiol A* 119:569–573
54. Lin K-C, Cross HR, Smith SB (1992) Esterification of fatty acids by bovine intramuscular and subcutaneous adipose tissues. *Lipids* 27:111–116
55. Chen Z-Y, Menard CR, Cunnane SC (1995) Moderate, selective depletion of linoleate and  $\alpha$ -linolenate in weight-cycled rats. *Am J Physiol* 268:R498–R505

Nudibranch mollusks unprotected by a shell and named sea slugs are striking by beauty of their forms and colors and also by wide species diversity and a significant contribution into the ecology of southern seas [5]. The morphology, biology and ecology of the tropical nudibranch species have been purely described in details until now [5, 6]. Knowledge on their biochemistry is scrappy. The chemical ecology of nudibranchs is particularly appealing. Most nudibranchs contain the secondary metabolites that are active in chemical defenses against predators. Bioactive metabolites from opisthobranchs have been shown to possess feeding-deterrent, cytotoxic and ichthyotoxic properties, to have antibacterial, antifungal activity, and to act as sexual pheromones [7, 8]. These compounds exhibit a high variety of chemical structures including diterpene diacylglycerols [9]. Nudibranchs are capable of biosynthesizing the defensive compounds or accumulate them from their dietary sponge. No information is available on the lipid and FA composition of these invertebrates. To the best of our knowledge, only one paper concerning the fatty acid composition of the eggs of four nudibranchs from southwestern Spain exists; high concentration of n-3 PUFA, especially, 20:5n-3 and 22:6n-3 was reported [10].

The present study was carried out to examine lipid classes, phospholipids (PL) and FA compositions of the *Chromodoris* sp. and *Phyllidia coelestis*, representatives of the most common genera of tropical nudibranchs, in order to acquire data for lipid biochemistry of mollusks of the order Nudibranchia: Opisthobranchia: Mollusca that had not been studied earlier.

## Materials and Methods

Two species of nudibranchs, *Chromodoris* sp. and *P. coelestis* (Phylum: Mollusca, Class: Gastropoda, Subclass: Opisthobranchia, Order: Nudibranchia) were collected from the R.V. *Akademik Oparin* by SCUBA divers in the Nha Trang Bay of the South China Sea, Vietnam in January 2005 at 2–5 m depth.

Lipids were extracted according to method of Bligh and Dyer [11]. The total lipid content was determined gravimetrically. Lipid class separation was performed by one-dimensional TLC on silica-gel plates [12]. The primary solvent system was hexane/diethyl ether/acetic acid (80:20:1, by volume), a mobile phase resolving nonpolar compounds. After development, the TLC were dried under air flow. A second polar solvent system chloroform/methanol/acetone/acetic acid/water/benzene (70:30:5:4:1:10, by vol) was also used to partly resolve polar lipids. For this purpose, the TLC were developed on 20% of the plate

length. Lipids were detected on the TLC using 10% H<sub>2</sub>SO<sub>4</sub>/MeOH with subsequent heating to 180 °C. Lipid class concentrations were determined by analyzing a scanned image of the TLC plate using a Sorbfil TLC Videodensitometer DV program (Krasnodar, Russia). Preparative separation of lipid classes was performed by TLC on silica acid using a solvent system resolving nonpolar compounds mentioned above. After development, the zone of the polar lipids (this includes mainly PL) and the zone of neutral lipids (which include mainly TAG, DAGE, LCA and ES) were immediately scraped off and eluted with chloroform/methanol (1:1, by vol).

Polar lipids were separated by two-dimensional silica gel TLC in the solvent systems: chloroform/methanol/28% NH<sub>4</sub>OH/benzene (65:30:6:10, by volume) for the first direction, chloroform /methanol/acetone/acetic acid/water/benzene (70:30:5:4:1:10, by volume) for the second one. Lipids were detected on TLC plates using 10% H<sub>2</sub>SO<sub>4</sub>/MeOH with heating to 180 °C and by specific reagents for PL [13], amino-containing lipids (0.2% ninhydrin in acetone) and choline lipids (Dragendorff's reagent). PL were quantified by the method of Vaskovsky et al. [13].

FAME were prepared according to the method of Carreau and Dubacq [14] and purified by TLC in benzene. *N*-acylpyrrolidides of FA were prepared by heating FAME with 1 mL pyrrolidine and 0.1 mL of acetic acid at 100 °C for 30 min in capped vial followed by extraction with chloroform of the acidified solution and purification by TLC in chloroform/acetone (9:1, by vol) [15]. GC analysis was performed on a Shimadzu GC-17A gas chromatograph (Kyoto, Japan) equipped with a flame ionization detector and SUPELCOWAX 10 (Supelco, Bellefonte, PA, USA) capillary column (25 m × 0.25 mm i.d.), 210 °C and, additionally, SPB-5 (Supelco) capillary column (25 m × 0.25 mm i.d.), 230 °C was used. Helium was the carrier gas. Individual components of FAME were identified by comparing retention time data with those obtained for authentic standards and by using the ECL data, and confirmed by GC-MS of MEFA and their *N*-acylpyrrolidide derivatives. GC-MS analyses of FAME were performed on a Shimadzu GCMS-QP5050A instrument (Kyoto, Japan) fitted with a MDN-5S (Supelco) capillary column (30 m × 0.25 mm i.d.). Samples were injected at an oven temperature 160 °C. After 1 min, the oven temperature was raised at 3 °C min<sup>-1</sup> to 240 °C, which was held for 40 min. Injector and detector temperatures were 250 °C. GC-MS of *N*-acylpyrrolidides was performed on the same GC-mass spectrometer; the column temperature was 210 °C with a 3 °C min<sup>-1</sup> ramp to 270 °C, which was held for 60 min; injector and detector temperatures were 270 °C.

Mass spectral data are as follows:

*7,13-heneicosadienoic acid methyl ester*. MS  $m/z$  (relative intensity, %): 336 ( $M^+$ , 13), 318 (0.1), 305 (3), 287 (3), 276 (0.5), 262 (1), 252 (0.6), 238 (2), 224 (6), 210 (4), 194 (10), 178 (11), 164 (8), 150 (16), 135 (14), 123 (21), 109 (35), 95 (75), 81 (96), 67 (91), 55 (100).

*7,13-heneicosadienoic acid pyrrolidide*. MS  $m/z$  (relative intensity, %): 375 ( $M^+$ , 9.8), 363 (0.3), 346 (1), 332 (1.7), 318 (1), 304 (2), 290 (3.2), 276 (3), 262 (2.5), 250 (2.7), 236 (8), 222 (4.5), 208 (7.4), 194 (6), 180 (13.5), 168 (6.8), 154 (6.7), 140 (6), 126 (53), 113 (100).

## Results

The lipid content of the mollusks studied was high (14.7–19.5 mg g<sup>-1</sup> wet weight). PL was the major lipid class in both species (85.7 and 54.9% of the total lipids, Table 1). ST were also an abundant lipid class and constituted about 13% of the total lipids. FFA were the minor components. NL were distinguished between species with respect to the composition of TAG, DAGE, LCA and ES, which were present only in *P. coelestis*. The content of TAG was higher than that of DAGE (9.6 and 4.6%, respectively). Among PL classes, PC was predominant, accounting for nearly half of the total PL (Tables 2, 3). PE was also a major class. Other PL–PS and CAEP (sum of ceramide aminoethylphosphonate and ceramide methylaminoethylphosphonate)—were detected in almost equal concentrations. The proportions of individual PL classes were similar for both species.

In the case of *P. coelestis*, FA were analyzed separately for NL and PL. FA composition of PL and NL of *P. coelestis* was distinguished with higher concentrations of PUFA, NMID and VLC FA in PL (29.1, 9.5 and 9.4% in

**Table 1** Lipid classes (% of total lipids) of Nudibranchs *Chromodoris* sp. and *Phyllidia coelestis*

Lipid classes	Percentage composition			
	<i>Chromodoris</i> sp.		<i>Phyllidia coelestis</i>	
	Mean	SD	Mean	SD
Polar lipids	85.7 ± 1.5		54.9 ± 2.5	
Sterols	13.0 ± 1.0		12.5 ± 2.3	
Long-chain alcohols	–		10.2 ± 0.7	
Free fatty acids	1.4 ± 0.4		3.3 ± 0.4	
Triacylglycerols	–		9.6 ± 0.6	
Diacylglyceryl ethers	–		4.6 ± 0.4	
Sterol esters	–		5.1 ± 1.0	

Values are mean ± SD,  $n = 3$

**Table 2** Phospholipid composition (% of total PL) of Nudibranchs *Chromodoris* sp. and *Phyllidia coelestis*

Phospholipids	Percentage composition	
	<i>Chromodoris</i> sp.	<i>Phyllidia coelestis</i>
Phosphatidylcholine	45.3 ± 1.6	50.4 ± 2.0
Phosphatidylethanolamine	22.3 ± 2.1	23.4 ± 2.9
Phosphatidylserine	15.6 ± 2.1	12.5 ± 0.6
Ceramide aminoethylphosphonates	16.5 ± 3.5	14.2 ± 0.8

Values are mean ± SD,  $n = 3$

PL versus 11.5, 4.1 and 2.5% in NL). The saturated FA (SFA) was twice higher in NL than in PL (38.8 and 16.9% of the total FA, respectively). The enrichment of NL by 18:1n-9 was observed, whereas in PL the concentration of 7–21:1 was higher.

Considering that acyl-producing lipids of *Chromodoris* sp. consisted only of the PL with exception of minor amounts of FFA, it is more correctly to compare the FA composition of *Chromodoris* sp. with that of in particular PL of *P. coelestis*. The studied species had differences in their FA profiles. The dominant FA (more than 5%) of *Chromodoris* sp. were 17:0, 18:2n-6, 18:1n-7, 20:4n-6, 7–21:1, 22:4n-6 and 5,9–26:2; these seven components accounted for about 50% of the total FA. The main FA of *P. coelestis* were 15:0, 17:0, 18:1n-9, 20:4n-6, 7–21:1 and 22:4n-6, all together 41%.

In the sea slugs, the total SFA accounted, respectively, for 16.0 and 16.9% of the total FA. Among them, the common 16:0 and 18:0 as well as the odd chain 15:0 and 17:0 were found; the input of the last was especially noticeable in *P. coelestis*. The rare branched FA, 6-methyl-14:0, 10-methyl-16:0, 11-methyl-18:0 and *iso*-21:1n-5, were identified in *P. coelestis* lipids. The MUFA content was high in both species: 26.0 and 24.2% of the total FA, among them isomers of 18:1, 20:1 and 21:1 were the main. FA 7–21:1 was identified by MS–GC. A molecular ion peak  $m/z$  338 and major ion at  $m/z$  306 was obtained from the MS of MEFA indicating the presence of 21:1. A molecular ion peak of pyrrolidine derivative appeared at  $m/z$  377. Double bond at C7 was recognized from irregular interval of  $m/z$  12 between C6  $m/z$  168 and C7  $m/z$  180. These fragments offer further corroborating evidence for the structure of 7–21:1. The sea slugs contained a considerable content of this FA (about 6% of the total FA).

Both species had various NMID FA with C20, C21 and C22 chain (in sum 12.0 and 9.5% of the total FA). The most important NMI FA characteristic of the sea slugs were 5,11–20:2 and 5,13–20:2; as well as 7,13–22:2 and 7,15–22:2 and the novel FA 7,13–21:2. FA, which was tentatively identified according to retention time and ECL

**Table 3** Fatty acid composition (wt.%) of Nudibranchs *Chromodoris* sp. and *Phyllidia coelestis*

	<i>Chromodoris</i>	<i>Phyllidia coelestis</i>		
	sp. Total lipids	Total lipids	Phospho- lipids	Neutral lipids
14:0	0.9 ± 0.1	1.1 ± 0.2	0.6 ± 0.2	1.8 ± 0.4
<i>iso</i> -15:0	2.6 ± 0.1	1.9 ± 0.8	0.9 ± 0.1	2.6 ± 0.5
<i>anteiso</i> -15:0	0.1 ± 0.1	0.4 ± 0.0	0.2 ± 0.1	0.7 ± 0.2
6-methyl-14:0	–	2.5 ± 0.3	1.4 ± 0.1	1.5 ± 0.3
15:0	1.4 ± 0.1	7.9 ± 1.8	4.5 ± 0.5	11.5 ± 0.7
<i>iso</i> -16:0	0.4 ± 0.1	1.1 ± 0.3	0.6 ± 0.3	1.5 ± 0.2
<i>anteiso</i> -16:0	1.1 ± 0.1	0.1 ± 0.1	0.2 ± 0.1	0.4 ± 0.1
16:0	3.5 ± 0.4	4.8 ± 1.3	2.8 ± 0.6	8.0 ± 0.5
16:1n-9	0.8 ± 0.1	1.1 ± 0.3	1.1 ± 0.1	3.5 ± 0.3
16:1n-7	0.6 ± 0.1	1.8 ± 0.6	0.8 ± 0.1	1.2 ± 0.2
<i>iso</i> -17:0	1.0 ± 0.4	1.3 ± 0.4	0.8 ± 0.2	2.2 ± 0.2
<i>anteiso</i> -17:0	–	1.6 ± 0.4	0.9 ± 0.2	2.6 ± 0.5
10-methyl-16:0	–	2.0 ± 1.1	1.0 ± 0.2	1.6 ± 0.3
17:0	5.2 ± 0.4	7.3 ± 1.5	3.8 ± 0.7	9.2 ± 0.8
17:1n-8	0.6 ± 0.1	1.9 ± 0.4	1.5 ± 0.2	2.0 ± 0.3
18:0	4.3 ± 0.6	4.8 ± 0.5	4.0 ± 0.6	5.9 ± 0.6
18:1n-9	2.9 ± 0.1	7.1 ± 0.7	5.4 ± 0.8	9.8 ± 1.1
18:1n-7	5.6 ± 0.4	1.8 ± 0.3	1.4 ± 0.4	2.1 ± 0.3
18:2n-6	6.3 ± 0.8	2.6 ± 0.6	3.5 ± 0.6	2.1 ± 0.4
19:0	0.8 ± 0.1	0.9 ± 0.2	0.7 ± 0.2	1.4 ± 0.2
11-methyl-18:0	–	1.3 ± 0.9	1.1 ± 0.4	1.0 ± 0.1
19:1n-8	0.9 ± 0.2	1.1 ± 0.4	1.2 ± 0.3	1.8 ± 0.2
19:1n-6	1.1 ± 0.2	1.7 ± 0.7	1.3 ± 0.4	0.4 ± 0.1
20:1n-13	4.4 ± 0.5	3.2 ± 1.0	3.4 ± 0.9	1.9 ± 0.3
20:1n-7	1.4 ± 0.1	0.7 ± 0.2	0.5 ± 0.2	0.5 ± 0.2
5,11–20:2	1.3 ± 0.1	0.8 ± 0.5	0.7 ± 0.2	0.5 ± 0.1
5,13–20:2	2.5 ± 0.1	2.0 ± 0.2	2.5 ± 0.4	1.4 ± 0.2
20:4n-6	8.9 ± 0.8	6.5 ± 1.2	11.4 ± 0.8	3.3 ± 0.2
20:5n-3	0.6 ± 0.3	0.6 ± 0.3	0.8 ± 0.3	0.4 ± 0.1
<i>iso</i> -21:1n-5	–	1.0 ± 0.4	2.6 ± 0.5	0.8 ± 0.2
21:1n-5	1.1 ± 0.2	–	–	–
7–21:1	5.8 ± 0.4	5.5 ± 0.8	6.2 ± 0.4	3.0 ± 0.3
7,13–21:2	1.5 ± 0.1	2.1 ± 0.8	3.9 ± 0.7	1.6 ± 0.2
22:1n-9	–	0.5 ± 0.3	0.8 ± 0.2	0.5 ± 0.1
22:1n-7	0.7 ± 0.3	0.2 ± 0.1	0.2 ± 0.1	0.2 ± 0.1
7,13–22:2	3.4 ± 0.1	1.8 ± 0.7	2.1 ± 0.5	0.6 ± 0.2
7,15–22:2	3.4 ± 0.1	0.4 ± 0.1	0.3 ± 0.1	–
22:4n-6	10.7 ± 0.1	5.5 ± 1.0	9.4 ± 0.4	4.1 ± 0.3
22:5n-3	1.1 ± 0.4	0.4 ± 0.2	0.6 ± 0.3	0.3 ± 0.1
22:6n-3	1.0 ± 0.2	1.0 ± 0.3	1.5 ± 0.4	0.1 ± 0.1
5,9–24:2	1.0 ± 0.1	1.8 ± 0.5	2.2 ± 0.5	0.5 ± 0.2
5,9–25:2	4.0 ± 0.2	1.7 ± 0.6	2.6 ± 0.4	0.7 ± 0.2
<i>iso</i> -5,9–25:2	–	1.4 ± 0.8	2.5 ± 0.5	0.7 ± 0.1
<i>iso</i> -5,9–26:2	0.8 ± 0.1	0.2 ± 0.1	0.4 ± 0.1	0.1 ± 0.1
5,9–26:2	6.0 ± 0.4	0.9 ± 0.4	1.0 ± 0.3	0.4 ± 0.1

**Table 3** continued

	<i>Chromodoris</i>	<i>Phyllidia coelestis</i>		
	sp. Total lipids	Total lipids	Phospho- lipids	Neutral lipids
Sum SFA	16.0 ± 1.6	27.0 ± 3.8	16.9 ± 1.8	38.8 ± 3.2
Sum MFA	26.0 ± 2.6	27.0 ± 3.1	24.2 ± 2.1	27.5 ± 2.2
Sum PUFA	28.8 ± 2.7	18.1 ± 2.5	29.1 ± 2.9	11.5 ± 1.8
n-6	26.0 ± 2.0	15.4 ± 2.4	25.3 ± 2.2	10.2 ± 1.2
n-3	2.7 ± 0.6	2.8 ± 0.8	3.7 ± 0.7	1.3 ± 0.5
VLC FA	12.0 ± 0.9	6.2 ± 1.7	9.4 ± 1.1	2.5 ± 0.5
NMID FA	12.0 ± 0.5	7.1 ± 1.3	9.5 ± 1.9	4.1 ± 0.9
Bacterial FA	15.7 ± 2.1	34.4 ± 4.6	21.6 ± 3.5	41.7 ± 4.5

Values are mean ± SD, n = 3. “Bacterial” refers to sum of odd and branched FA

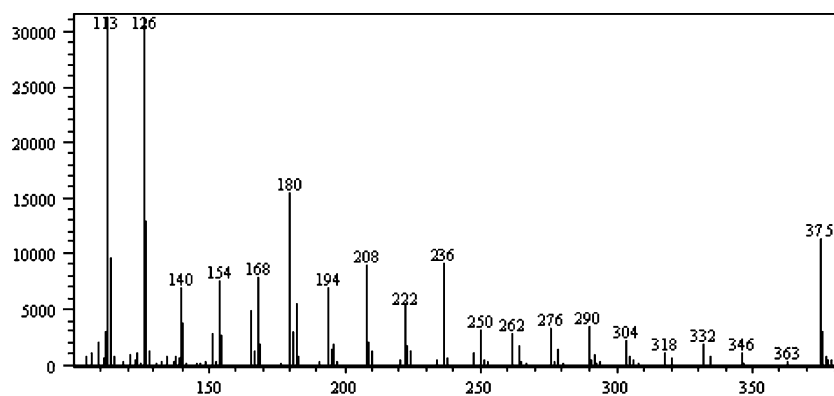
Other FA identified include *iso*-13:0, 17:1n-6, 17:2, *iso*-18:0, 18:3n-6, 18:3n-3, 18:4n-3, *iso*-19:0, *anteiso*-19:0, 19:2, 20:0, 20:1n-9, 20:3n-6, 22:5n-6, 5,9–23:2, 24:4n-6, *iso*-25:0 and *iso*-26:0, which were present in trace amounts (<0.2%)

value as 21:2, reached 3.9% of the total FA in PL of *P. coelestis*. MS of the methyl ester of this FA gave a molecular ion at  $m/z$  336, indicating the presence of two double bonds in C21 FA. Neither a peak of  $m/z$  108, which is characteristic for the MS of n-3 PUFA nor a peak  $m/z$  150 characteristic for n-6 PUFA were present. Double bonds were located by GC–MS of pyrrolidine derivatives of FAME (Fig. 1). A molecular ion peak  $m/z$  375 was present. The presence of irregular interval of  $m/z$  12 between the most intensive peaks  $m/z$  168 and 180 and between  $m/z$  250 and 262 indicated the positions of double bonds at C7 and C13, respectively.

PUFA were presented mainly by 18:2n-6, 20:4n-6 and the most important 22:4n-6, which was 10.0–9.5% of the total FA. The common marine FA, 20:5n-3 and 22:6n-3, were minor components (0.6–0.8 and 1.0–1.5%, respectively).

Numerous VLC FA with straight and branched chain (*iso*-), saturated and dienes with  $\Delta$ 5,9 group were identified in both species (12.0 and 9.4% of the total FA). The major VLC FA were identified based on the MS. The molecular ions at  $m/z$  364, 378, 392 and 406 corresponded to the molecular weight of FAME of 23:2, 24:2, 25:2 and 26:2. Their MS of pyrrolidides had a diagnostic ion at  $m/z$  180 that is typical when two double bonds are located at the 5 and 9 positions. Hence, these proved that 5,9–23:2, 5,9–24:2; 5,9–25:2 and 5,9–26:2 were present. Additionally, the molecular ion of the pyrrolidine derivatives at  $m/z$  431 was consistent with 25:2 although the GC retention times were appreciably less than that of corresponding straight chain isomers. The gap of 28 amu between  $m/z$  388 and 416 was indicative of an *iso*-methyl branch, while the abundant ion

**Fig. 1** Mass spectra of the pyrrolidide derivatives of 7,13–21:2



at  $m/z$  180 is a characteristic marker for double bonds in the positions  $\Delta 5,9$ . Consequently, 5,9–25:2-*iso* was identified.

## Discussion

Although lipids and fatty acids of marine mollusks from different taxons have been extensively studied, it is the first report on the analysis for lipid composition of nudibranchs.

Our lipid analysis indicated that the nudibranchs comprised mainly PL, which are known to be major constituents of cell membranes. ST, another structural lipid, was also abundant. The concentrations of FFA reported here 1.4 and 3.3% of the total lipids is in agreement with results reported for other marine invertebrates [16, 17] and seemed unlikely to be due to enzymatic hydrolysis of the lipids. The proportion of the lipid classes varied according to the species mainly due to high values of NL in *P. coelestis*. In contrast to *Chromodoris* sp, lipids of *P. coelestis* comprised high concentrations of TAG, DAGE, LCA, and ES. This may be attributed to the differences in diet and biochemistry of the species, because lipids stored in the animals are likely to be of dietary origin. The level of the neutral storage lipids are known to be species specific and depends on mainly a life history strategy and food availability. For example, amounts of TAG are highly variable between different species of *Cnidaria* and *Ctenophora* [16]; its level in the sea butterfly *Limacina helicina* varies throughout the stages of the spawning cycle and seasons [17]. DAGE, which is also used as an energy store, have been previously mentioned for all classes of mollusks [4] and, indeed, some other marine invertebrates. Extraordinary large amounts (up to 40% of the total lipids) were reported for the pteropod *Clione limacine* [18]. PL were constituted of PC, PE, PS and CAEP. A similar distribution is reported for mollusks [4, 19]. Our PL data for nudibranchs are in a good agreement with the results published earlier. A high

concentration of CAEP was noticeable. Phosphonolipids are widely distributed in the phylum Mollusca and, in some cases, comprise the major PL class [4]. Phosphatidylinositol and diphosphatidylglycerol, the usual minor components of marine invertebrates [20], were not found in the species studied. Both species were similar in their PL distribution. The absence of a species-specific pattern in PL classes was suggested as an evidence for the similarity of the nature of biological membranes.

The species studied exhibited a wide diversity of FA, including common SFA, MUFA and PUFA, as well as NMID FA described firstly in mollusks [2, 21], and VLC FA specific for sponges [22, 23]. The FA profiles of the sea slugs distinguished in most respects from those described earlier for other gastropods and mollusks [4, 24].

Distribution of FA among PL and NL in *P. coelestis* reveal the known pattern, namely, NL were rich in SFA. Though the amount of MUFA was similar in the lipids, they differ in isomer ratio. Isomers of 16:1 and 18:1 were more abundant in NL whereas 20:1 isomers were prevalent in PL. It apparently indicates the structural role of the 20:1 along with NMID, PUFA and VLC FA which prevailed in PL in comparison with NL of *P. coelestis*. The acid 20:1(n-11) together with NMID were found to associate with aminophospholipid plasmalogens (PE and PS) in bivalve mollusks [20].

The FA composition of marine mollusks is considered to be characterized by predominance of n-3 PUFA, 20:5n-3 and 22:6n-3 [4, 24] which constitute usually near a half of total FA. In contrast, the sea slugs did not exhibit this specific feature; these two marine PUFA were minor components and in sum constituted 1.6 and 2.1% of the total FA. In the studied species, n-6 PUFA were dominant (26.0 and 25.3% of the total FA); their amounts were an order of magnitude higher than the concentration of n-3 PUFA. The content of the components decreased in the line of 22:4n-6, 20:4n-6 and 18:2n-6. High values of n-6 relative to n-3 PUFA are unusual in marine organisms. An



elevated level of 20:4n-6 was also found in two snails, *Littorina littorea* and *Lunatia triseriata*, (up to 8% of the total FA), but it was lower than that of 20:5n-3 [2, 21]. A prevalence of n-6 PUFA over n-3 was found in the asteroids [25] and in the PL of gorgonian corals [26], but the amounts of n-3 PUFA were also abundant.

The various NMI FA were found, their content reached 12.0% in *Chromodoris* sp. and 9.5% in PL of *P. coelestis*. Among them, 20:2 and 22:2 NMI FA, first found in the oyster *Crassostrea virginica* [2] and the clam *Arctica islandica* [3], were present also in the sea slugs. Their structures as shown by MS–GL analysis, were identical to those previously isolated from lipids of *C. virginica* and characterized as 5,11–20:2 and 5,13–20:2, as well as 7,13–22:2 and 7,15–22:2 [20]. Of particular interest was the finding of a novel NMI FA identified as 7,13–21:2. It amounted to 3.9% of the total FA in PL of *P. coelestis* and 1.5% in *Chromodoris* sp. This unusual NMI FA might be biosynthesized by the sea slugs rather than be of dietary origin, similar to that shown for 22:2 NMI in bivalves [27, 28]. The bivalve mollusks are able to synthesize the NMI FA 7,13–22:2 and 7,15–22:2 by a  $\Delta 5$  desaturation of corresponding precursors, 11–20:1 and 13–20:1, respectively, and a further elongation reaction [27]. Although isomer 7–21:1 was the main one (up to 6.2%) in the sea slugs, it is improbable that it might be the precursor of 7,13–21:2. An alternative pathway of this odd NMI FA production may be similar to that of NMI FA in bivalve mollusks. Probably, biosynthesis of 7,13–21:2 can occur via a  $\Delta 5$  desaturase acting upon the appropriate precursor 11–19:1 and further chain elongation of 5,11–19:2. It is possible that 11–19:1 might be derived from the diets of the sea slugs or arises from the chain elongation of 9–17:1. The potential precursors 9–17:1 and 11–19:1 were abundant in the sea slugs and, apparently, are of bacterial origin. FA 19:2 was also identified in both species at least in trace amounts. Unfortunately, too small quantity of 19:2 did not allow to establishing the position of double bonds in the isomer. Thus, biosynthesis of 7,13–21:2 in the nudibranchs entirely probable occurs in the following way: 9–17:1  $\rightarrow$  11–19:1– $\Delta 5$  desaturase  $\rightarrow$  5,11–19:2  $\rightarrow$  7,13–21:2.

The biological role and function of NMI FA are not clear. However, they were found in high concentrations in PL of the mollusks, and their amounts were in a reverse relation to common n-3 PUFA, 20:5n-3 and 22:6n-3 and therefore they are proposed as being important for membrane structure and function [20, 29].

The FA profile of *Chromodoris* sp. and *P. coelestis* differed from those for other gastropods and, indeed, for other mollusks by the presence of significant amounts of VLC FA specific of sponges [22, 23]. Distribution of the demospongiac FA was different for the species studied. VLC FA with double bonds at  $\Delta 5,9$ , among them 5,9–24:2,

5,9–25:2 and 5,9–26:2 and *iso*-5,9–25:2 were found in high concentrations; additionally, 5,9–23:2 and branched: *iso*-5,9–26:2, *iso*-25:0 and *iso*-26:0 were identified in *P. coelestis* in trace amounts. Their amounts were higher in PL in comparison with TAG, 9.4 and 2.5%, respectively, in *P. coelestis*. FA with  $\Delta 5,9$  pattern are typical for many sponges [22, 23]. Nudibranchs are carnivorous and majority of species are specialized feeders on sponges [5]. Utilization of this food source seems to be responsible for a high level of the VLC FA found in the nudibranchs.

Another unique feature of the FA composition of these two sea slugs concerned a high abundance (15.7 and 34.4% of the total FA) of the odd-chain and branched FA, predominantly *iso*- and *anteiso*-usually named bacterial FA. The dominant odd-chain FA were 15:0 and 17:0, which enriched especially in NL of *P. coelestis* (11.5 and 9.2% of the total). They are normal also as minor metabolites in most animals and can be derived from amino acid precursors which are freely available in marine mollusks. The presence of a high abundance of bacterial FA, especially in NL of *P. coelestis* (up to 41.7% of the total FA), is intriguing. It is obvious that different odd and branched FA were detected in many species of sponges [22, 23] which are a commonly part of nudibranchs diet. Therefore, the bacteria associated with sponges seem to be one of the suppliers of these FA for sea slugs. However, the contribution of these FA was so high that it seems unlikely that bacteria from the sponges are their only source in the sea slugs. The elevated levels of bacterial FA have been reported for some benthic invertebrates, for example, in tunicate [30] and asteroids [25]. The occurrence of odd-chain FA dominated by 17:1n-8 and 15:0, in exceptional amounts (up to 18 and 8.3%, respectively) have been found in the pteropode *Clione limacine* and assumed that 17:1n-8 could be synthesized via propionate de novo [18]. It is uncertain that the sea slugs can synthesize odd chain FA since the precursors of these compounds are accumulated from phytoplankton [18]. More probable they are of a dietary origin. It may suggest that odd-chain and branched FA may have come from bacteria in the food chain or from bacteria living in symbiosis with the sea slugs. More research has to be done to answer this question. The occurrence of odd and branched FA in PL in high level (15.7 and 21.6%) implies a possible structural requirement for them. In conclusion, the lipid and FA composition of the nudibranchs is determined by taxonomic relationships of the species, food supply and internal biosynthetic activities.

**Acknowledgments** The author would like to thank Dr. Alexei V. Chernyshev for the identification of the species and Dr. Svetlana A. Rodkina for the assistance in the mass spectrometry.

## References

- Gardner D, Riley JP (1972) The component fatty acids of the lipids of some species of marine and freshwater molluscs. *J Mar Biol UK* 52:827–838
- Ackman RG, Hooper SN (1973) Non-methylene-interrupted fatty acids in lipids of shallow-water marine invertebrates: a comparison of two molluscs (*Littorina littorea* and *Lunatia triseriata*) with the sand shrimp (*Crangon septemspinus*). *Comp Biochem Physiol* 46B:153–165
- Ackman RG, Epstein S, Kelleher M (1974) A comparison of lipids and fatty acids of the Ocean Quahog, *Arctica islandica*, from Nova Scotia and New Brunswick. *J Fish Res Board Can* 31:1803–1811
- Joseph JD (1982) Lipid composition of marine and estuarine invertebrates: Mollusca. *Prog Lipid Res* 21:109–153
- Thompson TE, Brown GH (1984) Biology of opisthobranch mollusks, vol 2. The Ray Society, London
- Gosliner TM (1994) Gastropoda: Opisthobranchia, Chap. 5, In: Harrison FW, Kohn AJ (eds) *Microscopic anatomy of invertebrates*, vol 5: Mollusca I. Wiley-Liss Inc., New York, pp 253–356
- Avila C (1995) Natural products of opisthobranch molluscs: a biological review. *Oceanogr Mar Biol* 33:487–559
- Wagele H, Ballesteros M, Avila C (2006) Defensive glandular structures in opisthobranch mollusks—from histology to ecology. *Oceanogr Mar Biol* 44:197–276
- Iken K, Avila C, Fontana A, Gavagnin M (2002) Chemical ecology and origin of defensive compounds in the Antarctic Nudibranch *Austrodoris kerguelensis* (Opisthobranchia: Gastropoda). *Mar Biol* 141:101–109
- Martinez-Pita I, Garcia F, Pita ML (2005) Fatty acid composition and utilization in developing eggs of some marine Nudibranchs (Mollusca: Gastropoda: Opisthobranchia) from southwest Spain. *J Shellfish Res* 24:1209–1216
- Bligh EG, Dyer WJ (1959) A rapid method of total lipid extraction and purification. *Can J Biochem Physiol* 37:911–918
- Svetashev VI, Vaskovsky VE (1972) A simple technique for thin-layer micro-chromatography of lipids. *J Chromatogr* 67:376–378
- Vaskovsky VE, Kostetsky EY, Vasendin IM (1975) A universal reagent for phospholipids analysis. *J Chromatogr* 114:129–142
- Carreau JP, Dubacq JP (1979) Adaptation of the macroscale method to the micro-scale for fatty acid methyl transesterification of biological lipid extracts. *J Chromatogr* 151:384–390
- Anderson BA (1978) Mass spectrometry of fatty acid pyrrolidides. *Prog Chem Fats other Lipids* 16:279–308
- Nelson MM, Phleger CF, Mooney BD, Nichols PD (2000) Lipids of gelatinous Antarctic zooplankton: Cnidaria and Ctenophora. *Lipids* 35:551–559
- Gannefors C, Boer M, Kattner G, Graeve M, Eiane K, Gulliksen B, Hop H, Falk-Petersen S (2005) The Arctic sea butterfly *Limacina helicina*: lipids and life strategy. *Mar Biol* 147:169–177
- Kattner G, Hagen W, Graeve M, Albers C (1998) Exceptional lipids and fatty acids in the pteropod *Clione limacine* (Gastropoda) from both polar oceans. *Mar Chem* 61:219–228
- Dembitsky VM, Kashin AG, Stefanov K (1992) Comparative investigation of phospholipids and fatty acids of freshwater mollusks from the Volga River Basin. *Comp Biochem Physiol* 102B:193–198
- Kraffe E, Sounant P, Marty A (2004) Fatty acids of Serine, ethanolamine, and choline plasmalogens in some marine bivalves. *Lipids* 39:59–66
- Paradis M, Ackman RG (1975) Occurrence and chemical structure of nonmethylene-interrupted dienoic fatty acids in American oyster *Crassostrea virginica*. *Lipids* 10:12–16
- Morales RW, Litchfield C (1976) Unusual C24, C25, C26 and C27 polyunsaturated fatty acids of the marine sponge *Microciona prolifera*. *Biochim Biophys Acta* 431:206–216
- Bergquist PR, Lawson MP, Lavis A, Cambie RC (1984) Fatty acid composition and the classification of the Porifera. *Biochem Syst Ecol* 12:63–84
- Ackman RG (1983) Fatty acid metabolism of bivalves. In: Pruder GD, Langdon CJ, Conklin DE (eds) *Biochemical and physiological approaches to shellfish nutrition. Proceedings of the second international conference on aquaculture nutrition*. Baton Rouge
- Sargent JR, Falk-Petersen IB, Calder AG (1983) Fatty acid composition of neutral glycerides from the ovaries of the asteroids *Ctenodiscus criptus*, *Asterias lincki* and *Pteraster militaris* from Balsfjorden, Northern Norway. *Mar Biol* 72:257–264
- Carballeira NM, Shalabi F, Stefanov K, Dimitrov K, Popov S, Kujumgiev A, Andreev S (1995) Comparison of the fatty acids of the tunicate *Botryllus schlosseri* from the Black Sea with two associated bacterial strains. *Lipids* 30:677–679
- Zhukova NV (1986) Biosynthesis of non-methylene-interrupted dienoic fatty acids from [<sup>14</sup>C] acetate in molluscs. *Biochim Biophys Acta* 878:131–133
- Zhukova NV (1991) The pathway of the biosynthesis of non-methylene-interrupted dienoic fatty acids in molluscs. *Comp Biochem Physiol* 100B:801–804
- Klingensmith JS (1982) Distribution of methylene and non-methylene-interrupted dienoic fatty acids in polar lipids and triacylglycerol of selected tissues of the hard shell clam (*Mercenaria mercenaria*). *Lipids* 17:976–981
- Carballeira NM, Miranda C, Rodriguez AD (2002) Phospholipid fatty acid composition of *Gorgonia mariae* and *Gorgonia ventalina*. *Comp Biochem Physiol* 131B:83–87